SPIE. OPTICS + PHOTONICS

CONNECTING MINDS.
ADVANCING LIGHT.

2017 TECHNICAL SUMMARIES.

WWW.SPIE.ORG/OP

Conferences & Courses
6–10 August 2017

Exhibition
8–10 August 2017

San Diego Convention Center
San Diego, California, USA

CONTENTS

NanoScience + Engineering

Symposium Chairs

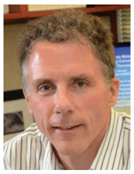

Harry A. Atwater,
California Institute of Technology (USA)

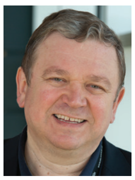

Nikolay I. Zheludev,
Univ. of Southampton (United Kingdom) and Nanyang Technological Univ. (Singapore)

Co-chairs:

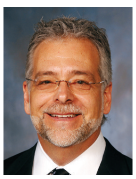

James G. Grote,
Air Force Research Lab. (USA)

David L. Andrews,
Univ. of East Anglia (United Kingdom)

Organic Photonics + Electronics

Symposium Chairs

Zakya H. Kafafi,
National Science Foundation, ret (USA)

Ifor D. W. Samuel,
Univ. of St. Andrews (United Kingdom)

Click on the Conference Title to be sent to that page

NanoScience + Engineering

Organic Photonics + Electronics

Optical Engineering + Applications

Return to Contents

10343-1, Session 1

Real and imaginary properties of epsilon-near-zero materials *(Invited Paper)*

Mark I. Stockman, Georgia State Univ. (United States)

From the fundamental principle of causality we show that epsilon-near-zero (ENZ) materials with very low (asymptotically zero) intrinsic dielectric loss do necessarily possess a very low (asymptotically zero) group velocity of electromagnetic wave propagation. This leads to the loss function being singular and causes high non-radiative damping of optical resonators and emitters (plasmonic nanoparticles, quantum dots, chromophore molecules) embedded into them or placed at their surfaces. Rough ENZ surfaces do not exhibit hot spots of local fields suggesting that surface modes are overdamped. Reflectors and waveguides also show very large losses both for realistic and idealized ENZ.

1. Introduction

Recently, materials at frequencies close to the bulk plasmon frequency, which are characterized by dielectric permittivity being small enough, and are usually referred to as Epsilon Near Zero (ENZ) materials, have attracted a great deal of attention, see, e.g., [1-3].

Their optical properties are expected to be quite remarkable: ENZ should totally reflect light at all angles, the phase velocity of light tends to infinity and, correspondingly, the light wave carries almost constant phase, the density of photonic states diverges at, a waveguide formed inside an ENZ material can confine light at deep sub-wavelength dimensions, there is no reflections even at sharp bands, and the unavoidable roughness of the waveguide walls does not significantly spoil the wave-guiding. As in many other cases in nanooptics cite[4], dielectric losses present a significant problem deteriorating these unique properties and limiting useful applications of ENZ materials.

2. Results

Following Ref. [5], we show that the fundamental principle of causality [as given by dictates that any ENZ material with a very low (asymptotically zero) loss at the observation frequency has necessarily asymptotically zero group velocity at that frequency. Physically, this leads to enhanced scattering and dissipative losses as given by the diverging energy-loss function. Paradoxically, a reduction of the intrinsic loss, leads to an increase of energy-loss function and further deterioration of performance of reflectors and waveguides built from ENZ materials. Both analytically and numerically we have shown that a realistic ENZ material ITO at the bulk plasma frequency causes high reflection and propagation losses. The singular loss function is also responsible for anomalously strong optical damping of resonant systems (plasmonic nanoparticles, dye molecules, quantum dots, etc.) embedded into or positioned at the surfaces of ENZ materials. In contrast to plasmonic metals, there are no pronounced hot spots of local fields at rough ENZ surfaces. Structured dielectric media with practically zero loss in the optical region cannot function as true ENZ materials because of the singular response; they necessarily are diffractive photonic crystals, and not refractive effective media. Obviously, this anomalous loss of ENZ materials can be gainfully used in energy absorbers, which begets analogy with heating of plasmas at plasma frequency with charged particles or electromagnetic waves. These losses and singularities are fundamental, local properties of the ENZ media, which cannot be eliminated by micro- or nano-structuring.

4. References

1. N. Engheta, Pursuing near-Zero Response, Science 340, 286-287 (2013).

2. R. Marques, J. Martel, F. Mesa, and F. Medina, Left-Handed-Media Simulation and Transmission of Em Waves in Subwavelength Split-Ring-Resonator-Loaded Metallic Waveguides, Phys. Rev. Lett. 89, 183901-1-4 (2002).

3. M. Silveirinha and N. Engheta, Tunneling of Electromagnetic Energy through Subwavelength Channels and Bends Using Epsilon-near-Zero Materials, Phys. Rev. Lett. 97, 157403 (2006).

4. M. I. Stockman, Nanoplasmonics: Past, Present, and Glimpse into Future, Opt. Express 19, 22029-22106 (2011).

5. M. H. Javani and M. I. Stockman, Real and Imaginary Properties of Epsilon-near-Zero Materials, Phys. Rev. Lett. 117, 107404-1-6 (2016).

10343-2, Session 1

Universal spin-momentum locking of light *(Invited Paper)*

Todd Van Mechelen, Farid Kalhor, Ward D. Newman, Zubin Jacob, Purdue Univ. (United States)

We show the existence of an inherent property of evanescent electromagnetic waves: spin-momentum locking, where the direction of momentum fundamentally locks the polarization of the wave. We trace the ultimate origin of this phenomenon to complex dispersion and causality requirements on evanescent waves. We demonstrate that every case of evanescent waves in total internal reflection, surface states and optical fibers/waveguides possesses this intrinsic spin-momentum locking. We also introduce a universal right-handed triplet consisting of momentum, decay and spin for evanescent waves. We derive the Stokes parameters for evanescent waves which reveal an intriguing result - every fast decaying evanescent wave is inherently circularly polarized with its handedness tied to the direction of propagation. We also show the existence of a fundamental angle associated with total internal reflection (TIR) such that propagating waves locally inherit perfect circular polarized characteristics from the evanescent wave. This circular TIR condition occurs if and only if the ratio of permittivities of the two dielectric media exceeds the golden ratio. Our work leads to a unified understanding of this spin-momentum locking in various nanophotonic experiments and sheds light on the electromagnetic analogy with the quantum spin hall state for electrons.

10343-3, Session 1

High order plasmonic resonances in time-varying media *(Invited Paper)*

Alessandro Salandrino, E. Alexander Ramos, The Univ. of Kansas (United States)

The optical response of noble-metal nanoparticles in the visible spectrum is characterized by the presence localized surface plasmon resonances. Localized surface plasmons are non-propagating coherent oscillations of free-carriers coupled to the electromagnetic field arising as a consequence of confinement effects in sub-wavelength nanoparticles. Plasmonic nanoparticles in general support an infinite discrete set of orthogonal localized surface plasmon modes, yet in the case of structures of deep-subwavelength dimensions only the lowest order resonances of dipolar nature can be effectively excited by an incident electromagnetic wave. By reciprocity such high-order modes tend to be subradiant and therefore difficult to observe in far-field.

Here we discuss the novel localized surface plasmon dynamics that emerge when the electromagnetic properties of the plasmonic particle or of the background medium vary in time. We show in particular that such temporal permittivity variations lift the orthogonality of the localized surface plasmon modes and introduce coupling among different angular momentum states. Exploiting such dynamics we show how surface plasmon amplification of high order resonances can be achieved under the action of a spatially uniform optical pump of appropriate frequency. In addition we discuss the signature of the excitation of these high-order surface plasmon resonances in the temporal profile of the pump field. Possible implementations and potential applications are also presented, as well as extensions to other physical systems.

10343-4, Session 1

Index retrieval of finite thickness fishnet metamaterials tracking the phase accumulation

Eyal Feigenbaum, Anna M. Hiszpanski, Lawrence Livermore National Lab. (United States)

Currently used methods for effective index retrieval of a metamaterial (MM) are based on calculating the transmission and reflection of a MM slab. This 'black-box approach' leads to an uncertainty as to the number of cycles that have passed and as a result to a multi-branch uncertainty in the real part value of the effective index. Multiple approaches have been proposed to determine the correct branch. However, the validity of these existing methods is limited with respect to some currently studied MM implementations, e.g.: MM with a small number of layers; MM where the light transmission decreases with increasing optical wavelength (e.g., fishnet MM (FMM), especially for the negative index domain). Here we propose to depart from the 'black-box' retrieval approach and track the phase accumulation through the structure to avoid the multi-branch uncertainty. This approach is possible for structures where the energy flow through the structure is predominantly carried across the slab by only a single propagation mode, as in the case of the FMM, and other resonant guided waves networks (RGWNs). The algorithm is implemented based on FDTD and validated. It provides a look into the phase accumulation inside the structure, showing that the negative index is a net effect of positive and dominating negative phase accumulation at the metal and dielectric layers, accordingly. The details of the algorithm, as well as the newly revealed underlying physics would be further discussed.

This work was performed under the auspices of the U.S. Department of Energy by Lawrence Livermore National Laboratory under Contract DE-AC52-07NA27344. LLNL-ABS-718700.

10343-5, Session 1

Dynamic properties of large light filament arrays for complex photonic meta-structures in air

Wiktor T. Walasik, Univ. at Buffalo (United States); Shermineh Rostami, Daniel Kepler, CREOL, The College of Optics and Photonics, Univ. of Central Florida (United States); Matthieu Baudelet, CREOL, The College of Optics and Photonics, Univ. of Central Florida (United States) and Univ. of Central Florida (United States); Martin C. Richardson, CREOL, The College of Optics and Photonics, Univ. of Central Florida (United States); Natalia M. Litchinitser, Univ. at Buffalo (United States)

High-power femtosecond filaments—laser-light beams capable of kilometer-long propagation—attract interest of nonlinear-optics community due to their numerous applications in remote sensing, lightning protection, virtual antennas, and waveguiding. Specific arrangements of filaments, into waveguides or hyperbolic metamaterials, allow for efficient control and guiding of electromagnetic radiation, radar-beam manipulation, and resolution enhancement. These applications require spatially uniform distribution of densely packed filaments.

In order to address this challenge, we investigate the dynamic properties of large rectangular filament arrays propagating in air depending on four parameters: the phase difference between the neighboring beams, the size of the array, separation between the beams, and excitation power. We demonstrate that, as a result of the mutual interaction between the filaments, the arrays where the nearest neighbor beams are out-of-phase are more robust than the arrays with all the beams in phase.

Our analysis of the array stability reveals that there exist certain trade-offs between the stability of a single filament and the stability of the entire array. We show that in the design of the experiment, the input parameters have to be chosen in such a way that they ensure a sufficiently high filling fraction, but caution has to be used in order not to compromise the overall array stability.

In addition, we show the possibility of filament formation by combining multiple beams with energies below the filamentation threshold. This approach offers additional control over filament formation and allows one to avoid the surface damage of external optics used for filamentation.

10343-6, Session 2

Meoscopic optics of two-dimensional random media *(Invited Paper)*

Hui Cao, Yale Univ. (United States)

In disordered media there are many fascinating counter-intuitive effects resulting from interferences of multiply scattered waves. One of them is the creation of transmission eigenchannels which can be broadly classified as open and closed. In general, the penetration depth and energy density distribution of multiply scattered waves inside a disordered medium are determined by the spatial profiles of the transmission eigenchannels that are excited by the incident light. The distinct spatial profiles of open and closed channels suggest that selective coupling of incident light to these channels enables an effective control of total transmission and energy distribution inside the random medium. Since the energy density determines the light-matter interactions inside a scattering system, manipulating its spatial distribution opens the door to tailoring optical excitations as well as linear and nonlinear optical processes such as absorption, emission, amplification, and frequency mixing inside turbid media.

We demonstrate experimentally an efficient control of light intensity distribution inside a random scattering system. The adaptive wavefront shaping technique is applied to a silicon waveguide containing scattering nanostructures, and the on-chip coupling scheme enables access to all input spatial modes. By selectively coupling the incident light to open or closed channels of the disordered system, we not only vary the total energy stored inside the system by 7.4 times, but also change the energy density distribution from an exponential decay to a linear decay and to a profile peaked near the center. This work provides an on-chip platform for controlling light-matter interactions in turbid media.

10343-7, Session 2

Space-time super-resolution imaging *(Invited Paper)*

Evgenii E. Narimanov, Andrei Rogov, Purdue Univ. (United States)

We present a new approach to super-resolution imaging, that allows to offset the performance loss due to material absorption by engineering the profile of the light source waveform.

10343-8, Session 2

Laser scanning using spatiotemporal beam dynamics in metasurfaces

Amr M. Shaltout, Konstantinos Lagoudakis, Soo Jin Kim, Jelena Vuckovic, Stanford Univ. (United States); Vladimir M. Shalaev, Purdue Univ. (United States); Mark L. Brongersma, Stanford Univ. (United States)

Laser scanning through controlled deflection of beam is a key element in various applications including 3D printing, rapid prototyping, LIDAR, autonomous vehicles, and imaging applications. Typical laser scanners require the utilization of a rotating mirror, or optical phased-array using electro-optic modulators which provides faster scanning speed (scanning

time ~microseconds). Current efforts are also taking place to implement metasurface based ultra-compact laser scanners using tunable nano-antennas exhibiting voltage-controlled free carrier modulation. This would dramatically reduce the size of the device keeping the speed of operation limited by the electronic control signal bandwidth as previous phased-array technologies.

To further enhance the scanning time, we present a novel methodology of beam steering based on light-matter interaction between metasurfaces and mode-locked lasers with a frequency-comb spectrum (i.e., equally-spaced phased-locked frequency lines). Over the past few years, metasurfaces interacting with CW lasers were successfully used to engineer far-field optical patterns through coherent interference of light scattered from an array of nano-antennas. Nevertheless, dynamic patterns can be generated if CW laser is replaced with a frequency-comb source. In this case, we demonstrate that coherent interference of light in the far-field is a 4D space-time process. A metasurface is thoughtfully designed to produce a constructively interfered laser beam at a narrow angle in the far-field leading to directivity of the beam. The temporal interference of phase-locked frequency comb causes the direction of the constructed beam to be at a time-dependent rotating angle, leading to laser scanning of ~90-deg angle-of-view over ~100ps time interval.

10343-9, Session 2

Removing material singularities in Schwarz-Christoffel coordinate transformations

Sophie Viaene, Vrije Univ. Brussel (Belgium) and Chalmers Univ. of Technology (Sweden); Vincent Ginis, Jan Danckaert, Vrije Univ. Brussel (Belgium); Philippe Tassin, Chalmers Univ. of Technology (Sweden)

Transformation optics has led to the design of impressive photonic devices that reproduce the desired effects of coordinate transformations by making use of tailored material properties. Unfortunately, these material properties are often required to take on extreme values which are difficult to implement without compromising the performance of the device. This is especially true for coordinate transformations that rely on singularities, such as those leading to invisibility cloaks and beam splitters. Previous work has shown that the detrimental effects due to material singularities may be mitigated by adding anisotropy to the initial design. However, this technique cannot be applied to devices that crucially rely on isotropy and symmetry, as is the case for our metamaterial slab waveguides that implement two-dimensional coordinate transformations of guided modes. Therefore, we mitigate the detrimental effects due to isolated singularities in an isotropic way. First, we systematically study the effect of isolated singularities, representing each of them as a local power map that induces vanishing or infinite material parameters. Second, we propose a beam splitter design consisting of a collection of local power maps, also known as a Schwarz-Christoffel coordinate transformation. By making use of full-wave numerical simulations, we show that the strategic replacement of singular power maps with analytic curve-factors allows for the removal of optical singularities without affecting the functionality of the design. The resulting waveguide devices have no need of extreme material properties to efficiently manipulate guided waves.

10343-10, Session 2

Experimental validation of tunable features in laser-induced plasma metamaterials

Roberto A. Colon Quinones, Mark A. Cappelli, Stanford Univ. (United States)

Measurements are presented which validate the use of gaseous plasma metasurfaces (MTS) as highly tunable reflectors. The plasma MTS considered here is an n x n array of laser produced plasma kernels generated by focusing the fundamental output from a 2 J/p Q-switched Nd:YAG laser through a multi-lens array (MLA) and into a gas of varying pressure. The tunability of these surfaces stems from the dispersive nature of plasmas arising from their variable electron density and electron momentum transfer collision frequency, and the concommitant effect on their Mie scattering resonance. Experiments were carried out in the low GHz regime to characterize the impedance or reflectivity of these surfaces for different values of electron density and collision frequency. The results of these experiments are compared to Mie scattering and effective-medium theory, and with finite element method (FEM) electromagnetic simulations to account for finite array dimensions.

10343-11, Session 3

Widely tunable semiconductor antennas for reconfigurable metasurfaces *(Invited Paper)*

Jon A. Schuller, Univ. of California, Santa Barbara (United States)

The ability to engineer the optical phase at subwavelength dimensions has led to metasurfaces that provide unprecedented control of electromagnetic waves. To reach their ultimate potential, metasurfaces must incorporate reconfigurable functions. The central challenge is achieving large tunability in subwavelength elements. Here, we describe two different approaches for achieving order-unity refractive index shifts: free-carrier refraction and thermo-optic tuning. We experimentally demonstrate wide tuning of single-particle infrared Mie resonances through doping, and demonstrate simulations of electrically reconfigurable III-V heterojunction metasurfaces based on these effects. We conclude with recent experimental demonstrations of dyamic, ultrawide tuning of Mie resonators based on two distinct thermo-optic effects: 1) modifying the electron mass and carrier density in InSb and 2) exploiting the anomalous temperature-dependent bandgap of PbTe.

10343-12, Session 3

All-dielectric photonic topological metamaterials and metasurfaces *(Invited Paper)*

Alexander B. Khanikaev, The City College of New York (United States)

The past few years have witnessed the discovery of photonic topological insulators, which transformed our views on propagation and scattering of electromagnetic waves. Here we show that judiciously designed all-dielectric photonic metamaterials and metasurfaces can exhibit a topological photonic state. The bianisotropy of the metamaterial is shown to result in emergence of a topological photonic band gap in the bulk and photonic states guided by edges and interfaces which appear to be one-way spin-polarized and immune to sharp bending. Experimental realizations of photonic topological metamaterials and metasurfaces for microwave and optical domains are used to test and confirm the topological properties.

10343-13, Session 3

Light concentration in subwavelength volume by dielectric transducer and local sensing of plasmonic systems

Andrey Karlovich Sarychev, Institute for Theoretical and Applied Electrodynamics (Russian Federation); Sergey Vergeles, L.D. Landau Institute for Theoretical Physics (Russian Federation) and Moscow Institute of Physics and Technology (Russian Federation); Gennady Tartakovsky, Advanced Systems and Technologies, Inc. (United States)

The main achievement of the modern plasmonics is the concentration of light into nanospots that are much smaller than the wavelength. Nanospot concentration is beneficial for various applications: biomedical imaging and sensing, optical microscopy with single-molecule resolution, heat assisted magnetic recording (HAMR), QED studies, nanolasing, etc. Until now, plasmonic metal nanoantennae, sub-wavelength apertures or metallic near field concentrators (NFCs) are used for this purpose. The main advantage of the metal NFC is their capabilities to localize plasmonic modes, which can be excited by the incident transverse em wave. However, the metal NFCs have large optic loss so we propose a novel all-dielectric NFC, which allows focusing the light into a sub-wavelength hot nanospot, without the dissipative loss. The detrimental dephasing and thermal effects almost vanishes in the dielectric NFC opening new opportunities in the magnetic recording and quantum plasmonics. The ability to concentrate light is important not only to fundamental physics studies, but also to practical device applications. For example, microcavities can force the atoms or quantum dots to emit spontaneous photons in a desired direction or can provide an environment, where dissipative mechanisms such as spontaneous emission are overcome. The electric field is much enhanced in the proposed new device at the vertex of the dielectric beak, which is attached to the tablet dielectric resonator. The resonator in turn is pumped through the plane waveguide. The electric field is enhanced due to longitudinal polarization of the beak vertex, which is excited by em field of the pumped resonator.

10343-14, Session 3

High-Q resonances with low azimuthal indices in all-dielectric high-index nanoparticles

Kirill Koshelev, ITMO Univ. (Russian Federation) and The Academic Univ. (Russian Federation); Andrey A. Bogdanov, Zarina Sadrieva, ITMO Univ. (Russian Federation); Kirill B. Samusev, Mikhail V. Rybin, Mikhail F. Limonov, Ioffe Institute (Russian Federation); Yuri S. Kivshar, The Australian National Univ. (Australia)

Resent progress in all-dielectric nanophotonics opens many opportunities for the enhanced resonant phenomena with applications in nanophotonics [1]. However, usually dielectric resonators demonstrate low values of the quality factor (Q-factor) and low efficiencies of the Purcell effect for Mie-type resonant modes [2]. Here we report on a novel approach to achieve high-Q optical resonators based on all-dielectric high-index nanoparticles. We demonstrate that high-quality states could be formed through a mechanism of the hybridization of Mie resonances with low azimuthal indices (0, 1) leading to the substantial suppression of far-field radiation and high Q features of the resonators. This mechanism is somewhat related to the concept of bound states in the continuum [3] demonstrated recent for some optical structures.

We analyse the Q-factors of all-dielectric high–index resonators in two ways: (i) as a ratio of real and imaginary parts of complex eigenfrequencies [4], and (ii) by fitting the Fano type resonance in the numerical simulation of the scattering problem. Both methods give consistent results. We predict that for the ceramic resonators with permittivity 40, the Q-factor of the mode with a low azimuthal index could reach 5000.

10343-15, Session 3

Metasurface axicon lens design at visible wavelengths

Saleimah Alyammahi, Qiwen Zhan, Univ. of Dayton (United States)

The emerging field of metasurfaces is promising to realize novel optical devices with miniaturized flat format and added functionalities. Metasurfaces have been demonstrated to exhibit full control of amplitude, phase and polarization of electromagnetic waves. Using the metasurface, the wavefront of light can be manipulated permitting new functionalities such as focusing and steering of the beams and imaging. One optical component which can be designed using metasurfaces is the axicon. Axicons are conical lenses used to convert Gaussian beams into non-diffraction Bessel beams. These unique devices are utilized in different applications ranging from optical trapping and manipulation, medical imaging, and surgery. In this work, we study axicon lens design comprising of planar metasurfaces which generate non-diffracting Bessel beams at visible wavelengths. Dielectric metasurfaces have been used to achieve high efficiency and low optical loss. We measured the spot size of the resulted beams at different planes to demonstrate the non-diffraction properties of the resulted beams. We also investigated how the spot size is influenced by the axicon aperture. Furthermore, we examined the achromatic properties of the designed axicon. Comparing with the conventional lens, the metasurface axicon lens design enables the creation of flat optical device with wide range of depth of focus along its optical axis.

10343-16, Session 4

Nonlinear frequency conversion with all-dielectric nanoantennas *(Invited Paper)*

Dragomir N. Neshev, Sergey S. Kruk, Mohsen Rahmani, Maria del Rocio Camacho-Morales, Lei Wang, Lei Xu, Daria A. Smirnova, Alexander S. Solntsev, Yuri S. Kivshar, The Australian National Univ. (Australia)

Dielectric nanoantennas and metasurfaces have proven to be able to manipulate the wavefront of incoming waves with high transmission efficiency. The important next question is: Can they enable enhanced interaction with the light to transform its colour or to be able to control one light beam with another? Here we show how a dielectric nano-resonator of subwavelength size can enable enhanced light matter interaction for efficient nonlinear frequency conversion. In particular, we show how AlGaAs or silicon nanoantennas can enhance second and third harmonic generation, respectively. Importantly, by controlling the size of the antennas, we can achieve control of directionality and polarisation state of the emission of harmonics. Our results open novel applications in ultra-thin light sources, light switches and modulators, ultra-fast displays, and other nonlinear optical metadevices based on low loss subwavelength dielectric resonant nanoparticles.

10343-17, Session 4

Active and tunable Mie-resonant semiconductor metasurfaces *(Invited Paper)*

Isabelle Staude, Friedrich-Schiller-Univ. Jena (Germany)

Nanoparticles composed of high refractive index semiconductors can support electric and magnetic multipolar Mie-type resonances that can be tuned by the nanoresonator design [1]. Furthermore, such semiconductor nanoresonators can exhibit very low absorption losses at optical frequencies. Based on these properties, semiconductor nanoresonators represent versatile building blocks of functional photonic nanostructures with tailored optical response.

This talk will review our recent advances in controlling the generation and propagation of light with metasurfaces composed of high-index semiconductor nanoresonators. Such metasurfaces can impose a spatially variant phase shift onto an incident light field, thereby providing control over its wave front with high transmittance efficiency [2]. However, there are two important limitations: most semiconductor metasurfaces realized so far are passive, and their optical response is permanently encoded into the structure during fabrication. This talk will concentrate on strategies to integrate emitters into the metasurfaces and to obtain dynamic control of the metasurface optical response.

In particular, two approaches for active tuning of the metasurface response will be discussed, namely integration of the metasurface into a nematic-liquid-crystal cell [3] and ultrafast all-optical tuning based on the nonlinear optical response of the constituent semiconductor materials. Furthermore, I will show that Mie-resonant semiconductor metasurfaces allow for spatial and spectral tailoring of spontaneous emission from various types of emitters.

[1] M. Decker & I. Staude, J. Opt. 18, 103001 (2016).

[2] K. E. Chong et al., Nano Lett. 15, 5369–5374 (2015).

[3] J. Sautter et al., ACS Nano 9, 4308–4315 (2015).

10343-18, Session 4

Directional second harmonic generation from AlGaAs nanoantennas

Maria del Rocio Camacho Morales, Mohsen Rahmani, Sergey S. Kruk, Lei Wang, The Australian National Univ. (Australia); Lei Xu, The Australian National Univ. (Australia) and Nankai Univ. (China); Daria A. Smirnova, Alexander S. Solntsev, Andrey E. Miroshnichenko, Hark Hoe Tan, Fouad Karouta, Shagufta Naureen, Kaushal D. Vora, The Australian National Univ. (Australia); Luca Carletti, Costantino De Angelis, Chennupati Jagadish, Univ. degli Studi di Brescia (Italy); Yuri S. Kivshar, Dragomir N. Neshev, The Australian National Univ. (Australia)

Optical nanoantennas possess great potential for controlling the spatial distribution of light in the linear regime as well as for frequency conversion of the incoming light in the nonlinear regime. However, the usually used plasmonic nanostructures are highly restricted by Ohmic losses and heat resistance. Dielectric nanoparticles like silicon and germanium can overcome these constrains [1,2], however second harmonic signal cannot be generated in these materials due to their centrosymmetric nature. GaAs-based III-V semiconductors, with non-centrosymmetric crystallinity, can produce second harmonic generation (SHG) [3]. Unfortunately, generating and studying SHG by AlGaAs nanocrystals in both backward and forward directions is very challenging due to difficulties to fabricate III-V semiconductors on low-refractive index substrate, like glass. Here, for the first time to our knowledge, we designed and fabricated AlGaAs nanoantennas on a glass substrate. This novel design allows the excitation, control and detection of backwards and forwards SHG nonlinear signals. Different complex spatial distribution in the SHG signal, including radial and azimuthal polarization originated from the excitation of electric and magnetic multipoles were observed. We have demonstrated an unprecedented SHG conversion efficiency of 10-4; a breakthrough that can open new opportunities for enhancing the performance of light emission and sensing [4].

References

[1] A. S. Shorokhov et al. Nano Letters 16, 4857 (2016).

[2] G. Grinblat et al. Nano Letters 16, 4635 (2016).

[3] S. Liu et al. Nano Letters 16, 7191 (2016).

[4] R. Camacho et al. Nano Lett. 16, 7191 (2016).

10343-19, Session 4

Characterization of Si-disk magnetic nanoprobe by photoinduced force microscopy

Jinwei Zeng, Mohsen Rajaei, Mahsa Darvish, Mohammad Albooyeh, Brian Albee, Hemantha K. Wickramasinghe, Eric O. Potma, Filippo Capolino, Univ. of California, Irvine (United States)

Due to the weak magnetic responsibility of natural existing materials at optical frequency, optical magnetism remains a “dark state” of light which is largely unexplored. However, optical magnetism is also very desirable because of the many splendid possibilities it may lead to, including ultra-compact opto-magnetic storage devices, high speed magnetic imaging, magnetic tweezers etc. Here we design a Si nano-disk structure as the magnetic nanoprobe which supports magnetic resonance in visible range with the incident azimuthally polarized beam (APB). APB features a donut shape beam profile, with a strong longitudinal magnetic field and a vanishing electric field at the beam axis. Therefore, on the magnetic resonance while the probe is aligned to the APB axis, a longitudinal magnetic dipole is excited in the probe, and interacts with the incident APB inducing an exclusive magnetic force. Making such magnetic nanoprobe under APB illumination serves as an important first step to realize the proposed photoinduced magnetic force microscopy (PIMFM), which selectively exploits the interaction between matter and the magnetic field of light to characterize the optical magnetism in nanoscale. Such investigation of the optical magnetism in samples is dearly needed in many mechanical, chemical, and life-science applications.

10343-20, Session 4

Dynamically tunable topologically protected edge-states in silicon photonic crystals with liquid crystal background

Mikhail I. Shalaev, Wiktor T. Walasik, Sameerah Desnavi, Natalia M. Litchinitser, Univ. at Buffalo (United States)

Topological insulators are materials that conduct on the surface and insulate in its interior, while having non-trivial topological order. Remarkably, the edge states on the surface between topological (non-trivial) and conventional (trivial) materials are topologically protected from scattering on structural defects and disorders. First, these materials were theoretically predicted and then experimentally demonstrated in the field of electronics. However, most of the electronic materials exhibit topological properties only at very low temperatures.

Recently, it was shown that very similar topologically protected materials can be made in bosonic systems using photonic crystals. In conventional photonic crystals, imperfections, structural disorders, and surface roughness often lead to significant losses. To solve this problem, topologically protected photonic crystals might be used. At the same time, it is highly desirable to be able to control light propagation on optical chip. One way to facilitate such dynamic control is to use liquid crystals. Liquid crystals allow one to modify the refractive index with external electric field.

Here, we demonstrate dynamic control of topologically protected edge states by modifying refractive index of liquid crystal background media. Background index is changing depending on orientation of liquid crystal while preserving the topological order of the system. As a result of changing the refractive index, the spectral position of photonic bandgap and edge states change as well. Proposed concept might be implemented using conventional semiconductor technology and can be used for highly robust photonic energy transport in optical communication systems.

10343-21, Session 5

Polariton lasing in organic semiconductor microcavities *(Invited Paper)*

David G. Lidzey, The Univ. of Sheffield (United Kingdom)

A semiconductor-microcavity is an optical structure composed of two mirrors separated by a layer of semiconducting material. If the energy of the confined photon and excitonic transition are degenerate, interactions can occur in the strong-coupling regime, with the eigenstates of the system being cavity polaritons (a coherent superposition between light and matter).

Due to their bosonic nature, cavity polaritons are able to undergo condensation to a macroscopically occupied coherent state. Polariton condensates can be optically pumped and then undergo decay by emitting coherent light, very much like an optically pumped laser. Here, we demonstrate evidence of polariton condensation in a microcavity containing a dispersed molecular dye.

Our structures are based on two dielectric-mirrors placed either side of a film of the transparent matrix polymer polystyrene containing the fluorescent molecular dye BODIPY-Br. We first show using CW photoluminescence measurements that weakly-coupled excimer-like states in the BODIPY-Br, together with emission from the (0,1) vibrational transition are responsible for optically pumping polariton states along the lower polariton branch.

We then explore the non-linear emission from control thin-films and cavities using pulsed laser excitation. We obtain strong evidence of non-linear photoluminescence with increasing excitation density, associated with a six-fold linewidth narrowing and a continuous blue-shift attributed to polariton interactions with other polaritons and the exciton reservoir. We believe that there is a large number of molecular dyes that could dispersed into a polymer matrix allowing polariton condensation to be realised at wavelengths spanning the entire visible and near infrared.

10343-22, Session 5

Control of vibration-cavity polaritons in the frequency domain *(Invited Paper)*

Blake S. Simpkins, Kenan P. Fears, Adam Dunkelberger, U.S. Naval Research Lab. (United States); Wonmi Ahn, National Research Council (United States); Walter J. Dressick, Igor Vurgaftman, Jeffrey C. Owrutsky, U.S. Naval Research Lab. (United States)

We will focus on approaches which make use of light-matter interactions to alter the chemical behavior of a target molecular species. This is done through cavity coupling to a molecular vibration. Coupling vibrational transitions to resonant optical modes creates vibrational polaritons shifted from the uncoupled molecular resonances and provides a convenient way to modify the energetics of molecular vibrations. This approach is a viable method to explore controlling chemical reactivity and energy relaxation. Here, we demonstrate frequency domain results for vibrational bands strongly coupled to optical cavities. We experimentally and numerically describe strong coupling between a Fabry-Pérot cavity and several molecular species (e.g., poly-methylmethacrylate, thiocyanate, hexamethyl diisocyanate). We investigate strong and weak coupling regimes through examination of cavities loaded with varying concentrations of a urethane monomer. Rabi splittings are in excellent agreement with an analytical description using no fitting parameters. We show that coupling strength is a function of molecule/cavity mode overlap by systematically altering the position of a molecular slab throughout a first order cavity with results agreeing well with analytical and transfer matrix predictions. Further, remote molecule-molecule interaction will be explored by placing discrete and separated molecular layers throughout a cavity. In addition to establishing that coupling to an optical cavity modifies the energy levels accessible to the coupled molecules, this work points out the possibility of systematic and predictive modification of the excited-state kinetics of vibration-cavity polariton systems. Opening the field of polaritonic coupling to vibrational species promises to be a rich arena amenable to a wide variety of infrared-active bonds that can be studied in steady state and dynamically.

10343-23, Session 5

Effect of strong coupling on the photodegradation of poly(3-hexylthiophene)

Vanessa N. Peters, Md. Omar Faruk, Norfolk State Univ. (United States); Rohan Alexander, Univ. of Michigan (United States) and Norfolk State Univ. (United States); D'Angelo A. Peters, Norfolk State Univ. (United States) and Purdue Univ. (United States); Mikhail A. Noginov, Norfolk State Univ. (United States)

The effect of strong coupling on a chemical reaction, photodegradation of poly-3-hexylthiophene (p3ht), has been studied in a resonant cavity. The Fabry-Perot silver cavity was made to be resonant with the strong absorption band of the p3ht polymer. In comparison to a reference sample, p3ht film deposited on glass, the p3ht film inside the resonant cavity showed significant reduction in the rate of photodegradation (at tungsten lamp illumination, after proper normalization to the absorbed light intensity). No such effect was observed at excitation with the UV-enhanced xenon lamp.

10343-24, Session 5

Directional spontaneous emission of dye on top of thin silver grating

Ekembu K. Tanyi, Soheila Mashhadi, Norfolk State Univ. (United States); Sahana Das Bhattacharyya, Tal Galfsky, Vinod M. Menon, The City College of New York (United States); Natalia Noginova, Norfolk State Univ. (United States); Viktor A. Podolskiy, Univ. of Massachusetts Lowell (United States); Mikhail A. Noginov, Norfolk State Univ. (United States)

We studied angular distribution of spontaneous emission of dye (R6G) embedded in the polymer (PMMA) spin-coated on top of a thin silver grating. We found that while the vertically polarized (TE) emission had a characteristic double-crescent pattern (with minimum of emission intensity in the normal direction), the horizontally polarized (TM) emission was confined to a narrow range of angles centered around the normal direction. The surface modes of the grating structure supporting out-coupled spontaneous emission have been studied in the angular reflectance experiments and COMSOL simulations. The correlation between the surface modes and the observed emission patterns will be discussed at the conference.

10343-25, Session 5

Vibrational energy relaxation of vibration-cavity polariton modes

Adam Dunkelberger, Kenan P. Fears, U.S. Naval Research Lab. (United States); Bryan T. Spann, National Institute of Standards and Technology (United States); Blake S. Simpkins, Jeffrey C. Owrutsky, U.S. Naval Research Lab. (United States)

Steady-state and transient infrared studies have been used to investigate coherent coupling between the vibrational modes of polymers, liquids, and solvated species and a Fabry-Perot optical cavity mode. The coupling is characterized in terms of the Rabi splitting that scales with the absorption strength of the vibrational band of the molecular species in the cavity. We use pump-probe infrared spectroscopy to identify how the vibrational energy relaxation of the mixed, cavity-vibration polarition states are modified compared to the vibrational bands for materials outside the cavity. For W(CO)¬6 in hexane, we observe so-called Rabi oscillations at early times due to quantum beating between the two polariton states. Transient infrared studies are used to observe excited-state absorption from both polariton modes and uncoupled reservoir modes. The polariton mode relaxes significantly more quickly than the uncoupled vibrational mode and the lifetime depends on the angle of incidence with respect to the IR pulses. The incoherent lifetime is also modified for anions (NCS-) in polymers. The experiments demonstrate that energy transfer and relaxation of molecular vibrational bands can be altered by coupling to optical cavities, which may be an avenue for controlling nonequilibrium excited state population and chemical reactivity.

10343-26, Session 5

Reconfigurable Mie resonators embedded in a tunable ENZ cavity

Prasad P. Iyer, Mihir Pendharkar, Chris J. Palmstrøm, Jon A. Schuller, Univ. of California, Santa Barbara (United States)

Reconfigurable Mie resonator metasurfaces may give rise to new classes of programmable optical devices. Large phase and amplitude modulations can be achieved with high-Q resonances that are tunable by at least one line-width. We experimentally demonstrate narrow linewidth, reconfigurable Mie resonators comprising undoped InSb wires embedded inside a highly doped InSb Epsilon-Near-Zero (ENZ) cavity. We demonstrate a Q-factor increase of 400% by embedding a high index resonator within, instead of atop, an ENZ substrate. Systematic studies of varying width resonators reveal significant differences in coupling to the ENZ media for TM and TE resonators. A large refractive index modulation (μn ≥1.5) is achieved with heating (80-575K), stemming from variations in the effective mass of free-carriers. Thermally tuning the ENZ wavelength of the cavity by >2μm (13-15.5μm) emables reconfigurable tuning by multiple line-widths. This ultra-wide thermal tunability of high-Q embedded resonators may enable new class of active metadevices in the mid-infrared wavelength regime.

10343-27, Session 6

Active tuning of surface-phonon polariton resonances *(Invited Paper)*

Adam Dunkelberger, Chase T. Ellis, Daniel Ratchford, Alexander J. Giles, U.S. Naval Research Lab. (United States); Mijin Kim, Sotera Defense Solutions, Inc. (United States); Chul Soo Kim, U.S. Naval Research Lab. (United States); Bryan T. Spann, National Institute of Standards and Technology (United States); Igor Vurgaftman, Joseph G. Tischler, Jeffrey C. Owrutsky, Joshua D. Caldwell, U.S. Naval Research Lab. (United States)

The infrared spectra of SiC and InP are dominated by highly reflective reststhralen bands that occur between the transverse and longitudinal optical phonons. Through the LOPC effect, free carriers shift the reststrahlen band to higher frequencies. We have previously shown that photoinjected carriers transiently and reversibly modify the infrared reflectivity of bulk SiC. Within the reststrahlen band, SiC and InP nanostructures can exhibit surface-phonon polariton resonances. Here we report, for the first time, active tuning of SiC and InP surface-phonon polariton resonances via carrier photoinjection, achieving better modulation depths than active tuning in plasmonic systems. In SiC, ultraviolet excitation with femtosecond laser pulses induces >10 cm-1 shifts in the transverse dipole resonance (width = 7 cm-1). Time-resolved infrared reflection spectroscopy reveals that the photoinduced shifts decay in tens of ps, depending on the initial carrier density. Our results suggest that spatial redistribution of photoexcited carriers dominates the time dependence of the active tuning. In InP, continuous-wave visible excitation produces qualitatively similar resonance shifts. Substrate heating appears to limit the extent of the active tuning in InP. This work lays the foundation for further studies of the physics of active tuning and optimization of the tuning for infrared nanophotonics applications.

10343-28, Session 6

Harnessing the metal-insulator transition for tunable metamaterials *(Invited Paper)*

Nicholas A. Charipar, Heungsoo Kim, U.S. Naval Research Lab. (United States); Nicholas Bingham, National Research Council (United States); Ryan Suess, Nova Research (United States); Kristin M. Charipar, U.S. Naval Research Lab. (United States); Scott A. Mathews, U.S. Naval Research Lab (United States); Raymond C. Y. Auyeung, Alberto Piqué, U.S. Naval Research Lab. (United States)

The control of light-matter interaction through the use of subwavelength structures known as metamaterials has facilitated the ability to control electromagnetic radiation in ways not previously achievable. A plethora of passive metamaterials as well as examples of active or tunable metamaterials have been realized in recent years. However, the development of tunable metamaterials is still met with challenges due to lack of materials choices. To this end, materials that exhibit a metal-insulator transition are being explored as the active element for future metamaterials because of their characteristic abrupt change in electrical conductivity across their phase transition. The fast switching times (?t < 100 fs) and a change in resistivity of four orders or more make vanadium dioxide (VO2) an ideal candidate for active metamaterials. It is known that the properties associated with thin film metal-insulator transition materials are strongly dependent on the growth conditions. For this work, we have studied how growth conditions (such as gas partial pressure) influence the metal-insulator transition in VO2 thin films made by pulsed laser deposition. In addition, strain engineering during the growth process has been investigated as a method to tune the metal-insulator transition temperature. Examples of both the optical and electrical transient dynamics facilitating the metal-insulator transition will be presented together with specific examples of thin film metamaterial devices.

10343-29, Session 6

Dynamic metasurfaces for the near to long-wave infrared *(Invited Paper)*

Jason G. Valentine, Zachary Coppens, Zhihua Zhu, Vanderbilt Univ. (United States); Philip G. Evans, Oak Ridge National Lab. (United States); Richard F. Haglund, Vanderbilt Univ. (United States)

I will first discuss simultaneous spatial and temporal control of a metamaterial that is activated with spatially patterned ultraviolet (UV) light. The use of an all-optical modulation approach allows us to transfer the complexity associated with pixel-level control to the illumination source or an intermediate masking layer. Doing this dramatically reduces the nanophotonic material fabrication complexity and when combined with a projection system can allow optical property control over large areas. Modulation is achieved through photocarrier doping of zinc oxide (ZnO) which increases optical losses in the metamaterial and causes a transition from low to high absorption. Importantly, the ZnO layer has a long photo-carrier lifetime allowing for modulation of the metamaterial with low power continuous wave illumination.

I will then discuss phase-change based dynamic metasurfaces. By minimizing the thermal mass of the vanadium dioxide phase-change material (PCM) and placing the PCM at the nexus of a bowtie field concentrator, we realize a highly efficient metadevice in a perfect-absorber configuration, which enables an experimental tunable range up to 360 nm, as well as modulation depth of 37% at the resonant wavelength. Instead of complex optical pump-probe triggering or bulky temperature control stage, this tunable device uses the optical antennas as integrated heating elements leading to fast temporal and spatial management. This device could be a competitive candidate for signal processing, memory units, security recognition, holography and imaging.

10343-30, Session 6

Controlling metasurfaces on demand *(Invited Paper)*

Jonathan Bar David, Jacob Engelberg, Liron Stern, Noa Mazurski, Uriel Levy, The Hebrew Univ. of Jerusalem (Israel)

In this talk we demonstrate a variety of dielectric metasurfaces and show mechanisms for controlling their transfer function. We also discuss their spectral properties

10343-31, Session 7

Optoelectronic device applications of metafilms *(Invited Paper)*

Mark L. Brongersma, Geballe Lab. for Advanced Materials (GLAM) (United States)

Many conventional optoelectronic devices consist of thin, stacked films of metals and semiconductors. In this presentation, I will demonstrate how one can improve the performance of such devices by nano-structuring the constituent layers at length scales below the wavelength of light. The resulting metafilms and metasurfaces offer opportunities to dramatically modify the optical transmission, absorption, reflection, and refraction properties of device layers. This is accomplished by encoding the optical response of nanoscale resonant building blocks into the effective properties of the films and surfaces. To illustrate these points, I will show how nanopatterned metal and semiconductor layers may be used to enhance the performance of solar cells, photodetectors, and enable new imaging technologies. I will also demonstrate how the use of active nanoscale building blocks can facilitate the creation of active metafilm devices.

10343-32, Session 7

Laser printing of flat optics metasurfaces *(Invited Paper)*

Anders Kristensen, Xiaolong Zhu, Marcus Schultz Carstensen, Oseze Ester Mobolanle Iyore, DTU Nanotech (Denmark); Rodolphe Marie, Technical Univ. of Denmark (Denmark); Mehdi K. Hedayati, DTU Nanotech (Denmark); N. Asger Mortensen, DTU Fotonik (Denmark); Uriel Levy, The Hebrew Univ. of Jerusalem (Israel)

This paper describes digital printing of flat optics metasurfaces, by holographic laser post-writing on nano-textured, metal-coated optical metasurfaces. Holographic laser printing with a spatial light modulator (SLM) has several advantages over conventional raster-writing and dot-matrix display (DMD) writing: multiple pixel exposure, high power endurance and existing software for computer generated holograms (CGH). We present a technique for design and manufacturing of plasmonic Fresnel zone plates (FZP) based on ultrafast laser printing with a SLM. Here the design is scalable, such that tailoring a plasmonic FZP with different wavelengths and focus lengths is done with ease.

10343-33, Session 7

High-angle light bending and ultra-high NA lenses achieved through resonance interference effects in dielectric metasurfaces *(Invited Paper)*

Ramon Paniagua-Dominguez, Egor Khaidarov, Ye Feng Yu, Hanfang Hao, Reuben M. Bakker, Xinan Liang, Vytautas Valuckas, Yuan Hsing Fu, Arseniy I. Kuznetsov, A*STAR - Data Storage Institute (Singapore)

Optically resonant dielectric nanostructures represent a new and rapidly developing research direction in nanophotonics [1]. They show plenty of useful functionalities and can complement or even substitute resonant plasmonic nanoparticles for many potential application directions. The main advantages over conventional plasmonics are low losses, wide range of applicable dielectric materials and strong magnetic resonant response. In particular, the last feature opens a broad range of opportunities to control light scattering, transmission, reflection and phase characteristics through designed interference between electric and magnetic resonant modes. This has already led to demonstrations of low-loss dielectric Huygens' metasurfaces operating with very high efficiencies in transmission mode and generalized Brewster effect showing unconventional behaviour of dielectric metasurface in reflection mode [1]. In this presentation, we will review recent magnetic resonant phenomena obtained with high-index dielectric nanoantennas and metasurfaces and show how this might lead to new functionalities, which cannot be achieved neither with conventional metasurface approaches nor with conventional bulk optics. In particular, we demonstrate how the resonance interference effect can be used to control energy distribution between diffraction orders in a nanoantenna array, which leads to light bending at very high angles of >82 degrees with efficiency >50%. This property is used to design and experimentally demonstrate flat lenses having a free-space numerical aperture (NA) of >0.99, which strongly exceeds NA of existing flat lenses and bulk optics analogues. Applications of these new, ultra-high NA, flat dielectric lenses will also be discussed.

References:

1) A. I. Kuznetsov et al., "Optically resonant dielectric nanostructures", Science 354, aag2472 (2016).

10343-34, Session 7

Solar metadevice with enhanced absorption, scattering, and spectral control

Richard M. Osgood III, Yassine Ait-El-Aoud, U.S. Army Natick Soldier Research, Development and Engineering Ctr. (United States); Lalitha Parameswaran, Vladimir Liberman, Mordechai Rothschild, MIT Lincoln Lab. (United States); Andrew Luce, Nicholas LeGrand, Michael Okamoto, U.S. Army Natick Soldier Research, Development and Engineering Ctr. (United States); Steven E. Kooi, MIT Institute for Soldier Nanotechnologies (United States); Diane M. Steeves, U.S. Army Natick Soldier Research, Development and Engineering Ctr. (United States); Richard P. Kingsborough, MIT Lincoln Lab. (United States); Stephen A. Giardini, U.S. Army Natick Soldier Research, Development and Engineering Ctr. (United States)

Light scattering from nanoparticles has been shown to strongly influence optical properties of many diverse systems, including monolayer arrays of plasmonic particles [1] and cuttlefish chromatophores, where large scattering effects have recently been observed from unusual nanostructured granules [2]. Random and ordered arrays of plasmonic particles have produced larger nanoscopic field enhancements responsible for the Surface Enhanced Raman Scattering effect. We explore metadevices, consisting of monolayers of patterned or semi-random plasmonic (Al and Ag) particles, to enhance scattering into and enhanced absorption of thin photovoltaic films. Without this nano-enhancement, absorption is limited by film thickness in the long-wavelength region. With lithographically patterned arrays of Al nano-islands, we observe a solar-weighted absorption enhancement of greater than 35% in 200-nm thick amorphous silicon layers on glass, and obtain absorption enhancement data from semi-random spuncast Ag nanoparticle arrays as well as arrays on glass. We model scattering and enhanced absorption, discussing how to scale to large areas.

Lightweight, portable thin-film solar blankets are of great economical value, providing size, weight and logistics advantages over heavy, brittle, standard solar cells. Typically two m2 in area, these solar blankets almost satisfy specifications, but still have limited absorption, and are too large and heavy. Our metadevice will enable the broader use of these solar blankets for commercial and military applications.

[1] M. K. Kinnan and G. Chumanov, J. Phys. Chem. C.114 (2010) 1796.

[2] S. R. Dinneen, R. M. Osgood III, M. E. Greenslade, L. F. Deravi, J. Phys.

Chem. Lett. 8 (2017) 313-317.

10343-35, Session 7

Sensitivities of large aperture multi-element plasmonic metasurface lenses

Bryan Adomanis, Stephen E. Nauyoks, Air Force Research Lab. (United States); D. Bruce Burckel, Sandia National Labs. (United States); Michael A. Marciniak, Air Force Research Lab. (United States)

Development of metasurface lenses has rapidly advanced in the few years since the first experimental demonstration, due to the excitement of full control of a propagating wavefront through an interface on the order of a wavelength or less. Lenses based on polarization conversion via plasmonic antennas are inherently limited in efficiency, and so a preponderance of recent efforts focus on more efficient dielectric-based designs. As a result, plasmonic metasurface lenses have been sparsely characterized. However, it has been found that expanding the design beyond a single interface offers hope for plasmonic structures, thanks to improvements such as adding impedance-matched layers and additional functional layers for polarization conversion. Before continuing development of these multi-layer structures, we wish to better understand dependencies of plasmonic designs. Thus, here we demonstrate the spectral, geometrical, angular and polarization sensitivities of 19 large-scale (5mm) variants of the original V-antenna lens design at 5μm and 8μm. Focal ratios of our cylindrical lenses range from F/5-F/40. Results are measured for several optical systems, including a single lens, a Keplerian beam expander, and a two-lens relay.

10343-36, Session 8

Merging micro- and nanooptics *(Invited Paper)*

Harald Giessen, Simon Thiele, Univ. Stuttgart (Germany)

We demonstrate miniaturized micro- and nano-optics. Our approach uses femtosecond 3D direct laser writing. Aberration-corrected performance for large angles of incidence is achieved, and our approach solves the common problem of off-axis coma in metasurfaces.

An inherent property of metasurfaces for optical imaging is coma [1]. Despite excellent on-axis performance, metasurfaces based on TiO2 nanoantennas that use dielectric Mie resonances do not give good imaging quality when going away from the optical axis or using large angles of incidence [2].

Using femtosecond 3D direct laser writing, we manufactured complex freeform microoptics with different diameters below 1 mm [3], see figure 1. The optical design and layout, the mechanical model, the manufactured lens, and the resolution performance are shown. A resolution of 780 nm with excellent contrast is even possible for large angles of view. Miniature phase plates are also possible [4]. Our smallest compound microscope objectives are as small as 100 μm in diameter and were fabricated directly on an imaging fiber with 125 μm diameter and 1600 single mode imaging strands [5]. Our systems can also be printed directly onto CMOS imaging sensors with sub-micron pixel sizes [5]. Furthermore, printing onto LED is also possible for illumination shaping [6]. It is also possible to print several lenses with different focal lengths and fields of view onto a single sensor, creating a foveated image that comprises teleeohoto-, normal- and wide angle-lenses [7]. One can also combine the lenses with quantum dots as integrated single photon source device [8]. We demonstrate further how to combine these structures with suitable nano-optics.

Acknowledgements This work has been supported by ERC Advanced Grant Complexplas, by DFG, BMBF (Printoptics), and BW-Stiftung.

References

[1] F. Aieta, P. Genevet, M. Kats, and F. Capasso, Opt.Express 21, 31530 (2013).

[2] M. Khorasaninejad, F. Capasso, Science 352, 1190 (2016).

[3] T. Gissibl, H. Giessen, et al., Nature Comm. 7, 11763 (2016).

[4] T. Gissibl, M. Schmid, and H. Giessen, Optica 3, 448 (2016).

[5] T. Gissibl, H. Giessen, et al., Nature Phot. 10, 554 (2016).

[6] S. Thiele et al., Opt. Lett. 41, 3029 (2016).

[7] S. Thiele, K. Arzenbacher, T. Gissibl, H. Giessen, and A. Herkommer, Science Advances 3, e1602655 (2017).

[8] M. Sartison, T. Gissibl, S. Portalupi, P. Michler, and H. Giessen, Scientific Reports 7, 39916 (2017).

10343-37, Session 8

Optoelectronic metasurfaces *(Invited Paper)*

Pierre Berini, Univ. of Ottawa (Canada)

Metasurfaces constructed from metallic nanostructures such as optical antennas and sub-wavelength gratings can be designed to operate efficiently as coupling structures for incident optical beams to surface plasmon polaritons (SPPs) propagating thereon. On a semiconductor, metallic metasurfaces can act simultaneously as a device electrode while ensuring strong optical field overlap with the active region. Additionally, SPP fields thereon can be confined to sub-wavelength dimensions and significantly enhanced relative to the exciting field. These features are very attractive for nanoscale optoelectronic device applications, such as photodetectors and modulators, as the excitation of SPPs alters conventional trade-offs between responsivity and speed, or modulation and speed, respectively. This is due to the facts that sub-wavelength confinement enables the active region to be shrunk to nano-scale dimensions, while good optoelectronic performance is maintained due to SPP field enhancement. We discuss recent progress on optoelectronic metasurfaces, particularly recent device demonstrations for high-speed reflection modulators based on a metal-oxide-semiconductor capacitor structure exploiting the carrier refraction effect in Si [1,2], and for Schottky contact sub-bandgap hot-hole infrared photodetectors on p-Si [3,4]. Potential application to non-contact Si CMOS electronic wafer testing will be discussed.

References

1. S. Hassan, E. Lisicka-Skrzek, A. Olivieri, R. N. Tait and P. Berini, “Fabrication of a Plasmonic Modulator Incorporating an Overlaid Grating Coupler,” Nanotechnology, Vol. 25, 495202, 2014.

2. A. Olivieri, C. Chen, S. Hassan, E. Lisicka-Skrzek, R. N. Tait, P. Berini, “Plasmonic nanostructured metal-oxide-semiconductor reflection modulators,” Nano Letters, Vol. 15, 2304, 2015.

3. M. Alavirad, A. Olivieri, L. Roy, P. Berini, “High-responsivity sub-bandgap hot-hole plasmonic Schottky detectors,” Optics Express, Vol. 24, 22544, 2016.

4. M. Alavirad, A. Olivieri, L. Roy, P. Berini, “Sub-bandgap photodetection with electrically-contacted plasmonic nano-antennas on silicon,” Submitted

10343-38, Session 8

Cloaking of contact fingers on solar cells and OLEDs using free-form surfaces designed by coordinate transformations *(Invited Paper)*

Martin F. Schumann, Malte Langenhorst, Karlsruher Institut für Technologie (Germany); Michael Smeets, Kaining Ding, Forschungszentrum Jülich GmbH (Germany); Ulrich W. Paetzold, Benjamin Fritz, Karlsruher Institut für Technologie (Germany); Ralph Eckstein, Karlsruher Institut für Technologie (Germany) and InnovationLab GmbH (Germany); Guillaume Gomard, Martin Wegener, Karlsruher Institut für Technologie (Germany)

In transformation optics, coordinate transformations are usually mapped onto equivalent (meta-)material parameter distributions. In 2015, we introduced an approach mapping coordinate transformations onto dielectric free-form surfaces. We presented model experiments on cloaking of reflective contact fingers on solar cells. We now report on the fabrication of masters by 3D laser lithography used for soft imprinting. For prototype silicon heterojunction solar cells investigated under 1-sun illumination, we demonstrate the predicted 9% relative efficiency increase. We additionally show that our approach is adaptable to Lambertian sources, thereby cloaking light-emitting diode contacts to achieve spatially homogeneous emission.

10343-39, Session 8

Integrating quantum-dots and Mie resonators into a 2D metamaterial for sunlight downconversion

Antonio Capretti, Arnon Lesage, Tom Gregorkiewicz, Univ. van Amsterdam (Netherlands)

Dielectric Mie resonators and quantum-confined semiconductors enable an unrivaled control over light absorption and excited electron states, respectively. Here, we embed photoluminescent silicon nanocrystals (Si-NCs) into a planar array of SiO2 nanocylinders, and experimentally demonstrate a powerful concept: the resulting metamaterial preserves the Si-NC radiative properties and inherits the spectrally-selective absorption properties of the nanocylinders. This hierarchical approach provides increased photoluminescence (PL) intensity, without utilizing lossy plasmonic components.

Our metamaterial enables tunable absorption peaks up to 50% in the visible spectrum, when freestanding, and is predicted to reach total absorption by using an impedance-matched substrate. These absorption peaks occur in correspondence of the nanocylinder Mie resonances and of the grating condition in the array. We experimentally detect extinction peaks, driving enhanced absorption in the Si-NCs. Therefore, the metamaterial features increased PL intensity, obtained without affecting the PL properties such as lifetime, angular pattern and extraction efficiency. Remarkably, our best-performing metamaterial shows +30% PL intensity achieved with a lower amount (43%) of Si-NCs, compared to a planar film without nanocylinders. This results in a 3-fold average PL enhancement.

This spectral selectivity of absorption paves the way for an effective light down-conversion scheme to increase the efficiency of solar cells. The demonstrated principle is completely general and the Si-NCs can be replaced with other semiconductor quantum dots, rare-earth ions or organic molecules. Similarly, the dielectric medium can be adjusted on purpose. We envision the use of this hierarchical design for efficient photovoltaic, photocatalytic and artificial photosynthetic devices with enhanced efficiency.

10343-40, Session 8

A Monte Carlo approach for investigating the fabrications imperfections for metasurfaces

Li-Yi Hsu, Univ. of California, San Diego (United States)

In this paper, we introduce a method to compare the quality of concentrators in the realm of metasurfaces. Specifically, we generalize the concepts of the slope error and the intercept factor in the realm of ray-optics. After proposing definitions valid in physical optics, we put forward an approach to calculate them. As examples, we design in the optical domain three metasurfaces based on three different unit cells: cylindrical, rectangular and ellipsoidal elements. The concept allows for the comparison of the efficiency of the metasurfaces, their sensitivities to fabrication imperfections and can provide a guidance to design large scale and highly efficiency metasurface concentrators.

10343-42, Session 9

Nonlinear metasurfaces: materials and directional generation *(Invited Paper)*

Augustine M. Urbas, Air Force Research Lab. (United States)

Plasmonic and metamaterial systems are enabling to many relevant technologies. Detecting optical signals in the mid and long wave infrared, and the generation, detection and conversion of single photons for quantum information applications are significant to a range of Air Force technologies and drive the research to increase performance and functionality. We explore how nonlinear properties of metasurfaces can be engineered for quanutm information applications. We show that nonlinear multipole interference allows both a non-reciprocal and unidirectional nonlinear generation from nanoelements or their periodic arrangement, with the direction of nonlinear generation preserved with respect to a fixed laboratory coordinate system when reversing the direction of the fundamental field.. These effects arise due to the nonlinear response of the component materials and we are actively pursuing novel materials systems and growth procedures to produce structures with controlled response. A significant part of this work focuses on the characterization of time resolved nonlinear response in plasmonic and dielectric materials. We employ the beam deflection method to measure the nonlinear refraction and absorption of thin films. Beam deflection is a pump probe technique which offers extreme sensitivity to nonlinear response in materials. This allows us to measure the response of films at the dimensions relevant to our dimer designs deposited using the same techniques and reveal thickness and process dependent changes in the properties of nonlinear materials. This system is a useful example of where the engineering of materials response through structure to achieve desired optical properties can enable new potential technolgies.

10343-43, Session 9

Engineering optical nonlinearities in plasmonic titanium nitride thin films

Nathaniel Kinsey, Virginia Commonwealth Univ. (United States); Heather J. Ferguson, Univ. of Michigan (United States); Jennifer M. Reed, Air Force Research Lab. (United States); Manuel R. Ferdinandus, Air Force Institute of Technology (United States); Clayton T. DeVault, Urcan Guler, Alexei S. Lagutchev, Purdue Univ. (United States); Theodore Norris, Univ. of Michigan (United States); Vladimir M. Shalaev, Alexandra Boltasseva, Purdue Univ. (United States); Augustine M. Urbas, Air Force Research Lab. (United States)

Recently, the development of alternative plasmonic materials has provided several candidates that possess optical properties that mimic those of gold, but are able to withstand temperatures in excess of 2800 °C before melting. These so-called refractory plasmonic materials, e.g. TiN, ZrN, HfN, and TaN, may provide a good solution for nonlinear plasmonics applications as they are able to support surface plasmon oscillations with competitive losses while maintaining a larger damage threshold than similar noble metals. Of the transition metal nitrides, TiN has received attention for applications in photovoltaics, data storage, waveguiding, and metamaterials.

Recently, it was shown that the effective third-order nonlinear optical properties of TiN were similar in strength to those found in silver or gold films but TiN is able to withstand a significantly higher irradiance. However, the mechanism and temporal response of the nonlinearity were not well understood. In this work, we extend the study of TiN to include the effect of material quality, as well as the temporal dependence, to highlight the design space for potential applications. By observing the dynamics of the various nonlinear mechanisms as a function of the film quality/stoichiometry, we were able to identify several distinct contributions to the observed response through the material's linear properties and band structure. Specifically, we observe both an instantaneous semiconductor-like response as well as a delayed hot-electron response whose sign, speed, and magnitude can be engineered by controlling the growth conditions. Consequently, the flexibility in both the linear and nonlinear optical properties offered by TiN combined with its competitive plasmonic response and enhanced damage threshold make it a promising material for future nonlinear nanophotonic applications.

10343-44, Session 9

Chiral metamaterials in the nonlinear regime: harmonic generation, multiphoton luminescence, and intensity-dependent optical activity *(Invited Paper)*

Wenshan Cai, Georgia Institute of Technology (United States)

The past few years have witnessed an explosive development of chiral photonic metamaterials that exhibit circular dichroism and optical rotation orders of magnitude larger than conventional materials. Though chirality is most commonly applied in linear optical regime, opposing circularly polarized waves can also display parity as a property of higher order optics. In this talk, we present a set of photonic metamaterials that possess pronounced chiroptical features in the nonlinear regime. In additional to the gigantic chiral properties such as the circular dichroism and polarization rotation, the metamaterials demonstrate a distinct contrast between harmonic responses from the two circular polarizations. These nano-engineered structures are further exploited for chiral-selective two-photon luminescence from quantum emitters and a photon-drag effect with helicity-sensitive generation of photocurrent. Finally, we report a noticeable shift in the circular dichroism and optical activity under a modest level of excitation power.

Reference:

[1] Y. Cui, ... W. Cai, “Giant chiral optical response from a twisted-arc metamaterial,” Nano Lett. 14, 1021 (2014).

[2] S. P. Rodrigues, ... W. Cai, “Nonlinear imaging and spectroscopy of chiral metamaterials,” Adv. Mater. 26, 6157 (2014).

[3] S. P. Rodrigues, ... W. Cai, “Metamaterials enable chiral-selective enhancement of two-photon luminescence from quantum emitters,” Adv. Mater. 27, 1130 (2015).

[4] L. Kang, ... W. Cai, “An active metamaterial platform for chiral responsive optoelectronics,” Adv. Mater., 27, 4377 (2015).

[4] S. P. Rodrigues, ... W. Cai, “Intensity-dependent modulation of optically active signals in a chiral metamaterial,” Nat. Comm., in press (2017).

10343-45, Session 9

Organic molecular epsilon-near-zero ultrathin film: toward enhanced nonlinear optical response in visible spectral range

Yeon Ui Lee, Ewha Womans Univ. (Korea, Republic of); Hyo Jung Kim, Pusan National Univ. (Korea, Republic of); Jean-Charles Ribierre, Ewha Womans Univ. (Korea, Republic of); Young Chul Jun, Ulsan National Institute of Science and Technology (Korea, Republic of); Kenji Kamada, National Institute of Advanced Industrial Science and Technology (Japan); Jeong Weon Wu, Ewha Womans Univ. (Korea, Republic of); Anthony D’Aléo, Ewha Womans Univ. (Korea, Republic of) and Aix Marseille Univ. (France) and Ctr. National de la Recherche Scientifique (France)

Epsilon-near-zero (ENZ) materials exhibit optical response such as directional emission, modification of dipole radiation behavior and enhancement of third-order optical nonlinearity. Doped semiconductors and transparent conducting oxides are known to have ENZ response in mid-IR and near-IR spectral ranges, which is determined by the maximum density of carrier doping still maintaining good optical property. Here we introduce organic molecular materials showing an efficient ENZ response in visible spectral range. Organic molecular films of squaraine and cyanine are prepared by spin-coating to obtain high optical quality ultrathin films. Squaraine is dissolved in organic solvent while cyanine is prepared in aqueous polymer. Linear optical spectrum and spectroscopic ellipsometry measurements of both films evidenced ENZ in 500-600nm. Attenuated total internal reflection measurement further identified spectral ranges of negative dielectric constant. Third-order optical nonlinearity is known to be enhanced in ENZ regime, demonstrated in mid-IR and near-IR spectral ranges. We demonstrate an enhancement of third-order optical nonlinearity in visible wavelength by femtosecond Z-scan measurement. Both samples showed third-order nonlinear response enhanced at ENZ when compared with off-resonant value. In open-aperture measurement squaraine film showed both two-photon and saturable absorptions, while cyanine film showed saturable absorption only. In closed-aperture measurement squaraine film showed a well-behaved response while cyanine film signal was erratic presumably due to a break-down of J-aggregate at high intensity of optical field. Furthermore, molecular packing structure of both films is studied by grazing-incidence synchrotron radiation scattering measurement to relate ENZ properties and packing structure.

10343-46, Session 10

Plasmonic metasurfaces by evolutionary design *(Invited Paper)*

Teri W. Odom, Northwestern Univ. (United States)

Metasurfaces are an emerging class of flat optics that can manipulate light via subwavelength phase elements. Their 2D structures are usually determined by (1) calculating the phase change required at each location to obtain far-field properties from analytical equations and (2) structuring each building block to produce that wavefront change. However, computational or digital approaches to design metasurfaces based on search heuristics offer advantages in targeting and realizing properties not possible by analytical expressions. This talk will describe an evolutionary approach to design flat lenses based on subwavelength plasmonic building blocks. Our lattice evolution algorithm can achieve desired optical responses by tuning the arrangement of the phase units on a discrete square lattice. We will discuss two different systems with different classes of building units—holes and particles—to realize achromatic lattice lenses at up to three wavelengths and flat lenses in semiconductor plasmonic materials such as titanium nitride. We will describe prospects for scaling the production of these lenses as well as their ability to achieve dynamic optical responses.

10343-47, Session 10

Subwavelength Pancharatnam-Berry phase controlled metasurface for imaging with instantaneous SHG

Christian Schlickriede, Univ. Paderborn (Germany); Naomi Waterman, The Univ. of Birmingham (United Kingdom); Bernhard Reineke, Philip Georgi, Univ. Paderborn (Germany); Guixin Li, Southern Univ. of Science and Technology (China); Shuang Zhang, The Univ. of Birmingham (United Kingdom); Thomas Zentgraf, Univ. Paderborn (Germany)

We design and experimentally investigate a new plasmonic metasurface, which is able to work as a lens for nonlinear imaging with simultaneous frequency conversion for the incident near-infrared light. With our approach, we take advantage of the nonlinear Pancharatnam-Berry phase originating from the arrangement of meta-atoms with threefold rotational geometry. Due to the strong light-matter interaction of the plasmonic nanoantennas, the lenses have only a thickness of 30 nm. Furthermore, the nonlinear metalens shows different operation modes, which depend on the spin angular momentum of light. By using a particular polarization state, the nonlinear lens can either work as a focusing or defocusing lens while simultaneously converting the illumination light to SHG light. We investigate the beam propagation of our nonlinear metalens and determine the evolution of the real and virtual focal planes for illumination with Gaussian beams. To underline the strength and the design flexibility we fabricated and analyzed different types of more complex nonlinear devices featured by different focusing abilities. In addition to that, we present intriguing spin angular momentum depending nonlinear imaging abilities giving rise to real and virtual SHG images of real objects as well as nonlinear Fourier transformations. The images are thereby generated at visible wavelength, which enables this device for revealing new avenues in integrated nano-optoelectronics, quantum communication technologies or other future device applications. Nonlinear metalenses feature a symbiotic relationship between generation and modulation of frequency conversion within an ultrathin element.

10343-48, Session 10

Ultra-high refractive index in deep subwavelength coupled bi-layer free-standing flexible metamaterials

Leena Singh, Oklahoma State Univ. (United States)

We demonstrate an order of magnitude enhancement in refractive index of artificially designed metamaterials by exploiting the deep subwavelength coupling in a free-standing, thin-film metal-dielectric-metal checkboard structure. A record high refractive index of 183.2 is characterized at terahertz frequencies. The detailed investigations reveal that the enhancement of the effective refractive index of the structure via deep subwavelength coupling in a bilayer design is governed by a power law, which is an effective and simpler approach to design high index metamaterials. The approach relies on deep subwavelength coupling to obtain extremely high refractive index values that can lead to many practical applications in the field of imaging, lithography, design of delay lines and interferometers.

10343-49, Session 10

Bianisotropy: a new route towards non-reciprocal optical metasurfaces

Mark Lawrence, Jennifer A Dionne, Stanford Univ. (United States)

Directional light flow is fundamental to the development of photonic information processors. One all optical way of generating such nonreciprocal transport involves exploiting the nonlinear Kerr effect within an asymmetric arrangement of high Q resonators. However, current demonstrations involve optical paths that are tens to hundreds of microns in length.

Here, we show that Kerr based nonreciprocal devices can be further miniaturized to the nanoscale by working with Silicon nanoantenna-based metasurfaces. In the subwavelength regime structural asymmetry alone isn't enough to generate directionally-dependent field amplification. We overcome this limitation by overlapping a sub-radiant electric dipolar mode with a perpendicular super-radiant magnetic dipole. In this case, breaking out-of-plane inversion symmetry leads to nearfield coupling between the two excitations. Because of interference between nearfield and far field magneto-electric coupling, the electric dipole is suppressed (enhanced) for a normally incident plane wave propagating in the backward (forward) direction. When the metasurface is illuminated with powers of a few 100kW/cm2, the electric field strength within the Si becomes sufficient to change its refractive index, red-shifting the narrow transmission dip. For forward excitation the resonance is shifted by a significant portion of the FWHM, making the metasurface transparent. For backward excitation the much smaller shift renders the transmission very low.

We show, for the first time, that bianisotropy provides a means to achieve optical nonreciprocity at the nanoscale. Relying simply on collocated dipolar excitations, our scheme has, in principle, no lower size limitation and could be miniaturised further by making use of gain assisted plasmonics.

10343-50, Session 10

Nonlocal metasurfaces enable perfect anomalous reflection

Viktar S. Asadchy, Aalto Univ. (Finland) and Francisk Skorina Gomel State Univ. (Belarus); Andreas Wickberg, Karlsruher Institut für Technologie (Germany); Ana Díaz-Rubio, Aalto Univ. (Finland); Martin Wegener, Karlsruher Institut für Technologie (Germany); Sergei A. Tretyakov, Aalto Univ. (Finland)

Recently introduced generalized Snell's law provides wide possibilities for wavefront manipulations using metasurfaces. In contrast to conventional blazed gratings, their metasurface-based counterparts are planar (no grooves) and do not require complicated fabrication techniques. However, all previously demonstrated metasurfaces for anomalous reflection have revealed their deficiency due to parasitic energy coupling into non-desired diffraction modes. This negative effect becomes especially pronounced for metasurfaces designed to have a large separation angle between the incident and reflected beams. The reason is the used inaccurate approach for metasurface synthesis. It approximates that the surface is uniform on the sub-wavelength scale and the phase of the local reflection coefficient follows the linear profile dictated by the generalized reflection law. While the former assumption could be made, the latter one, as we show in the presentation, is incorrect. Moreover, the conventional synthesis approach does not take into account requirements on the amplitude of the local reflection coefficient. In the presentation, we will demonstrate an original alternative design scheme for metasurface gratings based on the generalized surface impedance model. It appears that perfect coupling of an incident plane wave into a single reflected plane wave requires energy channeling along the metasurface plane. To verify our design approach, we fabricate and measure an optical metasurface that reflects a normally incident beam at a very steep angle of 80 deg. The comparison of the two approaches shows that our new scheme provides double increase in the efficiency and complete absence of parasitic reflections.

10343-51, Session 10

Metasurface-based holograms and vortices

Cheng-Wei Qiu, National Univ. of Singapore (Singapore)

We experimentally report our recent progress on developing high-capacity and advanced holographic metasurfaces and vortex metasurfaces. Compared with traditional lens, such flat devices take the advantage from its ultrathin trait to realize the helicity-dependent optical vortex focusing metalens (consisting of 306,306 rotating nano-voids) that focuses three longitudinal vortices with distinct topological charges at different focal planes. The designed metasurface may find potential applications in multi-plane simultaneously particles manipulation, angular-momentum-based quantum information processing and integrated nano-optoelectronics. In the meantime, on-chip discrimination scheme of detecting the orbital angular momentum of light was experimentally demonstrated to focus the surface plasmons to different lateral positions, with reliable 120nm lateral shift between any two neighbouring topological charges of the incident vortex light. On the other hand, we also demonstrate how to incorporate multiple holographic images into one metasurface, via nonlinearity, spatial multiplexing, random phase mask, etc. Overall, those two major applications of metasurface may serve as competitive alternative to generate OAMs and holograms from traditional methods.

10343-72, Session 10

Embedded eigenstates and virtual absorption using metamaterials *(Invited Paper)*

Alexandr E. Krasnok, The Univ. of Texas at Austin (United

States); Francesco Monticone, Cornell Univ. (United States); Andrea Alù, The Univ. of Texas at Austin (United States)

We discuss the possibility of confining electromagnetic energy and enhancing the interactions of light and matter in nanostructures, based on the concept of embedded eigenstates within the radiation continuum. We discuss how metasurfaces and metamaterials may be able to trap light in plain sight, and how lossless structures may be able to store energy in the transient by engaging complex zeros in the scattering response of the system. We also shed light on the role that reciprocity plays in the response of these systems, and how these functionalities may play a pivotal role in low-energy nanophotonic opto-electronic and bio-sensing devices.

10343-52, Session 11

Reconfigurable chiroptical nanostructures *(Invited Paper)*

Nicholas A. Kotov, Univ. of Michigan (United States)

Chiral nanomaterials represent one of the most dynamic research areas in photonics. High values of polarization rotation observed for assemblies of plasmonic nanoparticles inspire the development of new chiroptical nanomaterials. Transition of this new physical phenomena to photonics technologies requires active modulation of the degree of polarization rotation. In this presentation I will demonstrate the possibility of reconfigurable chiroplasmonic systems based on three different platforms: scissor-like nanoparticle pairs, chiroptical nanocomposites, and kirigami optics. Advantages and disadvantages of the three platforms will be discussed using practical applications in biosensing and chiral photonics.

10343-53, Session 11

Towards all-optical chiral resolution with achiral plasmonic and dielectric nanostructures *(Invited Paper)*

Jennifer A. Dionne, Stanford Univ. (United States)

Light can exert differential forces on left- and right-handed enantiomers, promising an all-optical route towards chiral resolution and controlled assembly of chiral nanostructures. However, enantioselective optical forces on nano-specimens are challenging to both control and quantify, since their magnitudes are predicted to be sub-piconewton-scale with nanometer-scale spatial variation. Here we demonstrate new methods to both strengthen and visualize these forces using achiral nanostructures. First, we show how plasmonic optical tweezers can enable selective optical trapping of enantiomers. Our technique combines plasmonic optical tweezers with a chiral atomic force microscope (AFM) probe. Illumination of the plasmonic tweezers with left- and right- circularly polarized light (CPL) results in distinct forces on the chiral AFM tip: the total optical forces exerted on a left-handed chiral tip are 10 pN stronger when illuminated with left-CPL than with right-CPL. Additionally, the transverse optical forces on this chiral tip are attractive with left-CPL, but repulsive with right-CPL. We use the AFM tip to map such chiral optical forces over the plasmonic tweezers with 2 nm lateral spatial resolution, showing distinct force distributions in all three dimensions for each handedness. Then, we show how high-index dielectric nanostructures and metasurfaces can increase enantiomer separation yields more than 50 times beyond CPL in free space. Mie theory and a local optimization algorithm indicate that magnetic multipolar Mie resonances supported by sub-micron silicon spheres increase both the circular dichroism signal and Kuhn's dissymmetry factor compared to CPL in free space. Importantly, these enhancements maintain the total molecular absorption rate, enabling efficient selective photoexcitation. Combined, our results suggest that achiral photonic nanostructures can significantly enhance chiral light-matter interactions, potentially enabling controlled enantiopure chemical syntheses, single molecule chiral spectroscopy, and dynamic monitoring of structural changes of chiral molecules with sub-nanometer resolution.

10343-54, Session 11

Symmetry induced topological Weyl points in chiral nanophotonic metamaterials *(Invited Paper)*

Ortwin Hess, Imperial College London (United Kingdom)

No Abstract Available

10343-55, Session 11

Realizations of Weyl points in reciprocal metamaterial

Meng Xiao, Qian Lin, Stanford Univ. (United States); Wenjie Chen, Che Ting Chan, Hong Kong Univ. of Science and Technology (Hong Kong, China); Shanhui Fan, Stanford Univ. (United States)

Weyl points as monopoles of Berry curvature in momentum space are stable under any perturbation which preserve the translational symmetry. Their experimental realizations like gyroid photonic crystals, on the other hand are quite complex. Here we show two experimentally feasible systems with Weyl points. We break the inversion symmetry in these systems and does not need any external magnetic field. In the first system, we show the existence of Weyl points in a class of non-central symmetric metamaterials. Here the inversion symmetry is broken by utilizing the chiral coupling between the electric and magnetic fields. The exploration of Weyl point in metamaterials as described by homogeneous effective material parameters is of fundamental interest since the wavevector space of such meta-material is non-compact, which is in contrast with the wavevector space of periodic systems which is always topologically compact. We find that such metamaterial can be realized with a simple system consisting of an array of metal wire in the shape of elliptical helix. Experimental detection of Weyl points in this system is also discussed. The second system we consider goes beyond the effective medium description. It is a chiral stacking of layered honeycomb structure. This system possesses both single Weyl points (including type-II nodes) and multiple Weyl points with topological charges of 2 and 3. We also experimentally show the robustness of the surface states against kz-preserving scattering in this system.

10343-56, Session 12

Experiment of synthetic Weyl points in optical regime

Hui Liu, Qiang Wang, Nanjing Univ. (China); Meng Xiao, Stanford Univ. (United States); Shi Ning Zhu, Nanjing Univ. (China); Che Ting Chan, Hong Kong Univ. of Science and Technology (Hong Kong, China)

Weyl fermions have not been found in nature as elementary particles, but they emerge as nodal points in the band structure of electronic and classical wave crystals. Novel phenomena such as Fermi arcs and chiral anomaly have fueled the interest in these topological points which are frequently perceived as monopoles in momentum space. We demonstrate that generalized Weyl points can exist in a parameter space and we report the first observation of such nodal points in one-dimensional photonic crystals in the optical range. The reflection phase inside the band gap of a truncated photonic crystal exhibits vortexes in the parameter space where the Weyl points are defined and they share the same topological charges as the Weyl points. These vortexes also guarantee the existence of interface states, the trajectory of which can be understood as "Fermi arcs" emerging from the Weyl nodes.

10343-57, Session 12

Multiplexing of adjacent vortex modes with the forked grating coupler

Christopher T. Nadovich, Derek J. Kosciolek, William D. Jemison, David T. Crouse, Clarkson Univ. (United States)

For OAM multiplexing in vortex fiber to reach practical commercial viability, simple silicon photonic interfaces with vortex fiber will be required. These interfaces must support multiplexing. Toward this goal, an efficient single-fed multimode Forked Grating Coupler (FGC) for coupling two different optical vortex OAM charges to or from the TE0 and TE1 rectangular waveguide modes has been developed. A simple, apodized device implemented with e-beam lithography and a conventional dual-etch processing on SOI wafer exhibits low crosstalk and reasonable mode match. Advanced designs using this concept are expected to further improve performance.

Forked Grating Couplers retain many of the advantages of conventional grating couplers, including convenience of placement, reasonable bandwidth, small size, and CMOS fab compatibility. Herein we propose a new kind of single-fed FGC design that can simultaneously couple to a pair of OAM modes, connecting these modes one-to-one onto a pair of TE modes in a “bus” waveguide on a photonic IC. The bussed modes can then be split/combined with an asymmetric coupler or other on-chip multiplexing techniques.

The simple multi-mode FGC concept presented can be applied for different multiplexed OAM charges so long as their integer charges must differ by +/-1. A basic, apodized device implemented with e-beam lithography and a conventional dual-etch processing of SOI wafer exhibits better than 20 dB crosstalk isolation and mode match efficiency better than 3 dB. Advanced designs using this concept are expected to further improve performance.

10343-58, Session 12

Singular optical beams enabled by photonic meta-structures *(Invited Paper)*

Natalia M. Litchinitser, Liang Feng, Pei Miao, Jingbo Sun, Zhifeng Zhang, Mikhail I. Shalaev, Wiktor T. Walasik, Univ. at Buffalo (United States); Stefano Longhi, Politecnico di Milano (Italy)

Recent developments in the field of nanostructured optical materials enable unprecedented control over light propagation and a possibility of “tailoring” the space for light propagation. In particular, the emergence of novel optical materials opens a new paradigm in studies of singular optics (or structured light), which is a fascinating emerging area of modern optics that considers spin and orbital angular momentum (OAM) properties of light and brings a new dimension to optical physics. We will discuss fundamental optical phenomena at the interface of singular and nonlinear optics in novel optical media and show that the unique optical properties of optical nanostructures open unlimited prospects to “tailor” light itself.

We present theoretical and experimental studies of light-matter interactions of vector and singular optical beams in optical nanostructures and microcavities. In particular, by exploiting the emerging non-Hermitian photonics design at an exceptional point, we demonstrate a microring laser generating a single-mode OAM vortex lasing with the ability to precisely define the topological charge of the OAM mode. We show that the polarization associated with OAM lasing can be further manipulated on demand, creating a radially polarized vortex emission. Such OAM microlaser could find applications in the next generation of integrated optoelectronic devices for optical communications in both quantum and classical regimes.

10343-59, Session 12

Conversion of optical spin-to-orbital angular momentum on metasurfaces

Feng Lin, Peking Univ. (China)

Abstract: The optical spin-orbit interaction is that a coupling of the intrinsic angular momentum (photon spin) and the extrinsic momentum (orbital angular momentum) [1-2]. The effect is usually observed when the light passes through an anisotropic and inhomogeneous medium. For instances, the optical spin Hall effect, beam displacement and momentum shift due to the optical spin, was observed at the medium interface. In metasurface structures, the surface plasmons travel along the path that can be defined to within a subwavelength scale by the geometric patterns of the structures, which generate a significant optical orbital angular momentum. In our work, on the Au thin film deposited on glass substrates, we fabricated the subwavelength holes by focused ion beam, which form the ring shape. Using the scanning near-field optical microscope, the different propagation modes of surface plasmons has been observed for the excitation light with the left and right handed circular polarization, respectively. Based on the conservation of total optical angular momentum in this circular system, the conversion effect of the spin and orbital angular momentum can be deduced from the measured and simulated distribution of electric fields.

References:

[1] Shitrit, N.; Bretner, I.; Gorodetski, Y.; Kleiner, V.; Hasman, E. Nano Lett. 2011, 11, 2038.

[2] Shitrit, N.; Yulevich, I.; Maguid, E.; Ozeri, D.; Veksler D.; Kleiner, V.; Hasman, E. Science 2013, 340, 724.

10343-60, Session 12

Chiral nanophotonics of plasmonic and dielectric nanoclusters: from Landau-Lifshitz constraint to flat blazed gratings *(Invited Paper)*

Gennady B. Shvets, Cornell Univ. (United States)

Interference between multiple resonances can dramatically modify the optical response of plasmonic and dielectric nanoclusters. The coupling between resonances is often mediated by symmetry breaking, and the arising from it chirality. I will describe two photonic platforms that take advantage of intrinsic and extrinsic chirality: (a) asymmetric plasmonic nanoclusters that exhibit direction-dependent scattering, and (b) all-dielectric metasurfaces that exhibit highly asymmetric scattering into different diffractive orders. Platform (b) is also used to experimentally characterize “optical magnetism” that is prohibited by the Landau-Lifshitz constraint, and to separately extract magneto-electric and magnetic optical polarizability of asymmetric plasmonic nanoclusters.

10343-61, Session 13

Long range light matter interactions at hyperbolic meta surfaces *(Invited Paper)*

Girish Agarwal, Texas A&M Univ. (United States)

We show how long range light matter interactions can be realized at hyperbolic metasurfaces. We concentrate on the dipole-dipole interactions which are important for energy transfer studies and in quantum entanglement between qubits at metasurfaces. We apply this to get the electromagnetically induced transparency in artificial atoms at large distances. We will present experimental evidence for large range energy transfer.

Return to Contents

10343-62, Session 13

Enhanced superconductivity in hyperbolic metamaterials *(Invited Paper)*

Vera N. Smolyaninova, Christopher Jensen, William Zimmerman, Towson Univ. (United States); Joseph C. Prestigiacomo, Michael S. Osofsky, Heungsoo Kim, Nabil D. Bassim, U.S. Naval Research Lab. (United States); Zhen Xing, Mumtaz Qazilbash, The College of William & Mary (United States); Igor I. Smolyaninov, Univ. of Maryland, College Park (United States)

One of the most important goals of condensed matter physics is materials by design, i.e. the ability to reliably predict and design materials with a set of desired properties. A striking example is the deterministic enhancement of the superconducting properties of materials. Recent experiments have demonstrated that the metamaterial approach is capable of achieving this goal, such as tripling the critical temperature Tc in Al-Al2O3 epsilon near zero (ENZ) core-shell metamaterials and hyperbolic metamaterial superconductors. Here, we demonstrate that an Al/Al2O3 hyperbolic metamaterial geometry is capable of a similar TC enhancement, while having superior transport and magnetic properties compared to the core-shell metamaterial superconductors. We will also report the Tc enhancement in hyperbolic metamaterials based on Sn/CaF multilayers. Reflectivity measurements were made to confirm the hyperbolic character of the fabricated metamaterials. Effect of metamaterial cell size on Tc will be discussed.

10343-63, Session 13

Loss compensation in metamaterials with extraordinary high- and low-momentum plasmic modes

Anatoliy O. Pinchuk, Univ. of Colorado at Colorado Springs (United States)

Hyperbolic metamaterials can propagate electromagnetic modes with unusually large wave numbers (extraordinary high-momentum modes). The extraordinary high-momentum modes are non-propagating or evanescent modes in common optical media. On the other hand, hyperbolic metamaterials can sustain propagating electromagnetic waves with unusually low wave numbers (extraordinary low-momentum modes). Both extraordinary high- and low-momentum modes are of special interest for a number of applications. For example, the development of these exotic modes, which are fundamental to the operation of hyperlenses, might lead to unprecedented sub-diffraction optical imaging systems. Hyperbolic metamaterials are also of special interest for radiative decay engineering.

The inevitable trade-off between optical mode confinement and the optical losses inherent to the metal component is a fundamental challenge for plasmonics and metamaterials. We have carried out numerical analysis of Rytov's dispersion equations to model loss-compensation in metal-semiconductor hyperbolic metamaterials with extraordinary high- and extraordinary low-momentum modes. Numerical results provide a framework for the design of loss compensation schemes in hyperbolic metamaterials with extraordinary high- and extraordinary low-momentum modes.

10343-64, Session 13

Hyperbolic metamaterial filter for angle-independent TM transmission in the infrared regime

Golsa Mirbagheri, Kaitlin J. Dunn, Derek J. Kosciolek, Clarkson Univ. (United States); Igor Bendoym, Phoebus Optoelectronics, LLC (United States); David T. Crouse, Clarkson Univ. (United States)

In this project we propose and fabricate a hyperbolic metamaterials-based narrowband notch filter for the infrared regime with a center wavelength that remains fixed as the angle of incidence changes from 0 to 30 degrees for TM polarization. This novel device modifies a conventional Bragg reflector by including a middle resonance layer that opens up a narrow, highly transmissive band. To achieve angular independence, a subwavelength sized array of silver wires are inserted in a vertical orientation and permeate all 7 Si and SiO2 layers of the structure.

In this work the theoretical underpinnings are explored using Maxwell-Garnett Theory, and simulated with 3D finite element full wave electromagnetic modeling software. Simulations demonstrate that the device is capable of up to 60% transmission at a fixed center wavelength for TM polarization in the infrared.

The device is fabricated using typical microfabrication techniques. The silver nanowires are fabricated via DC electrodeposition. The angle and polarization dependent transmission, reflection and absorption of the device are experimentally measured, and scanning electron microscopy images of the structure are shown.

Though the experimental validation of this device is performed for the infrared regime, scaling the structural sizes can extend the operating regime to higher and lower wavelengths. Whether used as a stand-alone filter, or integrated into a hyperspectral array, the angle-independent response of this filter has many uses in remote sensing applications.

10343-65, Session 13

Non-local effect of hyperbolic metamaterial structure on photo-induced intramolecular charge transfer emissions

Kwang Jin Lee, Yeon Ui Lee, Ewha Womans Univ. (Korea, Republic of); Fre?de?ric Fages, Aix-Marseille Univ. (France) and Ctr. National de la Recherche Scientifique (Gabon) and CINaM - Ctr. Interdisciplinaire de Nanoscience de Marseille (France); Jean-Charles Ribierre, Jeong Weon Wu, Ewha Womans Univ. (Korea, Republic of); Anthony D'Aléo, Ewha Womans Univ. (Korea, Republic of) and Aix Marseille Univ. (France) and Ctr. National de la Recherche Scientifique (France)

Metamaterial is one example of optical material system where non-local effect of optical response can be realized via effective medium description. Non-local effect based on hyperbolic metamaterial (HMM) has been utilized in manipulating the photophysical processes such as intramolecular charge transfer (ICT) dynamics, photodegradation and emission rate. Here, we report an example of non-local effect on spectral shift of emission. There are two different kinds of emissions, namely, emissions from local excited (LE) state and charge transfer (CT) state which are distinguished based on the excited state dipole moment of organic chromophore. In particular, we inspected the photophysical properties of 4-dicyanomethylene-2-methyl-6-(p-dimethylaminostyryl)-4H-pyran (DCM) dye dispersed in polymethylmethacryate (PMMA) matrix in order to identify the effect of non-local effect of HMM on spectral shift of charge transfer emission. There occurred around 6 nm blue shift of ICT emission from DCM fluorophore when located inside of PMMA matrix on top of HMM structures. Image dipole interaction dominant in CT state is responsible for the blue shift, which arises from a non-local dielectric constant surrounding the fluorophore, which is modified by HMM structure nearby. The amount of spectral shift was related to the variation of non-local dielectric constant and ionic radii of donor and acceptor in terms of Lippert-Mataga formalism. Furthermore, high energy LE state and low energy ICT state are identified by time resolved spectroscopy by taking into account of a change in Purcell factor at the same time.

10343-66, Session 14

Active plasmonic devices and processes *(Invited Paper)*

Naomi J. Halas, Rice Univ. (United States)

While graphene plasmonics has been well-studied in the IR, shifting the plasmon resonance of graphene to the visible region of the spectrum would require extremely small graphene structures with dimensions smaller than can be fabricated by the best currently available top-down fabrication methods. This is the length scale of polycyclic aromatic hydrocarbon (PAH) molecules, which can be regarded as picoscale versions of graphene, edge-passivated with hydrogen atoms. Recent theoretical studies have predicted that charged PAH molecules with partially filled orbitals can possess molecular plasmon resonances. While neutral PAH molecules exhibit large energy gaps, rendering them transparent in the visible region of the spectrum, the addition of removal of one or more electrons leads to strong absorption features in the visible wavelength range. Experimentally, PAHs can be incorporated into planar device geometries where they show outstanding potential as low-voltage, fast electrochromic media suitable for applications ranging from nanoscale optical components to large-area, color-changing walls or windows. There has been growing interest in the solar illumination of nanoparticles and nanostructured materials that capture light energy efficiently, enabling localized, confined heating at the liquid-vapor interface to vaporize liquids at high efficiency. Just as there are many fundamental aspects of this problem to investigate there are an increasing number of applications for this process, such as solar distillation. We will discuss how nanoparticle-mediated, light-induced phase separation can be used for water purification, transforming membrane distillation, an energy-intensive conventional process, to a far higher-efficiency, scalable, all-solar process.

10343-67, Session 14

Plasmonic nanofocusing facilitates ultrafast point-projection electron microscopy *(Invited Paper)*

Christoph Lienau, Carl von Ossietzky Univ. Oldenburg (Germany)

Ultrafast optical spectroscopy is now able of tracking even the fastest elementary processes such as the motion of electrons and/or holes in biomolecules or organic solar cells. Despite tremendous progress in sub-diffraction optical microscopy, a direct spatially resolved imaging of such processes is still out of reach since the spatial resolution of even the most advanced near-field imaging techniques is far beyond the Angström-resolution achieved, e.g., in aberration-corrected electron microscopy. As such, numerous efforts are currently ongoing in combining ultrafast optics and electron microscopy.

Recently, point-projection electron microscopy, realized by placing an object directly behind a nanoscopic electron source and recording a diffraction image on a distant screen, emerged as an interesting concept for improving the time resolution in ultrafast electron microscopy into the regime of few tens of femtoseconds or possibly even beyond. It avoids the need for electron lenses, makes the experimental setup compact and simple and minimizes temporal dispersion of the electron pulses.

Sharp metal tips, illuminated with few cycle laser pulses, are interesting electron sources for such experiments. Since direct laser illumination of their apex limits is necessarily diffraction limit, the tip-sample distance, however, is ultimately limited. We will show that nanofocusing of surface plasmons on a metal nano taper can circumvent this limitation by moving the far-field illumination to a grating coupler located several tens of microns away from the sharp taper apex acting as a point-like electron emitter. Here, we demonstrate for the first time the potential of this new technique for probing the dynamics of local electromagnetic fields at the surface of nanostructures with 10-nm spatial resolution and a temporal resolution of better than 30 fs.

10343-68, Session 14

Hybrid perovskite metamaterials *(Invited Paper)*

Cesare Soci, Nanyang Technological Univ. (Singapore)

We engineered the optical response of solution-processed metal-halide perovskite films using metamaterial design concepts. As a proof of principle we fabricated both, all-perovskite dielectric metasurfaces and hybrid metal-perovskite metamaterials, showing significantly enhanced luminescence and control of the spectral response throughout the visible region. Focused ion beam milling was used to directly engrave all-dielectric metamaterials onto thin films of methylammonium lead iodide perovskite (CH3NH3PbI3), spin-coated on quartz substrates: the resulting perovskite metasurfaces display rich structural color tuning and strong field enhancement, dependent on the geometrical parameters of the nanometer sized metamolecules. Photo- and cathodo-luminescence emission from such metasurfaces exhibit up to a five-fold Purcell enhancement with respect to the unstructured films. We also explored hybridization of perovskite films with plasmonic metamaterials and metal-semiconductor-metal slab waveguides to provide higher control over spectral enhancement and light extraction. These results suggest that sub-wavelength structuring and plasmonic hybridization are viable routes to engineer radiative emission properties and tunable structural colour in large-area photovoltaic and light-emitting perovskite devices.

10343-69, Session 14

Light manipulation with metasurface and meta-device *(Invited Paper)*

Pin Chieh Wu, Research Ctr. for Applied Sciences - Academia Sinica (Taiwan); Wei-Yi Tsai, Hui-Hsin Hsiao, National Taiwan Univ. (Taiwan); Hui Jun Wu, Research Ctr. for Applied Sciences - Academia Sinica (Taiwan); Chun Yen Liao, Hsiang-Chu Wang, National Taiwan Univ. (Taiwan); Ai Qun Liu, Nanyang Technological Univ. (Singapore); Greg Sun, Univ. of Massachusetts Boston (United States); Din Ping Tsai, Research Ctr. for Applied Sciences - Academia Sinica (Taiwan)

The functionalities of traditional optical component are mainly based on the phase accumulation through the propagation length, leading to a bulky optical component such as converging lens and waveplate. Metasurfaces composed of planar structures with artificial design have attracted a huge number of interests due to their ability on controlling the electromagnetic phase as well as amplitude at a subwavelength scale. The feasible applications based on metasurfaces include nonlinear dynamics, light beam shaping, quantum interference etc. Beside those promising characteristics, people now intend to discover the field of meta-devices, where we can attain optical properties and functionalities through changing the feature characteristics of metasurfaces in demand. They therefore pave a potential way for the development of flat optical devices and integrated optoelectronic systems and toward the far-reaching applications which are impossible previously. In this talk, four research topics for photonic applications with metasurfaces and meta-devices will be performed and discussed: high efficiency anomalous beam deflector, highly dimensional holographic imaging, versatile polarization control and metadevices with active property.

10343-70, Session 14

Isotropic metamaterial perfect light absorber using 3D split ring resonator in the mid IR region

Renilkumar Mudachathi, Takuo Tanaka, RIKEN (Japan)

Electromagnetic metamaterials have been the subject of intense research

in the recent past owing to their exotic optical properties such as negative or zero refractive index and independently tailorable magnetic and electric response to the incident electromagnetic radiation. Unusual properties like these resulted in devices like electromagnetic cloak and flat super lenses. Metamaterials are often encountered with losses arising from metal and dielectric inclusions, which deteriorates its performance. By taking advantage of this intrinsic loss, the metamaterial could be designed to absorb electromagnetic radiation at any frequency of interest, which has huge potential in many applications like emitters, sensors, spatial light modulators, IR camouflage, thermophotovoltaics and wireless communication to name a few.

We present a perfect light absorber in the mid IR region of the spectrum with wide angle operation. The metamaterial absorber is essentially a three layer structure comprising of an impedance matching layer made up of 3D SRR, a dielectric dissipation layer realised using SiN and a metal ground plane of thickness 100nm which cancels any transmission. The 3D SRR is realised by the self folding of patterned metal strips on the release of residual stress. The SiN layer acts as a sacrificial layer to release the gold arms of length 2?m, width of 100nm and thickness of 50nm to form the ring structures using reactive ion etching. The SRR are then hovered on top of the gold ground plane by the unetched SiN pillars of height 200nm. The 3D SRR directly couples to the incident magnetic field, which generates an oscillating current in the ring which induces an anti parallel current in the metal ground plane. This creates a strong magnetic field coupling in the rings to form a dip in the reflection spectrum. We demonstrate the absorbance of more than 90% at a wavelength of 12.5?m and more than 96% at a wavelength of 8?m for the design with a cut at the metal ground plane.

10343-88, Session PWed

Tunable plasmon induced transparency in a graphene-based waveguide structure and it's applications in sensing

Tao Wang, Xu Han, Huazhong Univ. of Science and Technology (China)

The plasmon induced transparency (PIT) effect, which generates a transparency window within a broad absorption spectrum, has attracted enormous attention because it's potentially important applications in the field of filters, sensors, and slow light. Various plasmonic structures have been proposed to realize the PIT effect, e.g. metamaterials, plasmonic waveguide side-coupled with nanocavities, metallic nanowire grating coupled with a dielectric waveguide layer. However, there are rarely related reports on the realization of dynamically tunable PIT effect and sensor in graphene nanoribbon waveguide structure based on the plasmonic edge modes coupling. In this paper, we propose dynamically tunable PIT in a graphene-based nanoribbon waveguide structure by changing the chemical potential of graphene. It is the direct destructive interference between the propagating plasmonic edge mode in the graphene nanoribbon waveguide and the rectangular resonators gives rise to the PIT effect. We calculate the transmission spectrum for the two-resonator-coupled system with different relaxation times and the Fermi levels. Moreover, a novel plasmonic refractive index sensor (RIS) has been proposed and investigated numerically based on the PIT effect in the mid-IR range. Our calculated results exhibit that large wavelength sensitivity as high as 2500 nm/RIU and a high figure of merit (FOM) of 10.50 can be achieved in this ultra-compact structure (< 0.05 ?m2) with large fabrication tolerance. This work not only paves a new way towards the realization of graphene-based integrated nanophotonic devices, but also has important applications in multi-channel-selective filters, sensors, and slow light.

10343-89, Session PWed

Structural metamaterials with Saint-Venant edge effect reversal

Eduard Karpov, Larry Danso, Univ. of Illinois at Chicago (United States)

When a usual material is loaded statically at surfaces, fine fluctuations of surface strain diminish fast in the material volume with the distance to the surface, a common phenomenon known as the Saint-Venant edge effect. In this presentation, we explore highly nonlocal discrete lattices to demonstrate structural metamaterials featuring reversal of the Saint-Venant edge effect. In these materials, certain coarse patterns of surface strain may decay faster than the finer ones. This phenomenon is rooted in an anomalous behavior of Fourier modes of static deformation in the material, and creates opportunities for blockage, qualitative modification and in-situ recognition of surface load patterns. Potential applications and useful practical techniques of spectral analysis of deformation, density of states and phase diagram mapping are outlined.

10343-90, Session PWed

Bistability and thermal coupling in elastic metamaterials with negative compressibility

Michelle Chen, Johns Hopkins Univ. (United States); Eduard Karpov, Univ. of Illinois at Chicago (United States)

When elastic metamaterials are subjected to tension they may respond by undergoing contraction instead of expansion as an ordinary material would, and vice versa. This negative compressibility behavior can only occur if the system moves from one stable state to a different stable state as the force is applied, i.e., displays bistability. With a simple interatomic potential, we demonstrate that this negative behavior leading to a pinched hysteresis on the stress cycle diagram is a solid-to-solid condensation-type polymorphic phase transformation. In addition, we show that the negative compressibility may disappear in realistic dynamical systems, unless coupling with an external heat sink is strong enough to stabilize the newly formed phase. Such a material is an open thermodynamical system where the condensation process is accompanied by a fast return of the released heat into the ambient. Molecular dynamics with Verlet integration is used to study the dynamics of this behavior.

10343-91, Session PWed

Non-reciprocal manipulation of light with metamaterials in the deep UV light range

Hiroyuki Kurosawa, Shin-ichiro Inoue, National Institute of Information and Communications Technology (Japan)

We numerically studied the directional birefringence induced by the magneto-chiral (MCh) effect. The MCh effect gives rise to nonreciprocal transmittance, which is a key phenomenon to realize highly functional devices such as a one-way mirror. The MCh effect has been investigated in natural materials. However, several conditions such as low temperature and high magnetic fields are required to realize the MCh effect in the natural materials, which is not preferable for practical application. Recently, metamaterials with chirality and magnetism (magneto-chiral metamaterials) at microwave region exhibited an enhanced MCh effect at room temperature and convenient magnetic field strength. In the MCh metamaterial, the coupling of chiral and magnetic resonances plays the key role in realizing the enhanced MCh effect. However, the enhanced MCh effect is not realized in higher frequency region more than the microwave frequency. This is because the magnetic resonance does not exist in the higher frequency regions such as the optical region.

In this paper, we focus on the deep ultra-violet (DUV) light range. In the range, there are magnetic resonances associated with the optical transition. In order to realize the enhanced MCh effect in the DUV light range, both chiral and magnetic resonance are required. As the chiral resonance, we introduce plasmonic resonance of gammadion shaped nanostructure which consists of Aluminum. Combining the magnetic resonance and plasmonic chiral resonance, we for the first time demonstrate numerically that an enhancement of the MCh effect is realized in the DUV light range.

10343-92, Session PWed

LiTaO3 microcubes based metamaterial perfect absorber

Nishant Shankhwar, Reena Dalal, Yogita Kalra, Ravindra K. Sinha, Delhi Technological Univ. (India)

In this paper we present the design of a metamaterial perfect absorber made up of an array of dielectric microcubes grown on a metallic substrate. The fundamental principle of operation of the proposed structure is Mie Resonance occurring in high permittivity particles in combination with the negative permittivity provided by the metallic substrate. The proposed structure is simpler than all other existing metamaterial perfect absorber structures. The geometrical parameters of the structure are between 1μm and 10 μm, hence it is not supposed to pose any challenge during fabrication. Moreover, the structure has been designed for terahertz spectrum which is the most unexplored part of the spectrum. The structure is made up of an array of microcubes of LiTaO3 whose permittivity is very high (~100) for wavelength range from 70 μm to 80 μm. This gives rise to Mie resonance in dielectric microcubes. The microcubes are arranged on a metallic (silver) substrate which provides a negative permittivity and ensure negligible transmission of light through the structure. Furthermore, structure has been optimized to the match the impedance of the free space so as to minimize the reflection as well.

10343-93, Session PWed

Ultrabroadband polarization-independent absorber based on hyperbolic metamaterial

Igor Leonardo Gomes de Souza, Vitaly F. Rodriguez-Esquerre, Univ. Federal da Bahia (Brazil)

We present an ultrathin ultraviolet spectrum absorber composed of multilayers of metal and dielectric with half-cylinder cross-section. The dielectric layers are SiO2 while the metallic ones are niquel, the structure has optimized characteristics of high absorption for both modes. Total absorbance of more than 94% for both electric and magnetic (TM) polarization at normal incidence is observed over a wide range of wavelengths. This property is retained well over a wide range of incidence angles up to approximately 70 degrees. The structure can maintain optimized absorption characteristics even with possible errors in the manufacturing process.

10343-94, Session PWed

Plasmonic nanoballs comprised of gold nanoparticle shells

Hiroshi Yabu, Tohoku Univ. (Japan)

Many efforts have been done to create three-dimensional (3D) metamaterials with piling up two-dimensional (2D) of metallic nanopatterns fabricated by state-of-art lithography techniques. This method is powerful and realizes electromagnetic responses to visible-near infrared (NIR) region of lights, but it has high angler dependency and requires fabrication elaborations. Bottom-up approaches including 3D arrangements of metal nanoparticles have been also one of the challenging to create 3D metamaterials. Nanoparticle arrangements based on DNA self-assembly, block-copolymer phase separation and other techniques have been developed, however, it is quite difficult to create useful "meta-atoms" for realizing 3D metamaterials.

We have demonstrated a simple fabrication method for SERS-active plasmonic nanoballs, which consisted of Au nanoparticles (NPs) and core-shell polystyrene and amino-terminated poly(butadiene) particles, by self-assembly. The amount of Au NPs introduced into the core-shell particles increased with the concentration of Au NPs added to the aqueous dispersion of the core-shell particles. When the amount of Au NPs increased, closely packed, three-dimensionally arranged and close-packed Au NPs arrays were formed in the shells. Strong SERS signals from para-mercaptophenol adsorbed onto this "plasmonic nanoballs" with multilayered Au NPs arrays were obtained by NIR light illumination.

10343-95, Session PWed

Automated design of infrared digital metamaterials by genetic algorithm

Yuya Sugino, Atsushi Ishikawa, Yasuhiko Hayashi, Kenji Tsuruta, Okayama Univ. (Japan)

We demonstrate automated design scheme of infrared (IR) digital metamaterials and experimentally characterize their IR properties. The unit cell of a metamaterial consisted of 7 x 7 Au nano-pixels with an area of 200 nm x 200 nm, and their placements were coded as binary genes in the Genetic Algorithm (GA). The arrangement of each pixel was then searched by the GA combined with 3D electromagnetic numerical analysis to automatically construct the targeted metamaterial. The evaluation function in the optimization process was predefined such that three types of the metamaterials would exhibit pronounced resonant dips at 50, 60, and 75 THz, respectively in their transmission spectra. The GA optimization with a population size of 20 was repeated until the 50th generation where the fitness was fully converged. Based on the numerical results, the metamaterials were fabricated on a Si substrate over an area of 1 mm ? 1 mm by using an EB lithography, Cr/Au (2/20 nm) depositions, and liftoff process. In the FT-IR measurement, clear transmission dips of each metamaterial were observed near the targeted frequencies, although the synthesized pixel arrangements of the metamaterials were seemingly random. The corresponding numerical simulations revealed the important resonant behavior of each pixel and their hybridized systems. Our approach is fully computer-aided without artificial manipulation, thus paving the way toward the novel device design for next-generation plasmonic device applications.

10343-96, Session PWed

Phase modulation in ultrathin lossy material

Tsung Lin Chung, Jia-Wern Chen, Hsiang-Chu Wang, Yu Han Chen, Chun Yen Liao, Mu-Ku Chen, National Taiwan Univ. (Taiwan); Cheng Hung Chu, Pin Chieh Wu, Research Ctr. for Applied Sciences - Academia Sinica (Taiwan); Yi Chieh Lai, National Taiwan Univ. (Taiwan); Din Ping Tsai, National Taiwan Univ. (Taiwan) and Research Ctr. for Applied Sciences - Academia Sinica (Taiwan)

In metasurface optics, electromagnetic wave front can be modified by changing its phase, amplitude and polarization in a desired manner. Arrays of sub-wavelength optical antennas is the major method to control and reshape the wave front of reflection or refraction light. These antennas can take many forms such as metallic or dielectric nanostructures on top of metallic films. By adjusting the separation of arrays and spatial geometric parameters (shape, size, and orientation), the wave fronts can be designed at will. Recently metasurface based on ultra-thin films is proposed because of its abrupt change of optical properties with the film thickness far below the incident wavelength. For instance, the spectrum, leading to various color, can be tuned by adjusting the thickness of lossy material on the metallic mirror. Ultra thin film metasurface can be achieved only by lossy materials (imaginary part of the complex refractive index comparable to the real part). The phase difference of light on reflection or transmission at the interfaces between lossy materials can be more than 0 and ?. This optical property enables the phase modulation with thickness far below the incident wavelength. In this work, the idea using thickness of lossy material in few nanometers to modulate the phase of reflection light is demonstrated.

10343-97, Session PWed

Aluminum plasmonic metasurfaces for control in reflection

Elena I. Chaikina, Ctr. de Investigación Científica y de Educación Superior de Ensenada B.C. (Mexico); Liliana Avalon Murillo, Efren Garcia, Univ. Autónoma de Baja California (Mexico); Eugenio R. Mendez, Ctr. de Investigación Científica y de Educación Superior de Ensenada B.C. (Mexico)

Unlike silver and gold, aluminum has material properties that present strong surface plasmon resonances in the ultraviolet that also span much of the visible region of the spectrum. This spectrally extended response, combined with its natural abundance, low cost, and amenability to manufacturing processes, makes aluminum a highly promising material for nanophotonic applications. In this work, we investigate numerically and experimentally the influence of the geometrical parameters of aluminum covered nanostructures on its optical properties.

The detailed comparison of numerical calculations with the results obtained with fabricated of Al-based nanostructures can be however quite challenging, due to remarkably sensitivity the plasmonic resonance to the presence of oxide on the metal. Here, we model the growth and stabilization of the aluminum oxide film and investigate their influence on the fabricated nanostructures. The nanostructures were fabricated by electron beam lithography method.

10343-98, Session PWed

Guided modes analysis in metamaterial bounded optical waveguides

Juarez Caetano da Silva, Davi Araújo de Figueiredo, Vitaly F. Rodriguez-Esquerre, Univ. Federal da Bahia (Brazil)

We study the propagation characteristics of plasmonic waveguides employing analytical and numerical approaches. The analyzed structures are made of metallic nanowires or metal and dielectric thin layers claddings surrounding a semiconductor or dielectric core. The main parameters to be computed are the propagation distance, the confinement of the fields and the penetration distance into the metamaterial cladding. These structures are intended to exhibit low loss propagation guided modes from visible light to optical communication infrared radiation.

10343-99, Session PWed

Low-loss modes in a hyperbolic metamaterial

Samantha Koutsares, Ekembu K. Tanyi, Michael Admassu, Norfolk State Univ. (United States); Ilya V. Shadrivov, The Australian National Univ. (Australia); Roman Saveliev, ITMO Univ. (Russian Federation); Mikhail A. Noginov, Norfolk State Univ. (United States)

Metamaterials with hyperbolic dispersion have developed a significant amount of interest in the scientific community because they can propagate electromagnetic waves with very large wavevectors. Slabs of lamellar metal-dielectric hyperbolic metamaterials (HMMs) were shown to have the waveguide modes, termed volume plasmons or bulk plasmons, supported by the whole metamaterial structure. These modes, confined to the volume of the lamellar metal-dielectric stack, are of potential importance for signal propagation in plasmonic nanocircuits and stimulated emission at the nanoscale. At this time, we have studied coupling to the HMMs' volume modes in the Kretschmann geometry and shown that light can penetrate through tens of metallic and dielectric layers without substantial loss.

10343-100, Session PWed

Control of electric and magnetic dipole emission with metasurfaces

Soheila Mashhadi, David M. Keene, Antoine C. Hardy, Natalia Noginova, Norfolk State Univ. (United States)

Effect of plasmonic metasurfaces on spontaneous emission of Eu 3+ ions has been studied in patterned metal surfaces of various periodicity and geometry of the surface profile.Both electric and magnetic dipole transitions show strong modification of the angular radiation pattern with specific features determined by metasurface geometry.

10343-101, Session PWed

Spectral shifts of the first and second excited state transitions in R6G dye coupled with the cavity

Ekembu K. Tanyi, Norfolk State Univ. (United States); Erin Harrison, Univ. of Delaware (United States); Cansu On, Mikhail A. Noginov, Norfolk State Univ. (United States)

We have studied strong coupling of silver and aluminum Fabry-Perot cavities with the first (S0-->S1) and the second (S0-->S2) excited state transitions in R6G dye and analyzed the effect of the ENZ dielectric permittivity in Ag. We studied several cavities with different thicknesses in order to vary the level of coupling of the (S0-->S1) transition with the cavity, which according to perturbation theory, should affect the second (S0-->S2) excited state transitions as well. We observed a significant change of the (S0-->S2) excitation band for the Ag cavity of 182 nm: The maximum of the excitation band was shifted from 345 nm to 329 nm. This was not observed in the Al cavities of the same thickness, and we conclude that this strong spectral shift is due to its coupling with the cavity, supporting "full standing wave" resonance and not due to coupling of the (S0-->S1) transition with the cavity.

10343-102, Session PWed

Optically tunable Fano-resonant filter based on graphene

Alexander Grebenchukov, Anton Zaitsev, Mikhail M. Novoselov, Egor Kornilov, Mikhail K. Khodzitsky, ITMO Univ. (Russian Federation)

The ability to narrowband filtering in terahertz (THz) frequency range with effective tunability in terms of resonance frequency is important for many potential applications, such as biomolecule sensing or switching [1]. Currently, for THz filtering planar metamaterials with low quality factor are used [2], which impairs filter performance. Moreover majority of such metasurfaces exhibit static characteristics [3], which also limit their utilization. To overcome mentioned above drawbacks of planar metamaterials the reconfigurable metasuface that supports Fano resonance can be used. In this work, the hybrid graphene-metal Fano resonator is proposed and theoretically investigated. The Fano resonance was obtained by using asymmetric metal split ring covered by graphene as a unit cell of the filter. Tunability is reached by using graphene as reconfigurable medium. Graphene properties and, accordingly, properties of whole composite structure can be efficiently controlled by infrared optical pumping. The simulations of proposed graphene-based filter were performed by solving Maxwell's equations using finite element method for frequency range of 0.1-1 THz. As a result of modeling the high-Q dip in transmission spectrum of proposed filter with fine tuning of resonance frequency by varying the intensity of optical pump was obtained.

References:

1. B. Luk'yanchuk, et al. "The Fano resonance in plasmonic nanostructures and metamaterials," Nat. Mater. V. 9, 707–715 (2010).

2. H.T. Chen, et al. "Experimental demonstration of frequency-agile terahertz metamaterials," Nat. Photonics. V. 2(5), 295–298 (2008).

3. W.J. Padilla, et al. "Electrically resonant terahertz metamaterials: theoretical and experimental investigations," Phys. Rev. B. V. 75, 041102R (2007).

10343-103, Session PWed

A numerical investigation of difference frequency generation in nonlinear multilayered metamaterials

Surawut Wicharn, Srinakharinwirot Univ. (Thailand); Jakkapol Visessamit, Prathan Buranasiri, King Mongkut's Institute of Technology Ladkrabang (Thailand)

In this paper, a second-order nonlinear interaction, difference-frequency generation (DFG), based on three-wave mixing (TWM) process in nonlinear multilayered metamaterials (NMMs) structure has been investigated numerically. The NMMs have been composed of two periodically alternated linear positive-index material (PIM) and nonlinear negative-index material (NIM) layers. To enhance DFG, the pump frequency (µ1) and the signal frequency (µ3) have been tuned into the negative-index and the positive-index regions, respectively, of NIM dispersion for satisfy a backward phase-matching (BPM) condition and meanwhile PIM layer thickness has been optimized to creating field enhancement effect inside the structure. Therefore, the pump and signal fields can efficiently generate a strong idler at frequency µ2 = µ3 x µ1 in backward direction. The numerical results have also confirmed that a conversion efficiency of this idler component is maximized when both conditions being achieved. According to this parametric interaction, the NMMs can be applied as a nonlinear meta-mirror for using as an important part of nonlinear frequency converters and optical signal amplifiers.

10343-104, Session PWed

Interscale mixing microscopy: towards 2D imaging beyond the diffraction limit

Bo Fan, Christopher M. Roberts, Univ. of Massachusetts Lowell (United States); Nicolas Olivier, William P. Wardley, King's College London (United Kingdom); Sandeep Inampudi, Univ. of Massachusetts Lowell (United States); Wayne Dickson, Anatoly V. Zayats, King's College London (United Kingdom); Viktor A. Podolskiy, Univ. of Massachusetts Lowell (United States)

The detection and visualization of subwavelength objects have numerous applications in imaging, spectroscopy, material science, biology, healthcare and security. However, resolution of conventional optical microscopes is fundamentally limited by diffraction to ?/(2NA). Several techniques based on first-order diffraction can enhance resolution of imaging of non-florescent objects with far field measurements to ~?/4. Interscale Mixing Microscopy (IMM) employs diffractive elements in the near field proximity of objects to fold information from the evanescent field into the propagation zone, and uses computer reconstruction to recover the properties of the object based on far field measurements. We have recently reported an analytical implementation and experimental realization of IMM for 1D objects with resolution of the order of ?/10 based on a single measurement. In this work we generalize the developed paradigm to imaging and spectroscopy of two-dimensional objects. In particular, we consider various 2D objects located in the proximity of finite 2D periodic gratings and explore the effect of size, shape, and position of the object as well as size, and shape of the gratings' openings on the accuracy of the imaging and spectroscopy. We demonstrate that 2D IMM can recover the position, and transparency of the subwavelength objects.

10343-105, Session PWed

Design of fan-out diffractive optical elements based on dielectric geometric metasurfaces

Guoxing Zheng, Zile Li, Song Li, Ping'an He, Wuhan Univ. (China)

Previous demonstrated phase-only diffractive optical elements (DOEs), which control the phase by etching different depth into a transparent substrate, suffer from a contradiction between the complexity of fabrication procedures and the performance of DOEs. In this paper, we propose a novel metasurface-based DOEs, whose pixels are replaced by orientation-controllable silicon nanobrick arrays sitting on a transparent substrate. Such so called geometric metasurfaces (GEMS) can act as continuous-phase DOEs whilst only using structures of two-step-depth, which has great promise for designing high-performance DOEs. With the above principle, we report the realization of two different fan-out DOEs based on dielectric GEMS working in C-band fiber telecommunications window (1530-1565 nm) and visible range, respectively. In the first design, uniform 4x4 spot arrays with an extending angle of 59°x59° can be obtained in the far field. In the second design, visible spot arrays with different grayscale form a holographic image with high fidelity in the far field. Because of these advantages of the single-step fabrication procedure, continuous and accurate phase manipulation, and high conversion efficiency, GEMS-based fan-out DOEs could be utilized for various practical applications such as laser holographic keyboard, random spots generator for body motion, optical anti-counterfeiting, laser beam shaping and many other potential fields requiring phase control.

10343-106, Session PWed

Ultra-broadband absorption with gradient metasurface

Tiancheng Han, Southwest Univ. (China)

Due to the advantages of perfect absorption and ultrathin structure, metamaterial absorber (MA) as an important branch of metamaterial-based devices, has been attracting great interest and making great progress in the past several years. For most practical applications, the absorption bandwidth is one of the most important performance metrics. Here, we demonstrate two kinds of ultra-broadband MAs that function in microwave and infrared spectrum, respectively. We first designed an ultra-broadband microwave absorber by combing four different metal-dielectric multilayered quadrangular frustum pyramids within a subwavelength period. Compared with the prior work [Appl. Phys. Lett. 100(10), 103506 (2012)], the proposed absorber demonstrates nearly the same performance (the total absorption exceeds 90% from 8 to 12 GHz and the full width at half maximum is 54.5%) with only 9 layers (at a total thickness of 4.122 mm), showing a great advantage compared to the former that has 20 layers at a total thickness of 5.05 mm. In addition, the absorption remains quasi-constant up to 60°. Then, we designed an ultra-broadband infrared absorber by combing four different pentagon patch metal-insulator-metal (MIM) resonators within a subwavelength period. Both the metal and dielectric thicknesses are very thin (<?/20) and are the same for each resonator of the patchwork. Compared with the previous infrared absorber [Opt. Express 22(S7), A1713-A1724 (2014)], the proposed absorber shows more than twice the absorption bandwidth. The total absorption exceeds 80% from 5.2 to 13.7 um and the full width at half maximum is 95% (from 5.1 to 14.1 ?m), much greater than those previously reported for infrared spectrum. Figure 1 demonstrates the simulation results of the proposed ultra-broadband absorbers. These pave the ways to the design of ultra-broadband efficient plasmonic absorbers from microwave to optical spectrum.

10343-107, Session PWed

Compact three-layered film of passive radiation cooling for LED heat dissipation

Yung-Chiang Lan, Po Jui Chiu, Bo-Han Cheng, National Cheng Kung Univ. (Taiwan); Din Ping Tsai, Research Ctr. for Applied Sciences - Academia Sinica (Taiwan) and National Taiwan Univ. (Taiwan)

In this work, a three-layered (Si-Ni3Si-Al) compact film with heat dissipation based on the method of passive radiation cooling for light emitting diode (LED) are developed and analyzed. The proposed film is designed with the feature of high absorptance at atmospheric transmission region (i.e. 8 um – 13 um). According to Kirchhoff's law of thermal radiation, the emissivity of the film will be equal to its absorptivity at thermal equilibrium. The corresponding admittance diagram and absorption spectra are also explored to elucidate the reason of high absorption. Electromagnetic and heat diffusion simulations based on the finite element method (COMSOL) are accomplished to verify that the design of proposed film can effectively decrease the temperature of LED with various input powers. Considering the typical LED in work (e.g. 1 mm square surface area with heat generation of 1 watt), the proposed film can achieve lower temperature with significantly reduced size as compared to LED with traditional heat sink. This work has potential applications in the field of thermal emitter, photovoltaic-based device and high power devices.

10343-108, Session PWed

A highly efficient and broadband photonic circular polarizer in optical range

Hossein Alizadeh, Björn M. Reinhard, Boston Univ. (United States)

Miniaturization of bulky optical devices to micro and nano scales, has been at the forefront of cutting-edge research in the photonics community. The core idea of this line of research is to move towards ever smaller photonic components that can function even more efficiently than their bulky counterparts. One of such optical elements are Quarter Wave Plates, which convert a linearly polarized light to a circularly polarized light. Upon realization of nanoscale circular polarizers, they would find immediate applications in various areas, from Quantum information processing to nanoscale integrated chips and on-chip photonic communications. In this context, we present a novel nano-sized photonic element, that can function as a circular polarizer in the visible range of spectrum and with very high efficiency. More specifically, we demonstrate that when light impinges on two closely fabricated silicon nanowires, the optical modes of these structures interact and the subsequent lifting of degeneracy of the degenerate fundamental modes of subwavelength nanowires, induces a phase shift in the modes and converts the incident linearly polarized light to a circularly polarized one.

10343-109, Session PWed

Design and analysis of tip slotted square patch nanoantenna

Shubhanshi Sharma, Nishant Shankhwar, Yogita Kalra, Ravindra K. Sinha, Delhi Technological Univ. (India)

In this paper, Tip slotted square patch nanoantenna has been designed and analysed to test its near field enhancement capabilities for implementation in infrared region. Here, near field resonant properties and far field characteristics of a tip slotted square patch nanoantenna have been studied. In this design, a gold square patch has been grown over a silica substrate. Being, chemically inert gold is the most suitable metal to make the patch. At higher frequency, metals cease to behave as perfect conductors and facilitate the formation of surface plasmons. Another advantage of using gold is that it offers low ohmic losses. The data for permittivity of silica has been taken from Palik (1999) and for Gold Drude's model has been used. Complete frequency domain analysis has been performed in COMSOL Multiphysics. As a result of which electric field intensity plots have been obtained which show that near-field enhancement within the slots are substantially high. Moreover, complete far field analysis has been performed and three-dimensional plots of the radiation pattern have been obtained. On account of simple geometry, the proposed structure is not supposed to pose any difficulty during fabrication. The design has been optimised to operate in infrared region to create scope for implementation in IR detection, solar energy harvesting and sensing application.

10343-110, Session PWed

A hybrid phononic waveguide using multilayer structure at mid-infrared

Asma Al-Amri, Michael F. Finch, Claudio Augusto Barreto Saunders Filho, Brian A. Lail, Florida Institute of Technology (United States)

Surface phonon polaritons, SPhPs, results from the coupling or interaction of light with phonon resonance. There has been extensive research into utilizing surface plasmon polaritons, SPPs, for subwavelength confinement of propagating waveguide modes for photonic integrated circuits. This work investigates the use of a multilayer system or insulator-metal-insulator (IMI) heterostructure as a SPhP-enhanced infrared waveguide where the metal response is due to phonons in a polar dielectric's Reststrahlen band. In addition, an IMI heterostructure supports types of modes: an even mode and odd mode that have their own unique trade-offs. For the odd mode as the metal film thickness decreases the confinement of the SPhPs decreases, and thus resulting in an increase in the SPhPs propagation length. Conversely, the even mode shows the opposite behavior with decreasing metal film where the confinement increases as propagation length decreases. This endeavor investigates the trade-off between the even and odd IMI modes, and the characterization of propagation length and model confinement, as applied to a hybrid phononic waveguide.

10343-111, Session PWed

Electrically controlled free space THz polarization modulation using vanadium dioxide metasurfaces

Muhammad Tayyab Nouman, Ji Hyun Hwang, Jae-Hyung Jang, Gwangju Institute of Science and Technology (Korea, Republic of)

We propose a metasurface device design to electronically control polarization of free space terahertz (THz) waves. The proposed metasurface device employs horizontally connected split ring resonators (SRR) on top of a 100-nm-thick Vanadium dioxide (VO2) film grown on a sapphire substrate. The horizontally connected SRRs offer a bandstop resonant transmission for horizontal polarization and a bandpass resonant transmission for the vertical polarization. The proposed design exploits insulator to metal transition (IMT) in VO2 films to electrically tune the resonant response of the THz metasurface. By applying a bias voltage across the top and bottom half of SRRs, the IMT in VO2 at the split gap of the SRRs can be triggered. Without an applied electric field, the VO2 acts as insulator with resistivity on the order of 10-1 ?-cm. Upon application of a large electric field, VO2 exhibits metallic property having resistivity of nearly 10-3 ?-cm. We demonstrate via full wave electromagnetic simulations that above resistivity modulation can significantly vary the SRR response for horizontal polarization while not affecting the response for vertical polarization. The variation of SRR resonant response results in phase modulation as large as 90° for horizontally polarized waves. Thus the polarization of transmitted waves can be switched between linear or circular polarization by applying a bias voltage. The proposed metasurface based modulator can offer huge improvement in modulation speed, compactness and integration capability compared to the previous designs mostly based on liquid crystal devices.
This work is supported by Samsung Research Funding Center of Samsung Electronics under Project Number SRFC-IT1401-08.

10343-112, Session PWed

THz beam-steering using VO2 deep-subwavelength metamaterials

Sara Arezoomandan, Berardi Sensale-Rodriguez, Univ. of Utah (United States)

The demand for bandwidth is close to reach its limits if employing GHz-frequency carriers; from this perspective resorting to THz carriers for future wireless communication links seems inevitable. In this context, many researchers are trying to develop different components for THz communications, being one of those an efficient THz beam-steerer. Based on the generalized laws of reflection and refraction it is possible to employ metamaterial phase modulators so to construct a beam-steerer. By actively controlling the phase gradient imposed by the metasurface, the angle of transmission can be arbitrarily controlled thus beam-steering is possible. In this work, such phase gradient metasurface is constructed using unit-cells that are much smaller than a tenth of a wavelength and employing VO2, a phase-changing material as the reconfigurable material.

To systematically study the effect of the unit-cell dimensions, we introduce a variable, the unit-cell to wavelength ratio, design phase modulators by varying it, and study its effect on the directivity of the transmitted beam (under normal incidence of an incoming excitation). By decreasing the unit-cell to wavelength ratio, the directivity of the array can be improved. However, there is a compromise between this and loss, which is augmented. Overall, a good tradeoff occurs for unit cell dimensions in the order of lambda/20. VO2 when undergoing its insulator to metal transition can provide for the phase modulation required to practically implement such arrays.

10343-113, Session PWed

Magneto-optical nanowire metamaterials

Bo Fan, Univ. of Massachusetts Lowell (United States); Mazhar E. Nasir, Anatoly V. Zayats, King's College London (United Kingdom); Viktor A. Podolskiy, Univ. of Massachusetts Lowell (United States)

Plasmonic nanowire metamaterials have been shown to enable multiple applications in sensing, emission modulation, and in nonlinear optics, in part due to unique dispersion of the modes propagating in metamaterials. In this work, we analyze the perspectives of incorporating magneto-optical (MO) materials into plasmonic nanowire platform. As illustrative purpose, we consider metamaterial on the glass substrate, where gold nanowires with Ni shell are submerged into alumina matrix. With the presence of static external magnetic field, optical response of the MO component of the composite can be described by the permittivity tensor with non-trivial off-diagonal components. External magnetic fields parallel and perpendicular to the wires were considered separately. Starting from the extension of Maxwell-Garnett formalism to wire media with large inclusion concentrations, we have developed an effective medium description of magneto-optical (MO) nanowire platform. The developed effective medium theory (EMT) was verified by comparing the predictions for transmission and reflection through a layer of MO nanowires to full-vectorial solutions of Maxwell equations with commercial finite-element solver. Results show that, similar to other lossy MO composites, combination of anisotropy, lossess and gyrotropy, yields non-reciprocal transmission in the metamaterial, providing the utility of the proposed material platform in the new emerging subfield of optics. The developed formalism can be readily used to calculate optical response of a wide variety of nanowire composites that incorporate MO components as well as to design such composites for particular applications.

10343-115, Session PWed

Mass production compatible fabrication techniques of single-crystalline silver metamaterials and plasmonics devices

Ilya A. Rodionov, Bauman Moscow State Technical Univ. (Russian Federation) and All-Russian Research Institute of Automatics (Russian Federation); Ilya A. Rizhikov, Institute for Theoretical and Applied Electrodynamics (Russian Federation) and Bauman Moscow State Technical Univ. (Russian Federation); Alexander S. Baburin, Bauman Moscow State Technical Univ. (Russian Federation); Alexey P. Vinogradov, Institute for Theoretical and Applied Electrodynamics (Russian Federation) and All-Russian Research Institute of Automatics (Russian Federation); Alexander V. Baryshev, All-Russian Research Institute of Automatics (Russian Federation); Elena V. Ryzhova, Bauman Moscow State Technical Univ. (Russian Federation); Nikolay A. Orlikovsky, All-Russian Research Institute of Automatics (Russian Federation); Alexander M. Merzlikin, Institute for Theoretical and Applied Electrodynamics (Russian Federation); Igor V. Trofimov, Alexander V. Zverev, Bauman Moscow State Technical Univ. (Russian Federation); Sergey S. Maklakov, Institute for Theoretical and Applied Electrodynamics (Russian Federation); Anton I. Ivanov, Ivan A. Philippov, Aidar Gabidulin, Alina Dobronosova, Bauman Moscow State Technical Univ. (Russian Federation)

During last 20 years great results were obtained in metamaterials and plasmonics nanostructures fabrication. However, large ohmic losses in metals and mass production compatibility still represent the most serious challenges which impede progress in the fields of metamaterials and plasmonics. Many recent researches primarily focused on developing low-loss alternative materials, such as nitrides, II–VI semiconductors oxides, high-doped semiconductors, or two-dimensional materials. In this talk, we demonstrate that perfectly fabricated silver films could be an effective low-loss material system, as theoretically well-known. We present our research of silver films optical properties with various crystalline structure (from nanocrystalline to single-crystalline) and our new sub-50nm single-crystalline continuous low-loss low-cost silver film technology, which was optimized to give optical losses below ones reported by Jonson-Christy and sub-nm roughness to maximize SPP propagation length. Films were characterized by AFM, SEM, XRD, profilometry, spectroscopic ellipsometry and SPP propagation length. We manufacture a number of plasmonics and metamaterials nanodevices on transparent (quartz, sapphire, mica) and non-transparent (silicon) substrates using e-beam lithography and dry etch instead of common-used FIB technology. Furthermore, the developed technology is compatible with multilayer device manufacture. We eliminate negative influence of litho-etch steps on silver films quality and fabricate millimeter square devices with different topologies and perfect sub-100nm dimensions reproducibility. The technology is tried out on trial manufacture of spasers, plasmonic sensors and waveguides, metasurfaces, etc. These results could be used as a flexible device manufacture platform for a broad range of practical applications in optoelectronics, communication, photovoltaic and biotechnology.

10343-116, Session PWed

Polarizing properties of chiral metasurface based on gammadion crosses with different geometry in THz frequency range

Maxim S. Masyukov, Anna V. Vozianova, Alexander Grebenchukov, Mikhail K. Khodzitsky, ITMO Univ. (Russian Federation)

Last decade the advances in application of terahertz (THz) technologies for wireless communications, biomedicine, remote sensing, imaging, etc. require the development of new optical components to simplify further progress [1]. Novel devices based on artificial materials (metamaterials) being developed to efficiently control terahertz electromagnetic radiation include frequency-selective surfaces, absorbers, polarization converters, cloaks, etc. Of particular interest is the creation of terahertz components for THz time-domain polarimetry to apply in new diagnostic methods of cancer and diabetes. Chiral metasurfaces may be overcompensated the lack of THz polarizing components due to through the availability of such properties as optical activity, circular dichroism, negative index of refraction, etc [2]. In this work the properties of chiral metasurfaces made from 2-D array of twisted gammadion crosses with different relation of ellipse semi axes of cross were considered in the frequency range of 0.1-1 THz. The total scattering matrixes for the metasurfaces were obtained by Finite Difference Time Domain method. The polarization azimuth rotation angle and ellipticity of structures were calculated from transmission coefficients. The influence of design of metasurface unit cell on polarizing properties was observed. It was shown that the changing of semi axes relation of ellipses of gammadion cross allows tuning operational frequency and creating multiband polarizer.

1. T. Seifert et. al., Nature Photonics 10, 483-488 (2016)

2. G. Kenanakis et al., Optics Express 22, 10, 12149-12159 (2014)

3. Korolenko S.Y. et al., Journal of Physics: Conference Series 735, 1, 1-5 (2016)

10343-71, Session 15

Interscale mixing microscopy: far field imaging beyond the diffraction limit *(Invited Paper)*

Viktor A. Podolskiy, Christopher M. Roberts, Univ. of Massachusetts Lowell (United States); Nicolas Olivier, William P. Wardley, King's College London (United Kingdom); Bo Fan, Univ. of Massachusetts Lowell (United States); Sandeep Inampudi, Univ. of Massachusetts Lowell (United States) and Northeastern Univ. (United States); Wayne Dickson, Anatoly V. Zayats, King's College London (United Kingdom)

Optical characterization of subwavelength objects is important for biology, nanotechnology, chemistry, and materials science. Unfortunately, the information about interaction of an isolated subwavelength object with light is contained in evanescent waves that exponentially decay away from the source. Numerous techniques have been proposed to access or restore this information. In interscale mixing microscopy (IMM), a diffraction grating positioned in the near field proximity of the object is used to convert the originally-evanescent waves into propagating modes that can be detected with far-field measurements. However, far-field signal needs to be post-processed to un-couple the diffraction-limited and subwavelength responses. Several techniques, based on multiple measurements, have been previously proposed. Here, we show that with simple Fourier-transform based post processing can be used to characterize position, and optical size of the object based on a single measurement. To verify the proposed formalism, three finite diffraction gratings were fabricated. Two of these gratings contained pre-engineered "defects" that played the role of "unknown objects", while the remaining grating was used as a reference. We demonstrate that we can identify the position and size of ~wavelength/10 object with far-field characterization. The same measurement provides a platform to analyze optical spectrum of the object. Although demonstrated in this work on example of 1D grating, IMM can be extended to 2D subwavelength imaging

10343-73, Session 15

Surface-assisted carrier excitation in plasmonic nanostructures

Tigran V. Shahbazyan, Jackson State Univ. (United States)

We present a quantum-mechanical model for surface-assisted carrier excitation by optical fields in plasmonic nanostructures of arbitrary shape. We obtain an explicit expression, in terms of local fields inside the metal structure, for surface absorbed power and surface scattering rate that determine the enhancement of carrier excitation efficiency near the metal-dielectric interface. We show that surface scattering is highly sensitive to the local field polarization and can be incorporated into metal dielectric function along with phonon and impurity scattering. We also show that the obtained surface scattering rate describes surface-assisted plasmon decay (Landau damping) in nanostructures larger than the nonlocality scale. Our model can be used for calculations of plasmon-assisted hot carrier generation rates in photovoltaics and photochemistry applications.

10343-74, Session 15

Fano metamaterial absorber for controlling mechanical resonances *(Invited Paper)*

Ertugrul Cubukcu, Hai Zhu, Univ. of California, San Diego (United States); Fei Yi, Huazhong Univ. of Science and Technology (China)

Resonant light absorption in photonic metamaterials can efficiently convert optical energy into heat based on the photothermal effect. Here, we present a plasmomechanical metamaterial that simultaneously supports thermomechanically coupled optical and mechanical resonances for controlling mechanical damping with light. In this metamaterial absorber with voltage tunable Fano resonances, we experimentally achieve optically pumped coherent mechanical oscillations based on a plasmomechanical parametric gain mechanism over a ~4 THz bandwidth. Via the reverse effect, optical dampening of mechanical resonance is also achieved. Our results provide a metamaterial based approach for optical manipulation of the dynamics of mechanical oscillators.

10343-75, Session 15

Mechanical metamaterials: recent advances and opportunities

Eduard Karpov, Univ. of Illinois at Chicago (United States)

Mechanical metamaterials and metastructures show responses to static loads that can be interpreted as a negative elastic modulus or a negative Poisson ratio by a combination of simple mechanical elements, bars and springs. One recent study [1-2], also uses a structural bistability at the unit cell level to deploy a load-induced polymorphic phase transformation in the entire sample. When properly designed, this phase transformation can lead to a contraction of the sample in the direction of an increasing load, a manifest of the negative extensibility phenomenon. In this presentation, we overview recent developments in mathematical analysis of mechanical metamaterials, discuss the paths toward design and fabrication of these interesting materials, and outline their opportunities for structural health monitoring and intelligent structures applications. [1] Nicolaou ZG, Motter AE. Nature Materials 11, 608, 2012. [2] Chen ML, Karpov EG. Physical Review E 90, 033201, 2014.

10343-76, Session 15

Electric field distribution on surface of the artificial magnetic conductor: miniaturization process

Welyson Tiano Dos Santos Ramos, Renato Cardoso Mesquita, Elson José da Silva, Univ. Federal de Minas Gerais (Brazil)

Artificial Magnetic conductor (AMC) are a kind of metamaterial. In contrast metamaterials have properties that are not commonly found in nature. The use of the AMC brings new perspectives of application in solve antennas problems, such as growth of gain and reduction of the back lobe in the radiation pattern [1], obtaining antennas with low profile (0.019?) [2] , procurement multiband devices [3] and the physical and electrical miniaturization of the system [4].This paper presents a detailed study of the role of the geometric shape at resonance frequency of the Artificial Magnetic Conductor (AMC) through the analysis of the electric field distributions on the surface metallic patch inside the unit cell. The device has illuminated by a plane wave with polarization in the y direction. As reference, a square patch with a unit cell of size 10 mm x 10 mm has simulated and a resonance frequency of 5.75 GHz has obtained. The following geometric shapes were performed: square, circular, hexagonal, dipole, cross dipole, Cross of Jerusalem, meander and bowtie. We observed that the electric field distribution, due to polarization of the charges on metal surface of the High impedance surface, strongly contribute to the electrical miniaturization of the AMC. In particular, we propuse some simple geometries that provided considerable electrical miniaturization compared with square patch, about 1.5 GHz. The results are supported by finite element method (FEM), using the commercial software COMSOL Multiphysics and MATLAB.

[1] A. Kamalaveni and M.G. Madhan, " A compact TRM antenna with high impedance surface for SAR reduction at 1800 MHz," AEUE – International Journal of Electronics and Comunications, vol. 70, no. 9, pp. 1192-1198, September 2016.

[2] C. Yen-Sheng and T. Ku, "A low-profile wearable antenna using a miniature high impedance surface for smartwatch applications," IEEE Antennas and Wireless Propagation Letters, vol. 15, pp. 1144-1147, 2016.

[3] Z. Shuai, "Novel dual-band compact his and its application of reducing array in-band RC," Microwave and Optical Technology Letters, vol. 58, no. 3, pp. 700-704, 2016.

[4] M. E. de Cos, Y. Álvarez, R. C. Hadarig, and F. Las-Heras, "Novel SHF-Band uniplanar artificial magnetic conductor," IEEE Antennas and Wireless Propagation Letters, VOL. 9, 2010.

10343-77, Session 16

Graphene metamaterials

F. Javier García de Abajo, ICFO - Institut de Ciències Fotòniques (Spain)

The extraordinary optical, opto-electronic, and magneto-optical properties of graphene render this material an excellent choice for the design of metamaterials with extraordinary capabilities. I will review in this presentation some of them, including the a new strategy for molecular sensing that relies on the strong plasmon-driven nonlinearity of nanographenes; a scenario in which radiative heat transfer is the fastest cooling mechanism, even beating relaxation to phonons; the generation of intense high harmonics from graphene, assisted by its plasmons; and the possibility of strong electro-optical modulation in the visible regime by combining ultrathin metal layers and graphene.

10343-78, Session 16

Near-field study in graphene/hBN moiré superlattices

Guangxin Ni, Univ. of San Diego (United States); Haomin Wang, Shanghai Institute of Microsystem and Information Technology (China); Jhih-Sheng Wu, Zhe Fei, Alexander S. McLeod, Univ. of California, San Diego (United States); Fritz Keilmann, Ludwig-Maximilians-Univ. (Germany); Xiaoming Xie, Shanghai Institute of Microsystem and Information Technology (China); Michael M. Fogler, Dimitri Basov, Univ. of California, San Diego (United States)

Moiré patterns are periodic superlattice structures that appear when two crystals with a minor lattice mismatch are superimposed. A prominent recent example is that of monolayer graphene placed on a crystal of hexagonal boron nitride (hBN). As a result of the moiré pattern superlattice created by this stacking, the electronic band structure of graphene is radically altered, acquiring satellite sub-Dirac cones at the superlattice zone boundaries. To probe dynamical response of the moiré graphene, we use infrared (IR) nano-imaging to explore propagation of surface plasmons, collective oscillations of electrons coupled to IR light. We show that interband transitions associated with the superlattice minibands in concert with free electrons in the Dirac bands produce two additive contributions to composite IR plasmons in graphene moiré superstructures. This novel form of collective modes is likely to be generic to other forms of moiré-forming superlattices, including van der Waals heterostructures.

10343-79, Session 16

Fractal metasurface enhanced graphene photodetector on glass substrate

Di Wang, Jieran Fang, Clayton T. DeVault, Ting-Fung Chung, Yong P. Chen, Alexandra Boltasseva, Vladimir M. Shalaev, Alexander V. Kildishev, Purdue Univ. (United States)

Graphene has been demonstrated to be a promising photodetection material because of its atomic-thin nature, broadband and uniform optical absorption, etc. Photovoltaic and photothermoelectric, which are considered to be the main contributors to photo current/voltage generation in graphene, enable photodetection through driving electrons via built-in electric field and thermoelectric power, respectively. Graphene photovoltaic/photothermoelectric detectors are ideal for ultrafast photodetection applications due to the high carrier mobilities in graphene and ultrashort time the electrons need to give away heat. Despite all the advantages for graphene photovoltaic/photothermoelectric detectors, the sensitivity in such detectors is relatively low, owing to the low optical absorption in the single atomic layer. In the past, our research group has used delicately designed snowflake-like fractal metasurface to realize broadband photovoltage enhancement in the visible spectral range, on SiO_2 thin film backed by Si substrates. We have also demonstrated that the enhancement from the proposed fractal metasurface is insensitive to the polarization of the incident light. In this current work, we have carried out experiments of the same fractal metasurface on transparent SiO_2 substrates, and obtained higher enhancement factor on the fractal metasurface than that achieved on SiO_2/Si substrates. Moreover, the device allows more than 70% of the incident light to transmit during the detection, enabling photodetection in the optical path without any significant distortion. Another possibility to make use of the large portion of transmitted light is to stack multiple such devices along the optical path to linearly scale up the sensitivity.

10343-80, Session 16

Highly confined phonon polaritons in atomically thin interfaces

Alexander M. Dubrovkin, Bo Qiang, Harish N. S. Krishnamoorthy, Nanyang Technological Univ. (Singapore); Nikolay I. Zheludev, Nanyang Technological Univ. (Singapore) and Optoelectronics Research Ctr. (United Kingdom); Qi Jie Wang, Nanyang Technological Univ. (Singapore)

We report the first observation of highly confined polaritons with wavelength two orders of magnitude shorter than the free space wavelength that propagates on the surface of silicon carbide crystals covered by a few atomic layers of molybdenum disulfide.

Confined surface polaritons attract increasing attention as a promising platform for nanoscale opto-electronic integrated circuits enabling strong light-mater interactions. Recently, a new approach for confining surface phonon-polaritons (SPhPs) in bulk polar crystals by ultrathin capping layer has been experimentally demonstrated in quartz/GST system. However, the ultimate performance of the device was limited by the film quality on few-nm thickness scale, and would also require a stronger polar crystal. In this work, we meet these requirements by placing nanometric layers of two-dimensional dielectric materials on a bulk silicon carbide substrate. To experimentally excite SPhPs we use mid-IR radiation of CO2-gas laser at frequencies between 930 and 897 cm-1. Scattering-type scanning near-field optical microscopy (s-SNOM) revealed deeply subwavelength confinement of SPhPs in the MoS2-SiC interface down to bi-layer of the layered dielectric. The confinement factor is highly sensitive to both the MoS2 thickness and the spectral line of excitation. We experimentally perform a systematic study of thickness and spectral dependency of the confinement, and fit the data with theoretically calculated dispersion.

Approach discussed in our work enables realization of ultimate light-matter interaction on the interface of nanometric layered dielectrics supported by bulk polar crystals down to the fundamental atomic limit, opening a new avenue on the surface polaritons confinement at nanoscale.

10343-81, Session 16

Plasmonic MXene for broadband absorber

Krishnakali Chaudhuri, Purdue Univ. (United States); Mohamed Alhabeb, Drexel Univ. (United States); Zhuoxian Wang, Vladimir M. Shalaev, Purdue Univ. (United States); Yury Gogotsi, Drexel Univ. (United States); Alexandra Boltasseva, Purdue Univ. (United States)

MXenes are a new family of 2D layered nanomaterials with chemical form of Mn+1XnTx (M is a transition metal, X is carbon and/or nitrogen). Due to its surface functional groups T (-OH, -O or -F), MXene shows surface hydrophilicity, in addition to high metallic conductivity, excellent mechanical and variable electronic properties. The limited exploration of this material class in the context of plasmonics and nanophotonics motivates the current discussion.

Application area of broadband absorbers has seen versatile use of plasmonics as well as new materials, but often in very complex geometries. Here, a simple, planar absorber structure has been developed, utilizing the resonances of nanostructured Ti3C2Tx, with a polarization-insensitive, extremely large bandwidth operation.

Aqueous dispersion of 2D sheets of Ti3C2Tx with lateral dimensions of 1-2 ?m is spin coated and dried in nitrogen to form a continuous film on desired substrate. Using the measured optical data for these films, we perform FEM simulations of Ti3C2 disks/pillar-like structures showing signatures of localized surface plasmon (LSP) type resonances in the NIR, tunable with varying dimensions. These resonances are then optimized for maximum absorption efficiency in the NIR. This simple disk array (diameter & thickness 0.4 ?m) demonstrates ~80% absorption across ~0.5-1.6 ?m. A further improvement is shown with the disk array sitting on a bilayer stack of a dielectric spacer (SiO2) and a metal (TiN) creating stronger resonances at desired wavelengths, that enable large enhancement of absorption efficiency, especially around the NIR tail (~4x) and a large bandwidth of operation (~1.5 ?m).

10343-82, Session 16

Flat and conformal meta-sheets for controlling light

Samad Jafar-Zanjani, Sandeep Inampudi, Hossein Mosallaei, Northeastern Univ. (United States)

Optical metasurfaces are periodic or graded pattern arrays of ultra-thin plasmonic and/or dielectric nanostructures, which are intended to scatter light in manners that cannot be achieved with conventional stratified media. Recent advancements in the theoretical knowledge and fabrication methods of two-dimensional materials, such as graphene, have provided the opportunity to scale down the principles of metasurfaces to atomic dimensions and to offer graded pattern meta-sheets. We present here engineered nanostructures to tailor the beaming pattern of light scattered through such meta-sheets. We obtain designs to precisely control both the in-plane scattering of surface waves associated with the sheets and also out-of-plane scattered far-field beams into a desired direction. We then determine a set of conductivity-balancing conditions to completely confine the surface waves to the meta-sheets at highly scattering sites and demonstrate that under such criterion the propagation of guided surface waves can be described simply using Fresnel equations of plane waves. Furthermore, we cascade three sinusoidally modulated reactance surfaces to realize a broad-beam leaky-wave antenna to completely scatter the surface waves to far-field and also control the steering direction. In addition, conformal patterned 2D sheets will be explored for the first time and how to successfully design and manipulate the light wavefront. For fast and accurate designs of the flat and conformal meta-sheets, we take advantage of our superior auxiliary differential equation finite-difference time-domain (ADE-FDTD) method. Also, an integral equations (IE) model will be applied for large-area system platforms design investigation.

10343-83, Session 17

Quantum plasmonics *(Invited Paper)*

Peter Nordlander, Rice Univ. (United States)

Recently it has been demonstrated that quantum mechanical effects can have a pronounced influence on the physical properties of plasmons. Examples include the charge transfer plasmon enabled by conductive coupling (tunneling) between two nearby nanoparticles and nonlocal screening of the plasmonic response of small nanoparticles and narrow nanoscale junctions. I will discuss a multitude of recent hot quantum plasmonics topics such as: how to fundamentally distinguish plasmons from excitons in small systems; molecular plasmons in polycyclic aromatic hydrocarbons; plasmon-phonon coupling; plasmons in doped semiconductor nanocrystals; plasmons in two-component hole liquids; plasmon-induced luminescence; and plasmon-induced hot carrier generation.

10343-84, Session 17

Sources and detectors near metasurfaces *(Invited Paper)*

Meir Orenstein, Technion-Israel Institute of Technology (Israel)

Sources and detectors are modified substantially when operating near metasurfaces. Here we discuss light emission from various 2-photon sources when embedded in or near a well engineered metasurface including antennas, plasmon polaritons of HBN, superconductor, epitaxial semiconductor nanoflags and hyperbolic metamaterials. We reort on substantial emission rate enhancement and the discuss the quantum nature of the emission

10343-85, Session 17

Metasurface route to quantum photonics

Pankaj K. Jha, Nir Shitrit, Jeonmin Kim, Xuexin Ren, Yuan Wang, Xiang Zhang, Univ. of California, Berkeley (United States)

Entanglement-based quantum technology is an emerging field of science and engineering that exploits subtle properties of quantum mechanics into practical classical-limits-free applications such as quantum computing, sensing and metrology. The up-to-date route for modern quantum photonics applications, which calls for ultracompact, integrated and scalable architecture, is an atom chip, i.e., microfabricated solid-state device to trap and manipulate cold atoms near an interface. On-chip quantum entanglement in this platform is achieved using cold controlled collisions between the atomic qubits which are significant at subwavelength separations. However, as other manifolds of quantum state engineering require selective addressing and controlled manipulation of individual qubit, entanglement of qubits separated by macroscopic distances at the chip level is still an outstanding challenge. Here, we report on a novel platform for on-chip quantum state engineering by harnessing the extraordinary light-molding capabilities of judiciously designed metasurfaces. We demonstrate robust generation of quantum entanglement between two atomic qubits trapped on a chip and separated by macroscopic distances, by engineering their coherent and dissipative interactions via the metasurface functionality. The metasurface route to quantum state engineering opens a new paradigm for on-chip quantum technology at the nanoscale by integrating high-end custom-designed ultrathin optical elements in atom chips.

10343-86, Session 17

Lasing in arrays of metal nanoparticles

Heikki Rekola, Tommi K. Hakala, Aaro I. Väkeväinen, Jani-Petri Martikainen, Marek Ne?ada, Antti J. Moilanen, Päivi Törmä, Aalto Univ. (Finland)

Plasmonic resonances supported by metallic nanoparticles have extremely small mode volumes and high field enhancements, making them an ideal platform for studying nanoscale lasing. However, these good measures of plasmonic resonances also make them bad in terms of practical implementations, as Ohmic and radiative losses have to be compensated with gain available in the small mode volume of the resonances. Here we show a way around these limitations by utilizing arrays of nanoparticles, which support delocalized resonances called Surface lattice resonances (SLRs). The structures are combined with organic dye molecules and optical pumping to realize lasing at visible wavelengths in both bright and dark modes of an array of silver nanoparticles, with linewidths down to 0.2 nm. [1]

The SLR modes are hybrids of the localized surface plasmon resonances of the nanoparticles, and the diffractive orders of the periodic structure. Both bright and dark (sub-radiant) modes are supported by the arrays. These dark modes offer even further reduced losses, as radiation away from the structure is suppressed. We show lasing in both bright and dark modes of the arrays, with access to the dark modes provided by the finite size of the array structure. By varying the array size, we show spatial coherence over the whole structure. We expect the SLR modes, which are both photonic and plasmonics in nature to become important for also other applications of plasmonics.

[1] T.K. Hakala, et al. Lasing in dark and bright modes of a finite-sized plasmonic lattice. Nat. Comms. 8, 13687 (2017)

10343-87, Session 17

Valley photonic crystals

Jian-Wen Dong, Xiao-Dong Chen, Sun Yat-Sen Univ. (China)

Photonic crystals known as the periodic optical structures have been well exploited to manipulate the flow of light. For example, photonic net spin flow such as one-way transports and spin-directional locking have been realized in at the boundary of topologically-protected photonic crystals. But this is not the only way to achieve spin flow control. In this talk, without the assist of boundary, we will show the molding of spin flow of light in two kinds of valley photonic crystal by exploiting the valley degree of freedom. The coupled valley and spin physics in valley photonic crystal is illustrated through both analytical photonic Hamiltonian and bulk band structures. The photonic valley Hall effect, i.e., different spin states in two inequivalent but time-reversal valleys flow to opposite directions, is demonstrated in the bulk crystal. In addition, unidirectional spin flow is achieved by selective excitation of either spin or OAM chiral sources inside the topologically trivial valley photonic crystal instead of the assist of topologically non-triviality. We also show the independent control of valley and topology, resulting in a topologically-protected flat edge state in bianisotropic photonic metacrystal and a valley-protected back-scattering immune state in all-silicon photonic crystal. Valley photonic crystals may open up a new route towards the discovery of fundamentally novel states of light and possible revolutionary applications.

10343-117, Session 17

Quantum nanophotonics *(Invited Paper)*

Jelena Vuckovic, Jingyuan Zhang, Stanford Univ. (United States)

Nanophotonic structures that localize photons in sub-wavelength volumes are possible today thanks to modern nanofabrication and optical design techniques. Such structures enable studies of new regimes of light-matter interaction, quantum and nonlinear optics, and new applications in computing, communications, and sensing. The traditional quantum nanophotonics platform is based on InAs quantum dots inside GaAs photonic crystal cavities, but recently alternative material systems based on color centers in diamond and silicon carbide have emerged, which could potentially bring the described experiments to room temperature and facilitate scaling to large networks of resonators and emitters. Additionally, the use of inverse design nanophotonic methods that can efficiently perform physics-guided search through the full parameter space, leads to optical devices with properties superior to state of the art, including smaller footprints, better field localization, and novel functionalities.

10344-1, Session 1

Designing the metal nanoparticle (MNP)-non linear optical (NLO) material: future nanophotonics

Preeti Gupta, G.V. Pavan Kumar, Indian Institute of Science Education and Research Pune (India)

We have elucidated the role of plasmon resonance in the ETU system, and provides a straightforward method to directly measure the energy transfer rate and internal upconversion efficiency. We have also probe plasmon-coupled emission engineering of lanthanides using nano-optical tools and uniquely characterize and quantified the effects of size and shape on the plasmonic behaviour of nanoparticles, and allowed the study of properties inaccessible with bulk measurements, such as plasmon decay and polarization effects. We have unravel and provided quantitative information on the magnitude of the intrinsic polarization-induced scattering intensity variation and mode selectivity by single particle spectroscopy.

10344-2, Session 1

Nanoparticles induced light to vapor conversion for off-grid water purification: full multiphysics modeling *(Invited Paper)*

Alessandro Alabastri, Pratiksha Dongare, Seth Pedersen, Rice Univ. (United States); Katherine Zodrow, Montana Tech (United States); Nathaniel J. Hogan, Oara Neumann, Jinjian Wu, Qilin Li, Peter Nordlander, Naomi J. Halas, Rice Univ. (United States)

In the world, 1.1 billion people lack practical access to a fresh water supply. Membrane Distillation (MD) is a promising technique employed to purify or desalinize water. However the process is highly energy demanding due to water relatively large latent heat leading, at ambient conditions, to a limited evaporation rate. Broadly absorbing metal or carbon nanoparticles (NPs), when mixed with water, greatly enhance the evaporation rate if the solution is placed under focused sun irradiation. MD can be improved by including a thin layer of light-absorbing NPs on top of the membrane which separates salty and fresh water providing a sun powered, electrical energy free heat source along the whole device. In the process, only the water in contact with the NPs is heated, leading to an effective layer-by-layer vaporization effect. To prove the concept, alongside experiments, a full multiphysics model has been realized including the main physical mechanisms playing a role in the NP induced vaporization and water transport process. At this purpose, a Finite Element Method (FEM) approach was employed to analyze and predict the efficacy of the system, fully reproducing the employed device. Light-to-vapor conversion efficiencies of about 20% below 1 Sun of illumination and salt rejection of more than 99.5% have been found in desalination experiments and confirmed by theoretical investigations.

10344-3, Session 1

Photocurrent generation from TiN nanostructures by visible light *(Invited Paper)*

Satoshi Ishii, Satish L. Shinde, Tadaaki Nagao, National Institute for Materials Science (Japan)

Titanium nitride is a highly conductive ceramic which has been gaining tremendous attentions in plasmonics community. While the applications of titanium nitride for plasmonic metamaterials and photothermal effects have been studied, generation of hot electrons from titanium nitride has been elusive. Here we demonstrate experimentally that hot electrons can be optically excited from titanium nitride. We confirm the generation of hot electrons up to 800 nm in wavelength by measuring the photocurrent from titanium nitride thin films deposited on a zinc oxide thin film. A control sample where the titanium thin film is replaced with a gold thin film having the identical thickness is also fabricated and its photocurrent is much weaker than the titanium nitride sample in whole visible spectrum. Hence our results show that titanium nitride is superior than gold in generating hot electrons in visible range. Since titanium nitride is chemically stable and less expensive than gold, we anticipate that titanium nitride can replace gold in photoelectric applications such as visible light photocatalysis and solar water splitting.

10344-4, Session 1

Plasmonics: transformed quantum emitters *(Invited Paper)*

Ajay Singh, Jennifer A. Hollingsworth, Los Alamos National Lab. (United States)

Nanocrystal plasmonics enjoy scientific attention for enhancement of optical processes, such as luminescence, Raman scattering, optical switching, and absorption. In plasmonic nanomaterials, free carriers are driven to oscillate collectively at a resonate frequency in response to the oscillatory electromagnetic field of incident light, which is characterized as the localized surface plasmon resonance (LSPR). The excitation of LSPR are strongly confined to the size, shape, and composition of plasmonic nanocrystal. As a result, the resonant dipolar polarization modes (longitudinal and transverse) of the nanocrystals are dominant and correspond to strongly enhanced electric fields (hot spots) within and especially just outside the nanocrystals vicinity. This near field enhancement in the nanocrystal can be exploited to enhance (by coupling) the inherent properties (luminescence, absorption, vibrational state transitions etc.) of nearby molecules or materials such as the quantum emitters (QE). In case of quantum emitters, the LSPR resonance coupled to the emitter in the range from weak (Purcell effect quickens QE's emission rate) to strong (reversible exchange between field and emitter – Rabi oscillation) coupling. In order to understand these coupling regime (plasmon-photon interactions), we performed series of experiment by varying the QE (emission) and plasmonic nanocrystal size, shape, resonance frequency and studied their effect on the emission rate of the exciton.

10344-5, Session 1

Heat dissipation control in plasmonic systems

Alessandro Alabastri, Rice Univ. (United States); Andrea Toma, Mario Malerba, Eugenio Calandrini, Francesco De Angelis, Remo Proietti Zaccaria, Istituto Italiano di Tecnologia (Italy)

Metallic nanostructures can be utilized as heat nano-sources which can find application in different areas such as photocatalysis, nanochemistry or sensor devices. Here we apply a temperature dependent dielectric function model to different nanoparticles finding that the optical responses are strongly dependent on shape and aspect-ratio. Depending on the structures geometry, absorption efficiency can either increase or decrease with temperature. The electric permittivity, which dictates the optical response, is modified by the temperature which depends on the electric fields and currents induced in the metallic medium. When the intensity of the incident electromagnetic field is sizable, the induced non-linearity plays a major role and the effect on the final electric fields and temperature can be substantial. Moreover, the background temperature itself can be used to tune an antenna optical and thermal properties. In particular it was found that, by properly designing arrays of nano-antennas, the temperature dependence

of the heat released by each single antenna can be tailored and can exhibit opposite trends for different structures aspect ratio. In fact, high aspect ratio antennas exhibit a decreasing heat dissipation for increasing temperature. This effect may lead to materials with self-limiting heating properties which reduce the dissipation upon reaching high temperature values.

The calculation method employed here is flexible and matched experimental measurements. The same approach was used to successfully predict the role of the thermal boundary resistance in gold nanowires at low temperatures, thus confirming its validity as a tool for thermoplasmonic applications.

10344-6, Session 2

Large area fabrication of robust plasmonic color metasurfaces by a high-speed roll-to-roll method

Swathi Murthy, Inmold (Denmark); Henrik Pranov, Heliac (Denmark); Guggi Kofod, Inmold (Denmark); Rafael J. Taboryski, Technical Univ. of Denmark (Denmark)

Lab-scale plasmonic color printing using nano-structured and subsequently metallized surfaces has been demonstrated to provide vivid colors on structured surfaces. However, upscaling these structures for large area manufacturing is extremely challenging due to the requirement of nanometer precision of metal thickness. Here, we report for the first time, a novel plasmon resonance mode which is a hydridization between surface and gap plasmon resonances in Al nanostructures, for obtaining plasmonic colors. The existence of this hybrid mode makes the colors insensitive to the thickness of the metal layer, when this thickness exceeds the depths of the nano-pits on the surface. Thus, allowing for a robust high speed fabrication of plasmonic color metasurfaces. We have also demonstrated the feasibility of fabrication of these plasmonic color surfaces by a high-speed roll-to-roll method. First nanostructured polymer foils, comprising of 100nm deep nano-pits of varying diameter and pitch were fabricated by roll-to-roll extrusion coating at 10 m/min, followed by roll-to-roll metallization with 100 nm of Al at 350 m/min by a high vacuum thermal evaporation process and finally, a roll-to-roll lacquering process for protection of the metalized nanostructures. This can pave way for plasmonic meta-surfaces to be implemented in applications such as memory, SERS, flexible displays, photovoltaics, security, product branding etc.

10344-8, Session 2

Precipitation and spectral characteristics of silver nanoparticles and rare-earth ion doped oxide nanocrystals inside borate glasses

Ki-Soo Lim, Chang-Hyuck Bae, Chungbuk National Univ. (Korea, Republic of)

We prepared CaO-K2O-B2O3-ZnO-Al2O3 glass system doped with Ag2O, Eu2O3, and Yb2O3 using conventional melt-quenching method. Femtosecond laser irradiation and the following proper annealing produced silver nanoparticles showing surface plasmon band in the absorption spectra of the glass. The enhancement of the photoluminescence from Eu3+ ions was observed due to the local field effect. We also synthesized glass-ceramics containing ZnO nanocrystals by further thermal annealing in an electric furnace and observed much enhanced visible emission of Eu3+ ions due to the environment of nanocrystals instead of glass. Instead of this traditional furnace annealing, we used CO2 laser annealing by slow-speed scanning for the glass and obtained another oxide nanocrystals of ZnAl2O4 on the surface. Spectral characteristics of the enhanced down- and up-conversion emissions in the glass-ceramics under 365 nm and 980 nm excitation were explained by cross-relaxations, excited state absorptions, and energy transfer processes between Eu3+ and Yb3+ ions. TEM analyses revealed the size and presence of silver nanoparticles and oxide nanocrystals. XRD analysis showed the phase appearance of ZnO and ZnAl2O4 crystals and we discussed the effects of the annealing temperature and duration time for furnace and laser treatments.

10344-9, Session 2

DNA-assembled large-scale responsive multicomponent nanoparticle metamaterials *(Invited Paper)*

Qingyuan Lin, Jarad Mason, Vinayak P. Dravid, Chad A. Mirkin, Northwestern Univ. (United States)

The assembly of large-scale multicomponent nanoparticle superlattices with programmable geometries and arrangements remains a grant challenge in the field of colloidal nanocrystal synthesis. Here we combine top-down lithography and bottom-up DNA assembly to construct structurally sophisticated responsive three-dimensional multicomponent nanoparticle superlattices that are inaccessible with conventional solution assembly and lithographic techniques. Six designs of large-area ternary superlattices consisted of up to three different types of nanoparticle shapes were synthesized, demonstrating the versatility of such assembly strategy. In addition, the placement of each individual nanoparticles at the nano-scale and the crystal symmetry and size at the macro-scale were precisely defined at the same time, offering unprecedented control over the superlattice architectures. This general approach have potential to further extend to the assembly of superlattices with more than three elements, providing a powerful platform for the construction of metamaterials for optical, electronic, magnetic, and catalytic applications.

10344-10, Session 3

3D femtosecond laser printing for angular momentum generators *(Invited Paper)*

Xuewen Wang, Swinburne Univ. of Technology (Australia)

We propose to use femtosecond laser direct writing technique to realise dielectric optical elements from photo-resist materials for the generation of structured light from purely spin-orbital conversion transformations. This is illustrated by the fabrication and characterisation of spin-orbital optical angular momentum couplers generating optical vortices of topological charge from 1 to 20. The elements achieved using this techniques also were demonstrated its capabilities to working in the whole visible range with efficiency up to 85%. We also firstly demonstrated the abilities to combine the dynamic phase and geometric phase using the 3D fabrication capability of laser direct writing to create elements that generate different topological charges of optical vortices simultaneously with the shared aperture.

10344-11, Session 3

Formation and multi-imaging analysis of nascent surface structures generated by femtosecond laser irradiation in silicon

Felice Gesuele, Jijil J. J. Navas, Pasqualino Maddalena, Salvatore Amoruso, Univ. degli Studi di Napoli Federico II (Italy)

The formation of surface structures (both ordered and random) by means of femtosecond laser micro-structuring is a striking and extensively studied phenomenon at the base of several applications. Due to its great technological importance, silicon is one of the most investigated material forming a realm of surface structures depending on the processing conditions.

Here we report on the formation of periodic structures on the (100) crystalline silicon surface after irradiation with a low number of 1055 nm, 850 fs laser pulses, in high vacuum conditions. We focus our analysis on the nascent stage of surface structures formation. We employ a wide variety of microscopy techniques to retrieve the mechanical, optical and structural properties of realized structures. Sample topography is measured by means of an Atomic Force Microscope. Sample structural phase and amount of defects are revealed by performing a Raman micro-analysis carried out through a scanning confocal optical microscope, while confocal reflection images of the sample surface are also registered with the same optical setup.

Our analyses clearly show the creation of grating structures of near-wavelength (1.02μm) period consisting of alternating amorphous and crystalline periodic lines, with almost no material removal. The gratings originate from defects acting as scattering centres and generating energy modulation patters propagating along the direction of laser polarization.

A comparative analysis, carried out with silicon samples processed in ambient air at atmospheric pressure under the same experimental conditions, allows to gain insights on the fs laser surface structuring process of silicon.

10344-12, Session 3

Spectral analysis of volume holograms in materials with diffusion-based formation mechanisms by means of coupled wave theory and Kramers-Kronig relations

Vladimir N. Borisov, Aleksandr E. Angervaks, Aleksandr I. Ryskin, Andrey V. Veniaminov, ITMO Univ. (Russian Federation)

Volume holography has a potential in terms of production of precise optical diffraction elements and photonic-crystalline structures, and analysis of such structures is of considerable interest. The key role in that analysis is to obtain spectral dependences of optical parameters modulation. Solid materials with diffusion-based formation mechanisms of holograms (like PQ-PMMA or calcium fluoride crystals with color centers) are in a great interest since they potentially allow for large refractive index modulation. However, due to the complexity of photochemical and photophysical processes occurring during the recording of holograms, their spectral analysis is a challenging task.

In this research volume holograms were studied by capturing selectivity hypercontours (2D spectral and angular dependences of diffraction efficiency) and analyzing them by means of Kogelnik coupled wave theory. Selectivity hypercontours provide the most informative picture of the hologram properties, including spectral dependences of absorbance and refractive index modulation profiles. Measurements made at different times showed a hologram transformation in PQ-PMMA due to diffusion processes: holograms converted from predominantely amplitude to almost phase ones in the course of postexposure diffusion of PQ molecules. Thus, this technique allows for studying processes that are involved in the formation of holograms.

While absorbance modulation is in direct connection with the absorption spectra of the materials, an adequate description of phase modulation through Kramers-Kronig dispersion relations discovered in colored crystals. Kramers-Kronig relations are operable tool in cases where the nature of holograms formation is well studied. In turn, testing holograms formation hypotheses using Kramers-Kronig relations can prove their validity.

10344-13, Session 4

Long-range exciton transport in cesium lead halide perovskite nanocrystals organized in ordered nanoscale assemblies *(Invited Paper)*

Erika Penzo, Lawrence Berkeley National Lab. (United States); Anna Loiudice, Ecole Polytechnique Fédérale de Lausanne (Switzerland); Edward S. Barnard, Nicholas Borys, Lawrence Berkeley National Lab. (United States); Raffaella Buonsanti, Ecole Polytechnique Fédérale de Lausanne (Switzerland); Adam M. Schwartzberg, Stefano Cabrini, Alexander Weber-Bargioni, Lawrence Berkeley National Lab. (United States)

Fully inorganic cesium lead halide perovskite nanocrystals (NCs) are a novel colloidal material displaying remarkably bright photoluminescence (PL) characterized by high quantum yield (QY) of 50-90% and narrow emission line widths of 12-42 nm. In addition, compositional control and quantum-size effects allow for the precise and continuous tuning of bandgap energies over the entire visible spectral region.

The cubic perovskite crystal structure results in NCs with cubic shape, 4-15 nm in side length. Taking advantage of their affinity for hydrophobic surfaces, these NCs can be assembled in highly ordered monolayers in which the cubic NCs are organized in arrays with parallel edges. The close proximity of this arrangement and the high polarizabilty of these NCs allow for efficient exciton migration between adjacent NCs through Förster Resonant Energy Transfer (FRET). The monolayer layout confines the available paths for exciton transport in two dimensions, enabling the accurate study of the transport effects and mechanism using super-resolution based optical imaging techniques combined with steady-state and time-resolved spectroscopy. Evidence of FRET-like transport is found in accelerated relaxation times and spatial expansion of the excited state ensemble. FRET-mediated long-range exciton migration exceeding 200 nm is observed, and the impact of the inter-nanocrystal energetic disorder on the observed optical signatures is discussed.

This system allows for the first demonstration of such long-range exciton transport in NCs solids opening up new possibilities for high functionality optoelectronic devices based on cesium lead halide perovskite NCs.

10344-14, Session 4

Possibility of cost effective and energy efficient high quality natural white light sources with a new nano-phosphor

Dilip De, Covenant Univ. (Nigeria) and Sustainable Green Power Technologies (United States); Ikorya De, Univ. of the Free State (South Africa)

In this paper we present results authors' published initially on the white light emission with broad band (330-465 nm) excitation of the specially prepared nano-phosphor: Eu^{3+}:ZnS which is capped with sodium methyl carboxylate and on pure red-light emission from the nano-phosphor when capped with alpha methyl acrylic acid and prepared in a different method. Then we discuss possible methods of future improvement of the white light emission from the nano-phosphor. We then present the cost effective and energy efficient method of obtaining highest quality natural white light sources using such nano-phosphor and blue or near UV blue light emitting diodes. The latter discussion includes the driving circuit for the white LED and powering the LED by concentrated solar photovoltaics for completely clean energy natural white lighting sources.

10344-15, Session 4

Quantum-confined and pseudo Stark effects in the semiconductor conical quantum dot

Karen G. Dvoyan, Ani Tshantshapanyan, Branislav Vlahovic, North Carolina Central Univ. (United States); Gregory J. Salamo, Univ. of Arkansas (United States)

Electronic states and direct interband light absorption in GaAs conical quantum dot (QD) are theoretically investigated within the framework of the geometric adiabatic approximation both in strong and weak quantum confinement regimes. For the lower levels of the spectrum, the localization of the electron in the vicinity of the QD center of gravity is proved. The QD conical symmetry leads to appearance of an atypical linear term in the effective confining potential. The influence of a uniform electrical field on the system is also considered, and both quantum-confined and pseudo Stark

effects are discussed. For weak quantum confinement regime, the motion of the exciton center-of-gravity is quantized, which leads to appearance of additional Coulomb sub-levels. Dependencies of the absorption edge on the QD geometric parameters are obtained, and corresponding selection rules for quantum transitions are revealed.

10344-29, Session PWed

VOx nanofibers for IR detection

Seong Hyun Kim, Su Jae Lee, Electronics and Telecommunications Research Institute (Korea, Republic of); Bong-Jun Kim, Mobric Co. Ltd. (Korea, Republic of)

Various materials have been used for infrared detection. They are also manufactured in various structures. Among them, vanadium oxide is widely used in non-cooling type infrared image sensors. Among them, V_2O_5 type is used most commonly, and recently VO_2 is being studied. The vanadium oxide is not easy to make single phase because the phase varies considerably and the production conditions are complicated. The mix of these phases leads to performance degradation. At present, thin film vanadium oxide is mainly used. In the manufacturing process, since the thin film must be floated in the air, the process is difficult and the defect rate is high.

In this study, vanadium oxide in nanofiber form was studied. Fabricated nanofibers were able to change the phase according to the process conditions and space between the material and the substrate spontaneously occurred in the manufacturing process without artificially floating in the air. We also discuss the fabrication process using a random structure.

10344-30, Session PWed

Luminescence and transient lifetime studies for energy transfer of PbS QD films

Joanna S. Wang, Bruno Ullrich, Chandriker K. Dass, Air Force Research Lab. (United States); Anirban Das, Chien M. Wai, Univ. of Idaho (United States); Gail J. Brown, Joshua R. Hendrickson, Air Force Research Lab. (United States)

Nanoparticle colloidal solutions of quantum confined semiconductor materials have drawn great attention in scientific communities due to the size-tunability of their optical properties arising from the effect of quantum confinement. PbS quantum dots (QDs) are exciting candidates for quantum optics, particularly, due to size controllable parameters in the synthetic process which provides precisely tunable emission properties in the infrared region. PbS QDs in different sized pairs are deposited onto glass substrates to form thin films using supercritical fluid CO_2 (sc-CO_2) deposition and solvent deposition methods. Fluorescence and photoluminescence (PL) spectra of PbS QDs obtained from these closely packed films prepared by the sc-CO_2 method reveal effective Förster resonance energy transfer (FRET) between two different sized dots, while the films composed of three different sizes of dots show an even more effective FRET from the smallest to the largest ones. Energy transfer can be observed more directly by spectrally resolved PL decay of mixed dots. A mixed PbS film with 3.1 and 4.8 nm QDs was studied for FRET by time correlated single photon counting for transient lifetime measurements. The PL is quenched at the short wavelength, which decays faster than that recorded for the radiative emission decay of the long wavelength peak. The lifetime (decay constant)$^{-1}$ for the shorter wavelength is best fit using a biexponential equation. The long wavelength decay is best fit by a monoexponential equation. More theoretical and experimental work is required for a thorough understanding of the radiative lifetimes of PbS QDs in mixed QD systems.

10344-31, Session PWed

Magnetic field influence on the intensity of ZnO random lasing and exciton luminescence

Andrey P. Tarasov, Moscow Institute of Physics and Technology (Russian Federation) and Kotel'nikov Institute of Radio Engineering and Electronics of Russian Academy of Sciences (Russian Federation); Charus M. Briskina, Alexey Saveliev, Valery M. Markushev, Kotel'nikov Institute of Radio Engineering and Electronics of Russian Academy of Sciences (Russian Federation); Mikhail Shiryaev, M.V. Lomonosov Moscow State Univ. (Russian Federation)

There are a lot of theoretical and experimental investigations devoted to the influence of magnetic field on the exciton, particularly, in the case of ZnO, but they are mainly focused on very low temperatures and single crystals or heterostructures (such as quantum dots and wells). In our opinion, it is useful to perform such investigation at room temperature (RT) and using structures which are easier to prepare.

In our investigation, the influence of magnetic field on the exciton luminescence of ZnO microfilms at RT was studied. The samples had a disordered nanorod structure with nanorod diameter ~200 nm and length ~1 um. Nanorods were almost randomly oriented, diverging from the normal to the Si-substrate surface up to ~50 degrees.

The excitation of samples luminescence was performed by 3rd harmonic of pulsed Nd:YAG laser (pulse duration is ~10 ns, repetition rate is 15 Hz). Constant magnetic field with magnitude of 0.9 T was generated by a rather portable magnetic system. The excitation levels in the experiment lay in the range 5-39 μJ. Random lasing started appearing in the area of exciton band peak at the excitation of 5 μJ. Inserting the sample in magnetic field leaded to the increase of random lasing and the luminescence intensity. The value of enhancement is approximately 15-20% and varies only slightly with the excitation level rise.

The experimental results were analyzed on the base of the concept of the Zeeman effect and by estimation of exciton recombination probability using Schrödinger equation.

10344-32, Session PWed

Optical properties of cyanine dyes in nanotubes of chrysotile asbestos

Anton A. Starovoytov, ITMO Univ. (Russian Federation); Vladimir I. Belotitskii, Yuri A. Kumzerov, Anna A. Sysoeva, Ioffe Institute (Russian Federation); Tigran A. Vartanyan, ITMO Univ. (Russian Federation)

Incorporation of organic dye into porous materials has received increasing attention in recent years due to its potential application potential in lasers, artificial light-harvesting antennas, optical switches and sensors. The dye molecules embedded in nanopore system are well-isolated in comparison with molecules in thin films or solutions. Thus, photophysical properties of the dye molecules in nanoporous material would provide insights for fundamental understanding of such system.

We studied the absorption, linear dichroism, fluorescence (emission, anisotropy and decay lifetime) for monocarbocyanine dye embedded in chrysotile asbestos which consists of a regular arrangement of cylindrical nanopores (nanotubes) that form a one-dimensional nanopore system.

The Stokes shift for dye in asbestos is smaller than for the molecules in the ethanol solution. This circumstance reflects smaller polarity of the nanopore environment. The absorption and fluorescence spectra of dye in asbestos and solution have the similar shapes, but they have blue shift. We conclude that organic molecules in asbestos are well-isolated as monomer and free from aggregation.

For the studied monocarbocyanine the dipole moment of transition S0

? S1 is directed along the conjugated chain. According linearly polarized absorption and fluorescence spectra we conclude that the molecules oriented predominantly along asbestos nanotubes.

We investigated the fluorescence decay lifetime of dye molecules in asbestos and thin film. For asbestos samples the lifetime is longer due to the decrease of the nonradiative decay process. The main pathway of this process for cyanine is photostereoisomerization, which is hindered in pores.

10344-33, Session PWed

Biocompatible Er, Yb co-doped flouroapatite upconversion nanoparticles for imaging applications

Anjana R., Jayaraj M. K., Cochin Univ. of Science & Technology (India)

Design and characterization of new luminescent nanomaterials is an interesting area while considering its potential applications in display screens, solid state lasers, imaging, security printing and bio-assays. Upconversion luminescencent materials gives visible or NIR emission on NIR excitation. It is a multi-photon process in which more than one photon combines to give a single photon. The real energy levels of rare earth ions like Er3+, Tm3+, Ho3+ are involved in the energy transition and emission. In order to increase NIR absorption cross-section it is co-doped with ions like Yb3+ having higher NIR absorption cross section. Selection of suitable host lattice is also important for achieving efficient upconversion luminescence. The properties of host lattice and crystal field interaction with dopant ion will have strong influence on upconversion process.

Recently upconversion luminescent materials are widely being studied towards imaging applications. The biocompatibility of many of the common host is a major concern for imaging applications. Apatite crystals like hydroxyapatite [Ca10(PO4)6(OH)2] and fluorapatite [Ca10(PO4)6F2] are well known biomaterials and are components of bone and teeth. Also they are excellent host materials for lanthanide doping since the ionic radii of lanthanide is similar to that of Ca2+ hence successful incorporation of dopants within the lattice is possible. Er3+, Yb3+ co-doped fluorapatite nanoparticles were prepared by precipitation method. The particles show intense visible emission when excited with 980 nm laser. The crystal structure and morphology of the particle were determined using X-ray diffractometer and SEM. These particles with surface fictionalized can be used for imaging.

10344-34, Session PWed

ITO-Si heterojunction solar cell with nanocrystal line CdTe thin films

Andrii Pocherpailo, Sergii Kondratenko, Taras Shevchenko National Univ. of Kyiv (Ukraine)

ITO-Si heterojunction solar cell with nanocrystal line CdTe thin films grown by magnetron sputtering are studied. The electrical and optical properties of these solar celldevices, as determined by current–voltage and photovoltage spectroscopy, were found to change with temperature over a range of 80–300 K. The electron traps present in devices with a different morphology of the CdTe films have been investigated using transient photovoltage techniques with 650 nm pulse excitation. Solar cells with CdTe films with a thickness of 24 nm exhibits the highest efficiency of 11 % as compare with 9,4% for the reference ITO-Si cells without CdTe. We have proposed the model that explains the increase achieve of efficiency due to increase of the photovoltage while short-circuit current exhibits a week lowering. Also we have established the physical mechanism of the observed increase in the lifetime of photoexcited charge carriers.

10344-18, Session 5

Optical transmittance of metallic nanowires

Mazen S. Nairat, Mousa Imran, Al-Balqa Applied Univ. (Jordan)

Wave optical simulation has been performed to study the optical transmittance of an array of metallic nanowires. Comsol multiphysics is used to briefly analyze polarization dependency of an incident light on the transmittance of nickel nanowires. Parallel polarization along to the nanowires makes the array almost appears as opaque metal sheet. On the other hand, normal polarization perpendicular to the nanowires not only makes the array transparent but also causes dipolar coupling between the nanowires. Our results provide briefly transmittance as well as reflectance of specific layer of nickel nanowires. The determined unique feature of the nanowires could be implemented in several applications and technologies, for instance: developing nanosolar cells.

10344-19, Session 5

Precise control over the morphology and dopant distribution in colloidal metal oxide nanocrystals

Ajay Singh, Los Alamos National Lab. (United States); Delia J. Milliron, The Univ. of Texas at Austin (United States)

Colloidal synthesis of doped metal oxide nanocrystals provides a great opportunity and easy route to generate materials that has unique optoelectronic properties with promising applications such as smart windows, displays, sensing and photo-catalysis etc. By introducing the free carriers with different type of dopants (n- or p-type) in the metal oxide nanocrystals, their surface plasmon resonance can be tuned precisely from near IR to mid-IR range. Similarly like metals, the optical response of plasmonic metal oxide nanocrystals can be manipulated by controlling the shape, size of the nanocrystal and free electron concentration. The effect of nanocrystal shape and size on the enhancement of their local electrical field strength and surface plasmon resonance have paved the way for new technologies and better sensing opportunities. The sharp faceted nanocrystals exhibit enhanced electric fields at corners and edges, which give us an opportunity to explore different morphologies of the NC for sensing application. Here, we will be presenting a solution route to synthesize plasmonic metal oxide nanocrystal (doped Indium Oxide) with defined shape, size and radial distribution of dopant in the nanocrystals. Also, with co-doping (cation, anion or both) in these nanocrystals, we can shift the surface plasmon resonance to higher energies and can also influence the shape of the nanocrystals. Further, we will present near field enhancement property of single nanocrystals via EELS mapping and quantify both near field and far field plasmon property via COMSOL electromagnetic simulations.

10344-20, Session 5

Controlling the emission spectra of white CdSe quantum dots by growth time

Yu-Sheng Su, Shu-Ru Chung, National Formosa Univ. (Taiwan)

In the recent years, the phosphor-converted light emitting diodes (pc-WLEDs) applies to solid state lighting (SSL) due to their high efficacy and reliability. However, the color rendering index (CRI) of the current commercial WLED is not enough. Because that quantum dots (QDs) possess controllable emission wavelength, broad excitation band, and high quantum yield (QY). Therefore, QDs is seemed as alternative materials to replace traditional phosphors. Moreover, in order to enhance the color rendering index (CRI) of WLED, blending QDs with different emission wavelengths, such as G- and R-QDs, has been used frequently. Unfortunately, these procedures are complex and time-consuming, and the emission energy of smaller QDs can be reabsorbed by larger QDs, resulting in decreasing the emission intensity in green region. Therefore, creating a process to produce white light emission QDs with high QY is important. In this study, we have demonstrated a facile chemical route to prepare CdSe QDs with white light emission in low temperature at 180 oC, and the performance of white CdSe-based WLED is also exploded. An organic oleic acid (OA) is used to form Cd-OA complex first and hexadecylamine (HDA) and 1-octadecene (ODE) is used as surfactants. Meanwhile, by varying the reaction time from 1 s to 60 min, CdSe QDs with white light can be obtained. The result shows that the luminescence spectra compose two obvious emission peaks and entire visible light from 400 to 700 nm, when the reaction time less than 10 min. The wide emission wavelength combine two particle sizes of CdSe, magic and normal, and the magic-CdSe has band-edge and surface-state emission, while normal size only possess band-edge emission. The TEM characterization shows that the two different sizes with diameter of 1.5 nm and 2.7 nm for magic and normal size CdSe QDs can be obtained when the reaction time is 4 min. We can find that the magic size of CdSe is produced when the reaction time is less than 3 min. In the time ranges from 3 to 10 min, two sizes of CdSe QDs are formed, and with QY from 20 to 60 %. Prolong the reaction time to 60 min, only normal size of CdSe QD can be observed due to the Ostwald repining, and its QYs is 8 %. Based on the results we can conclude that the two emission peaks are generated from the coexistence of magic size and normal size CdSe to form the white light QDs, and the QY and emission wavelength of CdSe QDs can be increased with prolonging reaction time. The sample reacts for 2 (QY 30 %), 4 (QY 32 %) and 60 min (QY 8 %) are choosing to mixes with transparent acrylic-based UV curable resin for WLED fabrication. The Commission International d'Eclairage (CIE) chromaticity, color rendering index (CRI), and luminous efficacy for magic, mix, and normal size CdSe are (0.49, 0.44), 81, 1.5 lm/W, (0.35, 0.30), 86, 1.9 lm/W, and (0.39, 0.25), 40, 0.3 lm/W, respectively.

10344-21, Session 5

Tuning graphene photonic properties with a self-assembled molecular monolayer *(Invited Paper)*

Sylvain Le Liepvre, Tessnim Sghaier, CEA-Ctr. de SACLAY (France); Ping Du, David Kreher, Fabrice Mathevet, André-Jean Attias, Univ. Pierre et Marie Curie (France); Céline Fiorini-Debuisschert, Ludovic Douillard, Fabrice Charra, CEA-Ctr. de SACLAY (France)

Graphene, as a flexible 2D conductor with broadband transparency, has potential photonic applications in optical modulators, photodetectors, light harvesting or emitting devices. However, its zero-bandgap electronic structure limits graphene to a narrow range of roles centered on that of transparent electrode. Graphene needs to be combined with a complementary photonic material to create a hybrid component with novel properties for advanced photonics.

The molecular self-assembly is an original bottom-up approach toward novel materials displaying unusual properties. 2D self-organized molecular networks obtained on the graphene surface reach sufficiently high surface packing density (typically 0.5 molecules/nm2) to add macroscopic properties to the graphene layer.

The photonic properties of closely packed dye assemblies can be drastically altered compared with the isolated or diluted specie due to charge transfer processes, collective excitations, or conformational changes in the dye molecule. Hence, the possible fine tuning of inter-constituents distances and orientations offered by the design of self-assembling building blocks makes the self-assembly approach very appealing for adjusting graphene photonic properties.

By controlling the interactions between dye molecules, we obtained a nanostructured hybrid graphene/dye 2D material that displays an absorption peak in the visible range. Adjusting the dye-graphene distance through a molecular spacer thanks to a specifically designed dual-functionalized self-assembling building block, we demonstrated a fluorescent self-assembled monolayer on graphene.

This experimental proof of concept shows the suitability of self-assembly techniques for the development of multi-functional hybrid dye/graphene 2D materials for nanophotonics, optoelectronics, light emitting or harvesting devices.

10344-22, Session 5

All-dielectric cylindrical nanoantennas in the visible range

Reena Dalal, Nishant Shankhwar, Yogita Kalra, Ajeet Kumar, Delhi Technological Univ. (India); Ravindra K. Sinha, Delhi Technological Univ. (India) and Central Scientific Instruments Organisation (India)

All-dielectric nanoparticles have attained a lot of attention owing to the lesser loss and better quality than their metallic counterparts. As a result, they perceive applications in the field of nanoantennas, photovoltaics and nanolasers. In the dielectric nanoparticles, the electric and magnetic dipoles are created in dielectric nanoparticles when they interact with the light of a particular frequency. Kerker's type scattering is obtained where electric and magnetic dipoles interfere. In our design, Silicon cylindrical nanoparticles having radius of 70 nm and length 120 nm have been considered. The propagation of light is taken along the length of the cylinder. The scattering cross section has been obtained and plotted with respect to the wavelength. At the peaks of scattering spectra, electric and magnetic dipoles are created at the wavelengths of 500 nm and 600 nm, respectively. Both dipoles interfere at the wavelengths of 564 nm and 676 nm. At these wavelengths, far field scattering pattern has been calculated. At the wavelength 676 nm, forward scattering takes place because electric and magnetic dipoles are in phase at this wavelength. Further, directivity is enhanced by taking the planar array of the nanoparticles. It has been observed that directivity increases by increasing the size of the array. Also, there is an increase in the directivity by increasing the gap between the nanoparticles. This enhancement of directivity can lead to the design of all dielectric cylindrical nanoantennas

10344-35, Session 5

Third order optical nonlinearity investigation of germanium quantum dots embedded in silicon matrix

Liangmin Zhang, David Bishel, William Cheung, Joseph Mini Jr., Salvador Montes, California State Univ., Stanislaus (United States)

Germanium (Ge) nanoscrystals have smaller electron and hole effective masses and a larger dielectric constant than silicon (Si) nanocrystals. The effective Bohr radius of excitons is also much larger than that of Si, therefore, comparing with Si nanocrystals, the quantum confinement effect will be more prominent in Ge nanocrystals. In addition, the melting point (938.3°C) of Ge is lower than that of Si (1414°C), which implies that Ge nanocrystals can form at lower temperature during annealing process. The synthesis and characterization of Ge nanocrystals may open new possibilities for theoretical investigations and applications to optoelectronics and microelectronics.

The common way to investigate the properties of Ge nanocrystals is to incorporate these nanoclusters in a matrix using thermal deposition or sputtering techniques. We use the conventional radio frequency magnetron co-sputtering and post-annealing techniques to embed Ge nanocrystals into a silicon matrix. The thickness of thin films fabricated by these techniques varies from 150 – 300 nm. After fabrication, the samples are annealed inside a quartz tube for several minutes at 750oC - 800oC under nitrogen environment.

The samples are then characterized by X-ray diffraction, high resolution transmission electron microscopy (HRTEM), Raman scattering spectroscopy, and open-aperture z-scan techniques. These measurements clearly show the Ge nanocrystals are formed in the Si matrix. The average size of Ge nanocrystals is estimated to be 5.5 nm by HRTEM and X-ray diffraction. The average imaginary part of third-order susceptibility of these films is measured to be 2.9 x 10^(-10) esu using a femtosecond laser system.

10344-24, Session 6

Tuning the optical properties of colloidal quantum nanocrystal/Al2O3 composite films by atomic layer deposition

Milan Palei, Vincenzo Caligiuri, Stefan Kudera, Prachi Rastogi, Roman Krahne, Istituto Italiano di Tecnologia (Italy)

Colloidal semiconductor nanocrystal (NCs) are promising building blocks for electronics and optoelectronics devices such as LEDs, photodetectors, and solar cells.1 They possess shape tunable optical and electronic properties that can be controlled via the synthesis process. 2 This make them a promising material for light emitting, lasing and photovoltaic application. However, nanocrystal films typically suffer from surface oxidation, stability issues, and physico-chemical changes when exposed to ambient conditions.3 Hence it is essential to protect the NCs from such chemical and physical changes using surface coatings. Here we used low temperature atomic layer deposition (ALD) to deposit a dielectric material like alumina (Al2O3) on CdSe/CdS core-shell NC films.4 The infilling and over coating of the NC film with alumina changes the dielectric and optical properties of the layer, and can be used to prevent photoluminescence quenching. In this work, we study the dielectric constants of composite CdSe/CdS nanocrystal/alumina films by ellipsometry and correlate the results to changes in optical emission. The enhancement in photoluminescence of ALD coated NC films can be an important step towards potential applications in the field of optoelectronic devices.

1. D.V. Talapin, J.S. Lee, M.V. Kovalenko and E.V. Shevchenko, Chemical reviews, 2009, 1, 389-458.

2. A.M. Smith, A.M. Mohs and S. Nie, Nature Nanotechnology, 2009, 1, 56-63

3. M.A. Boles, D. Ling, T. Hyeon and D.V. Talapin, Nature Materials, 2016, 2, 141-153.

4. Y. Liu, M. Gibbs, C.L. Perkins, J. Tolentino, M.H. Zarghami, Jr, J. Bustamante and M. Law, Nano Letters, 2011, 11, 5349-5355.

10344-25, Session 6

Nanostructured organosilicon luminophores for efficient and fast elementary particles photodetectors

Sergey A. Ponomarenko, Institute of Synthetic Polymeric Materials (Russian Federation) and Lomonosov Moscow State Univ. (Russian Federation) and Luminescent Innovation Technologies LLC (Russian Federation); Oleg V. Borshchev, Nikolay M. Surin, Maxim S. Skorotetcky, Institute of Synthetic Polymeric Materials (Russian Federation) and Luminescent Innovation Technologies LLC (Russian Federation); Elena A. Kleymyuk, Institute of Synthetic Polymeric Materials (Russian Federation); Tatyana Y. Starikova, Institute of Synthetic Polymeric Materials (Russian Federation) and Lomonosov Moscow State Univ. (Russian Federation); Alexey S. Tereshenko, Luminescent Innovation Technologies LLC (Russian Federation)

Organic luminophores are widely used in various optoelectronic devices, which serve for photonics, nuclear and particle physics, quantum electronics, medical diagnostics, etc. Improving their spectral-luminescent characteristics for particular technical requirements of the devices is a challenging task. In this work, we report on a convenient solution of this problem by design, synthesis and application of nanostructured organosilicon luminophores (NOLs), which consist of two types of covalently bonded via silicon atoms organic luminophores with efficient Forster energy transfer between them. NOLs combine the best properties of organic luminophores and inorganic quantum dots: high absorption cross-section and photoluminescence quantum yield, fast luminescence decay time, good processability and low toxicity [S.A. Ponomarenko, et al., Sci. Rep. 2014, 4, 6549; T.Yu. Starikova, et al., J. Mater. Chem. C, 2016, 4, 4699]. A variety of organic luminophores allowed to design and synthesize a library of NOLs, absorbing from VUV to visible region and emitting at the desired wavelengths with maxima varying from 390 to 650 nm. Using NOLs in plastic scintillators and scintillating optical fibers, widely utilized for elementary particles detection, led to their high light output and fast decay time. Thin films of NOLs or their composites with optical plastics are transparent [M.S. Skorotetcky, et al., Silicon, 2015, 7, 191], which leads to efficient conversion of UV light in different types of photodetectors [N. Surin, at al., NIM A, 2014, 766, 160; Y. Jin, et al., NIM A, 2016, 824, 691]. Properties of NOLs and their constituent organic luminophores will be compared and discussed.

10344-26, Session 6

Structural and optical characterization of highly anisotropic low loss Al:ZnO/ZnO multilayered metamaterial with hyperbolic dispersion grown by pulsed layer deposition *(Invited Paper)*

Priscilla N. Kelly, San Diego State Univ. (United States); Wenrui Zhang, Mingzhao Liu, Brookhaven National Lab. (United States); Lyuba Kuznetsova, San Diego State Univ. (United States)

Transparent conductive oxide materials have shown unique optical properties, such as negative refraction [1], hyperbolic dispersion [2], and epsilon-near-zero dispersion [3] for incoming TM polarized light. In particular, aluminum-doped zinc oxide (Al:ZnO) has shown the most promising results over traditionally used noble metals. Pulsed layer deposition (PLD) is a popular technique due to its fast and controlled growth rate, as well as the stoichiometric target-to-substrate material transfer. But since it uses large and inhomogeneous kinetic energy, samples could be prone to macro- and microscopic defects. In this work, we investigate multilayered samples of Al:ZnO/ZnO grown by PLD with the goal of developing a low loss metamaterial with hyperbolic dispersion. Different fabrication conditions, such as Al:ZnO/ZnO ratio, the thickness of an individual layer, different substrates and deposition temperatures were investigated. Results of the cross-sectional Transmission Electron Microscopy indicate a clear layer-by-layer structure. Results of the ellipsometry analysis, based on fitting spectroscopy data using the Berreman formalism, show that the hyperbolic dispersion transition (Re ??>0, Re ??< 0) is achieved at ?c=1857 nm wavelength (Im (??)~0.03) for samples with 1:4 Al:ZnO/ZnO deposition ratio. The fitted dielectric functions for samples with various parameters show that a lower deposition temperature leads to a shorter transition wavelength. Results will be compared to our previous work [4] on designing Al:ZnO/ZnO multilayered metamaterial using atomic layer deposition. Potential applications for Al:ZnO/ZnO multilayered metamaterial will be discussed.

References

[1] PNAS 109, 8834 (2012)

[2] Science 336, 205(2012)

[3] Nature Communications 5, 5638(2014)

[4] Applied Optics 55, 2993(2016)

10344-27, Session 6

Integrated freestanding two-dimensional transition metal dichalcogenides *(Invited Paper)*

Gilles Lérondel, Univ. de Technologie Troyes (France)

Two-dimensional transition metal dichalcogenides (TMDs), which are atomically thin semiconductors consisting of transition metals M-(Mo, W, Sn, etc.) covalently bonded to chalcogens X-(S, Se, Te), have recently been the focus of extensive research activity due to their remarkable properties and especially emission properties. Nevertheless, such remarkable properties can strongly be altered once the atomically thin layer is deposited on a support.

In this study, we report on the integration of freestanding TMDs. Monolayer (1-L) MoS2, WS2, and WSe2 as representative TMDs are transferred on ZnO nanorods (NRs), used here as nanostructured substrates. The photoluminescence (PL) spectra of 1-L TMDs on NRs show a giant PL intensity enhancement, compared with those of 1-L TMDs on SiO2. The strong increases in Raman and PL intensities, along with the characteristic peak shifts, confirm the absence of stress in the TMDs on NRs. In depth analysis of the PL emission also reveals that the ratio between the exciton and trion peak intensity is almost not modified after transfer. The latter shows that the effect of charge transfer between the 1-L TMDs and ZnO NRs is here negligible. Furthermore, confocal PL and Raman spectroscopy reveal a fairly consistent distribution of PL and Raman intensities. These observations are in agreement with a very limited points contact between the support and the 1-L TMDs. The entire process reported here is scalable and may pave the way for the development of very efficient ultrathin optoelectronics.

10345-1, Session 1

Novel nanophotonic light sources *(Keynote Presentation)*

Marin Soljacic, Massachusetts Institute of Technology (United States)

Nanophotonic systems can support a wide variety of states of unusual properties. I will describe how some such states discovered recently could be useful for a variety of novel light sources.

10345-2, Session 1

On-chip and planar optics with alternative plasmonic materials *(Invited Paper)*

Soham Saha, Krishnakali Chaudhuri, Aveek Dutta, Clayton T. DeVault, Purdue Univ. (United States); Nathaniel Kinsey, Virginia Commonwealth Univ. (United States); Vladimir M. Shalaev, Alexandra Boltasseva, Purdue Univ. (United States)

Plasmonic interconnects as well as metasurfaces manipulating the phase and amplitude of reflected and/or transmitted light, have attracted significant attention in the fields of planar optics and on-chip nanophotonics. The application space of plasmonics has recently been expanded by new materials classes including transparent conducting oxides (TCOs) and refractory transition metal nitrides (TMNs). These materials offer superior thermal stability, robustness, tailorability and CMOS compatibility, thus outperforming the conventional plasmonic components (e.g. gold and silver) in application-specific requirements. Here, we discuss recent progress in the areas of plasmonic interconnects, modulators and metasurfaces realized using TMNs and TCOs.

Ultrafast nonlinear responses near the epsilon near zero (ENZ) region have been recently demonstrated for Al doped zinc oxide (AZO) (TCO). This has spurred the development of ultrafast, on-chip modulators with TCOs as an active material. Building from on our previous work on LRSPP waveguides with ultrathin Titanium Nitride (TiN) (5.5mm propagation length) and Zirconium Nitride (ZrN), we will report solid-state hybrid mode waveguides using TiN as well as a modulator based on this waveguide which provides all-optical tunability, low optical losses at the telecommunication window, and CMOS-compatibility.

Successful integration of these alternative plasmonic components into the phase gradient metasurfaces platform without loss of performance have also been demonstrated. A metasurface employing ZrN brick antennas shows the photonic spin Hall Effect (PSHE), by reflecting the two circular polarizations in different directions. In another device, a metasurface based on nanostructures of Ga doped ZnO (TCO), functioning as a quarter-wave plate, have been realized.

10345-4, Session 1

Ultrafast carrier capture and Auger recombination in individual III-nitride nanowires *(Invited Paper)*

Stephane A. Boubanga Tombet, Los Alamos National Lab. (United States); Jeremy B. Wright, Ping Lu, Sandia National Labs. (United States); Michael R. C. Williams, Los Alamos National Lab. (United States); Changyi Li, George T. Wang, Sandia National Labs. (United States); Rohit P. Prasankumar, Los Alamos National Lab. (United States)

Group III-nitride (III-N) semiconductors are widely used in commercial optoelectronic devices to efficiently produce light, making them very attractive materials for solid-state lighting. III-N semiconductor nanowires (NWs) have garnered particular attention recently, as they can be synthesized with higher structural quality than conventional heteroepitaxial planar films, making them promising unconventional platforms for the growth of nonpolar QWs with low dislocation densities. The implementation and optimization of these GaN/InGaN NW heterostructure-based devices will require a detailed understanding of their physical properties, on which one can gain insight by studying the mechanisms governing dynamic processes in these nanosystems, such as carrier capture and recombination.

This can be done using ultrafast optical microscopy (UOM), which has previously been used to reveal the fundamental properties (both static and dynamic) of single NWs and NW heterostructures, as well as other nanomaterials. Here, we used UOM to study carrier dynamics in single GaN and GaN/InGaN nonpolar MQW core?shell NWs. We find that the time scale for initial carrier relaxation into the quantum wells strongly depends on the photoexcitation fluence, indicating that intraband Auger carrier?carrier scattering may govern carrier capture. The relaxation dynamics are also density dependent; three-carrier Auger recombination dominates the dynamics at high densities, while at lower densities bimolecular recombination is shown to be the main channel governing carrier relaxation. Our results thus shed new light on carrier dynamics in III-N MQW NW heterostructures, particularly by revealing the processes governing carrier capture and relaxation, which should impact future applications of these unique nanosystems.

10345-84, Session 1

Quantum well intermixed tunable wavelength single stripe laser diode

Thamer Tabbakh, Patrick L. LiKamWa, CREOL, The College of Optics and Photonics, Univ. of Central Florida (United States)

A single-quantum-well strained InGaAs/GaAs design grown on a n-doped GaAs substrate is used to fabricate a single waveguide laser diode consisting of two sections with different bandgap energies. In this experiment, half of the sample is coated with a 50nm thick silicon nitride film using plasma enhanced chemical vapor deposition, photolithography and reactive ion etching. Then a 200nm thick silicon dioxide layer is deposited by PECVD on the entire surface of the sample. After a rapid thermal annealing at 925°C for 30s, the silicon nitride coated section (A) is protected from the intermixing while the section (B) whose surface is in contact with silicon dioxide experiences a blue shift in the bandgap energy. A ridge waveguide stripe is then delineated by photolithography and wet chemical etching such that it passes through both sections. The device is then planarized using BCB resin and segmented gold contacts are deposited on top of the two sections of the waveguide top p-layer. After depositing the n-contacts on the back of the thinned down polished substrate, the device is cleaved to an overall length of 1450?m of which, 800μm of the waveguide length is in section A. By injecting 3mA in section B of the device, lasing is obtained at a wavelength of 950nm when the current in section A exceeds 18.8mA. While fixing the current in section A at 4.5mA, leads to a lasing threshold of 26mA at 910nm. The slope efficiencies are 0.06W/A and 0.18W/A for sections A and B respectively.

10345-5, Session 2

Metamaterial infrared detectors *(Invited Paper)*

Sanjay Krishna, The Ohio State Univ. (United States)

There is an increasing demand for high performance long wave infrared (LWIR) detectors with multispectral capability. Meta-materials and antenna based concepts offer some interesting solutions to win the signal to noise ratio and provide enhanced functionality at the pixel level. The long wave infrared region is appealing due to the low metallic loss, large penetration depth of the localized field and the larger feature sizes compared to the visible region. I will discuss approaches to realize multispectral detectors with examples of double metal meta-material design combined with Type II superlattice absorbers (collaboration with Padilla group at Duke University).

10345-6, Session 2

A random metasurface for an all polarizations flat lens

Matthieu Dupre, Junhee Park, Boubacar Kante, Univ. of California, San Diego (United States)

We consider gold plasmonic nanorods in the infrared domain. Such elements are very anisotropic and only polarizable along their longer dimension. Varying the nanorod length from 150 to 500 nm changes the resonant frequency of the element, which allows us to tune the phase-shift provided to an incident plane wave which electric field is parallel to the long axis. On the contrary, the nanorod is transparent to an incoming plane wave with a polarization perpendicular to its main axis. In order to provide a 0 to 2pi phase shift, we chose to work in reflection with metasurfaces made of elements with random positions and orientation. We emphasize that the length of each nanorod is not random, but strongly depends on the position of the element. It is chosen accordingly so that the reflected phase shift follows a parabolic law.

The focusing efficiency strongly depends on the density of nanorods but also of the dimensionality and of the symmetry of the metasurface. Using full wave simulations, we design ordered and random metalens and compare their characteristics. Unfortunately, simulating 2D large area metasurface is numerically challenging. Hence, we extract the transmission matrix parameters for single elements from our FDTD simulation, and model the metasurface as an array of two level atom scatterers

Finally, we present an experimental realization of such random metalens. The latter is made with conventional top-down fabrication techniques and e-beam lithography. We will show that the resulting lens focus light on diffraction limited focal spots for the two polarizations.

10345-7, Session 2

Saturation of magnetic response of parallel slabs Metamaterials

Mona H. Alsaleh, Raj K Vinnakota, Dentcho A Genov, Louisiana Tech Univ. (United States)

Metamaterials are nanocomposite materials i.e. metal- dielectric resonators in the form of split ring resonators (SRRs), parallel wires or slabs. These materials show unique optical responses such as strong magnetism at high frequency range. It is so important to have a material with negative permeability at optical frequency which is not available in nature. Decreasing the size of resonators is a crucial step toward increasing the magnetic resonance frequency (MRF), however, this scaling breaks down at high frequencies range causing a saturation of MRF. In this work, we present a transmission line theory to model the magnetic response for pair of metallic nanostripes separated by a dielectric material. The magnetic response of parallel stripes system is due to antiparallel current in the stripes which forms a circular current that induces a magnetic moment. The predicted model represents the magnetic response by a magnetic susceptibility and MRF. The theoretical results show excellent agreement with the exact numerical simulations calculated by utilizing commercial software (Comsol Multiphysics). Specifically, we studied MRF as a function of the resonator's sizes and our parametric study of the MRF shows that scaling down the resonator sizes increases MRF and as we further decreases the resonator's size, the MRF saturates at frequency ranging from (150 – 600) THz. This is explained by the fact that at high frequencies, within the infrared and optical range, the metal strips behave as capacitive elements which precludes the excitation of magnetic resonances for frequencies higher than the surface plasma frequency of the system.

10345-8, Session 2

Fluorescence enhancement in fluidic nanochannels for dynamic molecular optical detection *(Invited Paper)*

Pablo A. Postigo, Raquel Alvaro, Instituto de Microelectrónica de Madrid (Spain); Aritz Juarros, IK4 Tekniker (Spain); Santos Merino, IK4 Tekniker (Spain) and Instituto de Microelectrónica de Madrid (Spain)

We show the fabrication of a novel optofluidic chip that uses a a network of nanochannels optimized for the transport of DNA-stretched molecules. The molecules can move through the nanochannels in the femto-liter per second. The nanochannels are optically accessible via a transparent cover of pyrex, allowing fluorescence microscopy imaging of the travelling molecules. The nanochannels are surrounded by photonic crystal structures to enhance the emission of the fluorescent light. The photonic crystal structures provide an enhancement up to 2.5 times in the light emitted by fluorescent molecules in motion inside the nanochannels which increases to around 250 when normalized to the area of the nanochannels emitting fluorescence. The results may help to the detection of fluorescent molecules (like marked-DNA) in series by speeding it or allowing the use of less sophisticated equipment.

10345-9, Session 2

Whispering gallery mode polymer fiber refractive index sensors fabricated by near-field electrospinning

Joseph E. Cheeney, Stephen T. Hsieh, Nosang V. Myung, Elaine D. Haberer, Univ. of California, Riverside (United States)

Because of their ability to serve in chemical and biological applications, there is a growing need for sensitive, compact, readily fabricated, and inexpensive refractive index sensors. In recent years, devices that utilize whispering gallery modes (WGMs) have proven versatile in many such applications, however, these reports have typically used fabrication techniques that are either complex, do not produce sensitive devices, or are expensive. One possible solution is to use polymer materials in conjunction with near-field electrospinning (NFE). This direct-write fabrication approach enables fast, yet precise positioning of micron-sized fibers for low-cost, scalable sensor manufacturing. Moreover, NFE can be used to incorporate additional functionality such as emitters for optically active sensing or receptors for enhanced selectivity. Here, fluorescent dye-doped polymer fiber refractive index sensors that support WGMs within the fiber cross-section were demonstrated. Resonators were fabricated using NFE to draw fibers from a 25 wt% poly(vinyl) alcohol polymer solution doped with 0.38 mM rhodamine 6G onto a substrate patterned with deep trenches. The suspended fibers ranged from 2 to 22 μm in diameter and displayed circular cross sections. Using microphotoluminscence, high-Q resonant peaks were observed in the emission range of the dye, from 540-630 nm. Using size-dependent mode spacing predicted by finite-difference time domain simulations and polarized optical microscopy, the resonances were identified as first order WGMs. Refractive index sensing was evaluated using a range of glucose solution concentrations. The WGM resonators fabricated here have demonstrated the potential of near-field electrospun polymer-based fibers for sensitive sensing applications.

10345-10, Session 2

Active plasmonic antennas

Kai Braun, Florian Laible, Alfred J. Meixner, Monika Fleischer, Eberhard Karls Univ. Tübingen (Germany)

Within the last decade gap antennas have been widely studied and are commonly used due to the strongly enhanced coupled electrical fields within their gaps. Many emerging nanophotonic technologies depend on the careful control of this plasmonic coupling, including optical nanoantennas for high-sensitivity sensors and Raman enhanced applications. Typically the distances between the metallic nanostructures range from several tens of nm down to a few nm. Only recently several groups managed to produce and measure ultra narrow gaps, which show new phenomena such as coherent quantum tunneling and improved luminescence enhancement or additional radiative recombination channels. These effects will become crucial in nanoscale optoelectronics and may pave the way to single molecule opto-electronics.

In this work, we will present an approach based on tunneling feedback, which therefore offers excellent distance control down to several angstrom. In this configuration the shape of the plasmonic tips in the gap region is preselected. This way, the junction region and the plasmon resonances of the plasmonic tips can be changed, while the tunneling feedback gives rise to a controlled approach to sub-nanometer distances. Additionally the tunneling junction allows for further manipulation of the antenna via the applied bias voltage. We will present variations of different geometries under defined polarized illumination and show the dependency of the plasmon resonances on varied distances and the applied bias voltages.

10345-11, Session 3

Quantum dot light-matter interactions in complex nanophotonic environments *(Keynote Presentation)*

Stephen Hughes, Queen's Univ. (Canada)

No Abstract Available.

10345-12, Session 3

Anapole-mode-based nanolaser in integrated optical chips *(Invited Paper)*

Juan Sebastian Totero Gongora, King Abdullah Univ. of Science and Technology (Saudi Arabia); Andrey E. Miroshnichenko, Yuri S. Kivshar, The Australian National Univ. (Australia); Andrea Fratalocchi, King Abdullah Univ. of Science and Technology (Saudi Arabia)

No Abstract Available.

10345-13, Session 3

Low-threshold lasing in coupled resonator optical waveguides with exceptional points of degeneracy

Mohamed A. K. Othman, Mohamed Y. Nada, Mehdi Veysi, Alexander Figotin, Filippo Capolino, Univ. of California, Irvine (United States)

Burgeoning interest in slow-light based photonic devices has spawned the concept of exceptional points in optical devices leading to many intriguing applications. In essence, exceptional points of degeneracy (EPD) are points in the spectrum of systems at which state eigenvectors coalesce. Aside from the EPD emergence in gain and loss balanced non-Hermitian systems such as those obeying the PT-symmetry; EPDs can still occur in lossless periodic structures without the presence of gain and loss. We demonstrate for the first time the emergence of EPDs in the eigenstates of lossless coupled resonator optical waveguides (CROWs) which enhance the performance of many devices, in particular optical amplifiers and lasers. Moreover, EPDs of various order can also be designed in CROWs by engineering the geometric parameters. First, we report a design of CROWs with periodic coupling and geometrical-symmetry breaking, in which EPDs of various orders can be found, and we investigate realistic considerations including losses and imperfections. We then show anomalous scaling law of the quality factor operating near a fourth order EPD, namely the degenerate band edge (DBE). We demonstrate that EPDs are associated with slow-light, in the sense that the group velocity of waves near EPD vanishes implying large local density of states. Furthermore, we demonstrate low threshold lasing operation and high slope efficiency when using a fourth EPD in laser cavity supporting the degenerate band edge (DBE). In fact, we also report that EPDs with various orders would lead also to unique scaling of the lasing threshold which can be beneficial for boosting the performance of lasers and sensors. As an example, we show a CROW design based on Silicon-on-insulator (SOI) technology and report the lasing action in such configuration using finite-different time domain (FDTD) along with the nonlinear rate equations in a four-level energy system describing the gain medium inside the CROW.

10345-14, Session 3

Ultrafast and quantum dynamics of plasmonic nanolasing and surface-plasmon polariton condensation *(Invited Paper)*

Ortwin Hess, Imperial College London (United Kingdom)

Nanoplasmonic stopped-light lasing is a recently established principle [1] that not only opens the door to ultrafast cavity-free nanolasing, ultra-thin lasing sufaces exploiting van Hove singularities [2] and cavity-free quantum-electrodynamics but also provides an entry point to quantum gain in quantum plasmonics. We show that engineered singularities in the density of optical states realised in a metal-dielectric-metal nano-waveguide structure lead to a stopped-light feedback mechanism that is the basis for the dynamics of the observed cavity-free photonic and surface-plasmon polariton nanolasing. The condensed surface plasmon polaritons are characterised by ultrafast spatio-temporally oscillating amplified surface-plasmon polaritons on ultrafast timescales <5 femtoseconds and with spatial periods on the nanoscale <100 nm.

[1] T. Pickering, J. M. Hamm, A. F. Page. S. Wuestner and O. Hess, "Cavity-free plasmonic nanolasing enabled by dispersionless stopped light", Nature Communications 5, 4972 (2014).

[2] J. M. Hamm and O. Hess, "Two Two-Dimensional Materials Are Better Than One", Science 340, 1298 (2014)

[3] S. Wuestner, T. Pickering, J. M. Hamm, A. F. Page, A. Pusch and O. Hess, "Ultrafast dynamics of nanoplasmonic stopped-light lasing", Faraday Discuss., 178, 397 (2015).

10345-15, Session 4

Controlled and tunable multi-modal lasing from plasmonic superlattices *(Invited Paper)*

Teri W. Odom, Northwestern Univ. (United States)

Band structure engineering is critical for controlling the emission wavelengths and efficiency in electronic and photonic materials. Single band-edge states that show trapped slow light have been used as high-quality optical feedback for lasing from photonic bandgap crystals and metal-dielectric waveguides. Recently, we demonstrated that single band-edge lattice plasmons in periodic metal nanoparticle arrays could contribute to single-mode lasing at room-temperature with directional emission. However, the manipulation of more than a single band-edge mode for nanolasing has not been possible because of limited cavity designs. This talk will describe a new architecture based on plasmonic superlattices—finite-arrays of nanoparticles grouped into microscale arrays—to achieve tunable and controllable multi-modal lasing. The underlying mechanism was found to depend on trapped slow light at both zero and non-zero wavevectors. We will discuss how the spectral separation and spatial emission angles of the lasing modes can be exquisitely manipulated by changing patch periodicity.

Such characteristics may enable multi-frequency multiplexing and fast-processing of nanoscale coherent light for on-chip photonic integration.

10345-16, Session 4

Nanolasers based on high-quality factor plasmonic resonators

Amit Agrawal, Wenqi Zhu, Henri J. Lezec, Shawn Divitt, National Institute of Standards and Technology (United States); Ting Xu, Nanjing Univ. (China)

Coherent optical sources with small device footprints, narrow-linewidth, and room-temperature operation are desirable for potential applications in on-chip optical communications. Surface plasmons, under the form of both stationary localized surface plasmons or propagating surface plasmon polaritons (SPPs), offer an effective route towards achieving lasing at micro- and nano-scale dimensions when integrated with a suitable optical gain medium. However, intrinsic absorption and scattering losses limit the quality factors (Q) associated with plasmonic cavity resonators to <10, thereby deteriorating the threshold properties and emission linewidth of plasmonic lasers or requiring low-temperature operation. Recent publications utilizing the template-stripping approach to achieve ultra-smooth metal surfaces have pushed the Q-factors of plasmonic resonators beyond 300, resulting in successful room-temperature lasing operation. Here, we demonstrate novel plasmon resonator geometries consisting of ultra-smooth metal surfaces that support surface plasmon polariton modes exhibiting record-high quality factors (>750) in the visible frequency range. The resonators are utilized to achieve record narrow-linewidth, low-threshold surface-plasmon-polariton lasing at optical frequencies, as well as exhibit high figure-of-merit sensing. The open-cavity architecture of the plasmonic resonators also makes them suitable for high figure-of-merit optical sensing; for example, the evanescent interaction between analytes and localized electromagnetic fields within a lasing cavity can result in their detection with high sensitivity in a label-free manner.

10345-17, Session 4

Spatial intensity of plasmonic distributed feedback lasers

Ke Guo, Femius Koenderink, FOM Institute for Atomic and Molecular Physics (Netherlands)

Depending on the strength of diffractive coupling, distributed feedback (DFB) lasers can support different lasing modes with distinctive spatial intensity distributions. Compared with conventional DFB lasers, a plasmonic DFB laser can have quite different coupling strength due to the much stronger scattering from the plasmonic lattice and the metallic losses. Here we study the spatial intensity distribution and coupling strength of plasmonic DFB lasers depending on the size of the plasmonic nano-particles. We show that the plasmonic resonance supported by the nano-particles allows us to achieve large and complex coupling strength values with small lattices, offering easy approaches to the optimization of the plasmonic DFB lasers.

10345-18, Session 4

Dynamics and coherence of metal-clad nanolasers

Si Hui Pan, Univ. of California, San Diego (United States); Qing Gu, The Univ. of Texas at Dallas (United States); Abdelkrim El Amili, Felipe Vallini, Univ. of California, San Diego (United States)

Metal-clad nanolasers with high spontaneous emission factors (?) represent a class of ultra-compact light emitters with applications in fiber-optic communications, hybrid and all optical computing, imaging and sensing. In-depth studies on both the coherence and dynamical properties of these emitters are necessary before practical applications can be realized. However, the coherence characterization of a high-? nanolaser using the conventional measurement of output light intensity versus input pump intensity (L-L curve) is inherently difficult due to the diminishing kink in the measurement curve. We conducted the second order intensity correlation measurement, or g2(?) — a more definitive method to confirm coherence — on a high-? metallo-dielectric nanolaser under nanosecond optical pulse pumping. Our result indicates that full coherence is achieved at three times the threshold conventionally defined by the kink in the L-L curve. Additionally, we observed that the g2(?) peak width shrinks below and broadens above threshold. Rate-equation analyses reveal that the above-threshold broadening is due to the delayed threshold phenomenon, providing the first observation of dynamical hysteresis in a nanolaser. We propose that this dynamical phenomenon can be exploited to determine the lasing regimes of a unity-? nanolaser, whose threshold is inherently ambiguous and difficult to observe.

10345-19, Session 4

Large Purcell enhancement in perovskite plasmonic nanolaser

Sui Yang, Wei Bao, Xiaoze Liu, Jeongmin Kim, Rongkuo Zhao, Yuan Wang, Xiang Zhang, Univ. of California, Berkeley (United States)

Halide perovskite semiconductors are an emerging class of materials that have shown great promise as nanophotonic and optoelectronic devices owing to their remarkable properties such as high radiative efficiency and low trap-state density. For applications in optical information processing and communications, however, the challenging requirements that must be met simultaneously are compact size, ultrafast, scalability, and room temperature operation. Here we demonstrate a deep subwavelength perovskite plasmonic nanolaser at room temperature with ultralarge Purcell enhancement by a scalable solution process. The nanalser enables a strong optical confinement by hybridizing perovskite single crystals with surface plasmon. It thus not only downscales the device but also facilitates its emission efficiency dramatically exhibiting a clear single mode lasing behavior at room temperature. With such superior lasing activity, more importantly, the perovskite plasmonic nanolaser enables an expedited emission dynamics of the device and achieves experimental Purcell enhancement over 200, the largest experimental value in reported lasers so far. Such significantly accelerated spontaneous dynamics inherently enhances stimulated emission and facilitates laser gain compensation due to the intrinsic relationship between Einstein's coefficients. The capability to combine plasmonic confinement with ultrafast amplification through perovskites not only promises fundamental physics for accelerating light–matter interactions but also opens new avenues for applications from ultrafast integrated optical communications to implantable computing microchips.

10345-20, Session 4

Hybrid photonic crystal lasers for wavelength division multiplexing *(Invited Paper)*

Liam O'Faolain, Cork Institute of Technology (Ireland) and Univ. of St. Andrews (United Kingdom) and Tyndall National Institute (Ireland)

The last decade has seen huge growth in the use of optical datacommunications. Silicon Photonics has produced high speed modulators, photodetectors and the associated electronics and is proving itself to be one of the most promising technologies for cost-effective fabrication of photonic components and integrated circuits. However, there are some major challenges in terms of device performance and, in particular, the development of efficient light emission from silicon has been the subject of a large body of research. The need for Wavelength

Division Multiplexing in the datacenter is stimulating significant research efforts into unconventional lasers. Here we demonstrate a hybrid external cavity laser architecture that provides a high performance, cost-effective silicon photonics compatible laser. A photonic crystal cavity is used as a resonant reflector and due to the enhanced light-matter interaction in the high Q-factor Photonic Crystal (PhC) reflectors, the device operates in a highly non-linear mode. With suitable design, a self-tuning effect is realised that reduces the laser's sensitivity to external temperature fluctuations. PhC cavities provide very precise control of their resonant wavelengths by lithographic tuning. Hybrid integration provides a means to combine the III-V and silicon components. Flip-chip bonded versions of these lasers are suitable for integration with our previously demonstrated active and passive PhC components for the realization of more complex power-efficient Si photonic systems

10345-21, Session 4

Fabrication of low-threshold ZnO nanorod array random lasers

Hideki Fujiwara, Ryo Niyuki, Keiji Sasaki, Hokkaido Univ. (Japan)

Random lasers (RLs) have recently expected as unique speckle-free laser light sources for sensors and imaging. To improve the controllability of RLs, we have proposed a novel resonance-controlled RL, which were composed of agglomerated mono-dispersed spherical ZnO nanoparticles. Although the resonance-controlled RL has unique features such as quasi-single-mode and low lasing threshold, there is an issue that an optical input-output becomes difficult due to its randomness. In contrast, because a two-dimensional nanorod array can also induce light localization via in-plane multiple light scattering, the accessibility of excitation and lasing light in the vertical direction could be expected to be improved comparing with agglomerated nanoparticles. As the fabrication method of nanorod array structures, a laser-induced hydrothermal synthesis using a local heating by laser irradiation on a gold thin film has recently been proposed. Because, unlike the conventional hydrothermal synthesis method, this method can easily control the size of nanorods by the control of irradiated laser power and time, we attempted to realize the resonance-controlled two-dimensional RL in nanorod array structures, like our previous study. In the presentation, we will introduce our recent progress on resonance-controlled ZnO nanorod array RLs. In the experiments, we succeed to induce random lasing in ZnO nanorod array structures fabricated by a laser-induced hydrothermal synthesis, and find that their thresholds strongly depend on the growth time (nanorod size). These results suggest the possibility to control the RL properties simply by tuning the irradiated laser conditions.

10345-87, Session 4

Nanowire array lasers on silicon for optical links

Diana L. Huffaker, Cardiff Univ. (United Kingdom); Hyunseok Kim, Univ. of California, Los Angeles (United States); Wook-Jaee Lee, Cardiff Univ. (United Kingdom)

Semiconductor nanowire lasers have recently gained attention as ultra-compact coherent light sources in the field of nanophotonics. Because nanowires can be grown on lattice-mismatched substrates, directly integrating nanowires on silicon is regarded as one of the promising ways to monolithically integrate functional light sources on silicon photonic platforms. Here, we report InGaAs/InGaP core/shell nanowire array lasers directly grown on a silicon-on-insulator (SOI) platform operating at room temperature. The growth platform is prepared by dry etching SOI(111) substrates to pattern waveguides, output grating couplers, and mesas. Nanowires are then grown on silicon mesas as a one-dimensional photonic crystal array by selective-area epitaxy using metal-organic chemical vapor deposition (MOCVD). InGaAs nanowires are passivated by InGaP shells to enhance the radiative efficiency by reducing non-radiative surface recombination. Vertical InGaAs/InGaP core/shell nanowire arrays are grown on SOI platform, where the nanowire array is directly connected to a conventional SOI waveguide to demonstrate coupling characteristics. The nanowire array cavity is optically pumped by a pulsed laser with 660 nm wavelength, 30 ps duration, and 78 MHz repetition rate at room temperature. Photoluminescence measurements reveal that the lasing peak dominates other peaks be increasing the pump power, resulting in the lasing threshold of 90 uJ/cm2 and the side-mode suppression ratio (SMSR) of 16.7 dB at the pump fluence of 131 uJ/cm2. These results suggest that the proposed nanowire array lasers could be the enabling technology for ultracompact and energy-efficient optical links.

10345-22, Session 5

High temperature hyperbolic metamaterial for selective thermal emitters in thermophotovoltaic (TPV) systems *(Invited Paper)*

Manfred Eich, Technische Univ. Hamburg-Harburg (Germany) and Helmholtz-Zentrum Geesthacht (Germany); Alexander Y. Petrov, Technische Univ. Hamburg-Harburg (Germany); Pavel N. Dyachenko, Technische Univ Hamburg-Harburg (Germany); Sean Molesky, Univ. of Alberta (Canada); Zubin Jacob, Purdue Univ. (United States); Michael Störmer, Helmholtz-Zentrum Geesthacht (Germany); Tobias Krekeler, Martin Ritter, Technische Univ. Hamburg-Harburg (Germany)

In order to tailor thermophotovoltaic emitters to match specific photovoltaic receivers a spectrally selective emitter is required that has a close to black body emission at short wavelengths and substantially reduced emission at long wavelengths. We propose a hyperbolic metamaterial for this purpose which changes its emission properties close to the topological transition of its isofrequency surface. At short wavelengths the metamaterial has a permittivity close to one and thus efficiently absorbs and emits radiation. At longer wavelength, beyond the topological transition, the thermally excited hyperbolic modes have large wave vectors and radiation thus cannot leave metamaterial due to total internal reflection. To emit significant power at wavelengths usable for photovoltaic conversion (<2 μm) the far-field emitter should be heated to high temperatures and thus must be thermally stable.

We demonstrate selective band-edge emitters based on a W-HfO 2 layered metamaterial. The thicknesses of the tungsten and hafnium oxide are 20 and 100 nm correspondingly. The metamaterial selectivity comes from the change in effective permittivity and does not rely on the phase matching condition. Thus the metamaterial exhibits almost angle independent selective emission. Stability up to 1000°C is demonstrated in vacuum conditions. At higher temperature residual oxygen in vacuum diffuses through the HfO 2 cap layer and oxidizes the upper W layer of the metamaterial leading to degradation of the selective emission.

10345-23, Session 5

Perfect and tunable electromagnetic absorption using epsilon-near-zero metamaterials and graphene-polymer heterostructures *(Invited Paper)*

Michaël Lobet, Bruno Majérus, Luc Henrard, Michaël Sarrazin, Philippe Lambin, Univ. of Namur (Belgium)

No Abstract Available.

10345-24, Session 5

3D gradient refractive index micro-optics *(Invited Paper)*

Paul V. Braun, Christian Ocier, Univ. of Illinois at Urbana-Champaign (United States)

Via electrochemical etching of silicon, followed by materials conversion, 3D gradient refractive index micro-optics including flat lenses, Bragg mirrors, polarization sensitive optical splitters and structures with nearly arbitrary refractive index distributions were formed with a particular focus on micro-optics important for solar energy harvesting. The conversion from silicon to silica and titania enabled the optics to operate in the visible with minimal loss, something particularly important for solar energy harvesting applications. A detailed model was developed which enabled tight control over optical properties based only on the electrochemical etch conditions.

10345-25, Session 5

Near-unidirectional superemitters enabled by cascaded phonon-polariton resonances

Ganga C. R. Devarapu, Cork Institute of Technology (Ireland); Stavroula Foteinopoulou, The Univ. of New Mexico (United States)

Phonon-polariton (Reststrahlen-band) materials have been hitherto little explored for photonic applications, since they are near-perfect reflectors in bulk form. Judicious microstructures comprising these materials can support localized resonances, with a large infrared field enhancement, as their plasmonic counterparts do in the visible. We propose here a SiC micropyramid paradigm, which by virtue of a strongly-asymmetric cascaded coupling to these resonances, behaves as a near-unidirectional superemitter, with an emissivity enhanced by as much as fifteen times with respect to bulk SiC. Our proposed platforms will benefit the design of infrared sources and detectors as well as passive radiative cooling devices.

10345-26, Session 5

Measuring and exploiting optical anisotropies in nanophotonic photovoltaics

Jon A. Schuller, Univ. of California, Santa Barbara (United States)

Nanophotonic coatings and structures provide an attractive approach for enhancing light-matter interactions in advanced photovoltaics. A little-discussed aspect of many photonic architectures is the presence of strong anisotropies in the electromagnetic field enhancements. These anisotropies are of particular importance in relation to nanostructured materials that possess intrinsic structure-dependent optical anisotropies. In this talk, we describe a novel class of momentum-resolved spectroscopies that provide new insight into structure-dependent optical properties of thin-film material and discuss approaches to exploit these effects in photovoltaic devices that incorporated nanophotonic enhancements.

Specifically, we use Fourier imaging techniques to measure or control the momentum distribution of in-coming or out-going light rays respectively. These techniques are applied to test-case organic photovoltaic materials that can be deposited with distinct morphologies depending on processing conditions. Using momentum-resolved photoluminescence, we determine the morphology-dependent orientation of transmission and absorption dipoles. We subsequently demonstrate the use of momentum-resolved reflectometry to perform "model-free" measurements of optical constants. The approach provides precise and accurate optical constants with quantified error estimates, obviating the complications associated with highly model-dependent, multi-parameter spectral fitting procedures used in ellipsometry. We conclude by describing ongoing efforts to exploit optical anisotropies to enhance light absorption in nanostructured photovoltaics.

10345-27, Session 5

Effectively infinite optical path-length created using a simple-cubic photonic crystal for extreme light-trapping *(Invited Paper)*

Shawn-Yu Lin, B. J. Frey, Rensselaer Polytechnic Institute (United States); Mei-Li Hsieh, National Chiao Tung Univ. (Taiwan); Ping Kuang, Rensselaer Polytechnic Institute (United States); J.-H. Jiang, Sajeev John, Univ. of Toronto (Canada)

In this talk, I will describe the fabrication of a TiO2 simple cubic photonic crystal and its use to experimentally validate a newly-discovered mechanism for extreme light-bending. Absorption enhancement was observed extending 1-2 orders of magnitude over that of a reference TiO2 film. Several enhancement peaks in the region from 600-950 nm were identified, which far exceed both the ergodic fundamental limit and the limit based on surface-gratings, with some peaks exceeding 100 times enhancement. These results are attributed to radically sharp refraction where the optical path length approaches infinity due to the Poynting vector lying nearly parallel to the photonic crystal interface. The observed phenomena follow directly from the simple cubic symmetry of the photonic crystal, and can be achieved by integrating the light-trapping architecture into the absorbing volume. These results are not dependent on the material used, and can be applied to any future light trapping applications such as phosphor-converted white light generation, water-splitting, or thin-film solar cells, where increased response in areas of weak absorption is desired.

1. A. Chutinan & S. John "Light trapping and absorption optimization in certain thin-film photonic crystal architectures". Phys. Rev. A 78, 023825 (2008).

2. S. Y. Lin, VM Hietala, L Wang, ED Jones, "A highly dispersive photonic band gap prism", Optics Letters, 21, p. 1771 (1996).

3. H. Kosaka, T. Kawashima, A. Tomita, M. Notomi, T. Tamamura,T. Sato, and S. Kawakami, Phys. Rev. B 58, R10096 (1998).

4. P. Kuang, A. Deinega, M.L. Hsieh, S. John & S.Y. Lin, "Light trapping and near unity solar absorption in a three-dimensional photonic-crystal". Opt. Lett. 38, 4200-4203 (2013).

5. B. J. Frey, P. Kuang, S.Y. Lin, J.H. Jiang & S. John, "Large area fabrication of a simple cubic metal-oxide photonic crystal for light trapping applications". J. Vac. Sci. Technol. B 33, 021804 (2015).

6. B. J. Frey, P. Kuang, M.L. Hsieh, S.Y. Lin, J.H. Jiang & S. John, "Effectively infinite optical path-length created using a simple-cubic photonic crystal for extreme light-trapping". Nature Scient. Report, under revision (2017).

10345-28, Session 6

Extra-ordinary modulators with 2D photonic materials *(Invited Paper)*

Volker J. Sorger, The George Washington Univ. (United States)

We show that nanophotonic device performance scales non-monotonically with critical length. Such scaling can be synergistic with the atomistic-scale of 2D materials. The naturally-low modal overlap factor can be engineered to approach 1% for electric in-plane field polarization waveguides, i.e. slot-waveguides. Moreover, we show that a polaritonic mode character (i.e. plasmonic) improves the modulator performance by about 10x due to (i), a lower contact resistance from synergistic use of one contact, and (ii) the higher modal group index. As an example we discuss our demonstration of the 1st sub-1Volt electro-optic modulator based on 2D material plasmonic hybrid integration on Silicon.

10345-29, Session 6

Fast and highly sensitive ionic polymer gated WS2-graphene photodetectors

Jake Mehew, Selim Unal, Elias Torres Alonso, Gareth F. Jones, Saad Fadhil Ramadhan, Monica Craciun, Saverio Russo, Univ. of Exeter (United Kingdom)

Student Contribution: The combination of graphene with semiconductor materials in heterostructure photodetectors, has enabled amplified detection of femtowatt light signals using micron-scale electronic devices. Presently, the speed of such detectors is limited by long-lived charge traps and impractical strategies, e.g. the use of large gate voltage pulses, have been employed to achieve bandwidths suitable for applications, such as video-frame-rate imaging.

In this work, we report graphene-few layer WS2 heterostructure photodetectors encapsulated in an ionic polymer, which are uniquely able to operate at bandwidths up to 1.5 kHz, whilst maintaining internal gain as large as 10^6. Highly mobile ions and a nanometre scale Debye length of the ionic polymer are used to screen charge traps and tune the Fermi level of graphene over an unprecedented range at the interface with WS2. We observe a responsivity R = 10^6 A/W and detectivity D* = 3.8x10^11 Jones, approaching that of single photon counters.

The combination of both high responsivity and fast response times makes these photodetectors suitable for video-frame-rate imaging applications.

10345-30, Session 6

MoS2 exciton-polaritonics in dielectric photonic structures *(Invited Paper)*

Ertugrul Cubukcu, Xingwang Zhang, Univ. of California, San Diego (United States)

Direct bandgap transition metal dichalcogenides such as monolayer MoS2 offer interesting optical properties arising from room-temperature stable excitons in these materials. In this talk, we will present our results on 1000 times enhanced and highly directional (~5 degrees) excitonic emission coupled to photonic Fano resonances of a dielectric system. We will also talk about electrical and dynamic control of coupling between charged excitons of MoS2 and photonic resonances. In the last part, we will discuss some recent results on waveguiding in monolayer materials based on leaky modes and exciton-polaritons and exciton diffusion effects.

10345-31, Session 6

Ultrafast radiative heat transfer

Renwen Yu, ICFO - Institut de Ciències Fotòniques (Spain) and The Barcelona Institute of Science and Technology (Spain); Alejandro Manjavacas, The Univ. of New Mexico (United States); F. Javier García de Abajo, ICFO - Institut de Ciències Fotòniques (Spain) and The Barcelona Institute of Science and Technology (Spain) and ICREA-Institució Catalana de Recerca i Estudis Avançats (Spain)

Light absorption in conducting materials produces heating of their conduction electrons, followed by relaxation into phonons within picoseconds, and subsequent diffusion into the surrounding media over longer timescales. This conventional picture of optical heating is supplemented by radiative cooling, which typically takes place at an even lower pace, only becoming relevant for structures held in vacuum or under extreme thermal isolation. Here, we reveal an ultrafast radiative cooling regime between neighboring plasmon-supporting graphene nanostructures in which noncontact heat transfer becomes a dominant channel. We predict that more than 50% of the electronic heat energy deposited on a graphene disk can be transferred to a neighboring nanoisland within a femtosecond timescale. This phenomenon is facilitated by the combination of low electronic heat capacity and large plasmonic field concentration in doped graphene. Similar effects should occur in other van der Waals materials, thus opening an unexplored avenue toward efficient heat management.

10345-32, Session 6

Electrical properties of SiO2-based graphene under monochromatic visible light irradiation

Xiangdi Li, Xianming Liu, Xueying Cao, Peng Zhang, Xiaohua Lei, Weimin Chen, Chongqing Univ. (China)

Graphene with atomic scale thickness is film material of optically transparent and electrically conductive, which can be typically used as electrodes when a situation calls for low resistance electrical contacts without blocking light (e.g. touch panels, photovoltaics). There were many reports about the electrical conductivity change when the graphene irradiated under ultraviolet light, which were not the actual working environment. It is necessary to understand the stability of electrical properties of graphene film under visible light irradiation.

The purpose of this study is to investigate the electrical properties of graphene transparent conductive film under visible light irradiation. Samples in the study were chemical vapor deposition (CVD) growth graphene on the surface copper foils and then transferred to the SiO2 substrate. The electric resistance measurements were performed using a two-probe configuration on the graphene films placed inside a vacuum chamber with optical windows. Three monochromatic visible lights with wavelength of 635nm, 520nm and 450nm representing red(R), green(G) and blue(B) lights were used as irradiation sources, which were widely used in back lit displays. The irradiated power density on the samples could be adjusted in the experiments. Results show that the graphene resistances increased slowly under light irradiation with all the three different wavelengths, while decreased slowly as well after the light was switched off. The relative rates of resistance change were different under irradiation with the same density but different wavelength. Blue light irradiation may result in the largest resistance change.

10345-33, Session 7

Enhanced nonlinearities in transparent conducting oxides for ultrafast photonics *(Keynote Presentation)*

Clayton T. DeVault, Purdue Univ. (United States); Nathaniel Kinsey, Virginia Commonwealth Univ. (United States); Lucia Caspani, Heriot-Watt Univ. (United Kingdom); Matteo Clerici, Heriot-Watt Univ. (United Kingdom) and Univ. of Glasgow (United Kingdom); Kaipurath Muhammad Rishad, Thomas Roger, Enrico Carnemolla, Heriot-Watt Univ. (United Kingdom); Jongbum Kim, Amr M. Shaltout, Purdue Univ. (United States); Monica Pietrzyk, Andrea Di Falco, Univ. of St. Andrews (United Kingdom); Daniele Faccio, Heriot-Watt Univ. (United Kingdom); Alexandra Boltasseva, Purdue Univ. (United States); Marcello Ferrera, Heriot-Watt Univ. (United Kingdom); Vladimir M. Shalaev, Purdue Univ. (United States)

Coherent control of nonlinear and ultrafast plasmon-polariton mediated interactions has attracted wide attention for its potential for enhancing functionality in nano-scale photonic devices and applications. Contemporary research in ultrafast and nonlinear plasmonics primarily utilizes noble metals, such as gold and silver, as material platforms because of their high performance both in linear and nonlinear optical properties. Unfortunately, noble metals possess numerous drawbacks including low melting points, chemical instabilities, and an incompatibility with standard CMOS processing techniques, all of which hamper their incorporation into functional plasmonic devices. Here we investigate the mid-infrared ultrafast and nonlinear properties of the alternative plasmonic material, aluminum-doped zinc oxide (AZO). By performing time-resolved pump-probe spectroscopy, we observe an unprecedentedly large and ultrafast (sub-picosecond) response in AZO thin films for both intra- and inter-band pumping frequencies. These two nonlinearities arise from distinct electron excitation dynamics and, as such, can be controlled simultaneously and independently to provide a novel method of dynamic tunability. We demonstrate this phenomenon with two-color excitation and find our AZO films exhibit a THz modulation bandwidth. We also probed the nonlinear response of AZO films at the epsilon-near-zero (ENZ) frequency and observed a dramatic increase in the Kerr nonlinearity with an induced refractive index change on the order of unity. In summary, our ultrafast and nonlinear studies strongly support AZO as an alternative plasmonic material with qualities pertinent to the development and realization of practical plasmonic technologies.

10345-34, Session 7

Molding optical wavefronts with nonlinear active photonic platforms *(Invited Paper)*

Xiang Zhang, Nir Shitrit, Univ. of California, Berkeley (United States)

The emerging photonic platform of gradient metasurfaces has paved the way for new era of light manipulation. By incorporating meta-atoms with strong nonlinear light-matter interactions, nonlinear gradient metasurfaces takes the molding of optical wavefronts to a higher level, enabling new functionalities that cannot be achieved with linear metasurfaces. Moreover, by harnessing nonlinear dynamics in active photonic waveguides, on-chip light control of complex wavefronts is accessible with nanoscale cross-sectional area in stark contrast with metasurface platforms. In this talk, we will review the recent progress in nonlinear gradient metasurfaces and active photonic waveguides for extreme molding of light.

10345-35, Session 7

Tunable chiral metasurfaces based on the transfer of electromagnetic angular momentum

Sophie Viaene, Vrije Univ. Brussel (Belgium) and Chalmers Univ. of Technology (Sweden); Vincent Ginis, Jan Danckaert, Vrije Univ. Brussel (Belgium); Philippe Tassin, Chalmers Univ. of Technology (Sweden)

Chiral metasurfaces are widely recognized for their realization of strong optical activity and asymmetric transmission. Unfortunately, their use in photonic applications is limited by the fact that most chiral metasurface designs are static, i.e., it is not possible to tune the chiral response with an external time-dependent signal. In this contribution, we investigate whether the electromagnetic torque due to a circularly polarized pump beam provides a viable mechanism for the active control of chiral torsional metasurfaces. Our torsional metasurface consists of two cross-wire surfaces, connected by filaments in such a way that elements within one unit cell can rotate with respect to each other. We show that, in presence of friction and restoring torques due to the filaments, a microwave pump beam may use its torque to temporally modify the angular orientation between the right and the left layers. In particular, we provide a full analysis of the nonlinear dynamics of the rightmost layer to determine the equilibrium orientations and their bifurcations as a function of the power and the frequency of the beam. A subsequent parameter sheet retrieval of the chiral response explicitly demonstrates its tunability in terms of the input power and frequency. Overall, our work shows that an electromagnetic torque due to circularly polarized microwaves may sufficiently tune the chiral response of the torsional metasurfaces with realistic pumping powers.

10345-36, Session 7

Enhanced nonlinear optical interactions in 2D-3D heteromaterials *(Invited Paper)*

Nicolae Coriolan Panoiu, Jian Wei You, Univ. College London (United Kingdom)

We briefly discuss some theoretical concepts and methods widely used in the study of optical nanostructures and explain how they can be extended to incorporate quadratic and cubic nonlinear optical effects in 2D materials. We illustrate how these tools can be used to design nonlinear photonic devices containing 2D materials in which orders-of-magnitude nonlinearity enhancement is achieved. Specifically, we demonstrate strongly enhanced nonlinear optical interactions in photonic nanostructures via resonant excitation of nonlinear waveguide modes, enhanced optical nonlinearity of nanostructures containing graphene and transition-metal dichalcogenide nanomaterials, and tunable Fano resonances for increased frequency conversion efficiency of hybrid 2D-3D photonic heteromaterials.

10345-37, Session 7

Nonlinear tuning of resonance in metamaterial absorbers *(Invited Paper)*

Subramaniam Anantha Ramakrishna, Sriram Guddala, Indian Institute of Technology Kanpur (India)

Metamaterials are structured composite materials that give rise to unique properties due to the resonant interaction of the structure with electromagnetic waves. As an example, arrays of structures can be tailored to have electric and magnetic resonances so as to have optimized impedance matching for high absorption at selected bands of frequency from visible to microwaves. The resonant structures have large localized fields that can enhance nonlinear responses of the constituent materials. The nonlinear response allows one to dynamically tune the resonance of the metamaterial structure and change its response.

Two cases of nonlinear and switchable resonant metamaterial absorbers will be presented:

(i) a metamaterial perfect absorber made of structured aluminum, where the nonlinearity originates in the change of conductivity of aluminum with increased temperatures. The thermal nonlinearity changes the behaviour of the metamaterial due to heating caused by the absorption of light.

(ii) a nonlinear metamaterial made of an array of gold discs separated from a continuous gold thin film by a thin film of ZnS, where the Kerr-nonlinearity of gold plays a defining role. This metamaterial acts as a reflective clamp whereby the reflected intensity does not increase beyond a point, for intense picosecond laser pulses. Strong local field enhancements in the ZnS film result in multi-photon fluorescence from ZnS and enhance the nonlinear response of ZnS. The enhanced nonlinear response of ZnS contributes an equal amount to the phenomenon although its intrinsic nonlinearity is four orders of magnitude smaller than that of gold.

10345-38, Session 8

Graphene terahertz photonics *(Invited Paper)*

Philippe Tassin, Chalmers Univ. of Technology (Sweden)

Graphene is an interesting material for terahertz photonics, because of its gate voltage tunability and its support of surface plasmon polaritons. I will review our recent work on graphene terahertz photonics. First we have studied the scattering behavior of graphene with an externally modulated conductivity and we show that this leads to a mechanism for tunable terahertz frequency combs. Second, we study the nonlocal response of graphene and its implications on surface plasmon excitations. Third, I discuss the potential of graphene plasmons, which are sensitive to the index of refraction of tiny amounts of an analyte on their surface.

Return to Contents

10345-39, Session 8

Terahertz transitions in quasi-metallic carbon nanotubes and graphene nanoribbons *(Invited Paper)*

Mikhail E. Portnoi, Vasil A. Saroka, Univ. of Exeter (United Kingdom); Richard R. Hartmann, De La Salle Univ. (Philippines)

No Abstract Available

10345-40, Session 8

Instantaneous and transient nonlinearities of graphene plasmons

Joel D. Cox, ICFO - Institut de Ciències Fotòniques (Spain); F. Javier García de Abajo, ICFO - Institut de Ciències Fotòniques (Spain) and ICREA-Institució Catalana de Recerca i Estudis Avançats (Spain)

Graphene exhibits a remarkably high intrinsic nonlinearity that can be pushed even further when the optical frequency is tuned to the plasmon resonances of the material. Atomistic simulations provide an accurate description of these phenomena, although their computational cost is prohibitive for large graphene nanostructures. In the weak-field, cw regime, an alternative formalism consists in relying on classical electromagnetism, using the local nonlinear conductivities extracted from perturbative models of extended graphene. We show that both of these approaches are in excellent agreement for sufficiently-large structures (10s of nm in lateral size) when describing second- and third-harmonic generation, as well as the Kerr nonlinearity. Additionally, we exploit an eigenmode decomposition of the optical field in the classical formalism to obtain analytical expressions for the plasmon-driven response of graphene ribbons and finite islands, in excellent agreement with atomistic calculations.

In contrast to the instantaneous nonlinear response, where input and output fields maintain relative coherences, a delayed nonlinearity also takes place as a consequence of the strong dependence of the graphene response on the temperature of its conduction electrons. Here we show that transient plasmons arising from the elevated electronic temperature in graphene upon ultrafast optical pumping can produce strong modulations of the optical absorption. Our nonperturbative time-domain simulations indicate that the strong incoherent nonlinearity associated with plasmons in doped graphene nanostructures can be used for all-optical switching in nonlinear optical devices.

10345-41, Session 8

Electromagnetic properties of multilayered nanostructured 2D materials: application to graphene

Bruno Majérus, Michaël Lobet, Mirko Cormann, Nicolas Reckinger, Philippe Lambin, Univ. of Namur (Belgium); Jérémy Butet, Gabriel D. Bernasconi, Raziman Thottungal Valapu, Olivier J. F. Martin, Ecole Polytechnique Fédérale de Lausanne (Switzerland); Luc Henrard, Univ. of Namur (Belgium)

The determination of the electromagnetic properties of 2D materials is of primary interest for applications in biosensing, shielding and optronics. Various methods have been proposed to numerically evaluate the electromagnetic response of nanostructured 2D materials. These methods generally model graphene either as an isotropic material with a given thickness or as a surface current.

In this work, we have compared several methods such as the surface current method, the discrete dipole approximation, the finite-difference time-domain method and rigorous coupled wave analysis to study graphene and graphene multilayers. We highlight the role of the layer thickness and of the anisotropy on the electromagnetic properties of graphene. We have also shown that a modification of the Brewster angle is observed, linked with the conducting nature of a graphene layer transferred to dielectric substrate. We propose a way to measure the surface conductivity of a conducting 2D material by optical measurement [1].

We then study the electromagnetic response of graphene nanostructures. The second-harmonic generation by graphene disk dimers has been investigated [2]. We show that SHG is greatly enhanced when the symmetry of this system is broken. In particular, applications such as nanorulers are suggested. Other features as the electron energy loss spectroscopy spectrum of nanostructured graphene are also explored.

[1] Modified Brewster angle on 2D materials: a way to optically characterize bidimensionnal conductivity. M. Lobet et al. In preparation.

[2] Optical second harmonic generation from nanostructured graphene: a full wave approach. B. Majérus et al. Submitted to PRB.

10345-42, Session 9

On-chip phase-change photonic memories and computing *(Invited Paper)*

Zengguang Cheng, Carlos A. Rios, Harish Bhaskaran, Univ. of Oxford (United Kingdom)

No Abstract Available.

10345-43, Session 9

Switchable infrared nanophotonic elements enabled by phase-change materials *(Invited Paper)*

Thomas Taubner, RWTH Aachen Univ. (Germany)

The strong confinement and enhancement of light when coupled to surface waves or nanoparticles is key for various applications in nanophotonics such as sensing, imaging or the manipulation of light fields. In the mid-infrared spectral range, metallic nanoantennas and materials supporting surface phonon polaritons (SPhPs) can be used as building blocks of such devices. Often, their optical functionality is only obtained at a fixed wavelength, determined by the geometric design and the material properties.

By using phase-change materials (PCMs) as tunable environment for nanophotonic resonators, their resonance frequency can be altered in a non-volatile, reversible way. PCMs offer a huge change in refractive index due to a phase transition from their amorphous to crystalline state, which can be thermally, optically or electrically triggered. We present results on thermal and optical switching, as well as addressing of individual IR resonances of both systems, metallic nanoantennas and resonators for SPhPs. SPhPs on polar dielectrics exhibit lower losses and larger Q-values compared to metallic nanoantennas, and their confinement can be even increased by adding ultrathin, switchable PCM layers. We show the all-optical, non-volatile, and reversible switching of the SPhPs by controlling the structural phase of the PCM [1], opening the door for re-configurable metasurfaces.

[1] P. Li et al., Nat. Mat. 15, 870 (2016).

10345-44, Session 9

Chalcogenide active photonics *(Invited Paper)*

Robert Simpson, Weiling Dong, Hailong Liu, Sreekanth K. Valiyaveedu, Li Liu, Singapore Univ. of Technology & Design (Singapore); Tun Cao, Dalian Univ. of Technology

(China); Joel Yang, Singapore Univ. of Technology & Design (Singapore)

Chalcogenides are materials that substantially consist of sulfur, selenium, or tellurium. Their dielectric properties can be tuned by thermally induced structural phase transitions, photostructural transitions, and dissolution of metal dopants. We have designed active photonic structures using a range of 'tuneable' chalcogenides. The resonant frequency of aluminium plasmonic structures was tuned over a 100 nm band in the visible, metal-chalcogenide-metal structures provide tuning of over a band of 0.5 μm in the mid-infrared, and hyperbolic metamaterials incorporating chalcogenides provide a means to alter the radiative decay rate of fluorescent photons.

10345-45, Session 9

Thermal homeostasis using nanophotonic phase change materials *(Invited Paper)*

Michelle L. Povinelli, Shao-Hua Wu, Mingkun Chen, The Univ. of Southern California (United States); Michael Barako, Vladan Jankovic, Philip W. C. Hon, Luke A. Sweatlock, NG Next Northrop Grumman Corp. (United States)

We consider the design of nanostructured materials for thermal homeostasis, or the ability to maintain a temperature within a fixed range despite externally varying heat input. Our design uses nano- and microstructured phase-change materials to achieve a sharp change in thermal emission at a particular phase-transition temperature. We use electromagnetic simulations to calculate the thermal infrared absorption spectra for metal and insulator phases of the phase-change material. The results indicate a large increase in thermal emission at the phase transition. We then use numerical simulations of the heat equation to show that the sharp change in emission results in thermal homeostasis. For a varying external heat source, the material experiences much smaller temperature fluctuations than an unstructured or bulk material.

10345-46, Session 10

Optical modulation in silicon-vanadium dioxide photonic structures *(Invited Paper)*

Kevin J. Miller, Kent A. Hallman, Richard F. Haglund, Sharon M. Weiss, Vanderbilt Univ. (United States)

In principle, Tbps optical signal modulation could be achieved by integrating an ultrafast phase-change material into silicon photonics devices. Here we demonstrate high-speed all-optical and electro-optic hybrid silicon-vanadium dioxide (Si-VO2) ring resonator and waveguide modulators. The thermally induced insulator-to-metal transition (IMT) suggests that 10 dB modulation depths are achievable, although the dynamics of the IMT enforces a tradeoff between modulation depth and response time. The effects of placing VO2 atop or within the Si photonic structures will also be discussed.

10345-47, Session 10

Dynamic control of infrared optical absorption and thermal emission using phase-transition materials *(Invited Paper)*

Mikhail A. Kats, Univ. of Wisconsin-Madison (United States)

No Abstract Available.

10345-48, Session 10

Photoinduced optical dynamics of phase-change vanadium oxides

Nardeep Kumar, Armando Rúa, Lee R. Chevres, Larry Theran, Brian Ayala, Félix E. Fernández, Sergiy I. Lysenko, Univ. de Puerto Rico Mayagüez (United States)

Using time- and angle-resolved hemispherical elastic light scattering technique we reveal complex pathways of photoinduced ultrafast insulator-to-metal and metal-to-insulator phase transition in VO2, V2O3 and V3O5 thin films. The structural dynamics was monitored with extraordinary detail by novel ultrafast diffraction conoscopy technique. The evolution of insulating and metallic phases in these correlated oxides is substantially different and significantly depends on optical excitation, temperature, size of grains and domains. Strong optical nonlinearity along with its complex transient dynamics makes vanadium oxides attractive for high-contrast all-optical switches, high-speed optical data storage and holographic devices. The characteristic time of optical nonlinearity can be tuned from ~500 fs to several picoseconds by altering the excitation fluence and wavelength, film thickness and size of grains and domains. Additional control of ultrafast phase transition dynamics can be achieved by photoacoustical generation of strain waives. In V2O3 at room temperature the strain wave produces metal-to-insulator transition, while in VO2 and V3O5 it triggers insulator`-to-metal one. Depending on material morphology and level of optical excitation, the optical signal shows coherent oscillations caused by photoacoustic wave at picosecond and nanosecond time scales. Complex nonlinear dynamics of correlated vanadium oxides can provide a way for precise tuning of transient optical and electronic properties of photonic devices.

10345-49, Session 10

Electrically driven hybrid photonic metamaterials for multifunctional control *(Invited Paper)*

Lei Kang, Liu Liu, Sawyer D. Campbell, Taiwei Yue, Qiang Ren, Theresa S. Mayer, Douglas H. Werner, The Pennsylvania State Univ. (United States)

The unique light-matter interaction in metamaterials, a type of artificial medium in which the geometrical features of subunits dominate their optical responses, have been utilized to achieve exotic material properties that are rare or nonexistent in natural materials. To enable practical applications, active materials have been introduced into metamaterial systems to advance tunability, switchability and nonlinearity, which has given rise to the concept of metadevices proposed recently. Nevertheless, practical examples of versatile photonic metamaterials remain exceedingly rare for two main reasons. On the one hand, in sharp contrast to the broad material options available at lower frequencies, it is much more uncommon to find active media that can provide pronounced dielectric property changes in optics under external stimuli, such as electric and magnetic fields. Vanadium dioxide (VO2), offering a large refractive index variation over a broad frequency range, due to its near room temperature insulator-to-metal transition (IMT), has been favored in recent studies on tunable metamaterials. On the other hand, it turns out that regulating responses of hybrid metamaterials to external forces in an integrated manner is not a straightforward task. Recently, metamaterial-enabled devices (i.e., metadevices) with 'self-sufficient' or 'self-contained' electrical and optical properties have enabled complex functionalities. Here, we present a design methodology along with the associated experimental validation of a VO2 thin film integrated optical metamaterial absorber as a hybrid photonic platform for electrically driven multifunctional control, including reflectance switching, a rewritable memory process and manageable localized camouflage. The nanoengineered topologically continuous metal structure simultaneously supports the optical resonance and electrical functionality that actuates the phase transition in VO2 through the process of Joule heating. This work provides a universal approach to creating self-sufficient and highly-versatile nanophotonic systems.

10345-50, Session 11

Topological photonics: from macro- to nano-scale *(Keynote Presentation)*

Gennady B. Shvets, Univ. of Texas at Austin (United States)

The 2016 Nobel Prize in Physics was awarded to Kosterlitz, Thouless, and Haldane for their pioneering theoretical work on the novel and counter-intuitive phases of matter that are now referred to as topological phases. Almost half a century after these researchers applied powerful mathematical techniques of topology to condensed matter systems, a new rapidly developing area is taking shape, now in the field of photonics. I will provide an overview of the field, with special emphasis on the photonic emulation of the canonical quantum topological phases such as the Hall, spin-Hall, and valley-Hall phases. The prospects for bringing topological photonics to nanoscale using 2D materials will also be discussed.

10345-51, Session 11

Self-induced topological solitons for nonlinear optical isolation *(Invited Paper)*

Yidong Chong, Daniel Leykam, Xin Zhou, You Wang, Nanyang Technological Univ. (Singapore)

No Abstract Available.

10345-52, Session 11

Topological steering of the lasing beam in surface lasers

Babak Bahari, Junhee Park, Felipe Vallini, Ricardo Tellez Limon, Ashok Kodigala, Thomas Lepetit, Yeshaiahu Fainman, Boubacar Kante, Univ. of California, San Diego (United States)

Steering the beam of a wave source has been demonstrated using mechanical and non-mechanical techniques. While mechanical techniques are bulky and slow, non-mechanical techniques rely on breaking the symmetry of the refractive index profile either using asymmetric structure or injecting a non-uniform current. In this contribution, we theoretically and experimentally demonstrated a new type of topological steering of light sources in which the phase offset is provided by Floquet-Bloch phase in periodic structure. It was shown that in periodic structures, there exist singular states in the radiation region of the band diagram that exhibit diverging quality factor. Thus light sources can operate at these states with lower power threshold. The existence of these singular states are topologically protected, and their momentum are very sensitive to any small perturbations, which is used to control the steering angle. By uniformly controlling some parameters in the system, such as a physical dimension or injecting current uniformly, the beam of the light source steers. Our experimental demonstrations open new paradigm in the implementation of light steering with applications in data communications, bio imaging and sensing.

10345-53, Session 11

Index ellipsoids at arbitrary k-points *(Keynote Presentation)*

Che Ting Chan, Wenjie Chen, Hong Kong Univ. of Science and Technology (Hong Kong, China)

The index ellipsoid gives the orientation and relative magnitude of refractive indices in a crystal. In all natural materials, the index ellipsoid is centered at k=0. This is expected to be true even for man-made crystals such as photonic crystals and metamaterials. For photonic crystals, we are used to see photonic band structures that are either gapped at low frequency (for metallic structures) or those having a linear dispersion emerging at k=0 (for dielectric structures). Metamaterials can have exotic values of permittivity and permeability that cannot be found in natural materials, and as such, they can have unconventional index ellipsoids. However, in most of the previously designed metamaterials, the equi-frequency surface either forms an ellipsoid (e.g. in double negative medium) or hyperboloid (hyperbolic medium) centered at k=0. If the local effective permittivity and permeability are well defined, we expect a linear dispersion at low frequency in the long wave limit, and ?-->0 as k-->0.

Here, we propose a new type of photonic crystal structure that possess one or more index ellipsoids positioned at nonzero k-points. Linear bands that go to zero frequency emerge from non-zero k-points as a consequence of artificial gauge potentials provided by the microscopic structure possessing special geometries. The number of ellipsoids and their positions within the Brillouin zone can be engineered by changing the connectivity of the metallic components. This gives us a new degree of freedom to tailor the optical response of man-made materials, leading to unusual wave propagation behaviors.

10345-54, Session 12

Topology emerging from photonic graphene *(Keynote Presentation)*

Xiao Hu, National Institute for Materials Science (Japan)

No Abstract Available.

10345-55, Session 12

Topological photonics research at Sandia Lab

Ganapathi S. Subramania, Sandia National Labs. (United States); P. Duke Anderson, Sandia National Labs. (United States) and The Univ. of Southern California (United States)

Topological photonic structures in analogy to their electronic counterparts can provide new functionalities in nanophotonics. In particular, they can possess topologically protected photonic modes that can propagate unidirectionally without scattering and can have an extreme photonic density of states (PDOS). These unique properties can directly impact many photonic systems used in communications and quantum information processing applications such as single photon transport. Several theoretical works and experimental demonstrations of topological states have been done on macroscopic systems such as optical fiber arrays and microwave structures. Enabling such properties at optical frequencies and on chip-scale will be very important for practical applications of such phenomena. We present work conducted at Sandia lab towards the goal of optical frequency chipscale nanophotonic structures with topological properties. We will discuss implementation of topological photonic structures in semiconductor based systems (e.g. Si, GaAs and GaN).

Sandia National Laboratories is a multi-mission laboratory managed and operated by Sandia Corporation, a wholly owned subsidiary of Lockheed Martin Corporation, for the U.S. Department of Energy's National Nuclear Security Administration under contract DE-AC04-94AL85000.

10345-56, Session 12

Topological edge states of distorted photonic Kagome lattices

Xiang Ni, The City College of New York (United States); Andrea Alù, The Univ. of Texas at Austin (United States); Alexander B. Khanikaev, The City College of New York (United States)

We demonstrate that the distorted Kagome lattice formed by 2d array of dielectric rods embedded in air exhibits a new class of topological states characterized by a topological invariant number in Pauli vector space. The Kagome lattice can be considered as a two dimensional analogy of Su-Schrieffer–Heeger (SSH) which displays the topological transition by detuning the relative amplitudes of the inter-cell and intra-cell hopping terms. The surface d(k) as k sweeps through the whole Brillouin zone will enclose the origin in Pauli vector space and the topological number be nonzero if the inter-cell hopping amplitude is larger than the intra-cell hopping amplitude. While d(k) will exclude the origin and the topological number be zero if the case is reversed. The topological transition is accompanied by the opening of complete band gap in Brillouin zone, which may host topological edge states on either truncated end of the lattice or at the domain walls between topological nontrivial and trivial domains. To further validate the above conclusion, quasi 1d Kagome lattice is built by rolling 2d Kagome lattice sheet into cylinder and revealed to have SSH-like edge states at the ends of cylinder by Dimensional reduction method. The first-principles simulations based on the full wave finite element method (FEM) are used to design the lattice and confirm the analytic prediction.

10345-57, Session 12

Non-Hermitian defects in topologically protected photonic crystals *(Invited Paper)*

Tsampikos Kottos, Wesleyan Univ. (United States)

The development of non-Hermitian photonics and the implementation of spatio-temporal symmetries in optics has led to new avenues for the manipulation of light. Two of the most prominent subfields which utilize the above two developments are parity-time symmetric optics and topological photonics. In this presentation we will focus at the second framework and investigate the scattering properties of non-Hermitian photonic crystals with topologically protected defect modes. We will discuss two specific applications associated with perfect absorbers and topologically protected power switches.

10345-58, Session 13

Dipolar second order nonlinear effects from goldnano-antennas by controlling radiation phase *(Invited Paper)*

Sylvain D. Gennaro, Vincenzo Giannini, Themistoklis P. H. Sidiropoulos, Imperial College London (United Kingdom); Miguel Navarro-Cía, The Univ. of Birmingham (United Kingdom); Stefan A. Maier, Rupert F. Oulton, Imperial College London (United Kingdom)

No Abstract Available.

10345-59, Session 13

Shaping of higher harmonic radiation in dielectric nanoantennas

Massimiliano Guasoni, Univ. of Southampton (United Kingdom); Luca Carletti, Univ. degli Studi di Brescia (Italy); Dragomir N. Neshev, The Australian National Univ. (Australia); Costantino De Angelis, Univ. degli Studi di Brescia (Italy)

Higher harmonic generation (HHG) at nanoscale is of paramount importance for a plethora of applications.To overcome the issue of ohmic losses in plasmonic devices, last years have seen the development of dielectric nanoantennas that are in principle loss-free. In this framework, careful design of the antenna geometry is essential: different geometries lead indeed to different higher harmonic (HH) radiation patterns.Despite the efforts made in the last decade, most of the theoretical works on this subject have been limited to spherical particles or short cylinders with circular cross-section and in the limit of low refractive index difference between the antenna and the surrounding environment. These constraints are not realistic when dealing with high-index materials like AlGaAs (extremely suitable for HHG) and do not cover complex geometries that may reveal useful radiation features. In this work, we develop a novel theoretical model for the study of HHG in cylindrical nanoantennas. Our model applies whatever the cross-section shape and the refractive index of the material. The key idea is the decomposition of the electromagnetic field over the complete set of transverse modes of the antenna. For a given incident field at the fundamental harmonic we can predict the modes excited at the HH, each one related to a peculiar modal radiation pattern for which an analytical or semi-analytical formulation is provided. In conclusion, these results find useful application in the design of optimal geometries leading to ad-hoc HH radiation patterns at the nanoscale.

10345-60, Session 13

Reconfigurable silicon photonics: shaping light on a chip *(Invited Paper)*

Otto L. Muskens, Roman Bruck, Nicholas Dinsdale, Univ. of Southampton (United Kingdom); Kevin Vynck, Philippe Lalanne, Lab. Photonique, Numérique et Nanosciences (France); Goran Z. Mashanovich, Graham T. Reed, Univ. of Southampton (United Kingdom)

Defining elements with reconfigurable input-output characteristics is of importance to achieve flexible circuitry where light can be manipulated and routed using external control signals. We have developed an experimental approach for shaping of the transmission function of multimode silicon photonic waveguides by projecting a pattern of local nonlinear perturbations induced by an ultrafast laser pulse. Making use of the degrees of freedom offered by a spatial light modulator, the technique offers a new approach for studying light transport, for controlling its flow on ultrafast time scale, and for programming functions on a photonic chip.

10345-61, Session 14

Topological and complex birefringent metamaterial *(Keynote Presentation)*

Shanhui Fan, Alex Cerjan, Meng Xiao, Luqi Yuan, Qian Lin, Stanford Univ. (United States)

We discuss novel electromagnetic effects in topological metamaterial and in complex birefringent meta material. In particular, we discuss the creation of novel topology using meta-material geometry., We also discuss three-dimensional meta-materials with balanced gain and loss for the purpose of achieving arbitrary control of a pair of polarization states.

10345-62, Session 14

Topological and non-reciprocal photonics *(Keynote Presentation)*

Andrea Alù, The Univ. of Texas at Austin (United States)

In this talk, we will review our recent progress towards the concept, design and realization of magnet-free non-reciprocal photonic devices and arrays of them with strong topological protection, aimed at realizing reconfigurable, broadband isolators and circulators. We will discuss our approaches to design topological photonic metasurfaces based on spatio-temporal modulation, nonlinearities, and/or opto-mechanical interactions, and discuss our vision towards new transport phenomena for light, and new nanophotonic devices with enhanced non-reciprocal properties.

10345-64, Session 14

Entangled photons in 2D topological photonic systems *(Invited Paper)*

Sunil Mittal, Venkata Vikram Orre, Joint Quantum Institute, Univ. of Maryland (United States) and National Institute of Standards and Technology (United States); Mohammad Hafezi, Joint Quantum Institute, Univ. of Maryland (United States) and National Institute of Standards and Technology (United States)

Topological photonic systems using synthetic gauge fields have now been implemented using a variety of platforms, for example, using coupled ring resonators and helical waveguides in the optical domain, and also using metamaterials in the microwave domain. Edge states, a hallmark of topological phenomena, have been observed and the robustness of edge state transport against disorder has been quantitatively established. However, recent explorations of edge state physics have relied on measuring classical transport properties, such as transmission and delay statistics. Here, we discuss quantum transport of entangled photons in a 2D topological photonic system of coupled ring resonators. In particular, we consider transport of time-bin entangled photons through the system. Using numerical simulations, we show that in the presence of disorder, edge state transport preserves temporal correlations of input photons whereas bulk transport can lead to significant bunching or anti-bunching of photons. We present our experimental progress in this direction. Moreover, we discuss generation of entangled photons in this 2D topological system. The topological robustness of edge states could be used for efficient on-chip generation of wavelength-entangled photons.

10345-3, Session PWed

Polarization driven supramolecular chirality in soft-printed dielectric microstructures

Angelo Angelini, Politecnico di Torino (Italy); Federica Pirani, Politecnico di Torino (Italy) and Istituto Italiano de Tecnologia (Italy); Federico Ferrarese Lupi, Istituto Nazionale di Ricerca Metrologica (Italy); Francesca Frascella, Serena Ricciardi, Politecnico di Torino (Italy); Natascia De Leo, Luca Boarino, Istituto Nazionale di Ricerca Metrologica (Italy); Emiliano Descrovi, Politecnico di Torino (Italy)

The interaction of light with periodic and quasi-periodic dielectric structures has gained novel interest since the fabrication techniques have enabled the fabrication of large area surface patterns in which each element can be shaped to provide additional degrees of freedom over the emerging light. Such surfaces allow finely engineering the wave-front of visible light with an unprecedent degree of control, enabling the fabrication of ultrathin optical elements with complex optical functionalities. Polarization sensitive holographic patterns and dielectric meta-surfaces are examples of what can be done with those kinds of surfaces.

A fundamental limit of pre-patterned surfaces comes from the impossibility to modify their optical behavior after the initial structuration. Here we propose the use of photo-responsive dielectric materials to dynamically control the polarization state of light emerging from individual surface elements. We make use of a commercial azo polyelectrolyte (Pazo) dispersed in a passive polymeric matrix (PMMA) that is patterned in an array of micro-pillars. When a single pillar is exposed to UV-visible radiation, a supramolecular chirality is induced within the pillar, and light emerging from it takes memory of the writing beam polarization. A direct experimental observation of such effect and the fully reversibility of the induced chirality will be provided. The method proposed may enable the fabrication of optically active metasurfaces as well as fabrication of dynamically tunable holographic patterns.

10345-82, Session PWed

Incident femtosecond pulse chirp influence on nonlinear localization of laser energy in layered photonic crystal

Vyacheslav A. Trofimov, Tatiana M. Lysak, Evgenii M. Trykin, M.V. Lomonosov Moscow SU (Russian Federation)

We investigate laser energy localization in a layered photonic crystal with Kerr nonlinear response in dependence of chirp of an incident femtosecond pulse. Such kind of energy localization appears due to soliton formation in certain layers of photonic crystal. Layers position, in which a solitons appear, depend on the pulse chirp and the incident pulse intensity essentially. It is important to emphasize that a soliton occurs in separate layers. Therefore, its width must be less than a layer thickness. Consequently, an intensity of the incident pulse must be greater than its crucial value. A process of energy localization strongly depends on relation between the wave packet carrier frequency and a frequency characterizing a photonic crystal.

The problem under consideration is described by a nonlinear Schrödinger equation with respect to amplitude slowly varying in time. We investigate a femtosecond pulse interaction with photonic crystal numerically and analytically.

10345-83, Session PWed

Self-similar chirped laser pulse propagation in a medium with TOD and non-resonant TPA

Vyacheslav A. Trofimov, Aleksey A. Kalinovich, Irina G. Zakharova, M.V. Lomonosov Moscow SU (Russian Federation)

In this report we derive a self-similar both shape and chirp of a pulse propagating in a medium with non-resonant TPA under the condition of a TOD influence. The main feature of this soliton-like propagation of the laser pulse is a pulse chirp presence. In the frame-work of nonlinear Schrödinger equation we derive an approximate pulse shape and its chirp evolution in time. Consideration is shown that self-similar shape of a pulse is asymmetrical one and nonlinear time dependence of the pulse carrier frequency.

To confirm the results of our analytical consideration and to clarify its frame-work validity we make computer simulation. We show that the analytical result is valid along long distance propagation.

10345-85, Session PWed

Magnetic and magneto-optical properties on sub-micrometer thick Bi-doped iron garnets grown by liquid phase epitaxy

Nathan Beaulieu, Souren P. Pogossian, Univ. de Bretagne Occidentale (France); Lucile Soumah, Abdelmadjid Anane, Paolo Bortolotti, Vincent Cros, Unité Mixte de Physique CNRS/Thales (France); Jamal Ben Youssef, Univ. de Bretagne Occidentale (France)

Iron based garnets have unique magneto-optical (MO) properties that make them interesting for photonic applications such as the non-reciprocal Mach-Zehnder Interferometer [1]. The integration of garnets on the photonic circuit can be performed either by direct deposition on Si or by molecular bonding [2]. This second approach requires growing very smooth garnet films in order to obtain uniform bonding properties. The growth of thin films (thinner than 100 nm) is critical to perform nanostructuration on these materials, as they are very resilient to standard etching techniques. Usually, the growth of thin garnet films is performed by PLD [3], or off axis

sputtering [4]. Liquid phase epitaxy (LPE) is a well-established industrial process that can produce rapidly large area and uniform films, but the control of the growth rate is critical to obtain layers thinner than 100 nm.

Here we report on the growth and the characterization of submicrometer thick garnets with optimized MO characteristics using LPE. The study of the structural and magnetic properties as a function of the garnet film thickness revealed a dependence on the roughness, on the anisotropy and on the damping parameter. We measured the magneto-optical response using Faraday rotation at different wavelengths ranging from 635 to 1550 nm on samples from 40 nm to 1 μm thick. This study showed an enhanced Faraday rotation at lower thicknesses (thinner than 100 nm). Future cladding based photonic devices could be more compact using thin Bi-doped garnets. We also studied the magnetization dynamics of those films using broadband ferromagnetic resonance and observed a significant increase in the Gilbert damping for the thinnest films.

[1] Y.Shoji et al.,Japanese Journal of Applied Physics53,022202, (2014).

[2] Pantzas K.,et al.,APL105,141601 (2014)

[3] d'Allivy-Kelly et al.,APL103,082408 (2013)

[4] Wang et al.PRB88,100406(R) (2013)

10345-86, Session PWed

Modeling and simulation analysis of graphene integrated silicon waveguide

Swati Joshi, Brajesh Kumar Kaushik, Vikas Nehra, Indian Institute of Technology Roorkee (India)

The modern high density on-chip electrical interconnects are not able to meet current technology demands due to inherent RC limitation. Silicon photonics is an emerging technology with the prospects of combining electronics with photonics on a single chip to improve system performance and open up numerous design opportunities. Optical waveguides are the basic elements of photonic circuits for transmission of light over various distances. The potential of optical interconnects has been investigated immensely for the parameters such as compact design, strong light confinement, high bandwidth, low crosstalk, low loss propagation, in design of high density next-generation on-chip system. The performance of these parameters is a key factor for the growth of silicon photonics. Graphene, an allotrope of carbon with unique optoelectronic properties and silicon compatibility has prompted intense research in graphene based electrical and optical applications ranging from the terahertz to the visible spectral region. The fermi level of the graphene can be electrically and chemically controlled to modulate its conductivity. Graphene has been shown as a promising candidate in planar photonic circuit design to pave the way for realistic applications. The transmission properties of the waveguide are directly affected by its geometry, location, and tunability of graphene refractive index. This paper analyzes the graphene integrated waveguide properties such as mode profiles, effective index, propagation loss, bending behavior. We propose an optimized waveguide design to have mode field concentrated near graphene layer to maximize absorption through graphene for the compact electro-absorption modulator. The simulation results show agreement with the analytical models.

10345-65, Session 15

Photonic crystal Fano resonances for realizing optical switches, lasers, and non-reciprocal elements *(Invited Paper)*

Dagmawi A. Bekele, Jesper Mork, Yi Yu, Aurimas Sakanas, Luisa Ottaviano, Elizaveta Semenova, Kresten Yvind, Technical Univ. of Denmark (Denmark)

No Abstract Available.

10345-66, Session 15

Metawaveguide for asymmetric interferometric light-light switching *(Invited Paper)*

Han Zhao, Univ. at Buffalo (United States); William S. Fegadolli, California Institute of Technology (United States); Jiakai Yu, Zhifeng Zhang, Univ. at Buffalo (United States); Li Ge, The City Univ. of New York (United States); Axel Scherer, California Institute of Technology (United States); Liang Feng, Univ. at Buffalo (United States)

Here we report an experimental demonstration of a metawaveguide that operates exactly in the opposite way in a linear regime, where an intense laser field is interferometrically manipulated on demand by a weak control beam with a modulation extinction ratio up to approximately 60 dB. This asymmetric control results from operating near an exceptional point of the scattering matrix, which gives rise to intrinsic asymmetric reflections of the metawaveguide through delicate interplay between index and absorption. The designed metawaveguide promises low-power interferometric light-light switching for the next generation of optical devices and networks.

10345-67, Session 15

Quantum optical circulator controlled by a single chirally coupled atom *(Invited Paper)*

Juergen Volz, Vienna Ctr. for Quantum Science and Technology (Austria)

In our experiment, we implement a quantum optical circulator by coupling a single rubidium atom to a whispering-gallery-mode microresonator which is interfaced by two optical nanofibers. Due to the chiral (direction dependent) interaction between the atom and the resonator light, this realizes a four port optical circulator with a strong nonreciprocal behavior. The operation direction of the device is controlled by the atomic quantum state. This, in principle, allows the preparation of the circulator in a coherent superposition of its operational states and renders it a key element for routing and processing quantum information in integrated optical circuits.

10345-68, Session 15

Non reciprocal light propagation in a YIG based magnetic waveguide

Lucile Soumah, Unité Mixte de Physique CNRS/Thales (France); Lilia Qassym, Thales Research & Technology (France); Cécile Carretero, Eric Jacquet, Unité Mixte de Physique CNRS/Thales (France); Jamal Ben Youssef, Nathan Beaulieu, Univ. de Bretagne Occidentale (France); Richard Lebourgeois, Alfredo De Rossi, Sylvain Combrie, Thales Research & Technology (France); Paolo Bortolotti, Abdelmadjid Anane, Unité Mixte de Physique CNRS/Thales (France)

Magneto-optical (MO) materials are key elements for non-reciprocal photonic functionalities such as optical isolation. Commercial optical isolators are based on the Faraday effect of Yttrium Iron Garnet (YIG) single crystals. Integrating such materials on a photonic chip has proven to be challenging. Most studies have been using cladding effects where a MO material (usually YIG) is put in close proximity to a silicon photonic waveguide using either direct deposition or molecular bonding [1]. In the present work, we study an alternative configuration where the MO material is used as the optical wave guide medium for light propagation.

Using the Pulsed Laser Deposition technique we have grown Bi:YIG layers with thickness up to 120 nm on YAG (111) substrates. The structural, magnetic and magneto-optical properties have been fully characterized. They show the good quality and the large MO effect (Faraday rotation) of the films. Using spectroscopic ellipsometry, we obtained the refractive index of both, the film and the substrate, the contrast between those two values, respectively 2.3 and 1.8 is sufficient to induce confined propagation of the TM mode. The low film thickness allows for wave guide structuration using standard lithography technics and ion beam etching. Non reciprocal propagation experiments will be presented on 0.7 to 2 μm wide waveguides; we discuss the potential of this approach for compact optical isolators despite the large insertion losses in our first generation devices.

[1] B. J. H. Stadler and T. Mizumoto, IEEE Photonics Journal 6, 1 (2014).

10345-69, Session 15

Non-PT-symmetric plasmonic waveguide-cavity systems: unidirectional reflectionlessness and broadband near total light absorption *(Invited Paper)*

Georgios Veronis, Louisiana State Univ. (United States); Yin Huang, Central South Univ. (China); Changjun Min, Shenzhen Univ. (China)

No Abstract Available.

10345-70, Session 15

Structure-induced asymmetry between counterpropagating modes and the reciprocity principle in whistle-geometry ring lasers *(Invited Paper)*

Marek Osinski, The Univ. of New Mexico (United States)

A key feature of the whistle-geometry semiconductor ring lasers is their unidirectionality, caused by an asymmetry between the counterpropagating modes. The asymmetry between modal losses results in different lifetimes for the two counterpropagating modes, which might be misconstrued as a violation of the Helmholtz reciprocity principle and the time-reversal symmetry of Maxwell's equations. We have verified the unidirectionality of the whistle-geometry configuration through rigorous three-dimensional finite-difference time-domain simulations. An explanation will be given why this result does not violate the reciprocity principle.

10345-71, Session 16

Active parity-time symmetric systems *(Invited Paper)*

Mercedeh Khajavikhan, Demetrios N. Christodoulides, CREOL, The College of Optics and Photonics, Univ. of Central Florida (United States)

In recent years, non-Hermitian degeneracies, also known as exceptional points (EPs), have emerged as a new paradigm for engineering the response of optical systems. Among many different non-conservative photonic configurations, parity-time (PT) symmetric arrangements are of particular interest since they provide an excellent platform to explore the physics of exceptional points. In this talk, I will present some of the work in our group, where the intriguing properties of exceptional points that are arising in judiciously designed parity-time-symmetric systems are utilized to address two of the long standing challenges in the field of integrated photonics: enforcing single mode lasing in intrinsically multimode cavities, and enhancing sensitivity of micro-resonators.

10345-72, Session 16

Towards nanoscale optical nonreciprocity with PT-symmetric metamaterials

David R. Barton III, Stanford Univ. (United States); Hadiseh Alaeian, Northwestern Univ. (United States); Mark Lawrence, Jennifer A. Dionne, Stanford Univ. (United States)

Optical nonreciprocity is critical for the function of optical isolators and circulators, but is challenging to achieve in nanophotonic systems using conventional methods. Here, we investigate a nonlinear parity-time (PT)-symmetric plasmonic metamaterial as a novel diode structure. A metamaterial with 150 nm unit cell composed of five alternating layers of Silver and a high index dielectric (n=3.2) is used as a model system; the structure is made PT-symmetric by inclusion of loss or gain in alternating dielectric layers. Analytical calculations reveal a bandstructure and band gap tunable with the amount of loss and gain. In the linear regime, the structure exhibits unity transmission at a wavelength of 500 nm near the optical band gap; further, internal electric field intensities vary based on the illumination direction (i.e., illumination from the "loss" or "gain" side of the metamaterial) by up to an order of magnitude. To make this structure nonreciprocal, saturable gain and absorption are introduced in the dielectric layers. These nonlinearities allow for intensity-based tuning of the bandgap such that illumination from the loss side is in the band gap, but is in the band pass from the gain side. Full field finite element simulations reveal nonreciprocal transmission with a transmission difference of nearly 10 dB within three free space optical wavelengths. The angular response of this material is additionally studied for possible applications in nonreciprocal negative index lensing. This sub-two-micron PT metamaterial represents a new approach in designing nanoscale nonreciprocal elements based on planar plasmonic and high-index dielectric films.

10345-74, Session 16

Higher-order exceptional points in photonic systems

Hossein Hodaei, Absar U. Hassan, Steffen Wittek, Midya Parto, Hipolito Garcia-Gracia, CREOL, The College of Optics and Photonics, Univ. of Central Florida (United States); Ramy A. H. El-Ganainy, Michigan Technological Univ. (United States); Demetrios N. Christodoulides, Mercedeh Khajavikhan, CREOL, The College of Optics and Photonics, Univ. of Central Florida (United States)

Student contribution: In recent years, non-Hermitian degeneracies, also known as exceptional points (EPs), have emerged as a new paradigm for engineering the response of optical systems. This class of degeneracies represents points in parameter space where the eigenvalues and their corresponding eigenvectors simultaneously coalesce [1,2]. Among the large set of non-conservative photonic systems, parity-time (PT) symmetric arrangements are of particular interest since they provide an excellent platform to study the physics and properties of non-Hermitian degeneracies [3,4]. So far, the abrupt nature of the phase transitions at EPs has led to a number of new functionalities such as loss-induced transparency [5], unidirectional invisibility [6,7], and single mode lasing [8-11]. In addition, it has been suggested that the bifurcation properties associated with second-order exceptional points can be utilized to achieve enhanced sensitivity in micro-resonator arrangements [11]. Of interest is to use even higher-order exceptional points that in principle could further amplify the effect of perturbations. While such higher-order singularities have been theoretically studied in a number of recent works [13,14], their experimental realization in the optical domain has so far remained out of reach. In this paper, for the first time, we show the emergence of third order exceptional points in ternary parity-time-symmetric coupled resonator lasers by judiciously designing the gain/loss distribution and coupling strengths following a recursive bosonic quantization procedure. Subsequently, the nature of the third order exceptional point is confirmed through the cubic root response

of this ternary system to external perturbations. Our work may pave the way towards the utilization of higher order exceptional points in designing ultrasensitive photonic arrangements.

References

[1] W. D. Heiss, J. of Phys. A: Mathematical and Theoretical 45, 444016 (2012).

[2] N. Moiseyev, Non-Hermitian Quantum Mechanics. (Cambridge University Press, 2011).

[3] K. G. Makris, R. El-Ganainy, and D. N. Christodoulides, Phys. Rev. Lett. 100, 103904 (2008).

[4] C. E. Rüter, K. G. Makris, R. El-Ganainy, D. N. Christodoulides, M. Segev, and D. Kip, Nat. Phys. 6, 192 (2010).

[5] A. Guo et al., Phys. Rev. Lett. 103, 093902 (2009).

[6] B. Peng et al., Nat. Phys. 10, 394 (2015).

[7] A. Regensburger, C. Bersch, M.-A. Miri, G. Onishchukov, D. N. Christodoulides, and U. Peschel, Nature 488, 167 (2012).

[7] M. Miri, P. Likamwa, D. N. Christodoulides, Opt. Lett. 37, 764 (2012)

[8] H. Hodaei, M.-A. Miri, M. Heinrich, D. N. Christodoulides, and M. Khajavikhan, Science 346, 975 (2014).

[9] L. Feng, Z. J. Wong, R.-M. Ma, Y. Wang, X. Zhang, Science 346, 972 (2014).

[11] H. Hodaei et al., Laser & Photon. Rev. 10, 494 (2016).

[12] J. Wiersig, Phys. Rev. Lett. 112, 203901 (2014).

[13] G. Demange, and E.-M. Graefe, J. Phys. Math. Theor. 45, 25303 (2012).

[14] M.H. Teimourpour, R. El-Ganainy, A. Eisfeld, A .Szameit, D.N. Christodoulides, Phys. Rev. A 90, 053817 (2014).

10345-75, Session 16

PT symmetry in Kagome photonic lattices *(Invited Paper)*

Gia-Wei Chern, Univ. of Virginia (United States); Avadh Saxena, Los Alamos National Lab. (United States)

Photonic lattices composed of balanced gain and loss waveguides have attracted considerable attention due of their potential applications in optical beam engineering and image processing. These photonic lattices belong to a larger class of intriguing active metamaterials that exhibit the parity-time (PT) symmetry. Kagome lattice is a two-dimensional network of corner-sharing triangles and is often associated with geometrical frustration. In particular, the frustrated coupling between waveguide modes in a kagome array leads to a dispersionless flat band consisting of spatially localized modes. Recently, a PT-symmetric photonics lattice based on the kagome structure has been proposed by placing PT-symmetric dimers at the kagome lattice points. Each dimer corresponds to a pair of strongly coupled waveguides. With balanced arrangement of gain and loss on individual dimers, the system exhibits a PT-symmetric phase for finite gain/loss parameter up to a critical value. Here we discuss the linear and nonlinear optical beam propagations in this novel PT-symmetric kagome system. The linear beam evolution in this complex kagome waveguide array exhibits a novel oscillatory rotation of optical power along the propagation distance. Long-lived local chiral structures originating from the nearly flat bands of the kagome structure are observed when the lattice is subject to a narrow beam excitation. We further show that inclusion of Kerr-type nonlinearity leads to novel optical solitons.

10345-76, Session 17

Measuring photon non-classicality using quantum-dot light sources *(Invited Paper)*

Glenn S. Solomon, Joint Quantum Institute, Univ. of Maryland (United States) and National Institute of Standards and Technology (United States)

No Abstract Available.

10345-77, Session 17

Quantum dots in photonic crystals for Integrated quantum photonics *(Invited Paper)*

Je-Hyung Kim, Univ. of Maryland, College Park (United States); Christopher J. K. Richardson, Richard P. Leavitt, Lab. for Physical Sciences (United States); Edo Waks, Univ. of Maryland, College Park (United States)

Future quantum information processing will rely on solid-state architectures that integrate quantum emitters, channels, beamsplitters, and detectors so all excitation, extraction, processing, and detection is efficiently possible on a chip. Quantum dots have attracted much attention for bright solid-state quantum emitters with high single photon purity and indistinguishability, and slab-type photonic crystal structures have an ability to integrate these emitters to cavities and waveguides on a chip. By combining these systems, quantum dots in photonic crystals have played important roles in the rapidly growing field of integrated quantum photonics. However, achieving quantum devices incorporating multiple quantum dots on a chip is a quite challenging task due to the spectral randomness of quantum dots and fabrication errors in photonic crystals. Here, we demonstrate multiple, identical quantum emitters in photonic crystal devices that generate indistinguishable single photons on the same chip. Integration of photonic crystal cavities enhances both radiative recombination rates and off-chip collection efficiency of quantum dots, resulting in bright single photons at telecom wavelength. To address the challenge of spectral randomness, we design thermally-isolated multiple photonic crystal structures with optical heating pads. Together with local thermal tuning, local gas tuning techniques enable us to control multiple cavities and dots. We perform Hong-Ou-Mandel interference measurements to verify indistinguishable single photons from individual dots. In addition, we suggest the way for on-chip quantum interference between multiple quantum dots in photonic crystals. Our devices and techniques paves the way for the scalable, controllable quantum devices involving multiple, identical quantum emitters on a chip.

10345-78, Session 17

Entanglement optimization in plasmonically coupled quantum dots *(Invited Paper)*

Matthew A. Pelton, Univ. of Maryland, Baltimore County (United States)

Although the enhanced near fields produced by plasmon resonances in metal nanoparticles can enable strong local light-matter interactions, the strong dissipation of plasmon resonances would seem to be incompatible with quantum-mechanical phenomena such as entanglement. Counter to this intuition, the dissipation can in fact lead to the production of transient entanglement between the occupation states of dots coupled to a common plasmonic system. Building on previous results that showed entanglement between pairs of dots, we scale to larger systems of two, three, and more closely spaced dots. Moreover, we show that tuning the degree of coupling between each dot and the common plasmonic nanostructure enables entanglement to be created in the case where the entire system begins in its

ground state and is excited by a single laser pulse. Entanglement is achieved without the need for the dots to be individually addressable, and without the need for controlled quantum gates, postselective measurements, or engineering of the dissipative environment. Through analytical solutions and numerical simulation of a model Hamiltonian based on a cavity-quantum-electrodynamics approach, we determine system configurations that maximize pairwise entanglement among the quantum dots, illustrating in principle the potential for true "quantum plasmonics.

10345-79, Session 18

Quantum self-organized criticality and nonequilibrium light localization *(Invited Paper)*

Kosmas L. Tsakmakidis, Univ. of Ottawa (Canada); Pankaj K. Jha, Xiang Zhang, Univ. of California, Berkeley (United States); Hatice Altug, Ecole Polytechnique Fédérale de Lausanne (Switzerland); Robert W. Boyd, Univ. of Ottawa (Canada)

Self-organized criticality emerges in dynamical complex systems driven out of equilibrium, and characterizes a wide range of classical phenomena in physics, geology and biology. However, for decades now, it remains a fundamental open question whether this broad property also finds a place in the quantum regime. In the talk, we shall present the first example of quantum self-organized criticality, emerging from quantum fluctuations and controlled by quantum coherence. We shall introduce a many-body quantum-coherently driven nanophotonic system where heavy photons interact in the presence of active nonlinearities. In this system, we shall show how quantum self-organized criticality emerges in an inherently new type of light localization, arising from two first-order phase transitions and being robust to dissipation, fluctuations and many-body interactions. The observed localization exhibits emergence of scale-invariant power laws and absence of finely-tuned control parameters. In analogy with the regime of quantum criticality at Tc = 0 in equilibrium static systems, we find that for our nonequilibrium dynamical system there exists a range of parameters for which the effective critical 'temperature' drops to zero, at which point we enter a fundamentally new regime of phase transitions – the quantum self-organized critical regime. We shall also approach the problem from a thermodynamic and information-theory perspective, deriving the multidimensional-state-vector Fokker-Planck (FP) equation for the distribution function of our problem, applying the maximum information entropy principle to make unbiased estimates on the probability distribution of microscopic states of our active nanosystem, and finally determining and analyzing the information gain and efficiency of the complex nanosystem close to its critical points.

10345-80, Session 18

All-dielectric transparent metasurfaces for holography and quantum tomography *(Invited Paper)*

Sergey S. Kruk, Lei Wang, Kai Wang, Matthew Parry, The Australian National Univ. (Australia); Hung-Pin Chung, The Australian National Univ. (Australia) and National Central Univ. (Taiwan); Hanzhi Tao, The Australian National Univ. (Australia) and Nanjing Univ. (China); Ivan I. Kravchenko, Andrey Sukhorukov, Dragomir N. Neshev, Yuri S. Kivshar, The Australian National Univ. (Australia)

Metasurfaces are ultra-thin patterned photonic structures that emerged recently as planar metadevices capable of reshaping and controlling incident light. They are composed of resonant subwavelength elements distributed across a flat surface. Due to the resonant scattering, each element can alter the phase, amplitude and polarization of the incoming light. Many designs and functionalities of metasurfaces suggested so far are based on plasmonic planar structures, however most of these metasurfaces demonstrate low efficiencies in transmission due to losses in their metallic components. In contrast, all-dielectric resonant nanophotonic structures avoid absorption losses, and can drastically enhance the overall efficiency, especially in the transmission regime. Here we utilize this platform to create flat optical elements such as vector beam q-plates, holograms and quantum polarization tomography devices. Holograms, in particular, showcase a potential of the metasurface platform as they rely on a complex wavefront engineering. Metasurface platform enables a new way to create highly efficient holograms with single-step patterning. Here, we design and realize experimentally greyscale meta-holograms with superior transmission properties. Another promising area for implementation of all-dielectric metasurfaces is quantum optics. We suggest and develop experimentally a new concept of quantum-polarization measurements with a single all-dielectric resonant metasurface. A metasurface enables full reconstruction of the state of entangled photon pairs based on the photon correlations with single-photon detectors. The subwavelength thin structure provides an ultimate miniaturization, scalability to a larger number of entangled photons, and gives the possibility to study the dynamics of quantum states in real-time.

10345-81, Session 18

Photonic band control in a quantum metamaterial *(Invited Paper)*

Didier Felbacq, Emmanuel Rousseau, Univ. Montpellier (France)

In the present work, we present a metamaterial made of a periodic collection of dielectric resonators in which a quantum oscillator (denoted QO in the following) is inserted.

The geometry at stake here is much more complicated than the textbook 1D cavity usually dealt with theoretically in quantum optics. We do provide a treatment essentially based on the scattering matrix non-perturbative approach, in order to investigate the various effects that could be expected to exist in such structures.The theoretical methods used are the Feshbach projection method associated with multiple scattering theory.

First, the phenomenology for one scatterer with a QO inserted is presented, then the collective behavior of a finite periodic set of such scatterers is investigated and it is shown that it is possible to open and close a conduction band according to the state of the oscillators when the inserted quantum oscillators are put in the inversion regime by means of a pump field. They add gain to the system, allowing to reach the amplification regime in the vicinity of the Mie resonances of the dielectric resonators. When the transition frequency is situated at the photonic band gap edge, it creates switchable conducting modes within the bandgap.

10346-1, Session 1

Plasmon-induced hot carrier generation and applications *(Invited Paper)*

Peter Nordlander, Rice Univ. (United States)

Plasmons can serve as efficient generators of hot electrons and holes that can be exploited in light harvesting applications. The physical mechanism for plasmon-induced hot carrier generation is plasmon decay. Plasmons can decay either radiatively or non-radiatively with a branching ratio that can be controlled by tuning the radiance of the plasmon mode. Non-radiative plasmon decay is a quantum mechanical process in which one plasmon quantum is transferred to the conduction electrons of the nanostructure by creating an electron-hole pair, i.e., excitation of an electron below the Fermi level of the metal into a state above the Fermi level but below the vacuum level. I will discuss the time-dependent relaxation of plasmon-induced hot carriers including electron-electron scattering, fluorescence, and electron-phonon coupling. I will also discuss recent applications of plasmon-induced hot carrier generation such as photocatalysis, and how photocatalytic efficiencies can be enhanced and quantified by placing catalytic reactors in the nearfield of a plasmonic antenna in an Antenna/Reactor geometry.

10346-2, Session 1

Novel numerical method for electron energy-loss spectroscopy calculation: EELS-FDTD *(Invited Paper)*

Nicolas Large, The Univ. of Texas at San Antonio (United States)

Electron energy-loss spectroscopy (EELS) is a unique tool that is extensively used to investigate the plasmonic response of metallic nanostructures since the early works in the '50s. To be able to interpret and theoretically investigate EELS results, a myriad of different numerical techniques have been developed for EELS simulations: boundary element method (BEM), discrete dipole approximation (DDA), finite-element method (FEM), Galerkin discontinuous time-domain method. Although these techniques are able to predict and reasonably reproduce experimental results, they possess significant drawbacks and are often limited to highly symmetrical geometries, non-penetrating trajectories, free-standing nanostructures, small nanostructures, and may present some complexity in their implementation and use.

Here, we present a novel approach for EELS calculations using the finite-difference time-domain (FDTD) method that goes beyond these limitations [1]. We benchmark our EELS-FDTD implementation by direct comparison with results from the well-established BEM and published experimental results. In particular, we compute EELS spectra for spherical nanoparticles, nanoparticle dimers, nanodisks supported by various substrates, and supported gold bowtie antennas. The flexibility our EELS-FDTD method allows for easily extending to more complex geometries and configurations. To illustrate this we investigate the plasmonic properties of (i) high density sub-10-nm-gap homo- and hetero-dimers, (ii) encapsulated gold nanoparticle chains, and (iii) hollow gold nanorods [2,3]. This implementation can also be directly exported beyond the FDTD framework and implemented within other numerical methods.

[1] Cao et al, ACS Photonics 2015, 2, 369

[2] Zhang et al, ACS Nano 2015, 9, 9331

[3] Yazdi et al, Nano Letters 2016, 16, 6939

10346-3, Session 1

Femtosecond dynamics of plasmon-induced hot electrons in nanostructured titanium nitride

Brock Doiron, Yi Li, Andrei P. Mihai, Lesley F. Cohen, Peter K. Petrov, Neil M. Alford, Rupert F. Oulton, Stefan A. Maier, Imperial College London (United Kingdom)

Due to its high melting point and comparable optical properties to gold, titanium nitride (TiN) is a promising replacement for gold in high-energy plasmonic applications. This would not only pave the way to more durable plasmonic devices but facilitate the study of light-metal interactions in regimes once thought impossible. However, thin films of TiN are challenging to grow consistently due to their susceptibility to oxidation during growth. Here we report on the optical properties of high-quality TiN films achieved through a detailed analysis of the growth conditions on oxide formation. These TiN films are then used to explore the ultrafast hot electron relaxation dynamics. Although hot electron generation in TiN films has been investigated previously, the effects of plasmon-enhanced absorption on the excitation and relaxation of the hot electrons has yet to be explored. Using time-resolved pump-probe differential transmission measurements, the electron relaxation process is studied under both resonant and non-resonant conditions to determine the plasmon's influence on the energetics of the electron distribution and their interaction with the phonons of the material. Pump-probe studies used a Ti:Sapphire laser and optical parametric oscillator (OPO) with pulse widths of 150fs at 850nm (pump) and 1100nm (probe). Differential transmission is observable for several hundred picoseconds after a pump pulse in TiN compared to just a few picoseconds in Au. Preliminary results indicate plasmon-enhanced absorption increases the maximum electron temperature, causing a longer electron relaxation time due to the finite electron-phonon energy transfer rate.

10346-4, Session 1

Enabling new regimes of nanoparticle resonances through beam engineering

Jon A. Schuller, Univ. of California, Santa Barbara (United States)

Optical resonances in sub-wavelength nanoparticles enable a variety of plasmonic phenomena and devices. Conventionally, researchers tune the resonant properties of nanoparticles (NPs) by manipulating their size, shape, and composition. However, these light-matter interactions depend on two critical factors: 1) the physical properties of the nanostructure, and 2) the properties of the illuminating radiation. Here, we concentrate on the latter and demonstrate via electromagnetics calculations how unconventional light sources can be used to to selectively excite, enhance, and engineer resonant light-matter interactions in nanostructures. Specifically, we show how azimuthally and radially polarized light sources can be used to couple to "dark" modes and to achieve unprecedented magnetic field enhancements in single and dimer nanostructures.

10346-5, Session 2

3D plasmonic nanoarchitectures for extreme light concentrating *(Invited Paper)*

Wei-Chuan Shih, Univ. of Houston (United States)

Plasmon resonance, the collective oscillation of conduction band electrons, can be excited by shining light on some metallic nanostructures. Localized

surface plasmon resonance (LSPR). LSPR-based detection provides a sensitive reporting mechanism of the local refractive index changes due to surface binding. LSPR also provides a "boost" to light matter interactions near the surface of metallic nanostructures, typically known as "surface enhancement" in various spectroscopy. Over the past few decades, numerous studies have led to the current state of knowledge by largely attributing the enhancement to nanostructural "singularities", e.g., small gaps and sharp protrusions on the order of 10 nm. However, most of these studies relied on advanced lithography or colloidal surface chemistry to produce nanostructural singularities, aka "hot spots". Lithographic techniques such as focused ion beam is time-consuming and cost-prohibitive for scaling up. Colloidal surface chemistry produces assays that are challenging to translate into a "biochip".

My group has developed highly porous yet monolithic plasmonic nanostructures that feature intense and high-density hot spots, large surface area, and high structural integrity and reproducibility. We have applied them to several analytical Chem/Biosensing platforms for a range of sensing targets by various spectroscopic and imaging techniques. In this talk, I will mainly emphasize on the design, fabrication, modeling and simulation, and characterization of nanoporous gold nanoparticles and arrays.

10346-6, Session 2

Plasmonic nanogap structures studied via cathodoluminescence imaging

Stephen J. Bauman, Qigeng Yan, Mourad Benamara, Joseph B. Herzog, Univ. of Arkansas (United States)

Cathodoluminescence (CL) makes use of the beam raster capabilities of a scanning electron microscope to excite electrons in a sample and collects the luminescent light to produce images or obtain spectra that can reveal useful information about the sample. This technique has been shown to be particularly interesting for studying the plasmonic oscillations of metallic nanostructures. A recently developed fabrication technique has allowed for the creation of sub-10 nm gaps between metallic nanostructures for use as plasmonically active samples that can be tailored for various potential applications. The high degree of control over the geometries capable of being fabricated via this nanomasking technique allow for unique types of structures that are otherwise difficult to fabricate. In this work, the plasmonic response of metallic structures separated by sub-10 nm gaps is studied via CL imaging. Hyperspectral images can demonstrate the effectiveness with which various geometries produce specific wavelength resonances. The results can be helpful in determining which structures are optimal for specific applications based on these resonances. Also, the images can help to guide future fabrication, as the plasmon modes become better understood.

10346-8, Session 2

Maskless patterning using surface plasmon enhanced electron beamlets

Zhidong Du, Chen Chen, Liang Pan, Purdue Univ. (United States)

Optical lithography transfers fixed geometric patterns from a photo mask to photoresist wafers. Current tools cost more than 50 million US dollars each, and much more for the masks. To keep up with Moore's law, future tools and processes will become increasingly expensive. The next-generation extreme-UV tools have sufficient resolution, but current pilot tools will need substantial upgrades in source and process infrastructures to have sufficient throughput and yield. Patterning using parallel electron beams has emerged as a potential approach to meet the industry's patterning needs at advanced nodes, however researchers have not been able to find a robust method to generate and utilize a massive number of beamlets with satisfactory brightness and uniformity.

Here we report our recent research progress aiming to enable massively-parallel electron-beam lithography by using a novel nanoscale electron beam source array. We use plasmonic lenses to excite and focus surface electron waves to generate massively-parallel electron beamlets. Specifically, the proposed SPEP device consists of an array of plasmonic lens and electrostatic micro-lens pairs. Each pair independently produces a beamlet. During lithography, optical modulator dynamically controls the light incident onto the plasmonic lenses. The photons incident onto each plasmonic lens are concentrated into a diffraction-unlimited spot to excite the local electrons above their vacuum levels. Meanwhile, the electrostatic micro-lens extracts the excited electrons to form a focused beamlet to perform lithography. We investigate the fundamentals of localized electron excitation, build a proof-of-concept system and demonstrate lithography.

10346-9, Session 3

Tunable plasmonics and metasurfaces for applications in optical switching and space technology *(Invited Paper)*

Otto L. Muskens, Kai Sun, Christoph A. Riedel, Bigeng Chen, Cornelis Hendrik De Groot, Univ. of Southampton (United Kingdom)

Plasmonic nanoantennas are of interest because of their capability to enhance light-matter interactions. We present new results where antennas are used to obtain nanoscale devices with tunable characteristics. Applications of these devices include electrically controlled antennas, antennas integrated on silicon waveguides, and optical solar reflectors for spacecraft. By using tunable materials such as vanadium dioxide and doped-metal oxides, we demonstrate precise control and active tunability of the optical response. Experimental results are supported by combined electro-optical modelling at the nanoscale.

10346-10, Session 3

Measurement of Stokes parameters using plasmonic metasurface *(Invited Paper)*

Chih-Ming Wang, National Dong Hwa Univ. (Taiwan)

Recently, a plasmonic metasurface is proposed to generate versatile polarization. It is demonstrated that left-handed, right handed and linear polarization with various polarization angle can be generated using a single metasurface device. This fancy result makes a miniaturized stokes polarimeter possible. In this paper, a broadband plasmonic metasurface with Pancharatnam-Berry phase distribution is proposed to measure the polarization state of light through a birefringent plastic tape. It is shown that the polarization state of light through birefringent tape measured by plasmonic metasurface has a fair agreement with that measured by commercial polarimeter. This result shows that the metasurface has a potential as a miniaturized stokes polarimeter, meta-polarimeter.

10346-11, Session 3

Plasmon resonance sensors for compact plasmonic integrated device *(Invited Paper)*

Masanobu Haraguchi, Shun Kamada, Tokushima Univ. (Japan); Hiroyuki Okamoto, Nagaoka Univ. of Technology (Japan); Toshihiro Okamoto, Salah E. El-Zohary, Tokushima Univ. (Japan)

Surface plasmon polariton (SPP) provide the field enhancement and localization beyond the diffraction limit of light. By using SPP, we have numerically designed tiny resonance sensors as plasmonic integrated devices with silver or gold as metal material for near infrared region of light. We will present our recent work for the sensors. The sensors are the combination of the plasmon resonator and MIM channel plasmon waveguide with the gap of ~150 nm and the hight of ~1.5 micron. The typical area size of

sensor is order of 1 square micrometers and their sensitivity for temperature or stress change is comparable to current optical sensors. We have fabricated some fundamental structure of the device by using the electron beam lithography and will show experimental optical characteristics for IR region.

10346-12, Session 4

Metal-dielectric resonances in tip silicon metasurface and SERS based nanosensors *(Invited Paper)*

Andrey K. Sarychev, Andrey N. Lagarkov, Irina A. Boginskaya, Institute for Theoretical and Applied Electrodynamics (Russian Federation); Igor V. Bykov, Institute for Theoretical and Applied Electromagnetics (Russian Federation); Andrey V. Ivanov, Ilya A. Ryzhikov, Marina V. Sedova, Institute for Theoretical and Applied Electrodynamics (Russian Federation); Ilya N. Kurochkin, N.M. Emanuel Institute of Biochemical Physics (Russian Federation)

We investigate the optical metasurface made of silicon tip-shaped grating. The geometric parameters are: period 3.0 μm, diagonal period 2.12 μm, height 0.3-0.7 μm, the tip angle 30º, tip curvature radius ≤ 10 nm, the effective area of the metasurface 2?2 mm. The metasurface can be considered as a diffraction grate. The diffraction pattern for red laser revivals 37 modes. The total reflection estimates as 0.32, where 0.26 corresponds to zero order reflectance and 0.06 - to the diffraction. In other words 19% of the reflected energy goes to the diffraction beams. The silicon tips cover only 8% of the total area of the metasurface. Hence, they provide very effective diffraction, which could be called the extraordinary optical diffraction. Our computer simulation gives very effective metal-dielectric resonances in the metal nano-particles placed on the silicone tips. The dielectric resonances in the cone are hybridized with plasmon modes. The conjugate of Au nanoparticles + DTNB molecules are deposited on pyramid grating. The conjugate has series of the well-defined Raman peaks, which we use as an effective SERS indicator.

10346-13, Session 4

Design of a colorimetric sensing platform using reflection mode plasmonic color filters

Renilkumar Mudachathi, Takuo Tanaka, RIKEN (Japan)

Extraordinary optical transmission (EOT) exhibited by nano hole arrays in plasmonic metasurfaces have been explored for the realization of colorimetric sensors which are useful for many applications like rapid diagnostics of infectious diseases and monitoring of food and environmental quality. We present a colorimetric sensing platform based on reflection mode plasmonic colour filter realized using aluminum as functional material. The plasmonic metasurface is designed in such a way that it produces intense narrow reflective peaks, which are highly sensitive to the ambient refractive index change. We demonstrate sharp colour changes for varying concentrations of sugar solutions.

In order to realize reflection mode plasmonic filter with narrow reflection peaks, we fabricated 2D arrays of aluminum nano square patches raised on top of PMMA nano pillars in the back ground of a perforated back reflector by systematically varying the metal patch size (D) and periodicity (P). In the single layer fabrication process the PMMA nano pillars were defined by electron beam lithography and subsequently aluminum thin film was deposited by thermal evaporation to form both the metal square patches and the fishnet like back reflector. The colour formation is based on the excitation of plasmonic light absorption at two distinct wavelengths leaving a central reflective peak that is coherently scattered by coupling to a strongly radiating dipole resonance. Pure colours both in the RGB and CMY colour schemes with extreme reflective peaks of high quality factor (FWHM of 100nm) across the visible spectrum are optimized. Sugar solutions of varying concentration is then introduced to the nano structures to produce visible colour changes to demonstrate the refractive index sensing using the proposed colorimetric sensing platform.

10346-14, Session 4

Nanoporous gold decorated with silver nanoparticle as large area efficient SERS substrate

Eugenio Calandrini, Paolo Ponzellini, Matteo Ardini, Istituto Italiano di Tecnologia (Italy); Sandro Cattarin, CNR-IENI (Italy); Francesco De Angelis, Denis Garoli, Istituto Italiano di Tecnologia (Italy)

In the last decade, the research efforts was focused on the quest of novel plasmonic materials. In particular metal nanostructure films can act as plasmonic platform embedding hot spots that are perfect for surface enhanced Raman scattering (SERS) with considerable signal improvements. Usually, hot spots confined within the interstices between the adjacent metal nanostructures are essential to enable highly sensitivity detection due to near-field coupling of localized surface plasmon resonance (LSPR). Unfortunately, such substrates have competing geometrical requirements including the narrowest interstice between neighboring units to provide maximum near-field coupling, and sufficient space to accommodate the target probes. Due to the exponential decay of electromagnetic fields normal to the metal surface, strong near-field coupling prefers to be obtained within the interstices with 1–2 nm separation. On the other hand, such small gaps are not favorable for the insertion of target molecules dissolved in the solvents. Numerous efforts have been made to address these issues and different nanostructures including nanoparticles, nanowires, nanopores, and their conjugations have been used as the precursors.

Herein, we fabricate hybrid nanostructure that addresses the issues discussed above and exhibits giant enhancement in Raman scattering. It consists of nanoporous gold (NPG) films decorated by silver nanoparticles that provide extremely narrow interstitial spaces contributing to significant near-field coupling and enhance Raman scattering by several orders of magnitude.

10346-15, Session 4

Refractive index sensing with graphene plasmons

Tobias Wenger, Giovanni Viola, Jari Kinaret, Mikael Fogelström, Philippe Tassin, Chalmers Univ. of Technology (Sweden)

We report on our theoretical work investigating graphene plasmons for refractive index sensing at room temperature. We have found that graphene plasmons are very sensitive to the index of refraction of the material in their immediate neighbourhood. This is the result of the strong field confinement of graphene in a volume that stretches about 100 nm away from the graphene sheet. We compare the sensitivity of graphene-plasmon-based refractive index sensors to gold-based plasmonic index sensors, and we find that graphene has a much stronger surface sensitivity.

10346-16, Session 4

Labeling and imaging brain tumor cells with Raman tags *(Invited Paper)*

Li-Ching Huang, Yung-Ching Chang, Shiuan-Yeh Chen, National Cheng Kung Univ. (Taiwan)

Glioblastomas (GBM) are highly lethal brain tumors which arise from astrocytes. These tumors are highly malignant due to quick reproduce rates and are extremely resistant to radiation and chemotherapies. The median survival of GBM patients is less than 16 months. In addition to strong resistance to conventional treatments, the other fundamental difficulty in removing GBM cells is their highly infiltrative nature. Therefore, imaging and locating these tumor cells is a challenging task. In this work, plasmonic nano-tags with stable Raman signals are fabricated and utilized to label GBM cells. The backbone of the Raman tags is a plasmonic core-satellite assembly which produces highly internal concentrated field for Raman enhancement. Compared to the conventional fluorescent dyes, the Raman tags are more stable and robust under laser illumination. The fabrication and functionalization of Raman tags is described and the Raman images of the labeled GBM cells are demonstrated.

10346-17, Session 5

Ultra-thin transition metal nitrides for plasmonic applications *(Invited Paper)*

Harsha Reddy, Deesha Shah, Purdue Univ. (United States); Nathaniel Kinsey, Virginia Commonwealth Univ. (United States); Vladimir M. Shalaev, Alexandra Boltasseva, Purdue Univ. (United States)

With continuing advances in nanofabrication methods, the sizes of metal components in plasmonic devices have been shrinking, now approaching only a few monolayers in thickness. The strong spatial confinement in such thin films is expected to lead to quantum and nonlocal effects. These ultra-thin films serve as ideal material platforms for probing various classical to quantum transitions. More importantly, they are extremely sensitive to external electrical and optical perturbations, making them an attractive platform to tune light-matter interactions at the nanoscale. However, a key to the study of these exotic light-matter interactions lies in producing metallic films only a few monolayers in thickness.

Producing such thin films with noble metals is extremely challenging due to the well-known issues of island formation. On the other hand, ultra-thin TiN films with thicknesses down to only 2 nm can be routinely grown, which is critical for enabling enhanced control over the plasmonic properties. We have experimentally characterized the optical constants of ultra-thin TiN films (<10 nm) of various thicknesses. All the films remained highly metallic with a carrier concentration on the order of 1022 cm-3 even in the thinnest film (2 nm). The ability to grow such thin films is the first step towards realizing the potential electrical and optical control of plasmonic properties. Furthermore, the extreme light confinement that can be achieved in ultra-thin films could enable several forbidden light-matter interactions. Together with its refractory properties and CMOS compatibility, ultra-thin TiN shows great promise for realizing various quantum and nonlocal nanophotonic applications.

10346-18, Session 5

Light twists around plasmonic nanowires *(Invited Paper)*

Laurens Kuipers, Kavli Institute of Nanoscience Delft (Netherlands)

We use a near-field microscope to visualize the nanoscale light patterns, both electric and magnetic fields [1,2]. The interplay between the various components of either the magnetic or the electric fields leads to optical entities that, in their size, put nanophotonics to shame: these optical singularities have a size zero. Interestingly, optical singularities near nanoscale structures exhibit a markedly different behavior from those in macroscopic beams [3,4]. We observe a distinctly different behavior around plasmonic nanowires to that above photonic crystal waveguides [5]. Moreover, we show that these singularities and their associated local helicity can be applied for new quantum technology as they can be used to deterministically couple a spin-transition to emission direction [6], useful for novel quantum technology [7]. In addition we show that plasmonic nanowires are better than dielectric waveguides for the transmission of ultrashort pulses [8]. This can also be used to induce nonlinear phenomena [9].

[1] B. le Feber, et al., Nature Photonics Vol. 8, 43-46, (2014).

[2] N. Rotenberg and L. Kuipers, Nature Photonics Vol. 8, 919-926, (2014).

[3] N. Rotenberg, et al., Optica 2, 540-546 (2015).

[4] L. De Angelis, et al., Phys. Rev. Lett. 117, 093901 (2016).

[5] I.V. Kabakova, et al., Scientific Reports 6, 22665-1/9 (2016)

[6] B. le Feber, et al., Nature Communications 6, 6695 (2015).

[7] A. B. Young, et al., Phys. Rev. Lett. 115, 153901 (2015).

[8] M. Wulf, et al., ACS Photonics 1, 1173?1180 (2014).

[9] A. de Hoogh, et al., ACS Photonics 3, 1446-1452 (2016).

10346-20, Session 5

Numerical simulation of nonlocal optical response in light scattering by nanoparticle on the substrate

Ivan V. Lopushenko, M.V. Lomonosov Moscow SU (Russian Federation)

Thorough analysis of the plasmonic phenomena requires proper account for such effects as size dependent surface plasmon resonance shifts and intensity changes observed in metal nanoparticles, especially in systems with small feature sizes [1]. Recent theoretical advances, including Generalized Nonlocal Optical Response (GNOR) approach, allow to very accurately resolve these effects within the classical electromagnetics [2], thus paving the way for implementation of efficient low cost computational techniques.

We present a new GNOR-based numerical scheme of the flexible Discrete Sources Method [3] for analysis of light scattering by single plasmonic nanoparticle in the layered medium with rigorous account for both substrate-particle interaction and nonlocal effects. Key features of the proposed surface oriented approach include meshless algorithm without any surface integration procedures involved, the ability to track the real convergence of the solution via a posteriori error estimation, and the ability to consider very small plasmonic nanoparticles with size under 5nm.

Numerical simulations have been carried out in order to appropriately verify the created mathematical model and investigate the influence of nonlocal effect on the scattering properties of various plasmonic nanoparticles. We show that proposed method enables to accurately study the significant influence of such parameters as substrate material, size, shape and material of the particle on the position and intensity of plasmon resonance peak.

[1] B.Gallinet et al. Laser Photonics Rev., Vol.9, No.6, 577–603,2015.

[2] S.Raza et al. J. Phys.: Condens. Matter, Vol.27, No.18, 183204, 2015.

[3] Yu.A. Eremin, I.V. Lopushenko. Moscow Univ. Comput. Math. Cybern., Vol.40, No.1, 1-9,2016.

10346-21, Session 5

Revealing the femtosecond dynamics of metallic and molecular nanostructures *(Invited Paper)*

Benjamin Stadtmueller, Martin Aeschlimann, Technische Univ. Kaiserslautern (Germany)

The extensive effort to study and understand the optical response of metallic nanostructures is motivated by their potential to act as essential building blocks in novel electronic devices with nano-optical circuits. For instance, nanoscale antennas can act as source for the propagation of surface plasmon polariton (SPP) waves. These SPPs are coherent hybrid modes of the collective electronic motion and the electromagnetic fields and have the potential to mediate a coherent energy transfer between different nanostructures acting as source and receiver of a nanoscale device. Moreover, the optical excitation of nanostructures can lead to long lasting electronic coherences in these structures which can be manipulated by the phase properties of the external light field.

An ideal tool to study ultrafast phenomena in nanostructures on a nanoscale is time-resolved photoemission electron microscopy (PEEM) which allows us to investigate their ultrafast optical response with a spatial resolution far beyond the optical diffraction limit [1-3].

In a first work, the long-range energy transfer mechanism between two coupled plasmonic whispering gallery nano-antennas in an elliptical cavity has been investigated. Only one gold antenna is excited selectively when the structure is illuminated under grazing incidence. We demonstrate periodic energy transfer back and forth over a distance of twice the excitation wavelength mediated by the SPPs. The experimentally observed ultrafast dynamics is in accordance with simulations as well as a coupled-oscillator model and suggests the feasibility of long-range coherent coupling of pairs of quantum emitters.

In a second project, we move from metallic to molecular nanostructures and investigate the coherent electron dynamics of the metal-organic hybrid interface formed between the organic semiconductor Alq3 and the ferromagnetic Co surface. This interface is of particular interest for the field of molecular spintronics since it possess states with long spin-dependent relaxation times [4,5]. After optical excitation with visible light, we observe a coherence response in the interferometric correlation traces. Using two-dimensional spectroscopy in combination with PEEM, we can clearly identify two excited resonances with an energy spacing of about 77 meV and a linewidth of 11 meV and 48 meV, respectively. These homogeneous linewidth of these states correspond to coherence lifetimes of about 370 fs and 87 fs. These results underline the potential of organic molecules to significantly enhance coherent lifetimes of metallic surfaces.

[1] J. Lange et al, Proc. SPIE Vol. 6195, (2006) 61950Z

[2] M. Aeschlimann et al, Science 333, 1723-1726 (2011)

[3] M. Aeschlimann et al, Nature Photo. 9, 663 (2015)

[4] S. Steil et al. Nature Phys. 9, 242 (2013)

[5] A. Droghetti et al., Nature Commun. 7, 12668 (2016)

10346-22, Session 6

A link between the superconducting transition and the optical range plasmonics of niobium *(Invited Paper)*

Chun Yen Liao, Univ. of Southampton (United Kingdom); Harish N. S. Krishnamoorthy, Nanyang Technological Univ. (Singapore); Vassili Savinov, Jun-Yu Ou, Univ. of Southampton (United Kingdom); Chunli Huang, Giorgio Adamo, Nanyang Technological Univ. (Singapore); Eric Plum, Kevin F. MacDonald, Univ. of Southampton (United Kingdom); Yidong Chong, Cesare Soci, Nanyang Technological Univ. (Singapore); Feodor V. Kusmartsev, Loughborough Univ. (United Kingdom); Din Ping Tsai, National Taiwan Univ. (Taiwan) and Academia Sinica (Taiwan); Nikolay I. Zheludev, Univ. of Southampton (United Kingdom)

Superconductivity is commonly expected to be insignificant in optics, where photon energy is orders of magnitude higher than the binding energy of the Cooper pairs, the superconducting charge carriers. By experimentally studying optical range plasmonic response of niobium, a conventional low-temperature superconductor, we show that, contrary to this expectation, superconductivity does affect plasmonic behaviour at optical frequencies. Our results shed a new light on properties of superconductors, suggesting that superconductivity may play a role in forming the optical dielectric response near the superconducting transition.

We study the temperature-induced changes in the optical properties of a nanostructured superconducting metamaterial as well as unstructured superconductor film. In the non-superconducting metamaterials, the temperature-related variations in the optical response have been shown to saturate below temperature 50K. In contrast, we show that both the position and the strength of niobium metamaterial resonances exhibit a pronounced dependence on temperature down to a few Kelvin, with a sharp change in behaviour around the superconducting transition temperature at 9K. Equivalently dramatic changes are also observed in the temperature-dependence of the dielectric constant of unstructured niobium film, measured in a separate experiment.

10346-23, Session 6

Mimicking general relativity through plasmonic spin hall effect

Hui Liu, Nanjing Univ. (China)

Based on the concept of drawing equivalence between different configurations in transformation optics, we introduce a conceptual framework to investigate radiation from accelerating particles using chains of metamaterial atoms with SOI on a metasurface. The framework allows a global geometric picture in visualizing different one-dimensional space-times in general relativity using our two-dimensional metasurface. In particular, chains of metamaterial atoms along different curved lines in generating a common SPP caustic represent the same particle motions observed in difference reference frames, with relative motion through a general-relativistic transformation, such as a Rindler transformation from a reference Minkowski space-time. Such a tool allows us to study particle motions in different space-times in general while the particular geometric understanding provides us unique ways in generating SPP.

10346-24, Session 6

Novel platforms for plasmonics *(Invited Paper)*

Alejandro Manjavacas, The Univ. of New Mexico (United States)

Photonic systems containing active and passive elements with balanced gain and loss, usually known as PT-symmetric systems, are attracting increased attention due to their exceptional properties including, to cite some, asymmetric propagation and reflection, unidirectional invisibility, switching, or extraordinary nonlinear behaviors. Here, we will discuss the optical response of finite nanostructures composed of pairs of active and passive nanospheres operating close to the PT-symmetry condition. We will show that, despite their highly regular geometry, these systems present very anisotropic optical response. We will also discuss how the geometrical arrangement of ensembles of nanostructures can give rise to unexpected collective modes displaying strongly localized responses. We will analyze different types of ordered arrays containing either a finite or an infinite number of structures.

10346-25, Session 7

Surface plasmon manipulated Smith-Purcell radiation on metallic periodic and gradient gratings *(Invited Paper)*

Yung-Chiang Lan, Yi-Chieh Lai, Bo Han Cheng, Hsin-Yu Kuo, Tzu Cheng Kuang, National Cheng Kung Univ. (Taiwan)

An electron beam passing over metallic gratings can emit Smith-Purcell radiations (SPRs). The emission frequency and angle of SPRs strongly depend on the period of gratings which is previously designed. The electron beam can also excite surface plasmons (SPs) at the metallic surface. Therefore, the electron beam excited SPs may affect SPRs when the frequencies of SPs are within the emission bands of SPRs. In this work, SPs manipulated SPRs on metallic periodic and gradient gratings are explored by FDTD simulation and theoretical analyses. Our investigations indicate that, for periodic gratings, the SPRs can be enhanced by exciting SP and mimic SP on the gratings if their frequencies are within the emission bands of SPRs. When using periodic metallic disk arrays as the gratings, the SPRs can also be enhanced and inhibited by exciting the resonant surface plasmon (RSP) modes on the top and bottom, respectively, of the metal disk. For gradient gratings, SPs enable the SPRs at designed frequencies to be focused or divergent in space by changing the incident direction of the electron beam. This work provides a way toward practical applications on frequency-selected devices such as multi-wavelength optoelectronic device, communication security and compact and tunable visible light source.

10346-26, Session 7

Instantaneous spatial variation of Green's tensor in complex nanostructures via eigenmode expansion *(Invited Paper)*

Parry Chen, David J. Bergman, Tel Aviv Univ. (Israel); Yonatan Sivan, Ben-Gurion Univ. of the Negev (Israel)

The spatial variation of Green's tensor of micro-structured media in both source and detector position and orientation over all 3D space on arbitrarily fine grid is obtained without repeated simulation. Total radiated fields even for arbitrary extended sources are simulated by simply projecting onto the structure's source-free eigenmodes. Eigenmodes are obtained from a linear eigenvalue problem, and is easily implemented on COMSOL. Maxwell equations are solved rigorously, thus circumventing implementation and interpretation issues associated with quasi-normal eigenmode methods. Rapidly converging results are obtained, facilitating analytic calculations involving Green's tensor, such as radiative heat transfer and van der Waals forces.

10346-27, Session 7

Plasmon-exciton energy transfer in nanoparticle-molecule aggregates

Maicol A. Ochoa, Univ. of Pennsylvania (United States); Abraham Nitzan, Univ. of Pennsylvania (United States) and Tel Aviv Univ. (Israel)

Plasmon-plasmon coupling in nanoscopic structures permits the manipulation of light at sub-wavelength distances, promising novel technological applications that span from medicine to quantum computing. In the presence of molecular media, plasmon-exciton interactions introduce additional complexities for the control and manipulation of light in plasmonic nanowaveguides. In this work, we have theoretically investigated within semiclassical models the energy transfer process between plasmonic spherical nanoparticles mediated by molecular media. In particular, we have characterized the lineshape for these complexes, as determined from measurements of scattered radiation and heating rate, and their dependence on molecular properties such as transition energy, relaxation and dephasing. In situations where the energy transfer mechanism is dominated by plasmon-exciton coupling, the effect of molecular density, distance, geometry and orientation were also evaluated. Our results indicate that the molecular media can dramatically change the linear response of plasmonic aggregates when the molecular energy gap is in resonance (or nearly in resonance) with the optically active hybrid states and can potentially activate dark modes from the aggregate.

10346-29, Session 7

Light conrol metasurfaces with randomly dispersed silver nanoparticles *(Invited Paper)*

Masayuki Naya, Takeharu Tani, Hideki Yasuda, Shinya Hakuta, Hirotoshi Yoshizawa, FUJIFILM Advanced Research Labs. (Japan)

We propose metasurfaces using randomly dispersed silver nano discs [1]. Wavelength of optical response can be artificially controlled by changing aspect ratio (diameter/thickness) and dispersion density of silver nano discs. These structures are easy to fabricate in a large area using conventional wet-coating methods. We applied these structures to a transparent solar insulation film and an anti-reflection film for visible light. Utilizing reflection wavelength selectivity of this structure, we have developed a transparent solar insulation film which strongly reflects infrared light whereas transmit visible light. We also have developed silver nanodiscs metasurface for anti reflection film for visible light. We show that the effective refractive index of metasurcface layer was about 0.5 in the visible wavelength. The reflectance of 0.3% at wavelength of 550nm, which is 25 times smaller than the reflectance of normal glass, was demonstrated in the experiment.

We also propose ring-like silver particles randomly dispersed structure for controlling far infrared light. The properties were calculated by employing an electromagnetic optical simulation based on the finite difference time domain (FDTD) method. It was confirmed by calculation that the reflectance of optimized structure is 80% at wavelength of 5500nm and the visible light transmittance is 80% at wavelength of 500nm. Preliminary experimental results qualitatively agree with the simulation.

[1] T. Tani, S. Hakuta, N. Kiyoto, and M. Naya, Optics Express, 22, 9262(2014)

10346-30, Session 8

New material platforms for dielectric nanoantennas and metasurfaces *(Invited Paper)*

Naresh K. Emani, Hanfang Hao, Egor Khaidarov, Ramon Paniagua-Dominguez, Yuan Hsing Fu, Reuben M. Bakker, Vytautas Valuckas, Arseniy I. Kuznetsov, A*STAR - Data Storage Institute (Singapore)

Optically resonant dielectric nanostructures is a new direction in nanophotonic research which gives a strong promise to compliment or substitute plasmonics in many potential application areas [1]. The main advantages of resonant dielectric nanostructures over conventional plasmonics are low losses, wide range of applicable dielectric materials and strong magnetic resonant response. So far most of research in this field has been conducted with silicon as a material for nanostructures due to its one of the highest value of refractive index at optical frequencies and CMOS compatibility. However, while silicon is an excellent material of choice for operation in the near-IR spectral range its applicability for visible frequencies is limited by increasing losses inside the material. Also, being an indirect bandgap semiconductor it is not a suitable material for making active nanoantenna devices. For these reasons in recent studies research focus starts shifting towards other appropriate materials such as III-V semiconductors, e.g. GaAs or GaP, and wide-bandgap semiconductors such as TiO_2. In this presentation we will discuss applicability of different dielectric/semiconductor material platforms for obtaining resonant nanoantennas and metasurfaces operating in the visible frequency range. We will first show that titanium dioxide metasurfaces can be designed to obtain sharp resonances and full phase control at all three RGB wavelengths through Huygens' metasurface approach, which pave the way towards realization of thin multi-layer metasurfaces with multi-colour operation. Then we will introduce a new III-V material platform based on GaN, which is highly transparent through the whole visible spectrum, and show high-efficiency operation of GaN metasurfaces in the blue and green parts of the visible spectrum. Finally we will discuss active nanoantennas based on GaAs and show the path towards achieving laser emission from resonant semiconductor nanoantenna structures.

References:

1) A. I. Kuznetsov et al., "Optically resonant dielectric nanostructures", Science 354, aag2472 (2016).

10346-31, Session 8

Mode-matched multi-resonant 2.5D plasmonic nano-terrace array for surface-enhanced spectroscopy

Weihua Zhang, Shuang Zhou, Jie Bian, Nanjing Univ. (China)

Plasmonic nanostructures can function as a resonant optical antenna, which can trap the far-field propagating field into nanoscale spots in the near-field regime with a large field enhancement and vice versa.[1] This unique property makes plasmonic nanostructures a powerful platform for enhancing both the excitation and emission processes of various optical effects. However, most of the applications are based on the large local field enhancement at the excitation frequency, despite that the total enhancement is also dependent on the enhancement at the emission frequency. This severely limits the performance of the plasmonic substrates.

To tackle this issue, we designed and numerically studied a new type of multi-resonant plasmonic nanostructure, the tri-level plasmonic nano-terrace array (3L-PNTA), which is a 2.5D structure consisting of an array of vertically coupled plasmonic nanotiles on dielectric nanoterrace substrate. [2] The results show that the 3L-PNTA supports multiple resonances, which can be independently tuned by changing different geometrical parameters. On the resonances, local light intensity can be enhanced by more than two orders of magnitude in the nanogaps between the plasmonic nanotiles due to the strong vertical couplings. Moreover, the enhanced fields associated with different resonant modes are spatially overlapped, allowing the 3L-PNTA to enhance optical processes at both excitation and emission wavelengths, simultaneously. This makes the 3L-PNTA a perfect multi-resonant plasmonic nanostructure for enhancing various optical processes.

[1] W. Zhang, F. Ding, S. Y. Chou, Adv. Mater. 24, OP236 (2012)

[2] S. Zhou, J. Bian, W.-D. Li, W. Zhang, Opt. Mater. Express 7, 503 (2017)

10346-32, Session 8

Multimode metasurfaces: from direct observation of the phase front to advanced optical functions *(Invited Paper)*

Chen Yan, Xiaolong Wang, Kuang-Yu Yang, Luc Driencourt, T. V. Raziman, Olivier J. F. Martin, Ecole Polytechnique Fédérale de Lausanne (Switzerland)

Planar photonic metasurfaces, exhibiting artificial optical effects at the interface, are enabling a broad variety of possibilities as optical elements, communications, and signal processing. The signal we perceive from a metasurface is determined by the phases of the different nanostructures that compose the system. This phase controls the spatial radiation distribution following Huygens'principle and has been utilized in planar optical devices exhibiting negative refraction, cloaking, and holographic elements to name a few.

In this presentation, we will first demonstrate the quantitative direct measurement of the phase front produced by a metasurface using digital holography microscopy. We will then show that by designing and tuning the multipolar components of the nanostructured building blocks, it is possible to also control the spectral response as well as the polarization state of the system. By composing a metasurface with such complex nanostructures fabricated in silver, we are able to control the scattered light and channel different colors into different directions. In the second series of experiments, we specifically study the multipolar radiation of a bianisotropic scatterer and use it for the efficient splitting of circularly polarized light, similar to a photonic spin Hall effect. Since the near-field enhancement and circularly polarized scattering in this case occur at the individual antenna level, this planar surface is capable of extracting the fluorescence and controlling the spin-polarized emission from nearby emitters, as will be demonstrated experimentally. These results have practical implications for controlling the optical activity and can potentially enable new polarization-dependent light-emitting devices for applications in imaging, optical communication, and optical displays.

10346-33, Session 9

Surface plasmon polaritons for opto-mechanical control of nanoparticles *(Invited Paper)*

Mihail I. Petrov, Aliaksandra Ivinskaya, Natalia Kostina, Andrey A. Bogdanov, ITMO Univ. (Russian Federation); Sergey Sukhov, CREOL, The College of Optics and Photonics, Univ. of Central Florida (United States); Pavel Ginzburg, Tel Aviv Univ. (Israel) and ITMO Univ. (Russian Federation); Alexander S. Shalin, ITMO Univ. (Russian Federation) and Institute of Radio Engineering and Electronics (Russian Federation) and Ulyanovsk State Univ. (Russian Federation)

The talk will be focused on new concepts of opto-mechanical manipulation of nanoparticles mediated by their coupling to propagating surface plasmon polariton (SPP) modes. This approach gives a broad range of new opportunities for opto-mechanics, which will be illustrated by several important effects. In particular, we will show that one can achieve optical pulling force acting on nanoparticle due to its coupling to SPP mode [Laser and Photonics Reviews, 10(1), 116–122]. The unidirectional excitation of SPP modes controlled by the optical spin-orbital locking effect results in strong recoil force, which pulls it in the direction of laser beam incidence. Moreover, the generation of SPP modes allows getting unique trapping and anti-trapping regimes when nanoparticles is placed near metal surface in the Gaussian beam [Light: Science & Applications (2017) 6, e16258]. The switching of the trapping regimes strongly depends on the wavelength of light, and on the nanoparticle sizes, which make it prospective for optical sorting near flat metallic interfaces. We also suggest utilizing the efficient generation of SPP modes for transverse optical binding effect, which is usually attributed to the interference of photons in homogenous space. We show that strong transverse optical binding can be observed near planar metallic surface due to the SPP interference. As the result the nanoparticles will form bounded states (nanoparticle molecules) at the distances defined by the SPP wave vector. The discussed results show the new opportunities for opto-mechanical control and manipulation through SPP modes generation.

10346-34, Session 9

Tuning the characteristics of surface plasmon polariton nanolasers by tailoring the dispersion relation *(Invited Paper)*

Tien-Chang Lu, National Chiao Tung Univ. (Taiwan)

Nanolasers with ultra-compact footprint are able to provide high intensity coherent light, which have various potential applications in high capacity signal processing, biosensing, and sub-wavelength imaging. Among various nanolasers, those lasers with cavities surrounded with metals have shown to have superior light emission properties due to the surface plasmon effect providing better field confinement capability and allowing exotic light-matter interaction. In this talk, we report robust ultraviolet ZnO nanolaser by using silver (Ag) [1] and aluminum (Al) [2] to strongly shrink the mode volume. The nanolasers operated at room temperature and even high temperature (353K) shows several distinct features including an extremely small mode volume, large Purcell factor and group index. Comparison of characteristics between Ag- and Al-based will also be made.

References

[1] Yu-Hsun Chou, et. al, "Ultrastrong Mode Confinement in ZnO surface Plasmon Nanolasers," ACS Nano, 9(4), pp 3978–3983 (2015).

[2] Yu-Hsun Chou, et al., "High-operation-temperature surface plasmon polariton nanolasers on single crystalline aluminum," Nano Letters, 16, 3179-3186, (2016)

10346-35, Session 9

Ultrafast carrier dynamics in bimetallic nanostructures-enhanced methylammonium lead bromide perovskites

Rizia Bardhan, Holly Zarick, Vanderbilt Univ. (United States); Abdelaziz Boulesbaa, Alexander A. Puretzky, Oak Ridge National Lab. (United States); Eric M. Talbert, Naiya Soetan, Vanderbilt Univ. (United States); David B. Geohegan, Oak Ridge National Lab. (United States)

An unprecedented rise in efficiency has been observed in methylammonium lead trihalide (MAPbX3, X=I, Cl, Br) perovskite solar cells (PSCs) reaching >20% recently. While MAPbI3 perovskites have been the primary focus in PSCs, the poor stability and rapid degradation in humidity has remained a major obstacle in MAPbI3. MAPbBr3 is a promising alternative to MAPbI3 with a large 2.2 eV bandgap which gives rise to a high open circuit voltage, long exciton diffusion length (>1.2 ?m) enabling good charge transport in devices, and higher moisture stability due to its stable cubic phase and low ionic mobility relative to the pseudocubic MAPbI3. However, a relatively large exciton binding energy (76 meV) and poor light absorption beyond its band edge at 550 nm has limited the efficiencies for MAPbBr3 solar cells. In this work, we examine the impact of hybrid bimetallic Au/Ag core/shell plasmonic nanostructures on the carrier dynamics of methylammonium lead tribromide (MAPbBr3) mesoporous PSCs.1 Plasmon-enhanced PSCs incorporated with Au/Ag nanostructures demonstrated improved light harvesting and increased power conversion efficiency by 26% relative to reference devices. Two complementary spectral techniques, transient absorption spectroscopy (TAS) and time-resolved photoluminescence (trPL), were employed to gain a mechanistic understanding of plasmonic enhancement processes. TAS revealed a decrease in photobleach formation time which suggests that the nanostructures improve hot carrier thermalization to an equilibrium distribution, relieving hot phonon bottleneck in MAPbBr3 perovskites. TAS also showed a decrease in carrier decay lifetimes indicating nanostructures enhance photoinduced carrier generation and promote efficient electron injection into TiO2 prior to bulk recombination. Further, nanostructure-incorporated perovskite films demonstrated quenching in steady-state PL and decreases in trPL carrier lifetimes, providing further evidence of improved carrier injection in plasmon-enhanced mesoporous PSCs.

1. H. F. Zarick, A. Boulesbaa, A. A. Puretzky, E. M. Talbert, Z. Debra, N. Soetan, D. B. Geohegan, and R. Bardhan*, Nanoscale, 2017, DOI: 10.1039/C6NR08347A

10346-36, Session 9

Enhanced photovoltaics in metamaterial devices using transparent conducting oxides

Nicholas Sharac, Heungsoo Kim, Chase T. Ellis, Alexander Vlasov, Jeffrey P. Calame, Joshua D. Caldwell, Joseph G. Tischler, Marc Curry, U.S. Naval Research Lab. (United States)

The cost effectiveness, flexibility, and lightness of weight of future photovoltaic devices can be achieved by utilizing surface plasmons to enhance solar cell efficiencies of thin film devices. By tuning the plasmon resonance, enhanced light concentration can occur at frequencies complimentary to those of traditional devices such as Si, so as to optimize light trapping from the sun. Here, we present light trapping metamaterial structures consisting of metallic gratings which couple light through a thin insulating dielectric layer and into a thin doped transparent conducting oxide (TCO) film, which forms a Schottky contact with Si. This configuration absorbs light in the visible through interband transitions (normal operation) and uses hot electrons in the IR. Reflectance data for two different configurations (top and bottom side gratings) show pitch dependent resonances in the visible and IR, which exhibit modes, shown from simulations, to be localized to the ITO film. Current-voltage curves show increased electrical activity under both white light and IR broad band, suggesting plasmon enhanced absorption in the IR as a result of our metamaterial structure. By tailoring the geometric properties of the grating in addition to the thickness and doping of the ITO film, the optical properties of the structure can be tuned to maximize light absorption. By also utilizing a bottom side configuration, we show that the metal gratings can be used in conjunction with TCO films without obstructing any potential collected sunlight.

10346-37, Session 9

Infrared localized surface plasmon polariton nanostructures for various applications *(Invited Paper)*

Min-Hsiung Shih, Academia Sinica (Taiwan)

In the presentation, we will present and discuss the localized surface plasmon polariton (LSPP) resonances in the Ag/SiO2/Ag nanostructures for narrow-band emitters, tunable polarizer and high performed biosensor. The Ag/SiO2/Ag sandwich nanostructure was designed and fabricated to exhibit the LSPP modes in an infrared wavelength regime. By manipulating the geometry, the high-performance, wide-angle, polarization-independent LSPP resonant waves are flexible for various applications.

The two-dimensional metallic broadband absorbers with the Ag/SiO2/Ag multi-sized nanodisk structures will be first presented. The absorptivity of such structure can be increased by tailoring the ratio of disk size to the unit cell area. The metallic disk exhibits a localized surface plasmon polariton (LSPP) mode for both TE and TM polarizations. By manipulating the ratios and disk sizes, a high-performance, wide-angle, polarization-independent multiple band absorber was experimentally achieved. The metallic nanodisk structure can be also applied an efficient narrow-band thermal emitter in the IR region. The metallic nanodisk would be a perfect thermal emitter at a specific wavelength, which can be tuned by varying the diameter of the disk.

We also discuss that oval-shape nanodisk LSPP structure can be used as an efficient angle-independent polarizer in the mid-infrared wavelength regime. For the optimum design, we can obtain a degree of polarization of 99% both experimentally and theoretically. A high extinction ratio between 20 and 40 dB can be obtained by changing the axis ratio of the oval disc between 0.65 and 0.85. The wavelength of polarized light can be tuned in a wide range by changing the structural parameters.

10346-38, Session 10

Plasmonic nonlinear optical components *(Invited Paper)*

Euclides Almeida, Yehiam Prior, Weizmann Institute of Science (Israel)

The ability to control the amplitude, phase and polarization states of light on subwavelength scales established metasurfaces as miniaturized alternatives to standard, the relatively large optical components. So far, most of these ultrathin elements operate in the linear regime, and do not change the frequency of the light transmitted or reflected from them. Using our better control over the response of the metasurfaces, we demonstrate a special class of metasurfaces that act as frequency-converting optical components [1-3]. Through nonlinear generation, plasmonic meta-atoms are used as the metasurfaces' building blocks and a 2ϖ phase shift can be imparted on the nonlinear wave. Similar to the linear metasurfaces case, the laws governing nonlinear optics can be generalized to include nonlinear phase gradients. In phase matched interactions for example, the anomalous signal generated in a collinear wave mixing scheme is emitted into another direction [2]. We demonstrate optical elements such as blazed gratings and lenses operating through four-wave mixing and third-harmonic generation. Additionally, we devise a novel type of computer-generated hologram that can reconstruct complex images at the third harmonic frequency of the reading beam [3]. Polarization-multiplexed, three-dimensional and dynamical

nonlinear holograms are fabricated in ultrathin elements by multilayer nanolithography, paving the way to a class of devices that can manipulate optical beams in unprecedented ways.

[1] E. Almeida and Y. Prior. Scientific Reports 5, 10033 (2015)

[2] E. Almeida, G. Shalem and Y. Prior, Nature Communications 7, 10367 (2016)

[3] E. Almeida, O. Bitton and Y. Prior, Nature Communications 7, 12533 (2016)

10346-39, Session 10

Femtosecond controlling mechanism of surface plasmon polaritons

Kuidong Wang, Long Chen, Haijuan Zhang, Jie Chen, Shanghai Jiao Tong Univ. (China)

Femtosecond controlling of surface plasmon polaritons (SPPs) has become a promising route for the development of high-speed plasmonic switches. However, the applications of femtosecond plasmonic modulation are limited by the relatively slow modulation speed and the requirements of high optical powers, such as in high speed integrated plasmonic circuits. Moreover, the mechanism of the femtosecond modulation remains unresolved. With time-resolved optical pump-probe technique, two sets of experiments were performed to improve the modulation speed and minimize the requirement of the optical power for femtosecond plasmonic modulation. In the first set of experiments, an ultrafast plasmonic modulation with a 70-fs switching time on an aluminum-coated grating was achieved in frequency degenerate experiments via light-SPP interaction, which is about one-third of the value reported previously. We found that the high-speed plasmonic modulation primarily results from the coherent nonlinearities which are related to the anharmonicity of the SPPs. The switching time was measured experimentally with a range of laser pulse widths and estimated theoretically to be even shorter and ultimately limited by the plasmon damping time. In the second set of experiments, the modulation depth of 8.66% was achieved with pump fluence of 1.5 mJ/cm2 via plasmon-enhanced optical nonlinearities, which is 7 times higher than that achieved from light-SPP interaction. This preliminary results suggest that the plasmonic effects could strongly enhance the modulation depth in plasmonic switching.

10346-40, Session 10

Adiabatic nanofocusing in hybrid gap plasmon waveguides

Michael P. Nielsen, Lucas Lafone, Aliaksandra Rakovich, Themistoklis P. H. Sidiropoulos, Mohsen Rahmani, Stefan A. Maier, Rupert F. Oulton, Imperial College London (United Kingdom)

We present an experimental demonstration of a silicon hybrid gap plasmon waveguide for efficient adiabatic nanofocusing. Formed of a gap in a thin metal film atop an unetched silicon-on-insulator (SOI) substrate, a recent theoretical proposal showed that these waveguides had unique advantages for nanofocusing applications. A schematic of the structure can be seen in Figure 1(a). At large gap widths, in excess of 100nm, the mode propagates primarily in the underlying silicon away from the metallic films, leading to propagation lengths of tens or even hundreds of micrometres. When the waveguide width is reduced below 100nm, the mode becomes concentrated in the gap, leading to mode areas far below the diffraction limit. This provides a new degree of freedom in waveguide dispersion engineering as the localisation of the mode is purely controlled by the gap width. Moreover, one can imagine filling the gap region with a functional nonlinear material and with the metal films acting as natural electrical contacts, creating a plasmonic phase or absorption modulator.

In this work we will give evidence of extreme nanofocusing through the use of a photoluminescent material in the gap with a three photon absorption process. Furthermore, by incorporating a nonlinear material into the gap, the high intensities gained through this nanofocusing process were utilized for nonlinear frequency conversion through both theoretical and experimental studies.

10346-41, Session 11

Fabrication and characterization of coupled ensembles of epitaxial quantum dots and metal nanoparticles supporting localized surface plasmons *(Invited Paper)*

Tigran A. Vartanyan, ITMO Univ. (Russian Federation); Vladimir Chaldyshev, Ioffe Institute (Russian Federation) and Saint-Petersburg State Polytechnical Univ. (Russian Federation); Nikita A. Toropov, Igor A. Gladskikh, Polina V. Gladskikh, ITMO Univ. (Russian Federation); Valeriy V. Preobrazhenskiy, Mikhail A. Putyato, Boris R. Semyagin, A.V. Rzhanov Institute of Semiconductor Physics (Russian Federation); Alexander Kosarev, Saint-Petersburg State Polytechnical Univ. (Russian Federation)

Epitaxial quantum dots (QDs) find numerous optoelectronic applications ranging from intermediate band solar cells to optical memory devices. Coupling of the epitaxial quantum dots to metal nanoparticles may improve their performance due to the field enhancement provided by the localized plasmon excitation. In this contribution we report on coupling an array of InAs quantum dots in the GaAs matrix to silver nanoparticles.

A stack of five layers of epitaxial InAs QDs separated by 10 nm thick GaAs barriers was grown by molecular beam epitaxy using Stranski-Krastanow mechanism. In the stacks the QDs were vertically self-aligned. The upper layer of QDs was capped by 3nm-GaAs/3nm-AlAs/4nm-GaAs layer sequence. Then, a thin silver layer was added via physical vapor deposition in a vacuum chamber at the residual pressure of 10 7 Torr. The equivalent thickness of the silver layer was set at 20 nm. Scanning electron microscopy reveals a dense labyrinth structure of silver deposits. After annealing at 200°C for two hours, isolated silver nanoparticles with broad size distribution in the range of 20 to 100 nm were formed above the layer of buried InAs quantum dots.

We studied interplay of the exciton resonance in InAs QDs and plasmon resonance in Ag nanoparticles. In particular, we observed more than two-fold enhancement of the exciton photoluminescence intensity from the InAs QDs when they were coupled to the silver nanoparticles. It seems to be due to the influence of the plasmon near fields on the radiative exciton recombination rate.

10346-42, Session 11

In-plane plasmonic antenna arrays resolve nanoscopic phase separation in model lipid membranes

Pamina Winkler, ICFO - Institut de Ciències Fotòniques (Spain); Raju Regmi, Institut Fresnel, Ctr. National de la Recherche Scientifique (France) and ICFO - Institut de Ciències Fotòniques (Spain) and Aix-Marseille Univ. (France); Valentin Flauraud, Ecole Polytechnique Fédérale de Lausanne (Switzerland); Hervé Rigneault, Institut Fresnel, Ctr. National de la Recherche Scientifique (France) and Aix-Marseille Univ. (France); Jürgen Brugger, Ecole Polytechnique Fédérale de Lausanne (Switzerland); Jérôme Wenger, Institut Fresnel, Ctr. National de la Recherche Scientifique (France) and Ctr. National de la Recherche Scientifique (France); María F. Garcia-Parajo, ICFO - Institut de Ciències Fotòniques (Spain) and

Institució Catalana de Recerca i Estudis Avançats (Spain)

Resolving the various interactions of lipids and proteins in the plasma membrane of living cells with high spatiotemporal resolution is of upmost interest [1]. Here we introduce an innovative design of plasmonic nanogap antennas to monitor single-molecule events on model biological membranes at physiological relevant concentrations by means of fluorescence correlation spectroscopy. Our design involves the fabrication of in-plane plasmonic nanogap antennas arrays embedded in nanometric-size boxes to provide full surface accessibility of the hotspot-confined region. Using these antennas we recently reported fluorescence enhancement factors of 104-105 times on individual molecules diffusing in solution, together with nanoscale detection volumes in the zeptoliter range [2]. In principle, the planarity of these antennas should enable similar studies on biological membranes without unwanted membrane curvature effects.

To show their applicability, we recorded the diffusion of individual molecules inserted in multi-component lipid bilayers as a simple mimetic system that recapitulates some of the most important features of cell membranes. We prepared membranes of different compositions: saturated phospholipids, sphingolipids and cholesterol and used antennas of different gap sizes (10-45 nm). The diffusion of individual molecules on membranes consisting of phospholipids and/or in a mixture with sphingolipids resulted Brownian, confirming homogenous lipid distribution. Interestingly, the strong confinement of antennas revealed the formation of transient (<1ms lifetime) nanoscopic domains of ~11 nm in size upon cholesterol addition. These results indicate that in-plane antennas represent a highly promising non-invasive tool to investigate the nanoscale dynamic organization of biological membranes and its impact in biological function.

References:

[1] D. Lingwood, K. Simons, Science 327, 46 (2010).

[2] V. Flauraud et al, submitted.

10346-43, Session 11

UV fluorescence modification by aluminum bowtie nanoantennas

Emmanuel Lotubai, Yunshan Wang, Steve Blair, The Univ. of Utah (United States)

UV plasmonic nanostructures have applications in enabling label free native fluorescence biosensing and enhancing efficiency of UV light emitting diode. Aluminum nanostructures such as nanoaperture, bulleye aperture, dipole antenna have been shown to modify emission properties of UV fluorescence molecules. However, these structures demonstrate small radiative enhancement and total decay rate enhancement factors (less than 10x), which hinders the application of UV plasmonic structures. In this paper, we report FDTD simulation results on excitation and emission enhancement factors of a pair of aluminum bowtie antenna in ultraviolet region. The structure was chosen because they exhibit larger LDOS (local density of states) than aforementioned geometries based on calculations. The sizes and apex angles of bowtie antennas pairs are varied to determine the optimal geometries. Our results show that increasing the size of the antennas red shifts the excitation and emission resonance peak and increases the resonance peak intensity. Increasing the apex angles (20 degree to 60 degree) slightly blue shifts the excitation and emission peak and increase the peak intensity. Thus the optimal geometry is a pair of small bowtie (radius 20nm) with apex angle 60 degrees. The gap of bowtie antennas was kept constant. The highest radiative enhancement we can achieve is 25x (~340nm) and highest total decay rate enhancement is 100x, which is higher than previously studied geometries, but still 10 times lower than the limit predicted by LDOS. Those results can be used to make better antennas for UV fluorescence modification.

10346-44, Session 11

UV plasmonic enhancement through three dimensional nano-cavity antenna array in aluminum

Jieying Mao, Yunshan Wang, Steve Blair, The Univ. of Utah (United States)

Metallic nanostructure can enhance fluorescence through excited surface plasmons which increase the local field as well as improve its quantum efficiency. When coupling to cavity resonance with proper gap dimension, gap hot spots can be generated to interact with fluorescence at their excitation/emission region in UV.

Recently, A new SER substrate architecture has been demonstrated and investigated to greatly enhance immunoassay's fluorescence and detection sensitivity in visible and infrared region.[5,6] In this work, two distinct plasmonic structure of 3D resonant cavity nanoantenna has been studied and its plasmonic response has been scaled down to the UV regime through finite-difference-time-domain (FDTD) method. Two different strategies for antenna fabrication will be conducted to obtain D-coupled Dots-on-Pillar Antenna array (D2PA) through Focus Ion Beam (FIB) and Cap-Hole Pair Antenna array (CHPA) through nanosphere template lithography (NTL). With proper optimization of the structures, D2PA and CHPA square array with 280nm pitch have achieved distinct enhancement at fluorophore emission wavelength ~350nm and excitation wavelength ~280nm simultaneously. Maximum field enhancement can reach 20 and 65 fold in the gap of D2PA and CHPA when light incident from substrate, which is expected to greatly enhance fluorescent quantum efficiency that will be confirmed in fluorescence lifetime measurement.?

10346-46, Session 11

Optical bistability and optical response of an infrared quantum dot hybridized to VO2 nanoparticle

Ali Hatef, Nipissing Univ. (Canada); Naser Zamani, Department of Physics, College of Sciences, Shiraz University, 71946-84795, Iran (Iran, Islamic Republic of); Hamid Nadgaran, Department of Physics (Iran, Islamic Republic of); Alireza Keshavarz, Department of Physics, Shiraz University of Technology (Iran, Islamic Republic of)

Vanadium dioxide (VO2) features a semiconductor to metal phase change characteristic below and above a critical temperature that leads to an abrupt change in the particle's optical properties. These VO2 optical variations lead to alter this martial from a relatively transparent semiconductor to an opaque metal in the infrared region. Recently, VO2-based nanoparticles have been synthesised with a variety of different chemical and physical techniques where the value of critical temperature can be decreased to room temperature. In this work, we theoretically show that a hybrid system consisting of semiconductor quantum dot (SQD) and vanadium dioxide nanoparticle (VO2NP) can support the coherent coupling of exciton-polaritons and exciton-plasmon polaritons in the semiconductor and metal phases of the VO2NP, respectively. In our calculations the VO2NP phase transition is modelled with a filling fraction, representing the fraction of the VO2NP in the metallic phase. Our results show that detuning an infrared CW laser around the SQD resonance frequency results in the enhancement or suppression of the SQD's linear absorption for different values of the filling fraction. We also demonstrate that the strong coupling between SQD and VO2NP can result in optical bistability of the SQD absorption where the switch-up threshold for optical bistability can be strongly controlled by filling fraction without changing the structure of the hybrid system. These results suggest that such a process allows a SQD-VO2NP to act as coherent nanoantenna, offering novel ways in order to monitor local temperature variation at the nanoscale.

10346-47, Session 12

Topological features of plasmon polaritons *(Invited Paper)*

Meir Orenstein, Technion-Israel Institute of Technology (Israel)

Plasmon Polariton and similar fields of nanostructures, although reduced to two dimensions compared to light propagating in the bulk - can carry topological features that may be crucial for light matter interactions, We will discuss the surface plasmon polariton topological - non local characteristics, showing and measuring a different type of "plasmonic" modes' manifold, discussing the topological nature of perfect lensing, and show in real time how to generate and manipulate high order topologicalyl charged plasmons.

10346-48, Session 12

Excitation of dark modes in plasmonic clusters by focused cylindrical vector beams

Tian-Song Deng, John A. Parker, Nolan Shepherd, Norbert F. Scherer, The Univ. of Chicago (United States)

Control of the spatial polarization of light allows tailoring the electromagnetic response of plasmonic nanostructures. In this work, we show that focused cylindrical vector beams (CVBs) can be used to efficiently excite dark plasmon modes in highly symmetric gold nanoparticle (AuNP) dimers. Specifically, we use single particle spectroscopy and FDTD simulations to study the response of AuNP dimers excited by linearly (LP), azimuthally (AP), and radially (RP) polarized beams. Under LP excitation, the resonances correspond to in-phase coupling of the dipolar moments of the particles, with dipolar moments parallel or perpendicular to the dimer axis. These resonances are known as bright modes, as they can easily couple to light. By contrast, the field distribution of focused AP or RP beams indicates that the fields acting on the AuNPs is primarily perpendicular or parallel to the dimer's axis, but with opposite directions at each particle. Therefore, the resonances here are out of plane coupling of dipolar moments, or so called "dark modes". In addition, multipolar expansion of the fields associated with each scattering spectrum shows that the resonances excited by LP beams are dominated by electric dipole modes. By contrast, CVB excitation causes new modes, such as magnetic dipole and electric quadrupole modes, to be driven and that they even dominate the scattering spectra. This work opens new opportunities for spectroscopic investigation of dark modes and Fano resonances in plasmonic nanostructures, which are difficult or impossible to be excited by conventionally polarized light.

10346-49, Session 12

Suppression of infrared absorption in nanostructured metals by controlling Faraday inductance and electron path length

Sang Eon Han, Samuel M. Clark, The Univ. of New Mexico (United States)

Nanostructured metals have been intensively studied for optical applications over the past few decades. However, the intrinsic loss of metals has limited the optical performance of the metal nanostructures in diverse applications. In particular, light concentration in metals by surface plasmons or other resonances causes substantial absorption in metals. Moreover, if the device operates over a broad band as in many photovoltaic devices, metal absorption needs to be controlled over the whole spectrum of interest and this poses a significant scientific and engineering challenge. Here, we avoid plasmonic excitations for low loss in infrared optoelectronics and investigate methods to further suppress loss in nanostructured metals. We demonstrate that parasitic absorption in metal nanostructures can be significantly reduced over a broad band by increasing the Faraday inductance and the electron path length. Surprisingly, we find that nanostructured metals, when cleverly designed, can behave almost like a vacuum with a negligible optical loss in the infrared region. For an example structure, the loss is reduced in comparison to flat films by more than an order of magnitude over most of the very broad spectrum between short and long wavelength infrared. For a photodetector structure, the fraction of absorption in the photoactive material increases by two orders of magnitude and the photoresponsivity increases by 15 times because of the selective suppression of metal absorption. Further, we investigate how the physics of loss suppression can be realized in 2-dimensionally patterned metal nanostructures. In this case, we increase the electron path length by using serpentine nanostructures. These nanostructured metals become transparent with optical loss of less than 7% in the infrared even at a large metal area fraction of 30%. The loss suppression effect in the serpentine structures far exceeds that in metal grid structures or straight wire arrays. These findings could benefit many metal-based applications that require low loss such as photovoltaics, photoconductive detectors, solar selective surfaces, infrared-transparent defrosting windows, and other metamaterials.

This talk is based on the following papers:

[1] S. E. Han, "Suppression of infrared absorption in nanostructured metals by controlling Faraday inductance and electron path length," Opt. Express 24, 2577-2589 (2016).

[2] S. M. Clark and S. E. Han, "Two-dimensional metamaterial transparent metal electrodes for infrared optoelectronics," Opt. Lett. 39, 3666-3669 (2014).

10346-50, Session 12

Magneto-plasmonic properties of metal nanostructures as novel functional nanomaterials for bio and gas sensing

Roberto Rella, Istituto per la Microelettronica e Microsistemi (Italy)

Metallic nanostructures supporting Localized Surface Plasmon Resonances (LSPR) are characterized by their unique ability to control and manipulate light at the nanoscale. In this work we demonstrate that gold nanostructures can exhibit magneto-optic activity in the presence of modulated magnetic field of low intensity at room temperature in transversal configuration (T-MOKE). The MO response derives from a torque in the electrical polarizability of the gold nanoparticles in resonance condition due to an external magnetic field. In this condition the resonance is modulated out of the plane of the sample and a switch-off of the plasmonic hot-spots takes place and can be monitored by measuring the intensity of the reflected light in Kretschmann configuration. In order to validate our experimental results and obtain further insight of the physical mechanism underlying these effects, numerical simulations, based on Finite Element Method (FEM) techniques, have been performed. The optical and magneto-optical properties of the investigated gold nano-particles were theoretically analysed confirming the experimental outcomes. Finally, the MO signal was used as a new transducing signal for refractive index sensing in liquid phase. An increase of sensitivity and limit of detection was registered with respect to traditional plasmonic sensors, giving proof of concept of the potential biosensing applications of this sensing mechanism

10346-51, Session 13

Functional multi-layered composite metasurfaces *(Invited Paper)*

Yehiam Prior, Euclides Almeida, Weizmann Institute of Science (Israel); Ori Avayu, Tal Ellenbogen, Tel Aviv Univ. (Israel)

Recent years have shown major advances in light manipulation capabilities offered by metasurfaces. Different configurations of metasurfaces were studied, based on metallic inclusions or all-dielectric, working in transmission or in reflection [1]. Some of these metasurfaces function differently at different polarizations or different frequencies, but the degree of functional multiplexing in a single metasurfaces was rather limited. Here [2] we use a configuration of vertically stacked metasurfaces where each layer is constructed from a different optimal building block, e.g. different inclusion material and geometry, and is designed to perform a different functionality. This scalable approach allows us to demonstrate experimentally functional spectral multiplexing of visible light. We specifically show an aberration corrected metasurface-based triplet lens for RGB colors in the visible, integrated elements for STED microscopy, and elements with anomalous dispersive focusing.

In our design, the nanoparticles dimensions and inter-particle spacing were chosen in such a way to cover the entire visible spectrum, with minimal crosstalk between the layers. Metasurface based Fresnel lens elements, composed of different disc-shaped nanoparticles of gold, silver and aluminum were optimized for working at wavelengths of 650 nm, 550 nm, and 450 nm, respectively, and full RGB achromatic operation was demonstrated. As a further demonstration of functional element, a two-layer STED element was designed - consisting of one layer silver lens, focusing green light at 1 mm, and a second spirally shaped gold lens layer, creating a red vortex beam at the same focal spot.

The potential of the stacked architecture for realizing complex and multifunctional metasurface-based optical components will be discussed.

[1] N. Yu and F. Capasso, “Flat optics with designer metasurfaces,” Nat. Mater. 13, 139–150 (2014).

[2] Ori Avayu, Euclides Almeida, Yehiam Prior, and Tal Ellenbogen, “Composite functional metasurfaces for multispectral achromatic optics”, Submitted, and arXiv:1609.08275 (2016).

10346-52, Session 13

Light tunable fano resonnance in metal-dielectric multilayer structures

Zouheir Sekkat, Moroccan Foundation for Advanced Science, Innovation and Research (Morocco)

High-Q optical Fano resonances realized in a variety of plasmonic nanostructures and metamaterials are very much promising for the development of new potent photonic devices, such as optical sensors and switches. One of the key issues in the development is to establish ways to effctively modulate the Fano resonance by external perturbations. Dynamic tuning of the Fano resonance applying the mechanical stress and electric filds has already been demonstrated.I will discuss another way of tuning, i.e., photo-tuning of the Fano resonance. We used a simple metal-dielectric multilayer structure that exhibits a sharp Fano resonance originating from coupling between a surface plasmon polariton mode and a planar waveguide mode. Using a dielectric waveguide doped with azo dye molecules that undergo photoisomerization, we succeeded in shifting the Fano resonance thorough photo-modulation of the propagation constant of the waveguide mode. The present work demonstrates the feasibility of phototuning of the Fano resonance and opens a new avenue towards potential applications of the Fano resonance.

10346-53, Session 13

Plasmonic nano-shaping and nano-manipulation *(Invited Paper)*

Keiji Sasaki, Masaki Ide, Shutaro Ishida, Kyosuke Sakai, Hokkaido Univ. (Japan)

We clarified that multipolar plasmons of metal nano-disks can be selectively excited by circularly-polarized optical vortex beams. The orbital and spin angular momenta are transferred from Laguerre-Gaussian (LG)-mode photons to localized surface plasmons. Unfortunately, the mode volume of this plasmonic nanodisk resonator is sub-micrometer dimension that is restricted by the diffraction limit of the surface plasmon wave. In order to realize single-nanometer-sized cavities, we design the tailored plasmonic structure consisting of metal multimer surrounding a nano-gap. This metal structure makes it possible to localize the optical vortex field into the gap space with conserving the orbital and spin angular momenta. We discuss on the relations between the degrees of freedom in the multimer structures and the transferable angular momenta. The transfer of orbital angular momentum from nano-vortex photons to molecules or nanoparticles induces rotational radiation pressure, i.e., optical torque, which induces nano-vortex flow of molecules/particles and may lead to chiral structuring of molecule/particle assemblies. We experimentally demonstrate rotational manipulation of a 100-nm polymer bead with a gold nano-prism trimer structure. The plasmonic structure is illuminated with a circularly polarized beam of a near-infrared laser, so that the nano-sized field with the angular momenta is formed within the gap. The result shows orbital rotational motion of the particle with 25-nm diameter. We will also show detailed analyses of the rotational motions and their relations to the chirality of the plasmonic fields.

10346-54, Session 14

Nonlinear optics based on hybrid 2D semiconductor-plasmonic metasurfaces *(Invited Paper)*

Shangjr Gwo, National Tsing Hua Univ. (Taiwan); Jinwei Shi, National Tsing Hua Univ. (Taiwan) and Beijing Normal Univ. (China); Wei-Yun Liang, National Chiao Tung Univ. (Taiwan); Yanrong Wang, National Tsing Hua Univ. (Taiwan) and Beijing Normal Univ. (China); Soniya S. Robert, Chun-An Chen, Cheng-Tse Chou, National Tsing Hua Univ. (Taiwan); Hyeyoung Ahn, National Chiao Tung Univ. (Taiwan); Yi-Hsien Lee, National Tsing Hua Univ. (Taiwan)

Plasmonic metasurfaces consist of two-dimensional (2D) arrays of plasmonic nanoresonators (plasmonic “meta-atoms” or “meta-molecules”), which exhibit collective and tunable surface plasmon polariton (SPP) resonance controlled by electromagnetic near-field coupling between meta-atoms or meta-molecules. These man-made surfaces can produce a range of unique optical properties unattainable with natural materials. However, the intrinsic lossy nature of plasmonic materials limits their potential uses. The recent discovery of transition metal dichalcogenide (TMDC; MX2, M = Mo, W and X = S, Se, etc.) monolayers as promising 2D semiconductor materials for novel photonic applications offer an interesting hybrid scenario, alternative to pure plasmonic approaches. It is well known that the fundamental optical excitation of 2D semiconductor monolayers is based on excitons (bound pairs of electron–hole) owning to the remarkably large exciton binding energies in monolayer TMDCs, making them relevant even at room temperature. Therefore, the realization of hybrid 2D semiconductor–plasmonic metasurface systems lies in the ability to control and manipulate the light–matter interactions, especially those between SPPs and excitons. In this talk, I will focus on the emerging applications of plasmonic metasurfaces with precisely engineered properties for nonlinear optics using monolayers of TMDCs as the nonlinear media.

10346-55, Session 14

Optical transition and amplification of organic phosphor coupling with graphene plasmon

Seokho Kim, INHA Univ. (Korea, Republic of); Sunjong Lee, Korea Institute of Industrial Technology (Korea, Republic of); Dong Hyuk Park, INHA Univ. (Korea, Republic of); Bo-Hyun Kim, DGIST (Korea, Republic of)

Light-matter interactions in two dimensional (2D) materials have given new momentum to nano optoelectronics since the observation of localized surface plasmons interacting with the excitons. Graphene, a typical metallic

2D crystal with high optical absorbance, can provide surface plasmon effects to proximate molecules as nanostructured metals do. The spontaneous emission rate can be enhanced by the coupling of plasmonic modes with the emission frequencies of organic molecules. However, most experimental and theoretical studies report graphene plasmonics in the terahertz to mid-infrared range. Here, we demonstrate the optical transition and significant amplification of singlet emission from phosphoric molecule on a graphene substrate, with simultaneous enhancement of triplet emission in the visible regime. The spectroscopic investigations ascribe these phenomena to the coupling of graphene plasmonic modes with molecular transient dipole. The modulation of emission channel and quantum efficiency is achieved by specifically controlling the organic molecular surface density on graphene. The single layer graphene is the most efficient substrate for plasmon coupling, however, remarkable strong PL intensity is achieved by forming multi-stacks of the organic molecule-graphene hybrid layer. This work suggests a novel route for the manipulation of organic molecular emissions using graphene plasmonics, and can be applied in developing photonic devices with high quantum efficiency.

10346-56, Session 14

Modification of UV surface plasmon resonances in aluminum hole-arrays with graphene

Yunshan Wang, Sourangsu Banerji, Jieying Mao, Sara Arezoomandan, Berardi Sensale-Rodriguez, Steve Blair, The Univ. of Utah (United States)

Active optical devices enabled by plasmon resonances have gained increasing interest during recent years. Tunable UV devices can enable enhanced functionalities such as multiplexed sensing, wavelength-tunable light emission, and so on. Interestingly, in the UV range, graphene shows an abnormal optical absorption due to pi-plasmon resonance, which can be tuned by electric bias or chemical doping. Here we report our studies on the interaction of graphene pi-plasmons with the surface plasmon resonance on Al hole-arrays. Hole periodicities of 240, 280, 320 nm are employed. Transmittance though the Al hole-array was measured before and after graphene transfer. Two important features are noticed across all the measured samples: (i) the longer-wavelength resonant dip, which has its origin on SPRs in the Al/substrate interface, is not altered when adding graphene. This is a result of the placement of the graphene layer being on top of the Al film. On the other hand, (ii) the short-wavelength resonant dips, which are associated with SPRs at the top-interface, do red-shift when graphene is added. This is a result of interaction of graphene pi-plasmon with Al SPR. Moreover, it is observed that a maxima occurs in the 280 nm to 310 nm wavelength range (i.e. 4.3 to 4.0 eV). This is attributed to an enhanced graphene optical conductivity owed to pi-plasmons. This maxima is red-shifted from the UV peak in pristine graphene because our graphene has a large unintentional doping during the transfer process.

10346-57, Session 14

Resonant coupling between molecular vibrations and localized surface plasmon resonance of faceted metal oxide nanocrystals

Ajay Singh, Los Alamos National Lab. (United States); Delia J. Milliron, The Univ. of Texas at Austin (United States)

Colloidally synthesized doped metal oxide nanocrystals has recently got great scientific attention for their ability to manipulate the localized surface plasmon resonance (LSPR) by varying their composition. Due to highly variable carrier concentration in these material, it enables plasmon frequency over entire infrared region and has facilitated a new class of tunable plasmonic materials with potential applications in the fields of photocatalysis, sensors, smart windows and surface enhanced Infrared absorption spectroscopy (SEIRA). In particular, SIERA exploits the signal enhancement to increase the sensitivity of spectroscopic feature exerted by the plasmon resonance of nanostrucrtured/nanocrystal thin films. To date, most of the studies based on plasmon- molecular vibration coupling have been focused on the plasmonic metal nanocrystal. Here, we will present the doped Indium Oxide as prototypical material. Dopant driven nanocrystal shape evolution and thereby plasmon property of colloidally synthesized octahedron , cubo-octaherdron and cubic will be emphasized. We will further describe the size dependent plasmon property of doped Indium Oxide, map the near field enhancement property of single cubic nanocrystals via EELS and quantify both far field and near field plasmon property via COMSOL electromagnetic simulations. Furthermore, we show how C-H molecular bonds (2800-3200 cm-1) couples to periodic film doped Indium Oxide nanocrystal both experimentally and computationally. This development of metal oxide plasmonic platform for molecular sensing could lead to easy to make, electrically tunable surface enhanced infrared absorption spectroscopy substrates.

10346-58, Session 14

Symbiotic plasmonic behavior of bimetallic Ag-Co nanoparticles in the conductive regime

Abhinav Malasi, Jigxuan Ge, Ritesh Sachan, Humaira Taz, Mikayla Ehrsam, The Univ. of Tennessee Knoxville (United States); Jesse Goodwin, Webb School of Knoxville (United States); Gerd Duscher, The Univ. of Tennessee Knoxville (United States); Hernando Garcia, Southern Illinois Univ. Edwardsville (United States); Ramki Kalyanaraman, The Univ. of Tennessee Knoxville (United States)

The interaction between plasmonic nanostructures in the conductive (i.e. touching) and non-conductive regimes has lead to identifying new types of resonances as well as new functionalities. Conductive regime nanoparticles made from combinations of plasmonic metals with non-plasmonic metals such as Au-Ag, Au-Pd and Au-Co have been explored for applications in sensing, catalysis and magneto-optics. Here we show that the interaction of Ag-Co in the conductive regime shows a novel symbiotic plasmonic behavior. Ag-Co nanoparticles with a segregated microstructure were prepared by pulsed laser dewetting of bilayer films on optically transparent substrates as well as on electron transparent carbon membranes. Electron energy loss spectroscopy (EELS) investigations in a TEM showed that the Co region contained ferroplasmons, i.e. strong localized surface plasmons, which are not present in pure Co. Similar ferroplasmonic behavior was also evidenced in bimetals of Ag-Fe and Ag-Ni, though with markedly different intensities compared to Ag-Co. Far field spectroscopy from a collection of nanoparticles revealed that the plasmon bandwidth from Ag-Co can be equal to or larger than pure Ag of comparable volumes. By performing a volume dependent study using Ag triangles prepared by nanosphere lithography we determined that the radiative damping in Ag could be reduced by the contact with Co. Consequently bimetallic nanoparticles can show comparable or better plasmonic quantum efficiencies than pure Ag. In addition, since Ag in the bimetal is galvanically stabilized by Co, this bimetal has many promising attributes as a new plasmonic material, including more stable extraordinary optical transmission devices.

10346-76, Session PWed

Directional and enhanced emission from a fluorescent nano-diamond

Guowei Lu, Peking Univ. (China)

We demonstrated experimentally unidirectional enhanced emission of a fluorescent nanodiamond coupled to a gold nanorod which was assembled via atomic force microscope nanomanipulation. The emission patterns can be controlled by adjusting the configurations, i.e., the gold nanorod orientation and separation with respect to the nanodiamond. Numerical

simulation results reveal that the unidirectional emission can be ascribed to the interference between the electromagnetic fields produced by the dipole like source and the out-of-phase dipole induced in the gold nanorod. The proposed hybrid nanostructures remarkably exhibit highly unidirectional emission even when the emitter is positioned up to 50 nm away from the nanorod antenna and present a broad working spectral bandwidth of ~ 200 nm.

10346-77, Session PWed

Broadband enhancement of infrared absorption using Ag nanocrystals

Jae Hong Park, National Nanofab Ctr. (Korea, Republic of)

High performance microbolometers are widely sought for thermal imaging applications. In order to increase the performance limits of microbolometers, the responsivity of the device to broadband infrared (IR) radiation needs to be improved. In this work, we report a simple, quick, and costeffective approach to modestly enhance the broadband IR response of the device by evaporating Ag nanocrystals onto the light entrance surface of the device. When irradiated with IR light, strong fields are built up within the gaps between adjacent Ag nanocrystals. These fields resistively generate heat in the nanocrystals and underlying substrate, which is transduced into an electrical signal via a resistive sensing element in the device. Through this method, we are able to enhance the IR absorption over a broadband spectrum and improve the responsivity of the device by 11%. including electrodes of secondary batteries, fuel cells, solar cells, and energy harvesters, biological devices including biochips, biomimetic or biosimilar structured devices, and mechanical devices including micro- or nano-scale sensors and actuators.

10346-78, Session PWed

Resonance modes in unbalanced Mach-Zehnder interferometers embedded in plasmonic waveguides

Shun Kamada, Toshihiro Okamoto, Masanobu Haraguchi, Tokushima Univ. (Japan)

Plasmonic waveguides (PWGs) are widely proposed for compact components of integrated circuits. We proposed an unbalanced Mach-Zehnder interferometer (MZI) for optical modulators or sensors devises by using Metal/Insulator/Metal (MIM) PWGs. Transmission spectra of the MZI were calculated by Finite difference time domain (FDTD) method. MIM PWGs of numerical simulation model is comprised of Ag/PMMA/Ag. Thickness of PMMA is 100nm. Incident light that has polarization of perpendicular to PWGs is irradiated for excite the gap plasmon mode.

We observed oscillation of transmission and transmission dips in calculated transmission spectra of an unbalanced MZI. To confirm the mechanism of the oscillation, analytical solution was calculated at an unbalanced MZI that has different path length. The numerical structures of oscillation of transmission and analytical solution have been found to be in good agreement. Therefore, oscillation of transmission is due to different path length of an unbalanced MZI. And we also calculated the field distributions of the MZI with incident light of continuous wave at dip wavelength. As a result, standing wave was observed at each airs of MZI. Those transmission dips are due to resonance in unbalanced MZI. Standing wave was appeared when wavelength of the gap plasmon mode is equal to the integral multiple of PWG length of resonance area. Therefore, an unbalanced MZI serves as a ring resonator.

In this study, it is found that an unbalanced MZI by MIM PWGs is appeared transmission properties as a ring resonator and a MZI.

10346-79, Session PWed

Nano-metallic-planar-apex metamaterials

Dong Wei, Qing Tong, Yu Lei, Huazhong Univ. of Science and Technology (China); Zhaowei Xin, Huazhong Univ. of Science and Technology (China); Xinyu Zhang, Haiwei Wang, Changsheng Xie, Huazhong Univ. of Science and Technology (China)

We present the results of numerical simulations and preliminary experiments to investigate the nano-focusing effect of incident light based on the surface plasmon polaritons (SPPs) over the nano-metallic-planar-apex metamaterials (NMPAM). The NMPAM are prepared by electron-beam lithography(EBL) and a set of nanoscale fabrication tools. The NMPAM can be used to remarkably enhance the strength of the surface evanescent and thus lead to a remarkable excitation of several SPP modes on the nano-metal-film surface. The interaction of different SPPs will result in a unique near-field optical properties for imaging and optical storage, because incident beams can focus light into a nano-size point and thus enhance the light power greatly. The energy flow and electromagnetic field distribution is calculated by finite-difference time-domain (FDTD) method. The nano-spot position and intensity is experimentally shown based on careful controlling the arrangement of apexes. In our experiments, we fabricate a 10?10 array by EBL, and then the scanning near-field optical microscopy(SNOM) is used to observe the optical power distribution in nano-scale at the air-metal interface in infrared region. We find that the incident light can be focused into ~100nm-scale and consequently enhance the light power up to several times than before common focusing method. The principle of nano-focusing based on nano-planar-apex is theoretically explained. The NMPAM can be utilized for coupling with infrared photosensitive pixels to enhance the incident light converging so as to improve signal to noise ratio of infrared detection.

10346-80, Session PWed

Flow-through nanohole array based sensor implemented on a smartphone

Juan Gomez, Univ. Nacional Autónoma de México (Mexico); Srijit Nair, Queen's Univ. (Canada); Gabriel Ascanio, Univ. Nacional Autónoma de México (Mexico); Carlos Escobedo, Queen's Univ. (Canada)

Mobile communications have massively populated the consumer electronics market over the past few years and it is now ubiquitous, providing a timeless opportunity for the development of smartphone-based technologies as point-of-care (POC) diagnosis tools.1 The expectation for a fully integrated smartphone-based sensor that enables applications such as environmental monitoring, explosive detection and biomedical analysis has increased among the scientific community in the past few years.2, 3 The commercialization forecast for smartphone-based sensing technologies is very promising, but reliable, miniature and cost-effective sensing platforms that can adapt to portable electronics in still under development. In this work, we present an integrated sensing platform based on flow-through metallic nanohole arrays. The nanohole arrays have 260 nm in diameter and 520 nm in pitch, fabricated using Focused Ion Beam (FIB) lithography. The nanohole arrays are integrated with a microfluidic chip that is used to deliver analytes to the sensing surface. An LED from a smartphone serves as light source to excite surface plasmons and the signal is recorded via a spectrometer and a CCD module. The sensing abilities of the integrated sensing platform is demonstrated for the detection of (i) changes in bulk refractive index (RI), (ii) real-time monitoring of monolayer self-assembly formation and (iii) real-time biosensing of a protein.

1. O. Tokel, F. Inci and U. Demirci, Chemical Reviews, 2014, 114, 5728-5752.

2. C. Escobedo, S. Vincent, A. I. K. Choudhury, J. Campbell, A. G. Brolo, D. Sinton and R. Gordon, Journal of Micromechanics and Microengineering, 2011, 21, 115001.

3. A. M. Foudeh, T. F. Didar, T. Veres and M. Tabrizian, Lab on a Chip, 2012, 12, 3249-3266.

10346-81, Session PWed

Excitation of plasmonic waveguide modes using principles of holography

Anton I. Ignatov, All-Russia Research Institute of Automatics (Russian Federation); Alexander M. Merzlikin, All-Russia Research Institute of Automatics (Russian Federation) and Institute for Theoretical and Applied Electromagnetics (Russian Federation)

One of methods for excitation of plasmonic surface waves and modes of plasmonic waveguides is using of periodic gratings on a metal surface or in dielectric parts of plasmonic waveguides. For particular examples of dielectric-loaded plasmonic waveguides, principles of holography were employed for development of such gratings to make the gratings more efficient and more compact. Holograms in the form of spatial modulations of refractive index of the dielectric of waveguides were theoretically analyzed. The modulations were determined by spatial distribution of intensity of the sum of exciting light beam (incident on a waveguide from free space) and excited wave (plasmonic mode of a waveguide). It was shown that such holographic gratings may have considerably higher (to several times) efficiency of coupling of the exciting light into plasmonic waves compared to the efficiency of usual strictly periodic one-dimensional gratings with optimized parameters. The advantage of holographic gratings over one-dimensional periodic gratings is most pronounced in the cases when intensity distributions of either exciting or excited waves are not uniform of when phase fronts of the waves are strongly curved in the area of a hologram. The suggested holographic method of excitation of plasmonic waveguide modes is rather universal. We expect this may be used for development of tapers with gratings to effectively excite plasmonic modes in dielectric-loaded waveguides with subwavelength aperture and for other types of plasmonic waveguides.

10346-82, Session PWed

Using split ring resonators to generate nanoscale hotspot for heat assisted magnetic recording

Anurup Datta, Xianfan Xu, Purdue Univ. (United States)

In this work, we explore the use of a split-ring resonator (SRR) type of nanostructure for the purpose of generating a nanoscale hot spot. Subwavelength focusing of light has a wide range of potential applications, one of which is heat-assisted magnetic recording (HAMR), considered to be one of the next generation data storage technologies that can address the potential challenges of increasing the areal data storage density. A typical HAMR system consists of a plasmonic nanostructure also called as near field transducer (NFT) which helps in focusing light down to a sub diffraction volume and locally heat the recording medium to temporarily decrease its coercivity during the write cycle.

In the past we have studied extensively various types of nanostructures including bowtie antenna, C-shaped antenna, and E-shaped antenna for NFT in HAMR. SRR offers another possibility as an NFT. In addition to Mie resonance peaks, SRR has been shown to possess LC-circuit type of resonance in the infrared and optical frequency range. These resonance modes, when coupled with localized surface plasmons, can be utilized to design a hot spot near the gap of the SRR structure. The relation between the geometric dimensions of the SRR NFT and the different resonance peaks is established and the coupling efficiency of the incident radiation to the storage medium is computed. The performance of an SRR NFT is compared with other types of plasmonic NFTs. We believe this work provides an insight into the design of plasmonic nanostructures which can be of significance to the development of HAMR technology.

10346-83, Session PWed

Surface plasmons on periodically corrugated surface

Eugene Chubchev, Igor Nechepurenko, Dukhov Research Institute of Automatics (Russian Federation); Alexey P. Vinogradov, Dukhov Research Institute of Automatics (Russian Federation) and Moscow Institute of Physics and Technology (Russian Federation) and Institute for Theoretical and Applied Electromagnetics (Russian Federation); Alexander A. Lisyansky, Queens College (United States) and The Graduate Ctr. (United States)

We have shown that there is a specific kind of strongly localized surface plasmon modes that exist only on periodically corrugated surface. These modes exist in the frequency range where the sum of the real parts of permittivities of metal and adjacent dielectric is positive. This frequency range is prohibited for conventional surface plasmon polaritons in case of flat metal surface. The reason why these modes arise is the surface-shape resonances [1] of single surface defect on flat surface. If such defects are periodiacally distributed on the surface than interaction among them leads to formation of nanoparticle chain waveguide [2, 3]. If the distance between defects is much smaller than free space wavelengths the eigenmodes of this chain waveguide are strongly localized.

[1] P. C. Das and J. I. Gersten, Phys. Rev. B 25, 6281 (1982)

[2] M. Quinten, A. Leitner, J. R. Krenn, and F. R. Aussenegg, Optics Letters, Vol. 23, ? 17, p. 1331 (1998)

[3] D.G. Baranov, A.P. Vinogradov, A.A. Lisyansky, JOSA B, Vol.32, ?2, p. 281 (2015)

10346-85, Session PWed

Universal characterization of plasmons satellites in photoemission from nanostructures

Sandra de Vega, ICFO - Institut de Ciències Fotòniques (Spain); F. Javier García de Abajo, ICFO - Institut de Ciències Fotòniques (Spain) and Institució Catalana de Recerca i Estudis Avançats (Spain)

Our understanding of the electronic structure of material surfaces has greatly relied on photoemission spectroscopy [1]. Photoelectrons additionally constitute an excellent source of information on optical modes, which are excited by Coulomb interaction with both the electron and the hole that is left behind [2]. In particular, plasmons have been extensively observed as satellite features in the emission spectra from planar surfaces [3]. Here, we explore the potential of plasmon satellites to render information on these excitations when photoelectrons are emitted from nanostructured materials.

Our study relies on a quantum-mechanical treatment of the plasmons and a semiclassical description of their interaction with the electron and the hole. We identify two interaction parameters that allow us to obtain universal multiple-plasmon probability distributions: the hole-plasmon and the transient electron-plasmon coupling coefficients. We further investigate characteristic values of those parameters for metallic spheres and graphene nanoislands. Our results support the ability of photoelectrons to resolve plasmons in these structures.

References:

[1] S. M. Bose, S. Prutzer and P. Longe, Phys. Rev. B 26, 729-735 (1982).

[2] F. J. García de Abajo, ACS Nano 7, 11409-11419 (2013).

[3] A. Bostwick et al., Science 328, 999-1002 (2010).

10346-86, Session PWed

Ultrafast transient dynamics of optical loss mitigation in aggregated gain-plasmon hybrid systems

Alireza Rahimi Rashed, Bilkent Univ. (Turkey); Mohamed El Kabbash, Case Western Reserve Univ. (United States); Betul Kucukoz, Ankara Üniv. (Turkey); Quang Nnguyen, Case Western Reserve Univ. (United States); Ahmet Karatay, Halime Gul Yaglioglu, Ankara Üniv. (Turkey); Giuseppe Strangi, Case Western Reserve Univ. (United States) and Univ. della Calabria (Italy); Ekmel Ozbay, Humeyra Caglayan, Bilkent Univ. (Turkey)

The extraordinary properties of the plasmonic systems arise from the confining of the electromagnetic wave beyond the diffraction limit, as a result of surface plasmons. However, oscillating plasmons can be damped due to electron scattering events. One of the most successful approaches to compensate the optical losses, while maintaining the electromagnetic sub-wavelength confinement, is to incorporate gain material in plasmonic systems. In this work, we report on systematic and detailed study utilizing transient pump-probe absorption spectroscopy on hybrid systems consisted of the aggregates of core-shell quantum dots (QDs) and Au nanoparticles (NPs). Our study provides a clear understanding of the ultrafast gain-plasmon dynamics to control optical losses in plasmonic nanostructures, paving the way towards further promising scientific research aimed to enable their practical applications. We highlight that generating hot electrons in plasmonic NPs contribute to the transient differential absorption spectrum under optical excitation and is of great significance. The results suggest modifying the way of analyzing the transient absorption spectra of loss mitigated systems. Furthermore, a frequency pulling like effect of the transient bleach signal towards the emission maximum of the gain material is reported as an evidence of loss mitigation process. Additionally, we study the implications of the coupling strength between the electron oscillation frequency and the phonon modes of aggregated NPs on loss mitigation efficiency of gain-plasmon hybrid systems, based on the observed TA properties. Finally, we investigated the transient kinetics of all systems and showed that hybrid gain-plasmon systems have unique decay kinetics.

10346-87, Session PWed

Bright off-axis directional light harvesting with plasmonic corrugations

Alireza Rahimi Rashed, Bilkent Univ. (Turkey); Hamed Sattari, Ecole Polytechnique Fédérale de Lausanne (Switzerland) and Bilkent Univ. (Turkey); Ekmel Ozbay, Humeyra Caglayan, Bilkent Univ. (Turkey)

Enhancing the photon collection efficiency and narrowing the emission directivity of sub-wavelength diffracted light sources are two critical aspects for their practical applications. These features can be attained by creating symmetric or asymmetric periodic corrugations on the exit side of a single aperture in a metallic substrate. In this approach the emitted light of nano-emitter is coupled into the antenna plasmonic modes, resulting in the emission rate enhancement and the far field radiation in the oriented direction. Here, we propose a new design of bulls-eye antenna by introducing a metallic sub-plate and dielectric layer below conventional structure. Our proposed design provides high degree of directionality and out-coupled far field intensity of the emitted light from florescence sources as compared to conventional designs. The parameters are optimized for the emission peak of diamond NV centers. In our model, we have considered diamond NV centers to be doped to PMMA and placed inside the central cavity. We have optimized the design by considering the underlying physics of a dielectric layer sandwiched between metal layers. Proposed bulls-eye configuration provides higher out-coupled intensity efficiency even better than double side corrugated antenna. Moreover, we have studied trends for steering the radiated beam over the plate of the antenna. We have introduced a modification on the design of our proposed structure, with considerable off-axis beaming angle retaining high out-coupled light intensity. Our model shows that by introducing optimal asymmetries to grooves and ridges of the structure we can achieve high degree two dimensional off-axial steering angle.

10346-88, Session PWed

Handheld highly selective plasmonic chem/biosensor using engineered binding proteins for extreme conformational changes

Derek J. Kosciolek, Ajay V. Sonar, Clarkson Univ. (United States); Lori A. Lepak, Phoebus Optoelectronics, LLC (United States); Peter Schnatz, The City College of New York (United States); Igor Bendoym, Phoebus Optoelectronics, LLC (United States); Mia C. Brown, The City Univ. of New York (United States); Ronald L. Koder, The City College of New York (United States); David T. Crouse, Phoebus Optoelectronics, LLC (United States)

We develop and fabricate a handheld, portable, highly selective and sensitive chem/biosensor that has potential applications in both airborne and water-based environmental sensing. The device relies on a plasmonic chip of subwavelength-scale periodic gold pillars engineered to resonate in the near infrared. The chip is functionalized with a novel class of proteins that exhibit extremely large conformational changes upon binding to a specific target analyte. The subsequent change in local refractive index near the surface of the gold is one to two orders of magnitude greater than current conventional methods, which produces a readily measurable 5 to 10 percent difference in light transmission. This allows us to forgo traditional, bulky tabletop setups in favor of a compact form factor. Both theoretical and measured changes in refractive index of the protein are presented here, as well as numerical and experimental results of the functionalized plasmonic chip. We then integrate these components into a fully stand-alone module, with discussions on the optical train, temperature tuning of the laser diode to obtain the plasmonic chip's spectral response, and methods to introduce airborne analytes onto the functionalized chip. While we present data on heme as the analyte, the functionalized protein can be engineered to pair with a wide variety of analytes with minimal alterations to the plasmonic chip or device design. Such flexibility allows for this device to potentially meet the needs of first responders and health care professionals in a multitude of scenarios.

10346-89, Session PWed

Ultrafast room temperature dynamic modulation of spontaneous emission in plasmonic nano-cavities

Mohamed El Kabbash, Case Western Reserve Univ. (United States); Ermanno Miele, National Univ. of Singapore (Singapore); Ahmad K. Fumani, Northwestern Univ. (United States); Michael Wolf, Elisha Haber, Jesse Berezovsky, Case Western Reserve Univ. (United States); Francesco De Angelis, Istituto Italiano di Tecnologia (Italy); Giuseppe Strangi, Case Western Reserve Univ. (United States)

The spontaneous emission (SE) of an emitter can be modified by changing its electromagnetic environment. Particularly, embedding an emitter in a high Q cavity e.g. photonic crystal, or small modal volume cavity, e.g. plasmonic nanocavity (PNC) increases its SE rate due to the Purcell effect. However, dynamically modifying the SE rate is challenging due to the ultrafast lifetime properties of emitters of ~ 1ns. Here we show, for the first time, that by using PNCs we can dynamically modify the SE rate at room temperature. Our approach relies on compensating the plasmonic optical

losses via resonantly coupled gain which dynamically modify the PNC Q factor.

Compensating plasmonic optical losses shares the same physics of enhancing the SE rate of an emitter coupled to a PNC. Both phenomena rely on non-radiative resonant energy transfer between the gain (donor) and plasmonic nanostructure (acceptor). In our work, we embedded quantum dots in an out of plane PNC and showed that by changing the gain excitation power we control the SE rate. Exciting more gain compensate more plasmonic losses, i.e. increases the Q factor of the PNC which increases the SE rate. The loss compensation of a single PNC was experimentally demonstrated by pump-probe confocal scattering spectroscopy. Very recently, modifying the SE rate was shown in photonic crystals at cryogenic temperatures using complicated photonic devices. The simplicity of our approach opens the route for further utilization of plasmonics in cavity quantum electrodynamics applications, quantum information applications and nano-scale optical communication sources.

10346-90, Session PWed

Dislocated double-layered metal gratings: an efficient unidirectional coupler/ beamsplitter

Yang Shen, Wenjie Liu, XiaoYi She, Chongjun Jin, Sun Yat-Sen Univ. (China)

Surface plasmon polaritons (SPPs) show great promise in providing an ultracompact platform for integrated photonic circuits. However, challenges remain in easily and efficiently coupling light into and subsequently routing SPPs. We propose theoretically and demonstrate experimentally a one-dimensional dislocated double-layered metal grating (DDMG) structure, which operates as a unidirectional coupler capable of launching surface plasmon polaritons in a desired direction under normal illumination. The experimental results demonstrate a coupling efficiency of 36% and a contrast ratio of 43[1]. Moreover, we theoretically propose and experimentally demonstrate a switchable unidirectional coupler/ beamsplitter which can simultaneously perform both tasks using a two-dimensional version of DDMG[2]. The core of device is a 3?3 um2 periodic array of slanted gold 'mushrooms' (SGMA) composed of angled dielectric pillars with gold caps extruding from a periodic array of perforations in a gold film. The unidirectional coupling results from the interference of the in-plane guided modes scattered by the pair of dislocated gold gratings, while the output channel is determined by the polarization of the incident beam. This device, in combination with dynamic polarization modulation techniques, has the potential to serve as a router or switch in plasmonic integrated circuits.

[1] Liu, T. R.; Shen, Y.; Shin W. et al. Nano Lett. 2014, 14, 3848–3854.

[2] Shen, Y.; Fang G. S. et al. Nanoscale. 2016, 14, 3848–3854.

10346-91, Session PWed

Plasmonic Fano resonances in novel nanostructure consisting of two rings with different diameter

Maojin Yun, Tongtong Liu, Qingdao Univ. (China)

In this paper a novel metallic nano-structure consisting of two rings with different diameter is proposed to generate intense plasmonic Fano Resonances (FRs). In this nano-structures, the FRs is explained by the interference between spectrally overlapping narrow subradiant (dark) and broad superradiant (bright) plasmonic modes and is simulated by COMSOL Multiphysics based on Finite Element Method. The simulations shows that dipolar resonance only occur in the small-diameter ring as a bright plasmon mode, other than the large-diameter ring.- It can be found that the resonant wavelength will be red-shift with the change of the radius of rings. Such structure will have many potential applications in the field of chemical and biological sensors in the future.

10346-92, Session PWed

Infrared detector based on cross-shape nano-antenna

Maojin Yun, Weipeng Hu, Qingdao Univ. (China)

In this paper the cross-shape nano-antenna composed of a cross metal film and a dielectric film in which the cross-metal film is deposited on the dielectric film is proposed and theoretically analyzed. It is found that this structure can effectively confine and dramatically enhance electromagnetic radiation. Meanwhile a infrared detector based on the cross-shape nano-antenna is presented and numerically analyzed with Finite Element Method (FEM) with wide-angle for infrared frequencies. The simulation shows that the design offers several times enhancement in absorption compared the performance of cross-shape nano-antenna detector with a bulk metal layer or nano-trip antennas, and is less affected by the incident angle and the resonance wavelength can be tuned by utilizing coupled different sizes. This design provides many practical potential applications for high flexible infrared detectors.

10346-93, Session PWed

Polarizing filter based on anisotropic absorption of graphene ribbons with varying width

Maojin Yun, Peng Sun, Qingdao Univ. (China)

In this paper, we theoretically demonstrate a polarizing filter consisted of graphene ribbon arrays with varying width placed on the top surface of dielectric and a metal reflector rested at the bottom of the structure. It is found that proper ribbon width, which corresponds to resonant frequency of graphene plasmons, is a crucial factor that can significantly influence the absorption effect. The results of fullwave numerical simulations indicate that total absorption of more than 90% for TE polarization and approaching to 1% for TM polarization can be achieved at normal incidence in the infrared range. Therefore, this characteristic can be applied into polarizing filter by adjusting the coupling effect between the graphene ribbon arrays. Such structure will be beneficial to the manufacture of infrared nanophotonic devices for optical filtering and selective absorption.

10346-94, Session PWed

Plasmonic waveguides based and optical logic gate

Sonia Tomer, Nishant Shankhwar, Yogita Kalra, Ravindra K. Sinha, Delhi Technological Univ. (India)

In this paper, a design of plasmonic waveguides based optical AND gate has been proposed. Various designs of Photonic crystal based optical logic gates have already been envisioned and proposed during the past decade, in which, wavelength of operation is comparable to the geometrical parameters. On the contrary, the proposed structure consists of plasmonic waveguides whose thickness is much smaller than the wavelength of operation. This may pave the way for large scale integration for the development of all optical circuits for optical computing systems. Moreover, the proposed design is simple and easy to fabricate using techniques like thin-film technology and lithography.The thickness of the waveguides is 50 nm and chosen wavelength of operation is 650 nm. The waveguides used are actually Insulator-Metal-Insulator structures in which metal region is made of silver and insulator is a dielectric material of permittivity ? = 4 . The data for refractive index of silver has been taken from Palik (1999). The design has been numerically analyzed in COMSOL Multiphysics® and the truth table for AND gate has been verified.

10346-95, Session PWed

Tunable sub-10nm metal gap by manipulating PDMS substrate

Wenjie Liu, Yang Shen, Chongjun Jin, Sun Yat-Sen Univ. (China)

Manipulating light in sub-10-nm or subnanometer metal nanogaps is crucial to study the strong interaction between electromagnetic waves and matters. However, the fabrication of metallic nanogaps with precisely controlled size and high-throughput still remains a challenge.?In this work, taking advantage of the shrink effect of the PDMS, we developed a feasible and cost-effective method to mechanically tune the metal gap distance as well as the property of localized surface plasmon resonances (LSPR). Large tunable range from 140 nm to sub-10-nm or even 0 nm gap distance were achieved, transmission spectra show a remarkable red shift of the dipole resonance with narrowing gap. Importantly, a universal scaling law between the gap distance in nanoscale and the stretching amount of PDMS substrate in macroscopic scale were demonstrated experimentally and theoretically. The results reveal that, tuning of the gap distance in nanoscale region can be linearly transferred to the tuning of the PDMS length in macroscopic scale and the resonant wavelength which depended strongly on the gap distance could be easily tuned by the applied strain. We also developed an analytical method to explain a universal scaling law between the gap distance in nanoscale and the stretching amount of PDMS substrate in macroscopic scale.

10346-96, Session PWed

Polarization-independent multi-peak plasmonic absorber

Igor Leonardo Gomes de Souza, Vitaly F. Rodriguez-Esquerre, Univ. Federal da Bahia (Brazil)

The effect of selective absorption of the spectrum of a metal-dielectric grating structure is studied. We propose a selective metamaterial absorber (MMs) of independent polarization spectrum based on a diffraction grating with trapezoidal geometry for the frequencies of the visible spectrum (400-700nm). Quasi-unit absorption with polarization independence is observed under normal incidence with three absorption peaks (blue, green and red). The understanding of a perfect selective absorption mechanism is illustrated by investigating the electric and magnetic field distributions at each resonant wavelength. The manufacturing tolerance of the device is also analyzed by varying the geometric parameters of the diffraction absorber grid.

10346-97, Session PWed

Quasi-normal mode expansion of the interaction between light and dispersive nano-objects: a theoretical platform for nanoplasmonics

Mathias Perrin, Ctr. National de la Recherche Scientifique (France) and Univ. Bordeaux 1 (France)

One tough task in nanophotonic is to carry heavy numerical simulations – typically Finite Element Methods, or Finite Difference in Time Domain –, in order to compute some key physical quantities (absorption and extinction cross sections, Purcell factor), for different excitation parameters (wavelength, polarization, ...).

To overcome this problem, the Quasi – Normal Mode (QNM) expansion seems promising both in quantum and classical physics, and has received much attention in recent years. Indeed, the QNMs of the device under study need to be computed only once. Then, if excitation is changed (wavelength, polarization, ...) only the expansion coefficients have to be recalculated, and this is done quickly, using an analytic expression even for dispersive and dissipative systems.

In the present work, we derive a corrected QNM expansion that removes the hypothesis of weakly dispersive materials implicitly used in previous works [1]. This leads to more accurate predictions in the near IR range, as an Eigen-energy correction now appears in the expansion [2] and permits a better description going farther from the pole frequency. This analytic formulation has been extended to several non-orthogonal QNMs without using the complex concept of PML integration.

At the conference, we will discuss the interest of this method in topical problems of nanophotonics (Quantum plasmonics, Nonlinear Plasmonics, Bio sensing).

[1] Q. Bai et al. Opt. Exp. 21 27371 – 27382 (2013).

[2] M. Perrin, Opt. Exp. 24 27137 – 27151 (2016).

10346-98, Session PWed

Plasmon-driven design of bimetallic catalysts with nanoscale resolution

Evgenia Kontoleta, Lai-Hung Lai, Erik C. Garnett, FOM Institute for Atomic and Molecular Physics (Netherlands)

It is well-known that plasmonic nanostructures have resonances that depend strongly on the particle shape and size. Here we use optical simulations and single particle experiments to show that the location of optical field “hot spots” corresponding to such localized resonances can be controlled by the illumination wavelength and polarization. We show that the optical field concentration can drive local chemical reactions with nanometer-level spatial control even using a uniform illumination source. As a first test platform we use gold nanotriangles with controllable edge length and thickness. We see that Pt can be photodeposited selectively on the triangle corners or edges depending on the illumination conditions. We investigate the three possible mechanisms leading to such localized deposition: local heating, local field enhancement and local hot electron generation. The gold nanotriangles were excited at their plasmon resonance frequency in a photoelectrochemical cell with variable bias to control the solution electrochemical potential. We verify plasmon-driven reduction of chloroplatinic acid to platinum nanoparticles only under illumination and investigate the bias-dependent deposition rate to determine the energy of these hot carriers for various illumination conditions and sample dimensions. We also study the deposition rate with and without electron and hole acceptors adjacent to the Au nanotriangles, which provides further evidence for a hot-electron mechanism. Our approach provides fundamental insights into hot-electron reactions and opens up a new synthetic pathway for hierarchical nanostructures with both simple synthesis and high spatial control. Such highly controlled nanostructures could find applications in single-molecule spectroscopy, photoelectrochemical water splitting and CO_2 reduction.

10346-99, Session PWed

Polarization dependent second harmonic generations of equilateral triangular Au nanorods at localized surface plasmon resonances

Atsushi Sugita, Hirofumi Yogo, Atsushi Ono, Yoshimasa Kawata, Shizuoka Univ. (Japan)

Nonlinear plasmonics, the technologies of mixing multiple photons in localized surface plasmon (LSP) enhanced fields, have drawn great attentions. Most of the previous studies about the nonlinear plasmonics employed centrosymmetric metal nanoparticles, such as nanospheres, nanorods, or nanodisks, and they were forbidden for electric dipolar even-order nonlinear susceptibilities. However, the resultant nonlinearities were pretty small. In the present study, the second-order nonlinear optics were investigated for noncentro-symmetric equilateral triangular Au nanoprisms at the LSP resonances.

The model systems consisted of the Au nanotriangles arrayed two-dimensionally on the SiO2 substrates. The geometry of the system was C3v point symmetry. The scattering spectrum demonstrated that the linear optics of the systems were isotropic. The second-order nonlinearities were examined by the polarized second harmonic generation (SHG) spectroscopies. There were six robes in the polar plot of the SHG signals against the excitation light polarizations. The SHG intensities were the highest at the excitation light polarizations vertical to the edges of the triangles, while they were the lowest at the polarizations parallel to the edges.

The anisotropy in the polarized SHG signals were not reproduced with the second-order nonlinear susceptibility tensors imposed on the C3v point symmetry and it was explained by taking account of the fourth-order nonlinearities. The first two photons induced the electrostrictions and the other two were converted into the SHG waves on the transiently deformed nanoprism. The photo-induced anisotropies were dependent on the polarization directions, which resulted in the anisotropy in the polarized SHG signals against the excitation polarization.

10346-100, Session PWed

Theoretical analysis of near-field distribution by point dipole source located on metallic surface

Changhoon Park, Jae W. Hahn, Yonsei Univ. (Korea, Republic of)

Conceptual and experimental demonstration of extraordinary transmission in subwavelength hole arrays perforated on metallic film attracts much interests in plasmonics. For the physics of single hole, near-field distribution by single hole is mainly composed of surface plasmon polaritons(SPPs) and diffracted fields. Diffracted field is called creeping wave or quasi-cylindrical wave in 1D object and it has asymptotic attenuation rate with respect to distance from aperture. However, theoretical derivation of diffracted field in 2D object is not investigated well. For the 2D aperture on metallic film, light from 2D aperture can be replaced with light from point dipole source due to excitation of local plasmon. Thus, near-field distribution by 2D aperture is replaced with field distribution from point dipole source. In this paper, we investigate near-field distribution based on SPPs and diffracted fields or quasi-spherical waves(QSWs) in 2D aperture. For obtaining characteristics of QSW and SPP, we solved Sommerfeld type integral for the case of horizontal electric dipole source and obtained closed-form solution for SPP and QSW. In the process of derivation, we used the modified steepest descent method described in literature to consider impact of SPP pole. With the closed-form solution for point dipole source, we investigate decay characteristics of near-field by point dipole source and we found that QSW asymptotically falls off as x-q where q ranges from 1 to 2. We expect that our closed-form solution is helpful to design plasmonic device such as sensor, lithography, etc.

10346-101, Session PWed

Broadband coherent perfect absorber based on symmetric layered thin films using indium tin oxide in epsilon-near-zero wavelength regime

Tae Young Kim, Seoyoung Kim, Wonyoung Kim, Minsuk Kim, INHA Univ. (Korea, Republic of); Young Chul Jun, Ulsan National Institute of Science and Technology (Korea, Republic of); Chang Kwon Hwangbo, INHA Univ. (Korea, Republic of)

Coherent perfect absorption (CPA) is an optical phenomenon occurring in an absorbing thin film or in a subwavelength periodic structure by the interaction of two counter-propagating coherent waves; Incident light is trapped in a cavity, bouncing back and forth, until it is completely absorbed. In this study, we propose a new broadband CPA scheme based on epsilon-near-zero (ENZ) multilayer films. Using the admittance matching method, we designed a symmetric three-layer CPA device of [ZnSe / ITO-2 (9.93 nm) / ITO-1 (14.66 nm) / ITO-2 / ZnSe] using the different ENZ wavelengths of ITO thin films; The incident light is 1550 nm wavelength at a 45o incident angle and two media are prisms of ZnSe. This configuration was chosen to realize near infrared (NIR) broadband CPA while keeping the structure as simple as possible. The output irradiances in two exit media show a broadband CPA phenomenon in the wavelength region of 1442 nm ~ 1576 nm; It is much broader than the single-layer CPA. At CPA, the transverse magnetic field profile of the symmetric-ENZ-ITO-multilayer CPA was simulated using the finite-difference time domain (FDTD) method; When two input fields are incident at CPA, complete constructive interference patterns appear in the ENZ ITO films and there are not any transmitted and reflected waves in both incident and substrate media. Our design for ENZ thin film CPA devices can be used in optical switches, modulators, filters, sensors and thermal emitters.

10346-102, Session PWed

Design of dielectric to plasmonic waveguide power transfer couplers

Emanuela Paranhos Lima, Univ. Federal da Bahia (Brazil) and Co. de Eletricidade do Estado do Bahia (Brazil); Vitaly F. Rodriguez-Esquerre, Univ. Federal da Bahia (Brazil)

Efficient directional couplers composed by parallel dielectric and metallic waveguides have been analyzed in details. The results show that an efficient power conversion of optical dielectric modes to long range plasmonic ones is possible in such devices. Low insertion losses in conjunction with short coupling length as well as a broadband operation can be obtained under certain conditions. This kind of couplers has potential applications for the design of photonic integrated circuits and for signal routing between dielectric and plasmonic waveguides.

10346-103, Session PWed

Polarization independent asymmetric light absorption in plasmonic nanostructure

Davi Franco Rego, Univ. Federal da Bahia (Brazil) and Instituto Federal da Bahia (Brazil); Igor Leonardo Gomes de Souza, Vitaly F. Rodriguez-Esquerre, Univ. Federal da Bahia (Brazil)

The directional dependency of the optical coefficients, such as absorbance and reflectance, of a periodic hole plasmonic structure is numerically simulated and investigated. The tridimensional structure, which is composed of a metallic thin layer on a semiconductor matrix, is polarization independent and exhibits wide angle tolerance. It is found that the optical coefficients of the simulated structure have strong dependency to the radii of the holes due to cavity modes resonance and surface plasmon resonance. Simulations were carried out using gold and silver, varying the holes radii ranging from 40 to 70nm, as well as its depth, from 30 to 60nm of the metallic thin layer and from 100 to 200nm of the semiconductor matrix. A maximum contrast ratio of a unit was obtained for a broadband over above 100nm with 10-fold contrast in absorbance peak asymmetry. The resonant modes excited in the structure and excitation of surface plasmon polaritons in the metallic side illumination favors absorption, which explains the asymmetric behavior. We also investigate the structure's fabrication sensitivity by randomizing the generation of center of the holes in a supercell as well as the incident illumination angle dependency. These findings are significant for a diverse range of applications, ranging from optical integrated circuits to solar and thermovoltaics energy harvesting

10346-104, Session PWed

Strong terahertz wave coupling to plasmons in grating-grate GaN HEMT arrays

Hugo Condori, Ashish Chanana, The Univ. of Utah (United States); Jimy Encomendero, Mingda Zhu, Cornell Univ. (United States); Yu Cao, IQE (United States); Ajay Nahata, The Univ. of Utah (United States); Huili Grace Xing, Cornell Univ. (United States); Berardi Sensale-Rodriguez, The Univ. of Utah (United States)

Electron plasma wave based devices have attracted significant attention during recent years for terahertz generation, detection and amplification. Efficient coupling of external terahertz radiation into and out of plasmons in a semiconductor hetero-structure is essential for the performance of such devices. Here, we report on mechanisms leading to an enhanced terahertz to electron plasma wave coupling in periodic grating-gate structures. This is achieved via the addition of source and drain (S/D) contacts as theoretically proposed by Popov [APL 89(12), 2006], which can properly synchronize electron plasma waves excited across each unit-cell when placed in close proximity to the gate fingers.

The analyzed hetero-structures consist of a 4.5um thick AlN buffer layer, followed by a 200nm GaN layer and a 20nm AlGaN barrier, which are grown on Si(111). A 2DEG is formed at the AlGaN/GaN interface. After definition of the S/D contacts and gate fingers in a periodic pattern, the back-side of the sample is etched employing DRIE so to get rid of the substrate. The resulting samples are ultra-thin membranes (thickness ~5um) and thus do not exhibit any substrate-related effects. The fabricated devices show a geometrically-defined resonance at 0.56 THz (77K), which is in close agreement with predictions from electromagnetic simulations (HFSS). Moreover, samples with S/D contacts show significantly stronger resonant responses when compared to structures without. Overall, our results demonstrate a simple way in which to enhance the electromagnetic coupling and thus improve the performance in electron plasma wave based devices.

10346-105, Session PWed

Surface plasmon-polaritons in graphene: antiferromagnet structure

Igor V. Bychkov, Dmitry A. Kuzmin, Chelyabinsk State Univ. (Russian Federation) and South Ural State Univ. (Russian Federation); Valentin A. Tolkachev, Ivan Y. Biryukov, Chelyabinsk State Univ. (Russian Federation); Vladimir G. Shavrov, Kotel'nikov Institute of Radio Engineering and Electronics of Russian Academy of Sciences (Russian Federation)

Nowadays, in plasmonics great researchers attention is paid to investigation of graphene-based nanostructures and perspectives of its applications in data processing and storage devices. In our recent works we have considered some graphene-containing structures. Some interesting results on speckle-pattern rotation in graphene-coated optical fibers, surface plasmon manipulation by magnetic field in the planar gyrotropic waveguide formed by two graphene layers, plasmonically induced magnetic field and Faraday rotation of high order modes in graphene-covered nanowires have been obtained.

In this work surface plasmon-polaritons in dielectric – graphene – antiferromagnet structure is investigated. We assume that dielectric is non-dispersive one, antiferromagnet is centrosymmetric few-sublattice magnet (of rhombic symmetry) with exchange spin excitations of electroactive type. Eigen frequencies of exchange modes correspond to infrared and visible spectrum ranges (for example, YBa2Cu3O6+x, ?-Fe2O3). Frequency-dependence of graphene conductivity is taken into account.

Calculations are carried out in assumption of decaying length of surface electromagnetic wave is much greater than the lattice constant and phenomenological method may be used. Properties of the structure are depending on dielectric permittivity tensor of antiferromagnet and graphene conductivity.

Different propagation directions of electromagnetic wave with respect to antiferromagnet crystal orientation are considered. Dispersion equations and conditions of excitation of TM- and TE- waves and components of electromagnetic field are obtained. It is shown, that TE- waves, which are non-existing without graphene, may propagates in the structure when some relations between parameters of mediums are satisfied in frequency ranges of exchange modes of antiferromagnet.

10346-106, Session PWed

3D multifocal metalens

Bo-Han Chen, National Taiwan Univ. (Taiwan); Pin Chieh Wu, Cheng Hung Chu, Academia Sinica (Taiwan); Mu-Ku Chen, Wei-Yi Tsai, Jia-Wern Chen, Tsung Lin Chung, National Taiwan Univ. (Taiwan); Din Ping Tsai, Academia Sinica (Taiwan)

Optical metasurface has attracted wide attentions because of its ability on the control of electromagnetic wave properties such as phase, amplitude as well as polarization in a subwavelength resolution. This characteristic profit the metasurfaces developing flat optical components like color filter, planar metalens, meta-hologram, polarimetry and so on. Take metalens as an example, the impinging light is converging into a single spot through 2ϖ phase modulation along a metasurface interface. Beside the compact dimension, integrated functionality is also possible in metalens that provides an additional dimension for designing devices. Although several lectures have demonstrated spatial functionalities like off-axis focus and multispectral lenses that are impossible via traditional optical components, the generalization of converging metalens in a three dimension scheme is still missing.

In this work, we present a design principle for a multifocal metalens in which the focal point can be designed at arbitrary position on a sphere at free space. To realize metalenses working in the visible light, gallium nitride (GaN) is implemented as the material composition. The results show that the non-coplanar focal points can be realized at will for three wavelengths corresponding to red, green and blue colour. Furthermore, a metalens which is able to focus three colours simultaneously at different positions is also achieved by integrating three components into a single meta-device. This study provides a promising way for the development of a variety of applications like miniature optical systems, multispectral camera and CMOS image sensor, just named a few.

10346-107, Session PWed

Intrinsic exciton-plasmon coupling at polar surfaces of ZnO in the epsilon-near-zero region

Munise Cobet, Johannes Kepler Univ. Linz (Austria); Markus R. Wagner, Axel Hoffmann, Technische Univ. Berlin (Germany)

High resolution ellipsometry of the complex dielectric function of polar ZnO surfaces are presented which show the existence of an additional propagation mode in the interface formed by an 1s-exciton-free layer (dead layer) at the Zn-terminated surface and the 2D-electron accumulation zone of the n-type material . This natural "intrinsic" layer formation fulfills ATR-like conditions for simple reflection geometries in a certain frequency window so that no prism is required. In the energy range around the longitudinal B-exciton, where epsilon is near zero, enhanced exciton-plasmon coupling generated by the p-polarized light mimics a negative effective refractive index and non-linearities comparable with metamaterials.

In order to verify the conclusions, calculations of the optical response are performed, which theoretically show the effect of a Drude-like thin surface layer on a semiconductor with exciton-polaritons. Results of this simulations are rather high carrier concentration and strong localization.

10346-108, Session PWed

Wideangle plasmonic filter for visible light applications

Igor Leonardo Gomes de Souza, Vitaly F. Rodriguez-Esquerre, Univ. Federal da Bahia (Brazil); Davi Franco Rego, Univ. Federal da Bahia (Brazil) and Instituto Federal da Bahia (Brazil)

We proposed and designed angle insensitive color filter based in metal/dielectric multilayers structures for red electromagnetic radiation (620-750nm). The thickness of the dielectric in the structure is calculated according to the physical theory and the omnidirectional resonance occurs when the reflection phase shift cancels the propagation displacement. The thickness of the metal is chosen analyzing a transmission properties in an interval of thicknesses previously described in the literature. We obtain analytically a highly stable filter with a transmission peak greater than 70% in approximately 634nm. This device can keep the same perceived transmitted color when the incidence angle changes from 0° to 50°, especially for TM polarized light.

10346-109, Session PWed

Optics of multiple grooves in metal: transition from high scattering to strong absorption

Enok J. H. Skjølstrup, Thomas M. Sondergaard, Thomas G. Pedersen, Kjeld Pedersen, Aalborg Univ. (Denmark)

This paper studies theoretically how the optics of multiple grooves in a metal change as the number of grooves is increased gradually from a single groove to infinitely many arranged in a periodic array. In the case of a single groove the out-of-plane scattering (OUP) cross section at resonance can significantly exceed the groove width. On the other hand a periodic array of identical grooves behaves radically different and is a near-perfect absorber at the same wavelength. When illuminating multiple grooves with a plane wave the OUP cross section is found to scale roughly linearly with the number of grooves and to significantly exceed the physical array width even for widths of many wavelengths. The normalized OUP cross section per groove even exceeds that of a single groove, which is explained as a consequence of surface plasmon polaritons generated at one groove being scattered out-of-the-plane by other grooves. In the case of illuminating instead with a Gaussian beam, and observing the limit as the incident beam narrows and is confined within the multiple-groove array, it is found that the total reflectance becomes very low and that there is practically no out-of-plane scattering. The well-known result for periodic arrays is thus recovered. All calculations were carried out using Greens function surface integral equation methods taking advantage of the periodic nature of the structures. Both rectangular and tapered grooves will be considered.

10346-110, Session PWed

Analysis of near-field thermal energy transfer within nanoparticles

Anil Yuksel, Michael Cullinan, Edward T. Yu, Jayathi Y. Murthy, The Univ. of Texas at Austin (United States)

Nanoscale size effects bring additional near-field thermal considerations when heating under high laser power. In this paper, we apply a Finite Difference Frequency Domain method to nanoparticles in a bed with Gaussian and Log-normally distributed particles to understand near-field thermal radiation energy effect. The nanoparticles are generated by using Discrete Element Model in which certain number of particles are generated by defining a position and radius. The solid particles interacting with the neighbouring particles are to be distributed randomly into the bed domain with an initial velocity and a boundary condition, which creates the particle packing within a defined time range under gravitational and Van der Waals forces. Finite Difference Frequency Domain, which allows electromagnetic field distribution, is applied by solving the Maxwell's equations to obtain thermal properties such as effective absorption and extinction coefficient. We show that different particle distributions create different plasmonic effects in the bed domain which results in non-local heat transport. We calculate the surface plasmon effect due to the electromagnetic coupling between the nanoparticles and the dielectric medium under the different distributions. This analysis helps to understand how sintering quality can be enhanced by creating stronger laser-particle interactions for specific groups of nanoparticles.

10346-111, Session PWed

Reducing back scattering of plasmonic scattering nanostructures for enhancing light absorption inside perovskite solar cells

Omar A. M. Abdelraouf, The American Univ. in Cairo (Egypt) and Ain Shams Univ. (Egypt); Ahmed Shaker, Ain Shams Univ. (Egypt); Nageh K. Allam, The American Univ. in Cairo (Egypt)

The efficiency of the organic perovskite solar cells has remarkable rapid increase in last decade, which make perovskite material a good candidate for cheap photovoltaic. Plasmonic scattering nanostructure could concentrate, scatter or absorb electric field at the nanometer scale.

Using these nanophotonic structures in perovskite solar cells, light absorption percentage inside active layer could be increased. For best performance using plasmonic nanostructures, we need to reduce light losses due to absorption inside metal. Also, we aim to scatter all light inside active layer and reduce backscatter light.

Herein, theoretically, we studied how to minimize backscattering effects of metallic nanostructures deposited on top perovskite active layer. Backscattering causes reflection of incident light and would reduce the amount of light inside active layer.

We studied the effect of using different silver nanostructure shapes like sphere, cone, cube, and cylindrical. Also, we examined changing dimensions of sphere radius from 50nm to 125nm, cone height, cube side length, and cylindrical radius from 50nm to 200nm.

Our results show that backscattering is highly depending on shape and dimension. So, after changing these parameters, we could suggest some shapes and appropriate dimensions with lowest value of backscattering over active perovskite wavelength.

All calculations of this work built based on Mie theory. For verifying our results, we start by modeling silver sphere in air, which gave excellent matching with Mie theory results. All models are done using COMSOL a three-dimensional, finite element method simulation tool.

Finally, using suggested nanostructures, efficiency of perovskite solar cells could be enhanced.

10346-112, Session PWed

Second harmonic generation from metal-dielectric-semiconductor nanoresonator

Anatoly Khomenko, Paulina Segovia Olvera, Pamela Mastranzo-Ortega, Elena I. Chaikina, Ctr. de Investigación Científica y de Educación Superior de Ensenada B.C. (Mexico)

In this work numerically and experimentally studied second harmonic generation (SHG) and field enhancements of two-dimensional periodical structures based on a metal nanostrips separated from semiconductor block by a small dielectric gaps. The numerical study has been conducted using the commercially available finite element software Comsol Multiphysics.

Field enhancement effects on the metal and semiconductor surface were analyzed at different incident angles of pump light. We show that by varying the gap size, dielectric constant of gap material and metal strip width the optimal wavelength for SHG can be tuned over a wide spectral range.

The numerical results were used to optimize the configuration of experimental samples, which were fabricated by electron beam lithography method. Each sample sized 1?1 mm2 consists of grating of gold strips deposited on an oxidized silicon surface. The thickness of the naturally grown oxide was measured as 2 nm.

We performed the measurements of second harmonic diffraction efficiency and its dependence on the state of polarization of the pump beam with the different period of Au strips. As a pump source a mode locked Ti:Sapphire laser delivering pulses at 83.3 MHz repetition rate and temporal FWHM 140 fs was used in the experiments. The experimental results are in good agreement with the numerical data and demonstrate up to two-order increase in SH diffraction efficiency from the Si-surface after deposition of Au-strips.

10346-113, Session PWed

SPP-assisted sub-wavelength reflection-type THz imaging with THz time-domain spectrometer

Senfeng Lai, Yanghui Wu, Wen Wu, Wenhua Gu, Nanjing Univ. of Science and Technology (China)

THz imaging has become a hot research topic in recent years, thanks to its merits of non-contact, strong penetration, immunity to hostile environments, and nondestructive detection. However, its spatial resolution is limited by the relatively long wavelength, so the location and measurement precision can only reach the level of the imaging wavelength, which has become a severe limitation of THz imaging. A simple way using surface plasmon polaritons (SPPs) to improve the location and measurement precision of THz by one order of magnitude was proposed in this manuscript, which can also realize subwavelength THz imaging.

10346-114, Session PWed

Orientational imaging of single plasmonic nanocube using dark-field hyperspectral imaging

Manas R. Gartia, Nishir S. Mehta, Georgios Veronis, Amirreza Mahigir, Louisiana State Univ. (United States)

Knowing the orientation of plasmonic nanostructures is important for catalyst, biosensors for DNA, protein detections, hotspot of surface enhanced Raman spectroscopy (SERS), and fluorescence resonant energy transfer (FRET) experiments. However, due to diffraction limit, it is challenging to obtain the exact orientation of the nanostructure using standard optical microscope. Hyperspectral Imaging Microscopy is a state-of-the-art visualization technology that combines modern optics with hyperspectral imaging and computer system to provide the identification and quantitative spectral analysis of nano- and microscale structures.

In this work, initially we use transmitted dark field imaging technique to locate single nanoparticle on a glass substrate. Then we employ hyperspectral imaging technique at the same spot to investigate orientation of single nanoparticle. No special tagging or staining of nanoparticle has been done, as more likely required in traditional microscopy techniques. Different orientations have been identified by carefully understanding and calibrating shift in spectral response from each different orientations of similar sized nanoparticles. Wavelengths recorded are between 300 nm to 900 nm.

Validation of the experimentally obtained results with finite difference time domain (FDTD) electrodynamics calculations and electron microscopy techniques allows us to confirm the correctness of our orientation assignments. The combination of high resolution nanometer-scale imaging techniques and the modern numerical modeling capacities thus enables a meaningful advance in our knowledge of manipulating and fabricating shaped nanostructures.

This work will advance our understanding of the behavior of small nanoparticle clusters useful for sensing, nanomedicine, and surface sciences.

10346-115, Session PWed

Exceptional points in hybridized plasmonic systems

Ashok Kodigala, Thomas Lepetit, Boubacar Kante, Univ. of California, San Diego (United States)

Plasmonics and its applications have garnered ample attention over the years. These applications range from chemical and biological sensors to enhanced photovoltaics.We design for the first time 3D plasmonic structures with exceptional point (EP) singularities. Exceptional Points (EPs) are singularities of open systems where at least two complex eigenmodes coalesce. They manifest themselves by the simultaneous degeneracy of both resonant frequencies and linewidths. These points are highly sensitive to external perturbations as even a tiny variation will lift the degeneracy and cause splitting of both resonant frequencies and linewidths. These results make it possible to envision a highly sensitive molecular sensor.

10346-116, Session PWed

Investigation of electron and ion beam exposures on a new HfO2 based hybrid resist

Paolo Ponzellini, Istituto Italiano di Tecnologia (Italy); Gioia Della Giustina, Univ. degli Studi di Padova (Italy); Matteo Ardini, Eugenio Calandrini, Francesco De Angelis, Istituto Italiano di Tecnologia (Italy); Denis Garoli, Univ. degli Studi di Padova (Italy)

During the recent years there was a growing interest in the application of nanostructured ceramic coatings. Several materials such as transition metals oxides: Hafnia Oxide (Hf2O3), Titania (TiO2), Zirconia (ZrO2), Alumina (Al2O3), Silica (SiO2), Indium Tin Oxide (ITO) and Lead Zirconate Titanate (PZT) can be applied in a wide variety of fields thanks to their chemical and thermal stability, mechanical resistance and advanced optical, structural and electrical properties. In order to extensively apply these materials in nanofabrication processes, it's of great interest to engineer the material in order to make it directly patternable. In fact, the traditional lithography and nanopatterning of inorganic films consists in complicated and time consuming processes. These comprises physical deposition onto a pre-patterned organic resist which is then removed by the lift-off process leaving the patterned structures. Among the different materials Hafnium dioxide (HfO2) is a well-known optical material due to its relatively high refractive index, high transparent from infrared (IR) to ultraviolet (UV) wavelength range, and low reflectivity in the visible and near IR regions. It has been used in several applications such as high-index optical coatings and as high -k gate dielectric in microelectronic next generation devices. Here we present the development of a negative tone sol-gel resist based on HfO2. Exposures under electron and ion beam have been investigated.

10346-117, Session PWed

Efficient OAM generation at the nanoscale level by means of plasmonic vortex lens

Yuri Gorodetski, Ariel Univ. (Israel); Pierfrancesco Zilio, Paolo Ponzellini, Matteo Ardini, Xavier Zambrana-Puyalto, Andrea Jacassi, Eugenio Calandrini, Denis Garoli, Istituto Italiano di Tecnologia (Italy)

Structured light beams have been the subject of an intense work in the last years due to the numerous potential applications they may offer in several disparate technological and research fields. The possibility to produce and analyze singular optical beams at the micro and the nanoscale led to focus on the interaction of light with metallic nanostructures, resulting in Surface Plasmon Polaritons (SPPs) carrying angular momentum (AM).We will refer to these waves as Plasmonic Vortices (PVs). Such modes are generally surface confined helical electromagnetic distributions with a field singularity. The strength of the singularity, termed the topological charge of a vortex, is defined by the phase ramp acquired in one round trip about the singularity center. This charge is proportional to the AM carried by the field.

PVs can be generated by coupling AM-carrying beams to the plasmonic modes of metallic films using particular chiral grating couplers, which have been sometimes called plasmonic vortex lenses (PVLs). Several examples of these couplers have been presented so far. A feature common to most of them is the Archimede's spiral shaped grooves or slits milled in a noble metal film.

Here we theoretically and experimentally demonstrate an approach to the efficient PV coupling to the free space, by means of a single-layer PVL structure with a smoothed-cone tip at its center. We show that, by properly shaping the tip geometry, the PV excited by the spiral structure can be adiabatically coupled to the far-field mode, carrying well defined AM.

10346-119, Session PWed

Ultrafast energy transfer between excitons and plasmons from weak to ultrastrong coupling regime

Sinan Balci, Turk Hava Kurumu Univ. (Turkey); Betul Kucukoz, Ankara Üniv. (Turkey); Osman Balci, Bilkent Univ. (Turkey); Ahmet Karatay, Ankara Üniv. (Turkey); Co?kun Kocaba?, Bilkent Univ. (Turkey); Halime Gul Yaglioglu, Ankara Üniv. (Turkey)

We investigate ultrafast energy transfer between excitons and plasmons in ensembles of core-shell type nanoparticles consisting of metal core covered with a concentric thin J-aggregate shell. The high electric field localization by the Ag nanoprisms and the high oscillator strength of the J-aggregate allow us to probe this interaction in the ultrastrong plasmon-exciton coupling regime. Transient absorption spectroscopy experiment revealed that the hybrid system shows half-plasmonic and half-excitonic properties. The tunability of the nanoprism plasmon resonance provides us a flexible platform to study the dynamics of the hybrid state in a broad range of wavelengths. Besides, we present a new method for the ?synthesis of plexcitonic nanoparticles to ?control the number of dye molecules self-assembled on Ag?-nanoprisms where, individual dye molecules? self-assemble into J-aggregates on Ag-nanoprisms. We observed a transition from weak coupling to the ultrastrong coupling regime. Ultrafast energy transfer of the hybrid system as a function of Rabi splitting energy revealed that the lifetime of the polariton states increases with the coupling strength and the upper polaritons are short-lived, whereas the lower polaritons are long-lived. Hybrid metal?organic nanoparticles presented in this study (i) have tunable Rabi splitting energies, (ii) are easy to prepare in large quantities in aqueous medium, (iii) can be uniformly assembled on solid substrates, (iv) have resonance frequencies in the visible spectrum, and (v) have small mode volume, thus making them an excellent model system for studying light?matter interaction at nanoscale dimensions from the weak to ultrastrong coupling regime.

10346-120, Session PWed

Experimentally quantifying losses of Fano resonances

Junhee Park, Ashok Kodigala, Abdoulaye Ndao, Boubacar Kante, Univ. of California, San Diego (United States)

A multilayered periodic array of coupled gold bars is experimentally shown to exhibit inversion between their hybridized modes in the near-infrared domain. Placing two bars hybridizes their individual plasmon modes. The resulting two fundamental modes of the system resemble symmetric (?+) and anti-symmetric (?-) modes investigated. Spatially displacing one of the bars with respect to the other can be used to modify the spectral position of these two fundamental modes even leading to resonance inversion contingent on near-field coupling. The multilayered nanostructures were fabricated by high resolution electron beam lithography (EBL), metal deposition and lift-off process on a glass substrate. SU-8 photoresist was planarized and the first layer of gold bars on the glass substrate are embedded in SU-8 which also serves as a dielectric spacer EBL, metal deposition, and lift-off steps for the second layer are carried out in a similar manner. The transmittance and reflectance spectra were acquired using a Fourier-transform infrared spectrometer (FTIR, Vertex 70, Bruker Inc.) system coupled with an optical microscope (Hyperion 2000) operated in the near infrared. The measured transmittance and reflectance spectra are normalized with a glass substrate with SU-8 spacer and with a gold mirror, respectively. Moreover, experimentally, the decay (radiation) rates of plasmonic modes are quantitatively estimated. This is of practical importance for sensing applications as it pertains and allows for loss engineering. The challenging fabrication and characterization of these multilayered structures are detailed. We highlight the importance of fabrication quality and its effect on device performance dependent on added losses.

10346-121, Session PWed

Photoluminescence of fullerene C60 thin film in plasmon coupled Au NPs monolayer, C60 film, Al film nanostructure

Oleg A. Yeshchenko, Viktor Kozachenko, Nataliya Berezovska, Yurii Liakhov, Taras Shevchenko National Univ. of Kyiv (Ukraine)

The optical properties of plasmon coupled Au NPs monolayer – C60 film – Al film nanostructure were studied in dependence of the fullerene film thickness varied in the range of 10 – 95 nm. Effects of the fullerene spacer thickness on plasmonic coupling of Au NPs with Al film were analyzed basing on the dependences of the intensity, wavelength and width of SPR extinction peak of Au NPs and the intensity of C60 PL on the fullerene film thickness.

The red shift, non-monotonic dependences with maxima of the intensity and width of SPR in Au NPs at the decrease of the spacer thickness were observed and considered as the result of thickness dependent plasmon coupling between Au NPs monolayer and Al film. The non-monotonic dependence with minimum of the PL intensity of C60 film on its thickness was also observed. The extrema of the thickness dependences of SPR extinction peak intensity and width and fullerene PL intensity occur at the same thickness value of 50 nm that allows to assume the same physical mechanism of such non-monotonic dependences. We assume that such mechanism is the excitation of the propagating SP-polaritons in Al film by the plasmonic near field waves from the Au NPs. The SP-polaritons excitation leads to additional radiative damping of SP oscillations in Au NPs. The increase of radiative damping causes the weakening of the plasmonic field of Au NPs in the gap between the Au NPs monolayer and Al film that leads to decrease of the fullerene PL intensity.

10346-122, Session PWed

Gold nanoparticle plasmon resonance in near-field coupled Au NPs monolayer / dielectric spacer / Al film nanostructure: tuning by variation of spacer thickness

Oleg A. Yeshchenko, Viktor Kozachenko, Yurii Liakhov, Taras Shevchenko National Univ. of Kyiv (Ukraine); Anatoliy O. Pinchuk, Univ. of Colorado at Colorado Springs (United States)

Effects of plasmonic coupling between the metal nanoparticles and thin metal film separated by thin dielectric film-spacer have been studied by means of the light extinction in three-layer planar Au NPs monolayer / dielectric (shellac) film / Al film nanostructure. An influence of coupling on the spectral characteristics of SPR extinction peak in Au NPs has been analyzed at spacer thickness varied in the range of 3 – 200 nm. The main observed features are strong red shift (160 nm), non-monotonical behavior of the magnitude and width of SPR at the decrease of the spacer thickness. An appearance of the intensive quadrupolar SPR peak has been observed at spacer thickness smaller than about 30 nm that is caused by the hybridization of dipolar and quadrupolar SPR modes in Au NPs in the presence of Al film. The appreciable enhancement (in 5.6 times) of light extinction by Au NPs monolayer in presence of Al film has been observed. It has been revealed that a certain value of dielectric spacer thickness (70 nm) exists at which such enhancement is maximal.

10346-123, Session PWed

Plasmonic detection of possible defects In multilayer nanohole array consisting of essential materials in simplified STT-RAM cell

Parinaz Sadri Moshkenani, Qiancheng Zhao, Mohammad Wahiduzzaman Khan, Ilya N. Krivorotov, Mikael Nilsson, Nader Bagherzadeh, Ozdal Boyraz, Univ. of California, Irvine (United States)

Plasmonic nanostructures are highly used for sensing purposes since they support plasmonic modes which make them highly sensitive to the refractive index change of their surrounding medium. Therefore, they can also be used to detect changes in optical properties of ultrathin layer films in a multilayer plasmonic structures. Here, we investigate the changes in optical properties of ultrathin films of macro structures such as STT-RAMs. Among the highest sensitive plasmonic structures, nanohole array has attracted many research interest because of its ease of fabrication, small footprint, and simplified optical alignment, and hence they are more suitable for defect detection in STT-RAM geometries. Moreover, the periodic nanohole pattern in the nanohole array structure makes it possible to couple the light to the surface plasmon polariton (SPP) mode supported by the structure. To assess the radiation damages and defects in STT-RAM cells we have designed a multilayer nanohole array based on the layers used in STT-RAM structure, consisting 4nm-Ta/2nm-CoFeB/2nm-MgO/1nm-CoFeB/5nm-Ta layers, all on a 300nm silver layer on top of a PEC boundary. The nanoholes go through all the layers and become closed by the PEC boundary on one side. The nanoholes are of 314nm depth, 350nm diameter, and 700nm period. Here, we consider the normal incidence of light and investigate zeroth-order reflection coefficient to observe the resonance. Our simulation results show that a 10% change in refractive index of the 2nm-thick MgO layer leads to about 123.2 GHz shift in SPP resonance in reflection pattern.

10346-59, Session 15

Self-assembly for plasmonic structures on large scale *(Invited Paper)*

Nobuyuki Takeyasu, Okayama Univ. (Japan) and RIKEN (Japan)

Metallic nano-structures exhibit plasmonic properties, which are different from bulk metals. For some practical applications, large amount of such structures are required over bulk scale. Self-assembly is a key platform for a large-scale fabrication of metallic nano/micro structures. However, the shape control is not easy even though their plasmonic properties are determined by their shapes. Here, I show different approaches for the shape controls of plasmonic structures with metallic atoms and nanoparticles (NPs), resulting silver nano-trees, gold NP dimers, and NP array. Silver fractal structures were formed through the assembly of silver atoms reduced from the silver ions in acetone/water solution under diffusion-limit condition. Gold NP dimers were formed through hydrophobic assembly, where hydrophobic point decorations were performed at the surface of each gold NP using Langmuir-Blodgett film. Over a wide area, NP array was formed using oil-in-water emulsion, which collected NPs dispersed in a solution and brought them into the oil/water interface through coalescence of oil droplets. I would like to show their applications to surface-enhanced Raman spectroscopy as well.

10346-60, Session 15

Plasmonic nanoparticle lithography

Zhenying Pan, Ye Feng Yu, Vytautas Valuckas, Guillaume G. Vienne, Arseniy I. Kuznetsov, A*STAR - Data Storage Institute (Singapore)

The fast development of nanoscience, especially in the field of nanoelectronics, nanophotonics and plasmonics, has shown a great demand for new nanofabrication techniques to fulfil diverse requirements. The nanolithographic methods, e.g conventional photolithography, focused electron beams lithography (EBL), and focus ion beams (FIB), all exhibit the capability for nanostructure fabrication but most of them inherently suffer from their nature, which limit the size of nanostructures, fabrication area, and throughput at reasonable costs. The limitations of these conventional lithographic techniques have motivated the development of alternative approaches such as micro-contact printing, scanning probe lithography and nanoimprinting lithography (NIL). In this paper, we propose a new alternative laser based approach which could satisfy the requirements of high resolution, fast processing speed for large area fabrication of sub-wavelength nanohole and nanoparticle arrays with feature size controllably varied from a few tens to a few hundreds nanometers. The technique, named as plasmonic nanoparticle lithography, effectively combines the laser induced transfer (LIT) [1, 2] and light-induced near-field nanomodification [3, 4] relying on the optical enhancement and thermal effect in near-field under spherical plasmonic nanoparticles. It allows producing ordered sub-wavelength nanohole arrays in a thin mask layer (e.g. Chromium film) upon laser exposure. Subsequent post-processing allows transferring the nanohole array into a desired substrate or converting it into an array of pillars made out of a desired material.

References:

1. A. I. Kuznetsov, A. B. Evlyukhin, M. R. Gonçalves, C. Reinhardt, A. Koroleva, M. L. Arnedillo, R. Kiyan, O. Marti, and B. N. Chichkov, "Laser fabrication of large-scale nanoparticle arrays for sensing applications", ACS Nano., 5(6),4843-9 (2011).

2. A. I. Kuznetsov, R. Kiyan, and B. N. Chichkov, "Laser fabrication of 2D and 3D metal nanoparticle structures and arrays", Optics Express, 18(20), 21198-21203 (2010).

3. P. G. Kika, S. A. Maiera and H. A. Atwater, Plasmon Printing - a New Approach to Near-Field Lithography, 2001 MRS Fall Meeting, MRS Proceedings, Volume 705 (2001).

4. A. Plech, V. Kotaidis, M. Lorenc and J. Boneberg, "Femtosecond laser near-field ablation from gold nanoparticles", Nature Physics, 2, 44- 47 (2006).

10346-62, Session 15

Electrohydrodynamic flow as a driving force for the directed chemical assembly of plasmonic meta-molecules

William Thrift, Regina Ragan, Mahsa Darvishzadeh-Varcheie, Filippo Capolino, Univ. of California, Irvine (United States)

Advances in understanding chemical and physical driving forces in self-assembly allow the fabrication of unique nanoarchitectures with subwavelength building blocks as the basis for plasmonic and metamaterial devices. Directed assembly of colloidal nanospheres has been shown as a

promising method for producing large area plasmonic metasurfaces. Still, self-assembly often faces significant challenges with fabrication precision, especially for metasurface applications. In this work, electrohydrodynamic (EHD) flow and chemical crosslinking are combined to form dense meta-molecules in the 2-dimensional plane of a working electrode immersed in Au nanosphere colloid solution. EHD provides a long range driving force to bring nanospheres together and crosslinking yields small, uniform gap spacings which yield strong light-matter interactions. This work represents a novel use of EHD flow for directed assembly to improve assembly kinetics with nanoparticles as small as 40nm. Selective chemical crosslinking is used to ensure selective deposition onto templates, reducing defects and nonspecific deposition. Circular meta-molecules are fabricated using directed assembly to produce strong magnetic resonances. We investigate the magnetic near field enhancements via dark field scattering spectroscopy assisted by full wave finite difference time domain simulations. Understanding long range (EHD flow) and short range (chemical crosslinking) driving forces provides the control for assembling colloidal nanoparticles in architectures for large area plasmonic metasurfaces as the basis of novel biosensing techniques and for achieving negative permeabilities at optical frequencies.

10346-63, Session 15

Large-scale nanofabrication of three-dimensional chiral nanostructures using a method combining nanospherical-lens lithography and hole mask lithography *(Invited Paper)*

Chang-Han Wang, Research Ctr. for Applied Sciences - Academia Sinica (Taiwan); Jyun-De Wu, National Taiwan Univ. (Taiwan); Zhan-Hong Lin, Yi-Hsin Chien, Chi-Ching Liu, Research Ctr. for Applied Sciences - Academia Sinica (Taiwan); Yang-Fang Chen, National Taiwan Univ. (Taiwan); Yun-Chorng Chang, Research Ctr. for Applied Sciences - Academia Sinica (Taiwan)

Plasmonics is a research field that has been under intense researches during the last decade and many interesting and new research topics have been discovered. One of the new and hot research topics in Plasmonics is Chiral Plasmonics, which studies the different responses to incident light with different handedness. Although many new and novel findings in this topic have been reported so far, however, it is still limited to the available chiral nanostructures that can be fabricated. It is hard enough to fabricated planar nanostructures with chiral optical properties. It is even harder to fabricate three-dimensional chiral nanostructures using standard lithography processes.

In this study, we will demonstrate he fabrication of various three-dimensional chiral nanostructures using a method combining Nanospherical-Lens Lithography (NLL) and Hole Mask Lithography. NLL is a technique that uses polystyrene nanospheres to focus the incoming ultraviolet light and exposure the underlying photoresist (PR) layer. PR hole arrays form after developing. We subsequently covered the PR holes with oblique angle deposited Cr to form Cr metal holes. These holes are then used with Hole Mask Lithography for angled metal deposition. By the proposed procedures, we are able to fabricate chiral nanostructures that covers a large area with very high fabrication throughput.

In the final part of this study, we will also present theoretically and experimentally obtained results to demonstrate the optical properties of the fabricated nanostructures. The properties of the chiral structures are detailed investigated and we will propose several possible applications.

10346-64, Session 16

Ultrafast nonlinearities of semiconductor metasurfaces *(Invited Paper)*

Maxim R. Shcherbakov, M.V. Lomonosov Moscow SU (Russian Federation) and Cornell Univ. (United States)

Samples were fabricated using combinations of electron beam lithography, plasma-enhanced chemical vapor deposition of silicon, dry etching, molecular beam epitaxy of Al(x)Ga(1-x)As heterostructures, and wet oxidization of AlGaAs to AlGaO. Reflectance and transmittance spectra were measured using white light spectroscopy. Ultrafast transient traces were obtained using either single frequency pump-probe (Ti:Sap at 780 nm and 45 fs) or supercontinuum IR probe pumpr-probe. Experimental data are supported by fullwave simulations in either Lumerical FDTD or COMSOL Multiphysics.

10346-65, Session 16

Graphene-plasmon lenses for enhanced harmonic generation

José Ramón Martínez Saavedra, ICFO - Institut de Ciències Fotòniques (Spain); F. Javier García de Abajo, ICFO - Institut de Ciències Fotòniques (Spain) and Institució Catalana de Recerca i Estudis Avançats (Spain)

Plasmons —the collective oscillations of electrons in metals— are one of the most promising phenomena for the design of photonic devices, thanks to its appealing properties such as strong field enhancement and energy concentration [1]. These capabilities make plasmonic materials the perfect ground for the enhancement of optical nonlinear effects, which typically require very high field intensities to be noticeable [2]. Among the plethora of plasmonic materials suitable for nonlinear effects, graphene arises as one of the most promising candidates, thanks to its active tunability properties and its linear dispersion relation, which makes it inherently nonlinear [3]. When the propagating plasmons exhibit long propagation distances, geometry can be exploited to accumulate them at focal hotspots, thus providing an additional mechanism for enhancing the nonlinear response.

In this work, we combine both the nonlinear properties of graphene and the geometrical nonlinear enhancement of a designated graphene structure to enhance harmonic generation to unprecedented limits. We analyze second- and third-order harmonic generation emission patterns from this device. We also perform a systematic study of its nonlinear properties as a function of the different material and geometrical parameters. We also explore the effect of different environments on the nonlinear effects, showing an enhancement of the second- and third-order responses of the lens. These results pave the way toward the realization of efficient, graphene-based nonlinear devices.

References

[1] F. H. L. Koppens, D. E. Chang, and F. J. García de Abajo, Nano Letters 11, 3370-3377 (2011)

[2] M Kauranen and A. V. Zayats, Nature Photonics. 6, (2012)

[3] J. D. Cox, I. Silveiro, and F. J. García de Abajo, ACS Nano 10, 1995-2003 (2016)

10346-66, Session 16

Nonlinear plasmonic sensing with nanographene

Renwen Yu, Joel D. Cox, ICFO - Institut de Ciències Fotòniques (Spain) and Barcelona Institute of Science and Technology (Spain); F. Javier García de Abajo, ICFO - Institut de Ciències Fotòniques (Spain) and Institució Catalana de Recerca i Estudis Avançats (Spain) and Barcelona Institute of Science and Technology (Spain)

Plasmons provide excellent sensitivity to detect analyte molecules through their strong interaction with the dielectric environment. Plasmonic sensors based on noble metals are, however, limited by the spectral broadening of these excitations. Here we identify a new mechanism that reveals the presence of individual molecules through the radical changes that they produce in the plasmons of graphene nanoislands. An elementary charge or a weak permanent dipole carried by the molecule are shown to be sufficient to trigger observable modifications in the linear absorption spectra and the nonlinear response of the nanoislands. In particular, a strong second-harmonic signal, forbidden by symmetry in the unexposed graphene nanostructure, emerges due to a redistribution of conduction electrons produced by interaction with the molecule. These results pave the way toward ultrasensitive nonlinear detection of dipolar molecules and molecular radicals that is made possible by the extraordinary optoelectronic properties of graphene.

10346-67, Session 16

Extreme nonlinear plasmonic phenomena in nanostructured graphene

Joel D. Cox, Andrea Marini, ICFO - Institut de Ciències Fotòniques (Spain); F. Javier García de Abajo, ICFO - Institut de Ciències Fotòniques (Spain) and Institució Catalana de Recerca i Estudis Avançats (Spain)

The realization of efficient high-harmonic generation (HHG) in solid-state systems is anticipated to pave the way for compact ultraviolet and ultrafast light sources, and to provide fundamental insight into quantum many-body electron motion [1-3]. Here we argue that the large light intensity required for HHG to occur can be reached by exploiting localized plasmons in doped graphene nanostructures. In particular, we demonstrate that the synergistic combination of strong plasmonic near-field enhancement and a large intrinsic nonlinearity originating from the anharmonic charge-carrier dispersion of graphene result in efficient broadband high-harmonic generation within a single material [4]. We extract this conclusion from rigorous time-domain simulations using complementary nonperturbative approaches based on atomistic one-electron density matrix and massless Dirac-fermion Bloch-equation pictures, where the latter treatment is supplemented by a classical electromagnetic description of the plasmonic near-field enhancement produced by the illuminated nanostructure.

High harmonics are predicted to be emitted with unprecedentedly large intensity by tuning the incident light to the localized plasmon resonances of ribbons and finite islands, which in turn can be actively modulated via electrical gating. In contrast to HHG in atomic systems, we observe no cutoff in harmonic order, while a comparison of graphene plasmon-assisted HHG to recent measurements in solid-state systems suggests that the HHG yields from bulk semiconductors can be produced by graphene plasmons using 3-4 orders of magnitude lower pulse fluence. Our results support the strong potential of nanostructured graphene as a robust, electrically-tunable platform for HHG.

10346-68, Session 17

Ultrafast dynamics of plasmonic nanostructures *(Invited Paper)*

Stephan Link, Rice Univ. (United States)

Aluminum nanostructures support tunable surface plasmon resonances and have become an alternative to gold nanoparticles. While gold is the most-studied plasmonic material, aluminum has the advantage of high earth abundance and hence low cost. In addition to understanding the size and shape tunability of the plasmon resonance, the fundamental relaxation processes after photo-excitation must be understood to take full advantage of aluminum nanostructures in various applications including photocatalysis and photodetection. In this work, we investigate the energy relaxation after ultrafast pulsed excitation and the launching of acoustic vibrations in individual aluminum nanodisks with varying diameters using single-particle transient extinction spectroscopy. We find that the transient extinction signal can be assigned to a thermal relaxation of the photoexcited electrons and phonons. The ultrafast heating induced launching of in-plane acoustic vibrations reveal moderate binding to the glass substrate and are affected by the native aluminum oxide layer as demonstrated by theoretical calculations. We furthermore compare the behavior of aluminum nanodisks to that of similarly prepared and sized gold nanodisks.

10346-69, Session 17

Superresolution imaging of the local density of states in plasmon lattices

Ke Guo, FOM Institute for Atomic and Molecular Physics (Netherlands); Marc A. Verschuuren, Philips Research (Netherlands); Femius Koenderink, FOM Institute for Atomic and Molecular Physics (Netherlands)

Periodic plasmonic nanostructures have been found promising in controlling photoluminescence directivity and efficiency for a wide variety of applications. Because of the inhomogeneous spatial distribution of the photonic resonances of periodic plasmonic nanostructures, their influence on emission is strongly dependent on the position of emitters relative to the nanostructures. Therefore, mapping the local dependence of directivity, efficiency, and emission rate enhancements is key to understanding and optimizing the devices. We introduce a method of mapping the local enhancement of spontaneous emission rates of emitters coupled to periodic nanostructures based on stochastic superresolution imaging. As an example, we show superresolved measurements of the local density of states (LDOS) at 605 nm induced by a hexagonal lattice of aluminum nanoantennas with a spatial resolution of 40 nm. Comparison with electrodynamic simulations indicates that the variation of the decay rate of the emitters in the investigated sample is hardly influenced by the lattice modes and mainly governed by single-particle LDOS variations and nearest-neighbor interactions.

10346-70, Session 17

Necklace beams in engineered nonlinear media *(Invited Paper)*

Natalia M. Litchinitser, Jingbo Sun, Salih Z. Silahli, Wiktor T. Walasik, Univ. at Buffalo (United States); Eric G. Johnson, Clemson Univ. (United States)

Colloidal suspensions offer as a promising platform for engineering polarizibilities and realization of large and tunable nonlinearities. Previous studies of Gaussian beams propagation in various colloidal suspensions predicted in a number of remarkable optical phenomena and applications, including initiation and regulation of chemical reactions, sorting different species of nanoparticles and imaging through highly scattering media. As compared to the conventionally used Gaussian beams, optical vortices that are characterized by the doughnut-shaped intensity profile and a helical phase front offer even more degrees of freedom for, in particular, optical trapping or imaging applications. In our earlier work, we predicted, using the linear stability analysis and numerical simulations, that the perturbations with an orbital angular momentum of a particular charge will be amplified and lead to the formation of a necklace beam with a particular number of peaks, or "beads." Here, we performed detailed experimental studies of such necklace beam formation that show an excellent agreement with the analytical and numerical predictions. This work might bring about new possibilities for dynamic optical manipulation and transmission of light through scattering media as well as formation of complex optical patters in colloids.

10346-71, Session 17

Plasmonic toroidal excitation with engineering metamaterials *(Invited Paper)*

Pin Chieh Wu, Research Ctr. for Applied Sciences - Academia Sinica (Taiwan); Hui-Hsin Hsiao, Chun Yen Liao, Tsung Lin Chung, Pei Ru Wu, National Taiwan Univ. (Taiwan); Vassili Savinov, Nikolay I. Zheludev, Univ. of Southampton (United Kingdom); Din Ping Tsai, Research Ctr. for Applied Sciences - Academia Sinica (Taiwan)

Natural toroidal molecules, such as biomolecules and proteins, possess toroidal dipole moments that are hard to be detected, which leads to extensive studies of artificial toroidal materials. Recently, toroidal metamaterials have been widely investigated to enhance toroidal dipole moments while the other multipoles are eliminated due to the spacial symmetry. However, to effectively excite a toroidal dipole, a specific excitation method is necessary since a closed-loop of induced magnetic dipoles in a toroidal metamaterial weakly interact with the external wave. Moreover, most of generated toroidal dipole moments are either aligned vertically to the substrate surface or embedded in a dielectric, which is another constraint for further applications.

In this talk, we will show several cases on the plasmonic toroidal excitation by engineering the near-field coupling between metamaterials. The gain-assistant toroidal resonance is subsequently studied for realizing toroidal lasing spaser. In addition, a novel design for a toroidal metamaterial with multi-layered structures is also studied. Because the induced toroidal dipole moment is oscillating at the interface between metallic structure and free space, this design overcomes the challenge in detecting the scattering of the induced toroidal dipole and provides a possibility of coupling with other dipolar moments. Besides, the non-radiating anapole mode results from the destructive interference between toroidal and electric dipoles are realized through such proposed toroidal metamaterials. To our best knowledge, this is the first proof-of-concept demonstration of anapole mode though coupled plasmonic metamaterials which offers a promising way for the investigation of optical properties with complicated electromagnetic fields.

10346-72, Session 18

Catching light in-flight: reshaping nanosecond laser pulses using active metasurfaces *(Invited Paper)*

Gennady B. Shvets, Cornell Univ. (United States)

One of their most appealing features of graphene-integrated metasurfaces is their ability to change their optical properties on a nanosecond time scale. I will describe our experiments showing temporal reshaping of an optical pulse through its interaction with a metasurface evolving on the time scale of the pulse itself.

10346-73, Session 18

A three-dimensional negative index medium and a miniature surface plasmon polariton amplitude modulator *(Invited Paper)*

Ta-Jen Yen, National Tsing Hua Univ. (Taiwan); Chu-En Lin, National Chin-Yi Univ. of Technology (Taiwan); Chih-Jen Yu, Chang Gung Univ. (Taiwan); Tsung-Yu Huang, Ting-Tso Yeh, Cheng-Wei Chang, National Tsing Hua Univ. (Taiwan)

In this talk, I introduce two plasmonic devices. Firstly, we design and construct a three-dimensional (3D) negative index medium (NIM) composed of gold hemispherical shells to supplant an integration of a split-ring resonator and a discrete plasmonic wire for both negative permeability and permittivity at THz gap. With the proposed highly symmetric gold hemispherical shells, the negative index is preserved at multiple incident angles ranging from 0° to 85° for both TE and TM waves, which is further evidenced by negative phase flows in animated field distributions and outweighs conventional fishnet structures with operating frequency shifts when varying incident angles. Finally, the fabrication of the gold hemispherical shells is facilitated via standard UV lithographic and isotropic wet etching processes and characterized by -FTIR. The measurement results agree the simulated ones very well. Secondly, we present a miniature surface plasmon polariton amplitude modulator (SPPAM) by directing and interfering surface plasmon polaritons on a nanofabricated chip. Our results show that this SPPAM enables two kinds of modulations. The first kind of modulation is controlled by encoding angular-frequency difference from a Zeeman laser, with a beat frequency of 1.66 MHz; the second of modulation is validated by periodically varying the polarization states from a polarization generator, with rotation frequencies of 0.5-10k Hz. In addition, the normalized extinction ratio of our plasmonic structure reaches 100. Such miniaturized beat-frequency and polarization-controlled amplitude modulators open an avenue for the exploration of ultrasensitive nanosensors, nanocircuits, and other integrated nanophotonic devices.

10346-74, Session 18

Giant nonlinearity arising from the vertical split ring resonators *(Invited Paper)*

Hui-Hsin Hsiao, Hui Jun Wu, Research Ctr. for Applied Sciences - Academia Sinica (Taiwan); Tsung Lin Chung, Wei-Yi Tsai, Ren Jie Lin, Wei Hou Lee, National Taiwan Univ. (Taiwan); Din Ping Tsai, National Taiwan Univ. (Taiwan) and Research Ctr. for Applied Sciences - Academia Sinica (Taiwan)

Increasing the nonlinear optical response at nanometer length scale is a very important issue due to the wide applications in various disciplines such as information science, bio-medicine and quantum computation technology. Second harmonic generation (SHG) arising from the metal nanostructures has provide a very powerful tool in studying the surface and interface properties of these materials. The SHG from various kinds of asymmetric geometric configurations such as V and L shape structures, imperfect nano-spheres, metal/insulator/metal multilayer structures, and planar split ring resonators have been proposed. However, all the previous studies in plasmonic nonlinear optical behavior rely on the enhancement of the electric field and seldom considered the magnetic field effect.

In this work, we present a vertical split ring resonator (SRR) based metamaterial to generate SHG. By adopting such a novel structure, both the electric and magnetic field will be significantly enhanced due to the localized surface plasmon resonance, hence the generation of the second-harmonic and its re-emission into the far field are dramatically increased several orders comparing with that of the planar SRR. We simulated and fabricated the reflective type vertical SRR, and optimized the aspect ratio to maximize the SHG signal. We further systematically studied the nonlinear optical response in the vertical SRR dimers and trimers and found that the gap distance between two SRRs plays a very important role in the SHG intensity. This work paves a new way in increasing the nonlinear transition quantum efficiency and provides a new insight in designing new nonlinear sources.

10346-75, Session 18

Periodic metal nanoparticle arrays for large-area enhanced light-trapping

Yassine Ait-El-Aoud, U.S. Army Natick Soldier Research, Development and Engineering Ctr. (United States) and Univ. of Massachusetts Lowell (United States); Alkim Akyurtlu, Univ. of Massachusetts Lowell (United States); Richard M. Osgood III, U.S. Army Natick Soldier Research, Development and Engineering Ctr. (United States)

Due to the unique properties of the electromagnetic interactions of light with metal nanoparticles, these particles can exhibit large optical field enhancements, resulting in large enhancements in the absorption or scattering of the incoming light. Thin film solar cells based can greatly benefit from this phenomenon. In this work, we have examined the effect of incorporating large-scale periodic arrays of these nanoparticles, fabricated using advanced patterning techniques that can be scaled up to large areas,onto an hydrogenated amorphous silicon thin film to determine their effect on light scattering. Samples were fabricated using the popular self assembly process method: dip coating, combined with nanosphere lithography, polystyrene spheres with 500 nm, 400 nm, and 200 nm diameter. The optical measurements, including the forward and backward scattering, were collected using the 150 mm integrating sphere UV-Vis-NIR spectrophotometer.

Conference 10347: Optical Trapping and Optical Micromanipulation XIV

SPIE. OPTICS+ PHOTONICS NANOSCIENCE+ ENGINEERING

Sunday - Thursday 6 –10 August 2017

Part of Proceedings of SPIE Vol. 10347 Optical Trapping and Optical Micromanipulation XIV

10347-1, Session 1

Machined multicore optical fibers for on-chip optical manipulation

Georgia Anastasiadi, Mark Leonard, Lynn Paterson, William N. MacPherson, Heriot-Watt Univ. (United Kingdom)

Optical Tweezing is a powerful technique enabling a variety of single cell experiments. However, tweezing experiments tend to be based on a high numerical aperture microscope objective to simultaneously deliver the tweezing light and image the sample, introducing restrictions in terms of system flexibility.The development of a single optical fibre-based probe, capable of manipulating microparticles under a variety of microscope objective lens, has been demonstrated. The working principle of the probe is based upon two crossed beams to create an intensity profile that can trap particles in the intersection. Forming these beams requires the light to exit the fibre at an angle to the fibre axis. To realize this, a cleaved multicore fibre is modified using Focused Ion Beam machining (FIB) to form the angled mirrors in two cores, such that the light coming out these cores is deflected and crosses at a point close to the fibre end. The effectiveness of this approach has been tested by trapping yeast cells of 5-10?m diameter for three different repeats of the design.

By using a multicore fibre instead of separate fibres glued together, results in simplified probe, suitable for use in a wider range of applications, including on-chip manipulation. The beam intensity profile of the probe has been simulated to predict the trapping area in the sample medium and compared with experimental results. Three dimensional manipulation of cells has been achieved and the trapping force has been estimated.

10347-2, Session 1

Revealing the micromechanics driving cellular division: optical manipulation of force bearing substructure in mitotic cells

Matthew D. Ono, Daryl Preece, Michelle L. Duquette, Univ. of California, San Diego (United States); Michael W. Berns, Univ. of California, San Diego (United States) and Beckman Laser Institute and Medical Clinic (United States)

Proper cellular division underlies the natural development and repair processes in living tissues. In the anaphase stage of division, a motility force separates genetic material in the form of chromosomes; failure to separate chromosomes can result in tumor development and birth defects. Current estimates of this motility force based on viscous drag do not reflect forces from direct measurements. As such a more complete understanding of cellular substructure is needed to reconcile measurement with theory. During anaphase, chromosomes can be understood as elastic bodies whose deformations reflect physical forces and strains. Anaphase chromosome elongation has widely been attributed to viscous drag. However, LaFountain et. al found a physical element connecting sister chromosome ends in crane-fly spermatocytes such that a tethering force elongates chromosomes. Laser microsurgery was used to deduce the mechanistic basis for chromosome elongation in mammalian PtK2 cells. In half of tested chromosomes, laser microsurgery directed between separating chromosome ends reduced elongation by ~7.5%, suggesting a source of chromosome strain independent of viscous drag. When laser microsurgery was used to cut chromosomes in transport, the kinetochore attached fragments continued normal poleward travel while half of end fragments travelled to the opposite pole and the remaining fragments either stagnated or segregated normally. For fragments traveling towards the opposite pole, laser microsurgery directed between chromosome ends always ceased cross-polar travel suggesting the laser severed a physical linkage responsible for transmitting force to the fragment. Optical trapping of cross-polar moving fragments places an upper bound on the tethering force of ~1.5 pN.

10347-3, Session 1

Assessment of influence of nano-particles on the red blood cell aggregation *(Invited Paper)*

Alexey P. Popov, Tatiana I. Avsievich, Alexander Bykov, Igor Meglinski, Univ. of Oulu (Finland)

The red blood cell (RBC) aggregation is an intrinsic property of blood, which influencing significantly the blood microcirculation with a great potential in clinical applications. The ultimate understanding of the fundamental mechanism of the cells adhesion is essential for further proper applications. Presently there are two hypotheses of the 'cross-bridges' and 'depletion layer' to describe the cells interaction while either is still to be experimentally proven. Current study is aiming to obtain the experimental evidence toward the cells interaction mechanism. Optical tweezers were used to measure the RBC adhesion forces and energies. The cells interaction was examined in different solutions, including plasma, serum and model solutions with dextran or proteins, and nano-particles. The experimental result shows that the cells adhesion forces get stronger as they are separated in all solutions except dextran. The adhesion energy is found to be increasing few times, while in dextran the adhesion force decreases as the cells are separated and corresponding adhesion energy is constant. The obtained results are clarifying the mechanism of the RBC adhesion, confirming the 'cross-bridge' migration model to describe properly the cells interaction.

10347-4, Session 1

Manipulating mutant bacterial cells by tug-of-war multi-trap tweezers

Josh Lamstein, San Francisco State Univ. (United States); Anna S. Bezryadina, Univ. of California, San Diego (United States) and San Francisco State Univ. (United States); Daryl Preece, Univ. of California, San Diego (United States); Joseph C. Chen, San Francisco State Univ. (United States); Zhigang Chen, San Francisco State Univ. (United States) and Nankai Univ. (China)

We design and demonstrate multi-trap tug-of-war (TOW) optical tweezers with object-adapted optical potentials for trapping and manipulating asymmetric particles and biological samples such as mutant bacterial cells. While dual TOW tweezers can effectively trap rod-shaped objects and even stretch them laterally, triangular TOW tweezers enable in-plane trapping of larger asymmetric objects which do not necessarily have mirror symmetry. When trapping with the dual TOW tweezers, we previously demonstrated that they are more stable than Gaussian beam-based dual traps, and the strong lateral pulling forces from the TOW optical tweezers can stretch and even break apart cellular clusters. Here we show multi-trap TOW (with 3 and 4 arms) optical tweezers can be employed to control and manipulate mutant Sinorhizobium meliloti bacterial cells, which are typically multi-pronged. We discuss the advantage of such TOW beam-based optical tweezers over traditional Gaussian beam-based holographic tweezers, and the potential applications of these TOW tweezers in studying cellular viscoelasticity, biomechanics, motility, and intercellular interactions.

Return to Contents

10347-5, Session 1

Optical measurements of cell adhesion *(Invited Paper)*

Josef A. Käs, Steffen Grosser, Univ. Leipzig (Germany)

We demonstrate that the optical stretcher, a fully automated dual-beam laser trap for probing single-cell mechanics, can also be used to trap pairs of cells and manipulate them. More specifically, we can press cells against each other and tear them apart again, enabling us to measure cell adhesion/ dissociation dynamics.

We show that we can see differences in adhesion behaviour between cell lines and we see single-molecule dissociation processes. We calculate the forces which we exert on the cells, which are in the pN range.

This "optical micromanipulator" provides high-throughput adhesion measurements with about 50 cell pairs per hour, while allowing for full optical inspection of the cell dissociation process. The method can be combined with other characterization methods readily available in the stretcher such as fluorescence imaging and cell rheology evaluation.

10347-6, Session 1

Hydrodynamic stretching for analysing urological cancer cells

Yuri Belotti, Tianjun Huang, Stephen J. McKenna, Ghulam Nabi, David McGloin, Univ. of Dundee (United Kingdom)

Prostate cancer (PCa) is one of the most common types of cancer in the world, with especially high rates of incidence in the United States and Western Europe. The current diagnostic gold standards are controversial can lead to issues in diagnosis. Blood tests are commonly used to check the level of the prostate specific antigen (PSA), when in fact this antigen is organ-specific but not cancer-specific with the outcome that many unnecessary procedures with significant side effects are carried out. We therefore need new methods to improve clinical diagnostics in this area.

Here we outline how one might be able to distinguish between different cellular phenotypes using a label-free measurement technique based on the mechanical stiffness of a cell. Our technique makes use of microfluidic devices which can act as hydrodynamic stretchers, squashing cells in a very high-throughput manner. Here we demonstrate that we can correctly classify two different prostate cell lines, DU145 (cancerous) and PNT2 (healthy) with a high degree of confidence. Our system involves a very high speed camera (~300,000 frames per second) and bespoke image processing to classify cell roundness coupled with machine learning to classify the cells. We will contrast the current system with attempt to extract the same data using optical stretching techniques, and outline developments of the technique to extract dynamic deformation in a time-resolved manner.

10347-7, Session 2A

Coherent control of light transmission and focusing in strong scattering medium *(Invited Paper)*

Hui Cao, Yale Univ. (United States)

Strongly scattering media usually look opaque, even though the material has little absorption. Due to the diffusion of light, the average transmission varies as one over the thickness of the medium. It poses a severe limitation for biomedical imaging and telecommunication. We experimentally demonstrate that the total transmission through a multiple-scattering sample can be varied by one order of magnitude by shaping the incident wavefront of a monochromatic laser beam. Our theoretical analysis reveals that the mesoscopic correlations are essential to significantly modify the total transmission.

In recent years wavefront shaping has been widely used to focus light to wavelength-scale regions (speckles) inside or behind a turbid medium. Increasing the size of focal spot to contain many speckle grains is of great interest for several applications. We show with optical wavefront-shaping experiments that long-range correlations substantially increase the dynamic range of control over light transmitted onto larger target regions, when the number of targeted speckles inside the focal area exceeds the dimensionless conductance.

Finally, we study the optimal diffusive transmission of broadband or polychromatic light in a disordered medium. A single input wavefront can exhibit strongly enhanced total transmission across a bandwidth that is orders of magnitude broader than the spectral correlation width of the medium. This is attributed to the long-range spectral correlations in coherent diffusion.

10347-9, Session 2A

Gaussian vs. Bessel light-sheets: performance analysis in live large sample imaging *(Invited Paper)*

Michael P. MacDonald, Sascha L. Reidt, Ricardo B. C. Correia, Cornelis J. Weijer, Univ. of Dundee (United Kingdom)

Light-sheet microscopy was selected as the Nature Method of the Year 2014 and has become a fundamental imaging technique in modern biology. Conventional Gaussian light-sheets are inherently limited by the trade-off between the beam waist and its depth of field, resulting in a non-uniform excitation across the field of view. Lately, Bessel and Airy lightsheets have been proposed because of their larger depth of field and their stability towards on-axis obstructions.

Recent studies describe the advantages of using Bessel beams and report an improved image quality, for example when imaging Arabidopsis root or when imaging cellular dynamics. Lightsheet microscopy is particularly suited to imaging the in toto development of live large samples, and Bessel beams have been applied for imaging organs of transgenic zebrafish. However, for the study of large scale and coordinated cell movements in embryonic development a quantitative analysis of its performance is still missing.

In our paper, we describe a novel application to Bessel beam light-sheet microscopy on large, living and highly scattering chick embryos and its potential use in answering important biological questions regarding coordinated cell movements, cell ingression and cell shape changes. We show that whilst using Bessel illumination can be of significant help when imaging thicker samples due to the increased depth of field, there is little or no benefit for overcoming light scattering during gastrulation in chick embryos.

10347-10, Session 2A

3D microscopy with scattering media *(Invited Paper)*

Laura Waller, Univ. of California, Berkeley (United States)

This talk will describe new methods for computational 3D microscopy with coded illumination and detection systems that use simple hardware modifications combined with efficient computational algorithms.

10347-11, Session 2A

Sculptured light for control and measurement on microscales *(Invited Paper)*

Alexander B. Stilgoe, Anatolii V. Kashchuk, Timo A. Nieminen, Halina H. Rubinsztein-Dunlop, The Univ. of Queensland (Australia)

Dynamic manipulation (using beam shaping) of light is an important tool with wide ranging applications in image analysis and optical micro-manipulation. We use dynamic manipulation of incident and scattered light to determine the properties of both resting/naturally moving and optically trapped particles. The application of specialized beam modes and careful analysis of scattered light can extract particular information from the system to determine the fundamental properties of objects under investigation. With appropriate choice of detector, improved sensitivity and bandwidth is also possible. We will overview measurements of position, force and angular momentum transfer and current research developments.

Dynamic manipulation (beam shaping) of light is an important tool with wide ranging applications in image analysis and particle manipulation. The use of dynamic manipulation of light enables very extensive determination of the properties of optically trapped particles. The archetypal measurement of a trapped particle is to detect aggregate properties of the light that it scatters, such as the change in average scattering direction to measure optical forces. Total angular momentum transfer could also be measured as an aggregate property of the scattered light. We investigate the performance changes in measurements of the properties of objects using optical mode shaping and the filtering of sculptured light fields. We demonstrate that position measurement performance can be significantly increased when specific modes are optimized. Through the appropriate choice of filter and detector, measurements can be performed with both high-bandwidth and sensitivity. We demonstrate measurements using both liquid crystal spatial light modulators and digital micromirror devices and discuss a specific behavior in each experiment and their performance. We further discuss challenges that occur in development of these techniques as well as their use when applied in specific experiments and more broadly outline possible uses of the methods in practical applications. This presentation will give an overview of both past successes in measurement of position, force and angular momentum transfer as well as current research developments.

10347-12, Session 2B

High fidelity beam shaping for optical neuroscience

Wolfgang Losert, Mitchell Weikert, Samira Aghayee, Univ. of Maryland, College Park (United States)

Optical neuroscience has surged in recent years. Advances in fast fluorescent calcium indicators and optically addressable ion channel now allow for two-photon imaging and perturbations of neuronal activity. Since most meaningful neuronal activity involves firing of multiple neurons, beam shaping with Phase-only Spatial Light Modulators (SLM) is emerging as a powerful approach for photo-stimulation of selective neurons in the brain. The ability to form any desired illumination pattern and to modify the wavefront at high speeds is essential to trigger neuronal activity in meaningful ways. Since the wavefront is aimed at modulating brain activity, it is important to minimize imperfections in beam shaping, in particular speckles and non-uniformities in intensity. Here we present an optical arrangement that allows for the removal of the unmodulated light from the path at the Fourier plane. The proposed configuration is effective enough to eliminate the need for removing the unmodulated light in two-photon applications. We find that this modified beam path not only removes speckles, but also increases the uniformity of peak intensities.

10347-13, Session 2B

Probing mechanobiology with laser-induced shockwaves

Christopher Carmona, Daryl Preece, Veronica Gomez-Godinez, Linda Z. Shi, Michael W. Berns, Univ. of California, San Diego (United States)

Traumatic Brain Injury (TBI) occurs when an external force injures the brain. According to the Center of Disease Control and Prevention, TBI is a contributing factor to a third of all injury-related deaths in the United States. Those that survive TBI can face temporary or permanent effects that significantly impact thinking or memory, movement, sensation, or emotional functioning. While clinical outcomes of TBI can vary widely in severity, few mechanisms of neurodegeneration following TBI have been identified for treatment. We propose a model for studying TBI using laser-induced shockwaves (LISs). To further our understanding on the way that cells respond to shear stress, an optical system was developed that allows single cells to be studied in response to a sudden but short application of shear stress. This system can generate LISs at a specified time and location. The LIS exerts a shear stress between 0 - 50 kPa depending on the distance from the shockwave epicenter. Our system utilizes an optically-coupled force measurement component that allows for the visualization of shockwave dynamics. Here, the force measurement system is characterized by imaging stages of the approximately 40 ns period of violent expansion and collapse of microbubbles responsible for shockwave generation. Ultimately, this system's capacity to quantitatively study shockwave dynamics permits the study of the spatiotemporal details occurring in cells in response to shear stress. Thus, TBI can be further studied and subsequent results could reveal the molecular basis for neurodegeneration and potential therapeutic avenues for treatment.

10347-14, Session 2B

Printing hydrogel based living neural networks

Anna M. Linnenberger, Meadowlark Optics, Inc. (United States)

We investigate holographic optical tweezing combined with step-and-repeat projection micro-stereolithography for fine control of live cell positioning within a three-dimensional (3D) hydrogel microstructure. Samples are fabricated using NT2 cells, which have been pre-differentiated into NT2-N human neurons. A twisted nematic 256x256 pixel SLM is used to pattern the supporting hydrogel structures. Neurons are shown to grow along printed hydrogel channels, demonstrating that the structure can be used to pre-determine the path of cellular growth. Sample viability is assessed for a variety of hydrogel geometries. This work demonstrates biocompatibility of the printing method. The samples fabricated with this system are a useful model for future studies of neural circuit formation, neurological disease, cellular communication, plasticity, and repair mechanisms.

10347-15, Session 3A

Nanohole optical tweezers in hetergeneous mixture analysis

Reuven Gordon, Gurunatha K. Laxminarayana, Noa Hacohen, Timothy S. DeWolf, Univ. of Victoria (Canada)

Since 2012, we have been studying the use of double nanohole optical tweezers in the trapping of proteins and other nanoparticles. This talk will overview recent developments in using the platform to analyze heterogeneous samples, such as egg-white. We will also describe recent advances in the setup, including thermal control which has allowed for probing transitions in the dynamics of proteins. I will also overview our work on the analysis of acoustic Raman modes of proteins and quantitative comparison with elastic network models.

10347-16, Session 3A

Optical trapping and Raman spectroscopy of single nanostructures using standing-wave Raman tweezers

Mu-ying Wu, Lin He, Gui-hua Chen, Guang Yang, Dongguan Univ. of Technology (China); Yong-Qing Li, East Carolina Univ. (United States) and Dongguan Univ. of Technology (China)

Optical trapping integrated with spectroscopic techniques is attractive for manipulation and characterization of nanoscale structures, and opens up new possibilities for assembly and control of nanodevices and biomolecules. Optical tweezers integrated with Raman spectroscopy allows analyzing a single trapped micro-particle, but is generally less effective for individual nano-sized objects in the 10-100 nm range. The main challenge is the weak gradient force on nanoparticles that is insufficient to overcome the destabilizing effect of scattering force and Brownian motion. Here, we present standing-wave Raman tweezers for stable trapping and sensitive characterization of single isolated nanostructures with a low laser power by combining a standing-wave optical trap (SWOT) with confocal Raman spectroscopy. SWOT is formed by the interference of a tightly focused Gaussian beam with the reflected beam by a dichroic mirror. This scheme has stronger intensity gradients and balanced scattering forces, and thus is more stable and sensitive in measuring nanoparticles in liquid with 4-8 fold increase in the Raman signals. It can be used to analyze many nanoparticles that cannot be measured with single-beam Raman tweezers, including individual single-walled carbon nanotubes (SWCNT), graphene flakes, biological particles, polystyrene beads (100 nm), SERS-active metal nanoparticles, and high-refractive semiconductor nanoparticles with a low laser power of a few mW. This would enable sorting and characterization of specific SWCNTs and other nanoparticles based on their increased Raman fingerprints.

10347-17, Session 3A

Interfacial resistances and other thermal effects in plasmonic optical tweezers and their implications for nano-biomolecule manipulation

Steven Jones, Pawel Karpinski, Daniel Andrén, Mikael Käll, Chalmers Univ. of Technology (Sweden)

An emerging technique for the optical manipulation of nanoparticles is the method of plasmonic optical tweezers. This technique is particularly interesting for its potential applications in the study of small biomolecules such as proteins or DNA. Plasmonic optical tweezers utilize the plasmonic resonance of noble metal nanostructures to confine electric fields to deeply subwavelength length scales. Because of this extreme field confinement, the optical gradient forces generated are strong enough to stably trap sub 100 nm dielectric nanoparticles.

It is well known that these plasmonic structures also exhibit significant heat generation due to Ohmic resistance of the oscillating electrons. This heat generation is detrimental when attempting to study optically trapped bio-molecules, which are extremely sensitive to their thermal environment. Because of this conflict between the optical forces generated by plasmonic structures and the associated temperature increase, a detailed understanding of nanoscale thermal transport phenomena is crucial to designing plasmonic optical trapping systems for applications in bionanophotonics. In this work we utilize Raman scattering to directly observe the temperature of the plasmonic antennae; as well as Brownian motion analysis, and temperature dependent fluorescent techniques to determine the temperature of the surrounding environment and the nanoparticle itself. Interesting thermodynamic phenomena are investigated, such as the Kapitza resistance, which can cause discrete temperature discontinuities at the boundary between dissimilar materials. Combined with finite element method simulations this work provides a clearer understanding of the thermal environment experienced by optically trapped nanoparticles, and outlines strategies that can be employed to mitigate temperature increases allowing for these systems to be effectively utilized in the study of delicate bionanoparticles.

10347-18, Session 3A

Probing of biomolecular films with colloidal nanomotors

Hana Sipova, Lei Shao, Nils Odebo Länk, Mikael Käll, Chalmers Univ. of Technology (Sweden)

Advanced design of nanomaterials requires a large amount of control over the properties of nanoscale components, including nanostructured substrates as well as biomolecular components. While properties of solid-state nanostructures can be assessed with numerous imaging methods available, probing biomolecular ensembles is much more difficult to perform because of their small dimensions and high sensitivity to environmental changes. There is, therefore, a great need for nanoscopic probes to biomolecular layers in their native, aqueous environment.

Here we demonstrate an ultra-sensitive method for probing of thin biomolecular films with rotary nanomotors. Single-crystal gold nanorods are trapped in 2D against a glass surface in a laser focus and rotated extremely fast in aqueous solutions through optical torques dominated by plasmonic resonant scattering of circularly polarized light. The rotational dynamics of the nanorods is found to be highly dependent on the properties of adsorbed biomolecular layers, such as the length or conformation of adsorbed molecules. Moreover the localized heating in the vicinity of the nanomotors generated by light absorption is employed in manipulating temperature at the nanoscale and monitoring of the temperature-induced transitions of molecular films. By tracking of rotational dynamics of the nanorods in real time we can observe kinetics of biomolecular interactions and temperature-induced molecular transitions.

We believe, that the method developed based on rotary nanomotors could meet a wide range of applications in nanobiotechnology, such as design of new functional materials, investigation of fast temperature-induced molecular transitions, as well investigation of nanoscale properties of biomolecular films and ultra-sensitive biomolecular detection.

10347-19, Session 3A

Electrostrictive in-situ nanoparticle detection with coherent Rayleigh-Brillouin scattering *(Invited Paper)*

Alexandros Gerakis, Princeton Plasma Physics Lab. (United States); Mikhail N. Shneider, Princeton Univ. (United States); Yevgeny Raitses, Brentley C. Stratton, Princeton Plasma Physics Lab. (United States)

We report on the development and application of coherent Rayleigh-Brillouin scattering for the in situ detection of large molecules and nanoparticles. This four wave mixing diagnostic technique relies on the creation of an electrostrictive optical lattice in a medium due to the interaction between polarized particles and the intense electric field gradient created by the optical interference of two intense pulsed laser beams. Though this interaction, we can detect the temperature, pressure, relative density, polarizability and speed of sound of a gas and gas mixture. This diagnostic was already successfully demonstrated in atomic and molecular gaseous environments, where the different gas polarizabilities and pressures were successfully measured. We are currently conducting in situ measurements with large molecules and nanoparticles produced in an arc discharge, the results of which will be presented in this meeting.

10347-20, Session 3B

Reflective inverse diffusion method for dynamic compensation of small optical system perturbations

Kenneth W. Burgi, Michael Marciniak, Air Force Institute of Technology (United States)

Reflective inverse diffusion uses phase front modulation to refocus light after reflective scattering. A spatial light modulator (SLM) is used to shape the wave front of a HeNe laser at 632.8-nm wavelength to produce a converging phase front after reflection. The reflection matrix (RM), measured from rough-surface reflectors, contains the phase information of the light from each SLM segment to every segment in the observation plane. This phase information can be used to produce phase maps that can refocus light to any segment in the observation plane. Phase maps created from

an RM refocused light to a single segment in the observation plane with demonstrated enhancements up to 25 times over the background speckle. The measurement of an RM requires the optical system to be completely static. Small perturbations in the laboratory setup cause significant decreases in enhancement performance. We present a method for reflective inverse diffusion that improved enhancement performance by dynamically compensating for small perturbations in the optical system. A continuously optimized phase map is used to update a diffraction-based propagation model. This model then determines the proper phase map to produce a single focused spot or multiple foci at any location in the observation plane.

10347-21, Session 3B

Beam shaping by the transport-of-intensity equation

Soheil Mehrabkhani, Thomas Schneider, Technische Univ. Braunschweig (Germany)

In this paper, a novel unified approach for beam shaping based on a phase retrieval technique by the use of the transport-of- intensity equation is presented. In principle, an arbitrary target profile can be generated by an appropriate phase modification of the input profile. The necessary phase information can be calculated by the transport-of-intensity equation. The axial intensity derivative of the equation is a fundamental requirement for its solvability. Although it can be easily calculated for the near distance between input and target planes, the determination of the intensity derivative for a far distance still has been reminded an open problem. For a solution of this obstacle, an intensity distribution in an auxiliary plane at an infinitesimal distance from the input plane has been used. The new intensity distribution is obtained from the given intensity information in two planes and consequently, the desired intensity derivative can be calculated by the difference of the intensity values in the first and auxiliary plane. Finally, from the transport-of-intensity equation, the phase information might be achieved. Thus, the target profile can be reconstructed by the phase and intensity values in the input plane. To verify the validity of this approach, the reconstructed and original target profiles are compared based on the correlation method. For a practical implementation, a phase shaper can be used to generate the required phase distribution in the input plane.

10347-22, Session 3B

Optimal trapping beam for spherical micro-particles

Michael Mazilu, Univ. of St. Andrews (United Kingdom)

Scattering is one of the simplest light mater interactions possible. For spherical particles, this process can be described using the Lorenz-Mie theory, which makes use of vector spherical harmonic solutions of Maxwell's equations to represent the fields involved. Using these solutions it is possible to describe the light field scattered from microscopic spherical particles and thus represent the field around a scattering object as a function of the incident fields. These solutions also allow us to determine the optical momentum transfer to the scattering object. This can be calculated using Maxwell stress tensor. Here, we use this approach to calculate the quadratic relationship between the incident field and the optical forces acting on the scattering objects. This relationship defines also a set of orthogonal optical eigenmodes, which delivers a natural basis to describe momentum transfer in light-matter interactions. Using this natural description of the momentum transfer it is possible to define, for each numerical aperture, particle size or geometry the optimal trapping beam in 1, 2 or 3 dimensions. We present a study as a function of the particle parameter and conclude on the maximum achievable trapping stiffness enhancement factor as a function of these parameters.

10347-23, Session 3B

Multi-focus beam shaping of high power multimode lasers

Alexander V. Laskin, AdlOptica Optical Systems GmbH (Germany); Joerg Volpp, Bremer Institut für angewandte Strahltechnik GmbH (Germany); Vadim V. Laskin, AdlOptica Optical Systems GmbH (Germany); Aleksei B. Ostrun, ITMO Univ. (Russian Federation)

Beam shaping of powerful multimode fiber lasers, fiber coupled solid-state and diode lasers is of great importance for improvements of industrial laser applications. Welding, cladding with millimetre scale working spots benefit from "inverse-Gauss" intensity profiles; performance of thick metal sheet cutting, deep penetration welding can be enhanced when distributing the laser energy along the optical axis as more efficient usage of laser energy, higher edge quality and reduction of the heat affected zone can be achieved. Building of beam shaping optics for multimode lasers encounters physical limitations due to the low beam spatial coherence of multimode fiber coupled lasers resulting in big Beam Parameter Products (BPP) or M? values. The laser radiation emerging from a multimode fiber presents a mixture of wavefronts. The fiber end can be considered as a light source which optical properties are intermediate between a Lambertian source and a single mode laser beam. Imaging of the fiber end, using a collimator and a focusing objective, is a robust and widely used beam delivery approach. Beam shaping solutions are suggested in form of optics combining fiber end imaging and geometrical separation of focused spots either perpendicular to or along the optical axis. Thus, energy of high power lasers is distributed among multiple foci. In order to provide reliable operation with multi-kW lasers and avoid damages the optics are designed as refractive elements with smooth optical surfaces. The paper presents descriptions of multi-focus optics, intensity profile measurements of beam caustics and experimental results of welding technology improvement.

10347-24, Session 3B

Generation of arbitrary vector beams

Benjamin Perez-Garcia, Tecnológico de Monterrey (Mexico); Carlos López-Mariscal, Underwater Photonics (Mexico); Raul I. Hernandez-Aranda, Julio C. Gutiérrez-Vega, Tecnológico de Monterrey (Mexico)

Optical vector beams arise from point to point spatial variations of the electric component of an electromagnetic field over the transverse plane. In this work, we present a novel experimental technique to generate arbitrary vector beams, and provide sufficient evidence to validte their state of polarization. This technique takes advantage of the capability of a Spatial Light Modulator to simultaneously generate two components of an electromagnetic field by halving the screen of the device and subsequently recombining them in a Sagnac interferometer. Our experimental results show the versatility and robustness of this technique for the generation of vector beams.

10347-25, Session 4A

Single-cell and single-molecule biosensing with optical nanosensors *(Invited Paper)*

Qimin Quan, The Rowland Institute at Harvard (United States)

Fluorescence imaging provides a powerful approach to study fundamental life processes and has become an integral part of the toolbox for biologists. In this talk, I will present optical nanosensors as a new tool; and how we push it to the limit for the applications of translational medicine. Two examples will be given to represent two distinct architectures to solve medical problems at single molecule and single cell level, respectively. The

first example is a "lab-on-a-chip" device that can measure binding kinetics between two single molecules without fluorescent labeling. The second example is a "lab-on-a-tip" device that monitors protein expressions in single living cells over time. These nanosensor approaches, complementary to fluorescent imaging, will broaden our understanding of basic life processes at molecular level and will provide new ways for drug discovery and disease diagnostics.

10347-26, Session 4A

An ultra-fast EOD-based force-clamp detects rapid biomechanical transitions

Michael S. Woody, E. Michael Ostap, Yale E. Goldman, Pennsylvania Muscle Institute (United States)

We assembled an ultra-fast infrared optical trapping system to detect mechanical events that occur less than a millisecond after a ligand binds to its filamentous substrate, such as myosin undergoing its 5 – 10 nm working stroke after actin binding. The instrument is based on the concept of Capitanio et al. (Nat Meth 9, 1013–1019, 2012), in which a bead-actin-bead dumbbell is held in two force-clamped optical traps. An applied force from the traps causes the filament to move at a constant velocity as the force from hydrodynamic drag resists the applied load. When the ligand binds, the filament motion stops within 100 ?s as the applied force is transferred to the attachment. Subsequent translations signal active motions, such as the magnitude and timing of the motor's working stroke. In our instrument, the beads defining the dumbbell are held in independent force clamps utilizing a field-programmable gate array (FPGA) to update the beam positions at 250 kHz. We found that in our setup, the acousto-optical deflectors (AODs) steering the beams were unsuitable for this purpose due to a slightly non-linear response in the beam intensity and deflection angle, likely caused by low-amplitude standing acoustic waves in the deflectors. These aberrations caused instability in the force feedback loop leading to artefactual ~20 nm jumps in position. This type of AOD non-linearity has been reported to be absent in electro-optical deflectors (EODs) (Valentina et al. Opt Lett 33, 599–601, 2008). We demonstrate that EODs improve the performance of our instrument. Combining the superior beam-steering capability of the EODs, force acquisition via back-plane interferometry, and the dual high-speed FPGA-based feedback loops, we smoothly and precisely apply constant loads to study the dynamics of interactions between biological molecules such as actin and myosin.

10347-27, Session 4A

Jamming of a single DNA molecule during nanoscale 3D confinement with attractive self interactions

Douglas E. Smith, Nicholas A. Keller, Univ. of California, San Diego (United States)

We use optical tweezers to study viral DNA packaging, a model for studying the physics of charged polymers under tight 3D confinement. Single DNA molecules ~6600 nm in length are translocated into a ~50 nm-diameter phage phi29 capsid through a nanochannel by a molecular motor. Theories and simulations predicted that attractive DNA-self interactions mediated by +3 or +4 ions would facilitate faster packaging with less force resisting confinement. However our experiments found the opposite—packaging stalls at much lower densities than achieved in purely repulsive conditions. We present studies that suggest that packaging stalls because the DNA undergoes a nonequilibrium jamming transition of the type used describe colloidal and granular systems in soft-matter physics. An abrupt deceleration is observed before stalling, indicating that a transition in DNA conformation causes an abrupt increase in resistance. Experiments in which conditions are changed during packaging also show that the dynamics are history-dependent. Our findings suggest that the concept of a jamming transition can be applied to a single polymer molecule.

10347-28, Session 4A

Evanescent single-molecule biosensing with quantum limited precision

Nicolas P. Mauranyapin, Lars Madsen, Michael A. Taylor, Muhammad Waleed, Warwick P. Bowen, The Univ. of Queensland (Australia)

Evanescent optical biosensors that operate label-free and can resolve single molecules have applications ranging from clinical diagnostics, to environmental monitoring and the detection and manipulation of viruses, proteins and antibodies.

Here, we demonstrate an optical nanofibre-based approach to evanescent detection and tracking of unlabelled biomolecules that utilises a combination of heterodyne interferometry and dark field illumination. This greatly suppresses technical noise due to background scatter, vibrations and laser fluctuations that has limited previous experiments, allowing operation at the quantum noise limit to sensitivity introduced by the quantisation of light.

We apply our biosensor to the detection of single unlabelled biomolecules, an application that has not previously been demonstrated using a nanofibre sensor. We perform measurements on low concentration solution of BSA and anti-E.coli antibody. BSA, in particular, has a 3.5 nm radius, and is among the smallest biomolecules detected using plasmonic and cavity-enhanced techniques. By achieving quantum noise limited performance, we increase the information that is extracted per scattered photon and we achieve state-of-the-art sensitivity with optical intensities five orders of magnitude lower than has been possible previously. This opens the door to apply quantum correlated photons to enhance the precision of single molecule biosensors. Moreover, the reduction of intensity enables studies of molecules behaviour for an extended period of time and can lead to the understanding of biological phenomena at the single molecule level, such as cell membrane formation and molecular motor motion with high sensitivity, in real time.

10347-29, Session 4A

Trapping-assisted analysis of single particles using integrated nanopores *(Invited Paper)*

Holger Schmidt, Mahmud Rahman, Mark Harrington, Univ. of California, Santa Cruz (United States); Matthew A. Stott, Aaron R. Hawkins, Brigham Young Univ. (United States)

Nanopores are nanoscale openings in thin membranes that have shown the potential for advanced electrical detection of single molecules based on ionic current blockades resulting from individual particles translocating through the pore. This technology is a forerunner for next generation sequencing. However, nanopores can form the basis of more advanced integrated sensors that can respond to a multitude of different targets and can be integrated with other detection modalities. Recently, we have demonstrated the combined electro-optical detection of single viruses and single nucleic acids on optofluidic chips that incorporate solid-state nanopores [1-3]. Here, we discuss the addition of optical trapping to further increase the functionalities of these devices. Examples include the use of a loss-based dual beam trap [4,5] for increasing translocation rates, and the combination of feedback controlled particle gating into an optofluidic channel with a waveguide-based ABEL trap [6] for high-throughput single bioparticle analysis.

[1] S. Liu, Y. Zhao, J.W. Parks, D.W. Deamer, A.R. Hawkins, and H. Schmidt, "Correlated Electrical and Optical Analysis of Single Nanoparticles and Biomolecules on a Nanopore-Gated Optofluidic Chip", Nano Letters, 14, 4816-4820 (2014).

[2] S. Liu, T.A. Wall, D. Ozcelik, J.W. Parks, A.R. Hawkins and H. Schmidt, "Electro-optical detection of single ?-DNA", Chemical Communications 51, 2084 (2015).

[3] S. Liu, A.R. Hawkins and H. Schmidt, "Optofluidic devices with integrated solid-state nanopores", Microchimica Acta 183, 1275 (2016).

[4] S. Kühn, P. Measor, E.J. Lunt, B.S. Phillips, D.W. Deamer, A.R. Hawkins, and H. Schmidt, "Loss-based optical trap for on-chip particle analysis", Lab on Chip, 9, 2212 (2009).

[5] S. Kühn, P. Measor, E.J. Lunt, B.S. Phillips, A.R. Hawkins, and H. Schmidt, "Optofluidic particle concentration by a long-range dual-beam trap", Optics Letters, 34, 2306-2308 (2009).

[6] S. Kühn, E.J. Lunt, B.S. Philips, A.R. Hawkins, and H. Schmidt, "Ultralow power trapping and fluorescence detection of single particles on an optofluidic chip", Lab Chip 10, 189 (2010).

10347-30, Session 4A

Direct measurement of a nonequilibrium system entropy using a feedback trap *(Invited Paper)*

Momcilo Gavrilov, John Bechhoefer, Simon Fraser Univ. (Canada); Raphael Chetrite, Univ. de Nice Sophia Antipolis (France)

The entropy function for an equilibrium system has a Gibbs-Shannon form; however, there is a long, sometimes contentious debate as to whether the Gibbs-Shannon form applies to systems out of equilibrium. Here, we report the first direct measurement of the entropy function for a system out of equilibrium. In a feedback trap, we confine a silica bead immersed in water in a virtual double-well potential that models a two-state system capable of storing one bit of information. By measuring the average work to erase a controlled fraction of the information, we isolate directly the change in entropy in a nonequilibrium system and show its compatibility with the Gibbs-Shannon form.

10347-31, Session 4B

Programmable diffractive optic for multi-beam processing: applications and limitations

Patrick Gretzki, Arnold Gillner, Fraunhofer-Institut für Lasertechnik (Germany)

A wide range of materials can be processed with ultra-short laser pulses with minimal thermal stress. These processes are used for the specific ablation and surface structuring in many applications. Due to low productivity, a direct processing on an industrial scale is not economical, so these processes are limited to indirect procedures like the structuring of injections molds. The available average laser power for modern laser source can no longer be used efficiently, so new optical systems are needed. In this paper we will discuss the field of applications and limitations for multi-beam processing based on diffractive optics. Especially the utilization of spatial light modulators (SLMs) for dynamic beam shaping and division will be shown. The possibility for high quality beam splitting with a closed loop feedback system will be presented. For industrial applications the suitability of the system has been evaluated for high average laser powers and it could be confirmed, that the modulation properties of the SLM can be held constant with an adapted cooling system. In combination with a galvanometer scanner the optics can be used for applications like thin film structuring, drilling of sieves and filters. A detailed analysis of the bottleneck regarding processing speed for different applications shows, that with suitable laser sources the yield of current applications can be significantly increased.

10347-33, Session 4B

Vectorial field propagation through high NA objectives using polarized Gaussian beam decomposition

Norman Girma Worku, Herbert Gross, Friedrich-Schiller-Univ. Jena (Germany)

Scalar fields can be propagated through non-paraxial systems using the Gaussian beam decomposition method. However, for high NA objectives, this scalar treatment is not sufficient to correctly describe the electromagnetic fields inside the focal region due to high ray bendings, which result in a significant change in the polarization state of light. To model these vectorial effects, the Gaussian beam decomposition method has to be extended to include the polarization state of light. In this work we have combined it with three dimensional polarization ray tracing in order to propagate vectorial fields through high NA optical systems. During Gaussian beam decomposition, each individual beamlet has a polarization vector [Ex,Ey,Ez] associated with its central ray. Individual Gaussian beams are then propagated through the system using the complex ray tracing method. The effect of the optical system on the polarization state of each beam is computed by applying the three dimensional polarization ray tracing of the corresponding central rays. Finally the individual beams are superposed coherently in the plane of interest resulting in the complete vectorial field. We apply the proposed method to compute the vectorial field inside the focal region of a high NA microscope objective lens and compare our result to the Richards-Wolf integral method. We find that the Gaussian beam decomposition method overcomes serious limitations of algorithms relying on Fourier transforms, i.e. the field sampling requirements are less critical in high NA focusing and in the presence of large aberrations. However, sharp edges in the amplitude profile are difficult to handle as they should be replaced with smooth Gaussian edge.

10347-34, Session 4B

Fraunhofer and Fresnel diffraction pattern of a Mathieu-Gauss beam through rectangular aperture

Cristian Hernando Acevedo Cáceres, Yezid Torres Moreno, Univ. Industrial de Santander (Colombia); Angela M. Guzmán , CREOL, The College of Optics and Photonics, Univ. of Central Florida (United States)

The Mathieu-Gauss beams are unique and exhibit remarkable behavior in a variety of 3D applications such as optical manipulation of matter. These beams are characterized by the ellipticity parameter q, and the integer m, which is termed the mode order or charge. In these beams the total orbital angular momentum l is distinct of the value of the parameter m, i.e. physically be stressed . In this work we analyze the diffraction pattern in the Fraunhofer and Fresnel regime of a Mathieu-Gauss beam through a rectangular aperture theoretically and experimentally. This work allow describe how the orbital angular momentum and the topological charge of a beam are different concepts but are equal them for field distributions with azimuthal symmetry.

10347-35, Session 4B

Arbitrary manipulation of micro-particles in three dimensions by steering of multiple orbital angular momentum modes

Ting Xie, Huihui Wang, Fei Yuan, Shengqian Chang, Peng Sun, Siman Zhang, Huaye Li, Zhenrong Zheng, Zhejiang Univ. (China)

Optical tweezers is an increasingly important technique for controlling

and probing particles since computer-generated holography (CGH) make steering of multiple traps individually possible. In addition, the dark focus of orbital angular momentum (OAM) beams is increasingly widely used in trapping reflecting, absorbing or low-dielectric-constant objects. In this paper, we present a method to create arbitrary three-dimensional configurations of orbital angular momentum modes to achieve manipulation of micro-particles. Compared with conventional optical tweezers, this method can steer mixed patterns of traps individually and randomly by producing three-dimensional structure of optical vortices. These optical traps we used was formed by a CGH generated complex phase mask, which has three components: 1) a helical phase mask to change the transverse phase structure, 2) a blazed grating phase mask to vary the propagation direction of the incident beams, and 3) a modulated grating phase mask to divert the focal plane from the planar configurations. The latter one ensure that we can form three-dimensional trapping patterns. The trap patterns can also be generated dynamically by holographic display system based on liquid crystal on silicon (LCoS). The experimental results show that the refresh frequency of reconfiguring achieves 24fps. Our method is effective and promise an exciting new opportunity to be used as a valuable non-contact manipulation tool in various applications.

10347-36, Session 4B

Propagation of transverse linear and orbital angular momenta of beam waves

Mikhail I. Charnotskii, Consultant (United States)

We show that for paraxial propagation of scalar waves classic electromagnetic theory definitions of transverse linear (TLM) and orbital angular (OAM) momenta of beam waves are simply related to the wave coherence function in the coherent wave case. This allows the extension of the TLM and OAM density concepts to the case of partially coherent waves when phase is indeterminate. We introduce a general class of Radial Irradiance-Angular Phase (RI-AP) waves that includes the Laguerre-Gaussian (LG) beams, and similar to LG beams has discrete OAM to power ratio, but have more complex phase shape than simple helices of LG beans. We show on several examples that there no direct connection between the intrinsic OAM and optical vorticity. Namely, neither the presence of the optical vortices is necessary for the intrinsic OAM, nor the presence of the optical vortices warrants the non-zero intrinsic OAM. We examine OAM for two classes of partially-coherent beam waves and show that the common, Schell-type coherence, does not add variety to the TLM and OAM in comparison to coherent waves. However, Twisted Gaussian beam has an intrinsic OAM with per unit power value that can be continuously changed by varying the twist parameters. This analysis suggests an intrinsic OAM creation method based on rotation of tilted Gaussian beam. Using the parabolic propagation equation for the coherence function, we show that both total TLM and OAM are conserved for the free space propagation, but not for propagation in inhomogeneous medium. In the presence of the random inhomogeneous medium the total TLM and OAM are conserved in average, but the OAM fluctuations grow with the propagation path. This growth appears to be slower for the beams with rotation-symmetric irradiance.

10347-37, Session 5

Angular momentum exchange between light and small particles

Masud Mansuripur, College of Optical Sciences, The Univ. of Arizona (United States)

We present a few simple examples to illustrate certain fundamental properties of the EM field. Using elementary physical concepts, we explain the nature of interactions that involve exchanges of energy, linear momentum, and angular momentum between EM fields and material media. First, the radiation force experienced by a small, polarizable particle which has a predetermined dielectric susceptibility will be examined. The dielectric susceptibility of small spherical particles will be related to their refractive index (with proper accounting for the effects of radiation resistance). We describe the relation between the energy and orbital angular momentum of a cylindrical harmonic EM wave trapped inside a hollow cylindrical cavity, and explore the relations among the energy, linear momentum, and angular momentum picked up by a small particle under illumination by a cylindrical harmonic EM wave. In light of this analysis, it becomes clear why a small particle spins around its own axis when illuminated by a light beam that carries spin angular momentum, whereas the same particle tends to orbit around an axis of vorticity when exposed to a beam (such as a vector cylindrical harmonic) that possesses orbital angular momentum.

10347-38, Session 5

Hybrid entanglement for quantum communication and information applications

Isaac M. Nape, Bienvenu I. Ndagano, Univ. of the Witwatersrand (South Africa); Benjamin Perez-Garcia, Tecnológico de Monterrey (Mexico); Stirling Scholes, Melanie McLaren, Univ. of the Witwatersrand (South Africa); Raul I. Hernandez-Aranda, Tecnológico de Monterrey (Mexico); Filippus S. Roux, National Metrology Institute of South Africa (South Africa); Thomas Konrad, Univ. of KwaZulu-Natal (South Africa); Andrew Forbes, Univ. of the Witwatersrand (South Africa)

Combining the multiple degrees of freedom of photons has become topical in quantum communication and information processes. This provides advantages such as increasing the amount of information that is be packed into a photon or probing the wave-particle nature of light through path-polarisation entanglement. Here we present two experiments that show the advantages of using hybrid entanglement between orbital angular moment and polarisation. Firstly, we present results where high dimensional quantum key distribution with spatial modes that have non-separable polarisation-OAM DOF called vector modes. Secondly, we show that through OAM-polarisation entanglement, the traditional 'which-way' experiment can be performed without using the traditional physical path interference approach.

10347-39, Session 5

Dynamics of optically levitated microparticles in vacuum placed in 2D and 3D optical potentials possessing orbital angular momentum

Yoshihiko Arita, Michael Mazilu, Mingzhou Chen, Tom Vettenburg, Juan M. Auñón Garcia, Univ. of St. Andrews (United Kingdom); Ewan Wright, College of Optical Sciences, The Univ. of Arizona (United States); Kishan Dholakia, Univ. of St. Andrews (United Kingdom)

We demonstrate the transfer of orbital angular momentum to optically levitated microparticles in vacuum. We prepare two-dimensional (2D) and three-dimensional (3D) optical potentials. In the 2D case the microparticle is placed within a Laguerre-Gaussian beam. We explore the particle dynamics as a function of the topological charge of the levitating beam. Our results reveal that there is a fundamental limit to the orbital angular momentum that may be transferred to a trapped particle, dependent upon the beam parameters and inertial forces present. Whilst a Laguerre-Gaussian beam scales in size with azimuthal index, recently we have created a "perfect" vortex beam whose radial intensity profile and radius are both independent of topological charge. As the Fourier transform of a perfect vortex yields a Bessel beam, imaging a perfect vortex, with its subsequent propagation thus realises a complex 3D optical field. In this scenario we load individual silica microparticles into this field and observe their trajectories. The optical gradient and scattering forces interplay with the inertial and gravitational forces acting on the trapped particle, including the rotational degrees of

freedom. As a result the trapped microparticle exhibits a complex 3D motion that includes a periodic orbital motion between the Bessel and the perfect vortex beam. We are able to determine the 3D optical potential in situ by tracking the particle. This first demonstration of trapping microparticles within a complex 3D optical potential in vacuum opens up new possibilities for fundamental studies in levitated optomechanics.

10347-40, Session 5

Highly birefringent, liquid-crystalline microspheres are tuneable rotational probes for optical tweezers

Avin Ramaiya, Basudev Roy, Erik Schäffer, Eberhard Karls Univ. Tübingen (Germany)

Birefringent particles serve as probes for rotation measurements using optical tweezers. However, current probes are often difficult to fabricate, have a limited size range, are unstable in aqueous solutions, or have a small birefringence. Here, we used spherical microspheres composed out of the liquid-crystal precursor RM257 that were solid at room temperature and stable in aqueous solutions. The microspheres were produced in wide range of different sizes by a standard precipitation protocol. For large microspheres, the liquid crystal was in the nematic state and had a very high birefringence. When trapped with circularly polarized optical tweezers, microspheres rotated. Interestingly, the rotation peak in the rotational power spectrum had a shape corresponding to a sum of Gaussian and a Lorentzian function. We attribute this shape to a combination of thermal fluctuations and inertial effects of entrained water. Furthermore, we measured the birefringence as a function of particle size and discovered a topological radial-bipolar phase transition at a diameter of about 500,nm. For microspheres with a diameter of 1.2,mum, we measured rotation rates exceeding 7,kHz in aqueous solutions using a laser power of 1.2,W in the laser focus. This high rotation rate corresponds to a Reynolds number of 0.08 implying that inertial effects start to be relevant for a microscopic system. Among others, the particles are useful to study the rotational motion of biological, molecular machines.

10347-41, Session 5

Elliptical orbits of microparticles driven by an evanescent field *(Invited Paper)*

Lulu Liu, Harvard School of Engineering and Applied Sciences (United States); Andrea Di Donato, Univ. Politecnica delle Marche (Italy)

We report the elliptical motion of microparticles driven by a periodic evanescent field. We have fully characterized this motion experimentally and created a theoretical model based on the dynamics of Mie-particles under influence of near field optical forces and surface-induced hydrodynamic effects. The agreement between our model and experiments is confirmed by a series of measurements at an unprecedented level of precision. Our method offers an alternative to structured-light optics for inducing orbital motion in microparticles, with the inherent advantage of easy integration into lab-on-a-chip devices.

10347-42, Session 5

Speckles of an optical vortex and a perfect optical vortex: a comparative morphological study

Cristian Hernando Acevedo Cáceres, Univ. Industrial de Santander (Colombia); Sergey Sukhov, Aristide Dogariu, CREOL, The College of Optics and Photonics, Univ. of Central Florida (United States)

Optical vortex (OV) beams are electromagnetic waves with a helical wave front due to phase singularities, which are characterized by an integer topological charge related to the spatial distribution of their wavefront. The diameter of an optical vortex is related with its topological charge. This property causes difficulties to achieve a high spatial accuracy and high orbital angular momentum coupling optical vortices into a fiber. To solve these requirements, the concept the perfect optical vortex (POV) has been introduced as optical waves whose ring width size and average ring diameter (the arithmetic average of the inner and outer ring-diameters) are both independent of the topological charge. In this work we study theoretically and experimentally the speckle formation produced by scattering the OVs and POVs through a diffuser. It is found that the speckle size of the OVs decreases with the order of the topological charge in free space propagation and it do not have a appreciable cluster form. Also it is found that the speckle size of the POVs is independent of topological charge in free space propagation and the speckle size remains the same over a long propagation when a lens is placed at focal distance from the diffuser. In addition, we showed that the speckle grains generated by using the POVs form cluster with ringing correlation tails in the speckle intensity distribution. Finally, we proved experimentally that the Shannon entropy value is similar in the OVs and POVs speckle patterns.

10347-43, Session 6

Avoiding induced heating in temperature sensing by optical trapping

Patricia Haro-González, Paloma Rodriguez Sevilla, Univ. Autónoma de Madrid (Spain); Yuhaix Zhang, National Univ. of Singapore (Singapore); Francisco Sanz-Rodríguez, Francisco F. Jaque, José García Solé, Univ. Autónoma de Madrid (Spain); Xiaogang Liu, National Univ. of Singapore (Singapore); Daniel Jaque, Univ. Autónoma de Madrid (Spain)

The trap heating during optical manipulation is an important issue mainly when optical tweezers are applied in biological studies. Temperature increase at the laser focus could be produced either by medium (water) absorption of the trapping wavelength (980 nm) or by heating release of the trapped particle after trapping light absorption. This is not a negligible effect and, indeed, it has been the subject of study of a number of papers appearing in the field of optical trapping. In those cases, alternatives should be found to minimize this effect.

A control of the intra trap temperature could be performed by photothermal sensors, such as NaYF4:Er3+,Yb3+ upconverting particles. This thermometer allows for real time determination of the optical trap temperature. Two methods have been proposed to reduce the temperature loading due to medium absorption of the trapping wavelength or by the optically trapped particle itself: shift of the trapping wavelength out of the water absorption band, and use of time-modulated laser trapping beams. By using the mentioned thermometers, both approaches have been proved to reduce temperature heating at the trap position.

10347-44, Session 6

High-speed position and force measurements in optical tweezers

Anatolii V. Kashchuk, Alexander B. Stilgoe, Timo A. Nieminen, Halina H. Rubinsztein-Dunlop, The Univ. of Queensland (Australia)

Position measurements of the light spot are used in a large variety of applications: from laser guidance and beam alignment to atomic force microscopy and tracking of microparticles. It is also an important procedure in optical tweezers for most quantitative measurements. For example, we track the position of the trapped particle by calculating the centroid and determine the optical force by measuring the change in the momentum of the trapping beam. The existing detectors provide either

accurate measurements, like in duo-lateral photodetectors, or high-speed measurements, such as quadrant photodiodes. Here we propose a detection method for performing ultrafast accurate beam tracking at high bandwidth. The idea of the method is to use a filter with a linear transmittance in order to modulate the amplitude of the input beam in such a way that the transmitted intensity of the light is proportional to the displacement of the trapping beam. After the linear filter, the intensity of the beam is detected by a high-speed photodetector. As the task of finding the position of the centroid reduces to an intensity only measurement, it is possible to use smaller and faster photodetectors. By varying the gradient of the filter, we can also tune the sensitivity of our position detector. We compare the approach experimentally with both duo-lateral and quadrant detectors. We show that our method provides versatile and accurate measurements while ensuring high bandwidth in the measurement of the beam position and optical force.

10347-45, Session 6

Multi-modal microscopy platform including optical tweezers and the need to perform spherical wave vectors decompositions for optical force and signal intensity calculations *(Invited Paper)*

Carlos Lenz Cesar, Univ. Federal do Ceara (Brazil) and Instituto de Física “Gleb Wataghin” (Brazil); Wendel L. Moreira, Petrobras (Brazil); Antonio A. R. Neves, Univ. Federal do ABC (Brazil); André A. de Thomaz, Univ. Estadual de Campinas (Brazil); Diogo B. Almeida, Univ. of Michigan (United States); Adriana Fontes, Univ. Federal de Pernambuco (Brazil); Hernandes F. Carvalho, Vitor B. Pelegati, Univ. Estadual de Campinas (Brazil)

We will present the multi-modal photonic platform including Optical Tweezers, linear and non linear optics techniques in a single instrument to allow parallel information gathering during single cell processes. The platform includes the following techniques: multipoint Optical Tweezers; Laser cutting; multi/single photon fluorescence, Fluorescence Lifetime Imaging (FLIM); Förster Resonant Energy Transfer (FLIM-FRET); Fluorescence Correlation Spectroscopy (FCS); Raman; Second/Third Harmonic Generation (SHG/THG); Coherent AntiStokes Raman Scattering (CARS) and cascade CARS; Near field tip-enhancement and 1 and 2 photons Photoluminescence Excitation Spectroscopy (1-2 PLE). Next, we will discuss the issue of spherical wave vectors decomposition of any optical beam in the Fourier space without any approximation solving the problem of spherical Bessel functions cancellation in both sides of the expansion. This expansion is the necessary first step to perform optical forces, as well as optical signals intensities, of scattering/absorbing particles. The limit of Rayleigh regime is easily obtained.

10347-122, Session 6

Optical trapping of rare earth-doped nanorods using an optical fiber tweezers approach

Jochen Fick, Institut NÉEL (France); Godefroy Leménager, Maud Thiriet, Lahlil Khalid, Thierry Gacoin, Ecole Polytechnique (France); Francisco Valdivia-Valero, Gérard Colas des Francs, Univ. de Bourgogne (France)

$NaYF_4$:(Er,Yb,Gd) nanorods of different size were trapped using our original optical tweezers consisting of two fiber tips facing each other. Trapping properties were found to depended drastically on the actual particle size. Small rods were efficiently trapped whereas long rods were strongly attracted by the fiber tips and their stable trapping position was situated at the apex of one single fiber tip. In the case of the long particles the trapped particle modified the fiber tip emission properties and trapping of a second nanorod at distances of some microns from the first one is observed. These experimental results will be explained by numerical simulations using the exact Maxwell Stress Tensor approach.

10347-46, Session 7

Hybrid 3D optical and acoustic trapping *(Invited Paper)*

Monika Ritsch-Marte, Medizinische Univ. Innsbruck (Austria)

Optical trapping is a very precise and versatile method for the contactless manipulation of microscopic particles, but the rather weak optical forces pose some limitations on the size and number of particles that can be handled. Acoustic radiation forces induced by ultrasound in the MHz range offer alternative means for particle trapping, which are well suited for dealing with many or large particles, due to the much longer wavelength and lower energy density.

We present a hybrid setup comprising optical and acoustic trapping, by which the strengths of the individual methods can be united. As a particular feature we have implemented 3D acoustic trapping with independent control of the trapping strength in each direction. Optical trapping played a crucial role as a tool to characterize and optimize the acoustic forces when developing this device. It also helped to investigate experimental challenges due to the close contact of the objective lens with the device, which affects the acoustic resonances.

This device is designed to study the contactless formation and trapping of large cell clusters, while offering the ability to image and probe mechanical properties by optical forces on the single cell level.

10347-47, Session 7

Optically enhanced acoustophoresis

Michael P. MacDonald, Craig McDougall, Paul O’Mahoney, Univ. of Dundee (United Kingdom); Alan McGuinn, Nicholas A. Willoughby, Heriot-Watt Univ. (United Kingdom); Yongqiang Qiu, Univ. of Glasgow (United Kingdom); Christine E. M. Demore, Univ. of Toronto (Canada)

One of the most powerful tools available to a life scientist is the ability to use antibody labelling to achieve highly specific cell sorting. However, there are some applications where it is not possible to use labels for regulatory, cost or efficacy reasons. One such application is in cell therapy where the sorted cell product is to be introduced into a patient. Hence there is an unmet demand for scalable label free sorting methodologies capable of meeting the future needs of cell therapy bioprocessing.

Acoustic control of cells is well suited to handling large volumes of cells but does not have the specificity/selectivity available from optical manipulation. Here we present a method for enhancing the acoustophoretic effect through the use of the optical selection of particles in an acoustically confined analyte flow, combining the bulk handling abilities of acoustics with the specificity of optics.

Axially periodic dispersion of acoustically confined particles within a simple microcapillary, arising from the effects of the finite length of the capillary, are used to achieve acoustophoretic particle separation. This effect is by itself insufficient to lead to complete particle separation but, through the introduction of optical selection within the narrow acoustophoretic fractionation column, efficient and scalable sorting can be achieved. We will show examples of this hybrid sorting approach, which is particularly well suited to extracting rare-species from a flow, as will be needed for future cell therapy bioprocesses.

10347-48, Session 7

Simultaneous optical trapping and imaging in axial plane

Yansheng Liang, Ming Lei, Zhiliang Cao, Yue Wang, Shaohui Yan, Manman Li, Dan Dan, Yanan Cai, Zhaojun Wang, Baoli Yao, Xi'an Institute of Optics and Precision Mechanics, CAS (China)

Optical tweezers has demonstrated great success in widespread applications, such as in life science, atom cooling and fundamental physics. Since most existing optical tweezers systems use single objective lens for both trapping and imaging, the trapping and imaging planes are confined to the same focal plane. To track the trapped micro-particles along axial direction, different volumetric imaging and tracking techniques have been developed to extract the axial information from the 3D image stacks, but at the cost of complex measurement schemes and challenging calibration procedures [1]. Therefore, a direct visualization method of trapped objects is highly desirable in many studies. G. Thalhammer et al. [2] employed a right-angle prism to directly image the trapped particles in axial plane in 2011, but the method was limited in macro-trapping with low magnification. Here, we further advance this approach by implementing the prism into a tight-focusing holographic optical tweezers setup combined with fluorescent imaging. Simultaneous optical trapping and imaging in axial plane are demonstrated with several types of optical traps structured by spatial light modulator. We have successfully trapped 3 silica beads along axial direction with Gaussian traps array of 1?3, and axially aligned the silica beads like a chain with focused Bessel beam. Moreover, the trajectory of the transported micro-particle driven by an Airy beam has been obtained. The technique proposed here may provide a new angle of view in optical trapping and imaging, and promote the combination of optical trapping and microscopic imaging.

10347-49, Session 7

Optical vortex response to introduced phase objects

Mateusz M. Szatkowski, Agnieszka Popiolek-Masajada, Jan Masajada, Wroclaw Univ. of Science and Technology (Poland)

Optical Vortex Scanning Microscope (OVSM) uses focused laser beam with embedded optical vortex to scan the sample. The optical vortex can be moved inside the focused light spot by shifting the vortex lens (which generates optical vortex). This new scanning method was tested experimentally with simple phase micro-objects. It was shown that our system is sensitive to small phase disturbances which have an impact on both optical vortex position and phase profile. One of the challenges for the OVSM is finding the effective procedures for surface topography reconstruction. We proposed a new experimental setup to support the works focused on this problem. The Spatial Light Modulator (SLM) is used as an object generator. SLM allows to generate any phase disturbance with specified value and size, which can be easily introduced into the beam carrying optical vortex. Our system gives an opportunity to measure optical vortex response due to phase modifications introduced by the SLM as well as vortex sensitivity. We tested how object position, size, phase value affects phase distribution around vortex and position of vortex point inside the beam. Phase retrieval algorithm, noise analysis and results of experiments will be presented. These results show the way in which the OVSM should be developed.

10347-50, Session 8

Tutorial on optomechanics

James Millen, Univ. Wien (Austria)

In the last few years a remarkable field of study has emerged, in which we study the interaction of light with the mechanical motion of massive objects: optomechanics. With the introduction of an optical resonator, cavity optomechanical systems have been cooled to their motional ground state. This means that objects many microns in size have been observed exhibiting quantum behaviour.

Optomechanical systems can be used to coherently transduce quantum signals, or store them for long times, indicating that in the future they will be essential components in quantum networks. They also offer the potential for ultra-precise sensing, and the on-chip nature of many nanomechanical systems points the way to technological integration.

In this lecture I will introduce the basic mathematical structure of optomechanical systems, how they can be cooled, several detailed examples, and the major results from the field. I will also discuss the future implications, and the relevance to studying fundamental physics and the limits of quantum mechanics. There will be a particular focus on systems where the nanomechanical oscillator is levitated and isolated from the environment, due to its relevance to the Optical Trapping and Micromanipulation community.

10347-51, Session 9

Laser refrigeration of levitated nanocrystals

A. T. M. Anishur Rahman, Peter F. Barker, Univ. College London (United Kingdom)

Levitated optomechanics has seen significant progress over the last five years. While a considerable control over the centre-of-mass motion has been achieved, the internal temperature of levitated particles remains at best at room temperature. Here we report on the demonstration of internal cooling of levitated ytterbium doped yttrium lithium fluoride (Yb^{3+}: YLF) nanocrystals. Using anti-stokes laser refrigeration we demonstrate that trapped particles can be cooled from room temperature to 130 K. By controlling the amount of trapping power, and exploiting the interaction between polarised light and the particles natural birefringence, we demonstrate that the Yb^{+3}: YLF nanocrystals can be aligned along the direction of the trapping laser's electric field enhancing the refrigeration. We show that both the spectral emission from the levitated particle induced by the trapping laser and a modification to the damping rate of the particle in the trap, can be used to determine the temperature of the levitated particle.

10347-52, Session 9

Optical and magnetic measurements of a frequency-locked graphene nanoplatelet in a quadrupole ion trap

Joyce E. Coppock, Univ. of Maryland, College Park (United States); Pavel Nagornykh, The Univ. of Texas at Austin (United States); Jacob P. J. Murphy, Bruce E. Kane, Univ. of Maryland, College Park (United States)

Extremely sensitive force measurements can be performed on electrically charged nanoscale materials by levitating them in a quadrupole ion trap in high vacuum. In this talk, we discuss recent results[1] and ongoing investigations on the magnetic properties of a few-layer, micron-scale, rotating graphene nanoplatelet. To facilitate such measurements, we have developed a method of frequency-locking a nanoplatelet to a radio-frequency electric field, making use of the fact that the intrinsic electric dipole moment of the irregularly-shaped platelet couples to the applied electric field. The rotation frequency has been varied up to 100 MHz,

with higher frequencies expected to be possible. The particle's motion is detected optically, via the scattering of a low-power 532 nm laser.

We observe the dynamics of the frequency-locked platelet in response to applied magnetic fields. From frequency- and field-dependent measurements, we observe one magnetic moment arising from diamagnetism and another arising from the rapid rotation of the platelet, and we estimate their magnitudes and compare them to proposed theoretical properties of graphene. We determine a gyromagnetic ratio corresponding to the rotational moment, which is larger than would be expected for charge fixed to the outside of the platelet. We hypothesize that the excess magnitude of the gyromagnetic ratio may arise from the Barnett effect, in which a spinning object develops a magnetic moment even in the absence of net charge.

[1] Nagornykh et. al. (2016) https://arxiv.org/abs/1612.05928

10347-53, Session 9

Optomechanics of a levitated helium drop *(Invited Paper)*

Florian Marquardt, Friedrich-Alexander-Univ. Erlangen-Nürnberg (Germany)

Inside a levitated helium drop, one can have optical whispering gallery modes of very high finesse. These can couple to the vibrations of the drop surface. I will describe our theoretical predictions for both the case of Helium-4 (in its superfluid state), as well as Helium-3. In the latter case, there is an interesting additional coupling between vibrations and rotations which would eventually permit quantum non-demolition measurements of the drop's angular momentum.

10347-54, Session 9

Cooperative effects between color centers in diamond: applications to optical tweezers and optomechanics *(Invited Paper)*

Mathieu L. Juan, Institut für Quantenoptik und Quanteninformation (Austria)

Both an atom and a lump of dielectric material are polarizable objects that can be manipulated with optical light, a feature exploited separately in the fields of ultracold atoms and optical tweezers. In a recent experiment we have shown that the force from quantum emitters (Nitrogen-Vacancy colour centres, NVs) embedded in a dielectric nanosphere (nano-diamond) can be observed, even in liquid. Remarkably, the magnitude of this effect suggests that due to the large density of centres, cooperative effects between centres significantly contribute to the observed modification of the trapping strength. Along with experimental data, I will present the underlying mechanisms allowing for cooperative effects to be observed at room temperature and in the presence of large dephasing. This work enables the study of cooperativity in nanoscale solid-state systems and the use of atomic physics techniques in the field of nano-manipulation. In particular, by controlling such effects we envision various promising applications in the field optical tweezers where it may be possible to significantly enhance the optical forces acting on small nano-objects with embedded quantum emitters. In the context of optomechanics, we argue that it is experimentally feasible to have a scenario where the optical dipole force due to the embedded quantum emitters is stronger that the bulk dipole force acting on the dielectric host. This would allow to use repulsive optical potentials for dielectric nanospheres, by using the internal structure of the quantum emitters, to levitate them in evanescent fields analogously to what can be done with ultracold atoms.

10347-55, Session 9

Coherent control of single spins in optically levitated nanocrystals

Robert M. Pettit, Univ. of Rochester (United States); Levi P. Neukirch, Los Alamos National Lab. (United States); Yi Zhang, A. Nick Vamivakas, Univ. of Rochester (United States)

Nitrogen-vacancy (NV) centers in diamond provide a platform for room temperature spin manipulation, making them a strong candidate for inclusion in optical levitation experiments seeking to couple mechanical and spin degrees of freedom. Here, we report progress on the coherent manipulation of single NV center spins contained within optically levitated nanodiamond in a free-space optical dipole trap. The NV center spin is coherently manipulated at both atmospheric pressure and low vacuum, and while the trapping beam causes a reduction in the fluorescence emitted by the center, no reduction in the spin coherence is observed. Further, after an initial exposure to low vacuum, the nanodiamond remains at near room temperatures at all pressures and trapping powers considered in these experiments.

10347-56, Session 10

MilliKelvin cooling of the center of mass motion of a levitated nanoparticle

Nathanaël P. Bullier, Antonio Pontin, Peter F. Barker, Univ. College London (United Kingdom)

Many recent experiments have brought optomechanics one step closer for testing quantum mechanics at nanoscales and probing nonclassical motions. These breakthroughs include cooling oscillators to their quantum ground state [1], performing quantum non-demolition measurements [2] and measuring squeezed states of mechanical motion [3]. Levitated optomechanics has the advantages over previous experimental set-ups of providing greater isolation, higher mechanical Q factor and longer coherence times [4]. We use a hybrid electro-optical trap to levitate silica nanoparticles in a Fabry-Pérot cavity [5]. The Paul trap provides a deep potential that enables trapping at lower pressures. Once trapped, the particle can then be localized in an optical well. The optomechanical interaction between the trapped particle and the cavity field can currently be used to cool the centre-of-mass motion to milli-Kelvin temperatures [6]. To date these measured temperatures have been limited by technical noise in our system. We report on our latest measurements that implement a low noise homodyne detection scheme which probes the motion of the particle near the ground state.

[1] Laser cooling of a nanomechanical oscillator into its quantum ground state, Chan et al., Nature 478 (2011)

[2] Mechanically Detecting and Avoiding the Quantum Fluctuations of a Microwave Field, Suh et al., Science 344 (2014)

[3] Quantum squeezing of motion in a mechanical resonator, Wollman et al., Science 349 (2015)

[4] Cavity opto-mechanics using an optically levitated nanosphere, Chang et al., PNAS 107 (2010)

[5] Cavity Cooling a Single Charged Levitated Nanosphere, Millen et al., PRL 114 (2015)

[6] Nonlinear Dynamics and Strong Cavity Cooling of Levitated Nanoparticles, Fonseca et al., PRL 117 (2016)

10347-57, Session 10

Optical trapping and control of nanospheres inside hollow core photonic crystal fibers

David Grass, Nikolai Kiesel, Univ. Wien (Austria); Daniel R. Ladiges, John E. Sader, The Univ. of Melbourne (Australia); Markus Aspelmeyer, Univ. Wien (Austria)

We report a hollow core photonic crystal fiber based optical conveyor belt for levitated nano-particles in vacuum. An optical read-out allows monitoring the three-dimensional motion of the particle over the entire fiber length and is used for radiation pressure based feedback cooling. Besides the target application of controlled and clean delivery of nano-particles into ultra-high vacuum for levitated optomechanical systems we utilize read-out and feedback cooling to investigate the local pressure along the fiber when a pressure gradient is applied. We compare the measurements with predictions from a direct simulating Monte Carlo method of the nonlinear Boltzmann equation.

10347-58, Session 10

Developing optomechanical inertial sensors using whispering gallery mode resonances *(Invited Paper)*

Ying Lia Li, Peter F. Barker, Univ. College London (United Kingdom)

Experiments in cavity optomechanics readily obtain measurements of displacement and force with unprecedented sensitivity, and many now approach or surpass quantum limits. In the work presented here, the optomechanical coupling between a whispering gallery mode (WGM) optical resonance and the centre-of-mass mechanical motion of the WGM cavity itself is exploited for inertial sensing. This system is shown to detect micro-g accelerations (g=9.81 ms^(-2)), with prospects towards obtaining quantum limited sensing. The development of an automated, portable prototype is described and results from field testing will be presented.

10347-59, Session 10

Rotational optomechanics with levitated nanorods

Stefan Kuhn, Univ. Wien (Austria); Benjamin A. Stickler, Univ. Duisburg-Essen (Germany); Alon Kosloff, Fernando Patolsky, Tel Aviv Univ. (Israel); Klaus Hornberger, Univ. Duisburg-Essen (Germany); Markus Arndt, James Millen, Univ. Wien (Austria)

Optical control over nano-mechanical structures has become a valuable tool for tests of fundamental physics and force sensing applications. In order to achieve optimal performance of such devices, their dissipation to the environment needs to be minimized. Levitating nanoparticles in external fields is a possible solution which opened up the growing field of levitated optomechanics. Here we extend this work to the rotational degrees of freedom of optically levitated silicon nanorods[1]. We track and manipulate their linear and rotational motion by exploiting the polarization of two counter-propagating, focussed laser beams. This allows us to gain full control over the ro-translational dynamics of the rod. We will discuss the prospects of our levitated system for sensing applications as well as for realising rotational optomechanics and cavity cooling [2,3] which may be an important step towards high-mass matter-wave interference experiments with nanoparticles.

[1] Kuhn, S., Kosloff, A., Stickler, B. A., Patolsky, F., Hornberger, K., Arndt, M., and Millen, J., Full Rotational Control of Levitated Silicon Nanorods. arXiv:1608.07315 (2016)

[2] Kuhn, S., Asenbaum, P., Kosloff, A., Sclafani, M., Stickler, B. A., Nimmrichter, S., Hornberger, K., Cheshnovsky, O., Patolsky, F., and Arndt, M., Cavity-Assisted Manipulation of Freely Rotating Silicon Nanorods in High Vacuum. Nano Lett., 15(8), 5604–5608 (2015)

[3] Stickler, B.A., Nimmrichter, S., Martinetz, L., Kuhn, S., Arndt, M., and Hornberger, K., Rotranslational cavity cooling of dielectric rods and disks. Phys. Rev. A, 94, 033818 (2016)

10347-60, Session 11

Translational and rotational motion of Janus particles trapped in optical tweezers *(Invited Paper)*

Honglian Guo, South China Univ. of Technology (United States); Jing Liu, Institute of Physics, Chinese Academy of Sciences (China); Baoqin Chen, South China Univ. of Technology (China)

We study the rotation behavior of gold-coated Janus colloidal particle in optical traps. The Janus particle is observed to stably rotate in the optical trap. Both the direction and the rate of rotation can be experimentally controlled. Numerical calculations reveal that the rotation is the result of spontaneous symmetry breaking induced by the uneven curvature of the coating patterns on the Janus particle. In addition, we report the cyclic round-trip motion of Janus particles in static line optical tweezers . Both experiment and simulation show that this cyclic translational and rotational motion is a consequence of the collective action of the gold-face orientation dependent scattering optical force, the gradient optical force, and the spontaneous symmetry breaking induced optical torque in di?erent regions of the line optical tweezers. This study indicates a novel way to construct large quantities of fully functional motors for nano- or microdevices.

10347-61, Session 11

Maximum likelihood estimation in optical tweezers-based force sensing

Robert Meissner, Cornelia Denz, Westfälische Wilhelms-Univ. Münster (Germany)

Quantitative estimation of optical forces with artificial microprobes in optical tweezers is typically used to determine micro-rheological and biomechanical properties of living cells in both viscous and viscoelastic media. In viscous media, force calibration is performed by fitting the measured power spectrum density of Brownian motion of a microprobe with a Lorentzian function yielding friction coefficient and a so-called corner frequency, the latter being the ratio of the friction coefficient and the trap stiffness. Thus, the desired trap stiffness is directly obtained. Theoretical requirements of calibration are demanding, and a variety of error sources such as aliasing, drift or parameter bias have been treated. However, there is an increasing demand in fitting sparse or low signal-to-noise data as they represent the typical situation in biophysical analysis of cells.

In our contribution, we focus on the influence of user-biased initial conditions, i.e. frequency range or averaging techniques employed in biophysical settings. These conditions control the amount of data and noise included in fitting. By comparing state-of-the-art least squares estimation (LSE) with a novel approach based on maximum likelihood estimation (MLE), we show numerically that MLE is more robust than LSE, especially when the corner frequency is close to the Nyquist frequency or when noise limits the available range of frequencies. We observe a biased corner frequency of LSE when frequency ranges and number of averages change. We compare features of LSE and MLE, and demonstrate how MLE increases the applicability of optical tweezers for in vitro and in vivo biometrology.

10347-62, Session 11

Dynamics of a driven two-particle system coupled by hydrodynamic interactions in optical tweezers

Shuvojit Paul, Indian Institute of Science Education and Research Kolkata (India); Abhrajit Laskar, Ronojoy Adhikari, Institute of Mathematical Sciences (India); Ayan Banerjee, Indian Institute of Science Education and Research Kolkata (India)

A single trapped mesoscopic particle in optical tweezers in a viscous fluid behaves as an overdamped harmonic oscillator subjected to stochastic forces arising from thermal fluctuations in the fluid. The large viscosity of the fluid damps out the inertial response of the particle entirely, so that even if it is driven by an external sinusoidal force, no motional resonance is observed. However, if two particles are trapped at separations comparable to their radii, the near-field hydrodynamic interactions lead to unexpected effects. Here, we measure the amplitude and phase response of a weakly trapped particle (probe) to the hydrodynamically mediated forcing from a nearby strongly trapped particle driven at a fixed frequency. The amplitude response shows a clear resonance as a function of the driving frequency of the strongly trapped particle, while the phase behavior emulates the velocity response to the driving force in damped driven harmonic oscillators – which is expected since the colloidal particles in our case are dissipatively coupled. We validate our experimental results by analytically solving the hydrodynamically coupled equations of motion of the two particles and obtain good matches between theory and experiment. The amplitude response of the probe is a sensitive function of the fluid viscosity suggesting the use of this setup for two-point microrheology. Indeed, we are able to measure the viscosity of different glyecerol-water solutions with good accuracy using our technique. Our technique can now be extended to study near-field hydrodynamic effects in viscoelastic fluids where the retarded hydrodynamic interactions will produce surprising responses.

10347-63, Session 11

Optically driven colloidal microscopic Taylor-Couette cell

Antonio Ortiz-Ambriz, Pietro Tierno, Univ. de Barcelona (Spain)

We present an optically driven colloidal microscopic rheometer based on the recent work of Williams et al. [1]. With optical tweezers, we create a colloidal corral that confines a highly packed system of particles. In addition, we introduce an inner triplet of superparamagnetic particles which we can drive by applying an in plane rotating magnetic field. The interplay between magnetic and optical forces allows us to experimentally build a two dimensional Taylor-Couette cell, in which the outer wall and inner wall move independently of each other. Such a system can be used to explore the rheological properties of confined colloidal suspensions at a microscopic scale. The small scale of this rheometer allows us to explore how deformations in the structure lead to shear thinning, and how the coexistence of ordering phases leads to depinning transitions. Despite the discrete nature of the system, we observe local instabilities in the response of the layers' flow to the applied shear, which is a characteristic of shear banding in larger systems. Besides the rheological phenomena, we believe that these type of experiments can be useful to develop the understanding of non-equilibrium many body systems.

Williams I. et al. Transmission of torque at the nanoscale. Nature Physics 12, 98–103 (2016)

10347-64, Session 11

Optical torques on upconverting particles for intracellular microrheometry

Paloma Rodriguez Sevilla, Univ. Autónoma de Madrid (Spain); Yuhai Zhang, National Univ. of Singapore (Singapore); Nuno de Sousa, Manuel I. Marqués, Francisco Sanz-Rodríguez, Daniel Jaque, Univ. Autónoma de Madrid (Spain); Xiaogang Liu, National Univ. of Singapore (Singapore); Patricia Haro-González, Univ. Autónoma de Madrid (Spain)

Upconverting particles (UCPs) are a new class of optical nanomaterials that are able to convert infrared excitation into visible light output, a unique attribute that has been exploited in a large variety of research fields ranging from energy harvesting to biomedicine. Their starring role has been further boosted by the recent demonstration of their three dimensional control and tracking by single beam infrared optical traps. Such possibility has opened the door for exciting new applications and, at the same time, it has raised new fundamental questions regarding light-matter interactions at the nanoscale.

We have demonstrate that, once a single UCP is incorporated into an optical trap, particle dynamics cannot be only described in terms of optical forces, since optical torques (OTQs) need to be considered. We have demonstrated that OTQs are responsible of the stable orientation of the UCP inside the trap. The combination of single-particle polarized spectroscopy and numerical simulations has evidenced the dominant role of magnetic dipole torques.

Moreover, numerical calculations and experimental data allowed us to use rotation dynamics of a optically trapped single UCP for environmental sensing. In particular, we have shown for the first time that cytoplasm viscosity could be measured by using the rotation time and thermal fluctuations of an intracellular optically trapped UCP.

Our study constitutes a groundbreaking contribution within the emerging areas of optical manipulation and bioapplications of UCPs. Furthermore, the dominant role of OTQs as well as the potential use of rotation dynamics for intracellular studies will be of great interest for the large scientific community working on particles as remote biosensors.

10347-65, Session 11

Optical measurements of nanoparticle vibrations for fluid mechanics on the nanoscale

Matthew A. Pelton, Univ. of Maryland, Baltimore County (United States)

Optical measurements of acoustic oscillations in metal nanoparticles provide a sensitive probe into the mechanical properties of materials at GHz frequencies and nanometer length scales. In these experiments, an incident pump laser heats the nanoparticles, leading to their expansion and the excitation of mechanical vibrations. The vibrations produce oscillations in the plasmon resonance frequency of the nanoparticles, which are monitored by measuring the change in transmission through the sample of a second, probe laser pulse. By making these measurements on a highly monodisperse sample of bipyramidal gold nanoparticles, we were able to determine both the frequency and the decay rate of the vibrations. Measurements on nanoparticles in different solvents made it possible to determine the portion of damping and the vibrational frequency shift that are due to coupling to the surrounding liquid environment. Viscous damping could account for results at low viscosities, but significant discrepancies were observed for higher viscosities. The discrepancies were ultimately resolved by accounting for the viscoelastic nature of the surrounding liquids. For more viscous liquids, relaxation times are higher, and thus more of the vibrational energy is stored as elastic energy in the surrounding liquid. This reduces damping, and the restoring force provided by the stored energy increases the vibrational frequency, the opposite of what would occur for an ordinary

Newtonian fluid. These measurements demonstrate that metal nanoparticles can serve as nanoscale rheometers, with the picosecond response times required to reveal viscoelastic effects in conventional liquids.

10347-66, Session 11

Absolute temperature measurements in optical tweezers by synchronized position and force measurement

Anatolii V. Kashchuk, Alexander B. Stilgoe, Timo A. Nieminen, Halina H. Rubinsztein-Dunlop, The Univ. of Queensland (Australia)

Optical tweezers as a tool for contactless manipulation of the micro- and nanoparticles are widely used to apply and measure forces in biological systems. Precise temperature measurements are crucial for biological objects, such as bacteria or cells, as they are highly sensitive to the heating effects. It is also an important parameter for calibrating an optical trap for force measurements.

It is difficult to measure the exact temperature of a trapped object. Temperature can be obtained from viscosity measurements as it is a temperature dependent parameter. A particle is tracked by a CMOS camera and the optical force is determined directly by measuring the change of the momentum of the laser beam. We shift the trapped particle from the equilibrium position by moving the stage. The Stokes drag forces the particle out of the focal spot and balances the optical force. The temperature can be obtained using known data of the viscosity of water or by measuring the viscosity of the bulk liquid with other methods. In this proposed method we combine viscosity measurements with optical force detection and measure a temperature in the optical trap with 0.2K precision.

The absolute nature of the force detection method makes it suitable for measuring optical forces in a non-linear region of the optical trap and in various environments with known viscosity-temperature dependency, increasing the signal-to-noise ratio and expanding the applicability of the temperature measurements. The proposed method does not require a precalibration of the force detector and, therefore, can be used for temperature independent calibration.

10347-67, Session 12

Flow through oil nanothreads *(Invited Paper)*

Colin Bain, Alex Hargreaves, Joshua Bull, Durham Univ. (United Kingdom); Buddhapriya Chakrabarti, Sheffleld Univ. (United Kingdom)

The oil-water interfacial tension in emulsions of heptane/AOT/brine are reduced to ultralow values (< 10 micronewtons/m) by control of the salinity and temperature. Under these conditions, the dimensionless ratio of the force constant of an optical trap to the interfacial tension is O(1) so optical tweezers can be used to deform oil droplets. We have shown previously (Soft Matter 7, 2517 (2011)) that if an oil drop is pulled apart with a pair of tweezers, the two daughter droplets remain attached by an invisible oil thread of nanometric thickness. Optical pressure induced on the trapped droplets can be used to pump oil through the nanothreads. In this paper we will show how the bending rigidity stabilises the nanothreads and that the spontaneous curvature results in stable nanothreads on only one side of the phase inversion point. Flow through the nanothreads is analysed in the slender approximation for fixed radius by matching a parabolic flow profile within the thread to the solution for flow past a rigid cylinder. The internal flow accounts for a minor part of the mass transport between two droplets: most of the volumetric flow arises from motion of the whole thread. Relaxing the assumption of fixed radius in order to balance the normal stresses results in a singularity in the thread radius, placing an upper limit on the length of the thread through which oil can be pumped at a given flow rate.

10347-68, Session 12

Development of a Bessel-beam-based optical guide of aerosolized nanoparticles for femtosecond x-ray diffractive imaging

Andrei V. Rode, Woei Ming Lee, The Australian National Univ. (Australia); Salah Awel, Xiaoyan Sun, Daniel Horke, Ctr. for Free-Electron Laser Science (Germany); Richard A. Kirian, Arizona State Univ. (United States); Jochen Ku?pper, Henry N. Chapman, Ctr. for Free-Electron Laser Science (Germany)

The manipulation of airborne particles by light driven by photophoretic forces arise from uneven thermal gradient imposed upon a particle. In this work, we constructed a funnel-shaped hollow-core laser beam that can stably utilised these thermal gradients and controllably manipulate graphite particles over different heights based on their masses. By measuring the trapped particles of different mass at different heights inside the optical funnel, we show a direct relationship of the force that acted on the particles at each position in the laser beam. This allows for calibration, and prediction of the trajectories of objects in the optical funnel depending on laser intensity, size and air pressure.

Furthermore, we combined a spatial light modulator (SLM) and an electrically tunable lens to construct a variable-divergence aberration-free vortex beam to facilitate the dynamic and stable axial and azimuthal positioning of optically levitated micrometer-size particles under normal atmospheric pressure. In addition, modulation of the beam divergence with a predicted oscillatory movement and resulted particle move into a different equilibrium position provides a measure of the mass of a single, isolated particle. Such touch-free positioning could potentially be useful in guiding biomolecules at the focus of an x-ray free electron laser, for the recording of its structure in femtosecond coherent diffractive imaging experiments. The driving signal of oscillatory motion can potentially be phase-locked to an external timing signal enabling synchronization of particle delivery into the x-ray focus with XFEL pulse train.

10347-69, Session 12

Optical fabrication and trapping of superconducting nanoparticles in superfluid helium

Masaaki Ashida, Yosuke Minowa, Osaka Univ. (Japan); Mitsutaka Kumakura, Univ. of Fukui (Japan); Yuta Takahashi, Fusakazu Matsushima, Yoshiki Moriwaki, Univ. of Toyama (Japan)

Laser ablation in liquids provides us a unique opportunity to fabricate novel nano-materials. Among chemically inactive liquids, superfluid helium having extremely low temperature, negligibly small viscosity, huge thermal conductivity, and high transparency in visible region generates an ideal cryogenic space for the fabrication of nano-materials and the optical manipulation of their motion. Recently, we successfully fabricated nano- and micro-particles by the laser ablation in superfluid helium with a nanosecond Nd:YAG laser. Surprisingly, we found single-crystalline microspheres of semiconductors, such as ZnO, CdSe, etc., with high sphericity and their efficient lasing of whispering gallery modes. [Scientific Reports 4, 5186 (2014).] Here we applied this method to metals, such as indium and rhenium. At low temperature these metals show superconductivity, of which dependence on the size has attracted much attention for a long time. To select superconducting particles, we utilized perfect diamagnetism caused by Meissner effect. Namely, we designed a magnetic trap with two permanent magnets for the superconducting particles. Thus we fabricated and trapped a single or several superconducting particles after the laser ablation in superfluid helium, and then we measured the temperature dependence of the trapping force by changing the temperature of liquid helium and examined the size dependence of the superconductivity.

10347-70, Session 13

Thermodynamics of radiation pressure and photon momentum

Masud Mansuripur, College of Optical Sciences, The Univ. of Arizona (United States)

Theoretical analyses of radiation pressure and photon momentum in the past 150 years have focused almost exclusively on classical and/or quantum theories of electrodynamics. In these analyses, Maxwell's equations, the properties of polarizable and/or magnetizable material media, and the stress tensors of Maxwell, Abraham, Minkowski, Chu, and Einstein-Laub have typically played prominent roles. Each stress tensor has subsequently been manipulated to yield its own expressions for the electromagnetic force, torque, energy, and linear as well as angular momentum densities of the electromagnetic field. We will present an alternative view of radiation pressure from the perspective of classical thermodynamics, invoking the properties of blackbody radiation in conjunction with gas-filled cavities that contain electromagnetic energy in thermal equilibrium with the container. In this type of analysis, Planck's quantum hypothesis, Einstein's A and B coefficients, the entropy of the gas, and the spectral distribution of the trapped radiation play the central roles.

10347-71, Session 13

Thermophoretic levitation of generic objects

Cheng Chin, Frankie Fung, Benjamin Foster, Mykhaylo Usatyuk, B. J. DeSalvo, Anita Gaj, The Univ. of Chicago (United States)

The levitation machine we demonstrate is based on pure thermophoretic force. At the center of a vacuum chamber is a 1-cm gap between a warm copper plate at room temperature and a stainless steel bucket filled with liquid nitrogen at T= 77?K. In the presence of a large temperature gradient, particles are levitated and trapped near the mid-plane between the top and bottom plates. A careful tuning of the pressure ensures the levitation force is stronger than gravity below the particle and weaker than gravity above the particle. Horizontal stability is provided by a inward radial heat flow toward the trap center. Such three-dimentional trapping stability offered by our system overcomes the Earnshaw's theorem for a static temperature field. We conducted quantitative comparison between the levitation force and the theoretical calculations. A good agreement with two theoretical models is concluded. We will report our system design, the performance of the levitation and address on future potential to levitation macroscopic objects.

10347-72, Session 13

Hopping hither and thither-examining Kramer's law and stochastic resonance with a levitated nanoparticle *(Invited Paper)*

Jan Gieseler, Harvard Univ. (United States) and ICFO - Institut de Ciències Fotòniques (Spain); Francesco Ricci, ICFO - Institut de Ciències Fotòniques (Spain); Loic Rondin, ETH Zurich (Switzerland); Raúl A. Rica, ICFO - Institut de Ciències Fotòniques (Spain); Marko Spasenovic, ICFO - Institut de Ciències Fotòniques (Spain) and Univ. of Belgrade (Serbia); Christoph Dellago, Univ. Wien (Austria); Lukas Novotny, ETH Zurich (Switzerland); Romain Quidant, ICFO - Institut de Ciències Fotòniques (Spain) and Institució Catalana de Recerca i Estudis Avançats (Spain)

Noise activated bistable systems are ubiquitous in nature since the dynamics of vastly different systems can be described by a fictitious particle hopping between two potential wells. Systems that fall into this class include quantum emitters, protein folding, phase transitions and neural signaling. Thus bistable systems play a prominent role in quantum and biophysics, chemistry and nanotechnology. However, given the complexity of the above mentioned systems, it does not surprise that results based on this model tend to be qualitative.

To gain further insight into the predictive power of theories based on noise activated dynamics in a double well potential, we investigate the bistable dynamics of an optically levitated particle in high vacuum with and without externally added noise. The high degree of control we have with this experimental platform allows us to tune and to calibrate all the system parameters. This allows us to compare our measurements quantitatively with the theoretical models.

We find excellent agreement with analytical models for the escape rate (Kramer's law) and the switching between the two potential wells and observe a clear signature of stochastic resonance. This demonstrates that a levitated nanoparticle in high vacuum is a versatile experimental platform for studying and simulating a wide range of stochastic processes and testing theoretical models and predictions.

10347-73, Session 13

A realization of an information machine with temporal correlations *(Invited Paper)*

Yael Roichman, Tamir Admon, Tel Aviv Univ. (Israel); Saar Rahav, Technion-Israel Institute of Technology (Israel)

We realize experimentally and in simulation an information machine which converts information to work. In our realization, a single particle is diffusing in a one dimensional channel. Fluid flow in the channel causes the particle to drift along one direction preferentially. A barrier placed at the end of the channel confines the particle to one side of the channel. If the fluid flow is weak in comparison to thermal forces, the particle is able to diffuse upstream, against the fluid flow, occasionally. During the machine's operation the particle is monitored continuously, each time it diffuses far enough upstream, away from the barrier, a feedback mechanism moves the barrier slightly closer to the particle, without acting on the particle or the fluid. Experimentally, this is realized using a low refractive index colloidal particle diffusing in a microfluidic channel and the barrier is made of a repelling laser beam. The particle is tracked using video microscopy, and holographic optical tweezers are used to control the barrier position. In a quasi-static mode of operation of the amount of used information is easily calculated through the Shannon entropy of uncorrelated steps. However, at faster rates of operation temporal correlations arise and their full characterization is required for assessment of the information used to operate the machine. We develop a scheme to calculate information at steady-state operation based on measured temporal correlations. We use this calculation to characterize the output power and efficiency of our information machine as a function of feedback cycle time.

10347-74, Session 13

New insights into barrier crossing processes using driven optical matter *(Invited Paper)*

Norbert F. Scherer, The Univ. of Chicago (United States)

No Abstract Available

10347-75, Session 14

Particle trapped by a non-conservative force under Brownian motion

Jack Ng, Hong Kong Baptist Univ. (Hong Kong, China);

Yongyin Cao, Hong Kong Baptist Univ. (Hong Kong, China) and Harbin Institute of Technology (China); Xiao Li, Hong Kong Baptist Univ. (Hong Kong, China); Che TIng Chan, Hong Kong Univ. of Science and Technology (Hong Kong, China)

A particle trapped by light typically also undergoes Brownian motion. This problem can be solved by solving the Langevin equation. We analytically and numerically solved the Langevin equation for a generalized harmonic oscillator with non-conservative forces, which governs the motion of an optically trapped particle under Brownian motion. It is shown that with non-conservative forces, equipartition theorem is no longer held because the non-conservative optical force keeps pumping energy into the system. However the equipartition theorem is still approximately valid in a heavily damped environment like water. The role of the parity-time symmetry and other symmetries in the stability of the optically trapping will also be discussed.

10347-76, Session 14

Short-time Brownian motion *(Invited Paper)*

Mark G. Raizen, The Univ. of Texas at Austin (United States)

Brownian motion has been the benchmark for classical transport in a disordered system for many years, and is characterized by diffusion. In 1907, Albert Einstein predicted that particle motion should be ballistic on very short time scales, rather than diffusive. Einstein concluded that this instantaneous velocity would be impossible to measure in practice, a prediction that held for over 100 years.

We report experiments with micron-sized beads held in optical tweezers. We developed novel methods for fast, shot-noise limited detection of laser-beam deflection. Using this system, we have resolved the instantaneous velocity of a Brownian particle in air and in liquid [1,2,3]. We use the velocity measurements to test the energy equipartition theorem. In liquid, we observe complex effects such as memory loss, and an anti-correlated thermal force. This work opens the possibility of studying the microscopic origins of dissipation due to viscosity of the fluid, and the onset of the arrow of time.

[1] T. Li, S. Kheifets, D. Medellin, and M. G. Raizen, Science 328, 1673 (2010).

[2] S. Kheifets, A. Simha, K. Melin, T. Li, and M. G. Raizen, Science 343, 1493 (2014).

[3] M.G. Raizen and T. Li, Physics Today 68, 56 (2015).

10347-77, Session 14

High bandwidth optical tracking of micro/nanoparticles

Muhammad Waleed, Lars Madsen, Catxere Andrade Casacio, Michael A. Taylor, Nicolas P. Mauranyapin, Warwick P. Bowen, Queensland Quantum Optics Lab. (Australia)

Since Einstein's explanation of Brownian motion of particles in the fluid in 1907, hydrodynamic interactions between particles and fluid have been studied extensively. For this purpose, optical tweezers is the fastest available tool to measure the displacement fluctuation of an optically trapped particle. In optical tweezers, the particle is trapped using a tightly focused laser beam. The particle scatters light both in even and odd modes of Gaussian beam and usually its position is detected by detecting both modes. Using this standard detection scheme, a major breakthrough appeared in 2011, where particle position was tracked at MHz speed which led to the observation of particle diffusion transition from normal to the ballistic Brownian motion. However, high power photodetectors are required to track particles in MHz regime.

In this work, we take a different approach to the high power detection problem. The information about the particle displacement is primarily in the odd spatial modes, while the trapping field is in the even spatial mode. Hence we can reduce the intensity without reducing the information by filtering out the even spatial modes. We perform the filtering using a split waveplate, which turns all the odd modes even, and a single mode fiber, which only transmits the first even mode (TEM00). This spatial mode filter detection would allow high power optical trapping and high bandwidth detection of particles without requiring high power photodetectors. This high-bandwidth optical tweezers system will be useful to better understand the fluid dynamics especially in biological fluids that are occurring at very short times scales (< microseconds).

10347-78, Session 14

Manipulating single and multiple biomolecules with dynamic temperature fields

Tobias Thalheim, Univ. Leipzig (Germany); Katrin Günther, TU Dresden (Germany); Michael Mertig, TU Dresden (Germany) and Kurt-Schwabe-Institut für Mess- und Sensortechnik e.V. (Germany); Frank Cichos, Univ. Leipzig (Germany)

One of the challenges of single molecule experiments in solution is the ability to trap and manipulate one or even multiple molecules against the erratic Brownian motion. Brownian fluctuations are fueled by thermal energy and increase in strength with increasing temperature. Therefore, it is at first glance counterintuitive to confine Brownian fluctuations with the help of elevated temperatures. In thermal non-equilibrium, however, temperature gradients induce thermo-phoretic and thermo-osmotic drifts, which provide our means for single particle and single molecule manipulation in solution.

We describe experiments which use optically heated metal nanostructures and metal films to create dynamical temperature profiles in solution. These temperature fields induce thermo-phoretic drift fields that act as effective potentials for objects suspended in liquids. As compared to their optical tweezers counterparts, thermophoretic trapping is force free. Combined with optical feedback mechanisms, such effective potentials can be shaped almost arbitrarily to store and manipulate single molecules. The inhomogeneous nature of the generated temperature fields further allows a trapping of a well defined number of molecules for interaction studies and the compression of conformational fluctuations of macromolecules. Dynamic reshaping of the virtual effective trapping potentials also provides access to fundamental principles of non-equilibrium statistical mechanics in thermal non-equilibrium such as the Jarzynski relation.

10347-100, Session PWed

Diffracted optical vortices by an angular aperture

Angela M. Guzmán , Univ. Nacional de Colombia (Colombia); Paula López, Jesús Herman Mendoza Castro, Zayda Paola Reyes Quijano, Yezid Torres Moreno, Univ. Industrial de Santander (Colombia)

The measurement of the topological charge of laser beams with orbital angular momentum (OAM) is key to deciphering information encoded in several AOM channels. Current techniques useful for that purpose are interferometry, diffraction through triangular apertures [1], diffraction through pentagonal apertures, and azimuthal and radial decomposition [2].

A less explored issue is the effect of diffraction of OAM beams through circular sectors. Jack et al. [3] studied the angular diffraction of Gaussian beams (whose OAM is zero) through a circular sector. By means of a Fourier transform of the truncated Gaussian they showed that the orbital angular momentum spectra of the transmitted beam has a sinc-shaped envelope centered at zero orbital angular momentum, the width of which increases as

the central angle of the circular sector decreases.

We analyze here the spectra of a laser beam with integer OAM that has been diffracted by a circular sector. We present results for circular sectors of different central angles. For a circular ϖ-sector, we also study the influence of the transmittance in the OAM spectra of the transmitted beam, using intensity attenuators consisting of nanometric thin films of titanium oxide with different thicknesses.

We use a spatial light modulator to generate the incoming OAM beam [1] and measure the evolution of the intensity profile of the diffracted beam as it propagates away from the circular sector. The spectra of the diffracted OAM beams are shown numerically and experimentally to have a sinc-shaped envelope centered at the OAM value of the incoming OAM wave.

References

[1] C.H. Acevedo Cáceres, C.F. Díaz Meza y Y. Torres Moreno, Intensidad en campo lejano de un haz de luz con momento angular orbital entero o no entero, Revista Científica Ingeniería y Desarrollo, Vol.32, No.2, Julio-diciembre, pp.161-178, (2014).

[2] C. Schulze, A. Dudley, R. Brüning, M. Duparré and A. Forbes, "Measurement of the orbital angular momentum density of Bessel beams by projection into a Laguerre–Gaussian basis", Appl. Opt. Vol.53, No.26, pp.5924-5933 (2014).

[3] B. Jack, M.J. Padgett and S. Franke-Arnold, Angular Diffraction, New Journal of Physics Vol.10, No.103013, 8pp. (2008).

10347-101, Session PWed

Angle-dependent rotation of calcite in elliptically polarized light

Catherine M. Herne, Natalie A. Cartwright, Matthew T. Cattani, State Univ. of New York at New Paltz (United States)

Calcite crystals trapped in an elliptically polarized laser field exhibit intriguing rotational motion. In this presentation, we show measurements of the angle-dependent motion, and discuss how the motion of birefringent calcite can be used to develop a reliable and efficient process for determining the polarization ellipticity and orientation of a laser mode. The crystals experience torque in two ways: from the transfer of spin angular momentum (SAM) from the circular polarization component of the light, and from a torque due to the linear polarization component of the light that acts to line up the optic axis of the crystal with the polarization axis of the light. These torques alternatingly compete and amplify each other, creating an oscillating rotational crystal speed. We model the behavior as a rigid body in an angle-dependent torque. We experimentally demonstrate the dependence of the rotational speed on the angular orientation of the crystal by placing the crystals in a sample solution in our trapping region, and observe their behavior under different polarization modes. Measurements are made by acquiring information simultaneously from a quadrant photodiode collecting the light after passing through the sample region, and by imaging the crystal motion onto a camera. We finish by illustrating how to use this model to predict the ellipticity of a laser mode from rotational motion of birefringent crystals.

10347-102, Session PWed

Uncovering the radial modes of vortex beams

Bereneice Sephton, Council for Scientific and Industrial Research (South Africa) and Univ. of the Witwatersrand (South Africa); Angela Dudley, Council for Scientific and Industrial Research (South Africa); Andrew Forbes, Univ. of the Witwatersrand (South Africa)

Beams carrying orbital angular momentum (OAM) are ubiquitous in many experiments carried out today and cover a wide range of research, from surface micro-structure processing to optical tweezers and communications. It follows that these beams are a significant factor in the outcome of these research areas. They are often generated through the use of phase-only modulation with elements such as spatial light modulators and q-plates due to the simplicity of the approach. Interesting consequences result from this generation principal which include the introduction of radial modes as they propagate. We experimentally demonstrate how this effects the distribution of power where a notable decrease in the desired fundamental mode power occurs with higher OAM beams in addition to an expansion in the power across these radial modes. This research additionally affirms their mathematical description as the recently introduced Hyper-Geometric Gaussian beams.

10347-103, Session PWed

Progress on optical trapping assay to measure DNA folding pathways in sperm

Ashley R. Carter, Luka Devenica, Amherst College (United States)

DNA undergoes a dramatic condensation in sperm nuclei. During this condensation, the DNA rapidly folds into a series of toroids when protamine proteins replace histone proteins. Measuring the mechanics and folding pathway for this incredible condensation is an important goal. Here, we report on progress to use an in vitro, optical trapping assay to measure the DNA folding dynamics for this process. In this assay, a single DNA molecule with its associated histone proteins is attached to a cover slip and to an optically trapped bead. Movement of the trapped bead applies a force on the DNA, stretching it to a particular DNA extension. When protamine is added the extension changes, allowing us to measure the preliminary folding dynamics for the process.

10347-104, Session PWed

Investigation on unwinding motion of papillomavirus, E1 helicase with force spectroscopy

Sihwa Joo, Korea Research Institute of Bioscience and Biotechnology (Korea, Republic of); Seung-Jae Lee, Seoul National Univ. (Korea, Republic of); Bong Hyun Chung, Korea Research Institute of Bioscience and Biotechnology (Korea, Republic of); Arne Stenlund, Cold Spring Harbor Lab. (United States); Mina Lee, Korea Research Institute of Standards and Science (Korea, Republic of); Tai Hwan Ha, Korea Research Institute of Bioscience and Biotechnology (Korea, Republic of)

Like other viruses, papillomavirus replicates its genetic information using its own helicase, E1. Especially at the early stage of infection of papillomavirus, multiple copy of the viral episome by E1 is related to the success of infection. Therefore, E1 has been studied as one of the anti-viral drug targets. In addition, E1 belonging to the SFIII family is the representative helicase to study eukaryotic replication system with SV40, large T-antigen helicase. Recently, single-molecule force spectroscopies have been in the spotlight for manipulating biomolecules and mimicking in vivo environment existing tension and torque. Therefore, magnetic tweezers is a robust tool to study enzymes like helicase interacting with DNA. E1 is the mono-hexameric DNA helicase. It is known to be assembled into a hexameric form and unwind the DNA strand in the 3' to 5' direction when ATP is present. However, it is controversial whether E1 grips single strand or both strands when E1 is the active form, and it is unrevealed for the unwinding motion of E1 particularly on the long range DNA scale. Therefore, we studied dynamic motion of E1 with the hairpin constructs under tension by magnetic tweezers on various DNA length scales.

10347-105, Session PWed

Photoionization of water molecules by a train of attosecond pulses assisted by a near-infrared laser: delay and polarization control

Lara Martini, Diego I. R. Boll, Omar A. Fojón, Consejo Nacional de Investigaciones Científicas y Técnicas (Argentina)

Basic reactions involving water molecules are essential to understand the interaction between radiation and the biological tissue because living cells are composed mostly by water. Therefore, the knowledge of ionization of the latter is crucial in many domains of Biology and Physics. So, we study theoretically the photoionization of water molecules by extreme ultraviolet attopulse trains assisted by lasers in the near-infrared range. We use a separable Coulomb-Volkov model in which the temporal evolution of the system can be divided into three stages allowing spatial and temporal separation for the Coulomb and Volkov final state wavefunctions. First, we analyze photoelectron angular distributions for di?erent delays between the attopulse train and the assistant laser field. The water molecule bound states are represented using the Moccia's monocentric wavefunctions. We compare our results for water and Ne atoms as they belong to the same isoelectronic series. Moreover, we contrast our calculations with previous theoretical and experimental work for Ar atoms due to the similarities of the orbitals involved in the reaction. Second, we study the effect of varying the relative orientations of the attopulse and laser field polarizations and we compare our predictions with other theories and experiments. We expect these studies contribute to the improvement of polarization experiments and the development of the attopulse trains and assistant laser fields technologies. Finally, we hope our work promote progress on the control of the chemical reactivity of water molecules since this could be useful in different fields such as radiobiology and medical physics.

10347-106, Session PWed

A single-molecule study of mutual relation between the vaccinia virus E3L protein and Z-DNA by magnetic tweezers

Mina Lee, Korea Research Institute of Standards and Science (Korea, Republic of); Sihwa Joo, Bong Hyun Chung, Korea Research Institute of Bioscience and Biotechnology (Korea, Republic of)

The vaccinia virus E3L protein plays an important role in viral infection to the host and suppression of the host immune response. It contains a dsRNA binding domain and a Z-DNA binding domain at its C-terminal and N-terminal regions, respectively. Z-DNA binding motif is known to be crucial for viral pathogenesis. Since sequences capable of forming Z-DNA are frequently found in promoter region of genes and Z-DNA formation alters the transcription activity, it is likely that E3L modulates the host gene expression by binding to Z-DNA and, thus, affecting its dynamics and stability. However, the effect of E3L on the properties of Z-DNA has not been studied well yet. To address this, we used magnetic tweezers which can apply torsion and tension to biomolecules. Negative supercoiling by magnetic tweezers generated Z-DNA in physiological condition. The dynamics of Z-DNA in the presence of E3L was monitored at various tensions and torsions. Interestingly, we found that superhelical density onset for Z-DNA formation was lowered by E3L. It indicates that E3L facilitates Z-DNA formation, probably by capturing transiently formed Z-DNA. Our result suggests that E3L might alter metabolic pathway of the host genome by pushing conformational bias to Z-DNA.

10347-107, Session PWed

Super-resolution plasmonic tweezers utilizing optical nonlinearity

Masayuki Hoshina, Nobuhiko Yokoshi, Hajime Ishihara, Osaka Prefecture Univ. (Japan)

As the laser technology advances, the targets of the laser manipulation have been shifting to nanoscale objects. One of the effective schemes to manipulate nanoparticles (NPs) such as single molecules is plasmonic tweezers, which utilizes localized surface plasmon resonance. If we create an array of metallic structures with many nanogaps (hot spots), it might be possible to trap NPs changing a trapping spot one by one with moving a laser beam. However, it will be difficult to choose a particular hot spot in the array because a number of spots are included in the beam cross-section though each spot is strongly localized beyond the diffraction limit. In order to overcome this limitation, we propose a super-resolution trapping scheme, where NPs are trapped only at a selected hot spot among multi spots in the beam cross-section.

We theoretically evaluate the radiation force exerted on a NP on the periodic metallic array assuming that the metallic array is irradiated concurrently with Gaussian and Laguerre Gaussian (LG) beams. We demonstrate that the NP is trapped only in a hot spot located at the beam center and at all the other spots covered by both the Gaussian and LG beams, NPs are repelled from the spots due to the resonant optical nonlinearity. This scheme is based on the principle similar to the stimulated emission depletion (STED) microscopy. The realization of the proposed super-resolution plasmonic tweezers will open a new avenue to develop a novel reaction field of single molecules.

10347-108, Session PWed

Manipulation of micro-bubbles in water by CW laser

Peter P. Maksimyak, Oleg V. Angelsky, Andrew P. Maksimyak, Elena I. Kurek, Yuriy Fedkovych Chernivtsi National Univ. (Ukraine)

Gas and vapor bubbles of nano- and micrometric sizes in aqueous solutions are interesting for many fundamental and applied research problems: thermodynamic studies of liquid superheating and phase transitions in nano-scale, microhydraulic and micromachinery manipulation, microoptics, diverse biomedical applications including the cell investigations, precise drug delivery and therapy

In this work we demonstrate a simple scheme for generation of microbubbles and their ensembles in water suspension containing colloidal light-absorbing nanoparticles (diluted suspension of the black ink for jet printers) based on the suspension heating by the moderately focused beam of the near-IR laser. The bubbles are formed around the ink particles due to the superheated water evaporation; however, the great number of closely situated heating centers (particles) provides macroscopic collective effects of the inhomogeneous temperature distribution which can be suitably regulated by the incident laser power. As a result, we demonstrate the possibility of controllable growth of bubbles up to sub-millimeter size. Under special heating regimes, based of the special temporal variation of the incident laser power, generation of spatially-ordered systems of bubbles with controllable size distribution is shown. The bubbles obtained and their ensembles show high stability and can exist long time provided that the illumination conditions are maintained. Their spatial localization is fixed within the bright spot, and the bubbles can be transported over the liquid volume together with the focal region of the beam.

10347-109, Session PWed

Microbubble trapping in inverted optical tweezers

Thomas J. Smart, Univ. College London (United Kingdom); Mehmet B. Ünlü, Bogaziçi Univ. (Turkey); Philip H. Jones, Univ. College London (United Kingdom)

Microbubble-enhanced ultrasound-induced sonoporation increases the permeability of cell membranes to bioactive materials. Since the cell membrane typically acts as an impenetrable barrier to water-soluble molecules, this enhanced uptake has clear implications for drug delivery and gene therapy. In order to better understand the role of microbubbles in sonoporation or to be able to develop efficient theranostic applications for microbubbles, it is crucial to have a means of manipulating and observing individual bubbles.

We have developed an inverted microscope optical tweezers for trapping and manipulation of microscopic gas bubbles. Trapping is achieved by a time-averaged optical trap using a rapidly-scanning Gaussian laser beam. Unlike holographic optical tweezers for microbubbles that employ a Laguerre-Gaussian beam, in this configuration the backwards-directed optical gradient force is sufficient to confine a microbubble against both the optical scattering force and the microbubble buoyancy. We have calibrated the optical trapping forces for microbubbles with a range of sizes, and determined the scanning trap configuration that produces the strongest confinement. These results are compared with a ray optics calculation of optical trapping force on microbubbles. Our system also includes a real-time "point-and-click" user interface for interactive selection, capture and isolation of individual microbubbles from a polydisperse population with optimal trap stiffness.

10347-110, Session PWed

Controllable rotation of microsphere chain in dual-beam fiber-optic trap with transverse offset

Xinlin Chen, Guangzong Xiao, Xiang Han, Wei Xiong, Hui Luo, Kaiyong Yang, National Univ. of Defense Technology (China)

Controllable rotation of the trapped microscopic objects has traditionally been thought of one of the most valuable optical manipulation techniques. The controllable rotation of a microsphere chain is achieved by the dual-beam fiber-optic trap with transverse offset. The experimental device is made up of a PDMS chip housing two counter-propagating fibers across a microfluidic flow channel. Each fiber is coupled with different laser diode source to avoid the generation of coherent interference, both operating at a wavelength of 980 nm. Each fiber is attached to a translation stage to adjust the transverse offset distance. The polystyrene microspheres with diameter of 10 μm are chosen as the trapped particles. The microfluidic flow channel of the device was flushed with the polystyrene microspheres solution by the mechanical fluid pump. At the beginning, the two fibers were strictly aligned to each other. Five microspheres were captured as a chain parallel to the axis of the fibers. When introducing a transverse offset to the counter-propagating fibers by adjusting the translation stages, the microsphere chain was observed to rotating in the trap center. When the offset distance was set as 9 μm, the rotation frequency was estimated to be 0.9Hz. Experiment shows that the rotation speed increases with the offset distance. the rotation speed could be accurately controlled by adjusting the translation stages. A comprehensive analysis has been presented of the characteristics of the rotation. The functionality of rotated chain could be extended to applications requiring microfluidic mixing or to improving the reaction speed in a localized environment, and is generally applicable to biological and medical research.

10347-111, Session PWed

Analysis of acceleration sensing in a dual-beam fiber-optic trap

Wei Xiong, Guangzong Xiao, Xiang Han, Xinlin Chen, Hui Luo, Kaiyong Yang, National Univ. of Defense Technology (China)

Optical fiber trapping is a technique utilized for manipulating micron-sized dielectric particles such as microspheres and biological cells. A dual-beam fiber-optic trap is designed to measure the acceleration in this article, which is created by the beams emerging from two coaxially aligned optical fibers. Acceleration of the system results in microparticle displacement along the sensitive axis, which is subsequently measured by optical detection to provide an acceleration measurement. We have analyzed the amplitude-frequency characteristics of the acceleration sensing system. The detection bandwidths of the system with the trapped polystyrene particles in various medium are discussed. Influences of thermal noise, detecting noise and laser noise act on the system are then analyzed. The acceleration sensing bandwidth is demonstrated to be dependent on the viscosity coefficient of the medium. The bandwidth is 1 kHz with the particle trapped in air atmosphere. And that is reduced to 1 Hz when the particle is in water. The computed results show that thermal noise (~1mg/√Hz) is the main factor that affects the acceleration-sensing ability. That can be reduced by lowering temperature and changing a low-viscosity medium. A limited sensitivity of several ?g/√Hz can be achieved when the thermal noise is ignored. Thus a low-noise and high-bandwidth acceleration sensing system based on dual-beam fiber-optic trap will be achieved with the particle in a vacuum environment.

10347-112, Session PWed

Pancharatnam-Berry phase optical elements fabricated by 3D printing for shaping terahertz beams

Arturo I. Hernandez-Serrano, Enrique Castro-Camus, Centro de Investigaciones en Óptica, A.C. (Mexico); Dorilian Lopez-Mago, Tecnológico de Monterrey (Mexico)

The design, fabrication and characterization of space-variant Pancharatnam-Berry phase optical elements (PBOEs) is presented for the terahertz regime (THz). These PBOEs are made out of polystyrene and were fabricated by commercially available three-dimensional printers, providing a simple and inexpensive solution for the generation of THz vector beams. The polarization structure was characterized by using a THz time-domain imaging system. These devices can find applications in future THz technologies and provide new tools for the study of polarization morphologies.

10347-113, Session PWed

Analysis of the geometric phase produced by homogeneous and inhomogeneous Jones matrices for applications in space-variant polarized beams

Arturo A. Canales-Benavides, Dorilian Lopez-Mago, Raul I. Hernandez-Aranda, Julio C. Gutiérrez-Vega, Tecnológico de Monterrey (Mexico)

If light travels a set of anisotropic elements, it acquires a dynamic and a geometric phase. The former is produced by the optical path length and the latter by the evolution of the polarization state on the Poincaré sphere. Here, we provide a practical formulation to evaluate both type of phases for any polarization state entering an optical system characterized by a Jones matrix. By employing an automated and robust interferometric experiment,

we observe characteristic behaviors depending on whether the system is homogeneous, with orthogonal eigenpolarizations, or inhomogeneous, with nonorthogonal eigenpolarizations. The results apply either for classical or quantum states of light and can be used for the design of Pancharatnam-Berry phase optical elements.

10347-114, Session PWed

Formation of optical energy flows using the biaxial crystal

Peter P. Maksimyak, Oleg V. Angelsky, Andrew P. Maksimyak, Elena I. Kurek, Yuriy Fedkovych Chernivtsi National Univ. (Ukraine)

Separate particles of micro- or nano-scale or the ensembles of such particles merged into complex (inhomogeneous in intensity, polarization and coherence) optical field can be used for detection and diagnostics of fine effects, viz. the presence of internal energy flows at such fields determined by various factors. This problem is among topical ones at the epoch of moving from micro-optics to nano-optics.

Optical fields with rich structure of the internal energy flows we using a biaxial crystal. Propagation of a slightly divergent (conical) light beam with prescribed linear polarization generates a complicated optical field with spatially inhomogeneous distributions of the intensity, phase and polarization, that is accompanied by the intricate pattern of the transverse energy flows. Such fields offer a variety of possibilities for microparticles' trapping and control, for example:

a) the intensity minima (maxima) form natural traps for absorbing (dielectric) particles due to the gradient forces;

b) phase singularities associated with the amplitude zeros are coupled with the vortex-like orbital flows able to induce the rotation of the particles trapped;

c) both the orbital and spin flows can induce directional motion of particles in the transverse plane;

d) the spin angular momentum density of the field may induce controllable spinning motion of particles depending on their position within the beam cross section;

e) the output field pattern can be easily modified via the controllable input and output polarization, which provides suitable means for fine spatial positioning of the trapped particles.

10347-115, Session PWed

Optical trapping with femtosecond laser pulses

Arijit K. De, Indian Institute of Science Education and Research Mohali (India); Anita Devi, Shaina Dhamija, Indian Institute of Science Education & Research Mohali (India)

Our group were the first to propose repetitive instantaneous trapping [1] and nonlinear optical effects [2] for trapping of nanoparticles. We also extended this work to Ray optics limit [3] and to arbitrary size limit (using generalized Lorentz-Mie theorem) [4, 5]. Using a home-built versatile femtosecond laser tweezer set-up, we also carried out experiments the results of which will be presented along with a discussion on the underlying theory.

References:

1. Applied Optics, 54, 7002-7006 (2015).

2. Optics Express, 24, 21485-21496 (2016).

3. Journal of Optics, under review.

4. Photonics 2016, OSA Technical Digest, Th4A.3 (2016).

5. Physical Review A, under review.

10347-116, Session PWed

Sorting and measurement of single gold nanoparticles in an optofluidic chip

Yuzhi Shi, Xiong Sha, Lip Ket Chin, Nanyang Technological Univ. (Singapore); Jiuhui Wu, Tianning Chen, Xi'an Jiaotong Univ. (China); Ai Qun Liu, Nanyang Technological Univ. (Singapore)

Gold nanoparticles have sparked strong interest owing to their unique optical and chemical properties. Their size-dependent refractive index and plasmon resonance are widely used for optical sorting, biomedicine and chemical sensing. However, there are only few examples of optical separation of different gold nanoparticles. Only separating 100-200 nm gold nanoparticles using wavelength selected resonance of the extinction spectrum has been demonstrated. This paper reports an optofluidic chip for sorting single gold nanoparticles using loosely overdamped optical potential wells, which are created by building optical and fluidic barriers. It is the first demonstration of sorting single nanoparticles with diameters ranging from 60 to 100 nm in a quasi-Bessel beam with an optical trapping stiffness from 10?10 to 10?9 N/m. The nanoparticles oscillate in the loosely overdamped potential wells with a displacement amplitude of 3–7 ?m in the microchannel. The sizes and refractive indices of the nanoparticles can be determined from their trapping positions using Drude and Mie theory, with a resolution of 0.35 nm µm?1 for the diameter, 0.0034 µm?1 and 0.0017 µm?1 for the real and imaginary parts of the refractive index, respectively. Here we experimentally demonstrate the sorting of bacteria and protozoa on the optofluidic chip. The chip has high potential for the sorting and characterisation of nanoparticles in biomedical applications such as tumour targeting, drug delivery and intracellular imaging.

10347-117, Session PWed

Parallel alignment of bacteria using near-field optical force array for cell sorting

Haitao Zhao, Yi Zhang, Lip Ket Chin, Peng Huat Yap, Nanyang Technological Univ. (Singapore); Kuan Wang, Academia Sinica (Taiwan); Wee Ser, Ai Qun Liu, Nanyang Technological Univ. (Singapore)

This paper presents a near-field approach to align multiple rod-shaped bacteria in parallel. The conventional optical tweezer requires complex configurations, such as a dual-beam setup, to align a bacterium in-plane for direct observation, and also has limitations in parallel bacterial manipulation. In order to solve the problem, a near-field approach is proposed based on the interference pattern in silicon nano-waveguide arrays. This method is a promising toolbox for parallel single-cell analysis and is anticipated to benefit the research of single-cell biophysical characterization, cell-cell interaction, etc.

The waveguide array is composed of 101 silicon waveguides (width: 300 nm, height: 220 nm, gap: 200 nm). When a focused light (wavelength: 1550 nm, power: ~300 mW) is applied to the central waveguide, it is coupled evanescently to the adjacent waveguides and forms an interference pattern. The patterned optical field exerts two forces on the particle: a gradient force toward the surface and an overall scattering force toward the direction of light propagation. When a rod-shaped bacterium flows through the optical field, one end could be first trapped by the gradient force and then acts as an "anchor" on the surface. Thereafter, the bacterium is rotated both in the x-y plane by the scattering force to the equilibrium position, and in the x-z plane by the gradient force until contacting the surface. In the experiment, the Shigella bacteria is rotated 90 deg and aligned to horizontal direction in 9.4 s. Meanwhile, ~150 Shigella is trapped on the surface in 5 min and 86% is aligned with angle < 5 deg.

10347-118, Session PWed

Force tracing: a method to sculpt the optical force

Alireza Akbarzadeh, Foundation for Research and Technology-Hellas (Greece); Christophe Caloz, Ecole Polytechnique de Montréal (Canada)

One of the long-lasting controversies in the electrodynamics of light-matter interaction is the problem of optical momentum in a medium, which has engendered an enormous number of debates for more than a century. Aside from the prominent canonical controversy, optical force has played a crucial role in different applications such as optical trapping, optical microscopy, optical holograms, and optical tractor beams. In this presentation, we will briefly recapitulate the Abraham-Minkowski dilemma and the suggested expressions for the optical force in a medium. Then, we will describe how the fundamental connection between the energy and momentum conservation equations leads to the recently developed "force tracing" technique, which is basically a method to trace optical force fields along the trajectories of light rays. Furthermore, we will show that the force tracing technique not only significantly simplifies the conventional force computation procedure, but also offers the opportunity to sculpt the optical force in a reverse engineering approach. Accordingly, we will examine the validity of force tracing through several examples and illustrate that the Lorentz optical force density is directly proportional to the curvature of light rays. Moreover, based on the force-tracing method, we will demonstrate how graded-index lenses can be employed for interesting designs, which are offering versatile platforms for various sorts of optical manipulation such as optical sensing, space isolation, particle trapping. In this regard, we will go over the design procedures in detail and envision how optical force can lead to the formation of stable self-aligning systems made of graded-index devices.

10347-119, Session PWed

The total energy-momentum tensor for electromagnetic fields in a dielectric

Michael E. Crenshaw, U.S. Army Aviation & Missile Research, Development & Engineering Ctr. (United States)

Optically induced forces are under intensive investigation for micromanipulation and nanofabrication technology. A wide variety of physical principles have been applied to resolve issues related to momentums and optically induced forces for electromagnetic fields in dielectric media. Typically, one assumes some fundamental physical principle and the correctness of the results are affirmed by the fundamental nature of the principles that are used as the basis of the analyses. Although many well-founded theories have been advanced to resolve the physical issues, the theories are not all in agreement with each other and this leads to confusion and a lack of progress.

In a thermodynamically closed system, the total momentum, like the total energy, is a known quantity that is uniquely determined by temporal invariance. Then the construction of the unique total energy--momentum tensor resolves the Abraham--Minkowski controversy. Applying the four-divergence operator to the total energy—momentum tensor, one obtains conservation laws for the total energy and the total linear momentum. It is easily argued that the conservation law for the total energy, so obtained, cannot be incommensurate with the Poynting theorem that is systematically derived from the Maxwell field equations. It is also easily proven that the energy conservation law, derived from the four-divergence of the total energy--momentum tensor, is: 1) incommensurate with the Poynting theorem and 2) self-inconsistent because it's two non-zero terms depend on different powers of the refractive index. We discuss implications for resolution of the Abraham—Minkowski momentum controversy.

10347-79, Session 15

Probing chemical transformation in pL volume aerosol droplets

Anatolij Miloserdov, Calum P. F. Day, Antonia E. Carruthers, Newcastle Univ. (United Kingdom)

Aerosol droplets are a viable and exciting approach to probing chemical transformation and for use as chemical and environmental sensors. The nature of the air-liquid interface created through microscopic droplets existing in air can be exploited as micro-reactors to impose kinetic limitation and for fine control over reactions that require hazardous, expensive or reactive components.

Raman tweezing of aerosol is demonstrated as a route to quantify chemical and environmental change through measurement of single microscopic droplet dynamics and physical characteristics. Raman spectroscopy provides detailed insight into induced change in droplet chemistry and environment providing size, refractive index, composition, morphology, phase and mixing state information. Droplet solvent exchange mechanisms can be probed in situ through discrete control over the relative humidity of the localized environment where morphology dependent resonances provide insight into droplet physical characteristics. Aerosol equilibrated through uptake and transfer from water to heavy water is reversible and controllable allowing water diffusivity mechanisms in droplets to be studied through observation of OH and OD Raman stretches. Raman peaks arising due to the presence of solute can be exploited to extract temperature information through measurement of Stokes and anti-Stokes Raman. The relationship between these peaks are explored indicating reduced temperature as a result of the trapping laser and probe beams, and is dependent on chosen solvent.

10347-80, Session 15

Photoacoustic absorption spectroscopy of single optically trapped aerosol droplets

Ruth Signorell, Johannes Cremer, Paul Covert, ETH Zurich (Switzerland)

Within a narrow particle size distribution, the photoacoustic response from aerosols scales linearly with the particle number density. Yet, theoretical considerations indicate that particle heating and evaporation during the photoacoustic process could damp the measured response [1,2], which implies that it does not scale linearly with increases in the particle absorption cross-section that result from increases in the droplet size. To date, these effects of particle heating and evaporation upon the photoacoustic response have not been experimentally quantified.

We present the first measurements of the droplet-size-dependence of the photoacoustic response obtained from single optically-trapped aerosol droplets using our single-droplet photoacoustic spectrometer [3]. Measurements were made for a simple model system. As expected, our results show a significant nonlinearity between the magnitude of the photoacoustic signal and the absorption cross section calculated by Mie theory, especially for particles with a radius larger than 1 μm. This effect can be explained by local heat transfer processes at the surface of the particle.

The results give an experimental confirmation of the theoretical framework, improving confidence in photoacoustic absorption measurements of fine soot aerosols and opening up the possibility to correct photoacoustic field and laboratory measurements for the bias experienced when measuring the absorption of larger aerosol particles.

[1] Murphy D.M. (2009) Aerosol Sci. Tech. 43, 356–363.

[2] Raspet R., Slaton W.V., Arnott W.P., and Moosmüller H. (2003) J. Atm. Ocean. Tech. 20, 685–694.

[3] Cremer J.W., Thaler K.M., Haisch C., and Signorell R. (2016) Nature Comm. 7, 10941.

10347-81, Session 15

Optical trapping, pulling, and Raman spectroscopy of airborne absorbing particles based on negative photophoretic force

Gui-hua Chen, Lin He, Mu-ying Wu, Guang Yang, Dongguan Univ. of Technology (China); Yong-Qing Li, Dongguan Univ. of Technology (China) and East Carolina Univ. (United States)

Capture and characterization of small objects in air using lasers are attractive for the collection and analysis of atmospheric particles and biological aerosols. Optical pulling is the attraction of objects back to the light source by the use of optically induced “negative forces”. It is commonly expected that when illuminated by a light beam, a particle will be accelerated along the light propagation direction by radiation pressure. The idea of using laser beams to attract particles back to the light source is counterintuitive and has long been attractive to scientists. Here, we demonstrate that micron-sized absorbing particles can be optically pulled and manipulated towards the light source over a long distance in air with a collimated Gaussian laser beam based on negative photophoretic force. We also demonstrated that a variety of airborne absorbing particles can be pulled by this optical pipeline to the region where they are optically trapped with another focused Gaussian beam and their chemical compositions are characterized with Raman spectroscopy. The laser-induced photophoretic force is generated by the momentum transfer between the heating particles and surrounding gas molecules and can be several orders of magnitude larger than the radiation force and gravitation force. We found that micron-sized particles are pulled at a constant speed of 1-10 cm/s in the optical pulling pipeline and its speed can be controlled by changing the laser intensity. Optical pulling over large distances with lasers in combination with Raman spectroscopy opens up potential applications for the collection and identification of atmospheric particles.

10347-82, Session 15

Robust optical trapping and manipulation of absorbing particles in air by single dual-mode optical fiber-based tweezers

Souvik Sil, Tushar Kanti Saha, Ayan Banerjee, Indian Institute of Science Education and Research Kolkata (India)

Optical trapping of particles in air presents a challenge since the viscosity of air is extremely low so that the diffusivity of the particles is very high requiring steep confining potentials. Trapping with optical fibers should prove to be even tougher since fibers have much lower numerical aperture compared to microscope objectives, and additionally, single fibers are unable to trap particles in three dimensions using dipole forces. Photophoretic forces provide a solution towards trapping particles in air by virtue of their far stronger magnitude compared to dipole forces. In a vertical configuration trap, these forces easily balance gravity to provide stable axial trapping, and also generate a restoring force in the radial direction due to the spontaneous rotation of the trapped particle. Here, we develop a dual-mode single optical fiber based tweezers where mesoscopic absorbing particles can be trapped and manipulated employing photophoretic forces. We generate a superposition of Gaussian and Hermite-Gaussian beam modes from the optical fiber, by the simple innovation of coupling a lower wavelength laser into a commercial optical fiber designed to be single mode for a higher wavelength. The superposition mode is more effective in trapping and manipulation compared to the pure Gaussian mode, and we achieve robust trapping of the absorbing particles for hours with large manipulation velocities of 5 mm/s in the axial direction and 0.75 mm/s in the radial direction. The work has promising implications for trapping and spectroscopy of aerosols in air using simple single optical fiber-based traps.

10347-83, Session 15

A versatile system for optical manipulation experiments

Dag Hanstorp, Kelken Chang, Göteborgs Univ. (Sweden); Alvin Varghese, Cochin Univ. of Science & Technology (India); Ana Maria Gallego, Univ Nacional Autónoma de México (Mexico); Oscar K. Isaksson, Jonas Enger, Göteborgs Univ. (Sweden)

The development of a versatile experimental system for optical levitation will be presented. Microscopic liquid droplets are produced using a drop-on-demand dispenser based on piezo-driven inkjet printing technology. The vertically oriented dispenser releases the droplets towards a vertically focused 532 nm laser beam, where they are trapped. The size and position (in 3D) of trapped droplets are measured using two orthogonally placed high speed cameras, and the droplets charge is measured by recording its motion when an AC electric field is applied. Further, the charge can be altered by exposing the droplet to a radioactive source or UV light. Spectroscopic information of the trapped droplet is obtained by imaging the droplet on the entrance slit of a spectrometer. Raman spectra are obtained using the 532 nm trapping light, whereas laser induced fluorescence spectra are recorded by exciting the droplet using a cw Ti:Sa laser. Finally, the trapping cell can be evacuated, allowing investigations of droplet dynamics in vacuum and in control environments.

This system will be used to a variety of different applications. The set-up allows detailed studies of collisions of droplets, which will be used to investigate droplet coalescence for the application of rain drop formation in the atmosphere. Studies with the aim to investigate the spectroscopic signature of contaminants in droplets will be presented. Finally, the use of the system for didactic purposes as a means to demonstrate a variety of physical phenomena will be discussed.

10347-84, Session 16

Optical binding of two microparticles levitated in vacuum

Yoshihiko Arita, Univ. of St. Andrews (United Kingdom); Ewan Wright, College of Optical Sciences, The Univ. of Arizona (United States); Kishan Dholakia, Univ. of St. Andrews (United Kingdom)

Optical binding refers to an optically mediated inter-particle interaction that creates new equilibrium positions for closely spaced particles. Optical binding of mesoscopic particles levitated in vacuum can pave the way towards the realisation of a large scale quantum bound array in cavity-optomechanics. Recently we have demonstrated trapping and rotation of two mesoscopic particles in vacuum using a spatial-light-modulator-based approach to trap more than one particle, induce controlled rotation of individual particles, and mediate interparticle separation. By trapping and rotating two vaterite particles, we observe intensity modulation of the scattered light at the sum and difference frequencies with respect to the individual rotation rates. This first demonstration of optical interference between two microparticles in vacuum has lead to a platform to explore optical binding. Here we demonstrate for the first time optically bound two microparticles mediated by light scattering in vacuum. We investigate autocorrelations between the two normal modes of oscillation, which are determined by the centre-of-mass and the relative positions of the two-particle system. In situ determination of the optical restoring force acting on the bound particles are based on measurement of the oscillation frequencies of the autocorrelation functions of the two normal modes, thereby providing a powerful and original platform to explore multiparticle entanglement in cavity-optomechanics.

10347-86, Session 16

Towards large-scale optically bound nanoparticles

Fei Han, Zijie Yan, Clarkson Univ. (United States)

Optical matter is a unique class of materials formed by pure electrodynamic interactions of colloidal particles in an optical field, yet previous research on optical matter was almost limited to microparticle systems. Some recent experimental studies, including ours, have extended the boundary of optical matter into nanometer regime, but it remains a significant challenge to build large-scale optical matter with even more than 10 nanoparticles. Here we report our ongoing work on light-driven self-organization of plasmonic nanoparticles into mesoscale clusters and arrays. We use advanced laser beam shaping techniques and the significant electrodynamic interactions among strongly scattering Ag nanoparticles to stabilize the self-organization. By simultaneously controlling the intensity, phase and polarization of light, we can design and tailor the optical field to assemble stable optical matter with more nanoparticles, and reveal new structures arising from optical binding interactions.

10347-87, Session 16

Dynamics of optically bound knotted and chiral nanoparticles

Simon Hanna, Univ. of Bristol (United Kingdom); Stephen H. Simpson, Institute of Scientific Instruments of the ASCR, v.v.i. (Czech Republic)

We use computer simulations to explore the dynamical behaviour of optically bound assemblies of knotted and chiral nanoparticles. The knotted nanowire is not naturally occurring, but may be fabricated using two-photon polymerisation. Collections of such knots in circularly polarised counter-propagating plane waves form ordered arrays which rotate through interaction with the angular momentum of the beams. However, different types of behaviour are observed, depending on the size of the nanoparticles, their separation and the number of particles involved. Individual knotted or chiral particles will spin about their centres of mass while, at the same time, orbiting about each other. The sense of the spin and orbital motion (clockwise or anti-clockwise) can be the same or opposite in a given system, and can change with the sizes of the particles, which appears to be a consequence of the overlap between the particles and the intense regions of the optical field. Rotational synchronisation effects are also observed. Potential applications of the system as an optically-driven micro-machine are explored.

10347-88, Session 17

Nanoparticle size selection using near-field microphotonic array traps

Aravind Krishnan, Shao-Hua Wu, Michelle L. Povinelli, The Univ. of Southern California (United States)

Our experiments have used arrayed traps in the near field of a photonic crystal to selectively capture nanoparticles by size. The photonic crystal is designed to support a guided resonance mode, and the incident laser is tuned to the resonance wavelength. Each hole of the photonic crystal acts as a trapping site.

In this work, we use simulations of particle dynamics to determine the optimal experimental conditions for size selection. We include the effects of optical forces, fluid flow, and Brownian motion and explicitly track the trajectories of particles near an array of trapping sites. We study the effects of varying chamber height, flow rate, and particle concentration on size selectivity and trapping yield. We further present photonic crystal designs for selectively trapping smaller or larger particles out of mixed-particle solutions.

10347-89, Session 17

Particle trapping and hopping in an optofluidic lattice

Yuzhi Shi, Xiong Sha, Lip Ket Chin, Nanyang Technological Univ. (Singapore); Jiuhui Wu, Tianning Chen, Xi'an Jiaotong Univ. (China); Ai Qun Liu, Nanyang Technological Univ. (Singapore)

Particle jumping between optical potentials has attracted much attention owing to its extensive involvement in many physical and biological experiments. In some circumstances, particle jumping indicates escaping from the optical trap, which is an issue people are trying to avoid. Nevertheless, particle jumping can facilitate the individual trap in each laser spot in the optical lattice and enable sorting and delivery of nanoparticles. Particle hopping has not been seen in fluid because Fluidic drag force dramatically reduce the dwell time of particle or break the potential well. Here, we observe particle hopping in the microchannel by three reasons, e.g., particle collision or aggregation, light disturbing by pre-trapped particle and fake trapping position. We show that commonly ignored particle influence to the light could create a new isolated trapping position, where particle hops to the adjacent potential well. The hopping happens in an optofluidic fishnet which is comprised of discrete hotspots enabling 2D patterning of particles in the flow stream for the first time. We also achieve a 2D patterning of cryptosporidium in the microchannel. Our observed particle hopping in the flow stream completes the family of particle kinetics in potential wells and inspires new interests in the particle disturbed optical trapping. The 2D patterning of particles benefits the parallel study of biological samples in the flow stream and have potential on cell sorting and drug delivery.

10347-90, Session 17

Tracking Brownian particles in a standing-wave Bessel beam 2D optical trap

Keith D. Bonin, Chad McKell, Wake Forest Univ. (United States)

Optical traps are useful for manipulating small particles in fluid media. The motion of a particle in a fluid is determined by the viscoelastic properties that characterize the fluid as well as the proximity of nearby surfaces, especially in the case of microfluidics, where structural features are small. We have been working toward the goal of developing a method for loosely trapping particles in a plane, so that they can be readily tracked in a microscope, and stay in the imaging plane because of their 2D confinement. Our initial experiments, which we report here, use a standing wave optical trap formed by counter-propagating Bessel beams. A Bessel beam was chosen to produce a trapping region that is larger, with reduced center-zone diffraction, than a typical Gaussian beam. We will report on our initial characterization of the standing wave Bessel beam trap using latex sphere probes of 3 different diameters: 100, 200, and 300 nm. We will demonstrate that we can successfully trap such small particles in a 2D region, and track the motion of the beads within the 2D trap.

10347-91, Session 17

Dielectrophoretic focusing integrated pulsed laser activeted cell sorting

Xiongfeng Zhu, Yu-Chun Kung, Univ. of California, Los Angeles (United States); Ting-Hsiang Wu, NantWorks, LLC (United States); Michael A. Teitell, Pei-Yu E. Chiou, Univ. of California, Los Angeles (United States)

We present a pulsed laser activated cell sorter (PLACS) integrated with novel sheathless size-independent dielectrophoretic (DEP) focusing. Microfluidic fluorescence activated cell sorting (?FACS) systems aim to

provide a fully enclosed environment for sterile cell sorting and integration with upstream and downstream microfluidic modules. Among them, PLACS has shown a great potential in achieving comparable performance to commercial aerosol-based FACS (>90% purity at 25,000 cells sec?1). However conventional sheath flow focusing method suffers a severe sample dilution issue. Here we demonstrate a novel dielectrophoresis-integrated pulsed laser activated cell sorter (DEP-PLACS). It consists of a microfluidic channel with 3D electrodes laid out to provide a tunnel-shaped electric field profile along a 4cm-long channel for sheathlessly focusing microparticles/cells into a single stream in high-speed microfluidic flows. 10?m polystyrene beads can be focused at a particle speed up to 16 cm/s in high conductivity media (1 S/m). All focused particles pass through the fluorescence detection zone along the same streamline regardless of their sizes and types. Upon detection of target fluorescent particles, a nanosecond laser pulse is triggered and focused in a neighboring channel to generate a rapidly expanding cavitation bubble for precise sorting. DEP-PLACS has achieved a sorting purity of 91% for polystyrene beads at a throughput of 1,500 particle/sec.

10347-92, Session 17

Nanoparticle sorting in silicon waveguide arrays

Haitao Zhao, Yi Zhang, Lip Ket Chin, Peng Huat Yap, Nanyang Technological Univ. (Singapore); Kuan Wang, Academia Sinica (Taiwan); Wee Ser, Ai Qun Liu, Nanyang Technological Univ. (Singapore)

This paper presents a near-field approach to sort nanoparticles. The far-field approach, such as optical lattice, has difficulty in sorting nano-sized particles due to the large spot size limited by the diffraction barrier, while the conventional near-field approach generally has small light-particle interaction area and hence cannot manipulate nanoparticles massively. In order to avoid these drawbacks, a near-field approach is proposed based on the interference pattern in silicon waveguide arrays. This method has high potential in nanoparticle and biomolecule sorting.

The interference pattern is generated in waveguide arrays which are composed of 101 silicon nano-waveguides. When a focused light (? = 1550 nm, power = ~300 mW) is applied to the central waveguide, it is coupled to the adjacent waveguides and forms the interference pattern. The optical field will exert two forces on particles: the gradient force perpendicular to the waveguide surface and the scattering force along the light propagation. The vertical gradient force, induced by the evanescent wave, is large enough to trap both small and large particles onto the waveguide surface. Whereas the scattering force is only sufficient to push large particles toward the waveguide end. Therefore, the small and large particles can be separated efficiently. In the experiment, 300-nm and 500-nm polystyrene particles are separated as a demonstration. In a duration of 3 min, 93% of the 300-nm particles are trapped on the surface and move slightly near to the trapping position. Meanwhile, all the 500-nm particles are trapped and 85% of them are pushed to the waveguide end with an average lateral velocity of 7 ?m/s.

10347-93, Session 18

Optothermal assemblers and tweezers

(Invited Paper)

Yuebing Zheng, The Univ. of Texas at Austin (United States)

We exploit optothermal effects to realize versatile assembly and manipulation of colloidal particles and biological cells at low optical power and with simple optics. In this talk, I will present working principles and applications of the optothermal assemblers and tweezers that we have developed over the past three years. These include bubble-pen lithography, thermophoretic tweezers, reversible particle assembly, reversible particle printing, and colloidal lego.

10347-95, Session 18

Blue- and red-detuned laser trapping of individual dye-doped polystyrene particles

Tetsuhiro Kudo, National Chiao Tung Univ. (Taiwan); Hajime Ishihara, Osaka Prefecture Univ. (Japan); Hiroshi Masuhara, National Chiao Tung Univ. (Taiwan)

Optical trapping using the laser whose energy is resonant to electronic transition of the objects, leads to the manipulation of molecules, quantum dots, metal nanoparticles and various nanomaterials based on their quantum mechanical properties. Based on linear optical response theory with two-level model, it has been conventionally believed that attractive force is exerted on the object with the laser red-detuned from its electronic resonance peak, and the blue-detuned one induces the repulsive force.

However, there are experimental reports tell us blue-detuned laser can trap the dye molecules and nanoparticles efficiently. Motivated by these facts and in order to elucidate this contradiction, previously we proposed the nonlinear optical response theory of optical force with three-level system dyes, and we found blue-detuned laser provides the deeper optical potential compared with red-detuned one. Here, we experimentally demonstrate the resonance optical trapping of individual dye-doped polystyrene particles with the blue- and red-detuned lasers. We confirm that irradiation of blue-detuned laser can trap the particle much longer compared with that by red-one. The present study is very important step toward resonance optical trapping, and it will be possible to selectively trap the specific molecules, quantum dots and metal nanoparticles with tuning the wavelength of trapping laser.

10347-96, Session 19

A compact multi-trap optical tweezer system based on CD-ROM technologies

Thomas J. McMenamin, Woei Ming Lee, The Australian National Univ. (Australia)

Existing beam steering/shaping methods using acoustic optical deflectors, spatial light modulators and rapid scanning mirror has provided the ability to multiplex a single beam optical trap. This multiplexing ability offer users the ability to exert several trapping positions in the sample. However, these beam steering methods require extensive 4-f configurations. In this work, we demonstrate that a compact lens-scanning based system, based on an optical pickup unit (OPU), can be engineered to generate multiple optical traps. The crux of the technique is to alternate the pulsing of the compact laser diode at a rate synchronised with the oscillation of the objective lens, and compensating for the varied speed of the lens oscillation. By using this, we are also able to create a mixture of line and point trap geometries, and have these traps change position and shape over time as required by typical trapping experiments. The OPU used contains laser diode sources of multiple wavelengths (405nm, 650nm, 780nm) as well as a scanning objective lens of sufficient NA (0.65) for optical trapping. In addition, we constructed a compact darkfield system to visualise scattering light. The system has been demonstrated by experiments where microparticles and giant unilamellar vesicles (GUVs) have been optically trapped, moved and clearly imaged.

10347-97, Session 19

A biophotonics platform based on optical trapping of photonic membranes

Blair C. Kirkpatrick, Univ. of St. Andrews (United Kingdom); Tomá? ?i?már, Univ. of Dundee (United Kingdom); Kishan Dholakia, Andrea Di Falco, Univ. of St. Andrews (United Kingdom)

We present a biophotonics platform based on the optical manipulation of

photonic membranes via holographical tweezers. We review the fabrication and manipulation protocol which grants full six-degrees-of-freedom control over these membranes. This is despite the membranes having extreme aspect ratios, being 90 nm in thickness and 15 - 20 microns in side length.

The photonic properties of the trapped membranes can be tailored to very specific applications, by structuring their topology carefully. Our method merges the flexibility of photonic design of optical meta-surfaces with the advanced manipulation capability offered by holographic optical tweezers.

Here we demonstrate the validity of our approach, discussing the peculiar mechanical properties of trapped photonic membranes. Specifically, we focus on imaging and surface-enhanced Raman spectroscopy applications.

10347-98, Session 19

Photochemical tweezing of films of polymer

Zouheir Sekkat, Moroccan Foundation for Advanced Science, Innovation and Research (Morocco)

In this talk, I will discuss optical micro/nanomanipulation of films of photosensitive polymers in gradients of light Intensity. The polymers contain an azo dye molecule that undergo reversible photoisomerization, i.e. a molecular machine, and move in gradients of light intensity; a motion which is fuelled by a photochemical potential. The latter leads to a photochemical force that opposes the “classical” optical tweezing force, and the polymer moves away from the light into the dark.

10347-99, Session 19

Photonic arms, legs, and skin *(Invited Paper)*

Diederik S. Wiersma, LENS - Lab. Europeo di Spettroscopie Non-Lineari (Italy)

In this contribution we will report on a new adventure in the field of photonics, combining the optical control of photonic materials with that of true micro meter scale robotics. We will show how one can create complex photonic structures using polymers that respond to optical stimuli, and how this technology can be used to create moving elements, photonic skin, and even complete micro meter size robots that can walk and swim. using environment light as the only source of energy. The materials that we have developed to that end can also be used to realise tunable photonic components that respond to light and adapt their photonic response on the basis of the illumination conditions.

Conference 10348: Physical Chemistry of Semiconductor Materials and Interfaces XVI

SPIE. OPTICS+ PHOTONICS NANOSCIENCE+ ENGINEERING

Sunday - Wednesday 6 –9 August 2017

Part of Proceedings of SPIE Vol. 10348 Physical Chemistry of Semiconductor Materials and Interfaces XVI

10348-1, Session 1

Electronic processes, morphologies, and structural-functional correlations in conjugated oligomers and polymers for OPV *(Invited Paper)*

Lin X. Chen, Northwestern Univ. (United States) and Argonne National Lab. (United States)

Conjugated polymers with charge transfer characters in a large extend are responsible for the recent advancement in organic photovoltaic (OPV) applications in bulk heterojunction (BHJ) devices. We have carried out collaborative studies on electronic processes and in-situ morphological development of these low bandgap polymers and small molecules using ultrafast optical spectroscopy and in-situ grazing incident X-ray scattering (GIXS). Conventional organic photovoltaic models, in which donor molecules are treated as anonymous electron sources and charge carrier diffusion channels, are challenged by near-infrared transient absorption results of low bandgap polymers indicating strong correlations between intramolecular donor dynamics in < 100 fs and corresponding device power conversion efficiencies. The other conventional model being challenged is the driving force for exciton splitting in the bulk heterojunction environment which has been described by the LUMO-LUMO energy off-set between conjugated polymer electron donor and fullerene derivative electron acceptor. Our study suggests the intramolecular charge transfer characters must be combined with local and global conformations of conjugated polymer chains to achieve the low band gap. Moreover, the morphology of the BHJ films is also investigated by in-situ GIWAS/GISAX methods including the effects of additives which suggest the interplays of the additives and the polymers in solution. The morphology of the heterojunction films has been correlated directly with the yield of the charge separation on time scales from femtosecond to microsecond. In addition, new photophysical studies are also carried out on a series of metal chelating conjugated polymers showing the capability and potential in photocatalytic hydrogen generation.

10348-2, Session 1

Nanoscale energetic mapping of bulk heterojunction solar cells

Sukumar Dey, Hanlin Hu, Weimin Zhang, Iain Macculloch, Aram Amassian, King Abdullah Univ. of Science and Technology (Saudi Arabia)

The nanoscale organization and corresponding electronic properties of a photoactive donor-acceptor blend layers based on regioregular poly (3-hexylthiophene) (RR-P3HT) donor with fullerene and non-fullerene acceptors on Au(111) substrate has been studied using scanning tunneling microscopy and spectroscopy (STM/STS). Subsequent to annealing treatment, STM topography and dI/dV images are observed as a combination of phase-separated donor-rich, acceptor-rich, and mixed donor-acceptor domains. This technique permits to explore simultaneously the quantitative linkage between the nanoscale morphologies and corresponding local electronic properties. We determine the HOMO and LUMO-edges at the individual domains and interfacial band alignments of the donor-acceptor interface. We have observed a noteworthy deeper HOMO energy of RR-P3HT in mixed-region associated primarily with the degree of disorder-induced band gap widening of the polymer and donor:acceptor intermolecular interactions. Similarly, LUMO of the acceptor in the mixed region is also raised due to intermolecular interaction. These energetic difference in the mixed phase is likely to be responsible for the reduced recombination in bulk heterojunction (BHJ). Hence, this characterization provides nanoscale insight to the annealing-induced morphological organization and corresponding local electronic properties account for an impressive increase of the charge generation, transport and corresponding device performance of the BHJ solar cells.

10348-3, Session 1

Electronic structure and ion migration in lead-halide perovskites: a first-principles perspective *(Invited Paper)*

Leeor Kronik, Weizmann Institute of Science (Israel)

Power-conversion efficiencies of lead-halide perovskite (LHP) solar cells have rapidly improved and already well-surpassed 20%. This is impressive, especially because high-quality LHP crystals can be synthesized by relatively simple means, potentially offering new routes to cheaper high-efficiency cells. However, the microscopic origins and present limitations of the impressive photovoltaic and charge-transport properties of LHPs are far from being fully understood.

Here, I will briefly discuss the electronic-structure properties of LHPs based on a comparison between density functional theory (DFT) and direct and inverse photoemission spectroscopy (PES) and discuss how it is conducive to photovoltaic performance. I will then show, based on nudged-elastic band calculations, that ion migration may also play a key role, both positive and negative, in LHP properties in general and stability in particular.

10348-4, Session 2

In situ transient absorption of thin film formation *(Invited Paper)*

Cathy Y. Wong, Kelly S. Wilson, Univ. of Oregon (United States)

The electronic structure and exciton dynamics of solution deposited thin films are principal factors which determine the utility of a film for photovoltaic, transistor, or solid state lighting applications. These properties are typically measured in films after they have been prepared, but rarely during their preparation. Transient absorption spectroscopy can report on exciton dynamics by probing a sample at different delay times after a pump beam photogenerates a population of excitons. Transients are typically accumulated sequentially, with an individual differential absorption spectrum measured at each pump-probe delay time. This precludes the measurement of any system which changes during the collection period, which can span many minutes. In this work, we reveal the exciton dynamics of evolving chemical systems using a novel implementation of transient absorption whereby entire transients can be collected in a few laser shots. The exciton dynamics measured during the solution deposition of a thin film are validated by comparing the initial dynamics of the solution and the final dynamics of the dry film to traditional sequential transient absorption measurements. The dynamics during the film formation process will be presented for the first time. The information gained using this technique can be used to modify environmental parameters during the film formation process to enable the production of materials with tailored exciton dynamics.

10348-6, Session 2

Intra- and inter-molecular energy transfer in organic semiconductors: insights from nonadiabatic dynamics simulations *(Invited Paper)*

Sergei Tretiak, Los Alamos National Lab. (United States)

Using non-adiabatic excited-state dynamics simulations framework, we study ultrafast dynamics and exciton transport in several molecular systems. These simulations reveal an interplay of conformational vibrational

dynamics, internal conversion and energy transfer processes followed photoexcitation, which have specific spectroscopic signatures. For example, an efficient through-bond energy transfer occurs in the absence of spectral overlap between the donor and acceptor units being assisted by a transient delocalization of the wavefunction. Observed relationships between spatial extent/properties of electronic excitations and electronic functionalities allow us to understand excited state dynamics and energy transfer pathways in a number of organic molecular materials.

10348-7, Session 3

Optoelectronic properties of Ruddlseden-Popper phase halide perovskites *(Invited Paper)*

Adiitya D. Mohite, Los Alamos National Lab. (United States)

Understanding and controlling charge and energy flow in state-of-the-art semiconductor quantum-wells has enabled high-efficiency optoelectronic devices such as multijunction solar cells and light emission devices. Two-dimensional Ruddlesden-Popper perovskites are solution-processed quantum-wells wherein the bandgap can be tuned by varying the perovskite layer thickness, which modulates the effective electron-hole confinement. In my talk, I will describe new results on Ruddlesden-Popper phase perovskites based devices. In our first few attempts, we fabricated solar cells with efficiency approaching 13% as compared to the previous best of 4.5%. This phenomenal increase in efficiency is attributed to the near single-crystalline quality thin-films with a strongly preferential out-of-plane alignment of the inorganic perovskite component that facilitates efficient charge transport. Photovoltaic devices exhibit no hysteresis or degradation in performance under continuous operation and withstand an illumination intensity up to 4-Suns. Importantly, these devices with layered perovskites exhibit extraordinary, technologically relevant stability with no loss in performance with for ~2000 hours under humidity and 1-SUN full spectrum illumination. Finally, I will describe results on using these novel materials for light-emission applications and also discuss exciton dissociation mechanisms and how they vary with dielectric confinement.

10348-8, Session 3

Energy level alignment in hybrid perovskite solar cells *(Invited Paper)*

Philip Schulz, National Renewable Energy Lab. (United States)

The ongoing development of hybrid organic inorganic perovskite photovoltaics has revealed that the numerous interfaces in perovskite solar cells (PSC) play crucial roles for device efficiency and stability. Importantly, many critical interfacial properties are still poorly understood, a deficiency that often limits efforts to improve device performance. In this talk I will present our most recent results exploring the mechanisms by which transition metal oxide and carbon nanotube layers enable or suppress charge carrier extraction from the absorber.

We use photoemission spectroscopy and optical spectroscopy to probe the energetic alignment between a set of various lead halide based perovskite absorber films and different charge transport layers. We find that for comparable charge transport layers the energetic alignment can vary as a function of the halide composition in the perovskite which has further implications on the implementation in the device geometry. In one example, we show that ground state charge transfer between perovskite and transport material can lead to band bending in the transport layer such as a film of single-walled carbon nanotubes which is beneficial for charge transport away from the interface. Thus, we demonstrate, that integrated as a thin interlayer, carbon nanotubes can facilitate rapid charge carrier collection and thus improve PSC performance. In contrast to this observation, band bending induced in the perovskite film by the charge transport material such as high work function oxides can be detrimental for charge carrier collection and thus impede device functionality.

10348-9, Session 3

Colloidal APbX3 nanocrystals [A=Cs+, CH3NH3+, CH(NH2)2+] with bright photoluminescence spanning from ultraviolet to near-infrared spectral regions *(Invited Paper)*

Maksym V. Kovalenko, ETH Zurich (Switzerland)

Chemically synthesized inorganic nanocrystals (NCs) are considered to be promising building blocks for a broad spectrum of applications including electronic, thermoelectric, and photovoltaic devices. We have synthesized monodisperse colloidal nanocubes (4-15 nm edge lengths) of fully inorganic cesium lead halide perovskites (CsPbX3, X=Cl, Br, and I or mixed halide systems Cl/Br and Br/I) using inexpensive commercial precursors [1]. Their bandgap energies and emission spectra are readily tunable over the entire visible spectral region of 410-700 nm. The photoluminescence of CsPbX3 NCs is characterized by narrow emission line-widths of 12-42 nm, wide color gamut covering up to 140% of the NTSC color standard, high quantum yields of up to 90% and also low thresholds for stimulated emission [2]. Post-synthetic chemical transformations of colloidal NCs, such as ion-exchange reactions, provide an avenue to compositional fine tuning or to otherwise inaccessible materials and morphologies [3]. Similar synthesis methodologies are well suited also for hybrid perovskite nanocrystals based on methylammonium (MA) and formamidinium cations (FA): MAPbX3 [4], FAPbBr3 [5], Cs1-xFAxPbI3 and FAPbI3 [6]. In particular, Cs- and FA-based NCs (Figure below) are highly promising for luminescence downconversion (bright and narrow emission at 530 and 640 nm), for infrared light-emitting diodes and as precursors/inks for perovskite solar cells. In this talk, we will discuss the synthesis methodologies and optical properties of these novel APbX3 NCs.

1. L. Protesescu et al. Nano Letters 2015, 15, 3692–3696

2. G. Nedelcu et al. Nano Letters 2015, 15, 5635–5640

3. S. Yakunin et al. Nature Communications 2015, 9, 8056.

4. O. Vybornyi et al. Nanoscale 2016, 8, 6278-6283

5. L. Protesescu et al. J. Am. Chem. Soc. 2016, 138, 14202–14205

6. L. Protesescu et al. submitted

10348-10, Session 3

High efficiency OLEDs enabled by molecular rotation *(Invited Paper)*

Dan Credgington, Univ. of Cambridge (United Kingdom)

Excitonic spin plays a crucial role in the design of organic light emitting diodes (OLEDs). The random spin statistics of recombining charge sets a limit of 25% on the fraction of singlet (spin-0) excitons formed by electrical excitation. Without efficient emission from triplet (spin-1) excitons, the same limit applies to the internal quantum efficiency (IQE) of fluorescent OLEDs. Phosphorescent OLEDs, utilising the heavy atom effect to render triplets emissive, and TADF OLEDs, based on thermally-assisted triplet-to-singlet up-conversion, are currently the most promising routes for triplet emission.

Here we demonstrate a different approach. The effective exchange energy in a family of linear copper and gold carbene metal amide compounds can be tuned via rotation about the metal-amide bond from positive to negative values. The energetic ordering of spin-states can therefore be inverted, enabling triplet-to-singlet down-conversion. The availability of degenerate states with high oscillator strength allows emission via triplets to occur on sub-microsecond timescales. Using such materials as emissive dopants in solution-processed OLEDs leads to extremely efficient devices with near 100% IQE (external quantum efficiencies >27%), and current efficiency, power efficiency and brightness comparable to or exceeding those of state-of-the-art vacuum-deposited OLEDs and quantum dot LEDs.

We describe the experimental and theoretical evidence for rotationally accessed spin-state inversion. Using time-resolved spectroscopy we show how the resulting emission depends strongly in the interplay between

rotational energetics, temperature, oscillator strength and the morphology of the emissive layer.

10348-11, Session 4

Determining charge carrier extraction in lead sulfide quantum dot near infrared photodetectors

Epimitheas Georgitzikis, IMEC (Belgium) and KU Leuven (Belgium); Pawel E. Malinowski, IMEC (Belgium); Mehedi Mamun, IMEC (Belgium) and Univ. Gent (Belgium); Oscar Enzing, IMEC (Belgium); Jorick Maes, Zeger Hens, Univ. Gent (Belgium); Paul Heremans, IMEC (Belgium) and KU Leuven (Belgium); David Cheyns, IMEC (Belgium)

Colloidal quantum dots (QDs) based on lead sulfide (PbS) have acquired scientific interest for infrared optoelectronic devices with potential bandgap tunability and ease of fabrication on arbitrary substrates. In this work, we show how device analysis data feed back into process optimization, towards the realization of high performance QD NIR photodetectors. Using the combination of transient PL, carrier transport and CV measurements we obtain the carrier density, lifetime and diffusion length in the layers. From the measured short diffusion length of the minority carriers, we deduce the need to achieve a wide depletion region to minimize recombination and thus enhance the carrier harvesting. Process optimization lead to a depletion region of more than 150 nm, resulting in high photon to carrier conversion. Furthermore, the complex index of refraction of all layers is characterized using ellipsometry and reflection/transmission, and these values are used as input for a transfer matrix method. Using the first interference peak, we show that a maximum EQE of 25% can be expected from optical modeling, a value that we almost reach experimentally (20%). Combining all of the above, we demonstrate 1450-nm photodetectors with dark current in the range of ?A and specific detectivity (D*) of 10^11 Jones.

10348-12, Session 4

Engineering hybrid interfaces in organic and perovskite optoelectronic devices *(Invited Paper)*

Yana Vaynzof, Heidelberg Univ. (Germany); Paul Hopkinson, Yunus Sevinchan, Carsten Hinzmann, Qingzhi An, Yvonne Hofstetter, Paul Fassl, David Backer-Koch, Ruprecht-Karls-Univ. Heidelberg (Germany); Osnat Magen, Technion-Israel Institute of Technology (Israel); Artem A. Bakulin, Imperial College London (United Kingdom); Nir Tessler, Technion-Israel Institute of Technology (Israel)

Hybrid interfaces such as organic/inorganic or inorganic/perovskite are commonly found in organic and perovskite optoelectronic devices. Many fundamental processes (e.g. charge separation, charge injection and extraction) take place at hybrid interfaces and have a significant impact on the device performance.

We will present three examples in which engineering of hybrid interface properties results in improvements in the device performance. In the case of hybrid organic-inorganic photovoltaic devices, we show that such improvements may be achieved by either organic or inorganic modifiers, or alternatively by introducing a dopant into the inorganic layer. These modifications result in an enhancement in the photo-induced charge separation efficiency, which is related to the density of the sub-bandgap states in the inorganic layer.

Next, we will demonstrate that interfacial sub-bandgap states at an inorganic/organic interface can influence charge injection in organic light-emitting diodes. By combining experimental results and modelling we show that not only the density, but especially the energetic position of these states determines the overall charge injection efficiency.

Finally, we will present how modifying both the bulk and interfacial properties of a metal oxide electron extraction layer can enhance the performance of perovskite solar cells. In this case, we find that surface modification by a self-assembled monolayer results in an improved perovskite film formation, while doping of the metal oxide improves its stoichiometry and as a result, enhances electron extraction.

10348-13, Session 4

Ion migration in organo lead halide perovskite based photovoltaic devices *(Invited Paper)*

Sven Huettner, Univ. Bayreuth (Germany)

The fundamental physics in organic-inorganic metal-halide perovskites, is still not sufficiently understood. Applied in photovoltaic devices, organolead halide based solar cells may suffer from hysteresis, that is the difference of the I-V curve during sweeping in two directions. This behaviour significantly influences the large-scale commercial application and seems to have its origin in ionic migration and directly affects stability and device performance. To investigate the mechanisms, we employ a combination of methods that help to identify the origin and effect of ion migration. We use electroabsorption spectroscopy, to explore the built-in potential, track the temperature dependent J-V behaviour and related current relaxation processes and perform X-ray photoemission spectroscopy experiments, showing the redistribution of iodine after applying a constant voltage. In addition, we carry out fluorescence microscopy under an electrical field which allows us to directly track the migration and accumulation of ions. This experiment allows to study the dynamic process of – in this case - iodide ions under an external electrical field and lets us estimate their mobility and diffusion constan. We associate the migration/accumulation of iodide ions with the modulation of interfacial barrier between perovskite and electrodes which gives rise to the shift of the built-in potential. We investigate the influence of PCBM on the migration of ions, which appears to be impeded by the presence of interdiffused PCBM molecules. Furthermore, photoluminescence microscopy gives access to interesting phenomena which are related to the presence of ions, such as blinking or long-term intensity changes in the emission signal.

10348-14, Session 4

Impact of band structure on recombination and efficiency in halide perovskite solar cells close to the radiative limit *(Invited Paper)*

Thomas Kirchartz, Uwe Rau, Forschungszentrum Jülich GmbH (Germany)

Some metal-halide perovskites have exceptionally good optoelectronic properties that make the materials attractive for applications in photovoltaics and other optoelectronic applications. Among the most remarkable properties are the extremely long charge-carrier lifetimes and high open-circuit voltages that are observed in thin films of CH3NH3PbI3. Recently, several explanations have been brought forward that connect the high lifetimes and Vocs with peculiar properties of the band structure of perovskites, in particular (i) the combination of a direct and an indirect band gap with a small energy offset and (ii) the low effective density of states. Here, we show how the direct-indirect combination of band gaps can indeed lead to longer lifetimes but the recombination rate, which is proportional to the ratio of the equilibrium carrier concentrations and the lifetime is likely to remain constant or constant. Therefore, the direct-indirect combination can explain good charge carrier collection but not high open-circuit voltages. This is different for the second feature of the band structure, namely the low effective density of states, which is combined with a high absorption coefficient. This is only possible of the matrix transition elements are high in perovskites. While for a given absorption coefficient, the effective density of states is irrelevant in the radiative limit at high mobilities, this is not the case if non-radiative recombination is present. This means, the high absorption at

low densities of states can indeed help the open-circuit voltage come closer to its radiative limit.

10348-54, Session 4

Heavy atom organic semiconductors *(Invited Paper)*

Dwight Seferos, Univ. of Toronto (Canada)

For over 7 years my group has been fascinated by how tellurium and selenium can influence the optoelectronic properties of conjugated electronic materials. Some of our work has focused on the development of conjugated polymers that self organize at the nanoscale by spontaneous phase-separation. We have been interested in conjuged block copolymers where each block contains a distinct heterocycle. These polymers are fundementally important for testing the limits of polymer phase separation. They are also useful in optoelectronic devices where nanoscale structure is important, such as solar cells. In this context we have developed selenophene-thiophene block copolymers and discovered that these copolymers undergo a significant amount of phase separation. This is surprising given the chemical similarity of the repeat units, however we have uncovered several properties, including crystal packing, that differ in these polyheterocycles. By increasing the compatibility of the selenophene and thiophene units and we observe co-crystallization in statistical copolymers. These statistical copolymers form nanowires and when fabricated into nanowire solar cells they operate with a greater efficiency than cells composed of homopolymer nanowires. We have also learned how to synthesize polymers and delocalized molecules based on tellurophene, and identified several unexpected properties in these materials including reversible binding of small molecules, and the ability to photo-reductively eliminate halogens. The synthesis, properties and optical applications of these materials will be discussed.

10348-15, Session 5

Mechanisms underlying emission quenching in conjugated polymers: the role of inter-chain interactions

Linda A. Peteanu, Eric C. Wu, Carnegie Mellon Univ. (United States); Matthew Y. Sfeir, Brookhaven National Lab. (United States)

Applications of conjugated polymers in photovoltaics and displays drive the need to understand how morphology and aggregation affect emission yields, spectra, and the facility with which charges are generated and migrate through the sample. It is known that solvent-polymer interactions in solution critically affect the properties of thin films formed when these solutions are evaporated onto substrates. Our work demonstrates that the propensity of conjugated oligomers and polymers to form emissive versus non-emissive aggregates in solution and in thin films is likewise governed by the solvent properties. Fluorescence correlation spectroscopy is used as a tool to identify both emissive and non-emissive species in dilute solutions while dynamic light scattering (DLS) is used to measure diffusion properties. In some solvents, such as toluene, conjugated materials form non-emissive aggregates even at picomolar concentrations. Under similar conditions, the same materials exhibit single-emitter properties in more polar solvents such as tetrahydrofuran (THF). These distinctions persist when the molecules are forcibly aggregated by addition of poor solvent and are correlated to variations in chain packing within the aggregate due to differences in their preferred conformation. Transient absorption spectroscopy is used to understand the impact of altering chain packing on the propensity for energy transfer and charge separation in the aggregated state and in films.

10348-16, Session 5

Intermolecular charge-transfer states for organic opto-electronics *(Invited Paper)*

Koen Vandewal, TU Dresden (Germany)

Intermolecular charge transfer (CT) states at the interface between electron-donating and electron-accepting (A) materials in organic thin films are characterized by absorption and emission bands within the optical gap of the interfacing materials. Depending on the used donor and acceptor materials, CT states can be very emissive, or generate free carriers at high yield. The former can result in rather efficient organic light emitting diodes, via thermally activated delayed fluorescence, while the latter property is exploited in organic photovoltaic devices and photodetectors. In this contribution, we will discuss the fundamental properties of CT states and link them to organic opto-electronic device performance. Furthermore, we introduce a new device concept, using an optical cavity resonance effect to boost CT absorption at photon energies below the optical gap of both donor and acceptor, enabling narrow-band, near infrared (NIR) photo-detection. This new type of photodetector can compete with standard organic photodetectors but extends their detection range to longer wavelengths.

10348-17, Session 5

Strategies for reducing energy loss and increasing efficiency of organic solar cells *(Invited Paper)*

Barry P. Rand, Princeton Univ. (United States)

Unique to the function of organic PVs are the creation of tightly bound excitons that can only be efficiently separated at a donor/acceptor (D/A) interface capable of providing the necessary energetic driving force for dissociation. At the D/A interface, the presence of charge transfer (CT) states, ground state complexes between the donor and acceptor materials, set the upper bound for the potential that can be extracted from a given D/A pair, but their role in photogeneration is not completely understood. Furthermore, the consequences of extreme levels of order in highly crystalline heterojunctions have not been conclusively determined.

We have recently been exploring organic semiconductor-based thin films that feature crystalline grains of up to 1 mm in extent. We have found that CT states from these films are highly delocalized, contributing to noticeably lower energy losses. Also, we have discovered that relative energies of CT states with respect to singlet and triplet energy levels are critical when considering devices that exploit multiple exciton processes such as singlet fission and its complement, triplet-triplet annihilation (or triplet fusion). We will discuss these aspects and their implications for more efficient organic solar cell function.

10348-18, Session 5

Optics and photo-physics of hybrid perovskites revealed via multi-scale modeling *(Invited Paper)*

Andrew M. Rappe, Liang Z. Tan, Univ. of Pennsylvania (United States); Fan Zheng, Lawrence Berkeley National Lab. (United States); Shi Liu, Carnegie Institution for Science (United States); Omer Yaffe, Weizmann Institute of Science (Israel); Yinsheng Guo, Louis E Brus, Columbia Univ. (United States); Jasmine P. H. Rivett, Felix Deschler, Univ. of Cambridge (United Kingdom); Maya Isarov, Efrat Lifshitz, Technion-Israel Institute of Technology (Israel)

The lead halide perovskites have recently demonstrated excellent photovoltaic power conversion efficiencies, but the physical explanation

underlying this success is still unknown. Part of the difficulty lies in the complex spatio-temporal fluctuations of the atomic structure and their interactions with carriers. In this talk, we show how the photo-physics of hybrid perovskites is understood in theory and manifested in experiments, focusing on the aspects of carrier relaxation, the nature of structural fluctuations, and the influence of spin-orbit effects. We show that a simple Debye-Waller picture is insufficient to describe the time-resolved nuclear response after photo excitation. Instead, the evolution of the pair distribution function indicates an activation of preferential sub-lattice motions over fully thermal motions, as supported by our molecular dynamics simulations and ultrafast electron diffraction experiments. We have examined the nature of structural fluctuations in DFT-MD simulations, finding that the organic molecules display significant displacive motion, and are not pure dipolar rotors.

The dynamics of electrons and holes is also very intricate. Our models of carrier relaxation, based on first-principles electron-phonon couplings, show that anisotropy is imprinted on the carrier distribution by polarized light. Time-resolved transient absorption experiments show that this anisotropy persists for several picoseconds, which is much longer than in other semiconductors. Spin-orbit coupling is predicted to affect carrier recombination rates, and affect the exciton splitting energies under a magnetic field. Our magneto-optical measurements on CsPbBr3 have shown how the Rashba effect results in non-linear Zeeman splitting of the excitons.

10348-19, Session 5

Understanding the device physics in polymer-based organic ratchets *(Invited Paper)*

Thuc-Quyen Nguyen, Univ. of California, Santa Barbara (United States)

Electronic ratchets, devices that can convert random AC signals into DC current, have been of great interest for years, in particular for applications in energy harvesting. In combination with an antenna, which absorbs electromagnetic waves from the environment and produces AC voltage at its terminals, electronic ratchets can be used to rectify AC signal into DC current that can be used to power small electronic devices. For many years, ratchets were not considered suitable for practical applications due to their complexity of fabrication, low output power, and, in some cases, their requirement of cryogenic operating temperatures. In this talk, I will discuss a simple ratchet device architecture that is able to transform random electrical noise signals to produce large DC currents at room temperature. Our ratchet has only three electrodes and can be fabricated via solution-processing methods and therefore has potential applications in low cost, flexible, and light-weight energy harvesting devices. It is possible to fabricate a working polymer ratchet using Scotch tape, pencil, and aluminum foil. The working mechanism of organic ratchets is based on the principle of a “charge pump”, which relies on the formation of rectifying junctions at metal/organic interfaces.

10348-20, Session 6

Field-induced exciton and CT-state dissociation probed by time-resolved luminescence quenching

Uli Lemmer, Karlsruhe Institute of Technology (Germany); Marina Gerhard, Philipps-Univ. Marburg (Germany); Andreas P. Arndt, Karlsruher Institut für Technologie (Germany); Martin Koch, Philipps-Univ. Marburg (Germany); Ian A. Howard, Karlsruher Institut für Technologie (Germany)

The microscopic mechanisms of exciton and charge-transfer-state dissociation in organic semiconductors play a major role for the efficiencies of organic solar cells [1]. One of the most direct experiments for probing the dynamics of these processes is luminescence quenching. Here, we present a comprehensive experimental and simulative study of the field and temperature dependence of the dissociation of singlet excitons in PTB7 and PC71BM, and from charge-transfer states generated across interfaces in PTB7/PC71BM bulk heterojunction solar cells. We deduce the relevant data from time-resolving the near infrared emission of the states from 10K to room temperature and for electric fields ranging from 0 to 2.5 MV/cm. To draw qualitative conclusions from our data, we use an analytical field-assisted hopping model in the presence of disorder [2]. We conclude that singlet excitons can be split by high fields, and that disorder plays a large role in broadening the critical threshold field for which singlet excitons are separated. Charge-transfer (CT) state dissociation can be induced by both field and temperature, and the data imply that a strong reduction of the Coulomb binding potential at the interface facilitates their separation. The observations provided herein of the field dependent separation of CT states as a function of temperature offer a rich dataset against which theoretical models of charge separation can be rigorously tested.

References: [1] H. Bässler and A. Köhler, Phys. Chem. Chem. Phys. 17, 28451 (2015) [2] O. Rubel, S. D. Baranovskii, W. Stolz, and F. Gebhard, Phys. Rev. Lett. 100, 196602 (2008).

10348-21, Session 6

Structure and function of bilayer organic photovoltaics *(Invited Paper)*

Mark E. Thompson, Peter I. Djurovic, Piyumie Wickramasinghe, The Univ. of Southern California (United States)

The exciton is a critical part of each of the processes leading to photocurrents in Organic PhotoVoltaics (OPVs), and being able to control the location, lifetime and energy of the exciton is essential to achieving high efficiency. I will discuss our most recent work with both organic dyes, such as squaraines and dipyrrins for OPVs. This involves a careful materials design study that leads to both low energy absorption (into the nearIR) and the efficient use of multiple absorbers to efficiently harvest photons through the entire visible spectrum. In particular, I will discuss the structure of bilayer films with these red/NIR absorbers and the role that fullerene diffusion into the donor layers plays on the properties of the photovoltaics. I will also discuss a new approach to designing materials for OPVs that involves symmetry breaking charge transfer. These materials are symmetric molecules that spontaneously form an intramolecular charge transfer complex, with nearly complete one electron transfer from one part of the molecule to another. This intramolecular CT state readily forms a charge separated state at the D/A interface of the OPV. We have explored these materials as both donors and acceptors in OPVs and found that they give good performance and high Voc.

10348-22, Session 6

Correlating microscale luminescent, electronic, and photovoltaic heterogeneity in perovskite thin films and solar cells *(Invited Paper)*

Giles E. Eperon, Univ. of Washington (United States)

Whilst perovskite solar cells have demonstrated an unprecedentedly rapid rise in power conversion efficiencies to over 22%, they are still far off their theoretical maximums of >30%.[1] Recently, several reports have emerged demonstrating that there is significant heterogeneity in the microscale properties of perovskite films – some grains seem to be of higher material quality than others, and grain boundaries show high densities of non-radiative defects.[2,3] It has been suggested that this heterogeneity could limit the performance of solar cells made from these films. However, the exact relations between film heterogeneity and device performance are still unclear.

Here, I will discuss our latest advances in correlative microscopy on perovskite thin films and devices. We conduct high-resolution scanning confocal photoluminescence microscopy, scanning kelvin probe microscopy, conductive atomic force microscopy, and laser beam induced current and voltage mapping to understand the origin and effects of local heterogeneity in perovskites. We find that heterogeneity can stem from both the perovskite itself and the perovskite-contact interfaces, and we go on to elucidate the role and impact of this on device performance.

I will go on to discuss the roles of grain boundaries and passivation techniques on heterogeneity in films and devices. Based on our results we elucidate rational routes to pushing the performance of perovskite solar cells closer to the thermodynamic limits.

References

(1) NREL. Best Research-Cell Efficiencies, http://www.nrel.gov/ncpv/images/efficiency_chart.jpg; 2016.

(2) Bischak, C. G.; Sanehira, E. M.; Precht, J. T.; Luther, J. M.; Ginsberg, N. S. Nano Lett. 2015, 150622162346003.

(3) de Quilettes, D. W.; Vorpahl, S. M.; Stranks, S. D.; Nagaoka, H.; Eperon, G. E.; Ziffer, M. E.; Snaith, H. J.; Ginger, D. S. Science (80-.). 2015, 348 (6235), 683–686.

10348-23, Session 6

Charge-carrier conduction and recombination mechanisms in hybrid metal halide perovskites *(Invited Paper)*

Laura Herz, Univ. of Oxford (United Kingdom)

Organic-inorganic metal halide perovskites have emerged as attractive materials for solar cells with power-conversion efficiencies now exceeding 21%. We discuss the fundamental photophysics that has enabled these materials to be such efficient light-harvesters and charge collectors. We demonstrate how parameters essential for photovoltaic operation are altered with perovskite composition [1], changes in electronic bandstructure [2,3] and dimensionality [4]. We further analyze distinct charge-carrier recombination and scattering mechanisms and their dependences on composition and temperature [2,3,5]. We use these insights to predict charge-carrier diffusion lengths and radiative efficiencies in the limit of ultra-low trap-related recombination and the presence of doping [6,7].

References:

[1] D. McMeekin et al., Science 351, 151 (2016).

[2] W. Rehman et al., Adv. Mater. 27, 7938 (2015)

[3] R. Milot et al., Adv. Func. Mater. 25, 6218 (2015)

[4] R. L. Milot et al., Nano Letters, 16, 7001 (2016)

[5] A. Wright et al., Nature Communications 7, 11755 (2016).

[6] R. L. Milot et al., J. Phys. Chem. Lett. 7, 4178 (2016).

[7] M. B. Johnston and L. M. Herz, Acc. Chem. Res. 49, 146 (2016).

10348-24, Session 7

Linker-dependent singlet fission in tetracene dimers

Jimmy Joy, Nadezhda Korovina, Mark E. Thompson, Stephen E. Bradforth, The Univ. of Southern California (United States)

Singlet fission is a process of generating two triplet excitons from a single photon that has the potential to increase the theoretical maximum efficiency of a solar cell. The rate of singlet fission is dependent on the coupling between the singlet state [S1S0] and the correlated triplet pair [1(T1T1)] in a chromophore. A series of ethynyl-tetraceme dimers linked via a phenyl bridge have been synthesized with the chromophore units at ortho-, meta- and para- configurations. Such dimers allow the investigation of the contributions of through-space and through-bond coupling to the rate of singlet fission. Transient absorption spectroscopy has been used to observe the singlet state, the correlated triplet state and the separated triplet states in these dimers. The spectral deconvolution of the transient absorption data shows that the only the para-dimer forms separated triplets while the ortho-dimer only forms the correlated triplet pair while the meta-dimer does not undergo singlet fission.

10348-25, Session 7

Measuring the electronic structure of buried organic semiconductor interfaces *(Invited Paper)*

Aaron P Moon, Univ. of Texas at Austin (United States); Ravindra Pandey, Aaron K. Le, Jon A. Bender, Daniel E. Cotton, Sean T Roberts, The Univ. of Texas at Austin (United States)

A primary source of energy loss within semiconductor photovoltaics is charge carrier thermalization, wherein carriers produced by high-energy photons relax to the semiconductor's band edge, giving up their excess energy as heat. In commercial silicon photovoltaics, this process accounts for nearly 50% of the energy lost by these cells. One strategy to combat this loss is to use a material that undergoes singlet exciton fission (SF) to capture high energy photons. SF, a process that occurs in select organic semiconductors, generates two spin-triplet excitons from a singlet photo-generated spin-singlet excitation. These triplet excitons can each transfer to a silicon layer resulting in a reduction of thermalization losses. However, efforts to couple SF materials with silicon have largely been hindered by inefficient triplet energy transfer across their junction. Currently, the physical basis underlying this result is unclear, and may be tied to poor orbital overlap as well as band edge mismatch. Differentiating between these scenarios and others is central to the design of SF-based photovoltaics. Herein, we use electronic sum frequency generation (ESFG) to probe how the electronic structure of perylenediimides, a family of promising SF materials, is altered at buried interfaces. ESFG measurements of perylenediimide thin films suggest that strain relaxation within crystalline grains can lead to exciton energy shifts of ~150 meV, affecting both their ability to undergo SF near interfaces and transfer triplet excitons to silicon. Our measurements suggest careful control of the arrangement of SF-materials at a semiconductor interface is critical to effecting energy transfer between them.

10348-47, Session 7

Picosecond light-induced rotational disordering in the hybrid perovskites *(Invited Paper)*

Aaron M. Lindenberg, Stanford Univ. (United States) and SLAC National Accelerator Lab. (United States)

Femtosecond resolution electron scattering techniques are applied to resolve the first atomic-scale steps following absorption of a photon in the prototypical hybrid perovskite methylammonium lead iodide. Following above-gap photo-excitation, we directly resolve the transfer of energy from hot carriers to the lattice by recording changes in the root-mean-square atomic displacements, on ten picosecond time- scales. Measurements of the time-dependent pair distribution function show an unexpected broadening of the iodine-iodine correlation function while preserving the Pb-I distance. This indicates the formation of a rotationally-disordered halide octahedral structure developing on picosecond time-scales. This work shows the important role of light-induced structural deformations within the inorganic sublattice in elucidating the unique optoelectronic functionality exhibited by hybrid perovskites and provides new understanding of hot carrier - lattice interactions which fundamentally determine solar cell efficiencies.

10348-27, Session 8

Interface and defect engineering of core-shell quantum dots

Ajay Singh, Jennifer A. Hollingsworth, Los Alamos National Lab. (United States)

Colloidal quantum dots (CQDs) are attractive materials for lasers, displays and light-emitting applications due to their narrow and brighter spectral emission bandwidth, size-tunable bandgap and high-photoluminescence quantum yield (PLQY). However, these CQDs undergo inevitable degradation of their unique optical properties overtime due to their sensitive surface chemistry. To overcome these limitations, several approaches have recently been used such as over coating with an inorganic semiconductor shell of a wider band gap (core-shell hetrostructures), surface functionalization with new ligands or polymer coating and composites etc. In particular, core-shell heterostructured quantum dots with thick shell (so called "giant" quantum dots (g-QDs)) has shown higher PLQYs and improved photochemical stability than traditional thin-shelled or core only CQDs. The outstanding properties of g-QDs essentially depend on both the structure (defects, surface chemistry etc.) and the properties of interfacial layer (sharp or smoothen core/shell interface). These structural and interfaces properties of g-QDs are strongly influenced and can be tailored by the synthetic parameters. Here, we will present our recent results on understanding the behavior of interfacial layer and structural defects on the photophysical properties of g-QDs.

10348-28, Session 8

Highly luminescent nanocrystals of formamidinium tin iodide (FASnI3) *(Invited Paper)*

Maryna Bodnarchuk, EMPA (Switzerland); Sergii Yakunin, Maksym V. Kovalenko, ETH Zurich (Switzerland)

During recent years lead-halide perovskite semiconductors have shown great potential in the field of optoelectronics; in particular, in photovoltaics and as versatile photon sources [1]. This progress is deeply rooted into unique defect-tolerant photophysics of the compounds. Colloidal organic/inorganic lead halide perovskite nanocrystals (NCs) are intensely pursued as highly promising, low-cost light-emitting materials with wide color gamut. The latter arises from the narrow-band photoluminescence, covering the entire visible spectral region and characterized by very high quantum yields of up to 90% [2]. However, the use of toxic Pb limits their broad applications and commercialization. Since the toxicity of lead is of great concern in most countries, a nontoxic substitute for perovskite materials is eventually required. The Pb(II) could be replaced with Sn(II), which is in the same group in the periodic table. Such replacement of lead with tin has been demonstrated in bulk films, but not in colloidal nanocrystals. We have developed solution-phase synthesis of colloidal formamidinium tin iodide (FASnI3) NCs with nearly cubic and platelet shapes, exhibiting tunable emission peak between 720-900 nm and with high quantum yields of 50% and above [3]. Structural analysis indicates orthorhombic crystal structure for FASnI3 NCs, that is in agreement with literature findings for the bulk material. These NCs exhibit higher stability than their MA- or Cs-based analogues of the same size and morphology. We also find that facile oxidation of Sn(II) limits the durability of these materials. We will discuss possible mitigation strategies for improving the oxidative stability via polymer encapsulation.

1. B. R. Sutherland, E. H. Sargent, Nat. Photon., 10, 5, 295.

2. L. Protesescu, S. Yakunin, M.I. Bodnarchuk, F. Krieg, R. Caputo, C. Holman Hendon, R.X. Yang, A. Walsh, and M.V. Kovalenko. Nano Lett., 2015, 15, 3692.

3. Bodnarchuk et al. in preparation.

10348-29, Session 8

The alkyl amines effect on the optical properties of inorganic perovskite quantum dot

Ya Zhu Yang, Shu-Ru Chung, National Formosa Univ. (Taiwan)

Perovskite quantum dots (QDs) is a new kind of optoelectronic materials in recent years. Compared with organic perovskite QDs (MAPbX3), inorganic perovskite QDs (CsPbX3) have a better stability. Inorganic perovskite QDs can be prepared at low temperature. Those novel QDs can be applied in solar cells, light-emitting diodes (LEDs), display, and biolables. Typical synthesis process to prepare CsPbX3 QDs is used oleic acid (OA) and cesium carbonate (Cs2CO3) to form Cs-oleate complex first. Moreover, the oleylamine (OLA) and octadecene (ODE) are used as capping agents. Cs-oleate complex then reacts with PbX2 to form CsPbX3 QDs (reacts for 5 s). As we know that the CsPbBr3 QDs emits green light, and its emission wavelength can be tuned by adding Cl- and I- ions to replace Br- ion. However, the reaction rate of CsPbX3 QDs is fast, and it is not easy to control the emission wavelength by particle size. In this study, we use the saturated alkyl amines with difference of carbon chain length such as dodecylamine (DDA), hexadecylamine (HDA), and octadecylamine (ODA) to prepare CsPbBr3 QDs. The result shows that the emission spectra for all samples range from 489 (ODA) to 514 nm (DDA), the full width at half-maximum (FWHM) is between 23 to 28 nm, the surface morphologies of all samples are nearly spherical, and the quantum yields (QYs) are higher up to 130 % (compared with R6G and the excitation wavelength is 450 nm). Based on emission spectra we can find that the emission peaks is fixed even under different excitation wavelength, imply that the particle size distribution of QDs is uniform. Moreover, the emission wavelength blue shifts with increasing carbon chain length of amines. The stability of alkyl amine-capped CsPbBr3 QDs is good, especially for DDA-capped sample. We also find that a small emission peak around 462 nm can be only observed for DDA-capped sample. Furthermore, this small peak also can be observed even prolong the reaction time to 10 min. The emission wavelengths of CsPbBr3 QDs can be controlled by carbon chain length of alkyl amines. The small FWHM and high QYs of CsPbBr3 QDs meaning that it is benefit to enhance the color gamut of display.

10348-30, Session 8

Colloidal perovskite nanocrystals: synthesis, optical properties, and applications *(Invited Paper)*

Alexander S. Urban, Ludwig-Maximilians-Univ. München (Germany)

Halide perovskites have emerged as an exciting material for photovoltaic and light-emitting applications due to their fascinating properties, including tunable optical band gaps, excellent absorption, and long charge carrier diffusion lengths. We review the current state of halide perovskite nanocrystals, focusing on our contributions to colloidal synthesis of hybrid and all-inorganic lead halide perovskites nanocrystals with controlled dimensionality, size and composition and on understanding their corresponding optical and electrical properties. We study the aspect of quantum-confinement and its effect on band-gap and exciton binding energies, quantum yield and photoluminescence decay rates. Based on the superb properties of the perovskite nanocrystals, we look at applicability, e.g. for amplified spontaneous emission (ASE), energy transfer and light-emitting devices.

Return to Contents

10348-31, Session 8

Photonic nanopatterns in organo-metal halide perovskites by thermal nanoimprint lithography *(Invited Paper)*

Neda Pourdavoud, Andre Mayer, Si Wang, Bergische Univ. Wuppertal (Germany); Ting Hu, Jie Zhao, Bergische Univ. Wuppertal (Germany) and Nanchang Univ. (China); Kai Brinkmann, Ralf Heiderhoff, Bergische Univ. Wuppertal (Germany); André Marianovich, Wolfgang Kowalsky, Technische Univ. Braunschweig (Germany); Hella-Christin Scheer, Thomas J. Riedl, Bergische Univ. Wuppertal (Germany)

The recently re-discovered class of organometal-halide perovskites hold great promise for solar cells, LEDs and lasers.[1] Today, their potential has not been fully unlocked partially because of the lack of suitable nano-patterning techniques, which are mandatory to create resonator structures, waveguides etc. with a maximum level of precision directly into perovskite layers. Their chemical and thermal instability prevents the use of established wet-chemical patterning techniques.[2] In contrast to conventional inorganic semiconductors, crystal binding in these perovskites includes significant contributions of van der Waals interactions among the halide atoms and Hydrogen bonding.[3] The formation enthalpy per unit cell is only about 0.1eV in MAPbI3.[4] Here, we take advantage of the "soft-matter properties" of organo-metal halide perovskites and demonstrate that photonic nano-structures can be prepared by direct thermal nano-imprint lithography in MAPbI3 and MAPbBr3 at relatively low temperatures (<150°C). The resulting periodic patterns provide distributed feedback resonators, which afford lasing in MAPbI3 with ultra-low threshold levels on the order of 1 ?J/cm2.[5] Moreover, our results also state the first DFB lasers based on MAPbBr3. We will discuss the applicability of thermal imprinting for perovskite solar cells and LEDs.

[1] B. R. Sutherland et al. Nat Photon 2016, 10, 295.

[2] D. Lyashenko et al. physica status solidi (a) 2017, 214, 10.1002/pssa.201600302.

[3] D. A. Egger et al. Journal of Physical Chemistry Letters 2014, 5, 2728.

[4] A. Buin et al. Nano Lett 2014, 14, 6281.

[5] N. Pourdavoud et al. Adv Mater 2017, 10.1002/adma.201605003.

10348-32, Session 9

Electron transfer and nonlinear activity in 2D semiconductors enhanced by nanoantenna through modeling and spectroscopy

Donald K. Roper, Gregory T. Forcherio, Mourad Benamara, Univ. of Arkansas (United States); Luigi Bonacina, Univ. de Genève (Switzerland); Jeremy R. Dunklin, Univ. of Arkansas (United States)

2D semiconductor heterostructures offer compelling new functionalities, e.g., gate tunability of p-n junction, valleytronics and anti-ambipolarity as well as unique optical, electronic and transport properties attributable to distinct atom-scale heterointerfaces. These features could enable atomically-thin flexible integrated circuits, field effect transistors and closed-loop resonators. However, present utility of 2D semiconductors is limited by difficulty in tuning their optoelectronic properties. This work examined nanoantenna (NA)-modulated electron transfer and nonlinear activity at heterointerfaces of monolayer (1L) transition metal dichalcogenides (TMD) exhibiting broken inversion symmetry. Heterostructures of 1LTMD and NA were self-assembled via exfoliation and dropcasting. Nanometer- and femtosecond-resolved electron energy loss spectroscopy (EELS) was used to simulate and measure low-energy NA plasmon modes, damping and electric near fields at heterointerfaces. Quantitated plasmon damping compared with computed inelastic population decay due to radiative and intraband mechanisms indicated electron injection through a Landau mechanism. Quantum efficiency of injection ranged from eight to over thirteen percent. Mid-bandgap edge states increased likelihood of nonlinear activity in exfoliated 1LTMD. A tunable femtosecond laser system for Hyper Rayleigh Scattering (HRS) was used to measure second order nonlinear coefficient of 1LTMD and NA-1LTMD heterostructure. A corollary novel computation method was used to validate measured values. Nonlinear susceptibilities for 1LTMD exceeding those of conventional materials by >102 pm/V with concomitant increases in second harmonic generation (SHG) intensity and two-photon absorption probability were investigated. Coordination of EELS and HRS offers a direct complementary measure of plasmon modes and damping, electric near-field and intrinsic nonlinear activity at high spatiotemporal resolution at heterointerfaces.

10348-33, Session 9

Organic micro-LEDs and cell-embedded lasers: new tools based on organic nanomaterials to advance physical understanding of biological systems *(Invited Paper)*

Malte C. Gather, Marcel Schubert, Anja Kämpf, Andrew Morton, Caroline Murawski, Klara C. R. Volckaert, Markus Karl, Nils M. Kronenberg, Philipp Liehm, Gareth B. Miles, Simon J. Powis, Stefan R. Pulver, Univ. of St. Andrews (United Kingdom)

The vast complexity of biological systems – even of single cells – poses enormous challenges for an in-depth understanding of their function and behaviour. In many cases, we simply lack the tools to observe the relevant processes or to perform deterministic experiments that reproducibly impose defined starting parameters, e.g. on a neuronal network. Here, we give two examples of microdevices that use organic nanomaterials to interface to biological systems. Organic micro-LEDs are used to optically control the behaviour of individual cells via optogenetic activation. We also show how organic microlasers can be embedded in live cells to facilitate long-term cell tracking.

10348-35, Session 9

Broadband excitation and nanoscale relaxation processes of excitons in monolayer MoS2 *(Invited Paper)*

Nicholas Borys, Lawrence Berkeley National Lab. (United States)

The tightly bound exciton complexes of monolayer MoS2 and other two-dimensional transition metal dichalcogenide semiconductors constitute an exciting class of electronic excitations for nanoscale optoelectronics. While it is tempting to assume that these states are analogous to excitons in conventional two-dimensional quantum wells, the atomically thin width, tunable many-body interactions and intricate band structure of monolayer MoS2 combine to produce a unique collection of unanticipated phenomena that defy such simplifications. Exploiting their strong light-matter interactions, a broad arsenal of near-field and conventional optical microscopy and spectroscopy tools has been used to explore and develop a better understanding of this rich suite of photoexcitations. Identified phenomena such as efficient broadband coupling, large renormalization of excitation energies and tunable relaxation dynamics set the stage for the incorporating monolayer MoS2 into a broad range of model optoelectronic systems where strong light-matter interactions and the precise control of energy transport are paramount. At microscopic to nanometer length scales, a striking diversity of photophysical behavior and distinct optoelectronic regions such as disordered peripheral edges, nanoscale charge puddles and defective grain boundaries are found in synthetic monolayer MoS2.

The spatially-dependent behavior, which can be traced to a combination of external stimuli, a complex interplay between excitons and defect states, as well as the temporal dynamics of the growth process, highlights the potential of using two-dimensional transition metal dichalcogenide semiconductors as a canvas in which specific excitonic functionalities can be patterned.

10348-36, Session 9

Strained relations: optical tuning of electronic dynamics in nanoparticle and molecular systems using ultrafast spectroscopy *(Invited Paper)*

Vanessa Huxter, The Univ. of Arizona (United States)

In colloidal metal and semiconductor nanoparticle systems, interface or surface strain can determine many of their optical and material properties including reactivity, catalytic activity and potential for energy and charge transfer. Strain can tune energy levels, raising and lowering the barriers to a variety of physical processes. The inherent strain in the material can be controlled synthetically by modifying the size or shape of the nanomaterial. We propose that strain can also be used as a dynamic, adjustable parameter. Using polarization controlled ultrafast electronic spectroscopy to selectively excite vibronic modes, we periodically enhance the interface strain. This enhancement has an optical readout in the oscillations that appear in the cross polarized anisotropy transient grating signal, providing a direct in-situ measurement of optically controlled strain. In semiconductor heterostructures, strain can be used to shift the relative separation of the levels and modify the rate of charge separation. In metal nanoparticles, the surface strain can be periodically enhanced, modulating their physical properties. Using strain as an adjustable parameter to control the optical properties of nanomaterials will provide new paths towards manufacturing robust, efficient solar cells and novel material systems. Moving from nanoparticle to molecular systems, I will also discuss ultrafast nonlinear spectroscopy measurements of new synthetic analogs of highly conserved natural light harvesting pigments. Relaxation in these tunable redox-active systems is driven by vibrational coupling and symmetry distortions, providing new pathways to controllable and efficient energy and charge transfer in artificial light harvesting systems.

10348-37, Session 10

Investigating ion migration via photoluminescence blinking in perovskite films

Gregory Tainter, Univ. of Cambridge (United Kingdom); Cheng Li, Univ. Bayreuth (Germany); Richard H. Friend, Hannah J. Joyce, Univ. of Cambridge (United Kingdom); Sven Huettner, Univ. Bayreuth (Germany); Felix Deschler, Univ. of Cambridge (United Kingdom)

Recent investigations have revealed spatial variation in photoluminescence (PL) emission of perovskite films. Other reports have found fluctuation in PL intensity in individual grains, i.e. blinking. Here we combine spatially, spectrally, and temporally resolved PL techniques to investigate the characteristic lifetime and emission energy of blinking grains within CH3NH3PbI3-XClX perovskite films. Histograms with millisecond resolution of PL intensity and energy variations are coupled with studies of the charge carrier lifetimes of blinking and non-blinking perovskite grains. These methods reveal a prolonged process, with the switching of increased to decreased emission intensity, and vice versa, taking up to tens of seconds. We investigate the influence on blinking activity of excitation density, while the difference between the influence of electrons and holes is investigated via the deposition of a film of phenyl-C61-butyric acid methyl ester (PCBM). We further investigate the influence of ion migration on blinking by applying an external voltage. The frequency of blinking events is found to be highly dependent upon excitation density. We investigate the scaling of PL intensity of a grain with ion concentration. We identify if the probability of a grain blinking is proportional to ion concentration or if blinking commences at a defined threshold value. These results give dynamic information on local ion migration between grains in perovskite films. From these results, the effect of migration and local over-abundance of ions on charge recombination is identified, which is a central question underlying the improvement of solar cell and LED performance.

10348-38, Session 10

Reversible laser induced amplified spontaneous emission from coexisting tetragonal and orthorhombic phases in hybrid lead halide perovskites *(Invited Paper)*

Anna Köhler, Univ. Bayreuth (Germany)

In the talk I will focus on the optical properties of lead halide perovskites and their dependence on the amount of excess PbI2. I shall first address that, at low temperature, it is possible to optically and reversibly induce a phase change from the orthorhomic to the tetragonal phase. By exploiting amplified spontaneous emission (ASE) from these phases, fully optical read-write-erase cycles can be conducted, as detailed in Adv. Optical Mater. 6 (2016) 917-928 . I shall then elaborate on how and why the photoluminescence features are modified in the presence of excess PbI2.

10348-39, Session 10

Excited state superposition in metal halide perovskites probed via two dimensional spectroscopy *(Invited Paper)*

Carlos Silva, Georgia Tech Research Institute (Canada)

Hybrid lead halide perovskites have emerged as promising materials for efficient opto-electronic technologies. Colloidal nanocrystals of these systems have shown remarkably high photoluminescence quantum yields, reaching upto 90% and have recently been proposed as inks to achieve high quality thin films [1]. Being virtually defect-free [2], these nanocrystals offer an ideal scenario to address some of the key issues in the photo-physical processes in these novel materials. Here, we use two dimensional phase modulation excitation spectroscopy to investigate coherent non-linear interactions in colloidal suspensions of CsPb(Br:I)3 nanocrystals. We observe a cross-peak close to the band-edge in the 2D spectrum within a population time of 50 fs, suggesting an evolution of coherent superposition of two distinct electronic states, that cannot be identified via conventional spectroscopies. Defects excluded, we attribute the presence of such a mixed-state to the weak but finite non-radiative decay channel for the primary photo-excitation. Such a superposition is quenched at higher excitation densities due to the presence of competing Auger interactions or via Coulomb screening by the high carrier density.

[1] Q. A. Akkerman, V. D'Innocenzo, S. Accornero, A. Scarpellini, A. Petrozza, M. Prato, and L. Manna, J. Am. Chem. Soc. 137, 10276 (2015).

[2] A. R. Srimath Kandada, S. Neutzner, V. D'Innocenzo, F. Tassone, M. Gandini, Q. A. Akkerman, M. Prato, L. Manna, A. Petrozza, and G. Lanzani, J. Am. Chem. Soc. 138, 13604 (2016).

10348-40, Session 10

Solid-state organic/nanocrystal films for infrared/visible photon conversion via excitonics *(Invited Paper)*

Mark W. B. Wilson, Univ. of Toronto (Canada) and Massachusetts Institute of Technology (United States);

Lea Nienhaus, Mengfei Wu, Massachusetts Institute of Technology (United States); Daniel Congreve, The Rowland Institute at Harvard (United States) and Massachusetts Institute of Technology (United States); Vladimir Bulovic, Moungi G. Bawendi, Marc A. Baldo, Massachusetts Institute of Technology (United States)

The ability to efficiently interconvert low-intensity light between the visible and infrared would be an enabling technology—particularly for applications such as 3rd-generation photovoltaics, biological imaging, and cost-effective cameras in the short-wave infrared (SWIR; ?:1?3μm). Here, we present a novel approach using multi-excitonic interactions in nanostructured materials that could enhance existing silicon-based detectors. Specifically, we show that two excitonic materials—organic semi-conductors and colloidal nanocrystals—can be combined to create passive thin-film devices that achieve broadband, non-coherent down- or up-conversion between the SWIR and the visible.

To achieve upconversion, we synthetically tune the bandgap of PbS nanocrystals to absorb SWIR photons (?>1 μm), and funnel these excitations to an organic semiconductor (rubrene). Here, their energy is combined to create visible light. We achieve an upconversion efficiency of 1.2±0.2% with ?=808 nm excitation at 12 W/cm2. Further, we show that there is no fundamental barrier to efficient performance at a thousandth of this excitation intensity (less than natural sunlight!)

Our hybrid approach to achieve non-coherent upconversion may prove broadly applicable in solar and SWIR-detection applications, where effective molecular phosphors are lacking—indeed, quantum dots are ideal SWIR sensitizers, as their excitons are functionally spin-mixed at room temperature, and both their optical gap and ionization energy can be tuned via colloidal synthesis.

10348-41, Session 11

Effects of surface and interface traps on exciton and multi-exciton dynamics in core/shell quantum dots

Renato Bozio, Univ. degli Studi di Padova (Italy) and Consorzio Interuniversitario Nazionale per la Scienza e Tecnologia dei Materiali (Italy); Marcello Righetto, Alessandro Minotto, Univ. degli Studi di Padova (Italy)

Exciton interactions and dynamics are the most important factors determining the exceptional photophysical properties of semiconductor quantum dots (QDs). In particular, best performances have been obtained for ingeniously engineered core/shell QDs. We have studied two factors entering in the exciton decay dynamics with adverse effects for the luminescence efficiency: exciton trapping at surface and interface traps, non radiative Auger recombination in QDs carrying either net charges or multiple excitons.

In this work we present a detailed study into the optical absorption, fluorescence dynamics [1] and quantum yield [2], as well as ultrafast transient absorption properties of CdSe/CdS, CdSe/Cd0.5Zn0.5S, and CdSe/ZnS QDs as a function of shell thickness. It turns out that de-trapping processes play a pivotal role in determining steady state emission properties. By studying the excitation dependent photoluminescence quantum yields (PLQY) in different CdSe/CdxZn1-xS (x = 0, 0.5, 1) QDs, we demonstrate the different role played by hot and cold carrier trapping rates in determining fluorescence quantum yields. The complementary use of global and inversion analysis allows us to untangle the complex ultrafast transient absorption signals. Smoothing of interface potential, together with effective surface passivation, appear to be crucial factors in slowing down both Auger-based and exciton trapping recombination processes.

[1] A. Minotto, F. Todescato, et al., J. Phys. Chem. C 118, 24117 (2014).

[2] M Righetto, A Minotto, R Bozio, J. Phys. Chem. C 121, 896, (2017).

10348-42, Session 11

Ultrafast energy transfer in photosynthetic light harvesting *(Invited Paper)*

Gabriela Schlau-Cohen, John Ogren, Ashley Tong, Minjung Son, Massachusetts Institute of Technology (United States)

In photosynthetic light harvesting, absorbed energy migrates through a network of light-harvesting complexes to reach a dedicated location for conversion to chemical energy. This energy flow gives rise to a remarkable near unity quantum efficiency through a series of rapid energy transfer steps. We measure these ultrafast energy transfer dynamics within light-harvesting complexes in a near-native environment using transient absorption spectroscopy. We quantitatively compare the energy transfer dynamics within this near-native environment to those within the typical detergent-solubilized environment for light-harvesting complex 2 (LH2), the primary light-harvesting complex in purple bacteria. Through this comparison, we identify the energy transfer steps that change with the surrounding environment and those that are protected by the protein structure of the light-harvesting complex. Thus, we identify the effect of the surrounding membrane in driving energy flow.

10348-43, Session 11

Dopant-enhanced photoluminescence in solution processed semiconducting single crystals *(Invited Paper)*

Dmitry Y. Paraschuk, Olga D. Parashchuk, Vladislav G. Konstantinov, M.V. Lomonosov Moscow SU (Russian Federation); Oleg V. Borshchev, Nicolay M. Surin, Institute of Synthetic Polymeric Materials (Russian Federation); Sergey A. Ponomarenko, Institute of Synthetic Polymeric Materials (Russian Federation) and M.V. Lomonosov Moscow SU (Russian Federation); Artur A. Mannanov, M.V. Lomonosov Moscow SU (Russian Federation) and Zernike Institute for Advanced Materials (Netherlands); Maxim S. Pshenichnikov, Zernike Institute for Advanced Materials (Netherlands)

Organic optoelectronics needs materials combining high luminescence and efficient charge transport. Organic single crystals demonstrate the best charge transport properties in organics; however, tight molecular packing in them usually results in luminescence quenching. Here we report on enhancement of luminescent properties of solution-processed organic semiconducting single crystals via doping by molecular energy acceptors. As host and dopant molecules we synthesized thiophene-phenylene co-oligomers (TPCOs) of different lengths and used the longer TPCOs (with lower band gap) as dopant to the shorter ones (with higher band gap). We grew TPCO host single crystals doped by longer TPCOs in the concentration range 0.01–3% and studied their photophysics by steady-state and time-resolved photoluminescence (PL) spectroscopy. For the best host-dopant single crystals, the PL is maximal at the doping level ~1%, and all the PL comes from the dopant with the PL quantum yield corresponding to that of dilute dopant solution. As the mechanisms of host-dopant energy transfer, we modelled exciton diffusion and Förster resonant energy transfer using Monte-Carlo simulations. Our results demonstrate that doping of organic semiconducting single crystals by highly luminescent dopant is a promising route to high performance materials for organic optoelectronics.

10348-26, Session 12

Effect of crystal packing on the electronic properties of molecular crystals *(Invited Paper)*

Noa Marom, Carnegie Mellon Univ. (United States)

Molecular crystals have applications in nonlinear optics, organic electronics, and particularly in pharmaceuticals, as most drugs are marketed in the form of crystals of the pharmaceutically active ingredient. Molecular crystals are bound by dispersion (van der Waals) interactions, whose weak nature generates potential energy landscapes with many shallow minima that are close in energy. As a result, molecular crystals often exhibit polymorphism, the ability of the same molecule to crystallize in several structures. Crystal structure may profoundly influence the bioavailability, toxicity, manufacturability, and stability of drugs. In the context of technological applications, crystal structure affects the electronic and optical properties.

We perform large scale quantum mechanical simulations to predict the structure of molecular crystals and investigate the effect of crystal packing on their electronic and optical properties. The massively parallel genetic algorithm (GA) package, GAtor, relies on the evolutionary principle of survival of the fittest to find low-energy crystal structures of a given molecule. Dispersion-inclusive density functional theory (DFT) is used for structural relaxation and accurate energy evaluations. The structure generation package, Genarris, performs fast screening of randomly generated structures with a Harris approximation, whereby the molecular crystal density is constructed by replicating the single molecule density, which is calculated only once. Many-body perturbation theory, within the GW approximation and the Bethe-Salpeter equation (BSE), is then employed to describe properties derived from charged and neutral excitations.

For tricyano-1,4-dithiino[c]-isothiazole (TCS3), we propose a layered crystal structure, which is only 20 meV higher in energy than the observed cyclic dimer structure, and may exhibit a smaller gap, better transport properties, and broader optical absorption. For rubrene, we predict that a lesser known monoclinic crystal structure may exhibit higher singlet fission efficiency than the orthorhombic form, possibly rivaling that of pentacene. Thus, the electronic and optical properties of organic semiconductors may by optimized by modifying the crystal packing.

10348-44, Session 12

Nanostructural engineering towards high quality luminescent giant quantum dots

Amita Joshi, Ajay Singh, Jennifer A. Hollingsworth, Los Alamos National Lab. (United States)

The inorganic fluorophores such as quantum dots have application ranging from opto-electronics to cell imaging in biology. But this important aspect (optical) of the QDs has always been challenged by the surface or chemical environmental instabilities in bulk and at single particle level. To overcome the problems with these systems different approached have been used such as surface passivation with ligands, over coating with polymers, core-shell heterostructures etc. The core-shell semiconductor nanocrystals, called giant quantum dot (gQDs) nanocrystal with their wide-bandgap chalcogenides based core-shell structure have exhibited improved photo-physical properties. With decreased non-radiative recombination, suppressed blinking and enhanced photo-stability, the core-shell gQDs provided more opportunities for applications such as single particle tracking, active biolables and stable light emitting diodes. But still the chalcogenides based shell systems can undergo photo-oxidized and lead to emission loss and instability. Here, we will present our approach to overcome this problem by exploring the oxide based shell and polymer matrix, as they are more stable in case of photo-oxidation process and can greatly reduce the surface recombinations. The oxide shell and polymer matrix not only prevent the core oxidation but also maintain the structural integrity and act as a protective layer to prevent the leaching out of the cation or anion from the cores. By carefully choosing the oxide material for the over coating not only the optical properties of bare quantum dots and giant quantum dots were improved but also other undesirable results like nucleation of metal oxide nanocrystals was avoided.

10348-45, Session 12

Structural dynamics in lead-halide perovskites from first-principles molecular dynamics *(Invited Paper)*

David A. Egger, Weizmann Institute of Science (Israel) and Univ. Regensburg (Germany)

The optical and transport properties of lead-halide perovskites (LHPs) have been used as a basis for new solar cell technologies showing record improvements in efficiencies. In the search for the microscopic origins of this success, many recent studies suggest that structurally dynamic effects, going far beyond small harmonic vibrations, are active already at room temperature and standard operating conditions.

Here, I explore this issue in several different LHP materials using first-principles molecular dynamics based on density functional theory. In particular, I will focus on dynamic polar distortions and an assessment of optical phonons. I will also comment on the possible relevance of these phenomena for charge-carrier dynamics.

10348-46, Session 12

Nanoscale structure measurements for flexible electronics manufacturing *(Invited Paper)*

Dean M. DeLongchamp, National Institute of Standards and Technology (United States)

Flexible electronics is an emerging additive manufacturing method in which electronics are made using functional inks that are printed or coated. Organic photovoltaics (OPV) is a flexible electronics technology for making low-cost solar cell modules. Although OPV has significantly matured over the past few years, there remain significant challenges in moving from lab-scale devices to real manufacturing. We address this gap using a blade coating process as a prototype for slot-die coating and observing the structure of films in-situ as they dry. Our measurements include synchrotron-based X-ray scattering and a variety of optical methods.

I will highlight our studies of organic photovoltaic (OPV) systems deposited by blade coating, which can achieve up to 9.5 % power conversion efficiency (PCE). Our methods reveal a diversity of solidification mechanisms among OPV systems. Some are dominated by the nanoscale crystallization of the components, whereas others appear to be dominated by liquid-liquid phase separation. Examples of good performance can be found for systems that obey either mechanism. Systems that maintain high PCE in active layers thicker than greater than ≈200 nm, however, are rare. We describe one such system, in which the salient traits appear not to be the nanoscale shape and orientation of the domains, but rather the relatively pure phases and relatively strong diffraction of the polymer component. The results are extended to pilot-scale R2R coating by demonstrating nominally identical morphologies for both piece blade-coating and continuous-web, slot-die coating.

10348-50, Session PWed

Self-powered active acetylene gas sensing based on triboelectric nanogenerator by the semimetallic PEDOT:PSS hole transport layer

Gwiy-Sang Chung, Univ. of Ulsan (Korea, Republic of)

We report an enhanced triboelectric nanogenerator (TENG) based on the

contact-separation mode between a patterned film of polydimethylsiloxane (PDMS) with a semi-metallic elastomer of poly(3,4-ethylenedioxythiophen e):poly(styrenesulfonate) (PEDOT:PSS) and a nylon fiber film. The addition of ethylene glycol to the PEDOT:PSS film improves the functionality of the TENG significantly, yielding promising applicability in both indoor and outdoor (i.e., under sunlight) environments, with the maximum instantaneous power of 0.09 mW (indoors) and 0.2 mW (outdoors) for the load resistance of 3.8 M?. The device can also generate 11.2 V and 0.08 μA cm?2 in response to the forearm movement of a human. Additionally, by replacing the bare nylon fiber in the TENG design with a Ag@ZnO/nylon fiber film, a self-powered active sensor (triboelectric nanogenerator–based sensor; TENS) has been realized to detect acetylene (C2H2) gas. The TENS exhibits excellent sensitivity of 70.9% (indoors) and 89% (outdoors) to C2H2 gas of 1000 ppm concentration. The proposed approach for harvesting energy and sensing can be advantageous in practical applications and may stimulate new research that will enhance nanogenerators as well as wearable, self-powered active sensors.

10348-51, Session PWed

Surface resistance change during nickel hydroxide phase transformations

Ricardo I. Tucceri, Univ. Nacional de la Plata (Argentina)

No Abstract Available.

10348-52, Session PWed

Optical properties in Al2O3-Y2O3 dielectric ultrathin multilayer stacks grown by atomic layer deposition

Javier Lopez, Hugo Borbón, Roberto Machorro, Univ. Nacional Autónoma de México (Mexico); Nicola Nedev, Univ. Autónoma de Baja California (Mexico); Mario Farias, Hugo Tiznado, Gerardo Soto, Univ. Nacional Autónoma de México (Mexico)

Ultrathin multilayer stacks based on Al2O3-Y2O3 bilayers were prepared via thermal atomic layer deposition (ALD) in order to study the behavior of refractive index and optical bandgap energy as a function of Y2O3 thickness layer. Ttotal thickness (?100 nm), Refractive index n(?) and optical bandgap Eg, of each multilayer were studied via spectroscopic ellipsometry (SE). Cross-sectional mode scanning electron microscope (SEM) images allowed to verify the multilayer total thickness and confirmed the accuracy of the optical model used for SE measurements. From the Single effective oscillator model (MSEO), it found that Eg gradually decreases from 5.45 to 4.24 eV as the bilayer thickness increases. The Eg change is ?Eg= 1.2 eV for thickness variation between 2.1 to 13.3 nm. These results reveal that refractive index and optical bandgap can be modulated systematically as a function of bilayer thickness and open the possibility for this material to be exploited for developing opto-electronic devices in nanotechnology.

Acknowledgments

This work was partially supported by Direcció General de Asuntos del Personal Académico (DGAPA-UNAM) through PAPIIT research projects IN105114 and IN107715 J. López kindly thanks DGAPA-UNAM for a 2-year postdoctoral fellowship. The authors also would like to thank valuable technical support and the collaboration of David Dominguez, Eduardo Murillo, Jose Juan Gervacio, Noemi Abundiz, David Mateos, Israel Gradilla, Francisco Ruiz, Jaime Mendoza, Jose Luis Cervantes and Eric Flores.

10348-53, Session PWed

Chemical and charge transfer studies on interfaces of a conjugated polymer and ITO

Sam-Shajing Sun, Tanya S. David, Norfolk State Univ. (United States)

Conjugated oligomers and polymers are very attractive for potential future plastic electronic and opto-electronic device applications such as plastic photo detectors and solar cells, thermoelectric devices, field effect transistors, and light emitting diodes. Understanding and optimizing charge transport between an active polymer layer and conductive substrate is critical to the optimization of polymer based electronic and opto-electronic devices. This study focused on the design, synthesis, self-assembly, and electron transfers and transports of a phosphonic acid end-functionalized polyphenylenevinylene (PPV) that was covalently attached and self-assembled onto an Indium Tin Oxide (ITO) substrate. This study demonstrated how atomic force microscopy (AFM) can be an effective characterization technique in conjunction with conventional electron transfer methods, including cyclic voltammetry (CV), towards determining electron transfer rates in polymer and polymer/conductor interface systems. This study found that the electron transfer rates of covalently attached and self-assembled films were much faster than the spin coated films. The knowledge from this study can be very useful for designing potential polymer based electronic and opto-electronic thin film devices.

10348-55, Session PWed

Spin-polarization effects upon light-Induced charge separation at BHJ interfaces

Oleg G. Poluektov, Jens Niklas, Argonne National Lab. (United States)

Organic Photovoltaic technology could provide sufficient energy to satisfy the global economic demands in the near future. Understanding the charge separation and electronic structure at a molecular level is crucial for improving the efficiency of OPV materials. In spite of the importance of this research a number of fundamental questions about how the organic bulk heterojunction cell enables efficient long-lived and long-range charge separation remain unanswered. Here we report on the relationship between efficiency of charge separation and spin-polarization phenomena. The detection of strong electron spin-polarization in the transient EPR spectra of organic photovoltaic materials points to the significance of electron spin dynamics and spin-quantum phenomena for the efficient charge separation in solar cells. Evidence for spin-dependent charge separation dynamics in OPV materials comes from the observation of spin-correlated radical pairs and triplet excitons generated by back recombination within primary CT-state. Important that spin-polarization in CT- and triplet-states can be detected only by transient EPR technique. The paper discusses possible pathways for spin-correlated radical pairs and triplet excitons formation. Correlation between manifestation of spin-polarization in radical pairs and triplets is reported. While the observation of the back recombination triplet indicates low charge separation efficiency, since back recombination competes with forward charge separation, there is no direct correlation with the OPV efficiency. One of the reason is that EPR experiments were done in the high magnetic field of the EPR spectrometer (versus the natural environment) where of singlet-triplet mixing is more efficient.

10348-56, Session PWed

Development of a single-shot transient absorption technique: studying exciton dynamics in non-static systems

Kelly S. Wilson, Cathy Y. Wong, Univ. of Oregon (United States)

Single-shot transient absorption (ssTA) spectroscopy is a novel technique that is capable of measuring exciton dynamics of non-static systems, such as molecules as they undergo drying-mediated aggregation. This allows us to correlate evolving exciton dynamics with the progress of molecular aggregation, which, to our knowledge, has not yet been measureable. TA measures exciton dynamics using transients obtained by varying the time delay between a pump and probe pulse. Typically, these time delays are generated using a back-reflecting mirror mounted on a motorized translation stage; as a result, data collection requires a significant amount of time which limits measurements to systems that are static for the duration of the experiment. ssTA overcomes this restriction by employing cylindrically focused pump and probe pulses that enable us to spatially encode time delays, thus permitting collection of an entire transient in a single shot. A time delay range of ~50 ps, which is dependent on the beam profile and wavefront angle, has been successfully implemented. We present the design of our ssTA instrument, including time delay calibration. ssTA is demonstrated by measuring exciton dynamics during solution deposition of copper phthalocyanine dye into a thin film and comparing initial and final transients with traditional TA measurements. We also reveal, for the first time, how these dynamics change as molecules interact with each other during aggregation. This technique will tighten the feedback loop on the development of designer materials with target photophysical properties, such as singlet fission in electron donor materials.

10348-57, Session PWed

Mechanism of fluorescent silicon nanoparticles

Woong Young So, Qi Li, Rongchao Jin, Linda A. Peteanu, Carnegie Mellon Univ. (United States)

Silicon (Si) is known to have an indirect bandgap transition, which means it has poor fluorescence properties. However, when engineered into sub-nm sized particles, Si nanoparticles become emissive due to quantum confinement. However, in unmodified Si particles, this effect is limited to generating red or near-infrared emission with low quantum yield. To resolve these limitations, surface-modification methods have successfully generated Si particles that emit in the blue, cyan, and green with quantum yields up to ~90%.[1,2] These modifications have also made the Si nanoparticles water-soluble, making them promising in biological applications. To date, the mechanism of emission in these species is still unclear although it has been speculated that charge transfer of SiON could be responsible. To investigate whether emission by these Si nanoparticles proceeds via a charge transfer mechanism, Stark spectroscopy is used. In this method, an external electric field is applied to the Si nanoparticles. Changes in the absorption and/or emission spectra due to the applied field can be taken as strong evidence for a charge transfer mechanism. From the results of Stark spectroscopy, Si nanoparticles are revealed to have ligand to metal charge transfer mechanism along with electric-field quenching, which is useful information for utilization into applications. Addition to the information found, a method of how to tune the emission maxima based on selection of ligands is prosed.

[1] J. Am. Chem. Soc., 2013, 135(40), 14924–14927

[2] ACS Nano, 2016, 10(9), 8385–8393

10348-58, Session PWed

Depth profile interface analysis on full photonic devices

Yan Busby, Univ. of Namur (Belgium); Lucio Ciná, Sara Pescetelli, Aldo Di Carlo, Univ. degli Studi di Roma “Tor Vergata” (Italy); Jean-Jacques Pireaux, Laurent Houssiau, Univ. of Namur (Belgium)

To develop advanced spectroscopies allowing for three-dimensional analysis of hybrid interfaced materials stacks is both highly desirable and challenging. This contribution aims illustrating recent progress in this field by applying depth profile interface analysis on full photonic devices including solar cells and light-emitting devices. Interesting results have been recently obtained in the analysis of devices based on bulk heterojunctions (P3HT:PCBM) or organometal halide perovskite absorbers. In this approach, the device functionality was correlated to the depth-resolved elemental composition and chemistry of interfaces by combining quantitative chemical analysis with high-resolution X-ray photoelectron spectroscopy (XPS) and 3D molecular imaging with time-of-flight secondary ion mass spectrometry (ToF-SIMS). Materials erosion was performed with low-energy (< 1 keV) ion beams (Ar+ or Cs+) to preserve both the chemical information and the interface quality.

In conventional P3HT:PCBM solar cells, the heterojunction components distribution have been resolved the chemical analysis on S2p and O1s peaks, showing a strong PCBM segregation toward the top metal electrode.[1] In mixed halide perovskite absorbers, Cl segregation have been resolved.[2] In organolead halide perovskite solar cells, the interfaces quality, perovskite composition and top electrode metal diffusion was correlated to the perovskite deposition procedure and conversion environment.[3] In mesoscopic perovskite based LEDs, the device lifetime was correlated to the degradation of the hole-transporting material (HTM) and to the perovskite?HTM interface quality.[4] Recent results on graphene-based perovskite solar cells will be also discussed.

References

[1] Y Busby; E List-Kratochvil; J-J Pireaux, Chemical analysis of the interface in bulk-heterojunction solar cells by xps depth profiling ACS Applied Materials & Interfaces 2017, DOI: acsami.6b14758

[2] M Ralaiarisoa; Y Busby; J Frisch; I Salzmann; J-J Pireaux; N Koch, Correlation of Annealing Time with Crystal Structure, Composition, and Electronic Properties of CH3NH3PbI3-xClx Mixed-Halide Perovskite Films Physical Chemistry Chemical Physics, 2016, DOI: 10.1039/c6cp06347k

[3] F Matteocci; Y Busby, J-J Pireaux; G. Divitini; S Cacovich; C. Ducati; A Di Carlo, Interface and Composition Analysis on Perovskite Solar Cells ACS Appl. Mater. Interfaces 2015, DOI: acsami.5b08038.

[4] A L Palma, L Cinà, Y Busby, A Marsella, A Agresti, S Pescetelli, J-J Pireaux, A Di Carlo, Mesoscopic perovskite light emitting diodes ACS Appl. Mater. Interfaces, 8, 2016, DOI: 10.1021/acsami.6b07750

10348-59, Session PWed

Growth method and mechanism formation of the InP nanostructured thin films

Orest Kvitsiani, Tinatin Laferashvili, Institute of Cybernetics (Georgia); Sch Lomithashvili, Georgian Technical Univ. (Georgia); Vladimer Mikelashvili, Institute of Cybernetics (Georgia) and Georgian Technical Univ. (Georgia)

InP is a direct bandgap semiconductor with bandgap width of 1.344 eV which gives strong near infrared emission; infrared photodetectors based on InP represent an important technology in the field of infrared detection. The nanostructured InP thin films exhibit unique properties, their emission wavelength can be tuned within the whole visible and near-infrared range by changing the size of nanocrystals (NCs).

An undoped n-type GaP wafers grown by the Czochralski method with the thickness of about 200-250 μm and the carrier concentration of

2?1016 - 4?1017 cm-3 were used in our experiments. The technology of electrochemical deposition of metallic thin films (20-25 nm thickness) on a semiconductor surface were used for fabrication of the In/GaP metal/semiconductor contacts with "near-ideal" photoelectric characteristics.

Dependence of the electric and photoelectric characteristics on the annealing temperature (100-350 0C) of In/GaP Schottky barrier was investigated. A new region of the strong photosensitivity in the 1.75-2.05 eV area was detected. The appearance of this region was attributed to the formation of a new nanostructured thin film on GaP surface, via the metal and semiconductor interaction.

Here we present new technology fabrication of InP nanostructured thin films, that differs from the Stranski-Krastanov growth mode, and from the formation of InP NCs by droplet epitaxy using molecular beam epitaxy, described in literature lately. The mechanism of the InP NCs formation on the GaP surface is discussed taking into account obtained experimental data and the publications.

10348-60, Session PWed

Effects of plasmonic metal films on the emission properties of organic films

Sikandar Abbas, Linda A. Peteanu, Carnegie Mellon Univ. (United States)

There is a growing demand to improve the operational lifetime of electroluminescent devices utilizing conjugated polymers which are often deposited over metal electrodes. Photo-degradation of emissive organic layer is one factor that decreases the overall efficiency and longevity of these devices. Therefore, it is important to investigate the underlying photochemistry at metal-polymer interface. Here, effects of metal films on the emission properties of organic polymers are studied using Total Internal Reflection Fluorescence (TIRF) microscopy and Fluorescence Lifetime Imaging (FLIM). Poly(phenylene vinylene) (MEHPPV) is spun cast over gold films of varying thickness (2 nm to 8 nm). While 8 nm gold films completely quench the MEHPPV fluorescence, thinner gold films (~ 2 nm) cause minimal quenching. More surprisingly, MEHPPV exhibits a remarkable increase in photo-stability when deposited on gold films relative to that on glass, even in the presence of molecular oxygen and under continuous laser illumination. When the gold film is replaced with non-plasmonic metal film, this enhanced stability is not observed suggesting it is induced by interactions of the molecules with the surface plasmon of the gold films. The gold films are prepared by sputter coating process. If these films are kept under ambient conditions for ~ 4-5 hours, these metal films behave differently. The photostability effects are not observed when MEHPPV is deposited on these aged films. Experiments are underway to investigate the aging effects.

10348-61, Session PWed

Ultrafast carrier dynamics in atomically thin 2D transition metal dichalcogenides

Felice Gesuele, Carlo Altucci, Pasqualino Maddalena, Univ. degli Studi di Napoli Federico II (Italy)

Two dimensional crystal are a new class of layered materials with novel and intriguing optical and electronic properties when reduced to single atomic layer. Several applications have been proposed in nanoelectronics, photodetection and photovoltaics; however the practical use of 2D crystals requires a detailed knowledge of the light matter interaction processes. As a consequence charge carrier dynamics is subject of intense studies in 2D crystals and requires ultrafast spectroscopies to be unveiled.

Here we employ hyperspectral ultrafast transient absorption spectroscopy based on supercontinuum probe: in this technique the samples are optically "pumped" using the femtosecond tunable pulse coming from an Optical Parametric Amplifier, and "probed" for changes in transmission with a "white light" laser-generated supercontinuum. We combine this technique with confocal microscopy in order to resolve the carrier dynamics with micron spatial resolution.

We prepare 2D crystals of transition metal dichalcogenides (MoS2 and WS2) by means of mechanical exfoliation (tape method) and characterize them by means of confocal microscopy, Atomic Force Microscopy, Raman and Photoluminescence spectroscopy to determine their number of layers, level of doping, presence of defects. We also compare results obtained with Chemical Vapor Deposition growth.

Transition Metal dichalcogenides are direct gap semiconductor, in the limit of single atomic layer. Our technique shows the presence of negative differential response (bleach) corresponding to the A and B exciton. Measured lifetimes are on the order of tens of picosecond for band-edge recombination mechanisms and depends on the pump fluence and, strongly, on the number of layers. Carrier dynamics in close proximity of flakes edges shows additional decay channel due to edge related defects and trap states.

Our results provide insights into the photophysics of these materials in view of their applications in optoelectronics and photovoltaics.

Conference 10349: Low-Dimensional Materials and Devices 2017

SPIE. OPTICS+ PHOTONICS NANOSCIENCE+ ENGINEERING

Wednesday - Thursday 9 –10 August 2017

Part of Proceedings of SPIE Vol. 10349 Low-Dimensional Materials and Devices 2017

10349-500, Session Plen

Science, engineering, and commercialization of flexible, printable 2D atomic materials and devices *(Invited Paper)*

Deji Akinwande, The Univ. of Texas at Austin (United States)

This talk will focus on the scientific progress, engineering achievements, and commercialization of flexible/printable atomically thin materials (graphene, TMDs, phosphorus, Xenes, etc.) and devices. A variety of advancements have been made in electronic, photonic, and passive devices over the past decade including the demonstration of 100GHz flexible transistors, discovery of novel switching properties, development of electronic tattoos, and understanding of interlayer coupling via high-pressure physics. In addition, nanomanufacturing advancements have enabled large-area materials which for the case of graphene has resulted in several commercial products. The talk will conclude with a perspective for the next decade of research.

10349-2, Session 1

Highly sensitive and high-speed imaging of grain boundaries in graphene by transient absorption microscopy *(Invited Paper)*

Chen Yang, Purdue Univ. (United States)

No Abstract Available.

10349-3, Session 1

Plasmon-enhanced photon emission and absorption in monolayer, two-dimensional semiconductors *(Invited Paper)*

Koray Aydin, Northwestern Univ. (United States)

Monolayer two-dimensional transition metal dichalcogenides (2D-TMDCs) have gained immense attention for their desirable transport properties and direct bandgap that have led to a plethora of studies on modern nanoelectronic and optoelectronic applications. These properties are known to occur exclusively in TMDCs when thinned down to one or few monolayers. However reduced dimensionality poses a significant challenge for photonics and optoelectronics applications due to poor light absorption and emission dictated by the volume of semiconductor material. Plasmonic nanostructures have been widely studied for enhancing light-matter interactions in wide variety of material systems resulting in increased emission and absorption properties. 2D Materials provide the ultimate lower limit in terms of material thickness, therefore investigation of plasmon/2D Material hybrid material systems with a specific aim to enhance light-matter interactions is essential for practical optoelectronic applications. In this talk, I will discuss increased photoluminescence emission from MoS2 using both periodic plasmonic nanodisc arrays as well as a single plasmonic optical antenna. I will also describe a method for understanding and identifying the contributions of excitation and emission field enhancements to the overall photoluminescence enhancement using a tapered gold antenna. Additionally, I will describe a systematic study in which we have demonstrated increased light absorption in a monolayer WS2 film.

10349-49, Session 1

Inkjet printed graphene-based field-effect transistors on flexible substrate

Mahmuda Akter Monne, Evarestus Enuka, Texas State Univ. (United States); Zhuo Wang, Chang'an Univ. (China); Maggie Y. Chen, Texas State Univ. (United States)

This paper presents the design and fabrication of inkjet printed graphene field-effect transistors (GFETs). The inkjet printed GFET is fabricated on a DuPont™ Kapton® FPC polyimide film with a thickness of 5 mill and dielectric constant of 3.9 by using a Fujifilm Dimatix DMP-2831 materials deposition system. A layer by layer 3D printing technique is deployed with initial printing of source and drain by silver nanoparticle ink. Then graphene active layer, doped with MoS2 monolayer/multilayer dispersion, is printed onto the surface of substrate covering the source and drain electrodes. Ion gel is adopted as the dielectric material due to the high dielectric constant. The dielectric layer is then covered with silver nanoparticle gate electrode. Characterization of GFET has been done at room temperature (25°C) using HP-4145B semiconductor parameter analyzer (Hewlett-Packard). The characterization result shows for a voltage sweep from -2 volts to 2 volts, the drain current changes from 949 nA to 32.3 μA and the GFET achieved an on/off ratio of 38:1, which is a milestone for inkjet printed flexible graphene transistor.

10349-4, Session 2

Correlated structural and optical properties of the MoTe2-WTe2 alloy system *(Invited Paper)*

Patrick Vora, George Mason Univ. (United States); Ryan Beams, National Institute of Standards and Technology (United States); Sean M. Oliver, Jaydeep Joshi, George Mason Univ. (United States); Sergiy Krylyuk, National Institute of Standards and Technology (United States) and Theiss Research (United States); Irina Kalish, Alina Bruma, National Institute of Standards and Technology (United States); Iris Stone, George Mason Univ. (United States); Arunima Singh, Francesca Tavazza, Stephan J. Stranick, Albert V. Davydov, National Institute of Standards and Technology (United States)

The structural polymorphism intrinsic to select transition metal dichalcogenides provides exciting opportunities for engineering novel devices. Of special interest are memory technologies that rely upon controlled changes in crystal phase, collectively known as phase change memories (PCMs). $MoTe_2$ is ideal for PCMs as the ground state energy difference between the hexagonal (2H, semiconducting) and monoclinic (1T', metallic) phases is minimal. This energy difference can be made arbitrarily small by substituting W for Mo on the metal sublattice, thus improving PCM performance. Therefore, understanding the properties of $Mo_{1-x}W_xTe_2$ alloys across the entire compositional range is vital for the technological application of these versatile materials.

We combine Raman spectroscopy with aberration-corrected scanning transmission electron microscopy and x-ray diffraction to explore the $MoTe_2$-WTe_2 alloy system. The results of these studies enable the construction of the complete alloy phase diagram, while polarization-resolved Raman measurements provide phonon mode and symmetry assignments for all compositions. Temperature-dependent Raman measurements indicate a transition from 1T'-$MoTe_2$ to a distorted orthorhombic phase (T_d) below 250 K and facilitate identification of the anharmonic contributions to the optical phonon modes in bulk $MoTe_2$

and Mo$_{1-x}W$_xTe_2$ alloys. We also identify a Raman-forbidden MoTe$_2$ mode that is activated by compositional disorder and find that the main WTe$_2$ Raman peak is asymmetric for x<1. This asymmetry is well-fit by the phonon confinement model and allows the determination of the phonon correlation length. Our work is foundational for future studies of Mo$_x$W${1-x}$Te$_2$ alloys and provides new insights into the impact of disorder in transition metal dichalcogenides.

10349-5, Session 2

Characterization of few-layer 1T' MoTe2 using polarization resolved Raman scattering and second harmonic generation *(Invited Paper)*

Ryan Beams, National Institute of Standards and Technology (United States); Luiz Gustavo Cancado, Univ. Federal de Minas Gerais (Brazil); Sergiy Krylyuk, Irina Kalish, Berc Kalanyan, Alina Bruma, National Institute of Standards and Technology (United States); Arunima Singh, Lawrence Berkeley National Lab. (United States); Kamal Choudhary, National Institute of Standards and Technology (United States); Patrick Vora, George Mason Univ. (United States); Francesca Tavazza, Albert V. Davydov, Stephan J. Stranick, National Institute of Standards and Technology (United States)

We study the crystal symmetry of few-layer MoTe2 in the metallic 1T' phase using polarization resolved Raman scattering and second harmonic generation (SHG). The bulk 1T' crystals were grown using chemical vapor transport and subsequently exfoliated onto an Si/SiO2 surface. Group theory analysis of the polarization dependence of the Raman scattering for crystals with various number of layers allowed for definitive assignment of the modes and resolves a discrepancy in the literature. The results were also compared to density-functional theory simulations. While bulk 1T' MoTe2 is known to be inversion symmetric, we find that the inversion symmetry is broken for crystals with even numbers of layers, resulting in a strong SHG signal comparable to other transition metal dichalcogenides. The layer-dependence and wavelength dependence of the nonlinear susceptibility was also measured. Finally, the measurements also determine the relationship between the crystal axes and the polarization-dependence of the SHG and Raman scattering, which now allows the anisotropy of polarized SHG or Raman signal to independently determine the crystal orientation.

R. Beams, et. al. ACS Nano 10, 9626 (2016).

10349-6, Session 2

Laser treated molybdenum disulfide nanosheets: towards engineering better 2D photodetectors

Moh Amer, Univ. of California, Los Angeles (United States) and King Abdulaziz City for Science and Technology (Saudi Arabia); Frank DelRio, National Institute of Standards and Technology (United States); Fadhel Alsaffar, Abdullah Alrasheed, King Abdulaziz City for Science and Technology (Saudi Arabia)

Transition Metals Dichalcogenide (TMDC) materials have attracted the scientific community due to their unique optical, mechanical, and electronic properties. Molybdenum disulfide (MoS2), an emerging 2D material, exhibit a tunable band gap that strongly depends on the numbers of layers, which makes MoS2 an attractive candidate for optoelectronic applications. However, recent reports have shown that engineering a monolayer using laser thinning can be an effective method without oxide formation, which can be a promising technique for various applications. Here, we investigate this laser thinning process using Raman spectroscopy, μ-XPS, and AFM measurements. Our results show that laser thinned multilayer MoS2 exhibit a large oxide on the surface of the nanosheet, contrary to previous reports. This oxide cannot be detected using μ-Raman spectroscopy. We also show that monolayer and bilayer MoS2 nanosheets exhibit distinctive phonon behavior compared to multilayer MoS2 nanosheets after prolonged laser treatments. This behavior is reflected on the steep intensity decrease for E2g mode, while the intensity of A1g mode slightly changes. This behavior can be interpreted as localized non-equilibrium temperature change due to the formation of anomalous particles on the surface of monolayer and bilayer MoS2 nanosheets. We show that these anomalous particles have a significant effect on the measured Raman properties of pristine monolayer and bilayer MoS2 nanosheets, unlike multilayer MoS2 nanosheets. Our results shed some light on the behavior of MoS2 nanosheets when laser treated for future photodetector applications.

10349-7, Session 3

Two-dimensional van der Waals materials based nonvolatile memory field-effect transistors

Do Kyung Hwang, Young Tack Lee, Won-Kook Choi, Min-Chul Park, Korea Institute of Science and Technology (Korea, Republic of)

Two-dimensional van der Waals (2D vdWs) materials are a class of new materials that can provide important resources for future electronics and materials sciences due to their unique physical properties. Molybdenum disulfide (MoS2) is one of the most promising n-type TMD semiconductors. Several research groups reported on MoS2 nanosheet based transistors that exhibit satisfactory carrier mobility values with high on/off current ratios. On the other hand, a newly discovered 2D vdWs material, called black phosphorous (BP), has generated considerable scientific and technological interest in the research community. 2D BP also has considerable potential for electronic and optoelectronic applications. This is evidenced by recent research on FETs, diodes, and photodetectors involving few-layered BP flakes.

Here, we report on a high performance MoS2 and BP nanosheet based nonvolatile memory transistors with a poly(vinylidenefluoride-trifluoroethylene) (P(VDF-TrFE)) ferroelectric top gate insulator. The MoS2 ferroelectric field-effect transistor (FeFET) shows a highest linear electron mobility value of 175 cm2/Vs with a high on/off current ratio more than 107, and a very clear memory window over 15 V. The program and erase dynamics and static retention properties are also well demonstrated. Our BP ferroelectric FETs (FeFETs) also exhibit a clear memory window of 15 V and a highest linear mobility value of 1159 cm2V-1s-1 with a 103 on/off current ratio at room temperature in ambient air. In order to explore advanced memory applications beyond unit memory devices, we implement two kinds of memory inverter circuits: a resistive-load inverter circuit and a CMOS inverter circuit combined with n-type MoS2.

10349-8, Session 3

Atomic layer deposition of tunable ZnO films for the application in resistive memory *(Invited Paper)*

Ruomeng Huang, Kai Sun, Kian S. Kiang, Kees de Groot, Univ. of Southampton (United Kingdom)

No Abstract Available.

10349-9, Session 3

Highly efficient strain energy harvester through electrochemical cointercalation into few layered graphene *(Invited Paper)*

Cary L. Pint, Nitin Muralidharan, Adam P. Cohn, Karl Zelik, Vanderbilt Univ. (United States)

Ambient human interactions are mechanical stimuli of low frequencies <1Hz; if efficiently captured could effectively power next generation smart wearable devices and sensors without ever requiring an external power supply. The best present day energy harvesting devices rely on low energy density piezoelectric materials which can only operate efficiently in moderate to high frequencies >10Hz. These limitations can be effectively overcome by taking advantage of the mechano-electrochemical coupling observed in high energy alkali metal electrodes used in traditional energy storage devices. Using two such identical electrodes separated by an electrolyte soaked separator, high energy alkali metal cations can be shuttled between them in response to ambient mechanical stimuli. Here we utilize the non-destructive, ultrafast co-intercalation chemistry of sodium ions into few layered graphene observed in the presence of glyme based solvents. Applying small bending motions which create tension in one electrode and compression in the other sets up a chemical potential gradient causing the migration of solvated sodium ions across the separator creating an electric current. The characteristic rapid ion insertion kinetics and the significantly high volume expansion of the multilayered graphene (~250%) observed during co-intercalation enables effective stress-voltage coupling of ~40 mV even at moderate bending radius of 20 mm at frequencies <0.1 Hz to >1 Hz thus significantly outperforming all known previous devices described in the literature. These results provide a design framework for developing efficient devices to harness energy from ambient human interactions such as exercising, walking, or running, which can be stored or used to power wearable technologies and sensing devices.

10349-10, Session 3

Interfacial dynamics during lateral epitaxy of one-dimensional (1D) nanocrystals over 2D membranes *(Invited Paper)*

Babak Nikoobakht, National Institute of Science and Technology (United States)

Interfacing mismatched low-dimensional materials is an important step in development of hybrid and complex heterostructures. At nanoscale size regimes, interfacial bonding strength and strain energy can very well define the structural integrity and physiochemical properties of semiconductor junctions changing fundamental properties such as distribution of electron-hole wave functions, carrier charge density, etc. Here, we present some of our results on structural behavior of 2D membranes and their overgrowth with laterally grown 1D nanocrystals. Based on the surface energy of 2D layered materials, we hypothesize different bonding scenarios between 1D and 2D nanocrystals. Using experimental results such as structural changes at the interfaces as well as electro-optical properties, we identify some of the interfacial forces involved, and discuss their significance in controlling the properties of the heterojunctions. We use the metal-catalyzed Surface-directed Vapor-Liquid-Solid (SVLS) process for the lateral growth of 1D nanocrystals

10349-11, Session 4

Superionic conductivity in low-dimensional polyborate nanocages *(Invited Paper)*

Vitalie Stavila, A. Alec Talin, Sandia National Labs. (United States); Terrence Udovic, National Institute of Standards and Technology (United States)

Low-dimensional anionic polyborate nanocages such as B12H122-, B10H102-, CB11H12-, and CB9H10-can enable high lithium and sodium conductivity in their corresponding salts. These solid-state materials display entropically driven order-disorder phase transitions with dramatic enhancements in conductivity (e.g., up to ~0.03 S cm-1 for NaCB9H10 at 297 K [1]). The increase in conductivity is due to a vacancy-rich cation sub-lattice, coupled with the high reorientational mobility of the quasi-spherical anionic nanocages (1-2 nm in size). This talk will focus on polyborate nanocage materials design strategies to achieve superionic conductivity at device-relevant temperatures. We will show examples of superionic-conducting phases near room-temperature, which can be further enhanced via doping and nanostructuring. Specifically, results of X-ray diffraction, quasielastic neutron scattering, differential scanning calorimetry, NMR, and AC impedance measurements on promising superionic materials will be presented. The possible relationship between the high reorientational mobilities of the anionic polyborate nanocages and the cationic conductivities will be discussed. Finally, an outlook on further improving the remarkable conductive properties of this class of materials will be presented, and the potential of superionic boron nanocages to meet the requirements of future all-solid-state energy storage devices.

[1] W. S. Tang, M. Matsuo, H. Wu, V. Stavila, W. Zhou, A. A. Talin, A. V. Soloninin, R. V. Skoryunov, O. A. Babanova, A. V. Skripov, A. Unemoto, S. Orimo, T. J. Udovic, Adv. Energy Mater. 6, 1502237 (2016).

10349-12, Session 4

The challenge of dimensional scaling of the non-volatile redox transistor to achieve ultrafast switching

Elliot Fuller, Francois Leonard, A. Alec Talin, Sandia National Labs. (United States)

The rapid performance gains and cost reductions derived from the downscaling of transistor dimensions have nearly come to a stop, signaling the end of Moore's Law. To address the need for novel logic and memory devices with vastly improved energy efficiency, we recently demonstrated a solid-state switch that uses facile ion insertion to modulate the electronic conductance of transition metal oxides. Our device, a non-volatile redox transistor (NVRT), achieves switching voltages as low as 5 mV. However, for the NVRT to be competitive with conventional or emerging electronic devices such as memristors it will have to achieve fast switching times on the order of 10s of nanoseconds or faster. In my presentation, I will describe our recent experimental and modeling efforts to understand how the NVRT, a solid-state electrochemical device, can be downsized to nanoscale dimensions and whether sufficiently fast switching times are possible using presently available materials.

10349-13, Session 4

Revealing interphases in all-solid-state batteries through time-of-flight secondary ion mass spectroscopy *(Invited Paper)*

Marina S. Leite, Univ. of Maryland, College Park (United States)

Mapping where Li preferentially accumulates during cycling in all-solid-state batteries can resolve critical open questions in the field, related to the undesired chemical reactions that causes capacity fade. Here, we implement time-of-flight secondary ion mass spectroscopy (ToF-SIMS) in oxygen free and controlled environment. We determine the spatial distribution of Li-ions in batteries formed by Si/LiPON/LiCoO2, an ideal model system. We directly map Li spatial distribution within all active layers of the batteries upon cycling. We deconvolute Li diffusion from the formation of a solid-electrolyte interphase (SEI) at the LiPON-LiCoO2 interface after the first lithiation step. ToF-SIMS can be applied to directly map Li in a variety of Li-ion energy storage systems, enabling the precise identification of the chemical reactions taking place during cycling, critical for the design of long-life and stable devices.

10349-14, Session 4

Reversible intercalation of lithium and sodium ions into layered and tunnel structured manganese oxides: one-dimensional versus two-dimensional diffusion

Bryan W. Byles, Ekaterina Pomerantseva, Drexel Univ. (United States)

Manganese oxides are attractive electrode materials due to their environmental friendliness, low cost, and high electrochemical activity. We study two different magnesium containing manganese oxides: the first is a material with layered buserite crystal structure (Mg-BUS) and open 2D ion diffusion pathways, and the second material is a tunnel structured phase with todorokite crystal structure (Mg-TOD) containing well-defined 1D diffusion pathways. The characteristic size of the square structural tunnels in Mg-TOD (the length of the tunnel wall) is ~9.6 Å, which is equal to the interlayer spacing in Mg-BUS crystal structure. Benefiting from the similar chemical composition and crystal structure dimensions of these two materials, we have studied the role of diffusion channel geometry in electrochemical reactions of reversible ion intercalation.

It was found that in both Li-ion and Na-ion batteries, the two materials have similar initial capacities of ~120 mAh/g. With continued cycling, the Mg-TOD maintained a greater amount of its initial capacity, indicating superior cycling stability. At a higher current rate, Mg-TOD maintains a higher capacity in a Li-ion battery, while in a Na-ion battery, Mg-BUS maintains a higher capacity, suggesting the layered structure allows for more facile diffusion of the larger and heavier Na+ ions. These results indicate that the tunnel walls, while impeding ion diffusion for the larger Na+ ions, provide structural stability during electrochemical cycling, a finding which can help guide the design of electrode materials for intercalation-based batteries.

10349-15, Session 4

The ion dependent change in the mechanism of charge storage of chemically preintercalated bilayered vanadium oxide electrodes

Mallory Clites, Ekaterina Pomerantseva, Drexel Univ. (United States)

Chemical pre-intercalation is a soft chemistry synthesis approach that allows insertion of inorganic ions into the interlayer space of layered battery electrode materials prior to electrochemical cycling. Previously, we have demonstrated that chemical pre-intercalation of Na+ ions into the structure of bilayered vanadium oxide (?-V2O5) results in record high initial capacities above 350 mAh g-1 in Na-ion cells. This performance is attributed to the expanded interlayer spacing and predefined diffusion pathways achieved by the insertion of charge-carrying ions. However, the effect of chemical pre-intercalation of ?-V2O5 has not been studied for other ion-based systems beyond sodium. In this work, we report the effect of the chemically preintercalated alkali ion size on the mechanism of charge storage of ?-MxV2O5 (M = Li, Na, K) in Li-ion, Na-ion, and K-ion batteries, respectively.

The interlayer spacing of the ?-MxV2O5 varied depending on inserted ion, with 11.1 Å achieved for Li-preintercalated ?-V2O5, 11.4 Å for Na-preintercalated ?-V2O5, and 9.6 Å for K-preintercalated ?-V2O5. Electrochemical performance of each material has been studied in its respective ion-based system (?-LixV2O5 in Li-ion cells, ?-NaxV2O5 in Na-ion cells, and ?-KxV2O5 in K-ion cells). All materials demonstrated high initial capacities above 200 mAh g-1. However, the mechanism of charge storage differed depending on the charge-carrying ion, with Li-ion and Na-ion cells demonstrating predominantly pseudocapacitive behavior and K-ion cells revealing diffusion limited intercalation processes. We will highlight how the size of chemically preintercalated, charge-carrying ions affects electrochemical properties and the mechanism of charge storage of the bilayered vanadium oxide electrodes.

10349-16, Session 4

Reversibility of water intercalation in potassium- and magnesium-intercalated Mxenes

Ilia N. Ivanov, Eric S. Muckley, Michael Naguib, Jagjit Nanda, Oak Ridge National Lab. (United States)

High electrical conductivity and high surface area of thermodynamically stable inorganic MXenes, two-dimensional layered carbide or nitrides materials showed promising performance in energy storage devices including Li- and Na- ion batteries and supercapacitors. We investigated the effect of water vapor intercalation in thin membrane of K+ and Mg2+ intercalated T3C2 MAxenes (Ti3C2-K and Ti3C2-Mg) using gravimetric technique and electrical resistance measurements.We demonstrate that Ti3C2-K and Ti3C2-Mg interact with water vapor differently, probably because of difference in size of intercalated cation (150 and 85 pm radium of K+ and Mg2+ ions respectively). Water remains partially trapped inside MAxenes layers even after prolong exposure of samples to vacuum on recovery stage. The recovery of Mxene resistive response in the vacuum on dehydration is an order of magnitude slower than the recovery time of the gravimetric response.

We used neutron total scattering experiments on hydrated MXenes and DFT-MD simulations of to develop a model of water interaction with Ti3C2-K and Ti3C2-Mg.

We show that Ti3C2-K and Ti3C2-Mg can be used as water vapor sensors in 0-85% relative humidity range, achieving detection thresholds of ~0.8%. This is comparable with the performance of metal oxides, graphene oxide and conjugated polymers based RH sensors.

10349-17, Session 4

Structural and optical studies of ZnO:Mn nanostructures

Arun Aravind, Univ. of Kerala (India); Jayaraj M. K., Cochin Univ. of Science & Technology (India)

ZnO has great potential in a wide range of applications such as microelectronics, optoelectronics and sensors. Hydrothermal method has proven to be an effective method for the growth of nanostructured materials. Dilute magnetic semiconductors (DMS) gained much more attention due to their wide applications in spintronics. A large number of research works is published after the theoretical prediction on the room temperature ferromagnetism (RTFM) in transition metals doped ZnO. Manganese doped ZnO nanostructures were prepared by hydrothermal method. An appropriate amount of ammonium hydroxide was added to the mixture of zinc acetate (0.3M - 1M) and manganese acetate (0.001M-0.1M) solution to adjust the pH value above 9. These solutions were transferred into Teflon lined stainless steel autoclave and maintained at various temperatures in the range of 100-200oC for 3 to 6 h under autogenous pressure. The formation of ZnO:Mn nanostructures were confirmed by scanning electron microscopy (SEM), x-ray diffraction (XRD), Raman scattering and EDAX analysis. Optical absorption studies confirms the red shift of ZnO:Mn nanostructures with TM doping. The broad green-yellow-orange photoluminescent emission from ZnO nanostructures originates from the oxygen vacancy or ZnO interstitial related defects. The presence of non-polar E2high and E2low Raman modes in nanostructures indicates that TM doping didn't change the wurtzite structure of ZnO.

10349-35, Session PWed

Comparison of structural properties of iron nano-particles prepared by sol-gel method and spin coating technique

Sunil Dehipawala, Queensborough Community College

(United States); Pubudu Samarasekara, Univ. of Peradeniya (Sri Lanka); Harry D. Gafney, Queens College (United States)

Small scale magnets have very high technological importance today. Instead of traditional expensive methods, scientists are exploring new low cost methods to produce micro magnets. We synthesized thin film magnets containing iron and nickel oxides. Films were synthesized using sol-gel and spin coating methods. Several different precursor concentrations were tested to find out the ideal concentrations for stable thin films. Structural properties of iron particles were investigated using Mossbauer spectroscopy, X-ray absorption spectroscopy including Extended X-ray Absorption Spectroscopy, X ray Absorption Near Edge Structure, and pre-edge feature appears before the main absorption edge. The variation in oxidation state and other structural parameters were deduced. It appears the oxidation state of iron particles prepared by sol-gel method is very stable up to annealing temperatures of 6000C. The iron particles prepared by spin coating method exist in two different chemical environments with slightly different oxidation states.

10349-36, Session PWed

Visible light irradiation-induced conductivity change for CVD-grown graphene on different substrates

Xiangdi Li, Xianming Liu, Yun Luo, Peng Zhang, Xiaohua Lei, Weimin Chen, Chongqing Univ. (China)

Transparent conductive films (TCFs) play important roles in applications such as touch panels, liquid crystal displays, solar cells, and organic light emitting diodes. Graphene with atomic scale thickness has been investigated widely as potential replacements for ITO in TCFs. The TCF should conduct electricity effectively under visible light irradiation. However, some previous works show that the conductivity of graphene may change. It is necessary to understand the stability of electrical properties of graphene electrodes under visible light irradiation.

This research examines the influence of lighting on the electrical properties of graphene on different substrates, including PET, glass and SiO2, which were the most widely used materials represent the flexible and rigid applications. The graphene sheets were prepared by CVD and subsequently transferred to the three different substrates. Samples were placed inside a vacuum chamber with optical windows. The resistances of graphene under periodic visible light irradiation were measured. Results show that the resistances for graphene samples on all substrates increased slowly under lighting, while decreased slowly as well after the light was switched off. The degree and pace of the change were different for graphene on different substrates, which were influenced as well by the illumination time, environment atmosphere and irradiation power. Graphene on flexible PET substrate is more stable than that on other substrates. Photo-desorption of small molecules on the graphene surface may be the main reason resulting in the graphene resistance increasing.

10349-37, Session PWed

Hydrogen sensing properties based on self-assembly monolayer film of Pt/Pd core-shell nanocrystals

Gwiy-Sang Chung, Univ. of Ulsan (Korea, Republic of)

This report presents the synthesis of Pt/Pd core-shell nanocrystals and their monolayer distribution as a resistivity-type sensor that can be utilized for implementing a fast-response hydrogen (H2) sensor. Pd nanocubes with an average size of 40 nm were synthesized via a chemical route, subsequently, Pt/Pd core-shell nanocrystals as colloids were synthesized using these Pd nanocubes via a facile chemical route and were then carefully assembled on a SiO2/Si substrate using the self-assembly monolayer (SAM) technique. Three different Pt/Pd core-shell nanocrystals with varied Pt shell thicknesses were synthesized for the SAM process. The short diffusion length of Pt/Pd due to the thin Pt shell layer and the monolayer distribution of the Pt/Pd core-shell preferentially accelerated the adsorption-desorption of the H2 molecules on the sensing interface, resulting in a very quick response to H2 gas. At an optimum operating temperature of 150oC, the sensor showed a fast-response time of 6 sec, a maximum response of 3.6% to 1 vol% gas concentration, and a broad detection range of 0.001-4 vol% H2 concentrations. The aforementioned outcomes of the as-fabricated sensor demonstrate the possibility of implementing an efficient H2 sensor for safety applications.

10349-38, Session PWed

Formation properties of two-dimensional atomic layers for high-efficiency multi-layer-nanostructure smart packages

Sungwon Hwang, Kyung-Jin Yeum, Konkuk Univ. (Korea, Republic of)

Two dimensional (2-D) atomic layers have several advantages such as flexibility in choosing substrates, easy fabrication, large package area, minimum change of components, enhanced expiration date, and reduced defects by oxygen blocking structure for smart packages. The formation of 2-D atomic layers preventing oxygen penetration is crucial for enhancing the efficiency of multi-layer-nanostructures(MLNs). The nanostructures of two types of packages containing defect-free MLNs with atomic layer and defective thin film were determined by scanning electron microscopy and high-resolution transmission electron microscopy. The defective thin film has a porous structure, whereas the defect-free MLNs with atomic layer had a single crystal structure. These results suggest that the well-defined 2-dimensional atomic layer of MLNs can be utilized for the high- efficiency smart packages.

10349-39, Session PWed

Molecular dynamics modeling and simulation on graphene nanoribbon trench for fullerene shuttle device

Jeong-Won Kang, Korea National Univ. of Transportation (Korea, Republic of)

The position controlling C60 fullerene encapsulated into a graphene-nanoribbon trench is investigated via classical molecular dynamics simulations. The graphene-nanoribbon trench can provide nanoscale empty spaces, and a C60 encapsulated therein can be considered as media for a nanoelectromechanical shuttle device. The classical molecular dynamics simulations presented here provide information on the potential application of a graphene-nanoribbon trench in a C60 shuttle device. Driving forces applied to C60 resulted in its motion toward the edges of the graphene-nanoribbon trench, the suction forces induced at both edges were balanced with the driving forces, and finally, the C60 fullerene gradually settled on the edges of the graphene-nanoribbon trench after several oscillations. The results of the present simulation suggest the importance of graphene-nanoribbon trenches encapsulating fullerenes in a wide range of applications in the field of nanotechnology.

10349-40, Session PWed

The performance of quantum dots-based white light-emitting diodes

Kuan Lin Chen, Shu-Ru Chung, National Formosa Univ. (Taiwan)

Recently, the investigation of quantum dots (QDs) as a color converter for white light-emitting diodes (WLEDs) application has attracted a great deal of attention. Because that the narrow emission wavelength can be controlled by their particle sizes and compositions, which is facilitated to improve the color gamut of display as well as color rendering index (CRI) and the correlated color temperature of WLEDs. In a typical commercially available LCD display, the color gamut is approximately to 92 % of the National Television System Committee (NTSC). In order to enhance NTSC, the full width at half-maximum (FWHM) of color converter should be less than 30 nm. Therefore, the QDs are the best choice for display application due to the FWHM of QDs is less than 30 nm. In this study, the hot injection method with one-pot process is used to synthesis of colloidal ternary ZnCdSe green (G-) and red-emission (R-) QDs with a narrow emission wavelength around 530 and 613 nm. By controlling the complex reagents-steatic acid (SA) and lauric acid (LA), high performance of G- and R-QDs can be prepared. The quantum yields (QYs), particle sizes and FWHM for G- and R-QDs are 70, 30 %, 3.2 ± 0.5, 4.1 ± 0.5 nm and 25, 26 nm, respectively. In order to explore the performance of QDs-based WLEDs, mixing ratios effect between G-QD and R-QD are studied and the WLED is packed as conformal-type. Different ratios of G-QD and R-QD (10:1, 20:1 and 30:1) are mixed and fill up the 3020 SMD blue-InGaN LED. After that, UV curable gel is deposited on the top of QD layer to form WLED and named as LED-10, LED-20 and LED-30. The results show that the Commission International d'Eclairage (CIE) chromaticity coordinates, color rendering index (CRI), luminous efficacy of LED-10, LED-20 and LED-30 are (0.27, 0.21), 53, 1.9 lm/W, (0.29, 0.30), 72, 3.3 lm/W and (0.25, 0.34), 45, 6.8 lm/W, respectively. We can find that the positions of CIE can be controlled simply by adjusting the ratios of G- and R-QDs. Besides, the LED-20 device shows the high CRI, implying that it has great potential for application on backlight of display technology and solid-state lighting.

10349-41, Session PWed

Layer-number-dependent optical properties and application for thickness determination in 2D graphene-like materials

Li Xiaoli, Wang Ying, Hebei Univ. (China)

2D graphene-like materials (2DMs) can be usually exfoliated from layered materials (LMs), which form strong chemical bonds in-plane but display weak van der Waals (vdW) bonding out-of-plane. The remarkable properties of 2DMs make them to be the ideal materials for promising applications in nanoelectronics and optoelectronics devices. However, the properties of 2DMs are highly related to their thickness, i.e., layer number (N), and thus the N determination of 2DM flakes is critical to cater to quality appraisals for the 2DM industrial products. Layer-number-dependent optical properties of 2DMs have been widely probed by several optical techniques, such as optical absorption, Raman spectroscopy, photoluminescence. The definite relations between the optical properties and N by different optical techniques can be demonstrated for rapid and accurate identification of the thickness or N of 2DM flakes. This paper will be expected to pave the ways to construct N-identification techniques of 2DM flakes based on optical techniques, benefit the whole 2DM community for fundamental study, practical applications and quality appraisal for industrial products.

10349-42, Session PWed

Carrier transfer in coupled quantum dot-quantum well hybrid structure

Ying Wang, Qinglin Guo, Suheng Zhang, Xiaoli Li, Baolai Liang, Shufang Wang, Guangsheng Fu, Hebei Univ. (China)

The carrier coupling and transfer in InAs QDs and In0.15Ga0.85As QW hybrid structures grown by molecular-beam epitaxy are investigated by using photoluminescence (PL) spectroscopy. The samples contains a layer of 1.8 ML self-assembled InAs QDs and a QW of 15 nm In0.15Ga0.85As separated by a GaAs spacer of 3 nm or 170 nm. At the low temperature of 10 K, PL spectra are measured as a function of laser excitation intensity in the range of 0.01 W/cm2 ~ 10000 W/cm2. As indicated by figure (a), the QW is strongly coupled with the QDs and carriers can transfer from the QW into InAs QDs though the 3 nm thin GaAs spacer, but not for the 170nm spacer sample. The strong carrier transfer enhance the carrier injection for QD ground states (GS) and subsequently lead to a coulomb effect in the 3 nm spacer sample, which enable the PL peak from the QD GS to display a blueshift while the laser excitation intensity is over 100 W/cm2. Further temperature-dependent PL measurements in figure (d) show that the integrated intensity of QD peak has almost no changes under 170 K for the coupled hybrid structure. However, a clear increase of QD PL integrated intensity is found for the uncoupled structure, likely due to carrier thermal excitation from QW to QDs. In summary of PL results, the coupled hybrid structure has a better PL performance than the uncoupled one in consideration of carrier collection efficiency, temperature stability, and exciton localization effect.

10349-43, Session PWed

PECVD growth of high quality graphene on interdigital electrodes of MEMS supercapacitor

Azrul Azlan Hamzah, Hafzaliza E. Zainal Abidin, Mohd A. Mohamed, Burhanuddin Y. Majlis, Univ. Kebangsaan Malaysia (Malaysia)

MEMS supercapacitor with vertical graphene layers grown via Plasma Enhanced Chemical Vapor Deposition (PECVD) at different deposition times has been investigated in this work. Graphene attracts much attention in supercapacitor research due to its exceptional properties such as high electrical conductivity, good electrochemical stability and excellent mechanical behavior. The fabrication of direct growth graphene nanolayers on MEMS supercapacitor interdigital electrodes is achieved via several subsequent Plasma-Enhanced Chemical Vapor Deposition (PECVD) deposition, E-beam evaporation and spin coating processes. PECVD has been chosen in this work due to its high growth selectivity and excellent nanostructure patterning. PECVD graphene was grown at 1000°C at times ranging from 2 to 10 minutes, with 40 Watt power. All samples were analyzed using Raman spectroscopy, Field Emission Scanning Electron Microscope (FESEM) and Atomic Force Microscopy (AFM). Raman analysis shows that at growth time of 2 minutes, only D band and G band peaks appear. In absence of the 2D peak, amorphous carbon formation was confirmed. At growth time of 6 minutes, D band, G band and 2D band were detected. The ratio I2D/IG is 0.36 and the value of full width at half maximum (FWHM) is 52.57 cm-1, which confirmed that multilayer graphene was formed on the MEMS supercapacitor. High quality graphene layers has been deposited for growth time of 10 minutes, in which the Raman spectra exhibits I2D/IG value of 0.43. The value of FWHM is calculated to be 60.48 cm-1, indicating a highly structured graphene layers, useful for increasing the efficiency of MEMS supercapacitor.

10349-44, Session PWed

Enhanced performance in quantum dot light-emitting diodes by adopting interfacial layer on ZnO

Jinyoung Yun, Kukjin Lee, Hokyun Jang, Korea Univ. (Korea, Republic of); Jeonghun Kwak, The Univ. of Seoul (Korea, Republic of); Gyutae Kim, Korea Univ. (Korea, Republic of)

Since the first quantum dot (QD) light-emitting diodes (QLEDs) were introduced about two decades ago, QLEDs emerge as a next generation flat-panel display because of their unique optical characteristics such as the narrow spectral emission, easy control of the emission wavelength by changing their size and composition. However, the performance of QLEDs is still lacking compared with other light-emitting devices. Thus, more research in material synthesis, device design, and processes are required to improve the efficiency and lifetime. Balancing electrons and holes in QLEDs is one of the important factors to improve the performance. Particularly, using a metal oxide electron transport layer (ETL) and an organic hole transport layer (HTL) in QLEDs leads to severe imbalance of electrons and holes due to intrinsic difference of electrical properties between organic and inorganic materials. In this work, we introduce enhanced performance of inverted red-emitting QLEDs by adopting a non-conjugate polymer monolayer onto the ZnO ETL. The interfacial polymer layer can tune the work function of the metal oxide surface. Also, the device showed reduced leakage current and improved device performance compared to those without the interfacial layer. It means that electrons and holes were balanced well by controlling the electron injection into the QLEDs with the interfacial layer. The performance of the QLEDs and the analysis on charge balance will be presented.

10349-45, Session PWed

Synthesis and characterization of Au-MWCNT/PEDOT: PSS composite film for optoelectronic applications

Jasna Mannayil, Anjana R., Jayaraj M. K., Cochin Univ. of Science & Technology (India)

Recently, flexible organic optoelectronics have got great attention because of their light weight, mechanical flexibility and cost effective fabrication process. Conjugated polymers like PEDOT: PSS are widely used for the transparent electrode applications due to its chemical stability, high conductivity, flexibility and optical transparency in the visible region. Conductivity of the PEDOT: PSS polymer can be enhanced by adding organic solvents or conducting nano fillers like CNT, graphene, etc. Carbon nanotubes are good nano fillers to enhance the conductivity and mechanical strength of PEDOT: PSS composite film. In the present work, the effect of gold nano particles in PEDOT: PSS/CNT composite is studied. The conductivity enhancement in PEDOT: PSS/CNT thin films can be attributed to the formation of CNT network in the polymer matrix and conformational change of the PEDOT from benzoid to quinoid structure. Even though the conductivity was enhanced, the transparency of the composite thin films decreased with increase in CNT concentration. To overcome this problem, gold nano particles were attached to CNT walls via chemical route. Au-MWCNT/PEDOT: PSS composite films were prepared by spin coating method. TEM images confirmed the decoration of gold nano particles on CNT walls. Electrical and optical properties of the composite films were studied. This simple solution processed conducting films are suitable for optoelectronic applications

10349-46, Session PWed

Photon-trapping micro/nanostructures for high linearity in ultra-fast photodiodes

Hilal Cansizoglu, Yang Gao, Cesar B. Perez, Soroush Ghandiparsi, Ekaterina Ponizovskaya Devine, Univ. of California, Davis (United States); Mehmet F. Cansizoglu, The Univ. of Texas Southwestern Medical Ctr. at Dallas (United States) and Univ. of California, Davis (United States); Toshishige Yamada, Univ. of California, Santa Cruz (United States); Aly Elrefaie, Shih-Yuan Wang, Saif M. Islam, Univ. of California, Davis (United States)

Photodetectors (PDs) in datacom and computer networks where the length of the links are a few meters only, need to handle higher than typical input power used in communication links. A thin absorption region can limit the maximum power handling capability of the high-speed PD, contributing to nonlinearity in the currents that can contribute to high order harmonic generations and degrade the signal-to-noise ratio. Nonlinearity is caused by a decrease in the electric field under intense illumination that reduces the carrier velocity due to a space-charge effect or an electric-field screening effect in a thin photo-absorption region. Photon-trapping micro/nanostructures can effectively bend the light in-plane to the direction of the PD surface and avoid current crowding in a PD. Consequently, the photocurrent per unit volume remains at a low level contributing to high linearity in the photocurrent. We present the effect of design and lattice patterns of micro/nanostructures on the linearity of ultra-fast silicon PDs designed for high speed multi gigabit data networks.

10349-47, Session PWed

Highly efficient silicon photovoltaic using photon trapping micro/nano structures

Yang Gao, Hilal Cansizoglu, Ahmet Kaya, Ahmed S. Mayet, Soroush Ghandiparsi, Cesar B. Perez, Univ. of California, Davis (United States); Ekaterina Ponizovskaya Devine, W&WSens Devices, Inc. (United States); Toshishige Yamada, Univ. of California, Santa Cruz (United States); Aly Elrefaie, Shih-Yuan Wang, W&WSens Devices, Inc. (United States); Saif M. Islam, Univ. of California, Davis (United States)

Crystalline silicon (c-Si) remains the most commonly used material for photovoltaic (PV) cells in the current commercial solar cells market. However, current technology requires “thick” silicon due to the relative weak absorption of Si in the solar spectrum. We demonstrate several CMOS compatible fabrication techniques including dry etch, wet etch and their combination to create different photon trapping micro/nanostructures on very thin c-silicon surface for light harvesting of PVs. Both the simulation and experimental results show that these photon trapping structures are responsible for the enhancement of the visible light absorption which leads to improved efficiency of the PVs. Different designs of micro/nanostructures via different fabrication techniques are correlated with the efficiencies of the PVs. Our method can also drastically reduce the thickness of the c-Si PVs, and has great potential to reduce the cost, and lead to highly efficient and flexible PVs.

10349-48, Session PWed

InAs/GaAs quantum dot lasers monolithically grown on Si substrates

Mingchu Tang, Jiang Wu, Siming Chen, Mengya LIao, Alwyn Seeds, Huiyun Liu, Univ. College London (United Kingdom)

As a future driving force technology, Si photonics can improve the low-cost and high speed inter-chip communication by using optical transmission instead of electrical connection. However, Si based light-emitting sources have been considered as “holy grail” for silicon photonics due to bulk Si has in-direct bandgap. Using InAs/GaAs quantum dots (QDs) as active region in laser structure, could bring high performance light emitting sources on Si platform. The challenge of monolithic growth is that high density of threading dislocations will propagate into laser active region due to the lattice mismatch between GaAs and Si. In this paper, we have optimised the III-V buffer layer includes GaAs buffer layer and InGaAs/GaAs strained-layer superlattices (SLSs) defect filter layers (DFLs), which sufficiently reduce the density of threading dislocations.

The laser devices with optimised GaAs buffer layers and DFLs have been fabricated as broad-area laser with 50 μm ridge width without any facet coating. the maximum operation temperature is 75 °C under continuous-wave (CW) operation mode with threshold current density at 62.5 A/cm2 at room temperature. A 29.7% drop in power after 3,100 h is observed during the lifetime test. These results indicate that a reliable Si based laser device has been demonstrated, and has the capable to be integrated on Si opto-electronic integration circuits.

10349-50, Session PWed

Modified Richardson Dushman thermionic emission equation for metals and nano-materials

Olukunle Charles Olawole, Dilip K. De, Sunday O. Oyedepo, Covenant Univ. (Nigeria)

Ordinary Richardson Dushman equation fails to explain many experimental observations, of thermionic emission including temperature variation of work function in metals. Recently it has been shown that it does not fit very well either thermionic emission data from graphene and carbon nano-tube. In this paper we show that Modified Richardson Dushman (MRD) equation derived on the basis of temperature variation of Fermi levels, explains very well thermionic emission data from many materials, including temperature variations of work function, except for alkali metals. It is found that it not only explains thermionic emission data of graphene and carbon nano-tube better than ordinary Richardson Dushman (RD) equation but also explains some physical parameters such as effective thermionic mass, values of work function and its temperature variation which RD equation cannot.

10349-18, Session 5

2D emerging devices: from ordinary to extra-ordinary *(Keynote Presentation)*

Deji Akinwande, The Univ. of Texas at Austin (United States)

This talk will present our latest research advances on 2D nanomaterials towards greater scientific understanding and advanced engineering applications. In particular the talk will highlight our work on topological 2d materials, zero-power devices, wearable sensors, straintronics, and new topological semiconductor transistor concepts. Finally, recent commercial electronic products employing graphene and related materials will be featured.

10349-19, Session 5

Monolithic integration of III-V nanostructures for electronic and photonic applications *(Invited Paper)*

Benedikt Mayer, IBM Research - Zürich (Switzerland); Stephan Wirths, Svenja Mauthe, IBM Research - Zürich (Swaziland); Lukas Czornomaz, Heinz Schmid, Marilyne Sousa Petit, IBM Research - Zürich (Switzerland); Clarissa Convertino, IBM Research - Zürich (Swaziland); Yannick Baumgartner, IBM Research - Zürich (Switzerland); Heike Riel, IBM Research - Zürich (Swaziland); Kirsten E. Moselund, IBM Research - Zürich (Switzerland)

At IBM we have recently developed a novel III-V integration scheme, Template-Assisted-Selective-Epitaxy (TASE), where III-V material is grown directly on top of Si within oxide nanotubes or microcavities which control the geometry of nanostructures. This allows us to grow III-V material non-lattice matched on any crystalline orientation of Si, to grow arbitrary shapes as well as abrupt heterojunctions and to gain more flexibility in tuning of composition. In this talk applications for heterojunction tunnel FETs, MOSFETs as well as microcavity III-V lasers monolithically integrated on Si will be discussed along.

10349-20, Session 5

Self-aligned nanoscale processing solutions via selective atomic layer deposition of oxide, nitride, and metallic films *(Invited Paper)*

Necmi Biyikli, Utah State Univ. (United States); Ali Haider, Petro Deminskyi, Mehmet Yilmaz, Bilkent Univ. (Turkey)

Controlling the lateral dimensions of thin films by patterning is an essential requirement for microelectronics industry for continuous device miniaturization. Conventionally, thin film patterning is achieved by photolithography which includes several processing steps. During the atomic layer deposition (ALD) process, film nucleation is critically dependent on the surface chemistry of the substrate which makes it possible to achieve selective ALD (SALD) by chemically modifying the substrate surface. Local modification of substrate surface opens up possibilities to achieve lateral control over film growth in addition to robust thickness control during ALD process. SALD offers numerous advantages in nanoscale device fabrication such as reduction of the lithography steps required, elimination of complicated etching processes, and minimization of expensive and poisonous reagent use.

In this work, we report detailed investigation to select the most compatible inhibition layer among poly(methyl methacrylate) (PMMA), polyvinylpyrrolidone (PVP), and ICP-polymerized fluorocarbon layers for SALD of metal-oxide and metallic thin films. In addition, multi-layer graphene layers are explored as plasma-compatible inhibition layers for selective deposition of III-nitride materials. Extensive materials characterization efforts are carried out to correlate the ALD recipe parameters with the selective deposition performance. The robust albeit rather simple and straightforward technique presented in this work overcomes various challenges associated with previous methods of SALD and provides an alternative route towards nano-patterning particularly for the sub-10 nm technology nodes.

10349-21, Session 6

Triangle-lattice InGaN/GaN nanocolumn arrays exhibiting photonic crystal effect *(Invited Paper)*

Katsumi Kishino, Shunsuke Ishizawa, Yuzo Matsui, Jun Yoshida, Sophia Univ. (Japan); Ai Yanagihara, Sophia Univ. (Jordan)

GaN nanocolumns are extensively studied as promising nano-materials for high-performance visible emitters because of their dislocation filtering and strain relaxation effects. The size and position of nanocolumns were precisely controlled using Ti-mask selective-area growth (SAG) by RF-MBE, fabricating uniform arrays of pn-junction InGaN/GaN nanocolumns. The periodic arrangement in the nanocolumn arrays led to nanocolumn photonic crystal (PhC) effect. It is however, necessary to integrate a wave-guiding scheme in the nanocolumn system to activate efficiently the PhCs. In the experiment, triangle-lattice GaN nanocolumn arrays with the lattice constant from 280 to 350 nm were grown, followed by the growth of InGaN/GaN superlattice buffer, MQW, and p-type GaN cladding layers. In the upper region of pn-junction nanocolumns from SL to p-GaN, the nanocolumn diameter increased and introduced the increase in the equivalent refractive index, which acts to confine the optical field there. Thus, the optical mode propagated laterally, interacting with the nanocolumn PhC. The diffraction at the photonic band edge resulted in high-directional beam radiations from the nanocolumn system. The photonic band edge was systematically investigated for various nanocolumn arrays with L=280–250 nm. The experimental photonic band diagram for the triangular-lattice pn-junction InGaN/GaN nanocolumn array exhibited a clear photonic band edge.

10349-22, Session 6

Top-down etching of GaN nanostructures for optoelectronics and beyond *(Invited Paper)*

George T. Wang, Benjamin Leung, Sandia National Labs. (United States); Miao-Chan Tsai, Changyi Li, Ganesh Balakrishnan, The Univ. of New Mexico (United States)

Chemical etch processes for GaN materials and devices are significantly underdeveloped due to its apparent inertness to common wet etchants. To fully realize the potential of the III-nitrides in new opto-electronic devices, such as in optical nano- and microcavity lasers, more complete knowledge and development of techniques with anisotropic etching are needed. Here, we explore the etch characteristics of GaN using the general geometric principles of crystallographic dissolution processes to enable the prediction of facet-determined etch structures. We perform the first complete orientation-dependent etch rate measurements, clearly showing fast a-plane etch rate relative to m-plane, and use them to predict the faceting of pillar structures with good agreement with experiment. Finally, we use these developments in GaN wet etching to fabricate functional optical nanowire and microcavity structures, where faceting enables smooth sidewalls for a high quality cavity structure. Control over the lasing properties of nanowires fabricated using this method, including single-mode lasing, polarization control, wavelength tuning, and beam shaping, will also be highlighted.

This work was performed, in part, at the Center for Integrated Nanotechnologies, a U.S. Department of Energy, Office of Basic Energy Sciences user facility. Sandia National Laboratories is a multi-mission laboratory managed and operated by Sandia Corporation, a wholly owned subsidiary of Lockheed Martin Corporation, for the U.S. Department of Energy's National Nuclear Security Administration under contract DE-AC04-94AL85000.

10349-23, Session 6

Controlling reabsorption effect of Bi-color CdSe quantum dots-based white light-emitting diodes

Cyuan-Bin Siao, National Central Univ. (Taiwan); Shu-Ru Chung, National Formosa Univ. (Taiwan); Kuan-Wen Wang, National Central Univ. (Taiwan)

Because the traditional white light-emitting diode (WLED) composed of YAG: Ce phosphor shows low color quality due to lack of red color emission, the colloidal semiconductor quantum dots (QDs) have the potentials to be used in WLED as a down-converting component to replace incandescent lamps. Among various QDs, CdSe has been extensively studied because it possesses attractive characteristics such as high quantum yields (QYs), narrow emission spectral bandwidth, as well as size-tunable optical characteristics. However, in order to enhance the color rendering index (CRI) of WLED, blending materials with different emission wavelengths has been used frequently. Unfortunately, these procedures are complex and time-consuming, and the emission energy of smaller QDs can be reabsorbed by larger QDs, resulting in decreasing the excitation intensity in yellowish-green region. Therefore, in this study, in order to decrease the reabsorption effect and to simplify the procedures, we have demonstrated a facile thermal pyrolyzed route to prepare bi-color CdSe QDs with dual-wavelengths. The emission wavelengths, particle sizes, and QYs of QDs can be tuned from 537/595 to 537/602 nm, 2.59/3.92 to 2.59/4.01 nm, and 27 to 40 %, for GR1 to 3 samples, respectively when the amount of Se precursor is decreased from 1.5 to 0.75 mmol. Meanwhile, the area ratio of green to red (Ag/Ar) in fluorescence spectra is gradually increased, due to the increase in growth rate, decrease in nuclei formation in red emission. The GR1, GR2, and GR3 QDs are then encapsulated by convert types to form the LED, in which the QDs are deposited on the blue-emitting InGaN LED chip (?em = 450 nm). After encapsulation, the devices properties of Commission International d'Eclairage (CIE) chromaticity and Ag/Ar area ratio are (0.40, 0.24), 0.28/1, (0.40, 0.31), 0.52/1, and (0.40, 0.38), 1.02/1, respectively for GR1, GR2, and GR3. The results show that the green emission intensity are strongly reabsorbed by red emission, as the Ag/Ar area ratios are gradually increased and the CIE are dramatically shift to white light region, suggesting that the Se amount not only can tune the red emission intensity but also can decrease the reabsorption effect. Based on the above results, the GR3 is suitable to be applied for WLED against the reabsorption effect. Therefore, the GR3 QDs are further blended with different transparent acrylic-based UV resin (UV resin/QDs=15/85, 30/70, and 45/55) and the CIE, CRI, and luminous efficacy are (0.37, 0.36), 70, 2.85 lm/W, (0.35, 0.34), 73, 2.98 lm/W, and (0.29, 0.29), 70, 3.26 lm/W, respectively. As a result, by simply adjusting the concentration of Se precursor, QDs with dual-wavelengths can be prepared and the reabsorption effect can be avoided to show promising lighting properties for the application in WLED.

10349-24, Session 7

Semiconducting nanowires self-assembly towards solution processed electronics for sensing and RF applications *(Invited Paper)*

Maxim N. Shkunov, Marios Constantinou, Univ. of Surrey (United Kingdom); Sergiy Krylyuk, Theiss Research (United States); Grigorios-Panagiotis Rigas, Bobur Mirkhaydarov, Kaspar Snashall, Michael P. Hughes, Univ. of Surrey (United Kingdom); Brian A. Korgel, The Univ. of Texas at Austin (United States); Philippe Caroff, The Australian National Univ. (Australia)

Single crystalline inorganic nanowires (NWs) are exceptional semiconducting components for solution-processed, low-cost printed electronic devices. Their excellent charge-carrier mobility, high surface-to-volume ratio and solution processability make them ideal building blocks for flexible circuits, chemical/biological sensors and RF switch elements. The key challenge in nanowire printed electronics is the controllable deposition of nanowires with selected properties on pre-defined locations. NWs selective assembly based on their morphological and electrical properties remained mainly unexplored, with NWs being deposited as-synthesised, thus dramatically affecting the reproducibility and reliability of NW-based devices.

In this work we address the above challenge and demonstrate high quality solution processable nanowire assembly platform, targeting field-effect transistor for flexible electronics for chemical and biological sensor applications utilising Si nanowires, and RF switch devices for reconfigurable antennas with InAs nanowires. For reproducible printable NW FETs, we have developed a method for one-step nanowire positioning, alignment, purification and selection by using dielectrophoresis (DEP) and impedance spectroscopy to isolate the highest conductivity and lowest defect density Si nanowires at 5-20MHz DEP signal range. The method also provides ordered monolayer assembly of NWs with desired lengths and controlled number of NWs in the device channel area, ranging from a few NWs to hundreds per device.

Finally, functionalised Si NW FETs are developed with highly sensitive response to volatile organic compounds with sub-ppm detection level, with high prospects for both environmental monitoring and early stage cancer related diagnostics. Using the same methodology, very–low impedance InAs nanowire FETs are demonstrated for RF applications.

10349-25, Session 7

Fabrication of single crystalline stripe in Si and Ge film on rolled flexible glass substrate by UV cw micro-chevron laser beam *(Invited Paper)*

Wenchang Yeh, Shimane Univ. (Japan)

No Abstract Available.

10349-26, Session 7

Thermal transport and thermal management by silicon nanostructures *(Invited Paper)*

Jaeho Lee, Univ. of California, Irvine (United States)

Thermal transport in low-dimensional materials with dimensions scaling below the phonon mean free path and even close to the phonon wavelength poses significant challenges for thermal management of semiconductor devices. While phonons can display both wave-like and particle-like behaviors, the dominant mechanism for thermal conductivity reductions in silicon nanostructures remains unclear. The interpretation has been complicated by the coupled effects of phonon coherence, boundary scattering, backscattering, and contact resistance. Here, we isolate the wave-related coherence effects by comparing periodic and aperiodic silicon nanomeshes, and quantify the particle-related backscattering effect by comparing variable-pitch silicon nanomeshes. Based on the combination of thermal conductivity measurements and phonon ray-tracing simulations, we conclude phonon coherence is unimportant for thermal transport when periodicities are greater than the dominant wavelengths but smaller than inelastic mean free paths. We also show that phonon backscattering, as manifested in the classical size effect, is responsible for the thermal conductivity reduction in silicon nanomeshes. Based on the new understanding, we demonstrate a novel thermoelectric cooling design utilizing the unique thermal transport properties in silicon nanomeshes. Due to the strong anisotropy including the ultralow in-plane thermal conductivity and the high cross-plane thermal conductivity, the silicon nanomesh provides effective thermoelectric cooling performance even at a confined lateral space, which is unachievable by conventional isotropic materials. This work helps bridge the gap between fundamental materials research and device engineering and provides new pathways of utilizing low-dimensional materials and their unique properties for advancing breakthroughs in thermal management of semiconductor devices

10349-27, Session 7

Fabrication of effective photon trapping and light manipulating micro/nano structures

Yang Gao, Hilal Cansizoglu, Ahmet Kaya, Ahmed S. Mayet, Soroush Ghandiparsi, Cesar B. Perez, Univ. of California, Davis (United States); Ekaterina P. Devine, W&WSens Devices, Inc. (United States); Toshishige Yamada, Univ. of California, Santa Cruz (United States); Aly Elrefaie, Shih-Yuan Wang, W&WSens Devices, Inc. (United States); Saif M. Islam, Univ. of California, Davis (United States)

We present a CMOS compatible fabrication technique to create micro/nanostructures on silicon and germanium surfaces for effective photon trapping and enhanced absorption. We achieved more than 10 times absorption enhancement enabled by these photon trapping micro/nanostructures compared to bulk silicon and germanium counterparts. This method can lead to designing both highly efficient photovoltaics, ultra-fast photodetectors and highly sensitive photon counting devices with dramatically reduced device thickness. We also demonstrate that different fabrication techniques (dry etch, wet etch, and their combination) and different design/geometries of these micro/nanostructures can affect the ability and extent of the photon trapping and light manipulation in semiconductors. .

10349-28, Session 7

Extreme bandwidth and efficiency in silicon photodetectors using photon-manipulating micro/nanostructures

Hilal Cansizoglu, Yang Gao, Soroush Ghandiparsi, Ahmet Kaya, Cesar B. Perez, Ahmed S. Mayet, Ekaterina Ponizovskaya Devine, Univ. of California, Davis (United States); Mehmet F. Cansizoglu, The Univ. of Texas Southwestern Medical Ctr. at Dallas (United States) and Univ. of California, Davis (United States); Toshishige Yamada, Univ. of California, Santa Cruz (United States); Aly Elrefaie, Shih-Yuan Wang, Saif M. Islam, Univ. of California, Davis (United States)

Nanostructures allow broadband and near-unity optical absorption and contributed to high performance low-cost Si photovoltaic devices. Despite considerable research and tangible progress in the field of nanostructures enhanced solar cells, photodetectors (PDs) did not receive similar attention until the recent demonstration of a micro/nanohole integrated and CMOS-compatible Si PD that enables above 20 Gb/s data rate with 52% quantum efficiency (QE) at 850 nm. Integration of micro/nanoholes maximizes the QE by bending the light to efficiently couple to in-plane direction. Such Si PDs can be further designed to enhance the bandwidth (BW) of the PDs by reducing the device capacitance with etched holes in an axial pin junction. Here we present the ultimate limit of BW and QE of Si PDs with micro/nanoholes based on a combination of empirical evidence and device modeling. Higher than 50 Gb/s data rate with above 40% QE at 850 nm is conceivable in transceivers designed with such Si PDs that are integrated with photon trapping micro and nanostructures.

10349-29, Session 8

Every atom counts: solving the structure of ligand protected Au102 nanoparticles using electron microscopy and diffraction *(Invited Paper)*

Alina Bruma, National Institute of Standards and Technology (United States)

The Au102(p-MBA)44 nanoclusters recently became the subject of study in biolabeling analyses for site-specific covalent conjugation to viral surfaces, photodynamics and nanocatalysis. The single crystal X-ray method, which is one of the most direct and decisive analytical tools - has been applied with limited success in the case of ligand-protected Au nanoclusters. Using this technique, only a few species have been successfully crystallized and their structure unambiguously determined: Au25[SR]18, Au38[SR]24, Au102[SR]44 (where SR=thiol ligands). Other direct characterization techniques such as electron microscopy prove to be extremely cumbersome for these systems due to the electron beam induced irradiation. In this talk we report a technique for acquiring nanobeam (NBD) electron diffraction patterns acquired at millisecond rate, involving an ultralow electron dose, which can be used for nanoscale systems susceptible to electron beam damage. The acquired electron diffraction patterns show stability for several milliseconds, suggesting that they are the representative patterns and emphasize that the thiolate ligands on the surface of the nanoclusters are not damaged during the electron-beam interaction. We demonstrate that the method can be directly correlated with structural predictions previously obtained with the help of Density Functional Theory (DFT). The strength of this method demonstrated its ability to build a structural “atlas” in reciprocal space for nanoparticles and quantum dots whose structure cannot be otherwise determined using X-ray techniques.

10349-30, Session 8

Chroplasmonic and chiroexcitonic photonics *(Invited Paper)*

Wenchun Feng, Univ. of Michigan (United States); Chuanlai Xu, Jiangnan Univ. (China); Nicholas A. Kotov, Univ. of Michigan (United States)

Several types of plasmonic and excitonic nanoparticles (NPs) and their assemblies had been discovered over the last decade. The origin of the giant polarization rotation in chiroplasmonic systems will be elaborated. NP assemblies organized by DNA will be used to discern different geometries contributing to photon adsorption and emission. Chiroexcitonic systems will be considered using nanoscale helices from semiconductors. Preparation of nanoscale helices with near unity enantiomeric excess enabled elucidation of the effect of their geometry on the spectral position and intensity of the chiroptical bands. Applications of chiroplasmonic and chioexcitonic materials for biosensing and photonic devices will be demonstrated.

10349-31, Session 8

Broadband graphene optical modulator with 35 GHz speed and athermal performance

Yang Xia, Univ. of California, San Diego (United States); Hamed Dalir, Yuan Wang, Xiang Zhang, Univ. of California, Berkeley (United States)

Ultra-compact, wide-band and complementary metal-oxide semiconductor (CMOS)-compatible optical modulators with athermal high-speed operation are highly desirable in optical interconnection systems. However, conventional optical modulators usually suffer from the trade-off between footprint and optical bandwidth due to weak light-matter interaction. And the limited temperature stability constrains their application in modern optical interconnection systems. The tunable absorption in graphene is intrinsically wide band, high speed and temperature insensitive, with extremely strong light-matter interaction. In this work, we experimentally demonstrate a graphene optical modulator with 35 GHz modulation speed. This is achieved by placing the graphene layers in a planar structure and adjusting the interlayer distance so that the resistance and capacitance are both reduced. In addition, the modulation covers 1500-1640 nm bandwidth and exhibits speed stability in a wide range of temperatures (25-145 °C). Our results indicate the potential of the graphene modulator in advanced optical interconnection systems.

10349-32, Session 8

Silver film grain boundary pinning by ion bombardment decreases surface plasmon resonance absorption

David M. Fryauf, Juan J. Díaz León, Univ. of California, Santa Cruz (United States); Andrew C. Phillips, Univ. of California Observatories (United States); Nobuhiko P. Kobayashi, Univ. of California, Santa Cruz (United States)

Telescope mirrors based on highly reflective silver films must be protected from atmospheric corrosion with dielectric overlayers. Reflectivity is optimized when the silver surface is extremely smooth and uniform prior to dielectric overlayer deposition. Silver thin films were deposited on glass slides by electron beam evaporation using a custom deposition system at the University of California Observatories Astronomical Coatings Lab. The silver thin films were subsequently covered with a stack of dielectric films utilizing silicon nitride and titanium dioxide deposited by ion assisted electron beam evaporation to fabricate protected mirrors. In-situ argon ion bombardment was introduced after silver deposition prior to the deposition of dielectric films to assess its effects on the performance of the mirrors. Effectiveness of the ion bombardment was systematically studied for different holding time in vacuum, the time between the end of the silver thin film deposition and the start of the ion bombardment, related to the changes in the surface morphology of silver films and resulting reflectivity spectra. Reflectivity at wavelengths in the range of 350nm – 800nm was found to improve due to ion bombardment, which was qualitatively interpreted to result from decreased surface plasmon resonance coupling. The decrease in the coupling is explained by asserting that the ion bombardment slows down silver surface diffusion and pins grain boundaries, preventing post-deposition grain growth, forming smoother silver-dielectric interfaces.

10349-33, Session 8

Multi-physics simulation of monolithic tantalum oxide memristor-selector structures illustrating negative differential resistance

John F. Sevic, Nobuhiko P. Kobayashi, Univ. of California, Santa Cruz (United States)

Self-assembled niobium dioxide (NbO_2) thin-film selectors self-aligned to tantalum dioxide (TaO_2) memristive memory cells are studied by a multi-physics simulation of the mass transport equation coupled to the current continuity equation and heat equation. While a compact circuit model can resolve quasi-static negative differential resistance (NDR), a self-consistent coupled transport formulation provides a non-equilibrium picture of NbO_2-TaO_2 selector-memristor operation ab initio. By employing the drift-diffusion transport approximation, a finite element method is used to study dynamic electrothermal behavior of our experimentally obtained selector-memristor devices, showing bulk conditions exist favorable for electroformation of NbO_2 selector thin-films. Simulation results suggest Poole-Frenkel defects introduce negative differential resistance, in agreement with our measured results.

10349-34, Session 8

Study of thin film oxidation kinetics using a combination of simulations and advanced characterization

Juan J. Díaz León, David M. Fryauf, Nobuhiko P. Kobayashi, Univ. of California, Santa Cruz (United States)

No Abstract Available.

Conference 10350: Nanoimaging and Nanospectroscopy V

Sunday - Tuesday 6 –8 August 2017

Part of Proceedings of SPIE Vol. 10350 Nanoimaging and Nanospectroscopy V

10350-1, Session 1

Recent progress in the study of surface chemistry on various noble metal surfaces by ultrahigh vacuum tip-enhanced Raman spectroscopy *(Invited Paper)*

Nan Jiang, Univ. of Illinois at Chicago (United States)

Tip-Enhanced Raman Spectroscopy (TERS) affords the spatial resolution of traditional Scanning Probe Microscopy (SPM) while collecting the chemical information provided by RAMAN spectroscopy. This system, further aided by the benefits of Ultra-High Vacuum, is uniquely capable of obtaining surface data that would otherwise be unobtainable with less-specialized methods. Large polyatomic molecular adsorbates on various single crystal surface (Ag, Cu and Au) will be explored in this talk. By investigating substrate structures, superstructures, and the adsorption orientations obtained from vibrational modes, we extract novel surface-chemistry data at an unprecedented spatial (<1nm) and chemical resolution.

10350-2, Session 1

Tip-enhanced Raman scattering monitoring of a nanoscale pH at a solution/solid interface by chemically modified tip-enhanced Raman scattering tip *(Invited Paper)*

Prompong Pienpinijtham, Chulalongkorn Univ. (Thailand); Sanpon Vantasin, Yasutaka Kitahama, Kwansei Gakuin Univ. (Japan); Sanong Ekgasit, Chulalongkorn Univ. (Thailand); Yukihiro Ozaki, Kwansei Gakuin Univ. (Japan)

Thus far, TERS measurements have been carried out for dry samples, and relatively few studies have been reported for TERS measurements in solution/liquid systems due to a number of limitations including problems with laser focusing, sample preparation, the feedback system of SPM, and adsorbed contaminants on the TERS tip. In the present study, a TERS tip was chemically modified with pH sensitive molecules i.e., p-mercaptobenzoic acid (pMBA) and paminothiophenol (pATP), which have received much attention in pH/chemical probes using SERS techniques. In pMBA, a ?COOH group is converted to a ?COO? moiety when an acidic solution becomes alkaline. For pATP, in an alkaline solution, two pATP molecules react each other to form an azo (N=N) dimer, i.e., 4,4?dimercaptoazobenzene (DMAB), while a pATP molecule is stable in acidic environments.

We developed a nanoscale pH profile on a 4 ? 4 ?m2 area of NH2-anchored glass slide in an aqueous solution using chemically modified TERS. pMBA and pATP are bonded to the tip surface. A pH profile can be developed by a peak at 1422 cm?1 due to the ?COO? stretching vibration of pMBA and that at 1442 cm?1 due to the N=N stretching vibration due to the formation of 4,4?-dimercaptoazobenzene (DMAB) on the pATP-modified tip. The pMBA- and pATP-modified tip can be used to determine pH in the range of 7?9 and 1?2, respectively. This technique suggests a possibility for the pH sensing in wet biological samples.

10350-4, Session 1

Evaluation of probes for tip-enhanced Raman scattering by darkfield microspectroscopy and calculation

Yasutaka Kitahama, Shohei Uemura, Ryota Katayama, Kwansei Gakuin Univ. (Japan); Yuko S. Yamamoto, Kagawa Univ. (Japan); Toshiaki Suzuki, UNISOKU Co., Ltd. (Japan); Tamitake Itoh, National Institute of Advanced Industrial Science and Technology (Japan); Yukihiro Ozaki, Kwansei Gakuin Univ. (Japan)

Tip-enhanced Raman scattering (TERS) can be observed highly sensitive spectral image with high spatial resolution. However, it shows low reproducibility due to difference and change in optical properties of the metallic tips. For surface-enhanced Raman scattering (SERS), the spectra have been related with the scattering spectra due to localized surface plasmon resonance (LSPR) of the individual metallic nanostructures, which observed by a darkfield illumination, and the calculated electromagnetic (EM) field around the nanostructures. In the present study, we tried to relate TERS spectra with the LSPR spectra and the calculation in a similar way of SERS. By conventional darkfield illumination, LSPR scattering spectra at the apex of the tip were measured and were compared with the corresponding scanning electron microscope (SEM) images and TERS spectra. The LSPR peak from the apex with smaller curvature was red-shifted. By excitation using polarization parallel to the tip, the polarized LSPR peak was stronger than that by perpendicular polarization. Also in the case of TERS, the similar trend was observed. It was confirmed whether the vertical polarization to the sample plane (z-polarization) is effective or not by the polarized LSPR and TERS spectra. By excitation at different wavelengths, moreover, TERS enhancement factors were compared. In the calculation for TERS, the nanostructure like a monopole antenna was adopted, because the EM field is enhanced not at both sides, but at only apex. The dependence on taper and curvature of the tip were compared with the calculated results for the nanostructure like a conventional dipole antenna.

10350-18, Session 1

Hierarchical plasmonic metamaterials and metasurfaces for ultrasensitive, reproducible SERS *(Invited Paper)*

Dangyuan Lei, Jiyan Dai, The Hong Kong Polytechnic Univ. (Hong Kong, China)

In this talk I will present our recent research on the design and preparation of three-dimensional (3D) hierarchical metamaterials and two-dimensional (2D) hierarchical metasurfaces as novel SERS substrates with ultrahigh sensitivity and reproducibility. The former substrate consists of close-packed arrays of nanoholes and uniformly distributed mesopores over the bulk and the second comprised of sub-wavelength-sized conical nanopores and sub-5-nm nanogrooves. Both substrates employ a cascaded field enhancement mechanism, leading to the ultrahigh sensitivity, and have a (quasi)periodic arrangement of plasmonic near-field hot-spots, ensuring excellent structural and signal reproducibility. In particular, the latter substrate is highly mechanically flexible, allowing for extreme adaptability to complex working conditions such as build-in real-time monitoring of trace level molecules.

References:

[1] X. Zhang, Y. Zheng, X. Liu, W. Lu, J. Dai, D. Y. Lei* & D. R. MacFarlane*, "Hierarchical porous plasmonic metamaterials for reproducible ultrasensitive surface-enhanced Raman Spectroscopy", Advanced Materials 27, 1090-1096 (2015).

[2] C. Xu, Y. Zhou, S. Lyu, Y.-L. Zhang, H. Yao, D. Mo, J. L. Duan* & D. Y. Lei*, "Highly flexible, hierarchical porous plasmonic metasurfaces for reproducible, ultrasensitive surface-enhanced Raman spectroscopy", under preparation (2017).

[3] K. Chen, X. Zhang, Y.-L. Zhang, D. Y. Lei, H. Li, T. Williams & D. R. MacFarlane, "Highly ordered Ag/Cu hybrid nanostructure arrays for ultrasensitive surface-enhanced Raman spectroscopy", Advanced Materials Interfaces 3, 1600115 (2016).

10350-5, Session 2

Wavefront correction for superresolution microscopy *(Invited Paper)*

Peter Kner, Kayvan F. Tehrani, Benjamin Thomas, Abhijit Marar, The Univ. of Georgia (United States)

Superresolution microscopy is rapidly becoming an essential tool in the biological sciences allowing imaging biological structure at length scales below 250 nm. Currently, superresolution microscopy has been applied successfully on single cells achieving resolutions of 100nm down to 20nm over a few microns of depth. When superresolution microscopy is applied in thicker samples the resolution rapidly degrades. Optical aberrations and scattering distort and reduce the point spread function causing different superresolution techniques to fail in different ways. I will discuss our work on combining structured illumination microscopy and stochastic optical reconstruction microscopy with adaptive optics to achieve sub-diffraction resolution in thick tissue.

10350-6, Session 2

Fluorescence scanning microscopy with SPAD array *(Invited Paper)*

Marco Castello, Giorgio Tortarolo, Istituto Italiano di Tecnologia (Italy); Mauro Buttafava, Federica A. Villa, Politecnico di Milano (Italy); Sami Koho, Alberto Diaspro, Istituto Italiano di Tecnologia (Italy); Alberto Tosi, Politecnico di Milano (Italy); Giuseppe Vicidomini, Istituto Italiano di Tecnologia (Italy)

In a typical fluorescence laser scanning microscope (i) an excitation laser beam is focused on a small (usually diffraction-limited) region of the sample, (ii) the fluorescence arising from the molecules located in this region is registered by a photodetector and (iii) the beam is sequentially scanned across the whole sample to reconstruct its (3D) image. Comparing to camera-based (wide-field) microscope systems, scanning systems have a limited temporal resolution (frames per second) and typically a reduced field-of-view. However, the fast photodetectors employed in laser-scanning microscopes make them extremely well suited for studying the molecular dynamics, with temporal resolution way beyond the possibilities of camera-based systems. In classical single element detectors, such as photomultiplier tubes (PMTs) or single photon avalanche diodes (SPADs), the temporal resolution spans from tens to hundreds picoseconds, giving access to information regarding molecular diffusion and photophysical dynamics. The single element detectors however lack in spatial information, as all the photons arriving from the excitation spot are accumulated into a single detector; by replacing the single element detector with a detector array it is possible exploit the photon positions to decipher spatial information about the position of the molecules within the excitation spot, thus refining the spatial resolution. High sensitivity bi-dimensional array of SPAD (SPAD array) detector is ideal for such a task, as it maintains the high temporal resolution of single element SPADs, while providing additional spatial information on the location of molecules within the excitation spot. Here we present a novel SPAD array optimized for fluorescence scanning microscopy. It consists of a 5?5-pixel array with 50 μm pixel size, 75 μm pixel pitch, < 200 ps temporal resolution and <1% pixel crosstalk. In the context of spatial resolution we demonstrate the integration of the SPAD array into a confocal scanning microscope obtaining the most straightforward implementation of image scanning microscopy. In the context of temporal resolution we show its potentiality for time-resolved microscopy/spectroscopy.

10350-7, Session 2

Tomographic STED microscopy

Jennifer-Rose Krüger, Laser-Lab. Göttingen e.V. (Germany); Jan Keller-Findeisen, Max-Planck-Institut für Biophysikalische Chemie (Germany); Claudia Geisler, Alexander Egner, Laser-Lab. Göttingen e.V. (Germany)

Far-field optical microscopy represents a well-established method in the life sciences. Due to diffraction, the resolution is limited to lambda/2 in the focal plane. This constraint can be surpassed by nanoscopic techniques. Amongst others, STED microscopy provides a resolution of up to 20 nm. By definition, resolution enhancement in STED microscopy is achieved by narrowing the effective fluorescent area. This reduction of detection volume depends on the factor of resolution enhancement and is directly linked to a decrease in fluorescence signal which limits the acquisition rate in many cases.

Here, we present a STED technique based on a rotating 1D depletion pattern. This novel STED variant can achieve a higher resolution for a given depletion light intensity as compared to the classical implementation. Furthermore, the overall fluorescence signal detected is higher than for conventional STED microscopy working at the same resolution. Consequently, not only identical super resolution conditions can be realized at lower depletion laser powers but also the acquisition can be sped up. Moreover, both aspects have the potential to drastically reduce photobleaching and sample damage.

10350-8, Session 2

Beam shaping for superresolution nonlinear lifetime and Raman microscopy

Ryan Beams, Stephan Stranick, National Institute of Standards and Technology (United States)

We experimentally and theoretically investigate various phase-masks for superresolution nonlinear microscopy. By applying a Toraldo-style phase-mask to the excitation beam, we can reduce the size of the center of the point-spread function at the expense of increasing the intensity of the side lobes. In order to utilize the central spot for imaging, the side lobes have to be suppressed. This can be accomplished by either engineering the collection volume to only collect the central spot or by exploiting the multiplicative nature of nonlinear microscopy. The first case has the advantage of being a general approach any signal. In the later case, the shape of the second beam is chosen such that it only overlaps with the central lobe. Therefore, by controlling the shape of both beams the nonlinear signal, such as coherent Raman processes, is only generated in the overlap region leading to an improved spatial resolution. To illustrate this technique, we use fluorescence lifetime imaging and coherent Raman scattering with a spatial resolution of ≈ ?/7. These results are compared to analytical calculations of the point-spread function from strongly focused fields.

10350-9, Session 3

Tip-enhanced Raman spectroscopy of semiconductor nanostructures *(Invited Paper)*

Edward T. Yu, The Univ. of Texas at Austin (United States)

Raman scattering can serve as a powerful probe of local bonding, strain, temperature, and other properties of molecular and solid-state materials via their influence on vibrational modes or optical phonons. Raman scattering interactions are typically very weak, however, making characterization of materials with high spatial resolution extremely challenging. We have used tip-enhanced Raman spectroscopy (TERS), in which optical excitation of plasmonic modes at the apex of a metal-coated scanning probe tip enables Raman scattering signals to be detected from nanoscale volumes with precise positional control, to characterize a variety of semiconductor nanostructures. In studies of Ge-SiGe core-shell nanowires, we measure

spatially resolved Raman spectra along the length of a tapered nanowire to demonstrate the ability to measure local strain distributions with nanoscale spatial resolution. In addition, we observe tip-induced shifts in Raman peaks associated with the interaction of optical phonon modes with inter-valence band carrier transitions, enabling local carrier distributions to be probed and interactions among plasmon, phonon, and carrier excitations to be elucidated. In tip-induced resonant Raman studies of single- and few-layer transition metal dichalcogenide materials, we observe large enhancements in Raman signal levels measured for MoS2 associated with excitation of plasmonic gap modes between an Au-coated probe tip and Au substrate onto which MoS2 has been transferred, and significant differences in Raman spectra for monolayer compared to bilayer MoS2. The origins of these differences in terms of strain, altered vibrational modes, and other factors will be discussed.

10350-10, Session 3

Enabling strain-sensing at the nanoscale with TERS *(Invited Paper)*

Erin Wood, Yanfei Yang, Will Gannett, Gordon A. Shaw, Randolph E. Elmquist, Mark Keller, Angela Hight Walker, National Institute of Standards and Technology (United States)

This talk will present three primary ideas: The first will be the use of test structures between laboratories and instrumentation as a tool to aid in understanding of the results from tip-enhanced Raman scattering (TERS) results. This test structure was designed to be used to help enable comparability between backscattering instrumentation, although it also is particularly useful for establishing the limitations of instrumentations. This test structure has been presented at a previous SPIE meeting, although we go into great detail of the data analysis, not the manufacturing process as previously presented. Secondly, we discuss advanced in tips including commercially available metal dielectric tips that have a broad-spectrum enhancement. Most of this talk, however, will focus on our work on graphene-based systems such as epitaxially-grown graphene on SiC, exfoliated graphene, and CVD graphene on copper. This work will focus on the use of TERS to both sense mechanically applied strain and expand our understanding of strain in 2-D materials. Finally our recent work on highly purity carbon nanotubes will be presented.

10350-11, Session 3

Multimodal tip-enhanced microscopy *(Invited Paper)*

Kai Braun, Anke Horneber, Dai Zhang, Alfred J. Meixner, Eberhard Karls Univ. Tübingen (Germany)

Electromagnetic coupling between plasmonic resonances of two closely spaced metal particles can lead to a strongly enhanced optical near field in the gap between. It is the leading amplification mechanism for surface- and tip-enhanced Raman scattering (SERS/TERS) or enhanced molecular luminescence and has widespread applications in nanoplasmonics. Scanning near-field optical microscopes (SNOM) have the ability to correlate local optical properties with topography at the nanometer scale. Collecting correlated signals of photoluminescence (PL) and Raman as well as topography, tip-enhanced hyperspectral imaging is able to provide a thorough map of the chemical and morphology-related optical properties in multi-component material systems. Introducing new microscope functions offer us insights into various aspects, such as morphology related photophysical and photochemical processes.

Despite its attractive capabilities, developing a tip-enhanced near-field microscope providing reliable and reproducible performance is demanding. Stringent requirements have to be met, such as precise positioning of a nanometer-sized tip apex inside the laser focus, capability of maintaining the tip-sample distance with an accuracy of some angstroms and reproducibly locate the tested species with ultrahigh accuracy etc. In the last years great efforts have been made in our lab to develop stable, reproducible and reliable near-field optical microscopes, which largely meet the above requirements. They successfully demonstrated their capability in high-resolution optical imaging and spectral mapping, or using the tip as local probe for enhanced coupled fields. Furthermore we demonstrate the direct manipulation and measurement of surface properties via electrical charging or injection of charge carriers and ultrafast non-linear optical microscopy.

10350-12, Session 3

Reproducible plasmon nanofocusing on optimized plasmonic tip structure for optical nano-imaging

Takayuki Umakoshi, Misaki Tanaka, Osaka Univ. (Japan); Yuika Saito, Gakushuin Univ. (Japan); Prabhat Verma, Osaka Univ. (Japan)

Optical nano-imaging technique using plasmon nanofocusing has a great potential to achieve near-field measurements background-free from far-field incident laser, since plasmon nanofocusing enables to generate near-field light by propagating plasmon excited at a coupler far from the apex with adiabatically condensing its light energy. Since Raschke et al. reported plasmon nanofocusing on a metallic tip in 2007, increasing interest in this topic has been seen. In the most cases, metallic tips were fabricated through electrochemical etching, which produced gold conical tip. Practically, this is the only way reported so far to fabricate tips that works for plasmon nanofocusing.

In this work, making an important development in tip fabrication for the plasmon-nanofocusing-based near-field microscopy, we optimized configurations and fabrication processes of plasmonic tips for plasmon nanofocusing, so that 100% reproducible plasmon nanofocusing was achieved on fabricated tips. We first deposited an atomically smooth silver layer (thickness: 40 nm, roughness: less than 1 nm) on an oxidized silicon pyramidal tip through thermal evaporation. We then fabricated a grating by focused ion beam, whose structure was optimized by FDTD simulation. Through these optimizations, we observed light spots appeared at apexes of more than 20 fabricated tips with reproducibility of 100% by illuminating the grating with laser of 642 nm wavelength. Owing to such efficient plasmon nanofocusing, we have also proposed a completely new and unique broadband nano-imaging technique, the details of which as well as the details of tip fabrication tricks will be included in the presentation.

10350-13, Session 4

Imaging nanoscale nuclear architecture in cancer development *(Invited Paper)*

Yang Liu, Jianquan Xu, Hongqiang Ma, Univ. of Pittsburgh (United States); Wei Jiang, West China Second Univ. Hospital, Sichuan Univ. (China) and Univ. of Pittsburgh (United States)

Alteration in nuclear architecture remains one of the most striking abnormalities in cancer cells and remains the gold standard in cancer diagnosis. However, microscopically defined nuclear architecture in cancer often do not unambiguously distinguish early-stage aggressive cancers from benign lesions, or identify proper cancer patients who can benefit from treatment. Super-resolution fluorescence microscopy revolutionizes the file of light microscopy by overcoming the diffraction limit. We will present the use of single-molecule localization microscopy to investigate how nanoscale organization of nuclear architecture is altered at various stages of cancer development in cancer progression cell line models, animal models of carcinogenesis and human patients.

10350-14, Session 4

Multiple emitter fitting using reversible jump Markov chain Monte Carlo *(Invited Paper)*

Keith A. Lidke, The Univ. of New Mexico (United States)

In single molecule based super-resolution imaging, high labeling density or the desire for greater data collection speed can lead to clusters of overlapping PSFs in the raw super-resolution image data. Multi-emitter fitting algorithms can identify and localize the particles in those dense regions of the data. In this work, we improve upon the state-of-the art in multi-emitter fitting by employing Reversible Jump Markov Chain Monte Carlo (RJMCMC). Markov Chain Monte Carlo (MCMC) can be used to find the posterior distribution of a set of parameters, which in the multi-emitter fitting problem consists of the particle positions and intensities and a local background. RJMCMC takes this concept further and allows jumps between parameter spaces, in this case allowing the addition or subtraction of emitters in the model. We allow four mechanisms to make jumps between spaces of various models, called birth, death, merge and split. Birth (death) allows the addition (deletion) of an emitter anywhere in the sample. Split allows the possibility that an existing particle can be actually two or more neighboring particles. Merge allows the chance of two adjacent particles to join into a single particle. RJMCMC averages over the possible models, weighting them by their probabilities. This Bayesian approach also allows prior knowledge on intensity, background and particle density to be easily input in a principled manner. Although demonstrated here in 2D, the approach can be easily extended to analysis of 3D data with arbitrary PSFs.

10350-15, Session 4

An ultra-fast algorithm for high-density localization microscopy

Hongqiang Ma, Yang Liu, Univ. of Pittsburgh (United States)

High-density localization of multiple fluorescent emitters is a common strategy to improve the temporal resolution of super-resolution localization microscopy. In recent years, various high-density localization algorithms have been developed. Despite their rigorous mathematical model and the subsequent improvement in image resolution, they still suffer from high computing complexity and the resulting extremely low computation speed, thus limiting the application to either small dataset or expensive computer clusters. It is still impractical as a routine tool for a large dataset. With the recent advance of high-throughput localization microscopy with sCMOS cameras that can produce a huge amount of data in a short period of time, fast processing now becomes even more important. Here, we present a simple algebraic algorithm based on our previously developed method, gradient fitting, for fast and precise high-density localization of multiple overlapping fluorescent emitters. Through numerical simulation and biological experiments, we showed that our algorithm can yield comparable localization precision and recall rate as DAOSTORM in various densities and signal levels, but with much simpler computation complexity. After being implemented on a GPU device (NVidia GTX1080) for parallel computing, it can run over three orders of magnitude faster than DAOSTORM implemented on a high-end workstation.

Therefore, our method presents a possibility for online reconstruction of high-speed super-resolution imaging with high-density fluorescent emitters.

10350-16, Session 4

Single marker switching microscope with isotropic resolution over large axial range

Haugen Mittelstädt, Claudia Geisler, Alexander Egner, Laser-Lab. Göttingen e.V. (Germany)

Single marker switching (SMS) based nanoscopy techniques overcome the resolution limit by utilizing molecular switching events in conjunction with localization of sufficiently separated point-shaped emitters. The typically inferior axial resolution due to detection through a single objective lens can be improved by employing two opposing lenses for detection. Interference of the fluorescence signal then enables a resolution of better than 20 nm in all three spatial directions. However, the volume in which markers can be localized is restricted to thin optical layers around the focal plane of ~0.25 µm (iPALM [1]) or ~1 µm thickness (4Pi-SMS [2], W-4PiSMSN [3]), thereby necessitating scanning steps to image thicker structures.

Here, we present a 3D-SMS microscope based on the stereo view principle which clearly overcomes this axial restriction and makes detection point spread function modifications and delicate interference patterns obsolete. By simultaneously observing an emitter through four low numerical aperture (NA) lenses which are oriented in a tetrahedron-like shape, our microscope allows to acquire super-resolved 3D-images of an axially extended volume of several micrometer thickness without axial scanning. The image quality benefits from the significantly enhanced solid angle as compared to detection through a single standard high NA lens. Our system not only enables imaging within fluorescently labeled whole cells, but also permits to track individual fluorescent markers.

[1] Shtengel, G. et al., Proc. Natl. Acad. Sci. USA, 106, 3125 (2009)

[2] Aquino, D. et al., Nat. Methods, 8, 353 (2011)

[3] Huang, F. et al., Cell, 166, 1028 (2016)

10350-3, Session 5

In-situ electrochemical tip-enhanced optical spectroscopy and imaging *(Invited Paper)*

Taka-aki Yano, Masahiko Hara, Tokyo Institute of Technology (Japan)

Tip-enhanced optical spectroscopy has been nowadays recognized as a powerful tool for nano-imaging and nano-analysis with a nanoscale spatial resolution far beyond the diffraction limit of light. In this study, we utilized a plasmonically-active metallic probe tip to apply DC voltage to sample surfaces through the tip, enabling us to locally initiate electrochemical reactions. Reversible oxidation and reduction reactions were observed with organic self-assembled monolayers, which was in-situ characterized through tip-enhanced Raman spectral changes. The tip-applied DC voltage was also utilized to measure local diffusion of lithium ions on a lithium-ion battery cathode.

10350-17, Session 5

Physical chemistry of Nanogap-Enhanced Raman Scattering (NERS) *(Invited Paper)*

Yung Doug Suh, Korea Research Institute of Chemical Technology (Korea, Republic of) and Sungkyunkwan Univ. (Korea, Republic of); Hyun Woo Kim, Korea Research Institute of Chemical Technology (Korea, Republic of)

Plasmonic coupling-based electromagnetic field localization and enhancement are becoming increasingly important in chemistry, nanoscience, materials science, physics, and engineering over the past decade, generating a number of new concepts and applications. Among the plasmonically coupled nanostructures, metal nanostructures with nanogaps have been of special interest due to their ultrastrong electromagnetic fields and controllable optical properties that can be useful for a variety of signal enhancements such as surface-enhanced Raman scattering (SERS). The Raman scattering process is highly inefficient, with a very small crosssection, and Raman signals are often poorly reproducible, meaning that very strong, controllable SERS is needed to obtain reliable Raman signals with metallic nanostructures and thus open up new avenues for a variety of Raman-based applications. More specifically, plasmonically coupled metallic nanostructures with ultrasmall (?1 nm or smaller) nanogaps can generate very strong and tunable electromagnetic fields that can generate strong SERS signals from Raman dyes in the gap, and plasmonic nanogap-enhanced

Raman scattering can be defined as Raman signal enhancement from plasmonic nanogap particles with ?1 nm gaps. However, these promising nanostructures with extraordinarily strong optical signals have shown limited use for practical applications, largely due to the lack of design principles, high-yield synthetic strategies with nanometer-level structural control and reproducibility, and systematic, reliable single-molecule/single-particle-level studies on their optical properties. All these are extremely important challenges because even small changes (<1 nm) in the structure of the coupled plasmonic nanogaps can significantly affect the plasmon mode and signal intensity. In this Account, we examine and summarize recent breakthroughs and advances in plasmonic nanogap-enhanced Raman scattering with metal nanogap particles with respect to the design and synthesis of plasmonic nanogap structures, as well as ultrasensitive and quantitative Raman signal detection using these structures. The applications and prospects of plasmonic nanogap particle-based SERS are also discussed. In particular, reliable synthetic and measurement strategies for plasmonically coupled nanostructures with ?1 nm gap, in which both the nanogap size and the position of a Raman-active molecule in the gap can be controlled with nanometer/sub-nanometer-level precision, can address important issues regarding the synthesis and optical properties of plasmonic nanostructures, including structural and signal reproducibility. Further, single-molecule/single-particle-level studies on the plasmonic properties of these nanogap structures revealed that these particles can generate ultrastrong, quantifiable Raman signals in a highly reproducible manner.

10350-19, Session 5

3D plasmonic architectures for ultrasensitive Raman spectroscopy *(Invited Paper)*

Manohar Chirumamilla, Aalborg Univ. (Denmark); Remo Proietti Zaccaria, Andrea Toma, Istituto Italiano di Tecnologia (Italy)

The fabrication of innovative plasmonic architectures supporting extremely large electric field enhancement has gained increasing attention over the last few years, especially for the detection of molecules in highly diluted liquids, and/or the spectral signature collection of single/few molecules concentrated in nanogaps. The application of the “hot-spot” concept, induced by localized surface plasmon resonances, has been successfully exploited for surface-enhanced infrared absorption and surface-enhanced Raman spectroscopy. Within this context, we have conceived and developed novel 3D plasmonic architectures, endowed with multiple tips and detached from the substrate by means of standing silicon pillars. By exploiting the localization and enhancement capabilities of the proposed configurations, we have investigated the Raman signal of different biomolecules, approaching the single/few units detection limit. Raman spectra have been observed for p-Aminothiophenol and Rhodamine-6G molecules under very low concentrations (below 1 fM) in order to statistically ensure only single/few molecules per hot-spot. Finally, we have shown how the 3D configurations can be recycled for multiple uses in a cost effective way, still preserving high reproducible SERS enhancement performances.

10350-20, Session 5

TiO2-enhanced Raman spectroscopy and its relevance to electromagnetic and chemical enhancements

Yusuke Tanaka, Taka-aki Yano, Masahiko Hara, Tokyo Institute of Technology (Japan)

Plasmonic nanoparticles have been commonly utilized for surface-enhanced Raman spectroscopy (SERS) because of the strong field enhancement effect. Here, we propose to utilize titanium dioxide (TiO2) nanoparticles as an alternative to plasmonic ones. Since TiO2 possesses a relatively high refractive index, TiO2 nanoparticles with diameters of 150-250 nm exhibit strong electromagnetic resonances in the visible region, enabling us to employ them as an efficient field enhancer for SERS. We performed dark-field spectroscopy of individual TiO2 nanoparticles with various diameters, and determined the optimal size of the nanoparticle providing the strongest enhancement of Raman scattering from sample molecules attached on the nanoparticle surface. More interestingly, the SERS spectrum was found to be significantly different from the neat spectrum in terms of peak position and peak-to-peak intensity ratio, indicating the chemical enhancement effect caused by interfacial charge-transfer transition between sample molecules and TiO2.

10350-21, Session 6

Nanometer resolution imaging and tracking of fluorescent molecules with minimal photon fluxes *(Invited Paper)*

Klaus Gwosch, Francisco Balzarotti, Yvan Eilers, Max-Planck-Institut für Biophysikalische Chemie (Germany); Arvid H. Gynnå, Uppsala Univ. (Sweden); Volker Westphal, Max-Planck-Institut für Biophysikalische Chemie (Germany); Fernando D. Stefani, Univ. de Buenos Aires (Argentina); Johan Elf, Uppsala Univ. (Sweden); Stefan W. Hell, Max-Planck-Institut für Biophysikalische Chemie (Germany)

We introduce MINFLUX, a concept for localizing photon emitters in space. By probing the emitter with a local intensity minimum of excitation light, MINFLUX minimizes the fluorescence photons needed for high localization precision. In our experiments, 22 times fewer fluorescence photons are required as compared to popular centroid localization. In superresolution microscopy,MINFLUXattained ~1-nanometer precision, resolvingmolecules only 6 nanometers apart. MINFLUX tracking of single fluorescent proteins increased the temporal resolution and the number of localizations per trace by a factor of 100, as demonstrated with diffusing 30S ribosomal subunits in living Escherichia coli. As conceptual limits have not been reached,we expect this localization modality to break new ground for observing the dynamics, distribution, and structure of macromolecules in living cells and beyond.

10350-22, Session 6

Angstrom resolution using Cryogenic Optical Localization in 3D (COLD) *(Invited Paper)*

Daniel Böning, Siegfried Weisenburger, Max Planck Institute for the Science of Light (Germany); Benjamin Schomburg, Karin Giller, Stefan Becker, Christian Griesinger, Max-Planck-Institut für Biophysikalische Chemie (Germany); Vahid Sandoghdar, Max Planck Institute for the Science of Light (Germany)

The significance of super-resolution microscopy beyond the diffraction barrier was honored by the Nobel Prize in Chemistry last year. One such popular method employs pinpointing the position of single fluorophores, whereby the center of the point-spread function can be determined with arbitrary localization precision depending on the available signal-to-noise ratio. At room temperature, the signal of a fluorophore is limited by photobleaching resulting in typical localization precisions on the order of ten nanometers. We have already demonstrated Angstrom localization precision made possible by the substantial enhancement of the molecular photostability at cryogenic temperatures. We also verified the feasibility of colocalization and cryogenic distance measurements by resolving two fluorophores on the backbone of a double-stranded DNA at nanometer separation.

Here, we present our results on resolving the positions of multiple fluorophores attached to proteins using cryogenic colocalization microscopy. By applying algorithms borrowed from cryogenic electron microscopy, we can reconstruct a three-dimensional density map for the positions of the fluorescent labels with a resolution of several Angstrom, yielding excellent agreement with the expected crystal structure (Figure 1). Our technique pushes optical resolution by nearly two orders of magnitude beyond the state-of-the-art conventional super-resolution microscopy. It allows us to gain structural information that might not be accessible via existing analytical methods such as x-ray scattering or magnetic resonance spectroscopy. We discuss the potential of the technique for further improvement and its important challenges.

10350-23, Session 6

High-speed localized plasmonic structure illumination microscopy for biological imaging

Anna S. Bezryadina, Junxiang Zhao, Joseph L. Ponsetto, Yang Xu, Univ. of California, San Diego (United States); Xiang Zhang, Univ. of California, Berkeley (United States); Zhaowei Liu, Univ. of California, San Diego (United States)

We developed localized plasmon structured illumination microscopy (LPSIM) for high-speed super-resolution imaging. This new plasmonic technique was applied to observe biological specimens' movement with video speed imaging, 50nm resolution and wide field of view at the same time. LPSIM method was based on controlled plasmonic excitations from laser on a periodic 2-D array of nano-discs as a structured illumination pattern to excite a fluorescently tagged biological sample and achieve 3 times resolution improvement over standard microscopy. The LPSIM sapphire substrates have hexagon lattice array of 60 nm silver discs with 150 nm pitch and PMMA layer on top to protect array from oxidation or damaging bio-sample. Since the localized plasmonic field provides strong near-field enhancement of fluorescence particles, the LPSIM imaging process requires lower illumination laser power and shorter exposure time, thus provides faster imaging speed and longer observation time.

Our LPSIM method is very easy to implement for biological samples by drop-casting prepared cells in a solution, pressing down slice of tissue, or directly growing sample on the substrates. We tested our super-resolution imaging performance by using microtubules, fluorescent beads, neuron cells, and human tissues. By taking sequence of images at high speed we could create a video and observe dynamic of movements over wide field of view. As of today the LPSIM has higher speed than STORM or PALM, better spatial resolution than other SIM methods, and broader field of view and lower laser damage than STED.

10350-24, Session 6

Nanoscale Photoacoustic Tomography (nPAT) for label-free super-resolution 3D imaging of red blood cells

Pratik Samant, Armando Hernandez, Shelby Conklin, Liangzhong Xiang, The Univ. of Oklahoma (United States)

Here we present a novel imaging technique, nanoscale photoacoustic tomography (nPAT) for label-free super-resolution imaging of in vivo samples in 3D. This imaging modality uses a focused ultrashort (~7ps) laser pulse durations in order to generate photoacoustic (PA) waves, which are then detected and used to construct an image. These PA waves are high frequency (~GHz) signals that cannot be detected by a typical ultrasound transducer. In order to maximize bandwidth and obtain high-resolution, we use a pump-probe detection method in order to detect signals in the GHz range. This allows us to achieve a theoretical resolution on the order of ~10nm in the axial direction. The calculated sensitivity of this system is ~25Pa of the photoacoustic wave. The amplitude of the generated PA signal is directly proportional to the concentration of the absorber, in our case hemoglobin. Therefore, we can generate 3D absorption coefficient maps of our sample by raster scanning at different points. We present in the letter the simulations and experimental work that we have done so far in making this imaging modality a reality.

10350-36, Session PMon

Turning Ag/PDA/CuO into a 3D glass microfiber as the SERS platform for monitoring the photoinduced surface catalytic coupling reaction of 4-nitrothiophenol to 4,4'-dimercaptoazobenzene

Gongchun He, Jyunde Chen, Pei-Ying Lin, Worasaung Klinthong, National Sun Yat-Sen Univ. (Taiwan); Shuchen Hsieh, National Sun Yat-Sen Univ. (Taiwan) and Kaohsiung Medical Univ. (Taiwan)

A silver/polydopamine/copper oxide film decorated glass microfiber (Ag/PDA/CuO@GMF) was successfully fabricated using a simple preparation method and served as a 3D SERS substrate. The electron was found to transfer from silver nanoparticles to CuO through PDA, which served as an electron donor, facilitating a strong improvement of the electromagnetic field, leading to the enhancement of SERS intensity. The enhancement factor of Ag/PDA/CuO@GMF was as high as 1.07?106, which is suitable for a single molecule detection. Furthermore, the Ag/PDA/CuO@GMF was applied to monitor the photoinduced surface catalytic coupling reaction for converting 4-nitrothiophenol (4-NTP) to 4,4'-dimercaptoazobenzene (DMAB) in situ. The metal–semiconductor nanocomposite, which combined Ag nanoparticles and CuO in Ag/PDA/CuO@GMF, exhibited the highest catalytic activity over the individual Ag or CuO as the SERS substrate. The pseudo first-order reaction kinetics with the reaction rate constant of 0.1679?0.0022 min-1 explained the conversion of 4-NTP to DMAB. Thus, CuO/PDA/Ag@GMF proved to be a promising SERS substrate for application in biosensing and catalyst fabrication.

10350-37, Session PMon

Three-dimensional nanoscale optical vortex profilometry

Bogdan V. Sokolenko, Dmitrii Poletaev, V.I. Vernadsky Crimean Federal Univ. (Russian Federation)

The geometry of surface can be analyzed with optical vortices due to the high sensitivity of singular beam phase to the small distortions of the wavefront. The interference of the reference beam and the Laguerre-Gaussian beam transmitted through the isotropic thin plate coated with a wedge-shaped layer of 500 nm thickness makes possible to analyze the rotation of the spiral phase, depending on the thickness of the applied layer, as well as a surface topology in reflected beam regime. Evaluation of phase sensitivity shows that the distinguishable spiral phase rotation occurs at the isotropic plate thicknesses equals to wavelength300. The overall resolution of vortex profilometer based on phase-shifted singular beam is determined by shift - retrievement algorithm and may exceed diffraction limits for lens systems.

10350-38, Session PMon

Dynamic modeling of AFM piezoelectric MC in liquid with various percentages of glycerin in the presence of rough surface in nanoscale

Alireza Habibnejad Korayem, Iran Univ. of Science and

Technology (Iran, Islamic Republic of)

One of the most useful applications of an AFM is imaging of biological ?particles in a liquid medium. The increase of the topography accuracy in a liquid ?medium requires accurate dynamic modeling of a Microcantilever (MC). This article ?investigates the accurate dynamic modeling of the non-uniform AFM piezoelectric ?MC with rectangular geometry in the amplitude mode in liquid medium for rough ?surfaces. To increase the accuracy of the modeling, the Modified couple stress ??(MCS) theory in the liquid medium according to the Timoshenko beam model has ?been used. Moreover, for solving equations, the differential quadrature (DQ) method ?has been used, because in comparison with the other methods it has a high speed in ?solving equations and it is accurate in the number of fewer elements. In addition, the ?accurate force modeling has been established by considering the shear forces caused ?by liquid on the sides of the piezoelectric MC by solving the Navier-Stokes ?equations, and by considering the hydrodynamic force, squeeze force and applied ?forces between the sample surface and the MC tip. The results illustrate that utilizing ?higher vibration modes effects on the quality of rough surface topography with the ?rectangular roughness in the liquid medium and increase the quality of surfaces ?topography in the tapping mode, especially in the second MC vibration mode. ?Moreover, it should be noted that the sensitivity of the MC vibration amplitude to ?the piezoelectric MC angle is higher in comparison with other investigated ?parameters.?

10350-25, Session 7

Hyperspectral mapping of optoelectronic properties at length scales that matter in 2D semiconductors *(Invited Paper)*

James P. Schuck, The Molecular Foundry (United States)

Transition metal dichalcogenide semiconductors such as monolayer MoS2 are atomically thin direct band gap semiconductors which host a compelling combination of crystalline order and tightly bound exciton complexes with intense light-matter interactions. I will discuss our efforts aimed at the nano-optical investigation of these materials, where we uncover new optoelectronic regions and spatially-varying features that were hidden in prior optical studies. In addition, hyperspectral photoluminescence-excitation (PLE) mapping of TMDCs is enabling us to directly probe excited state properties, revealing charge puddling, unexpectedly-large binding energies, "anomalous" high-energy absorption features, and the first direct determination of band-gap renormalization as a function of carrier density in MoS2. Directly quantifying the fundamental exciton properties and carrier-dependent renormalization effects is essential for developing exciton-based optoelectronic devices in monolayer TMDC semiconductors that capitalize on their remarkable ability to tune the underlying many-body interactions.

10350-26, Session 7

Efficient plasmonic tip for nano Raman microscopy *(Invited Paper)*

Atsushi Taguchi, Osaka Univ. (Japan)

Tip-enhanced Raman spectroscopy (TERS) is recently becoming indispensable as a nano-imaging technique for analyzing advanced nano-devices and nano-materials because it allows strong enhancement of weak Raman signals from the nanometric volume of a sample. However, consistent enhancement in TERS is still an issue, and scientists have been struggling to fabricate good tips for a reliable, strong and reproducible enhancement. Here, I show that discretely arranged metal nano-grains work as an efficient optical antenna with large scattering cross section [1]. TERS image of graphene and carbon nanotubes are shown with enhancement factor of 5,500 and spatial resolution of 14 nm. This finding will bring TERS to a new level, where it can be utilized with more confidence of large reproducible enhancement for those nano-sized samples that have extremely weak Raman scattering. [1] A. Taguchi, et al., Nanoscale 7, 17424 (2015).

10350-27, Session 7

Near-field visible light absorption imaging by Raman-nano-light source

Ryo Kato, Osaka Univ. (Japan); Yuika Saito, Gakushuin Univ. (Japan) and Osaka Univ. (Japan); Takayuki Umakoshi, Prabhat Verma, Osaka Univ. (Japan)

In aperture-less near-field scanning optical microscopy (NSOM), when the apex of a sharp silicon nano-tip is illuminated with an incident laser, a strong Raman signal of silicon (LO phonon mode) is created at the tip apex. This silicon Raman signal can be partially absorbed by the sample while passing through it when the nano-tip is placed on the sample. Since the silicon Raman light is highly confined at the only tip apex, this absorption occurs only in near-field. In terms of inherent optical properties of the sample, because the total amount of absorption is dependent on sample topography as well as absorption coefficient of the sample, it is required to remove the effect of sample thickness from absorption measurements to observe only absorption properties of the sample. For this purpose, we employed two excitation lasers with wavelengths of 488 nm and 594 nm. We took the absorbance ratio between two Raman signals of silicon excited by two different wavelengths, which allowed the contribution of sample topography to be neglected. To verify the success of this technique, we observed two types of carbon nanotubes (CNTs) that have different absorption properties (semiconducting and metallic CNTs). An absorbance ratio image (A613nm / A502nm) allowed us to distinguish the two kinds of CNTs clearly due to the difference of their absorption coefficients. The present results demonstrate the flexibility of aperture-less NSOM, not only for vibrational spectroscopies, such as tip- enhanced Raman spectroscopy, but also for electronic energy state analysis.

10350-28, Session 7

Sharply focused azimuthally polarized beam characterized by photoinduced force microscopy

Jinwei Zeng, Fei Huang, Caner Guclu, Mehdi Veysi, Hemantha K. Wickramasinghe, Filippo Capolino, Univ. of California, Irvine (United States)

A sharply focused azimuthally polarized beam (APB) presents a strong longitudinal magnetic field with a vanishing electric field at its beam axis, forming an effective magnetic dominant region at the vicinity. This magnetic dominance is extremely desirable in the proposed high-speed ultra-compact optical magnetic force manipulation and microscopy, where the interaction between matter and the magnetic field of light can be exclusively exploited. However, direct characterization of such beam is challenging due to its subwavelength features. Here we show for the first time a direct characterization on a sharply focused APB in nanoscale using the novel Photoinduced Force Microscopy (PIFM) technique, which simultaneously excites and detects incident beam in near-field. Comparing to the Scanning Near-field Optical Microscopy (SNOM) which has near-field excitation and far-field detection, PIFM boasts a much smaller background noise and a more robust system. Based on the measured force-map, we develop a theoretical model to retrieve the corresponding electric and magnetic field distribution, and correct the distortion caused by the imperfect probe-tip of the PIFM. This research pioneers the exploration in the experimental investigation on the sharply focused structured light, unveiling its potentials in a plethora of optoelectronics, chemical, or biomedical applications.

10350-29, Session 8

Improving axial resolution in nanoscopy with supercritical angle fluorescence emission *(Invited Paper)*

Nicolas Bourg, Clement Cabriel, Iván Coto Hernández, Institut des Sciences Moléculaires d'Orsay (France); Siddharth Sivankutty, Sandrine Lévêque-Fort, Guillaume Dupuis, Univ. Paris-Sud 11 (France); Emmanuel Fort, Institut Langevin (France); Sandrine Lévêque-Fort, Institut des Sciences Moléculaires d'Orsay (France)

We propose to take advantage of Supercritical Angle Fluorescence (SAF) emission, also called forbidden light, to extract axial information in super-resolution microscopy. When a fluorophore is located in the vicinity of the coverslip interface, its near-field component can become propagative and be emitted above the critical angle. As this SAF emission decreases exponentially with the fluorophore/interface distance, absolute nanometric axial position of each fluorescent emitter can be extracted. To take advantage of the axial information hold by SAF, only the detection of the microscope need to be modified. Different pupil engineering strategies can be implemented depending on the super-resolution approach. In combination with dSTORM, an absolute axial localization precision of 15 nm within an axial range of ~150 nm above the coverslip can be achieved, allowing to investigate adhesion structures. Associated to STED microscopy, membrane imaging specificity can achieved.

10350-30, Session 8

Development of integrated optical nanoscopy using photonic chips *(Invited Paper)*

Balpreet S. Ahluwalia, Øystein I. Helle, Jean-Claude Tinguely, David A. Coucheron, Marcel Lahrberg, Firehun Tsige Dullo, Cristina I. Øie, UiT The Arctic Univ. of Norway (Norway)

Photonic integrated circuits (PIC) reduce the footprint, cost and complexity of optical systems. PIC technology enables on-chip integration of several optical functions. The compatibility with standard optical fibre components enable high-speed light coupling into PICs. Advancement of PIC technology has revolutionized several optical systems, while optical nanoscopy using photonic-chip has not been explored. Here, we discuss the integrated platform and the optical functions necessary for developing chip-based nanoscopy. By retrofitting a standard microscope with appropriate photonic-chip we convert it into an advanced nanoscope. The development of chip-based optical nanoscopy would enable wide-penetration of cost-effective, miniaturized multi-modality optical nanoscopy.

10350-31, Session 8

Chip-based nanoscopy: towards integration and high-throughput imaging

David A. Coucheron, Øystein I. Helle, Christina I. Øie, Firehun Tsige Dullo, Balpreet S. Ahluwalia, UiT The Arctic Univ. of Norway (Norway)

The advent of optical nanoscopy has opened up new research possibilities in the field of life sciences. Although optical nanoscopy provides unprecedented resolution, it suffers from a low throughput. This poses a major limitation to applications requiring large screening, such as in pathology and pharmaceutical research. Here, we report high-throughput integrated optical nanoscopy based on a photonic chip. The photonic chips are used to generate, steer and deliver the illumination, while a standard microscope is used to collect the signal. The sample is placed directly on top of waveguide chip and is illuminated by the evanescent field generated at the top of the waveguide surface. Chip-based nanoscopy decouples illumination and collection optics, enabling high-throughput imaging. As the entire laser illumination is integrated, an array of waveguides can be employed to simultaneously illuminate large areas. Here we demonstrate the high-throughput capabilities of the chip-based nanoscopy through large field of view imaging.

For optical nanoscopy, high intensity in the evanescent field is preferred. This is achieved by fabricating thin (100-200 nm) waveguides made of high-refractive index contrast. The waveguide material is transparent in the visible light region (405-660 nm) for fluorescence imaging. Chip-based optical nanoscopy would enable widespread availability of affordable optical nanoscopes by retrofitting any standard fluorescence microscope with the photonic chip. The optical fibre-compatibility with the photonic chips enables light delivery with commercially available telecom optical devices, which may enhance the imaging speed.

10350-32, Session 9

Dynamics of surface plasmon polaritons and excitons in ultrastrong coupling regime *(Invited Paper)*

Remo Proietti Zaccaria, Istituto Italiano di Tecnologia (Italy) and Chinese Academy of Sciences (China); Hai Wang, Haiyu Wang, Hong-Bo Sun, Jilin Univ. (China); Andrea Toma, Istituto Italiano di Tecnologia (Italy)

The interaction of quantum emitters with surface plasmon polaritons (SPPs) has attracted tremendous attention due to the possibility of controlling light–matter interactions at the nanoscale [1-5]. Recently, with the introduction of photochromic molecules and organic semiconductors with inhomogeneous broadened absorption spectra, the light–matter interaction has entered a completely new regime, in which the Rabi splitting values are remarkably enhanced. In the so-called ultrastrong coupling regime, the Rabi splitting energy becomes an appreciable fraction of the exciton transition energy, which has been experimentally and theoretically observed in a variety of systems.

In the present work, ultrastrong exciton-plasmon coupling in squaraine dye filled gold nanoholes array is investigated both from a static and dynamic point of view. A Rabi splitting energy of 860 meV, corresponding to ?50% of the exciton transition energy, is observed in steady-state reflection measurements. Moreover, transient absorption experiments were performed to understand the dynamics of the ultrastrong coupled exciton-plasmon states. It is found that the lower hybrid band is characterized by a shorter lifetime than the uncoupled exciton states, phenomenon which can be attributed to the very strong radiative damping of SPPs modes.

[1] H. Wang et al., Appl. Phys. Lett. 98, 251501 (2011)

[2] P. Vasa et al., Nat. Photonics 7, 128 (2013)

[3] H. Wang, et al., The Journal of Phys. Chem. Lett. 7, 4648 (2016)

[4] H. Wang et al., Nanoscale 8, 13445 (2016)

[5] H. Wang et al., Adv. Funct. Mat. 26, 6198 (2016)

10350-33, Session 9

Nanoplasmonic multiplexing of optical angular momentum from the visible to terahertz range *(Invited Paper)*

Min Gu, Haoran Ren, RMIT Univ. (Australia)

Similar to the other physical dimensions of light, such as time, space, polarization, wavelength, and intensity, optical angular momentum (AM) is another physically-orthogonal dimension of light. Owing to an unbounded set of orbital angular momentum (OAM) modes carried by helically-phased beams, the availability of using AM-carrying beams as information carrier to generate, transport and detect optical signals has recently been largely explored in both classical and quantum optical communications, suggesting that AM is indeed a promising candidate to dramatically boost the optical multiplexing capacity. However, the extrinsic nature of OAM modes restricts conventional OAM multiplexing to bulky phase sensitive elements, imposing a fundamental limit for realizing on-chip OAM multiplexing. Recently, we demonstrate an entirely-new concept of nanoplasmonic multiplexing of AM of light, which for the first time enables AM multiplexing to be carried out by an integrated device with six orders of magnitude reduced footprint as

compared to the conventional OAM detectors. We show that nanoring slit waveguides exhibit a distinctive outcoupling efficiency on tightly-confined plasmonic AM modes coupled from AM-carrying beams. More intriguingly, unlike the linear momentum sensitivity with a typical sharp resonance, the discovered AM mode-sorting sensitivity is nonresonant in nature, leading to an ultra-broadband AM multiplexing ranging from visible to terahertz wavelengths. This nanoplasmonic manipulation of AM of ultra-broadband light offers exciting avenues for future on-chip AM applications in highly-sensitive bio-imaging and bio-sensing, ultrahigh-bandwidth optical communications, ultrahigh-definition displays, and ultrahigh-capacity data storage.

10350-34, Session 9

Plasmon-enhanced light-matter interactions on nanoporous gold nanoparticles and arrays *(Invited Paper)*

Wei-Chuan Shih, Univ. of Houston (United States)

Light matter interaction can provide rich compositional information from various types of samples in a non-destructive fashion. Our laboratory has developed a broad range of opto-analytical spectroscopy, imaging, and sensing technologies with core innovations in nanomaterial, device, and instrumentation. In this talk, I will report our work in light-based sensing and imaging using various plasmon-enhanced light-matter interactions as contrast mechanisms, e.g, Raman, fluorescence, extinction, and near-infrared absorption. Over the past few decades, numerous studies have led to the current state of knowledge by largely attributing the enhancement to nanostructural “singularities”, e.g., small gaps and sharp protrusions on the order of 10 nm. However, most of these studies relied on advanced lithography or colloidal surface chemistry to produce nanostructural singularities, aka “hot spots”. Lithographic techniques such as focused ion beam is time-consuming and cost-prohibitive for scaling up. Colloidal surface chemistry produces assays that are challenging to translate into a “biochip”.

To overcome these issues, I will present our efforts in engineered nanostructures with high-density plasmonic hot spots and their use in chemical and biosensing – in some cases at the single molecule level. I will discuss their potential uses in biomedical and environmental applications, in particular, the potential translation into point-of-care, low-cost, distributed, and wearable devices. I will also discuss our early results of plasmon-enhanced nanoimaging and colorimetric detection by DotLens smartphone microscopy.

10350-35, Session 9

Planar plasmonic nano antennas explore membrane nanoscale heterogeneities in living cells

Raju Regmi, Institut Fresnel (France) and ICFO - Institut de Ciències Fotòniques (Spain); Pamina Winkler, ICFO - Institut de Ciències Fotòniques (Spain); Valentin Flauraud, Ecole Polytechnique Fédérale de Lausanne (Switzerland); Kyra J. E. Borgman, Carlo Manzo, ICFO - Institut de Ciències Fotòniques (Spain); Jürgen Brugger, Ecole Polytechnique Fédérale de Lausanne (Switzerland); Hervé Rigneault, Jérôme Wenger, Institut Fresnel (France); María F. Garcia-Parajo, ICFO - Institut de Ciències Fotòniques (Spain)

The spatiotemporal architecture of the cell membrane and diffusion dynamics of its constituents (lipids and proteins) are critical for many cellular processes such as signaling, trafficking and cell adhesions. Sub-diffraction photonics based on plasmonics offer new opportunities to follow such events as they can confine electric fields in nanoscale hotspots with spatial dimensions comparable to single molecules (~5 nm). In this work, we propose in-plane plasmonic nanogap antenna arrays and study the diffusion characteristics of phosphoethanolamine (PE) and sphingomyelin (SM) in Chinese hamster ovary cells by incorporating fluorescent lipid analogs.

The enhanced electric fields in nanoscale probe areas yield a sub-diffraction spatial resolution ultimately making it possible to follow single molecule events at physiological expression levels. Fluorescence correlation spectroscopy and burst analysis of these events show free 2D Brownian diffusion for PE (with both confocal and nanogap antennas). However the diffusion dynamics of SM at the nanoscale indicates extremely heterogeneous behavior which was otherwise hidden in the confocal ensemble.

The findings presented here are crucial to understand the spatiotemporal and heterogeneous organization of live cell membranes at the nanoscale. In addition, the proposed technique is fully biocompatible and thus provides various opportunities in biophysics and live cell research.

Conference 10351: UV and Higher Energy Photonics: From Materials to Applications 2017

SPIE. OPTICS+ PHOTONICS NANOSCIENCE+ ENGINEERING

Sunday - Monday 6 –7 August 2017

Part of Proceedings of SPIE Vol. 10351 UV and Higher Energy Photonics: From Materials to Applications 2017

10351-1, Session 1

Research on AlGaN deep UV lasers and B-III-N alloys *(Invited Paper)*

Xiaohang Li, King Abdullah Univ. of Science and Technology (Saudi Arabia)

Deep-ultraviolet (DUV) emitters with wavelengths shorter than 280 nm have numerous applications such as high-density optical storage, disinfection, and biochemical identification. However, most of the commercially available DUV emitters including mercury lamps, quadrupled Nd:YAG lasers, and excimer lasers have limitations in many applications due to their large footprint, poor reliability, or toxicity. Recently, the III-N semiconductor-based UV light emitters have drawn great attention, as the AlInGaN direct bandgap covers the entire DUV range (200–280 nm), which can lead to efficient, compact, and reliable DUV emitters. Compared to other group-III-nitride wide bandgap ternary alloys, the BAlN alloy has not been studied extensively. A detailed understanding of BAlN-AN heteroepitaxy is motivated by achieving DUV light sources. Recently, theoretical and experimental studies have shown that boron-containing nitrides are promising for UV application. BAlN has a similar bandgap as AlN that does not vary significantly as a function of boron content, thereby being transparent to the UV spectrum. In addition, it has been shown that wurtzite BAlN layers with small amounts of boron incorporation (i.e. less than 5%) could introduce strong refractive index contrasts. Therefore, higher boron-content and high-quality wurtzite BAlN layers are desirable in UV distributed Bragg reflectors (DBRs). In this presentation, we will cover the latest progress regarding the DUV lasers and B(Al)N materials.

10351-2, Session 1

Challenges and breakthroughs in the development of AlGaN-based UVC lasers

Ramon Collazo, North Carolina State Univ. (United States); Ronny Kirste, Adroit Materials, Inc. (United States); Zlatko Sitar, North Carolina State Univ. (United States) and Adroit Materials, Inc. (United States)

Despite the rapid progress in III-nitride-based laser diodes, sub-300 nm UV semiconductors lasers have not been realized yet, mainly due to the lack of proper crystalline substrates and poor defect control in the wide bandgap semiconductors. Al-rich AlGaN alloys are the building blocks for these deep UV optoelectronics devices with the highest crystalline quality Al-rich AlGaN films obtained on AlN single crystal substrates. Furthermore, reduction in non-radiative centers and compensating point defect is required to achieve high IQE. Recently, UV LEDs emitting at 265 nm exceeding 80 mW, as well as low-threshold, optically pumped lasers emitting at wavelengths between 230–280 nm have been demonstrated. Nevertheless, issues related to the performance and further improvement of the heterostructure-based active regions as related to quantum efficiencies and emission polarization is desired. These issues to be discussed are classified in two main categories: (1) growth, crystallography and surface morphology control and (2) identification and control of point defects. In addition to this, results on electrically-pump laser structures will be discussed, showing the very near possibility of the first ever demonstration of deep UV semiconductor lasers. Such devices will find direct and immediate uses in health care, bio-defense and other commercial and defense applications. The use of light sources in the deep UV will lead to detection systems of different chemical and biological aerosols, providing for detection of a variety of pollutant agents among other effluents, in addition to help in increasing the availability of clean potable water through efficient UV disinfection.

10351-3, Session 1

Broadband ultraviolet light emitter based on GaN quantum dots on truncated pyramids

Jong-Hoi Cho, Seung-Hyuk Lim, Min Ho Jang, KAIST (Korea, Republic of); Samuel Matta, Julien Brault, Ctr. de Recherche sur l'Hétéro-Epitaxie et ses Applications (France); Yong-Hoon Cho, KAIST (Korea, Republic of)

Broadband ultraviolet (UV) light sources have been used for many applications such as UV curing, UV spectrophotometry and phototherapy. However, traditional UV light sources such as mercury-vapor lamps remain with some challenging issues. The mercury-vapor lamps are bulky systems and present environmental issues coming from the use of mercury. In this respect, UV light emitting diodes (LEDs) have been suggested to replace mercury-vapor lamps. Because of compact size, the phototherapy using UV LEDs can treat location of lesions without damage of adjacent normal skin. However, narrow spectrum range of conventional UV LEDs makes utilization limited since some applications such as UV spectrophotometry require a broad UV spectrum. Moreover, in AlxGa1-xN-based UV LEDs (x > ~0.25), UV light laterally propagates since the top of the valence band can be converted to crystal field split-off hole band. It has out-of-plane polarized light, which consequently has limited light extraction efficiency. In this study, we demonstrated broadband UV light source from UV-A to UV-C using GaN QDs on hexagonal truncated pyramids. Since the built-in electric fields and growth rates are different depending on regions such as (0001) polar facet, {101¯1} semipolar facets and its boundary, various UV emission wavelengths can be observed from each region, which leads to a broadband UV light source. In addition, most of the UV light source was emitted from GaN QDs, which have predominantly in-plane polarized light. This result presents a potential for solid-state based broadband light sources.

10351-4, Session 1

A design of energy detector for ArF excimer lasers

Zebin Feng, Academy of Opto-Electronics, CAS (China) and Univ. of Chinese Academy of Sciences (China); Xiaoquan Han, Yi Zhou, Lujun Bai, Academy of Opto-Electronics, CAS (China)

ArF excimer lasers with short wavelength and high photon energy are widely applied in the field of integrated circuit lithography, material processing, laser medicine, and so on. Excimer laser single pulse energy is a very important parameter in the application. In order to detect the single pulse energy on-line, one energy detector based on photodiode was designed. The signal processing circuit connected to the photodiode was designed so that the signal obtained by the photodiode was amplified and the pulse width was broadened. The amplified signal was acquired by a data acquisition card and stored in the computer for subsequent data processing. The peak of the pulse signal is used to characterize the single pulse energy of ArF excimer laser. In every condition of deferent pulse energy value levels, a series of data about laser pulses energy were acquired synchronously using the Ophir energy meter and the energy detector. A data set about the relationship between laser pulse energy and the peak of the pulse signal. Then, by using the data acquired, a model characterizing the functional relationship between the energy value and the peak value of the pulse was trained based on an algorithm of machine learning, Support Vector Regression (SVR). By using the model, the energy value can be obtained directly from the energy detector designed in this project. The result shows that the relative error between the energy obtained by the energy detector and by the Ophir energy meter is less than 3%.

10351-5, Session 1

Formation of p-type ZnO through cocktail implantation *(Invited Paper)*

Wei-Yen Woon, National Central Univ. (Taiwan)

We present a study on the. formation of p-type ZnO thin film through ion implantation. Group V dopants (N, P) with different ionic radii are implanted into chemical vapor deposition grown ZnO thin film on GaN/sapphire substrates prior to thermal activation. It is found that monodoped ZnO by N+ implantation results in n-type conductivity under thermal activation. Dual-doped ZnO film with a N: P ion implantation dose ratio of 4:1 is found to be p-type under certain thermal activation conditions. Higher p-type activation levels (1019 cm(-3)) under a. wider thermal activation range are found for the N/P dual-doped ZnO film co-implanted by additional oxygen ions. From high resolution x-ray diffraction and x-ray photoelectron spectroscopy it is concluded that the observed p-type conductivities are a result of the promoted formation of P-Zn-4N(O) complex defects via the. concurrent substitution of nitrogen at oxygen sites and phosphorus at zinc sites. The enhanced solubility and stability of acceptor defects in oxygen co-implanted dual-doped ZnO film are related to the reduction of oxygen vacancy defects at the surface. Our study demonstrates the prospect of the. formation of stable p-type ZnO film through co-implantation.

10351-6, Session 2

Performance stability of reflection-mode AlGaN photocathode under different preparation methods

Junju Zhang, Yijun Zhang, Nanjing Univ. of Science and Technology (China)

Solar-blind detectors have received widespread use in manufacturing and space detection due to their spectral response wavelength. The widebandgap semiconductor AlGaN could be an outstanding selector because of its physical and chemical stability, high solar rejection, and detectivity performance. In addition, the image intensifier and vacuum photodiode based on an AlGaN photocathode has the distinctive characteristics of low dark current and high sensitivity. Nevertheless, the performance stability of the AlGaN photocathode was rarely reported. It is known that the traditional activation method of the III-nitride photocathode is that the cesium(Cs) source is kept continuous and the oxygen(O) source is introduced periodically. To investigate the attenuation performance of the AlGaN photocathode, three samples with the same structures grown by metalorganic chemical vapor deposition were activated with three different activation methods, which are called Cs-only, Cs–O, and Cs–O–Cs activation, respectively. The spectral responses and attenuated photocurrents of the three AlGaN photocathodes were measured. The results show that the Cs–O activated AlGaN photocathode exhibits the lowest attenuation speed in the first few hours, and the attenuation speed of the Cs-only activated one is fastest. After attenuating for 90 min, the attenuation photocurrent curve of the Cs–O–Cs activated sample is coincident with that of the Cs–O activated one. The main factor affecting the photocurrent attenuation is related to Cs atoms desorbed from the photocathode surface.

10351-7, Session 2

FUV-DUV spectra of graphene, carbon nanotubes, and polymer nanocomposites

Kenta Kobashi, Kwansei Gakuin Univ. (Japan); Yusuke Morisawa, Kindai Univ. (Japan); Krzysztof Bec, Kwansei Gakuin Univ. (Japan); Ichiro Tanabe, Osaka Univ. (Japan); Masahiro Ehara, Institute for Molecular Science (Japan) and Kyoto Univ. (Japan); Harumi Sato, Kobe Univ. (Japan); Yukihiro Ozaki, Kwansei Gakuin Univ. (Japan)

The far-ultraviolet (FUV) region, which is the region of 120-300 nm, provides unique information about the electronic transitions and structure of a molecule. We have recently succeeded in measuring electronic spectra of graphene, carbon nanotubes, and polymer nanocomposites down to 150 nm using a newly developed attenuated total reflection (ATR)-UV spectrometer. The spectra of graphene show a thickness dependence. A thin graphene sample with the thickness of 1-2 nm shows a small peak near 155 nm. Single-wall carbon nanotubes with the thickness of 1-2 nm yields a similar peak. We investigate band assignments for these peaks including theoretical calculation. In the case of polymer nanocomposites a polymer gives rise to major peaks below 200 nm while nano carbon part does not show a peak in the whole region because the content of nanocarbon is very small compared with the polymer. We compared an FUV-DUV spectrum of PHB (poly(hydroxybutyrate))-graphene nanocomposites with that of PHB. A peak near 171 nm shows a longer wavelength shift by ca. 2 nm upon the formation of nanocomposites, indicating a change in electronic structure in the polymer. We investigate the cause of the shift by using quantum chemical calculations.

10351-8, Session 2

Extended polariton condensate of GaN microwire with whispering gallery mode at room temeperature

Hyun Gyu Song, Min Kwan Kim, Min-Sik Kwon, Sunghan Choi, Kie Yong Woo, Yong-Hoon Cho, KAIST (Korea, Republic of)

Exciton cavity polaritons (polaritons) are bosonic quasi-particles providing a unique semiconductor-state system for research of interacting condensate. Surviving temperature of polaritons is determined by Bohr radius and binding energy of exciton and phonon energy. Especially, the temperature upper limit for wide bandgap semiconductor like GaN is expected to be above room temperature (RT) due to large exciton binding energy and oscillator strength. Up to now , strain-induced potential fluctuation due to lattice misfit for two-dimensional cavity of GaN have prevented the construction of long-range off-diagonal term necessary for any quantum control. Especially as-grown GaN microwire could be free for lattice misfit due to strain bending and no observable dark spot. In addition, long- range off-diagonal term can be stable at RT because of reduced interaction with phonon result from large spatial overlap between exciton and photon. In this work, using a single hexagonal microwire grown by selective area method of metalorganic chemical vapor deposition, we show the condensates can propagate over microscopic distances from the excitation area because of no microscopic potential fluctuation, while preserving their spatial coherence at RT due to large Rabi splitting energy. The extension of the condensate is related to the repulsive local potential induced by excitons generated by off-resonance pumping within small excitation area. To our knowledge , the characteristics of RT extended polariton condensate of single GaN microwire systems remain unexplored until now. The single microwire structure with the manipulation of this local excitation provide a versatile method to control the extended state at RT.

10351-9, Session 2

Tunnel junctions based ultra-violet light emitting diodes *(Invited Paper)*

Siddharth Rajan, Yuewei Zhang, Jamal-Eddine Zane, Fatih Akyol, The Ohio State Univ. (United States)

We report on the design, demonstration and current status of tunnel junction-based UV LEDs. III-Nitride ultraviolet light emitting diodes (UV LEDs) are promising in various applications including sterilization, water purification and medical sensing. However, both the light extraction efficiency and electrical efficiency face fundamental challenges for the conventional UV LED structures. This stems from the poor p-type conductivity and high p-type contact resistance. Hole injection using interband tunneling provides an elegant solution to the fundamental issues of UV LEDs, and can resolve both the hole injection and light extraction issues that have been the primary problems for UV LEDs.

In this talk, we will discuss in detail the heterostructure and polarization engineering needed to realize efficient interbank tunneling in ultra-wide band gap devices. We will then outline some of the growth and fabrication challenges, and our approaches to overcome these. Finally, we will present our results on tunnel-injected UV LEDs that have enabled us to achieve efficient UV light emission in the UVA and UVB wavelength ranges with on-wafer efficiency comparable to state-of-the-art values [1,2,3].

1. Zhang, Yuewei, et al. "Interband tunneling for hole injection in III-nitride ultraviolet emitters." Applied Physics Letters 106.14 (2015): 141103.

2. Zhang, Y., Krishnamoorthy, S., Akyol, F., Allerman, A.A., Moseley, M.W., Armstrong, A.M. and Rajan, S., 2016. Design and demonstration of ultra-wide bandgap AlGaN tunnel junctions. Applied Physics Letters, 109(12), p.121102.

3. Zhang, Yuewei, et al. "Enhanced light extraction in tunnel junction-enabled top emitting UV LEDs." Applied Physics Express 9.5 (2016): 052102.

10351-10, Session 3

Recent advances in metals for plasmonics applications in the UV range *(Invited Paper)*

Yael Gutiérrez, Francisco González, José M. Saiz, Rodrigo Alcaraz de la Osa, Univ. de Cantabria (Spain); Juan M. Sanz, Textil Santanderina SA (Spain) and Univ. de Cantabria (Spain); Dolores Ortiz, Univ. de Cantabria (Spain); Henry O. Everitt, U.S. Army Aviation and Missile Command (United States) and Duke Univ. (United States); Fernando Moreno, Univ. de Cantabria (Spain)

Extending plasmonics to the UV range is a hot topic due to the many challenges arising in fields such as biology, chemistry (photocatalysis) or spectroscopy techniques. A recent study considered several metals for this task by comparing their plasmonic performance (PP) to those of gold and silver in the visible. The main conclusion was that Mg, Al, Ga and Rh can be considered promising metals for UV-plasmonics. However, nanoparticles (NPs) made of Mg, Al and Ga suffer from the formation of a native oxide layer whose thickness strongly depends on the ambient conditions and that affects its plasmonic behavior. A more recent numerical study presented Rh as one of the most promising metals for UV-plasmonics not only for its good PP but also for its low tendency to oxidation. Moreover, the easy fabrication through chemical means of Rh NPs with sizes smaller down to 10 nm, and its potential for photocatalysis applications, makes this material very attractive for building plasmonic tools for the UV.

In this contribution, we will make an overview of our recent research in metals for UV plasmonics. We will pay special attention to our studies on the plasmonic properties of NPs made of Rh and two of the synthesized geometries: tripod stars and nanocubes. The role of shape, polarization of the incident radiation on the performance and generation of LSPRs in the UV will be explored as well as the possibility of generating hot spots with NPs aggregates located on flat substrates for applications in SERS experiments.

10351-11, Session 3

Reduction of plasmon damping in aluminum nanoparticles with rapid thermal annealing

Feifei Zhang, Julien Proust, Davy Gerard, Jérôme Plain, Jérôme Martin, Univ. de Technologie Troyes (France)

Aluminum is now widely regarded as a promising plasmonic material, especially in the ultraviolet spectrum. In this presentation, we propose rapid thermal annealing (RTA) as a simple method to significantly decrease the amount of intrinsic losses in aluminum nanoparticles. We study the structural and optical properties of aluminum nanodisks before and after RTA at different temperatures.

Our results unveil how RTA affects the plasmonic properties of Al nanoparticles through the competition between the reduction of the number of grain boundaries and oxidation. If RTA is performed below a threshold temperature of 400oC, oxidation is extremely weak and the plasmonic resonances sustained by Al nanodisks are blue shifted with a diminution of their full width at half maximum. This improvement is due to a diminution of the number of grain boundaries inside the metal core. Hence, RTA appears as a simple, cost-effective and up-scalable technique to improve the plasmonic properties of aluminum. In contrast, above the threshold temperature, oxidation becomes predominant, resulting in a detrimental effect on the plasmon resonance. This effect should be taken into account in any industrial process involving heated Al nanoparticles

10351-12, Session 3

Aluminum plasmonics for UV nanooptics *(Invited Paper)*

Jérôme Martin, Davy Gerard, Jérôme Plain, Dmitry Khlopin, Feifei Zhang, Julien Proust, Univ. de Technologie Troyes (France)

An electromagnetic field is able to produce a collective oscillation of free electrons at a metal surface. This allows light to be concentrated in volumes smaller than its wavelength. The resulting waves, called surface plasmons can be applied in various technological applications such as ultra-sensitive sensing, Surface Enhanced Raman Spectroscopy (SERS), or metal-enhanced fluorescence, to name a few. For several decades plasmonics has been almost exclusively studied in the visible region by using nanoparticles made of gold or silver as these noble metals support LSPR only in the visible and near-IR range. Nevertheless, emerging applications will require the extension of nano-plasmonics toward higher energies, in the UV range. Aluminum is one of the most appealing metal for pushing plasmonics up to ultraviolet energies. The subsequent applications in the field of nanooptics are various. This metal is therefore a highly promising material for commercial applications in the field of ultraviolet nano optics. As a consequence, aluminum (or UV) plasmonics has emerged quite recently. Aluminium plasmonics has been demonstrated efficient for numerous potential applications including non-linear optics, enhanced fluorescence, UV-SERS, optoelectronics (plasmonic assisted lasing, by coupling Al with wide bandgpap semiconduc-tors such as GaN), photocatalysis, structural colors and data storage. In this talk, we will discuss about the recent advances in aluminum plasmonics. Different preparation methods developed in the laboratory to obtain aluminum nanostructures will be presented with their optical and morphological characterizations. Both advantages and issues of aluminum as a plasmonic material will be part of the presentation.

10351-13, Session 4

Sample photodegradation and protection in UV resonance Raman spectroscopy

Yasuaki Kumamoto, Kyoto Prefectural Univ. of Medicine (Japan)

Raman spectroscopy enables a sensitive, label-free molecular analysis of a biological sample. Employing UV light for the Raman excitation allows tremendous scattering enhancement of molecules up to 108 due to the electronic resonance, as well as fluorescence-free spectral acquisition thanks to the wavelength separation of Raman scattering and fluorescence of a sample. In UV Raman spectroscopy, however, sample photodegradation often occurs due to absorption of the UV light by molecules in the sample. This is the serious limitation of the technique in biomedical sciences. Here we present three approaches for sample protection from UV-induced photodegradation. Trivalent ions of three lanthanide group elements, terbium, europium, and thulium, were added to a buffer solution immersing fixed cells so that molecular photodegradation of the cells during Raman measurement were significantly suppressed. Utilizing such protective effects

of lanthanide ions, I successfully achieved repetitive, twice higher signal-to-noise ratio UV Raman imaging of cells. The underlying mechanisms of the protection effect can be explained as energy relaxation of the excited molecules by the lanthanide ions. Removing oxygen from the sample environment also suppressed molecular photodegradation of the cells during UV measurement, by avoiding generation of reactive oxygen species around the excited molecules. Combination of these two techniques further suppressed the UV-induced photodegradation of the cellular molecules. Cooling the sample is the other approach for suppressing the molecular photodegradation under UV exposure, by decelerating the rates of photoreactions. The presented three techniques can extend applications of UV resonance Raman spectroscopy in biomedical sciences.

10351-14, Session 5

The role of light interference in the formation of laser-induced shallow pits from metal micro-particles on glass

Eyal Feigenbaum, Omer Malik, Alexander M. Rubenchik, Manyalibo J. Matthews, Lawrence Livermore National Lab. (United States)

In high power laser systems the presence of metal particulate contamination on the exit surface of silica glass was recently reported to result in sub-micron deep laser-induced shallow pits (LSPs), which appear in high densities and result in light scattering thus limiting the optics lifetime. In the LSP formation process the incident laser beam deposits heat into the skin depth of the metal particle, which in turn ejects a plasma plume towards the substrate surface, propelling the particle away from the substrate, and etching a LSP into it. We present here a model that predicts the laser-induced plasma pressure exerted on a surface-bound micron-scale metal spherical particle, resulting in the modification of the glass substrate under the particle by etching. The model starts with a full-wave FDTD electromagnetic simulation of the geometry which results in the absorption distribution in the metal particle, leading to the plasma emitted from the particle and to the projected plasma pressure on the surface. The model predications provide an explanation to the puzzling observed 'shoulder' signature in LSP profiles, as well as agreeing with other experimentally observed trends. The model highlights the significance of the interference of the incident light in the open cavity geometry formed between the micro-particle and the substrate in the resulting LSPs shape, and provides an understanding of the geometry dependence. These results contribute to the current understanding of laser-induced damage science and can enable high resolution controlled machining of silica surfaces using plasma etching jets.

This work was performed under the auspices of the U.S. Department of Energy by Lawrence Livermore National Laboratory under Contract DE-AC52-07NA27344. LLNL-ABS-718628.

10351-15, Session 5

Changes in electronic states of molecules resulted from interactions in the condensed phase *(Invited Paper)*

Yusuke Morisawa, Nami Ueno, Kindai Univ. (Japan); Shin Tachibana, Kwansei Gakuin Univ. (Japan); Masahiro Ehara, Institute of Molecular Science (Japan); Yukihiro Ozaki, Kwansei Gakuin Univ. (Japan)

The wavelength region shorter than 200 nm, far-ultraviolet (FUV) region, is very rich in information about the electronic states and structure of a molecule. We have recently developed a totally new UV spectrometer based on attenuated total reflection (ATR) that enables us to measure spectra of liquid and solid samples in the 140–280 nm region. This paper shows the studies by the attenuated total reflection far-ultraviolet (ATR-FUV) spectroscopy. Intermolecular interactions between alkyl chains such as CH---HC should be reflected in the phase behavior of organic compounds. We measured the attenuated total reflectance spectra in the far-UV region (145–300 nm) of n-tetradecane (Tm = 5.9 °C) from 15 to -38 °C to determine its temperature dependency. With decreasing temperature, the absorption band at 153 nm in the liquid phase becomes weaker and new bands appear at around 200 and 230 nm. These results suggest that an unusually compressed structure might be generated at the surface at low temperatures, and this phase change, which is reversible, is responsible for the unusual absorption observed in the ATR-FUV spectra. We have also investigated composite polymer electrolytes (CPE). ATR-FUV spectra of CPEs composed of Poly(ethylene oxide) (PEO) and Li salt were observed and its variation of anions for the CPEs are studied.

10351-16, Session 5

A measurement validated model for an infrared laser induced filament damage formation in fused silica glass

Eyal Feigenbaum, Ted A. Laurence, Lawrence Livermore National Lab. (United States)

Here we measure and develop a model for filament formation in silica glass especially suitable for picosecond laser pulses, which is simplified with respect to the model for ultrashort pulses and enables the derivation of closed form expressions. This is critical for high power laser systems where the beam has to be directed through optics, e.g., thin debris shields. The experimental measurements of filamentation damage in fused silica induced by infrared ps pulses laser will be detailed. An analytical model adjusted to picosecond pulse-lengths is derived, resulting in expressions for the expected field intensities and carrier densities in the filament, and thus also the energy loss. The analytical expressions are validated with split-step beam-propagation-method numerical simulations, and compared to the experimental data. We have found that simulations and calculations of the propagation of high intensity laser beams through fused silica are able to capture the essential effects and features of experiments with ps pulses of 1053 nm. An upper limit of approximately 5 TW/cm^2 for the propagation intensity in the filament is found. For 1-5 ps pulses the beam decays and is dissipated rapidly off the front surface, while for longer pulses a filament of finite length is formed, followed for some cases by a second filament after a longer distance. Further cases and details of the model and measurements will be discussed.

This work was performed under the auspices of the U.S. Department of Energy by Lawrence Livermore National Laboratory under Contract DE-AC52-07NA27344. LLNL-ABS-718742.

10351-17, Session 6

Multiphoton ultraviolet excitation allows label free ratiometric imaging of neurotransmitters *(Invited Paper)*

Sudipta Maiti, Tata Institute of Fundamental Research (India)

Multiphoton ultraviolet excitation provides unprecedented access to the naïve fluorescence of physiological chromophores. This has been exploited to image neurotransmitters, e.g. serotonin and dopamine in live cells. Here we extend the technique to perform ratiometric imaging of neurotransmitters in live neurons. Ratiometric imaging provides quantitative measure of the change of concentrations of cellular analytes, but is usually achievable for only a few analytes using specially designed reporter molecules added externally. Here we describe a label free ratiometric imaging technique for direct detection of changes in intra-vesicular serotonin concentration. At higher concentrations of serotonin, there appears a growing longer wavelength tail with an isoemissive point at 376 nm due to formation of oligomers. So we split the emission signal into two channels to determine the intra-vesicular concentration of serotonin using multi-photon microscopy. We first generate a calibration curve and show that our technique is sensitive to alterations in the range of ~ 10-150 mM of serotonin. As a proof of principle study, we then show an increase in

intra-vesicular serotonin concentration upon addition of external serotonin. In brief, our label free ratiometric imaging technique can be utilized to investigate conditions affecting vesicular serotonin packaging and content.

10351-18, Session 6

Enhanced thermoelectrical properties of new doped conjugated polymers

Jiae Lee, Han Young Woo, Korea Univ. (Korea, Republic of)

Thermoelectric (TE) materials have attracted growing attention due to their potential to convert vast amounts of waste heat directly into electricity, therefore reducing the dependence on fossil fuel. Because of mechanical flexibility, solution processability, and low thermal conductivity, organic thermoelectric materials are of great interest.1 For improving thermoelectric properties, enhanced electrical properties are required by chemical doping of conjugated polymers.The electrical conductivity can be also modulated by carrier mobility from morphology changes.

In this contribution, we synthesized two kinds of p-type thermoelectric polymers based on cyclopentadithiophene (CDT) and benzothiadiazole (BT) moieties with different solubilizing side chains. To increase the chain planarity, dialkylmethylene substituents were attached (CPDTSBT) at 4 position of CDT via double bond where the first carbon (next to the main backbone) in the side chain is sp2 hybridized and located in the same plane of the main chain. For comparison, the bis(ethylhexyl) substituted polymer was also prepared (CPDTBT). The film morphology, i.e., interchain ordering and orientation was investigated by Grazing-Incidence Wide-Angle X-ray Scattering (GIWAXS) and the electrical conductivity was measured by 4 point probe with changing the concentration of dopant (tris(pentafluorophenyl) borane).In the UV-vis spectra, the increase of the polaronic peak in the range of 800 to 1100 nm was observed with increasing concentration of dopant. Furthermore,by adjusting the amount of dopant, the electrical conductivity was increased up by 6 orders of magnitude and the resulting power factor up to 6.15?W/mK2 was measured. CPDTSBT shows the higher crystalline morphology, electrical conductivity and the resulting power factor, compared to CPDTBT. Finally, it will be discussed in detail how the molecular structure and morphology can affect the electrical and thermoelectrical properties.

References

(1) Heeger, A. J. Semiconducting and Metallic Polymers: The Fourth Generation of Polymeric Materials. J. Phys. Chem. B 2001, 105, 8475-8491.

10351-19, Session 6

DNA methylation detection using nano bowtie antenna enhanced Raman spectroscopy *(Invited Paper)*

Shuang Fang Lim, Ling Li, Robert E. Riehn, Hans D. Hallen, North Carolina State Univ. (United States)

We show that methylated-DNA (m-DNA) can be distinguished from non-methylated (n-DNA) with bowtie enhanced Raman spectra. Raman energies in both DNA samples are found at 1324, 1407 (weak), 1473, and 1567 cm-1. The primary differences are two additional Raman peaks in the 1200 – 1700 cm-1 band with methylation: one at 1239 cm-1 and the other at 1639 cm-1. We also show distinct Raman peaks attributed to the state of the m-DNA. A comparison between dried/denatured and liquid state m-DNA, show a general broadening of the larger lines and a transfer of spectral weight from the ~1470 cm-1 vibration to the two higher energy lines of the dried m-DNA. We attribute the new peaks to DNA denaturing under high salt conditions.

10351-20, Session PMon

Smartphone incorporated on-site crude oil analyzer based on CMOS image sensor

Sangwoo Oh, Korea Research Institute of Ships and Ocean Engineering (Korea, Republic of); Kiyoung Ann, Dongmin Seo, Sanghoon Shin, Euijin Han, Korea Univ. (Korea, Republic of); Moonjin Lee, Korea Research Institute of Ships and Ocean Engineering (Korea, Republic of); Sungkyu Seo, Korea Univ. (Korea, Republic of)

Crude oil is a mixture composed of various hydrocarbons such as saturated hydrocarbons, unsaturated hydrocarbons, resins, and asphaltenes. Among them, the unsaturated hydrocarbons consist of alkenes, alkynes, and aromatic hydrocarbons, and the aromatic hydrocarbons contain chemicals with one or more benzene rings, which emit fluorescence upon receiving an ultraviolet light. Conventional instrument for detecting the emitted fluorescence from the crude oil usually utilize an expensive light source, e.g., halogen lamp, and an expensive detector, e.g., photomultiplier tube (PMT), to measure the intensity of the emitted fluorescence and to quantify the crude oil concentration. While this established instrument can provide high sensitivity with a high-end detector, i.e., PMT, this relatively expensive, bulky, and single pixel detector has many limitations to be widely accepted in on-site instruments. To address this issue, we propose a crude oil fluorescence analyzer composed of low-cost and compact optoelectronic elements, i.e., light emitting device (LED) for light source and complementary metal oxide semiconductor (CMOS) image sensor for detector. Since this device employs multi-million pixels of CMOS image sensor, it can minimize the fluorescent noise by selective data collection, enabling low concentration (~ 1 ppb) crude oil fluorescence detection as an on-site platform. Furthermore, the proposed device also improves the user convenience by integrating a remote system that enables operation and analysis on a smartphone. This low-cost, compact, and highly sensitive crude oil fluorescence analyzer holds great promise in many applications requiring fluorescence detection and quantification.

10351-21, Session PMon

Real-time label-free detection and sizing of protein molecules using a deep UV microfluidic platform

Pavankumar Challa, Quentin Peter, Maya A. Wright, Yuewen Zhang, Jacqueline A. Carozza, Tuomas P. J. Knowles, Univ. of Cambridge (United Kingdom)

Optical detection has become a convenient and scalable approach to read out information from microfluidic systems. For the study of many key biomolecules, including peptides and proteins, that have low fluorescence at visible wavelengths, however, this approach typically requires the labelling of the species of interest with extrinsic fluorphores to enhance the optical signals obtained, a process which can be time-consuming, requires purification steps, and has the propensity to perturb the behaviour of the systems under study due to interactions with the labels themselves. As such, the exploitation of the intrinsic fluorescence of protein molecules in the deep UV is an attractive path to allow the study of unlabelled biomolecules, yet deep UV detection has to date required the use of coherent sources with frequency multipliers and devices fabricated out of materials that are incompatible with widely used soft-lithography techniques. Here, we develop a deep UV-LED platform that allows the visualisation in real time of unlabelled proteins within microfluidic channels fabricated into PDMS doped with carbon nanoparticles using soft-lithography. Using this platform, we demonstrate intrinsic fluorescence detection of proteins at nanomolar concentrations on chip and combine detection with micron-scale diffusional sizing to measure the sizes of proteins in solution in a label free manner by exploiting a microfluidic co-flow geometry. These results open up the possibilities for routine use of label-free measurements of a key class of biomolecules in lab-on-chip devices.

10351-22, Session PMon

Probing Li-ion transport at carbon anode/solid electrolyte interfaces using in operando SEM

Alexander Yulaev, National Institute of Standards and Technology (United States) and UMD (United States); Vladimir Oleshko, Paul Haney, National Institute of Standards and Technology (United States); A. Alec Talin, Sandia National Laboratories (United States); Marina S. Leite, Univ. of Maryland, College Park (United States); Andrei Kolmakov, National Institute of Standards and Technology (United States)

Today all-solid-state lithium-ion batteries (SSLIBs) offer a promising alternative basis to substitute liquid counterparts in many industrial applications owing to their high specific energy and power densities, improved cycle life, and reduced safety risks of a thermal runaway. Despite all advantages mentioned above, the dearth of techniques enabling spatially resolved characterization of ionic transport at battery interfaces remains a key challenge to understand the interplay between their structure and performance during operation. Here, we implement scanning electron microscopy (SEM) in conjunction with Auger electron spectroscopy (AES) to probe Li-ion transport at the anode-solid electrolyte interface in operando conditions. We fabricate a model SSLIB sample made of $LiCoO_2$ cathode, LiPON electrolyte, and (i) ultra-thin amorphous carbon or (ii) single-layer graphene anodes. Altering the charging current and oxidizing conditions at the amorphous carbon anode, we observe the variation in Li plating morphology between in-plane and out-of-plane growth behavior. We experimentally quantify the nucleation density of Li deposits as a function of current during cycling under UHV conditions and confirm the observed dependence using a 2D nucleation/growth model. In addition, AES data reveal that battery cycling leads to appreciable capacity losses even under UHV conditions. Finally, using graphene as an electron transparent anode, we directly probe the lithium transport at the anode-electrolyte interface. We foresee that our findings will shed light on details of Li-ion battery transport inhomogeneity and help elucidate a risk-free parameter space.

Conference 10352: Biosensing and Nanomedicine X

SPIE. OPTICS+ PHOTONICS NANOSCIENCE+ ENGINEERING

Sunday - Monday 6 –7 August 2017

Part of Proceedings of SPIE Vol. 10352 Biosensing and Nanomedicine X

10352-1, Session 1

Upconverting nanoparticles as optical sensors of nano- to micro- Newton forces

Alice Lay, Derek S. Wang, Michael D. Wisser, Yang Zhao, Randy D. Mehlenbacher, Yu Lin, Stanford Univ. (United States); Holger Fehlauer, Stanford School of Medicine (United States); Michael Krieg, Wendy L. Mao, Miriam B. Goodman, Jennifer A. Dionne, Stanford Univ. (United States)

Nearly all diseases trace back to improper mechanotransduction, but few sensors have the nanoscopic size and stable signal to measure these sub-microNewton forces in vivo. We investigate sub-25nm lanthanide-doped nanoparticles (NPs) as optical force sensors, which provide several biocompatible features: sharp emission peaks in upconversion (UC) and photoluminescence (PL), high signal-to-noise by virtue of near infrared illumination in UC, and photostability. To increase force sensitivity, we introduce d-metal doping; the d-metal energetically couples to the lanthanides with an efficiency that varies with pressure. Using a diamond anvil cell and atomic force microscopy to probe nanoNewton to microNewton forces, we perform force-dependent spectroscopy on NaYF4: Er3+,Yb3+ nanoparticles doped with 0% to 5% Mn2+. We find that color, quantitatively defined as the red-to-green emission ratio, varies linearly with force and is highly dependent on crystal structure. Namely in UC, cubic-phase NPs change from orange to red, while optimized hexagonal-phase NPs change from yellow-green to green. These color responses are not only reproducible over several compression and release cycles, but provide stable signal for over 24 hours. Compared to current mechanobiology tools, these optical force sensors provide nanoscopic size, large dynamic range (i.e. nN to N), and a ratiometric signal (i.e. color) that is robust to systematic errors. To demonstrate in vivo imaging capabilities, we feed water-soluble NPs (5mg/mL concentration) to C. elegans. Using two-photon confocal microscopy, we image the NPs along the digestive tract, correspond their color to force, and quantify mechanical processes within key anatomical features like the pharynx and grinder.

10352-2, Session 1

Plasmonic active rotary nanomotors for tunable biochemical release, removal, and microfluidic manipulation *(Invited Paper)*

Donglei Fan, The Univ. of Texas at Austin (United States)

In this talk, we will discuss our recent progress on design, assembling and operation of an innovative type of rotary nanomotors made from micro/nanoscale building blocks, such as nanowires, nanodisks, nanodots, and microrods. Arrays of nanomotors can be efficiently assembled and rotated with controlled angle, chirality and speed to 18,000 rpm, the same level of that of jet engine. The nanomotors are one of the smallest rotary Nanoelectromechanical System (NEMS) Devices, having all dimensions less than 1 ¬m. They can operate for 80 hours over 1.1 million cycles. The micro/nanomotors are further equipped with plasmonic sensing components. The motorized sensors can readily realize tunable biochemical release and its real time monitoring, enhanced chemical removal, and microfluidic manipulation. This work can inspire a new concept of robotized nanosensors that offer unprecedented precision and control for research in single cell stimulation, cell-cell communication, and system biology.

10352-3, Session 1

Plasmonic biosensors for resource-limited settings *(Invited Paper)*

Srikanth Singamaneni, Washington Univ. in St. Louis (United States)

Plasmonics is expected to make a tremendous impact in the field of life sciences, with applications in bioimaging, biosensing, targeted delivery and externally-triggered locoregional therapy. Plasmonic biosensors are considered to be highly promising for the development of simple, portable, sensitive, on-chip biodiagnostics for resource-limited settings such as at-home care, rural clinics, developing countries with low and moderate incomes and battle-field. While there has been a tremendous progress in the rational design of nanotransducers with high sensitivity and the development of hand-held read-out devices, the translation of these biosensors to resource-limited settings is hindered by the poor thermal, chemical, and environmental stability of the biorecogntion elements. "Cold-chain", which is employed in the affluent parts of the world for reagent transport, storage, and handling, is expensive (capital cost of freezers, recurring cost of liquid nitrogen), environmentally unfriendly, and simply not feasible in resource-limited settings where electricity and refrigeration are not reliable or even available. Degradation of the sensitive reagents and biodiagnostic chips outside the cold-chain, compromises analytical validity, preventing accurate and timely diagnosis. We will present a novel class of plasmonic biosensors that rely artificial antibodies or peptide recognition elements with excellent thermal and chemical stability. In addition, we have recently introduced silk and metal-organic frameworks as protective coatings to stabilize natural antibodies bound to nanotransducers against thermal denaturation and loss of biorecognition. This multi-pronged approach overcomes the poor stability of existing plasmonic biosensors and takes them closer to real-world applications in resource-limited settings.

10352-4, Session 1

Novel approaches towards practical applications of CMOS-compatible integrated surface enhanced Raman scattering sensors

Cuong Nguyen, William Thrift, Qiancheng Zhao, Mahsa Darvishzadeh-Varcheie, Arunima Bhattacharjee, Allon I. Hochbaum, Filippo Capolino, Ozdal Boyraz, Regina Ragan, Univ. of California, Irvine (United States)

Quick diagnosis via the ability to monitor bacterial metabolic activity over time would allow physicians to make informed decisions regarding patient treatment at an unprecedented level; unfortunately, the bottom line in healthcare is often cost. Thus our Surface enhanced Raman Scattering (SERS) platform is being developed as a low-cost biosensing system to provide new tools for metabolomics to positively impact healthcare. Here, the fabrication of an integrated device composed of silicon nitride trench waveguides, microfluidic channels, and self-assembled Au nanoantennas will be presented. Nanofabrication of SERS sensors with reproducible response over device-relevant areas is achieved by utilizing electrohydrodynamic flow as driving force in colloidal assembly. Au nanoentannas assembled on waveguides enhance the nonlinear refractive index by approximately 10-fold to be 7.1x10-19m2/W. An average SERS enhancement factor of 1.4x109 and signal standard deviation of 10% over 1mm2 area are obtained for the known analyte benzenethiol using excitation wavelength of 785 nm. Uniform 1nm interparticle spacing allows for parts-per-billion detection limits of bacterial metabolites. When using SERS surfaces for pyocyanin, a metabolite released by pseudomonas aeruginosa (PA) during biofilm formation, 100 parts-per-trillion detection limit and 1 part-per-billion quantification limit are achieved in pure gradients. Furthermore, in vitro detection of pyocyanin

in microfluidic channels was quantified during PA biofilm formation down to 10 parts-per-billion and correlated with biofilm growth stages using fluorescence imaging. When untreated bacteria-free supernatant is used as samples, SERS sensors were able to detect pyocyanin after 2 hours of growth, compared to 8 hours for UV-Visible spectroscopy.

10352-5, Session 2

Exploring plasmonic nanoantenna arrays as a platform for biosensing *(Invited Paper)*

Kimani C. Toussaint Jr., Univ. of Illinois at Urbana-Champaign (United States)

In recent years, the PROBE Lab at the University of Illinois at Urbana-Champaign has made significant developments in plasmonic nanoantenna technology by more closely exploring the rich parameter space associated with these structures including geometry and material composition, as well as the optical excitation conditions. Indeed, plasmonic nanoantennas are attractive for a variety of potential applications in nanotechnology, biology, and photonics due to their ability to tightly confine and strongly enhance optical fields. This talk will discuss our work with arrays of Au bowtie nanoantennas (BNAs) with an emphasis on how their field enhancement properties could be harnessed for particle manipulation and sensing. We also present our work with pillar-supported BNAs (pBNAs) and discuss their potential for sensing applications, particularly when adapted for responses in the near-IR. The talk will conclude with a brief discussion of some of the future work pursued by the PROBE lab, including adapting BNAs for lab-on-a-chip applications.

10352-6, Session 2

Real-time label-free detection and sizing of protein molecules using a deep UV microfluidic platform

Pavankumar Challa, Quentin Peter, Maya A. Wright, Yuewen Zhang, Jacqueline A. Carozza, Tuomas P. J. Knowles, Univ. of Cambridge (United Kingdom)

Optical detection has become a convenient and scalable approach to read out information from microfluidic systems. For the study of many key biomolecules, including peptides and proteins, that have low fluorescence at visible wavelengths, however, this approach typically requires the labelling of the species of interest with extrinsic fluorphores to enhance the optical signals obtained, a process which can be time-consuming, requires purification steps, and has the propensity to perturb the behaviour of the systems under study due to interactions with the labels themselves. As such, the exploitation of the intrinsic fluorescence of protein molecules in the deep UV is an attractive path to allow the study of unlabelled biomolecules, yet deep UV detection has to date required the use of coherent sources with frequency multipliers and devices fabricated out of materials that are incompatible with widely used soft-lithography techniques. Here, we develop a deep UV-LED platform that allows the visualisation in real time of unlabelled proteins within microfluidic channels fabricated into PDMS doped with carbon nanoparticles using soft-lithography. Using this platform, we demonstrate intrinsic fluorescence detection of proteins at nanomolar concentrations on chip and combine detection with micron-scale diffusional sizing to measure the sizes of proteins in solution in a label free manner by exploiting a microfluidic co-flow geometry. These results open up the possibilities for routine use of label-free measurements of a key class of biomolecules in lab-on-chip devices.

10352-9, Session 3

An automatic holographic adaptive phoropter *(Keynote Presentation)*

Gholam A. Peyman, Nasser N. Peyghambarian, Jim Schwiegerling, Babak Amirsolaimani, College of Optical Sciences, The Univ. of Arizona (United States)

Phoropters are the most common instrument used to detect refractive errors. During a refractive exam, lenses are flipped in front of the patient who looks at the eye chart and tries to read the symbols. The procedure is fully dependent on the cooperation of the patient to read the eye chart and provides only a subjective measurement of visual acuity and can at best provide a rough estimate of the patient's vision. Phoropters are difficult to use for mass screenings requiring a skilled examiner, and it is hard to screen young children and the elderly etc.

We have developed a simplified, lightweight automatic phoropter that can measure the optical error of the eye objectively without requiring the patient's input. The automatic holographic adaptive phoropter is based on a Shack-Hartmann wave front sensor and three computer-controlled fluidic lenses for each channel of a binocular system. The fluidic lens system is designed to be able to provide power and astigmatic corrections over a large range of corrections without the need for verbal feedback from the patient in less than a minute.

10352-10, Session 3

Simultaneous multimodal ophthalmic imaging with spectrally encoded scanning laser ophthalmoscopy and optical coherence tomography at 400 kHz *(Invited Paper)*

Mohamed T. El-Haddad, Ivan Bozic, Joseph D. Malone, Jianwei D. Li, Amber M. Arquitola, Shriji N. Patel, Karen M. Joos, Yuankai K. Tao, Vanderbilt Univ. (United States)

Multimodal ophthalmic imaging systems that combine concurrent scanning laser ophthalmoscopy (SLO) and optical coherence tomography (OCT) have demonstrated utility for aiming, tracking and compensation of bulk motion, and mosaicking. However, these systems suffer from added cost and complexity because both modalities often require separate sources, scanners, optics, and electronics. Here, we demonstrate a novel approach for swept-source spectrally-encoded SLO and OCT (SS-SESLO-OCT) for simultaneous imaging in vivo. A 200 kHz Axsun wavelength-swept laser was buffered to achieve a line-rate of 400 kHz. Buffered output was shared between SESLO, OCT, and 1.2 GHz linear-in-wavenumber clock. The detected signals were digitized on a dual-channel AlazarTech card with 4 GS/s maximum sampling rate. SESLO and OCT shared the imaging optics and the fast-axis scanner, which guaranteed inherently co-registered fields-of-view. In vivo performance was demonstrated by imaging the cornea and the retina of a healthy volunteer. Additionally, aiming with live SESLO display enabled mosaicking of ultrawide-field retinal images (>90o). Imaging was performed at 200 frames-per-second with >2 GPix/s throughput, enabling three-dimensional motion tracking with high spatial and temporal resolutions. Finally, A modular scan-head was designed and rapidly-prototyped, that can be coupled to ophthalmic surgical microscope-integrated and slit-lamp imaging optics for intraoperative guidance or clinical diagnostics. Our design reduces the complexity, cost, and maintenance required for clinical translation of these technologies. We believe SS-SESLO-OCT may benefit intraoperative imaging by allowing for real-time surgical feedback, instrument tracking, and overlays of computationally extracted biomarkers of disease, and slit-lamp imaging by enabling aiming, image registration, and multi-field mosaicking.

10352-11, Session 3

Multiplexed surface-enhanced Raman immunoimaging in vivo with gold nanoantennas

Rizia Bardhan, Yu-Chuan Ou, Joseph Webb, Vanderbilt Univ. (United States)

The upregulation of immune checkpoint programmed death protein-1 (PD-1) expressed on CD8+ activated T cells, and interaction of PD-1 with its ligand, PD-L1, strongly contributes to an immunosuppressive tumor microenvironment. Blockade of PD-L1 pathway with therapeutic antibodies have shown long-term survival in many cancer patients and several clinical trials are currently ongoing. However, <30% of patients respond to PD-L1 blockade, in part due to inaccurate identification of PD-L1 expression in tumors incurring high costs of immunotherapy and toxicities in patients. Therefore, an unmet clinical need exists for high resolution noninvasive detection techniques. Surface-enhanced Raman scattering (SERS) based imaging mediated by gold nanostructures has gained tremendous interest as a pre-clinical noninvasive diagnostic tool due to the high cellular-level spatial resolution delineating tumor margin from healthy tissue, multiplexed biomarker detection enabled by the narrow linewidths of vibrational signatures of molecules, portability, low cost, and exceptional temporal resolution.

In this work, we demonstrate the use of multibranched gold nanoantennas (MGNs) conjugated with Raman reporter molecules for multiplexed SERS imaging enabling the simultaneous diagnosis of PD-L1 and EGFR (epidermal growth factor receptor) in a breast cancer model in vivo. Nanoantennas conjugated with anti-PDL1 antibodies/ DTNB Raman molecule, and nanoantennas conjugated with anti-EGFR antibodies/pMBA Raman molecules were concurrently introduced in MDA-MB-231 breast cancer tumors, which are known to overexpress EGFR and have a high intrinsic expression of PD-L1. Longitudinal SERS analysis demonstrated maximum accumulation of nanoantennas occur 6 h post IV delivery. Ex-vivo SERS spatial maps correlated well with histological analysis and clearly show nanoantennas primarily accumulate in the tumor vasculature. Transmission electron microscopy (TEM) micrographs demonstrated that nanoantennas maintain their structural integrity in vivo. The gold content in tissues was quantified with inductively coupled plasma mass spectrometry (ICPMS) to evaluate their pharmacokinetics and uptake in tumor relative to other tissues. ICPMS analysis showed nanoantennas accumulation in tumors as well as the reticuloendothelial system and substantial clearance within 72 h. This work shows gold nanoantenna mediated SERS imaging provides a quantitative measure of PDL1 to allow predictive and personalized immunotherapies with minimal toxicities.

10352-12, Session 3

Nanophotonics-enhanced intraocular pressure sensor for glaucoma management *(Invited Paper)*

Hyuck Choo, Jeong Eon Lee, Haeri Park, Vinayak Narasimhan, Blaise Ndjamen, California Institute of Technology (United States); Juan Du, David W. Sretavan, Univ. of California, San Francisco (United States)

Glaucoma is a leading cause of irreversible blindness with 60 million cases worldwide. An elevated intraocular pressure (IOP) level has been identified as a major risk factor, and all the glaucoma therapies are aimed at lowering the IOP level. Moreover, in a recent large-scale NIH-sponsored study, researchers have found that IOP of an individual patient fluctuates largely over the course of the day, and continuous monitoring and aggressively lowering IOP in a timely manner is crucial for optimal disease management.

My research group has been developing a nanophotonics-enhanced implantable pressure sensor with remote optical readout. The sensor is compact for easy implantation, and its operation requires only a broadband light source, such as a tungsten light bulb. Bench testing has demonstrated that the sensor tracks pressures ranging from 0-40 mmHg within +/-1 mmHg, and we have been successfully performing short- and long-term in vivo IOP monitoring in live rabbits over two years now.

This presentation will describe our nanophotonics-enhanced IOP-sensor development and up-to-date progresses. I hope to leave you convinced that our approach will allow us to solve the long-standing challenge in glaucoma research and patient management.

10352-13, Session 4

Enabling rapid, quantitative detection of bacteria in blood with high resolution DNA melting, microfluidics, and machine learning *(Invited Paper)*

Stephanie Fraley, Daniel Ortiz Velez, Hannah Mack, Julietta Jupe, Sinead Hawker, Ninad Kulkarni, Behnam Hedayatnia, Yang Zhang, Shelley Lawrence, Univ. of California, San Diego (United States)

We report the development of an integrated platform enabling the identification and absolute quantification of bacterial DNA in blood samples in less than four hours. The system incorporates a 20,000 reaction digital PCR chip with sensitive imaging and controlled heating to produce for the first time high resolution melt (HRM) curves of pathogen DNA within picoliter scale reactions. Clinically relevant concentrations of bacteria are spiked into blood; then DNA is extracted and the molecules separated by digitization across 20,000 picoliter scale reactions. Pathogen DNA is amplified with universal primers targeting the bacterial 16S gene. Amplification is followed by HRM sequence fingerprinting in all reactions simultaneously using our custom device. The resulting bacteria-specific melt curves are identified by Support Vector Machine learning, and individual pathogen loads are quantified. The platform reduces reaction volumes by 99.995% and achieves a greater than 200-fold increase in dynamic range of detection compared to traditional PCR HRM approaches. Type I and II error rates are reduced by 99% and 100% respectively compared to intercalating dye-based digital PCR (dPCR) methods. This technology could impact a number of quantitative profiling applications, especially infectious disease diagnostics.

10352-14, Session 4

Nanostraw mediated non-perturbative cell access and transfection *(Invited Paper)*

Nicholas A. Melosh, Yuhong Cao, Martin Hjort, Stanford Univ. (United States)

The cell's lipid membrane is one of the most vital cell components as the gate-keeper in and out of the cytoplasm and a critical barrier to integrating technology with biological cells. Newly discovered forms cancer therapy and future biological technologies rely upon manipulating chemical or electronic flow across this membrane. Unfortunately, artificially controlling access through the lipid layer is surprisingly difficult; current techniques often involve harsh chemicals or creating holes that cause cell cytotoxicity. Here we investigate how scaling fluidic technology to the nanoscale can provide non-perturbative access through the cell wall and into biological cells, providing a long-term communication channel for chemical or biological signals. We achieved high-efficiency chemical delivery and control by mimicking natural gap junction proteins, creating arrays of 'nanostraws'. These nanoscale (100-500 nm) diameter straws are formed by templating high-aspect ratio pores, allowing precise control of height, diameter and thickness. The nanostraws deliver a wide variety of materials that could normally not pass through the cell wall, yet do not disturb natural cell function. Models of how these materials penetrate the lipid bilayer show that a simple impaling mechanism is insufficient, but instead rely upon cellular traction forces to drive membrane rupture.

Surprisingly, we discovered that these nanoscale conduits can not only deliver material into cells, but also can extract minute quantities of cellular proteins and small molecules out. Our data shows that intracellular contents from thousands of cells down to even a single cell can be non-destructively sampled and quantitatively analyzed multiple times over the course of one week, a feat which has not been previously possible. This advance enables new studies of how cells temporally evolve within fully interconnected cell monolayers in response to different therapies and lineage drivers. These, and other similar nanofluidic technologies, open a new area for engineered devices to play a leading role in future biological technologies and healthcare.

10352-15, Session 4

Double emulsion electrospun nanofibers as a growth factor delivery vehicle for salivary gland regeneration

Zahraa I. Foraida, SUNY Polytechnic Institute (United States); Alexander T. Khmaladze, Deirdre A. Nelson, Melinda Larsen, Univ. at Albany (United States); James Castracane, SUNY Polytechnic Institute (United States)

Sustained delivery of growth factors, proteins, drugs and other biologically active molecules is necessary for tissue engineering applications. Electrospun fibers are attractive tissue engineering scaffolds as they partially mimic the topography of the extracellular matrix (ECM). However, they do not provide continuous nourishment to the tissue. In search of a biomimetic scaffold for salivary gland tissue regeneration, we previously developed a blend nanofiber scaffold composed of the protein elastin and the synthetic polymer polylactic-co-glycolic acid (PLGA). The nanofiber scaffold promoted in vivo-like salivary epithelial cell tissue organization and apicobasal polarization. However, in order to enhance the salivary cell proliferation and biomimetic character of the scaffold, sustained growth factor delivery is needed. The composite elastin-PLGA nanofiber scaffold was optimized to act as a growth factor delivery system using epidermal growth factor (EGF) as a model protein. The nanofiber/EGF hybrid nanofibers were synthesized by double emulsion electrospinning where EGF is emulsified within a water/oil/water (w/o/w) double emulsion system. Ethyl cellulose was used as an emulsifying and release retardant agent. Successful incorporation of EGF was confirmed using fluorescence spectroscopy, Fourier transform infrared spectroscopy (FTIR) and Raman spectroscopy. EGF loading efficiency and release profile was characterized using fluorescently-labelled EGF/nanofibers and compared to standard blend electrospinning technique. Submandibular immortalized mouse salivary epithelial cells (SIMS) were cultured on the proposed EGF/nanofiber scaffolds where the cell proliferation was observed. We demonstrated the potential of the proposed double emulsion electrospun nanofiber scaffold for the delivery of growth factors and/or drugs for tissue engineering and pharmaceutical applications.

10352-16, Session 4

Magnetoresistive biosensors for quantitative proteomics *(Invited Paper)*

Xiahan Zhou, Chih-Cheng Huang, Drew Hall, Univ. of California, San Diego (United States)

Superparamagnetic magnetic nanoparticles (MNPs) exhibit a relaxation response due to a pulsed magnetic field, enabling a new time-domain magnetorelaxometry biosensing scheme. Giant magnetoresistive (GMR) sensors were used to detect this phenomenon due to their high transduction efficiency and small size. We report a novel biosensor system consisting of a GMR sensor array, a Helmholtz coil, an electromagnet driver, and an integrator-based analog front-end for magnetorelaxometry biosensing. The custom electromagnet driver reduces the switch-off time to < 10 ?s by applying a large negative voltage during switching enabling the system to monitor fast relaxation processes of 30 nm MNPs. Magnetic correlated double sampling is proposed to eliminate sensor-to-sensor variation, temperature drift, circuit offset, and non-linearity. An optimum integration time is calculated and experimentally verified to maximize the SNR. Lastly, experiments with dried MNPs show successful relaxation detection and immunoassay experiments demonstrate the binding kinetics.

10352-17, Session 4

Micro-array isolation of circulating tumor cells: the nanotube-CTC chip

Balaji Panchapakesan, Farhad Khosravi, Worcester Polytechnic Institute (United States); Eric Wickstrom, Thomas Jefferson Univ. (United States); Shesh N. Rai, Univ. of Louisville (United States); Alison Zibelli, Thomas Jefferson Univ. (United States); Goetz Kloecker, Univ. of Louisville (United States)

We demonstrate the rapid and label-free capture of breast cancer cells spiked in blood using nanotube-antibody micro-arrays. 76-element single wall carbon nanotube arrays were manufactured using photo-lithography, metal deposition, and etching techniques. Anti-epithelial cell adhesion molecule (anti-EpCAM), Anti-human epithelial growth factor receptor 2 (anti-Her2) and non-specific IgG antibodies were functionalized to the surface of the nanotube devices using 1-pyrene-butanoic acid succinimidyl ester. Following device functionalization, blood spiked with SKBR3, MCF7 and MCF10A cells (100/1000 cells per 5 ?l per device, 170 elements totaling 0.85 ml of whole blood) were adsorbed on to the nanotube device arrays. Electrical signatures were recorded from each device to screen the samples for differences in interaction (specific or non-specific) between samples and devices. A zone classification scheme enabled the classification of all 170 elements in a single map. A kernel-based statistical classifier for the 'liquid biopsy' was developed to create a predictive model based on dynamic time warping series to classify device electrical signals that corresponded to plain blood (control) or SKBR3 spiked blood (case) on anti-Her2 functionalized devices with ~90% sensitivity, and 90% specificity in capture of 1000 SKBR3 breast cancer cells in blood using anti-Her2 functionalized devices. Screened devices that gave positive electrical signatures were confirmed using optical/confocal microscopy to hold spiked cancer cells. Confocal microscopic analysis of devices that were classified to hold spiked blood based on their electrical signatures confirmed the presence of cancer cells through staining for DAPI (nuclei), cytokeratin (cancer cells) and CD45 (hematologic cells) with single cell sensitivity. We report 55%–100% cancer cell capture yield depending on the active device area for blood adsorption with mean of 62% (~12 500 captured off 20 000 spiked cells in 0.1 ml blood) in this first nanotube–CTC chip study.

10352-18, Session 5

Multi-area distributed network of implanted neural interrogators *(Invited Paper)*

David A. Borton, Marc Powell, Brown Univ. (United States)

Electrophysiological interrogation of the nervous system is today limited by our inability to simultaneously probe many areas of the brain with high spatial and temporal resolution to discriminate single neurons and their interactions. For example, countless microfabricated electrode arrays (MEAs) have been developed to densely record populations of single neurons and capture full spike waveforms, but have been limited to recording from a miniscule, mm3 volume of the cortex. Alternatively, electrocorticography (ECoG) and electroencephalography (EEG) can record from multiple cortical sites, but integrate the activity of many neurons together, obscuring the intricacies of the underlying circuit dynamics. There is a fundamental need to develop long lasting implantable devices that bridge the gaps between scale and scope. In this presentation, we will describe a platform technology for accessing a network of independently addressable neural interrogators, or nodes, each capable of recording from 100 individual channels with high temporal precision, distributed across the cortical surface. The system will enable clinicians and researchers to place nodes ad libitum on the cortex, agnostic to location and therefore customized to the specific needs of the treatment or research question, alleviating the surgical challenges currently faced while implanting traditionally tethered MEAs. The platform eliminates transdural cables, reducing surgical implantation site limitations and more importantly removing pathways for long-term infection directly to the meninges and damage due to micromotion between the interface

and the skull. Nodes are powered, and communicate, wirelessly enabled by the application of novel electromagnetically transparent ?hermetic ASIC packaging techniques for extended functionality.

10352-19, Session 5

Advances in flexible optrode hardware for use in cybernetic insects *(Invited Paper)*

Joe Register, Dennis Callahan, Carlos Segura, John LeBlanc, Charles Lissandrello, Parshant Kumar, Chris Salthouse, Jesse Wheeler, Aaron Stoddard, Draper Lab. (United States)

Optogenetic manipulation is widely used to selectively excite and silence neurons in laboratory experiments. Recent efforts to miniaturize the components of optogenetic systems have enabled experiments on freely moving animals, but a completely new approach is required to apply the same techniques to freely flying insects.

We present the design of lightweight optogentic hardware and supporting electronics for the untethered steering of dragonfly flight. The system is designed to enable autonomous flight and includes processing, guidance sensors, solar power, and light stimulators. The system will weigh less than 200mg and be worn by the dragonfly as a backpack. The flexible implant has been designed to provide stimuli around nerves through micron scale apertures of adjacent neural tissue without the use of heavy hardware. We address the challenges of lightweight optogenetics and the development of high contrast polymer waveguides for this purpose.

10352-20, Session 5

Electronic, optical, and chemical interrogation of neural circuits with multifunctional fibers *(Invited Paper)*

Andres Canales, Seongjun Park, Chi Lu, Yoel Fink, Polina O. Anikeeva, Massachusetts Institute of Technology (United States)

Despite recent advances in microfabrication and nanofabrication, integrating multiple modes of communication with the brain into a single biocompatible neural probe remains a challenge. These multifunctional neural probes may further our understanding of normal and disrupted functions of neural circuits manifested in neurological conditions, such as Parkinson's disease. Here, we present a novel family of probes fabricated using a thermal drawing process. In this process, a macroscopic template (preform) containing the desired features is drawn by applying heat and tension into a fiber that conserves the original geometry of the preform but at a much smaller scale. Being composed of soft materials, such as polymers, conductive composites, and low melting temperature metals, fiber based neural probes minimize the damage to the surrounding tissue when implanted. Furthermore, fiber drawing enables straightforward integration features allowing for simultaneous electrical, optical and chemical interrogation of the brain. We demonstrate the utility of these probes for one-step optogenetics, in which a viral vector carrying opsin genes is injected through the same device then used to optically stimulate neurons and record their response as electrical activity. With these probes, we also show, for the first time, recordings of electrical activity in the spinal cord of freely moving mice.

10352-21, Session 5

Neural signal transmission through brain tissue with high spatial and temporal resolution using near infrared light *(Invited Paper)*

Iman Hassani Nia, Skylar Wheaton, Michael Adoff, Daniel Dombeck, Hooman Mohseni, Northwestern Univ. (United States)

Interferometric optical methods have great potential to discern small changes in refractive index at each voxel of brain space with high speed. In this regard, various types of optical coherence tomography systems (OCTs) have been developed and improved such that shot-noise limited sensitivity is currently being pursued with scan rates close to a billion voxels per second. Therefore, there is tremendous potential for OCT to aid in the detection of neural activity in vivo. Here we introduce the idea of a novel optically linked implanted microprobe. When combined with a slightly modified OCT system, the approach could provide two-way communication with hundreds of thousands of neurons with high temporal and spatial resolution. We present our experimental methodology, including methods for implanting the microprobes and implementing our OCT apparatus. We then present the results of our in-vitro experiments, which are consistent with our optical simulations and in-vivo experiments. The in-vitro experiments demonstrate that action potential signals with 100mV amplitude could be retrieved through ~300 ?m of brain tissue, with high fidelity (SNR~18) and with less than 10 micro-Watt of optical power. Based on these results, we present our prediction for the performance limit of the proposed approach.

10352-22, Session 5

Inorganic semiconductor nanorods for neural voltage sensing

Yung Kuo, Joonhyuck Park, Univ. of California, Los Angeles (United States); Shvadchak Volodymyr, Institute of Organic Chemistry and Biochemistry (Czech Republic); Kyoungwon Park, Antonino Ingargiola, Jack Li, Shimon Weiss, Univ. of California, Los Angeles (United States)

Monitoring membrane potential in neurons requires sensors with minimal invasiveness, high spatial and temporal (sub-ms) resolution, and large sensitivity enabling detection of sub-threshold activities. While organic dyes and fluorescent proteins have been developed to possess voltage-sensing properties, photobleaching, cytotoxicity, low sensitivity and low spatial resolution have obstructed further studies. Semiconductor nanoparticles, as prospective voltage sensors, have shown large sensitivity based on Quantum confined Stark effect (QCSE), at room temperature and at single particle level. Both theory and experiment have shown their voltage sensitivity can be increased significantly via material, bandgap and structural engineering. We synthesized one of the optimal voltage sensors predicted by calculation: 10nm type-II ZnSe/CdS nanorods (NRs), with asymmetrically located seed. The voltage sensitivity and spectral shift were characterized in vitro using spectrally resolved microscopy and electrodes either lithographically patterned or grown by thin film deposition, which "sandwich" the nanoparticles. We characterized multiple batches of such NRs and iteratively modified the synthesis to achieve higher voltage sensitivity (?F/F>10%), larger spectral shift (5nm), higher quantum yield (~30%), better homogeneity, better colloidal stability and longer fluorescence lifetime. Furthermore, the NRs were functionalized with transmembrane alpha-helical peptides for membrane insertion. TEM images of the peptide-coated NRs (pcNRs) inserted in lipid vesicles and fluorescence image of cultured cells stained with pcNRs in the membrane ascertain their membrane insertion capacity. The voltage sensing feasibility of pcNRs was tested using spontaneously spiking HEK cells and voltage clamped HEK at single particle level.

10352-23, Session 5

Shedding light to sleep studies *(Invited Paper)*

Alper Bozkurt, James Dieffenderfer, North Carolina State Univ. (United States)

We present our efforts on development of a miniaturized wireless bandage with near-infrared spectroscopy (NIRS) capability to perform biophotonics based at-home or clinical sleep analysis. The smart bandage has dimensions of 25x15x5 mm3. It is capable of performing NIRS with 660nm, 850nm and 940nm wavelengths for up to 11 hours continuously. The system is placed on the forehead to measure from the prefrontal cortex and the raw data is continuously streamed over Bluetooth Low Energy to a nearby smartphone for post processing analysis. We performed traditional polysomnography simultaneously with the device to train a supervised machine-learning algorithm. Ultimately, this algorithm will generate a scored hypnogram based on optical data. The extracted features are heart rate, respiratory rate, tissue oxygenation, relative change in local oxy- and deoxy-hemoglobin concentrations, posture, and skin temperature. Preliminary results show significant feature variations for transitions from one sleep stage to another. We also added 2-channel wireless EEG functionality to the electronic bandage in parallel to the NIRS; in the event that the algorithm is unable predict sleep stages accurately with solely biophotonics data and motion. This small bandage serves as a potential alternative to traditional polysomnography and future work will determine the accuracy of the automated sleep scoring algorithm.

10352-24, Session 6

Dynamic materials inspired by cephalopods *(Invited Paper)*

Alon Gorodetsky, Univ. of California, Irvine (United States)

Cephalopods (squid, octopuses, and cuttlefish) have captivated the imagination of both the general public and scientists for more than a century due to their visually stunning camouflage displays, sophisticated nervous systems, and complex behavioral patterns. Given their unique capabilities and characteristics, it is not surprising that these marine invertebrates have recently emerged as exciting sources of inspiration for the development of unique materials. Within this context, our laboratory has explored the properties of structural proteins known as reflectins, which play crucial roles in the functionality of cephalopod skin. In this talk, I will discuss our work on new types of photonic and protonic devices fabricated from reflectin-derived and reflectin-inspired materials. Our findings hold implications for the development of adaptive camouflage systems, sensitive bioelectronic platforms, and renewable energy technologies

10352-25, Session 6

Microfluidic body-on-a-chip platforms for mimicking the human drug metabolism *(Invited Paper)*

Mandy Esch, Hidetaka Ueno, National Institute of Standards and Technology (United States); Yang Yang, Syracuse Univ. (United States)

Patients with incurable diseases often participate in clinical trials hoping to benefit from a drug that has cured the disease in animals. However, drugs that cure diseases in animals often do not work in human patients. Unless we develop better mimics of the human body, patients will continue to be disappointed.

We have developed body-on-a-chip systems that replicate key aspect amiss in animals: the devices can mimic part of the human metabolism. We demonstrate that by simulating the oral uptake and metabolism of acetaminophen using the developed devices. Our platforms also feature integrated sensors that can monitor tissue health throughout a drug exposure. Sensor elements are optical (for estimating the toxicity of a drug), and electrical (for estimating the transepithelial resistances of tissues). The platform allowed us to monitor tissues during a drug exposure.

10352-26, Session 6

On-demand drawing of high aspect-ratio, microsphere-tipped elastomeric micropillars

Qiang Li, Tara Mina, Jaeyoun Kim, Iowa State Univ. of Science and Technology (United States)

High aspect-ratio elastomeric micropillars are widely used in a plethora of applications, such as functional surfaces, smart windows, actuators, and sensors. Their fabrication at arbitrary positions on non-planar substrates, however, has rarely been reported. Here we demonstrate a new technique for facile fabrication of high aspect-ratio, microsphere-tipped elastomeric micropillars based jointly on controlled dispensing of elastomer droplets and direct drawing of micropillars induced by vacuum-assisted pipetted microspheres with in situ UV light curing. It enables on-demand realization of elastomeric micropillars on various structures with uncommon geometries, such as the curved outer surface of a cylinder or end facet of an optical fiber. The new technique also facilitates arrayed fabrication of micropillars with different heights on the glass substrate and micropillars with different heights and orientations on the curved outer surface of a cylinder, further strengthening the micropillars' potential for collective operation. The tapering index (ratio of the difference in diameters of base and tip to height) can also be controlled with the UV light on/off during pulling process. As a proof-of-concept exemplary application, a fiber optic contact sensor is realized by integrating a micropillar onto the end facet of an optical fiber. Overall, both the fabrication technique and the resulting outcomes of this work will add new tools to the toolbox of soft-MEMS and soft-robotics.

10352-27, Session PMon

Modeling electrical response of biofluids

Anays Acevedo Barrera, Univ. Nacional Autónoma de México (Mexico); Augusto García Valenzuela, Ctr. de Ciencias Aplicadas y Desarrollo Tecnológico (Mexico); Asur Guadarrama Santana, Univ. Nacional Autónoma de México (Mexico)

Physical and chemical properties of biofluids can be assessed by optical, electrical and acoustics measurerments. In particular, electrical and optical measurements can usually be implemented in a single device and their results are complementary, being the first at low frecuencies and the later at high frecuencies. In this work, we focus on electrical properties of biofluids in the range of tens of kilohertz to megahertz. A simplified model is proposed to study the electrical response of biofluids . This model facilitates interpreting the results in complex impedance measurements. The model consist of a biphasic system, a suspension of micrometric spheres embedded in an homogeneous fluid. Both mediums are considered electrolytes of different conductivities. An effective medium theory is used to analyze the composite as if it were an homogeneous medium. We find the equivalent circuit of the biofluid inside a parallel plate capacitor and obtain mathematical expressions for the equivalent capacitance and resistance. The behavior and sensitivity of electrical parameters to the density of free charges (ions and counterions) in both phases is studied. The application of our model to the characterization of osmotic fragility in human blood cells, as well as for sedimentation monitoring in a colloidal suspension of particles is presented. Measurements are realized using a low noise system based on differential capacitive sensor.

10352-28, Session PMon

Scale-selective polarimetry of the birefringence distribution of myocardium tissue

Olexander V. Dubolazov, Alexander Ushenko, Vladimir Ushenko, Yuriy Fedkovych Chernivtsi National Univ. (Ukraine)

Among the numerous areas of optical diagnostics of biological tissues structure are widely used techniques that using laser polarized radiation. Particularly, laser polarimetry of microscopic images of polycrystalline protein networks was formed as a separate approach in the study of optically anisotropic component ?f different biological tissues biopsy.

Our research is aimed at designing the experimental method Fourier's polarimetry and spatial-frequency selection of parameter distributions of linear and circular birefringence of the biopsy of the myocardium in order to differentiate causes of death due to coronary heart disease (CHD) and acute coronary insufficiency (ACI).

The results of optical modeling of biological tissues polycrystalline multilayer networks have been presented. Algorithms of reconstruction of parameter distributions were determined that describe the linear and circular birefringence. For the separation of the manifestations of these mechanisms we propose a method of space-frequency filtering. Criteria for differentiation of causes of death due to coronary heart disease (CHD) and acute coronary insufficiency (ACI) were found.

A set of criteria for differentiation of CHD and ACI conditions of the myocardium has been revealed and substantiated:

- statistical moments of the 1st – 4th order which characterize a distribution of the phase shift between orthogonal components of the amplitude laser radiation, stipulated by linear birefringence of myosin fibers of the myocardium layer;

- statistical moments of the 1st – 4th orders which characterize a distribution of plane rotations of laser radiation polarization, stipulated by circular birefringence of the network of myosin fibrils of the myocardium layer.

10352-29, Session PMon

Wavelet analysis of myocardium polarization images in problems of diagnostic of necrotic changes

Olexander V. Dubolazov, Alexander Ushenko, Vladimir Ushenko, Yuriy Fedkovych Chernivtsi National Univ. (Ukraine)

This research presents the results of investigation of laser polarization fluorescence of biological layers (histological sections of the myocardium). The polarized structure of autofluorescence imaging layers of biological tissues was detected and investigated. Proposed the model of describing the formation of polarization inhomogeneous of autofluorescence imaging biological optically anisotropic layers. On this basis, analytically and experimentally tested to justify the method of laser polarimetry autofluorescent. Analyzed the effectiveness of of this method in the postmortem diagnosis of infarction. The objective criteria (statistical moments) of differentiation of autofluorescent images of histological sections myocardium were defined. The operational characteristics (sensitivity, specificity, accuracy) of these technique were determined.

On the basis of the model of generalized optical anisotropy myocardium analytically grounded and experimentally tested method of laser polarization autofluorescence.

Within the applied approach the interconnections between the statistical moments characterizing wavelet coefficients distributions polarization maps of laser autofluorescent images of histological sections of myocardium and the peculiarities of its pathological states were found.

Clinical efficiency of the technique of wavelet analysis of polarization of laser autofluorescence myocardium in the task of posthumous diagnosis is demonstrated.

10352-30, Session PMon

Electrical characteristics of Graphene Based Field Effect Transistor (GFET) biosensor for ADH detection

Azrul Azlan Hamzah, Reena S. Selvarajan, Burhanuddin Y. Majlis, Univ. Kebangsaan Malaysia (Malaysia)

FET biosensor could be utilized to detect antidiuretic hormone (ADH) in blood in order to regulate amount of urine production in artificial kidney. For this application, the most sensitive FET biosensor to date is graphene based field effect transistor (GFET) biosensor. The monoatomic structure of graphene biosensor offers unique properties such as high mechanical strength, distinctive electronic properties, high carrier mobility, high saturation velocity, and low charge scattering. Owing to these properties GFET has been used in sensitive detection of analytes. In this paper, GFET was designed using Lumerical software to obtain the I-V characteristics of GFET for ADH detection. P-doped Si was used as substrate, and active graphene layers are deposited on top of SiO_2 insulator layer. Aluminium electrodes were then deposited as source and drain, respectively. Highly conductive silver and silver nitride were used as gate and gate oxide respectively. Effect of gate characteristics on conductivity was observed by sweeping gate voltage from -1V to 1V at minimal electric field, V_{drain}= 0.1 V and 0.2 V respectively. It is observed that variation in drain current (Id) changes the conductivity of the graphene layer. At zero gate voltage, drain current of $9.90597e^{(-5)}$A was recorded. Drain current varies as ADH are attached to the aptamers on the graphene layers. The corresponding change in graphene resistivity is utilized to detect the presence of ADH molecules. The highly sensitive GFET makes it the most prominent biosensor in the detection of ADH, thus enables efficient control of fluid in artificial kidney.

10352-31, Session PMon

System of Mueller matrix polarization correlometry of biological polycrystalline layers

Olexander V. Dubolazov, Alexander Ushenko, Yuriy Fedkovych Chernivtsi National Univ. (Ukraine)

Biological tissues represent structurally heterogeneous optical anisotropic media with absorption. To describe interactions of polarized light with such complex systems more generalized approximations are required based on Mueller-matrix formalism. Nowadays many practical techniques based on the measurement and analyses of Mueller matrices of the investigated samples are applied in biological and medical research. A separate direction – laser polarimetry – was formed in matrix optics within 10-15 years. The work consists of investigation results of diagnostic efficiency of a new azimuthally stable 3D - Mueller-matrix method which using coherent reference wave. A new model of generalized optical anisotropy of biological tissues protein networks is proposed in order to define the processes of the formation of three-dimensional elements of the Mueller matrix. The influence of complex mechanisms of both phase anisotropy (linear birefringence and optical activity) and linear (circular) dichroism is taken into account. The interconnections between the series of layers of azimuthally stable Mueller-matrix imaging that characterizing different mechanisms of optical anisotropy are determined. The statistic analysis of coordinate distributions of such Mueller-matrix rotation invariants is proposed. Thereupon the quantitative criteria (statistic moments of the 1st to the 4th order) of differentiation of human prostate polycrystalline layers for the sake of diagnosing and differentiating benign (adenoma) and malignant (cancer) tumors are estimated.

10352-32, Session PMon

Two-point Stokes vector parameters of object field for diagnosis and differentiation of optically anisotropic biological tissues

Olexander V. Dubolazov, Alexander Ushenko, Yuriy Fedkovych Chernivtsi National Univ. (Ukraine)

A new method of Stokes-corellometric evaluation of polarization-inhomogeneous image histological sections of optically-anisotropic biological tissues with different morphological structure is developed. Algorithms of analytical description and experimental determination of coordinate distributions of "two-point" Stokes vector parameters is defined. Within statistical (Statistical moments 1st - 4th order), correlation (half-width and sharpness of the peak of the autocorrelation function) and fractal (dispersion of distributions of logarithmic dependence of power spectra) analysis the objective criteria is defined, which describing the distribution of the module and the phase size of "two-point" Stokes vector parameters of polarization-inhomogeneous microscopic images of three groups of biological tissues samples with ordered and disordered birefringence-fibrillar networks. A comparative analysis of "single-point" distributions and "two-point" distributions of Stokes vector parameters of polarization-inhomogeneous images of histological sections is conducted. A higher sensitivity (2-5 times) of Stokes-correlometry method to variations in orientation-phase structure of biological tissues with different morphological structure is demonstrated.

10352-33, Session PMon

Photochemically synthesized heparin-based silver nanoparticles antimicrobial activity study

Pilar Rodriguez-Torres, Laura Susana Acosta Torres, Univ. Nacional Autónoma de México (Mexico); Luis Armando Díaz Torres, Centro de Investigaciones en Óptica, A.C. (Mexico); Paloma Netzayelli Serrano Díaz, Univ. Nacional Autónoma de México (Mexico)

The antimicrobial activity of silver nanoparticles has been extensively studied in the last years. Such nanoparticles constitute a potential and promising approach for the development of new antimicrobial systems especially due to the fact that several microorganisms are developing resistance to some already existing antimicrobial agents, therefore making antibacterial and antimicrobial studies on alternative materials necessary to overcome this issue. Silver nanoparticle concentration and size are determining factors on the antimicrobial activity of these nano systems.

Heparin is a polysaccharide that belongs to the glycosaminoglycans (GAGs) family, molecules formed by a base disaccharide whose components are joined by a glycosidic linkage that is a repeating unit along their structure. It is highly sulfated making it a negatively charged material that is also widely used as an anticoagulant in Medicine because its biocompatibility besides it is also produced within the human body, specifically in the mast cells. Heparin alone possesses antimicrobial activity although it has not been studied very much in detail, it only has been demonstrated that it inhibits E. coli, P. aeruginosa, S. aureus and S. epidermidis, so taking this into account, this study is dedicated to assess UV photochemically-synthesized (?=254 nm) heparin-based silver nanoparticles antimicrobial activity using the agar disk diffusion method complemented by the broth microdilution method to estimate de minimum inhibitory concentration (MIC), that is the lowest concentration at which an antimicrobial will inhibit visible growth of a microorganism. The strains used were the ones aforementioned to assess the antimicrobial activity degree these heparin-based nanoparticles exhibit.

10352-34, Session PMon

Jones matrix polarization-correlation mapping of biological crystals networks

Olexander V. Dubolazov, Yuriy Fedkovych Chernivtsi National Univ. (Ukraine)

The theoretical background of azimuthally stable method of Jones-matrix mapping of histological sections of biopsy of myocardium tissue on the basis of spatial frequency selection of the mechanisms of linear and circular birefringence is presented. The diagnostic application of a new correlation parameter – complex degree of mutual anisotropy – is analytically substantiated. The method of measuring coordinate distributions of complex degree of mutual anisotropy with further spatial filtration of their high- and low-frequency components is developed. The interconnections of such distributions with parameters of linear and circular birefringence of myocardium tissue histological sections are found. The comparative results of measuring the coordinate distributions of complex degree of mutual anisotropy formed by fibrillar networks of myosin fibrils of myocardium tissue of different necrotic states – dead due to coronary heart disease and acute coronary insufficiency are shown. The values and ranges of change of the statistical (moments of the 1st – 4th order) parameters of complex degree of mutual anisotropy coordinate distributions are studied. The objective criteria of differentiation of cause of death are determined.

10352-35, Session PMon

Surface enhanced Raman spectroscopy in the prescense of hydroquinone assisted by gold nanorods

Rodrigo Cabrera Alonso, Francisco Javier González, Univ. Autónoma de San Luis Potosí (Mexico)

In particular, there are non-invasive analytical sciences to biomedical research in optical techniques. Which provide detailed information on the molecular composition, structure and interaction of the relationship between diseases and biochemical changes. One of the techniques most used today is Raman spectroscopy, which provides a "fingerprint" of the molecular structure of the sample that can be used to identify the material being analyzed.

However a disadvantage is that small amounts of clinically significant substances in biological samples beyond the detection limit of conventional Raman spectrometers, making them difficult or impossible to detect. Due to this low intensity in the Raman signal for biological samples, a variety of agents have been manufactured metal nanoparticles with unique optical properties for diagnostic and medical treatment. To perform Raman amplification of this signal, it is necessary to implement the technique known as surface enhanced Raman spectroscopy (SERS). A molecule of interest is an aromatic organic compound called hydroquinone. It is a substance found in skin lightening creams, which, when applied in high concentrations, it can be the cause of skin cancer. By means of Raman spectroscopy, a qualitative analysis for subsequent medical diagnosis is made.

SPIE. OPTICS+ PHOTONICS NANOSCIENCE+ ENGINEERING

10352-36, Session PMon

Photonic-plasmonic hybrid single molecule nanosensor measures the effect of fluorescence labels to DNA-protein dynamics

Feng Liang, The Rowland Institute at Harvard (United States); Yuzheng Guo, Swansea Univ. (United Kingdom); Qimin Quan, Shaocong Hou, The Rowland Institute at Harvard (United States)

Photonic-plasmonic hybrid single molecule nanosensor

In single molecule research, the subject molecules are labeled with fluorescent reporters. The effect of the labels on molecular dynamics has not been quantified due to lack of alternative methods. Here we develop a hybrid photonic-plasmonic antenna-in-a-nanocavity system to achieve real-time kinetic measurement on single molecule interactions. We trap a single 50 nm gold particle in a photonic crystal nanobeam cavity. The nanoparticle acts as an optical antenna, which confines photons in a deep sub-wavelength mode volume while maintaining a high-quality factor of the photonic crystal nanobeam cavity. This hybrid structure improves the Q/V ratio by two orders of magnitude over previous systems, thus pushing the sensitivity to the single molecule level. Our system has several other advantages. First, it utilizes resonantly trapped photons to probe molecular interactions, thus is not limited by low photon counts or photobleaching. Second, current technique does not need any fluorescent labels, hence the measurement is genuinely reflecting the molecular dynamics. Third, our current implementation has time resolution at millisecond scale level, fast enough to study single molecule interactions.

As an example, we used our nanosensor to study DNA-protein (XPA) interactions. We measured the DNA-XPA binding kinetics using unlabeled DNA, FITC-labeled DNA and GFP-labeled DNA. We discovered that FITC and GFP can affect the DNA-XPA binding affinities up to 3 and 18 times, due to weakened electrostatic interactions.

10352-37, Session PMon

Biocompatibility and toxicity of colloidal plasmonic titanium nitride nanoparticles in epithelial cells

Tejaswini Ronur Praful, Norfolk State Univ. (United States); Urcan Guler, Alexandra Boltasseva, Vladimir M. Shalaev, Purdue Univ. (United States); Nicholas A. Kotov, Univ. of Michigan (United States); Govindarajan T. Ramesh, Norfolk State Univ. (United States)

Titanium nitride (TiN) is an emergent plasmonic material with unique properties that promise solutions to existing challenges in a variety of applications including hyper-thermal medical treatment. In this work, we have studied biocompatibility of TiN nanoparticles. Studies from dynamic light scattering (DLS) indicated that the size of TiN nanoparticles was around 50 nm, and thus facilitates easier cellular uptake. This makes TiN promising material for bioelectrochemical sensing electrodes and a promising plasmonic photothermic and photocatalytic material. Gold nanoparticles were used as positive control. The biocompatibility was tested using 3-(4,5-dimethylthiazol-2-yl)-2,5-diphenyltetrazolium bromide (MTT) and live dead assay on epithelial cells. The TiN nanoparticles showed viability similar to that of control until 50x10^7 nanoparticles/ml concentration and dropped by several folds later.

10352-38, Session PMon

Innovative strategies in hepatic tissue engineering

Laila M. Montaser M.D., Menoufia Univ. (Egypt); Sherin M. Fawzy, Society for Research on Nicotine and Tobacco (Egypt)

Failure of human body organs is believed to be one of the most important health problems all over the world. Tissue engineering aims at developing functional substitutes for damaged tissues and organs.

The application of stem cells in human regenerative medicine could be an alternative to organ transplantation, avoiding the problem of donor shortage and rejection. There is an increasing range of potential applications of stem cells in liver diseases. The great challenge for tissue engineers is to optimize suitable systems to separate, proliferate and differentiate the cells so that they can set out to create tissue. Stem cell-based therapy has received attention as a possible alternative to organ transplantation, owing to the ability of stem cells to repopulate and differentiate at the engrafted site.

Advancements in the fields of stem cell biology and biomaterials science and engineering have been combined to produce strategies by which stem cell attachment; proliferation and differentiation in vitro are supported and enhanced. Before transplantation, cells are generally seeded on biomaterial scaffolds that recapitulate the extracellular matrix and provide cells with information that is important for tissue development. Degradation of excess liver scar is thus a suitable target for cell therapy. In this manuscript, we offer our view on the applying nanotechnology and present current and emergent approach in the field of hepatic tissue engineering for specific application. The application of nanotechnology to stem cell biology would be able to address the challenges of the failure of injected cells to engraft to target tissues.

Conference 10353: Optical Sensing, Imaging, and Photon Counting: Nanostructured Devices and Applications 2017

SPIE. OPTICS+ PHOTONICS NANOSCIENCE+ ENGINEERING

Wednesday - Thursday 9 –10 August 2017

Part of Proceedings of SPIE Vol. 10353 Optical Sensing, Imaging, and Photon Counting: Nanostructured Devices and Applications 2017

10353-1, Session 1

UV and IR photodetection in single GaN/AlN nanowires *(Invited Paper)*

Jonas Lähnemann, Paul-Drude-Institut für Festkörperelektronik (Germany) and Univ. Grenoble-Alpes (France) and Institut NÉEL (France); Martien I. den Hertog, Univ. Grenoble-Alpes (France) and Institut NÉEL (France) and CEA-INAC-PHELIQS (France); Akhil Ajay, Maria Spies, Jakub Polaczy?ski, Univ. Grenoble-Alpes (France) and CEA-INAC-PHELIQS (France) and Institut NÉEL (France); Pascal Hille, Justus-Liebig-Univ. Giessen (Germany); María de la Mata, Institut Català de Nanociència i Nanotecnologia (ICN2) (Spain); Jörg Schörmann, Justus-Liebig-Univ. Giessen (Germany); Jordi Arbiol, Institut Català de Nanociència i Nanotecnologia (ICN2) (Spain); Martin Eickhoff, Justus-Liebig-Univ. Giessen (Germany); Bruno Gayral, Eva Monroy, Univ. Grenoble-Alpes (France) and CEA-INAC-PHELIQS (France) and Institut NÉEL (France)

Almost defect-free semiconductor nanowires (NWs) grown by molecular beam epitaxy have potential applications as miniaturized photodetectors. GaN is a promising choice to cover the ultraviolet (UV) spectral range. Recently, we have investigated the photoconductive properties of single, contacted GaN NWs incorporating GaN/AlN nanodisks [1]. A significant dispersion in the magnitude of the photo- and dark currents for different single NWs was attributed mainly to the coalescence of NWs with displaced nanodisk stacks, reducing the effective length of the heterostructure. A larger number of active nanodisks and AlN barriers in the current path results in lower dark current and higher photosensitivity, and improves the sensitivity of the NW to variations in the illumination intensity (reduced sublinearity). Based on these results, we have devised an improved design with higher reproducibility of the characteristics of individual NWs. A n/n+ doping profile of the stem and cap segments results in an improved photovoltaic response at low bias.

Finally, we have demonstrated the feasibility of IR photodetection around the telecommunication wavelength in single GaN/AlN-nanowires based on intraband transitions in doped nanodisks. The spectral characteristics are in agreement with three-dimensional simulations of the transition energies in the investigated nanostructures. In contrast to the UV photocurrent, the response with IR illumination intensity is perfectly linear over several orders of magnitude, which can be related to the decoupling of the IR photoresponse from surface related effects predominant in the UV response.

[1] J. Lähnemann, et al., Nano Lett. 16, 3260 (2016).

10353-2, Session 1

Colloidal quantum dots for mid-IR detection and emission *(Invited Paper)*

Philippe Guyot-Sionnest, The Univ. of Chicago (United States)

No Abstract Available.

10353-3, Session 1

Infrared imaging using low-cost II-VI colloidal quantum dots *(Invited Paper)*

Richard E. Pimpinella, Christopher Buurma, Anthony J. Ciani, Christoph H. Grein, Sivananthan Labs., Inc. (United States); Philippe Guyot-Sionnest, The Univ. of Chicago (United States)

II-VI colloidal quantum dots (CQDs) have made significant technological advances over the past several years, including the world's first demonstration of MWIR imaging using CQD-based focal plane arrays. The ultra-low costs associated with synthesis and device fabrication, as well as compatibility with wafer-level focal plane array fabrication, make CQDs a very promising infrared sensing technology. In addition to the benefit of cost, CQD infrared imagers are photon detectors, capable of high performance and fast response at elevated operating temperatures. By adjusting the colloidal synthesis, II-VI CQD photodetectors have demonstrated photoresponse from SWIR through LWIR. We will discuss our recent progress in the development of low cost infrared focal plane arrays fabricated using II-VI CQDs.

10353-4, Session 1

Interesting problems in superlattice detectors *(Invited Paper)*

Sanjay Krishna, The Ohio State Univ. (United States)

There has been significant progress on the development of Type II superlattice detectors in the past 15 years. As we have progressed in advanced heterostructure engineering of the devices, it has also provided insight into some of the challenges associated with the superlattices. In this talk, I will discuss some of our recent results on unipolar barrier detectors. I will also discuss some of the fundamental challenges that need to be addressed for the superlattice detectors such as vertical transport and surface passivation. I will also present some interesting problems including superlattice based avalanche photodiodes and the growth of metamorphic InAsSb absorbers.

10353-5, Session 1

ZnO: from material to unipolar devices *(Invited Paper)*

Maxime Hugues, Ctr. de Rechercher sur l'Hétéro-Epitaxie et ses Applications (France); Nolwenn Le Biavan, Denis Lefebvre, Ctr. de Recherche sur l'Hétéro-Epitaxie et ses Applications (France); Miguel Montes Bajo, Julen Tamayo-Arriola, Adrian Hierro, Univ. Politécnica de Madrid (Spain); Arnaud Jollivet, Maria Tchernycheva, François H. Julien, Univ. Paris-Sud 11 (France); Jean-Michel Chauveau, Ctr. de Recherche sur l'Hétéro-Epitaxie et ses Applications (France)

Although ZnO and its related heterostructures are really attractive for their potential application in optoelectronics, their developments have been limited by the p-type doping issue. Here, we will show why ZnO properties are also very attractive for unipolar structures, only dealing with electrons,

and how the material quality has been improved to reach these devices requirements.

First, the benefit of homoepitaxy through material quality improvement is presented. We will show that molecular beam epitaxy allows getting defect density, surface roughness, and residual doping, comparable to the state-of-the-art of GaAs. Moreover, (Zn,Mg)O alloy could be used to fabricate heterostructures with very good optical and transport properties.

In the second part, we will give a brief overview of the main transport results, especially bidimensional electron gas, reported in the literature. Few examples of possible applications will also be addressed. Then, we will focus on the potentialities of nonpolar ZnO heterostructures for unipolar devices based on intersubband transitions. Once the advantages of using ZnO for TeraHertz quantum cascade laser discussed, we will show that the structural properties of the ZnO/(Zn,Mg)O heterostructures fulfill the requirements of these devices operation. Moreover, we will finish with absorption measurements clearly showing intersubband transitions in agreement with the light polarization selection rule. The strong influence of physical parameters, like doping level, on the energy of these kind of transitions will also be discussed.

This work was funded by EU commission under the H2020 FET-OPEN program; project “ZOTERAC” FET-OPEN 6655107.

10353-6, Session 2

Single-photon detection and imaging by using superconducting nanowires *(Invited Paper)*

Karl K. Berggren, Qing-Yuan Zhao, Andrew E. Dane, Di Zhu, Massachusetts Institute of Technology (United States)

This talk will generally review the superconducting nanowire single-photon detector, explaining our current understanding of its performance capabilities and limitations. We will then discuss the applications of the technology to quantum information processing, in particular its integration with various optical waveguides for on-chip integrated photonic quantum-information processing. Beyond the review portion of the talk, this talk will also present our recent work in preparing a microwave-plasmonic transmission line that can be used to both time- and position-tag individual photons upon arrival at an imaging surface. The microwave plasmons are in practice simply the natural transmission character of thin superconducting films, and result in extraordinarily slow (~c/50 velocity) transmission of microwave signals along a co-planar on-chip microwave guide. Photon-incidence events send pulses propagating along the waveguide in both directions. The position and time of the photon arrival can be distinguished by considering the relative times of arrival of the pulses at the ends of the long transmission line.

10353-7, Session 2

Ultrafast single photon detectors *(Invited Paper)*

Wolfram Pernice, Simone Ferrari, Westfälische Wilhelms-Univ. Münster (Germany)

Nanophotonic integrated circuits are emerging as a promising platform for quantum photonics. A key building block are waveguide integrated detectors with superior performance. Detectors based on superconductor nanowires (SNSPDs) attached to optical waveguides have been shown to provide high efficiency and good timing performance, as well as broad bandwidth. To move towards applications in high bandwidth quantum communication and processing, ultrafast single-photon detectors with high efficiency are needed. The speed of meander type SNSPDs is limited because the required high absorption efficiency necessitates long nanowires deposited on top of the waveguide. This enhances the kinetic inductance and makes the detectors slow. We overcome this problem by aligning the nanowire perpendicular to the waveguide to realize devices with a length below 1?µm. By integrating the nanowire into a photonic crystal cavity, we recover high absorption efficiency, thus enhancing the detection efficiency by more than an order of magnitude. Our cavity enhanced superconducting nanowire detectors are fully embedded in silicon nanophotonic circuits and efficiently detect single photons at telecom wavelengths. The detectors possess sub-nanosecond decay (~?120?ps) and recovery times (~?510?ps), and thus show potential for GHz count rates at low timing jitter (~?32?ps).

10353-8, Session 2

Time jitter and time walk in SLiK APD: characterization, measurements and implications for single photon counting applications

Bernicy S. Fong, Excelitas Canada, Inc. (Canada); Murray Davies, Excelitas Canada Inc. (Canada); Pierre Deschamps, Excelitas Canada, Inc. (Canada)

Transit time (response time), timing jitter (or timing resolution) and time walk are three separate parameters associated with a detector’s response time. Studies have been done on mostly the time jitter of various single photon detectors. Being the designer and manufacturer of the ultra-low noise (?-factor) silicon avalanche photodiode the SLiK APD, which is used in many single photon counting applications, we often get inquiries and questions to better understand how this detector behaves under different operating conditions. Hence, here we will be focusing on the study of these three time related parameters specifically for the SLiK APD, as a way to provide the most direct information for users of this detector to help with its use more efficiently and effectively. We will be providing the study data on how these parameters can be affected by temperature (both intrinsic to the detector chip and environmental input based on operating conditions), operating voltage, wavelength of photons, as well as light spot size. How they can be optimized, the trade-offs from optimization of the desired performance and if adjusting one time aspect will affect the other will be presented. Subsequently we will outline the implications of each of these parameters on some of the key single photon counting applications such as Lidar and Lidar imaging, time correlated single photon counting, and quantum experiments.

10353-9, Session 2

Modeling single photon detection

Majeed M. Hayat, The Univ. of New Mexico (United States)

Single-photon avalanche diodes (SPADs) are important devices in photon counting systems employed by applications such as quantum cryptography, time resolved spectroscopy and photon counting optical communication, time-resolved reflectometry, quantum imaging and three-dimensional laser radar. SPADs convert each photo-generated electron hole pair to a measurable current via an avalanche of impact ionizations, thereby yielding a measurable photocurrent. In this talk we present a review of a generalized and rigorous analytical model for determining single-photon detection efficiency (SPDE) and dark-count rate (DCR) of SPADs. Both gated and free-running modes of operation are considered. The model assumes a general SPAD structure, with arbitrary absorber and avalanche regions, including nonplanar devices for which the avalanche region exhibits 3D electric fields for which the SPAD can be viewed as a continuum of SPADs in tandem. The model allows us to describe dependence of the SPDE versus DCR behavior on the structure and material of the avalanche region, temperature and over-bias. At the heart of the model is a generalized theory for breakdown probability in SPADs, which takes into account the random locations where dark and photo-generated carriers are produced. A simple analysis for the role of the SPDE and DCR on the information flow in a simple quantum communication system is also described using metrics such as the mutual information and channel capacity. Finally, the peculiar effects of negative feedback on the characteristics of the avalanche pulse and quenching time in a closed-loop avalanche system are also reviewed using a hybrid analytical and simulation-based approach.

10353-10, Session 3

Depth imaging using single photon detection *(Invited Paper)*

Gerald S. Buller, Aongus McCarthy, Ximing Ren, Aurora Maccarone, Rachael Tobin, Abderrahim Halimi, Yoann Altmann, Yvan R. Petillot, Stephen McLaughlin, Andrew M. Wallace, Heriot-Watt Univ. (United Kingdom)

Single-photon detection has emerged as a candidate for a number of depth imaging applications, including both free-space and underwater. This presentation will describe experiments and image processing analysis which highlight the virtues of the approach, including sensitivity, accuracy and resolution, long range and eye-safe capabilities. These applications include long-distance depth imaging (ie > 1km) where both superconducting and semiconductor-based single-photon detectors have been used to operate within the atmospheric windows around the 1550nm wavelength. We will also examine the possibilities of extending the operational wavelength to greater than 1550nm. In underwater applications, the operational wavelength is typically between 500nm to 700nm, within the high-efficiency band of high-performance, near-room temperature silicon-based single photon avalanche diodes. In underwater imaging, depth and intensity measurements were made at up to nine attenuation lengths between transceiver and target. Another area of emerging interest is the use of multiple wavelength single-photon LIDAR which may prove suitable for investigation of distributed targets. For example, an appropriate selection of wavelengths can reveal indications of the structural and physiological parameters of vegetation to provide a valuable insight into the carbon dioxide cycle for environmental research. Single photon lidar has also been used to both reconstruct and classify color detail of targets, even at low signal levels equivalent to less than 1 photon per pixel, on average.

10353-11, Session 3

Smart single-photon detectors in CMOS technology *(Invited Paper)*

Angel Rodríguez-Vázquez, Univ. de Sevilla (Spain)

The detection of single photons by CMOS-compatible structures opens new vistas for the implementation of low-light, photon counting image sensors, on the one hand, and Time-Flight sensors, on the other hand. Relevant applications include Flash-LIDAR cameras, PET scanners and ultra-fast laser spectroscopy, among others. CMOS-SPAD sensor arrays with combined 2D/3D imaging capabilities are also being explored for possible usage in automotive and are already being used for consumer applications. All these applications largely benefit from the compatibility with VLSI mixed-signal and logic circuits and the subsequent possibility to embed sensor intelligence along with the photo-sensors. This, imaging systems capable of single photon counting and time correlated single photon detection can be built with reduced SWaP (Size, Weight and Power) figures.

Sensor smartness starts at readout, includes sensor calibration and image error correction and progresses up to the extraction of information from the raw senor data. This talk presents architectures and circuits for embedding intelligence into SPAD-based arrays. Electrical interactions among photo-sensors and read-out circuits are addressed seeking for pixel optimization. Also, strategies for time-to-digital conversion are discussed. Results from TCAD tools and measurements from prototype chips for PET, Flash LIDAR and combined 2D/3D imaging are included for demonstration purposes.

10353-12, Session 3

Hot-spot relaxation time current dependence in niobium nitride waveguide-integrated superconducting nanowire single-photon detectors

Simone Ferrari, Wolfram Pernice, Westfälische Wilhelms-Univ. Münster (Germany)

We realize fast, efficient and small footprint niobium nitride superconducting nanowire single photon detectors atop of photonic waveguides. By reducing the bias current of the nanowire, in order to break the superconductivity and trigger a detection event, more than one photon needs to be absorbed in a localized section of the wire within a very short time delay (hot-spot relaxation time), making such devices promising also for multiphoton sensing applications. We adopt a near-infrared pump-probe technique in a cryogenic environment to investigate the bias current dependence of the hot-spot relaxation time. A minimum relaxation time of (22 ± 1) ps is obtained when applying a bias current of 50% of the switching current at a bath temperature of 1.7K. Our study reveals a strong increase of the picosecond relaxation time with increasing bias current. We further adopt the same technique for determining the multi-photon detection regimes of the detector, which are in agreement with standard quantum detector tomography. In this context, we introduce a practical model and reconstruction method for determining the detector sensitivity regimes. Our work provides a complete description of the detector working operation in both number photon threshold sensitivity and time-delay sensitivity. The results allow for implementing on-chip measurement architectures for the characterization of weak classical light emitters and fast single photon sources with only one detector, driven at different biasing currents, with a drastic reduction of the time uncertainty limitations of typical correlation measurement systems.

10353-13, Session 4

Electromechanically tunable photonic crystal sensors for integrated spectrometry and nanometrology *(Invited Paper)*

Zarko Zobenica, Rob W. van der Heijden, Maurangelo Petruzella, Francesco M. Pagliano, Technische Univ. Eindhoven (Netherlands); Rick Leijssen, FOM Institute for Atomic and Molecular Physics (Netherlands); Tian Xia, Leonardo Midolo, Michele Cotrufo, Yongjin Cho, Frank W. M. van Otten, Technische Univ. Eindhoven (Netherlands); Ewold Verhagen, FOM Institute for Atomic and Molecular Physics (Netherlands); Andrea Fiore, Technische Univ. Eindhoven (Netherlands)

An ultra-compact integrated optomechanical device is presented with a footprint of the order of 15x15 micronm^2, that operates as a spectrometer with sub-pm wavelength resolution. Alternatively, using a laser source with a known wavelength, it is converted to a displacement sensor with expected resolution of some tens of fm/Hz^1/2.

The device is based on a pin photodiode fabricated on two optically-coupled semiconductor membranes. Its absorption is controlled by quantum dots in the intrinsic layer. A photonic crystal cavity is defined in the double-membrane, acting as a narrowband filter (linewidth ~ 0.1 nm) to render the detector spectrally selective. The filter is tuned by changing the membrane separation by an electrostatic force from a voltage in a reversed biased diode configuration. Reversely, an unknown displacement of the top membrane can be measured from the peak photocurrent wavelength.

A cavity resonance modulation scheme, realized by applying an additional AC electrostatic tuning voltage, in combination with phase sensitive detection, greatly improves the resonant signal to nonresonant background ratio. It also enables a direct implementation of derivative spectroscopy, leading to a wavelength resolution orders of magnitude better than the cavity linewidth for wavemeter applications.

The operation as a spectrometer is proven by resolving the absorption line of a HF gas cell excited by a broadband source. The displacement sensing is demonstrated from the observation of the mechanical resonance excited by thermal Brownian motion.

The integrated manufacturing will lead to low-cost mass production or to massive parallelization with additional potential for hyperspectral imaging or increased-throughput.

10353-14, Session 4

Photodetector fabrication by dielectrophoretic assembly of GaAs nanowires grown by a two-steps method *(Invited Paper)*

Basilio J. García, Univ. Autónoma de Madrid (Spain); Carlos García Nuñez, Univ. Autónoma de Madrid (Spain) and Univ. of Glasgow (United Kingdom); Alejandro F. Braña, Univ. Autónoma de Madrid (Spain); Nair López, Univ. Politécnica de Madrid (Spain); José L. Pau, Univ. Autónoma de Madrid (Spain)

Mechanical manipulation of nanowires (NWs) for their integration in electronics is problematic because of their reduced dimensions. Contactless NW manipulation using electromagnetic fields is usually much softer than mechanical methods, often resulting less destructive.

We report on the growth of vertically aligned GaAs NWs by Ga-assisted chemical beam epitaxy on Si(111) substrates using triethylgallium and tertiarybuthylarsine as precursors. We have developed a novel two-steps growth method –by inserting an air oxidation process- to prevent the nucleation of parasitic structures during NW growth such as traces and nanocrystals, increasing the length of resulting NWs, and improving its aspect ratio for their easy integration in electronics.

We also describe a feasible and reproducible dielectrophoretic method to assemble a single GaAs NW on conductive electrodes with high assembly and alignment yields. The electrical characteristics of obtained contacts between the bare NW and the electrode have been measured, resulting in Schottky-like barrier contacts when Al-doped ZnO (AZO) or Al are used as electrode material. On the other hand, a low-resistance contact is formed between the Ga-droplet terminated NW tip and the AZO electrode. The current-voltage measurements of a single GaAs NW diode under different illumination conditions show a strong light responsivity of the forward bias characteristic mainly produced by a change on the NW series resistance.

10353-15, Session 4

Near-unity absorption in atomically thin optoelectronic devices with high quantum efficiency *(Invited Paper)*

Deep Jariwala, California Institute of Technology (United States)

The isolation of stable atomically thin two-dimensional (2D) materials on arbitrary substrates has led to a revolution in solid state physics and semiconductor device research over the past decade. While, graphene is the poster child of 2D materials family, a variety of other 2D materials (including semiconductors) with varying structures and opto-electronic properties have been isolated over the last few years raising the prospects for a new class of devices assembled by van der Waals forces. A fundamental challenge in using 2D materials for opto-electronic devices is enhancing their interaction with light, ultimately responsible for higher performance and efficiency in the devices.

In this seminar, I will show our recent work on photovoltaic devices from transition metal dichalcogenides of molybdenum and tungsten (MoS_2, WSe_2 etc.). We have recently demonstrated near-unity absorption in the visible part of the electromagnetic spectrum in < 15 nm films of these semiconductors by placing them on reflecting metal substrates such as gold and silver. We have further shown that these highly absorbing, ultrathin films can be further used for fabrication of simple Schottky junction photovoltaic devices with microfabricated metallic top contacts. While, this work helps solve the light-absorption problem, the external quantum efficiency (EQE) was < 10% for our Schottky junction devices Very recently, we have extended this early work to fabricate p-n heterojunctions (p-WSe_2/n-MoS_2) and use graphene as a transparent top contact to amplify our current collection efficiency and push the EQE up to 50%, approaching that of many emerging photovoltaic technologies with active layers in the 100s of nm range. This represents a significant development as both light-absorption and charge collection have been addressed in these devices. Finally, I will present scope for future work using just monolayers of materials to engineer near unity light absorption and collection.

10353-16, Session 4

Photonic waveguide based evanescent excitation and near-field collection for improved surface to bulk fluorescence separation

Md. Mahmud-Ul-Hasan, KU Leuven (Belgium) and IMEC (Belgium); Pieter Neutens, Rita Vos, IMEC (Belgium); Liesbet Lagae, Pol Van Dorpe, IMEC (Belgium) and KU Leuven (Belgium)

Fluorescence is a widely used transduction mechanism in bio-imaging, sensing or physical chemistry characterization applications. The ability to selectively excite desired molecules without generating considerable bulk background from nearby molecules is very important for all these applications. A near field excitation using an exponentially decaying evanescent field is often used to reduce the bulk background by selectively exciting molecules near to the surface. We propose an on-chip platform to improve the surface and bulk fluorescence separation by combining near-field excitation and near-field collection. We used the exponentially decaying evanescent tail of a Silicon Nitride rib waveguide to excite molecules and coupled the subsequent emission back via the same waveguide. We observe from the finite difference time domain simulation that both the excitation and coupling efficiency depend exponentially on the surface-molecule distance. Thus, combination of near field excitation and collection improves surface-bulk separation. A reduction by half in effective 1/e decay length was found experimentally for this combined near-field excitation and collection technique compare to the conventional only near-field excitation based technique.

An analytical model is derived to find the optimum device efficiency for bio-sensing applications and established a general condition for sensor length to maximize the device efficiency and validated by experimental data.

Finally, we used this platform for Fluorescence Correlation Spectroscopy and steady-state fluorescence anisotropy measurement.

In this talk, I will present the fabrication, characterization and experimental results obtained using this proposed waveguide based platform.

10353-32, Session PWed

Scalable nanoantennas

Dmitrii Poletaev, Bogdan V. Sokolenko, Anna Kovaleva, V.I. Vernadsky Crimean Federal Univ. (Russian Federation); Nikolay V. Petrov, Igor A. Shevkunov, ITMO Univ. (Russian Federation)

Nanoantenna are important elements of modern photonics, along with traditional oscillators and receivers of radiation. They are widely used for the detection and conversion of electromagnetic waves. But there is the problem of expanding the operating frequency band. The purpose of work is to construct a numerical model of nanoantenna and its optimization for the expansion of the operating frequency band. In the work developed numerical model, based on Vivaldi antenna. The analysis of the parameters of the antenna (radiation pattern, Purcell factor, gain) and their optimization are carried out in the work. The conclusions of it usability for wideband transducers and Raman spectroscopy were made.

10353-33, Session PWed

Etched multimode fiber Bragg gratings based refractometer

Umesh Kumar Tiwari, Central Scientific Instruments Organisation (India); Siddharth Kaushik, Central Scientific Instrumentation Organisation (India)

A Multimode Fiber Bragg Gratings for refractive index sensing has been demonstrated experimentally. The fabrication of Bragg gratings in the Standard step-index multimode fiber with a core diameter of 50 μm and a numerical aperture of 0.20 is carried out by phase mask method. The periodic modulation of refractive index in the core region of fiber is done by KrF excimer laser operating at 248 nm as ultraviolet (UV) light source with repetition rate of output pulses is 200 Hz and energy density per pulse of 3 mJ, respectively. The beam expander enlarges the UV beam, which is then projected by a mirror into the phase mask. Focussing of enlarged UV beam is achieved with a cylindrical lens onto the fiber. The period of the phase mask is 1064 nm. The etching of cladding portion of grating region (2 cm) is carried out by Hydrofluoric acid (48%) for 15 minutes. The etching process causes reduction of cladding diameter by 55 μm which further enhances the interaction of light propagating in core mode with higher cladding modes. Solutions of varied concentrations of glycerol were prepared having corresponding refractive index. Shift in wavelength in the reflection peak of high-order mode L1 is observed when glycerol solution is passed over the cladding surface of grating region. The proposed sensor with 1-pm resolution was successfully employed for sensing of different glycerol solutions and can be used as potential sensing platform for bio-chemical applications.

10353-34, Session PWed

HgTe quantum dot photovoltaic detector at 5 micron

Matthew Ackerman, Philippe Guyot-Sionnest, The Univ. of Chicago (United States)

Mid-infrared (MIR) imaging is a currently expensive technology largely restricted to military and surveillance. A lower cost technology with similar performance would open many new civilian applications in chemical identification, driverless vehicles, and biosensing. Recent advances with colloidal quantum dots (CQDs) indicate that they may lead to very significant cost reductions in the production of focal plane arrays, while also promising higher operation temperature. To investigate the basic potential of the CQD approach, we study single element photovoltaic (PV) devices for MIR detection in the 3-5 micron range. We use HgTe CQDs in an inverted photovoltaic architecture. Interfacial layers such as titanium, Ag2Te, and MoO3 are incorporated as electron and hole barrier materials, to optimize short-circuit current (Isc) and minimize thermal noise. PV devices are characterized by current-voltage-temperature measurements, spectral response, responsivity, and specific detectivity from 50K to 295K. Time-of-flight photoconductivity measurements on HgTe thin films in conjunction with the photovoltaic devices are used to elaborate on carrier transport and carrier lifetime, and their contribution to the device operation. Our present structures show improved quantum yield, up to 30%, specific detectivity up to 10^11 Jones at 80K, and background limited detection up to 120K, and much improved stability compared to the prior report of MWIR HgTe CQD PV devices.

10353-35, Session PWed

PbS quantum dots with long wavelength absorption for SWIR photodetectors

Chen Dong, Jaewoong Lee, Shuyi Liu, Franky So, North Carolina State Univ. (United States)

Lead Sulfide nanoparticles (PbS NPs) are widely used in short-wavelength infrared (SWIR) photodetectors and solar cells due to their excellent photosensitivity, bandgap tunability, and solution processability. By varying the size of quantum dots, PbS NPs photodetectors with light sensitivity from 900 nm to 2000 nm have been demonstrated. However, there has not been any report of PbS NPs SWIR photodetectors with light sensitivity beyond 2000 nm wavelength. Larger PbS NPs require a higher reaction temperature and longer reaction time, during which second nucleation and Ostwald Ripening readily occurs leading to highly dispersion of the NPs size. In this work, we report a successful synthesis of large mono-dispersed PbS NPs with an absorption peak over 2500 nm and diameter up to 15.8 nm with good mono-dispersity, resulting in a very small half-width-at-half-maximum (HWHM) of 12 meV. Our work paves the way for fabricating broadband photodetectors with photo-response covering almost the entire visible and SWIR region.

10353-17, Session 5

III-nitride terahertz photodetectors for the reststrahlen gap of intersubband optoelectronics *(Invited Paper)*

Roberto Paiella, Habibe Durmaz, Faisal F. Sudradjat, Denis Nothern, Gordie C. Brummer, Wei Zhang, Jeffrey Woodward, Theodore D. Moustakas, Boston Univ. (United States)

Terahertz light sources and photodetectors based on intersubband (ISB) transitions in GaAs/AlGaAs quantum wells (QWs) have been the subject of extensive research efforts in the past several years, and already offer excellent performance for many applications. The operation of these devices, however, is fundamentally limited to incomplete coverage of the THz spectrum, due to the prohibitively strong lattice absorption in the (Al)(Ga)As Reststrahlen band around 8-9 THz. Recently, it has been argued that this prominent gap in the spectral coverage of semiconductor optoelectronics can be overcome using GaN/AlGaN QWs, by virtue of their large optical phonon frequencies above 15 THz.

At the same time, however, the development of III-nitride ISB devices is complicated by the large internal electric fields that exist in GaN/AlGaN QWs grown along the polar crystallographic c-axis (the most common growth direction for these materials), due to spontaneous and piezoelectric polarizations. These internal electric fields tend to distort the QW lineups and blue-shift the ISB transition energies. Here we present two different approaches that we have recently employed to address this issue for the development of THz ISB photodetectors: the use of suitably designed double-step quantum wells, and epitaxial growth on semi-polar GaN substrates. In both cases, the deleterious effects of the intrinsic electric fields are strongly reduced and promising device characteristics are demonstrated, with responsivity spectra covering the entire Reststrahlen band of arsenide semiconductors.

10353-18, Session 5

Hybrid cavity for photo-conductive detectors with nanoantenna arrays and distributed Bragg reflectors *(Invited Paper)*

Oleg Mitrofanov, Univ. College London (United Kingdom)

Efficiency of photoconductive detectors is limited by the bulk optical properties of photoconductive materials. The absorption length is on the order of several hundred nanometers, which limits the device thickness. Optical absorption however in the photoconductive layer can be modified substantially by using the concept of hybrid cavity, which consists of nanoantennas and a Distributed Bragg Reflector. A hybrid cavity containing a GaAs photoconductive layer of just 50 nm can be used to absorb >75% of incident photons by trapping the light within the cavity. We will discuss an intuitive model, which describes the dependence of the optimum operation wavelength on the cavity thickness. We will also show that the nanoantenna size is a critical parameter, small variations of which lead to both wavelength shifting and reduced absorption in the cavity. This behavior suggests that impedance matching is key for achieving efficient absorption in the hybrid cavities.

10353-19, Session 5

Light polarization sensitive photodetectors with non-polar and semi-polar homoepitaxial ZnO/ZnMgO MQWs *(Invited Paper)*

Gema Tabares, Univ. Autónoma de Madrid (Spain); Adrian Hierro, Alejandro Kurtz, Elias Muñoz, Univ. Politécnica de Madrid (Spain); Borge Vinter, Jean-Michel Chauveau, Ctr. de Recherche sur l'Hétéro-Epitaxie et ses Applications (France)

In this work, light polarization-sensitive UV photodetectors (PSPDs) using non-polar and semipolar ZnMgO/ZnO multiple quantum wells grown both on sapphire and ZnO substrates have been demonstrated. For the PSPDs grown on sapphire with anisotropic biaxial in-plain strain, the responsivity absorption edge shifts by ?dE ~ 21 meV between light polarized perpendicular and parallel to the c-axis, and the maximum responsivity contrast is (RE\C/ RE c)max~ 6. For the PSPDs grown on ZnO, with strain-free quantum wells, ?dE ~ 30-40, and 21 meV for non-polar and semipolar heterostructures, and maximum (RE\C/ RE c)max ~ 10, for non-polar heterostructure was achieved. These light polarization sensitivities have been explained in terms of excitonic transitions between the conduction and the three valence bands.

10353-20, Session 5

High-sensitivity refractometric sensor in a cylindrical resonator

William Morrish, Peter West, Nathan West, Univ. of Alberta (Canada); Elizaveta Klantsataya, The Univ. of Adelaide (Australia); Kirsty Gardner, Stephen Lane, Raymond G. DeCorby, Univ. of Alberta (Canada); Alexandre François, Univ. of Adelaide (Australia); Al Meldrum, Univ. of Alberta (Canada)

Microcapillaries are well-known to support whispering gallery resonances that can be employed for refractometric sensing. Here we instead report on an optical sensor for liquids and gases based on cross-channel Fabry-Pérot resonances. The device is comprised of a capillary with a thin film coated on the channel walls. The films tested included a reflective metal (i.e., silver) or a high-index polymer (i.e., poly-pentabromophenyl acrylate) deposited on the channel. The optical boundaries perpendicular to the capillary axis resulted in multiple resonances that resemble Fabry-Pérot interferences between a set of nested cylindrical mirrors. The reflective films strongly enhanced the cross-channel modes in comparison to the case of a bare capillary. Due to the improved visibility of these channel modes, it is in principle possible to track changes in the refractive index of an analyte flowing through the capillary by monitoring the resonance wavelengths. Here we tested the sensitivity of the device to both liquid and gaseous analytes. For gases such as Ar and N2, we found a 3?? detection limit of (6.3 ± 1.1) x 10-6 as the minimum detectable change in the index of refraction. When used as a gas pressure sensor, the device was found to have a limit of detection of 3.3 ± 0.1 kPa based on the pressure dependence of the refractive index. For liquids with a refractive index close to that of water, the detection limit was (1.000 ± 0.002) x 10-5. These results were interpreted in terms of a simple model for a cylindrical Fabry-Pérot cavity.

10353-21, Session 6

Time-resolved cathodoluminescence for wide bandgap nanostructures *(Invited Paper)*

Gwénolé Jacopin, Mehran Shahmohammadi, Wei Liu, Jean-François Carlin, Nicolas Grandjean, Benoit Deveaud, Ecole Polytechnique Fédérale de Lausanne (Switzerland)

As demonstrated by our laboratory [1], the use of the picosecond time resolved cathodoluminescence (p-TR-CL) is suitable to locally study the dynamics of excitons. Indeed, by combining the spatial resolution of a scanning electron microscope and the temporal resolution of a streak camera, it becomes possible to investigate processes, which happen at such scales. In particular, I will present recent studies of wide bandgap nanostructures such as bent ZnO microwires [2–4] or InGaN nanowires [5] realized by using the TR-CL. Finally, I will present the exciton dynamics on single dislocations in GaN [6], providing critical information about the nature of dislocation as non-radiative centers.

[1] M. Merano et al., Nature 438, 479 (2005).

[2] X. Fu et al., ACS Nano 8, 3412 (2014).

[3] G. Jacopin et al., Appl. Phys. Lett. 104, 042109 (2014).

[4] M. Shahmohammadi et al., Appl. Phys. Lett. 107, 141101 (2015).

[5] M. Shahmohammadi et al., Nano Lett. 16, 243 (2016).

[6] W. Liu et al., Appl. Phys. Lett. 109, 42101 (2016).

10353-22, Session 6

Biaxial strain tuning of the optical properties of single-layer transition metal dichalcogenides *(Invited Paper)*

Riccardo Frisenda, Andres Castellanos-Gomez, David Perez de Lara, IMDEA Nanociencia (Spain)

Strain engineering has been proposed as a promising route to modify the electronic and optical properties of two-dimensional (2D) materials. These materials can stand to large mechanical deformations, of the order of 10%, while conventional 3D semiconductors tend to break at moderate deformations of 0.5-1.5%. Another key feature of strain engineering of 2D materials stands in the way in which they can be strained. In fact, while 3D systems are typically stressed by epitaxial growing them onto substrates with a certain lattice parameter mismatch, strain in 2D systems can be applied by stretching or bending. Experiments on MoS2 single-layer and few-layers flakes have already demonstrated that the optical band gap can be changed of 50 meV/% for uniaxial strain and of 100 meV/% for biaxial strain. Most of these strain engineering experiments to date, however, study uniaxial tensile strain under static conditions and, apart from few exceptions, are limited to MoS2. In this talk I will present results on biaxial straining, both tensile and compressive, of single-layer transition metal dichalcogenides (TMDC). We studied the effect of strain on mechanically exfoliated flakes of monolayer MoS2 deposited on different polymeric substrates. We apply the strain exploiting the large mismatch between the thermal expansion coefficients of the polymeric substrates and the fabricated TMDCs flake deposited on top. We studied the substrate dependency of the strain transfer efficiency and we find that for substrates with Young's modulus larger than 1 GPa, biaxial strain can be applied reproducibly without slippage. We investigate the effects of strain on the optical properties of single-layers MoS2, MoSe2, WS2 and WSe2 and we observe a redshift of the optical band gap of these 2D TMDCs for increasing tensile strain. The observed bandgap shifts as a function of substrate extension/compression follow the order MoSe2 < MoS2 < WSe2 < WS2, i.e. with WS2 providing the largest bandgap tunability and MoSe2 the lowest. This method can be readily applied to other 2D materials and be used to vary the strain in real time.

10353-23, Session 6

Multi-purpose highly sensitive room temperature nano based detector *(Invited Paper)*

Yossi Paltiel, The Hebrew Univ. of Jerusalem (Israel)

The ability to integrate electronics with Nanocrystals (NCs) allows utilizing their unique properties for a future optoelectronic device. Combing top down approach using self-assembled hybrid organic-NCs systems, with bottom up components can revolutionize devices in future. In my talk I will present an ultra-high light sensing device based on InAs NCs acting as an optical gate to high electron mobility transistor (HEMT) device. Using a very narrow channel the device quantum efficiency is high as 106V/W, while the single to noise ratio (SNR) enables high sensitivity photon detection. In addition a side gate detector will be present showing enhancement in the sensitivity for light and gas detection. The same concept can be used to develop tunable, simple and flexible detector for the IR range printing semiconducting/conducting carbon nanotubes layer mixed with doped semiconductor nanocrystals.

10353-24, Session 6

Ratiometric 2D temperature mapping around plasmonic nanoparticles with one CCD using directional anisotropy in fluorescence

Chen Chen, Zhidong Du, Liang Pan, Purdue Univ. (United States)

Optically measuring two-dimensional (2D) temperature fields around plasmonic structures is of great importance for their thermal management considering the strong energy dissipations along with the extraordinary abilities of light coupling. Among all the available methods, ratiometric studies are particularly desirable since they suppress the influence of trivial factors, such as temporal fluctuations in excitation and spatial non-uniform distributions of fluorescent species, and thus gives reliable temperature dependence. Typical ratiometric mapping methods measure fluorescence signals on the emission side. They require additional modification to the detection beam path so that two images can be recorded simultaneously. Here we report a new ratiometric thermometry that modifies the excitation side and only needs one detector. This thermometry measures fluorescent anisotropy based on the directionality of emission. With just one CCD, ratiometric measurements of temperature are achieved by alternating two orthogonal polarizations on the excitation side. We show that this thermometry shares the same advantages claimed for anisotropy based methods, including robustness against intensity variations, compatibility with biological tissues, suitability for two-dimensional imaging and readout rate comparable to the detector's framerate. Besides, it can be easily integrated into commercial microscope systems since only rotation of excitation polarization is needed. We foresee it to trigger interests of a large community who desire simultaneous thermal characterization along with the optical imaging. Moreover, it brings out a general idea to simplify ratiometric setups if inequalities exist on the excitation side, which may reach for a larger number of researchers.

10353-25, Session 6

Microring resonators for real-time study of antibody interaction

Tatevik Chalyan, Univ. degli Studi di Trento (Italy); Geert A. J. Besselink, Eric Schreuder, Lennart Wevers, Floris H. Falke, René G. Heideman, LioniX BV (Netherlands); Lorenzo Pavesi, Univ. degli Studi di Trento (Italy)

Integrated optical (IO) biosensors based on Mach-Zehnder Interferometers or microring resonators are widely used for food and drug monitoring and protein studies thanks to their properties such as high intrinsic sensitivity, easy integration, miniaturization, low cost [1, 2]. In this study we present a system to perform faster antibody interaction analysis using a photonic chip made of an array of six microring resonators (MRRs) based on TriPleX platform. The input light is generated by a Vertical Cavity Surface Emitting Laser (VCSEL) pigtailed to a single mode fiber operating at 850nm wavelength. The output signal is detected by PIN photodetectors placed in optical signal read-out module (the so-called OSROM) and processed by an easy-to-use Fourier Transform algorithm which optimized to use most of the available data, reducing the noise. Measured bulk sensitivity (Sb =104 ± 0.04 nm/RIU) and Limit of Detection (LOD = 2 ? 10-6 RIU) are very similar for the six MRRs in the same chip [3], which is a good precondition for using proposed system for multianalyte detection.

Analyses of anti-biotin interaction with immobilized biotin by using different concentrations of anti-biotin antibody is performed. Dependence of resonance wavelength shift from antibody concentration, as well as association and dissociation rate constants were calculated. For the average dissociation constant (KD) of anti-biotin antibody toward immobilized biotin, a value of 2.3?10-7 M is achieved, that is in the same order of magnitude with published results in literature [4]. Furthermore, the specificity of the interaction was confirmed by using negative control antibodies. In addition, the functional surface of the sensors could be regenerated up to ten times by using 10 mM glycine/HCl pH 1.5.

References:

1. Chalyan, T, Guider, R., Pasquardini, L., Zanetti, M., Falke, F., Schreuder, E., Heideman, R.G., Pederzolli, C. and Pavesi, L., "Asymmetric Mach-Zehnder Interferometer based biosensors for Aflatoxin M1 detection, " Biosensors 6(1), 1 (2016).

2. Heideman, R.; Hoekman, M. and Schreuder, E., "TriPleX-based integrated optical ring resonators for lab-on-a-chip and environmental detection, " IEEE J. Sel. Top. Quantum Electron., 18, 1583–1596 (2012).

3. Besselink GAJ*, Heideman RG, Schreuder E, Wevers LS, Falke F and Van den Vlekkert HH, "Performance of Arrayed Microring Resonator Sensors with the TriPleX Platform", J Biosens Bioelectron 7:2 (2016).

4. H. Jung, et al., "Impact of hapten presentation on antibody binding at lipid membrane interfaces", Biophys. J. 94 (8) (2008) 3094–3103.

10353-36, Session 6

InP-based platform for sensing using telecom building blocks

François Lelarge, Almae Technologies SAS (France)

In this contribution, we will introduce the Almae-Technologies InP platform proposing processed wafers for DFB and diffused APD wafers. This telecom based 3- and 4-in InP-based PIC platform is using Ebeam, GSMBE and MOCVD production tools for developing DFB lasers with extreme wavelength control. Al-based and Al-free MQWs epiwafers from 1,3μm up to 2μm are available, opening the way to cover most of sensing applications. The Almae-Technologies integration schemes for PIC will be illustrated and discussed.

10353-26, Session 7

Plasmonic bio-sensing based on highly doped semiconductors *(Invited Paper)*

Thierry Taliercio, María José Milla-Rodrigo, Fernando Gonzalez Posada Flores, Mario Bomers, Franziska B. Barho, Eric Tournié, Laurent Cerutti, Institut d'Électronique et des Systèmes (France)

Plasmonics is one of the best suited approaches for bio-sensing. Based on the concept of surface plasmon polaritons, electromagnetic waves strongly coupled to collective oscillation of free carriers, plasmonics offers the possibility to detect and identify the presence of biomolecules at a metal surface. Plasmonics is mainly based on gold but it was recently demonstrated that alternative materials, such as highly doped semiconductors (HDSC), can outperform the plasmonic properties of gold in the mid-infrared spectral range. In this work, we will present surface plasmon resonance (SPR) detection and surface enhanced infrared absorption (SEIRA) spectroscopy obtained on periodic arrays of nano-antennas developed on an InAsSb/GaSb platform. These nano-antennas of Si doped InAsSb alloy are able to sustain localised surface plasmon resonances (LSPR) used in SPR and SEIRA experiments exploiting the strong electric field enhancement appearing at the HDSC surface. Adjusting the carrier concentration in the HDSC by the doping level allows to control the value of the plasma frequency which is linked to the LSPR frequency. The smaller the plasma frequency, the smaller the LSPR frequency. The nano-antennas have been fabricated by optical lithography and wet etching. As expected, when changing the size and the shape of the nano-antennas it is possible to cover a large spectral range and to be sensitive to the polarization of the incident light. Additionally, monitoring the carrier concentration of the InAsSb, make possible to lead up the maximum field enhancement in the targeted spectral range of the biomolecular fingerprints.

10353-27, Session 7

Low-loss dielectric nanoantennas for surface-enhanced spectroscopies and nonlinear photonics *(Invited Paper)*

Gustavo Grinblat, Yi Li, Javier Cambiasso, Toshishiko Shibanuma, Michael P. Nielsen, Emiliano Cortés, Pablo Albella Echave, Aliaksandra Rakovich, Rupert F. Oulton, Stefan A. Maier, Imperial College London (United Kingdom)

The initial excitement about the use of plasmonic nanostructures for the development of nanophotonic devices operating in the optical regime was later partially eclipsed with the observation that losses could, in some cases, overtake actual radiative properties [1]. In this scenario, dielectric nanoantennas have recently emerged as promising alternative candidates to plasmonic systems in the visible range [2]. When excited above their bandgap energies, high-refractive-index dielectric nanostructures can highly concentrate electric and magnetic fields within subwavelength volumes, while presenting ultra-low absorption compared to metals [3]. In particular, by locally enhancing the incident light intensity, dielectric nanoantennas are expected not only to produce negligible heating, but also boost nonlinear phenomena and surface-enhanced spectroscopies, since their efficiencies increase with the excitation density.

In this presentation, Si, Ge, and GaP nanoantennas will be introduced as promising nanosystems for surface-enhanced fluorescence and Raman spectroscopies, as well as for generating efficient second and third harmonic light on the nanoscale at visible wavelengths [2,4-7]. It will be shown that their associated temperature increase at resonance can be over one order of magnitude lower than that corresponding to metals. At the same time, fluorescence enhancement factors of over 3000 and harmonic conversion efficiencies of nearly 0.01% will be demonstrated for suitably engineered dielectric nanostructures. Finally, hybrid dielectric/metallic nanoantennas will also be analyzed, and, in all cases, comparison will be made with reference plasmonic nanosystems.

[1] Khurgin, J. B. Nat. Nanotech. 2015, 10, 2-6.

[2] Caldarola, M. et al. Nat. Commun. 2015, 6, 7915.

[3] Albella, P. et al. ACS Photonics 2014, 1, 524–529.

[4] Grinblat, G. et al. Nano Lett. 2016, 16, 4635-4640.

[5] Grinblat, G. et al. ACS Nano 2017, DOI: 10.1021/acsnano.6b07568.

[6] Cambiasso, J.; Grinblat, G.; et al. Nano Lett 2017, DOI: 10.1021/acs.nanolett.6b05026.

[7] Shibanuma, T.; Grinblat, G.; et al. Submitted, 2017.

10353-28, Session 7

Surface plasmon enhanced FRET

Jennifer M. Steele, Chae Ramnarace, William Farner, Trinity Univ. (United States)

We demonstrate enhanced fluorescence from Förster Resonance Energy Transfer (FRET) paired fluorescent molecules on a single metal enhanced fluorescence (MEF) substrate. MEF substrates support two mechanisms of enhancement via surface plasmons (SPs). In the first mechanism, if the absorption spectrum of the fluorophore overlaps a SP wavelengths, the excitation of the fluorophore is increased from the enhanced electromagnetic field from the SP. Second, when in the excited state, the fluorophore can relax back to the ground state by exciting a SP instead of emitting a photon. This increases the number of decay channels available to the fluorophore, decreasing the lifetime of the excited state, and therefore increasing the quantum yield. Previous work has shown that the second mechanism dominates the enhancement.

For grating structures, the periodicity allows for a broad range of SP wavelengths following a dispersion relationship. This is in contrast to nanoparticles, which have a narrow range of SP wavelengths available. Here, gold wire nanogratings with a period of 500 nm were fabricated as the MEF substrate, ensuring SP modes throughout the visible spectrum. We used Atto 532 and Atto 633 as the donor and acceptor FRET molecules respectively. A thin layer of PVA containing different concentrations of the donor and acceptor FRET molecules was spin coated onto the gratings. The donor molecules were excited with a 532nm laser, and the fluorescence emission from both the donor and acceptor molecules were recorded. We found that the enhancement was consistent over all concentration combinations of donor and acceptor molecules.

10353-29, Session 7

Hydrogel-integrated plasmonic nanostructures on optical fiber facet for remote and real-time pH sensing

Shijie LI, Wen-Di LI, The Univ. of Hong Kong (Hong Kong, China)

Plasmonic optical fiber probes have particular merits to be in vivo sensors. Besides its excellent biocompatibility, it also has small cross-section size and is capable of remote sensing. By integrating pH-responsive hydrogel on the probes, human body pH value can be monitored in real-time, which is helpful for diagnosis of diseases such as stomach disorder and Gastroesophageal reflux.

In this work, we use double-transfer ultraviolet nanoimprint lithography (UV-NIL) to transfer metallic nanostructures from a polymer mold to the facet of the optical fiber with 200 ?m core diameter. Once a polymer mold carrying nanopillar array is fabricated by thermal embossing, a thin layer of gold is deposited on it by thermal evaporation. Then the metallic nanostructure is transferred onto fiber facet by the cross-linked UV-cured resist. The transferred metallic nanostructures feature closely spaced double layers of disks and holes. The electric field is enhanced in between the metal disk and hole and generates resonantly enhanced local electrical field as revealed by peaks/dips in reflection spectra.

By dipping the plasmonic fiber probe into hydrogel precursor, a small amount of hydrogel is cross-linked on fiber facet with 365nm UV light exposure through the fiber. Hydrogel shrinks in acid and swells in basic solutions by containing different amount of water and thus has a different refractive index. Resonant reflection peaks/dips of plasmonic fiber probe were responsive to refractive index changes. Our hydrogel fiber probe shows obvious spectrum response to solutions with pH values ranging from 1 to 8. And when hydrogel fiber probe is under cycling test its spectrum response remains stable for three cycles when switching between acid and basic solutions. pH sensing was performed with fixed ionic strength, and hydrogel fiber probe's response to ionic strength was also investigated.

10353-30, Session 7

Nanostructured diodes for the infrared detection through two photons absorption

Baptiste Fix, Julien Jaeck, ONERA (France); Benjamin Vest, Lab. Charles Fabry (France); Jean-Luc Pelouard, Ctr. de Nanosciences et de Nanotechnologies (France); Riad Haïdar, ONERA (France)

Two-photon absorption (TPA) in semiconductors has drawn much interest in the past 20 years, as it allows photo-current generation by absorption of sub-band-gap photons pairs. In particular it can be an alternative scheme of infrared detection, where mid-wave IR signal photons and pump photons of smaller wavelength are simultaneously absorbed in a wide band gap semiconductor, reducing the need for cryogenic cooling.

Such applications are currently limited by the low efficiency of TPA processes in conventional photodiodes. To obtain measurable levels of photocurrent we propose to enhance the electrical field in the photodiode with functionalized electrode. In this paper we demonstrate the use of a 1D nanostructure in an InP diode to detect a signal at 3.39µm through non degenerate TPA.

The device consists in a thin Indium Phosphide P-i-N photo-diode with a thickness of 580nm and both p and n-layer thickness of 50nm. The bottom electrode is a plain gold mirror and the top electrode is a grid nanostructure defined by a period of 1780nm, strips width of 700nm, and a thickness of 100nm. It generates a resonance at 3.39µm that amplifies the intensity of the signal wave by 40 as compared to the incident intensity. Using a dedicated experimental bench, we detect a two-photon photo-current with a SNR of 13. The spectral and polarization dependence of the diode reflectivity and photo-current confirm the origin of this photo-current.

Wednesday - Thursday 9 –10 August 2017

Part of Proceedings of SPIE Vol. 10354 Nanoengineering: Fabrication, Properties, Optics, and Devices XIV

10354-500, Session Plen

3D laser nanolithography

Martin Wegener, Karlsruher Institut für Technologie (Germany)

Three-dimensional (3D) laser lithography has become a versatile, reliable, and widespread workhorse for fabricating 3D micro- and nanostructures. I will illustrate the current state-of-the-art by selected examples, including free-form micro-optics, 3D optical and other metamaterials, as well as functionalized 3D scaffolds for biological cell culture. I will speculate about near-term industrial applications and outline remaining technological challenges regarding spatial resolution, scalability, and multi-material 3D nano-printing.

10354-1, Session 1

Large-scale fabrication of LP-CVD Si3N4 photonic crystal structures as freestanding reflectors with 1 mm aperture for Fabry-Pérot interferometers

Christian Helke, Karla Hiller, Technische Univ. Chemnitz (Germany); Marco Meinig, Steffen Kurth, Fraunhofer-Institut für Elektronische Nanosysteme (Germany); Christoph Nowak, Herberth Kleinjans, AMO GmbH (Germany); Thomas Otto, Fraunhofer-Institut für Elektronische Nanosysteme (Germany)

Further development of miniaturized spectrometry systems require tunable Fabry-Pérot-interferometers (FPI). A main part of the FPI is the reflector, which is usually realized as a stack of alternating dielectric layers with high and low refractive index. To achieve high reflectivity adequate material property homogeneity for each layer is needed. For stacks with larger number of layers, the integration with MEMS processes is challenging. Particularly, stack structuring and the achievement of process compatibility to moveable MEMS structures are important.

Alternative to the alternating layer stack reflector, nanostructured photonic crystal (PC) reflectors indicate equivalent performance by using only one layer leading to a minimized reflector complexity.

This contribution presents a novel PC reflector consisting of a 400 nm thin moveable nanostructured LP-CVD Si3N4 PC realizing an aperture of 1 mm for reflectivity in the VIS range. Manufacturing of the reflectors is done on 6" wafers. The array of nanostructures is designed as 1 mm circular dies consisting of 436 nm wide holes with 545 nm pitch. The circular dies are arranged in an 8x8 matrix with 7.5 mm pitch.

The manufacturing and integration of the PC reflector into MEMS is realized by eBeam lithography and nanoimprint lithography nanostructure replication on 50 µm thin pre-etched silicon membranes combined with further dry and wet etching processes. The fabricated PC reflectors showed 424 nm wide holes and pitch of 549 nm.

The measured reflectivity is above 90 % in the spectral range from 560 to 583 nm with a maximum reflectivity of 97 %.

10354-2, Session 1

Actuated polymer based dielectric mirror for visual spectral range applications

Pedro Pablo Vergara Gonzalez, Leda Lunardi, North Carolina State Univ. (United States)

Miniature dielectric mirrors are useful components for lasers, thin film beam splitters and high quality mirrors in optics. These mirrors usually made from rigid inorganic materials can achieve a reflectance of almost one hundred percent. Being structural components, as soon as fabricated their reflectance and/or bandwidth remains constant. Here it is presented a novel fabrication process of a dielectric mirror based on free standing polymer layers. By applying an electrostatic force between the top and the bottom layers the reflectance can be changed. The large difference between the polymers refractive index and the air allows to achieve a reflectance of more than 85% using only six pairs of nanolayers. Preliminary simulations indicate an actuation speed of less than 1ms. Experimental optical characterization of fabricated structures agrees well with simulation results. Furthermore, structures can be designed to reflect a particular set of colors and/or isolated by using color filters, so a color pixel is fabricated, where the reflectance for each isolated color can be voltage controlled. Potential applications include an active component in a reflective screen display.

10354-3, Session 1

Highly sensitive tunable room temperature infrared hybrid organic-nanocrystals detector

Avner Neubauer, Shira Yochelis, Yossi Paltiel, The Hebrew Univ. of Jerusalem (Israel)

The integration of nanostructures in electronic devices utilize their unique advantages of quantum properties for future discrete measuring systems. Using self-assembled organic monolayers with nano-crystals (NCs), together with bottom up components was proven as appropriate approach for future electronic devices. In our work, we present a wavelength tunable near-infrared detector device based on NCs acting as an optical gate on top of a high-mobility shallow two-dimensional electron gas channel.(1) By using shallow and very narrow channel, the device's quantum efficiency can go as high as 10^6V/W at room temperature, with a signal-to-noise ratio (SNR) that enables sensitivity for very low photon power.(2) Further improvement of light detection is achieved by applying horizontal electrical field resulting narrower the conductive channel. This approach, enhance the detector response and the SNR at different operation conditions. In addition, a new concept of AC electrical field modulation will be presented and compared to DC measurements by analyzing response, SNR and noise behavior. We find that our experimental results are compatible with simulation. Lastly, expanding to a non-binary logical device is achievable due to the detector wavelength tunability.

1. Neubauer, A. et al. J. Phys. Chem. C 116, 15641–15645 (2012).

2. Neubauer, A. et al. Sens. Actuators Phys. 229, 166–171 (2015).

10354-4, Session 1

Pixel-sized guided-mode resonance filters for multispectral infrared focal plane arrays

Antoine Bierret, ONERA (France) and Ctr. de Nanosciences et de Nanotechnologies (France); Grégory Vincent, ONERA (France); Fabrice Pardo, Lab. de

Photonique et de Nanostructures (France); Jean-Luc Pelouard, Ctr. de Nanosciences et de Nanotechnologies (France); Riad Haïdar, ONERA (France)

Multispectral imaging of an infrared scene allows better identification of objects and materials. Numerous strategies can be implemented, involving for example Fourier transform or multichannels optical architectures. Another strategy, which simplifies the conception of snapshot imagers, is the "colorization" of infrared pixels thanks to the integration of filters in the vicinity of the detectors. The most common filters at pixel-level in the infrared are interferential filters, such as multilayer Bragg filters and Fabry-Perot filters. Fabrication process becomes complicated when numerous spectral bands are required, because filters are made of numerous thick dielectric layers. Furthermore, edge-effects restrict the minimal accessible size and lead to photon loss.

In our contribution, we present the use of nanostructured spectral filters at pixel level for MWIR focal plane arrays, with 15µm x15µm sized pixel. In the case of an imaging optical system, we must investigate the response of the filters to various incidence angles at pixel level. We thus lead numerical simulations on nanostructured filters under focused beams. We report the optical and spectral properties of these filters, highlighting the crucial issue of the angular acceptance, and describe the fabrication process. Finally, we examine the features of a mosaic of such filters and address the issue of the crosstalk.

10354-5, Session 1

Slotted photonic crystal nanobeams for enhanced light-matter interaction and optical forces

Francis Afzal, Sharon M. Weiss, Vanderbilt Univ. (United States)

Enhancement of light-matter interaction is key for achieving higher efficiency and lower threshold power in optical signal processing, photovoltaics, optical sensing and optical trapping. An important metric for light-matter interaction is the ratio of the quality factor (Q) to the mode volume (V). Resonant photonic structures typically have Q/V metrics of order 10^5 - 10^6. By utilizing deterministic design to taper the cavity defect in a continuously slotted photonic crystal nanobeam, our calculations suggest that metrics of Q > 10^6 and V ~ 0.02 (?/n)^3 can be readily achieved in a one-dimensional photonic crystal structure. Furthermore, the enhanced light-matter interaction in this high Q/V platform can be used to amplify optical forces and efficiently couple the optical cavity to mechanical modes of the physical device. The optomechanical coupling coefficient, g = ∂?/∂x, is numerically calculated to be > 400 GHz/nm. The designed slotted photonic crystal nanobeams are fabricated by electron beam lithography and reactive ion etching, and then undercut using buffered oxide etch. Both in-line and side-coupled configurations of the slotted photonic crystal nanobeams are measured. Comparisons in the tradeoff between the loaded Q and device footprint will be discussed: in general, side-coupling enables the measurement of a higher Q but requires more real estate on chip. Loaded quality factors of order 10^4 have been measured. Due to the high Q/V and large optomechanical coupling coefficient of the slotted nanobeams, slight fabrication deviations can dramatically affect the cavity optical and mechanical properties, as will be discussed in detail.

10354-6, Session 1

Color-selective and versatile light steering structure designed for up-scalable fabrication

Giorgio Quaranta, Guillaume Basset, Benjamin Gallinet, Ctr. Suisse d'Electronique et de Microtechnique SA (Switzerland); Olivier J. F. Martin, Ecole Polytechnique Fédérale de Lausanne (Switzerland)

In planar optics, beam steering techniques is a widely used technique to create specific phase and amplitude profiles by micro and nano-structuring surfaces. Nevertheless, the integration of beam steering structures in a user-friendly device for visible light is still challenging, due to the intrinsic optical response and the low throughput fabrication. Here we present a new thin-film single-layer device that allows selectively color-filtering and beam steering, compatible with up-scalable fabrication processes such as roll-to-roll replication and therefore relevant for high-volume production. The structure works in any part of the visible spectrum and can steer white light from low coherent source without need of any filter or polarizer. Furthermore, it versatilely works in both reflection and transmission.

In particular, the unit cell consist of two adjacent finite-length and cross-talking resonant waveguide gratings (RWGs). Their guided wave allows a stronger color-selectivity with respect to the localized energy of a standard resonator due to the leaky propagation and accumulation in the RWGs. It is possible to steer the light in any desired direction by engineering particular pairs of impedance-matched RWGs, where the former acts as in-coupler and the latter acts as out-coupler. Finally, the structure is made by only one nano-imprint lithography replication and one thin-film layer deposition. Functional proof-of-concepts will be presented with complex patterns to provide optical security features for smartphone authentication.

Widespread applications are foreseen in a variety of fields, such as multifocal or monochromatic lenses, solar cells, biosensors, security devices and see-through optical combiners for near-eye displays.

10354-7, Session 2

Novel Light Effect Transistors (LET) based on hybrid Coupled Organic-Inorganic Nanostructures (COINs)

Kai Braun, Alexander Andre, Marcus Scheele, Alfred J. Meixner, Eberhard Karls Univ. Tübingen (Germany)

Since the last decades, various different types of Field Effect Transistors (FET) have been developed. Later developments focused on 2D Materials as active layers. One promising candidate is based on coupled organic inorganic nanostructures (COINs) [1] which are formed by quantum dots linked by numerous different molecules e.g. Phthalocyanines. Consequently the COINs show also interesting optical properties and distinct absorption maxima in the visible range, which allow the construction of so called Light Effect Transistors (LET). Such a device works similar to a FET but instead of a gate voltage, light illumination is used to modulate the current flow. To characterize the LETs we use confocal microscopy and spectroscopy with different laser wavelengths (633, 488, 532 nm) and measured the currents across the source drain junction as a function to the illumination power. On gold, the luminescence of the COIN monolayer is quenched and the electrodes appear dark, while on glass a weak signal is detected. We assume that the very low quantum efficiency of the optically excited states on glass is due to efficient charge carrier separation inside the COIN monolayer. Furthermore we measured drain current vs. drain-to-source voltage under illumination, were the devices show a clear linear regime with ohmic behavior. Since the absorption resonances have diverse strengths' for different wavelength each color could be used as single gate and allow for a multi-gate device on a single chip.

[1] M. Scheele et al ACS Nano 2014 8 (3), 2532-2540

10354-8, Session 2

Capacitive-based adiabatic logic

Yann Perrin, Gaël Pillonnet, CEA-LETI (France)

The Field-Effect Transistor (FET) might not be the adequate technology for improving the energy-efficiency of logic devices. Nowadays, the lowest dissipation per operation is 6 to 10 decades higher than the theoretical limit predicted by Landauer [1]. Although this fundamental limitation is still discussed, there is room for decreasing the energy dissipation inherent to any logic operation. For this purpose, adiabatic computing based on FET has been introduced [2]. It consists of using slow transitions between logic

states. The charge and discharge of the capacitance of the FET gate through the resistance of the FET channel then become slower. Therefore, the energy dissipation decreases proportionally to the driving ramp duration. However, leakage and threshold voltage inherent to FET limit the energy saving to only one decade, compared to conventional FET circuits.

In this contribution, we introduce a new paradigm to implement logic gates. Instead of FET transistors, we use MEMS capacitors with a capacitance strongly influenced by its own polarization voltage. Each MEMS capacitor forms a building-block of a logic gate. This new type of logic is able to discriminate logic states by modulating capacitances values. In order to save energy, we use adiabatic transitions. We show how MEMS building-blocks can be cascaded and assembled, in order to form a logic capacitive unit. We describe the logic operation at the gate-level. We then focus on the energy transfer inside and between capacitors, during adiabatic charging and discharging phases. We finally suggest different MEMS devices suitable for adiabatic logic applications.

[1] P. Teichmann, "Adiabatic Logic: Future Trend and System Level Perspective," Springer, Berlin, Germany, 2012.

[2] G. Snider et al., "Minimum energy for computation, theory vs. experiment," IEEE Conf. Nanotechnology, pp. 478–481, Aug. 2011

10354-9, Session 2

Nanoimprinting optical fibers

Peipei Jia, The Univ. of Adelaide (Australia); Depeng Kong, Xi'an Institute of Optics and Precision Mechanics, CAS (China); Heike Ebendorff-Heidepriem, The Univ. of Adelaide (Australia)

Nanoimprinting has been applied on optical fiber tips to generate various nanostructures. In these techniques, additional layers are required to act as imprinting targets. However it is difficult to coat a thin layer on the micro-size fiber facets. Moreover these host layers might exfoliate in some harsh cases. Here, we develop a nanoimprint technique to directly pattern optical fiber facets without host layers. With this one-step method, nanohole arrays and nanoslit arrays can be imprinted into the plastic optical fiber end faces. These structures have high surface quality and uniformity due to the nature of replication. After metallization, these arrays are transformed to be functional devices such as plasmonic sensors and polarizers. Besides the depth of nanostructures can be adjusted by varying the imprinting pressure. Accordingly, their optical properties can be modulated through such topographic changes with one imprinting mold.

10354-10, Session 2

Development of highly sensitive holographic devices for metal ion detection

Sabad E. Gul, Suzanne Martin, John Cassidy, Izabela Naydenova, Dublin Institute of Technology (Ireland)

There is an urgent requirement for inexpensive mass producible clinical diagnostic devices that allow measurements on site. Biosensors are important tools in biomedical research. They are becoming an essential part of modern healthcare. The development of selective alkali metal ions sensors in particular is a subject of significant interest.

The research efforts in this area aim to increase sensitivity, reduce sample size, lower operating costs and make single-use disposable devices and improve portability. In this respect, the level of blood electrolytes, particularly H+, Na+, K+ and Cl- , is widely used to monitor aberrant physiologies associated with pulmonary emphysema, acute and chronic renal failure, heart failure, diabetes. Particularly K+ ions analysis attracts great attention due to interference from high concentrations of Na+ in blood.

The sensors reported in this paper are created by holographic recording of surface relief structures in a self-processing photopolymer material. The structures are functionalized by ionophores dibenzo-18-crown-6 and tetraethyl p-tert-butylcalix [4] in plasticised polyvinyl chloride. Interrogation of these structures by light allows indirect measurements of chemical analytes' concentration in real time. We present results on the optimisation and testing of the holographic sensor. Self-processing acrylamide-based photopolymer was used to fabricate the required photonic structures. The performance of the sensors for detection of K+ and Na+ was investigated. It was observed that the functionalisation with dibenzo-18-crown-6 provides a selective response of the devices to K+ over Na+. The sensor responds to K+ within the physiological ranges.

10354-11, Session 2

Pressure measurement using "photo-piezoelectric" effect: new MEMS design

Boris Oskolkov, Saint-Petersburg State Univ. of Aerospace Instrumentation (Russian Federation)

This work - a continuation of the previous one, which had shown perspective photovoltaic effects. In this paper we will explore one of the effects, namely "photopiezoelectric effect".

The effect begins to occur when compressed a doped semiconductor (silicon, for example) illuminated by light.

As a result of the new design of the sensor from the doped silicon is created and researched. Different designs and some of them will be most effective in measuring pressure are shown.

Own laboratory setup was collected. The laboratory setup consists of a sample, adjustable pressure screws, lamps illuminating the sample and the amplifier, from which readings are taken.

Such sensors will be in demand due to its low cost in the automotive industry, instrument making, in IoT systems in the field of portable electronics and so on.

10354-13, Session 3

Scalable maskless patterning of nanostructures using high-speed scanning electrical probe arrays

Chen Chen, Zhidong Du, Liang Pan, Purdue Univ. (United States)

Nanoscale patterning is the key process to manufacture important semiconductor products such as microprocessors and data storage devices. Many studies have shown that it has the potential to revolutionize the functions of a broad range of products for a wide variety of applications in energy, healthcare, civil, defense and security. However, tools for mass production of these devices usually cost tens of million dollars each and are only affordable to the established semiconductor industry. In this paper, we report a method, nominally known as "pattern-on-the-fly", that involves scanning an array of electrical probes at high speed to form nanostructures and offers a new low-cost approach for nanoscale additive patterning. Using this method, we show that silicon lines as thin as 25 nm using diphenylsilane as precursor molecules can be directly written on a silicon substrate coated with a self-assembled monolayer of phenethyltrichlorosilane (PETS). In addition, we propose a possible reaction pathway of the electro-chemical process and build up a multiphysics model in the commercial software COMSOL to study the corresponding reaction rates. The demonstrated results reveal the scalability potential of this maskless patterning method, which enables it to become a strong candidate for the next generation nano-manufacturing.

10354-14, Session 3

Self-catalyzed patterned growth of GaAs(Sb), GaAsSbN nanowires by molecular beam epitaxy

Manish Sharma, Joint School of Nanoscience and Nanoengineering (United States); Pavan K. Kasanaboina, North Carolina A&T State Univ. (United States); Md Rezaul Karim, Joint School of Nanoscience and Nanoengineering (United States); Shanthi Iyer, North Carolina A&T State Univ. (United States)

Nanowire (NW)-based optical devices have been enticing great interest due to its ability to enhance entrapment of light inside nanowire array and better strain accommodation due to its small footprint on the substrate. To achieve large scale homogeneous NW arrays with consistent device performance, it is important to have precise control in positioning, size and the alignment of the nanowires, in addition to high quality and compositional uniformity. The active sites on the silicon substrate for NWs growths are created by electron beam lithography. There have been numerous reports on patterned GaAs NWs [1, 2], with the primary focus on the growth parameters namely, Ga pre-deposition and V/III flux ratio to improve pattern coverage. In this work, the emphasis is on the effect of processing conditions along with growth parameters and their inter-dependency on the yield of self-assisted growth of vertical nanowires GaAs, using molecular beam epitaxy on patterned Si (111) substrate for different pitch size. The optimized processing condition for GaAs NW growths was then extended to the growth of patterned GaAsSb axial and GaAs/GaAsSb core-shell NWs. Further fine tuning of these parameters led to >90 % occupancy of patterned holes with nanowires. The observed pitch dependent optical absorption for NW array was correlated using, finite difference time domain (FDTD) simulation with wavelengths in the range of 400-1200 nm using Lumerical FDTD Solution software. The introduction of the dilute amount of N in the GaAsSb NWs on the patterning of the NW will also be presented.

Acknowledgment: This work is partially supported by the Army Research Office (Grant No. W911NF-15-1-0160), National Science Foundation (Grant No. 1649517) and the Office of Naval Research (Grant No. N00014?16?1?2720).

References

[1] S. Plissard, G.Larrieu, X. Wallart and P. Caroff, Nanotechnology, vol. 22, p. 2750602, 2011.

[2] S. J. Gibson, J. Boulanger and R. R. LaPierre, Semiconductor Science Technology, vol. 28, p. 105025, 2013.

10354-15, Session 3

Innovative patterning method for modifying few-layer MoS2 device geometries

Fernando Jiménez Urbanos, Andrés Black, IMDEA Nanoscience (Spain); Ramón Bernardo Gavito, Lancaster Univ. (United Kingdom); Manuel R. Osorio, Santiago Casado, Daniel Granados, IMDEA Nanoscience (Spain)

Mono-Layer and few-layer Tansition Metal Dichalcogenides (TMDCs) have attracted great interest since the discovery of graphene due to their oustanding properties. Semiconducting 2D Molybdenum Disulfide (MoS2) is considered a good candidate for opto-electronic applications due to its remarkable electrical and optical properties. However when mechanically exfoliated, these properties strongly depend on the geometry and number of layers present in the flake. In general, these properties cannot be modified once a device is fabricated out of an exfoliated flake. In this work we present a novel nano-patterning method for 2D material based devices, Pulsed eBeam Gas Assited Patterning (PEBGAP), that allows us to fine tune their properties once the device fabrication steps have been completed. This post-processing technique allows us to modify the channel geometry or thickness of MoS2 FETs.

PEBGAP post-processing technique is based on using a scanning electron microscope equiped with a gas injection system, and employing XeF2 as an etching agent. The etchant gas enters the chamber through a small nozzle situated in close proximity to the desired device, adsorbing locally on the substrate. The focused electron beam is then scanned and pulsed over the device to etch away the desired geometry onto the MoS2 flake.

Field effect devices were fabricated from mechanically exfoliated few-layer MoS2 flakes via optical beam lithography followed by a metal evaporation and lift-off process to define the gate-contact structures. The devices were characterised employing μ-Raman mapping spectroscopy, transport measurements and AFM/SEM microscopy. Afterwards, PEBGAP was utilized to alter device geometries and performance.

10354-16, Session 4

Update on bio-refining and nanocellulose composite materials manufacturing *(Invited Paper)*

Michael T. Postek, Dianne L. Poster, National Institute of Standards and Technology (United States)

Nanocellulose is a high value material that has gained increasing attention because of its high strength, stiffness, unique photonic and piezoelectric properties, high stability and uniform structure. One of the factors limiting the potential of nanocellulose and the vast array of potential new products is the ability to produce production quantities of this nano-material. However, recent research has demonstrated that nanocellulose can be produced in large volumes from wood at relatively low cost via ionizing radiation processing. Ionizing radiation causes significant break down of the polysaccharide and leads to the production of potentially useful gaseous products such as H2 and CO. Ionizing radiation processing remains an open field, ripe for innovation and application. This presentation will review the strong joint collaboration between NIST and its academic partners pursuing the demonstration of applied ionizing radiation processing to plant materials for the manufacturing and characterization of novel nanomaterials.

10354-17, Session 4

All dielectric metasurface nano-fabrication based on TiO2 phase shifters

Jeong Yub Lee, Jae Kwan Kim, Kiyeon Yang, Byonggwon Song, Yongsung Kim, Chang Seung Lee, Samsung Advanced Institute of Technology (Korea, Republic of)

Recently, various optical elements at infrared ranges have been developed using silicon and plasmonic metasurfaces. However, optical loss of silicon dielectric or plasmonic nanostructures restricts realization of highly efficient metasurfaces in visible wavelengths (400nm-700nm).

In this study, all dielectric metasurface of low loss TiO2 in visible wavelength was devised forming subwavelength-scale nanostructures. Because crystalline anataze-TiO2 layer has a rough surface of 11nm Ra, amorphous phase of TiO2 is essential to fabricate nano-scale patterns by reducing surface roughness to 1.35nm Ra. Compared to DC reactive sputtering by Ti target materials resulting anataze-TiO2 for all the process ranges and RF sputtering of low deposition rate (5nm/min, 1kW power), DC magnetron sputtering of oxygen-reduced conductive TiOx (x=1.67) target with reactive oxygen gas has advantages of amorphous phase formation and high rate deposition (21nm/min, 1kW power), therefore makes dense amorphous TiO2 thin films. We investigated density variations of TiO2 according to oxygen gas contents for high refractive index, and stoichiometric composition control of TiO2 for loss reduction. A 380 nm-thick TiO2 thin film was obtained having low extinction coefficient (k) under 1x10-5 and transparency of 98.33% as well as high refractive index (n) of 2.55 at 485nm wavelength. Highly precise patterning was performed for TiO2 meta-atoms by mass productive ICP-RIE etching, forming nano posts, grating array patterns of 100nm-300 nm size. Phase shift properties at visible wavelength of TiO2

metasurface were matched well with designed value. Finally, we constructed dielectric metaphotonic platform for various optical devices such as band pass filters, flat lens and beam deflectors in visible ranges.

10354-18, Session 4

A nanostructure based on metasurfaces for optical interconnects

Shulang Lin, Huarong Gu, Tsinghua Univ. (China)

Optical-electronic Integrated Neural Co-processor takes vital part in optical neural network, which is mainly realized by optical interconnects. Because of the accuracy requirement and long-term goal of integration, optical interconnects should be effective and pint-size. In traditional solutions of optical interconnects, holography built on crystalloid or law of Fresnel diffraction exploited on zone plate was used. However, holographic method cannot meet the efficiency requirement and zone plate is too bulk to make the optical neural unit miniaturization. Thus, this paper aims to find a way to replace holographic method or zone plate with enough diffraction efficiency and smaller size. Metasurfaces are composed of subwavelength-spaced phase shifters at an interface of medium such as TiO_2. Metasurfaces allow for unprecedented control of light properties. They also have advanced optical technology of enabling versatile functionalities in a planar structure. In this paper, a nanostructure is presented for optical interconnects. The comparisons of light splitting ability and simulated crosstalk between nanostructure and zone plate are also made.

10354-19, Session 4

Nanostructures for commercial approaches

Jae Hong Park, National Nanofab Ctr. (Korea, Republic of)

One of the two main processes of engineering nanostructures is the top down method, which is a direct engineering method for Si-type materials using photolithography or e-beam lithography. The other method is the bottom-up method, using nano-imprinting. However, these methods are very dependent on the equipment used, and have a high process cost. They are also relatively inefficient methods in terms of processing time and energy. Therefore, some researchers have studied the replication of nano-scale patterns via the soft lithographic concept, which is more efficient and requires a lower processing cost. In this study, accurate nanostructures with various aspect ratios are created on several types of materials. A silicon (Si) nanomold is preserved using the method described, and target nanostructures are replicated reversibly and unlimitedly to or from various hard and soft materials. The optimum method of transferring nanostructures on polymeric materials to metallic materials using electroplating technology was also described. Optimal replication and demolding processes for nanostructures with high aspect ratios, which proved the most difficult, were suggested by controlling the surface energy between the functional materials. Relevant numerical studies and analysis were also performed. Our results showed that it was possible to realize accurate nanostructures with high depth aspect ratios of up to 1:20 on lines with widths from 50~500 nm.

In addition, we were able to expand the applicability of the nano structured mold by adopting various backing materials, including a rounded substrate. The application scope was extended further by transferring the nanostructures between different species of materials, including metallic materials as well as an identical species of material. In particular, the methodology suggested in this research provides the great possibility of creating nanostructures composed of various materials, such as soft polymer, hard polymer, and metal, as well as Si. Such nanostructures are required for a vast range of optical and display devices, photonic components, physical devices, energy devices including electrodes of secondary batteries, fuel cells, solar cells, and energy harvesters, biological devices including biochips, biomimetic or biosimilar structured devices, and mechanical devices including micro- or nano-scale sensors and actuators.

10354-20, Session 4

Handling and assembling of low-density foam structures fabricated by two-photon polymerization

Ori Stein, Schafer Corp. (United States); Ying Liu, Univ. of Nebraska-Lincoln (United States)

The handling and assembling of micro-parts are usually considered as a main limitation in the fabrication process of microsystems. To support the research of High-Energy-Density Physics (HEDP), low-density materials (LDM, foams) were designed as a component of complex targets which are comprised of a range of materials (e.g., metals, polymers, glasses, ceramics, cryo-liquids, and gases) in various shapes and morphologies (e.g., capsules, enclosures, films, foams, composites, tubes, supports, etc.). In this work, laser direct writing of 2 mm x 0.25 mm x 0.3 mm (X x Y x Z) foam structures were carried out via two-photon polymerization (TPP) with high precision and submicron resolution. Commercially available TPP system (Photonic Professional GT, Nanoscribe GmbH) and commercially available photoresists (IP series, Nanoscribe GmbH) that are optimized for TPP were used for three-dimensional laser direct writing (LDW). The targets fabricated were then released from glass substrates by etching of a sacrifice layer followed by a subsequent lift-off process. Supercritical extraction and drying with liquid CO_2 were used in the developing and drying processes to minimize the mechanical deformation of components by post process shrinkage, stitching mismatch, bending, buckling and/or shearing. Although the foam's pore size is micron sized, capillary pressure developed within nano-sized cracks in the structure's struts during the drying process may cause the internal collapse of the structures.

Several log-pile configured foam structures were printed and assembled on specially designed holder in order to serve as a target for laser induced shock propagation experiments. The procedure developed for removing, handling, and assembling the printed foams into the final configurations laser targets will be discussed.

10354-21, Session 4

Carbon films on silicon substrates made from polydopamine films at the air/water interface

Hiroya Abe, Tomokazu Matsue, Hiroshi Yabu, Tohoku Univ. (Japan)

Polydopamine (PDA), easily formed by the oxidative polymerization of dopamine, is expected to the material sciences due to its spontaneous adhesion properties to the universal surface. PDA is known to form hollow particles, nanofilms, and fibers with sacrificial templates, such as solid substrates, micelles, and oil droplets in an emulsion, at the solid / liquid (S / L) interface or the liquid / liquid (L / L) interface. It is known that a PDA thin film spontaneously forms at the A / L interface under a non-stirred condition. The films formed twice as quickly as the film formation at the S / L interface.?In this study, we report a method of scooping up the PDA films formed at the A / W interface. And we succeeded in a preparation of a conductive thin film by calcinating of the PDA film. The thin films are expected to applied to new carbon materials.

PDA films were formed at the A / W interface under alkaline and non-stirring conditions, and scooped up on SiO_2 / Si substrate by Langumuir – Blodgett method. From atomic force microscopy, an average thickness of the PDA films was 39.1 ± 1.9 nm. Carbon films can be fabricated by calcinating the PDA films under nitrogen atmosphere at 1000 °C. A conductivity of the calcinated PDA films is 1100 ? / sq. A patterning of calcinated PDA films were fabricated by using masked the SiO_2 / Si substrate with a sacrificial layer before scooping up the films.

10354-37, Session PWed

Design and calibration of a nano dimensional standard

Junjie Wu, Guoqing Ding, Xin Chen, Tao Han, Shanghai Jiao Tong Univ. (China); Yuan Li, Shanghai Institute of Measurement and Testing Technology (China)

A nano dimensional standard named SIMT100 is designed and fabricated. The standard consists of a tracking area, a step height area, a 1D grating area and a 2D grating area. All the structures are fabricated with a height of 100 nm in a 3 ? 3 mm silicon substrate. To calibrate the standard, a white light interference microscope is constructed and integrated to the nano measuring machine (NMM). The height of a 10 µm width step measured by the white light interference (WLI) microscope is 100.2 nm with a standard deviation of 0.41 nm. Due to low lateral resolution of the optical microscope, a metrological atomic force microscope (AFM) is used as an auxiliary tool to measure the 1D and 2D gratings. The period length of the 1D grating evaluated by using the fast Fourier transform (FFT) method is 2999.7 nm with a standard deviation of 0.36 nm. The FFT method is also expended for evaluation of the 2D grating. The calibrated value of 2D grating along the x- and y-axes are 3001.2 and 3000.7 nm with standard deviations of 0.73 and 0.64 nm, respectively. All the measurement results are traceable because the data are recorded by three stabilized laser interferometers embedded in the NMM.

10354-38, Session PWed

Influence of electron interference effects on reflection of electron waves from potential barrier in 2D semiconductor nanostructures

Victor Petrov, Institute of Radio Engineering and Electronics (Russian Federation); Andrey V. Nikitin, Kotel'nikov Institute of Radio Engineering and Electronics of Russian Academy of Sciences (Russian Federation)

The influence of the interference of electron waves in the case of their reflection from potential barrier on the spatial distribution of the density of quantum-mechanical current ej?(x,z) (e – electron charge) in 2D semiconductor nanostructure which is represented by rectangular narrow (x < 0, QW1) and wide (x > 0, QW2) quantum wells (QWs) sequentially oriented along the direction of the propagation of electron wave (x-axis) has been studied theoretically. We investigated behavior of the ej? (x, z) at falling of the electron wave on rectangular semi-infinite potential barrier in height V0 . We have considered a situation when in such a nanostructure at the left, from QW1 the electron wave of unit amplitude with energy ?x < V0 on the barrier in QW2 falls. It has been analytically demonstrated that in case of an electron wave falling along the lower quantum-dimensional subband in QW1 and Ex being less than the energy positions of all the other subbands in QW1 (i.e., the undamped propagation of the wave reflected from the barrier with real quasi-momentum is possible only along this lower subband) ejx(1) (x,z) in QW1 and ejx(2) (x,z) in QW2 are equal to zero. However, if a particle has such the energy that the refection of the wave with real quasi-momenta is possible along more than one subband, then the situation completely changes due to the interference of the reflected waves. In this case the interference leads to an existence of a complicatedly oscillating spatially inhomogeneous distribution ?jx(1)(x,z). Under the barrier ?jx(2) ≠ 0 and its amplitude exponentially dumped at ? ? ∞.

10354-39, Session PWed

Extreme-ultraviolet and electron beam lithography processing using water-developable resist material

Satoshi Takei, Toyama Prefectural Univ. (Japan)

Extreme-ultraviolet (EUV) and electron beam (EB) lithography processing using a resist material has been carried out for the manufacture of advanced application such as semiconductor, MEMS, NEMS, and photomask. This study indicates fundamental progress of developing the high-sensitive and resolution negative type of water-developable resist material using pure water instead of spin coating solvent and alkaline developer. EB and EUV lithography techniques using a new type of inedible biomass-based resist material derived from woody biomass with beta-linked disaccharide unit for environmental affair, safety, easiness of handling, and health of the working people. 80 nm dense line patterning images with exposure dose of 20 ?C/cm2 and CF4 etching selectivity of 1.8 with hardmask layer were provided by specific process conditions.

10354-40, Session PWed

Bi-based Pb-free ceramic multilayer actuators using composite inner electrodes

Jae-Shin Lee, Univ. of Ulsan (Korea, Republic of)

Multilayer ceramic actuators (MLAs) including Nb-doped Bi1/2(Na,K)1/2TiO3 (BNKT:Nb) ceramic layers with electrically conducting AgPd-ABO3 thick films were prepared using tape-casting and screen-printing. The co-firing induced defects in the MLAs were analyzed by examining co-firing induced deflections and microcracks as a function of sintering temperature as well as the composition of the inner electrode. It was found that co-firing induced deflections were significantly relieved by employing AgPd-ABO3 composite layers as inner electrodes instead of pure AgPd via reducing thermal mismatch between the electromechanical and electrode layers. We have successfully fabricated lead-free electrostrictive multilayer actuators with normalized strain Smax/Emax of 350 pm/V. The results are believed to be very promising for lead-free precision actuator applications.

10354-41, Session PWed

Physical and micro-mechanical properties of nanocomposites: iron-copper and iron with carbon nanotubes

Mykola Kyruata, Sergey Revo, Mykola M. Melnichenko, Catherine Ivanenko, Taras Shevchenko National Univ. of Kyiv (Ukraine)

The use of high-energy mechanical-chemical activation of metal powders and mixtures of powders in planetary ball mills opens wide prospects for creation of new nanocomposite materials.

The structure of composite nanomaterials is characterized by the presence of the second phase, the particle size of a few (1-100) nanometers. The properties of the final nanocomposite material depend on the nature of the interaction between the phases and structure of interphase volume fraction which is extremely high.

The nanocomposites possess superior physical and chemical properties due to its structure and can be used in a variety of areas, including electronics manufacturing and new materials, in medicine and in ecology, in the aerospace and automotive industries.

In this work the technique of obtaining and processing of nanocomposite materials in the iron-copper and iron with multi-walled carbon nanotubes is presented. The structure and morphology of the obtained samples of the nanocomposite materials was studied by transmission electron microscopy.

Microhardness was determined by two methods a static method of Vickers and the method of continuous indentation with plotting the load-depth of indentation.

The method allows to obtain uniform distribution of components in volume of the composition, efficient pulverization of agglomerates of multi-walled carbon nanotubes and to optimize the characteristics of the nanocomposite materials.

10354-42, Session PWed

Modularized and water-cooled photo-catalyst cleaning devices for aquaponics based on ultraviolet light-emitting diodes

Henglong Yang, Louis Lung, Yu-Chien Wei, Yi-Bo Huang, Zi-Yu Chen, National Taipei Univ. of Technology (Taiwan); Yu-Yang Chou, National Taipei Univ of Technology (Taiwan)

The feasibility of applying ultraviolet light-emitting diodes (UV-LEDs) as triggering sources of photo-catalyst based on titanium dioxide (TiO2) nano-coating specifically for water-cleaning process in an aquaponics system was designed and proposed. The aquaponics system is a promising eco-environmental system in the future. It integrates aquaculture and hydroponics into a single system to establish an environmental-friendly and lower-cost method for farming fish and vegetable all together in a modern building. The uniqueness of aquaponics system is that water circulated from the fish tank can also be nutritious for vegetable. Proper water treatments are still required in this system to avoid mutual contamination. One of the critical treatments is to remove organic contaminant. Traditionally it can be done by UV tubes with proper coating. However, this approach consumes higher energy with relatively lower treatment efficiency. We proposed an electro-optical device benefited from photo-catalyst effect triggered by UV-LEDs on TiO2 nano-coating. This modularized and water-cooled device consists of two hollowed cylindrical pipes to form a coaxial structure. The LED module equipped with UV-LED arrays on outer surface and water-cooling mechanism on inner surface. The nano-coating module is on the external transparent pipe coated by TiO2. As the device submerges in circulating water, the coaxial structure allows UV radially emitted from LED arrays on internal pipe can efficiently reach the TiO2 coating on outer surface to trigger photo-catalyst effect for water treatment. The quantitative analysis will be conducted by analyzing the quantity of organic dye decomposed by photo-catalyst effect as the function of time.

10354-44, Session PWed

A study on high sensitivity planar waveguide Bragg grating sensor on Fabry-Perot cavity

Junhan Park, Sang-Mae Lee, Bo-Sung Shin, DanHee Yun, Gyeong Ju Je, Pusan National Univ. (Korea, Republic of)

Two types of evanescent field-based refractive index sensor having a Fabry-Perot(FP) cavity between dual bragg grating were fabricated and spectra of light reflected from bragg grating were measured.

One of sensor is embedded structure polymeric sensor and the other is rib structure SOI sensor.

To fabricate polymeric waveguide, we used ZPU 13-436(n=1.436 at 1550nm, Chemoptics, Korea) as clad and ZPU 12-480(n=1.480 at 1550nm, Chemoptics, Korea) as core.

Waveguide having 8um width was fabricated by photolithography and bragg grating on core layer was fabricated by two-beam interference lithography. Also, SOI sensor was fabricated by e-beam lithography. The period of the bragg grating was designed to be 528 nm and 226nm for polymeric and SOI sensor respectively, so that the Bragg wavelength of the Bragg grating should be obtained to be around 1550 nm.

When refractive index of the surrounding medium on the bio-sensitive area is changed, Bragg wavelength is changed by change of effective index of effective optical length.

To measure sensitivity of sensors, water, isopropyl alcohol was dropped on cavity between the two Bragg gratings and bragg wavelength shift measured. And, to confirm sensor can be used to biosensing, biotin was held on cavity and attenuated streptavidin was dropped on biotin to measure bragg wavelength shift by change of refractive index from biotin-streptavidin reaction.

10354-45, Session PWed

Octopus-frog inspired programmable hierarchical architectures for skin patches and medical applications

Da Wan Kim, Sang Yul Baik, Changhyun Pang, Sungkyunkwan Univ. (Korea, Republic of)

Nanoscale observation of attachment systems of animals has revealed various exquisite multiscale architectures for essential functions such as gecko's locomotion, beetles' wing fixation, octopuses' sucking and crawling. In particular, the hierarchical 3-dimensional hexagonal architectures in the tree frog's adhesion is known to have the capability of the enhancement of adhesion forces on the wet or rough surfaces due to the conformal contacts against rough surfaces and water-drainable micro channels. Here, we report that octopus-frog inspired patches using octopus sucker-like 3-dimensional nanostructures on unique artificial 3-dimensional hierarchical hexagonal structures can be exploited to form reversibly enhanced adhesion and peeling off energy against various highly curved and rough surfaces in dry and wet condition. To investigate the adhesion effect of micro-channels, we changed the arrangement of microstructure and spacing gaps between micro-channels. In addition, we introduced the 3-dimensional hexagonal hierarchical architectures to artificial patches to enhance to conformal contacts on the various rough surfaces such as skin and organs. Using the robust adhesion properties, we demonstrated the self-drainable and comfortable skin-attachable devices. As a result, bio-inspired hierarchical architectures can be applied in versatile devices such as, medical patches, skin-attachable electronics etc., which would shed light on future smart, directional and reversible adhesion systems.

10354-46, Session PWed

Meniscus-controllable hierarchical architectures for wet and dry adhesion

Sang Yul Baik, Jiwon Kim, Ui Dam Jung, Changhyun Pang, Sungkyunkwan Univ. (Korea, Republic of)

Adhesion strategies that rely on mechanical interlocking or molecular attractions between surfaces and interface can suffer when coming into contact with liquids. To improve wet and dry adhesion, some approaches have been investigated, including the employment of hierarchical structures, supramolecular structures, and catechol chemistries. In this work, we present reversible wet and dry adhesion system having meniscus-controllable hierarchical architectures inspired by dome-like protuberances found in the suckers of octopi. Based on a simple model, the doom-like structures in artificial suction-cup can be controllable by changing various parameters such as the applied pressure, curing-time, and surface properties of a patterned mould during the processes. As a result, our bio-inspired programmable architectures can be applied in versatile devices such as medical patches, skin-attachable electronics, micro-robots, which would shed light on future smart, directional and reversible adhesion systems in various wet and dry rough surfaces.

10354-47, Session PWed

High resolution patterning of ultraviolet cross-linked resins using gas permeable mold derived from cellulose in nanoimprint lithography

Shinya Nakajima, Satoshi Takei, Makoto Hanabata, Toyama Prefectural Univ. (Japan); Naoto Sugino, Takao Kameda, Sanko Gosei Ltd. (Japan); Yoko Matsumoto, Atsushi Sekiguchi, Litho Tech Japan Co., Ltd. (Japan)

A cellulose-based gas permeable mold having thermal crosslinking group for nanoimprint lithography has been developed to prevent transcriptional defects by volatile solvents from nanoimprinting materials. 3 wt.% of thermal initiator was required for producing the cellulose-based gas permeable mold. The void on 10 μm line structure of imprinted UV cross-linked resin with acetone as volatile solvents in nanoimprint lithography process using non-gas permeable mold was significantly removed using the cellulose-based gas permeable mold due to its high oxygen gas permeability. The cellulose-based gas permeable mold allows the employment of solvent including imprinting materials such as compounds and alloy particle.

10354-48, Session PWed

High resolution optical system for the magnetic characterization of thin films by longitudinal magneto-optic Kerr effect

Iulian Ionita, Mircea Bulinski, Univ. of Bucharest (Romania); Victor Kuncser, National Institute for Materials Physics (Romania)

We report about development of a high resolution scanning magnetometer based on longitudinal magneto-optic Kerr effect (MOKE). Due to the high sensitivity to the skin region magnetization MOKE is already well established technique to study magnetization properties of nano-layers. Longitudinal MOKE was found to be the most sensitive in order to measure a small rotation angle of polarization as happens in nano-layers. Due to the miniaturization race of devices the magnetic domains become smaller and smaller (micron range) and their characterization is a real challenge for optical system of the magnetometer that is near the diffraction limit.

We describe the performances required to the optical system and solutions we have found to overpass the contradictions. It is about lateral resolution, numerical aperture, working distance, spectral range, keeping a high degree of polarization, and the signal to noise ratio of entire measurement system (light source, optics, detector, amplifier). Another challenging feature of the system is the sample scanning capability in order to obtain a map of its magnetization.

Our main objective is to build a reliable and performant device with a submicron lateral resolution that will become a powerful tool for magnetic characterization of thin films and multilayers.

10354-49, Session PWed

The challenge of screen printed Ag metallization on nano-scale poly-silicon passivated contacts for silicon solar cells

Lin Jiang, Heraeus Inc. (United States)

Passivated contacts can be used to reduce metal-induced recombination for higher energy conversion efficiency for silicon solar cells, and are obtained increasingly attention by PV industries in recent years. The reported thickness of passivated contact layers are mostly within tens of nanometer range, and the corresponding metallization method are realized by plating/evaporation technology majorly. This high cost of metallization can't compete with screen printing technology, and may affect its market potential compared to present dominant solar cell technology. Very few work has been reported on screen printing metallization on passivated contact solar cells. Hence, there is a rising demand to realize screen printing metallization technology on this topic. In this work, we investigate modifications of screen printing metallization paste on various thickness of poly-silicon passivated contacts. The critical challenge for us is to build low contact resistance competitive to standard technology and meanwhile restrict the paste penetration within the thin nano-scale passivated contact layers. The contact resistivity of 1.1mohm-cm2 and open circuit voltages > 660mV are achieved, and the most appropriate thickness range is found around 50-100nm.

10354-50, Session PWed

Temperature dependency of mechanical properties for crystalline cellulose added to silicone elastomer

Takao Kameda, Naoto Sugino, Sanko Gosei Ltd. (Japan); Makoto Hanabata, Satoshi Takei, Toyama Prefectural Univ. (Japan)

In recent years, development has been actively conducted targeting electronic devices such as solar cells, antennas, and conductive films using cellulose nanofibers. In the parts for the car, the development of the electronic device is prosperous.??In case of the car, as a change of the atmosphere temperature is large, it is demanded that the stable properties of material with a widespread temperature change.

In this study, crystalline cellulose (hydroxypropyl cellulose; HPC) is mixed with silicone elastomer . We have obtained elastic material. In order to obtain high modulus of the composite material, the nanofibers is added in matrix material. The shear elasticity modulus of a provided sample was 2 (MPa) at room temperature. The shear elasticity modulus did not change from a room temperature to 140 (deg. C). The elasticity modulus of the sample fell to half when we increased to 200 (deg. C).

10354-51, Session PWed

Temperature dependence of viscoelasticity of crystalline cellulose with different molecular weights added to silicone elastomer

Naoto Sugino, Takao Kameda, Sanko Gosei Ltd. (Japan); Satoshi Takei, Makoto Hanabata, Toyama Prefectural Univ. (Japan)

There are many reports that cellulose is mixed with resin and used as a composite material.

It is expected that these composite materials will be used as parts for automobiles (exterior / interior parts to engine peripheral parts) as a substitute for metals.

Therefore, in this study, crystalline cellulose (hydroxypropyl cellulose; HPC) with different viscosity is mixed with silicone elastomer with good flowability, the temperature dependence of the elastic modulus was investigated.

As a result, the storage modulus of the crystalline cellulose having a high viscosity was lower than the storage modulus of the crystalline cellulose having a low viscosity.

10354-52, Session PWed

Amorphous InWO oxide for resistive random access memory application

Wei-Chiao Chang, Che-Chia Chang, National Chiao Tung Univ. (Taiwan); Wen-Tzu Chen, National Chiao Tung Univ. (Taiwan) and Institute of Electro-Optical Engineering (Taiwan); Po-Tsun Liu, Chung-Hao Tien, National Chiao Tung Univ. (Taiwan)

The conductive bridge random access memory (CBRAM) is considered to be a promising candidate or complementary component to the traditional charge based memory. In this study, we fabricated a bilayer CBRAM device based on a novel In-W-O Transparent-Amorphous- Oxide-Semiconductor (TAOS) material. Optimize this device in order to understand the mechanism of the Cu accumulation inside the filament. Based on the clarified physical picture, applicable approaches for performance optimization can be developed, ranging from material tailoring to structure engineering.

10354-53, Session PWed

Formation of thin metal silicide (Ni, Ti) film by nano-second Nd:YAG laser annealing with Gaussian and flat-top beam profiles

Sang Min Jung, Chul Jin Park, Jin Hwan Kim, Moo Whan Shin, Yonsei Univ. (Korea, Republic of)

The thin metal silicide has been widely investigated for contact materials in microelectronic devices. The formation of metal silicide thin film determines mainly the contact resistance between metal layer and p-type silicon substrate. As the device scaling becomes more important, the metal silicide must become thinner to achieve the more shallow contact junction depth for avoiding high contact leakage.

The laser thermal annealing (LTA) is considered as an effective method to form thin metal silicide and reduce annealing time. In this study, we have formed thin metal silicide (< 10nm) at p-type (100) silicon wafer using LTA process and investigated phase of various metal silicide by various analysis. The temperature distribution of laser annealed sample is calculated by COMSOL. The LTA system consisted of ND:YAG laser (532 nm, 355 nm) with 6 ns pulse width. The samples were annealed by laser energy density was 100 – 1000 mJ/cm2 at N2 ambient chamber. The sheet resistance was measured by a four point probe method. The specific contact resistance was measured the circular transmission line method (CTLM). The inner radius is 50? and gap spacing ranging from 2 to 48?. To analyze formation of metal silicide, X-ray photoelectron spectroscopy (XPS) and Raman spectroscopy were performed. Metal diffusion profiles were analyzed by secondary ion mass spectrometry (SIMS). In this work, thin metal silicide was formed by laser annealing with two different beam shapes. We achieved small metal diffusion into the silicon with thin metal silicide thickness.

10354-54, Session PWed

One-dimensional metallodielectric photonic crystal (tantalum and aluminum oxide) as selective thermal emitter for thermophotovoltaic systems

Jin Hwan Kim, Sang Min Jung, Chul Jin Park, Moo Whan Shin, Yonsei Univ. (Korea, Republic of)

Because of its simplicity, one-dimensional metallodielectric photonic crystal (1D MDPhC) is a promising nanostructure for the selective thermal emitter of thermophotovoltaic systems. Because it is high-temperature application (typically exceeding 1200 K), thermal stability of the nanostructure must be ensured. Coefficient of thermal expansion (CTE) matching among the substrate and adjacent materials is essential, and thus we select Ta, Al2O3 sputtered layer and Al2O3 substrate that are similar in CTE and thermally stable at the high temperatures. We optimize the multilayer structure by using transfer matrix method (TMM). Further, we fabricate the optimized structure by alternately depositing the Ta and Al2O3 by using DC and RF sputter, respectively on sapphire substrates. The emissivity of the samples is calculated from measurement data of UV-Vis-NIR spectrophotometer. In order to minimize plasma damage on the films during the sputtering process, we insert a few nm-thick Al2O3 layer deposited by Atomic Layer Deposition (ALD) at each interface of the sputtered Ta and Al2O3. The fabricated structures with and without ALD layer are compared in terms of thermal stability at 1200 K, 1300 K, and 1400 K under high vacuum condition (low 10-5 torr). It is demonstrated from cross-sectional observation via transmission electron microscope (TEM) that the ALD layer minimize inter-diffusion of Ta and Al2O3 at the high temperatures as well.

10354-55, Session PWed

Mechanical performance of SiC based MEMS capacitive microphone for ultrasonic detection in harsh environment

Azrul A. Hamzah, Siti A. Zawawi, Burhanuddin Y. Majlis, Univ. Kebangsaan Malaysia (Malaysia); Faisal Mohd-Yasin, Griffith Univ. (Australia)

In this work, we develop a SiC based MEMS capacitive microphone for detecting gas leak in extremely harsh environment such as coal mines and petroleum processing plants. The microphone detects gas leaks via ultrasonic detection. The MEMS capacitive microphone consists of two parallel plates; top plate (movable diaphragm) and bottom (fixed) plate, separated by an air gap. Vent holes were fabricated on the back plate to release trapped air and reduce damping. In order to withstand high temperature and pressure, a 1.0 μm thick SiC diaphragm was utilized as the top membrane. The SiC can withstand a temperature up to 1400°C. A 3 μm air gap is fabricated between the top membrane and the bottom plate via wafer bonding. COMSOL Multiphysics was used for design optimization. Various diaphragms with sizes of 600 μm2, 650 μm2, 700 μm2, 750 μm2 and 800 μm2 are loaded with external pressure. Performance of microphones with circular and square diaphragms are also compared. It is observed that SiC microphone with diaphragm width of 650 μm2 produces optimal surface vibrations, with first-mode resonance frequency of approximately 35 kHz. The maximum deflection value at resonance frequency is less than the air gap thickness of 3 μm, thus eliminating the possibility of shortage between plates during operation. It is also observed that circular membrane produces less stress as compared to its square counterpart. The designed SiC capacitive microphone is suitable to be used in ultrasonic gas leak detection at harsh environment.

10354-56, Session PWed

MoS2 thin films prepared by sulfurization

Michaela Sojkova, Institute of Electrical Engineering SAS (Slovakia)

The discovery of graphene has stimulated an extensive research on other 2D materials. The 2D structure determines the electronic properties that may exhibit correlated electronic phenomena such as charge density waves and superconductivity. Especially transition metal dichalcogenides (TMDs) with the formula MX2, where M is a transition metal (Mo, W, and so on) and X is a chalcogen (S, Se or Te), have attracted much attention due to their layer structure and semiconducting properties.

Among metal dichalcogenides, molybdenum sulfide (MoS2) material has been extensively investigated for its interesting properties including enhanced optical absorption, thermoresponsive photogeneration, efficient hydrogen evolution reaction capability, valley polarization and high on/off ratio with low subthreshold swing, which can lead to ultrathin and highly efficient photovoltaics, photo-thermoelectrics, and catalysis for sustainability.

A large effort has been made to develop methods for growing high quality layers. Recently, methods of physical vapor deposition; especially pulsed laser deposition (PLD) and sulfurization have successfully been used for the fabrication of ultrathin films. Sulfurization is very simple and effective method for the preparation of a few layers films.

Here we present fabrication of MoS2 thin films using sulfurization of Mo and MoO3 films on c-plane sapphire and silicon substrates. As-prepared films were characterized by number of techniques including XRD, AFM, SEM, Raman, Auger and Rutherford backscattering spectroscopy, transport and optical measurements. From thorough analyses we can assess the advantages and disadvantages of the source films as well as the substrate on the properties and quality of the final films.

10354-57, Session PWed

Damage-free laser annealing process via heat transfer layer

Chul Jin Park, Sang Min Jung, Jin Whan Kim, Moo Whan Shin, Yonsei Univ. (Korea, Republic of)

Laser thermal annealing (LTA) has received substantial attention as it has been regarded as the most suitable annealing method for next generation semiconductor manufacturing process. However, laser annealing process using intensive photon energies, induces thermal and optical stress on the silicon substrates. Furthermore, directly incident laser pulse on the surfaces of silicon produces a variety of melting patterns and laser-induced damages that are crucial problems on next fabrication steps. For this reason we investigated heat transfer layer which conducts generated heat to silicon surfaces deposited on the silicon substrates because of indirectly incident laser pulse avoiding optical and thermal stress. We present an experimental characterization of the laser-induced damages after LTA with and without heat transfer layer by using atomic force measurement (AFM), scanning electron microscopy (SEM) and transmission electron microscope (TEM). Also, numerical simulations are carried out by using COMSOL multiphysics based on heat transfer equations in order to predict surface and interface temperature profiles. According to optical and thermal properties of materials, several candidates as the heat transfer layer are selected and the thickness of heat transfer layers are optimized by the simulations. Concretely, heat transfer layer consisted of SiO2, Si3N4, and Al2O3 is deposited on silicon wafer and then, based on simulation results, LTA (532nm, 5ns) with flat-top beam profiles was executed. Finally, this heat transfer layers are removed with etchants. The observed results clearly show that through this in-direct laser annealing process with heat transfer layer, the surfaces of silicon can be efficiently annealed without remarkable damages, melting patterns and with LTA's merits. This approach could improve the feasibility of LTA in semiconductor manufacturing process such as ultra shallow junction (USJ) formation, laser crystallization, and low resistant metal contact formation.

10354-58, Session PWed

The diffraction patterns of the output light from the tapered fiber tips

Fang-Wen Sheu, National Chia Yi Univ. (Taiwan); Jiun-An Chen, National Chiayi Univ. (Taiwan)

There are many kinds of wavelength-tunable fiber lasers. A tapered fiber tip can also be used as a spatial filtering device in a fiber ring laser system to tune the output wavelength by a butt joint method. In order to explore its spatial filtering mechanism when used in a wavelength-tunable fiber laser, here we try to observe the variation in the diffraction pattern of the output light from the tapered fiber tip by displacing the imaging lens or changing the tapering ratio of the tapered fiber tip.

10354-59, Session PWed

Complementary methods of study for Zr1-xCexO2 compounds for applications in medical prosthesis

Alina Bruma, National Institute of Standards and Technology (United States); Adriana Savin, National Institute of Research & Development for Technical Physics (Romania); Mihai-Liviu Craus, Vitalii Turchenko, Joint Institute for Nuclear Research (Russian Federation); Pierre-Antoine Dubos, Sylvie Malo, ENSICAEN (France); Tatiana Konstantinova, Valerii Burkhovetsky, The National Academy of Sciences of Ukraine (Ukraine)

Zirconia (ZrO2)-based ceramics are preferred due to their advanced mechanical properties such as high-fracture toughness and bulk modulus, corrosion resistance, high dielectric constant, chemical inertness, low chemical conductivity and biocompatibility. The medical prosthesis components made from ZrO2 oxides present a very good biocompatibility as well as especially mechanical properties. In order to ensure implant safety of these prostheses, a wide range of examinations based on non destructive testing are imperative for these medical implants.

In this study, we aim to emphasize the improvement of Zr-based ceramics properties as a function of addition of Ce ions in the structure of the original ceramics. The substitution of the Zr with Ce in the Zr1-xCexO2 compounds, where x = 0.0–0.17, leads to a change of the phase composition, a gradual transition from the monoclinic to tetragonal structure, at room temperature. The structural investigations proposed in this paper are based on X-ray and neutron diffraction in order to establish a first indication of the variation of the phase composition and the structural parameters, as well as micro-hardness measurements and non-destructive evaluations in order to establish a correlation between the structural parameters and mechanical properties of the samples. These range of tests are imperative in order to ensure the safety and reliability of these composite materials which are widely used as hip-implants or dental implants/coatings. In combination of Resonant Ultrasound Spectroscopy, which makes use of the resonance frequencies corresponding to the normal vibrational modes of a solid in order to evaluate the elastic constants of the materials, we emphasize a unique approach on evaluating the physical properties of these ceramics, which could help in advancing the understanding of properties and applications in medical fields.

10354-60, Session PWed

Highly transparent phthalocyanine derivative nanocrystal dispersions and their photopatterning

Yutaro Hirai, Tohoku Univ. (Japan); Toshihiko Takaki, Sawano Bunji, Yamamoto Chemicals, Inc. (Japan); Yasutaka Matsuo, Hokkaido Univ. (Japan); Hiroshi Yabu, Tohoku Univ. (Japan)

Metal phthalocyanines (PCs) and their derivatives (PCDs) have been considered for applications in color filters, photovoltaic cells and photodynamic therapy, owing to their unique optical properties, high chemical and thermal stabilities and good electron mobility. Nano-crystals (NCs) of metal PCDs have received much attention, because the optical and electronic properties of metal PCDs are considerably improved by reducing their sizes to the nanoscale. In the present study, we revealed that metal PCD NCs having various pi-conjugated substituents (tetra-2,3-pyridoporphyradine and naphthalocyanine) could be synthesized in nano-micells with UV irradiation to prevent micelle from breaking due to conventional heating process.

The resulting metal PCD NCs were found to form stable dispersions in an aqueous PEG solution and these dispersions exhibited significant visible light absorption from 500 to 800 nm as well as high transparency at

wavelengths in the non-absorption region.

These results indicate that these PCD NCs can be applied to such as the pigments for color filters.

We also demonstrated photo-patterning of PCDs. Precursors of PCDs were dispersed in polyvinylbutyral methanol solution, casted on glass and UV was irradiated through photo mask. PCD patterns were clearly evident in their precursor solutions. The patterning of PCDs may be applicable to the fabrication of photoelectric conversion layers in organic thin-film solar cells.

10354-61, Session PWed

Designer metamaterials using graphene for integrated nano-photonic applications

Xinbo Wang, Berardi Sensale-Rodriguez, The Univ. of Utah (United States)

During recent years, graphene-based waveguide-integrated electro-optic modulators have been demonstrated to attain very good modulation depth as well as fast speed. By electrically tuning the Fermi level on a graphene sheet, it is possible to change its absorption at infrared wavelengths. Our work aims to explore the feasibility of employing the recently proposed "designer metamaterial" concept so to dramatically reduce the footprint of such devices. Designer metamaterials offer a new degree of design freedom that can enable unique and efficient integrated-photonic applications in very compact areas. The premise of this approach is that via nanofabrication, one can control the local refractive index of the device. By spatial engineering of the refractive index, it is possible to design devices with much higher performance than what is otherwise achievable. In order to show the applicability of this design approach, we applied nonlinear optimization so to design an optical modulator with very small footprint. A silicon ridge-waveguide couples light in and out of the device, which consists of a nano-pattern with graphene on top. The nano-pattern contains multiple "pixels", i.e. regions which may be comprised entirely of silicon or air. For given nano-pattern dimensions, we selected "seed" geometries from a pool of randomly generated patterns. After that, a search algorithm was ran. Because of the enhanced local fields in the optimized nano-pattern, the light-matter interaction in graphene is enhanced thus leading to a superior modulation performance and a reduced footprint.

10354-62, Session PWed

Organic-inorganic hybrid resist materials in advanced lithography

Satoshi Takei, Naoto Sugino, Makoto Hanabata, Toyama Prefectural Univ. (Japan)

Organic-inorganic hybrid resist materials on photoreactive underlayer material were reported to modify the film surface chemical adhesion between resist material and photoreactive underlayer material during ultraviolet irradiation of nanoimprint lithography. This procedure is proven to be suitable for material design and the process conditions of Organic-inorganic hybrid resist materials on photoreactive underlayer material for the defect reduction by mold contamination when the mold was removed from the organic-inorganic hybrid resist resist materials after ultraviolet irradiation. The developed organic-inorganic hybrid resist resist material with ultraviolet crosslinking groups produced high resolutions nanopatterning, and excellent film properties for nanoelectronic, nano-MEMS, and biological devices.

10354-63, Session PWed

Study of the change in electrical properties of mechanically vibrating FET device with graphene

Sungbae J. Lee, Gwangju Institute of Science and Technology (Korea, Republic of)

Graphene is a single layer of graphite, the honeycomb lattice structure of carbon allotrope. Most of the existing studies about graphene is performed with FET devices. The structure of typical FET devices is composed by graphene placed on the oxide layer substrate. Because of the interaction between the graphene and the substrate, studying the electric properties of genuine graphene itself is limited. The pure electric properties of graphene can be measured by suspending the graphene over the substrate. The suspended graphene is free to vibrate so the effect of mechanical vibration to the electric properties becomes important. In this study, the preliminary calculation is performed for the device to detect the effect of vibration before the measurement. The CVD growth graphene sheet is positioned over 50 nm thick metal electrode. The effect of quantum capacitance is negligible because it is about 100 times bigger than geometric capacitance. The typical doubly fixed beam model for natural frequency and spring constant does not match well for the 2 dimensional material so the thickness-modifying is necessary. The effect of mechanical vibration can be detected as difference between measured current and theoretic current calculated with calibrated and modified mechanical properties.

10354-64, Session PWed

Zig-zag grating with quasi-random array for single order diffraction

Ziwei Liu, Tanchao Pu, Lina Shi, Changqing Xie, Hailiang Li, Institute of Microelectronics (China)

We present the design of a novel single order diffraction grating with quasi-random array of zigzag grating. The fundamental structure consists of a series of quasi-random spaced slits along a 150nm thick Cr grating on a glass substrate. Both numerical simulation results and the experiment prove the effectiveness of single order diffraction. The 2n, 3n and 5n (n=1, 2, 3...) order diffractions can be completely suppressed. Especially, the critical dimension is kept to 1/2 of the grating period, which is highly advantageous to the spectrum measurement from the infrared to the x-ray region. The 1st order diffraction can be achieved to 24.26% in theory. We noted that the critical dimension is kept to 1/2 of the grating period. The simpler shape structure is much easier to fabricate in applications, especially the measurement in short wavelength. As a crucial factor for applying this grating to practical applications, we discuss the angle factor in fabrication error can be allowed and study the tolerance budget for the critical parameters. In addition, we further investigate dependences of these parameters on the suppression and derive a useful relation based on the Fraunhofer diffraction theory. Based on the theory, the parameters can be properly optimized with the special relation with a_1=1/3P_x , a=1/2P_x , d=1/10P_x. Our study provide an efficiency grating realization with high line density employing today's nanofabrication technology, and be of great significance to extend a wide range of spectrum.

10354-65, Session PWed

N-state random switching based on quantum tunnelling

Ramón Bernardo Gavito, Lancaster Univ. (United Kingdom); Fernando Jiménez Urbanos, IMDEA Nanociencia (Spain); Jonathan Roberts, Lancaster Univ. (United Kingdom); James Sexton, The Univ. of Manchester (United Kingdom); Benjamin Astbury, Hamzah Shokeir, Thomas McGrath, Yasir J. Noori, Christopher S. Woodhead, Lancaster Univ. (United Kingdom); Mohamed Missous, The Univ. of Manchester (United Kingdom); Utz Roedig, Robert J. Young, Lancaster Univ. (United Kingdom)

Random number generation is important for many computational processes, including cryptography. True random number generation (TRNG) is desirable but it is difficult to achieve in practice. Systems based on quantum physics are guaranteed to be random, as the fundamental laws governing their behaviour are fundamentally probabilistic. Random number generation based on quantum physics has been demonstrated previously, but commercial solutions are bulky, inefficient and unsuitable for integration.

In this work, we show that a compact semiconductor device, the resonant tunnelling diode (RTD), can be employed as a practical TRNG. The diodes in our demonstration contain a single quantum well, the most basic structure to exhibit quantum confinement. A pair of tunnelling transport mechanisms through the active region of the diode result in the voltage measured across it being a multivalued function of current. Thus, when driven with current pulse trains, the output voltage will be in one of two possible states, which is a randomly chosen value. The voltage measured across the RTD then depends on whether the electrons are resonantly tunnelling through the quantum well, or are subject to thermionic emission over the barriers – a naturally probabilistic outcome.

We show results from the physical characterisation of RTDs operating in a random number generating regime. A security analysis of the RTDs acting as a source of true randomness for on-chip cryptographic applications will also be presented.

10354-66, Session PWed

Three-dimensional printing and deformation behaviour of low-density target structures by two-photon polymerization

Ying Liu, Univ. of Nebraska-Lincoln (United States); Ori Stein, Schafer Corp. (United States); Yongfeng Lu, Univ. of Nebraska-Lincoln (United States)

Two-photon polymerization (TPP) is of increasing interest due to its unique combination of truly Three-dimensional (3D) fabrication capability and ultrahigh spatial resolution. The technique enables the fabrication of customized polymeric low-density materials (“foams”) over a large volume (up to millimeter scale in lateral sizes) with sub-micrometer resolution which could find practical applications as laser target components. Foam structures of 2 mm ? 0.25 mm ? 0.3 mm (X ? Y ? Z) size, in a log-pile structure with covered with 15 µm high fully- densified layer were fabricated using a commercial TPP system (Photonic Professional GT, Nanoscribe GmbH) and commercially available photoresists (IP series, Nanoscribe GmbH) that are optimized for TPP.

Deformation control of low-density structures with large dimensions during the development and subsequent drying processes still remains to be a challenge. In this work, deformation behaviors, including side-shrinkage, arc-shape deformation, stitching mismatch, bending, buckling and/or shearing, have been identified. The mechanical strength of polymeric foam structures depends on the photoresist properties, the foam density, the structure designs as well as the developing and drying processes. Methods to control deformation by using photoresist with high mechanical strength, optimized structure design, and developing process with supercritical drying were studied. The results obtained show obviously reduced deformation in large foam structures. These findings, coupled with the superior resolution of TPP technique, makes the foam structures an excellent target component designed to study plasma physics and high-energy-density (HED) conditions important to astrophysics, planetary science, shock physics, and radiation transport.

10354-67, Session PWed

Implement of multi-channel spectral sensor by hybrid-coating and a related algorithm

Yu-Jen Chen, Yu-Kuan Hsiao, VisEra Technologies, Inc. (Taiwan)

A four-channel spectral sensor is implemented by the optical filers based on integrated organic–inorganic layers. The multi-channel spectrum is provided by the unique M-I-M structure which is deposited on the whole photo-diodes on chip. Four photo-diodes are grouped as a four-channel spectral sensor, i.e. the spatial resolution is one fourth of the photo-diode density. Three specific photo-resists are applied on the set of four-diodes in different arrangements, so that each photo-diode catches one or more channel signal. A specific algorithm is also proposed to separate signals of the four channels. An Intuitive process of n-channel sensor consists of n photo-resists and procedures. Although this article demonstrates the process strategy and algorithm to build four-channel spectral sensor by three photo-resists, it presents a common rule to build n-channel spectral sensor by (n-1), or less, photo-resists and procedures.

10354-68, Session PWed

Nanofiber optic force transducers for high-resolution mechanical studies

Donald J. Sirbuly, Univ of California San Diego (United States)

Ultrasensitive force transducers such as the atomic force microscope (AFM) and optical/magnetic tweezers have been instrumental in quantifying fine nanomechanical events in static and dynamic environments. However, as more detailed information is sought after deep inside of systems such as the body, it becomes apparent that new technologies are needed given the difficulty in scaling down the size of the feedback mechanisms associated with the aforementioned techniques. In this talk we describe a novel approach to intercept small forces and quantify them with a pure optical read-out. The platform leverages a nanofiber optic equipped with a compressible plasmonic cladding that modulates the guided light when forces as low as 200 femtonewtons interact with the fiber. The device operates through a non-interferometric transduction mechanism and relies on strong plasmon-dielectric coupling effects in the near-field to achieve angstrom-level distance sensitivity. The distance-sensitive optical signals are converted into force by placing a mechanically compliant polymeric coating between the plasmonic structures and fiber. The ability of the nanofiber system to probe the local nanomechanical environment is first demonstrated by detecting forces generated by bacteria motion without physically touching the organisms. With their high force resolution, the nanofibers can also listen to acoustic signature generated by nearby biomechanical sources and pick up sound waves with a sensitivity of -30 dB in solution. With the ability to tune the mechanical response and detect forces independently from multiple sites on a single fiber, these devices should become a valuable tool for cellular mechanics and stethoscopic applications.

Summary: A novel nanofiber optic force transducer is discussed that leverages near-field plasmon-dielectric interactions to detect local nanomechanical events with sub-piconewton force resolution. A pure, non-interferometric optical read-out of the mechanical environment is achieved by placing a compressible polymer cladding between the waveguide and plasmonic nanoparticles and tracking the distant-dependent scattering in the far-field. The performance of the nanofiber platform is demonstrated through various experiments including the monitoring of bacterial motion and hear-cell beating as well as detecting infrasound power in solution.

10354-69, Session PWed

High throughput fabrication of transparent anti-reflective polymer foils by roll-to-roll extrusion coating

Swathi Murthy, Inmold (Denmark); Henrik Pranov, Heliac a/s (Denmark); Peter Johansen, Danapak Felxibles A/S (Denmark); Guggi Kofod, Inmold a/s (Denmark)

We investigated fabrication and performance of broadband and omnidirectional anti-reflective (AR) polymer foils, in visible range, consisting of inverted moth eye structures formed as tapered nano-pits with sub-wavelength size originated by electron beam lithography and reactive ion-etching in Si. The AR foils were fabricated by a novel, high throughput roll-to-roll extrusion coating process that allowed subsequent structuring with the AR relief on both sides at a rate of 60 m/min, with a web width of 45 cm. The highest, average total transmittance obtained in visible range, was (98 ± 1) %, with minimal scattering and absorption losses. For comparison, the unstructured foil has an average transmittance of (92 ± 1) %. The broad-band reduction in reflection is documented by transmittance measurements, in visible range (400 nm - 800 nm). The AR foils showed good omni-directional performance, with no significant difference in transmittance between normal incidence and incidence up to at least 60?, higher angles could not be measured due to limitation of the set-up. The AR performance of the foil was also investigated for different depth (Dp) and shape of the nano-pits. The transmittance initially increased with Dp and reached a maximum at Dp ~ 120 nm. For process parameters yielding higher depths, we found that other shape factors along with the depth played a critical role for the AR properties.

10354-22, Session 5

Direct laser writing of carbon nanotubes

Kentaro Yamada, Makoto Nakazumi, Satoru Odate, Koichiro Iwahori, Nikon Corp. (Japan)

Carbon nanotubes (CNTs) have been expected for applications in many future electronic devices. To fabricate CNT structures on substrates, several techniques such as spray coating, spin coating and vacuum filtration have been proposed so far. In this work, we report a very simple and efficient method to deposit CNTs on a glass substrate by only scanning a focused light in CNT dispersion. This fabrication technique can provides a bottom up method for the deposition of CNTs in arbitrary shape on the substrate.

We placed the dispersion of single-walled carbon nanotubes (SWCNTs) on a glass substrate. From the back side of the substrate, a laser (?=975 nm; 100 mW) was focused on the interface between the substrate and the SWCNT dispersion by an oil immersion objective lens (Nikon 100X 1.25NA). Once the focal spot of the light is in focus on the substrate, it began to deposit SWCNTs around the spot (~1 um). Then, the linewidth of the deposition of SWCNTs was approximately 30um, and its electrical conductivity was 12.5 S/cm. We measured the Raman spectrums of the SWCNT dispersion and the deposited SWCNTs. Their G/D ratios were the same value, which indicated that any lattice defects were hardly occurred to SWCNTs in this process. Hence, this method can be useful application for fabrication processes of a variety of CNT devices. We have built the prototype of CNT field-effect transistors. In this presentation, we will show that a collimated light instead of the focused light can be applicable also.

10354-23, Session 5

Low contact resistance of the MWCNTs ohmic contact to p-GaN and its application for high power LED

Toshiya Yokogawa, Yamaguchi Univ (Japan); Syota Miyake, Yamaguchi Univ. (Japan)

Recently optoelectronic devices and electronic power devices using GaN-based materials have attracted much attention because they exhibit high optical and electrical power with high efficiency due to the wide band-gap. These power devices are generally used in high temperature operation by the heat dissipation. For high device reliability, it is important to design the mounting structure for heat sink to obtain efficient heat spreading. Carbon nanotube is expected to be excellent heat conductor for heat spreading because of extremely high thermal conductivity. Therefore, it is thought that carbon nanotube is very useful for electrode material with high thermal conductivity in the GaN device.

We confirmed the large workfunction of metallic multi-wall carbon nanotubes (MWCNTs). The work function of metallic MWCNTs was determined to be 4.84 eV as high as that of Au, Pd and Ni which are generally used for the p-GaN contact. We concluded that there is possibility to exhibit ohmic property to p-GaN. Finally, the specific contact resistance of the MWCNTs electrode was as low as 2.6?10-3 ?cm2. We obtained low contact resistance of the MWCNTs ohmic contact to p-GaN. And we demonstrate LEDs using the MWCNTs ohmic contact for p-GaN. Low operation voltage and high optical power was successfully obtained. Threshold voltage was as low as about 2.7 V, and high optical power more than 1 W was also realized. Stable operation and good reliability of the LED were also obtained.

10354-24, Session 5

High aspect ratio CNT structures produced by energetic ion bombardment

Gregory A. Konesky, National Nanotech, Inc. (United States)

Earlier research has sought to utilize the exceptional thermal conductivity of CNTs to produce a heat spreader by bulk cross-linking the CNTs into an interpenetrating network. An isotropic thermal conductivity of 2150 W/m-K was measured in a 5 ?m thick MWCNT film which had been subject to argon ion bombardment with an ion energy of 4 keV and a fluence on the order of 10^17 ions/cm2. While energetic ions will randomly bombard the entire CNT network, on occasion, one will strike a junction where two or more CNTs are touching, momentarily disrupting them. CNTs have the remarkable ability to self-heal, and in doing so, the disrupted junction self-heals into a new interpenetrating junction. However, practical heat spreader applications require films at least 100 times thicker than this initial demonstration. In an attempt to achieve this, substantially higher ion energies and fluence were applied. But rather than forming interpenetrating junctions deeper into the bulk of a CNT thick film, an interesting new form of high aspect ratio structure results, where groups of CNTs are now vertically aligned, even though the original CNT thick film was randomly oriented. There is also a sharp transition at the base of these structures from the new aligned form to the original randomly oriented form. We consider various aspects of ion-induced sputter dynamics coupled to the growth processes of CNTs to account for these new aligned high aspect ratio structures. The role of ion channeling within and between CNTs is also considered.

10354-25, Session 5

Time-domain finite-difference based analysis of induced crosstalk in multiwall carbon nanotube interconnects

Amit Kumar, Brajesh K. Kaushik, Vikas Nehra, Indian Institute of Technology Roorkee (India)

Graphene rolled-up cylindrical sheets i.e. carbon nanotubes (CNTs) is one of the finest and emerging research area. Carbon nanotubes can be classified as single walled known as single-walled carbon nanotubes (SWCNTs) or multi-walled known as multi-walled carbon nanotubes (MWCNTs). The diameter of an SWCNT can be in the range from 1nm to 5nm while for MWCNT the diameter can range from few nanometers to several tens of nanometers. MWCNTs have been given intensive importance as compared to SWCNTs due to their better conduction properties, and ease

of fabrication. CNTs can be conducting or semiconducting depending on their chirality. MWCNTs will have better conductance than SWCNTs due to more number of conduction channels in comparison to SWCNTs. The ITRS reports have projected that beyond 8nm technology node, conventional copper interconnect technology will not be able cop-up with the device performance requirements. Thus, researchers have started looking for alternative interconnect technologies, and CNT seems to be one of the most prominent interconnect technology to replace conventional on-chip interconnect technology.

This paper presents the investigation of induced crosstalk in coupled on-chip multiwall carbon nanotube interconnects using finite-difference analysis (FDA) method in time-domain. The exceptional properties of versatile MWCNTs profess their candidacy to replace conventional on-chip copper interconnects. Time delay and crosstalk noise have been evaluated for coupled on-chip MWCNT interconnects. With a decrease in CNT length, the obtained results for an MWCNT shows that transmission performance improves as the number of shells increases. It has been observed that the obtained results using the finite-difference time domain (FDTD) technique shows very close match with the HSPICE simulated results.

10354-26, Session 5

Optical models for atomically thin sheets

Jessica R. Piper, Exponent (United States)

Over the last decade, the proliferation of experimental and theoretical interest in atomically thin materials, such as graphene and monolayer transition metal dichalcogenides, has lead to a great interest in the optics of ultra-thin films.[1] Two formalisms are generally used in electromagnetics to account for the properties of thin layers: the permittivity/thickness model, and the conductive sheet model. For atomically thin layers, the sheet conductor model feels intuitively correct. However, for convenience many electromagnetic simulation codes represent such layers using a finite thickness (often chosen based on a simulation grid size), and an effective permittivity. We show that for non-magnetic media, the permittivity-thickness model directly reduces to the sheet conductance model for very thin layers. Likewise, we show that an atomically thin sheet conductor can be represented as a thicker layer with an effective permittivity, and quantify the realm of applicability of this approximation. Finally, we compare our results with the polarization sheet models of Felderhof and Marowsky,[2] and of Sipe.[3]

[1] For example, many references are contained in: Piper and Fan (2014). Total Absorption in a Graphene Monolayer in the Optical Regime by Critical Coupling with a Photonic Crystal Guided Resonance. ACS Photonics, 1(4), 347–353. doi:10.1021/ph400090p

[2] Felderhof and Marowsky (1987). Linear Optics of Polarization Sheets, App. Phys. B 43, 161-166.

[3] Sipe (1987). New Green-function formalism for surface optics, J. Opt. Soc. Am. B 4, 481-489.

10354-27, Session 5

Surface plasmon resonance based electro optic measurement of SBN thin films

Surbhi Gupta, Ayushi Paliwal, Vinay Gupta, Monika Tomar, Univ. of Delhi (India)

Surface plasmon resonance (SPR) technique is a versatile tool for investigating the optical properties of different materials [1]. Among the known photo-refractive materials, strontium barium niobate (SBN) possesses a large value of diagonal electro-optic (EO) coefficient making it suitable for wide range of EO applications [2]. An effort has been made in the present work for the measurement of EO effect in SBN thin films using SPR technique. The $Sr_{0.6}Ba_{0.4}Nb_2O_6$ (SBN:60) thin films were positioned in Otto configuration for studying the variation in refractive index with the incident light using SPR. For application of electric field, LSCO has been grown using Pulsed Laser Deposition (PLD) technique providing epitaxial growth of SBN. The SPR resonance angle for prism/air-gap/gold/Si system was observed to be at 47.27° which increase to 52.05° for prism/air-gap/gold/SBN/LSCO/Si system. This may be due to change in dielectric media for the system which does not allow maximum light to couple with the SPR mode leading to increase in resonance angle. Further, the value of SPR reflectance was obtained by fixing the system in resonance angle and varying the applied electric field to monitor change in refractive index. Also, SPR reflectance curves were obtained by keeping the value of applied electric field to be constant.

References:

1. X. C. Yuan, B. Hong, Y. G. Tan, D. W. Zhang, R. Irawan, and S. C. Tjin, J. Opt. A 8, 959 (2006).

2. Y. Y. Zhu, R. F. Xiao, and G. K. L. Wong, J. Appl. Phys. 82, 4908 (1997).

10354-28, Session 6

Symmetry-breaking in light-trapping nanostructures on silicon for solar photovoltaics

Seok Jun Han, Swapnadip Ghosh, Omar Abudayyeh, Brittany Hoard, Ethan Culler, Jose Bonilla, Sang M. Han, Sang Eon Han, The Univ. of New Mexico (United States)

While various materials have been investigated for photovoltaics, solar cells based on crystalline silicon (c-Si) dominate the current photovoltaics market. To reduce the cost of c-Si cells, wafer manufacturing companies have produced competitively priced thin c-Si films, ranging from a few microns to tens of microns, using a kerfless process. In such thin-film c-Si cells, light absorption becomes poorer than in thick films and light trapping is crucial to increase the photovoltaic efficiency. Han et al. have demonstrated that, among various light-trapping schemes, symmetry breaking in photonic nanostructures can approach the Lambertian light-trapping limit very closely. However, fabricating symmetry-breaking nanostructures in a scalable, cost-effective, manufacturable manner remains elusive. Here, we introduce a new approach to systematically break the symmetry in photonic nanostructures on c-Si surface. Using our approach, we fabricate low-symmetry inverted nanopyramid structures. Our method makes use of low-cost, manufacturable wet etching steps on c-Si(100) wafers without relying on expensive off-cut wafers. Our experiment and computational modeling demonstrate that the symmetry breaking can increase the detailed balance efficiency from 27.0 to 27.9% for a 10-micron-thick c-Si film. Further, our computation reveals that this improvement would increase from 28.1 to 30.0% with over-etching for a 20-micron-thick c-Si film.

10354-29, Session 6

Chromatic mechanical response in 2D layered Transition Metal Dichalcogenide (TMDs) based nanocomposites

Balaji Panchapakesan, Vahid Rahneshin, Worcester Polytechnic Institute (United States)

The ability to convert photons of different wavelengths directly into mechanical motion is of significant interest in many energy conversion and reconfigurable technologies. Here, using few layer 2H-MoS2 nanosheets, layer by layer process of nanocomposite fabrication, and strain engineering, we demonstrate a reversible and chromatic mechanical response in MoS2-nanocomposites between 405?nm to 808?nm with large stress release. The chromatic mechanical response originates from the d orbitals and is related to the strength of the direct exciton resonance A and B of the few layer 2H-MoS2 affecting optical absorption and subsequent mechanical response of the nanocomposite. Applying uniaxial tensile strains to the semiconducting few-layer 2H-MoS2 crystals in the nanocomposite resulted in spatially varying energy levels inside the nanocomposite that enhanced the broadband optical absorption up to 2.3?eV and subsequent mechanical response. The unique photomechanical response in 2H-MoS2 based nanocomposites is a result of the rich d electron physics not available to

nanocomposites based on sp bonded graphene and carbon nanotubes, as well as nanocomposite based on metallic nanoparticles. The reversible strain dependent optical absorption suggest applications in broad range of energy conversion technologies that is not achievable using conventional thin film semiconductors.

10354-30, Session 6

Luminescence studies of laser MBE grown GaN on ZnO nanostructures

Sheetal Dewan, Monika Tomar, Univ. of Delhi (India); Ashok K. Kapoor, Solid State Physics Lab. (India); Ram Pal Tandon, Vinay Gupta, Univ. of Delhi (India)

Gallium Nitride (GaN) thin films and nanostructures feature highly promising material properties which have revolutionized the field of Photonics in last few decades. Growth of good quality defect free GaN films is of utmost importance for the development of high performance photonic devices, which inherently depends on the choice of substrates. GaN grown directly on sapphire (lattice mismatch-14%) usually suffers from cracks and high density of threading dislocations, which is circumvented by employing buffer layers like AlN, ZnO, etc. In the present work, GaN films have been fabricated on bare sapphire and ZnO nanostructures decorated Si substrates for luminescence studies.

ZnO nanostructures were grown using Excimer Laser (?=248 nm) assisted Pulsed Laser Deposition technique at optimized processing parameters. FESEM images of the ZnO nanostructures revealed a nano-columnar morphology with hexagonal facets. An Ultra High Vacuum-Laser MBE system equipped with RF Cell for Nitrogen dissociation was used for the growth of GaN films at 500?C.

The ?-2? mode X-Ray diffraction studies confirmed the formation of highly (002) plane oriented wurtzite GaN films on nitridated sapphire. However, the (002) peak intensity of GaN was significantly enhanced for GaN/ZnO/Si system owing to low lattice mismatch (1.8%) between GaN and ZnO. Subsequently, the near band edge emission in Photoluminescence studies of GaN film was found to be superior (high UV emission intensity and narrow FWHM) when grown on ZnO nanostructures. The hexagonal nucleation sites provided by the ZnO nanostructures strategically enhanced the emission characteristics of GaN film grown at relatively lower temperature. The obtained results are attractive for the realization of highly luminescent GaN films on Si for photonic devices.

10354-31, Session 6

Ultra low reflectivity black silicon surfaces and devices enable unique optical applications

Karl Y. Yee, Victor E. White, Kunjithapatham Balasubramanian, Daniel J. Ryan, Jet Propulsion Lab. (United States)

Optical devices with features exhibiting ultra low reflectivity on the order of 1e-7 specular reflectance and 0.1% hemispherical TIR in the visible spectrum enable unique applications in astronomical research and instruments such as coronagraphs and spectrometers. Nanofabrication technologies have been developed to produce such devices with various shapes and feature dimensions to meet these requirements. Infrared reflection is also suppressed significantly with chosen wafers and processes. Very low levels of specular and scattered light are achievable over a very broad spectral band. We present some of the approaches, challenges and achieved results in producing and characterizing such surfaces and devices currently employed in laboratory testbeds and instruments. The level of blackness achievable in relation to basic material properties such as conductivity and process variables are discussed in detail.

10354-32, Session 6

Quasi-triangle array of hexagonal aperturesboardband binary transmission gratings

Tanchao Pu, Ziwei Liu, Lina Shi, Changqing Xie, Hailiang Li, Institute of Microelectronics (China)

We propose a novel binary transmission grating based on a membrane with quasi-triangle array of hexagonal apertures based on the Fraunhofer diffraction theory. The shift of every unit's centers in the array positions follow a uniform distribution, keeping its absolute value <1/10, resulting in a sinusoidal average diffractive effect that suppresses high-frequency components. A grating on a quartz substrate for the visible light region was fabricated using laser beam direct writing technique. Through this quasi-triangle array grating, the normal incident light, with only 0th and +1st /-1st orders on the observation line, show good correlation with the theoretical predictions. The dependence of the high order diffraction property on the holes shape and size was investigated and the simpler shape and free-standing structure make it easy to fabricate. This compact method enables higher-order suppression be easily extended to other wavelength ranges of radiations, for example, microwave, infrared rays, Gamma rays, etc. We also discuss the tolerance of the parameters due to the fabrication errors in practical application. Furthermore, our design is optimized by selectingdifferent parameters of the gratings to get a more stable grating for the further application in soft X-ray. It offers a new opportunity for the grating monochromator with harmonics suppression. This idea can be scalable from X-rays to far infrared wavelengths and of great significance the grating application. Especially, our gratings can form free-standing structure which is highly desired for nanofabrication.

10354-33, Session 7

Subwavelength 2D segmented waveguide taper light coupling optimization by evolutionary algorithms

Anderson Dourado Sisnando, Vitaly F. Rodriguez-Esquerre, Univ. Federal da Bahia (Brazil); Cosme Eustaquio Rubio Mercedes, Univ. Estadual de mato Grosso do Sul (Brazil)

We propose a design for light coupling optimization between an optical fiber and a sub-micrometer waveguide using a subwavelength segmented waveguide taper with subwavelength periodicity. The power coupling and light coupling of the output waveguide are calculated, optimized and compared with other designs and values found in the literature. The optimized tapers has been successfully and efficient designed using evolutionary algorithms based on artificial immune system (AIS), the genetic algorithm (GA) and ant colony optimization (ACO). Power coupling above 75 % have been obtained with the evolutionary algorithms.

10354-35, Session 7

Narrow line-width reflection infrared filter using subwavelength metal-dielectric grating structure

Ziyi Wang, The Univ. of Alabama in Huntsville (United States); Rong-Jun Zhang, Fudan Univ. (China); Junpeng Guo, The Univ. of Alabama in Huntsville (United States)

It has been well-known that subwavelength metal slits grating structures function as extraordinary optical transmission filters due to excitation of surface plasmon-polaritons. In this work, we show that complex metal-dielectric subwavelength grating structures can also be designed to function as reflection-type optical filters with narrow spectral line-width in the infrared regime. Unlike extraordinary transmission filters, the new reflection optical filters with sharp spectral profiles can be designed within the entire infrared range by adjusting the height and period of the subwavelength grating structure. Detailed analysis has shown that the contrast of refractive indices of two dielectric materials embedded in the metal-dielectric structure is critical for giving sharp reflection spectral profiles.

10354-36, Session 7

Design of binary patterns for speckle reduction in holographic display with compressive sensing and direct-binary search algorithm

Thibault Leportier, Korea Institute of Science and Technology (Korea, Republic of) and Korea Univ. of Science and Technology (Korea, Republic of); Do Kyung Hwang, Korea Institute of Science and Technology (Korea, Republic of); Min-Chul Park, Korea Institute of Science and Technology (Korea, Republic of) and Korea Univ. of Science and Technology (Korea, Republic of)

One problem common to imaging techniques based on coherent light is speckle noise. This phenomenon is caused mostly by random interference of light scattered by rough surfaces. Speckle noise can be avoided by using holographic imaging techniques such as optical scanning holography. A more widely known method is to capture several holograms of the same object and to perform an averaging operation so that the signal to noise ratio can be improved. Several digital filters were also proposed to reduce noise in the numerical reconstruction plane of holograms, even though they usually require finding a compromise between noise reduction and edge preservation. In this study, we present the design of a digital filter based on compressive sensing algorithm. Our proposed method gives results equivalent to the average of multiple holograms, but only a single hologram is needed.

Filters for speckle reduction are applied on numerical reconstructions of hologram, and not on the hologram itself. Then, optical reconstruction cannot be performed. We propose a method based on direct-binary search (DBS) algorithm to generate binary holograms that can be reconstructed optically after application of a speckle reduction filter. Since the optimization procedure of the DBS algorithm is performed in the image plane, speckle reduction techniques can be applied on the complex hologram and used as a reference to obtain a binary patterns where the speckle noise generated during the recording of the hologram have been filtered.

10354-43, Session 7

Vanadium dioxide switchable components based on wiregrids for mid-infrared applications

Pengfei Guo, David Lombardo, Andrew M. Sarangan, Univ. of Dayton (United States)

Vanadium dioxide (VO2) is a polycrystalline material that exhibits reversible transition from a monoclinic semiconducting phase to a tetragonal metallic phase in the temperature range of 55 – 68 °C. The refractive index of VO2 (both real and imaginary parts) also undergoes a dramatic change during this phase change. Furthermore, the finite conductivity of the wiregrids in both phases allows for ohmic heating as the source of the temperature change, circumventing the need for an external heat source. This provides an attractive means for designing switchable optical components such as polarizers and beam steerers. In this work, we study the optical properties of vanadium dioxide wire grid structures in the mid-infrared region using the Rigorous coupled-wave analysis (RCWA). The polarizers' extinction and transmission performance was modeled as a function of temperature using measured data of the refractive index and sheet resistance as a function of temperature for various wire grid periods and heights. For the fabrication, the VO2 films were grown by ion-assisted deposition (IAD) using electron beam evaporation on sapphire substrates. The films were then patterned with interference lithography and etched using a fluorinated plasma to create the wiregrid structures.

Conference 10355: Nanobiosystems: Processing, Characterization, and Applications X

SPIE. OPTICS+ PHOTONICS NANOSCIENCE+ ENGINEERING

Wednesday - Thursday 9 –10 August 2017

Part of Proceedings of SPIE Vol. 10355 Nanobiosystems: Processing, Characterization, and Applications X

10355-1, Session 1

Bio-plasmonic and bio-electronic devices for human health and performance *(Keynote Presentation)*

Rajesh R. Naik, Air Force Materiel Command (United States); Steve Sang Nyon Kim, Joseph M. Slocik, Zhifeng Kuang, Air Force Research Lab. (United States)

No Abstract Available

10355-2, Session 1

DNA scaffold nanostructures for efficient and directional propagation of light harvesting cascades *(Invited Paper)*

Carl W. Brown III, Anirban Samanta, Sebastián A. Diaz, Susan Buckhout-White, Scott A. Walper, Ellen R. Goldman, Igor L. Medintz, U.S. Naval Research Lab. (United States)

The development of light harvesting systems for directed, efficient control of energy transfer at the biomolecular level has generated considerable interest in the past decade. Molecular fluorophores provide a straightforward mechanism for determining nanoscale distance changes through Förster resonance energy transfer (FRET), and many systems seek to build off of this simple yet powerful principle to provide additional functionality. The use of DNA-based integrated biomolecular devices offer many unique advantages towards this end. DNA itself is an excellent engineering material – it is innately biocompatible, quickly and cheaply synthesized, and complex structures can be readily designed in silico. It also provides an excellent scaffold for the precise patterning of various biomolecules. Here, we discuss the systems that have been recently developed which have added to this toolbox, including nanostructural dye patterning, photonic wires, and the incorporation of alternative energy propagation modalities, such as semiconductor quantum dots and the bioluminescent protein luciferase. In particular, we explore the incorporation of luciferase into various nanostructural conformations, providing the capability to efficiently control energy flow directionality. We discuss the nature of this system, including unexpected spectral complexities, in the context of the field.

10355-3, Session 1

Enhanced NLO response of lanthanides in DNA matrix *(Invited Paper)*

François Kajzar, Cosmina Andreea Lazar, Ana-Maria Manea, Ileana Rau, Univ. Politehnica of Bucharest (Romania)

Novel deoxyribonucleic acid (DNA) based materials, functionalized with hexadecyltrimethylammonium chloride (CTMA) and two lanthanide compounds: europium – (1.10 – phenanthroline) triazotate complex [Eu(NO3)3phen] and, separately, with terbium – bis – (2.2' – bipyridine) triazotate complex [Tb(NO3)3(bpy)2], were synthesized and characterized for their linear and nonlinear optical properties. The obtained complexes were processed into good optical quality thin films by spin coating method. The measured absorption spectra and fluorescence bands of studied solutions indicated the incorporation of Eu(NO3)3phen into DNA-CTMA backbones. The third-order nonlinear optical (NLO) properties of thin films were determined by the optical third-harmonic generation technique at 1 064.2 nm fundamental wavelength. For both compounds a large third-order NLO susceptibilities are observed. These enhanced NLO response of the studied compounds are due to highly polarisable 4f electrons of lanthanides showing their interest for application in third-order nonlinear optics.

10355-4, Session 2

Thin film DNA-complex-based dye lasers fabricated by immersion process *(Invited Paper)*

Yutaka Kawabe, Yuki Suzuki, Chitose Institute of Science and Technology (Japan)

Strong fluorescence enhancement of dyes was induced by their coupling to DNA or DNA-surfactant complex in hemicyanine and other dye systems, prompting the development of efficient thin film laser devices. Because fluorescence characteristics of the dyes were very sensitive to the interaction mode, laser performance can be optimized by the modification of preparation method. In this study, dye-DNA-surfactant complex films were fabricated with multiple methods and their lasing and ASE (amplified spontaneous emission) performance were investigated.

High quality dye-doped films were obtained with 'immersion method' where DNA-surfactant complex films were stained by immersing them into an acetone solution including hemicyanine dye. Because of strong electrostatic coupling established previously in the films, the interaction between DNA and the dye was supposedly not very direct as inferred from absorption spectroscopy results. Thus, it indicated the importance of the interaction between the dye and surfactant.

Laser oscillation was demonstrated with optical pumping by two nanosecond green laser beams interfering on the sample surface forming population grating. ASE was also obtained by the pumping with one of the two beams. Lasing was observed in three types of hemicyanines, and the typical laser threshold value obtained for pHemi1 (4-[4-(dimethylamino) stylyl]-1- methylpyridinium iodide) films was 0.35 mJ/cm2. The oscillation continued several minutes, although ASE has did for an hour. Lasing from other hemicyanines and wavelength tuning were also demonstrated.

10355-5, Session 2

DNA-based frequency selective electromagnetic interference shielding *(Invited Paper)*

Michael M. Salour, IPITEK, Inc. (United States); Fahima Ouchen, James G. Grote, Air Force Research Lab. (United States)

No Abstract Available.

10355-6, Session 2

Vegetable extracts embedded in biological matrices for applications in photonics

Ana-Maria Manea, Sorin Axinte, François Kajzar, Ileana Rau, Aurelia Meghea, Univ. Politehnica of Bucharest (Romania)

Limited mineral materials resources associated with their pollution problems push at present the interest of scientists onto biological materials which originate from renewable resources and are biodegradable. Among them the biopolymers like deoxyribonucleic acid (DNA) and collagen show very interesting properties as possible matrices for active molecules, being able to replace synthetic polymers [1] and bring more. These biopolymers are extracted from the waste of food processing industry and their sources are practically unlimited. However, their degradation time, if unprotected, is much faster than that of synthetic polymers in similar conditions.

On the other hand, the scientists turn their attention to natural photosensitive materials, which can be extracted from flowers or fruits, like

anthocyanines [2] showing some photosensitive properties for biophotonic applications. In this presentation we will describe and discuss the results of our study on bio-active molecules present in sea buckthorn, cranberries and blueberries extracts. It is well known that they exhibit a significant antioxidant activity.

In this context, the deoxyribonucleic acid (DNA) was functionalized with vegetable extracts in aqueous solution. The obtained material is soluble in water and form good optical quality thin films by spin coating and solution casting. The optical properties were characterized by UV –VIS spectroscopy.

The nonlinear optical (NLO) properties of functionalized thin films and membranes were studied by the optical third harmonic generation (THG) technique at 1064.2 nm fundamental wavelength. The results of spectroscopic studies and THG measurements indicate that the studied complexes are promising material for biophotonics.

[1] Grote J., Biopolymer materials show promise for electronics and photonics applications, SPIE newsroom, DOI 10.1117/2.1200805.1082(2008)

[2] I. Iosub, F. Kajzar, M. Makowska-Janusik, A. Meghea, A. Tane, I. Rau, Electronic structure and optical properties of some anthocyanins extracted from grapes, Opt. Mater. 34(10), (2012), pp. 1644-1650.

10355-7, Session 3

Nanocrystal pinning for green perovskite distributed feedback lasers *(Invited Paper)*

Jonathon R. Harwell, Guy L. Whitworth, Graham A. Turnbull, Ifor D. W. Samuel, Univ. of St. Andrews (United Kingdom)

There is great interest in organic and hybrid lasers because of the scope they offer for simple tuning of the materials properties, and their potential for simple fabrication. For example both conjugated polymers and perovskites can be deposited on nanoscale gratings to make distributed feedback lasers. By using methyl ammonium lead bromide, the emission of perovskites can be tuned into the green, making such lasers a candidate to fill the "green gap." We find that by using nanocrystal pinning perovskite lasers emitting at 550 nm with a threshold of 6 kW/cm2 can be made and can operate in both transverse electric and transverse magnetic modes.

10355-8, Session 3

Fluorescent noncovalent functionalization of graphene by surface-confined supramolecular self-assembly: towards nano-optics on graphene *(Invited Paper)*

Sylvain Le Liepvre, Commissariat à l'Énergie Atomique (France); Ping Du, Fabrice Mathevet, David Kreher, Univ. Pierre et Marie Curie (France); Fabrice Charra, Commissariat à l'Énergie Atomique (France); André-Jean Attias, Univ. Pierre et Marie Curie (France)

The realization of light-emitting devices based on emitters-graphene assemblies remains challenging, since graphene is known as a strong quencher of electronic excited states through excitation transfer between the adsorbed emitters and the graphene. Hence, a strategy is needed to avoid this transfer through introduction of an accurately controlled emitter–to-graphene electron barrier, for which planar flat-lying molecules are inefficient.

Here, the quenching of the fluorescence of the adsorbed dye by the adjacent graphene is hindered at the molecular scale based on a spacer approach, through a specifically designed dual-functionalized self-assembling building block. This 3D tecton presents two faces, one forming a noncovalent graphene-binding pedestal and the other carrying a dye group linked by a spacer to the pedestal. The spontaneous ordering of the adsorbed layer is investigated by scanning tunneling microscopy, whereas the resulting optical properties of the whole graphene–dye hybrid system are characterized by absorption and fluorescence spectroscopies.

10355-9, Session 3

Next polymer nanofibers: merging light emission and piezoelectric properties *(Invited Paper)*

Luana Persano, Andrea Camposeo, Istituto Nanoscienze (Italy); Dario Pisignano, Univ. del Salento (Italy)

Polymer nanofibers are one-dimensional nanostructures exhibiting smart physicochemical properties which enable their use as building blocks of more complex architectures with applications ranging from photonics and biotechnology to optoelectronics and energy harvesting. Such systems are characterized by high surface to volume ratio, large area coverage, and availability of low-cost production technologies. In particular, the electrospinning method, which is based on the uniaxial elongation of a polymer jet with sufficient molecular entanglements in the presence of an intense electric field, is a versatile and high-throughput technique which empowers materials capability by tailoring shape, size and functional properties of the resulting fibers. In this paper we review our recent results on electrospun nanofibers for photonics and energy harvesting applications. Material optimization aspects, processing parameters, and light-emission performances as well as piezoelectric behavior are studied and optimized in view of realizing a new generation of multi-functional nanofiber materials and components. Applications of the new species of nanofibers for achieving new sensing schemes are presented and discussions. The research leading to these results has received funding from the European Research Council under the European Union's 7th Framework Programme (FP/2007-2013)/ERC Grant Agreement n. 306357 (ERC Starting Grant NANO-JETS).

10355-10, Session 4

Colloidal photonic crystals: from lasing to microfluidics *(Invited Paper)*

Koen Clays, KU Leuven (Belgium) and Washington State Univ. (United States); Kuo Zhong, KU Leuven (Belgium); Kai Song, Chinese Academy of Sciences (China)

Colloidal photonic crystals are photonic crystals made by bottom-up physical chemistry ciomimetic strategies from monodisperse colloidal particles. The self-assembly process is automatically leading to inherently three-dimensional structures with their optical properties determined by the periodicity, induced by this ordering process, in the dielectric properties of the colloidal material. The best-known optical effect is the photonic band gap, the range of energies, or wavelengths, that is forbidden for photons to exist in the structure and is eminent from irridescence or opalescence in nature. The photonic band gap is similar to the electronic band gap of electronic semiconductor crystals.[1] We have previously shown how with the proper photonic band gap engineering, we can insert allowed pass band defect modes and use the suppressing band gap in combination with the transmitting pass band to induce spectral narrowing of emission and improved energy transfer.[2] We show now how with a high-quality narrow pass band in a broad stop band, it is possible to achieve photonic crystal lasing in self-assembled colloidal photonic crystals with a planar defect.[3] In addition, with proper surface treatment in combination with patterning, we prepare for addressable integrated photonics. Finally, by incorporating a water in- and outlet, we can create optomicrofluidic structures on a photonic crystal allowing the optical probing of microreactors or micro-stopped-flow in the lab-on-an-optical-chip.[4]

References

1) L. Gonzalez-Urbina, K. Baert, B. Kolaric, J. Pérez-Moreno, and K. Clays, Chemical Reviews, 2012, 112(4), 2268-2285.

2) O. Kruglova, P.-J. Demeyer, K. Zhong, Y. Zhou, and K. Clays, Soft Matter, 2013, 9, 9072-9087.

3) K. Zhong, L. Liu, X. Xu, M. Hillen, A. Yamada, X. Zhou, N. Verellen , K. Song, S. Van Cleuvenbergen, R. Vallée, and K. Clays, ACS Photonics, 2016, 3, 2330-2337.

4) K. Zhong, M. Khorshid, J. Li, K. Markey, P. H. Wagner, K. Song, S. Van Cleuvenbergen, and K. Clays, J. Mater. Chem. C., 2016, 4, 7835-7858.

10355-11, Session 4

Charge carrier blocking layers for polymer-based electro-optic devices *(Invited Paper)*

James G. Grote, Fahima Ouchen, Air Force Research Lab. (United States); Michael M. Salour, IPITEK, Inc. (United States)

No Abstract Available

10355-12, Session 4

Photoelectronic application of DNA associated with metal complex *(Invited Paper)*

Norihisa Kobayashi, Chiba Univ. (Japan)

No Abstract Available

10355-13, Session 4

DNA thin film fluorination for lower index of refraction *(Invited Paper)*

Fahima Ouchen, Perry P. Yaney, James G. Grote, Air Force Research Lab. (United States)

No Abstract Available.

10355-20, Session PWed

Electrical performances of straight and castellated dielectrophoresis electrodes for biological molecules separation

Azrul Azlan Hamzah, Farahdiana Wan Yunus, Muhamad R. Buyong, Jumril Yunas, Burhanuddin Y. Majlis, Univ. Kebangsaan Malaysia (Malaysia)

Dielectrophoresis (DEP) exerts force on a dielectric particle using non-uniform electric field. DEP is utilized in separation of biological molecules in MEMS artificial kidney. In this work, interdigitated DEP electrodes are interwoven on the nanopores of silicon filtration membrane to act as anti-clogging mechanism for the MEMS nanofiltration system. Negative DEP is utilized to repel the larger molecules, in order to prohibit them from clogging the nanofilters. The intensities and distribution of electric fields generated by various electrode designs were studied using COMSOL software. Straight and castellated electrode designs were compared. The MEMS DEP electrodes were fabricated using aluminium, with total device area of 3500 μm x 3500μm. Spacing between the interdigitated electrodes for the straight and castellated designs were 100μm and 300μm respectively. The input voltage between the electrodes was 2V AC. It was observed that the electric field varies from positive to negative across the alternating electrodes for both designs. The castellated electrodes exhibited higher electric field, with a maximum value of 27.14kV/m at compared to 9.54 kV/m for the straight electrodes. Similar results were observed along the length of the electrodes, where the castellated design produced 1.85 kV/m of highly clustered electric field, compared to scattered field with maximum value of less than 100 V/m for the straight electrodes. These results suggest that the castellated design would cluster and separate biological molecules better compared to straight electrodes, thus making it more suitable to be used in artificial kidney nanofiltration system.

10355-21, Session PWed

Effect of different AFM micro cantilever in fluid on the rough surface topography quality close to the surface

Alireza Habibnejad Korayem, Moharam Habibnejad Korayem, Iran Univ. of Science and Technology (Iran, Islamic Republic of)

The use of higher vibration modes and different geometries of the AFM ?piezoelectric MC is affected by the surface topography quality in a liquid medium. ?Therefore, utilizing an appropriate geometry and vibration mode is of a great importance. ?This paper analyzes AFM MC types with rectangular, dagger and V-shaped geometries in ?the noncontact and tapping modes in a liquid medium for rough surfaces in Nanoscale. The ?modified couple stress theory (MCS) in a liquid medium according to Timoshenko beam ?theory is used in order to enhance the accuracy of equations. In addition, the differential ?quadrature (DQ) method has been used to solve the equations. Identification of ?environmental forces helps an exact investigation of the system vibration amplitude. ?Investigating the effect of geometric and force parameters on the MC vibration behavior ?leads to understanding the system and to design it properly in a liquid medium. Also, due to ?oscillating the MC near the sample surface, the effect of interaction forces between the ?sample surface and the MC, including van der Waals, contact and squeeze forces is ?analyzed in a liquid medium in addition to the hydrodynamic forces. Furthermore, due to ?the sever reduction of the MC amplitude caused by the squeeze force; the MC is angled in ?comparison with the horizontal surface. ?

10355-14, Session 5

Increasing electric field strength in polymer capacitors

James G. Grote, Fahima Ouchen, Air Force Research Lab. (United States); Michael M. Salour, IPITEK, Inc. (United States)

No Abstract Available.

10355-15, Session 5

Influence of the biomatrix on fluorescence efficiency of luminophores

François Kajzar, Ana-Maria Manea, Cosmina Andreea Lazar, Ileana Rau, Univ. Politehnica of Bucharest (Romania)

Our recent studies on fluorescence of different luminophores embedded in deoxyribonucleic acid (DNA) matrix show that their fluorescence quantum efficiency is usually larger than in the case of a synthetic polymer matrix [1-4] This is due to the particular environment created by DNA, which behaves like a ionic liquid creating an important electric field exerted on embedded chromophores, modyfying their electronic structure. Several observations with different luminophores will be presented and discussed.

[1] J. Massin, S. Parola, C. Andraud, F. Kajzar, I. Rau, Enhanced fluorescence of isophorone derivatives in DNA based materials, Opt. Mat., 10, 1810-1816(2013).

[2] A.-M. Manea, I. Rau, F. Kajzar and A. Meghea, Fluorescence, spectroscopic and NLO properties of green tea extract in DNA, Opt. Mat.,, 36 (1), 140-145(2013). http://dx.doi.org/10.1016/j.optmat.2013.04.016

[3] A.-M. Manea, I. Rau, F. Kajzar and A. Meghea, Preparation, Linear and NLO properties of DNA-CTMA-SBE complexes, Proceed. SPIE, vol. 8901, (2013).

[4] C. A. Lazar, F. Kajzar, M. Mihaly, A. E. Rogozea, A. R. Petcu, N. L. Olteanu and I. Rau, Novel materials based on DNA-CTMA and lanthanide (Ce3+, Pr3+), Biopolymers, 105(9), 613-617(2016)

10355-16, Session 5

Fabrication of biomimetic sensing devices using bacteriorhodopsin via an inkjet printing method *(Invited Paper)*

Hiroyuki Hasegawa, Katsuyuki Kasai, Toshiki Yamada, Shukichi Tanaka, Yukihiro Tominari, Takahiro Kaji, Akira Otomo, National Institute of Information and Communications Technology (Japan); Yoshiko Okada-Shudo, The Univ. of Electro-Communications (Japan)

Bacteriorhodopsin is known as a photoreceptive membrane protein obtained from a cell membrane of Halobacterium salinarum. In the device fabrication using this material, the process that needs post-processing to remove a part of the film unused has been utilized such as dip-coating or spin coating method. However, it is difficult to apply some processes for semiconductor industry such as lithography to the material due to its chemical stability. Therefore, an on-demand and pinpoint 'soft' patterning is required to realize highly integrated device fabrication using such biomaterials. Here, we present an attempt of the soft patterning using a material printer in the device fabrication.

The details of device fabrication via the ink-jet patterning, and characteristics of the devices will be presented.

10355-17, Session 6

Conjugated polymer thin films for dynamic generation of photothermal patterns *(Invited Paper)*

Eunkyoung Kim, Yonsei Univ. (Korea, Republic of)

Near infrared (NIR) photothermal pattern on conjugated polymer film enabled unique approaches to harvest thermal energy with various patterns. The NIR photothermal pattern was generated from a patterned optical lens (POLs), which created dynamic Near IR light pattern (NLP) and the corresponding photothermal pattern (PTP) on the conjugated polymer thin film. The POL was prepared from transparent polydimethylsiloxane (PDMS) designed to generate various light patterns. The PTPs allowed a wet transfer of films coated on top of the PTPs in aqueous media. Various PTPs were generated by the diffraction of NIR light through POLs having different micro-patterns, which afforded wet transfer with a desired pattern. This provided cell sheet patterns without changing the original cell morphology at cultured state. Further optical engineering of the wet transfer system allowed multiple transfer of active thin films and productions of multiple cell sheets with one dose of light.

10355-18, Session 6

DNA-based electromagnetic interference shielding *(Invited Paper)*

Michael M. Salour, IPITEK, Inc. (United States); Fahima Ouchen, James G. Grote, Air Force Research Lab. (United States)

No Abstract Available.

10355-19, Session 6

DNA brush-assisted vertical alignment of gold nanorods and those chiral plasmonics *(Invited Paper)*

Hideyuki Mitomo, Satoshi Nakamura, Hokkaido Univ. (Japan); Andrew Pike, Newcastle Univ. (United Kingdom); Yasutaka Matsuo, Kuniharu Ijiro, Hokkaido Univ. (Japan)

Control over the assembly of metal nanorods are important for creating high-performance nanomaterials. Alignment of gold nanorods in one direction was observed by adsorbing gold nanorods on a double stranded DNA brush through electrostatic interactions. Those ordered structures were attributed by optimizing the density of positive charge on gold nanorods and the density of grafted DNA chains. In agreement with a theoretical simulation, the resultant structure exhibit plasmonic properties depending on the orientation of the gold nanorods relative to the direction of oscillating electric field. We observed those gold nanorods condugated with DNA provided CD bands due to chiral plasmonic effects. Our approach is new one utilizing a conformation of a polymer chain for control over the assembly of metal nanorods and could form ordered matal nanorods not only in a large area but also on a non-flat surface.

10356-1, Session 1

Ultrahigh field enhancements from nanostructured metal thin films *(Keynote Presentation)*

Ibrahim Abdulhalim, Ben-Gurion Univ. of the Negev (Israel) and Nanyang Technological Univ. (Singapore)

Enhancing the optical fields near metal nanostructures is of high importance for sensing, energy harvesting and improving the efficiency of optoelectronic devices. Surface enhanced spectroscopies such as Raman scattering (SERS), fluorescence (SEF) and infrared absorption (SEIRA) are enhanced significantly thus allowing lower detection limit and supresolved imaging. Solar energy harvesting can be improved by designing structures that enhance the local optical field over wide spectral and angular ranges covering the whole solar spectrum. Detectors for the short wave and mid-IR ranges with higher efficiencies started to appear following an optimum designs incorporating plasmonic nanostructures.

During the last few years we have been investigating several plasmonic nanostructured thin films for improved biosensors and lately for energy harvesting devices using variety of configurations: standard Kretchmann-Raether configuration, grating coupling, free space excitation of localized plasmons (LSPs) from nanosculptured thin films, and lately excitation of LSPs via extended surface plasmons (ESPs). The later configuration was shown both theoretically and experimentally (using SEF and SERS) to reveal extraordinary enhancement when the matching conditions between the ESP and the LSP are met. Several configurations for improved SPR biosensors and ultrahigh enhancement of local optical fields will be presented with the potential applications in sensing, solar energy harvesting and optoelectronic devices.

Acknowledgments:

This research was conducted partially by NTU-HUJ-BGU Nanomaterials for Energy and Water Management Programme under the Campus for Research Excellence and Technological Enterprise (CREATE), that is supported by the National Research Foundation, Prime Minister's Office, Singapore.

References

1. Atef Shalabney, C. Khare, Jens Bauer, B. Rauschenbach, and I. Abdulhalim, J. Nanophoton. 6 (1), 061605 (2012).

2. Alina Karabchevsky, Chinmay Khare, Bernd Rauschenbach, and I. Abdulhalim, J. NanoPhotonics 6, 061508-1, 12pp (2012).

3. I. Abdulhalim, Small 10, 3499-3514 (2014).

4. S.K. Srivastava, A. Shalabney, I. Khalaila, C. Grüner, B. Rauschenbach, and I. Abdulhalim, Small 10, 3579-3587 (2014).

5. Sachin K. Srivastava, H. Ben Hamo, A. Kushmaro, R. S. Marks, C. Gruner, B. Rauschenbach and I. Abdulhalim, Analyst, 140, 3201-3209 (2015).

6. Sachin K. Srivastava, C. Grüner, D. Hirsch, B. Rauschenbach, and I. Abdulhalim, Opt. Exp., Accepted (2017).

7. Anran Li, Sivan Isaacs, Ibrahim Abdulhalim, Shuzhou Li, J. Phys. Chem. C 119, 19382-9 (2015).

8. Anran Li, Sachin Srivastava, Ibrahim Abdulhalim, Shuzhou Li, Nanoscale 8, 15658-664 (2016).

9. Sachin K. Srivastava, Anran Li, Shuzhou Li, Ibrahim Abdulhalim, J. Phys. Chem. C 120, 28735-42 (2016).

10356-2, Session 2

Optical liquid monitoring with sculptural multilayers Bragg microcavities incorporated to microfluidic chips *(Invited Paper)*

Francisco Yubero, Manuel Oliva, Jorge Gil-Rostra, Agustín R. Gonzalez-Elipe, Instituto de Ciencia de Materiales de Sevilla (Spain)

Porous Bragg microcavities (BMs) formed by the successive stacking of sculptural SiO_2 and TiO_2 layers with slanted and zig-zag configurations are prepared by glancing angle deposition (PVD-GLAD). These BMs act as wavelength dependent optical retarders. This optical behavior is attributed to a self-nanostructuration mechanism involving a fence-bundling association of nanocolumns as observed by Focused Ion Beam- Scanning Electron Microscopy (FIB-SEM). The retarder response of these optically active BMs can be modulated by dynamic infiltration of their open porosity with liquids or solutions with different refractive indices. The unprecedented polarization and tunable optofluidic properties of these nanostructured photonic systems have been successfully simulated with a simple model that assumes a certain birefringence for the individual stacked layers and accounts for the light interference phenomena developed in the BM. This type of self-associated nanostructures has been incorporated to microfluidic chips for free label liquid sensing. Several examples of the detection performance (experimental sensitivity to variations below 0.001 liquid refractive index units) of these chips, working either in reflection or transmission configuration, for the optical characterization of liquids of different refractive index and aqueous solutions of glucose flowing through the microfluidic chips are described.

10356-3, Session 2

High efficient light absorption and nanostructure-dependent birefringence of a metal-dielectric symmetrical layered structure

Yi-Jun Jen, Yi-Ciang Jhang, Wei-Chih Liu, National Taipei Univ. of Technology (Taiwan)

A multilayer that comprises ultra-thin metal and dielectric films has been investigated and applied as a layered metamaterial. By arranging metal and dielectric films alternatively and symmetrically, the equivalent admittance and refractive index can be tailored separately. The tailored admittance and refractive index enable us to design optical filters with more flexibility. The admittance matching is achieved via the admittance tracing in the normalized admittance diagram. In this work, an ultra-thin light absorber is designed as a multilayer composed of one or several cells. Each cell is a seven-layered film stack here. The design concept is to have the extinction as large as possible under the condition of admittance matching. For a seven-layered symmetrical film stack arranged as Ta_2O_5 (42 nm)/ a-Si (13 nm)/ Cr (20 nm)/ Al (30 nm)/ Cr (20 nm)/ a-Si (13 nm)/ Ta_2O_5 (42 nm), its mean equivalent admittance and extinction coefficient over the visible regime is 1.2+0.08i and 2.04, respectively. The unit cell on a transparent BK7 glass substrate absorbs 98.26% of normally incident light energy. On the other hand, a transmission-induced metal-dielectric film stack is investigated by considering the dielectric film as a bi-deposited thin film. The equivalent birefringence of the structure varied with wavelength and nanostructure are investigated here

10356-4, Session 2

Third order non-linear response as function of the laser power in SiO2:DR1 mesostructured and amorphous films

Jorge A. García-Macedo, Gerardo S. Gámez, Univ. Nacional Autónoma de México (Mexico)

Non-linear optical behavior can be obtained in materials exposed to laser radiation. There are no much results of these properties as function of the structure of the samples. In our case we prepared SiO2;DR1 amorphous samples by sol-gel method, and mesostructured ones by using cethylmethyamonium bromide (CTAB). The hexagonal structure was evidenced by X-ray diffraction. The transmittance of a focused Helium-Neon 394nm laser light was studied in these samples when moving around the focal point. With the results and using the Sheik-Bahae model the third order non-linear optical absorption coefficient ? and refractive index n2 were obtained. The dependence of ? as function of the laser power is shown in Figure 1 for both samples. They can be fit with an exponential curve that reaches saturation. It is clear the hexagonal structured helps to increase the sensitivity of the sample. In the case of the refractive index as function of the laser power the response is similar, but in this case the mesostructure does not give a strong difference, as shown in Figure 2.

10356-5, Session 3

Exotic nanophotonic behavior in systems of reduced dimensionality *(Invited Paper)*

Marin Soljacic, Massachusetts Institute of Technology (United States)

Systems of reduced dimensionality can enable a variety of novel nanophotonic phenomena. Some of our recent investigations in this field will be presented.

10356-6, Session 3

Engineered metasurface of gold funnels for microwave filtering

Shayan Moghaddas, Masih Ghasemi, Pankaj K. Choudhury, Burhanuddin Y. Majlis, Univ. Kebangsaan Malaysia (Malaysia)

Surface plasmon polariton (SPP) excitation of the coupled light at small contact area of chromium pillars as the interface of metastructured gold funnel layer and silicon medium can be enhanced locally in the gold meta-funnel-structured filter. The structure of this filter is comprised of three layers, namely gold meta-funnels, nanostructured chromium pillars and silicon as the substrate. The quantum energy of microwave field in the range of 0.01 eV to 0.04 eV, coupled with the excited plasmon at the first and second layers, form an excitation, known as deformed plasmon polariton. Asymmetric distribution of localized SPPs takes place owing to the inherent converging plasmonic feature of the gold funnel structure. The nano-sized thick chromium pillars act as interface medium for better adherent for the gold metasurface and silicon substrate. The formation of sharp reflection peaks with different magnitudes at different incident angles of the polarized wave in the spectral characteristics makes the structure prominent for filtering microwaves and infrared waves. Moreover, the gold meta-funnel-structured filter possesses the additional feature of distinguishing the type of polarized incident wave. It has been found that the transmission spectrum corresponding to the TM polarized waves over the same wavelength range are almost blocked at any incident angle. However, the transmission peaks corresponding to the TE waves greatly demonstrate another application of this device as a meta-polarizer filter.

10356-7, Session 3

Amorphous Fe-Dy-Tb-O (FDTO) thin films with transparent, magnetic, and semiconducting behaviors

Abhinav Malasi, Humaira Taz, The Univ. of Tennessee Knoxville (United States); Tamil Sakthivel, Univ. of Central Florida (United States); Rama Vasudevan, Oak Ridge National Lab. (United States); Connor Carr, The Univ. of Tennessee Knoxville (United States); Nano Yamoah, North Carolina A&T State Univ. (United States); Benjamin J. Lawrie, Raphael C. Pooser, Oak Ridge National Lab. (United States); Hernando Garcia, Southern Illinois Univ. Edwardsville (United States); Dhananjay Kumar, North Carolina A&T State Univ. (United States); Gerd Duscher, The Univ. of Tennessee Knoxville (United States); Art P. Baddorf, Oak Ridge National Lab. (United States); Sudipta Seal, Univ. of Central Florida (United States); Ramki Kalyanaraman, The Univ. of Tennessee Knoxville (United States)

Functional amorphous thin films are attractive because they can be made at low temperatures and have smooth films over large areas. In the past decade amorphous oxide semiconducting thin films combining transparency and conductivity, such as In-Ga-Zn-O have been used in display devices, solar energy harvesting, and flexible electronics. We discuss here a new class of amorphous thin film materials made from Fe-Dy-Tb-O that display extraordinary multifunctional properties. Thin films in the range of 9 to 70 nm were deposited by pulsed laser deposition (PLD) or by e-beam co-evaporation at room temperature onto a variety of substrates. Films deposited by PLD from terfenol-D target showed a combination of high optical transparency (>90% for 9 nm films @ 500 nm wavelength), very large n-type carrier mobility (>30 cm^2/V-s) and large conductivity. Films with different Fe to lanthanide (Tb+Dy) ratio were prepared by e-beam co-evaporation. Lower Fe/(Tb+Dy) ratio films showed semiconducting behavior, optical transparency, low sheet resistance (<200 Ohm-sq) and room temperature ferromagnetism. Higher Fe/(Tb+Dy) content films showed metallic behavior. Energy dispersive spectrometry, X-ray photoelectron spectroscopy, x-ray diffraction and electron microscopy investigations were used to determine the mcirostructure and chemical composition. Amorphous films with generally homogenous distribution of metal and oxygen was found. The properties of the films appears to be critically linked to the oxidation state of the cations and the metal to oxygen ratio. This material could be a promising new option as a transparent conductor or a ferromagnetic semiconductor for applications in energy harvesting and spintronics.

10356-8, Session 3

Topology controlled functional nanoclustered thin films with tendency to superconductivity

Sergey M. Arakelyan, Alexey O. Kucherik, Stella V. Kutrovskaya, Anton V. Osipov, Vladimir State Univ. (Russian Federation)

The physical properties of nanocluster/granular systems are very sensitive to the form, size and distance between their composing elements. The thin films can be easily modified both in necessary direction and by controlled way in femto- nanophotonics experiments under normal environmental conditions.

The variation of the enumerated above topology parameters can result in new type of quantum correlation states for charged particles. Moreover, the electronic energetic bands/gaps of the materials in such system can vary dramatically for the case resulting in new physical behavior of the system.

We used different laser ablation and deposition technique to induce the topology controlled nanoclustered thin films of semiconductor (PbTe), monometallic (Au, Ag, Cu, Ni) and bimetallic (Au+Ag, Au+Cu, Ag+Ni) materials deposited (thickness 5-100nm) on solid substrate.

In experiment, we have seen competition between increase conductivity while opening new channels in a spatially inhomogeneous charged structure and increase the resistance by increasing of the area between the conductive grains.

Such electrical transport properties (due to tunnel and quantum correlated states resulting in jumps electroconductivity in experiment) may be presented as a tendency to high temperature superconductivity due to special type of topological surface structures (both localized and delocalized coupled states for charge carriers).

Obtained results give us an opportunity to establish the basis of new physical principles to create the functional elements for the optoelectronics and photonics in hybrid set-up (optics + electrophysics) by the different topology control nanoclusters with dramatic increase of electroconductivity vs spatial structure of nanoclusters at room temperature.

10356-26, Session PWed

Development of batch producible hot embossing 3D nanostructured surface-enhanced Raman scattering chip technology

Chu-Yu Huang, Ming-Shiuan Tsai, National Chung Hsing Univ. (Taiwan)

To date, the major drawback of the existing Surface-Enhanced Raman Spectroscopy (SERS) active chip design is the need for complicated and expensive microfabrication process. The complexity of the production process lead to the SERS active substrate quality is hard to control. Therefore, the measurement results are different each time, repeatability is not good. In addition, the fabrication cost of these SERS active chips is too expensive to be widely used.

The main purpose of this project is to develop a batch producible hot embossing 3D nanostructured surface-enhanced Raman chip technology for highly sensitive label-free plasticizer detection. This project utilizing the AAO self-assembled uniform nano-hemispherical array barrier layer as a template to electroforming a durable nanostructured nickel mold. With the hot embossing technique and the durable nanostructured nickel mold, we were able to mass produce the 3D Nanostructured PC (Polycarbonate) substrates with consistent quality. Gold nanodots array were formed uniformly by the spontaneous separation and coalescence of gold ultrathin film when deposited onto the 3D Nanostructured PC substrate. It provides high spatial density of hot spots. The FDTD (Finite-difference time-domain method) simulation and experiments were conducted to study how the geometric parameters such as: pitch distance of gold nanodots and diameter of the nano-hemisphere affect the resulting SERS enhance factor. The optimized the 3D nano composite structured SERS active chips were able to detect the type and the concentration of the plasticizers from food and beverages samples.

The batch producible hot embossing 3D nanostructured SERS chip proposed in this study possess many advantages such as high sensitivity, low cost, and high consistency over currently available SERS chips. It is very promising to be widespread and extensively use in many rapid detection applications, such as food safety, environmental monitoring, and pathogen detection.

10356-27, Session PWed

The effect of ion-beam etching on the sol-gel coating in the preparation of tri-wavelength antireflection coating

Siyu Dong, Lingyun Xie, Tao He, Hongfei Jiao, Jinlong Zhang, Bin Ma, Zhanshan Wang, Xinbin Cheng, Tongji Univ. (China)

In high power laser system, it is highly desirable to develop antireflection (AR) coatings exhibiting high transmittance simultaneously at 355, 532, and 1064nm. Its realization usually needs multilayers and the film thickness and refractive index of each layer must be controlled precisely to ensure the transmittance in these specific wavelengths. Besides, in order to improve the laser damage resistance of AR coating, sol-gel process provides a preferable choice due to the great advantage on the damage characteristic. Unfortunately, it is challenging to prepare tri-wavelength AR coating by sol-gel method for its low controlling accuracy of film thickness. To modify the sol-gel film thickness, ion-beam etching process has been proposed by us to remove the redundant material at a low rate. However, owing to the characteristics as porous structure and relaxed texture, the nanostructure of sol-gel coating will be changed under the ion-beam, resulting in the change of refractive index. The key challenge lies in obtaining the relationship between the refractive index and etching depth. In this work, a systematic and comparative study was designed to reveal the evolution of nanostructure and refractive index of the SiO_2 sol-gel coating under the ion-beam etching. Based on the above findings, a hybrid approach that combined conventional sol-gel process with ion-beam etching was successfully applied to prepare the sol-gel coating with both the controllable thickness and refractive index. Finally, after modifying the thickness and refractive index of each layer, a tri-wavelength AR coating featured excellent AR properties was achieved, and its laser-induced damage threshold (LIDT) was increased significantly.

10356-28, Session PWed

Transition from Dyakonov and Dyakonov-Tamm surface waves to surface-plasmon-polariton waves induced by temperature

Tom G. Mackay, The Univ. of Edinburgh (United Kingdom); Francesco Chiadini, Univ. degli Studi di Salerno (Italy); Vincenzo Fiumara, Univ. degli Studi della Basilicata (Italy); Antonio Scaglione, Univ. degli Studi di Salerno (Italy); Akhlesh Lakhtakia, The Pennsylvania State Univ. (United States)

Temperature-induced changes in the propagation of electromagnetic surface waves, guided by the planar interface of a temperature-sensitive isotropic material (namely, InSb) and a temperature-insensitive anisotropic material were investigated theoretically in the terahertz frequency regime. Two types of anisotropic partnering material were considered: (i) a homogeneous material and (ii) a periodically-nonhomogeneous material. As the temperature increases, the isotropic partnering material is transformed from a weakly dissipative dielectric material to a metal. As a consequence, the surface waves change from Dyakonov surface waves to surface-plasmon-polariton waves for (i), and change from Dyakonov--Tamm surface waves to surface-plasmon-polariton waves for (ii). Numerical investigations demonstrated that dramatic changes in the numbers of propagating Dyakonov or Dyakonov--Tamm surface waves, their angular existence domains, their propagation constants, and their decay constants, could arise from modest changes in temperature.

10356-29, Session PWed

Non-linear and linear optical techniques for identification of functional groups on plasma treated surfaces on the monolayer level

Munise Cobet, Matthias Kehrer, David Stifter, Johannes Kepler Univ. Linz (Austria)

We present a comprehensive study of the plasma modification of metals and polymers by combining non-linear and linear optical techniques as complementary sources of information. The used plasma is of a novel type of atmospheric pressure jet plasma, where also liquids can be ignited into the ionized state in a defined manner.

Among non-linear optics, IR-visible sum-frequency-generation (SFG) is used to obtain the vibrational spectral resonances of the treated surfaces which are not readily accessible by other optical methods. Since at surfaces the inversion symmetry is broken (centrosymmetric bulk) , spectroscopic features are highly sensitive to molecular adsorbates, such as small functional groups attached to the very surface and bond orientation. For a sufficiently intense illumination for this 2nd-order process, a pulsed IR-tunable laser source is used which overlaps with the second harmonic output from the 1064nm-laser. The orientation of molecules can be obtained by variation of polarization for the excitation and signal light beams.

While SFG is probing molecular adsorbates induced by the plasma, linear optics like confocal Raman and ellipsometry provide valuable information about the oxidation of metals, i.e. the formation of amorphous transparent layers on the surface and the degree of crystallinity in polymers.

The plasma processed species show a high level of functionalization with hydroxy-, carboxyl-, and carbonyl-groups as well as amino- and nitro-groups.

SFG, Raman and Ellipsometry optical responses are crosschecked with chemical composition obtained by X-ray photoelectron spectroscopy and HREELS in order to give a certain quantification of the found features.

10356-30, Session PWed

Oblique angle deposition of Al films on nanopatterned substrates for wire grid polarizers

Wonyoung Kim, Sungmin Hwang , Tae Young Kim, Won Gyu Ham, Myung Hoe Koo, Minbaek Lee, Chang Kwon Hwangbo, INHA Univ. (Korea, Republic of)

Wire grid polarizers (WGPs) comprised of 1D metal nanograting structures are drawing attention to industrial applications in display and optics. A WGP transmits the transverse magnetic (TM) wave and reflect the transverse electric (TE) wave. It is well-known that the realization of WGPs with a large area requires high-cost facility such as E-beam lithography, serial etching, and deposition. In this study, we employed oblique angle deposition (OAD) and nanoimprint lithography (NIL) methods to fabricate the broadband Al WGPs in visible and infrared wavelength regime. Firstly, polymer nanostructures were patterned by NIL, which resulted in nanopatterns with a pitch of 120 nm, width of 50 nm, and height of 160 nm. And then, Al was selectively deposited on the ridge of polymer nanopatterns by OAD. The result shows that the average transmittance of TM wave is 67% and the polarization extinction ratio is 22 dB in the visible and near infrared wavelength regime. Finite differential time domain simulation and SEM images were employed to analyze the various Al structures shaped by the different OAD conditions on top of the nanopatterns. The analysis and experimental results in this study may afford a simple and effective way for fabrication of large-scale and high-performance WGPs and can be applied to non-conformal deposition of metamaterials in near future.

10356-31, Session PWed

Non-exhibition of Bragg phenomenon by chevronic sculptured thin films: experiment and theory

Vikas Vepachedu, Patrick D. McAtee, Akhlesh Lakhtakia, The Pennsylvania State Univ. (United States)

A sculptured thin film (STF) is an array of parallel nanocolumns separated by a void network. If the individual nanocolumns take on the form of a zig-zag as they grow, then the resulting STF is known as a chevronic STF. To grow a chevronic STF, a collimated vapor flux is directed towards a substrate in vacuum. The plane of the substrate is oriented so that the vapor flux is directed towards it at a specified angle chi_v. Once a deposition of thickness h is over, the substrate is rapidly rotated about its normal axis by 180 deg and a second deposition of the same thickness is made, thereby completing a chevron. Multiple chevrons are deposited to yield a thin film that is periodically nonhomogeneous in the thickness direction.

We experimentally investigated the exhibition of the Bragg phenomenon for light incident normally as well as obliquely on a 10-period thick chevronic STF of zinc selenide. The period of this thin film was 330 nm and it was fabricated with chi_v = 20 deg. Measurements of the four linear reflectances and four linear transmittances were made as functions of both the free-space wavelength and the angle of incidence. The absence of the Bragg phenomenon for a wide range of angles of incidence was observed and compared with previous theoretical work of Maksimenko and Slepyan for normal incidence. Additional calculations were carried out at non-normal incidence.

10356-32, Session PWed

Electrophysical and gas-sensing properties of the nanoscale thin films of tin dioxide modified with silver and yttrium and with catalytic additives (Pt/Pd, Ag, Au or Pt/Pd/Au) on the surface

Aleksei V. Almaev, Stanislav Kim, National Research Tomsk State Univ. (Russian Federation)

The results of researches of the electrophysical and gas-sensing properties of the nanoscale thin polycrystalline tin dioxide films with a thickness of 120 nm are presented. It is shown that the introducing of the silver and yttrium in the bulk of tin dioxide control temporal drift of the characteristics of sensor based on these materials, but the resistivity and gas sensing properties of the films are determined by the dispersed layers of the catalysts (Pt/Pd, Ag, Au or Pt/Pd/Au) deposited on the surface of tin dioxide. The dispersed double layers of Pt/Pd on the surface of these films increase the resistivity, the response to hydrogen and decrease the operating temperature of the sensors. Replacement of catalytic layers of platinum and palladium on Ag or Au leads to a decrease of resistivity of the films, but also increase the operating temperature of the sensors. Deposition of the gold in the case of the triple catalyst Pt/Pd/Au also helps to reduce the resistivity of the films and increase the operating temperature of the sensors. Measurements of the conductivity in the thermo-cyclic operation mode show that the behavior of the films is caused by the dependence of the surface density of chemisorbed oxygen ions on the type of catalyst on the surface of tin dioxide films.

10356-33, Session PWed

Enhanced water stability and thermoelectric properties of PEDOT:PSS films via a glycerol vapor treatment

Sung Hyun Kim, Wonkwang Univ. (Korea, Republic of)

Thermoelectric (TE) energy harvesting devices, which recovered energy from waste heat, has been attracted much interest as environmentally friendly devices. The performance of TE is evaluated by the figure of merit (ZT) which is expressed as ZT = S2?T/? where S, ?, and ? is the Seebeck coefficient, electrical conductivity, thermal conductivity. The power factor (PF) is given by S2?. In order to achieve high a high ZT, thermoelectric materials have to show high power factor and low thermal conductivity. PEDOT:PSS has been considered as one of the most promising thermoelectric materials owing to its high electrical conductivity, high Seebeck coefficient, and low thermal conductivity. Especially, the value of Seebeck coefficient is easily fluctuated by water. Only a few research focusing on water stability of TE devices were reported. Therefore, the effect of water on the TE devices and the relationship between water-related TE performances are required to develop in the field of organic TE devices.

In this work, we reported a simple method using vapor treatment of glycerol, simultaneously leading to enhanced PF which was increased from 0.03 to 5.93 ?V/mK2 at optimal treatment condition as well as water stability compared to control device. We systematically investigated the effect of glycerol on PF by using IR, AFM, and XRD analysis. Based on that results, we found that glycerol induced morphological change of PEDOT:PSS film originating from cross-linking reaction where sulfonic ester formed between glycerol and PSS. In addition, the modified PSS induced lowering hygroscopic property of PEDOT:PSS thus the resultant films shows better water stability in highly humidity condition.

10356-34, Session PWed

Photonic nanostructure design for high efficiency light absorber

Yi-Fan Huang, National Taipei Univ. of Technology (Taiwan) and Institute of Atomic and Molecular Sciences - Academia Sinica (Taiwan); Yi-Jun Jen, National Taipei Univ. of Technology (Taiwan)

An ideal light-absorbing surface is able to collect light energy from wide ranges of wavelengths and angles of incidence. It has been reported that photonic and plasmonics structures can manipulate and couple light on the nanoscale surface. The properties of nanostructures which can enhance light absorption and improve solar energy conversion also have been expected. In this report, we design two types of photonic nanostructure for light absorption surfaces, metal nanohelices array on glass substrate and antireflecting structures on semiconductor substrates (moth eye's surface). The optical properties of these two types of structures were been analyzed using finite difference time domain (FDTD) calculations. FDTD simulation demonstrates that the aluminum-silver nanohelices array with thickness about ~500 nm have strong rod to rod localized surface plasmons which can absorb wavelength of light from UV to NIR region and angle of incidence up to 70 degree. Antireflecting structures utilize design parameters of spacing/wavelength and length/spacing, which could be expected exhibiting ?99% optical absorption over wavelength from UV-vis region and angle of incidence up to 60 degree in low-index and high-index semiconductor materials.

10356-35, Session PWed

Influence of the crystal potential on the energetic spectrum of the vicinal superlattices in the quantum: confined films

Victor Petrov, Kotel'nikov Institute of Radio Engineering and Electronics of Russian Academy of Sciences (Russian Federation)

As is known, the existence of superlattice effects in quantum - confined films (QCFs) on vicinal planes initiated with the appearance in these systems of a new crystallographic translation period in the plane of the film A >>a0 (a0 - lattice constance). The emergence in these QCF of the periodic system of atomic steps on the high-index Miller boundaries allows explain in the effective mass approximation the appearance of minigaps (MGs) in the energetic spectrum of particles in such QCF by the scattering of electrons on such steps. At the same time it is evident that the contribution to the MGs formation should also be made by all crystallographic planes in the area of localization of the particle wave function. In this work shows theoretically that the consideration of only crystal potential and of the potential locating the particle in QCF on high-index Miller vicinal planes results in the appearance of MGs even without taking into account of the step structure of the film boundaries. A method has been developed that makes it possible to calculate the energetic spectrum of this QCFs for the arbitrary localizing potential by leaving the effective mass approximation in single-valley semiconductors of the GaAs - type. For the cases of the rectangular quantum well analytical expressions have been obtained for MGs magnitudes which depend on the parameters of the crystal potential and localizing potentials as well as on angles that define the orientation of the QCFs in the crystal.

10356-36, Session PWed

Photo-excited carrier dynamics of CuPc/C60 organic thin film structure

Mitsuru Inada, Tomoki Miyake, Nozomi Isobe, Tadashi Saitoh, Kansai Univ. (Japan)

The structure of the sample was ITO/CuPc(30 nm)/C60(40 nm)/BCP(5 nm)/Al. These layers were deposited on SiO2 substrate by using vacuum evaporation. After the depositions, the sample was taken out into the atmosphere, and then, it was immediately sealed with epoxy resin.

Optical absorption spectra for each thin film layer were measured by ultraviolet to visible light absorption spectrometer (JASCO V-630). Current density-voltage characteristics of the sample were measured by using YOKOGAWA GS820 source measure unit with conventional two-terminal method. The spectral sensitivity characteristics were measured using a lock-in amplifier (Stanford Research SR830) and a xenon lamp as the irradiation source. The transient photocurrent properties were investigated irradiating third harmonic (532 nm) of pulsed Nd-YAG laser light (Quantel CFR200, pulse width: 7 ns) and the current decay characteristics were observed on a screen of digital oscilloscope. All measurements were carried out at room temperature and in air.

The obtained carrier lifetime is much longer than that of estimated lifetime from the mobility of thin-film layers. This means the carrier transport cannot be described by a general carrier drift model. In addition, the carrier lifetime become short under white halogen light illumination. The results suggest that the photo-excited carrier transport is affected by trapping levels in the organic layers.

10356-39, Session PWed

Photoelectric properties of ITO-pSi structures

Tetiana Batsko, Sergiy Kondratenko, Taras Shevchenko National Univ. of Kyiv (Ukraine)

Study photoelectric effects in semiconductors occupies an important place in the analysis of the properties of semiconductors. Photocurrent spectroscopy and photo EMF is a powerful method for studing of nonequilibrium processes in semiconductors.

Purpose of the work was to study photovoltaic properties of structures ITO-Si and Ge-Si and mechanisms of spatial separation of nonequilibrium charge carriers in the space charge barrier.

Current-Voltage (I-V) characteristics, photovoltage spectra and kinetics of decline for two series of samples SiO2-pSi and iSi-pSi with different thicknesses deposition layer ITO was studied.

It was established that the formation of the ITO film on the surface of SiO2-pSi structures and iSi-pSi leads to the formation of a potential barrier, which causes the straightening of I-V curves and observation Photovoltage. It is shown that an increase in film thickness the value of the barrier increases.

10356-40, Session PWed

Optical and structure properties of crystalline silver nano-layers with ultra-smooth surfaces

Husam Abu-Safe, German Jordanian Univ. (Jordan); Hameed Naseem, Univ. of Arkansas (United States)

Thin metal films with ultra-low scattering and ohmic losses are needed for plasmonic applications. Fabrication of noble metal nano-layers with ultra-smooth surfaces remains a challenge for this purpose. In this paper, silver layers of 3, 29, 60 and 122 nm thickness deposited directly on c-Si(111) substrates without any wetting layer are examined. The films were prepared at room temperature using electron beam evaporation with 0.5 Å/sec deposition rate. The optical and structural properties of the nano-layers depend on the experimental parameters of deposition process and the film thickness. The complex permittivity of the silver layers were parametrized using spectroscopic Ellipsometry measurements. The oscillatory patterns obtained from the x-ray reflectivity measurements indicated crystalline structure with ultra-smooth surfaces for all fabricated films.

10356-9, Session 4

Broadband perfect absorption of epsilon-near-zero thin films *(Invited Paper)*

Chang Kwon Hwangbo, INHA Univ. (Korea, Republic of)

Epsilon-near-zero (ENZ) metamaterials have been studied in various research areas such as wavefront engineering, supercoupling effect, strong coupling, nonlinear optics, and perfect absorption. An ideal ENZ material of ?=0 is highly omnireflective at any angle of incidence. For a real ENZ material of Re(?)≈0 the imaginary part Im(?) is not zero from the causality principle. At an ENZ wavelength at Re(?)≈0, the normal electric field (E_z) in an ENZ thin film with a very small Im(?) becomes very strong and the group velocity slows down; E_z is inversely proportional to the thickness of the film and the imaginary part of ?, resulting in a large light absorption in a low optical loss ENZ thin film. We investigate the tunable ENZ wavelength of indium tin oxide (ITO) thin films in the NIR wavelength regime which are controlled by the film growth conditions and demonstrate the broadband perfect absorption (PA) using the ITO multilayers of different ENZ wavelengths.

Coherent perfect absorption (CPA) is an optical phenomenon occurring in an absorbing thin film by the interaction of two counter-propagating coherent waves. We propose a new broadband CPA scheme based on ENZ multilayer films and investigate the multi-wavelength optical switching, indicating that the on- and off-states can be controlled by the phase shift and wavelength of the two incident waves.

In this lecture we provide design principles and fabrication guidelines for thin film ENZ devices for PA and CPA, which can find various applications in optical switches, modulators, filters, sensors, and energy harvesting devices.

10356-10, Session 4

Asymmetric metal-insulator-metal (MIM) structure formed by pulsed Nd:YAG laser deposition with titanium nitride (TiN) and aluminum nitride (AlN)

Yasushi Oshikane, Osaka Univ. (Japan)

A novel nanostructured end cap for a truncated conical apex of optical fiber has been studied experimentall and numerically. The peculiar cap is composed of asymmetric metal-insulator-metal (MIM) structure coupled with sabwavelength holes. The MIM structure may act as reflective band cut filter or generator of surface plasmon polariton (SPP). And nano holes in the thicker metal layer could extract the SPP from the MIM structure and lead it to outer surface of the metal layer. For the purpose, the author has started to create the asymmetric MIM structure with TiN and AlN by pulsed laser deposition (PLD). TiN is one of the candidates for alternative plasmonic materials in these days, and it seems that there are many difficulties to bring out its good plasmonic property as subwavelength thin film. In this research, hot pressed disc target, made of TiN powder, is irradiated by 355 nm laser pulses in high vacuum. A series of trial shots rerulted several passable films on glass slides which shows x-ray diffraction (XRD) and x-ray photoelectron spectroscopy (XPS) peaks related to TiN. But residual oxygen in high vacuum space got mixed in with the PLDed films. To avoid oxygen and lack of nitrogen, the PLD process is done in nitrogen based atmosphere at around several Pa. Desirable material of the insulator layer in MIM structure by PLD would be transparent nitrides in visible region because of the nitrogen atmosphere. Therefore AlN was selected as the material of insulator layer. Spectroscopic characteristic of the MIM will be reported.

10356-11, Session 4

An advanced plasmonic cermet solar absorbers for high temperature solar energy conversion applications

Maryna Bilokur, Angus R. Gentle, Matthew D. Arnold, Geoffrey B. Smith, Michael B. Cortie, Univ. of Technology, Sydney (Australia)

We examine the use of plasmonic cermet coatings based on nanoparticles of Au or Ag embedded in a dielectric medium including AlN and SiO2. The intended application is for enhancing solar absorption in solar-thermal conversion devices. For this application, coatings must have both the appropriate spectral selectivity and must be stable at high temperature. The nanoparticles in these materials provided a broad absorption peak due to localized surface plasmon resonances while the surrounding dielectric medium red-shifted the absorption range and provided mechanical support. Spectral tuning was also achieved by controlled variation of the thicknesses of individual layers in cermet-dielectric multilayer thin film stacks. These were produced by magnetron sputtering and possessed absorption efficiencies ranging between 91% and 97% with low thermal emittance. Thermal stability was assessed by annealing in vacuum at 800K while monitoring any changes in optical properties using high temperature ellipsometry. The results showed that this type of composite solar absorber exhibits very competitive solar absorptance and thermal stability. Thermal stability is also influenced by the stack profile. They are thus suitable for use in solar energy conversion applications at elevated temperatures.

10356-12, Session 4

Optical and electronic functionality of 2D crystal-metal hybrids: computation and microscopy

Donald K. Roper, Gregory T. Forcherio, Mourad Benamara, Univ. of Arkansas (United States); Luigi Bonacina, Univ. de Genève (Switzerland); Jeremy R. Dunklin, Univ. of Arkansas (United States); Drew DeJarnette, U.S. Dept. of Energy (United States); Claudia Backes, Yana Vaynzof, Ruprecht-Karls-Univ. Heidelberg (Germany)

Two-dimensional (2D) nanocrystals (NC) offer superior electron mobility, thermal conductivity, mechanical strength and broken inversion symmetry that could enable advanced sensors or quantum computing. But challenges in fabrication, assembly, and tunable coordination of optical and electronic activity have constrained their implementation in functional devices. This work examined optical modulation of carrier injection and second harmonic generation (SHG) in 2DNC, i.e., graphene and transition metal dichalcogenide (TMD) via localized plasmon modes. Monolayer 2DNC used were chemical vapor deposited (graphene) or liquid exfoliated from bulk (TMD). 2DNC were decorated by gold (Au) and silver (Ag) plasmonic structures through three methods (i) evaporation, (ii) drop-casting and (iii) direct reduction. Electron energy loss spectroscopy

(EELS) was used to predict and induce plasmon bright, dark, and hybrid modes. EELS enabled quantitative femtosecond-scale measurement of spectroscopic plasmon dephasing and nanometer-resolved mapping of electric fields on the 2DNC-metal hybrids. Coupled and discrete dipole simulations were used to characterize radiative and intraband dephasing in order to distinguish carrier injection. X-ray photoemission spectroscopy was used to contrast physicochemical metal-2DNC bonds vs. polyvinylpyrrolidone coatings representating alternate pathways for carrier injection. A tunable laser scanning confocal microscope (LSCM) was used to measure second harmonic generation of metal-2DNC hybrids. A computational scaffold supporting analysis spanning atom to nanometer scales was used to develop compact structure-function relations in order to rationalize measured values. Coordination of EELS, XPS, and LSCM offers a comprehensive approach to characterize plasmon-induction of carrier induction and SHG at high spatiotemporal resolution in metal-2DNC hybrids.

10356-13, Session 4

Angular-insensitive plasmonic filters based on ultrathin metal patch array

Chenying Yang, Weidong Shen, Yueguang Zhang, Xu Liu, Zhejiang Univ. (China); Jing Zhou, Chengang Ji, L. Jay Guo, Univ. of Michigan (United States)

We proposed a new scheme of omnidirectional plasmonic filters using ultrathin metal patch array structure. The two plasmonic filters comprised by single-layer of ultrathin metal patch array and three-layer of dielectric-metal-dielectric (DMD) patch array both can be used as reflective RGB filters as well as transmissive CMY filters simultaneously, which maintain the same perceived reflection/transmission color at unpolarized illumination for a broad range of incidence angles. The reflection/transmission curves are coincident at different angles and the color difference characterized by CIE DE2000 formula is inconceivably small, implying that no color variation can be observed for a large angle up to 60 degree. Various colors can be obtained by simply tuning the dimension of the patch structure and the thicknesses of the two dielectric layers for the DMD filter. The simulated reflectance/transmittance and electric field distribution profile of the plasmonic filter was performed by Finite-Difference Time-Domain (FDTD) method, while the color devices were fabricated by steps of sputtering deposition and focus ion beam (FIB) milling. The angle insensitive color filtering feature of this plasmonic filters is resulted from the localized surface plasmonic resonance excited in the single metallic patch. And as a result, great feature that patch array with as few as two periods were sufficient to demonstrate color filtering can be obtained.

10356-14, Session 5

Advanced light management for liquid phase crystallized silicon thin-film solar cells *(Invited Paper)*

Klaus Jäger, Helmholtz-Zentrum Berlin für Materialien und Energie GmbH (Germany) and Konrad-Zuse-Zentrum für Informationstechnik Berlin (Germany); Grit Köppel, David Eisenhauer, Helmholtz-Zentrum Berlin für Materialien und Energie GmbH (Germany); Duote Chen, Helmholtz-Zentrum Berlin (Germany); Martin Hammerschmidt, Sven Burger, Konrad-Zuse-Zentrum für Informationstechnik Berlin (Germany); Bernd Rech, Christiane Becker, Helmholtz-Zentrum Berlin für Materialien und Energie GmbH (Germany)

Liquid phase crystallized (LPC) silicon thin-film solar cells are a promising novel approach with a current efficiency record of 13.2%. The LPC process is performed on a nanocrystalline Si layer on an interlayer stack on glass. The high refractive index of crystalline silicon requires anti-reflective measures to maximize in-coupling of light from the glass superstrate into the c-Si absorber. Ideally, these nanotextures also scatter the incident light in order to trap more light in the absorber – especially at long wavelength. Light trapping is of special importance here because the absorber in LPC-Si solar cells is only 5 – 20 μm thick. Nanotextures for light management at the glass-Si interface can only be placed prior to the LPC process. Hence, they must be smooth in order to ensure LPC-Si with a high electronic quality.

In this contribution we discuss two types of nanostructures situated between glass and LPC-Si: (1) sinusoidal nanotextures and (2) smooth anti-reflective three-dimensional textures (SMART). Both textures are fabricated with nanoimprint lithography and enhance the optical performance of the solar cells. LPC-Si solar cells on these textures have excellent material qualities and hence electric properties, such that open circuit voltages exceeding 615 mV or even 640 mV are measured for sinusoidal or SMART structures, respectively. Numerical results obtained with the finite element method (FEM) match well with experimental data. This was achieved with a numerical correction, which is applied to FEM results a posteriori and allows to adequately take the thick glass superstrate into account at negligible numerical cost.

10356-15, Session 5

Wave front design using multi-scale metasurfaces

Didier Felbacq, Univ. Montpellier (France); Emmanuel Kling, Safran Electronics & Defense (France)

Metasurfaces are the bidimensional analog of metamaterials. There are made of resonant elements deposited on a thin film. They have been shown to allow for the control of polarization of light, in particular through topological effects and to make possible the transmission of a light beam under generalized refraction laws. In the present work, metasurfaces whose period is made of several resonant elements with both electric and magnetic dipoles are considered. A general theory of diffraction is developed and the possibility of optimization towards designing a predifined wavefront are investigated.

To do so, we use multiple scattering theory as well as a singular perturbation approach that allows us to obtain a simple setting of the scattering problem in terms of a generalized impedance operator. This formulation is then used within an optimization algorithm in order to investigate the range of parameters over which a fine control of the transmitted beam can be obtained.

10356-16, Session 5

Asymmetries in surface waves and reflection/transmission characteristics associated with topological insulators

Tom G. Mackay, The Univ. of Edinburgh (United Kingdom); Francesco Chiadini, Univ. degli Studi di Salerno (Italy); Vincenzo Fiumara, Univ. degli Studi della Basilicata (Italy); Antonio Scaglione, Univ. degli Studi di Salerno (Italy); Akhlesh Lakhtakia, The Pennsylvania State Univ. (United States)

Three numerical studies were undertaken involving plane-wave interactions with topological insulators. In each study, the topologically insulating surface states of the topological insulator were represented by a nonzero surface admittance. Canonical boundary-value problems were solved for the following cases: (i) Dyakonov surface wave propagation supported by the interface of a columnar thin film and an isotropic dielectric topological insulator; (ii) Dyakonov-Tamm surface wave propagation supported by the interface of a structurally chiral material and an isotropic dielectric topological insulator; and (iii) reflection and transmission at the planar interface of a topologically-insulating columnar thin film and vacuum. For studies (i) and (ii) the nonzero surface admittance resulted in asymmetries in the wave speeds and decay constants of the surface waves, while in study (iii) the nonzero surface admittance resulted in asymmetries in the reflectances and transmittances.

10356-17, Session 5

On optical-absorption peaks in a nonhomogeneous dielectric material over a two-dimensional metallic surface-relief grating

Faiz Ahmad, The Pennsylvania State Univ. (United States); Thomas H. Anderson, Benjamin J. Civiletti, Peter B. Monk, Univ. of Delaware (United States); Akhlesh Lakhtakia, The Pennsylvania State Univ. (United States)

The rigorous coupled-wave approach was used to calculate the optical absorption in a dielectric material deposited over a two-dimensional metallic surface-relief grating. The dielectric material was taken to be nonhomogeneous in the direction normal to the mean plane of the grating. The grating corrugations were chosen to be hillocks on a hexagonal grid. The chosen structure should support two types of guided-wave modes: surface-plasmon-polariton (SPP) waves and waveguide modes (WGMs). The absorption varies with the direction, polarization state, and the free-space wavelength of the incident light.

The peaks of absorption were correlated with the excitations of SPP wave modes and WGMs predicted by the underlying canonical boundary-value problems for guided wave propagation. Two cases were considered: (i) a periodic photonic crystal made from layers of silicon oxynitrides of differing composition, and (ii) a solar cell comprising three amorphous-silicon p-i-n junctions.

10356-18, Session 6

New generation all-silica based optical elements for high power laser systems

(Invited Paper)

Tomas Tolenis, Lina Grineviciute, Ctr. for Physical Sciences and Technology (Lithuania); Andrius Melninkaitis, Vilnius Univ. (Lithuania); Algirdas Selskis, Rytis Buzelis, Ctr. for Physical Sciences and Technology (Lithuania); Lina Ma?ule, Vilnius Univ. (Lithuania); Ramutis Drazdys, Ctr. for Physical Sciences and Technology (Lithuania)

Laser resistance of optical elements is one of the major topics in photonics. Various routes have been taken to improve optical coatings, including, but not limited by, materials engineering and optimisation of electric field distribution in multilayers. During the decades of research, it was found, that high band-gap materials, such as silica, are highly resistant to laser light. Unfortunately, only the production of anti-reflection coatings of all-silica materials are presented to this day. A novel route will be presented in materials engineering, capable to manufacture high reflection optical elements using only SiO_2 material and GLancing Angle Deposition (GLAD) method. The technique involves the deposition of columnar structure and tailoring the refractive index of silica material throughout the coating thickness. A numerous analysis indicate the superior properties of GLAD coatings when compared with standard methods for Bragg mirrors production. Several groups of optical components will be presented including anti-reflection coatings, Bragg mirrors, spectral filters and etc. Structural and optical characterisation of the method have been performed and compared with standard methods. All researches indicate the possibility of new generation coatings for high power laser systems.

10356-19, Session 6

Pulsed laser deposition of multiferroic complex oxide superlattices

John G. Jones, Air Force Research Lab. (United States); Zhongqiang Hu, Universal Technology Corp. (United States); Krishnamurthy Mahalingam, UES, Inc. (United States); Lawrence Grazulis, Univ. of Dayton Research Institute (United States); Matthew P. Zielewski, Wright State Univ. (United States); Gerald R. Landis, Univ. of Dayton Research Institute (United States); Yalin Lu, U.S. Air Force Academy (United States); Gail J. Brown, Air Force Research Lab. (United States)

Oxide layered structures that exhibit both polarization and magnetization properties simultaneously at room temperature are of intense interest for applications in information processing, data storage, sensors, actuators and tunable filters. One approach to creating a naturally layered heterostructure of very thin FE and FM layers is to use an Aurivillius phase oxide. The bulk ceramic version of $Bi_5Fe_{0.5}Co_{0.5}Ti_3O_{15}$ has shown the co-existence of polarization and magnetization at temperatures well above room temperature. $Bi_5Fe_{0.5}Co_{0.5}Ti_3O_{15}$ (BFCTO) ceramics exhibits a naturally forming layered structure of perovskite-like layers separated by Bi_2O_2 layers. These bulk ceramic properties led to an interest in further exploring the material's potential for electronic and photonic applications when deposited as crystalline thin films. Using pulsed laser deposition (PLD) and a $Bi_5Fe_{0.5}Co_{0.5}Ti_3O_{15}$ target, desired thicknesses of 30 or 70 nm was achieved using a 248 nm KrF excimer laser, an energy of 450 mJ per pulse, and a background pressure of oxygen. Trends in material properties were identified by systematically varying growth conditions and using in-situ spectroscopic ellipsometry, ex-situ XRD and AFM measurements. A representative TEM with EDS measurement was measured for the sample with best corresponding XRD. The thin films replicated the oxide superlattice structure formed in the bulk ceramic targets.

10356-20, Session 6

Optical anisotropy due to perpendicular azimuth serial bi-deposition onto tilted substrates

Matthew Tai, Matthew D. Arnold, Angus R. Gentle, Geoffrey B. Smith, Univ. of Technology, Sydney (Australia)

Angled columnar structures produced by oblique angle deposition (OAD) possess optical polarization effects useful for filters, retarders and polarimeters. The anisotropy of these thin films is intriguing: it arises from the structures formed and is influenced by many factors including bulk refractive index, temperature, deposition rate and tilt angle. Serial bi-deposition (SBD) is an extension of the growth processes involved in OAD, by alternating deposition of thin layers with azimuthal substrate rotation. SBD typically increases the in-plane birefringence, but the relative importance of underlying processes requires further investigation. In this work, silicon nanostructures were constructed by modified SBD with perpendicular azimuths at a tilt angle range 50-80°. The silicon nanostructures were formed off-axis, meaning they did not develop along the deposition axes. The optical anisotropy and void fractions were compared with varying tilt angles to determine the greatest birefringence in these off-axis films. Growth processes and possible applications are discussed.

10356-21, Session 6

Graphene oxide reduction induced by femtosecond laser irradiation

Maren Kasischke, Stella Maragkaki, Evgeny L. Gurevich, Andreas Ostendorf, Ruhr-Univ. Bochum (Germany)

Abstracts should contain enough detail to clearly convey the approach and the results of the research. Accepted abstracts may be published and made available at the meeting. Please submit only 250-word abstracts for review.

Large-scale and low-cost fabrication of graphene is of great interest for employing it in diverse applications due to the outstanding electrical properties of the graphene layers. A promising fabrication method is

the reduction of graphene oxide (GO), which results in a graphene-like material. Beside thermal and chemical methods, reduction of GO can also be achieved photochemically by laser irradiation. In this study, we examine the efficiency of latter method with a fiber laser (1030 nm, 280 fs) in inert atmosphere varying following parameters: laser repetition rate, overlapping rate and fluence. The chemical properties of the irradiated areas were analyzed with Raman and X-ray photoelectron spectroscopy (XPS) while electrical properties were evaluated using contact resistance measurements. We found that, within a wide range of fluences at high overlapping rates, photochemical oxygen reduction can be achieved. However hybridization transition of sp3 to sp2 graphene-like structures only takes place at the upper fluence window of the mentioned range. This finding is in agreement with an existing hypothesis that heat deposition into the material is necessary for structural reorganization of GO.

10356-22, Session 7

Zero-contrast silicon-based metasurfaces: resonance physics and applications *(Invited Paper)*

Yeong Hwan Ko, Robert Magnusson, The Univ. of Texas at Arlington (United States)

Nanopatterned surfaces and films with subwavelength periodicity sustain striking resonance effects as input light couples to leaky Bloch-type waveguide modes. In 1990, we coined the term “guided-mode resonance (GMR)” to clearly communicate the fundamental physics at play. In recent years, traditional GMR resonance devices are often called metasurfaces or metamaterials. These devices can have 1D or 2D periodicity as the resonance is not dependent on the type of periodicity in any fundamental ways. By design, a plethora of differing spectral expressions is available with this device class. Wide parametric design spaces allow control of light amplitude, phase, polarization, near-field intensity, and light distribution on surfaces and within device volumes. Here, we review principles and applications of resonant nanophotonic devices, addressing the considerable divergence in the literature regarding their operational principles. In many cases, the fundamental Bloch-mode aspect of wave propagation in periodic media is dismissed or ignored. The coupling of evanescent diffraction orders that drive the resonant leaky modes is often misunderstood. Rather, local Fabry-Perot or Mie-type modes, naturally generated by the fundamental resonance effects, are taken to be the causal entities behind the observed spectral characteristics. Here, we discuss device design and optimization with rigorous mathematical methods while properly noting the physical processes in play. We present flat-top bandpass filters applying cascaded 1D or 2D GMR structures achieving spectra that are comparable to those found with hundreds of stacked layers. At the resonance wavelength, strong phase dispersion causes flatting of the transmission spectrum. Moreover, wideband unpolarized reflectors are enabled by sequentially arranged GMR devices; we provide both theoretical and experimental spectra pertinent to these. Finally, we present tunable narrow bandpass filters with double GMR structures. For polarization independence, the device is designed by identical orthogonal 1D GMRs. The compact nature and high-efficiency operation of this device class renders attendant technology particularly interesting for applications where minimal, robust, and lightweight devices are desired. The guided-mode resonance concept applies in all spectral regions, from the visible band to the microwave domain, with available low-loss materials.

10356-23, Session 7

Nitrogen doped silicon-carbon multilayer protective coatings on carbon obtained by TVA method

Victor Ciupina, Univ. Ovidius Constanta (Romania) and Academy of Romanian Scientists (Romania) and Univ. of Bucharest (Romania); Eugeniu Vasile, Univ. Politehnica of Bucharest (Romania); Corneliu Porosnicu, National Institute for Laser, Plasma and Radiation Physics (Romania); Gabriel C. Prodan, Univ. Ovidius Constanta (Romania); Cristian P. Lungu, National Institute for Laser, Plasma and Radiation Physics (Romania); Rodica Vladoiu, Univ. Ovidius Constanta (Romania); Ionut Jepu, National Institute for Laser, Plasma and Radiation Physics (Romania); Aurelia Mandes, Virginia Dinca, Aureliana Caraiane, Univ. Ovidius Constanta (Romania); Virginia Nicolescu, Ovidiu Cupsa, Ceronav (Romania); Paul Dinca, National Institute for Laser, Plasma and Radiation Physics (Romania); Agripina Zaharia, Univ. Ovidius Constanta (Romania)

Protective nitrogen doped Si-C multilayer coatings on carbon, used to improve the oxidation resistance of carbon, were obtained by Thermionic Vacuum Arc (TVA) method. The initial carbon layer having a thickness of 100nm has been deposed on a silicon substrate in the absence of nitrogen, and then a 3nm Si thin film to cover carbon layer was deposed. Further, seven Si and C layers were alternatively deposed in the presence of nitrogen ions, each having a thickness of 40nm. In order to form silicon carbide at the interface between silicon and carbon layers, all carbon, silicon and nitrogen ions energy has increased up to 150eV. The characterization of microstructure, electrical and tribological properties of as-prepared N-Si-C multilayer structures were done using Transmission Electron Microscopy (TEM, STEM) techniques, Energy Dispersive X-Ray Spectroscopy (EDXS), Thermal Desorption Spectroscopy (TDS), electrical and tribological measurements. N-Si-C multilayer samples were investigated up to 1000oC. Oxidation protection of carbon is based on the reaction between oxygen and silicon carbide, resulting in SiO2 and CO2, and also by reaction involving N, O and Si, resulting in silicon oxynitride (SiNXOY) with a continuously variable composition, and on the other hand, since nitrogen acts as a trapping barrier for oxygen. The tribological measurements reveal that the friction coefficient on the N-Si-C structures used is smaller than friction coefficient on uncoated carbon layer. To perform electrical measurements, 80% silver filled two-component epoxy-based glue ohmic contacts were attached on the N-Si-C samples. Electrical conductivity was measured in constant current mode. The experimental data show the increase of conductivity with the increase of the nitrogen content. To explain the temperature behavior of electrical conductivity we assumed a thermally activated electric transport mechanism.

10356-24, Session 7

Thin film grating reflector for high power lasers

Jinlong Zhang, Shuaikai Shi, Hongfei Jiao, Bin Ma, Xinbin Cheng, Zhanshan Wang, Tongji Univ. (China)

High reflection (HR) coatings are one of the key components in high power laser systems, and the stress and the thermal effect of HR coatings are always difficult to control and influence the quality of output laser pulse. In this paper we present approaches to realize the HR components based on the concept of thin film gratings. These gratings are composed with the nanostructured thin films of HfO2 and Ta2O5, which is proved to possess quite high laser damage threshold. We discuss the design of such HR gratings with broad bandwidth and optimized electric-field distribution. Several HR gratings will be fabricated and the spectral properties will be measured. Moreover, we will investigate the stress and laser damage characteristics. The possible damage mechanisms of NIR HR gratings are then discussed. Finally, we compare the advantages and challenges of these thin film gratings reflectors with HR coatings for applications in high power laser systems.

10356-25, Session 7

Advanced design of UV waveplates based on nano-structured silica thin films

Lina Grineviciute, Tomas Tolenis, Rytis Buzelis, Ctr. for Physical Sciences and Technology (Lithuania); Mindaugas Andrulevicius, Algirdas Lazauskas, Kaunas Univ. of Technology (Lithuania); Algirdas Selskis, Ramutis Drazdys, Ctr. for Physical Sciences and Technology (Lithuania)

Polymers, solid or liquid crystals and other materials with anisotropic refractive index can be used for production of waveplates. Unfortunately, most of aforementioned materials are fragile, unstable when environmental conditions changes, difficult to apply in microsystems and has low resistance to laser radiation. Retarders, fabricated by evaporation process, do not consist any of these drawbacks. A waveplate can be deposited on micro optics or other optical elements, essentially improving compact optical systems. The range of available materials is limited by absorption losses for waveplates in UV spectral region. Therefore, the full-scale investigation was accomplished with three eligible candidates – LaF_3, Al_2O_3 and SiO_2. Structural (XPS, XRD, SEM) and optical (spectrophotometry, elipsometry) analysis have shown superior properties of silica material for UV waveplate production. Previous researches indicate that the continuous deposition of nano-structured amorphous layer results in considerable optical losses. The expansion and coalescence of individual columns causes significant light scattering in UV spectral region. A novel approach was devised to overcome this drawback. Combination of homogenous and anisotropic all-silica thin films resulted in multilayer waveplate with low optical losses. The design enables to produce transparent (T~99%) UV waveplate with high laser induced damage threshold.

10357-1, Session 1A

Swapping spin currents and spin Hall magnetoresistance *(Invited Paper)*

Michel I. Dyakonov, Univ. Montpellier (France)

Two topics related to spin currents and the Spin Hall Effect [1] will be discussed.

Swapping spin currents [2] is a transformation of spin currents in which the direction of spin and the direction of flow are interchanged. Like the spin Hall effect and the anomalous Hall effect, this phenomenon is caused by spin-orbit interaction. It opens a way of re-directing spin currents.

Spin Hall magnetoresistance [3] is an effect of second order in spin-orbit interaction. It is a result of the combination of the direct and inverse spin Hall effects, and of the Hanle effect (depolarization by magnetic field).

Both effects have aroused considerable interest in recent years. The experimental results (mostly for metals) and the relevant theoretical ideas will be reviewed, open questions and related problems will be discussed

[1] M.I. Dyakonov and V.I. Perel, JETP Lett. 13, 467 (1971); Phys. Lett. A 35, 459 (1971)

[2] M.B. Lifshits and M.I. Dyakonov, Phys. Rev. Lett. 103, 186601 (2009)

[3] M.I. Dyakonov, Phys. Rev. Lett. 99, 126601 (2007)

10357-2, Session 1A

Spintronic phenomena arising from bulk and interface spin-orbit interaction *(Invited Paper)*

Kazuya Ando, Keio Univ. (Japan)

Spin-orbit coupling (SOC) in solids plays a crucial role in modern spintronics. When a charge current passes through a heavy metal with strong SOC, electrons with opposite spins are deflected in opposite directions, resulting in the generation of a transverse spin current, which is known as the spin Hall effect. Another source of the charge-spin conversion is the Rashba-Edelstein effect, where a charge flow in a Rashba two-dimensional electron gas results in the creation of a non-zero spin accumulation. Here, we show that the Rashba-Edelstein effect drives a new type of magnetoresistance in a metallic heterostructure: the Rashba-Edelstein magnetoresistance [1]. We show that the simultaneous action of the direct and inverse Rashba-Edelstein effects in a Bi/Ag/CoFeB trilayer couples the current-induced spin accumulation to the electric resistance. We further show that, even when the magnetization is saturated, the resistance increases with increasing the magnetic-field strength, which is attributed to the Hanle magnetoresistance in this system. We also discuss recent experimental observation of enhanced spin-torque generation efficiency in a naturally-oxidized Cu, which is evidenced by measuring the spin-torque ferromagnetic resonance for Py/Cu bilayers [2].

[1] H. Nakayama, Y. Kanno, H. An, T. Tashiro, S. Haku, A. Nomura, and K. Ando, Phys. Rev. Lett. 117, 116602 (2016).

[2] H. An, Y. Kageyama, Y. Kanno, N. Enishi and K. Ando, Nature Communications 7, 13069 (2016).

10357-3, Session 1A

Theory of angular momentum transport *(Invited Paper)*

Shufeng Zhang, The Univ. of Arizona (United States)

The angular momentum currents have three distinct forms known as the electron spin current, the incoherent magnon current and the coherent macroscopic magnon current. We present a unified theory to correlate these different angular momentum currents in magnetic multilayered structures by using semi-classical approaches for electrons and magnons. Within each layer, which could be magnetic or non-magnetic and metallic or insulating, the non-equilibrium electron or magnon distributions satisfy the Boltzmann equations for fermions and bosons. The momentum and angular momentum transfer among electrons, incoherent magnons, and order parameters are explicitly taken into account via collision terms. By establishing boundary conditions for spin chemical potentials and the angular momentum current at the interfaces, we determine the distributions and subsequently find the spatial dependence of angular momentum currents. The formalism is applied to various multilayer systems and a few predictions are outlined.

10357-4, Session 1B

Ferromagnetism and spin-dependent transport in NdTiO3/SrTiO3 heterostructures *(Invited Paper)*

Vlad S. Pribiag, Univ. of Minnesota, Twin Cities (United States)

Complex oxide interfaces are a promising platform for studying a wide array of correlated electron phenomena in low-dimensions, including magnetism and superconductivity. The microscopic origin of these phenomena in oxide interfaces remains an open question. Evidence for magnetic order at oxide interfaces has been reported using various experimental techniques, including vibrating sample magnetometry, superconducting quantum intereference magnetometry, neutron scattering, and magneto-transport. Here we investigate electron transport in MBE-grown NdTiO3/SrTiO3 heterostructures as a function of magnetic field and time, at temperatures down to 150 mK. The magnetoresistance (MR) reveals steady-state signatures of ferromagnetic order below ~1.5 Kelvin. Moreover, the MR also shows transient hysteretic features with a characteristic timescale of ~100 seconds. We discuss the importance of time-dependent measurements for distinguishing signatures of magnetism from other effects that can produce hysteretic MR in experiments at low temperatures.

10357-5, Session 1B

Spin-dependant tunnelling in ultrathin Schottky junctions based on La0.66Sr0.33MnO3 / SrTiO3:Nb interfaces *(Invited Paper)*

Philippe Lecoeur, Univ. Paris-Sud 11 (France); Georg Kurij, Ctr. de Nanosciences et de Nanotechnologies (France); Aurélie Solignac, CEA-Ctr. de SACLAY (France); Thomas Maroutian, Institut d'Électronique Fondamentale, Univ. Paris-Sud II (France); Guillaume Agnus, Univ. Paris-Sud 11 (France); Ruben Guerrero, IMDEA Nanociencia (Spain); Laurie E. Calvet, Ctr. de Nanosciences et de Nanotechnologies (France); Myriam Pannetier-Lecoeur, CEA-Ctr. de SACLAY (France)

Since the first observation of tunnelling effect in La0.7Sr0.3MnO3 based magnetic structures, the search for high TMR values has been the main goal of research in this field, aiming at developing high sensitive magnetic sensors. Nevertheless, oxides TMR often have high level of noise when using SrTiO3 as insulating barrier drastically reducing the interest of such devices [1]. Recently we introduced the use of heavily doped n-type semiconductor SrTi0.8Nb0.2O3 as fully depleted layer to form the insulating barrier [2-3]. Magneto-transport properties of the MTJs were studied as a function of applied bias, temperature and barrier thickness. It is found that using semiconducting barrier at the place of the standard insulator, leads to a significantly improved reproducibility of results and in the spectral noise density reduced by three orders of magnitude at low temperature. We ascribe that fact to a strongly reduced amount of defects, such as oxygen vacancies, in doped SrTi0.8Nb0.2O3. This results brings novel opportunities to develop high sensitive magnetic devices working at low temperature.

[1] A. Solignac, G. Kurij, R. Guerrero, G. Agnus, T. Maroutian, C. Fermon, M. PArnnetier-Lecoeur, Ph. Lecoeur, SPIE Proceedings Series, 2015, 9551, pp.95512F (2016)

[2] G. Kurij, A. Solignac, T. Maroutian, G. Agnus, R. Guerrero, L. E. Calvet, M. Pannetier-Lecoeur, and Ph. Lecoeur, Appl. Phys. Lett. 110, 082405 (2017)

[3] G. Kurij, L. E. Calvet, R. Guerrero, T. Maroutian, G. Agnus, A. Solignac, and Ph. Lecoeur, Thin Solid Films vol. 716, part B, 82-85 (2016)

10357-6, Session 2A

Theory of unidirectional magnetoresistance *(Invited Paper)*

Giovanni Vignale, Steven S. L. Zhang, Univ. of Missouri (United States)

Recent experiments have detected nonlinear unidirectional magnetoresistance (UMR) in metallic bilayers consisting of a heavy metal (HM) and a ferromagnetic metal (FM). That is to say, a small change in the longitudinal resistance of the bilayer has been observed when reversing the direction of either the applied in-plane current or the magnetization. We attribute such nonlinear transport behavior to the spin-polarization dependence of the electron mobility in the FM layer acting in concert with the spin accumulation induced in that layer by the spin Hall current originating in the bulk of the HM layer. An explicit expression for the nonlinear UMR is derived based on a simple drift-diffusion model, which shows that the nonlinear magnetoresistance appears at the first order of the spin Hall angle, and changes sign when the current is reversed, in agreement with the experimental observations. We point out that nonlinear UMR is quite generally expected to arise in non-magnetic spin-orbit coupled electronic materials from the concerted action of current-induced spin polarization and spin-polarization-dependent mobilities. Nonlinear UMR in spin-momentum-locked bands, such as surface states of three-dimensional topological insulators will also be discussed.

10357-7, Session 2A

Spin Hall magnetoresistance and spin orbit torques in metallic heterostructures *(Invited Paper)*

Masamitsu Hayashi, The Univ. of Tokyo (Japan)

Strong spin orbit effects in metallic heterostructures with broken structural inversion symmetry have opened new paradigms to control magnetic moments electrically. In particular, generation of spin current or spin accumulation via the spin Hall effect and/or the Rashba Edelstein effect has attracted great interests as its degree determine the efficiency of current induced control of magnetization via the spin orbit torques. We have studied the spin Hall magnetoresistance and the resulting spin orbit torque in metallic heterostructures to estimate the effective spin Hall angle and the spin mixing conductance of the interface. A large spin Hall magnetoresistance is found in structures that include W and Pt. We have also studied the spin Hall magnetoresistance caused by a temperature gradient applied across the films. We find signatures of the so-called spin Nernst effect in W. Spin current generated from other material systems including chiral antiferromagnets will be discussed.

Acknowledgement: JSPS Grant-in-Aid (16H03853, 15H05702), Spintronics Research Network of Japan

10357-8, Session 2A

Nonlocal spin diffusion driven by giant spin Hall effect at oxide heterointerfaces *(Invited Paper)*

Jung-Woo Yoo, Mi-Jin Jin, Ulsan National Institute of Science and Technology (Korea, Republic of); Seon Young Moon, Korea Institute of Science and Technology (Korea, Republic of); Jungmin Park, Junhyeon Jo, Ulsan National Institute of Science and Technology (Korea, Republic of); Shin-Ik Kim, Hyun Cheol Koo, Byoung-Chul Min, Korea Institute of Science and Technology (Korea, Republic of); Hyun-Woo Lee, Pohang Univ. of Science and Technology (Korea, Republic of); Seung-Hyub Baek, Korea Institute of Science and Technology (Korea, Republic of)

The conductive interface at LaAlO3/SrTiO3 (LAO/STO) can be designed to exhibit high mobility with tunable carrier concentration and exhibits various unique electronic behaviors. This interface could be also interesting playground for "spin-orbitronics" as the structure itself strongly couple the spin and orbital degree of freedom through the Rashba spin-orbit interaction. One of core experiments toward this direction is the nonlocal spin transport measurement, which has remained elusive due to the low spin injection efficiency to this system. Here we bypass the problem by generating a spin current not through the spin injection from outside but instead through the inherent spin Hall effect and demonstrate the nonlocal spin transport. The Hall-bar (H-bar) like geometry was employed to generate a transverse spin polarized current, which in turn can be detected by the inverse spin Hall effect. Our results clearly demonstrated the non-local spin diffusion as well as effective spin charge conversion at this oxide heterointerface. The non-local spin resistance was confirmed through the signature of a Larmor spin precession and its length dependence. The analysis on the non-local spin voltage displays that both D'yakonov-Perel' and Elliott-Yafet mechanisms involve in the spin relaxation. Our results show that the oxide heterointerface is highly efficient in spin-charge conversion with exceptionally strong spin Hall coefficient ? ? 0.15 ± 0.05 and could be an outstanding platform for the study of coupled charge and spin transport phenomena and their electronic applications.

10357-9, Session 2A

Conditions for the existence of spin to charge current conversion in spin-Hall devices: the Hall bar versus the Corbino disk *(Invited Paper)*

Jean-Eric Wegrowe, Robert Benda, Ecole Polytechnique (France); Miguel Rubi, Univ. de Barcelona (Spain)

We investigate the compatibility of the concept of "charge to spin current conversion" with the second law of thermodynamics in the context of the spin-Hall effect (SHE).

This investigation is performed in the framework of the two spin channel model of the SHE.

It is first shown that the spin-accumulation due to spin-flip scattering at the interface is independent of the We investigate the compatibility of the electric charge to spin current conversion with the second law of the thermodynamics in the spin-Hall effect (SHE).

This investigation is performed in the framework of the two spin channel model of the SHE.

It is first shown that the spin-accumulation due to spin-flip scattering at the interface is independent of the spin-accumulation due to SHE, if the spin-flip scattering length is much larger than the electrostatic screening length [1].

A variational technique based on the least dissipation principle is then applied. We show that, for a bulk paramagnet with spin-orbit interaction, in the case of the Hall bar geometry the principle of minimum dissipated

power prevents the generation of transverse spin and charge currents while in the case of the Corbino disk geometry, transverse currents can be produced. More generally, we show that electric charge accumulation prevents the stationary spin to charge current conversion to occur inside the device [2].

[1] J.-E. Wegrowe, "Stationary state and screening equations in spin-Hall effect", arXiv:1701.0601 (2017)

[2] J.-E. Wegrowe, R. V. Benda, and J. M. Rubi, Conditions for the generation of sin current in spin-Hall devices, arXiv :1609.03916v1 [cond-mat.mes-hall] 2016.

10357-10, Session 2B

Control of ferromagnetism and transport by material growth and wavefunction engineering in ferromagnetic semiconductors and heterostructures

(Invited Paper)

Masaaki Tanaka, The Univ. of Tokyo (Japan)

Ferromagnetic semiconductors (FMSs) have been intensively studied for decades as they have novel functionalities that cannot be achieved with conventional metallic materials, such as the ability to control magnetism by electrical gating or light irradiation [1-3]. Prototype FMSs such as (Ga,Mn) As, however, are always p-type, making it difficult to be used in real spin devices. Here, we demonstrate that by introducing Fe into InAs, it is possible to fabricate a new n-type electron-induced FMS with the ability to control ferromagnetism by both Fe and independent carrier doping. The studied (In1-x,Fex)As layers were grown by low-temperature molecular beam epitaxy on semi-insulating GaAs substrates. Electron carriers in these layers are generated by independent chemical doping of donors. The ferromagnetism was investigated by magnetic circular dichroism (MCD), superconducting quantum interference device (SQUID), and anomalous Hall effect (AHE) measurements. With increasing the electron concentration (n = 1.8?1018 cm-3 to 2.7?1019 cm-3) and Fe concentration (x = 5 - 8%), the MCD intensity shows strong enhancement at optical critical-point energies E1 (2.61 eV), E1 + ?1 (2.88 eV), E0' (4.39 eV) and E2 (4.74 eV) of InAs, indicating that the band structure of (In,Fe)As is spin-split due to sp-d exchange interaction between the localized d states of Fe and the electron sea. SQUID and AHE measurements are also consistent with the MCD results. The Hall and Seebeck effects confirm the n-type conductivity of our (In,Fe)As samples. The electron effective mass is estimated to be as small as 0.03-0.175m0, depending on the electron concentration. These results reveal that the electrons are in the InAs conduction band rather than in the impurity band, allowing us to use the conventional mean-field Zener model of carrier-induced ferromagnetism [4]. This band picture is different from that of GaMnAs [5][6]. Our results open the way to implement novel spin-devices such as spin light-emitting diodes or spin field-effect transistors, as well as help understand the mechanism of carrier-mediated ferromagnetism in FMSs [7-14].

Furthermore, we demonstrate new phenomena in (In,Fe)As and its hetrerostructures: Novel crystalline anisotropic magnetoresistance with two fold and eight fold symmetry [7], and control of ferromagnetism by strain, quantum confinement, gate electric field and wavefunction engineering in quantum heterostructures with a (In,Fe)As quantum well [10-12]. Very recently, we have found a very intriguing phenomenon; sudden restoration of the band ordering associated with the ferromagnetic phase transition in the prototypical ferromagnetic semiconductor GaMnAs [15]. Also, we have successfully grown another narrow-gap p-type III-V-based FMS (Ga,Fe)Sb with high Curie temperature (TC>300K) [16]. Combining different n-type and p-type FMSs will lead to new spin-related functionalities and devices.

This work was carried out in collaboration with Drs. S. Ohya, P. N. Hai, I. Muneta, L. D. Anh, M. Kobayashi, S. Sakamoto, and A. Fujimori. This work was partly supported by Grants-in-Aid for Scientific Research, Project for Developing Innovation Systems of MEXT, and Spintronics Research Network of Japan (Spin-RNJ).

References

[1] S. Koshihara et al., Phys. Rev. Lett. 78, 4617 (1997).

[2] H. Ohno et al., Nature 408, 944 (2000).

[3] A. M. Nazmul, S. Kobayashi, S. Sugahara and M. Tanaka, Jpn. J. Appl. Phys. 43, L233 (2004).

[4] T. Dietl, H. Ohno, F. Matsukura, J. Cibert and D. Ferrand, Science 287, 1019 (2000).

[5] S. Ohya, I. Muneta, P. N. Hai, and M. Tanaka, Phys. Rev. Lett. 104, 167204 (2010).

[6] S. Ohya, K. Takata, and M. Tanaka, Nature Phys. 7, 342 (2011).

[7] P. N. Hai, L. D. Anh, S. Mohan, T. Tamegai, M. Kodzuka, T. Ohkubo, K. Hono, and M. Tanaka, Appl. Phys. Lett. 101, 182403 (2012).

[8] P. N. Hai, D. Sasaki, L. D. Anh, and M. Tanaka, Appl. Phys. Lett. 100, 262409 (2012).

[9] P. N. Hai, L. D. Anh, and M. Tanaka, Appl. Phys. Lett. 101, 252410 (2012).

[10] L. D. Anh, P. N. Hai, and M. Tanaka, Appl. Phys. Lett. 104, 042404 (2014).

[11] L. D. Anh, P. N. Hai, Y. Kasahara, Y. Iwasa, and M. Tanaka, Phys. Rev. B92, 161201(R) (2015).

[12] S. Sakamoto, L. D. Anh, P. N. Hai, G. Shibata, Y. Takeda, M. Kobayashi, Y. Takahashi, T. Koide, M. Tanaka, A. Fujimori, Phys. Rev. B93, 035203 (2016).

[13] L. D. Anh, P. N. Hai, and M. Tanaka, Nature Comm. 7, 13810 (2016).

[14] M. Tanaka, S. Ohya, and P. N. Hai (invited paper), Appl. Phys. Rev. 1, 011102 (2014).

[15] I. Muneta, S. Ohya, H. Terada, and M. Tanaka, Nature Commun. 7, 12013 (2016).

[16] N. T. Tu, P. N. Hai, L. D. Anh, and M. Tanaka, Appl. Phys. Lett. 108, 192401 (2016).

10357-11, Session 2B

Spin signals in Si non-local transport devices with giant spin accumulation

(Invited Paper)

Ron Jansen, Aurelie M. Spiesser, H. Saito, National Institute of Advanced Industrial Science and Technology (Japan); Y. Fujita, S. Yamada, K. Hamaya, Osaka Univ. (Japan); Shinji Yuasa, National Institute of Advanced Industrial Science and Technology (Japan)

As silicon, the mainstream semiconductor, exhibits only weak spin relaxation, it is the logical material of choice for spin-based semiconductor devices. The electrical injection of a spin accumulation in Si is achieved by ferromagnetic tunnel contacts, whereas non-local (NL) spin transport devices provide a powerful tool to electrically detect spins and determine the important spin-transport parameters. Unfortunately, the observed NL spin signals are usually much smaller (~ 2 orders of magnitude) than predicted by theory. Thus, achieving large spin signals in Si non-local devices is still a major challenge. Moreover, an in-depth comparison of non-local spin signals with theory is still lacking and the connection between non-local spin signals and local 3-terminal (3T) Hanle spin signals has not been established.

Here we report on the electrical signals produced by spin accumulation in Si-based non-local devices having ferromagnetic contacts of various sizes. First, we present the observation of NL spin signals that correspond to a giant spin accumulation of more than 17 meV in the Si channel, and show that the non-local spin signals are in excellent agreement with numerical calculations of spin injection and diffusion, but not with widely used analytical expressions. Secondly, we provide a comprehensive characterization of 3T Hanle spin signals in the same non-local devices, and compare the results with non-local spin-transport data and numerical calculations.

10357-12, Session 2B

Magnetic and superconducting proximity effects on the transport properties of hybrid heterostructures *(Invited Paper)*

Alex Matos-Abiague, Igor Zutic, Univ. at Buffalo (United States)

Interfaces between different materials provide versatile opportunities to study emergent behavior. With the lack of inversion symmetry, the formation of interfacial spin-orbit fields (SOFs) is crucial for novel phenomena, absent or fragile in the bulk. We theoretically investigate the interplay between SOFs and proximity-induced magnetism in hybrid SM/F heterostructures (SM and F stand for semiconductor and ferromagnet, respectively) as well as its effect on spectral and transport properties. The anisotropic spin-dependent transport leads to the emergence of novel magnetoresistive phenomena in planar SM/F multi-terminal devices, where both the longitudinal and transverse Hall-like responses become anisotropic with respect to the orientation of the proximity-induced magnetization. Strategies for increasing the anisotropy of the charge and spin transport are discussed. In order to enhance the device functionalities, we explore, in addition to interfacial SOFs, the role of non-Abelian fields produced by magnetic textures. We also investigate the superconducting proximity effect in SM/S heterostructures (S stands for superconductor), where the interfacial SOFs can lead to the emergence of triplet pairing even for s-type S materials. The signatures of interfacial triple pairs on the supercurrent are analyzed.

10357-13, Session 3A

Spintronics probed with soft x-rays *(Invited Paper)*

Elke Arenholz, Lawrence Berkeley National Lab. (United States)

The ever increasing importance of spintronics is based on our improved understanding spin based phenomena and our ability to engineer materials with specific materials properties. In this talk, we will highlight the contributions soft x-ray based characterization tools can make to the advancement of spintronics using two recent experiments.

Materials that exhibit simultaneous order in their electric and magnetic ground states hold promise for use in next-generation memory devices in which electric fields control magnetism. Such materials are exceedingly rare and engineering magnetoelectric multiferroic by interleaving two or more atomically thin layers is an intriguing new approach. A very recent example is establishing room temperature coexisting ferromagnetic and ferroelectric order in LuFeO3)m/(LuFe2O4)1 superlattices. [1]

Spin currents are mostly detected indirectly through measurement of spin-torque driven magnetization precession, spin-current induced second harmonic optical effects, inverse spin Hall effect (ISHE), etc. We have recently succeeded in monitoring a pure ac spin current through a Py/Cu/Co multilayer with by x-ray detected ferromagnetic resonance (XFMR) [2]

In both cases, the soft x ray based characterization techniques were crucial and will be discussed.

References

[1] J. A. Mundy et al., Nature 537, 523 (2016)

[2] J. Li et al., Phys. Rev. Lett. 117, 076602 (2016)

10357-14, Session 3A

Operando XMCD experiments: a tool for the investigation of magnetoelectric coupling in multiferroics *(Invited Paper)*

Piero Torelli, Istituto Officina dei Materiali, Consiglio Nazionale delle Ricerche (Italy)

In this work we present an experimental set-up which permits the simultaneous investigation of the magnetic and electronic structure of materials and nanostructures by performing XMCD under applied bias voltage at the APE-HE beamline at Elettra the Italian synchrotron radiation facility [1]. With this technique we investigated the magnetic properties of the Fe/BaTiO3 interface, which is probably the most representative Ferroelectric(FE)/Ferromagnetic(FM) interface. In this work [2] thanks to the chemical sensitivity of the operando XMCD we have observed the formation of iron oxide at the interface that surprisingly shows a magnetic phase transition driven by the FE state of the BaTiO3.

In a second example we investigated the magnetic properties of the LSMO/BTO interface as a function of temperature and of the ferroelectric polarization. In this experiment we were able to separate the effect of strain and of the electric charge of the substrate ferroelectric polarization on the magnetic properties of the FM overlayer. In fact the BTO substrate as a function of temperature change the crystallographic structure inducing different strain on the overlayer, while we have at the same time switched the FE polarization of the substrate while recording XMCD and thus we were able to observe the changes induced by the strain or the charge separately.

[1] G. Panaccione et al., Rev. Sci. Instrum. 80, 043105 (2009)

[2] G. Radaelli et al. Nature Communications 5, 3404 (2014)

10357-15, Session 3A

Magnetoelectroelastic coupling at artificial multiferroic interfaces probed with soft x-ray techniques *(Invited Paper)*

Rajesh V. Chopdekar, Univ. of California, Davis (United States)

I will present our recent work in studying strain- and charge- mediated magnetoelectric coupling at the interface of ferromagnetic thin films and relaxor ferroelectrics. By using soft x-ray spectroscopy and spectro-microscopy, we have disentangled changes in electric field-driven remanent magnetization states in ferromagnets such as cobalt, nickel, and Sr-doped manganites. X-ray magnetic circular dichroism allows for interrogation of magnetization orientation in an elementally resolved manner, while X-ray magnetic linear dichroism provides insight into anisotropy effects such as anisotropic strain or magneto-crystalline anisotropy orientation. These dichroism effects can be probed as a function of applied electric field, magnetic field, or temperature in a spatially averaged spectroscopy or spatially resolved microscopy geometry (e.g. X-ray photoemission electron microscopy), giving direct evidence of reproducible and reversible room temperature magneto-electric interactions in these systems. Density functional theory calculations give insight into the relative contributions that charge and strain effects have on such artificial multiferroic interfaces. We illustrate that in both metallic and complex oxide ferromagnetic heterostructures that strain-mediated and charge mediated coupling have different interfacial length scales but their co-action results in a strong room temperature magneto-electric interactions.

10357-16, Session 3B

Monolayer transition metal dichalcogenide spin valves *(Invited Paper)*

Bo Hsu, Zheng Yang, Univ. of Illinois at Chicago (United States)

Spin valves with as-grown single-crystalline two-dimensional MX2 (M = Mo, W; X = S, Se) monolayers as spacer layer were fabricated. Ferromagnetic metals Co and permalloy (Py) were used as top and bottom layers in the spin valve devices. The spin valve effects at room- and variable low-temperatures are studied. The tunneling magnetoresistance up to ~0.6%, ~0.7%, ~0.2%, and ~0.2% were observed at room temperature for MoS2,

WS2, MoSe2, and WSe2 spin valve devices, respectively. The tunneling magnetoresistance up to ~0.9%, ~1.4%, ~0.4%, and ~0.4% were observed at 16 K for MoS2, WS2, MoSe2, and WSe2 spin valve devices, respectively. The temperature dependence tunneling magnetoresistance of the spin valves is studied and analyzed. The layer dependence of tunneling magnetoresistance of the spin valves is studied. The PtMn antiferromagnetic-layer coupling effect with Py in the spin valve is studied. The magnetic field angle dependent effect is preliminary studied. The aging effect is studied for spin valve devices measured up to >104 times and for devices measured multiple times with a time span of > 6 months.

10357-17, Session 3B

Magneto-optical spectroscopy of excitons in semiconducting transition metal dichalcogenides *(Invited Paper)*

Ashish Arora, Westfälische Wilhelms-Univ. Münster (Germany)

Semiconducting transition metal dichalcogenides (TMDs) have set a new paradigm for exploring atomic scale phenomena and future spin and valleytronic device applications. In this talk, I will present our recent investigations on TMDs, such as monolayers of WSe2, WS2, and MoTe2 using high-field magneto-optical spectroscopy. We use photoluminescence, photoluminescence excitation and reflectivity measurements to study the valley Zeeman splitting and valley polarization of neutral and charged excitons in these materials under magnetic fields up to 30 T at cryogenic temperatures [1-5]. While in MoTe2, the neutral A and B excitons as well as the charged A excitons show similar valley Zeeman splittings (g-factor ~ -4) [1], a more involved behavior is observed for singlet and triplet charged excitons in WS2 [3,4]. I will also present high-field Zeeman spectroscopy of single-photon emission in WSe2 [5]. Our results shine light on the salient aspects of the spin- and valley-resolved band structure of TMDs.

[1] A. Arora et al., Nano Letters 16, 3624 (2016)

[2] R. Schmidt, A. Arora et al., Phys. Rev. Lett 117, 077402 (2016)

[3] G. Plechinger et al., Nat. Commun. 7, 12715 (2016)

[4] G. Plechinger et al., Nano Lett. 16, 7899 (2016)

[5] M. Koperski et al., Nat. Nanotech. 10, 503, (2015)

10357-18, Session 3B

Spin-valley properties in transition metal dichacogenides monolayers and heterostructures *(Invited Paper)*

Cedric Robert, Gang Wang, Fabian Cadiz, Bernhard Urbaszek, Xavier Marie, Lab. de Physique et Chimie des Nano-objets (France)

The choice of two-dimensional (2D) materials to engineer devices with atomically flat active regions is currently extending beyond graphene to a wide range of semiconductors, insulators, metals and superconductors. Among the various families of 2D materials, semiconductor transition metal dichalcogenide (TMDC) materials MX2 (where M stands for Mo or W and X stands for S, Se or Te) exhibit especially exciting properties when thinned down to one monolayer (ML). In particular, they are ideal systems to study the physics related to the coupled spin-valley degrees of freedom[1]. Indeed, the absence of inversion symmetry and strong spin-orbit coupling along with a direct optical band gap in the visible range enable to selectively excite carriers in the K+ or K- valleys by using polarized excitation.

Here, we will present our experimental results on the creation of valley pseudospin states, coherent superposition and manipulation [2,3,4] in WSe2 and MoS2 monolayers. The population and polarization dynamics of excitons, trions and single carriers will be discussed in regards to our latest measurements in high quality charge tunable devices

[1] K.F. Mak, Science 344, 1489 (2014)

[2] G. Wang et al. PRL 117, 187401 (2016).

[3] Z. Ye et al. Nat. Phys. 3891 (2016).

[4] R. Schmidt et al. PRL 117, 77402 (2016).

10357-19, Session 4A

Spintronic logic: from switching devices to computing systems *(Invited Paper)*

Joseph S. Friedman, The Univ. of Texas at Dallas (United States)

The most basic elements of a logical computing system are switching devices that can be cascaded to perform complex logic functions. This requires a circuit structure that provides a mechanism by which the output of each switching device can be used as the input to another switching device. This mechanism enables a logic family with the basic logic functions achieved by the switching devices. The unique switching mechanisms that characterize spintronic devices provide new opportunities and challenges for the development of computing systems. In particular, new mechanisms are required through which spintronic switching devices can modulate the switching behavior of other similar devices. The wide variety of physical phenomena underlying spintronic devices enable a range of potential strategies through which devices can be made to interact, including electrical and spin currents, magnetic fields, and voltages. However, it is often difficult to develop techniques that enable these interactions in a manner that permits cascaded logic gates, thus impeding the functionality of a computing system. Several techniques have been developed to cascade spintronic switching devices through a variety of different mechanisms. Many other spintronic switching devices have been proposed for which no cascading mechanism has been identified. The potential operation of several cascading mechanisms in a spintronic computing system is discussed here, particularly in relation to the following logic families: nanomagnet logic (NML), complementary magnetic tunnel junction logic (CMAT), spin-diode logic, emitter-coupled spin-transistor logic (ECSTL), magnetic domain-wall logic, domain-wall MTJ logic, and complementary spin-FET logic. For each logic family, the switching device and cascading mechanism is briefly described, followed by a discussion of the potential for integration into a computing system.

10357-20, Session 4A

Spintronics: a potential pathway to enable an exponential scaling for beyond-CMOS era *(Invited Paper)*

Jian-Ping Wang, Univ. of Minnesota (United States)

Many key technologies of our society, including artificial intelligence (AI) and big data, have been enabled by the invention of transistor and its ever-decreasing size and ever-increasing integration at a large scale. There is a clear scaling limit to the conventional transistor technology, however. Many recently proposed advanced transistors are also having an uphill fight in lab because of necessary performance tradeoffs and limited scaling potential. In this talk, we argue for a new pathway that could enable exponential scaling for multiple generations. This pathway involves layering multiple technologies that are beyond the available functions of conventional and newly proposed transistors. We believe that this potential pathway is becoming clear through recent worldwide effort. In this talk, I will brief you my group's recent progress on two selected topics along this line, one on the STT-RAM and one on spin logic. Meanwhile I will also introduce a team effort of C-SPIN Center of STARnet program, where systems designers, devices builders, materials scientists and physicist all work under one roof to tackle the scaling issue and overcome key technology barriers. Several successful examples such as the logic in memory, cognitive computing, probabilistic computing and reconfigurable information processing will be discussed.

10357-21, Session 4A

Challenges and opportunities with spin-based logic *(Invited Paper)*

Michael Niemier, X. Sharon Hu, Robert Perricone, Li Tang, Univ. of Notre Dame (United States)

In this presentation, we will discuss work with various spin-based devices that can be used to process information. We will highlight the challenges and opportunities associated with individual devices, as well as computing with spin-based devices in general. A particular focus of this talk will be on how various devices and use cases for said devices might be used to realize non-volatile processors — which may have significant utility in power constrained environments, etc. At the device-level we will focus on structures that have evolved from various SRC, DARPA, and/or NIST initiatives — including nanomagnet logic (NML), all-spin logic (ASL), composite-input magnetoelectric-based logic technology (CoMET), as well as different types of magnetic memories.

10357-22, Session 4A

Energy efficient switching of fixed magnetic skyrmions with an electric field for nanomagnetic computing devices *(Invited Paper)*

Dhritiman Bhattacharya, Md Mamun Al-Rashid, Jayasimha Atulasimha, Virginia Commonwealth Univ. (United States)

Computing device proposals involving the movement of skyrmions with a current have been proposed [1]. Further, stable skyrmions have been demonstrated at room temperature [2].

We propose a novel nanomagnetic computing paradigm based on electric field mediated switching of a fixed magnetic skyrmion through voltage control of magnetic anisotropy (VCMA) without using a magnetic field and establish its feasibility and energy efficiency with rigorous simulations [3]. Such a device is unique as it is based on reversal of fixed skyrmions [3, 4]. Additionally, our modeling shows that, when VCMA is used in conjunction with spin current, the critical current required for reversal can be significantly reduced [5]. Besides being extremely energy efficient, the density of such fixed skyrmions based computing devices can be high as its states can be directly read out by vertically integrating an appropriate magnetic tunneling junction (MTJ). Furthermore, we will discuss:

1) Switching error in memory devices based on reversal of fixed skyrmions in the presence of thermal noise.

2) Possible implementations of neuromorphic computing elements such as spin neuron and synaptic memory using such fixed skyrmion devices.

Acknowledgement: This work is partly funded by NSF CAREER grant CCF-1253370.

REFERENCES

[1] A. Fert et al, 2013, Nat. Nanotechnol. 8, 152–156, 2013.

[2] S. Woo et al, Nat. Materials 15, 501, 2016.

[3] D. Bhattacharya, M. M. Al-Rashid, J. Atulasimha, Sci. Rep. 6, 31272, 2016.

[4] Y. Nakatani et al, Appl. Phys. Lett. 108, 152403, 2016.

[5] D. Bhattacharya et al, arXiv:1611.03138, 2016.

10357-23, Session 4B

Spin-orbit and exchange proximity effects in 2D materials *(Invited Paper)*

Jaroslav Fabian, Denis Kochan, Univ. Regensburg (Germany)

Graphene and novel 2d materials offer new perspectives for spintronics [1]. Graphene can reach spin lifetimes of 1-10 ns, limited currently by spin flips off magnetic moments [2]. However, graphene has no band gap, so its spintronic applications will be limited as a highly efficient spin transfer channel. Heterostructures of graphene and two-dimensional transition-metal dichalcogenides (TMDC) are emerging as systems in which both orbital and spin properties can be controlled by gating, thus offering a materials basis for spintronic applications, such as bipolar spin devices [3]. We have proposed that graphene on TMDCs can be used in optospintronics [4], since the direct gap of TMDCs allows optical spin orientation, with the successive transfer of spin into graphene. But these van der Waals stacks also yield interesting fundamental physics. We have recently shown that graphene on WSe2 exhibits an inverted band structure, which leads to helical edge states in graphene nanoribbons on WSe2 [5], with a bulk spin-orbit gap of about 1 meV, which is giant when compared to 24 micro eV in pristine graphene. In the talk I will also mention our most recent results the proximity effects in bilayer graphene as well as on engineering the proximity exchange in graphene and TMDCs in tunnel junctions with ferromagnetic metals [6]. I acknowledge support from EU Graphene Flagship and the DFG SFB 689.

1. W. Han, R. Kawakami, M. Gmitra, and J. Fabian, Nature Nanotechnology 9, 794 (2014)

2. D. Kochan, S. Irmer, M. Gmitra, and J. Fabian, Phys. Rev. Lett. 115, 196601 (2015)

3. I. Zutic, J. Fabian, and S. Erwin, IBM journal of research and development 50, 121 (2006)

4. M. Gmitra and J. Fabian, Phys. Rev. B 92, 155403 (2015)

5. M. Gmitra, D. Kochan, P. Högl, and J. Fabian, Phys. Rev. B 93, 155104 (2016)

6. K. Zollner, M. Gmitra, T. Frank, and J. Fabian, Phys. Rev. B 94, 155441 (2016)

10357-24, Session 4B

First principles investigation of the Co(0001)/MoS2 and Ni(111)/WSe2 interfaces for spin injection in a transition metal dichalcogenide monolayer *(Invited Paper)*

Lionel Calmels, Ctr. d'Elaboration de Matériaux et d'Etudes Structurales (France); Thomas Garandel, Ctr. d'Elaboration de Matériaux et d'Etudes Structurales, Ctr. National de la Recherche Scientifique (France) and Lab* de Physique et Chimie des Nano-objets, Institut National des Sciences Appliquées de Toulouse (France); Rémi Arras, Ctr. d'Elaboration de Matériaux et d'Etudes Structurales (France); Xavier Marie, Lab. de Physique et Chimie des Nano-objets (France); Pierre Renucci, Institut National des Sciences Appliquées de Toulouse (France)

The valley index in two-dimensional semiconducting transition metal dichalcogenide (TMDC) monolayers (MoS2, WSe2 ...) [1] could constitute a novel degree of freedom to process information. Electrical generation and control of valley-polarized carriers, constitutes a key point for the use of this valley degree of freedom in nanoelectronics, and yet remains a formidable challenge [2]. Due the unique correlation between spin and valley indices of electric carriers in these materials [3], this crucial step is directly linked to the ability to electrically inject spin polarized carriers in the TMDC layer. Ferromagnetic metals constitute good potential candidates for such an injection. We used first principles methods based on the density functional theory to investigate the atomic and electronic structure at the Co(0001)/MoS2 and Ni(111)/WSe2 interfaces. Covalent bonding between the magnetic metal surfaces and S or Se atoms strongly modify the electronic structure of the TMDC layers, which behave like metals at the interface with Co or Ni. We give details on the magnetic moments, on the nature and spin-polarization of the electron states at the Fermi level and on the Schottky barrier height. These interfaces could be used to promote electrical spin-injection from a Co or Ni electrode to a single TMDC layer.

References:

[1] K.F. Mak et al., Phys. Rev. Lett. 105, 136805 (2010).

[2] A. Allain et al., Nat. Materials 14, 1195 (2015).

[3] D. Xiao et al., Phys. Rev. Lett 108, 196802 (2012).

10357-25, Session 4B

A comparative spectroscopic study of the charge density wave features in 2H-NbSe2 and 2H-TaS2 *(Invited Paper)*

Utpal Chatterjee, Junjing Zhao, Kapila Wijayaratne, Univ. of Virginia (United States)

Recent studies of incommensurate Charge Density Wave (CDW) order in TMDs, e.g., 2H-NbSe2 and 2H-TaSe2, have provided intriguing results. For example, spectroscopic measurements, using Angle Resolved Photoemission Spectroscopy (ARPES), have revealed that the CDW energy gap of 2H-NbSe2 opens up around selected regions of the Fermi surface (FS). FS nesting was shown not to drive the CDW instability in 2H-NbSe2. Moreover, particle-hole asymmetric CDW energy gap in 2H-NbSe2 persist even at temperatures (T's) greater than CDW transition temperature (Tcdw), reminiscent of the famous pseudogap behavior in underdoped cuprate high temperature superconductors (HTSCs).

In the light of the above described developments in our understanding of 2H-NbSe2 and 2H-TaSe2, and the close parallel between these systems and cuprate HTSCs, an important question emerges: which of the above described experimental observations are universal attributes of incommensurate CDW systems? In order to address this, we present here a comparative study of the CDW properties as a function of T and momentum (k) in 2H-TaS2 and 2H-NbSe2, which are two prototype incommensurate CDW systems.

Our conclusions are as follows: (i) like in 2H-NbSe2, the CDW gap in 2H-TaS2 is particle-hole asymmetric and it persists above Tcdw; (ii) in contrast to 2H- NbSe2, the gap in 2H-TaS2 is clearly visible along both K-centered FS barrels; (iii) the difference between the momentum anisotropy and FS specificity of energy gap in 2H-TaS2 and 2H-NbSe2 can be understood in terms of the difference in orbital selectivity of the electronic states responsible for their individual CDW orders.

10357-101, Session 4B

Nature of the electromagnetic force between classical magnetic dipoles *(Invited Paper)*

Masud Mansuripur, College of Optical Sciences, The Univ. of Arizona (United States)

The force exerted by one magnetic dipole on another is capable of performing mechanical work, which appears to be in violation of the Lorentz force law of classical electrodynamics. The discrepancy is resolved if one examines the model of a magnetic dipole as an Amperian current loop, which allows for the balancing of the translational kinetic energy gained (or lost) by the moving current loop against its rotational kinetic energy. This problem will be analyzed in some detail, where we show that the change in the loop's rotational kinetic energy is also related to its changing magnetic dipole moment in accordance with Larmor's diamagnetic susceptibility of the loop. We proceed to address the question of what would happen if a magnetic dipole failed to behave as an Amperian current loop. This brings up an alternative model of magnetism and magnetic dipoles, which will be treated in the context of the Einstein-Laub formulation of the classical theory. We examine the electromagnetic (EM) energy of an immobile magnetic dipole in the presence of an externally-applied static magnetic field. Two approaches to EM energy, the Lorentz approach (which considers magnetic dipoles as Amperian current loops), and the Einstein-Laub approach (which treats such dipoles as pairs of north-south magnetic monopoles) will be considered. We extend the discussion to the case of moving magnetic dipoles within a static magnetic field. The predictions of the Lorentz and Einstein-Laub formulations will turn out to be in complete agreement in all the cases considered.

10357-26, Session 5

Rashba effect on the photophysical properties of hybrid perovskites and topological insulators

(Invited Paper)

Andrew M. Rappe, Liang Z. Tan, Univ. of Pennsylvania (United States); Fan Zheng, Lawrence Berkeley National Lab. (United States); Shi Liu, Carnegie Institution for Science (United States); Youngkuk Kim, Univ. of Pennsylvania (United States); Maya Isarov, Efrat Lifshitz, Technion-Israel Institute of Technology (Israel)

In this talk, our focus is on the interplay of the Rashba effect with the photo-physics of semiconductors, including topological insulators. The influence of the Rashba effect on the electronic excited state is two-fold: firstly, the internal energy levels of the excited state (i.e. excitonic levels) may be modified by the spin-orbit interaction, and secondly, the lifetime of the excited state may change when a Rashba effect is present. Using first-principles electronic structure calculations and effective models, we show that both of these effects are present in the hybrid perovskites. Our magneto-optical measurements on CsPbBr3 reveal non-linear Zeeman splitting of the excitons as a result of the Rashba effect. We predict that carrier lifetimes are enhanced in the hybrid perovskites by opposing spin orientations of the conduction and valence Rashba bands.

We also consider the shift current bulk photovoltaic effect, which, like Rashba, only exists in non-centrosymmetric systems. We show that a crossing of Rashba bands results in a topological phase transition in a class of materials, including some halide perovskites, producing a ferroelectric topological insulator. At this band inversion transition, the magnitude of the shift current is sharply, and the direction of the shift current changes sign abruptly. We demonstrate that this effect is robust across different materials systems including layered BiTeI and perovskite CsPbI3.

10357-27, Session 5

Current-nonlinear magnetotransport and spin-orbit torque magnetization switching in a magnetic topological insulator *(Invited Paper)*

Kenji Yasuda, The Univ. of Tokyo (Japan); Atsushi Tsukazaki, Tohoku Univ. (Japan); Ryutaro Yoshimi, RIKEN (Japan); Kouta Kondou, RIKEN Ctr. for Emergent Matter Science (Japan); Kei S. Takahashi, RIKEN (Japan); YoshiChika Otani, Masashi Kawasaki, The Univ. of Tokyo (Japan); Yoshinori Tokura, RIKEN (Japan)

Efficient electrical reading and writing of the magnetization direction is one of the central research target in spintronic devices. Recently, topological insulator (TI) has attracted considerable attention because of the large spin Hall angle based on the spin-momentum locking at the surface state. Here, we report large current-nonlinear magnetotransport and efficient spin-orbit torque magnetization switching in magnetic/nonmagnetic TI heterostructures, $Cr_x(Bi_{1?y}Sb_y)_{2?x}Te_3/(Bi_{1?y}Sb_y)2Te_3$. Current-nonlinear, or current-direction dependent magnetoresistance is a recently discovered phenomenon called unidirectional magnetoresistance (UMR), which allows us to electrically read the magnetization direction with two-terminal geometry. The magnitude of the UMR is shown to be several orders of magnitude larger than those in other FM/NM heterostructures. From the angular, magnetic field and temperature dependence, the large

UMR is identified to originate from the asymmetric scattering of surface Dirac electrons by magnons, what we call asymmetric magnon scattering mechanism. Moreover, we find comparable magnitude of current-nonlinear Hall effect, or second harmonic Hall voltage. Although second harmonic Hall voltage has conventionally been attributed to the magnetization oscillation by spin-orbit torque (SOT), detailed study has revealed that the large voltage in TI heterostructure originates not from SOT but mainly from asymmetric magnon scattering mechanism without macroscopic magnetization oscillation. This means that the second harmonic Hall voltage method does not allow an accurate estimation of spin Hall angle. Instead, the SOT contribution in TI heterostructure is exemplified by current-pulse-induced non-volatile magnetization switching. The required current density is ~2.5 ? 10^{10} A/m^2, which is much smaller than other materials, showing its potential as spintronic materials.

10357-28, Session 5

Voltage-driven magnetization control in topological insulator/magnetic insulator heterostructures *(Invited Paper)*

Michael E. Flatté, The Univ. of Iowa (United States)

A major barrier to the development of spin-based electronics is the transition from current-driven spin torque, or magnetic-field-driven magnetization reversal, to a more scalable voltage-driven magnetization reversal. To achieve this, multiferroic materials appear attractive, however the effects in current materials occur at very large voltages or at low temperatures. Here the potential of a new class of hybrid multiferroic materi- als is described, consisting of a topological insulator adjacent to a magnetic insulator, for which an applied electric field reorients the magnetization. As these materials lack conducting states at the chemical potential in their bulk, no dissipative charge currents flow in the bulk. Surface states at the interface, if present, produce effects similar to surface recombination currents in bipolar devices, but can be passivated using magnetic doping. Even without conducting states at the chemical potential, for a topological insulator there is a finite spin Hall conductivity provided by filled bands below the chemical potential. Spin accumulation at the interface with the magnetic insulator pro- vides a torque on the magnetization. Properly timed voltage pulses can thus reorient the magnetic moment with only the flow of charge current required in the leads to establish the voltage. If the topological insulator is sufficiently thick the resulting low capacitance requires little charge current.

10357-29, Session 5

Superconductivity provides access to the chiral magnetic effect of an unpaired Weyl cone *(Invited Paper)*

Thomas O'Brien, Carlo W. J. Beenakker, Leiden Univ. (Netherlands); Inanc Adagideli, Sabanci Univ. (Turkey)

The massless fermions of a Weyl semimetal come in two species of opposite chirality, in two cones of the band structure. As a consequence, the current j induced in one Weyl cone by a magnetic field B (the chiral magnetic effect, CME) is cancelled in equilibrium by an opposite current in the other cone. Here we show that superconductivity offers a way to avoid this cancellation, by means of a flux bias that gaps out a Weyl cone jointly with its particle-hole conjugate. The remaining gapless Weyl cone and its particle-hole conjugate represent a single fermionic species, with renormalized charge $e^\ast$ and a single chirality $\pm$ set by the sign of the flux bias. As a consequence, the CME is no longer cancelled in equilibrium but appears as a supercurrent response $\partial j/\partial B=\pm(e^\ast e/h^2)\mu$ along the magnetic field at chemical potential μ.

10357-30, Session 5

Emergent nanoscale superparamagnetism and electronic phase separation at oxide interfaces *(Invited Paper)*

Eli Zeldov, Weizmann Institute of Science (Israel)

Atomically sharp oxide heterostructures exhibit a range of novel physical phenomena that do not occur in the parent bulk compounds including conducting, superconducting, and magnetic states. We present a new emergent phenomenon at the $LaMnO_3/SrTiO_3$ interface in which an antiferromagnetic insulator abruptly transforms into a superparamagnetic state. Above a critical thickness of $LaMnO_3$ of five unit cells, our scanning nanoSQUID-on-tip microscopy [1] shows spontaneous formation of isolated magnetic islands with in-plane moment of 10^4 to 10^5 ?_B with characteristic diameter of 10 to 50 nm [2]. The nanoscale islands display superparamagnetic dynamics of random moment reversals by thermal activation or in response to an in-plane magnetic field. We propose a charge reconstruction model of the polar $LaMnO_3/SrTiO_3$ heterostructure which describes a sharp emergence of thermodynamic phase separation leading to nucleation of metallic ferromagnetic islands in an insulating antiferromagnetic matrix. The model suggests that a gate tunable superparamagnetic-ferromagnetic transition can be induced, holding potential for applications in magnetic storage and spintronics.

[1] D. Vasyukov et al., Nature Nanotechnology 8, 639 (2013).

[2] Y. Anahory, L. Embon, C. J. Li, S. Banerjee, A. Meltzer, H. R. Naren, A. Yakovenko, J. Cuppens, Y. Myasoedov, M. L. Rappaport, M. E. Huber, K. Michaeli, T. Venkatesan, Ariando, and E. Zeldov, Nat. Commun. 7, 12566 (2016).

10357-31, Session 6

Spin-orbit splitting in quantum wells and 2D topological insulators *(Invited Paper)*

Mikhail Nestoklon, Ioffe Institute (Russian Federation)

We discuss the results of recent theoretical studies of the spin structure of free carriers in semiconductor structures. In addition to spin-orbit splitting of the spectrum of bulk materials, in 2D systems, the spin degeneracy of the levels is lifted in presence of lateral wave vector. The linear spin splitting of the energy levels is important for spin relaxation in quantum well structures because the dominant mechanism of spin relaxation in 2D structures relies on the connection between spin and electron momentum. Also, it is important for description of states in semiconductor-based 2D topological insulators because the structure of the levels strongly depends on the spin-orbit interaction.

Combining the envelope function theory and atomistic tight-binding approach, we calculate spin-orbit splitting constants for realistic quantum wells, study the relative importance of the interface and the bulk contributions to the spin splitting; show that the strain due to lattice mismatch is important in both conventional GaAs/AlGaAs and InGaAs/GaAs structures; and describe the fine structure of Dirac states in the HgTe/CdTe quantum wells of critical and close-to-critical thicknesses.

10357-32, Session 6

Dynamical quantum anomalous Hall effect in the intense optical field regime *(Invited Paper)*

Wang-Kong Tse, The Univ. of Alabama (United States)

Topological insulators are characterized by the quantum anomalous Hall effect on the topological surface states under time-reversal symmetry breaking. While this effect has been recently observed in a magneto-optical setup upon illumination of weak linearly polarized light, the influence of intense optical field remains largely unexplored. Using the Keldysh-Floquet

Green's function formalism, we develop a theory for the dynamical Hall conductivity for arbitrary incident optical frequency in the intense optical field regime. We apply our general theory to the adiabatic, low-frequency regime, and study the breakdown of the one-half Hall quantization under intense optical field. Our results reveal a strong nonlinear dependence of the dynamical Hall conductivity on the incident optical field, which is triggered by the formation of Floquet subbands and the transitions between them.

10357-33, Session 6

Emergent orbitronics and dissipationless magnetization control in complex magnets *(Invited Paper)*

Jan-Philipp Hanke, Institut für Fortgeschrittene Simulation, Forschungszentrum Jülich GmbH (Germany); Dongwook Go, Pohang Univ. of Science and Technology (Korea, Republic of); Patrick Buhl, Frank Freimuth, Stefan Blügel, Yuriy Mokrousov, Institut für Fortgeschrittene Simulation, Forschungszentrum Jülich GmbH (Germany)

The topological properties of magnets, encoded in the reciprocal space distribution of the Berry phase, have caused a revolution in our understanding of their transport properties.

The discovery that the non-trivial geometry of states in a solid is ultimately related to the orbital properties of electrons allows us to predict from theoretical arguments a pronounced orbital magnetism in various situations ranging from Rashba systems to Chern insulators. Moreover, we demonstrate that a combination of complex geometry in real and reciprocal spaces leads to an emergence of topological orbital magnetism in non-collinear magnets, which overall opens new vistas in large current-induced orbital magnetization response and magnetization manipulation in antiferromagnets. Finally, we predict that in insulating systems with non-trivial topologies the strength of the magneto-electric response as manifested in the magnitude of the current-induced spin-orbit torques and Dzyaloshinskii-Moriya interaction can exceed significantly that of conventional metallic magnets, which opens new perspectives in dissipationless control of magnetization in magnetic materials.

10357-35, Session 6

Spin to charge current conversion at surfaces and interfaces of Rashba systems and 3D topological insulators studied by spin pumping ferromagnetic resonance *(Invited Paper)*

Paul Noël, SPINTEC (France) and Univ. Grenoble Alpes (France); Edouard Lesne, Unité Mixte de Physique CNRS/Thales (France) and Univ. Paris-Sud (France) and Univ. Paris-Saclay (France); Yu Fu, SPINTEC (France) and Univ. Grenoble Alpes (France); Simón Oyarzún, Univ. de Santiago de Chile (Chile); Candice Thomas, MINATEC (France); Diogo C. Vaz, Juan-Carlos Rojas-Sánchez, Unité Mixte de Physique CNRS/Thales (France); Hiroshi Naganuma, Tohoku Univ. (Japan); Giuseppe Siccoli, CEA-INAC (France) and Univ. Grenoble Alpes (France); Serge Gambarelli, Commissariat à l'Énergie Atomique (France) and Univ. Grenoble Alpes (France); Jean-Philippe Attané, Commissariat à l'Énergie Atomique (France) and Ctr. National de la Recherche Scientifique (France) and Univ. Grenoble Alpes (France); Mathieu Jamet, SPINTEC (France) and Univ. Grenoble Alpes (France); Alain Marty, Commissariat à l'Énergie Atomique (France) and Ctr. National de la Recherche Scientifique (France) and Univ. Grenoble Alpes (France); Céline Vergnaud, SPINTEC (France) and CEA-INAC (France) and Univ. Grenoble Alpes (France); Eric Jacquet, Quentin Barbedienne, Jean-Marie George, Agnès Barthelemy, Unité Mixte de Physique CNRS/Thales (France); Yoshiyuki Ohtsubo, Osaka Univ. (Japan); Amina Taleb Ibrahimi, Patrick Le Fèvre, Synchrotron SOLEIL (France); Henri Jaffrès, Nicolas Reyren, Albert Fert, Unité Mixte de Physique CNRS/Thales (France); Tristan Meunier, Institut NÉEL, Ctr. National de la Recherche Scientifique (France) and Univ. Grenoble Alpes (France); Philippe Ballet, Commissariat à l'Énergie Atomique (France) and MINATEC (France); Manuel Bibès, Unité Mixte de Physique CNRS/Thales (France); Laurent Vila, CEA-INAC (France) and Univ. Grenoble Alpes (France) and SPINTEC (France)

In order to generate spin current in spintronic devices it is needed to find an efficient way to transform charge current into spin current and make the opposite conversion to detect spin current. Classical spintronics generally uses magnetic materials for such conversions but they can be obtained by exploiting the spin-orbit coupling in materials containing heavy atoms. An efficient current conversion can be obtained through Spin Hall Effect (and Inverse Spin Hall Effect) in heavy metals such as Pt or Ta. Yet a more efficient conversion can be obtained by exploiting the Rashba Edelstein Effect in two dimensional electron gas at surfaces and interfaces such as Rashba Interfaces and newly discovered materials topological insulators. Among these systems the Rashba interface STO/LAO and various topological insulators allows to obtain spin to charge current conversion one order of magnitude bigger than in Spin Hall Effect materials. These results suggest that surfaces and interfaces have a strong potential for spintronics, both for the generation or detection of spin currents through direct or inverse Edelstein effects.

An emerging direction in oxide research aims at discovering novel electronic phases at interfaces between two oxide materials. A well-known example is the STO/LAO system where a high-mobility two-dimensional electron system forms at their interface. Interestingly, LAO/STO possesses several remarkable extra functionalities, including a gate-tunable Rashba effect, which makes it particularly appealing for spintronics.

Another emerging field in spintronics is the conversion at the surface and interface states of Topological Insulator which are characterized by a locking between spin and momentum associated with a helical spin configuration of the Fermi contour. Recently discovered 3D topological insulators such as strained ?-Sn and HgTe could perform high spin to charge current conversion at room temperature.

10357-36, Session 7A

Evidence for a common origin of spin-orbit torque and the Dzyaloshinskii-Moriya interaction at a Py/Pt interface *(Invited Paper)*

Andrew Berger, Eric R. J. Edwards, Hans T. Nembach, Justin M. Shaw, National Institute of Standards and Technology (United States); Alexy D. Karenowska, Univ. of Oxford (United Kingdom); Mathias Weiler, Walther-Meissner-Institute (Germany); Thomas J. Silva, National Institute of Standards and Technology (United States)

Spin-orbit coupling (SOC) can drive non-equilibrium spin-charge conversion through the reciprocal processes of current-driven spin torque and spin precession-driven current in ferromagnet/heavy metal (FM/HM) bilayers. Both damping-like and field-like spin-orbit torques (SOT) have been observed in the forward process of current-driven SOT, but details of the underlying physics are still debated. SOC also underlies the equilibrium antisymmetric exchange coupling, a.k.a. the interfacial Dzyaloshinskii-Moriya

interaction (DMI). It was recently proposed that a Rashba Hamiltonian at FM/HM interfaces serves as a common origin for both SOT and DMI, with a simple quantitative relation between the two. Here, we verify this relation by comparing inverse SOT (iSOT) measurements with previous characterization of DMI via spin wave spectroscopy. To perform the iSOT measurements, we have developed a technique for quantitative vector network analyzer ferromagnetic resonance to inductively detect the AC charge currents produced by spin-charge conversion processes in FM/HM bilayers. Our findings reveal that Py/Pt bilayers exhibit both damping-like and field-like iSOT, consistent with the presence of inverse spin Hall effect and Rashba-Edelstein effect, respectively.

10357-37, Session 7A

Theory of spin loss at metallic interfaces *(Invited Paper)*

Kirill D. Belashchenko, Giovanni G. Baez Flores, Alexey A. Kovalev, Univ. of Nebraska-Lincoln (United States); Mark van Schilfgaarde, King's College London (United Kingdom)

Interfacial spin-flip scattering plays an important role in magnetoelectronic devices. Spin loss at metallic interfaces has usually been quantified by matching the magnetoresistance data for multilayers to the Valet-Fert model, while treating each interface as a fictitious bulk layer whose thickness is $delta$ times the spin-diffusion length. However, the relation between the parameter $delta$ and the scattering properties of the interface has been missing. We establish this relation using the properly generalized magnetoelectronic circuit theory, for both normal and ferromagnetic interfaces. It is found that the parameter $delta$ extracted from the measurements on multilayers scales with the square root of the probability of spin-flip scattering. The spin-flip scattering probabilities are calculated for several specific interfaces using the Landauer-Büttiker method based on the first-principles electronic structure, and the results are compared with experimental data.

10357-38, Session 7A

Green's function formulation of spin pumping *(Invited Paper)*

Gen Tatara, RIKEN Ctr. for Emergent Matter Science (Japan)

Current pumping by an external potential is studied on the basis of the Keldysh Green's function method, and a pumping formula written in terms of retarded and advanced Green's functions is obtained. The formula is used to study the spin pumping effect in the case of strong s-d exchange interaction, and the driving field is identified to be the spin gauge field. At the lowest order in the precession frequency of magnetization, the spin gauge field works as a constant potential, and the system is shown to reduce to a static problem of spin current generation by a time-independent potential with off-diagonal spin components.

We theoretically explore the optical properties of a bulk Rashba conductor by calculating the transport coefficients at finite frequencies. It is demonstrated that the combination of direct and inverse Edelstein effects leads to a softening of the plasma frequency for the electric field perpendicular to the Rashba field, resulting in a hyperbolic electromagnetic metamaterial. In the presence of magnetization, a significant enhancement of anisotropic propagation (directional dichroism) is predicted because of the interband transition edge singularity. On the basis of an effective Hamiltonian analysis, the dichroism is demonstrated to be driven by toroidal and quadratic moments of the magnetic Rashba system.

10357-39, Session 7A

Auto-oscillation and spin-wave propagation in ultra-thin YIG microstructures *(Invited Paper)*

Martin Collet, Paolo Bortolotti, Vincent Cros, Abdelmadjid Anane, Unité Mixte de Physique CNRS/Thales (France) and Univ. Paris-Sud 11 (France) and Univ. Paris-Saclay (France); José Luis Prieto, Instituto de Microelectrónica de Madrid (Spain); Manuel Muñoz, Instituto de Sistemas Optoelectrónicos y Microtecnología (Spain); Jamal Ben Youssef, Lab. de Magnétisme de Bretagne, CNRS, Univ. de Bretagne Occidentale (France); Vladimir Naletov, Commissariat à l'Énergie Atomique (France) and Ctr. National de la Recherche Scientifique (France) and Univ. Grenoble Alpes (France); Grégoire de Loubens, Commissariat à l'Énergie Atomique (France); Olivier Klein, Commissariat à l'Énergie Atomique (France) and Ctr. National de la Recherche Scientifique (France) and Univ. Grenoble Alpes (France); Michael Evelt, Westfälische Wilhelms-Univ. Münster (Germany); Vladimir Bessonov, M.N. Miheev Institute of Metal Physics, Ural Branch of Russian Academy of Sciences (Russian Federation); Sergej O. Demokritov, Vladislav E. Demidov, Westfälische Wilhelms-Univ. Münster (Germany)

In recent years, Spin Orbit interaction as a source of spin current has been widely used through the physics of Spin Hall Effect (SHE). The peculiar symmetry of SHE allows creating a spin accumulation at the interface between a spin-orbit metal and a magnetic insulator that could lead to a net pure spin current flowing from the metal into the insulator. This spin current will induce a torque on the magnetization and eventually could drive it into steady motion. As a ferromagnetic insulator with a very low Gilbert damping, Yttrium Iron Garnet (YIG) is a very promising candidate to investigate pure spin current phenomena. Only very recently, with the developments in preparation of high-quality nanometer-thick YIG films, the implementation of insulator-based spin-torque devices became practically feasible.

Here, we report on the excitation of auto-oscillations in microstructures of YIG(20nm)Pt(8nm) driven by Spin Orbit torque (SOT). By injection of a dc current in the adjacent Pt layer, we have been able to prove that the SOT due to SHE is sufficiently strong and efficient to drive the YIG magnetization dynamics at frequencies that closely follow the ferromagnetic resonance mode. These auto-oscillations have been detected either inductively using a spectrum analyzer or directly observed using micro-focus Brillouin Light Scattering. Furthermore, we achieved an efficient control of spin waves attenuation length in a YIG waveguide using the SHE in the sub-critical regime i.e. below the auto-oscillations threshold. We believe that our finding pave the path to active magnonics devices made out of YIG films.

10357-40, Session 7B

Understanding magnetization relaxation dynamics in half ferromagnet La0.66Sr0.33MnO3 *(Invited Paper)*

Giancarlo Panaccione, Consiglio Nazionale delle Ricerche (Italy)

We present a pump-probe Hard X-ray Photoemission (HAXPES) study of the magnetic relaxation dynamics of LSMO thin films. We study the structure of the Mn 2p core level and, in particular, the bulk-only screening satellites proportional to the metallic and ferromagnetic state in LSMO [7-10]. We observe a large and 'slow' reduced lineshape change up to 200 picoseconds after the IR pumping. By comparison with all-optical techniques (Time-Resolved Magneto-Optical Kerr effect, TRMOKE) we are able to attribute

the observed quenching to a collapse of magnetic order. The sudden demagnetization reduces the mobility of electrons in the solid, inducing a localization similar to a metal-insulator transition. We are able to follow the relaxation dynamics as the energy is first dissipated in the lattice and then in a reduction of the magnetic order.

10357-41, Session 7B

Ultrafast electrical switching of ferrimagnetic metals *(Invited Paper)*

Richard Wilson, Univ. of California, Riverside (United States); Yang Yang, Jon Gorchon, Univ. of California, Berkeley (United States); Charles-Henri Lambert, Univ. of California, Riverside (United States); Sayeef Salahuddin, Jeffrey Bokor, Univ. of California, Berkeley (United States)

When electrons in a magnetic metal are driven far from equilibrium via ultrafast heating of the electrons, the magnetic order undergoes radical changes within tens of femtoseconds due to massive flows of energy and angular momentum between electrons, spins, and phonons. In ferrimagnetic metals such as GdFeCo, ultrafast optical heating can deterministically reverse the magnetization in less than a picosecond. In this talk, I describe our experimental work to gain a better understanding of how energy is exchanged between electrons, phonon, and spins in a magnetic metal following ultrafast heating. We use time-resolved measurements of the magneto-optic Kerr effect to record the response of ferro- and ferri-magnetic metals to heating via ultrafast optical or electrical pulses. Picosecond electrical pulses are generated with photoconductive Auston switches. By comparing the magnetic dynamics that result from electrical vs. optical heating, we identify differences in the rate of energy transfer to phonons from thermal vs. nonthermal electrons. We also find that both optical and electrical heating are effective for ultrafast switching of ferrimagnetic metals. We observe deterministic, repeatable ultrafast reversal of the magnetization of a GdFeCo thin film with a single sub-10 ps electrical pulse. The magnetization reverses in ~10 ps, which is more than one order of magnitude faster than other electrically controlled magnetic switching mechanisms.

10357-42, Session 7B

Measuring ultrafast magnetisation dynamics in the sub 10 femtosecond regime *(Invited Paper)*

David Schmool, Univ de Versailles Saint-Quentin-en Yvelines (France); Helder M. Crespo, Ana S. Vieira Silva, David Navas, Francisco Silva, Univ. do Porto (Portugal); Miguel Miranda, Lund Univ. (Sweden); Aurelio Hierro Rodriguez, Univ. do Porto (Portugal); Cledson S. L. Gonçalves, Univ. Federal do Pará (Brazil)

Current time-resolution-limited dynamic measurements clearly show the necessity for improved techniques to access magnetic processes on the sub-10-femtosecond timescale. To access this regime, we have designed and constructed a state-of-the-art time-resolved magneto-optic Kerr effect apparatus, based on a new dual-color scheme, for the measurement of ultrafast demagnetisation and precessional dynamics in magnetic materials. This system can operate well below the current temporal ranges reported in the literature, which typically lie in the region of around 50 fs and above. We have used a dual-colour scheme, based on ultra broadband hollow-core fibre and chirped mirror pulse compression techniques, to obtain unprecedented sub-8-fs pump and probe pulse durations at the sample plane [1]. We will demonstrate the application of our system using ultrafast demagnetisation and precessional dynamics in thin magnetic films of GdCoFe and Ni. In particular we will show that a sub-10-fs laser pulse can be used to efficiently initiate magnetisation excitations.

[1] C. S. Gonçalves, A. S. Vieira, D. Navas, M. Miranda, F. Silva, H. Crespo and D. S. Schmool, Scientific Reports, 6, 22872, (2016).

10357-43, Session 7B

Non-equilibrium magnetic effects at interfaces for ultrafast dynamics *(Invited Paper)*

Ilya Razdolski, Alexandr Alekhin, Nikita Ilin, Fritz-Haber-Institut der Max-Planck-Gesellschaft (Germany); Jan P. Meyburg, Univ. Duisburg-Essen (Germany); Vladimir Roddatis, Institut für Materialphysik, Georg-August-Univ. Göttingen (Germany); Detlef Diesing, Uwe Bovensiepen, Univ. Duisburg-Essen (Germany); Alexey Melnikov, Fritz-Haber-Institut der Max-Planck-Gesellschaft (Germany)

Representing the future of spintronics, femtosecond spin current (SC) pulses constitute a versatile tool to transfer spin and control magnetization on the ultrafast timescale. It is therefore of paramount importance to understand the kinetics of these pulses and the fundamentals of their interaction with magnetized media. In our work, we demonstrate the key role of interfaces for the SC dynamics in Fe/Au/Fe multilayers. In particular, we argue that both (i) demagnetization caused by a pulse of hot electrons and (ii) spin transfer torque exerted by the orthogonal to the Fe magnetization projection of magnetic moment delivered by SC pulse are localized in the vicinity of the Fe/Au interface. We analyze both processes in details, showing that the SC-driven excitation of the sub-THz spin wave dynamics in Fe film is enabled by the spatial confinement of the exerted spin transfer torque. Moreover, a pulse of hot electrons leads to the efficient demagnetization of the Fe film. By disentangling the magneto-optical Kerr effect (MOKE) transients we demonstrate the strong spatial non-uniformity of this demagnetization. We argue that simultaneous recording of transient MOKE rotation and ellipticity is crucial for drawing such conclusions. Our findings have a twofold impact: firstly, they illustrate rich opportunities of utilizing SC pulses for manipulation of magnetization in ferromagnets and, secondly, they highlight the importance of spatial localization for understanding the ultrafast spin dynamics in multilayers.

10357-44, Session 8A

Studying pure spin currents in weakly spin-orbit coupled materials using the pulsed ferromagnetic resonance driven inverse spin-Hall effect *(Invited Paper)*

Christoph M. Boehme, Marzieh Kavand, Kipp J. van Schooten, Dali Sun, Hans Malissa, Chuang Zhang, Matthew Groesbeck, Z. Valy Vardeny, The Univ. of Utah (United States)

Spin-orbit coupling (SOC) and the spin diffusion length in condensed matter are crucial parameters for spintronics applications. In order to study these, we have succeeded in employing a pulsed spin-pumping method based on ferromagnetic resonance (FMR) to generate pure spin currents from ferromagnetic (FM) substrates into non-FM semiconductor layers [1] which can then be detected through the inverse spin-Hall effect (ISHE). When the FM is in FMR with a pulsed microwave (MW) excitation, a pure spin-current is generated in the non-FM layer which can circumvent potential impedance mismatches between the FM and the non-FM layer and, therefore generate a strong pulsed ISHE signal. Due to the low duty cycle of the pulsed excitation, MW excitation powers can be used that are strong enough to generate pronounced ISHE signals even in materials with weak SOC such as carbon-based materials. This sensitivity allows for the study of the quantitative nature of the ISHE and thus, to apply scrutiny to a number of questions about the ISHE effect in general, including how strongly FMR-driving field inhomogeneities affect a measured ISHE current, the relationship of ISHE voltages to the ISHE current in devices consisting of layers with different conductivities, as well the experimental conditions which have to be monitored during an ISHE experiment in order to ensure reproducibility.

This work was supported by the National Science Foundation (DMR-

1404634 – Sample preparation and Experiments) and the NSF-Material Science & Engineering Center (DMR-1121252- Polymer Synthesis and Facilities) at the University of Utah.

[1] D. Sun et al., Nature Materials 15, 863–869 (2016). doi:10.1038/nmat4618

10357-45, Session 8A

Spin transfer torque mechanisms in three terminal spin-torque oscillators *(Invited Paper)*

Emilie Jué, National Institute of Standards and Technology (United States)

The manipulation of magnetization by an electric current can be obtained thanks to the spin-transfer torque (STT) phenomenon. The two main mechanisms that give rise to this phenomenon are the spin filtering torque (SFT) and the spin-orbit torque (SOT). The former is obtained in multilayer systems by passing a spin-polarized current through the multilayers, whereas the latter is achieved through a direct transfer of angular momentum from the crystal lattice through the spin–orbit interaction. In this work, we study the influence of these two mechanisms on the magnetization dynamics of a three-terminal spin-torque oscillator. The device is composed of either a spin-valve (SV) or a magnetic tunnel junction (MTJ) on top of a Pt wire. The system can be excited either by SFT or by SOT depending on whether the current is applied through the magnetic structure (SV or MTJ) or through the Pt wire. Finally, each device is compared to a reference sample where the Pt wire is replaced by a Cu wire. Therefore, no SOT is expected in this second set of devices. In this presentation, we compare the different types of devices in order to understand the transport in the three terminal devices and study the role of the different mechanisms (SFT and STT) on the magnetization dynamics. Finally, we propose a method to compare the spin transfer efficiency of the two mechanisms on a single device.

10357-46, Session 8A

Perpendicular magnetic anisotropy in Bismuth substituted nanometers thick YIG films *(Invited Paper)*

Lucile Soumah, Unité Mixte de Physique CNRS/Thales (France); Lilia Qassym, Thales Research & Technology (France); Cécile Carretero, Eric Jacquet, Unité Mixte de Physique CNRS/Thales (France); Jamal Ben-Youssef, Univ. de Bretagne Occidentale (France); Richard Lebourgeois, Thales Research & Technology (France); Nathan Beaulieu, Univ. de Bretagne Occidentale (France); Vincent Cros, Paolo Bortolotti, Abdelmadjid Anane, Unité Mixte de Physique CNRS/Thales (France)

Pulsed laser deposition (PLD) of high quality nanometers thick (YIG) films have recently allowed to open the field of spintronics and magnonics nanostructured magnetic insulators[1,2]. YIG is a versatile material in term of anisotropy or magnetization as doping and growth induced strain can significantly change those properties. We present here the effect of Bi substitution on Bi:YIG PLD grown films with thicknesses ranging from 10 nm to 40 nm. By using lattice matched substituted GGG substrates (sGGG) it is possible to stabilize for specific growth conditions an out-of plane easy magnetization axis. We present comprehensive structural charcterisation using X-ray diffraction and squid magnetometry that shows the transition from an easy in-plane magnetization direction to an out-of plane magnetization. The effect of Bi doping is to significantly increase the Faraday rotation of the films. Using magneto-optical Kerr microscopy, it is therefore possible to observ the shape and the sizes of the magnetic domains for films thicknesses down to 10 nm. Using the Kooy and Enz model it is possible to extract a domain wall energy of 0.49 erg/cm2.

[1] O. D. Kelly et al., Applied Physics Letters 103, 4, 082408 (2013).

[2] M. Collet et al., Nature communications 7, 10377 (2016).

[3] C. Kooy and U. Enz, Philips Res. Rep., vol. 15, pp. 7-29(1960)

10357-47, Session 8B

Progress in the room temperature operation of GaAs-based lateral-type spin-LED and spin-PD in near-infrared wavelength region *(Invited Paper)*

Hiro Munekata, Ronel C. Roca, Kazuhiro Nishibayashi, Nozomi Nishizawa, Tokyo Institute of Technology (Japan)

Aiming at the incorporating spins in the future optical integrated circuit, we have been studying lateral-type spin photonic devices and memories. In this paper, we present recent progress in the room temperature operation of spin light-emitting diodes (LEDs) and photo-detectors (PDs). Our spin-LEDs consist of p-GaAs-based double heterostructures combined with Fe /crystalline AlOx contacts. Pure CP-EL occurs when a current of 100 A/cm2 or higher is sent to the device. This phenomenon arises due to the annihilation of minority-helicity EL component accompanied by slight narrowing in EL spectra, which lead us to the inference that the of minority helicity EL component is converted into that of the majority helicity in three steps: firstly, reversed spin polarization of the valence band resulting from injecting spin-polarized electrons into the conduction band; secondly, relatively strong re-absorption of minority helicity EL component; and thirdly, stimulated light emission of re-generated minority spin electrons in the relatively strong electromagnetic field of majority EL component. Spin-polarized rate equations will be discussed at the time of .presentation. Our spin-PDs consist of a Fe/crystalline AlOx/p-GaAs Schottky diode, and helicity-dependent photocurrent is yielded with the conversion efficiency F (the relative value of helicity-dependent photocurrent with respect to the total photocurrent) of 0.1 to 1 % for horizontal and oblique illuminations, respectively. The model calculation consisting of drift-diffusion and Julliere spin-dependent tunneling transports suggests that a possible cause of the reduced helicity-dependent photocurrent may be microscopic damages to the tunneling barrier at the cleaved edge.

10357-48, Session 8B

Efficient electrical spin injection into quantum dots at zero magnetic field *(Invited Paper)*

Fabian Cadiz, Delphine Lagarde, Lab. de Physique et Chimie des Nano-objets (France); Shiheng Liang, Institut Jean Lamour (France); Bingshan Tao, Institute of Physics, Chinese Academy of Sciences (China); Julien Frougier, Unité Mixte de Physique CNRS/Thales (France); Yuan Lu, Institut Jean Lamour (France); Bo Xu, Institute of Semiconductors, Chinese Academy of Sciences (China); Henri Jaffres, Unité Mixte de Physique CNRS/Thales (France); Zg Wang, Institute of Semiconductors, Chinese Academy of Sciences (China); X. Fhan, Institute of Physics, Chinese Academy of Sciences (China); Michel Hehn, Stephane Mangin, Institut Jean Lamour (France); Jean-Marie George, Unité Mixte de Physique CNRS/Thales (France); Thierry Amand, Xavier Marie, Bernhard Urbaszek, Lab. de Physique et Chimie des Nano-objets (France); Pierre Renucci, Institut National des Sciences Appliquées de Toulouse (France)

We have demonstrated for the first time at zero magnetic field a very efficient electrical spin injection into p-doped InAs/GaAs quantum dots (around one hole per dot in average) thanks to an ultrathin CoFeB (a few atomic planes)/MgO spin injector, presenting perpendicular magnetic

anisotropy. The circular polarization of the electroluminescence (EL) emitted by the Spin Light Emitting Diode (spinLED) follows the hysteresis cycle of the magnetic layer. At zero magnetic field, a Circular polarization as large as 22 percent is measured at low temperature, far above the values usually observed at zero magnetic field for spinLEDs. The dependence of the EL circular polarization rate on current intensity and on its duty cycle is investigated, in order to track the possible nuclear polarization of the nuclei in the dots. In addition, this structure is shown to operate also as a spin photodiode; spin polarized electrons are optically injected into the quantum dots, and then extracted towards theCoFeB layer.

The photocurrent is shown to be sensitive to the helicity of the incident light.

10357-49, Session 8B

Injection of sub-picosecond ultrashort spin current pulses in semiconductors *(Invited Paper)*

Marco Battiato, Technical Univ. Vienna (Austria)

The origin of the ultrafast demagnetisation has been a mystery for a long time. Recently we have proposed an approach based on spin dependent electron superdiffusion. [1-3] A number of experimental works have confirmed the importance and the amplitude of the superdiffusive spin transport for ultrafast magnetisation dynamics [4-7]. In particular the spin superdiffusion model predicted the transfer of magnetisation in the non-magnetic substrate and the possibility of increasing the magnetisation: both phenomena were experimentally confirmed. [4-5]

We predict the possibility of injecting ultrashort (sub-picosecond) spin current pulses from a ferromagnetic metallic layer undergoing ultrafast demagnetisation into a semiconducting substrate. [8] After laser excitation, energetic carriers can overcome the semiconductor bandgap. We address the complex interplay of spin diffusion, the formation of high electric fields at the metal/semiconductor interface, and the concomitant thermalisation of the laser excited carriers by ad hoc numerical techniques. We show that spin currents pulses hundreds of femtoseconds long are injected in the semiconductor and present a record spin polarisation.

Such spin current pulses have the possibility of becoming the carriers of information in future spintronics running at unprecedented frequencies above the THz regime.

[1] M. Battiato, K. Carva, P.M. Oppeneer, Phys Rev. Lett. 105, 027203 (2010).

[2] M. Battiato, K. Carva, P.M. Oppeneer, Phys Rev. B 86, 024404 (2012).

[3] M. Battiato, P. Maldonado, P.M. Oppeneer, J. Appl. Phys. 115, 172611 (2012).

[4] A. Melnikov et al., Phys. Rev. Lett. 107, 076601 (2011).

[5] D. Rudolf, C. La-O-Vorakiat, M. Battiato et al., Nature Comm. 3, 1037 (2012).

[6] A. Eschenlohr,* M. Battiato,* et al., Nature Mater. 12, 332 (2013).

[7] T. Kampfrath, M. Battiato, et al, Nature Nanotechnol. 8, 256 (2013).

[8] M. Battiato and K. Held, Phys Rev. Lett. 116, 196601 (2016).

10357-50, Session 9A

Modeling the negative magnetoresistance of ferromagnet-graphene-ferromagnet junctions *(Invited Paper)*

Olaf M. J. van 't Erve, Enrique Cobas, Berend T. Jonker, U.S. Naval Research Lab. (United States)

Ferromagnet – multilayer graphene – ferromagnet junctions are predicted to yield low resistance devices with a high magnetoresistance (MR) due to a metallic minority spin transport channel [1]. We fabricated arrays of such junctions via chemical vapor deposition of graphene on lattice-matched single-crystal NiFe(111) films with a bcc-Fe top contact. The junctions exhibit negative MR and metallic transport behavior attributed to minority spin filtering, and low resistance. Existing models fail to predict the negative MR observed in our metallic junctions. Here we develop a model based on the Mott two spin current approximation where the two spin channels are treated independently. The model incorporates spin current conversion, the minority spin filtering predicted for the high quality lattice matched NiFe(111) /graphene interface, as well as a diffusive interface for the graphene / e-beam deposited bcc-Fe layer that is not expected to result in spin filtering. This model correctly predicts the observed negative MR and gives a lower bound for the minority spin polarization in graphene, exceeding 80% at low temperatures, for junctions that exhibit an MR of -12% at 10K. The model quantitatively predicts the dependence of the MR on the RA product at room temperature, and is consistent with the high minority spin polarization inside the graphene junction as predicted by Karpan.

This work was supported by internal programs at NRL.

[1] Karpan, V. M. et al. Phys. Rev. Lett. 99, 176602 (2007).

10357-51, Session 9A

Microwave magnetization dynamics in room temperature organic-based magnets: from fundamental studies to emerging applications *(Invited Paper)*

Ezekiel Johnston-Halperin, The Ohio State Univ. (United States)

Organic and organic-based materials are attractive candidates for applications in magnetoelectronics and spintronics due to their low cost, ease of fabrication, and low spin-orbit coupling (and consequently long spin lifetimes). More recently, advances in these fields have highlighted the potential for dynamic excitations to drive new phenomena such as ferromagnetic resonance generated spin-pumping. Here we present a series of recent breakthroughs in the synthesis, encapsulation, and measurement of organic-based magnets that lay the foundation for all organic magnetoelectronic and spintronic devices. We will discuss advances in encapsulation strategies that allow lifetimes of up to 1 month in air, the use of ligand substitution to generate a library of related magnetic materials, the growth of all-organic and hybrid organic/inorganic magnetic heterostructures, and measurements of ferromagnetic resonance (FMR) linewidths of ~ 1 Oe (comparable to polished spheres of yttrium iron garnet; YIG). Finally, we demonstrate the potential for real world applications in the construction of a V[TCNE]2 based spin-wave resonance device with spectral tuning from 1 – 5 GHz and a quality factor in excess of 3,200 that operates under ambient conditions. These results establish the validity of organic-based magnets for applications in next-generation magnetoelectronics and provide unique leverage on long-standing challenges in the field of organic spintronics.

[1] H. Froning, M. Harberts, Y. Lu, H. Yu, A. J. Epstein and E. Johnston-Halperin, Appl. Phys. Lett 106, 122403 (2015).

[2] Yu Lu, Howard Yu, Megan Harberts, Arthur J. Epstein and Ezekiel Johnston-Halperin, RSC Advances 5, 82271-82275 (2015); Yu Lu, Howard Yu, Megan Harberts, Arthur J. Epstein and Ezekiel Johnston-Halperin, J. Mat. Chem. C 3 (28), 7363-7369 (2015).

[3]H. Yu, M. Harberts, R. Adur, Y. Lu, P.C. Hammel, E. Johnston-Halperin and A.J. Epstein, Appl. Phys. Lett. 105, 012407 (2014).

[4] Na Zhu, Xufeng Zhang, I.H. Froning, Michael E. Flatté, E. Johnston-Halperin, and Hong X. Tang Appl. Phys. Lett. 109, 082402 (2016).

10357-52, Session 9A

Spin to charge conversion in graphene and carbon nanotube mats *(Invited Paper)*

Yuichiro Ando, Sergey Dushenko, Ei Shigematsu, Masashi Shiraishi, Kyoto Univ. (Japan)

The small spin-orbit interaction of carbon atoms in nanocarbon materials such as graphene and carbon nanotubes (CNT) promises a long spin lifetime and potential for the creation of a spin transport devices. Actually, spin transport in graphene and CNT has been demonstrated even at room temperature to date, which enable us to quest for novel physics of the spin transport phenomena. However, graphene and carbon nanotube were largely overlooked as possible spin-charge interconversion materials. In this study, we demonstrated spin to charge conversion in a single-layer graphene and a single-walled carbon nanotube mats (SWCNT mats). A pure spin current were generated in graphene or SWCNT mats from a yttrium iron garnet (YIG) layer by means of spin pumping method. The spin current, flowing in the normal direction, was converted into an in-plane charge current. Clear electromotive forces due to spin-charge conversion were detected for both materials at room temperature. From electric gate tuning of the electromotive force in the single-layer graphene, we showed the dominance of the conventional inverse spin Hall effect over the inverse Rashba-Edelstein effect despite of two dimensional nature. We also revealed that the SWCNT mat exhibits negative spin Hall angle, the first discovery of organic materials which shows a negative spin Hall angle.

10357-53, Session 9A

Magnetically controllable graphene plasmonics *(Invited Paper)*

Dmitry A. Kuzmin, Igor V. Bychkov, Chelyabinsk State Univ. (Russian Federation) and South Ural State Univ. (Russian Federation); Vladimir G. Shavrov, Kotel'nikov Institute of Radio Engineering and Electronics of Russian Academy of Sciences (Russian Federation); Vasily V. Temnov, Institut des Molécules et Matériaux du Mans, Univ. du Maine (France)

Graphene is a unique material to study fundamental limits of plasmonics. Apart from the fact that it possesses the ultimate single-layer thickness, its carrier concentration can be tuned by chemical doping or applying a bias voltage. Thus, the electrodynamic properties of graphene can be varied from highly conductive to dielectric. Graphene supports strongly confined, propagating surface plasmon-polaritons (SPPs) from terahertz to mid-infrared frequencies, in a broad spectral range where conventional noble metal-based plasmonics usually does not work. On the other hand, the magnetooptical response of nanostructures can be much larger as compared to the bulk magnetooptic materials. The magnetic field allows for controlling SPPs properties and there are different ways to design magnetoplasmonic structures base on magneto-optical metals or dielectrics. Graphene has a strong magnetooptic response and thus provides an alternative to conventional magneto-plasmonics. Despite of a large number of works devoted to plasmonic properties and applications of graphene, little is known about the graphene-based magnetoplasmonics, which represents the main subject of this work. Here we will discuss recent strategies to enhance magnetoplasmonic effects by going to low-dimensional structures, i.e. graphene planar waveguides, graphene nanotubes, cylindric nanocavities and toroidal nanostructures. We will review how combining the topological properties of graphene-based meta-surfaces with topologically different closed surface landscapes.

10357-54, Session 9B

Spin orbit torque switching of compensated ferrimagnet *(Invited Paper)*

Luqiao Liu, Joseph Finley, Jiahao Han, Saima Siddiqui, Massachusetts Institute of Technology (United States)

There has been great interest recently in using antiferromagnetic materials (AFM) as opposed to ferromagnet (FM) to store information. Compared with FM, AFM exhibit fast dynamics as well as robust protection against external magnetic fields, which can enable spintronic devices with fast speed and high density. Rare earth (RE)–transition metal (TM) ferrimagnetic alloys have antiferromagnetically coupled sublattices. By varying the relative concentrations of the two species, one can reach the compensation points where the net magnetic moment or angular momentum is zero. Despite the appealing advantages close to the compensation point, few experimental works have explored this region, mostly due to the difficulty in controlling magnetic dynamics with external magnetic field. Here, we show that the spin orbit torque (SOT) provides the possibility of efficiently controlling the magnetic moment in CoTb ferrimagnet alloys. Current induced switching is demonstrated for both Co-rich and Tb-rich samples, including those near compensation point. We quantitatively measured the induced effective field in the domain wall motion regime and found that the largest effective field occurs near the magnetic compensation point. The strong SOT and the predicted fast magnetic dynamics in the ferrimagnet system could potentially lead to high speed spintronic applications.

10357-55, Session 9B

Spin-orbit fields at Fe/GaAs (001) interface *(Invited Paper)*

Lin Chen, Univ. Regensburg (Germany)

Interfacial spin-orbit torques (SOTs) enable manipulation of the magnetization through an in-plane charge current, which has drawn increasing attention for spintronic applications. In the search for material systems that can provide efficient SOTs, much work has been focused on polycrystalline ferromagnetic metal/non-magnetic metal bilayers [1-3]. Here the current flows in the non-magnetic layers and induces a torque at the interfaces via the spin Hall effect of the non-magnetic layer [1], the Rashba effect at the interface [2] or spin-momentum locking when a topological insulator is involved [3]. In this presentation, we report the observation of robust SOT occuring in a well characterized single crystalline Fe/insulating GaAs (001) interface at room temperature where the SOT is caused by the lack of space inversion symmetry at the interface. We find that the magnitude of the interfacial SOT per unit charge current density is comparable in strength with that in ferromagnetic metal/non-magnetic metal systems. This large magnitude also allows for the observation of spin-to-charge current conversion at the interface, which is known as spin-galvanic effect [4]. The results suggest that single crystalline Fe/GaAs interfaces may enable efficient magnetization manipulation through purely electric means [5].

References

[1] L. Liu, et al., Science 336, 555 (2012).

[2] I. M. Miron, et al., Nature 476, 189 (2011).

[3] A. R. Mellnik, et al., Nature 511, 449 (2014).

[4] S. D. Ganichev, et al., Nature 417, 153 (2002).

[5] L. Chen, et al., Nature Commun. 7, 13802 (2016).

10357-56, Session 9B

Phonon-induced superconductivity in a self-consistent Hubbard model *(Invited Paper)*

Enrique Munoz, Pontificia Univ. Católica de Chile (Chile); Edson Vernek, Univ. Federal de Uberlândia (Brazil); Victor Apel, Univ. Católica del Norte (Chile)

We have studied an infinite Hubbard chain with a spin-orbit coupling term, submitted to a uniform magnetic field as well as local phonons. By means of a Lang-Firsov transformation, we show that an effective interacting fermion model emerges. Moreover, a self-consistent mean-field theory of this model, formulated in terms of thermal Green's functions, shows that a BCS term emerges, thus leading to a superconducting phase transition at zero temperature. We find analytical expressions for the phase boundary, that agree well with exact numerical diagonalization of the Hamiltonian.

10357-57, Session 9B

Characterizing spin orbit torque effective fields *(Invited Paper)*

Wen Siang Lew, Sarjoosing Goolaup, Feilong Luo, Nanyang Technological Univ. (Singapore)

The spin coupling between spins of conduction electron in heavy metal (HM) and localized electrons in ferromagnetic (FM) material influences the magnetization of the FM layer via the spin-orbit torque (SOT). The two main phenomena contributing to SOT are bulk spin Hall effect arising from spin scattering in the heavy metal layer and Rashba effect, which is an interfacial spin orbit coupling at the FM/HM interface. The intensity of the SOT is generally characterized by two effective fields: field-like term and damping-like term. Various techniques have been used to quantify the two effective fields, such as current-induced domain wall motion, ferromagnetic resonance techniques, and SOT-assisted magnetization switching. However, the reported amplitude of the fields is highly dependent on the experimental technique.

We present our recent results on the effective fields measurements in multilayered ferromagnetic films and introduce a self-validating method, which simultaneously quantify both the field-like and damping-like terms in structures with in-plane magnetic anisotropy. An analytical expression is derived and experimentally verified using the harmonic Hall resistance measurement. The second harmonic Hall resistance is fitted with our derived equation, to extract both the field-like and damping-like effective fields. We show that in structures with in-plane magnetic anisotropy, the field-like term comprises of a constant component and an azimuth-angular-dependent term. For structures with perpendicular magnetic anisotropy, our analytical expression and experimental results reveals an angular dependence of the damping-like term. Finally, a novel approach to achieving field free bipolar SOT induced magnetization is presented.

10357-58, Session 10A

The engagement of optical angular momentum in nanoscale chirality *(Invited Paper)*

David L. Andrews, Univ. of East Anglia (United Kingdom)

Wide-ranging developments in optical angular momentum have recently led to refocused attention on issues of material chirality. The connection between optical spin and circular polarization, linking to well-known and utilized probes of chirality such as circular dichroism, has prompted studies aiming to achieve enhanced means of differentiating enantiomers - molecules or particles of opposite handedness. Newly devised schemes for physically separating mirror-image components by optical methods have also been gaining traction, together with a developing appreciation of how the scale of physical dimensions ultimately determines any capacity to select for material chirality. The scope of such enquiries has further widened on recognition that suitably structured, topologically charged beams of light can additionally convey orbital angular momentum. Understanding the full scope and constraints upon chiroptical interactions in the nanoscale regime involves the resolution of CPT symmetry conditions governing the fundamental interactions between matter and photons. The emerging principles provide a theory test-bed for new methodologies.

10357-59, Session 10A

Spin-orbit interaction of light on the surface of atomically thin crystals *(Invited Paper)*

Hailu Luo, Hunan Univ. (China)

Two-dimensional (2D) atomic crystals have extraordinary electronic and photonic properties and hold great promise in the application of photonic and optoelectronics. A fundamental understanding of the light-matter interaction in the 2D atomically thin crystals is therefore essential to optoelectronics applications. As a fundamental physical effect in light-matter interaction, spin-orbit coupling of light is attributed to the transverse nature of the photonic polarization. The photonic spin Hall effect (SHE) can be regarded as a direct optical analogy of the SHE in electronic systems where the spin electrons and electric potential are replaced by spin photons and a refractive index gradient, respectively. The analogy has been extensively demonstrated effective for the photonic SHE in 3D bulk crystals. However, the effective refractive index fails to adequately explain the light-matter interaction in 2D atomic crystals. It would be interesting how to describe the spin-orbit interaction on the surface of 2D atomic crystals.

In this paper, we examine the spin-orbit coupling of light on the surface of atomically thin crystals. First, we develop a general model to describe the spin-orbit interaction of light on the surface of 2D atomic crystals. We find that it is not necessary to involve the effective refractive index to describe the spin-orbit interaction and photonic SHE in the atomically thin crystals. The strong spin-orbit interaction and giant spin-dependent splitting in photonic SHE is predicted, which can be explained as the large polarization rotation of plane-wave components in order to satisfy the transversality of photon.

10357-60, Session 10A

Controlling angular momentum at the micro scale *(Invited Paper)*

Daryl Preece, Univ. of California, San Diego (United States)

Beams with angular momentum are often used for experiments at the micrometer and nanometer length scales. These include optical trapping of microscopic particles, STED microscopy, as well as plasmonic applications amongst others. But how much control do we actually have over such beams?

Focal parameters of microscopy systems can lead to separation of optical vortices as well a to spin-orbit coupling. These effects may produce undesirable outcomes when highly focused light is used for experimental research. However, such effects can be obviated with sufficient control over the properties of the focused laser beam. We examine the how beams with orbital and spin angular momentum are affected by focusing and how the associated momentum of such beans can be controlled in the focal region. We also show how control over vortex topology allows unique momentum states to be generated in highly focused beams.

10357-61, Session 10A

Active mid IR plasmonics using giant magneto resistance *(Invited Paper)*

Gaspar Armelles Reig, Instituto de Microelectronica de Madrid, Consejo Superior de Investigaciones Cientificas (Spain); Alfonso Cebollada, Instituto de Microelectrónica de Madrid, Consejo Superior de Investigaciones Científicas (Spain); Fernando García, Instituto de Microelectrónica de Madrid (Spain)

Plasmonics has proven as a powerful tool to improve the performance of mid-IR devices, resulting in plasmon assited quantum cascade lasers, plasmon enhanced light detection, plasmonic beam steering, plasmonic

thermal emiters or plasmonic nanoantenas for vibrational spectroscopy. In this scenario, the possibility of modulating the emission, propagation and/or detection of mid-IR radiation constitutes a promising aspect to expand the limits of the currently used technologies. In this sense, fast and contactless actuation on plasmon resonances via the Magneto-Optical (MO) effect has been put forward by the inclusion of ferromagnetic components into noble metal layers and nanostructures, yet up to now restricted to the visible and near-infrared ranges.

Here we present our proposal and initial results on the magnetic field control of plasmon resonances in the mid IR region by the use of the Magneto-Refractive (MR) effect, i.e., a change in the optical properties of the system by magnetic field controlled electrical resistivity. For this we select a Giant Magneto Resistance model system (a Au/Permalloy multilayer), which exhibits changes in resisitivity of the order of 10% by the application of small (of the order of 20 Oe) magnetic fields. The experiments are carried out in a dedicated FTIR spectrometer with magnetic field capabilities.

References

[1] S.Law, V.Podolsky, and D.Wasserman, Nanophotonics 2 (2013) 103

[2] J.C.Jacquet and T.Valet, Mat.Res.Soc.Symp. 384 (1995) 477

[3] S.S.P.Parkin et al., Physical Review Letters 72 (1994) 3718.

10357-62, Session 10A

Anomalous optical properties of Rashba conductor *(Invited Paper)*

Gen Tatara, RIKEN Ctr. for Emergent Matter Science (Japan)

We theoretically explore the optical properties of a bulk Rashba conductor by calculating the transport coefficients at finite frequencies. It is demonstrated that the combination of direct and inverse Edelstein effects leads to a softening of the plasma frequency for the electric field perpendicular to the Rashba field, resulting in a hyperbolic electromagnetic metamaterial. In the presence of magnetization, a significant enhancement of anisotropic propagation (directional dichroism) is predicted because of the interband transition edge singularity. On the basis of an effective Hamiltonian analysis, the dichroism is demonstrated to be driven by toroidal and quadratic moments of the magnetic Rashba system.

The effective theory of the cross-correlation effects has the same mathematical structure as that of insulating multiferroics.

10357-63, Session 10B

Acoustic driven magnonics *(Invited Paper)*

Ivan Lisenkov, Mikkel Hansen, Albrecht Jander, Pallavi Dhagat, Oregon State Univ. (United States)

Magnonics aims to utilize magnons (quanta of spin-waves) to process and transfer digital and analog information, promising high throughput, low power computing for the post-CMOS era. Any such future magnonic circuits will require spin wave signal sources and amplifiers. We propose that acoustic pumping of spin waves provides a mechanism to implement these functions in efficient and highly localized devices. In support of this, we have developed a general theoretical model of linear and parametric magneto-acoustic interactions, covering all possible polarizations of acoustic waves and spin wave modes. The model combines the predictive power of analytical techniques with numerical micromagnetic simulations and is thus well-suited for the design of complex physical devices. Based on this, we determine the configurations most amenable to spin wave generation and amplification. As an experimental prototype we demonstrate an acoustically-pumped amplifier for spin-waves. Our device consists of an yttrium-iron-garnet (YIG) film grown on a gallium gadolinium garnet (GGG) substrate, with a bulk acoustic waves (BAW) transducer fabricated on the top of the GGG substrate. We show experimentally that the amplitude of the propagating spin-waves increases with the application of the BAW. Moreover, this scheme can be used as a signal correlator, where the modulated spin-waves and acoustic waves serve as signal inputs and the resulting modulation of the amplified spin wave serves as the output.

10357-64, Session 10B

From non-linear magnetoacoustics and spin reorientation transition to magnetoelectric micro/nano-systems *(Invited Paper)*

Nicolas Tiercelin, Institut d'Electronique de Microélectronique et de Nanotechnologie (France); Vladimir Preobrazhensky, Institut d'Electronique de Microélectronique et de Nanotechnologie (France) and A. M. Prokhorov General Physics Institute of the Russian Academy of Sciences (Russian Federation); Olivier Bou Matar, Abdelkrim Talbi, Stefano Giordano, Yannick Dusch, Institut d'Electronique de Microélectronique et de Nanotechnologie (France); Alexey Klimov, Institute of Radio Electronics (Russian Federation) and Institut d'Electronique de Microélectronique et de Nanotechnologie (France) and Moscow Technological Univ. (Russian Federation); Théo Mathurin, Institut d'Electronique de Microélectronique et de Nanotechnologie (France); Omar Elmazria, Michel Hehn, Institut Jean Lamour (France); Philippe Pernod, Institut d'Electronique de Microélectronique et de Nanotechnologie (France)

The interaction of a strongly nonlinear spin system with a crystalline lattice through magnetoelastic coupling results in significant modifications of the acoustic properties of magnetic materials, especially in the vicinity of magnetic instabilities such as the spin-reorientation transition (SRT). The magnetoelastic coupling transfers the critical properties of the magnetic subsystem to the elastic one which leads to a strong decrease of the sound velocity in the vicinity of the SRT, and allows a large control over acoustic nonlinearities. The general principles of the non-linear magneto-acoustics (NMA) will be introduced and illustrated in 'bulk' applications such as acoustic wave phase conjugation, multi-phonon coupling, explosive instability of magneto-elastic vibrations, etc.

Then, the concept of the SRT coupled to magnetoelastic interaction has been later transferred into nanostructured magnetoelastic multilayers with uni-axial anisotropy. The high sensitivity and the non-linear properties have been demonstrated in cantilever type actuators, and phenomena such as magneto-mechanical RF demodulation have been observed. The combination of the magnetic layers with piezoelectric materials also led to stress-mediated magnetoelectric (ME) composites with high ME coefficients, thanks to the SRT.

The magnetoacoustic effects of the SRT have also been studied for surface acoustic waves propagating in the magnetoelastic layers and found to be promising for highly sensitive magnetic field sensors working at room temperature. The patterning of the magnetoelastic layer can more over allow the design of phononic crystals with tunable band gaps.

On the other hand, mechanical stress is a very efficient way to control the magnetic subsystem. The principle of a very energy efficient stress-mediated magnetoelectric writing and reading in a magnetic memory will be presented. Similar concepts are also applied to the magnetoelectric control of magnetic domain walls in microstructures. In conclusion, potential applications of 'magneto-electro-acoustic' devices in the field of plasmonics and photonics will be discussed.

10357-65, Session 10B

High field bipolar magnetic field sensors based on surface acoustic wave resonators *(Invited Paper)*

Vincent Polewczyk, Karine Dumesnil, Daniel Lacour, Mohammed Moutaouekkil, Hamid Mjadeh, Institut Jean Lamour (France); Nicolas Tiercelin, Institut d'Electronique de Microélectronique et de Nanotechnologie (France); Sébastien Petit Watelot, Institut Jean Lamour (France); Yannick Dusch, Institut d'Electronique de Microélectronique et de Nanotechnologie (France); Omar Elmazria, Institut Jean Lamour (France); Abdelkrim Talbi, Olivier Bou Matar, Institut d'Electronique de Microélectronique et de Nanotechnologie (France); Michel Hehn, Institut Jean Lamour (France)

Surface acoustic wave devices (SAW) have a major interest in sensor applications due to their ease of manufacturing, their sensitivity, small size, and wireless structures. Indeed, especially in SAW resonator geometry, the sensor can be wireless addressed and measured with any embedded power. Surface Acoustic Wave sensors have been used to measure a large variety of stimuli like temperature, pressure, constrain [ref]. It is also known that the velocity or resonant frequency of SAW devices including a magnetostrictive material can be changed by applying a magnetic field. By using magnetostrictive single materials or composites with enhanced magnetoelectric coefficients, various magnetic SAW sensors have been proposed during these last ten years. However, their use to sense magnetic fields is restricted to low magnetic fields and the capability to wireless measure bipolar fields and/or high fields is lacking. Furthermore, the occurrence of hysteresis in the SAW response has not been addressed. In this paper, we report magnetic Surface Acoustic Wave (SAW) sensors that consist of interdigital transducers made of a magnetostrictive material (Ni and $TbFe_2$) or based on exchange-biased multilayers (Co/IrMn and CoFe/IrMn). In the SAW resonator geometry, the wireless measure could be performed in a field range depending on the system studied. The intensity and sign of the applied field could be extracted. Finally, the control of the electrode magnetic properties insured reversible behavior in the SAW response.

10357-66, Session 10B

Traveling surface spin-wave resonance spectroscopy using surface acoustic waves *(Invited Paper)*

Praveen Gowtham, Univ. of California, Berkeley (United States)

Coherent gigahertz-frequency surface acoustic waves (SAWs) traveling on the surface of a piezoelectric crystal can, via the magnetoelastic interaction, resonantly excite traveling surface spin waves in an adjacent thin-film ferromagnet. These excited surface spin waves, traveling with a definite in-plane wave-vector, enforced by the SAW, can be detected by measuring changes in the electro-acoustical transmission of a SAW delay line. In this talk, we discuss how such measurements can be used as a precise and quantitative technique for spin-wave spectroscopy – providing a means to determine both isotropic and anisotropic contributions to the spin-wave dispersion and damping.

We also develop an analytical theory of the magnetomechanics of spin-wave resonance at the interface between the magnetic film and the piezoelectric. We use acoustical perturbation theory to find closed-form expressions for the back-action surface stress and strain fields and the resultant SAW velocity shifts and attenuation induced by elastically driven spin-wave resonance. The formalism can, with slight modification, be extended to magnetic thin films on top of various classes of acoustic resonators.

10357-67, Session 10B

Generation of ultrashort shear acoustic pulses by femtosecond laser demagnetization of highly magnetostrictive Terfenol *(Invited Paper)*

Thomas T. P. Pezeril, Univ. du Maine (France)

We experimentally and theoretically demonstrate that, upon femtosecond demagnetization of highly magnetostrictive Terfenol, the ultrafast release of the built-in strains generates ultrashort longitudinal and shear acoustic pulses. These ultrashort acoustic pulses gather new crucial information on the spin-lattice coupling at ultrafast timescale.

10357-68, Session 11A

Ultrafast terahertz spintronics *(Invited Paper)*

Dmitry Turchinovich, Max-Planck-Institut für Polymerforschung (Germany)

In this presentation we will review the spintronic terahertz (THz) phenomena such as ultrafast transient demagnetization [1], generation of spin waves via THz Zeeman torque [2,3], Mott scattering [4], and ultrafast inverse spin-Hall effect [5].

[1] E. Beaurepaire, G. M. Turner, S. M. Harrel, M. C. Beard, J.-Y. Bigot, and C. A. Schmuttenmaer, "Coherent terahertz emission from ferromagnetic films excited by femtosecond laser pulses," Appl. Phys. Lett. 84, 3465 (2004)

[2] T. Kampfrath, A. Sell, G. Klatt, A. Pashkin, S. Mahrlein, T. Dekorsy, M. Wolf, M. Fiebig, A. Leitenstorfer, and R. Huber, "Coherent terahertz control of antiferromagnetic spin waves," Nature Photonics 5, 31 (2011)

[3] Z. Jin, Z. Mics, G. Ma, Z. Cheng, M. Bonn, and D. Turchinovich, "Single-pulse terahertz coherent control of spin resonance in the canted antiferromagnet $YFeO_3$, mediated by dielectric anisotropy", Phys. Rev. B 87, 094422 (2013)

[4] Z. Jin, A. Tkach, F. Casper, V. Spetter, H. Grimm, A. Thomas, T. Kampfrath, M. Bonn, M. Kläui, and D. Turchinovich, "Accessing the fundamentals of magnetotransport in metals with terahertz probes", Nature Physics 11, 761 (2015)

[5] T. Seifert, S. Jaiswal, U. Martens, J. Hannegan, L. Braun, P. Maldonado, F. Freimuth, A. Kronenberg, J. Henrizi, I. Radu, F. Freimuth, E. Beaurepaire, Y. Mokrousov, P.M. Oppeneer, M. Jourdan, G. Jakob, D. Turchinovich, L. M. Hayden, M. Wolf, M. Münzenberg, M. Kläui, and T. Kampfrath, "Efficient metallic spintronic emitters of ultrabroadband terahertz radiation", Nature Photonics 10, 483 (2016)

10357-69, Session 11A

High performance THz emitters based on ferromagnetic/nonmagnetic heterostructures *(Invited Paper)*

Yang Wu, Mehrdad Elyasi, Mengji Chen, Hyunsoo Yang, National Univ. of Singapore (Singapore)

Terahertz spectroscopy is a powerful non-destructive and non-invasive characterization method, which can be applied for biological, medical, and chemical analysis applications. A low cost and versatile THz emitter is an important building block for a high performance THz system, which is lacking now. In this work, we report a THz emitter with excellent performances based on nonmagnetic (NM) and ferromagnetic (FM) heterostructures. The broadband THz waves emitted from our film stacks have a peak intensity exceeding 500 ?m thick ZnTe crystals (standard THz emitters). Our device is insensitive to the polarization of an incident laser beam which indicates the noise resistive feature. In contrast, the polarization

of THz waves is fully controllable by an external magnetic field. We have also fabricated the devices on flexible substrates with a great performance, and demonstrated that the devices can be driven by low power lasers. Together with the low cost and mass productive sputtering growth method for the film stacks, the proposed THz emitters can be readily applied to a wide range of THz equipment. Our study also points towards an alternative approach to characterize spintronic devices with NM/FM bilayers.

10357-70, Session 11A

Tunable THz emitters based on the magnetic heterostructure *(Invited Paper)*

Jingbo Qi, Univ. of Electronic Science and Technology of China (China) and The Peac Institute of Multiscale Sciences (China)

Terahertz (THz) wave, which lies in the frequency gap between infrared and microwave, has an electromagnetic spectrum conventionally defined in the range from 0.1 to 30 THz, which has a great potential in fundamental scientific research and other applications. Very recently, it was reported that the THz wave can be generated in heterostructure composed of ferromagnetic (FM) and non-FM metal films upon excitation of ultrafast laser pulses, which could open a new direction of ultrafast spintronics.

In this contribution, we report our study on the THz emission in Fe/Pt and Co/Pt magnetic heterostructures. We carried out a comprehensive investigation of THz emission from these magnetic heterostructures, employing time-domain THz spectroscopy. We revealed that by properly tuning the thickness of ferromagnetic or non-magnetic layer, THz emission can be greatly improved in this type of heterostructure. We further demonstrate that the THz field strength emitted from a newly designed multilayer [Pt/Fe/MgO]n can be strongly increased. Polarization of the emitted THz wave has been shown to follow the rotation of the applied magnetic field. In addition, the intensity and spectrum of THz wave is demonstrated to be tunable by the magnetic field applied on the patterned magnetic heterostructures. These findings thus promise novel approaches to fabricate powerful and tunable THz emitters based on magnetic heterostructure.

10357-71, Session 11A

Directly probing ultrafast spin dynamics in antiferromagnets using terahertz pulses *(Invited Paper)*

Pamela Bowlan, Stuart A. Trugman, Los Alamos National Lab. (United States); Xueyun Wang, Sang-Wook Cheong, Rutgers, The State Univ. of New Jersey (United States); Dmitry A. Yarotski, Antionette J. Taylor, Rohit P. Prasankumar, Los Alamos National Lab. (United States)

The ability to switch magnetization in a ferromagnet on an ultrafast timescale using femtosecond lasers is of longstanding fundamental interest, due to its potential applications in magnetic data storage. However, ultrafast control of antiferromagnetic (AFM) materials is arguably more promising, since a zero net magnetization makes it easier for the system to change while conserving spin, so that their spin dynamics should be much faster than in ferromagnets. Multiferroic materials, which are usually AFM, have coexisting and coupled magnetic and ferroelectric order, as well as the additional feature that ultrafast laser-induced changes to the ferroelectricity can change the magnetic order and vice versa. This leads to potential applications like ultrafast magnetoelectric switching. Although AFM materials could be quite useful, their magnetization, especially its temporal evolution, is more difficult to detect and therefore less well understood, since such experiments typically require x-ray pulses from large-scale free electron lasers.

We will discuss a new, relatively simple, table-top approach for probing the ultrafast dynamics of spin order in AFM manganites, using THz pulses resonant to magnons. Applying this method to two different AFM systems, hexagonal HoMnO3 and orthorhombic TbMbO3, clearly reveals picosecond spin dynamics in both cases, suggesting that this method is a rather general probe of spin dynamics in AFMs. Furthermore, our study of TbMnO3 shows that THz pulses are sensitive to both short and long range spin dynamics. Analysis of the measured dynamics, which show spin heating by phonon scattering, suggests a unique, direct exchange-mediated spin-phonon coupling mechanism in AFMs.

10357-72, Session 11B

The skyrmion switch: turning magnetic skyrmions on and off with an electric field *(Invited Paper)*

Anne Bernand-Mantel, Marine Schott, Laurent Ranno, Stéfania Pizzini, Jan Vogel, Institut NÉEL, Ctr. National de la Recherche Scientifique (France) and Univ. Grenoble Alpes (France); Helène Béa, Commissariat à l'Énergie Atomique (France) and Ctr. National de la Recherche Scientifique (France) and Univ. Grenoble Alpes (France); Claire Baraduc, Commissariat à l'Énergie Atomique (France) and Univ. Grenoble Alpes (France); Gilles Gaudin, SPINTEC, Ctr. National de la Recherche Scientifique (France) and Institut Nanosciences et Cryogénie, Commissariat à l'Énergie Atomique (France) and Univ. Grenoble Alpes (France); Stéphane Auffret, Commissariat à l'Énergie Atomique (France) and Ctr. National de la Recherche Scientifique (France) and Univ. Grenoble Alpes (France); Dominique Givord, Institut NÉEL, Ctr. National de la Recherche Scientifique (France) and Univ. Grenoble Alpes (France)

Magnetic skyrmions are nanoscale swirling spin structures with a non trivial topology. Recently several groups have reported the observation of magnetic skyrmions at room temperature (RT) in conventional transition-metal-based magnetic multilayers. This discovery has triggered a growing interest for the use of magnetic skyrmions as building blocks for memories which is reminiscent of the extensive research on magnetic bubble memories in the 1970s. The recent observation of current induced displacement of skyrmion bubbles using relatively low current densities reported at RT is very promising. The creation and annihilation of skyrmions have been addressed theoretically and experimentally by different techniques , however, those techniques are either energy consuming or difficult to integrate in functional devices. In this talk, we report on the room temperature switching of skyrmions bubbles with electrical gating, an energy efficient and easily integrable solution. The experiment is carried out on a Pt/Co/oxide trilayer which is imaged using magneto-optical Kerr microscopy under a transparent Indium Tin Oxide electrode. The spontaneous nucleation of skyrmion bubbles by thermal activation is observed. A classical magnetic bubble model, where the DMI interaction is directly imbedded in the domain wall energy, describes quantitatively the thermal nucleation and stability of the observed skyrmion bubbles. The observed efficient and reproducible electric field writing and deleting of skyrmion bubbles is well explaiend by our analytical isolated skyrmion bubble model. These results constitute an important milestone towards the use of skyrmions for memory or logic applications.

10357-73, Session 11B

Room-temperature skyrmion shift device for memory application *(Invited Paper)*

Guoqiang Yu, Pramey Upadhyaya, Qiming Shao, Univ. of California, Los Angeles (United States); Hao Wu, Institute of Physics, Chinese Academy of Sciences (China); Gen Yin, Xiang Li, Congli He, Univ. of California, Los Angeles

(United States); Wanjun Jiang, State Key Lab. of Low-Dimensional Quantum Physics, Tsinghua Univ. (China) and Collaborative Innovation Ctr. of Quantum Matter (China); Xiufeng Han, Institute of Physics, Chinese Academy of Sciences (China); Pedram Khalili Amiri, Kang L. Wang, Univ. of California, Los Angeles (United States)

Magnetic skyrmions are intensively explored for potential applications in ultralow-energy data storage and computing. To create practical skyrmionic memory devices, it is necessary to electrically create and manipulate these topologically-protected information carriers in thin films, thus realizing both writing and addressing functions. Although room-temperature skyrmions have been previously observed, fully electrically controllable skyrmionic memory devices, integrating both of these functions, have not been developed to date. In this talk, I will talk about our recent demonstration of a room-temperature skyrmion shift memory device, where individual skyrmions are controllably generated and shifted using current-induced spin-orbit torques. Particularly, it is shown that one can select the device operation mode in between: (i) writing new single skyrmions, or (ii) shifting existing skyrmions, by controlling the magnitude and duration of current pulses. Thus, we electrically realize both writing and addressing of a stream of skyrmions in the device. This prototype demonstration brings skyrmions closer to real-world computing applications.

10357-74, Session 11B

Electric field induced switching of magnetic skyrmions and strain relief effects *(Invited Paper)*

Aurore Finco, Pin-Jui Hsu, Niklas Romming, André Kubetzka, Kirsten von Bergmann, Roland Wiesendanger, Univ. Hamburg (Germany)

In ultrathin magnetic films deposited on heavy elements substrates, the interface-induced Dzyaloshinkii-Moriya interaction allows to stabilize non-collinear spin structures like magnetic skyrmions. These topologically protected objects are interesting for future data storage technologies like racetrack memories.

We present spin-polarized scanning tunneling microscopy investigations on a three-atomic-layer thick Fe film deposited on Ir(111). In this system, the large epitaxial strain is relieved by the formation of a dense dislocation lines network. This particular structure of the film induces a symmetry breaking with dramatic consequences on the magnetic state. In zero field, spin spirals propagate along the dislocations lines and their period depends on the spacing between these lines, i.e. on the strain relief, which is locally varying [1]. We attribute this effect on the spirals to modifications of the exchange coupling.

Single skyrmions appear in external magnetic field. We demonstrate that they can reliably be written and deleted by an STM tip [2]. The strong-bias polarity dependence and the linear behavior of the threshold voltage for switching with the tip-sample distance shows that electric field plays the dominant role in the switching mechanism. This switching between the topologically distinct magnetic states by electric fields may be beneficial in future spintronic devices employing skyrmions as information carriers.

We acknowledge financial support by the European Union via the Horizon 2020 research and innovation program under Grant No.665095.

[1] Finco et al, PRB 94, 214402 (2016)

[2] Hsu et al, Nat. Nanotech. (2016)

10357-75, Session 11B

Skyrmion motion in inhomogeneous magnetic multilayers *(Invited Paper)*

William Legrand, Unité Mixte de Physique CNRS/Thales (France); Davide Maccariello, Unite Mixte de Physique CNRS/Thales (France); Nicolas Reyren, Karin Garcia, Karim Bouzehouane, Unité Mixte de Physique CNRS/Thales (France); Horia Popescu, Jean-Yves Chauleau, Nicolas Jaouen, Synchrotron SOLEIL (France); Christoforos Moutafis, The Univ. of Manchester (United Kingdom); Simone Finizio, Carlos A. F. Vaz, Jörg Raabe, Swiss Light Source, Paul Scherrer Institute (Switzerland); Stephen McVitie, Univ. of Glasgow (United Kingdom); Vincent Cros, Albert Fert, Unité Mixte de Physique CNRS/Thales (France)

Magnetic skyrmions are magnetic textures, topologically different from the uniform ferromagnetic state, holding a lot of promise for applications as well as of fundamental interest. They have been observed for the first time in magnetic multilayers at room temperature only a couple of years ago. Since their stability has been demonstrated at relatively low magnetic field (1), the new challenge is to control their motion. Already in 2016, velocities up to about 100 m/s were reported, but many questions are still open. In particular, the so-called skyrmion Hall angle was not systematically observed, the threshold current density J0 for their motion can be much larger than expected, and finally effects of the edge repulsion were still not reported experimentally.

In this presentation, we report about observations of current-induced skyrmion motion close to J0, evidencing a motion apparently disordered (2). This motion is observed by different techniques: atomic force microscopy (MFM), scanning transmission x-ray microscopy (STXM) and holography. The advantages of the two last techniques are the sub-100nm spatial resolution together with sub-ns time resolution for reproducible periodic variation of the magnetic configuration in absence of perturbation by external probing fields (such as the magnetic tip in MFM). These observations are explained qualitatively and to some extent quantitatively by the presence of crystalline grains of about 20nm lateral size with a distribution of magnetic properties (Dzyaloshinskii-Moriya interaction and anisotropy).

1) C. Moreau-Luchaire et al, Nat. Nano. 11, 444.

2) W. Legrand et al, submitted.

10357-76, Session 12A

Nanodevices for bio-inspired computing *(Invited Paper)*

Julie Grollier, Unité Mixte de Physique CNRS/Thales (France)

In the last five years, Artificial Intelligence has made striking progress, and now defeating humans at subtle strategy games, such as Go, and even Poker. However, these algorithms are running on traditional processors which have a radically different architecture than the biological neural networks they are inspired from. This considerably slows them down and requires massive amounts of electrical power, more than ten thousand times what the brain typically need to function. This energy dissipation is not only becoming an environmental issue, but it also sets a limit to the size of neural networks that can be simulated. We are at a point where we need to rethink the way we compute, and build hardware chips directly inspired from the architecture of the brain. This is a challenge. Indeed, contrarily to current electronic systems, the brain is a huge parallel network closely entangling memory and processing.

In this talk, I will show that, for building the neuromorphic chips of the future, we will need to emulate functionalities of synapses and neurons at the nanoscale. I will review the recent developments of memristive nano-synapses and oscillating nano-neurons, the physical mechanisms at stake, and the challenges in terms of materials. Finally, I will present the first achievements of neuromorphic computing with novel nanodevices and the fascinating perspectives of this emerging field.

10357-77, Session 12A

Analogue spin-orbit torque device for artificial-neural-network-based associative memory operation *(Invited Paper)*

Shunsuke Fukami, William A. Borders, Aleksandr Kurenkov, Hisanao Akima, Satoshi Moriya, Shouta Kurihara, Yoshihiko Horio, Shigeo Sato, Hideo Ohno, Tohoku Univ. (Japan)

One of the great challenges of today's computer technology is a representation of the human brain in computers to execute complex tasks that the conventional von Neumann computers cannot efficiently complete. This has motivated many researchers to realize artificial neural networks, forming the field of artificial intelligence, or neuromorphic computing. So far, this trend has been mainly led by the software or CMOS based technologies, although it is difficult with such approaches to realize compactness and ultralow-power features as in the brain. Meanwhile, utilizing solid-state devices that function as artificial synapses is known to offer promising routes toward implementation of compact and ultralow-power neuromorphic computing. Here, we present an analog spin-orbit torque device based artificial neural network. The spintronics devices are nonvolatile and capable of virtually infinite read/write operation, which should be useful for edge computing with online learning capability. We will start from a brief description of the operation principle of the analog spin-orbit torque device with an antiferromagnet-ferromagnet structure [1]. Then, we will show a proof-of-concept demonstration of an associative memory operation using the analog spin-orbit torque device based artificial neural network [2].

This work is partly supported by ImPACT Program of CSTI and R&D Project for ICT Key Technology of MEXT.

[1] S. Fukami et al., Nature Mater. 15, 535 (2016).

[2] W. A. Borders et al., Appl. Phys. Express 10, 013007 (2017).

10357-78, Session 12A

Modulation and detection of single neuron activity using spin transfer nano-oscillators *(Invited Paper)*

Jose Miguel Algarin, Bharath Ramaswamy, Lucy Venuti, Matthew Swierzbinski, Pablo Villar, Univ. of Maryland, College Park (United States); Yu-Jin Chen, Univ. of California, Irvine (United States); Irving N. Weinberg M.D., Weinberg Medical Physics (United States); Jens Herberholz, Ricardo Araneda, Benjamin Shapiro, Edo Waks, Univ. of Maryland, College Park (United States)

The brain is a complex network of interconnected circuits that exchange electrical signals with each other. These electrical signals provide insight on how neural circuits code information, and give rise to sensations, thoughts, emotions and actions. Currents methods to detect and modulate these electrical signals use implanted electrodes or optical fields with light sensitive dyes in the brain. These techniques require complex surgeries or suffer low resolution. In this talk we explore a new method to both image and stimulate single neurons using spintronics. We propose using a Spin Transfer Nano-Oscillators (STNOs) as a nanoscale sensor that converts neuronal action potentials to microwave field oscillations that can be detected wirelessly by magnetic induction. We will describe our recent proof-of-concept demonstration of both detection and wireless modulation of neuronal activity using STNOs. For detection we use electrodes to connect a STNO to a lateral giant crayfish neuron. When we stimulate the neuron, the STNO responds to the neuronal activity with a corresponding microwave signal. For modulation, we stimulate the STNOs wirelessly using an inductively coupled solenoid. The STNO rectifies the induced microwave signal to produce a direct voltage. This direct voltage from the STNO, when applied in the vicinity of a mammalian neuron, changes the frequency of electrical signals produced by the neuron.

10357-79, Session 12B

Topological Hall effect in a system with magnetic skyrmions *(Invited Paper)*

Igor Rozhansky, Konstantin Denisov, Ioffe Institute (Russian Federation) and Lappeenranta Univ. of Technology (Finland); Nikita S. Averkiev, Ioffe Institute (Russian Federation); Erkki Lahderanta, Lappeenranta Univ. of Technology (Finland)

Topological Hall effect (THE) is a recently discovered transport phenomenon occurring in various magnetic systems due to free carriers interaction with chiral magnetization textures, such as magnetic skyrmions. THE mechanism is based on exchange interaction, thus it is fundamentally different from normal Hall effect and anomalous Hall effect. THE is considered as a very perspective tool to probe topologically nontrivial spin structures as well as for potential device applications based on topology-related properties of nanostructures, one of the most popular concepts in this field is racetrack memory based on magnetic skyrmions.

Despite its great importance for fundamental and applied research, the topological Hall effect has still lacked a proper theoretical description. The existing theories of THE consider two limiting cases of either infinitely strong exchange interaction when an adiabatic Berry phase approach is applicable or the case of a weak exchange interaction allowing for perturbation theory analysis. These two theoretical approaches are known to give qualitatively different results regarding THE.

The adiabatic Berry phase approximation has revealed that THE is accompanied with a pronounced transverse spin current, so the appearance of transverse charge Hall current requires spin polarization of the carriers in the sample, similarly to the anomalous Hall effect [1]. In the opposite case of a weak exchange the transverse charge current can occur in the absence of a spin current, in this regime THE is expected even for non-polarized carriers [2]. We have developed a theory of THE based on exact solution of a problem of electron scattering on a chiral spin field. The suggested theory fills the gap between the two limiting regimes of THE. We discovered a nontrivial crossover between the two regimes, the transverse pure charge current in the weak coupling case transforms into a pronounced transverse spin current in the adiabatic regime. Thus, the apparent contradiction between the results of adiabatic and perturbative theoretical approaches to THE have been eliminated for the first time [3].

[1] P.Bruno, V.K.Dugaev, M.Taillefumier, Phys.Rev.Lett. 63, 096806 (2004).

[2] K.S. Denisov, I. V. Rozhansky, N. S. Averkiev, E. Lähderanta, Phys.Rev.Lett, 117, 027202 (2016)

[3] K.S.Denisov, I.V.Rozhansky, N.S.Averkiev, E.Lähderanta, arXiv:1702.04985 (2017).

10357-80, Session 12B

Skyrmion Hall effect revealed by direct time-resolved x-ray microscopy *(Invited Paper)*

Kai Litzius, Johannes Gutenberg Univ. Mainz (Germany) and Max-Planck-Institut für Intelligente Systeme (Germany); Ivan Lemesh, Massachusetts Institute of Technology (United States); Benjamin Krüger, Pedram Bassirian, Johannes Gutenberg Univ. Mainz (Germany); Lucas Caretta, Massachusetts Institute of Technology (United States); Kornel Richter, Johannes Gutenberg Univ. Mainz (Germany); Felix Büttner, Massachusetts Institute of Technology (United States); Koji Sato, Tohoku Univ. (Japan); Oleg A. Tretiakov, Tohoku Univ. (Japan) and Far Eastern Federal Univ. (Russian Federation); Johannes Förster, Max-Planck-Institut für Intelligente Systeme (Germany); Robert M. Reeve, Johannes Gutenberg Univ.

Mainz (Germany); Markus Weigand, Iuliia Bykova, Hermann Stoll, Gisela Schuetz, Max-Planck-Institut für Intelligente Systeme (Germany); Geoffrey S. D. Beach, Massachusetts Institute of Technology (United States); Mathias Kläui, Johannes Gutenberg Univ. Mainz (Germany)

Magnetic skyrmions are nanoscale magnetic quasi-particles whose spin structure can be mapped continuously on a sphere. They are promising candidates for future spintronic devices such as the skyrmion racetrack memory.1 In interfacial systems, skyrmions are usually stabilized by the Dzyaloshinskii-Moriya interaction that favors a chiral spin canting.2,3 Additionally, these films can exhibit a significant spin Hall effect that leads to efficient spin dynamics, making thin film systems extremely promising for applications. Indeed, recently the possibility to move skyrmions efficiently in such geometries was reported by static imaging before and after pulse injection.4

In this work, we report the time-resolved pump-probe observation of magnetic skyrmion dynamics at room temperature in thin film devices by scanning transmission X-ray microscopy.5 Our findings reveal fully reproducible motion due to spin-orbit torques (SOT) and skyrmion velocities close to ideal micromagnetic predictions. We find that all skyrmions in the flow regime exhibit motion at an angle with respect to the current flow, demonstrating the presence of a drive dependent skyrmion Hall effect. One approach to explain this behavior is going beyond the rigid 1D-model and assumes a stronger influence of the field-like SOT than previously predicted, resulting in the insight that skyrmion dynamics might be more complex than expected.

References: 1. Tomasello et al., Sci. Rep. 4, 6784 (2014). 2. Dzyaloshinsky, J. Phys. Chem. Solids 4, 241–255 (1958). 3. Moriya, Phys. Rev. 120, 91–98 (1960). 4. Woo et al., Nat. Mater. 15, 501–506 (2016). 5. Litzius et al., Nat. Phys. 13, 170–175 (2017).

10357-81, Session 12B

Topological orbital magnetic moments *(Invited Paper)*

Manuel dos Santos Dias, Juba Bouaziz, Mohammed Bouhassoune, Stefan Blügel, Samir Lounis, Forschungszentrum Jülich GmbH (Germany)

The magnetic moment carried by electrons has two components: spin and orbital. The spin magnetic moment arises from the first of Hund's rule in most cases, also partially satisfied in magnetic solids. There are two well-known sources of the orbital magnetic moment: the second of Hund's rules, which applies only to localized electron orbitals, and spin-orbit coupling, which unquenches the orbital moment in a magnetic solid.

Here we discuss a third mechanism of orbital magnetic moment formation: magnetic structures with a special topology, where the spin magnetic moments do not all lie in the same plane. We illustrate the basic aspects considering magnetic trimers as model systems, e.g. Fe_3 on the Cu(111) surface. The symmetry of the effect is established, showing how to distinguish the topological and the spin-orbit contributions. We then focus on the implications of the topological orbital moments for single magnetic skyrmions formed in Pd/Fe/Ir(111) [1,2], using first-principles electronic structure calculations and a simplified tight-binding model. We propose that the topological orbital moments could enable detecting and distinguishing skyrmions from anti-skyrmions by soft x-ray spectroscopy [3], complementing transport measurements of the topological Hall effect [4], magnetic force microscopy [5] or scanning tunneling microscopy [2].

[1] D.M. Crum et al., Nat. Commun. 6, 8541 (2015)

[2] C. Hanneken et al., Nat. Nanotechnol. 10, 1039 (2015)

[3] M. dos Santos Dias et al., Nat. Commun. 7, 13613 (2016)

[4] A. Neubauer et al., Phys. Rev. Lett. 102, 186602 (2009)

[5] X.Z. Yu et al., Nature 465, 902 (2010)

10357-83, Session 13A

Memcomputing: a brain-inspired topological computing paradigm *(Keynote Presentation)*

Massimiliano Di Ventra, Univ. of California, San Diego (United States)

Which features make the brain such a powerful and energy-efficient computing machine? Can we reproduce them in the solid state, and if so, what type of computing paradigm would we obtain? I will show that a machine that uses memory to both process and store information, like our brain, and is endowed with intrinsic parallelism and information overhead - namely takes advantage, via its collective state, of the network topology related to the problem - has a computational power far beyond our standard digital computers [1]. We have named this novel computing paradigm "memcomputing" [2, 3]. As an example, I will show the polynomial-time solution of prime factorization and the NP-hard version of the subset-sum problem using polynomial resources and self-organizing logic gates, namely gates that self-organize to satisfy their logical proposition [4]. I will also demonstrate that these machines are described by a topological field theory and they compute via an instantonic phase where a transient long-range order develops due to the effective breakdown of topological supersymmetry [5]. The digital memcomputing machines that we propose are scalable and can be easily realized with available nanotechnology components, and may help reveal aspects of computation of the brain.

[1] F. L. Traversa and M. Di Ventra, Universal Memcomputing Machines, IEEE Transactions on Neural Networks and Learning Systems 26, 2702 (2015).

[2] M. Di Ventra and Y.V. Pershin, Computing: the Parallel Approach, Nature Physics 9, 200 (2013).

[3] M. Di Ventra and Y.V. Pershin, Just add memory, Scientific American 312, 56 (2015).

[4] F. L. Traversa and M. Di Ventra, Polynomial-time solution of prime factorization and NP-complete problems with digital memcomputing machines, Chaos: An Interdisciplinary Journal of Nonlinear Science 27, 023107 (2017).

[5] M. Di Ventra, F. L. Traversa and I.V. Ovchinnikov, Topological field theory and computing with instantons, arXiv:1609.03230.

10357-84, Session 13A

Neuromorphic computing with stochastic spintronic devices *(Invited Paper)*

Damien Querlioz, Adrien F. Vincent, Alice Mizrahi, Damir Vodenicarevic, Nicolas Locatelli, Univ. Paris-Sud 11 (France); Joseph S. Friedman, The Univ. of Texas at Dallas (United States); Jacques-Olivier Klein, Univ. Paris-Sud 11 (France); Julie Grollier, Univ. Paris-Sud (France)

Spin torque magnetic memory (ST-MRAM) is currently under intense academic and industrial development, as it features non-volatility, high write and read speed and high endurance. However, one of its great challenge is the probabilistic nature of programming magnetic tunnel junctions, which imposes significant circuit or energy overhead for conventional ST-MRAM applications. In this work, we show that in unconventional computing applications, this drawback can actually be turned into an advantage. First, we show that conventional magnetic tunnel junctions can be reinterpreted as stochastic "synapses" that can be the basic element of low-energy learning systems. System-level simulations on a task of vehicle counting highlight the potential of the technology for learning systems. We investigate in detail the impact of magnetic tunnel junctions' imperfections. Second, we introduce how intentionally superparamagnetic tunnel junctions can be the basis for low-energy fundamentally stochastic computing schemes, which harness part of their energy in thermal noise. We give two examples built around the concepts of synchronization and Bayesian inference. These results suggest that the stochastic effects of spintronic devices, traditionally interpreted by electrical engineers as a drawback, can be reinvented as an opportunity for low energy circuit design.

10357-89, Session 13A

Degree of match determination using coupled spin-torque oscillators *(Invited Paper)*

Matthew Pufall, National Institute of Standards and Technology (United States)

Determining a ranked list or degree of match is frequent computational task, and is one that does not require high numerical precision. A variety of methods for performing such calculations are being explored, such as hardware methods based on lower precision Boolean logic and threshold logic, among others. We have been exploring nonBoolean hardware methods of performing these calculations using phase locking of spin torque oscillator arrays. In this scheme, phase locking of the oscillators in the array maps on to a distance metric based on an L2 norm. We will discuss the progress and challenges of implementing larger (>4) arrays of independently controllable spin torque oscillators into microwave systems that exhibit phase locking, and require stable, high speed, phase sensitive detection. Finally, we will discuss how these results may impact the prospects for applying such oscillator arrays to computational schemes that are more bio-inspired or neuromorphic in nature.

10357-127, Session 13A

Implementation of energy efficient learning in neural networks based on synaptic devices *(Invited Paper)*

Yuhan Shi, Leon Nguyen, Duygu Kuzum, Univ. of California, San Diego (United States)

The biological brain has capability of learning, recognizing, and processing imprecisely defined data and execute extremely complex computational tasks with incredible computational efficiency. Inspired from biological counterparts, synaptic devices have been developed to enable new computational paradigms inspired from the unique features of the biological brain. The question of how to design and build compact synaptic devices for energy-efficient and robust neuromorphic architecture has been a challenge for industry and academia. Here we will describe desired device characteristics for the synaptic devices and potential programing techniques for system-level robustness and efficiency. Then we will discuss device-level and array-level approaches to implementation of multi-level resistance states and improvements in energy efficiency. We will also discuss future directions towards building computational systems with brain-like parallelism, computational efficiency and learning capability.

10357-85, Session 13B

High-frequency polarization dynamics in spin-lasers: pushing the limits *(Invited Paper)*

Nils C. Gerhardt, Markus Lindemann, Ruhr-Univ. Bochum (Germany); Tobias Pusch, Rainer Michalzik, Univ. Ulm (Germany); Martin R. Hofmann, Ruhr-Univ. Bochum (Germany)

While the high-frequency performance of conventional lasers is limited by the coupled carrier-photon dynamics, spin-polarized lasers have a high potential to overcome this limitation and to push the direct modulation bandwidth beyond 100 GHz. The key is to utilize the ultrafast polarization dynamics in spin-polarized vertical-cavity surface-emitting lasers (spin-VCSELs) which is decoupled from the intensity dynamics and its fundamental limitations. The polarization dynamics in such devices, characterized by the polarization oscillation resonance frequency, is mainly determined by the amount of birefringence in the cavity. Using an approach for manipulating the birefringence via mechanical strain we were able to push the polarization dynamics to resonance frequencies of more than 40 GHz. Up to now these values are only limited by the setup to induce birefringence and do not reflect any fundamental limitations. Taking our record results for the birefringence-induced mode splitting of more than 250 GHz into account, the concept has the potential to provide polarization modulation in spin-VCSELs with modulation frequencies far beyond 100 GHz. This makes them ideal devices for next generation fast optical interconnects.

Here we present our recent results for ultrafast polarization dynamics in spin-lasers and discuss different concepts to increase and control the amount of birefringence and thus the polarization dynamics of the laser. By comparing experimental and theoretical results we investigate the limitations for future polarization modulation concepts in spin-lasers and analyze the fundamentally important parameters.

10357-86, Session 13B

Quantum dot spin-V(E)CSELs: polarization switching and periodic oscillations *(Invited Paper)*

Nianqiang Li, Univ. of Essex (United Kingdom); Dimitris Alexandropoulos, Univ. of Patras (Greece); Hadi Susanto, Ian D. Henning, Michael J. Adams, Univ. of Essex (United Kingdom)

Spin-polarized vertical (external) cavity surface-emitting lasers, spin-V(E) CSELs are of interest since their output polarization can be manipulated by spin-selective pumping. Recently we reported [1] the first room temperature optically-pumped quantum dot (QD)-based spin-VECSEL operating at the telecom wavelength of 1300 nm. Under certain conditions it was found that the sign of the output polarization ellipticity could switch from following that of the pump to an ellipticity of the opposite sign. This was seen in experimental studies and theoretical simulations based on time?dependent solution of the rate equations for a spin-flip model (SFM) modified to apply to QD material [2]. The simulations also revealed regions of periodic oscillations at a frequency related to the birefringence rate.

A deeper level of understanding of these phenomena is gained by applying a stability analysis to the SFM equations used for simulations. The choice of in-phase and out-of-phase solutions that appear in a time-dependent simulation is found to be determined by the condition that the corresponding steady-state solutions are stable against small perturbations [3]. Whilst it is not yet possible to conclude that the observed behaviour in our 1300 nm device is caused by the same underlying physics as that of the model, it is nevertheless clear that stability analysis is a valuable theoretical tool for future studies of spin-V(E)SELs.

1. S.S. Alharthi et al, Appl. Phys. Lett. 107, 151109 (2015)

2. D. Alexandropoulos et al, Opt. Lett. 37, 1700 (2012)

3. N. Li et al, Electronics 5, 83 (2016)

10357-87, Session 13B

Theory of wurtzite-based spin lasers *(Invited Paper)*

Paulo E. Faria Junior, Univ. Regensburg (Germany); Gaofeng Xu, Univ. at Buffalo (United States); Yang-Fang Chen, National Taiwan Univ. (Taiwan); Guilherme M. Sipahi, Univ. de São Paulo (Brazil); Igor Zutic, Univ. at Buffalo (United States)

The injection of spin polarized carriers in semiconductor lasers greatly modifies the device operation. Although the vast majority of spin lasers are based on semiconductors with zinc-blende structure[1], there is a recent exception using nitride-based compounds with wurtzite structure[2], which still lacks a reliable theoretical description. In order to address such

deficiency, we investigated (In,Ga)N-based wurtzite quantum wells following typical device geometries[3]. The small spin-orbit coupling in such nitride materials allows the simultaneous spin polarization of electrons and holes, providing an unexplored path to control spin lasers. For instance, based on microscopic gain calculations[3,4] we found a robust gain asymmetry, one of the key signatures of spin laser operation. In addition, we combine these microscopic gain calculations with phenomenological rate equations[5] to investigate threshold reduction features. We show that the lasing threshold has a nonmonotonic dependence on electron spin polarization, even for a nonvanishing hole spin polarization. The complementary information of these theoretical frameworks provides a powerful predictive materials-specific tool to understand and guide the operation of semiconductor spin lasers. [1] Holub et al., PRL 98, 146603 (2007); Lindemann et al., APL 108, 042404 (2016); Rudolph et al., APL 82, 4516 (2003); Frougier et al., APL 103, 252402 (2013). [2] Cheng et al., Nat. Nanotech. 9, 845 (2014). [3] Faria Junior et al., arXiv:1701.07793 (2017). [4] Faria Junior et al., PRB 92, 075311 (2015). [5] Lee et al., APL 105, 042411 (2014).

10357-88, Session 13B

Eigenmodes of semiconductor spin-lasers with local linear birefringence and gain dichroism *(Invited Paper)*

Henri Jaffrès, Unité Mixte de Physique CNRS/Thales (France); Tibor Fordos, VŠB-Technical Univ. of Ostrava (Czech Republic) and Ecole Polytechnique (France); Kamil Postava, Jaromir Pištora, VŠB-Technical Univ. of Ostrava (Czech Republic); Arnaud Garnache, Univ. Montpellier (France); Henri-Jean Drouhin, Ecole Polytechnique (France)

We present a general method for modeling spin-lasers such as spin-polarized vertical cavity surface emitting laser (spin-VCSELs) with multiple quantum wells including anisotropic effects such as i) the emission of elliptically-polarized photons and originating from unbalanced spin-up and spin-down pumps, ii) the linear gain dichroism originating from the reduction from Td to C2v symmetry group at the III-V ternary interfaces and iii) the locally linear birefringence due to the anisotropic strain field at surface of ? VECSELs an optical birefringence of quantum wells from the Henry's factor. New recurrence calculations, together with analytically gain tensor derived from Maxwell-Bloch equations, enable to model emission from multiple quantum well active zones to find the laser resonance conditions and properties of eigenmodes.

The method is demonstrated on real semiconductor laser structures. It is used for the extraction of optical permittivity tensors of surface strain and of quantum wells (QWs). The laser structures are also experimentally studied via ellipsometry methods by measurement of the rotation spectra of complete Mueller matrix in the reflection geometry. The anisotropic optical permittivity constants in the spectral range from 0.73 to 6.4 eV are modeled in order to disantangle surface and QWs contributions to the linear optical birefringence of the structures.

10357-90, Session 14A

Mutually synchronized spin Hall nano-oscillators for neuromorphic computing *(Invited Paper)*

Mykola Dvornik, Ahmad A. Awad, Philipp Dürrenfeld, Afshin Houshang, Ezio Iacocca, Randy K. Dumas, Johan Åkerman, Göteborgs Univ. (Sweden)

Deep Machine Learning is the emerging brain-inspired computing approach that employs artificial neural networks to solve such important problems as image and voice recognition, market behavior prediction, etc. It however still relies on digital CMOS technologies that approach their fundamental limits. As a consequence, there is now significant research activity aimed at finding hardware platforms that would allow for the native implementation of the artificial neural networks. There are already models available that describe human brain operation via synchronization phenomena in complex networks of nonlinear oscillators. This research topic remains mostly theoretical, or numerical, since large-scale oscillator networks are needed, but not easily implemented. However, it was recently demonstrated that so-called spin torque and spin Hall nano-oscillators can act as artificial neurons [1], and their propensity for mutual synchronization on the nano-scale can open up for very large non-linear oscillator networks with different degrees of mutual interactions.

To this end, we here present the first experimental demonstration of mutual synchronization of nano-constriction spin Hall nano-oscillators (SHNOs) [2]. The mutual synchronization is observed both as a strong increase in the power and coherence of the electrically measured microwave signal. The mutual synchronization is also optically probed using scanning micro-focused Brillouin light scattering microscopy (μ-BLS), providing the first direct imaging of synchronized nano-magnetic oscillators. By tailoring the connection region between the nano-constrictions, we have been able to synchronize SHNOs separated by up to 4 micrometers. In addition, we have demonstrated mutual synchronization of as many as nine SHNOs. Our results opens up a direct route for the design of very large SHNO based oscillator networks and pave the way for the development of a spintronic brain-inspired computing technology.

[1] J. Grollier, D. Querlioz, M.D. Stiles, PIEEE 104, 2024 (2016)

[2] A. A. Awad, P. Dürrenfeld, A. Houshang, M. Dvornik, E. Iacocca, R. K. Dumas and J. Åkerman, Nature Physics 13, 292–299 (2017).

10357-91, Session 14A

Stochastic p-bits for invertible logic *(Invited Paper)*

Kerem Yunus Camsari, Purdue Univ. (United States)

Conventional logic/memory devices are built out of deterministic units such as MOS transistors, or nanomagnets with energy barriers in excess of ~40 kT. We show that unstable, stochastic units which we call "p-bits" can be interconnected to create correlations that implement Boolean functions with impressive accuracy, comparable to digital circuits. At the same time they are invertible, a unique property that is absent in digital circuits. When operated in the direct mode, the input is clamped, and the network provides the correct output. In the inverted mode, the output is clamped, and the network fluctuates among all possible inputs that are consistent with that output. We present an implementation of such an invertible gate to emphasize the key role of a "transistor-like" building block to construct p-bit networks. The results for this hardware implementation agree with those from a universal model for p-bits, showing that p-bits need not be magnet-based: any "transistor-like" tunable random bit generator should be suitable. We present an algorithm for designing a bi-directional p-bit network that implements a given truth table. We then show such bi-directional units, such as Full Adders, can be interconnected in a directed manner to implement 32-bit addition, that correlate hundreds of stochastic p-bits to pick a single state out of (~8 billion) possibilities. We also show that despite the directed interconnections, invertibility is largely preserved. This combination of digital accuracy and logical invertibility is enabled by the hybrid design using bi-directional BM units to construct circuits with directed inter-unit connections.

10357-92, Session 14A

Shock-waves and commutation speed of memristors *(Invited Paper)*

Marcelo Rozenberg, Ctr. National de la Recherche Scientifique (France) and Univ. of California, San Diego (United States)

Progress of silicon based technology is nearing its physical limit, as minimum feature size of components is reaching a mere 10 nm. The resistive switching behavior of transition metal oxides and the associated memristor device is emerging as a competitive technology for next generation

electronics. Significant progress has already been made in the past decade and devices are beginning to hit the market; however, it has been mainly the result of empirical trial and error. Hence, gaining theoretical insight is of essence. In the present work we report the striking result of a connection between the resistive switching and shock wave formation, a classic topic of non-linear dynamics. We argue that the profile of oxygen vacancies that migrate during the commutation forms a shock wave that propagates through a highly resistive region of the device. We validate the scenario by means of model simulations and experiments in a manganese-oxide based memristor device and we extend our theory to the case of binary oxides. The shock wave scenario brings unprecedented physical insight and enables to rationalize the process of oxygen-vacancy-driven resistive change with direct implications for a key technological aspect – the commutation speed.

10357-93, Session 14A

Reservoir computing with spin-torque nano-oscillators

Flavio Abreu Araujo, Mathieu Riou, Jacob Torrejon, Unité Mixte de Physique CNRS/Thales (France); Guru Khalsa, Mark D. Stiles, National Institute of Standards and Technology (United States); Sumito Tsunegi, Akio Fukushima, Hitoshi Kubota, Shinji Yuasa, National Institute of Advanced Industrial Science and Technology (Japan); Damien Querlioz, Univ. Paris-Sud 11 (France); Vincent Cros, Julie Grollier, Unité Mixte de Physique CNRS/Thales (France)

In this work, we prove that nanoscale magnetic oscillators called spin-torque nano-oscillators[1-3] can be used to emulate the oscillatory behavior of collections of neurons. We first highlight their two main assets for neuromorphic computing: their exceptional ability to synchronize and their well-controlled magnetization dynamics. We then demonstrate experimentally that a single spin-torque oscillator can realize neuromorphic tasks such as spoken digit recognition reaching state of the art performances.

For many tasks such as facial recognition, speech recognition or prediction, the brain processes information much faster and with much less power than any computer. Some models interpret the way brain process information treating the neurons as interconnected non-linear oscillators. In particular, reservoir computing is a recently introduced braininspired computing paradigm [4]. Its efficiency at dealing with complex cognitive tasks such as speech recognition or chaotic series prediction has already been demonstrated [5].

Reservoir computing can be implemented with a recurrent network (the reservoir) composed of an assembly of interconnected oscillators with fixed connections. A fast input signal, encoding the data to process, is applied to the network. The input signal modifies the frequency and amplitude of each oscillator. Different input waveforms will create different transient dynamics in the network, allowing for separation and classification. The responses of all the oscillators are recorded and recombined. This recombination corresponds to the output of the computation. When the input signal is applied to the reservoir of coupled oscillators, the initial problem (classifying the inputs) is projected non-linearly in a higher dimensional state where separation is easier. If the number of non-linear oscillators is sufficient, the projection of the initial problem in the reservoir state is linearly solvable. It is then sufficient to recombine linearly the response of the different oscillators of the reservoir in order to generate different outputs for different inputs. The optimum coefficients are determined using a training procedure, which consists in a simple linear regression. In other words the working principle of reservoir computing is to leverage non-linearity to transform the problem in another one that is easier to solve. Reservoir computing is one of the few neural network approaches demonstrated in hardware. However, existing implementations are restricted to FPGAs or optical systems, where the power consumption is high and oscillators are not nanometric [4,5].

In this context, spin-torque nano-oscillators are particularly promising building blocks for reservoir computing. They have a nanometric size and low energy consumption, they are compatible with CMOS and can be built in large quantities. In addition, these oscillators are highly non-linear and can synchronize to each other. They are therefore ideal candidates to mimic neurons [6]. Here we give the first experimental demonstration of neuromorphic computing with spin-torque nano-oscillators. We show that a single oscillator can emulate the behavior of a whole neural network. By time multiplexing the input waveform we create a temporal complexity which is the analog of the spatial complexity of a network. By exciting the oscillator with this preprocessed signal, we generate complex transient dynamics that we record and recombine. In order to have good performances in term of noise, we use vortex based spin-torque nano-oscillators with FeB free layer. The dynamics of our oscillator is controlled through the applied dc current and magnetic field. By changing these two parameters we have tuned the oscillator operating point to optimize the neural network-like behavior. By leveraging the transient dynamics of our spin-torque vortex oscillator, we have performed several cognitive tasks. First we have tested our system with a simple pattern recognition task, which consists in discriminating sequences of sine and squares randomly disposed in the input waveform. This task is not trivial since the recognition is piecewise, which means that at each moment the system should recognize if the input value belongs to a square or a sine. We achieved a perfect recognition of sines and squares. Then we moved to speech recognition task, which is more complex (Fig1). Our input signals are recorded digits said by 5 different speakers. After recombining the transients of the oscillator response, we were able to recognize which digit was said and which speaker said it with a success rate of 99,8%. Our results are comparable to the best results observed in hardware reservoir computing [4,5] and open the path to building large spintronics neural networks that exploit magnetization dynamics for computing.

[1] S.I. Kiselev et al., Nature 425, 380–383 (2003)

[2] W.H. Rippard et al., Phys. Rev. Lett. 92, 027201 (2004)

[3] B. Özyilmaz et al., Phys. Rev. Lett. 93, 176604 (2004)

[4] L. Appeltant et al., Nat. Commun. 2, 468 (2011)

[5] Y. Paquot et al., Sci. Rep. 2, 287 (2012)

[6] N. Locatelli et al., Nat. Mat. 13, 11-20 (2014)

10357-94, Session 14B

Dispersive elastic properties governing Dzyaloshinskii domain wall creep *(Invited Paper)*

Vincent Sokalski, James P. Pellegren, Derek Lau, Carnegie Mellon Univ. (United States)

Measuring asymmetric growth of chiral magnetic bubble domains has emerged as a popular technique for evaluating the interfacial Dzyaloshinskii-Moriya Interaction (DMI) in thin films, but the development of a complete theoretical model to explain the range of counterintuitive results has remained elusive. Here, we show that these anomalous trends are rooted in the highly anisotropic energy of Dzyaloshinskii domain walls (DWs), which has an immense impact on the governing elastic properties.[1, 2] Our model further suggests that there is a multitude of additional information built into the full asymmetric velocity measurements seen experimentally.

In the creep regime, velocity depends exponentially on the elastic energy, ?, often assumed to be equivalent to the wall energy, ?, which is strictly true only in the isotropic case. For the anisotropic case that emerges when the wall is subject to an external in-plane field, ? is given instead by the wall stiffness, ?(?)+?''(?), which adopts trends that are very different from ? itself including the striking result that higher energy walls are often more flexible than their low energy counterparts. We present analytic and numerical calculations of a dispersive stiffness that quantitatively predict many of the features seen experimentally including a reversal in the preferred expansion direction in magnetic bubbles. By fitting the full asymmetric velocity profile, it is now possible to, not only, measure DMI, but also estimate the lengthscale of the disorder; something notoriously difficult to study experimentally.

[1] J. P. Pellegren, D. Lau, and V. M. Sokalski, "Dispersive Stiffness of Dzyaloshinskii Domain Walls," arXiv:1609.04386 (2017).

[2] D. Lau, V. Sundar, J.-G. Zhu, and V. Sokalski, "Energetic molding of chiral magnetic bubbles," Physical Review B, vol. 94, 2016.

10357-95, Session 14B

Stabilization and control of Majorana bound states with skyrmions *(Invited Paper)*

Alexey A. Kovalev, Univ. of Nebraska-Lincoln (United States)

Majorana bound states (MBSs) are a promising candidate for a realization of topological quantum computer and memory, which uses non-Abelian anyons to encode and manipulate quantum information. Since Kitaev's toy model for creating MBSs using the unpaired sites at the ends of a spinless p-wave superconducting wire, it has been shown that a conventional s-wave superconductor with spin-orbit coupling (SOC) subject to Zeeman or proximity-induced exchange field has effective p-wave pairing and thus can also support these nonlocal quasiparticles. In systems lacking an extrinsic SOC, an effective SOC can be provided through a nonuniform magnetic texture or field. Here, we explore stabilization of MBSs through a proximity effect with a noncollinear ferromagnet supporting skyrmions. Skyrmions can be easily manipulated via currents or temperature gradients thus providing means for braiding and manipulation of MBSs. In particular, we demonstrate how a nonabelian statistics of MBSs can be revealed by moving proximity coupled skyrmions in a vicinity of a tri-junction with different superconducting phases.

10357-96, Session 14B

Charge-spin conversion in topological insulators and graphene *(Invited Paper)*

Ching-Tzu Chen, IBM Thomas J. Watson Research Ctr. (United States)

Topological insulators and graphene, the two representative 2D Dirac electron systems, have both been widely studied for spintronics applications. On the one hand, strong spin-orbit coupling in topological insulators makes them obvious spin source candidates. On the other hand, minute spin-orbit coupling in graphene makes it a promising spin transport channel. In this talk, I will first present our work on the charge-spin conversion in topological insulators. Our data demonstrate orders of magnitude improvement over conventional spin-Hall metals [1][2]. Furthermore, they indicate that the high spin generation efficiency originates from the spin-momentum locking of the topological surface states. In the second part of the talk, I will discuss the charge-spin conversion in graphene, when proximity coupled to a model magnetic insulator EuS. The interfacial exchange coupling produces a substantial Zeeman field (>= 14 T) in graphene, which yields orders-of-magnitude enhancement in spin generation by the Zeeman spin-Hall effect. Furthermore, the strong exchange field lifts the spin degeneracy in the graphene quantum Hall regime, which leads to novel spin-polarized edge transport features, potentially interesting for classical and quantum information processing [3].

[1] Luqiao Liu, A. Richardella, Ion Garate, Yu Zhu, N. Samarth, and Ching-Tzu Chen, Physical Review B 91, 235437 (2015).

[2] Luqiao Liu, Ching-Tzu Chen, and J. Z. Sun, Nature Physics 10, 561--566 (2014).

[3] Peng Wei, Sunwoo Lee, Florian Lemaitre, Lucas Pinel, Davide Cutaia, Wujoon Cha, Ferhat Katmis, Yu Zhu, Donald Heiman, James Hone, Jagadeesh S. Moodera, and Ching-Tzu Chen, Nature Materials 15, 711 (2016).

10357-123, Session PWed

AuCl3 doping-induced conductive unstability for CVD-grown graphene on glass substrate

Jiaqing Wang, Xianming Liu, Yun Luo, Peng Zhang, Xiaohua Lei, Weimin Chen, Chongqing Univ. (China)

Graphene is a candidate material for next-generation high performance transparent conducting film (TCF) to replace ITO materials. However, the sheet resistance of large area graphene obtained by the CVD method is higher than other kinds of TCFs. The main strategies for improving the electrical conductivity of graphene films have been based on various doping treatments. AuCl3 is one of the most effective dopants.

In the paper, we investigated the influence of AuCl3 doping on the conductive stability of CVD-grown graphene. Large area graphene film synthesized by CVD was transferred to glass substrates using poly(methyl methacrylate). AuCl3 in nitromethane was used to dope the graphene films to improve the electrical conductivity. A group of sample without doping were prepared for comparison. The resistances of graphene under periodic visible light irradiation with and without AuCl3 doping were measured. Results show that the resistances for all samples increased exponentially under lighting, while decreased slowly in an exponential form as well after the light was switched off. The change rate and degree for doped graphene were greater than that of undoped graphene. The relative resistance changes were up to 7% and 23% for undoped and doped samples under blue light irradiation with 80mW/cm2 in atmosphere. The corresponding value were 3.5% and 12.5% when the samples were in vacuum. It was evident from the experimental data that AuCl3 doping may induce conductive unstability for CVD-grown graphene on glass substrate.

10357-124, Session PWed

Excitons and magnetic properties of InP nanowires in wurtzite phase

Paulo E. Faria Junior, Univ. Regensburg (Germany); Davide Tedeschi, Sapienza Univ. di Roma (Italy); Marta De Luca, Sapienza Univ. di Roma (Italy) and Univ. Basel (Switzerland); Benedikt Scharf, Univ. Regensburg (Germany) and Julius-Maximilians-Univ. Würzburg (Germany); Antonio Polimeni, Sapienza Univ. di Roma (Italy); Jaroslav Fabian, Univ. Regensburg (Germany)

Spin-dependent phenomena in III-V wurtzite semiconductor nanowires have recently attracted great attention. Unlike their zinc-blende counterparts, some basic properties of these novel non-nitride wurtzite materials are still unknown. Starting with a robust 8x8 k.p Hamiltonian which includes the k-dependent spin-orbit coupling terms[1], we investigate the excitonic and magnetic properties of InP in wurtzite phase. At low magnetic fields, the Zeeman splitting is linear and our calculated values of effective g-factors are in good agreement with experimental data[2]. Furthermore, our calculations allow us to distinguish the independent contributions of electron and hole g-factors, typically entangled due to excitonic effects. We also investigated the interplay between Landau levels (orbital effects) and the Zeeman splitting by including the spatial dependence of the vector potential. For large magnetic fields, we showed that the nonlinear features of the Zeeman splitting found in experiments[2] arise from the interaction between the different valence bands, mainly heavy and light holes from different Landau level indices. Supported by: Capes, Alexander von Humboldt Foundation, DFG SCHA 1899/2-1, DFG SFB 1170, Awards2014 and Avvio alla Ricerca (Sapienza Università di Roma). [1] P. E. Faria Junior et al., Phys. Rev. B 93, 235204 (2016). [2] M. De Luca et al., Nano Lett. 14, 4250 (2014).

10357-125, Session PWed

Spinorbitronics and spin Hall effects in metallic multilayers for THz emission and THz applications

Thi-Huong Dang, Unité Mixte de Physique CNRS/Thales (France); Jérôme Tignon, Lab. Pierre Aigrain (France); Jean-Marie George, Sophie Collin, Unité Mixte de Physique CNRS/Thales (France); Henri-Jean Drouhin, Ecole Polytechnique (France); Gaetan Bracciale, Laurent Divay, Thales Research & Technology (France); Paolo Bortolotti, Unité Mixte de Physique CNRS/Thales (France); Sukhdeep Dhillon, Lab. Pierre Aigrain (France); Henri Jaffrès, Unité Mixte de Physique CNRS/Thales (France)

In this work, we will present our last results of THz emission provided by optimized growth spin-orbitronics metallic bilayers (Co/Pt, NiFe/Au:W) via dynamical spin-to charge conversion from interfacial spin-orbit coupling (SOC) or inverted spin-Hall effect (ISHE) through time-dependent spectroscopy (TDS) [1-3]. The bilayer systems represent state-to-the art model systems in experiments combining RF-spin pumping and spin-to-charge conversion by ISHE principles [4-5]. Here, experiments consist in exciting correlated (in-plane) magnetization and spin-currents within the ferromagnet (FM) in the bilayer, in the picosecond regime via femtosecond laser excitation and measuring, in the picosecond timescale, the relaxation of the correlated spin and charge currents responsible for THz dipolar emission. We will compare performances of the different bilayer SHE systems in terms of the superdiffusive current point-of-view [6] to compare with spin-pumping like models. In particular, we will emphasize from a theoretical (analytical) and computational approach to the extension of the theory of parameterized spin-pumping [7-8] adapted to shorter timescale in the case of a FM/SOC bilayers.

[1] T. J. Huisman et al, Nat. Nano., DOI 10.1038 (Nnano2015) 331 (2015)

[2] T. Seifert, and All Efficient metallic spintronic emitters of ultrabroadband t erahertz radiation Nature photonics 10:483488, (2016).

[3] D. Yang et al.. 'Powerful and tunable thz emmiters based on the Fe/Pt magnetic heterostructure', Adv. Opt. Mat. (2016).

[4] J. C Rojas Sanchez et al., Phys Rev Lett. 112, 106602 (2014)

[5] P. Laczowski, Applied Physics Letters 104 (14), 142403, 2014. 28, 2014.

[6] M. Battiato et al. Phys. Rev Lett. 105, 027203 (2010)

[7] P. Brouwer, Phys. Rev. 58, R10135 (1998)

[8] G. Tatara, Phys. Rev. B 94, 224412 (2016)

10357-97, Session 15A

Disentangling interface and bulk contributions to the anisotropic magnetoresistance in Pt/Co/Pt sandwiches *(Invited Paper)*

André Philippi-Kobs, Deutsches Elektronen-Synchrotron (Germany) and Univ. Hamburg (Germany); Hans Peter Oepen, Univ. Hamburg (Germany)

We report on interfacial contributions to the anisotropic magnetoresistance (AMR) in Co layers sandwiched between Pt. For that purpose we present the pure Co thickness dependence of the AMR in Pt(5nm)/Co/Pt(3nm) sandwiches at room temperature (Co thickness varied between 0.8 nm and 50 nm) obtained by a detailed analysis of the experimental data that were used to prove the existence of the anisotropic interface magnetoresistance (AIMR) effect [1]. The detailed analysis was triggered by a controversy that came up in a discussion about the properties of AIMR [2,3]. Utilizing the Fuchs-Sondheimer formalism interface contributions can be separated from bulk-like AMR. We demonstrate that for all-metal systems interfacial AMR is also present when varying the magnetization within the film plane [4]. This interfacial in-plane AMR is two times smaller than the contribution that arises when the magnetization is varied in the plane perpendicular to the current direction. This finding is in contrast to the spin Hall MR found for ferromagnetic insulator/Pt bilayers [5] revealing the existence of different MR effects at the interfaces of Pt with conducting and insulating ferromagnets.

Financial support by DFG via project OE 251/7-1 and SFB 668 is gratefully acknowledged. We thank S. Heße, A. Frauen, and A. Farhadi for technical support.

[1] A. Kobs and H. P. Oepen et al., Phys. Rev. Lett. 106, 217207 (2011). [2] A. Kobs, A. Frauen, and H. P. Oepen, Phys. Rev. B 90, 016401 (2014). [3] S. Y. Huang et al., Phys. Rev. B 90, 016402 (2014). [4] A. Kobs and H. P. Oepen, Phys. Rev. B 93, 014426 (2016). [5] H. Nakayama et al., Phys. Rev. Lett. 110, 206601 (2013).

10357-98, Session 15A

Engineering spin accumulation and giant magnetoresistance in metallic nanostructures *(Invited Paper)*

Gilles Zahnd, Laurent Vila, Van Tuong Pham, Paul Noël, CEA Grenoble (France); Alain Marty, Jean-Philippe Attané, Commissariat à l'Énergie Atomique (France)

Manipulation of spin accumulation has shown to be a versatile tool for both fundamental research and functional application since it enables to study spin injection and transport in non-magnetic materials, as well as spincaloritronics, spin-orbitronics effects and spin transfer torque [1].

In this presentation, we shows how spin accumulation can be engineered, and what functional behaviors can be obtain through spin accumulation control:

By manipulating spin accumulation in a lateral device through precession or absorption [2, 3], it is possible to extract independently transport parameters of a ferromagnetic material or of a heavy metal with strong spin orbit interaction. Anisotropic absorption in a ferromagnetic element notably enables to obtain both its spin diffusion length and its spin precession length.

Lateral devices are an adapted tool to manipulate spin accumulation for functional application thanks to the high flexibility of their geometry. Nevertheless, lateral devices had always been confined to fundamental research due to the smallness of the signal they emit. We briefly show that lateral devices can emit signal comparable to what is obtain from CPP geometry, as giant magnetoresistance exceeding 10% in an downscaled CoFe-based lateral spin valve [4,5]. We then highlight that the use of lateral devices enables many applicable functions as enhancing spin signal amplitudes, or engineering simultaneously several spin accumulation degrees of freedom. Finally, using a confined spin accumulation located between two tunnel barriers, we show that it is possible to observe a novel magnetoresistive effect that only requires one ferromagnetic element.

[1] Y. Otani et al., Phil. Trans. of the Royal Society of London A 369, 3136 (2011)

[2] F. J. Jedema, et al., Appl. Phys. Lett. 81, 5162 (2002)

[3] M. Isasa et al., Physical Review B 91, 2 (2015)

[4] Y. K. Takahashi, et al. Applied Physics Letters 100, 5 (2012)

[5] G. Zahnd, et al., IOP. Nanotechnology 27, 3 (2015).

10357-99, Session 15A

Temperature dependence of spin transport properties in Pt *(Invited Paper)*

Ryan Freeman, Andrei Zholud, Sergei Urazhdin, Emory Univ. (United States)

Despite extensive applications of Pt for spin-charge conversion in spintronics, its spin-dependent transport properties are still debated. We study spin transport in Pt by utilizing current perpendicular-to-plane (CPP) giant magnetoresistance (GMR) in nanoscale Permalloy (Py)-based spin valves with Pt inserted in the nonmagnetic spacer.

We will discuss our results for the temperature-dependent spin diffusion length (SDL) of Pt, extracted from the dependence of GMR on the Pt thickness and calculations based on the Valet-Fert model. By comparing samples with Pt sandwiched between Cu spacers and samples where Pt is in direct contact with Py, we determine that the spin relaxation rate at the Pt/Py interface is significantly smaller than at the Pt/Cu interface.

We interpret our results in terms of two relevant spin scattering mechanisms: spin flipping due to the orbital scattering (Elliot-Yafet mechanism, EY), and spin precession around the effective spin-orbit field (Dyakonov-Perel mechanism, DP). We argue that DP relaxation is suppressed at Pt/Py interfaces due to the dominance of the proximity-induced effective exchange field. By comparing the SDL as a function of temperature to the mean free path, we show that EY contribution to scattering in the bulk is dominant at temperatures above 150K. We also analyze samples with ultrathin Pt spacer, where scattering at interfaces should be dominant. Temperature dependence of GMR of these samples is consistent with the dominance of DP relaxation. Our results provide a pathway for the optimization of spin scattering and spin/charge current conversion in Pt-based spintronic devices.

10357-100, Session 15A

Imaging electrical rotation of antiferromagnetic domains *(Invited Paper)*

Sarnjeet Dhesi, Diamond Light Source Ltd. (United Kingdom)

Antiferromagnetic spintronics aims to exploit zero net magnetic moment materials as efficient generators, detectors and transmitters of spin current. Recently, it was predicted that the Néel vector of an antiferromagnet could be rotated using staggered current-induced effective fields when the local inversion symmetry is broken [1]. This prediction has now been experimentally confirmed, for the collinear antiferromagnet CuMnAs, using current pulses applied along two different crystallographic directions [2].The current-induced rotation of the Néel vector was monitored using anisotropic magnetoresistance (AMR) measurements which provided spatially averaged information over the probed area of the microdevice.

Here we use PhotoEmission Electron Microscopy (PEEM), with magnetic contrast arising from X-Ray Magnetic Linear Dichroism, to directly image changes in the antiferromagnetic domain structure after electrical rotation. The combined PEEM-AMR study allows a clear observation of the CuMnAs submicron domain pattern before and after rotation of the antiferromagnetic domains. We find that the domain structure is systematically modified, by current pulses applied along two orthogonal directions, with a clear correlation between the AFM domain structure and the AMR results. Reversible switching of several domain features was also observed. However, there are regions exhibiting no change in XMLD-PEEM contrast implying inhomogeneous switching and highlighting the complex nature of the switching process in multi-domain antiferromagnetic films.

[1] J. ?elezn? et al., Phys. Rev. Lett. 113, 157201 (2014).

[2] P. Wadley et al., Science 351, 587 (2016).

[3] M. J. Grzybowski et al., Phys. Rev. Lett. 118, 057701 (2017).

10357-102, Session 15B

Non-stationary spin-polarized tunneling currents tuning by means of applied bias changing *(Invited Paper)*

Vladimir N. Mantsevich, Natalia Maslova, M.V. Lomonosov Moscow SU (Russian Federation); Petr Arseyev, P.N. Lebedev Physical Institute (Russian Federation)

We analyzed time evolution of the opposite spin electron occupation for the single-localized state with the Coulomb interaction coupled to two reservoirs in the presence of applied bias voltage. We revealed that in the presence of the second reservoir with non-zero applied bias, "magnetic" state can be distinguished from the "paramagnetic" one by analyzing time evolution of the electron occupation numbers. Typical time scales strongly depend on the value of applied bias and initial conditions.

We revealed that non-stationary spin-polarized currents can flow in the both leads and their direction and polarization depend on the value of applied bias. We revealed, that spin polarization and the direction of the non-stationary currents in each lead can be simultaneously inverted by the sudden changing of the applied bias voltage. But in the stationary state occupation numbers for the electrons with the opposite spins have the same values. Spin polarized tunneling currents in each lead also become equal.

We also investigated the changes of the time evolution regimes when the second lead is switched on at the particular time moment. We found out that switching on of the second lead with the non-zero applied bias destroys long-living "magnetic" moment.

10357-103, Session 15B

Spin-dependent electrical transport at finite temperatures from the first principles *(Invited Paper)*

David Wagenknecht, Charles Univ. in Prague (Czech Republic) and Institute of Physics of Materials of the ASCR, v.v.i., The Czech Academy of Sciences (Czech Republic); Karel Carva, Charles Univ. in Prague (Czech Republic); Ilja Turek, Charles Univ. in Prague (Czech Republic) and Institute of Physics of Materials of the ASCR, v.v.i., The Czech Academy of Sciences (Czech Republic)

Finite-temperature electronic transport properties of materials suitable for spintronic applications like halfmetalic semi-Heusler NiMnSb are examined from the first principles. The influence of various structural defects on different sublatices will be discussed.

Inclusion of lattice vibrations to ab initio calculations is substantial, because real spintronic devices operate at finite temperatures. However, it represents a difficult analytical and numerical problem.

Numerical codes based on the tight-binding linear muffin-tin orbital method in atomic sphere approximation (TB-LMTO ASA) in combination with the relativistic Dirac equation and the coherent potential approximation (CPA) [1,2] are used. Thermal displacements of nuclei from their equilibrium positions are included by a frozen phonon approach and the multicomponent CPA can describe both chemical (different atoms) and thermal (random displacements) disorder. Used approximation of phonons is general and may be employed to study any material. The method is in a good agreement with experimental or other theoretical studies for good metals and random alloys; consequently, it opens a way to study more complex materials.

The results of our thermal dependent calculations of NiMnSb exhibit a good match with experimental data and the fully relativistic approach makes possible to examine phenomena like the anomalous Hall effect. Moreover, the calculated temperature dependence of quantities may be used as an additional information to, e.g., identify chemical defects in real samples.

[1] I. Turek et al.: Phys. Rev. B 86, 014405 (2012)

[2] K. Carva et al.: Phys. Rev. B 73, 144421 (2006)

10357-104, Session 15B

First-principles calculation of spin transport and relaxation in magnetic heterostructures *(Invited Paper)*

Zhe Yuan, Beijing Normal Univ. (China)

Manipulation of a spin current at nanoscale is desired in many proposed spintronics devices. Magnetic multilayers consisting of ferromagnetic, ferrimagnetic and nonmagetic materials show rich phenomena when a spin current propagates through the multilayers. An interface of ferromagnetic and nonmagnetic metals has been demonstrated to play an important role in the generation and dissipation of a spin current. Using first-principles scattering calculation, we study the transport and relaxation of spin currents in typical transition metals and alloys and their interfaces. In particular, we focus on identifying the correlation of spin transport and relaxation with the specific order parameters of magnetic materials. By examining the spin-Hall conductivity and spin-flip diffusion length as a function of conductivity (resistivity), we are able to distinguish different dominant physical mechanisms of the generation and dissipation of spin currents.

10357-126, Session 15B

Spin superfluid triggered domain-wall motion and spin-transistor action *(Invited Paper)*

Pramey Upadhyaya, Se Kwon Kim, Yaroslav Tserkovnyak, Univ. of California, Los Angeles (United States)

Spin superfluidity, that is a coherent flow of spin in the presence of rotational (U1) symmetry, enables possibility of uncovering a new class of spin-based dissipationless phenomenon and devices by mimicking well-established superfluid-like phenomenon, for example those observed in superconductors (charge-based superfluids). Motivated by this, recently, theoretical possibilities of room temperature excitation of spin superfluid-like transport, via exploiting interfacial spin-orbit torque, have been proposed in a number of easy-plane magnetic systems. In this work [1], we present how the angular momentum carried by these spin superfluids be utilized to construct low-dissipation spintronic devices. Specifically, we theoretically investigate the transfer of angular momentum between a spin superfluid and a domain wall in an exchange coupled easy-axis and easy-plane magnetic insulator. A domain wall in the easy-axis magnet absorbs spin angular momentum via disrupting the flow of a superfluid spin current in the easy-plane magnet. We derive analytical expressions for the resultant domain-wall motion in the geometry where spin superfluidity is actuated by spin-orbit torques. Furthermore, by controlling the pinning of the domain wall, the so-called zero voltage to finite voltage transition of superconducting Josephson Junctions can be mimicked, which we utilize to propose a reconfigurable spin transistor.

[1] P. Upadhyaya, Se Kwon Kim and Yaroslav Tserkovnyak "Magnetic domain wall floating on a spin superfluid", Phys. Rev. Lett. 118, 097201 (2017)

10357-105, Session 16A

Thermal generation of spin currents in oxides *(Invited Paper)*

Rafael Ramos, Takashi Kikkawa, Daichi Hirobe, Tohoku Univ. (Japan); Alberto Anadon, Irene Lucas, Univ. de Zaragoza (Spain); Ken-ichi Uchida, National Institute for Materials Science (Japan); Hiroto Adachi, Japan Atomic Energy Agency (Japan); Pedro Algarabel, Luis Morellon, Myriam Aguirre, Univ. de Zaragoza (Spain); Sadamichi Maekawa, Japan Atomic Energy Agency (Japan); Ricardo Ibarra, Instituto de Nanociencia de Aragon (Spain); Eiji Saitoh, Tohoku Univ. (Japan)

The spin-Seebeck effect (SSE) enables generation of a spin current in a magnetic material (F) by a temperature gradient. This spin current is injected in a contacting non-magnetic material (N) where it is electrically detected by means of the inverse spin-Hall effect (ISHE). The SSE offers a new paradigm for heat to electricity conversion, however, the main disadvantage of the SSE is the low value of the extracted voltage, with values significantly lower than conventional thermoelectrics.

Recently, we reported a substantial increase of the SSE thermoelectric voltage in magnetic multilayers formed by repeated growth of a basic Fe_3O_4/Pt bilayer structure [1]. As a consequence of the simultaneous increase in voltage and reduction of device resistance the multilayer system exhibits a two order of magnitude increase of the extractable thermoelectric power [2].

The observed enhancement of the SSE voltage, relative to its value in the single bilayer, monotonically increases as the temperature of the system is reduced [3]. This result can be possibly understood by an increase of the characteristic length for spin current propagation within the system, in qualitative agreement with the recently observed increase of the magnon diffusion length in Fe_3O_4 at lower temperatures [4]. Our results suggest that the thermoelectric performance of the SSE in multilayer system can be further improved by careful choice of materials with suitable spin transport properties.

During my talk, I will also introduce the results on spin current carried by spinons in a spin-liquid system [5] and the observation of magnon-phonon coupling by SSE [6]

[1] R. Ramos, T. Kikkawa, M. H. Aguirre, I. Lucas, A. Anadón, T. Oyake, K. Uchida, H. Adachi, J. Shiomi, P. A. Algarabel, L. Morellón, S. Maekawa, E. Saitoh, and M. R. Ibarra, Phys. Rev. B 92, 220407(R) (2015).

[2] R. Ramos, A. Anadón, I. Lucas, K. Uchida, P. A. Algarabel, L. Morellón, M. H. Aguirre, E. Saitoh, and M. R. Ibarra, APL Mater. 4 104802 (2016).

[3] R. Ramos, T. Kikkawa, A. Anadón, I. Lucas, K. Uchida, P. A. Algarabel, L. Morellón, M. H. Aguirre, E. Saitoh, and M. R. Ibarra, AIP Advances 7, 055915 (2017).

[4] A. Anadón, R. Ramos, I. Lucas, P. A. Algarabel, L. Morellón, M. R. Ibarra, and M. H. Aguirre, Appl. Phys. Lett. 109, 012404 (2016).

[5] D. Hirobe, M. Sato, T. Kawamata, Y. Shiomi, K. Uchida, R. Iguchi, Y. Koike, S. Maekawa, and E. Saitoh, Nat. Phys. 13, 30 (2017).

[6] T. Kikkawa, K. Shen, B. Flebus, R. Duine, K. Uchida, Z. Qiu, G. E. W. Bauer and E. Saitoh, Phys. Rev. Lett. 117, 207203 (2016).

10357-106, Session 16A

The contribution of the thermal Hall effect in the anomalous Nernst and spin Seebeck effects *(Invited Paper)*

Ssu-Yen Huang, Yi-Jia Chen, National Taiwan Univ. (Taiwan)

The Anomalous Nernst effect (ANE) and the spin Seebeck effect (SSE) in spin caloritronics are two of the most important mechanisms to manipulate the spin-polarized and pure spin current, respectively, through thermal excitation. The ANE in ferromagnetic metals and the SSE in magnetic insulators have been extensively studied, while a recent theoretical work suggests that the thermal Hall effect (THE), has been overlooked, and it may significantly contribute to the ANE and the SSE. [1] Most strikingly, the THE, which results in the anisotropic transverse temperature gradient, has the exact same magnetic-field angular dependence as the ANE and the SSE. This anisotropic transverse temperature gradient can be converted into an electric signal by the thermocouple effect. Therefore, it is vital to investigate the contribution of the THE in the ANE and the SSE.

In this work, we experimentally demonstrate that the thermocouple effect in the ANE and SSE measured geometry is indeed inevitable. [2] By designing several special measured geometries, we are able to systematically study the THE by the thermocouple effect in the ferromagnetic metal, permalloy (Py), and the magnetic insulator, yttrium iron garnet (YIG). Our results show that the contribution of the THE by thermocouple effect in the Py and YIG is negligibly small, if one includes the thickness dependence of the Seebeck coefficient. The spin-polarized current in the ANE and the pure spin current in the SSE remain important elements for exploring spin caloritronics phenomena.

Reference: [1] J.-E. Wegrowe, and H.-J. Drouhin, and D. Lacour. Phys. Rev. B 89, 094409 (2014).

[2] Y. J. Chen and S. Y. Huang, Phys. Rev. Lett, , 117, 247201 (2016).

10357-107, Session 16A

Spin-caloritronic nano-oscillator *(Invited Paper)*

Igor Barsukov, Univ. of California, Riverside (United States)

Energy-efficient generation of spin currents is an important step towards next-generation spintronics applications. In a nanowire, patterned from magnetic insulator/platinum (YIG/Pt) bilayer, electrical current generates a spin current due to the spin Hall effect (SHE). Furthermore, Ohmic heating in the Pt layer creates a large temperature gradient perpendicular to the YIG/Pt interface. The temperature gradient drives a spin current due to the spin Seebeck effect (SSE). Both spin currents exert spin torques, employed to reduce the magnetic damping of YIG. Different symmetries of the SHE and SSE can be used for their disentanglement. The SSE plays the dominant role in modification of the magnetization dynamics. With increasing temperature gradients, the damping can be compensated, leading to magnetic auto-oscillations and microwave emission from the nanowire. This result demonstrates that coherent magnonic condensates can be created by temperature gradients. It also points out that energy losses due to the Ohmic heating can be harvested by utilizing thermal spin currents in spintronics applications.

10357-108, Session 16A

Optimisation of Co2MnSi:Pt multilayers for giant spin Seebeck devices *(Invited Paper)*

Christopher Cox, Kelly Morrison, Michael D. Cropper, Loughborough Univ. (United Kingdom); Andrew Caruana, Loughborough Univ. (United Kingdom) and Science and Technology Facilities Council (United Kingdom); Christy Kinane, Science and Technology Facilities Council (United Kingdom); Timothy Charlton, Oak Ridge National Lab. (United States)

The spin Seebeck effect[1] is defined as the generation of a pure spin current (Js) when a magnetised material (such as Co2MnSi[2]) is subjected to a temperature gradient (?T). To detect it, a thin non-magnetic layer [NM] such as Pt, is deposited on top of the material of interest. This converts Js into an observable thermoelectric voltage (VSSE) by way of the Inverse Spin Hall Effect (ISHE). We are interested in how this phenomenon might be applied to harvesting waste heat (thermoelectric generators) or spintronics applications (spin current source).

Our work initially encompasses the thin film deposition of Co2MnSi on amorphous glass substrates using Pulsed Laser Deposition (PLD) and optimisation of the deposition parameters in order to produce L21 ordered films, which exhibit larger VSSE than B2 disordered films[3].

Additionally, we will present results on exploring the potential Giant Spin Seebeck Effect (GSSE)[4] in [Co2MnSi /Pt]_n/SiO2 multilayers, where the GSSE is an enhancement of VSSE due to the increase in the volume of the spin injector (Co2MnSi).

[1] K. Uchida et al., Nature 455, 778 (2008).

[2] S. Bosu et al., Phys. Rev. B 83, 224401 (2011).

[3] M. Jourdan et. al., Nat. Commun. 5, 3974 (2014).

[4] R. Ramos et al., APL Mater. 4, 104802 (2016).

10357-109, Session 16B

All-optical magnetization switching of FePt magnetic recording medium *(Invited Paper)*

Markus Münzenberg, Ernst Moritz Arndt Univ. Greifswald (Germany)

Magnetization manipulation is an indispensable tool for both basic and applied research [1]. The dynamics of the response depends on the energy transfer from the laser excited electrons to the spins within the first femtoseconds. This determines the speed of the ultrafast magnetization. A special material of interest for magnetic storage development is FePt [2]. In a seminal experiment all optical writing had been demonstrated for FePt nanoparticle of a magnetic hard disc media, completely surprisingly, by Lambert et al. in Science 2014 [3]. But, the mechanism remained unclear and it opened many questions about the extension of possibilities of all optical writing as a general mechanism. Meanwhile writing experiments by single laser spots point to an asymmetric writing per each shot. This is consistently observed by different groups [4,5,6]. These effects can be described within different rate models. I will review the current understanding of the interaction of ultrafast excitation and heating, influence of magnetic dichroism and the presence of the inverse Faraday effect and attempts of understanding of these processes so far. From the experimental side in especial single shot writing experiments, that show a kind of accumulation effects of the writing, allow to pinpoint the underlying mechanism of writing in these media. Together, ab-initio calculations of the optical effects (inverse Faraday effect and magnetic dichroism induced heating) and the thermal modeling, allow to calculate the switching rates of the individual FePt nanoparticles. The latter then provides a rate of switching of the ensemble. A careful experimental determination of the absorbed fluence in the spherical geometry of the nanoparticles gives us a complete picture of the competing effects, of heating and writing asymmetries, and we can trace the different processes from the beginning of the laser pulse impact. In addition, this theoretical description allows us to optimize the number of shots needed to write the magnetization of the FePt nanoparticles and to pinpoint how to optimize the all optical writing. In my talk, I will review these recent developments that may lead to address an individual nanosized magnetic element in the far future all optically, for writing magnetic memory and memory storage.

[1] J. Walowski and M. Münzenberg, Perspective: Ultrafast magnetism and THz spintronics, J. Appl. Phys. 120, 140901 (2016).

[2] J. Mendil et al., Resolving the role of femtosecond heated electrons in ultrafast spin dynamics, Sci. Rep. 4, 3980 (2014).

[3] C.-H. Lambert et al., All-optical control of ferromagnetic thin films and nanostructures, Science 345,1337-1340, (2014).

[4] R. John et al., Magnetization switching of FePt nanoparticle recording medium by femtosecond laser pulses, arxiv:1606.08723.

[5] M.S. El Hadri et al., Electrical characterization of all-optical helicity-dependent switching in ferromagnetic Hall crosses, Appl. Phys. Lett. 108, 092405 (2016).

[6] Y.K. Takahashi et al., Accumulative magnetic switching of ultra-high-density recording media by circularly polarized light, Phys. Rev. Applied 6, 054004 (2016).

10357-110, Session 16B

Transient THz spin dynamics by spin pumping *(Invited Paper)*

Lars Bocklage, Deutsches Elektronen-Synchrotron (Germany)

Experiments on THz magnetization dynamics provide insights into a yet unexplored time scale of transient magnetics and spintronics [1-3]. Coherent responses of the magnetization to THz pulses have been demonstrated [1,2]. Further, THz spin currents can be generated by non-equilibrium hot electrons [3]. These THz transients provide new ways to ultrafast spin control and its technical applications. Here, an analytical model is presented that describes transient magnetization dynamics up to the THz regime [4]. The model is used to determine the magnetization response to ultrafast multi and single-cycle THz pulses for a variety of parameters like carrier frequency, width, phase, frequency chirp, and polarization. The THz pulse shape and polarization provide a vectorial control of the magnetization on the sub-picosecond time scale. It is shown that an optimum timing for coherent magnetization control can be achieved.

Dynamics of the magnetization induce a spin current in an adjacent non-magnetic material. This effect s known as spin pumping [5]. Here, calculations of THz transient spin current generation by spin pumping are presented. An effective spin current generation is found far above the ferromagnetic resonance up to THz frequencies although dynamic magnetization amplitudes are very small at THz frequencies. At THz frequencies, the coherent reaction of the magnetization also causes a coherent spin current. In contrast to the dc spin current which scales with the susceptibility of the magnetization, the ac spin current does not vanish above the ferromagnetic resonance. Instead the THz ac spin current reaches a value that is comparable to the dc spin current at resonance. The behavior far above resonance can be used to efficiently generate ultrafast spin currents without the need for magnetic systems with very high resonance frequencies. Spin currents on picosecond time scales can be achieved by THz magnetization dynamics.

References:

[1] C. Vicario et al., Nat. Photonics 7, 720 (2013),

[2] T. Kampfrath et al., Nat. Photonics 5, 31 (2011)

[3] T. Kampfrath et al., Nat. Nanotechnl. 8, 256 (2013)

[4] L. Bocklage, Sci. Rep. 6, 22767 (2016) & ?J. Magn. Magn. Mater 429, 324 (2017)

[5] Y. Tserkovnyak, A. Brataas, and G. E. W. Bauer, Phys Rev. Lett. 88, 117601 (2002)

[6] D. Wei et al., Nat. Comm. 5, 3768 (2014)

[7] L. Bocklage, (submitted)

10357-111, Session 16B

Optically induced magnetization reversal dynamics in (Pt/Co)N multilayers *(Invited Paper)*

Roman Adam, Umut Parlak, Moritz Plötzing, Daniel E. Bürgler, Claus M. Schneider, Forschungszentrum Jülich GmbH (Germany)

The observation of optically-induced magnetization reversal in ferromagnetic alloys and ferromagnetic thin films raised many questions concerning the nature of the effect and triggered the search for fitting theoretical models describing the physical mechanism of the reversal. At the same time, the research is on the way to employ the effect for magnetic data-storage technology. Recent studies suggest that the interplay between light-induced heating of the electronic system and the polarization state of the laser beam plays a crucial role in achieving an efficient switching. We investigate the effect of laser pulse duration, laser fluence, multiple-pulse switching, and light polarization on the magnetization reversal in [Pt/Co]N multilayers, where N varies from 3 to 7. The multilayers were fabricated using magnetron sputtering at Ar gas pressure of 1?10-3 mbar. The response of the multilayers to the laser light was detected using a magneto-optical Kerr effect microscope combined with a Ti:Sapphire-based femtosecond laser amplifier generating a train of <70fs pulses with central wavelength of 800nm at 1kHz. Our results indicate that the optical pulses can trigger either demagnetization or magnetization reversal, and that the reversal process depends on extremely precise tuning of all the above-mentioned laser parameters. The dynamics of the reversal and demagnetization processes have been found to scale with laser fluence, external magnetic field, and multilayer repetition number N.

10357-112, Session 17A

Prolonging the coherence of spins in semiconductor quantum dots *(Invited Paper)*

Edwin Barnes, Virginia Polytechnic Institute and State Univ. (United States)

Future technologies based on electronic spins in semiconductor quantum dots require an unprecedented level of control over the spins. Achieving this level of control is made challenging by environmental decoherence and inhomogeneous dephasing. In this talk, I will present recent progress in understanding quantitatively the primary sources of noise for spins in semiconductor nanostructures, namely the hyperfine interaction with nuclear spins and charge fluctuations. I will present new theoretical techniques that capture the effects of multiple noise sources on the evolution of the spin coherence and show how they can be used to develop new ways to characterize and mitigate noise. I will then describe a new general theory for combatting decoherence and inhomogeneous dephasing by driving the system in a way that such adverse effects destructively interfere and cancel out, enabling precise and robust control of a broad range of coherent quantum systems. This theory generalizes and extends existing dynamical decoupling methods, making them much more precise and versatile for ultrafast spin manipulation.

10357-113, Session 17A

Optically probing spin qubit coherence without coherent control *(Invited Paper)*

Kai Müller, Alexander Bechtold, Walter Schottky Institut, Technische Univ. München (Germany); Fuxiang Li, Los Alamos National Lab. (United States); Tobias Simmet, Walter Schottky Institut, Technische Univ. München (Germany); Nikolai A. Sinitsyn, Los Alamos National Lab. (United States); Jonathan J. Finley, Walter Schottky Institut, Technische Univ. München (Germany)

We demonstrate an entirely new method to probe quantum measurement phenomena in semiconductor quantum dot (QD) spin qubits [1]. In addition to providing direct evidence for the quantum nature of solid state qubits, we show that our method has practical importance since it provides a completely alternative route for measuring ensemble and quantum dephasing times, T2* and T2, using only repeated projective measurements and without the need for coherent spin control.

Our approach is based on measuring time-correlators of a spin qubit in an optically active QD beyond the second order. We utilize a quantum dot spin-storage structure to initialize a single electron spin in a quantum dot subject to a magnetic field applied in Voigt geometry and perform repeated projective measurements of the spin at times t1 and t2. This measurement is repeated, corresponding to ensemble averaging, and the resulting third-order time correlations reveals rich physics: For times t1 or t2 < T2* Larmor precession is observed which reveals the ensemble dephasing time T2*. Importantly, even though the time-correlators were obtained through averaging many measurements for times t1 and t2 > T2* oscillations are observed that decay with the dephasing time T2 and allow its determination even without the need for coherent spin control. Finally, combining the third-order time correlator with the second-order time correlator allows to demonstrate a violation of Leggett-Garg type inequalities for certain times providing clear evidence for the quantum nature of the quantum dot spin.

[1] A. Bechtold et al. Phys. Rev. Lett. 117, 027402 (2016)

10357-114, Session 17A

Defects in SiC: electronic structure and spin-photon interfaces *(Invited Paper)*

Sophia Economou, Virginia Polytechnic Institute and State Univ. (United States)

The interest in quantum information processing and related technologies has largely driven spin and photonic research in recent years. Deep defect centers such as the NV center in diamond have shown great promise for quantum technologies, but diamond-based devices are not practical. Silicon carbide has emerged as a technologically viable material for such technologies, as it hosts defects that can be exploited both for spintronics and for photonics applications. I will present our recent work on the silicon vacancy defect in SiC. Through a combination of group theory and density functional theory, we have calculated the electronic structure of the multi-electron spin states in this defect. Based on our results, we have designed spin-photon interfaces for the generation of entangled photons in this and in other SiC defects. Using these interfaces, highly entangled 'graph' states of photons can be generated for applications in quantum computation and communication by pumping and manipulating appropriately the spin states of these defects.

10357-115, Session 17A

Coherent phenomena in ferromagnetic GaMnAs films *(Invited Paper)*

Brenden A. Magill, Giti A. Khodaparast, Virginia Polytechnic Institute and State Univ. (United States); Stephen A. McGill, National High Magnetic Field Lab. (United States); Hiro Munekata, Tokyo Institute of Technology (Japan); Gary D. Sanders, Chris J. Stanton, Univ. of Florida (United States)

The manipulation of spins in semiconductors without the application of external magnetic fields opens the door to next-generation spintronic devices, where the electronic computation and magnetic memory can be performed on the same chip. Ferromagnetic semiconductors such GaMnAs are excellent prototype materials for these classes of devices, as the strong coupling of their magnetic and elastic properties allows the magnetic anisotropy to be manipulated by applying external strain, electric/magnetic fields, or light pulses. In this work, we investigate ultrafast optical processes in ferromagnetic (III,Mn)V semiconductors induced by femtosecond laser pulses. We report on two-color, time-resolved magneto-optical spectroscopy on MBE grown GaMnAs with the Tc, as high as 110 K. Our measurements allow us to observe dynamical phenomena such as coherent phonon dynamics, where acoustic phonon wavepackets, between 40.9 – 42.9 GHz, can be generated in the ferromagnetic layer with strong tunability from external magnetic fields. In addition, time-resolved optically induced birefringence measurements display oscillations with a lower frequency (?10 GHz). We explain our experimental observation using theoretical models that include ferromagnetic couplings of the magnetic Mn ions with the conduction and valence bands in GaMnAs.

This work was supported by the AFOSR through grant FA9550-14-1-0376.

10357-116, Session 17A

Molecular engineering with artificial atoms: designing a material platform for scalable quantum spintronics and photonics *(Invited Paper)*

Matthew Doty, Xiangyu Ma, Joshua M. Zide, Univ. of Delaware (United States); Garnett W. Bryant, National Institute of Standards and Technology (United States)

Self-assembled InAs Quantum Dots (QDs) are often called “artificial atoms” and have long been of interest as components of quantum photonic and spintronic devices. Although there has been substantial progress in demonstrating optical control of both single spins confined to a single QD and entanglement between two separated QDs, the path toward scalable quantum photonic devices based on spins remains challenging. Quantum Dot Molecules, which consist of two closely-spaced InAs QDs, have unique molecular properties that can be engineered with the solid state analog of molecular engineering in which the composition, size, and location of both the QDs and the intervening barrier are controlled during growth. Moreover, applied electric, magnetic, and optical fields can be used to modulate, in situ, both the spin and optical properties of the molecular states. We will first describe the origin of a unique molecular spin property known as hole spin mixing, which provides opportunities for all-optical coherent control of a single hole spin without transverse magnetic fields that would prevent nondestructive readout. We will then describe computational and experimental progress toward the design of new molecules and devices that could maximize and leverage this effect by manipulating spin interactions at the atomic scale. In the second part of the talk, we will describe how the unique photonic properties of engineered Quantum Dot Molecules can be leveraged to overcome long-standing challenges to the creation of scalable quantum devices that manipulate single spins via photonics.

10357-117, Session 17B

Observation of current-induced, long-lived persistent spin polarization in a topological insulator: a rechargeable spin battery *(Invited Paper)*

Yong P. Chen, Purdue Univ. (United States)

Topological insulators (TIs), with their helically spin-momentum-locked topological surface states (TSS), are considered promising for spintronics applications. Several recent experiments in TIs have demonstrated a current induced electronic spin polarization that may be used for all-electrical spin generation and injection. Here, we report spin potentiometric measurements in TIs that have revealed a long-lived persistent electron spin polarization even at zero current. Unaffected by a small bias current and persisting for several days at low temperature, the spin polarization can be induced and reversed by a large “writing” current applied for an extended time. While the exact mechanism responsible for the observed long-lived persistent spin polarization remains to be better understood, we speculate on possible roles played by nuclear spins hyperfine coupled to TSS electrons and dynamically polarized by the spin-helical “writing current”. Such an electrically controlled persistent spin polarization with unprecedented long lifetime could enable a rechargeable spin battery and rewritable spin memory for potential applications in spintronics and quantum information.

10357-118, Session 17B

Helicity-dependent photocurrent generation in Bi2Se3 probed by THz emission spectroscopy *(Invited Paper)*

Jong Seok Lee, Sun Young Hamh, Soon Hee Park, Gwangju Institute of Science and Technology (Korea, Republic of); Sahng-Kyoon Jerng, Seung-Hyun Chun, Sejong Univ. (Korea, Republic of)

We investigate photocarrier dynamics in a Bi2Se3 thin film via terahertz (THz) emission spectroscopy. We observed strong modulations in amplitude and phase of the emitted THz wave under the variations in a polarization of an input laser beam and sample azimuth. In particular, photon-helicity-dependent responses are manifested in both time and frequency domains, and azimuth dependence of such circular anisotropy exhibits a clear threefold periodicity. We analyze these results based on the symmetry of the bulk and the surface of Bi2Se3 and demonstrate that the observed helicity-dependent photocurrent originates from the circular photon drag effect, namely, linear and angular momentum transfers from photons to photocarriers.

10357-119, Session 17B

Chiral magnetic monopoles in artificial spin systems *(Invited Paper)*

Yann Perrin, Ioan A. Chioar, Ctr. National de la Recherche Scientifique (France) and Institut NÉEL (France) and Univ. Grenoble Alpes (France); Hanna Riahi, Institut Jean Lamour (France); Van D. Nguyen, Univ. Grenoble Alpes (France); Aurélien Masseboeuf, Christophe Gatel, Ctr. d’Elaboration de Matériaux et d’Etudes Structurales (France); Stefan McMurtry, Institut Jean Lamour (France); Benito Santos Burgos, Tevfik Onur Mentes, Andrea Locatelli, Elettra-Sincrotrone Trieste S.C.p.A. (Italy); Jean-Christophe Toussaint, Ctr. National de la Recherche Scientifique (France) and Institut NÉEL (France) and Univ. Grenoble Alpes (France); François Montaigne, Daniel Lacour, Institut Jean Lamour (France); Nicolas Rougemaille, Benjamin Canals, Institut NÉEL, Ctr. National de la Recherche Scientifique (France); Michel Hehn, Institut Jean Lamour (France)

Complex architectures of nanostructures are currently routinely elaborated using bottom-up or nanofabrication processes. This technological capability allows scientists to engineer materials with properties that do not exist in nature, but also to manufacture model systems to explore fundamental issues in condensed matter physics. Two-dimensional frustrated arrays of magnetic nanostructures are one class of systems for which theoretical predictions can now be tested experimentally.

In particular, magnetic imaging techniques offer the appealing opportunity to observe a wide range of phenomena within the concept of lab-on-a-chip. For example, several exotic magnetic phases have been discovered in artificial frustrated spin systems. Besides, these systems allow the study of classical analogues of magnetic monopoles. These recent results have stimulated new research activities motivated by the quest for magnetic monopoles in condensed matter physics.

In this contribution, we'll show that the micromagnetic properties of the elements constituting artificial frustrated arrays of nanomagnets introduce the concept of chiral monopoles. Injecting and manipulating experimentally the chirality of a magnetic monopole provide a new degree of freedom in the system. This offers the opportunity to control their motion under an external magnetic field, thus allowing to envision applications in magnetronics.

10357-120, Session 17B

Massively degenerated ground state manifold in artificial square ice *(Invited Paper)*

Yann Perrin, CEA-LETI (France); Nicolas Rougemaille, Benjamin Canals, Institut NÉEL, Ctr. National de la Recherche Scientifique (France)

In physics, frustration appears in a system when it is impossible to minimise all pairwise interactions simultaneously. Frustration exists in some particular rare-earth based compounds, such as spin ices [1]. Their internal frustration gives rise to unusual properties, like a residual entropy at low temperature or the presence of monopole-like excitations [2]. However, experimental techniques are unable to probe each spin individually in these compounds.

In 2006, Wang and coworkers opened a new way for studying magnetically frustrated spin systems [3]. Using e-beam lithography, one can make arrays of nanomagnets with the desired design. The state of each nanomagnet can then be probed individually in real space at room temperature using magnetic imaging (eg. Magnetic Force Microscopy). In this context, the square geometry received a considerable interest, since it is closely related to condensed matter spin ice compounds. But for geometrical reasons, this system orders instead of showing a disordered low energy manifold

In this contribution, we explain how to bring back the massive ground state degeneracy in the square array of nanomagnets. We present the first experimental evidence of a Coulomb phase in this system [4]. We also report the presence of magnetic monopoles defects within the Coulomb phase. This study makes a new step toward a direct study of the dynamic of monopoles excitations (e.g. creation, annihilation or diffusion processes).

[1] M.J. Harris et al., Phys. Rev. Lett. 79, 2554 (1997).

[2] C. Castelnovo et al., Nature 451, 7174 (2008).

[3] R.F. Wang et al., Nature 439, 303 (2006).

[4] Y. Perrin et al., Nature 540, 410 (2016).

10357-121, Session 17B

Weyl node assisted conductivity switch in the interfacial phase change memory *(Invited Paper)*

Nicholas Kioussis, Jinwoong Kim, California State Univ., Northridge (United States); Ruqian Wu, Univ. of California, Irvine (United States); Young-Sun Song, Seung-Hoon Jhi, Pohang Univ. of Science and Technology (Korea, Republic of)

The interfacial phase-change memory (iPCM) GeTe/Sb2Te3 continues to attract a great deal of interest not only because they are promising candidates for the next generation non-volatile random-access memories but also for their fascinating topological properties. Depending on the atomic-layer-stacking sequence of the GeTe block the iPCM can be either in the “SET” (Ge-Te-Ge-Te) or “RESET” (Te-Ge-Ge-Te) states where the former exhibits a ferroelectric polarization and an electric conductivity which is two orders of magnitude higher than that of the RESET state. The presence of ferroelectric polarization which breaks the inversion symmetry and the fact that the system is close to the topological phase boundary raises the intriguing question of the emergence of a Weyl semimetal phase in the “SET” state between the topological and trivial insulator phases as proposed by Murakami. Ab initio electronic structure calculations reveal the emergence of a Weyl semimetal phase for the “SET” phase associated with a large electric conductivity due to the gapless Weyl nodes.

10358-1, Session 1

Super-resolution from single photon emission: toward biological application *(Invited Paper)*

Marco Genovese, Istituto Nazionale di Ricerca Metrologica (Italy)

Properties of quantum light represent a tool for overcoming limits of classical optics.

Several experiments have demonstrated this advantage ranging from quantum enhanced imaging to quantum illumination [1].

In this talk, after a general introduction discussing last developments in the field (as sub shot noise quantum microscopy) , I will present a work [2] where we experimentally demonstrate quantum enhanced resolution in confocal fluorescence microscopy. This is achieved by exploiting the non-classical photon statistics of fluorescence emission of single nitrogen-vacancy color centers in diamond. By developing a general model of super-resolution based on the direct sampling of the kth-order autocorrelation function of the photoluminescence signal, we show the possibility to resolve, in principle, arbitrarily close emitting centers.

Finally, possible applications in biology and future developments will be presented.

[1] “Real applications of quantum imaging”, M.Genovese, Journal of Optics, 18 (2016) 073002

[2] “Beating the Abbe Diffraction Limit in Confocal Microscopy via Nonclassical Photon Statistics” D. Gatto Monticone, K. Katamadze, P. Traina, E. Moreva, J. Forneris, I. Ruo-Berchera, P. Olivero, I.P. Degiovanni, G. Brida,M. Genovese; Phys. Rev. Lett. 113, 143602 (2014)

10358-2, Session 1

Preparation of single photon states with rising exponential shape *(Invited Paper)*

Christian Kurtsiefer, National Univ. of Singapore (Singapore); Bharat Srivathsan, National Univ. of Singapore (Singapore) and Max-Planck-Institut für die Physik des Lichts (Germany); Gurpreet Kaur Gulati, National Univ. of Singapore (Singapore) and Univ. of Sussex (United Kingdom); Mathias A. Seidler, Alessandro Cere, National Univ. of Singapore (Singapore)

e prepare single photons with a temporal envelope that resembles the time reversal of photons from the spontaneous decay process, based on a parametric conversion process in a cold atomic vapor. Photon pairs generated from from four-wave mixing inherit a particular time ordering from the atomic cascade decay in the atomic vapor. The detection of the first photon of the cascade is used as a herald after being time-reversed by reflection off an asymmetric Fabry-Perot cavity, reversing the temporal shape of the heralded photon to a rising exponential envelope. The photons have characteristic rise time of 12ns. Such a temporal single photon profile is ideal for absorption by a two level system. We demonstrate this in an experiment showcasing the absorption by a single atom.

10358-3, Session 1

From SHG to mid-infrared SPDC generation in strained silicon waveguides

Claudio Castellan, Alessandro Trenti, Univ. degli Studi di Trento (Italy); Mattia Mancinelli, Alessandro Marchesini, Univ. degli Studi di Trento (Italy) and Univ. degli Studi di Trento (Italy); Mher Ghulinyan, Georg Pucker, Fondazione Bruno Kessler (Italy); Lorenzo Pavesi, Univ. degli Studi di Trento (Italy) and Univ. degli Studi di Trento (Italy)

The centrosymmetric crystalline structure inhibits the existence of second order nonlinear optical processes in silicon. However, it has been recently reported on the possibility of breaking this symmetry with a stressing silicon nitride over-layer, inducing second order effects in silicon.

Here we report on Second Harmonic Generation (SHG) measurements on Silicon-On-Insulator (SOI) strained silicon waveguides designed to achieve multi-modal phase-matching between the pump and the SHG signal. Two-photon absorption effect was avoided using a laser source in the spectral region around 2.5 ?m, while walk-off effects were faced shaping the pulse temporal width from ?100 fs to ?13 ps. The pump laser externally triggered an InGaAs SPAD detector, determining a lowest detectable signal of ?0.01 fW. We realized a model for simulating the pulse propagation in waveguides, through which we estimated an effective strain-induced second order nonlinear coefficient of ?(2)=(0.304±0.025) pm/V. Due to experimental issues, this value is actually an underestimation. However, it agrees with high-frequency measurements of Pockels effect in strained silicon.

SHG observation provides a milestone for the Spontaneous Parametric Down Conversion (SPDC), where a single pump photon generates two entangled photons at a doubled wavelength. Here we report also on our preliminary results for measuring SPDC mid-infrared entangled photons generated in a strained silicon waveguide pumping at telecom wavelengths. The photon correlation properties are evidenced with a mid-infrared correlation set-up. This study is motivated by the great interest recently devoted to move quantum optics to the mid-infrared spectral region, where photons can be easily manipulated.

10358-4, Session 1

Quantum internet: the certifiable road ahead *(Invited Paper)*

Stephanie Wehner, QuTech (Netherlands)

No Abstract Available

10358-31, Session 1

Quantum optics with nanowires *(Invited Paper)*

Valery Zwiller, Technische Univ. Delft (Netherlands); Klaus D. Jöns, Ali W. Elshaari, M. Versteegh, Lucas Schweickert, KTH Royal Institute of Technology (Sweden)

Nanowires offer new opportunities for nanoscale quantum optics; the quantum dot geometry in semiconducting nanowires as well as the material composition and environment can be engineered with unprecedented freedom to improve the light extraction efficiency.

Quantum dots in nanowires are shown to be efficient single photon sources, in addition because of the very small fine structure splitting, we demonstrate the generation of entangled pairs of photons from a nanowire.

Another type of nanowire under study in our group is superconducting nanowires for single photon detection, reaching efficiencies, time resolution and dark counts beyond currently available detectors. We will discuss our first attempts at combining semiconducting nanowire based single photon emitters and superconducting nanowire single photon detectors on a chip to realize integrated quantum circuits.

10358-5, Session 2

Large-scale series-nanowire detectors packaged in a compact rack-mount cryostat *(Invited Paper)*

Vikas Anant, Photon Spot, Inc. (United States)

No Abstract Available

10358-6, Session 2

Quantum communication using amorphous SNSPDs *(Invited Paper)*

Félix Bussières, University of Geneva (Switzerland)

Progress in quantum communication has long been tied to the progress in single-photon detection technology. I will present some of the recent progress on superconducting nanowire single-photon detectors (SNSPDs) based on amorphous thin films such as WSi and MoSi, and the role this progress played in pushing limits in quantum communication. More precisely, I will discuss how such amorphous SNSPDs played an enabling role in the field of quantum repeaters with solid-state quantum memories. I will conclude with some remarks on the study of the detection mechanism in amorphous SNSPDs.

10358-7, Session 2

Towards integrated superconducting detectors on lithium niobate waveguides *(Invited Paper)*

Jan Philipp Höpker, Moritz Bartnick, Evan Meyer-Scott, Frederik Thiele, Stephan Krapick, Nicola M. Montaut, Matteo Santandrea, Harold Herrmann, Sebastian Lengeling, Raimund Ricken, Viktor Quiring, Torsten Meier, Univ. Paderborn (Germany); Adriana E. Lita, Varun B. Verma, Thomas Gerrits, Sae Woo Nam, National Institute of Standards and Technology (United States); Christine Silberhorn, Tim Bartley, Univ. Paderborn (Germany)

Superconducting detectors are now well-established tools for quantum optics, boasting high-efficiency, fast response and low noise. Similarly, lithium niobate is an important platform for second-order nonlinear optical process, such as high-speed electro-optic modulation and polarisation conversion, as well as frequency conversion and sources of quantum light. Combining these technologies completes the requirements for a single platform capable of generating, manipulating and measuring quantum light in many degrees of freedom, in a compact and potentially scalable manner.

We will report on progress combining tungsten transition edge sensors (TES) and amorphous tungsten silicide superconducting nanowire single photon detectors (SNSPDs) on titanium in-diffused lithium niobate waveguides. Crucial for quantum optics applications, our waveguides offer extremely low losses of <0.01dBcm-1, and support both polarisation modes. The ultimate goal is to couple the evanescent field from the waveguides into the superconducting absorber. We will report on simulations and measurements of the absorption, which we can characterise at room temperature prior to cooling down the devices. Independently, we show how the detectors respond to flood illumination, normally incident on the devices, demonstrating their functionality, and, in the case of the SNSPD structure, saturation of the internal detection efficiency. This result is assisted by the amorphous nature of the tungsten silicide, which is tolerant to the surface roughness of the lithium niobate waveguides, allowing us to demonstrate functional detectors deposited directly on top of the in-diffused structures. Finally, we report on efficient pigtailing at 77K from fibre to waveguide with 1dB interface loss.

10358-8, Session 3

Chip scale interactions of light and vapors *(Invited Paper)*

Uriel Levy, Liron Stern, Meir Grajower, Eliran Talker, Jonathan Bar David, The Hebrew Univ. of Jerusalem (Israel)

In this talk we will present our recent results related to chip scale integration of light with vapor cells. This include the interaction of vapors with waveguides, chip scale resonators and metasurfaces. We will also present the role of cell miniaturization. Linear and nonlinear effects will be demonstrated. The role of coherence will be explored. Finally, we will discuss applications such as all optical switching and frequency referencing.

10358-9, Session 3

Quantum nonreciprocal devices based on chiral light-matter coupling *(Invited Paper)*

Juergen Volz, Arno Rauschenbeutel, Vienna Ctr. for Quantum Science and Technology (Austria)

Nanophotonic components allow the control of the flow of light in integrated optical environments. Thereby, the light's strong confinement leads to an inherent link between its local polarization and propagation direction which fundamentally alters the physics of light-matter interaction and gives rise to phenomena such as directional emission and direction-dependent coupling strengths [1].

I will present the underlying principles of this chiral light-matter interaction and its consequences for integrated applications [1]. In particular, I will show how we employ this effect to control the direction of spontaneous emission [2] and to realize low-loss nonreciprocal transmission at the single-photon level through a silica nanofiber [3]. We use two different approaches where either an ensemble of spin-polarized atoms is weakly coupled to a nanofiber or a single atom is strongly coupled to the nanofiber via a whispering-gallery-mode resonator. The resulting optical isolators show a strong imbalance between the transmissions in forward and reverse direction and, at the same time, a forward transmissions exceeding 70%. We extended this system to a 4-port device, where a single atom routes photons nonreciprocally from one fiber port to the next. This realizes a quantum optical circulator [4] which can even be prepared in a superposition of its operational modes.

The demonstrated systems exemplify a new class of (quantum) nanophotonic devices that are ideally suited for photonic quantum information processing and quantum simulation.

[1] Nature 541, 473, (2017).

[2] Science 346, 67 (2014).

[3] Phys. Rev. X 5, 041036 (2015).

[4] Science 354, 1577 (2016).

10358-11, Session 3

Photostable molecules on chip: integrated single photon sources for quantum technologies *(Invited Paper)*

Costanza Toninelli, Istituto Nazionale di Ottica (Italy) and LENS - Lab. Europeo di Spettroscopie Non-Lineari (Italy); Pietro E. Lombardi, Consiglio Nazionale delle Ricerche (Italy) and LENS - Lab. Europeo di Spettroscopie Non-Lineari (Italy); Anna P. Ovvyan, Westfälische Wilhelms-Univ. Münster (Germany); Sofia Pazzagli, Giacomo Mazzamuto, LENS - Lab. Europeo di Spettroscopie Non-Lineari (Italy); Günter Kewes, Oliver Neitzke, Humboldt-Univ. zu Berlin (Germany); Nico Gruhler, Westfälische Wilhelms-Univ. Münster (Germany); Oliver Benson, Humboldt-Univ. zu Berlin (Germany); Wolfram H. P. Pernice, Westfälische Wilhelms-Univ. Münster (Germany); Francesco S. Cataliotti, LENS - Lab. Europeo di Spettroscopie Non-Lineari (Italy)

Efficient quantum light sources and non-linear optical elements at the few photon level are the basic ingredients for most applications in nano and quantum technologies. On the other hand, a scalable platform for quantum ICT typically requires reliable light matter interfaces and on-chip integration. In this work we demonstrate the potential of a novel hybrid technology which combines single organic molecules as quantum emitters and dielectric chips [1].

Dibenzoterrylene molecules in anthracene crystals (DBT:Ac) are particularly suitable quantum systems for this task, since they exhibit long-term photostability in thin samples [2], easy fabrication methods and life-time limited emission at cryogenic temperatures [3].

We demonstrate at room temperature the emission of single photons from DBT molecules into ridge waveguides with a branching ratio up to 40%. The overall single-photon source efficiency, including emission into the guided mode, propagation losses, and emission into a quasi-gaussian mode in free space, is estimated around 16%. These results are competitive with state-of-the-art single photon emission into propagating guided modes from solid state systems [4], while offering a novel platform with unprecedented versatility.

References

[1] P. Lombardi et al., Arxiv: 1701.00459v1 (2017).

[2] C. Toninelli et al., Opt. Express 18, 6577 (2010).

[3] A. A. L. Nicolet et al., ChemPhysChem 8, 1929 (2007).

[4] I. Zadeh et al., Nano Lett. 16, 2289 (2016); R. S. Daveau et al., Arxiv: 1610.08670v1 (2016).

[5] J. Hwang et. al., New J. Phys. 13, 085009 (2011); H.-W. Lee et al., Phys. Rev. A 63, 012305 (2000).

10358-12, Session 3

Superconducting atom chips *(Invited Paper)*

Rainer Dumke, Nanyang Technological Univ. (Singapore)

In recent years, microtraps for neutral atoms based on superconductors, i.e. 'superconducting atom chips' have become a subject of intensive research.

Motivated by the prediction of extremely low magnetic and thermal noise compared to normal conductors, superconducting atom chips have first been implemented in the expectation of improving the coherence of atomic quantum states close to surfaces by several orders of magnitude.

This boost in coherence time holds promising expectations for quantum information processing applications.

In particular, superconducting atom chips are ideal candidates for the realization of hybrid quantum systems between atomic and superconducting solid state qubits, merging the fast gate operation times for superconducting qubits with the long coherence times of atomic qubits.

In this talk I will discuss our work towards realizaing this hybrid quantun system via coupling ultracold atoms and superconducting circuits.

10358-13, Session 3

Integration of optically active neodymium (Nd) ions in niobium thin films by ion implantation: room temperature photoluminescence characteristics and photoconductivity

Patrick C. Sims, SPAWAR Systems Ctr. Pacific (United States); Brad Liu, SPAWAR Systems Ctr. Atlantic (United States); Saurabh Sharma, Carlos M. Torres, Lance Lerum, Mohammed Fahem, Sanja Zlatanovic, Vincent Dinh, Nenad Djapic, David Chao, Osama M. Nayfeh, Dave Rees, SPAWAR Systems Ctr. Pacific (United States)

We report on the integration of optically active rare earth Neodymium ions by implantation into 90 nm sputtered films of Niobium metal deposited on silicon-oxide wafers. The implantation conditions span doses of 1013 to 1014 ions/cm2 and energies of 10-60 keV. The resulting ion distribution and damage profiles were determined by ion implantation simulations. Energy-dispersive X-ray spectroscopy (EDX) measurements in a scanning electron microscope detects the signature of both the Neodymium and Niobium, and confirms a 1-3 % Nd concentration, where higher dose produces increased concentration. With laser confocal excitation at 785 nm, we observe photoluminescence (PL) emission in un-annealed samples at room temperature near ~850 nm and a robust peak at ~1064 nm. The PL wavelengths are consistent with the known 4F3/2 transitions of Nd3+ as well as an increased broad-wavelength co-contribution likely due to induced defects consistent with the implantation simulations. In comparison, Niobium control samples (i.e un-implanted) are devoid of pronounced peaks in the PL. We examine the effect of optical illumination on the electronic transport resistive properties of the films and find dependence between wavelength of excitation and modulating of the current conduction. We observe a selectivity in the resistance modulation when comparing excitation with an LED centered at 810 nm as compared to a broad-band Halogen lamp. We discuss use of these films as active elements in quantum memory.

10358-14, Session 4

Quantum light-matter interfaces based on rare-earth-doped crystals and nano-photonics *(Invited Paper)*

Andrei Faraon, Tian Zhong, Jonathan M. Kindem, Evan Miyazono, Ioana Craiciu, Jake H. Rochman, John G. Bartholomew, California Institute of Technology (United States)

Quantum light-matter interfaces that reversibly map the quantum state of photons onto the quantum states of atoms, are essential components in the quantum engineering toolbox with applications in quantum communication, computing, and quantum-enabled sensing. In this talk I present our progress towards developing on-chip quantum light-matter interfaces based on nanophotonic resonators fabricated in rare-earth-doped crystals known to exhibit some of the longest optical and spin coherence times in the solid state. We recently demonstrated coherent control of neodymium (Nd3+) ions coupled to yttrium orthosilicate Y2SiO5 (YSO) photonic crystal nano-beam resonator. The coupling of the Nd3+ 883 nm 4I9/2-4F3/2 transition to the nano-resonator results in a 40 fold enhancement of the transition rate (Purcell effect), and increased optical absorption (~80%) - adequate for realizing efficient optical quantum memories via cavity impedance matching. Optical coherence times T2 up to 100 ?s with low spectral diffusion were measured for ions embedded in photonic crystals, which are comparable to those observed in unprocessed bulk samples. This indicates that the remarkable coherence properties of REIs are preserved during nanofabrication process. Multi-temporal mode photon storage using stimulated photon echo and atomic frequency comb (AFC) protocols were implemented in these nano-resonators. Our current technology can be

readily transferred to Erbium (Er) doped YSO devices, therefore opening the possibility of efficient on-chip optical quantum memory at 1.5 ?m telecom wavelength. Integration with superconducting qubits can lead to devices for reversible quantum conversion of optical photons to microwave photons.

10358-15, Session 4

Engineering quantum emitters in wide bandgap semiconductors *(Invited Paper)*

Igor Aharonovich, Univ. of Technology, Sydney (Australia)

Solid State Single Photon Sources are vital components of integrated nanophotonic circuits. While research so far has been focused on quantum dots and color centers in diamond, other solid state platforms such as the nitrides and the oxides are of a great interest. In this talk I will show new results on engineering quantum emitters in wide range of materials including silicon carbide, gallium nitride and various oxides.

In the first part of my talk i will show new results on room temperature emitters in gallium nitride and silicon carbide. These emitters can be found in a variety of wafers and therefore offer a potential for scalable quantum photonic technologies. I will then show new ways to engineer emitters in oxides - including tungsten oxide and zinc oxide. I will summarize by highlighting the main challenges in the field of solid state single emitters and provide an outlook for further integration of these emitters with cavities and resonators.

10358-16, Session 4

Deterministic enhancement of coherent photon generation from a nitrogen-vacancy center in ultrapure diamond *(Invited Paper)*

Daniel Riedel, Immo Söllner, Brendan Shields, Sebastian Starosielec, Patrick Appel, Elke Neu, Patrick Maletinsky, Richard J. Warburton, Univ. Basel (Switzerland)

A key requirement for many applications in solid-state quantum sciences is a high fluence of indistinguishable photons. The spontaneous emission of these photons is governed by the coupling of an excited quantum system to electromagnetic vacuum fluctuations.

In our experiment, we enhance this coupling by engineering a tunable Fabry-Perot microcavity. The quantum system we study is the nitrogen-vacancy (NV) center in diamond, a workhorse for quantum science and engineering, due to its optical transitions and the coherent electron spin system it hosts. Our device consists of a high-quality, nano-fabricated, single-crystalline diamond membrane bonded to a planar mirror; the cavity is completed by a second, concave mirror. Using piezo positioners, we achieve full spectral and spatial tunability and freedom in selecting NVs with favorable emission properties in our low-temperature (4 Kelvin) experiments.

Upon tuning of the cavity into resonance, we find significant enhancement of the 637 nm zero phonon line for several individual NVs which is accompanied by a strong reduction of the overall photoluminescence (PL) lifetime. We infer a 30-fold enhancement of the zero-phonon transition rate at best. The fraction of the PL emission associated to this resonant transition is thereby increased from 3% to 46%.

Our results constitute a significant leap on the route towards the implementation of fast long-distance quantum networks, which are currently limited by the photon emission rate in their nodes. Furthermore, our versatile design is readily applicable to other solid-state quantum emitters like color centers in silicon carbide.

10358-17, Session 4

Formation of silicon carbide defect qubits with optically transparent electrodes and atomic layer deposited silicon oxide surface passivation

Brad Liu, Patrick C. Sims, Carlos M. Torres, Bradley M. Davidson, Lance Lerum, Hector Romero, Mohammed Fahem, Mark E. Lasher, Anna M. Leese de Escobar, Osama M. Nayfeh, Ken Simonsen, Ayax D. Ramirez, SPAWAR Systems Ctr. Pacific (United States); Hunter Banks, Sam G. Carter, D. Kurt Gaskill, Thomas L. Reinecke, U.S. Naval Research Lab. (United States)

Defect qubits in silicon carbide are an emerging system for quantum information science and technology. It is important to passivate and protect the surface to preserve the particular defect configurations as well as to provide means to tune the opto-electronic properties via electronic or opto-electronic gating. In this work, we construct defect qubit device structures that integrate Indium-Tin-Oxide (ITO) electrodes and a thin atomic layer deposited (ALD) silicon-oxide surface passivation. The devices are formed via 12C ion implantation and high temperature annealing of 4H and 6H silicon carbide. The process involves the integration of optically transparent indium tin oxide electrodes and a surface passivation film of silicon-oxide by atomic layer deposition. We find good contact is formed between ITO and SiC, and after complete processing, the measured broad-band photoluminescence (PL) with excitation at 785 nm in a scanning PL system is consistent with the formation of silicon vacancies. We find minimal change in the room temperature emission in regions beneath the ITO electrodes and the SiOx-SiC passivated surface. We evaluate the ability of electric field to tune the optically detected magnetic resonance (ODMR) response of the qubit system by simulations of the spectrum with a modified spin Hamiltonian that considers the Stark Effect. We quantify the simulated strength of the electric-field tuning of the energy levels and ODMR response for the various identified spin 3/2 transitions of the silicon vacancy

10358-19, Session 5

The COST action "Nanoscale Quantum Optics": implications for quantum photonics devices

Mario Agio, Univ. Siegen (Germany) and COST Action MP1403 (Germany); Costanza Toninelli, Istituto Nazionale di Ottica (Italy)

Several research efforts funded by national and EU projects in the last decades resulted into enormous progress in quantum physics and quantum optics, on the one hand, and in nano-optics and nanophotonics, on the other hand. The COST Action MP1403 "Nanoscale Quantum Optics" is the instrument to proactively increase the interaction among the communities of nanophotonics, quantum optics and materials science and to support them towards common objectives. The grand vision is the development of new ideas, materials, and techniques to control the interaction between light and matter at will, even down to the level of individual quanta. The potential breakthroughs will have profound implications in fields as diverse as classical and quantum information processing & communication, sensing & metrology, light sources, and energy harvesting. We have thus identified four research priorities that deal with problems and limitations in the operation of existing quantum technologies, and that may contribute to the discovery and understanding of novel quantum phenomena for future applications: Generation, detection & storage of quantum states of light at the nanoscale; Nonlinearities and ultrafast processes in nanostructured media; Nanoscale quantum coherence; Cooperative effects, correlations and many-body physics tailored by strongly confined optical fields. The first two priorities will also target technological aspects, such as performances and integrability of quantum photonics devices, whereas the other two include rather exploratory activities.

10358-20, Session 6

A universal quantum module for quantum communication, computation, and metrology *(Invited Paper)*

William J. Munro, NTT Basic Research Labs. (Japan) and National Institute of Informatics (Japan); Michael Hanks, Nicolò Lo Piparo, National Institute of Informatics (Japan); Michael Trupke, Jörg Schmiedmayer, Vienna Ctr. for Quantum Science and Technology (Austria); Kae Nemoto, National Institute of Informatics (Japan)

The development of devices that process information according to the principles of quantum mechanics is leading to a new technological revolution. There are many potential applications, ranging from sensing and metrology through to large scale quantum communication and computation, with various physical systems to realize them. Most physical are typically suited to a limited range of applications. In this presentation, we describe a simple module that could be ubiquitous for quantum information based applications, that is it can be used for metrology, communication and computation applications. Our basic modules, each comprising a single NV? center embedded in diamond embedded in an optical cavity, has the cavities mediate interactions between the photons and the electron spins (enabling entanglement distribution and efficient readout), while the nuclear spins constitute long-lived quantum memories capable of storing and processing quantum information. We will illustrate the design of such a module based on dipole induced transparency and its function using a single NV? center embedded in an optical cavity. Further we will show a network based architecture that while suitable for large scale fault tolerant computation can be easily used for communication and distributed metrology tasks. We will discuss these applications in detail. Finally, we will investigate the possible use of alternative newer diamond centers (for instance SiV/GeV) within our module and their applicability for our module based quantum information processing.

10358-21, Session 6

Towards fault-tolerant quantum computing with spins in diamond *(Invited Paper)*

Jiangfeng Du, Ya Wang, Univ. of Science and Technology of China (China)

The remarkable properties of spins in diamond make it promising candidate for quantum information processing. I will present our recent progress towards fault-tolerant quantum computing with the nitrogen-vacancy center in diamond. By using a hybrid electron-nuclear spin system we first demonstrate the three-qubit phase error correction protocol. We then provide advanced control techniques to realize fault-tolerant universal quantum gates. These results pave the way for fault-tolerant quantum computing.

10358-22, Session 6

Integrated single photon circuits with electrical light source *(Invited Paper)*

Wolfram Pernice, Westfälische Wilhelms-Univ. Münster (Germany)

Quantum photonic circuits based on nanophotonic components hold promise for overcoming scalability limitations in optical quantum systems. Functional systems will require the co-integration of single photon sources, detectors and tunable photonic components. Waveguide integrated single photon detectors based on superconducting nanowires (SNSPDs) have been shown to fulfill the demanding requirements for on-chip quantum photonics. Because they provide very wide optical detection bandwidth, their use with optically pumped single photon sources poses severe challenges for on-chip filtering. We overcome these challenges by co-integrating electrically driven single photon sources with superconducting detectors. Single photon sources with nanoscale footprint are realized by depositing electrically contacted carbon nanotubes (CNTs) across nanophotonic waveguides. CNTs under electrical current bias are shown to emit non-classical light which is coupled efficiently into the underlying photonic framework. The CNTs are shown to provide high count rates in the MHz range. The statistical characterization of the CNT light source crucially relies on the high timing resolution of the SNSPDs which allows for measuring photon statistics for emitters with sub-100ps lifetime. The combination of top-down nanofabrication with deposition by electrophoresis provides a waferscale approach for realizing non-classical circuits on chip. Such hybrid quantum photonic devices therefore hold promise for realizing complex integrated devices without additional optical input ports.

10358-23, Session 6

On-chip quantum photonics using quantum dots *(Invited Paper)*

Peter Lodahl, Niels Bohr Institute (Denmark)

Semiconductor quantum dots have excellent optical performance dramatically in recent years, and today a clear pathway is laid out for constructing a deterministic and coherent photon-emitter interface by embedding quantum dots in photonic nanostructures [1]. Such an interface can be employed as an on-demand single-photon source, but more generally enables deterministic quantum gates. We review the recent experimental progress on quantum dots coupled to nanophotonic waveguides including the internal single-photon coupling efficiency [2], coherence [3], and transfer efficiency to an optical fiber [4]. Currently, the first commercial products based on this technology are being brought to the market [5]. Finally the fundamental decoherence processes of a quantum dot single-photon source are discussed [6].

[1] Lodahl et al., Rev. Mod. Phys. 87, 347 (2015).

[2] Arcari et al., Phys. Rev. Lett. 113, 093603 (2014).

[3] Kirsanske et al., submitted, arXiv:1701.08131

[4] Daveau et al., Optica 4, 178 (2017).

[5] Single-photon chip technology is currently commercialized by the company Sparrow Quantum A/S, www.sparrowquantum.com

[6] Tighineanu et al., arXiv:1702.04812

10358-24, Session 6

A heterogeneous III-V / Si3N4 quantum photonic integration platform *(Invited Paper)*

Marcelo I. Davanco, National Institute of Standards and Technology (United States); Jin Liu, Sun Yat-Sen Univ. (China); Luca Sapienza, Univ. of Southampton (United Kingdom); Chen-Zhao Zhang, South China Normal Univ. (China); Jose V. De Miranda Cardoso, Univ. Federal de Campina Grande (Brazil); Varun B. Verma, Richard P. Mirin, Sae-Woo Nam, National Institute of Standards and Technology (United States); Liu Liu, South China Normal Univ. (China); Kartik Srinivasan, National Institute of Standards and Technology (United States)

Photonic integration is an enabling technology for photonic quantum science, offering greater scalability, stability, and functionality than traditional bulk optics. Here, we describe a scalable, heterogeneous III-V/silicon integration platform to produce Si3N4 photonic circuits incorporating GaAs-based nanophotonic devices containing self-assembled InAs/GaAs quantum dots. We demonstrate pure single-photon emission from individual quantum dots in GaAs waveguides and cavities - where strong control of spontaneous emission rate is observed - directly launched into

Si3N4 waveguides with > 90 % efficiency through evanescent coupling. To date, InAs/GaAs quantum dots constitute the most promising solid state triggered single-photon sources, offering bright, pure and indistinguishable emission that can be electrically and optically controlled.

Si3N4 waveguides offer low-loss propagation, tailorable dispersion and high Kerr nonlinearities, desirable for linear and nonlinear optical signal processing down to the quantum level. We combine these two in an integration platform that will enable a new class of scalable, efficient and versatile integrated quantum photonic devices.

10358-25, Session 7

Electromechanical semiconductor quantum structures *(Invited Paper)*

Hiroshi Yamaguchi, NTT Basic Research Labs. (Japan)

The use of compound semiconductor heterostructures allows us to fabricate micro/nanomechanical systems with novel functionalities. In this invited talk, we present examples of experimental results that we have recently demonstrated in our investigations of electromechanical resonators made of semiconductor-based low-dimensional quantum structures.

The mechanical motion can be coupled to the photo-excited carriers in compound semiconductors by piezoelectricity. Through the carrier-mediated optomechanical effects, the thermal motion can be optically controlled in similar way as that in cavity optomechanics. The amplification and the damping of thermo-mechanical vibration have been demonstrated by simply applying a laser light with a near-bandgap wavelength. We proposed to utilize the carrier-mediated optomechanical interaction for characterizing the properties of semiconductors. Optical absorption properties and carrier dynamics are studied through the mechanical resonance characteristic.

We also investigate the coupling between carriers and mechanical degrees of freedom in low-dimensional electron systems. The back-action on the mechanical motion mediated by electron systems is studied. In high mobility two-dimensional electron systems, electron localization induced by quantum Hall effects strongly suppresses the damping of mechanical motion, showing the electron-induced mechanical damping. The carrier-medicated back-action is also confirmed in quantum dots systems, where both damping and amplification were observed depending on the relative position of Fermi level to the quantized electron energy in QD.

10358-26, Session 7

Single photons from electrically driven reconfigurable photonic crystal cavities *(Invited Paper)*

Maurangelo Petruzzella, Simone Birindelli, Francesco M. Pagliano, Daniele Pellegrino, Zarko Zobenica, Michele Cotrufo, Frank W. M. van Otten, Rob W. van der Heijden, Technische Univ. Eindhoven (Netherlands); Lianhe H. Li, Edmund Linfield, Univ. of Leeds (United Kingdom); Andrea Fiore, Technische Univ. Eindhoven (Netherlands)

Due to their deterministic nature and efficiency, devices based on quantum dots (QD) are currently replacing traditional single-photon sources in the most complex quantum optics experiments, such as boson sampling protocols. Embedding these emitters into photonic crystal (PhCs) cavities enables the creation of an array of Purcell-enhanced single photons required to build quantum photonic integrated circuits. So far scaling of the number of these cavity-emitters nodes on a single chip has been hampered by practical problems such as the lack of post-fabrication methods to control their relative detuning and the complexity involved with their optical excitation. Here, we present a tuneable single-photon source combining electrical injection and nano-opto-electromechanical cavity tuning. The device consists of a double-membrane electromechanically tuneable PhC structure. A vertical p-i-n junction, hosted in the top membrane, is exploited to inject current in the QD layer and demonstrate a tunable nano LED whose cavity wavelength can be reversibly varied over 15 nanometers by electromechanically varying the distance between membranes. Besides, electroluminescence from single QD lines coupled to PhC cavities is reported for the first time. The measurement of the second-order autocorrelation function from a cavity-enhanced line proves the anti-bunched character of the emitted light. Since electrical injection does not produce stray pump photons, it makes the integration with superconducting single-photon detectors much more feasible. The large-scale integration of such tuneable single-photon sources, passive optics and waveguide detectors may enable the implementation of fully-integrated boson sampling circuits able to manipulate tens of photons.

10358-27, Session 7

On-chip hybrid quantum circuits *(Invited Paper)*

Klaus D. Jöns, Ali W. Elshaari, KTH Royal Institute of Technology (Sweden); Iman Esmaeil Zadeh, Andreas Fognini, Kavli Institute of Nanoscience Delft (Netherlands); Michael E. Reimer, Univ. of Waterloo (Canada); Dan Dalacu, Philip J. Poole, National Research Council Canada (Canada); Val Zwiller, KTH Royal Institute of Technology (Sweden)

Quantum communication applications require a scalable approach to integrate bright sources of entangled photon-pairs in complex on-chip quantum circuits. Currently, the most promising sources are based on III/V semiconductor quantum dots. However, complex photonic circuitry is mainly achieved in silicon photonics due to the tremendous technological challenges in circuit fabrication. We take the best of both worlds by developing a new hybrid on-chip nanofabrication approach. We demonstrate for the first time on-chip generation, spectral filtering, and routing of single-photons from selected single and multiple III/V semiconductor nanowire quantum emitters all deterministically integrated in a CMOS compatible silicon nitride photonic circuit. Wavelength and polarization filtering is performed using an electrically-controlled integrated ring resonator filter. We achieve more than 95dB on-chip excitation laser suppression, allowing for the detection of light down to the single-photon level without the need of additional filtering. Taking advantage of our new on-chip single-photon filtering and routing we are able to perform the first quantum wavelength division multiplexing and de-multiplexing. We realize a multi-frequency quantum channel comprising two independently selected and deterministically integrated quantum emitters. By tuning the ring resonator voltage, we can sift single-photons from one or the other nanowire into the drop-port. Our new approach eliminates the need for off-chip components, opening up new possibilities for large-scale quantum photonic systems with on-chip single- and entangled-photon sources.

References:

I. Esmaeil Zadeh et al., Nano Letters 16, 2289-2294 (2016).

A. W. Elshaari et al., submitted, see arXiv:1611.03245 (2016).

10358-28, Session 7

Fiber-integrated quantum switch

Ruixiang Guo, Charles M. X. Altuzarra, Ctr. for Disruptive Photonic Technologies, Nanyang Technological Univ. (Singapore) and The Photonics Institute, Nanyang Technological Univ. (Singapore); Angelos Xomalis, Optoelectronics Research Ctr. (United Kingdom) and Ctr. for Photonic Metamaterials, Univ. of Southampton (United Kingdom); Cesare Soci, Ctr. for Disruptive Photonic Technologies, Nanyang Technological Univ. (Singapore) and The Photonics Institute, Nanyang Technological Univ. (Singapore); Nikolay I. Zheludev, Ctr. for Disruptive Photonic Technologies, Nanyang Technological Univ.

(Singapore) and Optoelectronics Research Ctr., Univ. of Southampton (United Kingdom) and Ctr. for Photonic Metamaterials, Univ. of Southampton (United Kingdom)

We demonstrate the integration of a metamaterial coherent perfect absorption (CPA) switch with mainstream telecommunication optical fibres, an ideal scalable platform for quantum photonic devices. Using the recently demonstrated concept of CPA in a thin plasmonic metamaterial [1,2] we realized fibre-based dissipative non-local quantum gates for polarization- or phase- entangled photon pairs. Similar to the scheme we previously developed in free-space, here entangled photon pairs are generated by type-II spontaneous parametric down-conversion in a beta-barium borate (BBO) crystal and the signal photon is sent to a Sagnac-like interferometer, that contains the metamaterial absorber. The idler photon is used to control the mutual polarization/phase of the entangled photons via a polarizer or a geometric phase shifter, enabling non-local control of the dissipation of the signal photon. We obtained contrasts between perfect absorption and perfect transmission, measured by correlated photon counting, as high as 82%. This first demonstration of polarization and phase controlled CPA in fibre integrated quantum gates provides a practical solution to transfer and manipulate information between qubits.

[1] T. Rogers et al. “Coherent perfect absorption in deeply subwavelength films in the single-photon regime” Nat. Commun. 6, 7031 (2015)

[2] C. Altuzarra et al. “Nonlocal control of dissipation with entangled photons” arXiv:1701.05357 (2017)

10358-33, Session 7

Engineering of spectral correlations of telecom-wavelength photons

Maciej Gałka, Univ. of Warsaw (Poland); Michał Mikołajczyk, Michał Karpiłski, Faculty of Physics, University of Warsaw (Poland)

Time-frequency domain is a promising platform for optical quantum technologies due to large Hilbert space available for quantum information encoding. Moreover, photons appear as perfect candidates for interface between different quantum systems as they can be transmitted over large distances in a low-loss manner. Obviously mostly desired would be such link at telecommunication wavelengths, because it can be integrated with classical communication schemes.

We report on a tunable telecom-wavelength photon pair source based on bulk periodically poled potassium titanyl phosphate (PPKTP) pumped by femtosecond laser pulses. The pairs are produced via type-II spontaneous parametric down conversion (SPDC). The spectra of photons, which lies in telecommunication range, in our source can be affected via both changing the spectrum of pumping laser and changing the phase matching by using crystals of different lengths. By appropriate choice of these parameters either the pair of photons occupy single-mode in frequency and is in a separable state or is multimode and entangled [1].

Here we report on experimental active modification the photon pairs’ spectral properties. We employ fast electro-optic temporal phase modulation to induce a deterministic change of photons’ joint spectral intensity (JSI). Central wavelength of one photon is shifted by up to 0.2 nm. The measurement of the spectrum of single photons is based upon frequency to time mapping, implemented by large group delay dispersion (GDD) in chirped fiber Bragg grating (CFBG) [2]. An unprecedented sub-10 pm resolution of correlated single-photon spectral measurements has been achieved.

Further work will be done to modify not only the position, but also the shape of JSI by using techniques based on the time-lens principle [3].

References:

[1] P. G. Evans, R. S. Bennink, W. P. Grice, T. S. Humble, Phys. Rev. Lett. 105, 253601 (2010)

[2] A. O. C. Davis, P. M. Saulnier, M. Karpinski, B. J. Smith, arXiv:1610.03040 (2016)

[3] M. Karpi?ski, M. Jachura, L. J. Wright, B. J. Smith, Nature Photonics 11, 53–57 (2017)

10358-10, Session PMon

Quantum dynamics of confined modes of a metasurface

Didier Felbacq, Univ. Montpellier (France)

Meta—surfaces are the bidimensional analogues of metamaterials. They are made on resonant elements periodically disposed on a surface. In this work, we investigate the near-field properties of a metasurface whose basic elements possess an electric and a magnetic dipole resonance. We investigate the quantum dynamics of the coupling of a quantum emitter with Bloch surface modes localized on the meta—surface exist due the resonance of the dipoles. The strong coupling regime with a emitter can be reached when the Bohr frequency of the emitter is in resonance with the Bloch modes of the meta-surface. The approach is based on an impedance model for the metasurface allowing to obtain the dispersion relation for the electromagnetic modes below the light-cone, i.e. confined on the metasurface. The electromagnetic field can then be quantized canonically. The quantum oscillator is described as a two-level system situated in the vicinity of the metasurface and coupled with the electromagnetic field via a dipolar term. We are then able to describe the quantum electrodynamics of the coupled system and study the regime of weak and strong coupling.

10358-29, Session PMon

Optimal quantum teleportation of coherent states of light

Gerardo Adesso, Pietro Liuzzo-Scorpo, The Univ. of Nottingham (United Kingdom)

We consider quantum teleportation of ensembles of coherent states of light with a Gaussian distributed displacement in phase space. We address the following general question: given a certain amount of entanglement available as a resource, what is the maximal fidelity that can be achieved on average in the teleportation of such an ensemble of states? We answer the question analytically by means of an optimisation within the space of Gaussian quantum channels, which allows for an intuitive visualisation of the problem. We first show that not all channels are accessible with a finite degree of entanglement, and then prove that practical schemes relying on non-symmetric entangled states (i.e., unbalanced twin beams) enable one to reach the maximal fidelity at the border with the inaccessible region. We further extend our study to secure quantum teleportation by considering the role of Gaussian steering as a resource. Our results provide a rigorous quantitative assessment of entanglement as a resource for quantum communication. The schemes we propose can be readily implemented experimentally by a conventional continuous variable teleportation protocol involving homodyne detections and corrective displacements with an optimally tuned gain. These protocols can be integrated as elementary building blocks in quantum networks, for robust storage and transmission of quantum optical states.

10358-30, Session PMon

Tunable light superfluids using 4-level quantum atomic optical systems

Nuno Azevedo Silva, INESC Porto (Portugal) and Univ. do Porto (Portugal); Ariel Guerreiro, INESC TEC (Portugal)

In the paraxial approximation, the propagation of light in a bulk defocusing cubic nonlinear media is well described by a Nonlinear Schrödinger equation, which through the use of the Madelung transformation can be interpreted into a hydrodynamic description of light. In this description, the laser intensity maps into the light fluid density and the fluid velocity is related with the spatial phase gradient. Sharing similarities with the mean-field theory of Bose Einstein Condensates, the hydrodynamic description of light is capturing a lot of interest recently and opening new perspectives in different branches of physics by offering tabletop experiments of analogue many-body quantum systems with unprecedented control of the interactions which, in its turn, can model a wide range of phenomena in physics, ranging from superfluidity to Black Holes. Then, being able to tune the optical properties of the media is an important requirement of such analogue optical systems, in order to establish correct analogues of physical phenomena.

In this context, we will show theoretically how we can use a 4-level quantum atomic optical system to develop highly tunable optical media, with spatial control of both linear and nonlinear susceptibility. Also, we explore the superfluid behaviour of light in these atomic media and purpose a strategy to create connected geometries, discussing and investigating through GPU-enhanced numerical simulations the existence of quantized persistent currents, a phenomenon already observed in other superfluid systems such as liquid He or Bose Einstein Condensates.

10358-32, Session PMon

Highly-multimode photonic quantum memory in cold atoms

Mateusz Mazelanik, Micha? D?browski, Micha? Parniak, Wojciech Wasilewski, University of Warsaw (Poland)

Quantum memories are essential for the development of quantum information processing devices. Among others, they have been proposed as on-demand photon sources and key elements of quantum repeaters - devices allowing entanglement distribution on truly long distances.

We demonstrate a highly-multimode quantum memory which can generate, store and retrieve photons. The operation scheme relies on Raman scattering in cold rubidium-87 atomic cloud prepared in magneto-optical trap. In write-in process the Stokes photons are created in random direction together with atomic collective excitations - spin waves. During the readout the excitations are converted to anti-Stokes photons. The wave-vector of anti-Stokes photon is correlated with the Stokes one due to phase matching condition. We shot-by-shot register those photons on separate regions of a fast single-photon-sensitive camera. From single-photon counts statistics we calculated that we can store over than 1000 independent spin-wave modes. Such feature combined witch fast single photon switch could speed up single photon generation dramatically. To verify quantum nature of the stored states we measurred the normalyzed g_(S,aS)^((2)) cross-correlation of the Stokes and anti-Stokes fields. We obtained values of g_(S,aS)^((2)) reaching 100 which is indicative of a true quantum memory, since this parameter is classically bounded by 2.

10359-500, Session Plen

Controlling light at the atomic scale

F. Javier García de Abajo, ICFO - Institut de Ciències Fotòniques (Spain)

Atomically thin materials such as graphene and molecular aromatic hydrocarbon exhibit unique optical properties that allow us to control the flow of light down to the atomic scale. These materials can sustain collective electron resonances -plasmons- involving a relatively small number of electrons, therefore enabling unprecedented electrical, magnetic, optical, and thermal control of those properties. In this talk, I will review recent progress in this field and present illustrative examples of nonlinear, quantum, and ultrafast phenomena in these materials, along with applications to optical sensing, optoelectronics, and quantum optics.

10359-1, Session 1

Chiral quantum optics *(Invited Paper)*

Peter Lodahl, Niels Bohr Institute (Denmark)

Modern photonic nanostructures enable the full control of the interaction between a single quantum emitter and a single photon [1]. We will review the recent experimental progress on quantum dots coupled to nanophotonic waveguides offering a fully deterministic photon-emitter or photon-spin interface. We discuss how chiral light-matter coupling can be engineered enabling the construction of novel non-reciprocal photonic devices [2] and directional radiative coupling [3]. The light-matter coupling is inherently nonlinear and operational down to the level of single photons [4]. We finally discuss how chiral interaction may be advantageous for applications in quantum-information processing [5] and for scalable quantum network architectures [6]

[1] Lodahl et al., Rev. Mod. Phys. 87, 347 (2015).

[2] Söllner et al., Nature Nano. 10, 775 (2015).

[3] Lodahl et al., Nature 541, 473 (2017).

[4] Javadi et al., Nature Comm. 6, 8655 (2015).

[5] Ralph et al., Phys. Rev. Lett. 114, 173603 (2015).

[6] Mahmoodian et al., Phys. Rev. Lett. 117, 24501 (2016)

10359-2, Session 1

Unidirectional electron tunneling via asymmetric plasmonic resonances *(Invited Paper)*

Matthew T. Sheldon, Texas A&M Univ. (United States)

Optically excited plasmonic nanostructures display remarkable electron dynamics in the form of coherent electron displacement motion, as well as efficient generation of non-thermal 'hot electrons' with large kinetic energy. Here, we provide a theoretical and experimental overview of our studies of photo-induced charge transport across plasmonic tunneling junctions composed of nanoscale metallic gaps, as a strategy for taking advantage of such electron motion for optoelectronic energy conversion.

In symmetric plasmonic tunneling gaps the energetic distribution of electrons due to photo-induced thermalization and hot electron generation is insufficient for significant electrical currents, either through excitation over the interface potential barrier, or via tunneling that exhibits a net preference for the direction of charge transfer. However, asymmetric resonant structures can provide optical absorption, photo-excitation and time-dependent electric fields that induce significant temperature gradients and local variations in the hot electron population. Such asymmetry can be used to promote unidirectional tunneling transport currents with significant enhancement compared with conventional photoelectron and thermionic emission (~ 10^15 enhancement), and thus comprises an intriguing mechanism for providing electrical work. This presentation will introduce the theoretical framework of tunneling phenomena associated with photon-induced hot electrons in plasmonic structures, including principles of electron distribution under photon excitation, strategies for amplifying hot electron generation (e.g. manipulating hot spots in nano-antennas) and provide a mechanistic quantum model of power conversion devices based on unidirectional electron tunneling across nanoscale plasmonic junctions. We also report on initial transport measurements of plasmonic tunnel junctions that exhibit optical power conversion by this method.

10359-3, Session 1

Giant vacuum friction: PT symmetric spectral singularity and negative frequency resonance *(Invited Paper)*

Sarang Pendharker, Yu Guo, Farhad Khosravi, Univ. of Alberta (Canada); Zubin Jacob, Purdue Univ. (United States)

Vacuum consists of a bath of balanced and symmetric positive and negative frequency fluctuations. Media in relative motion or accelerated observers can break this symmetry and preferentially amplify negative frequency modes as in Quantum Cherenkov radiation and Unruh radiation. Here, we show the existence of a universal negative frequency-momentum mirror symmetry in the relativistic Lorentzian transformation for electromagnetic waves. We show the connection of our discovered symmetry to parity-time (PT) symmetry in moving media and the resulting spectral singularity in vacuum fluctuation related effects. We prove that this spectral singularity can occur in the case of two metallic plates in relative motion interacting through positive and negative frequency plasmonic fluctuations (negative frequency resonance). Our work paves the way for understanding the role of PT-symmetric spectral singularities in amplifying fluctuations and motivates the search for PT-symmetry in novel photonic systems.

[1] arXiv:1612.02050 [physics.optics]

10359-4, Session 2

Rb atomic vapor interaction with nanophotonic and plasmonic devices *(Invited Paper)*

Hadiseh Alaeian, Northwestern Univ. (United States)

Over the past decades, alkali atoms have been the subject of intensive and diverse research, ranging from fundamental studies on ultra-cold atoms and Bose-Einstein condensates to technological applications. Since they possess only a single valance s-electron, the alkali atoms manifest a simple low-lying electronic structure compared to other atoms. Moreover, unlike conventional solid state systems their dispersion-free features make them an ideal candidate for sensing applications and referencing tasks. These two features have introduced alkali atoms as promising quantum emitters for the new paradigm of hybrid quantum optics and quantum electrodynamics. This new concept benefits from the existing integrated photonics technology for squeezing and confining the light in sub-wavelength scales to substantially enhance the light-atom interaction. The hybrid chip is envisioned to have light sources, waveguides, devices, and detectors to realize a complex quantum network down to a single photon level.

In this talk I will discuss about our recent theoretical and experimental works on atomic vapor spectroscopy in the vicinity of the plasmonic and nanophotonic devices. I start from a density matrix-based formalism describing the evolution of Rb vapor atomic levels, excited with an incoherent pump and coupled to a plasmonic lattice. When designed properly, the lattice plasmon mode efficiently captures the spontaneously emitted photons from the excited Rb atoms and a coherent coupling between the lattice mode and the atomic levels would occur. I will elaborate on the effect of pumping rate and decoherence on the steady state of the hybrid system and the feasibility of achieving a lasing state. In the second part of the talk I will present the results of our experiments on Rb vapor coupled to such a plasmonic lattice. Starting from the pumping mechanism, I describe the collisional scheme we employed to transfer the excited Rb atoms from (_^5)P_(3/2) to(_^5)P_(1/2) , hence achieving a population inversion between P and S levels and an optical gain at 795 nm, eventually. I present the experimental results of this atomic vapor interaction with a plasmonic lattice resonating at 795 nm. The spectroscopy of Rb cloud modified with tightly squeezed and enhanced field of the lattice plasmons shows the clear signature of Fano resonances in the passive gas, followed by amplified spontaneous emission in the active gas and the lasing at higher pumping powers. The results of this study would pave the way toward hybrid atom-quantum photonic chips.

10359-5, Session 2

Quantum state reconstruction and photon statistics for coherent states interacting with few quantum dot states *(Invited Paper)*

Fabian Boehm, Nicolai B. Grosse, Mirco Kolarczik, Nina Owschimikow, Ulrike Woggon, Technische Univ. Berlin (Germany)

Quantum-dot devices have been of special interest for the quantum optics community, since they allow for the creation of quantum optical states used e.g. for single-photon emitters. To characterize the quantum optical properties of emitters, quantum state tomography is a technique to reconstruct the full state from the quantum statistical measurement of the field fluctuations. We demonstrate the interaction of a coherent state with few quantum dot-systems by investigating how a femtosecond laser pulse propagates through a quantum dot optical amplifier. Using a balanced detection scheme in a self-heterodyning setup, we achieve precise measurements of the quadrature components and their fluctuations at the quantum noise limit [1]. We time-resolve the photon number distribution and the thermal-to-coherent evolution as a laser pulse is travelling through a semiconductor optical amplifier. We reconstruct the Wigner function and the photon statistics of the coherent input state before and after propagation through the amplifier with very high temporal resolution. The detection sensitivity is at a level where the fluctuations of the vacuum field can be clearly measured. An efficiency is achieved that photon numbers of as little as 2-4 photons can be observed. We also combine the techniques with a pump-probe setup, which allows us to directly manipulate the state inside the amplifier at a picosecond timescale. Using both electrical and optical carrier injection we measure the photon statistics as a function of carrier injection and demonstrate gain modulation of few-photon states.

[1] N. B. Grosse et al., Opt. Express 22, 32520 (2014)

10359-6, Session 2

Quantum localization issues in nonlinear frequency conversion and harmonic generation

David L. Andrews, Kayn A. Forbes, Jack S. Ford, Univ. of East Anglia (United Kingdom)

Issues of a fundamentally quantum origin are involved in determining the mode structures and quality of output in optically parametric processes such as harmonic generation. Any theory with an implicit assumption that each frequency conversion event occurs in an infinitesimal volume necessarily leads to an uncertainty in the output wave-vector. However, it is possible to construct a rigorous, photon-based theory that explicitly provides for a finite conversion volume, and which also identifies the intricate electrodynamic mechanisms at play within the corresponding region of space and time, on an optical wavelength and cycle time scale. This paper reports recent work on the development of this theory, based on quantum electrodynamical analysis. It identifies the form of specific material parameters that are engaged in determining the extent and measure of delocalised frequency conversion, and it leads to equations whose implementation, provided with data on the input beam structure, can deliver detailed information on the optical mode structures in the output.

10359-7, Session 2

Engineering quantum light on photonic chips *(Invited Paper)*

Qiang Lin, Univ of Rochester (United States)

In this talk, we will discuss our recent progress in engineering micro/nanophotonic device structures for producing and manipulating photonic quantum states on chip.

Recent advances in quantum photonics have resulted in broad applications ranging from secure communication, metrology, sensing, to advanced computing. Chip-scale implementation would not only enhance the complexity and capacity of information processing, but also enable novel functionalities which are otherwise inaccessible in room-wide/table-top experiments.

Lying in the heart of these applications is the capability of generating versatile high-purity entangled photonic quantum states. In this talk, we will discuss our recent effort in engineering micro/nanophotonic device structures for producing and manipulating photonic quantum states on various chip-scale device platforms, by taking advantage of enhanced four-wave mixing and parametric down conversion processes, via the second-order and third-order optical nonlinearities.

10359-25, Session PMon

Quantum photoemission of confined nonlinear optical materials *(Invited Paper)*

Subhamoy Singha Roy, JIS College of Engineering (India)

The photo emission also exhibits oscillatory variation with changing electron concentration and field thickness, respectively, for all types of quantum confinement. The photo emitted current density is the greatest for QDs and the least for QWs. In addition, the well-known results for bulk specimens of wide-gap materials have also been obtained as special cases from our generalized expression under certain limiting conditions.

10359-8, Session 3

Nanophotonic enhanced quantum emitters *(Invited Paper)*

Xin Li, Univ. of St. Andrews (United Kingdom); Zhang-Kai Zhou, Ying Yu, Sun Yat-Sen Univ. (China); Malte C. Gather, Andrea Di Falco, Univ. of St. Andrews (United Kingdom)

Quantum dots are excellent solid-state quantum sources, because of their stability, their narrow spectral linewidth, and radiative lifetime in the range of 1ns. Most importantly, they can be integrated into more complex nanophotonics devices, to realize high quality quantum emitters of single photons or entangled photon sources. Recent progress in nanotechnology materials and devices has opened a number of opportunities to increase, optimize and ultimately control the emission property of single quantum dots. In this work we present an approach that combines the properties of quantum dots with the flexibility of light control offered by nanoplasmonics and metamaterials structuring.

Specifically, we show the nanophotonic enhancement of two types of quantum dots devices, based on a single layer of low density (In)GaAs QDs grown via molecular beam epitaxy. The quantum dots are decorated on the facets of core-shell GaAs/AlGaAs nanowires, fabricated with a bottom-up approach, or inserted into optical-positioned micro-pillar cavities.

In both cases, the metallic nanofeatures, which are designed to control the emission and the polarization state of the emitted light, are realized via direct electron beam ion deposition. This approach permits to create three-dimensional features with nanometric resolution and positional accuracy, and does not require wet lithographic steps and previous knowledge of the exact spatial arrangement of the quantum devices.

10359-9, Session 3

Ultrafast spontaneous emission from single quantum dots coupled to plasmonic nanocavities *(Invited Paper)*

Maiken H. Mikkelsen, Duke Univ. (United States)

In this talk, we will describe the observation of ultrafast spontaneous emission from a single quantum dot coupled to a plasmonic structure that acts both as a small mode volume nanocavity and a nanopatch optical antenna. The nanocavity is composed of a colloidally-synthesized silver nanocube separated from a gold film by a single colloidal quantum dot and polymer layers. A 3 nm polymer layer above and below the quantum dot create a ~12 nm gap between the metal film and the nanocube which supports a highly confined plasmonic cavity mode. From white light scattering measurements, the resonance wavelength for a nanocube with a side length of ~75 nm is found to be 630 nm and colloidal quantum dots are chosen with an emission at the same wavelength to provide maximum spectral overlap with the plasmonic mode. In this way, the plasmonic nanocavity coupled to a single quantum dot acts as a single photon source operating in the regime of ultrafast spontaneous emission. The detector limited emission lifetime of 13 ps corresponds to a 540-fold enhancement in the spontaneous emission rate of the quantum dot, and points towards a single photon source operating at an ~80 GHz rate. The ~1,900-fold enhancement in the emission intensity shows that the fast emission lifetime is due to enhancement of the radiative rate rather than quenching. Furthermore, antenna action of the cavity results in a directional radiation pattern and allows for high collection efficiency by free space optics or into a single mode fiber.

10359-10, Session 3

Two-photon bundles from a single two-level system

Lukas Hanschke, Walter Schottky Institut, Technische Univ. München (Germany); Kevin A. Fischer, Ginzton Lab., Stanford Univ. (United States); Jakob Wierzbowski, Tobias Simmet, Walter Schottky Institut, Technische Univ. München (Germany); Constantin Dory, Ginzton Lab., Stanford Univ. (United States); Jonathan J. Finley, Walter Schottky Institut, Technische Univ. München (Germany); Jelena Vuckovic, Ginzton Lab., Stanford Univ. (United States); Kai Müller, Walter Schottky Institut, Technische Univ. München (Germany)

We demonstrate the generation of two-photon bundles from a single quantum two-level transition in a semiconductor quantum dots [1]. Quantum two-level systems in the solid state are poised to serve the pivotal role of an on-demand single-photon source by converting laser pulses with Poissonian counting statistics to single photons. More recently, multi-photon quantum state generators have engendered strong interest as replacements for the single-photon source in many quantum applications. Here we investigate theoretically and verify experimentally that the same two-level system that has long been studied for single-photon generation can surprisingly operate in a two-photon bundling regime.

For on demand single-photon generation, the two-level system is typically excited with a resonant pulse of area pi. This prepares the two-level system in its excited state from where it spontaneously emits a single photon. In contrast, when exciting the system with a pulse of area 2pi, the system is expected to be returned to the ground state. However, if the ratio of pulse length to excited state lifetime is finite, photon emission during the presence of the laser pulse is possible. This is most likely to happen when the system is in its excited state - after an area of pi has been absorbed. If such an emission occurs, the Rabi oscillation is restarted with a pulse area of pi remaining in the pulse which re-excites the system and leads to the emission of a second photon within the excited state lifetime.

[1] K.A. Fischer et al. – to appear in Nature Physics

10359-11, Session 3

Quantum emitters in flatland *(Invited Paper)*

Igor Aharonovich, Univ. of Technology, Sydney (Australia)

Engineering solid state quantum systems is amongst grand challenges in engineering quantum information processing systems. While several 3D systems (such as diamond, silicon carbide, zinc oxide) have been thoroughly studied, solid state emitters in two dimensional (2D) materials have not been observed. 2D materials are becoming major players in modern nanophotonics technologies and engineering quantum emitters in these systems is a vital goal.

In this talk I will discuss the recently discovered single photon emitters in 2D hexagonal boron nitride (hBN). I will present several avenues to engineer these emitters in large exfoliated sheets using ion and electron beam techniques. Density functional theory calculations suggest that that the studied defects are the antisite nitrogen vacancy in hBN. The formed emitters in 2D hBN flakes have extremely promising properties – including high brightness (~ millions counts/s), stability up to high temperatuers and linear polarization at excitation and absorption. Those properties make these emitters extremely attractive for their integration with optical resonators and waveguides. Finally, I will discuss several challenges and promising directions in the field of quantum emitters and nanophotonics with 2D materials and other wide band gap materials.

10359-12, Session 3

External quantum efficiency research of GaN-based laser diodes

Pengyan Wen, Suzhou Institute of Nano-Tech and Nano-Bionics (SINANO) CAS (China)

The GaN-based laser diodes (LDs) have attracted much attention due to their wide applications in laser display and laser lighting. As an important parameter of the LDs, the external quantum efficiency not only influences the output power but also plays an important role in the reliability. In this study, we observed the external quantum efficiency of our blue LD decreases after aging, which is contrary to the conventionally reported results. Further characterization on the microstructure of the LDs was carried out by transmission electron microscope (TEM) technique. Dislocation like defects in the waveguide region of the LD structure was observed. Furthermore, the defects extended during the aging. We attributed the reduction of the external quantum efficiency to the dislocation like defects in the waveguide layer of the LDs.

10359-13, Session 4

Flat and conformal optics with dielectric metasurfaces *(Invited Paper)*

Andrei Faraon, California Institute of Technology (United States)

Flat optical devices based on lithographically patterned sub-wavelength dielectric nano-structures provide precise control over optical wavefronts, and thus promise to revolutionize the field of free-space optics. I discuss our work on metasurfaces composed of high-index nano-posts supported

by transparent substrates. Complete control of both phase and polarization is achieved at the level of single nano-post. Using this nano-post platform, we demonstrate lenses, waveplates, polarizers, arbitrary beam splitters and holograms. Devices providing multiple functionalities, like simultaneous polarization beam splitting and focusing are implemented. By embedding the metasurfaces in flexible substrates, conformal optical devices that decouple the geometrical shape and optical function are shown. Multiple flat optical elements are integrated in optical systems such as planar retro-reflectors and Fourier lens systems with applications in ultra-compact imaging systems.

10359-14, Session 4

High performance metasurfaces based on inverse design *(Invited Paper)*

Jonathan A. Fan, Stanford Univ. (United States)

Metasurfaces have traditionally employed building blocks with physically intuitive optical responses. Many of these concepts utilize dielectric posts, which serve as waveguides and are stitched together with sufficient spacing to minimize coupling between adjacent elements. These design principles can produce single wavelength devices with good performance, but are difficult to generalize to multi-wavelength devices with exceptional performance. We show that concepts in inverse design can be used to produce dielectric metasurfaces with capabilities that exceed the current state-of-the-art. With swarm and topology optimization, we incorporate optical coupling between waveguide elements in the device designs, which yield physically non-intuitive mode profiles and coupling dynamics. To demonstrate the power and versatility of our design approach, we fabricate silicon devices that can efficiently deflect light to 75 degree angles and multi-functional devices that can steer beams to different diffraction orders based on wavelength. We also show that single crystal silicon can be used to realize efficient metasurface devices across the entire visible spectrum, ranging from 480 to 700 nanometers. Alternative forms of silicon, such as polycrystalline and amorphous silicon, suffer from higher absorption losses and do not yield efficient metasurfaces across this wavelength range. We envision that metasurfaces based on inverse design will serve as a hardware platform for the efficient routing, sorting, and manipulation of single or few photons for quantum optics applications.

10359-15, Session 4

Surface-wave phenomena and anisotropic Photoluminescence in nano-film structures

Jan Heckmann, Karsten Pufahl, Philipp Franz, Nicolai B. Grosse, Ulrike Woggon, Technische Univ. Berlin (Germany)

Intrinsically absorbing materials can sustain low-loss surface-waves with long propagation length if prepared as thin films embedded in symmetric, low-absorbing cladding materials. Semiconductors, transition metals, metal oxides, dichalcogenides and even disordered materials can thus support long-range surface polaritons (LRSP). However, the most compelling aspect of absorbing materials—their intrinsic nonlinear susceptibility—have not yet been studied in the context of LRSP. We show experimental results and theoretical calculations of the dispersion relation of LRSPs in the VIS and NIR regime. We combine the Otto configuration with nonlinear k-space spectroscopy to investigate the field-enhancement properties of long-range surface polariton modes. The excitation of these modes in the near-infrared has allowed us to gauge the strength of the near-field on resonance where a boost in second-harmonic yield was found. In addition, we support the nonlinear data with angle-resolved white-light spectra of the attenuated total internal reflection. Even excitation of a long-range surface wave on a rough and disordered surface, e.g. a functional gold filled PNIPAM films, could be demonstrated. Our results show that the excited modes have superior propagation lengths compared to bulk metal surface plasmon polaritons. Our findings open up new possibilities by releasing the restriction of high surface qualities for subwavelength guiding and focussing of light.

10359-16, Session 5

Measurement and control of nanomechanical motion with photons confined at the nanoscale *(Invited Paper)*

Ewold Verhagen, Rick Leijssen, Giada R. La Gala, Lars Freisem, John Mathew, Juha T. Muhonen, FOM Institute for Atomic and Molecular Physics (Netherlands)

The creation of non-classical states of mechanical motion is a long-standing goal in experimental physics. One promising approach to achieve this is measurement-based state preparation, where sufficiently strong interaction with a measurement device is used to project the mechanics into an eigenstate of the measured observable. In order to prepare non-classical states, one needs to move away from linear continuous displacement measurements towards non-linear (e.g. quadratic) and/or non-continuous measurements that evade backaction. We employ nanophotonic optomechanical systems, in which nanomechanical resonators are coupled to optical fields with extreme strength. The combination of strong photon-phonon interactions and narrow optical linewidths results in record single-photon cooperativities of ~1000. This means optomechanical measurements become nonlinear even for minute thermal displacements at cryogenic temperatures. We exploit this intrinsic optomechanical nonlinearity to perform a quadratic measurement of position with unprecedented sensitivity, and discuss the potential of using such methods to prepare non-classical states in the quantum regime. Moreover, we demonstrate the use of fast, pulsed measurements of position to perform backaction-evading displacement measurement. Finally, we explore the use of this platform to couple and simultaneously control multiple mechanical resonators through light fields, with the potential to realize nonreciprocal and topological photon-mediated transport of acoustic signals.

10359-17, Session 5

Molecular optomechanics in plasmonic cavities *(Invited Paper)*

Mikolaj Schmidt, Ctr. de Fisica de Materiales (Spain); Alejandro Gonzalez-Tudela, Max-Planck-Institut fur Quantenoptik (Germany); Geza Giedke, Donostia International Physics Ctr. (Spain) and Ikerbasque, Basque Foundation for Science (Spain); Tomas Neuman, Ctr. de Fisica de Materiales (Spain) and Donostia International Physics Ctr. (Spain); Yao Zhang, Ctr. de Fisica de Materiales (Spain) and Donostia International Physics Ctr. (Spain); Rubén Esteban, Ctr. de Fisica de Materiales (Spain); Javier Aizpurua, Ctr. de Fisica de Materiales (Spain) and Donostia International Physics Ctr. (Spain)

Surface-Enhanced Raman Scattering (SERS) is a fundamental spectroscopic technique that allows to access the rich vibrational structure of molecules. A typical SERS configuration with a molecule located in a plasmonic cavity acting as an optical nanoantenna enhances the vibrational (Stokes or anti-Stokes) signal of the molecule. A number of recent implementations of Raman experiments in plasmonic nanocavities appear to provide results which escape the standard description of the Raman process based on the classical treatment of the electromagnetic fields enhancement inside the cavity.

We establish a novel analogy between non-resonant SERS in molecular spectroscopy and typical optomechanical processes. By adopting an optomechanical hamiltonian which describes the interaction between cavity plasmons and molecular vibrations, we are able to trace the quantum dynamics of both plasmons and vibrations in a SERS process. The solution of the master equation of this optomechanical hamiltonian allows to identify novel quantum effects such as the existence of different regimes of molecular vibrational build-up: a thermal vibrational regime, a vibrational pumping regime, and a strongly nonlinear vibrational regime, which emerge as a consequence of the quantum dynamics induced by the optomechanical

interaction. Correlations between the Stokes and anti-Stokes Raman signals can also be traced for different temperatures and pumping powers.

The presence of strong optomechanical effects in Raman has been recently addressed experimentally in special "picocavities" formed by a few metallic atoms in a plasmonic cavity. The strong optomechanical coupling achieved in this situation is found to activate the pumping regime in the Raman signal, thus corroborating the validity of this description.

10359-18, Session 5

Towards optomechanics with one-dimensional gallium phosphide photonic crystal cavities

Katharina Schneider, Pol Welter, Yannick Baumgartner, Herwig Hahn, Lukas Czornomaz, Paul F. Seidler, Simon Hönl, IBM Research - Zürich (Switzerland)

We describe the design, fabrication and characterization of one-dimensional photonic crystal cavities made of gallium phosphide (GaP). The large band gap (2.26 eV) and high refractive index (n≈3.1) make GaP a promising candidate for optomechanical devices. Compared to silicon, a reduced two-photon absorption is expected, which should mitigate heating of the devices in optical experiments.

We have developed a process flow for GaP devices that allows device integration on silicon dioxide (SiO2). GaP is grown by metal-organic chemical vapor deposition (MOCVD) on a bulk GaP wafer with an intermediate aluminum-gallium-phosphide (AlGaP) layer. A GaP-on-insulator substrate is then obtained by bonding the GaP-AlGaP-GaP stack on an oxidized silicon wafer. The sacrificial layers are removed with wet etch and dry etch processes selective to AlGaP or GaP. Finally, the device designs are transferred into the GaP by dry-etching. Structures, which are meant to be freestanding, are released by removal of the underlying SiO2.

Optical components such as grating couplers, waveguides and one-dimensional photonic crystal cavities have been designed for the GaP-on-SiO2 system. Photonic crystal cavities optimized with finite-element simulations yield optomechanical coupling strengths as high as g/2ϖ=900 kHz and optical quality factors Q>?10?^6. The optical performance of the fabricated devices is characterized and the optomechanical coupling of the trapped optical mode with the mechanical motion of the beam determined.

10359-19, Session 5

Optomechanical quantum non-demolition measurement of optical field fluctuations

Antonio Pontin, Univ. College London (United Kingdom); Michele Bonaldi, Istituto Nazionale di Fisica Nucleare (Italy) and Istituto per la Fisica Fondamentale e Applicazione, Istituto Nazionale di Fisica Nucleare (Italy); Antonio L. Borrielli, Istituto dei Materiali per l'Elettronica ed il Magnetismo (Italy) and Istituto per la Fisica Fondamentale e Applicazione, Istituto Nazionale di Fisica Nucleare (Italy); Lorenzo Marconi, Istituto Nazionale di Ottica, Consiglio Nazionale delle Ricerche (Italy); Francesco Marino, Istituto Nazionale di Fisica Nucleare (Italy) and Istituto Nazionale di Ottica, Consiglio Nazionale delle Ricerche (Italy); Gregory Pandraud, Technische Univ. Delft (Netherlands); Giovanni Andrea Prodi, Istituto Nazionale di Fisica Nucleare (Italy) and Univ. degli Studi di Trento (Italy); Pasqualina M. Sarro, Technische Univ. Delft (Netherlands); Enrico Serra, Istituto Nazionale di Fisica Nucleare (Italy) and Technische Univ. Delft (Netherlands); Francesco Marin, Univ. degli Studi di Firenze (Italy) and Istituto Nazionale di Fisica Nucleare (Italy) and Lab. Europeo di Spettroscopie Non-Lineari, Univ. degli Studi di Firenze (Italy)

In the framework of quantum mechanics there exists a class of observables for which is possible to confine the perturbation of a continuous measurement to the conjugate variable.

Experimental schemes exploiting this concept are referred to as quantum nondemolition measurements (QND) and can provide the means to estimate the observed variable with arbitrary accuracy or to prepare it in a well-known state. Among these observables there is the amplitude of the light field. Already in the mid-90s, it was proposed to exploit a movable mirror to implement a QND scheme(1). Indeed, intensity fluctuations of an optical field impinging on a mirror are not affected by the interaction. However, if the mirror is movable it can be excited by radiation pressure. The displacement of the mirror, in turn, affects the phase of the field. Thus, by measuring phase fluctuations of the optical field after its interaction with the movable mirror it is possible to gather information on the intensity quadrature.

We present an optomechanical experiment, in which the movable mirror is a high Q micro-mechanical device(2) and is the end mirror of Fabri-Pérot cavity. We have simultaneously measured intensity fluctuations of the field reflected by the cavity and the mirror motion imprinted in the phase fluctuations. By exploiting the correlations between these variables, we demonstrate a reduced uncertainty on intensity fluctuations actually reaching a sub-shot noise level.

(1) K. Jacobs, P. Tombesi, M. J. Collett, D. F. Walls, Phys. Rev. A, 1994, 49, 1961-1966.

(2) A. Borrielli, A. Pontin, F. S. Cataliotti, L. Marconi, F. Marin, F. Marino, G. Pandreaud, G. A. Prodi, E. Serra, M. Bonaldi, Phys. Rev. Applied, 2015, 3, 054009.

10359-20, Session 6

Towards integrated plasmonic quantum devices *(Invited Paper)*

Simeon Bogdanov, Mikhail Y. Shalaginov, Justus C. Ndukaife, Oksana A. Makarova, Purdue Univ. (United States); Alexey V. Akimov, Texas A&M Univ. (United States); Alexei S. Lagutchev, Alexander V. Kildishev, Alexandra Boltasseva, Vladimir M. Shalaev, Purdue Univ. (United States)

Integrated quantum photonics imposes very stringent and often contradictory requirements on the design of integrated optical components. Many material platforms have been proposed and developed to host the future quantum optical systems. All of them feature fundamental limitations that invite to consider more complex, hybrid platforms. In this talk, we focus on the use of plasmonic materials for realizing quantum devices that possess properties not available with only dielectric materials. We present our work on fast room-temperature single-photon sources and specifically address the problem of efficient outcoupling of the plasmonic modes to the far-field. We demonstrate optical spin-state readout from nitrogen-vacancies in nanodiamonds through surface plasmon-polaritons and show that quantum registers and sensors based on these color centers can operate within nanoscale optical circuits. We also discuss how our novel approach combining plasmonics with optofluidics helps achieving fast and deterministic positioning of nanodiamonds in the vicinity of plasmonic antennas. This result promises scalable assembly techniques for more complex nanophotonic systems. With these new functionalities, plasmonic devices could play a decisive role in the engineering of tomorrow's quantum photonic systems.

10359-21, Session 6

Inelastic-scattering tunnel electrons towards an electrically driven single-photon light source *(Invited Paper)*

Hasan Goktas, The George Washington Univ. (United States) and Harran Univ. (Turkey); Fikri Serdar Gökhan, Alanya Alaaddin Keykubat Üniv. (Turkey); Volker J. Sorger, The George Washington Univ. (United States)

We show that inelastically-scattering tunnel electrons are a source for electric plasmon generation. We experimentally demonstrate such electrically-driven light-emitting tunnel junction by forward biasing a Fermi sea against a doped semiconductor across a nanometer-thin tunnel oxide gap. Light emission at room temperature is found in the visible frequency range corresponding to a spectral power dependency of the tunnel current and the plasmonic mode. Light outcoupling, however is fundamentally weak since a top metal blocks emission. We studied the improvement in outcoupling in two ways; a) by gradually reducing the top-metal film thickness, and b) by introducing a grating coupler. Results show that the optimum metal thickness corresponds to the skin-depth of the metal at the emission frequency, while the grating allows for n 400x times increased relative to metal-blocking case. For the ~1-2eV observed emission, Heisenberg's uncertainty principle dictates an upper limit time response of the junction in the fs-range. Solving the current equation for both thermionic and tunnel event contributions, gives a response time (speed) scaling inverse exponentially with the tunnel gap thickness, approaching Tpbs for <0.5nm thin gaps. Lastly, since tunnel allows for single-charge events, the possibility for single-photon generation is expected.

10359-22, Session 6

Theory directions in excited-state quantum plasmonics *(Invited Paper)*

Prineha Narang, Harvard Univ. (United States)

The limits of electronic, optical and thermal performance of devices are determined by atomic-scale dynamics in their constituent materials. To enable technologies of the future, high-performance exascale computing, next factor-of-100 cost-effective capacity increases in optical networks and integrated quantum devices, conventional device concepts are insufficient. Non-equilibrium and excited state device architectures offer a fundamentally new pathway toward these technologies.

Surface plasmons, electromagnetic modes confined to the surface of a conductor-dielectric interface, have sparked recent interest because of their quantum nature and their broad range of applications in integrated nanophotonics, biosensing, photovoltaic devices, single photon transistors and single molecule spectroscopy. Despite more than a decade of intensive scientific exploration, new plasmonic phenomena continue to be discovered, including quantum interference of plasmons, observation of quantum coupling of plasmons to single particle excitations, and quantum confinement of plasmons in single-nm scale plasmonic particles.

Decay of surface plasmons to hot carriers is a new direction that has attracted considerable fundamental and application interest, yet a detailed theoretical understanding of ultrafast plasmon decay processes and the underlying microscopic mechanisms remain incomplete. In this talk I will provide a fundamental understanding of plasmon-driven hot carrier generation and relaxation dynamics in the ultrafast regime. I will report the first ab initio calculations of phonon-assisted optical excitations in metals as well as calculations of energy-dependent lifetimes and mean free paths of hot carriers, accounting for electron-electron and electron-phonon scattering, lending insight towards transport of plasmonically-generated carriers at the nanoscale. I will also discuss recent experimental observations of the injection of these nonequilibrium carriers into molecules tethered to the metal surface and into wide bandgap nitride semiconductors.

An unconventional direction in excited state quantum devices that I will discuss is based on quantum mechanical phenomena in natural energy conversion systems, namely photosynthesis. I will show recent results that probe the fundamental optical physics of cavities coupled to the elaborate topology of light-harvesting complexes. This understanding will enable rational control of photonic energy transfer at the molecular scale using spatially programmable nanoscale materials inspired by natural photosynthetic systems.

Finally I will give an outlook on the potential of excited state and non-equilibrium phenomena to deliver integrated quantum-engineered systems with diverse applications in quantum sensing and metrology, ultra-low power optoelectronic and electronic devices as well as energy conversion.

10359-23, Session 6

Plasmonic hot-carriers in the UV-VIS regime: experimental study of the internal quantum efficiency of generation and injection into GaN

Giulia Tagliabue, California Institute of Technology (United States); Ravishankar Sundararaman, Rensselaer Polytechnic Institute (United States); Adam S. Jermyn, Univ. of Cambridge (United Kingdom); Prineha Narang, Harvard Univ. (United States); Harry A. Atwater Jr., California Institute of Technology (United States)

The decay of surface plasmon resonances is usually a detriment in the field of plasmonics, but the possibility to capture the energy normally lost to heat has open new opportunities in photon sensors and energy conversion devices. In particular, the large extinction cross-section at a surface plasmon resonance enables nanostructures to absorb a significant fraction of the solar spectrum in very thin films and generate energetic carriers which could be exploited to drive photochemical processes.

Previously, we analyzed theoretically the quantum decay of surface plasmon polaritons, with and without phonons, and found that the prompt distribution of generated carriers is extremely sensitive to the energy band structure of the plasmonic material. In particular, the onset of interband transitions, occurring in the VIS regime (around 2 eV) for most common plasmonic metals (Au, Cu, Ag), is expected to significantly modify the hot-carriers distribution. Based on the theoretical work, we have designed an experimental system using GaN/noble-metal nanoscale heterostructures to investigate the photocurrent generated upon plasmon decay across the extended UV-visible regime. We indeed fabricated planar Schottky diodes where the Schottky contact was patterned with e-beam lithography to concurrently serve as plasmonic resonator. Using a super continuum Fianium laser as light source to cover the energy range from 3 eV to 1.2 eV, we measured the photocurrent as a function of photon energy. Thanks to the use of an optically transparent substrate which allows a direct experimental quantification of the absorption spectrum of our plasmonic structures, we can determine the internal quantum efficiency (IQE) spectrum of each device. By direct comparison with ab-initio calculations, we aim at assessing the contribution of direct and indirect transitions and identifying guidelines for engineering the generation of plasmonic hot-carriers in the UV-VIS regime.

10359-24, Session 6

Quantum phenomena with graphene plasmons *(Invited Paper)*

F. Javier García de Abajo, ICFO - Institut de Ciències Fotòniques (Spain)

Plasmons in atomic-scale structures exhibit intrinsic quantum phenomena related to both the finite confinement that they undergo and the small number of electrons on which they are supported. Their interaction with two-level emitters is also evidencing strong quantum effects. In this talk I will discuss several salient features of graphene plasmons in this context, and in particular their ability to mediate ultrafast heat transfer, the generation of high harmonics, their interaction with molecules and quantum emitters, and their extreme nonlinearity down to the single-photon level.

Conference 10360: Light Manipulating Organic Materials and Devices IV

SPIE. OPTICS+ PHOTONICS ORGANIC PHOTONICS+ ELECTRONICS

Sunday - Monday 6 –7 August 2017

Part of Proceedings of SPIE Vol. 10360 Light Manipulating Organic Materials and Devices IV

10360-1, Session 1

Light-induced plasmonic properties of organic materials: surface polaritons, bistability and switching waves *(Invited Paper)*

Boris D. Fainberg, Holon Institute of Technology (Israel) and Tel Aviv Univ. (Israel) and ITMO Univ. (Russian Federation); Nikolay N. Rosanov, ITMO Univ. (Russian Federation) and Vavilov State Optical Institute (Russian Federation); Nikolay Veretenov, ITMO Univ. (Russian Federation)

Recently Noginov et al. and Gentile et al. demonstrated that purely organic materials characterized by low losses with negative dielectric permittivities can be easily fabricated. And even the dramatic laser-induced change of the dielectric permittivity of organic dyes may be realized [1] that can enable us to control their "plasmonic" properties. Here we develop a theory of non-steady-state organic "plasmonics" with strong laser pulse excitation [2,3]. Our theory contains experimentally measured quantities that makes it closely related to experiment. The bistability response of the electron-vibrational model of organic materials in the condensed phase has been demonstrated [2]. Intermolecular interactions give rise to the excitation transfer along organic thin films. If the film transverse size exceeds the characteristic diffusion length, transverse phenomena such as switching waves (SW), known in optical bistability [4], should take place. We present the alternating-sign dependence of the SW velocity on pump intensity and the conditions for the spatial hysteresis realization [5]. As a mater of fact, in the case under consideration SW represents the wave of dramatic change of the dielectric permittivity of organic dye films that may have many applications. In particular, the SWs enable us to observe the bistability of surface polaritons.

1. G. Zhu et al, ACS Photonics 2, 622 (2015)

2. B.D. Fainberg, G. Li, Appl. Phys. Lett. 107 (2015) 053302 and 109902; arXiv: 1510.00205 (2015)

3. B.D. Fainberg, in preparation.

4. N. N. Rosanov, Spatial Hysteresis and Optical Patterns, Springer (Berlin), 2002

5. B. Fainberg, N. Rosanov, N. Veretenov, submitted.

10360-2, Session 1

Reverse saturable absorption (RSA) in fluorinated iridium derivatives

Michael J. Ferry, Ryan M. O'Donnell, Neal Bambha, Trenton R. Ensley, William M. Shensky III, Jianmin Shi, U.S. Army Research Lab. (United States)

Cyclometallated iridium compounds are widely studied in the organic light-emitting diode (OLED) community because of the large spin-orbit coupling constant of iridium which leads to efficient triplet state population. These photophysical properties are also advantageous for non-linear applications, such as the design of reverse saturable absorption (RSA) materials. We report on the photophysical characterization of a family of compounds of the form [Ir(pbt)2(LX)], where pbt is 2-phenylbenzothiazole and LX is a beta-diketonate ligand. Beta-diketonate ligands are referred to in the literature as "ancillary" ligands as they do not generally affect the photophysical properties of the material but allow for chemical manipulation. In particular, we investigate the effects of trifluoromethylation on compound solubility and photophysics compared to the parent acetylacetonate (acac) version. The non-linear optical properties, such as the singlet and triplet excited-state cross sections, of these compounds were measured using the Z-scan technique. We also round out the characterization with determination of the excited-state lifetimes and visible transient absorption spectroscopy from the picosecond to microsecond time scales.

10360-3, Session 1

Nonlinear management of the optical angular momentum of light from liquid crystals

Nina Kravets, Etienne Brasselet, Univ. Bordeaux 1 (France) and Ctr. National de la Recherche Scientifique (France)

Nowadays, complex light beam shaping is routinely achieved by the use of various kinds of linear optical devices enabling intensity, phase and polarization structuring of an incident light field. Less common are the situations where structured light results from a nonlinear process. Here we present recent experimental progress on the nonlinear management of the orbital angular momentum of light via spin-orbit interactoin of light. This is done by exploiting the self-induced light-driven generation of locally structured liquid crystal materials assisted by the photorefractive phenomenon. Two options are considered, namely the use of photorefraction under static and quasistatic applied voltage, while their application potential will be discussed.

10360-4, Session 1

On photochemical tweezing and photoassisted holography in azo dye containing polymers *(Invited Paper)*

Zouheir Sekkat, Moroccan Foundation for Advanced Science, Innovation and Research (Morocco)

Holographic storage is one of the most important applications in the field of optics, especially for recording and retrieving data, and information storage by interference patterns in photosensitive materials are no exception in this regard. In this talk, I will discuss the impact of photochemical tweezing on light-induced macroscopic movement in azopolymers whereby the photoisomerization force opposes the optical trapping force to form surface relief gratings, and I will give evidence that holograms recorded by interference of two coherent laser beams in azo dye doped polymer films can be controlled by a third incoherent assisting laser beam, and light diffraction can be increased or decreased by the assisting beam depending on the respective orientation of the polarizations of the recording and the assisting beams.

10360-5, Session 2

Dynamic amplification of light signals in photorefractive ferroelectric liquid crystal blends containing photoconductive chiral dopant *(Invited Paper)*

Takeo Sasaki, Tokyo Univ. of Science (Japan)

Effect of ferroelectricity on the photorefractive effect of ferroelectric liquid crystal blends was investigated. The photorefractive effect of ferroelectric liquid crystal blends is strongly dependent on the ferroelectricity of the blend. We have prepared a series of ferroelectric liquid crystal blends that contains several concentrations of a chiral compound while keeping a constant concentration of a photoconductive moiety. The photorefractive

properties of the ferroelectric liquid crystal blends were discussed with relations to the ferroelectric properties of the blends.

10360-6, Session 2

Silicon-organic hybrid devices for THz generation based on difference frequency generation

Manfred Eich, Technische Univ. Hamburg-Harburg (Germany) and Helmholtz-Zentrum Geesthacht (Germany); Marvin Schulz, Technische Univ. Hamburg-Harburg (Germany); Alexander Yu. Petrov, Technische Univ. Hamburg-Harburg (Germany) and ITMO Univ. (Russian Federation)

Here, we introduce a paradigm change in phase matching strategy and demonstrate how integrated waveguide optics can be used for wave mixing with large wavelength mismatch.

10360-7, Session 2

Measurement of the dynamics of nonlinear refraction and absorption via nonlinear beam deflection *(Invited Paper)*

David J. Hagan, Peng Zhao, Sepehr A. Benis, Eric W. Van Stryland, CREOL, The College of Optics and Photonics, Univ. of Central Florida (United States)

Many materials exhibit nonlinear refraction (NLR) and absorption (NLA) that has multifaceted temporal dynamics. As a result, measurements at one laser pulse width may not be fully predictive of the behavior at other pulse widths. We have recently developed a method, Nonlinear Beam Deflection, (BD) that allows sensitive time-resolved measurement of nonlinear refraction (NLR) and absorption (NLA) by using an excitation beam to create an index gradient deflecting a probe beam onto a quad-cell detector. The method has a demonstrated sensitivity to induced phase changes as small as 1/20,000 of a wavelength, which is sensitive enough to measure NLR in gases. By changing the relative polarization of the beams we can separate the bound-electronic response from the slower and different-symmetry nuclear contributions. In gases and liquids where reorientational nonlinearities are important, measurements at the magic angle allow isolation of the ultrafast nonlinearities. In isotropic solids the bound-electronic symmetry dictates a ratio of 1/3 for parallel to perpendicular polarizations which measurements confirm. This method also allows for measurements of nonlinearities using very different wavelengths for the excitation and probe. We have used this method to characterize the impulse response function for third-order nonlinearities in many transparent organic solvents. This allows accurate prediction of the nonlinear refraction for any pulse width longer than that used for the BD characterization. The method proves to be very useful in organic materials that may show strong nonlinear absorption, as it is able to resolve NLR in the presence of strong NLA better than other methods, such as Z-scan.

10360-8, Session 2

Enhanced optical limiting in 2D materials *(Invited Paper)*

Jitesh Kumar, Jayan Thomas, Sreekanth Varma, Katherine Layne, Univ. of Central Florida (United States); Yang Liu, Jingjie Wu, Pulickel M. Ajayan, Rice Univ. (United States)

Two dimensional (2D) graphene and transition metal dichalcogenides are an emerging class of extremely interesting materials showing unique physical properties, such as large third-order optical nonlinearity, offering potential applications in optical limiting. Materials which show high optical limiting can be used to protect sensors and human eyes against powerful laser irradiations. Here we report the optical limiting properties of graphene, titanium disufide (TiS_2) and molybdenum disulfide (MoS_2) sheets and their respective quantum dots measured using open aperture and photo-acoustic z-scan techniques. Our studies reveal that superior optical limiting is exhibited by 2D sheets and 2D quantum dots of TiS_2 at both low and high fluences compared to their graphene counterparts. Also, TiS_2 sheets and quantum dots show improved shelf life and stability upon irradiation with higher laser powers which demonstrates the feasibility of using them as potential candidates for optical limiting applications.

10360-10, Session 3

Reconfigurable micro-holes array by directional laser manipulation

Federica Pirani, Angelo Angelini, Francesca Frascella, Serena Ricciardi, Politecnico di Torino (Italy); Federico Ferrarese Lupi, Natascia De Leo, Luca Boarino, Istituto Nazionale di Ricerca Metrologica (Italy); Emiliano Descrovi, Politecnico di Torino (Italy)

In recent years, the ability to pattern large areas at the micro- and nano-scale with stimuli-responsive materials has opened the opportunity to engineer surface structures and trigger peculiar properties such as complex optical functionalities or surface properties by laser-matter interactions. The use of light-sensitive materials, such as azobenzene compounds, can open the opportunity to active manipulate in terms of morphology, physical and mechanical properties a pre-patterned architectures, which are intrinsically static once fabricated.

We employ azopolymers, in which the rapid and reversible photoisomerization reaction of azobenzene molecules can actuate mass transport phenomena typically parallel to the light polarization. The azopolymeric film is patterned by soft-imprinting as an array of micro-holes showing a well-defined isotropic round pores. Upon a linearly polarized illumination (365 nm, 150 W/cm2), we observe a deformation of the initial holes along the polarization direction, in such a way that the circular pores are transformed into long closed slits. A rotation of the polarization by 90° triggers a reconfiguration of the pristine round shape, with a good degree of control of the photo-induced pore reshaping. Due to the polarized-directionality of the photo-manipulation we demonstrate the possibility to tune the pristine morphology and properties along specific directions, providing a smart engineered platform with different reshaped micro-patterns. The light-induced contraction and expansion reshaping strategy of a porous polymeric structures shows exciting potential for a number of applications including microfluidics, lithography and tissue engineering. Tuning cells behavior in response to material manipulation cues is a promising goal in biology

10360-12, Session 3

Solution-processed organic bulk-heterojunctions in optical cavities for continuously tunable narrowband photodetection

Zheng Tang, Koen Vandewal, TU Dresden (Germany)

Spectroscopic photodetection, currently achieved through a combination of filters/prisms and broadband photodetectors, is the foundation of many modern technologies, such as environmental monitoring, biomedical materials analysis, imaging and surveillance. Low-cost arrays of filterless photodetectors with a continuously-tunable and selective spectral response would allow miniaturization of the used instrumentation.

Here, we use an organic bulk heterojunction in a resonant optical cavity device architecture to achieve solution-processed narrowband photodetectors. By making use of the weak CT absorption, and through optimizations on the molecular and the device level, we demonstrate a

spectral resolution down to 14 nm and a specific detectivity (over 10^13 Jones) comparable to commercial inorganic photodetectors lacking wavelength selectivity. Moreover, we achieve continuous wavelength tunability over a large part of the NIR spectral range, from 700 to 1700 nm. This excellent performance along with the advantages of organic materials, such as, flexibility, scalability, and easy-processibility makes this class of photodetectors highly demanded for future innovative areas of photodetection.

10360-13, Session 4

Simultaneous 10-fold brightness increase and emitted-light tunability in transparent ambipolar organic light-emitting transistor by integration with inorganic high-k photonic crystal

Stefano Toffanin, Istituto per lo Studio dei Materiali Nanostrutturati (Italy); Marco Natali, Istituto per lo Studio dei Materiali Nanostrutturati (Italy); Santiago D. Quiroga, Istituto per lo Studio dei Materiali Nanostrutturati (Italy); Luca Passoni, Luigino Criante, Istituto Italiano di Tecnologia (Italy); Emilia Benvenuti, Istituto per lo Studio dei Materiali Nanostrutturati (Italy); Gabriele Bolognini, Istituto per la Microelettronica e Microsistemi (Italy); Laura Favaretto, Manuela Melucci, Istituto per la Sintesi Organica e la Fotoreattività (Italy); Michele Muccini, Istituto per lo Studio dei Materiali Nanostrutturati (Italy); Francesco Scotognella, Politecnico di Milano (Italy); Fabio Di Fonzo, Istituto Italiano di Tecnologia (Italy)

In organic light-emitting transistors the structural properties such as the in-plane geometry and the lateral charge injection are the key elements which enable the monolithic integration of multiple electronic, optoelectronic and photonic functions within the same device [1]. In this contribution, we report on the realization of hybrid highly-integrated multifunctional optoelectronic organic device by introducing an inorganic high-capacitance photonic crystal [2] as a gate dielectric into a transparent single-layer ambipolar OLET. By engineering the photonic crystal multistack and band gap, we show that the integration of the inorganic photonic structure has a twofold effect on the optoelectronic performance of the device, i.e. (i) to modulate the spectral profile and outcoupling of the emitted light and (ii) to enhance the transistor source-drain current by a 25-fold factor. Consequently, the photonic-crystal integrated OLET showed an order-of-magnitude higher brightness with respect to the corresponding polymer-dielectric device, while presenting as-designed electroluminescence spectral and spatial distribution. Our results validate the efficacy of the proposed approach that is expected to unravel the technological potential for the realization of hybrid highly-integrated optoelectronic smart systems based on organic light-emitting transistors.

[1] M. Muccini el al, Laser & Photon. Rev., 6, 2, 258–275 (2012);

[2] L. Passoni et al. ACS Nano, 8, 12, 12167-12174 (2014).

10360-14, Session 4

A highly sensitive pyroresistive all-organic infrared bolometer

Raphael Pfattner, Victor Lebedev, Elena Laukhina, Institut de Ciència de Materials de Barcelona (Spain); Majid Ebrahim-Zadeh, Gerasimos Konstantatos, ICFO - Institut de Ciències Fotòniques (Spain); Vladimir Laukhin, Marta Mas-Torrent, Concepció Rovira, Jaume Veciana, Institut de Ciència de Materials de Barcelona (Spain)

The development of intelligent materials that can respond to the application of an external stimulus is of major interest for the fabrication of artificial sensing devices able to sense and transmit information about the physical, chemical and/or biological changes produced in our environment. In addition, if these materials can be deposited or integrated on flexible and transparent substrates and processed employing low-cost techniques their appeal is greatly increased. It is well known that single crystals of molecular conductors, consisting of ion-radical salts (IRSs), typically based on tetrathiafulvalene (TTF) derivatives, exhibit striking conducting properties. Such properties can be further tuned by choosing the nature of the IRSs enabling high sensitivity in sensors under applied pressure or temperature variations[1,2].

Bilayer (BL) films, composed of a thin-layer of pyroresistive submicrometer-sized crystals on top of a polymeric matrix can be used both as direct-contact thermometer and as passive infrared sensor (bolometer). These materials are capable of detecting, radiation of a wide range of wavelengths, from 532 to 6960 nm, very rapidly and reversibly, as well as recognizing distant objects[3].

This sensor platform enables the combination of high electrical performance of single crystals with the processing properties of polymers towards a simple, low-cost and highly sensitive sensor platform for applications in robotics, bio-medicine and human health care.

References

[1] E. Laukhina, et al. Advanced Materials, 21, 1-5, (2009).

[2] R. Pfattner, et al. Sensors & Transducers, Vol. 18, Special Issue, January, pp. 128-133 (2013).

[3] R. Pfattner, et al. Advanced Electronic Materials, 1, 1500090, (2015).

10360-15, Session 4

Organic crystals with long-period diffraction gratings engraved directly on their surfaces by focused ion beam lithography *(Invited Paper)*

Takeshi Yamao, Kyoto Institute of Technology (Japan)

Laser oscillations need a combination of gain media and optical cavities. We have used as the gain media crystals of thiophene/phenylene co-oligomers (TPCOs) that are composed of inline thiophene and benzene rings, and combined them with diffraction gratings acting as the optical cavities. We have fabricated these diffraction gratings on substrates as an external cavity.

Recently, we have directly engraved one-dimensional (1D) diffraction gratings on the surface of TPCO crystals by using focused ion beam (FIB) lithography. We regarded these diffraction gratings as a built-in cavity, and expected to be effective for producing narrowed emission peaks. However, the engraved parts of the crystals were quenched because the ion beam damaged the molecules. Engraving the diffraction gratings with a short period that is comparable in size to the beam spot caused weak emissions from the crystal.

In the present studies, we tried to keep wide unprocessed parts on the TPCO crystals with the FIB lithography. To this end, we fabricated diffraction gratings having a long period on the crystals. We chose one of the TPCOs that shows emission maxima at around 605 and 650 nm. We laminated vapor-phase-grown crystals on substrates. We engraved the equally-spaced 300 grooves with a period of 501 nm by precisely controlling FIB process conditions. We observed the emissions perpendicular to the grating grooves as well as parallel to the crystal surface under ultraviolet light illumination from a mercury lamp. We succeeded in observing a narrowed peak at 662 nm with the crystal with the 1D diffraction grating.

10360-16, Session 4

Low power optical switching by use of long-lived room-temperature triplet excitons *(Invited Paper)*

Toshiyuki Watanabe, Kenro Totani, Tokyo Univ. of Agriculture and Technology (Japan)

In general, all optical switching can be achieved under high-power pulsed laser irradiation. In this presentation, we will demonstrate low power all optical switching by use of metal free chromophore embedded into special polymer backbone. Persistent excited triplet state with a long lifetime (> 1 s) in special polymer can only be observed at a low temperature, because of the significant nonradiative deactivation pathway that occurs at room-temperature (RT). If polymer with persistent excited triplet state in air could be developed, they could potentially be utilized for optical modulation. Here, polymeric materials having long life time of excited triplet state are developed by minimizing the nonradiative deactivation pathway of triplet excitons. The nonradiative deactivation pathway is dependent on both nonradiative deactivation of chromophores and quenching by diffusional motion of the polymer. The rigidity and oxygen barrier properties of polynorbornene derivatives suppressed the quenching, and minimize nonradiative deactivation of chromophores. Accumulation by photosensitization of long-lived room-temperature triplet excitons with a large triplet–triplet absorption coefficient allows a nonlinear increase in absorbance also under low-power irradiation conditions that induce relatively large refractive index change in polymeric materials.

As a consequence, continuous exposure to weak light significantly decreases the transmittance of thin films fabricated with these compounds. Although, the response time of these systems are extremely slow, all optical modulation in these systems can be achieved under laser illumination in the intensity range between1 mW cm-2 to 100 mW cm-2.

10360-11, Session PMon

Flexible thin film polarizer with perylene-based reactive mesogens

Seok-in Lim, Ja-hyeon Koo, Seohee Park, Kwang-Un Jeong, Chonbuk National Univ. (Korea, Republic of)

Because the self-assembled lyotropic chromonic liquid crystal phase (LCLC) nanocolumns in LC phases can be uniaxially oriented in the macroscopic length scales, their applications have been dramatically magnified and expanded in various fields, such as dichroic light-polarizing materials, biosensing active materials, and electro-optic devices. However, LCLC water-based system have several disadvantages. To overcome this problem, we newly designed and synthesized a perylene-based reactive mesogen (PBRM) introducing the diacrylate functional groups at the both ends of perylene-diimide. Phase diagram of PBRM-H2O with different composition and temperature are observed by cross-polarized optical microscope (POM). The isotropic state (I) is observed under POM below 10 wt % at room temperature. Between 10 to 30 wt % at room temperature, it transforms to a typical columnar nematic (ColN) phase. Upon increasing the temperature of PBRM-H2O solutions between 10 and 30 wt %, its phase turns into the I phase by passing the biphase (ColN + I) state and it is the distinctive characteristic of LCLC compounds. After mechanically shearing the PBRM LCLC aqueous solution on the flexible polymer substrates, we successfully fabricated the patterned PBRM polarizer by etching the unpolymerized regions selectively blocked by a photomask during the photopolymerization process. The surface morphology was further investigated by optical microscopy, atomic force microscopy, and three-dimensional (3D) surface nanoprofiler. The fabrication of thin film polarizer on the flexible substrate may open the possibility of applications for the flexible devices. This work was supported by the BK21 Plus, the BRL 2015042417, Mid-Career Researcher Program (2016R1A2B2011041).

10360-17, Session PMon

To enhance OLED brightness by an extraction glass layer

Wei-Cheng Chien, Tatung Univ. (Taiwan); Chuang-Hung Chiu, Chunghwa Picture Tubes, Ltd. (Taiwan); Chao-Heng Chien, Yueh-Hao Chen, Tatung Univ. (Taiwan)

OLED has many advantages. For example, it is very thin, it can be self-luminous and has a fast reaction rate and so on. However, OLED has low life and optical loss and other issues. In organic light-emitting diodes (OLEDs), there are two major optical loss are related with glass layer. The two optical loss are waveguide mode and substrate mode, respectively. So the glass layer with the OLED light loss has a great impact.

In this research, an extraction layer is developed to enhance OLED brightness. The extraction layer could improve waveguide mode and substrate mode. A concave micro structure array was made on the glass substrate surface. A micro metal oxide particles was mixed with a transparent organic solution, which was filled into concave micro structure array. After baking process the transparent organic solution was cured. The cured glass layer was polished to get flat surface. Finally, the extraction layer was completed. The extraction glass layer was bonded on the OLED emitting surface to enhance luminance over 50 %.

10360-18, Session PMon

A remote-controllable light shutter by photochromic liquid crystalline amphiphile containing azobenzene

Ja-hyeon Koo, Seok-in Lim, Seohee Park, Kwang-Un Jeong, Chonbuk National Univ. (Korea, Republic of)

Systems showing photo-reversible phase transition have been considered to be promising in optical devices. By considering intramolecular conformations and intermolecular interactions, a photochromic liquid crystalline amphiphile containing a photo-isomerizable azobenzene (abbreviated as PLCA) is designed and synthesized for a remote-controllable light shutter. We investigated PLCA for demonstrating a remote-controllable light shutter by the photo-reversible isothermal phase transition induced by photo-isomerization of azobenzene. On the basis of diffraction results combined with thermal and microscopic ones, we confirmed the molecular packing structures of PLCA are transformed quickly upon alternating ultra-violet and visible lights. According to this, the direct photo-reversible phase transition between opaque crystalline solid and transparent isotropic liquid occur in 20 seconds at 25?. Therefore, PLCA films could be used as a remote-controllable light shutter. PLCA films were further investigated by transmittance test. The transmittance intensity of liquid state is about 40 times higher than that of solid state. The transmittance of solid state and liquid state is almost same under repeated and alternate irradiation of ultra-violet and visible lights. It is concluded that the relationship among the chemical structure, molecular packing structure and optical properties is very important to design the advanced photo-responsive materials for the practical applications in optical devices. This work was supported by the BK21 Plus, the BRL 2015042417, and Mid-Career Researcher Program (2016R1A2B2011041).

10360-19, Session PMon

Electronic structure at various substrates/ perovskite interface

Myung Joo Cha, Dong-A Univ. (Korea, Republic of)

The electronic properties of the interface formed between Au and organometallic triiodide perovskite (CH3NH3PbI3) were investigated using ultraviolet photoelectron spectroscopy (UPS) and X-ray photoemission spectroscopy (XPS). The CH3NH3PbI3 films were prepared onto the Au,

ITO and ITO / PEDOT:PSS surfaces by spin casting with various solution concentrations to control the film thickness and their morphology was examined using atomic force microscopy (AFM). The $CH_3NH_3PbI_3$ film exhibited a band gap of 1.70 eV and the maximum valence band edge of 6.31 eV. The best energy levels shift on Au downward by 0.26 eV with a perovskite coverage of 50 wt% upon it, indicating the band bending at the interface. The observed energy level shift means the presence of the interface dipole exists at the Au/$CH_3NH_3PbI_3$ interface. These findings are important for understanding how the perovskite materials function in electronic devices, and the design of new materials for use in perovskite-based optoelectronic devices.

10360-20, Session PMon

The study of polyelectrolyte-containing photoanisotropic compositions

Irakli Chaganava, Barbara N. Kilosanidze, George Kakauridze, Institute of Cybernetics (Georgia)

This paper presents the experiments on photoanisotropic organic media films based on the hydrophilic composition of the azo dye and polymer matrix with introduced different polyelectrolytes. In our previous works, we have repeatedly been observing that improved photoanisotropic properties of polarization-sensitive materials on the basis of azochromophores and polymers are essentially related to the integration of the material component molecules. As a part of an experiment to strengthen the cohesion of the matrix macromolecules, we individually added to the test compositions polyelectrolytes with a variation of quantity and with the different nature: polycation, polyanion and polyampholyte. The kinetic curves of the inducing photoanisotropy in the developing organic polarization-sensitive composition films are shown. According to our observations, the addition of the electrolyte to the composition of this type of materials contributes to an early manifestation of vector polyphotochromic effect at much lower exposures compared to the control samples without electrolytes, which in turn is a sign of improved photoanisotropic properties as this effect appears exclusively in high-performance polarization-sensitive materials.

10361-1, Session 1

Electro-optics of cholesterics with oblique helicoidal director *(Keynote Presentation)*

Oleg D. Lavrentovich, Olena Iadlovska, Kent State Univ. (United States); Sergij V. Shiyanovskii, Kent State Univ. (United States)

Liquid crystal materials with tendency to bend are capable of forming a unique type of a helicoidal structure in which the director is titled with respect to the helicoidal axis rather than orthogonal to it, as in regular cholecterics. The new state occurs in presence of an electric or magnetic field. It is called a cholesteric with oblique helicoidal structure or simply a twist-bend cholesteric, since both twist and bend deformations are characteristic of the ground state supported by the external field. Tilted configuration of the director and absence of density modulation makes the twist-bend cholesterics a unique material for various electro-optical applications. The presentation discusses electrically and magnetically tuned selective reflection of light as well as tunable lasing enabled by these materials. It is demonstrated that the electro-optical performance of the twist-bend cholesterics depends strongly on the type of anchoring conditions imposed by the boundaries of the cell. The work is supported by NSF grant DMR-1410378.

10361-2, Session 1

Self-assembly in chiral nematic LC *(Invited Paper)*

Julian S. Evans, Zhejiang Univ. (China); Nan Wang, Zhejiang Univ. (China); Sailing He, Zhejiang Univ. (China); Iam-Choon Khoo, The Pennsylvania State Univ. (United States)

Chiral nematic LC often contains a variety of defect lines which can cause aggregation of nanoparticles and other materials such as fluorescent dyes. While normal dyes suffer aggregation induced quenching a class of propeller-like dyes display aggregation induced emission (AIE), which makes them an ideal material for cholesteric lasers. Nanoparticle dispersion is necessary for switchability, while aggregation can be used as a tool to produce assembled structures. I will discuss strategies to promote or inhibit aggregation of various materials in chiral nematics.

10361-3, Session 1

Conditions for the formation of a uniformly lying helix structure induced by the electrohydrodynamic effect *(Invited Paper)*

Yu-Lin Nian, Po-Chang Wu, Wei Lee, National Chiao Tung Univ. (Taiwan)

The uniformly lying helix (ULH) state constitutes a class of cholesteric textures, showing unidirectionally aligned helices with their axes parallel to the plane of substrates. Unlike the generation of the well-known planar (P) and the focal conic (FC) states, a specific means is required to obtain a defect-free ULH structure in a cholesteric liquid crystal (CLC) cell. In this invited talk, we intend to discuss several key experimental conditions required to electrohydrodynamically induce a stable and well-aligned ULH state in CLC. Here the generation of the ULH structure stems from the low-frequency-electric-field-induced electrohydrodynamic (EHD) instability, attributable to the ionic movement. By means of dielectric spectroscopy and optical texture observation, clarified are the optimal frequency regime and three other significant parameters—field strength, ambient temperature and ion density and temperature—determining the formation of a well-structured ULH state.

10361-4, Session 1

Controlling optical phase in cholesteric and dye-doped liquid crystals *(Invited Paper)*

Stefania Residori, Aurélie Jullien, Umberto Bortolozzo, Institut Non Linéaire de Nice Sophia Antipolis (France); Jean-Pierre Huignard, Jphopto (France); Anis Alayet, Univ. of Tunis El Manar (Tunisia); Raouf Barboza, Tampere Univ. of Technology (Finland); Marcel G. Clerc, Univ. de Chile (Chile); Dong Wei, Beijing Genomics Institute (China)

We study the phase properties of dye-doped nematic and cholesteric liquid crystals. By using different mixtures and relative concentrations of chiral and dye dopants, we explore and characterize the phase shift as a function of the different relevant parameters : applied voltage, light-induced reorientation and optical phase shift, light polarization state. We study the dynamical response and degenerate two-wave mixing in both cw and pulsed regimes and we characterize the phase shift both in reflection and in transmission configuration. Then, by using cholesteric liquid crystals (CLC), which act as twisted Bragg reflectors, we demonstrate a novel type of geometric phase where the light-matter interaction is limited to the surface of reflection and the polarization state of the reflected light is unchanged. Even though planar CLC layers reflect circular polarized light with the same handedness as the helix without changing the polarization state, we demonstrate that the reflected light exhibits a geometric phase, ?(?)=??, where ? is the angle of the optical axis at the input face and ? the handedness of the polarization. The analytical predictions, derived from coupled wave theory in CLC, have been validated numerically and experimentally with planar CLC reflectors with piecewise uniform optical axis at the input interface. These findings open new routes to reflective geometric phase optical elements, with the possibility of designing asymmetric devices, as the front and the back reflective faces can have different optical axis patterns, as well as planar reflectors, refractive elements and gratings.

10361-5, Session 2

Optoelectronic applications of functional materials with aggregation-induced emissions *(Keynote Presentation)*

Ben Zhong Tang, Hong Kong Univ. of Science and Technology (Hong Kong, China)

Aggregation-induced emission (AIE) has drawn continuously growing attention due to its great potential in material science and biological techniques. The AIE effect is expected to conquer the notorious aggregation-caused quenching (ACQ) encountered by conventional luminescent materials, and thus realize the high-performance organic light-emitting diodes (OLEDs) without complicated doping method. Our recent studies have demonstrated that it is feasible. The solid-state luminescent materials created by melting AIEgens with conventional chromophores that suffer from ACQ problem at the molecular levels exhibit high photoluminescence efficiency up to unity, and function efficiently as light-emitting layers in non-doped OLEDs. Tunable electroluminescence colors from blue to red and excellent efficiencies approaching theoretical limit are attained by the devices. In addition, rational modifications on AIEgens with carrier-transporting functional groups can endow the luminescent materials with not only high solid-state emission efficiencies but also good hole- or electron-transporting abilities. The non-doped bilayer OLEDs fabricated by utilizing these multifunctional materials as light-emitting and hole-transporting (electron-transporting) simultaneously afford remarkably high efficiencies. These results clearly manifest the practical utility of the AIE effect in development of active materials for OLEDs.

10361-6, Session 2

Waveguiding with liquid crystal structures *(Invited Paper)*

Miha Ravnik, Univ. of Ljubljana (Slovenia) and Jo?ef Stefan Institute (Slovenia); Anja Bregar, Univ. of Ljubljana (Slovenia)

The birefringence of liquid crystal materials allows for the microscopic control of the-flow-of light. Here, we explore waveguiding by selected liquid crystal structures, including escaped nematic profiles and double-twist cylinders, by using numerical modelling. In order to realise stable waveguiding, these structures generally require negative liquid material birefringence, which is a notable materials' challenge. Methodologically, we use a combination of analytical approaches and Finite Difference Time Domain numerical calculations. Structure and properties of the waveguiding modes and their characteristics –especially polarization- are discussed. More broadly, this work is an attempt towards the development of soft matter photonics.

10361-7, Session 2

Functionalized liquid crystal polymers generate optical and polarization vortex beams *(Invited Paper)*

Moritsugu Sakamoto, Yuki Nakamoto, Tran Minh Tien, Kotaro Kawai, Kohei Noda, Tomoyuki Sasaki, Nagaoka Univ. of Technology (Japan); Nobuhiro Kawatsuki, Univ. of Hyogo (Japan); Hiroshi Ono, Nagaoka Univ. of Technology (Japan)

Optical and polarization vortex (OV and PV) beams, which have phase and polarization singularities, have much attracted attention from various research fields due to their unique physical properties. In general, for the study of vortex beams, a spatial light modulator is required to control the phase and polarization pattern of light waves between homogeneous into inhomogeneous, and advancement in the functions of them should be lead to evolution in photonics applications of vortex beams. In this presentation, we report our attempts for the vortex beam generation based on the photo-alignment technique of functionalized liquid crystal (LC) polymers.

We first report OV beam generation by using azo-dye-doped LC polymer (ADDLC). Due to the photo-isomerization of azobenzene molecules, LC director of ADDLC can be controlled by polarization illumination. Hence, when homogeneously aligned ADDCL is illuminated by the PV beam, three-dimensional helical LC alignment structure is formed since polarization states of light is continuously modulated in a propagation direction by an initial anisotropy. This LC structure shows OV generation properties. Phase singularity of generated OV can be temporally controlled by changing polarization pattern of illuminating PV. In addition, it has a potential for broadband OV generation with low dispersion.

Second, we also report PV beam generation by using photocrosslinkable polymer LC. Basic principle of this approach is based on the polarization holography. Proposed hologram spatially modulates not only polarization but also phase patterns of incident light, so that PV beam with helical phase is generated. Also, polarization, phase, and amplitude pattern of generated PV beam can be controlled by changing a polarization state of incident light.

10361-9, Session 2

Role of the order parameter, electric field, and geometric confinement on the dynamics of the photoinduced nematic-isotropic transition

Jayalakshmi Vallamkondu, National Institute of Technology, Warangal (India); Krishna Prasad Subbarao, Geetha G. Nair, Ctr. for Nano and Soft Matter Sciences (India); Gurumurthy Hegde, BMS College of Engineering (India)

The photoinduced phase transitions that we describe here are brought about by the photoisomerization driven shape transformation of photoactive molecules. The photoactive group is either covalently attached to the molecule or doped in a non-photoactive LC host material. The latter type, have the advantage of a wide choice of host materials that can be employed, the selection criterion being the required phase sequence, physical properties, etc. The guest photoactive material, present as a minority, adds the photoisomerization functionality to the system. Before presenting the results, the apparatus employed to investigate the photoinduced effects, is described in the thesis.

The thermal back relaxation of the photoinduced Z conformation of the photoactive molecule to its equilibrium E conformation is a matter of significant importance from the view point of basic as well as applied sciences. While the photochemical transition involving the change from E to Z form is fast, the TBR recovering the equilibrium phase is generally very slow ranging from few tens of minutes to as long as days although very fast (sub microsecond) time scales can be achieved with a pulsed laser source. In this chapter, we describe systematic studies of the influence of three different parameters, namely, (a) the nematic order parameter, (b) applied electric field and (c) geometric confinement, on the photochemical as well as TBR response times. The photoactive molecule serving as the guest dopant in all these studies is the 4-(4-ethoxyphenylazo)phenyl hexanoate (EPH). This compound also exhibits the nematic phase, a feature useful in obtaining homogeneous mixtures with host nematogenic compounds. The experiments were performed using an intensity-stabilized uv radiation with a peak wavelength of 365 nm and intensity of 1 mW/cm2.

10361-10, Session 3

Nano slippery interfaces in nematic gels -localization and lubrication of director motions *(Keynote Presentation)*

Jun Yamamoto, Kyoto Univ. (Japan); Isa Nishiyama, Dainippon Ink and Chemicals, Inc. (Japan)

We designed the fast switching & low driving voltage principle with nano slippery interfaces in nematic gels. Confinement effect by the gel network can accelerate the response time of nematic due the localization of director motion as similar way to the cholesteric blue phase. However, the anchoring of the director on the gel network induces the driving voltage. Slippery effect on the nano interface of the gel network can reduce the driving voltage due to the lubrication of the director motion. Since azo dye acrylates are co-polymerized with nematic gels (Azo-NGel), we can demonstrate the UV-switchable nano-slippery interface on the nematic gels.

Dynamic Light Scattering (DLS) provides us the information of the dynamics of director rotation. Dispersion relation of the pure 7CB-T15 mixture completely satisfies the prediction of hydrodynamic modes in the nematic. On the contrary, the relaxation frequency of the Azo-NGel keeps fast response in the low wave-number region due to the confinement effect.

Electro-Optic response (EO) of the Azo-Ngel without UV illumination shows the serious increase of the driving voltage compared to the pure 7CB-T15 mixture. When the Azo-Ngel is illuminated by UV-light Slippery interfaces can be created by the trans-cis isomerization of the Azo dye of the side-chain on the nano network of nematic gels. EO under UV illumination shows the drastic reduction of the driving voltage keeping the fast response time. We have also confirmed that the dispersion relation of the UV illuminated Azo-Ngel is almost the same as that of Azo-Ngel without UV illumination by the DLS measurement. Thus, the confinement effect for the nematic gels is still effective after the slippery interface is created by the UV illumination.

We success to demonstrates that the acceleration of the response time is compatible with reduction of the driving voltage by the localization and lubrication of director motions due to the design of the nano-slippery interfaces in the nematic gels.

10361-11, Session 3

Optically robust photoalignment materials for liquid crystal device applications in the near-UV region *(Invited Paper)*

Kenneth L. Marshall, Debra J. Saulnier, Tanya Z. Kosc, Univ. of Rochester (United States); Oleg Didovets, Optimax Systems, Inc. (United States); Shaw-Horng Chen, Univ. of Rochester (United States)

Photo-alignment technology is important for liquid crystal (LC) device applications where both high resistance to incident optical energy and spatially distributed alignment states over the device clear aperture are required. Coumarin-based photo-alignment materials developed at the Laboratory for Laser Energetics (LLE) possess near-IR laser damage resistance approaching that of fused silica and have been employed in the development and fabrication of a wide variety of LC high-peak-power laser optics. One example is a photo-patterned LC beam shaper, developed for use in LLE's four-beam, petawatt-peak-power OMEGA EP laser, that has demonstrated 1054-nm, 1 ns laser-damage thresholds approaching those of dielectric thin-film Brewster's angle polarizers (30 to 40 J/cm2). Achieving similar performance levels in LC devices for near-UV applications is challenging due to a scarcity of both UV-transparent LC materials and polymer alignment layers that can withstand repeated exposure to intense pulsed- or CW UV irradiation without degradation. Previously-employed alignment materials for UV-LC devices such as buffed polyvinyl alcohol (PVA) or Nylon 6/6 have limited usefulness; buffing embeds particulates and scratches into the alignment layer that reduce its UV damage thresholds to only a few J/cm2 and is incapable of producing highly resolved and spatially-distributed LC alignment states. In recent experiments, we have found that coumarin photoalignment materials are remarkably more resistant to damage from both incident 351 nm, 1 ns high-energy laser pulses [~11.42 J/cm2 (1-on-1) and ~15.70 J/cm2.(N-on-1)] and broad-band, continuous wave (CW) UV-visible light than would be expected due to their highly conjugated aromatic electronic structures. This finding opens a new chapter in the development of LC devices for UV applications in high-peak-power lasers (e.g. wave plates, polarization rotators, radial polarization converters, photo-patterned beam shapers) and other areas of optics and photonics where UV stability is important (e.g., space-based applications).

10361-12, Session 3

Template effect of twist structure liquid crystal and its photonic application *(Invited Paper)*

Jiangang Lu, Shanghai Jiao Tong Univ. (China)

The template effect of self-assembly twist structure liquid crystal (LC) is investigated. The anchoring energy of blue phase (BP) template containing different concentration of conventional polymer has been investigated that every different polymer system had its own threshold concentration to reconstruct the blue phase. The anchoring energy of the BP template increased with the polymer concentration resulting in the improvement of the reconstruction capacity. No matter with the same-handed or reverse-handed chiral materials refilling, there was a concentration range for the chiral dopant to reconstruct the blue phase by the polymer template. And the reconstruction range of the templates was extended as the polymer concentration of the template increased. It was demonstrated that the template anchoring energy has a threshold value to reassemble the double twist cylinder structure of BPLC by either refilling same-handed chiral materials or reverse-handed chiral materials which may help to improve the driving capacity of the polymer stabilized BPLC. Similar to the BPLC, a sphere phase template was proposed to improve the temperature range of sphere phase (SP) to more than 175?.By template processing, a wavelength tunable random lasing was demonstrated with dye doped SPLC. With different polymer concentrations, the reconstructed sphere phase random lasing may achieve more than 40nm wavelength shifting by electrical field modulation. And the threshold energy of SPLC random laser can be lowered to about 30% of that from the chiral nematic phase LC.

10361-14, Session 3

Fabrication of nearly-millimeter thick well aligned cholesteric liquid crystals for ultrafast pulsed laser modulation

Chun-Wei Chen, Iam-Choon Khoo, The Pennsylvania State Univ. (United States); Tsung-Hsien Lin, National Sun Yat-Sen Univ. (Taiwan)

We describe a technique that enables fabrication of nearly mm-thick stable well-aligned cholesteric liquid crystals (CLC) that possess very small scattering loss, large operating temperature range [~ 100 degrees Centigrade] and well-defined 1-D photonic crystal properties. Owing to the enhanced optical nonlinearity and dispersion near the photonic band-edges that result in velocity slow down, pulse chirping and nonlinear phase shifts, theory and experiments have been have shown that these CLC's can be used for femtoseconds -picoseconds laser pulse modulation [compression, stretching, variable pulse delay] purposes in compact photonic systems.

10361-24, Session 3

Smectic layer origami based on preprogrammed photoalignment *(Invited Paper)*

Yan-Qing Lu, Wei Hu, Nanjing Univ. (China)

Mesoscopic hierarchical superstructures bridge the micro and macro worlds and play vital roles in natural materials. To mimic hierarchical organization in nature, one promising strategy is the convergence of top-down microfabrication and bottom-up self-assembly. Much efforts have been devoted to this field, but till now, the precise realization and rational control of large-area perfect hierarchical superstructures is still challenging. On the other hand, Smectic liquid crystals (SLCs) are formed by flexible molecular layers of constant thickness. If the nanometer-thin smectic layers can be manipulated in an origami manner, a Japanese art that constructs various 3D objects via folding pieces of papers, brand new hierarchical superstructures possessing exceptional features then could be realized. In this work, the smectic layer origami is accomplished via preprogrammed photoalignment. The principle is rooted in the anisotropy of molecular interactions at interfaces, which makes the preset patterned alignment favoring a certain layer bending of adjacent SLCs, and subsequently dominating the configuration of entire family of smectic layers. Thanks to the excellent flexibility of photoaligning, the unit geometry (shape, size and orientation) as well as the clustering characteristic (lattice symmetry) of fragmented TFCDs can be rationally designed and freely manipulated over square centimeters. The obtained fragmented toric superstructures break the rotational symmetry while maintain the radially gradient director field, enabling metasurface-like direction-determined-diffraction. We believe this work is an important step toward extending the fundamental understanding of self-assembled soft materials and enhancing the construction of possible hierarchical superstructures. It may inspire extra possibilities in advanced functional materials and fantastic photonic applications.

10361-44, Session 3

Hidden LC/polymer gratings *(Invited Paper)*

Timothy J. Bunning, Air Force Research Lab. (United States); Luciano De Sio, Nelson V. Tabirian, BEAM Engineering For Advanced Measurements Co. (United States)

No Abstract Available

10361-15, Session 4

Single crystal blue-phase photonic crystal *(Keynote Presentation)*

Tsung-Hsien Lin, National Sun Yat-Sen Univ. (Taiwan); Iam-Choon Khoo, The Pennsylvania State Univ. (United States); Timothy J. Bunning, Air Force Research Lab. (United States); Chun-Wei Chen, The Pennsylvania State Univ. (United States)

Photonic crystals are one of the most attractive optical materials, in which the inherent periodic undulations of refractive indices give rise to novel reflection, transmission and emission characteristics. Blue Phase Liquid Crystal (BPLC), is introduced because of its self-assembled 3D photonic crystal make-up and controllable lattice spacing. Besides, the uniqueness of BP lies in their high susceptibility to external stimuli, opening up a new door of adaptive photonics.

Although BPLCs have been widely studied, the conventional approach to crystal growth of BP, normally results in polycrystalline texture with crystal size ranging from submicron (in diameter) to ~ 300 ?m at most. This is because, in such an approach, nuclei form at arbitrary positions in the isotropic melt and grow in almost all directions, eventually terminating when meeting the others. To break the limit of the size of a BP single crystal, we have developed new ways of growing single-crystal BPLC of macroscopic sizes by introducing spatial variations of temperature into crystal growth. Fabrication procedure, characterization and applications of millimeter-sized BP monocrystals will be reported at the meeting.

10361-16, Session 4

Ultrafast nonlinear photonic in cholesteric liquid crystals *(Invited Paper)*

Yikun Liu, Jianying Zhou, Sun Yat-Sen Univ. (China); Tsung-Hsien Lin, National Sun Yat-Sen Univ. (Taiwan); Iam-Choon Khoo, The Pennsylvania State Univ. (United States)

Cholesteric liquid crystals (CLC) has the advantage of large nonlinearity and fast response. This brings great convenience to its applications in ultrafast nonlinear photonic. Here, several kinds of nonlinear phenomenon and applications are reported, such as optical soliton, modulation instability, optical diode effect and pulse compression of cascade CLC samples.

10361-17, Session 4

Liquid-crystalline simple cubic blue phase stabilized via polymer networks *(Invited Paper)*

Suk-Won Choi, Kyung Hee Univ. (Korea, Republic of)

A polymer-stabilized siple cubic blue phase (BPII) possessing a wide temperature range has been scarcely reported. Here, we report a polymer-stabilized BPII over a temperature range of 50 °C including room temperature. The fabricated polymer-stabilized BPII is confirmed via polarized optical microscopy, Bragg reflection, and Kossel diagram observations. Furthermore, we demonstrate reflective BP liquid-crystal devices utilizing the reflectance–voltage performance as a potential application of the polymer-stabilized BPII. Our work demonstrates the possibility of practical application of the polymer-stabilized BPII to photonic crystals.

10361-18, Session 4

Investigation of polarization-independent optical phases in polymer-dispersed liquid crystals originating from Kerr effect and molecular orientations *(Invited Paper)*

Yi-Hsin Lin, Chia-Ming Chang, Jing Yi Wang, Po-Ju Chen, National Chiao Tung Univ. (Taiwan); Eunjeong Shin, Ramesh Manda, Seung Hee Lee, Chonbuk National Univ. (Korea, Republic of)

The anisotropic properties of nematic liquid crystals result in polarization dependency which leads to requirement of at least a polarizer in liquid crystal photonic devices; however, polarizer reduces optical efficiency. We have been developed many polarization-independent liquid crystal (LC) phase modulators. In 2015, we found that the optical phases in nano-PDLC(size~250 nm) come from LC molecular orientations and Kerr effect-induced birefringence. However, optical phase from Kerr effect is much smaller than the one from LC molecular orientations. As a result, in this paper, we would like to continue investigating that in nano-PDLC, is it possible to have optical phase from Kerr effect is comparable to the optical phase from LC molecular orientation or even larger? The experimental results show that the polarization-independent optical phases in nano-PDLC come from both of LC molecular orientation and Kerr effect as the droplet size is around 200 nm. At a small applied voltage, Kerr phase dominates. With an increase of voltages, optical phase from LC molecular orientation dominates. For droplet size larger than 350nm, the optical phases come from LC orientation, without any Kerr phase. In our study and optical analysis, we conclude that Kerr phase depends on the droplet size in nano-PDLC. Kerr phase and orientational phase indeed can be comparable. Experimental results also indicates that Kerr phase occurs as applied voltage (V) is less than the threshold voltage(Vth). At V> Vth. orientational phase increases and Kerr phase reduced.

10361-19, Session 4

Azo-blue phase liquid crystals for high efficiency holographic Bragg grating with optically prolonged memory

Tsung-Jui Ho, Chun-Wei Chen, Iam-Choon Khoo, The Pennsylvania State Univ. (United States)

We present the results of recent studies of holographic Bragg grating formation and relaxation dynamics in mm-thick azo-dye doped Blue phase liquid crystals (a-BPLC). Unlike their nematic counterparts which generally yield low efficiency in this regime due to strong nonlocal anchoring forces, we have observed [Sci. Rep. 6, 36148; doi: 10.1038/srep36148 (2016)] that these mm-thick a-BPLC ware capable of yielding polarization-independent grating diffraction efficiency as high as 50% for grating constant as small as ~ 1 micron. Furthermore, we have discovered a simple all-optical means of prolonging the lifetime of the written grating; by keeping the reference beam on when the other beam (input signal) is turned off, the lifetime of the written grating/hologram can be prolonged from its natural relaxation time of a few seconds to several minutes. The underlying mechanism is attributed to local and nonlocal BPLC lattice distortions following laser induced trans-cis isomorphism of the azo dopant molecules. Our studies show that these 'performance' characteristics can be optimized with appropriate choice of the a-BPLC constituent materials, sample thickness, azo-dye concentration, and many other material and optical parameter, thus making a-BPLC a highly promising candidate material for updateable holographic recording and display application.

10361-13, Session 5

Magneto-optical properties of liquid crystal dimers *(Invited Paper)*

Seyyed M. Salili, Matthew Murachver, Samuel N. Sprunt, James T. Gleeson, Antal I. Jákli, Kent State Univ. (United States)

We studied magneto-optical properties of various liquid crystal dimers with both odd and even number carbon atoms in their flexible linkages. Dimers with even and odd numbered carbons in their linkages have I-N-Cr and I – N –Ntb –Cr or I – N –Ntb –SmCmod-Cr phase sequences, respectively.

Measurements of the Iso-N-Ntb transition temperature as a function of applied magnetic field found to show an unprecedented magnetic field enhancement of the nematic order. At 25T magnetic induction the transition temperature is shifted by up to 15ºC for the odd-dimers1 and up to 8ºC for the even-dimers. The field induced birefringence is much weaker for the even-dimers and show anomalous temperature dependences. The shift of the N-Ntb transition for the odd-dimers can be both positive and negative depending on the material. The effect of the chiral dopants also had been studied and was found to enhance the field induced transition shift. Possible microscopic models will be considered to consistently explain the experimental observations.

Acknowledgement: This work was financially supported by NSF DMR No. 1307674 and utilized the facilities of the NHMFL, which is supported by NSF DMR-0084173, the State of Florida, and the US Department of Energy. We are grateful for M. G. Tamba, G. Mehl, C. Imrie and O. Parri for providing us the materials.

References:

[1] Salili, S. M., Tamba, M.-G., Sprunt, S. N., Welch, C., Mehl, G. H., Jákli, A.., Gleeson, J. T., “Anomalous Increase in Nematic-Isotropic Transition Temperature in Dimer Molecules Induced by Magnetic Field,” Phys. Rev. Lett. 116, 217801 (2016).

10361-20, Session 5

High quality alignment of the helical nanofilament phase by micro-confinement in polymer channels *(Keynote Presentation)*

David M. Walba, Eric Carlson, Lee M. Foley, Edward Guzman, Eva D. Korblova, Rayshan Visvanathan, Univ. of Colorado Boulder (United States); SeongHo Ryu, Min-Jun Gim, Dong Ki Yoon, KAIST (Korea, Republic of); Noel A. Clark, Univ. of Colorado Boulder (United States)

The helical nanofilament (HNF) phase is one of a small family of “low temperature dark conglomerate” phases seen in bent-core mesogens, exhibiting low birefringence and very high optical rotatory power in the visible. The HNF phase is unique, however, per our hypothesis that the phase is composed of twisted nanocrystals, approximately 30 nm in diameter, and up 100s of μm in length.

Several research groups have reported on somewhat successful efforts to align the HNF phase. To our knowledge, however, none of the known methods for HNF alignment has led to alignment quality approaching that achievable for more conventional molecular LC phases.

Here we report unprecedentedly high quality alignment of the HNF phase of NOBOW (P-9-O-PIMB) by simply allowing the isotropic liquid to cool to room temperature in microchannels of polydimethylsiloxane (PDMS) on glass. Removal of the PDMS “mold” leaves well-defined and indefinitely stable stripes of HNFs showing excellent extinction by polarized optical microscopy (crossed polarizer and analyzer) with the polarizer parallel or perpendicular to the stripes, and strong visible light transmission with the polarizer at 45 deg. 2-D X-ray scattering on these samples corroborates the proposed structure, where the HNFs run parallel to the microchannels, with the twisted smectic layers perpendicular to the HNF long axis (this requires negative Gaussan curvature of the layers).

This method is a form of lithography, and should provide an approach for obtaining well-aligned HNF “stripes” of arbitrary shape in one dimension (parallel to the HNF long axis).

10361-21, Session 5

Shape and size effects in chirality transfer from chiral-ligand-capped nanomaterials to nematic liquid crystals *(Invited Paper)*

Torsten Hegmann, Lin Li, Leah E. Bergquist, Ahlam Nemati, Kent State Univ. (United States)

To probe how chirality propagates from a chiral nanoscale surface, we studied gold nanoparticles functionalized with chiral ligands. To do so, we synthesized series of chiral ligand-capped gold nanoparticles (Au NPs) differing in size, shape, curvature, and ligand density that allowed us to tune the chirality transfer from these nanoscale solid surfaces to a bulk nematic liquid crystal medium.[1] Ultimately, we tested how far the chirality from a NP surface reaches into the bulk N-LC material.[2] The helical pitch values of the induced N*-LC phase were determined, and the helical twisting power (HTP) of the chiral Au NPs and nanorods calculated to elucidate the chirality transfer efficiency of the chiral ligand-capped Au NPs. Remarkably, the HTP increases with increasing diameter for the smaller nanoclusters (~1 to 2 nm in core diameter) and increase for larger nanoparticles (~5 nm in core diameter), i.e. the efficiency of the chirality transfer of the chiral ligands bound to the NP surface is size dependent. However, in comparison to the free ligands, per chiral molecule, all tested Au NPs induce helical distortions in a 10- to 50-times larger number of N-LC host molecules surrounding each NP, indicating a significantly enhanced chiral correlation length, which appears to be the largest for chiral ligand-capped gold nanorods as expected from their largest anisotropy factors.[3] We propose that both the helicity and the chirality transfer efficiency of chiral ligands can be efficiently and elegantly controlled at NP surfaces by adjusting the NP size, shape, and curvature as well as the number and density of the chiral ligands to ultimately measure and tune the chiral correlation length.

[1] T. Mori, A. Sharma, T. Hegmann, ACS Nano 2016, 10, 1552-1564.

[2] A. Sharma, T. Mori, H.-C. Lee, M. Worden, E. Bidwell, T. Hegmann, ACS Nano 2014, 8, 11966-11976.

[3] A. Nemati, T. Hegmann, tbs.

10361-22, Session 5

Light-melt adhesive based on a columnar liquid crystal *(Invited Paper)*

Shohei Saito, Kyoto Univ. (Japan)

Liquid crystal (LC) provides a suitable platform to exploit structural motions of molecules in a condensed phase. Amplification of the structural changes enables a variety of technologies not only in LC displays but also in other applications. Until very recently, however, a practical use of LCs for removable adhesives has not been explored, although a spontaneous disorganization of LC materials can be easily triggered by light-induced isomerization of photoactive components. The difficulty of such application derives from the requirements for simultaneous implementation of the following essential requisites: (i) adequate strength for a temporary bond (more than 1 MPa) even under heating conditions, (ii) significant reduction of the bonding strengths by light irradiation, and (iii) quick photoresponse for the separation of bonded materials. Here we present a liquid crystal (LC) material that satisfies all of the above-mentioned requisites for the light-melt adhesives, namely, (i) a shear strength over 1 MPa up to 110 °C for bonding glass plates, (ii) an 85% reduction of the strength by ultraviolet (UV) irradiation, and (iii) an instant photomelting of the LC film in a few seconds. Moreover, this material is reusable as an adhesive, and the transformation between the LC and melted phases is associated with an informative color change in fluorescence. We envision that composite materials with the light-melt function will further improve the performance in manufacturing processes, which will accelerate the on-demand photoseparation technology complementary to the other switchable adhesion approaches.

10361-23, Session 5

Structure modifications directed towards obtaining SmAPf phases with broad temperature ranges *(Invited Paper)*

Eva D. Korblova, Edward Guzman, Edgardo Garcia, Joseph E. Maclennan, Matthew A. Glaser, Ren-Fan Shao, Rayshan Visvanathan, Noel A. Clark, David M. Walba, Univ. of Colorado Boulder (United States)

The first successful design of SmAPF mesogens came from modification of structural elements of known SmAPA mesogens. Specifically, bent-core smectics with orthogonal director orientation and ferroelectric interlayer order were achieved by suppression of out of layer fluctuations, leading to anticlinic layer interfaces. Thus, placement of a tricarbosilane moiety at the end of the single tail of a known SmAPA structure produced the SmAPF mesogen known as W586. [1] In typical LC cells, these materials exhibit electrooptic phase only modulation with optical latching. [2]

In order to optimize the properties of SmAPF materials for a wide range of exciting applications, a search for new mesogens providing industrial grade phase temperature ranges and improved phase modulation depth is in progress.

Here, we present the design, synthesis, and characterization of new materials with fluorinated tails. The original SmAPF mesogens possess one long tricarbosilane-terminated alkyl tail, and one "short tail" (a cyano group or trifluoromethyl group). Synthesis and properties of new structures showing the SmAPF phase, where the tricarbosilane-terminated tale of the classic system is replaced by fluorinated oligoethyleneglycols or oligoethyleneglycol esters, will be discussed.

[1] Reddy, R. A.; Zhu, C.; Shao, R; Korblova, E.; Gong, T.; Shen, Y.; Garcia, E.; Glazer, M. A.; Maclennan, J. E.; Walba, D. M.; Clark, N. A., Science 332, 72-77(2011)

[2] United States Patent: Walba US 9,187,500 B2, Nov. 17, 2015

10361-25, Session 6

Photoalignment control of dye-doped and dye-free liquid crystal systems *(Keynote Presentation)*

Atsushi Shishido, Tokyo Institute of Technology (Japan)

Photoalignment control of liquid crystals has been developed for optical, photonic, mechanical and display applications. Photophysical molecular alignment based on nonlinear optical effect was reported first, and photochemical control due to axis-selective photoresponse of anisotropic dye molecules was developed. The photophysical process was enhanced in dye-doped liquid crystals around the same time. In this study, recent progress on photochemical and photophysical molecular alignment control in dye-doped liquid crystals are presented. Dye-free liquid crystal systems can be also controlled by masked photopolymerization.

10361-26, Session 6

Intrinsic and photo-induced optical properties of photoaligning azo-based materials coupled with liquid crystal systems *(Invited Paper)*

Nina Podoliak, Elena Mavrona, Univ. of Southampton (United Kingdom); Sakellaris Mailis, Optoelectronics Research Ctr., Univ. of Southampton (United Kingdom); Jordan R. E. Gill, Giampaolo D'Alessandro, Vasilis Apostolopoulos, Univ. of Southampton (United Kingdom); Nelson V. Tabirian, BEAM Engineering For Advanced Measurements Co. (United States); Malgosia Kaczmarek, Univ. of Southampton (United Kingdom)

Recent developments in photoalignment of liquid crystals (LCs) brought to the market photoreversible materials such as azobenzene-based PAAD complex dyes [1], which quickly found broad photonics applications for constructing diffraction elements and waveplates [2,3]. Despite extensive investigations of photoaligned LC systems, there is little information on the optical properties such thin PAAD layers.

Here we report an experimental investigation of optical properties, such as refractive indices and absorption coefficients for different PAAD materials, namely PAAD-22D, 22E and 22N. Photoinduced phase gratings were recorded in 20-50 nm thick PAAD layers with no evidence of a corresponding surface relief, which is a typical feature in thicker azobenzene films. Therefore, the formation of the gratings is attributed to optically induced birefringence. The investigated materials exhibited different values of birefringence, reaching 0.025, and significantly different temporal response to laser irradiation. Moreover, the diffracted power was observed to be very sensitive to the polarisation of the probe beam with respect to that of the pump beam.

We also studied photoinduced diffraction in PAAD-LC systems, where we observed the formation of a stable and strong diffraction pattern. The gratings can be rewritten by illumination with another light pattern or switched off by reorienting liquid crystals with a bias voltage. A diffraction efficiency of more than 5% was measured in a cell containing PAAD-22D in combination with 8?m thick LC-E7 layer. Finally, we compare the dynamics of light induced response in the PAAD layers and PAAD-LC cells and investigate their respective memory effects.

[1] Beam Engineering for Advanced Measurements Company, Winter Park, FL 32789.

[2] Vernon, J. P., et al., Opt. Express 21, 1645 (2013).

[3] Nersisyan, S. R., et al. Opt. Express 21, 8205 (2013).

10361-27, Session 6

Computational chemistry modeling and design of photoswitchable alignment materials for optically addressable liquid crystal devices II: Transition state modeling in azobenzene and spiropyran oligomers

Kenneth L. Marshall, Unni Kurumbail, Akif Hosein, Univ. of Rochester (United States)

Computational chemistry tools such as density functional theory (DFT) have seen increasing application in the design and development of new organic optical materials, organic light emitting diodes (OLED) and liquid crystals. In previous work, we employed DFT to model the trans–cis isomerization state energies in a series of methacrylate and acrylamide photoswitchable polymer alignment materials functionalized with azobenzene pendants connected through a flexible alkyl chain (tether). Such photoswitchable alignment materials are of interest for LC devices for beam shaping due to their remarkable 1054 nm, 1 ns laser damage thresholds (28 to 67 J/cm2) and their ability to support spatially-varying write-erase capability. These modeling efforts were confined to a small representative section of the photoaligment polymer (an oligomer) composed of one tethered chromophore and four repeat backbone segments to reduce the large amounts of computational resources and time that would be required to accurately model a complete polymer system. Twenty-two different terminal functional groups were evaluated computationally to determine their individual effects on the trans and cis isomerization-state energies of the methacrylate and acryamide oligomers when used as substituents on azobenzene cores linked through a four-carbon tether to methacrylate and acrylamide backbones. The contribution of the alkyl tether to the isomerization-state energies of the methacrylate and acrylamide oligomers was also investigated computationally. This work extends the previous study by using DFT to evaluate the effect of molecular structure and tether length on the transition state energy barrier separating the pendant's isomeric switching states, which can have a large effect on bistability, write-erase fatigue, and switching energy requirements. Both oligomers containing azobenzene and spiropyran photoswitchable pendants were modeled in this study.

10361-28, Session 6

Liquid crystal elastomers presenting a homochiral building block

Elda Hegmann, Liquid Crystal Institute, Kent State Univ. (United States); Marianne Prévôt, Kent State Univ. (United States)

We have previously synthesized SmA LCEs using D,L-lactide as one of the building blocks. This resulted in a biodegradable and biodegradable scaffold for supporting the attachment and growth of cells. Here we present the use of enantiomically pure L-lactide, which is found naturally abundant in the human body, as a replacement to the previously used racemic D,L-lactide to affect its chirality. These racemic new biocompatible liquid crystal elastomers (LCE) showed enhanced mechanical properties promoting superior, stimuli-responsive surface properties for cell attachment and growth. LCE properties can also be tuned to vary in hydrophobicity, tensile strength, surface properties, biodegradation rate, cell adhesion, and response to external stimuli. We will discuss how this chirality change can affect the morphology as well as the mesomorphic behavior, and could potentially affect cell-elastomer interactions.

10361-29, Session 6

Relative permittivity imaging based on a liquid crystal sensor

Amir Aizen, Ibrahim Abdulhalim, Ben-Gurion Univ. of the Negev (Israel)

A new method and system for sensing and imaging objects based on sensing their relative permittivity values at low frequencies of a few kHz is presented. To the best of our knowledge, there is no system that can provide an image of an object's relative permittivity values at frequencies below the microwaves regime. The system's sensor is a parallel plate capacitor made from three main layers: a liquid crystal cell, a buffer layer and a cavity into which the imaged samples are inserted. When applying AC voltage of a few kHz on the sensor, the relative permittivity values of the samples will cause a unique voltage drop pattern on the liquid crystal cell. The voltages will create a retardation pattern in the liquid crystal cell that is then read by a light beam and being imaged. An image of the relative permittivity values of the samples can then be calculated using a few images taken at different voltages.

10361-30, Session 7

High power 4G optics *(Keynote Presentation)*

Nelson V. Tabiryan, David E. Roberts, Sergiy Kaim, Svetlana V. Serak, Sarik Nersisyan, Haiqing Xianyu, BEAM Engineering For Advanced Measurements Co. (United States); Timothy J. Bunning, Air Force Research Lab. (United States); Diane M. Steeves, Brian R. Kimball, U.S. Army Natick Soldier Research, Development and Engineering Ctr. (United States)

The optical power of diffractive waveplate structures is limited not as much by fabrication technology issues as by the fundamental features of light propagation in complex anisotropic structures. The infinitely thin two-dimensional film approximation does not apply, and the efficiency of 4G lenses, prisms, etc., is reduced for geometries corresponding to sharp focusing lenses and large diffraction angles. Due to thin-film nature, these films can be combined to reduce effective focal length, increase effective diffraction angle, topological charge, etc. Along with this, we will discuss the opportunity of increasing optical power of 4G lenses, prisms, etc. without compromising efficiency.

10361-31, Session 7

The Nematicon: A highly nonlocal regime wave singularity with ultra-sharp profile and random walk trajectory *(Invited Paper)*

Hélène Louis, Lab. de Physics des Laser, Atomes, et Molécules (France); Mustapha Tlidi, Univ. Libre de Bruxelles (Belgium); Eric Louvergneaux, Univ. des Sciences et Technologies de Lille (France)

We investigate light propagation within liquid crystals with focusing-like reorientational nonlinearity. This medium is "an excellent playground" for the study of spatiotemporal dynamics [1] such as localized states or modulational instability. Applications such as all optical routing is also a subject of intense research.

We focus here on the highly nonlocal regime (transverse beam extension "smaller" than the transverse nonlocality length). This regime is well known to depict solitary-like wave state [2]. We show experimentally that this state (known as "nematicon") has a "cusp"-like profile together with a trajectory that continuously wanders erratically with time [4]. In addition, we demonstrate that the highly nonlocal regime avoid wave collapse [3].

[1] A. Alberucci, G. Assanto, J. M. L. MacNeil, and N. F. Smyth, "Nematic liquid crystals: An excellent playground for nonlocal nonlinear light localization in soft matter", J. Nonlinear Opt. Phys. Mater. 23, 1450046 (2014).

[2] G. Assanto, "Nematicons Spatial Optical Solitons in Nematic Liquid Crystals", John Wiley & sons, INC., Publication (2013).

[3] H. Louis, M. TLidi, and E. Louvergneaux, " Experimental evidence of dynamical propagation for solitary waves in ultra slow stochastic non-local Kerr medium", Opt. Express 24, 16206 (2016).

[4] O. Bang, W. Krolikowski, J. Wyller, and J. Rasmussen, "Collapse arrest and soliton stabilization in nonlocal nonlinear media", Phys. Rev. E 66, 46619 (2002).

10361-32, Session 7

Nonlinear optical measurement of the twist elastic constant in thermotropic and lyotropic chiral nematics *(Invited Paper)*

Liana Lucchetti, Univ. Politecnica delle Marche (Italy); Tommaso Fraccia, Univ. degli Studi di Milano (Italy) and Univ. Telematica San Raffaele (Italy); Fabrizio Ciciulla, Univ. Politecnica delle Marche (Italy); Tommaso Bellini, Univ. degli Studi di Milano (Italy)

We show that by adopting a simple geometry we can readily extract the twist coefficient for known thermotropic N*, obtaining the value expected from literature. In the geometry here adopted the optical field induces a pure twist deformation, enabling a direct comparison between optical and elastic coupling. Furthermore, due to the planar geometry in which chiral nematic planes are stacked parallel to the cell walls, the characteristic length entering the energy balance is not the cell thickness but the pitch periodicity of the N* phase. This successful test opens the possibility to extend this strategy to lyotropic N* phases, in which coupling with external fields is typically more difficult to exploit. In particular, we focused on the N* phase of oligomeric DNA.

While the thermodynamics of DNA LC has been extensively characterized and modeled, no data is so far available on their elastic properties. This lack of information is the result of a combination of difficulties: DNA LC are

intrinsically chiral, making it difficult to use typical light scattering based analysis; no strategy has emerged yet to control the surface alignment of DNA LC phases; coupling with electric fields is weak and disturbed by the large density of intrinsic counterions present in the solution. The strategy that we describe here bypasses these limitations by using an optical field and by exploiting a geometry in which surface alignment is not crucial.

10361-33, Session 7

Self-induced structured light transformations using liquid crystal topological defects *(Invited Paper)*

Nina Kravets, Etienne Brasselet, Univ. Bordeaux 1 (France)

We discuss the use of self-engineered liquid crystals topological defects as soft spin-orbit photonic tools for that may find application in various fields such as opto-mechanics, optical metrology, information coding, and optical imaging. Here we will present recent results based on the use of a liquid crystal light valve that is known to enable the light-assisted electrical generation of localized umbilic defects acting as vectorial phase masks. Several examples emphasizing the self-induced interplay between structured light and structured matter will be presented.

10361-34, Session 8

Responsive optical filters prepared from polymer stabilized cholesteric liquid crystals *(Keynote Presentation)*

Timothy J. White, Kyung Min Lee, Vincent P. Tondiglia, Air Force Research Lab. (United States)

This presentation will summarize the opportunities to reconfigure the selective reflection inherent to the cholesteric liquid crystal phase. Adjustments to the materials or preparation conditions can enable either red- or blue-shifting reflection tuning, asymmetric or symmetric bandwidth broadening, dynamic scattering, or combinations thereof.

10361-35, Session 8

Liquid crystal 3D periodic gratings based on photo-alignment *(Invited Paper)*

Kristiaan Neyts, Inge Nys, Varsenik Nersesyan, Jeroen Beeckman, Univ. Gent (Belgium)

By illuminating a photo-alignment layer with two interfering UV laser beams with opposite circular polarization, a periodic alignment pattern is obtained for nematic liquid crystal. In a liquid crystal cell two substrates are used with periodic photo-alignment, with the periodicities perpendicular to each other. After filling with nematic liquid crystal the director obtains a 3D pattern with period twice that of the photo-alignment. The resulting 3D structure depends on the cell thickness (between 3 and 20 ?m) and the periodicity of the photo-alignment (also between 3 and 20 ?m). The director pattern can be estimated by performing numerical simulation with a Q-tensor method. The simulation results can be verified by polarization optical microscopy or by observing the diffraction properties of the structure. For a long range periodicity combined with a small period, the light is efficiently distributed over a small number of diffraction orders. The director pattern can be reoriented by applying a potential difference between the two substrate electrodes. Optical and electrical steering is investigated for devices with different dimensions.

10361-36, Session 8

Intra-ocular accommodative implant using liquid crystal lenses *(Invited Paper)*

Tigran Galstian, Ctr. d'Optique, Photonique et Laser (Canada)

Loss of distance accommodation is a common disease and many approaches have been considered to solve this problem. Some of them are based on the use of mechanical force. However, we have developed an alternative approach using motion-free focusing based on liquid crystal lenses. Electrical distance triggering mechanism was also developed. The optical, energy and size characteristics will e presented.

10361-37, Session 8

Confined photovoltaic fields in a photo-responsive liquid crystal test cell *(Invited Paper)*

Atefeh Habibpourmoghadam, Lin Jiao, Faissal Omairat, Univ. Paderborn (Germany); Dean R. Evans, Air Force Research Lab. (United States); Liana Lucchetti, Univ. Politecnica delle Marche (Italy); Viktor Y. Reshetnyak, Taras Shevchenko National Univ. of Kyiv (United Arab Emirates); Alexander Lorenz, Univ. Paderborn (Germany)

Exciting experimental results on the response properties of hybridized photo responsive liquid crystal test cells are reported, where iron doped lithium niobate substrates were used to photo generate electric fields and indium tin oxide coated cover glasses were used to confine these photo generated fields in a liquid crystal layer.

Samples were investigated in a modified inverted optical polarizing microscope with white probe light (crossed polarizers) and exposed with a Gaussian laser beam focused to a small spot (14 μm FWHM).

Test cells filled with nematic LC showed homeotropic director alignment. Upon exposure, this alignment was maintained at the exposure spot center and the LC director was selectively realigned in a surrounding single ring. This ring had a thickness of a few microns and its diameter increased with increasing exposure intensity (112 μm at 0.7 mW, 204 μm at 1.1 mW). This characteristic director realignment was traced back to the optically generated electric field distributions by simulations.

In samples filled with chiral nematic LC, uniformly standing helix alignment was found. Textural transitions were induced at the focus position, which again led to the formation of well-defined circular defects. We could show that these defects can be permanently stored within the chiral nematic LC. Polarized optical microscopy of a rotated sample revealed that a point like defect with +1 topological charge was enclosed in each of these defects.

Photovoltaic fields generated in small lithium niobate particles dispersed in a LC were found to cause promising optical responses and particle movement.

10361-38, Session 8

Chromatic-aberration correction in geometric-phase lenses, for red, green, and blue operation *(Invited Paper)*

Jihwan Kim, Kathryn J. Hornburg, Michael J. Escuti, North Carolina State Univ. (United States)

All diffractive lenses manifest chromatic aberration/dispersion. If the focal length f0 at a given wavelength ?0 is known, then the focal length f(?) = f0 ?0 / ? at other wavelengths ?. This can be considerable, even for lenses of a few diopters. Geometric-phase lenses (GPLs), are no exception, which manipulate incident light's wavefront by the Pancharatnam-Berry phase

effect. Several years ago, we developed achromatic coatings based on photo-aligned chiral liquid crystals that achieve nearly 100% efficiency into the primary and conjugate waves, and more recently we demonstrated fast, defect-free GPLs down to F/1.5 for red light. Until now, no one has reported how to generally reduce chromatic aberration and ensure that two or more wavelengths can have the same focal length. Here, we report on a new approach to correct for chromatic aberration using a stack of GPLs and retarders to arrange red, green, and blue wavelengths to have precisely the same focal length. A simple arrangement of these elements results in a thin, monolithic, and flat GPL, which can either converge or diverge three wavelength sources (R/G/B) with the same focal length, positive or negative, depending on the handedness of the circular input polarization. Here, we describe the concept and characterize our first prototypes by evaluating focal lengths, efficiency, and polarization contrast. We also discuss the realistic opportunities and limitations for this approach.

10361-39, Session PMon

Compact optical device for measuring liquid crystal elastic and dynamic properties

Nina Podoliak, Elena Perivolari, Thomas P. Bennett, Matthew B. Proctor, Univ. of Southampton (United Kingdom); Thomas Regrettier, Thomas Heiser, Univ. de Strasbourg (France); Giampaolo D'Alessandro, Malgosia Kaczmarek, Univ. of Southampton (United Kingdom)

We present a prototype of compact device for all-optical measurements of the elastic and dynamic properties of nematic liquid crystals (LC). The device is based on a standard cross-polarized optical set-up and uses a combination of both amplitude and frequency of the driving AC electrical signal. Using a three-step measurement protocol and a corresponding fitting procedure, it simultaneously determines the following LC parameters: the splay and bend elastic constants, K1 and K3, the rotational viscosity ?1, and the combination of Leslie viscosity coefficients ?4+ ?5. Moreover, by taking sampled measurements across the area of a LC cell, the map profile of the LC layer thickness and average pre-tilt on the surfaces can be determined. All measurements are conducted using the same LC sample, which simplifies the measurement procedure and allows LC parameter testing in already assembled LC devices. We demonstrate the device performance using standard LC cells with commercially available nematic LCs such as E7 and TL205, as well as more complex LC-polymer samples containing photoconductive polymers such as C60 doped polyvinylcarbazole (PVK: C60), or poly(3-hexylthiophene) and phenyl-C61-butyric acid methyl ester (P3HT:PCBM).

10361-40, Session PMon

Light-driven liquid crystalline elastomeric devices: From micro-robotics to micro-photonics

Sara Nocentini, Daniele Martella, Lab. Europeo di Spettroscopie Non-Lineari (Italy); Dmitry Nunhdin, Lab. Europeo di Spettroscopie Non-Lineari (Italy) and Karlsruher Institut für Technologie (Germany); Simone Zanotto, Istituto Nazionale di Ottica (Italy); Camilla Parmeggiani, Lab. Europeo di Spettroscopie Non-Lineari (Italy) and Consiglio Nazionale delle Ricerche (Italy); Diederik S. Wiersma, Lab. Europeo di Spettroscopie Non-Lineari (Italy) and Univ. degli Studi di Firenze (Italy)

Liquid crystals have been recognized as a state of matter that characterize the technological applications of the last century not only in the display technology but also in the bio-medical field, photonic devices and robotic research. If the liquid crystalline molecules are combined with cross-linking units, a polymeric liquid crystalline elastomeric (LCE) material is formed. Polymer deformation controlled by the molecule alignment opens to bending, twisting or more complex movements. Light has been chosen as the external stimulus since it figures out as one of the more appealing energy source for micro and nano-robot actuation, enabling the remote spatial and temporal control on the material responses up to the nano-scale. In order to obtain a photoresponsive material, a dye, an azobenzene molecule, is added in the monomeric formulation. Moreover the possibility to pattern LCE in the microscale thanks to the lithographic technique of direct laser writing allows to design with nanometric precision different kind of photo-responsive micro-structure.

Depending on the photonic structure that should be addressed, the property tuning is achieved both on the chemical point of view and on the physical side, acting on the lithographic parameters. It has already been demonstrated how this optimized technique, based on a two-photon polymerization, leads to 3D walking and swimming micro-structures. We show here how the chemical and physical knowledge merged into the realization and characterization of optically tunable photonic devices as a grating beam steerer and micro-robots as a self-activated gripper of absorbitive nanoparticles.

10361-41, Session PMon

High resolution all-optical image processing with azobenzene-doped blue-phase liquid crystals

Tsung-Jui Ho, Chun-Wei Chen, Iam-Choon Khoo, The Pennsylvania State Univ. (United States)

In this presentation, we show by theory and experiment that dye-doped BPLCs are capable of all-optical edge enhancement, intensity conversion, hologram recording as well as optical wave front conjugation with aberration correction capability. Generally, these image processing operations can be performed with arbitrary polarization state of the light, and only requires low optical input powers. The underlying mechanism is laser induced lattice distortion that result from trans-cis isomorphism of the azo-dye molecules which, unlike laser induced crystalline axis reorientation in other LC phases, allow very high resolution [~ 1micron] image processing capabilities.

10361-42, Session PMon

Nonlinear optical logic circuits enabled by dye-doped twisted nematic liquid crystals

Cheng-Yu Wang, Chun-Wei Chen, The Pennsylvania State Univ. (United States); Hung-Chang Jau, National Sun Yat-Sen Univ. (Taiwan); Iam-Choon Khoo, The Pennsylvania State Univ. (United States); Tsung-Hsien Lin, National Sun Yat-Sen Univ. (Taiwan)

All-optical transistors and diodes enable a wide range of applications, such as direct logic processing of optical image, that were previously unachievable by traditional linear optical elements. In this presentation, we demonstrate how all-optical transistor and diode actions (including cascadability, signal fan-out, logic restoration) using dye-doped twisted nematic liquid crystals (DTN) by exploiting their non-reciprocal transmission responses enabled by the anisotropic absorption, polarization-rotation property, and collective optical nonlinearity of the DTN. By integrating these nonlinear optical elements, we have also demonstrated various logic-gate operations such as OR, AND, and NOT. It is noteworthy that these devices can be designed to fit a wide range of operation power owing to the controllable absorbance of DTN.

10361-43, Session PMon

The alignment of liquid crystalline nanowires using micropatterned elastomer molds

Eric Carlson, Lee M. Foley, Edward Guzman, Eva D. Korblova, Rayshan Visvanathan, Univ. of Colorado Boulder (United States); SeongHo Ryu, Min-Jun Gim, Dong Ki Yoon, KAIST (Korea, Republic of); Noel A. Clark, David M. Walba, Univ. of Colorado Boulder (United States)

The helical nanofilament (HNF) liquid crystal (LC) phase of NOBOW (9-O-PIMB) forms chiral nanofilaments, driven by a torsional strain between molecular halves within smectic layers that causes a saddle-splay deformation. Due to the high levels of crystallinity within each filament, the HNF phase can be described as a LC phase of nanowires—potentially perfect for use in organic electronics. Various methods have been used to align the HNF phase, yet effective alignment within an electronic device framework remains elusive. In this study, we use a lithographic technique, template assisted self-assembly, to align HNFs in microchannels. Polydimethylsiloxane (PDMS) molds containing channels ca. 5μm wide, 10μm high, and 1cm long are fabricated from an etched silicon master. These PDMS molds are placed on a glass substrate and the resultant cell is subsequently filled with isotropic NOBOW and cooled to room temperature. Removing the mold from the substrate reveals high quality alignment of HNFs within now free-standing channels as studied by polarized light microscopy, 2-D SAXS, and SEM. SAXS data also suggests the B2 and B3 phases of NOBOW are perfectly aligned in the molds, and thus their alignment is at least partially responsible for the alignment of HNFs. Mixtures with 8CB in the molds, unlike glass cells, promote the formation of the B2 phase, highlighting the influence PDMS has on phase formation. Not only does this study aid in the development of new organic electronic motifs using liquid crystal nanowires, but it also helps to better understand how HNFs and other LCs might align in this bulk system.

Return to Contents

Conference 10362: Organic Light Emitting Materials and Devices XXI

SPIE. OPTICS+ PHOTONICS ORGANIC PHOTONICS+ ELECTRONICS

Sunday - Tuesday 6 –8 August 2017

Part of Proceedings of SPIE Vol. 10362 Organic Light Emitting Materials and Devices XXI

10362-1, Session 1

The design and synthesis of n-dopants and TADF materials for OLED applications *(Invited Paper)*

Seth R. Marder, Georgia Institute of Technology (United States)

Organic semiconductors have attracted interest for electronic applications due to their potential for use in low-cost, large-area, flexible electronic devices. In this talk I will discuss the development of metallocenes-based dimers as n-dopants for use in semiconductors, 2D materials and electrodes, and their resulting impact on material properties and device performance. In particular I will focus on the application of photo-induced doping of low electron affinity compounds using air-stable organometallic compounds. The mechanism of doping and the application of the doping for fabrication of organic light emitting diodes (OLEDs) will be discussed. I will also briefly discuss recent work on the development of materials that have small excited state singlet-triplet energy gaps, which may be of interest as hosts or emitters for OLED applications.

10362-2, Session 1

Highly efficient pure blue-to-green emission from pyrimidine-based TADF emitters *(Invited Paper)*

Hisahiro Sasabe, Ryutaro Komatsu, Tatsuya Ohsawa, Kohei Nakao, Yuya Hayasaka, Junji Kido, Yamagata Univ. (Japan)

A series of pyrimidine-based pure blue-to-green emitters are developed, and investigated the structure–property relationships. A pure blue emitter realized a PE of 20 lm W–1 at CIE of (0.16, 0.15), and a green emitter exhibited a PE of over 110 lm W?1 at CIE of (0.36, 0.58).

10362-3, Session 1

Vibrational coupling in TADF and how molecular structure can control this complex triplet harvesting process *(Invited Paper)*

Andrew P. Monkman, Durham Univ. (United Kingdom)

The process of triplet harvesting is by thermally activated delayed fluorescence, 'TADF', i.e. E-type delayed fluorescence, is now well established. In this talk I shall discuss how this triplet harvesting mechanism is affected by molecular architecture.

Detailed photophysical measurements of intramolecular charge transfer (ICT) states have been made both in solution and solid state. Temperature dependent time resolved emission, delayed emission and photoinduced absorption are used to map the energy levels involved in molecule decay, and through detailed quantum chemical modelling, true electron exchange energies and other energy barriers of the systems are determined with the real states involved in the reversed intersystem crossing mechanism elucidated.

Using the vibronic coupling second order spin orbit interaction we go on to show how both D-A-D molecule structure and conformation control TADF and efficiency in a TADF OLED. By confirming the vibronic coupling mechanism of rISC (and ISC) we can now start to think about true molecular design for TADF emitters.

1. Etherington, M. K., Gibson, J., Higginbotham, H. F., Penfold, T. J. & Monkman, A. P. Revealing the spin-vibronic coupling mechanism of thermally activated delayed fluorescence. Nat Commun 7, 13680 (2016).

2. Gibson, J., Monkman, A. P. & Penfold, T. J. The Importance of Vibronic Coupling for Efficient Reverse Intersystem Crossing in Thermally Activated Delayed Fluorescence Molecules. ChemPhysChem 1–7 (2016). doi:10.1002/cphc.201600662

3. Dias, F. B. et al. The Role of Local Triplet Excited States in Thermally-Activated Delayed Fluorescence: Photophysics and Devices. Adv. Sci. 3, 1600080 (2016).

10362-4, Session 1

Efficient TADF OLEDs using active materials with both efficient internal generation and external extraction *(Invited Paper)*

Chung-Chih Wu, National Taiwan Univ. (Taiwan)

To achieve ultimately high external quantum efficiencies of OLEDs, OLED materials and device architectures that can achieve high internal quantum efficiencies and high optical out-coupling efficiencies are equally important. In this paper, we will present some of our recent works on OLED materials and devices that can provide high internal and optical out-coupling efficiencies. For instance, extremely efficient blue organic EL with external quantum efficiency (EQE) of ~37% is achieved in a conventional planar device structure, using a highly efficient TADF emitter based on the spiroacridine-triazine hybrid that simultaneously possesses nearly unitary (100%) photoluminescence quantum yield and strongly horizontally oriented emitting dipoles (with a horizontal dipole ratio of 83%). On the other hand, judicious use of low-index active organic materials in OLEDs can also effectively enhance optical coupling efficiency and EQEs of OLEDs even with isotropic emitters. This was demonstrated by efficient and tunable blue-green to yellow TADF OLEDs (with EQEs of >31%) based on TADF emitters having acridine donor units and CN-substituted pyridine/pyrimidine acceptor units.

10362-5, Session 1

High efficiency thermally activated delayed fluorescence through an excited-state intramolecular proton transfer *(Invited Paper)*

Masashi Mamada, Ko Inada, Takeshi Komino, William J. Potscavage Jr., Hajime Nakanotani, Chihaya Adachi, Kyushu Univ. (Japan)

Thermally activated delayed fluorescence (TADF) materials have shown great potential for highly efficient organic light-emitting diodes (OLEDs). While the current molecular design of TADF materials primarily focuses on combining donor and acceptor units, we present a novel system based on the use of excited-state intramolecular proton transfer (ESIPT) to achieve efficient TADF without relying on the well-established donor-acceptor scheme. In an appropriately designed acridone-based compound with intramolecular hydrogen bonding, ESIPT leads to separation of the highest occupied and lowest unoccupied molecular orbitals, resulting in TADF emission with a photoluminescence quantum yield of nearly 60%. High external electroluminescence quantum efficiencies of up to 14% in OLEDs using the material prove that efficient triplet harvesting is possible with ESIPT-based TADF materials. This work will expand and accelerate the development of a wide variety of TADF materials for high performance OLEDs.

10362-6, Session 2

Conventional fluorescent OLEDs toward EQE of 30% *(Invited Paper)*

Jang-Joo Kim, Seoul National Univ (Korea, Republic of); Hyun-Gu Kim, Seoul National Univ. (Korea, Republic of)

Harnessing triplet excited states resulting from electrical pumping by conventional fluorophores in organic light emitting diodes (OLEDs) is very attractive to overcome low stability and high-efficiency roll-off at high current density of phosphorescent and thermally activated delayed fluorescence (TADF) OLEDs. Here we demonstrate a method to increase the fraction of singlet excitons on a conventional fluorescent material by reverse intersystem crossing (RISC) of exciplex and sensitization effect. As a result, we realise a fluorescent OLED with the external quantum efficiency (EQE) of 26% and predict that EQE of 30% may be expected if all singlet excitons in the fluorescent emitter decay radiatively.

10362-7, Session 2

Molecular design and device architectures for high performance thermally activated delayed fluorescent OLEDs *(Invited Paper)*

Chun-Sing Lee, City Univ. of Hong Kong (Hong Kong, China)

Thermally activated delayed fluorescence (TADF) has attracted much recent attention for it application in high performance organic light-emitting devices (OLED). In this talk, approaches for enhancing performance of TADF based OLED in term of both molecular design and device architecture will be discussed.

10362-8, Session 2

High efficiency OLEDs based on exciplex *(Invited Paper)*

Ken-Tsung Wong, National Taiwan Univ. (Taiwan)

Organic materials with efficient thermally activated delayed fluorescence (TADF) are emerging as attractive OLEDs emitters because of the achievable 100% internal quantum efficiency. TADF can be achieved by the manipulation of HOMO-LUMO overlap by tailor-made molecular structure with subtle intramolecular charge transfer (ICT) between the electron donor and acceptor.

Many efficient TADF emitters have been reported, paving the way to make high efficiency OLEDs in much cost-effective ways. Alternatively, TADF can be achieved by an exciplex formed through the intermolecular charge transfer between a hole-transporting (HT) material and an electron-transporting (ET) material. The uses of exciplex as emitting layer or host for high efficiency phosphorescent or fluorescent OLEDs have been successfully demonstrated, indicating the potential of exciplex in OLEDs. The selection of suitable HT and ET materials not only can generate efficient exciplex but also can reduce the complexity of device structures. In this conference, our recent developments of new carbazole-based HT and triazine-based ET materials for high efficiency exciplex and their uses to achieve blue to yellow and tandem white OLEDs will be reported.

10362-9, Session 3

Blue OLEDs based on thermally activated delayed fluorescent emitters with improved stability *(Invited Paper)*

Lian Duan, Dongdong Zhang, Tsinghua Univ. (China)

Much effort has been devoted to boost the performance of thermally activated delayed fluorescence (TADF) devices; however, the stability of blue TADF emitters remains a constraint for their potential applications in displays and lightings. In our previous work, we have successfully added bulky substituents to protect the chromophore of blue TADF emitters and improved lifetime is attained. Here, we will also show some other methods to further improve their stability. The first one is to use host materials with TADF properties together with TADF emitters. Reduced STA, TTA, and also TPA can be achieved. The second one is to utilize stable transporting materials, especially electron transporting materials with extended conjugations. By incorporating all these techniques into one device, we have demonstrated blue OLEDs with EQE of over 20% and a T50 up to 1200 hrs at an initial brightness of 500 cd/m2, pushing the performance of blue TADF OLEDs closer to the requirements of real applications.

10362-10, Session 3

Towards commercialization: Blue TADF emitter materials for next-generation AMOLED-displays *(Invited Paper)*

Thomas Baumann, Daniel Volz, cynora GmbH (Germany)

Thermally activated delayed fluorescence (TADF) is an upcoming key technology for organic light-emitting diodes (OLEDs).

For the first time, OLED materials that combine efficiency, stability and a deep blue color point are available.

In this work, we introduce the TADF technology and give a status update and development roadmap towards commercialization. As a highlight, we will especially feature a status update for deep-blue emitters with high stability and good color point, which are useful for efficient OLED displays.

10362-11, Session 3

Understanding spin-dependent processes in TADF light-emitting materials based on magneto-optical studies *(Invited Paper)*

Bin Hu, The Univ. of Tennessee Knoxville (United States)

This presentation reports our recent studies on the understanding of spin-dependent processes in TADF (Thermally Activated Delayed Fluorescence) light-emitting materials based on magneto-optical studies. Recently, we have performed magneto-optical studies on TADF light-emitting molecules (DMAC-TRZ) by using magneto-photoluminescence (magneto-PL). Our magneto-PL studies provide the first evidence that the TADF is a spin-dependent process occurring in charge-transfer states. Essentially, the key spin-dependent process, namely spin mixing, necessarily required to activate the TADF, is determined by the competition between two critical parameters: (i) exchange interaction which functions as a resistance force to the TADF and (ii) spin-orbital coupling which acts as a driving force to the TADF. Therefore, controlling the exchange interaction and spin-orbital coupling becomes a critical issue in the development of highly efficient TADF light-emitting materials. By using magneto-PL studies, we further found that, doping soluble magnetic nanoparticles (surface-modified Fe_3O_4) can conveniently change the exchange interaction and spin-orbital coupling, and consequently alters the TADF rate. At low doping concentrations, the spin-orbital coupling is enhanced, leading to an increase on TADF rate. However, at high doping concentrations, the exchange interaction is increased, causing a decrease on the TADF rate. Furthermore, we studied the polarization effects of spin mixing in liquid TADF materials by using various solvents with different polarities. We observed that increasing the host polarization can directly weaken the spin mixing and leads to a decrease on the TADF rate. This experimental observation indicates that host polarization can weaken the spin-orbital coupling and thus decreases the driving force to TADF. Clearly, the magneto-PL studies provide an insightful understanding on the spin-dependent process to control the TADF rate in organic light-emitting materials.

10362-12, Session 3

Device approach for extended lifetime in triplet exciton harvesting organic light-emitting diodes *(Invited Paper)*

Wook Song, Si Hyun Han, Jeong Min Choi, Jun Yeob Lee, Sungkyunkwan Univ. (Korea, Republic of)

Lifetime of organic light-emitting diodes has been a challenging issue because of intrinsic instability of organic light-emitting materials. In particular, the lifetime of high efficiency organic light-emitting diodes such as phosphorescent organic light-emitting diodes and thermally activated delayed fluorescent organic light-emitting diodes is still shorter than that of conventional fluorescent organic light-emitting diodes. Therefore, the lifetime extension of those triplet exciton harvesting organic light-emitting diodes is important. There have been many material and device approaches to extend the lifetime of the triplet harvesting organic light-emitting diodes and one of effective methods was to manage triplet-polaron annihilation in the emitting layer. In this presentation, we discuss several methods to control the triplet-polaron annihilation in the phosphorescent and thermally activated delayed fluorescent devices

10362-13, Session 3

Enhanced photoluminescence from a molecular tunneling junction

Alfred J. Meixner, Kai Braun, Eberhard Karls Univ. Tübingen (Germany); Xiao Wang, Hunan Univ. (China); Dai Zhang, Eberhard Karls Univ. Tübingen (Germany)

We demonstrate enhanced photoluminescence (PL) from an optically pumped bias driven molecular tunneling junction (Au-substrate/self assembled molecular monolayer/Au-tip) with molecules chemically bound to the Au substrate. The gap between a sharp gold tip and a flat gold substrate covered with a self-assembled monolayer (SAM) of 5-chloro-2 mercaptobenzothiazole (Cl-MBT) molecules can be used as an extremely small optical gain medium. When a bias-voltage is applied between tip and sample such that electrons tunnel from the Cl-MBT's highest occupied molecular orbital (HOMO) to the tip, holes are left behind in the molecules. These can be repopulated by hot electrons that are created by the laser-driven plasmon oscillation on the metal surfaces enclosing the molecule. Emission of photons occurs from the recombination of plasmon excited hot electrons with holes in the HOMO of surface bound molecules below the tip. Varying the laser pump power or alternatively the applied bias voltage shows in both cases a distinct threshold above which enhancement of the optical signal occurs. Solving the rate equations for this system shows that optical feed-back by the gap mode's near field can efficiently stimulate the emission process. The system reflects many essential features of a superluminescent organic light emitting diode.

10362-14, Session 4

Highly efficient flexible OLEDs with the extraction enhancement *(Invited Paper)*

Jianxin Tang, Yanqing Li, Soochow Univ. (China)

Flexible organic light-emitting diodes (OLEDs) hold great promise for future bendable display and curved lighting applications. One key challenge of high-performance flexible OLEDs is to develop new flexible transparent conductive electrodes with superior mechnical, electrical and optical properties. The second is to extract the confined light in the devices due to different loss mechanisms. Herein, an effective nanostructured metal/dielectric composite electrode (NMDCE) on plastic substrate is applied to flexible OLEDs with an ultrathin metal alloy film for optimum optical transparency, electrical conduction and mechanical flexibility. By combining an light-extraction structure for broadband and angle-independent outcoupling of white emission, the waveguided light and surface plasmonic loss can be remarkably reduced in white flexible OLEDs, resulting in a substantial increase in the external quantum efficiency and power efficiency to ~70% and >160 lm/W.

10362-15, Session 4

Efficient light extraction of organic light-emitting diodes *(Invited Paper)*

Qibing Pei, Univ. of California, Los Angeles (United States)

Organic light-emitting diodes (OLEDs) typically suffers from limited light outcoupling efficiencies despite high internal quantum efficiencies because of light loss in the surface plasmon, waveguide and substrate modes. Using a nanocomposite substrate with embedded silver nanowire network to replace ITO/glass, the waveguide and substrate modes can be out-coupled from the device. White OLEDs were fabricated on the nanocomposite substrates, achieving a power efficacy external quantum efficiency significantly higher than control devices on ITO/glass. Furthermore, the reported nanocomposite substrate was fabricated by solution processes and are mechanically flexible, allowing them to be readily adaptable in the low-cost production of flexible OLEDs.

10362-16, Session 4

Enhanced outcoupling of light from OLEDs fabricated on corrugated polycarbonate and PET substrates *(Invited Paper)*

Chamika Hippola, Rajiv Kaudal, Eeshita Manna, Iowa State Univ. of Science and Technology (United States); Thomas Trovato, Trovato Mfg., Inc. (United States); Dennis Slafer, MicroContinuum, Inc. (United States); Rana Biswas, Joseph Shinar, Ruth Shinar, Iowa State Univ. of Science and Technology (United States)

Extracting the "internally waveguided" light from OLEDs, which together with losses to plasmons at the metal cathode typically account for > 50% of the light generated in the emission zone, has proven to be a particularly challenging problem. To address this problem, we fabricated devices on nano-patterned plastic substrates that disrupt the internal waveguiding. We describe thermally evaporated small molecule fluorescent and phosphorescent OLEDs fabricated on corrugated polycarbonate (PC) and polyethylene terephthalate (PET) substrates nanopatterned in a roll-to-roll process. We compare the devices fabricated on plastic/ITO to those on plastic/PEDOT:PSS and the effect of adding a μm-scale Cu honeycomb mesh to the integrated substrate/anode as well. Depending on the height and pitch of the pattern, up to a 2.5 fold increase in the outcoupling factor is observed relative to the flat substrate. Issues related to the fidelity of the conformal deposition of the various layers on the patterned plastic are also discussed, particularly the effect of the nanopatterns on device stability.

10362-17, Session 4

Molecular orientations and energy levels *(Invited Paper)*

Yiying Li, Zheng-Hong Lu, Univ. of Toronto (Canada)

The relative molecular orientation between two adjacent molecules plays an important role in device performance. For example, a horizontally orientated emitter molecule leads to a surface-aligned transition dipole moment which yields a much higher optical out-coupling efficiency than a vertically oriented dipole, and hence, it significantly improves the external quantum efficiency of the organic light emitting diode. Molecular orientation has significant influence on energy levels at organic heterojunctions. In this talk, we will discuss our recent experimental findings on correlations between energy levels and molecular orientation. The impact of molecular orientation on interface energy level alignment and on interface charge transfer will be discussed. The influence of a material's glass transition temperature on molecular orientation will also be discussed.

10362-18, Session 4

OLED light extraction with corrugated substrate and hemispherical lens

Xiangyu Fu, Cheng Peng, Univ. of Florida (United States); Dong-Hun Shin, Monica Samal, Franky So, North Carolina State Univ. (United States)

While the internal quantum efficiency of an OLED can reach 100%, its external quantum efficiency (EQE) is limited to 30% because of light trapped in waveguided mode, SPP mode and substrate mode. In this study, we achieve more than 2X enhancement in EQE by using a corrugated substrate and a hemispherical lens. Polarized angle-resolved electroluminescence spectroscopy is used to analyzed the EL data, and the results are compared with optical simulation. We find the efficiency enhancement mainly comes from the diffraction of the SPP mode towards air mode due to the corrugated substrate, and the hemispherical lens assists the light extraction by extending the air cone into the substrate mode.

10362-19, Session 4

Vacuum nanohole array embedded organic light emitting diodes for enhanced light extraction *(Invited Paper)*

Sohee Jeon, Jun-Ho Jeong, Korea Institute of Machinery & Materials (Korea, Republic of); Jang-Joo Kim, Seoul National Univ. (Korea, Republic of)

High-efficiency organic light emitting diode (OLED) approaching the theoretical limit was produced by using the highly effective extraction layer based on a vacuum nanohole array (VaNHA). A novel process called robust reverse-transfer was developed to transfer a nanohole array defined on a dielectric layer onto a substrate. The nanohole array remains vacant between the dielectric layer and the substrate after the transfer process, maximizing the refractive index (RI) contrast of the extraction layer for the dielectric material as the selected high RI. The extraction enhancement confirmed that VaNHA extracts the entire waveguide loss into the air by comparing experimentally measured results with those produced from optical modeling analysis. We will show that EQEs approaching 80% is achievable by extracting all the waveguided and substrate confined modes with a VaNHA structure and a half spherical lens as internal and external light extraction layers, respectively, and by minimizing surface plasmon polariton loss with increasing the thickness of the electron transporting layer.

10362-20, Session 5

Extending the lifetime of blue phosphorescent OLEDs *(Keynote Presentation)*

Stephen R. Forrest, Univ. of Michigan (United States)

Since its first demonstration in 1998, electrophosphorescence has yielded 100% internal quantum efficiency OLEDs (PHOLEDs) across the color gamut. This advance has given birth to a huge global OLED display industry, now estimated to be >$15B, or more than 10% of all displays made. While red and green devices have shown extraordinary operational lifetimes, blue PHOLEDs have had unacceptably short lifetimes. In this talk I discuss the fundamental origins of this deficiency1, and approaches to extending the lifetime of blue PHOLEDs. Indeed, recent results in our laboratory have already yielded a 10 fold improvement in lifetime, the first such major improvement in almost a decade2. The understanding gained from these experiments suggest that much longer lifetimes, even for very deep blue emitting PHOLEDs, is possible. In particular, I will discuss the use of hot excited state managers as a means to greatly extend the lifetime of blues for both displays and lighting.

1. N. C. Giebink, B. W. D'Andrade, M. S. Weaver, P. B. Mackenzie, J. J. Brown, M. E. Thompson and S. R. Forrest, J. Appl. Phys. 103, 044509 (2008).

2. Y. Zhang, J. Lee and S. R. Forrest, Nature Commun. 5, 5008 (2014).

10362-21, Session 5

Blue emitting square planar metal complexes for displays and lighting applications *(Invited Paper)*

Jian Li, Arizona State Univ. (United States)

The successful development of alternate low cost technology for current solid state lighting devices will have a significant impact on the U. S. economy and national security. White organic light emitting diodes (OLEDs) with potentially high power efficiency are considered as strong candidate for the next generation of illumination devices. Moreover, the use of environmentally benign organic materials in white OLEDs and their potentially low fabrication cost makes them an attractive technological prospect. In this presentation, we will discuss our continuing efforts on the design, synthesis and characterization of novel platinum complexes for displays and lighting applications. The photo-physics, electrochemistry, electroluminescent properties and operational stability of these novel metal complexes, including deep blue narrowband emitters, blue emitters with 6-membered chelate rings and blue MADF emitters, will be discussed, particularly including our 10-year effort in the design of blue emitting phenyl-pyridine based metal complexes. The rational molecular design enables us to develop cyclometalated metal complexes with both photon-to-photon (in thin film) and electron-to-photon (in device settings) conversion efficiency close to 100% for OLED applications. Our approaches to achieve high efficiency white OLED using a single emitter will be also included.

10362-22, Session 5

Recent advances in phosphorescent OLEDs: Molecular design for long lifetime and high color purity *(Invited Paper)*

Hirohiko Fukagawa, Takahisa Shimizu, Yukiko Iwasaki, Taku Oono, Toshihiro Yamamoto, NHK Japan Broadcasting Corp. (Japan)

OLEDs are key devices for realizing next-generation displays such as flexible displays. Although the emission mechanism along with new luminescence materials have been intensively studied with the goal of harvesting all excitons as emission, it has not been uncommon to hear of devices with internal quantum efficiencies of approximately 100% that use phosphorescent or thermally activated delayed fluorescent (TADF) emitters in recent years. Thus, the device performances directly related to practical applications, such as operational lifetime and color purity, have begun to attract much attention. Here, we report on recent advances in phosphorescent OLEDs (PHOLEDs) related to these two device performances. First, the molecular design of the host material to obtain an operationally stable PHOLED is clarified. By analysing the device characteristics of several PHOLEDs utilising similar TADF materials as hosts, a TADF material with a small molecular size is found to be suitable for the phosphorescent host. Second, we demonstrated efficient green OLEDs with high color purity utilising a platinum complex with a rigid molecular structure. A current efficiency of 84 cd/A was obtained from a bottom-emitting OLED with CIE x-y coordinates of (0.27, 0.67), which is much greater than that of a bottom-emitting green OLED using conventional iridium complexes with CIE x-y coordinates of (0.33, 0.62). Furthermore, the CIE x-y coordinates reached (0.18, 0.74) upon employing a top-emitting structure.

10362-23, Session 5

Realizing high-performance and low-cost fluorescent OLEDs *(Invited Paper)*

Shi-Jian Su, South China Univ. of Technology (China)

Organic light-emitting diodes (OLEDs) are being increasingly applicable in flat-panel displays, such as television and mobile phone, and have a great potential to become the next generation solid-state lighting sources. One of the most attractive strategies is to construct OLEDs with low cost purely organic materials, where high cost phosphorescent materials containing rare or noble metals are not involved in the device fabrication. We have proposed a simple strategy towards high-performance fluorescent OLEDs. The designed devices are merely composed of stacked p-type hole-transport layer and n-type electron-transport layer, resulting in a planar pn heterojunction configuration similar to their inorganic counterparts, namely light emitting diodes (LEDs). In this novel device, the excitons are generated and decay at the pn junction interface due to the synergetic interaction of p-type and n-type materials, finally giving the light emission. In addition, a novel strategy towards simultaneously low-driving voltage and high efficiency fluorescent OLEDs was also proposed using an active planar pn heterojunction as the exciton generation region and conventional fluorescent dye or thermally activated delayed fluorescence (TADF) material as the emitter. The current findings highlight the significance of the role of the organic active planar pn heterojunction in fabrication of high-performance and structure-simplified OLEDs with conventional fluorescent and TADF emitters, and also enlighten that organic active pn heterojunction should play a much more important role in electric-to-light conversion devices as it has done in the light-to-electric photovoltaic devices.

10362-24, Session 5

Active control of OLED beam shapes *(Invited Paper)*

Sebastian Reineke, Felix Fries, Markus Fröbel, Pen Yiao Ang, Simone Lenk, TU Dresden (Germany)

Organic light-emitting diodes (OLEDs) are scalable area light sources, allowing for highly efficient mono- or polychromatic emission. In standard configuration of the OLED architecture, the emission pattern can be approximated well with an Lambertian intensity distribution. Patterns deviating from this distribution can be achieved by fine-tuning of the interplay between emitter location and the strength of the micro-cavity. Here, we demonstrate a concept for an OLED-based concept that allows for actively controlled, variable beam shapes. This is achieved using a cavity optimized tandem architecture, comprising two red-emitting phosphorescent OLED units, which is driven with a pulse-width modulation to achieve the desired beam shapes. For an optimized side-emission, this device shows a 2.7 times higher emission at 56° with respect to the normal emission. The discussion of our experimental results is supplemented with state-of-the-art optical simulations. We also include geometrical considerations that are important to evaluate the potential of this concept. Finally, we demonstrate qualitatively, how external optical elements can be incorporated the alter the emitted beam shape.

10362-25, Session 6

Investigating the causes of the lower stability of solution-coated versus vacuum-deposited small-molecule organic light emitting devices *(Invited Paper)*

Hany Aziz, Yong Joo Cho, Hyeong Hwa Yu, Yingjie Zhang, Univ. of Waterloo (Canada)

Although the promise of realizing lower cost fabrication by means of solution-based processing techniques, such as spin coating, web coating or inkjet printing, has been one key driver behind the interest in OLEDs for the last two decades, the lower stability of devices made by these techniques has been a long standing issue. With recent advances in developing solution-processable small molecule materials, it is now possible to make OLEDs of the same small molecule materials by either solution coating or vacuum deposition. Despite this, there continues to be an intriguing stability gap.

In this work, we investigate this phenomenon with the purpose of identifying its root causes. Electroluminescence, delayed electroluminescence and photoluminescence measurements are used to study and compare between the aging behavior in OLEDs made by spin-coating versus vacuum-deposition. Hole-only devices are also utilized, and employed to study the effects of charges and excitons, separately and combined. The results reveal that the faster degradation of solution-processed devices relative to their vacuum-deposited counterparts under electrical stress is due to a faster molecular aggregation process. Excitons and interactions between them and polarons appear to play a leading role in inducing this phenomenon. Results from these investigations will be presented and discussed.

10362-26, Session 6

Addition of lithium 8-quinolate into polyethylenimine/zinc oxide electron-injection layer improving driving voltage and lifetime of OLEDs *(Invited Paper)*

Yong-Jin Pu, Takayuki Chiba, Takafumi Ide, Satoru Ohisa, Hitoshi Fukuda, Tatsuya Hikichi, So Kawata, Junji Kido, Yamagata Univ. (Japan)

Solution-processed electron injection layers (EILs) comprising lithium 8-quinolate (Liq) and polyethylenimine ethoxylated (PEIE) are highly effective for enhancing electron injection from ZnO to organic layers and improving device lifetime in organic light-emitting devices (OLEDs). Doping of Liq into PEIE further reduces the work function of zinc oxide (ZnO) by enhancing dipole formation. The intermolecular interaction between Liq and PEIE was elucidated by UV-vis absorption measurement and quantum chemical calculation. The OLEDs with ZnO covered with PEIE:Liq mixture exhibited lower driving voltage than that of the device without Liq. Furthermore, as doping concentration of Liq into PEIE increased, the device lifetime and voltage stability during constant current operation was successively improved.

10362-27, Session 6

Electroluminescent polymers for solution-processed PLEDs *(Invited Paper)*

Lixiang Wang, Changchun Institute of Applied Chemistry (China)

Polymer light-emitting diodes (PLEDs) is fabricated by solution process, and should be cheaper enough, however their performance so far remains inferior to that of the best vacuum deposited organic light-emitting diodes (OLEDs), such as power efficiency and stability, so the further research for PLED will be on the materials issue and device structure for improving the efficiency and stability.

This presentation will discuss two topics with most updated results: (1) Solution-processed multilayer polymer light-emitting diodes for high-efficiency blue, green, red and white emission; (2) Power efficient solution-processed white organic light-emitting diodes with high energy level blue-emitting iridium complexes and carbazole-based dendritic host.

Based on the solvent resistance tests for the dendritic dopants with different emission color and dendritic hosts, the multilayer polymer light-emitting diodes are fabricated by using alcohol-soluble electron-transporting materials. It is found that their performances are quite comparable with that of the corresponding device with the electron-transporting layer by vacuum-deposition process, which is favorable to construct white polymer light-emitting diodes with multilayer structure.

To reduce the driving voltage and realize high power efficiency, solution processed white OLEDs with the power efficiency of 64.5 lm W-1 are achieved by using high energy level blue-emitting iridium complexes to replace low energy level FIrpic and carbazole-based dendritic host H2 instead of the traditional PVK. This result represents an important progress in solution-processed WOLEDs, for the development of the next-generation WOLEDs device using the active layer with the barrier-free hole/electron injection features.

10362-28, Session 7

Highly efficient solution-processed small-molecule organic light-emitting diodes using novel electron transporting host *(Invited Paper)*

Tae-Woo Lee, Tae-Hee Han, Seoul National Univ. (Korea, Republic of); Mi-Ri Choi, Pohang Univ. of Science and Technology (Korea, Republic of); Chan-Woo Jeon, Yun-Hi Kim, Soon-Ki Kwon, Gyeongsang National Univ. (Korea, Republic of)

Multilayered small-molecule organic light-emitting diodes (OLEDs) have been commonly used for balanced charge transport and exciton confinement. However, standard method that uses high-vacuum deposition for multilayered OLEDs entails high material and fabrication cost, and it has been a critical impediment to low-cost production. Solution-processing of small-molecule OLEDs has been considered as a promising method, but limited luminous efficiency of solution-processed OLEDs have also been a hurdle for practical use. Therefore, high-efficiency in solution-processed small-molecule OLEDs with a simple device structure should be developed. Here, we report highly efficient solution-processed simplified OLEDs using novel electron-transporting host materials based on tetraphenylsilane with pyridine moieties. These host materials have high triplet energy levels (> 2.8 eV), wide band gaps (> 4.0 eV), and high glass transition temperature. We additionally used multifunctional polymeric hole injection layer and mixed-host emitting layer to achieve simple device architecture without hole transporting or electron blocking layer. Our novel electron transporting host materials which have higher electron transporting ability and triplet energy levels than that of conventional electron transporting host material (2,2?,2''-(1,3,5-Benzinetriyl)-tris(1-phenyl-1-H-benzimidazole)) provided more balanced charge transport and efficient energy transfer preventing backward energy transfer from phosphorescent dopants to host. Orange-red (~97.5 cd/A), green (~101.5 cd/A), and white (~74.2 cd/A) solution-processed phosphorescent OLEDs with simple device structure showed the highest recorded electroluminescent efficiencies of solution-processed OLEDs without additional light outcoupling structure reported to date. We also demonstrated a solution-processed flexible solid-state-lighting device as a potential application.

10362-29, Session 7

Elucidating the film structure in organic light-emitting diodes *(Invited Paper)*

Paul L. Burn, Claire Tonnele, Martin Stroet, Tom Lee, Andrew J. Clulow, Jake A. McEwan, Ian R. Gentle, Alan Mark, Ben J. Powell, The Univ. of Queensland (Australia)

Advances in light-emitting materials design and device manufacturing have brought the first organic light-emitting diodes (OLEDs) to market. The most efficient devices are a combination of layers within the active film designed to: 1) balance charge injection and transport; 2) maximise recombination of the singlets and triplets generated in the device; 3) achieve an emissive layer with a high PL quantum yield; and 4) provide enhanced out-coupling of the light generated in the device. Furthermore, during their lifetime time devices undergo electrical and thermal stress and hence it is important to understand what happens within a device during its lifetime. In this presentation we will discuss our approach to understanding the structure of films typically used in OLEDs and their fate under thermal stress. In particular we will focus on a computational approach to understand film structure as well as neutron reflectometry (NR) with in situ photoluminescence measurements for elucidating the relationship between physical structure and emissive properties under thermal stress.

10362-30, Session 7

Unified analysis of transient and steady-state electrophosphorescence: Establishing an analytical formalism for OLED charge balance *(Invited Paper)*

Kyle W. Hershey, Russell J. Holmes, Univ. of Minnesota, Twin Cities (United States)

Under steady-state operation, organic light-emitting devices (OLEDs) often suffer from a reduction in luminescence efficiency. This "efficiency-roll-off" has been previously considered by invoking losses due to bimolecular processes including exciton-exciton annihilation and exciton-polaron quenching. While these efforts have successfully reproduced the steady-state efficiency roll-off, the corresponding transient electroluminescence behavior has not been modeled as effectively using the same approach. Here, we examine steady-state and transient electroluminescence from the archetypical green phosphor tris[2-phenylpyridinato-C2,N]Iridium(III) (Ir(ppy)3). Both the steady-state and transient (rise and decay) behaviors are successfully reproduced by considering a dynamic polaron population in addition to conventional exciton dynamics. Injected polarons may form excitons or leak through the device emissive layer, reducing efficiency. This formalism permits a rigorous connection between exciton and polaron dynamics and OLED charge balance, with the charge balance defined as the exciton formation efficiency. In the devices considered here, charge leakage through the emissive layer dominates the roll-up in efficiency at low current density, while bimolecular quenching is responsible for the majority of the roll-off. This model thus provides a complete picture of the dynamics present during the electrical operation of an OLED, while elucidating the rate and efficiency of exciton formation. Both of these parameters will be of use in more quantitative analyses of device efficiency and operation lifetime.

10362-31, Session 7

Multiscale hopping-type charge transport simulation: the prediction and molecular-level analysis *(Invited Paper)*

Hironori Kaji, Kyoto Univ. (Japan)

Charge transport is one of the most important factors for various devices. However, for organic devices, such as organic light-emitting diodes, charges are transported in amorphous molecular aggregates, and the prediction and detailed analysis has been difficult so far. Here, we show our recent study on multiscale charge transport calculations based on our preceding works[1,2]; the combination of quantum chemical calculations, molecular dynamics simulations, and kinetic Monte Carlo simulations. The calculations are performed by explicitly considering organic molecules, which allows detailed molecular level analysis.

[1] Suzuki, F., Shizu, K., Kawaguchi, H., Furukawa, S., Sato, T., Tanaka, K. & Kaji, H., J. Mater. Chem. C 3, 5549 (2015). [2] Uratani, H., Kubo, S., Shizu, K., Suzuki, F., Fukushima, T. & Kaji, H., Sci. Rep. 6, 39128 (2016).

10362-32, Session 8

Highly efficient perovskite LEDs from nanoscale perovskite crystallites *(Invited Paper)*

Barry P. Rand, Princeton Univ. (United States)

Hybrid organic-inorganic perovskite materials such as methylammonium lead iodide (CH3NH3PbI3 or MAPbI3) or methylammonium lead bromide (CH3NH3PbBr3 or MAPbBr3) have garnered significant interest in the thin film optoelectronics community due to their outstanding optical and electrical properties. However, solution processed perovskites commonly suffer from poor thin film quality, reproducibility, stability, and scalability. Our work has determined that the fabrication of perovskite thin films displays all of the hallmarks of sol-gel processing, an aspect that we exploit to improve the quality of spin coated thin films. In particular, we realize films with roughness on the order of 1 nanometer that consist of nanoscale crystallites, formed by incorporating a bulky organoammonium halide in addition to the stoichiometric 3D perovskite precursors. These bulky ligands passivate the 3D crystal, lead to considerably enhanced luminescence quantum yields, and increase stability. LEDs produced in this way are capable of exceeding 10% external quantum efficiency and exhibit significantly improved stability.

10362-33, Session 8

Continuing to explore the unusual properties of hybrid perovskites

Jinsong Huang, Univ. of Nebraska-Lincoln (United States)

There have been many unique and unusual properties been discovered for organic–inorganic halide perovskites which explain the high performance and many unusual characteristics of hybrid perovskite electronic devices. Here I will present our recent advance in studying the several hypothesized properties of hybrid perovskite materials including photon-recycling and ferroelectricity. I will qualify the photon recycling efficiency in hybrid perovskite single crystals by studying the reabsorption and remission efficiency. The recent first observation of abnormal photovoltaic effect in the perovskite solar cells will also be presented, and its origin will be discussed. I will also discuss the verification of ferroelasticity property of hybrid perovskite, but not ferroelectricity.

10362-34, Session 8

Tunable light emitting diodes utilizing quantum-confined layered perovskite emitters

Dan Congreve, Massachusetts Institute of Technology (United States) and Harvard Univ. (United States); Mark Weidman, Michael Seitz, Watcharaphol Paritmongkol, Nabeel Dahod, William A. Tisdale, Massachusetts Institute of Technology (United States)

Organic-inorganic perovskites have revolutionized the optoelectronics field, providing materials with a wide range of properties for solving numerous applications. Indeed, much recent work has been focused on nanostructured perovskites, with quantum dots, nanowires, and nanoplatelets showing tremendous potential. Here, we utilize the unique tunability of 2D perovskite nanoplatelets to build LEDs that span the visible spectrum. Quantum confinement in the z direction drives a significant blueshift, allowing for blue devices utilizing the bromide system and orange devices utilizing the iodide system. We demonstrate that excess ligand addition is crucial to achieving this blueshift in thin films that otherwise suffer from energy funneling. We build devices that show electroluminescence from 440 nm to 650 nm, although they still suffer from low efficiencies due to low photoluminescence quantum yields. We finally demonstrate that these materials suffer from reversible degradation with an applied electric field, further limiting the efficiency. The favorable optoelectronic properties of perovskite materials, combined with the blueshift due to quantum confinement, shows the promise of these materials as a new class of low cost emitters.

10362-35, Session 8

Hybrid perovskite light-emitting field-effect transistors

Francesco Maddalena, Xin Yu Chin, Daniele Cortecchia, Annalisa Bruno, Cesare Soci, Nanyang Technological Univ. (Singapore)

We demonstrate AC-driven, top-contact methylammonium lead iodide perovskite light-emitting field-effect transistors (PeLEFETs) with large electron mobility, high electroluminescence efficiency, uniform emission across the channel area, and operating near room temperature.

Field-effect transistors provide a versatile architecture to increase charge carrier density, mobility and radiative recombination efficiency of light-emitting devices. Using this concept, we recently demonstrated PeLEFETs with balanced ambipolar charge transport and stable electroluminescence at low temperature (below 200 K) [1]. Ionic screening and poor charge transport are the critical issues affecting efficiency and reliability of these devices. Here we prove a tenfold improvement of the field-effect electron mobility (~0.1 cm2V-1s-1) by employing a top-contact FET architecture, and significant reduction of ionic drift/screening by applying AC-driven gate bias, resulting in brighter and more uniform electroluminescence respect to DC-driven PeLEFETs at comparable applied voltages. Most significantly, high-frequency AC operation enables electro-luminescence emission at significantly higher temperatures, approaching room temperature. These results constitute a significant leap forward toward the realization of stable perovskite PeLEFET devices with controllable emission pattern, to be used in active-matrix displays and solid state lighting.

[1] Chin et al., Nature Communications 6, 7383 (2015).

10362-36, Session 8

Halide perovskite/polymer composites for fully printed and multifunctional LEDs

Zhibin Yu, Florida State Univ. (United States)

Recently, astounding optoelectronic properties have been discovered in a group of halide perovskite materials. They share a general ABX3 chemical formula, in which A is a cesium (Cs+) or an aliphatic ammonium (RNH3+) cation, B is a divalent Pb2+ or Sn2+ cation and X is an anion such as Cl-, Br- or I-. Their crystal structures resemble the one commonly found in conventional oxide based perovskite (BaTiO3). The halide perovskites can be processed like polymeric semiconductor materials using solution based processes; and can be coated into large area thin films on arbitrary substrates; they can also be crystallized into three-dimensional periodic structures and behavior like conventional inorganic semiconductors including the superior charge transportation properties.

In this talk, our recent work of developing perovskite/polymer composites towards the realization of fully printable light-emitting diodes (LEDs) will be presented. The perovskite/polymer composites possess all the remarkable optoelectronic characteristics of pure perovskites. For instance, we have demonstrated their use for blue, green and red LEDs. In addition, the device efficiencies exceeded those of pure perovskite LEDs. The perovskite/polymer composites have shown advantages in improving the processability and quality of the perovskite thin films; and enhancing the structural stability of the perovskites especially at highly humid fabrication and service environments. By embedding the perovskite crystals inside a polymer matrix, the perovskites can be less toxic and more environmentally benign compared to pure perovskites. Applications of the perovskite/polymer composites will be discussed towards multifunctional LEDs with ultra-high luminance intensities.

10362-48, Session PMon

Quantitative analyses of photophysical processes in thermally activated delayed fluorescent emitters

Wei-Kai Lee, Kuan-Chung Pan, Shiu Yi Jiun, Chung-Chih Wu, National Taiwan Univ. (Taiwan)

In addition to phosphorescent transition metal complexes, metal-free luminophores showing efficient thermally activated delayed fluorescence (TADF) are also emerging as attractive and promising alternatives for harvesting both singlet and triplet excitons in organic electroluminescence (EL) to achieve ideal 100% internal quantum efficiency. In order to fully evaluate potentials of a TADF emitter, quantiative analyses of their rate constants for various photophysical processes are essential. In this work, by solving rate equations involving both singlet and triplet states, quantitative relationships between various photophysical rate constants of a TADF emitter and photophysical quantities (such as prompt and delayed fluorescence quantum yields and decay rates) experimentally determined from steady-state and transient photoluminescence measurements, are derived. These quantitative relationships are then used comprehensively to study and establish the correlation of photophysical properties with molecular structures for a few series of TADF emitters, and to provide further insights in design of more effective TADF materials.

10362-49, Session PMon

Conjugation-induced highly efficient thermally activated delayed fluorescence in polymer emitters

Qiang Wei, Leibniz-Institut für Polymerforschung Dresden e.V. (Germany); Paul Kleine, TU Dresden (Germany); Yevhen Karpov, Xianping Qiu, Hartmut Komber, Karin Sahre, Anton Kiriy, Leibniz-Institut für Polymerforschung Dresden e.V. (Germany); Ramunas Lygaitis, Simone Lenk, Sebastian Reineke, TU Dresden (Germany); Brigitte Voit, Leibniz-Institut für Polymerforschung Dresden e.V. (Germany)

Nowadays, thermally activated delayed fluorescence (TADF), used as a novel, efficient concept for light-emitting materials in organic light-emitting diodes (OLEDs) has seen tremendous research efforts. It is widely discussed as an alternative to phosphorescent emitter materials, assuring 100% internal quantum efficiency via effective reverse intersystem crossing (RISC) of barely radiative triplet to emissive singlet states. While many small molecules have been reported to show efficient TADF, reports on polymers sporting TADF are rare. Still, compared with small-molecules, the conjugated polymers excel in low-cost and large-area applications as they allow for “wet“ processability via ink-jet printing, roll-to-roll coating, etc. at low temperatures. However, so far the dominating and simultaneously restrictive strategy in designing of TADF polymers involves the incorporation of known TADF-active building blocks into polymer structures either as pendant groups, as main chain constituents or as core units.

By contrast, we report a novel strategy unlocking an additional molecular design rule reserved exclusively for polymeric materials. A TADF ϖ-conjugated cyclic polymer composed of non-TADF building blocks was developed. Conjugation induced HOMO destabilization leads to a decreased singlet-triplet splitting and efficient TADF in the polymer, while the repeating unit itself shows only inefficient phosphorescence. In comparison to known concepts for TADF-polymers, our work shows for the first time a methodology to design TADF polymers based on non-TADF building units, which significantly enlarges the chemical space for material development. Our research comprises synthesize, detailed quantum chemical calculations and considerations paired with an in-depths time resolved photophysical characterization.

10362-50, Session PMon

Highly efficient fluorescent organic light emitting diodes using a novel blue TADF dopant

Min Hyeong Hwang, Chil Won Lee, Byung-Doo Chin, Dankook Univ. (Korea, Republic of)

Highly efficiency blue organic Light Emitting Diodes (OLEDs) has been researched actively for an achievement of low power consumption at the application of full color display. Conventional fluorescent materials, which can only utilize singlet excitons, exhibit low efficiency characteristics due to the quantum mechanical probability limit of electron excitation. Thermally activated delay fluorescence (TADF) can provide higher efficiency by a management of energy gap between singlet and triplet excitons ; TADF materials with donor-acceptor moieties have a small singlet-triplet energy gap (ΔEST) below 0.3eV. In this study, we designed novel donor-acceptor structure for blue TADF emitters. We have employed carbazole derivative, 7,7-dimethyl-5,7-dihydroindeno[2,1-b]carbazole (DMICz), which has high triplet energy and electron donating properties. 2,4-diphenyl-1,3,5-triazine, 2,4-bis(4-(tert-butyl)phenyl)-1,3,5-triazine and 2,4-bis(4-fluorophenyl)-1,3,5-triazine were used as acceptor units and were connected with DMICz through the para position of the phenyl spacer to produce DMICzTrz, DMICztBTrz and DMICzFTrz, respectively. tert-butyl substituent weakens the electron withdrawing effect of the triazine, and fluorine atom is the substituent that enhances the electron withdrawing property. We synthesized structures that DMICz combined with modified triazine through Buchwald-Hartwig coupling reaction. Also, Optical and electrochemical properties of three TADF materials were examined by Uv-vis, photoluminescence (PL with transient data) and cyclicvoltammetry (CV). We have fabricated the blue OLED device with dopant system using Bis[2-(diphenylphosphino)phenyl]etheroxide (DPEPO) as a host material. As a result, device performance showed the maximum external quantum efficiency of 14.8% and luminous efficiency of 27.0cd/A. Our investigation might provide more chance to develop the high performance OLED device based on TADF blue dopants.

10362-51, Session PMon

Identification of degradation mechanism of organic light emitting diodes based on cyan color thermally activated delayed fluorescence emitter

Cheng Peng, Univ. of Florida (United States); Amin Salehi, Ying Chen, North Carolina State Univ. (United States); Georgios Liaptsis, cynora GmbH (Germany); Franky So, North Carolina State Univ. (United States)

Degradation mechanism is studied on organic light emitting diodes (OLEDs) based on a cyan color thermally activated delayed fluorescence (TADF) emitter with a hole dominant host and hole blocking layer. Photoluminescence (PL) intensity degradation of the OLED is measured during electrical operation at a constant driving current density. A difference is observed between the degradation in PL intensity and electroluminescence (EL) intensity. This difference is attributed to the smaller exciton formation zone compared to the emitting layer thickness. Based on the fitting of the PL and EL losses in a theoretical model, the exciton formation zone length is estimated and compared to same type of OLEDs based on common commercially available TADF emitter. Our results show that the device operational stability in these OLEDs is found to be limited by the narrow exciton formation zone near the emitting layer and hole blocking layer interface due to a poor electron injection or transport property of the emitter.

10362-52, Session PMon

Development of new dopant materials for OLED

Yun-Hi Kim, Soon-Ki Kwon, Gyeongsang National Univ. (Korea, Republic of); Jang-Joo Kim, Seoul National Univ. (Korea, Republic of)

Organic light emitting diodes (OLEDs) have evolved because of their low power consumption and the possibility to fabricate large flat panel displays. Recently, fluorescent dopants are used for blue light emission, and phosphorescent dopants are used for green or red light. In the case of the phosphorescent material as compared with the fluorescent material, both singlet and triplet excitons can be harvested for light emission, and the internal quantum efficiency can achieve 100 %. Recently, the efficient fluorescene blue emitters have been developed by using TTA and TADF. Our group developed various blue emitters. For example, we designed fluorescent emitters with horizontal emitting dipoles using interconnecting units between chromophores. As a result, the new blue fluorescence emitter showed EQE of 6.6% and CIE color coordinates of (0.145, 0.068). We also developed azasiline-based TADF blue emitters. A blue OLED based on azasiline derivatives display CIE coordinates of (0.149, 0.197) with EQE of 22.3%. In addition, we developed high efficient deep blue phosphorescene with EQE of 21.4% and CIE color coordinates of (0.152, 0.148). In here, we will introduce the design strategies for dopant materials for high-efficient and high-color pure OLED.

10362-53, Session PMon

A new class of hole-transporting material for simple-structured phosphorescent OLEDs

Jaemin Lee, Hyejin Na, Korea Research Institute of Chemical Technology (Korea, Republic of); Byung-Jun Jung, The Univ. of Seoul (Korea, Republic of)

With the growth of the OLED industry, there is a growing market demand for various types of organic materials, and development of good hole-transporting materials (HTMs) is still an important issue in OLED research. Especially, in order to prepare effective HTMs for phosphorescent OLEDs, a high enough triplet energy level that can block triplet exciton quenching as well as a well-aligned HOMO energy level with adjacent emitting layer (EML) to facilitate hole-injection/transport should be considered. We have therefore introduced relatively less-explored phenoxazine moiety in designing new HTMs in this work. By adjusting the connection of such phenoxazine moieties, a new HTM candidate, HJ-01, could be successfully prepared. The basic chemical and physical properties of the new HTM were thoroughly investigated by NMR, UV-Vis./PL spectroscopy, cyclic voltammetry and etc. Finally, a series of phosphorescent OLED devices with a configuration of [ITO/HTL/CBP:Ir(ppy)2(acac)/BPhen/LiF/Al] with different HTLs, NPB, TAPC and HJ-01, have been fabricated and characterized. The device using NPB showed low efficiency due to exciton quenching at HTL/EML interface. On the other hand, despite the relatively simple device structure with a single HTL, devices using either TAPC or HJ-01 showed a sufficiently high efficiency of about 60 cd/A. But the maximum luminance of a device containing TAPC was less than one-tenth of that of HJ-01. These results show the superiority and potential of such phenoxazine derivatives including HJ-01 as a HTL. We believe our presentation about experimental procedures and detailed results and discussions can facilitate the development of new OLED materials.

10362-54, Session PMon

Highly efficient solution processed organic light emitting diode using low refractive index electron transport layer

Amin Salehi, North Carolina State Univ. (United States); Szuheng Ho, Univ. of Florida (United States); Ying Chen, North Carolina State Univ. (United States); Cheng Peng, Univ. of Florida (United States); Franky So, North Carolina State Univ. (United States); Daniel Volz, cynora GmbH (Germany); Hartmut Yersin, Univ. Regensburg (Germany)

A low refractive index electron transporting layer (ETL) can be very effective to enhance the out-coupling efficiencies of an organic light emitting diode (OLED). However, most organic films show a high refractive index close to 1.8. In this work, we discovered that tris-[3-(3-pyridyl)mesityl]borane (3TPYMB) has a low refractive index of 1.65 (at 550 nm), which is, to the best of our knowledge, the lowest refractive index among common used ETLs up to date. Using 3TPYMB as an ETL, we demonstrated a solution processed OLED using a novel copper based thermally-activated delayed florescence (TADF) emitter [(2-(Diphenylphosphino)-4-isobutylpyridine)(PPh3)2Cu2I2] (CuI-iBuPyrPHOS), resulting in nearly 80% enhancement in external quantum efficiency (EQE).

10362-55, Session PMon

Polarized light emitters

Kristiaan Neyts, Univ. Gent (Belgium)

No Abstract Available

10362-56, Session PMon

Stable core-shell copolymer-perovskite nanohybrids

Shaocong Hou, The Rowland Institute at Harvard (United States); Yuzheng Guo, The Rowland Institute at Harvard (United States) and Swansea Univ. (United Kingdom); Qimin Quan, The Rowland Institute at Harvard (United States)

The stability issue of the emerging lead halide perovskites has placed a grand challenge in their way to practical applications as optical and optoelectronic materials. Here, we demonstrate a facile synthesis approach to achieve core-shell perovskite nanocrystals at nanoscale via copolymer micelle template. In the nanosized micelle of copolymer ligands, the coordinating blocks of copolymer in the core uptake lead precursors and passivate the surface of as-reacted perovskite nanocrystals via multidentate coordinate bonds, while the hydrophobic blocks in the shell provide excellent colloidal stability and resistance from attacks from unfavorable environments.

10362-57, Session PMon

Optical and electric properties of lead iodide-based layered perovskite with self-organized quantum-well structure

Masanao Era, Saga Univ. (Japan); Kazuhiro Ema, Sophia Univ. (Japan); Yasunori Yamada, Saga Univ. (Japan); Kento Mori, Ryoka Systems Inc. (Japan); Norio Tomotsu, Idemitsu Kosan Co., Ltd. (Japan)

In our previous work1, we found that a lead iodide-based layered perovskite with cyclohexenylethyl ammonium molecular cation as an organic layer exhibits highly efficient PL originated from an exciton having large binding energy of several hundred meV. Further, efficient EL was observed in a device having emissive layer of the layered perovskite Here, we would like to present detailed optical properties, electric properties of the layered perovskite.

Kramers-Kronig transformation of reflection spectrum measured using a crystal sample of the layered perovskite demonstrated that an exciton band locates at 2.452 eV at RT. Polarization dependencies of its PL at 4 K revealed that emission bands assigned to singlet-dominant exciton and triplet-dominant exciton are located at 2.408 eV and 2.398eV, respectively. The PL excitation spectrum measured by detecting emission of the triplet-dominant exciton demonstrated the formation of an exciton-polariton in the crystal sample; L-T splitting = 94 meV, transverse exciton energy ET = 2.410 eV, and longitudinal exciton energy EL =2.504 eV. From the values, oscillator strength of the exciton band was estimated to be 0.74, and band gap Eg and binding energy Eb of the exciton were estimated to be 2.68 eV and 282 meV, respectively. The PL quantum efficiency was evaluated to be about 0.7 at 110 K from the quantum efficiency measurement using integrated optical sphere.

We also report electronic properties and properties expected from its band structure calculated by quantum mechanical calculation in this presentation.

1) M. Era el al., Appl. Phys. Lett., 65, 676 (1994).

10362-58, Session PMon

Charge-exciton interaction rate in organic field-effect transistors by means of transient photoluminescence electromodulated spectroscopy

Stefano Toffanin, Istituto per lo Studio dei Materiali Nanostrutturati (Italy); Wouter A. Koopman, Univ. Potsdam (Germany); Marco Natali, Giovanni P. Donati, Michele Muccini, Istituto per lo Studio dei Materiali Nanostrutturati (Italy)

Charge-exciton interaction is the main dominating mechanisms limiting the efficiency in Organic Light-emitting Transistors (OLETs). Thus, a comprehensive physical understanding of this detrimental process in charge accumulation devices is mandatory in order to unlock the technological potentiality of OLETs in real-setting applications. We have recently introduced a novel confocal microscopy method for mapping the charge density spatial distribution in OFETs based on the photoluminescence electro-modulation (PLEM) [1]. Here, we implement time-resolved PLEM spectroscopy on the picosecond timescale to investigate throughout the charge-exciton interaction in organic transistors [2]. The results show that the injected charges reduce the exciton radiative recombination in two ways: (i) charges may prevent the generation of excitons and (ii) charges activate a further non-radiative channel for the exciton decay. Moreover, the measurements clearly reveal that not only trapped charges, as it was already reported in literature, but rather the entire injected charge density contributes to the quenching of excitons. Finally, the kinetic model that we propose can be generalized to all the devices based on the field-effect transistor platform given that it relies on generic description of the charge accumulation and charge-exciton interaction processes.

Based on these insights we suggest possible measures to achieve high exciton density in OLETs, which might foster the development of high brightness OLETs.

[1] Koopman W., Toffanin S., Natali M., Troisi S., Capelli R., Biondo V., Stefani A., Muccini M. Nano Lett. 2014, 14, 4.

[2] Koopman W., Natali M., Donati G. P., Muccini M., Toffanin S. ACS Photonics DOI: 10.1021/acsphotonics.6b00573.

10362-59, Session PMon

Universal charge carrier generation layers for all-solution processed, highly efficient tandem OLEDs

Stefan Höfle, Min Zhang, Christian Kayser, Alexander Colsmann, Karlsruher Institut für Technologie (Germany)

Common tandem OLEDs comprise charge carrier generation layers (CGLs) from high-work function PEDOT:PSS and low-work function ZnO, only allowing the implementation of inverted device architectures (bottom cathode). Any attempt to incorporate a ZnO/PEDOT:PSS CGL into tandem OLEDs with regular architecture (bottom anode) would inevitably lead to a dissolution of ZnO in the acidic PEDOT:PSS. In this work, we developed novel CGLs based on solution processed metal oxides that simultaneously form a barrier for subsequently used processing agents and are robust towards the use of acidic components. Therefore, they can be universally employed in regular and inverted tandem OLEDs comprising fluorescent polymers as well as small-molecule triplet and TADF emitters. In total, 11 layers were sequentially processed from solution, including charge carrier injection, transport and blocking layers, yielding maximum current efficiencies of 200 cd/A.

Since every injected electron-hole pair generates two photons, the luminance and the current efficiency of the tandem OLED at a given device current are doubled (versus a reference single OLED) while the power efficiency remains constant. At a given luminance, the lower operating current in the tandem device reduces electrical stress and improves the device life-time.

10362-60, Session PMon

Transparent electrode of silver network fabricated by using cracks of polymers as templates

Beom Sun Choy, Jeong Hui Lee, Oh Young Kim, Ho Jong Kang, Dong Hyun Lee, Dankook Univ. (Korea, Republic of)

A highly transparent electrode was fabricated using silver networks embedded in an elastomeric substrate. To prepare the porous templates of silver(Ag) inks, a brittle silica-like layer was initially produced by UV/ozone treatment and sequentially bent with certain strain to create well-controlled cracks. Average crack spacing could be accurately controlled by changing bending strains. It was found that the crack spacing was influenced by relative thickness of the brittle layer to the flexible layer, UV/ozone dose and moduli of substrates. Then, conductive silver inks were filled into the cracks by sliding a glass blade on the surface and thermally sintered to create silver networks, which were directly used as electrodes. In addition, the silver networks were simply transferred to flexible substrates by placing adhesive tapes on the silver networks and immediately peeling them off. Finally, AC voltage-driven light-emitting devices based on an ECL electrolyte consisting of $Ru(bpy)_3^{2+}$ (ECL luminophore) and [EMI][TFSI] (ionic liquid) were demonstrated by applying the silver networks as electrodes.

10362-61, Session PMon

Organic light-emitting diodes with polyethylenimine as a solution-processed electron injection layer: Operational stability and degradation mechanisms

Sebastian Stolz, Karlsruher Institut für Technologie (Germany) and InnovationLab GmbH (Germany); Yingjie Zhang, Univ. of Waterloo (Canada); Ulrich Lemmer, Karlsruher Institut für Technologie (Germany); Gerardo Hernandez-Sosa, Karlsruher Institut für Technologie

(Germany) and InnovationLab GmbH (Germany); Hany Aziz, Univ. of Waterloo (Canada)

The fabrication of organic light-emitting diodes (OLEDs) by printing techniques requires the development of solution-processable electron injection layers (EILs). Over the last few years, amine-based EIL materials like Polyethylenimine (PEI) have received a lot of attention as they can be used with a multitude of electrode materials.1–3

In this work, we investigate the operational stability of OLEDs, which use PEI as EIL, and we show that the cathode metal that is in contact with the EIL plays a crucial role for the device lifetime. In case of Al, the primary degradation mechanism during electrical driving is caused by excitons which reach and subsequently degrade the emitter/PEI interface. At a current density of 20 mA cm-2, an LT50 lifetime of ~ 200 h is achieved. In contrast, in case of Ag, an additional mechanism degrades the OLEDs; during operation holes accumulate at the emitter/PEI interface and as a result the emitter quantum yield drops. Consequently, the operational lifetime of such OLEDs is significantly shorter with an LT50 value of < 10 h. Finally, we show that the degradation by excitons can be significantly slowed down by the use of a PEI:ZnO composite EIL. As a result, the LT50 lifetime of OLEDs with an Al cathode is increased by a factor of five, without adversely affecting OLED performance.

1: Zhou et al., Science 2012, 336, 327–332.

2: Stolz et al., ACS Appl. Mater. Interfaces 2014, 6, 6616–6622.

3: Stolz et al., ACS Appl. Mater. Interfaces 2016, 8, 12959–12967.

10362-62, Session PMon

To eliminate coffee ring effect during Inkjet printing of functional polymers for PLED

Yanchun Han, Changchun Institute of Applied Chemistry (China)

Organic/polymer light emitting diodes (O/PLEDs) have been attracting much attention due to their high brightness, wide viewing angle, low power consumption and good contrast. Inkjet printing is considered one of the most promising technology in the field of controlled deposition of polymers and functional materials in well-defined patterns, especially in relation to the fabrication of multicolor OLED displays. For OLED displays, the accuracy and uniformity of organic layer thickness is an important manufacturing issue. This talk will attempt to answer questions about how to eliminate coffee ring effect and improve film uniformity of inkjet printed films by low surface tension of PEDOT inks, suppression the outer-flow and edge deposition of poly (spirobifluorene) by the addition of co-solvent with high boiling point and high viscosity. By improving the uniformity of the film thickness, the performance of devices with ink-jet printed poly (spirobifluorene) film can reach 70% of the spin-coated devices.

10362-63, Session PMon

Simulation of exciton effects in OLEDs based on the master equation

Weifeng Zhou, Christoph Zimmermann, Christoph A. Jungemann, RWTH Aachen Univ. (Germany)

The luminous efficiency of OLEDs greatly depends on the doping profile in the emission layer (EL). To investigate this effect, occupancies of singlets and triplets are calculated with an extension to our numerical bipolar master equation model. Both Foerster and Dexter energy transfer of excitons are included and exciton energy equals the bandgap between LUMO and HOMO reduced by a binding energy. Exciton dissociation into free carriers involves an escape of the bound electron or hole at a donor-acceptor pair. Radiative and non-radiative decay, inter-system crossing, exciton-polaron quenching and triplet-triplet annihilation are all included with respective lifetimes. Based on appropriate parameters, the IV measurements of OLEDs, with a PH1 EL doped by Irppy and sandwiched between NPB and Alq as hole and electron transport layer (HTL and ETL) respectively, are well simulated in the space-charge-limited-current regime. For the OLEDs with higher constant dopant concentrations, excitons are produced in a broader region at the anode side of the EL, leading to lower exciton diffusion into the adjacent HTL and higher efficiencies. The efficiency roll-off of the OLED with 30% constant dopant may originate from exciton diffusion into the ETL and dopant-assisted dissociation. The best luminous performance is achieved by a graded dopant concentration from 30% at the anode to 0% at the cathode side of the EL with the merits of broad exciton distribution within and confined to the EL.

10362-64, Session PMon

Monte Carlo simulation of OLEDs by hopping conduction in the distributed density of state

Mun Chae Yoon, Il Hoo Park, Jinyoung Yun, Gyutae Kim, Korea Univ. (Korea, Republic of)

The light emission from organic light emitting diodes (OLEDs) is closely related to the electrical characteristics of the organic layers constituting OLEDs. Therefore, it is important to investigate and analyze the electrical parameters of the organic layers for improving the performance of OLEDs.

Unlike crystalline materials in conventional semiconductors, organic materials hardly form a continuous energy band. The analysis methods in conventional inorganic semiconductors cannot be applied to organic devices, requiring properly modified method considering the physical and chemical characteristics of organic materials.

However, carrier injection and transport mechanisms determining the electrical characteristics of OLEDs are not clearly confirmed. Especially, space charge limited conduction (SCLC) and hopping conduction are referred as dominant transport mechanism in organic materials. But, those studies are lack of enough explanation on the distribution of the highest occupied molecular orbital (HOMO) and lowest unoccupied molecular orbital (LUMO), which are closely related to electrical characteristics of organic materials.

In this paper, a Monte Carlo simulation model based on the hopping transport through organic layers is suggested. This model considers the distribution of HOMO/LUMO levels in OLEDs for the realistic disordered states. The tunneling event is considered as carrier injection or extraction with hopping of carriers among the HOMO/LUMO levels as carrier transports in the organic materials.

The validity of the model will be verified by comparing I-V curve, light spectrum and noise characteristic of the model with the real OLED devices.

10362-65, Session PMon

Boosting OLED efficiency by blending: spectroscopic identification of reduced charge trapping

Elham Khodabakhshi, Gert-Jan Wetzelaer, Paul W. M. Blom, Jasper Michels, Max-Planck-Institut für Polymerforschung (Germany)

Many polymeric semiconductors of use in organic light-emitting diodes (OLEDs) are known to suffer from a strongly suppressed electron current due to the presence of trap states within the bandgap. As a consequence, the electron current density may well be several orders of magnitude lower than the holes current density. This unbalanced charge transport limits the efficiency of the device. An important loss process is so-called trap-assisted recombination, where holes non-emissively recombine with trapped electrons. Very recently, we have experimentally shown that if the traps are distributed in energy or sufficiently deep, their negative effect can be eliminated by spatially separating the charge accommodation sites via dilution of the semiconductor in an insulating host material, such as polyvinyl carbazole (PVK) or polystyrene (PS). The observed increase in electron current and luminous efficiency validates long standing theoretical predictions. In this contribution, we present an analogous study based on the blue emitter poly(9,9-dioctylfluorene) (PFO), as it provides the possibility of directly visualizing the reduction of charge trapping green emission upon blending. This feature is obtained when the PFO contains a small fraction of fluorenenone monomers, which represent emissive trap states whilst integrated in the polymer backbone. Our results show that by blending disordered emitters with affordable insulating materials, electron and hole transport become balanced, leading to increased OLED efficiency by reducing both the radiative and non-radiative trap assisted recombination. Hence, our method may pave the way to cost-effective large scale production of highly efficient OLEDs.

10362-66, Session PMon

Effect of dopant polarity on the recombination mechanism in organic light-emitting diodes

Chang-Heon Lee, Jeong-Hwan Lee, Kwon-Hyeon Kim, Jang-Joo Kim, Seoul National Univ. (Korea, Republic of)

The recombination of charges is an important process in photonic devices such as organic light-emitting diodes (OLEDs) and organic photovoltaics because the process influences characteristics such as the driving voltage, efficiency and lifetime. Until now, trap depth has been considered the most important factor determining the recombination mechanism. Recombination at dopant becomes dominant if the dopant acts as deep trap site. Therefore, trap-assisted recombination is known as the dominant mechanism in phosphorescent dye-doped OLEDs (PhOLEDs) because the energy levels of the dopants are located deep compared with the host energy levels and act as trap sites. By contrast, there have been reports that some PhOLEDs with deep trap depths have Langevin-dominant characteristics. Unfortunately, the reason why Langevin recombination is dominant in these devices has not been determined. Here we report that the dipole moment of the dopant is a major factor influencing the recombination mechanism in dye-doped organic light-emitting diodes(OLEDs). Introducing dipole trap theory into the drift-diffusion model revealed that dipole moment becomes a major factor determining the recombination mechanism if trap depth is > 0.3 eV where any detrapping effect becomes negligible. Our experimental results showed that homoleptic Ir complexes possessing large dipole moments, exhibited trap-assisted recombination-dominant characteristics and that heteroleptic Ir complexes with small dipole moments exhibited Langevin recombination-dominant characteristics. Dopants with larger dipole moments can readily trap a charge with stronger Coulomb attraction, which in turn boosts trap-assisted recombination.

10362-67, Session PMon

Electrical degradation model of OLEDs depending on driving conditions

Ilhoo Park, Korea Univ. (Korea, Republic of)

OLEDs are widely used in display application because they are cheap and efficient in power consumption. By optimizing the materials and the designs, manufacturers can tune the electrical and opto-electronic properties of OLEDs. The opto-electronic properties of OLEDs are also changed by external conditions such as temperature, DC bias, defects, etc..

Reliability and lifetime are important issues in OLEDs, which have been improved by managing cleanliness and evaporation circumstance in fabrication. However, degradations occurs with the appearance of dark spots initiated by small pinholes, which is still the important problem to overcome. Therefore accurate evaluation of performance and lifetime is still required.

The researches on the degradation of OLEDs with secondary effects of dark spots were reported. The size of dark spot were reported linearly increase with the constant current through the OLEDs. The pinholes made during the process of the manufacture is known to play a major role in degradation phenomena owing to the possible intrusion of water and oxygen through the pinholes.

In this paper, we investigated the correlation of the degradation of OLEDs with the growth of dark spots under different conditions such as drive current, temperature, etc. By impedance analysis, the resistance and the capacitance of OLEDs are extracted depending on the bias condition. The resistance increased and the capacitance decreased as time increased.

We suggest more realistic model with environmental and time dependent parameters in the equivalent circuit model of OLEDs. By considering the growth effects of dark spots, we can evaluate and design the performance and lifetime more accurately.

10362-68, Session PMon

Achievement of long device lifetime by decreasing dipole moment of hole-blocking layer

Ko Inada, OPERA Ctr. for Organic Photonics and Electronics Research (Japan) and Japan Science and Technology Agency (JST), ERATO, Adachi Molecular Excton Engineering Project (Japan); Hiroshi Fujimoto, i3-OPERA (Japan) and OPERA Ctr. for Organic Photonics and Electronics Research (Japan); Masayuki Yahiro, Institute of Systems, Information Technologies and Nanotechnologies (ISIT) (Japan) and i3-OPERA (Japan) and OPERA Ctr. for Organic Photonics and Electronics Research (Japan); Satoshi Yukiwaki, i3-OPERA (Japan); Keiko Kusuhara, OPERA Ctr. for Organic Photonics and Electronics Research (Japan) and Japan Science and Technology Agency (JST), ERATO, Adachi Molecular Exciton Engineering Project (Japan); Nozomi Nakamura, OPERA Ctr. for Organic Photonics and Electronics Research (Japan) and International Institute for Carbon Neutral Energy Research (WPI-I2CNER) (Japan); Atula S. D. Sandanayaka, OPERA Ctr. for Organic Photonics and Electronics Research (Japan) and Japan Science and Technology Agency (JST), ERATO, Adachi Molecular Excton Engineering Project (Japan); Chihaya Adachi, OPERA Ctr. for Organic Photonics and Electronics Research (Japan) and International Institute for Carbon Neutral Energy Research (WPI-I2CNER) (Japan) and Japan Science and Technology Agency (JST), ERATO, Adachi Molecular Excton Engineering Project (Japan)

We applied extremely pure 2,4,6-tris(biphenyl-3-yl)-1,3,5-trazine (T2T) as the hole-blocking layer in organic light-emitting diodes (OLEDs) with an emission layer of 3,3-di(9H-carbazol-9-yl)biphenyl (mCBP) as host and (4s,6s)-2,4,5,6,-tetra(9H-carbazole-9-yl)isophthalonitrile (4CzIPN) as guest. Even though the current-density–voltage characteristics and external quantum efficiencies were the same as for devices using T2T with typical purities, the lifetimes were approximately nine-times longer for OLEDs with the extremely pure T2T. The dominant impurities affecting lifetime were determined to be chlorine-containing T2T derivatives having large dipole moments, which cause the charging of host and guest molecules in the emission layer near the interface with the hole-blocking layer. Density function theory calculations support that the degradation occurs through the charged host and guest molecules.

10362-69, Session PMon

High thermal stability OLEDs

Jared S. Price, Baomin Wang, Yufei Shen, Noel C. Giebink, The Pennsylvania State Univ. (United States)

Reliability remains an ongoing challenge for organic light emitting diodes

(OLEDs) as they expand in the marketplace. The ability to withstand operation and storage at elevated temperature is particularly important in this context, not only because of the inverse dependence of OLED lifetime on temperature, but also because high thermal stability is fundamentally important for high power/brightness operation as well as applications such as automotive lighting, where interior car temperatures often exceed the ambient by 50°C or more. Here, we present a strategy to significantly increase the thermal stability of small molecule OLEDs by co-depositing an additive that stabilizes their morphology and prevents crystallization. Using this approach, we demonstrate that the thermal breakdown limit of common electron and hole transport materials can be increased from typical temperatures of ~100°C to more than 200°C with minimal impact on their electrical transport properties. Similar enhancements are demonstrated in complete OLEDs ranging from simple bilayer fluorescent to multilayer phosphorescent devices. The generality of our approach points toward a new class of thermally robust and morphologically-stable organic electronic devices that are capable of operating or being stored in extreme thermal environments.

10362-70, Session PMon

Kirigami-based three-dimensional OLED concepts for architectural lighting

Taehwan Kim, Jared S. Price, Alex Grede, Sora Lee, Thomas N. Jackson, Noel C. Giebink, The Pennsylvania State Univ. (United States)

Dramatic improvements in white organic light emitting diode (OLED) performance and lifetime over the past decade are driving commercialization of this technology for solid-state lighting applications. As white OLEDs attempt to gain a foothold in the market, however, the biggest challenge outside of lowering their manufacturing cost arguably now lies in creating an architecturally adaptable form factor that will drive public adoption and differentiate OLED lighting from established LED products. Here, we present concepts based on kirigami (the Japanese art of paper cutting and folding) that enable intricate three-dimensional (3D) OLED lighting structures from two dimensional layouts. Using an ultra-flexible, encapsulated OLED device architecture on 25 ?m thick clear polyimide film substrate with simple cut and fold patterns, we demonstrate a series of different lighting concepts ranging from simple pyramidal shapes to more complex artistic designs such as stretchable window blind-like panels, multi-element globes, and candle flames. We only find slight degradation in OLED electrical performance when these designs are shaped into 3D and, because they naturally pack more OLED active area into the footprint of a traditional flat panel, these 3D OLED designs effectively enable higher luminance to be achieved at a given device current density. Our results point to an alternate paradigm for OLED lighting that moves beyond traditional 2D panels toward 3D designs that deliver unique and creative new opportunities for lighting.

10362-71, Session PMon

How to distinguish scattered and absorbed light from re-emitted light for solid-state lighting?

Maryna L. Meretska, Ad Lagendijk, Henri N. Thyrrestrup, Allard P. Mosk, Univ. Twente (Netherlands); Wilbert L. IJzerman, Philips Lighting B.V. (Netherlands); Willem L. Vos, Univ. Twente (Netherlands)

Energy efficient generation of white light has become an important issue in recent years. Technology of white-light emitting diodes (LEDs) is one of the promising directions. The main challenges in the LED production are understanding scattering, absorption and emission from ab-initio, and obtain chromaticity independent emission directions. Physical understanding of multiple light scattering in the LED can provide us with simple tools for extracting optical parameters of this system.

We have studied the transport of light through phosphor diffuser plates that are used in commercial solid-state lighting modules (Fortimo). These polymer plates contain YAG:Ce+3 phosphor particles that both elastically scatter light and Stokes shift light in the visible wavelength range (400-700 nm). We excite the phosphor with a narrowband light source, and measure spectra of the outgoing light. The Stokes shifted light is spectrally separated from the elastically scattered light in the measured spectra. Using this technique we isolate the elastic transmission of the plates. This result allows us to extract the transport mean free path ltr over the full wavelength range by employing diffusion theory. Simultaneously, we determine the absorption mean free path labs in the wavelength range 400 to 530 nm where YAG:Ce+3 absorbs. The diffuse absorption (μ_a=1/l_abs) spectrum is qualitative similar to the absorption coefficient of YAG:Ce+3 in powder, with the diffuse spectrum being wider than the absorption coefficient. We propose a design rule for the solid-state lighting diffuser plates.

10362-72, Session PMon

Semi-transparent vertical organic light emitting transistors based on a perforated indium-tin-oxide source electrode

Szuheng Ho, Univ. of Florida (United States); Hyeonggeun Yu, Nilesh Barange, Ryan Larrabee, Franky So, North Carolina State Univ. (United States)

Transparent or semi-transparent devices have found more versatile applications with the growing interest in smart gadgets. Vertical organic light emitting transistors (VOLETs), whose architecture features a vertical integration of a light emitting unit and the switching transistor, stand out as a novel device for transparent displays with high aperture ratio and low power consumption. However, the transparent VOLET hasn't been demonstrated because it is difficult to control the suitable roughness and obtain high transmittance from the thin metal source electrode. Herein, we for the first time fabricate semi-transparent VOLETs using indium tin oxide (ITO) source electrode. The maximum luminance and current efficiency are 500 cd/m2 and 8.8 cd/A on the bottom side, and 250 cd/m2 and 4.6 cd/A on the top side, which are the highest among the reported transparent organic light emitting transistors. With a porous ITO source electrode, the enhanced light extraction is observed and confirmed with a finite-difference time-domain simulation. Furthermore, the correlation between channel layer thickness and luminance ratio of bottom to top is investigated. The results presented here offer a new device approach for transparent displays.

10362-73, Session PMon

Experimental investigating distinguishable and non-distinguishable grayscales applicable in active-matrix organic light-emitting diodes for quality engineering

Henglong Yang, Wen-Cheng Chang, Yu-Hsuan Lin, Ming-Hong Chen, National Taipei Univ. of Technology (Taiwan)

The distinguishable and non-distinguishable grayscales of green and red organic light-emitting diode (OLED) with 64 (6-bit) grayscale control were experimentally investigated by using high-sensitive photometric instrument. The feasibility of combining external detection system for quality engineering to compensate the grayscale loss based on preset grayscale table as OLED degraded during operation was also investigated by SPICE simulation. Although active-matrix organic light-emitting diode (AMOLED) has been used in smart phones and TV, degradation phenomena caused by thin-film transistor (TFT) circuitry or OLED itself are major quality issues. The degradation loss of OLED deeply affects image quality as grayscales become inaccurate. The brightness of OLED is linearly dependent on driving current in general. The distinguishable grayscales are indicated as those brightness differences and corresponding current increments are differentiable by instrument. The grayscales may become non-distinguishable as current or voltage increments are in the same order of noise level in circuitry. The distinguishable grayscale tables for individual

red, green, blue, and white colors can be experimentally established as preset reference for quality engineering (QE) in which the degradation loss is compensated by corresponding grayscale numbers shown in preset table. The degradation loss of each OLED colors is quantifiable by comparing voltage increments to those in preset grayscale table if precise voltage increments are detectable during operation. The QE of AMOLED can be accomplished by applying updated grayscale tables. Our preliminary simulation result revealed that it is feasible to quantify degradation loss in terms of grayscale numbers by using external detector circuitry.

10362-74, Session PMon

White emission based on excimer emission control of triple core chromophores

Hyocheol Jung, Kyung Hee Univ. (Korea, Republic of); Jaehyun Lee, Kyoto Univ. (Japan); Hwangyu Shin, Joonghan Kim, The Catholic Univ. of Korea (Korea, Republic of); Daisuke Yokoyama, Yamagata Univ. (Japan); Hidetaka Nishimura, Atsushi Wakamiya, Kyoto Univ. (Japan); Jongwook Park, Kyung Hee Univ. (Korea, Republic of)

Three triple-core chromophore derivatives based on anthracene and pyrene or chrysene moieties were synthesized and characterized. All three materials showed highly twisted core structures and exhibited excimer emission when prepared as a film. Excimer emission makes single molecular white emission possible, and can be interpreted by anisotropic intermolecular alignment (orientation effect). The maximum wavelength of excimer emission was controlled by varying the core chromophore at the center position of the triple-core chromophore, with excimer emission of 1,6 DAP-TP, DAC-TP, and 2,7 DAP-TP occurring at 591 nm, 556 nm, and 537 nm, respectively. When the three materials were used as an OLED emitting layer, the CIE coordinate values of 1,6 DAP-TP, DAC-TP, and 2,7 DAP-TP were (0.37, 0.31), (0.30, 0.37), and (0.32, 0.44), respectively, indicating white emission. Especially, the device based on 2,7 DAP-TP acted as a WOLED with a high efficiency of 6.01 cd A-1 at 10 mA cm-2. The present findings demonstrate that triple-core chromophores composed of various chromophores can be applied in OLED lighting applications.

10362-75, Session PMon

High-efficiency orange-red organic electrophosphorescent devices with excellent operational stability

Pang-Chi Huang, Meng Hao Chang, Jin-Sheng Lin, Mei-Rurng Tseng, Industrial Technology Research Institute (Taiwan)

A novel orange-red phosphorescent iridium complex PR-24 has been successfully synthesized and characterized. By using this material, we demonstrated the high-efficiency OLED devices. The best efficiency was achieved for a device using PR-24 as the dopant, exhibiting 25.8 cd/A current efficiency, 20.0 lm/W power efficiency and 15.9% EQE at 1000 cd/m2. Moreover, when using the optimized co-host configuration, PR-24 shows a remarkable lifetime T50 of 211,000 h for an initial luminance of 1000 nits.

10362-76, Session PMon

White electroluminescence from single polymers with high power efficiency

Shiyang Shao, Changchun Institute of Applied Chemistry (China)

White electroluminescence from a single polymer represents an approach to realize low-cost plastic-based lighting application without the risk of phase segregation that is observed for the conventional physical blend systems. However, the molecular design of single white-emitting polymers (SWPs) is challenging and their performance is yet far from practical application.

This presentation will discuss some new design concepts toward high power efficiency SWPs: (1) non-conjugated polyarylether hosts showing both high triplet energy and bipolarity; (2) all-phosphorescent SWPs with power efficiency comparable with that of fluorescent lamps.

Different from the conventional conjugated polymer hosts (PFs, PCzs and so on) and PVK host, non-conjugated polyarylether hosts, namely poly(arylene ether phosphine oxide) hosts are designed for white phosphorescent OLEDs. These hosts feature a triarylphosphine oxide-containing main chain and carbazole-containing side chain, giving both high triplet energy (2.96 eV) and bipolarity.

On the basis of the polyarylether hosts, all-phosphorescent SWPs are designed by combining a high-energy-level blue phosphor with a high HOMO-level polyaryl ether host to achieve power efficiency comparable with that of fluorescent lamps (>40 lm/W). The role of the high-energy-level blue phosphor is to eliminate the hole scattering between the blue phosphors and polymer hosts, while the high HOMO-level polyaryl ether host is to reduce the hole injection barrier from the anode to the host, which both lead to a low driving voltage of <3.0 V.

10362-77, Session PMon

Controlling preferential alignment of heteroleptic phosphors in organic guest-host systems via film preparation parameters

Thomas Lampe, Philippe Linsmayer, Tobias D. Schmidt, Wolfgang Brütting, Univ. Augsburg (Germany)

The preferential alignment of organic small molecules in thin films is a very promising approach to increase the efficiency of organic light emitting devices. In this work we focus on the molecular orientation of heteroleptic Ir-complexes embedded in different organic host systems. While the underlying mechanism for the horizontal alignment in films prepared from evaporation techniques has already been described[1], we have recently performed experiments suggesting various contributing interactions, which can be identified from the preparation via solution processing. The results indicate dependence not only on the preparation technique itself but also on the dopant concentration as well as thermal post-deposition treatments. From the experiments we conclude on the contribution of three alignment mechanisms[1–3] to the film morphology, having different effects on the dye orientation. While the interaction of the heteroleptic complexes with the aromatic film surface is dominant during step-by-step deposition such as thermal evaporation[1], in solution processed films the alignment seems to be determined by host-dopant[2] and dopant-dopant[3] related processes. The results provide a better understanding of the orientation of heteroleptic Ir-complexes, thus having important impacts on the improvement of device efficiency.

[1] M. J. Jurow, C. Mayr, T. D. Schmidt, T. Lampe, P. I. Djurovich, W. Brutting, M. E. Thompson, Nature materials 2016, 15, 85.

[2] K.-H. Kim, S. Lee, C.-K. Moon, S.-Y. Kim, Y.-S. Park, J.-H. Lee, J. Woo Lee, J. Huh, Y. You, J.-J. Kim, Nature communications 2014, 5, 4769.

[3] A. Graf, P. Liehm, C. Murawski, S. Hofmann, K. Leo, M. C. Gather, J. Mater. Chem. C 2014, 2, 10298.

10362-78, Session PMon

Probing molecular orientation of organic molecules for organic light-emitting diode applications

Johnny K. W. Ho, Hong Kong Baptist Univ. (Hong Kong, China); Sai Wing Tsang, City Univ. of Hong Kong (Hong Kong, China); Shu Kong So, Hong Kong Baptist Univ. (Hong Kong, China)

Molecular orientation is found to be one of the factors in the out-coupling efficiency in organic light-emitting diodes. Studies based on optical methods are commonly used to measure the orientation order parameter and the preferred orientation, but the origin of such orientation is yet clear. We present here probing the preferred orientation with electrical approach by organic thin-film transistors (OTFTs). The carrier mobility of OTFT is dominated by the orientation of first few monolayers of the active layer in contact with the gate dielectric, which can be used to study the impact of molecular orientation. The interfacial dipoles of the gate dielectic plays a significant role in altering the molecular orientation. The influence of carrier mobility between different organic and iridium-based molecules with controlled ordered and random orientation was studied and the negative correlation between the carrier mobility ratio and degree of preferred molecular orientation was demonstrated.

10362-79, Session PMon

Controllable random nano-structures for organic light-emitting diodes

Yungui Li, TU Dresden (Germany); Milan Kova?i?, Univ. of Ljubljana (Slovenia); Paul-Anton Will, TU Dresden (Germany); Jasper Westphalen, Fraunhofer-Institut für Organische Elektronik, Elektronenstrahl- und Plasmatechnik (Germany); Manuela Junghähnel, Fraunhofer-Institut für Organische Elektronik, Elektronenstrahl- und Plasmatechnik FEP (Germany); Steffen Oswald, Leibniz-Institut für Festkörper- und Werkstoffforschung Dresden (Germany); Simone Lenk, Sebastian Reineke, TU Dresden (Germany)

Here, we report on controllable random nano-structures for light outcoupling in bottom-emitting organic light-emitting diodes (OLEDs). Wrinkle structures are generated by reactive ion etching (RIE) on polydimethylsiloxane (PDMS) and are randomly distributed on the entire surface with a periodicity distribution from 60 nm to more than 1000 nm. By optimizing the PDMS pretreatment conditions and RIE treatment recipes, we can reliably control the wrinkle geometry both in periodicity distribution and depth. We will discuss the physical reason why we can control the random wrinkle structures by using X-ray photoelectron spectroscopy of the RIE treated surface composition and dynamic mechanical analysis of various PDMS pretreatment conditions. We further obtain structures with a fixed periodicity distribution peaking at around 300 nm and different depth from 60 nm to 140 nm. OLEDs on wrinkle structures provide a better color stability with increasing viewing angle. To analyze the OLED emission, we bring together finite element method for thin organic films in the thick incoherent layers and at the structured surface. Therefore, the wrinkle structures are assumed to be a combination of sinusoidal wave patterns with different periodicity. OLEDs based on these wrinkle structures show enhanced light outcoupling. Simulation shows external quantum efficiency increases from about 20% for the planar device to 47% for buckled device.

10362-80, Session PMon

How high can the external quantum efficiency of OLEDs become by a scattering approach?

Jinouk Song, KAIST (Korea, Republic of); Kwon-Hyeon Kim, Seoul National Univ. (Korea, Republic of); Eunhye Kim, KAIST (Korea, Republic of); Jang-Joo Kim, Seoul National Univ. (Korea, Republic of); Seunghyup Yoo, KAIST (Korea, Republic of)

Increasing the external quantum efficiency (EQE) of OLEDs is a key agenda not only for display and general lighting but also for emerging applications such as automotive and wearable electronics. Several efforts have been made to realize OLEDs with high EQE by, for instances, using emitters with preferred horizontal dipole orientation or by taking advantage of cavity resonant effect [1,2]. However, these EQE values are still smaller than those of inorganic counterparts. In order to accomplish ultimately high EQEs yet without incurring too high fabrication cost, it is essential to introduce a light extraction structure that is practically viable and cost-effective. In this regard, an approach based on light-scattering layers has been of significant interest and proven quite effective. Nevertheless, there have been few studies that try to predict the maximum-achievable efficiency by considering both a base OLED structure and the effect of a scattering layer. Such study would be important because it is often challenging, even with a light-extraction structure, to further improve the EQE of already efficient OLEDs, which calls for more delicate and systematic design.

Hence, we here adopt a trans-scale simulation [3] to provide one with a global, bird-eye view on the EQE of OLEDs equipped with a scattering layer. The trans-scale simulation is done by combining a classical dipole model for a base, multilayer structure and a radiative transfer theory for the optical effect of a scattering layer. The latter, in particular, is based on equations rather than Monte-Carlo approach [3], making it easy to integrate two different domains and enable a fast, global simulation. Our study reveals that EQE over 50% is feasible when a scattering medium with forward-intensive scattering particles is combined with an emitter having a high horizontal dipole ratio.

Reference

[1] Kim, Kwon-Hyeon et al., Chemistry of Materials, 28 (20), 7505-7510 (2016)

[2] Lee, Jaeho et al. Nature Communications, 7, 11791 (2016).

[3] Kim, Eunhye et al. Advanced Materials, 27, 1624-1631 (2015, March)

10362-81, Session PMon

Inkjet-printed polymer-based scattering layers for enhanced light outcoupling from top-emitting organic light-emitting diodes

Armin Heinrichsdobler, OSRAM OLED GmbH (Germany) and Friedrich-Alexander-Univ. Erlangen-Nürnberg (Germany); Manuel Engelmayer, OSRAM OLED GmbH (Germany) and Univ. Augsburg (Germany); Daniel Riedel, OSRAM OLED GmbH (Germany) and Friedrich-Alexander-Univ. Erlangen-Nürnberg (Germany); Christoph J. Brabec, Friedrich-Alexander-Univ. Erlangen-Nürnberg (Germany); Thomas Wehlus, OSRAM OLED GmbH (Germany)

High refractive index polymer-based scattering layers used as internal light extraction layers are a promising low-cost approach to enhance the luminous efficacy of organic light-emitting diodes (OLEDs). In order to avoid damaging of the OLED layers a structured and contactless deposition method for the polymer-based scattering layers is required. For enhanced lifetime of the devices water diffusion through the scattering layer has to be eliminated by a structured patterning technique. Inkjet printing offers both a contactless and structured deposition.

In this study we evaluate inkjet printing of nanocomposite polymer-based scattering layers for OLEDs. A detailed view on the material and process development is given. This involves an optimization of ink formulation, printing parameters as well as layer formation. The resulting haze values of the scattering layers vary between 40% and 90% for different layer thicknesses. The gain in external quantum efficacy of top-emitting OLEDs induced by light scattering compared to reference devices peaks at a factor of 2.3

The obtained results are discussed and verified by an optical volume scattering simulation model which will be presented in full detail. Also a parameter variation study and its impact on extraction efficiency will be shown.

10362-82, Session PMon

Complex 3D photonic films used as external diffractive layer to improve blue OLEDs

Michal Mruczkiewicz, Univ. Bordeaux 1 (France); Frederic Dumur, Aix-Marseille Univ. (France); Mathias Perrin, Univ. Bordeaux 1 (France); Arthur Bertrand, Univ. de Pau et des Pays de l'Adour (France); Stéphane Reculusa, Institut des Sciences Moléculaires-NSysA (France); Christine Dagron-Lartigau, Antoine Bousquet, Univ. de Pau et des Pays de l'Adour (France); Lurence Vignau, Univ. Bordeaux 1 (France); Laurent Billon, Univ. de Pau et des Pays de l'Adour (France); Sophie Fasquel, Univ. Bordeaux 1 (France)

Blue OLEDs are essential to fabricate efficient color displays, but have a relatively low efficiency. Indeed, the produced light is strongly coupled to the optical modes of the metallo-dielectric stack waveguide, and tend to remain inside the medium of high optical index. Typically, only 20% of the electrogenerated photons are coupled to free space. To extract more light, several methods have been proposed, from the internal structuration of the organic layers, to the addition of an external diffractive layer made of micro-lenses or disordered structures.

Internal structuration of the OLED yields high improvements of the external quantum efficiency, but is complicate and costly to set up. We will present low cost techniques that can be easily scaled up to large surface OLEDs. These later uses dielectric films made either with the Langmuir-Blodgett technique [1], either using Breath Figure techniques [2]. We measured an improvement up to 40% of the EQE for a blue OLED emitting at 480 nm.

Besides, we will present a numerical model of this three-dimensional optical OLED cavity. This later extends the well-known one-dimensional formalism that is commonly used to model OLED stacks. It permits to link simply the electrical properties (exciton distribution) to the optical gain in an OLED caped with 3D photonic crystal, what enables global optimisation of 3D-OLED architectures. Eventually, we derive a simple criterion to optimize the photonic crystal shape and size, knowing the architecture of the planar OLED stack.

[1] Opt Express. 2016 Nov 28;24(24):27184-27198

[2] Soft Matter 2016 Jan 3;12(3):790-7.

10362-83, Session PMon

Cavity dependent Bragg scattering in red top-emitting organic LEDs

Paul-Anton Will, Elisabeth Schwarz, Cornelius Fuchs, Reinhard Scholz, Simone Lenk, Sebastian Reineke, TU Dresden (Germany)

We present a study of red top-emitting organic light-emitting diodes (OLEDs) comprising one dimensional nanoimprinted Bragg gratings beneath the opaque bottom electrode. The scattering of the trapped waveguide (WG) and surface plasmon polariton (SPP) modes is experimentally investigated and compared to results of a new sophisticated a-priori simulation of corrugated OLEDs. While the gratings properties are kept constant, a systematic variation of the cavity length is performed. Angular dependent spectral radiant intensity (SRI) measurements reveal that the cavity thickness strongly influences the occurring interference between the scattered non-radiative WG and SPP modes and the radiative cavity mode. Since an azimuthal symmetry of the corrugated OLED pixel is not given, an integrating sphere is used to determine the external quantum efficiencies (EQE). Compared to planar references, we find a decreased EQE for the 1st and 2nd optical maxima, but an eightfold enhanced EQE in the optical minimum for the OLED with Bragg grating. The enhancement originates mainly from a single scattered WG mode, which can be identified by comparing the SRI of the corrugated OLED to the simulated power dissipation spectra of the planar reference. Furthermore, we can qualitatively predict the SRI of the corrugated OLED in the optical minimum with our new simulation tool. We discuss the agreement between experiment and simulation in dependence of simulation parameters. Crucial quantities arise from the Bragg grating like period, height, and profile shape as well as from the OLED like layer thicknesses, coherence length, and optical constants.

10362-84, Session PMon

Towards continuous-wave operation of organic semiconductor lasers

Atula S. D. Sandanayaka, Toshinori Matsushima, Fatima Bencheikh, Kou Yoshida, Munetomo Inoue, OPERA Ctr. for Organic Photonics and Electronics Research (Japan); Takashi Fujihara, Institute of Systems, Information Technologies and Nanotechnologies (ISIT) (Japan); Kenichi Goushi, Jean-Charles Ribierre, Chihaya Adachi, OPERA Ctr. for Organic Photonics and Electronics Research (Japan)

The demonstration of continuous-wave lasing from organic semiconductor films is highly desirable for practical applications in the areas of spectroscopy, data communication and sensing but still remains a challenging objective. Here, we report low-threshold surface-emitting organic distributed feedback lasers operating in the quasi-continuous-wave regime at 80 MHz as well as under long pulse photoexcitation of 30 ms. This outstanding performance was achieved using an organic semiconductor thin film with high optical gain, high photoluminescence quantum yield and no triplet absorption losses at the lasing wavelength combined with a mixed-order distributed feedback grating to achieve low lasing threshold. A simple encapsulation technique greatly reduced the laser-induced thermal degradation and suppressed the ablation of the gain medium taking place otherwise under intense continuous-wave photo-excitation. Overall, this study provides evidence that the development of a continuous-wave organic semiconductor laser technology is possible via the engineering of the gain medium and the device architecture.

10362-85, Session PMon

High quality white OLEDs with LED efficiencies

Kyung-Hoon Han, Seoul National Univ. (Korea, Republic of); Sohee Jeon, Korea Institute of Machinery & Materials (Korea, Republic of); Sunghun Lee, Kwon-Hyeon Kim, Hyun Shin, Seoul National Univ. (Korea, Republic of); Jun-Ho Jeong, Korea Institute of Machinery & Materials (Korea, Republic of); Jang-Joo Kim, Seoul National Univ. (Korea, Republic of)

White OLEDs (WOLEDs) are considered as more attractive lighting sources than LEDs in terms of the quality of light, mechanical and design flexibility, free of blue hazard, and so on. However, WOLEDs with high luminous efficacy (LE) overcoming LEDs at high luminance are believed to be a distant goal at present even with large advances in light extraction during the last couple of decades. Here, we report novel WOLEDs approaching the theoretical limit by using the highly effective extraction layer based on a randomly dispersed vacuum nano-hole array (VaNHA). To obtain isotropic emission similar to the Lambertian emission profile, a random VaNHA was designed by dispersing the position of holes. The randomness of vacuum nanoholes is controlled not to show any symmetric emission patterns in the unit cell of 10*10 μm2. The WOLEDs in combination with a half spherical lens exhibited comparable performance with LED lighting with unprecedentedly high LE of 164 lm W–1 at 1,000 cd m–2 originating from high EQE (75.9%), low operating voltage (3.51 V) and low efficiency roll-off. In addition, the WOLEDs showed the maximum EQE of 78%, high color rendering index (CRI) around 80 and no color variation with viewing angle.

10362-86, Session PMon

Simulation and optimization for the optical performance of top emitting OLED

Shuwei Fan, Nana Chen, Zhaoxin Wu, Shenli Jia, Xi'an Jiaotong Univ. (China)

Top emitting Organic light-emitting diode(TEOLED) has been demonstrated to be suitable for next generation lighting and display application for high performance such as high efficiency and flexibility etc. The paper 's main work about TEOLED is as follow:

First, different anode structures of the TEOLED device was studied and the complex structure of Al (120nm) /MoO3 (4nm) /Al (4nm) was chosen as a reflective anode.

Second, with the help of software FDTD, the optimization design of the TEOLED device structures was completed. The light out coupling layer of the TEOLED had been modified to improve the light out coupling efficiency. The simulation of TEOLED with different microstructures on the surface of light out coupling layer was developed. And then the optimization design of TEOLED was carried out, which demonstrated that the average coupling-out efficiency could reach 75.8% near the wavelength of 525nm.

10362-87, Session PMon

Down-conversion white OLEDs with high performance color-conversion light outcoupling structures.

Joo Won Han, Siti Aisyah Nurmaulia Entifar, Pukyong National Univ. (Korea, Republic of); Chul Woong Joo, Jonghee Lee, Electronics and Telecommunications Research Institute (Korea, Republic of); Yong Hyun Kim, Pukyong National Univ. (Korea, Republic of)

White organic light-emitting diodes (OLEDs) have attracted considerable attention due to their important applications in flat panel displays, general lighting. The biggest challenge of conventional OLEDs is the limited light outcoupling efficiency about 20 % while the internal quantum efficiency of OLEDs approaches almost 100 %. In this respect, numerous light outcoupling techniques have been investigated to enhance the device efficiency. In contrast to most internal outcoupling structures, external outcoupling structures do not deteriorate the electrical functions of devices and can be readily introduced to the back side of substrate as a form of films. For external outcoupling, microlens array films and micro-sphere scattering layers have been extensively used. However, these external outcoupling structures typically need complex and expensive lithography process to form micro-shape patterns.

In this work, we develop a high performance down-conversion microlens array (DC-MLA) films for white OLEDs. The DC-MLA films are fabricated by a soft imprinting method with breath figure patterns, which are low-cost, simple and quick solution process. Blue OLEDs employing the DC-MLA films exhibit highly enhanced light outcoupling efficiency and high quality of white light. The DC-MLA films improve the external quantum efficiency (EQE) of white OLEDs by a factor of 1.45. In addition, high quality white light with a color rendering index of 84.3 is achieved for the white OLEDs with DC-MLA films. We anticipate that the novel solution-processable DC-MLA films based on breath figure patterns can be a simple, cost-effective approach to realize high performance down-conversion white OLEDs.

10362-88, Session PMon

The analysis of working mechanism for organic heterojunction charge generation layer

Feiping Lu, Tianshui Normal Univ. (China)

No Abstract Available

10362-89, Session PMon

The study of working mechanism of organic heterojunction charge generation layer

Feiping Lu, Tianshui Normal Univ. (China); Bo Yao, Yan Li, Shaoxing Univ. (China); Qin Liu, Yinglong Shi, Tianshui Normal Univ. (China)

The tandem organic light-emitting diodes (tandem OLEDs), which having two or more electroluminescence (EL) units vertically stacked in series through charge generation layer, were widely used in flatpanel displays and solid state lighting because of their advantages of enhanced current efficiency and luminance at low current densities, as well as their prolonged lifetime as compared to the conventional single unit devices. In a tandem OLED, the charge generation layer plays an important role, serving as the charge generation layer, and it is critical for the performance of tandem OLEDs. So the deep understanding the working mechanism of charge generation layer is the basis of fabrication high efficiency OLEDs. Organic heterojunction thin film layers were widely used in tandem OLEDs as charge generation layer, in order to undersdand the working mechanism of organic heterojunction charge generation layer, the device with the structure of glass/ITO/ tris(8-hydroxyquinoline) aluminum (Alq3) (60 nm)/C60(x nm)/ pentaence((40- x) nm)/ N,N'-bis(naphthalen-1-yl)-N,N'-bis (phenyl)-benzidine (NPB) (40 nm)/Al (100 nm) were successfully fabricated, here the organic heterojunction C60/pentaence was used as charge generation layer. The experiment results demonstrated that the organic heterojunction charge generation layer with the structure of C60(15 nm)/pentaence(25 nm) with the most effective charge generation ability. By the analysing the carrier transport characteristics in device, the device current can be attributed to the organic heterojunction charge generation layer. By numerical analysing the current-voltage (J-V) characteristics of devices, the results showed the charge generation mechanisem of organic heterojunction was in accord with quantum tunneling. The obtained results can help ones deeply understand the working mechanism of organic heterojunction charge generation layer and fabricat high efficiency OLEDs.

10362-90, Session PMon

Conductivity and injection ability enhancing of nickel (II) oxide hole injection layer for organic light-emitting diodes

Moohyun Kim, KAIST (Korea, Republic of); Chul Woong Joo, Byoung-Hwa Kwon, Electronics and Telecommunications Research Institute (Korea, Republic of); Wonseok Choi, Dodam Kim, Duk Young Jeon, KAIST (Korea, Republic of)

Sol-gel processed nickel (II) oxide (NiOx) is the one of the p-type metal oxide semiconductor materials which has widely used for hole transport layer (HTL) or hole injection layer (HIL) in optoelectronic devices. The NiOx film which fabricated with sol-gel process has many attractive electronic, optical and chemical properties. Based on these advantages of NiOx and disadvantages from PEDOT:PSS, NiOx is considered as great alternative for PEDOT:PSS. Consequently, NiOx film used optoelectronic devices like organic photovoltaic (OPV), organic light emitting diodes (OLEDs) and quantum-dot light emitting diodes (QLEDs) were demonstrated.

We introduce that the co-doping in NiOx with same Cu element but also different Cu oxidation number (Cu (I) and Cu (II)). There are only few studies in co-doping method for NiOx and that was limited to using distinct elements. The Cu2O (Cu (I)) and CuO (Cu (II)) have different crystal structures which are known as cubic structure and monoclinic structure. We assumed that Cu doping with two different lattice parameter led NiOx to more off-stoichiometric NiOx and this CuNiOx generates Ni2+ vacancies more effectively. Their modified chemical composition enhance conductivity and hole injection properties.

10362-92, Session PMon

The facile synthesis of 1,8-dibromo-9-heterofluorenes

Jinzhu Cao, Chuanhao Sun, China Electronics Standardization Institute (China); Yijiang Jiang, Beijing University of Technology (China)

The linking pattern of conjugated polymers was found to greatly influence their properties both in single molecular and aggregated states. For example, poly(1,8-carbazole) has been synthesized and has quite different properties in comparison with poly(2,7-carbazole) and poly(3,6-carbazole). Our previous theoretical investigations reveal that poly(1,8-silafluorene)s are very interesting optoelectronic materials with high bandgap, good hole and electron transport balance, and modest effective conjugation length for high-performance blue or deep-blue OLEDs. However, other poly(1,8-heterofluorenes) have not been synthesized due to the difficulties in the preparation of the monomers of 1,8-dibromo-9-heterofluorenes.

Recently,we successfully developed the critical premonitory compound of 1,8-dibromo-9-heterofluorenes via a new and facile synthetic route. The prepared compounds were fully characterized by NMR, GC-MS, and element analysis (EA).The successful preparation of 1,8-dibromo-9-heterofluorenes opens a door for a new kind of materials with high triplet state energy as excellent host materials and unique optical properties with tremendous potential in the field of organic electronics.

10362-93, Session PMon

Optical materials based on organometallic complexes and quantum dots loaded in solid matrices

Leandro P. Ravaro, Univ. of California, Santa Barbara (United States) and Univ. of São Paulo (Brazil); Peter C. Ford, Univ. of California, Santa Barbara (United States); Andrea S. S. de Camargo, Univ. of São Paulo (Brazil)

Optical materials based on organometallic copper (I) complexes and/or CdTe quantum dots displays rich photophysics properties that make them suitable candidates for technological applications including catalysis, OLEDs, cellular imaging, optical sensors, Photodynamic Therapy (PDT) and others. Due to the effect of quantum confinement, the CdTe semiconductor nanoparticles exhibit narrow and symmetrical fluorescence covering a broad spectrum of excitation and emission as a function of nanoparticle size. Many studies are focused on the characterization of these materials in solid state and solution, however there are few studies of them loaded into solid matrices. This work reports the photophysical properties of copper (I) complexes and CdTe QDs loaded in a mesoporous silica matrix obtained by sol-gel method with an average pore diameter of 10 nm. The colloidal suspension of CdTe, synthesized in aqueous phase, presents maximum excitation at 375 nm, maximum emission at 520 nm with full width at half maximum (FWHM) of 46 nm. While loaded into the solid SiO2 matrix, the QD emission had small shift, according to the type of incorporation strategy. The complexes Cu4I4py4 (1) and C30H28N2O2PCuI (2) incorporated on mesoporous silica showed a shift in emission of 580 nm to 720 nm and 660 nm to 575 nm, respectively. This shift of the emission is caused by distortion of the molecular complex, in the MLCT excited state, inside the matrix, known as rigidochromic effect [1]. Also, a sensitivity of these hybrids materials (1@SiO2 and 2@SiO2) was observed to oxygen. The mesoporous matrix dispersed the molecules of the complex, so as to enable a reversible interaction with oxygen in the center of the metal that quenches of luminescence[2] and provides a new functionality to the complex[3].

Already, the new complex C30H28N2O2PCuI (2) presented interesting properties. Exposed to dichloromethane its color alters from yellow to orange with shift the emission and returns the original color on exposure to acetone, indicating a reversible process. This color change was also observed for the complex 2 incorporated into a mesoporous silica matrix (2@SiO2). The x-ray data demonstrates that both compounds (yellow and orange) have the same crystalline structure (monoclinic), but with different lattice parameters and distorted angles. For example, for the yellow compound, the lattice parameter found was a = 17.769 Å, angle ? = 114.05 o and a smaller distance between Cu···Cu centers of 9.174 Å. While the orange compound, the lattice parameter found was a = 11.555 Å, angle ? = 92.70 o and a smaller distance between Cu···Cu centers of 7.197 Å. The change of color and shift of the emission must be related to the change of molecular packings after its recrystallization with referred organic solvent. The new functional materials proposed in this study have great potential for applications in optical materials devices.

[1] Ford, P. C.; Cariati, E.; Bourassa, J. Chem. Rev. 1999, 99, 3625.

[2] Quaranta, M.; Borisov, S. M.; Klimant, I. Bioanal Rev. 2012, 4, 115.

[3] Ravaro, L. P. and Almeida, T. R., Albuquerque, Rodrigo Q. and de Camargo, Andrea S. S. Dalton Trans. 2016, 45, 17652.

The authors would like to thank FAPESP (scholarship Post doctor 2016/17495-0; Cepid 2013/07793-6) and CNPq (Universal 479672/ 2012-1).

Figure 15 shows the emission spectrum for silica matrices incorporated with QDs obtained by the 4 different incorporation strategies.

10362-37, Session 9

Unraveling origin of phosphors doped in organic semiconducting layers

Chang-Ki Moon, Kwon-Hyeon Kim, Jang-Joo Kim, Seoul National Univ. (Korea, Republic of)

Emitting dipole orientation (EDO) is an important issue of emitting materials in organic light-emitting diodes (OLEDs) for an increase of outcoupling efficiency of light. The origin of preferred orientation of emitting dipole of spherically shaped iridium-based heteroleptic phosphorescent dyes doped in organic layers is revealed by simulation of vacuum deposition using molecular dynamics (MD) along with quantum mechanical (QM) characterization of the phosphors for a direct comparison with experimental observations of EDO. Consideration of both the electronic transitions in a molecular frame and the orientation of the molecules interacting with the environment at the vacuum/molecular film interface allows quantitative analyses of the EDO depending on host molecules and dopant structures. Interaction between the phosphor and nearest host molecules on the surface, minimizing the non-bonding energy determines the molecular alignment during the vacuum deposition. Parallel alignment of the main cyclometalating ligands in the molecular complex due to host interactions rather than the ancillary ligand orienting to vacuum leads to the horizontal EDO.

10362-38, Session 9

Charge transport and light emission in anisotropic media: the liquid-crystalline light-emitting diode

Changmin Keum, Shiyi Liu, Akram Al-Shadeedi, Vikash Kaphle, Robert J. Twieg, Antal I. Jákli, Björn Lüssem, Kent State Univ. (United States)

Alignment of emitter or transport molecules can have a profound influence on the efficiency of Organic Light-Emitting Diodes (OLEDs). A horizontal alignment of the emitter molecule is known to increase the overall external quantum efficiency (EQE) [Phys. Status Solidi 210, 44–65 (2013)]; an optical anisotropy in the transport layers can be used to tune the OLED microcavity [Opt. Express 23, 21128–21148 (2015)]; and finally, an increased order in the organic film enhances charge and exciton transport [Adv. Mater. 22, 1233–1236 (2010)].

Liquid-Crystalline (LC) semiconductors [Appl. Mat. & Interf. 7, 16374 (2015)] provide for new ways to control the orientation of functional molecules in organic thin films. In this presentation, a novel blading process is presented, which allows to change the orientation of the organic semiconductor C8-BTBT. Applying the blading process at elevated temperatures, i.e. in the LC phases of C8-BTBT, induces a more tilted alignment. The influence on the alignment of the semiconductor on electron and hole transport is studied in n-i-n and p-i-p devices and it is shown that the charge carrier mobility increases for a more tilted orientation.

To realize light emission inside the C8-BTBT layer, the semiconductor is doped by a red phosphorescent emitter. P-i-n type OLEDs show a promising EQE of up to 8%. Most importantly, both, annealing and blading lead to an increase in EQE. Hence, the presented results present a first step toward OLEDs employing LC layers, which opens new design possibilities to optimize OLEDs further.

10362-39, Session 9

Polymer gating white flexible field-induced lighting device

Junwei Xu, Wake Forest Univ. (United States); David Loren Carroll, Ctr. for Nanotechnology and Molecular Materials (United States)

The development of field induced electroluminescence (EL) devices holds great promise for the production of extremely flexible and efficient large-area light sources. Here, a novel flexible polymeric gate layer for alternating current (AC) driven organic electroluminescence (AC-OEL) devices is presented. The charge-valve mechanism of carrier manipulation in forward and reversed bias of the applied AC cycles is fully detailed. With a low-doping strategy of two phosphors in the fluorescent host, a flexible PET-based AC-OEL device with poly[(9,9-bis(3'-((N,N-dimethyl)-N-ethylammonium)-propyl)-2,7-fluorene)-alt-2,7-(9,9-dioctylfluorene)] (PFN-Br) gate exhibits incredible stability on EL performance with a superior color rendering index (CRI), over 81 at 2800K color temperature and a power efficiency of 2.8 lm/W at 1,000 cd/m2 with high bending ability (-90° to +90°).

10362-40, Session 9

Alternating current polymer electroluminescence for dynamic interactive display *(Invited Paper)*

Cheolmin Park, Yonsei Univ. (Korea, Republic of)

Field induced electroluminescence of either organic or inorganic fluorescent materials under alternating current (AC) has been of great attention as a potential candidate for next generation displays, lightings and sensors. Unique device architecture in which an emitting layer is separated with an insulator from electrode offers a new platform for designing and developing a variety of types of ELs. Here, we demonstrate high-performance field-induced AC polymer electroluminescence (AC-PEL) devices with high brightness, high efficiency and color-tunability. We also present a non-volatile EL memory in which arbitrarily chosen EL states are programmed and erased repetitively with long EL retention. Our memory is based on utilizing the built-in electric field arising from the remanent polarization of a ferroelectric polymer which in turn controls the carrier injection of an AC-PEL device. The device exhibits two distinctive non-volatile EL intensities at constant reading AC voltage, depending upon the programmed direct current (DC) voltage on the ferroelectric layer. DC programmed and AC read EL memories are also realized with different EL colors of R, G and B. Finally, we show that simultaneous sensing and visualization of the conductive substance is achieved when the conductive object is coupled with the light emissive material layer on our novel parallel-type AC-PEL device. A variety of conductive materials can be detected regardless of their work functions, and thus information written by a conductive pen is clearly visualized, as is a human fingerprint with natural conductivity.

10362-41, Session 9

Universal ohmic electron and hole contacts for organic light-emitting diodes and electronics *(Invited Paper)*

Peter Ho, Rui-Qi Png, Lay-Lay Chua, National Univ. of Singapore (Singapore)

An ohmic electrical contact is one that allows the largest possible current density limited by space-charge effects to be injected into the adjoining semiconductor. This is key to maximizing device efficiency and reliability, and thus fundamental to all semiconductor devices. A long-standing challenge for organic (and other solution-based) electronics is the lack of a general solution-based compatible strategy to fabricate ohmic contacts at will. To overcome these challenges, we have recently developed self-compensated heavily-doped polymers with ultrahigh and ultralow workfunctions, and polyelectrolyte interlayers for 2D interface doping. Unprecedented p- and n-doped conductive polymer films over an ultrawide work function range of 3.0 eV to 5.8 eV have been obtained, enabling solution-processed ohmic contacts for light-emitting diodes, solar cells, photodiodes and transistors. Self-aligned doped contacts have also become possible. We anticipate that these strategies will enable ohmic contacts to also be made to other advanced semiconductors, including quantum dots, nanotubes and 2D materials, and open up new and technologically interesting device architectures for various photonic and non-photonic applications. Using these materials, we have developed new understanding of the physics of work function and ohmic contacts relating to doped organic semiconductors. The localization of charge carriers in organic semiconductors, different from conventional band semiconductors, leads to important differences in the essential physics.

10362-42, Session 10

Recent advances in OLEDs on unconventional substrates *(Invited Paper)*

Bernard Kippelen, Xiaoqing Zhang, Canek Fuentes-Hernández, Felipe A. Larrain, Georgia Institute of Technology (United States)

The printed electronics industry offers a paradigm change in manufacturing, cost and environmental impact when compared to the conventional semiconductor industry. Printed electronic devices are expected to be mass-produced from less-energy-demanding processes over large areas and on flexible substrates with techniques that closely resemble the well-known mass production of printed media on paper. Organic light-emitting diodes (OLEDs) offer great versatility in the design of application-specific light sources; yet examples of OLEDs fabricated on exotic substrates that differ from glass and plastic are still scarce. In this talk we will present recent examples of OLEDs fabricated on unconventional substrates, including nanocellulose and shape memory polymers.

10362-43, Session 10

Highly efficient flexible OLEDs and their application to health-monitoring sensors *(Invited Paper)*

Seunghyup Yoo, Hyeonwoo Lee, Eunhye Kim, Jaeho Lee, KAIST (Korea, Republic of)

No Abstract Available

10362-44, Session 10

New materials for fabrication of efficient near infrared OLEDs and organic solid-state lasers *(Invited Paper)*

Anthony D'Aleo, CINaM - Ctr. Interdisciplinaire de Nanoscience de Marseille (France); Dae Hyeon Kim, Atula S. D. Sandanayaka, OPERA Ctr. for Organic Photonics and Electronics Research (Japan); Dandan Yao, Elena Zaborova, Gabriel Canard, CINaM - Ctr. Interdisciplinaire de Nanoscience de Marseille (France); Toshinori Matsushima, Youichi Tsuchiya, OPERA Ctr. for Organic Photonics and Electronics Research (Japan); Eunyoung Choi, Jeong Weon Wu, Ewha Womans Univ. (Korea, Republic of); Fre?de?ric Fages, Aix-Marseille Univ. (France) and CINaM - Ctr. Interdisciplinaire de Nanoscience de Marseille (France); Jean-Charles Ribierre, Chihaya Adachi, OPERA Ctr. for Organic Photonics and Electronics Research (Japan) and Japan Science and Technology Agency (Japan)

Thermally-activated delayed fluorescent (TADF) emitters have been successfully used in organic light-emitting diodes (OLEDs) with up to 100% internal quantum efficiencies and are now considered as the third generation of OLED materials.[1

]Here, we report on the fabrication of NIR TADF OLEDs with a maximum electroluminescence external quantum efficiency (EQE) of nearly 10%. The devices used a solution-processable heavy-metal-free do-nor-acceptor-donor borondifluoride curcuminoid derivative[2] as NIR emitter. This compound shows a rather high photoluminescence quantum yield (up to 69%) in solid matrices with an emission maximum wavelength typically in the range between 720 and 750 nm. Time-resolved photophysical measurements show that the TADF mechanism of this NIR emitter is due to a reverse intersystem crossing from triplet charge transfer (CT) to singlet CT excited states. In addition, the TADF emission wavelength and efficiency are found to strongly depend on the dye concentration in the emissive layer due to the large dipole moments of this compound. In the last part of this talk, we will demonstrate that this new TADF material exhibits amplified spontaneous emission in the NIR region, suggesting the possibility to harvest triplet excitons for stimulated emission.

[1] H. Uoyama, K. Goushi, K. Shizu, H. Nomura and C. Adachi, Nature 492, 234-238 (2012).

[2] A. Felouat, A. D'Aléo, F. Fages, J. Org. Chem. 78, 4446 (2013)

10362-45, Session 10

Fluorescent proteins and carbon nanotubes: unconventional materials for strong light-matter interaction and solid state lasers *(Invited Paper)*

Malte C. Gather, Univ. of St. Andrews (United Kingdom); Christof P. Dietrich, Univ. of St. Andrews (United Kingdom) and Julius-Maximilians-Univ. Würzburg (Germany); Arko Graf, Univ. of St. Andrews (United Kingdom) and Ruprecht-Karls-Univ. Heidelberg (Germany); Laura Tropf, Markus Karl, Anja Kämpf, Marcel Schubert, Nils M. Kronenberg, Univ. of St. Andrews (United Kingdom); Yuriy Zakharko, Ruprecht-Karls-Univ. Heidelberg (Germany); Sven Höfling, Julius-Maximilians-Univ. Würzburg (Germany); Jana Zaumseil, Ruprecht-Karls-Univ. Heidelberg (Germany)

Organic materials offer attractive properties for solid-state lasers, including large oscillator strength, high exciton binding energy, spectral tunability, and compatibility with low-cost fabrication processes. However, despite impressive proof-of-principle demonstrations and dramatic improvements in performance, important fundamental limitations remain. Particular challenges are concentration quenching and bi-molecular exciton recombination which limit the available gain under practical pumping conditions. For electrical pumping, there are further restrictions, including the low charge carrier mobility of most organic materials. Recently, it has been suggested that lasers operating in the regime of strong exciton-photon coupling may address some of these challenges.

Here, we will summarize key results from two current collaborations that both look at unconventional nano-scale organic materials for solid-state lasers: Biologically produced fluorescent proteins and single walled carbon nanotubes.

We found that the barrel-like molecular structure of fluorescent proteins prevents concentration-induced quenching of fluorescence and drastically reduces singlet-singlet annihilation at high exciton densities. This facilitates low-threshold lasing in various configurations and has recently enabled the realization of the first organic polariton laser that can be pumped in a quasi-continuous ns-regime.

In another collaboration, we have shown that the special photophysical properties of polymer-sorted semiconducting single-walled carbon nanotubes render them well-suited for strong light-matter coupling, possibly up to the ultra-strong coupling regime. Most recently, we found that the high charge carrier mobility and stability also enable efficient electrical generation of exciton polaritons. Using a light-emitting field effect transistor geometry, we achieved current densities up to 18,000 A/cm2 while maintaining strong coupling conditions.

10362-46, Session 10

Tunable solution processed metal organic perovskite distributed feedback lasers *(Invited Paper)*

Ulrich Lemmer, Philipp Brenner, Florian Mathies, Dorothee Kapp, Gerardo Hernandez-Sosa, Ian A. Howard, Karlsruher Institut für Technologie (Germany)

The use of metal halide perovskites for optoelectronic devices beyond solar cells is gaining growing attention.

Perovskites with different compositions are promising as tuneable light emitters for the whole visible spectral region [1]. We report solution processed perovskite laser devices that show amplified spontaneous emission and lasing. We have fabricated surface emitting perovskite distributed feedback lasers by spin-coating CH3NH3PbI3 precursor solutions in ambient atmosphere on nanoimprinted grating substrates [2]. These lasers exhibit narrow lasing linewidths below 0.2 nm and an excellent stability of more than 5?10^7 pulses at 1 kHz repetition rate. Lasing at different wavelengths could be achieved on a single substrate by integrating different grating periods on the same substrate. While the emission wavelength of CH3NH3PbI3 is in the deep red to infrared spectral region, the lasing emission can be shifted into the visible by a gradual exchange of iodine to bromine. By adapting the grating period to the emission spectra of the mixed halide perovskite, we achieved lasing in the visible. Furthermore, we demonstrate high-quality perovskites fabricated by ink-jet printing on flexible substrates. Such films show strong amplified spontaneous emission with a clear ASE intensity threshold.

References

[1] B. R. Sutherland and E. H. Sargent, “Perovskite photonic sources,” Nat. Photonics 10, 295–302 (2016).

[2] P. Brenner, M. Stulz, D. Kapp, T. Abzieher, U. W. Paetzold, A. Quintilla, I. A. Howard, H. Kalt, and U. Lemmer, “Highly stable solution processed metal-halide perovskite lasers on nanoimprinted distributed feedback structures,” Appl. Phys. Lett. 109, 141106 (2016).

10362-47, Session 10

Electrical simulation of organic light emitting diode under high current injection *(Invited Paper)*

Fatima Bencheikh, Atula S. D. Sandanayaka, Toshiya Fukunaga, Toshinori Matsushima, Chihaya Adachi, OPERA Ctr. for Organic Photonics and Electronics Research (Japan)

During the last two decades, organic semiconductor lasers (OSLs) have been attracted much attention due to their advantageous properties such as wavelength tunability in visible range [1], low cost, flexibility and large area fabrication [2]. These properties make them good candidates for a range of applications including sensing, spectroscopy and optical communication. However, only optically pumped organic lasers have been realized so far and the demonstration of an electrically-driven organic laser diode still remains a very challenging task. To achieve electrically pumped OSLs, much effort has been focused on the reduction of the energy threshold of optically pumped organic lasers by enhancing the gain media properties and optimizing the resonant cavities. The injection of high current density involves Joule heating which causes degradation and breakdown of the device. Moreover, the presence of high charge density induces multiple annihilation processes such as exciton-polaron quenching, polaron absorption and electric field dissociation which are ones of the causes of device external quantum efficiency rolloff. A fundamental understanding of the physical mechanisms governing the device operation is crucial to optimize the device performance and overcome the limitation processes to the achievement of an electrically driven OSLs. Electrical simulation of an organic light emitting diode under high current density is performed in order to predict the current at high voltage. The influence of the various annihilation processes is investigated by solving the exciton continuity equation.

1. O. Mhibik et al., Appl. Phys. Lett. 102, 41112 (2013).

2. C. Ge et al., Opt. Exp. 18, 12980–12991 (2010).

10363-1, Session 1

2D compact model to characterize phase separation in organic solar cell bulk heterojunctions

Franklin L. Lee, Amir Barati Farimani, Kevin L. Gu, Stanford Univ. (United States); Hongping Yan, Stanford Synchrotron Radiation Lightsource (United States); Zhenan Bao, Stanford Univ. (United States); Vijay S. Pande, Stanford Univ. (United States) and Andreessen Horowitz (United States)

The phase separation between donor and acceptor molecules within the active layer of an organic solar cells dictates the morphology and hence is key to the recombination rate and ultimately the performance of the organic solar cell. Molecular dynamics (MD) simulation is a suitable technique to understand this phenomenon; however, conventional all-atom MD simulations cannot reach the appropriate length and time scales to compare with macroscopic observation. Even with the many available coarse-grained MD models, it is difficult to reach these scales. Therefore, we introduce here a 2D compact model to overcome this challenge, built by multiscale coarse-graining. First, we simulate systems including conjugated polymers, fullerenes, and organic solvents using all-atom MD to extract information about molecular conformation and packing. This includes an analysis of polymer solution behavior, fullerene clustering, and binary and tertiary mixing properties. These results are then used to systematically parameterize the molecules used in 2D coarse-grained MD simulations. The 2D simulations probe experimentally relevant length scales that were previously intractable to sample by other MD simulation methods. Using this model, we explore ternary systems including polymer, fullerene, and solvent molecules to investigate the phase separation process between polymer donors and fullerene acceptors. In this scheme, we additionally introduce explicit solvent evaporation to emulate realistic processing conditions. We quantify phase separation domain sizes that are comparable to experimentally observed values from resonant soft x-ray scattering. In addition, we extend this framework to other chemical species to demonstrate the flexibility of the approach.

10363-2, Session 1

Quantitative structure-function relations in PSCs from soft x-ray scattering *(Invited Paper)*

Harald W. Ade, North Carolina State Univ. (United States)

Polymer Solar Cells (PSCs) continue to be a promising third generation, low energy-budget, lead-free PV technology. Efficiencies have now improved to over 12% and a new class of materials (small molecule acceptors) have recently provided rapid improvements that promise further advances. Significant effort in the field is being spent on synthetic efforts to tune the electronic structure and in understanding charge generation. In contrast, we explore the correlation of fill factor to the purity of domains as measured with soft x-ray scattering, and how said purity is controlled by thermodynamically metastable morphologies. We will argue that ideal materials systems will have a Flory Huggins interaction parameter ? that naturally leads to mixed domains that have a composition close the fullerene/SMA percolation threshold. Systems that are too miscible will have excessive bimolecular recombination. Systems too immiscible need to be quenched for best performance, are thus unstable and eventually produce fullerene islands that trap charges. Although some of these concepts are known and are indirectly referred to as "miscibility", quantitative relations remained largely elusive. Understanding molecular interactions is even more important for conventional ternaries devices. In some cases, the two donor polymer used can have unfavorable thermodynamic interactions (? = - 0.56 at 296 °C) that prevent improved performance due to lack of phase separation and alloying of the two donors. Overall, we advocate a program to measure ?(T) in model systems in order to develop a frame-work that will eventually lead to computational approaches that allow predictions of ? as a function of molecular tuning before synthesis of a targeted compound is attempted.

10363-3, Session 2

Triplet energy transfer and triplet exciton recycling in singlet fission sensitized organic heterojunctions

Ajay Pandey, Queensland Univ. of Technology (Australia)

Organics semiconductors such as tetracene, rubrene and pentacene have the unique ability of efficiently producing two electron-hole pairs per absorbed photon. This occurs due to the physical process of singlet fission where the excited singlet state breaks into two low energy triplets [1]. In this paper, we will present novel "triplet exciton management" strategies that are aimed at enhancing the yield of photocurrent generation and reduction of recombination losses in singlet fission active/sensitized organic photovoltaic diodes. Some latest results on ultrafast triplet exciton dynamics in donor-acceptor heterojunctions of rubrene and tetracene with C60 will be presented.

Example of squaraine as a triplet exciton reflecting layer in enhancing the photocurrent yield in pentacene/C60 diodes to values above 100% and triplet energy transfer (TET) from DCV3T to pentacene will be discussed. A successful case of triplet exciton recycling in the low optical gap polymer-fullerene bulk-heterojunctions of PCPDTBT:70-PCBM will be discussed where we have been successful in suppressing bimolecular recombination losses via TET that progresses through charge transfer intermediate and transfers its energy to the adjacent layer of pentacene.

In summary, through carefully designed experiments on operational photodiodes, we will discuss successful examples of Dexter type TET process in the organic photovoltaic cascades. We will make a strong case for strategic management of the triplet excitons in organic donor-acceptors and pitch new strategies for the material and device designs for realisation of next generation of organic photovoltaics.

References

1. Smith, M. B. and Michl, J. Singlet Fission. Chem. Rev. 2010, 110, 6891–6936.

2. Pandey, A. K. Highly efficient spin-conversion effect leading to energy up-converted electroluminescence in singlet fission photovoltaics. Scientific Reports, 2015, 5, 7787.

3. Ullah, M. et al. Singlet fission and Triplet Exciton Dynamics in Rubrene/Fullerene Heterojunctions: Implications for Electroluminnescence. Adv. Electron. Mater. 2015, 1, 1500229.

10363-4, Session 2

Ultrafast terahertz snapshots of excitonic Rydberg states and electronic coherence in an organometal halide perovskite

Liang Luo, Long Men, Zhaoyu Liu, Yaroslav Mudryk, Xin Zhao, Yongxin Yao, Joong-Mok Park, Ruth Shinar, Joseph Shinar, Kai-Ming Ho, Iowa State Univ. of Science and Technology (United States) and Ames Lab. (United States); Ilias E. Perakis, The Univ. of Alabama at Birmingham (United States); Javier Vela, Jigang Wang, Iowa State Univ. of Science and Technology (United States) and Ames Lab. (United States)

How photoexcitations evolve in time into Coulomb-bound electron and hole pairs, called excitons, and unbound charge carriers is a key cross-cutting issue in photovoltaic and optoelectronic technologies. Until now, the initial quantum dynamics following photoexcitation remains elusive in the organometal halide perovskite system. Here we reveal excitonic Rydberg states with distinct formation pathways by observing the multiple resonant, internal quantum transitions using ultrafast terahertz quasi-particle transport. Nonequilibrium emergent states evolve with a complex co-existence of excitons, unbound carriers and phonons, where a delayed build-up of excitons under various pumping conditions allows us to distinguish between the loss of electronic coherence and hot state cooling processes. The terahertz transport with rather long dephasing time and scattering processes due to discrete terahertz phonons in perovskites are distinct from conventional photovoltaic materials. In addition to providing implications for ultrafast coherent transport, these results break ground for a perovskite-based device paradigm for terahertz and coherent optoelectronics.

10363-57, Session PMon

Study the effects of thickness variation of different layers on the light spectrum reaching active layers of organic solar cells

Ronak Rahimi, Intel Corp. (United States)

Significant progress in fabrication and optimization of organic photovoltaics (OPVs) has been made during the last decade. The main reason for popularity of OPVs is due to their low production cost, large area devices and compatibility with flexible substrates. Various approaches including optimizing morphology of the active layers, introducing new materials as the donor and acceptor, new device structures such as tandem structure have been adapted to improve the efficiency of the organic photovoltaics. Power conversion efficiency of OPVs are affected by various parameters such as light absorption and charge carrier extraction. Among these parameters, light absorption strongly depends on the optical properties of the layers and the device structure. Solar cells with CuPC/PTCDI-C8 active layers were fabricated and their reflectivities were measured. Transfer matrix formalism was used to simulate the reflectivities of each layer and the final device structure. Simulated and measured reflectivities were compared and studied to determine the effects of thickness variation of different layers on the light spectrum reaching the active layers.

10363-58, Session PMon

EDOT-diketopyrrolopyrrole copolymers for polymer solar cells

Chao Wang, Christopher R. McNeill, Monash Univ. (Australia)

The photovoltaic properties of a series of diketopyrrolo[3,4-c]pyrrole (DPP) copolymers containing 3,4-ethylenedioxythiophene (EDOT) as a comonomer are reported. With use of different aryl flanking units on the DPP core, namely thiophene, pyridine or phenyl, optical gaps ranging from 1.91 eV to 1.13 eV are achieved. When blended with the fullerene derivative [6,6]-phenyl C71-butyric acid methyl ester (PC71BM), the thiophene-flanked copolymer PDPP[T]2-EDOT with an optical gap of 1.13 eV was found to have the best photovoltaic performance, with an efficiency of 2.5% in an inverted device architecture. Despite having the lowest open circuit voltage of the three polymers studied, PDPP[T]2-EDOT-based devices were able to achieve superior efficiencies due to the high short circuit current of up to ~ 15 mA/cm2. PDPP[T]2-EDOT-based devices also exhibit higher external quantum efficiencies which are associated with a superior microstructure as revealed by transmission electron microscopy (TEM) and grazing incidence wide-angle X-ray scattering (GIWAXS). In particular PDPP[T]2-EDOT:PC71BM blends were found to have a finer phase separated morphology with superior thin-film crystallinity. Surface morphology was also investigated with atomic force microscopy and near-edge X-ray absorption fine-structure spectroscopy.

10363-59, Session PMon

Modeling of trap assisted interfacial in planer heterojunction perovskite solar cells

Behzad Bahrami, Qiquan Qiao, South Dakota State Univ. (United States)

Based on our model, diffusion of electrons from compact TiO2 into the Mesoporous-TiO2 and electron injection from TiO2 into perovskite through the trap assisted processes have role in the case of dark current. Trap assisted mechanisms dominates the current flow at low defect densities. In contrast, at high defect density regime, diffusion through TiO2, overcomes the current flow. This explains the nearly higher sensitivity of J0 to NT in low defect density regime. In both the low and high defect density regimes VOC is sensitive to NT but Jsc is only sensitive to NT in the high defect density regime. The VOC and JSC of the simulated perovskite solar cell are dependent upon Dn and NT. These parameters, respectively, govern dispersive diffusion of electrons through shallow defect states in mesoporous TiO2 and trap-assisted injection of electrons into the perovskite. The simulation results show that VOC and JSC are independent of Dn at the low defect density regime. This means that the diffusion of electrons through the mesoporous TiO2 is much faster than the process of injection of electrons into perovskite through trap states for the entire range of Dn. VOC shows a weak decrease by increasing in Dn, at higher defect density regime because a smaller quasi-Fermi level separation due to fast diffusion leads to a lower density of electrons in the conduction band of TiO2. In contrast, JSC shows an important sensitivity to the Dn values because in the low diffusion coefficient and high defect density regime, injection time of photoelectrons into the perovskite is less than the time scale of their transit to reach the contact. This causes to too much recombination and decrease of JSC.

10363-60, Session PMon

Thick film high performance bulk-heterojunction solar cells retaining 90% PCEs of the optimized thin film cells

Hang Yin, Shu Kong So, Hong Kong Baptist Univ. (Hong Kong, China)

Amid looming concerns over the deteriorating environment and energy problems, organic photovoltaic (OPV) devices have gained considerable attention because of their high flexibility, light weight, and capability for large-area fabrication. Most optimized, high performance, bulk-heterojunction polymer solar cells have an active layer thickness of about 100nm. The thin active layer is unfavorable for optical absorption and film coating. This contribution employs a ternary cell to address this problem. We show that thick film BHJ cells can be fabricated that retain 90% of the optimized thin film cells. The BHJs under investigations are PTB7:PC71BM, PTB7-Th:PC71BM and P3HT:PCBM. Into these BHJs, a ternary component, p-DTS(fbtth2)2 (~5% for PTB7, PTB7-Th, and ~10% for P3HT by weight) is introduced. Without p-DTS(fbtth2)2, the binary BHJ devices have PCEs of 6.3%, 7.3% and 3.2% in thick films (~200nm, ~200nm and ~400nm). With p-DTS(fbtth2)2, the corresponding BHJs have markedly improved PCEs of 7.6%, 8.3% and 4.0%, respectively. The results are more than 90% the PCEs of the optimized binary BHJs. The origins of the improvement are investigated. Addition of the ternary component p-DTS(fbtth2)2 enhances hole mobility and reduces trap states. Both observations are well correlated with improved FFs of the ternary BHJ cells. We use 1H nuclear magnetic resonance (NMR) to trace the nano-scale interactions of the p-DTS(fbtth2)2 with the polymer and fullerene. Our results suggest the p-DTS(fbtth2)2 behave as conducting bridges in between two neighboring polymer segments.

10363-61, Session PMon

Enhanced photovoltaic performance of PTB7:PCBM bulk heterojunction solar cells with Al doped TiO2 interfacial layer

Jun Young Kim, Korea Institute of Industrial Technology (Korea, Republic of)

In inverted polymer solar cell, several n-type buffer layers such as cesium carbonate (Cs2CO3), titanium dioxide (TiO2), zinc oxide (ZnO) were used as an electron transport layer due to their relatively high electron mobility, environmental stability, and high transparency. Recently, in order to increase the device performance of inverted polymer solar cells, several groups have studied the use of metal doped n-type buffer layer. The metal doping is an effective procedure to modify the grain size, orientation, conductivity and could greatly influence the structural, optical and electrical properties of the n-type buffer layer. Especially, TiO2 films doped with impurities such as Al, Ga and In exhibit not only higher conductivities but also better stabilities compared to those of TiO2 films. In this work, we have investigated the effect of Al doping and properties of Al doped TiO2 thin films and have fabricated inverted polymer solar cells with doped TiO2 interfacial layer based on PTB7:PCBM bulk hetrojunction.

10363-62, Session PMon

Cationic dibenzothiophene-S,S-dioxide-bispyridinium-alt-fluorene copolymer as an efficient cathode modifier for polymer solar cells

Wei Yang, Zhicai He, Yong Cao, South China Univ. of Technology (China)

A novel n-type alcohol-soluble conjugated polymer containing dibenzothiophene-S,S-dioxide (FSO), bispyridinium, and fluorene scaffolds in the backbone (PFSOPyCl) was synthesized and used in the cathode interfacial layers (CILs) of conventional polymer solar cells (PSCs). The high electron affinities and large planar structures of the FSO and bispyridinium units endowed this polymer with good energy level alignments with [6,6]-phenyl-C71 butyric acid methyl ester (PC71BM) and metal cathode, and excellent electron transport and extraction properties. The bispyridinium salt donated to the polyelectrolyte nice solubility and processability in highly polar solvents, as well as versatile tunability of the cathode work function (WF). As a result, PSCs based on the poly[N-9''-heptadecanyl-2,7-carbazole-alt-5,5-(4',7'-di-2-thienyl-2',1',3'-benzothiadiazole)] (PCDTBT):PC71BM system with PFSOPyCl CIL exhibited simultaneous enhancements in open-circuit voltage, short-circuit current density, and fill factor, while the power conversion efficiency increased from 5.47% to 6.79%, relative to that of the bare Al device.

References

[1] Ye, H.; Hu, X.-W.; Jiang, Z.-X.; Chen, D.-C.; Liu, X.; Nie, H.; Su, S.-J.; Gong, X.; Cao, Y. J. Mater. Chem. A, 1 (2013), 3387-3394.

[2] Xiao, H.-P.; Miao, J.-S.; Cao, J.-Q.; Yang, W.; Wu, H.-B.; Cao, Y. Org. Electron. 15(2014), 758-774.

10363-64, Session PMon

Morphological effects of ZnO electron-collecting interlayers on the performance of organic solar cells

Jisoo Goo, Dongguk Univ. (Korea, Republic of); Do Kyung Hwang, Ju Won Lim, Korea Institute of Science and Technology (Korea, Republic of); Jae Won Shim, Dongguk Univ. (Korea, Republic of)

Organic solar cells (OSCs) with an inverted geometry, wherein transparent electron-collecting electrodes (ECEs) with a low work function (WF) sit at the bottom of the device, have been proposed to improve the air stability of OSCs. In such a structure, ITO, which is commonly used as a transparent electrode, is modified with low WF electron-collecting interlayers (ECIs) to serve as an efficient ECE. ZnO has been considered as a promising candidate for ECIs because of its electrical and optical properties. Even though many studies focusing on the characterization of inverted OSCs with various types of ZnO ECIs have been reported, only a few studies have been conducted to investigate the influence of the morphology-dependent effects of ZnO ECIs on the performance of OSCs.

Here, we examined the influence of the morphology-dependent effects of ZnO on the performance of PTB7:PC70BM-based inverted OSCs. To investigate the electrical, morphological, and optical properties of the ZnO layers in the OSCs, three different ZnO layers, sol-gel, nanoparticles, and nanorods, were employed as the ECI on the top of a glass/ITO substrate. All the ZnO layers showed a comparable WF value with the electron affinity of the PC70BM acceptor, allowing the ZnO-modified ITO electrode to function as an effective ECE. Among the ZnO layers, ZnO nanorods showed the strongest scattering effects and the most effective electron-collecting properties, resulting in an enhanced external quantum efficiency, and consequently, the highest efficiency (8.38±0.09%) under simulated AM 1.5G illumination. The optical effects were simulated by using a finite-difference time-domain method.

10363-66, Session PMon

Fluorinated PCPDTBT and its efficient polymer solar cells from sequential solution processing

Yong Zhang, Harbin Institute of Technology (China)

We reported a partially fluorinated low bandgap polymer, poly[2,6-(4,4-bis(2-ethylhexyl)-4H-cyclopenta [2,1-b;3,4-b?]dithiophene)-alt-4,7-(5-fluoro-[2,1,3]-benzothiadiazole)] (PCPDTFBT) was synthesized through a microwave-assisted Stille polymerization. It was found that PCPDTFBT has better ϖ–ϖ stacking in solution than its nonfluorinated analogue PCPDTBT, resulting in 2 times higher hole mobility. Power conversion efficiency (PCE) of the device using PCPDTFBT/PC71BM as active layer (5.51%) is much higher than the device using PCPDTBT/PC71BM (2.75%) that was fabricated under the same condition without using any solvent additive to modify the morphology. Further, by utilizing the solubility difference of PCPDTFBT and PC71BM in cold xylene and/or xylene/DCB mixture solvent, we are successfully fabricated the conventional and inverted solar cells by a sequential processing (SqP) method. With appropriate orthogonal solvents and thermal treatment, the SqP film can form an inter-diffused layer, and the SqP devices show efficient photovoltaic performance in both conventional and inverted layouts. The SqP inverted device was firstly demonstrated and the highest power conversion efficiency (PCE) of 5.84% with the enhanced Jsc of 16.4 mA cm-2 was able to be achieved with the high internal quantum efficiency (IQE). Photoluminescence quenching shows the SqP films can provide efficient exciton quenching. X-ray photoemission spectroscopy (XPS) and ellipsometry analysis shows a polymer-rich surface in SqP films after thermal annealing. The charge mobilities in the SqP films were significantly enhanced as measured by SCLC method. We believe that these results inspire a new way of forming the active layer with controllable morphology, efficient charge separation and collection in polymer solar cells.

10363-67, Session PMon

Fabrication of heterojunction film of lead halide perovskites by vacuum deposition using single crystal sources

Senku Tanaka, Natsuki Ueyama, Takuya Yoshitomi, Kindai Univ. (Japan); Toshihiko Kaji, Tokyo Univ. of Agriculture and Technology (Japan)

Vacuum deposition method is able to apply for the fabrication of a heterojunction film of lead halide perovskites. However, when the vacuum deposition is done by the co-deposition or the 2-step deposition of organic molecules and lead halides, the control of organic molecule deposition is relatively difficult because of the high vapor pressure of organics. As an alternative method to preparing perovskite films by vacuum deposition, we used single crystals as the deposition source. Using the single crystals of perovskite as the source of vacuum deposition improved controllability of vacuum deposition method significantly. The simplification of vacuum deposition conditions allows to fabricate various combinations of heterojunction films. As an example, we prepared a CH3NH3PbI3 (MAPbI3)/ CH3NH3PbBr3 (MAPbBr3) hetero-junction film. The MAPbI3 and the MAPbBr3 layer were deposited sequentially by the vacuum deposition using single crystal. The formation of heterojunction was confirmed by X-ray diffraction pattern of film. We observed the superimposed pattern of the MAPbI3 and the MAPbBr3 phase. However, the results of X-ray photoelectron spectroscopy indicated that a part of film surface was composed by a mixture of MAPbI3 and MAPbBr3 phase. We also explored the effect of deposition conditions and post-preparation on the physical and the chemical properties of perovskite films. The photovoltaic properties of solar cells with heterojunction perovskite layer will also be presented.

10363-68, Session PMon

Impact of 3D morphology on the performance of all-polymer solar cells processed by environmentally benign non-halogenated solvents

Hyeseung Jung, A-Ra Jung, Ewha Womans Univ. (Korea, Republic of); Seon-Mi Jin, Eunji Lee, Chungnam National Univ. (Korea, Republic of); Myung Hwa Kim, BongSoo Kim, Ewha Womans Univ. (Korea, Republic of)

Recently organic solar cells using halogenated solvents such as chlorobenzene and o-dichlorobenzene have recorded high efficiencies over 10%. However, halogenated solvents are very toxic to human health and environment. These solvents must be replaced with environmentally friendly non-chlorinated solvents. In addition, commonly-used n-type fullerene derivatives such as PC71BM are quite expensive, which spurred researchers to develop new soluble n-type organic materials. N-type polymers are a good alternative to fullerene derivatives because they renders many advantages including strong light absorption, good energy level tunability, and high mechanical stability. In these regards, we have investigated all polymer solar cells employing p-type PTB7-Th and n-type PNDI2OD-T2 polymers to find the dependence of photovoltaic properties on the processing solvent. We find that toluene and xylene are better processing solvents than halogenated solvents for the photovoltaic performance of PTB7-Th:PNDI2OD-T2 based devices. 3D TEM demonstrated that more ideal blend morphology in toluene and xylene-used active layer films was responsible for the solvent-property relationship.

10363-69, Session PMon

Interfacial engineering of hybrid perovskite solar cells via fullerene derivatives

Ka Kan Wong, Azhar Fakharuddin, Philipp Ehrenreich, Eugen Zimmermann, Michael Seybold, Carola Ebenhoch, Univ. Konstanz (Germany)

Extensive research activities on emerging organic-inorganic halide perovskite solar cells (PSCs) over the past few years brought them to deliver a certified photo-conversion efficiency (PCE) ~ 22 %, which is comparable to market dominating silicon and thin film solar cells. This remarkable improvement in PSCs, from 3.8% since their inception in 2009, has been due to unique optical (bandgap, high absorption coefficient) and electronic (high electron and hole mobility, low trap density) properties, their improved films processing and composition engineering, e.g., from a single cation to mixed cations that further broadened their optical absorption, and or eliminating charge-carrier recombination at the device interfaces via modification of electron/ hole transporting materials. Interface engineering has shown to significantly improve the charge carrier dynamics within the device as well as its stability. It is of particular importance as typical PSCs (those employing a low mobility electron transporting material, TiO2) results in notable interfacial recombination due to surface trap states and inferior electronic properties of TiO2. This not only limits the photovoltaic performance in PSCs but also induces a change in their current voltage profile dependent on voltage sweep directions. A remedy to resolve the trap-assisted recombination is to employ interfacial modifiers of high electronic mobility, e.g., fullerene-derivatives, where the fullerene, embedded into perovskite active layer, facilitates electron transfer to the TiO2. Herein, we employ two fullerene derivate such as fullerene-based PCBM-, and the self-assembling PCBA molecule, which anchors to TiO2 via a COOH-group. Additionally, benzoic acid has been used as interfacial modifiers to improve the charge carrier dynamics. Unlike the fullerene-based self-assembled molecules where anchoring group is chemically bonded to TiO2, PCBM is not, directly attached to TiO2 surface due to the absence of such an anchoring group. We investigate such different interactions with TiO2 surface via solar cells performance, steady-state and time-resolved spectroscopy studies, to understand charge extraction, and interfacial charge recombination.

10363-70, Session PMon

Driving intramolecular charge transfer by tuning molecular orbitals and dielectric constant

Melissa P. Aplan, Youngmin Lee, Jason M. Munro, Christopher Grieco, Ismaila Dabo, Qing Wang, John B. Asbury, Enrique D. Gomez, The Pennsylvania State Univ. (United States)

Fully conjugated block copolymers, consisting of an electron donor and an electron acceptor block, can serve as the active layer in organic photovoltaic devices. Incorporating the donor-acceptor interface within the chemical structure enables model studies of energy and charge transfer. We synthesized a series of block copolymers consisting of a P3HT electron donor and three different push-pull polymer electron acceptors, either poly-((9-(9-heptadecanyl)-9H-carbazole)-1,4-diyl-alt-[4,7-bis(3-hexylthiophen-5-yl)-2,1,3-benzothiadiazole]-2',2''-diyl) (PCT6BT), poly-((9,9-dioctylfluorene)-2,7-diyl-alt-[4,7-bis(3-hexylthiophen-5-yl)-2,1,3-benzothiadiazole]-2',2''-diyl) (PFT6BT), or poly-((2,5-dihexylphenylene)-1,4-diyl-alt-[4,7-bis(3-hexylthiophen-5-yl)-2,1,3-benzothiadiazole]-2',2''-diyl) (PPT6BT). By altering only the electron rich unit of the acceptor, we adjust the driving force for intramolecular charge transfer by tenths of an eV. Dynamic light scattering confirms that the synthesized block copolymers can be fully dispersed in dilute solutions, enabling studies of photoluminescence quenching within individual chains. The absorption and emission spectra of the block copolymers can be deconvoluted to extract the contributions from each of block, enabling us to quantify the yield of intramolecular charge transfer states. Taking the data from all block copolymers together, we find a critical driving force required to generate charge transfer states that depends on the dielectric constant of the solvent.

10363-71, Session PMon

Polarized soft x-ray scattering reveals chain orientation within block copolymer structures

Joshua H. Litofsky, Melissa P. Aplan, Thinh P. Le, Youngmin Lee, Enrique D. Gomez, The Pennsylvania State Univ. (United States)

Fully conjugated block copolymers, consisting of covalently bonded donor

and acceptor blocks, can serve as the active layer in organic photovoltaics (OPV) and other organic electronic devices. The use of Resonant Soft X-Ray Scattering (RSoXS) allows for studies into the molecular orientation and domain spacing of the polymers within lamellae by tuning the X-ray energy and polarization to examine various components of block copolymers. Using the conjugated block copolymer system of poly(3-hexylthiophene)-block-poly((9,9-dioctylfluorene)-2,7-diyl-alt-[4,7-bis(thiophen-5-yl)-2,1,3-benzothiadiazole]-2?,2?-diyl), P3HT-b-PFTBT, and PFTBT derivatives, we can examine the effects of various polymer blocks on the differences of morphology between the donor and acceptor. Polarized Soft X-Ray Scattering (PSoXS) allows us to quantify the type and the degree of orientation of chains within block copolymer domains in thin films. Our work suggests that within our conjugated block copolymers, the P3HT chains orient parallel to the block copolymer interface. Furthermore, examining the anisotropy in PSoXS data provides a clear signature of the block copolymer microstructure. Fourier transform calculations of ideal polymer structures corroborate this concept of block copolymer domains. Thus, we confirm that the domain spacing extracted from PSoXS scales with the end-to-end distance of the blocks. Based on our early findings, we believe that within our P3HT-b-PFTBT block copolymer films, the crystalline P3HT blocks orient parallel to the block copolymer interface.

10363-72, Session PMon

Photoluminescence dynamics in perovskites with different grain sizes

Hyung Do Kim, Yasunari Tamai, Hideo Ohkita, Kyoto Univ. (Japan)

Solution-processed organic–inorganic perovskites based on metal halides have shown considerable potential in application of photovoltaic devices because of their excellent properties, such as direct bandgap with high absorption coefficient, high charge carrier mobility, long diffusion length, and Wannier–Mott exciton. Currently, the power conversion efficiency (PCE) of perovskite solar cells has been improved dramatically from 3.8% in 2009 to more than 22% in 2016. Recently, we have fabricated highly efficient planar heterojunction CH3NH3PbI3 devices with different grain sizes by the fast deposition–crystallization procedure. All the photovoltaic parameters were improved as the grain size of perovskites increases.[1] The best PCE of 19.4% was obtained for a grain size of 500 nm: a short-circuit current density of 23.9 mA cm?2, an open-circuit voltage of 1.08 V and a fill factor of 0.750. In this study, we discuss the photoluminescence (PL) dynamics of perovskites with different grain sizes by measuring the time-resolved PL spectroscopy. As a result, we found that the lifetime is increased with increasing grain size of perovskites. By analyzing the lifetime dependence of excitation intensity, we also found that trap density is decreased with increasing grain size of perovskites. On the basis of these experimental data, we further discuss the relationship between the photovoltaic performance and the grain size of perovskites in terms of the charge carrier recombination dynamics.

Reference

[1] H. D. Kim, H. Ohkita, H. Benten, and S. Ito, Adv. Mater., 2016, 28, 917.

10363-74, Session PMon

Dual Förster resonance energy transfer and morphology control to boost the power conversion efficiency of all-polymer OPVs

Jiangang Liu, Changchun Institute of Applied Chemistry (China)

Broadening the absorption spectrum and efficiently harvesting photogenerated excitons are crucial tasks to realize high-efficiency polymer solar cells (PSCs). Recently, ternary PSCs with complementary absorptions into a single junction device have been emerging as a promising strategy to enhance the absorption of binary PSCs. However, the effect of ternary PSCs critically depends on the location of the third component according to different principles. Due to the hard control of the third component location, only limited high-performance ternary systems have been demonstrated previously. Here, we develop a new concept of dual Förster resonance energy transfer (dual-FRET), in which the third component acts as “energy donor” and the donor and acceptor act as “energy acceptor”. Thus, exciton energy of the third component could transfer energy to both the donor and the acceptor through the FRET principle. Consequently, the third component should only be dispersed uniformly in the binary film regardless of its location. Using this concept, the performance of ternary PSCs, i.e., PTB7-Th (donor) / P(NDI2OD-T2) (accepter) / PF12TBT (the third component), reaches to 6.07%, more than about 30% compared to the corresponding binary PSCs (4.70%). Our work provides a novel way for designing the ternary structure to boost the efficiency of PSCs.

10363-75, Session PMon

Proton radiation effects of conjugated polymer composite thin films

Sam-Shajing Sun, Harold O. Lee, Norfolk State Univ. (United States)

Polymeric thin film based electronic and optoelectronic materials and devices appear attractive for potential space and certain radiation related applications due to their inherent features such as lightweight, flexible, biocompatible, etc. Proton radiation is a major form of ionizing radiation in space, particularly in the so-called inner Van-Allen belt region where most near-earth satellites are orbiting, yet very few literature or data are available on proton radiation effects on conjugated polymer systems. In this study, the proton radiation effects on the electronic/optoelectronic properties of several conjugated polymers and their composites are briefly evaluated. Specifically, UV-Vis absorption spectra of several conjugated polymers and/or their composite thin films were studied and compared before and after the proton radiations at different dosages. The results revealed that proton radiation has very little or insignificant impact up to 800 Rads (corresponding to a dosage over an intense solar event in solar system) on the optoelectronic properties of P3HT, P3HT:PC60BM blend, a light harvesting donor-bridge-acceptor (DBA) and a novel donor-bridge-fluorinated-acceptor (DBfA) type block copolymer thin films. Results imply these conjugated polymers or their composites appear stable and durable for potential space and proton radiation related device applications.

10363-76, Session PMon

Dimethyl sulphoxide vapor annealing assisted morphology control for hysteresis-free organometal halide perovskite solar cells

Yu Wang, Ping Liu, Dongwei Han, Dongying Zhou, Feng Lai, Soochow Univ. (China)

Realizing high performance perovskite solar cells (PeSCs) requires that photons absorbed in the active layer and charges collected by the electrode be maximized. To this end, morphology control of perovskite films is very essential. Previous reports have revealed that dense pinhole-free perovskite films via one-step fabrication, having less recombination defects, generally contribute to high efficiency and negligible current-voltage hysteresis PeSCs. For such one-step fabrication of PeSCs, thermal annealing is routinely conducted to produce the crystallization of perovskite layers. However, due to their heterogeneous nucleation growth nature, discontinuous perovskite films are generally induced by the only treatment with thermal annealing. As an alternative method, solvent vapor annealing has been impressed for morphology control of perovskite films. For example, DMF and DMSO vapor annealing applied pre-/post- thermal annealing have been demonstrated for crystallization improvement of CH3NH3PbI3 films, respectively. In this regard, effects of solvent annealing onto the CH3NH3PbIxCl3-x based perovskite films still remain less studied.

In this work, we report that the use of DMSO vapor annealing followed by thermal annealing increases remarkedly the crystallinity and coverage of CH3NH3PbIxCl3-x film. Due to elimination of the film voids, DMSO solvent annealing effectively improves the electronic properties of CH3NH3PbIxCl3-x perovskite films by reducing recombination defects. Particularly, the perovskite solar cell using the DMSO vapor annealing yields a power conversion efficiency (PCE) of 13.14% under air mass global (AM 1.5 G) spectrum illumination, which shows a 14% improvement in PCE compared to the counterpart only treated by the thermal annealing (ca. a PCE of 11.51%).

10363-77, Session PMon

Inverted polymer solar cells with zinc oxide-modified vanadium-doped indium oxide as the electron-collecting electrode at room temperature

Sung-Jin Lim, Min-Jun Choi, Dongguk Univ. (Korea, Republic of); Keun Yong Lim, Korea Institute of Science and Technology (Korea, Republic of); Jisoo Goo, Young-Jun You, Dongguk Univ. (Korea, Republic of); Do Kyung Hwang, Korea Institute of Science and Technology (Korea, Republic of); Kwun-Bum Chung, Jae Won Shim, Dongguk Univ. (Korea, Republic of)

Recently, polymer solar cells (PSCs) with an inverted structure have received considerable attention for their improved air stability. In such a structure, tin-doped indium oxide (ITO)-modified with low-work function interlayers commonly serves as an electron-collecting electrode. However, a thermal annealing process is inevitable for high conductivity of ITO, which limits versatile use of ITO. Vanadium-doped indium oxide (IVO) is an attractive material for an alternative transparent conducting electrode (TCE), because of the excellent optical and electrical properties, and a variety of stoichiometric compositions of oxides VOX.

Here, we examined optical, electrical, and surface properties of the IVO films deposited by a radio frequency (RF) co-sputtering system using dual targets of V2O5 and In2O3 at room temperature as a function of V2O5 target RF power. The IVO film with the V2O5 target RF power of 8 W showed the optimal transparent conducting properties with the sheet resistance of 74.83 Ohm/square and an average transmittance of 89.4%. The energy band offset between Fermi level and conduction band minimum decreased to 1.02 eV without changes in the physical structure or surface property. The inverted PTB7:PC70BM-based PSCs with the IVO TCE fabricated at the V2O5 target RF power of 8 W yielded the highest power conversion efficiency of 4.7 ± 0.4 % under simulated air mass (AM) 1.5 global (G), 100 mW/cm2 illumination, which was above that of the reference PSCs fabricated using the ITO as the TCE.

10363-78, Session PMon

Perylene-3,4,9,10-tetracarboxylic acid tetracesium salt (Cs4PTA) as efficient and inexpensive cathode interfacial layer for inverted planar perovskite solar cells

Chen Wang, Ping Liu, Dongwei Han, Dongying Zhou, Lai Feng, Soochow Univ. (China)

Currently, perovskite solar cells (PeSCs) have attracted tremendous attention due to their boosting power conversion efficiency (PCE) up to 21%, allowing a promising application for solar-energy conversion in industry. Efforts have been devoted to developing efficient perovskite materials with improved photon absorption and exciton separation. More importantly, charge extraction from the perovskite to the electrodes also plays a critical role in the performance of PeSCs. Since diffusion length of electrons is generally shorter than that of holes, cathode interfacial layers (CILs) are very essential. For the inverted planer PeSCs, the electron transport layer, fullerene derivatives typically used, have the mismatch lowest unoccupied molecular orbitals with the work function of the cathode. Therefore, cathode interfacial layers (such as ZnO, BPhen, etc.) have been usually utilized between the fullerene derivatives and the cathode to reduce the electron extraction barriers.

In this work, we first report the use of perylene-3,4,9,10-tetracarboxylic acid tetracesium salt (Cs4PTA) as effective and low-cost cathode interfacial layer for perovskite solar cells. As a proof of concept, we impressed Cs4PTA to PeSCs having an inverted configuration of ITO/PEDOT:PSS/CH3NH3PbIxCl3-x/PCBM/CIL/Ag as the CIL. The PeSC with Cs4PTA yields a PCE of 12.55%, which is increased by 20% in comparison to the reference device without the CIL (ca. a PCE of 10.42%). The PCE value of PeSC with Cs4PTA is also higher than that of device with BPhen as the CIL (ca. a PCE of 11.94%).

10363-79, Session PMon

Controlling hybrid charge transfer exciton properties at nitride-organic semiconductor heterojunctions

Anurag Panda, Stephen R. Forrest, Univ. of Michigan (United States)

Analogous to polaron-pair states at excitonic HJs, hybrid charge transfer excitons (HCTEs) are at the heart of exciton-to-charge conversion and charge recombination processes at organic-inorganic heterojunctions (OI-HJs). In this work, we study HCTE formation and dissociation kinetics at junctions between inorganic semiconductors, gallium nitride ((In)GaN) with varying indium compositions, and organic semiconductors, boron subphthalocyanine chloride (SubPc), and tris(4-(5-phenylthiophen-2-yl) phenyl)amine (TPTPA). To study the HCTE dissociation efficiency as functions of temperature (T), from T = 294 K to T = 10 K, and voltage (V), from V = 1 V to V = -5 V, we measure external quantum efficiencies (EQE) of the OI devices. We find that nitride semiconductors with appropriate doping can dissociate organic semiconductor excitons with near unity efficiency at room temperature. We explain the voltage and temperature dependence of the EQE using our previously developed theory [1,2] of OI diode operation. We observe the HCTE spectra by electroluminescence, and find that the peak energy closely corresponds to OI-HJ offset energy. Further, we tune the spectra peak energy by changing the indium composition in the GaN layer. We use a quantum mechanical model [3] to elucidate the effects of semiconductor energy levels, dielectric constants, and interface confinement on the binding energy and oscillator strength of the HCTE.

[1] C. K. Renshaw, and S. R. Forrest. Phys. Rev. B 90, 045302 (2014).

[2] A. Panda and S. R. Forrest et al. Phys. Rev. B 90, 045303 (2014).

[3] A. Panda and S. R. Forrest et al. Phys. Rev. B 94, 125429 (2016).

10363-80, Session PMon

Hybrid tandem solar cells combining PbS quantum dot and organic subcells with complementary near infrared absorption

Taesoo Kim, Ru-Ze Liang, Hanlin Hu, King Abdullah Univ. of Science and Technology (Saudi Arabia); Banavoth Murali, Univ. of Hyderabad (India); Ahmad R. Kirmani, King Abdullah Univ. of Science and Technology (Saudi Arabia); Mingjian Yuan, Univ. of Toronto (Canada); Pierre M. Beaujuge, King Abdullah Univ. of Science and Technology (Saudi Arabia); Edward H. Sargent, Univ. of Toronto (Canada); Aram Amassian, King Abdullah Univ. of Science and Technology (Saudi Arabia)

We demonstrate monolithically integrated hybrid tandem solar cells that combine a solution-processed colloidal PbS quantum dot (CQD) and a solution-processed bulk heterojunction subcells with enhanced complementary absorption in the red and near infrared spectra. The hybrid tandem solar cell is electrically connected in series with a p and n type interconnecting layer (ICL) stack that includes a metal oxide layer and a conjugated polyelectrolyte with the incorporation of Au nano-islands. As the CQD subcell exhibits strong absorption at short wavelength and weaker absorption at longer wavelength (PbS QD; Eg = 1.34 eV), it is complemented with a polymer:fullerene top cell consisting of a blend of the low bandgap polymer (PDPP3T; Eg = 1.56 eV) and PC61BM, which is weakly absorbing in the visible to assure excellent spectral complementarity. The insertion of Au nano-islands into the ICL reduces the series resistance, increases the shunt resistance, enhances the fill factor and then achieves a power conversion efficiency (PCE) of 7.9%, superior to the efficiency of individual single cells. Additionally, we will discuss how QD subcell can be fabricated on the OPV subcell without damaging it and can help us achieve PCE approaching 10%.

10363-81, Session PMon

Optical excitations dynamics at quantum dots-fullerene heterointerface

Marcello Righetto, Alberto Privitera, Renato Bozio, Univ. degli Studi di Padova (Italy)

Colloidal quantum dots (QDs) display intriguing optoelectronic properties, such as broadband absorption, high oscillator strength, and size-tunable energy levels. These properties make them suitable candidates for photon harvesting. Due to generally high exciton binding energies, exciton-separating interfaces lay at heart of QDs photovoltaics.[1] The interaction of CdSe/CdS QDs with organic acceptors, such as PCBM, is complex and results in either exciton migration (energy transfer) or exciton dissociation (charge transfer). [2]

In this work, we exploit surface chemistry tools to tailor and direct QDs/PCBM interaction towards desired charge separation in blends, mimicking bulk hetero-junctions active layers. Indeed, changing ligands' chemical nature and length we achieved higher charge generation yields.

We monitored interaction dynamics on picosecond timescale using ultrafast transient absorption (TA) technique. Bleach signals in TA are associated with conduction band electrons and their dynamics is a quantitative probe of interactions dynamics. Moreover, electron paramagnetic resonance (EPR) provided a broader view on charge dynamics at hetero-interface. Indeed, time resolved and pulsed EPR allows tracking the dynamics of paramagnetic species on millisecond timescale. The fate of photo-generated charges plays a pivotal role in determining the efficiency of photovoltaic materials.

Noteworthy, short chain thiols ligands appear to greatly enhance charge generation and suppress geminate recombination of charges. The outcomes of this work suggest possible strategies for the implementation of QDs in hybrid organic-inorganic solar cells.

1. Kamat, P.V., Quantum Dot Solar Cells. The Next Big Thing in Photovoltaics. The Journal of Physical Chemistry Letters, 2013. 4(6): p. 908-918.

2. Stewart, M.H., et al., Competition between Förster Resonance Energy Transfer and Electron Transfer in Stoichiometrically Assembled Semiconductor Quantum Dot–Fullerene Conjugates. ACS Nano, 2013. 7(10): p. 9489-9505.

10363-82, Session PMon

Tuning charge transfer at organic/metal interfaces

Afaf El-Sayed, Al Azhar Univ. (Egypt); Elizabeth Goiri, Donostia International Physics Ctr. (Spain); Patrizia Borghetti, Institut des NanoSciences de Paris (France); Dimas G. de Oteyza, Donostia International Physics Ctr. (Spain); Enrique Ortega, Univ. del País Vasco (Spain)

Energy-level alignment at hetero-interfaces plays an essential role in the functionality of charge injection devices, such as organic solar cells, where the efficiency is largely determined by the relative band edge positions of all its constituents. In fact, an appropriate level alignment may drive the formation of hybrid interface states at the Fermi energy, trigger significant charge transfer and lower interface potential barriers. 1

In this work, we report how the electronic level alignment of fluorinated copper-phthalocyanines (F16CuPc) on metal surfaces [e.g. Au(111), Cu(111), and Ag(111)] can be tailored by changing the substrate work function. By doing this we show how the charge transfer into empty molecular levels can be triggered across the metal-organic interface. Remarkably, we report how we can finely tune the charge transfer within the very same organic-metal interface by making use of the supramolecular environment-dependent work function in molecular blends. 1-3

These intriguing observations are the outcome of a combination of surface-sensitive electron spectroscopies, e.g. x-ray photoemission spectroscopy (XPS), ultra-violet photoemission spectroscopy (UPS), and near edge x-ray absorption fine structure (NEXAFS). Such powerful techniques reveal a number of characteristic spectroscopic fingerprints that provide a fully coherent picture of the physical chemistry phenomena occurring at these relevant interfaces.

[1] A. El-Sayed et al., ACS Nano 7, 6914-6920 (2013)

[2] E. Goiri et al., Phys. Rev. Lett. 112, 117602-1-5 (2014)

[3] P. Borghetti et al., ACS Nano 8, 12786–12795 (2014)

10363-83, Session PMon

Fabrication of high coverage lead-free CH3NH3SnI3 perovskite films using modified solvent bathing method

Takashi Fujihara, Institute of Systems, Information Technologies and Nanotechnologies (ISIT) (Japan); Shinobu Terakawa, Toshinori Matsushima, Chuanjiang Qin, Masayuki Yahiro, Chihaya Adachi, OPERA Ctr. for Organic Photonics and Electronics Research (Japan)

Developing lead-free organic–inorganic perovskite absorbers for solar cells is a crucial issue for commercial use. Tin halide perovskites are alternative candidates for lead perovskites. However, they show unstable properties due to the low quality of their films. The film quality strongly depends on the formation speed of precursor solution to perovskite in a solution process. In this work, a modified solvent bathing method was used to fabricate MASnI3 perovskite films. The formation speed of the perovskite films was controlled by combining anti-solvents with miscibilities different from those of the precursor solvent. The coverage of the perovskite films was significantly improved by employing a mixed solvent in an appropriate ratio and at an appropriate temperature. The power conversion efficiency of a planar perovskite solar cell with a film prepared using this method was 2.1 ± 0.4%, which is higher than that of solar cells with a conventionally prepared active layer. Notably, an open-circuit voltage of 0.45 ± 0.01 V was obtained, which is relatively high for tin halide perovskites. Additionally, significant reproducibility was achieved in comparison with previously reported devices. Further, an unexpectedly long lifetime of over 200 h was observed for encapsulated solar cells under simulated 1 sun (AM1.5, 100 mW/cm2) continuous irradiation, which is in contrast to the expectation that tin perovskites degrade quickly. The high surface coverage of our tin halide perovskite film results in relatively high open-circuit voltage and stable photovoltaic properties.

10363-84, Session PMon

Practically viable strategy for efficient and reliable semi-transparent organic solar cells: Face-seal encapsulation embedded with color-filter functionality

Hyunwoo Lee, Jaewon Ha, Hyeonwoo Lee, Seunghyup Yoo, KAIST (Korea, Republic of)

Semitransparent solar cells are regarded as a photovoltaic (PV) technology in which organic solar cells (OSCs) can have a competitive edge over other PV technologies mainly due to their thin-film nature. Furthermore, the compatibility of OSCs with plastic substrates can even lead to semitransparent PV films that can be easily integrated with the existing building infrastructure at low cost, making semitransparent OSCs (ST-OSCs) even more attractive. To deploy ST-OSCs in real-world application such as solar windows in building-integrated or vehicle-integrated PV (BIPV or VIPV) applications, it is essential to establish an encapsulation method that effectively prevents water vapor or oxygen from infiltrating into cell active layers and interfaces while keeping the low manufacturing cost. From the efficiency perspectives, on the other hand, it will be highly useful if one can recycle a significant portion of the light that usually passes through ST-OSCs without being absorbed in active layers.

In this work, we propose an architecture for semi-transparent organic solar cells (ST-OSCs), wherein the cells are “face-seal” encapsulated with color-filtering barrier films. The color-filtering barrier film is designed based on transfer matrix formalism so that spectral components corresponding to major absorption band of active layers can be selectively reflected while the other spectral components are transmitted for see-through capability. Preparation of these color filters being independent of cell fabrication, the best material/ process composition can be utilized without worrying about damaging the organic active layers. By integrating the proposed plastic films having the embedded color filters with semi-transparent organic solar cells, we demonstrate ST-OSCs with power conversion efficiency of 7.3% under 100mW/cm2 (AM 1.5G) and with transmittance over 10% in the spectral range of 450-600 nm. Furthermore, we show that these devices can maintain over 90% of the initial efficiency even after being kept under highly damp condition (30°C, 90% relative humidity) for 120 hours.

Reference

[1] Zhang, Dan-Dan, et al. “Enhanced performance of semitransparent inverted organic photovoltaic devices via a high reflector structure.” ACS applied materials & interfaces 5.20 (2013): 10185-10190.

10363-85, Session PMon

Stability enhancement of organic-inorganic perovskite solar cells via thin film encapsulation

Nochang Park, Korea Electronics Technology Institute (Korea, Republic of); Jincheol Kim, Jae S. Yun, The Univ. of New South Wales (Australia)

This paper details an thin film encapsulation of perovskite solar cells to improve the stability from moisture. The perovskite solar cells were encapsulated with alumunum oxide (Al2O3) via atomic layer deposition (ALD) process. The process was performed at low temperatures (110°C, 150°C) to minimize thermal degradation. We achieved the 6.3 nm and 6.6 nm in thickness at 110°C and 150°C, respectively. There were little changes in electrical properties of perovskite solar cells after ALD process at 110°C. However, the power conversion efficiency (PSC) was decreased to about 10 % compared to initial PSC at 150°C. The encapsulated samples showed good stability at 25 °C, 50% RH for 2,000 hours. In addition, More than 200 hours in 45 °C, 85% RH testing has been observed without significant PSC decrease caused by moisture.

10363-86, Session PMon

Perovskite thin films on insulators and in thin-film transistors applications

Johnny K. W. Ho, Rocky K. H. Chan, Jenner H. L. Ngai, Sin Hang Cheung, Shu Kong So, Hong Kong Baptist Univ. (Hong Kong, China)

Methylammonium (MA)-based perovskite compounds are generally grown on conducting or semiconducting substrates. In this study, we explore the growth of these compounds on insulators. The key challenge is to find a surface that favors crystal growth of perovskites, but without compromising the adhesion of the crystals. A family of methacrylate-based polymers has been identified as the insulators. Onto these insulators, Pb-based MA iodide polycrystalline thin films are successfully grown. We found that PPMA, a derivative of a common commercial plastic poly(methyl methacrylate), produces the best perovskite films. To test the electronic quality of these films, we perform photothermal deflection spectroscopy to look into its subgap optical absorptions. The relation between the crystal quality and the hydrophobicity as well as microscopic interactions is investigated. Furthermore, we employ these films for thin-film transistor applications. Under optimal conditions, the thin-film transistors fabricated on PPMA produces the best device with electron mobility in excess of 0.1 cm2 V-1 s-1.

10363-87, Session PMon

Optoelectronic properties of CuO-Cu2O complex layers in MAPbI3 perovskite solar cells

Kuan-Lin Lee, Lung-Chien Chen, Kai-Chieh Liang, National Taipei Univ. of Technology (Taiwan)

The perovskite-based solar cells have high performance for power conversion efficiencies. The scientists had been searching new materials to fabricate a new structure of solar cells over the past 5 year. In this work, we report the optoelectronic properties of CuO-Cu2O complex layers in CH3NH3PbI3 (MAPbI3) perovskite solar cells. The nanostructured CuO-Cu2O films are made on the ITO-coated glass from cupper (Cu) target by AC sputtering. The CuO-Cu2O films were formed by oxidation method at different annealing temperature from 300 to 500° C. The CuO-Cu2O films were also applied into the MAPbI3 perovskite solar cells as a hole transport layer. In the cell structure, the C60 (Fullerene) is a n-type material that helps to inject electrons into the electrode. The BCP (Bathocuproine) not only is an exciton block layer but also the electron transport layer and active layer of the protective layer in the device. The evaporation method was employed to deposited C60 and BCP. The device structure is Ag / BCP / C60/ CH3NH3PbI3 / CuO-Cu2O / ITO / Glass which the C60 and BCP play electron transport layers (ETLs) and buffer layers, respectively. When the annealing temperature is 350° C, the PCE of the cell is the best value for 8.53%. With optimized annealing temperature and conditions, the solar cells have the highest efficiency, low J?V hysteresis and excellent stability. Therefore, the low-cost processed and stable nanostructured CuO-Cu2O will be an alternative hole transport layer materials for industrial production of the perovskite solar cells.

10363-88, Session PMon

Plasmon enhanced power conversion efficiency in inverted bulk heterojunction organic solar cell

Minu Mohan, Ramkumar Sekar, Manoj A. G. Namboothiry, Indian Institute of Science Education and Research Thiruvananthapuram (India)

P3HT:PCBM is one of the most studied polymer-fullerene system. However the reported power conversion efficiency (PCE) values falls within the range of 4% to 5%. The thin film architecture in OPVs exhibits low PCE compared to inorganic photovoltaic cells. This is mainly due to the low exciton diffusion length that limits the active layer thickness which in turn reduces the absorption of incident light. Several strategies are adapted in order to increase the absorption in the active layer without increasing the film thickness. Inclusion of metal nanoparticles into the polymer layer of BHJ solar cells is one of the promising methods. Incorporation of metal nanostructures increases the absorption of organic materials due to the high electromagnetic field strength in the vicinity of the excited surface plasmons.

In this work, we used ~ 60 nm Au plasmonic structures to improve the efficiency of organic solar cell. The prepared metal nano structures were characterized through scanning electron microscopy (SEM), and UV-Visible spectroscopy techniques. These prepared metallic nanoparticles can be incorporated either into the ETL or into the active P3HT:PC71BM layer. The effect of incorporation of plasmonic gold (Au) nanoparticle in the inverted bulk heterojunction organic photovoltaic cells (OPVs) of P3HT:PC71BM fabricated in ambient air condition is in progress. Initial studies shows an 8.5% enhancement in the power conversion efficiency (PCE) with the incorporation of Au nanoparticles under AM1.5G light of intensity 1 Sun.

10363-89, Session PMon

The intrinsic photoproducts and their dynamic balance revealed by density-resolved spectroscopic method

Shufeng Wang, Peking Univ. (China)

The highly efficient organolead trihalide perovskite based solar cells are the top interests in photovoltaics for the recent years. It is well known that their high efficiencies benefit from the rich photo-induced free carriers. It is also know that excitons co-exist with the free carriers. Are these two photoproducts has a fixed ratio after excitation, or they are of dynamic balance depending on the density? This fundamental question decides whether the exciton can convert to free carriers to improve the cell efficiency. It also decides the excited state dynamics since the ratio follows the total density, which decays in time. In addition, the dynamic balance of exciton and free carriers should be a very general question in many widely studied semiconductors. However, no method can be applied to see such density-dependent behavior until now. We developed a density-resolved spectroscopic method to directly observe the photoproduct types and their density-dependent interconversion. In perovskite, the dynamic co-existence of excitons and free carriers was experimentally verified for the first time. It is also revealed a exciton binding energy of 24±2 meV and an effective mass of electron-hole pair. Surprisingly, with the method, we found that the photoproduct system could be more complicated than above exciton-carrier system. Our spectroscopic method and the results profoundly enrich the understanding of the photophysics in perovskite materials for photovoltaic applications. In addition, our method can be widely applied to other semiconductors. (Ref: Physical Review B 94, 140302 (2016)).

10363-90, Session PMon

High efficiency printable polymer solar cell modules with a new simplified series connection architecture

Eunhag Lee, Jinho Lee, Soonil Hong, Kwanghee Lee, Gwangju Institute of Science and Technology (Korea, Republic of)

Despite the recent dramatic improvements in power conversion efficiencies resulting in values exceeding 12%, the fabrication of polymer solar cell modules (PSMs) via printing process is the important challenges. Conventional module architecture consisting of serially interconnected stripe-shaped patterned subcells requires highly sophisticated patterning techniques that significantly increase the complexity of manufacture process and lead to reduction in module efficiency due to so-called 'aperture loss' in series connection areas (SCAs). Here, we demonstrate the highly efficient PSM architecture without any patterning process by introducing innovative electric field-induced metal-nanofilament concept. To produce vertically connected metal nanoelectrodes within SCAs between the bottom indium tin oxide and top silver electrodes, we introduce the silver-nanoparticles (SNPs) and nonconjugated polyelectrolyte (NPE) into the photoactive bulk-heterojunction solar inks. The SNPs facilitate the formation of metal-nanofilament while amine-containing NPE performs dual function to construct simplified solar module architecture: (i) Self-assembly: NPE molecules are spontaneously migrate onto ITO surface and act as a work function modifier, thereby allowing ohmic contact. (ii) Stabilizer: amine group of NPE help to form and stabilize the SNP in solution. With the loss-free geometrical and electrical connection of subcells, we achieve a high module efficiency over 6.6% with a geometric fill factor of 90%.

10363-92, Session PMon

Femtosecond transient absorption spectroscopy of planar CH3NH3PbI3 perovskite films

In-Sik Kim, Cheol Jo, Gwangju Institute of Science and Technology (Korea, Republic of); Rira Kang, Korea Atomic Energy Research Institute (Korea, Republic of); Dong-Yu Kim, Do-Kyeong Ko, Gwangju Institute of Science and Technology (Korea, Republic of)

As an alternative to conventional inorganic solar cells, organo-metal halide perovskites (OMHPs) have caught considerable attention due to a high absorption coefficient, allowing photovoltaic devices to be thin and flexible, as well as low-cost solution processing methods. As a matter of fact, solution-processed perovskite solar cell technologies have reached power conversion efficiencies (PCEs) of over 20% in the past few years. This rapid progress in OMHP solar cells have realized by several approaches: a material development through varying consistent components of the perovskites, an optimization of device structure, and a development of sample preparation methodology. However, understanding of photo-induced carrier dynamics in the OMHPs remains still unclear.

We have fabricated methylammonium lead halide (CH3NH3PbI3) perovskite films using various methods for the solution processing, which affect crystal orientation, charge transfer in presence of electron transport layer, and PCE of planar perovskite solar cell devices. In this work, we demonstrate photo-generated dynamics in planar CH3NH3PbI3 perovskite films using a femtosecond transient absorption (TA) spectroscopy. The TA dynamics of perovskite shows a dependence on the preparation methods of the perovskite films.

10363-93, Session PMon

Crystalline MoOx thin-films as hole transport layer in organic photovoltaics

André L. F. Cauduro, Mehrad Ahmadpour, Univ. of Southern Denmark (Denmark); Roberto Moreno Souza dos Reis, Gong Chen, Lawrence Berkeley National Lab. (United States); Andreas K. Schmid, Lawrence Berkeley National Lab. (United States) and Univ. of Southern Denmark (Denmark); Christophe Méthivier, Léo Bossard-Giannesini, Hervé Cruguel, Nadine Witkowski, UPMC Sorbonne Univ. (France); Horst-Günter Rubahn, Morten Madsen, Univ. of Southern Denmark (Denmark)

Molybdenum-oxide (MoOx) thin-films have attracted a lot of attention in the past years due to their unique ability to act as interfacial layers in electronics and energy applications. In the work presented here, large tuning possibilities in the electronic and optoelectronic properties of MoOx thin-films deposited by reactive sputtering are demonstrated, along with the implementation of the films in organic photovoltaics. A large tuning range in the conductivity of thin MoOx films of around 10 orders of magnitude is demonstrated via tuning of the oxygen partial pressures during the growth process, which also lead to drastic changes in the optical absorption (0.60 eV - 2.50 eV) of the films. The observed effects are attributed to changes in the electron density at the defect band: as the oxygen partial pressure increases, electrons are released and empty out the defect band [1].

Ultraviolet (UPS) and X-Ray (XPS) Photoelectron Spectroscopy investigations are conducted for accessing information about the work function and surface composition of the thin-films. Importantly, the work function of the films increase strongly with annealing temperature, and span a tuning range of almost 2 eV. Low Energy Electron Microcopy (LEEM) is applied to extract the spatially resolved work function values from the sputtered MoOx thin-films [2]. Application of the MoOx thin-films in novel organic optoelectronic devices is demonstrated by employing them as hole transport layers in DBP:C70 based small molecule solar cells.

[1] Fernandes Cauduro et al., Applied Physics Letters 106, 202101 (2015).

[2] Fernandes Cauduro et al., Submitted (2016).

10363-94, Session PMon

Role of energy transfer for charge generation at organic-inorganic interfaces

Philipp Ehrenreich, Eugen Zimmermann, Lukas Schmidt-Mende, Univ. Konstanz (Germany)

Hybrid solar cells promise large potential for solar cell application by bringing together mechanical as well as chemical stability of an inorganic metal-oxide on the one hand, with unlimited design possibilities for organic semiconductors on the other hand. For efficient charge generation, not only comprehensive light absorption is needed but also charge separation and charge collection should take place efficiently. These properties, however, have turned out to be limited for hybrid interfaces compared to their fully organic opponents. In this contribution we highlight major challenges that are responsible for such limitations. Beside the role of trap states in the metal oxide we focus on the influence of polymer morphology and the role of Förster resonant energy transfer in a charge generation process. Both electronic measurements on solar cell devices as well as spectroscopic results with respect to exciton dynamics are presented and reveal design rules for future developments on hybrid solar cell materials.

10363-95, Session PMon

Multiscale study of the formation of the PFI:PSS:PEDOT super structure and its HOMO-LUMO energies

Min Huang, Tongji Univ. (China)

The vertically self-organized concentration profile of the PSS:PEDOT:PFI layer from mesoscale DPD simulations presented in the previous contribution were inversely mapped back into atomistic scale. DFT quantum calculations were then performed to understand the nature of the formation of the PFI:PSS:PEDOT complex. Hydrogen bond bonding energy and deprotonation energy were obtained accordingly. The charge states of PSS polymer chain in this complex and its effects on the HOMO-LUMO (the work function) were discussed. The DFT quantum calculation revealed the formation of complex hydrogen bonding networks leading to the formation of super PFI:PSS:PEDOT structure. PFI was found to be a stronger H donor than PSS. The adding of PFI was found to have the effect of lowering the energy of deprotonated PSS chain, as the result pushing HOMO, LUMO of the PFI:PSS:PEDOT ternary structure to lower than those of the original PSS:PEDOT binary structure. The increasing of the work function from the bottom to the top of the film can therefore be understood as the result of the combining effects of increasing PSS:PEDOT and PFI:PSS ratio in the vertical direction induced by PFI led phase segregation.

10363-96, Session PMon

Design of novel triphenylamine-based donor-acceptor oligomers for stable organic photovoltaics

Sergey A. Ponomarenko, Institute of Synthetic Polymeric Materials (Russian Federation) and M.V. Lomonosov Moscow SU (Russian Federation); Yuriy N. Luponosov, Alexander N. Solodukhin, Institute of Synthetic Polymeric Materials (Russian Federation); Artur L. Mannanov, M.V. Lomonosov Moscow SU (Russian Federation) and Institute of Synthetic Polymeric Materials (Russian Federation); Oleg V. Kozlov, Zernike Institute for Advanced Materials (Netherlands) and M.V. Lomonosov Moscow SU (Russian Federation); Dmitry Y. Paraschuk, M.V. Lomonosov Moscow SU (Russian Federation) and Institute of Synthetic Polymeric Materials (Russian Federation); Maxim S. Pschenichnikov, Zernike Institute for Advanced Materials (Netherlands); Christoph J. Brabec, i-MEET (Germany)

A library of linear and star-shaped donor-acceptor oligomers having triphenylamine (TPA)-based electron-donating unit linked through (oligo) thiophene ϖ-conjugated spacers to 1, 2 or 3 terminal alkyl- or phenyl-substituted dicyanovinyl (DCV) or 3-ethylrhodanine electron-withdrawing groups was designed, synthesized and investigated [S.A. Ponomarenko et al., Faraday Discuss., 2014, 174, 313; Y.N. Luponosov at al., Organic Electronics, 2016, 32, 157]. Systematic variations of the number and chemical nature of the acceptor units, length of both the solubilizing alkyl chains and oligothiophene ϖ-bridges allowed elucidating the structure-properties relationships in this series of organic semiconductors. We have shown that the analog of TPA with methoxy-substitutes (m-TPA) increases solubility and crystallinity of the star-shaped molecules, making m-TPA as attractive intramolecular donor unit [Y.N. Luponosov at al., J. Mater. Chem. C, 2016, 4, 7061]. Our studies revealed that oligomers with alkyl- or phenyl- substituted DCV groups demonstrate significantly better solubility, electrochemical and oxidation stability as compared to their analogues with common H-containing DCV groups. Ultrafast photoinduced absorption spectroscopy, using a visible pump to mimic the sun photons and broadly tunable IR probe to monitor concentration of hole polarons at the conjugated system allowed to study the charge separation dynamics [O.V. Kozlov et al., Adv. Energy Mater., 2015, 5, 1401657]. Right choice of TPA-based oligomers as donors and fullerene-based acceptors allowed preparation of bulk heterojunction organic solar cells achieving PCE of 4.0 – 5.4% with high (0.9 - 1.0 V) open circuit voltage, which are fairly stable without any encapsulation. This work was supported by Russian Science Foundation (grant 14-13-01380).

10363-97, Session PMon

Single phase high mobility Cu2O film as efficient and robust hole transporting layer for organic solar cells

Yaxiong Guo, GuoJia Fang, Wuhan Univ. (China); Gang Li, The Hong Kong Polytechnic Univ. (Hong Kong, China)

Carrier transport material plays critical role in solution processed advanced solar cells such as organic polymer solar cell and hybrid perovskite solar cells. Comparing to "standard" PEDOT:PSS hole transporting material (HTM)/ layer, inorganic HTMs such as MoO3, V2O5, NiOx etc. showed improved environmental stability and also high performance. High mobility, earth-abundant, environmentally-stable and nontoxic are the focus of HTMs research. This presentation will show highly transparent, high mobility and phase pure Cu2O nano-crystal films, which are synthesized by reactive magnetron sputtering at room temperature, are promising HTMs for efficient OSC applications.

In classical PTB-7 based solar cell system, we show that polymer solar cell with phase pure Cu2O HTM layer has over 10% enhancement in PCE, comparing to that with standard PEDOT:PSS solar cell. Better energy level alignment and reduced series resistance are believed to responsible for the improvement. The improved photovoltaic performance suggest Cu2O is a promising HTM for future low temperature roll to roll organic polymer solar fabrications.

10363-98, Session PMon

Minimizing beam damage in the electron microscope to enable new imaging approaches for conjugated polymers

Brooke Kuei, Enrique D. Gomez, The Pennsylvania State Univ. (United States)

Transmission electron microscopy (TEM) of conjugated polymers has remained a challenge because resolution is limited by the electron dose the sample can handle. We have characterized the effects of beam damage on poly(3-hexylthiophene) (P3HT) and poly[(5,6-difluoro-2,1,3-benzothiadiazol-4,7-diyl)-alt-(3,3’’’-di(2-octyldodecyl)-2,2’;5’,2’’;5’’,2’’’-quaterthiophene-5,5’’’-diyl)] (PffBT4T-2OD) via electron diffraction and scanning TEM electron energy-loss spectroscopy (STEM-EELS). Critical dose DC values were calculated from the decay of diffraction and low-loss EELS peaks as a function of dose rate, accelerating voltage, and temperature. Importantly, DC increases with dose rate in the low dose rate regime, likely due to the limited diffusion of ions. This diffusion-limited argument is further explored by studying beam damage in P3HT with the antioxidant butylated hydroxytoluene (BHT), as well as through beam blanking experiments in which ions are given time to move between short exposures to the beam. STEM-EELS spectrum imaging also revealed that damage occurs even in areas untouched by the beam, likely due to a local rise in temperature caused by the beam. Altogether, our results suggest that although local heating can be important, other factors such as the dose rate must also be tuned to minimize beam damage. This improved understanding of beam damage in conjugated polymers will allow for new TEM techniques that were previously difficult for this class of beam sensitive materials, such as low-loss electron energy loss spectroscopy imaging and high resolution imaging.

10363-99, Session PMon

On the ferroic properties of methylammonium lead iodide thin-films

Tobias Leonhard, Holger Röhm, Alexander Colsmann, Karlsruher Institut für Technologie (Germany)

The quest for alternative, non-toxic and long-term stable Perovskites is partly hampered by a lack of fundamental understanding of the MAPbI3 properties and energy conversion mechanisms. As part of this process, the scientific community controversially discusses the importance of ferroic properties for the exceptional performance of MAPbI3, including claims of non-ferroelectricity, anti-ferroelectricity, ferroelectricity and ferroelasticity. Some simulations have predicted ferroelectricity in MAPbI3 with alternating polarized domains ruling the vertical charge carrier transport. Any experimental evidence towards ferroelectricity will therefore provide helpful guidance for the quest to find non-toxic MAPbI3 replacements.

We explore the ferroic properties of methylammonium lead iodide (MAPbI3) perovskite solar cells by Piezoresponse Force Microscopy. We find domains of alternating polarization with a diameter of 90 nm which we identify as in-plane polarized ferroelectric domains. High-resolution photo-conductive atomic force micrographs under illumination also show an alternating charge carrier extraction pattern which we attribute to a small vertical polarization component. The correlation of the sample properties with Atomic Force and Kelvin Probe Force Micrographs evidence the piezo-electric nature of the domains.

10363-100, Session PMon

Porphyrin-based donor materials for highly efficient organic photovoltaics

Xunjin Zhu, Hong Kong Baptist Univ. (China)

To mimic the natural photosynthetic systems utilizing chlorophylls to absorb light and store light energy, a series of symmetrical ϖ-conjugated small molecules have been constructed from meso-alkyl substituted porphyrins as the central unit and rhodanine derivatives as the terminal group. At first, we synthesized three new unsymmetrical push-pull A-D-A small molecules (CS-I, CS-II and CS-III) consisting of meso-alkyl substituted porphyrins 5,15-bis(2-octylundecyl)-porphyrin, 5,15-bis(3-octyl-1-tridecyl)-porphyrin and 5,15-bis(4-octyl-1-tetradecyl)-porphyrin as electron rich donor (D) units, ethynylbenzene as ϖ-linkage, and 3-ethylrhodanine (RH) as electron deficient acceptor (A), and applied them as electron donors in solution-processed bulk-heterojunction solar cells, leading to high power conversion efficiencies up to 6.49%.[1] And further detailed studies indicated that small molecules based 10,20-bis(2-hexylnonyl) aliphatic peripheral substituted porphyrin core performed much better than those with aromatic peripheral substituted porphyrin cores (4a, 4b and 4c), mainly due to the decreased steric hindrance and increased intermolecular ϖ-ϖ interactions.[2] Very recently, to extend the backbone conjugation and enhance intermolecular ϖ-ϖ interaction, we designed and prepared two porphyrin-based small molecules (PTTR and PTTCNR) in which 3,3’’-dihexyl-terthiophene were symmetrically conjugated to 10,20-bis-(2-octylundecyl)-porphyrin core. The conjugation of terthiophene and 2-octylundecyl peripheral substitutions on porphyrin-core, can not only effectively increase the solar flux coverage, but also can simultaneously facilitate stronger intermolecular ϖ-ϖ stacking and higher charge transfer mobility in the film. The processing engineering for their blend films with PC71BM afforded the highest power conversion efficiency of 8.21%, corresponding to a JSC of 14.30 mA cm?2, VOC of 0.82 V, and FF of 70.01%.[3]

References

1. Chen, S., Xiao, L., Zhu, X., Peng, X., Wong, W. K., Wong, W. Y. Chem. Comm., 2015, 51(77), 14439-14442.

2. Wang, H., Xiao, L., Yan, L., Chen, S., Zhu, X., Peng, X., Wang, X., Wong, W. K. Wong, W. Y. Chem. Sci., 2016, 7, 4301-4307.

3. Xiao, L., Chen, S., Gao, K., Peng, X., Liu, F., Cao, Y., Wong, W. Y., Wong, W. K., Zhu, X. ACS Appl. Mater. Inter., 2016, 8, 30176?30183.

10363-101, Session PMon

Effect of Cu2O inorganic hole conducting material in flexible perovskite based heterojunction solar cell

Md. Asaduzzaman, Ali Newaz Bahar, Mawlana Bhashani Science and Technology Univ. (Bangladesh); Mohammad Maksudur R. Bhuiyan, Univ. Grants Commission of Bangladesh (Bangladesh)

The device modeling of a methyl ammonium lead iodide (CH3NH3PbI3) perovskite sensitized heterojunction solar cell has been carried out in this study. Cuprous oxide (Cu2O), an inorganic hole conducting material (HCM) has been proposed to use in the device structure consisting of Sn2O: F (FTO)/TiO2/perovskite absorber/HCM/Au stack. The thicknesses of the p-type Cu2O HCM, the n-type FTO, and the perovskite absorber have been optimized the crucial performance parameters including short circuit current density (Jsc), open circuit voltage (Voc), fill factor (FF), and energy conversion efficiency (?) of the perovskite solar cell have been computed using ADEPT 2.1 simulator. In addition, the effects of hole mobility and doping concentration of the HCM in corporations with the defect states of the Cu2O/interface have been analyzed. A higher open circuit voltage of 937.64 mV and a high energy conversion efficiency outstripping 23% have been recorded from the simulation. Moreover, the use of Cu2O as a hole transport layer substantiates the enhancement of the cell performance by reducing the degradation occurred due to using conventional Spiro-OMeTAD organic hole conducting layer. In addition, the replacement of moisture sensitive and costly Spiro-OMeTAD hole conducting material by Cu2O layer can provide double benefits to reduce the cost and to improve the stability.

10363-102, Session PMon

Role of morphology in exciton dissociation and charge extraction in dilute donor-acceptor blend organic heterojunctions

Kan Ding, Univ. of Michigan (United States)

The performance of mixed-heterojunction (HJ) organic photovoltaic (OPV) cells show a significant dependence on device morphology. Here, we study HJs comprising blends of tetraphenyldibenzoperiflanthene (DBP) and C70. OPVs with this material combination is maximum at a very low (< 10%) DBP concentration in C70[1][2]. It is unclear how hole polarons in DBP

created on the dissociation of excitons at donor-acceptor junctions can be extracted from such a dilute system, yet the high efficiencies achieved suggests that charge extraction is unimpeded in the dilute mixtures. By studying the photoluminescence emission of two discrete charge transfer (CT) states [3] in structures comprising alternating, ultrathin layers of C70 and DBP, we precisely control the layer morphology, and it influence on the charge dissociation process. A kinetic Monte Carlo (KMC) simulation model is applied to understand the nanoscopic morphology of the multilayers and blends. The model quantitatively explains the charge extraction process and the CT emission spectra in the dilute active regions. We find that planar DBP molecules form ϖ-ϖ stacks that result in continuous percolation pathways to enable hole extraction even in the most dilute blends. We provide an explanation to the high performance of DBP/C70 photovoltaics at surprisingly low donor concentrations.

References:

[1] X. Xiao, J. D. Zimmerman, B. E. Lassiter, K. J. Bergemann, and S. R. Forrest, A hybrid planar-mixed tetraphenyldibenzoperiflanthene/C70 photovoltaic cell, Appl. Phys. Lett. 102, 073302 (2013).

[2] X. Xiao, K. J. Bergemann, J. D. Zimmerman, K. Lee, and S. R. Forrest, Small-molecule planar-mixed heterojunction photovoltaic cells with fullerene-based electron filtering buffers, Adv. Energy Mater. 4, 1301557 (2013).

[3] X Liu, K Ding, A Panda, and SR Forrest, Charge Transfer States in Dilute Donor-Acceptor Blend Organic Heterojunctions, ACS Nano, 10 (8), pp 7619–7626 (2016).

10363-103, Session PMon

Hybrid solar cell based on a-Si/polymer flat heterojunction on flexible substrates

Antonio J. Olivares-Vargas, Svetlana Mansurova, Ismael Cosme-Bolaños, Andrey Kosarev, Carlos Alberto Ospina, Hiram Enrique Martinez, Instituto Nacional de Astrofísica, Óptica y Electrónica (Mexico)

An alternative to pure organic PVs is the class of organic-inorganic hybrid solar cells, where heterojunction is formed between inorganic semiconductors and organic compounds. An advantage of hybrid PVs over organics PVs lies in the high carrier mobility of the semiconductor and the light absorption at longer wavelengths than for organic compounds. In addition, band gap engineering can be a useful instrument in the design of the hybrid solar cell architecture since rather developed deposition process of inorganic semiconductors allows to tune the important structural and electronic parameters such as optical gap, Fermi level position, localized states distribution, etc. On the other hand, the chemical functionalizing of the organic component (by introduction of reducing or oxidizing groups in the chemical structure) is capable of significantly affecting their performance.

In this work, we present the results of investigation of thin film hybrid organic-inorganic photovoltaic structures based on flat heterojunction hydrogenated silicon (Si:H) and poly(3,4 ethylene dioxythiophene):poly(4-styrenesulfonate) (PEDOT:PSS) fabricated on different types of flexible substrates, namely, polyethylene naphthalate (PEN) and poly (4,4'-oxydiphenylene-pyromellitimide) (Kapton). Scanning electron microscopy (SEM) and atomic force microscopy (AFM) imaging have been used in order to study morphological characteristics of different layers in the structure. Spectral dependence of short circuit current has been analyzed aiming to reveal contribution of substrate on the electrical properties of the films grown on it. Performance characteristics of fabricated photovoltaic structures have been measured and analyzed for different thicknesses of the transparent electrodes and different substrate types.

10363-104, Session PMon

Investigation of charge generation and transport in fullerene-free ITIC-based organic solar cells

Xueping Yi, Iordania Constantinou, Erik D. Klump, Bhoj Gautam, Sofia Garakyaraghi, Franky So, North Carolina State Univ. (United States)

Over the past several years, considerable efforts have been dedicated to the synthesis of new non-fullerene small molecule acceptors but device efficiencies remained low compared to PC71BM-based devices. Recently, polymer solar cells using a non-fullerene acceptor, ITIC, reached efficiencies over 11%. In fullerene devices, it has been well understood that a large LUMO-LUMO offset (> 0.3 eV) between the donor polymer and the acceptor molecule is necessary for efficient exciton dissociation. On the other hand, devices using ITIC have been able to perform efficiently with much smaller LUMO-LUMO offsets.

To understand the difference between ITIC and traditional fullerene acceptors, we fabricated PTB7-Th devices with either ITIC or PC71BM. We found that these devices had similar performances, with a smaller short circuit current in the ITIC devices resulting from less short wavelength absorption. Surprisingly, while the LUMO of ITIC is 3.8 eV and PC71BM's LUMO is 4.3 eV, the open circuit voltage (VOC) observed in the devices was almost identical, indicating a larger voltage loss in the PTB7-Th:ITIC devices. To understand this difference, we probed the charge transfer state dynamics via transient photoluminescence. In this we found that the exciton lifetime was comparable in both ITIC and PC71BM systems, indicating that charge dissociation was efficient in both systems. Additionally, we measured sub-bandgap external quantum efficiency spectra in order to determine the energy level of the CT states. From these results, we found that despite the shallower LUMO energy of ITIC, both ITIC and PC71BM devices have the same CT energy level. Therefore, we conclude that while a smaller LUMO-LUMO offset is needed in ITIC based devices to achieve efficient exciton dissociation, the CT states form at a lower energy than the predicted energy level resulting in a significant VOC loss.

10363-105, Session PMon

Effect of polar sidechains on high efficiency organic solar cells

Xueping Yi, North Carolina State Univ. (United States); Bing Xu, Georgia Institute of Technology (United States); Erik D. Klump, Franky So, North Carolina State Univ. (United States); John R. Reynolds, Georgia Institute of Technology (United States)

It is commonly believed that a high dielectric constant is required to lower the exciton binding of a photovoltaic polymer. A common strategy is to add a polar side group to the polymer, as it will not affect the energy levels of the backbones. In this study, we compare the device performance of two polydithienosilole-thienopyrrolodione (DTS-TPD) based donor polymers. These two polymers are identical except DTS-TPD-CN has a side chain containing a cyano group while DTS-TPD does not. Surprisingly, despite the measured higher dielectric constant due to the polar cyano group, the device characteristics of the cyano containing devices were significantly worse than those of the devices made with the cyano polymer.

Atomic force microscopy images revealed very similar domain sizes for the two polymer-fullerene blends and suggested polar groups does not impair the intermixing of the polymer and fullerene. The measured space charge limited current mobilities showed the hole mobility of DTS-TPD-CN was two magnitudes lower than that of DTS-TPD indicating the cyano groups hinder the hole transport, contributing to a significant reduction in JSC and fill factor for the DTS-TPD-CN device. The energetic disorder of the hole transport was investigated by temperature dependent mobility measurements. It was found that the energetic disorder of DTS-TPD-CN:PC71BM was higher compared to that of DTS-TPD:PC71BM. We believe the high energetic disorder is due to local variations in the potential caused by the permanent dipoles on the cyano group.

10363-106, Session PMon

Ultrashort pulsed laser-dicing of silicon wafers for the decollating of conventional and hybrid solar cells

Christian J. Hördemann, Christian Fornaroli, Arnold Gillner, Fraunhofer-Institut für Lasertechnik (Germany)

In order to cut and to decollate silicon for the manufacturing of solar cells and electronic components, commonly blade sawing or nanosecond-based laser processes are used. If the cut needs to be carried out with high precision and without causing thermal damage to the surrounding material, ultrashort pulsed laser cutting can deliver a fine and small cutting kerf. The reduction of the kerf width leads to a higher yield per wafer, if single elements need to be cut out. By this, marginal heat affected zones and minimal edge damaging are attainable.

Ultrashort-pulsed lasers reach from pico- to femtoseconds. In order to demonstrate which pulse duration and ablation strategy is the best for the singling of silicon wafers, the ablation threshold for pulse durations from pico- to femtoseconds is determined with the method of Liu. During the method, the diameter of the ablated geometry is measured, squared and plotted against the peak fluence in logarithmic scale. With decreasing pulse durations the surface of the silicon seems to be smoother and the ablation is characterized by a sharp ridge. With knowledge of the ablation threshold, different cutting strategies are compared in order to create a minimal cutting kerf with a reduced heat affected zone. The ablation threshold of silicon depends on the temperature, so a second laser beam for the pre-heating of the silicon material is coupled coaxially with the cutting beam, which can improve the ablation behaviour of silicon significantly.

10363-107, Session PMon

Determination of transport parameters of organic thin film based on PTB7:PCBM mixture

Miriam Cuatecatl Tlapapatl, Nikolay Korneev, Svetlana Mansurova, Julio C. Carrillo Sendejas, Andrey Kosarev, Ismael Cosme-Bolaños, Antonio J. Olivares Vargas, Instituto Nacional de Astrofísica, Óptica y Electrónica (Mexico)

Organic semiconductors based on a mixture of poly[[4,8-bis[(2-ethylhexyl)oxy]benzo[1,2-b:4,5-b']dithiophene-2,6-diyl][3-fluoro-2-[(2-ethylhexyl)carbonyl]thieno[3,4-b]thiophenediyl]] (commonly known as PTB7) and [6,6]-phenyl-C61-butyric acid methyl ester (PCBM) give some of the highest reported efficiencies for polymer:fullerene solar cells due to the polymers extended absorption into the near infra-red and lower HOMO level.

Photoconductive properties of organic blend, and in particular its transport parameters (mobilities and diffusion lengths) are crucial factors determining the performance of photovoltaic structure based on it. As the blend of two different material types cannot be described by a simple superposition of the single properties material, a prediction of its photoconductive characteristic in a solar cell is not straightforward. In this context, the experimental data on donor/acceptor ratio dependent characteristics would have been of particular interest and a considerable amount of work has been devoted recently to this problem On the other hand, the change of photoelectric parameters of organic blend as a function of temperature is a widely used method to elucidate the material electronic structure.

In this work we present the results of detailed experimental study of photoelectric properties of organic thin film based on PTB7:PCBM bulk heterojunction for different ratios of the component. Temperature dependencies of dark and photoconductivity, as well as modulated photocurrent and non-steady-state photo-EMF technique have been used in order to elucidate materials photoelectric parameters, such as charge carriers motilities, their lifetime and the diffusion lengths.

10363-108, Session PMon

Organic solar cells based on graphene derivatives and eutectic alloys free-vacuum deposited as cathodes

Álvaro Daniel Romero-Borja, Ctr. de Investigación en Química Aplicada (Mexico) and Centro de Investigaciones en Óptica, A.C. (Mexico); J. Oracio C. Barbosa-García, Centro de Investigaciones en Óptica, A.C. (Mexico); Enrique Pérez-Gutiérrez, Consejo Nacional de Ciencia y Tecnología (Mexico) and Benemérita Univ. Autónoma de Puebla (Mexico); Mario A. Rodríguez, Centro de Investigaciones en Óptica, A.C. (Mexico); Arxel de León, Centro de Investigaciones en Óptica, A.C. (Mexico) and Ctr. de Investigación en Química Aplicada (Mexico); Salvador Fernández, Ctr. de Investigación en Química Aplicada (Mexico); Canek Fuentes-Hernández, Georgia Institute of Technology (United States); José-Luis L. Maldonado, Centro de Investigaciones en Óptica, A.C. (Mexico)

We present the use of two graphene derivatives in organic photovoltaic devices (OPVs) based on PTB7:[70]PCBM as active layer. First, reduced graphene oxide (rGO) was compared with PEDOT:PSS as hole transport layer (HTL) [1]. Second, solution-processable functionalized graphene (SPFG) was incorporated as a third component in the active layer [2]. Furthermore, we propose the use of two eutectic alloys as non-conventional cathodes: Field's metal (FM): Bi/Sn/In and BS: Bi/Sn, that melt at 65 and 138 ºC, respectively, which are deposited at room conditions by drop coating [3]. In OPVs with rGO as HTL, thin films were prepared by reiterative spin-deposition and thermal reduction of GO after each deposition. The best results were achieved for 8-rGO as HTL, where the PCE = 6.7% was as high as 95% of the obtained in reference devices (PEDOT:PSS as HTL, PCE = 7.0%). On the other hand, ternary active layers were prepared by blending SPFG at different weight ratios (0, 2, 4, and 6 wt. %) with PTB7:[70]PCBM (1:1.5 w/w). Our results show an increment in PCE for OPVs devices with 4 wt. % of SPFG that is 10% higher than that of the reference device (0 wt. % of SPFG). Finally, FM and BS were used as novel cathodes in OPVs devices reaching very acceptable PCEs (around 7.0%), for both eutectic alloys, in comparison with the PCE of those OPVs cells fabricated with the non-stable and costly high-vacuum evaporated Al.

References

[1] Da-Young Lee, et al., Nanoscale, 8, 1513-1522, 2016.

[2] Li Nian, et al., Adv. Mater., 28, 8184-8190, 2016.

[3] Daniel Romero-Borja, et al., Synth. Met., 200, 91-98, 2015.

10363-109, Session PMon

Hybrid perovskite/polymer composite for moisture stability in the absorber layer

John P. Murphy, Montana Tech (United States); Jessica M. Andriolo, Montana Tech (United States) and Univ. of Montana (United States); Jack L. Skinner, Montana Tech (United States)

Hybrid perovskite solar cells (PSCs) have climbed rapidly in power conversion efficiency in recent years and represent the future in low-cost photovoltaics. Facile fabrication of PSCs and the low cost of precursor chemicals have resulted many variations in materials synthesis and ultimately device design. A common goal across device architecture is the improvement of chemical stability of the hybrid perovskite material, particularly in resistance to degradation onset by moisture exposure. The research proposed herein will be directed at the improvement of moisture/UV stability in a PSC through utilization of a polymer/hybrid perovskite composite material in the active layer of the device. Perovskite

microcrystallites are synthesized via a simple solution method utilizing an organic ligand to control size and facilitate dispersion in toluene. Perovskite colloidal solutions can then be mixed into solutions of optical polymers and utilized as an active layer in a PSC. The dependency of the active-layer thickness, perovskite-crystallite size, and perovskite-crystallite loading in the composite on the device performance of PSCs will be parametrically analyzed using an AM 1.5G class ABA solar simulator and a Keithley 2450 sourcemeter. Device performance over time and in high humidity (~90% RH, ~20 °C) environments will be evaluated. Photocurrent will be minimized in the composite active layer cell due to a smaller heterojunction area. However, if device lifetime can be improved using composite active layers, PSCs may be able to reach an energy payback point necessary to allow implementation in the solar energy marketplace.

10363-110, Session PMon

Analysis of the aging/stability process of organic solar cells based on PTB7:[70] PCBM and an alternative free-vacuum deposited cathode: The effect of active layer scaling

Mirna D. Barreiro Argüelles, Gabriel Ramos-Ortiz, José-Luis L. Maldonado, Centro de Investigaciones en Óptica, A.C. (Mexico); Álvaro Daniel Romero-Borja, Centro de Investigaciones en Óptica, A.C. (Mexico) and Ctr. de Investigacíon en Química Aplicada (Mexico); Marco-Antonio Meneses-Nava, Centro de Investigaciones en Óptica, A.C. (Mexico); Enrique Pérez-Gutiérrez, Consejo Nacional de Ciencia y Tecnología (Mexico) and Benemérita Univ. Autónoma de Puebla (Mexico)

In this work the PV performance and aging/stability of organic photovoltaic (OPV) devices based on the well-known system PTB7:[70]PCBM are fully studied when the active area is scaled by a factor of 25. The cells configuration was: ITO/PEDOT:PSS/PTB7:PC71BM/PFN/Field's metal (FM), where FM is an alternative air-stable electrode deposited by doctor blade technique at room conditions. The average power conversion efficiency (PCE) for devices with the small active area of 0.09 cm2 is 7.4±0.8%, similar to that obtained for OPVs cells comprising Al as traditional cathode [1]. On the other hand, a decrease of 60% in efficiency for the scaled OPVs was measured. The aging/stability processes were also studied through single diode model, impedance spectroscopy and light-beam induced current (LBIC) measurements in accordance with the established ISOS-D1 (dark storage) and ISOS-L1 (illumination conditions) protocols [2]. Here it is found that the time to reach 50% of the initial PCE (T50) is >1500 h under ISOS-D1 protocol, which represent about 1000 h more than previously reported devices [3, 4]. In addition it was observed an improvement in stability for the scaled devices. However, for devices tested under ISOS-L1, T50 is reached in ~14 h independently of the device area. A discussion on the origin of these behaviors is presented. Finally, these results are a good indication that FM cathode works as an encapsulating material and provides excellent PV performance comparable with the common and costly high-vacuum evaporated Al cathode.

[1] D. Barreiro-Argüelles, et al. IEEE J. Photovolt., 7, 191, 2017.

[2] M. O. Reese, et al., Sol. Ener. Mat. Sol. Cells, 95, 1253, 2011.

[3] E. A. A. Arbad, et al. J. Mod. Opt., 61, 1749, 2014.

[4] W. Kim, et al. J. Phys. Chem. C, 119, 5954, 2015.

10363-112, Session PMon

Formation and diffusion of metal impurities in perovskite solar cell material CH3NH3PbI3: implications on the choice of electrode and solar cell degradation

Mao-Hua Du, Wenmei Ming, Oak Ridge National Lab. (United States); Dongwen Yang, Lijun Zhang, Jilin Univ. (China)

CH3NH3PbI3-based solar cells have shown remarkable progress in recent years but have also suffered from structural, electrical, and chemical instabilities and the resulting degradation. It was shown recently in CH3NH3PbI3 thin film solar cells that Au atoms from Au electrode can diffuse through hole transport layer and CH3NH3PbI3 layer at 70 °C, leading to significant degradation of the solar cell. We performed density functional theory calculations to study the formation and diffusion of a number of noble and transition metal impurities (Au, Ag, Cu, Cr, Mo, W, Co, Ni, and Pd) in CH3NH3PbI3. The purpose is to find a metal that has low resistivity, an appropriate work function, and does not diffuse into CH3NH3PbI3. We find that the oxidation state of the metal impurity affects its diffusion barrier. Au, Ag, and Cu have low resistivities but their ions with the +1 oxidation state can diffuse easily into CH3NH3PbI3. In particular, Au on a Pb site induces deep levels inside the band gap, which may be efficient nonradiative recombination centers. Cr, Mo, W, Co, Ni, and Pb impurities usually take the 2+ oxidation in CH3NH3PbI3 and their diffusion barriers are much higher. Mo, W, and Co have relatively low resistivities and Co has a work function that is most appropriate for hole extraction. These metals should deserve further experimental studies for their potential as stable back contact materials for CH3NH3PbI3 solar cells.

10363-113, Session PMon

Transparent wide bandgap metal halides for bifacial hybrid solar cells

Karunakara Moorthy Boopathi, Chintam Hanmandlu, Chih-Wei Chu, Academia Sinica (Taiwan)

The main objective of photovoltaic materials research is to find low-cost semiconductor materials with facile fabrication routes for efficient photovoltaic devices. Here, solution processable wide bandgap lead iodide semiconductor has been investigated as light absorbing material with different organic polymers as electron transport materials. Wide intrinsic bandgap of 2.6 eV was found for PbI2 thin film from Tauc plot and X-ray diffraction suggested the hexagonal crystalline structure with preferable orientation along (001) plane. Light intensity dependence of Voc and Jsc was studied to investigate the charge recombination mechanism for fabricated devices. The power conversion efficiency of 2.1% was achieved with opaque electrode (Ca/Al), while transparent electrode (BCP/Ag/MoO3) yielded 0.75% and 0.67% from bottom and top illumination, respectively. Using of wide bandgap light absorber materials opens up a new path for fabricating efficient and transparent photovoltaic devices for building integrated window applications.

10363-114, Session PMon

Solution processable lead free antimony based perovskite materials for photovoltaic applications

Chih-Wei Chu, Karunakara Moorthy Boopathi, Anupriya Singh, Academia Sinica (Taiwan); Gang Li, The Hong Kong Polytechnic Univ. (Hong Kong, China)

Organic–inorganic metal halide perovskites have recently emerged as highly competitive light absorbing materials for low cost solution-processable

photovoltaic devices. With the high efficiency already achieved, removing the toxicity, i.e., lead-free and stability are the key obstacles for perovskite solar cell. Here, we report the synthesis of antimony (Sb)-based hybrid perovskites having the crystal structure of A3Sb2I9 [A = CH3NH3 (MA), Cs] and an investigation of their potential photovoltaic applications. The Sb-based perovskite materials exhibited attractive absorbance properties, with the band gaps of MA3Sb2I9 and Cs3Sb2I9 measured as 2.2 and 2.3 eV, respectively. The band gaps of these materials are suitable for their use in solar cells, and also make them good choices for other optoelectronics applications. X-ray photoelectron spectroscopy confirmed the formation of stoichiometric perovskites from appropriate precursor molar ratios. Planar hybrid perovskite solar cells were fabricated with the device structure of glass/ITO/PEDOT:PSS/A3Sb2I9/PCBM/C60/BCP/Al and exhibited negligible hysteresis and reproducible power output under working conditions. A power conversion efficiency of 1.11% was achieved by MA3Sb2I9 perovskite device—the highest reported to date for a Sb-based perovskite solar cell.

10363-115, Session PMon

Phase stability of perovskite nanocrystals

Olivia Ashton, Henry J. Snaith, Univ. of Oxford (United Kingdom)

There are a wide variety of perovskite compositions, each with differing thermal and phase stability. For the bulk material, stabilising the perovskite phase has been widely researched across a range of these compositions. This has allowed for optimal materials and processing procedures to develop for photovoltaic devices.

Perovskite nanocrystals have recently shown great promise for both optoelectronic devices and photovoltaics. To date however there has been little research into the phase stability of the nanocrystals and how that could relate to device performance.

Here we present a study which investigates the phase stability of perovskite nanocrystals and how this changes relative to the composition of the material. We present emission and absorbance spectra along with structural characterisation from X-ray diffraction and transmission electron microscopy, to support our findings.

We also make a comparison to their bulk counterparts, exploring how the structural confinement that the nanocrystals undergo affects their stability in relation to an infinite lattice.

Coupled with the lifetime of carriers in these materials, extrapolation to potential device performances can be made.

10363-116, Session PMon

Improved efficiency of silicon nanoholes/gold nanoparticles/organic hybrid solar cells in both ultraviolet and visible regions

Ling Xu, Nanjing Univ. (China)

Silicon is the most widely used material for solar cells due to its abundance, non-toxicity, reliability, and mature fabrication process. We fabricated silicon nanoholes (SiNHS)/gold nanoparticles (AuNPS)/organic hybrid solar cells and investigated their spectral and opto-electron conversion properties. SiNHS nanocomposite films were fabricated by metal-assisted electroless etching (EE) method. Then, we modified the surface of the nanocomposite films by exposing the samples in the air. After that, polymer poly(3,4-ethylenedioxythiophene):poly (styrenesulfonate) (PEDOT:PSS) blended with AuNPS were spin-coated on the surface of the SiNHS nanocomposite films as a hole-transporting layer. The external quantum efficiency (EQE) values of the solar cells with AuNPS are higher than that of the samples without AuNPS in the spectral region of 600–1000 nm, which were essential to achieve high performance photovoltaic cells. The power conversion efficiency (PCE) of the solar cells incorporating AuNPS exhibited an enhancement of 27 %, compared with that of the solar cells without AuNPS. We thought that the improved efficiency were attributed to localized surface plasmon resonance (LSPR) triggered by gold nanoparticles in SiNHS nanocomposite films.

10363-117, Session PMon

K-space optoelectronic properties of organic-inorganic hybrid methylammonium lead halide crystals

Hye Ri Jung, Trang T. T. Nguyen, Hye-Jin Jin, Bich Phuong Nguyen, Gee Yeong Kim, Seokhyun Yoon, William Jo, Ewha Womans Univ. (Korea, Republic of); Won Seok Woo, Chang Won Ahn, Shinuk Cho, Ill Won Kim, Univ. of Ulsan (Korea, Republic of)

Organic-inorganic lead halide perovskite, CH3NH3Pb(Br,I)3 is taking the spotlight with outstanding performance for photovoltaic, light-emitting, and memristic devices. Most studies of all, examination on single crystals are demanded to comprehend the intrinsic physical characteristics. Grain growth in perovskite is not fully interpreted with regards to compositions, textures, and even believed as a trapping source of ionic migration. We confirm the structural systems and phase purity by using transmission electron microscopy and Raman scattering spectroscopy. We verify the details of the crystal structure in terms of configuration of the methyl-ammonium ligands. Thus, we evaluate the exposed surface of the perovskite crystals in terms of surface potential with Kelvin probe force microscopy. Calculated work function exhibits distribution around 4.6 eV, which is a similar value with thin film perovskite thin film. We also measured its photoluminescence and temperature dependent resistivity in order to estimate electronic structure and transport behaviors of the crystals. There are the deformations of the perovskite materials to the methyl- ammonium halide and lead halide on the surface partially by the deconvolution of the surface potential and it imply the alternative electrical characteristics depending on the surface doping. Synthetically, we obtained a stereographic schematic picture for the electronic band structures, which reveal the possible semiconducting nature of the materials by consolidating the information of the band gap and work function.

10363-119, Session PMon

Implications of ferroelectric polarization on ionic migration and hysteretic behaviors on hybrid perovskite absorber solar cells with mesoscopic and planar electron transport layers

Hye Ri Jung, Bich Phuong Nguyen, Juran Kim, Hye-Jin Jin, Wiiliam Jo, Ewha Womans Univ. (Korea, Republic of)

Hybrid lead halide perovksite, MAPbX3(MA=CH3NH3+, X=Br- or I-) have risen to prominence with remarkable efficiency increasing and examination on its physical properties are of particular concern. One of the issues is hysteresis phenomenon with ionic migration. Current-voltage curves tend to differ depending on the sweep rate and

direction. Several mechanisms have been proposed including difference in trapping efficiency, ion migration, imbalance between electron and hole fluxes into an electron transfer layer and a hole transfer layer, and ferroelectricity of the perovskites. We report our observations on the piezoelectricity in the perovskite thin-films grown on TiO2 mesoscopic and planar bottom electrodes by measuring piezoelectric responses and ferroelectric property using piezoelectric force microscopy which is one of atomic force microscopy techniques. In addition, we investigated for the distribution of the surface electric potential and current transport by Kelvin probe force microscopy and conductive atomic force microscopy, respectively. We propose a device model to enhance charge transfer with in the perovskite solar cells when we have a preferred polarization in the materials through examination for the nature of the hysteresis properties.

10363-121, Session PMon

Excited state polarizability in polymer:fullerene blends via electroabsorption

Erik D. Klump, Xueping Yi, Iordania Constantinou, Amin Salehi, North Carolina State Univ. (United States); Kin Lo, John R. Reynolds, Georgia Institute of Technology (United States); Franky So, North Carolina State Univ. (United States)

The interaction between donor polymers and fullerene in organic solar cells has been a topic of extensive study. However, detail understanding of this complex interface is still lacking. To further our understanding of the nature of the interface between fullerene and polymers, we sought to characterize the excited state polarizability and difference in dipole moment between the ground and excited states in blend films. To accomplish this, we utilized electroabsorption (EA) spectroscopy. This sensitive technique relies on modeling of the Stark effect to fit the measured EA signal at the band edge of polymer:fullerene blends. To attain the accurate absorption data necessary for good fits and confidence in the extracted parameters, we utilized photothermal deflection spectroscopy to extract the optical absorption data.

We were able to quantify the difference in excited state polarizability and dipole moment between the ground and excited states in a number of systems. We found that the charge transfer states in the polymer were greatly affected by the mixing with fullerene. Specifically, the difference in excited state polarizability was shown to significantly increase in blends with optimal morphology to several times that of the pristine polymer. This dramatic increase was found to closely correlate with exciton dissociation efficiency. Thus, we conclude that the mixing of polymer with fullerene not only creates charge transfer states, but also changes the polarizability of excited polymer states. In turn, this increased polarizability and thus delocalization of the charge transfer states facilitates the efficient exciton dissociation process necessary for highly performing organic solar cells.

10363-122, Session PMon

Optimization of regioregular polymer structure through synthesis and characterization of benzothiazole (BT)-based polymers

Na Gyeong An, Ulsan National Institute of Science and Technology (Korea, Republic of); Mohammad Afsar Uddin, Yuxiang Li, Korea Univ. (Korea, Republic of); Seyeong Song, Ulsan National Institute of Science and Technology (Korea, Republic of); Hwasook Ryu, Han Young Woo, Korea Univ. (Korea, Republic of); Jin Young Kim, Ulsan National Institute of Science and Technology (Korea, Republic of)

Three types of photoactive terpolymers (random, regular and block) were synthesized by incorporating two electron deficient and one electron-rich moieties based on two parent donor polymers, poly[(2,5-bis(2-decyltetradecyloxy)phenylene)-alt-(5,6-difluoro-4,7-di(thiophen-2-yl)benzo[c][1,2,5]thiadiazole)] (PPDT2FBTDT) and poly[(2,5-bis(2-decyltetradecyloxy)phenylene)-alt-(5,6-dicyano-4,7-di(thiophen-2yl) benzo[c][1,2,5]thiadiazole)] (PPDT2CNBT). All three terpolymers showed a broad light absorption in the range of 300-850 nm covering the absorption of two parent polymers. Their optical, electrochemical, morphological and photovoltaic properties were compared and investigated in detail. The power conversion efficiencies (PCEs) of 5.63, 4.45 and 3.13% were obtained for PPDT2FBTDTrandom-PPDT2CNBT, PPDT2FBTDT-regular-PPDT2CNBT and PPDT2FBTDT-block-PPDT2CNBT based photovoltaic devices, respectively. Through intensive investigation on charge carrier mobility, photocurrent and light intensity dependence of JSC, the random structure was proved to be most effective molecular design in this series of terpolymers to show weaker charge recombination and enhanced charge transport/extraction with well distributed blend morphology. The fine modulation of different arrangement and composition of three monomers in a main chain is crucial for optimizing the terpolymeric structures as an efficient photoactive material.

10363-125, Session PMon

Morphological characterization of fullerene and fullerene-free organic photovoltaics by combined real and reciprocal space techniques

Subhrangsu Mukherjee, Andrew A. Herzing, National Institute of Standards and Technology (United States); Donglin Zhao, Qinghe Wu, Luping Yu, The Univ. of Chicago (United States); Harald W. Ade, North Carolina State Univ. (United States); Dean M. DeLongchamp, Lee J. Richter, National Institute of Standards and Technology (United States)

The performance of a bulk heterojunction (BHJ) solar cell is sensitive to the details of the morphology that include the sub-100 nm domain size, shape, connectivity, orientation of components and composition. Recently molecular acceptors have showed promise to replace fullerene derivatives in BHJs and have achieved >10% efficiencies in single junction devices. However, a key challenge for the organic photovoltaics community has been to develop measurements of these aspects of structure for the newer systems. The similar mass/electron densities between the donor and acceptor results in poor material contrast compared to fullerene-based BHJs. Therefore, morphology characterization using techniques that rely on mass/electron density variations poses a challenge. Using two efficient fullerene-based (PTB7-Th:PC71BM) as well as a recent non-fullerene-based (PTB7-Th:a-TPB) BHJ systems it will be demonstrated that low-angle annular dark field scanning transmission electron microscopy (LAADF-STEM) and resonant soft X-ray scattering (R-SoXS) form a set of complementary tools that can provide quantitative characterization of fullerene as well as non-fullerene based organic photovoltaic systems. Excellent agreement was obtained between the Fourier analysis of LAADF-STEM images and R-SoXS profile shapes as well as size scales between the two techniques for both systems. The optimized non-fullerene blend prepared with additive DPE is found to have a higher average phase purity compared to the no additive sample. Furthermore, the strong differences between the phase separation characteristics of the identically prepared no additive fullerene and non-fullerene blends likely indicate different miscibilities of the acceptor materials in the donor (PTB7-Th) matrix and therefore different Flory-Huggins interaction parameters.

10363-126, Session PMon

Over 11%-efficiency fullerene-free organic solar cells enabled by benign solvents

Long Ye, North Carolina State Univ. (United States); Wenchao Zhao, Institute of Chemistry (China); Masoud Ghasemi, Yuan Xiong, North Carolina State Univ. (United States); Jianhui Hou, Institute of Chemistry (China); Harald W. Ade, North Carolina State Univ. (United States)

Owing to the recently developed nonfullerene small molecule acceptors, the best power conversion efficiency (PCE) of solution-processable organic solar cells (OSCs) has been boosted up to over 12%[1], which makes this technology an economically viable contender for commercialization. Along with the steady progress in PCE achieved by spin-coating photovoltaic materials with chlorinated solvents in protective atmosphere, a central issue in the development of OSCs is pursuing a greener and simpler manufacturing protocol[2], which particularly allows for large-area

processing in ambient air. Particularly, it is still a great challenge to replace halogenated solvents with halogen-free, low-toxicity solvents to achieve high-efficiency nonfullerene OSCs.

Here we show that ~11.6% efficiency is achieved in nonfullerene OSC device based on PBDB-T:IT-M[3] by using a non-halogenated solvent combination. Moreover, the device parameters were correlated to the morphology investigated by synchrotron radiation grazing-incidence wide-angle X-ray scattering (GIWAXS), resonant soft X-ray scattering (R-SoXS), and differential scanning calorimetry (DSC). We observed a monotonic correlation between the average composition variations and photovoltaic device characteristics across all processing protocols in this record-efficiency material system. This correlation is indeed universal for OSC, irrespective of acceptor materials used (fullerenes, nonfullerene molecular acceptor, or conjugated polymers) and fabrication methods used (spin-coating or blade-coating).[1-5] We believe this nonhazardous solvent approach will be also applicable in the large area roll-to-roll coating and industrial scale printing of high-efficiency OSCs in air.

Reference

[1] Li, S.; Ye, L.; Zhao, W.; Zhang, S.; Mukherjee, S.; Ade, H.; Hou, J., Energy-Level Modulation of Small-Molecule Electron Acceptors to Achieve over 12% Efficiency in Polymer Solar Cells. Adv. Mater. 2016, 28 (42), 9423-9429.

[2] Ye, L.; Xiong, Y.; Yao, H.; Gadisa, A.; Zhang, H.; Li, S.; Ghasemi, M.; Balar, N.; Hunt, A.; O'Connor, B. T.; Hou, J.; Ade, H., High Performance Organic Solar Cells Processed by Blade Coating in Air from a Benign Food Additive Solution. Chem. Mater. 2016, 28 (20), 7451-7458.

[3] Ye, L.; Zhao, W.; Li, S.; Mukherjee, S.; Carpenter, J. H.; Awartani, O.; Jiao, X.; Hou, J.; Ade, H., High-Efficiency Nonfullerene Organic Solar Cells: Critical Factors that Affect Complex Multi-length Scale Morphology and Device Performance. Adv. Energy Mater. 2017, 7, 1602000.

[4] Ye, L.; Jiao, X.; Zhang, S.; Yao, H.; Qin, Y.; Ade, H.; Hou, J., Control of Mesoscale Morphology and Photovoltaic Performance in Diketopyrrolopyrrole-Based Small Band Gap Terpolymers. Adv. Energy Mater. 2017, 7, 1601138.

[5] Ye, L.; Jiao, X.; Zhao, W.; Zhang, S.; Yao, H.; Li, S.; Ade, H.; Hou, J., Manipulation of Domain Purity and Orientational Ordering in High Performance All-Polymer Solar Cells. Chem. Mater. 2016, 28 (17), 6178-6185.

10363-127, Session PMon

Revealing the high stability of non-fullerene polymer solar cells

Masoud Ghasemi, Long Ye, Harald W. Ade, North Carolina State Univ. (United States)

The rapid increase in the power conversion efficiency (PCE) along with high stability in non-fullerene polymer solar cells (PSCs) is mostly attained through emerging novel non-fullerene acceptors. In this work we investigate the effect of vitrified morphology of non-fullerene small molecule acceptors on device stability of a binary blend comprised of a benchmark donor poly(3-hexylthiophene) (P3HT) with a non-fullerene acceptor O-IDTBR[1], as the morphological stability of such devices is an essential consideration for technological implantations. Further consideration of molecular miscibility of the polymer:non-fullerene blends provides an new insight into morphology-function correlation in non-fullerene PSCs. The diffusion experiments done with secondary ion mass spectroscopy (SIMS), and thermodynamic investigations by differential scanning calorimetry (DSC), complemented with X-ray scattering experiments together show that diffusion of non-fullerene acceptor in the polymer network is prohibited due to vitrified morphology of the non-fullerene acceptor when the temperature is below 140 °C. Furthermore, the maximum concentration of diffused O-IDBR into the polymer layer, by annealing the thin bilayer films at elevated temperatures, is found to be limited by the molecular miscibility in the blend. In conclusion, the vitrified morphology of non-fullerene acceptors well explains the excellent long-term stability of non-fullerene PSCs, due to prevention of formation of micro sizes crystals in the thin films. Our findings may pave a way to understand an important question that why non-fullerene PSCs are more stable compared with their fullerene counterparts.

10363-128, Session PMon

Critical factors that affect complex morphology and device performance of multiple cases of organic solar cells

Long Ye, Subhrangsu Mukherjee, North Carolina State Univ. (United States); Jianhui Hou, Institute of Chemistry (China); Harald W. Ade, North Carolina State Univ. (United States)

In the organic solar cell field, thousands of new polymer donors along with hundreds of emerging small molecule acceptors create an incredibly large pool of polymer:acceptor pairs that would be difficult to optimize without a complete characterization and fundamental understanding of the complex and often multi-length scale morphology[1-2]. The recent demonstration of multilength scale morphology brings many questions critical to the operation of these novel organic devices into focus: What are the critical factors that affect the complex morphology and device performance of organic solar cells? Through detailed characterizations (hard/soft X-ray scattering), we show that a linear correlation between the average composition variations at the smallest length scale and photovoltaic device characteristics in a PBDTTPD:fullerene[3] system and two state-of-the-art nonfullerene material systems[4]. The degree of molecular mixing in the amorphous mixed domains is shown to control fill factors (FFs) and needs to be precisely controlled for designing new polymer:nonfullerene acceptor pairs with even higher FFs. More significantly, we further correlate the thermodynamic interaction parameters to morphology and performance in these record-efficiency nonfullerene devices, which allows us to understand the optimal processing temperature for the 12%-efficiency PBDB-T:IT-M blend[4]. We propose that the precise determination of temperature dependent interaction parameters will aid in establishing property-performance relationships and screening new material combinations/optimal processing conditions creating a morphology that can support high performance.

Reference

[1] Mukherjee, S.; Proctor, C. M.; Bazan, G. C.; Nguyen, T. Q.; Ade, H. Significance of Average Domain Purity and Mixed Domains on the Photovoltaic Performance of High-Efficiency Solution-Processed Small-Molecule BHJ Solar Cells. Adv. Energy Mater. 2015, 5, 1500877.

[2] Ye, L.; Jiao, X. C.; Zhang, H.; Li, S. S.; Yao, H. F.; Ade, H.; Hou, J. H. 2D-Conjugated Benzodithiophene-Based Polymer Acceptor: Design, Synthesis, Nanomorphology, and Photovoltaic Performance. Macromolecules 2015, 48, 7156-7163.

[3] Mukherjee, S.; Jiao, X.; Ade, H. Charge Creation and Recombination in Multi-Length Scale Polymer:Fullerene BHJ Solar Cell Morphologies. Adv. Energy Mater. 2016, 6, 1600699.

[4] Ye, L.; Zhao, W.; Li, S.; Mukherjee, S.; Carpenter, J. H.; Awartani, O.; Jiao, X.; Hou, J.; Ade, H. High-Efficiency Nonfullerene Organic Solar Cells: Critical Factors that Affect Complex Multi-length Scale Morphology and Device Performance. Adv. Energy Mater. 2016, 6, 1602000.

10363-129, Session PMon

Effect of immerse an organic layer in isopropyl alcohol on characteristics of hybrid photovoltaic structures

Antonio J. Olivares-Vargas, Ismael Cosme-Bolaños, Svetlana Mansurova, Andrey Kosarev, Adrian Itzmoyotl Toxqui, Instituto Nacional de Astrofísica, Óptica y Electrónica (Mexico)

Solar cells based on crystalline silicon offer high efficiency but the manufacturing process is very costly, due to requirement of high temperatures and high vacuum to produce the p-n junction. Organic materials have become very important in recent years due to their potential use for photovoltaic applications. Among the main advantages of organic

semiconductors are their functional and mechanical flexibility, as well as fabrication simplicity. However, these materials usually afford moderate efficiency. Hydrogenated amorphous silicon (a-Si:H) is another material suitable for large area fabrication of potentially flexible devices at low cost. The idea of combining organic semiconductors and amorphous silicon films in hybrid photovoltaic devices is very attractive due to the possibility to complement the useful properties of both material systems.

The photovoltaic devices that we study in this work consist of a p-i-n structure, which is also commonly used in inorganic solar cells. In such kind of structures, the light is mainly absorbed in the intrinsic silicon film and the p- and n-type films are used to create an electric field that separates electrons and holes to produce a photocurrent. In this work, we use an organic material (PEDOT:PSS) to replace the p-type inorganic film in amorphous silicon p-i-n structure. It is widely known, that PEDOT:PSS based organic film is highly transparent and its conductivity can be modified e.g. immerse in a solvent type. Here we present the results of experimental investigation of the effect of isopropanol (IPA) treatments of p-type (PEDOT:PSS) organic layer in characteristics of hybrid solar cell structure.

10363-130, Session PMon

18% high-efficiency air-processed perovskite solar cells made in a humid atmosphere of 70% RH

Sai Wing Tsang, Yuanhang CHENG, City Univ. of Hong Kong (Hong Kong, China)

Despite the advanced progress in power conversion efficiency (PCE), developing air-processed high-efficiency perovskite solar cells (PVSCs) for future commercialization is still challenging. Here we report that, besides the general wisdom of the effect of moisture, oxygen in air has severe impact on the quality of the solution-deposited perovskite films. Interestingly, different from moisture that induces fast crystallization of PbI2 upon deposition, oxygen exacerbates the wetting of the PbI2 solution on substrates. To eliminate the impact of oxygen and moisture on the formation of PbI2, we preheat the substrate and PbI2 solution to build up a shield of organic vapor from the solvent during PbI2 film formation. Using this simple method, an air-processed PVSC made under a humid atmosphere of 70% RH has a record PCE of 18.11%. Our work not only reveals the origin of the detrimental effects on perovskite film formation in ambient air, but also provides a simple practical strategy to develop air-processed high-efficiency PVSCs for future commercialization.

10363-131, Session PMon

On the study of exciton binding energy with direct charge generation in photovoltaic polymers

Sai Wing Tsang, Ho-Wa LI, City Univ. of Hong Kong (Hong Kong, China)

Overcoming the strong excitonic effect in organic photovoltaics (OPVs) is one of the key strategies for the design of materials and device structures. Approaches to measure the binding energy in organics are, however, not readily available. Here, we systematically studied the electrical and optical quantum efficiencies of a series of conjugated photovoltaic polymers. We find that there is generally a secondary onset in external quantum efficiency (EQE) spectrum at high excitation energy, independent of optical absorbance of the materials. Combining photoluminescence quantum yield measurement and adding a small amount (1 wt%) of fullerene acceptor in polymer blends, it further confirms the pristine polymer EQE spectrum has a transition from exciton to free-charge generation with increased excitation energy. Strikingly, by comparing the reported photoemission spectroscopy results, the secondary onsets in the EQE spectra have excellent agreement with the transport gap (Eg) in corresponding materials. Consequently, the exciton binding energies of the polymers can be obtained with the smallest 0.6 eV in PCE10 to the largest 1.2 eV in MEHPPV. Our results demonstrate a facile access to the transport gap and exciton binding energies in organic semiconductors. This provides valuable information for further understanding the strong excitonic effect in photovoltaic cells.

10363-132, Session PMon

Understanding of electronic and ionic transport at metal halide perovskites interfaces

Ashwith Chilvery, Xavier Univ. (United States); Padmaja Guggilla, Alabama A&M Univ. (United States)

Over the past 5 years, perovskites have revolutionized optoelectronics and photonics with the discovery of organometal halide perovskite materials. These class of materials have displayed promising results for advanced and efficient photovoltaics (PV). However, some of the urgent issues associated with these materials such as hysteresis, lead toxicity, and poor stability are yet to be resolved. Hysteresis in these halide perovskite PV devices is a combination of multiple factors, that impact transport within the material. These relate to fundamental question regarding the transport of carriers and mobile ions that are of direct technological importance. In addition, the impact of non-reversible changes at interfaces under conditions of increased carrier density or field strength may couple these behaviors. In this project, we propose to examine basic interface interactions at metal halide perovskite interfaces with technological relevant contact materials. More specifically we will look at metal, metal oxide and select chalcogenide materials interfaced with solar relevant halide perovskites. This project will develop the several test structures in which these interface combinations can be examined. Specifically, to undertake this we intend to develop test structures in which contact resistance, and stability of these technologically relevant interfaces can be assessed.

10363-133, Session PMon

Solution-processable benzo[1,2-b:4,5-b’] dithiophene-6,7-difluoroquinoxaline small molecule donors with solar cell efficiency >8%

Ru-Ze Liang, Kai Wang, Jannic Wolf, Maxime Babics, Philipp Wucher, Pierre M. Beaujuge, King Abdullah Univ. of Science and Technology (Saudi Arabia)

Solution-processable small molecule (SM) donors are promising alternatives to their polymer counterparts in bulk-heterojunction (BHJ) solar cells with fullerene and nonfullerene acceptors. In particular, SM donors benefit from favorable spectral absorption, self-assembly patterns, crystalline thin-film morphologies, and high carrier mobilities in BHJ active layers with the electron-acceptor component. Our recent developments on rational pendant-group substitutions in a broad set of SM donors, and in benzo[1,2-b:4,5-b’]dithiophene–6,7-difluoroquinoxaline SMs specifically, proves that well-chosen substituents can help narrow the optical gap (Eopt) of the SM donors, without altering their propensity to order and form favorable thin-film BHJ morphologies with fullerenes. Systematic device examinations with benzo[1,2-b:4,5-b’]dithiophene–6,7-difluoroquinoxaline SMs show that power conversion efficiencies (PCEs) >8% and open-circuit voltages (VOC) nearing 1V can be achieved with the narrow-gap SM donor analogues (Eopt= 1.6 eV). Meanwhile, our concurrent effort to find solution-processable SM donor and nonfullerene acceptor combinations indicate that BHJ solar cells PCEs >6% and VOC values >1.1V can be achieved with selected nonfullerene acceptors (to be discussed in our presentation). In general, we find that in some of the best BHJ active layers, charge transport proceeds with minimal, nearly trap-free recombination. Detailed device simulations, light intensity dependence and transient photocurrent analyses will be used to emphasize how carrier recombination impacts BHJ device performance upon optimization of active layer thickness and morphology.

10363-136, Session PMon

Probing chemistry and structure of organic semiconductors with soft x-rays

Gregory Su, Isvar Cordova, Michael Brady, Cheng Wang, David Prendergast, Lawrence Berkeley National Lab. (United States)

Continued advances in the performance of organic electronics depends on an understanding of the connections among chemistry, structure, and device performance. These relationships are difficult to probe in these complex systems. Soft X-rays span an energy range that covers the core-level transitions of the most common elements found in organic materials, allowing for sensitivity not only to certain elements, but also specific functional groups and moieties. Additionally, scattering and microscopy at these energies provides spatial distribution information, making soft X-ray spectroscopy, scattering, and microscopy a unique set of tools that can probe both chemistry and structure in organic semiconductors. Here, we show recent advances in developing the groundwork for leveraging first-principles simulations of X-ray absorption spectroscopy that reveal details of electronic structure and molecular orientation that are needed to understand and interpret experimental results. Semiconducting polymers including polythiophenes and donor acceptor polymers poly[4-(4,4-dihexadecyl-4H-cyclopenta[1,2-b:5,4-b']dithiophen-2-yl)-alt-[1,2,5]thiadiazolo[3,4-c]pyridine], PCDTPT, and [N,N-9-bis(2-octyldodecyl) naphthalene-1,4,5,8-bis(dicarboximide)-2,6-diyl]-alt-5,59-(2,29-bithiophene), P(NDIOD-T2), will be used as examples to illustrate effects of chain length, backbone tilt and alignment, and side chains on resulting X-ray absorption spectra. Furthermore, developments to enable in situ and operando studies of organic semiconductors with soft X-rays will also be presented.

10363-137, Session PMon

Optical probes of amplitude modes in PTB7 copolymer

Shai Vardeny, College of Optical Sciences, The Univ. of Arizona (United States); Sangita Baniya, Evan Lafalce, The Univ. of Utah (United States); Nasser N. Peyghambarian, College of Optical Sciences, The Univ. of Arizona (United States); Z. Valy Vardeny, The Univ. of Utah (United States)

We measured the spectra of resonant Raman scattering (RRS) and doping induced absorption of pristine films of the ϖ-conjugated donor-acceptor copolymer, namely Thieno[3,4 b]thiophene- alt-benzodithiophene (PTB7), as well as photoinduced absorption spectrum in blend of PTB7 with fullerene PCBM molecules. We found that the copolymer contains six strongly coupled vibrational modes having relatively strong Raman scattering intensity, which are renormalized upon adding charges onto the copolymer chains either by doping or photogeneration. Since the charge polaron absorption band overlaps with the renormalized modes, the strongly coupled vibrations appear as anti-resonance lines superposed onto the induced polaron absorption band in the photo-induced absorption spectrum, but less so in the doping induced absorption spectrum. We show that the RRS, doping- and photoinduced absorption spectra of PTB7 are well explained by the amplitude mode model, where a single vibrational propagator describes the renormalized modes and their related intensities in detail. From the relative strengths of the induced infrared activity of the vibration and electronic transitions we calculated the polaron effective kinetic mass in PTB7 using the amplitude mode model to be ~3.8m*, where m* is the electron effective mass. This relatively small mass stems from the weak polaronic relaxation energy and indicates a rigid chain structure for PTB7.

10363-138, Session PMon

Fabrication of semi-transparent and flexible organic solar cells

Yeongjin Lee, Gwangju Institute of Science and Technology (Korea, Republic of); Hongkyu Kang, Imperial College London (United Kingdom) and Gwangju Institute of Science and Technology (Korea, Republic of); Nara Kim, Seok Kim, Jinho Lee, Kwanghee Lee, Gwangju Institute of Science and Technology (Korea, Republic of)

Organic solar cells (OSCs) have many advantages such as solution processability, high power-to-weight ratio, cost efficiency, transparency and flexibility. Transparency and flexibility are superior characteristics for organic solar cells than inorganic solar cells. However, semi-transparent and flexible OSCs have not get been explored because they need special electrodes which have high conductivity, transparency and flexibility at the same time. In this work, we demonstrated semi-transparent and flexible OSCs using transparent and flexible electrodes with high conductivity. Polymer-Ag (PA) electrodes were fabricated as bottom electrodes on polyethylene naphthalate (PEN) flexible substrates. Then, the H2SO4-treated PEDOT:PSS electrodes were transferred on the devices as top electrodes after coating interfacial and photoactive layers on PA electrodes. In addition, to investigate a relationship between the transmittance of PA electrodes and PCEs, we controlled the thickness of PA electrodes. Our semi-transparent and flexible solar cells achieved a PCE of 4.9% with an average transmittance (AVT) of 39%, and PCE of 7.4% with an AVT of 18% corresponding to the highest values in reported semi-transparent and flexible OSCs. Our device structure presents the guideline for promising applications of OSCs with the transparency, flexibility and high performance.

10363-139, Session PMon

Multi-colored luminescent configuration with versatile nanopatterns for advanced photovoltaics

Minwoo Nam, Jaehong Yoo, Doo-Hyun Ko, Kyung Hee Univ. (Korea, Republic of)

The conversion and manipulation of light via luminescent down-shifting (LDS) show promise in optoelectronic applications. In this study, we introduce a novel concept of multifunctional LDS platform bearing subwavelength nanopatterns. The lanthanide complexes, such as the down-shifting dopants terbium and europium, were incorporated into a polymer derived ceramic matrix, perhydropolysilazane (PHPS). The prompt formation of nanoscale photonic structures enhanced both absorption and emission characteristics, while retaining the material's optical transparency. The LDS template was a realistic strategy to enhance the efficiency of photovoltaic devices as their performance is determined by manipulating the incident light. The organic photovoltaics (OPVs) involving the LDS ceramics exhibited considerably enhanced efficiency. The LDS ceramic protected the OPV components against UV-induced degradation, resulting in the significantly better stability compared to that of the bare OPV. Double imprint technique was devised by superpositioning two LDS nanopatterned arrays to efficiently combine two lanthanide emissions. Colors could, therefore, be coded within a single layer via the double print approach. The outcome was a large-scale spectrum-matching window that was nearly transparent in the day light, while a vivid mosaic pattern with different colors emerged under UV illumination. Combined with the multi-functionality such as prominent LDS properties, self-cleaning capability, and color tunability, the developed LDS platform offers promise for future building-integrated photovoltaics (BIPVs).

10363-140, Session PMon

Air-stable organic solar cells using an iodine-free solvent additive

Seongyu Lee, Jaemin Kong, Kwanghee Lee, Gwangju Institute of Science and Technology (Korea, Republic of)

The organic photovoltaic cells have been researching after the discovery of charge transfer with two materials for the couple of decade. Among the many of research, the introducing additive for control of the morphology has been leading a high power conversion efficiency (PCE) over 10%, which seems to be one of powerful technique. In spite of advantages from additive for high PCE, however, the reproducibility and devices life time which fabricated from additives dramatically decrease rather than one without. Here, we found that the degradation of photoactive layer is very close to the residue of common additive, 1,8-diiodooctane (DIO), by making fullerene-Iodide intermediate compounds leading the oxidation of electron acceptor even without any illumination. By introducing iodine-free reagent 1,2,4-tricholorobenzene (TCB) as a solvent additive, photovoltaic organic layer secures the air stability showing no difference in J-V performance between processing in nitrogen filled glove box and processing in ambient air. Moreover, the device lifetime significantly extended by 10 times longer than that that by DIO without any encapsulation.

10363-303, Session Plen

The History and Progress of Halide Perovskite Photovoltaics

Nam-Gyu Park, Sungkyunkwan Univ. (Korea, Republic of)

Since the first report on the solid-state perovskite solar cell with power conversion efficiency (PCE) of 9.7% in 2012 by our group, its certified PCE now reaches 22%. It is believed that perovskite solar cell is promising next-generation photovoltaics (PVs) due to superb performance and very low cost. In this talk, the history of perovskite photovoltaics will be briefly presented along with their scientific progress. Methodologies to achieve hysteresis-free, stable and high PCE perovskite solar cells will be introduced. Lewis acid-base adduct approach has been found to be very reliable and reproducible method to get high quality perovskite layer minimizing non-radiative recombination. Non-stoichiometric precursor in adduct process demonstrated grain boundary healing effect, which further improved voltage and fill factor due to long carrier life time of perovskite and improved charge transporting at grain boundary as well. Grain boundary healing process yields PCE as high as 20.4%. Moisture was effectively protected and hysteresis was significantly reduced by introducing 2-dimensioanl perovskite at grain boundary of 3-dimensional perovskite grains. Ion migration is one of factors affecting stability and hysteresis, which can be deactivated by 2-dimensional perovskite with higher barrier energy for ion migration. Thermal stability of perovskite material was found to be stable up to 120°C in the absence of moisture, but that of full device was sensitive to selective contacts, indicating that thermally stable selective contacts are equally important. Universal method to remove hysteresis will be also given in this talk.

10363-304, Session Plen

Mesoscopic Photosystems for the Generation of Electricity and Fuels from Sunlight

Michael Grätzel, Ecole Polytechnique Fédérale de Lausanne (Switzerland)

A planetary emergency has arisen from the continued depletion of fossil fuels, producing green house warming and unprecedented environmental pollution. Future energy options for renewable and carbon-free sources will need to fill the terra-watt gap that will open up during the next few decades due to the growth of the world population. A promising development is the recent emergence of a new generation of highly efficient photovoltaic converters based on molecular dyes or perovskite pigments as light harvesters. Mesoscopic photosystem that mimic the primary process of natural photosynthesis also offer the prospect of low cost fuel generation from sunlight.

10363-5, Session 3

Hybrid metal halide perovskites: optoelectronic properties and stability *(Keynote Presentation)*

Laura Herz, Univ. of Oxford (United Kingdom)

Hybrid metal halide perovskites (stoichiometry AMX3) have recently emerged as low-cost active materials in PV cells with power conversion efficiencies in excess of 21%. We discuss how parameters essential for photovoltaic operation, such as crystallinity, photostability, charge carrier mobility and diffusion lengths are altered with substitutions of the organic A cation (e.g. methylammonium versus formamidinium), the metal M cation (e.g. Pb2+ or Sn2+) and the halide X anion (I- versus Br-). We focus on two 3D perovskite systems that have attracted interest lately, lead-free ASnI3 (optical bandgap ~1.3 eV) and the mixed organic lead iodide/bromide system APb(BryI1-y)3 whose band gap can be tailored between ~1.5 eV (FAPbI3) and ~2.3 eV (FAPbBr3). We show that unintentional hole doping in tin iodide perovskites introduces fast recombination pathways that can be moderated by crystal structure [1] and introduces a radiative quasi-monomolecular charge recombination channel [2]. In addition, we demonstrate that charge-carrier diffusion and recombination in FA1-xCsxPb(BryI1-y)3 depends on a complex interplay between changes in morphology and electronic bandstructure with bromide fraction y [3,4,5].

References

[1] Parrott, Milot, Stergiopoulos, Snaith, Johnston, Herz, J. Phys. Chem. Lett. 7, 1321 (2016).

[2] Milot, Eperon, Green, Snaith, Johnston, Herz, J. Phys. Chem. Lett. 7, 4178 (2016).

[3] Rehman, Milot, Eperon, Wehrenfennig, Boland, Snaith, Johnston, Herz, Adv. Mater. 27, 7938 (2015).

[4] McMeekin, Sadoughi, Rehman, Eperon, Saliba, Hörantner, Haghighirad, Sakai, Korte, Rech, Johnston, Herz, Snaith, Science 351, 151 (2016).

[5] Rehman, McMeekin, Patel, Milot, Johnston, Snaith, Herz, Energy Environ. Sci. 10, 361 (2017).

10363-6, Session 3

Oligomer-like small molecule based tandem solar cells with >12% PCEs *(Invited Paper)*

Yongsheng Chen, Nankai Univ. (China)

Polymer/organic photovoltaic has been thought as one of the promising technology to face the increasing energy and environmental issues. In this talk, a series of high performance oligomer-like organic small molecules and their OPV devices will be discussed. Particularly, tandem cells using all small molecules with >12% PCEs will be presented in details.

[1] "Solution-processed organic tandem solar cells with power conversion efficiencies >12%", Nature Photon, 2016, doi:10.1038/nphoton.2016.240

[2] "A Series of Simple Oligomer-like Small Molecules Based on Oligothiophenes for Solution-Processed Solar Cells with High Efficiency", J. Am. Chem. Soc., 2015, 137, 3886

[3] "Small-molecule solar cells with efficiency over 9%", Nature Photon., 2015, 9, 35.

[4] "High performance photovoltaic applications using solution processed small molecules", Acc. Chem. Res, 2013, 46, 2645.

[5] "Solution-Processed Organic Solar Cells Based on Dialkylthiol-Substituted Benzodithiophene Unit with Efficiency near 10%", J. Am. Chem. Soc., 2014, 136, 15529.

10363-7, Session 3

How are charge carriers protected in lead halide perovskite? *(Invited Paper)*

Xiaoyang Zhu, Columbia Univ. (United States)

The feverish research activity on lead halide perovskites has been fueled by their exceptional optoelectronic properties, e.g., in solar cells and light-emitting devices. Hybrid lead halide perovskites exhibit carrier properties that resemble those of pristine nonpolar semiconductors despite static and dynamic disorder, but how carriers are protected from efficient scattering with charged defects and optical phonons is unknown. We have recently put forward the large polaron model to explain the carrier protection [1-3]. We find that nascent charge carriers are screened by "solvation" or large-polaron formation on time scales ≤ 0.3 ps, leading to protected carriers with dramatic suppression of electron- LO phonon scattering. This results in long-lived energetic electrons with excess energy ~ 0.25 eV above the conduction band minimum and with lifetime on the order of 100 ps, which is ≥103 time longer than those in conventional semiconductors. The exceptionally long-lived energetic carriers lead to hot fluorescence emission. The protection of energetic carriers is directly correlated with the liquid-like motion of the lattice, as revealed by femtosecond Kerr-effect spectroscopy. In contrast to that of energetic carriers, the protection of long-lived bandedge carriers do not require the presence of organic cations and is an intrinsic property of the soft perovskite lattice [4].

[1] X.-Y. Zhu, V. Podzorov, "Charge carriers in hybrid organic-inorganic lead halide perovskites might be protected as large polarons," J. Phys. Chem. Lett. 2015, 6, 4758-4761.

[2] Haiming Zhu, Kiyoshi Miyata, Yongping Fu, Jue Wang, Prakriti P. Joshi, Daniel Niesner, Kristopher K. Williams, Song Jin, X.-Y. Zhu, "Screening in crystalline liquids protects energetic carriers in hybrid perovskites," Science, 2016, 353, 1409-1413.

[3] Haiming Zhu, M. Tuan Trinh, Yongping Fu, Jue Wang, Prakriti P. Joshi, Kiyoshi Miyata, Song Jin, X.-Y. Zhu, "Organic cations might not be essential for the exceptional properties of bandedge carriers in lead halide perovskites," Adv. Mater. 2017, 29,1603072.

[4] Daniel Niesner, Haiming Zhu, Kiyoshi Miyata, Prakriti Joshi, Tyler J. Evans, B. J. Kudisch, M. Marks, X.-Y. Zhu, "Persistent energetic electrons in methylammonium lead iodide perovskite thin films," J. Am. Chem. Soc. 2016, 138, 15717?15726.

10363-8, Session 3

A simple processing technique for the electrical doping of organic semiconductors *(Invited Paper)*

Bernard Kippelen, Georgia Institute of Technology (United States)

Organic photovoltaics (OPV) can lead to a low cost and short energy payback time alternative to existing photovoltaic technologies. However, to fulfill this promise, power conversion efficiencies must be improved and simultaneously the architecture of the devices and their processing steps need to be further simplified. In this talk we will present a simple solution-based technique that leads to the electrical doping of semiconducting polymer films over a limited depth. We will also show how that new processing technique can be employed to fabricate efficient single layer organic photovoltaic devices in which the functions of hole-and electron-collection are integrated in specific regions of the active layer near the electrodes.

"Solution-based electrical doping of semiconducting polymer films over a limited depth," V. A. Kolesov, C. Fuentes-Hernandez, N. Aizawa, F. A. Larrain, W.-F. Chou, M. Wang, A. Perrota, S. Choi, S. Graham, G. C. Bazan, T.-Q. Nguyen, S. R. Marder and B. Kippelen, Nature Materials (2016). Doi: 10.1038/nmat4818

10363-9, Session 4

On the challenge to scale perovskite photovoltaic devices from mm-scale cells to 6-inch modules *(Invited Paper)*

Sjoerd C. Veenstra, Energy Research Ctr. of the Netherlands (Netherlands); Francesco Di Giacomo, Santhosh Shanmugam, Henri Fledderus, Holst Ctr. (Netherlands); Weiming Qiu, IMEC (Belgium); Wiljan J. H. Verhees, Energy Research Ctr. of the Netherlands (Netherlands); Dibyashree Koushik, Technische Univ. Eindhoven (Netherlands); Valerio Zardetto, Holst Ctr. (Netherlands); Mehrdad Najafi, Energy Research Ctr. of the Netherlands (Netherlands); Yinghuan Kuang, Technische Univ. Eindhoven (Netherlands); Dong Zhang, Energy Research Ctr. of the Netherlands (Netherlands); Marcel A. Verheijen, Technische Univ. Eindhoven (Netherlands) and Philips Research (Netherlands); Maarten Doorenkamper, Energy Research Ctr. of the Netherlands (Netherlands) and Technische Univ. Eindhoven (Netherlands); Robert Gehlhaar, IMEC (Belgium); Yulia Galagan, Herbert Lifka, Holst Ctr. (Netherlands); Ruud E. I. Schropp, Mariadriana Creatore, Technische Univ. Eindhoven (Netherlands); Tom Aernouts, IMEC (Belgium); Ronn Andriessen, Holst Ctr. (Netherlands)

Organometallic halide perovskite are extremely promising novel materials for thin-film photovoltaics, exhibiting efficiencies over 22%. This presentation will focus on the current status of one of the main challenges in the industrial development of this novel PV technology: going from small cells (~0.01 cm2) to sheet-to-sheet processed modules (6 inch2).

As a first step perovskite absorbers, contact layers and device architectures were evaluated, and a planar n-i-p structure was selected. The stack consists of: Glass/ITO/TiO2/CH3NH3PbI3/Spiro-OMeTAD/Au. The perovskite absorber layer is prepared in a single deposition step based on a mixed Pb source (Pb(CH3COO)2.3H2O and PbCl2).[1] The deposition process allows a relatively fast crystallization, leading to a high PCE. TiO2 was e-beam evaporated, Spiro-OMeTAD spin coated and gold was thermally evaporated.

Secondly, laboratory deposition methods like spin coating and atomic layer deposition (ALD)[2] were replaced by scalable deposition methods like slot die coating and spatial ALD. Care is take to identify and quantify efficiency losses caused by upscaling. The cells fabricated with slot die coated perovskite and Spiro-OMeTAD layer exhibit an average PCE of 14.6 ± 1.3 %. The Jsc measured is confirmed by EQE.

In a third step, a monolithic laser interconnection is introduced yielding modules with 95% geometrical fill factor. These modules were encapsulated with flexible water barrier and PCE on aperture area (reverse JV scan) up to 10-11% were measured.

References

1. Qiu, W. et al. Pinhole-free perovskite films for efficient solar modules. Energy Environ. Sci. (2016). doi:10.1039/C5EE03703D

2. Koushik, D.et al. High-efficiency humidity-stable planar perovskite solar cells based on atomic layer architecture. Energy Environ. Sci. (2016). doi: 10.1039/c6ee02687g

10363-10, Session 4

Up-scaling perovskite solar cell manufacturing from Sheet-to-Sheet to Roll-to-Roll: Challenges and solutions

Francesco Di Giacomo, Yulia Galagan, Santhosh Shanmugam, Harrie Gorter, Fieke van den Bruele, Gerwin Kirchner, Ike de Vries, Henri Fledderus, Herbert Lifka, Holst Ctr. (Netherlands) and Solliance (Netherlands); Sjoerd C. Veenstra, Energy Research Ctr. of the Netherlands (Netherlands) and Solliance (Netherlands); Tom Aernouts, IMEC (Belgium) and Solliance (Netherlands); Pim Groen, Holst Ctr. (Netherlands) and Solliance (Netherlands); Ronn Andrissen, Solliance (Netherlands) and Holst Ctr. (Netherlands)

Organometallic halide perovskite are extremely promising novel materials for thin-film photovoltaics, exhibiting a photo conversion efficiency , PCE, of over 22% on glass and over 17% on foil [1,2]. The compatibility with flexible substrate paves the way to a roll to roll production if the coating and crystallization process can be tuned properly.

Starting from a Sheet-to-Sheet production of perovskite solar cells and modules on 152x152 mm2 substrates that involve a combination of sputtering, e-beam evaporation TiO2, slot die coating of perovskite and hole transport material (HTM) and thermal evaporation (average PCE of 14.6 ± 1.3 % over 64 devices, 14.2 ± 0.4 % with 300 s of tracking, more than 10% initial PCE on modules), the steps towards a roll-to-roll production will be analysed. First of all the stack was further optimized to make it compatible with a faster production at low temperature (max 5 minutes @ 145°C for each layer), by also keeping the PCE over a threshold value of 15%.

Two option were chosen and investigated for the electron transport layer (ETL): either a spatial Atomic Layer Deposition (R2R sALD) of TiO2 or slot die coating of a ETL ink.

A water based commercial SnO nanoparticles dispersion was used as coatable ETL, and the ink was up-scaled from spin coating on a 30x30 mm2 (with stabilized PCE of 17%+), to S2S slot die coating on 152x152 mm2 substrates to R2R coating of a 300 mm wide roll of PET/ITO without using hazardous solvent and materials.

While the S2S production is carried out in a highly controlled environment, the R2R production is often carried out in atmosphere and can consume much larger quantities of materials. Thus a first important point is the development of a green solvent and precursor system for the perovskite layer to prevent the emission of toxic compound. The use of DMSO with a surface energy modifier and the use of methylammonium free perovskite allow to have a R2R coatable ink and a safe production environment, without releasing toxic vapour in the environment (> 1 km coated so far) .

The solvent also massively influenced the film crystallization, that occur in a wet phase rather that in a dry phase as for the spin coated samples. We will show how a modification of the furnace condition (i.e. air flow and temperature profile) allowed to steer the crystallization of the layer in different manners.

The first results on device fabrication are encouraging, with R2R produced flexible PSC with stabilized PCE of 12.6%, a remarkable value for this novel devices. The perovskite layer show an high coverage of the substrate with large grain domains. This result can be considered an important milestone towards the production of efficient, low cost, lightweight, flexible PSC on large area.

References

[1] NREL chart, http://www.nrel.gov/ncpv/images/efficiency_chart.jpg

[2] Yoon, Jungjin, et al. "Superflexible, high-efficiency perovskite solar cells utilizing graphene electrodes: towards future foldable power sources." Energy & Environmental Science (2017).

10363-11, Session 4

Roll-to-roll production of organic solar cells *(Invited Paper)*

Christian L. Uhrich, Heliatek GmbH (Germany)

Heliatek GmbH produces organic solar cells using roll to roll processes in vacuum and inert atmospheres. In this talk, we will present the latest results from our first roll to roll manufacturing machine with a maximum size of 30cm width and a length of up to 6 meters. Tandem Solar Cells from this production line show efficiencies above 7% (active area). The solar cells are deposited on a flexible PET substrate in a continuous fully integrated vacuum process. These small molecule solar cells can be semitransparent and can be produced in various colors. Due to their low weight of only 500 g/m? and the very low thickness Heliatek's HeliaFilm® can be used in numerous fields of application such as between glass, in facades or on inflatable air domes. By using doped transport layers it is easy to stack two or more individual sub cells on top of each other.

We will report about the latest news from this production process including results on lifetime and pilot installations from around the world. Furthermore, we will discuss the progress from our labs including a detailed loss mechanism analysis of our world record 13.2% efficient multi-junction cell on glass.

Currently, Heliatek is setting up a second production line with a capacity of one million m? p.a. of solar films when fully ramped up.

10363-12, Session 4

High performance roll-to-roll printed PTB7-Th/PCBM solar cells

Kevin L. Gu, Stanford Univ. (United States); Xiaodan Gu, Stanford Univ. (United States) and Univ. of Southern Mississippi (United States); Yan Zhou, Stanford Univ. (United States); Hongping Yan, Stanford Univ. (United States) and SLAC National Accelerator Lab. (United States); Michael F. Toney, SLAC National Accelerator Lab. (United States); Zhenan Bao, Stanford Univ. (United States)

Despite having surpassed 10% power conversion efficiency (PCE), widely held as the threshold for commercial viability, high performance organic photovoltaics (OPVs) are still mostly constrained to lab-scale devices fabricated by spin coating. Efforts to produce scalable printed OPVs trail significantly in efficiency, highlighting the need to better understand the processing-morphology-performance relationship in the context of linear printing processes. Here we investigate the OPV system PTB7-Th/PC71BM, which has demonstrated >10% PCE via spincoating but only exhibits ~1% PCE when roll-to-roll printed. Of particular interest is the ubiquitous alcohol wash post-treatment applied to the dried active layer, which induces a significant improvement in device performance, and its crucial role for printed films. While it has been speculated that the primary utility of the alcohol post-treatment is to remove the additive 1,8-diiodooctane (DIO) residue in the dried film, we find here that the wash process itself dramatically impacts morphology in printed films regardless of the presence of DIO. Here we employ various x-ray characterization techniques to probe phase separation, crystallinity, and molecular orientation, as well as in-situ grazing-incidence x-ray diffraction (in-situ GIXD) to monitor morphological evolution during the isopropanol post-treatment process. It is discovered that isopropanol induces significant donor polymer alignment and enhanced ϖ-ϖ degree of crystallinity. Through the understanding gained in this study, we are able to achieve a roll-to-roll printed OPV with 5% PCE, which is to our knowledge the highest reported performance for a roll-to-roll printed single junction photoactive layer on a flexible substrate.

10363-13, Session 4

Self-doped n-type interfacial materials for high-performance polymer/perovskite solar cells *(Invited Paper)*

Fei Huang, South China Univ. of Technology (China)

The performance of polymer/perovskite solar cells (PSCs/PVKSCs) is highly dependent on the interfacial contact between the active layer and electrodes. Water/alcohol soluble interfacial materials, which enable orthogonal processing of high-performance multi-layer PSCs can greatly improve the interfacial contact as well as device performance. Traditional interfacial materials are not compatible with the large-area processing of PSCs using roll-to-roll techniques. Here, we present a series of self-doped interfacial materials with controlled doping properties and high mobility for the interface optimization of PSCs. Self-doped interfacial materials containing n-type conjugated backbone and polar side chains are prepared. It was shown that neutral amino groups undergo photo-induced doping process while the bromide-quaternized groups employ a self-doped mechanism.1 Further study on the counterions of the self-doped interfacial materials shows that the counterions can also induce different self-assembling and doping behavior with different strength, leading to varied charge-transporting properties. 2 More importantly, these self-doped interfacial materials can enable high-performance (>10%) PSCs and still work efficiently in varied thickness, which match well with the requirement of the fabrication of large-area PSCs. Based on the development of self-doped interfacial materials, a high-performance interconnecting layer for tandem solar cells was also developed, which can boost the power conversion efficiency (PCE) of tandem solar cells to 11.35%.3 Moreover, these interfacial materials can passivate the surface traps of perovskite to improve the electron extraction properties of PVKSC, leading to high-performance PVKSCs even when the thickness of interfacial material is more than 200 nm.4 The successful development of self-doped interfacial materials offers a better processing window for potential fabrication of PSCs/PVKSCs using large-area processing method.

1 J. Am. Chem. Soc. 2016, 138, 2004-2013.

2 Mater. Horiz. 2017, 4, 88-97.

3 Adv. Mater. 2016, 28, 4817-4823.

4 Adv. Energy Mater. 2016, 1501534.

10363-14, Session 4

A new series connection architecture for large area printed organic solar cell modules

Soonil Hong, Jinho Lee, Hongkyu Kang, Kwanghee Lee, Gwangju Institute of Science and Technology (Korea, Republic of)

The fabrication of organic photovoltaic modules via printing techniques has been the greatest challenge for their commercial manufacture. Current module architecture, which is based on a monolithic geometry consisting of serially interconnecting stripe-patterned sub-cells with finite widths, requires highly sophisticated patterning processes that significantly increase the complexity of printing production lines and cause serious reductions in module efficiency due to so-called 'aperture loss' in series connection regions. In this study, we demonstrate an innovative module structure that can simultaneously reduce both patterning processes and aperture loss. By using a charge recombination feature that occurs at contacts between electron/hole transport layers, we devise a series connection method that facilitates module fabrication without patterning the charge transport layers. With the successive deposition of component layers using slot-die and doctor-blade printing techniques, we achieve a high module efficiency reaching 7.5% with area of 4.15 cm2.

10363-15, Session 5

Fullerene-free polymer solar cells with over 12% efficiencies *(Invited Paper)*

Sunsun Li, Wenchao Zhao, Institute of Chemistry (China); Shaoqing Zhang, Univ. of Science and Technology Beijing (China); Jianhui Hou, Institute of Chemistry (China)

In polymer solar cells (PSCs), molecular design and modulation of chemical composition of the active layer materials are of critical importance for enhancing power conversion efficiencies (PCEs). In our previous work, a PCE of 11.2% was demonstrated by using a new combination of a polymer donor named PBDB-T and a small molecular acceptor (SMA) named ITIC. In order to optimized photovoltaic performance of the PBDB-T:ITIC-based PSCs, subtle chemical modifications of end-groups (EGs) were applied to precisely optimize the molecular energy level of ITIC. By successively introducing one- and two- methyl substituents, the lowest unoccupied molecular orbital (LUMO) levels of the two new acceptors (IT-M and IT-DM) were raised by 0.04 eV and 0.08 eV, respectively, compared to ITIC. Hence, improved open-circuit voltages (VOC) of 0.94 V and 0.97 V were obtained in the corresponding PSCs. Benefiting from the optimized molecular energy levels in the PBDB-T:IT-M-based blend, a PCE of 12.05% was obtained. Furthermore, we also introduced the third component Bis-PCBM[70] to enhance light absorption of the PBDB-T:IT-M blend in the short wavelength region. In the ternary PSCs based on PBDB-T:IT-M:Bis-PCBM[70], a higher PCE of 12.2% was achieved.

10363-16, Session 5

RAMP-ing the discovery of high-performance organic photovoltaic materials

Andrew J. Ferguson, Bryon W. Larson, Bertrand J. Tremolet de Villers, Wade A. Braunecker, Ross E. Larsen, National Renewable Energy Lab. (United States)

Organic semiconductors (OSCs) have found numerous applications in thin film electronic devices, including displays, sensors, lighting, and solar cells. OSCs offer the advantage that they can be modified by synthetic chemists to fulfill specific needs, and that they are not limited to being made from single elements or compositional alloys. For example, organic photovoltaics (OPVs) have reached nearly 13% power conversion efficiency (PCE) in small area devices using traditional polymer-fullerene blends, yet non-polymer and non-fullerene composites are now also showing PCEs above 10%. The flexibility offered by synthetic manipulation also presents a challenge: progress towards the discovery of next-generation, high-performance materials can be stifled by the bottleneck of device optimization through process engineering. High-throughput screening techniques that provide high fidelity performance metrics can circumvent this problem and will become important tools to accelerate material development. Here, we introduce such a tool, based on unique microwave conductivity capabilities, and illustrate a cost- and time-effective approach to evaluate the potential of promising new materials, independent of their bulk (i.e., device optimized) thin-film performance. We demonstrate the power of this approach, by correlating figures of merit from our screening tool to the OPV device performance for a library of current state-of-the-art OSCs, based on both polymer and small molecule chemical structure motifs. Finally, in the context of polymeric materials, we highlight the sensitivity of the screening process to physicochemical properties (e.g., molecular weight) and suggest that our tool can be employed for batch-to-batch quality control.

10363-17, Session 5

Charge generation in non-fullerene donor-acceptor blends for organic solar cells *(Invited Paper)*

Paul E. Shaw, Nasim Zarrabi, Dani Stoltzfus, Paul L. Burn, Paul Meredith, The Univ. of Queensland (Australia)

The continued improvement in organic solar cell efficiency has been the result of materials development and the optimization of the bulk heterojunction morphology. While a broad range of donor materials have been devised, the choice of acceptor material remains dominated by fullerenes derivatives such as PC60BM and PC70BM. Although some non-fullerene acceptors deliver blends with performance in devices approaching that of fullerene-containing blends, many do not. Given the potential benefits of non-fullerene acceptors it is important to understand what properties are required to give rise to high performance cells.

We report a photophysical study on a series of novel acceptor materials that share the same chromophore, and thus energetics, but vary in terms of their shape and chromophore number per molecule. Using ultrafast transient absorption spectroscopy, we have probed the process of singlet exciton quenching and polaron formation in blends with the polymer PTB7 across acceptor concentrations varying by two orders of magnitude and compare the results with those of PC70BM-based blends.

The results show that the structural differences between the non-fullerene acceptors had no significant impact on their performance. However, the loss of polarons to geminate recombination in the non-fullerene blends was approximately twice that of the blends containing PC70BM across a broad range of acceptor concentrations. This suggests that the choice of acceptor chromophore, which will determine the nature of the interface with the donor, is critical for minimising geminate losses and achieving high performance solar cells.

10363-18, Session 5

Impact of exciton transfer dynamics on charge generation in polymer/nonfullerene solar cells

Kenan Gundogdu, Harald W. Ade, Bhoj Gautam, North Carolina State Univ. (United States); He Yan, Hong Kong Univ. of Science and Technology (Hong Kong, China); Robert Younts, North Carolina State Univ. (United States); Shangshang Chen, Hong Kong Univ. of Science and Technology (Hong Kong, China)

The initial steps in organic photovoltaic cell (OPV) operation involve the formation of neutral excitons through photo absorption, exciton diffusion to and separation into free charges at the donor acceptor interface.1, 2As the usable solar spectrum spans a large range from the visible to the infra-red (IR), an obvious direction for improved light harvesting is to synthesize donor and acceptor materials with complementary absorption. In such devices, specifically those involving polymer donors and small molecule acceptors, both charge transfer from donor and acceptor moieties, and energy (exciton) transfer from high band gap to low band gap material are possible. Here we show that when charge and exciton transfer processes are present, the co-existence of excitons in both domains can cause a loss mechanism. Charge separation of excitons in a low band-gap polymer is hindered due to exciton population in the larger band-gap acceptor domains. Our results further show that excitons in the lower bandgap material should have a relatively long lifetime compared to the transfer time of excitons from the higher band gap material, in order to contribute to the charge separation. These observations provide significant guidance for design and development of new materials in OPV applications.

10363-19, Session 6

Perovskite tandem solar cells with greater than 25% efficiency and enhanced stability *(Invited Paper)*

Michael D. McGehee, Stanford Univ. (United States)

We have deposited perovskite solar cells with a bandgap of 1.68 eV onto heterojunction silicon solar cells that by themselves have an efficiency of 21% to create a 1 square centimeter monolithic tandem solar cell with an efficiency of 25.3%. We have also made all-perovskite tandems using a new ABX3 perovskite composition containing a mixture of tin and lead on the B site that have greater than 20% efficiency. With solar cells packaged between two sheets of glass with rubber edge seals, we have passed the industry standard 1000 hour 85°C 85% humidity damp heat test as well as 200 cycles between 85°C and -40°C. One of the keys to obtaining high efficiency and stability was optimizing the composition of cesium and formamidinium on the A site and iodine and bromine on the X site. We will show how light -induced phase separation occurs when there is too much bromine in the films. Another crucial step towards improving stability is the use of atomic layer deposition to deposit a tin oxide buffer layer on the perovskite that enables the sputter deposition of an indium tin oxide transparent electrode. ITO is less reactive with perovskites than the metals that are typically used in perovskite solar cells. The ALD layer has minimal parasitic absorption and prevents shunting. Our progress towards achieving 30% power conversion efficiency and passing even more aggressive stability tests will be presented.

10363-20, Session 6

Towards a reliable measurement protocol for perovskite solar cells

Eugen Zimmermann, Ka Kan Wong, Michael Müller, Hao Hu, Philipp Ehrenreich, Carola Ebenhoch, Thomas Pfadler, Lukas Schmidt-Mende, Univ. Konstanz (Germany)

The rapid rise of power conversion efficiency of metal-halide perovskite solar cells beyond 20 % has drawn huge attention. Recent certified efficiencies, however, have been marked as "unstabilized" as perovskite solar cells tend to show a hysteretic behaviour during current density-voltage (J-V) measurements. This leads to deviating results for varying scan parameters and conditions, which challenges reliable and comparable results. In particular, the extent of this behaviour is highly dependent on device preparation method, architecture, device history, and more importantly on measurement preconditions and scan rate. Thus, the demand for reliable stabilized values arises which are reproducible and comparable among different laboratories. Here we introduce an adaptive tracking of the maximum power point and the open circuit voltage. We compare these values with device characteristics derived from standard J-V measurements. Furthermore, we discuss the challenges of a correct efficiency determination and provide the algorithms for easy implementation in existing measurement systems.

10363-21, Session 6

Solution-processed inorganic-organic halide perovskite and charge transport layers for highly efficient and stable perovskite solar cells *(Invited Paper)*

Sang Il Seok, Ulsan National Institute of Science and Technology (Korea, Republic of)

We have analyzed microstructures of perovskite layers deposited with different composition by controlling X-ray incident angle from 0.05 to 0.5, corresponding to near-surface and full-depth from surface, respectively. The patterns in the perovskite layers will be discussed in detail by combing with a high resolution TEM. In addition, alternative materials for electron- and hole-transporting layers will be introduced, because it would be important to solve several practical issues such as stability and flexibility. Sn-based oxides for the use in electron-transporting layer (ETL) and a low temperature solution-processed copper thiocyanate (CuSCN) as an inorganic HTL were applied to PSCs

10363-22, Session 6

Perovskite materials for LED and solar cells

Ana F. Nogueira, Rodrigo Szostak, Adriano S. Marques, Emre Yassitepe, Univ. Estadual de Campinas (Brazil); Jilian N. Freitas, Ctr. de Tecnologia da Informacao Renato Archer (Brazil)

Perovskite materials have been extensively investigated as thin films or colloidal nanoparticles in several technological applications, such as photovoltaic cells (PV), lasers, photodetectors and light emitting diodes (LED).

Perovskite is the name given to materials that have the general formula ABX3 with a structure similar to the mineral CaTiO3. In perovskite materials for PV, the monovalent cation "A" is an organic cation such a methylammonium (CH3NH3+, MA) or formamidinium (CH(NH2)2+, FA). For LED applications, "A" is an inorganic cation as Cs+. In both applications, "B" is a divalent cation Pb2+ or Sn2+, and "X" a halogen anion Cl-, Br- or I-. The optoelectronic properties that make perovskites attractive are their direct and tunable band gap (that can be varied due to quantum confinement or composition), high absorption coefficient (similar to GaAs), ambipolar transport of charges, high mobility of electrons and holes compared with organic semiconductors, and electron diffusion lengths that can exceed micrometers in large crystals.

In this presentation we will discuss some aspects that limit or need to be improved in both PV and LED development.

Perovskite solar cells (PSC) are very sensitive to moisture and the highest reported efficiencies are for tiny devices assembled under very controlled conditions. A dry atmosphere found in glove boxes significantly increases equipment and operational costs for industrial processes; so ambient perovskite fabrication is much less expensive and thus more attractive. In our laboratory we prepare PSC under ambient conditions with efficiency of 13% by the intramolecular exchange method. We will discuss in more details how, by changing the deposition parameters, perovskite formation occurs immediately, or thermal annealing is required to promote the full conversion. A new formation mechanism is proposed for perovskite materials prepared at ambient conditions.

Colloidal perovskite nanocrystals are promising for LED applications., The most used synthetic method to prepare them relies on a mixture of oleylamine and oleic acid (OA) as surfactants. The resulting nanocrystals exhibit poor colloidal stability due to facile proton exchange between the oleate and amine surfactants and they readily precipitate from the crude solution. Oleylamine itself can also accelerate the degradation of the nanocrystals. We will discuss an amine-free synthesis that utilizes tetraoctylammonium halides (TOAX) for preparation of OA-capped CsPbX3 PQDs without the need of post-anion exchange methods. The nanocrystals show PLQY of 70%, narrow emission spectra and enhanced colloidal stability. We will show the results of red, green and blue (RGB) LEDs with utilizing solution-processed polymer based hole transport layers

10363-23, Session 6

Understanding the upper efficiency limit and stability in perovskite solar cells *(Invited Paper)*

Jinsong Huang, The Univ. of North Carolina at Chapel Hill (United States)

I will update the strategies in developing efficient and long lifetime perovskite solar cells in our group with material and interface engineering. I will discuss the factors which limit the enhancement of p-i-n structure perovskite solar cell efficiency, particularly the open circuit voltage in wide bandgap solar cells. The realistic upper-limit efficiency of the p-i-n structure perovskite solar cells will be discussed. I will also present the impact of material morphology, electrode materials on the stability of perovskite solar cells.

10363-24, Session 6

New low-temperature approach for forming high performance CH3NH3PbI3 solar cells with good productivity and stability

Wallace C. H. Choy, The Univ. of Hong Kong (China)

Recently, researchers have focused more to design highly efficient flexible perovskite solar cells (PVSCs), which enables the implementation of portable and roll-to-roll fabrication in large scale. Here, we demonstrated that vacuum-assisted thermal annealing can be used to control the composition, morphology, and thus the quality of the perovskite films formed from the precursors of PbCl2 and CH3NH3I. Using our vacuum-assisted thermal annealing approach to completely remove the chlorine byproduct, pure, pore-free planar CH3NH3PbI3 films with enhanced morphology can be readily formed for high efficiency PVSCs with high stability and reproducibility. In addition, we will report new room temperature approaches for forming PVSCs. Regarding the hole transport layer (HTL), NiOx is a promising material for candidate for fabricating efficient PVSCs. Here, we demonstrate the flawless and surface-nanostructured NiOx film from a simple and controllable room-temperature solution process. Meanwhile, we will propose a new room temperature scheme formation of perovskite films with the features of PbI2 residue-free, large grain-sizes, and highly crystalline. We further layout the design rules for the broad, rational extension of our scheme to form high-quality perovskite films. Using our approach, a room-temperature processed PVSC is obtained with no hysteresis, high power conversion efficiency of about 18%, which is the best of the PVSCs fabricated by low-temperature techniques to date. Additionally, the device is very stable with performance maintance of 95% after 1000 hours. This work contributes to the large-sale and low-cost production of PVSCs with high device performances.

10363-25, Session 7

Two-dimension-conjugated polymer donor materials for polymer solar cells *(Invited Paper)*

Yongfang Li, Institute of Chemistry (China)

Polymer solar cells (PSCs) have attracted great attention in the past decade, because of the advantages of simple device structure, light weight and capability to be fabricated into flexible and semitransparent devices. The key photovoltaic materials of PSCs are conjugated polymer donors and the fullerene or non-fullerene acceptors. For the conjugated polymer donor materials matching with the fullerene and nonfullerene acceptors, the two-dimension (2D)-conjugated polymers play a very important role in obtaining high power conversion efficiency (PCE) of the PSCs, because of its advantages of broad absorption and higher hole mobility. Recently, the nonfullerene n-type organic semiconductor (n-OS) (such as the low bandgap n-OS ITIC) acceptors have attracted great attention for their high photovoltaic performance. To match with the low bandgap ITIC acceptor, we developed a series of medium bandgap 2D-conjugated D-A copolymer donors based on bithienyl-benzodithiophene (BDTT) as donor unit and fluorobenzotriazole (FBTA) as acceptor unit. The D-A copolymer donors possess complementary absorption spectra and matching electronic energy levels with ITIC acceptor. By side chain engineering (alkyl, alkylthio or trialkylsilyl substitution) on the thiophene conjugated side chains of the medium bandgap polymers, the power conversion efficiency (PCE) of the PSCs with the polymers as donor and ITIC as acceptor reached 9~11%. By side chain isomerization of ITIC, the PCE of the nonfullerene PSCs was further improved to 11.77%. The results indicate that the side chain engineering of the 2D-conjugated polymer donors and n-OS acceptors are efficient way to improve photovoltaic performance of the nonfullerene PSC.

10363-26, Session 7

Electron-donating polymers containing pyrrolo[3,4-f]benzotriazole-5,7-dione unit for all-polymer solar cells

Lei Ying, South China Univ. of Technology (China)

We report a series of wide bandgap conjugated polymer consisting of a new electron-deficient building block of 4,8-di(thien-2-yl)-6-alkyl-2-alkyl-5H-pyrrolo[3,4-f]benzotriazole-5,7(6H)-dione (TzBI). This building block allows for incorporating solubilizing alkyl side chains into both triazole or imide moiety, both of which will not disturb the electronic structure of conjugated backbone. The resulting copolymers exhibited relatively wide bandgap of about 1.8 eV, with relevant absorption onset of 650-700 nm. The relatively short absorption profile provide an interesting opportunity to integrating this polymer with various recently emerged non-fullerene acceptors, presenting a remarkable power conversion efficiency over 10%. This series of copolymers can pair with electron-accepting polymer to fabricate the all-polymer solar cells with a remarkable power conversion efficiencies over 8%. Of particular interest is that these copolymers allow for the processing of high-quality films from non-chlorinated solvent, exhibiting dramatically improved stability with respect to the fullerene based devices. Detailed morphology studies on the blend film indicated that a fibrillar network can be formed and the extent of phase separation can be manipulated by thermal annealing. These results indicated the great potential of utilizing TzBI as a new building block for polymer solar cells.

10363-27, Session 7

UV-visible-near-infrared absorption dimeric porphyrin donor for highly efficient organic solar cell applications

Song Chen, Hong Kong Baptist Univ. (Hong Kong, China)

In our previous works, a serial of porphyrin-based small molecules substituted with a strongly electron-withdrawing group were exhibited a high cell performance of >8%.[1] Therefore, we have designed and synthesized an efficient push-pull A?ϖ?D?D?ϖ?A type dimeric porphyrin (CS-Dimer) based on an highly efficient porphyrin-based small molecule (4c) through coupling of two zinc porphine cores via an acetylene bridge at the meso-position to extend the absorption spectrum effectively into the near infrared region. To overcome the aggregation state caused by its nearly co-planar structural nature, the key structural feature of CS?Dimer involves long alkyl side-chains attached to the peripheral porphyrin ring so as to decrease the degree of disordered aggregation and enhanced solubility in organic solvent. This dimeric porphyrin-based small molecule possesses exceptional light harvesting capability with high extinction coefficients (?2.65?105 M?1 cm?1 in solutions) and broad absorption spectra up into the near-infrared region. The light-harvesting ability of the device exhibits a panchromatic IPCE action spectrum in the region from 300 nm to 1000 nm, and the devices displayed power conversion efficiencies as high as 8.23% with JSC/mA cm−2=15.14, VOC/mV=0.781 and FF=69.8% under AM 1.5G solar irradiation. This performance is superior to what is obtained from the individual near-infrared small molecule based single-layer devices systems.

References

1. Wang, H., Xiao, L., Yan, L., Chen, S., Zhu, X., Peng, X., Wang, X., Wong, W. K. Wong, W. Y. Chem. Sci., 2016, 7, 4301-4307.

10363-28, Session 7

Low bandgap conjugated polymers with high hole mobility for efficient thick-film polymer solar cells

Junwu Chen, South China Univ. of Technology (China)

Polymer solar cells (PSCs) are one of the most attractive ways to use solar energy – an inexhaustible renewable clean energy. Large area roll-to-roll printing is a remarkable advantage of PSCs. Low reliance of power conversion efficiency (PCE) of PSCs on large thickness variations of active layer should be a major concern toward good quality or yield control. We developed low bandgap polymer donors with high hole mobility to accelerate hole transport in thick active layer, so as to decrease recombination of holes and electrons and maintain high fill factor for highly efficient thick-film PSCs. A series of D-A conjugated polymers comprising oligothiophenes as the D-units and 5,6-difluorobenzothiadiazole (FBT), dithienobenzothiadiazole (DTfBT), and dithienobenzooxadiazole (DTfBO) as the A-units were synthesized. The polymers could show very strong interchain aggregation and result in high hole mobility. For example, field-effect hole mobilities based on neat polymer films could be higher than 2 cm2/(V s). The polymers also displayed high SCLC hole mobilities. PSCs were fabricated with varied thickness of the active layers. Delightedly, the PSCs based on the polymer donors exhibited very power conversion efficiency (PCE) with thick active layers of 200 nm or beyond. The PCE variations were relatively small for different thickness of active layers. For some FBT-based polymer, PSCs with over 400 nm thick active layer could show PCE higher than 10%. The polymers would be promising for large area printing with high speed and supply big potential for PSC modules with good quality or yield control.

10363-29, Session 7

Regioregular narrow bandgap conjugated polymers for solar cell and field effect transistor applications *(Invited Paper)*

Guillermo C. Bazan, Univ. of California, Santa Barbara (United States)

Regioregular conjugated polymers typically exhibit better pi-stacking than their regiorandom counterparts. A classic example involves regioregular poly(3-alkylthiophene), for which higher crystallinity, red-shifted optical absorption, and larger charge carrier mobilities are observed when the monomers are arranged in a head-to-tail configuration. This presentation will cover the synthesis and design of regioregular narrow bandgap conjugated polymers with donor/acceptor structural units with asymmetric acceptor units. Specifically, regioregular polymers with the pyridyl[2,1,3] thidiazole (PT) unit can be readily accessed because of the preferential reactivity of substituents in the electron-poor heterocycle. The resulting polymers have been used to fabricate thin film transistors with high hole mobilities ~6 V/cm s). Specific regioregular polymer systems have also been prepared that perform much better than their regiorandom counterparts with respect to the power conversion efficiencies (PCEs) of bulk heterojunction (BHJ) solar cells. For example, a regioregular narrow-band-gap (Eg ~1.5 eV) conjugated polymer (PIPCP) comprised of CPDT-PT-IDT-PT repeat units (CPDT = cyclopentadithiophene, IDT = indacenodithiophene) and strictly organized PT orientations, such that the pyridyl nitrogen atoms point toward the CPDT fragment was prepared. We find that PIPCP:PC61BM blends yield devices with an open circuit voltage (Voc) of 0.86 V, while maintaining a PCE of > 7%. Comparison against a range of analogous narrow band-gap conjugated polymers reveals that this Voc value is particularly high for a BHJ system with band-gaps in the 1.4-1.5 eV range thereby indicating a very low Eg-eVoc loss. We will discuss mechanistic insights into how PIPCP functions under a low enthalpic driving force for charge carrier generation and how structural variations impact solar cell performance.

10363-30, Session 8

Stable perovskite solar cells by 2D/3D interface engineering *(Invited Paper)*

Mohammad Khaja Nazeeruddin, Giulia Grancini, Cristina Roldán Carmona, Iwan Zimmermann, Ecole Polytechnique Fédérale de Lausanne (Switzerland)

Despite the impressive photovoltaic performances, perovskite solar cells are poorly stable under operation, failing by far the requirements for a widespread commercial uptake.1-3 Various technological approaches have been proposed to overcome the instability problem, which, while delivering appreciable improvements, are still far from a market-proof solution.4-5 In this talk we demonstrate stable perovskite devices by engineering an ultra-stable 2D/3D HOOC(CH2)2NH3)2PbI4/CH3NH3PbI3 perovskite junction. The 2D/3D composite delivers an exceptional gradually organized multidimensional structure that yields up to 12.9% photovoltaic efficiency in a low cost, hole-conductor free architecture and 17% in standard mesoporous solar cells. To demonstrate the up-scale potential of this technology we fabricate 10x10 cm2 solar modules by a fully printable, industrial-scale process delivering 11.2% efficient devices which are stable for >8,500 hours with zero efficiency loss measured under controlled standard conditions. This innovative architecture will likely enable the timely commercialization of perovskite solar cells.

References

1. National Renewable Energy Laboratory, N.R.E.L. http://www.nrel.gov/ncpv/images/efficiency_chart.jpg.

2. M. Saliba, T. Matsui, J. Seo, K. Domanski, J.-P. Correa-Baena, Md.K. Nazeeruddin, S.M. Zakeeruddin, W. Tress, A. Abate, A. Hagfeldt, M. Grätzel Energy Environ. Sci. 9, 1989-1997 (2016).

3. X. Li et al., Improved performance and stability of perovskite solar cells by crystal crosslinking with alkylphosphonic acid ?-ammonium chlorides. Nat. Chem. 7, 703–711 (2015).

4. I. C. Smith, E. T. Hoke, D. Solis-Ibarra, M. D. McGehee, H. I. Karunadasa, A Layered Hybrid Perovskite Solar-Cell Absorber with Enhanced Moisture Stability. Angew. Chem. 126, 11414–11417 (2014).

5. K. Domanski et al., Not All That Glitters Is Gold: Metal-Migration-Induced Degradation in Perovskite Solar Cells. ACS Nano. 10, 6306–6314 (2016).

10363-31, Session 8

Interlayer engineering for high Voc perovskite solar cells

Paul L. Burn, Qianqian Lin, Dani Stoltzfus, Ardalan Armin, Ravi Nagiri, Wei Jiang, Shanshan Zhang, Paul Meredith, The Univ. of Queensland (Australia)

Lead-based organohalide perovskites are promising for thin film solar cell technologies as they can be solution processed or deposited by low-temperature evaporation techniques, their opto-electronic properties can be tuned, and they have been shown to be capable of power conversion efficiencies (PCEs) of >20%. A factor that has led to the improvement in perovskite solar cell efficiency has been the use of interfacial engineering to control the open-circuit voltage (Voc). In principle, perovskites can work efficiently in a very simple device architecture – a high quality absorbing layer sandwiched between work function modified anodes and cathodes. In an inverted architecture the holes are collected at the transparent conducting electrode. For inverted solar cells, the hole transport/interlayer material needs to modify the anode such that its work function is close to the ionisation potential of the organohalide perovskite junction to maximise Voc. Poly(3,4-ethylenedioxythiophene):poly(styrenesulfonate) (PEDOT:PSS) can act as an anode work function modifier and is a sufficiently hydrophilic hole transport material to enable the deposition of good quality perovskite films. However, PEDOT:PSS has a relatively low work function, which limits the open-circuit Voc. In this presentation, we will discuss two different methods to modify the work function of the ITO anode to increase the Voc as well as providing a surface energy suitable for depositing a good quality perovskite film. Using these methods Vocs > 1 V and and PCEs of up to 16.5% can achieved for simple solution processed perovskite cells.

10363-32, Session 8

Pushing the lifetime of perovskite solar cell beyond 4500 h by the use of impermeable tin oxide electron extraction layers

Kai Oliver Brinkmann, Bergische Univ. Wuppertal (Germany); Jie Zhao, Ting Hu, Bergische Univ. Wuppertal (Germany) and Nanchang Univ. (China); Tim Becker, Neda Pourdavoud, Bergische Univ. Wuppertal (Germany); Selina Olthof, Klaus Meerholz, Univ. zu Köln (Germany); Lukas Hoffmann, Tobias Gahlmann, Ralf Heiderhoff, Bergische Univ. Wuppertal (Germany); Marek Oszajca, Nanograde (Switzerland); Detlef Rogalla, Ruhr-Univ. Bochum (Germany); Norman A. Lüchinger, Nanograde (Switzerland); Yiwang Chen, Baochang Cheng, Nanchang Univ. (China); Thomas J. Riedl, Bergische Univ. Wuppertal (Germany)

Perovskite solar cells (PSCs) suffer from decomposition of the active material in the presence of moisture or heat. In addition, the corrosion of metal electrodes due to halide species needs to be overcome.[1,2]

Here, we introduce ALD-grown tin oxide (SnOx) as impermeable electron extraction layer (EEL), which affords air resilient and temperature stable MAPbI3 PSCs. Being conductive, SnOx is positioned between the metal electrode and the perovskite. Its outstanding permeation barrier properties protect the perovskite against ingress of moisture or migrating metal atoms, while simultaneously the metal electrode is protected against leaking halide compounds.[2] Therefore, SnOx is also excellently suited to sandwich and protect ultra-thin metal layers (Ag or Cu) as cost efficient Indium-free semitransparent electrodes (SnOx/metal/SnOx) in PSCs. Using photoelectron spectroscopy, we unravel the formation of a PbI2 interfacial layer between a SnOx EEL and the perovskite. The resulting interface dipole between SnOx and the PbI2 depends on the choice of oxidant for ALD (water, ozone, oxygen plasma). SnOx grown by using ozone affords hysteresis-free devices with a stable efficiency of 16.3% and a remarkably high open circuit voltage of 1.17 V.[3] Finally, we fabricated semitransparent PSCs with efficiency >11% (Tvis = 17%) and an astonishing stability > 4500h under ambient conditions (>50% RH) or elevated temperatures (60°C).[4]

[1] Y. Kato et al., Adv. Mater. Interf. 2015, 2, 150019

[2] K. Brinkmann et al., Nat. Commun. 8, 13938

[3] T. Hu et al. Adv. Mat. (submitted)

[4] J. Zhao et al. Adv. Energ. Mat. (in press)

10363-33, Session 8

Tailored interfaces in halide perovskite thin films and nanocrystals *(Invited Paper)*

David S. Ginger, Univ. of Washington (United States)

Halide perovskite are being explored for optoelectronics applications ranging from solar cells to LEDs. Recent work suggests that electrical heterogeneity in both the perovskite active layer, as well as the perovskite/electrode interface can affect carrier diffusion and non-radiative recombination processes within perovskite active layers. In this talk, we will discuss both ligand exchange, and cation exchange experiments, for tailoring the properties of halide perovskite thin films and nanocrystals. We show that with controlled Lewis base passivation of the perovskite surfaces that we are able to obtain carrier lifetimes and PL intensities in thin films that rival those in the best single crystals, achieving quasi-Fermi level splittings that approach the Shockley-Queisser limit under illumination. In addition to controlling surface chemistry, we also demonstrate facile control over the perovskite chemical composition through metal B-site cation exchange of the ABX3 lattice, a process which enables control over composition of the perovskite lattice in perovskite nanocrystals, as well as perovskite thin films.

10363-34, Session 8

Enhancement of efficiency for mixed metal Sn/Pb perovskite solar cells from the view point of hetero-interface traps

Yuhei Ogomi, Daiki Yamasuso, Ayumu Yonaha, Kengo Hamada, Daiki Yamasuso, Erina Yamaguchi, Kyushu Institute of Technology (Japan); Qing Shen, Taro Toyoda, The Univ. of Electro-Communications (Japan); Kenji Yoshino, Univ. of Miyazaki (Japan); Takashi Minemoto, Ritsumeikan Univ. (Japan); Shuzi Hayase, Kyushu Institute of Technology (Japan)

Absorption edge of perovskite (PVK) solar cells consisting of MAPbI3 is 800nm. According to our simulation, light harvesting in the area of near IR is also necessary for enhancing the efficiency more. We have already reported that mixed metal perovskite (MAPbSnI3) shows photo-conversion in IR region (1-6). The short circuit current (Jsc) was high, reaching to 30 mA/cm2 because of the wide range of light harvesting. However, the open-circuit voltage (Voc) was lower than 0.3 V and the estimated voltage loss was 0.6-0.7 V, which was much larger than that of MAPbI3 (0.4 V), suggesting the presence of high density charge recombination center. We found that Ti-O-Sn bonds formed at the interface between Tiania and MAPbSnI3 layer, create trap states, resulting in increasing charge recombination at the interfaces. The surface trap density and the trap depth was quantitatively monitored by thermally stimulated current methods. When the Ti-O-Sn linkage was formed at the interface between TiO2 and PVK, the trap density increased by one order of magnitude. The interface was analyzed by XPS and confirmed that Ti-O-Sn linkage was formed. After removing the Ti-O-Sn bond at the interface between TiO2 and MAPbSnI3, the efficiency drastically increased from 4.0 % to 13.8 % and the stability was improved. It was proved that interface architecture is quite important for enhancing the MAPbSnI3 solar cells.

References

1. S. Nakabayashi, et al., J. Photonics for Energy; 2015, 5, 057410. 2. Y. Ogomi, et al., J. Phys. Chem. Lett. 2014, 5, 1004-1011.

10363-35, Session 8

Interface engineering for large-area planar perovskite solar cells

Jinho Lee, Soonil Hong, Eunhag Lee, Hongkyu Kang, Kwanghee Lee, Gwangju Institute of Science and Technology (Korea, Republic of)

The formation of pinhole-free perovskite photoactive films with full surface coverage has been a tremendous challenge for up-scaling planar perovskite solar cells (PSCs) while maintaining their high power conversion efficiencies (PCEs). Particularly, a significant mismatch between the surface energies of a hydrophilic perovskite precursor solution and a hydrophobic organic charge transport layer (CTL) has been a major cause for the poor and random surface coverage of perovskite photoactive films, which drastically reduces the scalability and reproducibility of PSCs. Here, we report a universal method to create extremely compact perovskite photoactive films on a variety of hydrophobic CTLs. By introducing an amphiphilic conjugated polyelectrolyte as an interfacial compatibilizer, we succeed in improving the wettability of perovskite precursor solutions on hydrophobic CTLs and fabricating perovskite photoactive films over large areas. Our approach enables the scalable fabrication of planar PSCs with large areas (1 cm2, PCE of 17%) while preserving nearly 90% of the PCEs of the corresponding small-area devices (PCE of 19%).

10363-36, Session 8

Advanced plasmonic and perovskite solar cells

Dong-Ha Kim, Ewha Womans Univ. (Korea, Republic of)

Plasmonics have also been recognized as promising platform that may premise the enhanced performance of next-generation photovoltaic devices. Plasmonic effects have been proposed as a solution to overcome the limited light absorption of thin film photovoltaic devices and diverse types of plasmonic solar cells have been developed. Recently, we made a comprehensive overview of the state-of-the-art progress on the design and fabrication of plasmonic solar cells as well as the understanding of the enhancement mechanism (Chem. Rev. 2016). In this presentation, we propose a few strategies to develop viable plasmonic DSSCs and OPVs based on metal-graphene oxide core-shell nanostructures (ACS Energ. Lett. 2017) or lithographically-induced plasmonic nanopatterns (ACS Nano 2016).

Very recently metal halide perovskites have been attractive as solar energy harvesters due to efficient ambipolar transport and strong light absorption. They have rapidly advanced thin film photovoltaic performance; as a result, the observed instabilities urgently require a solution. We report the reduced-dimensionality (quasi-2D) perovskite films that exhibit improved stability in solar cell performance while retaining the high performance of conventional three-dimensional perovskites. We achieve the first certified hysteresis-free solar power conversion in a planar perovskite solar cell, obtaining a 15.3% PCE, and observe greatly improved performance longevity (J. Am. Chem. Soc. 2016). The quasi-2D perovskites were also employed to develop limiting emitting diodes with the most bright and highest EQE (Nat. Nanotech. 2016).

10363-37, Session 9

Relating material properties to charge recombination mechanisms in solution processed solar cells *(Invited Paper)*

Jenny Nelson, Imperial College London (United Kingdom)

In any photovoltaic device, efficient energy conversion results from a competition between light harvesting, charge separation and transport, and charge recombination. Devices based on disordered materials such as solution processed molecular, inorganic and hybrid semiconductors, despite showing impressive advances in performance recently, typically show greater recombination losses than traditional crystalline semiconductor devices. The impact of non-radiative recombination on open-circuit voltage can be quantified precisely using luminescence techniques, but the method does not indicate the microscopic origin of the recombination nor its impact on overall solar cell performance. In this work, we use a variety of complementary experimental techniques and simulation to correlate the measured voltage losses to the underlying recombination mechanism in different types of solar cell including organic heterojunctions, lead halide perovskites and solution processed inorganic devices. We will focus on the impact of structural and energetic disorder, selectivity of contacts, density and energy of defect states and the competition of charge separation with recombination. We will comment on the extent to which disorder controls the losses to recombination, and address the question of whether large recombination losses are unavoidable in molecular materials.

10363-38, Session 9

Reducing voltage losses in multilayer organic solar cells while keeping high external quantum efficiencies

Vasileios C. Nikolis, Johannes Benduhn, Felix Holzmueller, TU Dresden (Germany); Fortunato Piersimoni, Dieter Neher, Univ. Potsdam (Germany); Christian Körner, Donato F. Spoltore, Koen Vandewal, TU Dresden (Germany)

High photon energy losses (Eloss) constitute a major performance limiting factor for organic solar cells (OSCs), limiting significantly their open-circuit voltage (Voc) and power conversion efficiency (PCE). Reduction of Eloss, while a keeping a high external quantum efficiency (EQE), can lead OSCs into a new PCE regime, beyond 12%.

In this work, we report a multilayer cascade device architecture which increases Voc through the insertion of discontinuous interlayers between electron donor (D) and electron acceptor (A). We systematically study the influence of adding various interlayers in a sequentially deposited ?-6T/interlayer/SubNc/SubPc cascade OSC, resulting in a Voc which increases from 0.98 V to 1.16 V. We show that this remarkable Voc-increase of 0.18 V is due to the suppression of non-radiative recombination, as a consequence of a reduced physical contact between ?-6T (D) and SubNc (A). The electroluminescence quantum yield of 0.9??-4 for our highest voltage device corresponds to non-radiative losses of 0.23 eV, which are the lowest reported for OSCs. Comprising the sum of non-radiative and radiative losses, we achieve an Eloss of 0.58 eV from the optical gap (Eopt) to Voc. The loss from the low energy peak of the EQE spectrum to Voc is 0.61 eV, due to a steep absorption onset. Most importantly, the low energy (700 nm) EQE peak remains high at 79%, despite a minimal driving force for charge transfer of less than 10 meV.

Our work shows that a low Eloss can be efficiently combined with a high EQE in organic photovoltaic devices.

10363-39, Session 9

Intrinsic non-radiative voltage losses in fullerene-based organic solar cells

Johannes Benduhn, TU Dresden (Germany); Kristofer Tvingstedt, Julius-Maximilians-Univ. Würzburg (Germany); Fortunato Piersimoni, Univ. Potsdam (Germany); Sascha Ullbrich, TU Dresden (Germany); Dieter Neher, Univ. Potsdam (Germany); Donato F. Spoltore, Koen Vandewal, TU Dresden (Germany)

For organic solar cells (OSCs), the open-circuit voltage is low as compared to the optical gap of the absorber molecules, indicating high energy losses per absorbed photon. These voltage losses arise only partly due to necessity of an electron transfer event to dissociate the strongly bound excitons. A large part of these voltage losses is due to recombination of photo-generated charge carriers, including inevitable radiative recombination. In this work, we study the voltage losses caused by non-radiative recombination and we find that they increase when the energy difference between charge transfer (CT) state and ground state decreases. This observed trend is in agreement with the "Energy-Gap Law for non-radiative transitions", which implies that a non-radiative decay of a CT state is facilitated by skeletal molecular vibrations. This intrinsic loss mechanism, which until now has not been thoroughly considered for OSCs, is different in its nature as compared to the commonly considered inorganic photovoltaic loss mechanisms of defect, surface, and Auger recombination. As a consequence, the theoretical upper limit for the power conversion efficiency of a single junction OSC reduces by ~25% as compared to the Shockley-Queisser limit for an optimal optical gap of the main absorber between (1.45-1.65) eV.

10363-40, Session 9

Transport and recombination considerations for charge generation efficiency in organic solar cells *(Invited Paper)*

Paul Meredith, Swansea Univ. (United Kingdom); Ardalan Armin, The Univ. of Queensland (Australia); Martin Stolterfoht, Safa Shaoi, Univ. Potsdam (Germany); Ivan Kassal, The Univ. of Sydney (Australia); Paul L. Burn, The Univ. of Queensland (Australia)

The efficiency with which photogenerated free carriers are extracted in excitonic solar cells is governed by the interactions between a number of material specific and device level properties and parameters: recombination dynamics, faster and slower carrier mobilities, contact potentials, etc. This complexity is inherent in disordered excitonic semiconductors, and understanding the underlying structure-property relationships is an ongoing endeavour in the field of organic solar cells. Questions such as – do higher mobility semiconductors necessarily deliver improved charge collection; how does supressed bimolecular recombination lead to fill factor maintenance especially at higher input irradiances [1]; or, how do we achieve high fill factors and efficiencies in thick junctions more suited to viable manufacturing [2]?

In my talk I will examine some of the latest thinking in this area [3], and present data from a suite of emerging experimental techniques such as intensity dependent photocurrent, resistant dependent photovoltage and related extraction methodologies. I will also discuss recent findings on the interrelationship between the efficiency with which free charges are extracted and charge separated state formation – the two possibly connected through entropic considerations [4].

[1] "The impact of hot charge carrier mobility on photocurrent losses in polymer-based solar cells", B. Philippa, M. Stolterfoht, P. L. Burn, G. Juska, P. Meredith, R. D. White & A. Pivrikas, Scientific Reports, 4, 5695 (2014).

[2] "Efficient, large area, and thick junction polymer solar cells with balanced mobilities and low defect densities." A. Armin, M. Hambsch, P. Wolfer, H. Jin, J. Li, Z. Shi, P. L. Burn, and P. Meredith, Advanced Energy Materials, 5, 1401221 (2015).

[3] "Impact of charge transport on current-voltage characteristics and power conversion efficiency of organic solar cells", U. Wurfel, D. Neher, A. Spies & S. Albrecht, Nature Communications, 6:6951 (2015).

[4] "Slower carriers limit charge generation in organic semiconductor light harvesting systems", M. Stolterfoht, A. Armin, S. Shoaee, I. Kassal, P.L. Burn & P. Meredith, Nature Communications, 7, 11944 (2016).

10363-41, Session 9

Carbon dangling bonds in photodegraded polymer:fullerene solar cells

Fadzai Fungura, William Robin Lindemann, Joseph Shinar, Ruth Shinar, Iowa State Univ. of Science and Technology (United States)

Intrinsic photodegradation of organic solar cells, theoretically attributed to C-H bond rearrangement/breaking, remains a key commercialization barrier. This work presents, via dark electron paramagnetic resonance (EPR), the first experimental evidence for metastable C dangling bonds (DBs) formed by blue/UV irradiation of polymer:fullerene blend films in nitrogen. The DB density increased with irradiation and decreased ~4 fold after 2 weeks in the dark. The dark EPR also shows increased densities of other spin-active sites in photodegraded polymer, fullerene, and polymer:fullerene blend films, consistent with broad electronic measurements of fundamental properties, including defect/gap state densities. The EPR and electronic measurements enable identification of defect states, whether in the polymer, fullerene, or at the donor/acceptor (D/A) interface. Importantly, the EPR results indicate that the DBs are at the D/A interface, as they were present only in the blend films. The role of polarons in interface DB formation will also be discussed.

10363-42, Session 9

Limits for photocurrent generation in polymer solar cells consisting of near-IR polymers

Yasunari Tamai, Shun Yamaguchi, Kota Tsujioka, Hideo Ohkita, Kyoto Univ. (Japan)

Near-IR polymers with the bandgap Eg below 1.5 eV have recently attracted considerable attention. Since achievable short-circuit current density JSC

increases with lowering the Eg, polymer solar cells (PSCs) consisting of the near-IR polymers potentially overcome state-of-the-art PSCs based on conventional low-bandgap polymers with Eg ~1.5–1.6 eV. Various near-IR polymers with the Eg around 1.2 eV have been developed and tested for PSCs. Nevertheless, PSCs consisting of the near-IR polymers routinely lagged in JSC behind their conventional low-bandgap polymer based analogues. Here, we study limits for photocurrent generation in PSCs consisting of near-IR polymers with the Eg around 1–1.2 eV. We performed transient absorption measurements for these polymer films, and find that exciton lifetimes of these polymers are very short. This finding suggests that PSCs consisting of the near-IR polymers suffer from poor exciton harvesting to the heterojunctions. We will discuss the origin of the short exciton lifetimes for the near-IR polymers.

10363-43, Session 10

Lead halide perovskites of different dimensionalities: growth, properties, and applications in optoelectronics *(Invited Paper)*

Osman M. Bakr, King Abdullah Univ. of Science and Technology (Saudi Arabia)

Three-dimensional (3D) lead halide perovskites exhibit impressively long carrier diffusion lengths and low trap densities, while reduced-dimensionality perovskites, such as two-dimensional (2D) and zero-dimensional (0D) perovskite derivatives, possess large exciton binding energies and high photoluminescence quantum yields. These characteristics make the diverse class of perovskite materials ideal for photovoltaics, photodetection, and light emission. Here we discuss our latest advances in growing and understanding the properties of monocyrstalline 3D perovskites, as well as 0D and 2D perovskite derivatives. We also demonstrate the integration of these materials in a range of optoelectronic applications including: monocrystalline perovskite solar cells; simultaneously fast and sensitive photodetectors that can operate in both broadband and narrow-band regimes; and efficient light-emitting diodes. Thus, in these device prototypes, we showcase the importance of crystallinity, dimensionality, and composition for tailoring materials properties, and realizing novel and efficient perovskite optoelectronics.

10363-44, Session 10

Mapping structural properties of lead halide perovskites by scanning nanofocus x-ray diffraction

David G. Lidzey, The Univ. of Sheffield (United Kingdom)

To date, the most widely employed technique to investigate the crystal structure and morphology of perovskite films have been SEM and X-ray diffraction. Most perovskite films are highly polycrystalline and thus traditional imaging techniques cannot easily isolate single crystallites or determine the statistics of lateral grain size or crystal size and morphology. A further limitation is that both SEM and other scanning probe microscopy techniques are surface-sensitive, with the bulk of the material being largely inaccessible using conventional imaging methods.

To gain better insight into a perovskite film, we scan an X-ray beam focused to 400 nm across a sample, while simultaneously recording wide-angle X-ray scattering patterns. Such scanning nanofocus x-ray diffraction (nXRD) techniques have been employed to resolve local variations in structure across a broad range of materials and research fields, however this is the first time they have been applied to a perovskite film.

We describe a method to in which each scattering pattern is analysed, allowing a classification to be made of individual perovskite grains according to a specific Miller plane. Using this method, we show that nXRD is able to resolve the extent of individual perovskite grains buried within a polycrystalline film (grain segmentation). We then use nXRD and SEM to demonstrate that the perovskite film coverage can be controlled by varying the temperature of the substrate during spin-coating. We conclude by showing that solar cells with a perovskite layer cast on a substrate held at a relatively high temperature result in devices with higher PCE.

10363-45, Session 10

Introduction of benzoquinone additive for efficient and stable planar perovskite solar cells

Chuanjiang Qin, OPERA Ctr. for Organic Photonics and Electronics Research (Japan) and Japan Science and Technology Agency, ERATO (Japan); Toshinori Matsushima, OPERA Ctr. for Organic Photonics and Electronics Research (Japan) and Kyushu Univ. (Japan) and Japan Science and Technology Agency, ERATO (Japan); Takashi Fujihara, Institute of Systems, Information Technologies and Nanotechnologies (ISIT) (Japan); Chihaya Adachi, OPERA Ctr. for Organic Photonics and Electronics Research (Japan) and Kyushu Univ. (Japan) and Japan Science and Technology Agency, ERATO (Japan)

Organic-inorganic perovskites have emerged as an interesting class of materials that have excellent photovoltaic properties for application to solar cells. The power conversion efficiency of perovskite solar cells over 20% has already been realized through systematic optimization of materials and fabrication processes. However, the long-term stability of perovskite solar cells still need to be improved for practical applications. In this study, we introduced a multifunctional benzoquinone (BQ) additive into a precursor solution containing methylammonium iodide (MAI) and lead iodide (PbI2) used for spin-coating of perovskite films. Resulting spin-coated perovskite films containing BQ had the improved perovskite morphology and crystal quality because of intermolecular interaction between MAI and BQ slowing the rate of perovskite crystal formation. Therefore, we obtained the greatly enhanced power conversion efficiency from 10.7% to 15.6%. The reduced charge recombination loss by electron transfer from perovskite to BQ is another source of the improved efficiency. In addition to the efficiency enhancement, the BQ addition led to the extended lifetime about twenty-six times. The lifetime, at which efficiency reduces to 80% of the initial under the one-sun condition (100 mW/cm2 and AM1.5G), reached about 4000 h, one of the longest lifetimes ever reported in perovskite solar cells. The extended lifetime can be explained by the reduced formation of carrier traps originating from metallic lead during solar irradiation as the results of thermally stimulate current measurements. We believe that the present findings offer insight to help obtain efficient, stable organic-inorganic perovskite solar cells for future applications.

10363-46, Session 10

A surface science approach to perovskite material and solar cell research *(Invited Paper)*

Yabing Qi, Okinawa Institute of Science and Technology Graduate Univ. (Japan)

In recent years, perovskite solar cells have been attracting enormous attention from academia as well as industry. To fabricate high performance perovskite solar cells, surfaces and interfaces are of paramount importance. My group at OIST is making concerted efforts to investigate relevant surfaces and interfaces in these materials and devices and to develop innovative strategies to improve their performance [1]. In this talk, I will introduce our research progress on real-space atomic-scale imaging of organic-inorganic hybrid perovskite [2], the vapor-based methods that can be used to fabricate large-area perovskite solar cells and modules [3-5], and degradation of perovskite [6, 7].

[1] L. K. Ono, Y. B. Qi*, J. Phys. Chem. Lett. 7, 4764 (2016).

[2] R. Ohmann, L. K. Ono, H.-S. Kim, H. Lin, M. V. Lee, Y. Li*, N.-G. Park*, Y. B. Qi*, J. Am. Chem. Soc. 137, 16049 (2015).

[3] L. K. Ono, S. Wang, Y. Kato, S. R. Raga, Y. B. Qi*, Energy Environ. Sci. 7, 3989 (2014).

[4] M. R. Leyden, Y. Jiang, Y. B. Qi*, J. Mater. Chem. A 4, 13125 (2016).

[5] L. K. Ono, M. R. Leyden, S. Wang, Y. B. Qi*, J. Mater. Chem. A 4, 6693 (2016).

[6] E. J. Juarez-Perez, Z. Hawash, S. R. Raga, L. K. Ono, Y. B. Qi*, Energy Environ. Sci. 9, 3406 (2016).

[7] S. Wang, Y. Jiang, E. J. Juarez-Perez, L. K. Ono, Y. B. Qi*, Nature Energy 2, 16195 (2016).

10363-47, Session 10

Unraveling the improved electronic and structural properties of methyl ammonium lead iodide deposited from acetonitrile

Alexandra Ramadan, Nakita Noel, Univ. of Oxford (United Kingdom); Sarah Fearn, Imperial College London (United Kingdom); Neil Young, Univ. of Oxford (United Kingdom); Marc Walker, The Univ. of Warwick (United Kingdom); Luke Rochford, The Univ. of Birmingham (United Kingdom); Henry J. Snaith, Univ. of Oxford (United Kingdom)

Perovskite-based photovoltaics are an emerging solar technology, with device efficiencies of up to 22.1 % and significant steps are being made towards their commercialisation. The conventional high efficiency active layers of perovskite solar cells are fabricated using solution film growth techniques employing high boiling point, polar aprotic solvents with N,N-dimethylformamide (DMF) one of the most frequently used solvents. However, toxicity associated with the use of each of such solvents on an industrial scale represents an insurmountable barrier to large scale manufacturing, thus the substitution of these solvents is vital for industrial upscaling of perovskite solar cells to be realised. Our recent work has established acetonitrile (ACN), in the presence of methylamine, as a viable alternative for fabrication of methylammonium lead iodide (MAPbI3) photovoltaic devices with efficiencies of >18%.

Films prepared from ACN and DMF based processing routes have been investigated using X-ray photoemission spectroscopy (XPS), ultraviolet photoemission spectroscopy (UPS), secondary ion mass spectrometery (SIMS), low energy ion scattering (LEIS) and scanning probe microscopy (SPM). The ACN processing route results in MAPbI3 based devices with higher efficiencies than those formed using DMF routes. Significant differences in the composition and electronic structure of MAPbI3 films, formed via the two different solvent routes, are observed. These differences suggest that the use of ACN as a solvent produces films with improved electronic and structural properties thereby resulting in more efficient photovoltaic devices.

10363-48, Session 10

Understanding the role of titanium dioxide (TiO2) surface chemistry on the nucleation and energetics of hybrid perovskite films

R. Clayton Shallcross, The Univ. of Arizona (United States); Selina Olthof, Klaus Meerholz, Univ. zu Köln (Germany); Neal R. Armstrong, The Univ. of Arizona (United States)

We demonstrate how amino-terminated silane monolayers alter the chemical and energetic composition of the TiO2 surface, which controls the interfacial nucleation, growth and energetics of device-relevant, hybrid perovskite (PVSK) thin films. The surface chemistry and energetics of compact TiO2 thin films are modified with a 3-aminopropyltriethoxysilane (APTES) monolayer that can either weakly coordinate Pb2+ ions (–NH2/free base form) or act as a surrogate organic cation (–NH3+/acid form) at the TiO2/PVSK interface, providing for significant differences in the nucleation free energy for the PVSK active layer as a function of NH3+/NH2 ratio. XPS spectra of amine-modified TiO2 surfaces (N 1s core level) demonstrate that we can achieve NH3+/NH2 ratios of between 3:1 and 1:3 depending upon subsequent acid and base treatment, respectively. Methylammonium lead triiodide (MAPbI3) films are incrementally co-evaporated on TiO2, TiO2/APTES-NH3+ and TiO2/APTES-NH2 interfaces, and the chemical composition, growth dynamics and energetics are systematically investigated using in situ X-ray photoelectron spectroscopy (XPS) and UV photoelectron spectroscopy (UPS). The XPS and UPS results reveal that initial nucleation and subsequent growth of the MAPbI3 PVSK film strongly depends on the chemical functionality of the TiO2 surface. The evaporated films display island-like growth on the bare TiO2 surface, which hinders nucleation of the PVSK phase until ca. 15 nm of precursor material is deposited. Conversely, film growth is more layer-by-layer on the amine-modified TiO2 interfaces, which promote nucleation of the PVSK phase within the first ca. 5 nm of deposition. In addition to vacuum evaporated thin films, we show how these TiO2 surface modifications control the morphology and crystallinity of solution-processed PVSK films based on formamidinium and methylammonium organic cations. These studies elucidate the role of TiO2 surface chemistry on the formation mechanism of hybrid PVSK active layers and the interfacial and bulk energetics, which have significant consequences related to the processing and operation of next-generation optoelectronic device platforms.

10363-49, Session 11

Molecular orientation-dependent photovoltaic performance in organic solar cells *(Invited Paper)*

Kilwon Cho, Pohang Univ. of Science and Technology (Korea, Republic of)

Photovoltaic performance of organic solar cells is highly dependent on the anisotropic nature of optoelectronic properties of photoactive materials. Here, we demonstrate an approach for highly efficient planar heterojunction solar cells by tuning the molecular orientation of the organic semiconducting materials. A monolayer graphene inserted at anode interface served as a template for quasi-epitaxial growth of pentacene crystals with lying-down orientation, which was favorable for overall optoelectronic properties including light absorption, exciton diffusion, charge transport, and interfacial energetics. The lying-down orientation persisted until ~100 nm in thickness, significantly enhancing the photon harvesting within the photoactive layer due to its increased absorption range and exciton diffusion length. The resultant photovoltaic performance showed a remarkable increase in Voc, Jsc, FF and consequently a 5 times increment in power conversion efficiency than the devices without graphene layers. The effect of molecular orientation at donor-acceptor interface was further investigated by using a planar heterojunction structure with orientation-controlled P3HT thin films. In this case, even though the P3HT layers showed similar optoelectrical properties regardless of the orientation, the photocurrent generation was more efficient in the case of the face-on donor-acceptor interface than the edge-on interface. Photophysical analyses revealed that the charge pair dissociation at the face-on interface was more efficient and resulted in smaller geminate recombination loss. These results imply that the molecular orientation in photoactive layers is a critical factor that should be elaborately controlled for future high performance organic solar cells.

10363-50, Session 11

Innovative architecture design for high performance organic and hybrid multi-junction solar cells

Ning Li, i-MEET (Germany); George D. Spyropoulos, Bayerisches Zentrum für Angewandte Energieforschung e.V. (Germany); Christoph J. Brabec, i-MEET (Germany) and Bayerisches Zentrum für Angewandte Energieforschung e.V. (Germany)

The multi-junction concept is especially attractive for the photovoltaic (PV) research community owing to its potential to overcome the Schockley-Queisser limit of single-junction solar cells. Tremendous research interests are now focused on the development of high-performance absorbers and novel device architectures for emerging PV technologies, such as organic and perovskite PVs. It has been predicted that the multi-junction concept is able to boost the organic and perovskite PV technologies approaching the 20% and 30% benchmarks, respectively, showing a bright future of commercialization of the emerging PV technologies.[1]

In this contribution, we will demonstrate innovative architecture design for solution-processed, highly functional organic and hybrid multi-junction solar cells.[2-4] A simple but elegant approach to fabricating organic and hybrid multi-junction solar cells will be introduced. By laminating single organic/hybrid solar cells together through an intermediate layer, the manufacturing cost and complexity of large-scale multi-junction solar cells can be significantly reduced.[3] Moreover, hybrid triple-junction solar cells based on organic and perovskite absorbing layers are exploited and analysed. In this hybrid triple-junction configuration, solution-processed silver nanowires are served as an intermediate electrode to efficiently extract the charge carriers from both organic and perovskite sub-cells.[4] This smart approach to balancing the photocurrents as well as open circuit voltages in multi-junction solar cells will be demonstrated and discussed in detail.

References:

1) N. Li, D. Baran, G. D. Spyropoulos, et al., Adv. Energy Mater. 2014, 4, 1400084.

2) N. Li, C. J. Brabec, Energy Environ. Sci. 2015, 8, 2902.

3) G. D. Spyropoulos, C. O. Ramirez Quiroz, M. Salvador, et al., Energy Environ. Sci. 2016, 9, 2302.

4) F. Guo, N. Li, F. W. Fecher, et al., Nat. Commun. 2015, 6, 7730.

10363-51, Session 11

Ternary blend polymer solar cells with wide-range light harvesting *(Invited Paper)*

Hideo Ohkita, Ryosuke Shimizu, Yasunari Tamai, Kyoto Univ. (Japan)

Polymer-based solar cells have made rapid progress in the last decade and are currently attracting a great deal of attention as a next-generation solar cell. Very recently, they have shown a power conversion efficiency (PCE) of more than 10%, which is comparable to that reported for amorphous silicon solar cells. However, it is still required to improve the photovoltaic performance furthermore for practical applications. In this talk, I will demonstrate ternary blend polymer solar cells, which are a new approach to improving the photocurrent generation. We have recently developed ternary blend polymer solar cells based on a wide-bandgap polymer, poly(3-hexylthiophene) (P3HT), a fullerene derivative (PCBM), and a near-IR dye molecule such as a silicon phthalocyanine derivative (SiPc). Such near-IR dye addition can easily expand the light-harvesting wavelength range up to the near-IR region, and hence can boost the photocurrent furthermore. I will demonstrate how molecular design of near-IR dye molecules can control the location in ternary blend solar cells to improve the photocurrent generation effectively. We also have fabricated ternary blend polymer solar cells based on a wide-bandgap polymer, a low-bandgap polymer, and PCBM. This two-donor polymer blend can also expand the light-harvesting wavelength and hence can boost the photocurrent effectively. Efficient exciton harvesting and charge collection can be designed by combining a wide-bandgap crystalline polymer and a low-bandgap amorphous polymer.

10363-52, Session 11

Flexible polymer solar cells with synergistic light harvesting enhancement

Yanqing Li, Jianxin Tang, Soochow Univ. (China)

To fully unlock the potential of metallic electrodes in flexible polymer solar cells (PSCs), tuning their optical properties is urgently required. Here we report an efficient light harvesting scheme involving the combination of silver mesowire grid-based front transparent electrode and plasmonic meta-mirror-based back reflector electrode. As an alternative to the indium-tin-oxide transparent conductor, the silver mesowire grid on plastic substrate enables the reduced Ohmic loss with competitive mechanical, electrical and optical properties, verifying its superiority in large-area flexible devices. The further implementation of plasmonic meta-mirror back reflector allows the broadband enhancement of light harvesting efficiency over the entire visible wavelength range, yielding a power conversion efficiency of 9.5% due to a 23.2% increase in photocurrent compared to the reference flat device. Experimental and theoretical analysis of light propagation in PSCs elucidates that the optical harvesting enhancement benefits from the synergistic effects of wide-area redistribution of optical field induced by silver mesowire grid electrode and broadband recovery of photon loss via surface plasmon and scattering enabled by the meta-mirror back reflector. This method provides a convenient and scalable way for developing high-performance flexible PSCs towards the future photovoltaic applications.

10363-53, Session 12

The importance of molecular packing, orientation and morphology control in performance and stability of all-polymer solar cells *(Invited Paper)*

Bumjoon Kim, KAIST (Korea, Republic of)

Non-ideal bulk-heterojunction morphology (BHJ) of all-polymer solar cells (all-PSCs), i.e., large-scale polymer domain size, reduced ordering of polymer chains, is one of the critical hurdles for producing efficient all-PSCs. To address this issue, we focused on developing the correlation between the polymer microstructure, BHJ morphology and the photovoltaic properties of high performance all-PSCs. As model systems of modulating the molecular weight and the alkyl side chain of polymers, the polymer microstructure and the BHJ blend morphology of all-PSCs are systematically controlled, and thereby we produced high-performance all-PSCs system with 6.7% efficiency, which is the highest value reported to date. More importantly, our all-PSCs exhibited dramatically enhanced strength and flexibility compared with polymer/PCBM devices, with 60x and 470x improvements in elongation at break and toughness, respectively. The superior mechanical properties of all-PSCs afford greater tolerance to severe deformations than conventional polymer-fullerene solar cells, making them much better candidates for applications in flexible and portable devices.

10363-54, Session 12

Enhanced thermal stability of ternary bulk-heterojunctions

Dominik Landerer, Adrian Mertens, Dieter Freis, Robert Droll, Daniel Bahro, Alexander Schulz, Tobias Leonhard, Alexander Colsmann, Karlsruher Institut für Technologie (Germany)

After enhancing the power conversion efficiencies of organic solar cells beyond 10%, their long term stability became the most urgent challenge in order to eventually integrate organic solar cells into end-user products. Even worse, the devices have to endure harsh conditions when fabricating tiles or façade elements, typically requiring lamination temperatures up to 120°C for 2 hours.

In this work, we demonstrate ternary high-performance bulk-heterojunctions with significantly enhanced thermal stability at 120°C, clearly outperforming the thermal stability of common binary polymer/fullerene bulk-heterojunctions. All solar cells were deposited from eco-compatible solvents as required by industry standards. [1] The binary bulk-heterojunctions comprise either of the BDT donor polymers PTB7 or PTB7-Th as well as the industrially more relevant (less expensive) fullerene acceptor PC61BM. The binary blends exhibit only moderate thermal stability by losing more than 30% of their initial performance, originating from crystallization and aggregation of the fullerene. In contrast, binary polymer:fullerene blends with the infrared absorber polymer PDTP-DFTB show practically no degradation but retain their initial performance. We found that the PTB7-Th:PC61BM bulk-heterojunctions can be stabilized by including 10 wt% of PDTP-DFTB (or more), thereby inheriting the thermal stability of PDTP-DFTB:PC61BM bulk-heterojunctions.

Besides the superior energy conversion of the ternary bulk-heterojunction over binary bulk-heterjunction, this device concept demonstrates how to suppress unfavourable morphological changes by using ternary blends. After 2 hours of thermal annealing at 120°C, the respective solar cells still exhibit 90% of their initial performance, here yielding PCEs of 6%.

10363-55, Session 12

Estimating the surface recombination velocity at contacts in organic devices using charge extraction by linearly increasing voltage

Oskar J. Sandberg, Mathias Nyman, Staffan Dahlström, Ronald Österbacka, Åbo Akademi Univ. (Finland)

The kinetics at contacts plays a crucial role in sandwich-type thin-film devices based on organic semiconductors. This is of particular importance in organic and perovskite solar cells where selective contacts that are able to efficiently collect majority carriers, simultaneously blocking minority carriers, are desired. Despite the vast progress made, a comprehensive understanding, needed for developing new electrode materials to improve and optimize device performance is still lacking.

A key parameter for obtaining information about processes taking place at the contacts is the effective surface recombination velocity.[1] However, means to quantitatively measure surface recombination velocities at contact interfaces in sandwich-type thin-film devices based on organic semiconductors are lacking.

The Charge Extraction by a Linearly Increasing Voltage (CELIV) technique is one of the most common methods to measure the charge transport properties in organic semiconductor devices. In this work, we show how CELIV can be used to determine surface recombination velocities at selective and/or blocking contacts in thin-film devices. The analytical framework behind the method is presented, and confirmed by numerical drift-diffusion simulations. We furthermore demonstrate the method on organic semiconductor devices, employing TiO_2 and SiO_2 as cathode buffer layers. The method allows for an increased understanding of contact properties in sandwich-type thin-film devices based on organic semiconductors.

[1] O. J. Sandberg, A. Sundqvist, M. Nyman, and R. Österbacka, Phys. Rev. Appl. 5, 044005 (2016).

10363-56, Session 12

Stabilizing organic solar cells using antioxidants, radical scavengers and light stabilizers

Vida Engmann, Univ. of Southern Denmark (Denmark); Sebastian Engmann, National Institute of Standards and Technology (United States); Nikos Tsierkezos, Technische Univ. Ilmenau (Germany); Harald Hoppe, Friedrich-Schiller-Univ. Jena (Germany); Uwe Ritter, Gerhard Gobsch, Technische Univ. Ilmenau (Germany); Morten Madsen, Horst-Günter Rubahn, Univ. of Southern Denmark (Denmark)

Record efficiencies of OPV devices nowadays reach well above 10%. However, their organic nature makes them strongly sensitive to oxygen, light, heat and humidity.

We report on long-term stabilization by ternary blending the active layers with small amounts of stabilizing compounds of different classes of antioxidants[1,3], radical scavengers[1] and light stabilizers[2]. Lifetime testing was conducted under ISOS3-degradation conditions on bulk-heterojunction cells containing a wide selection of stabilizers. Microscopic and spectroscopic methods were applied to monitor chemical degradation over time, and the observed differences are discussed in terms of energetic trap states formation within the HOMO/LUMO gap of the photoactive material, morphological and structural changes.

Both antioxidants and UV absorbers yielded an increase of the accumulated power generation by over a factor of 3 compared to the reference devices without additive. In both cases, stability improvement was caused by significant reduction of radicals within the photoactive layer, which in turn stabilizes the performance by decreasing exciton recombination. However, stabilization mechanisms of these two classes are quite different, as reflected in the burn-in. While antioxidant-stabilized cells manifested a simultaneous increase of the burn-in period and decrease of decay magnitude, UV-absorber-stabilized cells retained the same burn-in period as the reference.

[1] Turkovic V. et al, ACS Applied Materials & Interfaces 6, p 18525 (2014); http://dx.doi.org/10.1021/am5024989

[2] Turkovic V. et al, Journal of Physics D: Applied Physics 49, p 125604 (2016); http://dx.doi.org/10.1088/0022-3727/49/12/125604

[3] Turkovic V. et al, Applied Physics A 122:255 (2016); http://dx.doi.org/10.1007/s00339-016-9758-7

Conference 10364: Organic Sensors and Bioelectronics X

Sunday - Monday 6 –7 August 2017

Part of Proceedings of SPIE Vol. 10364 Organic Sensors and Bioelectronics X

10364-1, Session 1

Pushing the detection limit of organic and hybrid perovskites detectors to light and x-ray *(Invited Paper)*

Jinsong Huang, Univ. of North Carolina at Chapel Hill (United States)

I will present two materials and device structures which can further push down the detection limit of existing solution process non-cooled photodetectors. In one case, a modified organic phototransistor architecture for detecting ultraviolet–visible light down to 100 fW/cm^2 at room temperature is demonstrated. The exceptional sensitivity stems from an amplification process triggered by incident light. A responsivity of ≈10^7 A/W is achieved. The other type of detectors use the perovskite single crystals as absorber for incident visible and x-ray photons. The interfacial engineering allows the great suppress of noise, and thus the combination of high gain and low noise enabled the sensitivity enhancement by 10 to 1000 times over the state-of-the-art photodetectors and X-ray detectors based on perovskite materials. The imaging capability of the perovskite detector array will be reported.

10364-2, Session 1

Organic plasmonic Schottky barrier photodetectors

Ji-Ling Hou, Axel Fischer, Sheng-Chieh Yang, Johannes Benduhn, Daniel Kasemann, Johannes Widmer, Robert Brückner, Ronny Timmreck, Koen Vandewal, Karl Leo, TU Dresden (Germany)

Organic near-infrared (NIR) photodetectors are in the focus for developing low-cost optical-sensing devices.[1] In this work, a new device architecture for organic photodetectors is demonstrated to overcome the lack of efficient NIR absorbing organic semiconductors. We propose an organic Schottky barrier photodetector with an integrated plasmonic nanohole electrode. [2] Photons with energies below the gap of the organic semiconductor are detected via internal photoemission processes (IPE) over a metal/organic Schottky barrier, generating photocurrent. The intrinsically low IPE yield is significantly improved through the use of a nanohole electrode, enabling the excitation of surface plasmon resonances. Within the nanohole-metal/organic/metal device configuration, these SPRs are found to couple with the out-of-plane Fabry-Pérot cavity, further enhancing the responsivity. The responsivity can be easily modulated by an external field to affect the Schottky barrier, enabling selective control of individual pixels. A large (>1000) on/off ratio and a responsivity of 0.1 mA/W at 830 nm is achieved by forming a Schottky contact between Ag and a wide energy-gap (3.3 eV) organic semiconductor. Photodetection based on this mechanism allows tuning of the detector wavelength, for example by manipulating the nanohole geometry, independent of the absorption properties of the organic semiconductors used. This concept opens up new design and application possibilities for organic NIR photodetectors.

[1] Baeg, K. J. et al. Adv. Mater. 25, 4267 (2013).

[2] Hou, J. L. et al. Adv. Funct. Mater. 26, 5741 (2016)

10364-3, Session 1

Organic infrared photodiodes with charge blocking layers

Gijun Seo, Vishal Yeddu, Do Young Kim, Oklahoma State Univ. (United States)

Organic infrared photodetectors are attractive because of compatibility with flexible substrates, low-cost process, and large area applications. On the other hand, a low dark current is quite important in photodetector for obtaining high detectivity. In this study, we report infrared organic photodetectors with various charge blocking structures for reducing a dark current, thus resulting in enhancement in detectivity. Tin(IV) 2,3-naphthalocyanine dichloride (SnNcCl2) with an absorption band in the 650 ~ 1200 nm of the spectrum was used for infrared sensing. Various hole transporting materials including N,N?-Bis(naphthalen-1-yl)-N,N?-bis(phenyl)benzidine (NPB) and 4,4?,4??-Tris[phenyl(m-tolyl)amino] triphenylamine (m-MTDATA) were used as the electron blocking layer, and various electron transporting materials including bathocuproine (BCP) and Bathophenanthroline (BPhen) were used as the hole blocking layer. With both electron and hole blocking layer structure, the dark current density decreases significantly without sacrificing the photo-generated charge carrier extraction, thus resulting in the enhancement in detectivity. A systematic study of these devices and the underlying mechanism will be presented.

10364-4, Session 1

Characterization of novel organic short wavelength infrared photosensors

Weichuan Yao, Zhenghui Wu, Univ. of California, San Diego (United States); Jason D. Azoulay, The Univ. of Southern Mississippi (United States); Tse Nga Ng, Univ. of California, San Diego (United States)

Short wavelength infrared (SWIR) sensors are important to applications in environmental monitoring, medical diagnosis and optical communications, but there are only a few organic semiconductors that show optoelectronic response in the SWIR region. Recently we demonstrated a family of novel donor-acceptor polymers with narrow bandgap responsive in the SWIR region, and the bulk heterojunction photodiodes based on these polymers show detectivity up to 1E11 Jones at a wavelength of 1.37 micron, with absorption edge extending out to 1.7 micron. A SWIR photodiode was incorporated into the etalon-array reconstructive spectroscopy system to demonstrate its imaging capabilities.

As the initial performance is very promising, we proceed to investigate the stability of the encapsulated devices and to infer the degradation mechanisms. The performance of photodiodes were monitored by IV measurement, external quantum efficiency (EQE) and electrochemical impedance spectroscopy. The IV measurement and electrochemical impedance spectroscopy were conducted both in the dark and under illumination, to track over several weeks the change in charge generation and recombination processes under the short circuit and open circuit conditions. The characteristics from band-to-band absorption and from absorption in charge-transfer states were compared to quantify the lifetime and recombination losses of photogenerated carriers in these devices.

10364-5, Session 1

Photoresponse characteristics of small molecule organic photodetectors for image sensor applications *(Invited Paper)*

Dong-Seok Leem, Gae Hwang Lee, Kwang-Hee Lee, Sungyoung Yun, Seon-Jeong Lim, Younhee Lim, Hye Sung Choi, Moon Gyu Han, Kyung-Bae Park, Yeong Suk Choi, Yong Wan Jin, Sangyoon Lee, Samsung Advanced Institute of Technology (Korea, Republic of)

Organic photodetectors (OPDs) are attracting interest as various sensing platforms such as photo/chemical sensors, healthcare sensors, x-ray scanner, and image sensors. In particular, a distinct advantage of organic materials, i.e., orthogonal photosensitivity to the specific wavelength such as blue (B), green (G), red (R), and even infrared has recently facilitated promising applications to organic full colour image sensors. For instance, vertical stacks of G-wavelength selective organic photoconversion layers on conventional Si CMOS imagers with B/R color filters have been made to realize highly sensitive image sensors by doubling the light detecting area compared to the planar R/G/B pixel structure.

Our recent investigations on small molecule OPDs with bulk heterojunction structure have shown high peak external quantum efficiencies over 60% and extremely low dark current densities below 0.1 nA/cm2 at reverse bias of 3V, which are comparable to the typical performance of Si-based PDs. On the other hand, their photoresponse characteristics have not been systematically studied. For example, the Si PD exhibited the rising time of photoresponse speed as fast as 10 us at 99.9% of the peak photocurrent, whereas the OPD showed 20 times slower response time plausibly due to the reduced charge carrier mobility. Thus, in order to investigate the practical use of OPDs as image sensor applications, we will present the current status of dynamic characteristics of OPDs in terms of photoresponse speed, frequency response, and transient photocurrent. Further, the possible origin of photoresponse characteristics of OPDs will be described.

10364-6, Session 2

Microvolt-signal amplification circuitsbased on organic thin-film transistors *(Invited Paper)*

Tsuyoshi Sekitani, Osaka Univ. (Japan)

Organic thin-film transistors (OTFTs) are promising electrical components for biomedical applications because of their unique properties for lightweight, mechanical flexibility and cost effective processability. To realize a precise biosignal detecting, flexible and biocompatible electrodes should be tightly placed to the biological target surface. Also, it is desired to amplify the detected small signals nearby the electrodes for minimizing background noise. For this reason, ultra-flexible organic amplifier circuits combined with biocompatible electrodes are suitable for a reliable biosignal sensing.

We have developed ultra-flexible voltage amplifier system using an organic pseudo-CMOS inverter, which consists of four p-type OTFTs. The TFTs show the mobility is 1.5 cm2/Vs, the subthreshold slope is 92 mV, and the on/off ratio is 10^8. The voltage amplifier system, which includes a pseudo-CMOS inverter, feedback resistance, and input capacitor. Small input voltage for 10 μVpp at 3 Hz sine wave is amplified to 10 mVpp, which means the voltage gain is 60 dB. The large voltage gain is quite beneficial for detecting small biological signals. Especially, since the signal amplitude for electroencephalogram (Brain wave) is in the order of μV, which is three orders smaller than the other biological signals, the voltage amplifier system is effective for precise sensing of the electroencephalogram.

10364-7, Session 2

High sensitive biosensors based on water-stable organic field-effect transistors

Amir Foudeh, Raphael Pfattner, Celine Liong, Desheng Kong, Chao Wang, Wen-Ya Lee, Stanford Univ. (United States)

There is a big need for electronic biosensors that can be operated in water for biomedical applications and environmental monitoring. Devices based on organic materials are currently attracting great attention for applications where low-cost, large area coverage and flexibility are required. Water is an aggressive medium and due to its chemical activity the operational voltage window for stable sensor operation is limited. Related to that, in the past, degradation under both ambient and aqueous environments have limited their application in bio sensors for portable, label-free detection in the field of healthcare and environmental monitoring.

Quite recently, our group has demonstrated stable FET device operation based on organic active materials directly exposed to water and more interestingly, even sea water.[1-3] By pattering an array of gold nano-particles on top of the organic semiconductor but close to the transistor channel, the developed structure was able to sense low concentrations of mercury ions in sea water.[2,3]

Here we would like to present the second generation of this highly sensitive bio-sensor platform based on organic field-effect transistors developed in our group able to operate at even lower voltages which is a necessary condition for stable device operation in water based environments.[4,5] Functionalization is a powerful tool to attach receptor units close to the transistor channel which are able to detect its corresponding analytes. This methodology allows preparing a scalable, easy producible and high performing sensor platform suitable for portable biosensing in aqueous media.

[1] M. E. Roberts et. al., PNAS, 105, 12134 –12139, 2008.

[2] M. L. Hammock et al., ACSNano, 6, 3100-3108, 2012.

[3] O. Knopfmacher et. al. Nature Communications, 5, 2954, 2014.

[4] C. Wang, et al. Scientific Reports, 5, 17849, 2015.

[5] D. Kong, et al. Advanced Functional Materials, 26, 4680–4686, 2016.

10364-8, Session 2

Rylenediimide derivatives as a new molecular platform for n-type WG-OFETs: the role of thin-film 3D growth modality in engineering the electrolyte-semiconductor interface

Stefano Toffanin, Federico Prescimone, Emilia Benvenuti, Marco Natali, Andrea Lorenzoni, Istituto per lo Studio dei Materiali Nanostrutturati (Italy); Zhihua Chen, Northwestern Univ. (United States); Franco Dinelli, Istituto Nazionale di Ottica (Italy); Fabiola Liscio, Silvia Milita, Institute for Microelectronics and Microsystems (Italy); Francesco Mercuri, Michele Muccini, Istituto per lo Studio dei Materiali Nanostrutturati (Italy); Antonio F. Facchetti, Northwestern Univ. (United States)

The Water-Gated Organic Field-Effect Transistor (WGOFET) is one of the most promising device architecture for stimulating and recording cell electrophysiological activity given the possibility of biofunctionalization of the organic/electrolyte interface [1]. Here we present for the first time the use of two electron-transporting PDI derivatives, named PDIF-CN2 and PDI8-CN2 [2], as active materials in WGOFETs. The two materials have identical solid-state arrangement but show two different growth mechanisms: almost-2D layer by layer for PDIF-CN2 and 3D for PDI8-CN2. The electron mobility of PDI8-CN2 shows a saturation with increasing the semiconductor layer thickness (~10-4 cm2/Vs at 10-15 nm). Differently from other semiconductors used in WGOFETs, whose mobility saturates after 1-2 monolayers from the interface, the PDIF-CN2 mobility increases unexpectedly with the semiconductor film thickness up to 35 nm while preserving an almost-2D growth modality, thus reaching values comparable to state-of-the-art p-type semiconducors (~10-3 cm2/Vs). From the cross-correlation of experimental and theoretical investigations, we can suggest that the charge mobility increase is likely correlated to a bulk conduction contribution to the field-effect charge transport. Moreover, the electron-rich end-substituents of PDIF-CN2 organize into an ordered and dense interlayer at the interface with the electrolyte, which increases the surface hydrophilicity while avoiding water molecules percolation. These insights may enable the definition of a new material paradigm for the realization of performing WGOFETs for use in biological signal transduction.

[1]S. Toffanin et al., J.Mater.Chem.B 1 (2013) 3850–3859

[2] X. Zhanet al., Adv.Mater.23 (2011) 268–284

10364-9, Session 2

Prototype all solid state bioelectronic interfaces *(Invited Paper)*

Paul Meredith, Swansea Univ. (United Kingdom); Albertus B. Mostert, Margarita Sheliakina, The Univ. of Queensland (Australia); Adam P. Micolich, Damon J. Carrad, The Univ. of New South Wales (Australia)

One of the critical tasks in realising a bioelectronic interface is the transduction of ion and electron signals at high fidelity, and with appropriate speed, bandwidth and signal-to-noise ratio [1]. This is a challenging task considering ions and electrons (or holes) have drastically different physics. For example, even the lightest ions (protons) have mobilities much smaller than electrons in the best semiconductors, effective masses are quite different, and at the most basic level, ions are 'classical' entities and electrons 'quantum mechanical'. These considerations dictate materials and device strategies for bioelectronic interfaces alongside practical aspects such as integration and biocompatibility [2].

In my talk I will detail these 'differences in physics' that are pertinent to the ion-electron transduction challenge, and outline how DC and AC electrical measurements can isolate the different 'timescales' of transport. From this analysis, I will summarise the basic categories of device architecture that are possibilities for transducing elements, and give recent examples of their realisation including a novel all-solid-state electrochemical transducer that operates by so-called volumetric gating. Ultimately, transducing elements need to be combined to create 'bioelectronic logic' capable of signal processing at the interface level. In this regard, I will extend the discussion past the single element concept, and discuss our recent progress in delivering all-solids-state logic circuits based upon transducing interfaces [3].

[1] "Ion bipolar junction transistors", K. Tybrandt, K.C. Larsson, A. Richter-Dahlfors & M. Berggren, Proc. Natl Acad. Sci., 107, 9929 (2010).

[2] "Electronic and optoelectronic materials and devices inspired by nature", P Meredith, C.J. Bettinger, M. Irimia-Vladu, A.B. Mostert & P.E. Schwenn, Reports on Progress in Physics, 76, 034501 (2013).

[3] "Hybrid nanowire ion-to-electron transducers for integrated bioelectronic circuitry", D.J. Carrad, A.B. Mostert, A.R. Ullah, A.M. Burke, H.J. Joyce, H.H. Tan, C. Jagadish, P. Krogstrup, J. Nygard, P. Meredith & A.P. Micolich, Nanoletters doi:10.1021/acs.nanolett.6b0407s (2017).

10364-10, Session 3

Sensing of non-nitro group containing explosive vapours *(Invited Paper)*

Paul L. Burn, Shengqiang Fan, Paul E. Shaw, The Univ. of Queensland (Australia)

Detection of explosives can play an important role in combating terrorism and humanitarian de-mining in war-torn countries. Many detection systems used for identifying the presence of explosives are cumbersome or not portable. Luminescent conjugated polymers have been successfully used in portable detectors where the presence of the analyte is detected by a decrease in the luminescence. We have also discovered that light-emitting dendrimers can be used for effective detection of nitro-containing explosive analytes with them showing rapid and selective sensing. However, there are other explosives that are also important to detect. In this presentation we will discuss the development of sensing materials for non-nitro containing group explosives. We will show the properties of the materials and explain the method of sensing.

10364-11, Session 3

Nitroaromatic explosive vapor detection using a digitally printed sensor array *(Invited Paper)*

Carsten Eschenbaum, Karlsruher Institut für Technologie (Germany) and InnovationLab GmbH (Germany) and Institut für Mikrostrukturtechnik, Karlsruher Institut für Technologie (Germany); Nico Bolse, Karlsruher Institut für Technologie (Germany); Ralph Eckstein, Karlsruher Institut für Technologie (Germany) and InnovationLab GmbH (Germany); Tobias Rödlmeier, Karlsruher Institut für Technologie (Germany) and InnovationLab GmbH (Germany); Anne Habermehl, Karlsruher Institut für Technologie (Germany); Gerardo Hernandez-Sosa, Karlsruher Institut für Technologie (Germany) and InnovationLab GmbH (Germany); Ulrich Lemmer, Karlsruher Institut für Technologie (Germany) and InnovationLab GmbH (Germany) and Institut für Mikrostrukturtechnik, Karlsruher Institut für Technologie (Germany)

We report on a fluorescent optoelectronic nose for the trace detection of nitroaromatic explosive vapors. The sensor arrays, fabricated by aerosol-jet printing, consist of six different polymers as transducers. We demonstrate the nose's ability to discriminate between several nitroaromatics including nitrobenzene, 1,3-dinitrobenzene and 2,4-dinitrotoluene at three different concentrations using linear discriminant analysis (LDA). We assess the within-batch reproducibility of the printing process and we report that the sensor polymers show efficient fluorescence quenching capabilities with detection limits of a few parts-per-billion in air.

Our approach enables the realization of highly integrated optical sensor arrays in optoelectronic noses for the sensitive and selective detection of nitroaromatic explosive trace vapors using a potentially low-cost digital printing technique suitable for high-volume fabrication. An important challenge is temperature-dependence which is often neglected even though organic emitters are strongly affected by temperature. For some materials, even small changes of a few Kelvin can lead to large changes in the emission intensity making a temperature-control for sensing applications inevitable. Therefore, the temperature-dependence of these sensors is investigated via a heated transparent thin film on the back of such sensors allowing the active layer to be temperature controlled. All of these led to the development of a portable system.

10364-12, Session 3

Poly(dendrimers) for explosives sensing

Kinitra Hutchinson, Paul E. Shaw, Dani Lyons, Paul L. Burn, The Univ. of Queensland (Australia)

Trace detection of explosives and explosive-related compounds is crucial for countering terrorism and providing homeland security. Current technologies for doing this include ion mobility spectrometry , mass spectrometry, colorimetric detectors, electrochemical sensing, and surface acoustic wave devices. However, the best way to detect explosives is to use a stand-off detection method so as to minimize physical contact and risk to personnel. One method of achieving this goal is to use a luminescence-based system to detect explosive vapours. Luminescent conjugatged polymers and dendrimers have been developed for the detection of explosives in handheld sensors. Recently, luminescent dendrimers that incorporate triarylamine units have been shown to have good selectivity for nitro-containing explosives and taggants.[1]

In this presentation a new class of sensing material, namely luminescent poly(dendrimers), will be introduced. The poly(dendrimers) consist of triarylamine-based chromophores (dendrons) linked via a non-conjugated polymeric backbone. Such a structural motif combines the versatile

processability of polymeric materials as well as an alternative route to controlling the packing of the luminescent chromophores and thus reducing intermolecular ϖ-ϖ interactions that can cause quenching of the luminescence. Furthermore, the poly(dendrimer) can in principle give rise to a less dense film structure, which would facilitate diffusion of analytes into the sensing film. We discuss the synthesis of the materials as well as the sensing performance for the detection of nitroaromatics, such as 2,4-dinitrotoluene, and the nitroaliphatic taggant 2,3-dimethyl-2,3-dinitrobutane (DMNB) by fluorescence quenching. Stern-Volmer measurements show enhanced quenching of the poly(dendrimers) relative to the monomers. We will also discuss the potential for using poly(dendrimers) as a sensing material in a handheld detector.

[1] Geng, Y.; Ali1, M. A.; Clulow, A. J.; Fan, S.; Burn, P. L.; Gentle, I. R.; Meredith, P.; Shaw, P. E. Unambiguous detection of nitrated explosive vapours by fluorescence quenching of dendrimer films. Nat. Commun., 2015, 6, 8240.

10364-13, Session 3

Organic semiconductor sensing of explosives *(Invited Paper)*

Ifor D. W. Samuel, Ross Gillanders, James Glackin, Paulina Morawska, Graham A. Turnbull, Univ. of St. Andrews (United Kingdom)

The fluorescence of conjugated polymers is quenched by electronegative materials such as explosives. This can be used to make a sensor for explosive vapor, which can then give chemical information to help identify explosive devices, and complements other approaches such as metal detectors and ground penetrating radar. Whilst the principle has been known for some time, its practical implementation requires considerable development of instrumentation and materials. We will report our work to address these challenges, with particular emphasis on humanitarian demining.

10364-14, Session 4

Organic temperature sensor using 3D printed polymer surfaces

Kyu-Sung Lee, Electronics and Telecommunications Research Institute (Korea, Republic of) and Korea Univ. of Science and Technology (Korea, Republic of); Yong Suk Yang, Ji-Young Oh, Electronics and Telecommunications Research Institute (Korea, Republic of); Seung Eon Moon, Electronics and Telecommunications Research Institute (Korea, Republic of); Myoung-Woon Moon, Korea Institute of Science and Technology (Korea, Republic of); ChangWoo Lee, Korea Institute of Machinery & Materials (Korea, Republic of)

Recent development of 3D printing technologies would provide the variety of electronic devices including environmental sensors and bio-applications. Polymer-based sensors are compatible with human-body parts or prostheses to monitor the body status of surfaces or surroundings such as temperature, humidity, and pressure. Conventional 1D or 2D fabrication processes are effective for mass production. However, specific shapes such as curvy or 3D pathways would require the 3D printed sensors to expand the possible applications.

In this study, organic temperature sensors fabricated on 3D printed surfaces are investigated to improve the device properties. 3D structures were fabricated using a DLP (direct light processing) 3D printer with photo-polymers. Sensor electrodes based on conductive carbon materials were printed on 3D shape structures. The resistances of organic temperature sensors were measured by the temperature variations. As the environmental temperature increased from 29 to 54?, the resistance was decreased from 8.57 to 8.23 k? with the certain linearity, respectively. To further improvements, polymer composites comprising the inorganic nanoparticles were introduced to control the interfacial properties and the conductivity of composite carbons were improved.

10364-15, Session 4

Active matrix type large area flexible sensor arrays *(Invited Paper)*

Emil J. W. List-Kratochvil, Humboldt-Univ. zu Berlin (Germany)

Electrically tunable resistors realized in two terminal structures seem to be one of the most versatile innovations in the semiconductor industry with many possible applications such as logic circuitry or neuromorphic systems. In particular, inorganic resistive switching devices utilized as non-volatile memory are close to commercialization. Also, resistive switching effects in organic and hybrid devices have been presented in a multitude of devices and novel materials. [1] Recently the fabrication of organic resistive switches using environmentally friendly inkjet-printing methods and their integration into fully functional hybrid crossbar array structures has been demonstrated. [2]

[1] S. Nau, C. Wolf, K. Popovic, A. Blümel, F. Santoni, A. Gagliardi, A di Carlo, S. Sax, E. J. W. List-Kratochvil, “Inkjet-printed Resistive Switching Memory based on Organic Dielectric Materials: From Single Elements to Array Technology “, Adv. Electr. Mater, 1, 1400003 (2015)

[2] S. Nau, C. Wolf, S. Sax, E. J. W. List-Kratochvil, “Organic Non-Volatile Resistive Photo-Switches for Flexible Image Detector Arrays “, Adv. Mater. 27, 1048 (2015), also featured in Nat. Mater., 14, 134, (2015)

10364-16, Session 4

Synthesis and characterization of bioinspired organic nanowires and nanoribbons *(Invited Paper)*

Alon Gorodetsky, Univ. of California, Irvine (United States)

One-dimensional organic nanowires and nanoribbons represent idealized model systems for investigating charge transport mechanisms at molecular length scales. However, there are significant difficulties associated with the synthesis of organic nanowires and nanoribbons with precisely defined sequences, lengths, geometries, and terminal functionalities. By drawing inspiration from biological systems, we have developed facile strategies for the covalent assembly of organic semiconductor building blocks into well-defined one-dimensional ensembles. We have investigated the properties of these nanowires with a suite of spectroscopic, electrochemical, and computational techniques, discovering unique emergent properties for our constructs. Such findings hold significance both for fundamentally understanding nanoscale charge transport phenomena and for the ultimate development of next-generation molecular electronic devices.

10364-34, Session 4

Graphene electronic tattoo sensors *(Keynote Presentation)*

Nanshu Lu, The Univ. of Texas at Austin (United States)

Tattoo-like epidermal sensors are an emerging class of truly wearable electronics owing to their thinness and softness. While most of them are based on thin metal films, silicon membrane, or nanoparticle-based printable inks, we report the first demonstration of sub-micron thick, multimodal electronic tattoo sensors that are made of graphene. The graphene electronic tattoo (GET) is designed with filamentary serpentines and fabricated by a cost- and time-effective “wet transfer, dry patterning” method. It has a total thickness of 463 ± 30 nm, an optical transparency of ~85%, and a stretchability of more than 40%. GET can be directly laminated on human skin just like a temporary tattoo and can fully conform to the

microscopic morphology of the surface of skin via just van der Waals forces. The open mesh structure of GET makes it breathable and its stiffness negligible. Bare GET is able to stay attached to skin, for several hours, without fracture or delamination. With liquid bandage coverage, GET may stay functional on skin up to several days. As a dry electrode, GET-skin interface impedance is on par with medically used silver/silver-chloride (Ag/AgCl) gel electrodes, while offering superior comfort, mobility and reliability. GET has been successfully applied to measure electrocardiogram (ECG), electromyogram (EMG), electroencephalogram (EEG), skin temperature, and skin hydration. Graphene represents a new facile route for ultra-conformable multifunctional electronic tattoos, and paves the path for the introduction of other two dimensional materials for future advanced tattoo systems.

10364-17, Session 5

Ultra-sensitive bio-markers detection with an electrolyte gated organic transistor *(Keynote Presentation)*

Luisa Torsi, Univ. degli Studi di Bari Aldo Moro (Italy)

Organic bio-electronics represents one of the most exciting directions in printable electronics, promising to deliver new technologies for healthcare and human well?being. Among the others, organic field-effect transistors have been proven to work as highly performing sensors.1 Selectivity is achieved by integrating a layer of functional biological recognition elements, directly coupled with an electronic interface.

In this lecture novel developments in the field of organic and printable electronics implemented to probe biological interfaces will be discussed. It will also be shown that applications can lead to label-free electronic biosensors with unprecedented detection limits and selectivity. Notably, the extremely good sensing performance level can be rationalized by quantifying electrostatic and capacitance contributions characterizing the surface confined biological recognition elements interacting with their affinity ligands. Examples of the detection of clinical relevant biomarkers will be provided too.

10364-18, Session 5

Sulphonated mesoporous silica as proton exchanging layer in solid state organic transistors for bio-sensing

Soniya D. Yambem, Queensland Univ. of Technology (Australia)

Electronic devices that can interface with the human body are highly desirable for sensing of physiological parameters and for smart prosthetics. This is particularly challenging since the mechanism of signalling in most electronic materials is different from the mechanism of signalling in the human body. Most electronic devices in our daily life send signals through flow of electrons while body signals are carried via the exchange of ions and protons. There is a considerable interest in developing bioinspired proton conducting materials and solid-state devices for bio-electronic applications [1, 2, 3].

In this work, we will present a new class of proton conducting gate materials, sulphonated mesoporous silica nanoparticles (SMSN) [4], that are able to sense conduction of protons in all solid state, low voltage operating organic thin film transistors (OTFTs). Ordered mesoporous silica nanoparticles with various functional groups have been investigated for applications in catalysis, gas adsorption and drug delivery. SMSN have also been successfully investigated for applications in fuel cell membranes [4]. In this presentation, we will describe the OTFT operation of solution processable SO3H-MCM-41 films that have highly ordered pore structures. The OTFTs fabricated maintained low voltage transistor output characteristics for operating source-drain voltages 0 > Vds > -1.25 V.

We will also present results that demonstrate the application of our low voltage operating OTFTs in sensing proton exchange, where a drop of H2O2 dropped on top of the SO3H-MCM-41 gate electrode captures strong modulation in the current flow. H2O2 breaks down to oxygen, protons and electrons when a voltage above a threshold voltage is applied between source and drain. The Ids increases immediately by ~ 3-fold and continues to increase to a maximum value of ~ 5-fold, demonstrating that these OTFTs are highly applicable in advanced biomedical sensing applications.

1. L. Herlogsson, X. Crispin, N.D. Robinson, M. Sandberg, O.-J. Hagel, G. Gustafson, M. Berggren, Adv. Mater. 19, 97-101 (2007).

2. C.J. Wan, L.Q. Zhu, Y. H. Liu, P. Feng, Z.P. Liu, H.L. Cao, P. Xiao, Y. Shi, Q. Wan, Adv. Mater. 28, 3557-3563 (2016).

3. C. Zhong, Y. Deng, A.F. Roudsari, A. Kapetanovic, M.P. Anantram, M. Rolandi, Nature Comm. 2, 476 (2011).

4. R. Marschall, I. Bannat, A. Feldhoff, L. Wang, G.Q. Lu, M. Wark, Small 5 (7), 854-859 (2009).

10364-19, Session 5

Low voltage organic charge modulated FETs: A flexible approach for the fabrication of high sensitive biosensors *(Invited Paper)*

Piero Cosseddu, Andrea Spanu, Fabrizio Viola, Stefano Lai, Univ. degli Studi di Cagliari (Italy); Brunella Tedesco, Sergio Martinoia, Univ. degli Studi di Genova (Italy); Annalisa Bonfiglio, Univ. degli Studi di Cagliari (Italy)

Charge Modulated OTFTs represent a versatile tool for the realization of a wide range of sensing applications. The architecture is based on a floating gate organic transistor whose sensitivity to a specific target is obtained by properly functionalizing a part of the floating gate with a sensing layer that can be chosen according to the specific external stimulus to be sensed.

In this work we will show that such devices can be routinely fabricated on highly flexible, ultra-conformable thin films and that they can be employed, with no need of any chemical modification of the sensing area, for monitoring pH variations featuring a super-nernstian sensitivity. Interestingly, we will also show that the proposed approach has been applied for monitoring cell metabolic activity, demonstrated with a preliminary validation. In addition this device can be used for monitoring electrical activity of excitable cells, thus giving rise to a new family of highly sensitive, reference-less, and low-cost devices for a wide range of bio-sensing applications.

Finally, we will also demonstrate that using a different sensing layer it is possible to employ the same device architecture for the realization of matrices of multimodal tactile transducers capable to detect at the same time temperature and pressure stimuli, and that being fabricated on sub-micrometer thin film can be conformably transferred on whatever kind of surface allowing the reproduction of the sense of touch.

10364-20, Session 6

Large-scale organic neural interface devices *(Invited Paper)*

Dion Khodagholy, Columbia Univ. (United States)

As our understanding of the brain's physiology and pathology progresses, increasingly sophisticated technologies are required to advance discoveries in neuroscience and develop more effective approaches to treating brain disease. There is a tremendous need for advanced materials solutions at the biotic/abiotic interface to improve the spatiotemporal resolution of neuronal recording. Organic electronic devices offer a unique approach to these challenges, due to their mixed ionic/electronic conduction, mechanical flexibility, enhanced biocompatibility, and capability for drug delivery. We designed, developed, and characterized conformable organic electronic devices in the form of transistors and electrodes to efficiently interface with the brain and acquire neurophysiological activity not previously accessible with recordings from the brain surface. These devices have facilitated large-scale rodent neurophysiology experiments and uncovered a novel hippocampal-cortical oscillatory interaction. The biocompatibility of the devices allowed intra-operative recording from patients undergoing epilepsy surgery, highlighting the translational capacity of this class of neural interface devices

This multidisciplinary approach will enable the development of new devices based on organic electronics, with broad applicability to the understanding of physiologic and pathologic network activity, control of brain-machine interfaces, and therapeutic closed-loop devices.

10364-21, Session 6

A printed electronic platform for the specific detection of biomolecules

Amadou Doumbia, Michelle Webb, Michael L. Turner, The Univ. of Manchester (United Kingdom); Jonathan Behrendt, Richard J. Wilson, Cambridge Display Technology Ltd. (United Kingdom)

The rapid detection of disease specific biomarkers in a clinically relevant range using a low cost sensor can facilitate the development of individual treatment plans for a given patient, known as the precision, personalized or genomic medicine. In the recent decade Electrolyte Gated Organic Field Effect Transistors (EGOFETs), a subtype of OFETs where the dielectric is replaced by an electrolyte, have attracted a great deal of attention from both industry and academia for sensing applications. This is due to their capacity to operate at low voltage (< 1 volt) in physiological like media (water, phosphate saline solution, etc.) with high sensitivity and specificity. Although EGOFET based biosensors have demonstrate their capacity to specifically detect biomolecules with high sensitivity; the stability, reproducibility and performance required to reach the desired market are not yet achieved. In this contribution we describe a platform for the fabrication of stable and reproducible EGOFET sensors that are able to detect biomolecules rapidly with high selectivity and sensitivity in real time. Facile and scalable techniques are used to prepare arrays of these devices with patterned active layers. The influence of the electrode geometry (channel length to width ratio) on the device performance and sensitivity is examined. The selectivity of individual EGOFETs is investigated by immobilization of specific ligands to the target molecule of interest on the gate electrode or the active layer within a microfluidic flow cell. Finally calibration and control experiments show how the developed sensor arrays are capable of specifically determining the analyte concentration in real time

10364-22, Session 6

Microfluidics and BIO-encapsulation for drug- and cell-therapy *(Invited Paper)*

Rosaria Rinaldi, Univ. del Salento (Italy) and Istituto per la Microelettronica e Microsistemi, CNR (Italy); Alessandra Aloisi, Istituto per la Microelettronica e Microsistemi (Italy); Chiara Toma, Univ. del Salento (Italy)

We present the construction and the application of biocompatible micro- and nano-structures that can be administered systemically and transport in a targeted and effective way drugs, small molecules, stem cells or immune system cells. These polymeric nano-systems represent a primary goal for the treatment of a wide family of neurological/systemic disorders, as well as tumors and/or acute injuries As natural, biocompatible, biodegradable and non-immunogenic building blocks, alginate and chitosan are been currently exploited. Ionotropic pre-gelation of the alginate core, followed by chitosan polyelectrolyte complexation, allow to encapsulate selected active molecules by means of physical entrapment and electrostatic interactions within sub-micron sized hydrogel vesicles. Here we present a microfluidic-assisted assembly method of nano- and micro-vesicles -under sterile, closed environment and gas exchange adjustable conditions- a critical issue, when the cargo to be upload is very sensitive. Polymer/polymer and polymer/drug mass ratio relationship are crucial in order to attain the optimum in terms of shuttle size and cargo concentration. By modulating polymer reticulation conditions, it become possible to control drug loading efficiency as well as drug delivery dynamics. Recent results on the application of the vesicles for the encapsulation and delivery of Inhibin-A and Decorin secreted by Human Adult Renal Stem/Progenitor Cells for Renal tubular cell regeneration will be presented.

Finally, the impact of these polysaccharide sub-micron vesicles on Human Immune cells and the metabolic activity of cells embedded in the micro vesicles will be presented and discussed.

10364-23, Session 6

Microfluidic methods in organic electronics and organic bioelectronics *(Invited Paper)*

John C. de Mello, Imperial College London (United Kingdom)

Microfluidic methods have a critical role to play in the production of electronic and bioelectronic materials and their subsequent deployment in analytical devices. Here we describe several different aspects of microfluidic technology that are relevant to organic electronics research in general and organic bioelectronics research in particular, focusing on the optimisation and manufacturing of functional materials at scale, and their integration into self-contained analytic devices.

10364-24, Session 7

Vertical organic transistors for optoelectronic and ferroelectric applications *(Invited Paper)*

Hyeonggeun Yu, Franky So, North Carolina State Univ. (United States)

Direct integration of an infrared-sensing quantum dot film and an organic light-emitting diode (OLED) offers pixel-free infrared imaging. However, the infrared-to-visible conversion efficiencies of the devices are low due to the low photon-to-electron conversion efficiency of the quantum dot photodetector. Here, we report a novel vertical infrared phototransistor with 105 % external quantum efficiency (EQE). By integrating a phosphorescent OLED with this phototransistor, an infrared-to-visible up-conversion light-emitting phototransistor with an EQE over 1,000% is demonstrated. In addition, by employing a ferroelectric gate insulator for the vertical transistor, a flexible low voltage non-volatile memory is demonstrated with 10 years of retention extrapolated.

10364-25, Session 7

Effect of water adsorption on ionic and electronic transport in PEDOT:PSS

Eric S. Muckley, Christopher B. Jacobs, Rajeev Kumar, Ilia N. Ivanov, Oak Ridge National Lab. (United States)

Progress in bionic sensing and bio-electronic interfacing requires a thorough understanding of electronic and ionic transport in functional bio-compatible materials. The well-known polymer mixture poly(3,4-ethylenedioxythiophene) polystyrene sulfonate (PEDOT:PSS) is central to many optoelectronic applications which necessitate flexible, transparent biocompatible materials. While PEDOT:PSS is traditionally studied for its hole transport properties and resistive H_2O response, research interest has recently turned to ionic transport in the context of bio-electronic interfacing and sensing. Cations Na^+ and K^+ are often present in PEDOT:PSS as byproducts from industrial production. Uptake of water into PEDOT:PSS disrupts hydrogen bonding that maintains rigidity of the PSS matrix, causing film swelling and hydronium production due to water interaction at the hydrophilic SO_3^- moiety. As water uptake increases, mobility of Na^+, K^+, H_3O^+ and other ions may become hindered due to the formation of

electrical double layers and hydration shells around ions. At the same time, water-induced swelling of the PSS matrix increases the distance between adjacent conductive PEDOT domains, which reduces electronic mobility. Despite its widespread use as a hole transport material in a variety of organic optoelectronic devices, the effect of water on electronic and ionic transport in PEDOT:PSS remains unclear. To probe both electronic and ionic response during water uptake, we perform ultra-wide range dielectric spectroscopy from sub-Hz to optical frequencies while changing humidity conditions in a controlled environment. We correlate the frequency-dependent measurements with those of a PEDOT:PSS-coated quartz crystal microbalance (QCM) to estimate the mass of adsorbed H2O in the film. We show that the presence of water has an effect on electronic and ionic mobility in the film and both electronic and ionic transport play a role in defining the optoelectornic properties of PEDOT:PSS under a wide range of humidities.

10364-26, Session 7

Designing organic mixed conductors for bioelectronic applications *(Invited Paper)*

Jonathan Rivnay, Northwestern Univ. (United States)

Direct measurement and stimulation of electrophysiological activity is a staple of neural and cardiac health monitoring, diagnosis and/or therapy. Such bi-directional interfacing can be enhanced by the low impedance imparted by organic electronic materials that show mixed conduction properties (both electronic and ionic transport). Many high performance bioelectronic devices are based on conducting polymers such as poly(3,4-et hylenedioxythiophene):poly(styrenesulfonate), PEDOT:PSS. By investigating PEDOT-based materials and devices, we are able to establish a set of design rules for new formulations/materials. Introducing glycolated side chains to carefully selected semiconducting polymer backbones, for example, has enabled a new class of high performance bioelectronic materials that feature high volumetric capacitance, transconductance >10mS (device dimensions ca. 10um), and steep subthreshold switching characteristics. A sub-set of these materials outperform PEDOT:PSS and shows significant promise for biocompatible, low power in vitro and in vivo biosensing applications.

10364-27, Session PMon

An enzyme-based lactate sensor incorporating a three-dimensional complementary inverter for high sensitivity

Sanghoon Baek, Jimin Kwon, Pohang Univ. of Science and Technology (Korea, Republic of); Hiroyuki Matsui, Shizuo Tokito, Yamagata Univ. (Japan); Sungjune Jung, Pohang Univ. of Science and Technology (Korea, Republic of)

Enzyme-based biochemical sensors based on organic field-effect transistor (OFET) have gained attention for their potential applications as low-cost, disposable, wearable sensors. They take advantage of inducing drain current change in OFET from enzymatic reaction, however, the induced current signal is not stable and signal-to-noise ratio is not large enough to be easily detected. In this study, we propose a new strategy of an extended-gate type inverter incorporating three-dimensional complementary organic field-effect transistors (3D-COFETs) for lactate detection with higher sensitivity. In the device structure of 3D-COFETs, a bottom-gate p-type OFET is vertically integrated on a top-gate n-type OFET with the gate shared in-between, and complementary inverter is implemented with this transistor-on-transistor structure. For lactate detection, enzyme-functionalized gold electrode is used as an extended-gate of complementary inverter, and it composes biofuel cell with Ag/AgCl reference electrode in aqueous media. We have observed that the enzymatic redox chain reaction of lactate occurring in the biofuel cell causes potential difference between the two electrodes which results in switching voltage shift in the complementary inverter. The proposed 3D-COFETs structure itself has advantages in sensing applications within complementary integrated circuit systems thanking to its higher transistor density. The output signal from the detection of lactate levels using the proposed 3D-COFETs inverter is expressed in voltages which is more stable than current signals and sensitivity is higher compared with that of single OFET-based biochemical sensors because the voltage shift induced from enzymatic reaction is amplified by the gain of the inverter. It is expected that the proposed biochemical sensor incorporating 3D-COFETs is a promising candidate for highly sensitive biosensors in practical applications.

10364-28, Session PMon

Porous silicon photoluminescence biosensor for rapid and sensitive detection of toxins

Yuliia Melnyk, Karyna Pavlova, Valerii Myndrul, Valentyn Smyntyna, Odessa I.I. Mechnikov National Univ. (Ukraine); Roman Viter, Univ. of Latvia (Latvia); Igor Iatsunskyi, Adam Mickiewicz Univ. (Poland)

Mycotoxins are toxic secondary metabolites produced by some fungal species. Among all mycotoxins, ochratoxin A (OTA) and aflatoxin (AF) have received much attention due to severe health effects in animals and humans. Porous silicon (PSi) has become one of the most popular materials for the biosensor technology in the last years. In the present study, we have developed a sensitive, cost-effective, and comparatively fast method for OTA and AF detection. PSi samples fabricated by metal-assisted chemical etching (MACE) were used to develop photoluminescence (PL) biosensor for OTA/AF detection. PSi samples were characterized by X-ray diffraction (XRD), scanning electron microscopy (SEM), reflectance and PL spectroscopy. The main structural and chemical parameters of PSi were obtained. We explored the ability of PSi samples, as a new material to enhance the performance of optical biosensors for OTA and AF detection. This biosensing system using PSi and PL signal analysis was proposed in our knowledge for the first time for OTA/AF detection. The PL biosensor exhibited a wide detection range from 0.094 to 100 ng/mL (linear range from 0.001 to 100 ng/mL) of toxins. Immobilization of the biosensitive layer onto PSi surface was found to decrease the intensity of PL. A phenomenon of changes in PL of PSi samples upon the interaction with toxins was proposed to be used as a platform for the optical biosensor development.

10364-29, Session PMon

Au-Ag alloy nanoislands for high-sensitive localized surface plasmon resonance biochemical analytes detection

Guangyu Qiu, Siu Pang Ng, Chi-Man L. Wu, City Univ. of Hong Kong (Hong Kong, China)

Nanoislands of Au and Ag alloy were synthesized by self-assembly thermal annealing method. The nanoparticles show not only the combination of plasmonic properties related to the presence of two individual metal elements, but also have improved and tunable plasmonic sensing performance. The Au-Ag alloy nanoislands were optimized in two aspects: 1) the atomic ratio of Au and Ag, and 2) the size of synthesized nanoislands. UV-visible absorption spectroscopy was utilized to investigate the plasmonic effect of transmitted light, and achieved tunable light absorption ranging from 420 nm to 570 nm by changing the atomic ratio of Au and Ag. Among the various atomic ratios investigated, the Au60Ag40 (in atomic ratio) nanoislands exhibited the sharpest and strongest absorption. In virtue of the common-path interferometric sensing system, the optimized Au60Ag40 nanoislands showed improved refractive index sensitivity than pure Au nanoislands, together with better corrosion resistance properties over pure Ag nanoparticles.

The synthesized Au-Ag alloy nanoislands were successfully functionalized with various protocols, i.e. 1) conventional Au functionalization protocol with 11-Mercaptoundecanoic acid (11-MUA); 2) dielectric functionalization method to immobilized organic receptors onto glass substrate; and

3) direct functionalization with synthetic copolymer such as poly(m-Phenylenediamine-co-Aniline-2-sulfonic acid) nanoparticles. The functionalization efficiency and biochemical sensing performance toward various analytes of synthetic homodispersed Au60Ag40 nanoislands were compared with previously reported Au nanoislands. Further, it was demonstrated that the self-assembly Au-Ag alloy nanoislands showed improved plasmonic sensing performance. These results indicated that the Au-Ag alloy nanoislands have great potential for its sensing applications.

10364-30, Session PMon

Development of fully organic moisture sensor

Aramis A. Sanchez Juárez, Univ. Técnica Particular de Loja (Ecuador)

A fully organic moisture sensor was developed, the active substance is a natural organic dye contained in the species Hibiscus Sabdariffa and the support material is a natural biopolymer made from three different species Canna indica, Cavendish Valery and Arracacia xanthorrhiza. Characterization and accuracy results depending on the biopolymer are presented in this paper. The sensor was characterized by the correlation between color changes ranging from violet to blue and humidity levels varying from 5% to 100%, another study was the lifetime of the sensor under different storage conditions. An important result for an organic moisture sensor is that it exhibits reversibility when exposed to extreme moisture values. Additionally, the effects of temperature, UVA exposure and ionizing radiation on sensor performance with respect to time are studied.

10364-31, Session PMon

Fully organic pH sensor development

Aramis A. Sanchez Juárez, Johanna E. Jaramillo Q., Univ. Técnica Particular de Loja (Ecuador)

A fully organic pH sensor was developed, the active substance is a natural organic dye contained in the species Prunus Salicifolia and the support material is a natural biopolymer by an independent study carried out for the manufacture from three different species Canna indica, Cavendish Valery and Arracacia xanthorrhiza. Characterization and accuracy results depending on the biopolymer are presented in this paper. The sensor was characterized by the correlation between color changes ranging from green to red and pH levels varying from 1 to 12, another study was the lifetime of the sensor under different storage conditions. An important result for an organic moisture sensor is that it exhibits reversibility when exposed to extreme pH values. Additionally, the effects of temperature, UVA exposure and ionizing radiation on sensor performance with respect to time are studied.

10364-32, Session PMon

Novel biomimetic light-harvesting molecular architecture based on porphyrin-peptoid conjugates

Jiwon Seo, Gwangju Institute of Science and Technology (Korea, Republic of)

The energy flow during natural photosynthesis is controlled by maintaining the spatial arrangement of pigments, employing ?-helices as scaffolds. The natural photosynthetic mechanism can be better elucidated by developing a synthetic molecular system that can establish a pigment array with the precision of natural systems. Herein, we have developed porphyrin-peptoid conjugates that can tune the donor-acceptor energy transfer efficiency with exceptional precision by controlling the inter-porphyrin distances and orientations. Peptoids, or oligo-N-substituted glycines, with ?-helical conformation were used as scaffolds for porphyrin display; two porphyrins can have strong to minimal intramolecular excitonic couplings depending on their relative placement in the helix. The unique structural characteristics and synthetic accessibility of peptoids can be further utilized to develop artificial light-harvesting proteins and tunable photosensitizers.

10364-33, Session PMon

Fabrication and characteristics of composite metals for 3D printed electronics

Yong Suk Yang, Hyun-Woo Dang, Bonjin Koo, Electronics and Telecommunications Research Institute (Korea, Republic of); ChangWoo Lee, Korea Institute of Machinery & Materials (Korea, Republic of)

- This presentation contains the materials and processes of 3D printing for printed sensors and transistors.

- The metals for the 3D printing were based on eutectic materials such as GaIn, InAg, SnBi, and SnAgCu

and were utilized to achieve 3D printing.

- The 3D printed metals were applied to electrodes and wirings.

Conference 10365: Organic Field-Effect Transistors XVI

Monday - Wednesday 7 –9 August 2017

Part of Proceedings of SPIE Vol. 10365 Organic Field-Effect Transistors XVI

10365-1, Session 1

Programmable and coherent crystallization of semiconductors *(Invited Paper)*

Aram Amassian, King Abdullah Univ. of Science and Technology (Saudi Arabia)

Crystalline order determines the electronic properties of semiconducting materials, determining their functionality, performance and technological utility. Polycrystalline thin films are typically grown directly from vapour or solution phases, but crystalline films can also be formed by annealing a disordered film. We demonstrate that the stochastic nucleation of crystallites within disordered media proceeds via homogeneous nucleation. A key implication of this finding is that unlike heterogeneous nucleation, the crystallization behavior is proportional to the volume of material and thus to local variations in film thickness. We utilize this breakthrough to harness the nucleation and growth of the crystalline phase by creating deliberate thickness variations. This leads to fully programmable crystallization behavior which we utiize to fabricate organic thin film transistors (OTFTs) with superior transport properties as well as dramatically improved device to device reproducibility. This method provides significant new pathways for controlling material structure and patterning functional properties for use in electronic devices, circuits and beyond.

10365-2, Session 1

Formation and growth of organic semiconductors with mm-scale grains *(Invited Paper)*

Barry P. Rand, Princeton Univ. (United States)

While record mobilities have been reported for organic semiconductors in their single crystal form, the bulk nature of such crystals prohibit their practical application. Here, we discuss our efforts to realize pinhole free films of the organic semiconductor rubrene with grains of up to 1 mm in extent. We will show our efforts to understand their formation, epitaxy, and transistors. Homoepitaxial studies uncover evidence of point and line defect formation in these films, indicating that homoepitaxy is not at equilibrium or strain-free. Point defects that are resolved as screw dislocations can be eliminated under closer-to-equilibrium conditions, whereas we are not able to eliminate the formation of line defects. We are, however, able to eliminate these line defects by growing on a bulk single crystal of rubrene, indicating that the line defects are a result strain built into the thin film template, indicating that, in general, organic crystalline thin films may not adopt the exact lattice of a bulk crystal.

10365-3, Session 1

Large-area solution-processed monolayer single crystals for organic field-effect devices

Anastasia V. Glushkova, M.V. Lomonosov Moscow SU (Russian Federation); Elena Y. Poimanova, Donetsk National Univ. (Ukraine); Vladimir V. Bruevich, M.V. Lomonosov Moscow SU (Russian Federation); Yuriy N. Luponosov, Sergei A. Ponomarenko, Institute of Synthetic Polymeric Materials (Russian Federation); Dmitry Y. Paraschuk, M.V. Lomonosov Moscow SU (Russian Federation)

Single-crystal organic filed effect transistors (OFETs) can provide electrical performance exceeding that of a-Si devices. Solution-processed devices could be more advantageous enabling low production costs. For industrial applications of organic single crystals, their high morphological homogeneity and thickness uniformity on large areas are needed. As charge transport in OFETs occurs within a few monolayers of organic semiconductor, ultrathin devices are beneficial from the viewpoint of low material consumption, mechanical flexibility and optical transparency. Herein, we report on solution-processed oligothiophene-based monolayer single crystals with sizes up to a few mm and study their performance as OFET active layers. As materials, we used oligothiophenes and oligothiophene-phenylenes with five conjugated rings and different terminal linear alkyl substituents, which were proved to be crucial for 2D crystallization in monolayers. The monolayer single crystals were grown on various surfaces, both with high and low surface energies, and studied by optical polarization microscopy, atomic-force microscopy, spectroscopic ellipsometry, and x-ray diffraction. Our in situ studies of crystal growth allowed us to suggest a possible growth mechanism. The OFET mobility was tenfold higher for the oligomers with longer alkyl substituents. The best devices showed the charge mobility exceeding by an order of magnitude the highest reported mobilities for oligothiophene-based monolayer OFETs [1]. We discuss correlation between the OFET performance and the oligomers molecular structure. We conclude that large-area solution-processed monolayer single crystals can be a promising platform for ultrathin organic electronic field-effect devices.

1. Smits E.C.P., et al., Nature, 2008, v.455 p.956.

10365-4, Session 1

Robust design and fabrication of three-dimensional printed dual-gate organic circuits on a flexible plastic film

Jimin Kwon, Pohang Univ. of Science and Technology (Korea, Republic of); Yasunori Takeda, Rei Shiwaku, Shizuo Tokito, Yamagata Univ. (Japan); Sungjune Jung, Pohang Univ. of Science and Technology (Korea, Republic of)

The direct printing of organic thin-film transistors (TFTs) gives us a facile and fast route to fabrication of freeform electronic applications on a flexible substrate. However, despite the significant improvement in the performances of organic semiconductors, electronics industry still has not adopted the printed organic TFTs for manufacturing electronic applications. The low resolution, large feature size and variation of inkjet printing have limited the implementation of organic integrated circuits with reasonable transistor densities and uniformity. To overcome these problems, we have developed a robust inkjet design rule optimized for high-yield circuit patterning, and fabricate a three-dimensional (3D) printed dual-gate (DG) organic TFT where n- and p-type TFTs are stacked in transistor-on-transistor manner halving the transistor foot print. In this work, all the functional layers including electrodes and semiconductors are fully printed except a parylene dielectric that is formed by chemical vapor deposition. The design rule has been developed via a systematic study on the influence of inkjet printing parameters such as substrate temperature, drop spacing) on the minimum width, smoothness, and reproducibility of vertically or horizontally printed metal lines. The stacked DG TFTs showed average carrier mobilities of around 0.2 and 0.7 cm?/(V·s) for the n-type and p-type, respectively, showing exceptional uniformity and long-term stability at 5 V operation voltage. We successfully demonstrated 7-stage ring-oscillator on a flexible PEN film with the maximum frequency of 200 Hz and a gate delay of 340 ?s. Our 3D printing approach provides a path for achieving high transistor density, high yield, high uniformity, and long-term stability, which are critical for the realization of printed organic electronics applications.

10365-5, Session 1

High-density polyethylene, an inert additive stabilizing organic field-effect transistors *(Invited Paper)*

Natalie Stingelin, Georgia Institute of Technology (United States)

Polymer blends and in general multicomponent systems represent an interesting platform for organic electronics. Semiconducting:insulating polymer blends can, for instance, be useful to address specific mechanical requirements in addition to fulfilling the required electronic performance. Here we will focus on how addition of an 'inert' additive polymer can increase the stability of thin-film transistors subjected to bias-stress. It also allows to minimise high and parasitic off-currents. Stabilization of n-type operation for usually p-type materials will be demonstrated. We will discuss the interplay within structure, property and processing providing guidelines on how to further develop blend systems and electronic devices in the area of organic electronics. Future challenges and opportunities will be addressed.

10365-6, Session 2

All-printed organic transistors: integrating devices for flexible circuits *(Invited Paper)*

Mahsa Sadeghi, Lilian Cardoso, Ana Claudia Arias, Univ. of California, Berkeley (United States)

Over the past several decades, conventional electronic circuits have been used for both analytical and digital logic circuits. Printed electronics has the potential to reduce fabrication complexity of electronic circuits and using lower-cost and large area manufacturing techniques. The performance of film transistors (OTFTS) has also improved and these devices could be applied to circuit applications where the high performance, high speed, and high energy consumption offered by conventional electronics is not needed. Amongst many factors that govern circuit design, the scale factor (W/L) serves as a crucial variable for tuning a circuit performance. Here we present printing techniques developed in order to adjust aspect ratios of printed transistors using solution processed electronic materials on to flexible substrates. By combining high-speed doctor blade and surface energy patterning we can demonstrate arrays of OTFTs that are later integrated to form circuits. In the surface energy patterning process, a hydrophobic self-assembled monolayer is deposited on a plastic substrate, and plasma etching is used to create hydrophilic regions. The desirable ink is deposited on the hydrophilic regions using doctor blading and only hydrophilic regions are patterned with the ink. Device aspect ratios are increased and controlled by patterning intermitted SD electrodes and controlling the size of the semiconductor island. We utilize screen printing method to interconnect devices to demonstrate several circuit designs such as enhancement-load Inverter, NAND and NOR on the same printing batch. We will discuss how machine learning is used to train this circuits and applied to sensing applications.

10365-7, Session 2

Printed organic short wavelength infrared photo-transistors

Moran Amit, Hyunwoong Kim, Zhenghui Wu, Univ. of California, San Diego (United States); Jason D. Azoulay, The Univ. of Southern Mississippi (United States); Tse Nga Ng, Univ. of California, San Diego (United States)

Low-cost infrared photo-transistors with improved detectivity (i.e. higher signal-to-noise ratio) could find further use in spectral analysis, which is important for chemical identifications, as well as other applications from environmental monitoring to optical communications. Accordingly, the main goal of this research is to advance printed, flexible photo-transistors by using a family of novel donor-acceptor polymers with narrow bandgap that are responsive in the short wavelength infrared (SWIR) region. In particular, the transistors show optical response extending out to a wavelength of 1.8 micrometer. The external quantum efficiency and the rectification ratio are used to characterize the performance of devices with different polymer layer thickness, in order to optimize detectivity. The individual transistors could further be exploited for the fabrication of integrated arrays for bio-medical and/ or robotic applications. It paves the way to large-area, conformal designs that are currently not achievable with conventional inorganic SWIR materials.

10365-8, Session 2

Organic thin-film transistor fabrication using a laser printer

Peter J. Diemer, Angela F. Harper, Wake Forest Univ. (United States); Muhammad Rizwan Khan Niazi, King Abdullah Univ. of Science and Technology (Saudi Arabia); John E. Anthony, Univ. of Kentucky (United States); Aram Amassian, King Abdullah Univ. of Science and Technology (Saudi Arabia); Oana D. Jurchescu, Wake Forest Univ. (United States)

Organic electronic materials are desirable due to facile and low-cost manufacturing through solution deposition. However, the inherit difficulties of reproducibility and solvent compatibility, as well as the hazards associated with the solvents, have stifled the progress of realizing practical solution-deposition methods. As a result, organic thin-films used in industry are typically produced by thermal evaporation techniques, which largely negate the benefits due to the higher cost and complexity of vacuum and evaporation equipment. Here we report the use of a conventional office laser printer to electrophotographically deposit the organic semiconductor layer in thin-film transistors. We have successfully used this solvent-free, low-cost method to produce the first laser-printed organic semiconductor layer in thin-film transistors. We printed on flexible and transparent polyethylene terephthalate (PET) substrates. We used the highly hydrophobic fluoropolymer Cytop as the dielectric in a bottom-gate, bottom-contact configuration, a feat that is not possible with traditional solution-deposition. The organic semiconductor layer consisted of a toner powder based on triisopropylsilylethynyl pentacene (TIPS Pn). Grazing incidence wide-angle X-ray scattering (GIWAXS) images indicated both edge- and face-on orientations of the semiconductor for these devices while electrical measurements revealed field-effect mobilities up to 10-3 cm2V-1s-1 and on/off current ratio of 103.

Our method has the combined advantages of low temperature and ambient pressure deposition while eliminating the drawbacks of solvents or the high cost of evaporation equipment. Further, as a digital printing method, the laser-printed layer is easily patternable as designed by any convenient graphics software. Since the powder is transferred in a dry state, surface dewetting is no longer an issue, which opens the door to even more substrate/dielectric materials that would otherwise reject solutions from adhering.

10365-9, Session 2

Inkjet-printed intrinsically stretchable conductors and interconnects

Ulrike Kraft, Francisco Molina-Lopez, Chenxin Zhu, Yue Wang, Zhenan Bao, Boris Murmann, Stanford Univ. (United States)

Future electronics will be wearable and in close contact to the skin. However, to accommodate for deformations such as twisting and stretching, these next-generation electronics need to be stretchable. One viable approach towards stretchable electronics is the development of intrinsically stretchable electronic materials, devices and circuits. Recently, the first

intrinsically stretchable transistors have been demonstrated. However, for the realization of stretchable circuits, stretchable interconnects that connect the circuit components, such as transistors or capacitors, are very important. Therefore, intrinsically stretchable, conductive films based on doped PEDOT:PSS are also being investigated (Y. Wang, Z. Bao et al., Science Advances, accepted). Ionic additives act as dopants and plasticisers in this approach.

For the deployment of highly stretchable materials as interconnects and electrodes, patterning is crucial. Therefore, we developed a process for inkjet printing of intrinsically stretchable PEDOT:PSS-based interconnects and conductors and also via holes. A customized ink was printed on stretchable polymeric substrates (SEBS, styrene-ethylene-butadiene-styrene) and optimized to achieve a smooth morphology of the printed features by adjusting the surface tension and suppressing the coffee stain effect. The printed interconnects have a conductivity of 700 S/cm, sustain strains above 100% and show good stability in 1000-cycle stretching experiments. Besides the morphology, the electrical properties and the stretchability, we also investigated the bias-stress stability, the long-term stability in ambient air and the cycling stability.

With these findings, we will be able to connect individual transistors and build intrinsically stretchable circuits, such as health monitoring devices that can be directly attached to the skin.

10365-10, Session 2

Organic vapor-jet printing with reduced heat transfer for low-cost flexible organic electronics

Sungyeon Kim, Jung-Min Choi, Hanul Moon, Hyukyun Kwon, Jaehyeok Park, Seunghyup Yoo, KAIST (Korea, Republic of)

Organic vapor-jet printing (OVJP) is a promising organic thin-film deposition method that combines the advantages of mask-free, on-demand printing technologies and field-proven vacuum thermal evaporation techniques for small molecules [1]. However, its applications have been limited mostly to rigid substrates due to the excessive heat transfer from the heated nozzle head to the substrate. Hence, this study aims at reducing the radiative heat transfer to the underlying medium and thus broadening the use of OVJP even to temperature-sensitive cases. In particular, we focus on high-resolution flexible device fabrication, in which a small substrate-to-nozzle gap is necessary. To this end, we apply a low-emissivity coating on the nozzle via electrochemical deposition. It turns out that the proposed method can exert a significant effect on mitigating the deformation of plastic films, while maintaining temperature conditions and the substrate-to-nozzle distance. Using the proposed nozzle, we have succeeded in fabricating devices on plastic substrates. As an example, we demonstrate a fabrication of flexible active-matrix sensor arrays and flexible signage-type organic light-emitting diodes (OLEDs) on polyethylene terephthalate (PET) substrates. Both devices showed performances comparable to devices fabricated with vacuum thermal evaporation. We believe the results shown in the present study indicate that OVJP can be used also in devices or systems involving flexible substrates or heat-sensitive elements, providing one with an opportunity to unlock its full potential as a reliable additive fabrication technology for low-cost flexible electronics.

Reference:

[1] Shtein, M., Peumans, P., Benziger, J.?B., Forrest, S.?R. (2004), Adv. Mater., 16: 1615–1620.

10365-37, Session PMon

A lattice-strained organic single-crystal nanowire array fabricated via solution-phase nanograting-assisted pattern transfer for use in high-mobility organic field-effect transistors

Kyunghun Kim, Yebyeol Kim, Pohang Univ. of Science and Technology (Korea, Republic of); Se Hyun Kim, Yeungnam Univ. (Korea, Republic of); Chan Eon Park, Pohang Univ. of Science and Technology (Korea, Republic of)

Crystal orientation and polymorphism of organic semiconductors (OSCs) are crucial factors in determining the electrical performance of organic field-effect transistors (OFETs). Herein, uniaxially-aligned and lattice-strained organic single crystal nanowire (NW) array is fabricated via a straightforward solution processing technique called as ‘nanograting-assisted pattern transfer’. 50 nm-wide 6,13-bis(triisopropylsilylethyn yl) pentacene (TIPS-PEN) NWs are grown while the solution is confined between a substrate and a flexible nanograted template. From UV-vis absorption and grazing incidence wide angle X-ray scattering experiments, NWs are found to be single crystalline and adopt an anisotropic crystal orientation for efficient charge transport. Notably, the crystal growth under nano-confined spaces results in lattice-strained packing motif of NWs with close ϖ-ϖ stacking distance. TIPS-PEN NW OFETs yield extremely high field-effect mobilities (?FETs) up to 9.71 cm2/(V?s) with narrow ?FET distribution. In addition, the nanograting-assisted pattern transfer technique is applied on flexible substrates, demonstrating high-performance flexible OFETs. From these findings, it is expected that the nanograting-assisted pattern transfer technique provides a general method for realization of high ?FET OFETs, and also a facile soft lithographic method for nanoscale patterning of well-grown crystallites.

10365-38, Session PMon

Understanding doped organic field-effect transistors

Shiyi Liu, Akram Al-Shadeedi, Vikash Kaphle, Changmin Keum, Björn Lüssem, Kent State Univ. (United States)

Organic field-effect transistors (OFETs) have the potential to become the basic building block of a flexible electronics technology used e.g. in displays with novel form factors or low-cost or wearable sensors systems. Doping these transistors can make them not only more reliable and reproducible [Applied Physics Letters 104, 013507 (2014)], but opens new ways to tune their characteristics or even realize novel transistor concepts [Nature communications 4, 2275 (2013)].

To realize the full advantages of doping, a detailed understanding of the influence of doping on the flatband voltage, the pinch-off voltage, and the threshold voltage of the OFET has to be developed. In this presentation, pentacene-based organic field effect transistors (OFETs) and metal insulator semiconductor (MIS) junctions are studied by current-voltage (I-V) and capacitance-voltage (C-V) measurements. Based on the experimental results, a new analytical model of doped OFETs is presented that describes the influence of a shift in the flatband voltage due to doping on the pinch-off voltage and saturation in OFETs quantitatively.

Meanwhile, it is shown that OFETs become much less sensitive to gate bias stress by inserting a doped layer in the channel region of OFETs. By a series of carefully designed transistors, it is shown that this increase in stability originates from a change at the organic semiconductor/gate insulator interface.

Overall, the presented results provide for a detailed understanding of doping related effects on OFET behavior. It opens new approaches to optimize OFETs or even develop new organic transistor concepts.

10365-39, Session PMon

Enhanced performance in n-type organic field-effect transistors using non-conjugated polyelectrolytes

Yu Jung Park, Dong-A Univ. (Korea, Republic of)

To enhance electron injection in n-type organic field-effect transistors (OFETs), a non-conjugated polyelectrolyte (NPEs) layer was interposed between a [6,6]-phenyl-C61-butyric acid methyl ester (PCBM) layer and Au electrodes. Novel NPEs with various counterions (Cl-, Br-, I-) improved the electron mobilities up to ~10-2 cm2V-1s-1 and on-off ratios (Ion/Ioff) of 105. Ultraviolet photoemission spectroscopy (UPS) indicates that reduced electron injection barrier at NPE/metal interface was induced by dipole formation and led the improved electron injection and transport. These findings are important for understanding how NPEs function in devices, improve the device performance, and design of new materials for use in optoelectronic devices.

10365-41, Session PMon

Submicron-channel-length n-channel organic thin-film transistors fabricated by stencil-mask lithography

Ute Zschieschang, James W. Borchert, Max-Planck-Institut für Festkörperforschung (Germany); Florian Letzkus, Joachim N. Burghartz, Institut für Mikroelektronik Stuttgart (Germany); Hagen Klauk, Max-Planck-Institut für Festkörperforschung (Germany)

Using high-resolution stencil-mask lithography, we have fabricated bottom-gate, top-contact (inverted staggered) n-channel organic thin-film transistors that have a channel length of 0.3 μm, gate-to-source and gate-to-drain overlaps of 20 μm and channel widths ranging from 5 to 100 μm. As the semiconductor we used the commercially available small-molecule material Polyera ActivInkTM N1100 (bis(heptafluorobutyl)-dicyano-perylene tetracarboxylic diimide). The gate dielectric is a combination of oxygen-plasma-grown aluminum oxide and a fluoroalkylphosphonic acid self-assembled monolayer with a total thickness of 5.7 nm. Owing to the small channel length, the transistors have a large channel-width-normalized transconductance of 0.09 S/m, despite the relatively small electron mobility of 0.03 cm2/Vs. The transistors also have an on/off current ratio of 5?107 and a subthreshold slope of 160 mV/decade, which are to our knowledge the largest on/off ratio and the steepest subthreshold slope reported to date for submicron-channel-length n-channel organic transistors.

10365-42, Session PMon

Optimization of a hydroxyl-containing polymer mixture as gate dielectric for low-temperature, solution-processed organic thin-film transistors and logic circuits on a flexible substrate

Hyunjin Park, Jimin Kwon, Sungjune Jung, Pohang Univ. of Science and Technology (Korea, Republic of)

A polymer gate dielectric is one of the key elements of high-performance solution-processed organic thin-film transistors (OTFTs) for low-cost, large-area, flexible electronic applications. For decades, a hydroxyl-containing mixture of poly(4-vinylphenol) (PVP) and poly(melamine-co-formaldehyde) (PMF) has been widely used as gate dielectric in OTFTs due to its low gate leakage current, high dielectric constant, and good chemical compatibility. However, the polymer mixture has been compatible only with suitably engineered expensive plastic substrates due to its high curing temperature for crosslinking (typically higher than 175 °C) to remove hydroxyl groups that might cause hysteretic device characteristics. In this work, we report OTFTs with negligible hysteresis, low gate leakage current, and high on/off drain current ratio, even though the dielectric film was cured at 100 °C. We investigated the influence of various PVP:PMF mixture conditions such as weight ratio (0.2:1 to 5:1) and curing temperature (100 to 200 °C) on the performances of 6,13-bis(triisopropylsilylethynyl) OTFTs. We found that the OTFT using a PVP:PMF mixture with the weight ratio of 0.5:1 cured at 100 °C showed the best device performance for hysteresis, gate leakage current, and on/off drain current ratio. Fourier transform infrared spectroscopy results provided the evidence that device performances were influenced by PVP:PMF mixture related to non-hydrogen-bonded hydroxyl groups which might evoke water absorption.. Finally, we demonstrated OTFTs and diode-connected inverters on a 3-?m-thick flexible parylene film. This work shows that PVP:PMF mixture is a suitable dielectric material to fabricate flexible electronic devices and circuits on inexpensive plastic substrates.

10365-43, Session PMon

Thermal annealing effect on the stability of C60 thin-film transistor with a lithium fluoride protective layer

Bo Yao, Yan Li, Zebo Fang, Shaoxing Univ. (China)

Organic thin-film transistors (OTFTs), compared to the traditional inorganic transistors, demonstrate attractive advantages of light-weight, low cost and flexibility, and are the best candidates for large-scale flexible display, sensors and organic integrated circuit. A high-performance complementary logic circuit requires p-type and n-type transistors with high and balanced hole and electron mobilities. However, stable n-type organic semiconductors are rare and the current level of electron mobility of n-type organic semiconductors remains much lower than that of p-type organic semiconductors. At present, the field-effect mobility of single crystal C60 TFTs has reached 6 cm2/Vs, which has already exceeded than that of amorphous silicon TFTs. However, the air stability of C60 based n-type TFTs needs to be improved for possible industrial applications. In this paper, bottom-gate top-contact C60 TFTs with a lithium fluoride (LiF) protective layer was investigated. It is shown that the performances of C60 TFT with a LiF protective layer has been improved by vacuum annealing at 120 ? during various long-time annealing treatments. With the increase of annealing time, the saturated drain current and the on/off current ratio of the devices are significantly increased, the output characteristics are more stable. This shows that n-type OTFTs' stable performance can be enhanced by encapsulated a LiF protection layer with an appropriate annealing treatment.

10365-11, Session 3

Exploring disorder and polymorphism in small-molecule organic semiconductors *(Invited Paper)*

John E. Anthony, Univ. of Kentucky (United States)

Along with the precise orientation of crystals in the solid state determined from the crystal structure, the electronic performance of small molecule organic semiconductors is also influenced by a variety of disorder parameters common to soft materials. In chromophores of reduced symmetry, variations in orientations of the chromophore can yield subtle changes in intermolecular interactions that impact both crystal packing and the quality of films grown from such materials. Using weakly interacting supramolecular synthons, we can tune chromophores to enhance or diminish these subtle forms of disorder, to explore their impact both on calculated electronic coupling and on the transport properties observed in organic field-effect transistors. More recently, we have shown how certain vibrational modes can be highly detrimental to transport properties in materials functionalized across the short axis of a high-aspect-ratio chromophore. I will present our recent approaches to mitigate these vibrations, to determine whether short-axis functionalization strategies can yield processable ultra-high-mobility organic semiconductors.

10365-12, Session 3

Electronic and morphological traps in conjugated polymers *(Invited Paper)*

Alberto Salleo, Stanford Univ. (United States)

Efficient charge transport is needed in all electronic devices. For instance, the fill factor of solar cells is lowered when charge extraction is not efficient. In transistors, carrier mobility is directly linked to the transit time across the channel and therefore to switching speed. Carrier mobility is adversely affected by electronic traps, which are regions where charge delocalization is suppressed. By combining sensitive spectroscopy in the IR with theory, we can infer the degree of delocalization of the polarons and relate it to microstructural features. The delocalization of the polaron depends on charge density, as fixed by the gate voltage in a transistor architecture. A second type of trap, which is purely morphological, is unique to macromolecules. The polymer conformation dictated by the rigidity of the chain, induces kinks. When these kinks push charges against the direction of the field, a morphological trap is created. I will show how these traps affect charge transport. The effect of field and molecular weight will be described in more detail.

10365-13, Session 3

Highly reproducible single-crystalline organic thin-film transistors by minimizing morphological defects in crystalline templating layers

Robby Janneck, IMEC (Belgium) and KU Leuven (Belgium); Nicolas Pilet, Paul Scherrer Institut (Switzerland); Satya P. Bommanaboyena, IMEC (Belgium); Benjamin Watts, Paul Scherrer Institut (Switzerland); Paul Heremans, Jan Genoe, IMEC (Belgium) and KU Leuven (Belgium); Cedric Rolin, IMEC (Belgium)

Organic thin films transistors based on single-crystalline thin films offer great potential for the realization of high-performance, low-cost large area electronics. The fabrication of these films directly on the substrate with limited morphological defects pose one of the biggest challenge for their commercial application. Even though tremendous progress has been made in optimizing fabrication techniques, the resulting layers nevertheless typically show defects such as cracks, voids or ribbon-like growth. Here we employ a two-step fabrication method that yields single-crystalline layers with negligible morphological defects. We use a commonly used solution coating technique to fabricate a crystalline layer showing the typical ribbon-like growth. This layer acts as a templating layer for the subsequent deposition step, which repairs most of the morphological defects. In our case this results in a mobility increased by a factor of three and a relative spread in device characteristics improved by almost half an order of magnitude. In particular, for the case of C8-BTBT, we reproducibly achieved average thin film mobilities of 10cm2/Vs with device-to device parameter spreads of only 10%. This double step method is easily adoptable to different coating techniques and small molecules, enabling a route towards the fabrication of highly reproducible, high-performance large area electronics.

10365-14, Session 3

1D versus 2D growth of TIPS-pentacene in TIPS-pentacene/insulating polymer blends

Wi Hyoung Lee, Konkuk Univ. (Korea, Republic of)

Organic semiconductor/insulator polymer blends have been widely used in the manufacturing process of field-effect transistors (FETs) to overcome the disadvantages of FETs based on organic semiconductor. In this study, phase-separation characteristics and structural developments of 6,13-bis(triisopropylsilylethynyl)-pentacene (TIPS-pentacene)/insulating polymers were examined to enhance electrical properties of their blends for uses in active layers of FETs. Especially, phase-separation characteristics of TIPS-pentacene/insulating polymer blends were greatly affected by the processing condition such as spin coating time. Although TIPS-pentacene-top/insulating polymer-bottom vertically phase separated structures were formed onto the substrate regardless of spin-time, spin coating time governed growth mode of phase-separated TIPS-pentacene onto phase-separated insulating polymer. Excess residual solvent in short spin-coating time induces convective flow in a drying droplet, thereby resulted in one-dimensional (1D) growth of TIPS-pentacene crystals. On the other hand, optimum residual solvent in moderate spin coating time led to two-dimensional (2D) growth of TIPS-pentacene crystals. These 2D spherulites onto insulating polymer was quite advantageous for increasing field-effect mobility of FETs because of higher perfectness and coverage of TIPS-pentacene crystals compared to those of 1D crystals. In addition, when TIPS-pentacene was blended with various types of insulating polymers, critical spin-coating time was changed due to the different surface energy of the insulating polymers. Insulating polymer with lower surface energy was advantageous for increasing film formation time, thereby increasing time for phase-separation and crystallization.

10365-15, Session 3

Transport pathways in organic semiconducting polymers *(Invited Paper)*

Michael L. Chabinyc, Univ. of California, Santa Barbara (United States)

Thin film transistors with semiconducting polymers can exhibit high hole and electron carrier mobilities. There is a clear connection between microstructure and carrier mobility because of the need for carriers to move along and between single polymer chains. While local order is readily observed by methods such as wide angle X-ray scattering, significantly less is known about the detailed structure on longer length scales (100s nm) in thin films. We have studied the structural order in well-performing p-type semiconducting polymers using high resolution transmission electron microscopy (HR-TEM) to reveal how regions of ordered chains are connected. In a series of N-alkylthieno[3,4-c]pyrrole-4,6-dione (TPD)-based polymers, examination of the structure of nanoscale domains reveals multiple polymorphic structures, rather than typically assumed paracrystalline domains. The structure of the crossings of ordered domains observed in HR-TEM also suggests a rationale for changes, or lack thereof, in texture of the conjugated backbone upon thermal annealing in these systems. We will discuss a new computational framework that improves the analysis of HR-TEM images of soft materials and provides statistically robust information about percolation pathways for charge transport.

10365-16, Session 4

Multi-component organic blend semiconductors for transistor applications *(Invited Paper)*

Thomas D. Anthopoulos, King Abdullah Univ. of Science and Technology (United Kingdom)

The increasing demand for thin-film transistors (TFTs) technologies with improved carrier mobility and operating stability has been the driving force behind the tremendous progressed witnessed in recent years in the field of organic TFTs (OTFTs). A common approach towards this goal has been the development of new compounds with improved electronic and processing characteristics. In this presentation I will discuss an alternative strategy to materials, and ultimately OTFT and integrated circuits, development based on the use of molecular additives in combination with semiconducting blends. I will describe how the incorporation of different types of additives can lead to semiconducting systems and OTFTs that combine highly attractive features such as solution processability, high carrier mobility and enhanced bias stability. The role of the molecular additives and the

underlying mechanism responsible for the performance enhancement observed in several different blend systems will also be discussed.

10365-17, Session 4

Polarization-induced transport in organic field-effect transistors: the role of ferroelectric dielectrics *(Invited Paper)*

Suchi Guha, Amrit Laudari, Univ. of Missouri (United States)

The tuning of the dielectric constant in polymer-ferroelectric dielectrics with temperature offers a platform for monitoring changes in interfacial transport with the polarization strength in organic field-effect transistors (FETs). The charge transport mechanism in an organic semiconductor often occurs at the interface of bandlike coherent motion and incoherent hopping through localized states. By choosing two small molecule semiconductors, pentacene and 6,13 bis(triisopropylsilylethynyl)pentacene (TIPS-pentacene), which have distinct differences in their bulk transport properties, we show that ferroelectric dielectrics such as poly(vinylidene fluoride-co-trifluoroethylene) (PVDF-TrFE) allow an observation of bandlike transport with a negative temperature coefficient of the mobility in FETs, when the semiconductor shows discrete-trap space-charge-limited conduction. Pentacene-based FETs show a weak temperature dependence of the charge carrier mobility in the ferroelectric phase of PVDF-TrFE, which is attributed to polarization fluctuation driven transport resulting from a coupling of the charge carriers to the surface phonons of the dielectric layer [1]. By comparing single layer PVDF-TrFE pentacene FETs with stacked PVDF-TrFE/inorganic dielectric FETs, the contribution from Froehlich polarons is extracted. TIPS-pentacene based FETs using PVDF-TrFE show bandlike transport beyond 200 K. The polarization fluctuation dominant transport inherent to a ferroelectric dielectric, in conjunction with the nature of traps, results in an effective de-trapping of the shallow-trap states into more mobile states in TIPS-pentacene [2].

This work is supported through the National Science Foundation Grant No. ECCS- 1305642.

[1] A. Laudari and S. Guha, J. Appl. Phys. 117, 105501 (2015).

[2] A. Laudari and S. Guha, Phys. Rev. Applied 6, 044007 (2016).

10365-19, Session 4

Significance of the double-layer capacitor effect in solution-processable polymeric dielectrics and exceptionally stable low-voltage organic transistors

Raphael Pfattner, Amir Foudeh, Celine Liong, Chao Wang, Wen-Ya Lee, Desheng Kong, Zhenan Bao, Stanford Univ. (United States)

High-performance FETs based on organic active materials are of particular interest due to their compatibility with low-cost, high-throughput processing and mechanical compliance with soft tissues. Due to the relatively low charge carrier mobilities of organic materials, often high operational voltages have to be applied and result in severe limitations. To overcome these issues high gate capacitance materials are needed. One appealing approach is the fabrication of ultra-thin dielectric layers, which, however, are technologically very challenging to make and suffer often from high leakage problems.

Here, we discovered that a polar fluorinated PVDF-HFP dielectric, despite of a low ion concentration, is able to induce an electric double-layer charging effect under an applied gate voltage. This polymer dielectric is solution-processable with a high static capacitance of about 0.3 ?F/cm2, even at a thickness of several micrometers. Furthermore it is highly compatible with solution processing of various organic semiconductors. Remarkably, the resulting devices showed both high current output and low bias stress in both ambient and aqueous conditions making it the ideal candidate for low-voltage and stable device operation.[1,2] Furthermore, based on this novel dielectric material, some proof of concept BioSensor devices with the capability of working in complex physiological liquids have been developed.

References

[1] C. Wang, R. Pfattner, et al. Scientific Reports, 5, 17849, 2015.

[2] D. Kong, R. Pfattner, et al. Advanced Functional Materials, 26, 4680–4686, 2016.

10365-20, Session 5

Developing theory-driven approaches to design organic semiconducting materials *(Invited Paper)*

Chad Risko, Univ. of Kentucky (United States)

Semiconducting materials derived from organic, ϖ-conjugated molecules or polymers have drawn the attention of materials chemists for decades because of the potential to modulate material (opto)electronic properties through well-established synthetic chemistry methods. Unfortunately, materials design remains highly Edisonian, due to limited knowledge among the intimate relationships that connect chemical composition and molecular architecture, material processing, and the solid-state packing arrangements that define the underlying physicochemical processes that determine material performance. We seek to address these connections through the development and application of multiscale, theoretical materials chemistry approaches that build upon principles from organic and physical chemistry, condensed matter physics, and materials science. In this presentation, we will focus on how these models can reveal the striking influence of seemingly modest changes in chemical structure on the solid-state packing of organic semiconducting active layers and resulting characteristics of importance to charge-carrier transport. The chemical insight developed through these investigations is beginning to refine and offer novel design paradigms essential to the development of next generation organic semiconducting active layers, and is opening new pathways for in silico materials development.

10365-21, Session 5

Indolo-naphthyridine-6,13-dione thiophene building block for conjugated polymer electronics: Molecular origin of ultrahigh n-type mobility *(Invited Paper)*

Kealan Fallon, Univ. College London (United Kingdom); Nilushi Wijeyasinghe, Imperial College London (United Kingdom); Eric Manley, Tobin Marks, Northwestern Univ. (United States); Thomas D. Anthopoulos, King Abdullah Univ. of Science and Technology (Saudi Arabia); Hugo A. Bronstein, Univ. College London (United Kingdom)

We present the synthesis and characterization of four conjugated polymers containing a novel chromophore for organic electronics based on an indigoid structure. These polymers exhibit extremely small band gaps of ?1.2 eV, impressive crystallinity, and extremely high n-type mobility exceeding 3 cm2 V s–1. The n-type charge carrier mobility can be correlated with the remarkably high crystallinity along the polymer backbone having a correlation length in excess of 20 nm. Theoretical analysis reveals that the novel polymers have highly rigid nonplanar geometries demonstrating that backbone planarity is not a prerequisite for either narrow band gap materials or ultrahigh mobilities. Furthermore, the variation in backbone crystallinity is dependent on the choice of comonomer. We find that electron mobility can be correlated to the degree of order along the conjugated polymer backbone. Finally, we use this novel system to begin to understand the complicated effect of alkyl chain variation on the solid state packing in all 3 dimensions.

10365-22, Session 5

Truxenones on coinage metal surfaces: structure and epitaxial templating

Luke A. Rochford, The Univ. of Birmingham (United Kingdom); Alexandra J. Ramadan, Univ. of Oxford (United Kingdom); Christian Nielsen, Queen Mary, Univ. of London (United Kingdom)

The interface between organic molecules and metallic surfaces is integral to the performance of organic optoelectronic devices. Considerable efforts have been focused on the synthesis and processing of novel donor and acceptor materials for high performance devices. Despite this, there is little understanding of the fundamental behaviour of these molecules at relevant metallic surfaces. The truxenone family of small molecule semiconductors exhibit three-fold symmetry, have stabilised lowest unoccupied molecular orbital (LUMO) energy levels, independently conjugated branches from the core and have been shown to exhibit promising properties as electron acceptors in organic solar cells. Our recent work has demonstrated that Truxenones self-assemble to form epitaxial open-pored structures on Cu (111), a highly unusual observation in semiconducting organic molecules. This assembly is affected by the choice of metal substrate and data from analogous Ag (111) and Au (111) interfaces will be compared and contrasted. In addition the use of a commensurate epitaxial truxenone template to direct the growth of commensurate epitaxial C60 layers will be shown. This strategy imparts the structural symmetry and in-plane structural order of the substrate into the molecular template and subsequent C60 layers and has implications for the growth of single-crystalline organic interfaces and devices.

10365-23, Session 5

Organosilicon derivatives of BTBT for monolayer organic field effect transistors

Sergey A. Ponomarenko, Institute of Synthetic Polymeric Materials (Russian Federation) and M.V. Lomonosov Moscow State Univ. (Russian Federation); Oleg V. Borshchev, Elena V. Agina, Marina S. Polinskaya, Alexey S. Sizov, Askold A. Trul, Institute of Synthetic Polymeric Materials (Russian Federation); Viktoria P. Chekusova, Bauman Moscow State Technical Univ. (Russian Federation) and Institute of Synthetic Polymeric Materials (Russian Federation); Maxim A. Shcherbina, Institute of Synthetic Polymeric Materials (Russian Federation) and Russian Research Ctr. Kurchatov Institute (Russian Federation); Sergei N. Chvalun, Russian Research Ctr. Kurchatov Institute (Russian Federation) and Institute of Synthetic Polymeric Materials (Russian Federation)

Development of efficient self-assembled monolayer field-effect transistors (SAMFETs) is a great challenge for organic electronics. Recently we reported organosilicon derivatives of oligothiophenes capable to monolayer formation on the water-air interface, which were used for fast and efficient SAMFETs fabrication by Langmuir-Blodgett (LB) and Langmuir-Schaefer (LS) techniques [A.S. Sizov, et al., Langmuir, 2014, 30, 15327; E.V. Agina, et al., Proc. SPIE, 2015, 9568, 95680Z]. In this work we synthesised novel organosilicon derivatives of mono- and dialkyl substituted [1] benzothieno[3,2-b][1]-benzothiophene (BTBT) containing flexible aliphatic spacers linked to chlorosilane or disiloxane anchor groups [O.V. Borshchev, et al., Chem. Commun., 2017, 53, 885]. They were successfully used for LB and LS SAMFETs preparation, which showed the charge carrier mobilities up to 0.02 cm2/Vs, threshold voltage close to 0 V and On/Off ratio up to 10,000. The results obtained confirmed that the presence of covalent bonds between a semiconducting monolayer and a substrate is not crucial for the monolayer OFETs performance. In this report, influence of the chemical structure of the molecules synthesized (type of the anchor group, spacer length, presence or absence of hexyl end-group) on the morphology, molecular 2D ordering in the monolayers and their semiconducting properties will be considered. Different methods of the ultrathin layer preparation, such as LB and LS, as well as spin coating and doctor blade, and their effect on the OFET performance will be compared and discussed.
This work was supported by Russian Foundation for Basic Research (grants 16-29-05321 and 17-03-00222).

10365-24, Session 5

On the importance of alkyl chains in organic semiconductors *(Invited Paper)*

Bob C. Schroeder, Queen Mary, Univ. of London (United Kingdom)

Organic semiconductors are an intriguing class of materials because of their facile processability and good charge carrier properties. In order to employ conventional large scale printing techniques such as roll-to-roll or inkjet printing, it is important to understand how the viscosity of conjugated polymer solutions can be tweaked in order to be suitable for a wide variety of printing techniques. In many organic semiconductors the processability and the electronic properties are intimately intertwined, making it difficult to change one without negatively affecting the other. Decorating high performing conjugated polymers with long alkyl side chains is one of the most popular approaches to enhance the material's processability, however often at the expense of lower charge carrier mobilities. Gaining a fundamental understanding on how alkyl side chains affect transport characteristics is a key requirement to develop more processable and ye high performing semiconducting polymers suitable for industrial printing techniques.

In this talk, we will present a series of alternative approaches to incorporate electrically insolating alkyl side chains into semiconducting polymers, whilst maintaining excellent charge carrier mobilities. Our findings highlight that a better understanding of side chain geometry and architecture, cannot only lead to significantly enhanced material properties, but also allows to control the molecular packing and orientation down to the nanoscale.

10365-25, Session 6

Fast unipolar and complementary circuits based on organic thin-film transistors on flexible substrates *(Invited Paper)*

Hagen Klauk, Max-Planck-Institut für Festkörperforschung (Germany)

Organic thin-film transistors (TFTs) can typically be fabricated at temperatures below 150 °C and thus not only on glass, but also on unconventional substrates, such as plastics and paper. This makes organic TFTs potentially useful for flexible, large-area electronics applications, such as rollable or foldable displays and conformable sensor arrays. In some of the more advanced applications envisioned for organic TFTs, the TFTs have to control electrical signals of a few volts at frequencies of several megahertz. The first requirement for achieving high switching frequencies is efficient charge transport in the semiconductor. This requirement can be met by choosing organic semiconductors that provide good molecular ordering and large carrier mobilities, even when processed at low temperatures. Examples are the thienoacene DNTT and its alkylated or phenylated derivatives for p-channel TFTs and the core-cyanated perylene diimide derivative Polyera ActivInk N1100 for n-channel TFTs. The second requirement is a small channel length. To meet this requirement, we have developed a process in which the TFTs are patterned using high-resolution silicon stencil masks. With this process, bottom-gate, top-contact organic TFTs with a channel length of about 1 μm can be fabricated on plastic substrates. For 11-stage complementary and unipolar ring oscillators based on TFTs with a channel length of 1 μm, signal propagation delays per stage as short as 6.6 μs and 420 ns have been measured at a supply voltage of 3 V.

10365-26, Session 6

Understanding and improving the operational stability of polymer field-effect transistors *(Invited Paper)*

Thuc-Quyen Nguyen, Univ. of California, Santa Barbara (United States)

Polymer field effect transistors (PFETs) have potential applications in large-area flexible displays, sensors, radiofrequency identification tags, and logic circuits with low-cost processability. However, they are still inadequate for commercialization and practical implementation due to their operational instability. We investigated the mechanism of the electrical instability of high performing PFETs that show a certain degree of ambipolarity and unraveled the effect of electron conduction on the stability of hole current and the double-slope behavior. The model polymer used in this study is regioregular D-A copolymer poly[4-(4,4-dihexadecyl-4H-cyclopenta[1,2-b:5,4-b']dithiophen-2-yl)-alt-[1,2,5]thiadiazolo[3,4-c]pyridine] (PCDTPT). While performing current-voltage measurement, we found that consecutive sweeping of gate voltage changed the shape of the transfer curves. We conducted a thorough study of bias-stress of the system and found that electron trapping at the gate dielectric/polymer interface greatly alters the device characteristics including the occurrence of the double-slope. We provide several solutions to improve the device operational stability.

10365-27, Session 6

Understanding the working mechanisms of organic permeable-base transistors

Akram Al-Shadeedi, Changmin Keum, Shiyi Liu, Vikash Kaphle, Kashi Subedi, Björn Lüssem, Kent State Univ. (United States)

Organic Permeable Base Transistors (OPBTs) [J. Phys.: Condens. Matter 27, 443003 (2015)] show excellent performance, which make them a viable option for high-speed flexible electronics. They operate at low voltages (<2V), reach large ON-state currents (>1A/cm2), and can be processed without the need for high-resolution patterning techniques [Appl. Phys. Lett. 101, 213303 (2012); Adv. Mater. 27, 7734 (2015)]. However, despite some progress during the last years [J. Appl. Phys. 120, 094501 (2016)], the precise working mechanism of is still under discussion, in parts due to a lack of systematic experimental data.

In this presentation, we discuss the influence of the device area, thickness of base electrode, and annealing conditions on the OPBT performance. Based on a thorough optimization of the individual diodes the OPBT consists of, the ON/OFF ratio, transconductance, and amplification of the devices is optimized. Best devices reach an ON/OFF ratio of larger than 10^6, a transconductance above 2 S/cm^2, and an amplification of 10^2.

Based on this larger experimental effort, a 2D numerical model is developed that describes the experimental trends correctly. Strategies are presented to improve the performance of OPBTs further. In particular, it is argued that the current gain of the OPBT can be significantly increased without reduction in device performance by a reduction of charge injection at the base electrode. Experimental strategies to reduce base currents are proposed and first experimental data that validates these strategies is presented

10365-28, Session 6

Probing the origins of temperature dependence of charge transport in organic single crystal transistors

Emily G. Bittle, Adam J. Biacchi, Lisa Fredin, Andrew A. Herzing, Thomas Allison, Angela Hight Walker, David J. Gundlach, National Institute of Standards and Technology (United States)

Low temperature transport measurements of classical semiconductors are a well-defined method to determine the physics of transport behavior. These measurements are also used to evaluate organic semiconductors, though physical interpretation is not yet fully developed. The similar energy ranges of the various processes involved in charge transport in organic semiconductors, including excitonic coupling, charge-phonon coupling, and trap distributions, result in ambiguity in the interpretation of temperature dependent electrical measurements. The wide variety of organic semiconductors, ranging from well-ordered small molecule crystals to disordered polymers, manifest varying degrees of "ideal" device behavior and require intensive studies in order to capture the full range of physical mechanisms involved in electronic transport in this class of materials. In addition, the physics at electrical contacts and dielectric material interfaces strongly affect device characteristics and results in temperature dependent behavior that is unrelated to the semiconductor itself. In light of these complications, our group is working toward understanding the origins of temperature dependent transport in single crystal, small molecule organic semiconductors with ordered packing. In order to disentangle competing physical effects on device characterization at low temperature, we use TEM and Raman spectroscopy to track changes in the structure and thermal molecular motion, correlated with density functional theory calculations. We perform electrical characterization, including DC current-voltage, AC impedance, and displacement current measurements, on transistors built with a variety of contact and dielectric materials in order to fully understand the origin of the transport behavior. Results of tetracene on silicon dioxide and Cytop dielectrics will be discussed.

10365-29, Session 7

Interplay between processing and doping of organic semiconductors *(Invited Paper)*

Christian Müller, Chalmers Univ. of Technology (Sweden)

Molecular doping of organic semiconductors is an important tool for the optimization of electronic devices ranging from field-effect transistors to solar cells and thermoelectric generators. In this talk the interplay between processing and the solid-state nanostructure of molecularly-doped conjugated polymers will be discussed, and relevant structure-property relationships will be established. Design criteria that permit to mitigate the often encountered poor compatibility of molecular dopants and organic semiconductors will be introduced. As an example, co-processing of a polythiophene and common molecular dopants will be discussed, resulting in thermally stable films with a high electrical conductivity of 100 S/cm. Finally, the use of insulating matrix polymers will be revisited, which can be used to adjust the rheological and mechanical properties of electrically conducting plastics.

10365-30, Session 7

Thiol-treated palladium and platinum in pentacene bottom contact thin-film transistors *(Invited Paper)*

Marco R. Cavallari, Columbia Univ. (United States) and Univ. de São Paulo (Brazil); Jiho Yoon, Amrita V. Masurkar, Columbia Univ. (United States); Fernando J. Fonseca, Univ. de São Paulo (Brazil); Ioannis Kymissis, Columbia Univ. (United States)

The performance of organic Thin-Film Transistors (TFTs) with bottom contact electrodes is mostly limited by injection energy barrier and semiconductor thin-film lack of crystallinity from electrodes to conducting channel. This is often translated into series resistance effects. Despite its scarcity and cost, thiol-treated gold thin-films are widely-used as source and drain electrodes due to the lack of reliable alternatives. In this work, platinum and palladium noble metals were investigated to replace gold contacts. Furthermore, the effect of a pentafluorobenzothiol (PFBT) monolayer on top of these noble metals in pentacene transistor performance was investigated for the first time. A self-assembled monolayer was formed on both Pt and Pd, demonstrated by atomic force microscopy (AFM), ellipsometry, X-ray photoelectron spectroscopy, contact angle and Kelvin Probe techniques. Even though work function and surface energy varied, differences in pentacene morphology on top of electrode and channel areas persisted even after treatment. In the case of an untreated interface between semiconductor and dielectric, performance of TFTs from alternative metals was comparable to thiol-Au. However, after octadecyltrichlorosilane treatment of SiO2, the presence of a PFBT monolayer could further increase current modulation while achieving a hole mobility beyond amorphous silicon while decreasing series resistance.

10365-31, Session 7

A rational design of polymer semiconductors for high-resolution solution tandem electronics

Han Wool Park, Keun-Yeong Choi, Haejung Hwang, Soongsil Univ. (Korea, Republic of); Boseok Kang, Pohang Univ. of Science and Technology (Korea, Republic of); Kyung Ah Nam, Soongsil Univ. (Korea, Republic of); Yun-Hi Kim, Gyeongsang National Univ. (Korea, Republic of); Kilwon Cho, Pohang Univ. of Science and Technology (Korea, Republic of); Moon Sung Kang, Hojin Lee, Do Hwan Kim, Soongsil Univ. (Korea, Republic of)

Organic electronics has recently attracted a great deal of interest because of its solution-processed potential applications in flexible, wearble and even stretchable devices. Dissolvability of semiconducting organic materials in typical solvents potentially provides these materials with unique opportunities to acheive the electronics with cheaper and simpler manufacturing processes. This opportunity, however, serves as a trade-off when one tries to implement these processes in assembling practical electronic devices, since the as-deposited tandem layers would be defenceless to following solution processes. As a result, this controversial issue remains valid not only while applying advanced printing processes, but also while applying photolithography for semiconducting polymers.

Herein, we describe a whole new type of polymer semiconductors based on sol-gel chemistry, which is capable of remarkably showing chemical and mechanical reliability during sequential photolithography processes. The critical step in a sol-gel reaction is the formation of a highly cross-linked network out of molecular precursors through hydrolysis and condensation reactions. By carefully manipulating this step, we could prepare an orthogonal polymer semiconductor gel thin film with heterogeneous inter-penetrated polymer network (HIPN). The resulting structures yielded films that are highly tolerant against harsh external stimuli. Consequently, formation of high resolution patterns of various semiconductor polymers as well as fabrication of tandem devices and circuits based on multiple semiconducting materials could be readily attained using conventional photolithography processes, and finally fabricate high-resolution CMOS circuits with micron n- and p-type organic channels.

10365-32, Session 7

Self-organized (macro)molecular semiconducting materials for organic electronics and ambipolar charge transport *(Invited Paper)*

Yiming Xiao, Xiaolu Su, Univ. Pierre et Marie Curie (France); Martin Brinkmann, Institut Charles Sadron (France); Benoît Heinrich, Bertrand Donnio, Institut de Physique et Chimie des Matériaux de Strasbourg (France); Ji-Seon Kim, Imperial College London (United Kingdom); Jeong Weon Wu, Ewha Womans Univ. (Korea, Republic of); Jean-Charles Ribierre, EWHA Univ. (Japan); Emmanuelle Lacaze, Institut des NanoSciences de Paris (France); Thierry Barisien, David Kreher, André-Jean Attias, Fabrice Mathevet, Danli Zeng, Univ. Pierre et Marie Curie (France)

The self-organization of ϖ-conjugated organic materials forming highly ordered supramolecular architectures has been extensively investigated in the last two decades in view of optoelectronic applications. Indeed, the control of both the mesoscopic and nanoscale organization within thin semiconducting films is the key issue for the improvement of charge transport properties and achievement of high charge carrier mobilities. These well-ordered materials are currently either self-organized semiconducting polymers or liquid crystals.

In this context, we endeavored to investigate the self-organization of semiconducting liquid crystalline materials incorporating different kind of ϖ-conjugated systems in unique molecular or macromolecular architectures. Here we describe the design and synthesis of (i) dyads and triads combining discotic or calamitic ϖ-conjugated mesogens, and (ii) side-chain liquid crystal semiconducting polymers where the backbone is a ϖ-conjugated polymer and the side groups are ϖ-conjugated discotic mesogens.

In this work, we will give the details on the synthesis, structural characterization and morphology studied by Polarized-light Optical Microscopy (POM), Differential Scanning Calorimetry (DSC), Temperature-dependent small-angle X-ray diffraction, Grazing-incidence X-ray scattering (GIXS) and Atomic Force Microscopy (AFM). Moreover, their charge transport properties studied in OFET configuration will also be depicted.

10365-33, Session 8

Tailoring organic electrochemical transistors through form factor and materials selection *(Invited Paper)*

Jonathan Rivnay, Northwestern Univ. (United States)

Organic electrochemical transistors (OECTs) have gained considerable interest for applications in bioelectronics, neuromorphic computing, and logic circuitry. Their defining characteristic is the bulk-modulation of channel conductance owing to the facile penetration of ions into the (semi) conducting polymeric channel. In the realm of bioelectronics, OECTs have shown promise as amplifying transducers due to their stability in aqueous conditions and high transconductance. These devices can be fabricated in conformable form factors for in vivo stimulation/recording, and for cutaneous EEG and ECG recordings in human subjects. The performance of these devices, their operating conditions, and suitability for certain applications is linked intimately with their form factor and the transport properties of the active materials. In this work we show how thickness can be used to design optimal devices for a range of electrophysiological recording applications. Scaling of device performance with geometry reveals

the importance of the active material's mobility and charge storage capacity (per unit volume) in benchmarking new materials. Such findings have led to the development of a new class of polymers which outperform prototypical conducting polymers (i.e. PEDOT:PSS), and can potentially open new paths for the utility of OECTs in a number of application areas.

10365-35, Session 8

Anomalous behaviors of FeFETs based on polar polymers with high glass temperature

Vasileia Georgiou, National Institute of Standards and Technology (United States) and George Mason Univ. (United States); Dmitry Veksler, Jason P. Campbell, National Institute of Standards and Technology (United States); Pragya R. Shrestha, National Institute of Standards and Technology (United States) and Theiss Research (United States); Jason T. Ryan, National Institute of Standards and Technology (United States); Dimitris E. Ioannou, George Mason Univ. (United States); Kin P. Cheung, National Institute of Standards and Technology (United States)

The low processing temperature of polymeric materials and their wide range of applications make polar polymer based ferroelectric memory very promising and attractive. The typical configuration of the ferroelectric memory cell is the FeFET (Ferroelectric field-effect-transistor) with the polar polymer incorporated in the gate dielectric stack. The memory effect in these devices originates from the polarization of the ferroelectric polymer film and results in a hysteresis of the Id-Vg characteristics. In this study, we fabricated FeFETs based on ultrathin poly-Si channel and CP1-polymer (glass-transition temperature (Tg ~260 C) as the gate dielectric. We investigated the hysteresis of the Id-Vg curves over a wide range of temperatures and frequencies. We observed the effects of thermocycling on the device, such as the change of the hysteresis loop direction at temperatures close to Tg (associated with the change of the dominant hysteresis mechanism), and the simultaneous significant decrease in gate leakage current (which may indicate significant reduction of active defects in the polymer layer). The reversibility of the observed phenomena was also investigated through consecutive thermocycles. Soaking the chip in warm water (60 C) for 3 hours changes the magnitude of the hysteresis loop without changing the direction. The gate leakage current also remains very low. Thus, humidity may play some role in the hysteresis magnitude but not the loop direction, nor does it play any role in the leakage current. In this paper, we will discuss possible explanations of these observations.

Conference 10366: Hybrid Memory Devices and Printed Circuits 2017

Thursday 10–10 August 2017

Part of Proceedings of SPIE Vol. 10366 Hybrid Memory Devices and Printed Circuits 2017

10366-1, Session 1

Organic neuromorphic devices based on electrochemical concepts *(Invited Paper)*

Paschalis Gkoupidenis, Ecole Nationale Supérieure des Mines de Saint-Étienne (France) and Max-Planck-Institut für Polymerforschung (Germany); Dimitrios Koutsouras, Thomas Lonjaret, Shahab Rezaei-Mazinani, Esma Ismailova, Ecole Nationale Supérieure des Mines de Saint-Étienne (France); Jessamyn A. Fairfield, National Univ. of Ireland, Galway (Ireland); George G. Malliaras, Ecole Nationale Supérieure des Mines de Saint-Étienne (France)

Neuroinspired device architectures offer the potential of higher order functionalities in information processing beyond their traditional microelectronic counterparts. In the actual neural environment, neural processing takes place in a complex and interwoven network of neurons and synapses. In addition, this network is immersed in a common electrochemical environment and global parameters such as ionic concentrations and concentrations of various hormones regulate the overall behaviour of the network. Here, various concepts of organic neuromorphic devices are presented based on organic electrochemical transistors (OECTs). Regarding the implementation of neuromorphic devices, the key properties of the OECT that resemble the neural environment are also presented. These include the operation in liquid electrolyte environment, low power consumption and the ability of formation of massive interconnections through the electrolyte continuum. Showcase examples of neuromorphic functions with OECTs are demonstrated, including short-, long-term plasticity and spatiotemporal or distributed information processing.

10366-2, Session 1

Adaptive 2D memory-like devices with molecules and nanoparticles for unconventional computing *(Invited Paper)*

Dominique Vuillaume, Ctr. National de la Recherche Scientifique (France)

We have previously studied the photo-switching performances of azobenzene dithiophene derivative (AzBT) (1) inserted in nanoparticle self-assembled networks (NPSAN) nanodevices.(2) Here, we integrate AzBT-NPSAN in sub-100 nm 6-terminals devices (2 inputs, 4 outputs) and we demonstrate optically-driven reconfigurable Boolean operations associated to the light controlled switching of the molecules. Depending on the conductance pathways inside the AzBT-NPSAN, we identify 3 main output functions with a reconfiguration yield of 65%.(3) Contrary to previous results,(4) the devices work at room temperature and fully exploit the functionality of the molecules (and not Coulomb blockade in NPs). In addition, redox molecule NPSANs exhibit giant NDR (negative differential resistance) and memory effect.(5)

We also investigate how complex non-linearity in the AzBT-NPSAN leads to High Harmonics Generation (HHG), one of the prerequisites of reservoir computing (RC) approaches.(6,7) We show that HHG can be modified by UV illumination which paves the way for the processing of multi-input signals through a device that acts as a reservoir computer. Finally, temperature dependent measurements (4K) demonstrate light-driven increase of co-tunneling into these molecular networks.

References

1) K. Smaali et al., ACS Nano 2010, 4, 2411–2421; S.Karpe et al. Chem. Comm. 2010, 46, 3657–3659.

2) Y. Viero et al., J. Phys. Chem. C, 2015, 119 (36), 21173–21183.

3) Y. Viero et al., in preparation

4) S.K. Bose et al., Nature Nanotech. 2015, 10, 1048–1053.

5) T. Zhang et al., ACS Nano, submitted

6) W. Maass et al., Neural Computation, 2002, 14, 2531-2560.

7) Y. Viero et al.,in preparation.

10366-4, Session 1

The role of embedded nanoparticles in organic-based resistive nonvolatile memory devices

Giovanni Ligorio, Humboldt-Univ. zu Berlin (Germany); Sebastian Nau, Stefan Sax, NanoTecCenter Weiz Forschungsgesellschaft mbH (Austria); Marco Vittorio Nardi, Humboldt-Univ. zu Berlin (Germany); Norbert Koch, Humboldt-Univ. zu Berlin (Germany) and Helmholtz Zentrum Berlin für Materialien und Energie GmbH (Germany); Emil J. W. List-Kratochvil, Humboldt-Univ. zu Berlin (Germany)

Novel non-volatile memory devices are currently investigated to overcome the limitation of traditional memory technologies. New materials and architectures are being considered to address high-density, high-speed, low-fabrication costs and low power-consumption. Among the candidates competing for new-generation memories, resistive switching non-volatile memory (R-NVM) devices based on hybrid inorganic/organic materials (metal nanoparticles embedded in a conjugated organic host) are emerging. A R-NVM is a simple two-terminal device formed by two electrodes, separated by an active material, where the resistivity can be reversibly switched between two (high/low) states. Bistable electrical switching has been reported for a wide range of material combinations. Nonetheless, the switching mechanism is still under debate.

In unipolar R-NVMs, two distinct classes of switching mechanism have been proposed: one highlights the role of a space?charge field, controlling the current flowing in the device, thus the switching between the different conductive states is due to charging/discharging of the embedded metal NPs. A second reported mechanism is based on filamentary formation/destruction. The electrical switching is explained by the formation of highly conductive localized paths (filaments) within the organics.

In this contribution, we report on a series of carefully conducted experiments to rationalize the role of metal nanoparticles embedded into conjugated organic materials, and address whether the NPs' charging/discharging plays a role in the resistive switching of R-NVMs. The electronic and electric behaviour of the hybrid NP/organic materials was investigated via ultraviolet photoemission spectroscopy, as well as impendence spectroscopy.

Our results provide evidence that the most commonly proposed charging/discharging mechanisms can be excluded as the working mechanism, and there is solid evidence that resistive switching is due to the formation/rupture of filaments.

10366-5, Session 1

Spatial summation of pulse responses of a pair of organic heterogeneous junctions

Fei Zeng, Tsinghua Univ. (China)

Recent studies have found that responses to electrical stimulations in organic semiconductors and/or electrolytes heterogeneous junctions possess features in common with neural synaptic plasticity. Thus, we explore spatial summation of short-term plasticity by using a pair of such junctions. A simple integration of parallel connection displayed frequency selectivity

in the weight modification of charging peaks but not for discharging peaks. Significantly, the weight modification could be linearly summed from those of the two source devices though the absolute peak currents could not. Our system is feasible for synaptic computation including spatial summation and direction selectivity in artificial neural network.

10366-6, Session 2

Printed read-only memories and their operation in mobile readout system *(Invited Paper)*

Xiaojun Guo, Ruolin Wang, Sujie Chen, Wenjiang Liu, Shanghai Jiao Tong Univ. (China)

Printed read-only memory (ROM) would be a key component for many envisioned printed electronics applications such as item identification, anti-counterfeiting, brand protection and supply chain management. This paper will firstly introduce the electrical requirements on the memories to be operated in power constrained mobile readout systems for these targeted applications. Then, two types of printed ROMs, including polymer resistive type ROM and fuse-type electrically programmable write-once-read-many (WORM) ROM, will be presented. For the former, the instability issues associated with the conventional PEDOT: PSS and its interface with contact electrodes will be revealed. This work proves that, by removing the hydrophilic acidic groups in conventional PEDOT: PSS, these instability issues can be well addressed. The ROM tags fabricated based on the modified PEDOT: PSS of neutral pH and inkjet printed silver electrodes present extremely stable performance under both aging and electrical stress tests in air ambient. For the latter, fuse-type WORM ROMs are fabricated using a common material inkjet printer to form both the contact pads and the resistor tracks with the same silver ink and process settings. Based on the dependence of the fusing voltage on the length of the printed resistor track, a new cell structure is proposed to achieve multi-bit memories with greatly saved contact pad numbers for easier external electrical connections than the conventional design. The memory cells also present excellent long-term storage and operation stabilities. The function of the printed ROMs are finally demonstrated with mobile readout hardware systems.

10366-7, Session 2

Towards all inkjet printed electronics *(Invited Paper)*

Piero Cosseddu, Giulia Casula, Stefano Lai, Silvia Conti, Univ. degli Studi di Cagliari (Italy); Annalisa Bonfiglio, Univ degli Studi di Cagliari (Italy)

Organic electronics has been thoroughly investigated as technology for the fabrication of flexible devices enabling a wide range of applications including disposable electronics, smart cards, flexible displas, wearable electronics and sensors. However, in order to make such technology suitable for real applications, reliable, cost efficient approaches for large area fabrication, such as inkjet printing, have to be properly optimized. Moreover, in order to increase the final system portability, and as a consequence, its application range, such devices must be also operated at relatively low voltages.

In this work we present the different solutions we have developed for the routinely fabrication of inkjet printed organic transistors, operating a very low voltages and we report about their employment in the realization of different kinds of sensor devices for monitoring physical (pressure/temperature) and biochemical (eg. pH and/or DNA) stimuli and/or ionizing radiations.

Moreover, the development of organic electronics systems requires also the integration of such smart sensing systems with reliable data storage devices. Among several possible solutions, we will demonstrate that inkjet printing can be employed for the fabrication of high performing memory devices using different approaches, based on printed transistors and resistive switching elements, and that, such devices, can be easily integrated with electrical sensors for the fabrication of printed, flexible smart tags.

10366-8, Session 2

Non-volatile memory diodes based on organic ferroelectrics *(Invited Paper)*

Kamal Asadi, Paul W. M. Blom, Dago M. de Leeuw, Max-Planck-Institut für Polymerforschung (Germany)

Organic electronics has emerged as a promising technology for large-area micro-electronic applications, such as foldable displays, electronic papers, contactless identification transponders, and smart labels. Storing information is a key factor in many of the envisioned applications. A memory element is needed that retains its data in the absence of external power, hence non-volatile, and that further can be programmed, erased, and read-out electrically.

Organic ferroelectric memory diodes are promising candidates. A microstructure is needed that consists of bicontinuous columns of a semiconducting polymer embedded in the matrix of ferroelectric copolymer of vinylidenefluoride with trifluoroethylene (P(VDF-TrFE)). This microstructure can be realized either using a phase separated blends of a semiconducting polymer and P(VDF-TrFE) or using imprint patterning. Memory diode is realized by deliberately choosing an injection limited contact. Depending on the ferroelectric polarization, the current density is high and the diode is in the on-state or the current density is low and the diode is in the off-state. In this contribution we discuss state-of-the-art understanding of the device physics of the ferroelectric memory diodes by taking into account polarization dynamics, and confer the limits for the upscaling.

10366-9, Session 2

Organolead halide perovskites for low voltage resistive switching memories *(Invited Paper)*

Ho Won Jang, Seoul National Univ. (Korea, Republic of)

We report multilevel resistive switching using an organolead halide perovskite (OHP). Solution-processed 400 nm thick $CH_3NH_3PbI_3$ films with Ag top and Pt bottom electrodes exhibited electroforming-free resistive switching with a low SET voltage of ~0.13 V and high ON/OFF ratios of ≈10^6 under ±0.15 V pulses. Based on these extraordinary properties, four-level storage capability of the $CH_3NH_3PbI_3$-based devices was demonstrated. We attributed the high performance resistive switching behavior of the $CH_3NH_3PbI_3$-based devices to the energetically benign migration of anions defects, but further studies are needed to identify the mechanism responsible for the ultralow electric field resistive switching. Enhancements in switching speed, endurance, and retention are also necessary and may be achieved by controlling the doping concentration, crystallinity, and large area compositional uniformity of the OHP film. The inherent structural flexibility and the number of possible combinations for ABX_3-type OHPs will support intensive studies for other electronic device applications beyond resistive switching memories. Finally, we believe that the solution-processed $CH_3NH_3PbI_3$-based cells are promising for microelectronics built on flexible substrates.

10366-10, Session 2

Organic field-effect transistor nonvolatile memories: From fundamental understanding to prototype applications *(Invited Paper)*

Sui-Dong Wang, Soochow Univ. (China)

Organic nonvolatile memories can be key components toward future low-cost, light-weight, flexible and portable electronic products. The memories based on organic field-effect transistors (OFETs) possess advantages of nondestructive reading, capability to integrate data processing and storage,

and compatibility with various substrates. OFET nonvolatile memories face the challenge of simultaneously achieving large memory window, high air stability, long retention time and good rewritable endurance. We firstly elucidate the charge trapping/detrapping mechanism in the memories by a variety of approaches [1-9], including (1) in-situ surface potential mapping, (2) design and tailoring of nano-floating-gate, (3) characterization on memory ambient stability, (4) light response of memory behaviors and (5) probing of current transition point. The charge trapping/detrapping mechanism turns out to be a complex process dependent on both external electrical/optical fields and internal material properties. Secondly, the OFET nonvolatile memories are demonstrated to be promising in the applications of multibit data storage and solar-blind photodetection.

References:

[1] Wang, S.; Gao, X.; Zhong, Y. N.; Zhang, Z. D.; Xu, J. L.; Wang, S. D. Appl. Phys. Lett. 2016, 109, 023301.

[2] Liu, J.; Wang, C. H.; Liu, C. H.; Li, Q. L.; Gao, X.; Wang, S. D. Adv. Electron. Mater. 2016, 2, 1500349.

[3] Zhang, J. Y.; Liu, L. M.; Gao, X.; Liu, C. H.; Liu, J.; Dong, B.; Wang, S. D. Org. Electron. 2015. 25, 324-328.

[4] Cui, Z. Q.; Wang, S.; Chen, J. M.; Gao, X.; Dong, B.; Chi, L. F.; Wang, S. D. Appl. Phys. Lett. 2015. 106, 123303.

[5] Liu, J.; Liu, C. H.; She, X. J.; Sun, Q. J.; Gao, X.; Wang, S. D. Appl. Phys. Lett. 2014. 105, 163302.

[6] Gao, X.; Liu, C. H.; She, X. J.; Li, Q. L.; Liu, J.; Wang, S. D. Org. Electron. 2014. 15, 2486-2491.

[7] She, X. J.; Liu, J.; Zhang, J. Y.; Gao, X.; Wang, S. D. Appl. Phys. Lett. 2013. 103, 143302.

[8] She, X. J.; Liu, C. H.; Zhang, J. Y.; Gao, X.; Wang, S. D. Appl. Phys. Lett. 2013. 102, 053303.

[9] Gao, X.; She, X. J.; Liu, C. H.; Sun, Q. J.; Liu, J.; Wang, S. D. Appl. Phys. Lett. 2013. 102, 023303.

10366-11, Session 3

Hybrid electronic systems powered by printed thermoelectric generators *(Invited Paper)*

Ulrich Lemmer, Karlsruher Institut für Technologie (Germany); André Gall, Matthias Hecht, Karlsruher Institut für Technologie (Germany) and Otego GmbH (Germany); Silas Aslan, Karlsruher Institut für Technologie (Germany); Frederick Lessmann, otego GmbH (Germany) and Karlsruher Institut für Technologie (Germany); Verena Schendel, Karlsruher Institut für Technologie (Germany)

Thermoelectric generators (TEGs) transform heat to electricity without any movable parts. These devices are considered to be an important means of energy harvesting for wearables and sensor nodes for the Internet-of-Things (IoT). Organic semiconductors have recently demonstrated ZT-values approaching the same order of magnitude of those of the best established inorganic materials. Conjugated polymers as well as printable inorganic nanomaterials offer the unique advantage of being processable on printing machines. This opens a pathway for the fabrication of thermoelectric generators with unprecedented low costs thus enabling mass consumer applications. We have developed novel printable PEDOT formulations and a device layout which allow for a roll-to-roll printing process on ultrathin plastic foils. The TEGs are then subsequently fabricated by an automated folding process which allows to adapt the geometry of the devices such that the desired thermal resistance is optimum for the specific thermal boundary condition. Using this approach in combination with designed low power electronics forms the basis for several wireless sensor nodes.

10366-12, Session 3

Methods for fabrication of flexible hybrid electronics *(Invited Paper)*

Yong Zhang, Brent S. Krusor, Ping Mei, David E. Schwartz, Steve E. Ready, Robert A. Street, PARC, A Xerox Co. (United States)

Printed electronics (PE) is an emerging technology with potential applications in flexible displays, smart labels, wearable electronics, soft robotics, and prosthetics. While conventional electronics are fabricated on rigid, inorganic substrates, solution processed materials are compatible with plastic film substrates that are flexible, soft, and stretchable, thus enabling conformal integration with curvilinear objects. In addition, manufacturing by printing is scalable to large areas and is amenable to low-cost sheet-fed and roll-to-roll processes.

PE includes display and sensory components to interface with users and environments. On the system level, PE also requires electronic circuits for power, memory, signal conditioning, and communications. Those electronic components can be integrated onto a flexible substrate by either assembly or printing. PARC has been developing systems and processes for realizing both of these approaches. This talk will present PE fabrication methods with an emphasis on techniques recently developed for the assembly of off-the-shelf chips. A few examples of PE systems fabricated with this approach will also be described.

10366-13, Session 3

Printed soft-electronics for remote body monitoring *(Invited Paper)*

Matti Mantysalo, Tiina Vuorinen, Mahmoud Mosallaei, Vala Jeihani, Antti T. Vehkaoja, Tampere Univ. of Technology (Finland)

Wearable electronics has emerged into the consumer markets over the past few years. Wrist devices and textile integration are common technologies for unobtrusive measuring in sport and wellbeing sectors. Disposable bandages represents a paradigm shift in wearable electronics. Soft-electronics can conform to temporary transfer tattoo and deform with the skin without detachment or fracture.

In this presentation, we focus on printed soft-electronics for remote body monitoring. We will present fabrication and characterization of electrode bandage and temperature sensor. Components are fabricated on thin polyurethane film. Screen-printed interconnects for electrodes have sheet resistances of 36 m?/?, with a standard deviation of 4.5 m?/?, and it can be stretched up to 70% (single pull), and more than 1000 cycles (20% elongation). Stretchable interconnects are demonstrated in disposable electrode bandage. The measured ECG signals is fully satisfactory to compute important cardiac parameters. Temperature sensors are fabricated with inkjet-printed graphene/PEDOT:PSS ink. Sensor characterization was conducted both in inert and ambient atmosphere and the graphene/PEDOT:PSS temperature sensors (thermistors) were able reach higher than 0.06% per degree Celsius sensitivity in an optimal environment exhibiting negative temperature dependence.

10366-14, Session 3

Printed and Flexible Dual-color polymer light-emitting diodes (PLEDs) for optoelectronic sensors *(Invited Paper)*

Donggeon Han, Jonathan Ting, Ana Claudia Arias, Univ. of California, Berkeley (United States)

Here we demonstrate blade coated polymer light-emitting diodes (PLEDs) with different colors on a flexible substrate for optoelectronic sensor applications. Flexible electronics conform well to human body, which makes

them favorable for wearable application. Blade coating is an attractive printing scheme to fabricate electronic devices, in that it is simple to configure and has high throughput. Here, surface energy patterning (SEP) is used to blade coat solution at desired areas. This technique reduces the amount of solution wasted through the sides of the blade, as compared to bladecoating without SEP, which leads to highly homogeneous active layer film and relatively consistent device performance. Using this technique, PLEDs with individual colors, red, green and near infrared (NIR) which are known colors that can be used to detect the condition of haemoglobin, are separately fabricated with blade coating. Luminous Efficacy and EQE of the PLEDs at 1Wsr-1m-2 were 42.7mW/W, 10% for Red, 31.2mW/W, 6.3% for Green, and 8.6mW/W, 3.1% for NIR. Also, SEP is further utilized to bladecoat two PLEDs with different colors on one substrate with no significant changes in the performance of the PLEDs. Before fabricating PLEDs for optoelectronic sensors we assessed design parameters such as minimum required flux and ideal distance between the light source and the detector using solid-state components. Based on the experiment, the PLEDs are fabricated to be used in conjunction with a photodiode to perform pulsating photoplethysmogram (PPG) measurements. Furthermore, with the multicolor PLEDs we successfully demonstrate oxygenation measurement.

10366-15, Session 4

Development of printed large area organic transistors and integrated circuits *(Invited Paper)*

Yong-Young Noh, Dongguk Univ. (Korea, Republic of)

For at least the past 10 years, printed electronics has promised to revolutionize our daily life by making cost-effective electronic circuits and sensors available through mass production techniques, for their ubiquitous applications in wearable components, rollable and conformable devices, and point-of-care applications. In this presentation, I will give a talk on the recent progressive of my group on development of printed organic integrated circuits. I will mainly talk about on development of high performance inkjet printed unipolar and ambipolar polymer field-effect transistors (FETs), and applications to elementary organic complementary logic circuits by applying novel polymer dielectrics, new organic semiconducting and design new printing processes. In particular, we engineered and introduce new concept based for solution processed solid-state electrolyte gate insulators (SEGIs) by precise blending of P(VDF-TrFE) solution and P(VDF-HFP)-[EMIM][TFSI] gel solution resulting, after deposition of a thin film solid gate dielectric FETs, in ultrahigh field-effect mobility (?FET) and stable devices operating at low-voltage for several classes of unconventional semiconductors including ?-conjugated polymers, metal-oxides and other carbonaceous materials. By adding a minute amount (3% volume ratio for the optimal composition) of P(VDF-HFP)-[EMIM][TFSI] to the bulk fluorinated P(VDF-TrFE), high areal capacitance of > 4 µFcm-2 is reached thanks to the combined polarization of the -C-F interface dipoles and electrical double layers formation. To eliminate the integral complexity in differentiating field induced charge carriers from any possible carriers resulting from electrochemical doping of the semiconducting layer, we systematically measured the specific capacitance for each semiconductor/dielectric FET combination to avoid overestimation of the ?FET extraction in our SEGI devices - a major common issue in several publications. For instance, with our engineered SEGIs, unprecedented hole mobility increase from ~10-2 to 5 cm2V-1s-1 (corresponding ~37 cm2V-1s-1 by commonly used method) at ≤ 2 V operation is reached in commercially available poly(3-hexylthiophene-2,5-diyl) (P3HT) FETs, and ?FET exceeding 10 cm2V-1s-1 in others semiconductors.

10366-16, Session 4

Optogenetic electronic skins *(Invited Paper)*

Benjamin Tee, Institute of Materials Research and Engineering (IMRE) (Singapore)

Electronic sensor skins is an active area of research for many groups over the world due to its potential to enable dramatic changes in how we interact with the digital environment. For example, 'robots' can don on sensor active skins to shake human hands with comfortable pressure, measure our health biometrics and possibly aid in wound healing. In my talk, I will discuss the development of electronic sensor skins with some historical context, followed by showcasing of several force sensitive electronic skin technologies with high sensitivity, stretchability and bio-mimetic self-healing abilities. More recently, we demonstrated a power-efficient frequency encoded artificial mechano-receptor system inspired by biological mechano-receptors4. We further used a channelrhodopsin with fast kinetics and large photocurrents as an optical interface to neuronal systems for next generation opto-tactile prosthetic interfaces.

10366-17, Session 4

Large area processing and printing of conducting copper structures for use in (opto)electronics

Felix Hermerschmidt, David Burmeister, Humboldt-Univ. zu Berlin (Germany); Stefan Sax, Karl Popovic, JOANNEUM RESEARCH Forschungsgesellschaft mbH (Austria); Gerburg Schider, NanoTecCenter Weiz Forschungsgesellschaft mbH (Austria); Christine Boeffel, Fraunhofer-Institut für Angewandte Polymerforschung (Germany); Efthymios Georgiou, Stelios A. Choulis, Cyprus Univ. of Technology (Cyprus); Frank Peuckert, 3D-Micromac AG (Germany); Graham Gray, Richard Ward, Intrinsiq Materials Ltd. (United Kingdom); Emil J. W. List-Kratochvil, Humboldt-Univ. zu Berlin (Germany)

Most current electronics manufacturing technologies utilise subtractive processing that is expensive, wasteful and energy intensive. Printed electronics is revolutionising the electronics industry by enabling additive processing that significantly reduces expense, waste and energy consumption.

The EU-funded PLASMAS project demonstrates the capability of printed electronics based on novel nanoparticle Cu inks with favourable cost to performance ratios, through development of large area printed circuit boards and printed logic as well as OLED and OPV elements with printed Cu nanoparticle electrodes.

However, a number of challenges need to be overcome when printing these metal nanoparticle inks – the typical feature height of printed structures of several 100 nm tend to exhibit a rough surface, which can lead to shorts in the device after subsequent overcoating of the organic active layer materials. Furthermore, the sintering temperature of the nanoparticle inks needs to be low (< 130 °C) in order to allow deposition and curing on transparent flexible substrates such as PET.

We therefore present the process development of solution-processed electrodes based on inkjet-printed Cu grids, by embedding the inkjet-printed metal grids to yield ITO-free optoelectronic devices. Secondly, we present roll-to-roll inkjet-printed RFID antennas based on Cu inks. Finally, we demonstrate a truly low-temperature sintering route for a Cu nanoparticle ink by using a reducing atmosphere of formic acid, yielding stable highly conducting layers.

The results of the project highlight overall parameters for solution processing and implementation of novel metal nanoparticle materials and architectures in printed electronics.

10366-18, Session 4

Printed thin film transistors for flexible and transparent electronics applications *(Invited Paper)*

Yongtaek Hong, Seoul National Univ. (Korea, Republic of)

Printed electronics has been one of the hottest topics due to its potential low-cost, low-temperature, and facile fabrication of thin film transistors (TFTs) and circuits on various flexible platforms. Therefore, several types of the solution-process semiconducting materials, such as organic, oxide, single-walled carbon nanotube (SWCNT), have been widely studied. In addition, when organic conductor and dielectric are used, transparent TFTs and circuits can be also fabricated by using several printing processes. In this talk, technical issues of all inkjet-printed TFTs, including improvement of the source/drain (S/D) contacts for organic semiconductor and short channel printing process, will be addressed. Organo-compatible, single-step interface engineering with dimethylchlorosilane-terminated polystyrene (PS) (PS–Si(CH3)2Cl) has much improved the S/D contact properties of the bottom-contact organic TFTs with a poly(4-vinyl phenol) (PVP) gate dielectric, for both silver and poly(3,4-ethylenedioxythiophene):polystyre ne sulfonate (PEDOT:PSS) S/D electrodes. High transparency of the organic and SWCNT semiconducting thin films renders them feasible in transparent electronics applications. However, it should be noted that stability of TFT performances under illumination is key requirement in such applications. In fact, different behavior was observed for each semiconducting material under the visible light illumination and details of the illumination stability will be further discussed. Furthermore, by combining high-k aluminum oxide (Al2O3) and n-type indium gallium zinc oxide (IGZO), we obtained low voltage (< 5V) printed hybrid complementary metal oxide semiconductor (CMOS) circuits. This work was supported by the Center for Advanced Soft-Electronics funded by the Ministry of Science, ICT and Future Planning as Global Frontier Project (CASE-2015M3A6A5065309).

10366-19, Session 4

Toward solution processed magnetic nanoparticles for non-volatile memory applications

Hamed Sharifi Dehsari, Anielen Halda Ribeiro, Kamal Asadi, Max-Planck-Institut für Polymerforschung (Germany)

Iron oxide nanoparticles (IONPs) are among the most promising candidates for nano-scale magnetic memory applications due to their excellent magnetic properties. The information can be stored depending on the magnetization of the particles. The general drawback of IONPs however is the lack of ferromagnetism in IONPs at room temperature. To overcome this issue, doping of IONPs with cobalt is suggested. In this contribution we present a systematic study of Co doped IONPs using heat-up synthesis methods (thermal decomposition), wherein different synthesis parameters are surveyed and their effect on the particle size, stoichiometry of cobalt within the spinel ferrite nano crystals (CoxFe3-xO4) and magnetic properties are investigated. The synthesis was optimized to obtain sub-20 nm highly crystalline and monodisperse ferromagnetic nanoparticles with optimum magnetization and coercivity values. The particles were further modified by grafting polymerization from the surface of nanoparticles. Polymeric shells of different molecular weight are obtained, which allowed well dispersion of the ferromagnetic nanoparticles in common organic solvents. Nanoparticles can be solution processed to form a ferromagnetic thin-film. Solution processable magnetic films can open a new avenue in the low-cost non-volatile memory application.

10366-20, Session 4

Elucidation of light effects in organic nano-floating-gate nonvolatile memories

Xu Gao, Zhong-Da Zhang, Xiao-Jian She, Sui-Dong Wang, Soochow Univ. (China)

Organic nonvolatile memory based on OFET is an essential element in organic electronics, which integrates nondestructive data processing and reliable data storage [1,2]. It is reported the memory window is sensitive to light illumination. However, the fundamental of the light-assisted program, especially the photon energy dependence of memory performance, needs to be clarified with a clear physical picture. In our work, the charge trapping process in the organic nano-floating-gate memory was comparatively studied by light response measurements, where light sources with different wavelengths of 408 nm, 532 nm, and 652 nm were employed. The positive threshold voltage shift was observed for all lights and increased up raising the light intensity, while the negative threshold voltage shift was only observed under 408 nm light illumination. It is proposed that the light with photon energy higher than the HOMO–LUMO gap of pentacene can induce the minority multiplication effect, which leads to significant positive threshold voltage shift but no obvious impact on negative threshold voltage shift. Whereas the light with photon energy in excess of the injection barriers at the pentacene/PS interface can additionally cause the excitation-induced injection effect, corresponding to hole injection into floating gate from the HOMO of pentacene, which realizes further negative threshold voltage shift [3]. The photon-energy-dependent light effects could be utilized to reduce the operation voltage of organic nano-floating-gate nonvolatile memories, and motivate the development of organic energy-resolved photosensors.

References:

[1] Y. L. Guo, G. Yu, Y. Q. Liu, Advanced Materials, 2010, 22, 4427-4447.

[2] X. J. She, C. H. Liu, Q. J. Sun, X. Gao, S. D. Wang, Organic Electronics, 2012, 13, 1908-1915.

[3] X. Gao, C. H. Liu, X. J. She, Q. L. Li, J. Liu, and S. D. Wang, Organic Electronics, 2014, 15, 2486-2491.

Conference 10367: Light in Nature VI

Monday 7 –7 August 2017

Part of Proceedings of SPIE Vol. 10367 Light in Nature VI

10367-1, Session 1

Momentum of light

Michael Mazilu, Univ. of St. Andrews (United Kingdom)

There are many ways to calculate the optical forces acting on scattering particles such as Maxwell's stress tensor, Lorentz forces, gradient and scattering forces, Lorenz-Mie formalism, T-matrix. All these approaches use the electromagnetic field and define the amount of linear momentum transferred to the scattering particles. The resulting momentum transferred is proportional to the intensity of the incident fields, however, the momentum of single photons (hbar k) does not naturally appear in these classical expressions. Here, we discuss an alternative Maxwell's stress tensor based formalism that renders the classical electromagnetic field momentum compatible to the quantum mechanical one. This is achieved through the introduction of the quantum conversion which allows the transformation, including units, of the classical fields to wave-function equivalent fields.

10367-2, Session 1

Enhanced high-harmonic generation in photonics crystal: theoretical and experimental studies

Evgeny Gorbunov, Kirill I. Zaytsev, Egor Yakovlev, Arsen Zotov, Bauman Moscow State Technical Univ. (Russian Federation); Vladimir M. Masalov, Gennadi A. Emelchenko, Institute of Solid State Physics RAS (Russian Federation); Nikita Kruchkov, Stanislav O. Yurchenko, Bauman Moscow State Technical Univ. (Russian Federation)

The effect of strong localization of electromagnetic field in colloidal photonic crystals (PCs) is considered in our talk. It is shown theoretically that due to lateral modulation of dielectric permittivity of PC the sharp peaks of light's intensity arise at the band-gap pumping, and light field decays parametrically with depth. The light itself localises at the near-surface volume of the PC and enhances nonlinear light conversion. Theoretical model to explain generic physical picture is presented for two-dimensional PC, and the analytical results are compared with numerical simulations by finite-difference time-domein method to solve the Maxwell's equations. The fingerprints of enhanced high harmonic generation, which are observed in our experimental studies with globular opal PCs, justifyes the main theoretical predictions.

10367-3, Session 1

2D and 3D graphical representation of the propagation of electromagnetic waves at the interface with a material with general effective complex permittivity and permeability

Andres Diaz, Univ. Metropolitana (United States); Jonathan S. Friedman, Univ. Metropolitana (United States) and Arecibo Observatory (United States); Jose G. Ramos, Univ. Metropolitana (United States); Sarah C. Luciano, College of Optical Sciences, The Univ. of Arizona (United States)

One of the fundamental phenomena we need to understand about the nature of light is how it interacts with different types of materials and how it changes as it is reflected, absorbed, and refracted at an interface. With the collaboration of students in the Computer Science undergraduate program at Universidad Metropolitana, we developed a web-based instructional and research tool that addresses the need to visualize this physical phenomenon - usually only considered from a mathematical viewpoint - and that bridges the gap of inadequate or overly costly software in this area. From first-principle physics based on Maxwell's equations, the program analytically and graphically demonstrates the behavior of electromagnetic waves as they propagate through a homogenous medium and through an interface where the second medium can be characterized by an effective complex permittivity and permeability. Either p- or s-polarization wave components can be chosen, allowing a complete analysis of wave interaction with regular dielectric, ferromagnetic, metallic, and double-negative materials. Parameters such as amplitude, wavelength, frequency, direction of propagation, intensity, and phase velocity can be visualized. The graphical interface includes two-dimensional wave representation and three-dimensional component representations enabling the study of continuity (or lack thereof) of EM components, normal incidence, critical angle, Brewster angle, absorption and amplification, subunity and negative refractive indices, parallel and antiparallel behaviors of Poynting vector to phase velocity, and positive and negative Goos-Hänchen shifts.

10367-4, Session 1

Spectroscopic composition of corona discharge and some effects on materials

Jorge A. García-Macedo, Univ. Nacional Autónoma de México (Mexico); Giulio Fanti, Univ. degli Studi di Padova (Italy)

Corona-discharge CD is just the point at which the air breakdown begins to happen. This phenomenon is usually present when high voltage is applied between a needle and a metallic plate. The air molecules begin to ionizate, separation of their positive and negative charges occur and any minimum voltage increment produces a suddenly discharge between the electrodes. At this critical non-equilibrium point, some of the opposite separated charges are recombined and a light violet-blue emission is produced at the tip of the needle. The released energy can cause some kind of chemical transformation on the materials nearby. In this work we reported the composition of this emission captured from tip of the needle. We show the kind of change that this Corona-discharge produced on fabrics of cotton and linen. CD has been considered as one of the most probably effect that generate the image in the so called Turin Shroud. We present some image produced by controlled CD. Some discussion is given.

10367-5, Session 1

The generation, propagation, and absorption of photons

Nithin Kumar Goona, Priya Singh, Saidi Reddy Parne, Venugopal Reddy Barry, National Institute of Technology, Goa (India)

Photon can be treated as both particle and wave. Photon can also be treated as a spherical shell of information with its radius increasing with a rate of speed of light. It is equally likely for all other charges surrounding the charge to register this information with certain strength even when those are separated by huge distances. And so presence of photon at many places at same time in a double slit experiment can be explained which can also be extended to matter waves. Based on mutual separation between all charges and inverse square law, this paper discusses strength of information i.e quanta of energy to be registered at each charge, generation of new information after registering old information and its strength. This paper also discusses on the factors resulting in attenuation of information while it is propagating, maximum absorption of photon, single photon detector and the applications for renewable energy devices.

10367-6, Session 2

Not all butterflies have colorful wings *(Invited Paper)*

Akhlesh Lakhtakia, The Pennsylvania State Univ. (United States)

Fluttering from flower to flower, butterflies are nature's mobile flowers. Having evolved from moths, which are usually drab, butterflies must have developed brilliantly colorful wings some way down the evolutionary path. Pigments must have become brighter and scales must have developed ribbed reinforcements that doubled as diffraction gratings to produce structural color. Today, however, several species of glasswinged butterflies exist. Conspicuously large portions of their wings are transparent and colorless. Where did the colors go? Therein hangs a fascinating tale.

10367-7, Session 2

Nanophotonic structures discovered in wild comet moth

Norman Shi, Cheng Chia Tsai, Columbia Univ. (United States); Catherine Craig, Harvard Univ. (United States); Nanfang Yu, Columbia Univ. (United States)

This paper studies in detail the optical properties of the cocoons produced by a wild moth from the northern rainforest of Madagascar, the comet moth. Through detailed optical analysis and morphology studies of cocoon fibers, the first half of the paper demonstrates how the cocoon provides thermal regulation for the pupae through optical reflection in the visible and near-infrared, and radiative heat transfer in the mid-infrared. Cross sectional images prepared by focused ion beam milling show that the cocoon fibers contain a densely packed, random distribution of filamentary air voids with cross-sectional sizes ranging from 100 to 600 nm. Hemispherical reflection measurements at normal incidence on the cocoon shells show high reflectivity in the visible and near-infrared, and high emissivity in the mid-infrared. These properties allow the cocoon to act as a passive radiative cooling object that efficiently reflects solar radiation and meanwhile radiates heat away from the cocoon walls. The second half of the paper delves into the cocoon fibers' capabilities in waveguiding through transverse Anderson localization. Due to the unique longitudinal invariance (over tens of microns) of the filamentary voids inside these cocoon fibers, shorter-wavelength light (400-600 nm) that is launched from one end of the fiber is confined spatially through transverse Anderson localization as it propagates through the fiber. At times, there are strong confinements of certain propagating modes inside the localized region.

10367-8, Session 2

Light scattering optimization of chitin random network in ultrawhite beetle scales

Francesco Utel, LENS - Lab. Europeo di Spettroscopie Non-Lineari (Italy); Lorenzo Cortese, ICFO - Institut de Ciències Fotòniques (Spain); Lorenzo Pattelli, LENS - Lab. Europeo di Spettroscopie Non-Lineari (Italy); Silvia Vignolini, Univ. of Cambridge (United Kingdom); Matteo Burresi, Istituto Nazionale di Ottica (Italy); Diederik S. Wiersma, Univ. degli Studi di Firenze (Italy)

Among the natural white colored photonics structures, a bio-system has become of great interest in the field of disordered optical media: the scale of the white beetle Chyphochilus. Despite its low thickness, on average 7 ?m, and low refractive index, this beetle exhibits extreme high brightness and unique whiteness. These properties arise from the interaction of light with a complex network of chitin nanofilaments embedded in the interior of the scales. As it's been recently claimed, this could be a consequence of the peculiar morphology of the filaments network that, by means of high filling fraction (0.61) and structural anisotropy, optimizes the multiple scattering of light.

We therefore performed a numerical analysis on the structural properties of the chitin network in order to understand their role in the enhancement of the scale scattering intensity.

Modeling the filaments as interconnected rod shaped scattering centers, we numerically generated the spatial coordinates of the network components. Controlling the quantities that are claimed to play a fundamental role in the brightness and whiteness properties of the investigated system (filling fraction and average rods orientation, i.e. the anisotropy of the ensemble of scattering centers), we obtained a set of customized random networks. FDTD simulations of light transport have been performed on these systems, determining the values of the parameters that optimize brightness and whiteness. Moreover we demonstrated how the anisotropy is indeed a parameter that can strongly influence the system reflectance, even at such a low thickness.

10367-9, Session 2

Butterflies regulate wing temperatures using radiative cooling

Cheng Chia Tsai, Norman Nan Shi, Crystal Ren, Columbia Univ. (United States); Julianne Pelaez, Univ. of California, Berkeley (United States); Gary D. Bernard, Univ. of Washington (United States); Nanfang Yu, Columbia Univ. (United States); Naomi Pierce, Harvard Univ. (United States)

Butterfly wings are live organs embedded with a network of mechanical and temperature sensory neurons. For some butterfly species, their wings are equipped with pheromone-producing organs called scent pads or patches, which are filled with live cells. The proper function of butterfly wings thus demands a suitable range of temperatures. However, the wings have a small thermal capacity and correspondingly a very short time constant of temperature changes. Therefore, the wings are extremely thermally sensitive and can overheat quickly under exposure to strong solar radiation, while the head, thorax, and abdomen with much larger thermal capacities are still in their operation range of temperatures. We investigated the morphology of the butterfly wing scales and found that the non-uniform thickness of the wings and diverse wing scale nanostructures lead to a highly inhomogeneous distribution of radiative cooling, which determines the temperature distribution on butterfly wings. We developed an infrared technique to map butterfly wing temperatures by considering the spectral thermal emissivity distribution of butterfly wings. We discovered that despite the diverse visible colors and patterns, regions of wings that contain live cells are always the coolest. We also conducted a series of behavioral studies on live butterflies to show that their wings can function as sensitive and fast sensors of temperatures, and that the butterflies use a number of behavioral traits to prevent overheating and overcooling of their wings.

10367-10, Session 3

Contributions of early Arab scholars to color science and the role of Ibn al Haytham

Vasudevan Lakshminarayanan, Univ. of Waterloo (Canada)

The Islamic world made important discoveries in the field of color science during the medieval era. For example, al-Kindi proposed that it is the object rather than the medium that produces color (contrary to Aristotle). Ibn Sina, al Tusi and Nishaburi developed a two dimensional color order and described the partial hue scale. To Ibn al Haytham (whose publication of Kitab al Manzir, Book of Optics was celebrated during the International Year of Light) color was a percept and light and color were ontologically distinct. Al Haythm even discussed topics such as color contrast. Other contributions by these scholars include descriptions of the rainbow, color mixtures, color tops, etc. These contributions will be presented and discussed in this talk.

10367-11, Session 3

Effects of color in the learning of science

Aramis A. Sanchez Juárez, Johanna E. Jaramillo Q., Univ. Técnica Particular de Loja (Ecuador)

The teaching of science is a global problem, general studies have been carried out which take into account the effects of color in the educational environment and have had revealing results, however a study has not been made to measure the effects of color in the learning of the sciences, in this specific case of Physics and mathematics. A study of the effects of color on science teaching was conducted, controlling color of various materials such as slides used in class, markers on blackboard, pens, paper sheets, laboratory materials and teacher's clothing color. In this paper we present results of student academic performance, opinion about the subject, development of logical abilities and a comparison with the teaching of science in a free way, that is to say, without control of color. There is also a study of color effects in science education distinguishing between genders and finally comparing the general results in the educational field with those obtained in this work.

10367-12, Session 3

Non-visual biological effects of light on human cognition, alertness, and mood

Huaye Li, Huihui Wang, Junfei Shen, Peng Sun, Siman Zhang, Ting Xie, Zhenrong Zheng, State Key Lab. of Modern Optical Instrumentation, Zhejiang Univ. (China)

Light exerts non-visual effects on a wide range of biological functions and behavior apart from the visual effect. Light can regulate human circadian rhythms, like the secretion of melatonin and cortisol. Light also has influence on body's physiological parameters, such as blood pressure, heart rate and body temperature. However, human cognitive performance, alertness and mood under different lighting conditions have not been considered thoroughly especially for the complicated visual task like surgical operating procedure. In this paper, an experiment was conducted to investigate the cognition, alertness and mood of healthy participants in a simulated operating room (OR) in the hospital. A LED surgical lamp was used as the light source, which is mixed by three color LEDs (amber, green and blue). The surgical lamp is flexible on both spectrum and intensity. Exposed to different light settings, which are varied from color temperature and luminance, participants were asked to take psychomotor vigilance task (PVT) and Karolinska sleepiness scale (KSS) for alertness measurement, alphabet sheet test for cognitive performance measurement, positive and negative affect schedule (PANAS) for mood measurement. The result showed the participants' cognitive performance, alertness and mood are related to the color temperature and luminance of the LED light. This research will have a guidance for the surgical lighting environment, which can not only enhance doctors' alertness and efficiency during the operations, but also create a positive and peaceful surgical lighting environment.

10367-13, Session 4

Observing halos through airplane windows

Joseph A. Shaw, Montana State Univ. (United States)

A halo is one of the most frequent and impressive optical phenomena easily observable through an airplane window. Halos and related phenomena vary from a single spot of light formed by reflection of the sun from the tops of plate-shaped ice crystals to large rings with splashes of colors, caused by a combination of reflection and refraction in ice crystals. Even with extreme heat at the ground, an airplane quickly rises through sufficient altitude to find ice crystals in the clouds, enabling an alert passenger (or pilot) to see ice-crystal optical phenomena. This talk will briefly review these phenomena and explain them with photographs and diagrams. Photographs will include commonly seen halos, as well as one photo of Bottlinger's rings, which is a rare halo that is still not explained fully. The presentation will conclude with tips for how audience members can enhance their chances of seeing halos and understand them when they do.

10367-14, Session 4

Identifying the optical phenomena responsible for the blue appearance of veins

Spencer R. Van Leeuwen, Gladimir V. G. Baranoski, Univ. of Waterloo (Canada)

Blue in nature is often associated with beauty. It can be observed all around us, from captivating blue eyes to iridescent blue butterfly wings. While colours in nature are often the result of pigmentation, the majority of natural blue is produced by structural coloration. The colour of the sky, for example, is primarily caused by Rayleigh scattering. In this paper, we examine a single occurrence of blue in nature, specifically the blue appearance of veins near the surface of human skin. The most comprehensive investigation of this coloration to date showed that the blue light reflected by skin with an underlying vein is strongly dominated by the reflected red. Since these results imply that the vein should appear red, the authors suggested that we observe blue due to colour constancy, a feature of the visual perception system. However, in this previous work, the reflectance was only measured at three wavelengths which does not provide the full picture. In this paper, we employ in silico experiments, performed using first-principles light interaction models for skin and blood, to investigate the net effect of skin and vein optical properties on their aggregate reflectance across the visible range. We demonstrate that the blue coloration of veins results from Rayleigh scattering occurring within the skin. Furthermore, we show that veins can appear blue without considering colour constancy. The results of this paper, in addition to answering an old open question, have practical implications for performing non-invasive measurements of the physiological properties of skin and blood.

10367-15, Session PMon

Color vision tests comparison: Farnsworth D-15 versus Lanthony D-15

Marta A. Szmigiel, Malwina Geniusz, Wroclaw Univ. of Science and Technology (Poland)

Disorder of color vision in humans is the inability to perceive differences between some or all of the colors that are normally perceived by others. Color blindness is usually a birth defect, a genetically determined, inherited recessive in engagement with the chromosome X. For this reason it is much more common in men (approx. 8%) than women (approx. 0.5%). Different types of disorders color recognition are due to faulty or complete lack of functioning of the conesThe problem with color vision can be divided into: dichromacy - total absence of one of the types of cones, trichromacy - the difference of sensitivity to the color of one of the types of suppositories, or monochromacy - total inability to recognize colors.

This paper presents the results of the test FarnsworthD-15 and Lanthony D-15 on a group of volunteers, both adults and children. The study was conducted to compare the results of both tests, as well as the way of their execution (eg. the execution time of each test).

There is no known cure for color blindness. An essential part of adapting to the perceived defect is a change in the processing information about the world, eg. remembering the order and not the color of traffic lights on the road. It is very important that in the process of education to adapt teaching methods (eg images illustrating the contents of tasks) to a limited ability of recognizing colors.

10367-16, Session PMon

Color effect + motivation = learning and teaching

Darwin P. Castillo Malla, Aramis A. Sánchez Juárez, Univ. Técnica Particular de Loja (Ecuador)

The present work shows the teaching and motivation of children to study optics and color effects. The methodology consists of studying the different optical phenomena that occur through the sunsets and then do a correlation of this information with the phenomena and optical effects of the color of class presentations; to determine the motivation and attention of students.

References:

Retell, J. D., Becker, S. I., & Remington, R. W. (2016). An effective attentional set for a specific colour does not prevent capture by infrequently presented motion distractors. Quarterly Journal of Experimental Psychology, 69(7), 1340-1365. doi:10.1080/17470218.2015.1080738

10367-17, Session PMon

Determination of better protective eyeglasses depending on the shape and material

Aramis A. Sánchez Juárez, Johanna E. Jaramillo Q., Univ. Técnica Particular de Loja (Ecuador)

In the equatorial zone of the planet one suffers of a high degree of ultraviolet radiation, this is related to diseases of the skin and of the eyes, the solar blockers already do their part protecting the exposed skin and one has enough detailed information about the best one Sun cream protection, however when choosing sunglasses for sun protection, you end up choosing by style rather than utility. This study presents a study of the levels of protection offered by various products on the market, making a direct correlation between the shape of the glasses and the materials of the lenses. Also included are glasses for vision correction and spectacle performance on sunny days and cloudy days.

The results show small differences between expensive eyeglasses and cheap sunglasses regarding sun protection.

10367-18, Session PMon

Color vision deficiencies and the child's willingness for visual activity: preliminary research

Malwina Geniusz, Marta A. Szmigiel, Maciej Geniusz, Wroclaw Univ. of Science and Technology (Poland)

After a few weeks a newborn babys can recognize high contrasts in colors like black and white. They reach full color vision at the age of ca. six months. Matching colors is the next milestone. Most children can do it at the age of two. Good color vision is one of the factors which indicate proper development of a child.

The color vision of a group of children aged 3-8 was examined with saturated Farnsworth D-15 and desaturated Lanthony D-15. Fransworth test was performed twice - in a standard version and in a magnetic version. The time of completing standard and magnetic tests was measured. Furthermore, parents of subjects answered questions checking the children's visual activity in 1 - 10 scale. Parents stated whether the child is willingly to watch books, to color coloring books, to put puzzles or whether they like to play with blocks etc. Presented research shows the correlation between color vision and visual activity.

10367-19, Session PMon

Temporary effects of alcohol on color vision

Maciej Geniusz, Malwina Geniusz, Marta A. Szmigiel, Wroclaw Univ. of Science and Technology (Poland)

Color vision is an amazing and complex phenomenon. Despite numerous studies we still do not understand all the processes that affect the interpretation of colors. The concept of color itself is disputable: our brains create the perception of color from the spatial and temporal patterns of the wavelength and intensity of light.

It is well known that color vision seems to be very sensitive to several chemicals. This paper reviews the published literature that is concerned with color vision impairment from alcohol.

In general, most cases of congenital color vision impairment are red-green, and blue-yellow impairment is extremely rare. However, most of the acquired color vision impairment that is related to age, alcohol or environmental factors is blue-yellow impairment. Therefore, many studies have been performed to identify this relationship between alcohol addict and color impairment.

The present research reviews the published literature that is concerned with color vision impairment due to alcohol. Most of this research considers people under long-term effects of alcohol. However, there is little information about temporary effects of alcohol on color vision. A group of volunteers aged 20-40 was studied. During the study levels of alcohol in the body were tested with a standard breathalyzer while color vision were studied using Farnsworth and Lanthony D-15 Color Vision Tests. The extent of color vision loss was quantitatively assessed based on Bowman's color confusion index (CCI). The defect due to alcohol itself soon disappears during desintoxication.

10367-21, Session PMon

Six years of vision screening tests in pre-school children of Wroclaw

Ireneusz Szmigiel, Marta A. Szmigiel, Malwina Geniusz, Wroclaw Univ. of Science and Technology (Poland)

Detection of vision defects of a child without professional knowledge is not easy. Very often, the parents of a small child does not know that their child sees incorrect. Also the youngster, not knowing any other way of seeing, does not know that it is not the best.

While the vision of a small child is not yet fully formed, it is worth checking them very early. Defects detected early opportunity to give the correction anomalies, which might give the effect of the normal development of vision.

According to the indications the American Optometric Association (AOA) control eye examination should be performed at the age of 6 months, 3 years, before going to school and then every two years.

Members of SPIE Student Chapter, in cooperation with the Visual Optics Group working on the Department of Optics and Photonics (Faculty of Fundamental Problems, Wroclaw University of Science and Technology) for 6 years offer selected kindergartens of Wroc?aw performing visual screening test of children. Depending on the number of involved members of the student chapter and willing to cooperate students of Ophthalmology and Optometry, vision screening test was carried out in up toeight kindergartens every year.

The basic purpose of screening vision test is to detect visual defects to start the correction so early in life as possible, while increasing the efficiency of the child's visual potential. The surrounding community is in fact more than enough examples of late diagnose vision problems, which resulted in lack of opportunity or treatment failure.

Conference 10368: Next Generation Technologies for Solar Energy Conversion VIII

SPIE. OPTICS+ PHOTONICS OPTICAL ENGINEERING+ APPLICATIONS

Monday - Tuesday 7 –8 August 2017

Part of Proceedings of SPIE Vol. 10368 Next Generation Technologies for Solar Energy Conversion VIII

10368-201, Session Plen

A Brief History of Photovoltaics: Yesterday, Today, and Tomorrow

Charles Gay, U.S. Dept. of Energy (United States)

What can happen over the next 15 years, as photovoltaic (PV) power costs continue to decrease and markets expand? This talk will cover the range of opportunities associated with changes in energy supply in developed and developing economies. We will review the history of solar and discuss the key role of professionals in communicating a vision for the future. Our efforts to inform and educate a wide range of stakeholders will be essential to seeing the potential for wide adoption of PV become a reality. This talk will endeavor to convey some of the stories essential to enabling our outreach.

10368-202, Session Plen

Photovoltaics Moving into the Terawatt Age

Eicke R. Weber, Berkeley Education Alliance for Research in Singapore BEARS (Singapore) and Univ. of California, Berkeley (United States)

In the last few years, PV electricity became cost-competitive with electricity produced by conventional sources. Global PV production capacity will double within the next five years to 100-120 GWp/a, bringing PV installations into the Terawatt range. A key factor for this growth will be continuous technology advances aimed at higher efficiencies at reduced cost. In addition, cell efficiency will be even more important than lowest cost, to optimize energy harvest from a given area. Crystalline Silicon technology currently represents 90% of the global PV market. This technology is approaching a ceiling of 29% efficiency for a single-bandgap semiconductor. New approaches for higher efficiencies require heterojunctions, and several approaches will be discussed. These include heterojunctions on silicon, allowing to combine well-established large-scale Silicon PV technology with new technologies, such as low-cost III/V or Perovskite layers.

10368-203, Session Plen

Bankability of Novel Energy Technologies

Ralph Romero, Black & Veatch (United States)

New technologies are helping energy system owners improve performance and service to their customers while creating a sustainable energy future. But many of these new tools and processes are unproven and costly, which may hinder their large scale deployment. This talk will address the topic of new technology bankability and how owners, technology providers and financial institutions assess their risk exposure before embarking on significant projects. The talk will focus on the lessons learned from the rapid growth of the photovoltaic industry and discuss areas where technology risk should be further reduced.

10368-20, Session PMon

Power saving using amorphous transformers

Sarhan H. Hasan, Univ. of Denver (United States)

The large number of distribution transformer through any electrical network in any country result in a significant amount of losses .Low efficiency transformers effect the environment by requiring increased generation to supply increased transformer losses. The wasted generation causes increased carbon dioxide in the air and contribute to so called greenhouse effect. Alternatively, energy efficient transformers like amorphous transformers (AMDT) reduce the required generation and reduce the emission into the air. The purpose of this paper is to introduce amorphous material as alternative transformer core material in place of traditional silicon steel core, as it has excellent magnetic characteristics compared to silicon steel material. By using Amorphous as a transformer core material 70 % percent of transformer no load losses could be reduced due to amorphous low sheet thickness and its high resistivity. The economics of transformer replacement should be determined before replacement decision. The total owing cost (TOC) of both transformers the replacement and continuing operation transformer should be compared then the decision could be made. The total owing cost (TOC) is the transformer first price levelized over the life of transformer plus the cost of future transformer losses (no load losses and load losses) discounted to present value and levelized over the life of the distribution transformer. The electrical network in Libya is considered as case study in this paper where it contains about 5570 distribution transformer. The total owing cost (TOC) of some of them based on the data received from economical study center at the electrical department in ministry of energy in Libya is calculated to determine the replacement option, and then the power saving due to this replacement of the number of transformers that allowed to replace in the network is calculated.

10368-21, Session PMon

14.66%-efficient printing CIGS solar cells on stainless steel foil

Tung-Po Hsieh, Yu-Kuang Liao, Lung-Teng Cheng, Chia-Ming Chang, Wei-Sheng Lin, Chou-Cheng Li, Yu-Yun Wang, Wei-Tse Hsu, Jen-Chuan Chang, Sheng-Wen Chan, Song-Yeu Tsai, Industrial Technology Research Institute (Taiwan)

Efficiency of Cu(In,Ga)Se2 (CIGS) solar cells is pushing closer to silicon-based photovoltaic, outperforming silicon-based solar cells by its low material consumption, light weight, roll-to-roll production and wide variety of applications. In this work, we demonstrate a high quality, flexible CIGS absorber via mixed oxide particle ink for high efficiency flexible CIGS module. The ink was coated by Doctor Blade coator on a 2-?m-thick p-type contact metal (Mo/Cr), which was sputtered on stainless steel foils. The precursor film was prepared by the ink followed by hydrogen reduction. Sulfurization after selenization process are used for formation of CIGS absorber, which is followed by deposition of a CdS buffer layer on CIGS absorber by chemical bath deposition, and sputtering of an intrinsic ZnO, and a transparent conducting oxide (Al:ZnO). The device fabrication was terminated at top electrode prepared by screen printing of silver paste, and an MgF2 layer on AZO as anti-reflection layer.

Each CIGS absorber has been processed into CIGS module with two isolated CIGS solar cells, each with area of 100 cm2. From production of 56 devices, the yield rate of these 100 cm2 CIGS solar cells has reached 71 % for efficiency above 13 %, and 25 % for efficiency above 14 %. The champion 100 cm2 CIGS solar cell has reached 14.66 % efficiency. By series connection of these two devices, a 200 cm2, flexible CIGS mini-module has been successfully fabricated, and achieved 13.93 % efficiency.

10368-22, Session PMon

Fabrication of p-type monocrystalline germanium thin films on silicon wafer by magnetron sputtering

Cheng-Wei Luo, National Central Univ. (Taiwan)

The particular is p-type monocrystalline germanium thin films on silicon wafer by magnetron sputtering investigated in this research. Among the many types of solar cells, the conversion efficiency of III-V multi-junction solar cell is still the highest records of all kind of solar cells. But solar cell market gradually declining, we need to develop new battery technologies or structure. A silicon-based tandem solar cell is one of the possibility developments in the future. The III-V material is not suitable to grown on the silicon substrate, because the lattice constant is too different between III-V and Si, it will make the lattice mismatch to cause the threading dislocation density (TDD). Therefore, fabricating the epitaxial growth of Ge thin film on Si wafer substrate and applies it on tandem junction of Si and III-V group solar cells have great research potential to solve the problem of TDD. In order to overcome the current mismatch problem between the tandem junction of Si and III-V group solar cells, the single crystalline Ge thin film must have high carrier concentration as tunneling junction property.

This study, we use magnetron sputter system with B/Ge alloyed target to grow the p-type doped single crystal Ge films on Si (100) wafer. And the post annealing process was chosen to improve the Ge thin film qualities. For analysis of germanium film material analysis, we use XRD measurement verify crystallization of the single crystal Ge thin films. We also use Hall to measure the doped concentration and mobility of p-type Ge thin films.

10368-23, Session PMon

Using sputter epitaxial growth of SiGe films on mono-crystalline silicon substrate

Chiu-Yi Shih, National Central Univ. (Taiwan)

Monolithic integration is viewed as the most promising technique for the eventual realization of commercial wafer scale integration of III-V compound semiconductors on silicon. However, the large mismatches in lattice constant (~4.1%) and thermal expansion coefficient (~63%) , antiphase domains APDs and auto doping create difficulty for GaAs grown directly on Si negates the advantages of III–V/Si systems by generating large densities of dislocations in the III–V device layers. To reduce the dislocation density, We grown GexSi1-x thin films between Si and Ge as buffer layer since by increasing the Ge content (x) during growth of a GexSi1-x epitaxial layer on Si, the lattice constant can be increased from that of Si to Ge, providing a close lattice match for subsequent GaAs-based device growth. The general fabrication methods for epitaxial growth Ge were chemical vapor deposition (CVD) method and molecular beam epitaxy (MBE) method, however, the equipment costs of those methods were very expensive and needs use of extremely toxic raw materials in the CVD deposition processes. We use sputter meth to reduce hazardous substances and the cost. And improve competitiveness in the market.

This study we use sputter to epitaxy GexSi1-x on mono-crystalline silicon substrate. To measure

And analyze by X-ray diffraction (XRD) spectra, Raman spectra, and Electron backscatter diffraction (EBSD).

10368-1, Session 1

Energy migration, exchange and dissipation in ensembles of semiconductor nanocrystals for photovoltaic applications *(Invited Paper)*

Tom Gregorkiewicz, Univ. van Amsterdam (Netherlands)

The band structure of semiconductor nanocrystals (NCs) is modified by several effects which appear due to quantum confinement and surface eminence. When in an ensemble, individual NCs can couple with each other, depending on their proximity. In a dense dispersion of NCs, exchange of energy between proximal NCs can take place, profoundly influencing properties of the ensemble. In my presentation, I will discuss different processes of energy transfer between optically excited NCs in dense ensembles as induced by exciton concentration and/or bandgap gradients and facilitated by photon reabsorption, Förster and Dexter mechanisms, and specifically:

1. Exciton diffusion between Si NCs in SiO2 due to the Förster mechanism. I will show direct evidence of this process taking place in structures of different characteristics and evaluate the relevant transfer rates.

2. Dexter coupling between excited Si NCs. I will show that a highly excited NC can transfer energy to its neighbors, due to effective overlap of the highly delocalized character of the "hot" electron/hole states.

3. For a solid-state dispersion of Si NCs and Er3+ ions in SiO2, I will show how a combination of Förster and Dexter mechanisms operating in parallel facilitates efficient extraction of hot carrier excess energy.

4. Finally, I will discuss coupling between NCs of all-inorganic perovskite CsPbBr3. I will discuss how the bandgap energy of a particular NC is modified by the close proximity of its neighbors.

10368-2, Session 1

A metamaterial sunlight down-converter for improved photovoltaics

Antonio Capretti, Arnon Lesage, Tom Gregorkiewicz, Univ. van Amsterdam (Netherlands)

We tackle the requirements of sunlight down-conversion for improved photovoltaics by integrating semiconductor quantum-dots and dielectric nanocylinders, into a highly-optimized hierarchical metamaterial. Specifically, we utilize silicon nanocrystals (Si-NCs) supporting a form of multiple-exciton generation called space-separated quantum cutting, and embed them in SiO2 nanocylinders. We demonstrate that: i) total absorption can occur for photons with energy E > 2 Egap and ii) total transmission of photons with E < 2 Egap, where Egap is the cell bandgap (Egap ~ 1.11 eV for Si). This achievement solves the spectral selectivity needed for an effective down-conversion scheme.

Our efficient design supports metamaterial absorption peaks, whose spectral positions are tailored by geometrical design parameters. This peaks are due to both Mie resonances in the nanocylinders and grating resonances in the array. Our calculation predicts that the absorption can go up to 50% for a free-standing metamaterial, and it can reach total absorption by using an impedance-matched substrate. We experimentally prove that that the increased absorption directly couples to the Si-NC optical transitions, resulting in an enhancement of the photoluminescence intensity.

Although in this work we propose and use a specific material platform, the principle demonstrated is general and can be applied to other semiconductor quantum dots and emitting species, such as rare-earth ions and organic molecules. We envision the application of this principle to other applications in solar energy conversion, such as spectral shaping for photovoltaics, but also photocatalysis and artificial photosynthesis with higher efficiency.

10368-3, Session 1

Optical modeling of nanowire array tandem solar cell

Yang Chen, Johannes Svensson, Lund Univ. (Sweden); Oliver Höhn, Nico Tucher, Fraunhofer-Institut für Solare Energiesysteme (Germany); Mats-Erik Pistol, Lars-Erik Wernersson, Nicklas Anttu, Lund Univ. (Sweden)

A tandem solar cell consisting of a III-V nanowire top cell on a planar silicon bottom cell is a promising candidate for next generation photovoltaics. Here, we modeled the optical response of a III-V nanowire array on a silicon substrate with emphasis on varying processing layers. A conformal indium tin oxide (ITO) top contact lead to a 50% drop in the short-circuit current in the silicon cell. By instead using a planar ITO layer, this ITO absorption loss could be reduced by 90%. However, a ≈25% reflection loss showed up in such a planarized design. These reflection losses could be reduced by 80% with a 100 nm thick SiO_2 anti-reflection coating on top of the ITO layer and a 90 nm Si_3N_4 layer on top of the silicon surface between the nanowires. Regarding the absorption in the silicon bottom cell, we show that different approximate models can lead to a 15% variation in the estimated short-circuit current in the silicon subcell. Finally, we addressed the issue of weak absorption in small-diameter nanowires caused by electrostatic screening. We placed 16 nanowires in a cluster and coupled the nanowires optically with a dielectric coating. In this way, the clusters showed resonant absorption, and the absorption in the small-diameter nanowires was boosted by a factor of 200. Such a cluster design opens the door for using small-diameter nanowires for efficient absorption, while at the same time allowing for the inherent materials science benefits of small diameter nanowires like efficient strain relaxation in heterostructures.

10368-4, Session 1

Photovoltaic characteristics of organic-inorganic hybrid silicon quantum dot solar cell

Mitsuru Inada, Nozomi Isobe, Tomoki Miyake, Tadashi Saitoh, Kansai Univ. (Japan)

The sample structure is ITO/CuPc(20nm)/Si QDs(11nm)/C60(40nm)/BCP(5nm)/Al. The mean diameter of Si QD is 5nm. An indirect- and direct-optical band gap of Si QD obtained from UV-VIS absorption spectroscopy are 2.0eV and 3.5eV, respectively. An open-circuit voltage of 0.3V, a short-circuit current density of 0.032mA/cm2 and fill-factor of 0.23 are obtained from current-voltage measurements under AM1.5G sunlight irradiation. The result shows that the sample acts as a solar cell though the performance is not so good. Photocurrent characteristics are investigated by spectral responsivity measurements. The clear enhancement of resposivity at a photon energy of 3.5eV are observed, compared with a reference CuPc/C60 solar cell which does not include Si QD. These results shows that this inorganic-organic QD solar cell structure has a one of a new type of candidates of the QD solar cells.

10368-5, Session 1

Optimization of charge-carrier generation in amorphous-silicon thin-film tandem solar cell backed by two-dimensional metallic surface-relief grating

Benjamin J. Civiletti, Thomas H. Anderson, Univ. of Delaware (United States); Faiz Ahmad, The Pennsylvania State Univ. (United States); Peter B. Monk, Univ. of Delaware (United States); Akhlesh Lakhtakia, Pennsylvania State Univ. (United States)

The rigorous coupled-wave approach was used to calculate the three-dimensional charge-carrier-generation rate in an amorphous-silicon, thin-film tandem solar cell. The solar cell comprised a front coating, designed to reduce the reflection of incident light; three p-i-n junctions in tandem; and a periodically corrugated metallic back reflector (PBR). Indium-tin-oxide was chosen for the front coating. The p-i-n junctions were taken to be made from hydrogenated amorphous silicon alloyed with carbon or germanium. The silver PBR was assumed to possess hexagonal hillock texturing in order to couple the incident light with wave guide modes and surface-plasmon-polariton waves. The total charge carrier-generation rate in the three junctions, under illumination by the AM1.5G solar spectrum, was calculated at both normal and oblique incidence. The differential evolution algorithm was used to maximize this rate throughout the three junctions, with the design-parameter space including the PBR relief, the PBR duty cycle, front coating thickness, and the thicknesses of each of the i-layers. A one-dimensional, finite-element drift diffusion model, implemented in COMSOL, was used to predict the efficiency of the tandem solar cell at various locations in the parameter space. Each of the p-i-n junctions comprising the tandem solar cell was assumed to be electrically isolated.

10368-6, Session 2

Optimal indium-gallium-nitride Schottky-barrier thin-film solar cells

Thomas H. Anderson, Peter B. Monk, Univ. of Delaware (United States); Tom G. Mackay, The Univ. of Edinburgh (United Kingdom); Akhlesh Lakhtakia, Pennsylvania State Univ. (United States)

A two-dimensional model was developed to simulate the optoelectronic properties of indium-gallium-nitride (InGaN), thin-film, Schottky-barrier-junction solar cells. The solar cell comprises a front coating designed to reduce the reflection of incident light, Schottky and ohmic front contacts, an n-doped InGaN-wafer, and a periodically corrugated metallic back reflector. The ratio of indium to gallium in the wafer varies periodically in the thickness direction, and thus the optical and electrical properties also vary periodically. Empirical models for indium nitride and gallium nitride, combined with Vegard's law, are used to calculate the optical and electrical properties of these alloys. This material nonhomogeneity could be physically achieved by varying the fractional composition of indium and gallium during deposition. The periodic nonhomogeneity aids charge separation and, in conjunction with the periodically corrugated back reflector, enables incident light to couple to multiple surface plasmon-polaritons. The resulting charge-carrier-generation rate profile when the solar cell is illuminated by the AM1.5G spectrum was calculated using the rigorous coupled-wave approach. The steady-state drift-diffusion equations were solved using COMSOL, which employs finite-element methods, to calculate the current density as a function of the voltage. Mid-band Shockley-Read-Hall, Auger and radiative recombination rates were taken to be the dominant methods of recombination. This model was used to study the effects of the solar-cell geometry and the shape of the periodic material nonhomogeneity on efficiency. The solar-cell efficiency was optimized using the differential evolution algorithm.

10368-7, Session 2

Silicon-based infrared photodetectors enabled by hot electrons

Seok Jun Han, Sang Eon Han, The Univ. of New Mexico (United States)

Conventionally, photonic infrared (IR) detectors employ low band gap materials such as InGaAs, InSb, or HgCdTe. However, these materials include elements that are rare, expensive, or toxic. Past research indicates that crystalline Si (c-Si), which is a much cheaper and more abundant element, could be used for IR detection when metal electrodes are cleverly nanostructured. In this type of photodetection systems, the IR light with energies below the c-Si band gap is strongly absorbed by the metal

structures, rather than by c-Si. The photoexcited electrons in the metal can then be injected into the conduction band of c-Si before being thermalized and electric current can be generated. These non-thermalized electrons, called hot electrons, enable the detection of IR light with energies below the c-Si band gap. For efficient transport of electrons in the metal before thermalization, the metal layer should be as thin as approximately the electron mean free path. Accordingly, the metal layer thickness should be only a few tens of nanometers. To induce strong optical absorption in such a thin metal layer, surface plasmon polaritons (SPPs) can be excited at the metal surface. Previous studies on hot electron photodetection utilized small-scale metamaterials or deep trench resonators to have strong resonant absorption of SPPs in thin metal films on c-Si at the desired frequencies. However, these structures should be fabricated with a high precision because the metal structure sizes determine resonances. Accordingly, in many cases, expensive techniques such as electron beam lithography have been commonly used to fabricate the structures. However, for mass production, it is important to obtain metallic structures that do not require expensive techniques and tolerate practical fabrication errors. In this study, we use metal metasurfaces that can be fabricated by scalable, inexpensive techniques and achieve a broad-band IR absorption of over 95% in 15-nm-thick metal films. This unprecedented strong absorption, in terms of both the absorptance magnitude and the band width, is enabled by a new scheme where the light takes multiple passes within the c-Si substrate. During the passage, light is preferentially absorbed by the thin metal layer that is on one side of the substrate. Absorption on the other side is efficiently eliminated by using a dielectric layer. In our effort, the surface of the c-Si substrate where thin meal film is deposited is structured by a simple optical lithography. The structured surface admits the incident light into the substrate and prevents the light from leaking out of the substrate. In our scheme of multiple light passes, extremely strong resonances are not necessary and fabrication errors would not destroy the optical properties appreciably. In this talk, we will discuss the details of the optical absorption in our scheme. We will also present our experimental results on the electronic characteristics of our hot electron devices.

10368-8, Session 2

Highly efficient organic photovoltaics enabled by polymeric additives

Taeshik Earmme, Brian J. Worfolk, Kathy A. Repa, Hualong Pan, Alyssa B. Chinen, Kathy B. Woody, Phillips 66 (United States)

Organic photovoltaics (OPVs) are of current interest for providing a low-cost, scalable solar energy conversion technology. A typical photoactive layer for OPV consists of a light absorbing donor polymer and fullerene acceptor in a bulk heterojunction binary blend, where free charge carriers are generated by absorbed photons. Recently, the use of a ternary component in the active layer is emerging as a promising strategy to enhance device performance. The third component could be a quantum dot, small molecule or polymer. In addition to a complementary absorption with the primary donor material in the solar spectrum and cascade energy levels between HOMO and LUMO energy levels of the dominating donor polymer and fullerene acceptor to facilitate charge transport, improved nanomorphology over the binary device has been also reported.

In this study, incorporation of a non-conjugated polymeric additive to the polymer:PC70BM photoactive layer is demonstrated to enhance device performance. OPV devices with different ratios of polymeric additive were fabricated and investigated. The increase in the photovoltaic parameters by using polymeric additive is successfully demonstrated showing over 10% power conversion efficiency with very high current density (>19.0 mA/cm2). Results of a thermal stability test show that the additive suppressed a decrease in the fill factor, indicating the potential ability to stabilize morphological changes in the active layer caused from heat stress.

10368-9, Session 2

Enhanced optical absorption of amorphous silicon films modulated by silicon nitride (Si3N4) nanostructures

Hong Liu, Suzhou Univ. of Science and Technology (China) and Suzhou Thermoelectric Technology Co. (China)

The optical absorption of amorphous silicon (??-Si) films is enhanced by silicon nitride (Si3N4) nanostructures deposited on the films. The reflection of amorphous silicon (??-Si) films at the long wavelength side of localized phonon polaritons (LPPs) resonance originated from silicon nitride nanostructures is significantly decreased, i.e. the optical absorption is enhanced. The results show that the frequency of localized phonon polaritons depend on the sizes and shapes of cylindrical silicon nitride nanoparticles , and the average reflectivity of the amorphous silicon films in the wavelength range of 900–1200nm could be decreased by 20.5%. Moreover, the reduction of the reflection is found to be mainly dependent on the sizes and shapes of the silicon nitride nanostructures, which is related to nanoparticles sizes and shapes which result in the LPP's resonance peak position. The above results indicate that amorphous silicon films modulated by Si3N4 Nanostructures will be a ideal material for photo-thermal absorption.

10368-10, Session 3

Solar fuels *(Keynote Presentation)*

Tanja Cuk, Univ. of California, Berkeley (United States)

No Abstract Available

10368-11, Session 3

Reactive colloidal optics for passive tracking of the sun

Ido Frenkel, Avi Niv, Ben-Gurion Univ. of the Negev (Israel)

The growing need for cost effective renewable energy is hampered by the stagnation in solar cell technology. Concentrating photovoltaics (CPV) is a possible mean for increasing the module efficiency. CPV, however, requires cumbersome active tracking that reduces much of its cost effectiveness. Here we propose a passive tracking scheme based colloidal optical device. Here, tracking is achieved by exploiting the capacity of a new kind of colloidal material for light activated binary switching from opacity to transparency, switching that is based a new kind of opto-mechanical force. Being based on phase transition in water this approach is both cost-effective and efficient. We further show that combining this passive tracking approach with an external cavity results in what is possibly a groundbreaking optical approach for solar power conversion. Being external to the cell itself, the proposed approach is indifferent to the type of semiconducting material that is used, as well as to other aspects of the cell design. This, in turn, liberates the cell from optical constraints thus paving the way to higher efficiencies at lower module price.

10368-12, Session 3

Volume holographic lens spectrum splitting photovoltaic system for high energy yield with direct and diffuse solar illumination

Benjamin D. Chrysler, Yuechen Wu, Raymond K. Kostuk, The Univ. of Arizona (United States)

A flat-panel Volume Holographic Lens system is designed to 1) achieve

high conversion efficiency of sunlight at normal incidence, 2) convert diffuse sunlight, and 3) minimize system thickness. Spectrum splitting with a holographic lens is accomplished by focusing a transition wavelength to the junction between two solar cells. Longer wavelength light is dispersed to a narrow bandgap cell (Silicon) and shorter wavelength light to a wide bandgap cell (GaAs) allowing each spectral component to be more efficiently converted. Diffuse sunlight is not Bragg matched and is transmitted through the hologram, and converted to electricity by solar cells. This approach also allows flat-panel module configurations with depths less than 2.5cm. Two holographic lenses are cascaded to achieve efficient diffraction over a broad spectrum (450nm). The diffraction properties of the cascaded elements are optimized to maximize spectral bandwidth while minimizing cross-coupling effects. The holographic elements were fabricated in dichromated gelatin by ‘stitching’ or forming multiple holograms side by side to obtain the desired aperture. A prototype spectrum splitting system shows an increase in conversion efficiency relative to the more efficient cell in the system (GaAs). Experimental results are compared to simulation using non-sequential ray tracing and rigorous coupled wave analysis.

10368-15, Session 4

Transparent solar cell material processing using laser induced thin film epitaxial growth using laser beam holographic patterning and monitoring using RHEED

Mohammad Masum Anwar, Forever Living Products (Bangladesh)

Solar cell material processing is very important for generating efficient power supply from solar energy and this paper will focus on some kind of transparent solar cell that can be used as solar energy emf source and the material processing will be using laser beam induced thin film epitaxial growth by using holographic 3 d patterning and the epitaxial growth mode will be monitored using reflection high energy electron diffraction (RHEED) technique for precision and more efficiency in thin film growth. There are three different thin film epitaxial growth such as island growth , layer growth and island plus layer growth , we will use any mode of crystal growth suing vacuum technique where we will use laser beam holographic technique for crystal growth mode change and patterning and the process of thin film epitaxial growth will be monitored using reflection high energy electron diffraction technique.

10368-17, Session 4

Graphene for thermoelectronic solar energy conversion

Dilip De, Covenant Univ. (Nigeria) and Sustainable Green Power Technologies (United States); Olukunle C. Olawole, Covenant Univ. (Nigeria)

Graphene is a high temperature material which can stand temperature as high as 4600 K in vacuum. Even though its work function is high (4.6 eV) the thermionic emission current density at such temperature is very high. Graphene is a wonderful material whose work function can be engineered as desired. Kwon et al1 reported a chemical approach to reduce work function of graphene using K2CO3, Li2CO3, Rb2CO3, Cs2CO3. The work functions are reported to be 3.7 eV, 3.8 eV, 3.5 eV and 3.4 eV. Even though they did not report the high temperature tolerance of such alkali metal carbonate doped graphene, their works open a great promise for use of pure graphene and doped graphene as emitter (cathode) and collector (anode) in a solar thermionic energy converter. This paper discusses the dynamics of solar energy conversion to electrical energy using thermionic energy converter with graphene as emitter and collector. We have considered parabolic mirror concentrator to focus solar energy onto the emitter so as to achieve temperature around 4300 K. Our theoretical calculations and the modelling show that efficiency as high as 55% can easily be achieved if space-charge problem can be reduced and the collector can be cooled to certain proper temperature. We have discussed methods of controlling the associated space-charge problems. Richardson-Dushman equation modified by the authors have been used in this modeling. Such solar energy conversion would reduce the dependence on silicon solar panel and has great potential for future applications in enery conversion.

10368-18, Session 4

A solar powered device for chlorine generation

Enrico Chinello, Ecole Polytechnique Fédérale de Lausanne (Switzerland); Miguel Antonio Modestino, New York Univ. (United States); Laurent Coulot, Mathieu Ackermann, Insolight Sàrl (Switzerland); Christophe Moser, Ecole Polytechnique Fédérale de Lausanne (Switzerland)

The chlor-alkali process is employed to produce 60 million tons of chlorine each year, accounting for 1% of the overall global energy consumption. Currently, the process involves an electrochemical apparatus fed by almost exclusively grid electricity. Here we present a solar powered chlor-alkali device potentially able to decrease drastically the external energy demand. An innovative solar concentrator is utilized to focus sunlight on multi-junction solar cells, whose output voltage is sufficient to drive the reaction. The electrolyzer is constituted by a nickel-based cathode and a dimensionally-stable-anode (DSA), separated by a cation exchange membrane. The device shows a continuously stable operation when exposed to natural sunlight illumination, with performances that closely match the predictions based on the nearest weather station. Under the tested experimental conditions 16.1% sun-to-chlorine (STC) efficiency was recorded. The device was also tested in absence of direct sun. A typical summer day is reproduced in terms of illumination direction and intensity for each hour of the day; results show the capability of employing the innovative tracking strategy without angular limitations. Despite the relatively small input area of the device tested (5 square-centimeters), it holds the potential to be easily scaled up and be practically implemented.

10368-19, Session 4

A study of the penetration of photovoltaic generation into the Libyan power system

Abdulmunim Guwaeder, Oklahoma State Univ. (United States); Sarhan H. Hasan, Univ. of Denver (United States); Ibrahim Aldaouab, Univ. of Dayton (United States)

Current remarkable tendency in the cost of photovoltaic (PV) modules on a large scale has enhanced their deployment around the world. This paper presents a study of the penetration of photovoltaic generation on the Libyan power system. Further, it also presents a brief description of the Libyan power system with its past and current state of generation and transmissions infrastructure and potential solar power plans.

10369-1, Session 1

Nanostructured materials for selective solar absorbers and thermal emitters *(Invited Paper)*

Sheng Shen, Carnegie Mellon Univ. (United States)

In this talk, I will give two examples about utilizing nanostructured materials to develop selective solar absorbers and thermal emitters. First, I will demonstrate large-scale three-dimensional (3D) nanophotonic solar selective absorbers for solar thermal energy conversion. Compared with traditional photovoltaics, one major advantage of solar thermal energy conversion is the utilization of nearly the entire solar spectrum, enabling higher energy conversion efficiency. To maximize the conversion efficiency of the incident solar flux to heat, one important strategy is to employ spectrally selective solar absorbers that need to exhibit a near-blackbody absorption in the solar spectrum while suppressing infrared emission from the absorbers at elevated temperatures. The novel 3D nanophotonic solar selective absorbers developed in this work can significantly facilitate transformative advancements in the performance and design of solar thermal systems. Second, I will discuss our recent theoretical and experimental work about thermal emission from optical antennas. By carefully designing the thermal emission from optical antennas, we experimentally demonstrate a new type of perfect selective thermal emitters, which can be potentially used for thermal radiation control, high-performance infrared thermal sources and detectors.

10369-2, Session 1

Analysis of monthly solar radiation in Libya

Abdulmunim Guwaeder, Rama Ramakumar, Oklahoma State Univ. (United States)

The development of renewable energy sources generation capacity has increased rapidly over the years, as one of the most widely deployed renewable energy technologies, such as solar photovoltaic (PV), which is considered to be a promising energy source. In order to develop renewable energy sources technology such as photovoltaic, it's necessary to provide analysis at any area of suitability in its employment. Moreover the cost of renewable energy sources has decreased significantly in the last three decades. The amount of solar radiation data received for a specific area is one of the most important meteorological parameters for many application fields. This paper discusses the probability distribution functions (PDF) of a monthly insolation for four locations in Libya based on analysis of 30 years of historical weather data calculated by National Renewable Energy Laboratory (NREL), in order to get appropriate frequency distribution that best fits the data for a given month of the year. The frequency distributions used for solar irradiation data include Weibull, Normal, Lognormal and Gamma functions. The observed radiation at four locations in Libya on a monthly basis are analyzed to evaluate the suitability of the probability distribution functions based on mean square errors. The analysis showed all the probability functions are appropriate for all the locations where weather conditions are relatively steady throughout the year. From the analysis it is concluded that Normal and Weibull distribution give the best fit for observed solar radiation.

10369-3, Session 1

Tailoring nanomaterials for solar driven interfacial steam generation

Jia Zhu, Nanjing Univ. (China)

Water scarcity is one of the most pressing global challenges. Nanomaterials with carefully tailored properties can be used to manipulate the flow of phonons, electrons and photons, to enable unconventional solution to addressing this issue. In this talk, I will present our recent progress in solar steam generation for water treatment.

We report a plasmon-enhanced solar desalination device. This most efficient and broad-band plasmonic absorber is fabricated through self-assembly of metallic nanoparticles onto a nanoporous template by one step deposition process. Because of its efficient light absorption and strong field enhancement, it can enable very efficient and effective solar desalination by using low cost aluminum nanoparticles.

Inspired by the transpiration process in plants, we report an artificial transpiration device with a unique design of two dimensional water path. With efficient two dimensional water supply and suppressed heat loss, it can enables an efficient (80% under one-sun illumination) and effective (four orders salinity decrement) solar desalination device. More strikingly, the energy transfer efficiency of this artificial transpiration device is independent of water quantity and can be achieved without extra optical or thermal supporting systems, therefore significantly improve the scalability and feasibility of this technology.

Nature Photonics 10,393-398(2016)

Science Advances 2, e1501227(2016)

PNAS 113, 13953–13958(2016)

Advanced Materials DOI: 10.1002/adma.201604031(2016)

10369-4, Session 1

Spectrum splitting for thermal management in photovoltaic concentrators

Harry N. Apostoleris, Matteo Chiesa, Ibraheem Al-Mansouri, Masdar Institute of Science & Technology (United Arab Emirates)

Spectrum splitting between two or more cells of different band gaps is a well established way of enhancing the output of a photovoltaic system. Less widely explored is the impact of spectrum splitting on thermal management in PV concentrator systems. By dividing light between multiple cells, or between cells and thermal absorbers, cell heating can be significantly reduced. This is particularly relevant in certain proposed tracking-integrated systems, where the inclusion of internal sun-tracking mechanisms may require that cells be free to move within the module, and therefore be thermally isolated to only poorly contacted to a heat sink. We model several spectrum-splitting scenarios for a low-concentration trough-receiver and investigate the effects of different spectrum-splitting concepts on cell temperature and performance, using a combination of optical, thermal and PV-modeling software tools to capture the full process of solar energy collection, conversion and extraction. To corroborate the theoretical analysis we realize a spectrum-splitting system in an experimental prototype based on the 3D-printed trough concentrators that we have previously demonstrated, and compare the receiver temperature and cell performance for both split and broad band spectra. Finally we discuss in general terms the design principles that lead to the most effective thermal management in split-spectrum systems, and further steps that can be taken to minimize cell heating in unconventional module configurations.

10369-5, Session 2

Metasurfaces for angular and spectral control of thermal radiation *(Invited Paper)*

Luke A. Sweatlock, Katherine T. Fountaine, Northrop Grumman Aerospace Systems (United States)

Design of perfect absorbers and emitters has been a primary focus of the metamaterials community owing to their potential to enhance device efficiency and sensitivity in energy harvesting and sensing applications, specifically photovoltaics, thermal emission control, bolometers and photodetectors, to name a few. While reports of perfect absorbers/emitters for a specific frequency, wavevector, and polarization are ubiquitous, a broadband and polarization- and angle-insensitive perfect absorber remains a particular challenge. In this work, we report on directed optical design and fabrication of sparse III-V nanowire arrays as broadband, polarization- and angle-insensitive perfect absorbers and emitters. Specifically, we target response in the UV-Vis-NIR and NIR-SWIR-MWIR via two material systems, InP (Eg=1.34 eV) and InSb (Eg=0.17 eV), respectively.

Herein, we present results on InP and InSb nanowire array broadband absorbers, supported by experiment, simulation and analytic theory. Electromagnetic simulations indicate that, with directed optical design, tapered nanowire arrays and multi-radii nanowire arrays with 5% fill fraction can achieve greater than 95% broadband absorption (?InP=400-900nm, ?InSb=1.5-5.5μm), due to efficient excitation and interband transition-mediated attenuation of the HE11 waveguide mode. Experimentally-fabricated InP nanowire arrays embedded in PDMS achieved broadband, polarization- and angle-insensitive 90-95% absorption, limited primarily by reflection off the PDMS interface. Addition of a thin, planar VO2 layer above a sparse InSb nanowire array enables active thermal tunability in the infrared, effecting a 50% modulation, from 87% (insulating VO2) to 43% (metallic VO2) average absorption. These concepts and results along with photovoltaic and other optical and optoelectronic device applications will be discussed.

10369-6, Session 2

Thermal radiation management by metasurfaces

Sandeep Inampudi, Mohammad Mahdi Salary, Hossein Mosallaei, Northeastern Univ. (United States)

Controlling and confining the flow of thermal radiation is one of the key factors in most of the current nano-scale to macro-scale devices. While the existing principles of metasurfaces originally designed for coherent sources are not directly applicable here, we present by combining the principles of electromagnetic theory with the fluctuation-dissipation theorem, engineered nanostructures to manipulate thermal radiation emission from hot bodies. Utilizing the developed formulation, we design a composite structure consisting of both metamaterials and metasurfaces that simultaneously controls both the emission magnitude and direction of thermal radiation.

10369-7, Session 2

High temperature ENZ plasmonics and thermal graphene metamaterials *(Invited Paper)*

Zubin Jacob, Purdue Univ. (United States)

No Abstract Available

10369-8, Session 3

Amorphous metamaterials for large scale day-time radiative cooling *(Invited Paper)*

Xiaobo Yin, Univ. of Colorado Boulder (United States)

We demonstrate a 300-mm-wide, amorphous, organic-inorganic hybrid metamaterial manufactured on a roll-to-roll extruder for effective day-time radiative cooling. It has an infrared emissivity greater than 0.93 across the entire atmospheric window (8-13μm) while being fully transparent to solar irradiance, approaching the theoretical limit of spectroscopic performance for day-time radiative cooling. We also demonstrated an averaged noon-time (11 am-2 pm) radiative cooling power of 93 W/m2 and greater than 110 W/m2 averaged cooling power during a continuous three-day field test. The scalably manufactured metamaterial shows potential for large-scale cooling applications, such as cool roofs and the cooling of solar cell panels to improve cell efficiency.

10369-9, Session 3

Super-cool paints: Optimising composition with a modified four-flux model

Marc A. Gali Labarias, Matthew D. Arnold, Angus R. Gentle, Geoffrey B. Smith, Univ. of Technology, Sydney (Australia)

Optimization approaches to formulating paint able to create cool roofs is examined. Such paints maintain a roof under summer sun at temperatures close to or below ambient to reduce cooling demand in buildings and help to reduce peak urban air temperatures (the UHI problem). The aim is albedos in the range 90% to 96% so maximised spectral reflectance R(?) across the solar spectrum is required. 95% is easy to achieve at visible wavelengths but achieving best values also in the NIR remains a major challenge. Low cost for materials and a fast application process is also needed for city scale impacts and very large areas. At NIR wavelengths typical low cost, cool painted surfaces reduce NIR backscattering and raise NIR absorption. Composite structures that retain high visible reflectance while producing high NIR reflectance are possible. A variety of composite structures are studied and ranked according to their albedo.

Models and some data include impact of fill factors, particle size and material, size mix, and possible binder materials. The model used is a variation of the classical four-flux method, a differential method that solves the energy transfer problem through four balance equations. We use a different approach to the characteristic differential parameters to define the absorptance and scattering of the complete complex composite. This generalization allows extension to consider size dispersion of each type of particle used and various binders.

10369-10, Session 3

3D printable optical structures for sub-ambient sky cooling

Angus R. Gentle, Altay Nuhoglu, Matthew D. Arnold, Geoffrey B. Smith, Univ. of Technology, Sydney (Australia)

There has been continued recent interest in radiative sky cooling of flat surfaces, due to the ability to passively attain sub-ambient temperatures. As the clearest sky (lowest incoming infrared radiation) occurs at the zenith, ideally a surface will see this region of the sky, while limiting the view of the near horizon which has significantly more incoming radiation. Two approaches to this are angular selectivity, which limits outgoing as well as incoming radiation, and macroscopic reflectors which limit incoming sky radiation, while maximising the outgoing emitted radiation. This work focuses on the second of these techniques. Here we maximise the cooling potential via coated 3D printed structures which can passively maintain a thermal reservoir below ambient temperature throughout the night and day. We demonstrate novel design methods, to fabricate and test structures which maximise outgoing thermal radiation from a surface, while

minimising incoming radiation from the sky and sun. Preliminary results gave 10°C below both ambient both day and night during a Sydney summer. 3D printing allows the production of complex designed mirror cones with relatively low thermal conductivity. Post processing of the 3D printed structures allows the desired surface textures and optical properties to be created.

10369-11, Session 4

The superradiant effect in thermal emission *(Invited Paper)*

Zongfu Yu, Univ. of Wisconsin Madison (United States)

When wave effects of thermal photons become significant, thermal emitters can exhibit intriguing coherent effects. Here, we show that the superradiant emission, which was originally found in quantum emitters, can be realized in resonant thermal emitters. Similar to the superradiance in quantum emitters, the in-phase oscillation of resonant emitters reduces the lifetime of thermal photons in the emitters. Unlike the atomic superradiance, one remarkable consequence of the thermal superradiance is the anomalous power scaling, where the emission power can scale inversely with the number of thermal emitters. More thermal emitters generate less power due to the coherent interference of thermal photons.

10369-12, Session 4

Radiative cooling for concentrating photovoltaic systems

Yubo Sun, Zhiguang Zhou, Xingshu Sun, Muhammad Ashraful Alam, Peter Bermel, Purdue Univ. (United States)

Radiative cooling, merging as a unique but not widely used passive cooling method for devices operating outdoors, has been studied and demonstrated to be effective for photovoltaic thermal management. In this work, we investigate the effect of radiative cooling as a complementary to existing passive cooling methods like convective cooling for a system with much higher heat load, a concentrating photovoltaics (CPV) system, where severe thermal management challenges are encountered. A feasible radiative cooling enabled CPV system is proposed with its theoretical cooling limit calculated. Compared with a CPV system cooled via convective cooling only (with zero emittance), radiative cooling enables another temperature drop over ~36 K with an area ratio of ~800 at 1000 suns concentration and limited convection. A systematic simulation with realistic cooler design is then performed. The radiative cooler proposed in this work consists of low-iron soda-lime glass with a porous layer on top as an anti-reflection coating. It is found that a simple structure as proposed has strong mid-IR emittance as well as spectral selectivity that resembles an ideal cooler. Subsequently, the geometry of the radiative-cooled CPV system is optimized. The net result for a crystalline silicon PV is a relative increase in power production of at least 18% via radiative cooling and substantially higher reliability. Furthermore, the associated cooler volume can be substantially reduced relative to a finned convective heat sink.

10369-13, Session 4

Structure optimization of metallodielectric multilayer for high-efficiency daytime radiative cooling

Takahiro Suichi, Atsushi Ishikawa, Yasuhiko Hayashi, Kenji Tsuruta, Okayama Univ. (Japan)

Engineered metallodielectric nanostructures offer a new platform for controlling thermal emission in a desired manner, thus promise potential applications in passive cooling devices. Here, we present optimization design of metallodielectric multilayer structures for high-efficiency daytime radiative cooling and experimentally characterize their cooling performance. The device structure consisted of alternating layers of SiO2 and PMMA on an Al mirror, which worked as a selective thermal emitter at 8-13 μm with a high reflectance for sunlight. Automated design scheme based on simulated annealing method combined with photonic-thermal analysis was developed and applied to search the optimized number and thickness of each layer. The evaluation function in the optimization process was predefined such that a net emission power would be maximized at the ambient temperature of 300 K under the sunlight irradiation of AM1.5. The numerical results proved efficient radiative cooling to 2.5 K below the ambient temperature, corresponding to 13.5 K below the bare Al mirror temperature. Based on the optimized design, the device was fabricated on an Al mirror by using SiO2 deposition and spin-coating process over an area of 25 mm ? 25 mm. The reflectance and absorption properties of the fabricated device were characterized to demonstrate the selective thermal emission at the mid-infrared region. The equilibrium temperature of the device was also investigated to demonstrate the cooling performance under the direct sunlight irradiation.

10369-14, Session 5

High performance incandescent light bulb using a selective emitter and nanophotonic filters *(Invited Paper)*

Arny Leroy, Bikram Bhatia, Kyle Wilke, Evelyn N. Wang, Massachusetts Institute of Technology (United States)

While traditional incandescent light bulbs (ILB) are inefficient – reaching a luminous efficiency of just about 2% as most of the energy is radiated as infrared, they are still often preferred over alternatives because of their low price and high color rendering index (CRI). Previous approaches to improve the efficiency of ILBs have relied on tailoring the emitted spectrum using cold side interference filters that reflect the infrared energy back to the filament while transmitting the visible light. While this approach has, in theory, potential to surpass light-emitting diodes (LEDs) in terms of luminous efficiency while conserving the excellent CRI, system-level losses and challenges such as low view factor, high filament (>2800 K) and filter temperatures and tungsten evaporation have significantly limited the maximum efficiency. In this work, we propose combining a cold side filter with a selective emitter to further enhance the efficiency while preserving a near-perfect CRI. In particular, we analyze the effect of non-idealities of the cold side filter and the selective emitter on the luminous efficiency. On the cold side filter, we show that high reflectivity in the infrared and near unity view factor is critical. On the emitter side, we demonstrate that high emissivity in the visible combined with low emissivity in the infrared can lead to efficiencies higher than ILBs and even LEDs. Finally, we show that this approach can match the efficiency of LEDs while operating at much lower temperatures (2350 K) than conventional ILBs, thus alleviating the system-level challenges due to high temperatures.

10369-15, Session 5

Nanostructure enhanced near-field radiative heat transfer and designs for energy conversion devices

Bingnan Wang, Chungwei Lin, Koon Hoo Teo, Mitsubishi Electric Research Labs. (United States)

Near-field radiative heat transfer can exceed the blackbody limit, and this property has been explored toward energy transfer and conversion applications, such as thermophtovoltaic (TPV) devices, radiative cooling devices, and thermoradiative (TR) devices. The coupling of resonant modes between two surfaces is important in near-field heat transfer and near-field TPV systems. Recently, coupled-mode theory has been developed for the analysis and optimal design of TPV systems. In this paper, we show that all important parameters, including near-field emissivity of an emitter, the transmissivity from an emitter to an absorber, the radiation power from the emitter, the electric power generated by the photovoltaic (PV) cell, and eventually the power conversion efficiency of a near-field TPV system, can

be calculated from the resonant modes that are supported by the system. The calculation can be applied to both planar configurations, as well as nanostructured systems. While the frequency of surface plasmon polariton (SPP) resonance is fixed for a planar emitter, a nanostructured emitter supports additional resonances such as SPP or cavity modes with lower frequencies that are closer to the bandgap energy of a typical TPV cell. We show that this significantly improves the near-field radiative power transfer and electric power output for a TPV system.

10369-16, Session 5

Fabrication and thermal analysis of micro thermocouples for energy harvesting

Brhayllan Mora-Ventura, Gabriel González, Francisco Javier González, Univ. Autónoma de San Luis Potosí (Mexico)

We present the thermal study of micro thermocouples fabricated by electron beam lithography process, the micro thermocouples (MTCs) are based on a recently discovered thermoelectric effect in single-metal nanostructures with cross-sectional discontinuity, single-metal MTCs would simplify the fabrication process and allow the large-scale production of these devices using fabrication technologies such as nanoimprint lithography. In this work, we have investigated the temperature difference between the asymmetric unions of the micro thermocouples using Optotherm EL InfraSight 320 thermal imaging camera. Results show that single-metal MTCs are promising structures that could be used to harvest thermal radiation and generate electric energy through the Seebeck effect.

10369-17, Session 5

Demonstration of 24% efficient thermophotovoltaic energy conversion using 1055 C selective emitter

David Woolf, Physical Sciences Inc. (United States); Emil A. Kadlec, Don Bethke, Eric A. Shaner, Sandia National Labs. (United States); Joel Hensley, Physical Sciences Inc. (United States)

We demonstrated thermophotovoltaic (TPV) energy conversion using a selective thermal emitter whose emissivity was designed to match the external quantum efficiency of a 0.6 eV bandgap photovoltaic (PV) cell. Additional filtering of the transmitted radiation was achieved using a dielectric filter between the emitter and the PV cell. With the emitter at 1055 C, we measured 0.189 Watts/cm2 of power out of the PV cell. From a series of experiments, we were able to determine that the PV cell converted 24% of the power incident upon it into electricity.

Conference 10370: Reliability of Photovoltaic Cells, Modules, Components, and Systems X

SPIE. OPTICS+ PHOTONICS OPTICAL ENGINEERING+ APPLICATIONS

Sunday - Monday 6 –7 August 2017

Part of Proceedings of SPIE Vol. 10370 Reliability of Photovoltaic Cells, Modules, Components, and Systems X

10370-1, Session 1

Comparison of higher irradiance and black panel temperature UV backsheet exposures to field performance *(Invited Paper)*

Thomas C. Felder, William J. Gambogi, Steven W. MacMaster, Bao-Ling Yu, T. John Trout, DuPont Photovoltaic Solutions (United States)

Current IEC standard 61215 was adopted in 2005 and has been useful in revealing design flaws and manufacturing defects, but does not address long-term durability. The IEC is now developing a Weathering Technical Standard for backsheet qualification, IEC 62788-7-2, and an important component of this proposal is a higher irradiance and higher black panel temperature UV Xenon exposure (0.8W/sqm-nm and 90C BPT). Comparing results with field data is needed. We have tested polyester-based and PVF-based backsheets according to the proposed standard. Along with exposure, several specimen stuctures based on glass / EVA laminates are proposed to mimic the backsheet service environment. Samples were exposed as glass / EVA / EVA / backsheet laminates, and in the same structure with a transparent separator sheet between the backsheet and the EVA. Samples were exposed on both the airside and glass side.We find PET yellowing with no mechanical loss at the current 0.55 W/sqm-nm 70C BPT exposure condition. Increasing irradiance alone has no effect on yellowing, but leads to an observable drop in % elongation in the PET backsheets. Increasing black panel temperature with the higher irradiance increases both PET yellowing and mechanical loss. Comparative field results taken from a database of panels in the field 4 - 14 years. Results from the new exposure are closer to field data

10370-2, Session 1

Degradation analysis of field exposed photovoltaic modules with non-fluoropolymer-based backsheets

Andrew Fairbrother, National Institute of Standards and Technology (United States); Scott Julien, Kai-Tak Wan, Northeastern Univ. (United States); Liang Ji, Kenneth P. Boyce, Underwriters Labs. Inc. (United States); Sebastien Merzlic, Amy A. Lefebvre, Greg O'Brien, Arkema Research Ctr. (United States); Yu Wang, Laura S. Bruckman, Roger H. French, Case Western Reserve Univ. (United States); Michael D. Kempe, National Renewable Energy Lab. (United States); Xiaohong Gu, National Institute of Standards and Technology (United States)

The polymeric components of photovoltaic (PV) modules have changed little since the inception of the PV industry, with ethylene-vinyl acetate and fluoropolymer-based laminates being the most widely adopted encapsulant and backsheet materials, respectively. The backsheet in particular must serve as electrical insulation and to protect the solar cells from weathering. Due to continued downward pressure on cost, non-fluoropolymer-based materials are being modified to withstand outdoor exposure, including polyester- and polyamide-based backsheets. Because of their relatively recent deployment, less is known about their reliability and if they can stand up to the 25+ year warranty rated lifetimes of PV modules.

In that context this work presents a degradation analysis of field-exposed modules with polyester- and polyamide-based backsheets. Modules were exposed for up to five years in different geographic locations: USA (Ohio), Italy, China, and unexposed. Surface and cross-sectional analysis included visual inspection, colorimetry, gloss, Raman and Fourier-transform infrared spectroscopies, and scanning electron microscopy. Each module experienced different types and profiles of degradation depending on the exposure site, even for the same material and module brand. For instance, the polyamide-based backsheet experienced microcracking and greater yellowing in China, while in Italy it underwent macroscopic cracking and higher changes in gloss. Spectroscopic studies led to identification of degradation products and changes in polymer structure over time. Comparisons will be made to fielded modules with fluoropolymer-based backsheets, as well as materials in accelerated laboratory exposures. Implications for the service life prediction of the non-fluoropolymer-based backsheets will be discussed.

10370-3, Session 1

Comparison of PV module backsheet materials under multi-factor accelerated UV light exposures

Addison G. Klinke, Case Western Reserve Univ. (United States); Abdulkerim Gok, Case Western Reserve Univ. (United States) and Gebze Technical Univ. (Turkey); Roger H. French, Laura S. Bruckman, Case Western Reserve Univ. (United States)

Long term outdoor durability of photovoltaic module backsheets is critical to the module's power output over lifetime. The use of fluoropolymer-based backsheets or the addition of stabilizers to polyethylene-terephthalate (PET) and polyamide (PA) type backsheets can help extend the lifetime of these backsheets. In this study, the performance of 20 different types of backsheets under ASTM G154 Cycle 4 accelerated light exposures are presented. The backsheets were subjected to 4000 hours of high irradiance UVA light at 1.55 W/m2/nm at 340 nm at 70 oC with or without condensing humidity cycle. Backsheets were evaluated, with repeated measurements, using various evaluation techniques to identify and assess potential degradation mechanisms. These evaluations included the change in yellowness index (YI), gloss, UV-Vis absorbance, and Infrared spectroscopy. Fluoropolymer-based backsheets were found to withstand these exposure with only slight changes; however, PET and PA based backsheets showed serious yellowing and cracking under indoor exposures, and the stabilizer additives only helped protecting the polymers to some extent. Semi-supervised, generalized, network structural equation modeling (netSEM) analytics was then applied in order to explore statistically significant relationships describing the degradation of materials. In this stress | mechanism | response (< S|M|R>) framework, the type and level of multiple stressors (UV light, heat, humidity) and the observed physical and chemical responses are connected with statistical models to discover a network of mechanistic degradation pathways identifying factors contributing to overall degradation.

10370-4, Session 1

Characterizing the weathering induced changes in the optical performance and properties of poly(ethylene-terephthalate) via MaPd:RTS spectroscopy *(Invited Paper)*

Devin A. Gordon, Case Western Reserve Univ. (United States); Lin DeNoyer, Deconvolution & Entropy Consulting (United States); Corey W. Meyer, Noah W. Sweet, Case Western Reserve Univ. (United States); David M. Burns, 3M

Co. (United States); Laura S. Bruckman, Roger H. French, Case Western Reserve Univ. (United States)

Poly(ethylene-terephthalate) (PET) film is widely used in photovoltaic module backsheets for its dielectric breakdown strength, and in applications requiring high optical clarity for its high transmission in the visible region. However, PET degrades and loses optical clarity under exposure to ultraviolet (UV) irradiance, heat, and moisture. Stabilizers are often included in PET formulation to increase its longevity; however, even these are subject to degradation and further reduce optical clarity. To study the weathering induced changes in the optical performance and properties in PET films, samples of a UV-stabilized grade of PET were exposed to heat, moisture, and UV irradiance as prescribed by ASTM-G154 Cycle 4 for 168 hour time intervals. In a previous study it was found that material yellowing is dominant under exposure to UV light, while the addition of moisture to the exposure increases the light scattering behavior of the samples. UV-Vis reflection and transmission spectra were collected via Multi-Angle, Polarization-Dependent, Reflection, Transmission, and Scattering (MaPd:RTS) spectroscopy after each exposure interval. The resulting spectra were used to calculate the complex index of refraction throughout the UV-Vis spectral region via an iterative optimization process based upon the Fresnel equations. The index of refraction and extinction coefficient were found to vary throughout the UV-Vis region with time under exposure. The spectra were also used to investigate changes in light scattering behavior with increasing exposure time. The intensity of scattered light was found to increase at higher angles with time under exposure.

10370-5, Session 2

Comparison of modeled and experimental PV array temperature profiles for accurate interpretation of module performance and degradation

Teri Elwood, Kelly Simmons-Potter, The Univ. of Arizona (United States)

Quantification of the effect of temperature on photovoltaic (PV) module efficiency is vital to the correct interpretation of PV module performance under varied environmental conditions. However, previous work has demonstrated that PV module arrays in the field are subject to significant location-based temperature variations associated with, for example, local heating/cooling and array edge effects. Such thermal non-uniformity can potentially lead to under-prediction or over-prediction of PV array performance due to an incorrect interpretation of individual module temperature de-rating. In the current work, a simulated method for modeling the thermal profile of an extended PV array has been investigated through extensive computational modeling utilizing ANSYS, a high-performance computational fluid dynamics (CFD) software tool. Using the local wind speed as an input, simulations were run to determine the velocity at particular points along modular strings corresponding to the locations of temperature sensors along strings in the field. The point velocities were utilized along with laminar flow theories in order to calculate Nusselt's number for each point. These calculations produced a heat flux profile which, when combined with local thermal and solar radiation profiles, were used as inputs in an ANSYS Thermal Transient model that generated a solar string operating temperature profile. A comparison of the data collected during field testing, and the data fabricated by ANSYS simulations, will be discussed in order to authenticate the accuracy of the model.

10370-6, Session 2

Artifact-free coring of solar modules

Helio R. Moutinho, Steve Johnston, Bobby To, Chun-Sheng Jiang, Chuanxiao Xiao, Peter Hacke, John Moseley, Jerry Tynan, National Renewable Energy Lab. (United States); Neelkanth G. Dhere, Univ. of Central Florida (United States); Mowafak M. Al-Jassim, National Renewable Energy Lab. (United States)

Traditionally, researchers have studied solar panel performance and degradation by analyzing parameters such as efficiency and output power, which are measures of bulk properties. However, manufacturers would find it useful to know how these properties are related to local degradation that is associated with microscopic defects. The first requirement in performing this type of research is to develop procedures for removing (coring) small specimens from a solar panel without changing their properties during the process. Indeed, little information is available in the literature on this subject. In this work, we will describe our development of two coring procedures applied to Si, CdTe, and CIGS solar panels.

We developed the first procedure to accommodate most solar panels, which use tempered glass that shatters into small pieces when cut. In this case, we first shattered the glass and then cut the cores. Finally, we used a process to dissolve the ethylene vinyl acetate to obtain small pieces of the panel.

In the second procedure, we did a partial coring, i.e., we cored part of the panel, excluding the tempered glass. Then we attached a post with glue to the cored part of the panel and removed the sample from the panel.

To locate specific areas to be cored, we used electroluminescence and dark lock-in thermography. To investigate possible damage of structural and electro-optical properties during coring, we evaluated material quality by different analytical techniques, such as scanning electron microscopy, energy-dispersive X-ray spectroscopy, electron backscatter diffraction, scanning Kelvin probe force microscopy, and electron-beam induced current. In particular, to investigate changes in the defect structure, we analyzed some samples before coring by electroluminescence, and after coring by photoluminescence—on exactly the same area.

In this work, we describe in detail the two coring procedures applied to different kinds of modules, and show results of different analyses that prove the efficacy and reliability of our coring procedures.

10370-22, Session 2

Temperature coefficient of power (Pmax) of field aged PV modules: Impact on performance ratio and degradation rate determinations

Farrukh Mahmood, Hatif Majeed, Haider Agha, Saddam Ali, USPCAS-E, National Univ. of Sciences and Technology (Pakistan); Sai Tatapudi, Telia Curtis, GovindaSamy TamizhMani, Arizona State Univ. (United States)

The determinations of performance ratio (per IEC 61724 standard) and degradation rate (using slope of performance ratio over time) of photovoltaic (PV) modules in a power plant are computed based on the power (Pmax) temperature coefficient data of the unexposed modules or the exposed modules during the commissioning time of the plant. The temperature coefficient of Pmax is typically assumed to not change over the lifetime of the module in the field. Therefore, this study was carried out in an attempt to investigate the validity of this assumption and current practice. Several 15-20 years old field aged modules from four different manufacturers underwent baseline light I-V measurements and dark I-V measurements to determine the power temperature coefficient and series resistance for each module. Using the dark I-V and light I-V data, the series resistances (Rs) and shunt resistances (Rsh) were calculated in order to determine their impact on fill factor (FF) and hence on Pmax. The result of this work indicates a measurable drop in fill factor (FF) as the series resistance (Rs) increased which in turn increases the temperature coefficient of Pmax. This determination goes against the typical assumption that the temperature coefficient of (Pmax) for aged modules does not change over time. The outcome of this work has a significant implication on the performance ratio and degradation rate determinations based on the temperature coefficient of Pmax of new modules which is not an accurate practice for analyzing field aged modules.

10370-7, Session 3

Exposure of CIGS solar cells to negative, zero and positive electrical biases in a damp-heat Illumination environment *(Invited Paper)*

Mirjam Theelen, TNO (Netherlands) and Solliance (Netherlands); Klaas Bakker, Energy Research Ctr. of the Netherlands (Netherlands) and Solliance (Netherlands); Henk Steijvers, Gabriela De Amorim Soares, Soheyl Mortazavi, TNO (Netherlands) and Solliance (Netherlands); Jeroen Vink, ReRa Solutions B.V. (Netherlands); Nicolas Barreau, Institut des Matériaux Jean Rouxel (France); Erik Haverkamp, ReRa Solutions B.V. (Netherlands)

In earlier studies, unencapsulated CIGS solar cells were exposed to damp heat and illumination in an hybrid degradation setup, while their electrical parameters were real-time determined. In these studies, solar cells were kept under open circuit voltage, while operating solar cells perform at the maximum powerpoint, while shading can lead to negative voltages. Since it is known that exposure to small and large (reverse) bias voltages can modify [1,2,3] device performance, electrical loads were installed in the hybrid degradation setup.

Unencapsulated CIGS solar cells were exposed to damp heat and illumination, combined with open circuit, maximum powerpoint, short circuit and negative (-0.5V) voltage biases. In a preliminary study, differences could not be observed for the zero and positive voltages, while the solar cells under negative bias degraded faster. This was mostly caused by a more rapid decrease of the open circuit voltage of these cells.

In a second experiment, CIGS solar cells were exposed to the same conditions, which were changed after ~73 hours. Cells previously exposed to zero or positive biases, were set to -0.5V, while the cells exposed to -0.5V were exposed to -1.5V. These changes led to efficiency decreases of over 1 % point. It was therefore concluded that sudden negative bias exposure of these unencapsulated cells had a strong negative effect on their performance.

[1] K. Sinapis et al., Proc. 42th IEEE PVSC (2015) 1-5

[2] V. Fjällström et al., IEEE Journal of Photovoltaics 3 (3) (2013) 1-5

[3] S. Yamaguchi et al., Japanese Journal of Applied Physics 54 (2015) 08KC13

10370-17, Session 3

Ultrashort pulsed laser ablation for decollating of solid state lithium-ion batteries

Christian J. Hördemann, Hemanth Anand, Arnold Gillner, Fraunhofer-Institut für Lasertechnik (Germany)

Rechargeable lithium-ion batteries with liquid electrolytes are the main energy source for many electronic devices that we use in our everyday lives. But there are drawbacks of this energy storage technology as the liquid electrolyte impose a great danger to the user and the environment. Also lithium-ion batteries are limited in voltage, energy density and the range of operating temperature. One novel and promising battery technology are Solid-State Lithium-Ion Batteries (SSLBs) that can be produced without limitations to the geometry, are bendable in contrast to conventional batteries, have a high volumetric and gravimetric energy density and are intrinsically safe since no liquid electrolyte is used. However, manufacturing costs are still high and existing production-technologies are comparable to the processes used in the semiconductor industry. Single cells are produced in batches with masked-deposition at low rates. In order to decrease manufacturing costs and to move towards continuous production, Roll2Roll production methods offer the possibility to produce large quantities of substrates with deposited SSLB-layers. From this coated substrate, single cells can be cut out. For the flexible decollation of SSLB-cells from the substrate, new manufacturing technologies have to be developed since blade-cutting, punching or conventional laser-cutting lead to short circuits between the layers. Here, ultra-short pulsed laser ablation and cutting allows the flexible decollating of SSLBs. By selective ablation of individual layers, an area for the cutting kerf is prepared so that a shortcut-free decollation is possible. The approach can easily be transferred to the decollating of flexible electronics and flexible solar modules since the production process is similar.

10370-9, Session 4

Impact of PID on industrial roof-top PV-installations

Claudia Buerhop-Lutz, Frank W. Fecher, Tobias Pickel, Tirth Patel, Bayerisches Zentrum für Angewandte Energieforschung e.V. (Germany); Cornelia Zetzmann, Rauschert GmbH (Germany); Christian Camus, Jens A. Hauch, Bayerisches Zentrum für Angewandte Energieforschung e.V. (Germany); Christoph J. Brabec, Bayerisches Zentrum für Angewandte Energieforschung e.V. (Germany) and i-MEET (Germany)

Potential induced degradation (PID) causes severe damage and financial losses even in modern PV-installations. In Germany, approximately 19% of PV-installations suffer from PID [1] and resulting power loss. This paper focuses on the understanding of PID generation in real installations.

What promotes the unexpected inhomogeneous and fast development of PID on rooftop installations of industrial buildings? How does PID impact the module performance?

The analysis focuses exemplarily on a 314 kWp PV-installation in the Atlantic coastal climate. IR-imaging [2, 3] is used for identifying PID without operation interruption. Continuous historic electric performance data are available from a monitoring system on string level as well as punctually measured string IV-curves. Both data sets are combined for understanding the PID behavior of this PV plant.

The number of PID affected cells within a string varies strongly between 1 to 22% with the string position on the building complex after an operation period of just 3 years. With increasing number of PID-affected cells the performance ratio (PR) decreases down to 60%. Local differences in PID evolution rates are identified. A PR-reduction of 3.65% per year is found for the PV-plant.

The analysis reveals that PID generation and progress in rooftop installations on industrial buildings can be fairly complex. The results yield that local conditions, e. g. ambient weather conditions (solar irradiance, temperature, humidity, wind) as well as shading and influence of distinct roof installations, e. g. heat or dust emissions on an industrial building, seem to have a dominating impact on the PID degradation rate.

[1] M. Fuhs; PV magazine März (2016) 52.

[2] C. Buerhop, et al., SPIE Optics & Photonics (2016).

[3] T. Kaden, et al.; Solar Energy Materials and Solar Cells 142 (2015) 24.

10370-10, Session 4

Effect of bias application or light irradiation during PID tests of CIGS modules and crystalline silicon modules

Keiichiro Sakurai, Kinichi Ogawa, Hajime Shibata, Atsushi Masuda, National Institute of Advanced Industrial Science and Technology (Japan); Hiroshi Tomita, Darshan Schmitz, Shuuji Tokuda, Solar Frontier K.K. (Japan)

We experimentally studied the effects of forward bias application or light irradiation during PID tests of CIGS, as well as of some crystalline silicon (c-Si) modules. 96 hours of PID tests were conducted on modules after

300~1000 hours of damp heat testing. Some modules have shown lesser degradation by irradiating white LED (blue+yellow) light during PID tests. We would also report on effects of forward bias voltage during PID tests.

10370-21, Session 4

Mitigation of PID in commercial PV modules using current interruption method

Birinchi Bora, National Institute of Solar Energy (India) and TERI Univ. (India); Jaewon Oh, Sai Tatapudi, Arizona State Univ. (United States); Oruganty Sastry, Rajesh Kumar, National Institute of Solar Energy (India); Basudev Prasad, TERI Univ. (India); Govindasamy Tamizhmani, Arizona State Univ. (United States)

Potential induced degradation (PID) is known to have a very severe effect on the reliability of PV modules. PID is caused due to the leakage of current from the cell circuit to the grounded frame under humid conditions of high voltage PV systems. There are multiple paths for the current leakage. The most dominant leakage path is from the cell to the frame through encapsulant, glass bulk and glass surface. This dominant path can be prevented by interrupting the conductivity at the glass surface. In our previous works related to this topic, we demonstrated the effectiveness of glass surface conductivity interruption technique using one-cell PV coupons. In this work, we demonstrate the effectiveness of this technique using a full size commercial module susceptible to PID. The interruption of surface conductivity of the commercial module was achieved by attaching a narrow, thin flexible glass strips, from Corning, called Willow Glass® on the glass surface at the inner edges of the frame. The flexible glass strip was attached to the module glass surface by heating the glass strip with an ionomer adhesive underneath using a handheld heat gun. The PID stress test was performed at 60°C and 85% RH for 96 hours at ?600V. Pre- and post-PID characterizations including I-V and electroluminescence were carried out to determine the performance loss and affected cell areas. This work demonstrates that the PID issue can be effectively addressed by using this technique. An important benefit of this approach is that this interruption technique can be applied after manufacturing the modules and after installing the modules in the field as well.

10370-11, Session 5

Development of calibration standards for extremely low permeation measurement *(Invited Paper)*

Michael D. Kempe, Matthew O. Reese, Arrelaine A. Dameron, Dylan L. Nobles, Talysa R. Klein, Byron McDanald, National Renewable Energy Lab. (United States)

Flexible photovoltaic applications are typically made using thin film devices that are sensitive to moisture ingress. Because of this, there is a need to develop flexible barrier materials with permeation rates less than 10-4 g/m?/day. To put this in perspective, a permeation rate this low would be expected to pass enough water for a layer that is only 1 micron thick after 20 years. There are many methods suitable for measuring permeation rates this low but unfortunately, previously calibration standards suitable for validating these measurement methods below around 10-3 g/m?/day were not available.

In this work we demonstrate the development of a calibration standard suitable for measurement much less than 10-4 g/m?/day. These calibration standards are constructed by first drilling a ~2.3 mm diameter hole, inserting a glass capillary into the hole and sealing it using a low melting point glass solder creating a hermetic seal. The glass capillaries have an outer diameter of 2 mm and an inner diameter ranging between 0.025 mm and 1 mm. To further restrict moisture ingress through the capillary, it is filled with a polydimethyl siloxane elastomer. The moisture permeation properties of the silicone are known from transient permeation studies using conventional permeation equipment so that geometric considerations allow us to predict the moisture permeation rate through these standards and control it in the range from 1 g/m?/day to ~8·10-7 g/m?/day. This range of permeation rates is needed because it overlaps with conventional methods and NREL's custom method able to measure less than 10-6 g/m?/day to allow some inter-comparison with known and unknown permeation measurements.

10370-12, Session 5

Conducting paste based soldering process for thin crystalline silicon photovoltaic module

Hyung-Jun Song, Woo Gyun Shin, Ga Eon Jin, Gi-Hwan Kang, Korea Institute of Energy Research (Korea, Republic of)

Thin crystalline silicon photovoltaic (c-Si PV) module (< 100 um) will be dominant market owing to its low cost. However, high temperature soldering process for PV module to connect PV cells in serial and parallel induces bowing and crack of cells owing to different thermal expansion coefficient between silicon and ribbon. Moreover, it is expected that thermo-mechanical stress issues will deteriorate the performance of thin c-Si PV module. Thus, in this study, we demonstrated a low temperature soldering method based on conducting pastes (CP) for joint ribbon to C-Si PV. During the lay-up process, ribbon barely adhered to high viscosity CP printed busbar of PV cell. The temporally attached busbar and ribbon are securely connected each other at a low temperature (~ 150 °C) during the lamination process. The efficiency of module fabricated by our suggested method was similar to that of device based on high temperature process with soldering flux and tabbing. Especially, cell to module loss arising from increased resistance during the module process were at the same range in both cases. Furthermore, it was observed that bowing and micro-crack losses occurred in soldering process were suppressed in CP based module. Therefore, low temperature processed thin C-Si module with CP will reduce the losses and manufacturing cost without deteriorating its performance.

10370-13, Session 5

Data acquisition and PV module power production in upgraded TEP/AzRISE solar test yard

Whit Bennett, Asher Fishgold, Barrett G. Potter Jr., Kelly Simmons-Potter, The Univ. of Arizona (United States)

The Tucson Electric Power (TEP) and University of Arizona AzRISE (Arizona Research Institute for Solar Energy) solar test yard is continuing efforts to improve standardization and data acquisition reliability throughout the facility. Data reliability is ensured through temperature insensitive data acquisition (DAQ) devices with battery backups in the upgraded test yard. Software improvements allow for real-time analysis of collected data, while uploading to a web server. With no data failures over 365 days of data collection, the new loggers have proven to be both reliable and durable. In addition to improved DAQ systems, precision temperature monitoring has been implemented so that PV module backside temperatures are routinely obtained. Type-T thermocouples, shown to provide high measurement accuracy, have been applied in a standard, three-per-module sensor configuration. Sample data illustrates high fidelity monitoring of the burn-in period of a polycrystalline silicon photovoltaic module test string. Weather station data acquired at the test yard provide local ambient temperature, humidity, wind speed, and irradiance measurements that have been utilized to enable characterization of PV module performance over an extended test period.

10370-14, Session 5

Analyzing the degradation of pre-damaged PV-modules *(Invited Paper)*

Claudia Buerhop-Lutz, Sven Wirsching, Tobias Pickel, Christian Camus, Jens A. Hauch, Bayerisches Zentrum für Angewandte Energieforschung e.V. (Germany); Christoph J. Brabec, Bayerisches Zentrum für Angewandte Energieforschung e.V. (Germany) and i-MEET (Germany)

The presence of pre-damaged modules, especially with cell cracks and fractures, can be observed frequently in contemporary PV-installations which have been in service for some years [1, 2]. Up to now, most investigations, standards and test procedures focus on degradation of new, defect-free modules [3, 4]. Unknown/unclear is the degradation and lifetime of pre-damaged, cracked modules at real operating conditions.

This study highlights a twofold approach for the analysis of lifetime and degradation of pre-damaged PV—modules with cell cracks from a landslide claim: 1) Field monitoring and inspection data reveals information about real-life degradation of pre-damaged modules during 1 year of enduring outdoor exposure with highly temporarily resolved weather and performance data. Punctual EL-images visualize the new cracks – if observed - and their propagation. 2) For accelerated stress test a newly developed set-up for load testing is used. It allows the experimental simulation of planar load by under- or overpressure, which is typical for snow and wind loads. Simultaneous EL-imaging precisely records crack initiation and growth as well as crack opening under load and crack closure at unloaded stage.

This unique study yields information about load conditions on the degradation of pre-damaged modules, like load thresholds, crack orientation, most-affected cell positions, and statistics for crack appearance as well as the impact on the module performance.

[1] M. Köntges (2014) IEA.

[2] C. Buerhop, et al., SPIE Optics & Photonics (2016).

[3] U. Jahn, 11. Nationale Photovoltaik-Tagung (2013).

[4] Standard IEC 61215 1995, 2005.

10370-15, Session 5

Numerical simulation of wind flow over a photovoltaic solar panel using RANS equations

Andre Luiz Tenorio Rezende, Instituto Militar de Engenharia (Brazil) and Ctr. Univ. Augusto Motta - UNISUAM (Brazil); Katherine B. M. Leitão, Univ. Veiga de Almeida (Brazil); Neelkanth G. Dhere, Univ. of Central Florida (United States)

The aim of this study is the numerical simulation of wind flow over solar photovoltaic panels. At present there are 113 schools in Florida that use similar 10-kW photovoltaic (PV) solar energy systems installeds on their campus. The PV electricity is fed to the grid and reduces the consumption of grid electericity of the schools. Moreover, these schools serve as disaster relief shelters. During hurricanes or other disasters the grid electricity to the shelters may be cut for few weeks. The PV electricity can then serve to provide the minimum critical necessities during such periods. Because of strong winds and hurricanes in this region, it is essential to study the effect of flow of wind on photovoltaic panels. Such study can also be useful to design efficient protectors and supports to guard the panels. ypicals flows phenomena such as vortex shedding and boundary layer separation may influence the distribution of wind load on PV panels. Because of the similar PV system design and construction, the geometry of the solar panel installations and wind conditions would be similar in the PV systems in 113 Florida schools. The wind speed in critical conditions can reach 50 m/s. This work consists of a steady state and incompressible flow numerical simulation through the Reynolds Averaged Navier-Stokes equations (RANS). The turbulence closure model uses the shear stress transport (kw-SST).

The main results of the simulations are the pressure and velocity fields that are involved in loads that panels are being subjected to.

10370-16, Session PMon

Image analysis of PV module electroluminescence

Teh Lai, Claudia Ramirez, Barrett G. Potter Jr., Kelly Simmons-Potter, The Univ. of Arizona (United States)

Electroluminescence imaging can be used as a non-invasive method to spatially assess performance degradation in photovoltaic (PV) module. Cells, or regions of cells, that do not produce an infra-red luminescence signal under electrical excitation indicate potential damage in the module. In this study, an Andor iKon-M camera and an image acquisition tool provided by Andor have been utilized to obtain electroluminescent images of a full-sized multicrystalline PV module at regular intervals throughout an accelerated lifecycle test (ALC) performed in a large-scale environmental degradation chamber. Computer aided digital image analysis methods were then used to automate degradation assessment in the modules. Initial preprocessing of the images was designed to remove both background noise and barrel distortion in the image data. Image areas were then mapped so that changes in luminescent intensity across both individual cells and full module could be identified. Two primary techniques for image analysis were subsequently investigated. In the first case, pixel intensity was averaged over each individual PV cell and changes to the intensities of the cells over the course of an ALC test were evaluated. In the second approach, intensity line scans of each of the cells in a PV module were performed and variations in line scan data were identified during the module ALC test. In this presentation, both the image acquisition and preprocessing technique and the contribution of each image analysis approach to an assessment of degradation behavior will be discussed.

10370-18, Session PMon

Model development of degradation of PV modules backsheet with locating place of module

Yu Wang, Case Western Reserve Univ. (United States); Sebastien Merzlic, Arkema Research Ctr. (United States); Andrew Fairbrother, National Institute of Standards and Technology (United States); Lucas Fridman, Case Western Reserve Univ. (United States); Scott Julien, Northeastern Univ. (United States); Amy A. Lefebvre, Arkema Research Ctr. (United States); Xiaohong Gu, National Institute of Standards and Technology (United States); Liang Ji, Kenneth P. Boyce, Underwriters Labs. Inc. (United States); Michael D. Kempe, National Renewable Energy Lab. (United States); Kai-Tak Wan, Northeastern Univ. (United States); Roger H. French, Laura S. Bruckman, Case Western Reserve Univ. (United States)

Performance of photovoltaic modules under outdoor exposure is tightly related with the micro-environment around the module. The irradiance, temperature and humidity varies within a single array of modules. It is found that the position of a photovoltaic module within an array influences the yellowing and gloss-loss of its associated PV module backsheet, with PET outer layer, under exposure in Dfa climatic zone (Gaithersburg, MD). In this study, similar evaluation is conducted on modules with different backsheet materials exposed in the same climatic zone (Cleveland, OH). Stress/ Response models of yellowing and gloss-loss as function of module position, backsheet material and other related variables are under development. The chemical change of backsheet materials is investigated with FTIR spectroscopy and quantified with the intensity of selected peaks of normalized FTIR spectra. The selected peaks are also used as mechanistic variables to develop a Stress/ Mechanism/ Response model.

10370-20, Session PMon

Comparison of efficiency degradation in polycrystalline-Si and CdTe thin-film PV modules via accelerated lifecycle testing

Teh Lai, Barrett G. Potter Jr., Kelly Simmons-Potter, The Univ. of Arizona (United States)

Thin-film solar cells normally have the shortest energy payback time due to their simpler mass-production process compared to polycrystalline-Si photovoltaic (PV) modules, despite the fact that crystalline-Si-based technology typically has a longer total lifetime and a higher initial power conversion efficiency. For both types of modules, significant aging occurs during the first two years of usage with slower aging over the module lifetime. The PV lifetime and the return-on-investment for local PV system installations rely on long-term panel performance. Understanding the efficiency degradation behavior under a given set of environmental conditions is, therefore, a primary goal for experimental research and economic analysis. In the present work, in-situ measurements of key electrical characteristics (J, V, Pmax, etc.) in polycrystalline-Si and CdTe thin-film PV modules have been analyzed. The modules were subjected to identical environmental conditions, representative of southern Arizona, in a full-scale, industrial-standard, environmental degradation chamber, equipped with a single-sun irradiance source, temperature, and humidity controls, and operating an accelerated lifecycle test (ALT) sequence. Initial results highlight differences in module performance with environmental conditions, including temperature de-rating effects, for the two technologies. Notably, the thin film CdTe PV module was shown to be approximately 15% less sensitive to ambient temperature variation. After exposure to a five-month equivalent compressed night-day weather cycling regimen the efficiency degradation rates of both PV technologies were obtained and will be discussed.

10371-1, Session 1

Adhesive bonds for optics: analysis and trade-offs

John G. Daly, Vector Engineering (United States); Matthew D. Hawk, M. Hawk Consulting (United States)

Adhesives, normally epoxies are one of the most common solutions to mounting optical elements. This design decision can be considered a simple, low-cost fastening technique where a critical optical element must be attached to a metal (or plastic) structure. In most cases, especially commercial (room temperature) applications problem-free performance can be expected. However, in many cases a wide range of failures do occur. These include: adhesion failure, outgassing problems, movement during cure, movement after cure, optical distortion, stress birefringence, and even fracture of the lower strength optical element.

This paper will briefly touch on all aspects of the selection and application of an adhesive for fastening an optical element. The approach will attempt to derive a “rules of thumb” approach with general calculations to determine strength and predict stress situations. This provides set of analysis techniques that can be applied in each case to justify the proposed adhesive bond.

To support this analysis, 3D mechanical models are employed with finite element analysis where movement or distortion as well as stress can be predicted. Temperature changes are addressed where differential CTE (coefficients of thermal expansion) become a major concern. Shock and vibration loads as well as gravitational effects are also included. An accurate model is dependent upon not only the number of elements employed in the model, but also knowledge of all the mechanical properties and their changes with temperature.

The comparison using analysis and finite modeling will show trade-offs in selection of the optical material, the substrate, and the adhesive. This will be followed by bond geometry comparisons, that will lead into compensation designs with athermal bonds, monolithic designs, and flexure mechanical mounts.

10371-2, Session 1

Advancements in adhesive mounting of optics

Brian M. McMaster, Corning Tropel Corp. (United States)

Historic implementations of this method carried risk of UV degradation, photo contamination, long term stability, and long assembly cycle times. Others have developed non-adhesive friction/contact approaches to mount lenses but with significant compromises in durability and product cost. These two methods are contrasted and an optimal approach to achieve high lens mounting durability, low cycle time and negligible photo-contamination is demonstrated. Durability of this adhesive mounting solution will be established with examples including shock and vibration, mechanical stress decoupling factors, and optical stability over a wide range of shipping temperatures.

10371-3, Session 1

Use of composite housing materials in high-shock optical firearm environment

Rosa Seda, Leupold & Stevens, Inc. (United States)

Composite housing materials are available for many different optical applications but are not as common in optics for firearms. They are more prevalent in some night vision and thermal sights, but not as much in reflex or daytime optics. Reflex sight and daytime optics tend to use aluminum and magnesium housing due to their material and machining properties. Firearm optics need to pass a myriad of requirements including thermal, shock, drop and sealing. The challenges associated with composite housing are with bonding/adherence and molding. In this paper, the issues with bonding and mounting optics in a firearm reflex sight are studied, analyzed and tested.

In this study, two carbon fiber reinforced thermoplastic materials were studied and tested. The materials investigated were short carbon fiber reinforced PEEK (Polyether ether ketone) and PEI (Polyetherimide) materials. The first challenge associated with these materials was bonding them with optical material, electronic and other structural materials. The surface treatment of the composite was of great importance to increase bonded joint strength. In high shock environments, it is desirable to have good joint strength. In addition to this, other consideration were how absorbent the material was to UV, linear shrinkage, thermal coefficients and other mechanical properties. The second challenge is chemical compatability to firearm chemical cleaners and its effects on the composite. Other challenges included strength issues associated with shock. The optic needs to survive shock and drop test. To mitigate issues, finite element analysis with use of crack propagation theory was used to estimate stresses. The shock values are particularly high in this application, which will be tested and compared to the calculated values.

10371-4, Session 1

ZERODUR - bending strength: review of achievements

Peter Hartmann, SCHOTT AG (Germany)

Increased demand for using the glass ceramic ZERODUR with high mechanical loads called for strength data based on larger statistical samples. Design calculations for failure probability target value below 1: 100 000 cannot be made reliable with parameters derived from 20 specimens samples. The data now available for a variety of surface conditions, ground with different grain sizes and acid etched for full micro crack removal, allow stresses by factors four to ten times higher than before. The large sample revealed that breakage stresses of ground surfaces follow the three parameter Weibull distribution instead of the two parameter version. This is more reasonable considering that the micro cracks of such surfaces have a maximum depth which is reflects in the existence of a threshold breakage stress below which breakage probability is zero. This minimum strength allows calculating minimum lifetimes. Fatigue under load can be taken into account by using the stress corrosion coefficient for the actual environmental humidity. For fully etched surfaces Weibull statistics fails. The precondition of the Weibull distribution, the existence of weakest links, is not given anymore. ZERODUR with fully etched surfaces free from damages introduced after etching endures easily 100 MPa tensile stress. The possibility to use ZERODUR for combined high precision and high stress application was confirmed by the successful launch and continuing operation of LISA Pathfinder the precursor experiment for the gravitational wave antenna satellite array eLISA .

10371-5, Session 2

2-um optical time domain reflectometry measurements from novel Al-, Ge-, CaAlSi-doped and standard single-mode fibers

Jose Rodriguez-Novelo, Ctr. de Investigación e Innovación Tecnológica (Mexico); Abel Sanchez-Nieves, Instituto Politécnico Nacional (Mexico); Abraham Sierra-Calderon, Jose A. Alvarez-Chavez, Ctr. de Investigación e Innovación Tecnológica (Mexico)

The development of novel Al-, Ge- doped and un-doped standard single mode fibers for future optical communication at 2μm requires the integration of an optical time domain reflectometry (OTDR) technique for precise spectral attenuation characterization, including the well-known cut-back method. The integration of a state of the art OTDR at 2μm could provide valuable attenuation information from the aforementioned novel fibers. The proposed setup consists of a 1.7 mW, 1960nm pump source, a 30-dB gain Thulium doped fibre amplifier at 2μm, an 0.8mm focal length lens with a 0.5 NA, a 30 MHz acusto-optic modulator, a 3.1 focal length lens with a 0.68NA, an optical circulator at 2μm, an InGaAs photodetector for 1.2nm-2.6nm range, a voltage amplifier and an oscilloscope. The propagated pulse rate is 50KHz, with 500ns, 200ns, 100ns and 50ns pulse widths. Attenuation versus novel fibers types for lengths ranging from 400- to 1000- meter samples were obtained using the proposed setup.

Full description of the proposed state of art OTDR setup at 2μm, full reflectometry spectral results, and the spectral attenuation results of all fibers will be included in the presentation.

10371-6, Session 2

Large area of MCP electronic rinse system design

YaFeng Qiu, ChengXin Song, Nanjing Univ. of Science and Technology (China)

Through the reasonable arrangement of imported molecular pump and ion pump in vacuum System, to ensure that in 40 minutes to reach the vacuum degree of Pa to meet the requirement of electron rinse and test and to reach the ultimate vacuum degree of Pa. In this system, an efficient pumping device ensures that the vacuum system to reach the working environment for electron rinse as soon as possible. While the use of four-station design greatly improves efficiency of electron rinse and test of large area MCP.

An electronic surface-emitting source was redesigned in this system. The way it works is that the ultraviolet light source emits a uniform ultraviolet light on the gold cathode with voltage of several hundred volts, thus numerous uniform electrons are emitted from the surface of gold cathode. At the same time,0V ~ 700V adjustable high voltage is adopted between the gold cathode and the standard MCP(diameter of 105mm) to generate an accelerating electric field. After electrons are accelerated by the electric field, the high energy is obtained, and the standard MCP is bombarded. The number of electrons can be exponentially increased and controlled by the voltage applied between the input and output surface of the standard MCP.200v voltage is applied between the output surface of standard MCP and input surface of the MCP to be rinsed to lead the uniform electron beam to bombard the MCP to be rinsed, then the gas molecules and related impurities are cleared out in this process. In the original electron rinse system, which is suitable for the MCP with the diameter of 30mm,uniform emitted electrons are obtained by heating the planar spiral tantalum filament in the thermal electronic surface-emitting source in vacuum System. The largest effective emitting diameter of uniform electrons produced by such a thermal electronic surface-emitting source is 50mm, and it cannot meet the size requirement of the electron rinse of large area MCP. Meanwhile, prolonged use of this thermal electronic surface-emitting source causes the filament oxidation and deformation problems. And complexity of the tantalum filament production process and the design of the accelerating field makes difficult to guarantee the reliability of the uniformity of emission electrons. This successful design of the electronic surface-emitting source in the system not only overcomes the limitation of the thermal electronic surface-emitting source based on tantalum filament in use, but also the analysis of the results of the electronic uniformity testing experiment indicates the electronic uniformity of the electronic surface-emitting source has reached 98%,which is 5% higher comparing to the thermal electronic surface-emitting source based on tantalum filament in use.

10371-7, Session 3

LLIMAS: Revolutionizing integrated modeling and analysis at MIT Lincoln Laboratory

Keith B. Doyle, Gerhard P. Stoeckel, Justin J. Rey, MIT Lincoln Lab. (United States)

MIT Lincoln Laboratory is involved in the development of a broad array of optical systems including laser communications, directed energy, radiometric detectors, chemical sensing, laser radar, and imaging systems in support of science discovery and National security. LLIMAS (Lincoln Laboratory's Integrated Modeling and Analysis Software) was developed to optimize designs and enable new prototype systems to meet challenging SWaP and performance requirements while operating in harsh environments. LLIMAS utilizes a development philosophy that envelopes industry standard engineering tools in a unified framework. The software is highly extensible to provide custom analysis capabilities to support new program and technology needs. Current capabilities include the coupling of structural, thermal, optical, stray light, and CFD tools to provide unique insight into engineering performance and the interdisciplinary behavior typically unrealized by uncoupled simulations. Applications of LLIMAS on several optical system development efforts will be discussed.

10371-8, Session 3

The diffraction grating in Ivory's optomechanical constraint equations

Alson E. Hatheway, Alson E. Hatheway Inc. (United States)

The author's previous work (Proceedings of SPIE, 8840-16) describes the diffraction grating when the plane of incidence at the grating is orthogonal to the lay of the grating. This work develops the equations for the general case where the lay of the grating is rotated with respect to its surface normal so the direction of the desired diffraction order is a compound angle in the grating's coordinate system. The optomechanical constraint equations are developed and an example of their application is shown.

10371-9, Session 3

Linear analysis using secants for materials with temperature dependent nonlinear elastic modulus and thermal expansion properties

John W. Pepi, L-3 SSG (United States)

Thermally induced stress is readily calculated for linear elastic material properties using Hooke's law in which, for situations where expansion is constrained, stress is proportional to the product of the material elastic modulus and its thermal strain. When material behavior is nonlinear, one needs to make use of nonlinear theory. However, there are some situations in which we can avoid that complexity. For situations in which both elastic modulus and coefficient of thermal expansion vary with temperature, solutions can be formulated using secant properties. A theoretical approach is thus presented to calculate stresses for nonlinear, neo-Hookean, materials. This is important for high acuity optical systems undergoing large temperature extremes. The approach taken may not be new, but little information is available in the literature. While use of the secant coefficient of thermal expansion is well known, it is often misunderstood, and use of the secant modulus is even less understood and rarely used. The theoretical use defines a neo-Hookean law which can be used in a linear sense, making input for finite element analysis simplified, precluding the need for nonlinear modeling.

10371-10, Session 4

System engineering of complex optical systems for mission assurance and affordability

Anees Ahmad, Raytheon Missile Systems (United States)

Affordability and reliability are equally important as the performance and development time for many optical systems for military, space and commercial applications. These characteristics are even more important for the systems meant for global markets, where the competition from international suppliers is very real and intense, especially when it comes to total lifecycle costs. Most global customers are looking for high performance optical systems that are not only affordable but are designed with "no doubt" mission assurance, reliability and maintainability in mind. Both US military and commercial customers are now demanding an optimum balance between the performance and affordability. We must employ a disciplined systems design approach to meet the performance, cost and schedule targets while keeping affordability and reliability in mind. The Missile Defense Agency (MDA) now requires all of their systems to be engineered, tested and produced according to the Mission Assurance Provisions (MAP). These provisions/requirements are meant to ensure the system designs of large and expensive weapon systems are executed, designed, integrated, tested and produced with the reliability and total lifecycle costs in mind. This presentation will describe a system design approach based on the MAP document for developing sophisticated optical systems that are not only cost-effective but also deliver superior and reliable performance during their intended missions.

10371-11, Session 4

Optoelectronic methods and tools for pipeline's internal surface diagnosis

Radda A. Iureva, Evgenii O. Raskin, Nadezhda K. Maltseva, ITMO Univ. (Russian Federation); Alexandr V. Ilinsky, S.I. Vavilov State Optical Institute (Russian Federation)

Laser profiler includes a laser module, optical system, which deploys its radiation in the profile analysis' plane, and photodetector system with matrix detectors. The optical axis of the photodetector's lens system is located at a certain angle (viewing angle) to the analysis of the plane, so the photodetector array is formed by a distorted image of the profile of the analyzed surface. Under profile is meant the middle luminous tape's line, occurring at the surface under study by laser radiation. Obviously, the distortion of the picture profile will be minimal at an observation angle equal to 90 °. Computing system profiler on the distorted image profile can generate profilogram analyzed surface in digital form. Accuracy compliance profilograms profile particularly depends on the quality of laser illumination. Glowing tape investigated surface brightness may be asymmetrical in the transverse direction. This asymmetry can be caused by reflection ???? the heterogeneity investigated surface.

10371-12, Session 4

HabEx primary mirror trade studies

Jacqueline M. Davis, H. Philip Stahl, William R. Arnold Sr., W. Scott Smith, NASA Marshall Space Flight Ctr. (United States)

The Habitable Exoplanet (HabEx) is a NASA flagship mission to be considered for the 2020 Decadal Survey in Astronomy and Astrophysics. The concept is to develop an imaging system to detail the characteristics of planetary systems surrounding solar-type stars. The system must provide high contrast imaging and spectroscopy with a high signal-to-noise ratio and high stability. In this paper, we will present a point design for a 4 meter, off-axis, monolithic primary mirror to be used in the HabEx imaging system. An initial optimization of design parameters was performed to minimize distortions due to vibration while also maintaining a low areal density. Finite Element Models (FEM) of mirrors were created with varying mounting configurations, materials, depths, rib thicknesses, cell sizes, facesheet thicknesses, and depths. A harmonic analysis was performed on each model, and the corresponding displacements were output from the optical surface. The data from each model was imported into MATLAB and the distortion on the optical surface of each model was analyzed. Thus, the optimal design parameters were chosen based on the vibration performance of each design. The analysis and the chosen point design will be discussed further throughout the paper.

10371-13, Session 5

Design and test of precision vertical and horizontal linear nanopositioning flexure stages with centimeter-level travel range for x-ray instrumentation

Deming Shu, Barry Lai, Steven P. Kearney, Argonne National Lab. (United States); Jayson Anton, Argonne National Lab. (United States) and Univ. of Illinois at Chicago (United States); Wenjun Liu, Jörg Maser, Christian Roehrig, Argonne National Lab. (United States); Jonathan Z. Tischler, Oak Ridge National Lab. (United States)

The ever-increasing spatial resolution of nanofocusing hard x-ray optics, coupled with the need for long working distances and spectroscopic imaging, requires translating of optics and sample stages over millimeters with trajectory errors of 10 nm or less. To overcome the performance limitations of precision ball-bearing-based or roller-bearing-based linear stage systems, compact vertical and horizontal linear nanopositioning flexure stages, with centimeter-level travel range, have been designed and tested at the Advanced Photon Source (APS) for x-ray instrumentation applications. The mechanical design and finite element analyses of the flexural stages, as well as its detailed test results with laser interferometers are described in this paper.

10371-14, Session 5

Trajectory error analysis of a flexure pivot-type guide for linear nanopositioning

Steven P. Kearney, Deming Shu, Argonne National Lab. (United States)

With the current drive towards diffraction limited storage rings, hard x-ray optics will require subsequent increases in positioning accuracy over large travel ranges. Nanometer-level precision positioning requires the use of compliant mechanisms to remove friction and backlash type errors. Ideally, the compliant mechanism is compliant in the direction of desired travel and rigid in all other directions. However, in reality, there is still compliance in these other directions, particularly for flexure pivots, which lead to parasitic trajectory errors. In this paper we analyze the trajectory errors of a linear guiding mechanism, composed of commercially available C-FlexTM flexure pivots, using finite element analysis and experimental measurements. The guide is designed as an assembly of double parallel 4-bar type deformation compensated linear guiding mechanisms, and incorporates a novel 2:1 stabilizer unit to control the floating bar. The focus of the analysis is on the trajectory errors caused by rotation center shift, manufacturing tolerances, flexure pivot size, assembly tolerances, and includes a discussion of methods to mitigate these errors.

10371-15, Session 5

The development of alignment turning system for precision lens cells

Chien-Yao Huang, Cheng-Fang Ho, Wang Jung-Hsing, Lin Yi-hao, Chien-Kai Chung, Jun-Cheng Chen, Keng-Souo Chang, Kuo Ching-Hsiang, Wei-Yao Hsu, Instrument Technology Research Ctr. (Taiwan)

In general, the drop-in and cell-mounted assembly are used for standard and high performance optical system respectively. The optical performance is limited by the residual centration error and position accuracy of the conventional assembly. Recently, the poker chip assembly with high precision lens barrels that can overcome the limitation of conventional assembly is widely applied to ultra high performance optical system. ITRC also develops the poker chip assembly solution for high numerical aperture objective lenses and lithography projection lenses. In order to achieve high precision lens cell for poker chip assembly, an alignment turning system (ATS) is developed. The ATS includes measurement, alignment and turning modules. The measurement module including a non-contact displacement sensor and an autocollimator can measure centration errors of the top and the bottom surface of a lens respectively. The alignment module comprising tilt and translation stages can align the optical axis of the lens to the rotating axis of the vertical lathe. The key specifications of the ATS are maximum lens diameter, 400mm, and radial and axial runout of the rotary table < 2 ?m. The cutting performances of the AST are surface roughness Ra < 1 ?m, flatness < 2 ?m, and parallelism < 5 ?m. After measurement, alignment and turning processes on our ATS, the centration error of a lens cell with 200mm in diameter can be controlled less than 10 arcsec. This paper also presents the thermal expansion of the hydrostatic rotating table. A poker chip assembly lens cell with three sub-cells is accomplished with average transmission centration error in 12.45 arcsec by fresh technicians. The results show that ATS can achieve high assembly efficiency for precision optical systems.

10371-16, Session 5

Lithography lens mounting flexure design and aberration analysis

Ming-Ying Hsu, Ting-Ming Huang, Instrument Technology Research Ctr. (Taiwan)

The refraction lithography lens has many units, which are easily deformed by gravity forces. However, the lens mount flexure design can relieve lens surface gravity deformation. The lithography lens generically has more than 10 lens units, so with each unit, the gravity deformation sum will create large aberrations in the system. The flexure number can generate a relative aberration, such as trefoil, tetrafoil, and high-order aberrations. In addition, the lens flexure orientation can compensate for non-symmetric to symmetric aberrations from effects of gravity deformation. Thus, symmetric aberrations must resist magnitude in one or two lens units through the measurement data. This study attempts to calculate and predict lens gravity deformation; the results can assist with optical design and reoptimize system performance, as well as reduce the rework risk by measurement data.

10371-17, Session 5

Double Arm Linkage precision Linear motion (DALL) carriage: A simplified, rugged, high-performance linear motion stage for the moving mirror of an FTS (Fourier Transform Spectrometer) or other system requiring precision linear motion

Kendall B. Johnson, Greg Hopkins, Space Dynamics Lab. (United States)

The DALL (Double Arm Linkage precision Linear motion) carriage has been developed as a simplified, rugged, high performance linear motion stage. Initially conceived as a moving mirror stage for the moving mirror of an FTS (Fourier Transform Spectrometer), it is applicable to any system requiring high performance linear motion. It is based on rigid double arm linkages connecting a base to a moving carriage through flexures. It is a monolithic design. The system is fabricated from one piece of material including the flexural elements, using high precision machining. The monolithic design has many advantages. There are no joints to slip or creep and there are no CTE (coefficient of thermal expansion) issues. This provides a stable, robust design, both mechanically and thermally and is expected to provide a wide operating temperature range, including cryogenic temperatures, and high tolerance to vibration and shock. Furthermore, it provides simplicity and ease of implementation, as there is no assembly or alignment of the mechanism. It comes out of the machining operation aligned and there are no adjustments. A prototype has been fabricated and tested, showing superb shear performance and very promising tilt performance. This makes it applicable to both cube corner and flat mirror FTS systems respectively.

10371-29, Session PWed

Mirrors design, analysis, and manufacturing of the 550mm Korsch telescope experimental model

Po-Hsuan Huang, Yi-Kai Huang, Jer Ling, National Space Organization (Taiwan)

In 2015, NSPO (National Space Organization) began to develop the sub-meter resolution optical remote sensing instrument of FORMOSAT-5 follow-on and next generation optical remote sensing satellite.

Upgraded from the RC-Cassegrain telescope optical system of FORMOSAT-5, the experimental optical system of advanced optical remote sensing instrument was enhanced to off-axis Korsch Telescope optical system which consisted of five mirrors. It contains: (1) M1: 550mm diameter aperture primary mirror, (2) M2: secondary mirror (M2), (3) M3: off-axis tertiary mirror, (4) two folding flat mirrors (FM1 & FM2), for purpose of overall volume limitation, mass reduction, long focal length and excellent optical performance.

By the end of 2015, we implemented several important techniques including optical system design, opto-mechanical design, FEM & multi-physics analysis and optimization system to do preliminary study and began to developed and design these large size lightweighting aspheric mirrors and flat mirrors.

The lightweighting mirror design and opto-mechanical interface design had been completed in August 2016, then we manufactured and polished these experimental model mirrors in Taiwan, all five mirrors ware completed as sphere surface by the end of 2016. Aspherize figuring, assembling tests and optical alignment verification of these mirrors will be tested with a Korsch telescope experimental structure model in 2017.

10371-30, Session PWed

Optimization of a sixteen-inch diameter primary mirror assembly of a ground-based telescope

Yi-Kai Huang, Po-Hsuan Huang, National Space Organization (Taiwan); Chien-Wen Shen, Guan Sheng Optical Co., Ltd. (Taiwan)

This article presents the opto-mechanical design of a primary mirror assembly of a ground-based telescope with optimization algorithm. The prototype of ground-based telescope - RC16 with 16 inches diameter blank primary mirror has been manufactured in 2016. However, a telescope with a blank primary mirror is too heavy to carry on for the stargazer. Besides, deformations caused by temperature difference and gravity will do significant effect to the large aperture mirrors with high-optical performance requirements. In order to reduce the weight and maintain

the stiffness simultaneously, the lightweight design and mounting interface design are critical and important. There are four types of system architectures in this project, including (1) two types of lightweight mirror designs - honeycomb type segments and sector type segments; (2) two types of mounting interface designs - retainer type support and CFRP type support. The optimization results showed that (1) the lightweight ratio of the primary mirrors are greater than 70%; and (2) the PV value of the mirrors supported by optimal mounting interfaces with gravity effect as a tilt of about 45 degrees and ±20? temperature difference effectively less than 1/4 ?.

10371-31, Session PWed

Development of an athermalized optomechanical system of large-aperture remote sensing instruments

Chia-Yen Chan, Shenq-Tsong Chang, Ting-Ming Huang, Instrument Technology Research Ctr. (Taiwan)

An integrated optimum athermalization design and analysis system will be developed in the study. The distance between the primary and secondary mirrors for a remote sensing instrument (RSI) will be taken as the objective function to improve the influence of the environment temperature variation on the optical images. Under a developing RSI model, the athermalization design to the secondary mirror based on the established system integrating a computer-aided design software, materials library, finite element analysis, Zernike polynomial fitting and optimization program will be executed. The design variables of the barrel, supporting structure and shims will be carried under high and low temperature changes respectively. The displacements of the secondary mirror with respect to primary mirror with the optimum athermalization design can be reduced to almost zero from -196 ?m and 131 ?m for two extreme thermal boundary conditions separately.

10371-32, Session PWed

Removal of diamond turning marks on an off-axis optics with magneto-rheological finishing

Sangwon Hyun, Korea Basic Science Institute (Korea, Republic of); Min-Woo Jeon, Korea Basic Science Institute (Korea, Republic of) and Chungnam National Univ. (Korea, Republic of); Byeong-Joon Jeong, I. Jong Kim, Geon-Hee Kim, Korea Basic Science Institute (Korea, Republic of)

This paper suggests a magneto-rheological finishing process for the post-treatment of diamond turning to remove the periodic micro structures and sub-surface damages with improvement of the original figure and surface roughness. A workpiece used in experiment is an off-axis aspherical mirror that has the electro-less nickel-phosphorus plated surface. The workpiece was processed by SPDT and MRF. Fast Fourier Transformation (FFT) and Power Spectrum Density (PSD) were performed for identifying the residual diamond turning marks on the turned and polished surfaces. The experimental results indicate that MRF can be suitable for remove the repeated micro patterns caused by diamond turning process with progress of the original figure and surface roughness. The off-axis aspherical mirror used has a surface of electro-less nickel-phosphorus and a body of aluminum alloy, Al6061-T6. The desired mirror has been machined by SPDTM directly using STS technique, and finished with magneto0rheological fluid. The machined surfaces were examined by a low-coherence interferometer, and frequency domain analysis was performed through FFT. For the results of above process, the turning marks, clearly visible in diamond turned surface, were absolutely removed after MR process. Surface roughness, evaluated by a mean of four times measurement in 50% position of ±x and ±y direction of aperture, was improved from 6 nm Sa and 7 nm Sq of the turned surfaces to 2 nm Sa and 3 nm Sq of the polished surface.

10371-33, Session PWed

Method validation of measurement of power flux of a flame with a thermopile for flame test of materials

José G. Suárez-Romero, Instituto Tecnológico de Querétaro (Mexico)

Flame test of materials are required in aero-space industry and astronomy due to extreme environmental conditions of operation and transport. Flame test standards require the measurement of temperature and power flux per unit area radiated by the flame in order to implement a reference flame and assure the reproducibility and repeatability of the test. Some authors have reported pour reproducibility when two different fuels are used. The size, homogeneity and spatial distribution of the flame are also important parameters which depend of the fuel and burner used. The above shows that more information are necessary to correctly manipulate the test. In this work it is shown a method validation of the measurement of the power flux with a thermopile. Validation permits demonstrate equivalence between methods and can help to improve reproducibility.

10371-18, Session 6

Analysis technique for controlling system wavefront error with active optics

Victor L. Genberg, Gregory J. Michels, Sigmadyne, Inc. (United States)

The integration of a linear optics model with general purpose finite element models allows active control of system wavefront error in an optical system. The source of WFE may be due to distortions from environmental loads or due to an incoming WFE from external effects. Inequality equations provide realistic actuator stroke limits. A genetic algorithm allows optimal placement of actuators. Examples are provided.

10371-19, Session 6

Using integrated models to minimize environmentally induced wavefront error in optomechanical design and analysis

Victor L. Genberg, Gregory J. Michels, Sigmadyne, Inc. (United States)

An effective method for the analysis and design of optomechanical systems is discussed. The integration of a linear optics model with general purpose finite element models allows mechanical design to be optimized using environmentally induced system wavefront error as a design response to be minimized or constrained. The general approach applies to static, dynamic, and thermal environments. Examples are provided.

10371-20, Session 6

Using multidisciplinary optimization For CCD shim design in the transiting exoplanet survey satellite

Gerhard P. Stoeckel IV, Keith B. Doyle, MIT Lincoln Lab. (United States)

The Transiting Exoplanet Survey Satellite (TESS) is an instrument consisting of four, wide field-of-view CCD cameras dedicated to the discovery of exoplanets around the brightest stars, and understanding the diversity of planets and planetary systems in our galaxy. Each camera utilizes a seven-element lens assembly with low-power and low-noise CCD electronics.

Advanced multivariable optimization capabilities accommodating arbitrarily complex objective functions have been added to internally developed integrated modeling and analysis software and used to assess system performance. Various optical phenomena are accounted for in these analyses including full dn/dT spatial distributions in lenses and charge diffusion in the CCD electronics. These capabilities are utilized to design CCD shims for thermal vacuum chamber testing and flight, and verify comparable performance in both environments across a range of wavelengths, field points and temperature distributions.

10371-21, Session 7

Adaptive optics mounting method for higher second harmonic generation efficiency of large aperture KDP crystal

Zheng Zhang, Hui Wang, Menjiya Tian, Tsinghua Univ. (China); Xusong Quan, China Academy of Engineering Physics (China); Yiming Rong, South Univ. of Science and Technology of China (China)

In virtue of the superior nonlinear optical properties, KDP (potassium dihydrogen phosphate) crystals have been employed as the harmonic generation optics since 1960s. In inertial confinement fusion (ICF) facilities like NIF in America and SG-? in China, there are hundreds of KDP crystals utilized to convert the infrared laser (?=1053nm) to ultraviolet laser (?=351nm) in order to improve the energy absorption efficiency at the target point. Due to the large aperture (430mm?430mm) and small thickness (12mm) character of the KDP crystals, gravity-induced and mount-induced surface distortion always lead to severe wavefront aberration and phase mismatching which would decrease the harmonic generation efficiency significantly. Hence, a novel mounting configuration based on adaptive optics method is proposed in this article. Moreover, mechanical model of the KDP module is established according to thin plate bending theory, subsequently, numerical calculation of the stress and deformation distribution induced by the gravity and mount force on the crystal plate are conducted with FEM. Further, optical calculations including the effect of surface stress and deformation on phase mismatching and SHG (second harmonic generation) efficiency are performed. Finally, surface modification effect of the adaptive optics mounting configuration is analyzed in comparison with the original mounting configuration. The results could demonstrate the powerful surface adjustment and SHG improvement capacity of this new method.

10371-22, Session 7

Pre-construction results of giant steerable science mirror for TMT

Fei Yang, Hongchao Zhao, Qichang An, Peng Guo, Haibo Jiang, Changchun Institute of Optics, Fine Mechanics and Physics (China)

The Changchun Institute of Optics, Fine Mechanics and Physics (CIOMP) team is developing the Giant Steerable Science Mirror (GSSM) for Thirty Meter Telescope (TMT) which has got into the preliminary design phase in 2017. To develop the passive support structure system for the largest elliptic-plan flat mirror and a smoothest tracking mechanism for the gravity-invariant condition, CIOMP has developed a 1/4 scale, functionally accurate version of the GSSM prototype as the pre-construction of GSSM. The prototype incorporates the same optical-mechanical system and servo control system as the GSSM. The size of the prototype mirror is 898.5mm?634mm?12.5 mm with elliptic-plan figure and is supported by 18 points whiffletree on axial and 12 points whiffletree on lateral. The main objective of the preconstruction includes validate the conceptual design of GSSM and increase more confidence when meet the challenge during the development of GSSM. The assembly, integration and verification of the prototype have been completed based on the results in 2016. CIOMP has get the sufficient test results during the pre-construction phase and got into the preliminary design for GSSM.

10371-23, Session 7

WFE Testing of a large mounted germanium plano optical beam splitter for cryogenic infrared application

Trent Newswander, Tyrel Rupp, Space Dynamics Lab. (United States)

Mounting large reflective-refractive optical elements for cryogenic space application requires careful engineering. Optical wavefront error performance is balanced with surviving launch environments and cryogenic temperatures. Mounting and ground testing of a 25 cm by 15 cm plano germanium optical beam splitter element was completed. Cryogenic WFE testing was performed down to 115K predicting compliance to operational environment performance requirements. This paper discusses the mount engineering including detailed analysis, testing and the results.

10371-24, Session 8

Optomechanical design of TMT NFIRAOS subsystems at INO

Frédéric Lamontagne, Nichola Desnoyers, Martin Grenier, Pierre Cottin, Mélanie Leclerc, Olivier Martin, Louis Buteau-Vaillancourt, INO (Canada); Marc-André Boucher, OMP inc. (Canada); Reston Nash, California Institute of Technology (United States); Olivier Lardière, David Andersen, Jenny Atwood, Alexis Hill, Peter W. G. Byrnes, Glen Herriot, Joeleff Fitzsimmons, Jean-Pierre Véran, National Research Council of Canada (Canada)

The adaptive optics system for the Thirty Meter Telescope (TMT) is the Narrow-Field InfraRed Adaptive Optics System (NFIRAOS). Recently, INO has been involved in the optomechanical design of several subsystems of NFIRAOS, including the instrument selection mirror (ISM), the beam splitter (NBS), and the source simulator system (NSS) comprising the focal plane mask (FPM), the laser guide star (LGS), and natural guide star (NGS) sources. This paper presents an overview of these subsystems and the optomechanical design approaches used to meet the optical performance requirements under environmental constraints.

10371-25, Session 8

Recent advancements in robotic micro-optical assembly at Lockheed Martin Optical Payload Center of Excellence

David Hwang, Lockheed Martin Coherent Technologies (United States)

Lockheed Martin Space Systems Company Optical Payloads Center of Excellence is in process of standing up the Robotic Optical Assembly System (ROAS) capability at Lockheed Martin Coherent Technologies in Colorado. Once fully realized, Robotic Optical Assembly will enable LM to create world-leading, ultra-low-SWAP photonic devices using a closed-loop control robot to precisely position and align multi-material micro-optics with a potential fill factor of >25 optics per square inch. This presentation will discuss the anticipated applications and optical capability when ROAS is fully operational, as well as challenge the audience to update their “rules of thumb” and best practices when designing low-SWAP optical-mechanical systems that take advantage of LMSSC’s ROAS capability. This presentation will reveal demonstrated optical pointing and stability performance achievable with ROAS, and why we believe these optical specifications are relevant for the majority of anticipated applications. After a high level overview of the ROAS current state, the discussion will focus in on recent results of the “Reworkable Micro-Optics Mounting IRAD”. These results from these IRADs will be correlated to the anticipated optical specifications

presented at the opening of the presentation. The presentation will end with a review of near term next steps, and if time allows, a discussion on unidentified applications as well as any questions or advice for the ROAS team from the audience.

10371-26, Session 8

The optomechanical design process: from vision to reality

E. Todd Kvamme, David M. Stubbs, Michael S. Jacoby, Isaac Weingrod, Lockheed Martin Space Systems Co. (United States)

The design process for an opto-mechanical sub-system is discussed from requirements development through test. The process begins with a proper mission understanding and the development of requirements for the system. Preliminary design activities are then discussed with iterative analysis and design work being shared between the design, thermal, and structural engineering personnel. Readiness for preliminary review and the path to a critical design review are considered, with special focus on determining appropriate margins against the system level requirements prior to committing dollars to a production order. The value of prototyping and risk mitigation testing is examined with a focus on when it makes sense to execute a prototype test program. System level margin is discussed in general terms, and the practice of trading margin in one area of performance to meet another area is reviewed. Requirements verification and validation is briefly considered. A discussion of test and its relationship to requirements verification concludes the design process.

10371-27, Session 8

The theory of acousto-optical correlator the radio signals and generalized superposition principle

Georgy I. Korol, Saint-Petersburg State Univ. of Aerospace Instrumentation (Russian Federation)

Acousto-optic modulator is an input device of dynamic signals in optical information processing systems, acousto-optical methods, where one of the basic operations of the processed radio signals, is to calculate the correlation functions, which is a non-linear operation on correlatable radio signals. This assumes a linear mapping of each of the input in optical computing device processes the radio signals. This assumes a linear mapping of each of input to the optical the computing device being processed radio signal. The most important characteristic acousto-optic modulator is its transmission function, which is its a non-linear mapping spreading in the environment the acousto-optical interaction acoustic waves excited processed radio signals. This situation requires a decision questions on the linearization of the transmission function acousto-optic modulator. The nonlinear mapping propagating in a medium acousto-optical interaction acoustic wave described in the the form of action is non-linear operator on an acoustic wave. This non-linear map represented by the formula of finite increments. The linear part of this formula is given by the first derivative of Frechet, which defines a linear operator, and consequently, the linear approximation is introduced into the system optical correlation processing information radio signals. Acousto-optical devices processing radio signals contain two acousto-optic modulators. In this case we are talking about the processing of radio signals in the form of their work. At the same time one of the main tasks is to establish transmission functions a pair of acousto-optic modulators provided linearization of transmission function of each.

10371-34, Session 8

Comparison of lenses' thermal expansion formulation in Zemax versus ANSYS with SigFit post processing

Joao Faria, José Alves, Eduardo Pereira, Univerity of Minho (Portugal)

This paper describes an objective to be implemented in a 3D scanner system whose principle of operation is based on a time of flight (TOF) sensor. The objective is constituted by four even aspheric lenses made of a polymeric material with an aperture of 25 mm @ f/# = 1,0. Due to the environment in which the objective is going to be installed, the working temperature ranges from -40°C to 110°C. To ensure a proper optical quality of the objective, several simulations were performed to evaluate its performance over a wide range of temperatures. Initially, only Zemax was used to evaluate the objective. Zemax considers a linear geometric expansion of every optical surface, which is here proved to not be the best approach to find a deformed geometry after a thermal load. The second approach is to create a 3D model and perform a finite element simulation in Ansys software. The input data is the thermal variation and the output is the deformed geometry of both lenses and barrel. Using SigFit software, it was possible to generate new mathematical equations of the deformed lenses and import this data into Zemax to start a new ray tracing. The evaluated properties for both approaches are: MTF, focal plane shift, spot radius and geometry, optical path difference, and transverse ray fan. The new shape and location of lenses differs for both scenarios, and the difference in the focal plane shift is around 12% between both.

Conference 10372: Material Technologies and Applications to Optics, Structures, Components, and Sub-Systems III

SPIE. OPTICS+ PHOTONICS OPTICAL ENGINEERING+ APPLICATIONS

Monday 7 –7 August 2017

Part of Proceedings of SPIE Vol. 10372 Material Technologies and Applications to Optics, Structures, Components, and Sub-Systems III

10372-1, Session 1

High stability and low thermal expansion alloy (Fe36Ni) reinforced with Si3N4

Timothy A. Stephenson, NASA Goddard Space Flight Ctr. (United States)

The development of materials with improved properties over conventional materials is critical to improve performance for demanding space applications. Iron Nickel Alloys materials are commonly used in thermal structures for high stability applications in optics, detectors, and electronics. Fe36Ni has a low CTE value, but suffers from a high density and low thermal stability. This paper presents a new class of material, Fe36Ni reinforced with silicon nitride particles ceramic to improve strength, thermal stability and reduce density. Mechanical and physical properties will be presented and manufacturing technology will be discussed for precision components.

10372-2, Session 1

Mechanical alloyed aluminum metal matrix composites (MMC)

Don H. Hashiguchi, Materion Brush Beryllium & Composites (United States); David Tricker, Andrew D. Tarrant, Materion Aerospace Metal Composites Ltd. (United Kingdom)

Aluminum alloys reinforced with ceramic particles produce a low density metal matrix composite (MMC) with enhanced mechanical and physical properties including relatively high modulus and vibration loss. This paper will outline the capability through Powder Metallurgy processing techniques made by mechanical alloying (MA). MA enables production of MMC's with micron to submicron mean particulate reinforcement size which increases mechanical properties in comparison to larger reinforcement particle size. Smaller reinforcement particles also result in a material that fits well within established value streams enabling conventional post consolidation metalworking and machining methods. The microstructure and properties of MMC's mechanical alloyed with base aluminum alloys 6061B and 2124A will be presented.

10372-3, Session 1

Enhanced aluminum reflecting and metal-dielectric solar blind filter coatings for the far-ultraviolet

Javier Del Hoyo, Manuel A. Quijada, NASA Goddard Space Flight Ctr. (United States)

The advancement of far-ultraviolet (FUV) coatings is essential to meet the specified throughput requirements of the Large UV/Optical/IR (LUVOIR) Surveyor Observatory which will cover wavelengths down to the 100 nm range. The biggest constraint in the optical thin film coating design is attenuation in the Lyman-Alpha Ultraviolet range of 100-130 nm in which conventionally deposited thin film materials used in this spectral region (e.g.aluminum protected with magnesium fluoride) often have high absorption and scatter properties degrading the throughput in an optical system. We investigate the use of optimally deposited Aluminum (Al) and Aluminum tri-fluoride (AlF_3) materials for reflecting and metal-dielectric solar blind bandpass filter coatings for use in the FUV. Optical characterization of the deposited designs has been performed using FUV spectrometry while the surface quality of the film is analyzed using optical profilometry. The optical thin film design and optimal deposition conditions to produce superior optical properties in the FUV using Al and AlF_3 are presented.

10372-4, Session 1

Characterization of PDMS samples varying its synthesis parameters for tunable optics applications

Josimar Marquez-Garcia, Jorge González García, Angel S. Cruz-Félix, Agustín Santiago Alvarado, Univ. Tecnológica de la Mixteca (Mexico)

Nowadays the elastomer known as polydimethylsiloxane (PDMS Sylgard 184), due to its physical properties, low cost and easy handle, have become a frequently used material for the elaboration of optical components such as: variable focal length liquid lenses, optical waveguides, solid elastic lenses, etc. In recent years, we have been working in the characterization of this material for potential applications in visual sciences, in this work we describe the elaboration of PDMS made samples, also, we present a physical and optical characterization of the samples by varying its synthesis parameters such as the proportion of base - curing agent, and both, curing time and temperature. In the case of mechanical properties, tensile and compression tests are carried out through a universal testing machine to obtain the respective stress-strain curves and in order to obtain information regarding its optical properties, UV-vis spectroscopy is applied to the samples to obtain transmittance and reflectance curves. Index of refraction of the samples elaborated with different synthesis parameters, is obtained through Abbe refractometer. Preliminary results from the characterization will determine the proper synthesis parameters for the elaboration of tunable refractive surfaces to be implemented in a opto-mechatronic system used to imitate the objective performance of the human eye for potential applications in robotics.

10372-18, Session 1

Visualization of diffusion mixing in a micro-mixer with flow paths fabricated by photolithography

Toshiyuki Horiuchi, Yuta Morizane, Tokyo Denki Univ. (Japan)

How two liquids were mixed was investigated by visualizing the mixing when they were simultaneously injected in a micro-mixer with lithographically fabricated Y-shape flow paths, and the mixing phenomena was analyzed in detail. To visualize the mixing, flows were observed by an optical microscope, and a clearly detectable chemical reaction was utilized. As the two liquids, a transparent aqueous solution of a strong alkali and a phenolphthalein ethanol solution were used. When they were simultaneously injected in Y-shape flow paths of a micro-mixer, they flowed at first in parallel along the joined path as laminar flows. This is because the Reynolds' number became very small caused by the narrow flow-path widths of 50-100 μm. However, because two liquids were always contacted at the boundary, they were gradually mixed by diffusion, and the color of the mixed parts changed to vivid red. For this reason, it was able to measure the diffusion distance from the flow path center. Because the flow speeds were much faster than the diffusion speeds, the area colored in red did not depend on the time but depended on the distance from the joint point. It was known that the distance from the joint point corresponded to the time

for mixing the liquids by the diffusion. It was clarified that the diffusion distance was proportional to the square root of the diffusion time or the distance from the joint point. The calculated diffusion coefficient of 1.2?10^-9 m^2/s was relevant.

10372-6, Session 2

Interfacial studies of a metallurgical bond between "activated" ultrasonically applied solder and high purity fused silica

Lawrence W. Shacklette, Harris Corp. (United States); Donna L. Gerrity, E&S Consulting, Inc. (United States); Michael R. Lange, James C. Beachboard, Harris Corp. (United States); Ronald Smith, S-Bond Technologies, LLC (United States)

Packaging of optical devices often requires the need for creating strong bonds between metal and silica. The most convenient and cost effective approach would be to directly solder to both silica and metal without requiring pre-metallization of the silica. Soldering to oxides and oxidized surfaces has been accomplished with various solders containing metals with strong affinity for oxygen. In this work we investigate solders based upon a tin-bismuth eutectic with potential activating additives of cerium, gallium, and titanium. Each of these metals are energetically capable of competing for the oxygen in silica, and are therefore capable of reducing or forming mixed oxides with silica under appropriate conditions. The bond between such an "activated" solder and high purity fused silica (HPFS) has been characterized by Time-of-Flight Secondary Ion Mass Spectrometry (TOF-SIMS). Two variations of solder produced by S-Bond Technologies, S-Bond 140 and S-Bond 140 M1 were bonded to silica using a fluxless ultrasonic technique. TOF-SIMS was then used to characterize the bond interface by measuring the distribution of elements as a function of depth through the interface. The results show that the presumed activating elements concentrate at the interface and that their oxides form the interfacial layer between the HPFS and the bulk solder. The efficacy of these additives was established by demonstrating that the block shear strength of the bond to HFPS was trebled by the addition of the aforementioned reactive metals to the base Sn-Bi solder.

10372-7, Session 2

Comparison of material properties between ultra low thermal expansion ceramics and conventional low thermal expansion glasses

Tomohiro Kamiya, Tadahito Mizutani, Japan Aerospace Exploration Agency (Japan)

Material properties of ceramics, which have extremely low thermal expansion coefficients, were studied for space-based telescope mirror application. Numbers of the key mechanical and thermal properties for the application were investigated, such as Young's modulus, Poisson's ratio, bulk density, 3-point bending strength, coefficient of thermal expansion (CTE), thermal conductivity and specific heat capacity. They were intensively investigated at a normal temperature range (0 to 50 °C) and compared with that of conventional low thermal expansion glasses under exactly the same testing configurations. In this study, we selected four ceramics; NEXCERA-N117B and NEXCERA-CD107 (KUROSAKI HARIMA), CO-720 (KYOCERA) and ZPF-N (NTK CERATEC). As a characteristic result, the Young's modulus of 140 GPa, bulk density of 2.58 g/cm3, CTE of less than 0.03 ppm/K at 23 °C and thermal conductivity of 4.7 W/m?K were obtained for NEXCERA-CD107. This means that the specific stiffness was 1.5 to 2 times higher and temperature uniformity was 3 times higher than conventional low thermal expansion glasses while dimensional thermal stability was ensured to be almost the same as the competitive glass materials. In the previous paper, the long term dimensional stability of NEXCERA was reported as 0.01 ± 0.01 ppm over 13 months. In addition, the excellent processability of NEXCERA for lightweight rib structures and excellent polishing characteristics using Magnetorheological Finishing (MRF) technology were also reported in another paper. It was therefore revealed that the low thermal expansion ceramics have appropriate and attractive material properties for future space telescope applications.

10372-8, Session 2

Inverse problem of Bragg's scattering for measuring the spectrum surface roughness in the optical gradient waveguide

Anatoly N. Osovitsky, Natalia Grishaeva, Peoples' Friendship Univ. of Russia (Russian Federation); Nikolai D. Espinosa Ortiz, Christian Vega, Univ. de las Fuerzas Armadas-ESPE (Ecuador)

A new method for measuring the spectrum of surface roughness based on Bragg scattering, is proposed. This method is characterized by its high precision of measurement of the spatial amplitudes and frequencies. Was determined the rang of spatial frequencies (periods) of harmonics in the roughness spectrum surfaces (0,PI). When the rotation's angle of grid is (0,PI/4) will be a forward scattering or Bragg's deflector. At rotation's angle of grid is (PI/2,PI/4) or (-3PI/4,-PI/2) will a Bragg's mirror.

The measurements are made in a gradient waveguide, obtained by ion exchange method.

10372-9, Session 2

Thermal and mechanical properties of tellurite glasses for mid-IR molded lens applications

Ju Choi, Linganna Kadathala, Eui S. Lee, Ganesh L. Agawane, Korea Photonics Technology Institute (Korea, Republic of)

Systematic series of ternary zinc lanthanum tellurite glasses with molar composition of (1-x) TeO2-La2O3-xZnO, where x = 10, 20, and 30, were prepared by a conventional melt quenching technique and their thermal and mechanical properties have been investigated via differential scanning calorimeter, dilatometer and autovick techniques for mid-IR lens applications. The compatibility of molding process for IR lens will be investigated. First of all, it was found that the glass transition temperature (Tg), softening temperature (Ts) and Knoop hardness (Hk) significantly increased when ZnO content increases from 10 to 30 mol%. Glass stability factor (?T), which is most important factor for molding process, decreased as the ZnO content increased from 10 to 30 mol% due to loose packing structure which is result of increase of non-bridging oxygens (NBOs) in the tellurite Te-O-Te network. The thermal expansion coefficient (CTE) decreased from 11.26 to 12.6 (10-6/K) when ZnO content increases from 10 to 30 mol%. These results clearly indicate that the investigated glasses are attractive for device applications.

10372-10, Session 3

A review on the advances in 3D printing and additive manufacturing of ceramics and ceramic matrix composites for optical applications *(Invited Paper)*

William A. Goodman, Goodman Technologies, LLC (United States)

This paper provides a review of advances in 3D printing and additive manufacturing of ceramic and ceramic matrix composites for optical

applications. Dr. Goodman has been pioneering additive manufacturing of ceramic matrix composites since 2008. He is the inventor of HoneySiC material, a zero-CTE additively manufactured carbon fiber reinforced silicon carbide ceramic matrix composite which is now made by Fantom Materials. HoneySiC is briefly discussed here. More recently Dr. Goodman has turned his attention to the direct printing of ceramics for optical applications via various techniques including slurry and laser sintering of silicon carbide and other ceramic materials.

10372-11, Session 3

Nano-diamond polishing of super hard materials

Rajiv Singh, Arul Chakkaravarthi Arjunan, Sinmat, Inc. (United States)

A new nano-diamond based mechanical polishing process has been developed and optimized for polishing super hard materials such as SiC, sapphire and diamond samples. The nano-diamond based process uses specially engineered nano-diamond particles that has ability to react with super hard materials when used for polishing. Such a reactive nano-diamond process leads to removal rates of about an order higher than the base particles and yields ultra-smooth surfaces (RMS <0.5nm) on the super hard materials along with very low sub-surface damage. The process yielded surface roughness less than 1 nm for silicon carbide, sapphire and diamond materials. The process has been studied for single crystalline, poly-crystalline and composite materials. The removal rates for different materials with the newly developed nano-diamond process compared to base nano-diamond particles and the surface finish obtained with the use of atomic force microscope, optical interferometer and tropel flat master will be presented. The mechanism of nano-diamond process will be explained in the conference.

10372-12, Session 3

Time scales of radiation damage decay in five optical materials

Frank U. Grupp, Univ.-Sternwarte München (Germany) and Max-Planck-Institut für extraterrestrische Physik (Germany); Norbert Geis, Reinhard Katterloher, Max-Planck-Institut für extraterrestrische Physik (Germany); Ralf Bender, Max-Planck-Institut für extraterrestrische Physik (Germany) and Univ.-Sternwarte München (Germany)

Radiation damage has been doe at Paiul Scherrer Cyclotron. Damage result was measured by a precise in situ photometric setup at 1/2 exposure and after the exposure. 1 minute 1 hour 1 day 1 week -.-- 1 year after exposure.

10372-13, Session 4

A rigid and thermally stable all-ceramic optical support bench assembly for the LSST Camera *(Invited Paper)*

Matthias Krödel, ECM Engineered Ceramic Materials GmbH (Germany); J. Brian Langton, SLAC National Accelerator Lab. (United States); Bill Wahl, Brookhaven National Lab. (United States)

This paper will presenting the ceramic design, fabrication and metrology results and assembly plan of the LSST camera optical bench structure which is using the unique manufacturing features of the HB-Cesic technology. The optical bench assembly consists of a rigid “Grid” fabrication supporting individual raft plates mounting sensor assemblies by way of a rigid kinematic support system to meet extreme stringent requirements for focal plane planarity and stability.

10372-14, Session 4

Quality evaluation of spaceborne SiC mirrors: the effects on mirror accuracy by variation in the thermal expansion property of the mirror surface

Masaki Kotani, Tadashi Imai, Haruyoshi Katayama, Japan Aerospace Exploration Agency (Japan); Hidehiro Kaneda, Nagoya Univ. (Japan); Takao Nakagawa, Keigo Enya, Japan Aerospace Exploration Agency (Japan)

We studied a large-scale lightweight mirror constructed of reaction-bonded silicon carbide (SiC)-based material as a key technology in future astronomical and earth observation missions. One of the most important technical issues for large-scale ceramic components is the uniformity of the material’s property, depending on part and processing. It might influence mirror accuracy due to uneven thermal deformation.

To correlate the material property of a mirror body and the mirror accuracy, the authors evaluated all over the mirror surface deviation of a prototype mirror by inputting actually measured coefficient of thermal expansion (CTE) data into a finite element analysis (FEA) model. The computationally simulated contour diagrams well reproduced the mirror accuracy profile that the actual mirror showed in cryogenic testing. Density data were also useful for evaluating the mirror surface deviation because they had a close relationship with the CTE.

Besides, systematic case studies for the conditions of CTE by FEA were also conducted to know the typical influence of material property nonuniformity on mirror accuracy and a comprehensive empirical equations for the series of CTE’s main factors were derived.

Through all these studies, wide-range practical computational evaluation technology of mirror accuracy was acquired.

10372-15, Session 4

Dimensional stability performance of a CFRP sandwich optical bench for microsatellite payload

Nichola Desnoyers, Philippe Goyette, Bruno Leduc, INO (Canada); Marc-André Boucher, OMP Inc. (Canada)

Microsatellite market requires high performance while minimizing mass, volume and cost. Telescopes are specifically targeted by these trade-offs. One of these is to use the optomechanical structure of the telescope to mount electronic devices that may dissipate heat. However, such approach may be problematic in terms of distortions due to the presence of high thermal gradients throughout the telescope structure.

To prevent thermal distortions, carbon fiber reinforced polymer (CFRP) technology can be used for the optomechanical telescope material structure. CFRP is about 100 times less sensitive to thermal gradients and its coefficient of thermal expansion (CTE) is between 200 to 600 times lower than typical aluminium alloys. Unfortunately, designing with CFRP material is not as straightforward as with metallic materials. There are many parameters to consider in order to reach the desired dimensional stability under thermal, moisture and vibration exposures. Designing optomechanical structures using CFRP involves many challenges such as interfacing with optics and sometimes dealing with high CTE mounting interface structures like spacecraft buses.

INO has designed a CFRP sandwich telescope structure to demonstrate the achievable performances of such technology. Critical parameters have been optimized to maximize the dimensional stability while meeting the stringent environmental requirements that microsatellite payloads have to comply with. The telescope structure has been tested in vacuum from -40°C to +50°C and has shown a good fit with finite element analysis predictions.

10372-16, Session 4

Challenges of designing and testing a highly stable sensor platform: HB-Cesic solves MTG star sensor bracket thermo-elastic requirements

Matthias Krödel, ECM Engineered Ceramic Materials GmbH (Germany); Christoph Zauner, KRP-Mechatec Engineering GbR (Germany)

The Meteosat Third Generation's extreme pointing requirements call for a highly stable bracket for mounting the Star Trackers. Within the early design phase, HB-Cesic®, a chopped fibre reinforced siliconcarbide, was selected as a base material for the sensor bracket. The high thermal conductivity and low thermal expansion of HB-Cesic® were the key properties to fulfil the demanding thermo-elastic pointing requirements of below 1?rad/K for the Star Trackers mounting interfaces. ECM (Engineered Ceramic Materials GmbH) and KRP-M (KRP-Mechatec Engineering GbR) were selected by OHB System GmbH in mid-2014 to design, manufacture, and test the Star Sensor Assembly Bracket (SAB).

This paper/poster concentrates on the design and main test activities to achieve and to verify the thermo-elastic, thermal, and structural requirements. Special attention is paid on the development and application of the thermoelastic distortion measurement system. Dominated by thermoelastic stability requirements, the design and analysis of the Bracket requires a multidisciplinary approach with the focus on thermal and thermo-elastic analyses. A major aspect of the thermal analysis was the optimisation of conductive and radiative heat fluxes to minimize the temperature gradient and thus subsequent thermoelastic deformations within the Bracket. Further, it was found that for achieving the necessary high accuracy level for thermoelastic deformation results within this project, a highly accurate presentation of temperature distribution and thus a fine geometrical resolution of the thermal model is required. Therefore, in addition to the ESATAN thermal analysis (~1000 nodes), a FEM (ANSYS) thermal analysis (40000 DOF) was performed and correlated with the test results.

A key challenge of the thermo-elastic analysis was the optimization of the interfaces between Bracket and Star Tracker as well as to the satellite platform in order to minimize interface loads and still maintain sufficient stiffness to meet eigenfrequency requirements. Morphological optimization techniques have been applied for this as well for a further lightweighting of the Bracket.

Experimental verification of such thermo-elastic stable systems is a challenging design task of its own. It requires test platforms having a thermo-elastic stability higher by a factor of 10 being exposed to the same temperature load as the item under test. Within this project, a thermo-elastic distortion measurement rig was developed with a stability of <0.1?rad/K in all three rotational degrees of freedom. This was achieved by combining capacitive displacement sensors and ultra low expansion (ULE) glass-ceramics. Already low drift yet still off-the-shelf sensors (by Micro-Epsilon Messtechnik) were further optimised by dedicated tests and design improvements to achieve a sensor

drift of <10nm/K within a 40K temperature range. Fifteen of these sensors were mounted to a Clearceram® ULE rig in a special spatial configuration for measuring the relative rotation of all three Star Tracker interfaces in all three axis.

In conclusion, the MTG Star Sensor Bracket shows excellent thermo-elastic stability and presents a significant building block to the overall accuracy of the satellite pointing system.

10372-17, Session 4

Trade-off studies on LiteBIRD reflectors

Hajime Sugai, Tomotake Matsumura, Kavli Institute for the Physics and Mathematics of the Universe (Japan); Junichi Suzuki, Muneyoshi Maki, Masashi Hazumi, High Energy Accelerator Research Organization, KEK (Japan); Nobuhiko Katayama, Shin Utsunomiya, Shingo Kashima, Yuki Sakurai, Kavli Institute for the Physics and Mathematics of the Universe (Japan); Hiroaki Imada, Japan Aerospace Exploration Agency (Japan); Hirokazu Ishino, Okayama Univ. (Japan); Takenori Fujii, Cryogenic Research Ctr., The Univ. of Tokyo (Japan)

The LiteBIRD satellite aims at detecting a signature imprinted on the cosmic microwave background (CMB) by the primordial gravitational wave predicted in inflation, which is an exponentially expanding era before the hot big bang. The extraction of such weak spiral polarization patterns requires the precise subtraction of our Galaxy's foreground emission such as the synchrotron and the dust emission. In order to separate them from the CMB by using their spectral shape differences, LiteBIRD covers a wide range of observing frequencies. The main telescope, Low Frequency Telescope (LFT), covers the CMB peak frequencies as well as the synchrotron emission. Based on the required sizes of optical elements in the LFT, an order of one meter, the telescope will consist of reflectors rather than lenses since the latter is limited in size availabilities of the corresponding materials. The image quality analysis provides the requirements of reflector surface shape errors within 30um rms. The requirement on surface roughness of 2um rms is determined from the reflectance requirement. Based on these requirements, we have carried out tradeoff studies on materials used for reflectors and their support structures. One possibility is to athermalize with aluminum, with the expected thermal contract of 0.4% from room temperature to 4-10 K. Another possibility is CFRP with cyanate resin, which is lighter and has negligibly small thermal contraction. For the reflector surface shape measurements including in low temperature, photogrammetry is a strong candidate with suitable accuracy and dynamic range of measurements.

10372-5, Session PMon

Manipulation of microbubbles through the phenomenon of thermocapillarity

Julio Aurelio Sarabia-Alonso Sr., Univ. Politécnica de Tulancingo (Mexico); Jose Gabriel Ortega-Mendoza, Univ. Tecnológica de Tulancingo (Mexico)

We present a theoretical-experimental study of the movement that undergoes a bubble that is immersed in an aqueous medium due to the phenomenon of thermocapillarity. This phenomenon has its origin in the force of Marangoni generated by the presence of a temperature gradient. The temperature gradient is produced by the incidence of photons on nano silver particles immobilized on the tip of an optical fiber. The results show that it is possible to manipulate a bubble through two optical fibers, controlling the incidence of photons in each of them.

10372-19, Session PMon

Successful fabrication of GaN epitaxial layer on non-catalytically-grown graphene for smart packages

Sungwon Hwang, Kyung-Jin Yeum, Konkuk Univ. (Korea, Republic of)

Sapphire is widely used as a substrate for the growth of GaN epitaxial layer (EPI), but has several drawbacks such as high cost, large lattice mismatch, non-flexibility, and so on. Here, we first employ graphene directly grown on Si or sapphire substrate as a platform for the growth and lift-off of GaN-light-emitting-diode (LED) EPI, useful for not only recycling the substrate but also transferring the GaN-LED EPI to other flexible substrates. Sequential standard processes of nucleation/recrystallization of GaN seeds and deposition of undoped (u-) GaN/AlN buffer layer were done on graphene/substrate before the growth of GaN-LED EPI, accompanied by taping and lift-off of u-GaN/AlN or GaN-LED EPI. This approach can overcome the limitations by the catalytic growth and transfer of graphene, and make the oxygen-plasma treatment of graphene for the growth of GaN EPI unnecessary and smart packages.

10372-20, Session PMon

Characterization of ancient Chinese porcelains using optical coherence tomography

Song Liu, Qinghui Li, Shanghai Institute of Optics and Fine Mechanics (China); Yongqing Hu, Henan Provincial Institute of Cultural Relics and Archaeology (China)

Henan province is one of the few provinces which has many historical relics in China. Numerous clutural relics such as porcelains, bronzes, jades and so on have been excavated from the tombs and histortical sites of ancient times in Henan province. Porcelains with different kinds excavated from Baofeng county in Henan province and dated from Jin Dynasty to Yuan Dyansty have been analyzed by Optical Coherence Tomography (OCT). The phycial structures of glaze layer for different kinds of porcelains are obtained as 2D OCT images. The typical physical of glaze layer, such as glassy phase, heterogeneous phase, air bubbles and so on, are shown in OCT images. In order to distinguish the different types of glaze, the OCT images have been processed by Matlab software using image texture analysis technique. Parameters which are used to describe the OCT images are extracted based on image histogram and gray level co-occurrence matrix and appropriate parameters are determined to characterize and distinguish the glaze layer for different types of porcelains.

10372-21, Session PMon

Polishing aspheric mirrors of zero-thermal expansion cordierite ceramics (NEXCERA) for space telescopes

Jun Sugawara, Bumpei Mikashima, Krosaki Harima Corp. (Japan); Tomohiro Kamiya, Japan Aerospace Exploration Agency (Japan)

NEXCERA is an advanced cordierite ceramics with an extremely low thermal expansion coefficient of < 0.03 ppm/K at room temperature and superior mechanical properties. It has been used not only as structural components of LSI lithography, but also as optical reflecting mirrors in the precision metrology field requiring high accuracy and stability. Currently, it is regarded as a promising material essential for ultra-lightweight and thermally-stable optics for future optical missions that require extremely high observation performance because of its higher mechanical properties and higher stabilities compare to zero-thermal expansion glasses. To realize the high precision NEXCERA mirrors for space optics, it is important to develop a process for deterministic polishing of aspheric shape and a precise figure correction polishing for NEXCERA. This paper presents the results of mirror polishing for several shapes of NEXCERA such as plano, sphere, hyperbola and parabola. The plano mirror of 150 mm diameter was achieved a surface roughness of Ra around 0.3 nm. The convex hyperbolic mirror of 100 mm diameter was polished by MRF from a best-fit sphere and achieved a surface roughness of RMS 1 nm and a form accuracy of less than ?/10 in spite of an existence of sensitivity to sub-surface damage. The concave parabolic mirror of 250 mm diameter with 500 mm focal length was polished by computer-controlled asphere surface-finishing technology, and the results will be presented at the conference. Based on consequence of these work, it is expected that NEXCERA mirror will be applied to lightweight aspheric mirrors of space telescope.

Conference 10373: Applied Optical Metrology II

Tuesday - Wednesday 8 –9 August 2017

Part of Proceedings of SPIE Vol. 10373 Applied Optical Metrology II

10373-1, Session 1

Usefulness of orthogonal basis sets for predicting optical performance of wavefronts with mid-spatial frequency error *(Invited Paper)*

Zahra Hosseinimakarem, Angela Davies, Christopher J. Evans, The Univ. of North Carolina at Charlotte (United States)

Mid-spatial frequency texture on optical elements degrade their performance. Therefore, it is important to have a clear way of characterizing them and predicting the optical performance degradation. A Zernike polynomial representation of the wavefront can be used to predict the optical performance. The ability to generate very large orders of Zernike polynomials enables fitting and describing optical wavefronts all the way from low order form errors to mid-spatial frequencies. We will show decomposition of measured wavefronts into orthogonal bands of Zernike polynomials based on symmetry properties of these polynomials. Based on the filtering aspect of Zernike polynomials, we will present how different signatures affect optical performance differently. We will investigate the Strehl ratio as an optical performance metric for mid-spatial frequency and will see how the Strehl ratio of selected Zernike-filtered bands of a wavefront are related to the Strehl ratio of the entire wavefront. MTF is another useful metric for optical performance among optical designers. We will provide examples on how one can benefit from the linearity properties of MTF along with the orthogonality properties of Zernike polynomials to connect wavefront characterization representation to optical performance. We will present examples of both real and synthetic mid-spatial frequency textures to examine the approximation limitations of MTF when using linear systems formulation.

10373-3, Session 1

Improvement of accuracy in inner profile measurement of pipes and holes using an optical probe

Toru Yoshizawa, Tokyo Univ. of Agriculture and Technology (Japan) and NPO 3D Associates (Japan); Toshitaka Wakayama, Saitama Medical Univ. (Japan)

The requirements of inner profile measurement of pipes and tubes become recently larger and larger, and applications of inner profile measurement have rapidly expanded to various industrial fields such as mechanical engineering, automobile and heavy industries. We have proposed measurement method by incorporating a ring beam device that produces a circular beam and have developed various probe cameras for different inner profile measurement. In addition to measurement of mechanical components with inner diameter of 50 mm to 100 mm (typically such as car engine bores), in order to meet request of applying to smaller diameter pipes, we tried to improve the ring beam light source using a conical mirror and a laser diode. At the same time, we are trying to realize higher-sensitive probe on the basis of reducing noises due to speckles and others. One idea is proposed that is based on selective compliance applied method (SCAM). And the other is tried by checking the light source to get better result. Some examples are shown to verify availability of our trials in industrial applications.

10373-4, Session 1

Fusion of light-field and photogrammetric surface form data

Danny Sims-Waterhouse, Samanta Piano, Richard K. Leach, The Univ. of Nottingham (United Kingdom)

Photogrammetry based systems are able to produce 3D reconstructions of an object given a set of images taken from different orientations. In this paper, we implement a light-field camera within a photogrammetry system in order to capture additional depth information, as well as the photogrammetric point cloud. Compared to a traditional camera that only captures the intensity of the incident light, a light-field camera also provides angular information for each pixel. In principle, this additional information allows 2D images to be reconstructed at a given focal plane, and hence a depth map can be computed. Through the fusion of light-field and photogrammetric data, we show that it is possible to improve the measurement uncertainty of a millimetre scale 3D object, compared to that from the individual systems. By imaging a series of test artefacts from various positions, individual point clouds were produced from depth-map information and triangulation of corresponding features between images. Using both measurements, data fusion methods were implemented in order to provide a single point cloud with reduced measurement uncertainty.

10373-5, Session 1

Expansion of measurement area of three-dimensional deformation measurement speckle interferometry with same sensitivities in three directions under consideration of measurement sensitivity

Yasuhiko Arai, Kansai Univ. (Japan)

A novel in-plane and out-of-plane deformation simultaneous measurement method using only two speckle patterns grabbed before and after deformation of an object with rough surfaces has been proposed. In the new optical system, a phenomenon of the in-plane and the out-of-plane deformation can be simultaneously recorded by only one camera by using the multi-recording technology of speckle patterns. Furthermore, the same measurement sensitivities in three directions can be set in this system. Though the method can efficiently measure some deformation phenomena, the method has some area which cannot measure a deformation. The reason why there is such area is caused by the orthogonal laser beams as the coordinate system. In this paper, new optical system which is not based on the orthogonal laser beams is proposed in order to expand the measurement area of the method under consideration of measurement sensitivity. It is confirmed that the sensitivity of the deformation measurement system depends on the angles of vertices of coordinate system produced by laser beams. The sensitivity decreases sinusoidally as the angle decreases. In the experiments, the angle is defined as 80 degrees. At 80 degrees, it is also confirmed that the sensitivity is not changed drastically. The possibility of deformation measurement in the area where the deformation distribution cannot be measured by the conventional optical system is discussed. The situation of measurement accuracy in the extending of measurement area is investigated.

10373-6, Session 1

3D boundary extraction strategy using vector slices for the inspection of sheet parts

Liqun Ma, Changcheng Institute of Metrology & Measurement (China); Jingjing Fan, Yongqian Li, Northwestern Polytechnical Univ. (China); Zili Zhou, Changcheng Institute of Metrology & Measurement (China)

With the development of airplane manufacturing, too many bent sheet parts appear at the assembling segment. To improve the accuracy of the complete airplane assembling, many detecting methods of assembling accuracy have been employed. But the current methods aren't satisfied the requirement of rapid and accurate detection.

In this article, we put forward a project to extract the boundary of thin parts. The project is carried out after obtaining the discrete scanning points of sheet part, it can be divided into five parts: (1) constructing the complement relation of discrete points by methods of space division and K neighbor points searching, then triangle the discrete points based on the complement relation; (2) smoothing and simplifying the boundary points of scanning data of sheet part, fitting the simplified boundary points by B-spline, constructing the equal interval universal slices along the fitting boundary curve; (3) extracting the marginal data by solving the intersection between the surface of triangle and universal slices; (4) identifying the end points of arc chamfer and delete the linear segment, fitting the arc chamfer data by parabola and picking out the maximum curvature points, call these point ridge point; (5) obtaining the boundary points by fixed value compensation along the normal direction of ridge points. Comparing the extracted boundary points with measurement results of three coordinate measuring machine(CMM) and theoretical design line in SA software. In this article, we used a piece of 6mm thick board to compare with the results of CMM, used a piece of 2 mm thick board to compare with the theoretical design line, the comparing results show that the deviations of extracted points with reference data are in the range of 0.1mm, satisfying the required indicator.

10373-7, Session 2

Application of polarization in high-speed, high-contrast inspection

Matthew J. Novak, Technical Optics LLC (United States)

Industrial optical inspection requires high speed and high throughput of materials. Engineers use a variety of techniques to handle these inspection needs. Some examples include line scan cameras, high speed multi-spectral and laser-based systems.

High-volume manufacturing presents many challenges for inspection engineers. Often, manufacturers produce in quantities of millions per month, per week or even per day. Quality control of so many parts requires creativity to achieve the measurement needs. At times, traditional vision systems lack the contrast to provide the data required.

In this paper, we show how dynamic polarization imaging captures high contrast images. These images are useful for inspection tasks where optical contrast is low. We will cover basic theory of polarization. We show how to exploit polarization as a contrast enhancement technique. Finally, we show modeling for a polarization inspection application. The model shows how polarization can reveal low contrast materials such as adhesives on glass.

10373-8, Session 2

Deploying Mueller matrix polarimeter for characterizing diattenuation and retardation of subwavelength structure

Achyut Adhikari, Nanyang Technological Univ. (Singapore)

The essence of subwavelength structure measurement is in dire demand in advanced nanotechnology scenario. Mueller matrices for wire grid polarizer are measured experimentally using Mueller matrix polarimeter and validated with numerically simulated Lumerical Finite Difference Time Domain method. Wire grid polarizer are sub wavelength grating extensively used in display projection system attributable to its compact size; wide field of view and long term stability. Based on current state of art, where metrological equipment designed for nanometer level are quite expensive and complicated to use, this system and method has substantial scope. Experimentally calculated sub wavelength structure linewidth is validated with that of numerically simulated one by the aid of Mueller matrices. Further, intrinsic properties of the sample; diattenuation and retardance are experimentally calculated and verified by the numerical simulation.

10373-9, Session 2

Measurement of polarization state of light using in-plane spin splitting

Xiaodong Qiu, Zhaoxue Li, Zhiyou Zhang, Jinglei Du, Sichuan Univ. (China)

The measurement of polarization state of light, i.e., optical polarimetry, can provide essential information of the scattering objects. In this paper, we propose a precision method of polarization measurement using the in-plane spin splitting (IPSS). The IPSS, as a result of the spin-orbit interaction, manifests itself as the splitting in the incident plane of two circular polarized components of light beam reflected at an interface. By choosing a linear or elliptical incident polarization state, the IPPS can be observed in the coordinate or momentum spaces (i.e., spatial or angular IPSSs), respectively. Particularly, we find that the spatial (or angular) IPPS is extremely sensitive to the variation of the polarization direction (or ellipticity), when a horizontal polarized light beam is reflected at Brewster angle. Meanwhile, the spatial (or angular) IPPS is independent of the variation of the ellipticity (or polarization direction), when the polarization rotation angle and ellipticity are small. That is to say, the polarization direction and ellipticity of the light beam can be simultaneously estimated by measuring the spatial and angular IPSSs. In our experiment, we use a linear polarizer and a half-wave plate to produce the input polarization state. Then the light beam is reflected at the surface of a BK7 prism. Finally, the IPPSs are measured via the signal enhancement technique known from weak measurements with the built-in post-selection. Our results show that the input polarization state can be estimated with a high precision and may have applications in many fields, for example, magneto-optical effect and optical activity of chiral molecules.

10373-10, Session 2

The photonic spin Hall effect sensor

Linguo Xie, Zhiyou Zhang, Jinglei Du, Sichuan Univ. (China)

Refractive index sensing plays an important role in biological and chemical applications since a number of trace elements can be determined by measuring the refractive index. In this paper, we present an alternative refractive index sensing scheme based on the photonic spin Hall effect(PSEH). The PSHE manifests itself as opposite transverse displacements of left- and right-circular components when a linear polarized light beam is reflected or refracted at an interface between two media. We find that the spin splitting induced by the PSHE shows high sensitivity to the variation of the refractive index around the Brewster angle at a liquid-glass interface. Therefore, the refractive index sensing can be achieved by measuring the spin splitting. However, the spin splitting is of the order of several micrometers and it is difficult to detect using the conventional methods. In our case, the signal enhancement technique which is so-called weak measurement is employed to measure the spin splitting. We measure the amplified shift of spin splitting experimentally which can be several hundreds of micrometers. Our results show that the refractive index can be estimated with a precision of the order of 10-5 RIU. This method does not require the surface plasmon resonance structure based on noble metal films and the lock-in amplification technique, we believe that it is a robust, low-cost alternative to refractive index sensing.

10373-11, Session 3

Vibration-immune compact optical metrology to enable production-line quantification of fine scale features

Erik Novak, 4D Technology Corp. (United States)

Inspectors attempting to quantify defects and fine-scale features on precision machined surfaces such as turbine blades, drive train components, etc., are often limited by the capabilities and form factors of existing measurement techniques. For large components or to see features on complex geometries, inspectors most often rely on visual comparison tools or pin gauges to determine the geometry of surface features. These methods, however, are neither accurate nor precise, which can result in missed defects or rejection of good parts due to erring on the side of caution. Higher resolution metrology systems are are typically too expensive, slow and susceptible to environmental factors for use on the shop floor. Such instruments are also limited in their capability to measure defects on large components or in hard-to-reach areas. Inspectors must create plastic/rubber replicas of these surfaces, which can then be measured—a costly and time-consuming operation.

This talk will discuss a hand-held, video-rate, 3D optical metrology system for quantification of fine surface features for shop floor and in situ inspection and present critical performance tests including vertical and lateral resolution and gage capability.. With accurate, operator independent characterization, gage-capable measurements can be made on a variety of surfaces and geometries and proper determination of the severity of defects is possible. While the system cannot achieve the extremely high resolution of some optical systems, it bridges the gap between coarser coordinate measuring machines, stereoscopic imagers, and laser line projectors and such instruments. Various new applications will be discussed which are fundamentally enabled through access to a portable, vibration-immune, system that is both quantitative and easy-to-use.

10373-12, Session 3

Effective technique for evaluation of periodically-poled ferroelectric waveguide domains with nanoscale resolution based on frequency mixing

Pengda Hong, Yujie J. Ding, Lehigh Univ. (United States)

We have developed an effective technique for evaluating periodic domains of a ferroelectric waveguide including domain period, linear taper, and periodic domain depth. Such a technique is based on imaging of the surface-emitting second-harmonic beams generated generated by the waveguide. Using a periodically-poled lithium niobate domain waveguide, we have demonstrated that such a method has reached nanoscale spatial resolution.

10373-13, Session 3

Experimental investigation of natural convection in a rectangular cavity with two protruded half cylinders using a Mach-Zehnder interferometer

Akhil Krishnan Maliackal, Angarai R. Ganesan, Annamalai Mani, Indian Institute of Technology Madras (India)

Natural convection studies in an enclosure are very relevant since it spans a wide area of applications such as heat exchangers, chemical reactors, cooling of electronic equipment, etc. In the present study, an experimental investigation is performed in a rectangular cavity of dimension 46 mm x 23 mm with protruded copper half cylinders of diameter 15.8 mm (5/8 inch) each, placed in two different positions and two different configurations. Interferometry has always been a good technique for accurate measurements of temperature gradients. Mach-Zehnder interferometer is employed for visualising the isotherms and for quantitatively inferring the temperature gradient thereby local and average Nusselt number variation for the different configuration as well as the orientation of the test setup. The protruded half cylinders are maintained at constant temperature, ranging from 60 deg C to 120 deg C using an electric cartridge heater and associated temperature controller setup. A He-Ne laser with 24mm collimated beam size is used for experimental purposes. Further, it is planned to study the attributes associated with different aspect ratios along the length and breadth of the rectangular cavity for Rayleigh number varying from 10^3 to 10^4.

10373-14, Session 3

Authentication system using resonance evaluation spectroscopy (ASSURES)

Amit K. Lal, OMS Corp. (United States); James D. Trolinger, MetroLaser, Inc. (United States); Dave Dimas, Univ. of California, Irvine (United States)

This paper describes an ongoing instrument development project to distinguish genuine manufactured components from counterfeit components; we call the instrument ASSURES (Authentication System Using Resonance Evaluation Spectroscopy). The system combines Laser Doppler Vibrometry (LDV) with acoustical resonance spectroscopy (ARS) augmented with finite element analysis (FEA). Vibrational properties of components, such as resonant modes, damping, and spectral frequency response to various forcing functions, depend strongly upon the mechanical properties of the material, including its size, shape, internal hardness, tensile strength, alloy/composite compositions, flaws, defects, and other internal material properties. Although ARS has seen limited application, no one has fully exploited the information rich signals in the vibrational spectra of objects. Components with the same shape but made of different materials, different fatigue histories, damage, tampering, or heat treatment, will respond differently to high frequency stimulation. LDV offers high sensitivity and frequency bandwidth to measure the component's frequency spectrum, and overcomes many issues that limit conventional ARS, since the LDV beam can be aimed anywhere along the part as well as to multiple locations on a part. We have demonstrated ASSURES in a related application to detect manufacturing defects, specifications, and counterfeiting in similar parts. ASSURES is especially promising for use in added manufacturing technology AM because ASSURES signatures will act as digital codes that are unique to specific objects and even to specific locations on objects. We believe that such signatures can be employed to address many of the hypothetical and real vulnerability scenarios of importance to the manufacturing industry in general.

10373-15, Session 3

Optical mapping of surface roughnesses by implementation of a spatial light modulator

Laura M. Aulbach, Franziska Pöller, Min Lu, Shengjia Wang, Alexander W. Koch, Technische Univ. München (Germany)

It is well-known that the surface roughness of materials plays an important role in the operation and performance of technological systems. The roughness influences key parameters such as friction and wear and is directly connected to the quality and durability of the respective system. Tactile methods are widely used for the measurement of surface roughness, but a destructive measurement procedure or the lack of feasibility of online monitoring are crucial drawbacks. In the last decades, several non-contact, usually optical systems for surface roughness measurements have been developed, e.g., white light interferometry or speckle correlation. These techniques are in turn often unable to assign the roughness to a certain surface area or involve inappropriate adjustment procedures. One promising and straightforward optical measurement method is the surface roughness measurement by analyzing the fringe visibility of an interferometric fringe pattern. In our work, we employed a spatial light modulator in the interferometric setup to vary the fringe visibility and provide a stable and reliable measurement system. In previous research, the averaged fringe visibility or the fringe visibility along an observation profile have been analyzed. In this article, the analysis of the fringe visibility is extended to generate a complete roughness map of the measurement target. Thus, surface defects or areas of different roughnesses can be easily located.

10373-38, Session 3

Dimensional metrology of micro structure based on modulation depth in scanning broadband light interferometry

Yi Zhou, Yan Tang, Qinyuan Deng, Lixin Zhao, Song Hu, Institute of Optics and Electronics, Chinese Academy of Sciences (China)

Dimensional metrology for micro structure plays an important role in many science and industrial applications, such as integrated circuits (IC), medical cure, and chemistry. Broadband light interferometry is widely utilized in topography measurement due to its large measurement range, noncontact and high precision. In this paper, we propose a spatial modulation depth-based method to reshape the surface topography through analyzing the characteristics of both frequency and spatial domains in the interferogram. Due to the characteristics of spatial modulation depth, the method could effectively suppress the negative influences caused by light fluctuations and external disturbance. Both theory and experiments are elaborated to confirm that the proposed method can greatly improve the measurement stability and sensitivity with high precision. This technique can achieve a superior robustness with the potential to be applied in online topography measurement.

10373-16, Session 4

Phase measuring deflectometry for determining misalignment of segmented mirrors

Angela Davies, Trent Vann, Chris Evans, The Univ. of North Carolina at Charlotte (United States)

Alternative techniques for measurement of segment misalignment in a segmented mirror are of interest to the telescope community in the limit of large misalignment that precludes interferometric tracking. A variation of phase measuring deflectometry can be used to determine 5 degrees of freedom of the misalignment (DOF) with knowledge of the remaining 1 DOF. A camera and screen are positioned near the center of curvature, and the camera collects images of the screen pattern reflected from the mirror. In this application, the form of each segmented mirror is assumed known, so the misalignment contribution to the measurement can be separated. The approach is based on a Zernike analysis of distorted fringe patterns and their sensitivity to misalignment. We discuss simulation and experimental results in this paper.

10373-17, Session 4

Deflectometry for measuring mount-induced mirror surface deformations

Eric H. Frater, Ball Aerospace & Technologies Corp. (United States)

Deflectometry has been proven as a high precision and high dynamic range surface metrology technique. We report on the use of deflectometry to diagnose mount-induced optical surface deformations. A surrogate mirror from the OLI-2 earth-observing satellite mission is tested with deflectometry in a non-null configuration using only a CCD camera and an LCD computer monitor. Moments are mechanically induced at each flight-like mirror mount and the deformed surface is measured. Systematic errors in the surface measurements are significantly reduced by maintaining a consistent measurement geometry and evaluating moment-induced deformations differentially. The surface deformation modes from orthogonal moments at each mirror mount are compared to FEA predictions. The agility of this metrology sets the groundwork for in situ measurements of flight aspheric mirror surface deformations during component integration and prior to system testing.

10373-18, Session 4

General testing method for refractive surfaces based on reverse Hartmann test

Ping Xu, Daodang Wang, Zhidong Gong, China Jiliang Univ. (China); Rongguang Liang, College of Optical Sciences, The Univ. of Arizona (United States); Kong Ming, Jun Zhao, China Jiliang Univ. (China)

The testing of refractive wavefront enables the quantitative evaluation of refractive surfaces, such as the refractive lenses and glass bottles, and it plays a key role in the quality improvement of industrial products. The testing technique with high dynamic range is required to meet the measurement of refractive wavefront within large distortion range. In this paper, a general method based on reverse Hartmann test, a fringe-illumination deflectometry, is proposed to test the refractive surfaces. Ray tracing of the modeled test system is carried out to reconstruct the refractive wavefront from test refractive surface. To minimize the effect of geometrical error of test system, the computer-aided optimization of system geometry with iterative ray tracing is performed. According to the ray tracing result, the valid testing rays are obtained to reconstruct test wavefront, in which the TIR (total internal reflection) rays are removed from the acquired data to improve the measurement precision. Besides, the stitching method is applied to realize the full-aperture surface testing. To demonstrate the feasibility of the proposed method, experimental testing of glass bottles has been carried out and a good agreement is achieved, in which the RMS value of refractive wavefront is about 255 ?m and testing precision is better than 0.5 ?m. This testing method has preferable anti-interference ability, high dynamic range, low cost and character of suitable for field measurement. It is of great practicality for testing of transparent objects in industrial application.

10373-20, Session 4

Geometrical error calibration in reflective surface testing with reverse Hartmann test

Zhidong Gong, Daodang Wang, Ping Xu, China Jiliang Univ. (China); Rongguang Liang, College of Optical Sciences, The Univ. of Arizona (United States); Ming Kong, Jun Zhao, China Jiliang Univ. (China)

The development of deflectometry enables the high-precision testing of reflective surfaces with high dynamic range, such as the aspheric and freeform surfaces. In the fringe-illumination deflectometry based on reverse-Hartmann-test configuration, the reconstruction of test surface error is realized by ray tracing of the modeled test system. Careful calibration of system geometry is required to achieve high testing accuracy, and it is quite laborious and complicate. The calibration error of the geometrical relations among various components in the system, including the tilt angle deviations, lateral and longitudinal displacements, could introduce evident residual error in the testing result, even though the measurement accuracy of calibration device can reach the order of microns. For the convex surface with 2 inch aperture and 250 mm curvature radius, the RMS value of residual error corresponding to 1 ?m lateral displacement calibration error is about 0.080 ?m, and that for 0.01 degree tilt calibration error can reach 2.203 ?m. Thus, it places ultra-high requirement on the calibration devices.

To realize the high-precision reflective surface testing with reverse Hartmann test, a computer-aided geometrical error calibration method is proposed. The aberrations corresponding to various calibration errors of each component in test system are studied in detail. According to the aberration weights for various geometrical errors, the computer-aided optimization of system geometry with iterative ray tracing is carried out to calibrate the geometrical error. Both the numerical simulation and experiments have been performed to validate the proposed calibration method, and the accuracies in the order of sub-nanometer are achieved.

10373-21, Session 4

Study of annular sub-aperture stitching interferometry for aspheric surfaces

Zixin Zhao, Zhaoxian Xiao, Hangying Zhang, Xi'an Jiaotong Univ. (China)

Annular sub-aperture stitching interferometry (ASSI) has provided an alternative solution to measure rotationally symmetric aspheric surfaces with low cost and high flexibility. It is an effective way to test the aspheric surface with a larger aperture and larger relative aperture without null compensation. Currently, there are two main methods of full-aperture wavefront reconstruction. One is based non-overlapping sub-apertures and annular Zernike polynomial fitting, the full-aperture data is reconstructed by converting the fitting coefficients of sub-apertures into the fitting coefficients of full aperture. It is not suitable when there is a great local irregularity in some sub-aperture area, as the local irregular information may be missing. Another method is based on overlapping sub-apertures and the full-aperture data is obtained by minimizing the mismatch among all overlapping regions, which is more widely used. In this paper, two kinds of overlapping sub-aperture stitching algorithms, pairwise sequential stitching (PSS) and global synchronously stitching (GSS), were studied. The detailed mathematical expressions are shown in the form of matrix. Besides, the influence of the noise and number of sub-apertures to the two algorithms was also studied by simulation. At last, experimental results of a convex hyperboloid surface by using the two stitching algorithms are presented.

10373-22, Session 5

Development of an oxygen saturation measuring system using near-infrared spectroscopy

Kirara Kono, Doshisha Univ. (Japan)

Recently, the hypoxia imaging has been recognized as the advanced technique to detect cancers because hypoxia, which has a strong association to the biological features, is used for functional characterization of cancer. In previous studies, hypoxia imaging systems for endoscopic diagnosis have been developed. However, these imaging technologies can observe only blood vessels in mucous membrane in gastric because of visible light. Therefore, they could not detect scirrhous gastric cancer?which accounts for 10% of all gastric cancers and spreads rapidly into submucous membrane. To overcome this problem, we measured the blood oxygen saturation (SO2) in submucous membrane by using near-infrared (NIR) spectroscopy. NIR, which has high permeability for bio-tissues and high absorbency for hemoglobin, can image and observe blood vessel in submucous membrane. NIR system with LED lights and CCD camera module was developed to image blood vessel. We measured blood SO2 by optical density ratio (ODR) of two wavelengths, based on Lambert-Beer law. To image blood vessel clearly and measure blood SO2 accurately, we searched two optimum wavelengths by using a multilayer human gastric-like phantom which has same optical properties as human gastric one. By using Monte Carlo simulation of light propagation, we derived the relationship between ODR and blood SO2 and elucidated the influence of blood vessel depth on measuring blood SO2. These results were validated with experiments using our NIR system. Finally, it was confirmed that our system can detect SO2 in various depth blood vessels accurately.

10373-23, Session 5

Metrology of semiconductor structures using novel Fabry Perot fringe stretching system

Wojtek J. Walecki, Alexander Pravdivtsev, Frontier Semiconductor (United States)

Fabry-Perot (FP) fringes are widely used for measurement of thin optical films. Application of FP fringe method for very thick materials (such as silicon wafers) is limited since the spectral width of FP fringes decreases with thickness of a layer. Observation of thickness of wafers of silicon thicker than 50 mm is not possible using low resolution spectrometers.

We propose apparatus in which a reference etalon is introduced in the optical path of the beam between sample and spectrometer. In this arrangement, the low resolution spectrometer observes slow varying well separated fringes.

The frequency of these slow varying fringes corresponds to the difference of the FP fringes observed in the wafer alone and FP fringes observed in the etalon alone. Since thickness of the reference etalon is known, and since multiple etalons can be applied the thickness of the semiconductor wafer or other material can be established.

We present results of optical modelling, and characterization of the real life system. System is capable of measuring thicknesses of slabs of material having thicknesses from 0.5 to 10 mm. The reproducibility of the system is 0.01 um, and speed is limited by readout speed of 1D array detector and currently is about 10 ms (if thickness of the etalon is fixed).

In addition we present a simple solution transforming this system into Michelson interferometer and enabling slower phase sensitive measurements using this system, allowing easy identification of different layers and their optical properties in multilayer samples. The phase sensitive solution is used for easy generation of recipies in semiconductor metrology tool.

10373-24, Session 5

Rapid, automated, quality control of diffraction grating efficiency

Mark R. Fisher, Agilent Technologies, Inc. (United States)

A diffraction grating is found at the heart of every modern spectrophotometer and yet, despite being used for over 60 years, a practical and efficient characterization tool has proven to be elusive. Part of the challenge can be attributed to the unique angular dependent geometry (dispersion) of gratings. Here we demonstrate automated grating efficiency measurements of four reflection gratings (300, 1200, 1800 and 3600 grooves per mm). Total measurement time was less than 2 hrs at a maximum of 161 wavelengths per grating. This approach can reduce quality assurance, or design verification, test time from days to hours when compared to equivalent manually operated systems.

Multi-angle Photometric Spectroscopy (MPS) was used to measure the reflectance of gratings across a range of wavelengths and angles. A recent development by Agilent Technologies, the Cary 7000 Universal Measurement Spectrophotometer (UMS) combines both reflection and transmission measurements from the same patch of a sample's surface in a single automated platform. Angles of incidence range 5 deg ≤ |?i| ≤ 85 deg (i.e. angles on either side of beam normal noted as +/-) under s or p polarized light.

We describe the use of MPS on the Cary 7000 UMS by changing grating angle with respect to the incident beam (?i), from 20 deg to 80 deg and the fixed detector position (?d), user defined. This optical geometry replicates a typical monochromator design configuration where the entrance aperture represents the entrance slit of the monochromator and the detector the exit slit. Both s and p polarization efficiency profiles were collected within the range 250 nm to 2500 nm automatically without the need for user intervention.

This spectroscopic approach provides useful input into to quality assurance programs while simultaneously reducing test costs and enhancing part throughput.

10373-25, Session 5

Spatially and temporally resolved diagnostics of dense sprays using gated femtosecond digital holography

James D. Trolinger, MetroLaser, Inc. (United States); Derek Dunn-Rankin, Ali Ziaee, Univ. of California, Irvine (United States); Andrei K. Dioumaev, MetroLaser, Inc. (United States); Marco Minniti, Univ. of California, Irvine (United States)

This paper describes research that demonstrated that gated, femtosecond, digital holography enables 3D microscopic viewing inside dense, almost opaque sprays and can provide a new and powerful diagnostics capability for combustion researchers that enables seeing fuel atomization processes never seen before. The method works by exploiting the extremely short coherence and pulse length (approximately 30 micrometers in this implementation) provided by a femtosecond laser combined with digital holography to eliminate multiple and wide angle scattered light from particles surrounding the injection region, which normally obscures the image of interest. Photons that follow a path that differs in length by more than 30 micrometers from a straight path through the field to the sensor cannot contribute to the holographic recording of photons that travel in a near straight path (ballistic and "snake" photons). To further enhance the method, off-axis digital holography was incorporated to enhance signal to noise ratio an image processing capability in reconstructed images by separating the conjugate images, which overlap and interfere in conventional in-line holography. Because this is ground-breaking research, fundamental relationships and limitations were also examined in addition to demonstrating capabilities. The project is a continuing collaboration between MetroLaser and the University of California, Irvine.

10373-26, Session 6

Focusing schlieren systems using digitally projected grids

Drew L'Esperance, Benjamin D. Buckner, Spectabit Optics, LLC (United States)

Schlieren imaging has been an essential method for studying aerodynamic effects, particularly thermal convection, shock waves, and turbulent flows. This paper describes a compact portable digital focusing schlieren system that can be used to visualize relatively large fields for applications in ventilation design and aerodynamics research. Visualizing large fields is difficult using classical schlieren systems that employ collimated light because their field of view is limited by the size of the mirrors or lenses. Background-oriented schlieren systems are well-suited for visualizing large fields, but their sensitivity is limited by the need to simultaneously maintain focus on the background pattern and the test area. Lens and grid-based focusing schlieren systems are essentially hybrids between classical and background-oriented systems. They can visualize fields that are much larger than possible with comparably priced classical schlieren systems, while providing more sensitivity than background-oriented schlieren systems. Using commercially available camera lenses and optics, fields up to several square meters can be visualized. A key innovation in the system presented here is that digital display devices are used to display the background pattern, which simplifies the optical system and reduces its size. To calibrate the system, proprietary software is used to analyze images acquired by the system's digital camera, and then a background pattern is computed that is complementary to the cutoff grid. The calibration software also provides real-time background subtraction and contrast enhancement. The schlieren system is portable enough that it can be set up quickly in industrial facilities.

10373-27, Session 6

Application of the instrument transfer function to a fringe projection system for measuring rough surfaces

Bin Zhang, Angela Davies, John Ziegert, Christopher J. Evans, The Univ. of North Carolina at Charlotte (United States)

The fringe projection is a novel technique for surface inspection of the layered metal additive manufacturing (AM) process [1], [2]. When used as a surface texture/roughness measuring tool, this technology offers several benefits over the state-of-the-art interferometry methods. First, the instrument can be placed far from the measured object such that the measurements can be made in situ. Second, the fabrication cost is relatively lower than the interferometers because of the less rigid optical fabrication and alignment tolerances. However, fringe projection as a surface texture/roughness measuring technique is still immature. The spatial measurement performance is seldom mentioned by the commercial system vendors or in the literature. The instrument transfer function (ITF) has been proposed as a spatial resolution metric for topography measuring instruments [3], [4]. In this paper, we will investigate the application of ITF to a custom fringe projection system designed for measuring metal AM surfaces. We have found that the linear condition that is required for a meaningful use of ITF is approximately the case when the surface deviation is much smaller than (less than 1/10) the effective wavelength. These conclusions are supported by an analysis of the mathematical model of fringe projection and by extensive simulation. The relationships between ITF, the approximate validity, and optical diffraction will be discussed.

10373-28, Session 6

A three-dimensional scanning apparatus based on structured illumination method and its application in dental scanning

Jae Sung Ahn, Anjin Park, Korea Photonics Technology Institute (Korea, Republic of); Ju Wan Kim, Byeong Ha Lee, Gwangju Institute of Science and Technology (Korea, Republic of); Joo Beom Eom, Korea Photonics Technology Institute (Korea, Republic of)

We demonstrated a three-dimensional (3D) dental scanning apparatus based on structured illumination. A liquid lens was used for tuning focus of the 3D scanning apparatus and a piezomotor stage was used for shift of structured light. By incorporating the liquid tunable lens and the piezomotor stage into the 3D scanning apparatus, we fabricated a compact apparatus and reduced mechanical movement of optical parts inside the apparatus. A simple algorithm, which only detects intensity modulation, was used to perform optical sectioning with structured illumination. As an application in dental scanning, we reconstructed the 3D point cloud models of a dental gypsum cast by piling up sectioned images of the dental cast along the focal axis of the 3D scanning apparatus. We also performed 3D registration of the 3D point cloud models to exhibit a 3D model of the entire dental cast.

10373-29, Session 6

A calibration method immune to the projector errors in fringe projection profilometry

Ruihua Zhang, Shanghai Univ. (China); Yulin Shang, Xi'an Polytechnic Univ. (China)

Fringe projection profilometry is a typical three-dimensional (3D) shape measurement method, and has been extensively applied to many fields. In it, system calibration is a tedious task to establish the mapping relationship

between the object depths and the fringe phases. This paper presents an efficient calibration method based on cross-ratio invariance in the system geometry. In this procedure, we measure the phase maps corresponding to the reference board perpendicularly to three positions with known depths as the reference phase maps. And then calculating the cross-ratio of points along each incident light ray to determine the phase-to-depth relations. When measuring an object, the depth map is calculated from the reference and object phases by employing the pixel shifts on the image plane of the camera. This method is immune to the errors sourced from the projector, including the distortions in the geometric shapes and in the intensity profiles of the projected fringe patterns. Experimental results demonstrate the proposed method is feasible and valid.

10373-39, Session 6

Multimodal and synthetic aperture approach to full-field 3D shape and displacement measurements *(Invited Paper)*

Malgorzata Kujawi?ska, Robert Sitnik, Warsaw Univ. of Technology (Poland)

Recently most of the measurement tasks in industry, civil engineering, security and culture heritage applications require characterization and monitoring of 3D objects and structures and their performance under changing conditions. These requirements can be met if multimodal measurement (MM) strategy is applied. It rely on effective combining structured light method and 3D digital image correlation with laser scanning/ToF, thermal imaging, multispectral imaging and BDRF measurements. In the case of big size and/or complicated objects MMS have to be combined with hierarchical or synthetic aperture (SA) measurements. Both: MM and SA strategies are presented and their applicability is shown at interesting civil engineering and cultural heritage applications.

10373-30, Session PWed

Collimator focus check with interferometer

Ho-Lin Tsay, Yu-Chuan Lin, Sheng-Tsong Chang, Ting-Ming Huang, Instrument Technology Research Ctr. (Taiwan)

Collimator is popular used in optical testing in laboratory to simulate target in a distance. Glass plate or metal plate with pattern is fundamental constitute of collimator focal plane, which should be placed precisely with respect to its optics. For focal plane of collimator being in open space, collimating test is straightforward with a flat mirror. Reflection of the projected beam forms an image identical to focal plane pattern. Comparing pattern and its re-entrance image claims a simple way to check collimator's collimating properties.

However, most focal plane of collimator are surrounding by opto-mechanical structure. It is not possible to observe the pattern and its image simultaneously. A method mentioned in ISO-13485 standard using a penta-prism and theodolite can be used to check the collimating properties. This method measures relative angle in different aperture part of collimator to derive angle deviation of the collimating beam. This method is quantitative and suitable for large aperture collimator but time-consuming.

For small aperture collimator which focal plane is surrounding by opto-mechanical structure. We develop a method to check collimating properties with a Fizeau interferometer involving non-common path interferometry. Power element of interferometric analysis was used as an indicator for focus adjustment. As a result, a fast method to check focal plane position is developed.

Results derived from this method are compared with that derived from angle deviation measurement method.

10373-31, Session PWed

Characterizing the surface fluctuation of an epitaxial wafer by using the Shack-Hartmann wave-front sensor

Pao-Keng Yang, Yao-Kai Zhuang, Minghsin Univ. of Science and Technology (Taiwan)

By using a light-emitting diode as the probing light source and a Shack-Hartmann wave-front sensor to execute a relative measurement, we present a simple and sensitive method for characterizing the surface fluctuation of a nominally flat sample. We used an epitaxial wafer for test. The measured reflected wave front from the surface of the sample was first calibrated to be a planar surface. The surface fluctuation of the test sample could be estimated from the increment on the variance of the wave-front surface to its regression plane after the sample had been shifted by a small distance by using the Bienaymé formula.

10373-32, Session PWed

Fabrication and testing of a long-scale physically stitched diffraction grating using a compact laser interference lithography system with a blu-ray laser diode

Xinghui Li, Xiangwen Zhu, Qian Zhou, Graduate School at Shenzhen, Tsinghua Univ. (China); Haiou Lu, Tsinghua Univ. (China) and Graduate School at Shenzhen, Tsinghua Univ. (China); Kai Ni, Xiaohao Wang, Graduate School at Shenzhen, Tsinghua Univ. (China)

In this research, a technology enabling long-scale (>1000mm) sub-micron periodic diffraction gratings was investigated. Differing from the conventional metal belt type diffraction gratings fabricated by ruling engine, the long-scale grating presented here is formed by physically stitching multiple interference lithographied 20 mm order short-scale gratings, which dramatically simplifies the fabrication systems. Five such kinds of gratings are mounted on a plane substrate to form a 100 grating unit and multiple units are further connected. An interference lithography system for fabrication of these short-scale gratings was constructed by using a compact and cost-effective 405 nm blu-ray laser diode. Four-axis alignment errors that influence the uniformity of grating periods are thoroughly analyzed and a testing platform was established for calibration. Fabricated short-scale gratings were precisely evaluated and grating uniformity was verified to be higher than 95%. A 100 mm grating unit was assembled and tested. Alignment errors were controlled within comparable levels with the flatness of commercial optical glass. These performances proved that this unit is able to be connected for a 1000 mm order scale grating, which will greatly benefits precision positioning of linear motion stages based production engineering.

10373-33, Session PWed

Combined subminiature infrared particulate matter sensors with humidity sensors for reliable mass concentration outputs

Dong-Ik Kim, Han-Jung Kim, Taejoong Lee, Ctr. for Integrated Smart Sensors (Korea, Republic of)

In this paper, we propose a combined subminiature infrared particulate matter (PM) sensor with a capacitance type humidity sensor. In general, PM sensors show number or mass concentration of suspended PM2.5/PM10 in the air, but relative humidity can affect optical type PM sensors. In result,

the concentration of PM is a need for correction depending on the relative humidity. To correct PM concentration, a subminiature humidity sensor was installed inside the PM sensor and several correction factors were applied to a calibration process. Owing to the humidity sensor scale, there is a margin to reduce the PM sensor size also. Furthermore, we applied a specially designed aspheric lens pair with an effective focal length of 2.97 mm to the PM sensor for a subminiature dimension.

10373-34, Session PWed

Advanced polarization sensitive analysis in optical coherence tomography

Aleksandra Wieloszy?ska, Marcin R. Strakowski, Gdansk Univ. of Technology (Poland)

The optical coherence tomography (OCT) is an optical imaging method, which is widely applied in variety applications. This technology is used to cross-sectional or surface imaging with high resolution in non-contact and non-destructive way. OCT is very useful in medical applications like ophthalmology, dermatology or dentistry, as well as beyond biomedical fields like stress mapping in polymers or protective coatings defects detection. Standard OCT imaging is based on intensity images which can visualize the inner structure of scattering devices. However, there is a number of extensions improving the OCT measurement abilities. The main of them are the polarization sensitive OCT (PS-OCT), Doppler enable OCT (D-OCT) or spectroscopic OCT (S-OCT). Our research activities have been focused on PS-OCT systems. The polarization sensitive analysis delivers an useful information about optical anisotropic properties of the evaluated sample. This kind of measurements is very important for inner stress monitoring or e.g. tissue recognition. Based on our research results and knowledge the standard PS-OCT provide only data about birefringence of the measured sample. However, based on the OCT measurements more information including depolarization and diattenuation might be obtained. In our work, the method based on Jones formalism are going to be presented. It is used to determine birefringence, dichroism and optic axis orientation of the tested sample. In this contribution the setup of the optical system, as well as tests results verifying the measurements abilities of the system are going to be presented. The brief discussion about the effectiveness and usefulness of this approach will be carried out

10373-35, Session PWed

Optical stabilisation for time transfer infrastructure

Josef Vojtech, Ondrej Havlis, Pavel Skoda, Vladimír Smotlacha, Petr Munster, Michal Altman, Tomas Horvath, Jan Radil, Martin Slapak, Radek Velc, Lada Altmannova, CESNET z.s.p.o. (Czech Republic)

Transfer and distribution of precise time and stable frequency becomes an attractive alternative to satellite based methods for distances up to units of thousands of kilometers. We present developed of infrastructure for transfer of these precise quantities. Actually infrastructure over spans more than 1500 km reaches three countries. Infrastructure utilizes DWDM layer or creates overlay over this layer in optical network, using the available resources, i.e. reserved optical bandwidth in DWDM (Dense wavelength division multiplexing) CESNET network. Inside the Prague capital area, we also use a CWDM (Coarse wavelength division multiplexing) channel. These resources allow us to setup permanent bidirectional single fiber path between any two points of presence deployed in involved institutes. Now there are actively connected seven organizations in the Czech Republic and also one foreign institute – the Austrian national time and frequency laboratory BEV in Vienna. The infrastructure shares fibers with data channels at 10 or 100 Gbps without any measurable interactions. As transport delay significantly fluctuates (annul changes about 350ns for the longest link) mainly due to temperature influenced changes of fiber refractive index and length and also by vibrations it is important to stabilize the delay. We present practical issues of variety of optical methods for delay stabilization, ranging from different delay lines (free space tuned by distance change or fiber based tuned by temperature change) to change of transmission wavelength or chromatic dispersion of optical path.

10373-36, Session PWed

Demodulation of single carrier-frequency interferogram by pixel-level Lissajous figure and ellipse fitting

Fengwei Liu, Yongqian Wu, Fan Wu, Institute of Optics and Electronics (China)

In this paper, we present a novel method to demodulate the phase from single carrier frequency interferogram. It is based on pixel-level Lissajous figure and ellipse fitting (PLEF). Compared with FT method which is a global operation in frequency domain, the local demodulation in spatial domain mechanism makes it more flexible and accurate. The variation of phase distribution over a few pixels, i.e., local phase shifts , are considered with a more adaptable assumption. The mathematic model of demodulation is of interest. The correctness of the mathematic model is firstly demonstrated by simulations and the corresponding theoretical error of the phase demodulation is as less as 1e-4 rad level, followed by a comprehensively discussion on different influence factors. The experiments finally validate the effectiveness of proposed method.

10373-37, Session PWed

Robust phase unwrapping algorithm for 3D profile measurement applications

Meiqi Fang, Hong Zhao, Yueyang Ma, Xi'an Jiaotong Univ. (China)

Phase unwrapping is a significant procedure that has raised a great interest in many coherent imaging systems. What we believe to be a new phase unwrapping algorithm, is described and tested. The method starts from the fact that 2-D wrapped phase distribution can be regarded as a response to two orthogonal 1-D direction excitation signals. This suggests a cepstrum analysis to be implemented in the phase unwrapping problem. The simulated and real experimental results performed on fringe projection profilometry confirm the validity of our approach. In fact, this proposed method is possible to attain a fast and practical phase unwrapping solution with enhanced noise robustness.

10373-40, Session PWed

Measurement of vibration using phase-only correlation technique

Settu Balachandar, Vipin Karthikeyan, SRI Krishna College of Engineering & Technology (India)

A novel method for the measurement of vibration is proposed and demonstrated based on laser triangulation. Experiment involves, launching a Line-laser probe beam perpendicular to the axis of vibrating object. The reflected probe beam is recorded by high speed camera. The dynamic position of the line laser in image plane is governed by magnitude and frequency of vibrating test-object. Using phase correlation technique the maximum distance travelled by the probe beam in CCD plane is measured in-terms of sub-pixels using Matlab. The preliminary result of the proposed method is reported for the acceleration from 1g to 3 g, and the frequency from 6Hz to 26Hz.

Conference 10374: Optical Modeling and Performance Predictions IX

Monday - Tuesday 7 –8 August 2017

Part of Proceedings of SPIE Vol. 10374 Optical Modeling and Performance Predictions IX

10374-16, Session PMon

Measurements of the optical anisotropy parameter of Tb:CaF2 crystal

Alexey Yakovlev, Ilya L. Snetkov, Oleg V. Palashov, Institute of Applied Physics of the Russian Academy of Sciences (Russian Federation)

CaF2 crystals with Tb ions could be used as the magnetooptical material in Faraday isolators and rotators [1]. In such devices it is important to minimize of thermal depolarization that appears in magnetooptical element. One of the method of minimizing of thermal depolarization is based on its dependence on crystallographic axes [2]. Depolarization takes the minimum value in the optimal orientation of crystallographic axes, that is determined by the optical anisotropy parameter [3]. Because of weak absorption at 1070 nm, the depolarization in Tb:CaF2 (10at.% Tb) crystal does not show the dependence on laser power up to 1.5 kW [1] and it is not possible to apply the existing method of heating of the crystal to determine the optical anisotropy parameter [4].

In the experiment we used another method that is based on heating of the side surface of the cylindrical optical element. Obtained values for Tb:CaF2 were compared with data for CaF2 measured by both methods of heating of crystal. Using the obtained value of the optical anisotropy parameter at 1070 nm the optimal orientation of crystallographic axes for Tb:CaF2 was determined. Obtained value of the optical anisotropy parameter is necessary for numerical simulations and for minimizing of the thermal effects in such crystals.

References:

[1] D. S. Zheleznov, et.al., Opt. Mater. 46 526-9, 2015.

[2] W. Koechner et.al., J. Opt. Soc. Am. vol. 61, pp. 758-766, 1971.

[3] R. E. Joiner, et.al., Appl. Phys. Lett. 30, 485, 1977.

[4] I. L. Snetkov, et.al., Opt. Express 20, 13357, 2012.

10374-18, Session PMon

Aqueous ethanol detection using a fiber-optic sensor based on Fresnel reflection

Umesh Sampath, Dae-gil Kim, Minho Song, Chonbuk National Univ. (Korea, Republic of)

The measurement of ethanol concentrations in liquid environments is of vital importance for a variety of purposes such as food industry, ethanol production, chemical processing, fuel processing, and to use in forensic science and physiological research. Most common and commercial ethanol measurement techniques utilize semiconductor, electronic, and fuel cells. However, these systems are designed exclusively for vapor-phase measurements. Thus, they are usually bulky, and limited in range and selectivity. Also, the functionality is more limited than the required number of applications. These creates a demand for sensors to measure the ethanol concentrations in aqueous solutions with simple design and good accuracy.

Optical fiber sensors have a great potential for various biological and chemical solute concentration measurement applications. In recent years, optical sensors have also been studied to measure the ethanol concentration. Various configurations, which include U-bent multimode fiber and tapered optical fiber with Graphene Oxide (GO) coating, have provided successful results to measure wide range of ethanol concentration in aqueous solutions. In addition to these, we propose a novel fiber-optic ethanol sensor based on Fresnel reflections. The proposed sensor system is functionalized with a thin-layer of ethanol-sensitive graphene oxide (GO) coating on a single mode optical fiber end. The trace of ethanol concentration was measured by the variations in Fresnel reflection intensity and the optical properties of graphene oxide. Aqueous ethanol concentration from 10% to 100% was measured successfully with the sensor system. The proposed fiber end with GO film exhibited real-time, remote measurements of ethanol concentration with high precision.

10374-19, Session PMon

The optical schemes of head-mounted displays

Galina E. Romanova, Alexey V. Bakholdin, Vladimir N. Vasilyev, ITMO Univ. (Russian Federation)

Recently there is a growing interest to the head up and head mounted systems. There are many variants of implementation of the head-mounted display system for various purposes with different characteristics. The configuration of the system is highly affected by both type of the image generator and the type of the used combiner.

In many cases we need to design many variants of the scheme and even design new type to compare the characteristics and make a decision to manufacture and realize the system. We have considered several variants of the layout of the systems and compare their characteristics including the packaging and image quality. The systems were designed for operating with the same image generator.

10374-20, Session PMon

Optical system for UV-laser technological equipment

Yuri V. Fedosov, Galina E. Romanova, Maxim Y. Afanasiev, ITMO Univ. (Russian Federation)

Recently there is an intensive developing of intelligent industrial equipment. It can be rapidly adjusted for manufacturing and processing of certain details. This equipment can be robotic systems, automatic wrappers and markers, CNC machines and 3D printers.

The equipment considered in the work is the system for selective curing of the photopolymer using the UV-laser, and using the UV-radiation in such equipment leads to additional technical difficulties.

In many cases for transporting the radiation from the laser to the point processed multi-mirror system is used, but such systems are usually difficult to adjust. Additionally such multi-mirror systems are usually used as a part of equipment for laser cutting of metals using high-power IR-lasers. For the UV-lasers using many mirrors leads to crucial radiation losses because of many reflections .

So, during the development of the optical system for technological equipment using UV-laser, we need to solve two main tasks: to transfer the radiation for working point with minimum losses and to include the system for managing the radiation spot position.

We introduce the system for working with UV-laser with 1 W power and wavelength 423 nm based on fiber system.

The modeling has shown that the optical system gives the sizes of the light spot of about 300 ?m, the designed optical and mechanical systems (prototypes) were manufactured and assembled. In the paper we present the layout of the technological unit, the results of the theoretical modeling of the parts of the system and some experimental results.

10374-21, Session PMon

Optical modeling of light scattering for refractive-index detection of liquids in a microcapillary with low-coherence rainbow diffractometry

Grzegorz Swirniak, Wroclaw Univ. of Science and Technology (Poland)

Capillary electrophoresis (CE) is a technique that employs narrow capillary tubes (internal diameters from 2 μm up to approx. 700 μm) for the analysis of high-efficiency separations of large and small chemical compounds. Detection in CE is a challenge due to small dimensions of a measurement volume. Through the years, a variety of measurement techniques have been used to identify analytes of interest. CE detectors based on refractive index (RI) measurements allow to characterize micro-domain systems on-line with potentially high sensitivity of the measurement data to changes in RI. Importantly, RI detection allows to characterize samples with no deed of a chemical derivatization, so no pre-column workup is involved. Most of RI optical detectors for CE use a form of interferometric imaging and measure time-dependent concentration of separated ions. Common interferometric techniques include: amplitude splitting interferometry, holographic RI sensing, backscattering interferometry, whispering-gallery modes, and surface plasmon resonances sensing. The use of a lasers as measurement tools for this purpose is common due to both spatial and temporal coherence of laser light.

The aim of this manuscript is to present a different approach to RI sensing for CE which bases on the study of a rainbow phenomenon arising from light scattering by an unmodified glass capillary containing an analyte. Unlike most state-of-the-art interferometric techniques for RI detection, it uses a beam of light having low temporal coherence, which (i) reduces the detrimental sensitivity of the rainbow pattern to small changes in RI of the analyte, (ii) improves the stability of the inverse problem allowing to determine the RI of an analyte without the classical RI ambiguity problem related to morphology dependent resonances (MDRs), and (iii) offers a wide-range RI detection. A constant progress in developing light sources producing a high-intensity, polychromatic radiation (e.g. LED, SLD, etc.) as well as some optical elements capable of converting such light beams with minimal aberrations, makes a practical implementation of the described method feasible.

The main part of the work will be devoted to a numerical prediction of the sensitivity of the measurement data to changes of the refractive index with relative issues. However, as a qualitative understanding of the scattering mechanisms is necessary to extract the desired information, a detailed information about the scattering process will be also provided.

10374-22, Session PMon

Density of states of Cs3Sb calculated using density-functional theory for modeling photoemission

Daniel Finkenstadt, U.S. Naval Academy (United States); Samuel G. Lambrakos, Kevin L. Jensen, Andrew Shabaev, U.S. Naval Research Lab. (United States); Nathan A. Moody, Los Alamos National Lab. (United States)

An analysis is presented that provides a density of states (DOS or D(E)) factor for Cs3Sb in the calculation of its quantum efficiency QE and emittance using a Moments Approach. The analysis is based on density functional theory (DFT) adapted for the practical application of treating photoemission from bulk metal and semiconductor materials, and the interfaces between them. The Moments approach treats the processes of absorption, transmission and emission separately, for which DFT affects parameters and processes associated with each step, of which D(E), the optical constants n and k, and materials parameters such as effective mass m and band gap Eg are paramount. Such factors are required to provide the components of an evaluation similar to the Tsu-Esaki formula for calculating current density over and through and over barriers, and will become more important when a proper quantum mechanical treatment of the emission barrier is considered beyond the simplistic thermal model (transmission probability is unity only for energy levels in excess of the barrier height and zero otherwise). Such features are expected to be far more consequential if the barrier supports resonant levels, e.g., heterostructures.

10374-23, Session PMon

The effect of laser ablation parameters on optical limiting properties of silver nanoparticles

Irmak Gürsoy, Roketsan A.S. (Turkey); Halime Gul Yaglioglu, Ankara Üniv. (Turkey)

This paper presents the effect of laser ablation parameters on optical limiting properties of silver nanoparticles. The current applications of lasers like range finding, guidance, detection, illumination and designation have increased the potential for temporary or permanent damage on imaging systems or eyes. The ability of laser detection introduces the risks of sensors or eyes get harmed when laser power above the systems damage threshold level. There are some ways to protect these systems like neutral density (nd) filters, shutters, etc. But these limiters are reduced the total amount of light that gets into the system, response time may not be fast enough to prevent damage and caused precipitation in performance due to deprivation of transmission or contrast. In the present case, optical limiting filters are needed that is transparent for low laser intensities and limit or block the high laser intensities. We used silver nanoparticles for laser ablation and silver solutions were synthesized by Nd:YAG nanosecond laser at 532 nm of a high purity silver target immersed in pure water. UV-Vis spectrophotometer was employed to characterize the absorbance of silver nanoparticles. Laser power and ablation time was changed. The effect of altering these parameters on laser ablation efficiency of nanoparticles was investigated experimentally and optimum values were specified. These results are more useful indications for characterization of silver nanoparticles solutions for obtaining high performance optical limiters.

10374-24, Session PMon

Impact of the necking phenomenon on the spectral behavior of WO3 aggregates

Krzysztof Skorupski, Wroclaw Univ. of Technology (Poland)

Fractal-like aggregates are usually modelled as monodisperse particles positioned in point contact. However, this is a rough approximation which may lead to many inaccuracies in light scattering simulations. In reality, much more advanced connections between primary particles exist. Brasil studied the impact of the necking phenomenon on the morphological parameters of these geometries. He proposed a parameter for measuring the particle intersection level. It gives accurate results providing that investigated aggregates are composed of monodisperse, spherical particles. In this work, new parameters for measuring both the intersection level and the neck level were introduced. In contrast to the study be Brasil, they can be used regardless of the particle size and shape. Additionally, the impact of the connection type on the spectral behavior of WO3 aggregates was studied. Two cases were investigated: when the volume of the aggregate (or two connected primary particles) was constant regardless of the connection type, and when it was dependant on the connection size and shape. For light scattering simulations, the ADDA algorithm was used. The wavelength varied from 400nm to 800nm. The number of dipoles per wavelength was never smaller than 200. The refractive index for WO3 was adapted from the paper by Vourdas et al. The results prove that necks have strong impact on the spectral behavior of WO3 aggregates. For example, in some cases, the relative cross section error can be even larger than 50%. They also prove that connections, which exist between primary particles, should not be excluded from aggregate models.

10374-1, Session 1

Dynamic/jitter assessment of multiple potential HabEx structural designs

Joseph B. Knight, H. Philip Stahl, NASA Marshall Space Flight Ctr. (United States)

Dynamic analyses of multiple configurations of a proposed Habitable Exo-Planet (HabEx) 4 m off-axis telescope structure were performed to predict effects of jitter on primary mirror wave front error and primary/secondary mirror alignment. The dynamic disturbance used as the forcing function was the James Webb Space Telescope reaction wheel assembly vibration emission specification level. The objective of these analyses was to predict "order-of-magnitude" performance for various structural configurations which will roll into efforts to define the HabEx structural design's global architecture. Structural design parameters varied included structural vs. non-structural tube and secondary mirror (SM) to science instrument enclosure. Primary Mirror (PM) wave front error, PM/SM alignment, and overall mass of each configuration are reported.

10374-2, Session 1

Challenges in coronagraph optical design

Russell A. Chipman, James Breckinridge, College of Optical Sciences, The Univ. of Arizona (United States)

To accurately predict the performance of space-based terrestrial exoplanet coronagraphs, we have integrated several analysis methods: geometric ray tracing, polarized vector wave propagation and diffraction theory, and statistical optics. The space-based exoplanet coronagraph performance requires an accurate end-to-end (object to mask to detector) optical system model to guide science decisions, technology development to direct the optical system engineering needed to balance subsystem requirements and to define system ground & space calibration methodologies.

Due to the extreme specifications for exoplanet coronagraphs, such as the goal of resolving planets with a brightness less than 10^-9 of their star located within 3 Airy disk radii, geometric ray-tracing alone provides insufficient information to estimate contrast & SNR for exoplanet characterization. Using the Polaris-M polarization analysis program, we have analyzed how uncorrected coating polarization aberrations couple light around 10^-5 of the incident light into crossed polarized diffraction patterns about twice the size of the Airy disk. Since these orthogonal polarized components exiting with wavefront aberrations different from the principal uncoupled beams, their wavefronts not corrected by the deformable optics systems. Polarization aberrations expansions have shown how these polarization aberrations scale with mirror coatings, fold mirror angles, and numerical aperture. Form birefringence of the telescope mirrors is also analyzed to tolerance this poorly understood, but potentially damaging effect.

10374-3, Session 1

Improving wavefront estimation and control in high-contrast coronagraphy using a polarization compensation algorithm

Jessica Gersh-Range, N. Jeremy Kasdin, Princeton Univ. (United States)

Instrumental polarization is a concern for high-contrast coronagraphs because it introduces errors that cannot be corrected simultaneously with the current two-deformable-mirror wavefront estimation and control scheme, thereby degrading the final contrast. This problem cannot be solved by imaging in a single polarization because light that is initially in one polarization leaks into the orthogonal polarization as it propagates through the optical system; polarizers would be needed before and after the optical system, and this solution is impractical for a large telescope. Current mitigation schemes are hardware-oriented, seeking to cancel the instrumental polarization or minimize its sources. We have developed a complementary, algorithmic approach that compensates for instrumental polarization by subdividing the measured intensity based on the initial polarization and isolating the portion affected by wavefront control.

Our algorithm uses knowledge of the optical system and a set of final intensity measurements to estimate the composition of the incident light, then propagates the result through the optical system to estimate how each polarization component of the incident light contributes to the measured intensity. The estimates of these final intensity contributions are incorporated into a wavefront estimation and control scheme that considers only the estimates of the portions of the wavefront it can correct, and estimates of uncorrectable portions can be subtracted from the final image during postprocessing. In this paper, we present simulations that demonstrate the potential performance improvements that our approach provides, and we provide a preliminary discussion of the impact of model errors and uncertainties.

10374-4, Session 1

Optical performance prediction of space instruments using ray-tracing-based Earth system model

Dongok Ryu, Sug-Whan Kim, Yonsei Univ. (Korea, Republic of); Robert P. Breault, Breault Research Organization, Inc. (United States)

We report a new end-to-end computation model for performance evaluation of space optical instrument. The model combines the observing instrument, the global earth as an observation target and the sun as a light source in non-sequential ray tracing environment. Simultaneous imaging and spectroscopic results are provided using this model with fully resolved spatial, spectral, and temporal coverage of sub-models of Earth. Especially, the global earth system model is defined with a set of optical characteristics representing its 16 types of lands, a ocean and 3D atmosphere components. The incident sun-light interacts with the earth components in terms of reflection, refraction, transmission, absorption and scattering before it enters into the instrument aperture. This new model is capable of evaluating spectroscopic performance as well as imaging and radiometric performances of the optical instrument almost simultaneously from integrated ray tracing computation. We applied this technique to HRI-VIS instrument in EPOXI mission. A hypothetical two-mirror Cassegrain imager is designed with a 300 mm diameter aperture and 21.504 mm ? 21.504 mm focal plane. The simulation images are compared with observations from HRI-VIS meaurement for a day from UTC Mar.18, 2008. The surface scales are 55.0km/pixel for simulation and 54.9km/pixel for observation. Then we measured the defocus aberration of the instrument using a defocus mapping tool and edge spread function with six gradually defocused simulation images. The measuring result shows that optical path between primary and secondary mirror increases by 55.498 ?m from the diffraction-limited condition. This study shows the global Earth system model that includes an instrument model is new and powerful tool for evaluating the performance of an earth observing instrument when used in design, manufacturing and integration phases.

10374-5, Session 2

Augmented method to improve thermal data for the figure drift thermal distortion predictions during the JWST OTIS cryogenic vacuum test

Sang C. Park, Smithsonian Astrophysical Observatory (United States); Timothy M. Carnahan, NASA Goddard Space Flight Ctr. (United States); Lester Cohen, Smithsonian Astrophysical Observatory (United States); Cherie B. Congedo, SGT, Inc. (United States); Michael

J. Eisenhower, Smithsonian Astrophysical Observatory (United States); Wes Ousley, Genesis Engineering Solutions LLC (United States); Andrew Weaver, ATA Aerospace (United States); Kan Yang, NASA Goddard Space Flight Ctr. (United States)

The JWST Optical Telescope Element (OTE) assembly is the largest optically stable infrared-optimized telescope currently being manufactured and assembled, and is scheduled for launch in 2018. The JWST OTE, including the 18 primary mirrors, secondary mirror, and the Aft Optics Subsystems (AOS) are designed to be passively cooled and operate at near 45K. These optical elements are supported by a complex composite backplane structure. As a part of the structural distortion model validation efforts, a series of tests are planned during the cryogenic vacuum test of the fully integrated flight hardware at NASA JSC Chamber A. The successful ends to the thermal-distortion phases are heavily dependent on the accurate temperature knowledge of the OTE structural members. However, the current temperature sensor allocations during the cryo-vac test may not have sufficient fidelity to provide accurate knowledge of the temperature distributions within the composite structure. A method based on an inverse distance relationship among the sensors and thermal model nodes was developed to improve the thermal data provided for the nanometer scale WaveFront Error (WFE) predictions. The Linear Distance Weighted Interpolation (LDWI) method was developed to augment the thermal model predictions based on the sparse sensor information. This paper will encompass the development of the LDWI method using the test data from the earlier 'pathfinder' cryo-vac tests, and the results of the notional and as tested WFE predictions from the structural finite element model cases to characterize the accuracies of this LDWI method.

10374-6, Session 2

Propagation of polarization domain walls in standard optical fibers: beyond the Manakov model

Massimiliano Guasoni, Optoelectronics Research Ctr., Univ. of Southampton (United Kingdom) and Lab. Interdisciplinaire Carnot de Bourgogne, Univ. de Bourgogne (France); Pierre Yves Bony, Marin Gilles, Lab. Interdisciplinaire Carnot de Bourgogne, Univ. de Bourgogne (France); Josselin C. Garnier, Lab. de Probabilités et Modèles Aléatoires, Univ. Paris 7 (France); Antonio Picozzi, Julien Fatome, Lab. Interdisciplinaire Carnot de Bourgogne, Univ. de Bourgogne (France)

An optical polarization domain wall (PDW) is a localized structure of the kink type connecting two regions of space with different polarizations. Here we report a direct observation of PDW propagating within a standard optical fiber commonly used in optical communications. Furthermore, we exploit the topological properties of PDWs for optical data transmission beyond the Kerr limit of normally dispersive fibers. In order to generate a periodic train of PDWs, a 1555-nm continuous-wave is first intensity modulated by 30-ps square-shape pulses at a repetition rate of 14 GHz. This pulse train is then split in 2 out-of-phase, delayed and polarization multiplexed replica so as to obtain a pure orthogonal polarization flip-flopping at 28-GHz. After amplification, these PDWs are injected into a 10-km long normally dispersive fiber. When only one polarization component is injected into the fiber the output signal is strongly impaired by chromatic dispersion and self-phase modulation. In contrast, when both orthogonally polarized components propagate along the fiber the strong binding force imposed by cross-phase modulation compensate for the classical defocusing regime , leading to an undistorted propagation of PDWs. It is worth noting that the propagation of PDWs in km-long fibers question the validity of the Manakov model commonly accepted to describe light propagation in standard telecom fibers. In conclusion, these outcomes constitute the first experimental observation of kink–antikink solitary wave propagation in nonlinear fiber optics and open the way to new physical models describing light propagation in modern telecom fibers.

10374-7, Session 2

Coupled-fiber Bragg grating sensor structure for cryogenic conditions

Umesh Sampath, Dae-gil Kim, Minho Song, Chonbuk National Univ. (Korea, Republic of)

Fiber Bragg grating sensors have numerous advantages over other electro-mechanical sensors, such as zero electromagnetic interference, multiplexing capability, and can be embedded with less detrimental effects. Major drawback of the FBG sensors relies on cross sensitivity towards the applied temperature and the strain. Moreover, the low thermal sensitivity of silica at low temperatures creates additional difficulties in implementing FBG sensors at cryogenic conditions.

In this work, we present the possibilities of simultaneous sensing of the strain and the temperature by measuring the reflected wavelengths from coupled fiber Bragg gratings in cryogenic temperatures. We aimed to overcome the cross-sensitivity problem of FBG as well as improving the temperature sensitivity of gratings at cryogenic temperatures. For the purposes, we used polymer resin as a coating material for a FBG sensor. The polymer coated FBGs (PCFBGs) show high sensitivities to cryogenic temperatures because of the thermal expansion of polymer resin. The average temperature sensitivity of 42 pm °C-1 was obtained for a range -195 °C to 25 °C. To obtain strain free PCFBG, one PCFBG is encapsulated inside a glass capillary tube. Analogously, to eliminate the thermal expansion of capillary material at the one end, FBG is cleaved free and the other end is fixed with temperature resistant epoxy resin. The optical system readout simultaneously the applied strain and the temperatures successfully at cryogenic conditions.

10374-8, Session 3

Improved ray tracing simulation for aero-optical effect of a hypersonic projectile in wind tunnel using multiple gradient-index layer method

Seul Ki Yang, Yonsei Univ. (Korea, Republic of); Sehyun Seong, Dongok Ryu, Yonsei Univ. (Korea, Republic of) and SphereDyne Co., Ltd. (Korea, Republic of); Sug-Whan Kim, Yonsei Univ. (Korea, Republic of) and Ctr. for Galaxy Evolution Research (Korea, Republic of) and Yonsei Univ. Observatory (Korea, Republic of); Sang-Hun Jin, LIG Nex1 Co., Ltd (Korea, Republic of); Ho Jeong, Hyun Bae Kong, LIG Nex1 Co., Ltd. (Korea, Republic of)

We propose improved the simulation method of the aero-optical effect for a hypersonic projectile using multiple gradient-index (GRIN) layer method. The method discretizes anisotropic inhomogeneous media into multiple refractive index layers. Each layer constructs the refractive index distribution function derived from the flow field by Computational Fluid Dynamics (CFD) analysis. In this study, the target used the flow field in the hypersonic wind tunnel corresponds to Mach 7 in speed, 16km in altitude for density. The wedge shaped projectile has semi-vertex angle 12° and fused silica seeker window. The observation instrument inside the wind tunnel consists of a He-Ne fiber laser, a beam expander, a folding mirror, a beam reducer and a Shack-Hartmann sensor. The light source generated 2828 rays and numerical aperture (NA) is 0.12 with beam incident angle variation from 60° to 78°. The Shack-Hartmann sensor has 68?68 pixels and each pixel diameter is 0.108 mm. The simulation results show that the 2D optical path length (OPD) map was estimated in the real optical test measurement, the OPD change value was calculated by the difference OPD map between with and without the flow field. The RMS OPD had a tendency to decrease linearly as the beam incident angle increases and is 0.0141 ? at 78° in beam incident angle. For comparison with other method, we simulated ray equation methods and obtained comparable results.

10374-9, Session 3

The fluid field flow and optical system performance analysis

Ming-Ying Hsu, Ting-Ming Huang, Instrument Technology Research Ctr. (Taiwan)

Optical system performance is easily affected by variable surrounding conditions, including the precision optical system, as its performance is changed with flow field in the air or surrounding water. The air content of water vapor, carbon dioxide concentration, and dry air has a ratio that will affect the air refractive index. Water is another material of general optical systems, affected by surrounding conditions as well. Lithography and the microscope lens are commonly used for contact with water, with their refractive nature, changed by the pressure and density in the flow field. In addition, temperature and light wavelength are two important parameters of the air and water refractive index. This study calculates fluid field pressure and velocity distribution, and then transfers it to air and water refractive index differences in the optical system. We also evaluate optical performance variations with fluid field changes, which can improve optical design and system alignment progress by avoiding surrounding condition changes.

10374-10, Session 3

A fiber-optic ice detection system for large-scale wind turbine blades

Dae-gil Kim, Sampath Umesh, Minho Song, Chonbuk National Univ. (Korea, Republic of)

Recently, because of environmental issues, the demand for wind energy has rapidly increased world widely including colder and higher altitude regions. The cold weather operation of wind turbines, however, lead to problems, such as the ice accretion on surfaces and the impacts of low temperature on the materials of wind turbine blades. Due to imbalance, disrupted aerodynamics, or damages, icing can cause substantial problems in the reliability of large-scale wind turbines.

In this paper, for the purpose of detecting the ice growth, a fiber-optic sensor system is proposed. The system is based on the measurement of Fresnel-reflection intensities from the ends of single mode fibers, and it consists of a broadband light source, an AWG (arrayed waveguide grating), an optical circulator, and a spectrometer. The input broadband light illuminates the AWG via the optical circulator. After de-multiplexing by the AWG with different central wavelengths, the Fresnel-reflection signals from all channels are multiplexed again, detected, and analyzed by a spectrometer which consists of a volume phase grating and a photo-detector array. The intensity variation of each channel corresponds to the ambient refractive index variation of the measurement point. The transition in Fresnel-reflection intensity can identify the status of ambient medium, such as the ice, the water, and the air. Experimental results show that the proposed system can clearly detect the growth of ice in real time.

10374-11, Session 4

Balancing diffraction efficiency and laser damage in diffractive optics

Steven T. Glass, Thomas J. Suleski, The Univ. of North Carolina at Charlotte (United States)

Diffractive optics serve as an enabling technology for a host of applications requiring high power laser focusing and beam shaping, ranging from materials processing to military applications, among others. The ability of such components to resist damage under intense irradiation is of mounting importance as lasers attain ever higher power levels. Diffractive optics inherently contain sharp discontinuities that can enhance electric field distributions within the component, which can lead to increased laser damage. In many cases, diffractive optics are realized as multi- level step-wise approximations to an ideal shape. The increased number of phase levels increases the operating efficiency of the component, but also introduces additional surface discontinuities. As a consequence, it is useful to consider both diffraction efficiency as well as susceptibility to laser damage as performance criteria for diffractive optics in high-power laser systems. Researchers have previously analyzed subwavelength, AR gratings for geometrical field enhancement effects, but conventional diffractive elements with discontinuities have not received as much attention. In this paper, we apply FDTD simulations to determine a general relationship connecting field enhancement to basic grating parameters: period, depth, number of phase levels, step width, and step height. We discuss the results of these simulations, connecting them to diffraction efficiency, fabrication complexity, and laser damage thresholds in different optical materials.

10374-12, Session 4

Mounting and environmental effects on stress birefringence in silicon and zinc selenide windows

Kevin W. Peters, Thomas Yurovchak, Benjamin Dwyer, David E. Thompson, Robert T. Carlson, BAE Systems (United States)

Stress birefringence in an output window affects the performance of polarization dependent remote sensing instruments, such as polarimeter based systems and certain lidar systems. In such instruments, stress birefringence results in reduced signal to noise ratios. Understanding the impact of window stress birefringence is crucial to understanding system performance. This paper utilizes a finite element model (FEM) to analyze the stress in Silicon and Zinc Selenide Windows induced by mounting and environmental conditions. Specifically, the impact of mounting induced twisting modes due to over tightened screws from the window mount to the platform are investigated. Additionally, the impact of environmental pressure differentials across the window are analyzed. The nodal results of the FEM model are interpolated to a uniform grid inside the window in order to simplify a polarization ray trace. Using these interpolated stresses in the window, the stress induced index ellipsoid matrix is calculated. Using this matrix, a Jones calculus based propagation is performed for an arbitrarily polarized input beam passing through the window. Since the accuracy of this method depends on the sampling in the window, a nodal analysis is performed to determine the minimum number of analysis layers that are necessary to achieve an accurate prediction of the stress birefringence. Using the method outlined, the impact of mounting and environmental effects on window performance is predicted and presented for both Silicon and Zinc Selenide windows. This paper also presents experimental results which validate the analysis method and its predictions.

10374-14, Session 4

Modeling the extremely lightweight Zerodur mirror (ELZM) thermal soak test

Thomas Brooks, NASA Marshall Space Flight Ctr. (United States); Tony B. Hull, The Univ. of New Mexico (United States); Ron Eng, H. Philip Stahl, NASA Marshall Space Flight Ctr. (United States)

Schott's Extremely Lightweight Zerodur Mirror (ELZM) has been tested in the X-ray & Cryogenic Facility (XRCF) at Marshall Space Flight Center (MSFC). The mirror's surface was measured interferometrically at room temperature and at three soak temperatures (275K, 250K and 230K). The change in the mirror's figure caused by the change in the mirrors temperature is determined. A thermoelastic model was built and the change in the mirror's optical surface is estimated for thermal gradients, mount effects, and coefficient of thermal expansion (CTE) inhomogeneity. The predictions of this model are compared to the test results, and the model is correlated to the test results by adjusting the mirror's spatial CTE distribution. The surface figure change per mirror depth caused by changing the temperature of a Zerodur mirror is estimated.

10374-15, Session 4

Calculation of density of states for modeling photoemission using method of moments

Daniel Finkenstadt, U.S. Naval Academy (United States); Samuel G. Lambrakos, Kevin L. Jensen, Andrew Shabaev, U.S. Naval Research Lab. (United States); Nathan A. Moody, Los Alamos National Lab. (United States)

Modeling photoemission using the Moments Approach (akin to Spicer's "Three Step Model") is often presumed to follow simple models for the prediction of two critical properties of photocathodes: the yield or "Quantum Efficiency" (QE), and the intrinsic spreading of the beam or "emittance". The simple models, however, tend to obscure properties of electrons in materials, the understanding of which is necessary for a proper prediction of a semiconductor or metal's QE and emittance. This structure is characterized by localized resonance features as well as a universal trend at high energy. Presented in this study is a prototype analysis concerning the density of states (DOS) factor D(E) for Copper in bulk to replace the simple three-dimensional form currently used in the Moments approach. This analysis demonstrates that excited state spectra of atoms, molecules and solids based on density-functional theory can be adapted as useful information for practical applications, as well as providing theoretical interpretation of density-of-states structure, e.g., qualitatively good descriptions of optical transitions in matter, in addition to DFT's utility in providing the optical constants and material parameters also required in the Moments Approach.

10375-1, Session 1

New tools for the design of freeform mirrors

Donald C. Dilworth, Optical Systems Design, Inc. (United States)

Free-form mirrors offer design possibilities not possible with centered shapes, and are becoming more practical as manufacturing techniques improve. New design methods and algorithms are presented that can quickly lay out and optimize systems of mirrors, correcting image quality and distortion. Of special importance is the requirement that a given mirror must not block the beam between two others. This too can be managed automatically with these new methods.

10375-2, Session 1

Design of light guide sleeve on hyperspectral imaging system for skin diagnosis

Yung-Jhe Yan, Chao-Hsin Chang, Hou-Chi Chiang, Mang Ou-Yang, National Chiao Tung Univ. (Taiwan)

A hyperspectral imaging system is proposed for early study of skin diagnosis. A stable and high hyperspectral image quality is important for analysis. Therefore, a light guide sleeve (LGS) was designed for the embedded on a hyperspectral imaging system. It provides a uniform light source on the object plane with the determined distance. Furthermore, it can shield the ambient light from entering the system and increasing noise. For the purpose of producing a uniform light source, the LGS device was designed in the symmetrical double-layered structure. It has light cut structures to adjust distribution of rays between two layers and has the Lambertian surface in the front-end to promote output uniformity. In the simulation of the design, the uniformity of illuminance is about 92%. In the measurement of the actual light guide sleeve, the uniformity of illuminance is about 91%.

10375-3, Session 1

Imaging spectrometer design for high data fidelity *(Invited Paper)*

Pantazis Mouroulis, Jet Propulsion Lab. (United States)

This talk will review the design principles and techniques behind imaging spectrometer design leading to high spectroscopic data fidelity. These involve optical design, tolerancing and alignment, stray light, as well as methods of assessment and verification. Examples from deployed systems illustrate the methods. Some recent results on the use of freeform surfaces will also be shown.

10375-4, Session 1

Achieving linearity with an optical quadrant detector tracking system

Victor J. Doherty, Dina Aouani, EIDOLON Optical, LLC (United States); Michael S. Costello, Franklin W. Olin College of Engineering (United States)

Conventional round spot quadrant detector trackers are inherently non-linear. This non-linearity requires multiple iterations to converge onto perfect alignment with the object tracked. We created a system that generates a square spot. When convolved with a quadrant detector, this spot achieves perfect alignment in one iteration. This invention is thus essential to any system which requires speed and accuracy. In this paper, we introduce the theory behind the square spot as well as the design of our linear optical quadrant detector tracking technology.

10375-5, Session 2

Multi-band filter design with less total film thickness for short-wave infrared application

Yung-Jhe Yan, I-Pen Chien, National Chiao Tung Univ. (Taiwan); Po-Han Chen, National Central Univ. (Taiwan); Sheng-Hui Chen, Yi-Chun Tsai, Mang Ou-Yang, National Chiao Tung Univ. (Taiwan)

A multi-band pass filter array was proposed and designed for short wave infrared applications. The central wavelengths of the multi-band pass filters are located about 905 nm, 950 nm, 1055 nm and 1550 nm. By theory of the optical interference band pass based on H-L structure, the spectrum performance relies on the refractive index difference between the chosen high and low refractive indexes materials, and the repeated periods with the high and low refractive index thin film layers. When determining high and low refractive index materials, spectrum performance was improved by increasing repeated periods. Consequently, the total film thickness increases rapidly. In some cases, a thick total film thickness is difficult to process in practice, especially when incorporating photolithography liftoff. Actually the maximal thickness of the photoresist being able to liftoff will bound the total film thickness of the band pass filter. For the application of the short wave infrared with the wavelength range from 900nm to 1700nm, silicone was chosen as a high refractive index material. Different from other dielectric materials used in the visible range, silicone has a higher absorptance in the visible range opposite to higher transmittance in the short wave infrared. In other words, designing band pass filters based on silicone as a high refractive index material film could not obtain a better spectrum performance than conventional high index materials like TiO_2 or Ta_2O_5, but also its material cost would reduce about half compared to the total film thickness with the conventional material TiO_2. Through the simulation and several experimental trials, the total film thickness below 4 um was practicable and reasonable.

10375-6, Session 2

Multilayer interference coatings with the Gaussian profile for Nd:YAG lasers

Evgeni V. Kuznetsov, Vladimir V. Novopashin, Alexsandr V. Shestakov, JSC “Research Institute” POLYUS “them. M.F. Stelmaha” (Russian Federation)

The development of laser technologies defined the novel quality demands to optical interference coatings. For many technological applications is very important to use lasers with equal distribution of laser intensity across the beam. . These mirrors are used as output coupler in the laser cavity to form radiation close to the Gaussian distribution which using radially varying thickness that have been proved the most practical. Multilayer dielectric mirrors with a smooth changing reflection are used in various types of laser resonators. So, application of such mirrors, permit realize the selection of transverse modes in which the minimal losses possess the transverse mode with amplitude distribution close to distribution of mirror reflection. If mirror has Gaussian distribution, laser radiation generate arise on one or several limited transverse modes. Volumes mode in active media and output power decrease, however, brightness along axis, increase. Using such mirrors is

expedient inner unstable resonator of high power laser in this case we can provide the optimum correlation of the output signal functions. Uniform beams can be obtained by placing some optical elements such as refractive components, binary filters, and holographic systems outside a laser cavity. Intra-cavity optical elements have been demonstrated to be an approach to reducing the impact of edge diffraction in unstable resonators. Diffraction optical elements, a graded-phase mirror, two prisms and the Gaussian mirror are considered as intra-cavity modification accessories [1]. The dielectric graded reflectivity mirrors also minimizes losses, because its filtering action on the cavity field translates into useful output. Besides, optical coatings for laser components must have different requirements depending on the laser system. A common performance requirement is high laser-induced damage resistance, which depends on a number of factors involving optical, mechanical, thermal, and structural properties of the coating. Most of these characteristics are affected by the deposition properties. To maximize the damage threshold, the absorption within the layers has to be low and intensity of the electric field should be minimized. The damage occurs in the local electric field strength reaches its critical value at a weak point of the multilayer system. The electric field in the films must be as low as possible to avoid the film damage caused by the Joule effect and/or ionization process [2]. Since the absorbance is proportional to n?E?2, the high index layer will absorb more energy at the same electric field amplitude [3, 4]. So, the materials with high index must have the low absorption during deposition. In this work the ability of producing multilayer graded interference mirrors with smooth changing profile based on ZrO2 – SiO2 are considered. The processes are made by electron-beam evaporation with ion-beam source to assisted deposition and minimized absorption. In the multilayer dielectric graded mirror the thickness if only alternate layer must smooth varied along the cross section. The method of fixed mask are used which was remove at fixed definite distance. Masks that introduced between deposited material and substrate had various diameters and thickness, and distance to sample surface was varied too. The results of design analysis show that the height of the high reflection zone increases with the number of layers. Although, the main principal points of deposition multilayers graded mirrors had earlier publications, this paper show the ability simple method of obtaining such mirrors on a common vacuum set-up. Thus, in present paper, the design and fabrication of a dielectric graded reflectivity mirror for Nd:YAG laser were reported. The obtained results show that the fabrication graded mirror has maximum reflectance in the 1050 – 1270 nm wavelength range and can be used in the Nd:YAG laser applications, especially those requiring the uniform illumination.

References

1. S.P. Chang, J.M. Kuo, Y.P. Lee, C.M. Lu, K.J. Ling, Appl. Opt., 37, No. 4 747-752 (1998).

2. P.H. Lissberger, Opt. Acta, 28, No., 2, 187-200 (1981).

3. A.I. Braunstein, Thin Solid Films, 37, 181-184, (1981).

4. V.V. Novopashin, E.A. Levchuk, A.V. Shestakov, High performance dielectric interference coatings in a broad spectral range, Conference on Laser Optics, St. Petersburg 2012.

10375-7, Session 2

Introducing the quantum efficiency of fluorescence of SCHOTT optical glasses

Ralf Jedamzik, Frank Elsmann, Axel Engel, Uwe Petzold, Jana Pleitz, SCHOTT AG (Germany)

The fluorescence of optical glasses is a property that needs to be taken into account in optical designs for life science applications. Many optical glasses from SCHOTT have very low intrinsic fluorescence values. Usually this fluorescence depends on the excitation wavelength and the optical glass type. The fluorescence of optical glasses is usually defined as the quotient of the integral of the emission spectrum with the integral of the emission spectrum of a reference glass (e.g. SF1). This definition does not give any information about the actual quantum efficiency of the fluorescence. In this presentation recent data on the integral fluorescence of SCHOTT optical glasses are presented. Additionally, first measurements of the quantum efficiency of SCHOTT optical glasses are presented and compared to the standard method.

10375-8, Session 2

Cryogenic refractive index of Heraeus homosil glass

Kevin H. Miller, Manuel A. Quijada, NASA Goddard Space Flight Ctr. (United States); Douglas B. Leviton, Leviton Metrology Solutions, Inc. (United States)

This paper reports measurements of the refractive index of Homosil (Heraeus) over the wavelength range of 0.34—1.10 um and temperature range of 120—335 K. These measurements were performed by using the Cryogenic High Accuracy Refraction Measuring System (CHARMS) facility at the NASA's Goddard Space Flight Center. These measurements were in support of an integrated Structural-Thermal-Optical-Performance (STOP) model that was developed for a field-widened Michelson interferometer that is being built and tested for the High Spectral Resolution Lidar (HSRL) project at the NASA Langley Research Center (LaRC). The cryogenic refractive index measurements were required in order to account for the highly sensitivity performance of the HSRL instrument to changes in refractive index with temperature, temperature gradients, thermal expansion, and deformation due to mounting stresses. A dense coverage of the absolute refractive index over the aforementioned wavelength and temperature ranges was used to determine the thermo-optic coefficient (dn/dT) and dispersion relation (dn/d?) as a function of wavelength and temperature. Our measurements of Homosil will be compared with measurements of other glasses from the fused silica family studied in CHARMS as well as measurements reported elsewhere in literature.

10375-9, Session 3

Camera system MTF: combining optic with detector

Torben B. Andersen, Zachary A. Granger, Lockheed Martin Space Systems Co. (United States)

MTF is one of the most common metrics used to quantify the resolving power of an optical component. Extensive literature is dedicated to describing methods to calculate the Modulation Transfer Function (MTF) for stand-alone optical components such as a camera lens or telescope, and some literature addresses approaches to determine an MTF for combination of an optic with a detector. The formulations pertaining to a combined electro-optical system MTF are mostly based on theory, and assumptions that detector MTF is described only by the pixel pitch which does not account for wavelength dependencies. When working with real hardware, detectors are often characterized by testing MTF at discrete wavelengths. This paper presents a method to define a polychromatic detector MTF based on MTF measurements that are made at multiple discrete wavelengths within a defined passband. Additionally, it is shown how this assigned polychromatic detector MTF may be combined with a polychromatic optic MTF to describe the system MTF. This approach is compared to MTF predictions based solely on the monochromatic detector MTFs.

10375-10, Session 3

Diffraction and geometrical optical transfer function calculation time comparison

José Antonio Díaz, Univ. de Granada (Spain); Virendra N. Mahajan, College of Optical Sciences, The Univ. of Arizona (United States)

In a recent paper, we compared the diffraction and geometrical optical transfer functions (OTFs) of an optical imaging system, and showed that the GOTF approximates the DOTF within 10% when a primary aberration is about two waves or larger [Appl. Opt., 55 (12), 3241–3250 (2016)]. In this paper, we determine and compare the times to calculate the DOTF

by autocorrelation of the pupil function (that reduces to an integration of a complex exponential of the aberration difference function), 2D digital autocorrelation of the pupil function, and by a Fourier transform (FT) of the point-spread function (PSF); and the GOTF by a FT of the geometrical PSF (that reduces to an integration over the pupil plane of a complex exponential of the scalar product of the spatial frequency and transverse ray aberration vectors), and by a FT of the spot diagram. Our starting point for calculating the OTFs is the wave aberrations of the system in its pupil plane, and the ray aberrations in the image plane. Numerical results for primary aberrations and some typical imaging systems show that the direct integrations are slow, but the calculation of the DOTF by a FT of the PSF is as fast as the GOTF calculation by a FT of the spot diagram.

10375-11, Session 3

Polarisation effect on wide angle lens relative illumination

Simon Thibault, Zhengeng Zhuang, Univ. Laval (Canada); Jocelyn Parent, ImmerVision (Canada)

The consumer devices of tomorrow are evolving beyond capturing classic pictures and videos. The lenses of yesterday are narrow and restrictive. New generation of super wide angle lenses capture our surroundings in full 360°, allowing our friends and families to step inside our universe and experience it, live.

However, for such wide angle lens coverage, the relative illumination of the lens must take it account the vectorial nature of the light. Consequently, the light polarisation becomes a very important parameters. Custom coating exist to avoid light transmission polarisation fall off. But for consumer applications, complex coating is not a solution because it raises the cost.

In this talk, we will dicuss how to take care of the polarisation during the design and analysis of the lens design. We will also provide design tips to limit the polarisation impact.

10375-12, Session 3

Linear decomposition of the optical transfer function for annular pupils

Jim Schwiegerling, College of Optical Sciences, The Univ. of Arizona (United States)

A technique for decomposing the Optical Transfer Function (OTF) into a novel set of basis functions has been developed. The decomposition provides insight into the performance of optical systems containing both wavefront error and apodization, as well as the interactions between the various components of the pupil function. Previously, this technique has been applied to systems with circular pupils with both uniform illumination and Gaussian apodization. Here, systems with annular pupils are explored. In cases of annular pupil with simple defocus, analytic expressions for the OTF decomposition coefficients can be calculated. The annular case is not only applicable to optical systems with central obscurations, but the technique can be extended to systems with multiple ring structures. The ring structures can have constant area as is often found in zone plates and diffractive lenses or the rings can have arbitrary areas. Analytic expressions for the OTF decomposition coefficients again can be determined for ring structures with constant and quadratic phase variations. The OTF decomposition provides a general tool to analyze and compare a diverse set of optical systems.

10375-13, Session 3

Assembly of a micro-optical resonator based on silicon micro mirrors for use in gyroscopes

Ingmar Leber, Thalke Niesel, Technische Univ. Braunschweig (Germany); Christian Werner, Yu Liang, Physikalisch-Technische Bundesanstalt (Germany); Andreas H. Dietzel, Technische Univ. Braunschweig (Germany); Jens Flügge, Physikalisch-Technische Bundesanstalt (Germany)

For realization of a miniaturized optical gyroscope the precise assembly of optical micro optical components is crucial [1].To detect the rotation rate with such an optical gyroscopes the laser beam must circulate many times and not leave the resonator due to small misalignments. A passive free space triangular ring resonator shall be assembled in which the light is circulating by reflections at three mirrors. The beam path encloses an area of about 100 mm?. An external light source at 1550nm will be used to activate the resonator, because silicon is translucent at this wavelength and the light can couple into the resonator through the silicon mirrors. To achieve an inherent alignment two of the mirrors are fabricated with a micro technology manufacturing process within the same crystal by wet etching resulting in very perfect {111} facets. The etching solution was optimized with respect to process time and smoothness of the mirror surfaces. To further increase the reflectivity of the mirrors different kinds of coatings are tested. With these two well positioned mirrors the assembly challenge reduces to 3DOF alignment of the third {001} mirror for which a well-designed adjustable spacer is developed. In first tests resonance in a linear cavity test setup has been demonstrated already.

10375-43, Session 3

Wavefront analysis from its slope data

Virendra N. Mahajan, College of Optical Sciences, The Univ. of Arizona (United States); Eva Acosta, Univ. de Santiago de Compostela (Spain)

In the aberration analysis of a wavefront over a certain domain, the polynomials that are orthogonal over and represent balanced wave aberrations for this domain are used. For example, Zernike circle polynomials are used for analysis of a circular wavefront. When the data available for analysis are the slopes of a wavefront, as, for example, in a Shack-Hartmann sensor, the polynomials used are those that are orthogonal to the gradient of Zernike polynomials. Similarly, annular polynomials are used to analyze the annular wavefronts for systems with annular pupils, as in a rotationally symmetric two-mirror system such as the Hubble space telescope. In this paper we discuss the vector functions that are orthogonal to the gradient of aberration polynomials. Instead of integrating the wavefront slope data and then obtain the wavefront aberration coefficients, these vector functions can be used directly to obtain such coefficients.

10375-14, Session 4

Fabrication of multi-focal microlens array on curved surface for wide-angle camera module

Guig-Gu Pan, Guo Dung J. Su, National Taiwan Univ. (Taiwan)

In this paper, we presented a compact camera that consists of microlens arrays with different focal lengths. The design integrates the principle of an insect's compound eye and the human eye. It contains a curved hexagonal microlens array and a hemispherical lens. Compared with normal mobile phone cameras which usually need no less than four lenses, the proposed system use only two lenses. Furthermore, the diameter of our microlens is 400 um and the radius of curvature of curved surface is 2 mm. To make the critical microlens arrays, we used the inkjet printing to control the focal lengths of each microlens and use replication method to form a different curvature hexagonal microlens array.

10375-15, Session 4

The effect of optical system design for laser micro-hole drilling process

Chien-Fang Ding, Yin-Te Lan, Yu-Lun Chien, Hong-Tsu Young, National Taiwan Univ. (Taiwan)

Lasers are a promising high accuracy tool to make small holes in composite or hard material. They offer advantages over the conventional machining process, which is time consuming and has scaling limitations. However, the major downfall in laser material processing is the relatively large heat affect zone or amount of molten burrs it generates, even when using nanosecond lasers over high-cost ultrafast lasers. In this paper, we constructed a nanosecond laser processing system with a 532 nm wavelength laser source. In order to enhance precision and minimize the effect of heat generation with the laser drilling process, we investigated the geometric shape of optical elements and analyzed the images using the modulation transfer function (MTF) and encircled energy (EE) by using optical software Zemax. We discuss commercial spherical lenses, including plano-convex lenses, bi-convex lenses, plano-concave lenses, bi-concave lenses, best-form lenses, and meniscus lenses. Furthermore, we determined the best lens configuration by image evaluation, and then verified the results experimentally by carrying out the laser drilling process on multilayer flexible copper clad laminate (FCCL). The paper presents the drilling results obtained with different lens configurations and found the best configuration had a small heat affect zone and a clean edge along laser-drilled holes.

10375-16, Session 4

Focal tunable liquid crystal lens with floating ring electrode

Chi-Yen Huang, Che-Ju Hsu, National Changhua Univ. of Education (Taiwan); Jyun-Jia Jhang, National Changhua Univ of Education (Taiwan); Jia-Cih Jhang, National Changhua Univ. of Education (Taiwan)

Liquid crystal (LC) lenses have attracted much attention, owing to the light weight and an adjustable focal length without mechanically moving parts. Among the developed LC lenses, the hole-patterned LC lens has a convenient fabrication process, a simple addressing scheme, and widely tunable focal range. Nonetheless, a thick dielectric layer (TDL) has to be inserted between the hole-patterned electrode and the LC layer to distribute the fringing electric field throughout the center of the aperture hole (AH). However, the inserted TDL significantly increases the operation voltage of the LC lens. In this paper, we propose a hole-patterned LC lens with a wide diameter of 6 mm. In our design, a floating ring electrode (FRE) is embedded into the interface between the dielectric layer and the LC layer. This structure confines the electric field in the hole patterned area, therefore assists in distributing the fringing electric field throughout the LC layer and thus assists in tilting the LCs in the AH center of the lens. Therefore, the dielectric layer used in the conventional hole-patterned LC lens can be effectively decreased. The decreased thickness of the dielectric layer provides the FRE LC lens with the advantages of lower operation voltage and large tunable focal range. With a voltage of 40 V, the introduced floating ring electrode modulates the phase retardation of the LC lens in a nearly perfect quadratic form with wavefront error approaching 0.07 ?. The design principle, simulation and fabrication of the LC lens are demonstrated in this paper.

10375-17, Session 4

Zoom system without moving element by using two liquid crystal lenses with spherical electrode

Ren-Kai Yang, Guo Dung J. Su, Chia-Ping Lin, National Taiwan Univ. (Taiwan)

A traditional zoom system is composed of several elements moving relatively toward other components to achieve zooming. Unlike tradition system, an electrically control zoom system with liquid crystal (LC) lenses is demonstrated in this paper. To achieve zooming, we apply two LC lenses whose optical power is controlled by voltage to replace two lenses in traditional zoom system. The mechanism of zoom system is to use two LC lenses to form a simple zoom system. We found that with such spherical electrode, we could operate LC lens at low voltage range from 31V to 53 V for wide tunability in optical power. For each LC lens, we use concave spherical electrode which provide lower operating voltage and great tunability in optical power respectively. For such low operating voltage and compact size, this zoom system with zoom ratio approximate 3:1 could be applied to mobile phone, camera and other applications.

10375-18, Session 4

Tunable refractive power by mutual rotation of helical lens parts

Ingo Sieber, Thomas Martin, Peter Stiller, Karlsruher Institut für Technologie (Germany)

This paper describes a refractive optics consisting of two lens parts with helical surface structures which allows for tuning of the optical refraction power by means of a mutual rotation of the conjugated lens parts around the optical axis. Thus the refraction power can be tuned continuously in a designated range. The shape of the helical surfaces is formed by changing the radius of curvature subject to the polar angle. Combination of such two surfaces results in an optics with tunable refraction power by a mutual rotation. This optics is multifocal with at least two sectors with different individually tunable refraction power. To obtain a monofocal rotation optics, obscuration of the lens sector providing the unwanted refraction power is necessary.

Conventional lens systems providing tunable refraction power do so by mutual axial or lateral shift of the lenses or the lens parts. Hence additional space for lens movement is needed in the design. Since the rotational optics allows adjustment of the refraction power by a mutual rotation of the lens parts no displacement of lenses is needed allowing for a more compact design.

Optics with tunable refraction power by a mutual rotation of two or more diffractive optical elements have been examined and published appropriately. To our knowledge this is the first scientific publication of a varifocal optics with a continuously adjustable refraction power by means of mutual rotation of two refractive lens parts consisting of conjugated helical surface structures.

10375-27, Session PMon

A lazy way to design infrared lens

RongSheng Qiu, Jian Dong Wu, Long Jiang Chen, Kun Yu, Hao Jun Pang, Bai Zhen Hu, Shanghai Aerospace Control Technology Institute (China)

Optical system design in infrared band often brings more challenges than that in visible band. This is because: first, the quantity of the infrared lens design examples is much less than its visible counterpart; Second, infrared optical systems are often installed on UAV or other military electro–optical system, they are usually under a strictly limited space; Third, optical materials with useful transmission in the infrared region exhibit larger changes in refractive index with temperature (dN/dT) than optical glass used in visible band. This in turn introduces larger changes in focus or image quality over temperature for infrared systems compared to comparable focal length visual systems. Athermalization must be taken into account; Forth, compared to the cost-effective visible measurement instrument, infrared centration measurement instrument is too expensive to afford. As a result, each step in the alignment plan needs to pay enough attention; Fifth, stray light in infrared optical system is more complicated in such a way that stray light not only comes from outside but also inside of lens itself.

This essay proposed a stepwise design method of infrared optical system

guided by the qualitative approach. The method fully utilize the powerful global optimization ability, with a little effort to write code snippet in optical design software, frees optical engineer from tedious calculation of the original structure. An easy-to-assemble athermalized MWIR lens was designed based on this method. Because of its compactness, the lens has enough space for filter wheel installation, has the multispectral sensing ability.

10375-28, Session PMon

Design two-dimensional (crossed) diffraction grating in Czerny-Turner spectrometer using freeform mirrors

Yuri Bazhanov, Elena Demura, Rasima Chercashina, Precision Systems and Instruments Corp. (Russian Federation); Vadim Vlakhko, DynaOptics (Singapore)

The possibility of building a spectrometer based on a flat two-dimensional (crossed) grating is being considered. High-order spectres diffracted by such grating are located on the receiver sequentially in the form of horizontal lines, although there is no additional dispersive element. The most suitable layout for this is the Czerny - Turner, in which flat grating is located between the two concave mirrors. We selected one embodiment of this layout, when grating is located in parallel beams, and the distance from the grating to the second mirror was 0.85f, where f is focal length of the second mirror. In this case a spectral image lies in the plane and, with transverse aberrations minimization, can be recorded on receiver with high quality.

In this paper an attempt to compensate for the transverse aberrations is made by using a diffraction grating with variable spacing grooves in both sections and aspheric mirror elements of layout, including ones having a free-form surface.

Using crossed grating greatly simplifies the device layout and may be particularly effective when used in the ultraviolet and infrared regions of the spectrum, due to a small choice of transmissive materials for manufacturing spectral prisms. This paper gives examples of such case.

10375-29, Session PMon

Off-axial Gregory telescope design with freeform mirror corrector

Yuri Bazhanov, Precision Systems and Instruments Corp. (Russian Federation); Vadim Vlakhko, DynaOptics (Singapore)

In this paper a well-known approach is used for calculation of off-axis three-mirror telescope. It includes usage of conic cross-sections properties, each of the sections forming a stigmatic image. To create a compact optical system, a flat mirror aberration corrector is introduced, which is at later stage transformed into a free-form surface in order to compensate field aberrations. Similarly, one can introduce such a corrector in finalized layout for its further optimization and getting a suitable form, including the conversion of multimirrors axial optical system into decentered one.

As an example, off-axial Gregory telescope embodiment is used for infrared waveband region, due to the fact that, unlike the Cassegrain telescope, it provides a real exit pupil, and usage of the mirror corrector brings several advantages. Firstly, this feature may be used to include cold stop or adaptive mirror in the exit pupil, wherein corrector is introduced into a converging beam before the focus of the first mirror. Secondly, when placing corrector in the exit pupil of the optical system it is possible to eliminate high and low order aberrations of center point, which in turn improves optical system f-number, and minimize field aberrations. As another example, off-axial Ritchey-Chretien telescope embodiment is used as a good fit for visible region systems. Analysis and calculation results of optical systems with free-form correctors with surfaces, defined by Power polynomial series are presented in this paper. Advantages of different free-form surfaces usage depends on optical system layouts specifics.

10375-30, Session PMon

Comparative analysis of characterization techniques for SLM-LC using Jones matrices

Juan-Miguel Olvera-Angeles, Alfonso Padilla-Vivanco, Univ. Politécnica de Tulancingo (Mexico)

A comparative analysis between the Saleh and Yamauchi model is presented also a variation of the Yamauchi model for the characterization of SLM-LC (light space modulation - liquid crystal) is realized. The Jones matrices are used for these models. Broad phase modulation and linear transmission are obtained in comparison with the Yamauchi model. A high contrast is obtained from the variation of the transmission and phase modulation than in the Yamauchi model. The results presented are for SLM-LC LC 2012 Holoeye brand. The Mach-Zehnder interferometer is used for phase measurement. We present a more extensive phase modulation obtained using the Saleh method or the Yamahuchi method. Experimental results are presented.

10375-31, Session PMon

Optimization of wavefront coding imaging system using Heuristic algorithms

Enrique Gonzalez Amador, Alfonso Padilla Vivanco, Carina Toxqui Quitl, Univ. Politécnica de Tulancingo (Mexico)

An optimization process of a wavefront coding (WFC) imaging system is presented. This allows us to obtain high resolution images. This optimization is achieved by seeking the most appropriate linear superposition of Zernike polynomials. Heuristic algorithms are used to search for optimal parameters such as phase mask intensity and parameters of restoration filter to get the best restored image. This process is performed using a Wiener filter. Numerical and experimental results of the proposed system show invariance to defocus and astigmatism aberrations.

10375-32, Session PMon

Optical schemes for compact space objectives

Kseniia D. Butylkina, Galina E. Romanova, Alexey V. Bakholdin, ITMO Univ. (Russian Federation)

During last decades the number of space apparatus for the distant Earth monitoring is dramatically growing. The optical-electronic devices are comprised of the modern space units as the equipment on board and usually contain the optical system (objective) and the photodetector module. The most widely used objectives are the mirror systems and catadioptric systems because they can provide compact sizes together with the high image quality. The most widely used are the Ritchey-Chretien telescopes (with and without additional lens correctors) and Korsch systems.

The objectives for the space apparatus should have extremely small sizes (less than 0,4 of focal length) and wide angular field (more than 1 degree), high image quality to provide the resolution 1,5 – 4 meters (on the Earth surface) with the altitude 350 – 400 km and 600 – 700 km and work with wide spectral range.

The research of the schemes which can be used for the space apparatus for the Earth surveillance is carried out based on the third-order aberration theory. The derived equations can help for preliminary designing and researching of the three-mirror schemes of the Korsch-type and the systems without an intermediate image and also for the analysis of the two-mirror systems with lens correctors placed after the secondary mirror in the converging beam of rays.

In the work, we have considered several scheme types and compare them from the point of view of the future application as a part of the space equipment. The image quality and baffle configuration are also presented.

10375-33, Session PMon

Infrared simulation and performance validation of pinhole and 4-bar collimator targets for static performance evaluation of thermal imaging systems

Doruk Kucukcelebi, Roketsan A.S. (Turkey)

The minimum resolvable temperature difference (MRTD) and minimum detectable temperature difference (MDTD) are widely accepted static performance test parameters that best describe the field performance of thermal imaging systems. MRTD test is measured by determining the minimum temperature difference between the 4-bar target and the background required to resolve the thermal image of the bars by an observer. On the other hand, MDTD test is measured by determining the minimum temperature difference between the target and the background, which is required to detect the target from the thermal image. Different temperature differences between the target and the background and different target spatial dimensions were used while conducting both MRTD and MDTD measurements using collimator test systems. In this study, to evaluate the field performance of various thermal imaging systems, MRTD and MDTD tests were applied. Then, infrared simulations of pinhole and 4-bar collimator static test system targets were described based on the electro-optical parameters of unit under test (UUT) including detector resolution, system SiTF (Signal Transfer Function) and total optical transmission. With these inputs, the infrared simulation images of pinhole and 4-bar targets, which have adjustable temperature difference and different spatial frequency, were obtained in MATLAB environment. Then, the infrared simulations of pinhole and 4-bar target images were verified with various thermal imaging systems. Lastly, field performance results of the thermal imaging systems with respect to MRTD and MDTD static performance test parameters were provided.

10375-34, Session PMon

Mask in thickness uniformity for three coating materials

Cheng-Chung Jaing, Kai-Lun Wu, Jing-Han Xie, Jian-Wei Chen, Minghsin Univ. of Science and Technology (Taiwan); Yeuh-Yeong Liou, Chienkuo Technology Univ. (Taiwan); Pang-Shiu Chen, Minghsin Univ. of Science and Technology (Taiwan)

Uniform coatings are necessary for mass production. Masks are commonly adopted to obtain uniform coatings in e-beam evaporation chambers. The mask, located between the e-gun and the substrate inside the chamber, can correct the thickness distribution of thin films in the e-beam deposition. One mask is generally applicable to one material. However, there are few studies on the application of a mask to more than one material evaporated from one single e-beam source. In this study, a mask suitable for three materials evaporated from one single e-beam source is developed to obtain uniform thickness distribution on a substrate holder. The three coating materials are SiO_2, TiO_2 and Ag respectively. The design method is based on film thickness theory and the assumption that a substrate holder rotates about its central axis during the deposition of films. The emissive characteristics, which modify the cosine law of the surface source, of the three materials are characterized by thickness distributions of films deposited without a mask in an e-beam evaporation chamber. The form of a mask is decided by an optimized emissive characteristic which causes its thickness distribution to be closest to the three film thickness distributions described above. The uniform thickness distributions of the SiO_2, TiO_2 and Ag films deposited with the designed mask are achieved in an e-beam evaporation chamber. The design of a mask in thickness uniformity for three coating materials cuts the development time and requires less trial and error than traditionally experimental correction loops.

10375-35, Session PMon

Using the afocal compensator of the catadioptric systems for removal the thermal defocus

Galina E. Romanova, Alexey V. Bakholdin, ITMO Univ. (Russian Federation); Stepan E. Ivanov, ITMO Univ (Russian Federation)

The work associates with the ground-based catadioptric systems with two-component afocal achromatic compensator. The most catadioptric systems with afocal compensator have the power mirror part and the correctional lens part. The correctional lens part can be in parallel, in convergent beam or in both. One of the problems of this kind systems design is the thermal defocus by reason of the thermal aberration and the housing thermal expansion.

It is introduced the technique of thermal defocus compensation by choosing the optical material of the afocal compensator components. The components should be made from the optical materials with thermo-optical characteristics so after temperature changing the compensator should become non-afocal with the optical power enough to compensate the image plane thermal shift.

There is the requirement to Abbe coefficients of the components in view of achromatical properties of the compensator that reduces essentially the applicable optical materials quantity.

The catalogues of the most vendors of optical materials in visible spectral range are studied for the purpose of finding the suitable couples for the technique. In the result, it is shown the advantage of the plastic materials application.

The thermo-chromatical aberration is not considered in view of smallness.

The examples of the optical design are given.

10375-36, Session PMon

The improved optical setup for Abbe-Porter experiment

Volodymyr N. Borovytsky, Oleksii Hudz, Vytaliy Antonenko, National Technical Univ. of Ukraine (Ukraine)

The interesting experiments which have confirmed Abbe theory of image formation have been done by E. Abbe, A. Porter and L. Mandelshtam. These experiments have become the classical ones and they are widely used for explanation of Fourier optics. The principal disadvantage of them is difference in optical schemes for observation of an output images and observation of their spatial spectrums. The proposed optical setup makes possible demonstration of two stages of image formation – obtaining a spatial spectrum (Fourier analysis) and composing an output image (Fourier synthesis) – together. This setup contains two imaging channels that are separated by a beam splitter after a microscope objective. The first one forms a magnified image of a spatial spectrum, the second one – a magnified output image. These images can be observed on a screen, or via eyepieces or using image sensors. Any occluding of spectrum zones becomes visible and it leads to the corresponded changes in an output image. All technical details of the setup are described including calculations of a field of view and irradiance in an image plane. The images and their spatial spectrums registered using this setup are presented and discussed. This optical setup would be useful for optical education and conduction optical research.

10375-37, Session PMon

Development of surgical binoculars on the basis of polymeric lenses

Anna O. Voznesenskaya, ITMO Univ (Russian Federation); Alisa Ekimenkova, Artem Muratov, Lev Andreev, ITMO Univ. (Russian Federation)

In the modern world to carry out medical operations on the thin blood vessels, as well as in the manufacture of microelectronic circuits and manufacture of jewelry special optical systems (surgical binoculars) of a relatively small magnification are used. For the additional accommodation of the eye during the transition from observation with and without glasses an optical system which locates object and image in the same plane is necessary.

It can be a specially developed system that allows to change the base of the eye and the angle of convergence. At low magnifications one can use an ordinary spectacle frame, which is mounted on the ordinary glasses system.

The Galileo system is used for the binoculars design of relatively small magnification. Binoculars with prismatic system provide higher magnification. That allows the operator to see all of the items within the surgical field. Binoculars are manufactured strictly in accordance with the individual characteristics.

Key features of this systems are superior indicators of image clarity, lack of distortion and excessive fatigue of the eye. It could be achieved by application of high quality optics. Meantime the systems should have low weight and size. Lenses made of glass are much heavier construction.

The basis of this work is a modification of the modern design of surgical binoculars and the replacement of mineral glass with polymer lenses.

Specific weight of plastic is two times less than glass, so the glasses with polymer lenses are much lightweight. In addition, lightweight of plastic allows to use spectacle frame without rims or semi-rimless. Also in today's world strengthening coatings for polymeric lenses were developed to make them as scratch resistant as mineral. At the moment, glass has almost no advantages over plastic: plastic is lighter, more stable to impact and traumatic safe. Besides, polymers are better materials from an economic point of view.

In this article is presented the analysis of polymeric materials for the manufacture of lenses, and comparison of their optical properties. Using Zemax software and commercial catalogue of optical polymers and plastics optical systems of binoculars according to the Galileo scheme with polymeric materials for different magnifications were designed. To reduce aberrations and achieve high quality of the optical systems, mutual arrangement of materials is performed, and optical system optimization is realized.

Replace the minerals lens with the plastic ones helps to make binoculars convenient to use and makes easy the work of the operator as well as reduces the cost of the surgical bicnoculars and increases their availability on the world market without loss of image quality.

10375-38, Session PMon

Optical spherometer for measuring large curvature radii of convex surfaces

Jorge Alvarado-Martínez, Univ. Politécnica de Tulancingo (Mexico); Sergio Vazquez y Montiel, Univ. Tecnológica de la Huasteca Hidalguense (Mexico); César Joel Camacho Bello, Univ. Politécnica de Tulancingo (Mexico)

Measuring large curvature radii of convex surfaces with high precision is a challenge because the spherometer's focus must be positioned at the apex of the surface and at the center of curvature of the surface by moving the surface or the spherometer. If the center of curvature is greater than the distance from the focus to the spherometer, then measurement is not possible. In this work we propose to use the FOCOIVA system [1] to move the focus of the spherometer in longitudinal way without modifying the f number by moving two lenses inside it, with this mechanism it is possible to measure radii of curvature of several meters in length. The curves of movement of the lenses and the optical parameters of the lenses that compose the spherometer are presented.

References.

1. S. Vázquez Montiel, Tetsuya Susuki, Morio Hosoya, "Focoiva Lens: Scanner in Lateral and Longitudinal Directions", Applied Optics, vol. 40, 4547 a 556, 2001.

10375-39, Session PMon

Optimization of corneal topography maps by bio-inspired algorithms

Gerardo Diaz-Gonzalez, José Alfredo Jiménez-Hernández, Univ. Tecnológica de la Mixteca (Mexico); Marcelo David Iturbe-Castillo, Instituto Nacional de Astrofísica, Óptica y Electrónica (Mexico); Rigoberto Juarez-Salazar, Ctr. de Investigación y Desarrollo de Tecnología Digital (Mexico); Agustín Santiago-Alvarado, Univ. Tecnológica de la Mixteca (Mexico)

Nowadays, corneal topography mapping is a technique to detect and measure irregularities that appear in the human cornea surface. This technique is very useful for laser surgery planning or design of ophthalmic lenses. In this work, we propose a computational algorithm based on biological processes for refractive power optimization of corneal topography maps. The geometrical parameters of the cornea and other optical elements of the human eye are computationally optimized and analyzed by an intuitive graphic user interface.

10375-40, Session PMon

Ray tracing for inhomogeneous media applied to the human eye

Gerardo Diaz-Gonzalez, José Alfredo Jiménez-Hernández, Univ. Tecnológica de la Mixteca (Mexico); Marcelo David Iturbe-Castillo, Instituto Nacional de Astrofísica, Óptica y Electrónica (Mexico); Rigoberto Juarez-Salazar, Ctr. de Investigación y Desarrollo de Tecnología Digital (Mexico)

Inhomogeneous or gradient index media exhibit a refractive index varying with the position. This kind of media are very interesting because they can be found in both synthetic as well as real life optical devices such as the human lens. In this work, we present the development of a computational tool for ray tracing in refractive optical systems. Particularly, the human eye is used as the optical system under study. An inhomogeneous medium with similar characteristics to the human lens is introduced and modeled by the so-called slices method. The usefulness of our proposal is illustrated by several graphical results.

10375-41, Session PMon

Iterative paraxial design method based on an analytic calculation and its application to a three-group inner-focus zoom system

Euisam S. Lee, Juhyeon Choi, Yeon Hwang, Youngbok Kim, Korea Photonics Technology Institute (Korea, Republic of)

A paraxial design method based on an analytic calculation has been presented to overcome the problems of the conventional method for the design of initial zoom lens. We have theoretically derived the set of available zoom equations for three-group inner-focus zoom systems with infinite object distance, by using the matrix representation for paraxial ray tracing. Also we have made the program tool to calculate the first orders of lens

groups and zooming locus from the zoom equations using Matlab. The various constraints of three-group inner-focus zoom system could simply be described since the paraxial ray tracing equations are expressed in Gaussian brackets. The first orders of each group are used to calculate the zooming locus and then they are evaluated if the constraints are satisfied. If not, the first orders of each lens group should be changed to meet the constraints. The stability of this iterative paraxial design method has been confirmed and applied to the initial design for a three-group inner-focus zoom system having short total track of 12 mm and zoom ratio of 3x at all zoom positions.

10375-42, Session PMon

Analysis and design of a liquid-filled lens with controllable parameters and variable focus

Gerardo Diaz-Gonzalez, Agustín Santiago-Alvarado, Jorge González García, Univ. Tecnológica de la Mixteca (Mexico); Javier Munoz-Lopez, Instituto Nacional de Astrofísica, Óptica y Electrónica (Mexico)

We present the analysis and design of a liquid-filled lens made with two elastic membranes and a glass plate between them, in such a way that two controllable meniscus are formed. The parameters of the lens are proposed and analyzed in order to control the focal length and reduce the spherical aberration. A mechanical mount able to control the parameters of each meniscus is proposed.

10375-19, Session 5

Optical modeling of bullet-shaped LED for use in self-luminous traffic signs

Ted Liang-tai L. Lee, Yi-Chun Chen, Ming-Siou Tsai, Ching-Cherng Sun, National Central Univ. (Taiwan)

Bullet-shaped LEDs are commonly used in self-luminous traffic signs as LED dotted matrices due to their low cost, simplicity, robustness and ease of installation. This study aims to design a lens module on the bullet-shaped LEDs to reduce glare sensation by creating a desirable amount of backscatter onto the retroreflective sheets of traffic signs. Unfortunately, due to the high tolerance of the manufacturing process, the midfield modeling of bullet-shaped LEDs is a difficult task. In this paper, we use a proven modeling algorithm and expand its capabilities to model bullet-shaped LEDs, aiding us in designing beam-shaping lens in the midfield region.

A simple low-cost method that creates a model suitable for the high tolerance found in bullet-shaped LEDs is proposed, based on first measuring multiple one-dimensional intensity patterns at interested distances from multiple LEDs to form a database, including distances at 10, 14, 19, 24, 34, 49, and 100 mm. Their normalized cross correlations are then calculated to find the batch that has the most similarity and base our model off that batch. Finally, we validate the model via Monte Carlo simulations in comparison to the original one-dimensional intensity patterns in the database. Current work is mainly focused on building a fast and reliable measuring platform, and acquiring abundant data for the database.

The platform has been demonstrated to obtain an average of 97% in normalized cross correlation between different batches of the same model LED, and a model of that LED is currently under development. Future work will be focused on improving our model for the high tolerance bullet-shaped LEDs with the main goal to apply our model in designing a lens that directly covers the LED to provide a reasonable amount of backscatter for use in highway traffic signs.

10375-20, Session 5

Visual ergonomic evaluations on four different designs of LED traffic signs

Yi-Chun Chen, Ting-Yuan Huang, National Central Univ. (Taiwan); Tsung-Xian Lee, National Taiwan Univ. of Science and Technology (Taiwan); Ching-Cherng Sun, National Central Univ. (Taiwan)

Traffic signs are an indispensable part of our daily lives. However, traditional signs with retroreflective sheets and external lighting are almost invisible in severe weather such as heavy rains or fogs. Making traffic signs self-luminous with LEDs is a promising solution for longer legible viewing distance. To investigate the legibility and visual comfort of LED traffic signs, an ergonomic experiment is designed and performed.

Four different LED highway traffic signs are custom made, including three self-luminous ones as LED lightbox, LED backlight and regional LED backlight, and one non-self-luminous sign with external LED lighting. In our previous study, the luminance operating range of white texts on the self-luminous traffic signs has been identified to provide satisfactory legibility and visual comfort. The self-luminous signs in the present study are lit to the same luminance within that range. The illuminance of the external-lit one complies with the traffic-sign regulations. The four signs are hanged side-by-side and evaluated by observers through questionnaires. Four left-to-right hanging orders arranged by a Latin square are employed to compensate the possible viewing-order effect. Preliminary results from eight participants and four rounds show that the four designs have statistically significant differences in their legibility, visual comfort and user preference. The most preferred design is regional LED backlight, probably owing to its high contrast between the white texts and green background. Further evaluations with more observers are underway to verify the findings in the pilot study. The research outcome shall offer practical directions in designing LED traffic signs.

10375-21, Session 5

Smart lighting using a liquid crystal modulator

Alexandre Baril, Simon Thibault, Tigran Glastian, Univ. Laval (Canada)

Since the massive invasion of LED lighting over the illumination market, a clear trend of need appeared for a more effcient and targeted lighting. The project leads this trend by developing an evaluation board to test smart lighting applications with a new liquid crystal light modulator recently developed for broadening LED light beams. These modulator are controlled by electricals signals and they are characterised by a very linear working zone.

This feature allows the implementation of a closed loop control with a sensor feedback. We show that the use of computer vision is a promising opportunity for closed loop control. The developed evaluation board integrates the liquid crystal modulator, a camera, a LED light source and all the required electronics to implement a closed loop control with a computer vision algorithm.

10375-22, Session 5

High-efficiency zoom spotlight based on solid-state lighting

Shih-Kang Lin, Xuan-Hao Lee, Mao-Teng Ho, Tsung-Hsun Yang, Ching-Cherng Sun, National Central Univ. (Taiwan)

In this study, we propose an optical design for a high- efficiency zoom spotlight. The zoom spotlight has a reflector, a solid-state light source and a fixed lens. The solid-state light source of the zoom spotlight can be moved longitudinally so that the zoom spotlight can output a broad beam,

a collimated beam, or a beam ranging between the broad beam and the collimated beam. We also discuss the structure design for the solid-state light source to increase the output luminous flux. The simulation analysis and the corresponding experiment results are demonstrated.

10375-23, Session 5

Combining the transformation and the integration methods to design a refractive lens-array for signal lighting applications

Mahmoud Essameldin, Friedrich Fleischmann, Thomas Henning, Hochschule Bremen Univ. of Applied Sciences (Germany); Walter Lang, Univ. Bremen (Germany)

The design of a secondary optical lens for light beam shaping using the transformation method is performed by transforming the light source energy distribution using the concepts of energy conservation and light energy mapping. Using these concepts creates a dependency relation between the output optical performance and the luminous intensity distribution of the light source. This relation leads to errors on the optical performance due to the fabrication misalignment between the light source and the secondary optical lens. On the other hand, in the illumination applications, the integration method has been proved to be an efficient method for achieving a high degree of homogenized luminous intensity distribution by integrating and superimposing the light source energy over the illuminated objects.

In signal lighting applications, the luminous intensity distribution must meet the requirements regarding the brightness perception of users over the spatial angular distribution, not the illumination of objects. In this paper, the integration method is combined with the transformation method to design a refractive lens-array for signal lighting applications. The difference between the two methods is described, presenting the advantages of the combination process. Design procedures are explained in detail including the lens-array modeling. The optical performance is investigated using an optical ray tracing. Finally, the influence of the misalignment between the light source and the refractive lens-array is measured.

10375-24, Session 6

Development of the infrared instrument for gas detection

Ching-Wei Chen, Chia-Ray Chen, National Space Organization (Taiwan)

MWIR (Mid-Wave Infrared) spectroscopy shows a large potential in the current IR devices market, due to its multiple applications, such as gas detection, chemical analysis, industrial monitoring, combustion and flame characterization. It opens this technique to the fields of application, such as industrial monitoring and control, agriculture and environmental monitoring. However, a major barrier, which is the lack of affordable specific key elements such a MWIR light sources and low cost uncooled detectors, have held it back from its widespread use. In this paper an uncooled MWIR detector combined with image enhancement technique is reported. This investigation shows good results in gas leakage detection test. It also verify the functions of self-developed MWIR lens and optics. A good agreement in theoretical design and experiment give us the lessons learned for the potential application in infrared satellite technology. A brief discussions will also be presented in this paper.

10375-25, Session 6

Optical design of an athermalised dual field-of-view step zoom optical system in MWIR

Doruk Kucukcelebi, Roketsan A.S. (Turkey)

In this paper, the optical design of an athermalised dual field of view step zoom optical system in MWIR (3.7μm – 4.8μm) is described. The dual field of view infrared optical system is designed based on the principle of mechanical passive athermalization method not only to achieve athermal optical system but also to keep the high image quality within the working temperature between -40 ºC and +60 ºC. The infrared optical system used in this study had a 320 pixel x 256 pixel resolution, 30μm pixel pitch size cooled MWIR focal plane array detector. In this study, the step zoom mechanism, which has the axial motion due to consisting of a lens group, is considered to simplify mechanical structure. The optical design was based on moving a single lens along the optical axis for changing the optical system's field of view not only to reduce the number of moving parts but also to athermalize for the optical system. The optical design began with an optimization process using paraxial optics when first-order optics parameters are determined. During the optimization process, in order to reduce aberrations, such as coma, astigmatism, spherical and chromatic aberrations, aspherical surfaces were used. As a result, athermalised dual field of view step zoom optical design is proposed and the performance of the design using proposed method was verified by providing the focus shifts, spot diagrams and MTF analyzes' plots.

10375-26, Session 6

Contact lens design with slope-constrained Q-type aspheres for myopia correction

Wei-Jei Peng, Yuan-Chieh Cheng, Wei-Yao Hsu, Zong-Ru Yu, Cheng-Fang Ho, Instrument Technology Research Ctr. (Taiwan); Khaled Abou-El-Hossein, Nelson Mandela Metropolitan Univ. (South Africa)

The design of the rigid contact lens with slope-constrained Q-type aspheres for myopia correction is presented in this paper. The spherical contact lens is the most common type for myopia correction, however the spherical aberration (SA) caused from the pupil dilation in dark leads to the degradation of visual acuity which can't be corrected by spherical surface. The spherical and aspheric contact lenses are designed respectively based on Liou's schematic eye model, and the criterion is the normal vision on optical axis, that is defined as the resolution of one arc-minute. After optimization, the aspheric design is superior to the spherical design, and the aspheric surface corrects the SA for improving the visual acuity on retina. For avoiding the scratch caused from the contact profilometer, the aspheric surface is designed to match the measurability of the interferometer. The Q-type aspheric surface is employed to constrain the root-mean-square (rms) slope of the departure from a best-fit sphere directly, because the fringe density is limited by the interferometer. The maximum departure from a best-fit sphere is also controlled according to the measurability of the aspheric stitching interferometer (ASI). The inflection point is also removed in optimization for measurability and appearance. Therefore, the aspheric contact lens is successfully designed with Q-type aspheres for measurability of the interferometer. It not only corrects the myopia but also eliminates the spherical aberration for improving the visual acuity in dark based on the schematic eye model.

10376-1, Session 1

Curved sensors for compact high-resolution wide field designs *(Invited Paper)*

Christophe Gaschet, CEA-LETI (France); Emmanuel Hugot, Lab. d'Astrophysique de Marseille (France); Bertrand Chambion, Stéphane Gétin, Gaid Moulin, Stéphane Caplet, Aurélie Vandeneynde, CEA-LETI (France); David Henry, Commissariat à l'Énergie Atomique (France); Wilfried Jahn, Lab. d'Astrophysique de Marseille (France)

Over the recent years, a huge interest has grown for curved electronics, particularly for opto-electronics systems. Indeed, an optical system always has some aberrations, specifically for off-axis rays with Petzval Field curvature and astigmatism aberrations, which bend the focal plane. Usually, these aberrations are corrected with additional lenses, with the aim of coinciding the focal plane with a flat sensor. For more compact systems, this addition is impossible and corrections are made at the expense of the resolution. As the consequence, the main challenge is to obtain a compact system with a high resolution. In this paper, we proposed a new design architecture which has been developed specifically for a mechanically compatible curved image sensor. This type of optical design permits high performances and compactness without aspheric lenses, and has been evaluated in comparison with a benchmark system. For example, the gain of compactness is more than 50% compared to an equivalent system. Moreover, the role of different aberrations will be detailed, particularly for the Petzval curvature and astigmatism. We will also discuss trade-offs of several characteristics, such as stop shift, field of view of the system and chief ray angle at the edges of the sensors. Besides, curved sensors has also been studied, with results of its mechanical limits and electro-optical tests. All these experiments and results demonstrate the feasibility and the high performances at the entire optical system level.

10376-2, Session 1

Focus-induced photoresponse: a fundamentally novel approach to optical distance measurements

Christoph Lungenschmied, TrinamiX GmbH (Germany); Oili Pekkola, TrinamiX GmbH (Germany); Christian Lennartz, TrinamiX GmbH (Germany); Ingmar Bruder, TrinamiX GmbH (Germany)

Focus-Induced Photoresponse (FIP) is a patented monocular technology for optical distance measurements [1]. It relies on physical phenomena which are fundamentally different from established technologies such as time-of-flight, stereo vision, structured light or systems based on image processing. In this presentation, the underlying principles of the technology as well as application examples are introduced.

FIP exploits the nonlinear transient photoresponse of various organic as well as inorganic semiconductors when exposed to optical radiation. When a light-emitting (or reflecting) object moves in and out of focus, the size of the image that it creates on a sensor surface determines the magnitude of the photoresponse. As the focal point shifts with the distance between the collecting lens and the object, the sensor response yields a unique signature for every distance.

The device layout can hence be simple: the main components are modulated light sources, a lens and a non-pixelated sensor. Due to the unstructured sensor, resolution is not restricted by pixel size. FIP does not require large computational power as neither image processing nor stereo vision is required. By proper choice of optics and sensor type, the system can be adapted to any measuring task. We have successfully demonstrated functionality for wavelengths from visible light to IR and for distances up to 100 m.

[1] Bruder et al. (US 9,001,029 B2) DETECTOR FOR OPTICALLY DETECTING AT LEAST ONE OBJECT.

10376-3, Session 1

Ideal-lens stars

Jakub Bělín, Univ. of Glasgow (United Kingdom); Tomás Tyc, Masaryk Univ. (Czech Republic); Stephen Oxburgh, Johannes Courtial, Univ. of Glasgow (United Kingdom)

We recently showed how structures of ideal (thin) lenses can act as (ray-optical) transformation-optics devices. This was done by breaking the structure down into all sets of ideal lenses in the structure that share a common edge, and showing that these sets have very specific imaging properties.

In order to start the development of a general understanding of the imaging properties of sets of ideal lenses that share a common edge, we investigate here particularly simple and symmetric examples of combinations of ideal lenses that share a common edge. We call these combinations ideal-lens stars. An ideal-lens star is formed by N identical ideal lenses, each placed such that they share a principal point (which lies on the common edge) and such that the angles between all neighbouring lenses are the same.

We find that that passage through every single ideal lens in the ideal-lens star images any point to itself. Furthermore, light-ray trajectories in ideal-lens stars are piecewise linear approximations to conic sections. (In the limit of N approaching infinity, they are conic sections.) Finally, we show that light-ray trajectories in ideal-lens stars are closely related to the family of trajectories of particles with the same ratio of angular momentum and mass in the Kepler problem.

10376-4, Session 1

High-speed video analysis of ballistic trials to investigate the crack propagation in glass laminates

Arash Ramezani, Hendrik Rothe, Helmut-Schmidt Univ. (Germany)

In the security sector the partly insufficient safety of people and equipment due to failure of industrial components are ongoing problems that cause great concern. Since computers and software have spread into all fields of industry, extensive efforts are currently made in order to improve the safety by applying certain numerical solutions.

This work will focus on transparent armor consisting of several layers of soda lime float glass bonded to a layer of polycarbonate to produce a glass laminate. Details of ballistic trials on transparent armor systems are presented. Several targets of different laminate configurations were tested to assess the ballistic limit and the crack propagation for each design. Here, even the crack formation must precisely match later simulations. The crack propagation is analyzed using image processing software for highly accurate measuring functions. The goal is to evaluate the effects of ballistic glass with numerical simulations, promoting an effective development process. Due to the fact that all engineering simulation is based on geometry to represent the design, the target and all its components are simulated as CAD models. Using a CAD-neutral environment that supports direct, bidirectional and associative interfaces with CAD systems, the geometry can be optimized successively. The work will also provide a brief overview of ballistic tests to offer some basic knowledge of the subject, serving as a basis for the comparison of the simulation results. The objective of this work is to improve the safety of ballistic glasses. Instead of running expensive trials, numerical simulations should identify vulnerabilities of

structures. Contrary to the experimental result, numerical methods allow easy and comprehensive studying of all mechanical parameters. Modeling will also help to understand how the transparent armor schemes behave during impact and how the failure processes can be controlled to our advantage. By progressively changing the composition of several layers and the material thickness, the transparent armor will be optimized. There is every reason to expect possible weight savings and a significant increase in protection, through the use of numerical techniques combined with a small number of physical experiments.

10376-5, Session 1

Imaging with pairs of skew lenses

Jakub Bělín, Stephen Oxburgh, Univ. of Glasgow (United Kingdom); Tomáš Tyc, Masaryk Univ. (Czech Republic); Johannes Courtial, Univ. of Glasgow (United Kingdom)

Many of the properties of thick lenses can be understood by considering these as a combination of parallel ideal thin lenses that share a common optical axis. A similar analysis can also be applied to many other optical systems. Consequently, combinations of ideal lenses that share a common optical axis, or at least optical-axis direction, are very well understood. Such combinations can be described as a single lens with principal planes that do not coincide. However, in recent proposals for lens-based transformation-optics devices the lenses do not share an optical-axis direction. To understand such lens-based transformation-optics devices, combinations of lenses with skew optical axes must be understood.

In complete analogy to the description of combinations of pairs of ideal lenses that share an optical axis, we describe here pairs of ideal lenses with skew optical axes as a single ideal lens with sheared object and image spaces. The transverse planes are no longer perpendicular to the optical axis. We construct the optical axis, the direction of the transverse planes on both sides, and all cardinal points. We believe that this construction has the potential to become a powerful tool for understanding and designing novel optical devices.

10376-7, Session 2

Temporal focal plane filter arrays

Israel J. Vaughn, The Univ. of New South Wales (Australia); Andrey S. Alenin, Scott Tyo, UNSW Canberra (Australia)

We recently defined a new formalism for engineering spatial information channels for focal plane filter arrays (FPFAs) in a general way for any physical light property measured via irradiance including spectral bands, polarimetric bands, and general coherence. The formalism encompasses color filter arrays, micropolarizer arrays, and microantenna arrays over a pixelated irradiance sensor. The formalism derives the physical channels available from the parameters of the unit cell used to tile the focal plane array: the unit cell geometry, the filter transmission functions, the number of unit cells, and the unit cell filter weights. We also recently showed that switching the polarization measuring properties in time over a fixed micropolarizer array would perform well compared with snapshot systems, even given increased noise due to doubling the temporal framerate. We present preliminary results on the extension of our FPFA framework to include temporal effects. Instead of a 2D unit cell which completely defines the system channels, a 3D unit cell consisting of 3D attenuation functions on a 3D rectangular lattice in (x,y,t) is defined, and specific examples are shown for micropolarizer array systems with a ferroelectric variable retarder; and a color filter array system utilizing tunable etalons for color filter modulation.

10376-8, Session 2

Aberrations of temporally modulated optical wavefronts in dispersive optical systems *(Invited Paper)*

David H. Parker, Parker Intellectual Property Enterprises, LLC (United States)

Classical time-invariant lens aberrations, and methods for correcting them, are well known in the art. However, the design, analysis, and construction of optical components and systems for temporally modulated optical wavefronts--and in particular, wavefronts in optical time-of-flight or phase measurement instruments, such as laser trackers, heterodyne laser interferometers, and spherical retroreflectors, require additional considerations to correct for what will be called Optical Amplitude Modulation (OAM) aberrations. Ray tracing analysis is time-invariant and thus insensitive to temporal modulation of the rays. Secondary considerations must be given to the wavefront of the modulated envelope which is focused on a detector, i.e., while the rays converge to a focus, the phase of the modulated envelope will in general depend on the path of the rays. Elements from communications theory, including amplitude modulation (AM) and analysis in the Fourier transform frequency domain are unified with classical optics, where the optical wavelength of a laser is treated as a carrier signal and the AM produces two slightly offset sidebands. The sidebands produce the OAM aberration due to dispersion and different paths through the optical elements. Suggestions are made for methods for correcting OAM aberrations, such as lens designs that are achromatic at the two sidebands, the use of specific materials matched to the carrier wavelength, the use of corrector plates, and computer modeling tools. A review of relevant patent literature is included.

10376-10, Session 2

A novel surface plasmon-coupled tunable wavelength filter for hyperspectral imaging

John F. Turner II, Ajaykumar H. Zalavadia, Cleveland State Univ. (United States)

The development of ultra-compact handheld hyperspectral imagers has been impeded by the scarcity of small widefield tunable wavelength filters. The widefield modality is preferred for handheld imaging applications in which image registration can be performed to counter scene shift caused by irregular user motions that would thwart scanning approaches. Conventional widefield tunable filters like the liquid crystal tunable filter and acousto-optic tunable filter achieve narrow passbands across a wide spectral range by utilizing large interaction lengths, thereby increasing the thickness of the device along the optical path. In addition, these technologies rely on rather bulky external control circuitry and, in the case of acousto-optic filters, high power requirements. In the work presented here, we introduce a novel widefield tunable filter for visible and near infrared imaging based on surface plasmon coupling that can be miniaturized without sacrificing performance. The surface plasmon coupled tunable filter (SPCTF) provides diffraction limited spatial resolution with a ~10nm nominal passband and a spurious free spectral range of more than 300nm. Acting on the p-polarized component, the device is limited to transmitting 50 percent of unpolarized incident light. This is higher than the throughput of comparable Lyot-based liquid crystal tunable filters that employ a series of linear polarizers. The design of the SPTF is presented along with a comparison of its performance to calculated estimates of transmittance, spectral resolution, and spectral range.

10376-11, Session 3

Thermally tunable III-V photonic crystals for coherent nonlinear optical circuits

Ranojoy Bose, Hewlett-Packard Labs. (United States); Marina Radulaski, Hewlett Packard Labs. (United States); Tho Tran, Ray Beausoleil, Hewlett-Packard Labs. (United States)

We have developed a platform for low-energy, fast, nonlinear optical gates that can be coherently connected using low-index waveguides, with the idea of eventually scaling up to large nonlinear optical networks for applications in computation and sensing. The individual gates comprise of gallium arsenide photonic crystals designed at the edge of the photonic bandgap of the bulk material, thereby enhancing nonlinear effects, and allowing for switching using only a few femto Joules of energy. For scaling to multiple photonic crystal gates that are coherently connected, we surrounded the photonic crystal using glass cladding and designed bus waveguides running in a vertically displaced layer of low-index material. This design potentially allows us to connect multiple gates without the large lithographic constraints of photonic crystal waveguides that may be alternatively used. Any large network of optical gates also requires precise tuning of optical resonances. Some applications may require tuning of all gates to a single frequency, while others require tuning to precise known frequencies (DWDM is one example). We have achieved this by designing highly efficient chrome heaters on chip that can tune our photonic crystal resonances to nearly 6 nm, with a tuning efficiency of 1.5 nm/mW. This is well within our fabrication discrepancy of 5 nm in devices patterned with the same lithographic dose. With these capabilities, we have built photonic circuits comprising of 5 photonic crystal cavities connected to microheaters, and have characterized the linear performance of such a circuit pre-tuning.

10376-12, Session 3

Short range, >100Kbits/s, visible light communication protocol design for high-gamma smartphones

Jaime R. Ek-Ek, Ctr. de Investigación e Innovación Tecnológica (Mexico); Ponciano J. Escamilla-Ambrosio, Ctr. de Investigación en Computación (Mexico); Abraham Sierra-Calderon, Ctr. de Investigación e Innovación Tecnológica (Mexico); Abel Sanchez-Nieves, Escuela Superior de Ingenieria Mecanica y Electrica (Mexico); Abraham Rodriguez-Mota, Escuela Superior de Ingenieria Mecanica y Electrica, Unidad Zacatenco (Mexico)

High gamma smartphones based on Android operating system support the development of third-party applications. This kind of devices include subsystems such as sensors and actuators which can be used for diverse purposes. One example is the implementation of short range visible light communication (VLC) channels where the built-in light-emitting diode (LED) is the transmitter, and the complementary metal-oxide semiconductor (CMOS) camera works as the receiver. A major challenge for this communication channel is the modulation bandwidth of the light source which is limited to a few MHz, and the availability of a line-of-sight. The camera shutter is limited to a few frames per second (30 or 60 fps) for a few bits per second transmission, but the Rolling Shutter effect could allow the enhancement of the bit rate. In this work, we propose a VLC protocol design for the use of the built-in camera and the flash LED in order to implement a short range VLC channel, for high gamma mobile-to-mobile devices based on Android. The design is based on On-Off Keying (OOK) modulation for initially transmitting a few bits. Based on the rolling shutter effect in the CMOS image sensor, bright and dark fringes can be observed within each received frame, and the data can then be retrieved. Furthermore, two thresholding schemes for high fluctuation and large extinction ratio (ER) variations in each frame, are explored. Full protocol design and short range (5cm), >100Kbits/s, VLC demonstration and image processing results will be included in the presentation.

10376-13, Session 3

Experimental realisability of lens cloaks

Stephen Oxburgh, Jakub B?lín, Euan Cowie, Johannes Courtial, Univ. of Glasgow (United Kingdom)

We recently showed how to construct omni-directional ray-optical transformation-optics devices out of ideal thin lenses. These devices can be seen as theoretical generalisations of the paraxial, four-lens, “Rochester cloak”.

Here we investigate the practical realisability of such devices. We use ray-tracing simulations to compare real-lens cloaks in which the ideal lenses are replaced by glass lenses, by phase holograms of lenses, and by generalised confocal lenslet arrays (GCLAs, also known as telescope windows). We show that such devices can only work over a limited field of view.

10376-14, Session 3

Design and implementation of a large depth-of-field and large aperture optical system

Xiaohu Guo, China North Vehicle Research Institute (China); Lingqin Kong, Yijian Wu, Yuejin Zhao, Liquan Dong, Ming Liu, Beijing Institute of Technology (China)

In this paper, it presents a new imaging technology that could realize to extent the depth of field and contribute to receive the large iris aperture optical system. The new technology combines lenses assistance and the aberration modulation. Based on the method, we establish a new optical system. Simulation results indicate that the modulation transfer function (MTF) curves of this optical system have consistency feature during different object distances. According to the feature, we can restore ambiguous images to unambiguous ones. Compared with another normal optical system, the experimental results indicate that the new optical system has the large depth of field and large iris aperture features.

10376-15, Session 3

Dip-and-bake low-cost high-performance lenses for smartphone-based microscopy

Bhuvaneshwari Karunakaran, Joseph Tharion, Debjani Paul, Soumyo Mukherji, Indian Institute of Technology Bombay (India)

Low cost miniature lenses can transform smartphones into quality microscopes for use in low resource and low infrastructure settings. Such handheld microscopes can have potential applications in healthcare, forensics, surveillance, environmental monitoring and so on. The existing low cost techniques of fabricating miniature lenses require dispensing of polydimethylsiloxane (PDMS) in known quantity, which is challenging due to its high viscosity[1,2]. In this paper, we present a mould-free approach to fabricate high performance elastomer lenses reproducibly. A hanging drop of PDMS was formed by dipping a highly curved substrate (in our case, a 5mm diameter PDMS lens) in liquid PDMS and curing it. The resultant lens profile resembled a parabola and has improved light collecting ability[1]. The need for dispensing known quantities of PDMS was overcome, thus, resulting in reproducible lens fabrication. This action was repeated to obtain higher lens curvatures (radius of curvature down to 1.42±0.02mm). The focal length was measured to be 4.6±0.5mm, respectively, across three lenses fabricated. Further, we place a lens at the smartphone camera and transform it into a portable pocket microscope with ~80X magnification (without smartphone digital zoom) and ~2μm resolution (fringe visibility=0.07). We imaged various biological samples and compared the images to a conventional microscope. Also, we show that the micro-features on the Indian currency notes can be imaged using these microscopes in ambient light. This has potential impact in addressing the fake currency

determination.

[1] Lee, Biomedical optics express, 2014, 5, 1626.

[2] Sung, Journal of biomedical optics, 2015, 20, 47005.

10376-16, Session 4

Gait motion analysis using optical and inertial sensor fusion to design human kinetic energy harvesting systems *(Invited Paper)*

Oliver Kröning, Hendrik Rothe, Helmut-Schmidt Univ. (Germany)

Biomechanical energy harvesting converting kinetic energy from human motion into electrical energy appeared as a promising technology for powering mobile devices.

The optimization of these energy harvesting systems requires knowledge about human gait as an energy source to maximize the power output. Therefore, motions during walking and running have to be evaluated to determine the amount of available and convertible energy in several body parts. The efficiency of vibration energy harvesting systems is also dependent on the adjustment of the systems' dimensions and frequency characteristics to the driving force.

Thus, this paper presents a solution fusing optical sensors and inertial measurement units (IMU) to analyze human locomotion. High-speed cameras are used to track the positions and angles of the synchronized inertial body sensors in an earth frame while the IMUs acquire gyroscope, accelerometer and magnetometer data. This data is used to calculate linear acceleration and actual orientation represented in quaternions by applying an algorithm by Madgwick. The orientation gives major information about the effect of the driving force on moving masses of the system as energy harvesting devices are often designed as single-axis generators. Frequency responses of acceleration data from different body positions while gait cycles are analysed as well. Furthermore, prospects and issues converting acceleration into velocity and position data and vice versa are discussed.

10376-17, Session 4

Design, manufacture, and evaluation of prototype telescope windows for use in low-vision aids

Euan Cowie, Univ. of Glasgow (United Kingdom); Cyril Bourgenot, Durham Univ. (United Kingdom); Johannes Courtial, Univ. of Glasgow (United Kingdom); John Girkin, Gordon Love, David Robertson, Laura Young, Durham Univ. (United Kingdom)

Pixellated optics, a class of optical devices which preserve phase front continuity only over small sub areas of the device, allow for properties that would not be possible without this discretized phase continuity. One set of such devices are telescope windows (TWs), also known as generalised confocal lenslet arrays, where two arrays of lenslets are positioned confocally such that they are miniature telescopes. TWs allow for very general mappings between object space and image space and can be designed for a range of potential uses.

One such potential use is as low-vision aids (LVAs), where they are hoped to combine the function and performance of existing devices with the size and comfort of lower power eyewear. For these devices the TWs are designed to magnify objects, recreating the effect of traditional refracting telescope within a thin, planar device. Such devices can, therefore, be made significantly lighter than existing LVAs, increasing the comfort of the wearer.

We have developed a series of prototype TW devices to examine their real-world performance, focussing on the resolution, magnification and clarity attainable through the devices. It is hoped that these will form the basis for a future LVA devices. This development has required novel manufacturing techniques and a phased development approach centred on maximising performance. Presented here will be an overview of the development so far, alongside the performance of the latest devices.

10376-18, Session 4

Design of a three-view cooperative scanning handheld OCT probe for intraoperative microvascular imaging

Shizhao Peng, Yong Huang, Shaoyan Xia, Yuanzhen Jiang, Yanfeng Wu, Xiaodi Tan, Beijing Institute of Technology (China)

To meet the needs of real-time imaging in intraoperative microsurgical vessel anastomosis and to break through the bottleneck of limited penetration depth caused by absorption and scattering from blood, we present a novel design of three-view cooperative scanning handheld OCT probe. It is based on a low coherence source with 1.3?m central wavelength for extra-vascular imaging. Traditional OCT probe always scan from one direction and suffers from the problem of incomplete cross-sectional view of the vessel under investigation. We've designed an MEMS mirror based OCT handheld probe, which can be used to generate cross-sectional images from 3 view directions to increase the field of view in the depth direction. In addition, to adapt to vessels of different sizes, we've also designed a micro-stage to be used together with the handheld probe to solve the hand-trembling problem. The rectangle scanning range is about 3 * 3mm in three-view, which can meet the imaging demands of most vessels. We believe that application of the probe will greatly improve the quality of micro-vascular anastomosis success rate.

10376-19, Session 4

Research of the optical scheme for an endoscopic optical coherent tomography

Helen A. Tsyganok, Alina Dubrovskaya, ITMO Univ. (Russian Federation)

The method of the endoscopic optical coherent tomography (EOCT) allows carrying out noncontact diagnostics of organs in the scanning mode, to research a structure of an integumentary epithelium of a mucous membrane at a depth up to 2 mm, revealing its damages, to differentiate preinvazivny and microinvasive early cancer.

The EOKT method is based on the Michelson interferometer: illumination is generated by the superluminescent diode, passes through a lens, and gets on a beam splitter. In an object branch of the interferometer illumination going to optical fiber at the end of biological tissue is located. Illumination passes back on a beam splitter and gets on the receiver after reflection from the last.

In the reference branch illumination after a beam splitter passes through a lens, is reflected from system of mirrors, returns, getting to a lens, and then on the receiver. For safe and effective diagnostics the optimum wavelength of the radiation of 1300 nanometers based on a reversal spectrum of biological tissue was selected.

The optical probe represents the microscope objective consisting of two lenses and the swung mirror and protective plate made from leucosapphire. Scanning of tissue is carried out by rolling of a mirror by one degree from the basic provision. For the purpose of determination of complete physical losses in optical fiber theoretical calculation was made.

10376-35, Session 4

Thin head-mounted display utilizing reflective optics design

Chia-Ping Lin, Guo Dung J. Su, National Taiwan Univ. (Taiwan)

For wearable device, the most importance point for image system is miniaturization. In this paper, we present a head-mount display that reduce the distance between the eyeball to the lens and its thickness. In traditional, the thickness of head-mount display is not thin enough because of it is designed that the light source transmit a series of lenses. It make a large volume of head-mounted display. The system consists of three curve mirrors and a free-form lens. Mirrors and lens can form a reflective design. The image source is placed be next to the eyeball. We expect the image to go through the mirrors to the eyeball so that make the volume of head-mount display be thinner. The system is 60 mm thick and 140 mm wide. The field of view is designed to be 140 degree (V) and 110 degree (H).

10376-20, Session 5

Glasses-free 2D/3D switchable display using an integrated single lightguide plate (LGP) with a trapezoidal light-extraction (TLE) film

Jin-Ho Lee, Yoonsun Choi, Samsung Advanced Institute of Technology (Korea, Republic of); Igor Yanusik, Alexander Morozov, SAMSUNG R&D Institute Rus. (Russian Federation); Hyoseok Hwang, Samsung Advanced Institute of Technology (Korea, Republic of); Dongkyung Nam, SAMSUNG Electronics Co., Ltd. (Korea, Republic of); Du Sik Park, Samsung Advanced Institute of Technology (Korea, Republic of)

We present a 10.1-inch 2D-3D switchable display using an integrated single light guide plate (LGP) with a trapezoidal light-extraction (TLE) film. The integral single LGP is composed of inverted trapezoidal line patterns made by adding a TLE film on its top surface and straight lenticular lens patterns on its bottom surface. The TLE film is also bonded to the bottom surface of LCD panel to maintain the 3D image quality, which can be seriously deteriorated by the gap variations between the LCD panel and LGP. The inverted trapezoidal line patterns act as slit apertures of parallax barriers for 3D mode. Light beams from LED light sources placed along the left and right edges of LGP bounce between the top and bottom surfaces of the LGP, and when they hit the side edges of the inverted trapezoidal patterns, they are emitted toward the LCD panel. The lenticular lens patterns arranged along the horizontal direction scatter the light beams from LED light sources arranged on the top and bottom edges of LGP uniformly, together with a reflective film disposed under the LGP for 2D mode. Applying the integrated single LGP with a TLE film, we realized a 2D-3D switchable display prototype with a 10.1-inch tablet panel of WUXGA resolution (1,200x1,920). Consequently, we showed light-field 3D display and 2D display images without interference artifacts between both modes, and also achieved the brightness uniformity over 80%. This display easily generates both 2D and 3D images without increasing the thickness and power consumption.

10376-21, Session 5

Combining three wavelength illumination and parallel phase shift interferometry for high-speed high-resolution and real-time motion tracking and 3D imaging

Michael Ney, Ibrahim Abdulhalim, Ben-Gurion Univ. of the Negev (Israel)

Phase based imaging and sensing have been for decades effective optical methodologies for high resolution surface profiling. Several techniques for acquiring the phase information encoding the surface topography have been developed; the most prominent is phase shift interferometry (PSI) in which several phase shifted interference images are usually acquired in a sequence and are algebraically combined to extract the phase information. However, phase imaging is limited both by the 2ϖ phase modulo limiting the ability to map structures with heights only up to half the source's wavelength i.e. several hundreds of nm, and also by error induced by the movements of the sample between the acquisitions of phase shifted interference images. Several approached for dealing with these limitations have been developed that provided only a limited solution, e.g. using a beat wavelength interferogram by a two wavelength illumination but that is more sensitive to phase noise and thus less accurate and parallel PSI in which all phase shifted images are acquired simultaneously but that does not resolve the height limitation. We have developed a combined and improved technique for parallel PSI and three wavelength illumination enabling overcoming both limitations without elevating phase noise sensitivity and have set up two prototypes: the first allowing video rate 3D imaging of moving samples such as biological live samples or high throughput scanning of metrology samples with nm scale resolution, and the second allowing single point very high speed axial motion tracking and vibrometry with sub-nm scale resolution and max step height of 30μm.

10376-22, Session 6

Development of quadruplet-camera system for pipe thread measurement

Shudo Takenaka, Toshifumi Kodama, Takahiro Yamasaki, JFE Steel Corp. (Japan); Kingo Sawada, JFE Tubic Corp. (Japan)

Optical measurement of pipe thread has the problem of uncertainty below 1?m(?) at manufacturing plant level where object position and shape is not all same. The authors propose a measurement method by designing optical specification to suppress diffraction effect and adopting optical shading/aberration correction and sub-pixel edge-detection processing.

In this method, 4 CCD line Cameras are opposite to 4 Parallel light sources (Quadruplet-Camera system) in order to measure by four points of circumference on pipe. By moving those Quadruplet-Camera system in an axial direction of pipe, thread images are acquired.

In optical usual approach, Numerical Aperture(NA) of the lens is increased to acquire high optical resolution, however the diffracted rays which form a diffraction pattern is found in the edge area of the cylindrical object with increase of the NA, so that it causes measurement uncertainty. And increase of the NA which leads narrow depth of field (D.O.F.), causes instability on measurement results at manufacturing plant.

The authors design compatible optical specification, and result that stability on measurement which means eliminating diffraction effect and wide D.O.F. is taken precedence over high optical resolution for application at manufacturing plant, and adopt optical shading/aberration correction and sub-pixel edge-detection processing in order to supplement the image of low optical resolution.

In this manuscript, first, we explain the proposed method and confirmation experiments in the laboratory. We also explain a new optical measurement system based on the concept described above in a manufacturing plant to prove the effectiveness of the method. We concluded that the measurement system has sufficient performance which repeatability below 1?m (?) for use as a practical system.

10376-23, Session 6

Robust shearography system for inspection of defects in composite material using diffractive optics

Fabio A. da Silva, Mauro E Benedet, Analucia V. Fantin, Daniel P. Willemann, Armando A. Gonçalves Jr., Univ. Federal de Santa Catarina (Brazil)

The most commonly optical configuration used to produce the lateral shifted images, in a Shearography system, is the Modified Michelson interferometer, because of its simple configuration. Tests carried out in recent years have shown that the modified interferometer of Michelson is a device that presents good results in laboratory environment, but still presents difficulties in field. These difficulties were the main motivation

for the development of a more robust system, able to operate in unstable environments. The proposed configuration presents a diffractive optical element (DOE) positioned between the image sensor and the objective lens, producing a lateral displacement of the specimen image. The design using a DOE to generate the lateral shifted images is an attractive alternative compared to the Michelson interferometer. Besides the diffractive optical configuration to be more compact, the high efficiency, around 80%, allows a better utilization of the incident light. Another great advantage of the DOE configuration is the same intensity average from the two interference patterns, since the light intensity distributions in the +1 and -1 orders are very similar, resulting in high contrast fringes.

Since the pitch of a diffractive grid, which produces an acceptable lateral displacement for the measurement, is about 60 times greater than the wavelength of a green laser, the DOE configuration becomes much more robust to external influences compared to the Michelson Interferometer configuration.

This work describes the shearography system with DOE configuration, and presents phase maps results of specimens produced and coated with composite material.

10376-24, Session 6

540nm pulsed laser design for particle image velocimetry applications

Abraham Sierra-Calderon, Jaime R. Ek-Ek, Ctr. de Investigación e Innovación Tecnológica (Mexico); Abel Sanchez Nieves, Escuela Superior de Ingeniería Mecánica y Eléctrica (Mexico); Gabriel Plascencia-Barrera, Jose A. Alvarez Chavez, Ctr. de Investigación e Innovación Tecnológica (Mexico)

Different types of mechanical and digital devices for measuring the velocity of fluids such as rotameters, annubar tubes, orifice plates, are suitable options. A limitation of such devices is that the direct interaction with the flux causes unwanted perturbations affecting their results. In this work, the design of a 540nm pulsed fiber laser system for measuring the velocity of water as a fluid via the Particle Image Velocimetry (PIV) technique is proposed. In particle image velocimetry, the fluid motion is made visible by adding small tracer particles and from the position of these particles, at two instances of time, it is possible to determine the flow velocity. The proposed, made in-house, non-commercial PIV system consists of: a second harmonic generation Q-switched Yb-doped fiber laser emitting 540nm pulses, a CCD camera, a pair of cylindrical diverging lenses, reference beads, and the fluid under test. The Yb3+-doped fiber laser itself is capable of producing 540nm, 5 – 15ns, 400mJ pulses at 500Hz – 15kHz repetition rates, suitable for PIV flow field studies. Full fiber laser design, in-house PIV system integration and flow field measurement results will be included in the presentation.

10376-25, Session 6

A confocal microscope with programmable aperture arrays by polymer-dispersed liquid crystal

Ting-Jui Chang, Guo Dung Su, National Taiwan Univ. (Taiwan)

A programmable array microscope (PAM) is one kind of confocal microscopes which uses the spatial light modulator (SLM) to serve both the source and detection aperture as the scanning apertures. Usually, PAM uses the digital micromirror device (DMD) or liquid crystal based optical components (like LCOS) as the spatial light modulator. The latter one has no mechanical movement part in the system, but it needs polarizer in, and it will reduce the light utilization rate. We present a programmable array microscope (PAM) which uses the polymer-dispersed liquid crystal (PDLC) chip as the spatial light modulator. PDLC is a polarization-free material, so we can improve the light utilization rate twice as other liquid crystal based PAMs. Furthermore, in our system, the incident light is perpendicular to the PDLC chip, while others can't or need more SLMs. Therefore, our system will make the whole system more compact. Also, it can increase the dynamic range compare to other liquid crystal based PAMs.

10376-26, Session PWed

Imaging application based on an electrically tunable polarization-independent liquid crystal microlens array

Zhaowei Xin, Qing Tong, Yu Lei, Dong Wei, Xinyu Zhang, Haiwei Wang, Changsheng Xie, Huazhong Univ. of Science and Technology (China)

In this study, a polarization-independent liquid crystal microlens array (P-LCMLA) for imaging application is proposed and demonstrated. This device is composed of double layered nematic liquid crystal with orthogonal alignment, two aluminum deposited silica substrates and a double-sided indium-tin oxide (ITO) silica. The double-sided ITO glass is sandwiched between the two hole-patterned aluminum electrodes to separate the orthogonal liquid crystal (LC) layers. The experiment results show that a high beam utilization efficiency and a compound point spread function are obtained by this novel configuration with low applied voltages. The normalized focusing intensity is polarization-insensitive to the incident light under certain driving voltages applied on both LC layers. The cascaded microstructure provides a wide operation range in the manipulation of incident beams and also emerges multiple operation modes for imaging applications, such as conventional planar imaging with adaptive beam adjustment, polarization imaging mode, and polarization-independent imaging mode. Therefore, a big advantage of the device proposed by us is that it cannot only be used to obtain two orthogonal polarization images but also in conventional planar or 2-dimensional (2D) intensity imaging, dual-mode wavefront imaging, and 3-dimensinoal (3D) information measurement. Since the polarization-independent microlens array demonstrates high optical efficiency, low power consumption, multiple imaging modes and simple manufacture, this kind of microlens array has a potential to be used in imaging application and many other optical systems.

10376-27, Session PWed

Fast sub-wavelength imaging using scattering medium and computational phase mask

Shenghang Zhou, Nanjing Univ. of Science and Technology (China)

Recent studies have shown that the phase-modulated light (by SLM) can be focused perfectly by feedback process. Under the SLM made, sub-100nm scanning can be performed in a certain range surrounding the focus by the memory effect. But scanning other areas would be time-consuming for the repetition of focusing process that based on feedback. In this paper, we proposed a time-saving method to realize the whole process by a single feedback-based focusing process and computational phase mask.

10376-28, Session PWed

Focus-induced photoresponse: Insights into the microscopic mechanisms and optical features behind the novel technique for optical distance measurements

Oili Pekkola, TrinamiX GmbH (Germany); Christoph Lungenschmied, TrinamiX GmbH (Germany); Christian Lennartz, Ingmar Bruder, TrinamiX GmbH (Germany)

Focus-Induced Photoresponse (FIP) is a patented monocular technology for optical distance measurements [1]. It relies on physical phenomena which are fundamentally different from established technologies such as time-of-flight, stereo vision, structured light or systems based on image processing. This presentation gives insights into the microscopic mechanisms and optical features leading to the FIP effect.

FIP exploits the nonlinear transient photoresponse of various organic as well as inorganic semiconductors when exposed to optical radiation. When a light-emitting (or reflecting) object moves in and out of focus, the size of the image that it creates on a sensor surface determines the magnitude of the photoresponse. As the focal point shifts with the distance between the collecting lens and the object, the sensor response yields a unique signature for every distance.

The functional principle of FIP is illustrated with experimental results as well as optical and electrical simulations. The microscopic mechanisms leading to the nonlinear photoresponse under modulated excitation are illustrated. The essential role of the optics used in the system is demonstrated. Examples of sensors based on various semiconductors are introduced in order to show the broad applicability of the FIP technology. We have successfully demonstrated functionality for wavelengths from visible light to IR and for distances up to 100 m.

[1] Bruder et al. (US 9,001,029 B2) DETECTOR FOR OPTICALLY DETECTING AT LEAST ONE OBJECT.

10376-29, Session PWed

An optical chip aggregometer based on laser transmission to detect alterations in the aggregation of glycosylated RBC

Martín A. Toderi, CONICET-UNR (Argentina) and Univ. Nacional de Rosario (Argentina); Natalia Lerda, Patricia Buszniez, Univ. Nacional de Rosario (Argentina); Bibiana D. Riquelme, Univ. Nacional de Rosario (Argentina) and CONICET-UNR (Argentina)

The study of erythrocyte (RBC) aggregation is of great interest because of its implications on human health, alterations are observed in vascular pathologies such as hypertension and diabetes, as a consequence of a decrease in the erythrocyte surface electric charge. It is of great importance to develop techniques and equipment, which allows evaluation and characterization of the erythrocyte aggregation phenomenon. Human RBC tend to form aggregates which initially consist of face-to-face linear structures that resemble a stack of coins which are generally called rouleaux. RBC aggregation can be analyzed by recording the intensity of transmitted light through a blood sample in real time. The graphic of the variation of light intensity as a function of time is called syllectogram. Several syllectograms of altered blood samples were obtained with a low cost disposable-chip aggregometer based on laser transmission. Complementary parameters were assessed by an Erythrocyte Rheometer based on laser difractometry. Studies were carried out varying the erythrocyte surface electric charge by enzymatic and non-enzymatic glycosylation. A minimum sample volume of 15μL was used and the parameters, Parameters Amp_100 (the normalized light intensity at 100 s,) and t_12 (the time required to reach the 50% of the total amplitude of transmitted light) show sensibility to this alteration. Viscoelastic parameters DI (deformability index), μ (elastic module) and (surface viscosity of the membrane) are lower than control tests. These light-based devices are of interest for further applications in Clinical Medicine related to vasculopathies.

10376-30, Session PWed

Optical design of optical synthetic aperture telescope

Chenghao Zhou, Zhile Wang, Harbin Institute of Technology (China)

Optical synthetic aperture (OSA) is a promising solution for very high-resolution imaging while reducing its volume and mass. In this paper, first, the configuration of OSA systems are analyzed and the design methods of two types (Fizeau and Michelson) of OSA systems are summarized and researched. Second, Fizeau and Michelson OSA prototype systems are designed in detail. In the Michelson configuration, the instrument is made of sub-telescopes distributed in entrance pupil and combined by a common telescope via folding periscopes. The design of Michelson configuration is more difficult than that of Fizeau configuration.

In the design of Fizeau configuration, according to the third aberration theory two-reflective system is deigned. Then the primary mirror of the two mirror system is replaced by the synthetic aperture. The whole system was simulated by Zemax software to obtain the Modulation transform function (MTF).

In the design of Michelson configuration, the system is first divided into three parts: the afocal interferometric telescopes, beam combiner system and folding periscopes. The three parts are designed respective and then combined in Zemax software to obtain the MTF.

10376-31, Session PWed

Method for synthesis of high-accuracy dynamic non-linear control systems

Vladimir L. Kodkin, South Ural State Univ. (Russian Federation)

Optical Engineering + Application conference in 2016 had only few reports dedicated to high-accuracy position control systems for optical complexes. However, at SPIE Optics + Photonics Exhibition 2016 dozens of companies offered such projects. In that respect, this report may be of interest for academic community.

The main method for assessment of performance of automatic control systems is assessment of stability of a system as it allows the evaluation of dynamics and accuracy as well as the method for additional adjustment and technological capacity of the whole complex comprising the system. As a rule, complex systems do not reduce to linear systems or other known variants, so their analysis is normally based on modeling or simplified calculation. In the suggested paper the known criterion of stability for non-linear systems by Popov involves not frequency locus of linear part, but logarithmic frequency characteristics of the system, including non-linear frequency characteristics. It allows the development of conditions of stability and methods of adjustment for such complex systems as servo drives with non-rigid mechanics and alternating-current systems which cannot be analyzed with the help of known methods. In the systems where the stated methods are used accuracy and speed performance are increased fivefold at an average. All theoretical calculations are confirmed by experiments and modeling.

10376-32, Session PWed

Common-path holographic objective for conventional photographic camera

Vira R. Besaga, Nils C. Gerhardt, Ruhr-Univ. Bochum (Germany); Peter P. Maksimyak, Yuriy Fedkovych Chernivtsi National Univ. (Ukraine); Martin R. Hofmann, Ruhr-Univ. Bochum (Germany)

In this paper, we introduce a direct-view digital holographic camera objective for off-axis external white-light illumination, which is based on a standard photographic objective as the main component. The direct view operation is provided via a modified common-path point diffraction interferometer on a transmission diffraction grating (92 grooves/mm) basis. The spatial separation of the interacting beams is realized with a self-fabricated copper mask (465±5 ?m apertures) with a back-reflection suppressing coating. This ensures self-interference between the 0th and the 1st diffraction orders at the smallest possible overlapping angle. The objective system is matched for a conventional CMOS sensor, where a hologram is written. Due to the used photographic objective in the current system configuration, a compensation lens module is applied for reshaping the beam entering the interferometric module. The proposed system operates under external illumination with two standard photographic flashes synchronized between each other and providing homogeneous sample illumination from opposite directions. The system operability was proven as well for coherent (He-Ne laser, 632 nm) as for low-coherent (SLD, 850 nm) and several broadband (white LED, halogen lamp) sources. For the self-reference mode the copper mask has to be replaced by a pinhole based two-aperture spatial filter. Although, the initial design has been proposed for self-emitting and reflecting samples, the system independence on the illumination part enables operation in transmission mode as well. Modular assemblage ensures easy system scalability and up-grade possibilities. As a proof of system operability, reconstructed amplitude and phase information of test samples is presented.

10376-33, Session PWed

Computer tool for achromatic and aplanatic cemented doublet design and analysis

Tatiana Ivanova, Galina Romanova, Tatiana Zhukova, Olga Kalinkina, ITMO Univ. (Russian Federation)

Algorithm and computer tool for cemented doublet synthesis by Slusarev's methodology are presented. Slusarev's methodology is based on lookup tables that allow calculating doublet radii by given value of third-order coma, spherical aberration and chromatic aberration using specific algorithm. The most time consuming part of cemented doublet synthesis by Slusarev's methodology is selection needed parameters from lookup tables. This part is automated and presented in this paper.

The input parameters for tool are desired values of third-order coma, spherical aberration and chromatic aberration of cemented doublet. The tool looks up several appropriate pairs of optical glasses corresponding to specified value of chromatic aberration and then calculates radii of surfaces for each pair of glasses corresponding to specified third-order coma and spherical aberration. The resulted third-order aberrations and real aberrations (transverse, longitudinal, axial color and coma) are calculated for obtained system. Several doublets can be analyzed in result table and the chosen one can be imported into Zemax. The calculated cemented doublet parameters can be analyzed and optimized in optical system design software.

The tool allows making the first step of optical system design fast and simple. It allows to design not only the system which is free of the third-order spherical aberration, coma and axial color, but obtain necessary value of aberration for compensation of aberrations in another part of optical system. Possibility to automatically choose optical glasses and compare the real aberration of the preliminary designed system is especially important features of the developed software.

10376-36, Session PWed

Offset pixel aperture technique for extracting depth information

Byoung-Soo Choi, Myunghan Bae, Sang-Hwan Kim, Jimin Lee, Chang-Woo Oh, Kyungpook National Univ. (Korea, Republic of); Seunghyuk Chang, Jongho Park, Sang-Jin Lee, Ctr. for Integrated Smart Sensors (Korea, Republic of); Jang-Kyoo Shin, Kyungpook National Univ. (Korea, Republic of)

The 3-dimensional (3D) imaging is an important area which can be applied to face detection, gesture recognition, and 3D reconstruction. Many techniques have been reported for 3D imaging using various methods such as time of fight (TOF), stereo, and structured light. These methods have limitations such as use of light source, multi-camera, or complex camera system. In this paper, we propose the offset pixel aperture (OPA) technique which is implemented on a single chip so that the depth can be obtained without increasing hardware cost and adding extra light sources. 3 types of pixels including Red (R), Blue (B), and White (W) pixels were used for OPA technique. The aperture is located on the W pixel, which does not have a color filter. Depth performance can be increased with a higher sensitivity because we use white (W) pixels for OPA with Red (R) and Blue (B) pixels for imaging. The RB pixels produce a defocused image with blur, while W pixels produce a focused image. The focused image is used as a reference image to extract the depth information for 3D imaging. This image can be compared with the defocused image from RB pixels. Therefore, depth information can be extracted by comparing defocused image with focused image using the depth from defocus (DFD) method. Previously, we proposed the pixel aperture (PA) technique based on the depth from defocus (DFD). The OPA technique is expected to enable a higher depth resolution and range compared to the PA technique. The pixels with a right OPA and a left OPA are used to generate stereo image with a single chip. The pixel structure was designed, simulated and fabricated using 0.11 μm CMOS image sensor (CIS) process. Optical performances of various offset pixel aperture structures were evaluated using optical simulation with finite-difference time-domain (FDTD) method.

Conference 10377: Optical System Alignment, Tolerancing, and Verification XI

SPIE. OPTICS+ PHOTONICS OPTICAL ENGINEERING+ APPLICATIONS

Sunday - Monday 6 –7 August 2017

Part of Proceedings of SPIE Vol. 10377 Optical System Alignment, Tolerancing, and Verification XI

10377-1, Session 1

Sub-cell turning to accomplish micron-level alignment of precision assemblies

Jay Kumler, JENOPTIK Optical Systems, LLC (United States); Christian Buß, TRIOPTICS GmbH (Germany)

Higher performance expectations for complex optical systems demand tighter alignment requirements for lens assembly alignment. In order to meet diffraction limited imaging performance over wide spectral bands across the UV and visible wavebands, new manufacturing approaches and tools must be developed if the produces will be produced consistently in volume production.

This is especially applicable in the field of precision microscope objectives for life science, semiconductor inspection and laser material processing systems. We observe a rising need for the improvement in the optical imaging performance of objective lenses. The key challenge lies in the micron-level decentration and tilt of each lens element.

One solution for the production of high quality lens systems is sub-cell assembly with alignment turning. This process relies on an automatic alignment chuck to align the optical axis of a mounted lens to the spindle axis of the machine. Subsequently, the mount is cut with diamond tools on a lathe with respect to the optical axis of the mount. Software controlled integrated measurement technology ensures highest precision. In addition to traditional production processes, further dimensions can be controlled in a very precise manner, e.g. the air gaps between the lenses. Using alignment turning simplifies further alignment steps and reduces the risk for errors.

This paper describes new challenges in microscope objective design and manufacturing, and addresses difficulties with standard production processes. A new measurement and alignment technique is described, and strengths and limitations are outlined.

10377-3, Session 1

Photonic Doppler velocimetry probe used to measure grain boundaries of dynamic shocked materials *(Invited Paper)*

Robert M. Malone, Morris I. Kaufman, Daniel K. Frayer, Kevin D. McGillivray, National Security Technologies, LLC (United States); Steven A. Clarke, Saryu J. Fensin, David R. Jones, Los Alamos National Lab. (United States)

Material scientists have developed computational modeling to predict the dynamic response of materials undergoing stress, but there is still a need to make precision measurements of surfaces undergoing shock compression. Miniature Photonic Doppler velocimetry (PDV) probes have been developed to measure the velocity distribution from a moving surface traveling tens of kilometers per second. These probes use hundreds of optical fibers imaged by optical relays onto different regions of this moving surface.

While previous work examined large surface areas, we have now developed a PDV microscope that can interrogate 37 different spots within a field of view of <1 mm, with a standoff distance of 17 mm, to analyze the motion differences across grain boundaries of the material undergoing dynamic stress. Each PDV fiber interrogates a 10 μm spot size on the moving surface. A separate imaging system using a coherent bundle records the location of the PDV spots relative to the grain boundaries prior to the dynamic event. Designing the mounting structures for the lenses, fibers, and coherent bundle was a challenge. To minimize back reflections, the fibers are index matched onto the first relay lens, which is made of fused silica. The PDV fibers are aligned normal to the moving surface. The imaging probe views the surface at an 18° angle. The coherent bundle is tilted 11° to its optical relay. All components are assembled into a single probe head assembly. The coherent bundle is removed from the probe head to be used for the next dynamic event. Alignment issues will also be discussed.

10377-4, Session 1

Slope-based precision optical testing using portable laser coordinate measuring instruments

Manal Khreishi, NASA Goddard Space Flight Ctr. (United States) and The Univ. of Arizona (United States); Raymond G. Ohl, Theodore J. Hadjimichael, NASA Goddard Space Flight Ctr. (United States); Joseph E. Hayden, Sigma Space Corp. (United States)

High precision, portable coordinate measuring instruments such as laser radars (LR) and laser trackers (LT) have been used for optical system alignment and integration. The LR's ability to perform a non-contact scan of surfaces was previously utilized to characterize large spherical and aspheric mirrors. In this paper, we explore the use of an LR/LT as an accurate, fast, robust, and non-contact tool for prescription characterization of optical surfaces. Using Nikon's MV-224/350 LR and Leica's Absolute Tracker AT401/402 instruments, proof of concept measurements were performed to characterize a variety of optical components using "direct and through" measurements of calibrated metrology targets. The results were compared to the nominal parameters and were cross-checked using an LR scan and other approaches. Custom macros in metrology software and other data reduction code were developed to calculate the surface slopes from the "direct and through" target measurements. As with a typical slope-based technique, the slopes were integrated to obtain the optical surfaces being tested. We discuss potential applications across the fields of optical component fabrication and system alignment and testing.

10377-5, Session 1

Integrated confocal Raman probe combined with a freeform reflector-based lab-on-chip

Qing Liu, Vrije Univ. Brussel (Belgium); Giancarlo Barbieri, Univ. degli Studi di Pavia (Italy); Hugo Thienpont, Vrije Univ. Brussel (Belgium); Heidi Ottevaere, Univ. degli Studi di Pavia (Belgium) and Vrije Univ. Brussel (Belgium)

Traditionally, Raman spectroscopic analyses are done in a specialized lab, with considerable requirements in terms of equipment, time and manual sampling of substances of interest. In this paper we take a step from bulky, laboratory analyses towards lab-on-chip (LOC) analyses. We miniaturize the Raman spectroscopic analyses by combining a free-form reflector based polymer lab-on-chip (LOC) with a Raman probe. By using the confocal detection principle we aim to enhance the detection of Raman signals from the substance of interest due to the suppression of the background Raman signal from the polymer of the chip.

In a first step, we present the design of the free-form reflector and the optical simulation of the Raman excitation, scattering and collection system by means of non-sequential ray-tracing software (ASAP) combined with a mathematical code. In these simulations, the excitation laser emits at a wavelength of 785nm. A free-form reflector with a diameter of 1.6 mm and based on a parabolic mirror is optimized to ensure that all incident light is focused into a common focal point, especially for rays that are strongly bent which is the case due to the high NA of the reflector. Next, the Raman scattering is captured by a multimode fiber and sent to a spectrometer. Our simulations demonstrate that our system allows confocal measurements and that small physical displacements of the lab-on-chip result in a small collection loss. We can conclude that the polymer background signal is suppressed when collecting Raman signals from solutions under test in the fluidic channel resulting in a higher sensitivity.

In a next step, we miniaturized the external optical components, surrounding

the reflector embedding optofluidic chip, and assembled these in a Raman probe. Finally we demonstrated the proof-of-concept by measuring the Raman signature of urea solutions with different concentrations in pure water. The alignment errors between the Raman probe and lab-on-chip were measured and evaluated. We believe these confocal Raman based spectroscopic devices pave the way for the development of portable and robust lab-on-a-chip systems which can be mass-deployed for use in the field and for point-of-care diagnostic applications.

10377-15, Session 1

Tolerancing a lens for LED uniform illumination

Jieun Ryu, The Univ. of Arizona (United States); Jose Sasian, College of Optical Sciences, The Univ. of Arizona (United States)

We use a closed form surface used to produce LED uniform illumination to determine alignment and fabrication tolerances.

The effects of wavelength, lateral displacement, tilt, and surface errors are analyzed and tolerances are determined.

10377-7, Session 2

Understanding product cost vs performance through an in-depth system Monte Carlo analysis *(Invited Paper)*

Mark C. Sanson, Corning Incorporated (United States)

The manner in which an optical system is toleranced and compensated will greatly affect the cost to build it. By having a detailed understanding of different tolerance and compensation methods the end user can decide what criteria is most important to them cost or performance. A detailed phased approach Monte Carlo analysis can be used to demonstrate the tradeoffs between cost and performance. In complex high performance optical systems, performance is fine-tuned by making adjustments to the optical systems after they are initially built. This process allows one to achieve the overall best system performance without needing to fabricate components to stringent tolerance levels that can often be outside of a fabricator's manufacturing capabilities. A good performance simulation of as built performance can interrogate different steps of the fabrication and build process. This can help to determine if the measured parameters are within the acceptable range of the system build at that stage. Finding errors before an optical system progresses further into the build process saves both time and money. Having the appropriate tolerances and compensation strategy tied to a specific performance level will optimize the overall product cost.

10377-8, Session 2

Specifying tilts, decenters, and beam deviations using the new edition of ISO 10110-6

Ray Williamson, Ray Williamson Consulting (United States)

ISO 10110-6 is the international standard for specifying centration of optical components and systems. The original version addressed only surface tilt angles of individual spherical and rotationally-invariant aspheric components. Because the intent of ISO Standards is to facilitate commerce, additional expressions and situations were included in the update: 1) Axial and circular runout, beam deviation, and lateral decenter may more directly reflect the measurement technique of the inspector, the primary interest of the designer, or the concerns of the optomechanical engineer. 2) The relation of components within a system to each other and to their mechanical reference points must have a clear description. 3) The industry's capabilities now include previously unattainable forms, which must be clearly toleranced.

As a result of international collaboration over a decade, the 2016 edition now includes surface tilts, axial and circular runout, beam deviation, and decenter of components and systems, including aspheres, circular and non-circular cylinders, and general surface forms. This expansion necessitates a more detailed notation system, which this presentation describes.

10377-9, Session 2

Specification and tolerancing of bulk glass material imperfections with ISO standards

Allen Krisiloff, Triptar Lens Co., Inc. (United States)

Standards for the specification of tolerances for glass material imperfections have been evolving over the past 40 years. Today, several individual ISO Standards for drawings and drawing notation -- ISO 10110-2, ISO-10110-3, and ISO-10110-4, which were last revised in 1993 -- are being merged and re-written to incorporate technical improvements and enhance the clarity of presentation. The new standard, tentatively numbered ISO 10110-18, is on schedule for release in 2018. It will also provide notation to directly utilize concepts and quality classes defined in ISO 12123, the newly revised standard for raw glass material. New ways to specify striae and a way to specify raw material specifications on a finished part drawing are two additional highlights of the revised versions of this set of ISO standards. This paper will discuss the old shortcomings, their corrections, and the new features incorporated into the set of standards currently under final development and whose publication is expected next year.

10377-10, Session 2

Generalized surface contributions for misalignment sensitivity analysis

Mateusz Oleszko, Herbert Gross, Friedrich-Schiller-Univ. Jena (Germany)

In order to perform a misalignment sensitivity analysis of an optical system it is helpful to know what are the contributions of individual surfaces to the total wavefront aberrations. The expansion of wavefront aberration function is an analytic method used for that purpose.

An alternative numerical approach to describe wavefront aberrations of symmetry free optical systems is proposed. Data from the trace of multiple ray sets are used to determine surface contributions. Surface contributions are defined as modules bounded by reference spheres located at the successive surfaces. Further contributions are divided due to their origin into intrinsic, induced and transfer components. Each component is determined from the separate set of rays. Intrinsic part results from refraction of an ideal wavefront on the surface. It is therefore independent on the rest of the system. Induced and transfer parts are both the effect of incoming aberrations and error in mapping of intersection coordinate grids on reference spheres. Hence they both describe dependencies between individual surfaces and potential misalignments. Induced part is acquired by subtracting the intrinsic part from the complete refraction effect. Transfer term results from distortion of coordinates arising upon propagation of the aberrated wavefront between successive surfaces.

The method is combined with Zernike fringe decomposition approach, which allows to perform detailed analysis of system aberrations in respect to individual surfaces and their misalignments in a well known classification. Results are presented for single field point or in the form of full field displays.

10377-2, Session 3

SFR test fixture for hemispherical and hyperhemispherical camera systems

John M. Tamkin, Imaging Insights, LLC (United States)

Traditional methods for testing wide field lenses and cameras have either

used expensive projection systems, use targets on rotation stages, or have placed pre-distorted targets within box-like test fixtures. With all these methods, it is important to recognize that factory floor space is premium. For many applications, hemispherical camera lenses have short focal lengths (less than 3 mm), but still require reasonably small F-numbers to collect sufficient light and accomodate small pixel size (< 2.4 micron) sensors. This creates a hyperfocal distance that is reasonably short: 600 to 700mm. In this work, we fabricated a box from low cost and lightweight alumicore the box contains internal "leaves" with 600mm radius cutouts along vertical, horizontal and diagonal axes consistent with 16:9 camera formats. We then fabricated 24 2" backlit targets from PVC pipe, plastic fresnel lenses, low-cost sheet diffusers and 3D printed parts. which were attached to the leaves. along the edge of each leaf, we secured LED strip lights to provide "Almost point sources", which are accurately located in angle space. In this paper, we describe the design space where "reasonably" sized boxes with rear projection targets can be used, and where the design can be adapted to use low-cost projectors fabricated using the same techniques, thus achieving low cost and small factory footprint.

10377-11, Session 3

Optical alignment using a CGH and an autostigmatic microscope

Robert E. Parks, Optical Perspectives Group, LLC (United States); Chunyu Zhao, Arizona Optical Metrology LLC (United States)

It is often necessary to locate an optical or mechanical component precisely relative to another as in cementing a doublet or in aligning an off-axis parabola to a mount. We show that one way of making a fixture to do this is to make a computer generated hologram (CGH) that will produce foci or axes in space when illuminated with a point source of quasi-monochromatic light. An ideal instrument to use is an autostigmatic microscope (ASM) because it serves as a means of illuminating the CGH with a point source as well as viewing the reflected focused spot or line.

Once the reflected stigmatic image is located with um precision, the center of curvature of an optical surface or ball, or focus of an off-axis parabola, can be aligned to the image, again using the ASM with the same sort of precision.

We use this scheme to show how one would go about cementing a double or aligning an off-axis parabola to a mount using only the custom CGH and an ASM. It will become obvious from these examples that the same methodology can be used to create fixtures for a variety of alignment cases such as aligning balls to a CGH used for null testing to see that the CGH is precisely and repeatably located relative to a transmission sphere. The method makes full use of the flexible nature of patterning CGHs and of kinematic principles.

10377-12, Session 3

Measurement of low-order aberrations with an autostigmatic microscope

William P. Kuhn, Opt-E (United States)

Autostigmatic alignment tools are in common use for alignment and metrology of optical and mechanical systems. The autocollimator is the classical tool for alignment tasks at infinite conjugates involving flat optics or a collimated wavefront. The autocollimator is the common name for an autostigmatic telescope. Autocollimators in conjunction with auxiliary optics can be used for a variety of tasks including alignment of linear stage axes or finding the axis of rotation of a bearing. The autostigmatic microscope is a finite conjugate autostigmatic alignment tool and is sometimes referred to as a point source microscope (PSM). Autostigmatic microscopes are useful for locating optics via their center-of-curvature, while autocollimators locate the surface normal of flat optics.

The addition of a piezo-electric focusing stage and phase retrieval algorithms to a compact, adaptable autostigmatic microscope provides a means to introduce a precise amount of phase diversity (defocus) allowing one to collect in-focus and out-of-focus images. The images can be used in conjunction with phase retrieval algorithms to estimate the wavefront and low-order aberrations of the system being aligned. Since alignment errors introduce low-order aberrations, the emphasis is on low-order aberrations, to guide and ultimately qualify an optical system. A description of the instrument and initial results are reported.

10377-13, Session 3

Review of Zernike polynomials and their use in describing the impact of misalignment in optical systems *(Invited Paper)*

Jim Schwiegerling, College of Optical Sciences, The Univ. of Arizona (United States)

Zernike polynomials provide a generalized framework for analyzing the aberrations of non-rotationally symmetric optical systems with circular pupils. Even when systems are designed to be rotationally symmetric, fabrication and alignment errors will lead to non-rotationally symmetric aberrations. The properties of the Zernike polynomials are reviewed to illustrate their properties. Different indexing and ordering schemes are compared to demonstrate some of the potential pitfalls and limitations of using these functions. An example system with common misalignments such as tilt and decenter is analyzed to illustrate the changes in Zernike terms and how this information can provide feedback to the alignment process.

10377-25, Session 3

Ground to on-orbit alignment study of the WFIRST and resulting architecture changes in the telescope architecture

John G. Hagopian, Lambda Consulting (United States); Lisa Bartusek, NASA Goddard Space Flight Ctr. (United States); Thomas M. Casey, Sigma Space Corp. (United States); David A. Content, NASA Goddard Space Flight Ctr. (United States); Guangjun Gao, Sigma Space Corp. (United States); Alden S. Jurling, Catherine T. Marx, Bert A. Pasquale, Qian Gong, NASA Goddard Space Flight Ctr. (United States); Arthur L. Whipple, Conceptual Analytics, LLC (United States)

The Wide-Field Infrared Survey Telescope (WFIRST) mission is the top-ranked large space mission in the New Worlds, New Horizon (NWNH) Decadal Survey of Astronomy and Astrophysics. WFIRST will settle essential questions in both exoplanet and dark energy research and will advance topics ranging from galaxy evolution to the study of objects within the galaxy. The WFIRST mission uses a repurposed 2.4-m forward optical telescope assembly (FOA), which, when completed with new aft optics will be an optical telescope assembly (OTA). WFIRST is equipped with a Wide Field Instrument (WFI) and a Coronagraph Instrument (CGI). An Instrument Carrier (IC) meters these payload elements together and to the spacecraft bus (S/C). A distributed ground system receives the data, uploads commands and software updates, and processes the data.

A significant change to the OTA includes moving the tertiary mirror from the instrument package to a more conventional three-mirror anastigmat (TMA) telescope design that provides a wide 0.28-sq° instrumented field of view to the Wide Field Instrument (WFI). In addition, separate relays from the primary and secondary mirror feed the Wide Field Instrument (WFI) and CoronaGraph Instrument (CGI). During commissioning the telescope is aligned using wavefront sensing with the WFI. A parametric and Monte-Carlo analysis was performed, which determined that alignment compensation with the secondary mirror alone degraded performance in the other instruments. This led to the addition of a second compensator in the WFI optical train to alleviate this concern. This paper discusses the

trades and analyses that were performed and resulting changes to the WFIRST telescope architecture.

10377-16, Session 4

Simultaneous angular alignment of segment mirrors using sinusoidal pattern analysis

Heejoo Choi, Isaac Trumper, Dae Wook Kim, College of Optical Sciences, The Univ. of Arizona (United States)

We present a simultaneous angular alignment method for segmented mirrors, which are often utilized for advanced telescopes to achieve a large combined optical surface. Tip and tilt angles of the mirrors are measured with less than 10 ?rad resolution by monitoring the reflection of a displayed sinusoidal pattern off the mirrors under test. Because a single instrument concurrently covers multiple mirrors, all measured angles are with respect to a common origin, which enables precise angular control of each mirror.

10377-17, Session 4

Alignment and testing of the James Webb Space Telescope observatory vibration fixture and handling and integration fixture

Kyle McLean, NASA Goddard Space Flight Ctr. (United States); Paul Bagdanove, SGT, Inc. (United States); Joshua A. Berrier, Tech Innovations (United States); Emmanuel Cofie, SGT, Inc. (United States); Tiffany M. Glassman, Northrop Grumman Aerospace Systems (United States); Theodore J. Hadjimichael, Eric L. Johnson, NASA Goddard Space Flight Ctr. (United States); Joshua Levi, Amy Lo, Northrop Grumman Aerospace Systems (United States); Joseph C. McMann, Sierra Lobo, Inc. (United States); Raymond G. Ohl, NASA Goddard Space Flight Ctr. (United States); Dean Osgood, Sierra Lobo, Inc. (United States); James E. Parker, NASA Goddard Space Flight Ctr. (United States); Kevin W. Redman, Vicki Roberts, Sierra Lobo, Inc. (United States); Matthew Stephens, Genesis Engineering Solutions, Inc. (United States); Adam Sutton, Northrop Grumman Aerospace Systems (United States); Gregory W. Wenzel, Sierra Lobo, Inc. (United States); Jerrod L. Young, NASA Goddard Space Flight Ctr. (United States)

NASA's James Webb Space Telescope (JWST) is a 6.6m diameter, segmented, deployable telescope for cryogenic IR space astronomy. The JWST Observatory architecture includes the Primary Mirror Backplane Support Structure (PMBSS) and Integrated Science Instrument Module (ISIM) Electronics Compartment (IEC) which is designed to integrate to the spacecraft bus via six cup/cone interfaces. Prior to integration to the spacecraft bus the JWST observatory must undergo environmental testing, handling, and transportation. Multiple fixtures were developed to support these tasks including the vibration fixture and handling and integration fixture (HIF). This work reports on the development of the nominal alignment of the six interfaces and metrology operations performed for the JWST observatory to safely integrate them for successful environmental testing.

10377-18, Session 4

Metrology for trending alignment of the James Webb Space Telescope before and after ambient environmental testing

Theodore J. Hadjimichael, NASA Goddard Space Flight Ctr. (United States); Joshua A. Berrier, IntellecTechs (United States); Jeffery S. Gum, NASA Goddard Space Flight Ctr. (United States); Joseph E. Hayden, Sigma Space Corp. (United States); Manal Khreishi, Kyle McLean, Raymond G. Ohl, NASA Goddard Space Flight Ctr. (United States); Kevin W. Redman, Sierra Lobo, Inc. (United States); Joseph F. Sullivan, Ball Aerospace & Technologies Corp. (United States); Gregory W. Wenzel, Sierra Lobo, Inc. (United States); Jerrod L. Young, NASA Goddard Space Flight Ctr. (United States)

NASA's James Webb Space Telescope (JWST) is a 6.6m diameter, segmented, deployable telescope for cryogenic IR space astronomy. The JWST Observatory architecture includes the Optical Telescope Element (OTE) and the Integrated Science Instrument Module (ISIM) element which contains four science instruments (SIs). Prior to integration with the spacecraft, the JWST optical assembly is put through rigorous launch condition environmental testing. This work reports on the metrology operations conducted to determine any changes in subassembly alignment, including primary mirror segments with respect to each other, the secondary mirror to its support structure, the tertiary mirror assembly to the backplane of the telescope and ultimately to the Integrated Science Instrument Module (ISIM).

10377-19, Session 4

Assembly, alignment, and test of the Transiting Exoplanet Survey Satellite (TESS) flight optical assemblies

Gregory Balonek, Michael P. Chrisp, Kristin E. Clark, Christian D. Chesbrough, James E. Andre, Joshua J. Brown, Benjamin C. Richards, Michael Dalpiaz, Joseph Lennon, MIT Lincoln Lab. (United States)

The Transiting Exoplanet Survey Satellite (TESS) will carry four visible waveband, seven-element, refractive F/1.4 lenses, each with a 34 degree diagonal field of view. This paper describes the methods used for the assembly, alignment and test of the four flight optical assemblies. Prior to commencing the build of the four flight optical assemblies, a Risk Reduction Unit (RRU) was successfully assembled and tested. The lessons learned from the RRU were applied to the build of the flight assemblies. The main modifications to the flight assemblies include the inking of lens element number three for stray light mitigation, tighter alignment tolerances and making use of diamond turning for critical surfaces. Each one of the optical assemblies was tested interferometrically and measured with a non-contact profilometer to predict the optimal shim between the lens assembly and detector before -75C environmental testing. In addition to individual test data, environmental test results from prior assemblies allows for the exploration of marginal differences between each of the optical assemblies.

10377-20, Session 4

High-precision laser microcutting and laser microdrilling using diffractive beam-splitting and high-precision flexible beam alignment

Frank Zibner, Fraunhofer-Institut für Lasertechnik (Germany); Jens Holtkamp, Pulsar Photonics GmbH (Germany); Clemens Hönninger, Amplitude Systèmes (France); Arnold Gillner, Fraunhofer-Institut für Lasertechnik (Germany)

High-precision laser micro machining gains more importance in industrial applications every month. Optical systems like the helical optic offer highest quality together with controllable and adjustable drilling geometry, such as taper angle, aspect ratio and heat effected zone. The helical optic is based on a rotating Dove-prism which is mounted in a hollow shaft engine together with other optical elements like wedge prisms and plane plates. Although the achieved quality can be interpreted as extremely high the low process efficiency is a main reason that this manufacturing technology has only limited demand within the industry. The objective of the research studies presented in this paper is to dramatically increase process efficiency as well as process flexibility. Multi beam processing is used to parallelize the fabrication of periodic structures as most application only require a partial amount of the emitted ultra-short pulsed laser power. In order to achieve highest flexibility using multi beam processing the single beams are diverted and re-guided in a way that enables the option to process on different probes or semimanufactures with each single beam. Experiments are carried out using high power ultra-short pulsed laser sources such as a Trumpf TruMicro 5270 and a modified Amphos 400 system with an output power of almost 700W and a pulse duration of 2ps.

10377-21, Session PMon

Calculation of lens alignment errors using the ray transfer matrices for the lens assembly system with an autocollimator and a rotation stage

Jiyoung Chu, Sungwhi Cho, Won Don Joo, Sangdon Jang, SAMSUNG Electronics Co., Ltd. (Korea, Republic of)

One of the most popular methods for high precision lens assembly of an optical system is to use an autocollimator and a rotation stage. Some companies provide software calculating lens states along with their lens assembly systems, but calculation algorithms are unknown. In this paper, we suggest a calculation method for lens alignment errors using the ray transfer matrices. Alignment errors like decenter and tilt of a lens element can be calculated from tilts of front and back surfaces of the lens. Tilt of each surface can be obtained from a position of the reticle image on a CCD camera of the autocollimator. Rays from a reticle of the autocollimator are reflected from the target surface of the lens rotating with the rotation stage along an optical axis and imaged on the CCD camera. To get the clear image, a distance between the autocollimator and the first lens surface should be adjusted according to a focusing lens of the autocollimator and lens surfaces of the first to the target surface. Ray propagations for the autocollimator and the lens surfaces with tilts can be expressed effectively by using ray transfer matrices, so that lens alignment errors can be derived from them. This method is compared with Zemax simulation for various lenses with spherical or flat surfaces and its error is less than a few percent.

10377-22, Session PMon

Self-compensation for trefoil aberration of symmetric dioptric microlithographic lens

Wei-Jei Peng, Cheng-Fang Ho, Wei-Yao Hsu, Instrument Technology Research Ctr. (Taiwan)

The i-line microlithographic lens with unity magnification can be applied for the 3D integrated circuit steppers. The configuration of the microlithographic lens can be divided into three types: the dioptric type, the catoptric type, and both the catoptric and dioptric type mixed together. The dioptric type with unity magnification is typically designed as symmetry on both image and object sides to counterbalance aberrations on each side of the pupil effectively. The lens mounting is very critical for the diffraction-limit microlithographic lens because the mounting stress degrades image quality seriously. The three-point mounting is a semi-kinematic mounting without over constrain to decrease surface deformation obviously instead of the ring mounting, however, the disadvantage is significant trefoil aberration of the large-aperture lens due to gravity. The kinematic mounting is a method to make the surface deformation almost zero, but it's complicated and too expensive for the i-line microlithographic lens. Clocking of lens is a practical method of compensating the surface figure error for optimum wavefront error during pre-assembly phase, and then the yield rate of post-assembly for fine alignment increases. The three-point mounting of two pairs of symmetric lenses on both sides which crosses 60 degree is beneficial to compensate the trefoil aberration effectively, and it is a cost-effective method to approach the wavefront error close to the design nominal. In this study, the compensation method for the trefoil of the large-aperture lens employed in the symmetric dioptric microlithographic lens is verified in simulation.

10377-23, Session PMon

Research methodologies and justification of technical means of determining the accuracy characteristics of alignment control optical-electronic system

Maksim A. Kleshchenok, Valery V. Korotaev, Ivan S. Nekrylov, ITMO Univ. (Russian Federation)

Reconciliation of alignment - one of the most complex and demanding operations carried out during the maintenance of turbine unit and other mechanisms. Alignment largely determines the duration and complexity of major repairs. On the quality of these works depends largely on the duration of start-up, as well as the reliability and efficiency of turbine repaired.

Misalignment of shafts in a machine can cause following negative effects:

1) Emergence of moment causes generation forces reaction in the bearings of the machine

2) Overload of bearing shafts which leads to increase of distortions by 20% reduces bearing life estimated by 50%

3) Wear of seals, which in turn increases bearing damage risk due to penetration of dirt and grease leakage

4) Overload and vibration, those cause damage of couplings (overheating, weakened or broken bolts) and shafts

5) Power consumption engine may rise up to 20%, as a result of machine shafts warps.

For proper work of complex technological equipment its components need to be spatially positioned relative to assembly axis with high accuracy. As a result, the problem of contactless control of the position of objects relative to the extended linear base is relevant in many areas of technology. The task of object positioning is offer performed by means of optical – electronic measuring systems (OEMS), because of its high accuracy, remoteness and high level of automatization. OEMS determine the offset of basic parts of cylinders relative to the stage of turbine rotor axis with accuracy of 0.05 mm in the vertical and horizontal planes. The axis of the engine defined in the base bores (BB) during the measurement. OEMS allows recalculating

measurements relative to its own sighting line (SL) to given rotor axis, whereby there is no need "align" SL at predetermined coordinates, which is significantly automated of the measurement process.

In OEMS task of spatial positioning is implemented using the autoreflection and autocollimation techniques convergent beams, which allows for highly accurate measurement of linear offsets without determining the distance to the controlling element and provide power to the test object.

In this paper, we consider the influence of various factors and the noise on the invariant transformation of measurement information in autoreflection alignment control schemes. Theoretical and experimental research carried out for basic errors on bidiods and biprizms schemes.It is shown that the main influencing factors are non-linear transformations in optical systems and the impact of air path. Experimental studies were carried out on the basis of two opto-electronic control systems alignment, in which the control element is in the form of one or two corner-cube prisms.

10377-24, Session PMon

Raman laser spectrometer optical head: qualification model assembly and integration verification

Gonzalo Ramos Zapata, Miguel Sanz-Palomino, Andoni Moral Inza, Carlos Pérez, Tomás Belenguer-Dávila, Maria del Rosario Canchal, INTA Instituto Nacional de Técnica Aeroespacial (Spain); Jose Antonio Rodriguez Prieto, Amaia Santiago, Cecilia Gordillo, Ingeniería de Sistemas para la Defensa de España (Spain); David Escribano, INTA Instituto Nacional de Técnica Aeroespacial (Spain); Guillermo López-Reyes, Fernando Rull, Univ. de Valladolid (Spain)

Raman Laser Spectrometer (RLS) is the Pasteur Payload instrument of the ExoMars mission, within the ESA's Aurora Exploration Programme, that will perform for the first time in an out planetary mission Raman spectroscopy. RLS is composed by SPU (Spectrometer Unit), iOH (Internal Optical Head), and ICEU (Instrument Control and Excitation Unit). iOH focuses the excitation laser on the samples (excitation path), and collects the Raman emission from the sample (collection path, composed on collimation system and filtering system). Its original design presented a high laser trace reaching to the detector, and although a certain level of laser trace was required for calibration purposes, the high level degrades the Signal to Noise Ratio confounding some Raman peaks. So, after the bread board campaign, some light design modifications were implemented in order to fix the desired amount of laser trace, and after the fabrication and the commitment of the commercial elements, the assembly and integration verification process was carried out.

A brief description of the iOH design update for the qualification model (iOH EQM) as well as the assembly process are briefly described in this papers. In addition, the integration verification and the first functional tests, carried out with the RLS calibration target (CT), results are reported on.

Conference 10378: Sixteenth International Conference on Solid State Lighting and LED-based Illumination Systems

Tuesday - Wednesday 8 –9 August 2017

Part of Proceedings of SPIE Vol. 10378 Sixteenth International Conference on Solid State Lighting and LED-based Illumination Systems

10378-1, Session 1

Efficiency droop mitigation progress in blue and green III-nitride LEDs *(Invited Paper)*

Hee Jin Kim, Robert Armitage, Tsutomu Ishikawa, Isaac Wildeson, Parijat Deb, Lumileds, LLC (United States); Andrew M. Armstrong, Sandia National Labs. (United States); Zhibo Zhao, Akshay Singh, Silvija Gradecak, Massachusetts Institute of Technology (United States); Eric A. Stach, Brookhaven National Lab. (United States)

No Abstract Available

10378-2, Session 1

Challenges and new developments for conversion in solid state lighting *(Invited Paper)*

David O'Brien, JeKaterina Jurkova, Rainer Butendeich, Marcus Adam, Robert Schulz, Benjamin Gruber, Ralph Bertram, OSRAM Opto Semiconductors GmbH (Germany); Maria J. Anc, OSRAM SYLVANIA Inc. (United States); Britta Göötz, OSRAM Opto Semiconductors GmbH (Germany)

The careful control of LED spectral output is critical for a broad range of LED application areas. Optical down converters are the key technology in defining this spectral response and a number of recent advances in narrow band phosphors and quantum dot converters have the potential to improve existing applications as well as enabling new ones. Ultra-narrower spectral widths and finely tunable peak wavelengths have the potential to significantly improve current LED performance. Particularly in the area of solid state lighting these technologies have the potential to yield higher color rendering as well as higher overall efficiency.

10378-4, Session 1

Cryogenic characterization of LEDs for space application

Jerome Carron, Ctr. National d'Études Spatiales (France); Anne Philippon, Institut d'Astrophysique Spatiale (France); Lip Sun How, Audrey Delbergue, David Cillierre, AdvEOTec (France); Sahar Hassanzadeh, Institut d'Astrophysique Spatiale (France); Mathieu Boutillier, Pascale Danto, Ctr. National d'Études Spatiales (France)

In the frame of EUCLID project, the Calibration Unit of the VIS (VISible Imager) instrument must provide an accurate and well characterized light source for in-flight instrument calibration without noise when it is switched off. The Calibration Unit consists of a set of LEDs emitting at various wavelengths in the visible towards an integrating sphere. The sphere's output provides a uniform illumination over the entire focal plane. Some results about the radiation effects on LED properties are available in the litterature [1], but Light Emitting Diodes (LEDs) are not yet Space qualified at present. Therefore, a mission oriented full screening, qualification and EMC tests of some potential candidates Commercial Off The Shelf (COTS) LEDs has been carried out.

The calibration Unit will work at cryogenic temperature (136 K) for 6.25 years and uses a total of six different wavelengths. A total of 9 reference LEDs, coming from three different manufacturers (EPIGAP, EPITEX and OPTRANS), were selected, screened and submitted to a custom qualification plan in order to cover the needs of the mission.

The screening sequence includes thermal cycles between 323K and 136K under vacuum and Burn-in under atmospheric pressure. Based on screening results, a statistical method has been used to classify the LEDs into three subgroups per reference: Flight Models (25), Qualification Models (46) and Spares.

The qualification tests aimed to fulfill all the mission requirements : . The endurance subgroupat hot and cold temperatures simulated the thermal stress situations to which components will be subjected and took into account the number of LED ON/OFF operations. The environmental subgroup tested LEDs hardness versus on-ground and in-flight environments. Radiation subgroup using proton radiations has been performed at cryogenic temperatures. . Mechanical subgroup (destructive testing) aimed to construction defects, solderability and Electrostatic Discharge (ESD) sensitivity.

All the electrical and optical parameters of the LED have been monitored and recorded at ambient and cryogenic temperatures. These results have been compiled in order to show the total deviation of the LED electrical and electro-optical properties in the whole mission and to select the best suitable LED references for the mission.

The results of this complete qualification demonstrate the good reliability of most of the tested LEDs to withstand space environment and extreme conditions.

Then 6 wavelengths were selected and submitted to an EMC sensitivity test at room and cold temperature by counting the number of photons when LEDs drivers are OFF. Characterizations were conducted in the full frequency spectrum in order to implement solutions at system level to suppress the emission of photons when the LED drivers are OFF. LEDs impedance was also characterized at room temperature and cold temperature and no major difference has been detected.

10378-5, Session 1

Analysis of spectral power distributions for multi-channel platforms in a patient room application

James J. Kim, Tony Esposito, Patricia Rizzo, Dorene Maniccia, Philips Research Americas (United States)

A prototype innovative lighting system for a patient room application that integrates multi-channel luminaire platforms into indoor general area luminaires has been demonstrated. This system has spectrally tunable capabilities, and satisfies the visual and nonvisual needs of occupant, while providing an energy-efficient solution. We evaluated the performance of two different multichannel platforms in different luminaire types using a unique color processing algorithm. The LED modeling and simulations enabled optimization of spectral power distributions, color, light output, and efficacy. This paper discusses the complicated results of SPDs developed for the patient room application, especially how they are effective for positively impacting the visual and human circadian systems.

10378-35, Session 1

Opportunities and challenges for 3D printing of solid-state lighting systems *(Invited Paper)*

Nadarajah Narendran, Indika U. Perera, Xi Mou, Dinusha R. Thotagamuwa, Rensselaer Polytechnic Institute (United States)

Low energy use and reduced maintenance have made the light-emitting diode (LED), a solid-state light (SSL) source, the preferred technology for many lighting applications. With the explosion of LED products in the marketplace and subsequent price erosion, market transformation is expected to move quickly in the next few years. Manufacturers, therefore, are looking for lower cost materials and manufacturing methods to keep up with low price requirements. 3-D printing, also known as additive manufacturing, could be a potential solution to this need. During the past few years manufacturers in the automotive, aerospace, and medical industries have embraced 3-D printing for manufacturing parts and systems for their applications. This revolution could also pave the way for the lighting industry to step into the 3-D printing era for the production of lower cost, custom lighting systems that can be printed on-site to achieve on-time and on-demand manufacturing. One unique aspect of LED fixture manufacturing is that it requires thermo-mechanical, electrical, and optical components. This presentation will cover the current status of affordable 3-D printers capable of making mechanical, electrical, and optical components for the creation of lighting fixtures. Examples of printed components explored in our laboratory and their performance will be shown. Finally, this presentation will include a discussion of the improvements needed in the printer and materials technologies to enable 3-D printing to become a mainstream manufacturing tool for SSL fixtures.

10378-6, Session 2

A comparison of color fidelity metrics for light sources using simulation of color samples under lighting conditions *(Invited Paper)*

Hyeokjun Kwon, Yoojin Kang, Junwoo Jang, LG Display (Korea, Republic of)

Color fidelity has been used as one of indices to evaluate the performance of light sources. Since the Color Rendering Index (CRI) was proposed at the CIE, many color fidelity metrics have been proposed to increase the accuracy of the color fidelity. This paper focuses on a comparison of the color fidelity metrics in an aspect of accuracy with human visual assessments. To visually evaluate the color fidelity of light sources, we made a simulator that can make the color samples under lighting conditions. In this paper, eighteen color samples of the Macbeth color checker under test light sources and reference illuminants for each of them are simulated and displayed on monitor. With only a spectrum set of the test light source and reference illuminant, color samples under any lighting condition can be simulated. In this paper, the spectrums of the two LED and two OLED light sources that have similar values of CRI are used for the visual assessment. In addition, the results of the visual assessment are compared with the two color fidelity metrics that include the CRI and IES TM-30 (Rf), proposed by the Illuminating Engineering Society (IES) in 2015. Experimental results indicate that Rf is outperform CRI in terms of correlation with visual assessment.

10378-7, Session 2

Comparison of methods for measurement of HP-LEDs based on the junction temperature *(Invited Paper)*

Yuqin Zong, Noe V. Medina, National Institute of Standards and Technology (United States)

High power LEDs (HP-LEDs) are key building blocks of solid-state lighting products, therefore, it is important for LED manufacturers, lamp/luminaire manufactures, and testing/calibration laboratories to measure their optical and electrical properties with high accuracy. Measuring HP-LEDs has been difficult because they are highly sensitive to their junction temperatures, which rise rapidly when they are turned on. Various methods have been proposed and used to measure HP-LEDs, but most of them are only useful for particular applications and unable to produce accurate and reproducible measurement results. To address the measurement need, the Illuminating Engineering Society (IES) recently approved three methods that can be used for the measurement of HP-LEDs, which are the DC method, single-pulse method, and continuous-pulse method [1]. All three measurement methods refer to the junction temperature of an HP-LED as the thermal condition and thus, the measured results are considered to be equivalent as long as the junction temperature is set to be the same. However, our recent study shows that the difference in the measurement results of the three different methods can be significant (e.g., 5 % in total luminous flux) due to significant heating of the junction and/or phosphor material of the HP-LED during the period of a measurement. In this paper, we will describe the measurement of HP-LEDs using the three different methods, compare the measurement results, and discuss the cause that results in the significant difference.

[1] Illuminating Engineering Society, "IES LM-85-14: Approved Method: Electrical and Photometric Measurements of High-Power LEDs." (2014)

10378-9, Session 2

Low-NEP pyroelectric detector for calibration of UV and IR sources and detectors

George P. Eppeldauer, Vyacheslav B. Podobedov, Leonard M. Hanssen, Catherine C. Cooksey, National Institute of Standards and Technology (United States)

Pyroelectric radiometers with spectrally constant response have been developed in the last few years at NIST with the cooperation of several detector manufacturers. The new devices have noise-equivalent-power (NEP) values less than 1 nW/Hz^1/2 sufficiently low for use at the output of regular monochromators. Their response flatness is an order of magnitude better than that of filtered detectors and can be used to extend the reference responsivity scales of silicon-trap-detectors to both the UV and IR wavelength ranges. For the first time, the irradiance responsivity of a pyroelectric detector has been determined. Based on spectral reflectance measurements of the black coating of the pyroelectric detector, the relative spectral response was determined between 0.25 and 30 micrometers. This relative function was then converted into absolute spectral responsivity using absolute tie points from a silicon-trap-detector in the VIS range. Similarly, the flat response between 1.6 and 2.5 micrometers can also be utilized and a close to constant irradiance responsivity can be realized. This irradiance responsivity will be used as a reference scale for the NIST SIRCUS facility where tunable laser sources are used for the spectral responsivity calibration of detectors, instead of using a monochromator. The spectral power responsivity of the pyroelectric detector is the internal standard of the NIST VIS-IR detector calibration facility for the 0.6 to 24 micrometers wavelength range. The pyroelectric standard can be used to calibrate other types of detectors for spectral power responsivity using detector substitution. The flat pyroelectric standard calibrated for the spectral irradiance responsivity, was used to calibrate other irradiance measuring detectors and also to measure the broadband (integrated) irradiance from UV and blue LEDs without using any source standard. All the pyroelectric

detector based calibrations described here were performed in AC measurement mode with expanded uncertainties of about 2 % (k=2).

10378-10, Session 3

Ultra-high power semiconductor devices: heat-sinking using GaN-on-diamond *(Invited Paper)*

Martin Kuball, Univ of Bristol (United Kingdom)

GaN devices when operated at high powers are limited by excessive temperature rise in the device critical regions. Traditionally SiC, Si or sapphire substrates or homoepitaxy on GaN substrates is used, however the substrate thermal conductivity is rather limited. We review the use of diamond substrates with their ultra-high thermal conductivity for GaN devices, and the opportunities (and challenges) this offers.

10378-11, Session 3

Growth and characterization of GaN/InN/GaN heterostructures on GaN substrate templates using migration-enhanced, plasma-assisted MOCVD

Daniel Seidlitz, Brendan Cross, Viktoriia E. Babicheva, Yohannes Abate, Georgia State Univ. (United States); Axel Hoffmann, Technische Univ. München (Germany); Nikolaus Dietz, Georgia State Univ. (United States)

This contribution will present the structural and optoelectronic properties of GaN/InN heterostructures grown by Migration Enhanced Plasma-assisted Metal Organic Chemical Vapor Deposition (MEPA-MOCVD) on GaN/sapphire templates.

In comparison to conventional MOCVD, MEPA-MOCVD utilizes as nitrogen precursor plasma-activated nitrogen species (N*/NH*/NHx*) in the after-glow regime above the growth surface. The plasma-activated nitrogen species can generated by a hollow cathode plasma source (13.56 MHz, 50 – 600 W) at lower temperatures compared to the ammonia decomposition. The kinetic energies of the excited species stabilize the growth surface and reduce the partial pressure difference between InN and GaN binaries, enabling to potential stabilization of both binaries in the same temperature regime. Tailoring the kinetic energies and plasma activated nitrogen species are specific processing parameter, in addition to nitrogen flux through the plasma source, MO flows, and reactor pressure explored.

We will present characterization results (using Atomic Force Microscopy (AFM) and Raman) and optoelectronic (Fourier Transform Infrared - FTIR) studies on the formation of InN/GaN and GaN/InN/GaN heterostructures and interfaces by deposition of a thin InN/InGaN quantum well (QW) and GaN/InN/GaN layers in the same temperature range. High-resolution s-SNIN (scattering type scanning near-field infrared nanoscopy) studies will be presented on spontaneous polarization induced charge accumulations in GaN/InN/GaN interfaces as function of process parameters.

The influence of growth parameters such as growth temperature, plasma power, reactor pressure and pulsed supply of Metalorganic (MO) and plasma activated nitrogen precursors are examined by AFM, Raman and FTIR spectroscopy. A correlated analysis of the macro/microscopic/nanoscopic investigations on the structural properties, crystal quality, surface morphology, film thickness, and optoelectronic characteristics (free carrier concentration and high-frequency dielectric function) will be presented.

10378-12, Session 3

High-resolution spectroscopy and imaging of interfacial strain fields in InN/GaN and GaN/InN/GaN heterostructures

Yohannes Abate, Alireza Fali, Viktoriia E. Babicheva, Nikolaus Dietz, Georgia State Univ. (United States)

We investigate nanoscale interfacial properties of GaN/InN heterostructures grown on GaN/sapphire templates, using Migration Enhanced Plasma-assisted Metal Organic Chemical Vapor Deposition (MEPA-MOCVD). High-resolution s-SNIN (scattering type scanning near-field infrared nanoscopy) studies are utilized to study spontaneous polarization induced charge accumulations at GaN/InN/GaN interfaces. s-SNIN optical and infrared spectroscopic images are correlated with the process parameters and optimum values for maximum local charge accumulation are reported. An advanced theoretical model that uses realistic growth and imaging parameters is developed to guide the experimental results and interpret results.

10378-13, Session 3

Growth and characterization of GaN/GaAlN heterostructures on GaN substrate templates

Lance Hubbard, Pacific Northwest National Lab. (United States); Viktorriia E. Babicheva, Yohannes Abate, Georgia State Univ. (United States); Vincent T. Woods, Pacific Northwest National Lab. (United States); Nikolaus Dietz, Georgia State Univ. (United States)

This contribution will present the structural and optoelectronic properties of GaN/GaAlN heterostructures grown by Metal Organic Chemical Vapor Deposition (MOCVD) on GaN/sapphire templates. The target parameters for the materials heterostructures have been modeled for utilization in Avalanche Photodiode Detector Structures (APD) operating in the near UV region. Optical modeling has improved absorption within the heterojunction as well as maximized light trapping within the device. Electronic modeling has determined the optimal dopant concentrations for maximum impact ionization rate, as well as tolerance to defects and unintentional doping. This application will require advances in the defect densities, surface morphology, and interfaces. Surface morphological and structural properties of the GaN/GaAlN heterostructures are analyzed by Atomic Force Microscopy (AFM), Raman spectroscopy. The optoelectronic properties (phonon structures, free carrier concentrations, and carrier mobility) as well as layer thickness information, are determined by Fourier Transform Infrared Reflectance (FTIR) spectroscopy. High-resolution s-SNIN (scattering-type scanning near-field infrared nanoscopy) studies are utilized to study spontaneous polarization induced charge accumulations at GaN/GaAlN/GaN interfaces and how these impact the point- and extended defect formation and their evolution with layer thickness. A correlation of such interfacial defects (type and concentration) with microscopic/nanoscopic structural properties, surface morphology, and optoelectronic properties (free carrier concentration and high-frequency dielectric function) is attempted

10378-14, Session 3

The optical properties of phosphor converted white LED with adding Zirconium dioxide particles *(Invited Paper)*

Quang-Khoi Nguyen, Yu-Yu Chang, National Central Univ. (Taiwan); Benoit Glorieux, Institut de Chimie de la Matière Condensée de Bordeaux (France); Tsung-Hsun Yang, Ching-Cherng Sun, Chien-Hung Hsu, National Central Univ. (Taiwan)

Return to Contents

We performed the simulation and experiment to investigate the influence of Zirconium dioxide (Zirconia, ZrO_2) particles on the optical properties of phosphor converted white LED (pcW-LED). An efficient optical model was developed and applied to the incorporation diffuse particle of ZrO_2 into a hemisphere package containing YAG phosphors. The optical properties (chromaticity, packaging efficiency) were estimated as a function of phosphor and ZrO_2 particles, through the calculation of effective radius, refractive index, and absorption and conversion efficiency, in a range of correlated color temperature 4500 K to 6500 K. In the same way, the amount of phosphor and ZrO_2 can be calculated accurately to obtain a targeted optical property in a hemisphere LED design. Especially, the angular distribution of CCT was also diminished, and even almost inexistent for low CCT design. In addition, the adding of ZrO_2 particles allows clearly decreasing the amount of phosphor for an identical target CCT. It is really suitable in the context of decreasing the amount of phosphor or in some applications where the color uniformity is an important parameter, like indoor down-lighting.

10378-15, Session 3

Spectra control of RE doped calcium silicate through topochemical reduction strategy for white LED application

Jingshan Hou, Yongzheng Fang, Shanghai Institute of Technology (China)

In this work, europium-doped calcium silicate (abbreviated as C2S:Eu) was prepared by a topochemical reduction strategy with aluminum as a solid-state reducing agent at the calcination temperature from 300°C to 1000°C. The emission intensity ratio of Eu^{2+}/Eu^{3+} started to increase at 400°C, indicating the occurrence of the reduction of Eu^{3+}. Such prepared samples showed stronger emission intensity from Eu^{2+} centers than the ones prepared by traditional CO reduction. Especially, the Al-reduced C2S:Eu^{2+} calcinated at 1000°C exhibited PL intensity as 300% high as the CO-reduced C2S:Eu^{2+} prepared at the same temperature. This phenomenon is further explained from the standpoint of the different reduction reaction kinetics of solid state Al and vapor phase CO at the same temperature. This result suggested that this strategy can be used as an effective tool for the spectra control of the rare earth doped luminescent systems, thus opening up new avenues to develop novel optical materials for the white light emitting diodes applications.

10378-16, Session 3

Strong coupling between ordered Ag nanosphere and a-SiNx:O induced highly efficient blue LED

Zhongyuan Ma, Nanjing Univ. (China)

Developing a highly efficient blue light emission source has long been a major focus of Si-based optoelectronic integration as a sustainable solution of IC industry. In recent years, localized surface plasmon resonance (LSPR) from metal nanostructures has attracted great interest due to its unique application in increasing the luminescence efficiency of silicon light source. The energy match between LSPs from metal NPs and excitons in luminescent material is the key factor to achieve the enhancement of spontaneous radiations. As the wavelength of LSPR is highly dependent on the size and shape of metal nanostructures, a nanofabrication technique to produce metal nanostructures with controllable size and shape is vital important.

In this work we demonstrate ordered and controllable Ag nanosphere arrays with higher surface coverage in large region can be realized by laser annealing combined with self-assembled process of nanosphere lithography. Sharply enhancement of blue electroluminescence intensity can be obtained through strong coupling with the excitons of a-SiNx:O by tuning the size of Ag nanosphere from 170 to 300 nm. Finite-difference time-domain solution (FDTD) calculation confirms that the quadrupolar mode of the plasmon for Ag-sphere arrays play the dominant role in the coupling of Ag-sphere arrays with a-SiNx:O films. The successful fabrication of the Ag nanosphere arrays ensures the strongly localized character of quadrupolar mode, which prominently enhances the blue emission from a-SiNx:O via the effective energy coupling between the LSPs and the excitons. Our method supplies a new way for a-SiNx:O as a highly efficient blue LED in the future.

10378-17, Session 4

Next generation III-nitride materials and devices: From photonics to new applications *(Invited Paper)*

Nelson Tansu, Lehigh Univ. (United States)

No Abstract Available

10378-18, Session 4

Improving the thermal stability of $K_2SiF_6:Mn^{4+}$ red phosphor using atomic layer deposition in a fluidized bed reactor

Otmar M. Ten Kate, Technische Univ. Delft (Netherlands); Y. Zhao, Technische Univ. Delft (Netherlands) and Xiamen Univ. (China); H. T. Hintzen, J. R. van Ommen, Technische Univ. Delft (Netherlands)

In recent years, the Mn^{4+} doped K_2SiF_6 (KSF) phosphor has gained a lot of attention due to its efficient and narrow red line emission after blue light excitation, which makes it a very promising phosphor for phosphor converted white light emitting diodes (pc-wLEDs).[1,2] In pc-wLEDs a blue LED chip is combined with red and green-emitting phosphors to obtain warm-white light. However, the KSF:Mn^{4+} phosphor suffers from thermal degradation as a result of oxidation, severely limiting its lifetime and applicability. Recently, we demonstrated that YAG:Ce^{3+} phosphor particles can be protected against thermal degradation, by coating them with a thin Al_2O_3 layer using atomic layer deposition in a fluidized bed reactor (ALD-FBR).[3] ALD-FBR is a technique to deposit thin (several nm) closed layers on powder particles in a controlled way via sequential deposition of the reactants. Here we will report on the deposition of Al_2O_3 on KSF:Mn^{4+} phosphor particles using ALD-FBR with trimethylaluminium (TMA) and ozone as reactants. We will discuss the influence of water on the fluidization of KSF powders and its role in the deposition processes. In addition, the influence of thickness of the Al_2O_3 coating on the optical properties and thermal stability of the KSF:Mn^{4+} phosphor will be discussed.

[1] H. Zhu et al.; Nature Commun. 5 (2014) 4312.

[2] J.W. Moon et al.; Opt. Mater. Expr. 782 (2016) 782.

[3] Z. Zhou et al.; RSC Adv. 6 (2016) 76454.

10378-19, Session 4

New phosphors Eu^{2+} and Ce^{3+} doped $Sr_{4-x}(Si,Al)_{19+x}(N,O)_{29+x}$ for white LED applications

Chunyun Wang, Takashi Takeda, Hokkaido Univ. (Japan) and National Institute for Materials Science (Japan); Shiro Funahashi, Rong-Jun Xie, Naoto Hirosaki, National Institute for Materials Science (Japan)

Light-emitting diodes (LEDs) have been steadily consolidating their share in the lighting and display market. Phosphor-converted (pc) white LED becomes the preferred way to generate white light especially for general lighting, as it is much cheaper and simpler than RGB system. Phosphors are essential to high color quality and luminous efficacy. However, the number of commercially available phosphors is very limited. Therefore, developing

new phosphors suitable for various white LED applications is very important.

Recently, our group developed the single-particle-diagnosis approach [1-2] to discover new phosphors, with which a tiny luminescent microcrystalline particle down to 5-10 ?m can be selected from powder mixtures. In this work, we report a new green emitting Sr-sialon:Eu phosphor discovered by this approach. The crystal structure was solved and refined from single crystal X-ray diffraction data. Sr-sialon:Eu crystallizes in the trigonal space group P3m1 (no. 156) with a = b = 12.1054 Å, c = 4.8805 Å and Z = 1, and consists of a network of corner sharing (Si,Al)(N,O)4 tetrahedra. Upon doping with Eu2+, the emission band can be tuned from 487 nm to 541 nm with fwhm = 96-124 nm. Ce3+ doped Sr-sialon phosphor shows strong blue emission around 435 nm with a fwhm ≈ 90 nm after 355 nm light excitation. The blue luminescence exhibits a small thermal quenching behavior at high temperature. These performances show that the new Eu2+ and Ce3+ doped Sr-sialon phosphors are promising for white LED applications.

[1] N. Hirosaki, T. Takeda, S. Funahashi and R.-J. Xie, Chemistry of Materials, 2014, 26, 4280-4288.

[2] T. Takeda, N. Hirosaki, S. Funahashi and R.-J. Xie , Materials Discovery, 2015, 1, 29-37.

10378-20, Session 4

Selecting the optimal synthesis parameters of InP/Cd[x]Zn[1-x]Se quantum dots when combined with different broad band phosphors to optimize color rendering and efficiency of a remote phosphor white LED

Jana Ryckaert, António Correia, Kevin Smet, KU Leuven (Belgium); Mickaël D. Tessier, Dorian Dupont, Zeger Hens, Univ. Gent (Belgium); Peter Hanselaer, Youri Meuret, KU Leuven (Belgium)

Combining traditional phosphors with a broad emission spectrum and non-scattering quantum dots with a narrower emission spectrum can have multiple advantages for white LEDs. It allows to reduce the amount of scattering in the color conversion element (CCE), increasing the efficiency of the complete system. Furthermore, the unique possibility to tune the emission spectrum of quantum dots allows to optimize the resulting LED spectrum in order to achieve optimal color rendering properties for the light source. However, finding the optimal quantum dot properties to achieve the desired efficiency and color rendering is a non-trivial task. Instead of simply summing up the emission spectra of the blue LED, phosphor and quantum dots, we propose a complete simulation tool that allows an accurate analysis of the final performance for a continuous range of different quantum dot properties. A model is included that generates the absorption and emission spectrum of the considered InP/Cd[x]Zn[1-x]Se quantum dots as a function of certain quantum dot parameters that can be controlled during the synthesis, namely core size, shell size and cadmium fraction. The recycling of the reflected light from the CCE by the LED package is taken into account, as well as the reabsorption and the associated red-shift. This simulation tool is used to scan through these synthesis parameters and we find the ideal quantum dot for two specific broad band phosphors, in each case providing the optimal efficiency and color rendering for the white LED with a specific pumping LED, phosphor and recycling cavity, with the desired CCT.

10378-21, Session 4

Fabrication of CuInS2/ZnS quantum dots-based white light-emitting diodes with high color rendering index

Chih-Chun Hsiao, Shu-Ru Chung, Yu-Sheng Su, National Formosa Univ. (Taiwan)

Among solid-state lighting technology, phosphor-converted white light-emitting diodes (pc-WLEDs) are excellent candidates to replace incandescent lamps for their merit of high energy conservation, long lifetime, high luminous efficiency as well as polarized emissions. Semiconductor quantum dots (QDs) are emerging color tunable emissive light converters. They have shown significant promise as light emitters, as solar cells, and in biological imaging. It has been demonstrated that the pc-WLED devices integrated with red emissive ZnCdSe QDs show improved color rendering index of device. However, cadmium-based QDs have limited future owing to the well-known toxicity. Recently, non-cadmium luminescence materials, i.e. CuInS2-based QDs, are investigated as desirable low toxic alternatives. Particularly, CuInS2-based QDs exhibit very broad emissions spectra with full width at half maximum (FWHM) of 100-120 nm, large Stokes shifts of 200~300 meV and finely-tunable emissions. In order to adjust emission wavelengths and improved quantum yield (QY), CuInS2/ZnS (CIS/ZnS) core/shell structure was introduced. Therefore, CIS/ZnS QDs have been extensively investigated and be used as colour converter in solid-state lighting. Synthesis and application of CuInS2/ZnS core/shell QDs are conducted using a hot injection route. CIS/ZnS core/shell QDs with molar ratio of Cu:In equal to 1:4 are prepared. For WLED fabrication, the CIS/ZnS QD is dispersed in toluene first, and then it is blended with transparent acrylic-based UV resin. Subsequently, the commercial green-emitting Lu3Al5O12:Ce3+ (LuAG) phosphors are mixed with QD-resin mixture. After that, the QDs-phosphors-resin mixtures are put in the oven at 140 °C for 1 h to evaporate the toluene. Subsequently, the homogeneous QDs-phosphors-resin mixture is dropped on the top of a blue LED chip (InGaN). Then, the device is cured by 400 W UV light to form WLED. The emission wavelength of CIS/ZnS QD exhibits yellow region of 552 nm with QY of 76 %, and with relatively broad bandwidth of 86 nm. The structure of CIS/ZnS belongs to chalcopyrite phase and its average particle size is 3.2 nm. The luminous efficacy, color rendering index (CRI), correlated color temperature (CCT), and CIE chromaticity coordinate of WLED is 47.3 lm/W, 89, 5661 K, and (0.33, 0.29), respectively.

10378-22, Session 5

High lumen density sources based on LED-pumped phosphor rods: opportunities for performance improvement *(Invited Paper)*

Dick K. G. de Boer, Philips Research (Netherlands)

Recently, LED-based sources with high brightness (up to 10^9 lm/(m2 sr) have been developed [1,2,3,4]. These sources can be applied in projection systems, as well as in other applications requiring high brightness. The technology makes use of a transparent phosphor rod that is pumped by a multitude of blue LEDs. Most of the converted light is guided in the rod towards one of its small sides, where it is extracted using suitable extraction optics.

In this paper, the requirements for the optical materials for phosphors and extraction optics will be discussed. Because of the high lumen density inside these materials, special attention should be given to non-linear processes that limit the performance. Possibilities to overcome these limitations will be discussed.

1. D.K.G. de Boer, D. Bruls, H. Jagt, High-brightness source based on luminescent concentration, Optics Express 24 (2016) A1069.

2. C. Hoelen, D.K.G. de Boer, D. Bruls, J. van der Eyden, R. Koole, Y. Li, M. Mirsadeghi, V. Vanbroekhoven, J.-J. Van den Bergh, P. Van de Voorde, LED light engine concept with ultra-high scalable luminance, SPIE 9768 (2016) 9768-63.

3. D.K.G. de Boer, D. Bruls, H. Jagt, C. Hoelen, LED-based projection source based on luminescent concentration, SPIE 9896 (2016) 989606-1.

4. C. Hoelen et al., Progress in light sources with scalable brightness for projection systems, this conference.

10378-23, Session 5

Progress in extremely high brightness LED-based light sources *(Invited Paper)*

Christoph G. A. Hoelen, Philips Lighting B.V. (Netherlands)

Although the maximum brightness of LEDs has been increasing continuously during the past decade, their luminance is still far from what is required for multiple applications that now still rely on the high brightness of discharge lamps. In particular for high luminous flux applications with limited étendue, like in front projection systems, only very modest luminance values in the beam can be achieved with LEDs compared to systems based on discharge lamps or lasers. With dedicated LED architectures, phosphor converted green light emitters for projection may achieve luminance values up to ca 200 Mnit (108 lm/m2sr). In this paper we report on the progress made in the development of light engines based on a light converter rod pumped with blue LEDs. This concept, named ColorSpark High Lumen Density LED technology, has recently been introduced. These sources outperform the étendue and brightness limits of LEDs by multiple factors. In LED front projection systems, green LEDs are the main limiting factor. With our green modules, we now have achieved peak luminance values in excess of 1.5 Gnit, enabling LED-based projection systems with over 3500 ANSI lm. The green light source efficiency has been increased considerably, reaching 45-60 lm/W under application conditions. The module architecture as well as module and system performance characteristics are reviewed, and compared against alternative projection systems. Finally an extension of this concept to yellow light sources is presented, enabling a further breakthrough in the performance of LED-based projection systems and a wide variety of other high brightness applications.

10378-24, Session 5

The impact of the driving frequency on the output flux of high-power InGaAlP-LEDs during high-current pulsed operation

Benjamin Schulz, Stefan Morgott, OSRAM Opto Semiconductors GmbH (Germany)

Direct red light-emitting diodes based on InGaAlP comprise a strong temperature sensitivity regarding their output flux. In Étendue limited applications, like digital projectors, these LEDs are usually driven at current densities exceeding 3 A/mm? in pulsed mode. The losses inside the semiconductor lead to a large amount of heat, which has to be removed most efficiently by a heatsink to keep the junction temperature as low as possible and therefore to obtain the maximum output flux. One important performance parameter is the thermal resistance Rth of the LED, which has been improved during the last few years, e.g. by the development of new high-power chips and packages.

In our present approach, we investigated the influence of the driving frequency – which is closely related to the thermal impedance Zth – on the luminous and the radiant flux of red LEDs. A simulation model based on the electro-thermal analogies was implemented in SPICE and the optical and electrical characteristics of one LED type (OSRAM OSTAR Projection Power LE A P1W) were measured under application-related driving conditions while varying the parameters frequency, duty cycle, forward current, and heatsink temperature.

The experimental results show clearly that the luminous and the radiant flux go up when the driving frequency is increased while the other parameters are maintained. Moreover, it can be noticed that the degree of this effect depends on the other parameters. The largest impact can be observed at the lowest tested duty cycle (30 %) and the highest tested current density (4 A/mm?) and heatsink temperature (80 °C). At this operating point, the luminous and the radiant flux increase by 20 % and 14 % respectively when raising the frequency from 240 Hz to 1920 Hz.

10378-25, Session 5

Opto-thermal design of a white light point source based on high power blue laser diodes

António Correia, Peter Hanselaer, Youri Meuret, KU Leuven (Belgium)

When designing white light systems, using laser diodes allows for an accurate control of the intensity pattern when combined with optical components, but also imposes severe challenges regarding the thermal packaging of colour conversion element (CCE) used for the blue laser diode(s). Accounting for both optical and thermal effects is critical to correctly assess the performance of white light systems based on laser diodes. We propose an opto-thermal design that produces white light with a very small spatial extent, approaching a point source. We optimize this system’s performance with an opto-thermal simulation tool that adjusts its optical and thermal properties and allows estimating the maximum incident optical power that still results in a thermally stable white light system. We show that even when using high power laser diodes to excite a millimetre scale CCE, it is still possible to have a thermally stable white light system.

10378-8, Session PWed

Dome diagnostics system of optical parameters and characteristics of LEDs

Vladimir S. Peretyagin, Nikita A. Pavlenko, ITMO Univ. (Russian Federation)

The intensive development of LED technologies resulted in the creation of new, more efficient and high-power LEDs. Such LEDs are usually used in devices of the street lighting, industrial (decorative and accent) and domestic lighting. It was possible by the rapid increase their energy, spatial (viewing angle of LEDs ranges from 10 to 160 deg), spectral (colorimetric) and electrical characteristics as well as reliability and durability of quasi-monochromatic light sources.

Opportunities of using LEDs in these fields are connected with combination of a powerful LED light with practically any form of its spatial distribution as well as a wide variety of color shades. However, development and production (especially mass production) of LED lighting devices are impossible without a thorough analysis of its parameters and characteristics. So, design methods for developed lighting device, its structure, size and reliability, all of this depends on the results of analysis. The development of equipment for quality analysis of LED (assessment of parameters and characteristics of LEDs proposed by manufacturers) is an important problem for a variety of areas where LEDs are used today.

This work presents a diagnostic system of optical parameters and characteristics of LEDs. The main feature of this system is the presence of 55 RGB photodiodes. These photodiodes from a hemispherical structure (in the hemispherical frame). This structure allows analysis of spatial (angular) and energy parameters and characteristics of LEDs on all upper hemisphere of its radiation. Also the uses of RGB photodiodes will enable measure the color parameters of LEDs radiation. Such device allows us to analyze parameters of LEDs in three-dimensional space and to assess the quality of LED products.

10378-26, Session PWed

Universal fixture design for body mounted LED lights

Debdyut Hajra, B.P. Poddar Institute of Management & Technology (India)

Today LED headlamps, armbands and ankle-bands, shoe-lights etc. have become very popular. These find extensive use in search and rescue operations, mining, carving, etc. and are also used by individuals during

hiking, trekking, running, etc. during dark hours. They serve two main purposes: they provide sufficient illumination in low light conditions and they are used to indicate the presence of a person after dark. These have the same basic requirements. They must produce sufficient light, have high durability, long battery life, must be light weight and energy efficient. This paper discusses possibilities of designing a universal LED fixture can be designed so that it meets the respective needs of everyone irrespective of their background and industry. It discusses the materials to be used for its different body parts, innovative clip design for attachment with support structures like head and armbands, helmets, shoes, etc. It also discusses the energy efficiency that can be achieved and alternatives for charging like fast-USB charging and also integration of solar charger in the fixture. Discussions have also been made on controlling intensity level of illumination using ambient sensors and manually through integrated buttons. IOT integration with the fixture also been discussed. Using IOT allows remote control, data collection, measuring performance and efficiency of the device. It also emphasizes the importance of having a universal design. Effort has been made to standardize the fixture design in reference to methods specified by renowned bodies such as DOE, IES, BIS, etc.

10378-27, Session PWed

Self CCT stabilization for white LEDs from turn-on stage to thermal equilibrium

Tsung-Hsun Yang, Shin-Mei Wu, National Central Univ. (Taiwan); Benoit Glorieux, Institut de Chimie de la Matière Condensée de Bordeaux (France); Xuan-Hao Lee, Ching-Yi Chen, Yu-Yu Chang, Yeh-Wei Yu, Ching-Cherng Sun, National Central Univ. (Taiwan)

In this paper, a self-balancing method of the phosphor efficiency for pcW-LEDs from the initial turn-on state to thermal equilibrium is proposed and demonstrated. For the obtainment of a pcW-LED with stabilized CCT, we proposed a novel scheme about the selection of the suitable peak wavelength of the blue LED under normal operation condition during the defined life time. According to experiment results, expect an observation of the turning pint for CCT variation upon rising temperature, the self-balance group was obtained as small as 7K and 83K when the initial CCT of the pcW-LEDs was around 4700K and 6300K, respectively. Besides, we also proposed a new factor, guide number, to figure out the design and choose the matching blue LED die and phosphor pair for self-balancing.

10378-28, Session PWed

Modeling and simulation of a solar simulator with multi-wavelength high-power LEDs

Yoon Kim, Reuben T. Lewis, Calvin College (United States)

This paper presents the modeling and simulation of a solar simulator that is comprised of multiple- wavelength high-power LEDs.

A solar simulator is a light source which can provide optical power to measure the characteristics of solar panels indoors. For this application, the light source requires an optical spectrum and irradiance that is similar to solar rays. A high-power LED-based light source is considered to provide a light-weight design, higher luminous efficacy, and longer operating life. To match the solar spectrum, the light source in the form of an LED array needs various types of LEDs whose wavelengths and intensities are different from one another.

The proposed solar simulator includes a high-density LED fixture containing a 10 by 10 array of high-intensity LEDs. The square fixture measures 5 inches (127 mm) per side. Additional fixtures can be added seamlessly to provide optical power over an area of any desired size.

The goal of this work is to find the optimum layout for an array of high-power LEDs in order to generate an optical spectrum similar to solar rays with uniform irradiance. The fixture has 100 LEDs of 13 different types. Each LED in the fixture has a specific wavelength and intensity set by a 3D optical modeling tool.

This work presents the parameters that affect spectral match and uniformity of irradiance. The parameters are the number of different LEDs used, their intensities, spacing, and arrangement.

The number of LEDs and their intensities for a spectral match were computed by a developed algorithm. Modeling and simulation for uniformity of irradiance were carried out by a 3D optical modeling tool.

The results include the spectral and irradiance distributions of the light fixture.

10378-29, Session PWed

The color enhancement and collimation features of the multi-colored LEDs with different periodic microstructure on the top surface of TIR lens

Shang-Ping Ying, Minghsin Univ. of Science and Technology (Taiwan); Han-Kuei Fu, Industrial Technology Research Institute (Taiwan)

Due to the advantages, such as high efficiency, power consumption reduction, no mercury, pure saturated color, high reliability and long lifetime, the solid-state lighting based on light-emitting diodes (LEDs) has become very popular at this stage. In the lighting applications such as spot lighting, downlighting, architectural and show lighting, the color-tunable properties with collimating beam of LEDs are highly demanded. The color–tunable lighting is easily achieved using multi-colored LEDs instead of inefficient color filters. However, the applications of multi-colored LEDs usually appear the undesirable light patterns such as color separation or color fringes. At the meantime, the use of TIR (total internal reflection) lens for multi-colored LEDs to collimate the light from the LEDs with different color will introduce seriously undesirable artifacts. Thus, a periodic microstructure surface on the top surface of the TIR lens would be used to reshape the light from the different colored LED chips in the multi-colored LEDs, and then decrease the color separation and color nonuniformity. In this study, the TIR lens with periodic microstructure surface on the top surface would be used to collimate the light from multi-colored LEDs with low color separation or color fringes. The analysis of color enhancement and collimation features of the multi-colored LEDs with different periodic microstructure on the top surface of the TIR lens is presented.

10378-30, Session PWed

Analysis of stereo depth for 3D LED autostereoscopic displays based on physiological limitations

Shu An, Graduate School at Shenzhen, Tsinghua Univ. (China); Ping Su, Graduate School at Shenzhen Tsinghua Univ (China); Zehao He, Jianshe Ma, Graduate School at Shenzhen, Tsinghua Univ. (China)

Stereo depth is the most important factor for the 3D experience when viewing an autostereoscopic display. In this paper, we investigate the influence of viewing distance and viewing angle to the stereo depth . First, we build the ideal stereo depth model based on the physiological limitation. Second, we establish a wave aberration model based on diffraction theory. The simulation and experimental results agree with the theoretical analyses. The model is of significant importance for giving a guidance on display system designing.

10378-31, Session PWed

The fabrication and performance of laser light engine used in next-generation laser projector system

Yung-Peng Chang, National Chung Hsing Univ. (Taiwan) and Taiwan Color Optics, Inc. (Taiwan); Jin-Kai Chang, National Sun Yat-Sen Univ. (Taiwan); Wei-Chih Cheng, Taiwan Color Optics, Inc. (Taiwan); Chun-Nien Liu, Wood-Hi Cheng, National Chung Hsing Univ. (Taiwan)

A laser projector system usually includes a laser light engine (LLE) module The LLE module consists of optical mirrors, diffuser glasses, blue laser diode, and color phosphor. The color phosphor is a key component in the LLE module which consists of a micro motor and two glass-based yellow and green phosphor-converted layers. The conversion layers of the yellow Ce:YAG and green Ce:LuAG phosphors are bonded on an aluminum substrate. A blue laser array source is used to excite the color phosphpr and then release yellow and green lights. Then, the combinations of blue, yellow, and green lights become white-laser light for use in the LLE module. In this study, the fabrication of LLE with two glass-based yellow and green phosphor-converted layers is presented. The optical performance of the LLE including lumen, lumen efficiency, chromaticity, and transmission is detailed discussion. This study demonstrates the adapting glass as a phosphor-converted color phosphor in the LLE modules that provide high-reliability and better performance for use in the next-generation laser projector system.

10378-32, Session PWed

Light box for investigation of characteristics of optoelectronics detectors

Agnieszka Szreder, Gdansk Univ. of Technology (Poland)

In this paper, a light box for investigation of characteristics of optoelectronic detectors is described. The light box consists of an illumination device, an optical power sensor and a mechanical enclosure.

The illumination device is based on four types of high-power light emitting diodes (LED): white light, red, green and blue. The illumination level can be varied for each LED independently by the driver and is measured by optical power sensor. The mechanical enclosure provides stable mounting points for the illumination device, sensor and the examined detector and protects the system from external light, which would otherwise strongly influence the measurement results. Uniformity of illumination distribution provided by the light box for all colors is good, making the measurement results less dependent on the position of the examined detector.

The response of optoelectronic detectors can be investigated using the developed light box for each LED separately or for any combination of up to four LED types. As the red, green and blue LEDs are rather narrow bandwidth sources, spectral response of different detectors can be examined for these wavelength ranges.

The described light box can be used for different applications. Its primary use is in a student laboratory setup for investigation of characteristics of optoelectronic detectors. Moreover, it can also be used in various colorimetric or photographic applications. Finally, it will be used as a part of demonstrations from the fields of vision and color, performed during science fairs and outreach activities increasing awareness of optics and photonics.

10378-33, Session PWed

Smart street lighting solution for remote rural areas of India

Debdyut Hajra, B.P. Poddar Institute of Management & Technology (India)

Though many smart street lighting solutions are available for urban areas, comparatively fewer solutions exist for rural areas. In the recent times, village streets have been illuminated with artificial lights as a part of rural development drive undertaken by the governments of respective countries. But, vehicle and pedestrian traffic is quite low through village roads. Hence, if light remains on all night long on such roads, then there is a huge wastage of energy. This calls for solutions to reduce this energy loss in an efficient manner. There are a lot of factors which must be kept in mind while designing solutions. Many villages lack the proper infrastructure to support new technologies. Communication facilities are limited, lack of local technically skilled labor, lack of security, etc. After evaluating these opportunities and challenges, an attempt has been made to devise a smart street lighting solution tailored for remote rural areas in India. One part of the solution discusses how intensity of the LED street lights can varied according to the ambient lighting conditions using sensors and LED switching in LED matrix. An artificial intelligence (AI) has also been modelled to identify traffic conditions using PIR sensors and object identification through image processing and independently control the lights. It also tracks the performance and status of each light. It would send this data and necessary notifications to a distant control center for human evaluation. This solution is also applicable for other rural areas throughout the world.

10378-34, Session PWed

High-speed modulation of GaN-based light-emitting diode with embedded photonic crystals

Zi-Xuan You, Tung-Ching Lin, Jian-Jang Huang, National Taiwan University (Taiwan)

Using GaN-based light-emitting diodes (LEDs) as a radio source for visible light communication (VLC) is one of alternative choice in a high-speed data system. However, the spontaneous radiative recombination lifetime in the multiple quantum wells (MQWs) usually restrict the modulation bandwidth of LEDs. For LEDs accompanied photonic crystal (PhC) structure, the guided photonic modes can be extracted with a shorter radiative recombination lifetime; therefore improve the performance of the devices for VLC. In this paper, we compare various PhC structures with corresponding dynamic behaviors in both small- and large-signal modulation. Faster transient responses and higher efficiency of the out-coupled modes were obtained in the room-temperature time-resolved photoluminescence (TRPL) and Raman scattering measurement. Here, sub-GHz modulation of GaN-based PhCLED is demonstrated, and the PhCLED exhibits a higher bandwidth than the conventional LED structure. Our study also indicates that we can not just keep scaling down the masa size of LEDs to increase the operation frequency owing to the light output power may become dull and reduce the performance of VLC system.

Conference 10379: Nonimaging Optics: Efficient Design for Illumination and Solar Concentration XIV

Sunday - Monday 6 –7 August 2017

Part of Proceedings of SPIE Vol. 10379 Nonimaging Optics: Efficient Design for Illumination and Solar Concentration XIV

10379-3, Session 1

Étendue and angular acceptance of the asymmetric compound parabolic concentrator

Melissa N. Ricketts, Roland Winston, Jonathan Ferry, Univ. of California, Merced (United States)

While the use of the asymmetric compound parabolic concentrator (ACPC) for solar concentration has been addressed, documentation regarding the étendue and angular acceptance of the ACPC is absent from the literature. This paper delves into the 2D design of the ACPC and discusses its étendue and angular acceptance, offering a new design tool regarding such instances when symmetry is broken. It is found that unlike the compound parabolic concentrator (CPC) whose angular acceptance fills a symmetric ellipse, the ACPC's angular acceptance fills an asymmetric ellipse in some cases, and a folded ellipse in others. Both cases are dependent on the maximum acceptance angles of the design. Ray tracing is utilized to confirm both the angular acceptance ellipses and étendue, as well as to offer a visual representation of the intensity distribution for asymmetric designs in both angular and phase space.

10379-4, Session 1

How the Hilbert integral theorem inspired flowlines

Roland Winston, Lun Jiang, Univ. of California, Merced (United States)

The connection of the Hilbert integral theorem to nonimaging optics appears in the first book on the subject. (Welford and Winston, The optics of the nonimaging concentrators). The flowline design method in nonimaging optics came much later. We discuss in this talk the over arching connection between the two.

10379-15, Session 1

Optical design: Why perfect optics (inside the solar cell) are needed to approach the theoretical limit *(Invited Paper)*

Sarah R. Kurtz, Univ. of California, Merced (United States)

No Abstract Available

10379-27, Session 1

New frontiers in solar concentrator design enabled by optically transparent thermal insulators

Thomas A. Cooper, Massachusetts Institute of Technology (United States)

No Abstract Available

10379-2, Session 2

Why do we still care about CPV?

Marco Stefancich, Dubai Electricity and Water Authority (United Arab Emirates); Matteo Chiesa, Harry N. Apostoleris, Masdar Institute of Science & Technology (United Arab Emirates)

With PV module prices low and flat-plate technology dominating the market, the industry has taken a hard turn away from concentrator systems. This is unsurprising as CPV involves higher up-front costs and large balance of system, including dual-axis tracking and in some cases active cooling, and on-site output is compromised by factors including optical losses, spectral effects and soiling to a greater extent that flat-plate systems. Despite this, we believe that concentrators still have a role to play in the long-term sustainability of the PV sector, but these advantages are best realized by aggressively rethinking the way we design PV concentrators. Here we argue, based on an analysis of manufacturing, material supply and end-of-life issues, that CPV can mitigate the negative environmental affects associated with PV manufacturing and disposal. This will likely be the primary justification for concentrators going forward, and it addresses a major challenge which has not yet been fully confronted by the industry, as the amount of PV in production and use has been quite small until recently, and large-scale module retirement is still some years away. We propose a number of module solutions utilizing low-concentration optics, tracking integration and light splitting which can remove the cost barriers to CPV while retaining its positive sustainability impact.

10379-5, Session 2

Optical performance effects of the misalignment of nonimaging optics solar collectors

Jonathan Ferry, Melissa N. Ricketts, Roland Winston, Univ. of California, Merced (United States)

The use of nonimaging optics in the application of high temperature solar thermal collectors can be extremely advantageous in eliminating the need to track the sun. The stationary nature of nonimaging optics collectors, commonly called external compound parabolic concentrators (XCPC's), present a unique design challenge when orienting them to collect sunlight. Many facilities throughout the world that adopt XCPC's are not situated to orient the collectors in the ideal angle facing the sun. This North-South misalignment can adversely affect the optical and power performance of the XCPC collector. To characterize how this misalignment effects XCPC's, raytracing simulations are conducted for varying offset angles of the collectors from the North-South plane. Optical performance is analyzed for multiple nonimaging optics designs accounting for the daily and seasonal movement of the sun in the sky. These results are compared to an ideal compound parabolic concentrator (CPC) with no angular misalignment from the North-South plane. Using the CPC as a baseline, a correlation between angular misalignment and seasonal optical performance is determined.

10379-6, Session 2

Optimization of photovoltaic V-Trough concentrators through genetic algorithms based on the interactions with beam radiation

Andrés Arias-Rosales, Ricardo Mejía-Gutiérrez, Univ. EAFIT (Colombia)

V-Trough concentrators use simple and low-cost non-imaging optics, namely flat mirrors, to boost the performance of regular solar cells. To improve their collecting power, the geometrical parameters can be explored for specific radiation and tracking conditions. Given the amount of possible configurations, and the interdependence of the parameters involved, genetic algorithms are a suitable approach to navigate the space of possible solutions. This work performs a V-trough study through such algorithms with unprecedented design flexibility, since the parameters, such as lengths and tilting angles, can be individually defined as static or as dynamic in function of the solar elevation. This allows the assessment of novel V-trough configurations, such as asymmetric mirrors with tracking tilting or sliding. The genetic algorithms, based on an analytical beam radiation model, were designed with several modalities: Maximization of the effective optical concentration or the cost-effectiveness; minimization of the cost or the space needed to fulfill a given energy need; or multi-objective. The capacities of these algorithms are explored in a case study and different heuristics within the genetic functions are assessed. For the same case study, the set-ups obtained with the convergence of the algorithms are then compared against set-ups designed through an interactive software. This comparison suggests that genetic algorithms, such as the ones developed in this work, are effective tools for defining the V-Trough geometrical parameters under personalized conditions. The genetic solutions can be as competitive as the ones achieved by a qualified engineer with an interactive simulation software.

10379-7, Session 2

Broadband angular selectivity in solar concentrators

Harry N. Apostoleris, Masdar Institute of Science & Technology (United Arab Emirates); Yichen Shen, Duncan C. Wheeler, Thomas A. Cooper, Massachusetts Institute of Technology (United States); Matteo Chiesa, Masdar Institute of Science & Technology (United Arab Emirates); Marin Soljacic, Massachusetts Institute of Technology (United States)

In designing solar concentrator optics there are many parameters that must be optimized in order to create a useful system, such as compactness, number of elements or interfaces, and acceptance angle, among others. Using geometric optics, tradeoffs between these parameters become inevitable. For example, a lens, trough or dish may be compact but has low tolerance of angular misalignment; angular tolerance can be improved by adding secondary and tertiary optics, but this increases complexity and reduces optical throughput; nonimaging optics such as the CPC offer wide acceptance angles from as single element, but are too long to be practical, in most applications, above low concentrations. These tradeoffs can be avoided by using angle-selective photonic materials to exploit the equivalence between angular restriction and concentration. Recently, broadband angular selectivity in optical films has been demonstrated by the Soljacic group in MIT. In this collaborative work we use this material to experimentally demonstrate two visible-spectrum optical concentrators. We demonstrate that these concentrators are thermodynamically ideal when the material properties are ideal, and describe the material improvements most essential for improving device performance, and discuss how commercial solar concentrator systems could be improved by the use of angular-selective optics

10379-8, Session 3

Testing light concentrators prototypes for the Cherenkov Telescope Array

François B. Hénault, Pierre-Olivier Petrucci, Laurent Jocou, Institut de Planétologie et d'Astrophysique de Grenoble (France)

The Cherenkov Telescope Array (CTA) shall be the largest cosmic gamma ray detector ever built. Each MST focal plane consists in an array of 2000 photomultipliers equipped with their own light concentrating optics. Within the CTA Consortium, IPAG is in charge of designing, subcontracting the realization to industry, and testing CTA light concentrators. Prototypes were manufactured by different industrial companies and tested in our laboratory on a test bench specifically built for the project. Each type of concentrator has been submitted to extensive performance measurements, including radiometric efficiency at different wavelengths and rejection curves. The final selected concentrator is the CPC, although non-imaging lenses exhibit interesting radiometric performance

10379-9, Session 3

Synthesis of freeform refractive surfaces forming various radiation patterns using interpolation

Iana Mazur, Anna O. Voznesenskaya, Pavel Krizskiy, ITMO Univ. (Russian Federation)

Optical freeform surfaces are very popular today in such fields as lighting systems, sensors, photovoltaic concentrators, and others. The application of such surfaces allows to obtain systems with a new quality with a reduced number of optical components to ensure high consumer characteristics: small size, weight, high optical transmittance. This article presents the methods of synthesis of refractive surface for a given source and the radiation pattern of various shapes. The light beams of rays coming from the source passes through the optical element and form the radiation pattern of the necessary shape. Calculation of the refractive surface is reduced to solving the integrated differential equation, which uses a refractive index, the function describes of a given radiation pattern, the direction vector of the beam and the function characterizing the distance from the refracting plane to the origin. This algorithm is implemented for the refracting optical free-form element, using the Matlab program. The outcome is a set of points, which belong to the free-form surface, approximating them, we will get the necessary element. This was done with the help of a computer simulation of a freeform surface a cubic spline interpolation. Interpolation algorithm was implemented in C ++. The result is a 3-D profile of the required optical component.

10379-10, Session 3

Designing freeform reflectors using new source-target mapping method

Egor V. Byzov, Leonid L. Doskolovich, Evgeniy S. Andreev, Nikolay L. Kazanskiy, Image Processing Systems Institute, Russian Academy of Sciences (Russian Federation) and Samara Univ. (Russian Federation)

In this paper a new kind of source-target map for design mirrors generating prescribed two-dimensional line-shaped intensity distributions is presented. Line-shaped means that distribution is defined in region with a high aspect ratio, obtained from the line by direct replacement for each point on the segment perpendicular to the reference. This map is a generalization of the mapping, used in the well-known problem of reflective optical elements design generating one-parameter intensity distributions. Design examples show high performance of the proposed method, including for areas with a small aspect ratio. For rectangular and elliptical intensity distributions with

angular dimensions from 80°x20° to 40°x20° the relative standard error does not exceed 8.5%

10379-11, Session 3

Efficiency of geometric designs of non-tracing flexible solar panels: Mathematical simulation

Malgorzata Marciniak, Yasser Y. Hassebo, LaGuardia Community College (United States); Delfino Enriquez, Maria-Ignacia Serey-Roman, LaGuardia Community College, The City Univ. of New York (United States)

The purpose of this study is to analyze various surfaces of flexible solar panels and compare them to the traditional flat panels mathematically. We evaluated the efficiency based on the integral formulas that involve flux. We performed calculations for flat panels with different positions, a cylindrical panel, conical panels with various opening angles and segments of a spherical panel. Our results indicate that the best efficiency per unit area belongs to particular segments of spherically-shaped panels. In addition, we calculated the optimal opening angle of a cone-shaped panel that maximizes the annual accumulation of the sun radiation per unit area.

10379-12, Session 4

Shaping and homogenization of LED white light using aperiodic scattering cell arrays

Daniel Asoubar, Roberto Knoth, Hagen Schweitzer, LightTrans International UG (Germany); Frank Wyrowski, Huiying Zhong, Friedrich-Schiller-Univ. Jena (Germany)

Shaping of LED white light is of increasing interest for several industrial applications. There are several known design concepts available. However these concepts suffer from high uniformity errors, low efficiencies, chromatic aberrations and/or high tolerance sensitivity. To overcome these limitations we present a novel design concept which is based on the design of aperiodic scattering cell arrays. In a first design step, a unit scattering cell is designed. Afterwards this cell is periodically replicated. Finally the periodicity of the array is broken using parametric optimization. Obtained design results are compared with experimental data.

10379-13, Session 4

Compact collimators designed with a modified point approximation for light-emitting diodes

Tao Luo, Gang Wang, Sun Yat-Sen Univ. (China)

The refraction-internal reflection-reflection-refraction (RIXR) type lens which has been designed by SMS method is an ultra-compact collimator very close to ideal concentrator. However, the shapes of the lens are also sensitive to design conditions and all the curves designed are formed automatically and can't be pre-determined.

We present a novel freeform lens design method for an application to LED collimating illumination. A modified compact collimating lens design with point source approximation is presented to form compact air-gap RIXR type collimators. Two freeform surface of the lens are constructed simultaneously, with the point source approximation to get uniform luminous exitance at the exit surface. The method is derived from a basic geometric-optics analysis and construction approach. By using this method, a compact collimated lenses with Aspect Ratio = 0.219 is presented. With optimization of initial parameters, a highly collimating lens with Cree XP-E LED and optical simulation efficiency of 83.06% under a view angle of ± 1.5 deg is constructed. Moreover, the utility efficiency (UE) inside the angle defined by ideal concentrator hypothesis with different lens-to-LED size ratios for both the lens in this paper and Total-internal-reflection (TIR) lenses are presented that the UE of the lens in this paper has improved to more than 90% with lens-to-LED size ratio larger than 16:1 and the "size effect" is restrained compared with traditional TIR lenses. A prototype of the collimator lens is also made to verify the practical performance of the lens, which has light distribution very compatible with the simulation results.

10379-14, Session 4

Control of ray deflection angles in the design of secondary optics with multiple surfaces

Sergey V. Kravchenko, Kseniya V. Andreeva, Samara Univ. (Russian Federation) and Image Processing Systems Institute, Russian Academy of Sciences (Russian Federation); Mikhail A. Moiseev, Image Processing Systems Institute, Russian Academy of Sciences (Russian Federation) and Samara Univ. (Russian Federation); Leonid L. Doskolovich, Image Processing Systems Institute (Russian Federation) and Samara Univ. (Russian Federation)

The use of LEDs in the modern lighting devices makes the problem of designing secondary optics quite relevant. For the purpose of street, industrial and emergency lighting optical elements with two free-form surfaces are usually used. In this study the method for computation of such LED optics is proposed. In this approach the optical element surfaces are designed sequentially: firstly the inner surface is computed and then the outer one. At the beginning of each surface computation a piecewise smooth solution should be designed. Such a surface generates discrete intensity distribution that approximates the continuous one. In order to compute piecewise smooth solution we propose to utilize the supporting quadric method. After we have had piecewise smooth surface the smooth one is obtained by fitting NURBS-spline on it. Such a method allows controlling the balance of deflection angles between the inner and outer surfaces. It has been proven that in the case of point source, the maximal efficiency is obtained when each surface performs the half of the required ray deflection. As an example, the optical element with equal ray deflection part in each surface generating intensity distribution for ME1 class roadway lighting is designed. The simulation results of the luminance and illuminance distribution confirm good quality of the proposed method.

10379-1, Session 5

Thermodynamic foundation of nonimaging optics

Lun Jiang, Roland Winston, Univ. of California, Merced (United States)

Nonimaging Optics is the theory of thermodynamically efficient optics and as such depends more on thermodynamics than on optics. Hence in this paper a condition for the "best" design is proposed based on purely thermodynamic arguments, which we believe has profound consequences for the designs of thermal and even photovoltaic systems. This new way of looking at the problem of efficient concentration depends on probabilities, the ingredients of entropy and information theory while "optics" in the conventional sense recedes into the background. Much of the paper is pedagogical and retrospective. Some of the new development of flowline designs will be introduced at the end and the connection between the thermodynamics and flowline design will be graphically presented. We will conclude with some speculative directions of where the new ideas might lead.

10379-16, Session 5

Thermodynamic investigation of segmented CPC

Bennett K. Widyolar, Univ. of California, Merced (United States)

A new parameter Flux Efficiency (FE), which combines concentration ratio and optical efficiency, is introduced which directly relates to the maximum achievable flux on the absorber and allows comparison between ideal and non-ideal concentrators. The effect of approximating curved CPC profiles by a finite number of flat segments on the Incident Angle Modifier (IAM), optical efficiency, and newly defined Flux Efficiency is presented, providing new considerations for designing geometric concentrators under real world constraints.

10379-28, Session 5

Advances on geometric flux optical design method *(Invited Paper)*

Ángel García-Botella, Univ. Politécnica de Madrid (Spain); Antonio A. Fernandez-Balbuena, Daniel Vázquez-Moliní, Univ. Complutense de Madrid (Spain)

Nonimaging optics is focused on the study of methods to design concentrators or illuminators systems. It can be included in the area of photometry and radiometry and it is governed by the laws of geometrical optics. The field vector method, which starts with the definition of the irradiance vector E, is one of the techniques used in nonimaging optics. Called “Geometrical flux vector” it has provide ideal designs. The main property of this model is, its ability to estimate how radiant energy is transferred by the optical system, from the concepts of field line, flux tube and pseudopotential surface, overcoming traditional raytrace methods. Nevertheless this model has been developed only at an academic level, where characteristic optical parameters are ideal not real and the studied geometries are simple. The main objective of the present paper is the application of the vector field method to the analysis and design of real concentration and illumination systems. We propose the development of a calculation tool for optical simulations by vector field, using algorithms based on Fermat`s principle, as an alternative to traditional tools for optical simulations by raytrace, based on reflection and refraction law. This new tool provides, first, traditional simulations results – efficiency, illuminance/irradiance calculations, angular distribution of light- with lower computation time, photometrical information needs about a few tens of field lines, in comparison with million rays needed nowadays. On the other hand the tool will provides new information as vector field maps produced by the system, composed by field lines and quasipotential surfaces. We show our first results with the vector field simulation tool.

10379-29, Session 5

Point to point multispectral light projection applied to cultural heritage

Daniel Vázquez-Moliní, Antonio A. Fernandez-Balbuena, Univ. Complutense de Madrid (Spain); Ángel García-Botella, Univ. Politécnica de Madrid (Spain)

Regarding cultural heritage preservation and exhibition of art goods it is necessary to take into account social, cultural and economic needs that show opposing requirement. The use of new of light sources based on LED technology should allow the develop of systems that combine both requirements and allow to make these art goods available to the next generations according to sustainability principles. The goal of this work is to develop light systems and sources with an optimized spectral distribution for each specific point of the art piece. This optimization process implies to maximize the color fidelity reproduction and the same time to minimize the photochemical damage. Perceived color under these sources will be similar (metameric) to technical requirements given by the restoration team uncharged of the conservation and exhibition of the goods of art. Depending of the fragility of the exposed art objects (i.e. spectral responsivity of the material) the irradiance must be kept under a critical level. Therefore, it is necessary to develop a mathematical model that simulates with enough accuracy both the visual effect of the illumination and the photochemical impact of the radiation. Spectral reflectance of a reference painting The mathematical model is based on a merit function that optimized the individual intensity of the LED-light sources taking into account the damage function of the material and color space coordinates. Moreover the algorithm used weights for damage and color fidelity in order to adapt the model to a specific museal application. In this work we show a sample of this technology applied to a picture of Sorolla (1863-1923) a important Spanish painter title “woman walking at the beach”.

10379-17, Session 5

The error tolerance of nonimaging optic systems

Ali Hassanzadeh, Bennett K. Widyolar, Lun Jiang, Roland Winston, Univ. of California, Merced (United States)

In real world applications the nonimaging optics has the advantage of high error tolerance compared to conventional imaging optics. In this paper we present the result of a solar collector constructed with the nonimaging optics principles and the effect of off-positioning its absorbers on its optical efficiency. Thermal analysis of such effects are also presented.

10379-18, Session 5

Tracking and shape errors measurement of concentrating heliostats

Mathieu Coquand, Institut de Planétologie et d’Astrophysique de Grenoble (France) and PROMES-CNRS (France); Cyril Caliot, PROMES-CNRS (France); François B. Hénault, Institut de Planétologie et d’Astrophysique de Grenoble (France)

In solar tower power plants, the tracking accuracy, facets misalignment and surface shape errors of concentrating heliostats are of prime importance on the efficiency of the system. Methods enabling quick adjustment of a field with a huge number of heliostats are essential for the rise of solar tower technology. In this communication is described a new method for heliostat characterization that makes use of four cameras located near the solar receiver and simultaneously recording images of the sun reflected by the optical surfaces. Data processing then allows reconstructing the shape errors of the heliostats, including tracking and canting errors. The mathematical basis of the process is explained. Numerical simulations demonstrate that the measurement accuracy of this method is compliant with the requirements of solar concentrating optics. Finally, we present our first experimental results obtained on the THEMIS experimental solar tower plant.

10379-19, Session 5

Optimizing luminescent solar concentrators *(Invited Paper)*

Boaz Ilan, Univ. of California, Merced (United States)

This talk will review some of the challenges in making efficient luminescent solar concentrators, the modeling efforts, and how to optimize the performance of these devices.

10379-20, Session 5

Enhancing the light conversion efficiency in a luminescent solar concentrator by using a prism film

Pao-Keng Yang, Hua-Yu Tseng, Chia-Wei Lin, Min-Hsiu Chung, Tsung-Wei Huang, Minghsin Univ. of Science and Technology (Taiwan)

We present a method for enhancing the light conversion efficiency of a luminescent solar concentrator by putting a prism film on the upper surface for receiving the incoming light. The luminescent solar concentrator under study was composed of a thick glass with a luminescent film deposited on the top surface and a solar cell attached to the lateral surface. The prism film will deflect the incident light into two different directions. Dependence of the conversion efficiency on the incident angle of the sunlight and influence of the rotation of the prism film on the conversion efficiency were also investigated. Experimental results show that the prism film will increase the light falling on the solar cell in our luminescent solar concentrator.

10379-21, Session 5

The characteristics of luminescent solar concentrators (LSCs) using inorganic phosphors

Shang-Ping Ying, Bing-Mau Chen, An-Ting Li, Minghsin Univ. of Science and Technology (Taiwan)

The Luminescent Solar Concentrator (LSC) consists of a transparent plate with solar cells on one or more sides. The incoming sunlight is absorbed by the luminescent dyes or particles, which are embedded in the transparent plate or applied in a film on the top or bottom of the transparent plate. The absorbed light is re-emitted at a longer wavelength, and part of the re-emitting light is trapped in the transparent plate by total internal reflection (TIR). Then the solar cells attached to the edges of the transparent plate would collect the light and convert it to electricity. However, the luminescent dyes or particles used in the conventional LSC still suffer from reduced efficiencies and lifetimes, then the inorganic phosphors with relatively high quantum yields, good absorption properties and longer lifetime could be alternative materials used in the structure. In this study, the ray-tracing simulation is used to investigate the optical characteristics of the LSC with the inorganic phosphors embedded film on the top or bottom of the transparent plate. The simulation results will also be used to study the loss mechanisms in the LSC with inorganic phosphors embedded film.

10379-22, Session PMon

Optimization design of nonimaging Fresnel lens using total internal reflection prisms for light concentration

Perla M. Viera-González, Guillermo E. Sánchez-Guerrero, Edgar Martínez-Guerra, Univ. Autónoma de Nuevo León (Mexico); Daniel Enrique Ceballos-Herrera, Univ. Nacional Autónoma de México (Mexico)

The efficiency in Fresnel lenses is affected by three principal sources: energy lost due to material absorption; geometric losses such as chromatic dispersion or surface roughness; and reflectance losses at refracting surfaces. On this subject, the design of nonimaging Fresnel lenses integrated by refractive and total internal reflection (TIR) prisms is presented. This design method uses iterative calculations for design every prism and it selects the best option to avoid reflectance losses. An example of a Fresnel lens design and characterization is shown, including its spatial and angular distribution, and a comparison with a nonimaging Fresnel lens composed only by refraction prisms is performed, having as result the analysis of the cases when the TIR increases the efficiency of the Fresnel lenses. In addition, the study about how acceptance angle of the lens affects the iteration method in the selection of the prism with the minimal lost is included.

10379-23, Session PMon

Numerical analysis of lateral illumination lightpipes using elliptical grooves

Guillermo E. Sánchez-Guerrero, Perla M. Viera-González, Edgar Martínez-Guerra, Univ. Autónoma de Nuevo León (Mexico); Daniel Enrique Ceballos Herrera, Univ. Nacional Autónoma de México (Mexico)

Lightpipes are used for illumination in applications such back-lighting or solar cell concentrators due to the high irradiance uniformity, but its design requires several parameters. This work presents a procedure to design a square lightpipe that control the area of emission on its lateral face using commercial LEDs placed symmetrically in the lightpipe frontal face. We propose the use of grooves using total internal reflection placed successively in the same face of extraction to control the area of emission. The LED area of emission is small compared with the illuminated area, and, as expected, the lateral face total power is attenuated. These grooves reduce the optical elements in the system and can control areas of illumination. A numerical analysis is presented to show how the selected parameters affect in the area to illuminate.

10379-24, Session PMon

Design and manufacturing of cascaded DCG based holograms for spectrum-splitting PV systems

Yuechen Wu, Benjamin D. Chrysler, Silvana Ayala Pelaez, Raymond K. Kostuk, The Univ. of Arizona (United States)

In this work the technique of designing and manufacturing broad band volume transmission holograms using dichromate gelatin (DCG) is summarized for solar spectrum-splitting application. Spectrum splitting photovoltaic system uses a series of single bandgap PV cells that have different spectral conversion efficiency properties to more fully utilize the solar spectrum. In such a system, one or more high performance optical filters are usually required to split the solar spectrum and efficiently send them to the corresponding PV cells. An ideal spectral filter should have a rectangular shape with sharp transition wavelengths. DCG is a near ideal holographic material for solar applications as it can achieve high refractive index modulation, low absorption and scattering properties, and long term stability to solar exposure after sealing. In this research, a methodology of designing and modeling a transmission DCG hologram using RCWA for different PV bandgap combinations is described. To achieve a broad diffraction bandwidth and sharp cut-off wavelength, a cascaded structure of multiple thick holograms are used. Material and processing factors that are taken into consideration for the optimization process include: the grating variation during the wet development process, the film thickness, the grating vector, the index modulation, and the average and differential swelling. A set of experiments are also described to verify the design principles and optimization model.

10379-25, Session PMon

Impact of internal forced air cooling on radiative absorption of a gas-particle medium in a small particle solar receiver

James O'Hara, San Diego State Univ. (United States)

A high output solar receiver utilizing a specifically developed infrared-absorbing, air-particle mixture as the working fluid is being developed for a power plant. Solar radiation, redirected and focused by a heliostat field is concentrated into the receiver and absorbed by a "black" air particle mixture with flows through the receiver. The exiting mixture, now superheated, serves as the input to a gas turbine in a Brayton power cycle. Current efforts pertain to cooling of the receiver window as high levels of incident radiation heat the window directly through absorption within the glass and indirectly as the participating air-particle gas mixture serves to heat the internal face of the window beyond the material limits. The solution to lowering the operating temperature of the receiver window without sacrificing power level and system performance is to internally cool the internal surface of the window with jets of air. The cooling air mixes with the gas-particle mixture and has the effect of changing the optical path through the receiver by temporarily displacing, and impacting the density uniformity of the absorbing medium in the receiver, thus lowering the total mass of "black" particles that are exposed to incident radiation. This has a direct impact on the absorption of the working fluid for a given mass flow and therefore impacts system efficiency. Computational fluid dynamics coupled with a radiation simulation is employed to predict the impact of the forced-air convection on different aspects: effectiveness of window cooling, change in optical path length within the absorbing air-particle medium, and overall receiver efficiency. Transient effects are also studied.

10379-26, Session PMon

Optical coatings for luminescent solar concentrators

Cheng-Chung Jaing, Po-Chun Lu, Jian-Wei Chen, Wei-Gwo Yu, Jing-Han Xie, Pao-Keng Yang, Bing-Mau Chen, Minghsin Univ. of Science and Technology (Taiwan)

In this paper, the luminescent solar concentrator comprises a thick glass with a spectrally-selective optical coating deposited on the bottom surface and an inorganic phosphor layer stacked on the coating surface. A solar cell is attached to the lateral surface of the thick glass. Spectrally-selective coatings are applied to reflect and redirect the invisible solar radiation to the edges of luminescent solar concentrators. These coatings also transmit the visible solar light and the emission light of the inorganic phosphor. The short-circuit current of the solar cell is measured in a solar simulator with metal-dielectric heat mirrors and dielectric edge filters coated on the thick glass of the luminescent solar concentrators respectively. Experimental results show that the dielectric edge filter will increase the short-circuit current and the invisible light falling on the solar cell in our luminescent solar concentrator. The metal-dielectric coatings, silver-based transparent heat mirrors, will not increase the short-circuit current in our luminescent solar concentrator due to absorption of metal films.

10379-30, Session PMon

Real time 3D photometry

Antonio A. Fernandez-Balbuena, Daniel Vázquez-Moliní, Univ. Complutense de Madrid (Spain); Ángel García-Botella, Univ. Politécnica de Madrid (Spain); Jesus Romo, Valeo (Spain)

The photometry and radiometry measurement is a well-developed field. The necessity of measuring designed systems involve the use of several techniques like gonio-photometry. Actual goniophotometer are a precise measurement tool that is used in the lighting area like head car lighting, concentrator and collimator measurement and all the designed and fabricated optical systems that works with light.

There is one disadvantage in this kind of measurements that try to obtain the intensity polar curves and the total flux of the optical system. In the industry, there are good goniophotometers that are precise and reliable but they are very expensive and the measurement time is long. In industry the cost can be of minor importance but measuring time that is around 30 minutes is of major importance due to trained staff cost.

We have designed a system to measure photometry in real time, it consists in a curved screen to get a huge measurement angle and a CCD. The system to be measured projects light onto the screen and the CCD records a video of the screen obtaining an image of the projected profile.

A complex calibration permits to trace screen data (x,y,z) to intensity polar curve (I,??). This intensity is obtained in candels (cd) with an image + processing time below one second.

Conference 10380: Ultrafast Nonlinear Imaging and Spectroscopy V

Sunday - Monday 6 –7 August 2017

Part of Proceedings of SPIE Vol. 10380 Ultrafast Nonlinear Imaging and Spectroscopy V

10380-1, Session 1

Effects of cations and cholesterol with sphingomyelin membranes Investigated by high-resolution broadband sum frequency vibrational spectroscopy *(Invited Paper)*

Zhen Zhang, Yi-Yi Li, Rong-Juan Feng, Li-Li Lu, Yuan Guo, Institute of Chemistry, Chinese Academy of Sciences (China)

Sphingomyelin(SM) is specifically enriched in the plasma membrane of mammalian cells. Its molecular structure is compose by N-acyl-Derythro-sphingosylphosphorylcholine. The function of the SM related to membrane signaling and protein trafficking are relied on the interactions of the SM, cations, cholesterol and proteins. Therefore, the new techniques has to be applied to probe the detailed interactions of the molecules. In this report, the interaction of three different nature SMs, cations and cholesterol at air/aqueous interfaces are investigated by high-resolution broadband sum frequency vibrational spectroscopy(HR-BB-SFG), respectively. The Effects on the hydration of the headgroup and ordering of the alky chain of the SMs influenced by cations and cholesterol are studied systematically. Firstly, we focused on the sphingomyelin in the presence and absence of Ca2+, Na+ and K+ to characterize the specificity of cation binding to the headgroup of the sphingomyelin membranes in terms of molecular structure and the hydration. Secondly, we studied the sphingomyelin structural change in the present of different ratio of cholesterol, which reveals the role of hydrogen bonding in cholesterol's association with SM. Overall, the results demonstrate the importance of using HR-BB-SFG that can probe the nanoscale molecular interaction mechanism of SMs and cations and cholesterol are discussed in this report. Our results shed lights on understanding the relationship on the interactions of complex molecules at surfaces and interfaces.

10380-2, Session 1

High resolution vibrational sum frequency generation spectroscopy revealing new properties of the complex interfacial molecular systems: Spectral splitting, molecular symmetry, and supramolecular chirality *(Invited Paper)*

Zhou Lu, Yi-Yi Li, Rongjuan Feng, Jian Hou, Yingxue Ma, Zhen Zhang, Yuan Guo, Minghua Liu, Institute of Chemistry, Chinese Academy of Sciences (China)

The vibrational sum frequency generation spectroscopy (VSFG) has recently become a versatile characterization tool for the molecular interfaces owing to its unique surface selectivity and submonolayer sensitivity. In the past years, the applications of the VSFG technique have expanded into various research fields including biological sciences, environmental chemistry, heterogeneous catalysis, electrochemistry, and etc. However, the limited spectral resolution in the traditional VSFG techniques has hampered its further efforts to reveal the molecular details of the complex interfacial molecular systems. In this presentation, we will discuss the most recent progresses of our newly developed high resolution VSFG (HR-VSFG) spectrometer. With a 50-picosecond visible laser pulse synchronized and phase-locked with a ~35 femtosecond broadband infrared pulse, we can ultimately achieve a spectral resolution of <0.5 wavenumber using this HR-VSFG setup. The unprecedented high resolution, together with the powerful VSFG polarization dependent analysis, has enabled us to resolve the unpredicted spectral splitting for the commonly studied interfacial molecules. Assisted with the proper theoretical modeling, we can further infer the new molecular symmetry models used to describe the interfacial vibrational modes. These new spectroscopic data has helped bring new insights about the interfacial properties of the complex molecular systems such as the phospholipid membranes and macromolecular interfaces. The examples of new HR-VSFG studies on the interfacial supramolecular chirality will also be discussed.

10380-3, Session 1

Second-harmonic generation in semiconductor nanostructures and applications *(Invited Paper)*

Kai Wang, Huazhong Univ. of Science and Technology (China)

Second-harmonic generation (SHG) is a fundamental second-order nonlinear optical process, and it is quite sensitive to the polarization angle of the pumping light with respect to the crystallographic orientation of materials. In our works, we systematically studied SHG in single ZnS nanowires (NWs). The results indicate that the SHG response is quite sensitive to the orientations of c-axis as well as the (100) and (010) crystal-axis of ZnS NWs, thus all the three crystal-axis orientations of ZnS NWs are precisely determined by the SHG method. Secondly, we demonstrate a highly sensitive detection of the lattice distortion in single bent ZnO nanowires (NWs) by SHG microscopy. A high detection sensitivity of 10-3 nm on the bending distortion is obtained in our experiment. Thus, SHG microscopy provides a sensitive all-optical and non-invasive method for in situ detecting the lattice distortion under various circumstances. Thirdly, we studied the enhanced SHG in the hybrid nanostructures that a single ZnS nanobelt was half covered with aluminum (Al) film, which is an ideal platform for studying the SHG enhancement effects of the Al coating. The results indicate that the Al coating in the hybrid nanostructures not only confines the pumping laser in the ZnS effectively, but also concentrates the emitted SHG signal greatly, increasing the signal collection efficiency. The Al-based hybrid nanostructures open up new possibilities for low-cost, highly efficient and directional coherent nano-light sources at short wavelength.

10380-4, Session 1

Observation of polar domains in metallic layered oxides *(Invited Paper)*

Gregory A. Stone, Shiming Lei, Ke Wang, The Pennsylvania State Univ. (United States); Danilo Puggioni, Northwestern Univ. (United States); Zhiqiang Mao, Tulane Univ. (United States); James M. Rondinelli, Northwestern Univ. (United States); Venkatraman Gopalan, The Pennsylvania State Univ. (United States)

Recent studies of the systems Ca3B2O7 (B = Ti, Mn), have experimentally confirmed hybrid improper ferroelectricity, a geometrically induced displacement route to inversion symmetry breaking, in layered oxides. This approach does not require B-sites with a d0 configuration opening up the possibility phase coexistence within a single material, such as polarity and metallicity in a single material system as proposed by Anderson and Blount over fifty years ago and recently observed in LiOsO3. Despite the large amount of literature available on ferroelectric domains and domain walls in insulating materials, there have been no such reports for a polar metal system. Using a combination of nonlinear optical second harmonic generation (SHG) microscopy and atomic scale imaging we report for the first time direct observation of polar domains and walls the metallic system Ca3Ru2O7. SHG maps show the existence of 180o walls and 90o degree walls (simultaneously ferroelastic) which meander throughout the system

giving rise to both charged and neutral walls. Atomic-scale transmission electron microscopy confirms hybrid improper ferroelectricity the mechanism responsible for the polar behavior in this material. TEM images also show the presence of unique domain wall interactions that transform uncharged walls into energetically unfavorable charged walls and the role defects have on the domain structure.

10380-5, Session 1

Nonlinear characterization of two dimensional materials

Alexander S. Cocking, William Murray, Kazunori Fujisawa, Pennsylvania State Univ. (United States); Anna Laura-Elias, The Pennsylvania State Univ. (United States); Mauricio Terrones, Zhiwen Liu, Pennsylvania State Univ. (United States)

Two-dimensional materials have attracted significant interest recently for their unique optical properties compared to their bulk counterparts. Specifically, the family of transition metal dichalcogenides (TMD), such as MoS2 and WS2, have large second order nonlinear susceptibility. Extraordinary second harmonic generation and sum frequency generation have been observed. Here we investigate the second order nonlinearity of 2D materials, including TMD layered materials with dopants and defects. Experimental results and preliminary theoretical analysis will be discussed.

10380-6, Session 2

Supercontinuum generation using longitudinal z-polarized vectorial beam *(Invited Paper)*

Wenkai Zhang, Beijing Normal Univ. (China)

Broadband laser sources based on supercontinuum generation in femtosecond laser have been widely used for time-resolved absorption spectroscopy, material characterization, pulse compression, signal processing, three-dimensional imaging, ranging, atmospheric remote sensing, and medical diagnosis. Supercontinuum is generally generated by the strong non-linear effect when the narrow spectrum light pulse propagates in the nonlinear medium. Supercontinuum was first found in glass, followed by the generation of supercontinuum in solids, liquids, gases, and waveguides. The spectral broadening caused by self-phase modulation is related to many factors such as peak power, polarization, pulse shape and initial chirp of the input pulse. Researchers have put a lot of effort to extend the applicability of the supercontinuum. Here, we report the supercontinuum generation using the longitudinal z-polarized vectorial beam. Unconventional polarization states, also known as "vector beams," have become increasingly compelling in recent years. As we know, the conventional polarization states, such as linear, circular or elliptical polarizations, can be uniquely described by a specific point on the surface of the Poincaré sphere. However, the vector beams have a spatial inhomogeneous polarization state, and therefore cannot be described by a point, but rather by a number of points on the Poincaré sphere. In this article, the effect of the different polarization states on supercontinuum generation is studied.

10380-7, Session 2

Tunable optical source based on divided pulse soliton self-frequency shift

Chenji Zhang, Pennsylvania State Univ. (United States); Victor Bucklew, Perry S. Edwards, Atoptix, LLC (United States); Corey Janisch, The Pennsylvania State Univ. (United States); Zhiwen Liu, Pennsylvania State Univ. (United States)

We presented a broadly tunable, power scalable, multi-line, ultrafast source. The source is based on combining principles of pulse division with the phenomenon of the soliton self-frequency shift. By using this system, interferometric pulse recombination is demonstrated showing that the source can decouple the generally limiting relationship between output power and center wavelength in soliton self-frequency shift based optical sources. Broadly tunable multi-color soliton self-frequency shifted pulses are experimentally demonstrated. Simultaneous dual-polarization second harmonic generation was performed with the source, demonstrating one novel imaging methodology that the source can enable.

10380-8, Session 2

Iteratively-seeded mode-locking for high performance ultrashort pulsed lasers *(Invited Paper)*

Victor Bucklew, Atoptix, LLC (United States); William Renninger, Yale Univ. (United States); Perry S. Edwards, Atoptix, LLC (United States); Zhiwen Liu, Pennsylvania State Univ. (United States)

Ultrashort pulsed mode-locked lasers with exceptional performance qualities (e.g. short temporal widths or high peak powers) are desired for applications ranging from biomedical imaging to materials processing. Despite rapid progress in source development, evidence suggests that performance limits anticipated theoretically have not yet been reached. In this talk, we review recent progress and help resolve the discrepancy by presenting a limit to mode-locked laser performance based on the route taken to reach the desired steady-state pulse solution instead of on the pulse solution itself. Furthermore, we introduce an iteratively seeded method of mode-locking that allows this limit to be surmounted.

10380-9, Session 2

High power fiber laser pumped femtosecond optical parametric resources *(Invited Paper)*

Jintao Fan, Minglie Hu, Tianjin Univ. (China)

Wavelength tunable femtosecond laser sources are of great importance in many applications. Series examples of such a source used optical parametric generator, optical parametric oscillator and optical parametric amplifier are presented in this report.

10380-10, Session 3

Ultrafast MeV electron diffraction/ microscopy at SLAC *(Invited Paper)*

Xiaozhe Shen, Renkai Li, Jie Yang, Stephen P. Weatherspy, Xijie Wang, SLAC National Accelerator Lab. (United States)

SLAC recently launched the ultrafast electron diffraction and microscopy (UED/UEM) Initiative, with the goal to develop the world's leading ultrafast electron scattering instruments, which are complementary with x-ray free-electron lasers such as LCLS and LCLS-II. The first step of the Initiative is a MeV UED system which is now actively supporting an ultrafast science program, and at the same time serving as a testbed for instrumentation development.

In this talk, design of the SLAC MeV UED system will be briefly introduced. Key machine performance parameters will be reviewed, including machine stability and reproducibility, as well as reciprocal-space and temporal resolution. Ultrafast dynamics from a variety of samples, including 2D materials, thin nanofilms, nanoparticles, and gas-phase molecules have

been studied using this machine. Selected ultrafast science experiment results will be presented. In the meantime, much R&D efforts have been devoted for novel machine capabilities to enable new science opportunities. For example, we have experimentally demonstrated a femtosecond MeV electron microdiffraction, which is capable to resolve local structure from single crystal of ?m lateral size with 100 fs root-mean-square temporal resolution. Future developments include 10-fs temporal resolution UED, THz pumping capability, etc. We will also discuss R&D towards the next step of the Initiative, which is to develop key technologies for future UEM with unprecedented combined spatial-temporal resolution. This R&D will focus on a superconducting radio-frequency photocathode gun, which features high accelerating field hence high beam brightness, excellent energy stability, and outstanding flexibility in bunch length from picosecond to a hundred picoseconds.

10380-11, Session 3

Ultrafast imaging of molecular dynamics with electron diffraction *(Invited Paper)*

Martin Centurion, Univ. of Nebraska-Lincoln (United States); Jie Yang, SLAC National Accelerator Lab. (United States); Markus Guehr, Univ. Potsdam (Germany); Xiaozhe Shen, Renkai Li, SLAC National Accelerator Lab. (United States); Omid Zandi, Kyle J. Wilkin, Univ. of Nebraska-Lincoln (United States); Theodore Vecchione, Ryan N. Coffee, Jeff Corbett, Alan R. Fry, Nick Hartmann, Carsten Hast, Kareem Hegazy, Keith R. Jobe, Igor V. Makasyuk, Joseph S. Robinson, SLAC National Accelerator Lab. (United States); Matthew S. Robinson, Univ. of Nebraska-Lincoln (United States); Sharon Vetter, Stephen P. Weathersby, Chales Yoneda, Xijie Wang, SLAC National Accelerator Lab. (United States)

Ultrafast electron diffraction (UED) has the potential to capture changes in the structure of isolated molecules on the natural spatial and temporal scale of chemical reactions, that is, sub-Angstrom changes in the atomic positions that happen on femtosecond time scales. UED has the advantage that electron sources can easily reach sub-Angstrom spatial resolution, but so far femtosecond resolution had not been available for gas phase experiments due to the challenges in delivering short enough electron pulses on a gas target and the velocity mismatch between laser and electron pulses. Recently, we have used relativistic electron pulses at MeV energy to solve these challenges and reach femtosecond resolution. We have, for the first time, imaged coherent nuclear motion in a molecule with UED. In a proof-of-principle experiment, we captured the motion of a laser-excited vibrational wavepacket in iodine molecules. We are currently performing experiments in more complex molecules to capture laser-induced dissociation and conformational changes. We have also developed a table top 100 keV source that relies on a pulse compressor to deliver femtosecond electron pulses on a target and uses a tilted laser pulse to compensate for the velocity mismatch between the laser and the electrons. This source has a high repetition rate that will complement the high temporal resolution of the relativistic source.

10380-12, Session 3

Imaging electronic motions by ultrafast electron diffraction *(Invited Paper)*

Hua-Chieh Shao, Univ. of Nebraska-Lincoln (United States); Anthony F. Starace, Univ. of Nebraska-Lincoln (United States)

Recently ultrafast electron diffraction and microscopy have reached unprecedented temporal resolution, and transient structures with atomic precision have been observed in various reactions. It is anticipated that these extraordinary advances will soon allow direct observation of electronic motions during chemical reactions. We therefore performed a series of theoretical investigations and simulations to investigate the imaging of electronic motions in atoms and molecules by ultrafast electron diffraction. Two prototypical electronic motions were considered for hydrogen atoms. For the case of a breathing mode, the electron density expands and contracts periodically, and we show that the time-resolved scattering intensities reflect such changes of the charge radius. For the case of a wiggling mode, the electron oscillates from one side of the nucleus to the other, and we show that the diffraction images exhibit asymmetric angular distributions. If the energies of scattered electrons are resolved, our simulations show that additional details of the electronic motions can be obtained, enabling proper interpretations of electronic motions from energy-resolved diffraction images. Owing to the demonstrated abilities of ultrafast electrons to image these motions, we have proposed to image a coherent population transfer in lithium atoms using currently available femtosecond electron pulses. A frequency-swept laser pulse adiabatically drives the valence electron of lithium atoms from the 2s to 2p orbitals, and a time-delayed electron pulse maps such motion. Our simulations show that the diffraction images reflect this motion both in the scattering intensities and the angular distributions. This work is supported by NSF Grant No. PHYS-1505492.

10380-13, Session 3

Charge carrier dynamics in semiconductors studied by scanning ultrafast electron microscopy

Ebrahim Najafi, California Institute of Technology (United States)

With the continuous miniaturization of semiconductor devices, interfacial carrier dynamics have become essential to the device performance and efficiency. The disruption of the translational symmetry at the surfaces and interfaces makes the formation of interfacial barriers and defect states often inevitable. Despite such profound deviations from the bulk, there is only limited experimental evidence about how carriers behave at these boundaries, primarily due to the lack of a microscopy technique that can provide sufficient resolutions in both space and time. Scanning ultrafast electron microscopy (SUEM) is a recently developed technique that allows high resolution imaging of the electronic and structural dynamics at the femtosecond, picosecond and nanosecond timescales. In this work, we investigated the spatial dynamics of charge carriers in silicon by SUEM; specifically, we explored the initial super-diffusion of carriers after optical excitation which lasted tens of picoseconds and ultimately transitioned into the steady-state surface diffusion. Interestingly, at large excitation densities, electrons and holes showed non-linear transport behavior, resulting in the emission of plasma waves. Finally, we studied charge carrier dynamics at the silicon p-n junction which showed that charge separation was an ultrafast process which was not limited to the junction and began tens of micrometers away; in addition, the separated carriers remained localized in both space and time across the junction for tens of nanoseconds before they recombined to recover the ground state.

10380-14, Session 4

Serial single molecule electron diffraction imaging: A possible solution to the crystallization problem *(Invited Paper)*

Wei Kong, Oregon State Univ. (United States)

Serial single molecule electron diffraction imaging (ss-EDI) relies on signal accumulation of molecules oriented in the same direction to solve the problem of crystallization in atomic structure determination of molecules and nanoclusters. A critical issue in this approach is substrate free molecular orientation. Electric field induced alignment and/or orientation relies on effective suppression of thermal rotation, thus superfluid helium droplets with an equilibrium temperature of 0.4 K offer the desired cooling effect. However, the droplet matrix also introduces a diffraction background. Here

we demonstrate the practicality of electron diffraction of single molecules inside superfluid helium droplets. By taking advantage of velocity slip of a pulsed droplet beam, selective diffraction from monomers, dimers and even larger clusters can be obtained. To further extend this approach to macromolecular ions and nanoclusters, we also demonstrate doping of ions from electrospray ionization into superfluid helium droplets. Although the ultimate demonstration of ss-EDI is still steps away, steady efforts are being made toward the final goal.

10380-15, Session 4

Momentum-space imaging of ultrafast electron-phonon coupling in functional materials *(Invited Paper)*

Hermann A. Dürr, SLAC National Accelerator Lab. (United States)

The functional properties of materials often depend on the detailed interplay of electronic, spin and lattice degrees of freedom. The complexity of this interplay leads to some of the most technologically useful behavior. Effects from anomalous thermal expansion, through optical switching of magnetization, to superconductivity emerge from this complexity. However, understanding the details of this electron–spin –lattice interplay is perhaps the most challenging scientific problem in condensed matter physics. The availability of femtosecond lasers allowed the detailed study of electronic & spin scattering, thermalization, and electron-phonon energy transfer in real time. Ultrafast electron diffraction is a unique tool to probe the excitation of phonons on equal footing. In this talk I will give an overview of recent results for the momentum resolved detection of transient phonon populations in ultrathin films and nanoructures.

10380-16, Session 4

Spatiotemporal visualization of molecular rotational dynamics in femtosecond laser fields *(Invited Paper)*

Hui Li, Jian Wu, Heping Zeng, Peifen Lu, Kang Lin, Junyang Ma, Xiaochun Gong, Qinying Ji, Qiying Song, Wenbin Zhang, East China Normal Univ. (China)

A rotational wave packet (RWP) can be created when a molecule is nonresonantly excited by laser pulses with durations much shorter than the molecular rotational periods. More interestingly, a unidirectional molecular rotation at THz frequency can be initiated by optical kicking. Such phenomenon has attracted many interests in the fields of molecular deflection, generation of molecular vortices, and etc. However, a comprehensive physical picture of the spatiotemporal evolution of the impulsively excited molecular unidirectional rotation has lacked for more than 10 years since its first observation. Here, we directly visualize the spatiotemporal evolution of an impulsively created unidirectional spinning molecular RWP using the coincidence Coulomb explosion imaging technique (CCEIT) in an intense ultrafast laser field for the first time [1]. Both the experimental results and the numerical simulations show rich dynamical information. Depending on the timing or polarization of the pump pulses, the well-confined cigar- or disk-shaped RWP can be impulsively kicked to rotate clockwise or counterclockwise which afterwards disperses and exhibits field-free revivals owing to the time-dependent beating of the coherently populated rotational states. Very recently, the rotational echo of an impulsively excited RWP has been visualized using the CCEIT [2]. The quantum and classical dynamics of the echo phenomena will be discussed. These results will improve the understanding in other fields of physics and trigger the developments in many applications.

Refs:

[1] K. Lin et al., PRA 92, 013410 (2015).

[2] K. Lin et al., PRX 6, 041056 (2016).

10380-17, Session 5

Smartphone chloridometer for point-of-care diagnosis of cystic fibrosis

Chenji Zhang, Jimin Kim, Jian Yang, Zhiwen Liu, Pennsylvania State Univ. (United States)

Chloride is an essential electrolyte that maintains homeostasis within the body, thus evidence of various conditions and diseases can be presented in the chloride levels of biological fluids, such as in sweat chloride which is the primary diagnostic criteria for cystic fibrosis (CF). Yet the transition of chloride sensors from laboratories to the point-of-care has been hindered by prohibitive costs, such that analytical methods for sweat chloride is predominated by manual titration in almost 70% of clinical laboratories. Thus our primary objective in this work is the development of a low cost, point-of-care sweat diagnostics system for cystic fibrosis. We recently established a citrate-derived synthesis platform for the versatile design of new fluorescence chloride sensors with improved sensing properties. As a next step, we herein designed a smartphone operated fluorometer equipped with a citrate-derived chloride sensor such that chloride levels correspond to measurable changes in fluorescence emission. To evaluate clinical performance, we implemented clinical validation with sweat from individuals with or without CF. To our knowledge, this is the first clinical demonstration of a fluorescence-based chloridometer. Such advances in performance and cost-reduction may meet the clinical needs of a reliable point-of-care diagnostic system for CF, and may significantly improve diagnostic accuracy by reducing technical complexity in fast-paced clinical settings.

10380-18, Session 5

Step-index optical fiber based on citrate-based synthetic polymers

Chenji Zhang, Dingying Shan, Jian Yang, Zhiwen Liu, Pennsylvania State Univ. (United States)

The turbidity of biological tissue due to fundamental light-tissue interactions has been a long-standing challenge in biomedical optical technologies. Implanting fibrous optical waveguide into tissue and organ for light delivery and collection is one of the most effective way for alleviate this problem. In this manuscript, by taking advantage of the favorable designability and processibility of citrate-based synthetic polymers, two bio-elastomers with distinct optical properties but matched mechanical properties and similar biodegradation profiles were developed. Combining with an efficient two-step fabrication method, we created a new biodegradable and biocompatible step-index optical fiber. Benefited from this step-index structure and high tunability of citrate-based bio-elastomers, our optical fiber not only demonstrated outstanding optical performance (0.4dB/cm loss), but also had favorable mechanical and biodegradable properties. Apart from the fabrication and characterization of our optical fiber, we successfully demonstrated the functionalities of multimode fiber imaging, deep tissue light delivery and in vivo fluorescence detection of our newly designed optical fiber. We believe the flexible, biodegradable and low loss optical fiber designed in our work offers a valuable tool for optical applications including imaging, detecting, sensing, optogenetic stimulation, and treatment to target regions underneath deep tissue.

10380-19, Session 5

Measure the spatial distribution of corneal elasticity by combining femtosecond laser induced breakdown spectroscopy and acoustic radiation force elasticity microscope

Hui Sun, Xin Li, Zhongwei Fan, Academy of Opto-Electronics, CAS (China); Mingyong Hu, Hefei Univ. of Technology (China)

Purpose: The nonhomogeneous structure of the cornea suggests a unique spatial distribution of corneal elasticity. Non-invasive measurement of this distribution is critical to understanding how biomechanics control corneal stability and refraction. We show that the anterior cornea is more rigid than the underlying posterior stromal bed without disturbing the overall corneal structure.

Methods: Corneas from fresh porcine eyes (Sierra Medical, Whittier, CA) were excised from the globe leaving a 2 mm scleral rim intact. The corneal samples were suspended in collagen gelatin (10% w/w) within a water tank filled with deionized, degassed water. The water tank was attached to a 3-D mechanical stage allowing for precise control of cavitation bubble placement within the cornea. Femtosecond laser pulses induced optical breakdown and produced cavitation in the anterior and posterior cornea. A confocal ultrasonic transducer applied 6.5 ms acoustic radiation force-chirp bursts to the bubble at 1.5 MHz while monitoring bubble position using pulse-echoes at 20 MHz. A cross-correlation method was used to calculate bubble displacements. Maximum bubble displacements are inversely proportional to the Young's modulus. The laser induced breakdown spectroscopy (LIBS) were measured in the anterior and posterior cornea with the same femtosecond laser pulses to see whether the laser induced plasmas signals will show relationship to Young's modulus.

Results: Bubble displacement was 18-25% greater in the posterior cornea relative to the anterior cornea. This indicates a larger Young's modulus in the anterior cornea in the direction orthogonal to the corneal surface. But the laser induced breakdown spectroscopy from the same femtosecond laser source gave the similar results for different locations of cornea.

Conclusions: Our results show that the anterior cornea is stiffer than the posterior cornea and that ARFEM is capable of non-invasively measuring the distribution of corneal elasticity while the LIBS does not have such ability.

10380-20, Session 6

Infrared fingerprint spectroscopy of nanoscale molecules with graphene plasmons *(Invited Paper)*

Qing Dai, National Ctr. for Nanoscience and Technology of China (China)

Infrared (IR) spectroscopy is widely used for chemical identification in such as chemical detection, food safety and biosensing, due to its fast and noninvasive measurement of molecular vibrational fingerprints. In particular, in the molecular fingerprint region from 600 to 1500 wavenumber (corresponds to the wavelength range of 6-16 micrometer), complex vibrational characteristics of molecules in bulk materials can be effectively distinguished to enable unambiguous identification of molecular structures and species. However, molecular fingerprinting at the nanoscale level still remains a significant challenge, due to weak light–matter interaction between micron-wavelengthed infrared light and nano-sized molecules. We demonstrate molecular fingerprinting at the nanoscale level using our specially designed graphene plasmonic structure on 300 nm CaF2 nanofilm supported on doped silicon. This structure not only avoids the plasmon–phonon hybridization, but also provides in situ electrically-tunable graphene plasmon covering the entire molecular fingerprint region, which was previously unattainable. We enhance about 8-nm PEO film vibrational signatures up to larger than 20-fold. In addition, undisturbed and highly confined graphene plasmon offers simultaneous detection of in-plane and out-of-plane vibrational modes with ultrahigh detection sensitivity down to the sub-monolayer level, significantly pushing the current detection limit of far-field mid-infrared spectroscopy. Our results provide a platform, fulfilling the long-awaited expectation of high sensitivity and selectivity far-field fingerprint detection of nano-scale molecules for numerous applications.

10380-22, Session 6

Ultrafast optical spectroscopy of individual nano-materials *(Invited Paper)*

Kaihui Liu, Peking Univ. (China)

When the characteristic length of a material shrink to 1 nm scale, many distinct physical phenomena, such as quantum confinement, enhanced many-body interactions, strong van der Waals inter-material couplings and ultrafast charge separation, will appear. To investigate the related fascinating low-dimensional physics, we need a tool to quantitatively link the atomic structures to the physical properties of these very small nano-materials. In this talk, I will introduce our recently developed in-situ TEM + high-sensitive ultrafast nano-optical spectroscopy technique, which combines capability of structural characterization in TEM and property characterization in ultrafast nano-optical spectroscopy on the same individual nano-materials. Several examples of using this technique to study the 1D carbon nanotube and 2D atomic layered systems will be demonstrated.

10380-23, Session 6

Ultrafast imaging of microstructures and coherent transients in hybrid perovskite materials *(Invited Paper)*

Jigang Wang, Ames Lab., Iowa State Univ. (United States)

The most compelling principle beyond conventional wisdom is that a coherent photoexcitation and hot state delocalization on ultrafast time scales are responsible for a photocarrier generation and quasi-instantaneous probability of energy migration in highly efficient photovoltaic materials. Until now the origin is unclear in the new organic-inorganic perovskite systems despite they have emerged as new revolutionary materials for light-harvesting and electron-transporting applications. In this talk, I will discuss our measurements to image local carrier/exciton population, electronic coherence and charge transport across different grains and grain boundaries (~10-1000 nm). Our results demonstrate a quantitative, ultrafast microscopy spectroscopy tools and elucidate the impact of microstructure on coherent/incoherent charge transport in the hybrid perovskites.

10380-24, Session 6

Ultrafast pump-probe and Raman experiments of individual plasmonic junctions *(Invited Paper)*

Eric O. Potma, Alexander Fast, Kevin T. Crampton, Vartkess A. Apkarian, Univ. of California, Irvine (United States)

We present pump-probe and Raman measurements on individual plasmonic nano-junctions. The time-resolved measurements reveal differences between capacitive and conductive junctions, and paint a detailed picture of the ultrafast electrodynamics of the nano-junction. The insights gleaned from these measurements help interpret the ultrafast response of single molecules placed in the junction.

10380-25, Session 6

Efficient triplet exciton generation in hybrid perovskites *(Invited Paper)*

Kenan Gundogdu, North Carolina State Univ. (United States)

Triplet excitons (TE), bound electron-hole pairs with unity spin and long lifetime, form the basis for exploitation in applications including singlet oxygen generation, photodynamic therapy, and photochemical

Return to Contents

upconversion. As a result, an emerging theme in the realm of nanostructured inorganic semiconductors is the extraction of their transiently stored potential in the form of molecular triplet excited states. In some instances, the efficiency of the triplet energy transfer process approaches unity, leading to generation of surface-bound triplets with lifetimes on the millisecond time scale. These observations are mostly limited to molecular or reduced-dimensional structures, and most typically are pursued in solution phase. While organic-inorganic perovskites have attracted substantial attention for application to optoelectronics, the generation of TEs from the broad perovskite family (i.e., both 3D and lower-dimensional frameworks) remains largely unexplored. In the present work, efficient TE generation on picosecond time scales in a 2D perovskite $(CH_3NH_3)_2Pb(SCN)_2I_2$ is demonstrated using static and transient spectroscopic techniques.

10380-26, Session 7

Redox-sensitive heme imaging with transient absorption microscopy *(Invited Paper)*

Jesse W. Wilson, Erkang Wang, Colorado State Univ. (United States)

Ultrafast pump-probe microscopy enables visualization of non-fluorescent materials in biological tissue, such as melanin and hemoglobin. Whereas transient absorption has been primarily a physical chemistry technique, used to gain insight into molecular and electronic structure, pump-probe microscopy represents a paradigm shift in translating transient absorption into an analytical technique, which can clearly resolve pigments with nearly indistinguishable linear absorption spectra. Extending this technique to other important targets, such as mitochondrial respiratory chain hemes, will require new laser sources and strategies for selecting pump and probe wavelengths to optimize contrast. We will present recent developments on both of these fronts. The laser system we have developed to elicit a pump probe response of respiratory chain hemes is based on an amplified Yb:fiber ultrafast laser that uses modest spectral broadening followed by sum frequency generation to produce a tunable pulse pair in the visible region. Wavelength tuning is accomplished by changing quasi-phase matching conditions. We will present preliminary imaging data in addition to discussing how to manage sample heating problems that arise from performing transient absorption measurements at the high repetition rates needed for imaging microscopy. In the second part of the talk, we will present the use of a subset selection algorithm to choose pump-probe wavelength combinations to optimally measure redox in mixtures of heme proteins.

10380-27, Session 7

Simultaneous two-photon photoactivation and readout of brain activity in 3D with single neuron resolution *(Invited Paper)*

Nicolas C. Pegard, Alan Mardinly, Hillel Adesnik, Laura Waller, Univ. of California, Berkeley (United States)

Understanding how the brain processes information requires the ability to monitor and control neural activity with minimally invasive methods. Optogenetics offers a viable avenue towards large-scale neural control with photosensitive opsins and functional fluorescence markers that externally indicate or trigger action potentials with light.

Fast readout of neural activity in large volumes of brain tissue is made possible by 3D point scanning two photon holography. However, the limiting factor for two-way communication with the brain is photoactivation. Current techniques either suffer from poor spatial resolution, temporal resolution or only operate in small volumes. Precise photo-activation of large custom subsets of neurons such as those involved in a particular brain function remains impossible.

Our technique, 3D Scanless Holographic Optogenetics with Temporal focusing (3D-SHOT), combines temporal focusing, for single neuron spatial resolution, and 3D computer generated holography, for custom targeting within a large volume and with adequate temporal resolution. Temporal focusing and 3D holography are made compatible by giving up the ability to generate custom shapes. For this, we rely on a Custom-made Temporally-Focused Pattern (CTFP) adjusted to the characteristic dimensions of a neuron soma. We then implement point cloud holography, with an SLM in the Fourier domain to replicate the CTFP the desired locations in the volume of interest by all-optical convolution.

Here, by digitally aligning functional imaging and photostimulation, our technology is able to establish all-optical two-way communication with many neurons spatially distributed across a large volume of brain tissue.

10380-28, Session 7

Molecular spectroscopy and dynamics of novel FRET Sensors in crowded environments *(Invited Paper)*

Hannah Leopold, Jacob Schwarz, Megan Currie, Erin D. Sheets, Ahmed A. Heikal, Univ. of Minnesota Duluth (United States)

Macromolecular crowding affects numerous cellular processes including protein folding, biochemical reaction kinetics and transport. As a result, there is a need for new crowding probes, as well as integrated, noninvasive, and quantitative approaches to investigate those processes in heterogeneous, crowded environments, both in vivo and in vitro. In this contribution, we will highlight our recent findings on novel FRET probes (mCerulean—linkers—mCitrine), which can be genetically encoded in living cells with site specificity. Time-resolved fluorescence and anisotropy measurements were employed to characterize the spectroscopy and molecular dynamics of these probes as a function of biomimetic crowding (Ficoll-70 and glycerol at variable concentrations in PBS buffer). At the single molecule level, fluorescence fluctuation analyses were also used to quantify the translational diffusion coefficient of the probes in crowded environments as a means to quantify the hydrodynamic radii while elucidating the underlying diffusion mechanism. Our comprehensive studies of these FRET probes on multiple time scales would help understand the length/time scales associated with macromolecular crowding. Importantly, these results represent a first step towards quantitative, non-invasive studies of in vivo crowding.

10380-29, Session 7

Second harmonic generation chiral imaging in biological tissues *(Invited Paper)*

Shi-Wei Chu, National Taiwan Univ. (Taiwan)

Chirality plays a fundamental role in biomedical fields; many drugs, enzymes, and biomolecules cannot function unless their chiralities are correct. Since the conformation of a molecule, as well as the chirality, is very sensitive to the local microenvironment, it is vital to characterize molecular chirality without altering the surrounding conditions. To determine the chirality in materials, optical activity is the most common way. In linear optics, optical rotatory dispersion and circular-dichroism are the two well-developed methods for probing chirality. However, their weak contrast, poor optical sectioning, and low penetration depth constrain its application to study chirality in tissues and real bio-samples. Therefore, previous research has been mostly limited to surfaces or solutions.

In contrast to linear optics, there are several nonlinear optical activity effects in chiral materials, such as vibrational circular dichroism, Raman optical activity, two-photon absorption circular dichroism, and second-harmonic generation circular-dichroism (SHG-CD). The last one is the most studied nonlinear chiral effect since it shows significantly improved chiral contrast. An additional advantage of SHG-CD is its intrinsic optical sectioning due to nonlinearity. When combined with an infrared excitation, SHG-CD has

been demonstrated to provide high penetration depth for three-dimensional imaging. However, in recent studies, the signal origin of SHG-CD in biological tissue is ambiguous, since not only chirality, but also the anisotropy of molecules contribute to SHG-CD response. It will be of great importance to find an experimental skill that can distinguish the contribution between these two mechanisms.

Here we studied SHG-CD of collagen, which is the most abundant protein in human body. Inspired by linear CD where resonant wavelength is required to reveal chirality, we have carried out nonlinear microspectroscopy measurement and shown that when the excitation meets the resonant band of collagen, chirality-induced SHG-CD is strongly enhanced and can be easily identified versus the anisotropy-induced contribution. By slowly heating up the sample, we have further verified that there is a wavelength-independent anisotropy contribution of SHG-CD vanishing at around 40 – 50 degree Celsius, while the resonance-enhanced chirality component of SHG-CD remains until temperature rise to 60 degree. Our results feature the first quantitative identification of chirality-induced SHG-CD in an intact biological tissue, and will be a critical step toward nonlinear chiral microscopy.

10380-30, Session 8

Femtosecond pulse delivery through multi-core fibers for imaging and ablation *(Invited Paper)*

Demetri Psaltis, Eirini Kakava, Nicolino Stasio, Donald B. Conkey, Christophe Moser, Ecole Polytechnique Fédérale de Lausanne (Switzerland)

No Abstract Available.

10380-31, Session 8

Label-free mid-Infrared photothermal imaging: High spatial resolution beyond the mid-Infrared diffraction limit *(Invited Paper)*

Michelle Y. Sander, Boston Univ. (United States)

Photothermal spectroscopy in the mid-infrared can directly target vibrational modes in the fingerprint region and forms an attractive technique for label-free, bond-specific characterization of chemical and biological samples. Through a raster-scanning approach, local sample information can be combined with spectroscopic and spectral details. We will discuss how the spatial resolution of this technique benefits from the shorter wavelength fiber laser to obtain resolving powers beyond the diffraction limited mid-infrared pump wavelength. This is of particular interest to analyze biological tissue samples without a need for exogenous labels or thin-film samples at high spatial resolution. Studies based on the United States Air Force (USAF) resolution target patterned in PMMA as well as histopathological mouse brain tissue will be presented.

10380-32, Session 8

Practical masks for multimodel spatial frequency modulation imaging fabricated with femtosecond laser micromachining *(Invited Paper)*

Jeffrey A. Squier, Colorado School of Mines (United States); Randy A. Bartels, Colorado State Univ. (United States); Michael D. Young, Colorado School of Mines (United States); Jeffrey J. Field, Colorado State Univ. (United States); Nathan Worts, Colorado School of Mines (United States); Keith A. Wernsing, Patrick A. Stockton, Colorado State Univ. (United States); Alyssa M. Allende Motz, Colorado School of Mines (United States)

Spatial frequency modulation for imaging (SPIFI) is an important new imaging modality in linear and nonlinear microscopy. It uses an extended excitation source for optimal imaging speeds, and is compatible for use with scattering specimens. Significantly, this is a multimodal imaging modality: contrast can be achieved with the excitation laser or nonlinear excitation mechanisms such as second and third harmonic generation imaging and/or multiphoton excitation fluorescence. What is particularly exciting is that the SPIFI method can achieve enhanced resolution with any of the aforementioned modalities.

SPIFI requires a mask at an intermediate image plane to modulate the extended excitation source. We have been able to fabricate the masks used to achieve this modulation through femtosecond laser micromachining. Notably we have been able to create highly efficient masks that can be use in reflective or transmissive geometries. These masks produce high contrast images with enhanced resolution and can be produced inexpensively. Here we will show how a standard nonlinear microscope architecture can be adapted for use with these masks, making SPIFI conversion straightforward and easy to implement.

10380-33, Session 8

Sum frequency generation holography

Ding Ma, Pennsylvania State Univ. (United States); Christopher M. Lee, The Pennsylvania State Univ. (United States); Yizhu Chen, Nikhil Mehta, Seong H. Kim, Zhiwen Liu, Pennsylvania State Univ. (United States)

We demonstrate a sum frequency generation (SFG) holographic imaging method by integrating the capabilities of holography and SFG spectroscopy. SFG can probe the molecular vibrational resonance in non-centrosymmetric media. Holographic recording can capture both the amplitude and the phase of the SFG signal, thus leading to label-free spectroscopic three-dimensional imaging.

10380-34, Session 9

Non-degenerate two-photon excitation for increasing the fluorescence photon yield and maximum microscopy imaging depth *(Invited Paper)*

Mu-Han Yang, Christopher G. L. Ferri, Payam A. Saisan, Maxim Abashin, Univ. of California, San Diego (United States); Peifang Tian, John Carroll Univ. (United States); Yeshaiahu Fainman, Anna Devor, Univ. of California, San Diego (United States)

We investigate the utility of non-degenerate 2-photon excitation (ND-2PE) as a strategy for extending the 2-photon imaging depth. For the ND-2PE scheme, two pulsed, synchronized laser sources of different wavelength each provide a photon for the 2-photon absorption process. By independently tuning their wavelengths, we are able to tune the excitation to tissue transparency windows while maintaining resonant fluorescence excitation. These transparency windows reduce excitation power loss resulting from scattering. In addition, by having two sources we are able to displace the beams in space except at their common focus; thus, reducing background fluorescence excitation. Finally, we show that ND-2PE inherently results in increased 2-photon absorption cross sections, resulting in increased fluorescence intensity. By combining beam displacement, tissue transparency and increased absorption cross sections, we achieve increased imaging depths as compared to degenerate 2-photon excitation with commonly used fluorophores.

10380-35, Session 9

High resolution nonlinear imaging based on optical field engineering *(Invited Paper)*

Kebin Shi, Dashan Dong, Yanhui Cai, Wei Liu, Chendi Shao, Peking Univ. (China)

There have been increasing interests in nonlinear optical imaging technology, especially in biomedical and material research fields, where higher spatial resolution, better sensitivity, deeper penetration and faster data acquisition are always desired. Most recent examples include fluorescence microscopy, coherent Raman and nonlinear wave mixing imaging. In this talk, we will present our recent progresses on deep tissue fluorescence super-resolution and non-labeling chiral sum frequency generation imaging by utilizing optical field engineering mechanism.

10380-36, Session 9

Ultrafast all-optical laser scanning imaging with spatiotemporally encoded pulses *(Invited Paper)*

Kevin K. Tsia, The Univ. of Hong Kong (Hong Kong, China)

The holy grail of optical bioimaging is to gain quantitative understanding of the biological systems at different scales, from biomolecules to tissue, with high spatiotemporal resolution. However, this long-standing goal has been hampered by the intrinsic speed limit imposed by the prevalent image capture strategies, which involve the laser scanning technologies, (e.g. galvanometric mirrors), and/or the image sensors. Regarding live imaging, these factors explains the scarcity of video-rate volumetric microscopy and tomography platforms. Regarding high-throughput single-cell analysis, the speed-versus-sensitivity trade-off of the image sensor explains why the throughput of flow cytometry has to be scaled down from 100,000 cells/sec to 1,000 cells/sec when the imaging capability is incorporated.

This talk will describe our recent efforts on addressing these challenges by taking a generic imaging concept - ultrafast spatiotemporal encoding of laser pulses for all-optical laser-scanning. These techniques, including time-stretch imaging and free-space angular-chirp-enhanced delay (FACED) imaging, enable ultrahigh-throughput single-cell imaging with multiple image contrasts (e.g. quantitative phase and fluorescence imaging) at a line-scan rate beyond MHz (i.e. an imaging throughput up to ~100,000 cells/sec).

10380-37, Session 9

Coherence-domain imaging with harmonic holography *(Invited Paper)*

Ye Pu, Demetri Psaltis, Ecole Polytechnique Fédérale de Lausanne (Switzerland)

Observing the fast dynamics of specific molecules or targets in three-dimensional (3D) space and time inside a crowded and complex environment, such as living cells or tissues, remain one of the grand open challenges in modern science. Harmonic holography tackle this challenge by combining the 3D imaging capability of holography with the ultrafast, coherent optical contrast offered by second-harmonic radiating imaging probes (SHRIMPs). Similar to fluorescence, the second-harmonic signal emitted from SHRIMPs provides a color contrast against the uninterested background scattering, which can be efficiently suppressed by an optical filter. We review the latest developments in SHRIMPs and harmonic holography and discuss their further applications in fluidics and biofluidics.

10380-39, Session PMon

Research study of the treatment efficacy of staphylococcia in the palatine tonsils by using Raman-scattering spectroscopy method

Anna A. Asadova, Elena V. Timchenko, Pavel E. Timchenko, Elena G. Zarubina, Evgeniy S. Burenkov, Yuriy D. Ityaksov, Anna S. Tyumchenkova, Samara Univ. (Russian Federation)

These WHO statistics show that the world is suffering from tonsillitis from 10 to 15% of adults and from 20 to 25% of children. From 15 to 45% of cases is bacterial tonsillitis caused by ?-hematolytic streptococcus of group A. For the monitoring the effectiveness of treatment in medicamental practice was carried out a number of laboratory studies: common urine analysis and clinical blood analysis, and at the end of treatment: electrocardiogram and biochemical blood assay.

At the present time, optical methods in research are widely used in medical challenges. These methods are painless and fast, and can be performed in outpatient facilities. One of the alternative and promising methods of analysis of biological objects is Raman scattering method.

During the experiment, the 8 samples of different strains of staphylococcus ATCC ?25923 (Group I) and ATCC ?35591 (Group II) which are in the saliva of patients and normal saline. Half of the samples were subjected to treatment with antibiotics Amoxiclav dosage 500mg / 10ml, the second half was the control.

The spectral-response characteristics were studied using an experimental stand, which includes a high-resolution digital spectrometer Andor Shamrock sr-303i with built-in cooling chamber DV420A-OE, a fiber-optics probe for Raman spectroscopy RPB785, combined with laser module LuxxMaster LML-785.0RB-04 (with regulated power up to 500 mW, wavelength 785 nm).

The effectiveness of treatment of staphylococcus in the tonsils was analyzed using Raman spectroscopy (RS). The spectral changes were established in the treatment of palatine tonsils using antibiotic Amoxiclav. It is shown that at a dose of antibiotic 500mg / 10ml disappears lines at wave numbers 735 cm-1 and 783 cm-1, 986 cm-1 and 1635 cm-1, corresponding to adenine, cytosine, proteins and amide I, which indicates the treatment success. There are input optical criteria for evaluating the effectiveness of treatment.

10380-40, Session PMon

Research studies of aging changes of hyaline cartilage surface by using Raman-scattering spectroscopy

Anna S. Tyumchenkova, Elena V. Timchenko, Pavel E. Timchenko, Samara Univ. (Russian Federation); Larisa T. Volova, Dmitry A. Dolgyshkin, Samara State Medical Univ. (Russian Federation); Maria D. Markova, Elena F. Yagofarova, Samara Univ. (Russian Federation)

The articular hyaline cartilage is the unique tissue, which is due to its physical properties, is able to provide damper function throughout human life, supporting the possibility of movement in the joints. However, the destructive changes occur in cartilaginous tissue with aging. The ability to identify the characteristics of the cartilage surface using Raman spectroscopy makes it possible to carry out a comparative assessment of the spectral characteristics of the cartilaginous tissue of elderly people and children of 12 months and downwards.

For the research study were used cartilage samples of articular surface of knee joint of elderly people, obtained during the operations of endoprosthesis replacement and cartilaginous tissue of articular surfaces of the maniphalanx which children under 12 months of age were amputated because of polydactylia.

The research studies were carried out with the stand, actualized high-resolution digital spectrometer Shamrock sr-303i (Fig. 1), combined with a laser module LuxxMaster LML-785.0RB-04 (up to 500 mW, wavelength 785 nm), and built-in cooled chamber DV420A-OE, providing spectral resolution of 0.15 nm (spectral range 200-1200 nm). Isolation of the Raman spectra in the background of autofluorescence was carried out using polynomial approximation of fluorescence and its subtraction from recorded spectra in the program Wolfram Mathematica 9. In the chosen range 400-2200 cm-1 using an iteration algorithm [29] was determined approximating line (polynom of the fifth degree) of autofluorescence component then subtracted this component and obtained dedicated Raman spectrum. During treatment the experimental spectra was purified from the noise by smoothing median filter in 7 points.

The main differences of the spectral characteristics of cartilaginous tissue were observed in the lines 1244 cm-1 and 1660 cm-1 which corresponded to amide III and amide I. Optical coefficients that were input allow to allocate age features of hyaline cartilage surface.

10380-41, Session PMon

Research of vertical sections of rats' tubular bones in simulation of reduction bone tissue mineral density using Raman spectrum method

Yana V. Fedorova, Elena V. Timchenko, Pavel E. Timchenko, Samara Univ. (Russian Federation); Dmitry A. Dolgyshkin, Larisa T. Volova, Samara State Medical Univ. (Russian Federation); Anna A. Asadova, Anna S. Tyumchenkova, Samara Univ. (Russian Federation)

Density mineral reduction of bone tissue leads to the development of destructive processes in the bones and to reduction its mechanical strength, fracture. During preclinical study is needed to simulate animals' reduction bone tissue mineral density and to confirm the effectiveness of the various ways to treat this pathosis. One of the research methods to study bone tissue can be Raman spectroscopy.

24 rats' humeri were used as research materials. 12 of them were obtained from healthy animals and they became the first study group. Others were in the second group and were obtained from animals which at first we simulated density bone mineral reduction by doing ovariotomy, and then they were given a course of hydroxyapatite treatment. Bones were sawed longitudinally and measured in section. In each sample, Raman spectra were taken from three areas: the head area, neck and shaft of bone.

Experimental stand realizing the Raman spectroscopy method included a high-resolution digital spectrometer Shamrock sr-303i with built-in cooled chamber DV420A-OE, an optical fiber probe for Raman spectroscopy RPB785, combined with laser module LuxxMaster LML785.0RB-04 (with controlled output up 400 mW, wave length 785 nm). The radiation power of 400 mW did not cause any tissue destructive changes. The treatment of Raman spectra was carried out in program Wolfram Mathematica 9.

The spectrum analysis showed that the samples in the second group in comparison with the first group were observed the changes in intensity of the lines at wave numbers 956 cm-1 (phosphate ion PO43- (?1) (P-O symmetrical valent)), 1071 cm-1 (CO32- (?1) substitution of B-type (C-O valent planar)), 1246 cm-1 (amide III) and 1659 cm-1 (amide I).

10380-42, Session PMon

Optical surface evaluation of bone implants during its processing

Oleg O. Frolov, Pavel E. Timchenko, Elena V. Timchenko, Samara Univ. (Russian Federation); Larisa T. Volova, Dmitry A. Dolgyshkin, Violetta V. Boltovskaya, Samara State Medical Univ. (Russian Federation); Vadim D. Meshcheryakov, Yana Fedorova, Anna S. Tyumchenkova, Samara Univ. (Russian Federation)

Bone implants used in reconstructive surgery to restore structural integrity of bones and increase the osteogenetic potential of bone tissue. The quality of allogeneic bone tissue for transplantation depends on the way of its production, processing and keeping. Bone implants should be nonimmunogenic and bioresorbable.

The study objects were samples of spongy bone tissue (the size of 5 x 5 x 5 mm). In the manufacture process of bone bio-implants was carried out their low-frequency ultrasonic treatment, and as a result the samples deprived of fat and all the bone marrow cells were eliminated from interjoist bone spaces. Then, to obtain a demineralized biomaterial the bone tissue was placed in a spirit of salt.

In the capacity of essential method of biomplants research was used Raman spectroscopy method.

The features of the Raman spectra were studied for surfaces bone implants manufactured by different demineralization protocols. It has been established that the spectral characteristics of the surfaces bone implant manufactured by different demineralization protocols had difference at wavenumbers 428, 585, 960, 1065, 1243 and 1555 cm-1, corresponding to a significant for the implant quality of components. Raman-scattering spectroscopy can be used to evaluate the quality of the surface bone implants during its processing.

10380-43, Session PMon

Extension of supercontinuum spectrum, generated in photonic crystal fiber, by using chirped femtosecond pulses

Julius Vengelis, Vygandas Jarutis, Valdas Sirutkaitis, Vilnius Univ. (Lithuania)

We present results of experimental and numerical investigation of supercontinuum generation in polarization maintaining photonic crystal fiber (PCF) using chirped femtosecond pulses. The initial unchirped pump pulse source was a mode-locked Yb:KGW laser generating 52 nJ energy 110 fs duration pulses at 1030 nm with 76 MHz repetition rate. The nonlinear medium was a 32 cm long polarization maintaining PCF with zero dispersion wavelength at 800 nm manufactured by NKT Photonics A/S. The generated supercontinuum spanned through a wide spectral range ? from roughly 450 nm to 1400 nm. We showed the influence of various nonlinear phenomena on spectral characteristics of supercontinuum by changing unchirped pump polarization and pulse energy. Eventually, we experimentally demonstrated that by chirping pump pulses positively or negatively we can obtain broader supercontinuum spectrum than in case of unchirped pump pulses at the same peak power. The broadening of supercontinuum spectrum increases with the value of pump pulse chirp but the increase is different in cases of positively and negatively chirped pulses. In our case the supercontinuum spectrum width was extended by up to 115 nm (at maximum chirp value of +10500 fs2 that we could achieve in our setup) compared to the case of unchirped pump at the same peak power.

Numerical simulations of supercontinuum generation in PCF were also performed. The simulated supercontinuum spectra display the same qualitative features as the ones measured in the experiment. We also discuss possible physical mechanisms leading to additional spectrum broadening due to pump pulse chirp.

10380-44, Session PMon

Temporal focusing multiphoton excitation fluorescence imaging using the excitation wavelength-selected configuration

Fan-Ching Chien, National Central Univ. (Taiwan); Chi-Hsiang Lien, National United Univ. (Taiwan); Gerald Abrigo, National Central Univ. (Taiwan)

Temporal focusing multiphoton excitation microscopy (TFMPEM) has been presented the improvements in temporal and spatial resolutions of multiphoton excitation imaging by combined with the structured light illumination techniques and is a powerful platform for visualizing the dynamic distribution of molecules and cells and the architecture of subcellular structures in biotissues. However, TFMPEM is insufficient for performing efficient excitation of fluorophores with different two-photon absorption spectra in multifluorophore imaging through an illuminated configuration of fixed wavelength pulse light source. Therefore, TFMPEM with the fast excitation wavelength-selected configuration was implemented using an optical setup to change the incident angle of the light source at the diffraction grating depending on its central wavelength. The proposed system was used to observe two-photon excitation (TPE) fluorescent section images of the mouse muscle fibers through wavelength-selected excitation. Furthermore, the intensity enhancement of a TPE fluorescence image of multifluorophore-labeled specimens through optimum wavelength excitation in the proposed TFMPEM system was demonstrated.

10380-45, Session PMon

Imaging of thick, transparent samples by time-of-flight detection of optical pulse trains

Xing Lu, Jiarui Wu, Wentao Yu, Ziheng Ji, Qihuang Gong, Kebin Shi, Peking Univ. (China)

Imaging of transparent sample via optical phase contrast mechanism has been intensively investigated in biomedical and material science. Various methods were employed in this field, including Zernike phase contrast microscopy [1], Nomarski differential interference contrast microscopy [2], off-axis based digital holography (DH) imaging [3], diffraction phase microscopy (DPM) [4], common-path based Fourier phase microscopy (FPM)[5], quadriwave lateral shearing interferometry (QWLSI) [6], etc. While their axial resolution could reach nanometers, their axial imaging depth however is still limited to micrometers. In this paper, we report a novel imaging method that enables observing transparent specimen with thickness exceeding hundreds of micrometers. The new method employs 1550 nm femtosecond mode-locked fiber laser and is based on time of flight (TOF) detection of optical pulse trains. Although transparent sample is invisible under traditional bright-field microscope, its refractive index distribution exists. When optical pulse passes through different areas of the sample, the phase retardation is different. In this method, a new device – fiber loop optical-microwave phase detector (FLOM PD) [7] is employed. FLOM PD is capable of detecting optical-microwave phase, which is related to optical pulse delay, with high resolution and can help achieve tight synchronization between microwave and optical pulse train up to sub-femtosecond level [7]. And due to its microwave reference, this technique enables large detection range. In the experiment, we firstly use one FLOM PD to synchronize the optical pulse train and the microwave reference, and then use another identical FLOM PD to detect the optical-microwave phase (the same microwave signal acts as the reference) after the synchronized optical pulse passes through the sample. With the advantage of FLOM PD, we have achieved imaging of thick, transparent sample of hundreds of micrometers thick with sub-micrometer resolution.

[1] F. Zernike, "Phase contrast, a new method for the microscopic observation of transparent objects," Physica 9, 686-698 (1942).

[2] G. Nomarski, "Differential microinterferometer with polarized waves," J. Phys. Radium 16, 9S-11S (1955).

[3] P. Ferraro, S. Grilli, D. Alfieri, S. De Nicola, A. Finizio, G. Pierattini, B. Javidi, G. Coppola, and V. Striano, "Extended focused image in microscopy by digital holography," Optics Express 13, 6738-6749 (2005).

[4] C. Edwards, R. Zhou, S.-W. Hwang, S. J. McKeown, K. Wang, B. Bhaduri, R. Ganti, P. J. Yunker, A. G. Yodh, J. A. Rogers, L. L. Goddard, and G. Popescu, "Diffraction phase microscopy: monitoring nanoscale dynamics in materials science [Invited]," Applied Optics 53, G33-G43 (2014).

[5] G. Popescu, L. P. Deflores, J. C. Vaughan, K. Badizadegan, H. Iwai, R. R. Dasari, and M. S. Feld, "Fourier phase microscopy for investigation of biological structures and dynamics," Optics letters 29, 2503-2505 (2004).

[6] P. Bon, G. Maucort, B. Wattellier, and S. Monneret, "Quadriwave lateral shearing interferometry for quantitative phase microscopy of living cells," Optics Express 17, 13080-13094 (2009).

[7] K. Jung, and J. Kim, "Subfemtosecond synchronization of microwave oscillators with mode-locked Er-fiber lasers, " Optics letters 37, 2958-2960 (2012).

10380-46, Session PMon

Holographic imaging of two dimensional materials

Joshua Noble, Atriya Ghosh, Zhiwen Liu, The Pennsylvania State Univ. (United States)

Two-dimensional (2D) materials have recently attracted interest in the field of photonics. Here, we examine the phase response and thickness of 2D monolayers created by chemical vapor deposition onto Si/SiO2 substrates. These structures exhibit transverse dimensions on the order of tens of microns. Measuring the thickness along the axial direction, however, is much more challenging. We explore the feasibility of using digital holographic imaging to quantify the associated phase response.

10380-47, Session PMon

Tomographic diffractive microscopy for better 3D imaging

Dashan Dong, Yanhui Cai, Ziheng Ji, Hong Yang, Qihuang Gong, Kebin Shi, Peking Univ. (China)

Tomography imaging is one of the most developing imaging technology in recent years; it has great capability for biopsy and living cell imaging. Lately, the diffraction tomography imaging based on the scatting theory has greatly promote the resolution of tomographic imaging. The need to visualize three-dimensional (3-D) structures noninvasively using this method is growing rapidly. In this studying, based on a commercial microscope, a holographic tomography microscope is built by combined with digital holography. The imaging speed is greatly boosted by simultaneously controlling the rotation of light and raw imaging logging. In the image processing stage, a fast and robust algorithm is used to mapping the data in frequency domain to reconstruct the 3-D reflection index. The result shows a valid 3-D reflection index measurement of polystyrene microspheres and INS-1 cells.

10381-16, Session PMon

Molding and simulating of GaN step-up power switched capacitor converter

Ayoob Alateeq, Yasser A. Almalaq, Mohammad A. Matin, Univ. of Denver (United States)

According to the demand of low voltage DC-DC converter, a proposed step-up power switched capacitor converter (PSC) was designed and analyzed in this paper. The proposed two-level PSC converter has been proven to achieve high voltage gain by using fewer switches than other types of DC-DC switched capacitors converter. The proposed two-level PSC consist of 8 switches and 5 capacitors. The switches were selected to be GaN transistors in order to maintain the losses when either the switching frequency or the temperature increase. To validate the design outputs, the theoretical results were compared with LT spice simulator. Since the design combines semiconductor elements such (GaN transistor), then 10 % error is a reasonable difference between the mathematical and simulation results.

10381-18, Session PMon

Design and performance study of a DC-DC flyback converter based on wide bandgap power devices for photovoltaic applications

Salah S. Alharbi, Saleh S. Alharbi, Ali M. S. Al-bayati, Mohammad Matin, Univ. of Denver (United States)

This paper presents a high-performance dc-dc Flyback converter design based on GaN power devices for photovoltaic (PV) applications. The flyback converter is modeled with two different power devices: a GaN-transistor and a Silicon (Si) MOSFET. They are implemented individually in the flyback converter to describe the impact of these devices on the converter performance. The total power loss of the converter with different power devices is analyzed for various switching frequencies. The converter efficiency is evaluated at different operating conditions. The results show that the GaN-based converter has a higher efficiency level and lower total power loss compared to the conventional Si-based converter.

10381-19, Session PMon

Design of a high-performance cascaded boost converter with SiC power devices for photovoltaic applications

Saleh S. Alharbi, Ali M. S. Al-bayati, Salah S. Alharbi, Mohammad Matin, Univ. of Denver (United States)

This paper presents a comprehensive evaluation of the effects of Silicon Carbide (SiC) power devices on the performance of a dc-dc cascaded boost converter for photovoltaic (PV) applications. The converter is designed with SiC MOSFETs and compared to the conventional cascaded boost converter based on Silicon (Si) devices. The total power loss and efficiency of the converter are evaluated at different switching frequencies and load conditions. SiC power devices in the cascaded converter show a superior performance under wide switching frequency conditions. The results show that the cascaded converter with SiC devices significantly reduces total losses and improves the overall efficiency.

10381-20, Session PMon

Properties of reactively sputtered Alx Ny thin films for pyroelectric detectors

Nicholas P. Calvano, Philip C. Chrostoski, Andrew Voshell, Keesean Braithwaite, Delaware State Univ. (United States); Dennis W. Prather, Univ. of Delaware (United States); Murzy D. Jhabvala, NASA Goddard Space Flight Ctr. (United States); Mukti M. Rana, Delaware State Univ. (United States)

Pyroelectric detectors are class of uncooled infrared detectors whose polarization changes with change in temperature. Infrared radiation from objects falls on top of the sensing layer of the pyroelectric detector and absorbed radiation causes the temperature of to change. The polarization of the sensing layer changes this way. This work presents the deposition and characterization of Al_x N_y thin films for using them as pyroelectric detector material. To test the pyroelectric effect, capacitors of various sizes were fabricated. The diameter of the electrodes for capacitor used during testing of the device was 1100 ?m while the distances between these two electrodes was 1100 ?m. On a 3-inch diameter cleaned silicon wafer, 20 nm thick Ti adhesion layer was deposited followed by a 100 nm thick Au layer. On top of this Au layer, 100 nm Al_x N_y thin films were deposited. Finally, 100 nm thick Au layer was deposited and lifted off by conventional photo lithography to form the electrodes of capacitors. All the layers were deposited by radio frequency sputtering at room temperature. The thin film samples were annealed at 700 0C in N2 environment for 10 minutes. X-ray diffraction showed the films are poly-crystalline with peaks in (100), (002) and (101) directions. The pyroelectric current increased from 3.38 ? 10-14 A at 303 K to 1.75 ? 10-13 at 353 K. When the temperature varied between 303 K to 353 K, the pyroelectric coefficient was increased from 8.60 ? 10-09 C/m2K to 3.76 ? 10-08 C/m2K while the loss tangent remains almost constant to ~1.5 ? 10-5 when the temperature was varied in the same range. The room temperature pyroelectric coefficient, loss tangent, voltage responsivity figure of merit and detectivity figure of merit were found to be 8.60?10-9 C/m2K, 1.79?10-5, 1.25?10-4 C/m2K and 1.39?10-3 Pa-2 respectively.

10381-1, Session 1

Junction formation by laser irradiation through semiconductor substrate for CdTe and wide-band gap materials *(Keynote Presentation)*

Toru Aoki, Junichi Nishizawa, Jinwei Lee, Kento Tabata, Akifumi Koike, Shizuoka Univ. (Japan)

pn junction formation in the CdTe by laser irradiation doping has been developed. We could confirm the p-n diode can be formed by direct laser irradiation of CdTe-metal interface through semiconductor material irradiation and doping of CdTe and its performance as a gamma-ray detector with high reverse voltage bias. Moreover, it has been found that the number of irradiation and power of the laser affect condition of the doping. This method is suitable for wide-bandgap material for heavy doping and pn junction without high-temperature processes.

10381-2, Session 1

A study of the effect of surface pretreatment on atomic layer deposited Al2O3 Interface with GaN

Jianyi Gao, Wenwen Li, Srabanti Chowdhury, Univ. of California, Davis (United States)

Al2O3 has been an attractive gate dielectric for GaN power devices owing to its large conduction band offset with GaN (~2.13eV) [1], relatively high dielectric constant (~9.0) and high breakdown electric field (~10MV/cm). Due to exceptional control over film uniformity and deposition rate, atomic layer deposition (ALD) has been widely used for Al2O3 deposition. The major obstacle to ALD Al2O3 on GaN is its high interface-state density (Dit=1012~1013 eV-1cm-2) [2] caused by incomplete chemical bonds, native oxide layer and impurities at the Al2O3/GaN interface. Therefore, an appropriate surface pretreatment prior to deposition is essential for obtaining high-quality interface. In this study, we investigated the effect of TMA, H2O and Ar/N2 plasma pretreatment on Dit and border traps (Nbt). 5 cycles of TMA purge, 5 cycles of H2O purge and Ar (50sccm, 25W, 5min)/N2 (50sccm, 50W, 20min) plasma pretreatment were conducted respectively on MOCVD-grown GaN-on-sapphire consisting of 1µm n-GaN layer with doping of ~1?1017cm-3 on the top and 1µm n+ GaN layer with doping of ~3?1018cm-3 on the bottom prior to the Al2O3 deposition. Al2O3 was also deposited on as-received GaN for comparison. Au/Ni/Al2O3/GaN metal-oxide-semiconductor capacitors (MOS-C) were fabricated for the characterization of Dit and Nbt using UV-assisted capacitance-voltage (C-V) technique [3]. Integrated Dit over E-Ec=0.15eV to 1eV for as-received, TMA, H2O and Ar/N2 plasma pretreated samples were 1.09?1012cm-2, 1.48?1012cm-2, 1.77?1012cm-2 and 9.82?1011cm-2. Nbt for as-received, TMA, H2O and Ar/N2 plasma pretreated samples were 7.78?1012cm-2, 9.43?1012cm-2, 7.61?1012cm-2 and 1.66?1012cm-2. The results showed that TMA and H2O pretreatment had trivial effects on interface engineering whereas Ar/N2 plasma pretreatment slightly reduced Dit and significantly reduced Nbt.

Reference

[1] R. D. Long and P. C. McIntyre, Materials 5, 1297 (2012).

[2] A. M. Sonnet, C. L. Hinkle, H. Dawei, and G. Bersuker, IEEE Trans. Electron Devices 57, 2599 (2010).

[3] B. L. Swenson and U. K. Mishra, J. Appl. Phys. 106, 064902(2009).

10381-3, Session 1

3D analysis of thermal and electrical performance of wide bandgap VDMOSFETs

Mahesh Manandhar, Mohammad A. Matin, Univ. of Denver (United States)

Power electronics is based on the conversion and conditioning of electric power in its different forms. The need for higher operating voltages, temperatures and switching speeds have necessitated for the use of semiconductor materials more superior to Silicon for power electronics purposes. Wide bandgap (WBG) materials like SiC, GaN and Diamond have been known to demonstrate better material properties as compared to Silicon, like higher operating temperatures, higher breakdown voltages and reduced thermal and electrical resistances which make them ideal for high power electronic devices. This paper analyzes the thermal and electrical performance of WBG power MOSFETs, in particular the Vertical Double-diffused MOSFET (VDMOSFET) structure, modeled in the commercial simulation software COMSOL Multiphysics. VDMOSFETs are ideal for high power electronic applications owing to their higher voltage blocking capabilities as compared to the conventional lateral MOSFET structure. COMSOL uses Finite Element/Volume Analysis methods to approximate solutions to differential equations involved with complex geometries and physics. The 3D model investigated in COMSOL for this model solved for thermal and electrical variables for VDMOSFETs using SiC, GaN and Diamond as their semiconductor material. Only half of the 3D VDMOSFET structure was modeled for faster computational speed as the structure itself is symmetric about the vertical axis. The temperature profiles and current densities of each WBG material VDMOSFET were analyzed for different operating voltages. These profiles were compared with a Si VDMOSFET model to determine relative similarities and differences between each material.

10381-4, Session 2

Emission control of multilayered thin films of ZnO/CuO prepared by pulsed laser deposition *(Invited Paper)*

Hong-Kun Lyu, DGIST (Korea, Republic of); Bunyod Allabergenov, DGIST (Korea, Republic of) and Urgench State Univ. (Uzbekistan); Hyunseok Shim, Myoung-Jae Lee, Byeongdae Choi, DGIST (Korea, Republic of)

In this report, we present on a research result of the microstructural and optical properties of ZnO/CuO multilayered films. Three types of multilayer ZnO/CuO stacks were prepared by pulsed laser deposition (PLD) on amorphous SiO2/Si substrates, and then annealed at 500oC for 30 min to improve crystallinity. TEM and XRD analysis of the thin films revealed the formation of multiple crystallographic defects and modification of the dominant growth plane. Consequently, near-band-edge emission in ZnO can be controlled through the number of CuO layers. The detailed microstructure and electro optical properties of multilayered ZnO/CuO thin films will be discussed.

10381-6, Session 2

Development of an efficient DC-DC SEPIC converter using wide bandgap power devices for high step-up applications

Ali M. S. Al-bayati, Salah S. Alharbi, Saleh S. Alharbi, Mohammad A. Matin, Univ. of Denver (United States)

This paper presents the development of an efficient DC-DC single-ended primary-inductor converter (SEPIC) for high step-up applications. The SEPIC converter is designed using wide bandgap power devices and its performance is compared with the conventional silicon power device based converter. The behavior of the power devices is characterized and analyzed at the system level. The total power losses as well as the overall performance efficiency of the converter are measured and reported under different conditions. The analysis and results show the potential of the designed converter to operate efficiently and reliably at a wide range of operating conditions.

10381-7, Session 3

Defect-induced optical breakdown in aluminum nitride *(Invited Paper)*

Jae-Hyuck Yoo, Lawrence Livermore National Lab. (United States); Andrew Lange, Lawrence Livermore National Lab. (United States) and Univ. of California, Davis (United States); Selim Elhadj, Lawrence Livermore National Lab. (United States)

Aluminum nitride (AlN) has an extremely wide bandgap (~6 eV), making it a promising material for high power and deep ultraviolet applications. Aluminum nitride is also commonly used as a buffer layer for gallium nitride devices where its electrical breakdown characteristics can limit high voltage operation. The authors have investigated conductive gallium nitride on AlN films for use in high-power optoelectronics. It was found that damage

initiates in the AlN buffer or at the AlN-GaN interface when bi-layer films are exposed to sub-bandgap, high infrared laser fluences. Through subsequent optical damage studies, it was revealed that laser damage in single layers of intrinsic AlN occurs by either dielectric breakdown or discrete absorption processes thought to be initiated by extended defects. This understanding has motivated the use of laser-based probing to spatially resolve breakdown behavior in AlN over large areas for emerging power device applications.

This work was performed under the auspices of the U.S. Department of Energy by Lawrence Livermore National Laboratory under Contract DE-AC52-07NA27344

10381-8, Session 3

Comparison between dielectric and p-GaN gates for CAVETs with Mg ion-implanted current blocking layers

Saptarshi Mandal, Univ. of California, Davis (United States)

Gallium Nitride power electronics has witnessed significant technological development in the last decade [1]. Commercial GaN power electronic devices are based on lateral channel AlGaN/GaN high electron mobility transistors (HEMTs) [2]. Despite their high mobility and channel charge, lateral HEMTs have key limitations when compared to vertical transistors like the current aperture vertical electron transistor (CAVET). Unlike lateral HEMTs, CAVETs do not exhibit surface state induced current collapse or dynamic RON during switching, due to a buried peak electric field [3]. The breakdown voltage in a HEMT scales with gate to drain distance (BVd) whereas in vertical transistors BVd scales with drift layer thickness, resulting in a higher current density per unit chip area for the same breakdown voltage [4]. In this work, a study of two different types of CAVETs with Mg ion-implanted current blocking layer are presented. The device fabrication and performance limitation of a CAVET with a dielectric gate is discussed, and the breakdown limiting structure is evaluated using on-wafer test structures. The gate dielectric limited the device breakdown to 50V, while the blocking layer was able to withstand over 400V. To improve the device performance, an alternative CAVET structure with a p-GaN gate instead of dielectric is designed and realized. The p-GaN gated CAVET structure increased the BVd to over 400V. Measurement of test structures on the wafer showed the breakdown was limited by the blocking layer instead of the gate p-n junction. The devices also showed no dc-RF dispersion when pulsed using 80 ?s wide pulses.

[1] S. Chowdhury et al 2013 Semicond. Sci. Technol. 28 074014

[2] J. Millán, et al 2014 IEEE Transactions on Power Electronics, 29, 2155

[3] S. Chowdhury et al 2008 IEEE Electron Device Letters, 29 543

[4] N. Q. Zhang et al 2000 IEEE Electron Device Letters 21 421

10381-9, Session 3

Highly efficient GaN HEMTs transformerless single-phase inverter for grid-tied fuel cell

Khaled S. Alatawi, Fahad M. Almasoudi, Mohammad A. Matin, Univ. of Denver (United States)

The interest in distributed generation systems based on solar PV and fuel cells (Fcs) has increased recently due to their low cost and high efficiency. Fuel cells are electrochemical devices that generate electrical energy without the burning process. Fuel cells use hydrogen and Oxygen as fuels which make them safe for the environment and very efficient. Transformerless inverters are the most efficient approach to utilize renewable energy sources for grid tied applications. Removing transformers will increase the efficiency and reduce the size, cost and the complexity of the system. In this paper, a new transformerless inverter equipped with GaN HEMTs is proposed. The new topology is derived from conventional H5 inverter. GaN HEMTs are used to enable the system to switch at high frequency, which will reduce the size, volume and cost of the system even more. Moreover, inverter control is designed and proposed to supply real power to the grid and to work as DSTATCOM to mitigate any voltage sag and compensate reactive power in the system. The new topology is investigated and compared to H5 inverter in terms of efficiency and power losses. The switching strategy of the new topology creates a new current path which reduces the conduction losses significantly. The analysis of the proposed system was carried out using MATLAB/SIMULINK and PSIM. The proposed controller improves voltage stability and mitigates voltage sag and compensates reactive power. The simulation results prove the effectiveness of the system for grid-tied applications.

10381-10, Session 3

The wide bandgap of optical absorption coefficient for optoelectronic materials

Subhamoy Singha Roy, JIS College of Engineering (India)

In both the cases, the OAC exhibits the singularity when the incident photon energy ( ) tends to and the magnitude of the OAC depends to a large extent on the numerical values of the energy band constants of the said compounds. In addition, the simplified results of the OAC for materials having parabolic energy bands have also been obtained form the present generalized analysis under convinced restrictive circumstances.

10381-11, Session 4

?-Ga2O3 films grown via oxidation of GaAs substrates and their device demonstrations *(Invited Paper)*

Ahmet Kaya, Daniel M. Dryden, Howard Mao, Dewyani Patil-Chaudhuri, Andrew Philip Lange, Subhash Mahajan, Jerry M. Woodall, M. Saif Islam, Univ. of California, Davis (United States)

We present a simple and inexpensive method for growing ?-Ga2O3 films by heating GaAs wafers at high temperature in a furnace in both argon and air ambient. Prolonged heating was found to completely oxidize a GaAs wafer into ?-Ga2O3 while shorter heating duration contributes to large-area, high-quality ?-Ga2O3 nanoscale thin films that spontaneously delaminates from the GaAs substrate. The films are characterized using x-ray diffraction, energy dispersive spectroscopy, Raman spectroscopy, and scanning electron microscopy. The ?-Ga2O3 film's optical band gap and Schottky barrier height with gold are 4.8 eV and 1.03 eV, respectively. The photoconductance of the ?-Ga2O3 films was found to increase by more than three orders of magnitude under 270 nm ultraviolet (UV) illumination with respect to the dark current.

10381-12, Session 4

Simulation and performance comparison of Si and SiC-based interleaved boost converter

Yasser A. Almalaq, Ayoob Alateeq, Mohammad A. Matin, Univ. of Denver (United States)

In this paper, simulation and performance comparison of Si and SiC based interleaved boost converter is presented. Wide band gap devices such as silicon carbide and gallium nitride are desirable and recommended in high-power applications because of their capability of operating under high temperature, high switching frequency, and high voltage with reduced switching losses. The main advantage of using SiC materials in interleaved boost converter is the ability to increase the switching frequency which will reduce the size. However, their cost is high compared to Si. In this paper, 60V input voltage is used to get 120V output voltage under 100 KHz switching frequency and 0.5 duty cycle. With the help of LTSpice software,

a comparison between silicon and silicon carbide by considering interleaved boost converter are simulated and studied.

10381-13, Session 4

High efficiency H6 single-phase transformerless grid-tied PV inverter with proposed modulation for reactive power generation

Fahad M. Almasoudi, Khaled S. Alatawi, Mohammad A. Matin, Univ. of Denver (United States)

Implementation of transformerless inverters in PV grid-tied system offer great benefits such as high efficiency, light weight, low cost, etc. Most of the proposed transformerless inverters topologies in literatures are verified for only real power application. Currently, international standards such as VDE-AR-N 4105 has demanded that PV grid-tied inverters should have the ability of controlling specific amount of reactive power. Generation of reactive power cannot be accomplished in H6 topology because the existing modulation techniques are not adopted for freewheeling path in the negative power region. This paper enhances a previous high efficiency proposed H6 trnasformerless inverter with SiC MOSFETs and demonstrates new operating modes for the generation of reactive power. A proposed pulse width modulation (PWM) technique is applied to achieve bidirectional current flow through freewheeling state. A comparison of the proposed H6 transformerless inverter using SiC MOSFETs and Si MOSFTEs is presented in terms of power losses and efficiency. The results show that reactive power control is attained without adding any additional active devices or modification to the inverter structure by taking the advantage of SiC MOSFET's body diode with small reverse recovery current. Also, the proposed modulation provides low leakage current by maintaining constant common mode voltage (CM) during every operating mode. The performance of the proposed system verifies its effectiveness in grid-tied applications.

10381-14, Session 4

Low-crosstalk optimization in 2D segmented waveguide crossings by evolutionary algorithms *(Invited Paper)*

Cosme Eustaquio Rubio Mercedes, Maicon de Souza Alcântara, Univ. Estadual de mato Grosso do Sul (Brazil); Anderson Dourado Sisnando, Vitaly Felix Rodriguez Esquerre, Univ. Federal da Bahia (Brazil)

A rigorous analysis of two-dimensional segmented waveguide (2D-SWG) crossing using evolutionary algorithms in conjunction with the two-dimensional finite element method (2D-FEM) is presented. The power transmission and crosstalk of the waveguide crossings are calculated, optimized and compared with other designs in the literature. The optimized crossing has been successfully and efficient designed using evolutionary algorithms based on artificial immune system (AIS) and the genetic algorithm (GA). Power transmissions above 98 % and crosstalk below 40 dB over a broadband interval of wavelength have been obtained with both evolutionary algorithms.

10381-15, Session 4

III-nitride based N-polar current aperture vertical electron transistors

Saba Rajabi, Saptarshi Mandal, Univ. of California, Davis (United States); Haoran Li, Univ. of California, Santa Barbara (United States); Matthew A. Laurent, Univ. of California, Davis (United States); Stacia Keller, Univ. of California, Santa Barbara (United States); Srabanti Chowdhury, Univ. of California, Davis (United States)

Gallium nitride (GaN) based transistors have been of interest to power electronics community because of their high breakdown voltage, high sheet carrier density, and the high saturation velocity of GaN. The low switching losses of GaN enable high-frequency operation which reduces bulky passive components with negligible change in efficiency [1,2]. The most established GaN electronic devices are fabricated on the Ga-polar orientation of GaN. Recently, N-polar GaN based devices are being explored for high frequency applications due to their advantages over Ga-face, such as lower contact resistance since the 2DEG is contacted through a lower bandgap material and better electron confinement due to natural back-barrier provided by the charge inducing barrier [3]. In this work, the first N-polar GaN current aperture vertical electron transistor is presented. The samples were grown by metal-organic chemical vapor deposition on c-plane Sapphire substrate. Mg ions were implanted at 80keV (dose: 1??10?^15 ?cm?^(-2)) into the top GaN layer, everywhere except the current aperture to form the current blocking layer. A 7 A^0 AlN to reduce alloy scattering followed by 150nm UID N-polar GaN as channel were regrown on top of the implanted structure. The 2DEG density and the mobility of the as-grown sample, determined using Hall measurement, were 1.1??10?^13 ?cm?^(-2) and 1800 ?cm?^2/(V-S) , respectively. The CAVET showed excellent device modulation and a maximum current of 2 KA?cm?^(-2) at V_G=2V. The maximum transconductance per mm of source was 140 mS. The device had a very large pinch-off voltage of -14V as calculated due to the presence of high charge density in the channel.

[1] S. Chowdhury et al 2013 Semicond. Sci. Technol. 28 074014

[2] J. Millán, et al 2014 IEEE Transactions on Power Electronics, 29, 2155

[3] Uttam Singisettiet al 2013 IOP Semicond. Sci. Technol. 28 074006

Conference 10382: Photonic Fiber and Crystal Devices: Advances in Materials and Innovations in Device Applications XI

SPIE. OPTICS+ PHOTONICS OPTICAL ENGINEERING+ APPLICATIONS

Sunday - Monday 6 –7 August 2017

Part of Proceedings of SPIE Vol. 10382 Photonic Fiber and Crystal Devices: Advances in Materials and Innovations in Device Applications XI

10382-1, Session 1

Inorganic nanocomposite films with polymer nanofillers made by the concurrent multi-beam multi-target pulsed laser deposition *(Invited Paper)*

Abdalla M. Darwish, Abdel Aziz Mohammed, Shaelynn Moore, Wydglif Dorlus, Tyler Bastian, Dillard Univ. (United States); Sergey S. Sarkisov, SSS Optical Technologies, LLC (United States); Paolo Mele, Muroran Institute of Technology (Japan); Shrikant Saini, The Univ. of Utah (United States); Junichiro Shiomi, Susumu Yada, The Univ. of Tokyo (Japan); Darayas N. Patel, Oakwood Univ. (United States); Brent Koplitz, Xiaodong Zhang, Tulane Univ. (United States)

We report on the new class of inorganic nanocomposite films with the inorganic phase hosting the polymer nanofillers made by the concurrent multi-beam multi-target pulsed laser deposition of the inorganic target material and matrix assisted pulsed laser evaporation of the polymer (MBMT-PLD/MAPLE). We used the exemplary nanocomposite thermoelectric films of aluminum-doped ZnO known as AZO with the nanofillers made of poly(methyl methacrylate) known as PMMA on various substrates such as $SrTiO_3$, sapphire, fused silica, and polyimide. The AZO target was ablated with the second harmonic (532 nm) of the Nd:YAG Q-switched laser while PMMA was evaporated from its solution in chlorobenzene frozen in liquid nitrogen with the fundamental harmonic (1064 nm) of the same laser (50 Hz pulse repetition rate). The introduction of the polymer nanofillers increased the electrical conductivity of the nanocomposite films (possibly due to the carbonization of PMMA and the creation of additional channels of electric current) three times and reduced the thermal conductivity by 1.25 times as compared to the pure AZO films. Accordingly, the increase of the thermoelectric figure-of merit ZT would be ~ 4 times. The best performance was observed for the sapphire substrates where the films were the most uniform. The results point to a huge potential of the optimization of a broad variety of optical, opto-electronic, and solar-power nanocomposite inorganic films by the controllable introduction of the polymer nanofillers using the MBMT-PLD/MAPLE method.

10382-2, Session 1

Analysis of photonic spot profile converter and bridge structure on SOI platform for horizontal and vertical integration

Rajib Chakraborty, Saikat Majumder, Univ. of Calcutta (India); Amit K. Jha, Aishik Biswas, Debasmita Banerjee, Dipankar Ganguly, Techno India (India)

Presently, high index contrast SOI platform is extensively used for integrated photonic circuits due to its CMOS compatibility and better light confinement. In this work the simple matrix technique is used to design structures for horizontal and vertical integration in such a platform. The designed structures are horizontal spot profile converter required for horizontal light coupling and vertical bridge structure required for vertical integration. Both the structures are considered to be made with multimode interference couplers. Multimode interference coupler is a promising waveguide structure having wide application as splitter, multiplexer, photonic switch etc. Spot profile converter can be realized of successive integration of multimode interference structures with reducing dimension on horizontal plane, whereas an optical bridge structure is a combination of two vertical multimode interference structure connected by a single mode section. The analyses of these two structures are carried out for both TE and TM modes at 1550 nm wavelength using the semi analytical matrix method due to its simple nature and fastness in computation time and memory. The computational results obtained from matrix method have been compared with the results obtained from different numerical method like BPM, FEM etc with the other researchers. This work shows that the matrix method is equally applicable for horizontally integrated photonic circuit as well as vertically integrated photonic circuit. The proposed spot profile converter can be used for different sensing application and the bridge structure can be used for optical signal routing in optical communication systems.

10382-3, Session 1

Enhanced nonlinear light conversion in globular photonic crystals at the band-gap pumping

Arsen Zotov, Stanislav O. Yurchenko, Kirill I. Zaytsev, Egor Yakovlev, Evgeny Gorbunov, Bauman Moscow State Technical Univ. (Russian Federation); Gleb M. Katyba, Institute of Solid State Physics RAS (Russian Federation); Nikita V. Chernomyrdin, Bauman Moscow State Technical Univ. (Russian Federation)

The problems of nonlinear process enhancement and high optical harmonic generation are of great importance in optics. Recently, photonic crystals (PCs) have attracted considerable interest as prospective media for this purpose. The PC has a structure characterized by a spatially periodic distribution of optical properties, which leads to the appearance of numerous physical effects . These effects allows us employing the PC structures for highly efficient waveguiding nonlinear light conversion, or active media pumping .

In this talk, we would consider the results of experimental and theoretical study of the structural light focusing effects in PCs . This effect appears as a result of strong redistribution of electromagnetic field in 2D and 3D PCs at the bang gap-pumping owing to the curvature of its nodes. It leads to strong localization of electromagnetic wave in certain regions of the PC volume and, as a consequence to the enhancement of non-linear optical phenomena. We discuss theoretical background of the structural light focusing effect, the results of numerical simulations, as well as its application for enhanced nonlinear light conversion in artificial opal-based PCs, including generation of second and third harmonics, Raman light scattering, and fluorescence.

10382-4, Session 1

Terahertz waves and its interaction with ferroics and multiferroics, for the design of modulators

Moumita Dutta, Soutik Betal, Xomalin G. Peralta, Amar S. Bhalla, Ruyan Guo, The Univ. of Texas at San Antonio (United States)

With the advancements in femto-second laser technology and the coherent generation and detection of Terahertz(THz) radiation (ranging from 0.1?THz to 30?THz), this spectral region is finding applications in various disciplines like imaging, communications, explosive-detection, spectroscopy of molecular vibrations etc. However, in order to realize full-

fledged THz applications, efforts need to be directed towards the design and implementation of efficient THz modulators and switches. In this work we study interaction of THz-waves with different ferroic and multiferroic materials, excited by external fields, to exploit that knowledge for the design of THz modulators. These modulators can be envisioned to be the opto-electronic units for the future optical-communication/computing.

10382-5, Session 1

Magnetoelectric nanorobot for therapeutic applications

Soutik Betal, The Univ. of Texas at San Antonio (United States)

In this study we illustrate a novel device named magnetoelectric nanorobot (MENR) which is a core-shell magnetoelectric nanoparticle. We fabricated the MENR and proposed it as a bio-switch which can be controlled remotely by biased ac magnetic field. When a threshold attractive ac magnetic field (F1) is applied, this bio-switch can permeate in a series of aligned cells one by one. This process is called magneto-elasto-electroporation (MEEP), which is a unique technique of remotely controlled electrically excited, nanopore opening on a cell membrane and permeation using MENR. These MENR can also be dynamically targeted to a particular area of cells/single cell avoiding any of the untargeted cells on the path, under the influence of (F2) attractive ac magnetic field. It has also been experimentally confirmed that when a repulsive biased ac magnetic field (F3) ac excitation is applied, a group of MENR can induce motion and actuate a group of cells as well as can transport them to an unlimited distance and through narrow bifurcation such as blood vessels or veins with variable pressure gradient.

10382-6, Session 1

Nonlinear optical crystalline structures grown by laser precipitation in glass

Carl M. Liebig, Jonathan T. Goldstein, Air Force Research Lab. (United States); Sean A. McDaniel, Air Force Research Lab. (United States) and Leidos, Inc. (United States); Douglas M. Krein, Air Force Research Lab. (United States) and General Dynamics Information Technology (United States); Gary Cook, Air Force Research Lab. (United States)

Over the last decade it has been demonstrated that nonlinear optical (NLO) crystals can be grown by laser precipitation in customized glasses and used for electro-optic applications [1]. It has been further demonstrated that this novel crystal growth technique is capable of fabricating nonlinear waveguide structures, where the polar axis of the crystal is aligned along the growth direction [2]. Femtosecond precipitation of NLO crystals in glass has the potential to be a low-cost method of creating functional optical elements. In order to realize this goal, the orientation of the NLO crystals must be carefully controlled. In the present study, a widely used electro-optical crystal, Lithium Niobate, was precipitated in $33LiO_2$-$33Nb_2O_5$-$34SiO_2$ (mol%) (LNS) glass, forming NLO crystalline structures in an amorphous matrix. Glass fabrication techniques for making high quality glass, and the crystallization parameter space were explored to determine the optimal conditions for smooth and continuous crystal growth. The crystalline orientation of the precipitated lithium niobate was determined for a variety of writing conditions, and the growth technique was extended to multi-dimensional structures.

[1] T. Komatsu, et al., J. Solid State Chem. 184, 411 (2011)

[2] A. Stone, et al., Sci. Reports 5, 10391 (2015)

10382-7, Session 1

Characteristic study on circularly bent plastic optical fiber based refractometer

Mayank Upadhyay, Aman Kumar Srivatsava, National Institute of Technology, Warangal (India)

Many areas of research such as biomedicine, food safety, environmental monitoring, chemical and bio chemical sensing demand a precise measurement of refractive index (R.I) of various chemicals and fluids. Inherent advantages of Optical fibers such as small size, immunity from electromagnetic interference, low cost, high sensitivity, potential for remote sensing, and fast responsiveness offer an easy and cost effective solutions for refractive index measurement. POF sensors exhibit additional advantages which includes negative thermo-optic coefficients, high fracture toughness, flexibility to bending, high sensitivity to strain along with the inherent advantages of silica optical fibers. Moreover, they show excellent compatibility with organic materials, enabling them for chemical and biomedical applications.

In the present study, an investigation is made for the realization of plastic optical fiber based refractometer by evanescent field modulation techniques. Clad-removing, thermal tapering are some of the techniques for maximizing the evanescence field there by causing more interaction with the surrounding medium. In this study, plastic optical fiber is bent into circular shape of an optimized radius and etched to a suitable thickness in order to enhance the evanescent field. To characterize the sensors performance, it has undergone various experimental studies. It is observed that sensitivity of the sensor is increased in comparison with a straight etched optical fiber sensor. The sensitivity of the sensor is found to be 400 RIU. The sensor is very low cost, fast responsive and highly flexible.

10382-8, Session 1

Study on u-bent plastic fiber optic sensor for nitrite compounds detection by evanescent field modulation techniques

Aruna Gupta, National Institute of Technology, Warangal (India)

Recent decades has been witnessing a rapid growth of nitrite compounds in environment and drinking water. Nitrite is a notorious chemical, known for detrimental effects on human health. When consumed in excess quantities, it can cause methemoglobinemia which is medically called “Blue Baby Syndrome” and different types of stomach cancers. Nitrates and nitrites mainly enter into environment due to the anthropogenic activities such as excess use of pesticides in agriculture and from the drain waters of industries. World health organization (WHO) has set an upper limit of 3ppm for presence of nitrite compounds in drinking water. These reasons provoking for the development of accurate, high sensitive and specific low cost detection systems. Optical fiber based sensors has become an attractive alternative technology, due to its inherent advantages such as high sensitivity, low cost, immunity towards electromagnetic interference, remote monitoring and small size. Evanescent field techniques are well known low cost intensity modulated sensors. In the present article, an investigation on utilization of plastic optical fiber for nitrite sensing is discussed. A U-bent optical fiber sensor is designed for the purpose. The working principle in sensing the nitrite concentration is modulation of the evanescent field of the fiber being absorbed or scattered by ambient medium. The interaction between evanescent field and surrounding chemical is maximized by removing the cladding or etching the U-bent portion of the fiber by suitable techniques. Nitrite concentrations even in trace amounts as low as 100 ppb can be measured by the method.

10382-9, Session 2

Computation of the total number of particles in a spherical microbubble in optical trapping using an equation

Arjun Krishnappa, Univ. of Dayton (United States)

In the previous research, an optical force equation for microbubbles is derived to compute the force on a microbubble that is steered in a liquid using an Optical Field. To compute the total number of particles in the spherical microbubble, a tabular method is used. Although the tabular method is not complex and provides the approximate value, it is necessary to derive an equation for the precise value in computing the number of particles. This research paper has derived an equation for computing the total number of particles in the spherical microbubble. The equation provides the precise and reliable results in the computation of the total number of particles. By computing the number of particles using the equation instead of the tabular method, the precision of the optical force equation for the microbubble is increased. The equation for computing the total number of particles has been verified both theoretically and experimentally.

10382-11, Session 2

Organic-metal hybrid nanostructures for toward high-performance photonic devices: Photo-detector and waveguide

Sunjong Lee, Korea Institute of Industrial Technology (Korea, Republic of); Seokho Kim, INHA Univ. (Korea, Republic of); Bo-Hyun Kim, DGIST (Korea, Republic of); Dong Hyuk Park, INHA Univ. (Korea, Republic of)

Organic-metal hybrid nanotubes (NTs), nanowires (NWs), and nanoparticles (NPs) using ϖ-conjugated polymers and small molecules are introduced. The fabrications, characteristics, and applications of the hybrid nanostructures (NSs) using the organic nanomaterials are intensively covered. The hybrid NSs were visualized and confirmed through SEM, TEM, HR-TEM, and elemental analysis. We observed nanoscale laser confocal microscope (LCM) PL characteristics of the hybrid materials drastically varied with metal NSs. The LCM PL intensity of the single unit of the organic-metal hybrid NTs/NWs/NPs increased considerably. We analyze that the huge enhancement PL of the organic-metal hybrid NSs might originate from energy transfer and/or charge transfer in a surface plasmon resonance (SPR) coupling, supported by ultraviolet and visible absorption spectra. We investigated the photo-responsive electrical characteristics using the single unit of the hybrid NSs for the high sensitive and fast responsive photo-detector. In optical waveguiding experiments, the propagation characteristics of optical signals along the single hybrid material were dependent on the existence of the silver NPs. For the hybridized with silver NPs, the waveguiding PL signals of hybrid material had relatively higher output. Additionally, the waveguiding characteristics such as decay constant along the hybrid material considerably decrease the optical loss in hybrid materials. It is remarked that the effective SPR coupling between organic crystal and nanoscale silver NPs can be significantly activating PL propagate without optical loss. These outstanding photonic performances may be applied to photo-detector and photonic optical communication through SPR coupling effect.

10382-12, Session 2

Optical fiber Fabry-Perot sensing system based on Blackbody radiation in high temperature applications

Xiaohua Lei, Tao Chen, Lei Xie, Yijun Deng, Weimin Chen, Chongqing Univ. (China)

High-temperature sensing or strain sensing at high temperature in harsh environments is a challenging industrial task. Optical fiber sensors, especially Fabry-Perot sensors, have attracted much attention because of their promising characteristics, such as miniaturization, thermal stability, and a corrosion resistant nature. In an optical fiber sensing system, the broadband light source is often needed to supply energy for sensing and demodulation. While at high temperature, the blackbody radiation energy of materials is strong, so it has the great potential to become the light source of an optical fiber sensing system. In this way, the optical fiber sensing system architecture can be simplified and system cost can be reduced.

In this paper, a blackbody radiation model based on cylindrical cavity is presented and radiation coupling efficiency from blackbody into multimode fiber has been investigated. Fiber Fabry-Perot sensing system based on light source of blackbody radiation has been set up and strain sensing experiment has been carried out. Results show that blackbody radiation is strong enough to support sensing of fiber Fabry-Perot sensors in high temperature (800~1000ºC), a sensitivity around 10nm/?? has been achieved.

10382-13, Session 2

Fiber-optic refractive index sensor based on tapered single mode-thin core-single mode fiber structure

Ameni Ben Khalifa, Amine Ben Salem, Rim Cherif, SUP'COM (Tunisia)

The refractive index measurement based on all-optical-fiber technology play an important role in chemical and biotechnological applications due to their intrinsic advantages such as immunity to electromagnetic interference, low cost, compact size, high sensitivity and fast response. Recently, the inline fiber sensors based on thin-core fiber modal interferometers have been introduced because of the advantages of lower transmission loss, sharper filter bandwidth, and better resolution compared with single mode-multimode-single mode fiber structure.

In this paper, we propose the design of fiber optic refractive index sensor based on a thin core fiber, characterized by cladding and core diameters about 125 μm and 3 μm, respectively, sandwiched between an input and output single mode fiber. We investigate numerically the dependence of the surrounding refractive index of the sucrose solution to the shift of re-imaging resonant wavelength of the proposed sensor where we have a refractive index sensitivity of the proposed sensor about 179.65 nm/RIU.

In order to enhance the sensitivity of the thin core modal interferometer structure, we reduce the diameter of the cladding of the sensing region. To the best of our knowledge, this is the first time that a tapered single mode-thin core-single mode fiber structure is designed. The sensors with different waist-diameters (90, 60, 45, 30 μm) are investigated, as a result the sensitivity to the surrounding medium increases when the waist diameters decreases. We obtained an ultra-high sensitivity of the tapered sensor about 891.31 nm/RIU in the refractive index range of 1.3346-1.3899 achieved for a waist diameter equal to 30 μm and a taper length of 675μm.

The designed structure shows the merits of high sensitivity which is 5 times higher than that of the basic structure without tapering.

10382-14, Session 2

Anti-resonant hollow core fiber for precision timing applications

Amy Van Newkirk, The Pennsylvania State Univ. (United States); J. Enrique Antonio Lopez, Rodrigo Amezcua Correa, Axel Schülzgen, CREOL, The College of Optics and Photonics, Univ. of Central Florida (United States); John Mazurowski, The Pennsylvania State Univ. (United States)

Many applications rely on the ultra-precise timing of optical signals through fiber, such as fiber interferometers, large telescope arrays, in phase arrayed antennae, optical metrology, and precision navigation and tracking. Environmental changes, specifically those caused by temperature

fluctuations, lead to variations in the propagation delay of optical signals and thereby decrease the accuracy of the system's timing.

The cause of these variations in delay is the change in the glass properties of the optical fiber with temperature. Both the refractive index of the glass and the length of the fiber are dependent on the ambient temperature. Traditional optical fiber suffers from a delay sensitivity of 39 ps/km/K. We are reducing the temperature sensitivity of the fiber delay through the application of a novel design of optical fiber, Anti-Resonant Hollow Core Fiber. The major improvement in the thermal sensitivity of this fiber comes from the fact that the light is guided in an air core, with very little overlap into the glass structure. This drastically reduces the impact that the thermally sensitive glass properties have on the propagation time of the optical signal. Additionally, hollow core fiber is inherently radiation insensitive, due to the light guidance in air, making it suitable for space applications.

10382-15, Session 2

High light extraction efficiency (LEE) LEDs with asymmetric patterned sapphire substrate

Shizhuo Yin, Chang-Jiang Chen, Wenbin Zhu, Ju-Hung Chao, Haonan Zhou, The Pennsylvania State Univ. (United States)

This letter presents the recent advances of GaN light emitting diodes (LEDs) on asymmetric patterned sapphire substrate (PSS) with high light extraction efficiency (LEE). Compared to the conventional GaN LED on PSS with symmetric micro-pyramids, the asymmetric PSS-LED can further improve its LEE from 60% to 71% by optimizing the oblique angle of the asymmetric micro-pyramid. This improvement of LEE is mainly dedicated to the increased surface area and better randomization on the direction of transmitted/reflected light, which enhances the escaping probability after multiple reflections.

10382-16, Session 3

Characteristics of gold nanorods in volume holographic nanocomposites *(Invited Paper)*

Liangcai Cao, Shenghan Wu, Song Zong, Guofan Jin, Tsinghua Univ. (China)

Gold nanorod has generated great research interests due to its tunable longitudinal plasmon resonance. The mechanism of its localized surface plasmon resonance (LSPR) effect on the enhancements of holographic performance for the volume holographic polymer is not clear till now. In this work, a theoretical model for the gold nanorods has been set up and the LSPR effects between light and narorods could be successfully simulated. The obtained resonance wavelength is dependent on not only aspect ratio but also rod radius. The acquired data could be a good reference to design advanced nanocomposite of volume holographic material. Besides, the doped gold nanorods can also decrease the shrinkage of the photopolymer, which reduce the deformation of the multiplexed gratings. The experimental evaluation of the material in our lab suggests a novel candidate for potential applications in high-density optical data storage and high-resolution holographic display.

10382-17, Session 3

Intermodal four-wave-mixing and multimode parametric amplification in km-long fibers

Massimiliano Guasoni, Francesca Parmigiani, Peter Horak, Optoelectronics Research Ctr., Univ. of Southampton (United Kingdom); Julien Fatome, Lab. Interdisciplinaire Carnot de Bourgogne (France); David J. Richardson, Optoelectronics Research Ctr., Univ. of Southampton (United Kingdom)

Multimode amplifiers and wavelength converters are of paramount importance in spatial division multiplexing schemes. In this framework, intermodal four-wave-mixing (FWM) in km-long fibers may provide a suitable way to design efficient all-optical parametric amplifiers and converters, where large degrees of nonlinearity – and thus amplification - can be achieved thanks to long fiber lengths while keeping low input powers. However, long fibers undergo random birefringence fluctuations that can strongly affect the FWM and related amplification processes. While several works have addressed this issue in single-mode fibers, there are currently very few studies for multimode fibers. In this work we theoretically and numerically analyse the two main intermodal FWM processes, namely Bragg-Scattering (BS) and Phase-Conjugation (PC), when weak random birefringence fluctuations are present along the fiber length. In particular, we estimate the amplification impairments induced by these unavoidable fluctuations. The system configuration of the processes is the following: two input pumps P1 and P2, coupled respectively to two distinct spatial modes m1 and m2, and a seed signal S1, coupled to m1, nonlinearly interact giving rise to idler signals in m2 for both the PC (idler I2-PC) and the BS (idler I2-BS) processes. We analyze the amplification of both idlers, identifying several operation regimes depending on the main fiber features. Each one of the regimes discloses different amplification impairments for the BS and PC processes, which offers important guidelines for an efficient design of multimode parametric amplifiers and wavelength converters.

10382-18, Session 3

Moderate temperature-dependent surface and volume resistivity and low-frequency dielectric constant measurements of pure and multi-walled carbon nanotubes (MWCNT) doped polyvinyl alcohol thin films

Matthew E. Edwards Sr., Padmaja Guggilla, Angela Reedy, Alabama A&M Univ. (United States); Quratulann Ijaz, Troy Univ. (United States); Afef Janen, Alabama A&M Univ. (United States)

Previously, we have reported measurements of the temperature-dependent surface resistivity of pure and multi-walled carbon nanotubes doped amorphous Polyvinyl Alcohol (PVA) thin films. In the temperature range from 22°C to 40°C with a humidity-controlled environment, we found the surface resistivity to decrease initially but to rise steadily as the temperature continued to increase. Also, electric surface current densities (Js) were measured on the surface of pure and MWCNT doped PVA thin films. At low voltages, these densities were found to be produced analogously to ohmic conduction. However, unlike ohmic conduction in metals where free electrons exist, some captive electrons are freed to become conduction electrons from increased thermal vibration of constituent atoms in amorphous thin films. Finally, we present conventional volume resistivity measurements in the same temperature range, with the recognition that nano-dopants, microscopic structure, and environmental conditions contributed to the unique physical properties of these material systems.

10382-19, Session 3

Opposite virtual objective

Yeh-Wei Yu, Szu-Yu Chen, Che-Chu Lin, Chinng-Cherng Sun, National Central Univ. (Taiwan)

4-pi microscopy applies bi-directional illumination to create axial

interference fringe to improve the axial resolution. Since all the 4-pi-related techniques require two opposite objectives at each side of the tissues, their applications in optically-thick tissues have never been proposed. Besides, the information carried by backward and forward harmonic generation signals are also proved to be different. Limited by the penetration depth of light, imaging of intact or live bio-tissues can only be achieved by using an epi-detection microscopic geometry. Applications which are based on forward-emitted signals or bi-directional illumination are restricted due to the lack of the objective lens on the other side of the tissues. In this paper, we propose a novel concept of generating an opposite virtual objective (OV-Obj). The OV-Obj serves as an objective at the other side of the observed tissue that generates the desired backward illumination inside the tissue. The concept is stated as follows. A physical objective (P-Obj) is used to forward focus a laser beam in the tissue and to collect the backward scattering light from the tissue. The backward scattering light is sent to the holography-based optical phase-conjugate mirror (HOPCM) to generate a phase conjugate wave. When the phase conjugate wave illuminates the tissue, the tissue is activated to form an inverse focusing light. This process is regarded as an OV-Obj. Under this configuration, the forward and inverse focusing beams not only focus at the same point but also inherently possess the same phase at the focal plane. This autopositioning and auto-phase-matching can benefit 4-pi-related applications. The proposed method is compatible to current supper-resolution imaging technologies including coherent and incoherent methods. Therefore, it open a window for forward-emitted signals and bi-directional illumination in thick specimens.

10382-20, Session 3

Time: The enigma of space *(Invited Paper)*

Francis T. S. Yu, The Pennsylvania State Univ. (United States)

In this article we have based on the laws of physics to illustrate the enigma time as creating our physical space (i.e., the universe). We have shown that without time there would be no physical substances, no space and no life. In reference to Einstein's energy equation, we see that energy and mass can be traded, and every mass can be treated as an Energy Reservoir. We have further shown that physical space cannot be embedded in absolute empty space and cannot have any absolute empty subspace in it. Since all physical substances existed with time, our cosmos is created by time and every substance including our universe is coexisted with time. Although time initiates the creation, it is the physical substances presented to us the existence of time. We are not alone with almost absolute certainty. Someday we may find a right planet, once upon a time, had harbored a civilization for a short period of light years.

10382-21, Session 3

Rapid silicon carbide (SiC) crystal growth by laser heating in a vacuum chamber

Shizhuo Yin, Haonan Zhou, Chang-Jiang Chen, Wenbin Zhu, Ju-Hung Chao, The Pennsylvania State Univ. (United States)

This paper reports a rapid crystal growth technique to grow up to 50 micrometer silicon carbide (SiC) crystal from nano-size SiC powder. By heating the nano-size SiC powder with a high power CO2 laser beam in a vacuum environment, the silicon carbide nanosize powder is quickly heated to a temperature closing to the melting temperature in a few seconds. The laser beam is then held for one minute and then cooling down slowly. Since the outer SiC powder can be served as the protected shell during this rapid heating and cooling down process, the inner SiC powder is largely not decomposed and/or oxidized in the vacuum chamber even at the elevated melting temperature. Instead, SiC nano-size powder grows to micro size crystal in minutes.

10382-22, Session 3

Projected fringe profilometry for transparent objects

Wei-Hung Su, National Sun Yat-Sen Univ. (Taiwan); Chau-Jern Cheng, National Taiwan Normal Univ. (Taiwan)

A full-field method using fringe projection techniques to perform the 3D profile measurement for a transparent object is proposed. A fringe pattern is illuminated onto the transparent object, and a CCD camera is employed to record the transmitted fringes on the screen. Fringes on the obtained image are deformed both by the refractive index and the topography of the object, and are analyzable to retrieve the 3D shape.

10382-23, Session 3

A scanning approach using a binary grid pattern for 3D shape measurements

Nai-Jen Cheng, National Kaohsiung Univ. of Applied Sciences (Taiwan); Wei-Hung Su, National Sun Yat-Sen Univ. (Taiwan)

A scanning pattern projection technique for 3D shape measurements is proposed. A binary grid pattern is employed as the projected pattern. The limited depth-of-focus of the pattern projection system makes the surface on the focused area can be clearly observed. Thus, a 2D contour of the inspected surface addressed by the in-focused fringes was obtained. By assembling the surface contours with their corresponding depths, the 3D shape of the object cab retrieved.

10382-24, Session 4

Highly efficient cladding-pumped double-clad fiber laser based on a concentrically co-grown Yb:YAG/YAG crystal structure *(Invited Paper)*

Jun Zhang, Youming Chen, U.S. Army Research Lab. (United States); Shizhuo Yin, The Pennsylvania State Univ. (United States); Claire Luo, General Opto Solutions, LLC (United States); Mark Dubinskiy, U.S. Army Research Lab. (United States)

We investigated double-clad (DC) optical fibers for high power laser applications, with concentrically co-grown 'Yb:YAG/YAG' crystal structure, for which 'crystalline core/crystalline clad' = CCCC = C4 fiber term was coined. The fibers were fabricated using a liquid phase epitaxial growth (LPE) of undoped single-crystalline YAG cladding around the 100 μm single-crystalline Yb:YAG core separately grown by a laser heated pedestal growth (LHPG) technique. Laser testing of the low-loss C4 fibers with direct diode-clad-pumping at 969 nm has demonstrated over 40 W of core-guided (NA $\approx$ 0.025) multimode laser output at 1030 nm with over 60% slope efficiency.

10382-25, Session 4

A large capacity time division multiplexed (TDM) laser beam combining technique enabled by nanosecond speed KTN deflector

Shizhuo Yin, Ju-Hung Chao, Wenbin Zhu, Chang-Jiang Chen, Adrian Campbell, Michael Henry, The Pennsylvania State Univ. (United States); Mark Dubinskiy, Robert C.

Hoffman, U.S. Army Research Lab. (United States)

In this paper, a large capacity time division multiplexed (TDM) laser beam combining technique enabled by nanosecond speed potassium tantalate-niobate (KTN) crystal electro-optic (EO) deflector was reported. An array of pulsed lasers could be combined together via TDM, which resulted in a significantly increased average power but without sacrificing the quality of the combined laser beam. Thus, extremely high energy lasers with diffraction limited beam quality could be realized by harnessing this TDM beam combining technique.

10382-26, Session 4

Crystal fiber lasers

Woohong Kim, Brandon Shaw, Shyam Bayya, U.S. Naval Research Lab. (United States); Charles G. Askins, John R. Peele, Sotera Defense Solutions, Inc. (United States); Daniel L. Rhonehouse, Univ. Research Foundation (United States); Jason D. Myers, Syed Qadri, U.S. Naval Research Lab. (United States); Rajesh Thapa, Sotera Defense Solutions, Inc. (United States); Jasbinder S. Sanghera, U.S. Naval Research Lab. (United States)

Crystal fibers offer several advantages over traditional glass fibers such as silica fiber due to their higher thermal conductivity and excellent thermal stability, higher stimulated Brillouin scattering (SBS) thresholds, and higher doping concentrations. Here, we report on the recent progress in the development of cladded single crystal fibers for high power single frequency lasers. Various rare earth doped single crystal YAG and sesquioxide fibers have been drawn using a state-of-the-art Laser Heated Pedestal Growth (LHPG) system equipped with high power stabilized CO2 laser, fiber diameter monitoring and feedback, and continuous feed-pull mechanism. High quality thin and long crystal fibers were successfully drawn from the LHPG system. Rare earth thin crystal fibers were further cladded using specially developed glasses where optical and physical properties were precisely controlled to form rugged and efficient single and double clad fibers. All crystalline core/clad fibers where thermal and optical properties are superior over glass based fibers have been successfully fabricated using various crystal growth and deposition methods. We report on the optical characterization and gain measurements on these clad fibers.

10382-27, Session 4

Nanosecond KTN varifocal lens without electric field induced phase transition

Shizhuo Yin, Wenbin Zhu, Ju-Hung Chao, Chang-Jiang Chen, Adrian Campbell, Michael Henry, The Pennsylvania State Univ. (United States); Robert C. Hoffman, U.S. Army Research Lab. (United States)

This paper presents a nanosecond speed KTN varifocal lens. The tuning principle of varifocal lens is based on the high-speed refractive index modulation from the nanosecond speed tunable electric field. A response time on the order of nanosecond was experimentally demonstrated, which was fastest varifocal lens reported so far. The results confirmed that the tuning speed of the KTN varifocal lens could be significantly increased by avoiding the electric field induced phase transition. Such kind of nanosecond speed varifocal lens can be a great beneficial to a variety of applications that demand high speed z-scanning, such as high resolution 3D imaging and high speed 3D printing.

10382-28, Session 4

Ultrafast laser written arrayed waveguide gratings with integrated photonic lanterns

Glen Douglass, Simon Gross, Michael J. Withford, Macquarie Univ. (Australia)

Arrayed waveguide gratings (AWGs) are typically used by the telecommunications industry as (de)multiplexers. However, recently they have successfully been demonstrated as integrated sensors for applications such as biomedical and astronomical spectrographs. Unfortunately, advancement is generally stalled by development costs and time; or restricted to spectral regions covered by off-the-shelf lithographic produced AWGs. To broaden the potential applications of integrated spectrographs employing AWGs, we utilise the femtosecond laser direct write technique as a rapid-prototyping platform for fabricating AWGs. The AWGs fabricated operate at 633nm, have a free spectral range of 22.4nm, resolution of 1.35nm, resolving power of 468.7, a throughput of 11.47% across the 5 main orders, and 3.97% in the central 28th order. This mask-less process enables complete design freedom, takes approximately 2hours from completed design to finalized device, thus facilitating design feedback to easily fine tune the device specifications.

In some applications multimode fibres are used for efficient light collection, thus leading to large losses when coupling into single mode devices such as AWGs. A solution is to utilize a 3-dimensional photonic lantern. A photonic lantern converts multimode light into multiple single-mode waveguides that can then be individually launched into an AWG. While the AWG is only a 2-dimensional device the laser direct write technique enables 3-dimensional fabrication. Thus supporting the integration of a photonic lantern and AWG into a single monolithic chip, removing coupling losses while increasing the functionality of the AWG. Currently we have demonstrated the integration of a 3 port photonic lantern.

1One shot profile sensing using a 2D fringe-encoded pattern

Wei-Hung Su, Sih-Yue Chen, National Sun Yat-Sen Univ. (Taiwan)

A one-shot profilometry for surfaces with color or reflectivity variation is presented. It uses 2D fringe-encoded pattern to illuminate the inspected object and a monochromatic camera to observe the deformed fringes at another view angle. The encoded pattern provides additional to identify the fringe order. For spatially isolated objects or surfaces with large depth discontinuities, unwrapping can be identified without ambiguity. Even though the surface color or reflectivity varies rapidly with position, it distinguishes the fringe order as well.

10382-31, Session 4

Phase-shifting projected fringe profilometry using binary-encoded patterns

Sih-Yue Chen, National Sun Yat-Sen Univ. (Taiwan); Nai-Jen Cheng, National Kaohsiung Univ. of Applied Sciences (Taiwan); Wei-Hung Su, National Sun Yat-Sen Univ. (Taiwan)

A fringe projection profilometry is presented. It uses the phase-shifting technique perform the phase-extraction and use the binary-encoded patterns to identify the fringe orders. Only five-shot measurements are required for data processing. Experiments show that absolute phases could be obtained with high reliability.

10382-32, Session PMon

1 kW fiber cladding light stripper with 36 dB attenuation coefficient

Shuzhen Zou, Han Chen, Haijuan Yu, Zhiyan Zhang, Institute of Semiconductors, Chinese Academy of Sciences (China); Jingyuan Zhang, Institute of Semiconductors, Chinese Academy of Sciences (China) and Georgia Southern Univ. (United States); Jing Sun, Pengfei Zhao, Ling Zhang, Xuechun Lin, Institute of Semiconductors, Chinese Academy of Sciences (China)

High power fiber cladding light stripper is one of the key devices in the high fiber laser for stripping out the residual pump light and the signal light which is leaked from the fiber core into the fiber cladding. It eliminates the thermal effect and the damage on the key fiber devices and ensures the high beam quality of the fiber laser. We present a continuous gradient etching processing technique for fabricating a high power fiber cladding light stripper without significant temperature rise. An experimental device was designed for achieving continuous gradient etching of the fiber surface. The corresponding axial distribution of the fiber cladding etching time was obtained through ray tracing simulation and experimental tests. A stripper with axial uniform scattering power and a low temperature was fabricated, which provided an attenuation coefficient of 36 dB when the test pumping power was 1.01 kW with NA of 0.46. The highest temperature of the stripper was only 78.5 ? and the temperature rising rate was 0.05 ?/W when such a high cladding power was extracted. The temperature and the residual output power showed no significant fluctuation in the stability test for one hour. The performance of stripper by using this axial uniform power stripping technique shows that it is very suitable for the higher power fiber lasers at about 10-kilowatt level.

10382-33, Session PMon

The study of graphene thin film affects the heat conduction of HPLED

Ming Seng Hsu, Chinese Military Academy (Taiwan); Ching Yao Hsu, Cantwell-Sacred Heart of Mary High School (United States); Jen Wei Huang, Feng Lin Shyu, Chinese Military Academy (Taiwan)

Thin films were the best choice for microelectromechanical systems (MEMS) material. In this study, the graphene thin film was fabricated between the high power light emitting diodes (HPLED) source and 1070 aluminum alloy substrate by chemical reduction of exfoliated graphene oxide technology. It will be used to enhance both of the heat conduction and dissipation. In the process, thin films were characterized by several subsequent analyses to help the preparation of ggraphene thin films with high heat conduction. X-Ray photoelectron spectrometry (XPS), Raman spectra and atomic force microscopy (AFM) analyses reveal the ratio of carbon to oxygen (C/O) atoms, the ratio and the phase of sp2 bonds, and the morphology in the microstructure. The physical properties will characterized by Hardness measurement, Scratch test, and Sheet resistivity measurement. Thermal resistance test shall through the measurement of real work temperature of HPLED.

10382-34, Session PMon

FBG sensing system to study the bridge weigh-in-motion

Sravanthi Alamandala, Putha Kishore, L. N. Sai Prasad Ravinuthala, Mayank Upadhyay, Rathish Kumar P., National Institute of Technology, Warangal (India)

In this paper, a Fiber Bragg Grating (FBG) based Weigh-in-Motion (WIM) sensing system is designed by using two FBGs, each one attached to the center tension position of the beam with an angle of 45o between two piers of the Bridge. To study the response of the designed WIM system, the vehicle is moved over the bridge with varying velocities and loads. The temporal response of the FBG1 and FBG2 and wavelength shift is recorded using interrogator of resolution 1pm. The wavelength shift of the FBG illustrates two peaks and one dip, it represents the position of the vehicle at that point of the FBG over the bridge. The difference between these points of the two FBGs measures the velocity of the vehicle. The load of the vehicle can be measured from the height of the FBG dip at a particular velocity. The response of the sensor system for velocity and load shows linear of around 0.99 upto 150m/sec velocity and 5N weight respectively . The results reveals that the proposed system is capable to monitor the dynamic response of the load and velocity of the moving vehicle over the bridge.

10382-35, Session PMon

A dual tapered Mach- Zehnder interferometer for magnetic field sensing

Emmanuel A. Hernandez, Julián Moisés Estudillo-Ayala, Juan Manuel Sierra-Hernandez, Daniel Jáuregui-Vázquez, Roberto Rojas-Laguna, José Ramón Martínez Angulo, Univ. de Guanajuato (Mexico)

A magnetic field sensor based on a Mach-Zehnder interferometer (MZI) is proposed. Developed using tapered optical fiber technique in a SMF-28 optical fiber. In the SMF-28 Fiber the Mach- Zehnder interferometer is manufactured with two tapers, with a waist diameter of 40 um and a length of 5 mm, and a separation between the tapers about of 3~4 cm. The MZI will be covered by a fluid with magnetic proprieties inside a capillary tube. Performing experiments with coils and transformers, hoping that the proposed sensor offers a good option to measure the magnetic field in electrical devices and measurements electrical current in transmission lines.

10382-36, Session PMon

Detection of trace amounts of chromium (VI) using polymergel coated etched Fiber Bragg grating

Vayu Nandana Kishore Pabbisetti, National Institute of Technology, Warangal (India)

Chromium (VI) is a notorious metal ion well known for toxic and carcinogenic effects. In environment, chromium exists in two notable oxidation states, trivalent chromium (III) and hexavalent chromium (VI), of which hexavalent chromium ion Cr (VI) is known to be 500 times more toxic. Cr (VI) is highly active and easily binds with the DNA of human cells leading to various types cancers. The existing chromium sensors are suffering with drawbacks such as high time consumption, expensive instrumentation, and high maintenance costs. Thus eco-friendly, low cost, fast responsive and effective techniques are essentially required for the detection of Cr (VI) ion.

Stimulus responsive polymer gels swell or shrink in size in response to changes in surrounding physical and chemical parameters such as pH, electric and magnetic fields, light, salt concentrations and presence of specific ions. polymer gel coated FBG sensors, is an emerging area of research in which stimulus responsive property of hydrogels causes a swelling or contraction of the gel which in turn affects wavelength shift of FBG peak.

This article discusses a chemo- mechanical- optical sensing approach for detection of toxic chromium (VI) metal ion in environment. Stimulus responsive polymer gel which swell/deswell depending on ambient chromium ion concentrations is synthesized and agglutinated on an etched Fiber bragg grating (FBG) surface. To characterize performance of the sensor, it has undergone for various studies. The sensor shows good selectivity towards Chromium (VI) metal ion. Trace amount of chromium even down to 10ppb can be sensed by the method.

10382-37, Session PMon

Raman monitoring and evaluation of the aging effects of rocket propellant stabilizers

Jonathan A. Mills, Carlton W. Farley III, Aschalew Kassu, Michael Curley, Anup Sharma, Paul B. Ruffin, Alabama A&M Univ. (United States); Christopher A. Marshall, Jeremy Rice, Brian A. McDonald, U.S. Army Research, Development and Engineering Command (United States)

Stabilizers are added to nitrate ester based rocket motor propellants to form a stable product. The products added to stabilize the propellants react with NOx and are gradually exhausted over a period of time. In this paper, we demonstrate the efficacy of Raman spectroscopy technique for nondestructive, inexpensive, and rapid evaluation and monitoring of the depletion of rocket motor propellant stabilizers. The preliminary results show that, as low as 0.1% of both MNA and 2-NDPA dissolved in DMSO (Dimethyl sulfoxide) can easily be detected at 1 second integration time using a 785 nm wavelength Raman system. In addition, MNA concentrations between 0.37% and 0.54% are detected in live propellant samples using a 60 second integration time.

10382-38, Session PMon

An ultra-high contrast optical modulator with 30 dB isolation at 1.55 μm with 25 THz bandwidth

Mohsen Jafari, University of Michigan (United States); Mina Rais-Zadeh, University of Michigan (United States) and NASA Jet Propulsion Laboratory (United States)

Re-configurability employed in many optical shutters and modulators comes from either mechanical or optical change in the structure [1,2]. State-of-the-art electro-optical modulators use index changing materials such as liquid crystals [3], Germanium (Antimony) Telluride [4], [5], or Vanadium oxides [6]. Two significantly different refractive index values at two different phases available in these materials are exploited to achieve amplitude or phase modulation. Here, we present a high-contrast electro-optical modulator with record-breaking amplitude modulation index of 27 dB and forward loss of < 3 dB at 1.55 μm. The high contrast is achieved by utilizing slit and surface plasmon polariton (SPP) resonances in a two-layer stack of gold slits filled with a phase change material (Germanium Telluride-GeTe). Stacking multiple layers of the phase change plasmonic grating enabled the development of the high-index modulator in chip scale dimensions at telecommunication wavelengths. These sub-wavelength gratings are fabricated using two metal e-beam lithography (each 200 nm thick) separated with a thin (~300 nm) silicon nitride (Si_3N_4) spacing layer.

Extraordinary light transmission from the slit resonance in gratings [7] is employed to achieve high transmission (>50%) in the modulator OFF state when GeTe is amorphous. In the crystalline phase, however, the slit resonances are moved to longer wavelengths and the grating absorption is increased through coupling to SPPs. Each layer provides 14 dB isolation with a 27 dB total amplitude modulation for a two-layer device. Crystallographic phase transition of GeTe is achieved by applying a dc current through the same sub-wavelength array of gold lines (crystallization energy ~ 10 pJ @ 2 MHz switching frequency). FTIR spectroscopy of multiple fabricated devices verifies the theoretical transmission isolation of 30 dB.

References:

[1] Humar, M., et al., "Electrically tunable liquid crystal optical microresonators," Nature Photonics, 3(10), 595-600, 2009.

[2] Hosseini, P., Wright, C. D., and Bhaskaran, H. (2014). "An optoelectronic framework enabled by low-dimensional phase-change films". Nature, 511(7508), 206-211.

[3] Yang, Deng-Ke. "Fundamentals of liquid crystal devices," John Wiley and Sons, 2014.

[4] Nukala, P., et al. "Ultralow-power switching via defect engineering in germanium telluride phase-change memory devices." Nature communications ,7 (2016).

[5] Jafari, M., Rais-Zadeh, M., "Zero-static-power phase-change optical modulator," Opt. Lett. 41, 1177-1180 (2016).

[6] H. Wang, et al. "Fabrication of vanadium oxide micro-optical switches," Sens. and Act. A: (2005): 108-112.

[7] Ebbesen, T. W., Lezec, H. J., Ghaemi, H. F., Thio, T., & Wolff, P. A. (1998). Extraordinary optical transmission through sub-wavelength hole arrays. Nature, 391(6668), 667-669.

μ

10383-1, Session 1

Enhancement of terahertz generation in QD antennae by introduction of a silver nanoantennae pattern *(Invited Paper)*

Edik U. Rafailov, Sergei Lepeshov, Andrei Gorodetsky, Aston Univ. (United Kingdom)

Terahertz photoconductive antennae are one of the most promising sources of pulsed and CW THz radiation operated at room temperatures. However, antennae possess a low coefficient of optical-to-terahertz conversion due to the carrier screening effect and low quantum efficiency. To overcome these limitations, optical nanoantennae techniques can be used. Optical nanoantennae are resonant nanostructures capable of transforming incident optical waves in a strong near-field. Such nanoantennae can be used to enhance the electric field and increase the absorption cross section in the active layers of the antenna. We present results on pulsed and CW THz generation in quantum dot based photoconductive antennae (PCA) pumped by femtosecond and dual-wavelength semiconductor lasers. We also present results on enhancement of THz generation in QD-based log-periodic PCA with silver nanoantennae embedded in the antenna gap. 20-nm silver film was placed onto the surface of the antennae. Upon heating due to the thermal dewetting process the silver film folded into a disordered array of spheroid nanoparticles. By varying the thickness of the silver film, the size of the nanoparticles can be controllably changed. Our first results demonstrated that in the frequency range from 0.05 to 0.5 THz, the average output power gain value was 3, at the frequency of 0.5 THz there was no gain, and in the range from 0.5 to 1.1 THz, the average gain value was up to 5. Therefore, using silver spheroid nanoantennae fabricated by a relatively simple method can increase the coefficient of optical-to-terahertz conversion up to 4 times.

10383-2, Session 1

Backward wave oscillator for high power generation at THz frequencies *(Invited Paper)*

Diana Gamzina, SLAC National Accelerator Lab. (United States); Claudio Paoloni, Lancaster Univ. (United Kingdom); Ye Tang, Beijing Vacuum Electronics Research Institute (China); Xiang Li, Lancaster Univ. (United Kingdom); Xuejiao Hao, Yuan Zheng, Beijing Vacuum Electronics Research Institute (China); Branko Popovic, Logan Himes, Robert Barchfeld, Univ. of California, Davis (United States); Hanyan Li, Pan Pan, Beijing Vacuum Electronics Research Institute (China); Rosa Letizia, Lancaster Univ. (United Kingdom); Jinjun Feng, Beijing Vacuum Electronics Research Institute (China); Neville C. Luhmann Jr., Univ. of California, Davis (United States)

Generation of high power at Watt level in the sub-THz region remains a challenge. The advent of microfabrication techniques derived from MEMS technology and ultra-precision CNC milling with nanometric resolution are fostering the development of compact vacuum electron devices up to 1 THz with unprecedented output power level.

The Backward wave oscillator is one of the most promising vacuum THz sources. The physical mechanism is based on the transfer of energy from an electron beam traveling in a slow wave structure to an electromagnetic wave. It consists of an electron gun to generate the required electron beam, an interaction structure to support a wave at the operating frequency, a collector to collect the spent electron beam at the end of the tube, and a magnetic focussing field to keep the beam confined.

This paper describes the outstanding technological effort to design and realize a backward wave oscillator with 0.346 GHz operating frequency to be employed in fusion plasma diagnostics.

The dimensions of the parts require microfabrication processes with tolerance below a few microns and metal surface roughness below 50 nanometers. The latter constraint is fundamental to keeping the ohmic losses low.

In particular, the slow wave structure will be fabricated by nano CNC milling.

Different slow wave structures and beam shape are considered to produce a family of BWOs with different output power. In particular, the double corrugated waveguide is used with a cylindrical electron beam.

An output power higher than 0.5 W is obtained.

The BWO is in an advanced fabrication phase.

10383-3, Session 1

Coherent terahertz emission from nanomaterials without external bias *(Invited Paper)*

Lyubov V. Titova, Kateryna Kushnir, Worcester Polytechnic Institute (United States); Mengjing Wang, Brown Univ. (United States); Kristie J. Koski, Univ. of California, Davis (United States)

Recent theoretical studies predict that monolayer van der Waals mono-chalcogenides such as GeSe, GeS and SnS are ferroelectric, which makes them attractive candidates for bulk photovoltaic effect (BPVE), defined as production of a photocurrent at zero bias in the absence of traditional p-n junctions. The prevailing mechanism behind BPVE is a shift current, a zero-bias photocurrent resulting from excitation of quantum coherent carriers in noncentrosymmetric materials. We apply terahertz (THz) emission spectroscopy to probe shift currents in 2D chalcogenide nanomaterials. Shift current resulting from excitation with ultrafast pulses gives rise to THz emission, and detecting it allows electrical contact-free, all-optical monitoring of shift currents. In one example, we find that THz generation in GeS nanosheets is more efficient that in (110) ZnTe, which is a standard THz pulse source used for THz time-domain spectroscopy. Shift current photoexcitation in GeS nanosheets suggests applications of these new layered nanomaterials in third generation photovoltaics as well as in efficient, ultrathin THz sources.

10383-4, Session 2

To be announced *(Keynote Presentation)*

Manijeh Razeghi, Northwestern Univ. (United States)

No Abstract Available

10383-5, Session 2

Terahertz metasurface quantum-cascade VECSEL *(Invited Paper)*

Luyao Xu, Christopher A. Curwen, Daguan Chen, Univ. of California, Los Angeles (United States); John L. Reno, Sandia National Labs. (United States); Tatsuo Itoh, Benjamin S. Williams, Univ. of California, Los Angeles (United States)

Achieving high power in combination with high quality beam pattern is

a ubiquitous challenge for semiconductor lasers. The demonstration of vertical-external-cavity surface-emitting lasers (VECSELs) in 1997 for visible and near-infrared semiconductor lasers has been a very successful approach. Terahertz (THz) quantum-cascade (QC) lasers, also have the challenge of combining high power and good beam pattern into one device – even more so because they typically use sub-wavelength metallic waveguides. The concept of VECSEL has been impossible to implement for QC lasers, since the optical gain is based on intersubband transitions of electrons, which only interact with the electric field polarized perpendicular to the quantum wells plane according to the "intersubband selection rule". To address this issue, we have developed an amplifying metasurface reflector that can couple the incident THz wave with the QC gain medium via metal-metal micro-cavity antenna reflectarray. Pairing the active metasurface with an output coupler, we demonstrated the first VECSEL in the THz regime in 2015. Based upon the prototype design, we have achieved a number of improvements to the QC-VECSEL including designing an inhomogeneous focusing metasurface to achieve a near-diffraction limited beam pattern with M2 = 1.3 and high brightness of 1.86?106 Wsr-1m-2, designing compact cavities and optimizing metasurface bias area to achieve continuous-wave operation above 77 K, achieving record high slope efficiency of 745 mW/A, as well as extending the VECSEL concept to cover a broad frequency range from 2.5 - 4.4 THz.

10383-6, Session 2

High-performance broadly-tunable THz quantum cascade laser sources based on intracavity difference-frequency mixing on silicon substrates *(Invited Paper)*

Mikhail A. Belkin, The Univ. of Texas at Austin (United States)

We demonstrate that an application of a III-V-on-silicon hybrid concept to terahertz (THz) Cherenkov difference frequency generation (DFG) quantum cascade laser (QCL) sources (THz DFG-QCLs) can dramatically improve THz output power and mid-infrared-to-THz conversion efficiency. Completely processed THz DFG-QCLs grown on a InP substrate are transfer-printed onto a 1-mm-thick high-resistive Si substrate using a 100-nm-thick SU-8 as an adhesive layer. Room temperature device performance of the reference InP and hybrid Si THz DFG-QCLs of the same ridge width (22 µm) and cavity length (4.2 mm) have been experimentally compared. The target THz frequency of 3.5 THz is selected for both devices using the dual-period first order surface gratings to select the mid-infrared pump wavelength of 994 cm-1 and 1110 cm-1. At the maximum bias current, the reference InP and hybrid Si devices produced THz power of 50 µW and 270 µW, respectively. The mid-infrared-to-THz conversion efficiency corresponds to 60 µW/W2 and 480 µW/W2, respectively, resulting in 5 times higher THz power and 8 times higher conversion efficiency from the best-performing hybrid devices. A hybrid Si device integrated in a Littrow external-cavity setup showed wavelength tuning in the 1-6 THz range without THz beam steering.

10383-7, Session 3

Spintronic terahertz generation *(Invited Paper)*

Dmitry Turchinovich, Max-Planck-Institut für Polymerforschung (Germany)

In this presentation we will review the principles and applications of THz generation based on spintronic phenomena: coherent spinwave generation [1], Mott scattering [2], and inverse spin-Hall effect [3].

[1] Z. Jin, Z. Mics, G. Ma, Z. Cheng, M. Bonn, and D. Turchinovich, "Single-pulse terahertz coherent control of spin resonance in the canted antiferromagnet YFeO3, mediated by dielectric anisotropy", Phys. Rev. B 87, 094422 (2013)

[2] Z. Jin, A. Tkach, F. Casper, V. Spetter, H. Grimm, A. Thomas, T. Kampfrath, M. Bonn, M. Kläui, and D. Turchinovich, "Accessing the fundamentals of magnetotransport in metals with terahertz probes", Nature Physics 11, 761 (2015)

[3] T. Seifert, S. Jaiswal, U. Martens, J. Hannegan, L. Braun, P. Maldonado, F. Freimuth, A. Kronenberg, J. Henrizi, I. Radu, F. Freimuth, E. Beaurepaire, Y. Mokrousov, P.M. Oppeneer, M. Jourdan, G. Jakob, D. Turchinovich, L. M. Hayden, M. Wolf, M. Münzenberg, M. Kläui, and T. Kampfrath, "Efficient metallic spintronic emitters of ultrabroadband terahertz radiation", Nature Photonics 10, 483 (2016)

10383-8, Session 3

Tunable terahertz devices using graphene and metallic heterostructures

Yang Wu, Hyunsoo Yang, National Univ. of Singapore (Singapore)

Graphene is considered to be a promising candidate to replace indium tin oxide (ITO) as transparent conductive electrodes in optoelectronics applications. We use graphene films as transparent electrodes for THz applications such as phase shifters, reflector, and intensity modulators, leading to a low voltage operation and very small insertion loss.

First, we experimentally demonstrate the excellent performance of THz modulators based on graphene/ionic liquid/graphene sandwich structures. The modulation covers a broadband frequency range from 0.1 to 2.5 THz with the modulation depth of up to 99% by applying a small gate voltage of 3 V. To our knowledge, this is the highest modulation ratio from graphene based THz devices to date. We also report a highly efficient tunable THz reflector in graphene. By applying a small gate voltage (up to ± 3 V), the reflectance of graphene is modulated from a minimum of 0.79% to a maximum of 33.4% using graphene/ionic liquid structures at room temperature, and the reflection tuning is uniform within a wide spectral range (0.1 – 1.5 THz). In addition, we design and fabricate terahertz phase shifters based on thin liquid crystal cells sandwiched by two graphene layers. A maximum 10.8 degree phase shift is obtained with 5 V voltage. The proposed phase shifters are fully electrical controllable, continuous tunable, and require very low DC voltages for operation.

Finally, we show a high performance THz emitter based on ferromagnetic/nonmagnetic heterostructures. Our THz emitter based on nonmagnetic (NM) and ferromagnetic (FM) heterostructures has a peak intensity exceeding 500 ?m thick ZnTe crystals (standard THz emitters). We have also fabricated the devices on flexible substrates with a great performance, and demonstrated that the devices can be driven by low power lasers.

10383-9, Session 3

Design of a multistep phase mask for high-energy THz pulse generation in ZnTe crystal

Yuri H. Avetisyan, Armen Makaryan, Vahe Tadevosyan, Yerevan State Univ. (Armenia)

Optical rectification (OR) of the femtosecond laser pulses in nonlinear optical crystals has emerged as the most powerful way to generate high energy THz-pulses. The tilted-pulse-front pumping (TPFP) method is commonly used for phase-matched THz-pulse generation. By such way THz pulses with 0.4 mJ energy were obtained in lithium niobate crystal (LN) [1]. However, further increase of the THz energy is challenging due to many limiting factors. Recently it was shown that application of the grating on the surface of ZnTe crystal allows to overcome some of the limiting factors [2].

In this report we present a new design of THz source using a multi-step phase mask (MSPM) to provide discretely tilted pulse-front in ZnTe crystal. In essence, MSPM split a single input beam into many smaller time-delayed "beamlets", which together create a discretely tilted pulse front. In contrast to using of the gratings, here problems related to the introduction of large amounts of angular dispersion are eliminated.

We also calculate the steps horizontal and vertical dimensions that are needed to generate THz-pulse with maximal energy and high efficiency of

pump-to-THz conversion. The optimal number of the steps N is estimated taking in account the separate beamlets broadening in MSPM and problem of its fabrication. The proposed method is promising to realize highly efficient, monolithic, and alignment-free table-top THz source.

1. J. Fulop, et al. Opt. Express 22, 20155 (2014).

2. J. Fulop, et al. Optica 3, 1075 (2016).

10383-10, Session 3

THz nonlinearities in semiconductor superlattices *(Invited Paper)*

Mauro F. Pereira, Sheffield Hallam Univ. (United Kingdom)

This paper is focused on nonlinear optics for the THz range in semiconductor superlattices. A Nonequilibrium Green's Functions approach [A. Wacker et a, IEEE Journal of Sel. Top. in Quantum Electron.,19 1200611, (2013),T. Schmielau and M.F. Pereira, Appl. Phys. Lett. 95 231111, (2009)] is used to deliver input to analytical expressions for the nonlinear polarization for arbitrary orders. A complex balance between superlattice bias and input field power rule is demonstrated. The theory presented here predicts the nonlinear polarization in excellent agreement with experiments up to the 21st order. These results open the possibility of extending nonlinear optics to the THz range for a large number of applications based on superlattices as the basic nonlinear medium as well as for sources and detectors.

10383-11, Session 4

Temperature-driven massless fermions in HgCdTe heterostructures *(Invited Paper)*

Frédéric Teppe, Sergey Krishtopenko, Sandra Ruffenach, Univ. Montpellier (France)

Bulk films and heterostructures based on HgCdTe compounds can be engineered to fabricate "gapped-at-will" structures. Therefore, 1D , 2D and even 3D massless particles can be observed in topological phase transitions driven by intrinsic (quantum well thickness, Cd content) and external (magnetic field, temperature or pressure) physical parameters. So far, the phases of 2D and 3D topological insulator have already been experimentally demonstrated in HgCdTe-based heterostructures. More recently, clear experimental evidence of the existence of 3D electronic states with conical-like spectrum was obtained in HgCdTe bulk films at specific Cd content . These 3D massless particles, called Kane fermions, have unique symmetry properties, which are not equivalent to any well-known case of massless particles in the relativistic limit of the quantum electrodynamics.

In this work, we report on our recent experimental results obtained by Terahertz and Mid-Infrared magneto-spectroscopy, on topological phase transitions driven by temperature in HgCdTe-based QWs and bulk films. These transitions are accompanied with the appearance of 2D and 3D massless electrons called Dirac and Kane fermions, respectively.

10383-12, Session 4

Complex delay dynamics of high power quantum cascade oscillators *(Invited Paper)*

Frédéric Grillot, Télécom ParisTech (France); Timothy C. Newell, Air Force Research Lab. (United States); Athanasios Gavrielides, The Univ. of New Mexico (United States); Mathieu Carras, mirSense (France)

Quantum cascade lasers (QCL) are semiconductor lasers based on ultrafast intersubband transitions with picosecond timescale that have become the most suitable laser sources from the mid-infrared to the THz range, due to their compactness, efficiency and high room temperature performances. In particular, high-power QCLs are powerful sources for optical countermeasures, including night vision blinding and missile out steering. However, some drawbacks arise with high power lasers that usually lead to a strong degradation of the beam quality. In this paper, we examine the effects of external feedback in different high power mid infrared QCL structures and discover that the incident angle of the feedback wave can produce complex dynamics hence stabilization, destabilization into strong mode-competition or undamping nonlinear oscillations. More particularly, with a feedback above a few percent, the laser beam can be steered in the far-field using the mirror as the control parameter. In a second regime, very strong mode competition takes place while the last regime shows strong evidence of small amplitude external cavity oscillations. The laser is stable near threshold and a bifurcation occurs with increasing power exciting such external cavity oscillations. As a dynamical system, reinjection of external light back into the cavity also can also provoke possible apparition of chaotic oscillations which must be avoided for a stable operation. To this end, the paper will also review the limiting conditions leading to chaotic light at mid-infrared and THz wavelengths.

10383-13, Session 4

Characterization of THz wave generated from air plasma induced by two-color laser with long wavelength

Shijing Zhang, Beijing Institute of Technology (China); LiangLiang Zhang, Capital Normal Univ. (China); Tong Wu, Beijing Institute of Technology (China); Hang Zhao, Capital Normal Univ. (China); Yuejin Zhao, Beijing Institute of Technology (China); Xiaomei Yu, Peking Univ. (China)

Terahertz wave generation from laser-induced air plasma is widely used due to its high electric field and broad frequency bandwidth. The most popular and efficient laser-plasma scheme used for THz generation is the two-color scheme, in which a laser pulse at the fundamental frequency is supplemented by its second harmonic that is obtained with the use of a nonlinear crystal. The type-I ?-barium borate (BBO) crystal plays a very important role in second harmonic generation. In this research, we investigate the terahertz generation efficiency and polarization with changing the thicknesses of the BBO crystals (from 60um to 100um with an interval of 10um). Moreover, the wavelength of the excitation laser is tunable from 1200nm to 1600nm. The THz generation efficiency is characterized by rotating the BBO crystal with the same tilt angle, changing laser wavelength with invariant pump power. And we also record the polarization variation of THz wave by using a wire grid THz polarizer. We think that the thickness of BBO crystal affects the phase difference between the ordinary axis and the extraordinary axis component, which leads to the change of the polarization state of the fundamental. Meanwhile, the frequency doubling efficiency of BBO has an impact on the power ratio of the two-color laser. This provides a practical way to control the polarization of terahertz pulses for potential applications.

10383-14, Session 4

Terahertz and x-ray generation in nano-cluster jets: Origin of nonlinear interaction *(Invited Paper)*

Alexander P. Shkurinov, M.V. Lomonosov Moscow SU (Russian Federation)

We have found that the yield of THz and X-ray radiation from the argon cluster beam, excited by high-intensity femtosecond laser pulses, depends differently on the laser pulse duration. THz yield strongly decreases when laser pulse duration is the shortest, whereas X-ray yield is maximal under these conditions. The formation of spatial distribution under 30 is connected with the dynamics of radial oscillations and, therefore, has such complex dependence on the pulse duration. X-ray emission does not depend on such dynamics and grows proportionally to the growth of the laser intensity.The

difference in the optimal laser pulse duration for the efficient generation of X-ray and THz radiation can be explained by the different time periods required for the formation of electron subsystems in argon cluster. The population of outer electrons rises quickly during the first 50 fs and they are responsible for the generation of X-ray, which explains the maximal X-ray yield at the minimal pulse duration in our experiments. The inner electrons multiply slowly and their population reaches maximum at the time scale of about hundreds femtoseconds, which can be attributed to the enhancement of THz yield at ? approx250 fs in our experiments. At the later stages, the population of outer electrons begins to rise again that may cause the decrease in the THz signal. The use of dual-color excitation scheme results in 5-fold enhancement of the THz yield while the yield of the X-ray radiation remains the same and energy conversion efficiency to the K-line is about 7·10?6.

10383-15, Session 4

Generation of ultra-broadband terahertz radiation from LiNbO3 waveguides excited by femtosecond optical pulses

Brett N. Carnio, Abdulhakem Y. Elezzabi, Univ. of Alberta (Canada)

Terahertz (THz) electric field pulses covering the frequency range of 100 GHz to >100 THz allow for the ultra broad exploration of molecular dynamics, elementary excitations, nanostructure phenomenon, devices operation, and photonic component properties. Here, ultra broadband THz radiation generation is investigated in waveguide structures having a lithium niobate (LN) core and SiO2 cladding layers. These materials have sub wavelength dimensions and are sandwiched between two bulk Si layers, allowing wide band THz electric field pulses to be emitted at a nearly constant angle of 49? (as determined by the Si refractive index). When the waveguides are excited by laser pulses having a central wavelength of 780 nm and a duration of <10 fs, electric field pulses containing frequency components between 0.1 and 120 THz can be generated that have kV/cm amplitudes and short (<1 ps) durations. Notably, the sub wavelength dimensions of LN minimizes the amount of THz absorption in the lossy frequency regions of this material, permitting more efficient radiation generation in these waveguide structures, opposed to bulk LN THz generation arrangements. These sub wavelength LN based waveguides have the potential to be used for on chip applications demanding an ultra wide frequency spectrum.

10383-16, Session 5

Substance identification by pulsed THz spectroscopy in the presence of disordered structure *(Invited Paper)*

Vyacheslav A. Trofimov, Irina G. Zakharova, Dmitry Y. Zagursky, Svetlana A. Varentsova, M.V. Lomonosov Moscow SU (Russian Federation)

We discuss an effective method for the detection and identification of substance, covered by disordered structure, using the pulsed THz signal. The insufficiency of the standard THz-TDS method, based on comparison of the substance absorption spectra from database with the absorption spectrum of a substance under investigation, is demonstrated. The discussed method is based on time-dependent integral correlation criteria calculated using spectral dynamics of a medium response. A new type of the integral correlation criterion, which is less dependent on spectral characteristics of a noisy signal under investigation, is used for identification. To explain a physical mechanism for false absorption lines appearance in the signal we make a computer simulation using 1D Maxwell's equations and density matrix formalism.

For the detection and identification of substance we propose using a substance emission at high frequencies corresponding to high energy levels excitation due to cascade mechanism of their excitation under the THz pulse action.

10383-17, Session 5

Using ultrafast terahertz spectroscopy to study low energy excitations in quantum materials *(Invited Paper)*

Pamela Bowlan, Kamaraju Natarajan, Dmitry A. Yarotski, Antoinette J. Taylor, Rohit P. Prasankumar, Los Alamos National Lab. (United States)

Low energy excitations can shed light on the interplay between different degrees of freedom in complex materials. Ultrashort terahertz (THz) pulses can be used to both drive and probe these excitations. This is particularly useful in quantum and Dirac materials, since these materials exhibit novel magnetic and lattice excitations that can potentially be used to control their properties. Here, the use of ultrafast THz spectroscopy to probe the cyclotron resonance frequency in two-dimensional (2D) electron and hole gases and drive nonlinear phonon dynamics in the topological insulator Bi2Se3 will be discussed.

We used terahertz magneto-optical spectroscopy to study two-dimensional (2D) electron and hole gases in semiconductor quantum wells. Our measurements reveal a nonlinear scaling of the cyclotron resonance frequency with magnetic field in 2D hole gases, due to the non-parabolicity of the valence band structure. Furthermore, optical photoexcitation of a 2D electron gas reveals not only photoinduced changes at the cyclotron frequency, but also unexpected higher frequency modes that are likely due to internal hydrogen-like transitions of ionized donor atoms.

Intense THz pulses can also be used to drive low energy excitations in Dirac materials. We used intense THz pulses to resonantly drive an IR active phonon in Bi2Se3 and probed the resulting ultrafast changes in surface symmetry using optical second harmonic generation. We then coherently controlled the lattice vibrations with a pair of THz pulses. Our work thus demonstrates a versatile, table-top tool for probing and controlling phonon dynamics in a range of systems, particularly at surfaces and interfaces.

10383-18, Session 5

Dual THz comb spectroscopy *(Invited Paper)*

Takeshi Yasui, Tokushima Univ. (Japan)

Terahertz (THz) frequency comb has attracted attentions as a powerful tool for frequency metrology in THz region because a series of the comb teeth can be used as frequency markers traceable to a frequency standard for the broadband spectrum. Dual THz comb spectroscopy opens a new door for the high-resolution, high-accuracy, broadband spectroscopy because THz comb posses both characteristics of narrow-linewidth radiation and broadband spectrum. Furthermore, absolute frequency of comb tooth is secured by the frequency standard. However, too discrete distribution of the comb tooth limits the spectral sampling to the frequency spacing between the comb teeth although the linewidth of each tooth is sufficiently narrow. Here, we demonstrated combination of spectrally interleaved THz comb with dual THz comb spectroscopy by precise sweeping of frequency interval in dual THz combs. Furthermore, the spectrally interleaved THz comb was effectively applied for high-precision spectroscopy of water vapor in low pressure.

10383-19, Session 6

Using a gate electrode to control the tunneling current in a geometrically-asymmetric nanoantenna

Mohammad S. Khalifa, Zewail City of Science and

Technology (Egypt) and Cairo Univ. (Egypt); Ashraf H. Badawi, Zewail City of Science and Technology (Egypt); Tamer A. Ali, Cairo Univ. (Egypt) and Zewail City of Science and Technology (Egypt); Nadia H. Rafat, Ahmed A. Abouelsaood, Cairo Univ. (Egypt)

Geometrically asymmetric nanoantennas have been demonstrated to have a good ability to convert electromagnetic waves, in the optical range, into a rectified electric current. In this work, we focus on a nanostructure that consists of two metallic electrodes separated by a vacuum channel, with one of them supporting a nanotip. The asymmetry in the geometry introduced by the nanotip allows the electrons driven by the incident electromagnetic waves to tunnel through the vacuum channel in one direction more than the other, resulting in a rectified current. In this work, we investigate the potentials of integrating a gate electrode into the nanoantenna, in order to control the tunneling current through the vacuum channel. A three-dimensional analysis is used to model the quantum tunneling of the electrons driven by the electromagnetic field between the nanoantenna electrodes. The current transport through the nanoantenna is computed based on a transfer-matrix methodology. This approach enables studying this novel triode-structure nanoantenna at such a miniaturized scale for the first time. The obtained results demonstrate the current dependence on the voltage applied on the gate electrode. It is also shown that the rectification properties of the nanoantenna at optical frequencies can be significantly enhanced by exploiting the gate electrode.

10383-20, Session 6

Spectral emission control of terahertz quantum cascade laser via injection seeding technique *(Invited Paper)*

Hanond Nong, Feihu Wang, Lab. Pierre Aigrain (France); Tobias Fobbe, Ruhr-Univ. Bochum (Germany); Valentino Pistore, Sarah Houver, Lab. Pierre Aigrain (France); Sergej Markmann, Nathan Jukam, Ruhr-Univ. Bochum (Germany); Maria Amanti, Carlo Sirtori, Univ. Paris 7-Denis Diderot (France); Souad Moumdji, Raffaele Colombelli, Institut d'Électronique Fondamentale (France); Lianhe H. Li, Edmund H. Linfield, Giles A. Davies, Univ. of Leeds (United Kingdom); Juliette Mangeney, Jérôme Tignon, Sukhdeep Dhillon, Lab. Pierre Aigrain (France)

As applications such as heterodyne spectroscopy require only single mode operation, the selection, suppression and tuning of individual lasing modes in THz QCLs has received considerable attention over the last decade. By periodically patterning the QCL in one- or two dimensions (e.g. distributed feedback (DFB) or photonic crystal lasers), single mode emission can be enforced. An alternative approach which requires no modification of the QCL waveguide is based on injection seeding technique with tunable narrowband THz seeds. Using this technique, we will show how the same QCL can be operated in both multi-mode and single mode regimes.

On the other hand, short pulses allow for time-resolved measurements and the generation of frequency combs. As the duration of a pulse is limited by its spectral bandwidth, a multimode operation of the QCL is highly desirable. By addition of a microwave modulation at the round-trip frequency, where the spacing and phase of the QCL modes is consequently fixed, results in active modelocking. This leads to laser emission of a train of THz pulses separated by the round-trip frequency. Coupled to coherent detection and a novel application of dispersion compensation, we demonstrate the generation of a stable 4 ps train pulse train. This opens up the possibility to reach sub-picosecond pulses and potentially the single cycle regime.

To conclude, we will show two methods to control the THz QCL emission from single mode regimes to the generation of short THz pulses.

10383-21, Session 6

Wavefront phase modulation based on terahertz wave polyethylene lens

Tielin Lu, Instrumentation Technology and Economy Institute (China); Xiaohu Guo, China North Vehicle Research Institute (China); Yuejin Zhao, Jingshui Zhang, Lingqin Kong, Beijing Institute of Technology (China)

THZ wave modulator, due to its important value of research and application widely attention. In the paper?we discuss the Polyethylene lens based the terahertz wavefront modulation?which is benefit the terahertz image technology.We present a novel method to design the optical terahertz image root and simulation verifies the modulation results.IThe results could be applied in terahertz imaging and sensing.

10383-22, Session 6

Band engineering of metal/semiconductor nanocomposites for longer wavelength high performance terahertz photoconductive switches *(Invited Paper)*

Joshua M. Zide, Univ. of Delaware (United States)

We present our recent work on the band engineering of semiconductor matrix materials to extend the wavelength of photoconductive switches for terahertz generation and detection. Recent work has shown that ErAs:GaAs is an excellent material for photoconductive switches, with bandwidth and performance exceeding that typically obtained in materials such as low-temperature-grown GaAs. Briefly, the ErAs nanoparticles serve as deep recombination centers, increasing dark resistance and decreasing carrier lifetimes. While this material is highly effective, longer (optical) wavelength devices are desirable to capitalize on the availability of low-cost, compact, high-performance fiber-coupled lasers with operating wavelengths of 1064nm or 1550nm. While ErAs:In0.53Ga0.47As and other related materials have been studied, the band alignment between the nanoparticles and the matrix typically results in lower dark resistance, reducing the performance of photoconductive switches.

We report on the incorporation of ErAs into GaBiXAs1-X semiconductors. The incorporation of bismuth reduces the bandgap of the material, enabling longer wavelength pumps. Because the reduction in bandgap occurs primarily in the valence band, the band alignments remain favorable for high dark resistance. We present a promising material for terahertz devices operating at 1064nm and discuss approaches the further extension of this wavelength. We will discuss opportunities enabled by improved materials for terahertz devices at longer optical wavelengths.

10383-23, Session 6

Superconducting thin film nanostructures as terahertz and infrared heterodyne and direct detectors *(Invited Paper)*

Gregory N. Goltsman, Moscow State Pedagogical Univ. (Russian Federation)

The superconducting hot electron bolometer (HEB) mixers based on ultrathin films of NbN combine the best sensitivity at the frequencies well above 1 THz and a gain bandwidth of about 6 - 7 GHz which make them suitable for most sensitive instruments.

Direct detectors made from NbN films are operated in 0.3-3 THz range exhibit response time as low as 50 ps with noise equivalent power (NEP) of 3x10^-13 W Hz^-1/2. A promising type of the photon counting detector is superconducting single-photon detector (SSPD). The SSPD is patterned from 4-nm-thick NbN film as 120-nm-wide and meander-shaped strip that covers a square area of 10 x 10 ?m^2. At wavelength ?≤1.5 ?m quantum

efficiency (QE) of our best devices approaches 80% at 2 K with 35 ps timing jitter. The single-photon counting was observed at wavelength up to 5.6 ?m with QE of ~1%. Simultaneously, at 2K the SSPD has negligibly low dark counts of 2x10^-4 s^-1. It provides NEP value of 10-20 W/Hz^1/2 at ?≤1.3 ?m and 10^-18 W/Hz^1/2 at 5 µm.

In addition to the chip SNSPD with normal incidence coupling, we use the detectors with a travelling wave geometry design. In this case a NbN nanowire is placed on the top of a Si3N4 nanophotonic waveguide, thus increasing the efficient interaction length. Our approach is fully scalable and, along with a large number of devices integrated on a single chip can be adapted to the mid and THz ranges where photon-counting measurement may be beneficial as well.

10383-24, Session 7

Near-field wave transformation in THz super-resolution imaging

Mariano Flammini, Michele Ortolani, Sapienza Univ. di Roma (Italy); Valeria Giliberti, Sapienza Univ. di Roma (Italy) and Istituto Italiano di Tecnologia (Italy); Chiara Ciano, Emanuele Pontecorvo, Eugenio Del Re, Sapienza Univ. di Roma (Italy)

According to rigorous diffraction theory, monochromatic electromagnetic waves reflected from a material surface form a mixture of propagating and evanescent waves. During propagation, light fields suffer a progressive spatial filtering that depends exponentially on the size of the subwavelength image detail, a peculiar multiscale distortion in the image that spans the near-field of the sources, occurs in vacuum and with no dissipation, and has never been reported before.

Here we explore this transition from super-resolved to diffraction-limited imaging for THz frequencies (? =1 mm). The experiment is carried out at 300 GHz using a knife-edge scan that allows subwavelength beam profiling in the near-field of emitters, here enacted remotely to produce super-resolved images on planes at different distances from the emitters. Compared to visible light imaging, the millimetric wavelength expands the near-field region to the point that single near-field imaging planes can be scanned using a mechanical free-standing blade.

From a fundamental perspective, our study provides first experimental observation of the stepwise transformation with increasing scatterer-to-emitter plane distance from near-field imaging to diffraction-limited imaging. From an applicative perspective, our experiments introduce an innovative free-space delivery and detection scheme that achieves super-resolution for monochromatic THz light based on a knife-edge scan along one axis.

10383-25, Session 7

Terahertz imaging for subsurface investigation of art paintings

Alexandre Locquet, Junliang Dong, Georgia Tech-Lorraine (France); Marcello Melis M.D., Profilocolore Srl (Italy); David S. Citrin M.D., Georgia Institute of Technology (United States)

Terahertz (THz) reflective imaging is applied to the stratigraphic and subsurface investigation of oil paintings, with a focus on the mid-20th century Italian painting, 'After Fishing', by Ausonio Tanda. THz frequency-wavelet domain deconvolution, which is an enhanced deconvolution technique combining frequency-domain filtering and stationary wavelet shrinkage, is utilized to resolve the optically thin paint layers or brush strokes. Based on the deconvolved terahertz data, the stratigraphy of the painting including the paint layers is reconstructed and subsurface features are clearly revealed. Specifically, THz C-scans and B-scans are analyzed based on different types of deconvolved signals to investigate the subsurface features of the painting, including the identification of regions with more than one paint layer, the refractive-index difference between paint layers, and the distribution of the paint-layer thickness. In addition, THz images are compared with X-ray images. The THz image of the thickness distribution of the paint exhibits a high degree of correlation with the X-ray transmission image, but THz images also reveal defects in the paperboard that cannot be identified in the X-ray image. Therefore, our results demonstrate that THz imaging can be considered as an effective tool for the stratigraphic and subsurface investigation of art paintings. They also open up the way for the use of non-ionizing THz imaging as a potential substitute for ionizing X-ray analysis in nondestructive evaluation of art paintings.

10383-26, Session 7

All-dielectric metamaterial resonators for room temperature terahertz imaging *(Invited Paper)*

Willie J. Padilla, Kebin Fan, Jonathan Y. Suen, Duke Univ. (United States)

Metamaterial electromagnetic wave absorbers have demonstrated extreme properties across electromagnetic spectrum. Traditional metamaterials are based on metals and thus the performance of traditional designs is strongly tied to the electrical conductivity. Here we present a metamaterial absorber fashioned entirely from sub-wavelength dielectric resonators, which act as isolated 'metamaterial atoms'. Many dielectric materials exhibit thermal conductivities orders of magnitude smaller than those for metals, and thus our approach breaks the fundamental connection between thermal and electrical conductivity providing new opportunities for applications. Here we demonstrate dielectric absorbers for terahertz imaging and highlight the future of this exciting field.

10383-27, Session 7

Compact solutions for spectroscopic solid-state based terahertz imaging systems *(Invited Paper)*

Gintaras Valu?is, Rimvydas Venckevi?ius, Linas Minkevicius, Antanas Reklaitis, Vincas Tamo?i?nas, Irmantas Ka?alynas, Bogdan Voisiat, Dalius Seliuta, Gediminas Ra?iukaitis, Ctr. for Physical Sciences and Technology (Lithuania)

Convenience in use of room-temperature terahertz (THz) imaging systems, reduction of dimensions and presence of on-chip solutions remains one of prime interests for their direct implementation aims.

In this communication, we consider solid-state-based solutions in miniaturization of spectroscopic THz imaging systems including novel semiconductor nanostructures bias-free emitters, THz optics components relying on zone plates and their on-chip integration with THz detectors.

Pulsed optoelectronic terahertz emitter based on a {delta}-doped p-i-n-i GaAs/AlxGa1?xAs heterostructure was studied experimentally. It is shown that the heterostructure can serve as efficient antenna- and bias-free surface emitter which power, at certain conditions, exceeds the emission from InGaAs and InAs surfaces.

Compact THz optics solutions were demonstrated via conventional, inverted and combined zone plates with integrated band-pass filters. Components were designed numerically using the 3D finite-difference time-domain method and produced using laser direct writing technique. Spatial profiles of the concentrated radiation in the focal plane at the resonant frequencies are recorded, effects of focal depth influence are considered as well. Influence of Fabry-Perot resonances is resolved using phase zone plate fabricated on silicon substrates.

It is evidenced that on-chip integration of secondary diffractive optics and bow-tie InGaAs-based terahertz detectors enables one order of magnitude detection enhancement at 0.76 THz frequency.

Implementation of compact spectroscopic THz imaging is demonstrated in post packages scanning and medical imaging experiments employing bow-tie diodes, nanometric field-effect transistors and microbolometers.

10383-28, Session PMon

Organic conjugated material-based THz wave modulators

Joong-Wook Lee, Chonnam National Univ. (Korea, Republic of); Hyung Keun Yoo, SAMSUNG Electronics Co., Ltd. (Korea, Republic of); Chul Kang, Chul-Sik Kee, In-Wook Hwang, Gwangju Institute of Science and Technology (Korea, Republic of)

The characteristics of transmission modulation of terahertz (THz) wave transmission under photoexcitation were studied in organic/silicon hybrid structures, such as pentacene/silicon, TIPS-pentacene/silicon, PCBM/silicon, organic/metamaterial/silicon, etc. The organic/silicon hybrid structures show extremely high modulation efficiencies and broadband modulation of the THz waves. In addition, metamaterial-based organic/silicon hybrid structures enable selective modulation in the range of THz-wave frequencies. We've also investigated the optimization conditions for improving the properties of the modulation efficiency and for realizing various functionalities in organic-based active THz devices.

10383-29, Session PMon

Optical properties and relaxation times of oil and fuel in frequency range of 0.2-0.8 THz

Anna Simonova, Uliya Komarova, Petr Demchenko, Roman Grigorev, Roman Orlov, Mikhail K. Khodzitsky, ITMO Univ. (Russian Federation)

Currently, there are a number of physical and chemical methods used in the oil industry to implement quality control of petroleum products. Terahertz time-domain spectroscopy (THz-TDS) is not among the standardized control methods. The less scattering and the higher penetration depth are significant advantages of THz radiation unlike to IR, X-rays and visible radiation. The investigation on the determination of the water content in the crude oil and polyglycolic oil using the information about the dispersion of the refractive index for different concentrations of water in the THz frequency range was performed earlier in the [1,2] and other works.

In this paper, the optical properties and the relaxation times of crude oil and different marks of motor fuel in the frequency range of 0.2-0.8 THz have been investigated. The transmission spectra of the studied substances were obtained using THz-TDS spectrometer. Relaxation times were determined by means of multicomponent Debye model of permittivity. It was shown that terahertz time-domain spectroscopy allows the identification of different brands and types of motor fuel by optical properties and relaxation times in the studied frequency range. The differences between the obtained values indicate on the features of the fuels chemical structures, having the responses in the THz frequency range. Thus, the results of the present studies indicate the possibility of using a terahertz time-domain spectroscopy as a method of analysis of oil products to control.

1. Gorenflo S., Tauer U., et. al., Chem. Phys. Lett. 2006.

2. Jin Wu-Jun, Zhao Kun, et. al., Applied Geophysics. 2013.

10383-30, Session PMon

Frequency division multiplexing THz light field imaging

Xianshun Ming, Tsinghua Univ. (China); Willie J. Padilla, Duke Univ. (United States); Liqun Sun, Tsinghua Univ. (China)

We present a single pixel frequency division multiplexing imaging system with two metamaterial spatial light modulators (SLMs) for THz light field imaging. One SLM is used for slicing/modulating the 4D light field from various sub-apertures, while the second one together with a single pixel detector to implement 2D multiplexing measurement. The modulation signal and carrier signal at each pixel of the two SLMs is a square wave with specific frequency, and we computationally reconstruct the light field voxel information from the spectra of measured time signals. With the consideration of hardware restrictions, we show how to design the modulation frequencies to uniquely determine each voxel and alleviate the effect of high order harmonics crosstalk, the gaussian white noise and the frequency drift. Meanwhile, we design a prototype based on the THz source, off-axis parabolic mirror, TPX lens and SLMs.

Conference 10384: Optical Data Storage 2017: From New Materials to New Systems

Sunday 6 –6 August 2017

Part of Proceedings of SPIE Vol. 10384 Optical Data Storage 2017: From New Materials to New Systems

10384-1, Session 1

Optical technologies for the Internet of Things era *(Invited Paper)*

Philip N. Ji, NEC Labs. America, Inc. (United States)

The Internet of Things (IoT) is the network of interrelated physical objects that can collect and exchange data with one another through embedded electronics, software, sensors, over the Internet. It extends Internet connectivity beyond traditional networking devices to a diverse range of physical devices and everyday things that utilize embedded technologies to communicate and interact with the external environment. The IoT brings automation and efficiency improvement to everyday life, business, and society. Therefore IoT applications and market are growing rapidly.

Contrary to common belief that IoT is only related to wireless technology, optical technologies actually play important roles in the growth of IoT and contribute to its advancement. Firstly, fiber optics provides the backbone for transporting large amount of data generated by IoT network in the core , metro and access networks, and in building or in the physical object. Secondly, optical switching technologies, including all-optical switching and hybrid optical-electrical switching, enable fast and high bandwidth routing in IoT data processing center. Thirdly, optical sensing and imaging delivers comprehensive information of multiple physical phenomena through monitoring various optical properties such as intensity, phase, wavelength, frequency, polarization, and spectral distribution. In particular, fiber optic sensor has the advantages of high sensitivity, low latency, and long distributed sensing range. It is also immune to electromagnetic interference, and can be implemented in harsh environment.

In this talk, the architecture of IoT is described, and the optical technologies and their applications in the IoT networks are discussed with practical examples.

10384-2, Session 1

Big data innovation hubs: Opportunities for optical data storage partnerships *(Invited Paper)*

Meredith M. Lee, West Big Data Innovation Hub (United States)

Launched in November 2015 by the National Science Foundation, the four Regional Big Data Innovation Hubs (Northeast, Midwest, South, and West) build and strengthen public-private partnerships to address societal challenges. Focus areas include Smart Cities / Metro Data Science, Precision Medicine, Natural Resources and Hazards, and Education. By convening stakeholders from academia, industry, nonprofits, and government, the Big Data Innovation Hubs help the community to identify collaboration opportunities, share best practices, and advance the implementation of big data technologies.

This talk will introduce the flagship initiatives of the West Big Data Innovation Hub, describing a series of projects and applications that could leverage next-generation optical data storage systems. Design issues including the integration of hardware, software, and human-computer interaction elements will be discussed, emphasizing practical testbeds and pilot projects that bridge sectors and spark community engagement.

10384-3, Session 1

The possibility of the market expansion of large capacity optical cold archive *(Invited Paper)*

Ikuo Matsumoto, Emiko Sakata, Fujiwara-Rothchild, Ltd. (Japan)

The field, IoT and Big data, which is activated by the revolution of ICT causes rapid increase of distribution data of various business application. As a result, cold data with low access frequency has been rapidly increasing into a huge scale that human has never experienced before.

The cold archive storage should be suitable for long-term and low cost preservation, but a balance between cost and latency for read request is concerned. And the choice between an active archive warm storage and a cold archive storage is determined by whether performance or cost is emphasized. Consequently, storage for cold data is determined by the application's request including access frequency, response speed and cost. But the boundary is ambiguous.

HDDs, tapes, optical disks are utilized as devices of cold archive storage, and the development to increase the capacity by further increasing the recording density in order to reduce the storage cost has been proceeded. In this gray area, proposals of storages will be most activated in the future. For example, the object storage and SDS (software defined storage) are one of the candidates for this gray area. A Cloud storage is also the important way in this gray area.

Taking into consideration of TCO, large-capacity optical disc storage can be the promising candidate of cold archive storage by its performance enhancement in the future. How to demonstrate the superiority of optical storage in this area is an important issue in the future.

In this presentation, the issue of active archive / cold archive and the challenges of each storage are discussed.

10384-4, Session 1

A rack-based optical storage system with inline accessibility for long-term data preservation *(Invited Paper)*

Jie Yao, Changsheng Xie, Huazhong Univ. of Science and Technology (China)

The combination of the explosive growth in digital data and the need to preserve much of this data in the long term has made it an imperative to find a more cost-effective way than HDD arrays and more easily accessible way than tape libraries to store massive amounts of data. While modern optical discs are capable of guaranteeing more than 50-year data preservation without migration, individual optical disks' lack of the performance and capacity relative to HDDs or tapes has significantly limited their use in datacenters. This talk presents a Rack-scale Optical disc library System, or ROS in short, that provides a PB-level total capacity and inline accessibility on thousands of optical discs built within a 42U Rack. A rotatable roller and robotic arm separating and fetching the discs are designed to improve disc placement density and simplify the mechanical structure. A hierarchical storage system based on SSD, hard disks and optical discs are presented to hide the delay of mechanical operation. On the other hand, an optical library file system is proposed to schedule mechanical operation and organize data on the tiered storage with a POSIX user interface to provide an illusion of inline data accessibility. Besides, ROS is able to effectively hide and virtualize internal complex operational behaviors and be easily deployable in datacenters.

10384-5, Session 2

Cavity enhanced eigenmode multiplexing for volume holographic data storage

Bo E. Miller, College of Optical Sciences, The Univ. of Arizona (United States); Yuzuru Takashima, The Univ. of Arizona (United States)

Previously, we proposed and experimentally demonstrated enhanced recording speeds by using a resonant optical cavity to semi-passively increase the reference beam power while recording image bearing holograms. In addition to enhancing the reference beam power the cavity supports the orthogonal reference beam families of its eigenmodes, which can be used as a degree of freedom to multiplex data pages and increase storage densities for volume Holographic Data Storage Systems (HDSS). While keeping the increased recording speed of a cavity enhanced reference arm, image bearing holograms are multiplexed by orthogonal phase code multiplexing via Hermite-Gaussian eigenmodes in a Fe:LiNbO3 medium with a 532 nm laser at two Bragg angles for expedited recording of four multiplexed holograms. We experimentally confirmed write rates are enhanced by an average factor of 1.1, and page crosstalk is about 2.5%. This hybrid multiplexing opens up a pathway to increase storage density while minimizing modifications to current angular multiplexing HDSS.

10384-6, Session 2

Cavity enhanced eigenmode multiplexing with spatial light modulators for volume holographic data storage

Guanghao Chen, The Univ. of Arizona (United States); Bo E. Miller, College of Optical Sciences, The Univ. of Arizona (United States); Yuzuru Takashima, The Univ. of Arizona (United States)

Spatial Light Modulators (SLMs) are incorporated along with cavity enhanced eigenmode and angular hybrid multiplexing in Holographic Data Storage Systems (HDSS). Orthogonal reference beams supported as cavity eigenmodes are created by SLM and image bearing holograms are multiplexed by orthogonal phase code multiplexing via Hermite-Gaussian eigenmodes in a Fe:LiNbO3 medium with a 532 nm laser at multiple Bragg angles.

10384-7, Session 2

Analytic function expression of signal wave for data retrieve in holographic data storage

Daisuke Barada, Shaqueeb Sarwar, Toyohiko Yatagai, Utsunomiya Univ. (Japan)

Holographic data storage is a data storage with large data amount recorded by volume holography. Holography is well known as a method to record three-dimensional scenes. The principle is roughly established and major characteristics are well understood. In the case of three-dimensional scenes, some noises are acceptable because they are compensated by our brain. However, in the case of holographic data storage, the recording images are minute two-dimensional coded patterns so that the images are not robust for noises. Therefore, rigorous expressions of recording signal is required. In this study, the recording signal wave is expressed by Taylor expansion for small argument and asymptotic expansion for large argument. Then, the filling factor of pixels in a spatial light modulator (SLM), the size and the position shift of a rectangular aperture at a Fourier plane are considered. When the signal wave is ideally reconstructed, the signal wave at an image plane is captured by using an image sensor. Then, the signal wave is integrated by the area of pixels in the image sensor. In this study, the integral is analytically calculated whereas it is numerically calculated in general because the signal wave is expressed by analytic functions. Therefore, interpixel crosstalk is easily evaluated. In our previous study, high-density recording method of binary data pages is proposed by using four-step phase mask. The high-density recording characteristics are evaluated by analytic functions. When parameters such as the filling factor of pixels in a SLM and an image sensor and the size and the position shift of a rectangular aperture can be known, the analytic functions are obtained. Then, the analytic functions are expected for error corrections.

10384-8, Session 2

Temperature tolerance analysis on the volume holographic data storage

Liangcai Cao, Shenghan Wu, Song Zong, Guofan Jin, Tsinghua Univ. (China)

Volume holographic data storage has significant advantages of large theoretical storage density and high data transfer rate. Terabyte holographic optical disk system is one of the promising solutions for the future mass and green archival data storage. The unique advantages come from the multiplexing techniques due to the Bragg selectivity of the volume hologram. Since the Bragg grating is very sensitive to the grating deformation, the range of the working temperature for the storage system is relatively as small as several degrees. The temperature tolerance is one of the main constraints for the commercialization of the holographic optical data storage. In this work, the temperature characteristics for the holographic storage system are analyzed by theoretical modeling in order to extend the range of the working temperature. Adaptive compensation conditions are derived based on the refractive index change and material deformation caused by the temperature changing. Preliminary experimental test shows that the range of the working temperature could be extended effectively by applying the adaptive compensation method.

10384-9, Session 2

Effect of temperature change in microholographic recording

Ryuichi Katayama, Fukuoka Institute of Technology (Japan)

The effect of the temperature change in microholographic recording was investigated through a numerical simulation. The diffraction efficiency of a microhologram was calculated using the coupled wave theory. The wavelength of the laser was 405 nm, the numerical aperture of the objective lenses was 0.85, and the thickness of the recording medium was 300 um. The thickness change of the recording medium due to the temperature change of 10 deg. was 0.5%. When there was no compensation, the diffraction efficiency was almost 0. When the wavelength was changed by 0.5% to compensate for the temperature change, the diffraction efficiency increased but it was only about 16% of that without the temperature change. The reason is as follows. The beam consists of multiple plane waves and the microhologram consists of multiple diffraction gratings. Regarding the center of the beam, the corresponding wave vector of the plane wave and grating vector of the diffraction grating are perpendicular to the recording medium. Therefore, it is necessary to change only the wavelength of the plane wave to compensate for the Bragg mismatch due to the temperature change. On the other hand, regarding the periphery of the beam, the corresponding wave vector of the plane wave and grating vector of the diffraction grating are slanted to the recording medium. Therefore, it is necessary to change both the wavelength and angle of the plane wave to compensate for the Bragg mismatch due to the temperature change. The above two conditions cannot be satisfied simultaneously.

10384-10, Session 2

Research of circular polarized holography with a large crossing angle under a common condition

Yifan Hong, Jinliang Zang, Yiying Zhang, Fenglan Fan, Ying Liu, Guoguo Kang, Xiaodi Tan, Beijing Institute of Technology (China); Tsutomu Shimura, The Univ. of Tokyo (Japan); Kazuo Kuroda, Beijing Institute of Technology (China) and Utsunomiya Univ. Ctr. for Optical Research & Education (Japan)

Polarization holography is the coherent interference of the beams that can have the different polarized states. The early-stage theory of polarization holography is based on Jones matrix, where the paraxial approximation is assumed, while the theory of polarization holography represented by dielectric tensor can describe the case with a large crossing angle. And it also depicts the relationship between diffraction light and interference light. During the research people find some extraordinary phenomenon, such as null reconstruction and inverse polarizing effect. But there is a disadvantage in this new polarization holography theory, where only under a peculiar circumstance can we get a faithful reconstruction. The circumstance can be expressed as "A+B=0", where A and B refer to the coefficients for intensity and polarization holograms respectively. In this research, we calculate the formula of diffraction light's polarization, and extract the A+B factor in it. Then we establish a series of equations which can let the diffraction light faithfully reconstruct, no matter what value of A plus B is. From the result, we can use an artificial reference beam which is corresponding to the signal beam to generate the hologram. Under this condition, the polarization of the diffraction light is similar to the signal. For simplification, we only discuss the signal wave with circular polarization and experimentally verify the result.

10384-11, Session 3

Near-field coupling and readout of nano recording marks *(Invited Paper)*

Din Ping Tsai, Research Ctr. for Applied Sciences - Academia Sinica (Taiwan) and National Taiwan Univ. (Taiwan)

Near-field optical disk (NFOD) is a novel and demanded developments of optical storage technology. The nonlinear plasmonic coupling effect of the complete nano recording unit is important for increasing the near and far field optical readout contrast. Here, we present a simple plasmonic near-field coupling optical disk system. The near-field coupling effect between two nano-recording marks with various thickness of the dielectric spacer layer are investigated.

10384-12, Session 3

The reduction of graphene oxide induced by rare-earth doped nanocrystals towards super-resolution optical data storage *(Invited Paper)*

Simone Lamon, Qiming Zhang, RMIT Univ. (Australia); Yiming Wu, Xiaogang Liu, National Univ. of Singapore (Singapore); Min Gu, RMIT Univ. (Australia)

The growing amount of data generated every year creates an urgent need for improved methods and new storage media. Far-field super-resolution techniques have provided the foundation for nanoscale 3D optical data storage towards a petabyte-level capacity on DVD-sized discs. However, a suitable recording medium for high-density information storage over long-term periods and with low energy consumption is still lacking. Rare-earth doped nanocrystals, which feature ladder-like-arranged energy levels enabling emission from ultraviolet to near-infrared, have a fluorescence lifetime two to three orders of magnitude longer than that of other fluorophores and offer the potential for low-power super-resolution data reading. Moreover, the reduction of graphene oxide to reduced graphene oxide induces permanent changes in its chemical and optical properties which can be used for data recording. Here, we demonstrate the reduction of graphene oxide induced by rare-earth doped nanocrystals via FRET towards super-resolution optical data storage with ultra-high capacity, ultra-long lifetime and ultra-low energy consumption. Yb^{3+}/Tm^{3+}-doped core-shell nanoparticles were synthesized via co-precipitation method and their fluorescence spectrum was obtained using a home-built microscope. A solution of rare-earth doped nanocrystals and graphene oxide nanoflakes was spin-coated on coverslip glass and fluorescence lifetime measurements were conducted to confirm efficient FRET. The reduction of graphene oxide was attributed to the transfer of energy quanta from up-converting rare-earth doped nanocrystals under 980-nm laser excitation. High-contrast images of the data bits were generated by super-resolution optical microscopy based on rare-earth doped nanocrystals due to the different degree of fluorescence quenching between graphene oxide and reduced graphene oxide.

10384-13, Session 3

Nanophotonics mediated ultra-high capacity optical memory towards big data storage *(Invited Paper)*

Xiangping Li, Jinan Univ. (China)

Even though optical storage has been well heralded as green techniques, the conventional optical memories have been constantly challenged as they reached theirs physical limits imposed by nonlinear effects. Recently, nanophotonics harnesses light's interaction with materials at the nanoscale including the generation of nanoscale optical probes and the interaction with nanocomposite materials, offering bottom-up new approaches far superior to the conventional technology. In this regard, nanophotonics has emerged as a major propellant for the next generation of ultra-high capacity optical memories for big data. In this talk, we present the recent development of ultra-high capacity optical memories multiplexing information in the physical domain of the writing beams through tailoring the interaction between a tightly focused pulsed laser beam and plasmonic materials [1]. To circumvent the diffraction limit of light discovered by Ernst Abbe, tremendous research approaches have been developed including stimulated emission depletion (STED) microscopy [2]. Through coherently manipulating the distribution of excitons in the fluorophore molecules by a dual-beam approach, where one Gaussian shaped beam can pump the molecules into the excited state while the second doughnut shaped beam can inhibit the subsequent emission through stimulated emission processes, STED microscopy enables superresolved imaging as well as laser lithography [3, 4]. Based on this principle, superresolution optical memories enabled by the dual-beam approach has been demonstrated with an ultra-high equivalent capacity [5].

10384-14, Session 3

SIL-STED microscopy technique enhancing super-resolution of fluorescence microscopy *(Invited Paper)*

No-Cheol Park, Geon Lim, Wonsup Lee, Yonsei Univ. (Korea, Republic of); Hyungbae Moon, Asan Medical Ctr. (Korea, Republic of); Guk-Jong Choi, Young-Pil Park, Yonsei Univ. (Korea, Republic of)

We characterize a novel fluorescence microscope which combines the high numerical aperture (NA) optical head of a solid immersion lens (SIL) with that of stimulated emission depletion (STED) microscopy and it is named SIL-STED microscopy in this research. Advantage of this combination is that the lateral resolution is better than common STED microscopy because of

the higher NA of SIL. Thus, it promises advanced super-resolution imaging of the structure and function of cell surface or membranes with overcoming optical diffraction limit at the macro-molecular scale. Here we present the first implementation of higher NA illumination into STED microscopy which limits fluorescence lateral resolution down to about 40 nm. The material of the SIL is KTaO3 and the refractive index is about 2.23 at the wavelength of 633 nm. A full theoretical description of the SIL-STED microscopy is fulfilled based on the vector diffraction theory so that we could analyze numerical result of the point spread function of the microscopy and expected resolution. For the further investigation, we used both synthetic and biological samples to demonstrate that the performance of this new microscope technique is improved by using the SIL. The used samples were fluorescent bead test samples and cell stained with fluorophores which is appropriate to STED imaging, respectively. Moreover, the SIL-STED microscopy provides superior lateral resolution capabilities with the potential to reduce photo-bleaching and photo-damage in live cell imaging.

10384-15, Session 4

Active metasurfaces for optical data storage *(Invited Paper)*

Cheng Hung Chu, Pin Chieh Wu, Research Ctr. for Applied Sciences - Academia Sinica (Taiwan); Hui-Hsin Hsiao, Hsiang-Chu Wang, National Taiwan Univ. (Taiwan); Hui Jun Wu, Research Ctr. for Applied Sciences - Academia Sinica (Taiwan); Din Ping Tsai, Research Ctr. for Applied Sciences - Academia Sinica (Taiwan)

Metasurfaces, the two-dimensional (2D) sub-wavelength artificial structures, where light is not required to have a deep penetration, have shown the ability to tailor the amplitude, phase and polarization of light. The functionalities of various optical components can be realized by metasurface-based design, such as beam splitters, filters, waveplates, deflector, lens and holograms. However, the optical properties of conventional metasurfaces are typically permanent once the devices are fabricated. There is obviously a need to develop tunable metasurface where their optical responses can be actively controlled with external applied measures, such as force, heat, electric or magnetic field. In this paper, we will review the recent developments of active metasurface from fundamental theory to their potential applications. We also present our recent work in reconfigurable gradient metasurface, which exhibits different anomalous reflection angles by controlling the combination of Ge2Sb2Te5 rods with different geometries and phase states. Further, a gate-tunable metasurface that enables dynamic control by electrically modulating the complex refractive index of conducting oxide layers will be discussed. We foresee that these results provide great interest in applications toward metasurface-based optical storage system.

10384-16, Session 4

Mastering multi-depth bio-chip patterns with DVD LBR’s *(Invited Paper)*

Doug Carson, DCA, Inc. (United States)

LBR’s can expose the entire surface of a wafer much faster than XY lithography. Silicon wafers can be coated with PR, exposed, developed and then etched to a certain feature depth.

The challenge to using LBR’s is to accurately write a second pattern onto the wafer after the first pattern has been recorded and etched.

One concern is how to recoat the etched wafer with PR. Conventional optical disc production uses spin coating, which is not suitable. There are several other coating technologies used in semi-conductor industry including spray. This will not be the subject of this presentation.

The biggest challenge is due to the fact that LBR’s were not designed to mechanically mount the recording wafer in exactly the same XY and rotational position, relative to the turntable center of rotation each time. It is therefore not possible to record a second pattern onto a wafer perfectly aligned to the first pattern after the wafer has been removed for develop and etching and remounted.

The subject of this presentation is how to accurately write a second or subsequent patterns that aligns to previously written and etched patterns. Most bio-chip patterns require 2 different feature depths, with some requiring up to 8 different feature depths. This would require 8 different coating, mounting, recording, development and etch steps.

DCA has developed Virtual Image Alignment technology and equipment to virtually align each recording pattern to the center of the wafer as opposed to the center of the LBR rotation turntable.

10384-17, Session 4

An application of OFDM method to optical disc recording

Kimihiro Saito, Kindai Univ. Technical College (Japan)

An application of Orthogonal Frequency Division Multiplexing (OFDM) method to optical disc recording/readout is presented. OFDM has been widely used in the field of telecommunication owing to its highly efficient frequency usage. However OFDM has not been applied to optical disc recording because it is a multiple data transfer method and needs to record analog signals. Partial Response Maximum Likelihood (PRML) used in the current optical disc systems requires a certain kind of analog recording. Although optical recording usually creates binary marks, it is possible to obtain arbitrary analog readout signals by using PWM method. Another technique to generate analog signals using the oversampled binary recording is described and applied to multiple level recording. In addition, it is found that the level adjustment of multiple carriers for OFDM leads to the advantage when it is applied to the optical disc system. Using the simple transfer function model of the optical disc system, two types of readout signals using PRML and OFDM are calculated and then their qualities are compared. Since Quadrature Amplitude Modulation (QAM) method can be combined with OFDM, it is possible to increase the recoding density of optical disc systems. A method employing OFDM with 64-QAM and the pre-enhance method to the high frequency carrier shows an ability of 1.5 times recording density of the conventional Bru-ray Disc (BD).

10384-18, Session 4

Adaptive optics for data recovery on optical disk fragments

Thomas D. Milster, Young Sik Kim, College of Optical Sciences, The Univ. of Arizona (United States)

An adaptive optics system is designed and constructed to recover information from damaged optical media. The system is based on an Olympus IX70 microscope with custom illumination and detection. A scanning 408nm laser beam provides both the reference beam for the adaptive optics system and the data beam for imaging of data marks. A two-dimensional galvanometer system is used to scan the focused laser over the sample, and a precision z stage is used to change focus planes. The adaptive optics system is based on a Thorlabs AO kit with a Shack-Hartman wavefront sensor and a deformable mirror. A custom objective lens using a solid immersion lens is implemented that provides NA up to 1.5. Several types of data storage substrates are examined, including partial DVD and BD substrates, small 2cm-square pieces of DVD and BD substrates, and dust fragments on the order of 2mm in size. In order to view the dust fragments, they are collected on a microscope slide and melted to reflow the plastic and reveal data-containing flakes.

10384-19, Session 4

Optical mapping of oscillatory stresses in transparent media

Igor A. Sokolov, Mikhail A. Bryushinin, Alexander A. Petrov, Ioffe Institute (Russian Federation); Anatoli M. Balbashov, National Research University “MPEI” (Russian Federation)

The phase-modulated optical signal produced by the light propagation through the stressed transparent media is detected using the non-steady-state photoelectromotive force technique. The mechanical system including the glass plate and piezoelectric transducer demonstrates the resonant behavior in the vicinity of 100 kHz. The measured distribution of the optical phase is a bell-shaped surface for these frequencies. The simulation of the piezooptic response shows the qualitative coincidence with the experimental data and provides the maps of the stress field. The characterization of the Ga_2O_3 adaptive detector is performed for the light wavelength 532 nm.

10385-1, Session 1

Single shot Talbot imaging for wavefront sensing and x-ray metrology

Walan C. Grizolli, Xianbo Shi, Lahsen Assoufid, Argonne National Lab. (United States)

APS has recently developed and commissioned a portable X-ray grating interferometer system [1]. The instrument is suitable for different experimental techniques, for instance grating interferometry in Moiré, single-shot and phase-stepping modes, and near-field speckle tracking method. Special efforts have been made in using single-shot imaging using single phase gratings, also known as the Talbot imaging. This is a differential phase contrast technique that can be used for wavefront characterization and for imaging phase objects. In this work, we describe the latest results using this instrument for the wavefront characterization and for imaging compound refractive lenses.

[1] Assoufid, L. et al, (2016). Review of Scientific Instruments, 87(5), 52004.

10385-2, Session 1

High-performance at-wavelength metrology with an efficient high-order suppression system

Franz Schäfers, Andrey A. Sokolov, Andreas Gaupp, Martin Luettecke, Helmholtz-Zentrum Berlin für Materialien und Energie GmbH (Germany)

The At-Wavelength Metrology Station in a clean-room hutch at the BESSY-II storage ring is in operation now since two years. It consists of a plane grating monochromator beamline in collimated light (c-PGM) at a bending magnet and a versatile UHV-reflectometer with 11 axes. The energy range covers the UV, EUV and soft x-rays. It is primarily used for characterization of the efficiency of our in-house produced diffraction gratings, but also to develop novel optical concepts employing as reflection zone plate optics, multilayer mirrors or multilayer coated gratings. The use of off-plane bending magnet to deliver elliptically polarized light to the sample for ellipsometry and polarimetry applications has been recently established. High-quality metrology requires in particular a very high spectral purity of the incident beam. This is performed by (1) a set of filters with suitable absorption edges to suppress the second order radiation in a limited energy range and (2) by a High-Order Suppressor system (HiOS) consisting of 4 mirrors which can be inserted into the incident beam. The two pairs of mirrors are aligned parallel not to disturb the original beam path and are rotated clockwise and counter-clockwise, respectively. Three sets of coatings are available for the different energy ranges and the incidence angle is freely tunable to find the optimum figure of merit for maximum suppression at maximum transmission for each photon energy required. The status of the metrology station and recent results will be shown.

References

[1] F. Schäfers, P. Bischoff, F. Eggenstein, A. Erko, A. Gaupp, S. Künstner, M. Mast, J.-S. Schmidt, F. Senf, F. Siewert, A. Sokolov, Th. Zeschke, The At-Wavelength Metrology Facility for UV- and XUV-Reflection and Diffraction Optics at BESSY-II, Journal of Synchrotron Radiation, Proc. PhotonDiag workshop Trieste 23(1), 67-77 (2016)

[2] A. Sokolov, P. Bischoff, F. Eggenstein, A. Erko, A. Gaupp, S. Künstner, M. Mast, J.-S. Schmidt, F. Senf, F. Siewert, Th. Zeschke, F. Schäfers, At-Wavelength Metrology facility for XUV reflection gratings, Rev. Sci. Instrum. 87, 052005-1-7 (2016)

10385-3, Session 1

Speckle-based portable device for in-situ metrology of x-ray mirrors at Diamond Light Source

Hongchang Wang, Tunhe Zhou, Yogesh Kashyap, Kawal J. S. Sawhney, Diamond Light Source Ltd. (United Kingdom)

The successful exploitation of X-ray beams generated by modern third-generation synchrotron light sources depends to a significant extent on developments in X-ray mirrors. The push toward higher spatial resolution requires diffraction-limited and coherence-preserved beams which demand accurate metrology on X-ray mirrors. Moreover, it is important to perform in-situ characterization and optimization of X-ray mirrors since their ultimate performance is critically dependent on the working conditions. Therefore, it is highly desirable to develop a portable metrology device, which can be easily implemented on any beamline for in-situ metrology. A speckle-based portable device for in-situ metrology of synchrotron X-ray mirrors has been developed at Diamond [1]. Ultra-high angular sensitivity is achieved by scanning the speckle generator in the X-ray beam [2, 3]. In addition to the compact setup and ease of implementation, a user-friendly graphical user interface has been developed to ensure that characterization and alignment X-ray mirrors is simple and fast. The functionality and feasibility of this device will be presented including the first results of this device's use on different beamlines at Diamond.

[1] Y. Kashyap, H. Wang, and K. Sawhney, "Development of a speckle-based portable device for in situ metrology of synchrotron X-ray mirrors," Journal of Synchrotron Radiation, 23(5), 1131-1136 (2016).

[2] H. Wang, J. Sutter, and K. Sawhney, "Advanced in situ metrology for x-ray beam shaping with super precision," Optics Express 23(2), 1605-1614 (2015).

[3] H. Wang, Y. Kashyap, and K. Sawhney, "Speckle based X-ray wavefront sensing with nanoradian angular sensitivity," Optics Express 23(18), 23310-23317 (2015).

10385-4, Session 1

Investigation of HF-plasma-treated soft x-ray optical elements

Frank Eggenstein, Andrey A. Sokolov, Andrei Varykhalov, Maxim Krivenkov, Ivo Rudolph, Johannes Wolf, Mewael Giday Sertsu, Thomas Zeschke, Franz Schäfers, Helmholtz-Zentrum Berlin für Materialien und Energie GmbH (Germany)

Contamination of optical elements (mirrors and gratings) with carbon is still an issue using soft x-ray synchrotron radiation. With an in-house developed HF-plasma treatment we are able to decontaminate our optics in-situ very efficiently from carbon. The cleaning device, a simple Al-antenna, is mounted in situ inside the mirror- and grating vacuum chambers. A systematic study of the cleaning efficiency was performed using in-situ and ex-situ methods for monitoring: An atomic force microscope (AFM) and a scanning tunneling microscope (STM) were applied before and after the cleaning process to determine the surface roughness. Reflectivity scans ([theta]-2[theta]) with the reflectometer at the BESSY-II Metrology Station [1] [2] was used to estimate the thickness of the remaining C-layer after different cleaning steps and thereby the etching rate. Photon flux measurements in the range of 200 eV - 900 eV show the complete removal of C from the optics without contamination it with other elements created by the plasma treatment. The data will show that the plasma process improves the reflectivity and reduces the roughness. Moreover, the region of the optical surface where the carbon has been removed becomes passivated.

References:

1. A. Sokolov, P. Bischoff, F. Eggenstein, A. Erko, A. Gaupp, S. Künstner, M. Mast, J.-S. Schmidt, F. Senf, F. Siewert, T. Zeschke, F. Schäfers, At-Wavelength Metrology facility for XUV reflection gratings, Rev. Sci. Instrum. 87, 052005-1-7 (2016)

2. F. Eggenstein et al. A reflectometer at-wavelength charakterization of XUV-reflection gratings Proc. of SPIE 9206, Advances in Metrology for X-Ray and EUV Optics

10385-5, Session 2

Intrinsic resolving power of XUV diffraction gratings measured with Fizeau interferometry

Samuel Gleason, Jonathan Manton, Janet Sheung, Taylor Byrum, Cody Jensen, Lingyun Jiang, Inprentus, Inc. (United States); Joseph Dvorak, Ignace Jarrige, Brookhaven National Lab. (United States); Peter Abbamonte, Inprentus, Inc. (United States)

Measuring the intrinsic resolving power R = q/dq of high-resolution diffraction gratings with R = 10^4 - 10^5 is a challenge for benchtop diffractometers.

On the other hand, real-space measurements face the difficulty of correlating line-spacing errors across the entire grating surface, as local measurements of periodicity are not sufficient to determine R.

To overcome these challenges, we introduce a method for using Fizeau interferometry, a real-space probe of the entire grating, to measure R.

By translating the native Fizeau `height' map into a map of phase errors in the grating pattern, we are able to compute the resolution function of the grating and determine R.

Furthermore, we show that it is possible to isolate contributions to R from either ruling or substrate imperfections.

Our results show excellent agreement with direct measurements of R obtained with a visible-light diffractometer, and we demonstrate R = 50,400 for a mechanically-ruled, XUV grating from Inprentus, Inc.

10385-7, Session 2

Characterization of a 150-mm long variable line spacing plane grating through interferometry

Maurizio Vannoni, Idoia Freijo-Martín, European XFEL GmbH (Germany)

The European XFEL is a large facility under construction in Hamburg, Germany [1]. It will provide a transversally fully coherent X-ray radiation with outstanding characteristics: high repetition rate (up to 2700 pulses with a 0.6 milliseconds long pulse train at 10Hz), short wavelength (down to 0.05 nm), short pulse (in the femtoseconds scale) and high average brilliance (1.6?1025 photons / s / mm2 / mrad2/ 0.1% bandwidth). It will have initially three main beamlines, named SASE1, SASE2 and SASE3. The last one is considered a “soft X-ray” beamline, with energies that will span from 0.25 to 3 keV, delivering photon pulses to SQS (Small Quantum System) and SCS (Spectroscopy & Coherent Scattering) experiments. The optical transport of the almost diffraction-limited beam is done using 950 mm long mirrors, cooled with InGa eutectic bath and super-polished (50 nrad RMS slope error and less than 3 nm PV residual height error).

A VLS-PG (variable line spacing - plane grating) monochromator is installed to enhance the spectral coherence of the beam. The final specifications for the grating substrates are 530 mm length, InGa eutectic bath cooled and ion-beam polished with gravity sag compensation. For the initial commissioning of the beamline, a shorter grating (150 mm long) will be installed.

We recently received the 150 mm long grating and we present here its characterization performed using Fizeau Interferometry and White-Light-Interferometry [2]. The VLS parameters are especially investigated and characterized. The result can be summarized that most of the measured parameters are fulfilling the requirements, with some exceptions. This study can give an interesting insight in present status of European XFEL metrology applied to gratings, but also additional information for the future development of the final 530 mm long grating.

10385-8, Session 2

Metrology of variable-line-spacing x-ray gratings using the APS Long Trace Profiler

Janet Sheung, Argonne National Lab. (United States) and Univ. of Illinois (United States); Jun Qian, Argonne National Lab. (United States); Muriel Thomasset, Synchrotron SOLEIL (France); Jonathan Manton, Inprentus, Inc. (United States); Sunil Bean, Argonne National Lab. (United States); Peter Z. Takacs, Joseph Dvorak, Brookhaven National Lab. (United States); Lahsen Assoufid, Argonne National Lab. (United States)

As resolving power targets have increased with each generation of beamlines commissioned synchrotron radiation facilities worldwide, diffraction gratings are quickly becoming crucial optical components for meeting performance targets. However, metrology of variable-line-spacing (VLS) gratings for high resolution beamlines is not widespread; in particular, no metrology facility at any US DOE facility is currently equipped to fully characterize such gratings. To begin to address this issue, the Optics Group at the Advanced Photon Source at Argonne, in collaboration with SOLEIL and with support from Brookhaven National Laboratory (BNL), has developed an alternative beam path addition to the Long Trace Profiler (LTP) at Argonne's Advanced Photon Source. This significantly expands the functionality of the LTP to not only to measure mirrors surface slope profile at normal incidence, but also to characterize the groove density of VLS diffraction gratings in the Littrow incidence up to 79°, which covers virtually all diffraction gratings used at synchrotrons in the first order. The LTP light source is a 20mW HeNe laser, which yields enough signal for diffraction measurements to be performed on low angle blazed gratings optimized for soft X-ray wavelengths. We will present the design of the beam path, technical requirements for the optomechanics, and our data analysis procedure. Results for diffraction gratings to be installed in BNL's future Inelastic X-ray Scattering beamline will also be presented. Finally, we discuss challenges still to be overcome and potential limitations with use of the LTP to perform metrology on diffraction gratings.

*Work done at Argonne National Laboratory and Brookhaven National Laboratory was supported by U.S. Department of Energy (DOE) Office of Science, under Contracts No. DE-AC02-06CH11357 and DE-AC02-98CH10886, respectively.

10385-9, Session 3

Recent developments on nanoradian-angle metrology

Tanfer Yandayan, TÜBITAK UME (Turkey)

The demands for angle measurement-generation at the nanoradian precision for scientific and industrial applications continue to grow with various numerical applications; e.g., to monitor the angles of telescope mirrors in astrometry (0.1 nrad sensitivity), to tune the angle between a pair of silicon crystals in gamma ray spectroscopy (0.1 nrad resolution), to calibrate accelerometers for space missions (20 nrad accuracy) and to determine the constant of gravitation G by use of a torsion balance etc,. Autocollimators, optical measurement devices which measure the angular tilt of reflecting surfaces are good candidates for this and also used in slope measuring profilers for the inspection of ultra-precise X-ray optical components; particularly for applications in synchrotron radiation and X-ray

Free Electron Lasers (XFELs). An angle metrology project (SIB58 Angles) addressing the challenging issues related to performance of autocollimators in slope measuring profilers run for three years and was completed recently with cooperation of a wide range of partners. Outcomes of the project which are for interest to the X-ray optics community will be presented; new aperture centring device (ACenD) for the accurate centring of a beam-limiting aperture in front of an autocollimator (with a positional accuracy of ±0.1 mm), performance of autocollimators with varying distances to reflector at small apertures, developed guides for calibration of autocollimators and reference angle encoders, first 2D calibration of autocollimators, new devices and novel methods for traceable generation and measurement of angles at nanoradian precision.

10385-10, Session 3

A new ultra-high-accuracy angle generator: current status and future direction

Christian F. Guertin, Vermont Photonics Technologies Corp. (United States); Ralf D. Geckeler, Physikalisch-Technische Bundesanstalt (Germany)

Lack of an extreme high-accuracy angular positioning device available in the U.S. has left a gap in industrial and scientific efforts conducted here. Specifically, in x-ray mirror metrology the global research community is advancing the state-of-the-art to unprecedented levels. We aimed to fill this U.S. gap by developing a versatile high-accuracy angle generator as a part of the national metrology tool set for x-ray mirror metrology and other important industries. Using an established calibration technique to measure the errors of the encoder scale graduations for full-rotation rotary encoders, we implemented an optimized arrangement of sensors positioned to minimize propagation of calibration errors. Our initial feasibility research shows that upon scaling to a full prototype we expect to achieve uncertainties at the level of 50 nrad or better and offer the immense advantage of a highly automatable and customizable product to the commercial market. We will present the current status and future direction of the project.

10385-11, Session 3

A portable device for calibration of autocollimators with nanoradian precision

Tanfer Yandayan, TÜBITAK UME (Turkey)

Autocollimator-based surface measuring profilers offer the state of the art capability for the inspection of ultra-precise X-ray optical components; particularly for synchrotron radiation (SR), X-ray Free Electron Lasers (XFELs). Demands for sub-nanometre topography measurement by these profilers require calibration of autocollimators with expanded uncertainties less than 0.01 arcsec (50 nrad) in the range of ±1000 arcsec (5 mrad). Also, regular in-situ checks of the performance of these autocollimators in these applications become more and more important. Such in-situ checks are able to uncover differences in the angle response of autocollimators between the calibration at a laboratory and their subsequent application in the slope measuring profilers. Apart from subtle changes in the autocollimator's measuring conditions, shocks, particularly during their transportation, may affect the previous calibration values. This requires on-site/in-situ calibrations of autocollimators with low uncertainties. A large range small angle generator (LRSAG) has been developed in TUBITAK UME to calibrate high precision autocollimators with nanoradian precision. The portable device can operate in the range of ±4500" which is far enough for the calibration of the available autocollimators and can generate ultra-small angles in measurement steps of 0.0005" (2.5 nrad). Description of the device with the performance tests using the calibrated precise autocollimators and novel methods will be reported. The test results indicate that the device is a good candidate for application to on-site/in-situ calibration of autocollimators with expanded uncertainties of 0.01 arcsec particularly those used in slope measuring profilers.

10385-12, Session 4

A new optics metrology laboratory at CNPEM: metrology capabilities, performance, and future plans

Bernd C. Meyer, Murilo B. da Silva, Harry Westfahl Jr., Ctr. Nacional de Pesquisa em Energia e Materiais (Brazil)

A new metrology and assembly facility was constructed at CNPEM and turned recently into operation. The facility includes an assembly area of 100 m?, a high-precision mechanical metrology laboratory and an optical metrology laboratory (OML), both of 50 m?, and provide improved environmental and instrumental conditions. All three laboratories sit on inertial blocks with special foundations originally developed and tested as prototype for the SIRIUS tunnel floor. The inertial blocks perform very well in attenuation of external vibrations. The OML is cleanroom ISO7 and has temperature stability better than ±0.1 K. Measurements of the surface under test (SUT) using NOM, Fizeau-Interferometer (FI), Micro-Interferometer (MI) and AFM as the four instruments inside the OML cover the full required range of spatial frequencies. We report on the performance of the NOM and FI, the first instruments installed in the OML.

10385-13, Session 4

X-ray optics laboratory at the ALS: current capabilities, new challenges, and tasks for further development

Ian Lacey, Lawrence Berkeley National Lab. (United States); Gary P. Centers, Helmholtz-Institut Mainz (Germany) and Lawrence Berkeley National Lab. (United States); Gevork S. Gevorkyan, Sergey M. Nikitin, Brian V. Smith, Valeriy V. Yashchuk, Lawrence Berkeley National Lab. (United States)

The R&D work on the ALS upgrade to a diffraction limited electron ring, ALS-U, has brought to focus the need for near-perfect x-ray optics, capable of delivering light to experiments without significant degradation of brightness and coherence. The desired quality of the optics is illustrated by the residual surface slope and height errors of <50?100 nrad (rms) and <1?2 nm (rms), respectively. This catalyzes the development at the ALS new ultra-high accuracy metrology methods. Fundamental to the optimization of beamline performance of such x-ray optics, metrology must be capable of characterizing the optics with accuracy even better than the specification. The major limiting factors of the current absolute accuracy are systematic errors inherent to the metrology instruments. Here, we discuss details of work at the Advanced Light Source (ALS) X-Ray Optics Laboratory (XROL) on the development of advanced experimental methods and techniques to suppress, measure, and eliminate the instrumental systematic errors. With examples, we show how the implementation of these methods allows us to significantly improve the capabilities and performance of the existing lab equipment used for characterization and optimal tuning of high quality x-ray optics. We will also review the ALS XROL plans for instrumentation upgrades and development of sophisticated methods for metrology data processing and usage. The discussion will be illustrated with the results of a broad spectrum of measurements of x-ray optics and optical systems performed at the lab. Supported by the U.S. Department of Energy under contract number DE- AC02-05CH11231.

10385-14, Session 4

Status of the metrology laboratory for the LCLS II project

May Ling Ng, Corey L. Hardin, Josep Nicolas, Daniele Cocco, SLAC National Accelerator Lab. (United States)

Along with the demanding requirements for the extreme limit pushing LCLS II project, comes the challenge in metrology work for qualifying the optical and mechanical components. Besides qualifying the components against specifications, it is also crucial to study performance, repeatability and stability of the mirror systems designed for meeting the LCLS II conditions. Therefore a dedicated metrology laboratory has been jointly funded by LCLS II project and LCLS facility.

The laboratory, located close to the experimental hall of LCLS, is currently equipped with a 6" Fizaeau interferometer (Zygo DynaFiz) and a Zygo NewView 8300 white light interferometer. A profilometer, hosting a Long Trace Profiler optic head, an autocollimator (Moller Wedel) and a Shack Hartman head (SHArPer, Imagine Optics), is under assembling.

The combination of these instruments will enable us to measure spatial periods from the μm scale up to 1.5 m. Further implementation in progress are the implementation of a stitching method for the 6" interferometer and reduction of environmental noise.

The results obtained from measuring 1-m long flat mirrors, with sub-nm shape errors, produced by Jtec, show a very high sensitivity of the interferometer. These results, as well as the results obtained in testing the bender prototype and some diffraction gratings, will be presented.

10385-15, Session 5

New surface slope profiler reaching sub-millimeter spatial resolution

Fugui Yang, Ming Li, Quan Cai, Ya Du, Dingxiao Liu, Xiaowei Zhang, Yuhui Dong, Peng Liu, Institute of High Energy Physics (China)

We introduce a novel (to the best of our knowledge) slope measurement system for long X-ray mirror surface characterization with enhanced spatial resolution. Different from traditional long trace profiler, the focused instead of collimated light beam was used to sample the mirror surface placed in the conjugate plane of the light source (pinhole), which ensures the spatial resolution of the system same with image size of the pinhole. Experimental studies show that high spatial resolution (?0.1?mm) and high angular accuracy (< 0.1??rad) has been achieved. The scanning measurement gives a repeatability as high as 0.05 nm by integration the slope profile. Not only ex-situ measurement, but also this new profiler offers an inexpensive and robust way to perform in-situ measurement due to long distance between sample and optical head

10385-16, Session 5

Development of a high-performance surface slope profiler for two-dimensional mapping of x-ray optics

Ian Lacey, Lawrence Berkeley National Lab. (United States); Jérôme Adam, Ecole Nationale Supérieure d'Ingenieurs de Caen et Ctr. de Recherche (France); Gary P. Centers, Helmholtz-Institut Mainz (Germany); Gevork S. Gevorkyan, Sergey M. Nikitin, Valeriy V. Yashchuk, Lawrence Berkeley National Lab. (United States)

The research and development work on the Advanced Light Source (ALS) upgrade to a diffraction limited electron ring, ALS-U, has brought to focus the need for near-perfect x-ray optics, capable of delivering light to experiments without significant degradation of brightness and coherence. The desired surface quality is characterized with residual (after subtraction of an ideal shape) surface slope and height errors of <50?100 nrad (rms) and <1?2 nm (rms), respectively. The ex-situ metrology that supports the optimal usage of the optics at the beamlines has to offer even higher measurement accuracy. At the ALS X-Ray Optics Laboratory, we are developing a new surface slope profiler, the Optical Slope Measuring System (OSMS), capable of two-dimensional (2D) surface-slope metrology at an absolute accuracy below 50 nrad. In this article we provide the results of comprehensive characterization of the key elements of the OSMS, a NOM-like high-precision granite gantry system with air-bearing translation and a custom-made precision air-bearing stage for tilting and flipping the surface under test. We show that the high performance of the gantry system allows implementing an original scanning mode for 2D mapping. We demonstrate the efficiency of the developed 2D mapping via comparison with interferometric measurements performed with the same plane test mirror. The details of the OSMS design and the developed measuring techniques are also provided. This work was supported by the U. S. Department of Energy under contract number DE- AC02-05CH11231.

10385-17, Session 5

Optomechanical development progress of high-accuracy long-trace profiler at the planning HEPS

Shanzhi Tang, Ming Li, Institute of High Energy Physics (China)

High accuracy long trace profiler (LTP) is one most important of many sub-projects for the planning High Energy Photon Source (HEPS, Beijing), which is crucial to test and fabricate advanced X-ray mirrors. LTP at HEPS will be a metrological instrument with high accuracy of <0.1?rad rms for components of length ≥1m in this paper. The development progress is introduced in the overall, in which the precision instrument designing, optical and mechanical manufacturing, assembling have been discussed and carried out based on a novel scheme of LTP. The several considerations are emphasized to reduce systematic errors and to strengthen the anti-jamming capability. The prototype and test experiments are presented to validate it. It will play a key role to X-ray optics metrology and fabrication for the construction of HEPS coming soon.

10385-18, Session 5

Surface slope metrology of highly curved x-ray optics with an interferometric microscope

Gevork S. Gevorkyan, Lawrence Berkeley National Lab. (United States); Gary P. Centers, Helmholtz-Institut Mainz (Germany) and Lawrence Berkeley National Lab. (United States); Kateryna S. Polonska, Yuriy Fedkovych Chernivtsi National Univ. (Ukraine) and Lawrence Berkeley National Lab. (United States); Ian Lacey, Valeriy V. Yashchuk, Lawrence Berkeley National Lab. (United States)

The development of deterministic polishing techniques has given rise to vendors that manufacture high quality three-dimensional x-ray optics. The surface metrology on these optics remains a difficult task. For the fabrication, vendors usually use unique surface metrology tools, generally developed on site, that are not available in the optical metrology labs at x-ray facilities. At the Advanced Light Source X-Ray Optics Laboratory, we have developed a rather straightforward interferometric-microscopy-based procedure capable of sub microradian characterization of sagittal slope variation of x-ray optics for two-dimensionally focusing (such as ellipsoids) and collimating (paraboloids). In the paper, we provide the mathematical foundation of the procedure and describe the related instrument calibration. We also present analytical expressions describing the ideal surface slope variation in both directions of a spheroid specified by the conjugate parameters of the optic's beamline application. The expressions are useful when analyzing data obtained with such optics. The high efficiency of the developed measurement and data analysis procedures is demonstrated in results of measurements with a number of x-ray optics with sagittal radius of curvature between 56 mm and 480 mm. We also discuss potential areas of further improvement. This work is supported by the U.S. Department of Energy under contract number DE-AC02-05CH11231 and, in part, by DOE BES STTR grant number DE-SC0011352.

10385-19, Session 5

New twist in the optical schematic of surface-slope measuring long-trace profiler

Gevork S. Gevorkyan, Lawrence Berkeley National Lab. (United States); Wayne R. McKinney, Diablo Valley College (United States); Ian Lacey, Sergey M. Nikitin, Lawrence Berkeley National Lab. (United States); Peter Z. Takacs, Brookhaven National Lab. (United States); Valeriy V. Yashchuk, Lawrence Berkeley National Lab. (United States)

The advent of fully coherent free electron laser and diffraction limited synchrotron storage ring sources of x-rays is catalyzing the development of new, ultra-high accuracy metrology methods. To fully exploit the potential of these sources, metrology needs to be capable of determining the figure of an optical element with sub-nanometer height accuracy. Currently, the two most prevalent slope measuring instruments used for characterization of x-ray optics are the auto-collimator based nanometer optical measuring device (NOM) and the long trace profiler (LTP) using pencil beam interferometry (PBI). These devices have been consistently improved upon by the x-ray optics metrology community, but appear to be approaching their metrological limits. Here, we revise the traditional optical schematic of the LTP. We experimentally show that for the level of accuracy desired for metrology with state-of-the-art x-ray optics, the Dove prism in the LTP reference channel appears to be one of the major sources of instrumental error. Therefore, we suggest returning back to the original PBI LTP schematics with no Dove prism in the reference channel. In this case, the optimal scanning strategies [Yashchuk, Rev. Sci. Instrum. 80, 115101 (2009)] used to suppress the instrumental drift error have to be used to suppress a possible drift error associated with laser beam pointing instability. We experimentally demonstrate the usefulness of the suggested approach via measurements with a number of x-ray optics with both face up and face down orientations. This work is supported by the U.S. Department of Energy under contract number DE-AC02-05CH11231.

10385-29, Session 5

Fabrication and metrology of OSAKA MIRROR for synchrotron applications

Yoshio Ichii, Hiromi Okada, Shinya Aono, Shinsaku Shiroma, Akihiko Ueda, Takashi Tsumura, JTEC Corp. (Japan)

We, JTEC Corporation, have been fabricating OSAKA MIRROR using EEM, nano-fabrication, and RADSI and MSI, nano-measurements, developed by Osaka University [1], and have delivered nearly 400 Super Precision Mirrors to synchrotron radiation facilities worldwide.

We will give an overview of our production technologies and the potentialities. In addition, we will report some focusing results using our OSAKA MIRRORs installed in SPring-8 and SACLA [2][3]. Furthermore, we will show fabrications of challenging mirrors which are developed in collaboration with Osaka University and SPring-8.

[1] K. Yamauchi et al., Rev. Sci. Instrum. 73 (2002) 4028.

[2] H. Ohashi et al., J. Phys.: Conf. 425 (2013) 052018.

[3] H. Yumoto et al., Nature Photon. 7 (2013) 43.

10385-30, Session 5

Development of measurement system for ellipsoidal mirrors

Hiroki Nakamori, JTEC Corp. (Japan) and Osaka Univ. (Japan); Yoshio Ichii, Hiromi Okada, Akihiko Ueda, Takashi Tsumura, JTEC Corp. (Japan); Satoshi Matsuyama, Kazuto Yamauchi, Osaka Univ. (Japan)

We manufacture ultra-precise X-ray mirrors (plane, cylinder, elliptic cylinder, parabolic cylinder and etc.) for synchrotron radiation and free-electron laser facilities with subnanometer accuracy. Such high-precision mirrors are achieved with our unique metrology and polishing techniques: the relative angle determinable stitching interferometry (RADSI); the microstitching interferometry (MSI); and the elastic emission machining. In recent years, ellipsoidal mirrors have drawn strong attentions; however, it is difficult to measure sagittal-curved mirrors with subnanometer accuracy using RADSI and MSI. We, therefore, develop a new measurement system for measuring ellipsoidal mirrors.

10385-20, Session 6

Development of relative angle determinable stitching interferometry for high-accuracy x-ray focusing mirrors

Yingna Shi, Xudong Xu, Qiushi Huang, Zhanshan Wang, Tongji Univ. (China)

X-ray focusing mirrors with elliptical shape are widely used in synchrotron facilities for micro-, nano-scale focusing experiments. Surface interferometry plays an important role in the x-ray mirrors figuring with subnanometer accuracy. To avoid the second order error in stitching interferometry, relative angle determinable stitching interferometry (RADSI) is under development. This method was first developed by Yamauchi et al from Osaka University, which uses a planar mirror to correct the relative stitching angle between the neighboring subapertures. Here, we use RADSI to measure the x-ray spherical and elliptical mirrors with 300mm aperture Fizeau interferometer. The interferometer is combined with 4 accurate rotation and tilt stages for the stitching measurement. To ensure the stitching accuracy, we first studied the measurement accuracy within every single subaperture. Multiple measurement is used to decease the random error of single subaperture and 2-D shearing method is proposed to obtain the reference surface error. The subaperture positioning is also carefully corrected to ensure the pixels of the adjacent subapertures in overlapping areas can be matched well. Finally, the profile of the mirror is stitched and compared with the measurement results using Nanometer Optical Component Measuring Machine (NOM) at Shanghai synchrotron radiation facility (SSRF).

10385-21, Session 6

Fizeau stitching at the ESRF

Amparo Vivo, Raymond Barrett, ESRF - The European Synchrotron (France)

X-ray mirror figure errors are commonly measured in the synchrotron community using long trace profiler (LTP) or nanometer optical measuring machine (NOM) instruments, both providing 2D slope measurement. 3D reconstruction is possible but is time consuming, requiring a high stability of environmental conditions over long periods which is not easy to achieve. Characterization of the complete topography of mirror surface is particularly valuable to reveal stresses or deformations such as twist that could be introduced by optomechanical mounting.

At the ESRF metrology laboratory Fizeau stitching methods are under development. A full automated mechanical setup dedicated to stitching measurement of long flat mirrors is now operational. We have already demonstrated accurate reconstruction by stitching 2D profiles acquired from Fizeau sub-aperture measurements . The current work is focused on 3D reconstruction of flat mirror sur-faces up to one meter long. Repeatability, accuracy and in particular the influence of the transmission element will be discussed.

10385-22, Session 6

Three-dimensional shape measurement for x-ray ellipsoidal mirror

Takehiro Kume, Yoshinori Takei, Satoru Egawa, Gota Yamaguchi, Hiroto Motoyama, Hidekazu Mimura, The Univ. of Tokyo (Japan)

An x-ray ellipsoidal mirror requires nanometer-level shape accuracy for its internal surface. Because of the difficulty in processing the surface, electroforming using a high precision master mandrel has been applied to mirror fabrication. To investigate replication accuracy of electroforming, a measurement method for the whole internal surface of the mirror needs to be developed.

The purpose of this study is to evaluate shape replication accuracy of electroforming.

In this paper, a three-dimensional shape measurement apparatus for an x-ray ellipsoidal mirror is developed. The apparatus is composed of laser probes, a contact probe, reference flats, a z-axis stage and a rotation table. First, longitudinal profiles of a mandrel or a mirror vertically placed on the rotation table are measured at several angular positions, and straightness of the center axis and a deviation of the diameter at each height are estimated. Next, without realignment of the measured sample, circularity at every height is measured at regular intervals of 0.1 mm. During each measurement, an effect of motion errors is calculated and subtracted from each profile by referring to distances between probes and the reference flats. Combining the circularity data with information on the straightness of the center axis and the diameter deviation, the three-dimensional error distribution of the whole surface is obtained.

Using a mandrel with nanometer-level shape accuracy and a replicated mirror, performance of the measurement apparatus and the replication accuracy are examined. Measurement repeatability of 1 nm order and a replication accuracy of sub-100 nm order are confirmed.

10385-23, Session 6

Testing Resistive Element Adjustable Length (REAL) cooling for sub-nanometer figure preservation in high-heat load FEL optics

Corey L. Hardin, May Ling Ng, Venkat N. Srinivasan, Daniel S. Morton, Peter M. Stefan, Nicholas M. Kelez, Josep Nicolas, Lin Zhang, Daniele Cocco, SLAC National Accelerator Lab. (United States)

SLAC National Accelerator Laboratory is developing a new high repetition rate free electron laser, LCLS-II, a superconducting linear accelerator capable of a repetition rate up to 1 MHz over a wide energy range (200- 5000 eV). To deliver the FEL beam with minimal power loss and wavefront distortion, the mirrors for the system need height errors below 1nm rms in operational conditions across this spectrum.

In order to maintain this figure error, thermal load effects due to the high repetition rate must be minimized. The absorbed thermal profile is highly dependent on the beam divergence, and this is a function of the photon energy. This leads to a large variation in the beam footprint on the mirror, leading to a large variance in the thermal bump throughout the energy range. In order to correct for this error, first order curvature correction is performed with an off-axis bender. Past this, the cooling system is designed to minimize higher order error. A technique has been developed at SLAC called Resistive Element Adjustable Length (REAL) cooling. This method uses variable length heaters on the mirror cooling system to control the effective cooling width. This allows the cooling footprint to closely match the beam footprint on the mirror, minimizing the thermal bump across a wide range of photon energies. Modeling has been performed which shows this technique could produce height errors below 1nm rms under a FEL power of 200W.

We present the design features, thermo-mechanical analysis and results from metrology tests of a prototype assembly as well as the effects of mirror figure errors, thermal deformation, and bending errors on wavefront propagation through the system.

10385-24, Session PMon

Calibration devices and methods for soft x-ray detector at Beijing Synchrotron Radiation Facility (BSRF)

Mingqi Cui, Yidong Zhao, Lei Zheng, Institute of High Energy Physics (China)

There are two beamlines (4B7A & 4B7B) used for calibration at Beijing Synchrotron Radiation Facility (BSRF). The 4B7A is a medium energy x-ray double-crystal monochrometer (DCM) beamline. It includes three type crystals (KTP (111), InSb (111) and Si (111)). The energy range is from 1.2keV to 6keV. The 4B7B is a VLS plane grating monochrometer (PGM) soft x-ray beamline. The photon energy range is 0.05keV-1.7keV. The monochrometer can be used for two working modes, variable and fix included angle. The high energy resolution (E/?E~5000) and high spectral purity (higher-harmonics suppressor ratio: 0.1%) have been carried out with these working modes, respectively. A lot of sensors have been absolutely-calibrated with the beamlines. For example, XRD, mirror and multilayer, filter, transmission grating, CCD, crystal and image plate etc.. And have been used for other fields, too. They are optics, material, astronomy, metrology etc..

10385-25, Session PMon

X-ray multilayer mid-frequency characterizations using speckle scanning techniques

Hui Jiang, Shanghai Synchrotron Radiation Facility (China)

Determination of multilayer structure was developed so much, but most of studies focused on the relationship between structural imperfections and reflectivity. These imperfections, whether interfacial roughness and interdiffusion or surface feature, measured by grazing X-ray scattering, atomic force microscopy or electric microscopy, reflect relatively high-frequency characteristics. The mid-frequency figure errors were regarded as the main factor to produce large satellite peaks near the focusing spot in the multilayer K-B mirror and were found to produce stripes in the far-field imaging. We report novel method to study mid-frequency interface and layer growth characterizations of multilayer structure using at-wavelength speckle scanning technique. This work is beneficial for matching multilayer manufacture technology to the optimization of beam performances.

10385-26, Session PMon

Optimization of pencil beam F-Theta lens for high-accuracy metrology

Chuanqian Peng, Yumei He, Jie Wang, Shanghai Institute of Applied Physics (China)

Pencil beam deflectometric profilers are common instruments for high accurate surface slope metrology of X-ray mirrors in synchrotron facilities. F-theta optical system is a key optical component of deflectometric profilers used to perform linear angle-to-position converting. Traditional optimization procedures of f-theta systems are not directly related to the angle to position converting relation and performed with large size stop at fixed working distance, which means they may not suitable for the design of f-theta systems working with a small size pencil beam within a working distance range for ultra high accuracy metrology. If an f-theta system is not well designed, aberrations of the f-theta system will introduce lots of systematic errors to the measurement. In this paper we propose a

least square fitting procedure to optimize configuration parameters of an f-theta system. ZEMAX simulation shows that the optimized f-theta system significantly suppressed the angle-to-position converting errors caused by aberrations. Any pencil beam f-theta optical system might be optimized with the help of our optimization method.

10385-27, Session PMon

A novel scanning deflectometry based on secondary light source normal tracing method

Chuanqian Peng, Yumei He, Jie Wang, Shanghai Institute of Applied Physics (China)

Scanning deflectometric profilers, e.g. ESAD, NOM, LTP, which based on an f-theta system are typical optical tools for measurements of mirror profiles in many synchrotron facilities. Unlike these profilers which based on pencil beam, in this paper we use a secondary light source and a pinhole to make up a beam select system to automatically select a beam which will always pass through the pinhole and propagates along the normal direction of the measured area on the surface under test. By measuring the angle variation of the selected beam the slope variation of the surface under test could be measured. Manufacture defects and aberrations introduced systematic errors of optical elements due to big beam lateral motion, which greatly degrade the performance of traditional profilers could be minimized by using this method. A simple example demonstrated that the measurement accuracy of 60nrad within an angle range of 10mrad is readily accessible.

10386-1, Session 1

Pd-based multilayer mirrors for 8-12nm soft x-ray region

Zhanshan Wang, Qiushi Huang, Yiwen Wang, Wenbin Li, Tongji Univ. (China); Igor V. Kozhevnikov, A.V. Shubnikov Institute of Crystallography (Russian Federation); Zhong Zhang, Tongji Univ. (China)

Multilayer mirrors working at the waveband of 8-12 nm are of particular interest for space telescopes, plasma diagnostics and free electron laser sources. Pd/Y and Pd/B4C are promising candidate for this region due to the high theoretical reflectance. To realize the high reflectance experimentally, the interface structure, stress property and temporal stability of these multilayers are investigated. Pd and Y layers have poor interfaces due to severe intermixing and compound formation. This can be solved by adding B4C barrier layers or using reactive sputtering with nitrogen for the fabrication. The Pd/B4C/Y/B4C and Pd(N)/Y(N) multilayers show high reflectance of 44% and 30%, respectively, at around 9.5 nm under near normal incidence. The Pd/B4C multilayer is also fabricated with reactive sputtering using Ar+N2. Although the compressive stress is essentially reduced, the soft X-ray reflectance (32%) is lower than the sample fabricated with pure Ar (45%). Moreover, a distinct deterioration of the nitridated Pd/B4C multilayer is observed after stored in air for 6-17 months. A large part of the top layers of the nitridated samples is degraded with severe interdiffusion and significant decrease in d-spacing. The deterioration is less pronounced for the multilayers fabricated with a higher ratio of N2. A primitive model of upward diffusion of nitrogen and boron is proposed to explain the aging effects of the nitridated structure.

10386-2, Session 1

Double multilayer monochromators for upgraded ESRF beamlines

Christian Morawe, Damien Carau, Jean-Christophe Peffen, ESRF - The European Synchrotron (France)

Following the recent upgrade programme of the ESRF experimental facilities, several new beamlines have become operational. Some of them include Double Multilayer Monochromators (DMM), operating at photon energies between 20 keV and 70 keV. The motivation to deploy a DMM on a 3rd generation light source can be two-fold: reducing the heat load on downstream optics such as high-resolution crystal monochromators while maintaining the beam direction with little offset; taking benefit from the broader bandwidth to transmit more flux to the experimental end station. In the latter case the bandwidth of the DMM needs to be well controlled and, to comply with certain experimental requirements, it has to stay below 0.5%. Multilayers providing this energy resolution while maintaining a decent peak reflectance require the deposition of an elevated number of layers, the use of materials with moderate electron density, and a coating uniformity close to 0.1% over a substrate area of about 300 mm x 100 mm. These boundary conditions impose severe constraints on the performance of both the deposition system and the available characterization technique.

This work will summarize the outcome of recent DMM deposition projects carried out for the ESRF beamlines ID01, ID15, ID19, and ID31. Several NiV/B4C and W/B4C DMMs with up to 500 repetition periods were coated using DC magnetron deposition. The multilayers were characterized by x-ray reflectivity scans at 8048 eV. The paper will highlight successful results and discuss persisting issues and potential approaches for technical improvements.

10386-3, Session 1

Laterally-graded multilayer as x-ray mirror for the laser-induced plasma x-ray sources

Xianchao Cheng, China Academy of Engineering Physics (China)

The laser-induced plasma sources give instantaneous 4ϖ divergent x-ray beams. The x-ray source size and pulse duration depend on the properties of the high-energy laser. Copper is the typical target material giving characteristic photon energies around 8.4keV for the Cu He-like emission line. Different shapes of bent crystals are widely used as imaging and monochromatizing optics. Focusing and collimating are normally functioned by polycapillary x-ray lenses. Especially, the laterally-graded multilayers are applied as x-ray mirrors, which can reflect hard x-rays with big grazing angles, moderate energy resolution and high reflectivities. To get larger acceptance angel, a higher gradient of bilayer thicknesses from 2nm to 3.6nm within 80mm length scale is designed and experimentally used. An alignment precision of 10?m along the direction perpendicular to the central beam is required to select the correct photon energy. The reflected monochromatic x-rays can enhance the traverse coherence for the phase contrast imaging. By using two mirrors symmetrically arranged, the object can be illuminated from two different directions. Multi-frames of the same object can be obtained instantaneously. The laterally-graded multilayer x-ray mirrors are also used for the pinhole imaging of a Z-pinch target, which benefits from the flat reflection surface with much smaller aberration comparing to the reflection of logarithmic-spiral bent crystal.

10386-4, Session 1

Fabrication and characterization of W/B4C lamellar multilayer grating and NbC/Si multilayer phase-shift reflector

Paresh C. Pradhan, Raja Ramanna Ctr. for Advanced Technology (India) and Homi Bhabha National Institute (India); S. Bhartiya, Raja Ramanna Ctr. for Advanced Technology (India); A. Singh, National Institute of Science Education and Research (India) and Homi Bhabha National Institute (India); A. Majhi, Raja Ramanna Ctr. for Advanced Technology (India) and Homi Bhabha National Institute (India); A. Gome, UGC-DAE Consortium for Scientific Research (India); R. Dhawan, Raja Ramanna Ctr. for Advanced Technology (India); M. Nayak, Raja Ramanna Ctr. for Advanced Technology (India) and Homi Bhabha National Institute (India); Pratap K. Sahoo, National Institute of Science Education and Research (India) and Homi Bhabha National Institute (India); S. K. Rai, Raja Ramanna Ctr. for Advanced Technology (India); V. R. Reddy, UGC-DAE Consortium for Scientific Research (India)

We present fabrication and structural analysis of two different multilayer grating structures. W/B4C based lamellar multilayer grating (LMG) was studied for high resolution monochomator application near soft x-ray region. Whereas NbC/Si based multilayer phase-shift reflector (MPR) was studied for high reflection at normal incidence near Si L-edge (~99 eV) and simultaneously to suppress the unwanted vacuum ultraviolet / infrared radiation. The grating patterns of different periods down to D=10 micron were fabricated on Si substrates by using photolithography, and multilayers of different periodicity (d= 9.5 to 2 nm) and number of layer pairs (15 to 100) were coated using sputtering techniques by optimizing the process parameters. For LMG and MPR samples, XRR measurements were carried

out using both incident planes are perpendicular to the grating lines and parallel to the grating lines, respectively. XRR results show successive higher order Bragg peaks that reveal a well-defined vertical periodic structure in LMG, MPR and multilayer structures. The lateral periodicity of the grating and depth of the rectangular groves were analysed using atomic force microscopy (AFM). The AFM results show good quality of lateral periodic structures in terms of groove profile. The effect of the process parameters on the microstructure (both on vertical and lateral patterns) were analysed and optimized to obtain good quality of both LMG and MPR structures and will be presented.

10386-5, Session 1

Ruthenium growth on B, C, and B4C studied by LEIS

Andrey Zameshin, Andrey E. Yakshin, Marko Sturm, Eric Louis, Fred Bijkerk, MESA+ Institute for Nanotechnology (Netherlands)

Ruthenium is one of the frequently used materials in the design of multilayers for EUV optics of different wavelengths, for example in Ru/B4C, Ru/B or Ru/C multilayers for 7-9 nm or Ru/Si as a specular broadband option for 12.5-14 nm, as well as a capping layer for various multilayers. Ruthenium forms very broad interfaces with Si, B4C, B and C. In this work the growth of magnetron sputtered Ru thin films on these materials was investigated by using in situ Low Energy Ion Scattering (LEIS). This technique has a unique sensitivity to the topmost atomic layer. Combination of in-vacuum transfer of samples and outermost surface sensitivity of LEIS allows us to quantify the surface composition for different thicknesses of Ru and therefore compose a “deposition depth profile”, which gives us knowledge of interface width, as well as the surface segregation effects and changes in surface density during compound formation. This method provides a much better depth sensitivity than traditional sputter depth profiles, and allows to resolve details that could not be seen before.
After adding chemical interaction information from in-vacuum X-ray Photoelectron Spectroscopy (XPS), we propose growth mechanisms of Ru on these substrate materials. Among interesting effects found in this work is extremely strong surface segregation of C on Ru, persisting even after 30 nm of Ru deposited on a carbon substrate layer.

10386-6, Session 1

Growth of x-ray multilayer coatings on sculptured surfaces

Dmitriy L. Voronov, Farhad H. Salmassi, Lawrence Berkeley National Lab. (United States); Peter Gawlitza, Fraunhofer IWS Dresden (Germany); Eric M. Gullikson, Lawrence Berkeley National Lab. (United States); Stefan Braun, Fraunhofer IWS Dresden (Germany); Howard A. Padmore, Lawrence Berkeley National Lab. (United States)

Multilayers grown on substrates with sculptured surfaces offer new functionalities and allow novel advanced x-ray optics and instrumentation. For example, multilayers deposited on saw-tooth substrates enable high efficiency Multilayer Blazed Gratings (MBG) which are a key component for high throughput and high resolution EUV and soft x-rays spectrometers. Understanding the fundamentals of x-ray diffraction in a sculptured multilayer stack and investigation of the growth of the multilayers on highly corrugated surfaces are of great importance for design optimization and performance of the MBGs. We found by simulations and confirmed by experiments that diffraction in MBGs corresponds to asymmetric Bragg diffraction of x-rays with specific refraction effects which depend on diffraction geometry and might significantly differ from the ones for the symmetrical diffraction in plane multilayers. The asymmetrical refraction alters the resonance wavelength, bandwidth, effective blaze angle, and diffraction efficiency of MBGs. Growth of multilayers at incline deposition which corresponds to growth geometry for highly faceted surface of a saw-tooth substrates has been investigated. A new growth mode which results in highly periodic ripple patterns was discovered. Optimization of the deposition aimed to mitigate shadowing effects, roughening of interfaces of the multilayer stack, and excessive smoothing of the triangular groove shape has been performed. The optimal growth regime provided almost perfect replication of the saw-tooth substrate by the multilayer interfaces and allowed absolute diffraction efficiency close to the theoretical one.
This work was supported by the US Department of Energy under contract number DE-AC02-05CH11231.

10386-7, Session 2

Ultra-high-aspect multilayer zone plates for even higher x-ray energies

Markus Osterhoff, Christian Eberl, Jakob Soltau, Hans-Ulrich Krebs, Georg-August-Univ. Göttingen (Germany)

Penetration lengths in the millimetre range make hard x-rays above 60 keV a well-suited tool for non-invasive probing of small specimens buried deep inside their surroundings, and enable studying individual components inside assembled, complex devices (solar cells, batteries etc.). The real-space resolution of typical imaging modalities like fluorescence mapping, scanning SAXS and WAXS depend on the available beam size. Although routine in the 5-25 keV regime [1-4], spot sizes below 50 nm are very challenging at x-ray energies above 50 keV: Compound refractive lenses lack in refractive power, the multilayer thickness of coated mirrors is bounded by interfacial diffusion, and lithographic Fresnel Zone Plates loose their efficiency in the two-digit keV regime.

Multilayer Laue Lenses and Multilayer Zone Plates (MZP) are promising candidates for high-keV focusing to small spot sizes; compared to Fresnel Zone Plates, the aspect ratio comparing outermost layer width (~focal spot size) to optical thickness (efficiency) is virtually unlimited by the fabrication. Using Pulsed Laser Deposition on a rotating wire (several millimetre long), we have fabricated an MZP with 10 nm outermost zone widths and optical thickness of 30 μm (optimum phase shift at 60 keV), yielding an unprecedented ultra-high aspect ratio of 1:3000 (outermost zone width compared to optical thickness).

We present experimental results obtained at ESRF’s high energy beamline ID31, where for the first time scanning experiments with real-space resolutions well below 100 nm, but at x-ray energies of 60 keV and above 100 keV have been achieved.

[1] Kang et al, Applied Physics Letters 92 (2008).

[2] Mimura et al, Nature Physics 6 (2010).

[3] Huang et al, Scientific Reports 3 (2013).

[4] Döring et al, Optics Express 21 (2013).

10386-8, Session 2

Development of EUV focusing system based on ellipsoidal mirror

Hiroto Motoyama, Hidekazu Mimura, The Univ. of Tokyo (Japan)

World’s free-electron laser facilities, FLASH, FERMI, and SACLA, have generated the intense extra ultra violet (EUV) pulses to investigate especially the light-matter interaction. Intense EUV pulses offered possibility to observe the multiple ionization or saturable absorption in short-wavelength region. Accessible peak intensity mainly depends on the pulse energy and size of focus beam. Pulse energy is physically limited by the beamline parameters of facilities. On the other hand, size of focus beam still has a room for improvement. The nonlinear phenomena between further intense EUV pulses and matters will lead to deeper understanding of optics.

Ellipsoidal mirror is one of the most ideal focusing optic for EUV region. It has a high-reflectivity (>70%) and shows extremely low chromatic aberration. In recent years, unique fabrication processes have been developed and applied to fabricate an ellipsoidal mirror. The glass mandrel which has an inversed shape of ellipsoidal mirror is replicated to mirror by

using accurate electro forming process. Using highly accurate glass mandrel, highly precise ellipsoidal mirror with the figure accuracy of more than 100 nm (PV) is possible to fabricate.

To test the focusing performance of the ellipsoidal mirror, we have been developed the focusing system at table-top EUV light source which uses high-order harmonic generation. We succeeded in making a 0.5 um focal spot stably. In addition, we are now planning to focus the EUV pulses at free-electron facility, SACLA. In this presentation, we introduce the current status of the performance of ellipsoidal focusing mirror and focusing system.

10386-9, Session 2

Perfect x-ray focusing via corrective glasses made to measure

Frank Seiboth, Deutsches Elektronen-Synchrotron (Germany) and SLAC National Accelerator Lab. (United States); Andreas Schropp, Maria Scholz, Felix Wittwer, Deutsches Elektronen-Synchrotron (Germany); Christian Rödel, Martin Wünsche, Tobias Ullsperger, Stefan Nolte, Friedrich-Schiller-Univ. Jena (Germany); Jussi Rahomäki, Karolis Parfeniukas, Stylianos Giakoumidis, Ulrich Vogt, KTH Royal Institute of Technology (Sweden); Ulrich H. Wagner, Christoph Rau, Diamond Light Source Ltd. (United Kingdom); Ulrike Boesenberg, Jan Garrevoet, Gerald Falkenberg, Deutsches Elektronen-Synchrotron (Germany); Eric C. Galtier, Hae Ja Lee, Bob Nagler, SLAC National Accelerator Lab. (United States); Christian G. Schroer, Deutsches Elektronen-Synchrotron (Germany)

Modern synchrotron radiation sources and XFELs provide highly-brilliant X-ray beams that allow studying the structure and dynamics of matter from atomic distances and a few femtoseconds to macroscopic dimensions and seconds. To fully exploit the potential of these sources the creation of small and intense X-ray beams is crucial. However, due to the short wavelength of X-rays, the fabrication of X-ray optics is very challenging and requires the most advanced technologies. Consequently, most X-ray optics are limited by fabrication limitations, and trade-offs need to be made in terms of aberration-free performance and highest possible NA. Here, we present a general scheme to assess aberrations of an X-ray optical system under working conditions and correct them by introducing an appropriate X-ray phase plate into the optical path to achieve diffraction-limited focusing. The phase plate operates in transmission and is based on refraction. Hence, it is largely insensitive to small shape and surface inaccuracies of a few micrometers and can correct residual aberrations originating from surface errors of reflective optics, zone deformations in diffractive optics and accumulated surface errors in larger refractive lens stacks. The method can be applied very generally to achieve diffraction-limited focusing, thus solving the X-ray focusing problem at synchrotron radiation sources and XFELs.

10386-10, Session 2

Refractive optics to compensate x-ray mirror shape-errors

Kawal J. S. Sawhney, David Laundy, Diamond Light Source Ltd. (United Kingdom); Vishal Dhamgaye, Raja Ramanna Ctr. for Advanced Technology (India); Ian Pape, Diamond Light Source Ltd. (United Kingdom)

X-ray mirrors are extensively used on X-ray beamlines at all synchrotron facilities. Increasingly, beamline users are demanding variable beam sizes [1] and shapes at the sample position on one hand; and aberration-free optics to achieve diffraction-limited focusing on the other. At Diamond, we are developing custom-designed refractive optical elements that modify the wavefront to either broaden the focus of the X-ray mirror or which corrects the X-ray wavefront in order to cancel out the errors in the focusing optics [2]. The optics uses structures made by micro-fabrication which utilise the weak refraction of X-rays. The structures are fabricated using the LIGA deep X-ray lithography technique [3]. Development involves design with wavefront-propagation simulations, precise nano-metrology, accurate fabrication by LIGA and finally testing on synchrotron beamlines. The concept has been successfully tested by measurements on the Diamond Test beamline B16. Design details of this novel concept and representative examples of their use will be presented.

[1] D. Laundy , K. Sawhney, I. Nistea, S. G. Alcock, I. Pape, J. Sutter, L. Alianelli and G. Evans, “Development of a multi-lane X-ray mirror providing variable beam sizes”, Rev. Sci. Instrum., 87, 051802 (2016)

[2] Kawal Sawhney, David Laundy, Vishal Dhamgaye and Ian Pape, “Compensation of X-ray mirror shape-errors using refractive optics, Applied Physics Letters, 109, 051904 (2016)

[3] V. P. Dhamgaye, G S Lodha, B Gowri Sankar, C Kant, “BL07 Beamline at Indus-2: A Facility for Micro fabrication Research”, Journal of Synchrotron Radiation, 21, 259-263 (2014)

10386-11, Session 3

Development of precision Wolter mirrors for solar x-ray observations

Taro Sakao, Institute of Space and Astronautical Science (Japan) and The Graduate Univ. for Advanced Studies (Japan); Satoshi Matsuyama, Takumi Goto, Jumpei Yamada, Shuhei Yasuda, Kazuto Yamauchi, Osaka Univ. (Japan); Yoshiki Kohmura, RIKEN Harima Branch (Japan); Ayumi Kime, Japan Aerospace Exploration Agency (Japan); Yoshinori Suematsu, Noriyuki Narukage, National Astronomical Observatory of Japan (Japan); Shin-nosuke Ishikawa, Institute of Space and Astronautical Science (Japan)

Fine structures of the hot corona, whose angular scale reaching down to sub-arcseconds, play a crucial role for the dynamics and heating of plasmas there. However, X-ray imagery of the Sun with such resolution has never been conducted due to severe technical difficulty in fabricating precision Wolter mirrors with a wide field of view exceeding several 100”.

For future observations of the solar X-ray corona, we are attempting to realize precision Wolter mirrors with sub-arcsecond resolution by utilizing state-of-the-art surface polish and measurement methods to segmented mirrors which consist of a portion of an entire circle.

X-ray evaluation of an engineering mirror in 2015 with BL29XUL coherent X-ray beam line of SPring-8 synchrotron facility yielded FWHM size of ~0.2” for the PSF core at 8 keV while its HPD (half power diameter) size still remained at ~3” due to a large amount of small-angle scattering right outside the core. Furthermore, large astigmatism was identified for the mirror.

By carefully reviewing these results, improvements in the precision polish, especially in the spatial scale from 0.3 mm to 5 mm, were adopted together with nm-level characterization of the mechanical measurement system for the polish. Preliminary analyes from the subsequent evaluation at SPring-8/ BL29XUL in December 2016 indicate that improved focusing performance of ~0.1” FWHM and ~0.5” HPD has been achieved, without noticeable astigmatism.

Our development activities for precision Wolter mirrors will be reported including at-wavelength evaluation results.

10386-12, Session 3

Development of concave-convex imaging mirror system for a compact and achromatic full-field x-ray microscope

Jumpei Yamada, Satoshi Matsuyama, Shuhei Yasuda, Yasuhisa Sano, Osaka Univ. (Japan); Yoshiki Kohmura, RIKEN Harima Branch (Japan); Makina Yabashi, Tetsuya Ishikawa, SPring-8, RIKEN Harima Branch (Japan); Kazuto Yamauchi, Osaka Univ. (Japan)

A full-field X-ray microscope utilizing an advanced Kirkpatrick-Baez (AKB) optics, which comprises four concave mirrors, provides a high-resolution X-ray image without chromatic aberration. However, it has required long distance, e.g., 10-45 m, between the mirrors and the detector to obtain sufficiently high magnification factor. To overcome the problem, the novel X-ray imaging mirror system consisting of two pairs of concave and convex mirrors was proposed, which enables effective focal length to be short by shifting the principal surface.

We designed a pairs of elliptical concave and hyperbolic convex mirrors, which follow Wolter type III optics, for the demonstration of the imaging system. These mirrors possess numerical aperture of 1.6 x 10^-3 and magnification factor of more than 300 with a total length of ~2m. The mirrors were fabricated with an ion beam figuring system, developed by our group, with an accuracy of ~2 nm peak-to-valley. A one-dimensional demagnification imaging test was performed at SPring-8. The demagnified image of a slit with 10 micron width, which leads to the point spread function of the imaging mirrors, was characterized with the wire scanning method. Consequently, the full width at half maximum value of 42.7 nm was achieved at an X-ray energy of 10 keV, which can never be achieved with the conventional AKB optics because of the limitation of the magnification. We also investigated the wavefront aberration of the reflected X-ray using the single-grating interferometer. Few wavefront aberrations were observed. Additionally, the wavefront aberrations hardly changed when changing the incident angle of the mirror pair. The results indicate that the new imaging system has wide field of view thanks to correction of the coma aberration.

10386-13, Session 3

Advances toward micron resolution optics for x-ray instrumentation and applications

Mark Cordier, Benjamin Stripe, Wenbing Yun, S. H. Lau, Alan Lyon, David Reynolds, Sylvia J. Y. Lewis, Sharon Chen, Vladimir A. Semenov, Richard I. Spink, Sigray, Inc. (United States)

Although the bottleneck of laboratory x-ray source brightness is well-known and discussed, the need for improvements to develop higher efficiency and higher resolution optics is not as often considered. Without optics with excellent FWHM, ultrahigh brightness x-ray sources cannot be utilized efficiently.

We present our novel x-ray mirror lens designs, enabled by high precision and sophisticated manufacturing techniques to enable advanced micronanalytical capabilities for focusing x-rays to microns-scale spot sizes. These axially symmetric x-ray mirror lenses provide advantages over conventional focusing optics such as polycapillary lenses and Fresnel zone plates in key performance attributes such as focusing efficiency, numerical aperture (NA), FWHM of point spread function, working distance, focus chromaticity, energy bandpass, energy transmission, percent of source brightness preservation, and phase space acceptance. The design of these optics allows micron-scale spot sizes even at low x-ray energies, enabling research into low atomic number elements and allows increased sensitivity of grazing incidence measurements and surface analysis.

We will discuss advances made in the fabrication of double parabolic mirror lenses designed for use in laboratory x-ray applications. We will additionally present results from as-built double paraboloids, including surface figure error, slope error and focal spot size achieved to-date.

10386-14, Session 4

Development of x-ray optical components for DLSRs

Makina Yabashi, Inoue Ichiro, Taito Osaka, RIKEN SPring-8 Ctr. (Japan); Hiroshi Yamazaki, Japan Synchrotron Radiation Research Institute (JASRI) (Japan); Kenji Tamasaku, RIKEN SPring-8 Ctr. (Japan); Haruhiko Ohashi, Shunji Goto, Japan Synchrotron Radiation Research Institute (JASRI) (Japan)

We will present our preliminary R&D on x-ray optics and diagnostics for a diffraction-limited storage ring (DLSR). One of the key challenges is to achieve ultimate angular stability in a 10-nrad range for beamline optics including high heatload monochromators. For this purpose, we propose to utilize a double channel-cut crystal monochromator (DCCM), which combines two channel-cut crystals in a (+,-,-,+) configuration. A plasma etching technique (PCVM) is applied to remove lattice strains and to gain smooth surfaces on inner walls of CCs. As another key device, we are developing harmonic separator optics. An important function of this device is to extract a specific harmonic of undulator radiation, enabling utilization of intense pink beam especially in a short wavelength range. Design and evaluation results with coherent x-ray illumination will be reported.

10386-15, Session 4

Current status and future plan of the soft x-ray beamline at SACLA

Shigeki Owada, RIKEN Harima Branch (Japan); Kyo Nakajima, Kensuke Tono, Yasumasa Joti, Tadashi Togashi, Kazuaki Togawa, Japan Synchrotron Radiation Research Institute (JASRI) (Japan); Takahiro Inagaki, RIKEN Harima Branch (Japan); Toru Hara, Japan Synchrotron Radiation Research Institute (JASRI) (Japan); Takashi Tanaka, RIKEN Harima Branch (Japan); Mitsuhiro Yamaga, Yasunori Senba, Hirokatsu Yumoto, Takahisa Koyama, Haruhiko Ohashi, Hitoshi Tanaka, Makina Yabashi, Japan Synchrotron Radiation Research Institute (JASRI) (Japan)

SACLA was inaugurated in March 2012 with two beamlines: BL3 for hard X-ray FEL and BL1 for wide range spontaneous emission. To enhance the research opportunities in soft X-ray region, the SCSS test accelerator, which was a prototype linac of SACLA and decommissioned in 2013, was upgraded, relocated to the SACLA undulator hall, and connected to BL1. The commissioning of this upgraded BL1 had been started from September in 2015, and user operation was started from June 2016. Currently, SASE-FEL pulses in the photon energy range of 20 to 150 eV are available and average pulse energy is about 70 ?J at 100 eV. We are developing beam diagnostic systems such as an arrival timing diagnostics between the SXFEL and the synchronized optical laser. We have further upgrade plans of the accelerator and the beamline. In this presentation, I will report the latest status and future upgrade plans of this beamline.

10386-16, Session 5

REAL cooled mirror for FEL application: FEA modelling and wavefront propagation simulation

Lin Zhang, Corey L. Hardin, Daniele Cocco, SLAC National Accelerator Lab. (United States)

To preserve the full coherence of the FEL, the acceptance of the optics should be at least 2*FWHM of the X-ray beam. The LCLS-II soft X-ray experiments cover a photon energy range from 250 eV to 1300 eV. The

photon beam footprint on the flat and KB mirrors varies from 150 mm to 1000 mm. The length of the mirror is chosen as 1 meter. Resistive Element Adjustable Length (REAL) cooling technique has been proposed to minimize the thermal deformation [1] for LCLS-II mirrors when the power FEL is above 200 W. The water cooling of the mirror is applied on the top-up-side [2]. The additional electric heater is adjustable both in length and power density to cope with the variable X-ray beam footprint length. A R&D project including the prototype of this REAL cooling technique is funded by DoE for FY2017 & FY2018.

In this paper, we will present the modeling results of this REAL cooled prototype mirror. The two parameters of the electric heater (length and power density) are optimized for the thermal deformation minimization of the mirror Finite Element Analysis (FEA) with ANSYS. This optimization of two parameters within ANSYS is not straight forward and necessity large number of FEA calculations. SRW software is used for the wavefront propagation simulation to compare the performance of REAL cooled mirror with other frequently used cooling techniques.

1. Zhang L., Cocco D., Kelez N., Morton D.S., Srinivasan V. and Stefan P.M. - Optimizing X-ray mirror thermal performance using matched profile cooling, J. Synchrotron Rad. (2015). 22,1170–1181, doi: 10.1107/S1600577515013090

2. Zhang L. , Barrett R. , Friedrich K. , Glatzel P. , Mairs T. , Marion P. , Monaco G. , Morawe C. , Weng T. - Thermal distortion minimization by geometry optimization for water-cooled white beam mirror or multilayer optics, Journal of Physics : Conference Series 425, 052029-1-052029-4 (2013)

10386-17, Session 5

Finite element analysis for the Bragg crystal of D-line at SSRF

Zhongmin Xu, Limin Jin, Xiangjun Wei, Yajun Tong, Wei Li, Shanghai Institute of Applied Physics (China)

The Dynamic Beamline (D-line) is a combination of ED-XAS beamline and IR beamline. Among the D-line ED-XAS Branch, a Si (111) crystal with the thickness of 1 millimeter is used in Bragg geometry. The crystal has to be bent with a radius of curvature ranging from 2 to 20 m and receives heat load of 30 watts. To meet the need of dynamical focusing and heat cooling, the crystal is immersed in a water-cooled liquid eutectic In/Ga alloy bath. We perform bending and thermal analyses for the crystal, using Ansys software.

The size of crystal is 300mm*20mm and it is held in the four-point bender system. The footprint on the crystal is 0.46mm*78. To reduce its deformation, an indirect water cooled method is adopted. The water film coefficient is 3000W/mm2C, and the reference temperature is 17 degree Celsius. The thermal conductivity for Si and In/Ga is 149 W/mC and 28 W/mC, respectively. After thermal analysis, the maximum temperature is about 48 degree Celsius. By mean of structural analysis, the deformation and stress distribution of the crystal were calculated as well. The RMS tangential slope error of the centerline on the footprint is 5?rad or so, which can meet the need of beamline.

10386-18, Session 5

Development of hybrid adaptive x-ray focusing system based on piezoelectric bimorph mirror and mirror bender

Takumi Goto, Satoshi Matsuyama, Hiroki Hayashi, Osaka Univ. (Japan); Juniki Sonoyama, Kazuki Akiyama, TOYAMA Co., Ltd. (Japan); Hiroki Nakamori, JTEC Corp. (Japan); Yasuhisa Sano, Kazuto Yamauchi, Osaka Univ. (Japan)

In synchrotron radiation facilities and X-ray free-electron laser facilities, X-ray deformable mirrors have been used for X-ray beam conditioning and focusing. Various types of deformable mirrors based on mirror benders and piezoelectric bimorph mirrors have been reported. However, the existing deformable mirrors are not used widely because the bending systems do not have sufficient deformation accuracy at the high-spatial-frequency range and the piezoelectric bimorph mirrors lack long-term stability of deformation and suffer from the junction effect, i.e., deformation errors introduced by gaps between piezoelectric actuators. To overcome these problems, we proposed a hybrid adaptive focusing system based on a piezoelectric bimorph mirror and a bending system consisting of flexure hinges and a precise actuator. The flexure hinges can provide different bending moments to both ends of the mirror, which results in an approximate elliptical shape. The piezoelectric actuators attached on the mirror substrate correct with extreme precision the remaining deformation errors at the high-spatial-frequency range. We will present a simulation study of the mirror deformation and the performance test of a prototype bending system.

10386-19, Session 5

LCLS-II dynamically bendable and water-cooled KB mirrors

Lin Zhang, Daniel S. Morton, Daniele Cocco, Lance Lee, SLAC National Accelerator Lab. (United States)

The LCLS-II project will provide a 4 GeV superconducting (SC) linear accelerator to deliver high-repetition-rate FEL pulses, up to 1 MHz. The average power of the FEL beam from the SC linac will range from 20 to 200 W, and potentially to 600 W. The FEL beam has ultra-short pulse length (down to a few fs), narrow energy band width (down to less than 10-4, thanks to self-seeding technology), and is fully coherent beam. The preservation of the wavefront is essential to maintain the outstanding FEL beam properties. For the FEL beam focusing, we will use dynamically bendable and water cooled KB mirrors system. It is challenging to reach high performance bending of the mirror by minimizing the mechanical coupling with the water cooling.

In this paper, we will present the technical challenge of the KB design to preserve the FEL beam wave-front. We will discuss the aspects of cooling technology to minimize the thermal deformation, some preliminary test and modeling results in order to minimize the mechanical coupling between the mirror bending and the cooling. Finally, we will report some experiment results on a prototype mirror with bender.

10386-20, Session 6

Development of crystal-based split-and-delay optics with wavefront splitting at SACLA

Takashi Hirano, Osaka Univ. (Japan); Taito Osaka, Osaka Univ. (Japan) and RIKEN SPring-8 Ctr. (Japan); Yasuhisa Sano, Osaka Univ. (Japan); Yuichi Inubushi, Tadashi Togashi, Japan Synchrotron Radiation Research Institute (JASRI) (Japan); Ichiro Inoue, RIKEN SPring-8 Ctr. (Japan); Satoshi Matsuyama, Osaka Univ. (Japan); Kensuke Tono, Japan Synchrotron Radiation Research Institute (JASRI) (Japan); Kazuto Yamauchi, Osaka Univ. (Japan); Makina Yabashi, RIKEN SPring-8 Ctr. (Japan)

Ultra-intense and transversely coherent hard X-ray pulses with femtosecond duration provided from X-ray free-electron laser (XFEL) sources, such as SPring-8 Angstrom Compact free-electron LAser (SACLA) in Japan, are powerful tools to explore ultrafast phenomena at an atomic spatial scale. A split-and-delay optics (SDO), which produces two XFEL pulses with a time separation controlled with sub-femtosecond accuracy, have been developed for observing atomic scale dynamics at the time scale of up to hundreds picoseconds. The SDO is based on perfect diffraction of Si(220) single crystals, which enables the production of such a large time separation in a compact setup. We conducted performance tests of the SDO at SACLA, and investigated the capabilities for manipulating the split XFEL pulses in both space and time. In combination with the focusing mirror system, the two split pulses were successfully focused onto the same position with the focal spot size of 1 um. The almost ideal spot size confirmed that crystal components in the SDO had sufficiently high crystal perfection. Temporal overlapping of the split pulses was also achieved by observing interference fringes formed in a spatially overlapped area of the unfocused beams. It indicated that the time separation can be adjusted with a few femtosecond accuracy over the whole temporal range of the SDO.

10386-21, Session 6

Application of MEMS-based x-ray optics as tuneable nanosecond choppers

Pice Chen, Donald A. Walko, Il Woong Jung, Zhilong Li, Gao Ya, Daniel Lopez, Jin Wang, Argonne National Lab. (United States)

The fastest time-resolved synchrotron x-ray measurements rely on the isolation of a set of x-ray pulses. This functionality is often realized by a mechanical chopper. As an alternate method to manipulate x-ray beams, MEMS-based x-ray optics offer several advantages: they are compact, low-cost, and are adaptive in modulating the temporal, spatial and spectral characteristics of x-ray. In the application of x-ray pulse isolation, we recently achieved a pulse-picking time window of 1 ns, which is three orders of magnitude faster than mechanical choppers. The MEMS device consists of a comb-drive silicon micromirror whose resonance is at 67.88 kHz, a subharmonic of the cycling frequency at the Advanced Photon Source (APS). When operating the silicon micromirror at its 004 Bragg reflection, the brief period when the Bragg condition is met defines the pulse-picking window for incident x-rays. We will discuss the design we used to narrow down the temporal Bragg window to 1 ns. By tuning the driving voltage and thus the oscillation amplitude of the MEMS micromirror, we demonstrate the capability to select a set of several sequential pulses or even a single, isolated x-ray pulse out of a train of pulses with the densest fill pattern of the APS. The nanosecond pulse-picking window is far from the limit of the performance of MEMS optics. With a few technically accessible modifications, we expect to achieve a sub-100 ps window which will be a milestone for enabling slicing 100-ps x-ray pulses in synchrotron facilities.

10386-22, Session 6

The development of crystal fabrication in SSRF

Li Song, Shanghai Institute of Applied Physics (China)

In synchrotron field, single-crystal is key component for diffraction. There are huge demand for crystal in Shanghai Synchrotron Radiation Facility (SSRF) phase II project, ranging from simple rectangular plates to direct water cooling crystals and Bragg-Laue crystal wafers and nested channel-cut crystals. The requirement of crystal orientation accuracy is 1' , crystal surface slope error for crystal 2?rad and roughness 1nm(rms) . In order to meet the requirement of beamlines, SSRF will built a crystal fabrication lab, which can provide support, research and development in the field of crystal X-ray optics. The crystal fabrication lab will include crystal orientation, crystal surface grinding and polishing and chemical etching to remove the surface damage. Detailed crystal needs for SSRF Phase II, and the plan for the crystal lab are presented in this paper, some crystal we fabricated are also described.

10386-23, Session 7

Single-order diffraction grating for soft x-ray: state of the art and perspective

Leifeng Cao, China Academy of Engineering Physics (China)

All conventional x-ray dispersive elements including multilayers, crystals and diffraction gratings provide multi-order diffraction spectra, which bring problems in spectroscopy application especially in the region of from VUV to soft x-ray region. The emergence of the so-called soft x-ray single-order diffraction grating (SXSDG) changed such a situation and may bring promised big benefits in lots of fields such as laser plasma diagnostics, x-ray astronomy, synchrotron radiation beam monochromatic; laser generated high harmonics and etc.

In this presentation, the authors provid that the introduction of the concept of the so-called soft x-ray single-order diffraction grating, the evolution and development of such a new emergened dispersive elements, the state of the art and its application, the perspect and ets. A possible worldwide collaboration in future is also suggested.

10386-24, Session 7

Fabrication and test of quasiperiodic x-ray reflection gratings for high-order diffraction suppression

Yilei Hua, Lina Shi, Hailiang Li, Changqing Xie, Institute of Microelectronics (China)

X-ray diffraction gratings with periodic structures have been widely used in various x-ray instruments and systems, such as synchrotron radiation, x-ray interferometer, x-ray astronomy and plasma diagnostics in the field of laser fusion. However, conventional diffraction gratings suffer from so-called high order diffraction contamination. Here we present a large-area quasiperiodic x-ray reflection grating fabricated by high-speed electron beam direct writing technique. The grating consists of a large number of circular holes for the high order diffraction suppression. The 3rd and even order diffractions can be completely eliminated, and the 5th order diffraction is as low as 0.02% of the 1st order diffraction. Shipley SAL-601 with high-resolution, high sensitivity and good resistance is used for electron beam lithography, followed by dry silicon etching and Au thin film deposition using magnetron sputtering. Since the surface roughness and flatness of the x-ray reflection gratings have a great impact on the dispersion performance, we optimized the fabrication the inductively coupled plasma (ICP) silicon etching process, and tested the surface roughness and flatness of the x-ray reflection gratings by an atomic force microscope and a Zygo interferometer, respectively. The optical characterization of the fabricated quasiperiodic x-ray reflection gratings was performed at the spectral radiation standard and metrology beamline BL08B, national synchrotron radiation laboratory of China. The test results demonstrated the effectiveness of high order diffraction suppression. The capability of high order diffraction suppression and fabrication constraints and the limitation of the diffraction efficiency of the quasiperiodic x-ray reflection gratings are also discussed. The unique high order diffraction suppression properties of the quasiperiodic x-ray reflection gratings may provide a platform for x-ray spectroscopic instruments in laboratory sciences and synchrotron light sources.

10386-25, Session 7

Nanofabrication of free-standing spectroscopic photon sieves operating in soft-x ray region

Xiaoli Zhu, Institute of Microelectronics (China); Lai Wei, China Academy of Engineering Physics (China); Hailiang Li, Institute of Microelectronics (China); Leifeng Cao, China Academy of Engineering Physics (China); Changqing Xie, Institute of Microelectronics (China)

A hybrid lithographic method combining electron beam lithography (EBL), x-ray lithography (XRL) and ultra violet lithography (UVL) were adopted to realize a novel design of 1000 lines/mm x-ray spectroscopic photon sieves (SPS) which is able to eliminate the higher diffraction orders. SPS gratings consist of randomly distributed circular holes which form an approximately sinusoidal transmission function. The circularity of circular holes has effect on the far field diffraction pattern. Moreover, these gold holes must be free-standing without supporting membrane due to soft-x A hybrid lithographic method combining electron beam lithography (EBL), x-ray lithography (XRL) and ultra violet lithography (UVL) were adopted to realize a novel design of 1000 lines/mm x-ray spectroscopic photon sieves (SPS) which is able to eliminate the higher diffraction orders. SPS gratings consist of randomly distributed circular holes which form an approximately sinusoidal transmission function. The circularity of circular holes has effect on the far field diffraction pattern. Moreover, these gold holes must be free-standing without supporting membrane due to soft-x ray intensive absorption in any known material. In the process flow, an electron beam was focused to write patterns on membrane substrate to achieve a master mask. Using this mask XRL was performed to efficiently replicate SPS structures and followed by gold electroplating. After that, UVL was applied to define the supporting coarse mesh. In the replication process of XRL, the deviation of circle patterns caused by overheating problem in exposure has been resolved by inserting appropriate filter in x-ray beam path. The spectrum of x-ray source for exposure can be shifted to be higher, and in consequence less heat are produced in exposure due to less absorption of higher energy x-rays in resist. After the fabrication of SPS has been finished, the diffraction pattern was characterized using a soft x-ray beam line. The calibration results show that higher-order diffraction orders can be efficiently suppressed along the axis of symmetry. Our work has given the opportunity of SPS to replace the conventional transmission gratings in potential applications.

10386-26, Session 7

Soft x-ray grating compressors for free-electron-laser pulses

Paolo Miotti, Nicola Fabris, CNR-IFN Padova (Italy) and Univ. degli Studi di Padova (Italy); Fabio Frassetto, CNR-IFN Padova (Italy); Ennio Giovine, CNR-Istituto di Fotonica e Nanotecnologie (Italy); Luca Poletto, CNR-IFN Padova (Italy)

We discuss the design of grating compressors to be used for chirped pulse amplification on free-electron-laser (FEL) ultrashort pulses at energies higher than 100 eV. The compressor adopts gratings to introduce either positive or negative group-delay dispersion (GDD). The optical design originates from a compressor with plane gratings already tested at the FERMI FEL, that has been demonstrated capable to introduce tunable negative GDD to compress chirped FEL pulses in the extreme ultraviolet. Here, we compare two designs to be used in the 100-500 eV region : 1) the configuration with two plane gratings operated in an almost collimated beam, that gives only negative GDD, with an extended design able to operate at energies as high as 500 eV; 2) the configuration with two concave gratings and an intermediate focus between the twos, that is demonstrated capable to introduce positive GDD. Both the configurations are tunable in wavelength and GDD, by rotating and translating the two gratings. These instruments are designed for maximum throughput, since they have the minimum number of optical elements. The compressor efficiency is furthermore discussed, since it is one of the main parameters that is needed to calculate the final peak intensity at the output of the compressor. The transmission of the different configurations is calculated from measurements of grating efficiency done with synchrotron radiation in the 100-500 eV region. Laminar and blazed groove profiles have been measured to compare different gratings. The experimental results will be discussed.

10386-27, Session PWed

High-aspect ratio zone plate fabrication for hard x-ray nanoimaging

Karolis Parfeniukas, Stylianos Giakoumidis, Rabia Akan, Ulrich Vogt, KTH Royal Institute of Technology (Sweden)

High-resolution x-ray optics are of utmost importance for modern x-ray nanoimaging. High efficiency is also desirable to fully utilize the advantage of increased coherence on the optics at fourth generation synchrotron radiation facilities such as MAX IV. We will present our results in fabricating Fresnel zone plate optics for the NanoMAX beamline at MAX IV, to be used in the energy range of 6 – 10 keV.

We managed to manufacture diffraction-limited zone plates in tungsten with 30 nm outermost zone width and an aspect ratio of 21:1. These optics were successfully used for nanoimaging experiments at NanoMAX. However, we found it challenging to further improve resolution and diffraction efficiency for the tungsten process. Therefore, we started to investigate metal-assisted chemical etching (MACE) of silicon for nanofabrication of high-resolution and high-efficiency zone plates.

The first type of structures we manufactured use the silicon directly as the phase-shifting material. We could achieve etching of 5 um deep dense vertical structures 100 nm linewidth. The second type of optics use a heavy metal such as iridium as the phase material. The structures in the silicon substrate act as a mold for heavy metal coating via atomic layer deposition (ALD). A semi-dense pattern is used with line to space ratio of 3:1 for a so-called frequency-doubled zone plate. This way, it is possible to produce smaller structures with the tradeoff of the additional ALD step. We achieved 45 nm-wide and 3.6 um-thick silicon/iridium structures.

10386-28, Session PWed

Design and first commissioning results of the EMIL beamlines at BESSY-II

Stefan Hendel, Franz Schäfers, Helmholtz-Zentrum Berlin für Materialien und Energie GmbH (Germany); Michael Hävecker, Fritz-Haber-Institut der Max-Planck-Gesellschaft (Germany); Gerd Reichardt, Klaus Lips, Mihaela Gorgoi, Helmholtz-Zentrum Berlin für Materialien und Energie GmbH (Germany)

The beamlines for the Energy Materials In-Situ Laboratory Berlin (EMIL) at BESSY-II are currently under commissioning. They consist of two canted undulators, providing a wide energy spectrum of 70 – 10.000 eV, three monochromators (two plane grating monochromators and one LN2-cooled double crystal monochromator) and ten mirror chambers for radiation dispersion and focusing into two separate pathways of 65 m length. Split-mirror chambers distribute the desired photon energy to one (or simultaneously to two) of five experimental endstations. The maximum lateral distance between all beamline elements is less than one meter. This narrow design, selectable monochromators and several beam crossings require advanced modification of all vacuum chambers to enable variable beam routes. Long pathways demand a very high mechanical and thermal stability as well as a reproducible motion of all optical elements. The chosen constant strut-length hexapod design for the mirror chambers provides a wide range of movement in six degrees of freedom. We report on the optical and mechanical beamline design and present commissioning results.

10386-29, Session PWed

Design of the test beamline at SSRF

Zhongliang Li, Lian Xue, Zengyan Zhang, Hongxin Luo, Jie Wang, Shanghai Synchrotron Radiation Facility (China)

In order to ensure high performance beamline instruments & optics rapid successful operated, online measurement system, test beamline (09B) were designed. The beamline covers photon energy range from 4 to 30keV at a bending magnet, and it is highly flexible and versatile in terms of the available beam size and the range of energy resolution and photon flux. Four group 1D Compound refractive lens (CRL) were used for collimate 8, 12, 16 &20keV at a beamline aperture of 0.15?0.12 mrad2. A water cooling double crystal monochromator(DCM) were used Si(111) and Si(311), which could switched in vacuum chamber operates in a dynamic range of 4-20keV and 20-30keV, to produce monochromatic light. A cylindrical mirror with Rh film was bent to toroidal shape to focusing the monochromatic or white beam. The CRL, DCM & Toroidal mirror could combined to produce a white, monochromatic with and without focusing and collimation beam.

The focused light spot size at sample is 173?226?m2 with an acceptance divergence of 1.5?0.1mrad2 (H?V). The photon flux and resolution of the monochromatic light were 3?1011phs/s and 5?10-4 at 10keV. The white beam peak power density is 0.3W/mm2, that could positive incidence on optical components to study the deformation with high heat load. The test beamline could provide several operational modes, detectors and experimental techniques for the instruments and optics measurement. Details of the beamline optical design and its measured performance are presented in this paper.

10386-30, Session PWed

Thickness uniformity study on the ESRF multilayer deposition system

Damien Carau, Jean-Christophe Peffen, Christian Morawe, ESRF - The European Synchrotron (France)

The ESRF Multilayer Laboratory provides reflective X-ray optics using a deposition system where substrates are coated with well-defined multilayer stacks over a total length of up to 1 m. Such long coatings are obtained by moving the substrate in front of the sputter cathodes. The multilayer period is used to tune the photon energy of the reflected X-ray beam. In some applications, when high spectral resolution is required, the variation of the thickness profiles of the deposited materials must not exceed 0.1%. The aim of the study is to quantify the thickness uniformity of 1.2 m long single layer coatings with a spatial resolution of 10 mm or better.

Reflectivity spectra have been acquired with an X-ray reflectometer operating at 8048 eV and fitted using optical models. Genetic optimization algorithms have been employed to avoid converging to local minima.

The first coating under study consisted of a W single film. However, surface oxidation evolving with time had a considerable impact on the thickness measurements and limited their interpretation. To avoid surface oxidation effects, a similar Pt single layer coating was deposited. The measured thickness uniformity contained a relative standard deviation below 0.2% over the full length of 1.2 m. This value is probably overestimated, as it includes measurement uncertainty due to acquisition and modeling. Indeed, an investigation of a multilayer sample showing a d-spacing variation of about 0.05% over a length of 280 mm, has demonstrated the capability of the deposition system to respond to the present requirements.

10386-31, Session PWed

Development of multilayer-based reflection and diffraction optics for the XUV applications

Zhanshan Wang, Qiushi Huang, Zhong Zhang, Wenbin Li, Shengzhen Yi, Tongji Univ. (China); Igor V. Kozhevnikov, A.V. Shubnikov Institute of Crystallography (Russian Federation); Friedmar Senf, Alexei Erko, Helmholtz-Zentrum Berlin für Materialien und Energie GmbH (Germany); Hongchang Wang, Kawal J. S. Sawhney, Diamond Light Source Ltd. (United Kingdom); Eric Louis, Fred Bijkerk, Univ. Twente (Netherlands)

Multilayer-based optics are vital optical components in the extreme ultraviolet (EUV) and X-ray wavelength range which enable the reflection beyond the total reflection region. With the advancement of synchrotron radiation facility, space observation, dense plasma diagnostics, and EUV photolithography, new multilayer optics with higher performance are demanded. Here, some recent development of the multilayer optics and related system in the Institute of Precision Optical Engineering (IPOE) in Tongji University, China, will be presented.

High reflectance EUV mirrors are required below the Si-L edge (?=12.4nm) e.g. for EUV telescope and water window microscope. Pd/Y and Pd/B4C multilayers are promising candidates for the waveband of 8-12 nm. To improve the interface structure, interface engineering methods like reactive sputtering with nitrogen and B4C barrier layers are used and a high reflectance of 45% was measured at?=9.1nm. For the water window region, a new material combination of V/Sc is demonstrated working primarily at the Sc-L edge (?=3.11nm). The V/Sc multilayer with 1.59 nm d-spacing exhibits a reflectance of 18.4% at?=3.129 nm under near normal incidence of 9°. Besides the planar multilayer optics, three dimensional multilayer optics is explored. One notable example is the multilayer coated blazed grating for high efficiency soft X-ray monochromator. A 2000 line/mm blazed grating was coated with Cr/C multilayer which demonstrated a maximum efficiency of 35%-55% at 2-4 keV. Based on the good experimental results, a multilayer grating monochromator is designed for the soft X-ray imaging beamline. Multilayer based imaging system has also been developed for the diagnostics of high power laser produced plasma. Recently, an eight-channel KB microscope using multilayer mirrors was assembled and applied at the high power laser facility for real time X-ray imaging experiments.

10386-32, Session PWed

Spatial coherence measurement of hard synchrotron radiation using a combined pinhole and grating

Wenqiang Hua, Yuzhu Wang, Chunxia Hong, Fenggang Bian, Xiuhong Hong, Jie Wang, Shanghai Institute of Applied Physics (China)

A simple method to measure the spatial coherence of hard X-rays was developed. This method depends on the far-field Fraunhofer diffraction of a grating and the expansion ratio of diffraction peaks instead of the near-field diffraction of grating diffraction used in other available coherence measurements. According to optics, Fraunhofer fringes may be realized by confining an incident beam or observing at far enough location. The expansion effect of Fraunhofer fringes is a function of partial coherence, which in the case of synchrotron radiation can be simply described using a form of the Pythagorean theorem. As a result, transverse coherence can be obtained from the widths of the measured diffraction peaks of a grating with high accuracy and reliability. Good agreement between measurements and calculations based on the GSM in the horizontal direction verified the accuracy and reliability of this method, although there was some discrepancy between experimental and simulated results in the vertical direction. An advantage of the developed technique is that the influence of imperfections of the instrumentation on measurements is minimized. Furthermore, the theoretical analysis of the expansion effect is also expected to be useful for coherent X-ray experiments and coherence characterization of low-brilliance, high-energy X-ray sources despite their short coherence length and numerous distractions

10386-33, Session PWed

Diffraction effects in diamond x-ray refractive lenses

Maxim Polikarpov, Immanuel Kant Baltic Federal Univ. (Russian Federation); Irina Snigireva, Hermann Emerich, ESRF - The European Synchrotron (France); Nataliya Klimova, Anatoly A. Snigirev, Immanuel Kant Baltic Federal Univ. (Russian Federation)

Laser treatment nicely suits for the fabrication of diamond refractive lenses with large acceptance and high profile quality. Unique optical properties of diamond coupled with its excellent thermal stability allow such lenses to be applied as focusing, imaging and beam-conditioning elements at high-heat flux beams of today and future X-ray sources. However, as lenses are made from single crystal, the Bragg law can be satisfied, depending on crystallographic orientation of the lens substrate or on the photon energy of incident-to-lens X-rays. Due to the Bragg diffraction, transmitted intensity might be dramatically reduced. This problem is well known in X-ray spectroscopy and is called "glitch". In this paper, we demonstrate the existence of the diffraction in the focusing mode of the refractive lens and

measure the magnitude of the effect.

A corresponding experiment was done at the BM31 at the ESRF and we observed presence of X-ray spectral glitches by monitoring an intensity transmitted through the CRL. Predictably, the effect arises at certain energies and affects lens' gain factor while keeping invariable a transmitted wave front. We noticed that contribution of X-ray glitches may be minimized by manufacturing of single lenses from various diamond plates with slightly different crystallographic orientation. In such case, the intensity drops are relatively small and may be comparable to X-ray glitches from monochromators, which have the drop value of 2-3%. To summarize, one can say that X-ray glitches from single-crystalline X-ray lenses may only impact spectroscopy or like experiments while the main part of the experiments with refractive optics (focusing, imaging, microscopy and diffraction) should ignore this effect.

10386-34, Session PWed

Micromirror-based manipulation of synchrotron x-ray beams

Donald A. Walko, Pice Chen, Il Woong Jung, Daniel Lopez, Craig P. Schwartz, Gopal K. Shenoy, Jin Wang, Argonne National Lab. (United States)

Synchrotron beamlines typically use macroscopic, quasi-static optics to manipulate x ray beams. We introduce the use of dynamic microelectromechanical systems-based optics (MEMS) to temporally modulate synchrotron x-ray beams. We demonstrate this concept using single-crystal torsional MEMS micromirrors oscillating at frequencies of kHz and above. Such a MEMS micromirror, with lateral dimensions of a few hundred micrometers, can interact with x rays by operating in either grazing-incidence reflection geometry or high-angle diffraction geometry. X rays are deflected only when an x-ray pulse is incident on the rotating micromirror under appropriate conditions, i.e., at an angle less than the critical angle for reflectivity or at the Bragg condition for diffraction. The time window for such deflections depends on the frequency and amplitude of the MEMS rotation. We demonstrate that reflection geometry can produce a time window on the order of a microsecond, while the time window of diffraction geometry can be much shorter, even on the nanosecond scale. We compare the efficiency and the overall flexibility of the two geometries. We further demonstrate that these MEMS optics can be synchronized to the frequency of the Advanced Photon Source to reproducibly select x rays from a selected bunch or group of bunches. We discuss how such optics bring unprecedented design flexibility for future dynamic and miniature x-ray optics for focusing, wave-front manipulation, multicolor dispersion, and pulse slicing.

10386-35, Session PWed

A tool of X-LAB v1.5 for optical design and its application

Zuhua Yang, China Academy of Engineering Physics (China)

To design the monochorator beamlines of synchrotron radiation, XFEL and the X-ray diagnoses of inertia fusion, dynamic process in extreme physical conditions, we developed a useful tool and a platform for optical design, optimization and simulation, X-LAB v1.5 with the independent intellectual property rights. The present version, X-LAB v1.5 has more functions for only one optical element or optical system design and simulation than the old version. X-LAB v1.5 is a useful and friendly tool that comprises sequence ray-tracing, vector diffraction simulation and layout drawing of complex micro-structure optical element. Also, this tool is easy to operate and can provide accustomed service, characteristic functions for users to freely design, optimize an optical system. Currently, X-LAB v1.5 has been applied in designing and simulating of the 3B1 monochromatic beamline in Beijing synchrotron radiation facility with spectral resolution 1000, and spectral range 10eV~100eV, the X-ray diagnosis optical systems of inertia fusion and dynamic process in extreme physical conditions, the KB microscope with spatial resolution up to 6?m, and studying the single order diffraction property of grating photon sieves.

10386-36, Session PWed

Initial growth characteristics for Cr layer and Cr-based multilayers

Hui Jiang, Shanghai Synchrotron Radiation Facility (China)

Multilayers with short (several nm) or ultra-short (less than 2.5 nm) periods have particular applications from soft X-ray to X-ray regimes. Cr-based multilayers are one of most attractive material pairs for short periods to satisfying different energy ranges. In hard X-ray regime, Cr is the best material for energy lower than Cr K absorption edge (~6 keV) and important material for the energy higher than 20 keV. In water window regime, Cr has suitable optical constant as scattering layer and stable interface to combine with C, Sc, Ti and V to obtain high and uniform reflectivity. In this study, a series of Cr layers and Cr/C multilayers were deposited by magnetron sputtering and characterized by GIXR, AFM, XPS, XRF and XANES synthetically. The results reveal the evolution of Cr layer growth and interdiffusion in Cr-based multilayers.

10386-37, Session PWed

APS modular deposition system

Raymond P. Conley Jr., Argonne National Lab. (United States)

The APS Modular Deposition System has recently been commissioned. The equipment consists of a 4.7 meter long linear substrate translator which is housed inside a vacuum chamber. This substrate translator uses a state of the art direct-drive in-vacuum servo system with velocity stability better than 99.9975%. An absolute optical encoder provides 5nm resolution over the entire length of travel. The design revolves around modularity and adaptability; where sources, metrology, or other instrumentation are easily changed or upgraded to adapt to future needs. The goals for the machine are not only to produce a wide variety of multilayer and other thin-film based x-ray optics, but also to allow the APS to initiate an ion-beam figuring (IBF) based mirror surface correction capability. Off-line surface metrology can be utilized for iterative feedback into the fabrication process. However, the prospect of obtaining surface figure information without the need to extract the substrate from the vacuum chamber provides a number of performance advantages. Such in-situ measurement capability would not only increase throughput for standard ion-beam figuring, but would also allow quasi-real time deposition feedback and more frequent monitoring of the IBF process to study its variability. Additionally, removing the requirement of venting the process chamber; thereby exposing the sample to atmosphere, would allow the flexibility to work with reactive materials. By utilizing an on-axis interferometer in place of a more conventional off-axis Fizeau phase-shifting interferometer, the interferometry transmission flat can be remotely located within the UHV system. This configuration reduces certain measurement errors induced by environmental factors such as air turbulence and humidity. Provisions for a dynamically-actuated aperture will be used to explore methods for 3-D multilayer deposition intended to enable the use of new optical geometries and allow for higher efficiency and mirror figure correction. Machine capabilities will come online in phases. Multilayer deposition will be the first priority for the machine, while the other features related to metrology, figuring, and the dynamic aperture will be brought online later as they are developed.

Conference 10387: Advances in Laboratory-based X-Ray Sources, Optics, and Applications VI

Monday 7 –7 August 2017

Part of Proceedings of SPIE Vol. 10387 Advances in Laboratory-based X-Ray Sources, Optics, and Applications VI

10387-1, Session 1

The Lyncean Compact Light Source: x-ray synchrotron radiation for analytical and imaging applications

Michael Feser, Lyncean Technologies, Inc. (United States)

The Lyncean Compact Light Source (CLS) is a true miniature synchrotron x-ray source with undulator output x-ray characteristics (inherently monochromatic, tunable, high flux). The compact size (8m x 4m) is accomplished by employing a low energy (45 MeV) electron beam storage ring combined with a sub-micrometer period "laser undulator" replacing the permanent magnets of traditional undulators. The output beam of the Lyncean CLS is axially symmetric with 4 mrad beam divergence, a 4% bandwidth and tunable from 8 to 35 keV by changing the energy of the stored electron beam. It delivers 1010 photons per second to experimental end stations located outside of the CLS shielded enclosure.

The first commercial installation of a Lyncean CLS is at the Technical University Munich (TUM) in Germany. Applications pursued there are primarily Talbot grating based multi-modal imaging and tomography (quantitative absorption/phase contrast, dark field) and high-resolution x-ray tomography. The Lyncean CLS is very well matched to these measurements due to the inherent coherence property, Monochromaticity (no beam hardening + quantitation) and the high flux. Analytical applications using specifically developed multilayer focusing optics have been demonstrated at the Lyncean factory in the USA. Protein crystallography with freely selectable x-ray energy to enable advanced phasing techniques such as single wavelength anomalous dispersion (SAD) are possible. Other examples include powder diffraction and small angle scattering to name a few.

Operating the Lyncean CLS has been made extremely simple for users. The complexity of the system is packaged into easy to use interfaces enabling non-experts to run the machine after one week of training. The special characteristic of the Lyncean CLS of producing a truly symmetric and monochromatic beam without contamination by higher x-ray energies (compared to traditional synchrotrons) allows very simple beam transport systems and experimental stations with relaxed shielding requirements to be utilized.

10387-2, Session 1

Compact Linac-driven light sources utilizing mm-period RF undulators

Filippos Toufexis, Valery A Dolgashev, Cecile Limborg-Deprey, Sami G. Tantawi, SLAC National Accelerator Lab. (United States)

Conventional synchrotron light sources and Free-Electron Lasers (FELs) utilize permanent magnet undulators with periods on the order of a few centimeters, and therefore need GeV scale electron beam energies to operate. Such facilities are very large and expensive. Inverse Compton scattering sources use a laser beam as an undulator with micrometer periods and produce X-ray energies on the order of tens of keV. These sources operate with MeV scale beam energies, and therefore they could fit in a lab. However, their average photon flux is typically small, especially in the EUV and soft X-ray regime.

We present a novel compact linac-driven light source, which could produce both incoherent and FEL radiation depending on its configuration. This source is based on a mm-period RF undulator. The RF undulator is a mm-wave cavity resonating at a deflecting mode. The source operates as follows: a train of electron bunches is generated in a thermionic X-band RF injector. These bunches are accelerated in an X-band linac and then interact with the RF undulator. The RF power that feeds the undulator is extracted from the electron beam in a decelerating RF structure, located downstream of the undulator. As an example, a light source with a 91.392 GHz RF undulator and a 124 MeV electron beam can generate incoherent EUV radiation at 13.5 nm. Such a light source could be less than 6 m long, and be used for EUV mask metrology. Similar approach will enable soft X-Ray imaging.

10387-3, Session 1

Developments in compact sources of synchrotron radiation

Timur Shaftan, Brookhaven National Lab. (United States)

Modern synchrotron light sources deliver intense flux of X-rays to many tens of beam lines with reliability above 95%. While the light source is capable of serving photons to many user experiments at once they require large construction and operating budgets, facilities on the scale of a stadium and expert engineering team dedicated to their support.

Since decades ago compact versions of synchrotron light source, perhaps less bright but delivering the same photon spectrum with similar reliability, was in focus of research of several scientific and industrial groups worldwide. Footprint of an electron machine fitting into a large university room with low power consumption and only few experts of the support staff were the quality of merits of the research and development programs.

In this presentation I will go over several types of compact light sources developed and operating in comparison with their large sister facilities. A summary of the user programs for compact light sources will be discussed.

10387-15, Session 1

5th-generation light source development based on inverse Compton scattering

James B. Rosenzweig, Univ. of California, Los Angeles (United States)

We describe recent advances in the experimental development of a high average flux inverse Compton scattering (ICS) source. There are three novel aspects of this research: use of an inverse free-electron laser (IFEL) accelerator; use of laser intensities that yield non-negligible nonlinear electrodynamic effects; and development of recirculation systems for re-use of the laser. In this presentation we concentrate first on the progress made in single-shot measurements of nonlinear effects, and the implications of the methods used for spectral tailoring of ICS. We then describe the achievement of ICS produced from an IFEL-accelerated electron beam, where the IFEL and ICS systems are enabled by a single laser source. We discuss the implications of application of the high flux ICS source in national security and medicine.

10387-4, Session 2

New developments in ultra-high brightness microstructured x-ray sources for applications in Talbot-Lau imaging and dual-energy microanalytical/microXRF

Wenbing Yun, David Reynolds, Vladimir A. Semenov, Janos Kirz, Alan Lyon, Sharon Chen, Benjamin Stripe, Richard I. Spink, Sigray, Inc. (United States)

The limitations to achievable x-ray brightness within the laboratory1 for x-ray spectra is a well-known problem for improving the throughput, sensitivity, and resolution of a wide variety of x-ray techniques. Specific examples of such challenges include: throughput in Talbot-Lau interferometry for medical applications, limits to sensitivity in micro x-ray fluorescence (microXRF), and resolution in x-ray microscopy.

We will present our patented x-ray source technology and recent developments. The major innovations in our x-ray source are the x-ray anodes, which are comprised of arrays of microstructured metal x-ray emitters embedded within a diamond substrate. The diamond substrate enables highly localized large thermal gradients that passively and rapidly cool the metal microstructures as heat is generated under the bombardment of electrons. Electron power densities, 4X higher than conventional solid metal targets can be achieved on the target even greater for metals of lower thermal conductivity. The thermal advantages of the anode design enables the use of many elements that were previously unsuitable as x-ray source materials, and will enable access to new x-ray characteristic lines to optimize performance in monochromatic x-ray analysis.

In addition, we will review practical benefits of our patented FAASTTM (fine array anode source technology) x-ray source over both conventional x-ray sources and newer schemes such as liquid metal anodes2. Advantages include the ability to produce a patterned microbeam optimized for Talbot-Lau interferometry (phase contrast imaging) and the ability to produce various characteristic lines through the incorporation of novel materials (e.g. Au, Pt, Cr) for dual energy capabilities.

10387-6, Session 2

120-kV and 5-watt compact x-ray source

Eric Miller, Sterling W. Cornaby, G. Smith, R. Steck, B. Harris, Kris Kozaczek, Sanjay Kamtekar, MOXTEK, Inc. (United States)

Moxtek has developed a 1kg monoblock 120 kV tube with high voltage power supply which is meant for use in portable devices. This small device with photon energies ranging from 70keV to 120keV expands the accessibility of miniature x-ray sources available for XRF, NDT, and imaging applications. The radiation self-shielding and battery powered design make it ideal for portable handheld devices. The bi-polar transmission window eliminates the heal-effect and the associated detriments in some imaging applications that are typical of reflection stationary anodes. This also enables the output angles easily configured to either cone or fan beam while maintaining the brightness output.

10387-7, Session 2

1D heat transfer problems for a CNT as an electron emitter

Yozo Mikata, Bechtel (United States); Scott Price, GE Global Research (US) (United States)

This paper will discuss three 1D heat transfer problems associated with both conduction and radiation, which are mathematical models for a CNT used as a field electron emitter. CNT has attracted an increasing attention as a potentially excellent material for an electron emitter since around mid-90's. Predicting the current density and the temperature profile of CNT caused by the Joule heating associated with the current density is the key to understanding the physics of CNT as a field electron emitter. This is the focus of this paper.

10387-17, Session 2

The compact x-ray source ThomX

Pierre Favier, Lab. de l'Accelerateur Lineaire, Ctr. Scientifique d'Orsay (France)

Inverse Compton Scattering provides a unique way to produce quasi-monochromatic X-rays via the interaction of relativistic electrons with a laser pulse. This process has the advantage of producing very high fluxes of X-rays with energies above a few tens of keV. In addition the output beam divergence is much larger than in classical synchrotron light sources and the X- ray beam is thus easier to manipulate. We present an X-ray source under construction at Paris- Sud University, ThomX. This source uses a 50 MeV electron beam that collides at 16.7 MHz with a few picoseconds pulsed laser beam whose power is enhanced at the state of the art 600 kW average power to produce X-rays between 30 and 50 keV with a flux of 1013 ph/s. This energy range as well as the energy-angular dependence coming from the physical process are suitable for societal applications like radiotherapy or art history.

We use a prototype Fabry-Perot cavity to perform R&D for the ThomX source. Various diagnostics like real time finesse measurements or passive coupling enhancement are under study on this test cavity to increase the achievable stored power. We will present the ongoing developments along with the results we obtained. A very high finesse optical cavity (F > 28 000) is used, which is one of the highest finesse cavities in pulsed regime. The numerous challenges and solutions to mitigate the related issues will be presented.

10387-8, Session 3

X-ray metrology in the semiconductor industry *(Invited Paper)*

R. Joseph Kline, Daniel F. Sunday, National Institute of Standards and Technology (United States)

The semiconductor industry has advanced technology through the continual shrinking of feature sizes in their integrated circuits. The industry is currently manufacturing the 14 nm node and will soon transition to the 10 nm node. The exact size, shape, and chemical placement in 3D nanodevices determine the performance of the transistors. Each microprocessor can contain billions of these transistors and all of them have to operate similarly for proper operation. Detailed metrology is critical to both the development of new process technologies and in process control during the product manufacturing. We will discuss how high brightness compact X-ray sources can provide critical metrology solutions to the semiconductor industry. We will cover the source requirements for a variety of X-ray measurements and will focus on one particular X-ray measurement for dimensional metrology, critical dimension small angle X-ray scattering (CDSAXS). CDSAXS has been demonstrated at the synchrotron to provide sub-nm resolution in average feature size and errors in the lithography. Commercially available lab-based sources have insufficient flux to satisfy the high throughput and small target requirements of an in-line process control measurement. CDSAXS is particularly demanding because it requires both collimation and a small spot size.

10387-9, Session 3

New developments in laboratory-based x-ray sources and optics

Bernd Hasse, Jenss N. Schmidt-May, Frank Hertlein, Carsten Michaelsen, Incoatec GmbH (Germany)

Many applications in the field of X-ray analytics require an X-ray beam with a high flux density at the sample position. Examples are single crystal diffraction or microdiffraction. An X-ray system comprising of an X-ray source with a small spot size of the electron beam combined with a 2-dimensional multilayer mirror is the ideal source for these applications. In this presentation we will show new developments of X-ray tubes and multilayer optics to achieve higher flux densities at the sample. We will further show applications of X-ray diffractometry and SAXS to show the power of new X-ray sources.

10387-10, Session 3

High-energy radiography of dense material with high flux Inverse-Compton x-ray source

Shouyuan Chen, Ping Zhang, Grigory Golovin, Baozhen Zhao, Colton Fruhling, Daniel Haden, Wenchao Yan, Cheng Liu, Sudeep Banerjee, Univ. of Nebraska-Lincoln (United States); Cameron Miller, Shaun Clarke, Sara A. Pozzi, Univ. of Michigan (United States); Donald P. Umstadter, Univ. of Nebraska-Lincoln (United States)

We report the high energy radiography of dense material using MeV all-optical-driven inverse Compton x-ray source. The properties of the inverse-Compton x-ray source are controlled by means of electron energy, electron charge, scattering beam focal spot size and pulse duration to obtain optimized x-ray energy and high flux for dense material radiography. In this experiment, the x-ray has a photon energy of 8 MeV for maximal steel penetration depth, and a flux of 1011 x-ray photons per shot. With this novel x-ray source, we are able to demonstrate radiography of a 10 cm thick "kite" object through a steel shielding with thickness up to 40 cm in a single exposure. The radiography image of the "kite" object though the 40 cm steel has signal to noise ratio of 2 and image contrast of 0.1, and the "kite" object can be clearly distinguished in the image. Combining its tunability, ultrafast pulse duration and micron meter resolution, the all-optical-driven inverse Compton x-ray source provides unique capacities for flash radiography of dense material, and is of interest for ultrafast nuclear physics study.

10387-16, Session 3

Lobster eye as a collector for water window microscopy

Ladislav Pína, Czech Technical Univ. in Prague (Czech Republic); Veronika Marsikova, Rigaku Innovative Technologies Europe (Czech Republic); Alexandr Jancarek, Radka Havlikova, Czech Technical Univ. in Prague (Czech Republic); Adolf Inneman, Daniela Doubravova, Rigaku Innovative Technologies Europe (Czech Republic); Rene Hudec, Astronomical Institute of the ASCR, v.v.i. (Czech Republic)

Imaging in EUV, SXR and XR spectral bands of radiation is of increasing interest. Material science, biology and hot plasma are examples of relevant fast developing areas. Applications include spectroscopy, astrophysics, Soft X-ray Ray metrology, Water Window microscopy, radiography and tomography. Especially Water Window imaging has still not fully recognized potential in biology and medicine microscopy applications. Theoretical study and design of Lobster Eye (LE) optics as a collector for water window (WW) microscopy and comparison with a similar size ellipsoidal mirror condenser are presented.

10387-5, Session 4

High-energy XRF device for heavy metal identification utilizing the triboelectric effect

T. Lopez, Eli Van Cleve, Matthew Ibbotson, M. Dahl, Carlos G. Camara, Tribogenics, Inc. (United States)

In 2015 Tribogenics introduced a low cost XRF device utilized the triboelectric effect. This revolutionary device is capable of measuring the elemental composition of steel and aluminium alloys. Currently all XRF devices that are used to measure the concentration of heavy elements in materials, such as gold and lead, utilize radioactive decay to generate the x-rays. We have been able to generate x-rays at sufficient energy, above 120 keV, to utilize our current x-ray tube for concentration of gold and lead in materials. We are working to improve our flux output of these devices and by the end of this year we will be introducing this new device into the market. Our device will not only be cheaper than current heavy element XRF devices as well as safer because it does not utilize dangerous radioactive materials. This also reduces the cost and complexity of regulation for the devices.

10387-12, Session 4

Image processing methods for analyzer-based phase-contrast imaging

Oriol Caudevilla Torras, Illinois Institute of Technology (United States)

No Abstract Available

10387-13, Session 4

Strain-free polished channel-cut crystal monochromators: a new approach and results

Elina Kasman, Jonathan Montgomery, Xianrong Huang, Lahsen Assoufid, Argonne National Lab. (United States)

The use of channel-cut crystal monochromators has been traditionally limited to applications that can tolerate the rough surface quality from wet etching without polishing. We have previously presented and discussed the motivation for producing channel cut crystals with strain-free polished surfaces [1]. Afterwards, we have undertaken an effort to design and implement an automated machine for polishing channel-cut crystals. The preliminary effort led to inefficient results. We have since conceptualized, designed, and implemented a new version of the channel-cut polishing machine, the CCPM V2.0. The new machine design no longer utilizes Figure-8 motion that mimicked manual polishing. Instead, the polishing is achieved by a combination of rotary and linear functions of two coordinated motion systems. Here we present the new design of channel-cut polishing machine, its capabilities and features.

Multiple channel-cut crystals polished using the CCPM V2.0 have been deployed into several beamlines at the Advanced Photon Source. We present the measurements of surface finish, flatness, as well as topography results obtained at 1-BM of APS, as compared to results typically achieved when polishing flat-surface monochromator crystals using conventional polishing processes.

Limitations of the current machine design, capabilities and considerations for strain-free polishing of highly complex crystals will be also discussed, together with an outlook for future developments and improvements.

References:

[1] E. Kasman, et. al. "The best of both worlds: automated CMP polishing of channel-cut monochromators", Proc. SPIE 9590, Advances in Laboratory-based X-Ray Sources, Optics, and Applications IV, 95900D (September 3, 2015); doi:10.1117/12.2196034

10387-11, Session PMon

X-ray microscope with refractive x-ray optics and microfocus laboratory source

Dmitry Serebrennikov, Immanuel Kant Baltic Federal Univ. (Russian Federation); Yuriy I. Dudchik, Belarusian State Univ. (Belarus); Aleksandr Barannikov, Anatoly A. Snigirev, Nataliya Klimova, Immanuel Kant Baltic Federal Univ. (Russian Federation)

High penetration depth makes X-ray microscopy very useful research tool and enable to obtain information even inside the sample. The idea of X-ray microscope has already been proposed and even tested at synchrotron radiation sources and laboratory sources. However the majority of works is found Fresnel zone plates to be the best solution for focusing optics. The alternative is Compound Refractive X-ray Lens (CRL), which consists of several elementary biconcave elements. The CRL can be used either as a condenser lens for sample illumination or as an objective lens for imaging. Especial attention attracts two lens systems, which can operate in full-field X-ray microscopy mode or scanning X-ray microscopy mode.

This work demonstrates possibility of X-ray microscopy using CRL based on beryllium and bubble epoxy lens at laboratory microfocus X-ray Metajet source. The main feature of the source is a liquid-metal gallium anode that is able to support high electron-beam power and therefore generates microfocus X-ray source with higher flux than at conventional solid-metal anodes. Single lens and two lens schemes are considered. Images of Cu 2000-grid mesh recorded at different experimental setups are presented.

This work is supported by the Russian-Belarusian Research Grant RFBR (project 16-52-00212, F16R-070).

10387-14, Session PMon

Moxtek's compact x-ray sources

Rick Steck, Sterling W. Cornaby, B. Harris, T. Parker, Kris Kozaczek, C. Smith, Eric Miller, Sanjay Kamtekar, MOXTEK, Inc. (United States)

The XRF and XRD benchtop instrumentation face increasing demand for lowering the detection limits and increasing the accuracy and precision of the measurements. The x-ray tube is a vital component of XRF instruments, which affects the aforementioned characteristics. Moxtek is a leader in developing miniature X-ray sources for portable and handheld XRF instruments. We will present on our current x-ray sources which run from 4 to 70 kV and up to 12 watts. Additionally, we will presenting on prototype x-ray tubes listed below.

1. A compact 75 kV 350 watt x-ray tube, which provides an unprecedented x-ray flux from a compact, air cooled device.

2. A compact 60 kV 30 watt microfocal x-ray tube, with a 50 microns or less focal spot size, for close coupling with the polycapillaries, multilayer mirrors.

3. A portable and compact 120 kV & 5 Watt x-ray tube and high voltage power supply, an air cooled device in a hand size package for backscatter imaging.

In this presentation we will be covering some of the basic functionality of each one of these sources, as well as some of the intended applications.

Conference 10388: Advances in Computational Methods for X-Ray Optics IV

Wednesday - Thursday 9 –10 August 2017

Part of Proceedings of SPIE Vol. 10388 Advances in Computational Methods for X-Ray Optics IV

10388-1, Session 1

Computational methods in development of modern synchrotrons and their applications *(Keynote Presentation)*

Qun Shen, Brookhaven National Lab. (United States)

Advanced analysis and modelling methods has been an essential part of X-ray optics advances and X-ray techniques development at synchrotron light sources. These methods not only help researchers develop designs of X-ray sources and beamlines, diagnose and identify problems and issues in operations, but also enable advanced modelling and simulations of novel X-ray optics and experiments. Recent development rends in diffraction-limited sources and in coherence applications further illustrate the community interests and increased needs in advanced wavefront-based analysis and modelling capabilities. This presentation will provide an overview of this growing area of X-ray optics and techniques and its impact on synchrotron science in general.

10388-2, Session 1

Data handling at SACLA x-ray free electron laser facility and future SPring-8-II synchrotron radiation facility *(Keynote Presentation)*

Tetsuya Ishikawa, RIKEN (Japan)

Only one end-station of X-ray free electron laser or next-generation synchrotron radiation facilities will produce more than 10 TB data in a near future. At SACLA x-ray free electron laser facility, we have installed a acquisition/handling system to cope with the huge amount of data. We have developed a 60 Hz Multi-Port CCD detector for the image sensor of SACLA which is used for most applications. On the other hand, we are developing a new type of pixel detector for the future synchrotron radiation applications. Data handling system, including the dataway to K-computer, has been developed.

10388-4, Session 2

Recent progress of the synchrotron radiation calculation code SPECTRA *(Invited Paper)*

Takashi Tanaka, RIKEN (Japan)

SPECTRA is an application software to compute the optical properties of synchrotron radiation (SR) emitted from bending magnets, wigglers (conventional, elliptical) and undulators (conventional, helical, elliptical, figure-8, etc.). Computations of SR emitted from an arbitrary magnetic field distribution are also available. Parameters and specifications related to the electron beam and light source can be edited completely in fully graphical user interfaces (GUIs) and several methods to visualize the computation results are also implemented.

SPECTRA is written in standard C++ language, with the assistance of the wxWidgets GUI tool kit and OpenGL graphic library for the GUI part. Thanks to portability of these libraries, SPECTRA will run on most available operating systems such as Microsoft Windows, Mac OS X, Linux, and most unix-like operating systems. As of 2017, more than 2,000 users have downloaded SPECTRA.

Since the first official release in 2000, a lot of improvements have been made to the algorithms for faster and reliable computations and a number of new functions have been implemented to meet the increasing demands from the users. In this presentation, we focus on the new functions recently implemented, which we hope help the users to design the components in the SR beamline in the upcoming low-emittance storage rings.

10388-5, Session 2

Main functions, recent updates, and applications of Synchrotron Radiation Workshop code *(Invited Paper)*

Oleg Chubar, Maksim S. Rakitin, Brookhaven National Lab. (United States); Yu-Chen Chen-Wiegart, Brookhaven National Lab. (United States) and Stony Brook Univ. (United States); Yong S. Chu, Andrei Fluerasu, Dean Hidas, Lutz Wiegart, Brookhaven National Lab. (United States)

The presentation will include an overview of main functions of the “Synchrotron Radiation Workshop” (SRW) code, dedicated to calculation of different types of synchrotron radiation, and simulation of propagation of fully-coherent radiation wavefronts, partially-coherent radiation from a finite-emittance electron beam of a storage ring source, and time-/frequency-dependent radiation pulses of a free-electron laser, through X-ray optical elements of a beamline. A special attention will be paid to updates in the library of physical-optics “propagators” for different types of reflective, refractive and diffractive X-ray optics with its typical imperfections, enabling simulation of practically any X-ray beamline in a modern light source facility. High accuracy of calculation methods used in SRW allows for multiple applications of this code, not only in the area of development of instruments and beamlines for new light source facilities, but also in areas such as electron beam diagnostics, commissioning and performance benchmarking of insertion devices and individual X-ray optical elements of beamlines. Applications of SRW in these areas, facilitating development and advanced commissioning of beamlines at the National Synchrotron Light Source II, will be described.

10388-6, Session 2

Recent progress of the XRT: ray tracing and wave propagation toolkit *(Invited Paper)*

Roman Chernikov, Deutsches Elektronen-Synchrotron (Germany); Konstantin Klementiev, Max IV Lab. (Sweden)

Xrt is a python-based software library for beamline simulation and analysis in x-ray regime. We provide classes for many beamline elements, propagation engine in ray and wave approximations with full account for shapes and material properties, and high quality visualization capabilities. Recently added support for the GPGPU calculations via OpenCL not only allowed us to speed up the existing ray tracing routines but to qualitatively extend the limits of the theoretical models involved at all stages. As an example for the sources: we managed to increase the integration precision at high magnetic fields and high energies, which allows to calculate wigglers as undulators, an important case for the next-generation low-emittance synchrotrons. For the optics: wave propagation is implemented in the most general Kirchhoff integral form, therefore diffraction efficiency can be derived for multiple diffraction orders in gratings and zone plates. For the materials: reflectivity curves are calculated for the deformed crystals by solving the Takagi-Taupin equations numerically for each photon in the beam.

We also introduce an XML-based file format to store the ray tracing project parameters and an interactive GUI tool, xrtQook, which we recommend for the project configuration editing and automatic ray tracing script generation.

10388-7, Session 3

RAY, RAY-UI, and REFLEC: new developments *(Invited Paper)*

Franz Schäfers, Peter Baumgaertel, Helmholtz-Zentrum Berlin für Materialien und Energie GmbH (Germany)

The raytrace program RAY developed and continuously upgraded at BESSY since the 1980th is a well-known versatile synchrotron radiation simulation tool, well established since many years with comparable capabilities like the widely used SHADOW-program. Recently a comfortable and powerful graphical user interface RAY-UI has been added, which makes it an attractive and easy-to-use program for every-day use. Special helpful features have been added here like the mono-capillary optics and instantaneous calculation of mirror reflectivities and grating efficiencies of the central beam. A built-in DO-loop helps optimizing certain features such as focal spot or energy resolution as function of e.g. slope errors. The capabilities and new developments will be demonstrated with recent simulations ranging from complex soft x-ray elliptical undulator beamlines to hard x-ray beamlines at diffraction-limited storage rings. The Fresnel-reflectivity program REFLEC which accesses the same optics data-basis as RAY will also be shown. REFLEC is a program to calculate synchrotron radiation features, mirror or crystal reflectivities and grating efficiencies. It can easily be run as well as RAY in an outside DO loop (LOOPER) for optimizing e.g. grating design parameters or mirror reflectivities. Recent approaches to handle interference and coherence phenomena are also shown.

References

[1] F. Schäfers, RAY - The BESSY Raytrace Program, in: Modern Developments in X-Ray and Neutron Optics, Springer Series in Modern Optical Sciences, eds A. Erko, , M. Idir, Th. Krist, , A.G. Michette, , Vol. 137, 9-41 (2008)

[2] M. Sanchez del Rio, N. Canestrari, F. Jiang, F. Cerrina, SHADOW3: a new version of the synchrotron X-ray optics modelling package", J. Synchrotron Rad. 18, 708–716 (2011)

[3] P. Baumgärtel, M. Witt, J. Baensch, M. Fabarius, A. Erko, F. Schäfers, H. Schirmacher, RAY-UI: A Powerful and Extensible User Interface for RAY, AIP Conference Proceedings 1741-1-4, 040016 (2016) (SRI 2015)

10388-8, Session 3

Interoperability and complementarity of simulation tools for beamline design in the OASYS environment *(Invited Paper)*

Luca Rebuffi, Elettra-Sincrotrone Trieste S.C.p.A. (Italy); Manuel Sanchez del Rio, ESRF - The European Synchrotron (France)

In the next years most of the major synchrotron radiation facilities around the world will upgrade to 4th-generation Diffraction Limited Storage Rings using multi-bend-achromat technology. Moreover, several Free Electron Lasers are ready-to-go or in phase of completion. These events represent a huge challenge for the Optics physicists responsible of designing and calculating optical elements and systems capable to exploit the revolutionary characteristics of the new photon beams. Reliable and robust beamline design is only possible by lumping together different simulation tools. The OASYS (OrAnge SYnchrotron Suite) [1] suite drives several simulation tools providing new mechanisms of interoperability and communication within the same software environment. OASYS has been successfully used during the conceptual design of many beamline and optical designs for the ESRF and Elettra-Sincrotrone Trieste upgrades. Some examples are presented showing comparisons and benchmarking of simulations against calculated and experimental data.

[1] http://www.elettra.eu/oasys.html

10388-9, Session 3

McXtrace 1.4: latest developments in the new release

Erik B. Knudsen, Peter K. Willendrup, Technical Univ. of Denmark (Denmark)

We present the new features included in McXtrace 1.4 - the latest release of the open source x-ray tracing software package[1]. McXtrace is an open source ray-tracing package designed for simulating X.ray scattering experiments at synchrotrons, FELs, and lab sources, but recently it has found use in other areas such as the astrophysics community for telescope design.

Among the interesting new features are:

1. A set of synchrotron source models including Bending Magnet, Wiggler, and Undulator.
2. Several new optics modules.
3. Divergence monitors.
4. Flat & bent Darwin-limited Bragg-monochromator crystal components.
5. A new python/qt-based GUI.
6. Full-size mode of the DanMAX[2] beamline (in construction at the MAX IV synchrotron).
7. Full-size model of FXE[3] beamline at XFEL.
8. Redesigned and faster data-file reading lib.
9. SAS-view based SAXS-sample components.
10. Redesigned installation procedure.
11. A particle list output interface file-format (MCPL[4]) to enable simpler integration with other software packages such as SimEX[5] and MCNP6[6].
12. Generalized multilayer mirrors, with an option for graded profiles.
13. A Polycrystal model.

We will show examples of using these new features, and how they may be utilized in a beamline design process as has been done for the DanMAX[2] beamline.

[1] Knudsen et.al, Journal of Applied Crystallography, 2013.

[2] DanMAX – MAX IV, https://www.maxiv.lu.se/accelerators-beamlines/beamlines/danmax/

[3] European XFEL - Research - Instruments - FXE, www.xfel.eu/research/instruments/fxe

[4] MCPL: Kittelmann et. al., arXiv:1609.02792, 2016.

[5] SimEX: Fortmann-Grote et.al. arXiv:1610.05980, 2016.

[6] MCNP6: Los Alamos National Laboratory: MCNP Home Page, https://mcnp.lanl.gov

10388-10, Session 4

Application of x-ray simulations in development of instruments at Linear Coherent Light Source (LCLS) at National Accelerator Laboratory (SLAC) *(Invited Paper)*

Jacek Krzywinski, Lin Zhang, Gabriel Marcus, Yiping Feng, SLAC National Accelerator Lab. (United States)

Development of X-ray Free Electron Lasers (XFEL) opens new era in X-ray science. The full exploitation of unique properties of the XFEL radiation require challenging solutions that preserves radiation properties from a coherent, diffraction limited source under unprecedented instantaneous and average power load. We will present properties of simulated XFEL radiation such as coherence, source shape, divergence and longitudinal location inside the undulator. Recently, a construction of the LCLS II project has started as a major upgrade to the LCLS facility that will increase the average power of

the XFEL up to 1 kW level. We will show how the X-ray simulations are used for minimizing thermal distortions on focusing of the LCLS II X-ray beams by 1 meter long Kirkpatrick-Baez mirrors. We will discuss and compare accuracy of simulations using different simulation methods and packages applied to focusing optics. The design of instruments should mitigate the damage to the optics caused by the tremendous instantaneous XFEL power. We will present X-ray simulation of the damage to the diffraction grating coatings and compare it with experimental results obtained at LCLS. The self-seeded mode of the LCLS operation increases temporal coherence and reduces greatly the bandwidth of the X-ray radiation. The results of time dependent X-ray simulations of the LCLS radiation passing through the seeding monochromator will be presented. We will compare two different approaches: Fourier Optics and an approach based on a dispersive system described by 6x6 pulse ray matrixes.

10388-11, Session 4

European XFEL optics: current status *(Invited Paper)*

Liubov Samoylova, Harald Sinn, Maurizio Vannoni, European XFEL GmbH (Germany)

The European X-ray Free Electron Laser (XFEL) is a high repetition rate source that will deliver the most powerful hard X-ray short pulses in the world, up to 1e14 photons per 100 fs pulse. The end stations at the European XFEL are designed to carry out cutting edge scientific research in such areas as the deciphering the structure of biomolecules; studying ultra fast processes in real time, e.g. chemical reaction, dynamics of phase transitions; investigation of matter under extreme conditions; non-linear effects such as multi-photon ionization, etc. To enable such experiments, the optical components of 1 km beam transport and focusing optics downstream should provide ultra-short and almost fully transversely coherent laser pulses to experiments with minimal losses and distortions.

One of the main special features of the beam transport system is the use of 800 mm long mirrors to offset and distribute the beam at propagation distances many hundreds meters. Performance of the beamlines depends critically on these components, since profile errors and unwanted deformations at level of few nanometers, e.g. due to mounting and heat load, will cause severe beam distortions at experimental stations. In the talk we will present the up-to-date status of EuXFEL X-ray optics in the beam transport system and at specific experimental stations. We will present a thorough analysis of awaited beam parameters, calculated from metrology data for real optics components. Besides, we will discuss the modification of the beams after such mirrors by effects of spatial frequency filtering in free space propagation.

10388-12, Session 4

X-ray optics simulation and beamline design for the APS upgrade *(Invited Paper)*

Xianbo Shi, Ruben Reininger, Dean R. Haeffner, Argonne National Lab. (United States)

The upgrade of the Advanced Photon Source (APS) to a Multi-Bend Achromat (MBA) will increase the brightness of the APS by between two and three orders of magnitude. The upgrade project includes approximately eight feature beamlines that will take full advantages of the new machine. Many of the existing beamlines will be upgraded to profit from this significant machine enhancement. Optics simulations are essential in the design and optimization of the new and existing beamlines. In this presentation the simulation tools used and developed at APS, ranging from analytical to numerical methods, are summarized. Three general optical layouts are compared in terms of their coherence control and focusing capabilities. The concept of zoom optics, where two sets of focusing elements (e.g., CRLs and KB mirrors) are used to provide variable beam sizes at a fixed focal plane, is described in detail. Finally, simulation studies of a few APS upgrade beamlines are presented.

10388-13, Session 4

Simulation and optimization of the Sirius IPE soft x-ray beamline

Bernd C. Meyer, Tulio C. R. Rocha, Sergio A. L. Luiz, Artur Clarindo Pinto, Harry Westfahl Jr., Ctr. Nacional de Pesquisa em Energia e Materiais (Brazil)

The soft X-ray beamline IPÊ is one of the first phase SIRIUS beamlines at the LNLS, Brazil. Divided into two branches, IPÊ is designed to perform ambient pressure X-ray photo-electron spectroscopy (AP-XPS) and high resolution resonant inelastic X-ray scattering (RIXS) for samples in operando/environmental conditions inside cells and liquid jets. The aim is to maximize the photon flux in the energy range 200-1400 eV generated by an elliptically polarizing undulator source (EPU) and focus it to a 1 ?m vertical spot size at the RIXS station and 10 ?m at the AP-XPS station. In order to achieve the required resolving power (40.000 at 930 eV) for RIXS both the dispersion properties of the plane grating monochromator (PGM) and the thermal deformation of the optical elements need special attention. The grating parameters were optimized with the REFLEC code to maximize the efficiency at the required resolution. Thermal deformation of the PGM plane mirror limits the possible range of cff parameters depending of the photon energy used. Hence, resolution of the PGM and thermal deformation effects define the boundary conditions of the optical concept and the simulations of the IPÊ beamline. We compare simulations performed by geometrical ray-tracing (SHADOW) and wavefront propagation (SRW) and show that wavefront diffraction effects (apertures, optical surface error profiles) does not significantly change the beam spot size and shape.

10388-14, Session 4

Optical design and simulation of a new coherence beamline at NSLS-II

Garth J. Williams, Oleg Chubar, Ian K. Robinson, Brookhaven National Lab. (United States)

High spectral brightness X-ray sources, whose development and construction were driven in large part by demonstrable improvements to experimental efficiency, are now providing X-ray beams with unprecedented spatial and temporal characteristics. These beams, in turn, are driving the refinement and development of instrumentation capable of fully exploiting their novel properties. Whether the advanced instrumentation meets the need to provide very-high spatial or energy resolution through existing techniques or strives to explore new methods, our tools for its design must accurately account for the source properties and the effects of beamline optics on the X-ray probe.

We will discuss the optical design of a proposed beamline at NSLS-II, an optimized third generation storage ring source, designed to exploit the coherence of the X-rays to extract high-resolution spatial information from ordered and disordered materials through Coherent Diffractive Imaging (CDI), executed in the Bragg- and forward-scattering geometries. This technique offers a powerful tool to image sub-10 nm spatial features and, within ordered materials, to map deformation fields with sub-Angstrom sensitivity. Inspired by the opportunity to apply CDI to a wide range of samples, with sizes ranging from sub-micron to hundreds-of-microns, an optical design has been proposed and simulated under a variety of optical configurations using Synchrotron Radiation Workshop. The design, its goals, and the result of simulations of the beamline performance as a function of its variable optical components will be presented.

10388-15, Session 4

Theory of x-ray echo spectrometers *(Invited Paper)*

Yuri V. Shvyd'ko, Argonne National Lab. (United States)

X-ray echo spectroscopy is a recently proposed inelastic x-ray scattering

(IXS) technique, a space-domain counterpart of neutron spin-echo. X-ray echo spectroscopy involves imaging of the IXS spectra without requiring x-ray monochromtization. Due to this, the echo-type IXS spectrometers have a potential to simultaneously provide dramatically increased signal strength, reduced measurement times, and higher resolution compared to the traditional scanning-type IXS spectrometers. Here we develop further the theory of the x-ray echo spectrometers initially presented in [1] with an emphasis on questions of practical importance, which could help to design and assess feasibility and performance of the echo spectrometers such as: echo spectrometers tolerances, tuning up the refocusing condition, effective beamsize on the sample, spectral window of imaging and scanning range, the impact of the secondary source size on the spectral resolution, etc.

Examples of optical designs of the echo spectrometers with an 1-meV and 0.1-meV resolution will be presented as well.

[1] Yuri Shvyd'ko, Phys. Rev. Lett. 116, 080801 (2016).

10388-32, Session PWed

Numerical analysis of partially coherent radiation at soft x-ray beamline

Xiangyu Meng, Chaofan Xue, Huaina Yu, Yong Wang, Renzhong Tai, Yanqing Wu, Shanghai Synchrotron Radiation Facility (China)

A new model for numerical analysis of partially coherent x-ray at synchrotron beamlines is presented. The model is based on statistical optics. Four-dimensional coherence function, Mutual Optical Intensity (MOI), is applied to describe the wavefront of the partially coherent light. The MOI propagation through the beamline is developed. First, the plane is separated into many elements. It is assumed that in every element the beam has full coherence and constant complex amplitude, which is reasonable as long as the dimension of element is much smaller than the coherent length and beam spot size. Second, the propagation of MOI for every element can be analytical solved with Fraunhofer or Fresnel approximations. Finally, the total MOI propagation through free space can be obtained by summing the contribution of all elements. Local stationary phase approximation is implemented to simulate MOI propagating through ideal mirrors and gratings. In this theory, path length is used to describe the phase shift through the optics. The source is not necessary to be Gaussian Schell type. Any MOI distribution can be applied in this model. The STXM beamline at SSRF was analyzed with this model. The diffraction experiment of a single slit was performed and the diffraction pattern was simulated to get the coherence length, (31 ± 3.0) μm ? (25 ± 2.1) μm (H ? V), which had a good agreement with the theoretical results, (30.7 ± 0.6) μm ? (31 ± 5.3) μm (H ? V). It indicates that the model is applicable in the analysis of partial coherence propagation in soft x-ray beamlines.

10388-33, Session PWed

A fast and reliable approach to simulating the output from an x-ray tube used for developing security backscatter imaging

Anna Vella, Andre M. A. Munoz, Matthew J. F. Healy, David W. Lane, Cranfield Univ. (United Kingdom); Joseph G. Zhou, VJ Technologies, Inc. (United States); David Lockley, Defence Science and Technology Lab. (United Kingdom)

The PENELOPE Monte Carlo simulation code was used alongside the SpekCalc code to simulate X-ray energy spectra from a VJ Technologies' X-ray generator at a range of anode voltages. The PENELOPE code is often utilised in medicine but is here applied to develop coded aperture and pinhole imaging systems for security purposes. The greater computational burden of PENELOPE over SpekCalc is warranted by its greater flexibility and output information. The model was designed using the PENGEOM sub-tool and consists of a tungsten anode and five layers of window materials. The photons generated by a mono-energetic electron beam are collected by a virtual detector placed after the last window layer, and this records the spatial, angular and energy distributions which are then used as the X-ray source for subsequent simulations. The process of storing X-ray outputs and using them as a virtual photon source can then be used efficiently for exploring a range of imaging conditions as the computationally expensive electron interactions in the anode need not be repeated. The modelled spectra were validated with experimentally determined spectra collected with an Amptek X-123 Cadmium Telluride detector placed in front of the source.

10388-34, Session PWed

The use of simulation to optimize the pinhole diameter and mask thickness for an x-ray backscatter imaging system

Anna Vella, Andre M. A. Munoz, Matthew J. F. Healy, David W. Lane, Cranfield Univ. (United Kingdom); David Lockley, Defence Science and Technology Lab. (United Kingdom)

The PENELOPE Monte Carlo simulation code was used to determine the optimum thickness and aperture diameter of a pinhole mask for use in coded aperture backscatter security imaging. The thickness of the mask needs to be sufficient to prevent any X-ray leakage, and the pinhole diameter wide enough to maximise the field of view. The model consisted of an extended X-ray source, a pinhole mask, and a detector. The X-ray source was modelled as a thin wire emitter; the X-rays passed through the pinhole mask and were collected at a simulated 1040 x 1340 pixels' area detector, placed inside a lead lined aluminium camera housing. Each mask was model irradiated with X-rays with a flat energy distribution across a defined energy range. This artificial source was used to avoid being specific to a particular source technology. To generate the image, the integrated energy was calculated from the phase-space file to correlate the energy of the photons with their positions in the real pixels of the real detector. A MATLAB routine was written to accomplish this mapping and integration. The image contrast, signal to background ratio, spatial resolution, and collimation effect were calculated at the simulated detector as a function of the thickness and the pinhole diameter of three different mask materials: tungsten, tungsten/epoxy resin composite and a low melting point bismuth alloy.

10388-36, Session PWed

Alignment of KB mirrors with at-wavelength metrology tool simulated using SRW

Lei Huang, Brookhaven National Lab. (United States); Bo Gao, Shanghai Institute of Applied Physics (China) and Univ. of Chinese Academy of Sciences (China); Maksim S. Rakitin, Brookhaven National Lab. (United States); Junpeng Xue, Brookhaven National Lab. (United States) and Sichuan Univ. (China); Oleg Chubar, Mourad Idir, Brookhaven National Lab. (United States)

Synchrotron Radiation Workshop (SRW) is a powerful synchrotron simulation tool and has been widely used at synchrotron facilities all over the world. During the last decade, many types of x-ray wavefront sensors has been developed and used. In this work, we will present our recent effort on the development of at-wavelength metrology simulation based on SRW mainly focused on the Hartmann Wavefront Sensor (HWS). Various conditions have been studied to verify that the simulated HWS is performing as expected in terms of accuracy. This at-wavelength metrology simulation tool is then used to align KB mirrors by minimizing the wavefront aberrations. We will present our optimization process to perform an 'in situ' alignment using conditions as close as possible to the real experiments (KB mirrors with different levels of figure errors or different misalignment geometry). Present status of this simulation tools will be presented and future foreseen extensions will be discussed, like Grating Shearing

Interferometry (GSI) and the possibility to use Transport of Intensity Equation (TIE).

10388-37, Session PWed

Collaborative simulation of x-ray optics and electron beam dynamics

David L. Bruhwiler, RadiaSoft LLC (United States); Paul Moeller, RadiaSoft LLC (United States) and Bivio LLC (United States); Robert Nagler, RadiaSoft LLC (United States); Maksim S. Rakitin, Oleg Chubar, Brookhaven National Lab. (United States); Gerard Andonian, RadiaBeam Technologies, LLC (United States) and Univ. of California, Los Angeles (United States)

Modern synchrotron light sources are an efficient source of X-ray, UV and infrared beams, enabling scientific research with a wide range of applications. State-of-the-art low-emittance facilities like NSLS-II produce partially-coherent X-ray beams that enable new research with more sophisticated X-ray optics. We present a browser-based GUI for X-ray optics [1] and electron beam dynamics [2], which is available for beta testing. The open source code SRW [3,4] is used to simulate synchrotron radiation sources and the subsequent transport of coherent and partially-coherent radiation beams through optical systems of beamlines. We are presently implementing support for the open source code Shadow3 [5,6] to simulate incoherent synchrotron radiation via geometrical ray-tracing. Electron beam dynamics in the electron storage ring is simulated with the Pelegant code [7]. Examples will be presented and the open source cloud computing framework Sirepo [8] will be described, with emphasis on features that enable instantaneous collaboration. Lightweight and extensible, Sirepo could become a community resource for use with other codes.

[1] X-ray optics in the cloud, https://beta.sirepo.com/light

[2] Beam dynamics in the cloud, https://beta.sirepo.com/elegant

[3] O. Chubar and P. Elleaume, Proc. of EPAC, 1177 (1998).

[4] SRW, https://github.com/ochubar/SRW

[5] M. Sanchez del Rio et al., J. Synchrotron Rad. 18, 708 (2011).

[6] Shadow3, http://www.esrf.eu/Instrumentation/software/data-analysis/OurSoftware/raytracing

[7] Y. Wang and M. Borland, AIP Conf. Proc. 877, 241 (2006).

[8] Sirepo, http://sirepo.com

This material is based on work supported by the U.S. Department of Energy, Office of Science, Office of Basic Energy Sciences, under Award Numbers DE-SC0006284 and DE-SC0011237.

10388-38, Session PWed

Simulation of experiments with partially-coherent x-rays using Synchrotron Radiation Workshop

Oleg Chubar, Maksim S. Rakitin, Brookhaven National Lab. (United States); Yu-Chen Chen-Wiegart, Brookhaven National Lab. (United States) and Stony Brook Univ. (United States); Andrei Fluerasu, Lutz Wiegart, Brookhaven National Lab. (United States)

High-accuracy physical optics calculations methods used in the “Synchrotron Radiation Workshop” (SRW) allow for multiple applications of this code in different areas, covering development, commissioning, diagnostics and operation of instruments at light source facilities. This presentation will focus on applications of SRW for determining of important physical characteristics of micro-spectroscopy and coherent scattering beamlines, and on the simulation of experiments at these beamlines. The most complete and most detailed simulation of experiments with SRW is possible in the area of elastic coherent scattering, where the interaction of radiation with samples can be described with the same transmission-type “propagators” that are used for the simulation of fully- and partially-coherent radiation propagation through X-ray optical elements of beamlines. Besides the examples of forward-simulation of such experiments, performed at beamlines of NSLS-II, new developments in the SRW code, facilitating solution of the corresponding inverse problems, will be described.

10388-39, Session PWed

Hard x-ray FEL SASE pulses propagation through perfect single crystals diffracting in Bragg and Laue geometry

Angel Rodriguez-Fernandez, Paul Scherrer Institut (Switzerland); Liubov Samoylova, European XFEL GmbH (Germany); Alexey V. Buzmakov, A.V. Shubnikov Institute of Crystallography (Russian Federation)

With the commissioning of three new hard x-ray Free Electron Lasers (X-FEL), European XFEL (Hamburg), PAL (Pohang) and SwissFEL (Zurich), comes a time when a better knowledge of hard x-ray optics for high brilliant sources will be needed. Due to the high coherence and the femtosecond range of these types of photon pulses, the dynamical diffraction effects in perfect crystals, use as monochromators, have more relevance in the interaction between the crystal structure and the wave field under propagation. To tackle this problem, we have used Synchrotron Radiation Workshop (SRW), a well-known tool based on Fourier optics approach, to simulate the propagation of different FEL SASE pulses along perfect crystals in Laue and Bragg geometry. Different thicknesses (between 30 and 100 um) have been studied for two different photon energies 8 KeV and 12 KeV. The FEL SASE beams were generated by GENESIS and FAST code. These types of models could help in the understanding of the Self-Seeding modes of operation at FEL facilities, where the common large SASE bandwidth mode is reduced from the typical bandwidth on the order of 0.2-0.5 % of the fundamental energy (20 eV at 8 KeV) to 0.005% (0.4 eV at 8 KeV). This mode also introduce an increment of the brilliance power and an improvement of the jittering stability of the photon beam , which is of great interest for photon energy techniques as resonant x-ray scattering as well as observation of nonlinear x-ray–matter interactions.

10388-40, Session PWed

Simulation of x-ray images of an IXS echo spectrometer

Alexey Y. Suvorov, Oleg Chubar, Yong Q. Cai, Brookhaven National Lab. (United States); Yuri V. Shvyd’ko, Argonne National Lab. (United States)

A recently advanced concept of an X-ray echo spectrometer allows to overcome limitations of spectral resolution and weak signals of the traditional inelastic x-ray scattering (IXS) instruments [1]. The spectrometer illuminates a sample with a spatially expanded beam due to energy dispersion of its monochromator. After the sample, the spectrometer analyzer recombines the beam into an image in a detector plane. The enhanced strength of the spectrometer signal allows to speed up the acquisition process and obtain the IXS spectrum with a very high energy resolution. The design of the echo spectrometer is based on a combination of crystal and focusing optics. The spectrometer analyzer requires an X-ray focusing optics with a high numerical aperture which is capable to collect radiation scattered by the sample into a wide solid angle. The required numerical aperture can be achieved with a graded multilayer mirror. To collect the scattered intensity from a solid angle, we considered the mirrors with a single reflection 2D parabolic shape. We simulated the images and investigated the performance of the echo spectrometer with the above mentioned mirrors using numerical computations in the SRW software package.

10388-41, Session PWed

Advanced commissioning of the Soft Matter Interfaces Beamline at NSLS-II

Mikhail Zhernenkov, Elaine DiMasi, Oleg Chubar, Maksim S. Rakitin, Brookhaven National Lab. (United States)

We report on the results of the advanced commissioning of the Soft Matter Interfaces (SMI) beamline, a long energy range canted in-vacuum undulator (IVU) beamline at NSLS-II. We compare the complete beamline simulation results performed with SRW software and the beam parameters measured during the technical and scientific commissioning. In particular, we will present the outcome of the recent IVU optimization (spectrum-based alignment resulted in a considerable increase of flux at beamline), bimorph horizontal and vertical focusing mirror tuning and profile optimization, as well as the commissioning of the microfocusing CRL transfocator.

10388-16, Session 5

Modelling imperfect x-ray optics *(Invited Paper)*

David Laundy, Kawal J. S. Sawhney, Diamond Light Source Ltd. (United Kingdom)

Geometrical optics and physical optics simulations are two methods for modelling the transport of X-rays through optical systems. Physical optics simulations include the coherent wave properties of the radiation and allow modelling of focusing near to the diffraction limit and also where interference of the wave-field occurs. With reductions in source emittance at modern X-ray storage rings, there are greater demands placed on X-ray optical elements to minimize distortion of the X-ray wavefront. We have related the perturbation of the wavefront following reflection from elliptically profiled X-ray mirrors to the figure error of the mirror surface.

We show the results of geometrical and physical optics simulations of mirrors whose surface figure had been measured by nanometer optical metrology (NOM). Simulation results are compared with measurements carried out on the Diamond Test Beamline.

10388-17, Session 5

Mutual optical intensity propagation through non-ideal optics

Xiangyu Meng, Shanghai Institute of Applied Physics (China); Xianbo Shi, Argonne National Lab. (United States); Yong Wang, Shanghai Institute of Applied Physics (China); Ruben Reininger, Lahsen Assoufid, Argonne National Lab. (United States); Renzhong Tai, Shanghai Institute of Applied Physics (China)

We continue to develop MOI method to analyze the mutual optical intensity (MOI) propagation through non-ideal optics. Local stationary phase approximation is implemented to calculate the MOI propagating through a non-ideal mirror. The phase generated by the path length from the incident to exit plane is the key to solve the MOI propagation through the mirror. The effect of figure error can be expressed as phase shift. There are two methods to deal with the figure error, the analytical method and numerical one. The two methods are compared at different spatial frequency range of the figure error. An APS beamline is analyzed with the developed MOI model, in which a partially coherent beam with 10keV energy is focused to ~20nm by a non-ideal elliptical mirror. The MOI at the focal plane is acquired after propagation through the non-ideal mirror. The intensity profile, the wavefront and the global coherence degree can be get from the MOI. The results indicate that the figure error with low spatial frequency generates oscillations, redistributes coherence property and damages the wavefront on the image plane. However, the figure error does not change the global coherence degree. Comparison with other codes such as Hybrid and SRW was performed. The results show that MOI model and SRW have similar intensity profiles. The apparent oscillations from MOI model and SRW indicate high coherence. Limitation on the beam size by the BDA and mirror will increase the coherence, which can be quantitatively analyzed by global coherence degree from MOI.

10388-18, Session 5

Speckle-based at-wavelength metrology of x-ray optics at Diamond Light Source *(Invited Paper)*

Hongchang Wang, Tunhe Zhou, Yogesh Kashyap, Kawal J. S. Sawhney, Diamond Light Source Ltd. (United Kingdom)

Over the last few decades, significant progress has been made to improve both the optical quality and metrology accuracy of X-ray optics. Although ex-situ measurement of X-ray optics is routinely performed, the ultimate performance of X-ray optics is critically dependent on the exact nature of working conditions. Therefore, it is equally important to perform in-situ metrology at the optics' operating wavelength ('at-wavelength' metrology) to optimize the performance of X-ray optics and correct and minimize the collective distortions of upstream beamline optics, e.g. monochromator, windows, etc. Several at-wavelength metrology methods have been implemented and further improved at Diamond [1]. The method based on speckle scanning technique is the most promising as we have demonstrated that the angular sensitivity for measuring the slope error of an optical surface can reach accuracy in the range of two nanoradians[2, 3]. The recent development of the speckle-based at-wavelength metrology technique implemented at the Diamond will be presented [4, 5]. Representative examples of the application of the speckle-based technique will also be given – including in-situ at-wavelength metrology of X-ray mirrors and characterization of compound refraction lenses. Such a high-precision metrology technique will be extremely beneficial for the manufacture and in-situ alignment / optimization of x-ray mirrors for next-generation synchrotron beamlines.

[1] K. Sawhney, H. Wang, J. Sutter et al., "At-wavelength Metrology of X-ray Optics at Diamond Light Source," Synchrotron Radiation News, 26(5), 17-22 (2013).

[2] H. Wang, J. Sutter, and K. Sawhney, "Advanced in situ metrology for x-ray beam shaping with super precision," Optics Express 23(2), 1605-1614 (2015).

[3] H. Wang, Y. Kashyap, and K. Sawhney, "Speckle based X-ray wavefront sensing with nanoradian angular sensitivity," Optics Express 23(18), 23310-23317 (2015).

[4] Y. Kashyap, H. Wang, and K. Sawhney, "Development of a speckle-based portable device for in situ metrology of synchrotron X-ray mirrors," Journal of Synchrotron Radiation, 23(5), 1131-1136 (2016).

[5] H. Wang, Y. Kashyap, D. Laundy et al., "Two-dimensional in situ metrology of X-ray mirrors using the speckle scanning technique," Journal of Synchrotron Radiation, 22(4), 925-929 (2015).

10388-19, Session 5

Stochastic surface metrology analysis

Anastasia Y. Tyurina, Yury N. Tyurin, Second Star Algonumerix, LLC (United States); Valeriy V. Yashchuk, Lawrence Berkeley National Lab. (United States)

The design and evaluation of the expected performance of new optical systems requires sophisticated and reliable information about the surface topography for planned optical elements before they are fabricated. The problem is especially complex in the case of x-ray optics, particularly for the X-ray Surveyor under development and other missions. Modern x-ray source facilities are reliant upon the availability of optics with unprecedented quality (surface slope accuracy < 0.1?rad). The high angular resolution and throughput of future x-ray space observatories requires hundreds of square meters of high quality optics. The uniqueness of the

optics and limited number of proficient vendors makes the fabrication extremely time consuming and expensive, mostly due to the limitations in accuracy and measurement rate of metrology used in fabrication. We discuss improvements in metrology efficiency via comprehensive statistical analysis of a compact volume of metrology data. The data is considered stochastic and a new statistical model called Invertible Time Invariant Linear Filter (InTILF) is developed to provide compact description of the data. It captures faint patterns in the data and serves as a quality metric and feedback to polishing processes, avoiding x-ray high resolution metrology measurements over the entire optical surface. The modeling, implemented in our Beatmark software, allows simulating metrology data for optics made by the same vendor and technology. The forecast data is vital for reliable specification for optical fabrication, to be exactly adequate for the required system performance. Supported by NASA SBIR NNX16CM09C and the USDOE AC02-05CH11231.

10388-20, Session 6

Latest developments of x-ray refractive optics for coherent applications *(Invited Paper)*

Anatoly A. Snigirev, Immanuel Kant Baltic Federal Univ. (Russian Federation)

In the past two decades, there has been a rapid development in our ability to control, manipulate and focus x rays by refractive optics. The emergence of x-ray free electron lasers and diffraction-limited synchrotron radiation sources has increased demands on coherence compatible optics, where refractive lenses as in-line optics have obvious advantages. In addition, the past few years have been witness to significant advances in the development of new coherent techniques based on refractive optics: x-ray microscopy, diffraction imaging and interferometry. For utilizing these new techniques, scientists in the field are taking the first steps toward the development of new optical concepts of beamlines. Details of these developments are discussed.

10388-21, Session 6

Aberrations in compound refractive lens systems: analytical and numerical calculations

Markus Osterhoff, Georg-August-Univ. Göttingen (Germany); Carsten Detlefs, Claudio Ferrero, ESRF - The European Synchrotron (France)

Hard x-ray beams can be focused using refractive lenses, but depending on energy, a large number N of individual lenses stacked in a row is needed.

Such a stack can be either composed of single lenses in cartridges, or lithographically fabricated lenses in a row. With N in the three-digit regime, the question arises which tolerances on lens alignment and shape have to be met not to disturb the focus. Here we use analytical and numerical calculations based on a Zernike polynomial expansion to give such error bounds for typical set-ups.

10388-22, Session 7

Simulations of x-ray free-electron laser experiments with the SIMEX platform *(Invited Paper)*

Carsten Fortmann-Grote, European XFEL GmbH (Germany); Zoltan Jurek, Ctr. for Free-Electron Laser Science (Germany) and The Hamburg Ctr. for Ultrafast Imaging (Germany); Beata Ziaja-Motyka, Ctr. for Free Electron Laser Science (Germany) and The Hamburg Ctr. for Ultrafast Imaging (Germany) and Institute of Nuclear Physics (Poland); Robin Santra, Ctr. for Free-Electron Laser Science (Germany) and The Hamburg Ctr. for Ultrafast Imaging (Germany) and Hamburg Univ. (Germany); Adrian P. Mancuso, European XFEL GmbH (Germany)

We present a generic software platform for simulations of experiments at modern light sources, e.g. free electron lasers, synchrotrons, and optical laser facilities. In our complete start--to--end simulations, we track the radiation from the source through the beam transport optics to the sample under investigation, the photon-matter interaction within the sample, and detection of scattered or transmitted photons in a detector.

We apply our simulation tools to model coherent diffractive imaging of single biomolecules with x-ray free electron lasers. This technique is expected to yield new structural information about biologically relevant macromolecules thanks to the ability to study the isolated sample in its natural environment as opposed to crystallized or cryogenic samples.

Establishing the optimal experimental parameters (e.g. x-ray pulse duration, photon energy, and fluence) as well as the level of radiation damage acceptable for electron density reconstructions are among open questions that we address with our simulation capabilities as well as the effect of the solvent on the diffraction pattern and interpretability of the data. We present first results of calculations in which the solvent has been taken into account.

10388-23, Session 7

X-ray optical simulations supporting advanced commissioning of the coherent hard x-ray beamline at NSLS-II

Lutz Wiegart, Oleg Chubar, Andrei Fluerasu, Maksim S. Rakitin, Brookhaven National Lab. (United States)

The presentation will showcase the application of fully- and partially-coherent synchrotron radiation wavefront propagation simulation functions, implemented in the “Synchrotron Radiation Workshop” (SRW) computer code, to create a ‘virtual beamline’, mimicking the Coherent Hard X-ray (CHX) scattering beamline at NSLS-II. The beamline simulation includes all optical beamline components, such as the insertion device, mirror with metrology data, slits, double crystal monochromator and refractive focusing elements (compound refractive lenses and kinoform lenses). A specialty of the CHX beamline is the exploitation of X-ray beam coherence, boosted by the low-emittance NSLS-II storage-ring, for techniques such as X-ray Photon Correlation Spectroscopy (XPCS) or Coherent Diffraction Imaging (CDI). The key performance parameters are the degree of X-ray beam coherence and photon flux, and the trade-off between them needs to guide the beamline settings for the specific experimental requirements. Simulations of key performance parameters will be compared to measurements obtained during beamline commissioning, and will include the spectral flux of the undulator source, the degree of transverse coherence, focal spot sizes and simulated and measured coherent scattering patterns.

10388-24, Session 7

Nano-focused hard x-ray beam measured by ptychography

Xiaojing Huang, Hanfei Yan, Evgeny Nazaretski, Mingyuan Ge, Nathalie Bouet, Juan Zhou, Weihe Xu, Petr P. Ilinski, Yong S. Chu, Brookhaven National Lab. (United States)

With the progress of achieving diffraction-limited X-ray focus, ptychography offers a unique and powerful tool to provide quantitative reconstruction of the complex-valued wavefront of a focused beam. Propagation of the reconstructed wavefront essentially describes complete performance characterization of the optics. We will present the accumulated efforts at

NSLS-II on exploring the capability of ptychography to quantify focusing performance of a variety of hard X-ray optics, including K-B mirrors, zone plates, multilayer Laue lenses [1-3]. Presentation will also elaborate on our recent development of monolithically bonded MLLs as a signal optical component for scanning probe microscope applications [4,5].

References:

[1] X. Huang, et al., "Quantitative X-ray wavefront measurements of Fresnel zone plate and K-B mirrors using phase retrieval", Optics Express, 20, 24038-24048 (2012).

[2] X. Huang, et al., "11 nm hard X-ray focus from a large-aperture multilayer Laue lens", Scientific Reports, 3, 3562 (2013).

[3] X. Huang, et al., "Achieving hard X-ray nanofocusing using a wedged multilayer Laue lens", Optics Express, 23, 12496-12507 (2015).

[4] E. Nazaretski, et al., "Development and characterization of monolithic multilayer Laue lens nanofocusing optics"", Applied Physics Letters, 108, 261102 (2016).

[5] X. Huang, et al., "Hard x-ray scanning imaging achieved with bonded multilayer Laue lenses", submitted, (2017).

10388-25, Session 7

A Monte Carlo simulation of scattering reduction in spectral x-ray computed tomography

Matteo Busi, Ulrik L. Olsen, Erik B. Knudsen, Jan Kehres, Technical Univ. of Denmark (Denmark); Erik D. Christensen, Niels Bohr Institute (Denmark); Mohamad Khalil, Jeppe Revall Frisvad, Kristoffer Haldrup, Technical Univ. of Denmark (Denmark)

In X-ray computed tomography (CT), scattered radiation plays an important role in the accurate detection of the object's mass attenuation coefficients, leading particularly to a loss of contrast and streaking artifacts. We develop a Monte Carlo based simulation of a spectral CT tool, to predict the effect of different modes of collimation of a fan-beam geometry. The collimation is designed specifically to study and reduce the detected energy distribution of scattered radiation. Spectral CT is a novel technique implementing photon-counting detectors able to discriminate the energy of incoming photons, enabling real time spectral analysis of observables. It is therefore useful to efficiently extract more information on energy dependent quantities (e.g. mass attenuations) and processes (e.g. X-ray scattering, photoelectric absorption, etc.). Having a good knowledge of the spectral distribution of scattering is fundamental to establish methods for attempting to correct it. The simulations are then validated by real measurements with the use of different novel CdTe spectral detectors (Multix ME-100, Advacam Modupix). Notably, we found a shift of the scattered distribution towards lower energies, becoming of particular relevance in the energy range where the photoelectric absorption is dominant (i.e. below 50keV). We found a good match between simulations and experiments.

10388-26, Session 8

SPECTRA demonstration *(Invited Paper)*

Takashi Tanaka, RIKEN (Japan)

No Abstract Available

10388-27, Session 8

Sirepo: a web-based interface for physical optics simulations - its deployment and use at NSLS-II *(Invited Paper)*

Maksim S. Rakitin, Oleg Chubar, Brookhaven National Lab. (United States); Paul Moeller, RadiaSoft LLC (United States) and Bivio LLC (United States); Robert Nagler, David L. Bruhwiler, RadiaSoft LLC (United States)

"Sirepo" is an open source cloud-based distributed software framework which provides a convenient and user-friendly web-interface on the client side for scientific codes such as Synchrotron Radiation Workshop (SRW) running on the server side. SRW is a physical optics code allowing to simulate the synchrotron radiation from various insertion devices (undulators and wigglers) and bending magnets. Another feature of SRW is a support of high-accuracy simulation of fully- and partially-coherent radiation propagation through X-ray optical beamlines, facilitated by so-called "Virtual Beamline" module. In the present work, we will discuss the most important features of Sirepo/SRW interface with emphasis on their use for commissioning of beamlines and simulation of experiments at National Synchrotron Light Source II. In particular, "Flux through Finite Aperture" and "Intensity" reports, visualizing results of the corresponding SRW calculations, are being routinely used for commissioning of undulators and X-ray optical elements. Material properties of crystals, compound refractive lenses, and some other optical elements are dynamically obtained for the desired photon energy from the databases publicly available at Argonne National Lab (http://x-server.gmca.aps.anl.gov/x0h.html) and at Lawrence Berkeley Lab (http://henke.lbl.gov/optical_constants/). In collaboration with the Center for Functional Nanomaterials (CFN) of BNL, a library of samples for coherent scattering experiments has been implemented in SRW and the corresponding Sample optical element was added to Sirepo. Electron microscope images of artificially created nano-scale samples can now be uploaded to Sirepo to simulate scattering patterns created by synchrotron radiation in different experimental schemes that can be realized at beamlines.

10388-28, Session 8

OASYS (OrAnge SYnchrotron Suite): an open-source graphical environment for x-ray virtual experiments *(Invited Paper)*

Luca Rebuffi, Elettra-Sincrotrone Trieste S.C.p.A. (Italy); Manuel Sanchez del Rio, ESRF - The European Synchrotron (France)

The evolution of the hardware platforms, the modernization of the software tools, the access to the codes of a large number of young people and the popularization of the open source software for scientific applications drove us to design OASYS (ORange SYnchrotron Suite) [1], a completely new graphical environment for modeling X-ray experiments. The implemented software architecture allows to obtain not only an intuitive and very-easy-to-use graphical interface, but also provides high flexibility and rapidity for interactive simulations, making configuration changes to quickly compare multiple beamline configurations. Its purpose is to integrate in a synergetic way the most powerful calculation engines available. OASYS integrates different simulation strategies via the implementation of adequate simulation tools for X-ray Optics (e.g. ray tracing and wave optics packages). It provides a language to make them to communicate by sending and receiving encapsulated data. Python has been chosen as main programming language, because of its universality and popularity in scientific computing. Orange [2] is the high level workflow engine that provides the interaction with the user and communication mechanisms.[1] http://www.elettra.eu/oasys.html [2] http://orange.biolab.si/

10388-29, Session 8

RAY, RAY-UI, and REFLEC demonstration *(Invited Paper)*

Franz Schäfers, Helmholtz-Zentrum Berlin für Materialien und Energie GmbH (Germany)

No Abstract Available

10388-30, Session 8

McXtrace demonstration *(Invited Paper)*

Erik B. Knudsen, Technical Univ. of Denmark (Denmark)

No Abstract Available

10388-31, Session 8

XRT demonstration *(Invited Paper)*

Roman Chernikov, Deutsches Elektronen-Synchrotron (Germany)

No Abstract Available

10389-1, Session 1

Propagation-based phase-contrast imaging using laboratory sources *(Invited Paper)*

William Vågberg, Daniel H. Larsson, KTH Royal Institute of Technology (Sweden); Mei Li, Anders Arner, Laszlo Szekely, Jonas Persson, Karolinska Institutet (Sweden); Andre Yaroshenko, Technische Univ. München (Germany); Ali Önder Yildirim, Helmholtz Zentrum München GmbH (Germany); Hans M. Hertz, KTH Royal Institute of Technology (Sweden)

Liquid-metal-jet x-ray sources have vastly increased the achievable brightness from a laboratory microfocus source. This development has paved the way for bio-imaging that was previously only possible at synchrotrons. We describe three biomedical phase-contrast imaging applications: First, imaging of juvenile zebrafish to allow observation of sub-5 µm muscle structures. Secondly, imaging of human coronary arteries to evaluate the vulnerability of lipid-rich atherosclerotic plaques. Finally, short exposure and low dose imaging of whole mouse and mouse lungs.

10389-2, Session 1

Increasing spatial resolution in full-field soft x-ray nanotomography of cells *(Invited Paper)*

Eva Pereiro, ALBA Synchrotron (Spain); Joaquín Otón, Ctr. Nacional de Biotecnologia (Spain); Javier Conesa, ALBA Synchrotron (Spain); Javier Chichon, Ctr. Nacional de Biotecnologia (Spain); Ana Perez-Berna, Andrea Sorrentino, ALBA Synchrotron (Spain); Jose L. Carrascosa, Jose Maria Carazo, Ctr. Nacional de Biotecnologia (Spain)

We have explored two ways to improve the spatial resolution and/or visibility of cellular ultrastructure in full field soft X-ray nanotomography at the Mistral beamline (ALBA light source). The first one consists on a new data collection method and processing framework to computationally extend the depth of field (XTEND) of a Fresnel zone plate objective lens based on focal series projections and deconvolution. Visual details of a 3D-reconstructed eukaryotic cell that is affected by depth of field artifacts in standard tomographic reconstruction are recovered. The second one consists on diminishing the missing wedge inherent to flat sample supports (rotation range ±70deg) by performing dual axis tomography. Both strategies clearly show a spatial resolution and visibility improvement on the reconstructed volumes while complying with radiation dose limitation. Examples of these methods on relevant biological applications will be presented.

10389-3, Session 1

Coherent high-energy x-ray microscopy for mesoscopic materials

Irina Snigireva, ESRF - The European Synchrotron (France); Anatoly A. Snigirev, Immanuel Kant Baltic Federal Univ. (Russian Federation)

Coherent high energy X-ray microscope was employed to study the wide range of natural and artificial mesoscopic materials that are structured on scales of the order of a few to a few hundred nanometers. The microscope operates under a coherent illumination where a diffraction pattern of the specimen is formed in the back focal plane of the condenser and an inverted two-dimensional image of the object is formed by objective lens in the image plane. Functioning at 10 – 30 keV, the microscope consists of the condenser, the objective lens and two X-ray CCD cameras – large area detector for diffraction and high resolution CCD for imaging. Condenser and objective assemblies are comprised of Be parabolic refractive lenses. Switching from the diffraction mode to the imaging is achieved by placing the objective lens into the beam, and the chosen detector. The tunable objective lens offers full-field imaging with variable resolution and field of view.

The microscope was applied for study of natural and synthetic opals, metal inverted photonic crystals and colloidal suspensions. The combination of the direct-space imaging and high resolution diffraction provide a wealth of information on their local structure and the long range periodic order. The development of the hard x-ray microscope emerged concomitantly with the realization of the ESRF source upgrade which greatly enhanced brilliance and fraction of coherent light, and this will open entirely new frontiers in materials imaging.

10389-4, Session 1

The imaging and coherence beamline I13L at DIAMOND

Christoph Rau, Diamond Light Source Ltd. (United Kingdom) and Manchester Univ. (United Kingdom) and Northwestern Univ. (United States); Ulrich H. Wagner, Malte Ogurreck, Xiaowen Shi, Darren Batey, Silvia Cipiccia, Shashidhara Marathe, Andrew J. Bodey, Diamond Light Source Ltd. (United Kingdom); Marie-Christine Zdora, Diamond Light Source Ltd. (United Kingdom) and Univ. College London (United Kingdom); Irene Zanette, Diamond Light Source Ltd. (United Kingdom); Mirna Saliba, Diamond Light Source Ltd. (United Kingdom) and Univ. Zürich (Switzerland); Venkata S. C. Kuppili, Diamond Light Source Ltd. (United Kingdom) and Univ. College London (United Kingdom); Simone Sala, Stefanos H. Chalkidis, Univ. College London (United Kingdom); Pierre Thibault, Univ. of Southampton (United Kingdom) and Univ. College London (United Kingdom)

The Diamond Beamline I13L is designed to imaging on the micron- and nano-lengthsale with X-rays of energies between 6 and 30 keV [1]. Two independently operating branchlines and endstations have been built at distance of more than 200m from the source for this purpose. The imaging branch is dedicated for imaging in real space, providing In-line phase contrast imaging and grating interferometry with micrometre resolution and full-field transmission microscopy with 50nm spatial resolution.

On the coherence branch coherent diffraction imaging techniques such as ptychography, coherent X-ray diffraction (CXRD) and Fourier-Transform holography are currently developed. Because of the large lateral coherence length available at I13, the beamline hosts numerous microscopy experiments. The coherence branchline in particular contains a number of unique features. New instrumental designs have been employed such as a robot arm for the detector in diffraction experiments and a photon counting detector for diffraction experiments. The so-called 'mini-beta' layout in the straight section of the electron storage ring permits modulating the horizontal source size and therefor the lateral coherence length.

We will present the recent progress in coherent imaging at the beamline and the sciences addressed with the instrumental capabilities.

Reference:

[1] C. Rau, U. Wagner, Z. Pesic, A. De Fanis Physica Status Solidi (a) 208 (11). Issue 11 2522-2525, 2011, 10.1002/pssa.201184272

10389-5, Session 1

Development of full-field x-ray fluorescence microscope using total-reflection mirrors

Satoshi Matsuyama, Jumpei Yamada, Shuhei Yasuda, Osaka Univ. (Japan); Yoshiki Kohmura, Makina Yabashi, Tetsuya Ishikawa, RIKEN Harima Branch (Japan); Kazuto Yamauchi, Osaka Univ. (Japan)

A full-field X-ray fluorescence microscope was developed at SPring-8. It consists of advanced Kirkpatrick-Baez mirrors with four total-reflection mirrors as an objective and a CCD camera. The imaging optics has the following specifications: magnifications of 84 x 26 (horizontal x vertical), numerical aperture of 0.0015, whole length of ~6 m. In this system, the four total-reflection mirrors can also function as an energy filter that selectively reflects only low energy X-rays. This energy filter has reflectivity of 50 % at around 10 keV, but 3 x 10^-7 % at 20 keV, which can reduce excitation X-rays down to the weak fluorescence signal level. X-ray fluorescence imaging of a Siemens star chart (Ta) and micron-size particles (Ni, Cu, Zn, Ge and Bi) was demonstrated using excitation energy of 20 keV. The fluorescence signals were acquired with whole exposure time of 3.3 h, in which each exposure was selected to be 10 s to perform the photon counting method using the CCD. The samples were successfully visualized with a resolution of 500 ~ 1000 nm. Also, it was confirmed that the excitation X-rays were blocked well as expected.

10389-6, Session 2

Double-sided Fresnel zone plates for high-efficiency x-ray nanofocusing *(Invited Paper)*

Istvan Mohacsi, Deutsches Elektronen-Synchrotron (Germany) and Synchrotron SOLEIL (France) and Paul Scherrer Institut (Switzerland); Ismo Vartiainen, Paul Scherrer Institut (Switzerland) and Univ. of Eastern Finland (Finland); Manuel Guizar-Sicairos, Vitaliy A. Guzenko, Paul Scherrer Institut (Switzerland); Ian McNulty, Robert P. Winarski, Martin V. Holt, Argonne National Lab. (United States); Elisabeth Mueller, Paul Scherrer Institut (Switzerland); Andréa Somogyi, Synchrotron SOLEIL (France); Christian David, Paul Scherrer Institut (Switzerland)

Diffractive X-ray optics, like Fresnel zone plate lenses, are widely employed X-ray optics for collimation and focusing. While they are extremely versatile and easy to use optical elements, they generally suffer from limited efficiency due to limitations in fabrication possibilities. Near-field stacking is an established concept for overcoming fabrication limitations, yet its existing implementations suffer from issues regarding complexity and stability. In this work, an alternative stacking concept is explored, by patterning both the front and back sides of a single membrane. Such double-sided zone plates are shown to exchange conventional zone plate stacks in increasing the efficiency or resolution of conventional zone plate optics. In conventional stacking, they achieve 9.9% focusing efficiency at 9 keV with 30 nm smallest half-pitch and diffraction limited optical performance. Following the blazed stacking scheme, they are shown to provide up to 54.7% diffraction efficiency at 6.2 keV. Finally, using the novel concept of interlaced stacking, they demonstrate the feasibility of large aperture X-ray optics for sub-10 nm X-ray nanofocusing.

10389-7, Session 2

Development of 2D monolithic multilayer Laue lens nanofocusing optics for x-ray microscopy

Evgeny Nazaretski, Weihe Xu, Nathalie Bouet, Juan Zhou, Hanfei Yan, Xiaojing Huang, Yong S. Chu, Brookhaven National Lab. (United States)

We have developed an experimental approach to bond two independent linear Multilayer Laue Lenses (MLLs) together. A monolithic MLL structure was characterized using ptychography at 12 keV photon energy, and we demonstrated 12nm and 24 nm focusing in horizontal and vertical directions, respectively. Fabrication of 2D MLL optics allows installation of these focusing elements in more conventional microscopes suitable for x-ray imaging using zone plates, and opens easier access to 2D imaging with high spatial resolution in the hard x-ray regime. During the presentation technical steps of the fabrication and characterization process will be reviewed. Novel approach utilizing microfabrication methods suitable for the MLL bonding will be discussed.

10389-8, Session 2

Focus of a multilayer Laue lens with an aperture of 102 microns determined by ptychography at beamline APS/1-BM

Albert T. Macrander, Michael Wojcik, Jörg Maser, Argonne National Lab. (United States); Nathalie Bouet, Brookhaven National Lab. (United States); Raymond P. Conley, Argonne National Lab. (United States)

Ptychography was used to determine the focus of an MLL at beamline 1-BM at the Advanced Photon Source [1]. The MLL had a record aperture of 102 microns [2,3]. The focal length was 9.6 mm, and the outer-most zone was 4 nm thick. MLLs with ever larger apertures are under continuous development since ever longer focal lengths , ever larger working distances, and ever increased flux in the focus are desired. A focus size of 52 nm was determined by ptychographic phase retrieval from a gold grating sample with 1 micron lines and spaces over 6.0 microns horizontal distance. The probe function determined from the ptychography was used to measure the focus. The MLL was set to focus in the horizontal plane of the bending magnet beamline. A CCD having 13.0 micron pixels was used to collect data at 1.3 m downstream distance. The beam incident on the MLL was sized 10 micron (H) x 20 micron (V). 100 iterations of the difference map algorithm were sufficient to obtain a good reconstructed image as shown in the figure below. Here the amplitude and phase are represented by brightness and color, respectively. The units on the horizontal axis are 25.9 nm and the phase difference between lines and spaces is 2.00 radians corresponding to a gold thickness of 1.78 microns. The present work highlights the utility of a bending magnet source at the APS for performing coherence-based experiments. Use of ptychography at 1-BM on MLL optics opens the way to study other hard x-ray optics. We acknowledge the use of the ptychography tools of J. Clark and the assistance of R. Harder in implementing them. We also acknowledge T. Mooney for implementation of the software to scan over illumination views. This work was supported by the U.S. Department of Energy, Office of Basic Energy Sciences under contract No. DE-AC-02-06CH11357 for work at the APS and under contract No. DE-SC00112704 for work at NSLS II.

10389-9, Session 2

Commissioning of the Montel nano-optics for the x-ray nanoprobe at Taiwan Photon Source

Gung-Chian Yin, Shi-Hung Chang, Bo-Yi Chen, Chien-yu Lee, Bi-Hsuan Lin, Shao-Chin Tseng, Xiao-Yun Li, Huang-Yeh Chen, Jian-Xing Wu, Mau-Tsu Tang, National Synchrotron Radiation Research Ctr. (Taiwan)

The diffraction-limited Montel mirrors, equipped at the X-ray Nanoprobe (XNP) at Taiwan Photon Source (TPS), provide a 40 nm focal spot and working distance 55 mm under the total beamline length of 69 m. The underneath holder supporting for the Montel mirrors is a 12 axes flexure based manipulators in which 10 out of the 12 axes are motorized. To monitor the position and stability of individual holder motion, a monitoring system consisted of three optical encoders and three- axes laser interferometers for angle movement is implemented. The gap width between the two mirrors and their orthogonality can be adjusted by a tilting sensor and a high magnification optical microscope. The focusing properties, phase and amplitude, after the Montel mirrors will be investigated by means of coherent Ptychography, as well as by zone plate imaging. An SEM in close cooperation with laser interferometers is equipped to precisely position the samples and conduct the on-the-fly scan. A high speed FPGA based circuit is developed to address signal from XRF, XAS, XEOL and XRD. Data is in tag with position and time information and been processed by computers to allow 5nm precision stage scanning free from mechanical feedback. The XNP at TPS is under commissioning since February 2017. The commissioning result, particularly the performance of the Montel mirrors will be reported in this presentation.

10389-10, Session 3

Integration of ptychography with the nanoscale multimodality imaging instrument at HXN of NSLS-II *(Invited Paper)*

Xiaojing Huang, Hanfei Yan, Evgeny Nazaretski, Mingyuan Ge, Nathalie Bouet, Juan Zhou, Petr P. Ilinski, Yong S. Chu, Brookhaven National Lab. (United States)

Nano-focused hard X-ray probe offers a suite of analytic tools for quantitative characterization of specimen under investigation. Scanning probe operated in a multi-modality imaging mode evokes fluorescence, absorption, phase contrasts, and potentially diffraction contrast as well. Without introducing extra instrumental complexity, ptychography technique can be seamlessly integrated into the scanning probe imaging system, since it shares the same data collection procedure and even shares the exactly the same dataset with absorption- and differential-phase-contrast imaging. We will present our implementation of ptychography method for nano-Mii (Nanoscale Multimodality Imaging Instrument) at the Hard X-ray Nanoprobe (HXN) Beamline of the National Synchrotron Light Source II (NSLS-II). The ptychography reconstruction assist aligning optics to achieve diffraction-limited focus and provide quantitative images with enhanced resolution. The on-the-fly operation mode maximizes the experimental throughput, and make it timely realistic to conduct three-dimensional high-resolution imaging.

10389-11, Session 3

Multislice x-ray ptychography towards 3D high-resolution imaging

Kei Shimomura, Makoto Hirose, Osaka Univ. (Japan) and RIKEN SPring-8 Ctr. (Japan); Nicolas Burdet, RIKEN SPring-8 Ctr. (Japan); Yukio Takahashi, Osaka Univ. (Japan) and RIKEN SPring-8 Ctr. (Japan)

X-ray ptychography is a lensless imaging method to access inner information of a sample with high-spatial-resolution. In X-ray ptychography, the projection image of the sample is reconstructed by iterative phasing methods from multiple diffraction patterns. Moreover, X-ray ptychography combined with computed tomography provides high-resolution 3D images, which has been demonstrated with the 3D resolution of better than 20 nm. However, it is difficult to observe samples thicker than 1 ?m with the resolution of better than 10 nm due to the limitation of the depth of field. To eliminate this limitation, a new phase retrieval algorithm using multislice approach has been proposed and demonstrated in visible light and X-ray regime. Multislice approach models the object as multiple axial sections and calculates the wave propagation effects within a sample. In addition, mutlislice X-ray ptychography combined precession measurement has been demonstrated to improve the longitudinal resolution, in which a tilt-series diffraction patterns is collected and the multiple sections are reconstructed from them. Until now, precession multislice X-ray ptychography has been applied to a sample composed of discrete layers with a gap more than 10 ?m. To extend applications to discrete samples with a narrow gap between layers and continuous samples, we performed the feasibility study by numerical simulations using 2-?m-thickness sample composed of two Cu TEG tips and 3-?m-thickness Au nanoporous. In this presentation, we intend to show experimental results at SPring-8.

10389-12, Session 3

Nanoscale x-ray imaging using the GINIX Instrument: combining zoom-holography and nano-scanning

Markus Osterhoff, Georg-August-Univ. Göttingen (Germany); Michael Sprung, Deutsches Elektronen-Synchrotron (Germany); Tim Salditt, Georg-August-Univ. Göttingen (Germany)

The Göttingen Instrument for Nano-Imaging with X-ray (GINIX) is a holography endstation located at the P10 beamline at PETRA III, designed and operated by the University of Göttingen in close collaboration with DESY Hamburg [1-2]. GINIX is designed as a waveguide based holography experiment with a Kirkpatrick-Baez pre-nanofocus. Its versatility has stimulated a great manifold of imaging modalities. Today, users choose the GINIX setup not only for its few nm coherent waveguide beams (e.g. for ptychography or holography), but also to carry out scanning SAXS measurements to probe local anisotropies with sub-micron real-space and even higher reciprocal space resolution. In addition, it is possible to combine different detectors for e.g. simultaneous SAXS/WAXS and fluorescence measurements [3].

We present latest experimental results obtained with GINIX, focusing on the unique capabilities offered by its versatile and flexible design. The overview includes results from different imaging schemes such as waveguide based zoom-tomography and user examples in WAXS geometry. We show how to correlate complementary techniques like holography and scanning SAXS and present first results obtained using a new fast sample scanner for Multilayer Zone Plate imaging. We conclude by summarizing the ongoing upgrades and discussing new possibilities for our users.

[1] T. Salditt et al., Journal of Synchrotron Radiation 22 (2015).

[2] S. Kalbfleisch et al., AIP Conference Proceedings 1365 (2011).

[3] J. Wallentin et al., Journal of Applied Crystallography 48 (2015).

10389-13, Session 3

PtyNAMi: Ptychographic nano-analytical x-ray microscope at PETRA III

Christian G. Schroer, Deutsches Elektronen-Synchrotron (Germany) and Univ. Hamburg (Germany); Andreas Schropp, Ralph Döhrmann, Stephan Botta, Deutsches

Elektronen-Synchrotron (Germany); Dirk Samberg, TU Dresden (Germany); Maik Kahnt, Mikhail Lyubomirskiy, Juliane Reinhardt, Maria Scholz, Martin Seyrich, Felix Wittwer, Dennis Brückner, Jan Garrevoet, Gerald Falkenberg, Deutsches Elektronen-Synchrotron (Germany)

In recent years, ptychography has revolutionized x-ray microscopy in that it is able to overcome the diffraction limit of x-ray optics, pushing the spatial resolution limit down a few nanometers. However, due to the weak interaction of x-rays with matter the detection of small features inside a sample require a high coherent fluence on the sample, a high degree of mechanical stability, and a low background signal from an x-ray microscope. The x-ray scanning microscope PtyNAMi at PETRA III at DESY in Hamburg, Germany, is designed for high-spatial-resolution 3D imaging with high sensitivity. To optimize the coherent flux density on the sample, a two-stage focusing scheme matches the coherence length to the aperture of the nanofocusing optic. The sample is scanned (also continuously) with a high-precision scanner and the sample position is tracked interferometrically with respect to the x-ray optical axis, also under the rotation needed for tomographic scanning. Finally, the optical path behind the sample is evacuated up until the sensor of a four-megapixel pixel detector that is placed into the vacuum. In this way, parasitic scattering from air and windows close to the detector are avoided. A beamstop can be used to suppress scattering inside the detector in order to capture even weakest scattering signals from small features inside a sample. The new instrument is presented together with some applications.

10389-14, Session 3

High-energy cryo x-ray nano-imaging at the ID16A beamline of ESRF *(Invited Paper)*

Julio C. da Silva, Alexandra Pacureanu, Yang Yang, Florin Fus, Maxime Hubert, Leonid Bloch, Murielle Salome, ESRF - The European Synchrotron (France); Sylvain Bohic, ESRF - The European Synchrotron (France) and Grenoble Institut des Neurosciences (France); Peter Cloetens, ESRF - The European Synchrotron (France)

The ID16A nano-imaging beamline at ESRF offers unique capabilities for X-ray imaging at nanometer scale and currently produces the world's brightest diffraction-limited nanofocus. Such a nanoprobe was designed for quantitative 3D characterization of the morphology and the elemental composition of specimens at the nanoscale. As the endstation is located at 185 m from the source, the beamline is optimized for coherent hard X-ray imaging with very high photon flux (1012 photons/s at ?E/E~1%), at the ultimate spatial resolution (~20 nm). Billions of photons per second can be delivered in a diffraction-limited focus spot size of about 13 nm. The two discrete energies of operation, 17.05 keV and 33.6 keV, are well suited for applications in biomedicine, materials science and nanotechnology. Coherent X-ray imaging techniques, as magnified holographic tomography and ptychographic tomography, provide the distribution of the electron density at length scales ranging from ~130 nm down to ~10 nm, while keeping a relatively large field of view. Complementary, X-ray fluorescence microscopy delivers label-free highly efficient trace element quantification with detection limit down to ppm level. In addition, an integrated cryogenic system operating under high vacuum has been installed to preserve biological samples from radiation damage at temperatures close to 120 K. Finally, we will show the latest developments in coherent and spectroscopic X-ray nano-imaging implemented at our beamline and important applications.

10389-15, Session 3

X-ray fluorescence nanotomography of single cells at 20-nm voxel resolution

Tiffany W. Victor, Stony Brook Univ. (United States); Lindsey M. Easthon, Katherine H. O'Toole, Boston Univ. (United States); Hanfei Yan, Xiaojing Huang, Mingyuan Ge, Brookhaven National Lab. (United States); Karen Allen, Boston Univ. (United States); Barbara Imperiali, Massachusetts Institute of Technology (United States); Yong S. Chu, Lisa M. Miller, Brookhaven National Lab. (United States)

X-ray Fluorescence (XRF) microscopy is a powerful method for imaging trace element concentration, distribution, and speciation in biological cells at the nanoscale. Moreover, nanotomography provides the added advantage of imaging subcellular structure and chemistry in 3D without the need for staining or sectioning the cells. To date, technical challenges in X-ray optics, sample preparation, and detection sensitivity have limited the use of XRF nanotomography on biological cells.

In this work, XRF nanotomography was used to image individual E. coli bacterial cells for the first time at ~20 nm voxel resolution. The measurement was performed using nano-Mii (Nanoscale Multimodality Imaging Instrument) at the Hard X-ray Nanoprobe (HXN, 3-ID) beamline at NSLS-II. Typically, cryo-fixation is used to prevent radiation damage and preserve integrity of biological samples. Instead, we embedded cells in small (5-20 µm) NaCl crystals, which provided a nonaqueous matrix to retain the 3D structure of the E. coli while minimizing radiation damage. Tomography was performed from +/- 90 degrees in 3 degree increments with a dwell time of 100 ms per pixel.

Results showed the distribution of Ca, K, S, P, Fe, and Zn with sufficient resolution to visualize cell membranes. Our work demonstrates that XRF nanotomography can be performed on unfrozen biological cells to co-localize and quantify elements and show their distribution and speciation in whole cells at very high spatial resolution.

10389-16, Session 4

Rapid alignment of projection images in x-ray nanotomography: extension to phase-contrast imaging *(Invited Paper)*

Doga Gürsoy, Argonne National Lab. (United States); Young Pyo Hong, Kuan He, Karl Hujsak, Seunghwan Yoo, Northwestern Univ. (United States); Si Chen, Vincent De Andrade, Argonne National Lab. (United States); Kai He, Oliver Cossairt, Aggelos K. Katsaggelos, Chris J. Jacobsen, Northwestern Univ. (United States)

As x-ray tomography is pushed farther into the nanoscale, the limitations of rotation stages become more apparent leading to challenges in the alignment of the acquired projection images. We have developed an approach for rapid post-acquisition alignment of these projections based on a joint estimation of alignment errors, and the object, using an iterative refinement procedure, and have demonstrated it on x-ray absorption and fluorescence nanotomography. However, phase contrast offers a stronger signal for hard x-ray imaging than either absorption or fluorescence provide, and its potential for low-dose x-ray fluorescence tomography has already been explored in previous studies. We describe here our first tests of using our iterative re-projection approach with phase-contrast images included in the alignment iterate.

10389-17, Session 4

Self-absorption correction in x-ray fluorescence nanotomography

Mingyuan Ge, Xiaojing Huang, Hanfei Yan, Evgeny Nazaretski, Li Li, Petr P. Ilinski, Brookhaven National Lab. (United States); Wilson K. S. Chiu, Univ. of Connecticut (United States); Kyle S. Brinkman, Clemson Univ. (United States); Yong S. Chu, Brookhaven National Lab. (United States)

The Hard X-ray Nanoprobe (HXN) at NSLS-II provides a nanoscale 3D multi-modality imaging capability, useful for investigating diverse material systems. The multi-modality scanning-probe imaging utilizes a variety of imaging contrasts such as fluorescence, transmission, scattering, and diffraction. Images taken simultaneously using different contrast mechanisms can provide 3D visualization of a sample, producing complementary information about the sample. Such comprehensive 3D characterizations are extremely useful in studying materials with multiple phases or complex internal structures. An important scientific problem is to investigate phase or grain boundaries of multi-component materials during or after material processing such as sintering, since re-organization of these boundaries due to annealing or phase-separation often result in profound impact on material property or functionality. However, accurate quantification of 3D elemental concentration is hampered by a well-known self-absorption problem, particularly severe for the low energy fluorescence x-rays. Correcting absorption is non-trivial and requires an iterative and three-dimensional solution. In this presentation, we will describe our approach using experimental data taken from mixed ionic ceramic membrane samples and elaborate on how accurate absorption correction led to discovery of a new material phase in this material system.

10389-29, Session PMon

Faster scanning and higher resolution: New setup for multilayer zone plate imaging

Markus Osterhoff, Christian Eberl, Jakob Soltau, Hans-Ulrich Krebs, Georg-August-Univ. Göttingen (Germany)

Hard x-ray imaging methods are routinely used in two and three spatial dimensions to tackle challenging scientific questions of the 21st century, e.g. catalytic processes in energy research and bio-physical experiments on the single-cell level [1-3]. Among the most important experimental techniques are scanning SAXS to probe the local orientation of filaments and fluorescence mapping to quantify the local composition. The routine available spot size has been reduced to few tens of nanometres; but the real-space resolution of these techniques can degrade by (i) vibration or drift, and (ii) spreading of beam damage, especially for soft condensed matter on small length scales.

We have recently developed new Multilayer Zone Plate (MZP) optics for focusing hard (14 keV) and very hard (60 keV to above 100 keV) x-rays down to spot sizes presumably on 5 or 10 nm scale. Here we report our progress on a new MZP based sample scanner, and how to tackle beam damage spread. The Eiger detector synchronized to a piezo scanner enables to scan in a 2D continuous mode fields of view larger than 20 μm squared, or for high resolution down to (virtual) pixel sizes of below 2 nm, in less than three minutes for 255?255 points (90 seconds after further improvements). Nano-SAXS measurements with more than one million real-space pixels, each containing a full diffraction image, can be carried out in less than one hour, as we have shown using a Siemens star test pattern.

[1] M. Bernhardt et al., New Journal of Physics (accepted; 2017).

[2] C. Hémonnot et al., ACS Nano (2016).

[3] M. Priebe et al., Biophys Journal (2014).

10389-30, Session PMon

PyXRF: Python-based x-ray fluorescence analysis package

Li Li, Brookhaven National Lab. (United States)

We developed a python-based fluorescence analysis package (PyXRF) at the National Synchrotron Light Source II (NSLS-II) for the X-ray fluorescence-microscopy beamlines, including Hard X-ray Nanoprobe (HXN), and Submicron Resolution X-ray Spectroscopy (SRX). This package contains a high-level fitting engine, a comprehensive command-line/GUI design, rigorous physics calculations, and a powerful visualization interface. PyXRF offers a method of automatically finding elements, so that users do not need to spend extra time selecting elements manually. Moreover, PyXRF provides a convenient and interactive way of adjusting fitting parameters with physical constraints. This will help us perform sensitivity analysis, and find an appropriate initial guess for fitting. Furthermore, we also create an advanced mode for professional users to construct their own fitting strategies with a full control of each fitting parameter. PyXRF runs single-pixel fitting at a fast speed, which opens up the possibilities of viewing the results of fitting in real time during experiments. A convenient I/O interface was designed to obtain data directly from NSLS-II's experimental database. PyXRF is under open-source development and designed to be an integral part of NSLS-II's scientific computation library.

10389-31, Session PMon

Device for interferometric characterization of rotation stages for x-ray nanotomography

Stefan Kubsky, Synchrotron SOLEIL (France); Tomas Stankevic, Max IV Lab. (Sweden); Christer Engblom, Florent Langlois, Filipe Alves, Alain Lestrade, Nicolas Jobert, Gilles Cauchon, Synchrotron SOLEIL (France); Ulrich Vogt, KTH Royal Institute of Technology (Sweden)

State-of the art X-ray nanoanlyses in 3D, such as XRF, Ptychography and Tomography require not just brilliant and focussed x-rays, but also fine-positioning on a nm-level during experiment. A key difficulty is the need to rotate the sample by 360° to obtain a 3D reconstruction. We have designed and built a new, compact device which characterizes mechanical errors of rotation stages: we demonstrate that repeatable and non-repeatable radial- and angular errors (wobble) can be quantified without relying on a nm-level precise metrology standard-object. This approach comprises an optomechanical setup with several interferometric sensors and a mathematical method to separate the abovementioned errors of the rotation stage from the (non-perfect) cylindrical shape of the measuring object. Obtained precision with active feedback via additional correction stages yields down to 40nm, other examples show even much lower values, down to the nm-level. For less demanding applications, a fixed Look-up-table (LUT) can be employed, simplifying metrological requirements during experiment. Furthermore, the measurement procedure is fully automated and integrated into the SOLEIL software architecture (TANGO). Time requirements are compatible with systematic, repeated measurements (approximately 15 min. per scan). Nm-level precision on macroscopic lenght scales calls for dedicated thermal monitoring and stabilization (mK-level), which is integrated as well.

Applications include live-error correction during experiment, but also production of better rotation stages for industry.

10389-32, Session PMon

Quantitative analysis of the reoxidation stability of Ni-Fe anode for solid ox-ide fuel cells using x-ray nanotomography

Yong Guan, Yangchao Tian, Univ. of Science and Technology of China (China)

Ni-Fe alloy as anode for solid oxide fuel cells (SOFCs) has attracted much attention recently. Ni-Fe alloy anode has a better tolerance to redox cycling as compared to the Ni-YSZ cermet anode and porous Ni metal. X-ray nanotomography had been applied to investigate porous nickel-yttria-stabilized zirconia (Ni-YSZ) composite anode. The quantitative analysis methods had been devel-oped and used to characterize and quantify the key structural parameters. In the present work, the mechanisms of redox stability of Ni-Fe alloy anode had been studied by X-ray nanotomography at beamline 4W1A at the Beijing Synchrotron Radiation Facility (BSRF), China. The resolution is about 30 nm and field of view (FOV) is 15 um. The results indicated that a small amount of Fe ad-dition can affect the microstructure of anode during redox cycling. After a redox cycling, the microstructure of

Ni-YSZ anode was different from that of Ni-Fe-YSZ anode with 9.4 wt% Fe . For example, Ni grain in Ni-Fe-YSZ anode was smaller than that of Ni-YSZ anode. This can be said that the microstructure of Ni-Fe-YSZ anode was better compared to Ni-YSZ anode after a redox cycling, which had been further proved by the calculation on the three phase boundary length. This indicated that 9.4 wt% Fe can improve the redox stability of Ni-YSZ anode.

10389-33, Session PMon

An analytical method for extending the depth-of-focus in x-ray microscopy

Yangchao Tian, Yong Guan, Univ. of Science and Technology of China (China)

X-ray microscopy (XRM) as a powerful, nondestructive and three dimensional (3D) imaging tool has been applied in many fields. However, for the high-resolution X-ray microscopy, to image large size samples is restricted due to a limited depth of focus (DOF). In this study, an analytical method for extending the depth of focus of X-ray microscopy was proposed. By moving the ZP, many sets of projections are collected. Then these sets of projections are reconstructed respectively by filtered back-projection (FBP) reconstruction algorithm to get the 3D reconstructions. Based on the features of 3D reconstruction data, the slices of 3D reconstruction data are regarded as different focus-stacked images, which contain different in-focus and defocus information. By analyzing the slices stack of 3D reconstruction data along the optical axis, the slices are fused by the image fusion algorithm. Through the slices stack image fusion, the slices stack at same position are fused into a fully in-focus image. When all slices are fully in-focus, a new 3D reconstruction data with all-focused is achieved. The simulation and experimental results demonstrate the novel method is effective and reliable in extending the DOF of high-resolution X-ray microscopy and can be applied to image the large sample for high resolution X-ray microscopic system.

10389-34, Session PMon

Three-dimensional imaging of biological samples and nanomaterials using soft x-ray nanotomography

Gang Liu, Jianhong Liu, Yong Guan, Univ. of Science and Technology of China (China)

The full-field Transmission X-ray Microscopy beamline BL07W at NSRL is devoted to cryo nano-tomography for biological applications in the water window (284 - 530 eV) and for imaging of nanomaterials from 200 to 2500 eV. An ellipsoidal capillary used as condense to focus monochromatic light onto the sample. Two Ni zone plate (ZP) lenses made by Zeiss with 40 nm and 25 nm outer most zone widths, respectively, are available, giving spatial resolution in 2D of down to 40 nm and 30 nm, respectively. Hydrated biological specimens had been imaged in the water window photon energy range without chemical fixation, dehydration, chemical staining and physical sectioning. A tilt series images were collected from ? 60o + 60o at 1o intervals at 520 eV X-ray energy. Each projection was collected with an exposure time of 1 seconds. Alignment and reconstruction of the tilt series were carried out with filtered back-projection algorithm from Carl Zeiss X-ray Microscopy Inc and some algorithms developed in-house based on algebraic reconstruction techniques[1-2]. We had demonstrated cryo soft X-ray tomography of frozen hydrated biological samples in the water window energy range with spatial resolution down to 40 nm and the studies of nano-materials. The results shown that soft X-ray nanotomography can provide an alternative tool for people to study hydrated biological specimens and nano-materials.

Reference:

1. Zhiting Liang et al., Journal of synchrotron radiation (2016). 23, 606–616

2. Lei Wang et al., Journal of synchrotron radiation, accepted.

10389-35, Session PMon

Fully automatic sample alignment with VLM at the STXM beamline of SSRF

Xiangzhi Zhang, Zhi Guo, Limei Ma, Zijian Xu, Haigang Liu, Zhenhua Chen, Jiefeng Cao, Yong Wang, Renzhong Tai, Shanghai Institute of Applied Physics (China)

Three-dimensional fine structure of the sample with high spatial resolution is very important in many area. Nano-CT system based on the STXM BL08U soft X-ray spectromicroscopy station of Shanghai Synchrotron Radiation Facility has been developed. STXM is based on two dimensions image the focal length is about 2um, 1um accuracy is necessary for the beam direction. The scanning area of sample is several um scale sample which drifted seriously during the rotation, the accuracy and efficiency be reduced seriously which waste much beamtime. Fully automatic sample alignment involves the application of optical methods to identify the sample with Visible Light Microscope be founded. The relative axis positon of sample and rotation motor can be calculated by the VLM data, then make it two coincidence and move into the X-ray beam. All the alignment process can be completed before experiment automatic.This can be used in many other CT experiment.

10389-36, Session PMon

Detection limits for the inverse analysis of Bragg coherent diffraction data

Hande Öztürk, Xiaojing Huang, Hanfei Yan, Yong S. Chu, Brookhaven National Lab. (United States)

Bragg Coherent Diffraction has been an increasingly used, non-destructive imaging technique that can characterize the structure of isolated nanocrystals and their apparent strain distributions. Although numerous successful reconstructions of nanomaterial samples have been published in the literature, where nano-scale spatial resolution and ultimate sensitivity have been reported, there is currently no systematic study on the inherent limits of this technique.

In this presentation, I will introduce a framework that is capable of numerically simulating Bragg Coherent Diffraction Imaging (Bragg CDI) experiments. The three-dimensional rocking-curve diffraction data are generated using first-principle forward modeling algorithm that considers crystalline lattice structure, shape function and dislocation field inside an irradiated particle. The simulated data can then be inverted with established phase recovery techniques to deliver real-space images. By systematically investigating the performance of the Bragg CDI method using this framework, the detection limits of dislocation field under various oversampling conditions, noise levels and detection dynamic range are explored. These results have the potential to improve the assessment of reconstructed phases from Bragg CDI experiments and to optimize practical guidelines for experimental scenarios.

10389-38, Session PMon

Progress of ptychography method at STXM beamline of SSRF

Zijian Xu, Haigang Liu, Chunpeng Wang, Xulei Tao, Renzhong Tai, Shanghai Institute of Applied Physics (China)

We have been developing the methodology of soft X-ray ptychographic coherent diffraction imaging (PCDI) in recent years based on the STXM beamline of SSRF. A series of algorithmic and experimental studies of PCDI methodology were carried out in depth, and a PCDI platform with relatively low dose, high resolution and high efficiency have been developed at STXM endstation of SSRF. Compared to other FZP-based PCDI setups, we used a much larger illumination spot with 3-5 ?m diameter by moving

samples downstream from ZP focus, and a larger step size of 500-1000 nm in our platform, which would result in fewer scanning positions and lower radiation dose when imaging the same sample area, but leading to a more difficult reconstruction due to the highly curved wavefront of the probe. By combining the mixed-state method or up-sampling method with the position-correction algorithm in our home-developed ptychography reconstruction software, we can obtain high-quality images (10 nm resolution) from our PCDI platform with much lower radiation dose (1/12 of STXM) and less data acquisition time (1/3 of STXM). In addition, we systematically investigated the effects of beamstop-induced low frequency signal loss on both the PCDI and plane-wave CDI by simulations, finding that PCDI can tolerate much more low-frequency signal loss than plane-wave CDI, and the PCDI robustness to missing signals is further improved when a larger overlap or a smaller probe is adopted. This work suggests that a beamstop can be applied in PCDI to further improve the imaging resolution. We also developed practical background noise removal methods for ptychography datasets including the difference minimization, thresholding and local erasing techniques, which could notably improve the reconstruction image quality and would be helpful in most ptychography experiments.

10389-39, Session PMon

Complementing cryo x-ray microscopy with a compatible confocal microscope for biological applications

Si Chen, Oliver Schmidt, Argonne National Lab. (United States); Qiaoling Jin, Northwestern Univ. (United States); Amanda Petford-Long, Chris J. Jacobsen, Argonne National Lab. (United States)

Hard X-ray fluorescence microscopy (XFM) and visible light fluorescence microscopy (VLFM) provide complimentary information for biological studies. While XFM allows one to measure the distribution and total content of an element regardless of its valence and chemical binding state, VLFM enables imaging of certain elements in specific chemical states via fluorophore labeling. By using cryo specimen preparation, biological samples can be studied in a frozen hydrated state with both the ultrastructure and elemental distribution preserved closest to their natural state.

There is a rapid growth of activity in correlative cryo light and electron microscopy (CLEM)1,2, and this has been followed by correlative light and soft X-ray microscopy3-6. Compared to CLEM, where cryosections thinner than 100 nm are examined, or soft x-ray microscopy where depth of focus and absorption limit the sample thickness to ~10 ?m, XFM is particularly suitable for studies of thick samples such as tomography of whole cells or of tissues that are tens of microns thick. The Bionanoprobe (BNP)7 is the only cryo-XFM instrument in the US, dedicated to studying soft materials, in particular biological samples in a frozen hydrated state (other cryo XFM instruments have been demonstrated at Spring-8, ESRF, and Petra III). To complement the BNP, we are developing a correlative cryo confocal light microscope (C3LM), which we believe will be the first of its kind for studies alongside cryo XFM. The C3LM system incorporates a Nikon confocal system (340 nm lateral and 700 nm depth resolution) and a cryo sample cartridge and transfer system compatible with the BNP. Confocal imaging capability is important for imaging of thick samples, and will allow correlative 3D studies coupled with the BNP. In this presentation, we will discuss the design philosophy of the C3LM system and show progress towards its operation.

1. Sartori, A. et al. Correlative microscopy: Bridging the gap between fluorescence light microscopy and cryo-electron tomography. Journal of Structural Biology 160, 135–145 (2007).

2. Schwartz, C. L., Sarbash, V. I., Ataullakhanov, F. I., Mcintosh, J. R. & Nicastro, D. Cryo-fluorescence microscopy facilitates correlations between light and cryo-electron microscopy and reduces the rate of photobleaching. Journal of Microscopy 227, 98–109 (2007).

3. Le Gros, M. A., McDermott, G., Uchida, M., Knoechel, C. G. & Larabell, C. A. High-aperture cryogenic light microscopy. Journal of Microscopy 235, 1–8 (2009).

4. Schneider, G., Guttmann, P., Rehbein, S., Werner, S. & Follath, R. Cryo X-ray microscope with flat sample geometry for correlative fluorescence and nanoscale tomographic imaging. Journal of Structural Biology 177, 212–223 (2012).

5. Chichón, F. J. et al. Cryo X-ray nano-tomography of vaccinia virus infected cells. Journal of Structural Biology 177, 202–211 (2012).

6. Duke, E. M. H. et al. Imaging endosomes and autophagosomes in whole mammalian cells using correlative cryo-fluorescence and cryo-soft X-ray microscopy (cryo-CLXM). Ultramicroscopy 143, 77–87 (2014).

7. Chen, S. et al. The Bionanoprobe: hard X-ray fluorescence nanoprobe with cryogenic capabilities. J. Synchrotron Rad 21, 66–75 (2014).

10389-40, Session PMon

Streamlining data analysis for x-ray fluorescence microscopy

Arthur Glowacki, Argonne National Lab. (United States)

X-ray fluorescence microscopy (XFM) experiments involve attention and time to set up a proper experiment and analyze the results. The accurate analysis of XRF data requires multiple parameters and deep knowledge of the scanning equipment. While simple, fast approaches exist (eg, 'spectral ROIs') these tend not to do work well with more complex data (eg, overlapping peaks). We have implemented several different fast and more accurate analysis methods. To streamline the analysis, and make optimum use of dedicated analysis machines, we created a web interface to submit XRF analysis jobs, and give feedback on processing status and results of specific jobs. The interface significantly simplifies the analysis process and can be expanded to pass jobs from one technique to another such as tomography. Additional processes submit jobs automatically for user experiments that are in progress, as scans finish. Future work will utilize Globus to transfer results off site automatically for users, as well as allow users to remotely use analysis servers for additional processing.

10389-41, Session PMon

Fast hierarchical length-scale morphological, compositional, and speciation imaging at the Nanoscopium Beamline Synchrotron Soleil

Kadda Medjoubi, Gil Baranton, Synchrotron SOLEIL (France); Maria Sancho-Tomas, Synchrotron SOLEIL (France) and Institut de Physique du Globe de Paris (France); Pascal Philippot, Institut de Physique du Globe de Paris (France); Andréa Somogyi, Synchrotron SOLEIL (France)

The Nanoscopium [1] 155 m-long nanoprobe beamline of Synchrotron Soleil (St Aubin, France) is dedicated to scanning multi-modal imaging in the 5-20 keV energy range. It offers 2D/3D information on the elemental composition, speciation and morphology through the combination of complementary techniques such as X-ray fluorescence, X-ray absorption near edge structure spectroscopy (XANES), absorption, phase contrast and dark field imaging. The fast (down to 3 ms per pixel dwell time) and multi-technique Flyscan acquisition scheme [2] is implemented at the beamline and opens the possibility of hierarchical length-scale multi-technique imaging. Fast measurements also provide access to XANES imaging and 3D XRF tomography for user experiments.

The understanding of real complex geological and geo-biological processes depends increasingly on such in-depth chemical studies. We present here such a multi-technique, hierarchical length-scale approach, including the study of the variation of the elemental composition, morphology and chemical speciation combined with multivariate statistical data-treatment in order to understand the processes determining the sub-micron scale variation of As speciation in complex highly heterogeneous samples in natural conditions.

[1] Somogyi, A. et al. (2015). Journal of synchrotron radiation, 22(4), 1118-1129.

[2] Medjoubi, K. et al. (2013). Journal of synchrotron radiation, 20(2), 293-299.

10389-19, Session 5

Current status of the Hard X-Ray Nanoprobe beamline at the SSRF *(Invited Paper)*

Aiguo Li, Hui Jiang, Yan He, Hua Wang, Zhaohong Zhang, Gaofeng Zhao, Shanghai Institute of Applied Physics (China)

The hard X-ray nanoprobe beamline (HXN) designed at the Shanghai Synchrotron Radiation facility (SSRF) will be of capability to realize a focal spot size of 10 nm for hard X-rays to satisfy requirements in biology, environmental, material sciences and etc. The beamline includes two modes of operation, high energy resolution mode and high flux mode respectively. High energy resolution mode uses a total-reflection KB system to reach 50 nm with the energy of 5-25 keV. High flux mode utilizes the multilayer KB system to obtain high-flux diffraction-limited focusing of ~10nm. Diffraction-limited focusing requires an ultra-high-precision figure fabrication to satisfy the Rayleigh Criterion. In this case, the allowed PV roughness for KB mirror cannot be polished directly. An idea to overcome this problem is to introduce a phase compensator system [1] upstream of the KB system to compensate the wavefront errors in the beamline. At wavelength speckle-based method [2] will be used to measure the wavefront error in the beamline and feedback to the phase compensator to adjust the figure shape by PZT elements. Related studies were being carried out and demonstrated in our hard X-ray mirco-focusing beamline.

[1] H.Mimura, S.Handa, T.Kimura, Nature Physics 6, 2010, 122-125

[2] H.Wang, Y.Kashyap and K.Sawhney, Optics Express 23(18), 2015, 23310-7

10389-20, Session 5

First x-ray nanoimaging experiments at NanoMAX

Ulrich Vogt, Karolis Parfeniukas, KTH Royal Institute of Technology (Sweden); Tomas Stankevic, Sebastian Kalbfleisch, Zdenek Matej, Alexander Björling, Marianne Liebi, Gerardina Carbone, Max IV Lab. (Sweden); Anders Mikkelsen, Lund Univ. (Sweden); Ulf Johansson, Max IV Lab. (Sweden)

NanoMAX is a hard x-ray nanoprobe beamline at the new Swedish synchrotron radiation source MAX IV that became operational in 2016. Being a beamline dedicated to x-ray nanoimaging in both 2D and 3D, NanoMAX is the first to take full advantage of MAX IV's exceptional low emittance and resulting coherent properties. We will present results from the first experiments at NanoMAX that took place in December 2016. These did not use the final endstations that will become available to users during 2017, but a temporary arrangement including a zone plate and order-sorting aperture stage and a piezo-driven sample scanner. We used zone plates with outermost zone widths of 100 nm and 30 nm and performed experiments at 8 keV photon energy on x-ray fluorescence and ptychography, both in step-scan and fly-scan mode. Moreover, we investigated stability and coherence with a Ronchi test method. Despite the rather simple setup, we could demonstrate spatial resolution below 50 nm after only few hours of beamtime. The results showed that the beamline is working as expected and experiments approaching the 10 nm resolution level or below should be possible in the future.

10389-21, Session 5

Development of the PtychoProbe Beamline at the Advanced Photon Source

Volker Rose, Jörg Maser, Junjing Deng, Barry Lai, Argonne National Lab. (United States); Tonio Buonassisi, Massachusetts Institute of Technology (United States); David Fenning, Univ. of California, San Diego (United States); Ross Harder, Chris J. Jacobsen, Argonne National Lab. (United States); Rafael Jaramillo, Massachusetts Institute of Technology (United States); Antonio Lanzirotti, The Univ. of Chicago (United States); Eugene M. Lavely, BAE Systems (United States); Karen Mulfort, Argonne National Lab. (United States); Conal E. Murray, IBM Thomas J. Watson Research Ctr. (United States); Stephen R. Sutton, David Tiede, Curt A. Preissner, Argonne National Lab. (United States); Gayle Woloschak, Northwestern Univ. (United States); Stefan Vogt, Argonne National Lab. (United States)

The multiscale and multi-modal understanding of advanced materials via x-ray microscopy has been recognized as one of the great challenges of science end engineering in the coming decades. It will lead to dramatic changes in the ways materials, devices, and systems are understood and created. The goal of the PtychoProbe (Ptychography + Nanoprobe) beamline is to realize the highest possible spatial resolution in x-ray microscopy both for structural and chemical information with scan rates up to 1,000 times faster than currently possible. This will enable visualization across all relevant length scales, nanoscale, mesoscale, and macroscopic, using a single experimental technique. The unprecedented brightness of the future multi-bend achromat lattice for the Advanced Photon Source will be exploited to produce a nanoscale beam of focused hard X-rays (e.g., 5 nm in size) to achieve the highest possible sensitivity to trace elements. Ptychography will be used to further improve the spatial resolution for structural components to its ultimate limit at the 1-nm-scale, only limited by the radiation hardness of the sample. The proposed beamline will enable high-resolution two- and three-dimensional imaging of thick objects, and bridge the resolution gap between contemporary x-ray and electron microscopy. Pushing x-ray microscopy into the nanoscale is crucial for understanding complex hierarchical systems on length scales from atomic up to meso and macroscales, and time scales down to the microsecond level, and is applicable to scientific questions ranging from biology to earth and environmental materials science, to electrochemistry, catalysis and corrosion, and beyond.

10389-22, Session 5

The Velociprobe: A fast hard x-ray nanoprobe for ptychographic imaging

Junjing Deng, Curt A. Preissner, Christian Roehrig, Michael Wojcik, Shane Sullivan, Argonne National Lab. (United States); David J. Vine, Lawrence Berkeley National Lab. (United States); Barry Lai, Stefan Vogt, Argonne National Lab. (United States)

Motivated by the Advanced Photon Source Upgrade (APS-U), a new hard X-ray microscope called "Velociprobe" has been recently designed and built for fast ptychographic imaging with high spatial resolution. We are addressing the challenges of high-resolution and fast scanning with novel hardware/stage designs, new positioner control designs, and new data acquisition strategies, including the use of high bandwidth interferometric measurements. The use of granite, air-bearing-supported stages provides the necessary long travel ranges for coarse motion to accommodate real samples and variable energy operation while remaining highly stable during fine scanning. Scanning the low-mass zone plate enables high-speed high-precision motion of the probe over the sample. Our primary goal is to use

this instrument to demonstrate sub-10 nm spatial resolution ptychography over a 1-square-micron area in under 10 seconds. We have also designed the instrument to take advantage of the upgraded source when the APS-U is completed. This presentation will describe the unique designs and characteristics of this instrument, and some preliminary data obtained during the instrument commission.

10389-23, Session 5

High-resolution chemical imaging using hard x-ray spectro-ptychography

Makoto Hirose, Kei Shimomura, Osaka Univ. (Japan) and Japan Synchrotron Radiation Research Institute (JASRI) (Japan); Nicolas Burdet, Japan Synchrotron Radiation Research Institute (JASRI) (Japan); Yukio Takahashi, Osaka Univ. (Japan) and Japan Synchrotron Radiation Research Institute (JASRI) (Japan)

X-ray ptychography is a method for reconstructing the complex-valued image of an extended specimen from multiple diffraction dataset by using iterative phase retrieval calculation. Hard X-ray spectro-ptychography, which involves multiple-energy ptychogrphy measurements around the absorption edge of a specific element, allows us to visualize the chemical composition mapping of micrometer-sized bulk materials since X-ray absorption fine structure (XAFS) can be reconstructed. A major difficulty of hard X-ray spectro-ptychography is due to the weak absorption of hard X-rays. We here propose the use of the Kramers-Kronig relation as an additive constraint (KKR constraint) to improve the convergence of phasing method of spectro-ptychography. A proof-of-principle experiment was carried out at SPring-8 BL29XUL. A 600-nm-thick Mn_2O_3 layer was deposited on a 500-nm-thick SiN membrane, and then both a pattern comprising the characters of 'SPring-8' and a square hole were fabricated using a focused ion beam. Fourteen X-ray energies were selected between 6.530 keV and 6.588 keV, around the K absorption edge of Mn. The incident X-rays were two-dimensionally focused to a 500 nm (FWHM) spot size using a pair of Kirkpatrick-Baez mirrors. Ptychographic coherent diffraction patterns were collected in a 7 by 7 overlapping view with a 400 nm step width. Sample images were reconstructed with a spatial resolution of 41.1 nm and reconstructed XAFS was improved by using KKR constraint. Hard X-ray spectro-ptychography using KKR constraint can be applied heterogeneous bulk materials, such as oxygen storage/release particles used in three-way catalyst system.

10389-24, Session 6

Time-resolved x-ray diffraction microscopy at Advanced Photon Source

Zhonghou Cai, Yi Zhu, Haidan Wen, Martin V. Holt, Argonne National Lab. (United States)

The high tendency of structural response to external stimuli and the spontaneity in structural heterogeneity require that the investigation of the structural dynamics of a material to be performed both spatially and temporally. Phenomena such as solid-solid phase transition, colossal magnetoresistance, and ferroelectricity/ferromagnetism are often characterized by the spontaneous formation of spatially separated regions with distinct structures that support material properties. The length scales of such phase heterogeneities range from nanometers to micrometers and have roles in the dynamics of phase transition, electron transport, and structural response to applied fields. The dynamics of non-equilibrium heterogeneity including ferroelectric and magnetic domains, nucleation and growth, and short-range electronic ordering cover time scales from picoseconds to microseconds. Fast time-resolved X-ray nanoprobe techniques are thus necessary to address many questions in domain dynamics, nanoscale energy transport, and phase separation and competition. We will present recent development at several APS beamlines of time-resolved diffraction microscopy, their applications in studies of device materials, and its future in the layout of APS Upgrade.

10389-25, Session 6

A new cryo scanning transmission x-ray microscope at the Canadian Light Source

Jan Geilhufe, Adam F. G. Leontowich, Russ Berg, Chris Regier, Darwin M. Taylor, Jian Wang, John Swirsky, Chithra Karunakaran, Robert Peters, Canadian Light Source Inc. (Canada); Mirwais Aktary, Applied NanoTools Inc. (Canada); Adam P. Hitchcock, Brockhouse Institute for Materials Research (Canada); Stephen G. Urquhart, Univ. of Saskatchewan (Canada)

A new scanning transmission X-ray microscope (STXM) optimized for cryo-spectro-tomography with soft X-rays has been designed, built and commissioned at Canadian Light Source (CLS) beamline 10ID1 (130-2700 eV). It is controlled via a new python-based software package, pySTXM. A liquid N2 goniometer (Gatan 630, -80° to 80°), mounted on a computer controlled (x,y,Theta) tilt stage allows for spectro-tomographic measurements at cryogenic temperatures (-180°C) which reduces radiation damage. The CLS cryo-STXM is unique among the set of soft X-ray STXMs currently installed around the world. Details of the cryo-STXM design and examples of its performance will be presented.

10389-26, Session 6

New type of on-the-fly scanning data acquisition system for x-ray nanoprobe at Taiwan Photon Source

Chien-yu Lee, Gung-Chian Yin, Bo-Yi Chen, Bi-Hsuan Lin, Shao-Chin Tseng, Shi-Hung Chang, Jian-Xing Wu, Xiao-Yun Li, Mau-Tsu Tang, National Synchrotron Radiation Research Ctr. (Taiwan)

This on-the-fly scanning control system is for the x-ray nanoprobe endstation at Taiwan Photon Source(TPS) and built base-on the high speed Hardware (H/W), high throughput data stream and multi-channel control interfaces. The main idea is to tag each data with information of time and position, which generates by circuit and laser interferometer. The data is then processed by a computer to be analyzed and visualized.

By using high speed FPGA with embedded processer to process the input and output data which includes the DAC, ADC, Gigabit Ethernet (GbE), X-ray fluorescence (XRF) and laser interferometer control interfaces. Three DAC control the X,Y and Z axes of the flexure stage, four ADCs and sensor interfaces gather the data and packet it into data packet. GbE send data back to computer to do image processing then reconstruct the scanning image. The numerous data not only for rebuild the image but also good for information analysis. Including the vibration, time slide analysis.

Our demo system is built by an e-beam source, flexure stage and laser interferometer. The current maximum scanning speed is up to 5 lines/sec which is limited by the mechanical, the sample rate can be as high as 20M samples/sec which limited by laser interferometer, and the maximum data rate is close to 100M bytes/sec which is limited by the GbE. Interferometer information combine with position data in data packet, makes easy for data analysis and also for image stitching. The system is going to commission on beamline at March, 2017. The commission result for this system will be presented.

10389-27, Session 6

X-ray beam stabilization for nanoscale imaging

Yong S. Chu, Petr P. Ilinski, Hanfei Yan, Xiaojing Huang, Mingyuan Ge, Joseph Mead, Alfred Dellapenna, Anthony Caracappa, Brookhaven National Lab. (United States)

Achieving sufficient stability of the incidence beam is a major technical challenge for nanoscale x-ray imaging, in particular for scanning x-ray microscopy. A typical approach for guarding against beam instability is to create a secondary source in conjunction with a secondary source aperture. This method is highly effective against positional instability of an x-ray source but is only partially effective against angular instability. Since incidence wavefront typically contains contributions from imperfect optics, angular instability introduces undesired time-varying phase in nanoscale imaging experiments. Negative effects not only depends on the magnitude of the angular instability but also the type of nanoscale imaging methods. Negative impact is rather mild for nano-fluoresce imaging, since the measurement is performed at the nanobeam focus. On the other hand, the impact is much more significant for the imaging techniques analyzing the diffracted or transmitted beam. At the Hard X-ray Nanoprobe at NSLS-II, we have achieved angular stability better than 100 nrad in the horizontal direction and 20 nrad in the vertical direction. Presentation will illustrate the impact of the beam instability on different nanoscale imaging methods and describe instrumentation methods used for achieving a stable x-ray beam.

10389-28, Session 6

Beamline for extremely high-resolution Bragg coherent x-ray diffraction imaging with in-situ and operando capabilities

Wonsuk Cha, Evan Maxey, Ross Harder, Argonne National Lab. (United States)

A unique feature of Bragg Coherent Diffractive Imaging (BCDI) is extremely high sensitivity to strain and the ability to image local strain distributions in three dimensions with nanoscale spatial resolution. In-situ and operando imaging has been a major driver for BCDI in recent years. Chemistry and catalysis have been understood through the changes induced in the lattice of nanoscale crystalline materials. BCDI has also been used to study morphological changes in nano-diamond during annealing in-situ. Modern synchrotron x-ray sources, such as that proposed in the upgrade of the Advanced Photon Source (APS), will deliver two orders of magnitude greater coherent x-ray flux. As a result, there is a realistic opportunity for BCDI to reach toward atomic spatial resolution. In this talk, I will discuss current status of the 34-ID-C beamline at the APS. This instrument is dedicated for BCDI, and is pushing the limits of in-situ and operando imaging at high resolution. A new beamline, called ATOMIC, has been proposed as part of the upgraded APS. This new instrument and its potential to impact our sub-nanoscale understanding of science across many disciplines will be introduced.

10390-15, Session PMon

Implementation of the next-generation Gas Cherenkov Detector at the National Ignition Facility

Jorge A. Carrera, Arthur C. Carpenter, Hans W. Herrmann, Alex B. Zylstra, Bart V. Beeman, Hesham Y. Khater, Jose E. Hernandez, Lawrence Livermore National Lab. (United States); Frank E. Lopez, Jeffrey R. Griego, Yong Ho H. Kim, Los Alamos National Lab. (United States); E. Kirk Miller, National Security Technologies, LLC (United States); Steve A. Gales, Colin J. Horsfield, AWE plc (United Kingdom); James S. Milnes, Photek Ltd. (United Kingdom); Jonathan D. Hares, Kentech Instruments Ltd. (United Kingdom)

The Gas Cherenkov Detector version 3 (GCD-3) diagnostic has completed its phase one commissioning/milestone at the National Ignition Facility (NIF). Several key challenges to implementing GCD-3 at the NIF and their resolutions are discussed. In phase one GCD-3 required rigorous mechanical design efforts to prepare it to be installed in a 3.9m well at the NIF. Shielding solutions have been simulated, installed, and tested. Initial Photo Multiplier Tube (PMT) and Photo Diode (PD) measurements using a double and triple stacked Mach-Zehnder based recording system will be presented. Preliminary test results from the ultra-high bandwidth Pulse Dilation Photo Multiplier Tube (PD-PMT) will also be discussed.

This work performed under the auspices of the U.S. Department of Energy by Lawrence Livermore National Laboratory under Contract DE-AC52-07NA27344

10390-20, Session PMon

Solid-state streak camera prototype electronic performance testing and characterization

Yekaterina P. Opachich, Lawrence P. MacNeil, National Security Technologies, LLC (United States); John L. Porter, Sandia National Labs. (United States); Alicia Alarie, National Security Technologies, LLC (United States); Mark W. Kimmel, Joel Long, Quinn Looker, Sandia National Labs. (United States); Don Max, National Security Technologies, LLC (United States); John W. Stahoviak, Sandia National Labs. (United States); Vu Tran, National Security Technologies, LLC (United States); Caleb Wolf, Northwest Nazarene Univ. (United States); Thomas B. Waltman, National Security Technologies, LLC (United States)

Streak Cameras are an essential diagnostic tool used in shock physics and high energy density physics experiments. Such experiments require well calibrated temporally resolving diagnostics for studying events that occur on the nanosecond to microsecond time scales. Although streak cameras are the most common detectors used within the scientific community, they require routine calibration and typically lack reproducibility. A solid state device with similar performance characteristics could provide several advantages to current streak camera systems. NNSS has built a 24-channel solid state streak camera (SSSC) prototype, in collaboration with Sandia National Laboratories, as part of an ongoing project to develop the technology to a level competitive with analog streak cameras. The device concept and results from electronic testing will be discussed in this poster. These measurements will be used as a base for future SSSC development projects.

10390-1, Session 1

Design of a line-VISAR interferometer system for the Sandia Z-Machine

Justin D. Galbraith, John R. Celeste, Todd J. Clancy, Simon J. Cohen, Michael K. Crosley, Phillip S. Datte, Dayne Fratanduono, James Hammer, John L. Jackson, Lawrence Livermore National Lab. (United States); Michael C. Jones, Sandia National Labs. (United States); Don Koen, Jeremy Lusk, Thomas J. McCarville, Harry S. McLean, Kumar Raman, Samuel Rodriguez, Lawrence Livermore National Lab. (United States); Decker Spencer, Sandia National Labs. (United States); Paul T. Springer, Nan J. Wong, Lawrence Livermore National Lab. (United States); Kevin Austin, Jacob Baker, Drew Johnson, Sandia National Labs. (United States)

A joint team comprised of both Lawrence Livermore National Laboratory (LLNL) and Sandia National Laboratory (SNL) personnel is currently designing a line-VISAR (Velocity Interferometer System for Any Reflector) for the Sandia Z Machine, Z Line-VISAR. This system is composed of the following: a two-leg line-VISAR interferometer, an eight-channel Gated Optical Imager (GOI), and a fifty-meter transport beampath to the target of interest.

The Z Machine presents unique design constraints on the optomechanical design. The machine utilizes magnetically driven pulsed power to drive a target to high temperatures and pressures useful for high energy density science. Shock loads exceeding thirty g and a strong electromagnetic pulse (EMP) are generated during the shot event as the machine discharges currents of over twenty-five million amps. Sensitive optical components must be isolated from the shock load path, and electrical equipment must be adequately shielded from the EMP. Additionally, temperature and humidity fluctuations as well as airborne hydrocarbons present in the Z facility pose unique challenges to optical performance.

We will describe the engineering design and concept of operations of the Z Line-VISAR system. Focus will be on optomechanical design.

10390-2, Session 1

An optically passive method that rate doubles 2-GHz timing fiducials

Joshua D. Kendrick, Robert Boni, Charles Sorce, Univ. of Rochester (United States)

Solid-state optical comb-pulse generators provide a convenient and accurate method to include timing fiducials in streak-camera images for time-base correction. Commercially available vertical-cavity surface-emitting lasers (VCSEL's) emitting in the visible can be modulated up to 2 GHz. An optically passive method is presented to interleave a delayed path of the 2-GHz comb with itself, producing a 4-GHz comb. A fiber-delivered, randomly polarized 2 GHz VCSEL comb pulse is polarization split into s-pol and p-pol paths. One path is delayed relative to the other by twice the 2-GHz rate with ?1-ps accuracy, and the two paths recombine at the fiber coupled output. High throughput (>90%) is achieved through the careful use of polarization beam-splitting cubes, a total internal reflection beam path steering prism, and antireflection coatings. The glass path-length delay block and turning prism are optically contacted together. The beam-polarizer cubes that split and recombine the paths are precision aligned and permanently cemented into place. We expect the palm-sized, inline fiber-coupled, comb-rate doubling device to maintain its internal alignment indefinitely.

This material is based upon work supported by the Department of Energy National Nuclear Security Administration under Award Number DE-NA0001944, the University of Rochester, and the New York State Energy Research and Development Authority.

10390-3, Session 1

Using S-parameters for calibration of deployed cables on NIF

Alexander Wargo, California Polytechnic State Univ., San Luis Obispo (United States); Bart V. Beeman, Lawrence Livermore National Lab. (United States) and California Polytechnic State Univ., San Luis Obispo (United States)

Measuring the x-ray environment and other physics phenomena generated at the center of the NIF target chamber is a core capability required for understanding target implosions and other physics experiments. Many of these diagnostic systems include a detector at or near the target chamber with long cables transporting the signal to remote recording devices. As the cables cause distortions in the recorded signal a precise method of in-situ calibration is required. Scattering parameters (S-Parameters) are the gold standard for device characterization but can be difficult to obtain on deployed cables as both ends of the cable are usually required at the measuring instrument. We present an alternate method capable of gathering the required information for full characterization of deployed cables with the main recording instrument on one end and simple, small terminators at the remote end.

Lawrence Livermore National Laboratory is operated by Lawrence Livermore National Security, LLC, for the U.S. Department of Energy, National Nuclear Security Administration under Contract DE-AC52-07NA27344.

10390-4, Session 1

Recording system upgrade for the Dante x-ray diagnostic on NIF

Bart V. Beeman, Alastair S. Moore, Perry M. Bell, Klaus Widmann, Todd J. Clancy, Lawrence Livermore National Lab. (United States)

Measuring the X-ray environment generated at the center of the NIF target chamber is a core capability required for understanding target implosions and other physics experiments. Recently an upgrade was performed to the recording systems employing modern digital technology and additional remote control capabilities. Together significantly decreasing manual setup burdens, increasing accuracy, stability and availability while contributing to shot rate improvement, overall efficiency and cost of operations reduction on NIF. We present the systems chosen, improved calibration techniques employed and some of the key features including the addition of self-test capabilities.

Lawrence Livermore National Laboratory is operated by Lawrence Livermore National Security, LLC, for the U.S. Department of Energy, National Nuclear Security Administration under Contract DE-AC52-07NA27344.

10390-5, Session 1

Performance of a 2ns gated hybrid CMOS burst mode imager

Pratik Patel, Arthur C. Carpenter, Matthew S. Dayton, Brad T. Funsten, Jeremy Hill, Christopher C. Macaraeg, Brian Pepmeier, Lawrence Livermore National Lab. (United States); Brandon Mitchell, Liam D. Claus, Marcos Sanchez, Sandia National Labs. (United States)

An overview of a hybrid CMOS (hCMOS) image sensor, with nanosecond integration time, is presented.

This sensor named “Icarus” was developed with under the Ultra-Fast X-ray imager program collaborated with Sandia National Lab. It will be used for capturing images during high energy density experiments on NIF (National Ignition Facility) at Lawrence Livermore National Lab and on the OMEGA Laser at the Laboratory for Laser Energetics (LLE). The sensor is 1024x512 with 25umx25um pixel size. Same photodiode can be connected to multiple frames and thus ultra-fast frame rate is achieved. Gate profiles as short as 2ns were characterized. The sensor also has ability to time left and right hemisphere independently (so can be used as two sensors with one device). This paper gives basic architecture, function and some characterization and performance results such as gain, linearity, noise floor, full well, gate profile, and hemisphere skew and tuning.

10390-6, Session 1

Radiation effects on active camera electronics in the target chamber at the National Ignition Facility *(Invited Paper)*

Matthew S. Dayton, Arthur C. Carpenter, Hesham Y. Khater, Philip S. Datte, Perry M. Bell, Lawrence Livermore National Lab. (United States)

The camera electronics for Sandia’s nanosecond gated CMOS xray imager are exposed to a large neutron flux at NIF during high yield DT experiments. Most of the non-radhard components in the camera’s prototype were not expected to survive this radiation environment, however the fluence thresholds for failure were unknown. A good understanding of radiation tolerances for the components benefit the final design since non-radhard parts are typically lower cost and readily available. The first tests where done at Cobham Rad instead of the NIF chamber because high yield shots are not performed often at NIF and placing large sets of electronics near TCC can be challenging. Cobham Rad’s 14.1MeV neutron source produces a flux 20 neutrons/ns into 4pi. We were surprised to find that there were no component failures during an active test of the camera for a total fluence on the board of 1.4e12 neutrons/cm^2, which is equivalent to 28 NIF shots. During the experiment one hour was approximately equal to a single shot at NIF. The next set of tests made a link between test results taken at Cobham and test results taken in NIFs high flux environment of 5e15 neutrons/ns into 4pi. These test results combined with the performance of the boards in NIF provide insight into the development of a test strategy for qualifying commercially available components to survive in NIF.

10390-7, Session 2

X-ray Doppler velocimetry for diagnosis of fluid motion in ICF implosions *(Invited Paper)*

Jeffrey A. Koch, National Security Technologies, LLC (United States); John E. Field, Lawrence Livermore National Lab. (United States); Joseph D. Kilkenny, General Atomics (United States); Eric Harding, Gregory A. Rochau, Sandia National Labs. (United States); Aaron M. Covington, Univ. of Nevada, Reno (United States); Eric C. Dutra, Richard R. Freeman, National Security Technologies, LLC (United States); Gareth N. Hall, Lawrence Livermore National Lab. (United States); Michael J. Haugh, James A. King, National Security Technologies, LLC (United States)

We describe a novel technique for measuring bulk fluid motion in materials that is particularly applicable to very hot, x-ray emitting plasmas in the high energy density physics (HEDP) regime. This X-ray Doppler Velocimetry technique relies on monochromatic imaging in multiple closely-spaced wavelength bands near the center of an x-ray emission line in a plasma,

and utilizes bent crystals to provide the monochromatic images. Shorter wavelength bands are preferentially sensitive to plasma moving toward the viewer, while longer wavelength bands are preferentially sensitive to plasma moving away from the viewer. Combining multiple images in different wavelength bands allows for reconstruction of the fluid velocity field integrated along the line of sight. Extensions are also possible for absorption geometries, and for three dimensions. We describe the technique, and we present the results of simulations performed to benchmark the viability of the technique for implosion plasma diagnosis as well as of ongoing efforts to demonstrate the technique with experiments.

10390-8, Session 2

On the design of the NIF Continuum Spectrometer

Daniel B. Thorn, Andrew MacPhee, Jay J. Ayers, Justin D. Galbraith, Michael C. Hardy, Nobuhiko Izumi, David K. Bradley, Lousia A. Pickworth, Benjamin Bachmann, Otto L. Landon, Marilyn B. Schneider, Perry M. Bell, Hesham Y. Khater, Joseph D. Kilkenny, Lawrence Livermore National Lab. (United States)

On inertial confinement fusion (ICF) experiments on the NIF, measurements of average ion temperature using DT neutron time of flight broadening and of average electron temperature using time-integrated differentially-filtered x-ray images are sometimes discrepant. Some of this may be due to time and space dependent temperature profiles in the imploding capsule which are not taken into account in the analysis. As such, we are attempting to measure the electron temperature a second way, by recording the continuous electron bremsstrahlung spectrum from the tail of the Maxwellian temperature distribution. This new NIF Continuum Spectrometer (NCS) spans the x-ray range of 20 keV to 30 keV (where any opacity corrections from the remaining mass of the ablator shell are negligible) and will be sensitive to temperatures between 3 keV and 6 keV. The NCS is designed to be compatible with an x-ray streak camera to record time resolved free-free electron continuum spectra for direct measurement of the dT/dt evolution across the burn width of a DT plasma. The spectrometer is a conically bent Bragg crystal focusing geometry that allows for the dispersion plane to be perpendicular to the spectrometer axis and provides 1:1 imaging. Additionally, to address the spatial temperature dependence, both time integrated and time resolved pinhole and penumbral imaging will be provided along the same polar angle. The optical and mechanical design of the spectrometer is presented along with estimates for the dispersion, solid angle, photometric sensitivity, and performance.

*This work was performed under the auspices of the U.S. Department of Energy by LLNL under Contract DE-AC52-07NA27344.

10390-9, Session 2

Design and characterization of an improved 2-ns multi-frame imager for the Ultra-Fast X-ray Imager (UXI) program at Sandia National Laboratories

Liam D. Claus, Marcos Sanchez, Gideon A. Robertson, Mark W. Kimmel, John L. Porter, Lu Fang, Douglas Trotter, John W. Stahoviak, Troy England, Andrew Montoya, Brandon Mitchell, Gregory A. Rochau, Sandia National Labs. (United States); Arthur C. Carpenter, Matthew S. Dayton, Pratik Bhogilal, Lawrence Livermore National Lab. (United States)

The Icarus camera is an improvement on past imagers (Furi and Hippogriff) designed for the Ultra-Fast X-ray Imager (UXI) program to deliver ultra-fast, time-gated, multi-frame image sets for High Energy Density (HED) physics experiments. Icarus is a 1024 x 512 pixel array with 25 ?m spatial resolution containing 4 frames of storage per pixel. It has improved timing generation and distribution components and has achieved 2 ns time gating. Design improvements and initial characterization and performance results will be discussed.

10390-10, Session 3

X-ray penumbral imaging diagnostic developments at the National Ignition Facility *(Invited Paper)*

Benjamin Bachmann, Lawrence Livermore National Lab. (United States); Hatim Abu Shawareb, Neil B. Alexander, General Atomics (United States); Jay J. Ayers, Christopher G. Bailey, Perry M. Bell, Laura R. Benedetti, David K. Bradley, Laurent Divol, Tilo Doeppner, John E. Field, Lawrence Livermore National Lab. (United States); Andrew Forsman, General Atomics (United States); Justin D. Galbraith, Michael C. Hardy, Lawrence Livermore National Lab. (United States); Terance Hilsabeck, General Atomics (United States); Nobuhiko Izumi, Leonard C. Jarrot, Lawrence Livermore National Lab. (United States); Joseph D. Kilkenny, General Atomics (United States); Steve Kramer, Otto L. Landen, Tammy Ma, Andrew MacPhee, Nathan D. Masters, Sabrina R. Nagel, Arthur E. Pak, Pravesh K. Patel, Louisa A. Pickworth, Joseph E. Ralph, Lawrence Livermore National Lab. (United States); Christopher Reed, General Atomics (United States)

X-ray penumbral imaging has been successfully fielded on a variety of inertial confinement fusion (ICF) capsule implosion experiments on the National Ignition Facility (NIF). We have demonstrated sub-5 micrometer resolution imaging of stagnated plasma cores (hot spots) at x-ray energies from 6 to 30 keV [1, 2]. These measurements are crucial for improving our understanding of the hot deuterium-tritium fuel assembly, which can be affected by various mechanisms, including complex 3-D perturbations caused by the support tent, fill tube or capsule surface roughness. Here we present the progress on several approaches to improve x-ray penumbral imaging experiments on the NIF. We will discuss experimental setups that include penumbral imaging from multiple lines-of-sight, target mounted penumbral apertures and variably filtered penumbral images. Such setups will improve the signal-to-noise ratio and the spatial imaging resolution, with the goal of enabling spatially resolved measurements of the hot spot electron temperature and material mix in ICF implosions.

References

[1] B. Bachmann et al., Rev. Sci. Instrum. 85, 11D614 (2014)

[2] B. Bachmann et al., Rev. Sci. Instrum. 87, 11E201 (2016)

This work performed under the auspices of the U.S. Department of Energy by Lawrence Livermore National Laboratory under Contract DE-AC52-07NA27344. This work was also supported in part by General Atomics under Contract DE-NA0001808.

10390-11, Session 3

X-ray calibration and characterization at NNSS Livermore operations

James A. King, Michael J. Haugh, Richard R. Freeman, Kenneth D. Jacoby, Gabe Torres, Peter Torres III, Patrick W. Hillyard, Jeffrey A. Koch, National Security Technologies, LLC (United States)

X-ray calibration is a primary component of the services provided by the Nevada National Security Site / Livermore Operations (NNSS/LO). The four X-ray calibration labs at NNSS/LO provide characteristic and Bremsstrahlung

X-ray output ranging in energy from 500 eV to 110 keV. These labs are capable of calibrating a variety of X-ray detectors and components including CCD's, streak cameras, spectrometers, and filters. Many of the calibration measurements are NIST-traceable. Calibrations and characterizations include quantum efficiency, sensitivity, dynamic range, and flat field measurements. Historically these labs have performed calibrations for various institutions and national laboratories such as Lawrence Livermore National Laboratory, Los Alamos National Laboratory, and Sandia National Laboratories. In addition, NNSS/LO has in-house diagnostic development capabilities, resulting in new techniques, such as high-energy curved crystal X-ray imaging. This presentation will describe the services provided by these labs, the operation and layout of the labs, and in-house, NVLAP accredited calibration of the various X-ray sources and diagnostics used.

This work was performed by National Security Technologies, LLC, under Contract No. DE-AC52-06NA25946 with U.S. Department of Energy. DOE/NV/25946--3130

10390-12, Session 3

Offline metrology and alignment of a passive neutron imaging pinhole on the National Ignition Facility

Jay J. Ayers, Nick Shingleton, Robin L. Hibbard, David N. Fittinghoff, David A. Barker, Lawrence Livermore National Lab. (United States); Valerie E. Fatherley, Frank E. Merrill, Los Alamos National Lab. (United States); Daniel H. Kalantar, Lawrence Livermore National Lab. (United States)

Neutron imagers have been used on many ICF experiments at the National Ignition Facility. To complement the existing equatorial view on the NIF target chamber a North Pole view was added in FY16. The North Pole neutron imaging system is the first Diagnostic Instrument Manipulator (DIM) based system that is passively aligned. The North Pole neutron imager is a snout based instrument that is positioned approximately 200mm from target chamber center (TCC). The neutron imaging snout contains a set of pinholes along the center axis of the snout positioned 100mm from TCC that relay x-ray images onto a gated framing camera. The neutron imaging pinhole is positioned at 5.75° off the center axis of the snout and relays images onto image plate 8177mm away. The successful deployment of the North Pole neutron imaging system required careful attention to insure that both the neutron line of sight (LOS) and the x-ray LOS were both looking at the same point in space. Additionally it was critical that the neutron LOS be parallel to its nominal to enable small systematic alignment corrections without negative impact to the location of where the images fall at the image plane. This paper will discuss the offline alignment methodology which includes coordinate measurement machine (CMM), analysis using spatial analyzer software and laser tracking systems.

10390-13, Session 3

Pulsed x-ray sources for characterization of gated framing cameras

Catalin Filip, Jeffrey A. Koch, Richard R. Freeman, James A. King, National Security Technologies, LLC (United States)

Gated x-ray framing cameras are used to measure important characteristics of ICF implosions, such as size and symmetry, with ~ 50 ps time resolution in two dimensions. These detectors require a variety of tests and calibration exposures to allow quantitative data to be obtained and analyzed. A pulsed source of hard (> 8 keV) x-rays, other than the NIF laser, would be a valuable calibration device, for example for gain-droop measurements of the variation in sensitivity along the length of the gated strips. We have explored the requirements for such a source, and have explored a variety of source options that could meet these requirements. We find that a small-size dense plasma focus machine could be a practical single-shot x-ray source for this application if timing uncertainties can be overcome. We will present expected performance for a variety of sources compared with known requirements.

10390-14, Session 4

System design of the NIF neutron imaging system North pole *(Invited Paper)*

Valerie E. Fatherley, Los Alamos National Lab. (United States); Jay J. Ayers, David A. Barker, Lawrence Livermore National Lab. (United States); Steve H. Batha, Christopher R. Danly, Los Alamos National Lab. (United States); David N. Fittinghoff, Lawrence Livermore National Lab. (United States); Lynne A. Goodwin, Hans W. Herrmann, Los Alamos National Lab. (United States); Robin L. Hibbard, Los Alamos National Lab. (United States) and Lawrence Livermore National Lab. (United States); Justin J. Jorgenson, John I. Martinez, Frank E. Merrill, John A. Oertel, Derek W. Schmidt, Los Alamos National Lab. (United States); Nick Shingleton, Michael Vitalich, Lawrence Livermore National Lab. (United States); Petr L. Volegov, Carl H. Wilde, Los Alamos National Lab. (United States)

A new neutron imager, known as Neutron Imaging System North Pole, has been fielded to image the neutrons produced in the burn region of imploding fusion capsules at the National Ignition Facility. The resolution and alignment requirements and parameters that drive the design of this system are similar to the pre-existing equatorial system, there are significant changes. This work describes the parameters and limitations driving the design of this system. In addition discussion of the alignment and metrology solutions are discussed. This is intended as a full review of the characteristics of the NIS-NP.

10390-16, Session 4

Fielding the LANL Gas Cherenkov Detector (GCD-3) at the National Ignition Facility: The mechanical engineering challenges of designing, analyzing, fabricating, testing, and commissioning the next-generation GCD detector and WellDIM3.9m insertion manipulator within a 3.9 meter well on the National Ignition Facility target chamber

Frank E. Lopez, Hans W. Herrmann, Ramon J. Leeper, Steve H. Batha, John A. Oertel, Jeffrey R. Griego, Brian C. Steinfeld, Paul J. Polk, Lynne A. Goodwin, Valerie E. Fatherley, Thomas N. Archuleta, Robert J. Aragonez, Benjamin J. Pederson, Los Alamos National Lab. (United States); John R. Celeste, Robin L. Hibbard, Arthur C. Carpenter, Jose E. Hernandez, Jorge A. Carrera, Hesham Y. Khater, Lawrence Livermore National Lab. (United States); Justin J. Jorgenson, Los Alamos National Lab. (United States)

Abstract: The design and commissioning of the next-generation LANL Gas Cherenkov Detector (GCD-3) for fielding at the National Ignition Facility resulted in an array of unique engineering challenges. To field the GCD-3 Detector in an existing 3.9m Well on the NIF Target Chamber required a specialized deployment system. This deployment system transports the existing GCD-3 (currently fielded at LLE/OMEGA) within an existing 3.9m

conical Well (64-275) outside the NIF Target Chamber. The GCD-3, outfitted with additional shielding to mitigate higher NIF backgrounds, serves as the operational payload/prototype for the future, heavily shielded "Super-GCD".

The GCD-3 is a third-generation Gas Cherenkov Diagnostic that provides important information about Inertial Confinement Fusion (ICF) implosions including fusion burn and imploded capsule conditions. The GCD-3 converts gamma rays into Compton electrons, which generate Cherenkov photons inside of the pressurized gas cell. Pressurized gases include CO2, SF6 and C2F6. The Cherenkov photons are then focused onto a photomultiplier tube (PMT) using a Cassegrain optic. Conflat™ knife-edge, crushed-metal seals in conjunction with explosion-bonded Bi-metallic flanges became essential aspects of this vessel design to achieve a low leak-rate specification. The LANL Pressure Safety Program in compliance with DOE Order 10CFR851 invokes the ASME Boiler and Pressure Vessel Code, Section VIII, Division I/II for the design of all pressure vessels. As the B&PV Code can be characterized as a "one size fits all" standard, the tendency toward conservatism is typical. Vessel-wall and flange thicknesses are routinely robust, although inconsequential to refineries, are atypical of pressurized ICF diagnostics. A detailed review of these engineering challenges, correlated with the resulting experimental data, emphasizes the successful collaborative mix of engineering and physics expertise within the ICF Diagnostic Development arena.

10390-17, Session 4

Large-area solid radiochemistry collector (LASR) at the National Ignition Facility

Cory Waltz, Donald R. Jedlovec, Michael C. Hardy, Dawn Shaughnessy, Narek Gharibyan, Cal A. Smith, Lawrence Livermore National Lab. (United States)

The flux of neutrons and charged particles produced from inertial confinement fusion experiments at the National Ignition Facility (NIF) can induce measurable concentrations of nuclear reaction products in various target materials. The collection and radiochemical analysis of the post-shot debris can be utilized as an implosion diagnostic to obtain information regarding fuel areal density and ablator-fuel mixing. Furthermore, assessment of the debris from specially designed targets, material doped in capsules or mounted on the external surface of the target assembly, can support experiments relevant to nuclear forensic research.

To collect the shot debris, we have deployed the Large Area Solid Radiochemistry Collector (LASR) at NIF. LASR uses a main collector plate that contains a large collection foil with an exposed 20 cm diameter surface located ~50 cm from the NIF target. This covers ~0.12 steradians, or about 1% of the total solid angle. We will describe the design, analysis, and operation of this experimental platform as well as the initial results. To speed up the design process 3-dimensional printing was utilized. Design analysis includes the dynamic loading of the NIF target vaporized mass, which was modeled using LS-DYNA.

This work was performed under the auspices of the U.S. Department of Energy by Lawrence Livermore National Laboratory under Contract DE-AC52-07NA27344.

10390-18, Session 4

Measuring the down scattered neutron ratio using the NiToF detector system at the National Ignition Facility *(Invited Paper)*

Gary P. Grim, Lawrence Livermore National Lab. (United States); George L. Morgan, Carl H. Wilde, Los Alamos National Lab. (United States); Edward Hartouni, Robert Hatarik, Mark J. Eckart, Lawrence Livermore National Lab. (United States)

The National Ignition Facility neutron time-of-flight diagnostic suite is comprised of five independent detector systems, including the neutron imaging time-of-flight diagnostic, NIToF. Because of unique capability to measure both the foreground and background system with the NIToF system, a novel method for determining the neutron downscatter ratio (DSR), defined to be the ratio of the integrated flux of 10-12 MeV neutrons to the 13-15 MeV neutrons, has been developed. This constrained least squares unfold methodology will be described, along with current systematic uncertainty studies, and comparisons with other approaches.

10390-19, Session 4

Development of the Real-Time Neutron Activation Diagnostic System for NIF

Jaben Root, Phil Adams, Gordon K. Brunton, Ellen R. Edwards, Tony Golod, Jose E. Hernandez, Donald R. Jedlovec, Charles Yeamans, Lawrence Livermore National Lab. (United States)

The National Ignition Facility (NIF) is one of the highest-fluence 14.1 MeV neutron sources provided by the nuclear fusion of deuterium and tritium nuclei. One of the resultant products is 14.1 MeV neutrons, which provide key information to the conditions in which they were formed. The degree of polar and azimuthal symmetry of the neutron yield is a key metric for the performance of the capsule, thus a spatially-resolved measurement of the neutron distribution is critical. A suite of 48 lanthanum bromide detectors with zirconium activation samples around the target chamber is being implemented to measure the neutron distribution. The system provides rapid estimates of the neutron fluence distribution. It is designed to operate over six orders of magnitude of neutron yield, providing relative yield estimates precise to 1.3%. The system is designed to operate continuously through the NIF shot cycles, accommodating high data rates. We will describe the nuclear counting system, data acquisition and archiving, analysis, and results for some NIF high yield shots.

This work was performed under the auspices of the U.S. Department of Energy by Lawrence Livermore National Laboratory under Contract DE-AC52-07NA27344. Lawrence Livermore National Security, LLC.

Conference 10391: Developments in X-Ray Tomography XI

Tuesday - Thursday 8 –10 August 2017

Part of Proceedings of SPIE Vol. 10391 Developments in X-Ray Tomography XI

SPIE. OPTICS+ PHOTONICS OPTICAL ENGINEERING+ APPLICATIONS

10391-1, Session 1

Recent trends in high-resolution X-ray tomography

Bert Müller, Univ. Basel (Switzerland)

X-ray tomography is a non-destructive technique. It provides three-dimensional data with a spatial resolution down to the nanometer scale. There are several fields of improvement, which include (i) the detectors being more and more efficient and having an increasing number of pixels, (ii) the development of methods beyond the conventional attenuation contrast, (iii) the realization of fast set-ups to study processes such as loading of scaffolds, and (iv) the implementation of X-ray optics to reach a spatial resolution of about 10 nm. These developments will be discussed on the basis of current literature.

10391-2, Session 1

A comparison study: image-based vs. signal-based retrospective gating on microCT

Xuan Liu, Phil L. Salmon, Kjell Laperre, Alexander Sasov, Bruker microCT (Belgium)

Retrospective gating on animal studies with microCT has gained popularity in recent years. Traditionally, we use ECG signals for cardiac gating and breathing airflow or video signals of abdominal motion for respiratory gating. The 2 methods are adequate and work well for most applications. However, through the years, researchers have noticed some pitfalls in the method. For example, the additional signal acquisition step may increase failure rate in practice. X-Ray image-based gating, on the other hand, does not require any extra step in the scanning. Therefore we investigate image-based gating techniques. This paper presents a comparison study of the image-based versus signal-based approach to retrospective gating. The two application areas we have in mind are respiratory and cardiac gating.

Image-based respiratory gating on microCT is relatively straightforward and has been done by several other researchers and groups. This method retrieves an intensity curve of a region of interest (ROI) in the lung area. Our initial tests show very promising results. Further investigation will be done on the automatic or semi-automatic placing and definition of the ROI. A detailed comparison between image-based and signal-based methods will be made.

For cardiac gating, the image-based method is less obvious. The difficulty in cardiac gating is due to the relatively smaller amplitude of cardiac movements comparing to the respirational movements, and the higher heart rate. Higher heart rate requires high speed image acquisition. We have been working on our systems to improve the acquisition speed. Analysis techniques have been studied to separate cardiac and respirational signals. Comparison on image-based cardiac gating and ECG-based gating will be conducted.

10391-3, Session 1

Improving Material Identification by Combining X-ray and Neutron Tomography

Jacob M. LaManna, Daniel S. Hussey, Elias M. Baltic, David L. Jacobson, National Institute of Standards and Technology (United States)

X-rays and neutrons provide complementary non-destructive probes for the analysis of structure and chemical composition of materials. Contrast differences between the modes arise due to the differences in interaction with matter. Due to the high sensitivity to hydrogen, neutrons excel at separating liquid water or hydrogenous phases from the underlying structure while X-rays resolve the solid structure. Many samples of interest, such as fluid flow in porous materials or curing concrete, are stochastic or slowly changing with time which makes sequential imaging with X-rays and neutrons difficult as the sample may change between scans. To alleviate this issue, NIST has developed a system for simultaneous X-ray and neutron tomography by orienting a 90 keVpeak micro-focus X-ray tube orthogonally to a thermal neutron beam. This system allows for non-destructive, multimodal tomography of dynamic or stochastic samples while penetrating through sample environment equipment such as pressure and flow vessels. Current efforts are underway to develop methods for 2D histogram based segmentation of reconstructed volumes. By leveraging the contrast differences between X-rays and neutrons, greater histogram peak separation can occur in 2D vs 1D enabling improved material identification. This talk will discuss the simultaneous X-ray and neutron tomography system at NIST and current efforts in multimodal, 2D histogram segmentation with several case studies that have been conducted at NIST.

10391-4, Session 1

Nanoscale holographic tomography based on x-ray waveguide optics

Tim Salditt, Malte Vassholz, Mareike Toepperwien, Aike Ruhlandt, Markus Osterhoff, Georg-August-Univ. Göttingen (Germany)

We describe the optics and state-of-the-art applications of nanoscale holographic tomography based on x-ray waveguide optics. The combination of high gain x-ray nano-focusing with optimized coherence and wavefront filtering by waveguide optics, with recent improvements in phase retrieval and tomographic reconstruction have enabled full-field x-ray tomography at the nanoscale with unprecedented resolution and image quality. Compared to ptychography, the tomographic scans are faster, can easily cover larger volumes and are recorded at significantly reduced dose. In this contribution, we present state-of-the art examples, from materials characterisation to biomedical imaging, and discuss the optimum choice of optical parameters. To this end, the instrumental setting at the GINIX endstation of the PetraIII storage ring, waveguide optics and photon energy, as well as phase retrieval approaches are addressed in view of different experimental requirements: resolution, sensitivity, quantitative contrast, dose minimization, and high speed tomographic scan in view of time-resolved studies.

10391-5, Session 1

High energy near- and far-field ptychographic tomography at the ESRF *(Invited Paper)*

Julio C. da Silva, Alexandra Pacureanu, Leonid Bloch, Yang Yang, Peter Cloetens, ESRF - The European Synchrotron (France)

X-ray ptychographic imaging in synchrotron sources has already shown great potential for high-resolution quantitative microscopy. Such a technique, which can be implemented in the near- and far-field regimes, enables not only high-resolution imaging, but also high sensitivity to the electron density of the sample. A sequence of diffraction patterns in the far-field or holograms in the near-field is collected for different lateral translations of the sample with respect to an unknown illumination. The transverse diversity added to the phase retrieval enables the image reconstruction taking into account the incoming beam information. Iterative algorithms carry out the phase-retrieval. The combination with tomography makes 3D imaging possible via ptychographic X-ray computed tomography

(PXCT), which can provide a 3D map of the refractive index of the sample. To do so, several pre-processing steps are needed before the actual tomographic reconstruction. We present here the latest developments in near- and far-field PXCT implemented at the ESRF. We exploit the coherence of the X-ray at the ID16A beamline to perform such a technique at high energy (17.05 keV and 33.6 keV). We discuss the challenges of implementing PXCT with high energy and high flux and how we tackle them. The most recent algorithm developments enable us to circumvent the non-ideal experimental conditions and allow broad bandwidth coherent X-ray imaging. We will also show the results of applications of PXCT to important problems of materials science, for example, applications in heterogeneous catalysis and metallurgy.

10391-6, Session 2

Fast and low-dose phase contrast CT with non-microfocal laboratory x-ray sources *(Invited Paper)*

Alessandro Olivo, Paul C. Diemoz, Marco Endrizzi, Charlotte K. Hagen, Fabio A. Vittoria, Alberto Astolfo, Peter R. T. Munro, Peter Modregger, Gibril K. N. Kallon, Dario Basta, Ian Buchanan, Charlotte Maughan Jones, Anna Zamir, Univ. College London (United Kingdom)

The implementation of X-Ray Phase Contrast (XPC) imaging at synchrotrons has demonstrated transformative potential on a wide range of applications, from medicine and biology to materials science. However, translation to conventional laboratory sources has proven more problematic, because of XPC's stringent requirements in terms of spatial coherence. This has imposed the use of either micro-focal sources, or collimators (e.g. source gratings) where sources with extended focal spots were used. This reduces the available x-ray flux leading to long exposure times, which is often exacerbated by the use of additional optical elements that need to be scanned during image acquisition. Where these elements are placed downstream of the object, they also lead to an increase in the delivered dose.

XPC has also been successfully adapted to full 3D, computed tomography (CT) implementations, which has however exacerbated the above concerns in terms of acquisition times and delivered doses.

We tackled this problem by developing an incoherent approach to XPC that works with non micro-focal laboratory sources without requiring any additional collimation. The method uses one or two low aspect ratio x-ray masks that are built on low-absorbing graphite substrates for maximum transmission through the mask apertures. The combination of this with a "single-shot" phase retrieval algorithm has enabled the development of a lab-based XPC-CT system that can perform a full scan in a few minutes while delivering low radiation doses. The talk will briefly describe how the method works, then show application examples including direct comparisons with the synchrotron gold standard.

10391-7, Session 2

High-Resolution Grating Interferometer for Phase-Contrast Imaging at PETRA III

Alexander C. Hipp, Helmholtz-Zentrum Geesthacht (Germany); Matthias Vogelgesang, Jürgen Mohr, Andreas Kopmann, Karlsruher Institut für Technologie (Germany); Felix Beckmann, Helmholtz-Zentrum Geesthacht (Germany)

Phase-contrast imaging has proven to be a valuable tool for the investigation of weak absorbing materials like soft tissue, due to its increased contrast compared to conventional absorption-contrast imaging. While propagation-based phase-contrast is ideal to achieve highest resolution at a good contrast for almost non-absorbing material, it has limitations for demanding applications that require contrast with a high dynamic range. For those applications grating-based phase-contrast is preferable, although it lacks of spatial resolution compared to inline phase-contrast or attenuation-based microCT. To reduce the gap in spatial resolution we equipped the two PETRA III beamlines P05 and P07 with a customized mechanics to maximize the performance of the interferometer. The optimized system enables phase-contrast measurements in a continuous energy range between 10 keV and 80 keV. Dependent on the investigated material and energy the setup is capable to achieve a spatial resolution of 5 μm on a field of view of 6.5 mm. We will present our implementation of grating-based phase-contrast computed tomography for fast and high-resolution measurements at the PETRA III along with its recent optimizations, and demonstrate its performance for different kinds of applications.

10391-8, Session 2

Quantitative phase contrast and x-ray scattering micro-tomography with the 9.2 keV liquid metal jet anode: applications on materials and life science

Simon A. Zabler, Fraunhofer-Institut für Integrierte Schaltungen (IIS) (Germany); Andreas Balles, Jonas Dittmann, Julius-Maximilians-Univ. Würzburg (Germany); Christian Fella, Randolf Hanke, Fraunhofer-Institut für Integrierte Schaltungen (IIS) (Germany)

Grating-based X-ray phase contrast and scattering contrast tomography were pioneered by Pfeiffer and David at synchrotron beamlines as well as for laboratory applications [1]. While volume image reconstruction from the refractive phase contrast is straight forward, interpretation and appropriate reconstruction from scattering contrast (so called dark-field image contrast DIC) long remained an issue vividly discussed in the scientific community [2]. Based on its interpretation as ultra-small angle scattering by microscopic interfaces (e.g., fibers, pores or particles) we select filtered back-projection with an adaptive filter-kernel as the appropriate reconstruction method. The data which will be shown is acquired downstream of a liquid metal-jet Gallium anode which features quasi-monochromatic 9.2 keV radiation from the K-emission line. High spatial resolution is achieved through 2.7 μm/pixel and 0.6 μm/pixel indirect X-ray cameras coupled to a two-grating interferometer.

Examples of this three-contrast CT from various micro-structured materials are presented along with interpretation, in particular of the DIC signal with respect to the sub-pixel micro structure (e.g. pores in compresses, chloroplasts in plant cells and fibers in high-grade filter materials).

While most of our results confirm the abovementioned theories, we find some unexpected discrepancies, e.g. between propagation-based and grating-based phase contrasts. An additional experiment on a microscopic gradient structure clearly reveals the structural sizes which produce the strongest DIC signal. Such calibration samples might be used for absolute calibration of DIC in a large variety of X-ray interferometers.

[1] C. David et al. (2002) Appl. Phys. Lett. 81(17):3287

[2] V. Revol et al. (2011) J. Appl. Phys. 110(4):044912

10391-9, Session 2

Tomography with energy dispersive diffraction

John S. Okasinski, Russel Woods, Antonino Miceli, Argonne National Lab. (United States); David P. Siddons, Brookhaven National Lab. (United States); Jonathan D. Almer, Argonne National Lab. (United States); Stuart R. Stock, Northwestern Univ. (United States)

X-ray diffraction can be used as the signal for tomographic reconstruction and provides a cross-sectional map of the crystallographic phases and

related quantities. Diffraction tomography is typically performed with monochromatic x-radiation and an area detector. This paper reports tomographic reconstruction with polychromatic radiation and an energy sensitive detector array. The energy-dispersive diffraction (EDD) geometry, the instrumentation and the reconstruction process are described and related to the expected resolution. Results of EDD tomography are presented for two samples containing hydroxyapatite (hAp). The first is a 3D-printed sample with an elliptical cross-section and contains synthetic hAp. The second is a human second metacarpal bone from the Roman-era cemetery at Ancaster, UK and contains bio-hAp which may have been altered by diagenesis. Reconstructions with different diffraction peaks are compared. Prospects for future EDD tomography are also discussed.

10391-10, Session 3

Microanatomy of the cochlear hook
(Invited Paper)

Claus-Peter Richter, Changyow Claire Kwan, Xiaodong Tan, Stuart R. Stock, Northwestern Univ. (United States); Carmen Soriano Hoyuelos, Argonne National Lab. (United States)

To examine the cochlear hook of mice, micro-CT was carried out at beamline 2-BM of the Advanced Photon Source at Argonne National Laboratories. All cochleae were imaged using monochromatic radiation with photon energies of 22 keV. The separation between the detector and the tomography rotation axis was 600 mm for phase contrast. 5x and 10x objective lenses were used in the detector system. Specimens were placed such that they were in the visual field at all times. A series of X-ray projections were taken over a range of 180 degrees at increments of 0.12 degrees. The exposure time for a single image was 0.2-0.3 s. At the beginning and end of each image series, flat field images (no object in the beam path) were recorded; after the series, a dark field image (the X-ray beam was blocked) was captured. At the conclusion of the experiment, the projections were used to reconstruct the cochlear hook region. Custom written phase retrieval software was used for the reconstructions. Reconstructions were on a 2048 x 2048 grid. The reconstructions resulted in 1.45 μm / 0.78 μm isotropic voxels. Detailed evaluation of the bony and soft tissue structures showed for the first time specific configurations of the bony structures and the anchoring of the basilar and tectorial membranes at the very base of the cochlea. The data will be used in cochlear models to further describe linear and nonlinear processing of acoustical information in the inner ear.

10391-11, Session 3

Microcomputed tomography and x-ray diffraction of intact archeological human second metacarpal bones as a function of individuals' age at death

Stuart R. Stock, Northwestern Univ. (United States); J. S. Park, Argonne National Lab. (United States); Malene Laugesen, Aarhus Univ. (Denmark); Simon Mays, Historic England (United Kingdom); Jonathan D. Almer, Argonne National Lab. (United States); Henrik Birkedal, Aarhus Univ. (Denmark); Carmen Soriano Hoyuelos, Argonne National Lab. (United States)

Bones recovered from archeological sites provide information on past human health, and destructive sampling is often not an option, making x-ray methods invaluable. This paper uses two high energy x-ray methods to study human second metacarpal (Mc2) bones from Roman (Ancaster) and from medieval (Wharram Percy) Britain. MicroComputed Tomography (microCT) and position resolved x-ray scattering (wide angle – WAXS – and small angle – SAXS) provide quantitative data on six Mc2 from each site with two Mc2 from each of three age (at death) cohorts and on a modern Mc2 and two synthetic hAp phantoms.

Laboratory microCT imaged trabecular bone, and synchrotron microCT (2-BM, Advanced Photon Source - APS) imaged cortical bone from these Mc2. A series of WAXS and SAXS patterns covering the cross-section of these Mc2 and phantoms were collected simultaneously with a 50 ?m wide beam at 1-ID, APS. Rietveld refinement was applied to the WAXS patterns, and cAp lattice parameters and crystallite size and microstrain determined. From SAXS, collagen D-period was quantified.

We seek to answer the following questions: 1) How does the microCT and scattering data correlate in defining bone "quality"? 2) How much has diagenesis altered the bone material and changed quantities measured by x-ray scattering (cAp lattice parameters; crystallite size, microstrain; collagen D-period)? 3) If diagenetic changes are minor or non-existent, do the above quantities change with age in Roman and medieval era populations, and are these changes similar to those observed for bone from modern sedentary populations?

10391-12, Session 3

3D mapping grain morphology and grain orientations by laboratory diffraction contrast tomography

Christian Holzner, Carl Zeiss X-ray Microscopy, Inc. (United States); Nicolas Gueninchault, Florian Bachmann, Xnovo Technology ApS (Denmark); Hrishikesh Bale, Leah Lavery, Carl Zeiss X-ray Microscopy, Inc. (United States); Erik Lauridsen, Xnovo Technology ApS (Denmark)

Determining crystallographic microstructure of a given material in 2D can be challenging. Further extending such an investigation to 3D on meaningful volumes (and without sample sectioning) can be even more so. Yet reaching this insight holds tremendous value for 3D materials science since the properties and performance of materials are intricately linked to microstructural morphology including crystal orientation. Achieving direct visualization of 3D crystallographic structure is possible by diffraction contrast tomography (DCT), albeit only available at a limited number of synchrotron X-ray facilities around the world. Recent developments, however, have made DCT possible on an X-ray microscope with a laboratory source.

The introduction of diffraction contrast tomography as an additional imaging modality on the ZEISS Xradia 520 Versa laboratory X-ray microscope has opened up a whole new range of possibilities for studies of the effect of 3D crystallography on materials performance. The capability to link directly the crystallographic and grain microstructure information with that obtained via conventional absorption or phase contrast imaging, non-destructively in three-dimensions and all in the laboratory, creates a powerful and easy to access tool [1-2]. Using a polychromatic X-ray source, laboratory diffraction contrast tomography technique (LabDCT) takes advantage of the Laue focusing effect, improving diffraction signal detection and allows handling of many and closely spaced reflections.

Additionally, LabDCT opens the way for routine, non-destructive and time-evolution studies of grain structure to complement electron backscatter diffraction (EBSD). Crystallographic imaging is performed routinely by EBSD for metallurgy, functional ceramics, semi-conductors, geology etc. However, EBSD is an end-point characterization technique and prevents any investigation of microstructure evolution when subject to either mechanical, thermal or other environmental conditions.

Combination of grain information with microstructural features such as cracks, porosity, and inclusions all derived non-destructively in 3D presents new insights for materials characterization of damage, deformation and growth mechanisms. Furthermore, 3D grain orientation data is a valuable input into multi-scale, multi-layered modeling platforms that can virtually evaluate mechanical properties to produce high fidelity simulation results.

Recent developments of the LabDCT technique have extended its capabilities to include full reconstruction of the 3D grain structure including both grain morphology and crystallographic orientation, thereby making the LabDCT more comparable to conventional 3D-EBSD data – while still supporting 4D time dependent studies. We will present a selection of results of LabDCT with particularly emphasis on its non-destructive operation,

demonstrated through 4D evolutionary studies obtained by repeating the imaging procedure numerous times on the same sample. We will discuss the boundary conditions of the current implementation, point to the future of the technique and discuss ways in which this can be correlatively coupled to related techniques for a better understanding of materials structure evolution in 3D.

[1] McDonald, S.A. et al. Non-destructive mapping of grain orientations in 3D by laboratory X-ray microscopy. Scientific Reports 5, 14665 (2015). doi: 10.1038/srep14665

[2] C. Holzner et al., "Diffraction Contrast Tomography in the Laboratory – Applications and Future Directions," Micros. Today, vol. 24, no. 4, pp. 34–43, 2016.

10391-13, Session 3

In-situ observation of phase separation of polymer blend using x-ray Talbot-Lau interferometer

Yanlin Wu, Hidekazu Takano, Atsushi Momose, Tohoku Univ. (Japan)

X-ray phase tomography was used to follow the time evolution of the structure of polymer blend experiencing phase separation with respect to heating treatment.

In this work, we performed high-speed X-ray phase imaging and tomography with X-ray Talbot-Lau interferometer using synchrotron radiation white beam, which has the advantage that broad energy bandwidth X-rays can be used.

The X-ray Talbot-Lau interferometer consists of a source grating (30 ?m), a ϖ/2 phase grating (4.5 ?m) and an amplitude grating (5.3 ?m) and high speed camera. A polymer blend system of polystyrene (Mw = 76,500) and polymethylmethacrylate (PMMA) (Mw = 33,200) was used for the CT observations. A compound of PS and PMMA were made by a twin-screw extruder and put into an Al tube, which inner diameter was 5 mm. The sample temperature can be maintained at desired temperature sequence, and corresponding CT scans were repeated to track the changes in the sample structures.

The phase separation structure of PS / PMMA blends was observed during heating at a temporal time resolution of 5 seconds. PS-rich phase and PMMA-rich phase and their change with time evolution can be observed.

10391-14, Session 4

Numerical study on simultaneous emission and transmission tomography in the MRI framework

Lars Gjesteby, Wenxiang Cong, Ge Wang, Rensselaer Polytechnic Institute (United States)

Multi-modality imaging methods have greatly advanced diagnostic and therapy assessment capabilities in medicine. Specifically, hybrid systems that combine positron emission tomography (PET) with computed tomography (CT) and magnetic resonance imaging (MRI) respectively deliver valuable complementary functional and structural/morphological information. A novel imaging method was recently demonstrated that combines MRI principles with nuclear medicine techniques to reconstruct the concentration of a polarized ?-ray emitting radioisotope. The resultant images achieved better spatial resolution than standard nuclear imaging and higher sensitivity than MRI. In our work, we propose to acquire this form of MRI-modulated nuclear data for simultaneous image reconstruction in terms of both emission and transmission parameters, suggesting the potential for simultaneous CT-MRI-SPECT. The simultaneous information provides insight into tissue forms and molecular/cellular functions of features being imaged. We describe the methodology involving the system design with emphasis on the imaging protocol and the formulation for image inversion. Polarized radiotracers are used to serve as internal sources for attenuation-based imaging. In the presence of a main magnetic field with alteration by gradient coils, a region of radiotracers emitting directionally-specific x-rays can be targeted for measurement by collimated detectors. Initial numerical results demonstrate the feasibility of our technique for reconstructing concentration and attenuation images of a water phantom with various radio-labeled tissue types. Additional considerations regarding the radioisotope half-life, ?-branching ratio, and longitudinal relaxation are needed to find the best material.

10391-15, Session 4

A spectral CT reconstruction algorithm based on weighted block matching 3D filtering

Morteza Salehjahromi, Yanbo Zhang, Hengyong Yu, Univ. of Massachusetts Lowell (United States)

In spectral CT, an energy-resolving x-ray detector is capable of counting the number of received photons in different energy channels with appropriate post-processing steps. Because the received photon number in each energy channel is low in practice, the generated projections suffer from low signal to noise ratio. This makes it a challenging task to reconstruct spectral CT images. Because the reconstructed multi-channel images are technically from the same object but in different energies, there is a high correlation among these images and one can make full use of this redundant information. In this work, we propose a weighted block matching 3D (BM3D) filtering-based method for iterative spectral CT reconstruction. It is based on denoising of small 3D data arrays formed by grouping similar 2D blocks from the whole 3D data image. This method consists of the following steps in each iteration. First, a 2D image is updated by the OS-SART for each energy channel. Second, we perform the weighted BM3D filtering-based method to not only denoise each channel image but also exploit the correlation among the channel images. The proposed method is evaluated by using both numerical simulation and realistic preclinical datasets, and its merits are confirmed by the promising results.

10391-16, Session 4

Applications of compressed sensing image reconstruction to sparse-view phase tomography

Ryosuke Ueda, Hiroyuki Kudo, Jian Dong, Univ. of Tsukuba (Japan)

It is known that x-ray phase microscopy CT as well as x-ray phase micro CT require a long measurement time so that the so-called sparse-view CT data acquisition is an attractive way to shorten the measurement time. This paper applies two major compressed sensing (CS) approaches to image reconstruction in the x-ray sparse-view phase tomography where the projection data is undersampled. The first CS approach is the standard Total Variation (TV) regularization, in which the cost function for image reconstruction is expressed as f(x)=beta*TV(x)+|DAx-b|_W^2, where x is the image, b is the phase differential projection data, A is the projection matrix, and D is the differentiation operator. The major drawback of TV regularization is patchy artifact and loss in smooth intensity changes and textures due to the piecewise constant nature of image model. The second CS method is a relatively new approach of CS which uses a non-linear smoothing filter to design the regularization term. In this approach, the cost function is expressed as f(x)=beta*NL(x)+|DAx-b|_W^2 with the regularizer NL(x) having the form of |x-Mx|_1^1, where M is an arbitrary non-linear smoothing filter such as median, non-local mean (NLM), bilateral (BL), and anisotropic diffusion filter. The non-linear filter based CS is expected to reduce the major artifact in the TV regularization. The both cost functions can be minimized by using an iterative algorithm based on the so-called proximal gradient optimization method. However, in the past research activities, it is not clearly demonstrated 1) how much image quality difference occurs between the TV regularization and the non-linear filter based CS and 2) effect of used non-linear filter to image quality in the

non-linear filter based CS, with CT applications. We clarify these two points by applying the two CS applications to the case of x-ray tomography. We provide results with numerically simulated data as well as results with real data. The results demonstrate that the non-linear filter based CS using the NLM and BL filter significantly outperforms the TV regularization in terms of preserving edged, textures, and smooth intensity changes.

10391-17, Session 4

Deep learning for low-dose CT *(Invited Paper)*

Hu Chen, Yi Zhang, Jiliu Zhou, Sichuan Univ. (China); Ge Wang, Rensselaer Polytechnic Institute (United States)

The great biomedical utilities of the CT technology have led to an increasingly high number of CT scans, and at the same time an elevated public concern over the potential radiation damage to the patients. The well-known guiding principle is abbreviated as ALARA (as low as reasonably achievable), which is seriously taken in the medical community. The most common way to minimize the radiation dose is to reduce the x-ray flux, which can be implemented by adjusting the tube voltage, current, and operating time, process photon-limited raw data and/or reconstruct an image iteratively in a statistical and compressed sensing framework. Different from the sinogram-based filtering and iterative reconstruction methods, post image processing does not rely on the raw data format (normally unavailable) and the scanner imaging protocol (depending on vendors and protocols), and can be directly applied on low-dose CT images. This means that the denoising work can be easily integrated into the current CT workflow. The main problem of this post-processing method lies in that the distribution of the noise in the image domain cannot be statistically well modeled at this stage, which is a current challenge to achieve the optimal tradeoff between structure preservation and noise suppression. Fortunately, the machine learning approach is immune to this problem. Here we propose a deep neural network model for low-dose CT. While traditional convolutional neural network (CNN) with cascaded pooling operations will lose important details, we are inspired by the idea behind the auto-encoder, and include deconvolutional layers in the network to construct a symmetrical auto-encoder CNN model. Shortcut connections are used to compensate for the lost details and suppress the impact of gradient diffusion for training. Our results from both simulated and clinical data have demonstrated that the proposed scheme is promising for low-dose CT via image restoration.

10391-18, Session 4

Machine learning for micro-tomography *(Invited Paper)*

Dilworth Y. Parkinson, Daniela M. Ushizima, Daniel Pelt, Talita Perciano, Harinarayan Krishnan, Holden Parks, Alexander Hexemer, Harold S. Barnard, Alastair A. MacDowell, Lawrence Berkeley National Lab. (United States); James A. Sethian, Univ. of California, Berkeley (United States)

Machine learning has revolutionized a number of fields, but many micro-tomography users have never used it for their work. The micro-tomography beamline at the Advanced Light Source (ALS), in collaboration with the Center for Applied Mathematics for Energy Research Applications (CAMERA) at Lawrence Berkeley National Laboratory, has now deployed a series of tools to automate data processing for ALS users using machine learning. This includes new reconstruction algorithms, feature extraction tools, and image classification and recommendation systems for scientific image. Some of these tools are either in automated data pipelines that operate on data as it is collected. Others are deployed on computing resources at Berkeley Lab--from workstations to supercomputers--and made accessible to users through either scripting or easy-to-use graphical interfaces. I will present a progress report on this work.

10391-19, Session 5

Imaging human brain tissue using tomography with conventional and synchrotron x-ray sources *(Invited Paper)*

Anna Khimchenko, Georg Schulz, Christos Bikis, Simone E. Hieber, Marzia Buscema, Hans Deyhle, Univ. Basel (Switzerland); Gabriel Schweighauser, Jürgen Hench, Univ. Hospital Basel (Switzerland); Alexandra Pacureanu, ESRF - The European Synchrotron (France); Peter Thalmann, Natalia Chicherova, Bert Müller, Univ. Basel (Switzerland)

Brain tissue has a complex, multi-scale organization down to its individual sub-cellular components. Hard X-ray imaging is a powerful method for three-dimensional (3D) investigations, providing a (sub-)cellular resolution in a non-destructive and time-efficient manner. As recently shown, laboratory-based microtomography in absorption contrast of formalin-fixed paraffin-embedded (FFPE) human cerebellum yields an image contrast, comparable to conventional histological sections; even the individual Purkinje cells are clearly seen [1]. For the 3D visualization of soft tissues phase contrast yields better data quality compared to conventional absorption contrast mode. Synchrotron radiation based X-ray phase-contrast imaging enabled the visualization of non-stained Purkinje cells down to the sub-cellular level and their automatic counting [2]. In this communication, we present the study of brain tissue ultra-structure using magnified phase contrast holotomography. As an example, we present images of human cerebellum and cortex blocks embedded in JB-4 (water-soluble, GMA based, plastic resin), epoxy resin and paraffin in which structures at nanometer scale such as the nucleoli of Purkinje, granule or pyramidal cells are resolved. We expect that absorption and phase contrast tomography can provide valuable information on human tissues in health and disease for many medical applications as well as for basic research.

[1] A. Khimchenko et al., NeuroImage 139, 26-36 (2016).

[2] S.E. Hieber et al., Scientific Reports 6, 32156 (2016).

[3] A. Khimchenko et al., Proceedings of SPIE 9797, 97970B (2016).

10391-20, Session 5

Assessment of imaging quality in magnified phase CT of human bone tissue at the nanoscale

Boliang Yu, Max Langer, Institut National des Sciences Appliquées de Lyon (France); Alexandra Pacureanu, ESRF - The European Synchrotron (France); Remy Gauthier, Institut Francais des Sciences et Technologies des Transports de l'amenagement et des Reseaux (France); Cécile Olivier, ESRF - The European Synchrotron (France); Helene Follet, Institut National de la Santé et de la Recherche Médicale (France); David Mitton, Institut Francais des Sciences et Technologies des Transports de l'amenagement et des Reseaux (France); Peter Cloetens, ESRF - The European Synchrotron (France); Françoise Peyrin, Institut National des Sciences Appliquées de Lyon (France) and ESRF - The European Synchrotron (France)

The investigation of bone properties has a major impact on the prediction of fracture risk in disease such as osteoporosis. However, there are still few 3D quantitative data on bone tissue at the cellular scale. Here we propose to use magnified X-ray phase nano-CT to quantify bone ultra-structure in human bone, by using the new ID16A beamline at the ESRF to reach a voxel size of 10nm. Obtaining 3D images requires the application of phase retrieval prior to tomographic reconstruction. Phase retrieval is an ill-posed problem for which various approaches have been developed. Image quality being essential for the further quantification of bone tissue, our aim, here,

is to evaluate different phase retrieval methods for imaging bone samples at the nanoscale. Samples from femurs of female donors were scanned using magnified phase nano-CT at voxel sizes of 120 and 30 nm with an energy of 33 keV. Four CT scans at varying sample-to-detector distances were acquired for each sample. We evaluated three phase retrieval methods adapted to these conditions: Paganin method at single distance, Paganin method extended to multiple distances, and the contrast transfer function (CTF) approach for homogeneous objects. These methods were followed by an iterative refinement step. Our results based on visual observation and quantitative assessment show that the use of several distances (as opposed to one) decisively improves image quality and the two considered phase retrieval methods give similar results. First results on the segmentation of osteocyte lacunae and canaliculi from such images will be presented.

10391-21, Session 5

Micro-CT in situ study of carbonate rock porosity for CO2 storage

Yi Zheng, Technical Univ. of Denmark (Denmark); Melania Rogowska, Yi Yang, Univ. of Copenhagen (Denmark); Carsten Gundlach, Technical Univ. of Denmark (Denmark)

To achieve the 2?°C target made in the 2016 Paris Agreement, it is essential to stop emitting CO2 and the other greenhouse gases into the atmosphere. Carbon Capture and Storage (CCS) has been given increasing importance over the last decade. One of the suggested methods for CCS is to inject CO2 into geologic settings such as carbonate reservoirs in the North Sea. Micro-CT imaging is a non-destructed 3D method that can be used to study the storage properties of carbonate rocks. The advance in lab source based micro-CT has made it capable of in situ experiments. In this paper, we used a commercial bench top micro-CT (ZEISS Xradia 410 Versa) to study the change of porosity and permeability during CO2 injection in chalk. The aim is to determine an effective way to control the change of porosity during CO2 injection, such as by controlling the flow rate, injection pressure or chemical solutions. Fast CT technique is also being investigated during the study. The results show that the bench top CT system, combined with a specially designed pressure cell is capable in the in situ study of CO2 injection in chalk.

10391-22, Session 5

Establishment of metrological traceability in porosity measurements by x-ray computed tomography

Petr Hermanek, Simone Carmignato, Univ. degli Studi di Padova (Italy)

Internal porosity is an inherent phenomenon to many manufacturing processes, such as casting, additive manufacturing, and others. Since these defects cannot be completely avoided by improving production processes, it is important to have a reliable method to detect and evaluate them accurately. The accurate evaluation becomes even more important concerning current industrial trends to minimize size and weight of products on one side, and enhance their complexity and performance on the other. X-ray computed tomography (CT) has emerged as a promising instrument for this application offering several advantages over equivalent methods already established in the detection of internal defects. The main shortcomings of the conventional techniques pertain to too general information about total porosity content (e.g. Archimedes method) or the destructive way of testing (e.g. microscopy of cross-sections). On the contrary, CT is a non-destructive technique providing complete information about size, shape and distribution of internal porosity.

However, due to the lack of standards and the fact that it is relatively new measurement technique, CT as a measurement technology has not yet reached maturity. This study proposes a procedure for the establishment of measurement traceability in porosity measurements by CT including the necessary evaluation of measurement uncertainty. The traceability transfer is carried out through a novel reference standard calibrated by optical and tactile coordinate measuring systems. The measurement uncertainty is calculated following several methods and the results are compared upon. In addition, the accuracy of porosity measurements by CT with the associated measurement uncertainty is evaluated using the reference standard.

10391-23, Session 5

Biodegradable magnesium-based implants in bone studied by synchrotron-radiation microtomography *(Invited Paper)*

Julian Moosmann, Jörg U. Hammel, Felix Beckmann, Diana Krüger, Helmholtz-Zentrum Geesthacht (Germany); Silvia Galli, Malmö Univ. (Sweden); Regine Willumeit-Römer, Florian Wieland, Berit Zeller-Plumhoff, Helmholtz-Zentrum Geesthacht (Germany); Martin Bech, Niccolo Peruzzi, Lund Univ. (Sweden)

Permanent implants made of titanium or its alloys are the gold standard in many orthopedic and traumatological applications due to their good biocompatibility and mechanical properties. However, a second surgical intervention is required in order to remove the implant, e.g., in the case of children or because of detrimental effects due to stress shielding or wear debris. Here, magnesium-based materials which degrade under physiological conditions have become increasingly attractive due to their mechanical stability, biocompatibility, and degradation properties. A major challenge, however, is tailoring the degradation in a manner that is suitable for a biological environment and such that stabilization of the bone is provided until the bone defect is healed and implant removal can be avoided. In order to understand failure mechanisms of magnesium-based implants in orthopedic applications, bone-implant samples are studied under mechanical and cyclic load conditions by means of a push-out device installed at the imaging beamline (IBL) P05 at PETRA III at DESY. Implants from titanium and PEEK serve as control. The materials are implanted in bone and harvested after various healing times. Conventional absorption contrast microtomography and phase-contrast techniques are applied in order to monitor the bone-implant interface in three dimensions. Analyzing the morphological adaptations of bone and soft tissue and the degradation and biocompatibility of the screw material, we present results of how different materials influence the integration of implants into the bone.

10391-24, Session 6

The NOVA project: maximizing beamtime efficiency through synergistic analyses of SRuCT data *(Invited Paper)*

Sebastian Schmelzle, Technische Univ. Darmstadt (Germany); Vincent Heuveline, Ruprecht-Karls-Univ. Heidelberg (Germany); Jürgen Becker, Karlsruher Institut für Technologie (Germany); Michael Heethoff, Technische Univ. Darmstadt (Germany); Thomas van de Kamp, Karlsruher Institut für Technologie (Germany)

Beamtime and resulting SR?CT data are a valuable resource for researchers of a broad scientific community working with tomographic data. Most research groups, however are only interested in a specific organ and thus use only a fraction of their data. The rest of the data usually remains untapped. By using a new collaborative approach, the NOVA project (Network for Online Visualization and synergistic Analysis of tomographic data) aims to create possibilities, that allow for a more efficient use of the valuable beam time through the coordination of research on different organ systems. The biological partners in the project cover different scientific aspects and thus serve as model community for the collaborative approach. As prove of principle, different aspects of insect head morphology will be investigated (e.g., biomechanics of the mouthparts and neurobiology with the topology of sensory areas). This effort is accomplished by development of advanced analysis tools for the ever-increasing quantity of tomographic datasets. In the preceding project ASTOR, we already successfully demonstrated considerable progress in semi-automatic segmentation and classification of internal structures. Further improvement of these methods is essential for an efficient use of beamtime and will be refined in this project. Significant enhancements are also planned at the PETRA III instrumentation (phase contrast), on the reconstruction algorithms (based on intensity as well as absorption), and the tools for subsequent analyses and management of the data. All improvements made on key technologies within this project will be equally beneficial for all users of tomography instrumentations.

10391-25, Session 6

Detector response artefacts in spectral reconstruction

Ulrik L. Olsen, Jan Kehres, Yun Gu, Technical Univ. of Denmark (Denmark); Erik D. Christensen, Univ. of Copenhagen (Denmark); Mohamad Khalil, Technical Univ. of Denmark (Denmark)

Energy resolved detectors are gaining traction as a tool to achieve better material contrast. K-edge imaging and tomography is an example of a method with high potential that has evolved on the capabilities of photon counting energy dispersive detectors. Border security is also beginning to see instruments taking advantage of energy resolved detectors. The progress of the field is halted by the limitations of the detectors. The limitations include non-linear response for both x-ray intensity and x-ray spectrum. In this work we investigate how the physical interactions in the energy dispersive detectors affect the quality of the reconstruction and how corrections restore the quality. We have modelled detector responses for the primary detrimental effects occurring in the detector; escape peaks, charge sharing/loss and pile-up. The effect of the change in the measured spectra is evaluated based on the artefacts occurring in the reconstructed images. We also evaluate the effect of a correction algorithm for reducing these artefacts on experimental data acquired with a setup using Multix ME-100 V-2 line detector modules. The artefacts were seen to introduce 20% deviation in the reconstructed attenuation coefficient for the uncorrected detector. We performed tomography experiments on samples with various materials interesting for security applications and found the SSIM to increase >5 % below 60keV. Our work shows that effective corrections schemes are necessary for the accurate material classification in security application promised by the advent of high flux detectors for spectral tomography.

10391-26, Session 6

Simulated data for synchrotron radiation based microtomography at the imaging beamline P05/PETRA III

Felix Beckmann, Helmholtz-Zentrum Geesthacht (Germany)

The Helmholtz-Zentrum Geesthacht, Germany, is operating the user experiments for microtomography at the beamlines P05 and P07 using synchrotron radiation produced in the storage ring PETRA III at DESY, Hamburg, Germany. In recent years the software pipeline and sample changing hardware for performing high throughput experiments were developed. To test and optimize the different measurement techniques together with quantification of the quality of different reconstruction algorithms a software pipeline to simulate the experiment was implemented. Within this this talk the current status of the beamline P05 and a comparison of simulated data with measured data will be given.

10391-27, Session 6

Comparison of data processing techniques for single-grating x-ray Talbot interferometer data

Shashidhara Marathe, Diamond Light Source Ltd. (United Kingdom); Marie-Christine Zdora, Diamond Light Source Ltd. (United Kingdom) and Univ. College London (United Kingdom); Irene Zanette, Silvia Cippicia, Christoph Rau, Diamond Light Source Ltd. (United Kingdom)

For over a decade, the X-ray Grating Talbot interferometer (XGTI) has been at the forefront of X-ray phase-contrast imaging due to its ability to visualize very small density variations of bulk objects with the possibility of extracting three imaging modalities from a single interferogram image or a data set. Most widely used XGTI data acquisition techniques, namely the two grating phase-stepping and Moiré techniques, suffer from poor signal to noise ratio (SNR), which is mainly due to about 50% reduction in scattered sample signal by the second amplitude grating. Consequently, longer exposure times are required for an improved SNR, which comes at the cost of an increased dose to the sample.

To overcome this problem, we can use a setup with only a single phase grating in combination with a high-resolution detector system. Data acquisition and analysis can be performed either in phase-stepping mode or from a single reference and sample image. The latter technique makes use of the fact that a Talbot interferogram consists of carrier frequency spectrum of the grating overlapping with the sample spectrum and by Fourier transforming the interferogram we can separate the two. We will compare these two single grating data processing techniques using a single data set measured with mouse embryo heart and discuss advantages and disadvantages of each technique. These two techniques can be used as complementary; one for high resolution, and the other for high-speed imaging.

10391-28, Session 6

Micro- and nano-tomography at the DIAMOND beamline I13L imaging and coherence

Christoph Rau, Andrew J. Bodey, Malte Ogurreck, Shashidhara Marathe, Silvia Cipiccia, Marie-Christine Zdora, Irene Zanette, Ulrich H. Wagner, Xiaowen Shi, Darren Batey, Diamond Light Source Ltd. (United Kingdom)

The Diamond Beamline I13L is dedicated to imaging on the micron- and nano-lengthsale, operating in the energy range between 6 and 30 keV [1]. For this purpose two independently operating branchlines and endstations have been built. The imaging branch is fully operational for micro-tomography and in-line phase contrast imaging with micrometre resolution. Grating interferometry is currently implemented complementing the instrumental capabilities on the micron lengthscale. In addition, a full-field microscope providing 50nm spatial resolution over a field of view of 100microns is being tested. The instrument provides a large working distance between optics and sample to adapt a wide range of customised sample environments. On the coherence branch coherent diffraction imaging techniques such as ptychography, coherent X-ray diffraction (CXRD) are currently developed for three dimensional imaging.

The imaging branch is operated in collaboration with Manchester University, called therefore the Diamond-Manchester Branchline. The scientific applications cover a large area including bio-medicine, materials science, chemistry geology and more. We will present the current status of the beamline and an overview of the science addressed at the beamline.

Reference:

[1] C. Rau, U. Wagner, Z. Pesic, A. De Fanis Physica Status Solidi (a) 208 (11). Issue 11 2522-2525, 2011, 10.1002/pssa.201184272

10391-29, Session 7

Design of 4D x-ray tomography experiments based on reconstruction analysis *(Invited Paper)*

K. Aditya Mohan, Lawrence Livermore National Lab. (United States)

4D computed tomography (4DCT) using X-rays is widely used to perform non-destructive characterization of time varying physical processes in material and biological samples. The conventional approach to improving temporal resolution in 4DCT revolves around developing expensive and complex instrumentation that acquire views faster with reduced noise. It is customary to acquire fully sampled data that satisfy the Nyquist sampling criteria at a high signal to noise ratio. This approach is sub-optimal as there exist advanced iterative algorithms that are less sensitive to noise and limited data but can benefit from optimization of other experimental parameters. Guided by quantitative analysis of the sample reconstruction, these algorithms allow us to achieve significant gains by optimizing the view sampling strategy while reducing the number of view angles and/or the detector exposure time. Such algorithms can be formulated using the framework of model-based iterative reconstruction (MBIR). Most of the existing and widely used iterative algorithms can also be described and analyzed using the MBIR framework. This talk discusses the design of 4DCT experiments based on analysis of sample reconstructions.

10391-30, Session 7

Reduction of metal artifacts in x-ray CT images using fully convolutional networks

Yanbo Zhang, Ying Chu, Hengyong Yu, Univ. of Massachusetts Lowell (United States)

Patients usually contain various metallic implants (e.g. dental fillings, prostheses), causing severe artifacts in x-ray CT images. Although a large number of metal artifact reduction (MAR) methods have been proposed in the past four decades, MAR is still one of the major problems in clinical x-ray CT. Recently, deep learning methods have been successfully applied to various fields, where fully convolutional networks (FCN) is a powerful tool for semantic segmentation. In this work, we apply FCN to reduce metal artifacts. In specific, our method includes three consecutive steps. First, metals are segmented from the original uncorrected CT images, and a pre-correction procedure (e.g. linear interpolation) is carried out. Then, the original CT image, the pre-corrected image and the segmented metal image are combined as a multi-channel image. It is segmented into different types of tissues using FCN to generate a prior image. Finally, the metal contaminated projections are replaced by the forward projection of the prior image, and the corrected image is reconstructed. The merits of the proposed approach are threefold. First, this method is able to combine useful information in both the original and pre-corrected images. Second, because this method is based on big data, the larger the training database is, the better the artifacts removal performance is. Third, different from other MAR methods, the proposed algorithm is in an open framework, and the performance can be further improved by introducing other MAR corrected results into the multi-channel image. Our results show that the proposed method can remarkably suppress metal artifacts and avoid introducing new artifacts

10391-31, Session 7

Deep learning methods for CT image-domain metal artifact reduction

Lars Gjesteby, Qingsong Yang, Rensselaer Polytechnic Institute (United States); Yan Xi, Shanghai Jiao Tong Univ. (United States); Bernhard E. H. Claus, Yannan Jin, Bruno De Man, GE Global Research (United States); Ge Wang, Rensselaer Polytechnic Institute (United States)

Artifacts resulting from metal objects have been a persistent problem in computed tomography (CT) images over the last four decades. A common approach to overcome their effects is to replace corrupt projection data with values synthesized from an interpolation scheme or by reprojection of a prior image. Then, reconstruction of the corrected data is expected to yield better image quality than the original reconstructed image. A state-of-the-art interpolation and normalization-based algorithm is NMAR. In some clinical applications, methods like NMAR still do not produce sufficient results. Residual artifacts remain in challenging cases and even new artifacts can be introduced by the interpolation scheme. Radiation therapy planning is one task that is very sensitive to image reconstruction errors due to the high image quality needed for accurate tumor volume estimation. A possible new solution to the long-standing metal artifact reduction (MAR) problem is deep learning, which has been successfully applied to medical image processing and analysis tasks. Deep networks have the ability to extract detailed features from large datasets to map an input to an output. In this study, we combine a convolutional neural network (CNN) with the state-of-the-art NMAR algorithm to reduce metal streaks in critical image regions. The CNN is able to map metal-corrupted images to artifact-free monoenergetic images to achieve additional correction on top of NMAR for improved image quality. Our results indicate that deep learning is a novel tool to address CT reconstruction challenges, and may enable more accurate tumor volume estimation for radiation therapy planning.

10391-32, Session 7

Sliding ordered-subset algorithm for real-time x-ray tomography *(Invited Paper)*

Doga Gürsoy, Tekin Bicer, Daniel Ching, Vincent De Andrade, Argonne National Lab. (United States)

As the sophistication and speed of today's experiments grow, collecting the most informative data become of great relevance, necessitating development of algorithms that can provide good quality reconstructions from data streams. However, almost all conventional reconstruction algorithms work exclusively off-line, requiring for complete data to be collected and available before they can successfully be applied. We describe here a streaming algorithm, based on sliding ordered-subsets, and present our first tests of using it on tomography datasets generated at the Advanced Photon Source. We will also evaluate the quality of reconstructions live using multiple quality metrics, as data are being collected, and discuss ways of steering experiment based on the information gained during acquisition.

10391-33, Session 8

Recent Advance in grating-based x-ray phase tomography *(Invited Paper)*

Atsushi Momose, Tohoku Univ. (Japan) and Japan Science and Technology Agency (Japan) and Japan Synchrotron Radiation Research Institute (JASRI) (Japan); Hidekazu Takano, Tohoku Univ. (Japan) and Japan Science and Technology Agency (Japan); Yanlin Wu, Tohoku Univ. (Japan) and Japan Synchrotron Radiation Research Institute (JASRI) (Japan); Masato Hoshino, Japan Synchrotron Radiation Research Institute (JASRI) (Japan) and Japan Science and Technology Agency (Japan)

X-ray phase tomography based on grating interferometry is attractive because of its flexible optical configuration and the potential of various applications even with laboratory X-ray sources other than synchrotron radiation. Since grating interferometers functions with X-rays of a broad energy band, polychromatic X-rays are used for high-speed or four-dimensional X-ray phase tomography. We have recently installed a multilayer bandpass fileter to produce a pink beam sutable for a Talbot

interferometer at BL28B2, SPring-8. Pilot experimental results of four-dimensional X-ray phase tomography will be presented for revealing dynamical properties of samples, for instance under laser irradiation. Another activity is the development of nanoscopic phase tomography by comging FZP-based X-ray full-field microscopes and gratings both at SPring-8 and laboratory. An X-ray microscope with a spatial resolution around 200 nm with a field of view of 300 μm has been constructed at BL37XU, SPring-8. High-resolution phase tomograms of mouse bone samples will be presented. Another X-ray microscope (Zeiss Xradia 800 Ultra), whose best spatial resolution is 50 nm, has been combined with a Lau interferometer. The system is operated with an incoherent X-ray source at laboratory, and a twin phaes image rather than a differential phase image is obtained. A special algorithm is developed for generating a single phase image from the twin image, and a pilot result of nanoscopic phase tomography at laboratory will be presented.

10391-34, Session 8

Thomson scattering x-ray source: a novel tool for x-ray imaging *(Invited Paper)*

Yingchao Du, Zhijun Chi, Chuanxiang Tang, Wenhui Huang, Lixin Yan, Zhen Zhang, Tsinghua Univ. (China)

As a powerful complement of large scale synchrotron radiation and free electron laser (FEL) facilities, Thomson scattering x-ray source, also called inverse Compton scattering x-ray source, can produce quasi-monochromatic, continuously tunable, high brightness, small spot size, polarization precisely controllable, and ultrashort (ps or sub-ps) x-ray pulse in the energy regime ranging from tens keV to several MeV or even higher. The excellent beam quality combined with room scale or tabletop footprint and relative low cost provides the prospect for and will help to prosper a myriad of x-ray imaging applications, such as mono-chromatic, dual-energy and multi-energy computed tomography (CT), phase-contrast imaging and phase-contrast CT, x-ray fluorescence (XRF) or nuclear resonance fluorescence (NRF) analysis, pump-probe diagnostic of ultrafast processes, and new dimensional x-ray imaging (e.g. charge and spin orientation) with further use of the straightforward controllable polarization. In this paper, we will introduce recent progress of x-ray imaging based on Tsinghua Thomson scattering X-ray source (TTX). Based on the mono-chromaticity of x-rays generated by Thomson light source, beam hardening effect seen with commercial polychromatic x-ray source can be resolved fundamentally, and quantitative CT becomes possible. Monochromatic CT of a peanut (Arachis hypogaea L.) has been reconstructed, and different compositions of the peanut have been segmented by quantitative analysis of reconstructed attenuation coefficients. Taking advantage of the continuous tunable x-rays, dual energy x-ray imaging has been carried out, and the effective atomic numbers (i.e. Zeff) of different materials have been retrieved and compared with theoretical values. Since the small spot size of Thomson light source makes the x-ray pulse highly spatially coherent, phase-contrast x-ray imaging (PCI) of different sample (e.g. shrimp, fish, and peanut) and preliminary phase-contrast CT imaging of a simple Teflon sample have been accomplished. Clear edge-enhancement effect has been witnessed in in-line PCI, which provides an exact way for interface diagnosis between different materials. Besides, XRF imaging has also been carried out to quantitatively analyze the content of some trace elements. Our results demonstrate the potential of Thomson scattering x-ray source for a variety of x-ray imaging, and pave the way towards practical application of this type of x-ray source, such as preclinical radiography and tomography, and industrial material analysis.

10391-35, Session 8

High spatial resolution x-ray phase tomography based on laboratory source

Hidekazu Takano, Yanlin Wu, Atsushi Momose, Tohoku Univ. (Japan)

X-ray microscopy is important technique for X-ray tomography to increase the spatial resolution. Also, phase-contrast technique is important to increase the sensitivity. We developed phase quantitative method by using grating interferometer, and combined it to full-field X-ray microscope. These techniques are capable to apply for laboratory-based optics by introducing Lau interferometer.

Zeiss Xradia 800 Ultra, which can achieve 50 nm resolution with a laboratory source of Cu target, is adopted as a basic microscope to be installed the interferometer. The Lau interferometer consists of an absorption grating (G0) and a ϖ/2 phase grating (G1). G0, set in front of sample, is formed an image by the microscope objective. It functions as a source array to yield a spatial coherence. G1, set at behind of the image of G0, is magnified and projected on detector, which is set to form the self-image G1 by Talbot effect. The parameters are optimized so that the self-image projected by each source overlaps in phase. As the results, interference fringes with visibility better than 0.6 were obtained. By conventional fringe scanning procedure, phase-differential image, which is superposition of a separated image with opposite contrast, is obtained. Phase quantitative image can be retrieved by calculation, and the optical system can be applied for phase tomography.

In the presentation, we will introduce about results of evaluation in spatial resolution and sensitivity, and CT images with high resolution.

10391-36, Session 8

Seeing inhomogeneous buried layers and interfaces: image reconstruction from x-ray reflection projections *(Invited Paper)*

Jinxing Jiang, Univ. of Tsukuba (Japan) and National Institute for Materials Science (Japan); Keiichi Hirano, High Energy Accelerator Research Organization, KEK (Japan); Kenji Sakurai, National Institute for Materials Science (Japan) and Univ. of Tsukuba (Japan)

Exotic functions of thin films are quite often connected to the unique atomic and molecular features of buried layers and interfaces. In reality, they are far from uniform, but seeing such inhomogeneity is extremely difficult. The present talk describes how we have solved the difficulties. The novel technique developed is the X-ray reflectivity imaging. Ordinary X-ray reflectivity gives very precise information such as the number of layers, the density and the thickness of each layer, and the roughness of each interface. The method can have imaging capability, by combining with the image reconstruction scheme. While the illuminated area size is around 8 mm x 8mm, the obtained typical spatial resolution is below 20 micron. The inhomogeneity can be quantitatively imaged with very high depth-resolution of the order of Å. The present method can also provide X-ray reflectivity data for all points in the viewing area, even without the use of micro beam. Not only instrumental details but also many practical application will be reported.

10391-47, Session PWed

Development of high-energy micro-tomography system at SPring-8

Kentaro Uesugi, Masato Hoshino, Japan Synchrotron Radiation Research Institute (JASRI) (Japan)

A high energy X-ray micro-tomography system has been developed at BL20B2 in SPring-8. The available range of the energy is between 20keV and 113keV. The system enables us to image large or heavy materials such as fossils. The X-ray image detector consists of visible light conversion system and sCMOS camera. The effective pixel size is variable by changing a tandem lens between 12.2um/pixel to 25.5um/pixel discretely. The format of the camera is 2048 pixels x 2048 pixels.

As a demonstration of the system, a nodule from Bolivia was imaged. The experimental conditions are follows, X-ray energy: 73keV, exposure time: 200msec, number of projections: 900, single scan time: 20min, pixel size: 31um/pixel (2x2 binning mode) and field of view: 31.0mm x 5mm. The field of view is restricted by the beam size.

A Trilobite and some other fossils were successfully imaged without breaking the fossil.

At the conference, the detail of the system and some demonstration will be shown.

10391-48, Session PWed

Spectral CT material decomposition in the presence of poisson noise: a KL approach

Tom Hohweiller, Nicolas Ducros, CREATIS (France); Françoise Peyrin, CREATIS (France) and ESRF - The European Synchrotron (France); Bruno Sixou, CREATIS (France)

Spectral computed tomography (SPCT) is a new imaging modality able to measure the energy of the X-rays hitting the detector. This new information allows to identify the materials in an object since the attenuation of any atomic element depends on energy. A large number of methods have been proposed for SPCT. A conventional approach is to perform a decomposition step, followed by standard tomographic reconstructions of the decomposed projections.

Our group recently introduced a regularized weighted least square (WLS) decomposition algorithm that allows material-specific regularization of the projection images. However, the WLS data fidelity term is not optimal when low counts are measured in some of the energy bins of the detector.

In this work, we evaluate a data fidelity term based on the Kullback-Leibler (KL) distance, which is the metric adapted to Poisson noise. A nonlinear image formation model is considered. The cost function is minimized iteratively using the Gauss-Newton (GN) method. Our nonlinear KL-GN decomposition algorithm is evaluated on a numerical mouse phantom with two materials, namely soft tissue and bone. Our results show that the KL distance is more effective than the WLS data fidelity. For the same amount of time, it provides reduced material error when low numbers of photon counts are available. We also show that accurate 3D map of each material can be reconstructed from the decomposed projections.

10391-49, Session PWed

Evaluating the precision of intraoral scans by means of micro-computed tomography measurements and three-dimensional rigid registration

Christoph Vögtlin, Georg Schulz, Kurt Jäger, Univ. Basel (Switzerland); Dieter Müssig, Danube Private Univ. (DPU) (Austria); Bert Müller, Univ. Basel (Switzerland)

The preparation of prosthetic restorations and orthodontics appliances requires three-dimensional data on the patient's dentition. Previously, the dentition was replicated using impressions with dedicated mold materials. The disadvantages of the approach relate to the unfavorable flavor of the impression materials and the human choke impulse. In order to overcome these discomforts, the dentists currently employ scanners, which provide digital impressions of the patient's dentition. With these digital data the dentist simplifies the workflow and can reduce the costs. Many dentists, however, are afraid that the accuracy of the present oral scanners does not reach the precision of the replicas using the well-established, conventional protocol. In the present study, we investigate the accuracy of the intraoral scanner "True Definition Scanner" (3M Espe, Seefeld, Germany) taking advantage of high-resolution tomography. For this purpose, we produced five reference models with constant transversal dimension. We have considered five situations in the front region, which were scanned for three times. The reference models were imaged using the tomography system nanotom® m (GE Sensing & Inspection Technologies, Wunstdorf, Germany). The obtained 15 data sets were rigidly registered to the data of reference to extract parameters such as the mean and maximal deviations in order to characterize the precision of the oral scanners. Preliminary results indicate that the intraoral scanner used in the present study reaches a precision comparable to the conventional protocol.

10391-50, Session PWed

Characterization of a spectroscopic detector for application in x-ray computed tomography

Alex A. Dooraghi, Brian J. Fix, Jerel A. Smith, William D. Brown, Stephen G. Azevedo, Harry E. Martz, Lawrence Livermore National Lab. (United States)

Recent advances in cadmium telluride (CdTe) energy-discriminating pixelated detectors have enabled the possibility of Multi-Spectral X-ray Computed Tomography (MSXCT) to incorporate spectroscopic information into CT. MultiX ME 100 V2 is a CdTe-based spectroscopic x-ray detector array capable of recording energies from 20 to 160 keV in 1.1 keV energy bin increments. Hardware and software have been designed to perform radiographic and computed tomography tasks with this spectroscopic detector. Energy calibration is examined using the end-point energy of a bremsstrahlung spectrum and radioisotope spectral lines. When measuring the spectrum from Am-241 across 500 detector elements, the standard deviation of the peak-location and FWHM measurements are ±0.4 and ±0.6 keV, respectively. As these values are within the energy bin size (1.1 keV), detector elements are consistent with each other. The count rate is characterized, using a nonparalyzable model with a dead time of 64 ± 5 ns. This is consistent with the manufacturer's quoted per detector-element linear-deviation at 2 Mpps (million photons per sec) of 8.9% (typical) and 12% (max). When comparing measured and simulated spectra, a low-energy tail is visible in the measured data due to the spectral response of the detector. If no valid photon detections are expected in the low-energy tail, then a background subtraction may be applied to allow for a possible first-order correction. If photons are expected in the low-energy tail, a detailed model must be implemented. A radiograph of an aluminum step wedge with a maximum height of about 20 mm shows an underestimation of attenuation by about 10% at 60 keV. This error is due to partial energy deposition from higher-energy (> 60 keV) photons into a lower-energy (~60 keV) bin, reducing the apparent attenuation. A radiograph of a PTFE cylinder taken using a bremsstrahlung spectrum from an x-ray voltage of 100 kV filtered by 1.3 mm Cu is reconstructed using Abel inversion. As no counts are expected in the low energy tail, a first order background correction is applied to the spectrum. The measured linear attenuation coefficient (LAC) is within 10% of the expected value in the 60 to 100 keV range. Below 60 keV, low counts in the corrected spectrum and partial energy deposition from incident photons of energy greater than 60 keV into energy bins below 60 keV impact the LAC measurements. This report ends with a demonstration of the tomographic capability of the system. The quantitative understanding of the detector developed in this report will enable further study in evaluating the system for characterization of an object's chemical make-up for industrial and security purposes.

10391-51, Session PWed

Integrated high-throughput tomography experiment control environment

Igor Khokhriakov, Felix Beckmann, Lars Lottermoser, Helmholtz-Zentrum Geesthacht (Germany)

The initial design and implementation of such system was presented in the SPIE publication in 2014 [Proc. SPIE 9212, Developments in X-Ray Tomography IX, 921217]. In this paper an update to the system is presented. The paper will cover the following 4 topics. The first topic simply gives an overview of the system. The second topic presents the way how we integrate different software components to achieve simplicity and flexibility. As it is still in research and design phase we need a possibility to easily adjust the system to our needs introducing new components or removing old ones. The third topic presents a hardware driven tomography experiment design implemented at one of our beamlines. The basic idea is

that a hardware signal is sent to the instrument hardware (camera, shutter etc). This signal is emitted by the controller of the sample axis which defines the moment when the system is ready to capture the next image, i.e. next rotation angle. Finally as our software is in a constant process of evaluation a continuous integration process was implemented to reduce the time cost of redeployment and configuration of new versions.

10391-52, Session PWed

Innervation of the cow's inner ear derived from micro-computed tomography data

Loic Costeur, Bastien Mennecart, Naturhistorisches Museum Basel (Switzerland); Anna Khimchenko, Bert Müller, Georg Schulz, Univ. Basel (Switzerland)

The innervation of the inner ear has been thoroughly investigated in humans as well as in animal models including guinea pig, rabbit, cat, dog, rat, pig, and some monkeys. Ruminant inner ears are still poorly known. Despite the potential interest in phylogenetic reconstructions, the innervation was never investigated. Following earlier work on the ontogeny of the cow's ear (Costeur et al., 2016b), we expand our understanding of this delicate structure by reconstructing the fine innervation pattern of the inner ear of the cow in two ontogenetic stages, at seven months gestation and at an adult age. The micro computed tomography data were obtained using the advanced μCT-system nanotom m with a pixel length of 45 μm, an acceleration voltage of 120 kV and the electron beam current of 200 μA. Since we work on dry skeletal specimens, only the endocast of the innervation inside the petrosal bone was reconstructed up to the internal acoustic meatus. The facial and vestibulocochlear nerves could be reconstructed together with the spiral ganglion canal. The nerves have a fibrous pattern. The ampular and utricular branches of the vestibulocochlear nerve could also be reconstructed. Comparisons to the pattern in pig, another Artiodactyla and the closest animal for which the structure is known will be given. Preliminary observations indicate similar anatomical features known from pig.

L. Costeur, B. Mennecart, B. Müller, G. Schulz, Prenatal growth stages show the development of the ruminant bony labyrinth and petrosal bone, Journal of Anatomy 230 (2017) 347-353.

10391-37, Session 9

Sparse reconstruction methods in x-ray CT *(Invited Paper)*

Juan Felipe Perez Juste Abascal, Univ. de Lyon (France) and Univ. Jean Monnet Saint-Etienne (France) and CREATIS (France); Monica Abella, Univ. Carlos III de Madrid (Spain) and Instituto de Investigación Sanitaría Gregorio Marañón (Spain); Cyril Mory, Univ. de Lyon (France) and Univ. Jean Monnet Saint-Etienne (France) and CREATIS (France); Claudia de Molina, Univ. Carlos III de Madrid (Spain) and Instituto de Investigación Sanitaría Gregorio Marañón (Spain); Nicolas Ducros, Institut National des Sciences Appliquées de Lyon (France) and Univ. de Lyon (France) and Univ. Jean Monnet Saint-Etienne (France); Eugenio Marinetto, Univ. Carlos III de Madrid (Spain) and Instituto de Investigación Sanitaría Gregorio Marañón (Spain); Françoise Peyrin, CREATIS (France) and Univ. de Lyon (France) and Univ. Jean Monnet Saint-Etienne (France); Manuel Desco, Univ. Carlos III de Madrid (Spain) and Instituto de Investigación Sanitaría Gregorio Marañón (Spain) and Ctr. de Investigación en Red de Salud Mental (Spain)

Recent progress in X-ray CT is contributing to the advent of new clinical applications. A common challenge for these applications is the need for new image reconstruction methods that meet tight constraints in radiation dose and geometrical limitations in the acquisition. The recent developments in sparse reconstruction methods provide a framework that permit obtaining good quality images from drastically reduced signal-to-noise-ratio and limited-view data.

In this work, we present our contributions in this field. For dynamic studies (3D+Time), we have explored the possibility of extending the exploitation of sparsity to the temporal dimension: a temporal operator based on modelling motion between consecutive temporal points in gated-CT and based on experimental time curves in contrast-enhanced CT. In these cases, we also exploited sparsity by using a prior image estimated from the complete acquired dataset and assessed the effect on image quality of using different sparsity operators. For limited-angle CT, we evaluated the viability of exploiting sparsity on the spatial domain to use a convectional radiology system as a tomograph. For other emerging imaging modalities, such as spectral CT, the image reconstruction problem is nonlinear, so we are exploring new efficient approaches to exploit sparsity for multi-energy CT data.

In conclusion, we review our approaches to challenging CT data reconstruction problems and show results that support the feasibility for new clinical applications.

10391-38, Session 9

Spectral CT data reduction for material classification

Mina Kheirabadi, Wail Mustafa, Technical Univ. of Denmark (Denmark); Mark Lyksborg, Fingerprint Cards (Denmark); Ulrik Lund Olsen, Anders Bjorholm Dahl, Technical Univ. of Denmark (Denmark)

In the recent years, using of detectors which are able to allow imaging of many channels at once has been popular in many applications such as medical and security. They provide higher and more accurate discrimination for chemical component of materials. In this paper, we work with data acquired using MULTIX detectors that can give us the information for 128 different energy beams. It is clear that although the reconstruction of all channels of energy can reduce the number of errors in process of recognition of materials but on the other hand it can also be time consuming in the most of cases. Therefore, to ease the process of reconstruction, we can reduce the channels of energy as long as the large amount of information is not lost. We apply classical multi dimensional scaling for reduction of channels of energy which is followed by reconstruction using an iterative algebraic reconstruction (Kaczmarz method) with a total variation regularization. We will analysis the method for the data included aluminum and four liquids, i.e. water, hydrogen peroxide, sucrose solution, Pentaerythritol tetranitrate. We will show that the materials can be distinguished after reduction of energy channels as well as when we consider all of channels of energy. It can be considered an improvement in Multi-spectral CT reconstruction in term of time.

10391-39, Session 9

Removing ring artifacts from synchrotron radiation-based hard x-ray tomography data

Peter Thalmann, Christos Bikis, Georg Schulz, Univ. Basel (Switzerland); Pierre Paleo, Alessandro Mirone, Alexander Rack, ESRF - The European Synchrotron (France); Bert Müller, Univ. Basel (Switzerland)

Indirect detectors which are frequently used in synchrotron radiation-based micro computed tomography (SRμCT) using hard X-rays give rise to ring artifacts, which interfere with image details and reduce the image quality. Such ring artifacts arise, for example, from improperly working detector elements and defects in the scintillator screens such as scratches or dust particles [1]. We propose a method that corrects such artifacts before the

reconstruction algorithm is applied. The main steps of the pipeline are (i) registration of the reference images with the radiographs, (ii) integration of the flat-field corrected projection over the acquisition angle, (iii) high-pass filtering the integrated projection, (iv) subtraction of filtered data from the flat-field corrected projections. One advantage of the algorithm is that it mainly corrects the pixels affected, in comparison to the ones using wavelet-Fourier [2] or median filtering [3]. Furthermore, since the sinograms are mainly locally corrected, the correction method maintains the three-dimensional smoothness of the reconstructed data. The study includes the removal of ring artifacts from μCT-datasets acquired at ID19 (ESRF, Grenoble, France) in phase-contrast mode [4]. The results corroborate the fact that full and partial ring artifacts are effectively removed from the reconstructed slices while preserving the image details and without inducing any gradient in the tomograms.

[1] V. Titarenko et al. Proceedings of SPIE 7804, 78040Z (2010).

[2] B. Münch et al., Optical Express, 17, 8567 (2009).

[3] F. Sadi et al., Computers in Biology and Medicine, 40, 109 (2010)

[4] S. Lang et al., Journal of Applied Physics, 116, 154903 (2014).

10391-40, Session 9

Comparison of different phase retrieval algorithms

Rolf Kaufmann, Mathieu Plamondon, Jürgen Hofmann, EMPA (Switzerland)

X-ray phase contrast imaging techniques are developed for numerous applications today, ranging from biomedical research to security scans. First commercial systems are already on the market. Since the phase cannot be measured directly by a conventional detector an indirect method as to be applied, e.g. by a grating interferometer. A common implementation is the Talbot-Lau interferometer, which also works with polychromatic radiation from an industrial X-ray tube. To have enough sensitivity a phase-stepping approach is applied where one of the gratings is slightly shifted between several acquisitions. From such a phase-stepping series of images, typically 4-10, the phase shift of a sample (=phase of the phase-stepping curve), attenuation (=mean value of the phase-stepping curve) and the scattering coefficient (=amplitude of the phase-stepping curve) are extracted. Three different approaches are compared to do so. Besides the usually applied Fourier coefficient method also a fitting technique and series expansion method are applied and compared with respect to speed, accuracy and mechanical error tolerance.

10391-41, Session 9

Nonlinear problems in fast tomography *(Invited Paper)*

William Lionheart, The Univ. of Manchester (United Kingdom)

In this paper we formulate the non-linear problem of monochromatic CT. Of course polychromatic CT is already non-linear due to beam hardening but the important point we make is that it is non-linear even if monochromatic. We calculate the Frechet derivative of the non-linear method and show that it can be solved by a regularized Newton-Kantarovich method. We will include experimental data from the Bergen gamma tomography system to show that we can get quantitatively better images using the non-linear technique. We also show using a MC model that the effect we observe cannot be attributed to scattering. This work will be presented in a paper under preparation in collaboration with the Bergen group.

Non linear problems are common thought a variety of tomographic methods and a similar approach is often effective. As an illustrative example we touch on our work giving the first non-linear reconstructions of magnetic fields using Neutron spin tomography.

I could modify the talk if necessary. Graham wanted me to emphasise fast tomography but I would like to reflect some of my most recent work. However I do not know the interests of the audience.

10391-42, Session 10

Grating-based tomography applications in biomedical engineering *(Invited Paper)*

Georg Schulz, Univ. Basel (Switzerland)

For the investigation of soft tissues or tissues consisting of soft and hard tissues on the microscopic level, hard X-ray phase tomography has become one of the most suitable imaging techniques. Besides other phase contrast methods grating interferometry has the advantage of higher sensitivity than inline methods and the quantitative results. One disadvantage of the conventional double-grating setup (XDGI) compared to inline methods is the limitation of the spatial resolution. This limitation can be overcome by removing the analyser grating resulting in a single-grating setup (XSGI). In order to verify the performance of XSGI concerning contrast and spatial resolution, a quantitative comparison of XSGI and XDGI tomograms of a human nerve was performed. Both techniques provide sufficient contrast to allow for the distinction of tissue types. The spatial resolution of the two-fold binned data sets of (5.2 ± 0.6) μm and (10.7 ± 0.6) μm, respectively, underlies the performance of XSGI in tomography of soft tissues. Another application for grating-based X-ray phase tomography is the simultaneous visualization of soft and hard tissues of a plaque-containing coronary artery. The simultaneous visualization of both tissues is important for the segmentation of the lumen. The segmented data can be used for flow simulations in order to obtain information about the three-dimensional wall shear stress distribution needed for the optimization of mechano-sensitive nanocontainers used for drug delivery.

10391-43, Session 10

Displaying of the human tooth cementum ultrastructure of archeological teeth by non-invasive and high-resolution imaging techniques to determine age-at-death and stress periods

Gabriela Mani-Caplazi, Georg Schulz, Gerhard Hotz, Univ. Basel (Switzerland); Ursula Wittwer-Backofen, Univ. of Freiburg (Germany); Bert Müller, Univ. Basel (Switzerland)

The tooth cementum annulation (TCA) is used by anthropologists to decipher the age-at-death (Wittwer-Backofen 2012) and stress periods based on the yearly deposited incremental lines (Kagerer & Grupe 2001). The destructive aspect of the TCA, which requests to cut the tooth root in sections to display the incremental lines using transmitting light microscopy can be problematic for archaeological teeth and a non-invasive imaging technique would be preferred. The purpose of this study is to evaluate less or non-invasive high resolution 3D imaging techniques including laboratory μCT scanner nanotom® and synchrotron radiation based μCT (SRμCT) to explore the tooth cementum ultrastructure, display the incremental lines and to assess stress markers. Twelve archaeological teeth of the St. Johann hospital cemetery (1845-1868) have been selected for the μCT experiments. The identified skeletons of this collection are considered a worldwide unique reference series in the anthropological science community considering the high level of documented life history data in the medical files and the additionally collected and verified birth history by genealogists (Hotz & Steinke 2012). Before the SRμCT experiments, the specimens were to be measured using the nanotom® in order to select the teeth and to find interesting areas. The preliminary results demonstrate that the μCT and SRμCT display the cementum nanostructure corresponding to the incremental lines in the transmitting light microscope view. Hence these μCT techniques should allow to assess the age-at-death and stress periods in archeological teeth in a non-invasive fashion and display them in a 3D view improving the accuracy of the assessments.

Hotz G. Steinke H. 2012 Knochen, Skelette, Krankengeschichten. Spitalfriedhof und Spitalarchiv - zwei sich ergänzende Quellen. Basler Zeitschrift für Geschichte und Altertumskunde, 112, 105-138.

Kagerer P. Grupe G. 2001 Age-at-death diagnosis and determination of life-history parameters by incremental lines in human dental cementum as an identification aid. Forensic Sci Int. 118(1), 75-82.

Wittwer-Backofen U. 2012 Age estimation using tooth cementum annulation. Methods Mol. Biol. 915, 129-143.

10391-44, Session 10

High-contrast x-ray microtomography in dental research

Graham R. Davis, David Mills, Queen Mary, Univ. of London (United Kingdom)

X-ray microtomography (XMT) is a well-established technique in dental research. Using this technique, much insight has been gained into the complex morphology of the root canal system and to qualitatively and quantitatively evaluate root canal instrumentation and filling efficacy in extracted teeth; enabling different techniques to be compared. Densitometric information can be used to identify and map demineralized tissue resulting from tooth decay (caries) and again, in extracted teeth, the method can be used to evaluate different methods of excavation. More recently, high contrast XMT is being used to investigate the relationship between external insults to teeth and the pulpal reaction. When such insults occur, fluid may flow through dentinal tubules as a result of cracking or porosity in enamel. Over time, there is an increase in mineralization along the paths of the tubules from the pulp to the damaged region in enamel and this can be visualized using high contrast XMT. The scanner used for this employs time-delay integration to minimize the effects of detector inhomogeneity in order to greatly increase the upper limit on signal-to-noise ratio that can be achieved with long exposure times. When enamel cracks are present in extracted teeth, the presence of these pathways indicates that the cracking occurred prior to extraction. At high contrast, growth lines are occasionally seen in deciduous teeth which may have resulted from periods of maternal illness. Various other anomalies in mineralization resulting from trauma or genetic abnormalities can also be investigated using this technique.

10391-45, Session 10

The inside view of 3D photonic nanostructures

Diana A. Grishina, Univ. Twente (Netherlands); Peter Cloetens, ESRF - The European Synchrotron (France); Cornelis A. M. Harteveld, Univ. Twente (Netherlands); Alexandra Pacureanu, ESRF - The European Synchrotron (France); Pepijn W. H. Pinkse, Ad Lagendijk, Willem L. Vos, Univ. Twente (Netherlands)

In nanofabrication, it is important to characterize the structure of a fabricated sample, since optical properties of photonic structures are defined by their complex internal structure. It is particularly challenging to access the inside of the three-dimensional (3D) samples. X-ray techniques are promising tools for nanophotonics, in view of excellent penetration depth, non-destructive character, and nm spatial resolution. Here we study a 3D Si photonic band gap crystal with a cubic diamond-like structure by X-ray tomography.

Our crystals have an inverse woodpile structure that exhibits a complete 3D band gap. The crystals are made in silicon by CMOS-compatible means. Holotomography was performed at the ESRF (beamline ID-16NI): X-rays (17 keV photon energy) are focused before the sample. We collect 1500 images while rotating the crystal from 0 to 180° at four sample-to-detector-distances in Fresnel regime to cover all spatial frequencies. Phase maps are obtained at every angle, followed by tomographic reconstruction to obtain the 3D electron density distribution. We reconstruct the volume of the complete fabricated 3D photonic crystal and its surrounding with 20 nm resolution in a real space. The close inspection of the reconstructed volume reveals new insights for the fabrication process as well as for the optical properties of the nanophotonic structures. We conclude that 3D X-ray tomography has great potential to solve many future questions on optical metamaterials for much nanophotonic research and applications, including cavity arrays, physically unclonable functions, and precise localization of light emitters as qubits and for enhanced lighting efficiency.

10391-46, Session 10

Recovery of text from locked 17th-century letters

David Mills, Graham R. Davis, Queen Mary, Univ. of London (United Kingdom)

The Brienne letters archive offers a snapshot of life in the 17th century preserved in the undelivered letters of people of Europe. The archive has remained virtually untouched by historians until it was recently rediscovered. The letters are uncensored, unedited, and around 600 of them even remain unopened.

The letters pre-date the invention of the gummed envelope, so they have been folded and manipulated such that they form their own protective carriers. Very few historical letters are available in the un-opened state to investigate this letter locking technique.

It is these unopened letters we are imaging with high contrast X-Ray microtomography with the dual intention of revealing the writing inside without opening the letters and also to study the structue of the letters and their seals to revel metadata about the letter's authors.

Conference 10392: Hard X-Ray, Gamma-Ray, and Neutron Detector Physics XIX

Monday - Wednesday 7 –9 August 2017

Part of Proceedings of SPIE Vol. 10392 Hard X-Ray, Gamma-Ray, and Neutron Detector Physics XIX

10392-1, Session 1

History and current status of strontium iodide scintillators *(Invited Paper)*

Nerine J. Cherepy, Patrick R. Beck, Stephen A. Payne, Erik L. Swanberg, Peter A. Thelin, Scott E. Fisher, Steven L. Hunter, Brian Wihl, Lawrence Livermore National Lab. (United States); Arnold Burger, Fisk Univ. (United States); Kanai S. Shah, Rastgo Hawrami, Radiation Monitoring Devices, Inc. (United States); Lynn A. Boatner, Oak Ridge National Lab. (United States); Michael Momayezi, Bridgeport Instruments, LLC (United States); Kevin T. Stevens, Mark H. Randles, Denys Solodovnikov, Northrop Grumman SYNOPTICS (United States)

Since its discovery in 2008, the Europium-doped Strontium Iodide scintillator, SrI2(Eu), has become commercialized and is available from several companies worldwide. SrI2(Eu) offers high proportional light yield (>80,000 ph/MeV), high effective atomic number (Z=49), and relatively easy growth from melt due to is moderate melting point (5380C). High, uniform, proportional light yield requires single crystals which for uniform solid solutions with the activator concentration, as may be obtained for Cerium in Lanthanum Bromide, LaBr3(Ce) and Europium in Strontium Iodide, SrI2(Eu), in both cases the dopant having matched ionic radii with the host.

Establishment of high quality crystal growth feedstock has been key to decreasing the cost of SrI2(Eu) crystal growth and increasing yield of uncracked boules. Recently, high quality 1.5" and 2" diameter encapsulated crystals have become commercially available for integration of SrI2(Eu) into gamma spectrometers providing high resolution and no intrinsic radioactivity. Light-trapping by the Eu2+ dopant may be addressed by: (1) the use of a physical taper, where the top of the crystal has a slight taper for uniform light collection, and (2) the use of on-the-fly correction of scintillation pulses by digital readout electronics. With the digital correction technique, we have demonstrated reproducible energy resolution of R(662 keV) = 2.9% FWHM for multiple 2.5-4 in3 SrI2(Eu) crystals. Based on the digital readout technology, we have developed a detector prototype with greatly improved radioisotope identification capability compared to NaI(Tl).

10392-2, Session 1

Organic spectroscopic scintillators based on nanoparticles *(Invited Paper)*

Qibing Pei, Univ. of California, Los Angeles (United States)

Spectroscopic gamma-photon detection has widespread applications for research, defense and medical purposes. The dominant materials for the detection have been inorganic semiconductors, scintillation crystals, and plastics that are either prohibitively expensive for wide deployment or cannot produce characteristic gamma photopeak. We report the synthesis of transparent, ultra-high-loading (up to 60 wt%) nanoparticle/polymer nanocomposite monoliths for gamma scintillation. The energy transfer of the high-atomic-number nanoparticles to lower-band-gap organic dyes was studied relative to light yield. One nanocomposite system was demonstrated exhibiting simultaneous enhancements in both light yield and gamma attenuation. Synthesis of transparent monoliths capable of producing 662 keV gamma photopeak will be described.

10392-3, Session 1

Plastic scintillator enhancement through QD

Alan Tam, Mikael Nilsson, Univ. of California, Irvine (United States)

Enhancement of PVT scintillating polymer was observed under ionization radiation by suspension of nano-crystalline quantum dots under Förster-type energy transfer. Plastic polymers has the ability to be modified by loading various kinds of dopant to reinforce scintillation property. By loading scintillating polymer with luminescence nanoparticles, particularly wavelength tunable quantum dot, it is possible to shift the primary scintillation emission to the quantum dot through Förster Resonance Energy Transfer (FRET) and enhance scintillation. Unlike conventional wavelength shifters where energy transfers is done by emission and absorption, FRET is a non-radiative transfer between the donor and acceptor. As we observed, primary emission was shifted from PPO's emission at 360 nm to the oleic acid coated CdS quantum dot's emission at 426 nm under high UV excitation while the transfer effect was absent below an excitation threshold. Scintillation fluorescence of PPO with CdS loading at 0.5 wt% was enhanced by 2 to 5 times depending on the beta and gamma energy. A change in energy spectroscopy was also observed with a strong contrast from beta radio luminescence with presence of an energy partition. Even though QD can be seen as a moderate high Z material the low loading have limited impact as a gamma sensitizer in the polymer with small deviations in the gamma spectrum.

10392-4, Session 1

Design and development of position sensitive detector for hard x-ray using SiPM and new-generation scintillators

Shiv Kumar Goyal, Physical Research Lab. (India); Amisha P. Naik, Nirma Univ. (India); Santosh Vadawale, Mithun N. P. S., Neeraj K. Tiwari, Physical Research Lab. (India); Tanmoy Chattopadhyay, The Pennsylvania State Univ. (United States)

Silicon Photomultiplier (SiPM) is a new development in the field of photon detection and can be described as 2D array of small (hundreds of μm2) avalanche photodiodes. SiPM is a linear amplifier device, where the amount of output charge is linearly proportional to the number of incoming photons, as long as these numbers of incoming photons does not exceed the total number of APDs in detection area. SiPM is an alternate option of using conventional PMTs (Photo Multiplier Tubes), as this offers comparable photon detection efficiency, small size, feasibility of compact array, low cost, low operating voltage and insensitivity to the external magnetic field.

Here, we are developing a hard X - ray imaging detector using Scintillator and SiPM devices. In our experiment, we are using CeBr3 Scintillator crystals of size 25 mm x 25 mm x 5 mm, which is optically coupled to SiPM array of size 6 x 6. These SiPMs are SensL make, surface mount device of total size 4 mm x 4 mm with an active area of 3 mm x 3 mm. We are using this setup in two different modes; 1) Total charge output of all SiPMs added together to get the energy information. 2) In the imaging mode to get the X - Y position of the incoming X - ray. The readout of the SiPM is carried out using IDEAS make ASIC. ASIC has 64 channels independent analog readout for the SiPM with input charge range from -20pC to +55pC.

We will present the preliminary results from the experiment for low energy threshold and the achieved position accuracy. We also provide the comparison using CsI scintillator, readout using same SiPMs.

10392-5, Session 2

Implementation of accelerated crucible rotation (ACRT) in vertical Bridgman growth of CdZnTe *(Invited Paper)*

Kelvin G. Lynn, Washington State Univ. (United States); Jeffery J. Derby, Univ. of Minnesota (United States); Jedidiah J. McCoy, Saketh Kakkireni, Santosh K. Swain, Washington State Univ. (United States); Mia S. Divecha, Univ. of Minnesota (United States)

Modified vertical Bridgman based melt growth techniques have several advantages such as fast growth rates and provision for stoichiometry control, however, issues such as secondary phase particles, inhomogeneous zinc distribution and polycrystallinity are common. These issues originate due to growth instabilities triggered by thermal and compositional fluctuations near the solidification front. This paper will investigate the effect of accelerated crucible rotation in minimizing growth instabilities by promoting favorable flow patterns and melt mixing during CZT growth. A number of ACRT growth experiments with varying acceleration, deceleration and melt stoichiometry were performed. Highly uniform axial zinc distribution within 2% of the intended zinc concentration was obtained over the entire boule length. Solidification from a highly off stoichiometric melt (7.5 weight % excess Te) generally resulted in better carrier transport with resistivity >1010 ohm.cm and µ?e >10-3 cm2/V in planar detectors. In addition, the high excess tellurium growths were reproducibly better in terms of second phase particle size distribution. High single crystal yield was obtained in ACRT growths with growth rates exceeding 2mm/hr from a highly tellurium rich melt by implementing boron nitride crucible.

10392-6, Session 2

Spatial calibration of the CdZnTe hard x-ray detectors for textit{NuSTAR}

Brian W. Grefenstette, California Institute of Technology (United States); Varun Bhalerao, Indian Institute of Technology Bombay (India); Fiona A. Harrison, Kristin K Madsen, Hiromasa Miyasaka, Peter Mao, Vikram R. Rana, California Institute of Technology (United States)

Pixelated Cadmium Zinc Telluride (CdZnTe) detectors are currently flying on the Nuclear Spectroscopic Telescope ARray (NuSTAR) NASA Astrophysics Small Explorer. While the pixel pitch of the detectors is $approx$ 605 mum, we can leverage the detector readout architecture to determine the interaction location of an individual photon to much higher spatial accuracy. The sub-pixel spatial location allows us to finely oversample the point spread function of the optics and reduces imaging artifacts due to pixelation. In this paper we demonstrate how the sub-pixel information is obtained, how the detectors were calibrated, and provide in-orbit performance results.

10392-7, Session 2

Electronic and thermodynamic properties of CdZnTeSe alloys from first-principles calculations: candidate room temperature radiation detector materials

Joel B. Varley, Vincenzo Lordi, Lawrence Livermore National Lab. (United States); Utpal N. Roy, Brookhaven National Lab. (United States); Ralph B. James, Savannah River National Lab. (United States)

Room temperature gamma detectors based on Cadmium Zinc Telluride (Cd1–xZnxTe or CZT) have demonstrated the favorable charge transport properties and technological potential of these alloys. However, difficulties in achieving large, uniform CZT single crystals have limited the widespread adoption of CZT detectors due to higher costs from low yields. One solution is the incorporation of Se into CZT, which has recently been shown to improve the homogeneity and charge collection efficiency of CZT-based detectors by decreasing the concentration of Te precipitates and inclusions and sub-grain boundary networks in the crystals. Despite the promise of these alloys, an understanding of how the Se incorporation influences the electronic properties of CZT is lacking. Here we use hybrid functional calculations to computationally assess the properties of Cd1–xZnxTe1–ySey (CZTS) alloys as a function of composition to improve the development of alloys with favorable electronic properties. Our calculations characterize the band gaps, band edges, and thermodynamic properties of the solid solutions over the entire quaternary space and identify compositions that are candidate alternative alloys to pure CZT.

Prepared by LLNL under Contract DE-AC52-07NA27344 and funded by the U.S. DOE/NNSA Office of Defense Nuclear Nonproliferation R&D.

10392-8, Session 3

Towards the development of a SiPM-based module for the camera of the Schwarzschild-Couder Telescope prototype of the Cherenkov Telescope Array

Giovanni Ambrosi, Michelangelo Ambrosio, Carla Aramo, Istituto Nazionale di Fisica Nucleare (Italy); Elisabetta Bissaldi, Politecnico di Bari (Italy) and Istituto Nazionale di Fisica Nucleare (Italy); Alfonso Boiano, Carmela Bonavolontà, Istituto Nazionale di Fisica Nucleare (Italy); Leonardo Di Venere, Univ. degli Studi di Bari Aldo Moro (Italy) and Istituto Nazionale di Fisica Nucleare (Italy); Emanuele Fiandrini, Univ. degli Studi di Perugia (Italy) and Istituto Nazionale di Fisica Nucleare (Italy); Nicola Giglietto, Politecnico di Bari (Italy) and Istituto Nazionale di Fisica Nucleare (Italy); Francesco Giordano, Univ. degli Studi di Bari Aldo Moro (Italy) and Istituto Nazionale di Fisica Nucleare (Italy); Maria Ionica, Univ. degli Studi di Perugia (Italy); Francesco Licciulli, Istituto Nazionale di Fisica Nucleare (Italy); Serena Loporchio, Univ. degli Studi di Bari Aldo Moro (Italy); Vincenzo Masone, Istituto Nazionale di Fisica Nucleare (Italy); Riccardo Paoletti, Univ. degli Studi di Siena (Italy) and Istituto Nazionale di Fisica Nucleare (Italy); Vasile Postolache, Istituto Nazionale di Fisica Nucleare (Italy); Andrea Rugliancich, Univ. degli Studi di Siena (Italy) and Istituto Nazionale di Fisica Nucleare (Italy); Daniela Simone, Istituto Nazionale di Fisica Nucleare (Italy); Valerio Vagelli, Univ. degli Studi di Perugia (Italy) and Istituto Nazionale di Fisica Nucleare (Italy); Massimo Valentino, Consiglio Nazionale delle Ricerche (Italy) and Istituto Nazionale di Fisica Nucleare (Italy)

The Italian Institute of Nuclear Physics (INFN) is currently involved in the development of a prototype for a camera based on Silicon Photomultipliers (SiPMs) for the Cherenkov Telescope Array (CTA), a new generation of telescopes for ground-based gamma-ray astronomy. In recent years, SiPMs have proven to be highly suitable devices for applications where high sensitivity to low-intensity light and fast responses are required. Among their many advantages are their low operational voltage when compared with classical photomultiplier tubes, mechanical robustness, and increased photo-detection efficiency (PDE). Moreover, due to the possibility of operating them during bright moonlight, SiPMs can therefore considerably increase telescope duty cycle.

Here we present a full characterization of a particular type of SiPM produced in Italy by the Fondazione Bruno Kessler (FBK), which is suitable for Cherenkov light detection in the Near-Ultraviolet (NUV SiPMs). This device is a High-Density (HD) NUV SiPM, based on a micro cell of 30 μm x 30 μm and with an area of 6 mm X 6 mm, providing low levels of dark noise and high PDE peaking in the NUV band. NUV-HD SiPMs will be finally arranged in a matrix of 8x8 single units to become part of the focal plane of the Schwarzschild-Couder Telescope prototype (pSCT) for CTA. An update on recent tests of the front-end electronics based on signal sampling with the TARGET-7 chip will be given as well.

10392-9, Session 3

Anti-coincidence scintillation detector for the device “signal” of the spacecraft Interheliozond

Sergey E. Ulin, Alexander S. Novikov, Alexander E. Shustov, Valery V. Dmitrenko, Ziyaetdin M. Uteshev, Konstantin F. Vlasik, National Research Nuclear Univ. MEPhI (Russian Federation)

The device “Signal” intended for research of solar gamma-ray bursts and gamma-ray flares from the galactic objects is described. The device will be installed on board the spacecraft “Interheliozond”. The scintillation anticoincidence system to reject a charged component of cosmic rays is considered. The research results of the scintillation detector characteristics are shown. Major characteristics of silicon photomultipliers electrical signals, used for registration of scintillation flashes from polyvinyl toluene plates, are presented. Optimal number of silicon photomultipliers sufficient for the scintillation system to obtain maximal registration efficiency of these detectors is given.

10392-10, Session 3

Analysis of the energy gamma-spectrum measured by xenon gamma-spectrometer

Alexander S. Novikov, Sergey E. Ulin, Irina V. Chernysheva, Valery V. Dmitrenko, Konstantin F. Vlasik, Ziyaetdin M. Uteshev, Alexander E. Shustov, National Research Nuclear Univ. MEPhI (Russian Federation)

A Xenon gamma-ray spectrometer intended to measure gamma-ray spectra in the energy range 30 keV - 3 MeV is described. Software, which takes into account characteristics and features of the xenon gamma-ray spectrometer, has been developed for the analysis of gamma-ray spectra. The software “Acquisition and processing of gamma-ray spectra” created with the use of programming language DELPHI into IDE CodeGear ™ RAD Studio 2007 is presented. The program is a set of interactive windows for acquisition, visualization, calibration, processing and analysis of the energy spectra from gamma-ray sources. As a result of processing and analyzing the measured spectra, energies of the detected gamma-lines are determined. In order to identify the radioisotopes corresponding to these gamma-lines, a built-in library of radionuclides is used. The identified radionuclides’ activities are also calculated by means the program. The developed software can be used for processing of gamma-ray spectra obtained with other detectors, if their main characteristics are taken into account.

10392-11, Session 3

High-performance neutron spectrometer for planetary hydrogen

Masayuki Naito, Nobuyuki Hasebe, Hiroshi Nagaoka, Junya Ishii, Daisuke Aoki, Waseda Univ. (Japan); Kyeong J. Kim, Korea Institute of Geoscience & Mineral Resources (Korea, Republic of); José A. Matias Lopes, Univ. de Coimbra (Portugal); Jesús Martínez-Frías, Univ. Complutense de Madrid (Spain)

Neutron spectroscopy is regarded as important technique to obtain elemental information of planets such as average atomic mass and concentration of light elements, especially hydrogen. Moreover, to measure gamma-rays and neutron fluxes in thermal/ epithermal and high energy range are essential to derive elemental composition from gamma-ray flux. In future, small and miniature spacecraft to small planetary bodies such as asteroids and comets are expected. For such missions, the development of compact and light equipment is required. In this study, neutron spectrometer (NS) consisting of boron-loaded plastic scintillator (BLP) and lithium-glass scintillator (LiG) is experimentally and numerically studied. The LiG is sensitive to thermal neutron while BLP separately detects epithermal and fast neutrons by delayed coincidence. In experiments, neutrons emitted from 252Cf were injected toward the NS to test the detector response. Silicon photomultiplier (SiPM) and/or Miniaturized PMT are also tested to read out the signals from the NS. The use of SiPM will miniaturize the NS system. In numerical simulations, neutron fluxes emitted from some types of meteorite parent bodies (C, S, and M-type asteroids) were calculated by Monte Carlo simulations. Hydrogen concentration was also changed in the range of 0-20,000 ppm to confirm the effect to the neutron energy spectrum. The calculated neutron spectra were numerically injected toward the NS to estimate the count rate of BLP and LiG. The NS is found to be very sensitive to the existence of water hydrogen in the planetary surface. The results of experiments and simulations will be presented.

10392-12, Session 3

A pixelated x-ray detector for diffraction imaging at next-generation high-rate FEL sources

Luca Lodola, Istituto Nazionale di Fisica Nucleare (Italy) and Univ. degli Studi di Pavia (Italy); Daniele Comotti, Lorenzo Fabris, Univ. degli Studi di Bergamo (Italy); Marco Grassi, Univ. degli Studi di Pavia (Italy); Lodovico Ratti, Piero Malcovati, Univ. degli Studi di Pavia (Italy) and Istituto Nazionale di Fisica Nucleare (Italy); Massimo Manghisoni, Valerio Re, Gianluca Traversi, Univ. degli Studi di Bergamo (Italy); Carla Vacchi, Univ. degli Studi di Pavia (Italy); Giovanni Batignani, Stefano Bettarini, Francesco Forti, Istituto Nazionale di Fisica Nucleare (Italy) and Univ. di Pisa (Italy); Fabio Morsani, Istituto Nazionale di Fisica Nucleare (Italy); Antonio Paladino, Eugenio Paoloni, Giuliana Rizzo, Istituto Nazionale di Fisica Nucleare (Italy) and Univ. di Pisa (Italy); Gian-Franco Dalla Betta, Roberto Mendicino, Lucio Pancheri, Univ. degli Studi di Trento (Italy) and Trento Institute for Fundamental Physics and Applications (Italy); Giovanni Verzellesi, Univ. degli Studi di Modena e Reggio Emilia (Italy) and Trento Institute for Fundamental Physics and Applications (Italy); Hesong Xu, Univ. degli Studi di Trento (Italy) and Trento Institute for Fundamental Physics and Applications (Italy)

The state of the art of X-ray science is shaped by the use of large accelerator-driven X-ray sources such as synchrotron light sources and X-ray free-electron lasers (FELs), for which appropriate X-ray detectors have to be developed. The extremely high brilliance of these sources compensate for the lack of the Bragg peak amplification mechanism typical of crystal diffraction, so that the diffraction method can be extended to the analysis of small, non-periodic specimens. Also, their ultra-short X-ray pulses provide the needed resolution (<1ps) for the reconstruction of time-dependent processes when assisted by pump-probe techniques. Furthermore, operation at very fast rates (up to 5MHz) is foreseen in the next generation FELs. The PixFEL project aims at developing a multi-layer,

hybrid pixel detector for X-ray diffraction imaging applications, compliant with the challenging specifications set by the FELs in terms of input dynamic range, speed, amplitude resolution, energy range from 1 to 10keV and radiation hardness. The sensor consists of a slim edge silicon pixel detector to minimize the dead area. The front-end chip will result from the vertical integration of two layers, one devoted to the analog front-end and the ADC, the second one to memories used in applications with high X-ray pulse rates. A 65nm CMOS technology has been used to accommodate the needed functions in a pixel pitch of 110um. The characterization of the prototype front-end chip, consisting of 32x32 readout channels, is ongoing and the first measurements gave encouraging results in view of the interconnection with the sensor matrix.

10392-13, Session 4

Plastic scintillators for gamma spectroscopy and neutron radiography *(Invited Paper)*

H. Paul Martinez, Nerine J. Cherepy, Robert D. Sanner, Patrick R. Beck, Stephen A. Payne, Lawrence Livermore National Lab. (United States); Charles R. Hurlbut, Eljen Technology (United States)

Plastic scintillators are widely deployed for ionizing radiation detection, as they can be fabricated in large sizes, for high detection efficiency. However, commercial plastics are limited in use for gamma spectroscopy, since their photopeak is very weak, due to low Z, and they are also limited in use for neutron detection, since proton recoils are indistinguishable from other ionizing radiation absorption events in standard plastics. We are working on scale up and production of transparent plastic scintillators based on polyvinyltoluene (PVT) loaded bismuth metallorganics for gamma spectroscopy. When activated with standard organic fluors, PVT scintillators containing 8 wt% bismuth provide energy resolution of 11% at 662 keV. When Iridium complex fluors are used, we can load plastics up to 20 wt% bismuth, while obtaining energy resolution of 10% at 662 keV. Another formulation, activated with Ir fluors for use as neutron radiography scintillator may be used for high energy neutron radiography.

Acknowledgements

This work was performed under the auspices of the U.S. DOE by Lawrence Livermore National Laboratory under Contract DE-AC52-07NA27344, and has been supported by the US DOE National Nuclear Security Administration, Defense Nuclear Nonproliferation Research and Development under Contract No. DE-AC03-76SF00098

10392-14, Session 4

Directional gamma detection from the occlusion method and singular value decomposition *(Invited Paper)*

Rusty P. Trainham, National Security Technologies, LLC (United States)

Locating a gamma source can be done by a variety of methods, ranging from rotating shields, to inter-detector shadowing, to Compton and Coded aperture imaging. Directional information is usually available in spectra from detector arrays, but that information is often ignored. Compton data from an array can be exploited to yield precise source locations, but the technique is slow. Processing occlusion, or mutual shadowing, data is less precise, but much faster. Instruments currently implementing an occlusion method tend to focus only on azimuthal angles, but with some modification the technique can be extended to estimate elevation angles as well. We present a generalization of the occlusion method for estimating both azimuth and altitude of a source, and the method involves singular value decomposition. The method works even for ill-chosen detector array geometries, and we show results from several detector systems.

10392-15, Session 4

Applications of very fast inorganic crystal scintillators for future HEP experiments

Ren-Yuan Zhu, California Institute of Technology (United States)

In high energy physics (HEP) and nuclear physics experiments, total absorption electromagnetic calorimeters (ECAL) made of inorganic crystals are known for their superb energy resolution and detection efficiency for photon and electron measurements. A crystal ECAL is thus the choice for those experiments where precision measurements of photons and electrons are crucial for their physics missions. Future HEP experiments at the energy and intensity frontiers require very fast inorganic crystal scintillators to achieve excellent timing resolution at a level of a few tens ps and to face the challenge of unprecedented event rate. Very fast inorganic crystals may also find application for Gigahertz hard X-ray imaging. This paper reports recent progress in application of fast inorganic scintillators in HEP experiments, such as a thin LYSO crystal layer for fast timing for the CMS experiment upgrade at the HL-LHC, and the use of undoped CsI and rare earth doped BaF2 crystals for the Mu2e experiment and its upgrade at Fermilab. Applications of very fast crystal scintillators for Gigahertz hard X-ray imaging for the proposed Marie project at LANL will also be discussed.

10392-16, Session 4

Development of the LunaH-Map miniature neutron spectrometer

Erik B. Johnson, Radiation Monitoring Devices, Inc. (United States); Craig Hardgrove, The Univ. of Arizona (United States); Samuel Vogel, Rebecca Frank, Graham Stoddard, James F. Christian, Radiation Monitoring Devices, Inc. (United States)

There is strong evidence that water-ice is relatively abundant within permanently shadowed lunar surface materials, particularly at the poles. Evidence for water-ice has been observed within the impact plume of the LCROSS mission and is supported by data gathered from the Lunar Exploration Neutron Detector (LEND) and the Lunar Prospector Neutron Spectrometer (LPNS). Albedo neutrons from the Moon are used for detection of hydrogen, where the epi-thermal neutron flux decreases as hydrogen content increases. The origin on the concentration of water within permanently shadowed regions is not completely understood, and the Lunar Polar Hydrogen Mapper (LunaH-Map) mission is designed to provide a high-resolution spatial distribution of the hydrogen content over the southern pole using a highly elliptical, low perilune orbit. The LunaH-Map spacecraft is a 6U cubesat consisting of the Miniature Neutron Spectrometer (Mini-NS). Mini-NS is not collimated, requiring a low altitude to achieve a higher spatial resolution compared to previous missions. To develop a compact neutron detector for epi-thermal neutrons, the Mini-NS comprises of 2-cm thick slabs of CLYC (Cs2LiYCl6), which provide a sensitivity similar to a 10-atm, 5.7-cm diameter He-3 tubes, as used in LPNS. The Mini-NS digital processing electronics can discriminate by shape and height to determine signal (albedo neutrons) from background (cosmic rays). The Mini-NS achieves a total active sensing area of 200 cm2 and is covered with a cadmium sheet to shield against thermal neutrons. A review on the design for space flight and the instrument response with the readout scheme is presented.

10392-38, Session PMon

Effects of post-growth annealing on the properties of Cd1-xMnxTe crystals

Serhii Solodin, Petro Fochuk, Yuriy Fedkovych Chernivtsi National Univ. (Ukraine); Yevgen Nykonyuk, National Univ. of Water Management and Nature Resources Use (Ukraine); Zinaida Zakharuk, Serhii Dremlyuzhenko, Yuriy

Fedkovych Chernivtsi National Univ. (Ukraine); Aleksey E. Bolotnikov, Brookhaven National Lab. (United States); Ralph B. James, Savannah River National Lab. (United States)

The potential of Cd(Mn)Te solid solutions for fabrication of ?-detectors has been substantially restricted by the presence of high concentrations of point defects and impurities and by the presence of structural defects such as Te inclusions. To reduce the density of Te inclusions, we applied a special post-growth annealing method to the ingots. In this method a heater was moved along the ingot. The temperature of the heater was considerably less then the melting point of the Cd(Mn)Te crystals, but it exceeded the melting point of tellurium. Such a method for post-growth annealing (called «dry zone») leads to the following effects:

- Significant reduction in the density of Te inclusions within the crystals;
- Reduction in the concentration of shallow acceptors A1 (?A≈0.05??); and
- Increase in the degree compensation for acceptors A2(?A=0.17??).

10392-39, Session PMon

Vertical Bridgman growth and characterization of Cd0.95-xMnxZn0.05Te (x=0.20, 0.30) single-crystal ingots

Vasylyna Kopach, Oleh Kopach, Larysa Shcherbak, Petro Fochuk, Yuriy Fedkovych Chernivtsi National Univ. (Ukraine); Aleksey E. Bolotnikov, Brookhaven National Lab. (United States); Ralph B. James, Savannah River National Lab. (United States)

Solid solutions of Cd(Zn)Te are well known as materials for optoelectronics, nonlinear optics, solar cell and radiation detector applications. Substitution of Cd or Zn in the Cd(Zn)Te zinc-blende lattice by the magnetic impurity Mn promises more flexible properties arising from tailoring the alloy's enhanced chemical and structural peculiarities. Thus, quaternary chalcogenides based on Cd(Zn,Mn)Te arouse both scientific and technological interest.

Cd0.95-xMnxZn0.05Te alloys with x=0.20, 0.30 were investigated by differential thermal analysis (DTA) for determining their solid-liquid phase transitions at equilibrium temperature intervals. The heating/cooling rates were 5 and 10 K/min with a melt dwell time of 10, 30 and 60 minutes. Cd0.95-xMnxZn0.05Te (x=0.20, 0.30) single-crystal ingots were grown by the Vertical Bridgman method using the DTA results.

As commonly observed for CdTe and Cd(Zn)Te crystals, Te spherical inclusions (1-20 microns) were seen in these ingots by infrared transmission microscopy. Using current-voltage (I-V) measurements, the resistivity of the samples from each ingot was estimated to be about 105 Ohm•cm). The optical transmission analysis demonstrated that the band-gap values of the investigated ingots increased from 1.74 to 1.88 eV with the increase of the MnTe concentration from 20 to 30 mol. %.

10392-40, Session PMon

Improved pyroelectric x-ray generator for planetary active x-ray spectrometer

Masayuki Naito, Nobuyuki Hasebe, Hiroshi Nagaoka, Yusuke Oshima, Miho Mizone, Eido Shibamura, Haruyoshi Kuno, Waseda Univ. (Japan); Kyeong J. Kim, Korea Institute of Geoscience & Mineral Resources (Korea, Republic of); José A. Matias Lopes, Univ. de Coimbra (Portugal); Jesús Martínez-Frías, Univ. Complutense de Madrid (Spain)

Concentration of elements in planetary surface provides important clues to characterize geochemical restrictions and the geological evolution of the planetary bodies. As future missions, landing/roving on planetary surface are planned in Japan. The active X-ray spectrometer (AXS) , which consists of silicon drift detector, pyroelectric X-ray Generators (PXGs), and common electronics, is developed to measure the elemental composition on planetary surface. The AXS can measure major elements: Mg, Al, Si, Ca, and Fe; submajor elements: Na, K, P, S, Cl, Cr, and Ti. The previous missions such as Chang'E-3, MSL used radioisotopes to excite planetary surface materials. However, it is difficult to use radioisotopes for today's Japanese mission. Then, we adopted the PXG, which is composed by pyroelectiric crystal, peltier device, and metal target. The PXG yields X-rays in low pressure by utilizing spontaneous polarization of the crystal depending on temperature. Its characteristic features are light weight, compact size, and no radioisotopes. To obtain fluorescent X-rays effectively, selection of incident X-ray energy is important. For example, Mo L? line (2.29 keV) excites Si by ~20 times larger efficiency than Cu K? line (8.04 keV). By such a reason, the PXGs with different targets should be loaded on the AXS. In this study, PXGs with Cu and Mo targets are experimentally studied. Experimental configurations such as pressure surrounding the crystal, thickness of the target, distance between target and crystal, and shape of the target are changed to obtain high X-ray intensity. The results of experiments will be presented and discussed.

10392-41, Session PMon

Improved materials process for two promising semiconductors Rb3Bi2Br9 and Cs3Bi2Br9 for room-temperature gamma-ray detector applications

Duck Young Chung, Fang Meng, Mercouri G. Kanatzidis, Argonne National Lab. (United States)

A new class of metal chalco-halide compounds A3M2X9 (A = Rb, Cs; M = Bi, Sb; X = Br, I) was identified as good candidate materials for hard energy radiation detection. Particularly the fundamental physical properties of Rb3Bi2Br9 and Cs3Bi2Br9 well meet the requirements for gamma-ray detector materials with band gap 2.6 eV and 2.7 eV, high density 4.48 and 4.46 g/cm3, and low melting point 550 and 650 oC, respectively. These two compounds initially showed high resistivity near 10^12 ohm?cm but relatively low carrier mobility-lifetime product in 10^-5–10^-6 cm2/V For high responsiveness to the high energy radiation these should be further improved . To achieve high detection performance of these materials we focused on developing synthesis and purification process. By using solution process for synthesis of materials followed by a series of purification process and subsequent crystal growth by the Bridgman and Electro-Dynamic Gradient technique, we obtained highly pure single crystals and characterized. The crystals of Rb3Bi2Br9 and Cs3Bi2Br9 show the improved electrical resistivity and the mobility-lifetime products, in the range of 10^13–10^14 ohm.cm and 10^-4–10^-5 cm2/V, respectively. They also exhibit a strong spectroscopy counting response when exposed to Ag X-ray and a medium intense spectroscopy response to 57Co gamma-ray.

10392-42, Session PMon

Effect of cathode energy spectrum on the depth of interaction correction and anode signal recovery in CZT detectors

Mohan Li, Shiva Abbaszadeh, Univ. of Illinois at Urbana-Champaign (United States)

One electrode configuration frequently used in CZT detector is the cross-strip pattern. It is an efficient way to achieve multiplexing through the electrode pattern and it can achieve high spatial resolution in three dimensions (3-D) for imaging applications such as positron emission tomography. The intersection of the anode and cathode strips defines the x-y localization of photon interactions. The cathode-to-anode (C/A) signal ratio can be used to estimate the position of photon interaction in the z direction. In this work we evaluate the effect of cathode energy spectrum on the corrected depth dependent anode energy signal for a cross-strip

CZT detector. In the design investigated, the anode leverages the small pixel effect and the width of the cathode is comparable to the thickness of the CZT crystal. For converting the ADC counts to energy, 68Ge and 137Cs are used. The cathode energy spectrum is broad and does not have a well-defined peak. Therefore, the energy of the cathodes becomes sensitive to the user-selected ADC-to-keV fitting parameters, which affects the anode energy resolution through depth of interaction correction. The anode energy resolution is studied for a variation of cathode fitting parameters, and a method to automate calibration is investigated to improve the robustness of the calibration process, which is especially important for a system comprised of more than a hundred channels.

10392-43, Session PMon

Silicon grid collimator for CsI:Tl scintillator

Toru Aoki, Kento Tabata, Shizuoka Univ. (Japan); Akifumi Koike, ANSeeN Inc. (Japan); Hidenori Mimura, Junichi Nishizawa, Shizuoka Univ. (Japan)

Si grid type optical separator has been developed by using MEMS process. CsI:Tl was filled into the grid hole by evaporation method. Luminescence of CsI:Tl into the grid substrate was observed. The effect of the wall was confirmed by observing deposition of CsI:Tl into through hole substrate. Verification that photo-diode receive luminescence of CsI:Tl in the grid hole is conducted, and intensity and wavelength controlled by Tl concentration of luminescence is enough value for imaging detector. Measurement of spatial frequency is conduct by using test chart. Because the difference of amount of luminescence between pixels adhered test chart and pixels doesn't adhered was observed, the spatial frequency of the grid substrate filled CsI:Tl is 5.0LP/mm by MTF measurement.

10392-44, Session PMon

Characterization of CdTe x-ray detector with modulative depletion layer

Tsuyoshi Terao, Shizuoka Univ. (Japan); Akifumi Koike, ANSeeN Inc. (Japan); Katsuyuki Takagi, Toru Aoki, Shizuoka Univ. (Japan)

A novel method for realizing X-ray energy discrimination with conventional accumulation-type CdTe flat panel detector (FPD) has been proposed. Since the thickness of depletion layer in a diode detector depends on the bias voltage applied, the sensitivity of the detector to higher energy X-ray can be controlled by modulating the bias voltage. Measurements have been carried out to investigate the carrier transportation characteristics of Schottky CdTe detector at lower bias voltage.

10392-45, Session PMon

The development of a low-cost CsI(Tl)-SiPM detector for radiation monitoring by members of the public

Steven J. Bell, National Physical Lab. (United Kingdom); Craig Duff, Kromek (United Kingdom)

The accident at the Fukushima Daiichi NPP has increased interest amongst members of the public in the measurement and monitoring of radiation. Many simple radiation detectors have been developed and made freely available for public purchase and use; however these devices often lack a metrological underpinning and so their results are difficult to interpret. A collaboration between Kromek and the National Physical Laboratory has been established to develop and metrologically validate a CsI(Tl)-SiPM gamma radiation detector for on-line, geo-tagged radiation monitoring by members of the public. The device under development is based on the hybrid gamma/neutron detector; D3S, which was developed by Kromek for homeland security as a "wearable" networked detector carried by government agencies. The new device will contain a re-designed CsI(Tl)-SiPM gamma spectrometer and bluetooth for communication with the user's smartphone. A website will be developed to allow public sharing of radiation measurements. Presented is an overview of the project aims, details of the device design and a review of measurements made by the existing D3S device. This work is part of the EMPIR Preparedness project funded by EURAMET, BEIS and Kromek.

10392-46, Session PMon

Doping and metallization of the CdTe crystal surface by laser irradiation of the metal substrate through the semiconductor

Volodymyr A. Gnatyuk, V.E. Lashkaryov Institute of Semiconductor Physics (Ukraine); Kateryna Zelenska, Taras Shevchenko National Univ. of Kyiv (Ukraine); Toru Aoki, Shizuoka Univ. (Japan)

In fabrication of diode type CdTe-based X/gamma-ray detectors, a high barrier can be implemented by doping of a surface crystal layer and creation of a p-n junction or formation of a Schottky contact. Laser-assisted techniques have been studied for high resistivity p-like CdTe crystals to develop diode structures with high rectification properties and low leakage current. The key feature of the proposed method is irradiation of a CdTe crystal placed on the polished chemically pure metal (Al or In) plate with nanosecond pulses of the first harmonic (1064 nm) of a YAG:Nd laser. CdTe is transparent for this radiation which is strongly absorbed by only a thin layer of the substrate. Depending on energy density and number of laser pulses, irradiation of the metal through the CdTe causes such extreme conditions (high temperature, stresses, pressure, etc.) in the confined area at the metal-CdTe interface which can provide: (i) doping of the thin CdTe region adjoining to the substrate with Al (In) atoms and formation of a p-n junction; (ii) creation of a Schottky barrier by deposition of a thin Al (In) contact film; (iii) formation of a metal electrode. These technological procedures are realized as a result of laser-induced thermal extension of a thin layer of the substrate, melting of this layer and solubility of CdTe in the liquid metal, melting of both the semiconductor and metal layers near the interface, ablation of the metal with following deposition, respectively. The electrical properties of the formed CdTe-metal diodes are investigated.

10392-47, Session PMon

Challenges in the quantitative optical detection of radiation

Sean Fournier, Jeffrey B. Martin, Richard Harrison, Dora K. Wiemann, Sandia National Labs. (United States)

Modern ultraviolet (UV) cameras, when combined with UV-transmitting lenses/filter arrangements can be used to detect radiation dose in air. Ionizing radiation excites nitrogen molecules in ambient air resulting in decay by the emission of photons. The strongest emissions are in the 337 nm, 357 nm, 316 nm, 391 nm and 380 nm bands of the ultraviolet. This process is referred to as scintillation where roughly 17 photons are emitted per MeV of ionizing radiation deposited in the air. Previous work has proven this phenomenon is detectable using highly-sensitive electronically cooled cameras traditionally used in astronomy for low-background imaging. While the ability to detect the presence of radiation (i.e. qualitative measurement) has been demonstrated, there are several challenges in correlating images to known dose-fields (quantitative measurement). These challenges include: a low signal to background ratio, interferences due to electronic noise and direct radiation interactions with the camera, and a complex source-dependent detection efficiency. Based on measurements of low-level radioactive sources as well as high-level sources at several irradiation facilities at Sandia National Laboratories, researchers are building an understanding of these challenges in an attempt to engineer a system that can be used for quantitatively measuring radiation dose fields. This presentation will describe these efforts and share the lessons learned from several experiments.

10392-48, Session PMon

Characterization of Yb-doped silica optical fibre as real-time dosimeter

Ivan Veronese, Univ. degli Studi di Milano (Italy); Norberto Chiodini, Univ. degli Studi di Milano-Bicocca (Italy); Simone Cialdi, Edoardo D'Ippolito, Univ. degli Studi di Milano (Italy); Mauro Fasoli, Univ. degli Studi di Milano-Bicocca (Italy); Salvatore Gallo, Univ. degli Studi di Milano (Italy); Eleonora Mones, Azienda Ospedaliera Maggiore della Carità (Italy); Anna Vedda, Univ. degli Studi di Milano-Bicocca (Italy); Gianfranco Loi, Azienda Ospedaliera Maggiore della Carità (Italy)

Scintillator dosimeters (SD) have been a research topic by many groups over the last decade. The recent availability of a commercial system (ExradinW1) represents a significant accomplishment. The attractiveness of SD would be furtherly enhanced by a scintillator free from any spectral superposition with the Cherenkov light, so to avoid any sensitive calibration procedure for the stem effect correction. Yb-doped silica optical fibres, thanks to their near-infrared (NIR) emission, proved to be a promising option.

This study aims to characterize the dosimetric properties of Yb-doped fibers in radiotherapy and to compare their resultswith those obtained by various reference dosimeters like micro ion-chambers, the commercial SD, and diodes designed for small field dosimetry.

Yb-doped fibres were prepared by sol–gel. The scintillation was detected with a laboratory-made photon counting system based on an avalanche photodiode, using a long-pass filter at 950 nm. Irradiations were carried out with photons and electron beams generated by a Varian Trilogy accelerator.

The NIR scintillation proved to be unaffected by the stem effect, even in unfavorable large field irradiations. The system showed a satisfactory reproducibility, good sensitivity, linear dose-rate response, independence of the signal (total counts) of dose rate and impinging beam orientation. The results were in good agreement with reference dosimeters in terms of relative dose profiles and output factors.

We thus expect that our results will be of great interest for medical physicists involved in the complex issues of small field dosimetry and in-vivo dose monitoring in the new advanced radiation treatment modalities.

10392-17, Session 5

First report on printed contacts for CdZnTe detectors. *(Invited Paper)*

Arie Ruzin, Artem Brovko, Sergey Marunko, Tel Aviv Univ. (Israel)

This work reports on the first steps toward 3-D printed contacts to CdZnTe detectors. The three-dimensional printing is rapidly gaining new territories. This study is the first attempt to print silver contacts onto Cd1-xZnxTe crystals grown by horizontal Bridgman method. The contact printing technology is very promising since it enables mask-free design and fabrication of various contact configurations. It does not require vacuum deposition systems or chemical processes.

Although the printing process is relatively simple, it is not trivial and requires a review of surface preparation and optimization, as well as in contact annealing. The silver printing is done from a liquid phase of silver nano particles. In this study various surface treatments and post-printing annealing procedures were studies. The printed contacts are compared to evaporated contacts of the same metal.

10392-18, Session 5

Perovskite CsPbBr3 single crystals with improved physical properties for gamma-ray detector *(Invited Paper)*

Duck Young Chung, Fang Meng, Argonne National Lab. (United States); Christos Malliakas, Northwestern Univ. (United States); Gregory A. Bizarri, Tetiana Shalapska, Edith D. Bourret-Courchesne, Lawrence Berkeley National Lab. (United States); Mercouri G. Kanatzidis, Northwestern Univ. (United States); Anton S. Tremsin, Space Sciences Lab. (United States)

CsPbBr3 is a promising candidate for gamma-ray detector applications, as it has direct band gap (2.25 eV), high density (4.85 g/cm3), attenuation coefficient comparable to CZT, and high resistivity ~10^9 ohm?cm. CsPbBr3 exhibits the carrier mobility-lifetime product (??) in the order of 10^-5 - 10^-4 cm2/V, promising enough to further develop for practical applications. The major challenge is its detection performance limited by impurity phases and crystal defects that may act as carrier traps at a deep level of the energy gap. Here, we report new processes for synthesis and purification to obtain highly pure CsPbBr3 with reduced impurities, which improve the crystal quality and physical properties relevant to radiation detection. Compared to the conventional synthetic route which involves high temperature melting of precursors, the solution based route using aqueous HBr or organic solvent/anti-solvent mixture produced higher quality materials. After a series of purification process, large single crystals of CsPbBr3 were grown by the Bridgman and Electro-Dynamic Gradient (EDG) method. The crystals were characterized by optical and spectroscopic studies for crystal quality evaluation, charge transport and photo-response study using X-ray and gamma-ray sources for detection performance assessment, and carrier trap analysis. We report single crystals of CsPbBr3 with significantly improved properties such as reduced defects and low concentration of carrier trap high transmittance, high resistivity ~ 10^11 ohm?cm, and ?? ~ 10^-4 cm2/V. In addition, they exhibit the strong counting response to both Ag X-ray and 57Co gamma-ray irradiation.

10392-19, Session 5

Highly stable thallium bromide devices for long-term room temperature field applications *(Invited Paper)*

Amlan Datta, John Fiala, Piotr Becla, Shariar Motakef, CapeSym, Inc. (United States)

Thallium bromide (TlBr) is a wide bandgap, compound semiconductor with high gamma-ray stopping power and promising physical properties. However, performance degradation and the eventual irreversible failure of TlBr devices can occur rapidly at room temperature, due to "polarization", caused by the electro-migration of Tl+ and Br- ions to the electrical contacts across the device. In the previous studies we extensively explored and reported the defect nucleation and migration phenomena in TlBr devices.

With significantly better surface preparation, non-reactive electrodes, and optimized unique biasing switching schemes we have demonstrated that the room temperature long term performance of the detectors can be improved significantly. We have demonstrated spectroscopic performance of several devices under continuous bias and gamma irradiation for more than a year. This is close to ten times longer than other demonstrated room temperature lifetime for TlBr devices. This was achieved without the Cl-based heterojunctions between the TlBr matrix and the contact metal. Different bias-switching schemes and its effects would be discussed in this paper. These devices are stable within 2% standard deviation of the energy channels, which demonstrates the potential of TlBr detector modules for use in field applications. Effects of ambient atmosphere and applied detector bias on the long-term detector performance will be reported.

1 Conway et al, 2013.

**This work was supported in part by the U.S. Department of Homeland

Security, Domestic Nuclear Detection office contract SBIR HSHQDC-15-C-00044. This support does not constitute an express or implied endorsement on the part of the Government.

10392-20, Session 5

High-efficiency and high-sensitivity thermal neutron detectors based on hexagonal BN epilayers

Avisk Maity, Sam Grenadier, Jing Li, Jingyu Lin, Hongxing Jiang, Texas Tech Univ. (United States)

Due to the inherent nature of low flux of fission neutron emission from a potential fissile material and the fact that the neutron flux is inversely proportional to the square of the distance from the source, it is challenging to detect neutron signals at relatively large distances. Large size high efficiency detectors are desired to improve the detector performance and to provide a reasonable count rate. We have successfully synthesized by MOCVD wafer-scale 10B enriched hexagonal boron nitride (h-BN) epilayers with a thickness of about 50 microns [1-3]. We have realized recently vertical photoconductor-like thermal neutron detectors of 1 mm2 in size with 51.4% detection efficiency [1]. We report here the fabrication and characterization of 3 mm x 3 mm h-BN vertical detectors with 50% detection efficiency. The effects of resistivity, dark current density, and the carrier mobility-lifetime products on the device performance were monitored and optimized via MOCVD growth parameters. With improved material quality, the noise related dark counts have been significantly reduced. The work laid the groundwork for realizing large area detectors. Our results indicate that h-BN are highly promising for realizing highly sensitive solid-state thermal neutron detectors with expected advantages resulting from semiconductor technologies, including compact size, light weight, low operating voltage, and low cost.

[1] A. Maity, et al., Appl. Phys. Lett. 109, 072101 (2016).

[2] T. C. Doan, et al, Nuclear Inst. and Methods in Physics Research Section A, 748, 84 (2014).

[3] J. Li, et al., Appl. Phys. Lett. 101, 171112 (2012).

10392-21, Session 6

Neutron detector development for microsatellites *(Invited Paper)*

Julia G. Bodnarik, Dave Hamara, The Univ. of Arizona (United States); Arnold Burger, Fisk Univ. (United States) and Vanderbilt Univ. (United States); Vladimir Buliga, Joanna C. Egner, Michael Groza, Fisk Univ. (United States); Walter M. Harris, The Univ. of Arizona (United States); Liviu Matei, Fisk Univ. (United States); Thomas H. Prettyman, Planetary Science Institute (United States); Keivan G. Stassun, Vanderbilt Univ. (United States) and Fisk Univ. (United States); Ashley C. Stowe, Y-12 National Security Complex (United States)

The 3He supply shortage has spurred scientist to develop alternative neutron detectors for space science applications. One promising new neutron detector is 6LiInSe2, a room temperature semiconductor thermal neutron detector that also detects incident neutrons via scintillation [1]. It is an effective neutron detector due to the high neutron capture cross-section area of 6Li (935 barns). Although the thermal neutron cross section of 6Li is lower that of 3He, the atomic density of 6Li in a solid is higher, resulting in improved neutron absorption due to increased atomic density. This makes 6LiInSe2 a promising candidate for thermal neutron detection in space science applications.

6LiInSe2 has a response to both neutrons and gamma rays [2]. We investigate 6LiInSe2 in scintillation mode in the laboratory to determine this response and see if we can separate thermal neutrons, epithermal neutrons, and gamma rays in the resultant energy spectrum using moderating materials and digital signal processing if necessary. The results from our study will help us determine if 6LiInSe2 is a useful detector for space and planetary science missions.

References

[1] Wiggins, B. et al., “Scintillation Properties of Semiconducting 6LiInSe2 Crystals to Ionizing Radiation,” Nuclear Instruments and Methods in Physics Research, A: Accelerators, Spectrometers, Detectors and Associated Equipment, vol. 801, 2015, p.73-77.

[2] Stowe, A. C. et al., “Improving Neutron Detection in Semiconducting 6LiInSe2,” Proceedings SPIE 9213, Hard X-Ray, Gamma-Ray, and Neutron Detector Physics XVI, 92130B (September 5, 2014).

10392-22, Session 6

Lithium indium diselenide pressed ceramics *(Invited Paper)*

Ashley C. Stowe, Jeff Preston, Y-12 National Security Complex (United States); Joseph Bell, Vanderbilt Univ. (United States); Arnold Burger, Fisk Univ. (United States)

No Abstract Available.

10392-23, Session 6

Cs2LiCeCl6: An intrinsic scintillator for dual gamma and neutron detector applications

Utpal N. Roy, Giuseppe S. Camarda, Yonggang Cui, Rubi Gul, Brookhaven National Lab. (United States); Anwar Hossain, Brookhaven National Lab (United States); Ge Yang, Brookhaven National Lab. (United States); Ralph B. James, Savannah River National Lab. (United States); Steven L. Hunter, Patrick R. Beck, Nerine J. Cherepy, Stephen A. Payne, Lawrence Livermore National Lab. (United States)

Intrinsic materials can offer advantages over doped materials for some important applications. The doped material might suffer from non-uniform distribution of the dopant, such as fine-scale striations and larger scale segregation, which might affect the overall device response, especially for large-volume detectors such as those in demand for homeland security applications for gamma spectroscopy. Cs2LiCeCl6 (CLCC), being an intrinsic scintillator, can be grown in large volume to produce large detectors with good performance, provided the crystals are free from unwanted scattering centers. CLCC belongs to the elpasolite family and the structure is cubic, so large-volume ingots can be grown without the strains resulting from anisotropic thermal expansion coefficients. In this presentation, we will discuss extensive material characterization and device response of CLCC for gamma and thermal neutron detector applications.

10392-24, Session 7

Arrays of position sensitive virtual Frisch-grid detectors *(Invited Paper)*

Aleksey E. Bolotnikov, Giuseppe S. Camarda, Rubi Gul, Gianluigi De Geronimo, Jack Fried, Ge Yang, Anwar Hossain, Brookhaven National Lab. (United States); Luis A. Ocampo Giraldo, Brookhaven National Lab. (United States) and The Pennsylvania State Univ. (United States); Emerson Vernon, Brookhaven National Lab. (United States); Ralph B. James, Savannah River National Lab. (United States)

We present new results from testing a small array of position-sensitive virtual Frisch-grid gamma-ray detectors. Such arrays provide high-detection efficiency, excellent energy and position resolution. They can be used in compact hand-held instruments or in large-area gamma ray imaging cameras. The high granularity position sensing enables these detectors to correct the response non-uniformity caused by crystal defects. This important feature allows one to achieve high detection performance while using standard-grade (unselected) CZT crystals, which is expected to reduce the overall cost of field deployable high-resolution CZT gamma ray detection instruments. Here, we report the results of testing several array prototypes with configurations designed for different applications.

10392-25, Session 7

Bridgman growth of scintillator crystals via neutron imaging and finite-element modeling

Jeffrey J. Derby, Jeffrey H. Peterson, Chang Zhang, Jan Seebeck, Univ. of Minnesota (United States); Anton S. Tremsin, Univ. of California, Berkeley (United States); Didier Perrodin, Gregory A. Bizarri, Edith D. Bourret-Courchesne, Lawrence Berkeley National Lab. (United States); Sven Vogel, Mark A. M. Bourke, Los Alamos National Lab. (United States)

In this presentation, we discuss experiments that employ spallation neutrons to visualize, in situ, the compositional field that is developed during the growth of a mixed halide scintillator crystal via the Bridgman method. These measurements provide, for the very first time, a direct observation of melt crystal growth within a system large enough to display the complex interplay of heat transfer, fluid flow, segregation, and phase change characteristic of an industrially relevant process.

To understand the mechanisms at play during growth, we apply finite element models to predict the macroscopic transport of heat, mass, and momentum along with phase-change phenomena in the crystal growth system observed in these neutron imaging experiments. We discuss how ongoing synergies between modeling and experiment allow for unambiguous interpretation of growth experiments. This is particularly significant, since there is a lack of fundamental understanding of how microstructural defects arise during growth. If we can directly observe these phenomena via imaging and real-time measurements and correlate their behavior with growth conditions provided by the model, we have a path by which we can begin to understand and quantify the responsible mechanisms. Ultimately, the understanding obtained by model and experiment will truly allow the closing of the loop between materials quality, growth conditions, and process development, an undertaking that in the past has relied on empiricism and experience to typically achieve only incremental advances.

Supported by U.S. DOE/NNSA DE-NA0002514 and U.S. DOE/NNSA/DNN R&D (LBNL subcontract AC0205CH11231); no official endorsement should be inferred.

10392-26, Session 7

Real-time leakage current monitoring in two-step annealing process

Kihyun Kim, Seokjin Hwang, Hwanseung Yu, Korea Univ. (Korea, Republic of); Aleksey E. Bolotnikov, Brookhaven National Lab. (United States); Ralph B. James, Savannah River National Lab. (United States)

Te secondary phase defect is one of major limiting factor in the performance of CdZnTe(CZT) detectors. We want to get rid of Te secondary phase defects of CZT crystals through post-growth two-step annealing without creating new trapping centers. Two-step annealing (i.e. the first in Cd pressure, the second in Te pressure) demonstrated to be effective in order to preserve the resistivity of detector grade CZT. Leakage current of CZT detector during the two-step annealing was investigated with the help of real-time current monitoring system. First annealing of semi-insulating CZT under Cd pressure at 700/600 C (CZT/Cd) for 24 hours eliminated Te secondary phase defect completely but bring out low resistivity CZT of 2 Ohm cm. For example, second-step annealing of CZT under Te pressure at 550/350 C (CZT/Te) for 240 hours restored its resistivity to 8 x 10^8 ohm cm. In this research, we tried to find out proper annealing condition for restoring CZT's resistivity by using real-time leakage current monitoring system.

10392-27, Session 7

Transient current waveforms and electric-field profile in CZT detectors

Rubi Gul, Brookhaven National Lab. (United States) and Idaho State Univ. (United States); Aleksey E. Bolotnikov, Giuseppe S. Camarda, Anwar Hossain, Louis Iocampo, Brookhaven National Lab. (United States); Rene Rodriguez, Idaho State Univ. (United States); Utpal N. Roy, Ge Yang, Brookhaven National Lab. (United States); Ralph B. James, Savannah River National Lab. (United States)

We will present characterization data for the electric field and electrical transport properties of Bridgman- and THM- (travelling heater method) grown CZT detectors by using a transient current technique (TCT). The TCT system has an excellent position resolution and focused beam width; it has been routinely used for detailed study of the transient waveforms and the electric-field profile in II-VI radiation detectors. Four CZT gamma-ray detectors (two planar and two Frisch-grid designs) were characterized along the thickness of the detector extending from the top contact (cathode) to the bottom contact (anode). Transient current waveforms were collected for different applied bias conditions, and they were analyzed to determine the electron charge-carrier mobility and lifetime. In addition the data are used to calculate and plot the internal electric-field profile. The measured electric-field profile shows variations indicating creation of positive space charge induced by the laser illumination. The electric-field analysis indicates that the field strength decreases from the cathode towards the anode, which shows the strong positive space-charge region near the cathode and weaker space charge region towards the anode of the detector. A model based on the transient current waveforms will also be presented.

10392-28, Session 8

Mechanistic study of the accelerated crucible rotation technique (ACRT) applied to vertical Bridgman growth of CZT *(Invited Paper)*

Mia S. Divecha, Univ. of Minnesota (United States); Jedidiah J. McCoy, Saketh Kakkireni, Santosh K. Swain, Kelvin G. Lynn, Washington State Univ. (United States); Jeffrey J. Derby, Univ. of Minnesota (United States)

Current Bridgman crystal growth methods for cadmium zinc telluride (CZT) result in significant second-phase particle populations, the latter of which require lengthy annealing processes to remove. Additionally, spontaneous nucleation of new grains can occur at the solidification interface during growth, reducing the yield of single-crystal material. The application of the Accelerated Crucible Rotation Technique (ACRT) promises to reduce second-phase particles and improve monocrystallinity. However, there is little guidance on how this approach should be applied to the Bridgman growth of CZT.

We are applying a finite-element model for time-dependent flow, heat and mass transfer, and the crystal growth under realistic furnace thermal profiles. We are testing various ACRT strategies and their impact on melt flow and composition, interface morphology, and morphological stability of the growth interface. In this presentation, we summarize our effort to optimize the rotation schedule for ACRT Bridgman growth of CZT. We emphasize the underlying physical mechanisms that are expected to provide better growth conditions for single-crystal CZT with fewer second-phase tellurium inclusions. Comparison with ongoing growth experiments will also be featured.

This work is supported by the Department of Energy, National Nuclear Security Administration, under Award DE-NA0002565; no official endorsement should be inferred.

10392-29, Session 8

Through-Silicon Vias (TSVs) for 3D readout of ASIC for nearly gapless CdZnTe detector arrays

Jaesub Hong, Branden Allen, Jonathan Grindlay, Harvard-Smithsonian Ctr. for Astrophysics (United States); Sankgi Hong, Tezzaron Semiconductor Corp. (United States); Hiromasa Miyasaka, Jill Burnham, California Institute of Technology (United States); Robert Patti, Tezzaron Semiconductor Corp. (United States); Fiona A. Harrison, California Institute of Technology (United States); Scott Barthelmy, NASA Goddard Space Flight Ctr. (United States)

Wirebonds, although proven for space application and perceived necessary for hybrid sensors like CdZnTe detectors, introduce assembly complexity and undesirable gaps between detector units. Thus they poses a serious challenge in building a low cost large area detector. We are developing Through-Silicon Vias (TSVs) to make all connections (both power and data) through ASICs, which will eliminate wirebonds and enable a simple direct bonding between the ASIC and a substrate electronics layer. TSVs also enable a more compact layout of ASIC, which reduces the inactive area of the detector plane, and thus enables nearly gaplessly tilable detector arrays. We demonstrate the first successful TSV implementation on ASICs used for CZT detectors onboard the Nuclear Spectroscopic Telescope Array (NuSTAR) mission. We present the TSV development process, and the performance of CZT detectors using NuSTAR ASICs with TSVs.

10392-30, Session 8

Sub-pixel resolution in pixelated CdZnTe gamma ray detectors with different pixel sizes (0.5 mm to 1.72 mm) using a focused laser beam

Luis A. Ocampo Giraldo, The Pennsylvania State Univ. (United States); Aleksey E. Bolotnikov, Giuseppe S. Camarda, Gianluigi De Geronimo, Rubi Gul, Jack Fried, Anwar Hossain, Brookhaven National Lab. (United States); Kenan Unlu, The Pennsylvania State Univ. (United States); Emerson Vernon, Ge Yang, Brookhaven National Lab. (United States); Ralph B. James, Savannah River National Lab. (United States)

High-resolution position-sensing has been proposed to correct response non-uniformities in Cadmium Zinc Telluride (CZT) gamma ray detectors by virtually subdividing the area into small voxels and equalizing responses from each voxel. 3D pixelated detectors coupled with multichannel readout electronics are the most advanced type of CZT devices offering many options in signal processing and enhancing detector performance. The main hurdle in achieving high sub-pixel position resolution is the relatively low signal induced on the neighboring pixels because of the electrostatic shielding effect caused by the collecting pixel. In addition, to achieve high position sensitivity one should rely on time-correlated transient signals, which means that digitized output signals must be used. Previous results have shown the benefit of using a focused laser beam to study position resolution in 3D pixelated detectors. We present the results of our studies to measure the amplitude of the pixel signals so that these can be used to measure positions of the interaction points. This is done with the processing of digitized correlated time signals measured from several adjacent pixels taking into account rise-time and charge-sharing effects. In these measurements we used a focused pulsed laser to generate a 10-micron beam at one milliwatt (650-nm wavelength) over the detector surface while the collecting pixel was moved in cardinal directions. The results include measurements that present the benefits of combining conventional pixel geometry with digital pulse processing for the best approach in achieving sub-pixel position resolution with different pixel dimensions ranging from 0.5 mm to 1.72 mm.

10392-31, Session 8

Analysis of accelerated crucible rotation technique (ACRT) in the traveling heater method (THM) growth of CZT

Jeffrey H. Peterson, Jeffrey J. Derby, Univ. of Minnesota (United States)

The traveling heater method (THM) has enjoyed particular success for the growth of large, high-quality bulk crystals of cadmium telluride (CdTe) and cadmium zinc telluride (CZT) for radiation detector applications. However, the THM suffers from growth rates that are an order of magnitude slower than competing methods, such as Bridgman growth. Increasing THM growth rates would represent a major advance toward decreasing the very high cost of this material for use in large-volume gamma-ray spectrometers with high energy resolution.

In this presentation, we apply a rigorous, comprehensive computational model that couples phase equilibria with heat and species transfer, fluid mechanics, and interfacial dissolution and growth phenomena to faithfully describe the THM crystal growth process. We explain mechanisms that drive supercooling instabilities that limit THM growth rates. Specifically, we discuss the formation of melt flow structures (lee-wave vortices) near the growth interface that influence lateral transport in the melt and, in turn, promote concentration gradients in excess of the limit for morphological stability. In this presentation, we build on previous work to more carefully analyze the role of the lee-wave vortex in the onset of constitutional supercooling and investigate strategies for mitigation. Specifically, we consider the application of the accelerated crucible rotation technique (ACRT) to disrupt solute transport within the liquid zone that may alleviate constitutional supercooling and allow for faster growth rates.

This work has been supported in part by the National Science Foundation, under DMR-1007885, and no official endorsement should be inferred.

10392-32, Session 9

Recent advances in garnet scintillator gamma spectrometers *(Invited Paper)*

Erik L. Swanberg, Zachary M. Seeley, Patrick R. Beck, Brian Wihl, Nerine J. Cherepy, Stephen A. Payne, Steven L. Hunter, Scott E. Fisher, Peter A. Thelin, Lawrence Livermore National Lab. (United States); Todd Stefanik, Nanocerox, Inc. (United States); Joel Kindem, Cokiya, Inc. (United States)

Gadolinium Garnet transparent ceramics doped with Ce, ((Gd,Y,Ce)3(Ga,Al)5O12), for gamma-ray spectroscopy provide high density, high light yield, high energy resolution , high Z, mechanical robustness, and they are unreactive to air and water. Gadolinium garnet single crystals are costly to grow, due to their high melting points, and suffer from non-uniform light yield, due to Ce segregation. In contrast, transparent polycrystalline ceramic Garnets are never melted, and therefore are less costly to produce

and provide the uniform light yield required to achieve high energy resolution with a scintillator.

GYGAG(Ce) transparent ceramics offer energy resolution as good as R(662 keV) = 3.5%, in a pixelated detector utilizing Silicon photodiode array readout. We have developed a modular handheld detector based on pixelated GYGAG(Ce) on a photodiode array, that offers directional detection for point source detection as well as gamma spectroscopy. Individual modules can be assembled into detectors ranging from pocket-size to large panels, for a range of applications.

Large GYGAG(Ce) transparent ceramics in the 2-5 in3 size range have been fabricated at LLNL. Instrumentation of these ceramics with Silicon photomultipliers (SiPMs) and super bi-alkali PMTs has been explored and energy resolution as good as R(662 keV) = 5% has been obtained. Further improvements with SiPM readout will leverage their high quantum efficiency in the 500-650 nm range where GYGAG(Ce) emits, and implement electronics that minimize the effect of SiPM dark current and capacitance on the pulse height spectra.

This work was performed under the auspices of the U.S. DOE by Lawrence Livermore National Laboratory under Contract DE-AC52-07NA27344, and has been supported by the US Department of Homeland Security, Domestic Nuclear Detection Office, under competitively awarded IAA HSHQDC-12-X-00149 under Contract No. DE-AC03-76SF00098. LLNL-ABS-724480.

10392-33, Session 9

Crystal growth of CdZnTeSe (CZTS) gamma detectors: a promising alternative to CdZnTe *(Invited Paper)*

Utpal N. Roy, Giuseppe S. Camarda, Yonggang Cui, Rubi Gul, Ge Yang, Anwar Hossain, Brookhaven National Lab. (United States); Ralph B. James, Savannah River National Lab. (United States); Jakub Zázvorka, Václav Dedic, Jan Franc, Charles Univ. in Prague (Czech Republic); Vincenzo Lordi, Joel B. Varley, Lawrence Livermore National Lab. (United States)

Alloying of CdZnTe (CZT) with selenium has been found to be very promising and effective in reducing the overall concentration of secondary phases (Te precipitates/inclusions) and sub-grain boundary networks in the crystals. These two types of defects are the main causes for incomplete charge collection, and hence they affect the yield of high-quality CZT, resulting in a very high cost for large-volume, high-quality detector-grade CZT detectors. The addition of selenium was also found to very effective in increasing the compositional homogeneity along the growth direction of the CdZnTeSe (CZTS) ingots grown by the traveling heater method (THM) technique. The compositional homogeneity along the growth direction can enhance the overall yield of detector-grade CZTS, which should therefore be possible to produce at a lower cost compared to CZT. The electrical properties and detector performance of the CZTS crystals will be presented and discussed.

10392-34, Session 9

Stoichiometry and extended defects in Cd(Zn,Mn)Te and CdTeSe crystals

Anwar Hossain, Aleksey E. Bolotnikov, Giuseppe S. Camarda, Yonggang Cui, Utpal N. Roy, Ge Yang, Brookhaven National Lab. (United States); Ralph B. James, Savannah River National Lab. (United States)

We investigated the elemental distribution and extended defects in CdTe-based crystals with Zn, Mn or Se as the third element in a tertiary compound. The understanding and reduction of these defects in bulk crystals are vital for the manufacturing of high-quality large-volume detectors, as they have detrimental effects on detector performance. In this work, we obtained high spatial resolution X-ray fluorescence maps of the compositional elements, as well as the doping elements to determine elemental distributions along the both growth and radial directions of the crystals. We also used chemical etching and X-ray diffraction and fluorescence techniques to investigate the extended defects in crystals grown by Bridgman and traveling heater methods. We measured the shapes, sizes, and concentrations of these crystal defects to identify their nature. We evaluated areal densities and distributions of the etch pits associated with dislocations and other crystallographic defects using IR transmission microscopy and a scanning electron microscopy (SEM) combined with energy-dispersive x-ray spectroscopy (EDS). We performed a comparative assessment of the properties of different crystals and correlated our detailed data with detector response measurements to understand the influence of the material properties on detector performance.

10392-35, Session 9

Ionizing organic-based nanocomposites for efficient gamma-ray sensor

Narsingh B. Singh, Fow-Sen Choa, Bradley Arnold, Stacey Sova, Christopher Cooper, Jayati Bhavsar, Univ. of Maryland, Baltimore County (United States)

Single crystal based radiation detectors have been developed for semiconductor based radiation sensors. Materials such as cadmium zinc tellurides and its analogs have shown great promise. To reduce the cost a great deal of researches led by Khalil Arshak developed nickel oxide based sensors. But the sensors have low sensitivity. Our studies indicated that thickness and microstructure have pronounced effect on sensitivity. Since the interaction of gamma-ray with composites involves all three interaction processes; photoelectric effect, Compton scattering, and pair production, composites have better chance for enhancing sensitivity. The probability of the photoelectric effect where a gamma ray interacts with an atom resulting in the ejection of an electron from the atom is proportional to the atomic number (Z) of the absorbing element and inversely related to the energy of the gamma ray is most important for low energy gamma rays. In the composites of ionizing organics oxidation effect of unusual oxides changes much faster and hence increases the sensitivity of radiation. We expect that resistivity of the oxide composite will gradually increase following sequential irradiation processes because of the decrease in holes' concentration. In this presentation, we will present the effect of morphology and processing on sensing gamma-ray by oxides - ethylene carbonate composites.

10392-36, Session 10

Deep level analysis of CdZnTeSe radiation detectors: their effect on the internal electric field *(Invited Paper)*

Ge Yang, Utpal N. Roy, Yonggang Cui, Giuseppe S. Camarda, Anwar Hossain, Rubi Gul, Brookhaven National Lab. (United States); Ralph B. James, Savannah River National Lab. (United States)

We studied the defect-related deep levels in CdZnTeSe radiation detectors using low-temperature photoluminescence spectroscopy measurements. The outcomes are compared with the results of Pockels-effect measurements, which are coupled with external stimulation of light at different wavelengths to excite the deep levels. We discuss the correlation between the two measurements in detail. Our efforts help to understand better the effects of deep levels on the internal electric field of CdZnTeSe X- and gamma-ray detectors.

10392-37, Session 10

Three-dimensional mapping and analysis of mid-gap defect distributions in TlBr by a femtosecond two-photon photocurrent microscope

Drew Onken, Sergii Gridin, Kamil B. Ucer, Richard T. Williams, Wake Forest Univ. (United States); Shariar Motakef, Amlan Datta, CapeSym, Inc. (United States)

Thallium bromide is a promising semiconductor for room temperature radiation detection. One of the remaining challenges of this soft material is defects associated with strain. Defect states near mid-gap promote rapid loss of carriers at high densities by Shockley-Read-Hall bimolecular recombination. We describe 3-D mapping of nonlinear photoconductive response using femtosecond pulse trains at 840 nm, somewhat above mid-gap of TlBr. A confocal two-photon microscopy setup with photocurrent detection affords spatial resolution perpendicular to the surface. We report analysis of the irradiance dependence of the induced current as a function of depth in the sample. There are three separate contributions to the second-order current response. First is the intrinsic two-photon absorption of non-defective TlBr. As noted above, there will be a subtractive 2nd-order quenching term proportional to the local density of mid-gap states. Crucially for our technique, the same mid-gap states responsible for nonlinear carrier quenching also constitute a second-order source term causing resonantly enhanced two-photon absorption across the band gap in crystal regions where the mid-gap states are found. At moderately low irradiance, two-photon induced conductivity comes only from defective regions. At high irradiance, one finds normal 2-photon photocurrent from the nondefective regions and diminished response from nonlinear quenching in the defective regions. From such data, the spatial distribution of the defects is directly displayed and the cross section for bimolecular carrier quenching can be extracted. WFU acknowledges support of DNDO-ARI DHS-2014-DN-077-ARI077-04. This support does not constitute an express or implied endorsement on the part of the government.

Return to Contents

10393-1, Session 1

Threat detection of liquid explosives and precursors from their x-ray scattering pattern using energy dispersive detector technology

Jan Kehres, Mark Lyksborg, Ulrik Lund Olsen, Technical Univ. of Denmark (Denmark)

After the transatlantic Airplane plot in 2006 the maximum volume of liquids, aerosols and gels (LAG's) in carryon luggage was temporarily limited to 1 Liter, packed in individual bottles of max. 100 ml, until scanner technology emerges capable of identifying liquid threats. One approach to identify liquid threats in presence of complex electronics and without removing them from the luggage is the application of energy dispersive X-ray diffraction (EDXRD) on a by X-ray absorption contrast imaging pre identified object. To investigate the application an energy dispersive laboratory X-ray diffractometer using slit collimation and a CdTe detector has been developed. For the development of robust threat detection algorithms, EDXRD spectra of 11 liquid threats and 46 common LAGS at multiple angles and with limited count statistics, corresponding to realistic acquisition times in scanner applications, were recorded. The measurements were repeated 10 times, yielding a data set of 570 EDXRD patterns. Initial results from testing of threat detection algorithm, trained with the corrected, normalized and merged data acquired at multiple angles and in an energy window between 50 – 100 keV, which has been determined to be realistically usable with the limited count statistics and in presence of complex electronics in realistic luggage arrangements, detection levels as good as > 95 % true positive with < 6 % false positive alarms have been achieved.

10393-2, Session 1

Rapid and accurate detection of uranium in aqueous solutions

Gary Tepper, Brandon Dodd, Virginia Commonwealth Univ. (United States)

Elevated levels of uranium in water can be associated with activities such as uranium mining, enrichment and transport. Currently, water samples must be obtained and transported to a laboratory for analysis in order to determine the concentration of uranium. This costly and time-consuming method is inadequate for defense and security applications. This paper presents a new optical method for fast and accurate measurement of uranium in water. Water samples are circulated through a nanoporous silica gel material where dissolved uranium is accumulated and concentrated. The natural fluorescence of the dissolved uranium compounds is enhanced within the silica gel matrix allowing for rapid and highly sensitive measurement using a simple optical system. Uranium concentration is determined by controlling the flow-rate and measuring the kinetics of the fluorescent output signal.

10393-3, Session 1

Small unmanned aircraft system for remote contour mapping of a nuclear radiation field *(Invited Paper)*

Paul P. Guss, Karen McCall, Russell Malchow, Richard Fischer, Michael Lukens, Mark Adan, Ki Park, Roy Q. Abbott, Michael E. Howard, Eric Wagner, Rusty P. Trainham, Tanushree Luke, National Security Technologies, LLC (United States); Sanjoy Mukhopadhyay, International Atomic Energy Agency (Austria); Paul Oh, Pareshkumar Brahmbratt, Eric Henderson, Univ. of Nevada, Las Vegas (United States); Jinlu Han, Justin Huang, Casey Huang, Astro Flight, Inc. (United States); Jon Daniels, Univ. of Nevada, Las Vegas (United States)

For nuclear disasters involving radioactive contamination, small unmanned aircraft systems (sUASs) equipped with nuclear radiation detection and monitoring capability can be very important tools. Among the advantages of a sUAS are quick deployment, low-altitude flying that enhances sensitivity, wide area coverage, no radiation exposure health safety restriction, and the ability to access highly hazardous or radioactive areas. Additionally, the sUAS can be configured with the nuclear detecting sensor optimized to measure the radiation associated with the event. In this investigation, sUAS platforms were obtained for the installation of sensor payloads for radiation detection and electro-optical systems that were specifically developed for sUAS research, development, and operational testing. The sensor payloads were optimized for the contour mapping of a nuclear radiation field, which will result in a formula for low-cost sUAS platform operations with built-in formation flight control. Additional emphases of the investigation were to develop the relevant contouring algorithms; initiate the sUAS comprehensive testing using the Unmanned Systems, Inc. (USI) Sandstorm platforms and other acquired platforms; and both acquire and optimize the sensors for detection and localization. We demonstrated contour mapping through simulation and validated waypoint detection. We mounted a detector on a sUAS and operated it initially in the counts per second (cps) mode to perform field and flight tests to demonstrate that the equipment was functioning as designed. We performed ground truth measurements to determine the response of the detector as a function of source-to-detector distance. Operation of the radiation detector was tested using different unshielded sources.

10393-4, Session 1

International Radiation Monitoring and Information System (IRMIS)

Sanjoy Mukhopadhyay, Florian Baciu, Jan Stowisek, Gurdeep Saluja, Patrick Kenny, International Atomic Energy Agency (Austria); Franck Albinet, Independent Contractor - GIS & Data Analyst Consultant (France)

This article describes the International Radiation Monitoring Information System (IRMIS) which was developed by the International Atomic Energy Agency (IAEA) with the goal to provide Competent Authorities, the IAEA and other international organizations with a client server based web application to share and visualize large quantities of radiation monitoring data. The data maps the areas of potential impact that can assist countries to take appropriate protective actions in an emergency.

Ever since the Chernobyl nuclear power plant accident in April of 19861 European Community (EC) has worked towards collecting routine environmental radiological monitoring data from national networked monitoring systems. European Radiological Data Exchange Platform (EURDEP) was created in 19952 to that end – to provide radiation monitoring data from most European countries reported in nearly real-time.

During the response operations for the Fukushima Dai-ichi nuclear power plant accident (March 2011) the IAEA Incident and Emergency Centre (IEC) managed, harmonized and shared the large amount of data that was being generated from different organizations. This task underscored the need for a system which allows sharing large volumes of radiation monitoring data in an emergency.

In 2014 EURDEP started the submission of the European radiological data to the International Radiation Monitoring Information System (IRMIS) as a European Regional HUB for IRMIS.

IRMIS supports the implementation of the Convention on Early Notification of a Nuclear Accident by providing a web application for the reporting,

sharing, visualizing and analyzing of large quantities of environmental radiation monitoring data during nuclear or radiological emergencies.

IRMIS is not an early warning system that automatically reports when there are significant deviations in radiation levels or when values are detected above certain levels. However, the configuration of the visualization features offered by IRMIS may help Member States to determine where elevated gamma dose rate measurements during a radiological or nuclear emergency indicate that actions to protect the public are necessary. The data can be used to assist emergency responders determine where and when to take necessary actions to protect the public.

This new web online tool supports the IAEA's Unified System for Information Exchange in Incidents and Emergencies (USIE), an online tool where competent authorities can access information about all emergency situations, ranging from a lost radioactive source to a full-scale nuclear emergency.

10393-5, Session 2

Development and deployment of the Collimated Directional Radiation Detection System *(Invited Paper)*

Amber L. Guckes, National Security Technologies, LLC (United States); Alexander Barzilov, Univ. of Nevada, Las Vegas (United States)

The Collimated Directional Radiation Detection System (CDRDS) is capable of imaging radioactive sources in two dimensions. The detection medium of the CDRDS is a single $Cs_2LiYCl_6:Ce^{3+}$ scintillator enriched in Li-7 (CLYC-7). The CLYC-7 scintillator is surrounded by a heterogeneous ABS plastic and lead (Pb) collimator. These materials make-up a coded aperture inlaid in the collimator. The collimator is rotated 360 degrees by a stepper motor which enables time-encoded imaging of a measured radioactive source.

The measurements of a radioactive source are collected in discrete time steps that correlate to the angular rotation of the collimator. These measurements are collected in 360 degrees and recorded for post-measurement processing. The measurement results, combined with the decoding mask of the coded aperture, are convoluted to create an image of the measured radioactive source.

This collimator design allows for the directional detection of photons and fast neutrons by utilizing only one CLYC-7 scintillator. Directional detection of thermal neutrons can also be performed by utilizing another suitable scintillator. In addition to directional detection capabilities, the CDRDS is also capable of spectroscopy and pulse shape discrimination of photons and fast neutrons.

The CDRDS is portable, robust, and user friendly. This unit is capable of utilizing wireless data transfer for possible radiation mapping and network?centric CONOPS. The CDRDS is tested by performing laboratory directional measurements with various gamma-ray check sources and neutron sources. Field directional measurements are also performed to demonstrate the CDRDS's feasibility for deployment.

10393-6, Session 2

Performance of pulse-shape discriminating plastic scintillation modules using SiPMs for detecting fast neutrons

James F. Christian, Erik B. Johnson, Daniel E. Fernandez, Samuel Vogel, Rebecca Frank, Graham Stoddard, Radiation Monitoring Devices, Inc. (United States); Jorge Pereira, Remco Zegers, National Superconducting Cyclotron Lab. (United States); Christopher J. Stapels, Mathworks (United States)

The development of neutron detection systems is important to make further progress and complement the increased drive to explore very exotic nuclei systems, in particular with very large neutron excesses. Often, such experiments are performed in environments where background (gamma) radiation is high, or where strong magnetic fields are present. Traditional neutron-gamma separation techniques (using liquid scintillators) are expensive and employ photo-multipliers that cannot operate well in significant magnetic fields.

This work describes the development of detector modules, whose quantity accommodates large detector volumes, as well as the characterization of the modules at the National Superconducting Cyclotron Laboratory (NSCL). The approximately 1.8 cm x 1.8 cm x 2.5 cm plastic scintillation detector, coupled to a 1.2 cm x 1.2 cm SiPM, discriminates neutron from gamma events using the shape of the scintillation pulse. The LENDA Digital Data Acquisition System (DDAS) of the NSCL Charge-Exchange Group processed the signals from the detector module. This work compares the signal-to-noise performance of the detector module to a LENDA bar, which is a plastic scintillation material coupled to a PMT. Additionally, we present measurements of the PSD performance for the detector module in the relevant operating environment.

10393-7, Session 2

High-resolution photon spectroscopy with a microwave-multiplexed four-pixel transition edge sensor array

Paul P. Guss, National Security Technologies, LLC (United States); Mike Rabin, Mark Croce, Los Alamos National Lab. (United States); Nathan Hoteling, National Security Technologies, LLC (United States); Sanjoy Mukhopadhyay, International Atomic Energy Agency (Austria)

We demonstrate very high–resolution photon spectroscopy with a microwave-multiplexed 4-pixel transition edge sensor array. The readout circuit consists of superconducting microwave resonators coupled to radio frequency superconducting-quantum-interference devices (RF-SQUIDs) and transduces changes in input current to changes in phase of a microwave signal. We used a flux-ramp modulation to linearize the response and avoid low-frequency noise. The result is a very high-resolution photon spectroscopy with a microwave-multiplexed 4-pixel transition edge sensor (TES) array. We performed and validated a small-scale demonstration and test of all the components of our concept system, which encompassed microcalorimetry, microwave multiplexing, RF-SQUIDs, and software-defined radio (SDR). We shall display data we acquired in the first simultaneous combination of all key innovations in a 4-pixel demonstration, including microcalorimetry, microwave multiplexing, RF-SQUIDs, and SDR. We present the energy spectrum of a gadolinium-153 (153Gd) source we measured using our 4-pixel TES array and the RF-SQUID multiplexer. For each pixel, one can observe the two 97.4 and 103.2 keV photopeaks. We measured the 153Gd photon source with an achieved energy resolution of 70 eV, a full width half maximum (FWHM) of 100 keV, and an equivalent readout system noise of 90 pA/pHz at the TES. This demonstration establishes a path for the readout of cryogenic x-ray and gamma ray sensor arrays with more elements and spectral resolving powers. We believe this project has improved capabilities and substantively advanced the science useful for missions such as nuclear forensics, emergency response, and treaty verification through the explored TES developments.

10393-8, Session 2

Large-area CdTe imaging sensor and its applications *(Invited Paper)*

Tadayuki Takahashi, Shin Watanabe, Institute of Space and Astronautical Science (Japan); Shin'ichiro Takeda, Okinawa Institute of Science and Technology Graduate Univ. (Japan)

No Abstract Available

10393-9, Session 3

X-ray backscatter radiography with lower open fraction coded masks *(Invited Paper)*

Andre M. A. Munoz, Anna Vella, Matthew J. F. Healy, David W. Lane, Cranfield Univ. (United Kingdom); David Lockley, Defence Science and Technology Lab. (United Kingdom)

Single sided radiographic imaging would find great utility for medical, aerospace and security applications. While coded apertures can be used to form such an image from backscattered X-rays they suffer from near field limitations that introduce noise. Several theoretical studies have indicated that for an extended source the image's signal to noise ratio may be optimised by using a low open fraction (<0.5) mask. However, few experimental results have been published for such low open fraction patterns and details of their formulation are often unavailable or are ambiguous. In this paper we address this process for two types of low open fraction mask, the dilute URA the Singer set array. For the dilute URA the procedure for producing multiple 2D array patterns from given 1D binary sequences (Barker codes) is explained. Their point spread functions are calculated and their imaging properties are critically reviewed. These results are then compared to those from the Singer set and experimental exposures are presented for both type of pattern; their prospects for near field imaging are discussed.

10393-10, Session 3

Recent developments in high-speed proton radiography at LANSCE

Johnny Goett, Los Alamos National Lab. (United States)

Two recent developments in Proton Radiography at LANSCE's line C will be discussed.

The new pRAD2 10-frame hybridized focal plane array design offers much improved spatial and charge resolution, higher quantum efficiency, lower noise, and faster repetition rate over the current state of the art, with integration times below 50 ns. Characterization procedures and data, along with notable physics results will be shown.

Preliminary results from a single pixel proton time-of-flight measurement for energy resolved radiography will be presented along with device concepts for a multi-pixel imager. These advances, bringing tighter timing resolution, more frames and improved density resolution will significantly enhance pRad's capabilities for advances in materials and shock physics research.

10393-11, Session 3

New results from sub-3 MeV Compton spectrometer experiments *(Invited Paper)*

Amanda E. Gehring, Michelle A. Espy, Todd J. Haines, Los Alamos National Lab. (United States)

Our team at Los Alamos National Laboratory has successfully employed Compton spectrometers to measure the x-ray spectra of both continuous and flash, intense radiographic sources. In this method, a collimated beam of x-rays incident on a convertor foil ejects Compton electrons. A collimator may be inserted into the entrance of the spectrometer to select the angular acceptance of the forward-scattered electrons, which then enter the magnetic field region of the spectrometer. The position of the electrons at the magnet's focal plane is proportional to the square root of their momentum, allowing the x-ray spectrum to be reconstructed. A new samarium-cobalt spectrometer with an energy range of 50 keV to 4 MeV has been fielded at two facilities. The x-ray generating machines produced intense beams (> 4 rad at 1 m) of photons with spectral endpoints below 3 MeV. Recent experimental results will be presented.

10393-12, Session 3

Modeling charge collection in x-ray imagers

Giovanni Pinaroli, Univ. degli Studi di Udine (Italy) and Elettra-Sincrotrone Trieste S.C.p.A. (Italy); Pierpaolo Palestri, Luca Selmi, Alessandro Pilotto, Univ. degli Studi di Udine (Italy)

Biomedical and advance material research utilizing photons with energy range of some hundreds of eV to some keV, which are generated by high brilliance Light Sources such as new generation Synchrotron and Free Electron Lasers, put certain constrains on the utilized detection technology. Typical requirements in these applications are high frame and photon rates, single-photon counting capability with low probability of false positives, thus large dynamic range, high quantum efficiency, and (multi)-mega-pixels. To meet these requirements different detector strategies have been suggest and some have been implemented recently. Back-thinned, monolithic active pixel sensors (MAPS) based on standard CMOS technology and standard CMOS parameters are promising candidates for these applications. A priori it is important to understand if a generic photo-diode architecture where photo-generated carriers diffusion dominates the charge collection is suited to fulfill all the aforementioned requirements. A thorough simulation-based investigation of field line distribution, charge transportation and collection has been carried out on 3D-model of a generic pixel by utilizing the commercial TCAD tool Sentaurus.

Several aspects were observed in order to analyze the most relevant features of the photo-sensitive area of the sensor. Beside static simulations to determine the electric-field profile under different bias conditions and for different back-biasing strategies, charge collection was analyzed with transient simulations. Since these simulations are very time consuming when applied to 3D structures, we then investigated the possible use of Ramo's theorem to obtain reliable estimate of the trajectories of the generated carriers and of the associated currents at the device terminals.

10393-13, Session 3

A multi-purpose RTSD readout electronics for XRD and photon-counting x-ray imaging

Zhi Deng, Xiaobing Yue, Yuxiang Xing, Yinong Liu, Tsinghua Univ. (China)

RTSDs (Room-Temperature Semiconductor Detector) such as CdTe and CdZnTe have shown great potential power for X-ray detection in wide range of applications from medical imaging to security inspection. However the requirements of energy resolution, counting rate and efficiency are quite different, which bring big challenges not only for the detector technolgies, but also for the readout signal processing electronics.

A multi-purpose RTSD readout electronics was being developed mainly for linear array CdTe detectors and for luggage inspection systems. It can work at different modes, including high energy resolution at relatively low counting rate and high rate photon-counting (~10 Mcps per channel) with reduced energy resolution. Hence it can be used both for XRD (X-Ray Diffraction) and energy resolved photon-counting X-ray imaging. The multi-mode capability was implemented by using programmable digital signal processing. The linear array CdTe detector was firstly readout by a 32-channel analog front-end ASIC, which consisted of a charge sensitive preamplifier and a CR-(RC)^6 shaper with 100 ns peaking time for each channel. Then the analog signal was continuously digitized by commercial fast ADC cards and processed by different digital filters in FPGA. Only the final extracted information will be sent to the computer. Different digital signal processing algorithms will be verified and the test results will be compared and be present in the paper.

10393-14, Session 4

3D-printed coded apertures for x-ray backscatter radiography *(Invited Paper)*

Andre M. A. Munoz, Anna Vella, Matthew J. F. Healy, David W. Lane, Cranfield Univ. (United Kingdom); David Lockley, Defence Science and Technology Lab. (United Kingdom)

Many different mask patterns can be used for X-ray backscatter imaging using coded apertures, which can find application in the medical, industrial and security sectors. While some of these patterns may be considered to have a self-supporting structure, this is not the case for some of the most frequently used patterns such as uniformly redundant arrays or any pattern with a high open fraction. This makes mask construction difficult and usually requires a compromise in its design by drilling holes or adopting a 'no two holes touching' version of the original pattern. In this study this compromise was avoided by 3D printing a support structure that was then filled with a radiopaque material to create the completed mask. The coded masks were manufactered using two different methods, hot cast and cold cast. Hot casting involved casting a bismuth alloy at 80°C into the 3D printed acrylonitrile butadiene styrene mould which produced an absorber with density of 8.6 g cc-1. Cold casting was undertaken at room temperature, when a tungsten/epoxy composite was cast into a 3D printed polylactic acid mould. The cold cast procedure offered a greater density of around 9.5 to 10 g cc-1 and consequently greater X-ray attenuation. It was also found to be much easier to manufacture and more cost effective. A critical review of the manufacturing procedure is presented along with some typical radiographs. In both cases the 3D printing process allowed square apertures to be creating avoiding their approximation by circular holes when conventional drilling is used.

10393-15, Session 4

Leveraging multi-channel detector technology to improve quality metrics for industrial and security applications

Edward S. Jimenez, Kyle R. Thompson, Noelle M. Collins, Srivathsan Koundinyan, Sandia National Labs. (United States)

Sandia National Laboratories has recently developed the capability to acquire multi-channel radiographs for multiple research and development applications in industry and security. This capability allows for the acquisition of x-ray radiographs or sinogram data to be acquired at up to 300 keV with up to 128 channels per pixel. This work will investigate whether multiple quality metrics for computed tomography can actually benefit from binned projection data compared to traditionally acquired grayscale sinogram data. Features and metrics to be evaluated include the ability to distinguish between two di?erent materials with similar absorption properties, interface resolution of juxtaposed materials with wide absorption di?erences, and signal-to-noise for both raw data and reconstructed volumetric data. The impact of this technology to non-destructive evaluation, national security, and industry is wide-ranging and has to potential to improve upon many inspection methods such as dual-energy methods, material identification, object segmentation, and computer vision on radiographs. Sandia National Laboratories is a multi-program laboratory managed and operated by Sandia Corporation, a wholly owned subsidiary of Lockheed Martin Corporation, for the U.S. Department of Energy's National Nuclear Security Administration under contract DEAC0494AL85000.

10393-16, Session 4

Spectral correction algorithm for multispectral CdTe x-ray detectors

Erik D. Christensen, Niels Bohr Institute (Denmark); Yun Gu, Jan Kehres, Technical Univ. of Denmark (Denmark); Robert Feidenhans'l, European XFEL GmbH (Germany); Ulrik L. Olsen, Technical Univ. of Denmark (Denmark)

Compared to the dual energy scintillator detectors widely used today, pixelated multispectral X-ray detectors show the potential to improve material identification in various radiography and tomography applications used for industrial and security purposes. However, detector effects, such as charge sharing and photon pile up, distort the measured spectra in high flux pixelated multispectral detectors. These effects significantly reduce the detectors' capabilities to be used for material identification, which requires accurate spectral measurements. We have developed a semi analytical computational algorithm for multispectral CdTe X-ray detectors which corrects the measured spectra for severe spectral distortions coursed by the detector. The algorithm is developed for the Multix M100 CdTe X-ray detector, but could potentially be adapted for any pixelated multispectral CdTe detector. The calibration of the algorithm is based on simple attenuation measurements of commercially accessible materials using standard laboratory sources, making the algorithm applicable in any X-ray setup. The validation of the algorithm has been done using experimental data acquired with both standard lab equipment and synchrotron radiation. The experiments show that the algorithm is fast, reliable even at X-ray flux up to 4 Mph/s/pix, and greatly improves the accuracy of the measured X-ray spectra, making the algorithm very useful for both security and industrial applications where multispectral detectors are used.

10393-17, Session 4

Optimization of input parameters to improve big-data computed tomography reconstruction performance

Celia J. Flicker, Edward S. Jimenez, Sandia National Labs. (United States)

This work seeks to develop an autonomous optimization of input computational resource parameters for arbitrary big-data computed tomography (CT) configurations. It is well known that graphics processing units (GPU) have been a boon to many high-performance applications, including CT. The reconstruction task has both colossal computational and data throughput requirements that easily tax high-end GPUs to their limit. For big-data industrial and research applications, the burden is exacerbated through the use of high pixel count detectors (≥ 16 megapixels) and the large number of projections needed to meet Nyquist sampling requirements, resulting in datasets up to terabytes in size. Previous work has shown that the GPU kernels can be optimized to e?ciently handle big-data; however, as this work will show, some sensitivities exist with respect to the tunable input parameters that can exact an exaggerated toll on reconstruction performance. This work will investigate the input parameter space for various relevant and future-sized datasets and will present a calibration approach to optimize reconstruction performance for varying sized detectors, geometries, and graphics processing resources. This work has the potential to dramatically improve many non-destructive evaluation and inspection applications in industry, security, and research where reconstruction rate is the main bottleneck of the resource chain. Sandia National Laboratories is a multi-program laboratory managed and operated by Sandia Corporation, a wholly owned subsidiary of Lockheed Martin Corporation, for the U.S. Department of Energy's National Nuclear Security Administration under contract DEAC04-94AL85000.

10393-32, Session PWed

The dual-channel ultraviolet/low-light CMOS camera using image fusion technique

Yunsheng Qian, Xiangyu Kong, Xiaoyu Zhou, Xiaodong Tang, Yijun Zhang, Nanjing Univ. of Science and Technology (China)

Ultraviolet(UV) detection technology, as immediate area of research focus, has been adopted in the fields of fingerprint identification, corona detection and exhaust plume detection for its significant value and practical meaning. Low-light(LL) CMOS, which can work in even 10-3 lux, is used in visible light channel. The prominent advantage of the dual-channel UV/LL camera is the fusion of UV and wide dynamic range visible light information, which can enrich image details and help observers locate the UV targets in the complicated background around the clock rapidly. The paper studied on the component structure of ultraviolet ICMOS, imaging driving, the UV/LL images fusion algorithm and the photon counting algorithm. Firstly, the one inch and wide dynamic range CMOS chip with the coupling optical fiber panel are coupled to the ultraviolet image intensifier. The ultraviolet image intensifier adopts Te-Cs photocathode. Secondly, in consideration of the ultraviolet detection demand, the drive circuit of the CMOS chips is designed and the corresponding program based on Verilog language is written. Thirdly, after analysis and comparison of the characteristics of UV image and LL CMOS image, the improved Laplace pyramid fusion algorithm is applied. UV image and LL CMOS image are multiscale decompose, and the features in different frequency layer are chosen from either UV image or LL CMOS image. Weighted average fusion algorithm is also used as a contrast. Finally, the connected components labeling way is utilized for the ultraviolet detection and imaging. At last, the detection experiment of the ultraviolet signal in day and night is carried out, and the test results are given and analyzed.

10393-18, Session 5

Measurement of x-ray spectra using a recent YAP(Ce)-MPPC detector

Eiichi Sato, Yasuyuki Oda, Sohei Yoshida, Satoshi Yamaguchi, Yuichi Sato, Iwate Medical Univ. (Japan); Tomotaka Ishii, Osahiko Hagiwara, Hiroshi Matsukiyo, Toshiyuki Enomoto, Manabu Watanabe, Shinya Kusachi, Toho Univ. (Japan)

To measure X-ray spectra with high count rates, we developed a detector consisting of a cerium-doped yttrium aluminum perovskite [YAP(Ce)] crystal and a recent multipixel photon counter (MPPC). Scintillation photons are detected using the MPPC, and the photocurrents flowing through the MPPC are converted into voltages and amplified using a high-speed current-voltage (I-V) amplifier. The MPPC bias voltage was set to a maximum value at the pre-Geiger mode to perform zero-dark counting. The event-pulse widths were approximately 200 ns, and the X-ray spectra were measured using a multichannel analyzer (MCA) for pulse-height analysis. The photon energy was roughly determined by the four-point calibration using tungsten K photons, iodine K fluorescence, and bremsstrahlung maximum-energy photons. K-series characteristic photons from the tungsten target were observed using a 0.5-mm-diam lead pinhole at a tube voltage of 100 kV. Using the YAP(Ce)-MPPC detector, first-generation dual-energy computed tomography was accomplished using iodine and gadolinium contrast media.

10393-19, Session 5

Analysis of the effect of dielectric interlayer on modulation transfer function of granular x-ray scintillator detector

Hyeon Bo Shim, Jookwon Song, Jae W. Hahn, Yonsei Univ. (Korea, Republic of)

Modeling of visible light propagation through diffusive granular scintillator plate is important to predict optical properties of scintillators such as modulation transfer function (MTF). To estimate the diffusive light propagation, it is necessary to solve the radiative transfer equation (RTE) for photon. Therefore, there are various approaches to get the solution of RTE such as Monte-Carlo method and diffusion equation (DE). Although the most of the scintillators contain dielectric interlayer such as shields or adhesives between plate and detector, DE is not suitable to handle the light propagation in this layer because it ignores the propagation direction at an exit plane of the scintillator.

In this study, we suggest the light transport model for the scintillator with dielectric interlayer. From the RTE solution of homogeneous medium, we calculate the intensity distribution at exit plane under the propagation direction. This intensity, paired with specific point of the detector by refraction, is modulated by the rules of etendue conservation and Fresnel equation. The radiant power of the detector point comes from the product of solid angle of the detector mesh and the corresponding intensity. The point spread function (PSF), equivalent to the radiant power distribution of the detector plane, is calculated by numerical integration along the exit plane and the plate thickness. Finally, we analyze the MTF of the scintillator with different refractive index and layer thickness of the dielectric interlayer. We verify our modeling by comparing with the Monte-Carlo method (LightTools).

Acknowledgement: This work was supported by Vieworks Co. (No. 2016-11-0744).

10393-20, Session 5

Silicon strip photon-counting detectors for breast CT *(Invited Paper)*

William C. Barber, DxRay, Inc. (United States) and Interon AS (Norway); H. Ding, L. Singh, K. Habashi, Univ. of California, Irvine (United States); Nail Malakhov, Gregor Wawrzyniak, Interon AS (Norway); Neal E. Hartsough, DxRay, Inc. (United States); Eirik Næss-Ulseth, Interon AS (Norway); Jan Christopher Wessel, Interon AS (Norway) and DxRay, Inc. (United States); Jan S. Iwanczyk, DxRay, Inc. (United States); Sabee Molloi, Univ. of California, Irvine (United States)

We report on recent imaging experiments using edge illuminated silicon strip detectors for high resolution breast computed tomography (CT). The detector's throughput, energy resolution, and stability have been measured at a dynamic range suitable for breast CT at room temperature. The detectors have an array of pixels with a 0.1 mm pitch and can be tiled in one dimension on a single printed circuit board panel and multiple panels can be stacked in two dimensions. The detectors are have a 6 mm or 10 mm depth in the incident direction providing a dynamic range of up to 45 keV and 65 keV respectively. Each pixel has four energy discriminators with a linear energy response across the entire dynamic range. We have tiled the detectors in one dimension (1D) onto single printed circuit boards creating a 20 cm field of view panel. We have stacked two such 1D panels and measured; an output count rate of up to 100 Mcps/mm2 with a linear response up to 40 Mcps/mm2, an energy resolution of 2 keV full width at half maximum across the entire dynamic range, and a noise floor below 4 keV. Images of phantoms have been obtained under realistic breast CT conditions showing micro-calcification detection at a comparable dose as compared to conventional dual view mammography using a single 1D panel. Our future plans include imaging phantoms and post mortem breast tissue with the goal of demonstrating both micro-calcification detection and superior mass legion detection at a comparable dose as compared to conventional dual view mammography.

10393-21, Session 5

Scintillator performance considerations for dedicated breast computed tomography *(Invited Paper)*

Srinivasan Vedantham, The Univ. of Arizona (United States); Linxi Shi, Georgia Institute of Technology (United States); Andrew Karellas, The Univ. of Arizona (United States)

No Abstract Available

10393-22, Session 6

Optimized modeling of powder-based x-ray scintillator screen for improved total efficiency by double-layer scintillator design

Jookwon Song, Hyeon Bo Shim, Jae W. Hahn, Yonsei Univ. (Korea, Republic of)

Powder-based flat panel X-ray scintillator screen has been widely used in many medical fields for diagnosis and measurement. For the proper application in medical field, required dominant scintillator performances are total efficiency and resolution. We define total efficiency as a multiplication of conversion efficiency (X-ray to visible light energy) and light collection efficiency (ratio of detected visible light energy to emitted visible light energy). Even though high efficiency is required for low dose exposure to patient and high resolution is preferred to maintain each medical field's functional clinical task, both are in trade-off relation. A variety of powder-based flat panel scintillator designs have been proposed to improve its performance, however, because of the scintillator particle's isotropic radiation characteristics, collection efficiency cannot exceed over 50% within a single layer.

In this study, double-layer scintillator design is suggested for improving total efficiency with using theoretical x-ray absorption model and Mie-scattering-based Monte-Carlo (LightTools) analysis. Optimized scintillator layer design would be proposed with respect to the medical fields' clinical task, since image resolution quality requirement is quite different, individually. With selection of design parameters consisted of particle size and each layer's thickness, total efficiency can be improved with equal conversion efficiency while maintaining sufficient resolution-functionality in particular medical field without special complex fabrication technique. We expect that our double-layer scintillator design can be helpful and useful for the one who are in medical fields and scintillator manufacturers.

10393-23, Session 6

3D position-sensitive scintillation detectors for a high-resolution loco-regional PET imaging system *(Invited Paper)*

David Hsu, David Freese, Derek Innes, Craig S. Levin, Molecular Imaging Instrumentation Lab., Stanford School of Medicine (United States)

We are building a dual-panel positron emission tomography (PET) system prototype that enables focused imaging of local regions of interest of the body with 1 mm3 spatial resolution, The detector panels are built from novel 3D position sensitive scintillation (3DPSS) detectors comprising arrays of 1x1x1 mm3 LYSO scintillation crystal elements coupled to position-sensitive avalanche photodiodes (PSAPD). At the present state of system construction, the measured energy resolution over 98,304 crystal elements coupled to 1,536 PSAPDs is 11.34%, and 76.2% (74,938) of the system LYSO crystal elements are found to have greater than 99% event positioning accuracy. Imaging studies performed with a high-resolution phantom demonstrate resolution of the smallest (1.2 mm diameter) features. Besides enabling 1 mm resolution clinical PET studies, we describe other novel ways we are planning to exploit the 3DPSS detector information.

10393-24, Session 6

Applications of IQID cameras

Ling Han, Brian W. Miller, Harrison H. Barrett, H. Bradford Barber, Lars R. Furenlid, The Univ. of Arizona (United States)

iQID is an ionizing-radiation quantum imaging detector developed in the Center for Gamma-Ray Imaging (CGRI). Originally called BazookaSPECT, iQID was originally used for high-resolution gamma-ray imaging and preclinical single-photon emission computed tomography (SPECT). With the use of a columnar scintillator, an image intensifier, and modern CMOS visible light sensors, iQID cameras features outstanding intrinsic spatial resolution. In recent years, many advances have been achieved that greatly boost sensitivity and FOV of iQID, broadening its utility to include nuclear and particle imaging, preclinical and clinical imaging. This paper presents an overview of the recent advances of iQID technology and its applications in gamma-ray scintigraphy, preclinical SPECT, particle imaging (alpha, neutron, beta, and fission fragment), and autoradiography.

10393-25, Session 6

Pulse timing in edge-readout PET detectors

Xin Li, Maria D. Ruiz-Gonzalez, Lars R. Furenlid, Ctr. for Gamma-Ray Imaging, The Univ. of Arizona (United States)

No Abstract Available

10393-26, Session 7

A framework for optimizing micro-CT in dual-modality micro-CT/XFCT small-animal imaging system

Srinivasan Vedantham, Suman Shrestha, Univ. of Massachusetts Medical School (United States); Andrew Karellas, The Univ. of Arizona (United States); Sang Hyun Cho, The Univ. of Texas M.D. Anderson Cancer Ctr. (United States)

No Abstract Available

10393-27, Session 7

A compact energy-independent CZT-based gamma camera *(Invited Paper)*

Youngho Seo, Univ. of California, San Francisco (United States); Yonggang Cui, Paul O'Connor, Brookhaven National Lab. (United States); Qiu Huang, Shanghai Jiao Tong Univ. (China); Zhi Deng, Yu Chen, Tsinghua Univ. (China); Ralph B. James, Savannah River National Lab. (United States)

Conventional gamma cameras are heavy and occupy large volume for all required hardware components. Direct-conversion solid-state detectors like cadmium zinc telluride (CZT) enable a compact design of gamma camera. In addition, conventional gamma camera requires multiple collimators for different gamma-ray photon energies, and the change of collimators between studies sometimes disrupts the workflow. To ease this inconvenience (i.e., bulkiness and collimator change), we have recently developed a compact, CZT-based, energy-independent gamma camera that requires only one collimator to cover a broad range of photon energies.
In this presentation, we will show our design parameters and system specification as well as simulation studies that support our design principles.

10393-28, Session 7

Simulation modeling of a TlBr double-sided strip detector

Amanjot Gill, H. Bradford Barber, The Univ. of Arizona (United States); Leonard J. Cirignano, Hadong Kim, Radiation Monitoring Devices, Inc. (United States)

No Abstract Available

10393-29, Session 7

Investigation of a high-sensitivity near-infrared-ray computed tomography scanner

Eiichi Sato, Yasuyuki Oda, Sohei Yoshida, Yuichi Sato, Iwate Medical Univ. (Japan); Tomotaka Ishii, Toho Univ. (Japan); Osahiko Hagiwara, Iwate Medical Univ. (Japan) and Toho Univ. (Japan); Hiroshi Matsukiyo, Toshiyuki Enomoto, Manabu Watanabe, Shinya Kusachi, Toho Univ. (Japan)

To perform biomedical computed tomography (CT) for fundamental studies, we have constructed a first-generation near-infrared-ray (NIR) CT scanner. In the NIR-CT, NIR rays are produced from a light-emitting diode (LED), and the penetrating NIR rays are detected using an NIR phototransistor (PT) in conjunction with a long graphite collimator. The peak wavelengths of the LEDs are 850 and 940 nm. The photocurrents flowing through the PT are converted into voltages using an emitter-follower circuit, and the NIR sensitivity increases with increasing resistance between the emitter and the ground. The output voltages are sent to a personal computer through an analog digital converter. The X-ray projection curves for tomography are obtained by repeated linear scans and rotations of the object. The object rotates on the turn table, and the NIR scanning is conducted in both directions of its movement.

10393-30, Session 8

An integrated circuit readout for TOF-PET detectors for PET/MRI *(Invited Paper)*

Ilaria Sacco, Chen-Ming Chang, Stanford University (United States); Michael Ritzert, Peter Fischer, Heidelberg University (Germany); Craig Levin, Stanford University (United States)

The new generation positron emission tomography (PET) detectors for combined PET/magnetic resonance imaging (MRI) must achieve extremely good timing resolution while also being capable of simultaneous data acquisition in a high power, dynamic electromagnetic environment. SiPM-based detectors are a natural choice for this application, given the high gain and fast response of the SiPMs and their insensitivity to magnetic fields. We present the highly-integrated readout circuit “PETA”, specifically designed for SiPM readout and optimal timing resolution required for high performance TOF-PET. PETA is a bump-bonded chip, with pitch between bumps of 272 μm, suitable for compact detector design. It includes 36 readout channels, available with both single-ended and differential-ended front-ends. The event arrival time and energy are measured and digitized on chip with TDC/ADC circuits. The readout architecture is optimized for coping with high hit rate per channel. Two very compact MR-compatible TOF-PET detector modules based on PETA readout have been constructed and tested. Each is built on a single layer (ceramic and PCB substrate respectively), hosting the SiPM array and the readout electronics on opposite surfaces, and thermally decoupled with efficient integrated cooling. Coincidence measurements have shown coincidence time resolution of 230 ps FWHM using arrays of 2.25x2.25x10 mm3 LYSO crystals coupled to matching SiPMs.

10393-31, Session 8

Hardware strategies for adaptive molecular imaging

Lars R. Furenlid, Ctr. for Gamma-Ray Imaging, The Univ. of Arizona (United States)

No Abstract Available

10394-1, Session 1

Compressive hyperspectral time-resolved wide-field fluorescence lifetime imaging

Xavier Intes, Rensselaer Polytechnic Institute (United States)

No Abstract Available.

10394-2, Session 1

Recovering higher-dimensional image data using multiplexed structured illumination

Guoan Zheng, Univ. of Connecticut (United States)

No Abstract Available.

10394-3, Session 1

A sparsity-based simplification method for segmentation of spectral-domain optical coherence tomography images

William Meiniel, Institut Pasteur (France) and Télécom ParisTech (France); Jean-Christophe Olivo-Marin, Institut Pasteur (France); Elsa D. Angelini, Télécom ParisTech (France) and Imperial College London (United Kingdom)

No Abstract Available.

10394-4, Session 2

Direct and indirect photon pathway imaging: an information-theoretic perspective

Amit Ashok, Liang-Chih Huang, Eric W. Clarkson, The Univ. of Arizona (United States); Sumanta Pattanaik, Univ. of Central Florida (United States)

Typically, a camera only exploits the direct (line-of-sight) optical signal to infer information about the scene. However, the indirect (non-line-of-sight) optical signal, generated by interaction of ambient illumination with objects outside camera's field of view (FoV) and reflected or scattered into the camera FoV carries information about the extended scene, i.e. beyond the FoV. We use Fisher information and a physics-based ray tracing forward model to quantify the extended scene information embedded in the direct and indirect optical signal incident on the camera aperture. Our analysis uses a prototype "Hallway" scene to gauge the feasibility of indirect imaging (i.e. using non-line-of-sight optical signal) when reflector(s) in the scene range from fully diffuse (i.e. Lambertian surface) to fully specular (i.e. mirror surface). Our analysis indicates that under certain conditions, it is indeed theoretically possible to image objects in a scene that are fully obscured or outside the camera FoV.

10394-5, Session 2

Computational memory-effect imaging

Michael E. Gehm, Joel A. Greenberg, Xiaohan Li, Duke Univ. (United States)

No Abstract Available.

10394-6, Session 2

Photon-efficient super-resolution laser radar

Dongeek Shin, Jeffrey H. Shapiro, Massachusetts Institute of Technology (United States); Vivek K. Goyal, Boston Univ. (United States)

No Abstract Available.

10394-7, Session 2

Itertative back-projection techniques for non-line-of-sight imaging

Marco La Manna, Eric C. Breitbach, Jonathan Jackson, Fiona Kine, Andreas Velten, Univ. of Wisconsin-Madison (United States)

No Abstract Available.

10394-8, Session 3

Riemannian multi-manifold modeling and clustering in brain networks

Konstantinos Slavakis, Shiva Salsabilian, David S. Wack, Sarah F. Muldoon, Henry E. Baidoo-Williams, Univ. at Buffalo (United States); Jean M. Vettel, U.S. Army Research Lab. (United States); Matthew Cieslak, Scott T. Grafton, Univ. of California, Santa Barbara (United States)

No Abstract Available.

10394-9, Session 3

Probing the dynamics of resting-state cortical activities via wide field Ca+2 imaging in GCaMP6 transgenic mice

Li Zhu, Christian Lee, David Margolis, Laleh Najafizadeh, Rutgers, The State Univ. of New Jersey (United States)

No Abstract Available.

10394-10, Session 3

MR correlation spectroscopic imaging of multidimensional exponential decays: probing microstructure with diffusion and relaxation

Daeun Kim, Justin P. Haldar, The Univ. of Southern California (United States)

No Abstract Available.

10394-11, Session 3

A regularized clustering approach to brain parcellation from functional MRI data

Keith Dillon, Yu-Ping Wang, Tulane Univ. (United States)

No Abstract Available.

10394-12, Session 3

Joint fMRI analysis and subject clustering using sparse dictionary learning

Seung-Jun Kim, Univ. of Maryland, Baltimore County (United States)

No Abstract Available.

10394-13, Session 3

Detecting brain dynamics during resting state: a tensor based evolutionary clustering approach

Esraa Al-sharoa, Mahmood Al-Khassaweneh, Selin Aviyente, Michigan State Univ. (United States)

No Abstract Available.

10394-14, Session 4

Optimal transport-based dictionary learning and its application to Euclid-like Point Spread Function representation

Morgan A. Schmitz, CEA-Ctr. de SACLAY (France); Matthieu Heitz, Lab. d'InfoRmatique en Image et Systèmes d'information (France) and Univ. de Lyon 1 (France); Nicolas Bonneel, Univ. de Lyon 1 (France) and Lab. d'InfoRmatique en Image et Systèmes d'information, Ctr. National de la Recherche Scientifique (France); Fred-Maurice Ngolè-Mboula, CEA-Ctr. de SACLAY (France); David Coeurjolly, Univ. de Lyon 1 (France) and Lab. d'InfoRmatique en Image et Systèmes d'information, Ctr. National de la Recherche Scientifique (France); Marco Cuturi, École Nationale de la Statistique et de l'Administration Économique (France) and Ctr. de Recerche en Économie et Statistique, Univ. Paris-Saclay (France); Gabriel Peyré, Ecole Normale Supérieure (France); Jean-Luc Starck, CEA-Ctr. de SACLAY (France)

Optimal Transport theory enables the definition of a distance across the set of measures on any given space. This Wasserstein distance naturally accounts for geometric warping between measures (including, but not exclusive to, images). We introduce a new, Optimal Transport-based representation learning method in close analogy with the usual Dictionary Learning problem. This approach typically relies on a matrix dot-product between the learned dictionary and the codes making up the new representation. The relationship between atoms and data is thus ultimately linear. By reconstructing our data as Wasserstein barycenters of learned atoms instead, our approach yields a representation making full use of the Wasserstein distance's attractive properties and allowing for non-linear relationships between the dictionary atoms and the datapoints.

We apply our method to the PSF (Point Spread Function) spatial interpolation problem in the context of upcoming cosmological surveys, such as ESA's Euclid mission. Euclid will cover a large area of the sky in order to accurately measure the shape of billions of galaxies. PSF estimation and correction is one of the main sources of systematic errors on those galaxy shape measurements. Because of Euclid's large field of view, the PSF variation can be highly non-linear, while still retaining strong geometrical information, making the use of Optimal Transport distances an attractive prospect. By performing the interpolation within our new representation (that of barycentric weights), we can accurately reconstruct Euclid-like PSFs at any point in the field of view.

10394-15, Session 4

Localization of sound sources in a room by one microphone

Helena Peic Tukuljac, Hervé Lissek, Pierre Vandergheynst, Ecole Polytechnique Fédérale de Lausanne (Switzerland)

In this paper we introduce a method for the estimation of the location of multiple sound sources in a room by using only one microphone. Shape of the room is assumed to be known and the position of the microphone. The design guidelines and the limitations of the sensing matrix are given. The implementation is based on the sparsity in the terms of voxels in a room occupied by a source. What is especially interesting about our solution is the localization of the sound sources not only in the horizontal plane, but in the terms of the 3D coordinates.

Solution relies on the fact that the attenuation in the room transfer function at the resonant frequencies differs among different position in the room.

Once we have the location of the sound sources in a room, we can use it in numerous applications starting from hearing aids, robotics up to the investigation of creating anechoic conditions in a room by active noise removal.

10394-16, Session 4

Limited memory trust-region methods for sparse relaxation

Lasith Adhikari, Univ. of California, Merced (United States); Jennifer B. Erway, Wake Forest Univ. (United States); Omar DeGuchy, Univ. of California, Merced (United States); Shelby Lockhart, Wake Forest Univ. (United States); Marcia F. Roummel, Univ. of California, Merced (United States)

Sensing a sparse signal from underdetermined linear measurements is the main problem of compressed sensing. Sparse recovery is important in a variety of different applications such as medical imaging, photography, face recognition, and network tomography. Basis Pursuit and the Least Absolute Shrinkage and Selection Operator (LASSO) are few popular models for sparse recovery. In this paper, we minimize an objective function with a quadratic data-fidelity term (L2-norm) combined with a sparsity-promoting penalty function (L1-norm). There are various methods in the literature to solve this L2-L1 problem, many of which use a gradient decent-type approach. In our method, we propose to solve the L2-L1 sparse recovery problem by transforming the objective function into an unconstrained

differentiable function and applying a limited-memory trust-region method. Unlike gradient projection-type methods, which use only the current gradient, our method uses gradients from previous iterations to obtain a more accurate Hessian approximation. Moreover, we compute a global solution to the trust-region subproblem using a formula which makes use of an efficient partial spectral decomposition of the Hessian approximation via a QR factorization. Numerical experiments in 1- and 2-dimension show that our proposed approach is competitive with the well-known methods by eliminating spurious solutions and artifacts more effectively.

10394-17, Session 4

Underwater object classification using scattering transform of sonar signals

David Weber, Naoki Saito, Univ. of California, Davis (United States)

We present a novel method for underwater object classification using the Scattering Transform (ST) applied to sonar signals. The ST, developed by Mallat et al., performs consecutive layers of wavelet transforms followed by absolute values. The output from a given layer comes from averaging the wavelet transform with the father wavelet. A path corresponds to choosing different scales at each layer. We add paths until a discriminative measure on the classes, such as the earth mover's distance, is reached. We then use LASSO-based logistic regression to select a small number of these coefficients. We used a synthetic dataset generated using a fast solver for the Helmholtz equations, and real data from a semi-controlled experiments with 14 different objects. Our numerical experiments suggest the effectiveness of the ST compared to the results based on the Fourier transform. This is because the ST has more relevant invariants: It has been shown to be quasi-translation invariant and Lipschitz with respect to a very specific form of diffeomorphism, both in the signal domain. We examine the translation quasi-invariance of the ST on the synthetic dataset with respect to the object domain.

10394-18, Session 4

Non-convex Shannon entropy for photon-limited imaging

Lasith Adhikari, Omar DeGuchy, Marcia F. Roummel, Univ. of California, Merced (United States)

In compressed sensing, we acquire a sparse signal by solving an underdetermined linear system, which is typically penalized by a sparsity promoting penalty term. When the measurements are known to be corrupted by Gaussian noise, this optimization problem is known as the LASSO. However, there are many real-world situations such as astronomy, nuclear medicine, and night vision, where the measurement noise does not follow a Gaussian distribution. For example, in imaging, when a relatively low number of photons hits a camera detector, the imaging process is known to be photon-limited. Then the measurements at the detector are corrupted by Poisson noise and are typically modeled using Poisson noise statistics. There are different sparsity promoting optimization methods that have been employed to solve this photon-limited imaging problem. Recent work in nonconvex optimization has shown that sparse signals can be recovered accurately by minimizing the p-norm ($0 <= p < 1$) regularized negative Poisson log-likelihood function. The typical convex Shannon entropy also has been used in literature for imaging. For example, Skilling et al. maximized the Shannon entropy for image recovery in astronomy. In this paper, we propose to regularize the Poisson log-likelihood by the generalized nonconvex Shannon entropy function for recovering sparse signals. In our approach, the Poisson log-likelihood is approximated by a sequence of quadratic approximations and the non-separable Shannon entropy is approximated using its first-order Taylor series. We explore the effectiveness and efficiency of the proposed method using numerical experiments and compare with more recently proposed methods.

10394-19, Session 5

Binary channel codes with decoding by linear programming

Bernhard G. Bodmann, Univ. of Houston (United States)

No Abstract Available.

10394-20, Session 5

Finding the closest probabilistic Parseval frame

Desai Cheng, Univ. of Missouri (United States); Kasso A. Okoudjou, Univ. of Maryland, College Park (United States)

No Abstract Available.

10394-21, Session 5

Characterizing Grassmannian frames with a generalized simplex bound

John Haas, Univ. of Missouri (United States); Bernhard G. Bodmann, Univ. of Houston (United States)

No Abstract Available.

10394-22, Session 5

Equiangular tight frames from association schemes

John Jasper, Univ. of Cincinnati (United States)

No Abstract Available.

10394-23, Session 5

Optimal approximation by sparse deep neural networks

Philipp Grohs, Technische Univ. Wien (Austria); Gitta Kutyniok, Philipp Petersen, Technische Univ. Berlin (Germany)

No Abstract Available.

10394-24, Session 6

Real Phase Retrieval by Orthogonal Complements and Hyperplanes

Peter G. Casazza, Tin Tran, Sara Botelho-Andrade, Desai Cheng, John Haas, Janet C Tremain, Univ. of Missouri (United States)

No Abstract Available.

10394-25, Session 6

Methods for localized regression using graph Laplacians

Alexander Cloninger, Yale Univ. (United States)

No Abstract Available.

10394-26, Session 6

Harmonic equi-chordal and equi-isoclinic tight fusion frames

Matthew Fickus, Air Force Institute of Technology (United States); John Jasper, Univ. of Cincinnati (United States); Dustin G. Mixon, Cody E. Watson, Air Force Institute of Technology (United States)

No Abstract Available.

10394-27, Session 6

Soft recovery

Axel Flinth, Technische Univ. Berlin (Germany)

No Abstract Available.

10394-74, Session 7

Speeding up sparse signal recovery using sparse-graph codes *(Keynote Presentation)*

Kannan Ramchandran, Univ. of California, Berkeley (United States)

No Abstract Available

10394-28, Session 8

Optimal packings of many lines

John Haas, Univ. of Missouri (United States); Nathaniel Hammen, Dustin G. Mixon, Air Force Institute of Technology (United States)

No Abstract Available.

10394-29, Session 8

K?means clustering on the space of persistence diagrams

Joshua Mike, Andrew Marchese, The Univ. of Tennessee, Knoxville (United States); Vasileios Maroulas, The Univ. of Tennessee Knoxville (United States)

A recent cohort of research aims to apply topological and geometric theory to data analysis. However, more effort is needed to incorporate statistical ideas and structure to these analysis methods. To this end, we present persistent homology clustering techniques through the perspective of data analysis. These techniques provide insight into the structure of the underlying dynamic and are able to recognize important shape properties such as periodicity, chaos, and multi-stability. Moreover, introducing quantitative structure on the topological data space allows for rigorous understanding of the data's geometry, a powerful tool for scrutinizing the morphology of the inherent dynamic. Additionally, we illustrate the advantages of these techniques and results through examples derived from dynamical systems applications.

10394-30, Session 8

Phase retrieval from localized two-dimensional measurements

Mark Iwen, Michigan State Univ. (United States); Brian Preskitt, Rayan Saab, Univ. of California, San Diego (United States); Aditya Viswanathan, Michigan State Univ. (United States)

No Abstract Available.

10394-31, Session 9

Shearlet-based regularization in limited data and sparse tomography

Tatiana A. Bubba, Samuli Siltanen, Matti Lassas, Univ. of Helsinki (Finland)

This paper is invited to the LABATE LAEZZA session.

Over recent years, many novel medical imaging technologies employ sparse or limited sampling of the data space. While the use of sparse data may be motivated by different reasons, such as a lower exposure to X-ray radiation, or the need of a reduced scanning time (e.g., a faster sampling due to fast physiological changes), a common feature for such imaging technologies is the ill-posedness of the image reconstruction problem. The use of traditional CT reconstruction algorithms usually leads to poor reconstructions, which tend to be very unstable to noise.

We propose a novel method of promoting a priori information, that accounts for the missing information in the data, by using shearlets as regularization tool. The designed technique is tested on 2D synthetic and real data.

10394-32, Session 9

Detecting neuronal activity from calcium imaging data using FRI methods

Stephanie Reynolds, Jon Oñativia, Simon R. Schultz, Pier Luigi Dragotti, Imperial College London (United Kingdom)

Two-photon calcium imaging can be used to monitor the activity of thousands of neurons across multiple brain areas at single-cell resolution. To harness the power of this imaging technology, neuroscientists require algorithms to detect from the imaging data the time points at which each neuron was active. We present an algorithm based on Finite Rate of Innovation (FRI) theory to detect neuronal spiking activity from this data. By exploiting the parametric structure of the signal, the activity detection problem can be reduced to the classic FRI problem of reconstructing a stream of Diracs.

10394-33, Session 9

GASPACHO: a generic automatic solver using proximal algorithms for convex huge optimization problems

Bart Goossens, Hiêp Q. Luong, Wilfried Philips, Univ. Gent (Belgium)

Many inverse problems (e.g., demosaicking, deblurring, denoising, image

fusion, HDR synthesis) share various similarities: degradation operators are often modeled by a specific data fitting function while image prior knowledge (e.g., sparsity) is incorporated by additional regularization terms. In this paper, we investigate automatic algorithmic techniques for evaluating proximal operators. These algorithmic techniques also enable efficient calculation of adjoints from linear operators in a general matrix-free setting. In particular, we study the simultaneous-direction method of multipliers (SDMM) and the parallel proximal algorithm (PPXA) solvers and show that the automatically derived implementations are well suited for both single-GPU and multi-GPU processing. We demonstrate this approach for an Electron Microscopy deconvolution problem.

10394-34, Session 9

Adaptive windowing and windowless approaches to estimate dynamic functional brain connectivity

Maziar Yaesoubi, Vince D. Calhoun, The Mind Research Network (United States)

We discuss estimation of dynamic dynamic-connectivity among functional-networks in brain. Commonly used approaches are often based on a locality assumption (e.g. sliding-window) which can miss spontaneous changes due to blurring with local but unrelated changes. We discuss recent approaches to overcome this limitation including 1) a wavelet-space approach, essentially adapting the window to the underlying frequency content and 2) a sparse signal-representation which removes any locality assumption. The latter is especially useful when there is no prior knowledge of the validity of such assumption as in brain-analysis. Results on several large resting-fMRI data sets highlight the potential of these approaches.

10394-35, Session 9

Wavelet scattering transforms and machine learning for many particle systems

Matthew Hirn, Michigan State Univ. (United States)

Computing the energy and forces of many particle systems is a fundamental computational problem in quantum chemistry, materials science, and biochemistry. Machine learning algorithms do not simulate the physical system, but estimate solutions by interpolating values provided by a training set of known examples. However, precise interpolations may require a number of examples that is exponential in the system dimension. Tractable algorithms balance the flexibility of general machine learning architectures versus specific design choices that guarantee the learned model will obey fundamental physical laws. This delicate balance is the subject of an emerging body of research at the interface of machine learning and many particle physics. In this talk we give an overview of the field and discuss in some detail one approach based on wavelet scattering transforms.

10394-36, Session 9

Exploring neuronal synapses with directional filters with small support

Nikolaos Karantzas, Demetrio Labate, Manos Papadakis, Univ. of Houston (United States)

No Abstract Available.

10394-37, Session 10

Edge-augmented Fourier partial sums with applications to Magnetic Resonance Imaging (MRI)

Jade Larriva-Latt, Wellesley College (United States); Angela Morrison, Albion College (United States); Alison Radgowski, Goucher College (United States); Joseph Tobin, Univ. of Virginia (United States); Mark Iwen, Aditya Viswanathan, Michigan State Univ. (United States)

No Abstract Available.

10394-38, Session 10

Reconstruction of finite-valued sparse signals

Sandra Keiper, Technische Univ. Berlin (Germany)

No Abstract Available.

10394-39, Session 10

Tolerant compressed sensing with partially coherent sensing matrices

Tobias Birnbaum, Department of Electronics and Information Processing (Belgium); Yonina Eldar, Technion (Israel); Deanna M. Needell, Claremont McKenna College (United States)

No Abstract Available.

10394-40, Session 10

De-biasing one-step matrix completion

Yaniv Plan, The Univ. of British Columbia (Canada)

A simple and quick method for matrix completion is to fill in missing entries with zeros, take the low-rank projection of the result, and then rescale, thereby giving an estimate of all entries of the matrix. It is known that (amid noise) the estimate has near-optimal sample complexity. The simplicity and speed of creating this estimate makes it appealing to use as a warm start for other methods. However, a non-uniform sampling pattern can introduce bias, resulting in an unusable estimated matrix. We give a simple, data-dependent method to de-bias, which does not assume any knowledge of an underlying sampling distribution.

10394-41, Session 10

Energy decay in deep convolutional neural networks

Thomas Wiatowski, ETH Zurich (Switzerland)

No Abstract Available.

10394-42, Session 11

On distribution of a product of N Gaussian variables

Martin Kliesch, Univ. of Gda?sk (Poland); Daniel Suess, Zeljka Stojanac, Univ. zu Köln (Germany)

Although the product of N Gaussian variables appears naturally in many applications in probability theory and statistics, the distribution of this random variable has not yet been analyzed for generic $N>2$. It has been known that the probability density function of a product of N Gaussian variables can be expressed in terms of Meijer G-functions. First we show that also the complementary cumulative distribution function (ccdf) of the product of Gaussians can be written in terms of Meijer G-functions. Using the residue theorem and the theory developed for even more general Fox H-functions, we are able to expand the corresponding ccdf into power-log series. Numerically we show that for relatively small values of the argument, the ccdf of product of N Gaussians can be well approximated by the principal terms of the series. This bound becomes tighter, as N becomes larger.

This research is motivated by the reconstruction of rank-1 tensors from overlaps of rank-1 measurement tensors. If the latter are formed by products of vectors with independent standard normal components, the resulting measurements follow the product-of-Gaussians distribution. In ongoing work, we have shown that concentration inequalities for unbounded random variables such as Chernoff's inequality are not sufficient to prove recovery guarantees when the number of measurements scales polynomially.

10394-43, Session 11

Framed frames for data frames

Nathaniel Strawn, Georgetown Univ. (United States)

No Abstract Available.

10394-44, Session 11

You can have it all: rapid, robust, and rigorous algorithms for bilinear problems in signal processing and communications

Thomas Strohmer, Univ. of California, Davis (United States)

No Abstract Available.

10394-45, Session 11

A polynomial-time relaxation of the Gromov-Hausdorff distance

Soledad Villar, The Univ. of Texas at Austin (United States); Afonso S. Bandeira, New York Univ. (United States); Andrew Blumberg, Rachel A. Ward, The Univ. of Texas at Austin (United States)

No Abstract Available.

10394-46, Session 12

Structured sparse recovery with sparse sensing matrices

Bubacarr Bah, African Institute for Mathematical Sciences (South Africa) and Stellenbosch Univ. (South Africa)

No Abstract Available.

10394-47, Session 12

Blind demixing and deconvolution with noisy data at near optimal rate

Dominik Stöger, Technische Univ. München (Germany); Peter Jung, Technische Univ. Berlin (Germany); Felix Krahmer, Technische Univ. München (Germany)

No Abstract Available.

10394-48, Session 12

The scaling limit and dynamics of nonconvex algorithms for low-rank subspace estimation

Chuang Wang, Yue M. Lu, Harvard Univ. (United States)

We analyze, in the high-dimensional limit, the exact dynamics of a family of stochastic algorithms for nonconvex subspace estimation. We show that the time-varying empirical measures of the estimates given by the algorithms will converge weakly to a deterministic "limiting process" in the high-dimensional limit. Moreover, this limiting process can be obtained as the unique solution of a nonlinear PDE, and it provides exact information regarding the asymptotic performance of the algorithms. For example, performance metrics such as the MSE, the cosine similarity and the misclassification rate in sparse support recovery can all be obtained by examining the deterministic limiting process. A steady-state analysis of the nonlinear PDE also reveals interesting phase transition phenomena related to the performance of the algorithm. Although our analysis is asymptotic in nature, numerical simulations show that the theoretical predictions are accurate for moderate signal dimensions.

10394-49, Session 13

Convex relaxations of spectral sparsity for robust super-resolution and line spectrum estimation

Yuejie Chi, The Ohio State Univ. (United States)

No Abstract Available.

10394-51, Session 13

2D phaseless super-resolution

Myung Cho, The Univ. of Iowa (United States); Christos Thramboulidis, Massachusetts Institute of Technology (United States); Babak Hassibi, California Institute of Technology (United States); Weiyu Xu, The Univ. of Iowa (United States)

Super-resolution is concerned about recovering a signal in the continuous domain from limited measurement data. For the 1D signals, super-resolution often refers to the line-spectrum estimation problem, where we want to find frequency information in the [0,1) continuous domain from randomly or uniformly sampled time-domain data. Unlike the conventional super-resolution problem, in phaseless super-resolution, we only have magnitude measurements of the continuously-parameterized signals in a transform domain. Optic microscopy is one application where the phaseless super-resolution for 2D signals arise. In this paper, we propose algorithms for performing phaseless super resolution for 2D or higher-dimensional signals, and investigate their performance guarantees.

10394-52, Session 13

Recovery of continuous domain piecewise smooth images: theory, algorithms, and applications

Mathews Jacob, The Univ. of Iowa (United States); Gregory Ongie, Univ. of Michigan (United States); Sampurna Biswas, The Univ. of Iowa (United States) and Univ. of Michigan (United States); Arvind Balachandrasekaran, The Univ. of Iowa (United States)

No Abstract Available.

10394-53, Session 13

Learning-based low-rank Hankel structured matrix approach

Jong Chul Ye, KAIST (Korea, Republic of)

No Abstract Available.

10394-54, Session 13

Fast and provable algorithms for spectrally sparse signal reconstruction via low-rank Hankel matrix completion

Jian-Feng Cai, Hong Kong Univ. of Science and Technology (Hong Kong, China)

No Abstract Available.

10394-55, Session 14

Noise and outlier tolerance of RobustPhaseMax

Paul Hand, Rice Univ. (United States); Thang Huynh, Univ. of California, San Diego (United States)

In the phase retrieval problem, one attempts to find a vector from phaseless linear measurements. The first method with a recovery guarantee for this problem was the PhaseLift semidefinite program. Unfortunately, this approach is intractable for large problem sizes because it squares the problem's dimensionality. Subsequently, algorithms in the natural parameter space were invented, including Wirtinger Flow and several variants. Despite their convexity, these methods enjoy a recovery guarantee under idealized generic measurements, though the proofs are lengthy and technical. Because of the nonconvexity of these approaches, a careful initialization is often used and analyzed.

Recently, a convex formulation in the natural parameter space, called PhaseMax, was discovered independently by Bahmani and Romberg and by Goldstein and Studer. This formulation is a linear program that can be written provided some initialization that correlates with the true solution. The method provably recovers the exact signal under O(n) Gaussian measurements, and it is provably stable to bounded noise. Because of the structure of PhaseMax, it is susceptible to outliers. For example, if a fixed fraction measurements are arbitrary outliers, it is possible for the feasible set of PhaseMax to be trivial. Consequently, Hand and Voroninski recently introduced an L1 penalized version of PhaseMax called RobustPhaseMax. This version permits provably recovery in the presence of a fixed fraction of arbitrarily corrupted measurements. In the present paper, we empirically show the robustness of RobustPhaseMax to the simultaneous presence of outliers and dense noise under real and complex measurements.

10394-56, Session 14

Comparison of sampling strategies for 3D scene reconstruction from sparse multispectral lidar waveforms

Yoann Altmann, Rachael Tobin, Ximing Ren, Aongus McCarthy, Gerald S. Buller, Stephen McLaughlin, Heriot-Watt Univ. (United Kingdom)

No Abstract Available.

10394-57, Session 14

Semidefinite programming relaxations for inverse scattering, blind deconvolution, and matrix completion

Augustin Cosse, New York Univ. (United States)

No Abstract Available.

10394-58, Session 14

Faster PET reconstruction with a stochastic primal-dual hybrid gradient method

Matthias J. Ehrhardt, Univ. of Cambridge (United Kingdom); Pawel J. Markiewicz, Univ. College London (United Kingdom); Peter Richtárik, The Univ. of Edinburgh (United Kingdom); Antonin Chambolle, Ecole Polytechnique (France); Carola-Bibiane Schoenlieb, Univ. of Cambridge (United Kingdom)

No Abstract Available.

10394-75, Session 15

Sketchy decisions: convex optimization with optimal storage *(Keynote Presentation)*

Joel A. Tropp, California Institute of Technology (United States)

No Abstract Available

10394-60, Session 16

Local stationarity of graph signals: insights and experiments

Benjamin Girault, Shrikanth S. Narayanan, Antonio Ortega, The Univ. of Southern California (United States)

No Abstract Available.

10394-61, Session 16

Multiscale space-frequency analysis of functions defined on directed graphs

Harry Sevi, Ecole Normale Supérieure de Lyon (France) and Commissariat à l'Énergie Atomique (France); Gabriel Rilling, Commissariat à l'Énergie Atomique (France); Pierre Borgnat, Ecole Normale Supérieure de Lyon (France)

Over the last decade, numerous graph wavelet transforms have been proposed for functions defined on undirected graphs. Based on the diffusion wavelet framework of Coifman and Maggioni, Mhaskar has recently introduced a multi-scale transform for functions defined on directed graphs by studying the singular value decomposition of the random walk operator. One of the fundamental difficulties in the extension of wavelets to directed graphs is the absence of a suitable definition of frequency. In the undirected graph setting, the notion of frequency can be meaningfully related to the quadratic form associated to the Laplacian matrix. This gives properties similar to a Fourier basis to the eigenbasis of the Laplacian operator. However, in the directed graph case the definition of a Laplacian is not as straightforward and it is unclear how to define a meaningful notion of frequency. Using Diffusion wavelets as a starting point, we make a connection between the eigenvectors/eigenvalues of the Random walk matrix, usually non symmetric, with the directed graph Laplacian investigated by Chung, which is symmetric. That enables us to define a desirable notion of frequency on a directed graph and provide a frequency interpretation for the eigenvectors of the random walk matrix. This paves the way for a generalization of the diffusion wavelet approach based on spectral properties of the random walk operator instead of its singular value decomposition as in Mhaskar's work. The idea is developed to build both an orthogonal and a biorthogonal diffusion wavelet transform for directed graphs.

10394-62, Session 16

Extending classical multirate signal processing theory to graphs

Oguzhan Teke, Palghat P. Vaidyanathan, California Institute of Technology (United States)

No Abstract Available.

10394-63, Session 16

Semi-parametric, parametric, and possibly sparse models for multivariate long-range dependence

Vladas Pipiras, The Univ. of North Carolina at Chapel Hill (United States); Stefanos Kechagias, SAS Institute Inc. (United States); Changryong Baek, Sungkyunkwan Univ. (Korea, Republic of)

The focus of this talk is on multivariate (vector-valued) time series that exhibit long-range dependence (LRD) and, more specifically, on (semi-) parametric models that account for general phase parameters in the cross spectra of the series at the zero frequency. Several new multivariate LRD time series models are introduced and their estimation is discussed, possibly assuming sparsity of model parameters. Applications to several real time series are also presented.

10394-64, Session 17

Simultaneous sparse reconstruction using copula functions

Joao Mota, Heriot-Watt Univ. (United Kingdom); Evangelos Zimos, Vrije Univ. Brussel (Belgium); Miguel Rodrigues, Univ. College London (United Kingdom); Nikos Deligiannis, Vrije Univ. Brussel (Belgium)

Modern sensing devices often acquire multiple modalities of the same phenomenon, yielding necessarily correlated, but possibly heterogeneous, signals. In this paper, we address the problem of simultaneously reconstructing correlated sparse signals. We adopt the framework of Bayesian compressed sensing, specifically belief propagation, and model correlations between different signals through their sparse coefficients. Our main tool to learn correlations is copula functions, which allow treating dependent signals as if they were independent plus a small correction term. We illustrate the potential of the proposed scheme in simple image processing tasks.

10394-65, Session 17

A proximal Hamiltonian Monte Carlo algorithm: theory, method, and algorithm

Marcelo Pereyra, Heriot-Watt Univ. (United Kingdom)

No Abstract Available.

10394-66, Session 17

Recovery guarantees for low complexity models

Samuel Vaiter, Univ. De Bourgogne (France) and Ctr. National de la Recherche Scientifique (France)

No Abstract Available.

10394-67, Session 17

Non-convex blind deconvolution approach for sparse image processing

Audrey Repetti, Yves Wiaux, Heriot-Watt Univ. (United Kingdom)

No Abstract Available.

10394-68, Session 18

Analytic wavelets for multivariate time series analysis

Irène Gannaz, Institut National des Sciences Appliquées de Lyon (France); Sophie Achard, Ctr. National de la Recherche Scientifique (France); Marianne Clausel, Univ. Grenoble Alpes (France); François Roueff, Télécom ParisTech (France)

Many applications fields deal with multivariate long-memory time series. A challenge is to estimate the long-memory properties together with the coupling between the time series. Wavelets offer well-suited tools and many developments have been proposed in univariate settings. In multivariate framework, some recent works highlighted some good properties. Yet real

wavelets procedures present some limitations.

Phase phenomenons appear in multivariate analysis and real wavelets failed to well identify them. Indeed the presence of phase implies different behaviour of the spectral density for positive and negative frequencies around zero. A perspective is to use analytic wavelets to recover jointly long-memory properties, modulus of long-run covariance between time series and phases. Unfortunately it is impossible to construct exact analytic wavelets. Approximate wavelets Hilbert pairs of Selesnick (2002) fullfilled some of the required properties. The quality of analyticity yet has to be quantified. As an extension of Selesnick (2002)'s work, we present some results about existence and quality of these approximate analytic wavelets.

10394-69, Session 18

Laplacian embedding with tuned localization and spectral bandwidth using graph Slepians

Maria Giulia Preti, Dimitri Van De Ville, Ecole Polytechnique Fédérale de Lausanne (Switzerland)

No Abstract Available.

10394-70, Session 18

Change point detection in covariance/ network structures

Yi Yu, Univ. of Bristol (United Kingdom)

In this talk I will talk about change point detection in covariance/network structures with application in resting state fMRI data. The talk will be consist of motivation, methodology, as well as numerical and theoretical results.

10394-71, Session 19

Adaptive synchrosqueezing based on a quilted short-time Fourier transform

Alexander Berrian, Naoki Saito, Univ. of California, Davis (United States)

In recent years, the synchrosqueezing transform (SST) has gained popularity as a method for analyzing signals that can be broken down into multiple components determined by instantaneous amplitudes and phases. The central idea of SST is the usage of a reassignment frequency (RF) mapping to improve the concentration of a base time-frequency representation. One such version of SST, based on the short-time Fourier transform (STFT), enables the sharpening of instantaneous frequency (IF) information derived from the STFT, as well as the separation of amplitude-phase components corresponding to distinct IF curves. However, this SST is limited by the time-frequency resolution of the underlying window function used in the STFT, and may not resolve signals exhibiting diverse time-frequency behaviors with sufficient accuracy. In this work, we develop a framework for an SST based on a "quilted" short-time Fourier transform (SST-QSTFT), which allows adaptation to signal behavior in different time-frequency regions through the use of multiple windows. This motivates us to introduce a new discrete RF mapping for the SST, ensuring computational accuracy for a wider variety of windows. We develop a theoretical framework for the SST-QSTFT in both the continuous and the discrete settings, and describe an algorithm for the automatic selection of optimal windows depending on the region of interest. We also describe the potential usefulness of SST-QSTFT for problems in audio signal processing, and provide a Python implementation of our method.

10394-72, Session 19

Coupling wavelets and non-stationary Gaussian process models for the reconstruction of highly heterogeneous data

Sébastien Marmin, Jean Baccou, Institut de Radioprotection et de Surete Nucleaire (France); Jacques Liandrat, Ecole Centrale Marseille (France) and Institut de Mathématiques de Marseille (France); David Ginsbourger, Idiap Research Institute, Ecole Polytechnique Fédérale de Lausanne (Switzerland) and Univ. Bern (Switzerland)

Prediction of objective functions with highly heterogeneous behavior across the input space have various applications such as uncertainties analysis of complex computer codes. The wavelet transform is widely used to capture local variations in a signal or an image. It informs precisely about locations of breakdowns as well as their local frequencies. However, relying on a regular and dense grid of evaluations, it is expensive in some context.

Gaussian Process (GP) models do not require particular designs of experiments. Covariances determining GPs are usually stationary, but this is irrelevant when objective functions have high variations in subareas. Constructing non-stationary covariances, the non-linear map method estimates a warping of the input space. Classical estimation approaches are parametric and require a large set of evaluations which is often not affordable.

We exploit advantages of wavelets and GP models. The wavelet analysis is used in a new non-parametric method for estimating the warping involved in the non-stationary GP model. Stochastical wavelet transform have been studied for many applications with dense data points (image/sound). The originality of our contribution stands in an efficient coupling between wavelets with a non-stationary GP model for situations with only sparse and irregularly placed data points. We provide an algorithm estimating a warping focusing on high variation regions, and consequently the non-stationary GP can fit the data. Convergence is theoretically and numerically studied. The model estimation is incorporated in a sequential design of experiments. This approach show lower prediction errors compared with different methods on a mechanical case study.

10394-73, Session 19

Affine shear tight frames with two-layer structure

Zhihua Che, Xiaosheng Zhuang, City Univ. of Hong Kong (Hong Kong, China)

In this talk, we present the characterizations, construction, and applications of affine shear tight frames with 2-layer structure. First, affine shear tight frames are directional multiscale representation systems generated through operations of dilations, shears, and translations of bandlimited generating functions. Motivated by the successful applications of tensor product complex tight frames that are able to capture both edge and texture features of images, in this talk, we introduce affine shear systems with 2-layer structure that have generators splitting the frequency region at each scale into inner and outer layers, where the inner layer generators are used to capture edge-like features while the outer layer texture-like features. Second, we provide the characterizations of a sequence of affine shear systems with 2-layer structure to be a sequence of affine shear tight frames with 2-layer structure, based on which, smooth affine shear tight frames with 2-layer structure can be easily designed. Moreover, we show that affine shear tight frames with 2-layer structure naturally induce affine shear filter banks with 2-layer structure. Last but not least, based on the affine shear filter banks with 2-layer structure, we show that digital affine shear transforms can be implemented with low redundancy rate and with near-linear computational complexity (NlogN). Numerical experiments are conducted to demonstrate the advantages of our digital affine shear filter banks with 2-layer structure over many other state-of-the-art frame-based methods in image/video processing.

Conference 10395: Optics and Photonics for Information Processing XI

Monday - Tuesday 7 –8 August 2017

Part of Proceedings of SPIE Vol. 10395 Optics and Photonics for Information Processing XI

10395-1, Session 1

Real time adaptation of spatial resolution for high resolution space cameras

Ralf Reulke, Andreas Eckardt, Deutsches Zentrum für Luft- und Raumfahrt e.V. (Germany)

We expect commercial high resolution imaging systems, which are able to provide data with 25 cm ground sample distance (GSD) or better in the near future. For selling the data, it is necessary to re-sample it to 30 cm. The situation is similar when swinging out the satellite perpendicular to his flight direction. The GSD is then variable with the angle to Nadir direction. In this paper a method is proposed that the resolution adjusts adaptively according to the requirements.

10395-2, Session 1

Ronchigrams of parabolic concave mirrors by inverse ray tracing

Rigoberto Juarez-Salazar, Ctr. de Investigación y Desarrollo de Tecnología Digital (Mexico); Carlos I. Robledo-Sanchez, Fermin Guerrero-Sanchez, Benemérita Univ. Autónoma de Puebla (Mexico); Victor H. Diaz-Ramirez, Ctr. de Investigación y Desarrollo de Tecnología Digital (Mexico); Antonio Barcelata-Pinzón, Univ. Tecnológica de Puebla (Mexico); Gerardo Diaz-Gonzalez, Univ. Tecnológica de la Mixteca (Mexico)

An algorithm to generate ronchigrams of parabolic concave mirrors is proposed. Unlike the conventional direct ray-tracing method, which generates scattered pixels, the proposed algorithm returns regularly sampled images. This provides full compatibility with further fringe processing tasks such as phase demodulation and wavefront analysis. The theoretical principles of our proposal are explained in detail and the computer code is provided. The advantages of our proposal are highlighted by several experiments and computer simulations.

10395-3, Session 1

Radiometric calibration of digital cameras using neural networks

Michael Grunwald, Martin Schall, Pascal Laube, Georg Umlauf, Matthias O. Franz, Hochschule Konstanz (Germany)

Digital cameras are used in a large variety of scientific and industrial applications. For most applications, the acquired data should represent the real light intensity per pixel as accurately as possible. However, digital cameras are subject to physical, electronic and optical effects that lead to errors and noise in the raw image. Temperature-dependent dark current, read noise, optical vignetting or different sensitivities of individual pixels are examples of such effects. The purpose of radiometric calibration is to improve the quality of the resulting images by reducing the influence of the various types of errors on the measured data and thus improving the quality of the overall application.

In this context, we present a specialized neural network architecture for radiometric calibration of digital cameras. Neural networks are used to learn a temperature- and exposure-dependent mapping from observed gray-scale values to true light intensities for each pixel. In contrast to classical flat-fielding, neural networks have the potential to model nonlinear mappings which allows to accurately capture the temperature dependence of the dark current and to model cameras with nonlinear sensitivities. Both scenarios are highly relevant in industrial applications.

The experimental comparison of our network approach to classical flat-fielding shows a consistently higher reconstruction quality, also for linear cameras. In addition, the calibration is faster than previous machine learning approaches based on Gaussian processes.

10395-4, Session 1

An optimized knife-edge method for on-orbit MTF estimation of optical sensors using powell parameter fitting

Lu Han, Chen Gong, Kun Gao, Zhenyu Zhu, Yue Guo, Beijing Institute of Technology (China)

On-orbit Modulation Transfer Function (MTF) is an important indicator to evaluate the performance of the optical remote sensors in a satellite. There are many methods to estimate MTF, such as pinhole method, slit method and so on. Among them, knife-edge method is quite efficient, easy-to-use and recommended in ISO12233 standard for the whole-frequency MTF curve acquisition. However, the accuracy of the algorithm is affected by Edge Spread Function (ESF) fitting accuracy significantly, which limits the range of application. So in this paper, an optimized knife-edge method using Powell algorithm is proposed to improve the ESF fitting precision. Fermi function model is the most popular ESF fitting model, yet it is vulnerable to the initial values of the parameters. Considering the characteristics of simple and fast convergence, Powell algorithm is applied to fit the accurate parameters adaptively with the insensitivity to the initial parameters. Numerical simulation results reveal the accuracy and robustness of the optimized algorithm under different SNR, edge direction and leaning angles conditions. Experimental results using images of the camera in ZY-3 satellite show that this method is more accurate than the standard knife-edge method of ISO12233 in MTF estimation.

10395-5, Session 2

Generation of arbitrary complex phases by a spatial light modulator in a common path interferometer

Ceciibet Mendoza-Rodriguez, Rafael Rueda Ramos, Carlos I. Robledo-Sanchez, Areli Montes-Pérez, Benemérita Univ. Autónoma de Puebla (Mexico); Rigoberto Juarez-Salazar, Ctr. de Investigación y Desarrollo de Tecnología Digital (Mexico)

A method to generate arbitrary complex phases with a two-aperture common path interferometer is presented. The proposed optical setup is based on a 4f system. A transmissive Spatial Light Modulator generates two windows in the input plane. In the first window, the reference beam, a pattern of straight fringes with controlled phase shifts is displayed. In the second window, the test beam, a fringe pattern with curved fringes is displayed. In the Fourier plane, a mask and a Ronchi grating with an appropriate spatial frequency are fixed for diffraction order filtering and superposition of the reference and test beams, respectively. Preliminary experimental results and potential applications in optical metrology are discussed.

10395-6, Session 2

Complex amplitude modulation with a single phase-only spatial light modulator

Liangcai Cao, Dezhao Kong, Song Zong, Hao Zhang, Guofan Jin, Tsinghua Univ. (China)

Complex amplitude modulation is widely applied in optical information processing, optical communications, and laser engineering. The commercialized devices for complex amplitude spatial light modulator is rather limited till now. Two spatial light modulators could be combined to server as a complex amplitude modulator with a pixel-to-pixel superimposition. Several methods, such as phase-only elements and the double-pixel approach, may avoid a strict alignment for pixel-to-pixel superimposition. In this work, complex amplitude data page is encoded into two phase-only data pages by the vector stochastic decomposition algorithm. The two pages could be encoded as one phase-only page and uploaded in a single phase-only spatial light modulator. The experimental evaluation of our method suggests a simple yet effective solution for the applications of computer generated holography.

10395-7, Session 2

SF-FDTD analysis of a predictive physical model for parallel aligned liquid crystal devices

Andrés Márquez, Jorge Francés, Francisco J. Martínez-Guardiola, Sergi Gallego, Mariela L. Álvarez López, Eva M. Calzado, Inmaculada Pascual, Augusto Beléndez, Univ. de Alicante (Spain)

Recently we demonstrated a novel and simplified model enabling to calculate the voltage dependent retardance provided by parallel aligned liquid crystal devices (PA-LCoS) devices for a very wide range of incidence angles and any wavelength in the visible. To our knowledge it represents the most simplified approach still showing predictive capability. We demonstrated the good agreement between theoretical and experimental results, which enables to calculate and optimize the wavefront modulation capabilities of PA-LCoS devices for most of the photonics applications where these devices are applied to control the amplitude, phase and/or state of polarization (SOP) of light beams. Deeper insight into the physics behind the simplified model is necessary to understand if the parameters in the model are physically meaningful. Since the PA-LCoS is a black-box where we do not have information about the physical parameters of the device, we cannot perform this kind of analysis using the experimental retardance measurements. In this work we develop realistic simulations for the non-linear tilt of the liquid crystal director across the thickness of the liquid crystal layer in the PA devices. For these simulations we develop a rigorous method based on the split-field finite difference time domain (SF-FDTD) technique which provides realistic retardance values. These values are used as the experimental measurements to which the simplified model is fitted. From this analysis we learn that the simplified model is very robust to a large range of tilt angle profiles of the LC director across the cell. We also learn that some of the parameters in the model are physically meaningful, proving a useful reverse-engineering approach to probe into internal characteristics of the PA-LCoS device.

10395-8, Session 2

Particle field diagnose using angular multiplexing volume holography

Yu Zhao, China Academy of Engineering Physics (China)

The problem of particle field diagnosing using holography can be met in many areas. But single frame hologram can only catch one moment of the fast event, which can't reveal the change process of an unrepeatable fast event. For events in different time-scale, different solution should be used. We did this work to record a laser induced particle field in the time-scale of tens of micron seconds. A laser of pulse sequence mode is applied to provide 10 pulses, the energy and time interval of whom is 150mJ and 1?s. Four pockels cells are employed to pick up the last four pulses for holographic recording, the other pulses are controlled to pre-expose the photopolymer based recording material, the pre-exposure can enhance photosensitivity of the photopolymer during the moment of holographic recording. The angular multiplexing technique and volume holography is accepted to avoid shifting the photopolymer between each shot. Another Q-switch YAG laser (pulse energy 100mJ, pulse width 10ns) is applied to produce the fast event. As a result, we successfully caught the motion process of the laser induced particle field. The time interval of each frame is 1?s, the angular range of the four references is 14°, and the diffraction efficiency of each hologram is less than 2%. After a basic analysis, this optical system could catch more holograms through a compact design.

10395-9, Session 2

Design and manufacture of volume phase holographic gratings used in VIS/NIR wavebands

Qijing Mei, Peng Liu, Minxue Tang, Soochow Univ. (China)

Volume phase holographic gratings (VPHGs) recorded in dichromated gelatin (DCG) is a kind of hologram with periodic variation of refraction index. They have the characteristics of high diffraction efficiency, high signal-to-noise ratio, low scattering, with no ghosts, and good wavelength selectivity and angular selectivity. As the VPHGs are widely applied in the fields of holographic display, astronomical spectroscopy, optical communications, etc., the requirements for the diffraction properties of VPHGs are getting higher.

In this paper, reflective and transmission VPHGs with high diffraction efficiency that prospected to be used as components in a light beams combiner in VIS/NIR wavebands are designed by applying Rigorous coupled wave theory. By adjusting the process conditions of grating recording, chemical processing and packaging, a reflective VPHG with a frequency near 5000 lp/mm and Bragg wavelength at 633nm used as one element of the light beams combiner are manufactured. The diffraction efficiency and angular selectivity of the VPHG are tested and compared with the theoretical values. A method for improving the diffraction wave-front of the reflective VPHG is also explored. According to the initial diffraction wave-front measured by Zygo interferometer, it took a considerable amount of polishing on the surface of the glass-substrate of the above reflective VPHG and the diffraction wave aberration of the grating is reduced significantly. The experiment results in this paper will provides a technical support for further manufacturing VPHGs with high diffraction efficiency and wave-front quality.

10395-10, Session 3

On the use of video projectors for three-dimensional scanning

Rigoberto Juarez-Salazar, Victor H. Diaz-Ramirez, Ctr. de Investigación y Desarrollo de Tecnología Digital (Mexico); Carlos I. Robledo-Sanchez, Benemérita Univ. Autónoma de Puebla (Mexico); Gerardo Diaz-Gonzalez, Univ. Tecnologica de la Mixteca (Mexico)

Structured light projection is one of the most useful methods for accurate three-dimensional scanning. Video projectors are typically used as the illumination device. However, because video projectors are not designed for structured light systems, some considerations in the calibration procedure must be taken into account. In this work, we present a simple method for calibration of structured light projection systems with video projectors. The proposed method is applied in a fringe projection application.

10395-11, Session 3

Light output enhancement for a plastic scintillator using nano-fibers

Zhangkai Cheng, Samuel J. Blake, The Univ. of Sydney (Australia) and Ingham Institute (Australia); Philip Vial, Sydney South West Health Service (Australia) and The Univ. of Sydney (Australia) and Ingham Institute (Australia); Steven R. Meikle, The Univ. of Sydney (Australia); Minghui Lui, PerkinElmer, Inc. (United States); Zdenka Kuncic, Shaghik Atakaramians, The Univ. of Sydney (Australia)

Electronic portal imaging devices (EPIDs) are x-ray detector systems conventionally used for medical imaging applications in cancer radiotherapy. To improve upon current EPIDs, our group has developed a novel prototype EPID for simultaneous imaging and dose verification that utilises an array of plastic scintillating fibers in place of the standard copper and gadolinium oxysulfide phosphor components [1].

While our prototype EPID exhibits the tissue equivalent response needed for dose verification relative to commercial EPIDs, it suffers from reduced optical output. One contributing factor is the reduced optical coupling due to an air gap between the fiber array and the underlying photodetector. Here we investigate the effect of a layer of polystyrene nano-fibers placed at the end interface of the scintillator array on light extraction efficiency using finite element modelling. We demonstrate that when the nano-fiber diameter is on the order of optical wavelengths (670 nm) and the separation between the fibers is 150-200 nm, overall light extraction enhancement exceeding 10% is possible.

This enhancement stems from two effects: Bragg diffraction arising from the periodic arrangement of the fibers and whispering gallery modes formed at the cross-section of the fiber due to Mie resonances. We show that the nano-fibers increase the transmittance above the critical angle. Moreover, we demonstrate that the light extraction efficiency strongly depends on the polarization of the incident light (s- and p-polarizations), as well as the diameter and periodicity of the nano-fibers.

[1] Blake et al. Med. Phys. 2013, 40(9) 091902.

10395-12, Session 3

Development spectroellipsometric technology for the diagnosis of aquatic environments

Ferdenant A. Mkrtchyan, Vladimir V. Kovalev, Kotel'nikov Institute of Radio Engineering and Electronics of Russian Academy of Sciences (Russian Federation)

Spectroellipsometry methods used for non-destructive investigation of chemical and physical properties of solids and liquids. These methods are based on detection of optical polarization effects arising from the reflection or distortion of a light wave in the interaction with the analyte. In solid state physics spectroellipsometry allows simultaneous measurement of amplitude and phase characteristics of the test sample and accurately determine both film thickness and optical constants of the film material. In the diagnosis of liquids are given the opportunity to assess the concentration of dissolved and suspended chemicals, as well as to determine the spots of pollutants of the water surface. There are several major trends in modern ellipsomery. This spectroellipsometry polarization rotating elements with a photoelastic modulators speed and dividing the radiation beam reflected from the sample to multiple channels with different polarization states and several photodetectors. In V.A. Kotelnikov's Institute of Radioengiheering and Electronics, RAS developed spectroellipsometer a method with the binary modulation of the polarization state, based on the elemental base polarization optics for measurements in a wide spectral range and non-moving polarization elements. This approach provides spectral image of the test sample in a specific spectral range, which enables using mathematical techniques to evaluate the chemical and physical characteristics of this sample. In essence, it is necessary to solve the inverse problem of multi-channel.

In this paper, we propose a new method of ellipsometry measurements - ellipsometry with the binary modulation of the polarization state (BMPS), wherein the sample is alternately directed light with two polarization states and analyzes the signal to the photodetector. The work also explores the possibility of creating and using multi-channel LED spectroellipsometer based on ellipsometry method BMPS completely overlying a relatively broad spectral range 350-810 nm. In developed spectroellipsometer BMPS with no moving polarizing elements combined with high sensitivity, stability and measurement speed.

" The reported study was partially supported by RFBR, research project No. 17-07-00467".

10395-13, Session 3

Optical frequency comb generator using FWM for modern WDM system design

Abel Sanchez-Nieves, Escuela Superior de Ingeniería Mecánica y Eléctrica (Mexico); Ivan A. Aldaya-Garde, Univ. Estadual de Campinas (Brazil); Mauro A. Enciso Aguilar, Ctr. de Educación Continua (Mexico); Abraham Sierra-Calderon, Jose A. Alvarez-Chavez, Ctr. de Investigación e Innovación Tecnológica (Mexico)

Due to the high demand for bandwidth around the world, it is necessary to design optical communications systems with high capacity in addition to being low in cost. Wavelength Division Multiplexing systems are a good choice for such demands. Within WDM systems, Optical frequency comb generator is a technology that produces densely and equally spaced multiple optical subcarrier channels with the use of a minimum number of devices, offering bit rates from gigabits to even a few terabits per second. In this work, a novel optical frequency comb generator using Four Wave Mixing (FWM) for modern WDM systems is presented. The optical frequency comb generator is composed by a continuous wave (CW) laser at 1550.21 nm, a Mach-Zehnder modulator (MZM) fed by a sinusoidal signal at 12.5 GHz, an amplifier with 20 dB gain and a piece of 1.2 km highly nonlinear fiber (HNLF). The result is the generation of six subcarriers with 25 GHz spacing, spectral flatness of 0.71 dBm and transmission rate per subcarrier of 100 Gbps. Full design and characterization results will be included in the presentation.

10395-14, Session 3

A novel symmetric 40 Gbps RZ-DPSK-based colorless WDM-PON

Aftab Hussain, Swedish College of Engineering and Technology (Pakistan)

In this paper a novel Transmission approach regarding generation of simultaneous transmission of 40 Gbps RZ-DPSK data signal is simulated for both downstream & upstream directions. An OCS scheme is utilized for generation of second order dual side-band optical carrier by quadrupling a 50GHz clock-frequency with a 10GHz LN-MZM. The lower side second order band is used to generate an RZ-DPSK data signal at the OLT. At the receiving end 20 km apart, the higher side second order un-modulated band, coupled with the downlink transmitted signal is separated and used for uplink transportations of 40Gbps data in RZ-DPSK format. The proposed architecture eliminated the need of use of a pulse carver at either transmission ends. The proposed solution also eliminated the requirement of using a power splitting at the ONU. The proposed DWDM-PON architecture is seemed to be highly robust, cost effective as well as future proof design.

10395-15, Session 4

Restoration of degraded images using stereo vision

Jose Enrique Hernandez-Beltran, Victor H. Diaz-Ramirez, Ctr. de Investigación y Desarrollo de Tecnología Digital (Mexico)

Image restoration consists in retrieving an original image by processing a captured image of a scene which is degraded by noise or blurring. Commonly restoration algorithms utilize a single monocular image of the observed scene by assuming a known degradation model. In this approach, valuable information of the three dimensional scene is discarded. This work presents the design of a locally-adaptive algorithm for image restoration by employing a stereo camera. The proposed algorithm utilizes information of a three-dimensional scene as well as local image statistics to improve the quality of a single restored image by processing pairs of stereo images. Computer simulations results obtained with the proposed algorithm in terms of objective metrics are analyzed and discussed by processing stereo images degraded by noise and blurring.

10395-16, Session 4

Modeling apparent color for visual evaluation of camouflage fabrics

Scott Ramsey, Troy Mayo, Andrew Shabaev, Samuel G. Lambrakos, U.S. Naval Research Lab. (United States)

As the U.S. Navy, Army, and Special Operations Forces progress towards fielding more advanced uniforms with multi-colored and highly detailed camouflage patterning, additional test methodologies are necessary in evaluating color in these types of camouflage textiles. The apparent color is the combination of all visible wavelengths (380-760 nm) of light reflected from large (≥1m^2) fabric sample sizes for a given standoff distance (10-25ft). Camouflage patterns lose resolution with increasing standoff distance, and eventually all colors within the pattern appear monotone (the "apparent color" of the pattern). This paper presents an apparent color prediction model that can be used for evaluation of camouflage fabrics.

10395-17, Session 4

Restoration of motion blurred images

Leopoldo N. Gaxiola, Rigoberto Juarez-Salazar, Victor H. Diaz-Ramirez, Ctr. de Investigación y Desarrollo de Tecnología Digital (Mexico)

Motion blur estimation is a challenging problem in image restoration. Image degradation occurs due to various reasons like camera defocussing, atmospheric turbulence, and camera or object motion, among others. Satellite imaging, medical imaging, surveillance and target tracking are examples in where automatic motion blur estimation is required. In this work, we present a method to estimate linear uniform motion blur in an observed scene. The proposed approach is based on the spectrum of the blurred image to estimate the degradation parameters. The performance of the proposed method is evaluated in synthetic and real-life images. The obtained results are characterized in terms of accuracy of linear uniform motion blur estimation using objective metrics.

10395-18, Session 4

Computational reduction of the image sets required in conventional phase shifting methods applied to digital photoelasticity

Juan Carlos Briñez de León, Alejandro Restrepo Martínez, John W. Branch Bedoya, Univ. Nacional de Colombia Sede Medellín (Colombia)

In photoelasticity studies, phase shifting methods are highlighted for determining the principal stress directions, and principal stress differences. Notwithstanding, they require sets of images, whose acquisition process involves several rotations of the optical instruments, which makes complex their application.

Reducing the quantity of images represents an opportunity to decrease the time in the acquisition stage, and avoid errors introduced by the optic misalignment caused when the instruments are rotated.

In this paper, a conventional six phase shifting method is modified for evaluating the stress field using less images. Here, the light intensities that emerge from the optical arrangement are rescaled computationally to adjust the fringe patterns to the top and bottom values into the gray scale. There, the black color corresponds to the background light, and the white is the maximum transmitted light. With this process, the intensity equations for three of the phase shifted are expressed in function of the other three. This implicates that three of the images required by the method can be generated computationally from three acquired previously. The rest of the phase shifting process is performed according to traditional methods.

Our method is evaluated in synthetic images generated for the analytical model of a disk under diametric compression.

The results show that the new proposal evaluates the stress information with similar performance than the conventional method, using only a half of the images. This method can be useful for the industrial inspection area in which the image acquisition time is important into the process.

10395-19, Session 4

An adaptive template-matched filtering approach for object segmentation in real-life scenes

Kenia Picos Espinoza, CETYS Univ. Baja California (Mexico) and Ctr. de Investigación y Desarrollo de Tecnología Digital (Mexico); Victor H. Diaz-Ramirez, Ctr. de Investigación y Desarrollo de Tecnología Digital (Mexico)

Object segmentation is a basic task in computer vision that is required to assist several image processing applications such as object extraction, boundary detection, image retrieval, and target tracking for surveillance. Generally, the quality of image segmentation affects the overall performance of these systems. This work uses template matching filters in order to detect a target of interest within a scene. The system employs an adaptive strategy for the generation of space-variant filters which take into account several versions of the target and local statistical properties of the input scene. Template-matching filters has demonstrated that are able to yield a high performance in target recognition applications, given in terms of efficiency of target detection and accuracy in location estimation of the target in cluttered and noisy scenes. Moreover, the proposed method considers the geometric modifications of the target while is moving through a video sequence. The detection accuracy of the matched filter brings the location of the target of interest.

Furthermore, for the case of object segmentation, we implement an adaptive filtering procedure according to the geometrical changes of the target for the estimation of its current support region. The estimated location coordinates are used to compute the support area covered by the target. Then, a watershed segmentation technique is implemented in each frame using the estimated location in order to extract the area of the target from the remaining information of the scene. Experimental tests carried out in a video sequence show that the proposed system yields high detection accuracy, and object segmentation efficiency in real-life scenes.

10395-22, Session PMon

An improved silhouette for human pose estimation

Anthony H. Hawes, Khan M. Iftekharuddin, Old Dominion Univ. (United States)

We propose is a novel method of handling self-occlusion in human pose estimation (HPE) that exploits the dynamic range of a single image to infer the relative positions of limbs under self-occlusion. Specifically, self-occlusions in which the occluded parts are similar in appearance to the background are discussed. Errors caused by self-occlusion cause several modern human pose estimation methods to mis-identify body parts, complicating pose estimation algorithms. Techniques such as contour migration resolve ambiguity for rigid objects, however, require a database of known objects and are not suited for handling self-occlusion with non-rigid, deformable objects. More advanced methods of fitting 3D models to 2D silhouettes could be improved with knowledge of occluded limbs. While more effective algorithms exist for depth images, self-occlusion in 2D images remains a challenge. Our method is motivated by the variable aperture behavior of the human vision processing system: when viewing darker parts of a scene, our iris opens to allow more light, which gives humans more effective dynamic range compared to a single camera image. This method can be used to 1) help solve the inherent ambiguity of pose resulting from fitting a 3D human body model to a 2D silhouette obtained from background substitution, and 2) help initialize pose estimation algorithms. An intelligent edge detection algorithm based on the above principle can be used to provide an input superior to the silhouette for human pose estimation algorithms, which represents an essential step for model-based action recognition methods.

10395-36, Session PMon

Spectrum refinement and correction for laser Doppler velocimeter

Qiucheng Gong, Xiaoming Nie, Jian Zhou, National Univ. of Defense Technology (China)

In this paper, frequency spectrum refinement and frequency spectrum correction method for Doppler signal was proposed separately. Basic principle of frequency spectrum refinement and frequency spectrum correction algorithm was expounded. Spectrum simulation of different frequency ideal sinusoidal signal and real time Doppler signal were studied based on these theories. Theoretical analyses and experimental results demonstrated that, the Goertzel refinement algorithm has the least computing amount and the quickest computing speed; the ratio correction algorithm for frequency correction has simple correction formula, less computing amount and higher correction accuracy. Distinguishability of frequency spectrum can be improved by frequency spectrum refinement and correction technology, which is practical useful in frequency spectrum analyzing laser Doppler velocimeter.

10395-37, Session PMon

Influence of fiber-optic system of transmission of analyzed signals to spread function of diffraction grating spectral device

Vasily Kazakov, Oleg D. Moskaletz, Saint-Petersburg State Univ. of Aerospace Instrumentation (Russian Federation)

Fiber-optic system of transmission of analyzed signal is considered, which allow to transmit signals from optical sources with either impossible or undesirable contact. Diffraction grating spectral device is considered as investigated system. Moreover, the diffraction grating operates with transmitted light, not reflected. Influence of optical fiber is manifested in the distortion of the wave front incident on the spectral device. Front distortion leads to a broadening of the spread function of the device in all diffraction orders, and as a consequence, to a deterioration in resolution of the device. Under the complex spread function a reaction to the homogeneous plane monochromatic wave which clearly communicates the input-output of spectral device is understood. Accounting of fiber-optic system influence is made by introducing a fictitious transparency located directly in front of the diffraction grating.

Investigation of the influence of fiber-optic system to the spread function of the diffraction grating spectral device is made in two ways:

1. Mathematical model describing the influence of a single-mode optical fiber to a spread function of the diffraction grating spectral device is proposed. On the basis of the proposed model computer simulations of the analyzed signal transmission from the end of the optical fiber to the result of photodetection is performed. The calculations are performed for a single-mode optical fiber with a core diameter of 8 microns.

2. Experimental laboratory set up of the diffraction grating spectral device with a fiber optic transmission system is created.

Theoretical calculations are compared with the results of experimental studies.

10395-38, Session PMon

Acousto-optic modulator as an element of signal processing systems of radio and optical diapasons

Vasilisa Romashova, Oleg D. Moskaletz, Saint-Petersburg State Univ. of Aerospace Instrumentation (Russian Federation); Dmitriy Moskaletz, Saint Petersburg Electrotechnical Univ. “LETI” (Russian Federation)

Acousto-optic modulator is a device for input dynamic signals in the optical computing devices, which perform spectrum analysis of signals and calculate correlation functions of the signals.

The important characteristic of the acousto-optic modulator is a transparency function, which determines the quality of acousto-optic systems of information processing. Transparency function is determined by the acoustic wave, which propagating through the medium of acousto-optic interaction. In the idealized case, the action of acousto-optical devices is considered in the approximation of the acoustic wave in the form of acoustic column(parallelepiped form). The linearity of the input signal (linearization of the transparency function) was considered only for rarely used modes of diffraction of the Raman – Nath.

In real conditions it’s necessary to consider diffraction divergence of the acoustic column and the linearization of the transparency function of acousto-optic modulator in the General case of diffraction. In represented research is performed analysis of the diffraction divergence in the dissipative medium and application of methods of nonlinear functional analysis (the formula of finite increments of the Frechet derivative) for purposes of linearizing of transparency function.

The criterion of distinction of the diffracted field taken the increase in the radius of inertia of a plane figure, which describing a one-dimensional diffraction from the radius of inertia of the rectangle, which describing an undiffracted field.

Computer simulation of the diffraction pattern is realized by the method of calculation of the Fresnel integrals in Matlab software

10395-39, Session PMon

An edge detection method with boundary reserved based on non-subsampled contourlet transform for remote sensing imagery

Zizheng Hua, chen gong, Kun Gao, Yan Lu, su chen, Beijing

Institute of Technology (China); Yanqin Jia, Southwest Jiaotong Univ. (China)

During space reconnaissance applications, edge detection from remote sensing imagery plays an important role in the target recognition processing. However, traditional edge detection methods usually only utilize the high-frequency information in one image. Since low-frequency elements may be aliasing with high-frequency parts, the edges extracted may be unconnected under complex topography, different objects and imaging conditions. This paper proposes a novel image edge detection method based on Non-Subsampled Contourlet Transform (NSCT) to keep the object boundary continuously. It transforms the image into Contourlet domain in both high-frequency and low-frequency sub-bands respectively. Depending on the feature of flexible directivity reservation of an image during NSCT, the further edge extraction consists of 3 steps: firstly, the elements of the high-frequency coefficient matrix in Contourlet domain are filtered with high values left using adaptive thresholds. Then the low-frequency edge information is extracted via Canny operator from the low-frequency sub-band information. Finally, to achieve a more consistent edge image, the low-frequency edge image is achieved according to the low-frequency matrix and adopted to compensate the high-frequency image with the isolated noise points eliminated as well. The numerical simulation and practical test results show the higher effectiveness and robustness of the proposed algorithm when comparing with the classical edge detectors, such as Sobel operator, Canny operator, Log operator and Prewitt operator, etc.

10395-41, Session PMon

Security analysis of the first random phase mask in double random phase encryption

Lingfei Zhang, Thomas J. Naughton, National Univ. of Ireland, Maynooth (Ireland)

Double random phase encoding is one of the most studied techniques in optical encryption. It encrypts an input image to stationary white noise using two statistically independent random phase masks. When the input image is an amplitude image, the first mask is not required for decryption, and this has led to a preponderance in the literature to consider only the second mask (the Fourier plane mask) in security analysis. However, the first mask must also be kept secret because knowing the first mask and a plaintext-ciphertext pair allows one to directly solve for the second mask.

Any error in one's knowledge of the first mask leads to an imperfect estimation of the second mask. In this paper, we examine how the errors propagated to the second mask are amplified when decrypting previously unseen encrypted images. In particular, we find that with even 5% error in the first phase mask the decrypted images are completely unrecognisable (white noise).

The obvious approach to improve the quality of the first phase mask is to consider phase retrieval (given that the mask is already so close to the correct key). However, its convergence can slow considerably after the initial iterations. In this context, we introduce a greedy algorithm to improve the estimation of the first encryption key in order to better recover the second encryption key. We compare how accurately each of the phase retrieval and greedy approaches quantify the security implications of an attacker estimating the first phase mask.

10395-42, Session PMon

Imaging simulation for three-FOV daytime star sensors based on ray tracing

Feng Wu, Xifang Zhu, Ruxi Xiang, Xiaoyan Jiang, Qingquan Xu, Gong Chen, Tao Wu, Changzhou Institute of Technology (China)

Daytime star sensors provide accurate navigation information to air vehicles flying near the ground all day and all night. In order to resist the strong background irradiation disturbance in the atmosphere environment, daytime star sensors are made up of multiple star cameras working in the infrared band. They are called star sensors with multiple fields of view(FOV) and have become an important developing direction of modern star sensors. Huge amounts of star maps are demanded during the daytime star sensors development. Imaging simulation using computer programming is a shortcut to produce star maps efficiently. In this paper, an imaging simulation method of the three-FOV daytime star sensor is proposed. The structure of the three-FOV daytime star sensor is analyzed. Its working principle is introduced. Then, the simulation framework is designed which contains observed star catalog, observed star calculating module, ray tracing module and image output module. The observed star catalog is created after 2MASS (the Two Micron All-Sky Survey)star catalog is studied and processed. Procedures of tracing rays going through the optical systems of the three-FOV daytime star sensors made up of spherical or aspherical optical surfaces are described in detail. Then simulation star maps are output by calculating the pixel energy on the image plane. Finally, simulation experiments are implemented. Simulation star maps are compared with those produced by Sky chart. Observed stars in the maps are identified by applying Pentagram star pattern identification algorithm. Their results prove that the proposed imaging simulation method of the three-FOV daytime star sensor is satisfactory and appropriate.

10395-43, Session PMon

Optical-microstructures for read-only holograms

Joo Yeon Kim, Electronics and Telecommunications Research Institute (Korea, Republic of); Seung-Yeol Lee, Kyungpook National Univ. (Korea, Republic of); Yong-Hae Kim, Sanghoon Cheon, Seong-Mok Cho, Hojun Ryu, Tae-Youb Kim, Electronics and Telecommunications Research Institute (Korea, Republic of)

In recent years, optical micro-structures have become more important to be developed as optical components for security and authentication applications. The fabrication of these optical micro-structures, the compute-based holograms (CGHs) generating diffraction patterns in a space are attractive technology due to its difficulty in counterfeit. However, in order to generate certain images based on CGHs, it is challenge because of requiring a huge amount of calculation even for binary holograms.

Therefore, the consideration in terms of "mass-production" with an appreciate time and cost-efficient, replication technology is introduced in this work.

The developed binary CGHs generated by SiO_2 patterns on a transparent substrate were transferred onto polymeric layers, and their optical properties will be presented.

10395-44, Session PMon

Rapid and high-throughput microalgae monitoring platform based on lens-free shadow imaging technology

Dongmin Seo, Sanghoon Shin, Korea Univ. (Korea, Republic of); Sangwoo Oh, Korea Research Institute of Ships and Ocean Engineering (Korea, Republic of); Kiyoung Ann, Euijin Han, Korea Univ. (Korea, Republic of); Moonjin Lee, Korea Research Institute of Ships and Ocean Engineering (Korea, Republic of); Sungkyu Seo, Korea Univ. Sejong Campus (Korea, Republic of)

Microalgae have been employed and studied by various research fields including alternative energy, environmental science, pharmaceutics, or toxicology. Most of studies for microalgae analyzed them by counting the cells, determining the byproducts, or dissolving the cells to check internal materials. However, those analytical methods to date are extremely labor intensive and time consuming or require specialists and expensive equipment. In this study, we propose a rapid and high-throughput

microalgae monitoring platform based on LSIT, which utilizes the changes of diffraction or shadow patterns of micro-objects to count, differentiate, check viability, or evaluate other critical characteristics within a low-cost and compact platform mainly composed of light emitting diode (LED) light source and a complementary metal oxide semiconductor (CMOS) image sensor. In this platform, since the diffraction pattern changes sensitively to the change of an microalgae in shape and size, the change of growth state of the microalgae could be determined by analyzing the diffraction pattern in real time and by single cell basis. Dunaliella tertiolecta is an oval-shaped microalgae in healthy state (live) that turns into a circle shape (cyst) when exposed to stress, eventually losing its original shape (dead) and turning into a dead cell, and its small biological change was successfully quantified and determined by newly developed shadow parameters. Within this platform, automatic counting and analyzing of microalgae were performed with a single digital image rapidly and simultaneously for hundreds of the cells in real time. Therefore, this platform holds great promise in various research fields related with microalgae.

10395-45, Session PMon

Polarization characteristic pulse electromagnetic signals

Valentina Akperova, Oleg D. Moskaletz, Saint-Petersburg State Univ. of Aerospace Instrumentation (Russian Federation)

Polarization state is one of the important characteristics of signals in radio and optical ranges, and essentially influences on these signals receiving and processing. Propagation of electromagnetic signals is accompanied by polarization distortions; analysis of these distortions was performed in this paper. Vector models of electromagnetic signals and their polarization spectra is the basis of fulfilled research. Vector models and the polarization spectra of electromagnetic signals were introduced on the basis of Fourier integrals. These vector models and the polarization spectra are considered as a generalization of the spectra of scalar signals and as the most common characteristic of electromagnetic signal. All other characteristics of vector signal, including polarization properties, can be found from these vector models and polarization spectra.

The investigation techniques are based on the representation of polarization characteristics in the form Jones vector and the properties of propagation medium and reception system, which change polarization state are described by Jones matrices. Jones matrix, reflecting the properties of propagation medium is frequency dependent. This matrix is presented in form of matrix series, that allows in simplified form to consider polarization distortions with necessary degree of accuracy. On the base of Jones matrices formalism from polarization spectra following correlation functions: cross-correlation function between orthogonal components, cross-correlation function between received and referenced components, and autocorrelation function of every received component were derived.

10395-46, Session PMon

Optic fields transformation in acousto-optical signal processing systems

Aleksei Orlov, Oleg D. Moskaletz, Saint-Petersburg State Univ. of Aerospace Instrumentation (Russian Federation)

Major topic of our researches is optic fields transformation in the acousto-optical devices designed for spectral-correlation processing of radio signals based on generalized scheme, which includes an optical coherent Fourier-processor, dynamic and static transparents, which allows to input dynamic and static signals in optical coherent Fourier-processor, and a photodetector with photo-detector processing module. As a dynamic transparents we may use an acousto-optic modulators.

Transparents are making possible spatial and spatially-temporal modulation of laser radiation and can be characterized by the transmission functions. These transmission functions are represented in the form of two components: an unit and an additional modulating summand, which can be described in the case of dynamic transparent by a nonlinear representation of the acoustic wave. This wave propagates in the acousto-optical interaction medium. Linearity requirement of the processed dynamic signal inputting in the optical system can be satisfied by the linearization of additional modulating summand in the context of approximation of nonlinear operator by the formula of finite increments.

The distribution of laser light modulated by one, two and three transparents was investigated in the rear focal plane of optical coherent Fourier processor.

Photodetection and postdetector processing is considered both in the context of correlation functions receiving and radio signals spectrum analysis. The expressions for the correlation functions of cross-correlation of two radio signals and the correlation function with a fixed reference signal were obtained. The relation, expressing the radio signal energy spectrum estimation, was given.

10395-47, Session PMon

Diffractive lenses in biocompatible photopolymers using LCoS

Sergi Gallego, Roberto Fernández, Víctor Navarro-Fuster, Manuel Ortuño, Andrés Máquez, Cristian Neipp, Augusto Beléndez, Inmaculada Pascual, Univ. de Alicante (Spain)

The improving of the technology related to the Spatial Light Modulators (SLM), which can be used to modulate the wavefront of a light beam in many different applications in Optics and Photonics, has widespread their use in many new ways. In particular, the continue miniaturization of the pixel size let them be used as a master for Diffractive Optical Elements (DOE) recording applications. One of these displays is the parallel-addressed liquid crystal on silicon (PA-LCoS) microdisplay, which offers easily the possibility of phase-only modulation without coupled amplitude modulation, but can be use also as an amplitude master just rotating the angles of two polarizers. Together with the DOEs, the optic recording material is also one of the crucial components in the system. Photoresist has been used classically for this purpose. Recently some works provide results of the incorporation of photopolymers, initially used for holographic recording, to fabricate DOEs. Among photopolymers, polyvinil alcohol/acrylamide (PVA/AA) materials have been studied firstly due to the accurate control of their optical properties and the ease of fabrication. Nevertheless, this kind of photopolymer presents a high level of toxicity due mainly to the monomer, acrylamide. In this sense, we made efforts to search alternative “green” photopolymers, one of these is called “Biophotopol”. This material presents good optical properties; nevertheless, it has two principal drawbacks: its refractive index modulation is lower than for the PVA/AA one and the dye used presents very low absorption at 532 nm. In order to solve these problems for recording spherical diffractive lenses, in the present work we have explored different possibilities. On the first place, we have modified the fabrication technique of the solid layer to achieve thicker samples, on the second place we have introduce a biocompatible crosslinker monomer. These two actions provide us a higher value of the phase modulation capability. On the third place we have modified the dye to record DOE’s with the wavelength of 532 nm and obtain a direct comparison with the results obtained with PVA/AA materials.

10395-48, Session PMon

Laser radiation scattering by the cement in the process of setting and hardening

Peter P. Maksimyak, Mykhaylo P. Gorsky, Andrew P. Maksimyak, Yuriy Fedkovych Chernivtsi National Univ. (Ukraine)

Optical methods of concrete hydration diagnostics have a great potential. In this work we simulated the dynamics of intensity fluctuations in the process of coherent light scattering by the cement during its setting and hardening. Simulation was compared with experimental data.

Modeling of this process using transfer theory and Mie scattering indicatrix is impossible as they don't carry any information about scattered radiation phase. Strict modeling of this process is possible only with analytical theory of multiple scattering using. At present moment, there is an exact solution of this problem for a medium consisting of a set of spheres of equal radius, which is not suitable for our case.

The results show that the presented computer model of cement setting and hardening satisfactorily describes the initial stage of cement minerals hydration with calcium hydroxide formation in the interval 0 - 50 minutes, and the tobermoryth crystals formation and merging in the interval 0 - 300 min, when cement hardening finishes and cement stone begins to gain strength. The stage of further strengthening in the interval 300 - 600 minutes is worse described by this model, because it is not considered the possibility of solid porous structure formation. In addition, on the course of time dependence of speckle field fluctuations intensity of scattered radiation also effects the real shape of scattering particles, which in the framework of this model is not considered. Experimental studies show the optical examination perspectives of the process of cement setting and hardening and also good correlation with theoretical modeling.

10395-49, Session PMon

Phase-depth mapping in structured light field: analysis and application

Zewei Cai, Xiaoli Liu, Dingnan Deng, Xiang Peng, Shenzhen Univ. (China)

In the previous work, we proposed a method of structured light field combining the light field imaging with the structured illumination. In the structured light field, every ray carries not only the direction information but also the depth-modulated phase information, so that multidirectional depth estimation can be performed for high-dynamic-range 3D imaging. However, the projection axis was implicitly assumed to be perpendicular to the reference plane to obtain the mapping relationship between the phase and the depth. In this paper, we relaxed the implicit condition that the projection axis was not perpendicular to the reference plane, and then derived a universal phase-depth mapping in the structured light field, of which the previous mapping relationship was one special case. Based on this universal mapping relationship, nonlinear model used two coefficients and linear model used single coefficient were proposed. Each ray in the structured light field has its corresponding mapping coefficients that can maps the phase to the depth independently. Real and simulated experiments were implemented to compare the two models in different ranges of depth. Through error analysis, we found that the precision of the nonlinear model could keep consistent in a large range of depth. Consequently, the nonlinear model within a large range of depth was recommended to realize depth estimation, as demonstrated in our final experiment of the multidirectional scene reconstruction.

10395-50, Session PMon

Spectral analysis of a secure chaotic free space optical communication system

Marc M. Sepantaie, Nader M. Namazi, Amir M. Sepantaie, The Catholic Univ. of America (United States)

This paper aims to study the impact of Free Space Optical (FSO) channel on a transmitted chaotic signal infused by a random binary message [1, 2]. In particular, it examines and corroborates the numerical solution by analytical analysis of the chaotic communication system utilizing the autocorrelation function and power spectral density approach in the presence of multiplicative noise. The autocorrelation function of the multiplicative scintillation noise has been modeled by an exponential function as reported in [3]. Moreover, the transmitted chaotic signal was modeled by a telegraph signal as presented in [4].

The approach taken here renders the additive noise in the FSO channel as negligible, effectively employing the linear system concept to analyze the influence of the scintillation noise on the transmitted chaotic waveform. Consequently, the multiplicative term (scintillation noise) in the received signal can be converted to an additive term with respect to the received signal using a linear portion of the logarithmic operation. The subsequent signal, which consists of two additive terms was then passed through two cascaded Haar filters where a decision can be made using a static threshold to detect the original transmitted random binary message. Simulation experiments were performed in Matlab to validate the theoretical approach.

REFERENCES

[1] Sepantaie, M. M., Namazi, N. M., and Sepantaie, A. M., "Identical synchronization of chaotic secure communication systems with channel induced coherence resonance", Proceedings of SPIE 9842 (2016)

[2] Sepantaie, M. M., Bui, V., El-Araby, E., Sepantaie, A. M., Nehmetallah, G., and Namazi, N. M., "Secure Communication Systems Using Synchronized Lorenz Strange Attractor on Reconfigurable Hardware", Proceedings of SPIE 9478 (2015)

[3] Kolka, Z., Biolkova, V., and Biolek, D., "Channel Model for Monte-Carlo Simulation of Data Transmission on Terrestrial FSO Path", International conference on Emerging Trends in Engineering and Technology (2013)

[4] Anishchenko, V. S., Vadivasova, T. E., Okrokvertskhov, G. A., and Strelkova, G. I., "Correlation analysis of dynamical chaos", Elsevier Science B. V. (2003)

10395-52, Session PMon

Aerosol detection using Lidar-based atmospheric profiling

Mohamed I. Elbakary, Old Dominion Univ. (United States); Hossam M. Abdelghaffar, Virginia Polytechnic Institute and State Univ. (United States); Kwasi Afrifa, Old Dominion Univ. (United States); Hesham A. Rakha, Virginia Polytechnic Institute and State Univ. (United States); Mecit Cetin, Khan M. Iftekharuddin, Old Dominion Univ. (United States)

A compact light detection and ranging (LiDAR) is a system that provides aerosols profile measurements by identifying the aerosol scattering ratio as function of the altitude. The aerosol scattering ratios are used to obtain multiple aerosol intensive ratio parameters known as backscatter color ratio, depolarization ratio, and lidar ratio. The aerosol ratio parameters are known to vary with aerosol type, size, and shape. In this paper, we employed lidar measurements to detect the potential source of the aerosol around the campus of Old Dominion University. The lidar ratio and the color ratio are retrieved from collected data. To find the source of aerosol in the measurements, a tracking algorithm is employed to track the concentration of that pollution in the data. The results show that the source of soot pollution in the area of study is Hampton Blvd, a major street, in the area of the campus where the diesel trucks travel between the ports in the city of Norfolk.

10395-53, Session PMon

Phase demodulation for digital fringe projection profilometry: a review

Juana Martinez Laguna, Rigoberto Juarez-Salazar, Victor H. Diaz-Ramirez, Ctr. de Investigación y Desarrollo de Tecnología Digital (Mexico)

Phase demodulation is an essential image processing stage required by digital fringe projection profilometers. Currently, several approaches for phase demodulation have been proposed. In this work, a comprehensive review of the most successful phase demodulation methods useful for digital fringe projection profilometry is presented. This survey covers fringe pattern normalization, extraction of wrapped phase, and phase unwrapping. Experimental results obtained with a laboratory fringe projection system are analyzed and discussed. The accuracy of the reconstructed surfaces is measured by comparing with the digitized surfaces obtained by a commercial profilometer device.

10395-54, Session PMon

Polarimetric and diffractive evaluation of 3.74 micron pixel-size LCoS in the telecommunications C-band

Mi Wang, Huawei Technologies Duesseldorf GmbH (Germany); Francisco J. Martínez-Guardiola, Andrés Márquez, Univ. de Alicante (Spain); Yabin Ye, Huawei Technologies Duesseldorf GmbH (Germany); Liangjia Zong, Huawei Technologies Co., Ltd. (China); Inmaculada Pascual, Augusto Beléndez, Univ. de Alicante (Spain)

Liquid-crystal on Silicon (LCoS) microdisplays are one of the competing technologies to implement reconfigurable optical interconnects and more specifically wavelength selective switches (WSS) for optical telecommunications. These systems are the current promising solution for further increasing the traffic capacity in fiber networks. In order to increase the spatial bandwidth and resolution, last generation LCoS have decreased pixel size to values smaller than 4 microns, while increasing the number of pixel elements to more than 4 megapixels. This increases the port count number, thus enabling a superior manageable interconnection capacity bandwidth. However, for the LCoS to be applied in the telecommunication C-band (1.55 micron wavelength) the liquid-crystal layer needs to be significantly thicker than when used in the visible spectrum. The large ratio between the thickness with respect to the pixel size introduces important vicinity problems between neighbouring pixels due to the fringing-field and other cross-talk related phenomena. In the present work we proceed with an experimental evaluation of a 3.74 micron pixel size parallel-aligned LCoS (PA-LCoS) device. We evaluate its performance with well established techniques already applied to larger pixel size PA-LCoS microdisplays in the visible. We analyse with time-average Stokes polarimetry the retardance and its flicker magnitude as a function of voltage, and the existence of residual or induced twist of the LC director. Since the device performs as a beam steering device, diffraction efficiency evaluation is also fulfilled. Discussion of various trade-offs to optimize the performance for the range of steering angles is eventually done.

10395-55, Session PMon

Quantification of absolute blood velocity using LDA

Mariya A. Borozdova, Ivan Fedosov, Valery Tuchin, Saratov State Univ. (Russian Federation)

Abstract: We developed a novel type of laser Doppler anemometer (LDA) to measure absolute velocity of blood flow in superficial arterioles and venules. The instrument uses two laser beams to probe flow velocity and it is capable for measurement of velocity component perpendicular to its optical axis. Confocal detector with pinhole field filtering allows for registration of singly scattered light for measurements of velocity of blood in superficial vessels . When probing a blood vessel in a direction perpendicular to its axis, the result of velocity measurements almost does not depend on the small variations of angle of incidence. We propose novel method of signal processing to minimize the effect of undesirable light scattering on Doppler frequency shift estimation based on subtraction of low frequency components

10395-56, Session PMon

Research on characteristic of scattered light in laser Doppler velocimeter

Xiaoming Nie, Qiucheng Gong, Jian Zhou, National Univ of Defense Technology (China)

This paper introduced the principle of reference-beam laser Doppler velocimeter, analyzed the relationship between laser Doppler signal and the diameter of spot in theory, and investigated the effect of spot for laser Doppler signal, the polarization characteristic of scattered light and its intensity distribution. The result of theory and experiment showed that, first, the intensity of laser Doppler signal is proportional to the diameter of detector, and is inversely proportional to the diameter of spot, second, the scattered light is centrally distributed to the direction which follows the law of reflection, and the intensity of scattered light is related to coarseness of measured object, and the last, the signal is composed of linear polarization and natural light, and the rougher measured object is, the more seriously polarized light degenerate.

10395-57, Session PMon

Classification of cognitive systems dedicated to data sharing

Lidia Dominika Ogiela, Marek R. Ogiela, AGH Univ. of Science and Technology (Poland)

In this paper will be presented classification of new cognitive information systems dedicated to cryptographic data splitting and sharing processes. Cognitive processes of semantic data analysis and interpretation, will be used to describe new classes of intelligent information and vision systems. In addition, cryptographic data splitting algorithms and linguistic threshold schemes will be used to improve processes of secure and efficient information management with application of such cognitive systems. The utility of the proposed cognitive sharing procedures and distributed data sharing algorithms will be also presented. A few possible application of cognitive approaches for visual information management and encryption will be also described.

10395-20, Session 5

Unassisted reduction and segmentation of large hyperspectral image datasets

Leanna N. Ergin, John F. Turner II, Cleveland State Univ. (United States)

The information density in hyperspectral data is not uniform across the spectral and spatial dimensions, and the overall information sparsity is often high. While these non-uniformities underpin the sought-after image contrast, high sparsity generates unnecessarily long acquisition and data processing times. Conventional reduction techniques like those based on principal components analysis (PCA) sacrifice the contributions of minority pixel populations while retaining those representing a greater portion of the overall variability. The effect is that some regions in the reconstructed images achieve a higher degree of recovery than other locations, making it difficult to assess the meaning or relevance of the minority pixels, even when this information would reveal important sample defects or spectral inhomogeneities. In the work presented here, we introduce a novel user-unassisted data reduction and image segmentation method called reduction of spectral images (ROSI). The aim of ROSI is to achieve a threshold information density in the spectral dimension for all image pixels. The result effectively segments the image in a manner that provides rapid image contrast that is comparable to traditionally classified images, but does so without a priori information. In addition, ROSI results are suitable for subsequent data analysis enabling ROSI to be performed alone or as a preprocessing data reduction step. A full description of ROSI is presented along with results from both model and real hyperspectral data, and its performance is compared quantitatively to several conventional data reduction methods.

10395-21, Session 5

Visual environment recognition for robot path planning using template matched filters

Ulises Orozco-Rosas, Kenia Picos Espinoza, CETYS Univ. Baja California (Mexico); Victor H. Diaz-Ramirez, Oscar Montiel, Roberto Sepulveda, Ctr. de Investigación y Desarrollo de Tecnología Digital (Mexico)

Computer vision is an important task in robotics applications. Nowadays, there is a demand for autonomous mobile robots in various fields of application, such as driver assistance in automotive industry, logistics and transport of industrial materials, and object tracking for military applications. For robotics applications, the precise interaction with the environment is crucial to accomplish their tasks, in which is frequently changing or unforeseen. This work addresses the problem of environment recognition for path planning and robot navigation. We propose a computer vision system in order to sense a cluttered environment. This work includes template matching filtering approach for accurate obstacle detection and feasible path recognition. The autonomous mobile robot will have to interact with the environment and avoid collisions with obstacles, following the path planned to achieve its established mission. To achieve a smooth mobile robot navigation, an integration of a physics-based technique known as potential field functions is employed. Due to the robot, can move from the start to the goal by taking a single path between multiple possible ways, we use evolutionary computation in order to find an optimal path. Computer simulation results are presented and discussed in terms of accuracy of the recognition system, effectiveness of navigation, and computational efficiency.

10395-23, Session 5

Dynamic vehicle guidance by B-spline curves

Rigoberto Juarez-Salazar, Victor H. Diaz-Ramirez, Ctr. de Investigación y Desarrollo de Tecnología Digital (Mexico); Edgar Hernandez-Garcia, Jose Ramiro-Ramiro, Marcos A. Alvarez-Trejo, Instituto Tecnológico Superior de Zacapoaxtla (Mexico)

Path planning for autonomous vehicles is a challenging computer vision problem. In this work, we propose an algorithm to generate dynamically a smooth path for trajectory guidance of an autonomous vehicle. For this, we use B-spline curves and the perspective-distorted images obtained from an onboard camera. The theoretical principles of the algorithm are presented in detail. Preliminary results obtained with an experimental prototype are shown.

10395-24, Session 5

Road mark recognition using HOG-SVM and correlation

Ayman Alfalou, Yousri Ouerhani, C. Brosseau, ISEN Brest (France)

We present an innovative approach for identification and localization of road marks by making use of the VIAPIX® module [1,2]. In the identification step of this scheme, a perspective transform of the image is performed to get a global view of the road. Then, color segmentation is realized to keep only white color objects. Base on the calibration of the VIAPIX® module, the length and width of each detected object are evaluated. Next, a classification of the detected objects is performed using the correlation method [3]. Each road mark is detected and compared to a set of reference objects of a data base. To evaluate the degree of similarity between them, the peak-to-correlation energy (PCE) criterion is taken [3]. Such step of our scheme allows us to avoid considering detected objects with low PCE values. Additionally, other objects treated as false alarms are suppressed via the support vector machine (SVM) classifier [4] based on gradient histograms (HoG) [5]. In the localization step, the distance between road marks and the operating camera determined by Vincenty's approach [6] yields the GPS coordinates.

References

[1] ACTRIS VIAPIX solution, http://www.viapix.eu/

[2] ACTRIS Technologie & Innovation, http://www.actris.com/

[3] A. Alfalou and C. Brosseau, "Understanding Correlation Techniques for Face Recognition: From Basics to Applications," Face Recognition Book, Milos Oravec (Ed.), 354-380, ISBN: 978-953-307-060-5, INTECH, (April-2010). Available from:

http://sciyo.com/articles/show/title/understanding-correlation-techniques-for-face-recognition-from-basics-to-applications

[4] V. N. Vapnik. "The Nature of Statistical Learning Theory". Springer-Verlag, 1995

[5] N. Dalal and B. Triggs. "Histograms of oriented gradients for human detection ". In CVPR, 2005, pages 886-893

[6] T. Vincenty, "Direct and inverse solutions of geodesics on the ellipsoid with application of nested equations", Survey Review, 23, pages 88–93, 1975. addendum: Survey Review 23, 294, 1976, http://www.ngs.noaa.gov/PUBSLIB/inverse.pdf

10395-58, Session 5

Optical beam classification using deep learning: a comparison with rule and feature based classification

Md. Zahangir Alom, Univ. of Dayton (United States); Abdul A. S. Awwal, Roger R. Lowe-Webb, Lawrence Livermore National Lab. (United States); Tarek M. Taha, Univ. of Dayton (United States)

Deep Learning methods are becoming popular because of its state-of-the-art performance in image classification tasks. In this paper, we explore laser beam image classification using a novel deep learning approach. The National Ignition Facility (NIF) is the world's largest, most energetic laser which has nearly 40,000 optics that precisely guide, reflect, amplify and focus 192 laser beams onto a fusion target. NIF utilizes four petawatt lasers called the Advanced Radiographic Capability (ARC) to produce backlighting X-ray illumination to capture implosion dynamics of NIF experiments with picoseconds temporal resolution. In the current operational configuration, four independent short-pulse ARC beams are created and combined in a split-beam configuration in each of two NIF Apertures at the entry of the pre-amplifier. The sub-aperture beams then propagate through the NIF beam-path up to the ARC compressor. Each ARC beamlet is separately compressed with a dedicated set of four gratings and recombined as sub-apertures for transport to the parabola vessel where the beams will be focused using parabolic mirrors and pointed to the target. Small angular errors in the compressor gratings can cause the pointing of the sub-aperture beams to diverge from one-another and prevent accurate alignment through the transport section between the compressor and parabolic mirrors. This is an off-normal condition that must be detected and corrected. The goal of the off-normal check is to determine whether the ARC beamlets are sufficiently overlapped into a merged single-spot or diverged into two distinct spots. Thus, the objective of the current task is to explore the use of Convolutional Neural Network (CNN) for beam classification. The recognition results are compared with other approaches such as Deep Neural Network (DNN) and Support Vector Machine (SVM). The experiment results show around 96% classification accuracy using CNN that the CNN approach provides comparable recognition results compared to the present feature based off-normal detection. The misclassified results are further studied to explain the differences and discover any discrepancies or inconsistencies in current classification. The feature based solution is designed to capture the expertise of a human Physicist in classifying the images.

Short summary: The ARC beam is used to generate high energy X-rays for temporally recording the implosion dynamics of a NIF target. As an off-normal condition, we must determine if the beam has two or multiple spots instead of a single spot. Convolutional Neural Network (CNN), Deep Neural Network (DNN) and Support Vector Machine (SVM) are used.

10395-25, Session 6

Cognitive approaches for patterns analysis and security applications

Marek R. Ogiela, Lidia D. Ogiela, AGH Univ. of Science and Technology (Poland)

New generation information systems and security solutions are developing rapidly due to the application of the latest achievements in cognitive technologies, and biologically-inspired computational approaches. What are especially important in creation of such systems are techniques used for securing strategic or classified data, and allowing its intelligent transmission and management in distributed infrastructures or in the Cloud.

There is no doubt that all such technologies will become more important in the near future, as a result of the very dynamic development of new generation information systems dedicated for ubiquitous computing in cyberspace or ambient world.

In this paper will be presented new opportunities for developing innovative solutions for semantic pattern classification and visual cryptography, which will based on cognitive and bio-inspired approaches. Such techniques can be used for evaluation of the meaning of analyzed patterns or encrypted information, and involved such meaning into the classification task or encryption process. It also allows using some crypto-biometric solutions to extend personalized cryptography methodologies based on visual pattern analysis.

In particular application of cognitive information systems for semantic analysis of different patterns will be presented, and also a novel application of such systems for visual secret sharing will be described. Visual shares for divided information can be created based on threshold procedure, which may be dependent on personal abilities to recognize some image details visible on divided images.

10395-26, Session 6

Bimodal database classification

Mireya Saraí García Vázquez, Luis Miguel Zamudio Fuentes, Ctr. de Investigación y Desarrollo de Tecnología Digital (Mexico); Alejandro Álvaro Ramírez Acosta, MIRAL R&D&I (United States)

No Abstract Available.

10395-27, Session 6

A study of multiple correct keys and heuristic attacks in optical encryption

Lingfei Zhang, Thomas J. Naughton, National Univ. of Ireland, Maynooth (Ireland)

The strength of optical image encryption techniques, such as double random phase encoding, has been routinely measured using statistical and heuristic attacks. The most common attack scenario is a known-plaintext attack in which an attacker tries to infer the Fourier plane encryption phase key from a 'plaintext' input and 'ciphertext' encrypted image pair. For intensity-encoded inputs, it is well known that there are multiple perfect keys in the keyspace. This was previously considered an advantage to an attacker because finding any one of the keys or approximate solutions were sufficient. However, we propose that this is the reason for the well-documented performance limitations of heuristic attacks. For a small sample of inputs, we have observed that a class of heuristic attack performs suboptimally when its keyspace contains multiple equivalent solutions. We propose that a solution to the problem of underperforming heuristic attacks might be achieved by transforming the keyspace so that it contains only one correct solution. We illustrate this by introducing special circumstances that restrict the keyspace to one solution while keeping the size of the keyspace the same. We use the heuristic-based simulated annealing algorithm in a known-plaintext attack. In our limited tests, the performance of the heuristic attack is significantly improved. In particular, the accuracy of the heuristic-estimated decryption key far exceeds that found with any other simulated annealing attack when measured in terms of decrypting any subsequent decrypted images that were encrypted with the same key.

10395-28, Session 6

Performance evaluation of the multiple-image optical compression and encryption (MIOCE) method by increasing target images number

Ayman Alfalou, M. Aldossari, C. Brosseau, ISEN Brest (France)

In our earlier study [Opt. Express 22, 22349-22368 (2014)], we proposed and validated a compression and encryption mothed that simultaneous compress and encrypt closely resembling images. This multiple-image optical compression and encryption (MIOCE) method is based on a special fusion of the different target images spectra together in the spectral domain. To assess the capacity of the MIOCE method, we now evaluate and determine the influence of target images number on the MIOCE method. This analysis allows us to evaluate the performance limitation of this method. To achieve this goal, we use a new criterion based on root-mean-square (RMS) [Opt. Lett. 35, 1914-1916 (2010)] and compression ratio to determine the spectral plane area. Then, these different spectral areas are merged in a single spectrum plane. By choosing specific areas, we can compress together 38 images instead of 26 using the classical MIOCE method. The quality of reconstructed image is evaluated by making use of the mean-square-error criterion (MSE).

10395-29, Session 6

A low-light-level video recursive filtering technology based on the three-dimensional coefficients

Rongguo Fu, Shu Feng, Tianyu Shen, Hao Luo, Yifang Wei, Nanjing Univ. of Science and Technology (China); Qi Yang, Institute of Electric Science of Shanxi Province (China)

Low light level video is an important method of observation under low illumination condition, but the SNR of low light level video is low, the effect of observation is poor, so the noise reduction processing must be carried out. Low light level video noise mainly includes Gauss noise, Poisson noise, impulse noise, fixed pattern noise and dark current noise. In order to remove the noise in low-light-level video effectively, improve the quality of low-light-level video. This paper presents an improved time domain recursive filtering algorithm with three dimensional filtering coefficients.This algorithm makes use of the correlation between the temporal domain of the video sequence. In the video sequences, the proposed algorithm adaptively adjusts the local window filtering coefficients in space and time by motion estimation techniques,for the different pixel points of the same frame of the image, the different weighted coefficients are used.It can reduce the image tail, and ensure the noise reduction effect well. Before the noise reduction,,a pretreatment based on Boxfilter is used to reduce the complexity of the algorithm and improve the speed of the it. In order to enhance the visual effect of low-light-level video, an image enhancement algorithm based on guided image filter is used to enhance the edge of the video details. The results of experiment show that the hybrid algorithm can remove the noise of the low-light-level video effectively, enhance the edge feature and heighten the visual effects of video.

10395-500, Session Plen

Fast automated 3D modeling of building interiors

Avideh Zakhor, Univ. of California, Berkeley (United States)

In this talk, I will present a mapping and visualization platform for 3D modeling and documentation of indoor environments. Unlike existing mobile mapping systems with wheels, our proposed hardware acquisition devices are human wearable and hence must compensate for complex human gait. Furthermore, lack of GPS in indoor environments precludes us from applying existing outdoor mapping techniques indoors. We propose two distinct hardware systems to accomplish this task. The first one is an ambulatory backpack system equipped with a suite of sensors worn by an operator walking at normal speeds in and out of rooms inside a building in a continuous walk through. The second one is a handheld system carried by a human operator as s/he waives it at walls while walking inside the building. Both systems share a common software pipeline that results in 3D point clouds, texture mapped surface reconstructed 3D models, 3D architectural models and floor plans, and web based virtual navigation with tagging, annotation, and dimension measurement capability. We also describe a visual analytic platform that can be used to automatically recognize energy relevant assets such as windows, lights, and computers. The same walkthrough that generates 3D model can also be used to collect building sensor fingerprints which can later be used in a mobile app to locate building occupants, for example by first responders in emergency situations. I will describe some of the challenges in design and implementation of this platform and outline a number of open technical problems.

10395-30, Session 7

Audio classification

Mireya Saraí García Vázquez, Luis Miguel Zamudio Fuentes, Ctr. de Investigación y Desarrollo de Tecnología Digital (Mexico); Alejandro Álvaro Ramírez Acosta, MIRAL R&D&I (United States)

No Abstract Available.

10395-31, Session 7

Adaptive noise filtering of sinusoidal signals with unknown nonlinear phase

Rigoberto Juarez-Salazar, Victor H. Diaz-Ramirez, Ctr. de Investigación y Desarrollo de Tecnología Digital (Mexico)

A self-tuning filter for noise rejection useful for sinusoidal signals is proposed. Unlike the conventional sine fitting methods, no a priori knowledge of the encoded phase distribution is assumed. For this, an analytical model with two parameters (the amplitude of the sinusoid and the standard deviation of the noise) is used. The estimated standard deviation is used for adaptively tuning the noise filter. The results show the feasibility of the proposal for fringe pattern normalization.

10395-32, Session 7

Ultra-high-speed multiframe imaging with all-optical information shutters

Guanghua Chen, China Academy of Engineering Physics (China)

We have developed a multiframe imaging system with both ultra-high temporal resolution and diffraction lim-ited spatial resolution based on all-optical information shutter (AOIS). An AOIS consists of a signal beam and a strobe beam. The signal beam is a train of laser pulses which carry the movie information of the object, and the strobe beam is a single reference laser pulse. Using ultra-short pulse laser and multiple Mach-Zehnder interfer-ometer cavities, a group of AOIS were built and all-optical multiframe imaging was realized. The AOIS is not applied to control the energy transmission of light but to switch the optical information related to the specific process. By the AOIS, the multiframe images can be captured with interval of fs~ns. Moreover, the AOIS will not decrease the image resolution until the diffraction limit is reached. Experimentally, the ultra-fast physical processes such as air breakdown by intense laser radiation and laser ablation of Al foil were observed by the all-optical multiframe imaging system. The results of laser driven air experiments showed “point breakdown” and “serial breakdown” phenomenon induced by laser focusing in the air. In the diagnostics of laser driven Al foil, ultra-fast “jet” with apparent velocity of exceeding 9000 km/s were observed. These results confirmed that this method is effective for the ultra-high temporal and spatial resolution diagnosis of ultra-fast phenomenon.

10395-33, Session 7

Experimental demonstration of OFDM/OQAM transmission with DFT-based channel estimation for visible laser light communication system

Jing He, Jin Shi, Rui Deng, Lin Chen, Hunan Univ. (China)

Recently, visible light communication(VLC) based on light-emitting diodes (LEDs) is considered as a candidate technology for fifth-generation (5G) communications, VLC is free of electromagnetic interference and it can simplify the integration of VLC into heterogeneous wireless networks. Due to the data rates of VLC system limited by the low pumping efficiency, small output power and narrow modulation bandwidth, visible laser light communication(VLLC) system with laser diode(LD) has paid more attention. In addition, orthogonal frequency division multiplexing/offset quadrature amplitude modulation (OFDM/OQAM) is currently attracting attention in optical communications. Due to the non-requirement of CP and time-frequency domain well-localized pulse shapes, it can achieve high spectral efficiency. Moreover, OFDM/OQAM has lower out of-band power leakage so that it increases the system robustness against inter-carrier interference (ICI) and frequency offset.

In this paper, a Discrete Fourier Transform (DFT)-based channel estimation scheme combined with the interference approximation method (IAM) is proposed and experimentally demonstrated for VLLC OFDM/OQAM system. The performance of VLLC OFDM/OQAM system with and without DFT-based channel estimation is investigated. Moreover, the proposed DFT-based channel estimation scheme and the intra-symbol frequency-domain averaging (ISFA)-based method are also compared for the VLLC OFDM/OQAM system. The experimental results show that, the performance of EVM using the DFT-based channel estimation scheme is improved about 3dB compared with the conventional IAM method. In addition, the DFT-based channel estimation scheme can resist the channel noise effectively than that of the ISFA-based method.

10395-34, Session 7

The least-squares algorithm for interferograms with random phase shifts

Zhongsheng Zhai, Hubei Univ. of Technology (China)

Phase-shifting interferometry (PSI) is a useful technique in surface shape measurements with the advantages of non-contact, non-destruction, high accuracy and high resolution. The measurement correctness is relied on the extraction accuracy of initial phase. In traditional PSI, the phase shift between each interferogram is expected to keep constant. However, because of the influence of nonlinear phase shifter, mechanical vibration or air turbulence, there are some unavoidable phase shift errors. Therefore, the accuracy of the initial phase and phase-shifts is important but often difficult to be guaranteed.

In this paper, we propose a general least-squares algorithm to extract the parameters of interferograms: the initial phase, the background intensity and the modulation amplitude. It is a non-iterative algorithm, and it is also suitable for non-uniform phase shifts conditions. We express the phase-shift fringe patterns with the intensity of pixel index. With the rule of LS, we deduced the solution progress by extending the partial derivatives. With a single calculation, the parameter of the initial phase, the background intensity and the modulation amplitude can be extracted, and the solutions for the parameters are analytical. Numerical simulations and optical experiments are given to demonstrate the performance of the presented method, and the results show that the proposed method is rapid, effectively and accurate.The proposed method can accurately and rapidly present the solution of parameters of interferograms. Moreover, it is offer a way to solve the parameters of signal with sine feature in other domain.

10395-51, Session 7

Research on active polarization-based target detection on sea surface

Dongming Lu, Guohua Gu, Lixiang Geng, Jiang Xu, Nanjing Univ. of Science and Technology (China)

Under the sea-sky background, the optical characteristics of vessel target are influenced by many factors, such as atmospheric scattering, water reflecting, and the surface properties of the target, which blocks the objects being observed and discriminated. Since the polarization image contains abundant information of the object, the detecting ability of imaging system would be improved via observing the polarization features of this object. The active polarized imaging method is adopted, in which two beams of light with orthogonal polarization state are used to illuminate the target alternatively. While in the detecting part, two-channel CCD cameras are set in parallel, which are also fitted with orthogonal polarizer to acquire polarized images. Once the polarized data of various angle is collected, objects with different optical properties could be discriminated by the means of retrieval of the material's optical parameters. The PFR (Polarization Fresnel Reflection Coefficient) varies as the incident angle of the active polarized light changes which are demonstrated by the experimental results. Therefore by obtaining the PFR data at various angles could help to distinguish different material, which could enhance the discriminative ability. Since the PFR diversity of metallic material from the water, the proposed method could increase detection probability of vessel target under the sea-sky background.

Conference 10396: Applications of Digital Image Processing XL

Monday - Thursday 7 –10 August 2017

Part of Proceedings of SPIE Vol. 10396 Applications of Digital Image Processing XL

10396-2, Session 1

Joint denoising, demosaicing, and chromatic aberration correction for UHD video

Ljubomir Jovanov, Wilfried Philips, Univ. Gent (Belgium); Klaas Jan Damstra, Frank Ellenbroek, Grass Valley Nederland B.V. (Netherlands)

High-resolution video capture is crucial for numerous applications such as surveillance, security, industrial inspection, medical imaging and digital entertainment. In the last two decades, we are witnessing a dramatic increase of the spatial resolution and the maximal frame rate of video capturing devices.

In order to achieve further resolution increase, numerous challenges will be facing us. Due to the reduced size of the pixel, the amount of light also reduces, leading to the increased noise level. Moreover, the reduced pixel size makes the lens imprecisions more pronounced, which especially applies to chromatic aberrations. Even in the case when high quality lenses are used some chromatic aberration artefacts will remain. Next, noise level additionally increases due to the higher frame rates. To reduce the complexity and the price of the camera, one sensor captures all three colors, by relying on Color Filter Arrays. In order to obtain full resolution color image, missing color components have to be interpolated, i.e. demosaiced, which is more challenging than in the case of lower resolution, due to the increased noise and aberrations.

In this paper, we propose a new method, which jointly performs chromatic aberration correction, denoising and demosaicing. By jointly performing the reduction of all artefacts, we are reducing the overall complexity of the system and the introduction of new artefacts. In order to reduce possible flicker we also perform temporal video enhancement. We evaluate the proposed method on a number of publicly available UHD sequences and on sequences recorded in our studio.

10396-3, Session 1

A hardware architecture for real-time shadow removal in high-contrast video

Pablo Verdugo, Jorge E. Pezoa Nunez, Miguel Figueroa, Univ. de Concepción (Chile)

Broadcasting an outdoor sport event at daytime is a challenging task due to the high contrast present between areas in shadow and light within the same scene. Commercial cameras typically do not handle the high dynamic range of these scenes well, resulting in broadcast streams with very little shadow detail. We propose a hardware architecture for real-time shadow removal in high-resolution video, which reduces the effect mentioned above and improves shadow detail. The algorithm operates only on the shadow portions of each video frame, thus improving the results and producing more realistic images than algorithms that operate on the entire frame, such as simplified Retinex and histogram shifting. The architecture receives an input in the RGB color space, transforms it into the YUV space, and uses color information from both spaces to produce a mask of the shadow areas present in the image. The mask is then filtered using a connected components algorithm to eliminate false positives and negatives. The hardware uses pixel information at the edges of the mask to estimate the illumination ratio between light and shadow in the image, which is then used to correct the shadow area. Our prototype simultaneously processes up to seven video streams of 1920x1080 pixels at 60 frames per second on a Xilinx Kintex-7 XC7K325T FPGA.

10396-4, Session 1

High quality image recovery

Xiteng Liu, QualVisual Technology (Canada)

We introduce a new computing method for extracting essential data elements from data sets or data sources without loss of information. The full data sets may be recovered from the essential elements. Both extraction and recovery can be accomplished in real time. The invertible operations build a new type of equivalence between data sets and their subsets. This equivalence changes traditional concepts and methodologies in mathematics, data science and data processing engineering. The new method makes revolutionary improvement in technical performance than existing methods. It may greatly improve efficiency in data acquisition, compression and visualization, especially in resolution scalable applications. It may be extensively applied to image and video technologies, medical imaging, remote sensing, wireless communication and many other fields. Demo software and testing data are downloadable at http://qualvisual.net.

10396-5, Session 1

Image quality assessment for determining efficacy and limitations of image processing methods

Chris M. Ward, Joshua D. Harguess, Shibin Parameswaran, SPAWAR Systems Ctr. Pacific (United States)

Traditional metrics for evaluating the efficacy of image processing techniques do not lend themselves to understanding the capabilities and limitations of modern image processing methods - particularly those enabled by deep learning. When applying image processing in engineering solutions, a scientist or engineer has a need to justify their design decisions with clear metrics. By applying blind/referenceless image spatial quality (BRISQUE) and Structural SIMilarity (SSIM) index scores to images before and after image processing, we can quantify quality improvements in a meaningful way and determine the lowest recoverable image quality for a given method.

10396-6, Session 1

The role of optical flow in automated quality assessment of full-motion video

Joshua D. Harguess, Scott Shafer, SPAWAR Systems Ctr. Pacific (United States)

In real-world video data, such as that taken of full-motion-video (FMV) from unmanned vehicles, surveillance systems, and other sources, various corruptions to the raw data is inevitable. This can be due to the image acquisition process, noise, distortion, and compression artifacts, among other sources of error. However, we desire methods to analyze the quality of the video to determine whether the underlying content of the corrupted video can be analyzed by humans or machines and to what extent. Previous approaches have shown that motion estimation, or optical flow, can be an important cue in automating this video quality assessment. However, there are many different optical flow algorithms in the literature, each with their own advantages and disadvantages. We examine the effect of the choice of optical flow algorithm (including baseline and state-of-the-art), on motion-based automated video quality assessment algorithms using two standard optical flow databases.

10396-7, Session 2

Prediction of HDR quality by combining perceptually transformed display measurements with machine learning

Anustup Choudhury, Suzanne Farrell, Robin Atkins, Scott J. Daly, Dolby Labs., Inc. (United States)

We present an approach to predict overall HDR display quality as a function of key HDR display parameters. We first performed subjective experiments on a high quality HDR display (Pulsar) that explored five key HDR display parameters: maximum luminance, minimum luminance, color gamut, bit-depth and local contrast (backlight resolution). Subjects rated overall quality for different combinations of these display parameters: maximum luminance from 100 to 4000 nits; color gamut areas of BT. R. 709 and DCI-P3; minimum luminance from 0.005 to 0.1 nits; bit-depths from 7 to 12 bits; and backlight resolution ranging from the Pulsar's full backlight resolution to global dimming.

We explored two models – a physical model solely based on physically measured display characteristics and a perceptual model that transforms physical parameters using human vision system models. For the perceptual model, we use a family of metrics based on a recently published color volume model (ICtCp), which consists of the PQ luminance nonlinearity (ST2084) and LMS-based opponent color, as well as an estimate of the display point spread function.

To predict overall visual quality, we apply linear regression and other machine learning techniques such as SVM and RBF networks. We use RMSE and Pearson/Spearman correlation coefficients to quantify performance. We found that the perceptual model is better at predicting subjective quality than the physical model and that SVM is better at prediction than linear regression. We studied the significance and contribution of each display parameter. In addition, we found that combined parameters such as contrast do not improve prediction. Alternate perceptual models were also evaluated and we found that models based on PQ non-linearity are the best at prediction.

10396-8, Session 2

Low complexity reference frame selection in QTBT structure for JVET future video coding

Sang-hyo Park, Tianyu Dong, Euee S. Jang, Hanyang Univ. (Korea, Republic of)

In this paper, we propose a reference frame search method for JVET future video codec (FVC) that employs the quadtree plus binary tree (QTBT) structure. Among many new technologies proposed in FVC, QTBT poses a significant challenge since it contains the structural change of coding tree unit from HEVC. To reduce the encoding complexity of FVC with QTBT structure, we investigated some redundancy in motion estimation process—particularly, the reference frame search. In this paper, we present a method that effectively restricts the reference frame search range of general motion estimation as well as of affine motion estimation, exploiting the dependence within QTBT structure. The proposed method minimizes the maximum of the reference frame search ranges per each coding unit (CU) based on the prediction information of parents node. To be specific, the prediction direction and the index of reference frame of parent node were used. In addition, the proposed method utilizes the information of binary tree depth and of temporal layer to prevent undesired coding loss. The experimental results showed that the proposed method decreased the encoding time of motion estimation by 34% on average in comparison with joint exploration test model (JEM) 3.0, maintaining a reasonable coding efficiency (less than a 0.3% BD-rate loss).

10396-9, Session 2

Performance analysis of the AV1 video codec on 360 video coding

Adeel Abbas, Sandeep Doshi, GoPro, Inc. (United States); Pankaj Topiwala, Wei Dai, Madhu Krishnan, FastVDO Inc. (United States)

In this paper, we present performance evaluation of the AV1 codec from Alliance for Open Media (AOM) for virtual reality (VR) content. AV1 is a new codec which promises to offer compression efficiency beyond HEVC and VP9, with the benefit of being open and royalty free. From our experiments, AV1 achieves average bitrate savings of about X% compared to HEVC reference software HM.

10396-10, Session 2

Viewport analysis for omnidirectional videos

Adeel Abbas, Sandeep Doshi, GoPro, Inc. (United States); Pankaj Topiwala, Wei Dai, Madhu Krishnan, FastVDO Inc. (United States)

In this paper, we analyze viewport size considerations for Omnidirectional videos. As viewport size increases, rectilinear projection suffers from notable distortions along the edges of viewport. We attempt to classify and propose ways to correct some of these distortions. We present some results from subjective quality analysis to demonstrate effectiveness of the proposed scheme.

10396-11, Session 3

Verification testing of the HEVC screen content coding extensions

Gary J. Sullivan, Microsoft Corp. (United States); Vittorio A. Baroncini, GBTech (Italy); Rajan L. Joshi, Qualcomm Inc. (United States); Shan Liu, MediaTek USA Inc. (United States); Jizheng Xu, Microsoft Research Asia (China); Haoping Yu, Huawei Technologies Co., Ltd. (United States); Xiaoyu Xiu, InterDigital Communications, Inc. (United States)

This paper presents a verification test of the compression capability of the recently developed Screen Content Coding (SCC) extensions of the High Efficiency Video Coding (HEVC) standard. Formal subjective testing was conducted, and the results verify a major benefit in compression capability for the SCC extensions.

10396-12, Session 3

JPEG XS-based frame buffer compression inside HEVC for power-aware video compression

Alexandre Willème, Antonin Descampe, Univ. Catholique de Louvain (Belgium); Gaël Rouvroy, Pascal Pellegrin, intoPIX s.a. (Belgium); Benoît M. Macq, Univ. Catholique de Louvain (Belgium)

With the emergence of Ultra-High Definition video, reference frame buffers (FBs) inside HEVC-like encoders and decoders have to sustain huge bandwidth. The power consumed by these external memory accesses accounts for a significant share of the codec's total consumption. This paper

describes a solution to significantly decrease the FB's bandwidth, making HEVC encoder more suitable for use in power-aware applications. The proposed prototype consists in integrating an embedded lightweight, low-latency and visually lossless codec at the FB interface inside HEVC in order to store each reference frame as several compressed bitstreams. As opposed to previous works, our solution compresses large picture areas (ranging from a CTU to a frame stripe) independently in order to better exploit the spatial redundancy found in the reference frame. This work investigates two data reuse schemes namely Level-C and Level-D. Our approach is made possible thanks to simplified motion estimation mechanisms further reducing the FB's bandwidth and inducing very low quality degradation. In this work, we integrated JPEG XS, the upcoming standard for lightweight low-latency video compression, inside HEVC. In practice, the proposed implementation is based on HM 16.8 and on XSM 1.0 (JPEG XS Test Model). Through this paper, the architecture of our HEVC with JPEG XS-based frame buffer compression is described. Then its performance is compared to HM encoder. Compared to previous works, our prototype provides significant external memory bandwidth reduction. Depending on the reuse scheme, one can expect bandwidth and FB size reduction ranging from 50% to 83.3% without significant quality degradation.

10396-13, Session 3

Comparison and enhancements of JVET, AV1, and HEVC codecs

Pankaj Topiwala, Wei Dai, FastVDO Inc. (United States)

A brief comparative analysis of recent modern codecs is provided, covering HEVC, AV1, and JVET. Summary results for performance analysis are included. We also explore enhancements of current codecs, especially AV1. Our enhancements are in the areas of high performance image coding, coding of HDR content, and for 360 degree video.

10396-14, Session 3

Advanced single-stream HDR coding with SDR backward compatibility

Pankaj Topiwala, FastVDO Inc. (United States)

High dynamic range and wide color gamut (HDR/WCG, or briefly HDR) video is the current pinnacle of video transmission formats, and is already in use in streaming services such as Amazon and Netflix. Several formats for transmitting HDR content are currently in the market, including a standard called HDR10 (or PQ10), as well as proprietary technology called Dolby Vision. Neither of these formats offer what we called backward compatibility... the ability to render an SDR video straight from the bitstream, as well as to recreate an HDR by using embedded metadata. This paper presents an advanced approach that offers backward compatibility to SDR, yet has performance advantages over the current HDR10 approach.

10396-15, Session 3

Novel inter and intra prediction tools under consideration for the emerging AV1 video codec

Urvang B. Joshi, Debargha Mukherjee, Jingning Han, Yue Chen, Sarah Parker, Hui Su, Angie Chiang, Yaowu Xu, Google (United States); Zoe Liu, Google (United States); Yunqing Wang, Jim Bankoski, Google (United States)

Google has been developing new coding tools starting from VP9 as the baseline since early 2015, with a target to release a next generation codec by the end of 2017. Initially the plan was to release a successor codec to VP9, called VP10, but subsequently with the launch of the consortium called Alliance for Open Media, the efforts on VP10 merged into AV1 - the formal name of the first codec from the consortium.

As part of this effort, several new coding tools have been developed and already integrated into the Av1 codebase. In this paper we provide an overview of the new tools that aid prediction of pixel blocks. Specifically, we will describe the following: new block partition structures; a tool for ranking candidate motion vectors for available references; expanded intra prediction tools - including recursive filter intra prediction, extended directional prediction as well as new intra prediction modes; overlapped block motion compensation modes - including causal and non-causal; compound prediction modes - including wedge and smooth predictors - that combine two inter predictors as well as one inter and one intra predictor; expanded interpolation filter sets for inter prediction; warped motion modes including global and locally adaptive ones.

Results are presented on standard test sets to show up to 15% BDRATE reduction.

10396-16, Session 3

Novel intra prediction modes for AV1 codec

Ariel Shleifer, Ofer Hadar, Ben-Gurion Univ. of the Negev (Israel)

As the demand for high quality video data has been permanently increasing, the need and scope for compression has also been increasing due to increased spatial correlation of pixels within a high quality video frame. One basic feature that utilizes the spatial correlation of pixels for video compression is Intra prediction, which determines the compression efficiency of codec. Intra prediction enables significant reduction of the Intra frame (I frame) size and, therefore, contributes to efficient exploitation of bandwidth. In a recent work presenting video codec comparisonit was shown that the coding efficiency of VP9 is inferior to that of H.265/MPEG-HEVC. One possible reason for this result is that the HEVC's Intra prediction algorithm uses as many as 35 directions for prediction, while VP9 uses only 9 directions including the TM prediction mode. Therefore, there is high motivation to improve the Intra prediction scheme with new, original and proprietary algorithms that will enhance the total performance of the Google future codec and reduce the gap between its performance and that of HEVC. In this work, instead of using different angles for predictions, we introduce four unconventional intra-prediction modes for the AV1 codec and a new intra prediction concept called Intra prediction standard routes (IPSR).

Furthermore, we implement a new scanning method for inter/intra prediction in order to maximize the correlation and to reduce the sent data.

The following modes were developed and tested in the AV1 new platform:

Weighted CALIC (WCALIC), Intra-Prediction using System of Linear Equations (ISLE), Prediction of Discrete Cosine Transformations (PrDCT) Coefficients and Reverse Least Power of Three (RLPT).

10396-17, Session 3

Display of high dynamic range images under varying viewing conditions

Tim Borer, British Broadcasting Corp. (United Kingdom)

Recent demonstrations of high dynamic range (HDR) television have demonstrated that superb images are possible. With the emergence of an HDR television production standard (ITU Recommendation BT.2100) last year, HDR television production is poised to take off. Some programmes have already been made in HDR. However research to date has focused on image display only under "dark" viewing conditions. HDR television will need to be displayed at varying brightness and under varying illumination (for example to view sport in daytime or on mobile devices). We know, from common practice with conventional TV, that the rendering intent (gamma) should change under brighter conditions, although this is poorly quantified. For HDR the need to render images under varying conditions is all the more acute.

This paper seeks to explore the issues surrounding image display under

varying conditions. It presents results of the relationship between viewing conditions and the visibility of quantisation ("banding" artefacts). It also describes how visual adaptation is affected by display brightness, screen size and viewing distance, and surround illumination. Existing experimental results are presented and extended to try to quantify these effects. Using these results it is shown how HDR images may be displayed so that they are perceptually equivalent under different viewing conditions. In this way the consistency of HDR image reproduction should be improved, thereby better maintaining "creative intent" in television.

10396-18, Session 3

Spherical rotation orientation indication for HEVC and JEM coding of 360 degree video

Jill M. Boyce, Qian Xu, Intel Corp. (United States)

Omnidirectional (or "360 degree") video, representing a panoramic view of a spherical 360º x 180º scene, can be encoded using conventional video compression standards, once it has been projection mapped to a 2D rectangular format. When viewed with virtual reality devices such as head mounted displays, 360 degree video can provide an immersive experience, where users can dynamically change their viewport of the omnidirectional video. Because a much larger region of video is coded than is viewed, high resolution is required, leading to a large bitrate. Efficient compression of 360 degree video is thus highly desirable to facilitate storage and transmission.

Equirectangular projection is the most common format currently used for mapping 360 degree video to a rectangular representation using the HEVC standard, or the JEM under development by the JVET. However, video in the top and bottom regions of the image, corresponding to the "north pole" and "south pole" of the spherical representation, is significantly warped. Conventional HEVC codecs do not efficiently encode these regions. In this paper and in JCTVC-Z0025/JVET-E0075, we propose to perform spherical rotation of the input video prior to HEVC/JEM encoding in order to improve the coding efficiency, and to signal in an SEI message parameters that describe the inverse rotation process recommended to be applied following HEVC/JEM decoding, prior to display.

An encoder algorithm is presented that automatically determines pan, tilt, and roll spherical rotation parameters that can improve coding efficiency for some video sequences. For the Chairlift sequence, after a rotation of (0, 12, 79) degrees has been applied, 17.8% bitrate gain (using the WS-PSNR end-to-end metric) using HM16.14 and 12.3% gain using JEM 4.1, and an average gain of 2.9% for HM16.14 and 2.3% for JEM 4.1 for the full test set using the common test conditions described in JVET-D1030.

An SEI message has been adopted for a future edition of HEVC, as described in JCTVC-Z0051, to indicate the presence of equirectangular projection format omnidirectional video. Portions of our JCTVC-Z0025 contribution were incorporated into this SEI message, to accomplish the proposed spherical rotation operation.

10396-19, Session 3

Complexity and performance tradeoff for next generation video coding standard development

Elena A. Alshina, SAMSUNG Electro-Mechanics (Korea, Republic of)

New international standards for video coding come roughly once in 10 years. Typical requirement for the new standard is twice better compression efficiency compared to the predecessor. Unfortunately, each new video codec also increase implementation cost and power consumption a lot. This paper present analysis of performance and complexity for several key tools in HEVC standard and tools included into Joint Exploration Model which is used for potential of future video coding standard study. Suggestions and recommendation form industry on future video codec standardization are discussed.

10396-20, Session 3

Optimal design of encoding profiles for ABR streaming

Yuriy A. Reznik, Karl O. Lillevold, Abhijith Jagannath, Justin Greer, Manish Rao, Brightcove, Inc. (United States)

We discuss a problem of optimal design of encoding profiles for adaptive bitrate (ABR) streaming applications.

We show, that under certain conditions and optimization targets, this problem becomes equivalent to the problem of quantization of random variable, which in this case is bandwidth of a communication channel between streaming server and the client. But using such reduction to a known information-theoretic problem, we immediately arrive at class of algorithms for solving this problem optimally. We illustrate effectiveness of our approach by examples of optimal encoding ladders designed for different networks and reproduction devices.

Specific techniques and models utilized in this paper include:

- modeling of SSIM-rate functions for modern video codecs (H.264, HEVC) and different content

- adaptation of SSIM (by using scaling & CSF-filteing) to account for different resolutions and reproduction settins

- SSIM - MOS scale mapping

- CDF models of typical communication networks (wireless, cable, WiFi, etc)

- algorithms for solving quantization problem (Lloyd-Max algorithms, analytic solutions, etc)

10396-120, Session 3

Performance comparison of AV1, JEM, VP9, and HEVC encoders

Dan Grois, Tung Nguyen, Detlev Marpe, Fraunhofer-Institut für Nachrichtentechnik Heinrich-Hertz-Institut (Germany)

This work presents a performance evaluation of the current status of two distinct lines of development in future video coding technology: the so-called AV1 video codec of the industry-driven Alliance for Open Media (AOM) and the Joint Exploration Test Model (JEM), as developed and studied by the Joint Video Exploration Team (JVET) on Future Video Coding of ITU-T VCEG and ISO/IEC MPEG. As a reference, our study also includes reference encoders of the respective starting points of development, as given by the first encoder release of AV1/VP9 for the AOM-driven technology, and the HM reference encoder of the HEVC standard for the JVET activities. For a large variety of video sources ranging from UHD over HD to 360° video content, the compression capability of the different video coding technology has been evaluated by using a Random Access scenario along with the JVET common test conditions. As an outcome of our study, it was observed that the latest AV1 release achieved average bit-rate savings of around 12% relative to VP9 at the expense of a factor of 46 in encoder run-time. On the other hand, the latest JEM release provides an average bit-rate saving of around 28% relative to HM with a factor of approximately 10 in encoder run-time. When directly comparing AV1 and JEM for static quantization parameter settings, AV1 produces an average bit-rate overhead of more than 95% relative to JEM at the same objective reconstruction quality and a factor of approximately 1.5 in encoder run-time. Even when operated in a two-pass rate control mode, AV1 shows a significantly inferior compression performance relative to that of the one-pass JEM encoder for a static quantization configuration.

10396-63, Session PMon

Dynamic frame resizing with convolutional neural network in video codec

Jaehwan Kim, Youngo Park, Kwang Pyo Choi, Jong-Seok Lee, Sunyoung Jeon, Jeong-Hoon Park, SAMSUNG

Electronics Co., Ltd. (Korea, Republic of)

In the past, video codecs such as vc-1 and H.263 used a technique to encode reduced-resolution video and restore original resolution from the decoder for improvement of coding efficiency. The techniques of vc-1 and H.263 Annex Q are called dynamic frame resizing and reduced-resolution update mode, respectively. However, these techniques have not been widely used due to limited performance improvements that operate well only under specific conditions. In this paper, video frame resizing (reduced/restore) technique based on machine learning is proposed for improvement of coding efficiency. The proposed method does not show limited performance improvements in specific conditions like the existing techniques, but shows improved subjective performance over all the high resolution videos which are dominantly consumed recently. In order to assess subjective quality of the proposed method, Video Multi-method Assessment Fusion (VMAF) which showed high reliability among many subjective measurement tools was used as subjective metric. Moreover, to assess general performance, diverse bitrates are tested. Experimental results showed that BD-rate based on VMAF was improved by about 30% compare to conventional HEVC. Especially, VMAF values were significantly improved in low bitrate. Also, when the method is subjectively tested, it had better subjective visual quality in similar bit rate.

10396-64, Session PMon

Variable block Harris-based-features image watermarking

Issam J. Dagher, Univ. of Balamand (Lebanon)

Feature-based image watermarking schemes have gained important attention. Existing schemes have shown robustness against noise and geometrical attacks.

This paper proposes an improved feature-based watermarking algorithm. Robust feature points are detected using the Harris Detector. In the embedding stage, sequences are placed into regions located around feature points. The sequences used are PN, Gold and decimal. In the extraction process, image features are re-allocated using the same detector. Each feature point is used as a center of an N x N region. This region is moved horizontally and vertically within its neighboring pixels. Each move should be registered in a matrix as a correlation value of this region with the initial sequence. This procedure is repeated for all feature points till we find all the watermarked regions. The maximum correlation obtained will determine the center of the watermarked region. The proposed algorithm is compared to other feature-based watermarking schemes. Different variety of tests showed that this algorithm is more robust against noise and geometric attacks for grayscale images.

10396-65, Session PMon

A multi-scale segmentation algorithm for high resolution remote sensing images

Tingting Zhou, Lingjia Gu, Ruizhi Ren, Jilin Univ. (China)

In recent decades, with the rapid development of remote sensing technology, high resolution remote sensing images have been widely used in various fields due to their characteristics, such as rich spectral information and complex texture information. As a key step in the feature extraction, multi-scale image segmentation algorithm has been a hotspot currently. Traditional statistical region merging methods only consider spectral similarities but ignore the phenomenon that the same spectrums may represent different objects. Pixels' similarities rather than regions' are taken into account for traditional merging methods. That might lead to an over-merging problem for the regions with high regional and low pixel differences located in the fuzzy boundary. A multi-scale segmentation algorithm based on dynamic statistical region merging with texture information (DSRMT) for high resolution remote sensing images is proposed in this paper. In this algorithm, the segmental scale is controlled by an adjustable parameter Q. Meanwhile, the similarity function is redefined to guarantee that the most similar regions are merged each time. In addition, the texture information is introduced with the increasing of merging region area. Therefore, the algorithm is adjusted to apply for multi-band images easily. The experimental results demonstrated that the multi-scale segmentation algorithm based on DSRMT is more efficient and accurate for image segmentation of high resolution remote sensing.

10396-66, Session PMon

Automated extraction of complex shape buildings from high resolution imagery

Qiong Cao, Lingjia Gu, Ruizhi Ren, Tingting Zhou, Jilin Univ. (China)

Building extraction from the remote sensing imagery is one of the major application fields of remote sensing techniques since 1970s. In particular, high resolution satellites have practical significance in exploiting automatic, intelligent, accurate building extraction methods. Most methods are appropriate for rectangular building with regular shape, which cannot extract irregular building structures including arc lines. To address these problems, an extraction method for complex shape building is proposed in this paper. Considering that the high-resolution imagery can provide extensive information, including spectral and spatial information, building properties are analyzed. Subsequently, the decision tree for building information extraction is constructed by the analysis results. Finally, other features, such as Soil Adjusted Vegetation Index ?SAVI?, Normalized Difference Water Index (NDWI), texture analysis and morphological filtering are used to reduce interference from false information. The advantage of the proposed method is that it is applied to non-rectangular building extraction, not just the rectangular building.

In order to validate the proposed method, a comparative study is performed between the supervised method by the support vector machine (SVM) classification and the proposed method. The results demonstrate that the proposed method can achieve satisfactory correctness rates for complex shape buildings, and give better results than the supervised method.

10396-67, Session PMon

Blind image quality evaluation using the conditional histogram patterns of divisive normalization transform coefficients

Ying Chu, Shenzhen Univ. (China); Xuanqin Mou, Xi'an Jiaotong Univ. (China); Hengyong Yu, Univ. of Massachusetts Lowell (United States)

The performance of traditional machine learning based blind image quality assessment (BIQA) methods is sensitive to the contents of training samples, and it is easily influenced by the learning strategies. In this project, a novel blind image quality evaluation frame is presented to overcome the aforementioned drawbacks. Without complicated training and learning processes, the proposed method utilizes a clustering method to generate image quality code book. The idea comes from a property that image quality could be reflected by the degree of statistical independence among neighboring divisive normalization transform (DNT) coefficients. Specifically, it is observed that the patterns of combined conditional histograms among spatially adjacent DNT coefficients in degraded images could be used to represent image quality. Therefore, a high dimensional feature vector is constructed by using the conditional histogram patterns, and the code book is clustered and generated by combining the extracted feature vectors from sample database and the corresponding subjective score levels. Then, the distances between the image feature vectors and the code words are calculated and interpolated to construct the objective image quality score. Experiments are performed based on up to date databases (e.g. LIVE, CSIQ, TID2013 and CID 2013). The results show that the proposed metric outperforms the current no training BIQA methods for most cases. In cross database experiments, the proposed method is comparable to those metrics based on support vector machine. This implies that it is feasible and effective to evaluate image quality blindly by constructing code book through clustering image pattern of conditional histograms among adjacent DNT coefficients.

10396-68, Session PMon

An effective road extraction algorithm from high resolution remote sensing images

Yushan Zhang, Tingfa Xu, Beijing Institute of Technology (China); Tingting Zhou, Jilin Univ. (China)

Satellite remote sensing technology has become one of the most effective methods for land surface monitoring in recent years, due to its advantages such as short period, large scale and rich information. Meanwhile, road extraction is an important field in the applications of high resolution remote sensing images. An intelligent and automatic road extraction algorithm with high precision has great significance for transportation, road network updating and urban planning.The fuzzy c-means (FCM) clustering segmentation algorithms have been used in road extraction, but the traditional algorithms did not consider spatial information. An improved fuzzy C-means clustering algorithm combined with spatial information is proposed in this paper, which is proved to be effective for noisy image segmentation. Firstly, the image is segmented using the improved FCM algorithm. Based on the segmentation result, the center lines of the roads are extracted by the ridgeline tracking algorithm and then connected by the tensor voting algorithm. By using the characteristics of both sides of the road, the roads are reconstructed by shifting the center lines at final. The experimental results demonstrated that the improved fuzzy C-means clustering algorithm is more accurate for road extraction from high resolution remote sensing images. The problem of centerline fracture in the process of road extraction is effectively solved using the tensor voting algorithm. Meanwhile, the loss of the integrity of the road caused by obstacles is greatly compensated through the road reconstruction result using the centerline characteristic.

10396-69, Session PMon

Investigation of methods for construct a system of optical sensors for measure relative orientation of industrial robots for monitoring of the technosphere objects

Andrey V. Petrochenko, Igor A. Konyakhin, ITMO Univ. (Russian Federation)

Purpose: Developing of the methods of relative orientation of industrial robots and construction of three-dimensional scenes areas of interest using optical sensors. Results: Developed the method of construction of the relative orientation of industrial robots to meet the challenges of reconstruction of three-dimensional mapping and image-set received from the optical sensors. The basis of this technique is the problem of finding the solution of the global position of each industrial robot on the relative orientation of each of them. The global position of the industrial robot characterized by a matrix of rotation and transfer vector in a coordinate system (adopted as a global). As a result of the global positioning possible to solve the major problems of vision such as detection, tracking and classification of objects of the space in which these systems and robots operate. Practical significance: Continuous qualitative monitoring of technosphere objects.

10396-70, Session PMon

Siamese convolutional networks for tracking the lumbar spine

Yuan Liu, Nanjing Univ. of Science and Technology (China)

Deep learning models have demonstrated great success in various computer vision tasks such as image classification and object tracking. However, tracking the lumbar spine by digitalized video fluoroscopic imaging (DVFI), which can quantitatively analyze the motion mode of spine to diagnose lumbar instability, has not yet been widely applied in clinic due to the lack of steady and robust tracking method. In this paper, we propose a novel visual tracking algorithm of the lumbar vertebra motion based on a siamese convolutional neural network(CNN) model. We train a full-convolutional neural network offline to learn generic image features. The siamese network is trained to learn a similarity function that compares the labeled target in the first frame with the candidate patches in the current frame. And the similarity function returns a high score if the two images depict the same object. Once learned, the similarity function is used to track a previously unseen object without any adapting online. In the current frame, our tracker is performed by evaluating the candidate rotated patches sampled around the previous frame target position and presents a rotated bounding box to locate the predicted target precisely. Experiments indicate that the proposed tracking method can detect the lumbar vertebra steadily and robustly. Especially for images with low contrast and background clutter, the presented tracker can still achieve good tracking performance. Further, the proposed algorithm operates at real-time speed and achieves state-of-the-art performance in the online tracking benchmark (OTB) data set.

10396-71, Session PMon

Research on node extraction based on line feature

Xiaofeng Li, Sheng Chen, Weimin Li, Yuhai Zhang, Univ. of Science and Technology of China (China)

This paper is based on the FAST observatory fund project, whose panel surface is required to detect. The panel image is obtained by the camera and the panel nodes are extracted by the digital image processing method, finally ,the three-dimensional coordinates of the nodes are reconstructed to obtain the surface shape of the panel. The extraction of the relevant data information in the image, such as the intersection of two straight lines, which is a very important part in the machine vision learning, directly affects the quality of the experimental data. Based on the analysis of a large number of corner detection methods, the following detection method is proposed: first of all, the image down sampling and binaryzation are operated through the basic methods of digital image processing; secondly, Canny operator is used to detect the image to extract the best edge data; then, according to the corresponding threshold, the straight line data in the image is obtained by the cumulative version of the Hough transform, and duplicate removal and merging operations are carried out on the extracted straight lines to obtain optimized lines. Then on the basis of the relevant mathematical equations, the intersection of the lines optimized are solved; merging the near intersections according to the relevant threshold, the original matching results are obtained. Finally, through the experimental verification, the operation on the specified ROI region can achieve better experimental results, and achieve the optimal extraction of points.

10396-72, Session PMon

An efficient algorithm for coplanar feature points matching in binocular vision photogrammetry

Weimin Li, Siyu Shan, Yuhai Zhang, Gang Liu, Sheng Chen, Univ. of Science and Technology of China (China); Xiaofeng Li, Univ of Science and Technology of China (China)

Feature points matching, an important branch of machine vision, are frequently used in three-dimensional reconstruction, photogrammetry, camera calibration, object recognition and so on. In the system of binocular stereo vision, the prerequisite for three-dimensional reconstruction is the proper treatment of the feature point matching of images in the left and right cameras. Correct feature point matching functions as the groundwork to get accurate three-dimensional metric information. To solve the problem that feature points matching in the binocular vision measurement of plane workpiece, an efficient matching algorithm for coplanar feature points is presented in this paper. Firstly, the method utilize the existing algorithm

used for detection and recognition to obtain the high-precision center coordinates of the circular target. Then the proposed algorithm make use of the epipolar geometry to calculate the correlation values between the points in the left and right camera images. Next, sort these values and their corresponding points could obtain the initial matching sets. Finally, according to the above ordered sets, the presented method do correct the mismatching relationship of the initial matching sets to achieve the best matching which based on the reprojection errors of points and the plane constraint. Experimental results show that the mismatch can be eliminated effectively by the method, and the proposed algorithm is efficient, robust and high enough in accuracy. Compared with existing calibration methods, the proposed method is effective and simple to solve the above-mentioned problem.

10396-73, Session PMon

Real-time heartrate measurement for multi-people using compressive tracking

Ling Liu, Yuejin Zhao, Ming Liu, Lingqin Kong, Liquan Dong, Feilong Ma, Zhi Cai, Zongguang Pang, Yachu Zhang, Peng Hua, Ruifeng Yuan, Beijing Institute of Technology (China)

The rise of aging population has created a demand for inexpensive, unobtrusive, automated healthcare solutions. Image PhotoPlethysmoGraphy(IPPG) aids in the development of these solutions by allowing for the extraction of physiological signals from video data. However, the main deficiencies of the recent IPPG methods are non-automated, non-real-time and susceptible to motion artifacts(MA).To date, few works have studied this problem. In this paper, a real-time heart rate(HR) detection method for multiple subjects simultaneously is proposed, which consists of getting multiple subjects' facial video automatically through a Webcam, detecting the region of interest (ROI) in the video and reducing the false detection rate by our improved Adaboost algorithm, reducing the MA by our improved compress tracking algorithm, signal preprocessing for denoising and multi-threads for higher detection speed. For comparison, HR was measured simultaneously using an medical pulse oximetry device for every subject during all sessions. Experimental results on a data set of 30 subjects show that the max average absolute error of heart rate estimation is less than 8 beats per minute (BPM), and processing speed of every frame has almost reached real-time:the experiments with video recordings of ten subjects under the condition of the pixel resolution of 600? 800 pixels show that the average HR detection time of 10 subjects was about 17 frames per second (fps).

10396-74, Session PMon

Vision-based mobile robot navigation through deep convolutional neural networks and end-to-end learning

Yachu Zhang, Yuejin Zhao, Ming Liu, Liquan Dong, Mei Hui, Lingqin Kong, Xiaohua Liu, Beijing Institute of Technology (China)

In contrast to humans, who use only visual information for navigation, many mobile robots use laser scanners and ultrasonic sensors along with vision cameras to navigate. This work proposes a vision-based robot control algorithm based on deep convolutional neural networks. We create a large 15-layer convolutional neural network learning system and achieve the advanced recognition performance. Our system is trained from end to end to map raw input images to direction in supervised mode. The images of data sets are collected in a wide variety of weather conditions and lighting conditions. Besides, the data sets are augmented by adding Gaussian noise and Salt-and-pepper noise to avoid over-fitting. The algorithm is verified by two experiments, which are line tracking and obstacle avoidance. The line tracking experiment is proceeded in order to track the desired path which is composed of straight and curved lines. The goal of obstacle avoidance experiment is to avoid the obstacles indoor. Finally, we get 3.29% error rate on the training set and 5.1% error rate on the test set in the line tracking experiment, 1.8% error rate on the training set and less than 5% error rate on the test set in the obstacle avoidance experiment. During the actual test, the robot can follow the runway centerline outdoor and avoid the obstacle in the room accurately. The result confirm the effectiveness of the algorithm and our improvement in the network structure and train parameters.

10396-75, Session PMon

A locally adaptive algorithm for shadow correction in color images

Victor Karnaukhov, Vitaly Kober, Institute for Information Transmission Problems (Russian Federation)

Correction of color images distorted by nonuniform illumination usually uses the following degradation model: a part of the scene close to a directed light source is illuminated much brighter than the rest of the scene. A serious problem often arises in the case of nonuniform illumination of 3D objects of the scene; that is, extended heavily shadowed regions with a small area of transition from light to shadow are appeared in captured images. In this presentation, a locally-adaptive algorithm for correction of shadow regions in color images is proposed. The algorithm consists of segmentation of shadow areas with rank-order statistics followed by correction of nonuniform illumination with human visual perception approach. The performance of the proposed algorithm is compared to that of common algorithms for correction of color images distorted by nonuniform illumination and contained shadow regions.

10396-76, Session PMon

Tracking of multiple objects with time-adjustable composite correlation filters

Alexey Ruchay, Chelyabinsk State Univ. (Russian Federation); Vitaly Kober, Ctr. de Investigación Científica y de Educación Superior de Ensenada B.C. (Mexico); Ilya Chernoskulov, Chelyabinsk State Univ. (Russian Federation)

An algorithm for tracking of multiple objects in video based on time-adjustable adaptive composite correlation filtering is proposed. The object is selected at the beginning of the algorithm. For each frame a bank of composite correlation filters are designed in such a manner to provide invariance to pose, occlusion, clutter, and illumination changes. The filters are synthesized with the help of an iterative algorithm, which optimizes discrimination capability for each object. The filter is adapted to the objects changes online using information of current and past scene frames. Results obtained with the proposed algorithm using real-life scenes, are presented and compared with those obtained with state-of-the-art tracking methods in terms of detection efficiency, tracking accuracy, and speed of processing.

10396-77, Session PMon

Fast perceptual image hash based on cascade algorithm

Alexey Ruchay, Chelyabinsk State Univ. (Russian Federation); Vitaly Kober, Ctr. de Investigación Científica y de Educación Superior de Ensenada B.C. (Mexico); Evgeniya Evtushenko, Chelyabinsk State Univ. (Russian Federation)

In this presentation, we propose a perceptual image hash algorithm, which can be applied in image authentication, retrieval, and indexing. Image perceptual hash uses for image retrieval in sense of human perception against distortions caused by compression, noise, common signal processing and geometrical modifications. The main disadvantage of perceptual hash

is high time expenses. In the proposed cascade algorithm of image retrieval initializes with short hashes, and then a full hash is applied to the processed results. Computer simulation results show that the proposed hash algorithm yields a good performance in terms of robustness, discriminability, and time expenses.

10396-78, Session PMon

Removal of impulse noise clusters from color images with local order statistics

Alexey Ruchay, Chelyabinsk State Univ. (Russian Federation); Vitaly Kober, Ctr. de Investigación Científica y de Educación Superior de Ensenada B.C. (Mexico)

This paper proposes a novel algorithm for restoring images corrupted with clusters of impulse noise. The noise clusters often occur when the probability of impulse noise is very high. The proposed noise removal algorithm consists of detection of bulky impulse noise in three color channels with local order statistics followed by removal of the detected clusters by means of vector median filtering. With the help of computer simulation we show that the proposed algorithm is able to effectively remove clustered impulse noise. The performance of the proposed algorithm is compared in terms of image restoration metrics with that of common successful algorithms.

10396-79, Session PMon

Impulsive noise removal from color video with morphological filtering

Alexey Ruchay, Chelyabinsk State Univ. (Russian Federation); Vitaly Kober, Ctr. de Investigación Científica y de Educación Superior de Ensenada B.C. (Mexico)

This paper deals with impulse noise removal from color video. The proposed noise removal algorithm employs a switching filtering for denoising of color video; that is, detection of corrupted pixels by means of a novel morphological filtering followed by removal of the detected pixels on the base of estimation of uncorrupted pixels in the previous scenes. With the help of computer simulation we show that the proposed algorithm is able to well remove impulse noise in color video. The performance of the proposed algorithm is compared in terms of image restoration metrics with that of common successful algorithms.

10396-80, Session PMon

Application of white-light phase-shifting interferometry in white-light scanning interferometry

Yujing Wu, Yunsheng Qian, Nanjing Univ. of Science and Technology (China)

White–light scanning interferometry (WLSI) is an important technique, which has the advantages of high precision and noncontact testing, to measure surface profile when a test object contains discontinuous structures or microstructures. A series of algorithms is used to detect the peak position of a coherence envelope, which can estimate the profile. Phase-shifting interferometry (PSI) has a high precision. However, PSI suffers from phase-ambiguity problems, which limit the height difference between two adjacent data points to ?/4, where ? is the wavelength of the light. On the other hand, the coherence envelope techniques have a large dynamic range but are less precise. So a method that combines phase-shifting and coherence-peak-sensing techniques will provide the advantages of both, i.e., high precision and a large dynamic range. In this paper, an overlapping averaging four-bucket algorithm, which can eliminate phase shift errors caused by PZT in a large extent, is proposed to determine both the best-focus frame position and the fractional phase from the best-focus frame of the correlogram obtained from vertical scanning. Then a wavefront unwrapping algorithm is utilized to remove 2? phase ambiguities. Simulation and experimental results are presented to demonstrate the validity fo the proposed method.

10396-81, Session PMon

Edge detection for optical synthetic aperture based on deep neural network

Wenjie Tan, Mei Hui, Ming Liu, Lingqin Kong, Liquan Dong, Yuejin Zhao, Beijing Institute of Technology (China) and Beijing Key Lab. of Precision Photoelectric Measuring Instrument and Technology (China)

Synthetic aperture optics systems can meet the demands of the next-generation space telescopes being lighter, larger and foldable. However, the boundaries of segmented aperture systems are much more complex than that of the whole aperture. More edge regions mean more imaging edge pixels, which are often mixed and discretized. In order to achieve high-resolution imaging, it is necessary to identify the gaps between the sub-apertures and the edges of the projected fringes. In this work, we introduced the algorithm of Deep Neural Network into the edge detection of optical synthetic aperture imaging. According to the detection needs, we constructed image sets by experiments and simulations. Based on MatConvNet, a toolbox of MATLAB, we ran the neural network, trained it on training image set and tested its performance on validation set. The training was stopped when the test error on validation set stopped declining. As an input image is given, each intra-neighbor area around the pixel is taken into the network, and scanned pixel by pixel with the trained multi-hidden layers. The network outputs make a judgment on whether the center of the input block is on edge of fringes. We experimented with various pre-processing and post-processing techniques to reveal their influence on edge detection performance. Compared with the traditional algorithms or their improvements, our method makes decision on a much larger intra-neighbor, and is more global and comprehensive. Experiments on more than 2,000 images are also given to prove that our method outperforms classical algorithms in optical images-based edge detection.

10396-82, Session PMon

Accurate generation of the 3D map of environment with a RGB-D camera

Jose A. González-Fraga, Univ. Autónoma de Baja California (Mexico); Vitaly Kober, Ctr. de Investigación Científica y de Educación Superior de Ensenada B.C. (Mexico); Victor H. Diaz-Ramirez, Ctr. de Investigación y Desarrollo de Tecnología Digital-IPN (Mexico); Everardo Gutiérrez López, Omar Alvarez-Xochihua, Univ. Autónoma de Baja California (Mexico)

Simultaneous Localization and Mapping (SLAM) is one of the most fundamental problems in the field of robotics. The goal of a SLAM system is to determine the position of a moving camera in its environment, and at the same time, to construct a map representation of the explored workspace. With the development of RGB-D sensors, a new alternative for generation of 3D maps is appeared, because visual features are not robust enough in some situations. Thus, feature detectors and descriptors used in SLAM significantly affect the system performance. In this work, we propose a robust method for searching and selecting the minimum number of keypoints and keyframes to perform correct feature correspondences and to track the keypoints. The selected points and frames are utilized for generation of the 3D map of indoor environment with a help of the ICP algorithm. For tracking of the keypoints, we use composite correlation filters with adjustable training sets depending on appearance of indoor environment as well as relative position and perspective from the camera to environment components. The tracking algorithm is scale-invariant because it utilizes the depth information from RGB-D camera. The performance of

the proposed system is evaluated in terms of accuracy, robustness, and processing time and compared with classical RGB-D SLAM systems.

10396-83, Session PMon

Veterinary software application for comparison of thermograms for pathology evaluation

Gita Pant, Scott E. Umbaugh, Rohini Dahal, Norsang Lama, Southern Illinois Univ. Edwardsville (United States); Dominic J. Marino, Joseph Sackman, Long Island Veterinary Specialists (United States)

The bilaterally symmetry property in mammals can be used to detect pathologies where body parts on both sides can be compared. For any pathological disorder, thermal patterns differ compared to the normal body parts. A software application for veterinary clinics is under development to input two thermograms of body parts on both sides, one normal and the other unknown, and the application compares them on the basis of extracted features and appropriate similarity and difference measures and outputs the likelihood of pathology. Previous research has been used to determine the appropriate image processing, feature extraction and comparison metrics to be used. The comparison metrics used are the vector inner product, Tanimoto, Euclidean, city block, Minkowski and maximum value metric. Also, results from experiments with comparison tests are used to derive a potential threshold values which will separate normal from abnormal images for a specific pathology. In the first phase, the anterior cruciate ligament (ACL) pathology in dogs was considered and comparison tests were performed on 20 random leg pairs based upon texture, histogram and spectral features which suggested any thermogram variation below 50% of Euclidean distance is normal and above 50% is abnormal. Further experiments are ongoing with larger image datasets, and pathologies, new features and comparison metric evaluation for determination of more accurate threshold values to separate normal and abnormal images.

10396-84, Session PMon

Haze removal method based on decomposition

Xifang Zhu, Ruxi Xiang, Feng Wu, Qingquan Xu, Xiaoyan Jiang, Chunyu Zhao, Changzhou Institute of Technology (China)

In order to obtain a clear image with free haze, a new removing haze method is proposed, which effectively reconstructs the reflected image. Firstly, the image decomposed is easily formed by the monochrome atmospheric scattering model, and then it is decomposed two layers where one layer is smoother than the other by the constrained regularized total variance method .Thus the decomposition problem can be formulated as a constrained quadratic programming optimization problem, and the optimized solution of the layer contained more details can be obtained by effectively combining the Bregman method with half quadratic minimization method. Finally, the color of the reflectance image is adaptively adjusted according to the white balance theory. Compared with some existing methods, our experimental results show that the proposed method can effectively remove the haze from the bad weather condition and improve the image quality such as the contrast, sharpness and color.

10396-85, Session PMon

Texture analysis integrated to infrared light sources for identifying high fringe concentrations in digital photoelasticity

Hermes Fandiño Toro, Univ. Nacional de Colombia Sede Medellín (Colombia) and Instituto Tecnológico Metropolitano (Colombia); Juan Carlos Briñez de León, Alejandro Restrepo Martínez, John W. Branch Bedoya, Univ. Nacional de Colombia Sede Medellín (Colombia)

Digital photoelasticity allows to obtain the whole stress field of a birefringent sample undergone to mechanical loads. This technique provides stress information by processing fringe patterns observed in phase images, captured using optical arrangements named polariscopes. Such patterns are a function of the material optical coefficient, the sample thickness, the principal stress difference, and the wavelength. Thus, photoelasticity images vary with the material type, the applied load and the light source.

The polariscopes require a light source, polarizers and phase retarders, and a specific variant --phase shifting-- is a standard technique to implement the digital photoelasticity. However, images of phase shifting photoelasticity often show inconsistencies and phase wrappings, being a challenge to get the stress field. On the other hand, high stress concentrations points normally produce zones with high fringe densities, which affects isochromatic maps and phase unwrapping process.

In this work, we perform simulations of the diametral compression of birefringent discs in phase shifting photoelasticity. We evaluate the relevance of texture operators for recognizing regions with high fringe concentrations in photoelasticity images, when the wavelength of the light source change from visible to far infrared. Our results show that extending photoelasticity to the far infrared could help to reconstruct stress fields. Furthermore, we show that texture descriptors could be useful for dealing with difficulties associated to the phase-wrapping of the stress field in the visible spectrum, due to high fringe concentrations.

10396-86, Session PMon

Robot path planning algorithm based on symbolic tags in dynamic environment

Aleksandr Vokhmintcev, Andrey Melnikov, Aleksandr Kozko, Chelyabinsk State Univ. (Russian Federation)

Methods for solving the task of simultaneous localization and mapping (SLAM) do not account for information about semantic properties of investigated unknown environment. On the other hand, when building three-dimensional models of the virtual world, approaches based on the semantic labeling of investigated environment gained currency. Under a semantic marker a three-dimensional object in investigated space is meant, which can be detected based on methods of image recognition and object classification. The main focus of the research in this project will be aimed at developing new methods of deriving information about semantic properties of a 3D dynamic environment based on the depth and color of an analyzed scene, and on the use of this information for robot path planning on a dynamic scene. A new method of the “subtle” detection and classification of objects on images will be developed in the project, which employs the enthropic-optimal randomization of parameters of models of observed objects in conditions of uncertainty. Also, an algorithm will be developed of the search for the global minimum of the functional of the quality of detection and classification, which is based on Monte Carlo batch iterations and which permits obtaining probabilistic evaluations of accuracy through an analysis of real computational trajectories.

10396-87, Session PMon

Application of speckle-field images processing for concrete hardening diagnostics

Mykhaylo P. Gorsky, Peter P. Maksimyak, Yuriy Fedkovych Chernivtsi National Univ. (Ukraine)

This paper is devoted to processing of speckle field images dynamics during coherent light scattering by the cement surface in the process of hydration (hardening). Currently, optical methods aren't used in industry to determine concrete hardening stages. Traditional method for hardening diagnostics is mechanical Vicat apparatus, which has been used as referrer in our research. Coherent light scattering on concrete produces complex speckle-field which is changing during cement hardening. We tried to use these changes to determine concrete hardening stages. Experimentally obtained set of speckle-field images, were processed by different methods including Fourier transform, Wavelet analysis, statistical moments and deviation calculation. Results of each analysis were evaluated in order to select best image processing approach. Deviation method has been selected like most accurate and less resource consuming one. It allows fast and accurate determining of concrete hardening stages by optical method. Optical method allows "remote" and "not destructive" diagnostics in compare with Vicat apparatus.

10396-88, Session PMon

Transform extension for block-based hybrid video codec with decoupling transform sizes from prediction sizes and coding sizes

Jing Chen, Peking Univ. Shenzhen Graduate School (China)

In the block-based hybrid video coding framework, transforms are applied to the residual signal resulting from prediction. So we note that transform block sizes must be equal or smaller than prediction block sizes. Recent video coding techniques have allowed for decoupling of transform and prediction block structures. Such as in high efficient video coding (HEVC), transform block may overlap multiple prediction blocks with strict restrictions. Therefore in this paper, we propose an extension to the transform process in video coding. In our proposed method, transforms are operated not only within prediction blocks or coding blocks, but also span some prediction blocks or coding blocks which are in the same basic largest coding block (In H.264/AVC is macroblock, in HEVC is coding tree block and so on) and adjacent with each other. It's apparent in our method we will have to consider for boundary transition effects since the number of prediction blocks the extension transform span has increased largely. Overlapped block motion compensation (OBMC) has been verified effective to reduce blocking artifacts and thus can be used to improve the efficiency of large block transform. According to our experiment in some popular video coding platforms, we obtain consistent coding performance gains.

10396-89, Session PMon

A new cloud detection method based on CNN and SVM joint algorithm

Zhicheng Yu, China Academy of Space Technology (China)

Terrain information is difficult to obtain due to cloud cover, these regions will become blind in remote sensing images, which led to the remote sensing images can not play their due value. So we need to use some detection technology to detect the cloud in remote sensing images to avoid a lot of useless images captured by the satellite wastes a large amount of storage unit and transmission bandwidth.

In this paper, based on a delicate high-resolution earth observation satellite in synchronous orbit, I combined the CNN(convolutional neural network) with SVM(support vector machine) for cloud detection, and finally present a new algorithm which can be realized in remote sensing satellite video processing system to statistic the cloud coverage ratio in orbit. The new algorithm uses the deep learning algorithm to automatically abstract the effective features, and after that SVM classifier is used to recognize the thick cloud. The most important is that the CNN network is simple enough so that it can be realized in embedded system like Zynq platform . Final results show that this algorithm is much more accurate than traditional cloud detection such as threshold method or SVM.

10396-90, Session PMon

Robot mapping algorithm based on Kalman filtering and symbolic tags

Aleksandr Vokhmintcev, Tatiana Botova, Ilya Sochenkov, Chelyabinsk State Univ. (Russian Federation); Anastasia S. Sochenkova, RUDN Univ. (Russian Federation); Artyom Makovetskii, Chelyabinsk State Univ. (Russian Federation)

In the present project, a new method will be proposed of determining the dynamic position of a robot in a relative coordinate system based on Kalman filtering, on a history of camera positions and on the robot's movements, on symbolic tags. At each step, we can determine the displacement of the robot and predict its new position. On the other hand, we can single out the location of special signs from a new frame and calculate the position of the robot relative to them. Based on the difference between these two evaluations of the position of the robot, probabilities/weights for all special signs may be updated and the robot's poses and movement trajectory adjusted. In order to solve this problem, an approach based on Extended Kalman Filter will be employed, and on the orientation in an environment on the basis of symbolic tags. The Kalman filter enables one to obtain accurate and continuously updated evaluations of the position of a mobile robot based on a time series of inaccurate measurements of its location. To obtain an evaluation of a state vector during the robot's movement according to a series of noisy measurements and symbolic labels, it is necessary to present a model of this process in the form of a matrix equation of corresponding type. In order to track the robot's reiterated passage of one and the same place, it is necessary to carry out, at each step, the matching of the robot's position and state with the previous steps (the problem of "loop closure").

10396-91, Session PMon

An efficient point-to-plane registration algorithm for affine transformations

Artyom Makovetskii, Sergei Voronin, Chelyabinsk State Univ. (Russian Federation); Vitaly Kober, Ctr. de Investigación Científica y de Educación Superior de Ensenada B.C. (Mexico); Dmitrii Tihonkih, Chelyabinsk State Univ. (Russian Federation)

The problem of aligning of 3D point data is the known registration task. The most popular registration algorithm is the Iterative Closest Point (ICP) algorithm. The traditional ICP algorithm is a fast and accurate approach for rigid registration between two point clouds but it is unable to handle affine case. Recently, extensions of the ICP algorithm for composition of scaling, rotation, and translation have been proposed. A generalized ICP version for an arbitrary affine transformation also was suggested. These methods work with point-to-point approach. There is still no closed-form solution to the point-to-plane case for orthogonal transformations. In this presentation, a new iterative algorithm for registration of point clouds based on the point-to-plane ICP algorithm with affine transformations is proposed. At each iteration, a closed-form solution to the affine transformation is derived. This approach allows us to get a precise solution for transformations such as rotation, translation, and scaling. With the help of computer simulation, the proposed algorithm is compared with common registration algorithms.

10396-92, Session PMon

A generalized Condat's algorithm of 1D total variation regularization

Artyom Makovetskii, Sergei Voronin, Chelyabinsk State Univ. (Russian Federation); Vitaly Kober, Ctr. de Investigación Científica y de Educación Superior de Ensenada B.C. (Mexico)

Denoising has numerous applications in communications, control, machine learning, and many other fields of engineering and science. A common way to solve the problem utilizes the total variation (TV) regularization. Many efficient numerical algorithms have been developed for solving the TV regularization problem. Condat described a fast direct algorithm to compute the processed 1D signal. It is appropriate for real-time processing of incoming stream of data. Also there exists a direct algorithm with a linear time for 1D TV denoising referred to as the taut string algorithm. The Condat's algorithm is based on a dual problem to the 1D TV regularization. In this presentation, we propose a variant of the Condat's algorithm based on the direct 1D TV regularization problem. The usage of the Condat algorithm with the taut string approach leads to a clear geometric description of the extremal function. Moreover, the Condat's algorithm for some functions yields the quadratic complexity, while the performance of the proposed algorithm in terms of complexity is much better. Computer simulation results are provided to illustrate the performance of the proposed algorithm for restoration of degraded signals.

10396-93, Session PMon

Convolutional neural networks for face recognition

Ilya Sochenkov, Chelyabinsk State Univ. (Russian Federation) and RUDN Univ. (Russian Federation); Anastasiia S. Sochenkova, RUDN Univ. (Russian Federation); Artyom Makovetskii, Andrey Melnikov, Chelyabinsk State Univ. (Russian Federation)

Computer vision tasks are remaining very important for the last couple of years. One of the most complicated problems in computer vision is face recognition that could be used in security systems to provide safety and to identify person among the others. There is a variety of different approaches to solve this task, but there is still no universal solution that would give adequate results in some cases. Current paper presents following approach. Firstly, we extract an area containing face, then we use Canny edge detector. On the next stage we use convolutional neural networks (CNN) to finally solve face recognition and person identification task. This paper also contains analysis of obtained results. Furthermore there is additionally presented comparison of the described method performance to using CNN without Canny edge detection.

10396-94, Session PMon

System of multifunctional Jones matrix tomography of phase anisotropy in diagnostics of endometriosis

Alexander Ushenko, Vladimir Ushenko, Yuriy Fedkovych Chernivtsi National Univ. (Ukraine)

Historically, the optical methods of biological objects diagnostic may be divided into three groups. The spectrophotometric methods, which are based on analysis of spatial or time changes of radiation field intensity, scattered by biological tissues. Polarizing methods are based on usage of coherency matrix of complex amplitude. The correlation methods are based on the analysis of the correlation degree of the parallel polarization components of the light fluctuation at different points of object field.

For the complex azimuthally-stable analysis of polarizationally heterogeneous laser radiation fields a new approach was suggested, based on the generalization of coherence matrix by the polarization Jones matrix.

The theoretical background of azimuthally stable method Jones matrix mapping of histological sections of biopsy of uterine neck on the basis of spatial-frequency selection of the mechanisms of linear and circular birefringence is presented. The comparative results of measuring the coordinate distributions of complex degree of mutual anisotropy formed by polycrystalline networks of blood plasma layers of donors (group 1) and patients with endometriosis (group 2). The values and ranges of change of the statistical (moments of the 1st - 4th order) parameters of complex degree of mutual anisotropy coordinate distributions are studied. The objective criteria of diagnostics of the pathology and differentiation of its severity degree are determined.

The obtained results enable to state a rather high level of accuracy of azimuthally stable Jones matrix tomography.

10396-95, Session PMon

Azimuthally invariant Mueller-matrix mapping of biological optically anisotropic network

Olexander V. Dubolazov, Alexander Ushenko, Yuriy Fedkovych Chernivtsi National Univ. (Ukraine)

Biological tissues and fluids represent structurally inhomogeneous media with absorption. To describe interactions of polarized light with such complex systems the most general approaches based on Mueller-matrix formalism are required. Nowadays in biological and medical investigations many practical techniques based on measurement and analysis of Mueller matrices of investigated samples are used. In addition, laser polarimetry techniques require further development and generalization.

Firstly, not all elements of Mueller matrix prove to be convenient for characterizing biological samples. The reason of this is the azimuthally dependence of the majority of matrix elements – generally 12 of 16 elements change at rotation of the sample around the probing axis. Secondly, the spectrum of mechanisms of optical anisotropy of biological layers is not confined to linear birefringence only. Taking into consideration the impact of other mechanisms – circular birefringence, as well as linear and circular dichroism – is topical in the aspect of enlarging the range of diagnostic techniques.

The model of Mueller-matrix description of mechanisms of optical anisotropy typical for polycrystalline films of blood - optical activity, birefringence, as well as linear and circular dichroism - is suggested. Within the statistical analysis of such distributions the objective criteria of differentiation of films of blood from the healthy patients and patients with breast cancer. From the point of view of probative medicine the operational characteristics (sensitivity, specificity and accuracy) of the method of Mueller-matrix reconstruction of optical anisotropy parameters were found.

10396-96, Session PMon

Polarization-interference mapping of biological fluids polycrystalline films in differentiation of weak changes of optical anisotropy

Olexander V. Dubolazov, Alexander Ushenko, Yuriy Fedkovych Chernivtsi National Univ. (Ukraine)

Powered theoretical justification of method of polarization-interference mapping of optically thin polycrystalline films of human body fluids.

Investigated coordinate distribution of local contrast value of interference distributions of inhomogeneous polarization-microscopic images of polycrystalline films of human joints synovial fluid.

Within the statistical (statistical moments 1st - 4th order), correlation

(dispersion and kurtosis, describing autocorrelation function) and fractal (dispersion that characterizes the logarithmic dependence of power spectra) approaches set objective criteria of distributions of local contrast values.

The possibility of differentiation of weak optical anisotropy changes of synovial fluid films of patients with varying severity of the pathology of the knee joints.

A comparative study of accuracy of this method and traditional method of polarization mapping.

10396-97, Session PMon

Methods and means of 3D diffuse Mueller-matrix tomography of depolarizing optically anisotropic biological layers

Olexander V. Dubolazov, Alexander Ushenko, Yuriy Fedkovych Chernivtsi National Univ. (Ukraine)

This work contains the results:

1) Mueller-matrix description of phase anisotropy model of polycrystalline biological layers with linear and circular birefringence.

2) Justification of theoretical principles and experimental techniques of obtaining 3D distribution of Muller-matrix elements of biological layers.

3) Approval of 3D Mueller-matrix mapping methods of three-dimensional polycrystalline structure of biological layers.

4) Experimentally investigated statistical (statistical moments 1st - 4th order) correlation (autocorrelation function) and fractal (logarithmic dependence of power spectra) structure of Mueller-matrix images distribution of histological sections of biological tissues and polycrystalline films of biological fluids.

10396-98, Session PMon

Feature recognition of metal salt spray corrosion based on color spaces statistics analysis

Liqun Ma, Zhi Zou, Changcheng Institute of Metrology & Measurement (China)

Corrosion region and feature extraction is the key step of evaluating the metal material surface corrosion level. The color digital Images contains certain corrosion information. In this paper, we investigate a method on extracting the corrosion region and feature which is based on multi-color space feature analyzing and region growing. The object that we research is high strength alloy steel corrosion samples acquired from accelerating salt spray corrosion test. Through this method, 2 types corrosion can be extracted and recognized.

For the first type corrosion, the multi-color space statistics is applied. The working process of the extraction strategy is summarized as shown in figure 1. (1)Transform the image color RGB space to other spaces including HSV and YCbCr. Then analyze the histogram of each channel of each color space and calculate the statistics of each channel, the statistics include certain moments of the image such as skewness and kurtosis. Through analyzing these moments, choose the proper channel of image to process and extract. (2) A segmentation using Otsu threshold to process the single channel images from the last step.

For the second type corrosion which is mainly dim and surround by the first type corrosion, using the multi-color space statistics to choose the proper space and channel then segmenting would get some extra wrong regions, we using the region growing to amend and optimize the extraction which summarized as shown in figure 2. (1) Based on the image saturation mutation caused by procedure of the corrosion generation, we choose the local maximum in saturation channel as the initial pixels which are on the boundary between two type corrosion. (2) Use the initial pixels to execute the region growing algorithm, if any region from the extra regions hits the initial 8-neighbour, refresh the initial pixels to initial region, do the iterative refreshing until the initial region would not grow any more. Thus, the metal material salt spray corrosion which has strongly color mutation can be recognized. Through processing several sample color images of alloy steel, it is proved that the feature and region extracted by this procedure has more accuracy and the corrosion degree is quantifiable and the precision of discriminating the corrosion is improved. Fig 1 shows some results of this research.

10396-99, Session PMon

New opportunities of differential diagnosis of biological tissues polycrystalline structure using methods of Stokes correlometry mapping of polarization inhomogeneous images

Olexander V. Dubolazov, Yuriy Fedkovych Chernivtsi National Univ. (Ukraine)

A new method of Stokes correlometry evaluation of polarization-inhomogeneous images of optically anisotropic biological tissues histological sections of different morphological structure and physiological state was developed.

Algorithms and analytical description of experimental determination of the coordinate value distribution module and the phase of “two-point” Stokes vector parameters were determined.

Within statistic, correlation and fractal analysis was investigated the possibility of differential diagnosis of weak optical anisotropy changes in tissues and internal organs of healthy and with diabetes rats.

The research showed excellent precision (more than 90 percent) of differential diagnosis changes of optical anisotropy of internal tissues by rat using Stokes correlometry.

10396-100, Session PMon

Fuzzy logic for cognitive impairment prediction in structural imaging

Annarita Fanizzi, I.R.R.C.C.S. Oncologico di Bari (Italy); Nicola Amoroso, Univ. degli Studi di Bari (Italy) and Istituto Nazionale di Fisica Nucleare (Italy); Roberto Bellotti, Univ. degli Studi di Bari Aldo Moro (Italy) and Istituto Nazionale di Fisica Nucleare (Italy); Sabina Tangaro, Istituto Nazionale di Fisica Nucleare (Italy)

BBrain atrophy is a well-known biomarker for cognitive impairment related to several brain diseases, such as Multiple Sclerosis and Alzheimer’s Disease. Hippocampal atrophy is a well known biomarker for the Alzheimer’s disease (AD) progression state. We propose a novel methodology to drive features selection into prediction of conversion to brain disease. We define significant fuzzy classes of the hippocampal volume segmented by means of Hippocampal Unified Multi-Atlas-Networks (HUMAN). The proposed methodology is accurate, robust and can find a wide range of applications.

10396-101, Session PMon

Resolution analysis of archive films for the purpose of their optimal digitization and distribution

Karel Fliegel, Stanislav Vítek, Petr Páta, Czech Technical Univ. in Prague (Czech Republic); Jiri Myslík, Josef Pecák, Marek Jícha, Film and TV School of Academy of Performing Arts in Prague (Czech Republic)

With recent high demand for ultra-high-definition (UHD) content to be screened in high-end digital movie theaters but also in the home environment, film archives full of high-quality movies are in the scope of UHD content providers. Movies captured with the traditional film technology represent virtually unlimited source of UHD content. The goal to maintain complete image information is also related to the choice of scanning resolution. It might seem that scanning the film material in the highest possible resolution of the modern film scanners is the right choice. The information content of the film material is however limited, and various degradations moreover lead to its further reduction. Scanning and mainly exporting the content in the highest image resolution is therefore often unnecessary and uneconomical. In other cases, the highest possible resolution for digitization is inevitable if we want to preserve fine details and film grain structure. This paper deals with the information content analysis of archive film records. The theoretical limit in captured scene information and factors which make the final real resolution lower are discussed. Methods are proposed to determine the information content of the film material based on the analysis of its digitized image data. These procedures will allow determining the optimum resolution for scanning, followed by recommendations for optimal resolution for archiving or distribution of digitized video content intended for various display devices. Obtained results are illustrated using real examples of digitized film content and performance evaluation of the proposed techniques using this content is presented.

10396-102, Session PMon

An efficient direct method for image registration of flat objects

Dmitry Nikolaev, Artyom Makovetskii, Sergei Voronin, Chelyabinsk State Univ. (Russian Federation)

Image alignment of rigid surfaces is a rapidly developing area of research and has many practical applications. Alignment methods can be roughly divided into two types: feature-based methods and direct methods. Known SURF and SIFT algorithms are examples of the feature-based methods. Direct methods refer to those that exploit the pixel intensities without resorting to image features and image-based deformations are general direct method to align images of deformable objects in 3D space. Nevertheless, it is not good for the registration of images of 3D rigid objects since the underlying structure cannot be directly evaluated. In the article we propose a model that is suitable for image alignment of rigid flat objects under various illumination models. The brightness consistency assumptions used for reconstruction of optimal geometrical transformation. Computer simulation results are provided to illustrate the performance of the proposed algorithm for computing of an accordance between pixels of two images.

10396-103, Session PMon

Smoothing of astronomical images with Poisson distribution

Zuzana Krbcová, Univ. of Chemistry and Technology Prague (Czech Republic); Jaromir Kukal, Czech Technical Univ. in Prague (Czech Republic); Jan ?vihlík, Univ. of Chemistry and Technology Prague (Czech Republic); Karel Fliegel, Czech Technical Univ. in Prague (Czech Republic)

Images obtained from an astronomical digital camera are of integer nature as event counters in every pixel of its image sensor. The quality of the captured images is influenced mostly by the camera characteristics and photon noise caused by natural random fluctuation of observed light. We suppose the image pixel intensity as a mean value of the signal with Poisson distribution. The application of maximum likelihood method with image gradient regularization leads to variational task in continuous and discrete formulations. This variational task has only one unique solution on which the novel numerical method of image smoothing is based. The performance of the proposed smoothing procedure is tested using real images obtained from the digital camera in Meteor Automatic Imager and Analyzer (MAIA).

10396-104, Session PMon

A modified iterative closest point algorithm for noisy data

Dmitrii Tihonkih, Artyom Makovetskii, Aleksei Voronin, Chelyabinsk State Univ. (Russian Federation)

The ICP (Iterative Closest Point) algorithm has become the dominant method for aligning three dimensional models based purely on the geometry, of the points clouds. ICP starts with two clouds and an initial guess for their relative rigid-body or affine transform, and iteratively refines the transform by repeatedly generating pairs of corresponding points on the clouds and minimizing an error metric. The first step of the ICP algorithm is the selection of some set of points in one or both clouds. This paper proposes a new method of a realization of the selection step. We suppose that the values of the point coordinates are noisy by an additive noise. The cloud is divided into the smaller clouds by the smart approach. For each obtained subcloud is used RANSAC algorithm for finding the mean point. This step allows reduce the noise influence to the result. The set of obtained points is a new cloud. We get two new clouds with smaller quantity of points. For the new clouds are applied the matching ICP step based on the a previously described geometric similarity method. With the help of computer simulation, the proposed method is compared with common algorithms for the ICP matching step.

10396-105, Session PMon

Estimation of Poisson noise characteristics in wavelet domain

Jan ?vihlík, Univ. of Chemistry and Technology Prague (Czech Republic); Karel Fliegel, Czech Technical Univ. in Prague (Czech Republic); Jaromír Kukal, Zuzana Krbcová, Univ. of Chemistry and Technology Prague (Czech Republic)

This paper deals with modeling of astronomical images in the wavelet domain.

We consider astronomical light images contaminated by dark current which is modeled by Poisson random process. Dark frame image maps the thermally generated charge of the CCD sensor. In this paper, we solve the problem of linear filtering of the Poisson random variable. At first, the noise analysis of images obtained from the astronomical camera is performed. It allows estimating parameters of the Poisson probability mass function in every pixel of the acquired dark frame. Then the resulting distributions of the wavelet coefficients can be found. If the distributions of the coefficients are identified, then the denoising algorithm can be applied. The performance of the Bayesian approach is compared with the application of the Anscombe transform followed by denoising algorithm designed for the additive Gaussian noise.

10396-106, Session PMon

Discrete Fourier transform limitations regarding the MTF measurement of optoelectronic imaging systems

Oleg A. Perezyabov, ITMO Univ. (Russian Federation); Aleksandr V. Ilinski, S.I. Vavilov State Optical Institute (Russian Federation); Nadezhda K. Maltseva, ITMO Univ. (Russian Federation)

An important characteristic of every optoelectronic imaging system that determines its image final quality is resolution. This characteristic can be precisely determined using modulation transfer function (MTF).

The advantages of using MTF as the main characteristic to measure imaging system resolution are: the ability to measure the quality of the image

directly and quantitatively; objectivity and flexibility of the measurement (minimal influence of the human factor); the ability to measure the quality of the combined systems.

All the existing resolution measurement methods can be subdivided into several groups by the type of the pattern used: method using groups of bands of equal width or sinusoids of different frequencies; random target method; slanted edge pattern method.

Fourier Transform which decomposes a function of time (a signal) into the frequencies is used in all of this methods as MTF describes spatial frequency response of the imaging system.

Fast Fourier transform (FFT) is one of the most widespread algorithms of discrete Fourier transform (DFT) which is used to determine the MTF of an imaging system. Despite the fact this algorithm is much faster than the usual Fourier transform, it has some drawbacks. Speaking of finite signals, the DFT algorithm can be mistaken at the frequencies range next to Nyquist frequency.

Such behavior of MTF obtained by the FFT, can be explained by a small number of counts of some sine waves — components of the Fourier image.

The aim of the paper is to research the Fourier transform and FFT differences regarding the MTF measurement.

10396-107, Session PMon

Efficient encryption of image data in video sequences using discrete orthogonal moments

José Saúl Rivera López, Univ. Politécnica de Tulancingo (Mexico); César Joel Camacho Bello, Univ. Tecnológica de Tulancingo (Mexico)

Currently, new techniques have been implemented to provide data security, confidentiality, integrity and authentication. Orthogonal moments can be used for the watermark in small binary images. In this work we use this principle to encrypt a grayscale image in a video sequence. To validate our approach, we present a comparative analysis using different families of discrete orthogonal moments in terms of accuracy. Finally, results and conclusions are presented.

10396-108, Session PMon

High speed camera recording in the service of research of dependences between kinetics of eye pupil parameters and blood pulsation

Marta A. Szmigiel, Henryk T. Kasprzak, Wroclaw Univ. of Science and Technology (Poland)

The basis for the implementation of this study is high speed video recording of the pupil of human eye. With a use of optimum magnification it was possible to register images which accurately show the edge of the eye pupil. Synchronously with the pupil image the blood pulsation was recorded with the use of the oximeter - both with the frequency of 200Hz.

This study shows measurement and numerical analysis of variability of the eye pupil geometry in time, as well as its correlations with blood pulsation. Volunteers were asked to abstain from blinking while fixating their vision on a bright point. The head of the patient was stabilized in a rigid head rest. Number of video sequences of the pupil image for every subject were recorded. Each single image from a sequence was numerically processed. The contour of the pupil was detected and approximated with the best fitted ellipse. Selected geometrical parameters of the ellipse (area, lengths of both semiaxes, eccentricity, orientation angle of the axis, ellipse center) were calculated and processed. The main idea was to observe, how the parameters were changed in time and if there was any dependency between pupil parameters and blood pulsation signal. Spectral analysis of time variability of all calculated parameters was determined, as well as correlation and coherence analysis between pairs of those signals.

10396-109, Session PMon

The relation between the retinal image quality and the refractive index of defects arising in IOL: numerical analysis

Malwina Geniusz, Wroclaw Univ. of Science and Technology (Poland)

The best treatment for cataract patients, which allows to restore sharp vision is implanting an artificial intraocular lens (IOL). The image quality of the lens has a significant impact on the quality of patient's vision. After a long residence in the eye time of the implant various defects appear in the artificial lenses. The defects generated in the IOL have different refractive indices. For example, glistening phenomenon is based on light scattering on the oval microvacuoles filled with a aqueous humor, whose refractive index value is about 1.34. Calcium deposits are another example of lens defects and can be characterized by the refractive index 1.63. In the presented studies it was calculated how the difference between the refractive indices of the defect and the refractive index of the material, from which the lens is made ($\Delta n= |nm-nd|$), affects the quality of image.

The OpticStudio Professional program (from Radiant Zemax, LLC) was used for the construction of the numerical model of the eye with an artificial lens and to calculate the characteristics of the retinal image. Retinal image quality was described in such characteristics as Point Spread Function (PSF) and the Optical Transfer Function with amplitude and phase.

The results show a strong correlation between the refractive indices difference and retinal image quality.

10396-110, Session PMon

Analysis of image reconstruction artifacts in structured illumination microscopy

Jakub Pospíšil, Czech Technical Univ. in Prague (Czech Republic); Tomáš Lukeš, Czech Technical Univ. in Prague (Czech Republic) and Ecole Polytechnique Fédérale de Lausanne (Switzerland); Karel Fliegel, Miloš Klíma, Czech Technical Univ. in Prague (Czech Republic); Guy M. Hagen, Univ. of Colorado at Colorado Springs (United States)

Structured Illumination Microscopy (SIM) is a super-resolution technique which enables to enhance the resolution of optical microscopes beyond the diffraction limit. The final super-resolution image quality strongly depends on the performance of SIM image reconstruction. Standard SIM methods require precise knowledge of the illumination pattern and assume the sample to be stationary during the acquisition of illumination patterned images. In the case of imaging live cells, the movements of the cell result in the occurrence of image reconstruction artifacts. To reduce this kind of artifacts the short acquisition time is needed. However, short exposure time causes low signal to noise ratio (SNR). Moreover, a drift of the specimen may distort the illumination pattern properties in each image. This issue together with the low SNR makes the estimation of reconstruction parameters a challenging task. Inaccurate assessment of spatial frequency, phase shift or orientation of the illumination pattern leads to incorrect separation and shift of spectral components in Fourier space. This results in unwanted image reconstruction artifacts and hampers the resolution enhancement in practice. In this paper, we analyze possible artifacts in super-resolution images reconstructed using different SIM techniques. An overview of typical image reconstruction artifact types is presented. A metric is proposed for the quantitative evaluation of these artifacts in reconstructed images, which allows for performance comparison of different SIM reconstruction methods. Distinguishing image artifacts from newly resolved sample features is essential for future SIM applications in cell biology.

10396-111, Session PMon

FPGA implementation of image dehazing algorithm for real time applications

Rahul Kumar, Brajesh Kumar Kaushik, Indian Institute of Technology Roorkee (India)

Weather degradation such as haze, fog, mist, etc. severely reduces the effective range of the visual surveillance. This degradation is a spatially varying phenomena, which makes this problem non trivial. Dehazing is an essential preprocessing stage in applications such as long range imaging, border security, intelligent transportation system, etc. However, these applications require low latency of the preprocessing block. In this work, single image dark channel prior algorithm is modified and implemented for fast processing with comparable visual quality of the restored images/video. Although conventional single image dark channel prior algorithm is computationally expensive, it yields impressive results. Moreover, a two stage image dehazing architecture is introduced, wherein, dark channel and airlight are estimated in the first stage. Transmission map and intensity restoration are computed in the next stage. The algorithm is implemented using Xilinx Vivado software and validated with Xilinx zc702 development board, which contains an Artix7 equivalent FPGA and ARM Cortex-A9 dual core processor. Additionally, HDMI interface has been incorporated for video feed and display purposes. The results show that the dehazing algorithm attains 29 frames per second for the image resolution of 1920x1080 which is suitable for real time applications. It utilizes only 17% of the available resources.

10396-112, Session PMon

Radiometric calibration of wide-field camera system with an application in astronomy

Stanislav Vítek, Czech Technical Univ. in Prague (Czech Republic)

Camera response function (CRF) is widely used for the description of a relationship between scene radiance and image brightness. Most common application of CRF is High Dynamic Range (HDR) reconstruction of the radiance maps of imaged scenes from a set of frames with different exposures. CRF may be obtained by precise measurement of the digital camera, for example using a uniformly illuminated chart containing patches of known reflectance. However, this process is quite complicated and can be performed only under laboratory conditions. Numerous papers showed that set of differently exposed images of the same scene contain enough information to recover response using images themselves. The main goal of this work is to provide the comprehensive overview of CRF estimation algorithms. These algorithms, typically designed for multimedia data, are unfortunately quite useless with astronomical image data, mostly due to their nature - noise with a priori unknown statistical distribution, motion blur due to long exposures, and the shape of stellar objects close to point spread function (PSF) of the imaging system. Therefore, we propose an optimization of selected methods to use in the astronomical imaging application. An important part of this contribution is the description of CRF utilization in a non-linear camera system with the space-variant impulse response, used for detection and monitoring of faint meteor showers.

10396-113, Session PMon

Robust parameterization of time-frequency characteristics for recognition of musical genres of Mexican culture

Osvaldo Gerardo Perez Rosas, Ctr. de Investigación y Desarrollo de Tecnología Digital (Mexico); Luis Alejandro Maldonado Cano, Ctr. de Investigación y Desarrollo de Tecnología Digital (Mexico); Mario Lopez Rodriguez, Ctr. de Investigación y Desarrollo de Tecnología Digital-IPN (Mexico); Laura Mariel Amaya Reyes, Ctr. de Investigación y Desarrollo de Tecnología Digital-IPN (Mexico); Elizabeth Cano Martinez, Ctr. de Investigación y Desarrollo de Tecnología Digital (Mexico); Mireya Sarai García Vazquez, Ctr. de Investigación y Desarrollo de Tecnología Digital-IPN (Mexico); Alejandro Álvaro Ramírez Acosta, MIRAL R&D&I (United States)

The automatic identification and classification of musical genres based on the sound similarities to form musical textures, it is a very active investigation area. In this context it has been created recognition systems of musical genres, formed by time-frequency characteristics extraction methods and by classification methods. The selection of this methods are important for a good development in the recognition systems. In this article they are proposed the Mel-Frequency Cepstral Coefficients (MFCC) methods as a characteristic extractor and Support Vector Machines (SVM) as a classifier for our system. The stablished parameters of the MFCC method in the system by our time-frequency analysis, represents the gamma of Mexican culture musical genres in this article. For the precision of a classification system of musical genres it is necessary that the descriptors represent the correct spectrum of each gender; to achieve this we must realize a correct parametrization of the MFCC like the one we present in this article. With the system developed we get satisfactory detection results, where the least identification percentage of musical genres was 66.67% and the one with the most precision was 100%.

10396-114, Session PMon

Recognition of uncorrelated characters in maritime environment

Chris M. Ward, SPAWAR Systems Ctr. Pacific (United States)

Text detection and recognition in the wild present challenges where traditional Optical Character Recognition (OCR) methods fail: extreme skew, noise, target motion, and egomotion. Moreover, maritime environments present their own unique challenges in the analysis of motion imagery: haze, occlusion, high noise levels, poor ground truth, and moving targets. Much of the data under analysis consists of strings of non-correlated characters: Serial Numbers, Hull Identification Numbers, Vessel Names – algorithms that rely on fixed-typeface sets, dictionaries, and predictive language are not sufficiently robust in these conditions. Therefore, recognition must be accomplished on a character by character basis, under extreme optical conditions, with marginal sensor technology. This paper presents a methodology for identifying scene text in maritime environments using Text-Like Object Detection, Text-Object Tracking, Super Resolution Enhancement, and Convolutional Neural Networks (CNNs) for character classification.

10396-115, Session PMon

Text detection in natural scenes with phase congruency approach

Julia Diaz-Escobar, Vitaly Kober, Ctr. de Investigación Científica y de Educación Superior de Ensenada B.C. (Mexico)

In recent years, the importance of text detection in imagery has been increasing due to the great number of applications developed for mobile devices, such as document classification, image retrieval, language translator, assisting visually impaired, and augmented reality.

Text detection is one of the first stages of character recognition task. The fundamental goal is to determine whether or not there is text in a given image. Although text detection seems to be a simple task, it becomes complicated when backgrounds are complex, different types of fonts and sizes are presented or when captured conditions are not controlled (changes

of illumination, resolution, alignment).

To solve the problem, in this work a method for text detection in natural scenes is proposed. The method is based on the Phase Congruency approach, obtained via Scale-Space Monogenic Signal framework. The proposed method is robust to illumination, resolution and noise degradation, as well as geometrical distortions (rotations, scales and shearing). Finally, in order to verify the performance of the proposed scheme, experimental results are presented using a real natural scene dataset.

10396-116, Session PMon

Enhancing user experience by using multi-sensor data fusion to predict phone's Illumination

Asmaa H. A. Al-Marhoubi, Higher College of Technology (Oman)

The movement of a phone in an environment with different illumination changes makes the illumination prediction challenging. The ambient light sensor takes a time to modify the illumination of the screen based on the environment it is placed in. This causes an unsatisfactory user experience and delays in adjustment of the screen illumination. In this research, a method is proposed for enhancing the prediction of illumination using accelerometer, gyroscope and speed measurement technique. The speed of the phone is identified using Sum-of-Sine parameters along with the accelerometer and gyroscope sensors. The illumination is then fused with them to present more accurate illumination values for the ALS based on the movement of the phone. An investigation is made during the movement of the user in different lighting environments. This enhances the user experience and improves the screen brightness precision. The accuracy has given an R-Square value of up to 0.97.

10396-117, Session PMon

Global stereo matching algorithm based on disparity range estimation

Jing Li, Hong Zhao, Xi'an Jiaotong Univ. (China); Feifei Gu, Shenzhen Institutes of Advanced Technology (China)

The global stereo matching algorithms is of high accuracy for the estimation of disparity map, but the time-consuming in the disparity optimization still faces a curse, especially for the image pairs with high resolution and large baseline setting. To improve the computational efficiency of the global algorithms, a disparity range estimation scheme for the global stereo matching is proposed to estimate the disparity map of rectified stereo images in this paper. The projective geometry in a parallel binocular stereo vision is investigated to reveal a ratio relationship between the disparity values at each pixel in the rectified stereo images with different baselines, which can be used to quickly obtain a referenced disparity map in a large baseline setting estimated by that in the small one. Then, the drastically reduced disparity ranges at each pixel under a large baseline setting can be determined by the referenced disparity map. Furthermore, the disparity range estimation scheme is introduced into the graph cuts (GC) with expansion moves to estimate the precise disparity map, which can greatly save the cost of computing without loss of accuracy in the stereo matching, especially for the dense global stereo matching, compared to the traditional algorithm. Experimental results with the Middlebury stereo datasets are presented to demonstrate the validity and efficiency of the proposed algorithm.

10396-118, Session PMon

The error model of the handheld target in Target-based Vision Measurement System (T-VMS)

Yueyang Ma, Hong Zhao, Xi'an Jiaotong Univ. (China); Feifei Gu, Shenzhen Institutes of Advanced Technology (China); Meiqi Fang, Hehui Geng, Kejia Li, Xi'an Jiaotong Univ. (China)

The handheld Target-based Vision Measurement System (T-VMS) is advantageous in measuring inaccessible areas such as deep holes, occlusion regions, and internal surfaces that cannot be captured directly by traditional cameras. The handheld target performs the role of intermediary in the measurement process. The feature points mounted on the face of the handheld target can be positioned by two cameras, so the probe fixed at the bottom of the handheld target can be located by known spatial relations. The said process is called the calibration of the handheld target. Extracting feature points and establishing handheld target coordinate system, as essential part of the calibration of the handheld target, however, introduce extraction errors and handheld target coordinate system position errors, which degrades the positioning precision of the T-VMS. Therefore, in order to evaluate the handheld target' influence on the accuracy of visual measuring system in the process of measurement, we first analyzed the accuracy of the visual measurement system under some certain extrinsic parameters and established the corresponding precision model. We then studied the main error sources introduced by the handheld target during the measurement process: the extraction errors of feature points and the position errors of handheld target coordinate system, and quantified corresponding errors under some certain extrinsic parameters. Finally, we discussed the influence of the said errors on the measurement results under system precision model. We applied the precision model in an actual T-VMS to confirm its feasibility and effectiveness, and found that it indeed estimates the errors introduced by the handheld target effectively.

10396-119, Session PMon

Multiscale imaging of collagen

Michael Pinkert, Zachary J Simmons, University of Wisconsin-Madison (United States); Brittany L Woods, Appalachian State University (United States); Adib Keikhosravi, Bing Dai, Timothy J Hall, Jeremy Rogers, Paul Campagnola, Kevin Eliceiri, University of Wisconsin-Madison (United States)

Changes in tissue collagen organization accompany many major diseases, including a number of cancer types. Measuring this organization can give important clinically relevant information. The LINK multimodality imaging system integrates Second Harmonic Generation Microscopy, High-Frequency Ultrasound, Enhanced Backscattering Spectroscopy, and Optical Coherence Tomography onto a single platform. These four modalities are sensitive to different properties of collagen and operate across different spatial scales, with resolutions ranging from below the optical diffraction limit to the tissue mesoscale at tens of microns.

10396-21, Session 4

JPEG XS: a new standard for visually lossless low-latency lightweight image compression

Antonin Descampe, intoPIX s.a. (Belgium); Joachim Keinert, Fraunhofer-Institut für Integrierte Schaltungen (IIS) (Germany); Thomas Richter, Univ. Stuttgart (Germany); Siegfried Fößel, Fraunhofer-Institut für

Integrierte Schaltungen (IIS) (Germany); Gaël Rouvroy, intoPIX s.a. (Belgium)

JPEG XS is an upcoming standard from the JPEG Committee (formally known as ISO/IEC SC29 WG1). It aims to provide an interoperable visually lossless low-latency lightweight codec for a wide range of applications including mezzanine compression in broadcast and Pro-AV markets. This requires optimal support of a wide range of implementation technologies such as FPGAs, CPU and GPUs. Targeted use cases are professional video links, IP transport, Ethernet transport, real-time video storage, video memory buffers, and omnidirectional video capture and rendering. In addition to the evaluation of the visual transparency of the selected technologies, a detailed analysis of the hardware and software complexity as well as the latency has been done to make sure that the new codec meets the requirements of the above-mentioned use cases. In particular, the end-to-end latency has been constrained to a maximum of 32 lines. Concerning the hardware complexity, neither encoder nor decoder should require more than 50% of an FPGA similar to Xilinx Artix 7 or 25% of an FPGA similar to Altera Cyclon 5. This process resulted in a coding scheme made of an optional color transform, a wavelet transform, the entropy coding of the highest magnitude level of groups of coefficients, and the raw inclusion of the truncated wavelet coefficients. This paper presents the details of the standardization process, a technical description of the future standard, and the latest performance evaluation results. Finally, it also gives insight on the upcoming profiles and extensions that will soon be investigated.

10396-22, Session 4

Overview of the JPEG XS objective evaluation procedures

Alexandre Willème, Univ. Catholique de Louvain (Belgium); Thomas Richter, Univ. Stuttgart (Germany); Chris Rosewarne, Canon Information Systems Research Australia Pty. Ltd. (Australia); Benoît M. Macq, Univ. Catholique de Louvain (Belgium)

JPEG XS is an initiative conducted by the JPEG Committee, formally known as ISO/IEC SC29 WG1 group that aims at standardizing a low-latency, lightweight and visually lossless video compression scheme. This codec is intended to be used in applications where image sequences are usually transmitted or stored in uncompressed form such as in live production (through SDI or IP transport), display links, or frame buffers. It provides compression ratios ranging from 2:1 to 6:1 and therefore allows for significant bandwidth and power reduction. Through this paper, the objective quality assessment procedures conducted as part of the JPEG XS initiative are described. First, the focus is put on the objective part of the experiments that lead to the technology selection during the 73th WG1 meeting in late 2016. This assessment consists in PSNR measurements after a single and multiple compression decompression cycles at various compression ratios. After this assessment phase, two proposals among six candidates that answered the Call For Proposals were selected and merged to form the first JPEG XS test model (XSM). Eventually, this paper describes the core experiments that have been conducted so far on XSM. These experiments are intended to evaluate its performance in more challenging scenarios (insertion of picture overlay, robustness to frame edition), assess the impact of the different algorithmic choices, and measure its performance with the HDR VDP metric.

10396-23, Session 4

New procedures to evaluate visually lossless compression for display systems and mezzanine networks

Dale Stolitzka, SAMSUNG Electronics Co., Ltd. (United States); Tim Bruylants, Vrije Univ. Brussel (Belgium)

Visually lossless image coding in isochronous display streaming or plesiochronous networks reduces link complexity and power consumption and increases available link bandwidth. A new set of codecs developed within the last four years promise a new level of coding quality, but require new techniques that are sufficiently sensitive to the small artifacts or color variations induced by this new breed of codecs. This paper begins with a summary of the new ISO/IEC 29170-2, a procedure for evaluation of lossless coding and reports the new work by JPEG to extend the procedure in two important ways: for new high dynamic range (HDR) content and for evaluating the differences between still images, panning images and image sequences.

The ISO/IEC 29170-2 international standard relies on selecting and processing relevant images through a well-defined process chain for subjective, forced-choice psychophysical experiments. The procedure sets an acceptable quality level to one just noticeable difference. Traditional image and video coding evaluation techniques, such as, those used for television evaluation [Rec. ITU-R BT.500] have not proven sufficiently sensitive to the small artifacts or color variations induced by this new breed of codecs. In 2015, JPEG received new requirements to expand evaluation of visually lossless coding for high dynamic range images, slowly moving images, i.e., panning, and image sequences. The amended ISO/IEC 29170-2 procedures promise to be highly useful for the new content in television and cinema mezzanine networks.

The new amendments of this procedure are expected to pass their final ballots and should be published later this year.

10396-24, Session 4

JPEG XS call for proposals subjective evaluations

David McNally, Ecole Polytechnique Fédérale de Lausanne (Switzerland); Tim Bruylants, Vrije Univ. Brussel (Belgium) and IMEC (Belgium); Alexandre Willème, Univ. Catholique de Louvain (Belgium); Peter Schelkens, Vrije Univ. Brussel (Belgium) and IMEC (Belgium); Touradj Ebrahimi, Ecole Polytechnique Fédérale de Lausanne (Switzerland); Benoît M. Macq, Univ. Catholique de Louvain (Belgium)

This paper presents the details of how responses to JPEG XS call proposals were subjectively evaluated and how the content was selected and the evaluation methodologies were carried. It also details new interpretations that had to be brought to AIC-2 specifications in order to make JPEG XS evaluations more optimal. Results obtained are then presented together with a description of the statistical analyses that were carried out.

10396-25, Session 4

High-speed low-complexity video coding with EDiCTius: a DCT coding proposal for JPEG XS

Thomas Richter, Univ. Stuttgart (Germany); Joachim Keinert, Siegfried Fößel, Fraunhofer-Institut für Integrierte Schaltungen (IIS) (Germany)

In its 71th meeting, the JPEG committee issued a call for low complexity, high speed image coding, designed to address the needs of low-cost video-over-ip applications. As an answer to this call, Fraunhofer IIS and the Computing Center of the University of Stuttgart jointly developed an embedded DCT image codec requiring only minimal resources while maximizing throughput on FPGA and GPU implementations.

Objective and subjective tests performed for the 73rd meeting confirmed its excellent performance and suitability for its purpose, and it was selected as one of the two key contributions for the development of a joined test model. In this paper, its authors describe the design principles of the codec, provide a high-level overview of the encoder and decoder chain and provide evaluation results on the test corpus selected by the JPEG committee.

10396-26, Session 4

On a parallel rate control method for JPEG2000

Miguel Ángel Martínez del Amor, Volker Bruns, Heiko Sparenberg, Fraunhofer-Institut für Integrierte Schaltungen (IIS) (Germany)

Since the introduction of JPEG2000, several rate control methods have been proposed. Among them, post-compression rate-distortion optimization (PCRD-Opt) is the most widely used. The approach followed by this method is to first compress the entire image, and subsequently, optimally truncate the set of generated bit streams according to the maximum target bit rate constraint. The literature proposes various strategies on how to estimate ahead of time where a block will get truncated in order to stop the execution prematurely and save time. However, none of them have been defined bearing in mind a parallel implementation.

Today, multi-core and many-core architectures are becoming popular for JPEG2000. Therefore, in this paper, we analyze how some techniques for efficient rate control can be deployed in GPUs. In order to do that, the design of our GPU-based codec is extended, allowing to stop the process at a given truncation point. This extension also harnesses a higher level of parallelism on the GPU, leading to an average of 40% of speedup with 2K pictures and 60% with 4K. In a second step, three selected rate control methods are adapted and implemented in our parallel encoder. A comparison is then carried out, and used to select the best candidate to be deployed in a GPU encoder, which gave an extra 30% of speed-up in those situations where it was really employed.

10396-27, Session 4

Lossless medical image compression through lightweight binary arithmetic coding

Joan Bartrina Rapesta, Univ. Autònoma de Barcelona (Spain); Victor Sanchez, The Univ. of Warwick (United Kingdom); Joan Serra Sagrsità, Univ. Autònoma de Barcelona (Spain); Michael W. Marcellin, The Univ. of Arizona (United States); Francesc Aulí Llinàs, Ian Blanes, Univ. Autònoma de Barcelona (Spain)

A lightweight arithmetic coder is proposed for lossless compression of medical imagery. Context definition uses causal data from previous slices (components) and bitplanes, an inexpensive yet efficient approach. To further reduce the computational cost, a binary arithmetic coder with fixed-length codewords is adopted, thus avoiding the normalization procedure common in most implementations, and the probability of each context is estimated through bitwise operations. Experimental results are provided for several medical images and compared against state-of-the-art coding techniques, yielding improvements between 0.12 and 0.45 bps.

10396-28, Session 4

FBCOT: a fast block coding option for JPEG2000

David S. Taubman, Aous Naman, Reji Mathew, The Univ. of New South Wales (Australia)

Based on the EBCOT algorithm, JPEG2000 finds application in many fields, including high performance scientific, geospatial and video coding applications. Beyond digital cinema, JPEG2000 is also attractive as a mezzanine format for content delivery and for low-latency video communication. The main obstacle in some applications is the relatively high computational complexity of the block coder, especially at high bit-rates.

We propose a drop-in replacement for the JPEG2000 block coding algorithm, achieving much higher encoding and decoding throughputs, with only modest loss in coding effiency (typically < 0.5dB). High throughput derives from a vertical (all bit-planes at once) coding sequence, together with carefully optimized, vectorizable coding tools and multiple forward/backward growing bit-streams for each block, which enhance concurrency. The algorithm provides only limited quality/SNR scalability, but offers truly reversible transcoding to/from any standard JPEG2000 block bit-stream. Transcoding may be performed on a block-by-block basis, leading to interesting applications in which lightweight encoding and/or decoding is coupled with incremental communication via the fully scalable EBCOT algorithm.

The proposed FAST block coder can be used with EBCOT's post-compression RD-opimization methodology, allowing a target compressed bit-rate to be achieved even at low latencies, leading to the name FBCOT (Fast Block Coding with Optimized Truncation). We explain how FBCOT manages precise rate control in a complexity constrained low latency coding environment, with encoding and decoding throughputs well below 10 clock cycles per sample (each core) on a modern i7 CPU, at high bit rates such as 4bpp.

10396-29, Session 4

Advanced display stream compression for mobile applications

Natan Jacobson, Vijayaraghavan Thirumalai, Rajan L. Joshi, James Goel, Qualcomm Inc. (United States)

Digital displays are ubiquitous in our lives, and the display properties are constantly improving to provide a better viewing experience. These improvements include increased display resolution, high bit depth, and high refresh rate which enable new experiences such as 4K/8K, high dynamic range (HDR) and virtual reality (VR). Each of these display improvements brings a significant increase on the required transmission bandwidth, such that transmission may not be possible over existing display transmission links. To address this problem, we propose Advanced Display Stream Compression (ADSC), a novel fixed-rate intra-only codec supporting compression rates of 4:1 and beyond while maintaining visually lossless image quality. The ADSC codec is lightweight and is intended to be implemented in hardware (ASIC/FPGA) for real-time operation. The proposed ADSC is versatile, supporting both RGB and YCbCr input color formats with 4:4:4, 4:2:2, and 4:2:0 chroma subsampling and bit depths ranging from 8 to 16 bits/component. The ADSC codec therefore offers a cost-effective solution to enable new applications over existing display links – such as 4K/60 for mobile displays over DSI, 8K/120 for VR applications, and beyond.

10396-30, Session 5

A novel projection for omnidirectional video

Adeel Abbas, Sandeep Doshi, GoPro, Inc. (United States)

Omnidirectional video processing and compression techniques involve projection mapping of spherical data to 2D surface. There are a number of projections available e.g. Equirectangular, Cube Map and Segmented Sphere, and each projection offers multitude of frame packing arrangements. The best projection lies closer to sphere, with lower number of pixels contributing to geometric distortions. Additionally we want to minimize number of faces because face discontinuities present new challenges for encoders. In this paper, we present a new projection that attempts to address some of the limitations of existing projections. Our projection lies very close to the sphere, has small number of faces and offers practical advantages compared to existing projections. We have also tested performance of this projection with HM and found BD-rate gain up to X%.

10396-31, Session 5

Geometry padding for intra prediction in 360 video coding

Philippe Hanhart, Yuwen He, Yan Ye, InterDigital Communications, Inc. (United States)

This paper presents a new reference sample derivation method for intra prediction in 360-degree video coding. Unlike the conventional reference sample derivation method for 2D video coding, which uses the samples located directly above and on the left of the current block, the proposed method considers the spherical nature of 360-degree video when deriving reference samples located outside the current face to which the block belongs, and derives reference samples that are geometric neighbors on the sphere. The proposed reference sample derivation method was implemented in the Joint Exploration Model 3.0 (JEM-3.0) for the cubemap projection format. Simulation results for all intra configuration show that, when compared with the conventional reference sample derivation method, the proposed method gives on average luma BD-rate reduction of 0.3% in terms of the spherical PSNR (SPSNR), SPSNR weighted by latitude access frequency (L-SPSNR), and weighted spherical PSNR (WS-PSNR) metrics.

10396-32, Session 5

Segment scheduling method for reducing 360° video streaming latency

Yong He, InterDigital Communications, Inc. (United States); Srinivas Gudumasu, Aricent Technologies (India); Eduardo Asbun, Yan Ye, InterDigital Communications, Inc. (United States)

360° video is a rapidly growing new format emerging in the media industry enabled by the growing availability of VR devices. It is able to provide the viewer with a very new sense of presence and immersion. Comparing to the conventional rectilinear video (2D or 3D), 360° video poses a new and difficult set of engineering challenges on video processing and delivery. Enabling comfort and immersive user experience requires extreme high video quality and very low latency, while the large video size poses an impediment to delivering 360° video in a quality manner at scale.

Majority of 360° video applications and services available at present encode the entire 360° video into a standard compliant stream for progressive downloading or adaptive streaming. Delivering entire 360° video to the clients allows low-latency rendering (the client has access to the entirety of the 360° video content and can choose to render the portion he or she desire to see without further constraint). From the server's perspective, the same streams can support multiple users with possibly different viewports. On the down side, however, because the entire 360° video has to be encoded in high quality, e.g. 4K@60fps or even 8K@60fps, the coded video size would be tremendously high, incurring high transmission bandwidth when the video is delivered. At the client side, much of this high bandwidth consumption during delivery, as well as the power consumed to decode the video, will be wasted, because the user only watches a small portion (i.e., viewport) of the entire picture.

To solve these problems, tile based or layer based viewport adaptive streaming methods with essential signaling become common approaches to reduce the bandwidth utilization and power consumption and present high quality content to the users with low rendering latency. The tile-based viewport adaptive streaming approach divides a 360 video projection frame into a number of motion constrained tiles. Each tile can be independently encoded into multiple quality level representations. During streaming, the client may request tile segment that corresponds to the current viewing orientation at high quality, and request tiles that do not correspond to the current viewing orientation at low quality. This allows the client to utilize the available bandwidth efficiently and accommodate abrupt viewport changes with low rendering latency. In another layer-based approach, state-of-art scalable video coding standard called the Scalable High Efficiency Video Coding (SHVC) standard may be used to code the 360 video. SHVC encodes a video into a number of layers representing different qualities and/or resolutions: a base layer (BL) and one or more enhancement layers (EL), each incrementally enhancing the quality of the lower layers. With layer-based approach, the entire 360 video can be encoded into a low quality representation as base, and each individual viewport can be separately encoded at high quality levels as enhancement layers. In this approach, the client may request base representation to obtain the whole spherical video. Then, based on the current viewing orientation, an enhancement layer corresponding to the particular viewport can be requested and then overlaid on top of the base quality frame for rendering.

The conventional video streaming scheduling method can be deployed for viewport adaptive 360 video delivery, but it may increase the latency when switching between different viewports due to the segment length and head orientation detection. The start of video segments defines the random access point. Therefore, when a longer segment length is used, it takes a longer time to switch among different target viewports from low quality to high quality, as the next random access point is farther away. An early head orientation detection method to determine the corresponding viewport segment request may not be effective, since the user's head orientation may keep changing before rendering. It is ideal to have minimum segment length, such as one frame, in order to reduce the latency, but the video coding efficiency will drop significantly. An efficient segment scheduling scheme is critical to reducing the viewport switch latency and improve the orientation detection accuracy for 360° video delivery.

A dual buffer segment scheduling method is proposed to reduce the latency when switching between different viewports. In this approach the base buffer holds all lower quality tile segments and the viewport buffer stores the particular high quality viewport segments depending on the latest head orientation detection. The client can always request low quality tiles to fill the base buffer and request high quality tile(s) near to the playback time to improve the viewport prediction accuracy. The number of high quality tiles being requested depends on the available bandwidth and the number of tile(s) within the target viewport. The simulation results verify that the proposed tile based viewport adaptive streaming with dual buffer segment scheduling algorithm is able to utilize the bandwidth more efficiently. As a result, a more consistent high quality 360° video content viewing experience can be presented to the user.

10396-33, Session 5

An ROI multi-resolution compression method for 3D-HEVC

Chunli Ti, Yudong Guan, Guodong Xu, Yidan Teng, Xinyuan Miao, Harbin Institute of Technology (China)

3D High Efficiency Video Coding (3D-HEVC) provides a significant potential on increasing the compression ratio of multi-view RGB-D videos. However?the bit rate still rises dramatically with the improvement of the video resolution, which will bring challenges to the transmission network, especially the mobile network. This paper propose an ROI multi-resolution compression method for 3D-HEVC to better preserve the information in ROI on condition of limited bandwidth. This is realized primarily through ROI extraction and compression multi-resolution preprocessed video as alternative data according to the network conditions. At first, the semantic contours are detected by the modified structured forests to restrain the color textures inside objects. The ROI is then determined utilizing the contour neighbourhood along with the face region, foreground and the central area of the scene. Secondly, the RGB-D videos are divided into slices and compressed via 3D-HEVC under different resolutions for selection by the audiences and applications. Afterwards, the low-resolution videos are directly up-sampled via Laplace transformation and used to replace the non-ROI areas of the high-resolution videos. Finally, the ROI multi-resolution compressed slices are obtained by compressing the ROI preprocessed videos with 3D-HEVC. The temporal and special details of non-ROI are reduced in the low-resolution videos, so the ROI will be better preserved by the encoder automatically. Experiments indicate that the proposed method can keep the key high-frequency information with subjective significance while the bit rate is reduced.

10396-34, Session 5

Key factors for a high quality VR experience

Mary-Luc Champel, Technicolor S.A. (France)

For many years, Virtual Reality has been presented as a very promising technology which could deliver a truly new experience to users but until recently such promise was mostly met by the video game industry using computer Graphics images and with quite confidential success. With the recent invasion of VR headsets, the media & entertainment industry is now investigating the possibility to offer a video based VR 360 experience while using traditional production and delivery workflows. Whether such VR content is consumed on a head-mounted display, a tablet, a phone or a TV, there is no doubt that the immersion of the user within an audio video content offers a unique and never seen before experience. Nevertheless, there is a substantial risk that VR 360 could have the same fate as 3DTV if it cannot offer more than just being the next fad. The present paper aims at presenting the various quality factors that we believe need to be offered in a VR 360 content in order to ensure a high quality VR experience. More specifically, this paper will focus on the main three VR quality pillars: visual, audio and immersion.

10396-35, Session 5

Wider angle viewports for omnidirectional video

Adeel Abbas, Sandeep Doshi, GoPro, Inc. (United States)

Virtual Reality or 360-degree images and video often require one to extract a sub-region portion of video/image data (also called viewport) for rendering purposes. One of the most common method to extract viewport from omnidirectional video involves projecting video data in rectilinear projection. Rectilinear projection works for smaller FOV viewports e.g. 60°x60°, but as soon as FOV of viewport starts to increase, the corners of the viewport experience “stretching”. This is due to the geometric distortions introduced from projecting spherical data rectilinearly. In this paper, we present an alternate approach to creating viewports that overcomes some of the limitations of rectilinear viewports.

10396-36, Session 5

Depth map estimation using multiple captured images

José Luis López Martínez, Univ. Autónoma de Yucatán (Mexico); Vitaly Kober, Ctr. de Investigación Científica y de Educación Superior de Ensenada B.C. (Mexico); Joel Antonio Trejo Sánchez, Ctr. de Investigación en Matemáticas, A.C., CONACyT (Mexico)

The depth map of a scene has many applications like robot navigation, computer vision, 3D reconstruction, etc. In this presentation, we propose a novel algorithm of the depth map generation of a scene using three cameras. The proposed system utilizes a slight displacement between the cameras. The algorithm of the depth map estimation is based on optimization of an objective function. The proposed method yields a good accuracy of the map estimation, and it is robust to noisy data. The performance of the proposed method is compared with that of common depth map estimation algorithms in terms of accuracy.

10396-37, Session 5

Discontinuity minimization for omnidirectional video projections

Vladyslav S. Zakharchenko, SAMSUNG Electronics Co., Ltd. (Korea, Republic of); Elena A. Alshina, SAMSUNG Electro-Mechanics (Korea, Republic of)

Omnidirectional video processing, compression and rendering is actively and rapidly developed topic. Quality measurement is key part of development process. Several quality metrics for 360 video content are considered by MPEG and VCEG during international standardization. Adequacy of those metrics and suggestions on test methodology are discussed in this paper from view point of company actively working on 360 video market.

10396-38, Session 5

Measuring quality of omnidirectional high dynamic range content

Anne-Flore Perrin, Ecole Polytechnique Fédérale de Lausanne (Switzerland); Cambodge Bist, Institut de recherche technologique B-Com (France); Touradj Ebrahimi, Ecole Polytechnique Fédérale de Lausanne (Switzerland)

Although HDR content processing coding and quality assessment have been largely addressed in the last few years, little to no work has been concentrating on how to assess quality in HDR for 360 or omnidirectional content. This paper is a first address to answer to various questions in this direction. As a minimum, a new data set for 360 HDR content is proposed and a new methodology is designed to assess subjective quality of HDR 360 content when it is displayed on SDR HMD after applying various tone mapping operators. The results are then analyzed and conclusions are drawn.

10396-39, Session 5

True 3D digital holographic tomography for virtual reality applications

Alexander Downham, Ujitha A. Abeywickrema, Partha P. Banerjee, Univ. of Dayton (United States)

In our previous work, a spring has been reconstructed using digital holographic tomography by recording the holograms with a ‘on-axis’ system, while the object is rotated about a single axis. The recorded holograms are processed through MATLAB® using the multiplicative technique. In this work ‘off-axis’ Mach-Zehnder system is used to record holograms of each side of a die, by rotating the object along the x and y axes. Then the holograms of all six sides of the die are imported and reconstructed in MATLAB® using Fresnel techniques. Then the depth information of each side of the die is obtained by using phase unwrapping techniques. The unwrapped depth information is then converted into a n?3 array, which is then converted into a Point Cloud image. Finally, the true 3D image is constructed using Point Cloud image processing techniques. Once the true 3D image is constructed, the next step is to export the finale image into the Microsoft HoloLens. The HoloLens uses two holographic waveguides in a stereoscopic setting to generate a 3D image. The image can then be manipulated using hand gestures to rotate, zoom in and zoom out from the object. The HoloLens also, enables the user to spatially map their surroundings, which provided a virtual mesh for the true 3D image to use as an anchor point. With the use of the Microsoft HoloLens, the true 3D image is viewed in virtual reality while still containing the depth information, which is difficult to see with current virtual reality techniques used today.

10396-40, Session 6

Forming intermediate spatial resolution of microscopy images for continuous zooming on multi-resolution processing system

Evan Hutomo Eka Putranto, Tomohiro Suzuki, Shin Usuki, Kenjiro Takai Miura, Shizuoka Univ. (Japan)

Magnification is the main purpose of the microscope which uses to enlarging spatial area of the object appearance without make it physically large. There a many type and method that used by microscope to establish magnification. However, different acquisition on the same object which is done by different microscope might raise a problem to bring a better zooming transition. Hence, we propose a quasi-optical zooming transition by forming intermediate spatial resolution microscopy image using multi-resolution image processing and magnification of two kind physical microscope, optical microscope (OM) and scan electron microscope (SEM). In order to form quasi-optical zooming transition with multi-resolution images, it will involve three steps. The first, image con- formation, performing an image registration between the OM and SEM image which has the same magnification unit. We perform image correction one image with 100X maximum magnification on OM and image with 100X minimum magnification of the SEM and merge it. The second, forming intermediate multi-resolution image between the objective lens magnification that we used on both OM and SEM. The set of physical magnification both of microscope are S ={1X, 100X, 1000X}. We filled the magnification gap between 1X and 100X, 100X and 1000X with integer value of magnification from generated intermediate multi-resolution images. The third, perform a continuous image transition between all of generated spatial image.

10396-41, Session 6

Hough transform for microcalcification detection in digital mammograms

Annarita Fanizzi, I.R.C.C.S. Istituto Tumori “Giovanni Paolo II” (Italy); Teresa M. A. Basile, Univ. degli Studi di Bari Aldo Moro (Italy); Ubaldo Bottigli, Univ. degli Studi di Siena (Italy); Rosalba Dentamaro, Vittorio Didonna, I.R.C.C.S. Istituto Tumori “Giovanni Paolo II” (Italy); Alfonso Fausto, Azienda Ospedaliera Univ. Senese (Italy); Raffaella Massafra, I.R.C.C.S. Istituto Tumori “Giovanni Paolo II” (Italy); Marco Moschetta, Univ. degli Studi di Bari Aldo Moro (Italy); Liliana Losurdo, Pasquale Tamborra, I.R.C.C.S. Istituto Tumori “Giovanni Paolo II” (Italy); Sonia Tangaro, Istituto Nazionale di Fisica Nucleare (Italy); Roberto Bellotti, Univ. degli Studi di Bari Aldo Moro (Italy) and Istituto Nazionale di Fisica Nucleare (Italy); Daniele La Forgia, I.R.C.C.S. Istituto Tumori “Giovanni Paolo II” (Italy)

Many screening programs use mammography as principal diagnostic tool for detecting breast cancer at a very early stage. Despite the efficacy of the mammograms in highlighting breast diseases, the detection of some lesions is still doubtless for radiologists. In particular, the extremely minute and elongated salt-like particles of microcalcifications are sometimes no larger than 0.1 mm and represent approximately half of all cancer detected by means of mammograms. Hence the need for automatic tools able to support radiologists in their work. Here, we propose a computer assisted diagnostic tool to support radiologists in identifying microcalcifications in full (native) digital mammographic images. The proposed CAD system consists of a pre-processing step, that improves contrast and reduces noise by applying Sobel edge detection algorithm and Gaussian filter, followed by a microcalcification detection step performed by exploiting the circular Hough transform. The procedure performance was tested on 200 images coming from the Breast Cancer Digital Repository (BCDR), a publicly available database. The automatically detected (clusters of) microcalcifications were evaluated by skilled radiologists which asses the validity of the correctly identified ROIs as well as the system error in case of missed microcalcifications. The system performance was evaluated in terms of sensitivity and False Positives per images (FPi) rate resulting comparable to the state of the art approaches. The proposed model was able to accurately predict the micro-calcification clusters obtaining performances (sensibility = 92.03% and FPi rate = 3.74) which favorably compare to other state-of-the-art approaches.

10396-42, Session 6

Smartphone assisted microscopy for automated quantification of ER, PR, and Ki-67 molecular markers

Suman Tewary, Chandan Chakraborty, Indian Institute of Technology Kharagpur (India); Indu Arun, Rosina Ahmed, Sanjoy Chatterjee, Tata Medical Ctr. (India)

In cancer progression, alteration of molecular expression at tissue level is evaluated by Immunohistochemical (IHC) markers. Hormone receptors such as estrogen receptor (ER) and progesterone receptor (PR), and proliferative marker Ki-67 plays critical role in deciding future therapy of breast cancer patients. The routine pathological evaluation involves the staining of tissue with IHC markers followed by manual counting of positively (brown in color) and negatively (blue in color) stained cells in the tissue slide. The manual evaluation is tedious, time consuming and prone to inter-observer variability which may lead to errors in diagnostic and prognostic evaluation. Available digital image analyzers are not affordable for pathological centers, when most of these centers cannot even afford the facility for digital pathology and depends on manual observation by expert pathologists. In view of this, the presented work aims to develop smartphone assisted microscopic image analyzer. The separation of hematoxylin and diaminobenzidine (DAB) stains followed by quantification of positively and negatively stained cells are performed on smartphone. The application also provides different color balancing algorithms for the ease of user under various illumination conditions. The aim is to quantify the stained cells for population score and proliferation index generation which will assist the clinicians for automated report generation. The developed application is compared with the state-of-the-art web based software ImmunoRatio for a quantitative comparison and the results are promising. With the smartphone assisted IHC image analysis, cancer prognostic evaluation process would become faster, accurate and repeatable.

10396-44, Session 6

A multi-layer description of Parkinson’s disease

Marianna La Rocca, Nicola Amoroso, Roberto Bellotti, Univ. degli Studi di Bari Aldo Moro (Italy); Sabina Tangaro, Istituto Nazionale di Fisica Nucleare (Italy)

Magnetic resonance imaging (MRI) along with complex network is currently one of the most widely adopted techniques for detection of structural changes in neurological diseases, such as Parkinson’s Disease (PD). In this paper, we present a digital image processing study, within the multi-layer network framework, combining more classifiers to evaluate the informative power of the MRI features, for the discrimination of normal controls (NC) and PD subjects. We define a network for each MRI scan; the nodes are the sub-volumes (patches) the images are divided into and the links are defined using the Pearson’s pairwise correlation between patches. We obtain a multi-layer network whose topological features are used to feed a supervised multi-level random forest classifier which exploits this base of knowledge for accurate classification. Method evaluation has been carried out using T1 MRI scans of 356 individuals, including 177 PD subjects and 177 normal controls from the Parkinson’s Progression Markers Initiative (PPMI) database. The experimental results demonstrate that the features obtained from multiplex networks are able to accurately describe PD patterns and that a privileged scale for studying PD disease exists. In particular, this

method gives a comprehensive overview of brain regions statistically affected by the disease, an additional value to the presented study.

10396-45, Session 6

Machine learning for the assessment of Alzheimer's disease through DTI

Eufemia Lella, Nicola Amoroso, Roberto Bellotti, Univ. degli Studi di Bari Aldo Moro (Italy); Domenico Diacono, Istituto Nazionale di Fisica Nucleare (Italy); Tommaso Maggipinto, Univ. degli Studi di Bari Aldo Moro (Italy); Alfonso Monaco, Sabina Tangaro, Istituto Nazionale di Fisica Nucleare (Italy)

Digital imaging techniques have found several medical applications in the development of computer aided detection systems, especially in neuroimaging. Recent advances in Diffusion Tensor Imaging (DTI) aim to discover biological markers for the early diagnosis of Alzheimer's Disease (AD), one of the most widespread neurodegenerative disorders. We explore here how different supervised classification models provide a robust support to the diagnosis of AD patients. We use DTI measures, assessing the structural integrity of white matter (WM) fiber tracts, to reveal patterns of disrupted brain connectivity. In particular, we provide a voxel-wise measure of fractional anisotropy (FA) and mean diffusivity (MD), thus identifying the regions of the brain mostly affected by neurodegeneration, and then computing statistical and intensity features to feed supervised classification algorithms. In particular, we evaluate the accuracy of discrimination of AD patients from healthy controls (HC) with a dataset of 80 subjects (40 HC, 40 AD), from the Alzheimer's Disease Neurodegenerative Initiative (ADNI). In this study, we compare three state-of-the-art classification models: Random Forests, Naive Bayes and Support Vector Machines (SVMs). We use a repeated five-fold cross validation framework with nested feature selection to perform a fair comparison between these algorithms and evaluate the information content they provide. Results show that AD patterns are well localized within the brain, thus DTI features can support the AD diagnosis.

10396-46, Session 6

Association between MRI structural features and cognitive measures in multiple sclerosis

Nicola Amoroso, Univ degli Studi di Bari Aldo Moro (Italy) and Istituto Nazionale di Fisica Nucleare (Italy); Roberto Bellotti, Istituto Nazionale di Fisica Nucleare (Italy) and Univ. degli Studi di Bari Aldo Moro (Italy); Alfonso Monaco, Istituto Nazionale di Fisica Nucleare (Italy); Maria Liguori, Consiglio Nazionale delle Ricerche (Italy); L. Margari, Univ. degli Studi di Bari Aldo Moro (Italy); Marta Simone, Univ degli Studi di Bari Aldo Moro (Italy); R.G. Viterbo, Univ. degli Studi di Bari Aldo Moro (Italy); Sabina Tangaro, Istituto Nazionale di Fisica Nucleare (Italy)

Multiple sclerosis (MS) is an inflammatory and demyelinating disease associated with neurodegenerative processes that lead to brain structural changes. Magnetic Resonance Imaging (MRI) is generally used for diagnosis and follow-up in MS patients, however the conventional MRI measures (e.g. new or enlarging T2-weighted lesions, T1-weighted gadolinium-enhancing lesions) have often failed as surrogate markers of both physical and cognitive dysfunctions. Cognitive dysfunction is one of the most remarkable features of MS, and particularly in pediatric onset MS (POMS), the percentage of patients with cognitive deficit range from 30 to 80%. In order to investigate the association between cognitive measures and brain morphometry, in this work we present a fully automated pipeline for processing and analyzing MRI brain scans. Relevant anatomical structures are segmented with FreeSurfer; besides, statistical features are computed. Thus, we describe the data referred to 19 patients with POMS (mean age at MRI: 15.5 ± 2.7 years) with a set of 182 structural features. We perform an exhaustive investigation of association between single features and cognitive measurements, and exploring different abilities like the verbal and visuo-spatial learning, expressive language and complex attention. Different regression models and parameter configurations are explored to assess the robustness of the results, in particular Generalized Linear Models, Bayes Regression, Random Forests, Support Vector Regression and Artificial Neural Networks are discussed.

Funding: supported by FISM - Fondazione Italiana Sclerosi Multipla (Grant Cod. 2014/R/10)

10396-47, Session 6

Brain's tumor image proccessing using shearlet transform

Luis Cadena, Univ. de las Fuerzas Armadas-ESPE (Ecuador) and Siberian State Aerospace Univ. (Russian Federation); Franklin Cadena, Colegio Juan Suarez Chacon (Ecuador); Nikolai D. Espinosa Ortiz, Univ. de las Fuerzas Armadas-ESPE (Ecuador); Anna Korneeva, Alexey Kruglyakov, Alexander Legalov, Siberian Federal Univ. (Russian Federation); Alexey Romanenko, Novosibirsk State Univ. (Russian Federation); Alexander Zotin, Siberian State Aerospace Univ. (Russian Federation)

Brain tumor detection is well known research area for medical and computer scientists. In last decades there has been much research done on tumor detection, segmentation, & classification. Medical imaging plays a central role in the diagnosis of brain tumors and nowadays uses methods non-invasive, high-resolution techniques, especially magnetic resonance imaging and computed tomography scans. Edge detection is a fundamental tool in image processing, particularly in the areas of feature detection and feature extraction, which aim at identifying points in a digital image at which the image has discontinuities.

Shearlets is the most successful frameworks for the efficient representation of multidimensional data, capturing edges and other anisotropic features which frequently dominate multidimensional phenomena.

The paper proposes an improved brain tumor detection method by automatically detecting tumor location in MR images, its features are extracted by new shearlet transform.

10396-48, Session 6

Demyelinating disease and cerebral ischemia: detection algorithm through MRI

Darwin P. Castillo Malla, Univ. Técnica Particular de Loja (Ecuador); René Samaniego, Hospital UTPL (Ecuador); María José Rodríguez-Álvarez, Univ. Politècnica de València (Spain)

This work presents the development of an algorithm for automatic detection of demyelinating lesions and cerebral ischemia through magnetic resonance images, which have contributed in paramount importance in the diagnosis of brain diseases [1]. The sequences of images to be used are T1, T2, and FLAIR.

Brain demyelination lesions occur due to damage of the myelin layer of nerve fibers; and therefore this deterioration is the cause of serious pathologies such as multiple sclerosis (MS) [2], leukodystrophy, disseminated acute encephalomyelitis. Cerebral or cerebrovascular ischemia is the interruption of the blood supply to the brain, thus interrupting; the flow of oxygen and nutrients needed to maintain the functioning of brain cells [3]. The algorithm developed allows the differentiation between these lesions.

References:

[1] Daniel García-Lorenzo, Simon Francis, Sridar Narayanan, Douglas L. Arnold, D. Louis Collins, Review of automatic segmentation methods of

multiple sclerosis white matter lesions on conventional magnetic resonance imaging, Medical Image Analysis, Volume 17, Issue 1, January 2013, Pages 1-18, ISSN 1361-8415, http://dx.doi.org/10.1016/j.media.2012.09.004.

[2] Miller, D., Weinshenker, B., Filippi, M., Banwell, B., Cohen, J., Freedman, M., Polman, C. (2008). Differential diagnosis of suspected multiple sclerosis: a consensus approach. Multiple Sclerosis (Houndmills, Basingstoke, England), 14(9), 1157–1174. http://doi.org/10.1177/1352458508096878

[3] Ona Wu, Toshihisa Sumii, Minoru Asahi, Masao Sasamata, Leif Østergaard, Bruce R Rosen, Eng H Lo, and Rick M Dijkhuizen. Infarct Prediction and Treatment Assessment with MRI-based Algorithms in Experimental Stroke Models J Cereb Blood Flow Metab January 2007 27: 196-204, doi:10.1038/sj.jcbfm.9600328

10396-49, Session 6

Breast thermograms analysis in the search of temperature gradients linked with breast injuries

Osmond Abraham Zermeño Loreto, Carina Toxqui Quitl, Univ. Politécnica de Tulancingo (Mexico); Eber E. Orozco Guillen, Univ. Politécnica de Sinaloa (Mexico); Alfonso Padilla Vivanco, Univ. Politécnica de Tulancingo (Mexico)

Infrared thermography is a technique that allows us to measure the body temperature and represents it in an image without the need to have contact with the person. However the automatic calibration of the devices causes that the same color means a different temperature in each measuring, this increases the difficulty of manual analysis of these images. With digital image processing techniques based on edge detection and temperature thresholding, it is possible to highlight those areas of interest that have a temperature gradient that can be caused by breast injuries. Also, a statistical analysis of the region of interest is carried out to characterize and classify it through neural networks.

10396-50, Session 7

Weighted bi-prediction for light field image coding

Caroline Conti, Instituto de Telecomunicações (Portugal) and Instituto Univ. de Lisboa (Portugal); Paulo Nunes, Luís Ducla Soares, Instituto de Telecomunicações (Portugal) and Instituto Universitário de Lisboa (ISCTE-IUL) (Portugal)

Light field imaging based on a single-tier camera equipped with a microlens array – also known as integral, holoscopic, and plenoptic imaging – has currently risen up as a practical and prospective approach for future visual applications and services. However, successfully deploying actual light field imaging applications and services will require developing adequate coding solutions in order to efficiently handle the massive amount of data involved in these systems. In this context, self-similarity compensated prediction is a non-local spatial prediction scheme based on block matching that has been shown to achieve high efficiency for HEVC-based light field image coding1,2. As previously shown by the authors, this is possible by simply averaging two predictor blocks that are jointly estimated from a causal search window in the current frame itself, referred to as self-similarity bi-prediction. However, theoretical analyses for motion compensated bi-prediction (e.g., in Girod3) have suggested that it is still possible to achieve further rate-distortion performance improvements by adaptively estimating the weighting coefficients of the predictor blocks.

Therefore, this paper presents a comprehensive analysis of the rate-distortion performance for HEVC-based light field image coding when using different sets of weighting coefficients for self-similarity bi-prediction. Based on this analysis, an adaptive algorithm is proposed for estimating optimized weighting coefficients for each coding block. References:

[1] Conti, C., Soares, L. D.., Nunes, P., "HEVC-Based 3D Holoscopic Video Coding using Self-Similarity Compensated Prediction," Signal Processing: Image Communication 42, 59–78 (2016).

[2] Conti, C., Nunes, P.., Soares, L. D., "HEVC-Based Light Field Image Coding with Bi-Predicted Self-Similarity Compensation," 2016 IEEE International Conference on Multimedia & Expo Workshops (ICMEW), 1–4, Seattle, WA, US (2016).

[3] Girod, B., "Efficiency Analysis of Multihypothesis Motion-Compensated Prediction for Video Coding.," IEEE Transactions on Image Processing 9(2), 173–183 (2000).

10396-51, Session 7

A new framework for interactive quality assessment with application to light field coding

Irene Viola, Touradj Ebrahimi, Ecole Polytechnique Fédérale de Lausanne (Switzerland)

The paper describes a follow up and extended version of an interactive quality assessment approach to analyse user experience in interactive environments and provides enough information in order to make decisions either on the degree of impact of new tools or comparisons between different approaches aiming at the same objectives. The framework will be illustrated in the context of evaluation of codecs for light field image and video coding with analysis of results and as a by product the conclusions about which light field image coding are suitable to efficiently compress such data.

10396-52, Session 7

Liborg: a lidar-based robot for efficient 3D mapping

Michiel Vlaminck, Hiêp Q. Luong, Wilfried Philips, Univ. Gent (Belgium)

In this work we present a spatial mapping and localization system that is able to acquire 3D models in real-time by means of lidar data. To this end we mounted a Velodyne Lidar Puck (VLP-16) on a robot controlled by a Raspberry Pi to serve as an independent acquisition platform. The novelty of this work is in the way we organize the huge amount of data by using efficient multi-resolution maps based on octrees. The paper explains in which ways the proposed data structure can be exploited to speed up the estimation of the current pose of the robot. First, the known spatial relationship of the points in the map enables efficient nearest neighbor queries which on its turn facilitates correspondence estimation between newly acquired points and the current map. Second, an initial guess of the current pose can be estimated using a lower resolution representation of the scene, which can be refined using a higher resolution, yielding another speed-up. The paper further discusses how the octree serves as a compact representation of the scene that is useful to compress the 3D model for potentially streaming the data to a server or other device. Finally, we explain how the system facilitates the detection of changes in the environment and how it is easily updatable making it perfectly suitable for highly dynamic environments. An experimental study was conducted with our mobile acquisition platform and a thorough evaluation was done on both processing time, accuracy and memory usage.

10396-53, Session 7

On the performance of metrics to predict quality in point cloud representations

Evangelos Alexiou, David McNally, Touradj Ebrahimi, Ecole Polytechnique Fédérale de Lausanne (Switzerland)

This paper proposes a new approach to subjectively assess quality of point

cloud content and evaluates performance of state of the art point cloud objective metrics to predict the subjective quality of such content. The paper includes a rigorous methodology to generate various distortions, to display point cloud content, to run subjective protocols and to validate the results.

10396-54, Session 7

A new similarity measure for complex amplitude holographic data

Ayyoub Ahar, Tobias Birnbaum, Vrije Univ. Brussel (Belgium) and IMEC (Belgium); Christian Jäh, Loughborough Univ. (United Kingdom); Peter Schelkens, Vrije Univ. Brussel (Belgium) and IMEC (Belgium)

Simultaneous with rapid developments in the field of Digital Holography, new utilities for related data processing topics like perceptual quality assessment and data compression are highly desired. An efficient algorithm for perceptual quality prediction of holographic data, should be able to effectively analyze the recorded interferogram (the complex wavefield) and predict the perceived quality of the reconstructed object ideally without performing the reconstruction process. Such algorithms primarily require an efficient measure to compare the complex valued distorted holograms with the reference. To do so, one may use the conventional similarity measures defined for real valued data to separately evaluate the real and imaginary parts of holograms. However, that would discard any correlation between the two parts. Currently, Euclidean distance based error measures like Mean Squared Error (MSE) are widely utilized for measuring the dissimilarity of holograms since it is possible to apply them directly on complex data, even though MSE is not bounded and, most importantly, lacks local interpretability. In this research, a new versatile similarity measure specifically designed for complex values and adapted for holographic data will be presented.

This new measure benefits from nice mathematical properties like boundedness to [0;1], relative error weighting based on the magnitudes of the signals, steerable similarity between original and negative phase; symmetry with respect to ordering of the arguments and the regularity of at least a continuous function. We will also present a performance evaluation between the new measure and the MSE for analyzing a set of computer generated holograms.

10396-55, Session 7

Computer-generated holographic near-eye display system based on LCoS phase only modulator

Peng Sun, Fei Fei, Shengqian Chang, Siman Zhang, Ting Xie, Huaye Li, Liu Siqi, Wang Chang, Zhenrong Zheng, Zhejiang Univ. (China)

Augmented reality (AR) technology has been applied in various industries, such as large-scale manufacturing, national defense?healthcare, movie and mass media and so on. An important way to realize AR display is using computer-generated hologram (CGH), which is accompanied by large redundancy and heavy computing defects. In this paper, a fast calculation algorithm is given to improve the image resolution and reduce the speckle noise by multiplying the object light with virtual convergence light. Holograms are the complex far-field diffraction patterns of the desired objects and by this algorithm accurate holograms can be obtained without the need of iteration. 2D dynamic and 3D AR display with wide field of view (FOV) and high resolution are obtained utilizing this algorithm with LCoS. The undesired zero-order diffracted light is also eliminated easily with a digital raster after reconstructed image is shifted. The experimental results show that the FOV is broadened to 35 degree and refresh frequency of 2D dynamic display achieves 24 fps. This algorithm is effective and efficient, and is a promising method in practical applications.

10396-56, Session 8

A neighborhood vector PCA method for small defect target detection

Zhengzhou Wang, Xi'an Jiaotong Univ. (China); Bingliang Hu, Xi'an Institute of Optics and Precision Mechanics, CAS (China)

The LCM (Local Contrast Method) has many advantages in detecting the large defect targets of the optical component. However, it often suffers from low performance when the defect target is located in local bright region, which reduce the accuracy of defect detection. In this study, we proposed a new neighborhood vector PCA (NVPCA) method for small defect target detection. The main idea is that each pixel and its 8 neighborhoods of damage image are considered as a column vector to participate in matrix operations, a 9 dimensional data cube is reconstructed by all vectors of each pixel, and the main information of the data cube is concentrated in the first dimension being the PCA transform. When the NVPCA image is processed by LCM again, there is a great effect on the image enhancement. After extracting the feature of enhancing image, the important statistical information of each defect target, including coordinate, size, area, energy integral, can be obtained. Because the defect targets are segmented by the region growing method, rather than traditional methods of global threshold segmentation, this method has excellent precision in detecting small defect target with size of 1 pixel, and can detect the defect targets located in local bright region.

10396-59, Session 8

3D+T motion analysis with nanosensors

Jean-Pierre Leduc, Reliance Core Consulting (United States)

This paper addresses the problem of motion analysis performed in a digital signal sampled on an irregular grid spread in 3-dimensional space and time (3D+T). Practically, this analysis as described here can be performed on different kinds of fields for a large variety of applications with a ``smart dust'' composed of nanosensors. Applications relevant for this problem can be found in medicine, earth science, military, and neurophysiology.

A general setting of this problem can be described as follows. A source system is actively releasing nanosensors that shall spread randomly in the field. Once released, each nanosensor emits at its own fixed pace a signal which corresponds some physical variable measured in the field. The sampled signal is a digital number corresponding to a magnitude, and potentially a direction (real or complex number). Each nanosensor is supposed to have a limited lifetime given by a Poisson-exponential distribution after release. The source is supposed to diffuse nanosensors in the field as long as the experiment is carried on. Several antennas are located as an array around the perimeter of the measurement field to capture and transmit the signals to a central station where a computer processes the analysis.

At the central station, raw incoming data is processed in a two steps. The first step is data reconciliation. The second step is motion sensing and analysis. Motion analysis, as referred here for digital signals, proceeds through consecutive steps of detection, parameter estimation and tracking.

The data reconciliation consists in using the raw data captured from the different directional antennas to reconstitute the actual signal in 3D+T as sampled on a random grid. A computer will perform multiple triangulations for each received sample in order to derive triples made of parameter, spatial location and time. At this stage, an algorithm can track and determine the path of each nanosensor in the field until inactivation since each sensor is transmitting at a constant but slightly different pace. This motion analysis may be sufficient or would stop at this stage in cases where the nanosensors are just able and limited to sending their own signature.

The motion sensing analysis step can be considered as a so-called inverse problem where a physical model is inferred to estimate the parameters of interest. In this case, the model is classical mechanics on some given geometry. In classical mechanics, motion is ruled by a Lie group called the Galilei group. The Galilei group enables to perform motion parameter

estimation through the use of group representations. Additional parameters to motion can be added to end up with the following set of parameter of interest: spatial translation, dilation and orientation, and temporal translation. This extended Galilei group has representations in the space-time Hilbert space. Those representations have properties of unitarity, irreducibility and square-integrability that enable the existence of admissible continuous wavelets fit for motion analysis in 3D space and time. It is well-known that the Shannon sampling theory can be generalized to uniform sampling and that Fourier transform has generalized versions computing uniformly sampled frequency values from an unevenly sampled signal to enable convolution computations. Parameter estimation is performed as wavelet-based match filters minimizing the mean-square error with a steepest descent algorithm.

To conclude, the technique of motion analysis described in this paper is quite general, applicable to a smart dust setting and has the advantage to be suitable to neural networks and deep learning applications.

10396-60, Session 8

Low-complexity object detection with deep convolutional neural network for embedded system

Subarna Tripathi, Univ. of California, San Diego (United States); Gökçe Dane, Qualcomm Inc. (United States); Byeongkeun Kang, Truong Nguyen, Univ. of California, San Diego (United States)

In this work, we study low-complexity convolutional neural networks for embedded vision applications.

It is well-known that consolidation of an embedded system for CNN-based object detection is more challenging due to computation and memory requirement comparing with problems like image classification.

We design and develop an end-to-end TensorFlow-based fully-convolutional deep neural network for generic object detection task inspired by one of the fastest framework YOLO.

The proposed model predicts the localization of every object by regressing coordinates of the corresponding bounding box as in YOLO. Hence, the detection is not bounded by minimum object size in principle.

However, our detection layer is fully-convolutional unlike YOLO, where the penultimate layer and the final detection layer is fully-connected. The proposed network is optimized for modified weighted-L2 loss while exploiting the domain knowledge of dominant objects.

As a use case, we choose face detection and train the proposed model on images containing varying number of faces of different sizes. Our TensorFlow-Slim based network can predict up to 147 faces of different sizes and poses in a single frame. We evaluate the face detection performance on publicly available FDDB dataset. Our experimental results show that the proposed method achieves comparative accuracy comparing with state-of-the-art CNN-based face detection methods, while reducing the model size by 3x and memory-BW by 3-4x comparing with YOLO. Thus the proposed model becomes amenable for embedded implementations, and is generic to be extended to any number of categories of objects.

10396-61, Session 8

An embedded system for face classification in infrared video using sparse representations

Antonio Saavedra, Jorge E. Pezoa Nunez, Univ. de Concepción (Chile); Payman Zarkesh-Ha, The Univ. of New Mexico (United States); Miguel Figueroa, Univ. de Concepción (Chile)

We propose a platform for robust face recognition in infrared images using compressive sensing. In line with compressive sensing theory, the classification problem is solved within a sparse representation framework, where test images are represented as a linear combination of the training set. Because the training set constitutes an overcomplete dictionary, we identify new images by finding their sparsest representation based on the training set, using standard l1-minimization algorithms. Unlike conventional face-recognition algorithms, we perform feature extraction using random projections with a precomputed binary matrix, as proposed in the compressive sensing literature. This random sampling reduces the effects of image noise and various occlusions such as facial hair, eyeglasses and disguises, which are notoriously challenging in infrared images. Thus, the performance of our framework is robust to these noise and occlusion factors, reaching on average an accuracy of almost 90% using the UCHThermalFace database. For comparison, a combination of Ahonen's algorithm and linear discriminant analysis reaches 80% accuracy on the same data. We implemented a high-performance embedded digital system for face recognition using this framework, where the computation of the sparse representation of the images using the Orthogonal Matching Pursuit algorithm is performed by dedicated hardware using a deeply pipelined architecture on an FPGA, and the rest is executed in software in an embedded processor on the same chip.

10396-62, Session 8

BDVC (Bimodal Database of Violent Content): a database of violent audio and video

Jose L. Rivera, Mario Humberto Mijes Cruz, Ctr. de Investigación y Desarrollo de Tecnología Digital-IPN (Mexico); Abraham Montoya Obeso, Luis Rodriguez Espejo, Manuel Antonio Rodriguez Vazquez, Mireya García, Ctr. de Investigación y Desarrollo de Tecnología Digital-IPN (Mexico); Alejandro Álvaro Ramírez Acosta, MIRAL R&D&I (United States)

Nowadays there is a trend towards the use of unimodal databases for multimedia content description, organization and retrieval applications of a single type of content like text, voice and images, instead bimodal databases allow to associate semantically two different types of content like audio-video, image-text, among others. The generation of a bimodal database of audio-video implies the creation of a connection between the multimedia content through the semantic relation that associates the actions of both types of information. This paper describes in detail the used characteristics and methodology for the creation of the bimodal database of violent content; the semantic relationship is stablished by the proposed concepts that describe the audiovisual information. The use of bimodal databases in applications related to the audiovisual content processing allows an increase in the semantic performance only and only if these applications process both type of content. This bimodal database counts with 580 audiovisual annotated segments, with a duration of 28 minutes, divided in 41 classes. Bimodal databases are a tool in the generation of applications for the semantic web.

10397-1, Session 1

Modeling and measuring charge sharing in hard x-ray imagers using HEXITEC CdTe detectors

Daniel F. Ryan, Steven D. Christe, Albert Y. Shih, Andrew Inglis, Wayne H. Baumgartner, NASA Goddard Space Flight Ctr. (United States); Matthew D. Wilson, Paul Seller, STFC Rutherford Appleton Lab. (United Kingdom); Jessica A. Gaskin, NASA Marshall Space Flight Ctr. (United States)

There is an increasing demand for fine-resolution X-ray spectroscopic imaging to help better understand high-energy solar and astrophysical processes. Such observations require a new breed of solid-state hard X-ray (HXR) detectors. Small independent pixels are needed to sub-sample the point-spread function (PSF) of the X-ray optics in addition to rapid read-outs to provide fast timing or, in the case of solar observations, handle high count rates produced by solar flares. The Rutherford Appleton Laboratory (RAL) has developed the HEXITEC (High Energy X-ray Imaging Technology) ASIC, an 80x80 array of independent 1mm-thick 250-micron CdTe pixels sensitive down to ~3keV and with a full-frame read-out rate of 10kHz. HEXITEC's pixel size is well matched to the few-arcsecond FWHM provided by current HXR focusing optics. However, such small pixels increase the probability of charge-sharing, i.e. a single X-ray depositing its energy over multiple pixels. Charge-sharing can reduce the spectral and imaging performance of pixelated detectors but, if correctly understood, can be mitigated or even utilized, e.g. for obtaining sub-pixel resolution. NASA's Goddard and Marshall Space Flight Centers have been collaborating with RAL to measure and model charge-sharing in HEXITEC. A previous model of a single HEXITEC pixel's response to incident X-rays has been extended to a 2D multi-pixel model which includes diffusion of the charge cloud among neighboring pixels. This paper describes the model and compares it to observations. The results help us understand how spectral imaging of astrophysical sources is affected by charge-sharing and how to correct for it.

10397-2, Session 1

Developing monolithic CMOS detectors as x-ray imaging spectrometers

Almus T. Kenter, Thomas M. Gauron, Ralph P. Kraft, Stephen M. Amato, Harvard-Smithsonian Ctr. for Astrophysics (United States)

The Smithsonian Astrophysical Observatory (SAO) in collaboration with SRI has been developing monolithic CMOS detectors and associated camera and processing electronics optimized for x-ray astronomy. The goal of this multi-year program has been to produce CMOS x-ray imaging spectrometers that are Fano noise limited over the 0.1-10keV energy band while providing: radiation ``hardness'', high levels of integration, and very high read rates.

The latest detectors known as Big Minimal IIIs have been fabricated, back thinned, and are in the process of x-ray testing. These new detectors are fabricated on 9micron epitaxial silicon and have a 1k by 1k format. They incorporate 16 micron pitch, 6TPPD high "gain" (sensitivity) pixels. The devices incorporate a row-at-a-time analog CDS. The high sensitivity pixels have demonstrated read noise < 3 e rms.

Associated FPGA based camera and x-ray processing algorithms have been developed to clock the devices and to extract only those pixels with x-ray photon charge. The resulting x-ray data represents a great decrease in data volume.

Monolithic devices such as these, would be ideal candidate detectors for the focal planes of Solar, planetary and other space-borne x-ray astronomy missions. The high through-put, low noise and excellent low energy response, provide high dynamic range and good time resolution

We present details of our camera design and device performance with particular emphasis on those aspects of interest to single photon counting x-ray astronomy. These features include read noise, x-ray spectral response and quantum efficiency.

10397-3, Session 1

Recent x-ray hybrid CMOS detector developments and measurements

Sam Hull, Abe Falcone, David Burrows, Mitchell Wages, Tanmoy Chattopadhyay, Maria McQuaide, Evan Bray, The Pennsylvania State Univ. (United States); David Schendt, The Pennsylvania State Univ, (United States)

The Penn State x-ray detector lab, in collaboration with Teledyne Imaging Sensors (TIS), have progressed their efforts to improve soft x-ray Hybrid CMOS detector (HCD) technology on multiple fronts. In order to meet the demands of future high-throughput x-ray observatories, detectors with fast readout and small pixel sizes are being developed. Hybrid CMOS detectors were already capable of fast readout rates and they have now been scaled down to a 12.5 micron pixel pitch. We will report characteristics on these new small pixel HCDs that include in-pixel CDS circuitry and CTIA amplifiers for reducing crosstalk. In addition, PSU and TIS are developing a new large-scale array Speedster-EXD device. The original 64x64 pixel Speedster-EXD prototype used comparators in each pixel to enable the exclusive readout of pixels containing charge, while skipping the readout of pixels with no measurable signal. This event driven readout mode allows for order of magnitude higher effective readout rates and will now be implemented in a full sized device. Finally, PSU is involved in a sounding rocket mission that is slated to fly in 2018 with an off-plane grating array and an H2RG x-ray HCD. This H2RG includes a 36 micron pitch absorber array bonded to an 18 micron ROIC for reduced pixel crosstalk. We will report on the planned detector configuration for this rocket, which will increase the NASA technology readiness level of x-ray HCDs to TRL 9.

10397-4, Session 2

Kyoto's event-driven x-ray astronomical SOI pixel sensor

Takeshi Go Tsuru, Hideki Hayashi, Katsuhiro Tachibana, Makoto Itou, Shunichi Ohmura, Hideaki Matsumura, Hiroyuki Uchida, Takaaki Tanaka, Kyoto Univ. (Japan); Shinya Nakashima, Institute of Space and Astronautical Science (Japan); Yasuo Arai, Ikuo Kurachi, High Energy Accelerator Research Organization, KEK (Japan); Koji Mori, Ayaki Takeda, Yusuke Nishioka, Nobuaki Takebayashi, Shoma Yokoyama, Univ. of Miyazaki (Japan); Takayoshi Kohmura, Kouki Tamasawa, Yusuke Ozawa, Tadashi Sato, Tokyo Univ. of Science (Japan); Shoji Kawahito, Keiichiro Kagawa, Keita Yasutomi, Hiroki Kamehama, Sumeet Shrestha, Shizuoka Univ. (Japan)

We have been developing monolithic active pixel sensors, X-ray SOIPIXs based on a Silicon-On-Insulator (SOI) CMOS technology for future X-ray astronomy satellites (eg. Tsuru et al. 2014, Proc. SPIE, 9144, 914412 7pp., arXiv:1408.4556). Immediate readout of only the pixels hit by X-rays is available by an event trigger output function implemented in each pixel with its high time resolution of ~10 usec (event-driven readout). It allows us to do fast timing observation and also reduce non-X-ray background dominating at high X-ray energy band above 5-10 keV by adopting an anti-coincidence technique. We propose the X-ray SOIPIXs as a soft X-ray sensors of wide-band hybrid X-ray imagers of a next Japanese mission, FORCE (Focusing

On Relativistic universe and Cosmic Evolution), which is characterized by broadband (1-80 keV) X-ray imaging spectroscopy with high angular resolution (<15"), reaching to about 10 times the sensitivity compared to previous missions above 10 keV (See Mori et al. 2016, Proc. SPIE, 9905, id. 990510 10pp.). In this presentation, we report followings subjects. We here report (1) X-ray performances of newly fabricated 3-side buttable back-illumination devices with the size of 22mm x 14mm, (2) the source of dark current and its reduction, (3) the optimum device structure for low readout noise and high charge collection efficiency by using double SOI wafer, (4) dead layer thickness of back-illumination devices, (5) and future development plans.

10397-5, Session 2

Characterizing subpixel spatial resolution of a hybrid CMOS detector

Evan Bray, The Pennsylvania State Univ. (United States)

The detection of X-rays is a unique process relative to other wavelengths, and allows for some novel features that increase the scientific yield of a single observation. Unlike other photon energies, X-rays liberate a large number of electrons from the silicon absorber array of the detector. This number is usually on the order of several hundred to a thousand for moderate-energy X-rays. These electrons tend to diffuse outward into what is referred to as the electron cloud. This cloud can then be picked up by several pixels, forming a specific pattern based on the exact incident location. By performing a "mesh experiment", I have determined the responsivity of our hybrid CMOS detectors with subpixel resolution.

This test involved placing a thin mesh with precisely spaced holes directly over the detector and exposing it to a nearly parallel X-ray beam. The holes are spaced 144 ?m apart and have a diameter of 4 ?m, which is less than the 36 ?m pixel pitch of our detector. By limiting where the X-rays can strike the pixels with the mesh grid, it was possible to characterize the exact shape of these electron clouds through the resulting events seen on the detector. Since the shape of the electron cloud is known, we could then determine the exact location of the incident X-rays on the detector with subpixel resolution.

10397-6, Session 2

Overview of high-efficiency and low-noise solid-state detectors for future missions including the Habitable Exoplanet Imaging Mission and the Large UV/Optical/Infrared (LUVOIR) Surveyor

Shouleh Nikzad, Jet Propulsion Lab. (United States)

In preparation for the National Research Council's next Decadal Survey for Astrophysics, NASA is developing concepts for four flagship missions, including the Habitable Exoplanet Imaging Mission (HabEx) and the Large Ultraviolet/Optical/Infrared Survey Mission (LUVOIR). Science and Technology Definition Teams (STDT) have embarked on formulating the objectives, developing instrument designs and defining requirements and technology gaps.

These missions will depend on high performance detector arrays that will meet the exacting instruments' requirements and will be available affordably and with high yield. STDTs and the associated technology working groups have been identifying relevant detector technologies, their state of development, and plans for further development. In developing these matrices, they have been identifying technology gaps.

This talk focuses on potential solid state detector options and briefly reviews their performance and state of readiness. Silicon detectors as well as detectors using III-V and II-VI based IR, and III-N materials will be briefly discussed in terms of key performance metrics: detection spectral range, signal to noise performance, photon counting ability, pixel count, noise, quantum efficiency, TRL, and scalability in their production.

10397-7, Session 3

The VUV instrument SPICE for Solar Orbiter: performance ground testing

Martin E. Caldwell, Nigel Morris, Mark Anderson, Carmen Pastor, Davide Bruzzi, Samuel Tustain, Chris Howe, Jenny Davenne, Timothy Grundy, Roisin Speight, Paul Eccleston, Sunil D. Sidher, Alessandra Giunta, STFC Rutherford Appleton Lab. (United Kingdom); Douglas K. Griffin, Univ. of New South Wales (Australia); Anne Philippon, Frédéric Auchère, Donald M. Hassler, Institut d'Astrophysique Spatiale (France); Udo H. Schuehle, Stefan Meining, Max-Planck-Institut für Sonnensystemforschung (Germany); Joseph M. Davila, William T. Thompson, NASA Goddard Space Flight Ctr. (United States); Buddy Walls, P. Phelan, Greg Dunn, Southwest Research Institute (United States); Manfred Gyo, Physikalisch-Meteorologisches Observatorium Davos (Switzerland); Grant J. Munro, William Holmes, Peter Doyle, ESR Technology Ltd. (United Kingdom); Roman M. Klein, Thomas Reichel, Physikalisch-Technische Bundesanstalt (Germany)

SPICE (Spectral Imaging of Coronal Environment) is an imaging spectrometer operating at vacuum ultraviolet (VUV) wavelengths, 70.4 – 79.0 nm and 97.3 - 104.9 nm. It is a facility instrument on the Solar Orbiter mission, which carries 10 science instruments in all, to make observations of the Sun's atmosphere and heliosphere, at close proximity to the Sun, i.e. to 0.28 A.U. at perihelion. SPICE's role is to make VUV measurements of plasma in the solar atmosphere. SPICE is designed to achieve spectral imaging at spectral resolution ~1500, spatial resolution of several arcsec, and two-dimensional FOV of 11 x16arcmins. The many constraints on the instrument design imposed by the mission requirements, in particular the harsh thermal environment, prevent the imaging performance from exceeding those of previous instruments, but by being closer to the sun there is a gain in spatial resolution. The design constraints lead to some novel features in the design, which needed be proven by ground test programs. These include a dichroic solar-transmitting primary mirror to dump the solar heat, a high in-flight temperature (60deg.C) and gradients in the optics box, and a bespoke variable-line-spacing grating to minimise the number of reflective components used. The tests culminate in the system-level test of VUV imaging performance and pointing stability. We will describe how our dedicated facility with heritage from previous solar instruments, is used to make these tests, and show the results, firstly on the Engineering Model of the optics unit, and more recently on the Flight Model.

10397-10, Session 3

Photon counting type imaging spectrometer for solar soft x-rays

Noriyuki Narukage, National Astronomical Observatory of Japan (Japan); Shin-nosuke Ishikawa, Tomoko Kawate, Japan Aerospace Exploration Agency (Japan); Taro Sakao, Institute of Space and Astronautical Science (Japan); Lindsay Glesener, Univ. of Minnesota, Twin Cities (United States); Sasha Courtade, Space Sciences Lab. (United States); Säm Krucker, Univ. of California, Berkeley (United States) and Fachhochschule NordWestschweiz (Switzerland); Steven Christe, NASA Goddard Space Flight Ctr. (United States)

The imaging spectroscopic observations for solar soft X-rays are expected to provide us novel and valuable information about the plasma activity in the solar corona, e.g., particle acceleration, heating, shock, etc. However, this type of observations has not been performed yet with enough energy, spatial, and temporal resolutions. In this situation, we plan to realize the

imaging spectroscopic observations for solar soft X-rays with a high speed soft X-ray camera and grazing incidence mirrors. Our developing camera consists of a back-illuminated CMOS sensor. This censor has a sensitivity to soft X-rays (0.5 keV - 10 keV), and can perform continuous exposures of 1,000 frame per second for the imaging area of 1k x 100 pixels. We will mount this camera on the FOXSI-3 sounding rocket that is planned to be launched in the summer of 2018. By the combination of our camera and the X-ray mirror on the FOXSI, we can achieve an energy resolution of 0.2 keV, a spatial resolution of ~5 arcsec (1 arcsec sampling), and the temporal resolution of ~10 seconds in an energy range of 0.5 keV - 10 keV. In this presentation, we will explain the science goal, the instrumental design, and the developments of the solar soft X-ray imaging spectrometer.

10397-11, Session 4

Calibration of the hard x-ray detectors for the FOXSI solar sounding rocket

Subramania Athiray, Univ, of Minnesota (United States); Lindsay Glesener, Univ. of Minnesota, Twin Cities (United States); Sam Krucker, Univ. of California, Berkeley (United States) and Fachhochschule NordWestschweiz (Switzerland); Sasha Courtade, Univ. of California, Berkeley (United States); Steven D. Christe, NASA Goddard Space Flight Ctr. (United States); Shin-nosuke Ishikawa, Institute of Space and Astronautical Science (Japan); Tadayuki Takahashi, Shin Watanabe, Institute of Space and Astronautical Science (Japan) and The Univ. of Tokyo (Japan); Juan Camilo Buitrago Casas, Space Sciences Lab. (United States); Juliana Vievering, Sophie Musset, Kendra Bergstedt, Keith Goetz, Steven Monson, Univ. of Minnesota (United States)

The Focusing Optics X-ray Solar Imager (FOXSI) sounding rocket experiment conducts direct imaging and spectral observation of the Sun in hard X-rays, in the energy range 4 to 20 keV. These high-sensitivity observations are used to study particle acceleration and coronal heating. FOXSI is designed with seven grazing incidence optics modules that focus X-rays onto seven focal plane detectors kept at a 2m distance. FOXSI-1 was flown with seven Double-sided Si Strip Detectors (DSSD), and two of them were replaced with CdTe detectors for FOXSI-2. The upcoming FOXSI-3 flight will carry DSSD and CdTe detectors with upgraded optics for enhanced sensitivity. The detectors are calibrated using various radioactive sources. The detector's spectral response matrix was constructed using a Gaussian approximation with a spread (sigma) that accounts for the energy resolution of the detector. Spectroscopic studies of FOXSI flight data suggest that the inclusion of lower energy X-rays could better constrain the spectral modeling to yield a more precise temperature estimation of the hot plasma. This motivates us to carry out an improved calibration to better understand the finer-order effects on the spectral response, especially at lower energies. Here we report our attempts for improved calibration of FOXSI detectors using experiments and Monte-Carlo simulations.

10397-12, Session 4

Strontium Iodide Radiation Instrumentation (SIRI)

Lee Mitchell, Bernard Phlips, U.S. Naval Research Lab. (United States); Emily Jackson, National Research Council (United States); Neil Johnson, Praxis Inc. (United States)

The SIRI instrument was designed to test the performance of new gamma-ray detector technology for space-based astrophysical and military applications. This new technology offers improved energy resolution, lower power consumption and reduced size compared to similar systems. SIRI consists of europium-doped strontium iodide (SrI2:Eu) scintillator technology with improved energy resolution, 3% at 662 keV compare to 7% at 662 keV of traditional sodium iodide and was developed for terrestrial-based weapons of mass destruction (WMD) detection. The objective of SIRI's one year mission is to space qualify SrI2:Eu detector and silicon photomultiplier technology, study the internal activation of the SrI2:Eu material, and measure the performance of the SiPM readouts. The combined detector and readout measure the gamma-ray spectrum over the energy range of 0.04 - 8 MeV. The harsh radiation environment of space can present a challenge to new technology, often only developed for terrestrial uses. The SIRI mission payoff is a space-qualified compact, high-sensitivity gamma-ray spectrometer with improved energy resolution relative to previous sensors. Scientific applications in solar physics and astrophysics include flares, Gamma Ray Bursts, novae, supernovae, and the synthesis of the elements. DoD and security applications are also possible. Construction of the SIRI instrument has been completed, and it is currently awaiting integration onto the spacecraft. The expected launch date is November 2017. This presentation will discuss the design details, mission CONOPS, and expected science return of the SIRI spectrometer.

10397-13, Session 4

Modeling contamination migration on the Chandra X-ray Observatory: IV

Stephen L. O'Dell, NASA Marshall Space Flight Ctr. (United States); Douglas A. Swartz, Universities Space Research Association (United States); Neil W. Tice, Massachusetts Institute of Technology (United States); Paul P. Plucinsky, Smithsonian Astrophysical Observatory (United States); Herman Marshall, Massachusetts Institute of Technology (United States); Akos Bogdan, Smithsonian Astrophysical Observatory (United States); Catherine E. Grant, Massachusetts Institute of Technology (United States); Allyn F. Tennant, NASA Marshall Space Flight Ctr. (United States); Matthew T. Dahmer, Northrop Grumman (United States)

During its first 18 years of operation, the cold (about -60°C) optical blocking filter of the Advanced CCD Imaging Spectrometer (ACIS), aboard the Chandra X-ray Observatory, has accumulated a growing layer of molecular contamination, which attenuates low-energy x rays. Over the past five years or so, the accumulation rate, spatial distribution, and composition of the contamination have changed. This evolution has motivated further analysis of contamination migration within and near the ACIS cavity, in part to evaluate potential bake-out scenarios intended to reduce the level of contamination. This paper, the fourth on this topic, reports the results of recent contamination-migration simulations and their relevance to a decision whether to bake-out the ACIS instrument.

10397-14, Session 4

An update to the Chandra ACIS contamination model

Herman Marshall, Massachusetts Institute of Technology (United States); Akos Bogdan, Harvard-Smithsonian Ctr. for Astrophysics (United States); Paul P. Plucinsky, Smithsonian Astrophysical Observatory (United States)

We detail the steps used to arrive at a new release of the contamination correction file for use in Chandra ACIS data analysis. The update now reconciles a long-standing tension between imaging and grating spectral data. The update starts with fixing the O-K and F-K edge optical depths according to high spectral resolution LETG/ACIS spectra. Temporal and spatial models of the O-K and F-K variation are derived solely from LETG/ACIS data. Direct ACIS observations of galaxy clusters are then used to determine the C opacity above 0.5 keV after accounting for O-K and F-K opacity. The ACIS data are used to derive the spatial and temporal variation simultaneously. Finally, the C-K opacity dependence on energy was adjusted

near the K edge to obtain better agreement with LETG/ACIS-S spectra of blazars. The model was then tested against ACIS measurements of soft X-ray lines from the supernova remnant 1E 0102.2-7219, checking for temporal and spatial improvement when compared to the previous release.

10397-15, Session 4

The evaluation of the Hitomi (Astro-H)/ SXS spare beryllium window in 3.8-30 keV

Akio Hoshino, Yuki Yoshida, Shunji Kitamoto, Rikkyo Univ. (Japan); Ryuichi Fujimoto, Kanazawa Univ. (Japan); Noriko Y. Yamasaki, Institute of Space and Astronautical Science (Japan); Toshiaki Ina, Tomoya Uruga, Japan Synchrotron Radiation Research Institute (Japan); Megan E. Eckart, Maurice A. Leutenegger, NASA Goddard Space Flight Ctr. (United States)

During the Hitomi (Astro-H) commissioning observations the SXS dewar gate valve (GV) remained closed to protect the instrument from initial spacecraft outgassing. As a result, the optical path of the observations included the Be window installed on the GV. Both x-ray fluorescence (XRF) analysis and x-ray transmission measurements were performed in June 2016 on the flight-spare Be window which is from the same lot as the flight material at SPring-8 in Japan. The beamline operating range is 3.8– 30 keV. We used a beam spot size of 1 mm x 0.2mm to measure two positions on the Be window, at the center of the window and at one position 6.5 mm off-center. We used simultaneous transmission measurements of standard materials for energy calibration. The transmission data clearly showed Fe and Ni K-edges, plus a marginal detection of the Mn K- edge. We found that our transmission data was best fit using the following components; Be: 261.86pm 0.01mum, Cr:3nm(fixed), Mn:3.81pm0.05nm, Fe:10.83pm0.05nm, Ni:16.48pm0.03nm, Cu:5nm (fixed) The effective area is reduced 1$%$ at the Fe K-edge. The amount of contaminated materials are comparable to the values of the spec sheet. The surface transmission is constrained with $sigma=0.11%$ of the unbiased standard deviation. We also investigated additional measurement in the lower energy range at KEK-PF in Japan.

10397-16, Session 5

The gas pixel detector on board the IXPE mission

Carmelo Sgrò, Istituto Nazionale di Fisica Nucleare (Italy)

The Imaging X-ray Polarimetry Explorer (IXPE) has been selected by NASA to be the next mission dedicated to X-ray polarimetry. It is based on a Gas Pixel Detector that is able to add polarization measurement to imaging and spectroscopy, and will be placed at the focus of a conventional X-ray optics. The detector exploits the photoelectric effect in gas and a finely segmented ASIC as a collecting anode. In this talk I will describe the experimental technique and the details of the detector concept. I will than go through the detail of the detector construction and operation, the performance in laboratory tests and expected behavior in orbit at the focus of the IXPE telescope.

10397-17, Session 5

Calibrating IXPE from ground to space

Fabio Muleri for the IXPE team, INAF - Istituto di Astrofisica e Planetologia Spaziali (Italy)

The Imaging X-ray Polarimetry Explorer (IXPE) will be the next SMEX mission launched by NASA in 2020 in collaboration with the Italian Space Agency (ASI). IXPE will perform groundbreaking measurements of imaging polarization in X-rays for a number of different classes of sources with three identical telescopes, finally (re)opening a window in the high energy Universe after more than 40 years since the first pioneering results. The unprecedented sensitivity of IXPE to polarization poses peculiar requirements on the payload calibration, e.g. the use of polarized and completely unpolarized radiation, both on ground and in orbit. In this talk, we will present the IXPE calibration plan, describing both calibrations which will be performed on the detectors at INAF-IAPS in Rome (Italy) and the calibration on the mirror and detector assemblies which will be carried out at Marshall Space Flight Center in Huntsville, Alabama. In flight calibrations, performed with calibrations sources mounted on a filter wheel in front of each detector or with observations of well-characterized astrophysical sources, will be presented as well.

10397-18, Session 5

Imaging as a tool for the characterization of the gas pixel detector photoelectric polarimeter

Sergio Fabiani, INAF - Istituto di Astrofisica e Planetologia Spaziali (Italy)

The Gas Pixel Detector (GPD) is an X-ray polarimeter exploiting the photoelectric effect both to measure polarization and to obtain the image of astrophysical sources. This detector is on board the IXPE (Imaging X-ray Polarimetry Explorer) mission selected by NASA in the framework of the Explorer program for a launch in 2020. We report on the imaging capability of the GPD as a tool to perform a full detector characterization. X-ray photons are absorbed in a 1 cm thick gas cell and the absorption points are calculated by means of the analysis of the statistical momenta of the photoelectron ionization tracks. Imaging can be a useful tool to study the properties of gas diffusion and charge recombination along the drift if the image of the strip produced by an inclined X-ray beam is studied. The capability of track reconstruction can be studied along the depth of the drift because at each depth corresponds a position in the image plane along the strip. We report on the results of this measurement performed with the He 20% - DME 80 % filled detector foreseen on board the IXPE mission.

10397-19, Session 5

IXPE: The Imaging X-ray Polarimetry Explorer

Paolo Soffitta, INAF - Istituto di Astrofisica e Planetologia Spaziali (Italy)

IXPE, the Imaging X-ray Polarimetry Explorer, has been selected as a NASA SMEX mission to be flown at the end of 2020. It will perform polarimetry resolved in energy, in time and in angle as a break-through in High Energy Astrophysics.

IXPE will 're-open', after 40 years, a window in X-ray astronomy adding two more observables to the usual ones. It will directly measure the geometrical parameters of many different classes of sources eventually breaking possible degeneracies. The probed angular scales (30") are indeed larger than Chandra but nevertheless capable of producing the first X-ray polarization maps of extended objects with scientifically relevant sensitivity.

It will allow for mapping the magnetic fields in Pulsar Wind Nebualae and Super-Nova Remnants at the acceleration sites of 10-100 TeV electrons.

Finally it will probe vacuum birefringence effects in systems with magnetic fields far larger than those reachable with experiments on-Earth.

The payload of IXPE consists of three identical telescopes with mirrors provided by MSFC/NASA.

The focal plane is provided by ASI with the responsibility of the instrument by IAPS/INAF that includes the detector units with responsibility of INFN. ASI also provides, in kind, the Malindi Ground Station. The Mission Operation Center is at LASP while the Science Operation Center is at MSFC.

The operations phase lasts at least two years. All the data including those related to polarization will be made available soon to the general user.

In this paper we present the mission and the timelines its payload and we discuss few exemplary astrophysical targets.

10397-20, Session 6

The optomechanical design of the REDSoX sounding rocket experiment

Mark D. Egan, Timothy Hellickson, MIT Kavli Institute for Astrophysics and Space Research (United States); Herman Marshall, Massachusetts Institute of Technology (United States)

The Rocket Experiment Demonstration of a Soft X-ray Polarimeter (REDSoX) is an instrument proposed for launch on a Black Brant IX sounding rocket to carry out the first x-ray polarization measurement of an extragalactic source below 1 keV. The REDSoX instrument will consist of 4 major subsystems: the grazing incident optics, the grating assembly, the detector package with integrated polarizers, and the optical bench to which all components mount. The conventional, replicated nested shell mirror assembly houses a star tracker in the core and is protected prior to launch and upon descent/landing by a non-hermetic door assembly. Just past the x-ray optics there is a unique, staircase-like grating assembly attached to the space-frame optical bench organized in 3 sections with 120deg symmetry. The driving design challenge of this CAT-grating based assembly is the multiple-plane mounting: while minimizing obscuration by the support structure we need to provide a rigid frame that allows safe handling of the individual grating cells. The pattern of the grating assembly is matched on the focal plane by the location of the 3 polarizing laterally grated multi-layer mirrors (LGMLs) and the detectors, with a central detector that is used in 0th order for fine-tuning of the pointing. The central detector is shielded from optical light by an optical bandpass filter (OBF), while the other 3 are fully open but facing sideways and illuminated via the LGMLs oriented 45 degrees to the optical axis. The LGMLs work in concert with the gratings to produce a highly reflective and efficiently polarizing reflector, and the 120deg clocking allows for disentangling the 3 Stokes parameters. The sideways facing spectral detectors are baffled against direct and scattered light, and along with the on-axis CCD they are mounted in a small cooled vacuum enclosure at the end of the optical bench. The focal plane utilizes three titanium flexures that lift the focal plane and thermally isolate the detectors. The focal plane is passively cooled by LN2 before launch, and a gate valve to avoid condensation and contamination seals the vacuum volume. Trim heaters set the ideal CCD operating temperature. In this paper we present the opto-mechanical design derived from the mission requirements, including structures and initial thermal- and vibration analysis. We discuss the stress-free thermo-optical mounts, mechanisms, and the thermal management/control system.

10397-21, Session 6

The rocket experiment demonstration of a soft x-ray polarimeter

Herman Marshall, Norbert Schulz, Ralf K. Heilmann, Massachusetts Institute of Technology (United States); Brian Ramsey, NASA Marshall Space Flight Ctr. (United States); Sarah Heine, Massachusetts Institute of Technology (United States); Mark D. Egan, MIT Kavli Institute for Astrophysics and Space Research (United States); Timothy Hellickson, Massachusetts Institute of Technology (United States)

The Rocket Experiment Demonstration of a Soft X-ray Polarimeter (REDSoX Polarimeter) is a sounding rocket instrument that can make the first measurement of the linear X-ray polarization of an extragalactic source in the 0.2-0.8 keV band as low as 10%. We employ multilayer-coated mirrors as Bragg reflectors at the Brewster angle. By matching the dispersion of a spectrometer using replicated optics from MSFC and critical angle transmission gratings from MIT to three laterally graded multilayer mirrors (LGMLs), we achieve polarization modulation factors over 90%. We present a novel arrangement of gratings, designed optimally for the purpose of polarimetry with a converging beam. The entrance aperture is divided into six equal sectors; pairs of blazed gratings from opposite sectors are oriented to disperse to the same LGML. The LGML position angles are 120 degrees to each other. CCD detectors then measure the intensities of the dispersed spectra after reflection and polarizing by the LGMLs, giving the three Stokes parameters needed to determine the source polarization.

A current APRA grant is funding further development to improve the LGMLs. Sample gratings for the project have been fabricated at MIT and the development team continues to improve them under separate funding. Our technological approach is the basis for a possible orbital mission.

This work was supported in part by NASA grant NNX17AE11G to develop the design for a soft X-ray polarimeter.

10397-22, Session 6

Preparations for the Advanced Scintillator Compton Telescope (ASCOT) balloon flight

Tejaswita Sharma, Peter Bloser, Jason Legere, Christopher M. Bancroft, Mark McConnell, James M. Ryan, Alex M. Wright, The Univ. of New Hampshire (United States)

We describe our ongoing work to develop a new medium-energy gamma-ray Compton telescope using advanced scintillator materials combined with silicon photomultiplier readouts and fly it on a scientific balloon. There is a need in high-energy astronomy for a medium-energy gamma-ray mission covering the energy range from approximately 0.4 - 20 MeV to follow the success of the COMPTEL instrument on CGRO. We believe that directly building on the legacy of COMPTEL, using relatively robust, low-cost, off-the-shelf technologies, is the most promising path for such a mission. Fortunately, high-performance scintillators, such as Cerium Bromide ($CeBr_3$) and p-terphenyl, and compact readout devices, such as silicon photomultipliers (SiPMs), are already commercially available and capable of meeting this need. We are now constructing an Advanced Scintillator Compton Telescope (ASCOT) with SiPM readout, with the goal of imaging the Crab Nebula at MeV energies from a high-altitude balloon flight. We expect a ~4-sigma detection at ~1 MeV in a single transit. We present calibration results of the detector modules, and updated simulations of the balloon instrument sensitivity. If successful, this project will demonstrate that the energy, timing, and position resolution of this technology are sufficient to achieve an order of magnitude improvement in sensitivity in the medium-energy gamma-ray band, were it to be applied to a ~1 cubic meter instrument on a long-duration balloon or Explorer platform.

10397-23, Session 6

ximpol: a new x-ray polarimetry observation-simulation and analysis framework

Nicola Omodei, Stanford Univ. (United States) and MIT Kavli Institute for Astrophysics and Space Research (United States); Luca Baldini, Istituto Nazionale di Fisica Nucleare (Italy) and Univ. di Pisa (Italy); Niccolò Di Lalla, Melissa Pesce-Rollins, Istituto Nazionale di Fisica Nucleare (Italy)

We present a new simulation framework, ximpol, based on the Python programming language and the Scipy stack, specifically developed for X-ray polarimetric applications. ximpol is not tied to any specific mission or instrument design and is meant to produce fast and yet realistic observation-simulations, given as basic inputs: (i) an arbitrary source model including morphological, temporal, spectral and polarimetric information, and (ii) the response functions of the detector under study, i.e., the effective area, the energy dispersion, the point-spread function and the modulation factor. The format of the response files is OGIP compliant, and the framework has the capability of producing output files that can be directly fed into the standard visualization and analysis tools used by the X-ray community, including XSPEC---which make it a useful tool not only

for simulating physical systems, but also to develop and test end-to-end analysis chains.

In this contribution we will give an overview of the basic architecture of the software and present a few physically interesting case studies.

10397-24, Session 7

Development of digital system for the wide-field x-ray imaging detector aboard Kanazawa-SAT3

Yasuaki Kagawa, Daisuke Yonetoku, Tatsuya Sawano, Kanazawa Univ. (Japan); Tatehiro Mihara, RIKEN (Japan); Hirokazu Ikeda, Atsushi Harayama, Institute of Space and Astronautical Science (Japan); Makoto Arimoto, Waseda Univ. (Japan); Kazuki Yoshida, Masao Ina, Kaichi Ota, Yuki Minami, Kanazawa Univ. (Japan)

We are planning to launch a micro satellite, named KANAZAWA-SAT3, for a localization of gravitational wave sources with X-ray transients, for example short gamma-ray bursts originated from coalescence of neutron star-neutron star binaries and/or neutron star-black hole binaries. This satellite is designed to be a 50 cm cube and 50 kg class and going to be launched at the end of FY2018. Now we are developing a prototype model of wide field X-ray imaging detector aboard the satellite which covers the energy range of 1-20 keV with more than 1 str field of view.

This detector is composed of 1-dimensional coded aperture mask with tungsten and silicon strip detectors (SSDs) as X-ray imaging detector. The electric signals are read out by multi-channel ASICs controlled by FPGAs. In general, X-ray sky images are obtained by calculating the cross correlation function between the mask pattern and the detected X-ray intensity pattern. This pattern matching calculation with CPU is so easy but takes a lot of time because of many strips. Therefore, we newly designed a high speed X-ray imaging processor on FPGAs. This processor is able to make a 512 + 512 image (not 2-dimension but 2 set of 1-dimension) within 4 milliseconds at 8 MHz digital clock. Additionally we are developing a imaging trigger algorithm, which judges where X-ray came from and detect dim and long lasting X-ray transients from the X-ray sky images.

Using these systems, we also performed X-ray imaging experiments with six meter beamline in our laboratory, and confirmed the localization accuracy of 15 arcminutes. In our presentation, we report overview of the detector development, especially focusing on digital FPGA system, and show some results of X-ray imaging experiments.

10397-25, Session 7

The survey and time-domain astrophysical research explorer (STAR-X)

William W. Zhang, NASA Goddard Space Flight Ctr. (United States)

STAR-X was proposed in December 2016 as a MIDEX mission for launch in 2023. It is an X-ray telescope with the following characteristics: (1) large field of view; (2) excellent uniform PSF in the entire FOV; and (3) large effective area. STAR-X will catch and study transients, including those resulting from mergers of compact objects, supernova explosions, tidal disruptions, and gamma ray bursts. STAR-X will also conduct surveys to study the growth of compact objects, including stellar mass black holes in the Milky Way and nearby galaxies as well as distant, high-redshift supermassive black holes. The capabilities of STAR-X also enable the study of hot, low surface brightness diffuse emission from galaxy clusters and supernova remnants. STAR-X is facilitated by a spacecraft bus capable of autonomous and fast slewing to targets of opportunity. In this paper we will describe the STAR-X mission design, technology, and major science objectives and its synergy with other major observatories in the 2020s, including eROSITA, JWST, WFIRST, and Athena.

10397-26, Session 7

Performance of a double tilted-Rowland-spectrometer on ARCUS

Hans Moritz Günther, Massachusetts Institute of Technology (United States); The ARCUS Collaboration, Smithsonian Astrophysical Observatory (United States)

Spectroscopy of soft X-rays is an extremely powerful tool to understand the physics of the hot plasma in the universe but in many cases, such as kinematic properties of stellar emission lines or weak absorption features we have reached the limits of current instrumentation. Critical-angle transmission (CAT) gratings blaze the dispersed spectra into high orders and also offer a high throughput.

We present detailed ray-traces for the ARCUS mission, which promises an effective area > 0.5m^2 in the soft X-rays. It uses four modules of Athena-like silicon pore optics. Each module spans an azimuth of about 30 degrees and thus offers a point-spread function that is significantly narrower in one dimension than a full mirror would provide. The four channels are split into two pairs, where each pair has its own optical axis. For each pair, CAT gratings are arranged on a tilted Rowland torus and the two separate tori are positioned to overlap in such a way that the dispersed spectra from both pairs can be imaged onto a common set of CCD detectors, while at the same time keeping the requirement of the spectroscopic focus.

Our ray-traces show that a set of 16 CCDs is sufficient to cover both zeroths orders and over 90% of the dispersed signal. We study the impact of misalignment, finite size of components, off-axis sources, and spacecraft jitter on the spectral resolution and effective area and prove that the design achieves R > 3000 even in the presence of these non-ideal effects.

10397-27, Session 7

Arcus: Exploring the formation and evolution of clusters, galaxies, and stars

Randall K. Smith, Harvard-Smithsonian Ctr. for Astrophysics (United States)

The Large Scale Structure (LSS) of the Universe grew via the gravitational collapse of dark matter, but the visible components that trace the LSS–galaxies, groups and clusters–have a more complex history. Their baryons experience shock heating, radiative cooling and feedback from black holes and star formation, which leave faint signatures of hot (T~10^5-10^8 K), metal-enriched gas in the interstellar and intergalactic media (ISM and IGM). While recent Planck and X-ray studies support this scenario, no current mission possesses the instrumentation necessary to provide direct observational evidence for these "missing baryons." Arcus, a proposed MIDEX mission, leverages recent advances in critical-angle transmission (CAT) gratings and silicon pore optics (SPOs), using CCDs with strong Suzaku heritage and electronics based on the Swift mission; both the spacecraft and mission operations reuse highly successful designs. To be launched in 2023, Arcus will be the only observatory capable of studying, in detail, the hot galactic and intergalactic gas–the dominant baryonic component in the present-day Universe and ultimate reservoir of entropy, metals and the output from cosmic feedback. Its superior soft X-ray sensitivity will complement the forthcoming post-Hitomi and Athena calorimeters, which will have comparably high spectral resolution above 2 keV but poorer spectral resolution than XMM or Chandra in the Arcus bandpass.

10397-28, Session 7

The water recovery x-ray rocket (WRX-R)

Drew M. Miles, The Pennsylvania State Univ. (United States)

The Water Recovery X-ray Rocket (WRX-R) is a diffuse soft X-ray spectrometer that will launch on a sounding rocket from the Kwajalein Atoll. WRX-R has a field of view of >10 deg2 and will observe the Vela supernova remnant. A mechanical collimator, state-of-the-art off-plane reflection grating array and hybrid CMOS detector will allow WRX to achieve the most highly-resolved spectrum of the Vela SNR ever recorded. We present here an introduction to the instrument, the expected science return, and an update on the state of the payload as we work towards launch.

10397-29, Session 8

Lynx mission concept status

Jessica A. Gaskin, NASA Marshall Space Flight Ctr. (United States)

The Lynx Mission is a concept under study for prioritization in the 2020 Astrophysics Decadal Survey. Orders of magnitude increase in sensitivity over Chandra, Lynx will examine the first black holes and their galaxies, will map the large-scale structure and galactic halos, and shed new light on the environments of young stars and their planetary systems. This talk will present the concept development status and will highlight the optics and science instrument suite that will enable the next great X-Ray Observatory.

10397-30, Session 8

Conceptual design of the SMART dosimeter

Erik B. Johnson, Sam Vogel, Rebecca Frank, Graham Stoddard, Radiation Monitoring Devices, Inc. (United States); Alonzo Vera, COSMIAC (United States); David Alexander, David Alexander LLC (United States); James F. Christian, COSMIAC (United States)

Active dosimeters for astronauts and space weather monitors are critical tools for mitigating radiation induced health issues or system failure on capital equipment. Commercial spaceflight, deep space flight, and satellites require smarter, smaller, and lower power dosimeters. There are a number of instruments with flight heritage, yet as identified in NASA's roadmaps, these technologies do not lend themselves to a viable solution for active dosimetry for an astronaut, particularly for deep space missions. For future missions, nano- and micro-satellites will require compact instruments that will accurately assess the radiation hazard without consuming major resources on the spacecraft. RMD has developed the methods for growing an advanced scintillation material called phenylcarbazole, which provides pulse shape discrimination between protons and electrons. When used in combination with an anti-coincidence detector system, an assessment of the dose from charged ions and neutral particles can be determined. This is valuable as damage on a system (such as silicon or tissue) is dependent on the particle species. Using this crystal with readout electronics developed in partnership with COSMIAC at the University of New Mexico, the design of the Small Mixed field Autonomous Radiation Tracker (SMART) Dosimeter consists of a low-power analog to digital conversion scheme with low-power digital signal processing algorithms, which are to be implemented within a compact system on a chip, such as the Xilinx Zynq series. A review of the conceptual design is presented.

10397-31, Session 8

First results of Athena WFI prototype detectors

Wolfgang Treberspurg, Johannes Müller-Seidlitz, Robert Andritschke, Günter Hauser, Valentin Emberger, Annika Behrens, Norbert Meidinger, Max-Planck-Institut für extraterrestrische Physik (Germany)

The ATHENA observatory was selected as the second large-class mission in ESA Cosmic Vision 2015-2025, scheduled to be launch in 2028. To enable detailed explorations of the hot and energetic universe, two complementary focal-plane instruments are coupled to a high-performance X-ray telescope. One of these is the WFI (wide field imager). It features an unprecedented survey power by combining a large field of view of 40x40 arcmin2 with an excellent count rate capability (≥ 1 Crab). The large field of view is covered by four large arrays of monolithic 512x512 pixels sensors, while a second focal plane detector with fast readout enables observations of bright point sources. The energy resolution will be below 170 eV FWHM at 7 keV until the end of the nominal mission, with a readout time between 2.5 µs and 10 µs per sensor row.

This performance will be achieved with DEPFET (DEpleted P-channel FET) active pixel sensors. Each pixel contains a p-channel field effect transistor, which is integrated onto a fully depleted silicon bulk and provides a first amplification of the signal in the pixel itself. This is realized by creating an electrical potential minimum below the transistor gate in order to collect charge, generated inside the silicon bulk and modulate the channel conductivity.

To identify a detector concept, which optimally fulfils the scientific requirements, different variants of DEPFET sensors concerning the geometry and technology were implemented on a prototype production. Different concepts were studied and evaluated on small scale devices of 64x64 pixels with respect to the requirements of the WFI. Furthermore different readout mode were studied, in preparation of a fast operation of large detector devices.

10397-32, Session 8

The wide-field imager instrument for Athena

Norbert Meidinger, Kirpal Nandra, Markus Plattner, Arne Rau, Max-Planck-Institut für extraterrestrische Physik (Germany)

The WFI (Wide Field Imager) instrument is planned to be one of two complementary focal plane cameras on ESA's next X-ray observatory Athena. It combines unprecedented survey power through its large field of view of 40 arcmin x 40 arcmin together with excellent count-rate capability (≥ 1 Crab). High energy, spatial and time resolution are accomplished by the development of detectors using DEPFET active pixel sensors and custom-made control and readout ASICs. The large detector comprises 1024 x 1024 pixels and shall be operated with a frame rate of 200/s, whereas the high count-rate capable detector is planned to show a time resolution of 80 µs resulting in a throughput of more than 80% and a pile-up of less than 1% for an 1 Crab source intensity.

Prototypes of such detectors have been developed for the Athena project and tested. This included the development of electronics for operation of the detectors. In front of the camera head with the detectors is a filter wheel mounted which houses an ultra-thin optical blocking filter with a size of 16 cm x 16 cm.

Further subsystems of the instrument are the detector electronics and the instrument control and power distribution units.

We present the status of Athena's Wide Field Imager instrument including an outlook to the main future activities.

10397-33, Session 8

Updates on experimental grazing angle soft proton scattering

Sebastian Diebold, Sarah Hanschke, Emanuele Perinati, Eberhard Karls Univ. Tübingen (Germany); Randall K. Smith, Harvard-Smithsonian Ctr. for Astrophysics (United States); Christopher Tenzer, Andrea Santangelo, Josef Jochum, Eberhard Karls Univ. Tübingen (Germany)

Astronomical X-ray observatories are exposed to various kinds of orbital radiation that has the potential to compromise observations and to degrade the performance of the instruments. Particularly the soft proton component with energies below 10 MeV poses a major source for observational background and particle-induced damages in solid-state detectors. In-orbit experience has proven that soft protons are funneled much more efficient through Wolter-type X-ray optics than expected from simulations. In order to improve and validate simulations and, therefore, to enable a more realistic assessment of the soft proton flux near the focal plane of future X-ray telescopes, a series of grazing angle scattering experiments is being conducted at the University of Tübingen. In this contribution, the latest improvements of the experimental setup as well as preliminary results of the azimuthal scattering distribution on different targets are presented.

10397-8, Session PMon

An improved version of the Shadow Position Sensor readout electronics on board the ESA PROBA-3 Mission

Vladimiro Noce, Mauro Focardi, INAF - Osservatorio Astrofisico di Arcetri (Italy); Steve Buckley, SensL Technologies Ltd. (Ireland); François Denis, Ctr. Spatial de Liège (Belgium); Kevin O'Neill, SensL Technologies Ltd. (Ireland); Alessandro Bemporad, INAF - Osservatorio Astronomico di Torino (Italy); Silvano Fineschi, INAF - Osservatorio Astrofisico di Torino (Italy); Maurizio Pancrazzi, Federico Landini, Cristian Baccani, INAF - Osservatorio Astrofisico di Arcetri (Italy); Gerardo Capobianco, INAF - Osservatorio Astrofisico di Torino (Italy); Davide Loreggia, INAF - Osservatorio Astronomico di Torino (Italy); Marta Casti, INAF - Osservatorio Astrofisico di Torino (Italy); Marco Romoli, INAF - Osservatorio Astrofisico di Arcetri (Italy); Giuseppe Massone, Gianalfredo Nicolini, INAF - Osservatorio Astrofisico di Torino (Italy); Cédric Thizy, Ctr. Spatial de Liège (Belgium); Idriss Mechmech, Ctr. Spatial de Liège (Belgium); Etienne Renotte, Ctr. Spatial de Liège (Belgium)

PROBA3 is an ESA mission that consists of two satellites: the OSC (Occulter Spacecraft) and the CSC (Coronagraph Spacecraft) that will fly together in a rigid configuration. The two spacecraft will form together a giant (about 150 m) coronagraph instrument in space that will allow to study the solar corona closer to the limb than has ever before been achieved (1.02 Rsun). At the same time the mission will demonstrate the feasibility of precision formation-flying (FF) techniques.

The AOCS (Attitude and Orbit Control System) will keep the relative position of the two spacecraft with an unprecedented accuracy of 50 ?m transversal and 1 mm longitudinal ultimately relying on SPS (Shadow Position Sensor): a set of silicon photomultipliers (SiPM) that measures the light in the penumbra around the instrument opening and compares the readout to the expected illumination profile.

This paper presents the recent improvements adopted in the SPS electronics design that derive from the lessons learned during the first tests performed on the Evaluation Board and on the Development Model, the first two manufactured breadboards. The electronic amplification chain has been accurately reconsidered introducing e.g. precision components, a more stable voltage reference and reducing the dependency from temperature variations. Differential mode communication with the "external world" has been implemented as well as a system letting to operate contemporarily the two independent chains, either in the nominal and in the redundant case.

10397-9, Session PMon

Test plan for the PROBA3/ASPIICS scaled model measurement campaign

Federico Landini, INAF - Osservatorio Astrofisico di Arcetri (Italy); Cristian Baccani, Univ. degli Studi di Firenze (Italy); Sébastien Vives, Lab. d'Astrophysique de Marseille (France); Silvano Fineschi, INAF - Osservatorio Astrofisico di Torino (Italy); Marco Romoli, Univ. degli Studi di Firenze (Italy); Gerardo Capobianco, Giuseppe Massone, Marta Casti, INAF - Osservatorio Astrofisico di Torino (Italy); Alessandro Bemporad, INAF - Osservatorio Astronomico di Torino (Italy); Mauro Focardi, INAF - Osservatorio Astrofisico di Arcetri (Italy); Maurizio Pancrazzi, Univ. degli Studi di Firenze (Italy); Davide Loreggia, INAF - Osservatorio Astrofisico di Torino (Italy); Vladimiro Noce, INAF - Osservatorio Astrofisico di Arcetri (Italy); Alain Jody Corso, CNR-IFN Padova (Italy); Cédric Thizy, Etienne Renotte, Ctr. Spatial de Liège (Belgium)

PROBA3/ASPIICS (Association of Spacecraft for Polarimetric and Imaging Investigation of the Corona of the Sun) is the first formation flight solar coronagraph, scheduled by ESA for a launch and currently in phase C/D.

It is constituted by two spacecraft (one hosting the occulter, diameter 142 cm, and one with the telescope) separated by 144 m, kept in strict alignment by means of complex active and metrology custom systems.

The stray light analysis, which is always one the most critical work packages for a solar coronagraph, has been only theoretically investigated so far due to the difficulty of replicating the actual size system in a clean laboratory environment.

The light diffracted by the external occulter is the worst offender for the stray light level on the instrument focal plane, thus there is strong interest for scaling at least the occultation system of the coronagraph and test it in front of a solar simulator in order to experimentally validate the expected theoretical performance..

The theory for scaling the occulter, the occulter-pupil distance and the source dimension has been developed and a scaled model is being manufactured. A test campaign is going to be conducted at the OPSys facility in Torino in front of a solar simulator (conveniently scaled).

This work accounts for the description of the scaled model laboratory set-up and of the test plan.

10397-47, Session PMon

Transmission measurement of the spare Beryllium window of the SXS onboard the Hitomi satellite in 2.0-12 keV with KEK-PF

Yuki Yoshida, Akio Hoshino, Shunji Kitamoto, Jyuri Sugimoto, Ryouta Ishii, Yuki Ohgi, Sayaka Sato, S. Nukamori, Rikkyo Univ. (Japan); Ryuichi Fujimoto, Kanazawa Univ. (Japan); Noriko Y. Yamasaki, Institute of Space and Astronautical Science (Japan); Toshiaki Ina, Japan Synchrotron Radiation Research Institute (Japan); Tomoya Uruga, Japan Synchrotron Radiation Research Institute (Japan)

The Soft X-ray Spectrometer (SXS) onboard the Hitomi (ASTRO-H) satellite observed several celestial objects. All the observations were performed before the gave-vale(GV) opening and through the Be window installed on the GV. However, the Be window was not well calibrated before launching. Therefore, we measured the transmission of a spare Be window, which is from the same lot as the flight material. The measurements were preformed with BL01B1 for 3.8-30 keV range in SPring-8, and BL11B for 2.0-4.5 keV range and BL7C for 4.0-12 keV range in KEK-PF. The details of the SPring-8 experiment are reported as a separate paper. In this paper, we report the results of the KEK-PF experiment. With the BL7C, we measured five points of the Be window. Their estimated thicknesses are consistent with each other in 0.035% in the standard deviation. We detected absorption edges by Fe-K, Ni-K and Mn-K and four edge like features at 6057 eV, 6915 eV, 7590 eV and 9193 eV, which were interpreted as Bragg reflections by Be crystal. These are consistent with the results of the SPring-8 measurement. The edge-like feature at 8790 eV was detected only by KEK-PF experiment. The Be thickness obtained by experiment in range of 2.0-4.5 keV with BL-11C is also consistent with the results of the BL-7C and SPring-8 experiments.

10397-48, Session PMon

Semi-automated high-efficiency reflectivity chamber for vacuum UV measurements

James H. Wiley, Brian T. Fleming, Arika Egan, Univ. of Colorado Boulder (United States)

This paper presents the design and theory of operation for a semi-automated reflectivity chamber for ultraviolet optimized optics. A graphical user interface designed in LabVIEW controls the stages, interfaces with the detector system, takes semi-autonomous measurements, and monitors the system in case of error. Samples and an optical photodiode sit on an optics plate mounted to a rotation stage in the middle of the vacuum chamber. The optics plate rotates the samples and diode between an incident and reflected position to measure the absolute reflectivity of the samples at wavelengths limited by the monochromator operational bandpass of 70 nm to 550 nm. A fine steering tip-tilt motor on a collimating parabolic mirror enables beam steering for detector peak-ups. This chamber is designed to take measurements rapidly and with minimal oversight, increasing lab efficiency for high cadence and high accuracy vacuum UV reflectivity measurements.

10397-49, Session PMon

EXACT: The experiment for characterization and timing cubesat

Trevor Knuth, Univ. of Minnesota (United States); Lindsay Glesener, Univ. of Minnesota, Twin Cities (United States); Demoz Gebre-Egziabher, Univ. of Minnesota, Twin Cities (United States); Ryan Vogt, Hannah Weiher, Joel Runnels, Kale Hedstrom, Tim Kukowski, Maxwell Yurs, Kendra Bergstedt, Cynthia Cattell, Jeffrey Chaffin, Richard Linares, Gjerda RhodeHumphries, Univ. of Minnesota (United States)

The Experiment for X-ray Characterization and Timing (EXACT) mission will be a CubeSat based hard X-ray spectrometer used for measuring solar flares with high time precision. Solar flares and the related coronal mass ejections affect space weather and the near-Earth environment. EXACT can study the hard X-rays generated by the Sun in the declining phase of Solar Cycle 24 in order to probe electron acceleration in solar eruptive events while also serving as a precursor to future hard X-ray spectrometers that could monitor the Sun continuously.

EXACT will be a 3U CubeSat with 1U dedicated to a detector and 2U dedicated to avionics. The detector used will have a surface area of roughly 60 square cm. This allows for a large collecting area despite the spacecraft's small overall size. The detector, named the Gamma-Ray Incidence Detector (GRID), is a thallium-doped cesium iodide scintillator.

10397-50, Session PMon

The third flight of the Colorado high-resolution echelle stellar spectrograph (CHESS): improvements, calibrations, and preliminary results

Nicholas Kruczek, Lab. for Atmospheric and Space Physics (United States); Kevin C. France, Keri Hoadley, Nicholas Nell, Robert Kane, Brian T. Fleming, Univ. of Colorado Boulder (United States)

In this proceeding, we describe the scientific motivation and technical development of the Colorado High-resolution Echelle Stellar Spectrograph (CHESS), focusing on the hardware advancements and testing of components for the third launch of the payload (CHESS-3). CHESS is a far ultraviolet rocket-borne instrument designed to study the atomic-to-molecular transitions within translucent cloud regions in the interstellar medium. CHESS is an objective echelle spectrograph, which uses a mechanically-ruled echelle and a powered (f/12.4) cross-dispersing grating, and is designed to achieve a resolving power R > 100,000 over the band pass ?? 1000 - 1600 Å. Results from final efficiency and reflectivity measurements for the optical components of CHESS-3 are presented. CHESS-3 utilizes a 40mm-diameter cross-strip anode readout microchannel plate detector fabricated by Sensor Sciences LLC, to achieve high spatial resolution with high global count rate capabilities (~1 MHz). We present pre-flight laboratory spectra and calibration results, including wavelength solution and resolving power of the instrument. In support of the fourth launch of CHESS (CHESS-4), the CHESS-3 payload includes a photomultiplier tube, which will confirm the alignment of the CHESS-4 detector. An important role of sounding rocket experiments is the testing and verification of space-flight for experimental technologies. CHESS-4 will demonstrate a delta-doped CCD, assembled in collaboration with the Microdevices Laboratory at JPL and Arizona State University. CHESS-3 was scheduled to launch on 14 June 2017 aboard NASA/CU sounding rocket mission 36.323 UG. We present initial flight results for the CHESS-3 observation of the ? Sco? sightline.

10397-51, Session PMon

On-ground characterization of the IXPE polarization angle knowledge

Yuri Evangelista, INAF - Istituto di Astrofisica e Planetologia Spaziali (Italy)

The Imaging X-ray Polarimetry Explorer (IXPE) has been recently selected for development as part of NASA's Small Explorer program (SMEX), with a launch date in 2020.

IXPE is developed in a collaboration between NASA and the Italian Space Agency (ASI), and will perform groundbreaking measurements of imaging polarization in X-rays for a number of different classes of sources including isolated and accreting neutron stars, pulsar wind nebulae, stellar and supermassive black holes.

Combining 30-arcseond (HPD) grazing-incidence X-ray optics with the polarization-sensitive gas pixel detectors (GPDs) IXPE will provide two-orders of magnitude improvement in sensitivity over past flown instruments.

The IXPE requested precision on the measurement of the polarization angle (goal of 12') poses strict constraints

on the detector unit (DU) mechanical design and requires a specifically developed metrological procedure to meet the scientific performance.

In this paper we describe the design solutions that will be implemented in the DU flight models as well as a step-by-step metrology procedure that will ensure the fulfilment of the scientific requirement.

10397-52, Session PMon

The Marshall Grazing Incidence X-ray Spectrometer

Ken Kobayashi, Amy R. Winebarger, Sabrina Savage, NASA Marshall Space Flight Ctr. (United States); Patrick Champey, The Univ. of Alabama in Huntsville (United States); Peter N. Cheimets, Edward Hertz, Leon Golub, Smithsonian Astrophysical Observatory (United States); Brian Ramsey, ?Jaganathan Ranganathan, NASA Marshall Space Flight Ctr. (United States); Vanessa Marquez, Ryan Allured, Theodore Parker, Smithsonian Astrophysical Observatory (United States); Ralf K. Heilmann, Mark L. Schattenburg, Massachusetts Institute of Technology (United States)

The Marshall Grazing Incidence X-ray Spectrometer (MaGIXS) is a NASA sounding rocket instrument designed to obtain spatially resolved soft X-ray spectra of the Solar atmosphere in the 6-24 Å (0.5 - 2.0 keV) range. The instrument consists of a single shell Wolter Type-I telescope, a slit, and a spectrometer comprising a matched pair of grazing incidence parabolic mirrors and a planar varied-line space diffraction grating. The instrument is designed to achieve a 50 milli-Angstrom spectral resolution and 5 arcsecond spatial resolution along a 4-arcminute long slit, and launch is planned for 2018. We report on the status and our approaches for fabrication and alignment for this novel optical system. The telescope and spectrometer mirrors are replicated nickel shells, and are currently being fabricated at the NASA Marshall Space Flight Center. The diffraction grating is currently under development by the Massachusetts Institute of Technology (MIT); because of the strong line spacing variation across the grating, it will be fabricated through e-beam lithography.

10397-53, Session PMon

ART-XC/SRG: Joint calibration of mirror modules and x-ray detectors

Alexey Tkachenko, Mikhail N. Pavlinsky, Vasily Levin, Valeriy V. Akimov, Aleksandr Krivchenko, Alexey Rotin, Maria M. Kuznetsova, Igor Y. Lapshov, Alexander Yaskovich, Vladimir Alexandrovich Oleynikov, Space Research Institute (Russian Federation); Mikhail V. Gubarev, Brian Ramsey, NASA Marshall Space Flight Ctr. (United States)

The Astronomical Roentgen Telescope – X-ray Concentrator (ART-XC) is a hard x-ray instrument with energy response 6–30 keV that will to be launched on board of the Spectrum Roentgen Gamma (SRG) Mission. The ART-XC consists of seven co-aligned mirror modules coupled with seven focal plane CdTe double-sided strip detectors. The mirror modules had been fabricated and calibrated at the NASA Marshall Space Flight Center (MSFC). The Russian Space Research Institute (IKI) has been developed and tested the X-ray detectors. The joint x-ray calibration of the mirror modules and focal plane detectors was carried out at the IKI test facility. Details of the calibration procedure and an overview of the results will be presented.

10397-54, Session PMon

Characterization of the UV detector of Solar Orbiter/METIS

Michela C. Uslenghi, INAF - IASF Milano (Italy); Udo H. Schühle, Luca Teriaca, Max-Planck-Institut für Sonnensystemforschung (Germany)

METIS, one of the instruments of the ESA mission Solar Orbiter (to be launched in October 2018), is a coronograph able to perform broadband polarization imaging in the visible range (580-640 nm), and narrow band imaging in UV (HI Lyman-? 121.6nm) .

The detector of the UV channel is an intensified camera, based on a Star-1000 rad-hard CMOS APS coupled via a 2:1 fiber optic taper to a single stage Microchannel Plate intensifier, sealed with an entrance MgF2 window and provided with an opaque KBr photocathode. The qualification model and the flight UVDA (UV Detector Assembly) have been characterized and calibrated in the UV range using the Physikalisch-Technische Bundesanstalt (PTB) beamline at the BESSY-II synchrotron.

We present the description of the test setup and the results of the measurements carried out, which include:

- Spectral calibration in the range 115-300 nm
- Linearity of the response vs flux at 121.6 nm
- Linearity of the response vs exposure time
- Characterization of the gain vs intensifier voltages
- Response uniformity at 121.6 nm

10397-34, Session 9

Life testing of ALD-GCA MCPs: recent results

Mark A. Popecki, Christopher A. Craven, Till Cremer, William A. Worstell, Michael J. Minot, Bernhard W. Adams, Michael R. Foley, Alexey Lyashenko, Justin L. Bond, Michael E. Stochaj, Incom, Inc. (United States); Camden Ertley, Oswald H. W. Siegmund, Space Sciences Lab. (United States); Jeffrey W. Elam, Anil U. Mane, Argonne National Lab. (United States)

Microchannel plates have been made by combining glass capillary substrates with thin films. The films impart the resistance and secondary electron emission (SEE) properties of the MCP. This approach permits separate choices for the type of glass, the MCP resistance and the SEE material. For example, the glass may be chosen to provide mechanical strength, a high open area ratio, or a low potassium-40 concentration to minimize dark rates. The resistive film composition may be tuned to provide the desired resistance, depending on the power budget and anticipated count rate. Finally, the SEE material may be chosen by balancing requirements for gain, long term stability of gain with extracted charge, and tolerance to air exposure.

Microchannel plates have been fabricated by Incom Inc., in collaboration with Argonne National Laboratory and UC Berkeley. Glass substrates with microchannel diameters of 10 and 20 microns have been used, typically with a length to diameter ratio of 60:1. Thin films for resistance and SEE are applied using Atomic Layer Deposition (ALD). The ALD technique provides a film with uniform thickness throughout the high aspect ratio microchannels. MCPs have been made in sizes up to 8"x8". This three-component method for manufacturing MCPs also makes non-planar, curved MCPs possible.

Life testing results will be presented for 10 and 20 micron, 60:1 l/d ratio MCPs, with an aluminum oxide SEE film and two types of glass substrates. Results will include measurements of resistance, dark count rates, gain, and pulse height distributions as a function of extracted charge.

10397-35, Session 9

ALD-microchannel plates for cryogenic applications

Till Cremer, Bernhard W. Adams, Melvin Aviles, Justin L. Bond, Christopher A. Craven, Michael R. Foley, Alexey Lyashenko, Michael J. Minot, Mark A. Popecki, Michael E. Stochaj, William A. Worstell, Incom, Inc. (United States); Jeffrey W. Elam, Anil U. Mane, Argonne National Lab. (United States); Oswald H. W. Siegmund, Camden Ertley, Univ. of California, Berkeley (United States)

Atomic layer deposition (ALD) has enabled the development of a new technology for fabricating microchannel plates (MCPs) with improved performance that offer transformative benefits to a wide variety of applications. Incom uses a "hollow-core" process for fabricating glass capillary array (GCA) plates consisting of millions of micrometer-sized glass microchannels fused together in a regular pattern. The resistive and secondary electron emissive (SEE) functions necessary for electron amplification are applied to the GCA microchannels by ALD, which – in contrast to conventional MCP manufacturing– enables independent tuning of both resistance and SEE to maximize and customize MCP performance.

Incom is currently developing MCPs that operate at cryogenic temperatures and across wide temperature ranges. The resistive layers in both, conventional and ALD-MCPs, exhibit semiconductor-like behavior and therefore a negative thermal coefficient of resistance (TCR): when the MCP is cooled, the resistance increases, and when heated, the resistance drops. Consequently, the resistance of each MCP must be tailored for the intended operating temperature. This sensitivity to temperature changes presents a challenge for many terrestrial and space based applications.

The resistivity of the ALD-nanocomposite material can be tuned over a wide range. The material's (thermo-) electrical properties depend on film thickness, composition, nanostructure, and the chemical nature of the dielectric and metal components. We show how the structure-property relationships developed in this work can be used to design MCPs that operate reliably at cryogenic temperatures. We also present data on how the resistive material's TCR characteristics can be improved to enable MCPs operating across wider temperature ranges than currently possible.

10397-36, Session 9

Epitaxial deposition of high-efficiency GaN photocathodes on microchannel plates using lattice-matched metallic buffers

Amir Dabiran, Sara Rothwell, Stephenie Tandean, Robert J. Jorgenson, Lightwave Photonics, Inc. (United States); Anton S. TRemsin, Oswald H. W. Siegmund, Univ. of California, Berkeley (United States)

Negative electron affinity (NEA) semiconductor photocathodes are commonly used in combination with electron multipliers, such as microchannel plates (MCPs), to fabricate sensitive phototubes. In recent years, there have been significant improvements in the performance of these detectors by enhancing quantum efficiency (QE), and by advances in MCPs and readout techniques. In particular, robust GaN-based photocathodes have shown very high QE (> 80% in deep UV), for operation in opaque mode (front side illuminated). However, the QE values are much smaller for semitransparent (backside illuminated) GaN photocathodes, which are used in conjunction with MCP stacks in typical phototubes. Substantial improvements in QE, as well as spatial and temporal resolutions, for these detectors are expected if the high quality photocathode film can be directly deposited on the MCP surface. Previous attempts to deposit opaque p-type GaN cathodes on different MCP substrates have not resulted in high QE photoemission due to the much lower quality of GaN on these MCPs as compared to GaN grown on typical sapphire substrates. In this presentation, we will show performance of high quality p-doped GaN photocathodes deposited on standard MCPs using a lattice-matched transition metal-nitride buffer layer, all deposited by a low-temperature magnetron sputtering epitaxy (MSE) technique. In addition to a suitable buffer layer for epitaxial growth of GaN, the highly conductive transition metal-nitride layer acts as both the MCP electrode and as a blanket back-contact to improve the lateral conductivity of the thin p-GaN film in order to avoid charging effects away from periphery metal contacts.

10397-37, Session 9

Microchannel plate detector technology potential for LUVOIR and HabEx

Oswald H. W. Siegmund, Space Sciences Lab. (United States); Eric R. Schindhelm, Southwest Research Institute (United States); Camden Ertley, Space Sciences Lab. (United States); Brian T. Fleming, Kevin C. France, Univ. of Colorado Boulder (United States); Walter M. Harris, The Univ. of Arizona (United States); Alex Harwit, Ball Aerospace & Technologies Corp. (United States); Stephan R. McCandliss, Johns Hopkins Univ. (United States); John V. Vallerga, Space Sciences Lab. (United States)

Microchannel plate (MCP) detectors have been the workhorse detector of choice for ultraviolet (UV) instruments onboard many NASA missions. MCP UV detectors have many advantages, including high spatial resolution (<20 um), photon counting, radiation hardness, large formats (up to 20 cm), and ability for curved surfaces. We summarize the current state of the main component technologies; MCP substrates, photocathodes and anode/readout systems. Borosilicate glass microcapillary arrays with atomic layer deposition combine extremely low backgrounds, high strength, and tunable secondary electron yield. GaN and combinations of bialkali/alkali halide photocathodes show promise for broadband, higher quantum efficiency. Cross-strip anodes combined with compact ASIC readout electronics enable high spatial resolution over large formats and high dynamic range. Their technology readiness level are each being advanced through research grants for laboratory testing and rocket flights. Combining these capabilities would be ideal for a UV instrument onboard the Large UV/Optical/IR Surveyor (LUVOIR) or Habitable Exoplanet Imaging Mission (HabEx) concepts currently under study for NASA's Astrophysics Decadal Survey.

10397-38, Session 9

Microchannel plate life testing for UV spectroscopy instruments

Nathan Darling, Univ. of California, Berkeley (United States)

The Emirates Mars Mission (EMM) UV Spectrograph (EMUS) is a far ultraviolet (102-170 nm) imaging spectrograph for characterization of the Martian exosphere and thermosphere. Imaging is accomplished by a photon counting open-face microchannel plate (MCP) detector using a cross delay line (XDL) readout. A MCP gain stabilization (burn-in) followed by lifetime spectral line burn-in simulation has been completed at SSL. This has demonstrated gain and sensitivity stability of ≤ 5% for total dose of 2.3 x 10^12 photons cm-2 at ~6 kHz mm-2 counting rates after and initial burn in at low gain has been performed.

10397-39, Session 10

The LUVOIR Ultraviolet Multi-Object Spectrograph (LUMOS):instrument definition and design

Kevin C. France, Brian T. Fleming, Univ. of Colorado Boulder (United States); Garrett J. West, NASA Goddard Space Flight Ctr. (United States); Stephan R. McCandliss, Johns Hopkins Univ. (United States); John O'Meara, Saint Michael's College (United States); Jason Tumlinson, Space Telescope Science Institute (United States); David Schiminovich, Columbia Univ. (United States); Matthew R. Bolcar, NASA Goddard Space Flight Ctr. (United States); Walter M. Harris, The Univ. of Arizona (United States);

Leonidas A. Moustakas, Jet Propulsion Lab. (United States)

The LUVOIR Surveyor is being designed to pursue an ambitious program of exoplanetary discovery and characterization, cosmic origins astrophysics, and planetary science. The LUVOIR Ultraviolet Multi-Object Spectrograph, LUMOS, is being designed to support all of the UV science requirements of LUVOIR, from exoplanet host star characterization to tomography of circumgalactic halos to water plumes on outer solar system satellites. LUMOS offers point source and multi-object spectroscopy across the UV bandpass, with multiple resolution modes to support different science goals. The instrument will provide low (R = 5,000 – 15,000) and medium (R = 20,000 – 60,000) resolution modes across the far-ultraviolet (FUV: 100 – 200 nm) and near-ultraviolet (NUV: 200 – 400 nm) windows, and a very low resolution mode (R = 500) for spectroscopic investigations of extremely faint objects in the FUV. Imaging spectroscopy will be accomplished over a 2 ? 2 arcminute field-of-view by employing a holographically-ruled diffraction grating to control optical aberrations, microshutter arrays that build on the heritage of the JWST/NIRspec instrument, advanced optical coatings for high-throughput in the FUV, and next generation large-format photon-counting detectors. The spectroscopic capabilities of LUMOS are augmented by an FUV imaging channel (100 – 200nm, 30 milliarcsecond angular resolution, 2 x 2 arcminute field-of-view) that will employ a complement of narrow- and medium-band filters. We present an overview of LUMOS' observing modes and estimated performance curves for effective area, spectral resolution, and imaging performance. Example “LUMOS 100-hour Highlights” observing programs are presented to demonstrate the potential power of LUVOIR's ultraviolet spectroscopic capabilities.

10397-40, Session 10

The synergy instrument

Jonathan W. Arenberg, Northrop Grumman Aerospace Systems (United States); Carlton Wong, Xinetics Inc. (United States); Tom Mallen, Northrop Grumman Aerospace Systems (United States); Thomas Mooney, Materion Corp. (United States); John W. MacKenty, Jason Tumlinson, Space Telescope Science Institute (United States)

Synergy is an Explorer class mission concept to conduct a large area near-ultraviolet spectroscopic survey. This paper describes the optics and science instrument. The instrument has a wide field of view, 5 square degrees, and the capability of simultaneous imaging and low-resolution slitless spectroscopy in the 220-320 nm band and efficient rejection of out of band light. The wide FOV is achieved with an all reflective off-axis 4-mirror anastigmat, a dispersive element and an all-reflective reimaging system. The system level performance is sub-arcsecond level image quality and ?/d? from 200-600. The optical train mirrors are proven Silicon/Silicon Carbide technology. The high UV sensitivity is achieved through distributed out of-band rejection at each of the four telescope mirrors, achieving at least 104 and more typically105 rejection for out-of-band light, while maintaining more than 65% transmission in the near ultraviolet band onto six 4K x 4K CCDs with 15 micron pixels. A shutter and fused-silica dispersive element are located at the exit pupil of the telescope. The shutter can be positioned to enable the default imaging with spectra mode, a pure imaging mode and dark and flat field calibration modes. The operation of the instrument is also discussed.

10397-41, Session 10

The development and characterization of advanced broadband mirror coatings for the far-UV

Arika Egan, Brian T. Fleming, James H. Wiley, Univ. of Colorado Boulder (United States); Manuel A. Quijada, Javier G. Del Hoyo, NASA Goddard Space Flight Ctr. (United States); John Hennessy, Jet Propulsion Lab. (United States); Brian A. Hicks, Univ. of Maryland, College Park (United States) and NASA Goddard Space Flight Ctr. (United States); Kevin C. France, Nicholas Kruczek, Nicholas Erickson, Univ. of Colorado Boulder (United States)

We present a progress report on the development of new broadband mirror coatings that demonstrate > 80% reflectivities from 102 - 120 nm. We describe a multi-stage approach to the deposition and testing of these advanced coatings: First, the combination of high temperature physical vapor deposition developed at NASA Goddard Space Flight Center was used to coat the mirror with aluminum and a protective fluoride overcoat, and then an ultra-thin (10-30 angstroms) layer of a second fluoride was deposited via atomic layer deposition (ALD) at the Jet Propulsion Laboratory to increase durability. Second, a bench top system was fabricated at the University of Colorado to obtain the polarized reflectivities of the mirrors as a function of wavelength at optical and near-UV wavelengths. Polarized reflectivity into the far-UV was obtained in collaboration with the Synchrotron Ultraviolet Radiation Facility (SURF) at NIST. Third, we extrapolate on previous aging studies to assess the coating durability under exposure to controlled humidity. We find that our experimental coatings offer ~30% greater reflectivity than conventional Al+LiF, and that a protective ALD layer reduces the hygroscopic degradation of coatings such as LiF by as much as 35%, with further gains possible. We discuss the performance of these new coatings in the context of the requirements for the NASA concept missions LUVOIR and HabEx.

10397-42, Session 10

Optical measurements of the mirrors and of the interferential filter of the Metis coronagraph on Solar Orbiter

Paolo Sandri, Paolo Sarra, Paolo Radaelli, D. Morea, OHB Italia SpA (Italy); Radek Melich, Institute of Plasma Physics, TOPTEC department (Czech Republic); Arkadiusz Berlicki , Astronomical Institute, Academy of Sciences of the Czech Republic (Czech Republic); Ester Antonucci, INAF - Astrophysical Observatory of Torino (Italy); Marco M. Castronuovo, ASI - Agenzia Spaziale Italiana (Italy); Silvano Fineschi, INAF - Astrophysical Observatory of Torino (Italy); Giampiero Naletto, Dept. of Information Engineering - University of Padova (Italy) and CNR-IFN UOS Padova LUXOR (Italy); Gianalfredo Nicolini, INAF - Astrophysical Observatory of Torino (Italy); Marco Romoli, Dept. of Physics and Astronomy, University of Florence, (Italy)

The paper describes the wavefront error measurements of the concave ellipsoidal mirrors M1 and M2, of the concave spherical mirror M0 and of the flat interferential filter IF of the METIS coronagraph. METIS is an inverted occultation coronagraph on board of the ESA Solar Orbiter mission that will provide a broad-band imaging of the full corona in linearly polarized visible-light (580-640 nm) and a narrow-band imaging of the full corona in the ultraviolet Lyman ? (121.6 nm). METIS will observe the solar outer atmosphere from a close distance to the Sun as 0.28 A.U. and from up to 35deg out-of-ecliptic. The measurements of wavefront error of the mirrors and of the interferential filter of METIS have been performed in a ISO 5 clean room both at component level and at assembly level minimizing, during the integration, the stress introduced by the assembling of the optical items with the mechanical hardware. The wavefront error measurements have been performed with a digital interferometer for mirrors M0, M1 and M2 and with a Shack-Hartmann wavefront sensor for the interferential filter.

10397-43, Session 11

LRO-LAMP failsafe door-open performance: improving FUV measurements of dayside lunar hydration

Michael W. Davis, Thomas K. Greathouse, David E. Kaufmann, Kurt D. Retherford, Maarten H. Versteeg, Southwest Research Institute (United States)

The Lunar Reconnaissance Orbiter's (LRO) Lyman Alpha Mapping Project (LAMP) is a lightweight (6.1 kg), low-power (4.5 W), ultraviolet spectrograph based on the Alice instruments aboard the European Space Agency's Rosetta spacecraft and NASA's New Horizons spacecraft. Its primary job is to identify and localize exposed water frost in permanently shadowed regions (PSRs) near the Moon's poles, and to characterize landforms and albedos in PSRs. LRO launched on June 18, 2009 and reached lunar orbit four days later. LAMP operated with its failsafe door closed for its first seven years in flight. The failsafe door was opened in October 2016 to increase light throughput during dayside operations at the expense of no longer having the capacity to take further dark observations and slightly more operational complexity to avoid saturating the instrument. This one-time irreversible operation was approved after extensive review, and was conducted flawlessly. The improved throughput allows measurement of dayside hydration in one orbit, instead of averaging multiple orbits together to reach enough signal-to-noise. The new measurement mode allows greater time resolution of dayside water migration for improved investigations into the source and loss processes on the lunar surface. LAMP performance and optical characteristics after the failsafe door opening are described herein, including the new effective area, wavelength solution, and resolution.

10397-44, Session 11

Scattered light characterization of FORTIS

Stephan R. McCandliss, Anna Carter, Keith Redwine, Johns Hopkins Univ. (United States); Alexander S. Kutyrev, John G. Hagopian, Mary J. Li, Harvey H. Moseley, NASA Goddard Space Flight Ctr. (United States); Russell Pelton, Johns Hopkins Univ. (United States)

We describe our efforts to build a wide-field Lyman alpha geocoronal simulator (WFLaGs) for characterizing the end-to-end sensitivity of FORTIS (Far-UV Off Rowland-circle Telescope for Imaging and Spectroscopy) to scattered Lyman alpha emission from outside of the nominal (1/2 degree)^2 field-of-view (FOV). WFLaGs is a 50 mm diameter F/1 aluminum parabolic collimator fed by a hydrogen discharge lamp with a 80mm clear MgF2 window housed in a vacuum skin. It creates emission over a 10 degree FOV. WFLaGS will allow us to validate a recently developed scattered light model and verify our scatter light mitigation strategies, which will incorporate low scatter baffle materials, and possibly 3-d printed light traps, for covering exposed scatter centers. We present measurements of scattering intensity of Lyman alpha as a function of angle with respect to the specular reflectance direction for several candidate baffle materials. Initial testing of WFLaGs will be described. This work is supported by NASA grants to John Hopkins University, NNX11AG54G and NNX17AC26G.

10397-45, Session 11

Low-latitude ionospheric research using the CIRCE mission

Kenneth F. Dymond, Andrew C. Nicholas, Scott A. Budzien, Andrew W. Stephan, U.S. Naval Research Lab. (United States)

The Coordinated Ionospheric Reconstruction Cubesat Experiment (CIRCE) is a dual-satellite mission consisting of two 6U CubeSats actively maintaining a lead-follow configuration in the same orbit with a launch planned for the 2018-2019 time-frame. These nanosatellites will each feature two 1U ultraviolet photometers, observing the 135.6 nm emission of atomic oxygen at nighttime. The primary objective is to characterize the two-dimensional distribution of electrons in the Equatorial Ionization Anomaly (EIA). The methodology used to reconstruct the nighttime ionosphere employs continuous UV photometry from four distinct viewing angles in combination with an additional data source, such as in situ plasma density measurements or a wide-band beacon data, with advanced image space reconstruction algorithm tomography techniques. The COSMIC/FORMOSAT-3 (CF3) constellation featured six Tiny Ionospheric Photometers, a compact UV sensor design which served as the pathfinder for the CIRCE instruments. The TIP instruments on the CF3 satellites demonstrated detection of ionospheric bubbles before they had penetrated the peak of the F-region ionosphere. We present our mission concept, simulations illustrating the imaging capability of the sensor suite, and a range of science questions addressable using such a system.

10397-46, Session 11

The Colorado Ultraviolet Transit Experiment (CUTE): A dedicated cubesat mission for the study of exoplanetary mass loss and magnetic fields

Brian T. Fleming, Kevin C. France, Nicholas Nell, Richard A. Kohnert, Keri Hoadley, Jean-Michel Desert, Univ. of Colorado Boulder (United States); Pascal M. Petit, Univ. de Toulouse (France); Aline A. Vidotto, Univ. de Genève (Switzerland); Matthew Beasley, Planetary Resources, Inc. (United States); Luca Fossati, Austrian Academy of Sciences (Austria); Tommi T. Koskinen, The Univ. of Arizona (United States)

The Colorado Ultraviolet Transit Experiment (CUTE) is a near-UV (2500 – 3500 Angstrom) 6U cubesat mission designed to monitor transiting hot Jupiters for evidence of atmospheric mass loss and magnetic fields. CUTE maximizes the available cubesat space by means of an innovative optical system to achieve a projected effective area of ~22 cm^2, low instrumental background, and a spectral resolving power of R~2000 over the entire science bandpass. We present the CUTE optical and mechanical design, a summary of the science motivation and expected results, and an overview of the projected fabrication, calibration and launch timeline. CUTE will launch in 2020 and has a nominal baseline mission of 6 months.

Conference 10398: UV/Optical/IR Space Telescopes and Instruments: Innovative Technologies and Concepts VIII

SPIE. OPTICS+ PHOTONICS OPTICAL ENGINEERING+ APPLICATIONS

Sunday - Tuesday 6 –8 August 2017

Part of Proceedings of SPIE Vol. 10398 UV/Optical/IR Space Telescopes and Instruments: Innovative Technologies and Concepts VIII

10398-1, Session 1

The Habitable Exoplanet Imaging Mission (HabEx) *(Invited Paper)*

Bertrand P. Mennesson, Jet Propulsion Lab. (United States)

The Habitable-Exoplanet Imaging Mission (HabEx) is a candidate flagship mission being studied by NASA and the astrophysics community in preparation of the 2020 Decadal Survey. The HabEx mission concept is a large (~4 to 6.5m) diffraction-limited optical space telescope, providing unprecedented resolution and contrast in the optical, with likely extensions into the near UV and near infrared domains.

The primary goal of HabEx is to answer fundamental questions in exoplanet science, searching for and characterizing potentially habitable worlds, providing the first complete "family portraits" of planets around our nearest Sun-like neighbors and placing the solar system in the context of a diverse set of exoplanets.

At the same time, HabEx will enable a broad range of Galactic, extragalactic, and solar system astrophysics, from resolved stellar population studies that inform the stellar formation history of nearby galaxies, to characterizing the life cycle of baryons as they flow in and out of galaxies, to detailed studies of bodies in our own solar system.

We report here on our team's early efforts in defining a scientifically compelling HabEx mission that is technologically executable, affordable within NASA's expected budgetary envelope, and timely for the next decade. In particular, we present preliminary architectures trade study results, quantifying technical requirements and predicting scientific outcome for a small number of design reference missions, all with broad capabilities in both exoplanet science and cosmic origins science.

This research was carried out at the Jet Propulsion Laboratory, California Institute of Technology, under a contract with the National Aeronautics and Space Administration.

10398-2, Session 1

Habitable Exoplanet Imaging Mission (HabEx) initial flight system design

Farah Alibay, Gary M. Kuan, Keith R. Warfield, Jet Propulsion Lab. (United States)

The Habitable Exoplanet Imaging Mission (HabEx) is a concept for a mission to directly image planetary systems around Sun-like stars, being studied as part of a number of mission concepts for the upcoming 2020 Astrophysics Decadal Survey. HabEx would help assess the prevalence of habitable planets in our galaxy, searching in particular for potential biosignatures in the atmospheres of planets in habitable zones. More generally, HabEx would image our neighboring solar systems and characterize the variety of planets that inhabits them. Its direct imaging capability would also enable the mission to study the structure and evolution of debris disks around nearby stars, and their dynamical interaction with planets.

These science goals lead to a mission with a requirement for high contrast imaging requirements and the continuous spectral coverage. The baseline for HabEx is a 4-meter diameter off-axis telescope designed to both search for habitable planets and perform general astrophysics observations, possibly combined with a starshade. We present the initial flight system design for both the telescope and the starshade, focusing on the key and driving requirements and subsystems, as well as the trajectory and station keeping and formation flying technique. Furthermore, we discuss some of the initial design trades undergone, as well as the key challenges and enablers. Finally, we explore some of the future design and architecture trades to be performed within the flight system as part of the continuing effort in the HabEx study.

10398-3, Session 1

HabEx yield modeling with for systems engineering

Rhonda M. Morgan, Michael Bottom, Michael Turmon, Bertrand P. Mennesson, Keith R. Warfield, Jet Propulsion Lab. (United States); Dmitry Savransky, Christian Delacroix, Space Imaging and Optical Systems Lab., Cornell Univ. (United States) and Carl Sagan Institute (United States)

We present yield modeling results for the HabEx concept study using EXOSIMS. EXOSIMS (Exoplanet Open-Source Imaging Mission Simulator) provides a parametric estimate of science yield of mission concepts using contrast curves from physics-based diffraction model codes and Monte Carlo simulations of design reference missions using realistic observing constraints.

Two baseline architecture configurations and two extended configurations are compared. We compare a configuration with a coronagraph to a configuration with a starshade for both detection and spectral characterization. The input parameters, including astrophysical assumptions, are detailed. We show sensitivity to key design parameters around design space local to the point designs. The yield results provide an analysis of the relative performance of telescope and instrument design that enable system engineering decisions.

10398-4, Session 1

HabEx space telescope optical system

Stefan R. Martin, Mayer Rud, Daniel K. Stern, Jet Propulsion Lab. (United States); Paul A. Scowen, Arizona State Univ. (United States)

The HabEx study is defining a concept for a new space telescope with the primary mission of detecting and characterizing planetary systems around nearby stars. The telescope is designed specifically to operate with both a high contrast coronagraph and a starshade enabling the direct optical detection of exoplanets as close as 70 mas from their star. The telescope will be equipped both with cameras for exoplanetary system imaging and with spectrometers capable of characterizing exoplanet atmospheres. Gases such as oxygen, carbon dioxide, water vapor and methane have spectral lines in the visible and near infrared part of the spectrum and may indicate biological activity.

In addition to the study of exoplanets, HabEx enables general astrophysics with two dedicated instruments. One instrument is a camera enabling imaging on a 3 arc minute field of view in two bands stretching from the UV to the near infrared. The same instrument can also be operated as a multi-object spectrograph, with resolution of 2000. A second instrument will be a high resolution UV spectrograph operating near 100 nm with up to 60,0000 resolution. We discuss the preliminary designs of the telescope and the optical instruments for the observatory.

This work was conducted at the Jet Propulsion Laboratory, California Institute of Technology, under contract with the National Aeronautics and Space Administration.

10398-5, Session 1

Overview of a telescope concept design for the Habitable-zone Exoplanet Direct Imaging Mission

H. Philip Stahl, NASA Marshall Space Flight Ctr. (United States)

The Habitable-Exoplanet Imaging Mission (HabEx) engineering study team has been tasked by NASA with developing a compelling and feasible exoplanet direct imaging concept as part of the 2020 Decadal Survey. This paper summarizes a design concept for a 4-meter off-axis monolithic aperture HabEx telescope including launch vehicle accommodation, optical, structural and thermal design.

10398-6, Session 2

Science and architecture drivers for the HabEx Ultraviolet Spectrograph (UVS)

Paul A. Scowen, Arizona State Univ. (United States); Daniel K. Stern, Jet Propulsion Lab. (United States); Rachel Somerville, Rutgers, The State Univ. of New Jersey (United States); Mayer Rud, Stefan R. Martin, Jet Propulsion Lab. (United States); Matthew Beasley, Planetary Resources, Inc. (United States)

We have worked to define the compelling next generation General Astrophysics science that the 4m implementation of the HabEx mission concept might enable. These science drivers have been used to define requirements for a far ultraviolet (FUV) spectrograph design for the telescope design that meets the needs of these programs. We describe both the drivers and the baseline design for the instrument, the modes it might support, and the choices that were made to optimize the performance. The operational performance of the instrument in cooperation with the rest of the telescope design is also discussed.

10398-7, Session 2

Structural design of a 4-meter off-axis space telescope for the Habitable-zone Exoplanet Direct Imaging Mission

William R. Arnold Sr., a.i. solutions, Inc. (United States) and NASA Marshall Space Flight Ctr. (United States); Brent Knight, Jacqueline M Davis, H. Philip Stahl, NASA Marshall Space Flight Ctr. (United States)

The Habitable-Exoplanet Imaging Mission (HabEx) engineering study team has been tasked by NASA with developing a compelling and feasible exoplanet direct imaging concept as part of the 2020 Decadal Survey. This paper details the structural design for a 4-meter off-axis monolithic aperture HabEx telescope including primary mirror substrate and support system, ability to survive launch, telescope optical bench structure, and dynamic analysis of the structures ability to maintain stable optical alignment and wavefront error.

10398-8, Session 2

ATHENA: System design of the ATHENA x-ray telescope

Mark R. Ayre, Marcos Bavdaz, Ivo Ferreira, Eric Wille, David H. Lumb, Martin Linder, Alexander Stefanescu, European Space Research and Technology Ctr. (Netherlands)

ATHENA, Europe's next generation x-ray telescope, is currently under Assessment Phase study with parallel candidate industrial Prime contractors, after selection for the 'L2' slot in ESA's Cosmic Vision Programme, with a mandate to address the 'Hot and Energetic Universe' Cosmic Vision science theme. This paper will consider the main technical requirements of the mission, and their mapping to resulting design choices at both mission and spacecraft level.

The reference mission architecture and current reference spacecraft designs from each of the candidate Primes will then be described, with particular emphasis given to a detailed description of the Science Instrument Module (SIM) design, currently under the responsibility of the ESA Study Team. The SIM is a very challenging item due primarily to the need to provide to the instruments (i) a soft ride during launch, and (ii) a very large (~3 kW) heat dissipation capability at varying interface temperatures and locations.

Finally, a programmatic overview will be given of the on-going Assessment Phase leading up to adoption of the mission.

10398-9, Session 3

The Large UV/Optical/Infrared (LUVOIR) Surveyor: Decadal Mission concept design update *(Invited Paper)*

Matthew R. Bolcar, NASA Goddard Space Flight Ctr. (United States)

In preparation for the 2020 Astrophysics Decadal Survey, NASA has commissioned the study of four large mission concepts, including the Large Ultraviolet / Optical / Infrared (LUVOIR) Surveyor. The LUVOIR Science and Technology Definition Team (STDT) has identified a broad range of science objectives including the direct imaging and spectral characterization of habitable exoplanets around sun-like stars, the study of galaxy formation and evolution, the epoch of reionization, star and planet formation, and the remote sensing of Solar System bodies. NASA's Goddard Space Flight Center (GSFC) is providing the design and engineering support to develop executable and feasible mission concepts that are capable of delivering the identified science objectives. We present an update on the first of two architectures being studied: a 15-meter-diameter segmented-aperture telescope with a suite of serviceable instruments operating over a range of wavelengths between 100 nm to 2.5 ?m and beyond. Four instruments are being developed for this architecture, including: an optical / near-infrared coronagraph capable of delivering 10?10 contrast at inner working angles as small as 2 ?/D; the LUVOIR UV Multi-object Spectrograph (LUMOS), which will provide medium resolution multi-object spectroscopy in addition to near-UV imaging and high-resolution point-source spectroscopy; the High Definition Imager (HDI), a high-resolution wide-field-of-view NUV-Optical-IR imager; and a UV spectro-polarimeter being contributed by Centre National d'Etudes Spatiales (CNES). A fifth, empty instrument bay will also be available for future contributions. We provide an update on this architecture, as well as plans for the second architecture to be studied in late 2017.

10398-10, Session 3

The Large UV/Optical/Infrared (LUVOIR) surveyor: Decadal Mission concept technology development overview

Matthew R. Bolcar, NASA Goddard Space Flight Ctr. (United States)

The Large Ultraviolet / Optical / Infrared (LUVOIR) Surveyor is one of four large mission concept studies being developed by NASA for consideration in the 2020 Astrophysics Decadal Survey. LUVOIR will support a broad range of science objectives, including the direct imaging and spectral characterization of habitable exoplanets around sun-like stars, the study of galaxy formation and evolution, the epoch of reionization, star and planet formation, and the remote sensing of Solar System bodies. The LUVOIR Science and Technology Definition Team (STDT) has tasked a Technology Working Group (TWG), with more than 60 members from NASA

centers, academia, industry, and international partners, with identifying technologies that enable or enhance the LUVOIR science mission. The TWG has identified such technologies in the areas of Coronagraphy, Ultra-Stable Opto-mechanical Systems, Detectors, Coatings, Starshades, and Instrument Components, and has completed a detailed assessment of the state-of-the-art. We present here a summary of this technology assessment effort, as well as the current progress in defining a technology development plan to mature these technologies to the required technology readiness level (TRL). We also comment on the role these technology assessments and the technology development plan play in the overall mission concept study.

10398-12, Session 3

Dynamic stability with the disturbance-free payload architecture as applied to the Large UV/Optical/Infrared (LUVOIR) mission

Larry D. Dewell, Raymond M. Bell, Nelson Pedreiro, Richard L. Kendrick, Lockheed Martin Space Systems Co. (United States)

The need for high payload dynamic stability and ultra-stable mechanical systems is an overarching technology need for large space telescopes such as the Large Ultraviolet / Optical / Infrared (LUVOIR) Surveyor. Wavefront error stability of less than 10 picometers RMS of uncorrected system WFE per wavefront control step represents over a factor of 1000 improvement over current space-based telescopes being fielded. Previous studies of similar telescope architectures have shown that passive telescope isolation approaches are hard-pressed to meet dynamic stability requirements and usually involve complex actively-controlled elements and sophisticated metrology. To meet these challenging dynamic stability requirements, an innovative non-contact vibration isolation technology called Disturbance Free Payload (DFP) is applied to and analyzed for LUVOIR. In a non-contact DFP architecture, the payload and spacecraft fly in close proximity, and interact via non-contact actuators to allow precision payload pointing and isolation from spacecraft vibration. Because disturbance isolation through non-contact, vibration isolation down to zero frequency is possible, and high-frequency structural dynamics of passive isolators are not introduced into the system. In this paper, the performance of a DFP non-contact architecture is analyzed for LUVOIR, by quantifying the performance in metrics directly traceable to its science objectives, including astrophysics and the direct imaging of habitable exoplanets. Aspects of the non-contact isolation architecture and how they contribute to system performance are examined and tailored to the LUVOIR architecture and concept of operation.

10398-13, Session 3

First-order error-budgeting for LUVOIR mission

J. Scott Knight, Paul A. Lightsey, Ball Aerospace & Technologies Corp. (United States); Lee D. Feinberg, Matthew R. Bolcar, NASA Goddard Space Flight Ctr. (United States); Stuart B. Shaklan, Jet Propulsion Lab. (United States)

Future large astronomical telescopes in space will have architectures that will have complex and demanding requirements in order to meet the science goals. The LUVOIR mission concept being assessed by the NASA/Goddard Space Flight Center is expected to be 9 to 15 meters in diameter, have a segmented primary mirror and be diffraction limited at a 500 nanometer wavelength. The optical stability is expected to be in the picometer range for minutes to hours. Architecture studies to support the NASA Science and Technology Definition teams (STDTs) are underway to evaluate systems performance. JWST is closest analog to this mission concept but requires significant performance improvements to meet the science goals. In order to help define the technology needs and assess performance, a first order error budgets has been developed. Like the JWST error budget, the error budget includes the active, adaptive and passive elements in spatial and temporal domains. JWST performance is scaled using first order approximations where appropriate and includes technical advances in telescope control.

10398-14, Session 3

LUVOIR backplane thermal architecture development through the composite CTE sensitivity study

Sang C. Park, Harvard-Smithsonian Ctr. for Astrophysics (United States); Michael J. Eisenhower, Smithsonian Astrophysical Observatory (United States); Marcel Bluth, SGT, Inc. (United States); Matthew R. Bolcar, Lee D. Feinberg, NASA Goddard Space Flight Ctr. (United States); J. Scott Knight, Ball Aerospace & Technologies Corp. (United States); Joel A. Nissen, David C. Redding, Jet Propulsion Lab. (United States)

The Large UV/Optical/IR Surveyor (LUVOIR) is one of four 2020 Decadal Survey Missions, a concept for 'flag-ship' class space-borne observatory, operating across the multi-wavelength UV/Optical/NIR spectra. An Optical Telescope concept being considered is the segmented primary mirror architecture with composite backplane structure. In order to achieve the high-contrast imaging required to satisfy the primary science goals of this mission would require, roughly, 10 pico-meter wavefront RMS stability over a wavefront control time step of approximately 10 minutes. The LUVOIR primary mirror backplance support structure (PMBSS) requires active thermal management to maintain operational temperature while on orbit. Furthermore, the active thermal control must be sufficiently stable to prevent time-varying thermally induced distortions in the PMBSS. This paper describes a systematic approach to developing a thermal architecture of a modular composite section of the mirror support structure heavily guided by the sensitivity studies of the composite Coefficient of Thermal Expansion (CTE) values. Thermal and finite-element models, sensitivity studies against the absolute values and their variations of the composite CTE, the early findings from the thermal and thermal-distortion analyses are presented.

10398-27, Session 3

Ultra-stable segmented telescope sensing and control architecture

Lee D. Feinberg, Matthew R. Bolcar, NASA Goddard Space Flight Ctr. (United States); J. Scott Knight, Ball Aerospace & Technologies Corp. (United States); David C. Redding, Jet Propulsion Lab. (United States)

Large segmented space telescopes that can achieve 10^10 contrast are under consideration for both the Large Ultraviolet Optical InfraRed (LUVOIR) and Habex mission studies. The key challenge for this type of architecture is how to achieve sufficient stability to support this level of contrast. This paper will survey a few emerging sensing and control architectures and associated technologies that can potentially achieve the required stability. It will also provide a summary of the sensing and control portion of the LUVOIR segmented telescope architecture that has emerged from a recent design study and will provide a first look at the control methods that are being employed.

10398-15, Session 4

The LUVOIR coronagraph instrument: definition and design

Laurent Pueyo, Space Telescope Science Institute (United States)

We present the exo-earth imaging instrument concept for the Large Ultra Violet Optical Infra Red (LUVOIR) surveyor, one for the fours large missions concept studies being developed by NASA for the 2020 astrophysics decadal survey. This paper is an overview of the work of the LUVOIR Science and Technology Definition Team (STDT), working along with the GSFC study office and includes the outcomes of a yearlong discussion with the exoplanet community. It summarizes our group's design and findings regarding the LUVOIR Architecture A (~14 m class aperture). We first review the main science requirements underlying our design choices, and in particular our choice of wavelength coverage. We then present the architecture of the there channels selected for the coronagraph instrument: UV (~200 nm - 400 nm), optical (~0.4 to 1 micron) and near IR (1 to 2.4 microns). For each channel we discuss back end science instrument, coronagraph design and wavefront control. We present our current designs along with their performances based on high fidelity optical simulation. We discuss these performances in the context of their science yield for exo-earth detection, characterization and broader exoplanetary science. We finally summarize the current state of the art for coronagraph technology and discuss avenues towards maturing them.

10398-16, Session 4

Effects of space telescope primary mirror segment errors on coronagraph instrument performance

Mark T. Stahl, H. Philip Stahl, NASA Marshall Space Flight Ctr. (United States); Stuart B. Shaklan, Jet Propulsion Lab. (United States); Bijan Nemati, The Univ. of Alabama in Huntsville (United States)

Direct imaging of potentially habitable planets is challenging because of the relative proximity of the planet to the star and the low flux ratio (typically well under 1e-9 in the visible) of the planet relative to the star. Future exoplanet direct imaging telescopes like the Habitable Exoplanet Imaging Mission (HabEx) will hence require large collecting apertures with very low wavefront errors. The feasibility of these missions is in a large part dependent on the sensitivity of the achieved contrast at small working angles to imperfections and motions of the telescope optics. In past studies, we explored the effect of applying specific modes to segmented and monolith telescopes on the contrast leakage of a coronagraph. Here we extend the results to combined modes and incorporate some of the latest coronagraph designs.

10398-17, Session 4

Space technology for directly imaging and characterizing exo-Earths

Brendan P. Crill, Stuart B. Shaklan, Nicholas Siegler, Jet Propulsion Lab. (United States)

The detection of Earth-like exoplanets in the habitable zone of their stars, and their spectroscopic characterization in a search for biosignatures, requires starlight suppression that exceeds the current best ground-based performance by orders of magnitude. The required planet/star brightness ratio of 10^{-10} is obtained by blocking stellar photons with an occulter, either externally (a starshade) or internally (a coronagraph) to the telescope system, so as to directly image the reflected photons from the exoplanet. Coronagraph instruments require advancement with respect to telescope aperture (either monolithic or segmented), aperture obscurations (obscured by secondary mirror and its support struts), and wavefront error sensitivity (e.g. line-of-sight jitter, telescope vibration, polarization). A starshade has never been used in a science application and requires deploying a large structure (tens of meters to greater than 100m in diameter) that must be positioned precisely at a distance of tens of thousands of kilometers from the telescope. We describe in this paper a roadmap to achieving the technological capability to search for life in a Earth-like exoplanet from a future space telescope, in the context of the Decadal Survey mission concept studies. Two of these studies, HabEx and LUVOIR, include the search for habitable exoplanets as a central science theme.

10398-18, Session 4

Laser metrology for ultra-stable space-based coronagraphs

Joel A. Nissen, Alireza Azizi, Feng Zhao, Shannon Kian G. Zareh, Shanti R. Rao, Jeffrey B. Jewell, Jet Propulsion Lab. (United States)

Sensing starlight rejected from a coronagraph is essential in stabilizing the telescope's pointing and wavefront drift, but performance is degraded for dim stars. Laser Metrology (MET) provides a different, complementary sensing method, one that can be used to measure changes in the alignment of the optics at high bandwidth, independent of the magnitude of the host star. Laser metrology measures changes in the separation of optical fiducial pairs, which can be separated by many meters. The principle of operations is similar to the laser metrology system used in LISA-Pathfinder to measure the in-orbit displacement between two test masses to a precision of ~10 picometers. In closed loop with actuators, MET actively maintains rigid body alignment of the front-end optics, thereby eliminating the dominant source of wavefront drift. Because MET is not photon starved, it can operate at high bandwidth and feed-forward secondary-mirror jitter to a fast-steering mirror, correcting line-of-sight errors. In the case of a segmented, active primary mirror, MET provides 6 DOF sensing, replacing edge sensors. MET maintains wavefront control even during attitude maneuvers, such as slews between target stars, thereby avoiding the need to repeat time-consuming speckle suppression. These features can significantly improve the performance and observational efficiency of future large-aperture space telescopes equipped with internal coronagraphs. We evaluate MET trusses for various proposed monolithic and segmented space-based coronagraphs and present the performance requirements necessary to maintain contrast drift below 1e-11.

10398-19, Session 4

Design considerations for future far-IR observatories

Jonathan W. Arenberg, John Pohner, George M. Harpole, Michael B. Petach, Danny Chi, Perry J. Knollenberg, Northrop Grumman Aerospace Systems (United States)

This paper examines the architectural considerations for the development of a future far infra-red (~10-1000 μm) space-based observatory. These missions require their instruments and optics to operate at temperatures less than 10 Kelvin. Achieving these very low temperatures throughout the optical train in an executable and verifiable design is the defining architectural challenge for systems operating in the far-IR. This paper will discuss the necessary elements of the thermal design, cooling, parasitics and verification.

10398-20, Session 5

Technology advancements for future astronomical missions

J. Scott Knight, Paul A. Lightsey, Chip Barnes III, Alex Harwit, Ball Aerospace & Technologies Corp. (United States)

Future astronomical telescopes in space will have architectures have complex and demanding requirements in order to meet the science goals. The missions currently being studied by NASA for consideration in the next Decadal Survey range in wavelength from the X-ray to Far infrared; examining phenomenon from imaging exoplanet and characterizing their atmospheres to detecting gravitational waves. These missions have technical challenges that are near or beyond the state of the art from the telescope to the detectors. This paper describes some of these challenges and possible solutions. Promising measurements and future demonstrations are discussed that can enhance or enable the missions.

10398-21, Session 5

Stray-light field dependence for large astronomical space telescopes

Paul A. Lightsey, Ball Aerospace & Technologies Corp. (United States); Charles W. Bowers, NASA Goddard Space Flight Ctr. (United States)

Future large astronomical telescopes in space will have architectures that expose the optics to large angular extents of the sky.Options for reducing stray light coming from the sky range from enclosing the telescope in a tubular baffle to having an open telescope structure with a large sunshield to eliminate solar illumination. These two options are considered for an on-axis telescope design to explore stray light considerations. The tubular baffle design will limit the sky exposure to the solid angle of the cone in front of the telescope set by the aspect ratio of the baffle length to Primary Mirror (PM) diameter. The illumination from this portion of the sky will be limited to the PM and structures internal to the tubular baffle. The open structure will include direct sky illumination of the PM and Secondary Mirror (SM) and reflected or scattered light from sunshield and other structures onto the PM and SM coming from a large portion of the sky with only the portion of the sky shadowed by the sunshield not contributing. A Radiance Transfer Function (RTF) is calculated for the open architecture that determines the ratio of the stray light background radiance in the image contributed by a patch of sky having unit radiance. The full 4? steradian of sky is divided into a grid of patches, with the location of each patch defined in the telescope coordinate system. By rotating the celestial sky radiance maps into the telescope coordinate frame for a given pointing direction of the telescope, the RTF may be applied to the sky brightness and the results integrated to get the total stray light from the sky for that pointing direction. The RTF data generated for the open architecture may analyzed as a function of the expanding cone angle about the pointing direction. In this manner, the open architecture data may be used to directly compare to a tubular baffle design parameterized by allowed cone angle based on the aspect ratio of the tubular baffle length to PM diameter. Additional analysis has been done to examine the stray light implications for the fields near the image of a bright source. This stray light is shown to be dependent on the Bidirectional Reflectance Distribution Function (BRDF) characteristics of the mirrors in the optical train, with the mirrors closer to the focal plane dominating over the contributions from the PM and SM. Hence the near field stray light is independent of the exterior telescope baffle geometry.

10398-22, Session 5

Cryogenic system for the Origins Space Telescope: cooling a large space telescope to 4K with today's technology

Michael J. DiPirro, David T. Leisawitz, Edgar R. Canavan, Louis G. Fantano, Anel Florez, James W. Kellogg, NASA Goddard Space Flight Ctr. (United States)

The Origins Space Telescope (OST) concept is one of four NASA Science Mission Directorate, Astrophysics Division, observatory concepts being studied for launch in the mid 2030's. OST's wavelength coverage will be from the mid-infrared to the sub-millimeter, 6-600 microns. To enable observations at the zodiacal background limit the telescope must be cooled to about 4 K. Combined with the telescope size (currently the primary is 9 m in diameter) this appears to be a daunting task. However, simple calculations and thermal modeling have shown the cooling power required is able to be met with several already developed cryocoolers. Further, the telescope thermal architecture is greatly simplified, allowing simpler models, more thermal margin, and higher confidence in the final performance values than previous cold observatories. We will describe design principles to simplify thermal modeling and verification. We will argue that the OST architecture and design principles lower its integration and test time and reduce its ultimate cost.

10398-11, Session 6

APERTURE--a precise extremely-large reflective telescope using re-configurable element: a progress report

Melville P. Ulmer, Jian Cao, Yip-Wah Chung, Xiaoli Wang, David B. Buchholz, Northwestern Univ. (United States); Victoria L. Coverstone, Turgut B. Baturalp, Texas Tech Univ. (United States)

One of the pressing needs for the UV-Vis is a design to allow even larger mirrors than the JWST primary at an affordable cost. We report here the results of a NASA Innovative Advanced Concepts first year's Phase II study. Our project is called A Precise Extremely large Reflective Telescope Using Reconfigurable Elements (APERTURE). The idea is to deploy a continuous membrane-like mirror. The mirror figure will be corrected after deployment to bring it into better or equal lambda/20 deviations from the prescribed mirror shape. The basic concept is not new. What is new is to use a different approach from the classical piezoelectric-patch technology. Instead, our concept is based on a contiguous coating of a so called magnetic smart material (MSM). After deployment a magnetic write head will move on the non-reflecting side of the mirror and will generate a magnetic field that will produce a stress in the MSM that will correct the mirror deviations from the prescribed shape. In this progress report we give results of deformation vs in-plane stress, progress toward how long a deformation on Kapton or Mylar can be held in place my a magnetically hard material interacting with a MSM, and designs of a deployment, in-plane stress measurement of deployment and characterization of the deployed surface.

10398-23, Session 6

Highly-adjustable systems: an architecture for future space observatories

Jonathan W. Arenberg, Northrop Grumman Aerospace Systems (United States); Charles R. Lawrence, Robert A. Laskin, David C. Redding, John Steeves, Jet Propulsion Lab. (United States); Alberto Conti, Northrop Grumman Aerospace Systems (United States)

Mission costs for ground breaking space astronomical observatories are increasing to the point of unsustainability. We are investigating the use of highly adjustable or correctable systems as a means to reduce development and therefore mission costs. The paper introduces the promise and possibility of realizing a "net zero CTE" system for the general problem of observatory design. The discussion then introduces the basic systems architecture we are considering. This paper concludes with an overview of our planned study and demonstrations for proving the value and worth of highly adjustable telescopes and systems ahead of the upcoming decadal survey.

10398-24, Session 6

Revolutionary astrophysics using an incoherent synthetic optical aperture

Gerard L. Rafanelli, Susan B. Spencer, Douglas W.

Return to Contents

Wolfe, Raytheon Space and Airborne Systems (United States); Ronald S. Polidan, Polidan Science Systems & Technologies, LLC (United States)

Raytheon Space and Airborne Systems is exploring a paradigm shift for astronomical observatories that would replace circular apertures with rotating synthetic apertures. Rotating Synthetic Aperture (RSA) observatories can enable high value science measurements for the lowest mass to orbit, has superior performance relative to all sparse apertures, can provide the resolution of 20m to 30m aperture with the collecting area of an 8m to 12 m telescope with much less mass, risk, schedule, & cost. RSA is based on current, or near term technology and can be launched on a single, current launch vehicle to L2 (with much larger apertures possible using SLS).

10398-25, Session 6

The crisis in space astronomy: program structure and fatsats as a path to cheaper flagship missions

Martin Elvis, Harvard-Smithsonian Ctr. for Astrophysics (United States)

With an expected $5 B - $6 B to spend on large mission in the decade 2025-2035, NASA Astrophysics has a strategic problem. If JWST-like $9 B costs are the new normal, then the next large mission will launch ~2045, assuming no additional funds, or ~2035 if funding is doubled. No matching missions can join this mission until 10-20 years later yet. Individually impressive, these missions will inevitably narrow the scope of astrophysics for a generation or more. The alternative is to (1) take advantage of technological developments that allow 4 - 5 breakthrough missions to be built for 45 b - $6 B, and so by 3035; (2) take advantage of factor 3 – 5 lower launch costs to cut spacecraft costs, enabling a doubling of the number of breakthrough missions.

To put NASA Astrophysics on this expanding path, and avoid the constriction of the One Big Mission approach, requires policy changes. (1) the Statement of Task to the 2020 Astronomy Decadal should ask for a program that fits sensible design criteria, and avoids a prioritized list of large and medium missions. (2) Program choices should be explicitly tensioned against alternatives so that the opportunity cost is made visible. (3) studies of the gains to be had from using mass to solve problems rather than expensive design/test cycles should be made ahead of the 2020 Decadal. Other potential gains from commercial space on a 2030 timescale should be investigated.

10398-26, Session 6

An evolvable space telescope configured for NASA's Habex mission

Charles F. Lillie, Lillie Consulting LLC (United States); Howard A. MacEwen, Reviresco LLC (United States); James B Breckinridge, Breckinridge Associates, LLC (United States); Ronald S. Polidan, Polidan Science Systems & Technologies LLC (United States)

Previous papers have described our concept for a large telescope that would be assembled in space in several stages (in different configurations) over a period of fifteen to 20 years. Spreading the program cost over 20 years would minimize the impact on NASA's annual budget and drastically shorten the time between program start and "first light" for this space observatory.

The first Stage of that EST would consist of an instrument module located at the prime focus of three 4-meter hexagonal mirrors arranged in a semi-circle to form one-half of a 12-m segmented mirror. After several years three additional 4-m mirrors would be added to create a 12-m filled aperture. Later, twelve more 4-m mirrors will be added to this Stage 2 telescope to create a 20-m filled aperture space telescope. At each stage the telescope will have an unparalleled capability for UVOIR observations, and the results of these observations will guide the evolution of the telescope and its instruments.

This "Stage Zero" configuration will have only one 4-m mirror segment with the same 30-m focal length and a prime focus coronagraph with normal incidence optics to minimize polarization effects. Additional mirror segments and instruments would be added as the telescope evolves.

After augment and checkout in cis-lunar space, the telescope would transfer to a Sun-Earth L2 halo orbit and obtain high sensitivity, high resolution, high contrast UVOIR observations that address the scientific objectives of the UV/Optical/IR Surveyor and Habitable-Exoplanet Imaging Missions that NASA is studying for consideration by the 2020 Decadal Survey.

This "Stage Zero" configuration would have only one 4-m mirror segment with the same 30-m focal length and a prime focus coronagraph with normal incidence optics to minimize polarization effects. Additional mirror segments and instruments would be added as the telescope evolves.

After augment and checkout in cis-lunar space, the telescope would transfer to a Sun-Earth L2 halo orbit and obtain high sensitivity, high resolution, high contrast UVOIR observations that address the scientific objectives of the UV/Optical/IR Surveyor and Habitable-Exoplanet Imaging Missions that NASA is studying for consideration by the 2020 Decadal Survey.

10398-28, Session 6

Active optics for next-generation space telescopes

Vincent Costes, Lionel Perret, David Laubier, Christian Imbert, Laurent Cadiergues, Jean-Marc Delvit, Claude Faure, Ctr. National d'Études Spatiales (France)

High resolution observation systems need bigger and bigger telescopes. The design of such telescopes is a key element for the satellite design. In order to improve the imaging resolution with minimum impact on the satellite, a big effort must be made to improve the compactness of the telescope. Compactness is also important for the agility of the satellite and for the size and cost of the launcher. This paper shows how compact a high resolution telescope can be. A diffraction limited telescope can be less than ten times shorter than its focal length. The compactness impacts drastically the opto-mechanical sensitivity and the optical performances. Typically, a gain of a factor of 2 leads to a mechanical tolerance budget 6 times more difficult. The need to implement active optics for positioning requirements raises very quickly.

Moreover, the capability to compensate shape defaults of the primary mirror is the way to simplify the mirror manufacture, to mitigate the development risks and to minimize the cost. The larger the primary mirror, the more interesting it is to implement active optics for shape compensations .

Our active optics approach is to compensate primary mirror shape defaults with a deformable mirror located in the telescope exit pupil. Telescope positioning errors are corrected thanks to a mechanism located behind the secondary mirror.

Technological developments are ongoing at CNES for active optics demonstration. The aim is to achieve TRL5 for these new technologies and to validate the global performances of such a telescope. The present paper will describe these developments.

10398-29, Session 7

Recent developments in next-generation UV-visible space telescope planning and design

Paul A. Scowen, Arizona State Univ. (United States); Kevin C. France, Univ. of Colorado Boulder (United States); Jason Tumlinson, Space Telescope Science Institute (United States); Stephan R. McCandliss, Johns Hopkins Univ. (United States); Todd Tripp, Univ. of Massachusetts Amherst (United States); Jay C. Howk, Univ. of Notre

Dame (United States)

We discuss the recent input and development of next generation UV-visible space-based observatories, the science they have been designed to achieve, and the technological challenges and potential solutions that have been identified. This talk will cover community-driven needs and strategic goals and hopefully give some insight into what the next UV-visible space telescopes will look like and what they will be able to deliver. The discussion will focus on, but not be exclusive to, the ongoing studies for both LUVOIR and HabEx.

10398-30, Session 7

An innovative UV probe-class mission concept

Sara R. Heap, NASA Goddard Space Flight Ctr. (United States); Anthony B. Hull, The Univ. of New Mexico (United States); Stephen E. Kendrick, Kendrick Aerospace Consulting LLC (United States)

In the 2020's, current and future wide-field telescopes will survey the sky at wavelengths ranging from gamma rays to radio waves. These surveys will be highly synergistic, leading to new, important discoveries. But there is a glaring hole in the emerging global network of survey telescopes: the network lacks a UV-sensitive telescope capable of making surveys and following up on objects discovered in other surveys. We are therefore planning to develop a concept for a probe-class UV survey telescope. Such a telescope must have a wide field of view, high observing efficiency, and a suite of UV-sensitive cameras and spectrographs including a UV multi-object slit spectrograph. These requirements call for innovative telescope and instrument designs and technologies, which we will describe. These designs and technologies will help bridge the technology gap to future large space telescopes such as LUVOIR.

10398-31, Session 7

Medium UV/optical/IR observatory (MUVOIR) concept

Gary W. Matthews, ATA Aerospace, LLC (United States)

In preparation for the 2020 Decadal Survey, NASA has undertaken four general mission areas to assess the potential system configurations and the resulting science. The HabEx and LUVOIR mission concept teams are assessing observatories between 4-meters and 14-meters in size. The MUVOIR mission idea evaluates a modest sized, 6.5-meter mission which includes an additional political component that leverages the JWST investment in the national infrastructure and how that might be used to reduce the lead time for a post-WFIRST Exoplanet/UV and Visible band astrophysics mission. This would include how this new program can leverage the integration support equipment at Goddard Space Flight Center and the optical test facility at Johnson Space Center.

10398-32, Session 7

SYNERGY: An Explorer mission concept for a next-generation ultraviolet survey

John W. MacKenty, Jason Tumlinson, Space Telescope Science Institute (United States); Jonathan W. Arenberg, Craig Elder, Adam Gunderson, Steven Warwick, Terri O'Connell, Carlton Wong, Northrop Grumman Aerospace Systems (United States)

Synergy is an Explorer class mission concept to obtain a large-area, multi-tier near-ultraviolet sky survey with low-resolution, spatially resolved slitless spectroscopy (R = 200-600) and simultaneous arc-second imaging between 210-320 nm. It's Wide and Deep surveys will examine the co-evolution of more than 200 million galaxies, 500,000 AGN, and 30,000 gas halos between $0.8 < z < 2$ to constrain the multi-parameter physical relationships between gas, star formation history, mergers, AGN, and environment at the epoch when star formation peaked, half of galaxies transitioned from star-forming to passive, and the Hubble sequence first emerged. Many facilities in the 2020s will probe galaxies at this epoch, but the key tracers of diffuse gas over the 10 Gyr of cosmic time since $z = 2$ are in the ultraviolet.

Synergy employs a 100 Mpixel CCD focal plane to provide 0.75 arc second pixels over a 4.5 degree field of view. Its reflective optical system uses coatings optimized to pass near-ultraviolet light while rejecting visible light making Silicon CCD detectors ideal for this application. With a 63 cm aperture, this instrument achieves 27.8 AB mag (5 sigma) imaging and 23.8 spectroscopy sensitivity in the Deep Survey and 25.5/21.5 in the Wide Survey. Using a Northrop Grumman Eagle Spacecraft with components from the LCROSS and JWST mission, Synergy would fly in the same orbit as the TESS Explorer mission currently under development. This 100,000 by 400,000 km orbit is phase locked with the Moon and permits an efficient observing plan, cost effective communications, and avoids the geocoronal emission features present in low earth orbit.

10398-33, Session 7

Coatings for large-aperture UV optical infrared space telescope mirrors

Kunjithapatham Balasubramanian, John Hennessy, Shouleh Nikzad, Nasrat A. Raouf, Jet Propulsion Lab. (United States); Manuel A. Quijada, Javier G. Del Hoyo, NASA Goddard Space Flight Ctr. (United States)

Large space telescope concepts aiming for high throughput from far UV to near IR require advanced coating technologies to enable efficient gathering of light with important spectral signatures including those in far UV region down to 90nm. Typical Aluminum mirrors protected with MgF_2 fall short of the requirements below 120nm. New and improved coatings are sought to protect aluminum that oxidizes readily in normal environment causing severe absorption and reduction of reflectance in the deep UV. Besides choice of materials, the process of applying coatings has to be optimized and controlled accurately and reliably to ensure the coatings preserve the expected optical characteristics. This challenge is addressed here with experimental investigations at JPL and at GSFC. We present the progress achieved to date and discuss the path forward to achieve high reflectance in the spectral region from 90 to 130nm without degrading performance in the visible and NIR regions taking into account durability concerns when the mirrors are exposed to normal laboratory conditions. Requirements on other devices such as filters and beam splitters needed for the conceived large space telescope are also discussed.

10398-34, Session 7

Progress towards adding EUV reflectance to broadband Al mirrors for space-based observatories

David D. Allred, R. Steven Turley, Stephanie Thomas, Spencer Willett, Spencer B. Perry, Michael J. Greenburg, Brigham Young Univ. (United States)

We report on progress on vacuum removal of protective layers on aluminum mirror surfaces using hydrogen plasmas and/or heating. One of NASA's flagship astrophysical missions of the 2020's or 30's will likely be a LUVOIR (large, UV-optical-IR) telescope. This space-based observatory will employ the largest mirrors ever flown. The reflective coating will almost certainly be aluminum since such telescopes would profit from truly broad-band mirrors. The top surface of such aluminum mirrors, however, need to be bare without the oxide layers that naturally form in air. (The local space environment for the observatory should be sufficiently oxygen-free that a pristine surface should remain bare for decades.) We discuss protecting as-deposited aluminum mirrors before atmosphere exposure with a robust, protective layer, or layers, that could be deposited to coat the aluminum immediately after its deposition, before it meets air, and cleanly and relatively easily removed once the mirror is in space. This removal must be gentle enough to not roughen the mirror surface nor redepositing material removed from the protective layer on the mirror or other spacecraft components. Thus the choice of hydrogen plasmas. Both organic and inorganic (such as, Si, Cd-containing and Zn) films were evaporated onto the aluminum immediately after its deposition can be removed. Progress could open up the 11-15eV band and an EUV band such as 30.4 nm for space-based astrophysics without sacrificing IR, visible and UV reflectance.

10398-35, Session 7

Improved mirror coatings for use in the Lyman Ultraviolet to enhance astronomical instrument capabilities

Manuel A. Quijada, Javier G. Del Hoyo, NASA Goddard Space Flight Ctr. (United States)

Pure Aluminum (Al) exhibits a high reflectance over the proposed spectral range of the Large Ultraviolet Optical Infrared (LUVOIR) observatory (90-5000 nm). However, the Al has to be protected from the naturally occurring Al_2O_3 oxide layer (when exposed to oxygen) with a thin film of a transparent material for use below 130 nm. Aluminum protected with fluorides such as LiF or MgF_2 have been the most commonly used solutions. But below 102 nm down to 90 nm, no transparent material is available to protect Al and coating mirror reflectance stays well below 30%. But even above 102 nm, the reflectance of protected Al is limited by the residual absorption of the fluoride overcoats and the hygroscopic nature of the LiF overcoat. The low reflectivity of coatings in the Lyman Ultraviolet (LUV) range of 90-130 nm is one of the biggest constraints on FUV telescope and spectrograph design, and it limits the science return of FUV-sensitive space missions. In fact, to achieve high-reflectance in broadband coatings has been identified as an “Essential Goal” in the technology needs for the LUVOIR) surveyor observatory. Improved reflective coatings for optics, particularly in the LUV spectrum, could yield dramatically more sensitive instruments and permit more instrument design freedom. This paper aims at reporting recent developments to produce broadband mirror coatings with high performance that will extend from the infrared spectral region to LUV wavelengths. These mirror coatings would be realized by using a thin AlF_3 overcoat that will protect the aluminum from oxidation and, hence, realize the high-reflectance of this material down to its intrinsic cut-off wavelength of 90 nm. We present the progress achieved to date and discuss the path forward to achieve high reflectance in the spectral region from 90 to 130nm without degrading performance in the visible and NIR regions, taking into account durability concerns when the mirrors are exposed to normal laboratory conditions.

10398-37, Session PMon

James Webb Space Telescope optical simulation testbed IV: linear control alignment of the primary segmented mirror and the secondary mirror

Sylvain Egron, ONERA (France) and Space Telescope Science Institute (United States) and Lab. d’Astrophysique de Marseille (France); Rémi Soummer, Space Telescope Science Institute (United States); Vincent Michau, Aurelie Bonnefois, ONERA (France); Marc Ferrari, Emmanuel Hugot, Lab. d’Astrophysique de Marseille (France); Marshall D. Perrin, Laurent Pueyo, Space Telescope Science Institute (United States); Lucie Leboulleux, Space Telescope Science Institute (United States) and Lab. d’Astrophysique de Marseille (France) and ONERA (France)

The James Webb Space Telescope (JWST) Optical Simulation Testbed (JOST) is a tabletop experiment designed to study wavefront sensing and control for a segmented space telescope, including both initial alignment (commissioning) and maintenance activities. JOST is complementary to existing testbeds for JWST (e.g. the Ball Aerospace Testbed Telescope TBT) given its compact scale and exibility, ease of use, and colocation at the JWST Science & Operations Center. The design of JOST reproduces the physics of JWST’s three-mirror anastigmat (TMA) using three custom spheric and aspheric lenses. It provides similar quality image as JWST (80% Strehl ratio) over a field equivalent to a NIRCam module, but at 633 nm. An Iris AO segmented mirror stands for the segmented primary mirror of JWST. Actuators allow us to control (1) the 18 segments of the segmented mirror in piston, tip, tilt and (2) the second lens, which stands for the secondary mirror, in tip, tilt and x, y, z positions. We present the full linear control alignment infrastructure developed for JOST, with an emphasis on multi-field wavefront sensing and control. Our implementation of the Wavefront Sensing (WFS) algorithms using phase diversity is tested both in simulation and experimentally. The wavefront control (WFC) algorithms, which rely on a linear model for optical aberrations induced by misalignments of the secondary lens and the segmented mirror, are also tested and validated both experimentally and in simulations. The performance of the full active optic control loop is demonstrated by perturbing the testbed and analyzing the quality of the alignment correction.

10398-38, Session PMon

The afocal telescope of the ESA ARIEL mission: analysis of the layout

Vania Da Deppo, CNR-IFN Padova (Italy) and INAF - Osservatorio Astrofisico di Arcetri (Italy); Kevin F. Middleton, STFC Rutherford Appleton Lab. (United Kingdom); Mauro Focardi, INAF - Osservatorio Astrofisico di Arcetri (Italy); Gianluca Morgante, INAF - IASF Bologna (Italy); Emanuele Pace, Univ. degli Studi di Firenze (Italy); Riccardo U. Claudi, INAF - Osservatorio Astronomico di Padova (Italy); Giuseppina Micela, INAF - Osservatorio Astronomico di Palermo Giuseppe S. Vaiana (Italy)

ARIEL (Atmospheric Remote-sensing Infrared Exoplanet Large-survey) is candidate as an M4 ESA mission to launch in 2026. During its foreseen 3.5 years operation, it will observe spectroscopically in the infrared a large population of known transiting planets in the neighborhood of the Solar System. The aim is to enable a deep understanding of the physics and chemistry of these exoplanets.

ARIEL is based on a 1-m class telescope ahead of a suite of instruments: two spectrometer channels covering the band 1.95 to 7.8 microns and four photometric channels (two wide and two narrow band) in the range 0.5 to 1.9 microns.

The ARIEL optical design is conceived as a fore-module common afocal telescope that will feed the spectrometer and photometric channels. The telescope optical design is based on an eccentric pupil two-mirror classic Cassegrain configuration coupled to a tertiary paraboloidal mirror.

The temperature of the primary mirror (M1) will be monitored and finely tuned by means of an active thermal control system based on thermistors and heaters. They will be switched on and off to maintain the M1 temperature within +/-1K thanks to a proportional–integral–derivative (PID) controller implemented within the Telescope Control Unit (TCU), a Payload electronics subsystem mainly in charge of the thermal control of the two detectors owning to the spectrometer. TCU will collect the housekeeping data of the controlled subsystems and will forward them to the Instrument Control Unit (ICU), the main Payload’s electronic Unit linked to the spacecraft On Board Computer (OBC).

10398-39, Session PMon

Aligning the EUCLID NISP near infrared optics using a multi-zone hologram: stability of the set-up and achieved position readings

Frank U. Grupp, Univ.-Sternwarte München (Germany) and Max-Planck-Institut für extraterrestrische Physik (Germany); Andreas Bode, Jennifer Kaminski, Daniela Penka, Carolin Wimmer, Christof Bodendorf, Norbert Geis, Max-Planck-Institut für extraterrestrische Physik (Germany); Ralf Bender, Max-Planck-Institut für extraterrestrische Physik (Germany) and Univ.-Sternwarte München (Germany)

We did deeep analysis of our setup. encounterd the unexpected and where able to explainit .. we want to share this experiece with the community

10398-40, Session PMon

Predictive thermal control applied to HabEx

Thomas Brooks, H. Philip Stahl, NASA Marshall Space Flight Ctr. (United States)

The HabEx telescope will focus on directly imaging habitable exoplanets with the use of an internal coronagraph or external starshade. If an internal coronagraph is used, the telescope's wavefront may not change by more than 10pm over 10 minutes. Similarly, the line of sight cannot change by more than 2 mas over the integration time. Stringent pointing and wavefront error requirements result in stringent deflection and thermal stability requirements. Thermal and thermoelastic models of HabEx are used to determine whether requirements may be met with a proposed Predictive Thermal Control (PTC) system.

10398-41, Session PMon

ACCESS: integration, pre-flight performance, and calibration

Mary Elizabeth Kaiser, Matthew J. Morris, Johns Hopkins Univ. (United States); Jeffrey W. Kruk, Randy A. Kimble, Bernard J. Rauscher, NASA Goddard Space Flight Ctr. (United States); Edward L. Wright, Univ. of California, Los Angeles (United States); Robert Kurucz, Harvard-Smithsonian Ctr. for Astrophysics (United States); Stephan R. McCandliss, Russell Pelton, Lauren N. Aldoroty, Paul D. Feldman, H. Warren Moos, Johns Hopkins Univ. (United States); Adam G. Riess, Johns Hopkins Univ. (United States) and Space Telescope Science Institute (United States); Jonathan P. Gardner, NASA Goddard Space Flight Ctr. (United States); Ralph C. Bohlin, Susana E. Deustua, William V. Dixon, David J. Sahnow, Space Telescope Science Institute (United States); Saul Perlmutter, Univ. of California, Berkeley (United States) and Lawrence Berkeley National Lab. (United States)

Using SNeIa to distinguish dark energy models from one another levies a requirement for 1% precision in the cross-color calibration of the SNe Ia flux across a bandpass extending from 0.35 ? 1.7 ?m. The systematic errors in the flux calibration network spanning the visible through the NIR currently exceed 1%. ACCESS, Absolute Color Calibration Experiment for Standard Stars, is a series of rocket-borne sub-orbital missions and ground-based experiments that will leverage the significant technological advances in detectors, instruments, and the precision of the fundamental laboratory standards used to calibrate these instruments to enable improvements in the precision of the astrophysical flux scale through the transfer of absolute laboratory detector standards from the National Institute of Standards and Technology (NIST) to a network of stellar standards with a calibration accuracy of 1% and a spectral resolving power of 500 across the 0.35 to 1.7 micron bandpass. The ACCESS Cassegrain telescope feeds a compact (Rowland circle design) spectrograph with a cross dispersing Fery prism.

The detector, a HST/WFC3 heritage 1024x1024 HgCdTe array, is sensitive across the full 0.35 to 1.7 micron bandpass. Vibration and thermal vacuum testing of the detector have been successful. Ground-based detector characterization is on-going. The thermal vacuum system is being assembled and tested. Integration and alignment of the ACCESS telescope and spectrograph will be described. Calibration strategy and status, ground-based integration, vibration testing and instrument performance results will be presented. Launch is expected within the year. NASA sounding rocket grant NNX14AH48G supports this work.

10398-42, Session PMon

Technology pathways for a habitable-zone exoplanet direct imaging mission

Rhonda M. Morgan, Keith R. Warfield, Bertrand P. Mennesson, Jet Propulsion Lab. (United States); H. Philip Stahl, NASA Marshall Space Flight Ctr. (United States); Shouleh Nikzad, Joel A. Nissen, John E. Krist, Kunjithapatham Balasubramanian, Jet Propulsion Lab. (United States); Dimitri Mawet, California Institute of Technology (United States); Karl Stapelfeldt, Jet Propulsion Lab. (United States); Steven Warwick, Northrop Grumman Aerospace Systems (United States)

HabEx will be optimized for direct imaging and spectroscopy of potentially habitable exoplanets, and will also enable a wide range of general astrophysics science. Exoplanet detection and characterization drives the enabling core technologies. The STDT and Study Design Team have defined the driving technologies for a future HabEx mission, many of which are instrument-focused, and expand upon previous Technology Gap lists initiated by NASA's Exoplanet Exploration Program office. This paper presents initial assessments of these exoplanet-driven technologies, including elements of coronagraphs, starshades, mirrors, jitter mitigation, wavefront control, and detectors. By identifying high technology readiness solutions where ready, and identifying required technology development that can begin early, HabEx will be well position for assessment by the community in 2020.

10398-43, Session PMon

Monitoring solar irradiance from L2 with Gaia

Edmund Serpell, European Space Operations Ctr. (Germany)

Gaia is the European Space Agency's cornerstone astrometry mission to measure the positions of 1 billion stars in the Milky Way with unprecedented accuracy. Since early 2014 Gaia has been operating in a halo orbit around the second Sun-Earth Lagrange point that provides the stable thermal environment, without Earth eclipses, needed for the payload to function accurately. The spacecraft is constructed with a 10m diameter circular sun-shield which is equipped with a number of thermistors that provide a continuous measurement of the local temperature. As a consequence of the spacecraft design and operational conditions the Gaia sun-shield has been observed to behave as a bolometer that is measuring the solar output over a broad wavelength range.

In this paper we present analysis of temperature measurements made of the Gaia sun-shield at frequencies of up to 1Hz for the first 2.5 years of routine operations. We show that the Gaia sun-shield as a bolometer is capable of measuring the changes to the solar irradiance at a level of better than 0.1% with time constants of less than 1 hour.

Conference 10399: Optics for EUV, X-Ray, and Gamma-Ray Astronomy VIII

Tuesday - Thursday 8 –10 August 2017

Part of Proceedings of SPIE Vol. 10399 Optics for EUV, X-Ray, and Gamma-Ray Astronomy VIII

10399-1, Session 1

Cherenkov Telescope Array: the next-generation gamma ray observatory

Jan Ebr, Institute of Physics of the ASCR, v.v.i. (Czech Republic)

The Cherenkov Telescope Array (CTA) is a project to build the next generation ground-based observatory for gamma-ray astronomy at very-high energies in the range from 20 GeV to 300 TeV, which will both surpass the sensitivity of existing instruments in their energy domains and extend the limits of the observed energy spectrum. It will probe some of the most energetic processes in the Universe and provide insight into topics such as the acceleration of charged cosmic rays and their role in galaxy evolution, processes in relativistic jets, wind and explosions and the nature and distribution of dark matter. The CTA Observatory will consist of more than a hundred imaging atmospheric Cherenkov telescopes (IACT) of three different size classes, installed at two premier astronomical locations, one in each hemisphere. It is foreseen that the telescopes will use a variety of optical designs including parabolic primary mirrors, variations of the Davies-Cotton design and two-mirror setups such as the Schwarzschild-Couder telescope, and several camera designs, using both photomultiplier tubes (PMTs) and silicon photomultipliers (SiPMs) for detection of the nanosecond-scale Cherenkov flashes. Each telescope will feature a precise but lightweight and agile mount, allowing even the largest telescopes to change targets within 20 seconds, with systems of sensors and actuators actively controlling the shape of the reflecting surfaces. As an integral part, the Observatory will feature extensive calibration facilities, closely monitoring both the detectors themselves and the surrounding atmosphere. Several telescope prototypes already exist and the installation works at the northern site have started.

10399-2, Session 1

Aplanatic telescopes based on Schwarzschild optical configuration: from grazing incidence Wolter-like x-ray optics to Cherenkov two-mirror normal incidence telescopes

Giorgia Sironi, Paolo Conconi, Giovanni Pareschi, INAF - Osservatorio Astronomico di Brera (Italy)

Karl Schwarzschild introduced a method to design large-field aplanatic telescopes introducing radial polynomials in the optics profiles. Couder then refined the Schwarzschild solution correcting for the astigmatic aberration adding a curve focal plane. By the way, the lack of technological solutions to manufacture and test polynomial aspherical mirrors historically limited the applications of the Schwarzschild-like design. In 1952, Wolter extended the polynomial solution of Karl Schwarzschild to grazing incidence telescopes. The obtained design allowed to improve the Wolter-type grazing incidence optics, designed to bee free of spherical aberration, eliminating coma completely.

The resulting Wolter-Schwarzschild design for x-ray optics was adopted for telescopes already flown like the ROSAT WFC and the SOHO X-ray telescope, and for understudy missions like the wide field x-ray telescope (WFXT), designed assuming polynomials numerically optimized to get a flat field of view response. The Schwarzschild-Couder (SC) solution was recently proposed by Vassiliev and collaborators as a solution for Cherenkov telescopes.

The first Cherenkov telescope based on the SC configuration was realized and successfully characterized (the ASTRI telescope) by the Italian institute for Astrophysics (INAF), demonstrating the suitability of the SC configuration for the Cherenkov astronomy requirements. Moreover, another Cherenkov telescope based on a different SC solution is currently under construction at Fred Lawrence Whipple Observatory in southern Arizona, USA. In this paper we will review the Schwarzschild approach applied to grazing incidence and Cherenkov telescopes, discussing on future applications in the field of high energy astronomy.

10399-3, Session 1

The ASTRI SST-2M prototype for the Cherenkov Telescope Array: status after the commissioning phase of the telescope

Rodolfo Canestrari, INAF - Osservatorio Astronomico di Brera (Italy); Enrico Giro, INAF - Osservatorio Astronomico di Padova (Italy); Giorgia Sironi, INAF - Osservatorio Astronomico di Brera (Italy); Elisa Antolini, Univ. degli Studi di Perugia (Italy); Dino Fugazza, INAF - Osservatorio Astronomico di Brera (Italy); Salvatore Scuderi, INAF - Osservatorio Astrofisico di Catania (Italy); Gino Tosti, Univ. degli Studi di Perugia (Italy); Claudio Tanci, INAF - Osservatorio Astronomico di Brera (Italy); Federico Russo, INAF - Osservatorio Astrofisico di Torino (Italy); Daniele Gardiol, INAF - Osservatorio Astronomico di Torino (Italy); Carlos E. Fermino, Univ. de São Paulo (Brazil); Giovanni Pareschi, INAF - Osservatorio Astronomico di Brera (Italy); ASTRI collaboration, INAF Osservatorio Astronomico di Brera (Italy); CTA consortium, CTA observatory (Italy); Gianpietro Marchiori, Andrea Busatta, Enrico Marcuzzi, EIE Group s.r.l. (Italy); Ivan Folla, Galbiati Group (Italy)

ASTRI SST-2M is an imaging atmospheric Cherenkov telescope developed by the Italian National Institute of Astrophysics (INAF) in the framework of the Cherenkov Telescope Array (CTA) as an end-to-end prototype for the Small Size array. Large-, medium-, and small-sized telescopes will compose the CTA observatory that represents the next generation of imaging atmospheric Cherenkov telescopes and will explore the very high-energy domain from a few tens of GeV up to few hundreds of TeV.

The ASTRI SST-2M telescope has been installed at the INAF observing station at Serra La Nave, on Mt. Etna (Sicily, Italy) in September 2014. In these 3 years of open-air operations the telescope has been commissioned and its opto-mechanical performance is now well understood. The apparatus was made ready to host its main scientific instrument, the camera with a Silicon-Photomultiplier based detectors.

This contribution is a status report on the complete ASTRI SST-2M telescope assembly including the electro-mechanical structure, the optical system, the control software and on-board instrumentation.

10399-4, Session 1

The GCT small-sized dual-mirror telescopes for CTA

Tim Greenshaw, Univ. of Liverpool (United Kingdom)

The Gamma-ray Cherenkov Telescope (GCT) is one of the Small Size Telescopes (SSTs) proposed for the Cherenkov Telescope Array (CTA). The telescope is a Schwarzschild-Couder design of 2.3 m focal length, with aspherical primary and secondary mirrors of 4 m and 2 m diameter, respectively. It is planned to equip the GCT with Compact High-Energy Camera (CHEC) with about 2000 pixels of physical size about 6 times 6 mm^2, providing a field of view of over 8 degrees. The camera's TARGET-based readout electronics allows the GCT to trigger on and measure the cherenkov light images caused by photons entering the atmosphere of

energies above about 1 TeV. The camera digitises the signals recorded in its pixels at a rate of 1 Gs/s.

The GCT prototype in Meudon, Paris saw first Cherenkov light in late 2015, using a version of CHEC equipped with multi-anode photomultipliers, CHEC-M. This contribution presents the results of these and more recent tests of the prototype with CHEC-M and discusses the modifications to the telescope proposed before the first GCT is installed on CTA's southern site in Paranal, Chile. These include changes which further simplify the installation and maintenance of the telescope. Further, the design of a silicon photomultiplier-based version of the camera, CHEC-S, is presented. This will allow both better sensitivity and more robust operation to be achieved than is possible with CHEC-M.

10399-5, Session 1

First light on a new fully digital camera based on SiPM for CTA SST-1M telescope

Domenico della Volpe, Teresa Montaruli, Matthieu Heller, Victor Coco, Imen Al Samarai, Franck Cadoux, Yannick Favre, Cyril Alispach, Isaac Troyano Pujadas, Andrii Nagai, Theodore R. Njoh Ekoume, Roland Walter, Etienne Lyard, Andrii Neronov, Vitalii Sliusar, Univ. de Genève (Switzerland); Jacek Niemiec, Emil Mach, Jerzy Michalowski, Jacek Blocki, Jakub Rafalski, Krzysztof Skowron, Magdalena Stodulska, Institute of Nuclear Physics (Poland); Marek Stodulski, The Henryk Niewodniczanski Institute of Nuclear Physics (Poland); Marek Jamrozy, Michal Ostrowski, Lukasz Stawarz, Krzysztof Zietara, Jagiellonian Univ. in Krakow (Poland); Jerzy Borkowski, Mateusz Janiac, Adam Frankowski, Rafal Moderski, Nicolaus Copernicus Astronomical Ctr. (Poland); Tomasz Bulik, Mira Grudzi?ska, Univ. of Warsaw (Poland); Pawel Pa?ko, Karol Seweryn, Space Research Ctr. (Poland); Dusan Mandat, Miroslav Pech, Petr Schovánek, Institute of Physics of the ASCR, v.v.i. (Czech Republic); Krzysztof Lalik, Pawel J. Rajda, AGH Univ. of Science and Technology (Poland)

The single mirror small size telescope (SST-1M), one of the proposed solutions to become part of the small-size telescopes of the Cherenkov telescope array (CTA), will be equipped with an innovative camera.

The SST-1M has a Davies-Cotton optics with a mirror dish of 4 m diameter and focal ratio 1.4 focussing the Cherenkov light produced in atmospheric showers onto a 90 cm wide hexagonal camera providing a FoV of ~9 degree.

The camera features 1296 custom designed large area hexagonal silicon photomultipliers (SiPM) coupled to hollow optical concentrators to achieve a pixel size of almost 2.4 cm.

The SiPM is a custom design developed with Hamamatsu and with its active area of almost 1 cm^2 is one of the largest monolithic SiPM existing.

Also the optical concentrators are innovative being light funnels made of a polycarbonate substrate coated with a custom designed UV-enhancing coating.

The analog signals coming from the SiPM are fed into the fully digital readout electronics, where digital data are processed by high-speed FPGAs both for trigger and readout.

The trigger logic, implemented into an Virtex 7 FPGA, uses the digital data to elaborate a trigger decision by matching data against predefined patterns.

This approach is extremely flexible and allows improvements and continued evolutions of the system.

The prototype camera is being tested in laboratory prior to its installation expected in summer 2017 on the telescope prototype in Krakow (Poland).

In this contribution, we will describe the design of the camera, show the performance measured in laboratory and the early operations on the telescope.

10399-6, Session 2

Optics for the Imaging X-ray Polarimetry Explorer

Brian D. Ramsey, NASA Marshall Space Flight Ctr. (United States)

The Imaging X-ray Polarimetry Explorer (IXPE) was recently selected by NASA for flight in late 2020. IXPE features three identical x-ray telescopes each comprised of a 4-m-focal length mirror module assembly, fabricated at MSFC, that focuses x-rays onto a polarization-sensitive, imaging detector, contributed by Italy. Mirrors and detectors are separated by a deployable boom that sits atop a Ball-Aerospace-provided satellite bus. This presentation will give a brief overview of the IXPE mission with particular emphasis on the mirror module assembly design, fabrication approach, and expected performance. Trades performed to optimize the design within mass and launch-vehicle fairing constraints will be discussed, along with finite element analyses run to optimize the mechanical design. The presentation will also touch on modeling of leakage radiation from off-axis sources outside of the field of view.

10399-7, Session 2

The STAR-X X-Ray Telescope Assembly (XTA)

Ryan S. McClelland, Timo T. Saha, William W. Zhang, Peter M. Solly, Joeseph A. Bonafede, NASA Goddard Space Flight Ctr. (United States)

The STAR-X science goals are to discover what powers the most violent explosions in the Universe, understand how black holes grow across cosmic time and mass scale, and measure how structure formation heats the majority of baryons in the Universe. To achieve these goals, STAR-X requires a powerful X-ray telescope with a large field of view, large collecting area, and excellent point spread function. The STAR-X instrument, the XTA, meets these requirements using a powerful X-ray mirror technology based on precision-polished single crystal silicon and a mature CCD detector technology.

The XTA is composed of three major subsystems: an X-ray Mirror Assembly (MA) of high resolution, lightweight mirror segments fabricated out of single crystal silicon; a Focal Plane Assembly (FPA) made of back-illuminated CCDs capable of detecting X-rays with excellent quantum efficiency; and a composite Telescope Tube that structurally links the MA and FPA. The MA consists of 5,972 silicon mirror segments mounted into five subassemblies called meta-shells. A meta-shell is constructed from an annular central structural shell covered with interlocking layers of mirror segments. This paper describes the requirements, design, and analysis of the XTA subsystems with particular focus on the MA.

10399-8, Session 2

Miniature Lightweight X-ray Optics (MiXO) and CubeSat X-ray Telescope (CubeX) for solar system exploration

Suzanne E. Romaine, Jaesub Hong, Harvard-Smithsonian Ctr. for Astrophysics (United States); Brian D. Ramsey, National Space Sciences and Technology Ctr. (United States); Larry Nittler, Carnegie Institution for Science (United States); Keith Gendreau, NASA Goddard Space Flight Ctr. (United States); Daniele Spiga, INAF - Osservatorio Astronomico di Brera (Italy); Martin Elvis, Jonathan Grindlay, Harvard-Smithsonian Ctr. for Astrophysics (United States)

We report the recent progress in development of miniature X-ray optics

(MiXO), which can enable powerful, yet compact lightweight X-ray optics affordable for many future planetary missions.We also introduce a new concept of a CubeSat X-ray telescope (CubeX) capable of both X-ray fluorescence (XRF) imaging and X-ray pulsar timing based navigation (XNAV) by employing the MiXO and a novel focal plane configuration with no moving parts.

Comparative studies of surface variations in the elemental composition of diverse planetary bodies can provide clues to their formation and evolutionary history. XRF, intrinsic to atomic energy levels, carries a unique signature of the elemental composition of the emitting bodies. Unlike optical and infrared spectra that can be altered by space weathering, XRF can probe more than 10–20 ?m deep below the surface, thus it is a powerful diagnostic tool to understand the true chemical and mineralogical composition of the planetary bodies. X-ray Imaging spectroscopy can greatly improve our understanding of the origin and geological history of target bodies by identifying the elemental composition of individual surface features (e.g., boulders versus craters) and activities (e.g., outgassing).

Deep space navigation is a critical issue for small planetary missions. Millisecond pulsars (MSPs), whose spin rates range from a few to a few 10s of milliseconds, provide stable natural clocks in the sky comparable to precise atomic clocks. With recent technological advances of X-ray telescopes and discoveries of many new X-ray MSPs in the last decade, XNAV has become a plausible approach to greatly assist, or even outperform, NASA's Deep Space Network (DSN) or ESA's European Space Tracking (ESTRACK) and to realize low-cost autonomous deep space navigation. For instance, the Station Explorer for X-ray Timing and Navigation Technology (SEXTANT) program plans to test the feasibility of XNAV on the International Space Station (ISS) using the Neutronstar Interior Composition Explorer (NICER) mission.

10399-9, Session 2

The Lynx Optics Working Group: objectives and current status

Mark Schattenburg, MIT Kavli Institute for Astrophysics and Space Research (United States)

Lynx is one of four large mission concepts being developed by NASA for consideration by the 2020 Decadal Survey in Astronomy and Astrophysics. Lynx will observe in the traditional X-ray band (approximately 0.1 to 10 keV) with a sub-arcsecond grazing-incidence telescope of effective area exceeding a square meter.

Such a mission concept was identified in the 2013 NASA Astrophysics Roadmap "Enduring Quests, Daring Visions" and, since early 2016, has been developed by a community-selected Science and Technology Definition Team (STDT). The STDT convened several working groups to refine science objectives and to develop credible plans for maturing technologies needed to axhieve these science objectives. The Lynx Optics Working Group (OWG)---comprising more than 30 technologists from academia, research institutions, and industry---has been assessing current research and development efforts to identify key challenges to be overcome for Lynx to be successful. Here we discuss the OWG organization, its goals, and the current status of its work in support of the Lynx STDT.

10399-10, Session 3

The Athena telescope and optics status

Marcos Bavdaz, Eric Wille, Mark Ayre, Ivo Ferreira, Brian Shortt, Sebastiaan Fransen, European Space Research and Technology Ctr. (Netherlands); Maximilien J. Collon, cosine B.V. (Netherlands); Giuseppe Vacanti, cosine Science & Computing B.V. (Netherlands); Nicolas M. Barrière, Boris Landgraf, cosine B.V. (Netherlands); Jeroen Haneveld, Micronit Microfluidics B.V. (Netherlands); Coen van Baren, SRON Netherlands Institute for Space Research (Netherlands); Karl-Heintz Zuknik, OHB-System AG (Germany); Desirée Della Monica Ferreira, Sonny Massahi, Finn E. Christensen, DTU Space (Denmark); Michael Krumrey, Physikalisch-Technische Bundesanstalt (Germany); Vadim Burwitz, Max-Planck-Institut für extraterrestrische Physik (Germany); Giovanni Pareschi, Daniele Spiga, INAF - Osservatorio Astronomico di Brera (Italy); Giuseppe Valsecchi, Media Lario Technologies S.r.l. (Italy); Dervis Vernani, Thales Alenia Space (Switzerland); Paul Oliver, e2v technologies plc (United Kingdom)

The work on the definition and technological preparation of the ATHENA (Advanced Telescope for High ENergy Astrophysics) mission continues to progress. In parallel to the study of the accommodation of the telescope, many aspects of the X-ray optics are being evolved further.

The optics technology chosen for ATHENA is the Silicon Pore Optics (SPO), which hinges on technology spin-in from the semiconductor industry, and uses a modular approach to produce large effective area lightweight telescope optics with a good angular resolution.

Both system studies and the technology developments are guided by ESA and implemented in industry, with participation of institutional partners. In this paper an overview of the current status of the telescope optics accommodation and technology development activities will be provided.

10399-11, Session 3

Development of Athena mirror modules

Maximilien J. Collon, cosine B.V. (Netherlands); Giuseppe Vacanti, cosine Science & Computing B.V. (Netherlands); Nicolas M. Barrière, Boris Landgraf, cosine B.V. (Netherlands); Ramses Günther, Mark Vervest, Roy van der Hoeven, cosine Science & Computing B.V. (Netherlands); Marco W. Beijersbergen, cosine B.V. (Netherlands); Marcos Bavdaz, Eric Wille, Brian Shortt, European Space Agency (Netherlands); David Girou, cosine B.V. (Netherlands); Sebastiaan Fransen, European Space Agency (Netherlands); Jeroen Haneveld, Arenda Koelewijn, Karin Booysen, Maurice Wijnperle, Micronit Microfluidics B.V. (Netherlands); Coen van Baren, Alexander Eigenraam, SRON Netherlands Institute for Space Research (Netherlands); Peter Müller, Physikalisch-Technische Bundesanstalt (Germany); Michael Krumrey, European Space Agency (Netherlands) and Physikalisch-Technische Bundesanstalt (Germany); Vadim Burwitz, Max-Planck-Institut für extraterrestrische Physik (Germany); Giovanni Pareschi, Paolo Conconi, INAF - Osservatorio Astronomico di Brera (Italy); Sonny Massahi, Finn E. Christensen, DTU Space (Denmark); Giuseppe Valsecchi, Media Lario Technologies S.r.l. (Italy); Paul Oliver, Ian Checquer, Kevin Ball, e2v technologies plc (United Kingdom); Karl-Heinz Zuknik, OHB-System AG (Germany); Desirée Della Monica Ferreira, DTU Space (Denmark)

Silicon Pore Optics (SPO), developed at cosine with ESA and several academic and industrial partners, provides lightweight, yet stiff high resolution x-ray optics. This technology enables ATHENA to reach an unprecedentedly large effective area in the 0.2 - 12 keV band with an angular resolution better than 5''. After developing the technology for 50 m and 20 m focal length, this year has witnessed the first 12 m focal length mirror modules being produced. The technology development is also gaining momentum with three different radii under study: mirror modules for the inner radii (R_{min} = 250 mm), outer radii (R_{max} = 1500 mm) and middle radii (R = 737 mm) are being developed in parallel.

In this paper, we report on the current state of the Silicon Pore Optics technology, from the manufacturing of the stacks of mirror plates, to the

final characterization of mirror modules taking place at PTB's XPBF with synchrotron radiation and the PANTER test facility.

10399-12, Session 3

Silicon pore optics mirror module assembly process

Nicolas M. Barrière, Maximilien J. Collon, cosine B.V. (Netherlands); Giuseppe Vacanti, cosine Science & Computing B.V. (Netherlands); Boris Landgraf, cosine B.V. (Netherlands); Ramses Günther, Mark Vervest, Roy van der Hoeven, cosine Science & Computing B.V. (Netherlands); David Girou, Marco W. Beijersbergen, cosine B.V. (Netherlands); Marcos Bavdaz, Eric Wille, Sebastiaan Fransen, European Space Research and Technology Ctr. (Netherlands); Coen van Baren, Alexander Eigenraam, SRON Netherlands Institute for Space Research (Netherlands); Peter Müller, Michael Krumrey, Physikalisch-Technische Bundesanstalt (Germany); Giuseppe Valsecchi, Media Lario Technologies S.r.l. (Italy); Karl-Heinz Zuknik, OHB-System AG (Germany)

Silicon Pore Optics are produced as stacks of mirror plates, which are then paired to form X-ray Optics Units (XOUs). For ATHENA, in the current scheme, two XOUs are glued together in a set of brackets, leading to mirror modules (MMs) made of 4 stacks. The requirements regarding the positioning of the brackets with respect to the optical axis of the MM are very tight, in order to make the MMs integration in the mirror structure possible. MMs are integrated at the XPBF beamline of PTB (BESSY II synchrotron, Berlin), using a pencil X-ray beam and dedicated integration jigs. The relative orientation of the secondary stack with respect to the primary stack is fitted using the positions of the reflected beamspots onto the camera. This provides a deterministic way of orienting stacks with respect to each other within a XOU, and allows meeting with the stringent angular accuracy requirements. The same operation is then repeated for the second XOU composing a mirror module, with the additional constraint that it needs to be confocal with the first one. In this paper we review the process that is used to integrate stacks and brackets into mirror modules.

10399-13, Session 3

Optical integration of SPO mirror modules in the ATHENA telescope

Giovanni Bianucci, Giuseppe Valsecchi, Fabio Marioni, Media Lario Technologies S.r.l. (Italy); Daniele Gallieni, Paolo Lazzarini, A.D.S. International S.r.l. (Italy); Giancarlo Parodi, Matteo Ottolini, BCV Progetti S.r.l. (Italy); Maximilien J. Collon, cosine B.V. (Netherlands); Marta M. Civitani, Giovanni Pareschi, Daniele Spiga, INAF - Osservatorio Astronomico di Brera (Italy); Marco Nebiolo, Thales Alenia Space (Italy); Marcos Bavdaz, Eric Wille, European Space Research and Technology Ctr. (Netherlands)

ATHENA is the next high-energy astrophysical mission selected by ESA for launch in 2028. According to the current system studies, the 12 m focal length X-ray telescope is composed of 1062 SPO Mirror Modules (MM), arranged in a 3 m structure. The angular resolution requirement of the telescope is 5 arcsec half energy width, with an error budget allocation of 1.5 arcsec for the alignment and integration step of the entire mirror modules population.

This industrial and scientific team is developing, under an ESA contract, the alignment and integration process of the SPO mirror modules into the mirror structure. Besides the 1.5 arcsec angular resolution budget, the integration process meets the requirement of arbitrary integration sequence and MM exchangeability, independently of the already integrated population.

The integration is based on the 218 nm optical imaging of each MM at the 12 m focal plane, so that each module is precisely aligned in the telescope by measuring the photon counts and centroid position of its point spread function (PSF), and subsequently fixed to the structure by means of three dowel pins. This process does not require any vacuum infrastructure, but only a cleanroom laboratory, and has the great advantage of monitoring the telescope PSF during the 3-year integration time.

In this work, we will report on the design and demonstration of the integration of SPO mirror modules in a simplified mirror structure, including measurements showing that the position of the 218 nm centroid matches perfectly the X-ray values measured at PANTER.

10399-14, Session 3

Integration of the Athena mirror modules: development of indirect and x-ray direct AIT methods

Dervis Vernani, Thales Alenia Space (Switzerland); Thibault Seure, Steffen Blum, Thales Alenia Space (Switzerland); Eric Wille, Marcos Bavdaz, European Space Agency (Netherlands); Uwe Schaeffer, Airbus Deutschland (Germany); Nicolas Lièvre, MICOS (Switzerland); Adeeb Nazeeruddin, Micos Engineering GmbH (Switzerland); Maximilien J. Collon, Nicolas M. Barrière, cosine B.V. (Netherlands); Vadim Burwitz, Max-Planck-Institut für extraterrestrische Physik (Germany); Michael Krumrey, Peter Müller, Levent Cibik, Physikalisch-Technische Bundesanstalt (Germany)

Within the ATHENA optics technology plan, activities are on-going for demonstrating the feasibility of the mirror module integration. Each mirror module has to be accurately attached to the mirror structure by means of three isostatic mounts ensuring minimal distortion under environmental loads. This work reports on the status of one of the two parallel activities initiated by ESA to address this demanding task. In the study awarded to the industrial consortium, the integration relies on opto-mechanical metrology and direct X-ray alignment. For the first or "indirect" method the X-ray alignment results are accurately referenced, by means of a laser tracking system, to optical targets mounted on the mirror modules and finally linked to the mirror module structure coordinate system. With the second or "direct" method the alignment is monitored in the X-ray domain, providing figures of merit directly comparable to the final performance. The integration being designed and here presented, foreseen combining the indirect method to the X-ray direct method. The characterization of the single mirror modules is planned at PTB's X-ray Pencil Beam Facility (XPBF) at BESSY II, and the integration at Panter. It is foreseen to integrate and test a demonstrator with two mirror modules from Cosine. The final testing campaign at Panter shall be completed in December 2017.

10399-15, Session 3

Environmental testing of the ATHENA mirror modules

Boris Landgraf, David Girou, Maximilien J. Collon, cosine B.V. (Netherlands); Giuseppe Vacanti, cosine Science & Computing B.V. (Netherlands); Nicolas M. Barrière, cosine B.V. (Netherlands); Ramses Günther, Mark Vervest, Roy van der Hoeven, cosine Science & Computing B.V. (Netherlands); Marco W. Beijersbergen, cosine B.V. (Netherlands); Marcos Bavdaz, European Space Agency (Netherlands); Eric Wille, Sebastiaan Fransen, Brian Shortt, European Space Research and Technology Ctr.

(Netherlands); Coen van Baren, Alexander Eigenraam, SRON Netherlands Institute for Space Research (Netherlands)

The European Space Agency (ESA) is studying the ATHENA (Advanced Telescope for High ENergy Astrophysics) X-ray telescope, the second L-class mission in their Cosmic Vision 2015 – 2025 program with a launch spot in 2028. The baseline technology for the X-ray lens is the newly developed high-performance, light-weight and modular Silicon Pore Optics (SPO). As part of the technology preparation, ruggedisation and environmental testing studies are being conducted to ensure mechanical stability and optical performance of the optics during and after launch, respectively. At cosine, a facility with shock, vibration, tensile strength, long time storage and thermal testing equipment has been set up in order to test SPO mirror module (MM) materials for compliance with an Ariane launch vehicle and the mission requirements.

In this paper, we report on the progress of our ongoing investigations regarding tests on mechanical and thermal stability of MM components like single SPO stacks with and without multilayer coatings and complete MMs of inner (R = 250 mm), middle (R = 737 mm) and outer (R = 1500 mm) radii.

10399-16, Session 4

Optical simulations for design, alignment, and performance prediction of silicon pore optics for the ATHENA x-ray telescope

Daniele Spiga, INAF - Osservatorio Astronomico di Brera (Italy); FInn E. Christensen, DTU Space (Denmark); Marcos Bavdaz, European Space Research and Technology Ctr. (Netherlands); Giovanni Bianucci, Media Lario Technologies S.r.l. (Italy); Marta M. Civitani, INAF - Osservatorio Astronomico di Brera (Italy); Maximilien J. Collon, cosine B.V. (Netherlands); Paolo Conconi, INAF - Osservatorio Astronomico di Brera (Italy); Desirée Della Monica Ferreira, DTU Space (Denmark); Fabio Marioni, Media Lario Technologies S.r.l. (Italy); Sonny Massahi, DTU Space (Denmark); Giovanni Pareschi, Bianca Salmaso, INAF - Osservatorio Astronomico di Brera (Italy); Brian Shortt, European Space Research and Technology Ctr. (Netherlands); Kashmira Tayabaly, Politecnico di Milano (Italy); Giuseppe Valsecchi, Media Lario Technologies S.r.l. (Italy); Giuseppe Vacanti, cosine Science & Computing B.V. (Netherlands); Niels Joergen S. Westergaard, DTU Space (Denmark); Eric Wille, European Space Research and Technology Ctr. (Netherlands)

The ATHENA X-ray observatory is a large-class ESA approved mission, with launch scheduled in 2028. The technology of silicon pore optics (SPO) was selected as baseline to assemble ATHENA's optic with hundreds of mirror modules, obtained by stacking wedged and ribbed silicon wafer plates onto silicon mandrels to form the Wolter-I configuration. In the current configuration, the optical assembly has a 3 m diameter and a 2 m2 effective area at 1 keV, with a required angular resolution of 5 arcsec. The angular resolution that can be achieved is chiefly the combination of 1) the focal spot size determined by the pore diffraction, 2) the focus degradation caused by surface and profile errors, 3) the aberrations introduced by the misalignments between primary and secondary segments, 4) imperfections in the co-focality of the mirror modules in the optical assembly. A detailed simulation of these aspects is required in order to assess the fabrication and alignment tolerances; moreover, the achievable effective area and angular resolution depend on the mirror module design. Therefore, guaranteeing these optical performances requires: a fast design tool to find the most performing solution in terms of mirror module geometry and population, and an accurate point spread function simulation from local metrology and positioning information. In this paper, we present the results of simulations in the framework of ESA-financed projects (SIMPOSiuM, ASPHEA, SPIRIT), in preparation of the ATHENA X-ray telescope, analyzing the mentioned points: 1) we deal with a detailed description of diffractive effects in an SPO mirror module, 2) we show ray-tracing results including surface and profile defects of the reflective surfaces, 3) we assess the effective area and angular resolution degradation caused by alignment errors between SPO mirror module's segments, and 4) we simulate the effects of co-focality errors in X-rays and in the UV optical bench used to study the mirror module alignment and integration.

10399-17, Session 4

Optical design of the STAR-X telescope

Timo T. Saha, William W. Zhang, Ryan S. McClelland, NASA Goddard Space Flight Ctr. (United States)

Top-level science goals of the Survey and Time-domain Astrophysical Research eXplorer (STAR-X) include: investigations of most violent explosions in the universe, study of growth of black holes across cosmic time and mass scale, and measure how structure formation heats the majority of baryons in the universe. To meet these goals, the field-of-view of the telescope has to be about 1 square-degree, the angular resolution 5 arc-seconds across the field-of-view, and on-axis effective area at 1 KeV about 2,000 cm2.

Telescope design is based on a segmented meta-shell approach we have developed at Goddard Space Flight Center for the STAR-X telescope. The telescope shells are divided into 10-degree or 18-degree segments. Telescopes with meta-shells are nested inside each other in order to meet the effective area requirements in 0.5 – 6.0 KeV range. We consider Wolter-Schwarzschild, and Modified-Wolter-Schwarzschild telescope designs as basic building blocks of the nested STAR-X telescope. These designs offer excellent resolution over a large field of views.

Nested telescopes are vulnerable to stray light problems. We have designed a multi-component baffle system to eliminate direct and single-reflection light paths inside the telescopes. A large number of internal and external baffle vane structures are required to prevent stray rays from reaching the focal plane. We have developed a simple ray-trace based tool to determine the dimensions and locations of the baffles.

In this paper we present the results of our trade studies, baffle design studies, and optical performance analyses of the STAR-X telescope.

10399-18, Session 4

Methods for reducing ghost rays on the Wolter-I focusing figures of the FOXSI rocket payload

Juan Camilo Buitrago Casas, Space Sciences Lab. (United States); Lindsay Glesener, Univ. of Minnesota, Twin Cities (United States); Steven D. Christe, NASA Goddard Space Flight Ctr. (United States); Brian D. Ramsey, Ronald Elsner, NASA Marshall Space Flight Ctr. (United States); Sasha Courtade, Space Sciences Lab. (United States); Juliana Vievering, Univ. of Minnesota (United States); Athiray Subramania, Univ. of Minnesota, Twin Cities (United States); Säm Krucker, Stuart Bale, Space Sciences Lab. (United States)

In high energy solar astrophysics, imaging hard X-rays by direct focusing offers higher dynamic range and greater sensitivity compared to past techniques that used indirect imaging. The Focusing Optics X-ray Solar Imager (FOXSI) is a sounding rocket payload which uses seven sets of nested Wolter-I figured mirrors that, together with seven high-sensitive semiconductor detectors, observes the Sun in hard X-rays by direct focusing. The FOXSI rocket has successfully flown twice and is funded to fly a third time in summer 2018.

The Wolter-I geometry consists of two consecutive mirrors, one paraboloid, and one hyperboloid, that reflect photons at grazing angles. Correctly

focused X-rays reflect twice, once per mirror segment. For extended sources, like the Sun, off-axis photons at certain incident angles can reflect on only one mirror and still reach the focal plane, generating a pattern of single-bounce photons, or 'ghost rays' that can limit the sensitivity of the observation of focused X-rays. Understanding and cutting down the ghost rays on the FOXSI optics will maximize the instrument's sensitivity of the solar faintest sources for future flights. We present an analysis of the FOXSI ghost rays based on ray-tracing simulations, as well as the effectiveness of different physical strategies to reduce them.

10399-19, Session 4

Design and simulations of a short optical baffle for the Lightweight Asymmetry and Magnetism Probe (LAMP)

Yujie Xing, Zhanshan Wang, Tongji Univ. (China); Hua Feng, Tsinghua Univ. (China)

The Lightweight Asymmetry and Magnetism Probe (LAMP) is a micro-satellite based mission concept for soft X-ray polarimetry at 250 eV with a large aperture but a short focal length. Due to the very low energy response of the detector, the solar stray light must be well reduced. However, a long baffle is not favored for a micro-satellite with a limited geometry. In this paper, we propose a novel design of a short optical baffle with effective stray light suppression. With an optical aperture of 700 mm for LAMP, a baffle of 150 mm height can reduce the solar stray light by a factor of smaller than ~10-4 at incidence angles greater than 60?, justified with TracePro ray-tracing software. The design meets the requirement for LAMP and can also be used for other optical/UV/X-ray telescopes.

10399-20, Session 4

Optical design and simulations of the soft x-ray telescope for Einstein Probe mission

Yingyu Liao, Zhengxiang Shen, Qiushi Huang, Zhanshan Wang, Tongji Univ. (China)

The Einstein Probe (EP) mission, which aims at discovering transients and monitoring variable objects in 0.5-4 keV X-rays, is a small scientific satellite dedicated to time-domain high-energy astrophysics. For this purpose, the mission will employ a large instantaneous field-of-view (60°?60°) X-ray telescope (WXT), along with moderate spatial resolution (FWHM ~5') and energy resolution. It will also carry a follow-up observation X-ray telescope (FXT) with a smaller field-of-view (15'x15') — capable of much larger light-collecting power and better energy resolution than the main survey telescope. In this paper, we present the optical design and simulations of the FXT, which include the optimized structure parameters of the FXT and its focusing capabilities. The optical design and simulations are mainly performed based on MATLAB ray-tracing program. In our simulations, the FXT will employ conically-approximated Wolter-I structure with a focal length of 2 m. And the mirrors will employ thin glass with 100 mm in length and 0.3 mm in thickness. To obtain a large collective area, the FXT will consist of 66 shells tightly-nested, whose diameters range from 80 mm to 250 mm based on the center of secondary mirrors and three different kinds of coatings designed by utilizing IMD will be deposited. Based on such a kind of configuration, the effective area can be 238 cm2 at 1 keV and 152 cm2 at 4 keV, with an image quality to be approximately 55'' in half-power diameter (HPD), and with a field of view (FOV) to be approximately 15'.

10399-21, Session 5

Predicting silicon pore optics

Giuseppe Vacanti, cosine Science & Computing B.V. (Netherlands); Marcos Bavdaz, European Space Research and Technology Ctr. (Netherlands); Nicolas M. Barriére, Abdelhakim Chatbi, Maximilien J. Collon, D. Dekker, David Girou, cosine B.V. (Netherlands); Ramses Günther, cosine Science & Computing B.V. (Netherlands); Boris Landgraf, cosine B.V. (Netherlands); Roy van der Hoeven, Mark Vervest, cosine Science & Computing B.V. (Netherlands); Eric Wille, European Space Research and Technology Ctr. (Netherlands)

Continuing improvement of Silicon Pore Optics (SPO) calls for regular extension and validation of the tools used to model and predict their X-ray performance. In this paper we present an updated geometrical model for the SPO optics and describe how we make use of the surface metrology collected during each of the SPO manufacturing runs.

The new geometrical model affords the user a finer degree of control on the mechanical details of the SPO stacks, while a standard interface has been developed to make use of any type of metrology that can return changes in the local surface normal of the reflecting surfaces. Comparisons between the predicted and actual performance of samples optics will be shown and discussed.

10399-22, Session 5

Measuring silicon pore optics

Giuseppe Vacanti, cosine Science & Computing B.V. (Netherlands); Marcos Bavdaz, European Space Research and Technology Ctr. (Netherlands); Nicolas M. Barriére, Abdelhakim Chatbi, Maximilien J. Collon, D. Dekker, David Girou, cosine B.V. (Netherlands); Ramses Günther, cosine Science & Computing B.V. (Netherlands); Michael Krumrey, Physikalisch-Technische Bundesanstalt (Germany); Boris Landgraf, cosine B.V. (Netherlands); Peter Müller, Physikalisch-Technische Bundesanstalt (Germany); Roy van der Hoeven, Mark Vervest, cosine Science & Computing B.V. (Netherlands); Eric Wille, European Space Research and Technology Ctr. (Netherlands)

While predictions based on the metrology (local slope errors and detailed geometrical details) play an essential role in controlling the development of the manufacturing processes, X-ray characterization remains the ultimate indication of the actual performance of Silicon Pore Optics. For this reason SPO stacks and mirror modules are routinely characterized at PTB's X-ray Pencil Beam Facility at BESSYII. Obtaining standard X-ray results quickly, right after the production of X-ray optics is essential to making sure that X-ray results can inform decisions taken in the lab.

We describe the data analysis pipeline in operations at cosine, and how it allows us to go from stack production to full X-ray characterization in 24 hours.

10399-23, Session 5

Testing and calibrating the Athena optics at PANTER

Vadim Burwitz, Max-Planck-Institut für extraterrestrische Physik (Germany)

At the PANTER X-ray test facility of the Max-Planck-Institut für extraterrestrische Physik a lot of effort has and will be devoted to develop, test and calibrate the optics of ESA's Athena X-ray observatory. We will present and discuss the type of measurements that are and will be done at PANTER based on experience of testing and calibrating the optics of ROSAT, XMM-Newton as well as recently eROSITA. This encompasses the testing of single silicon pore optics and mini petals as part of Athena mirror assembly integration and testing efforts. Finally the testing of the complete Athena mirror during different stages of integration as well as the final calibration will have to be performed in a new upgraded X-ray test facility.

10399-24, Session 5

Calibration of the FOXSI sounding rocket x-ray optics

Steven D. Christe, NASA Goddard Space Flight Ctr. (United States); Brian D. Ramsey, Mikhail Gubarev, NASA Marshall Space Flight Ctr. (United States); Juan Camilo Buitrago-Casas, Space Sciences Lab. (United States); Lindsay Glesener, Univ. of Minnesota, Twin Cities (United States); Säm Krucker, Fachhochschule NordWestschweiz (Switzerland); Subramania Athiray, Univ. of Minnesota, Twin Cities (United States); Sasha Courtade, Space Sciences Lab. (United States); Shin-nosuke Ishikawa, The Univ. of Tokyo (Japan); Juliana Vievering, Univ. of Minnesota (United States)

We present the calibration of the Focusing Optics X-ray Solar Imager (FOXSI) sounding rocket X-ray optics. FOXSI consists of 7 telescope modules each with either 7 or 10 nested shells. These monolithic Wolter-I shells are fabricated at NASA MSFC using a nickel replication process wherein thin nickel-alloy shells are electroformed on figured and super-polished aluminum mandrels from which they are separated via differential thermal expansion. Concentric shells are then co-aligned to form a telescope module. FOXSI modules were calibrated at the MSFC Stray Light Facility. Performance metrics such as the point spread function (PSF), the half-power diameter (HPD), and the effective area as a function of energy and position on-axis and at multiple off-axis positions were measured. The PSF was found to have an FWHM of less than 7 arcsec (on-axis). The performance of individual telescope modules is consistent across many modules. The details of the calibration procedure and results are presented.

10399-25, Session 5

The Hitomi (ASTRO-H) Soft X-ray Telescope (SXT): current status of calibration

Yoshitomo Maeda, Institute of Space and Astronautical Science (Japan); Takashi Okajima, Yang Soong, Peter J. Serlemitsos, Hideyuki Mori, Lawrence G. Olsen, David Robinson, Richard G. Koenecke, William S. Chang, NASA Goddard Space Flight Ctr. (United States); Devin J. Hahne, Johns Hopkins Univ. Applied Physics Lab., LLC (United States); Ryo Iizuka, Manabu Ishida, Institute of Space and Astronautical Science (Japan); Toshiki Sato, Sho Kurashima, Nozomi Nakaniwa, Ryota Asai, Tokyo Metropolitan Univ. (Japan); Takayuki Hayashi, Tokyo Metropolitan Univ. (Japan); Takuya Miyazawa, Okinawa Institute of Science and Technology Graduate Univ. (Japan); Kazunori Ishibashi, Kenji Tachibana, Keisuke Tamura, Yuzuru Tawara, Nagoya Univ. (Japan); Akihiro Furuzawa, Fujita Health Univ. (Japan); Satoshi Sugita, Tokyo Institute of Technology (Japan)

We present latest results of the in-flight calibration of the SXT onboard the Hitomi satellite.

10399-26, Session 5

The Hitomi (ASTRO-H) Hard X-ray Telescope (HXT): current status of calibration

Hisamitsu Awaki, Ehime Univ. (Japan); Hideyo Kunieda, Hironori Matsumoto, Kazunori Ishibashi, Keisuke Tamura, Yuzuru Tawara, Ikuyuki Mitsuishi, Nagoya Univ. (Japan); Akihiro Furuzawa, Fujita Health Univ. (Japan); Takuya Miyazawa, Okinawa Institute of Science and Technology Graduate Univ. (Japan); Manabu Ishida, Yoshitomo Maeda, Ryo Iizuka, Institute of Space and Astronautical Science (Japan); Shigeo Yamauchi, Nara Women's Univ. (Japan); Yoshito Haba, Aichi Univ. of Education (Japan); Satoshi Sugita, Tokyo Institute of Technology (Japan); Tessei Yoshida, Ehime Univ. (Japan); Takashi Okajima, Hideyuki Mori, NASA Goddard Space Flight Ctr. (United States); Takayuki Hayashi, Nagoya Univ. (Japan) and NASA Goddard Space Flight Ctr. (United States)

The Japanese X-ray Astronomy Satellite, Hitomi (ASTRO-H) carries two hard X-ray telescopes (HXT), covering the energy band from 5 keV to 80 keV. Several targets were observed during the initial functional verification of the onboard instruments. The preliminary in-flight performance of HXT through the analysis of G21.5-0.9 observation was reported in the previous SPIE meeting.

We have updated the calibration of the Hitomi HXTs with Crab observation. The imaging performance of HXT have been estimated to be about 1.'7 (HPD) with X-ray emission originating from Crab pulsar.

The X-ray image of Crab Pulsar was obtained by subtracting on-pulse image from off-pulse image.

The HPD of HXT is better than those obtained from the extended source, G21.5-0.9. In the calibration of the energy response of HXTs, we found that a fine tuning of energy response of HXTs was required for the case of a bright source such as a Crab. Thus, we introduce a fudge factor to reproduce the effective area obtained from the ground calibration. The X-ray spectrum of Crab nebula is well reproduced with a simple power law model in the energy range from 8 keV to 80 keV.

The energy responses of HXTs are reflected in the latest calibration database of Hitomi.

10399-27, Session 6

Silicon mirror segments, meta-shells, and mirror assemblies for x-ray astronomy

William W. Zhang, NASA Goddard Space Flight Ctr. (United States)

Future X-ray observatories, from small Explorers to flagships, require telescopes of unprecedented performance in terms of angular resolution and effective area. Yet they must still fit under stringent launch and budgetary envelopes, which mean that these telescopes must be lightweight and of very low production cost per unit effective area. In this paper we describe a comprehensive approach to meet those manifold requirements. The approach is based on precision polishing of single-crystal silicon, which has the potential of achieving the highest possible angular resolution and lowest possible weight. In combination with a mass-production process, it also has the potential of achieving the lowest possible cost per unit effective area. Adopting the traditional philosophy of minimizing constraints, we align and bond each mirror segment at four locations, which are optimized for minimal distortion under gravity and after gravity release, to form meta-shells. The salient features of the meta-shells are that they are optically precise and structurally stiff modules and that they preserve the axial symmetry of X-ray optics, affording easy and accurate integration into final mirror assemblies. We will describe the motivation for this approach, its development status, and its prospects for enabling both near-term and long-term X-ray astronomical missions.

10399-28, Session 6

Progress on the fabrication of lightweight single-crystal silicon x-ray mirrors

Raul E. Riveros, NASA Goddard Space Flight Ctr. (United States) and Univ. of Maryland, Baltimore County (United States); Michael P. Biskach, NASA Goddard Space Flight Ctr. (United States); Kim D. Allgood, Marton V. Sharpe, John D. Kearney, Stinger Ghaffarian Technologies, Inc. (United States); William W. Zhang, NASA Goddard Space Flight Ctr. (United States)

Single crystal silicon is an excellent X-ray mirror substrate material due to its high stiffness, low density, high thermal conductivity, zero internal stress, and commercial availability. At NASA Goddard Space Flight Center, we are refining a manufacturing process for producing high resolution and lightweight X-ray mirror segments in a cost and time effective manner. Previous efforts demonstrated the possibility of producing X-ray mirrors that meet the high demands of a future X-ray mission such as STAR-X. Presently, we are producing paraboloidal and hyperboloidal mirror surfaces on the lightweight silicon segments in various optical prescriptions. This paper presents results from these recent investigations.

10399-29, Session 6

Kinematic alignment and bonding of silicon mirrors for high-resolution astronomical x-ray optics

Kai-Wing Chan, NASA Goddard Space Flight Ctr. (United States) and Univ. of Maryland, Baltimore County (United States)

We introduce a method in which a quasi-cylindrical mirror segment is mounted kinematically at 4 points, constrained in the radial direction when placed with its surface facing up or down. The segment is fully statically determined with additional constraints in axial translation and roll. Such alignment procedure is simple and precise when the radial constraints are precisely set. The mirrors are subsequently bonded into place. We address the precision of the process, the accuracy of the constraints, and the technical challenges in building up "meta-shells" of mirrors for lightweight x-ray optics to be used in the proposed STAR-X mission.

10399-30, Session 7

A hybrid concept (segmented plus monolithic fused silica shells) for a high-throughput and high-angular resolution x-ray mission (Lynx/X-Ray Surveyor like)

Giovanni Pareschi, Stefano Basso, Marta M. Civitani, Bianca Salmaso, INAF - Osservatorio Astronomico di Brera (Italy)

Lynx is a large area and high angular resolution X-ray mission concept for the next decade. It is a leap of two orders of magnitude in sensitivity over Chandra and ATHENA. The science of X-ray Surveyor requires a large-throughput mirror assembly with sub-arcsec angular resolution. These future X-ray mirrors have a set of requirements which, collectively, represents very substantial advances over any currently in operation or planned for missions other than X-ray Surveyor. Of particular importance is achieving low mass per unit collecting area, while maintaining Chandra-like angular resolution. Among the possible solutions under study, the direct polishing of both thin monolithic pseudo-cylindrical shells and segments made of fused silica are being considered as viable solutions for the implementation of the mirrors. Fused silica has very good thermo-mechanical parameters (including a very low CTE), making the material very attractive for the production of the Lynx mirrors. It should be noted that the use of close shells is very attractive, since the operations for the integration of the shells will be greatly simplified and the area lost due to the vignetting from the interfacing structures minimized. However the maximum diameter doable for close shells, according to the current technology, is of the order of 1.5 m, i.e. much smaller than the maximum diameter of the Lynx optic (3 m). In this paper we will discuss a possible layout for a hybrid concept (segmented plus monolithic shells made of fused silica) for the Lynx/XRS telescope, discussing preliminary results in terms of optical and mechanical performance.

10399-31, Session 7

Thin fused silica shells for high-resolution and large collecting area x-ray telescopes (like Lynx/XRS)

Marta M. Civitani, Stefano Basso, Oberto Citterio, Joanna Ho?yszko, Mauro Ghigo, Giovanni Pareschi, INAF - Osservatorio Astronomico di Brera (Italy); Giancarlo Parodi, BCV Progetti S.r.l. (Italy); Giorgio Toso, INAF - IASF Milano (Italy); Gabriele Vecchi, INAF - Osservatorio Astronomico di Brera (Italy)

The implementation on of a X-ray mission with high imaging capabilities, similar to those achieved with Chandra (< 1arcsec Half Energy Width, HEW), but with a much larger throughput (2.5m2 effective area @1keV), represents a compelling request by the scientific community. To this end the Lynx/XRS mission is being studied in USA, with the participation of international partners. In order to figure out the challenging technological task of the mirror fabrication, different approaches are considered, based on monolithic and segmented shells (possibly combined together). Starting from the experience done on the glass prototypal shell realized in the past years, the direct polishing of thin (2mm thick) fused silica monolithic shells is being investigated as a possible solution. A temporary stiffening structure is designed in order to support the shell during the figuring and polishing operations and to mange the handling up to its integration in the telescope supporting structure. After the grinding and the polishing phases, in order to achieve the required surface accuracy, a final ion beam figuring correction is foreseen. In this paper, we will present the technological process and the results achieved so far on a prototypal shell under development.

10399-32, Session 7

Fused silica segments: a possible solution for x-ray telescopes with very high angular resolution like Lynx/XRS

Bianca Salmaso, Stefano Basso, Marta M. Civitani, Mauro Ghigo, INAF - Osservatorio Astronomico di Brera (Italy); Joanna Holyszko, INAF - Osservatorio Astronomico di Bologna (Italy); Daniele Spiga, Gabriele Vecchi, Giovanni Pareschi, INAF - Osservatorio Astronomico di Brera (Italy)

In order to look beyond Chandra, the Lynx/XRS mission has been proposed in USA and is currently studied by NASA. The optic will have an effective area of 2.5 m2 and an angular resolution of 0.5 arcsec HEW at 1 keV. In order to fulfil these requirements different technologies are considered, with the approaches of both full and segmented shells (that, possibly, can be also combined together). Concerning the production of segmented mirrors, a variety of thin substrates (glass, metal, silicon) are envisaged, that can be produced using both direct polishing or replication methods. Innovative post-fabrication correction methods (such as piezoelectric or magneto-restrictive film actuators on the back surface, differential deposition, ion implantation) are being also considered in order to reach the final tolerances. In this paper we are presenting a technology development based on fused silica (SiO_2) segmented substrates, owing the low coefficient of thermal expansion of Fused Silica and its high chemical stability compared

to other glasses. Thin SiO2 segmented substrates (typically 2 mm thick) are figured by direct polishing combined with final profile ion figuring correction, while the roughness reduction is reached with pitch tools. For the profile and roughness correction, the segments are glued to a substrate with UV glue, thanks to the transparency of the Fused Silica to UV. In this paper we present the current status of this technology.

10399-33, Session 8

Thermal forming of glass substrates for adjustable optics

Vincenzo Cotroneo, Paul B. Reid, Ryan Allured, Vanessa Marquez, Casey T. DeRoo, Eric D. Schwartz, Kenneth L. Gurski, Harvard-Smithsonian Ctr. for Astrophysics (United States)

The proposed Lynx telescope is an X-ray observatory with Chandra-like angular resolution and about 30 times larger effective area. The technology under development at SAO is based on the deposition of piezoelectric material on the back of glass substrates, used to correct longer wavelength figure errors. This requires a large number (about 8000) of figured segments with sufficient quality to be in the range of correctibility of the actuators.

Thermal forming of thin glass offers a convenient approach, being based on intrinsically smooth surfaces (which doesn't require polishing or machining), available in large quantity and at a low cost from flat

display industry. Being a replica technique, this approach is particularly convenient both for development and for the realization of modular/segmented telescopes.

In this paper we review the current status and the most recent advances in the thermal forming activities at SAO, and the perspectives for the employment of these substrates for the adjustable X-Ray optics.

10399-34, Session 8

Indirect glass slumping of grazing incidence mirror segments for lightweight x-ray telescopes

Laura Proserpio, Peter Friedrich, Emanuel Madarasz, Elias Breunig, Vadim Burwitz, Max-Planck-Institut für extraterrestrische Physik (Germany); Thorsten Döhring, Anne-Catherine Probst, Hochschule Aschaffenburg (Germany)

The paper provides a description of recent progress in the development of lightweight, precision and high-throughput grazing-incidence mirrors for x-ray astronomy made by glass. In particular, the indirect slumping technology under investigation at the Max Planck Institute for Extraterrestrial Physics (MPE) is reviewed and recent activities are presented together with the research approaches. The glass slumping technique foresees several steps: a thermal forming process using a suitable mould; a reflective layer application; the alignment and integration of mirror segments into a supporting structure; and the final verification of prototype modules by X-rays. Each step is considered at MPE, with the involvement of partner institutes and universities. The last year of activities was mainly dedicated to the procurement of new moulds and to the application of Iridium coating. The main results will be presented.

10399-35, Session 8

Recent progress on experiments and numerical analysis of air bearing slumping for x-ray telescope mirror substrates

Heng Zuo, Brandon D. Chalifoux, Massachusetts Institute of Technology (United States); Michael D. DeTienne, Izentis LLC (United States); Ralf K. Heilmann, Youwei Yao, Mark L. Schattenburg, MIT Kavli Institute for Astrophysics and Space Research (United States)

Slumping of thin glass sheets onto high precision mandrels was used by NASA Goddard Space Flight Center to fabricate the NuSTAR telescope with spectacular success. Though this process generates mirrors with good resolution, it requires long thermal cycles and produces mid-range spatial frequency errors due to the anti-stick mandrel coatings.

Over the last few years, MIT Space Nanotechnology Lab has developed a slumping process which utilizes a pair of porous air bearing mandrels through which compressed nitrogen is forced, with the round flat glass sheet floating on a thin layer of nitrogen during the thermal cycle. A series of design and tests on horizontal slumping with improved control algorithm and fiber sensing techniques have shown results in glass with reduced mid-range spatial frequency errors that could be accomplished in much shorter thermal cycles. We examined the influence of the nitrogen pressure, the thickness of air gaps and the design of thermal cycles to the final shape of the wafers with this design. To complement the experiments and to understand the underlying mechanism, we utilized ADINA to carry out finite element analysis of the viscoelastic behavior of glass during the heating processes. We proved that for the 2D axisymmetric circular wafer, experimental approaches and numerical simulations have comparable results. We also discovered the crucial impacts of bearing permeability to the resulting shape of the wafers. A novel vertical slumping set-up is under test to eliminate the undesirable influence of gravity. 3D cylindrical air bearing simulations are also in development.

10399-36, Session 8

X-ray mirror prototype based on cold shaping of thin glass foils

Stefano Basso, Marta M. Civitani, Mauro Ghigo, Joanna Ho?yszko, Giovanni Pareschi, Bianca Salmaso, Daniele Spiga, Gabriele Vecchi, INAF - Osservatorio Astronomico di Brera (Italy)

The Slumping Glass Optics technology for the fabrication of astronomical X-ray mirrors has been developed in recent years in USA and Europe. The process has been used for making the mirrors of the Nustar, mission. The process starts with very thin glass foils hot formed to copy the profile of replication moulds. At INAF - Osservatorio Astronomico di Brera a process based on cold shaping is being recently developed, together with an integration method involving the use of inter-connecting ribs for making stacks. Each glass foil in the stack is shaped onto a very precise integration mould and the correct shape is frozen by means of glued ribs, that act as spacer between one layer and the adjacent ones (the first layers being attached to a thick substrate). Therefore, the increasing availability of flexible glass foils with a thickness of few tens of micron driven by electronic market for ultra-thin displays opens new possibilities for the fabrication of X-ray mirrors. This solution appears interesting especially for making hard X-ray mirrors based on multilayer coatings, taking advantage from the intrinsic low roughness of the glass foils that should grant a low scattering level. The stress on the glass due to the cold shaping is not negligible, but it is kept into account in the error budget in the design of X-ray optics. The simulations performed after FEM analysis are compliant with angular resolutions of the order of 15 arcsec HEW. As an exercise, we have considered the requirements and specs of the FORCE hard X-ray mission concept (being studied by JAXA) and we have designed the mirror modules assuming the cold slumping as a fabrication method. In the meantime, a prototype (representative of the FORCE mirror modules) is being design

and integrated in order to demonstrate the feasibility and the capacity to reach good angular resolution.

10399-37, Session 8

Lamination of ultra-thin silicon and glass wafers for producing high-quality and low-cost x-ray telescope mirrors

Youwei Yao, Mark L. Schattenburg, MIT Kavli Institute for Astrophysics and Space Research (United States)

We present a thin wafer lamination method for producing X-ray telescope mirrors. Future X-ray telescope missions require light weight optics with high resolution (<1'') and low fabrication cost. Traditional grinding/polishing and hot slumping methods find difficulty to meet the required figure accuracy when the mirror thickness is below 1 mm. In this paper, we introduce a new fabrication procedure to satisfy those requirements: first, we laminate flat and ultra-thin silicon or glass wafers on a well polished mandrel via direct bonding until the wafer stacking achieves the designed thickness. Second, we release the stacking from the mandrel since the direct bonding is temporary. Third, we anneal the stack to create permanent bonding and concrete the deformation. In such a manner, the intrinsic waviness of each wafer can be alleviated. Our FEA simulation shows the RMS slope error of the stacking surface released from a flat mandrel is improved by a factor of 6 when the layer number is doubled, regardless of the total thickness. In case of a cylindrical mandrel, the factor could be increased to 60, which indicates the lamination mirror is very promising to satisfy the requirements for future missions.

10399-38, Session 9

Diffraction efficiency of a replicated large-format x-ray reflection grating

Drew M. Miles, Jake McCoy, Randall L. McEntaffer, The Pennsylvania State Univ. (United States); Casey T. DeRoo, Harvard-Smithsonian Ctr. for Astrophysics (United States)

Future soft X-ray spectroscopy missions have science requirements that demand higher instrument throughput and higher resolution than currently available technology. A key element in such spectrometers are dispersive elements such as diffraction gratings. Our group at Penn State University develops and fabricates off-plane reflection gratings in an effort to achieve the level of performance required by future missions. We present here efficiency measurements made in the 0.2 – 1.3 keV energy band at the Advanced Light Source (ALS) at Lawrence Berkley National Laboratory for one such grating, which was fabricated to achieve the high-throughput required for future observatories. This grating was replicated from a grating master using UV-nanoimprint techniques which are suitable for mass-production and is coated in a layer of gold. Total absolute diffraction efficiency was measured to be ~55-65% across the energy range, with relative diffraction efficiency approaching 90%. These results represent the first successful demonstration of off-plane grating replicas produced via these fabrication techniques and exceed the grating efficiency requirements for future X-ray missions.

10399-39, Session 9

Critical-angle transmission gratings for high resolving power soft x-ray spectrometers on Arcus and Lynx

Ralf K. Heilmann, MIT Kavli Institute for Astrophysics and Space Research (United States); Alexander R. Bruccoleri, Izentis LLC (United States); Mark L. Schattenburg, MIT Kavli Institute for Astrophysics and Space Research (United States)

Soft x-ray spectroscopy with high resolving power (R) and large effective area (A) addresses numerous unanswered science questions about the structure and physics of our universe. In the soft x-ray band R > 500 can only be achieved with diffraction grating-based spectroscopy. Critical-angle transmission (CAT) gratings combine the advantages of blazed reflection gratings (high efficiency, use of higher diffraction orders) with those of conventional transmission gratings (relaxed alignment tolerances and temperature requirements, transparent at higher energies, low mass), resulting in minimal mission resource requirements. Diffraction efficiency > 33% and R > 10,000 have been demonstrated for CAT gratings. Last year the technology has been certified at TRL4 for a probe class mission concept.

An Explorer-scale (A > 500 sqcm, R > 2500) grating spectroscopy mission can be built with today's CAT grating technology and has been submitted to the current Explorer round as the Arcus mission. Its figure of merit for the detection of weak absorption lines will be an order of magnitude larger than current instruments on Chandra and XMM-Newton. Further CAT grating technology development and improvements in the angular resolution of x-ray optics can provide another order of magnitude improvement in performance, as is envisioned for the X-ray Surveyor/Lynx mission concept currently under development for input into the 2020 Decadal Survey.

We recently have fabricated the largest (32 mm x 32 mm) CAT gratings to date, and plan to increase grating size further. We report on our latest fabrication and x-ray efficiency, resolving power, and environmental testing results.

10399-40, Session 9

Toward measurement of period variation in Critical-Angle Transmission (CAT) gratings

Jungki Song, Ralf K. Heilmann, MIT Kavli Institute for Astrophysics and Space Research (United States); Mark L. Schatternburg, Massachusetts Institute of Technology (United States)

With the combined advantages of blazed reflection gratings and conventional transmission gratings, CAT grating technology is expected to meet the performance requirements for future x-ray missions. While resolving power > 10,000 has been experimentally demonstrated in a CAT grating spectrometer breadboard system, period variation, one of the potentially limiting factors for very high resolving power, has not been thoroughly studied. In this work we report progress towards developing a scanning laser reflection (LR) period measurement tool for generating high-precision grating period maps across CAT gratings. The LR tool operates on the same measurement principle as a tool built in 1994 for characterizing period variations of grating facets in Chandra X-ray Observatory, but with higher spatial resolution and enhanced measurement sensitivity (dp/p < 10 ppm rms). It uses a specularly reflected beam and a first-order diffracted beam to record local period variations, grating surface tilt and tip, and grating line orientation. The capability to measure small period variations was demonstrated by measuring grating samples that show only built-in period variations of the interference lithographic process. Preliminary results for period measurement of CAT grating samples will be presented.

10399-41, Session 9

Laboratory progress in soft x-ray polarimetry

Sarah Heine, Herman L. Marshall, Norbert Schulz, Massachusetts Institute of Technology (United States); Ralf K. Heilmann, MIT Kavli Institute for Astrophysics and Space Research (United States); David Windt, Reflective X-Ray Optics LLC (United States); Kyle A. Beeks, Massachusetts Institute of Technology (United States)

We present continued development of components for measuring linear

X-ray polarization over the 0.2-0.8 keV (15-62 A) band. We employ multilayer-coated mirrors as Bragg reflectors at the Brewster angle. By matching to the dispersion of a spectrometer, we take advantage of high multilayer reflectivities at these energies and achieve polarization modulation factors over 95%. We have constructed a source of polarized X-rays that operates at a wide range of energies with a selectable polarization phase. We will present results from measurements of new laterally graded multilayer mirrors and critical angle transmission gratings essential to the approach. While the lab is designed to verify components to be used in a soft X-ray polarimeter, it is reconfigurable and has been used to verify grating efficiencies with our new CCD detector. Our development work is the basis for a sounding rocket mission (Rocket Experiment Demonstration of a Soft X-ray Polarimeter) and future orbital missions.

10399-42, Session 9

REDSoX: Monte-Carlo ray-tracing for a soft x-ray spectroscopy polarimeter

Hans Moritz Günther, Mark D. Egan, Ralf K. Heilmann, Tim Hellickson, MIT Kavli Institute for Astrophysics and Space Research (United States); Jason Frost, Stanford Univ. (United States) and MIT Kavli Institute for Astrophysics and Space Research (United States); Herman L. Marshall, Norbert Schulz, Adam Theriault-Shay, Sarah M. Trowbridge Heine, MIT Kavli Institute for Astrophysics and Space Research (United States)

X-ray polarimetry o?ers a new window into the high-energy universe, yet there has been no instrument so far that could measure the polarization of soft X-rays (about 17-80 ˚A) from astrophysical sources. The Rocket Experiment Demonstration of a Soft X-ray Polarimeter (REDSoX Polarimeter) is a proposed sounding rocket experiment that uses a focusing optic and splits the beam into three channels. Each channel has a set of critical-angle transmission (CAT) gratings that disperse the x-rays onto a laterally graded multilayer (LGML) mirror, which preferentially reflects photons with a specific polarization angle. The three channels are oriented at 120 deg to each other and thus measure the three Stokes parameters: I, Q, and U. The period of the LGML changes with position. The main design challenge is to arrange the gratings so that they disperse the spectrum in such a way that all rays are dispersed onto the position on the multi-layer mirror where they satisfy the local Bragg condition despite arriving on the mirror at di?erent angles due to the converging beam from the focusing optics. We present a polarimeteric Monte-Carlo ray-trace of this design to assess non-ideal e?ects from e.g. mirror scattering or the finite size of the grating facets. With mirror properties both simulated and measured in the lab for LGML mirrors of 80-200 layers we show that the reflectivity and the width of the Bragg-peak are su?cient to make this design work when non-ideal e?ects are included in the simulation. Our simulations give us an e?ective area curve, the modulation factor and the figure of merit for the REDSoX polarimeter. As an example, we simulate an observation of Mk 421 and show that we could easily detect a 20% linear polarization.

10399-63, Session PWed

Readout electronics testing during mass production of FlashCam cameras for the Cherenkov Telescope Array

Sebastian Diebold, Felix Eisenkolb, Christoph Kalkuhl, Gerd Puehlhofer, Andrea Santangelo, Thomas Schanz, Chris Tenzer, Eberhard Karls Univ. Tübingen (Germany); the FlashCam Team, see F. Werner et al., NIM A, 2016, for all team members (Germany); the CTA Consortium, Full author and affiliation list on http://www.cta-observatory.org (Italy)

The Cherenkov Telescope Array (CTA) will be the future observatory for ground-based TeV gamma-ray astronomy. At two sites, one in the northern and one in the southern hemisphere, CTA will feature about one hundred telescopes of different size classes in order to significantly improve the sensitivity and energy range with respect to current Cherenkov facilities. FlashCam is a camera system proposed for the medium-sized telescopes of CTA that implements a fully digital readout and trigger processing, which allows the reconfiguration of parameters and routines for the trigger algorithm and the signal shaping. Extensive tests with a full-scale prototype yielded excellent performance and stability results, which surpass CTA requirements. For the mass production of a substantial number of FlashCam cameras, efficient and reliable testing routines have been developed. In this contribution the approach, the setups, and the procedures for the mass testing of the readout electronics are presented.

10399-64, Session PWed

McXtrace simulation of x-ray optics for astronomical telescopes

Desirée Della Monica Ferreira, DTU Space (Denmark); Erik B. Knudsen, Technical Univ. of Denmark (Denmark); Niels Joergen S. Westergaard, Sonny Massahi, Finn E. Christensen, DTU Space (Denmark)

We make use of the software package McXtrace to access the performance of X-ray telescopes concept designs. We consider the Athena X-ray telescope based on Silicon Pore Optics (SPO) technology as reference design to demonstrate the performance of individual pores within SPO mirror modules. After presenting our approach for simulations and concept designs, we present the effective areas generated from our studies for both SPO and concentric mirror shell optics.

10399-65, Session PWed

Development of the thermal shield with high x-ray transmission for PRAXyS x-ray telescopes

Yuzuru Tawara, Ikuyuki Mitsuishi, Ryoki Suganuma, Taisuke Futamura, Takafumi Onishi, Kazushi Tachibana, Kenji Tachibana, Ikuya Sakurai, Nagoya Univ. (Japan)

PRAXyS was proposed as a SMEX mission that observes X-ray polarization at 2 - 10 keV, and a Phase A study was conducted. The X-ray telescope for this mission is temperature-controlled by a heater and a thermal shield to realize a temperature environment of about room temperature. We developed a thermal shield using a plastic thin film with high X-ray transmission placed in front of and behind the telescope for this purpose. In addition to the above characteristics, the performance required for a thermal shield is resistance against the launch and orbital environment (acoustic vibration, aerodynamic heating, thermal vacuum, atomic oxygen). The basic structure of thermal shield consists of metal frame, film support mesh, aluminum-coated polyimide thin film following the XRT-TS of ASCA, Suzaku, Hitomi. Especially, we aimed at transmission of mesh higher than conventional, and newly developed an evaluation test apparatus for high temperature mechanical resistance accompanying acoustic and aerodynamic heating. In this paper, thermal shield design, temperature prediction by numerical simulation, prototype thermal shield sample, an evaluation test apparatus and details of its evaluation will be described.

10399-66, Session PWed

Industrialization of the mirror plate coatings for the Athena mission

Sonny Massahi, Finn E. Christensen, Desiree D. M. Ferreira, DTU Space (Denmark); Brian Shortt, European Space Research and Technology Ctr. (Netherlands); Maximilien J.

Collon, Boris Landgraf, cosine B.V. (Netherlands)

In the frame of the development of the Advanced Telescope for High-ENergy Astrophysics (Athena) mission, currently in phase A, ESA is continuing to mature the optics technology and the associated mass production techniques. These efforts are driven by the programmatic and technical requirement of reaching TRL 6 prior to proposing the mission for formal adoption, currently planned for 2020. A critical part of the current phase A preparation activities is addressing the industrialization of the Silicon Pore Optics mirror plates coating.

An essential part of this effort is the transfer of the well-established coating processes and techniques to an industrial scale facility suitable for coating the more than 100,000 mirror plates required for Athena.

In this paper we explain the work being undertaken in this area including, requirement specification, equipment and supplier selection, preparing the coating facility for the deposition equipment, designing and fabricating the deposition equipment.

10399-67, Session PWed

Characterization of multilayer coated replicated Wolter optics for fusion experiments at the Z Pulsed Power Facility

Andrew Ames, Harvard-Smithsonian Ctr. for Astrophysics (United States); David Ampleford, Sandia National Labs. (United States); Ricardo Bruni, Harvard-Smithsonian Ctr. for Astrophysics (United States); Chris Bourdon, Sandia National Labs. (United States); Bernard Kozioziemski, Lawrence Livermore National Lab. (United States); Suzanne E. Romaine, Harvard-Smithsonian Ctr. for Astrophysics (United States); Brian D. Ramsey, National Space Sciences and Technology Ctr. (United States); Michael J. Pivovaroff, Julia Vogel, Christopher Walton, Lawrence Livermore National Lab. (United States); M. Wu, Sandia National Labs. (United States)

Multilayer coatings can be applied to Wolter X-ray optics to extend the bandpass to high energies or to create a narrow high energy bandpass. For large diameter full shell optics these coatings can be directly applied to the inside surface of the optic and several such multilayer coated prototype telescopes have been fabricated and tested. However, for small diameter full shell optics direct deposition of the multilayers is not possible. Therefore we have developed a process for indirectly coating arbitrarily small diameter electroformed nickel replicated optics with multilayers to increase their response at high energy (i.e. > 10 keV). The multilayer coating is applied to the mandrel before the NiCo optic is electroformed onto the mandrel. The multilayer coating is then released along with the optic when the optic is separated from the mandrel. The ability to fabricate small diameter multilayer coated full shell Wolter X-ray optics with narrow bandpass opens the door to several applications within astronomy and also provides a path for cross-fertilization to other fields.

We report on the characterization and evaluation of the first two prototype X-ray Wolter optics to be tested at the Z Pulsed Power Facility at Sandia National Laboratory. The intent is to develop and field several optics as part of an imaging system with targeted spectral ranges.

10399-68, Session PWed

Development of a second generation SiLC-based Laue lens

David Girou, Nicolas M. Barrière, Maximilien J. Collon, cosine B.V. (Netherlands); Eric Ford, Univ. of Washington Medical Ctr. (United States); Ramses Günther, cosine Science & Computing B.V. (Netherlands); Lorraine Hanlon, Univ. College Dublin (Ireland); John Tomsick, Space Sciences Lab. (United States); Alexey Uliyanov, Univ. College Dublin (Ireland); Giuseppe Vacanti, cosine Science & Computing B.V. (Netherlands); Colin Wade, Univ. College Dublin (Ireland); Andreas Zoglauer, Space Sciences Lab. (United States)

cosine has been developing for more than a decade silicon pore optics (SPO), lightweight modular X-ray optic made of stacks of bent and directly bonded silicon mirror plates. This technology, which has been selected by ESA to realize the optics of ATHENA, can also be used to fabricate soft gamma-ray Laue lenses if Bragg diffraction through the bulk silicon is exploited, rather than grazing incidence reflection.

Silicon Laue Components (SiLCs) are made of stacks of curved, polished, wedged silicon plates, allowing the concentration of radiation in both radial and azimuthal directions. This greatly increases the focusing properties of a Laue lens since the size of the focal spot is no longer determined by the size of the individual single crystals, but by the accuracy of the applied curvature.

After a successful proof of concept in 2013, establishing the huge potential of this technology, a new project has been launched in Spring 2017 at cosine to further develop and test this technique. Here we present the latest advances of the second generation of SiLCs made from even thinner silicon plates stacked by a robot with dedicated tools in a class-100 clean room environment.

10399-43, Session 10

Design, development, and performance of x-ray mirror coatings for the Athena mission

Desirée Della Monica Ferreira, Sonny Massahi, Finn E. Christensen, DTU Space (Denmark); Brian Shortt, European Space Research and Technology Ctr. (Netherlands); Maximilien J. Collon, cosine B.V. (Netherlands); Chantal Silvestre, DTU Space (Denmark); Michael Krumrey, Levent Cibik, Swenja Schreiber, Physikalisch-Technische Bundesanstalt (Germany)

We report the latest results on coating design optimization and optics performance for the present Ir/B4C baseline coating and alternative designs and materials including bi/tri-layers and linear graded multilayers.

We make use of X-ray reflectometry (XRR) and atomic force microscopy (AFM), among other techniques, to test both coating performance and robustness.Deposition of coatings on Silicon Pore Optics substrates, evaluation of the coatings characteristics and long term stability are presented.

10399-44, Session 10

Development of multilayer coatings for hard x-ray optics at NASA Marshall Space Flight Center

Danielle N. Gurgew, The Univ. of Alabama in Huntsville (United States); David M. Broadway, Brian D. Ramsey, NASA Marshall Space Flight Ctr. (United States); Don Gregory, The Univ. of Alabama in Huntsville (United States)

In this work, we describe the development of multilayer coating capabilities of the X-ray astronomy group at NASA Marshall Space Flight Center (MSFC). A DC magnetron sputtering system has been constructed to deposit periodic, depth-graded and aperiodic multilayer coatings on flat silicon and glass substrates of various diameters. The main goal of this new area of research at MSFC is the development of coatings for use on future hard

X-ray astronomical telescopes, extending the reflected energy range into the hard X-ray to soft gamma ray band. Descriptions of the system geometry and calibration process as well as initial results from the first few months of deposition and coating recipe optimization are presented.

10399-45, Session 10

Cross-fertilization of multilayer coated Wolter optics: developing optics for fusion experiments at the Z Pulsed Power Facility

Suzanne E. Romaine, Andrew Ames, Harvard-Smithsonian Ctr. for Astrophysics (United States); David Ampleford, Chris Bourdon, Sandia National Labs. (United States); Bernard Kozioziemski, Lawrence Livermore National Lab. (United States); Ricardo Bruni, Harvard-Smithsonian Ctr. for Astrophysics (United States); Michael J. Pivovaroff, Lawrence Livermore National Lab. (United States); Brian D. Ramsey, National Space Sciences and Technology Ctr. (United States); Julia Vogel, Christopher Walton, Lawrence Livermore National Lab. (United States); M. Wu, Sandia National Labs. (United States)

Multilayer coatings can be applied to Wolter X-ray optics to extend the bandpass to high energies or to create a narrow high energy bandpass. For large diameter full shell optics these coatings can be directly applied to the inside surface of the optic and several such multilayer coated prototype telescopes have been fabricated and tested. However, for small diameter full shell optics direct deposition of the multilayers is not possible. Therefore we have developed a process for indirectly coating arbitrarily small diameter electroformed nickel replicated optics with multilayers to increase their response at high energy (i.e. > 10 keV). The multilayer coating is applied to the mandrel before the NiCo optic is electroformed onto the mandrel. The multilayer coating is then released along with the optic when the optic is separated from the mandrel. The ability to fabricate small diameter multilayer coated full shell Wolter X-ray optics with narrow bandpass opens the door to several applications within astronomy and also provides a path for cross-fertilization to other fields.

We report on the fabrication of the first two prototype X-ray Wolter optics to be tested at the Z-Pulsed Power Facility at Sandia National Laboratory (SNL). SNL and Lawrence Livermore National Laboratory are collaborating in the development of an x-ray imaging system for use on the Z Machine to image warm X-ray emission from Z pinches. The concept is to use multilayer mirror coatings on a cylindrical glancing incidence focusing mirror in a Wolter geometry. The intent is to develop and field several optics as part of an imaging system with targeted spectral ranges.

10399-46, Session 10

Simulation and optimization of a soft gamma-ray concentrator using thin film multilayer structures

Farzane Shirazi, Peter Bloser, James Krzanowski, Jason Legere, Mark McConnell, The Univ. of New Hampshire (United States)

We are reporting the investigation result of using multilayer thin film structures for channeling and concentrating soft gamma rays with energies greater than 100 keV, beyond the reach of current grazing-incidence hard X-ray mirrors. This will enable future telescopes for higher energies with same mission parameters already proven by NuSTAR. A suitable arrangement of bent multilayer structures of alternating low and high-density materials will channel soft gamma-ray photons via total external reflection and then concentrate the incident radiation to a point. We present the latest results of producing Si/Ir multilayers with the required thicknesses and smoothness by using magnetron sputter technique. In addition of experimental works, we have been working on gamma ray tracing model of the concentrator by IDL, making use of optical properties calculated by the IMD software. This modeling allows us to calculate efficiency and focal length for different energy bands and materials and compare them with experimental result. Also we describe combine concentrator modeling result and detector simulation by MEGAlib to archive a complete package of gamma-ray telescope simulation. This technology offers the potential for soft gamma-ray telescopes with focal lengths of less than 10 m, removing the need for formation flying spacecraft and providing greatly increased sensitivity for modest cost and complexity and opening the field up to balloon-borne instruments.

10399-47, Session 11

In-situ stress measurement of single and multilayer thin-films used in x-ray astronomy optics applications

David M. Broadway, Stephen L. O'Dell, Brian D. Ramsey, NASA Marshall Space Flight Ctr. (United States); Danielle N. Gurgew, The Univ. of Alabama in Huntsville (United States)

We report on the dependence of the stress and surface roughness of chromium and iridium single layer and bi-layer films deposited by magnetron sputter deposition for various process conditions such as argon pressure and substrate temperature. The stress is measured in-situ with a novel device developed at the NASA MSFC. The elegant device's capability and sensitivity are discussed and compared to other more complex current state-of-the-art optical stress measurement instruments such as the multiple beam optical stress sensor (MOSS). We further discuss the capability of in-situ stress measurement as a technique for the direct measurement of the physical thicknesses of the layers and the material profile at the interfaces of multilayer structures.

10399-48, Session 11

Development of iridium-coated x-ray mirrors for astronomical applications

Veronika Stehlíková, Max-Planck-Institut für extraterrestrische Physik (Germany) and Czech Technical Univ. in Prague (Czech Republic); Thorsten Döhring, Anne-Catherine Probst, Florian Emmerich, Manfred Stollenwerk, Hochschule Aschaffenburg (Germany); Laura Proserpio, Peter Friedrich, Max-Planck-Institut für extraterrestrische Physik (Germany)

Due to their excellent reflection properties iridium coatings are often applied for grazing incidence mirrors in astronomical X-ray telescopes. Future space-based X-ray observatories need to be very lightweighted for launcher mass constrains. Therefore they will use a reduced mirror thickness, which results in the additional requirement of low coating stress to avoid deformation of the initial precisely shaped mirror substrates. At Aschaffenburg University of Applied Sciences the coating of thin iridium films by an RF-magnetron sputtering technique is under development. The work is embedded in collaborations with the Max-Planck-Institute for Extraterrestrial Physics in Germany, the Czech Technical University in Prague, the Osservatorio Astronomico di Brera in Italy, and the French Institute Fresnel. Sputtering with different parameters, especially by variation of the argon gas pressure, leads to iridium films with different properties. The current work is focused on the microstructure of the iridium coatings to study the influence of the substrate and of the deposition parameters on the thin film growing process. Correlations between coating density, surface micro-roughness, crystalline structure of the iridium layers and the expected reflectivity as well as stress-induced deformation of the X-ray mirror will be presented and discussed. The final goal of the project is to integrate the produced prototype mirrors into an X-ray telescope module. On a longer timescale measurements of the mirror modules optical performance are planned at the X-ray test facility PANTER.

10399-49, Session 11

Effects of ion implantation in different substrate materials: stress, relaxation, and strength

Brandon D. Chalifoux, Graham Wright, Massachusetts Institute of Technology (United States); Youwei Yao, MIT Kavli Institute for Astrophysics and Space Research (United States); Claire Burch, Harvard Univ. (United States); Ralf K. Heilmann, Mark L. Schattenburg, MIT Kavli Institute for Astrophysics and Space Research (United States)

Ion implantation is a promising method of correcting figure errors in thin mirror substrates. For future high-resolution, high-throughput x-ray observatories, such figure correction may be critical. Ion implantation into both glass and silicon results in surface stress, which bends the substrate. In this paper we investigate three effects of ion implantation in several types of glass, as well as crystalline silicon. The first effect we report on is the stress resulting from the implanted ions, and the implications for figure correction with each material. Each material studied also shows some relaxation after the ion implantation is stopped; we report on the magnitude of this relaxation and its implications. Finally, the surface stress may affect the strength of implanted materials. We report on ring-on-ring strength tests we conducted on implanted samples.

10399-50, Session 12

Advancements in ion beam figuring of very thin glass plates

Marta M. Civitani, Mauro Ghigo, Joanna Ho?yszko, Gabriele Vecchi, Stefano Basso, INAF - Osservatorio Astronomico di Brera (Italy); Vincenzo Cotroneo, Ryan Allured, Paul B. Reid, Harvard-Smithsonian Ctr. for Astrophysics (United States)

The high-quality surface characteristics, both in terms of figure error and of micro-roughness, required on the mirrors of a high angular resolution x-ray telescope are challenging, but in principle well suited with a deterministic and non-contact process like the ion beam figuring. This process has been recently proven to be compatible even with very thin (thickness around 0.4mm) sheet of glasses (like D263 and Eagle). In the last decade, these types of glass have been investigated as substrates for hot slumping, with residual figure errors of hundreds of nanometres. In this view, the mirrors segments fabrication could be envisaged as a simple two phases process: a first replica step based on hot slumping (direct/indirect) followed by an ion beam figuring which can be considered as a post-fabrication correction method. The first ion beam figuring trials, realized on flat samples, showed that the micro-roughness is not damaged but a deeper analysis is necessary to characterize and eventually control/compensate the glass shape variations. In this paper, we present the advancements in the process definition, both on flat and slumped glass samples.

10399-51, Session 12

Improving x-ray optics via differential deposition

Kiranmayee Kilaru, Universities Space Research Association (United States)

Differential deposition is a means of figure correction in x-ray optics. In this technique physical vapor deposition is used to smooth out irregularities in an optic's figure, thereby significantly improving the imaging performance. A system has been developed to apply differential deposition to full-shell optics being developed for x-ray astronomy. Initial tests with a single stage of correction showed that a factor of three improvement in angular resolution was possible. Since that time, the coating system has been improved through increased automation so that the coating head more accurately tracks the tapering optic's surface. Here, we show new x-ray results for two stages of correction, the second stage addressing higher-frequency errors in the mirrors axial figure profile. We discuss challenges that must be addressed to achieve still higher angular resolution.

10399-52, Session 12

Additive manufactured x-ray optics for astronomy

Carolyn Atkins, UK Astronomy Technology Ctr. (United Kingdom); Charlotte H. Feldman, Univ. of Leicester (United Kingdom); David Brooks, Univ. College London (United Kingdom); Richard Willingale, Univ. of Leicester (United Kingdom); Peter Doel, Univ. College London (United Kingdom)

Additive manufacturing, more commonly known as 3D printing, has become a commercially established technology for rapid prototyping and the fabrication of bespoke intricate parts. Optical components, such as mirrors and lenses, are now being fabricated via additive manufacturing, where the printed substrate is polished in a post-processing step. One application of additively manufactured optics could be within the astronomical X-ray community, where there is a growing need to demonstrate thin, light-weight, high precision optics for a 'beyond Chandra' style mission.

This paper will follow a proof-of-concept investigation, sponsored by the UK Space Agency's National Space Technology Programme, into the feasibility of applying additive manufacturing in the production of thin, light-weight, precision X-ray optics for astronomy. One of the benefits of additive manufacturing is the ability to construct intricate light-weighting, which can be optimised to minimise weight while ensuring rigidity. This concept of optimised light-weighting will be applied to a series of polished additively manufactured test samples and experimental data from these samples, including an assessment of the optical quality and the magnitude of any print-through, will be presented. In addition, the finite element analysis optimisations of the light-weighting development will be discussed.

10399-53, Session 12

Design and modeling of an additive manufactured thin shell for x-ray astronomy

Charlotte H. Feldman, Univ. of Leicester (United Kingdom); Carolyn Atkins, UK Astronomy Technology Ctr. (United Kingdom); Richard Willingale, Univ. of Leicester (United Kingdom); David Brooks, Peter Doel, Univ. College London (United Kingdom)

Future X-ray astronomy missions require light-weight thin shells to provide large collecting areas within the weight limits of launch vehicles, whilst still delivering angular resolutions close to that of Chandra (0.5 arc seconds). Additive manufacturing, also known as 3D printing, is a well-established technology with the ability to construct or `print' intricate support structures, which can be both integral and light-weight, and is therefore a candidate technique for producing shells for space-based X-ray telescopes. The work described here is a feasibility study into this technology for precision X-ray optics for astronomy and has been sponsored by the UK Space Agency's National Space Technology Programme. The goal of the project is to use a series of test samples to trial different materials and processes with the aim of developing a viable path for the production of an X-ray reflecting prototype for astronomical applications. The initial design of an additive manufactured prototype X-ray shell is presented with ray-trace modelling and analysis of the X-ray performance. The polishing process may cause print-through from the light-weight support structure on to the reflecting surface. Investigations in to the effect of the print-through on the X-ray performance of the shell are also presented.

10399-54, Session 13

Experimental evaluation of solder bonding and actuation for thin-shell x-ray telescope mirror assembly

Michael D. DeTienne, Alexander R. Bruccoleri, Ross Tedesco, Massachusetts Institute of Technology (United States); Ralf K. Heilmann, Mark L. Schattenburg, MIT Kavli Institute for Astrophysics and Space Research (United States)

In past work, we demonstrated a new adjustable bonding technique utilizing solder to bond metal and glass, referred to as liquid metal actuation. The concept is to bond via solder, and then momentarily melt the solder surface with a laser while applying a force to compress or stretch the joint. We demonstrated sub 100 nm adjustments (0.2 arc seconds for a 200 mm mirror) via liquid metal actuation. This precision provides additional tools towards a sub-arcsecond telescope, such as the X-ray Surveyor mission concept. Further research and development of the technique is presented to evaluate the feasibility for mirror assembly.

At present, epoxy is used to bond thin-shell x-ray mirrors, which has several drawbacks including instability, time consuming application, shrinkage, creep, and sensitivity to ambient conditions such as humidity. Furthermore, epoxy bonds cannot be easily adjusted post curing and any errors in the initial bond are permanent. Preliminary structural testing was done comparing the strengths of solder to epoxy for Kovar pins and clips. Tin/silver solder joints were at least 4 times stronger than epoxy as measured via a Zwick mechanical tester.

We designed and built an in-house laser soldering and adjustment station. The apparatus is equipped with a 100 W infrared laser, and a suite of metrology tools. Preliminary experiments were focused on reproducing and understanding the results of past work. Specifically, we present more detailed experimental results for the joint adjustments, with a focus on understanding the heat transfer from the laser to the solder.

10399-55, Session 13

Adjustable optics applied to Laue lenses

Enrico Virgilli, Piero Rosati, Filippo Frontera, Univ. degli Studi di Ferrara (Italy); Ezio Caroli, John B. Stephen, Natalia Auricchio, Stefano Silvestri, Angelo Basili, INAF - IASF Bologna (Italy)

Given the unprecedented sensitivity level which is expected to be achievable in the hard X-/soft gamma-ray band using Laue lenses based on bent crystals (e.g., Frontera et al. 2013, SPIE Procs 8861; Virgilli et al. 2017, in preparation), great effort is being performed to refine the technology for assembling such a lens.

Indeed, the results so far obtained in the alignment process of a large number of crystal tiles for diffraction still require an improvement in order to achieve the limiting Point Spread Function (about 20 arcsec).

In our presentation we will discuss a modular approach for the realization of an entire Laue lens. Under this approach, the Laue lens comprises a significant number of sub-modules, each filled with accurately oriented crystals, which are mounted on the lens frame through an active alignment system. We will present the first results of this adjustment technology to demonstrate the capability of minimizing the alignment uncertainties.

10399-56, Session 13

Design and fabrication of adjustable x-ray optics using piezoelectric thin films

Julian Walker, Tianning Liu, Mohit Tendulkar, David Burrows, The Pennsylvania State Univ. (United States); Casey T. DeRoo, Ryan Allured, Edward Hertz, Vincenzo Cotroneo, Paul B. Reid, Eric D. Schwartz, Harvard-Smithsonian Ctr. for Astrophysics (United States); Thomas N. Jackson, The Pennsylvania State Univ. (United States); Susan Trolier-McKinstry, Harvard-Smithsonian Ctr. for Astrophysics (United States)

The Lynx X-ray telescope aims to have < 0.5 arc seconds resolution, large collection area and low weight. The development of adjustable X-ray optics is a potential method for facilitating this. Here we used 1.5μm thick, radio frequency RF deposited piezoelectric PbZr0.52Ti0.48O3 (PZT) thin films on the convex side of curved glass substrates to make adjustable X-ray mirrors. The electromechanical coupling of PZT allows the application of voltage to adjust the mirror figure. Double layer lithography by spray deposition and spinning was used to patterned top electrodes as separately controllable cells. ZnO-based thin film transistors (TFT) were developed as the control circuitry to modulate the applied voltage. Electrically conductive adhesive bonds (ACF bonding) were used to connect 112 electrodes on each mirror. 5 μm solution cast thin flex cables were used to minimize the impact of the bond on the mirror figure. After measurement of the change of the mirror figure due to the processing of the piezoelectric device layers, Cr and Ir layers were deposited on the concave side of the glass substrate to correct the X-ray mirror coating. The thickness of the Ir layer and the chamber pressure during deposition were modulated to balance the figure distortion resulting from the piezoelectric device layers.

This work will discuss the challenges involved with processing piezoelectric thin film devices on curved glass substrates, and detail the approaches being employed to overcome these for eventual application in flight quality adjustable X-ray optics.

10399-57, Session 13

Characterizing the poling process for piezoelectric cells in adjustable x-ray optics

Casey T. DeRoo, Ryan Allured, Sagi Ben-Ami, Paul B. Reid, Vincenzo Cotroneo, Daniel A. Schwartz, Edward Hertz, Harvard-Smithsonian Ctr. for Astrophysics (United States); Julian Walker, Tianning Liu, Mohit Tendulkar, David Burrows, Tom N. Jackson, Susan Trolier-McKinstry, The Pennsylvania State Univ. (United States)

The NASA large strategic mission candidate Lynx offers the opportunity to study the cosmological evolution of the large scale structure of the Universe in X-rays, performing observations of low surface brightness outflows in galaxy clusters and observing initial black hole seed masses at extreme redshift. To support Lynx, however, lightweight, high angular resolution (< 0.5") X-ray mirrors are needed. Fabricating adjustable X-ray optics is a potential method for realizing such mirrors; by constructing actuatable cells from a piezoelectric, thin-film layer of lead zirconate titanate (PZT), the figure of a thin-shelled mirror segment can be improved. In order to maximize the influence function of each actuator cell, the piezoelectric cells must first be "poled", which serves to orient polarization of the PZT domains with an applied electric field. In the present work, we report on the impact of variables in the poling process (temperature, applied field strength, etc.) on both the magnitude of the piezoelectric coefficient, and its stability over time. Using wavefront sensing metrology, we measure the stress induced by poling the discrete PZT cells on a fabricated adjustable X-ray optic. We also quantify the cell-to-cell variation of the piezoelectric coefficients produced by identical poling processes.

10399-58, Session 13

Deterministic figure correction of piezoelectrically adjustable slumped glass optics

Ryan Allured, Paul B. Reid, Casey T. DeRoo, Vincenzo Cotroneo, Alexey Vikhlinin, Edward Hertz, Vanessa Marquez, Eric D. Schwartz, Harvard-Smithsonian Ctr. for Astrophysics (United States); Susan Trolier-McKinstry, Julian Walker, Thomas N. Jackson, Tianning Liu, The Pennsylvania State Univ. (United States)

The Lynx (X-ray Surveyor) mission concept requires high resolution, lightweight X-ray optics. Our group has continued to advance cylindrical optics featuring thin film piezoelectric actuators as a viable technology to fulfill this need. For the first time, we have fabricated adjustable optics on thermally formed glass substrates and demonstrated absolute figure correction. Furthermore, we have quantified mirror correctability in terms of two dimensional orthogonal functions and extrapolated these results to larger format optics envisioned for the Lynx mission. Finally, we will discuss the limitations of our current approach and the facilities needed for fabrication of flight quality adjustable optics.

10399-59, Session 13

Controlling the shaping of Si and glass substrates via stresses in the coatings: via bias stress control and magnet fields

Melville P. Ulmer, Xiaoli Wang, Jian Cao, David B. Buchholz, Northwestern Univ. (United States); Lahsen Assoufid, Argonne National Lab. (United States)

We describe our progress in developing technologies that can be applied to making mirrors that could be used both at the Argonne National Laboratory's (ANL's) Advanced Photon Source (APS) as well as for X-ray astronomy. We have been able to apply enough controlled coating stress to a Si substrate so as to produce a radius of curvature of 17m. The Si substrates are also to be coated with Tefenol-D and then NiCo. The Terfenol-D (T-D)will be used to apply a magnetic field induced stress. The NiCo will retain the magnetic field. Progress has been made in producing nearly stress free T-D coatings. An update on how the entire process works will be presented along with results from shaping 50 mm x 50 mm coated glass substrates.

10399-60, Session 14

Characterization of x-ray lobster optics with a hybrid CMOS sensor

Tanmoy Chattopadhyay, Mitchell Wages, David Burrows, Evan Bray, The Pennsylvania State Univ. (United States); Adolf Inneman, Rene Hudec, Veronika Stehlikova, Czech Technical Univ. in Prague (Czech Republic); David Schendt, Sam Hull, Abe Falcone, Maria McQuaide, The Pennsylvania State Univ. (United States)

X-ray lobster optics provide a unique way to focus X-rays onto a small focal plane imager with wide field of view imaging. Such an instrument with angular resolution of a few arcminutes can be used to study GRB afterglows, as well as the variability and spectroscopic characteristics for other astrophysical objects. At Penn state University, we characterize these lobster optics with an H1RG CMOS sensor (100 ?m thick Silicon with 18 ?m pixel size), procured from Teledyne Imaging Sensors at its focal plane. The light-weight compact lobster optic with a 25 cm focal length provides two dimensional imaging with ~25 cm^2 effective area at 2 keV. We chose the hybrid CMOS detector (HCD) since X-ray HCDs offer several advantages (e.g. radiation hard, low power, faster and flexible readout rate) over CCDs for future X-ray missions. We utilize 47 m long X-ray beam line at Penn state University to do our experiments where we characterize the overall effective area of the instrument at 1.5 - 8 keV for both on-axis and off-axis angles.

In this presentation, we will describe the characterization test stand and methods, as well as the detailed results. We perform ray-tracing simulations to theoretically validate the results which would also be briefly discussed here. While this is simply a proof-of-concept experiment, such an instrument with significant collecting area can be explored for future rocket or CubeSat experiments.

10399-61, Session 14

Testing and modelling of the SVOM MXT narrow field lobster-eye telescope

Charlotte H. Feldman, James F. Pearson, Richard Willingale, Jonathan M. Sykes, Christopher L. Bicknell, Paul R. Houghton, Paul Drumm, Adrian Martindale, Julian P. Osborne, Paul T. O'Brien, Univ. of Leicester (United Kingdom); Ray Fairbend, Sylvain Petit, Romain Roudot, Emile Schyns, PHOTONIS France S.A.S. (France); Karine Mercier, Jean-Michel Le Duigou, Ctr. National d'Études Spatiales (France); Diego Gotz, CEA-IRFU (France)

SVOM is a French-Chinese space mission to be launched in 2021 with the goal of studying Gamma-Ray Bursts (GRBs), the most powerful stellar explosions in the Universe. The Microchannel X-ray Telescope (MXT) on-board SVOM, is an X-ray focusing telescope with a detector limited field of view of 1 degrees, working in the 0.2-10 keV energy band. The SVOM MXT is a narrow field lobster eye telescope, designed to detect and accurately locate GRBs, very soon after the initial GRB trigger. The MXT mirror comprises of an array of square pore Microchannel Plate Optics (MPOs) which are slumped to a spherical radius of 2m giving a focal length of 1m and an intrinsic field of view of 6 degrees. We present details of the baseline design and results from the on-going X-ray tests of the breadboard and STM MPOs performed at the University of Leicester (UoL) and Panter (MPE). In addition, we present details of modelling and analysis which reveals the factors that limit the angular resolution, characteristics of the point spread function (PSF) and the efficiency/collecting area of the currently available MPOs.

10399-62, Session 14

A principle for an x-ray defocusing telescope system with an angular resolution booster

Yoshitomo Maeda, Institute of Space and Astronautical Science (Japan) and The Graduate Univ. for Advanced Studies (Japan); Ryo Iizuka, Institute of Space and Astronautical Science (Japan); Takayuki Hayashi, Nagoya Univ. (Japan) and NASA Goddard Space Flight Ctr. (United States); Manabu Ishida, Institute of Space and Astronautical Science (Japan)

We present a novel concept to gives an opportunity to make a high resolution spectroscopy that is better than 0.5 arcsec of the Chandra HRMA. Since we concentrate X-rays with focusing optics, we can attain the high sensitivity such as the ASCA XRTs. Since our principle make available a small-size detector such as the X-ray CCD or the calorimeter, the telescope system gives an opportunity to make a high resolution spectroscopy with a good angular resolution and with a large effective area.

10400-1, Session 1

Science capabilities of the WFIRST coronagraph *(Invited Paper)*

Bruce A. Macintosh, Stanford Univ. (United States); Margaret Turnbull, SETI Institute (United States); N. Jeremy Kasdin, Princeton Univ. (United States); John H. Debes, Space Telescope Science Institute (United States); Tom Greene, NASA Ames Research Ctr. (United States); Nikole Lewis, Space Telescope Science Institute (United States); Mark S. Marley, NASA Ames Research Ctr. (United States); Bijan Nemati, Jet Propulsion Lab. (United States); Aki Roberge, NASA Goddard Space Flight Ctr. (United States); Tyler Robinson, Univ. of California, Santa Cruz (United States); Dmitry Savransky, Cornell Univ. (United States); Christopher C. Stark, Space Telescope Science Institute (United States)

The WFIRST mission was originally ended as a wide-field survey facility. With the change to a 2.4-m telescope, the mission is capable of carrying an effective coronagraph for exoplanet imaging. The baseline architecture allows use of a hybrid lyot or shaped pupil coronagraph, feeding a imager and integral field spectrograph. This will allow imaging and photometry of mature nearby planets and zodiacal disks in reflected light, as well as spectroscopy of the brightest targets. I will discuss the scientific motivations of the mission and show simulated science capabilities, and discuss the process towards definition of a science mission.

10400-2, Session 1

The WFIRST coronagraph instrument optical design update

Hong Tang, Richard Demers, John E. Krist, James McGuire, Mayer Rud, Feng Zhao, Jet Propulsion Lab. (United States)

The WFIRST Coronagraph Instrument will perform direct imaging of exoplanets via coronagraphy of the host star. It uses both the Hybrid Lyot and Shaped Pupil Coronagraphs to meet the mission requirements. The Phase A optical design fits within the allocated instrument enclosure and accommodates both coronagraphic techniques. It also meets the challenging wavefront error requirements. We present the optical performance includimg throughput of the imaging and IFS channels, as well as the wavefront errors at the first pupil and the imaging channel. We also present polarization effects from optical coatings and analysis of their impacts on the performance of the Hybrid Lyot coronagraph. We report the results of stray light analysis of our Occulting Mask Coronagraph testbed.

10400-4, Session 1

WFIRST coronagraph optical modeling

John E. Krist, Nikta Amiri, Gary Gutt, Luis Marchen, James McGuire, Bijan Nemati, Navtej Saini, Hong Tang, Jet Propulsion Lab. (United States)

WFIRST will include a coronagraphic instrument for high contrast imaging of extrasolar planets and circumstellar disks. It will utilize two methods, the Hybrid Lyot Coronagraph for detection in an imaging channel and the Shaped Pupil Coronagraph for characterization using an integral field spectrograph. Both have been optimized for the obscured (secondary mirror and spiders) WFIRST telescope. End-to-end numerical optical modeling incorporating wavefront sensing and control is used to determine the performance of the coronagraph with realistic errors, including pointing jitter and polarization. The coronagraphic designs are continually being optimized to improve tolerances to these errors and to improve the system throughput. We present the performance estimates of the current flight designs as predicted by modeling. We also describe the release of a new version of the PROPER optical propagation library, our primary modeling tool, which is now available for Python and Matlab in addition to IDL.

10400-5, Session 1

Wavefront control performance modeling with WFIRST shaped pupil coronagraph testbed

Hanying Zhou, Bijian Nemati, John E. Krist, Eric J. Cady, Brian D. Kern, Ilya Poberezhskiy, Jet Propulsion Lab. (United States)

NASA's WFIRST mission includes a coronagraph instrument (CGI) for direct imaging of exoplanets. To achieve and maintain high contrast for the desired science goal, CGI employs a dual wavefront sensing and control (WFSC) system: a low-order WFSC subsystem using a Zernike wavefront sensor and an electric field conjugation based high order subsystem. The system's ability to suppress star light and maintain a high contrast dark hole (<1e-8) in a simulated dynamic environment was recently demonstrated on the Occulter Mask Coronagraph (OMC) testbed at JPL. Parallel to this technology development is an effort to advance the CGI's model fidelity, as it will be crucial to inform the flight system's design, error budget, verification and validation, etc. Here we present our modeling method and some examples of predicted high-order wavefront correction performance for the shaped pupil coronagraph configuration of the OMC testbed. Significant improvement in model fidelity comes from: 1) incorporation of testbed-like operation features such as probing, deformable mirror voltage constraints, regular updates of the control model, etc., and 2) better understanding and inclusion of testbed imperfections in the model (e.g., chromatic pupil aberrations). Testbed error budget modeling and Monte Carlo modeling incorporating estimated uncertainties help to identify the most critical (or missing) testbed knowledge that impacts contrast floor and/or convergence. A better than a factor of 2 agreement between model prediction and testbed result has been consistently achieved in terms of contrast floor, chromaticity, and convergence. Testbed contrast performance enhancement from the modeling feedback further confirms the quality of model fidelity.

10400-6, Session 1

Sensitivity of WFIRST coronagraph broadband contrast performance to DM actuator errors

Erkin Sidick, Byoung-Joon Seo, Brian D. Kern, Ilya Poberezhskiy, Bijan Nemati, Jet Propulsion Lab. (United States)

The WFIRST/AFTA 2.4 m space telescope currently under study includes a stellar coronagraph for the imaging and the spectral characterization of extrasolar planets. The coronagraph employs sequential deformable mirrors to compensate for phase and amplitude errors. Using the optical model of an Occulting Mask Coronagraph (OMC) testbed at the Jet Propulsion Laboratory (JPL), we have investigated the sensitivity of a Hybrid Lyot Coronagraph (HLC) broadband contrast performance to DM actuator errors and actuator limits. Considered case include drifts in actuator heights, paired actuators, as well as the limits imposed by a neighboring-actuator rule. Actual data about the actuator drifts and the knowledge about the paired-actuators obtained in several DM characterization experiments

conducted at JPL, as well as the neighboring-actuator rule implement on the OMC testbed were used in simulations. In some cases we confirmed the theoretical predictions with the testbed measured results.

10400-7, Session 2

Sensitivity of the WFIRST coronagraph performance to key instrument parameters

Bijan Nemati, John E. Krist, Bertrand Mennesson, Jet Propulsion Lab. (United States)

Space coronagraphs offer the possibility of direct detection of light from extrasolar planets. The WFIRST space-based coronagraph, currently under development and slated for launch in the mid-2020's, will offer unprecedented starlight suppression and sensitivity, with contrast better than 1e-9 and the ability to directly detect and characterize extrasolar planets down to Jupiters and perhaps Neptunes. In addition, it will allow imaging of circumstellar disks. The main technical challenge in direct detection comes from three areas: starlight suppression, low flux detection, and speckle stabilization in the dark zone where the planet or disk light is to be detected. These three aspects in turn place requirements on key instrument parameters such as system throughput, raw contrast, detector noise, and thermal stability. The link between instrument limitations and instrument performance is captured in models, and balanced using error budgets. Instrument performance can be measured in terms of the science yield, which is itself limited by available mission time and the instrument sensitivity floor. In this paper, we present an overview of the modeling and methodology to assess the sensitivity of the coronagraph and some of the key results pertaining to the WFIRST coronagraph.

10400-8, Session 2

IMPipeline: an integrated STOP modeling pipeline for the WFIRST coronagraph

Navtej Saini, Kevin Anderson, Zensheu Chang, Gary Gutt, Bijan Nemati, Jet Propulsion Lab. (United States)

We have developed an automated software pipeline to perform Structural-Thermal-Optical Performance (STOP) analysis of the WFIRST coronagraph. The Coronagraph Instrument on the Wide Field InfraRed Survey Telescope (WFIRST) will search for exoplanets by controlling the diffraction of the host star light in order to suppress it and allow the planet light to become observable. Since the planet light is billions of times dimmer than the star light, precise control of the light is challenging and susceptible to even minute imperfections such as thermally induced deformations of the optics. The observatory STOP analysis is used to assess the impact of such perturbations. The pipeline integrates the thermal, structural, and optical analysis software to run a STOP analysis in a seamless manner, with the final output being optical wave-front errors for an input observational scenario. The pipeline is written in the Python high level language and uses the Luigi framework for dependency resolution, workload management, and visualization. The initial version uses Thermal Desktop for thermal analysis, NX NASTRAN for structural analysis, SigFit for optical surface fitting, and CODE V for optical analysis. The pipeline can be easily customized using configuration files and provides users with a web interface to monitor the submitted job. This paper will present results showing how the pipeline can be used to simulate different observational scenarios to generate optical wave-front errors. Which in turn are propagated through simulated WFIRST coronagraph optical system to generate realistic speckle patterns.

10400-9, Session 2

Current science requirements and planned implementation for the WFIRST-CGI Integral Field Spectrograph (IFS)

Avi M. Mandell, Tyler D. Groff, Qian Gong, Michael W. McElwain, Maxime J. Rizzo, Prabal Saxena, Neil T. Zimmerman, NASA Goddard Space Flight Ctr. (United States)

In this paper we describe the progress on defining the science requirements, the design implementation, and the current technology demonstration for the integral field spectrograph (IFS) camera baselined for Coronagraphic Instrument (CGI) on the NASA WFIRST flagship mission. The CGI is a technology demonstration instrument meant to demonstrate high-contrast direct imaging of exoplanets from space, with the goal of both characterizing the atmospheres of known giant exoplanets as well as discovering new planets. The WFIRST 2015 Science Definition Team (SDT) defined initial science requirements for the CGI IFS including a minimum spectral resolving power, instantaneous spectral bandwidth, and field of view, with updates by the WFIRST Science Investigation Teams (SITs) in preparation for the WFIRST Systems Requirements Review (SRR) in June 2017. In addition, GSFC was tasked with designing, integrating, and testing the Prototype Imaging Spectrograph for Coronagraphic Exoplanet Studies (PISCES) integral field spectrograph to demonstrate the technological capability to meet these science requirements. This paper will outline the current formulation and motivation for the IFS science requirements, describe how the current IFS baseline design meets these science requirements, and detail the current progress in demonstrating the required capabilities using the PISCES instrument.

10400-10, Session 2

Flight Integral Field Spectrograph (IFS) optical design for WFIRST coronagraphic exoplanet demonstration

Qian Gong, Tyler D. Groff, Avi M. Mandell, Michael W. McElwain, Maxime J. Rizzo, Prabal Saxena, NASA Goddard Space Flight Ctr. (United States)

Based on the experience from Prototype Imaging Spectrograph for Coronagraphic Exoplanet Studies (PISCES) for WFIRST, we have moved to the flight instrument design phase. The flight instrument is similar to PISCES, but there are important changes to its design as our requirements have evolved. Beginning with the science and system requirements, we discuss a number of critical trade-offs. Most significantly there are trades in the type of IFS, lenslet array shape and layout, detector sampling, and accommodating the larger Field Of View (FOV) and wider wavelength band for a potential Starshade. Finally, the traditional geometric optical design is also investigated and traded. We compare a reflective versus refractive design, and the telecentricity of the relay. The relay before the lenslet array controls the chief angle distribution on the lenslet array. Our previous paper1 has addressed how the relay design combined with lenslet array/pinhole mask can further suppress the residual star light and increase the contrast. Highlighting all of these design trades, we present the phase A IFS optical design for the WFIRST coronagraph instrument.

10400-11, Session 2

Simulating the WFIRST coronagraph Integral Field Spectrograph

Maxime J. Rizzo, Universities Space Research Association (United States) and NASA Goddard Space Flight Ctr. (United States); Ewan S. Douglas, Massachusetts Institute of Technology (United States); Timothy Brandt, Institute for Advanced Study (United States); Kerri L. Cahoy, Massachusetts Institute of Technology (United States); Qian Gong, Tyler D. Groff, NASA Goddard Space Flight Ctr. (United States); John E. Krist, Jet Propulsion Lab. (United States); Avi M. Mandell, Michael W. McElwain, NASA Goddard Space Flight Ctr. (United States); A. J. Eldorado Riggs, Jet Propulsion Lab. (United States); Aki Roberge, Prabal Saxena, Neil T. Zimmermann, NASA Goddard Space Flight Ctr. (United States)

A primary goal of direct imaging techniques is to spectrally characterize the atmospheres of planets around other stars at extremely high contrast levels. To achieve this goal, coronagraphic instruments have favored integral field spectrographs (IFS) as the science cameras to disperse the entire search area at once and obtain spectra at each location, since the positions of planets are not known a priori. These spectrographs are useful against confusion from speckles and background objects, and can also help in the speckle subtraction and wavefront control stages of the coronagraphic observation. We present a software package to simulate the WFIRST Coronagraph Instrument (CGI), and produce an end-to-end, realistic simulation of the CGI IFS. The software takes a broadband input science cube, transforms it into IFS detector maps using a CGI Shaped Pupil Coronagraph (SPC) model, and extracts the final cube from those maps. We validate the simulator by comparing to experimental data obtained from the PISCES instrument, a prototype IFS for the CGI-IFS, at JPL's High-Contrast Imaging Testbed. Simulated IFS cubes will be used to test data extraction techniques, refine sensitivity analyses and carry out design trade studies of the flight CGI-IFS. The open-source package is written in Python and designed to being user-friendly and fast.

10400-12, Session 3

Systematic errors and defects in fabricated coronagraph masks and laboratory scale star-shade masks and their performance impact

Kunjithapatham Balasubramanian, Eric J. Cady, Richard Muller, Bijan Nemati, Ilya Poberezhskiy, A. J. Eldorado Riggs, Daniel Ryan, Victor White, Daniel Wilson, Karl Yee, Hanying Zhou, Jet Propulsion Lab. (United States)

NASA WFIRST mission has planned to include a coronagraph instrument to find and characterize exoplanets. Masks are needed to suppress the host star light to better than 10-8 level contrast over a broad bandwidth to enable the coronagraph mission objectives. Such masks for high contrast coronagraphic imaging require various fabrication technologies to meet a wide range of specifications, including precise shapes, micron scale island features, ultra-low reflectivity regions, uniformity, wave front quality, etc. We present the technologies employed at JPL to produce these pupil plane and image plane coronagraph masks, and lab-scale external occulter masks, highlighting accomplishments from the high contrast imaging testbed (HCIT) at JPL and from the high contrast imaging lab (HCIL) at Princeton University. Inherent systematic and random errors in fabrication and their impact on coronagraph performance are discussed with model predictions and measurements.

10400-13, Session 3

Testbed demonstration of low-order wavefront sensing and control for WFIRST coronagraph

Fang Shi, Xin An, Kunjithapatham Balasubramanian, Randall Bartos, Eric J. Cady, Brian D. Kern, Raymond Lam, David S. Marx, Camilo Mejia Prada, Dwight Moody, Richard Muller, Keith Patterson, Ilya Poberezhskiy, A. J. Eldorado Riggs, Daniel Ryan, Byoung-Joon Seo, Chris Shelton, Joel Shields, Erkin Sidick, Hong Tang, John Trauger, Tuan Truong, Victor White, Daniel Wilson, Hanying Zhou, Robert Zimmer, Jet Propulsion Lab. (United States)

To maintain the required performance of WFIRST Coronagraph in a realistic space environment, a Low Order Wavefront Sensing and Control (LOWFS/C) subsystem is necessary. The LOWFS/C uses a Zernike wavefront sensor (ZWFS) with the phase shifting disk combined with the stellar light rejecting occulting mask, a key concept to minimize the non-common path error. For wavefront corrections, WFIRST LOWFS/C uses a fast steering mirror (FSM) for line-of-sight correction, a focusing mirror for focus drift correction, and one of two deformable mirrors (DM) for other low order wavefront error correction. As a part of technology development and demonstration for WFIRST Coronagraph a dedicated Occulting Mask Coronagraph (OMC) testbed has been built and commissioned. With its configuration similar to the WFIRST flight coronagraph instrument the OMC testbed consists of two coronagraph modes, Shaped Pupil Coronagraph (SPC) and Hybrid Lyot Coronagraph (HLC), a Low Order Wavefront Sensor, and an Optical Telescope Assembly (OTA) Simulator which can generate the realistic LoS drift and jitter as well as low order wavefront error that would be induced by the WFIRST telescope's vibration and thermal changes. In this paper we will present the recent testbed results of LOWFS/C and dynamic coronagraph tests in which we have demonstrated that LOWFS/C is able to maintain the coronagraph contrast with the presence of WFIRST like line-of-sight and low order wavefront disturbances.

10400-14, Session 3

Shaped pupil coronagraphy for WFIRST: high-contrast broadband testbed demonstration

Eric J. Cady, Kunjithapatham Balasubramanian, Jet Propulsion Lab. (United States); Jessica Gersh-Range, N. Jeremy Kasdin, Princeton Univ. (United States); Brian D. Kern, Raymond Lam, Camilo Mejia Prada, Dwight Moody, Keith Patterson, Ilya Poberezhskiy, A. J. Eldorado Riggs, Byoung-Joon Seo, Fang Shi, Hong Tang, John Trauger, Hanying Zhou, Jet Propulsion Lab. (United States); Neil T. Zimmerman, Space Telescope Science Institute (United States)

The Shaped Pupil Coronagraph (SPC) is one of the two operating modes of the WFIRST coronagraph instrument. The SPC provides starlight suppression in a pair of wedge-shaped regions, and is well suited for spectroscopy of known exoplanets. To demonstrate this starlight suppression in the presence of expected on-orbit input wavefront disturbances, we have recently built a dynamic testbed at JPL analogous to the WFIRST flight instrument architecture, with both Hybrid Lyot Coronagraph (HLC) and SPC architectures and a Low Order Wavefront Sensing and Control (LOWFS/C) subsystem to apply, sense, and correct dynamic wavefront disturbances. We present our best up-to-date results of the static SPC mode demonstration from the testbed, along with model comparisons and SPC performance under realistic dynamical conditions. HLC results will be reported separately.

10400-15, Session 3

Hybrid Lyot coronagraph for WFIRST: high-contrast broadband testbed demonstration

Byoung-Joon Seo, Eric J. Cady, Brian Gordon, Brian D. Kern, David S. Marx, Dwight Moody, Richard Muller, Keith Patterson, Ilya Poberezhskiy, Fang Shi, Erkin Sidick, John Trauger, Daniel Wilson, Jet Propulsion Lab. (United States)

Hybrid Lyot Coronagraph (HLC) is one of the two operating modes of the WFIRST coronagraph instrument. HLC can produce starlight suppression over full 360 degrees annular region and thus is particularly suitable for discovery of unknown exoplanets. Since being selected by National Aeronautics and Space Administration (NASA) in December 2013, the coronagraph technology is being matured to Technology Readiness Level (TRL) 6 by 2017. To demonstrate starlight suppression in presence of expecting on-orbit input wavefront disturbances, we have built a

dynamic testbed in JPL in 2016. This testbed, named as Occulting Mask Coronagraph (OMC) testbed, is designed analogous to the WFIRST flight instrument architecture: It has both HLC and Shape Pupil Coronagraph (SPC) architectures, and also has the Low Order Wavefront Sensing and Control (LOWFS/C) subsystem to sense and correct the dynamic wavefront disturbances. We are not reporting the dynamic test result or the SPC mode test in this paper. We present only up-to-date progress of HLC mode demonstration from the testbed. HLC occulter masks consisting of metal and dielectric layers have been fabricated and characterized. Wavefront control using two deformable mirrors is demonstrated in a vacuum testbed with 10% broadband light centered at 550 nm. As a result, we obtain repeatable convergence below 2E-9 mean contrast in the 360 degrees dark hole with working angle between 3 ?/D and 9 ?/D. We present the key hardware and software used in the testbed, the performance results and their comparison to model expectations.

10400-16, Session 4

Two deformable mirror methods for the correction of aperture discontinuities

Johan Mazoyer, Johns Hopkins Univ. (United States); Laurent Pueyo, Space Telescope Science Institute (United States); Mamadou N'Diaye, Observatoire de la Cote d'Azur (France); Kevin Fogarty, Johns Hopkins Univ. (United States); Rémi Soummer, Space Telescope Science Institute (United States); Neil T. Zimmerman, NASA Goddard Space Flight Ctr. (United States); Colin Norman, Johns Hopkins Univ. (United States); Stuart B. Shaklan, Jet Propulsion Lab. (United States)

The increasing complexity of the aperture geometry of the future space- and ground based-telescopes will limit the performance of the next generation of coronagraphic instruments for high contrast imaging of exoplanets. We propose here a new closed-loop optimization technique to use two deformable mirrors to correct for the effects of complex apertures on coronagraph performance, alternative to the ACAD technique previously developed by our group. This technique allows the use of any coronagraphs, designed for continuous apertures, with complex, segmented, apertures, maintaining high performance in contrast and throughput.
We present a numerical study on several pupil geometries (segmented LUVOIR type aperture, WFIRST, ELTs) for which we obtained high contrast levels with several deformable mirror setups (size, number of actuators, separation between them), coronagraphs (apodized pupil lyot and vortex coronagraphs) and spectral bandwidths, which will help us present recommendations for future coronagraphic instruments.

10400-17, Session 4

Optimization of coronagraph design for segmented aperture telescopes

Jeffrey B. Jewell, Jet Propulsion Lab. (United States); Garreth Ruane, California Institute of Technology (United States); Stuart B. Shaklan, Jet Propulsion Lab. (United States); Dimitri Mawet, California Institute of Technology (United States); David Redding, Jet Propulsion Lab. (United States)

The goal of directly imaging Earth-like planets in the habitable zone of other stars has motivated the design of coronagraphs for use with large segmented aperture space telescopes. In order to achieve an optimal trade-off between planet light throughput and diffracted starlight suppression, we consider coronagraphs comprised of a stage of phase control implemented with deformable mirrors (or other optical elements), pupil plane apodization masks (gray scale or complex valued), and focal plane masks (either amplitude only or complex-valued, including phase only such as the vector vortex coronagraph). We approach the coronagraph design problem from a function space perspective - an ideal coronagraph "rotates", with a unitary linear operator, the collection of telescope on-axis modes (the star or resolved stellar disc) into the null space of a singular linear operator blocking the starlight from reaching the science focal plane. Viewed in this setting, the coronagraph design problem involves a search for the phase control and focal or pupil plane masks to best approximate the ideal unitary and singular linear operators respectively. We apply this framework to the design of pupil plane apodization masks, as well as phase only beam-shaping, enabling vortex coronagraphs to be used with segmented aperture telescopes. We also provide examples of the optimization of complex-valued focal plane masks, and end-to-end joint coronagraph optimization.

10400-18, Session 4

Apodized/shaped pupil Lyot coronagraph designs for segmented aperture space telescopes

Neil T. Zimmerman, NASA Goddard Space Flight Ctr. (United States); Mamadou N'Diaye, Observatoire de la Côte d'Azur (France); Kathryn St. Laurent, Rémi Soummer, Christopher C. Stark, Laurent Pueyo, Anand Sivaramakrishnan, Marshall D. Perrin, Space Telescope Science Institute (United States); Robert J. Vanderbei, Princeton Univ. (United States)

Advanced Lyot coronagraphs of the apodized/shaped pupil variety are a candidate technology for directly imaging habitable exoplanets with future space telescopes. Until recently, the compatibility of this design family with segmented mirror telescopes was poorly understood. In support of the NASA Exoplanet Exploration Program's Segmented Coronagraph Design & Analysis effort, we are carrying out a comprehensive investigation on the performance of apodized/shaped pupil Lyot coronagraphs (APLC) with segmented and obscured telescope apertures. We have developed a software toolkit to automate the exploration of thousands of coronagraph design parameter combinations. This has enabled us to empirically establish relationships between planet throughput and telescope aperture geometry, inner working angle, bandwidth, and contrast level. Preliminary scientific yield evaluations based on design reference mission simulations indicate the APLC is a viable tool for surveying the local exoEarth population, producing detection tallies competitive with other starlight suppression concepts.

10400-19, Session 4

Performance and sensitivity of vortex coronagraphs on segmented space telescopes

Garreth Ruane, California Institute of Technology (United States); Jeffrey B. Jewell, Jet Propulsion Lab. (United States); Dimitri Mawet, California Institute of Technology (United States) and Jet Propulsion Lab. (United States); Stuart B. Shaklan, Jet Propulsion Lab. (United States)

The detection of molecular species in the atmospheres of earth-like planets orbiting nearby stars requires an optical system that suppresses starlight and maximizes the sensitivity to the weak planet signals at small angular separations. Achieving sufficient contrast performance on a segmented aperture space telescope is particularly challenging due to unwanted diffraction within the telescope from amplitude and phase discontinuities in the pupil. Apodized vortex coronagraphs are a promising solution that theoretically meet the performance needs for high contrast imaging with future segmented space telescopes. We investigate the sensitivity of apodized vortex coronagraphs to the expected aberrations, including segment co-phasing errors in piston and tip/tilt as well as low-order aberrations on individual segments. Telescope requirements are identified for notional HabEx and LUVOIR telescope designs.

10400-20, Session 4

Phase-induced amplitude apodization complex mask coronagraphy (PIAACMC) for large segmented apertures

Olivier Guyon, The Univ. of Arizona (United States) and Subaru Telescope, National Astronomical Observatory of Japan (United States); Brian D. Kern, Jet Propulsion Lab. (United States); Alexander T. Rodack, Justin M. Knight, The Univ. of Arizona (United States); Ruslan Belikov, Dan Sirbu, Stephen T. Bryson, Christopher E. Henze, NASA Ames Research Ctr. (United States); Johanan L. Codona, The Univ. of Arizona (United States); Stuart B. Shaklan, Jet Propulsion Lab. (United States)

High contrast imaging of exoplanets around nearby stars with future large segmented apertures requires starlight suppression systems optimized for such geometries, with the ability to control diffraction created by gaps between segments.

The PIAACMC approach is well-suited for high high efficiency coronagraphic imaging of exoplanets at small angular separations, offering an inner working angle (IWA) as small as 1 lambda/D. We show that PIAACMC can be designed for segmented apertures and present a few representative designs. The design process can mitigate leaks due to stellar angular size and chromatic diffraction by segment gaps by co-optimizing a multi-zone diffractive focal plane mask and a Lyot stop. The resulting performance is ultimately limited by stellar angular size, and the IWA must be carefully traded against contrast and throughput at small angular separations.

We show that PIAACMC's small IWA enables space-based near-IR imaging and spectroscopy of exoplanets around Sun-stars, and ground-based imaging and characterization of habitable planets around nearby M-type stars. We review the current status of PIAACMC laboratory development and near-term prospects for ground-based use.

10400-21, Session 4

Incorporating deformable mirrors into shaped pupil coronagraph optimizations to increase throughput

Jessica Gersh-Range, N. Jeremy Kasdin, Princeton Univ. (United States)

Shaped pupil and shaped pupil Lyot coronagraphs use a binary pupil mask to reduce the amount of starlight entering specific regions of the image plane. The advantages of these coronagraphs are their achromaticity, relative insensitivity to low-order aberrations and jitter, and low technical risk, which makes them attractive for missions such as the Wide-Field Infrared Space Telescope. The downside is that they have lower throughput than other coronagraph types because the binary pupil mask works by blocking selected patches of starlight in order to modify the diffraction pattern. To increase the throughput, we explore offloading some of the starlight suppression effort to the pair of deformable mirrors (DMs) in the wavefront control system. We first use a linear stroke minimization algorithm to determine DM settings that generate a dark hole with a specified contrast, with the shaped pupil mask omitted but all other coronagraphic masks present in the wavefront estimation and control model. We then calculate the corresponding amplitude and phase maps in the pupil plane and incorporate these into the shaped pupil optimization. With the optimized shaped pupil mask included, we determine updated DM settings, and we iterate until the shaped pupil design converges. We discuss the throughput gains that are possible with varying amounts of the final contrast generated by the DMs. We also preliminarily discuss the potential disadvantages of this modification to a shaped pupil Lyot coronagraph, which include greater technical risk and increased chromaticity and sensitivity to aberrations.

10400-22, Session 4

Sensitivity analysis for high-contrast missions with segmented telescopes

Lucie Leboulleux, ONERA (France) and Space Telescope Science Institute (United States) and Aix Marseille Université (France); Jean-François Sauvage, Thierry Fusco, ONERA (France) and Aix Marseille Univ. (France); Rémi Soummer, Laurent Pueyo, Space Telescope Science Institute (United States)

Segmented telescopes are a possible approach to enable large-aperture space telescopes for the direct imaging and spectroscopy of habitable worlds. However, the increased complexity of their aperture geometry, due to their central obstruction, support structures and segment gaps, makes high-contrast imaging very challenging.

In this context, we present a complete and comprehensive error budget allowing to evaluate the constraints on the segments and the influence of the error terms on the final image and contrast. Indeed, the optimal contrast of 10^10 to image Earth-like planets requires drastic conditions, both in term of segment alignment and telescope stability, since space telescopes have to evolve in unfriendly environments due to the flight conditions: vibrations and resonant modes of the segments.

In this communication, we study the impact of selected error terms on the final contrast, such as local or global, low order or higher order, correlated or non-correlated aberrations, in a static or dynamic environment. These results will then be compared to a theoretical model thanks to an analytic analysis of the image formation.

10400-23, Session 5

Electric field conjugation in the presence of model uncertainty

David S. Marx, Byoung-Joon Seo, Erkin Sidick, Brian D. Kern, Bijan Nemati, Ilya Poberezhskiy, Jet Propulsion Lab. (United States)

The Wide-Field Infrared Survey Telescope (WFIRST) is a 2.4m diameter space telescope NASA program. The payload will include a coronagraph instrument (CGI). The CGI designs under development use deformable mirrors (DM) to create a point spread function (PSF) with a dark region around the obscured star object. Electric field conjugation (EFC) is an iterative nonlinear optimization procedure that uses measurements of the electric field at the image to determine the DM displacements to modify the PSF to create the region of high contrast in the image. EFC requires a numerical model of the coronagraph to calculate the Jacobian of the system, which is used, along with regularization, to solve for the DM displacements for each iteration of the nonlinear optimization. Ideally, the coronagraph is aligned and calibrated, and the calibration data are used in the numerical model for calculating the Jacobian. However, calibration and alignment measurements always contain uncertainty resulting in calibration error. Therefore, the Jacobian calculated from the numerical model is not an exact representation of the physical coronagraph, and the resulting DM solution for an EFC iteration does not have the exact impact on the electric field of the coronagraph as predicted by the EFC. The result is slow convergence, and, as will be shown, drives the use of more restrictive regularization. Using Monte Carlo trials, we investigate the effect of calibration error on EFC convergence and regulatization. Comparison to results from the High Contrast Imaging Testbed Hybrid Lyot Coronagraph are also presented.

10400-24, Session 5

Wavefront control methods for high-contrast integral field spectroscopy

Tyler D. Groff, NASA Goddard Space Flight Ctr. (United

States); Olivier Guyon, Subaru Telescope, National Astronomical Observatory of Japan (United States); Camilo Mejia Prada, Eric J. Cady, Jet Propulsion Lab. (United States); Maxime J. Rizzo, Prabal Saxena, Avi M. Mandell, Qian Gong, Michael W. McElwain, NASA Goddard Space Flight Ctr. (United States); N. Jeremy Kasdin, Princeton Univ. (United States)

Direct imaging of exoplanets using a coronagraph has required the development of new technologies for both ground- and space-based observations. Key to the science of direct imaging is the spectroscopic capabilities of the instrument, our ability to obtain a spectrum of the exoplanet, which provides insights to the chemical composition, temperatures, atmospheric structure. Direct imaging instruments generally use an integral field spectrograph (IFS), which disperses each field point in an image plane onto the detector. The spatial and spectral content enhances detection and characterization capability, and the spectral information is critical to achieving detection limits below the speckle floor. The most mature application of these high contrast IFS techniques is at more modest contrast ratios on ground-based telescopes, achieving 5-6 orders of magnitude suppression. In space, where we are attempting to detect Earth-analogs, the contrast requirements are more severe and the IFS must be incorporated into the wavefront control loop to reach 1e-10 detection limits required for Earth-like planet detection. A new mathematical framework is presented that closes a control loop around the on the unprocessed IFS image for better computational efficiency, which considers sensitivity to the data pipeline accuracy. Experimental results and tested methodologies are presented using on-sky data from the Coronagraphic High Angular Resolution Imaging Spectrograph (CHARIS) and testbed data from the Prototype Imaging Spectrograph for Coronagraphic Exoplanet Studies (PISCES) at the JPL High Contrast Imaging Testbed. Efficient IFS wavefront control algorithms will be critical to the WFIRST IFS, which is currently in Phase A of its design.

10400-25, Session 5

Improved high-contrast wavefront controllers for exoplanet coronagraphic imaging systems

He Sun, N. Jeremy Kasdin, Princeton Univ. (United States); A. J. Eldorado Riggs, Jet Propulsion Lab. (United States); Tyler D. Groff, NASA Goddard Space Flight Ctr. (United States) and Princeton Univ. (United States); Robert J. Vanderbei, Princeton Univ. (United States)

All coronagraphs for exoplanet high-contrast imaging employ a wavefront estimation and control system to reject system aberrations and create sufficiently dark holes. Currently, two control schemes are being employed: electric field conjugation (EFC) and stoke minimization. Both of them are based on a linearized state transition model and both have achieved great success over the past decade. Mathematically, both controllers find the deformable mirror commands by balancing the final intensity in the dark holes and the mirror surface deformation in a quadratic minimization. In this paper, we introduce two new ideas to improve model-based wavefront controllers. Firstly, linear programming is applied to enable the use of inequality constraints. Then, without linearizing the system state transition model, we directly formulate the controller as a nonlinear optimization problem. Simulation and experimental results from Princeton High Contrast Imaging Lab (HCIL) are reported in this paper and the advantages and disadvantages of these new controllers are carefully investigated compared to the existing quadratic controllers. Both controllers reveal great potential for creating more uniform dark holes and increasing the correction speed.

10400-26, Session 5

Low-order wavefront sensing for coronagraphic telescopes

Hari Subedi, N. Jeremy Kasdin, Princeton Univ. (United States)

Space telescopes equipped with a coronagraph to detect and characterize exoplanets must have the ability to sense and control low-order wavefront aberrations. Most concepts for low-order wavefront sensing use the starlight rejected by the coronagraph to sense these aberrations. The sensor must be able to make precise estimates and be robust to photon and read noise. A thorough study of various differential low-order wavefront sensors (LOWFSs) would be beneficial for future space-based observatories designed for exoplanet detection and characterization. In this paper, we will expand on the comparison of different LOWFSs that use the rejected starlight from the coronagraphic focal plane to estimate these aberrations. We will also present the experimental results of the sparse aperture mask (SAM) LOWFS that we have designed at the Princeton High Contrast Imaging Lab (PHCIL). In addition, we will present simulation results of combined low-order and higher-order wavefront control loops.

10400-27, Session 5

Polynomial apodized vortex coronagraphs for obscured telescope pupils

Kevin Fogarty, Johns Hopkins Univ. (United States); Laurent Pueyo, Space Telescope Science Institute (United States); Johan Mazoyer, Johns Hopkins Univ. (United States) and Space Telescope Science Institute (United States); Mamadou N'Diaye, Lab. J.L. Lagrange (France) and Space Telescope Science Institute (United States)

Coronagraphs using vector vortex phase masks offer theoretically ideal starlight suppression when paired with telescopes with unobstructed, circular pupils, making them an attractive option for missions to directly image exoplanets. However, pupil obstructions in the form of secondary mirror central obscurations, primary mirror segmentation, and secondary mirror support struts all introduce diffraction artifacts that limit the performance offered by these instruments. We use an analytical prescription describing the propagation of starlight through a vortex coronagraph paired with a centrally obscured telescope pupil to derive polynomial pupil plane apodizations that compensate for the diffraction artifact introduced by central obscurations. The Polynomial Apodized Vortex Coronagraph (PAVC) provides theoretically ideal cancellation of on-axis starlight, with off-axis throughput that improves as the topological charge of the vortex increases. For a charge 6 vector vortex, PAVC provides 50% encircled energy throughput (nearly 70% total energy throughput) in the presence of a central obscuration that is 30% the radius of the pupil. These designs provide a large number of degrees of freedom, and we optimized these designs in combination with active methods to correct for pupil struts and segmentation. We also examine the sensitivity of PAVC designs to low order aberrations and finite stellar angular size, and discuss methods for mitigating these effects.

10400-28, Session 5

Patterned liquid-crystal optics for broadband coronagraphy and wavefront sensing

David Doelman, Frans Snik, Leiden Observatory (Netherlands); Zane Warriner, Michael Escuti, North Carolina State Univ. (United States)

The direct-write technology for liquid-crystal patterns allows for manufacturing of extreme geometric phase patterned coronagraphs that

are inherently broadband, e.g. the vector Apodizing Phase Plate (vAPP). The vAPP generates two coronagraphic PSFs with an efficiency, i.e. the amount of light in these PSFs, that depends on the retardance offset to half-wave. Three operational vAPPs have been installed with more than 96% efficiency from 2-5 micron on MagAO and LMIRCAM on LBT. We report a new liquid-crystal design for a broadband vAPP coronagraph with 10-5 raw contrast and more than 98% efficiency for a wavelength range of 1-2.5 micron. To decrease the leakage terms and increase efficiency for vAPPs with 360-deg dark holes, we introduce the double-grating vAPP, which consists of a standard "grating-vAPP", followed by another polarization grating. This combination has been tested on-sky with the LBT and decreases the relative leakage term of the vAPP to 10-4 and folds the two PFSs back on top of each other. Furthermore, we show new liquid-crystal designs for wavelength-selective devices that change between high coronagraphic efficiency and low efficiency for different wavelength ranges. The vAPP works as a coronagraph for selected wavelengths and transmits light unapodized for others. Therefore, a wavelength-selective vAPP can be used in a pupil plane before a WFS or used to feed multiple instrument arms. Any coronagraphic leakage can be used for focal plane wavefront sensing. Lastly, we present geometric phase patterns for advanced implementations of WFS (e.g. Zernike-type) that are enabled only by this liquid-crystal technology.

10400-29, Session 6

Optimal design of apodizing phase plate coronagraphs

Emiel Por, Leiden Observatory (Netherlands)

Direct observations of exoplanets require a stellar coronagraph to suppress the diffracted starlight. An Apodizing Phase Plate (APP) coronagraph consists of a carefully designed phase-only mask in the pupil plane of the telescope. This mask alters the point spread function in such a way that it contains a dark zone at some off-axis region of interest, while still retaining a high Strehl ratio (and therefore high planet throughput).

Although many methods for designing such a phase mask exist, none of them provide a guarantee of global optimality. Here we present a method based on generalization of the phase-only mask to a complex amplitude mask. Maximizing the Strehl ratio while simultaneously constraining the stellar intensity in the dark zone turns out to be a quadratically constrained linear algorithm, for which a global optimum can be found using large-scale numerical optimizers. This generalized problem yields phase-only solutions. These solutions are therefore also solutions of the original problem.

Using this optimizer we perform parameter studies on the inner and outer working angle, the contrast and the size of the secondary obscuration of the telescope aperture for both one-sided and annular dark zones. We reach Strehl ratios of >65% for a 10^{-5} contrast from 1.8 to 10 $lambda/D$ with a one-sided dark zone for a VLT-like secondary obscuration. This study provides guidelines for designing APPs for more realistic apertures.

10400-30, Session 6

High-contrast imaging in multi-star systems: progress in technology development and lab results

Ruslan Belikov, Eugene A. Pluzhnik, Eduardo A. Bendek, Dan Sirbu, NASA Ames Research Ctr. (United States)

We present the continued progress and laboratory results advancing the technology readiness of Multi-Star Wavefront Control (MSWC), a method to directly image planets and disks in multi-star systems such as Alpha Centauri. This method works with almost any coronagraph (or external occulter with a DM) and requires little or no change to existing and mature hardware. In particular, it works with single-star coronagraphs and does not require the off-axis star(s) to be coronagraphically suppressed. Because of the ubiquity of multistar systems, this method potentially multiplies the science yield of many missions and concepts such as WFIRST, Exo-C/S, HabEx, LUVOIR, and potentially enables the detection of Earth-like planets (if they exist) around our nearest neighbor star, Alpha Centauri, with a small and low-cost space telescope such as ACESat.

Our lab demonstrations were conducted at the Ames Coronagraph Experiment (ACE) laboratory and show both the feasibility as well as the trade-offs involved in using MSWC. We used a 32x32 Boston Micromachines deformable mirror both with and without a (PIAA) coronagraph, in monochromatic as well as broadband light. We show several tests corresponding to real targets and missions, including Alpha Centauri with ACESat and WFIRST, and others spanning a range of stellar separations, magnitude differences, and mission concepts. In addition, we demonstrate MSWC in Super-Nyquist mode, where the distance between the desired dark zone and the off-axis star is larger than the conventional (sub-Nyquist) control range of the DM.

10400-31, Session 6

High-contrast spectroscopy testbed for segmented telescopes (HCST)

Dimitri Mawet, Jason Fucik, California Institute of Technology (United States); James K. Wallace, Jet Propulsion Lab. (United States); Jacques-Robert Delorme, Nikita S. Klimovich, Garreth Ruane, California Institute of Technology (United States); Wenhao J. Xuan, Pomona College (United States); Daniel Echeverri, Princeton Univ. (United States); Reed Riddle, Richard G. Dekany, California Institute of Technology (United States); Michael Randolph, California Polytechnic State Univ., San Luis Obispo (United States); Gautam Vasisht, Bertrand Mennesson, Élodie Choquet, Jet Propulsion Lab. (United States); Ji Wang, California Institute of Technology (United States)

The High Contrast Spectroscopy Testbed for Segmented Telescopes (HCST) at Caltech is aimed at filling gaps in technology for future exoplanet imagers and providing the US community with an academic facility to test high contrast components and techniques for future segmented ground-based telescope (TMT, E-ELT) and space-based telescopes (LUVOIR, HDST, HabEx).

The HCST is capable of simulating any segmented telescope geometry up to 1000 segments and time-varying external wavefront disturbances. It also contains a wavefront corrector module based on two deformable mirrors and a Zernike wavefront sensor followed by a classical 3-plane single-stage coronagraph (entrance apodizer, focal-plane mask, Lyot stop), and a science instrument.

The back-end instrument will consist of an imaging detector and a high-resolution spectrograph, which is a unique feature of the HCST. The spectrograph instrument will utilize spectral information in exoplanet detection as a way to improve contrast down to the photon-noise limit as well as measure the chromaticity of new optimized coronagraph and wavefront control concepts, and test the overall scientific functions of high-resolution spectrographs on future segmented telescopes.

10400-32, Session 6

Utilizing active single-mode fiber injection for speckle nulling in exoplanet characterization

Nikita S. Klimovich, Dimitri Mawet, Garreth Ruane, Wenhao J. Xuan, Daniel Echeverri, Michael Randolph, Jason Fucik, Ji Wang, Richard G. Dekany, Jacques-Robert Delorme, California Institute of Technology (United States); James K. Wallace, Gautam Vasisht, Bertrand Mennesson, Élodie Choquet, Eugene Serabyn, Jet Propulsion Lab. (United States)

High dispersion coronagraphy is on the critical path to the full characterization of Earth-like exoplanet atmospheres, but such

measurements are still limited by the raw contrast between the remaining star speckle field and exoplanet. Using an adaptive optics system, the wave front of the starlight can be modified to create destructive interference at the planet location, further reducing the background from the star. We have demonstrated a new concept for speckle nulling via injecting the directly-imaged planet light into a single-mode fiber, linking a high-contrast adaptively-corrected coronagraph to a high-resolution spectrograph (diffraction-limited or not). The restrictions on the E-field that will couple into the single-mode fiber give the adaptive optics system additional degrees of freedom to suppress the speckle noise on top of destructive interference. Using this technique, we are able to show a significant improvement in starlight suppression at a given location.

10400-33, Session 6

Simulating instruments using the high-dispersion coronagraphy technique

Ji Wang, Dimitri Mawet, Garreth Ruane, Bjorn Benneke, California Institute of Technology (United States); Renyu Hu, Jet Propulsion Lab. (United States)

Direct imaging of exoplanets presents a formidable technical challenge owing to the small angular separation and high contrast between exoplanets and their host stars. High Dispersion Coronagraphy (HDC) is a pathway to achieve unprecedented sensitivity to Earth-like planets in the habitable zone. Here, we present a framework to simulate HDC observations and the corresponding data analyses. The goal of these simulations is to perform a detailed analysis of the trade-off between raw star light suppression and spectral resolution for various instrument configurations, target types, and science cases. We predict the performance of an HDC instrument at Keck observatory for characterizing two known, directly imaged planets (HR 8799 e and 51 Eri b) and investigate the potential for using HDC for new planet discoveries and molecular species detection in near infrared bands, in- cluding J, H, KS and L?. We also simulate HDC observations of an Earth-like planet using next-generation ground-based (TMT) and spaced-base telescopes (HabEx and LUVOIR). Potential targets for ground-based extremely large telescopes (ELTs) include Proxima Centauri b and habitable terrestrial planets around M dwarfs whereas space missions will target habitable planets orbiting solar-type stars. We conclude that ground-based ELTs are more suitable for HDC observations of an Earth-like planet than future space-based missions owing to the considerable difference in collecting area. For ground-based telescopes, HDC observations can detect an Earth-like planet in the habitable zone around an M dwarf star at 10?4 starlight suppression level. Compared to the 10?7 planet/star contrast, HDC relaxes the starlight suppression requirement by a factor of 103. For space-based telescopes, detector noise will be a major limitation at spec- tral resolutions higher than 104. Considering detector noise and speckle chromatic noise, R=400 and R=1600 are the optimal spectral resolutions for HabEx and LUVOIR. The corresponding starlight suppression requirement to detect a planet with planet/star contrast of 6.1 ? 10?11 is relaxed by a factor of 10 and 100 for HabEx and LUVOIR, respectively.

10400-34, Session 6

Optical tolerances for the PICTURE-C mission: Error budget for electric field conjugation, beam walk, surface scatter, and polarization aberration

Christopher B. Mendillo, Glenn A. Howe, Kuravi Hewawasam, Jason Martel, Susanna C. Finn, Timothy A. Cook, Supriya Chakrabarti, Univ. of Massachusetts Lowell (United States)

The Planetary Imaging Concept Testbed Using a Recoverable Experiment - Coronagraph (PICTURE-C) mission will directly image debris disks and exozodiacal dust around nearby stars from a high-altitude balloon using a vector vortex coronagraph. The mission contrast requirement is 10^-7 averaged over the inner 1.7-2.7 ?/D and covering a 20% bandpass centered at 600 nm. A comprehensive error budget has been developed to account for and set requirements on all sources of coronagraph leakage. Four leakage sources owing to the optical fabrication tolerances and metallic coatings are: electric field conjugation (EFC) residuals, beam walk on the secondary and tertiary mirrors, optical surface scattering, and polarization aberration. Simulations and analysis of these four leakage sources for the PICTURE-C optical design are presented here. These simulations utilize the PROPER optical propagation library for IDL, a dynamics simulation of the WASP balloon pointing system, an efficient surface scattering code, and a polarization raytrace of the complete optical system.

10400-35, Session 7

Characterization of low-mass deformable mirrors and ASIC drivers for high-contrast imaging

Camilo Mejia Prada, Jet Propulsion Lab. (United States); Li Yao, Yuqian Wu, Microscale, Inc. (United States); Lewis C. Roberts Jr., Chris Shelton, Jet Propulsion Lab. (United States)

The development of compact, high performance Deformable Mirrors (DMs) is one of the most important technological challenge for high-contrast imaging on space missions. With this technological need in mind, Microscale Inc. has fabricated and characterized piezoelectric stack actuator deformable mirrors (PZT-DM) and Application Specific Integrated Circuit (ASIC) drivers for direct integration. The DM-ASIC system is designed to eliminate almost all cables, enabling a very compact optical system with low mass and low power consumption. We report on the optical and electrical tests used to evaluate the performance of the DM and ASIC units. We also compare the results to the requirements for space-based high-contrast imaging of exoplanets.

10400-36, Session 7

Ferrofluid deformable mirror for high-contrast imaging: performance evaluation and design improvements

Aaron J. Lemmer, Princeton Univ. (United States); Tyler D. Groff, NASA Goddard Space Flight Ctr. (United States) and Princeton Univ. (United States); N. Jeremy Kasdin, Princeton Univ. (United States)

We report the current developmental status of a ferrofluid deformable mirror (DM) tailored for high-contrast imaging applications which demand high nominal optical surface quality, extreme-precision actuation at low strokes, and excellent low-spatial-frequency performance. Its optical surface is a flexible solid facesheet which is fixed along the perimeter and continuously supported across the aperture by a ferrofluid medium. There are two actuation modes for controlling the facesheet deflection. The nominal surface curvature may be tuned with hydraulic adjustments of the hydrostatic ferrofluid pressure. An array of current-controlled electromagnets beneath the ferrofluid reservoir create magnetic field gradients within the fluid medium which, in turn, determine the stress distribution on the facesheet and permit localized actuation. In this article we describe our experimental metrology method and present the performance of our 7-actuator ferrofluid DM prototype. The tunable focus capability is measured and compared with theoretical measurements, and the stroke precision for both the hydraulic and magnetic actuation modes are evaluated. Creating facesheet deflections with a useful degree of localization is a significant engingeering challenge for this DM concept. We outline our efforts, supported by theoretical predictions and computational multiphysics simulations, to modify the facesheet design and the magnetic actuation scheme to improve this aspect of the mirror's performance.

10400-37, Session 7

Design of the deformable mirror demonstration CubeSat (DeMi)

Ewan S. Douglas, Gregory Allan, Derek Barnes, Massachusetts Institute of Technology (United States); Ruslan Belikov, Eduardo A. Bendek, NASA Ames Research Ctr. (United States); Anne Marinan, Jet Propulsion Lab. (United States); John Merck, Aurora Flight Sciences Corp. (United States); Tenzin Ukyab, Kerri L. Cahoy, Massachusetts Institute of Technology (United States)

The Deformable Mirror Demonstration Mission (DeMi) was recently selected by DARPA to fly a 6U CubeSat with a wavefront sensor and Microelectromechanical system (MEMS) deformable mirror (DM) payload.

Space telescopes designed to make high-contrast observations using internal coronagraphs for direct characterization of exoplanets require the use of high-actuator density deformable mirrors. These DMs can correct image plane aberrations and speckles caused by imperfections, thermal distortions, and diffraction in the telescope and optics that would otherwise corrupt the wavefront and leaking allow starlight to contaminate coronagraphic images. There has not yet been long-term on-orbit performance qualification of MEMS deformable mirrors or closed loop wavefront sensing.

The DeMi mission has two operational modes, one mode that images an internal light source and another mode that uses external aperture that images stars to achieve its initial objectives, which are still being refined as the design matures. The objective of the internal source is measurement of the 140-actuator MEMS DM actuator displacement and to demonstrate close-loop correction of aberrations in the optical path. Using the external aperture to observe stars of magnitude 2 or brighter, and assuming 3-axis stability with > 0.1 degree of attitude knowledge and jitter < 10 arcsec DeMi will also demonstrate closed loop wavefront control on an astrophysical target. We will present an new payload design, and results from simulations and laboratory optical prototyping, as well as findings on accommodating high-voltage multichannel drive electronics for the DM on a CubeSat.

10400-38, Session 8

Combining angular differential imaging and accurate polarimetry with SPHERE/IRDIS to characterize young giant exoplanets

Rob van Holstein, Frans Snik, Leiden Observatory (Netherlands); Julien Girard, European Southern Observatory (Chile); Jozua de Boer, Christoph Keller, Leiden Observatory (Netherlands); Daphne Stam, Technische Univ. Delft (Netherlands); Jean-Luc Beuzit, David Mouillet, Institut de Planétologie et d'Astrophysique de Grenoble (France); Markus Kasper, European Southern Observatory (Germany); Maud Langlois, Ctr. de Recherche Astronomique de Lyon (France); Arthur Vigan, Lab. d'Astrophysique de Marseille (France); Alice Zurlo, Univ. Diego Portales (Chile) and Univ. de Chile (Chile); Remco de Kok, Leiden Observatory (Netherlands)

Young gas giants emit infrared radiation that can be linearly polarized up to several percent. This linear polarization reveals: 1) the presence of haze layers, 2) spatial structure, e.g. rotational flattening and bands, 3) the spin axis orientation and 4) the particle size and cloud top pressure. We introduce a novel high-contrast imaging scheme that combines angular differential imaging (ADI) and accurate near-infrared polarimetry to characterize self-luminous giant exoplanets. We implemented this technique at VLT/SPHERE-IRDIS and developed the corresponding observing strategies, the polarization calibration and the data-reduction approaches.

By combining ADI and polarimetry we can characterize planets that have already been directly imaged in intensity with high signal-to-noise ratio. We use the IRDIS pupil-tracking mode and apply Principal Component Analysis to reduce speckle noise. We take advantage of IRDIS' dual-beam polarimetric mode to eliminate differential effects that severely limit the polarimetric sensitivity (flat-fielding errors, differential aberrations and seeing), and thus further suppress speckle noise. We developed a detailed Mueller matrix model that describes the telescope and instrument and applied this model to correct for instrumental polarization effects. Our model has been validated with measurements using the internal source and observations of unpolarized standard stars, thereby reaching an absolute polarimetric accuracy ≤0.1%. The modular data-reduction software integrates ADI and polarimetry and incorporates the optimal order of data-reduction steps. We present first results of applying our methods to observations of the planets around HR 8799.

10400-39, Session 8

First light of the CHARIS high-contrast integral-field spectrograph

Tyler D. Groff, NASA Goddard Space Flight Ctr. (United States); Jeffrey K. Chilcote, Univ. of Toronto (Canada); Timothy Brandt, Institute for Advanced Study (United States); N. Jeremy Kasdin, Michael B. Galvin, Craig Loomis, Gillian Knapp, Princeton Univ. (United States); Olivier Guyon, Nemanja Jovanovic, Julien Lozi, Naruhisa Takato, Subaru Telescope, National Astronomical Observatory of Japan (United States); Masahiko Hayashi, Subaru Telescope, National Astronomical Observatory of Japan (Japan)

One of the leading direct Imaging techniques, particularly in ground-based imaging, uses a coronagraphic system and integral field spectrograph (IFS). The Coronagraphic High Angular Resolution Imaging Spectrograph (CHARIS) is an IFS that has been built for the Subaru telescope. CHARIS has been delivered to the observatory and now sits behind the Subaru Coronagraphic Extreme Adaptive Optics (SCExAO) system. CHARIS has 'high' and 'low' resolution operating modes. The 'high-resolution' mode is used to characterize targets in J, H, and K bands at ~R70. The 'low-resolution' prism is meant for discovery and spans J+H+K bands (1.15-2.37 microns) with a spectral resolution of ~R18. This discovery mode has already proven better than 15-sigma detections of HR8799c,d,e when combining ADI+SDI. Using SDI alone, planets c and d have been detected in a single 24 second image. The CHARIS team is optimizing instrument performance and refining ADI+SDI recombination to maximize our contrast detection limit. In addition to the new observing modes, CHARIS has demonstrated a design with high robustness to spectral crosstalk. CHARIS is in the final stages of commissioning, with the instrument open for science observations beginning February 2017. Here we review the science case, design, on-sky performance, engineering observations of exoplanet and disk targets, and specific lessons learned for extremely high contrast imagers. Key design aspects that will be demonstrated are crosstalk optimization, wavefront correction using the IFS image, lenslet tolerancing, the required spectral resolution to fit exoplanet atmospheres, and the utility of the spectrum in achieving higher contrast detection limits.

10400-40, Session 8

Subaru coronagraphic extreme adaptive optics (SCExAO): wavefront control optimized for high-contrast imaging

Olivier Guyon, The Univ. of Arizona (United States) and Subaru Telescope, National Astronomical Observatory of Japan (United States); Nemanja Jovanovic, Julien Lozi, Subaru Telescope, National Astronomical Observatory of Japan (United States); Jared Males, The Univ. of Arizona

(United States); Frantz Martinache, Observatoire de la Côte d'Azur (France); Ben Mazin, Univ. of California, Santa Barbara (United States); Barnaby Norris, The Univ. of Sydney (Australia); Prashant Pathak, Subaru Telescope, National Astronomical Observatory of Japan (United States)

The SCExAO system is a flexible high contrast imaging platform for exoplanet imaging on the 8-m Subaru Telescope. SCExAO's wavefront control architecture relies on both visible and infrared wavefront sensors to measure, correct and calibrate wavefront errors. The wavefront control loop, optimized for high contrast imaging, includes predictive control, sensor fusion and focal plane speckle control to address the performance limits of current extreme-AO systems: non-common path errors, time-lag and chromaticity. The control software is also designed to enable rapid prototyping of new wavefront algorithm, as one goal of the SCExAO project is to explore and validate new high contrast imaging approaches to guide the design of future ELT high contrast imaging systems.

We describe the SCExAO wavefront control architecture and its software implementation. Recent on-sky results are presented, and future steps are describbted. Current and future high contrast imaging performance are provided. We discuss findings (lessons learned) in the context of future exoplanet imaging instrument developments.

10400-41, Session 8

NIRPS: an adaptive-optics assisted radial velocity spectrograph to chase exoplanets around M-stars

François Wildi, Observatoire de Genève (Switzerland); François Bouchy, Lab. d'Astrophysique de Marseille (Switzerland); Rene Doyon, Étienne Artigau, Univ. de Montréal (Canada); Nicolas Blind, Observatoire de Genève (Switzerland); Vladimir Reshetov, NRC - Herzberg Astronomy & Astrophysics (Canada); Olivier Hernandez, Univ. de Montréal (Canada)

Since 1st light in 2002, HARPS has been setting the standard in the exo-planet detection by radial velocity measurements. Based on this experience, our consortium is developing is an high accuracy near-infrared radial velocity (RV) spectrograph covering YJH bands to detect and characterize low-mass planets in the habitable zone of M dwarfs. It will allow precise RV measurements at the 1?m/s level.

It will open up the path to look for habitable planets around M- type stars by following up the candidates found by the upcoming space missions TESS, CHEOPS and later PLATO.

NIRPS and HARPS, working simultaneously on the ESO 3.6m are bound to become a single powerful high?resolution, high?fidelity spectrograph covering from 0.4 to 1.8 micron,. NIRPS will complement HARPS in validating earth-like planets found around G and K-type stars whose signal is at the same order of magnitude than the stellar noise.

Because at equal resolving power the overall dimensions of a spectrograph vary linearly with the input beam etendue, spectrograph designed for seeing-limited observations are large and expensive. NIRPS will use a high order adaptive optics system to couple the starlight into a fiber corresponding to 0.4" on the sky as efficiently or better than HARPS or ESPRESSO couple the light 0.9" fiber.

This allows the spectrograph to be very compact, more thermally stable and less costly. Using a custom tan(?)=4 dispersion grating in combination with a start-of-the-art Hawaii4RG detector makes NIRPS very efficient with complete coverage of the YJH bands at 110'000 resolution.

NIRPS works in a regime that is in-between the usual multi-mode (MM) where 1000's of modes propagates in the fiber and the single mode well suited for perfect optical systems. This regime called few-modes regime is prone to modal noise- A significant R&D effort is made to characterize and circumvent the modal noise seen in the spectrum.

This paper will be the first presentation of NIRPS to the exo-planet instrumentation community.

10400-58, Session PWed

Commissioning and performance results of the PISCES instrument

Prabal Saxena, Maxime J. Rizzo, NASA Goddard Space Flight Ctr. (United States); Camilo Mejia Prada, Jet Propulsion Lab. (United States); Jorge D. Llop Sayson, California Institute of Technology (United States); Qian Gong, NASA Goddard Space Flight Ctr. (United States); Eric J. Cady, Jet Propulsion Lab. (United States); Avi M. Mandell, Tyler D. Groff, Michael W. McElwain, NASA Goddard Space Flight Ctr. (United States)

The Prototype Imaging Spectrograph for Coronagraphic Exoplanet Studies (PISCES) is a high contrast integral field spectrograph designed to demonstrate readiness of high contrast integral field spectroscopy for the WFIRST coronagraph instrument (CGI). PISCES was designed and built in the Goddard Integral Field Spectroscopy Laboratory as a prototype instrument for the WFIRST CGI and was integrated with a High Contrast Imaging Testbed at the Jet Propulsion Laboratory. We present results demonstrating the ability of PISCES to carry out flight-like data reduction and analysis that has enabled spectral retrieval at high contrast. Calibration and testing datasets were taken and analyzed using a modified version of the Gemini Planet Imager data reduction pipeline. The pipeline was used to generate IFS datacubes where wavefront control has been set to deconstructively interfere speckles in the image plane, producing a high contrast scene. Comparison with an imaging camera reveals change in contrast induced by non-common path optics in PISCES. Preliminary results using conventional wavefront control algorithms with the imaging camera have produced dark hole contrasts of ~1e-8 and indicate contrast achieved by PISCES is similar to that seen in the imaging camera (differing by ~3e-9). In the future, we will incorporate PISCES measurements into an automated wavefront control algorithm and demonstrate improvements in the achievable contrast in preparation for WFIRST flight IFS design. In spring of 2017, PISCES will be integrated with the Occulting Mask Coronagraph (OMC) testbed, enabling a dynamic stellar input to assess end to end high contrast wavefront control with representative pointing jitter.

10400-60, Session PWed

Development status and performance of the evanescent wave coronagraph testbed

Mary Angelie M. Alagao, Christophe Buisset, National Astronomical Research Institute of Thailand (Thailand); Yves Rabbia, Observatoire de la Côte d'Azur (France); Thierry Lépine, Lab. Hubert Curien (France); Saran Poshyachinda, Boonrucksar Soonthornthum, National Astronomical Research Institute of Thailand (Thailand)

The Evanescent Wave Coronagraph (EvWaCo) is a new specific kind of "Band-limited coronagraph" which mask involves the tunneling effect to separate the star and the planet beams thus producing the coronagraphic effect. The first advantage is that this mask adapts itself to wavelength due to the evanescent wave properties thus yielding a potential achromatization of the star extinction. The second advantage is that the star light can be collected for astrometry and/or wavefront analysis.

NARIT has developed a specific optical setup operating over the spectral band [800 nm, 1?m] to demonstrate high-level contrasts and inner working angles in line with the exoplanet direct detection requirements. Our aims are: to test and characterize EvWaCo performance in diffraction-limited regime, to install a simulator of turbulence and an adaptive optics setup to simulate on-ground observations and to define the best scheme for the wavefront correction. The preliminary results obtained in diffraction-limited regime demonstrated contrasts equal to few 10^-6 at a distance comprised between 10 and 20 ?/D from the PSF center with an unpolarized source emitting at ?≈880 nm with a relative spectral bandwidth ??/?≈6%.

In this paper, we first describe the setup and we present the results of the performance characterization that comprises: stability of the setup, variation of the contrast with the wavelength and with the polarization. Then, we describe the end-to-end numerical model of EvWaCo, we confront the experimental and the simulation results to identify the origin of the performance limitation. Finally, we discuss the future improvements to optimize the performance.

10400-61, Session PWed

Further exoplanet suppression using microlens/pinole mask for Luvoir coronagraph

Qian Gong, Lee Feinberg, Michael W. McElwain, Neil T. Zimmerman, Tyler D. Groff, Avi M. Mandell, Matthew R. Bolcar, Brian A. Hicks, NASA Goddard Space Flight Ctr. (United States); Rémi Soummer, Laurent Pueyo, Space Telescope Science Institute (United States)

Direct detection of habitable Earth-like exoplanets is a challenging problem that requires several components that exceed the current technical capabilities. Several approaches to starlight suppression are being developed and demonstrated in the laboratory, including external occulters, a shaped pupil coronagraph, hybrid-Lyot coronagraph, apodized pupil Lyot coronagraph, vector vortex coronagraph, phase induced amplitude apodization coronagraph, and the visible nulling coronagraph. We present an innovative method of starlight suppression using a microlens and pinhole mask, which can be incorporated as part of the integral field spectrograph to further suppress residual starlight by an additional 2-4 orders of magnitude. Most high contrast imaging architectures uses an integral field spectrograph (IFS) after the external or internal coronagraph to characterize the exoplanet atmosphere, with the ultimate goal of determining whether an exoplanet is inhabited. The microlens array is traditionally used in the focal plane input to the spectrometer. With a non-telecentric reimaging system onto the lenslet array, this optic can be used to introduce spatial diversity between the on-axis star and the off-axis planet. In this proceeding, we present an optimization of the design based on the desired starlight suppression and use this design do simulate a hybrid coronagraph and IFS that could be used as a future space instrument on the LUVOIR mission concept. The IFS is designed to be compatible with STScI's APLC design (Zimmerman, et al., 2016), creating an additional 2 – 4 orders of magnitude starlight suppression. This additional suppression can be used to offset existing technological challenges such as fabrication, assembly, alignment, and pointing stability. This method does add any additional complexity to the coronagraph itself and is compatible with all coronagraph suppression architectures proposed to date.

10400-62, Session PWed

Detection and characterization of exoplanets and disks in starshade mission

Mengya Hu, Anthony D. Harness, N. Jeremy Kasdin, Robert J. Vanderbei, Princeton Univ. (United States); Stuart B. Shaklan, Jet Propulsion Lab. (United States)

Direct imaging using a starshade is a powerful technique for exoplanet detection and characterization. While much work has been performed on the mechanical and optical designs of starshade, little attention has been paid to date on post-processing methods. In this paper we report on our recent efforts to develop a model of Starshade imaging considering the effects of various defects on the starshade and the dynamics of the system/telescope system. We adapt the image processing methods such as Locally Optimized Combination of Images (LOCI), KLIP, and inversion methods in a Bayesian framework and report on our preliminary results.

10400-63, Session PWed

Shape accuracy requirements on starshades for large and small apertures

Stuart B. Shaklan, Luis Marchen, Eric J. Cady, Jet Propulsion Lab. (United States)

Starshades can be designed to work with large and small telescopes alike. With smaller telescopes, the targets tend to be brighter and closer to the Solar System, and their putative planetary systems span angles that require starshades with radii of 10-30 m at distances of 10s of Mm. With larger apertures, the light-collecting power enables studies of more numerous, fainter systems, requiring larger, more distant starshades with radii >50 m at distances of 100s of Mm. Characterization using infrared wavelengths requires ever larger starshade radius, as does increasing the instantaneous bandwidth both on the blue and red ends of the bandpass. A mitigating approach is to observe planets between the petals. We compare the starshade shape requirements, including petal shape, petal positioning, and other key terms, for a range of starshade and telescope sizes, bandwidths, and working angles.

10400-64, Session PWed

Design, fabrication, and testing of stellar coronagraphs for exoplanet imaging

Justin M. Knight, John Brewer, Ryan Hamilton, Karen Ward, Thomas D. Milster, The Univ. of Arizona (United States); Olivier Guyon, The Univ. of Arizona (United States) and Subaru Telescope, National Astronomical Observatory of Japan (Japan)

Complex-mask coronagraphs destructively interfere unwanted starlight with itself to achieve the required contrast for direct imaging of exoplanets. This is accomplished using a device called a focal plane mask (FPM). A FPM can be a simple occulter mask, or it can be a multi-featured device designed to phase-shift starlight in a specific manner to have a desired interference effect in the science plane. Creating these masks requires nanofabrication techniques, yet many such methods remain largely unexplored in this context. In this paper we explore several nanofabrication methods for creating FPMs designed for Phase Induced Amplitude Apodization Complex-Mask Coronagraphs (PIAACMC). Previous FPM manufacturing efforts in the context of PIAACMC have concentrated on manufacturability of the devices as well as assessing broadband wavelength operation. Moreover, current fabrication efforts are concentrated on assessing achievable contrast given a single approach. We present FPMs fabricated from the lithographic and etching processes such as e-beam lithography, deep reactive ion etching, and focused ion beam etching using a Silicon substrate. The characteristic size of the mask features is five microns with depths ranging over a micron. The masks are characterized for manufacturing quality using equipment such as an optical interferometer and a scanning electron microscope. Ideal coronagraph performance is compared to experimental performance using the devices in the lab and with a PIAACMC coronagraph at SCExAO. Recommendations for improving the design and fabrication of these FPMs is outlined and discussed along with future experiments and potential applications.

A coronagraph focal plane mask (FPM) for exoplanet imaging typically requires a multi-featured device designed to phase-shift starlight in a specific manner to generate destructive interference in the science plane. We explore several nanofabrication methods for creating FPMs designed for Phase Induced Amplitude Apodization Complex-Mask Coronagraphs. We present PIAACMC FPMs fabricated from several lithographic and etching processes using Silicon. The characteristic size of the mask features is five microns with depths ranging over a micron. Ideal coronagraph performance is compared to simulated performance with the measured FPM errors as well as experiments using the devices in the lab.

10400-65, Session PWed

Starshade orbital maneuver study for WFIRST

Gabriel Soto, Dmitry Savransky, Christian Delacroix, Daniel Garrett, Amlan Sinha, Cornell Univ. (United States)

The Wide Field Infrared Survey Telescope (WFIRST) mission, scheduled for launch in the mid-2020s will perform exoplanet science via both a microlensing survey and direct imaging. An internal coronagraph is planned to perform starlight suppression for exoplanet imaging, but an external starshade could be used to achieve the required high contrasts with potentially higher throughput. This approach would require a separately-launched occulter spacecraft to be positioned at exact distances from the telescope along the line of sight to a target star system. We present a detailed study to quantify the ?v requirements and feasibility of deploying this additional spacecraft as a means of exoplanet imaging. The primary focus of this study is the fuel use of the occulter while repositioning between targets. Based on its designed IWA, the occulter is given an offset distance from the nominal WFIRST halo orbit. Target star systems and look vectors are generated using Exoplanet Open-Source Imaging Simulator (EXOSIMS); a boundary value problem is then solved between successive targets. On average, 50 observations are achievable with randomly selected targets with a 20-day transfer time. Minimizing ?v allows for more than 300 observations while exceeding the 6-year lifetime of the WFIRST mission; minimizing transfer time allows for 240 observations in a 1 year span while exceeding the expected fuel capacity of the occulter spacecraft. A comprehensive cost function conciliates these two constraints given two target stars from a target list. A method for determining the next best target given is also proposed.

10400-66, Session PWed

Line profile analysis of the laser frequency comb in FOCES

Liang Wang, Hanna Kellermann, Max-Planck-Institut für extraterrestrische Physik (Germany); Anna Brucalassi, European Southern Observatory (Germany); Frank U. Grupp, Max-Planck-Institut für extraterrestrische Physik (Germany) and Univ.-Sternwarte München (Germany); Ralf Bender, Univ.-Sternwarte München (Germany) and Max-Planck-Institut für extraterrestrische Physik (Germany)

The broad-band, optical laser frequency comb covers a wavelength range of 510 nm to 700 nm, spanning 30 dispersion echelle orders in the 2k x 2k CCD. Each comb mode is narrow compared to the pixel size. Therefore, the line shape represents the local instrumental profile (or line spread function). We isolate each comb line, and use Gaussian function plus a constant background to fit the profile. The full width at half maximums (FWHMs) of the Gaussian functions are ~2.2 pixels at the center of echelle orders, and show a steep increase towards one side of the CCD. Moreover, the residuals of Gaussian fittings shows a consistent pattern after normalizing by the amplitudes in their intensities and sigma in x direction. And their shapes slowly vary along the dispersion direction. Such deviations from the Gaussian profiles are reconstructed and all of the astro-comb lines are re-modelled with Gaussian functions plus the interpolation of these empirical shapes. The same model is also used to derive the radial velocities from a series of the overlapped spectra of the Sun and astro-comb. In the latter case, a high signal-to-noise ratio (S/N) template is obtained by stacking a series of solar spectra after removing the relative velocity drifts. This technique is of particular interest to the existing spectrographs of which the order spacing along the cross-dispersion direction are not large enough to accommodate an additional optical fiber carrying lights from a wavelength calibration source

10400-67, Session PWed

Performance evaluation of the frequency comb calibrated Echelle spectrograph FOCES

Hanna Kellermann, Liang Wang, Max-Planck-Institut für extraterrestrische Physik (Germany); Frank U. Grupp, Max-Planck-Institut für extraterrestrische Physik (Germany) and Univ.-Sternwarte München (Germany); Anna Brucalassi, European Southern Observatory (Germany); Florian Lang-Bardl, Ulrich Hopp, Univ.-Sternwarte München (Germany); Ralf Bender, Univ.-Sternwarte München (Germany) and Max-Planck-Institut für extraterrestrische Physik (Germany)

We present the first performance evaluation of the upgraded high-resolution spectrograph FOCES (Fiber Optics Cassegrain Échelle Spectrograph), which has been installed at the 2m Fraunhofer telescope at the Wendelstein Observatory in late 2016. FOCES has been successfully operated at the Calar Alto Observatory in southern Spain from 1995 to 2009 and brought back to Munich in 2010 for refurbishment and major upgrades. Among other improvements the spectrograph has been equipped with a laser frequency comb based system for simultaneous wavelength calibration and is now housed inside a pressure- and temperature- stabilized tank. The new system is designed to provide high-accuracy and long-term stability for precise radial velocity measurements as they are needed for discovering/characterizing earth-like extra-solar planets and for stellar atmosphere analyses.

10400-68, Session PWed

Optimization of high-inclination orbits using planetary flybys for a zodiacal light-imaging mission

Gabriel Soto, James Lloyd, Dmitry Savransky, Cornell Univ. (United States); Keith Grogan, Jet Propulsion Lab. (United States) and California Institute of Technology (United States); Amlan Sinha, Cornell Univ. (United States)

The zodiacal light caused by interplanetary dust grains is the second-most luminous source in the solar system. The dust grains coalesce into structures reminiscent of early solar system formation; their composition has been predicted through simulations and some edge-on observations but better data is required to validate them. Scattered light from these dust grains presents challenges to exoplanet imaging missions—resolution of their stellar environment is hindered by exozodiacal emissions and therefore sets the size and scope of these imaging missions. Understanding the composition of this interplanetary dust in our solar system requires an imaging mission from a vantage point above the ecliptic plane. The high surface brightness of the zodiacal light requires only a small aperture with moderate sensitivity; therefore, a 3cm camera is enough to meet the science goals of the mission at an orbital height of 0.1AU above the ecliptic. A 3U CubeSat is the target mass for this mission which will be a secondary payload detaching from an existing interplanetary mission. Planetary flybys are utilized to produce most of the plane change ?v; deep space corrective maneuvers are implemented to optimize each planetary flyby. We develop an algorithm that determines the minimum ?v required to place the CubeSat on a transfer orbit to a planet's sphere of influence, which maximizes the resultant inclination angle with respect to the ecliptic plane. Successive planetary flybys are computed to achieve the desired orbital height for imaging zodiacal light.

10400-69, Session PWed

Detected exoplanet population distributions found analytically

Daniel Garrett, Dmitry Savransky, Cornell Univ. (United States)

Predicting the distributions of planetary population parameters detected by direct imaging planet-finding missions may be accomplished by Monte Carlo simulation. When the assumed planetary parameters vary over a wide range, the number of simulated planets and computational cost to determine the detected distributions must increase. We present an analytical method of predicting the distribution of detected planetary parameters which is more accurate and less computationally expensive than Monte Carlo simulation.

A planet will be detected if its separation from its star is inside the annulus defined by the observing instrument's inner and outer working angles and if it is bright enough to be above the minimum contrast of the observing instrument. The relevant planetary parameters for detection by direct imaging are semi-major axis, eccentricity, geometric albedo, planetary radius, and phase angle (with associated phase function). An assumed planet population is formed by choosing probability density functions for each of these parameters.

We derive the detected planetary parameter distributions by first forming a joint probability density function from the assumed planet population probability density functions. To find the detected distribution of one of the planetary parameters, we marginalize the joint probability density function by all of the other parameters subject to the constraints imposed by the detection conditions of a given instrument. The resulting distributions are computed quicker and show good agreement with distributions determined by Monte Carlo simulations.

10400-70, Session PWed

The low-order wavefront control system for the PICTURE-C mission: preliminary testbed results from the Shack-Hartmann sensor

Glenn A. Howe, Christopher B. Mendillo, Kuravi Hewawasam, Jason Martel, Susanna C. Finn, Supriya Chakrabarti, Timothy A. Cook, Univ. of Massachusetts Lowell (United States)

The Planetary Imaging Concept Testbed Using a Recoverable Experiment - Coronagraph (PICTURE-C) mission will directly image debris disks and exozodiacal dust around nearby stars from a high-altitude balloon using a vector vortex coronagraph. We present experimental results of the PICTURE-C low-order wavefront control (LOWC) system utilizing a Shack-Hartmann (SH) sensor in an instrument testbed. The SH sensor drives both the alignment of the telescope secondary mirror using a 6-axis hexapod and a surface parallel array deformable mirror to remove residual low-order aberrations. The sensor design and actuator calibration methods are discussed and the preliminary closed-loop performance is presented.

10400-71, Session PWed

The low-order wavefront control system for the PICTURE-C mission: high-speed image acquisition and processing

Kuravi Hewawasam, Christopher B. Mendillo, Glenn A. Howe, Jason Martel, Susanna C. Finn, Supriya Chakrabarti, Timothy A. Cook, Univ. of Massachusetts Lowell (United States)

The Planetary Imaging Concept Testbed Using a Recoverable Experiment - Coronagraph (PICTURE-C) mission will directly image debris disks and exozodiacal dust around nearby stars from a high-altitude balloon using a vector vortex coronagraph. The PICTURE-C low-order wavefront control (LOWC) system will be used to correct time varying low-order aberrations due to pointing jitter, gravity sag, thermal deformation, and the gondola pendulum motion. We present the hardware and software implementation of the low-order Shack-Hartmann and reflective Lyot stop sensors. Development of the high-speed image acquisition and processing system is discussed with the emphasis on the reduction of hardware and computational latencies through the use of a real-time operating system and optimized data handling.

10400-72, Session PWed

Post-processing of the HST STIS coronagraphic observations

Bin Ren, Johns Hopkins Univ. (United States); John H. Debes, Laurent Pueyo, Marshall D. Perrin, Space Telescope Science Institute (United States); Élodie Choquet, Jet Propulsion Lab. (United States)

In the past 20 years, the STIS coronagraphic instrument has observed more than 80 stars with more than 4,000 exposures since its installment on the Hubble Space Telescope in 1997, and the numbers are still increasing. We focus on two occulting positions (WEDGEA0.6 and WEDGEA1.0), reduce the whole HST STIS coronagraphic archive at these positions with new post-processing methods, and present our method and results here.

We also explain our efforts in the calibration of STIS's new BAR5 occulting position for high contrast imaging, enabling STIS to explore inner regions as close as 0.2'' at a contrast of 10^4, and at 0.7'' at a contrast of 10^6 for point sources, indicating the 20-year-old STIS is able to compete with the best ground-based telescopes with extreme adaptive optics implemented. The detection limits of circumstellar disks with the BAR5 position is also investigated and reported.

The combination of the STIS results, with the HST/NICMOS results from the ALICE program, as well as other ground based high contrast imaging telescopes (e.g., GPI, P1640, and SPHERE) and future telescopes (e.g., JWST, and WFIRST), will provide us direct evidences in the understanding of planetary system formation and evolution.

10400-73, Session PWed

Shaped pupil coronagraph design developments for the WFIRST coronagraph instrument

A. J. Eldorado Riggs, Jet Propulsion Lab. (United States) and California Institute of Technology (United States); Neil T. Zimmerman, NASA Goddard Space Flight Ctr. (United States); Stuart B. Shaklan, Jeffrey B. Jewell, Jet Propulsion Lab. (United States) and California Institute of Technology (United States); Jessica Gersh-Range, Princeton Univ. (United States)

NASA's WFIRST Coronagraph Instrument (CGI) is planned to image and characterize exoplanets at high contrast. The CGI operating modes are the hybrid Lyot coronagraph for planet detection, a shaped pupil coronagraph for planet characterization, and another shaped pupil for disk imaging. Early CGI designs focused on overcoming the diffraction of the large pupil obscurations. Now that those designs have been proven to work in the lab, the design emphasis has been on achieving higher throughput and lower sensitivities to jitter and polarization-induced astigmatism. Here we present various coronagraph design and tolerancing studies to improve the performance of the CGI.

10400-74, Session PWed

Optimizing the regularization in broadband wavefront control algorithm for WFIRST coronagraph

Erkin Sidick, Byoung-Joon Seo, Brian D. Kern, David S. Marx, Ilya Poberezhskiy, Bijan Nemati, Jet Propulsion Lab. (United States)

The WFIRST/AFTA 2.4 m space telescope currently under study includes a stellar coronagraph for the imaging and the spectral characterization of extrasolar planets. The coronagraph employs sequential deformable mirrors to compensate for phase and amplitude errors. Using the optical model of an Occulting Mask Coronagraph (OMC) testbed at the Jet Propulsion Laboratory, we have investigated and compared through modeling and simulations the performance of several regularization-schemes in broadband wavefront control algorithm used to generate dark holes in an OMC, such as a Hybrid Lyot Coronagraph (HLC). Using the concept of Tikhonov filter constituting the G-matrix, we have explained what the different regularization schemes do to singular components during a wavefront control process called Electric Field Conjugation (EFC). In some cases we confirmed the numerical predictions with the testbed measured results.

10400-75, Session PWed

Mission design concept for detection of biosignatures of transiting planets

Jonathan W. Arenberg, Northrop Grumman Aerospace Systems (United States); Daniel Apai, The Univ. of Arizona (United States); Thomas D. Milster, College of Optical Sciences, The Univ. of Arizona (United States)

This paper discusses a feasibility argument for a mission concept to detect biosignatures in the spectra of transiting planets. Our design is based on the use of a large Fresnel optic based system operating from approximately 400-800 nm to collect the light from known transiting planet systems. The collected light is then analyzed for the presence of such gasses ozone and water. Use of a Fresnel lens system allows the construction of very large apertures for more modest cost than traditionally employed mirrors. We will discuss the science requirements and the basic design and options for our proposed mission.

10400-76, Session PWed

Focal-plane-based wavefront sensing with random DM probes

Eugene A. Pluzhnik, Dan Sibru, Ruslan Belikov, Eduardo A. Bendek, NASA Ames Research Ctr. (United States); Vladimir N. Dudinov, Kharkiv National Univ. of Radio Electronics (Ukraine)

An internal coronagraph with an adaptive optical system for wavefront control is being considered for direct imaging of exoplanets with upcoming space missions and concepts, including WFIRST, HabEx, LUVOIR, EXCEDE, and ACESAT.

The main technical challenge associated with direct imaging of exoplanets is to control of both diffracted and scattered light from the star so that even a dim planetary companion can be imaged. For a deformable mirror (DM) to create a dark hole with 10^-10 contrast in the image plane, wavefront errors must be accurately measured on the science focal-plane detector to ensure a common optical path.

We present here a method that uses a set of random phase probes applied to the DM to obtain a high accuracy wavefront estimate even in the case when the optical parameters/pupil plane phases of the system are dynamically changing.

The presented numerical simulations and experimental results show low noise sensitivity, high reliability, and robustness of the proposed approach. The method does not use any additional optics or complex calibration procedures and can be used during the calibration stage for any direct imaging mission. It can also be used in any optical experiment that uses the DM as the active optical element of the layout.

10400-77, Session PWed

Modeling of planetary signal detection through ray-tracing-based beam propagation

Dongok Ryu, Sug-Whan Kim, Yonsei Univ. (Korea, Republic of)

High contrast images of exoplanet are limited by diffraction from optical and optomechanical components of instrumentation. Therefore it needs optimized solution of these components design with accurate estimation of its optical performance. We are developing model of planetary signal detection through ray-tracing related beam propagation. Sun-like G-star with 695,500km in radius is a light source that emitting rays towards a planet and an instrument model. Earth-like planet with 6,400km in radius is composed with atmosphere, land, and ocean optical scattering model. The star and Earthlike planet are located 10-parsec away from hypothetic instrument model that has 6.5-meter diameter and F/20 telescope with spiders and Lyot coronagraph. Total 100,000,000 rays per spectral unit are emitted inside of the star surface and traced to directly instrument aperture or reflected and scattered through earth-like planetary model. The rays from emission to instrument aperture through star and planet model are traced by geometric optics condition. Then the rays passing through aperture in telescope model are traced with 8 additional para-basal rays that calculate beam propagation in order to wave optics properties. The model allows for simultaneous evaluations of the beam propagated imaging and radiometric performances for planetary signal detection with some cases of simulation. This simulation results would evaluate valuable information improving estimates space optical instrument in all phases of a space mission.

10400-78, Session PWed

The automated data processing architecture for the GPI Exoplanet Survey

Jason J. Wang, Univ. of California, Berkeley (United States); Marshall D. Perrin, Space Telescope Science Institute (United States); Dmitry Savransky, Cornell Univ. (United States); Pauline Arriaga, Univ. of California, Los Angeles (United States); Jeffrey K. Chilcote, Univ. of Toronto (Canada); Robert J. De Rosa, Univ. of California, Berkeley (United States); Maxwell A. Millar-Blanchaer, Jet Propulsion Lab. (United States); Jacob Shapiro, Cornell Univ. (United States); Julien Rameau, Univ. de Montréal (Canada); Schuyler G. Wolff, Johns Hopkins Univ. (United States) and Space Telescope Science Institute (United States); James R. Graham, Univ. of California, Berkeley (United States); Bruce A. Macintosh, Stanford Univ. (United States)

The Gemini Planet Imager Exoplanet Survey (GPIES) is a multi-year survey of 600 stars to discover and characterize young Jovian exoplanets and their planet-forming environments. We have developed an automated data architecture to uniformly process and index all data related to the survey. A back-end MySQL database indexes all files, which are synced to the cloud, and a front-end web server allows for easy browsing of all files associated with GPIES. An automated and flexible data processing framework which we term the GPIES Data Cruncher combines multiple data reduction pipelines together to intelligently process all spectroscopic, polarimetric, and calibration data taken with GPIES. With no human intervention, fully

reduced and calibrated data products are available in real-time less than an hour after the data is taken to expedite follow-up on potential objects of interest. All data of interest can be queried and reprocessed on a supercomputer as new algorithmic improvements are made to our data reduction pipelines. By uniformly processing all data with the most-updated data reduction techniques, we reduce our own workload, optimize our sensitivity to exoplanets, and also maintain a homogenously reduced dataset to study planet occurrence and instrument performance.

10400-79, Session PWed

Improving exoplanet sensitivity of the GPI Exoplanet Survey with a forward model matched filter

Jean-Baptiste Ruffio, Bruce A. Macintosh, Stanford Univ. (United States); Jason J. Wang, Univ. of California, Berkeley (United States); Laurent Pueyo, Space Telescope Science Institute (United States); Eric L. Nielsen, Stanford Univ. (United States); Robert J. De Rosa, Univ. of California, Berkeley (United States); Mark S. Marley, NASA Ames Research Ctr. (United States)

We developed a new matched filter based algorithm to detect point sources candidates for direct imaging of exoplanets. A forward model of the planet point spread function (PSF) is used as the matched filter template to account for distortions of the PSF of the planet due to the Karhunen-Loève Image Processing (KLIP) algorithm for stellar PSF subtraction. The new algorithm is optimized with respect to aggressiveness of KLIP and for exoplanet spectra by maximizing the Signal to Noise Ratio (SNR) of injected fake planet. We show that only two spectral templates are necessary to recover any young Jovian exoplanets with limited signal loss. We developed a complete pipeline for fully automated detection of point source candidates and the calculation of Receiver Operating Characteristic (ROC) curves, contrast curves and completeness contours. We uniformly processed more than 300 datasets from the Gemini Planet Imager Exoplanet Survey (GPIES) allowing for an unprecedented comparison of different detection algorithms with respect to both planet completeness and false positive rates.

To conclude, we show that the forward model matched filter allows the detection of 50% fainter objects in median compared to a conventional cross-correlation with a Gaussian PSF template at constant false positive rate.

10400-80, Session PWed

Fundamental limits to high-contrast wavefront control

Laurent Pueyo, Space Telescope Science Institute (United States)

In this paper we discuss fundamental limits associated with wavefront control with deformable mirrors in high contrast coronagraph. We start with an analytical prescription of wavefront errors, along with their wavelength dependence, and propagate them through coronagraph models. We then consider a few wavefront control architectures, number of deformable mirrors and their placement in the optical train of the instrument, and algorithms that can be used to cancel the starlight scattered by these wavefront errors over a finite bandpass. For each configuration we derive the residual contrast as a function of bandwidth and of the properties of the incoming wavefront. All errors, up to a finite spatial frequency set by the number of actuator on the deformable mirror, can be in principle perfectly cancelled under monochromatic light. However we show here that there exists modes of the wavefront that are uncorrectable under broadband light. We then carry out numerical simulations that illustrate these properties. This result has consequences when setting the wavefront requirements, along with the wavefront control architecture of future high contrast instrument both from the ground and from space. In particular we show that these limits can severely affect the effective Outer Working Angle that can be achieved by a given coronagraph instrument.

10400-81, Session PWed

Identification of the focal plane wavefront control system using E-M algorithm

He Sun, N. Jeremy Kasdin, Robert Vanderbei, Princeton Univ. (United States)

In a typical focal plane wavefront control (FPWC) system, such as the adaptive optics system of NASA WFIRST mission, all the efficient controllers and estimators in use are model-based. As a result, the modeling accuracy of the system influences the performance of the control and estimation. Currently, a linear state space model is used and calculated based on lab measurements using Fourier optics. Although the physical model is clearly defined, the calculated model is usually biased due to the incorrect distance measurements, imperfect diagnoses of the optical aberrations, and our lack of knowledge of the deformable mirrors (actuator gains and influence functions). In this paper, we present a new approach for measuring/estimating the linear state space model of a FPWC system using the expectation-maximization (E-M) algorithm. Simulation and lab results in the Princeton High Contrast Imaging Lab (HCIL) show that the E-M algorithm can well handle both the amplitude and phase errors and accurately recover the system. Using the recovered state space model, the controller creates dark holes with better contrast in the image plane and only needs around one-third the number of iterations compared to the experimental results using a physical model.

10400-82, Session PWed

A fiber injection unit for the Keck Planet Imager and Characterizer (KPIC)

Jacques-Robert Delorme, California Institute of Technology (United States); Dimitri Mawet, California Institute of Technology (United States) and Jet Propulsion Lab. (United States); James K. Wallace, Jet Propulsion Lab. (United States); Peter L. Wizinowich, W. M. Keck Observatory (United States); Garreth Ruane, Nikita S. Klimovich, Ji Wang, California Institute of Technology (United States)

Coupling a high-resolution spectrograph to a high-contrast imaging instrument is the next big step in the direct characterization of exoplanet atmospheres. In this scheme, the high-contrast imaging system serves as a spatial filter to separate the light from the star and the planet and the high-resolution spectrograph serves as spectral filter, which differentiates between features in the stellar and planetary spectra.

The Keck Planet Imager and Characterizer (KPIC) located downstream of the current Keck AO system will contain a fiber injection unit (FIU) capable of combing the high-contrast imaging system of KPIC with the current Keck high resolution infrared spectrograph (NIRSPEC). Thermal emission from young giant planets will be injected into a single mode fiber linked to NIRSPEC thereby allowing spectral characterization of exoplanet atmospheres. Moreover, the spectral resolution of NIRSPEC is high enough to enable spin measurements and Doppler imaging of atmospheric weather phenomenon.

Currently under development, the FIU design will be completed by the end Spring 2017. The module will then be integrated and tested at Caltech before being transferred to Keck in September 2017. During this presentation, I will present the design of the fiber injection unit, its science applications, and the expected results.

10400-83, Session PWed

Keck Institute for Space Studies. Report on exoplanet imaging and characterization: coherent differential imaging and signal detection statistics

Dimitri Mawet, California Institute of Technology (United States); Gautam Vasisht, Jet Propulsion Lab. (United States); Michael P. Fitzgerald, Univ. of California, Los Angeles (United States)

Here we report on the study recently held at the Keck Institute of Space Studies on the subject of Exoplanet Imaging and Characterization: Coherent Differential Imaging and Signal Detection Statistics. Direct imaging of a planet around another star is exceedingly challenging. For even the closest stars observed with the largest ground-based telescopes, the angular separation between star and planet will be near the classical diffraction limit. Moreover, a typical star will be about a billion times brighter than the planet to be imaged, a challenge even for the most stable telescope in space. The planetary image is also buried in "speckle noise," which is the result of uncorrected wavefront errors that propagate through the atmosphere and even the most accurately polished optical system. This speckle noise has complex properties which are different from planetary signals. While algorithms now exist that exploit some differences between the signal and noise characteristics, there has been little effort to address the full problem in a rigorous and comprehensive way. Our focus on speckle discrimination and control is motivated by key scientific measurements of exoplanetary systems:

Pure detection: Is there a planet present in the image(s)?

Astrometry: Where precisely is the planet located?

Photometry: How bright is the planet, and does its brightness vary with time?

Estimation of orbital parameters: How does it move relative to other bodies in the system?

Spectrometry: What are the spectral characteristics of the light from the planet?

Detection of life: Does the spectrum contain components consistent with living organisms?

Given the advent of high-precision focal plane wavefront control and low-noise fast-frame-rate detectors as well as the ongoing development of new facilities for exoplanet study, our KISS workshop sought to address several questions related to the development of statistically grounded strategies for detecting faint signals in the presence of both coherent and incoherent backgrounds:

What are the fundamental limits to focal-plane wavefront sensing and coherent differential imaging?

How is modulation best used in source-speckle discrimination and in speckle control?

How do ground-based focal-plane wavefront sensing and control differ from the space-based case?

What is the potential impact of new post-processing techniques, and rigorous statistical analyses on the next-generation instruments for extremely large ground- and space-based telescopes?

10400-42, Session 9

Modeling and performance predictions for the Princeton Starshade Testbed

Anthony D. Harness, N. Jeremy Kasdin, Robert J. Vanderbei, Yunjong Kim, Princeton Univ. (United States); Philip Dumont, Stuart B. Shaklan, Jet Propulsion Lab. (United States)

Starshades are a leading technology to enable the direct detection and spectroscopic characterization of Earth-like exoplanets. Two key aspects to advancing starshade technology are the demonstration of starlight suppression to the level required for flight and validation of optical models at this high level of suppression. These technologies are addressed in current efforts underway at the Princeton Starshade Testbed. We report on results from modeling the performance of the Princeton Starshade Testbed to help achieve the milestone 10-9 suppression. We use our optical model to examine the effects that errors in the occulting mask shape and external environmental factors have on the limiting suppression. We look at deviations from the ideal occulter shape such as over-etching during the lithography process, edge roughness of the mask, and random defects introduced during manufacturing. We also look at the effects of dust and wavefront errors in the open-to-atmosphere testbed. These results are used to set fabrication requirements on the starshade and constraints on the testbed environment. We use detailed measurements of the manufactured occulting mask to converge towards agreement between our modeled performance predictions and the suppression measured in the testbed, thereby building confidence in the validity of our optical models. We conclude with a discussion of the advantages and practicalities of scaling to a larger testbed to further advance the optical aspect of starshade technology.

10400-43, Session 9

Optical demonstration of a starshade at flight Fresnel numbers in the laboratory

Yunjong Kim, Anthony D. Harness, Princeton Univ. (United States); Dan Sirbu, NASA Ames Research Ctr. (United States); Mia Hu, Michael B. Galvin, N. Jeremy Kasdin, Robert J. Vanderbei, Princeton Univ. (United States); Stuart B. Shaklan, Jet Propulsion Lab. (United States)

A major science goal of exoplanet exploration is the direct detection and spectral characterization of Earth-like planets. The main challenge with the direct observation of Earth-like extra planets is that these planets are ten billion times fainter than the parent stars and the angular separation between the parent stars and the planets are less than a hundred milliarcseconds.

One of the main candidates for creating high-contrast for future Earth-like planet detection is a sharshade. The starshade is a spacecraft flown along the line-of-sight of a space telescope to suppress starlight and enable high-contrast direct imaging of exoplanets. However, optical testing of a full-scale starshade on the ground is impossible because of the long separations. Therefore, laboratory verification of starshade designs is necessary to validate the optical models used to design and predict starshade performance.

At Princeton, we have designed and built a testbed that allows verification of a scaled starshade at a flight-like Fresnel number whose suppressed shadow is mathematically identical to that of a space starshade. The goal of this experiment is to demonstrate a pupil plane suppression of better than 1e-9 with a corresponding image plane contrast of better than 1e-11. The starshade testbed uses a 77.2 m optical propagation distance to realize the flight Fresnel number of 14.5. Based on the first-light result we have added a gap at the inner tip region of the scaled starshade to minimize the effect of diffraction.

Here, we present lab result of the revised sample design operating at a flight Fresnel number. We compare the experimental results with simulations that predict the ultimate contrast performance.

10400-44, Session 9

Precise starshade stationkeeping and pointing with a Zernike wavefront sensor

Michael Bottom, Carl Seubert, Shannon K. G. Zareh, Stefan R. Martin, Eric J. Cady, Stuart B. Shaklan, Jet Propulsion Lab. (United States)

Starshades, large occulters positioned tens of thousands of kilometers in front of space telescopes, offer one of the few paths to imaging and characterization of Earth-like extrasolar planets. However, for the starshade to generate a sufficiently dark shadow on the telescope, the two must be coaligned to just 1 meter laterally at these large separations. The principal challenge to achieving this level of control is in determining the position of the starshade with respect to the space telescope. In this paper, we present numerical simulations and laboratory results demonstrating that a Zernike wavefront sensor coupled to a WFIRST-type telescope is able to deliver the stationkeeping precision required. The sensor can determine the starshade lateral position to centimeter level in seconds of open shutter time for stars brighter than eighth magnitude, with a capture range of ~10 meters. We discuss the potential for fast (ms) tip/tilt pointing control at the milli-arcsecond level by illuminating the sensor with a laser mounted on the starshade. Finally, we present early laboratory results validating the main components of the numerical simulations.

10400-45, Session 9

Starshade mechanical design for the Habitable Exoplanet Imaging Mission (HabEx)

Manan Arya, Jet Propulsion Lab. (United States); Steve Warwick, Northrop Grumman Aerospace Systems (United States); David Webb, P. D. Lisman, Stuart B. Shaklan, S. C. Bradford, John Steeves, Evan Hilgemann, Jet Propulsion Lab. (United States); Brian Trease, The Univ. of Toledo (United States); Mark Thomson, Northrop Grumman Aerospace Systems (United States); Neal Beidleman, Gregg Freebury, TENDEG, LLC (United States)

An external occulter for starlight suppression -- a starshade -- flying in formation with the Habitable Exoplanet Imaging Mission (HabEx) space telescope could enable the direct imaging and spectrographic characterization of Earth-like exoplanets in the habitable zone. This starshade is flown between the telescope and the star, and blocks stellar light while allowing the reflected planetary light through. This paper presents two mechanical architectures for this occulter, which must stow in a ~5 m diameter launch fairing and then deploy to a ~60-80 m diameter structure. The optical performance of the starshade requires that the edge profile is accurate and stable. The stowage and deployment of the starshade to meet these requirements present unique challenges that are addressed in these proposed architectures. The first mechanical architecture consists of a number of petals attached to a deployable perimeter truss, which is connected to central hub using tensioned spokes. The petals are furled around the stowed perimeter truss for launch. The second design uses telescoping booms to drive out each of the petals. The petal edges are stiff machined shapes with hinges between segments. These architectures demonstrate that there are identified mechanical design solutions that support an 80 m-class starshade for flight as part of the HabEx mission.

10400-46, Session 9

Prospects for exoplanet imaging in multi-star systems with starshades

Dan Sirbu, Ruslan Belikov, NASA Ames Research Ctr. (United States)

The main technical challenge associated with direct imaging of exoplanets is the control of diffracted and scattered light from the host star so that a dim planetary companion can be imaged at small angular separations and at high contrast ratios. Upcoming space missions including WFIRST, HabEx, and LUVOIR are currently exploring the usage of both internal coronagraphs and starshades to enable direct imaging of exoplanets. Multi-star systems pose additional challenges for both types of starlight suppression systems due to the combined off-axis star's diffraction and aberration leakage into the region of interest. As a result, many multi-star systems are considered unsuitable for direct imaging and not included in direct imaging survey target lists, even though the majority of (non-Mdwarf) stars belong to multi-star systems.

Here, we explore the capabilities of a starshade mission to directly image multi-star systems. A basic option is for additional starshades to block the off-axis stars. A more interesting option takes the form of operating a starshade in conjunction with internal starlight suppression. Two scenarios are considered. First, even without a coronagraph, a recent multi-star wavefront control (MSWC) technique can remove the off-axis star's leakage to enable a region of high-contrast around the on-axis star blocked by the starshade. Second, the coronagraph instrument blocking the on-axis star, with the starshade blocking off-axis starlight. We present simulation results of such starshade case studies to enable multi-star system imaging.

10400-47, Session 10

Gaia and exoplanets: a revolution in the making *(Invited Paper)*

Alessandro Sozzetti, INAF - Osservatorio Astrofisico di Torino (Italy)

The Gaia global astrometry mission is now headed towards the end of the third year of routine science operations. With the publication of the first data release in September 2016, it has begun to fulfil its promise for revolutionary science in countless aspects of Galactic astronomy and astrophysics. I will briefly review the Gaia mission status of operations and the scenario for the upcoming intermediate data releases, focusing on important lessons learned. I will then illustrate the Gaia exoplanet science case, and discuss how the field will be revolutionized by the power of micro-arcsecond (?as) astrometry that is about to be unleashed. I will conclude by touching upon future developments in the field of ultra-high precision astrometry that hold promise for much improved understanding of exoplanetary systems, particularly when seen in combination with other indirect and direct detection and characterization techniques.

10400-48, Session 10

The exoplanet program of the microarcsecond astrometric observatory Theia

Lucas Labadie, Univ. zu Köln (Germany); Fabien Malbet, Institut de Planétologie et d'Astrophysique de Grenoble (France); Alain Léger, Institut d'Astrophysique Spatiale (France); Céline Boehm, Durham Univ. (United Kingdom); Antoine Crouzier, Institut de Planétologie et d'Astrophysique de Grenoble (France); Alberto Krone-Martins, Univ. de Lisboa (Portugal)

The Theia mission, as a natural successor to Gaia, will be the first extremely-high-precision astrometric surveyor that may emerge from the last ESA M5 call in October 2016. A major objective of Theia in the context of this conference is the detection by astrometry of Earths and Super-Earths exoplanets in the habitable zone of nearby A to M stars. This can be done by astrometry from space if a motion of <1-microarcesec can be recorded (0.3 microarcsec for an Earth/Sun system at 10 pc). Such an accuracy can be reached by Theia in the form of an 0.8-m telescope with 0.5° FOV in orbit at L2 for 3,5 years and providing repeated differential astrometric measurements between the science target and background reference stars. The exoplanet program will use circa 10% of the mission lifetime and will be able to survey 63 nearby stars with a ~0.6 microarssec astrometric floor to eventually detect planets down to 0.2 M_earth over circa 50 visits. In order to measure a centroid position on the CCD with an accuracy of 1e-5 pixels, Theia's high-precision measurement relies on an on-board interferometric laser metrology unit to calibrate out the pixel's offset to the nominal position, as well as the inter- and intra-pixel quantum efficiency.

The preliminary Theia mission assessment allowed us to identify a safe and robust mission architecture that demonstrates the mission feasibility within the Soyuz ST launch envelope and a small M-class mission cost cap. We present here these features and the corresponding exoplanet program.

10400-49, Session 10

Results of the astrometry and direct imaging testbed for exoplanet detection

Eduardo A. Bendek, Ruslan Belikov, Eugene A. Pluzhnik, NASA Ames Research Ctr. (United States); Emily Finan, The Univ. of Arizona (United States)

Measuring masses of long-period planets around F, G, K or brighter stars is necessary to characterize exoplanets and assess their habitability. Imaging stellar astrometry offers a unique opportunity to solve radial velocity system inclination ambiguity and determine exoplanet masses.

The main limiting factor in sparse-field astrometry, besides photon noise, is the non-systematic dynamic distortions that arise from perturbations in the optical train. Even space optics suffers from dynamic distortions in the optical system at the sub-µas level. To overcome this limitation we propose to develop to use a diffractive pupil that uses an array of dots on the primary mirror creating polychromatic diffraction spikes in the focal plane, which are used to calibrate the distortions in the optical system. Combining this technology with a high-performance coronagraph allows measuring orbit and mass of planetary systems, faster and more accurately than using each technique separately.

In this paper, we will review the system architecture, milestones, and performance of the simultaneous astrometry and high-contrast imaging laboratory built at NASA Ames Research Center as part of a TDEM program. We will also discuss prospective technologies to enable an active diffractive pupil that would work on demand avoiding contaminating active the telescope field of view with diffracted light when precision astrometry is not required.

10400-50, Session 11

New technologies for nulling interferometry: laboratory demonstration of integrated optics beam combiners in the L and M bands

Lucas Labadie, Univ. zu Köln (Germany); Stefano Minardi, Friedrich-Schiller-Univ. Jena (Germany); Jan Tepper, Univ. zu Köln (Germany); Romina Diener, Friedrich-Schiller-Univ. Jena (Germany); Robert R. Thomson, Heriot-Watt Univ. (United Kingdom); Jörg-Uwe Pott, Max-Planck-Institut für Astronomie (Germany); Stefan Nolte, Friedrich-Schiller-Univ. Jena (Germany)

In the era of large telescopes and RV/Transit planetary missions, nulling interferometry remains a competitive technique for the characterization of Earths and Super-earths around Sun analogs in the mid-IR (Léger 2015, ApJ 808, 194). This is a spectral range where a number of bio-signatures can be accessed from space. One challenge of nulling is to benefit from well-established and qualified infrared fibers and integrated optics capable of mitigating the instrumental constraints on the beam combination and wavefront filtering to reach high extinction ratios. Such photonics devices have reached high maturity in the near-IR range as in the case of the integrated optics (IO) beam combiner of GRAVITY at the VLTI, leading to unprecedented interferometric accuracy.

Driven by the need of next-generation interferometers, we expand the photonic approach towards longer wavelengths and develop IO combiners based on the ultrafast laser writing technique. We developed single-mode, low-loss evanescent couplers in gallium lanthanum sulfide with a 50/50 splitting behavior around 3.4 µm and characterized the intrinsic chromaticity by FTS. High monochromatic and broadband contrasts are measured with unpolarized light at 3.39µm (>98%), over the L band (>95%), and over the M Band (4.5-4.8µm) (>95%). Our analysis of the interferometric visibilities and phase shows a small differential birefringence in the component and negligible differential dispersion. This results points out the promising properties of mid-infrared laser writing integrated optics devices to serve as high quality beam combiners. The extension to a four-aperture architecture appears plausible, with care to be taken about the impact of the design on the total throughput.

10400-51, Session 11

Segmented Aperture Interferometric Nulling Testbed (SAINT) II: component systems update

Brian A. Hicks, Univ. of Maryland (United States) and NASA Goddard Space Flight Ctr. (United States); Matthew R. Bolcar, NASA Goddard Space Flight Ctr. (United States); Michael A. Helmbrecht, Iris AO, Inc. (United States); Peter Petrone III, Sigma Space Corp. (United States) and NASA Goddard Space Flight Ctr. (United States); Jeffrey A. Bolognese, Mark Clampin, NASA Goddard Space Flight Ctr. (United States); James A. Corsetti, Univ. of Rochester (United States) and NASA Goddard Space Flight Ctr. (United States); Andrew Eberhardt, Univ. of Washington (United States); Corina Koca, NASA Goddard Space Flight Ctr. (United States); Andrew M. Lea, Stinger Ghaffarian Technologies (United States) and NASA Goddard Space Flight Ctr. (United States); Ron Shiri, Neil T. Zimmerman, NASA Goddard Space Flight Ctr. (United States)

This work presents updates to the coronagraph and telescope components of the Segmented Aperture Interferometric Nulling Testbed (SAINT). The project pairs an actively-controlled macro-scale segmented mirror with the Visible Nulling Coronagraph (VNC) towards demonstrating capabilities for the future space observatories needed to directly detect and characterize a significant sample of Earth-sized worlds around nearby stars in the quest for identifying those which may be habitable and possibly harbor life. Efforts to improve the VNC wavefront control optics and mechanisms towards repeating narrowband results are described. A narrative is provided for the design of new optical components aimed at enabling broadband performance. Initial work with the hardware and software interface for controlling the segmented telescope mirror is also presented.

10400-59, Session PWed

Phase-shifting coronagraph

François B. Hénault, Alexis Carlotti, Christophe Verinaud, Institut de Planétologie et d'Astrophysique de Grenoble (France)

With the recent commissioning of ground instruments and future space observatories, coronagraphy should become the most efficient the most efficient tool for identifying and characterizing extra-solar planets in the forthcoming years. Coronagraphic instruments are divided into sub-families such as Phase-mask coronagraphs spreading starlight outside the diameter of a Lyot stop. In this communication is investigated the capability of a PMC acting as a phase-shifting wavefront sensor. We propose an original design where phase-shifts are introduced in an image plane, and pupil images are acquired for wavefront sensing in presence of the coronagraphic mask. Numerical simulations allow for better understanding of the performance of the system. They demonstrate that the phase-shifting process is compatible with the most popular phase masks currently employed

10400-53, Session 12

ExEP yield modeling tool and validation test results

Rhonda M. Morgan, Michael Turmon, Jet Propulsion Lab. (United States); Dmitry Savransky, Christian Delacroix, Daniel Garrett, Cornell Univ. (United States); Patrick Lowrance, Xiang Cate Liu, California Institute of Technology (United States); Paul Nunez, Jet Propulsion Lab. (United States)

EXOSIMS is a modular, open-source simulation tool for parametric modeling of the detection yield and characterization of exoplanets. EXOSIMS has been adopted by the Exoplanet Exploration Program's Standard Definition and Evaluation Team (ExSDET) as a common yardstick for comparison of various exoplanet mission concept studies. To ensure trustworthiness of the tool, we developed a validation test plan that leverages the python unit-test framework, utilizes integration tests, and performs end-to-end cross-validation with other yield tools. Here we present the test results, with the physics-based tests such as photon counts and integration times treated in detail and the functional tests treated summarily.

The test case utilized a 4m unobscured telescope with an idealized coronagraph and exoplanets from the IPAC RV exoplanet catalog. The known RV planets were set at quadrature to allowed for deterministic validation of the calculation of physical parameters, such as photon counts and integration time. The observing keepout region was tested by generating a video of the targets in the keepout zone over a year; though the keepout integration test required the interpretation of a user, the test revealed several important errors in the L2 HALO orbit and the definition of keepout applied to other system bodies. The validation testing of EXOSIMS was performed iteratively with the Cornell developers of EXOSIMS and resulted in a more robust, stable, and trustworthy tool that the exoplanet community can use for simulating exoplanet direct detection missions from probe class to WFIRST to large mission concept such as HabEx and LUVOIR.

10400-54, Session 12

Multi-mission modeling for space-based exoplanet imagers

Dmitry Savransky, Christian Delacroix, Daniel Garrett, Cornell Univ. (United States)

In addition to the Wide-Field Infrared Survey Telescope Coronagraphic Imager (WFIRST CGI), which is currently scheduled for launch in the mid 2020s, there is currently an extensive, ongoing design effort for next-generation, space-based, exoplanet imaging instrumentation. This work involves mission concepts such as the Large UV/Optical/Infrared Surveyor (LUVOIR), the Habitable Exoplanet Imaging Misson (HabEx), and a starshade rendezvous mission for WFIRST, among others. While each of these efforts includes detailed mission analysis targeted at the specifics of each design, there is also interest in being able to analyze all such concepts in a unified way (to the extent that this is possible) and to draw specific comparisons between projected concept capabilities. Here, we discuss and compare two fundamental approaches to mission analysis---full mission simulation and depth of search analysis---in the specific context of simulating and comparing multiple different mission concept. We present results of mission analysis for various concepts at varying stages of definition and discuss useful metrics for cross-mission comparison, as well as strategies for evaluating these metrics.

10400-55, Session 12

Report on EXOPAG study analysis group 19: exoplanet imaging signal detection theory and rigorous contrast metrics

Dimitri Mawet, Rebecca Jensen-Clem, California Institute of Technology (United States)

As planning for the next generation of high contrast imaging instruments (e.g. WFIRST, HabEx, and LUVOIR, TMT-PFI, EELT-EPICS) matures, and second-generation ground-based extreme adaptive optics facilities (e.g. VLT-SPHERE, Gemini-GPI) are halfway through their large main surveys, it is imperative that the performance of different designs, post-processing routines, observing strategies, and survey results be compared in a consistent, statistically robust framework. SAG19, exoplanet imaging signal detection theory and rigorous contrast metrics, is overarching to all direct imaging instrument, strategies, and methods. The scope of SAG19 is:

1- To go back to the basics of Bayesian Signal Detection Theory (SDT).

2- To rebuild a solid set of usual definitions used for or in lieu of "contrast" in different contexts, such as astrophysical contrast or ground truth, instrumental contrast used for coronagraph/instrument designs, and the measured on-sky data-driven contrast.

3- To identify what we can learn and apply from communities outside our field (e.g. medical imaging). A good example is the widespread use of receiver operating characteristic curve (ROC) and area under the curve (AUC).

4- To define precise contrast computation and ROC curve computation recipes, a new "industry standard". The goal is to be able to compare results from surveys, instrument and/or telescope designs on a level-playing field.

5- To identify how the new metrics and recipes can be used to define confidence levels for detection (H1) and subsequently error bars for photometric, spectroscopic, astrometric characterization.

6- To perform a community data challenge before and after applying our proposed set of standardized SDT rules and recipes, and apply lessons learned.

10400-56, Session 12

Quantifying the impact of small statistics at small inner working angles

Stephen T. Bryson, Ruslan Belikov, NASA Ames Research Ctr. (United States)

The coronagraphic detection of exoplanets in the habitable zone requires the ability to detect exoplanets with small angular separation from their host star. Mawet et al. (ApJ 792, 2, 2014) pointed out that at such small inner working angles, small number statistics can have a significant impact on the delectability of exoplanets. We quantify the impact of small statistics by simulating the delectability of a standard set of exoplanets at small working angles. We describe a general method to estimate the impact on contrast curves as a function of inner working angle compared with the standard assumption of Gaussian noise after post-processing. To provide a specific example, we focus on the PIAACMC coronagraph designed for WFIRST, which features high throughput at small inner working angle. We find that for inner working angles as small as 1 lambda/D and a detection threshold of 5 sigma, 43% of the standard exoplanet test population is still detected after accounting for the small statistics effect of Mawet et al. We discuss mitigation strategies to recover lost planets, emphasizing observation strategies. We find that when multiple observations are possible over time, lowering the detection threshold to 3 sigma allows the detection of 89% of the test planets at small inner working angle.

10400-57, Session 12

Planet signal extraction from direct imaging using common spatial pattern filtering

Jacob Shapiro, Nikhil Ranganathan, Dmitry Savransky, Cornell Univ. (United States); Jean-Baptiste Ruffio, Bruce A. Macintosh, Stanford Univ. (United States)

The principal difficulty with detecting planets via direct imaging is that the target signal is similar in magnitude, or fainter, than the and structure compared to noise sources in the image . To compensate for this, several methods exist to subtract the PSF of the host star and other confounding noise sources. One of the most effective methods is Karhunen-Loève Image Processing (KLIP). The core algorithm within KLIP is Principal Component Analysis, which is a member of a class of algorithms called Blind Source Separation (BSS).

We examine another BSS algorithm that may potentially also be used for PSF subtraction: Common Spatial Pattern Filtering. The underlying principles of this algorithm are discussed, as well as the processing steps needed to achieve PSF subtraction. CSP is examined both as a primary PSF subtraction technique, as well as in comparison with KLIP.

These algorithms have been used onare applied to data from the Gemini Planet Imager, analyzing images of ? Pic b. To build a reference library, both Angular Differential Imaging and Spectral Differential Imaging arewere used. To compare to KLIP, three major metrics are examined: computation time, resulting signal-to-noise ratio, and astrometric biases in different image regimes (ie.eg., speckle-dominated compared to Poisson-noise dominated). Preliminary results indicate that CSP can achieve similar results to KLIP when used as the primary method of PSF subtraction.

10401-2, Session 1

NEO deflection by laser ablation: experimental results

Jessie Su, Jonathan A. Madajian, Philip M. Lubin, Travis R. Brashears, Nicholas Rupert, Univ. of California, Santa Barbara (United States); Gary B. Hughes, California Polytechnic State Univ., San Luis Obispo (United States)

Asteroids impact Earth daily. Some, like the Chelyabinsk Meteor that exploded over Siberia in 2013, can cause massive disruption to human enterprise (~$33M in damages) and thousands of injuries. To mitigate this potentially disastrous threat, our group has posited a phased laser array which would be used to direct energy towards approaching asteroids or other dangerous near Earth objects (NEOs). The laser array would ablate the NEO's surface, inducing mass ejection, that would then cause a reactant thrust on the NEO in the opposite direction of the laser. To verify this concept in a laboratory environment, this work quantitatively measured the thrust induced on basalt and other asteroid regolith simulant by a 350W laser array. By placing the sample target on a torsion balance and measuring its angle of deflection under ablation, it is possible to calculate the induced thrust per unit watt. This angular change is measured with a secondary laser that reflects off of the torsion balance into an optical position sensor. By comparing this paper's experimental results with prior theoretical and computational work, we can surmise a theoretical relationship between NEO size and required laser power for future NEO deflection missions.

10401-3, Session 1

Deflection of inert objects in comet-like orbits by laser ablation

Qicheng Zhang, Philip M. Lubin, Univ. of California, Santa Barbara (United States); Gary B. Hughes, California Polytechnic State Univ., San Luis Obispo (United States)

Planetary defense strategies have traditionally focused on the impact threat posed by near-Earth asteroids (NEAs). Typical NEAs follow prograde orbits with low inclination, low eccentricity, and short orbital periods—properties conducive to early detection and subsequent interception by spacecraft years or even decades in advance of any potential impact. Interception strategies, however, are ineffective against most comets which follow highly eccentric and highly inclined orbits, and are, moreover, often discovered only a few months before their encounters with Earth. Volatiles such as water ice on or near the surface of comets sublimate and perturb the comet's trajectory when heated, even naturally by solar heating, making comets particularly well-suited for deflection by directed energy laser heating. This method involves one or more laser arrays on or near the Earth which target and heat the threatening comet, shifting its trajectory to prevent an impact. Many comets, however, have depleted their surface volatiles after repeated perihelion passages and consequently become dormant or even extinct—effectively asteroids in comet-like orbits. These "inert comets" experience little if any measurable orbital perturbation from solar heating and will be similarly unresponsive to comparable levels laser illumination. Deflecting such an object demands a much greater laser flux than needed for active comets—one sufficiently high to vaporize the silicate materials that presumably comprise its surface. Strategies to divert inert comets are analyzed for a range of hypothetical scenarios.

10401-4, Session 1

High-beam quality all-solid-state nanosecond Nd:YAG laser system of high-repetition frequency for space-debris detection

Zhongwei Fan, Academy of Opto-Electronics, CAS (China)

Space debris endangers many space activities, therefore target detection has become an essential aspect of defensive and offensive strategies toward space debris management. Laser detection has good directivity, strong anti-jamming active-detection, and the advantage of around-the-clock operation. The main difficulty with laser-based space debris detection lies in that there are relatively few echo photons to measure due to small cross section of debris and long distance. The most direct and effective means to improve the accuracy of space debris detection is by improving the laser performance via higher pulse frequency and energy.

In order to develop our nanosecond Nd:YAG laser of high-repetition frequency and high-beam quality for space debris detection, we have achieved many key technologies and manufacturing processes like: stabilized frequency of single-frequency pulse, large-diameter high-uniform side-pump amplification, stimulated Brillouin scattering (SBS) phase conjugation, high-power LD driving source, etc. The single longitudinal-mode, nanosecond-pulse of our single-frequency oscillator achieves stable output up to 8 hours without mode hopping (RMS<2%). Ninety percent of the large diameter (?15mm) side-pump amplifier realizes high-uniform pump amplification with the relevant PV less than 5%. The stimulated Brillouin scattering phase-conjugate mirror (SBS-PCM) achieves near-diffraction-limit beam quality control and high-fidelity pulse-width compression. And, our high-power power supply achieves a maximum peak power output up to 100 kW, with the current stability less than 1% and the output efficiency up to 88%.

Our high-repetition frequency and high-beam quality Nd:YAG all-solid-state nanosecond laser adopts master oscillation power amplification (MOPA) technical solution including mainly four parts: a single longitudinal-mode oscillator, a pre-amplifier unit, a phase-conjugate beam-control unit and a power-amplification unit. The single longitudinal-mode oscillator adopts a high-stability, single-longitudinal-mode Q-switched laser as the seed laser with output pulse of?J level. The pre-amplifier unit amplifies the laser pulse up to mJ level. The phase-conjugate beam-control unit carries out real-time correction of the optical distortion caused by heating effects during the energy pre-amplification process. In the power amplifier unit, a split-amplify-combine solution is adopted to reduce the working current of the amplifier and achieve higher gain-saturated amplification. The total optical-to-optical conversion efficiency is up to 53%. The single longitudinal-mode oscillator—operating at a 100 Hz repetition frequency and a single pulse injection energy of 9.25?J—produces an output energy of 3.36J. The output laser-beam diameter is 25mm, the pulse width is 7.096ns, the far field intensity is 1.71 times the diffraction limit, and the energy stability (RMS) is 1.3%.

10401-5, Session 1

Deep-space laser communication hardware driver

Jonathan A. Madajian, Nicholas Rupert, Victoria Rosborough, Univ. of California, Santa Barbara (United States); Steven Estrella, Freedom Photonics, LLC (United States); Philip M. Lubin, Jonathan Klamkin, Univ. of California, Santa Barbara (United States)

Deep space exploration will require laser communication systems optimized

for cost, size, weight, and power. To improve these parameters, our group is developing a photonic integrated circuit (PIC) based on indium phosphide for optical pulse position modulation (PPM). A field-programmable gate array (FPGA) was programmed to serve as a dedicated driver for the PIC. The FPGA is capable of generating 2-ary to 4096-ary PPM with a slot clock rate up to 700 MHz.

10401-6, Session 1

Near-field optical model for directed energy-propelled spacecrafts

Gary B. Hughes, California Polytechnic State Univ., San Luis Obispo (United States); Lauren R. F. Busby, Univ. of California, Santa Barbara (United States)

Wafer-scale spacecraft are envisioned as interstellar probes. The spacecraft includes a reflective sail, and propulsion is achieved by focusing a directed energy beam onto the sail. The beam is created by a large array of phase-locked lasers, e.g. on the ground or in Earth orbit. In order to simulate spacecraft acceleration with directed energy, a near field intensity model of the laser array is required. This paper describes a near-field light propagation model that can be used to calculate intensity patterns for the near-field diffraction of a phased array. The model consists of an analysis of both the radiative and non-radiative near field intensities. The Rayleigh-Sommerfeld approach is used to approximate intensity distributions for lengths close to and including the aperture. Scalar diffraction theory is also employed to estimate intensity distributions in the Fresnel Regime. Ideally, the optical model will be combined with a physical model of the spacecraft, to investigate sail designs and beam patterns that optimize stability of the spacecraft during the acceleration phase.

10401-7, Session 2

Switchable optical materials for space propulsion and attitude control *(Invited Paper)*

Jeremy N. Munday, Univ. of Maryland, College Park (United States)

Radiation pressure from the sun can exert a force on spacecrafts that can either be beneficial, in the case of solar sails, or harmful, in the case of satellites in predefined orbits. As photons are reflected off a surface, they impart a momentum that pushes the object. For a solar sail, this momentum provides the necessary thrust for propulsion without the need for propellant. However, attitude control is still performed by traditional means, for example reaction wheels or propellant ejection, which limits mission lifetime. Similarly, this radiation pressure can affect satellite orbits, and a mechanism is needed to adjust them as a result. Here we present our latest work on switchable reflectivity materials to actively control the radiation pressure exerted on a spacecraft to enable real-time attitude control and steering. The devices are constructed from a polymer dispersed liquid crystal (PDLC), which can be switched between a high transparency state and a high reflectivity state with the application of an applied bias. Measurements of the reflectivity over the solar spectrum show a significant change in the momentum transferred to the spacecraft (more than a factor of two), enabling propellant-less attitude control [1]. We will discuss our first generation proof-of-concept devices, preliminary space environment testing, and provide a future outlook for this technology.

[1] Dakang Ma, Joseph Murray and Jeremy N. Munday, "Controllable Propulsion by Light: Steering a Solar Sail via Tunable Radiation Pressure" Advanced Optical Materials (in press and on the cover) DOI: 10.1002/adom.201600668

10401-9, Session 2

Evolution of wafer-scale space systems for terrestrial and deep-space missions

Nicholas Rupert, Philip M. Lubin, Univ. of California, Santa Barbara (United States); Gary B. Hughes, California Polytechnic State Univ., San Luis Obispo (United States); Russell Woods, Univ. of California, Santa Barbara (United States); Peter Ateshian, Naval Postgraduate School (United States); Prashant Srinivasan, California Polytechnic State Univ., San Luis Obispo (United States); Jonathan A. Madajian, Travis R. Brashears, Alexander Cohen, Qicheng Zhang, Jessie Su, Lauren R. F. Busby, Univ. of California, Santa Barbara (United States)

Innovation and technological advance within various fields, including microelectronics, integrated photonics and wafer based nanofabrication, has paved the way for a new class of space systems. In order to take full advantage of novel propulsion systems currently under development, a complete re-evaluation of space systems of today is required. The objective is to design, develop, assemble and characterize the initial prototypes of these robotic platforms, with focus on leveraging continued advances in semiconductor and photonics based technologies to recognize and efficiently address complexities associated with long duration autonomous robotic space flight. As with any complex system, wafer scale spacecraft technology can be projected to follow a steady evolutionary path. Initial prototypes have been based off of commercially available components and conventional printed circuit board (PCB) technologies. These systems are now roughly the size of a US quarter (24.26 mm), and despite their small size, contain a 9-axis inertial measurement unit, CMOS imaging chip, advanced photonic elements, and multiple other sensor systems. As these technologies are pushed to their extreme limits a transition to partial and eventually full wafer scale integration will be necessary. At this stage inorganic nanostructures and other various nanotechnologies will be employed to further miniaturize the spacecraft. Eventually these craft will have the ability to be mass manufactured using pre-existing techniques developed by the semiconductor industry. This evolutionary structure will produce a low cost, feature rich spacecraft which can be mass manufactured and utilized for both terrestrial and deep space applications.

10401-10, Session 2

Ions irradiation on bi-layer coatings

Enrico Tessarolo, Alain Jody Corso, CNR-IFN Padova (Italy); Alessandro Martucci, Univ. degli Studi di Padova (Italy); Marco Angiola, Maria Guglielmina Pelizzo, CNR-IFN Padova (Italy)

Optical components performances can be affected by the space environment agents and in particular by ions irradiation. The effect on bi-layers coatings of different materials induced by alpha particles implantation is under investigation. The dependence of the profiles implantation by ion energy is studied by TRIM software simulations. The experiment conceived foresees that the ions energy during experimental irradiation is selected in order to superimpose the maximum of the peak profile with the interface plane. Different optical, structural and morphological analysis are used to study the damage induced, and in particular to investigate the inter-diffusion at the bi-layer interface.

10401-11, Session 2

Systematic investigation of the optical coatings damages induced in harsh space environment *(Invited Paper)*

Alain Jody Corso, Enrico Tessarolo, CNR-IFN Padova

(Italy); Alessandro Martucci, Univ. degli Studi di Padova (Italy); Marco Angiola, Maria Guglielmina Pelizzo, CNR-IFN Padova (Italy)

Optical coatings are among the instrumental sub-systems which can highly suffer the agents in space environments. In particular, as recently demonstrated, the accelerated ions and particles can potentially jeopardize the coatings optical performances, with a consequent degradation of the overall functionality of an instrument. Despite its importance, this issue is still poorly investigated. In fact, the fragmentary knowledge of the space environments and the low number of systematic ground testing experiments complicates the definition of clear procedures to investigate the behavior of the optical coatings in space.

A systematic approach devoted to identify a methodology for the validation of optical coatings under ions irradiation is presented. Monte Carlo simulations are used to evaluate the effects induced by different ion species and energies on both layers and multilayers of different materials, getting an accurate overview of the main criticalities. Such results are then used to plan representative irradiation experiments and the subsequent analysis procedures needed for a proper characterization of the exposed samples.

10401-12, Session 3

Restoration of image distorted by atmospheric turbulence achieved by optical phase conjugation *(Invited Paper)*

Pengda Hong, Yujie J. Ding, Lehigh Univ. (United States)

In this proceeding, we systematically review our recent research results on reconstructing image quality by second order nonlinear crystal composites. The broadband and polarization-insensitive optical phase conjugated beams are generated with pretty low power, and they are demonstrated to successfully real time remove distortion caused by dynamic atmospheric turbulence. The unique features are realized by idler pair or signal pair simultaneously generated from periodically-inverted KTiOPO4 (KTP) plates and they overcomes disadvantages reported in previous literature, such as polarization sensitivity to pump, high pump power and low response speed. In this article, we demonstrated some of our preliminary results of novel configuration for removing distortion. Furthermore, we summarize our research on reflection and transmission configurations of image recovery. Compared with transmission configuration, reflection configuration can be more practically utilized in field deployment. With necessary modifications and miniaturization of setup, it can be potentially incorporated in satellite for space exploration.

10401-13, Session 3

Characterizing phase noise in long optical fibers *(Invited Paper)*

Prashant Srinivasan, California Polytechnic State Univ., San Luis Obispo (United States); Peter Krogen, Massachusetts Institute of Technology (United States); Gary B. Hughes, California Polytechnic State Univ., San Luis Obispo (United States); Philip M. Lubin, Peter Meinhold, Jonathan A. Madajian, Qicheng Zhang, Alexander Cohen, Benton Miller, Daniel Brouwer, Travis R. Brashears, Lauren R. F. Busby, Nicholas Rupert, Univ. of California, Santa Barbara (United States)

Effective transfer of energy to a spacecraft via optical requires that the source be accurately directed at the satellite with sufficient resolution to contain the beam within the absorbing area of the satellite. This can be achieved by coherently combining laser sources which are distributed throughout a kilometer-scale array. However, coherent beam combination requires that each source be synchronized with sub-wavelength accuracy over the entire array. In this work we investigate the phase and polarization noise in fiber optic links ranging from 1-25 km as could be used to synchronize such an array.

This scheme uses a 1060 nm laser source in a Mach-Zehnder interferometer where two orthogonal polarization modes are used to perform I/Q quadrature detection of the phase variations in the interferometer arms. The detectors are sampled at 250 kHz and, for spooled fibers, phase excursions on the order of 20 krad over 100 s were observed.

10401-14, Session 3

Anti-resonant hollow core fiber for precision timing applications *(Invited Paper)*

Amy Van Newkirk, The Pennsylvania State Univ. (United States); J. Enrique Antonio Lopez, Rodrigo Amezcua Correa, Axel Schülzgen, CREOL, The College of Optics and Photonics, Univ. of Central Florida (United States); John Mazurowski, The Pennsylvania State Univ. (United States)

Many applications rely on the ultra-precise timing of optical signals through fiber, such as fiber interferometers, large telescope arrays, in phase arrayed antennae, optical metrology, and precision navigation and tracking. Environmental changes, specifically those caused by temperature fluctuations, lead to variations in the propagation delay of optical signals and thereby decrease the accuracy of the system's timing.

The cause of these variations in delay is the change in the glass properties of the optical fiber with temperature. Both the refractive index of the glass and the length of the fiber are dependent on the ambient temperature. Traditional optical fiber suffers from a delay sensitivity of 39 ps/km/K. We are reducing the temperature sensitivity of the fiber delay through the application of a novel design of optical fiber, Anti-Resonant Hollow Core Fiber. The major improvement in the thermal sensitivity of this fiber comes from the fact that the light is guided in an air core, with very little overlap into the glass structure. This drastically reduces the impact that the thermally sensitive glass properties have on the propagation time of the optical signal. Additionally, hollow core fiber is inherently radiation insensitive, due to the light guidance in air, making it suitable for space applications.

10401-15, Session 3

Thermal assessment of sunlight impinging on OSIRIS-REx OCAMS PolyCam, OTES, and IMU-sunshade MLI blankets in flight *(Invited Paper)*

Michael K. Choi, NASA Goddard Space Flight Ctr. (United States)

The NASA Origins, Spectral Interpretation, Resource Identification, Security, Regolith Explorer (OSIRIS-REx) spacecraft was successfully launched into orbit on September 8, 2016. It is traveling to a near-Earth asteroid (101955) Bennu, study it in detail, and bring back a pristine sample to Earth for scientific analyses. At the Outbound Cruise nominal spacecraft (S/C) attitude, with Sun on +X, sunlight is incident on the following components on the payload deck: a) the OCAMS PolyCam sunshade multilayer insulation (MLI) with black polytetrafluoroethylene (PTFE), b) a portion of the PolyCam optics support tube (MLI with germanium black Kapton (GBK)), c) a portion of the OTES sunshade (MLI with GBK), and d) the canted panel of S/C IMU-sunshade (MLI with GBK). The black PTFE is diffuse. The specularity of GBK is 69%. Solar irradiance varies with the solar distance, which is in the 0.773 AU to 1.387 AU range in the Outbound Cruise mission phase. Sunlight is reflected by the MLIs above to the other components on the payload deck. It illuminates the payload deck. All three OCAMS cameras experienced scattered light when they were powered on for checkout. It was successfully removed from images by median filter. The amount of solar reflection varies with the solar distance. If the OCAMS PolyCam sunshade

MLI coating is GBK, instead of black PTFE, the solar flux reflected by this MLI will be much larger. In addition, the temperatures of the MLIs above vary with the solar distance. As a result, the thermal radiation from the MLIs above to the other components within their views also varies with the solar distance. This paper presents a detailed thermal assessment on the solar impingement and thermal implications for Proximity Ops at the asteroid and Touch-and Go sample acquisition.

10401-16, Session 4

SCHOTT optical glass in space

Ralf Jedamzik, Uwe Petzold, SCHOTT AG (Germany)

Optical systems in space environment have to withstand harsh radiation. Radiation in space usually comes from three main sources: the Van Allen radiation belts (mainly electrons and protons); solar proton events and solar energetic particles (heavier ions); and galactic cosmic rays (gamma- or x-rays). Other heavy environmental effects include short wavelength radiation (UV) and extreme temperatures (cold and hot). Radiation can damage optical glasses and effect their optical properties. The most common effect is solarization, the decrease in transmittance caused by high-energy radiation. This effect can be observed for UV radiation and also for gamma or electron radiation. Optical glasses can be stabilized against many radiation effects. SCHOTT offers radiation resistant glasses that do not show solarization effects for gamma or electron radiation. But a review SCHOTT optical glasses used in space missions shows that not only radiation resistant glasses are used in the optical designs, but also standard optical glasses, due to their good stability against UV radiation. This presentation gives an overview of space missions using SCHOTT optical glass over the last decades.

10401-17, Session 4

Homogeneity of the coefficient of linear thermal expansion of ZERODUR(R): a review of a decade of evaluations

Ralf Jedamzik, Thomas Westerhoff, SCHOTT AG (Germany)

The coefficient of thermal expansion (CTE) and its spatial homogeneity from small to large formats is the most important property of ZERODUR®. Since more than a decade SCHOTT has documented the excellent CTE homogeneity. It started with reviews of past astronomical telescope projects like the VLT, Keck and GTC mirror blanks and continued with dedicated evaluations of the production.

In recent years, extensive CTE measurements on samples cut from randomly selected single ZERODUR® parts in meter size and formats of arbitrary shape, large production boules and even 4 m sized blanks have demonstrated the excellent CTE homogeneity in production.

The published homogeneity data shows single ppb/K peak to valley CTE variations on medium spatial scale of several cm down to small spatial scale of only a few mm mostly at the limit of the measurement reproducibility. This review paper summarizes the results also in respect to the increased CTE measurement accuracy over the last decade of ZERODUR® production.

10401-18, Session 4

ZERODUR 4-m blank surviving up to 20 g acceleration

Thomas Westerhoff, Thomas Werner, Thorsten Gehindy, SCHOTT AG (Germany)

The glass ceramic ZERODUR® developed as astronomical telescope mirror substrate material has been widely used in many telescopes due to its excellent small coefficient of thermal expansion. Many large and medium sized mirror substrate blanks have been delivered in the almost 50 years of ZERODUR® business so far. Packaging and transportation of mirror substrates of 4 to 8 m in diameter with a weight between 3 and 20 tons requires special attention and sophisticated skills to successful deliver the blanks to their destination at polishing shops all over the world. Typically, a combination of road and sea transport needs to be organized. The requirements on the transport container are depending on the transport route and may vary from destination to destination. In any case the container needs to be able to sufficiently support the multi ton ZERODUR® blank to avoid breaking under gravity. Additionally, the configuration needs to be able to absorb shocks happening during transport and loading between truck trailer and ship. For insurance reasons the transport container is always equipped with a GPS trackable shock recorder allowing to download the recorded accelerations on the container and the blank throughout the entire journey. This paper reports on the event of a 4 m class ZERODUR® blank exposed to shocks up to 20 g during transport. The event will be discussed in detail together with lessons learned to avoid such events for future transports. Additionally, the 20 g acceleration will be discussed in respect to the data on bending strength for ZERODUR ground surfaces reported in numerous papers by Peter Hartmann et.al. in the last couple of years.

10401-19, Session 4

Parametric criteria for optimal selection of materials for spaceborne mirrors

Tony B. Hull, The Univ. of New Mexico (United States); Stephanie Behar-Lafenetre, Thales Alenia Space (France); Dominic Doyle, European Space Research and Technology Ctr. (Netherlands); Ralf Jedamzik, Thomas Westerhoff, SCHOTT AG (Germany)

Four primary criteria for spaceborne mirrors are 1) optical surface finish, 2) formable to mass-efficient structures 3) stable under mission thermal and other stimuli., and 4) thermally compatible with metering structure materials. We parametrically look at heritage and evolving mirror materials, all meeting the first criteria, that may be considered for telescope mirrors in the architecture of space missions. Materials will be graphed as specific stiffness (E/?) as a function of transient resilience (Thermal Diffusivity/ Coefficient of Thermal Expansion). We will discuss figures of merit contours as expressed on this plot, and how these can be used to optimize the passive performance of an optical telescope assembly or reflective instrument.

10401-20, Session 4

Review of space radiation interaction with ZERODUR

Antoine Carré, Thomas Westerhoff, SCHOTT AG (Germany); Tony B. Hull, The Univ. of New Mexico (United States)

Materials for space missions need to be evaluated according their behavior when exposed to radiation in their intended orbit. The extremely low thermal expansion glass ceramic ZERODUR® has been and is still being successfully used as mirror substrates for a large number of space missions. Two of those are the outstanding missions Hubble Space Telescope (HST) and the X-Ray Telescope CHANDRA. ZERODUR® was used for the secondary mirror in HST and for the Wolter mirrors in CHANDRA without any reported degradation of the optical image quality during the lifetime of the missions. Improvements in CNC machining at SCHOTT allow to achieve extremely light weighted substrates incorporating very thin ribs and face sheets. This paper is reviewing data published on the interaction of space radiation with ZERODUR®. Additionally, the paper will propose experiments in order to improve and extend the existing database and the model predicting the long lifetime behavior of ZERODUR® under space radiation. Special focus will be given on the question how to design radiation experiments to be performed in a reasonable and economic accessible time frame providing data for a long lifetime prediction. The model to be derived out of the new

experiments needs to be able to predict ZERODUR behavior under space radiation with a better accuracy as well as being applicable to the extremely light weighted ZERODUR structures described in numerous papers by Tony Hull et al. in the last recent years.

10401-21, Session 5

Design and component test results of the LSST Camera L1-L2 lens assembly

Allison A. Barto, Ball Aerospace & Technologies Corp. (United States); Scott E. Winters, Lawrence Livermore National Lab. (United States); James H. Burge, College of Optical Sciences, The Univ. of Arizona (United States); Deborah Davies, Heather A. Doty, Ball Aerospace & Technologies Corp. (United States); John Richer, Peter Seyforth, Alliance Spacesystems, LLC (United States)

The Large Synoptic Survey Telescope (LSST) camera will be the largest camera ever constructed for astronomy. When light enters the camera it will first pass through the two large lenses of the L1-L2 Lens Assembly. This assembly consists of a 1.6 m spherical lens and a 1.2 m aspheric lens held in critical alignment by a carbon fiber composite assembly which is mounted to the camera structure by six adjustable struts which provide the mechanism to align the L1-L2 Assembly to the rest of the camera optical system. Final optical performance of this assembly is based upon lens figure, lens alignment, and alignment stability. With manufacture of the individual components of the L1-L2 Lens assembly and testing of the integrated composite structure complete, design, design drivers, and test results from lens testing and deflection testing of the structure over the range of on-mountain operational camera orientations will be presented.

The L1-L2 Assembly is being designed and built by Ball Aerospace, under contract to LLNS, with major contributions from Arizona Optical Systems (lenses) and Alliance Spacesystems (composite structure to support each lens), with the lens mount design based on heritage from the Kepler program. Design drivers for this system include mass, seismic loading, and extremely tight volume constraints that greatly influenced the lens mounting and structure design. The test results presented will include final pre-coating Transmitted Wavefront Error (TWE) testing of the individual lenses and deflection testing of the structure assembly integrated with mass simulators to test the alignment shifts of each lens to each other and to the camera as the telescope slews through operational orientations.

10401-22, Session 5

Advanced mirror technology development (AMTD): year five status

H. Philip Stahl, NASA Marshall Space Flight Ctr. (United States)

The Advanced Mirror Technology Development (AMTD) project is a multiyear effort initiated in Fiscal Year (FY) 2012, to mature toward the next Technology Readiness Level (TRL) critical technologies required to enable 4-m-or-larger monolithic or segmented ultraviolet, optical, and infrared (UVOIR) space telescope primary-mirror assemblies for general astrophysics and ultra-high-contrast observations of exoplanets. AMTD Phase 2 concluded in 2017 with the thermal characterization testing of a low-temperature fusion 1.5-meter diameter ULE mirror that is a 1/3rd scale model of a 4-meter mirror.

10401-23, Session 5

Lightweight ZERODUR: Validation of mirror performance and mirror modeling predictions

Tony B. Hull, The Univ. of New Mexico (United States); H. Phillip Stahl, NASA Marshall Space Flight Ctr. (United States); Thomas Westerhoff, SCHOTT AG (Germany); Martin J. Valente, Arizona Optical Systems, LLC (United States); Thomas Brooks, Ron Eng, NASA Marshall Space Flight Ctr. (United States); Ralf Jedamzik, SCHOTT AG (Germany)

Upcoming spaceborne missions, both moderate and large in scale, require extreme dimensional stability while relying both upon established lightweight mirror materials, and also upon accurate modeling methods to predict performance under varying boundary conditions. We describe tests, recently performed at NASA's XRCF chambers and laboratories in Huntsville Alabama, during which a 1.2m diameter, f/1.29 88% lightweighted SCHOTT lightweighted ZERODUR® mirror was tested for thermal stability under static loads in steps down to 230K. Test results are compared to model predictions, based upon recently published data on ZERODUR®. In addition to monitoring the mirror surface for thermal perturbations in XRCF Thermal Vacuum tests, static load gravity deformations have been measured and compared to model predictions. Also the Modal Response (dynamic disturbance) was measured and compared to model. We will discuss the fabrication approach and optomechanical design of the ZERODUR® mirror substrate by SCHOTT, its optical preparation for test by Arizona Optical Systems (AOS), and summarize the outcome of NASA's XRCF tests and model validations.

10401-24, Session 5

Development of the camera lens system for total solar eclipse observation

Jihun Kim, Seonghwan Choi, Ji-Hye Beck, Jongyeob Park, Su-Chan Bong, Bi-Ho Jang, Korea Astronomy and Space Science Institute (Korea, Republic of); Heesu Yang, Seoul National Univ. (Korea, Republic of); Jinho Kim, Green Optics Co., Ltd. (Korea, Republic of); Geon-Hee Kim, Korea Basic Science Institute (Korea, Republic of); Kyungsuk Cho, Sung-Joon Park, Korea Astronomy and Space Science Institute (Korea, Republic of)

Korea Astronomy and Space Science Institute (KASI) has been developing the Camera Lens System (CLS) for the Total Solar Eclipse (TSE) observation. In 2016 we have assembled a simple camera system including a camera lens, a polarizer, bandpass filters, and CCD to observe the solar corona during the Total Solar Eclipse in Indonesia. Even we could not obtain the satisfactory result in the observation due to poor environment, we obtained some lessons such as poor image quality due to ghost effect from the lens system. For 2017 TSE observation, we have studied and adapted the compact coronagraph design proposed by NASA. The compact coronagraph design dramatically reduces the volume and weight and can be used for TSE observation without an external occulter which blocks the solar disk. We are in developing another camera system using the compact coronagraph design to test and verify key components including bandpass filter, polarizer, and CCD, and it will be used for the Total Solar Eclipse (TSE) in 2017. We plan to adapt this design for a coronagraph mission in the future. In this report we introduce the progress and current status of the project and focus on optical engineering works including designing, analyzing, testing, and building for the TSE observation.

10401-25, Session 5

ZERODUR expanding capabilities and capacity for future spaceborne and ground-based telescopes

Thomas Westerhoff, Thomas Werner, SCHOTT AG (Germany)

The glass ceramic ZERODUR® is well known for its extremely low coefficient of thermal expansion making it one of the key materials for ultra-precision application such as IC and LCD Lithography, High-end Metrology, Aviation and space born or ground based Astronomy. The steady growth of demand for more precision in those application together with a growing number of precision systems and components is requesting the ability to on first hand increase precision in manufacturing while on second hand in parallel increase volume in production of ZERODUR® CNC machined products. This paper reports on the measures SCHOTT is realizing to feed the continuously increasing demand on high precision material and components. Next to a second melting tank additional capacity is going to be installed along the entire value stream of ZERODUR® production. Features of new CNC machining capabilities in the two and four meter class will be reported allowing to provide tighter tolerance on mirror surface figure together with reduced sub surface damage in order to accelerate the polishing time. Examples will be discussed as the 4 m class secondary and tertiary mirrors for the ESO E-ELT. The new equipment will enable SCHOTT to light weight 4 m class mirror substrates for future space optics demand.

10401-26, Session 6

Instantaneous phase measuring deflectometry for dynamic deformable mirror characterization

Isaac Trumper, Heejoo Choi, Dae Wook Kim, College of Optical Sciences, The Univ. of Arizona (United States)

We present an instantaneous phase measuring deflectometry (PMD) system in the context of measuring a continuous surface deformable mirror (DM). Deflectometry has a high dynamic range, enabling the full range of surfaces generated by the DM to be measured. The recent development of an instantaneous PMD system leverages the simple setup of the PMD system to measure dynamic objects with accuracy similar to an interferometer. The previous instantaneous PMD system was developed on an iPhone platform. As a natural extension of this work to precision metrology, we are now using specialized hardware to increase spatial resolution and improve measurement quality. To demonstrate the capabilities of this improved technology, we perform a linearity measurement of the actuator motion in a continuous surface DM, which is critical for closed loop control in adaptive optics applications. We measure the entire set of actuators across the DM as they traverse their full range of motion, thereby obtaining the influence function. Given the influence function of each actuator, the DM can produce specific Zernike terms on its surface. We then measure the linearity of the Zernike modes available in the DM software. By obtaining this relationship, we can more accurately generate surface profiles composed of Zernike terms. This ability is useful for other dynamic freeform metrology applications that utilize the DM as a null component.

10401-27, Session 6

JWST center of curvature test method and results

David M. Chaney, Ball Aerospace & Technologies Corp. (United States); Babak N. Saif, NASA Goddard Space Flight Ctr. (United States); Perry E. Greenfield, Kyle Van Gorkom, Keira J. Brooks, Warren Hack, Space Telescope Science Institute (United States); Marcel Bluth, Josh Bluth, SGT, Inc. (United States); James Sanders, NASA Goddard Space Flight Ctr. (United States); Koby Z. Smith, Larkin B. Carey, Ball Aerospace & Technologies Corp. (United States); Sze M. Chaung, Orbital ATK (United States); Severine C. Tournois, Ritva Keski-Kuha, Lee D. Feinberg, NASA Goddard Space Flight Ctr. (United States); W. Scott Smith, NASA Marshall Space Flight Ctr. (United States)

The James Webb Space Telescope (JWST) recently saw the completion of the assembly of the Optical Telescope Element and Integrated Science Instrument Module (OTIS). This integration effort was performed at Goddard Space Flight Center (GSFC) in Greenbelt, Maryland. In conjunction with this assembly process a series of vibration and acoustic tests were performed. To help assure the telescope's primary mirror was not adversely impacted by this environmental testing an optical center of curvature (CoC) test was performed before and after to measure changes in the telescope performance. The primary is a 6.5 meter diameter mirror consisting of 18 individual hexagonal segments. Each segment is an off-axis asphere with a total of three prescriptions repeated six times each. As part of the CoC test each segment was individually measured using a high speed interferometer (HSI) designed and built specifically for this test. This interferometer is capable of characterizing both static and dynamic characteristics of the mirrors. Additionally, with the aid of a vibration stinger applying a very low level input force the dynamic characteristic changes to the PM backplane structure can also be ascertained. This paper describes the CoC test setup, an innovative alignment method, and both static and dynamic results for the test.

10401-28, Session 6

Slanted-edge MTF testing for establishing focus alignment at infinite conjugate of space optical systems with gravity sag effects

Trent Newswander, David W. Riesland, Duane Miles, Lennon Reinhart, Space Dynamics Lab. (United States)

For space optical systems that image extended scenes such as earth viewing systems, modulation transfer function (MTF) test data is directly applicable to system optical resolution. For many missions it is the most direct metric for establishing the best focus of the instrument. Additionally MTF test products can be combined to predict overall imaging performance. For fixed focus instruments, finding the best focus during ground testing is critical to achieving good imaging performance. The ground testing should account for the full imaging system, operational parameters and operational environment. Testing the full imaging system removes uncertainty caused by breaking configurations and the combination of multiple subassembly test results. For earth viewing, the imaging system needs to be tested at infinite conjugate. Operational environment test conditions should include temperature and vacuum. Optical MTF testing in the presence of operational vibration and gravity release is less straightforward and may not be possible on the ground. Gravity effects are measured by testing in multiple orientations. Many space telescope systems are designed and built to have optimum performance in a gravity free environment. These systems can have imaging performance that is dominated by aberration including astigmatism. This paper discusses how the slanted edge MTF test is applied to determine the best focus of a space optical telescope in ground testing accounting for gravity sag effects. Actual optical system test results and conclusions are presented.

10401-29, Session 6

Diffractive optics for precision alignment of Euclid space telescope optics

Jean-Michel Asfour, Frank Weidner, Dioptic GmbH (Germany)

We present a method for precise alignment of lens elements using specific

Computer Generated Hologram (CGH) with an integrated Fizeau reference flat surface and a Fizeau interferometer. The method is used for aligning the so called Camera Lens Assembly for ESAs Euclid telescope. Each lens has a corresponding annular area on the diffractive optics, which is used to control the position of each lens. The lenses are subsequently positioned using individual annular rings of the CGH. The overall alignment accuracy is below 1 μm, the alignment sensitivity is in the range of 0.1 μm. The achieved alignment accuracy of the lenses relative to each other is mainly depending on the stability in time of the alignment tower. Error budgets when using computer generated holograms and physical limitations are explained. Calibration measurements of the alignment system and the typically reached alignment accuracies will be shown and discussed.

10401-43, Session PWed

Customized broadband sloan-filters filters for the JST/T250 and JAST/T80 telescopes: summary of results

Ulf Brauneck, SCHOTT Suisse SA (Switzerland); Ruediger Sprengard, SCHOTT AG (Germany); Sébastien Bourquin, SCHOTT Suisse SA (Switzerland); Antonio Marín-Franch, Ctr. de Estudios de Física del Cosmos de Aragón (Spain)

The Centro de Estudios de Fisica del Cosmos de Aragon (CEFCA) will conduct a photometric sky survey with 2 recently setup new telescopes on the Javalambre mountain: the JST/T250 is a 2.55m telescope with a plate scale of 22.67" /mm and a 3° diameter field of view (FoV) and the auxiliary telescope JAST/T80 with a 82cm primary mirror and a FoV of 2deg diameter.

A multiple CCD (9k-by-9k 10μm pixel) mosaic camera is used together with filter trays or filter wheels each containing a multitude of filters in dimensions 101.7x96.5mm or 106.8x106.8mm.

For this project SCHOTT manufactured 56 specially designed narrow band steep edged bandpass interference filters and 5 broadband sloan-filters which were recently completed. We report here on the results of the broadband sloan-filters with transmission bands of 324-400nm (sloan-u), 400-550nm (sloan-g), 550-700nm (sloan-r), 695-850nm (sloan-i) and 830-1200nm (sloan-z). The filters are composed of SCHOTT colorglasses and clearglass substrates coated with interference filters and represent an improvement of broadband sloan filters commonly used in astronomy.

Inspite of the absorptive elements, the filters show maximum possible transmissions achieved by magnetron sputtered filter coatings. In addition the blocking of the filters is better than OD5 in the range 250–1050nm. A high image quality required a low transmitted wavefront error (<?/8 locally respectively <?/2 globally) which was achieved even by combining up to 2 substrates. We report on the spectral and interferometrical results measured on the filters.

10401-44, Session PWed

An empirical comparison of primary baffle and vanes for optical astronomical telescope

Taoran Li, Yingwei Chen, National Astronomical Observatories (China)

In optical astronomical telescopes, the primary baffle is a tube-like structure centering in the hole of the primary mirror and the vanes usually locate inside the baffle, improving the suppression of stray light. They are the most common methods of stray light control. In order to characterize the performance of primary baffle and vanes, an empirical comparison based on astronomical observations has been made with Xinglong 50cm telescope. Considering the convenience of switching, an independent vanes system is designed, which can also improve the process of the primary mirror cooling and the air circulation. The comparison of two cases: (1) primary baffle plus vanes and (2) vanes alone involves in-dome and on-sky observations. Both the single star and the various off-axis angles of the stray light source observations are presented. The photometrical images are recorded by CCD to analyze the magnitude and the photometric error. The stray light uniformity of the image background derives from the reduction image which utilizes the MATLAB software to remove the stars. The in-dome experiments results reveal the effectiveness of primary baffle and the independent vanes system. Meanwhile, the on-sky photometric data indicate there are little differences between them. The stray light uniformity has no difference when the angle between the star and the moon is greater than 20 degrees.

10401-46, Session PWed

A friction compensating method based on data fusion in telescope controller design

YongMei Huang, Qiang Wang, Dong He, ZhiJun Song, Institute of Optics and Electronics, Chinese Academy of Sciences (China)

In this paper, a friction identifier and compensator is proposed. Friction is a major disturbance of median or large volume telescope. But the dynamic friction can hardly be measured directly. This paper propose a method to observe the dynamic friction based on data fusion. And used the observed result to identify friction's parameters of LuGre model. A compensator based on these parameters is then designed to compensate the friction. Finally the experiment result is proposed.

10401-47, Session PWed

Advanced slicer design for integral field spectrograph

Shaojie Chen, Suresh Sivanandam, Univ. of Toronto (Canada)

Integral field spectroscopy, a form of spectral multiplexing, is one of the current innovations in astronomical instrumentation, which can improve the observation efficiency significantly by capturing imaging and spectral information over a large field with a single exposure. This concept is also broadly applicable and has commercial value. Image slicer-based integral field spectrographs (IFS) are one implementation of this type technology, and the key component, an image slicer, is used to rearrange the two-dimensional field of view along one dimension to form a long pseudo slit at the input of a spectrograph.

In this paper, we discuss the design of an advanced compact slicer for the IFS, which consists of slicer mirrors, pupil mirrors and field mirrors. The overall requirements and process are described, from the top level optical parameters to the detailed specifications. The geometric layout of slicer is designed first to fit a spectrograph, and then slicer-pupil-field mirrors are optimized to achieve a good quality pseudo slit at the input of a spectrograph. Besides, the performance of micro pupils and common pupil after the image slicer is considered. The slicer for the conceptual design of a high-throughput infrared IFS for the Gemini South telescope is presented, and the simulation of slicer performance is discussed.

10401-48, Session PWed

Optical design of pyramid wavefront sensor for multiple mirror telescope

Shaojie Chen, Suresh Sivanandam, Siqi Liu, Univ. of Toronto (Canada); Jean-Pierre Veran, NRC - Herzberg Astronomy & Astrophysics (Canada); Philip M. Hinz, The Univ. of Arizona (United States); Etsuko Mieda, Tim Hardy, Olivier Lardière, NRC - Herzberg Astronomy & Astrophysics (Canada)

We discuss the optical design of an infrared (1.0-1.8 μm) pyramid wavefront sensor (PWFS) that is designed for the Multiple Mirror Telescope (MMT)

to improve its existing adaptive optics system. Simulations have shown the sensitivity of PWFSs to faint stars are better than traditional Shack-Hartmann WFSs. As a result, the use of PFWSs can provide higher Strehl ratios, larger sky coverage and higher contrast imaging capability. Considering the challenge to manufacture the four-sided pyramid with a precisely sharp tip, this design employs the double-roof prism structure as the substitute of real pyramid to split light into four quadrants to form four micropupils on the detector. The wavefront error is calculated by comparing the intensities inside four pupil images, so the micropupil quality determines the accuracy of wavefront measurement for the adaptive optics system directly.

In this paper, we discuss the evaluation process of micropupils quality, and report the performance comparison between the different designs, including single pyramid, double-roof, double pyramid and two double-roof prisms. In order to decrease the chromatic aberrations, the achromatic pair is adopted for the double pyramid and two double-roof prisms. The two double-roof prism design has been adopted for the PWFS after considering the competitive performance and the challenges in manufacturing the pyramid. Finally, four high quality micropupils are imaged with sufficient fidelity on a low-noise, high frame-rate infrared avalanche photodiode image sensor.

10401-50, Session PWed

Design of large aspherical SiC mirror for spaceborne application

Il K. Moon, Young Ha Kim, Ho-Soon Yang, Yun Woo Lee, Korea Research Institute of Standards and Science (Korea, Republic of)

Optimal design study of large aspherical mirror made of SiC for a space-borne application has been conducted. By using the finite element analysis program NX NASTRAN we calculated the opto-mechanical performance of mirror and its support system under various design loads including gravity, temperature and dynamic loads. We also optimized a bi-pod type flexure bonded at the backside of the mirror with proper strength under environment of space-borne application. Optimized shape of 1.1 m lightweight SiC mirror shows good areal density and optical performance of RMS surface error. We also proposed the hybrid type bonding method between mirror and bi-pod flexure shown better bonding strength with proper flexibility to isolate the effect of environmental loads.

10401-51, Session PWed

Optical design of the long slit spectrograph for 1m telescope

Dmitry E. Sazonenko, Dmitriy E. Kukushkin, Alexey V. Bakholdin, ITMO Univ. (Russian Federation); Gennady G. Valyvin, Special Astrophysical Observatory (Russian Federation)

In this article we describe optical design of the long-slit spectrograph for the 1-m telescope in the Special Astrophysical Observatory Russian Academy of Science.

The spectral range is 350-750 nm. The spectrograph must provide few modes with a spectral resolution: R100; R1000; R4000. Moreover, removing of the spectral element from the devise must provide an observing mode. We used a CCD detector with a pixel size 13.5 μm. Size of detector 2000x4000 pix. As a dispersion element, we used a grysm for every mode. During design, we decided to divide R4000 mode to 3 spectral ranges: 350-450 nm; 450-580 nm; 580-750 nm. We did this for ability to design of projection camera. Light loses in the spectrograph must be less than 50% in all spectral range. We decided to use the Ohara glass catalog for achieving this condition. Features of this devise are ability to provide all modes in wide spectral range and using the projection camera without glued lenses. As a result, we designed multi-mode devise. Spot diagram size does not exceed 2 pixels size in all modes.

10401-52, Session PWed

Control code for laboratory adaptive optics teaching system

Moon-Seob Jin, Ryan J. Luder, Lucas R. W. Sanchez, Michael Hart, College of Optical Sciences, The Univ. of Arizona (United States)

By sensing and compensating wavefront aberration, adaptive optics (AO) systems have proven themselves crucial in large astronomical telescopes, retinal imaging, and holographic coherent imaging. Commercial AO systems for laboratory use are now available in the market. One such is the ThorLabs AO kit built around a Boston Micromachines deformable mirror. However, there are limitations in applying these systems to research and pedagogical projects since the software is written with limited flexibility. In this paper, we describe a MATLAB-based software suite to interface with the ThorLabs AO kit by using the MATLAB Engine API and Visual Studio. The software is designed to offer complete access to the wavefront sensor data, through the various levels of processing, to the command signals to the deformable mirror and fast steering mirror. In this way, through a MATLAB GUI, an operator can experiment with every aspect of the AO system's functioning. This is particularly valuable for tests of new control algorithms as well as to support student engagement in an academic environment. We plan to make the code freely available to the community.

10401-53, Session PWed

Design and simulation of image-based 2D BRDF measurement system using semicircular ring reflector

Seul Ki Yang, Yonsei Univ. (Korea, Republic of); Eunsong Oh, Yonsei Univ. (Korea, Republic of) and Korea Institute of Ocean Science & Technology (Korea, Republic of); Sug-Whan Kim, Yonsei Univ. (Korea, Republic of)

We've designed new measurement system for the 2-dimentional bidirectional reflectance distribution functions (2D BRDF) which is able to acquire images from all reflected angles with a semicircular ring type reflector simultaneously. The system simply consists of reference light source module, target material module, reflector, and imaging detector module. The light source with specific incidence angle scattered from the target material comes to the semicircular type reflector. Then, the reached rays on the reflector can be captured as images with detecting part. Theoretically, since the reflected angle by the semicircular ring is constant, it is possible to calculate the BRDF characteristic of the target material. The experiment condition consists of a 635nm laser, the semicircular ring reflector structure with diameter of 300 mm, and an imaging camera. In this study, we predicted performance of the proposed system through the dedicated ray tracing simulation. The incident angle of light source is generated as a parallel beam covering from 10 to 90°. The imaging detector module includes 8bit CMOS sensor with 768?576 pixels and a focusing lens. The target material with the BRDF of Lambertian and Harvey models were used to verify the performance of designed measurement system. The simulation results show that the BRDF of the Lambetian model tends to remain unchanged about all of beam incident angle. The BRDF of the Harvey model tends to have the highest value at the specular angle, and exponentially decrease at different angles. The technical detail of the new measurement system design and ray tracing simulations will be presented with the results and implication.

10401-54, Session PWed

Fused silica polishing and figuring using CO2 laser radiation

Ting He, Shanghai Institute of Optics and Fine Mechanics (China) and Univ. of Chinese Academy of Sciences (China);

Chaoyang Wei, Zhigang Jiang, Xiaoli Teng, Jianda Shao, Shanghai Institute of Optics and Fine Mechanics (China)

Laser polishing of glass by CO2 laser can achieve sub-nanometer scales surface roughness in a short processing time with no extra damage caused. With the assistance of laser figuring, the surface residual waviness and shape errors can be reduced. To understand the physics of melt layer temporal evolution of laser polishing, a 2D axisymmetric transient model that couples heat transfer and fluid flow was constructed. The results indicate that the fluid flows are dominated by thermo-capillary convection in the velocity of ?m/s magnitude. It is suggest that melt flows are capable of smoothing micro roughness in appropriate interaction time. To study CO2 laser local precision homogeneous ablation, we have experimentally tested depths of no-overlapped and overlapped local ablation. Simulation of fused silica heating through multiple pulses CO2 laser beam irradiate was applied to optimize processing parameters of repetition rate, scan speed.

10401-55, Session PWed

A fast measuring method of the small aperture convex hyperboloid surface reflector

Zhe Wang, Xueke Xu, Lingqi Wu, Chaoyang Wei, Jianda Shao, Shanghai Institute of Optics and Fine Mechanics (China)

In the reflective optical system, a convex aspherical mirror is often used for the secondary mirror. Hindle test is difficult to operate in actual measurement for convex hyperboloid usually?because during measuring, the star is extremely difficult to find, and the tilt and decenter of the compensating spherical mirror have great influence on the position of the star. It causes a long measurement time, the measured results will include coma, and low efficiency. This paper presents a method that can fast finding the star with specific gauge, by analyzing the aberration of the tilt and decenter according to the measurement results using self-compiled software ,we only need fine tuning to the compensating spherical mirror. Therefore, the measuring time is greatly shortened and the efficiency is improved.

10401-30, Session 7

Operation and performance of the New Horizons Long-Range Reconnaissance Imager during the Pluto encounter

Steven J. Conard, Harold A. Weaver, Jorge I. Núñez, Howard W. Taylor, John R. Hayes, Andrew F. Cheng, Johns Hopkins Univ. Applied Physics Lab., LLC (United States)

The LOng-Range Reconnaissance Imager (LORRI) is a high resolution imaging instrument on the New Horizons spacecraft. LORRI collected over 5000 images during the approach and fly-by of the Pluto system in 2015, including the highest resolution images of Pluto and Charon and the four much smaller satellites (Styx, Nix, Kerberos, and Hydra) near the time of closest approach on 14 July 2015. LORRI is a narrow field of view (0.29°), Ritchey-Chrétien telescope with a 20.8 cm diameter primary mirror and a three lens field flattener. The telescope has an effective focal length of 262 cm. The focal plane unit consists of a 1024 ? 1024 pixel charge-coupled device detector operating in frame transfer mode. LORRI provides panchromatic imaging over a bandpass that extends approximately from 350 nm to 850 nm. The instrument operates in an extreme thermal environment, viewing space from within the warm spacecraft. For this reason, LORRI has a silicon carbide optical system with passive thermal control, designed to maintain focus without adjustment over a wide temperature range from -100 C to +50 C.

LORRI operated flawlessly throughout the encounter period, providing both science and navigation imaging of the Pluto system. We describe the preparations for the Pluto system encounter, including pre-encounter rehearsals, calibrations, and navigation imaging. In addition, we describe LORRI operations during the encounter, and the resulting imaging performance. Finally, we also briefly describe the post-Pluto encounter imaging of other Kuiper belt objects and the plans for the upcoming encounter with KBO 2014 MU69.

10401-31, Session 7

High-performance integrated photonic spectrometers: arrayed waveguide gratings or echelle gratings

Andreas Stoll, Ziyang Zhang, Martin M. Roth, Leibniz-Institut für Astrophysik Potsdam (Germany)

Compact, efficient and high-performance optical components are desired in astrophotonics to reduce system cost and complexity. In particular, integrated photonic spectrometers (IPS) based on planar lightwave circuits are attractive since the compact and light-weight components also provide great robustness and flexibility in the design of spectrograph systems for airborne and space astronomy. Arrayed waveguide gratings (AWG) and integrated Echelle gratings (IEG) are the two most recognized candidates and both have been long developed for the wavelength division multiplexing (WDM) optical networks. The requirements for their practical application in astrophotonics, however, bring the design difficulty to a new level: high performances including extremely fine spectral resolution, broad free spectral range and ultra-low insertion loss often need to be achieved simultaneously. Depending on the operation principles, for AWG the difficulties lie in the arrangement of a large number of fan-out waveguides and the mode-overlapping with the free propagation region, while for IEG niche design is needed in the grating curvature (Roland circle or two stigmatic point trace) and the local facet arrangement (blazing angle, curvature and chirping) for the best performance within a reasonable footprint. This paper compares these two IPSs in detail, e.g. their sizes and performance limitations under a series of settings. The challenges for the respective device fabrication are also analyzed in terms of critical dimensions, structural conformity and material homogeneity. This paper may serve as a guideline in the design of high-performance IPS devices and provide insights in choosing AWG or IEG for astronomical application.

10401-32, Session 7

Adaptation of Dunn Solar Telescope for Jovian Doppler spectro imaging

Thomas A. Underwood, David G. Voelz, New Mexico State Univ. (United States); François-Xavier Schmider, Lab. J.L. Lagrange, Observatoire de la Côte d'Azur (France); Jason Jackiewicz, New Mexico State Univ. (United States); Julien Dejonghe, Yves Bresson, Lab. J.L. Lagrange, Observatoire de la Côte d'Azur (France); Robert Hull, New Mexico State Univ. (United States); Ivan Gonçalves, Lab. J.L. Lagrange, Observatoire de la Côte d'Azur (France); Patrick Gualme, New Mexico State Univ. (United States); Frédéric Morand, Olivier Preis, Lab. J.L. Lagrange, Observatoire de la Côte d'Azur (France)

This paper describes instrumentation used to adapt the Dunn Solar Telescope (DST) located in Sunspot, NM for observations using the Doppler Spectro Imager (DSI). The DSI is based on a Mach-Zehnder interferometer and measures the Doppler shift of solar lines to allow the study of atmospheric dynamics of giant planets and the detection of their acoustic oscillations. The instrumentation is being designed and built through a collaborative effort between a French team from the Observatoire de la Cote d'Azur (OCA) that designed the DSI and a US team at New Mexico State University. There are four major components that couple the DSI to the DST: a guider/tracker, fast steering mirror (FSM), pupil stabilizer and transfer optics. The guider/tracker processes digital video to centroid-track

the planet and outputs voltages to the DST's heliostat controls. The FSM removes wavefront tip/tilt components primarily due to turbulence and the pupil stabilizer removes any slow pupil "wander" introduced by the telescope's heliostat/turret arrangement. The light received at a science port of the DST is sent through the correction and stabilization components and into the DSI. The FSM and transfer optics designs are being provided by the OCA team and serve much the same functions as they do for other telescopes at which DSI observations have been conducted. The pupil stabilization and guider are new and are required to address characteristics of the DST.

10401-33, Session 7

An acquisition technology of optical ground station in satellite-ground QKD

Dong He, YongMei Huang, Qiang Wang, Bo Qi, WanSheng Liu, Institute of Optics and Electronics, Chinese Academy of Sciences (China)

In this paper, a method of acquisition between optical ground station and Mozi quantum communication satellite for establish optical links is proposed. The acquisition technological specification of the optical ground station system is analyzed. The acquisition strategy of optical ground station is designed. In order to point accurately to quantum satellite for optical ground station, system error modifying method is designed, using the telescope mount model to improve the absolute pointing precision. Finally the experiment result is proposed. Results show that the correction accuracy is better than 5urad. The capture time is less than 5 seconds.

10401-34, Session 7

Imaging and spectral performance of the New Horizons Ralph instrument during the 2015 Pluto encounter

Allen W. Lunsford, Dennis Reuter, Donald E. Jennings, NASA Goddard Space Flight Ctr. (United States); Catherine B. Olkin, S. Alan Stern, Southwest Research Institute (United States); Gerald E. Weigle, Big Head Endian, LLC (United States)

The Ralph instrument on New Horizons mission consists of a telescope that feeds two focal planes: the Multi-spectral Visible Imaging Camera (MVIC), and the Linear Etalon Imaging Spectral Array (LEISA). During the encounter with the Pluto system in 2015, Ralph collected numerous high spatial resolution images of the main components of the system, Pluto and Charon, as well as the four smaller objects Hydra, Kerberos, Nix and Styx.

The 75-mm aperture Ralph telescope uses an off-axis, three-mirror anastigmat design with an effective focal length of 657.5 mm. A dichroic beamsplitter transmits wavelengths longer than 1.1 micron to LEISA and reflects shorter wavelengths to MVIC. MVIC provides panchromatic (400 to 975 nm), blue (400-550 nm), red (540-700 nm), near IR (780-975 nm) and methane absorption (860-910 nm) spectral bands. The IFOV of MVIC is about 20x20 microradian^2. The cross-track FOV of is 5.7°.

LEISA images a scene through a linear variable filter, LVF that operates from 1.25-2.5 micron. The two segments of the LVF cover from 1.25 to 2.5 micron with a spectral resolving power of about 240 and 2.1 to 2.25 micron with a spectral resolving power of about 560. The LEISA IFOV is about 62x62 microradian^2 and the FOV is 0.91° x 0.91°.

Ralph operated as expected, returning a wealth of spectral imaging data. The data acquisition process, calibration procedures and data processing steps are presented here. We will also present the planned observations of the KBO 2014 MU69 that will occur during the Kuiper Extended Mission (KEM).

10401-35, Session 8

Reducing SOFIA's image jitter: an ongoing challenge

Friederike M. Graf, NASA Ames Research Ctr. (United States); Andreas Reinacher, Daniel Spohr, Holger Jakob, Deutsches SOFIA Institut (Germany); Stefanos Fasoulas, Univ. of Stuttgart (Germany)

The Stratospheric Observatory for Infrared Astronomy (SOFIA) has already successfully conducted over 350 flights. In its early science phase, SOFIA's pointing requirements and especially the image jitter requirements of less than 1 arcsec rms have driven the design of the control system. However, the increasing demands on the image size now require an image jitter of less than 0.4 arcsec rms to reach SOFIA's scientific goals.

The major portion of the remaining image motion is caused by deformation and excitation of the telescope structure in a wide range of frequencies due to aircraft motion and aero-acoustic effects. These disturbances are counteracted by the so-called Flexible Body Compensation system which uses a set of accelerometers to estimate the resulting image motion.

A new scheme of tests has been conducted by developing controlled and manually induced turbulent flight conditions. These tests clearly show the influence of several telescope Eigenmodes on the image motion and how the current control system performs. With these measurements a variety of opportunities for dramatic improvements on the image jitter have been revealed.

To better study these possibilities, a simulation tool has been developed which not only implements system identification data and FEM derived models, but also allows the inclusion of sensor data from inflight measurements.

Results of the simulation as well as inflight measurements will be presented and improvement strategies will be discussed.

10401-36, Session 8

A second-order spherical optoelectronic detector

Francesco Romano, Consultant (Italy)

Present Paper concerns a feasibility study about the 2nd order spherical or three dimensional Detector, for photonic radiation applications.

It has been developed in order to obtain a PARAXIAL approximation of the physical event observed under Coulomb gauge condition, which is essential to compute both the longitudinal and transverse rotational components of the observed 3-D Vortex field.

Generally those components are neglected by the conventional detection systems so far used.

Light and Laser are not fully Transverse and/or not-rotational phenomena. The 2nd order spherical (3-D) Detector purpose is to directly measure also the potential solenoidal energy (vortex) related to the Angular Momentum, in addition to the energy, mainly not-rotational, related to the Linear Momentum.

Direct 2nd order measure, enables a study development of a TEM + DEM monochromatic complex wave with a paraxial accuracy in the relativistic time-space domain.

This paper compares the performances of the innovative 2nd order detector technique proposed with the ones reached by a 1st order system.

The paper illustrates an innovative Matlab Model Detector which is quadratic spherical 3-D, here submitted in order to directly measure a light source power spectrum.

The paper summarizes the results of several test experiments lead by the authors, in cooperation with INAF astronomer of Arcetri (Firenze, Italy), focused on the telescopic observations of the inter-stellar electromagnetic radiations.

The innovative Quadratic Spheric 3-D Detector turns out to be optimal

for Optical and/or Radio Telescopes, Optical and Optoelectronic Sensors, Gravitational Wave 2nd order detectors.

10401-37, Session 8

4MOST optical system: presentation and design details

Nicolas Azais, Samuel C. Barden, Gregory A. Smith, Steffen Frey, Leibniz-Institut für Astrophysik Potsdam (Germany); Damien J. Jones, Prime Optics (Australia); Bernard-Alexis Delabre, European Southern Observatory (Germany)

The 4-meter Multi-Object Spectroscopic Telescope (4MOST) is a wide-field, high-multiplex spectroscopic survey facility under development for the Visible and Infrared Survey Telescope for Astronomy (VISTA) 4 meter telescope of the European Southern Observatory (ESO) at Cerro Paranal. The objective of 4MOST is to enable the simultaneous spectroscopy of a significant number of targets (>1600) within a field of view with of 2.5 degree diameter allowing high-efficiency all-sky spectroscopic surveys. A wide field corrector (WFC) is needed to couple targets across a field diameter of 2.5 degrees with the exit pupil concentric with the spherical focal surface where ~2400 fibres are configured by a fibre positioner (AESOP). It will correct optical aberrations of the primary (M1) and secondary (M2) VISTA optics across the field of view for optimal fibre optic coupling and active optics wavefront sensing, provide a well-defined and stable focal surface to which the acquisition/guiding sensors, wavefront sensors, and fibre positioner are interfaced, and compensate for the effects of atmospheric dispersion allowing good chromatic coupling of stellar images with the fibre optics over a wide range of telescope zenith angles. The fibres feed three spectrographs; two thirds of the fibres will go to two spectrographs with resolution R~4000-7500 and the remaining 812 fibres to a spectrograph with resolution R~18000-21000. The three spectrographs are fixed-configuration with three channels each. We will present the 4MOST optical system along with optical simulation of subsystems.

10401-38, Session 8

Voltage linear transformation circuit design

Lucas R. W. Sanchez, Randy P. Scott, Ryan J. Luder, Moon-Seob Jin, The Univ. of Arizona (United States); Michael Hart, The Univ. of Arizona (United States)

Many engineering projects require automated control of analog voltages over a specified range. We have developed a computer interface comprising of custom hardware and MATLAB code to provide real-time control at kilohertz rates. The hardware uses an op amp cascade to linearly shift and scale a voltage range, with the back end of the circuit allowing easy modification to accommodate any required linear transformation. In adaptive optics applications, the design is suitable to drive a range of different types deformable mirrors. Our original motivation and application was to control an Optics in Motion fast steering mirror (FSM) which requires the customer to devise a unique interface to supply voltages to the mirror controller in order to set the mirror's angular deflection.

The FSM is in an optical servo loop with a wavefront sensor, which controls the dynamic behavior of the mirror's deflection. The code reads in data from the wavefront sensor and fits a plane. The slope of the plane is then converted into its corresponding angular deflection. The OIM mirror provides +- 3 degree optical angular deflection for a +- 10 V voltage swing. Voltages are applied to the mirror via a National Instruments digital-to-analog converter followed by the op amp cascade circuit. This system will eventually be integrated into our Wide-Field Imaging Adaptive Optics Testbed. The plans and the code for our interface solution are freely available to the community, as well as our method to design virtually any level shifting circuit.

10401-45, Session 8

Design of the telescope controller rejecting ground-based disturbance based on data fusion

Qiang Wang, YongMei Huang, Dong He, Xiang Liu, Jin-ying Li, ShengPing Du, Yu Jiang, Institute of Optics and Electronics, Chinese Academy of Sciences (China)

In this paper, a telescope controller design method rejecting ground base disturbance based on data fusion is proposed. Telescope systems usually suffer some uncertain disturbances. One of these is the disturbance come from ground base. Unlike the other disturbances, such as wind load, friction etc. The ground base disturbance can hardly be rejected by improve the stiffness of control system. This paper gives the measurement of the influence to the telescope coming from ground base disturbance. The property of ground base disturbance to the control system is concluded. Then, a control method is proposed. Finally the experiment result is proposed.

10401-39, Session 9

Active optics as enabling technology for future large missions: current developments for astronomy and Earth observation at ESA

Pascal Hallibert, European Space Research and Technology Ctr. (Netherlands)

In recent years, a trend for higher resolution has increased the entrance apertures of future optical payloads for both Astronomy and Earth Observation most demanding applications, resulting in new opto-mechanical challenges for future systems based on either monolithic or segmented large primary mirrors. Whether easing feasibility and schedule impact of tight manufacturing and integration constraints or correcting mission-critical in-orbit and commissioning effects, Active Optics constitutes an enabling technology for future large optical space instruments at ESA and needs to reach the necessary maturity in time for future mission selection and implementation. We present here a complete updated overview of our current R&D activities in this field, ranging from deformable space-compatible components to full correction chains including wavefront sensing as well as control and correction algorithms. We share as well our perspectives on the way-forward to technological maturity and implementation within future missions.

10401-40, Session 9

Atomic layer deposition and etching methods for far ultraviolet aluminum mirrors

John Hennessy, Jet Propulsion Lab. (United States); Christopher S. Moore, Univ. of Colorado Boulder (United States); Kunjithapatham Balasubramanian, April D. Jewell, Shouleh Nikzad, Jet Propulsion Lab. (United States); Kevin C. France, Univ. of Colorado Boulder (United States)

High performance Al mirrors at FUV wavelengths require the use of transparent dielectric materials as a protective coating to prevent oxidation. Reducing the thickness of this protective layer can result in additional performance gains by minimizing absorption losses, and provides a path toward high Al reflectance in the challenging wavelength range of 90 to 110 nm. We have pursued the development of new atomic layer deposition processes (ALD) for the metal fluoride materials of MgF_2, AlF_3 and LiF. Using an anhydrous HF based approach, these films can be deposited at the

low temperatures required for large area surface-finished optics and can be incorporated onto polymeric diffraction gratings. We also report on the development and application of an atomic layer etching (ALE) procedure implemented to controllably etch native aluminum oxide. Our ALE process utilizes the same chemistry used in the ALD of AlF3 thin films, allowing a combination of high performance evaporated Al layers and ultrathin ALD encapsulation without requiring vacuum transfer or shared-chamber deposition systems. Progress in demonstrating the scalability of this approach, as well as the environmental stability of ALD/ALE Al mirrors will be discussed in the context of possible future applications for NASA LUVOIR and HabEx mission concepts.

10401-41, Session 9

A dense grid of narrow bandpass steep edge filters for the JST/T250 telescope: summary of results

Ulf Brauneck, SCHOTT Suisse SA (Switzerland); Ruediger Sprengard, SCHOTT AG (Germany); Sébastien Bourquin, SCHOTT Suisse SA (Switzerland); Antonio Marín-Franch, Ctr. de Estudios de Física del Cosmos de Aragón (Spain)

On the Javalambre mountain the Centro de Estudios de Fisica del Cosmos de Aragon (CEFCA) has setup a new wide field telescope, the JST/T250: a 2.55m telescope with a plate scale of 22.67" /mm and a 3° diameter field of view.

To conduct a photometric sky survey a 14 CCD large format mosaic camera is used together with filter trays each containing 14 filters of 101.7x96.5mm.

For this project SCHOTT manufactured 56 specially designed steep edged bandpass interference filters which were recently completed. The filter set consists of bandpass filters in the range between 348,5nm and 910nm and a longpass filter at 913nm. Most of the filters have a FWHM of 14.5nm and a blocking from 250 to 1050nm with OD5.

Absorptive color glass substrates in combination with interference filters were used to minimize the residual reflection to avoid ghost images. Inspite of the absorptive elements, the filters show maximum possible transmissions achieved by magnetron sputtered filter coatings. The most important requirement for the continuous photometric survey was the tight tolerancing of the central wavelengths and FWHM of the filters. This insures that each bandpass has a defined overlap with its neighbors. In addition the blocking of the filters is better than OD5 in the range 250–1050nm. A high image quality required a low transmitted wavefront error (<?/8 locally respectively <?/2 globally) which was achieved even by combining 2 or 3 substrates. We report on the spectral and interferometrical results measured on the whole set of filters.

10401-42, Session 9

The study of optimization on process parameters of high-accuracy computerized numerical control polishing

Wei-Ren Huang, Shih-Pu Huang, Tsung-Yueh Tsai, National Taiwan Univ. (Taiwan); Yi-Chun Lin, National Taiwan Univ. (Taiwan); Zong-Ru Yu, Instrument Technology Research Ctr., National Applied Research Labs. (Taiwan); Ching-Hsiang Kuo, Instrument Technology Research Ctr., National Applied Research Labs (Taiwan); Wei-Yao Hsu, Instrument Technology Research Ctr., National Applied Research Labs. (Taiwan); Hong-Tsu Young, National Taiwan Univ. (Taiwan)

Spherical lenses lead to forming spherical aberration and reducing the optical performance. Consequently, in practice optical system shall apply a combination of spherical lenses for aberration correction. Thus, the volume of the optical system increased. For modern optical system, aspherical lenses have been widely used because of its high optical performance with less optical components. However, aspherical surfaces cannot be fabricated by traditional full aperture polishing process due to its various curvature. Sub-aperture computer numerical control (CNC) polishing is adopted for aspherical surface fabrication in recent years. By using CNC polishing process, mid-spatial frequency (MSF) error is normally accompanied during this process. And the MSF surface texture of optics will decrease the optical performance for high precision optical system, especially for short-wavelength applications. Based on a bonnet polishing CNC machine, this study focuses on the relationship between MSF surface texture and CNC polishing parameters, which include feed rate, head speed, path pitch and path direction. The power spectral density (PSD) analysis is used to judge the MSF level caused by those polishing parameters. This study try to find out certain of polishing parameters without MSF surface texture, and the test results show that controlling the removal depth of single polishing path, through the feed rate, can efficiently reduce the MSF error. To verify the optimal polishing parameters, we divided a correction polishing process to several polishing runs with different direction polishing paths. Compare to one shot polishing run, multi-direction path polishing plan could producing better surface quality on the optics.

10401-56, Session 9

Lithographic manufacturing of adaptive optics components

R Phillip Scott, Michael Hart, Tom Milster, Madison Jean, Ryan Bronson, Lauren Schatz, Lee Johnson, University of Arizona (United States)

Adaptive optics systems and their laboratory test environments call for a number of unusual optical components. Examples include lenslet arrays, pyramids, and Kolmogorov phase screens. Because of their specialized application, the availability of these parts is generally limited, with high cost and long lead time, which can also significantly drive optical system design. These concerns can be alleviated by a fast and inexpensive method of optical fabrication. To that end, we are exploring lithographic techniques to manufacture three different custom elements. We report results from a number of prototype devices including 1, 2, and 3 wave Multiple Order Diffractive (MOD) lenslet arrays with 0.75 mm pitch, phase screens with near Kolmogorov structure functions with a Fried length r0 below 1 mm, and a diffractive pyramid that is smaller, lighter, and more easily manufactured than glass versions presently used in pyramid wavefront sensors. We describe how these components can be produced within the limited dynamic range of the lithographic process, and with a rapid prototyping and manufacturing cycle. We discuss exploratory manufacturing methods, including replication, and potential observing techniques enabled by the ready availability of custom components.

Conference 10402: Earth Observing Systems XXII

SPIE. OPTICS+ PHOTONICS OPTICAL ENGINEERING+ APPLICATIONS

Sunday - Thursday 6 –10 August 2017

Part of Proceedings of SPIE Vol. 10402 Earth Observing Systems XXII

10402-1, Session 1

A status update on EUMETSAT programmes and plans

K. Dieter Klaes, EUMETSAT (Germany)

The mandate of EUMETSAT is providing space observations for operational meteorology and climate monitoring. EUMETSAT operates geostationary and sun-synchronous polar orbiting satellites through mandatory programmes. Optional programmes provide further observations for altimetry and oceanography. EUMETSAT makes available data from partner agencies' satellites to the user community through third party programmes. The current fleet of operational geostationary spacecraft comprises Meteosat-7, which is the last satellite of the first generation and the four satellites of the Second Generation of Meteosat (MSG), Meteosat-8, Meteosat-9, Meteosat-10 and Meteosat-11. The EUMETSAT Polar System (EPS) provides data from sun-synchronous polar orbit with currently two satellites: Metop-B, the second of a series of three satellites, launched in September 2012 and currently the prime satellite, and Metop-A, the first of the series, in orbit since October 2006. These satellites are part of the Initial Joint Polar System (IJPS) together with the US. EUMETSAT's first optional programme continues to provide data from the Jason-2 satellite since summer 2008. The follow on satellite Jason-3 was successfully launched and commissioned in 2016 and is now providing the reference altimetry mission. To assure continuity in the mandatory missions the development of Meteosat Third Generation (MTG) is ongoing. The EPS-SG EPS Second generation) programme is now under full development. In the frame of the Copernicus Programme EUMETSAT operates the Sentinel-3A satellite, which was launched in February 2016. EUMETSAT is providing operational marine products from the Sentinel-3A satellite. Sentinel-3B, a second satellite, is scheduled to be launched end of 2017.

10402-2, Session 1

MTG-IRS: From raw measurements to calibrated radiances

Dorothee Coppens, Bertrand Theodore, K. Dieter Klaes, EUMETSAT (Germany); Stefano Gigli, European Organisation for the Exploitation of Meteorological Satellites (Germany)

The Meteosat Third Generation (MTG) series of future European geostationary meteorological satellites consists of two types of satellites, the imaging satellites (MTG-I) and the sounding satellites (MTG-S). The Infrared Sounder (IRS) is one of the two instruments hosted on board the MTG-S satellites. The scope of the IRS mission is to provide the user community with information on time evolution of humidity and temperature distribution, as function of latitude, longitude and altitude. Regarding time and space sampling, the entire Earth disk will be covered, with particular focus on Europe, which will be revisited every 30 minutes.

This paper presents a synthetic overview of the mission and the instrument, and will go through the level 1 processing chain which takes instrument raw data to obtain spectrally and radiometrically calibrated and geolocalised radiances, called level 1b products. A discussion will be presented around the radiances uniformisation in space, spectral range and time and its impact for the users community.

10402-3, Session 1

The EarthCARE mission BBR instrument: Ground testing of radiometric performance

Martin E. Caldwell, William Grainger, Martin S. Whalley, Anthony K. Ward, David Parker, John Delderfield, STFC Rutherford Appleton Lab. (United Kingdom); David Spilling, Nigel Wright, Thales Alenia Space UK Ltd. (United Kingdom); Evangelos Theocharous, National Physical Lab. (United Kingdom); Grant J. Munro, Oliver Poynz Wright, Matthew Hampson, David Forster, ESR Technology Ltd. (United Kingdom)

In ESA's EarthCARE mission the BBR (broad band radiometer) has the role of measuring the net Earth radiance (i.e. total reflected-solar and thermally-emitted radiances), from the same scene as viewed by the other instruments (aerosol lidar, cloud radar and spectral imager). For the methods to measure total Earth radiance the BBR is based on the heritage of previous Earth Radiation Budget (ERB) instruments, and the calibration of this type of sensor is technically similar to other EO instruments that measure in the thermal-IR, but with added challenges: (1) the thermal-IR has to have a much wider spectral range than normal thermal-IR channels, for the whole Earth-emission spectrum of around 4 to 50μm; and (2) the reflected-solar channel must also have a broad response, of around 0.3 to 4μm. Furthermore, this solar channel must be measured on the same radiometric calibration as the thermal channel, and in BBR this is achieved using the same radiometer for both channels. The radiometer has a very broad-band response of 0.3 to 50μm to cover both ranges, with a switchable 4μm short-pass cut-off filter used to separate the channels. The on-ground measurements required for the calibration of absolute responsivity in these channels are described: in the thermal-IR channel this is done using a calibrated black-body test source; and in the solar channel it is by means of a narrow-band (laser) measurement and reference radiometer. A calibration of relative spectral response is also made across this wide range, for the purpose of linking the two channels and converting the narrow-band solar channel measurements to broad-band.

10402-4, Session 1

Focal plane subsystem design and performance for atmospheric chemistry from geostationary orbit tropospheric emissions monitoring of pollution

Angelo S. Gilmore, Robert H. Philbrick, Josh Funderburg, Ball Aerospace & Technologies Corp. (United States)

Diurnal measurements of pollutants are enabled from a satellite in a geostationary orbit containing an imaging spectrometer encompassing the wavelength ranges of 290 - 490 nm and 540 - 740 nm. As the first of NASA's Earth Venture missions, the Tropospheric Emissions: Monitoring of Pollution (TEMPO) program will utilize this instrument to measure hourly air quality over a large portion of North America. The focal plane subsystem (FPS) contains two custom designed and critically aligned full frame transfer charge coupled devices (active area: 1028 x 2048, 18um) within a focal plane array package designed for radiation tolerance and space charging rejection. In addition, the FPS contains custom distributed focal plane electronics that provide all necessary clocks and biases to the sensors, receive all analog data from the sensors and perform 14 bit analog to digital conversion for upstream processing. Finally, the FPS encompasses custom low noise cables connecting the focal plane array and associated electronics. This paper discusses the design and performance of this novel focal plane subsystem with particular emphasis on the optical performance achieved including alignment, quantum efficiency, and modulation transfer function.

10402-5, Session 1

Landsat 9 - OLI 2 focal plane subsystem - design, performance, and status

Kevin J. Malone, Ronald J Schrein, M. Scott Bradley, Ronda Irwin, Barry N Berdanier, Eric Donley, Ball Aerospace & Technologies Corp. (United States)

The Landsat 9 mission will continue the legacy of Earth remote sensing that started in 1972. The Operational Land Imager 2 (OLI-2) is one of two instruments on the Landsat 9 satellite. The OLI-2 instrument is essentially a copy of the OLI instrument flying on Landsat 8. A key element of the OLI 2 instrument is the focal plane subsystem or FPS which consists of the focal plane array (FPA), the focal plane electronics (FPE) box and low-thermal conductivity cables. This paper presents design details of the OLI-2 FPS.

The FPA contains 14 critically-aligned focal plane modules (FPM). Each module contains 6 visible/near-IR detector arrays and three short-wave infrared arrays. A complex multi-spectral optical filter is contained in each module. Redundant pixels for each array provide exceptional operability. Spare detector modules from OLI were re-characterized after six years of storage. Radiometric test results will be presented and compared with data recorded in 2010.

Thermal, optical, mechanical and structural features of the FPA will be described. Special attention is paid to the thermal design of the FPA since thermal stability is crucial to ensuring low-noise and low-drift operation of the detectors which operate at -63°C.

The OLI-2 FPE provides power, timing and control to the focal plane modules. It also digitizes the video data and formats it for the solid-state recorder. Design improvements to the FPA-FPE cables will be discussed and characterization data will be presented. The paper will conclude with the status of the flight hardware assembly and testing.

10402-6, Session 1

Mission studies on constellation of LEO satellites with remote-sensing and communication payloads

Chia-Ray Chen, National Space Organization (Taiwan)

Revisiting time and global coverage are two major requirements for most of the remote sensing satellites. Constellation of satellites can get the benefit of short revisit time and global coverage. Typically, remote sensing satellites prefer to choose Sun Synchronous Orbit (SSO) because of fixed revisiting time and Sun beta angle. The system design and mission operation will be simple and straightforward. However, if we focus on providing remote sensing and communication services for low latitude countries, Sun Synchronous Orbit will not be the best choice because we need more satellites to cover the communication service gap in low latitude region. Sometimes the design drivers for remote sensing payloads are conflicted with the communication payloads. For example, lower orbit altitude is better for remote sensing payload performance, but the communication service zone will be smaller and we need more satellites to provide all time communication service. The current studies focus on how to provide remote sensing and communication services for low latitude countries. A cost effective approach for the mission, i.e. constellation of microsatellites, will be evaluated in this paper.

10402-7, Session 2

Pathway to future sustainable land imaging: The compact hyperspectral prism spectrometer

Thomas U. Kampe, William S. Good, Ball Aerospace & Technologies Corp. (United States)

NASA's Sustainable Land Imaging (SLI) program, managed through the Earth Science Technology Office, aims to develop technologies that will provide future Landsat-like measurements. SLI aims to develop a new generation of smaller, more capable, less costly payloads that meet or exceed current imaging capabilities. One projects funded by this program is Ball's Compact Hyperspectral Prism Spectrometer (CHPS), a visible-to-shortwave imaging spectrometer that provides legacy Landsat data products as well as hyperspectral coverage suitable for a broad range of land science products. CHPS exhibits extremely low straylight and accommodates full aperture, full optical path calibration needed to ensure the high radiometric accuracy demanded by SLI measurement objectives. Low polarization sensitivity in visible to near-infrared bands facilitates coastal water science as first demonstrated the exceptional performance of the Operational Land Imager. Our goal is to mature CHPS imaging spectrometer technology for infusion into the SLI program. Our efforts build on technology development initiated by Ball IRAD investment, and includes laboratory and airborne demonstration, data distribution to science collaborators, and maturation of technology for spaceborne demonstration. CHPS is a three year program with expected exiting technology readiness of TRL-6. The 2013 NRC report Landsat and Beyond: Sustaining and Enhancing the Nations Land Imaging Program recommended that the nation should "maintain a sustained, space-based, land-imaging program, while ensuring the continuity of 42-years of multispectral information." We are confident that CHPS provides a path to achieve this goal while enabling new science measurements while significantly reducing the cost, size, and volume of the VSWIR instrument.

10402-8, Session 2

Design and development of the CubeSat Infrared Atmospheric Sounder (CIRAS)

Thomas S. Pagano, Jet Propulsion Lab. (United States)

The CubeSat Infrared Atmospheric Sounder (CIRAS) will measure upwelling infrared radiation of the Earth in the MWIR region of the spectrum (4.08-5.13μm) with a spatial resolution of 13.5 km (3km in zoom mode) from space on a CubeSat. The observed radiances can be assimilated into weather forecast models and be used to retrieve lower tropospheric temperature and water vapor for climate studies. Multiple units can be flown to improve temporal coverage or in formation to provide new data products including 3D motion vector winds. The CIRAS is currently under development at NASA JPL under the NASA In-space Validation of Earth Science Technologies (InVEST) and scheduled for launch in 2019.

CIRAS incorporates three new instrument technologies. The first is a 2D array of High Operating Temperature Barrier Infrared Detector (HOT-BIRD) material, selected for its high uniformity, low cost, low noise and higher operating temperatures than traditional materials. The detectors are hybridized to a commercial ROIC and commercial camera electronics. The second technology is an MWIR Grating Spectrometer (MGS) designed to provide imaging spectroscopy for atmospheric sounding in a CubeSat volume. The MGS will be built at Ball Aerospace, has no moving parts, and is based on heritage spectrometers developed under the NASA Instrument Incubator Program (IIP) including the SIRAS-G. The third technology is an infrared blackbody developed using Black Silicon developed at JPL. Black silicon has a very high emissivity (<0.2%) over a broad spectral range including the CIRAS band. JPL will develop the mechanical, electronic and thermal subsystems for CIRAS. The spacecraft will be developed by Blue Canyon Technologies (BCT). The integrated system will be a complete 6U CubeSat capable of measuring temperature and water vapor profiles with good lower tropospheric sensitivity. This paper will discuss the design requirements for CIRAS and the current state of development of the instrument, including recent fabrication results for certain subsystems.

10402-9, Session 2

Snow and water imaging spectrometer (SWIS): A CubeSat-compatible instrument

Holly A. Bender, Justin M. Haag, Pantazis Mouroulis, Jet

Propulsion Lab. (United States); Christopher Smith, Sierra Lobo, Inc. (United States)

The Snow and Water Imaging Spectrometer (SWIS) is a fast, high-uniformity, low-polarization sensitivity imaging spectrometer and telescope system designed for integration on a 6U CubeSat platform. Operating in the 350-1700 nm spectral region with 5.7 nm sampling, SWIS is capable of simultaneously addressing the demanding needs of coastal ocean science and snow and ice monitoring. While the SWIS instrument benefits from a rich heritage of imaging spectrometer development at the Jet Propulsion Lab, certain adaptations are required to stay within CubeSat resources. New key technologies that facilitate the development of this instrument include a linear variable anti-reflection (LVAR) detector coating for stray light management, and a single drive on-board calibration mechanism utilizing a transmissive diffuser for solar calibration. We provide an overview of the optomechanical assembly, alignment and performance of the SWIS instrument.

10402-10, Session 2

Design and qualification of the STREEGO multispectral payload

Massimiliano Rossi, Luigina Arcangeli, Giovanni Bianucci, Ruben Mazzoleni, Sebastiano Spinelli, Marco Terraneo, Fabio Emilio Zocchi, Media Lario Technologies S.r.l. (Italy); Giuseppe Capuano, Giuseppe Formicola, Pasquale Longobardi, Techno System Developments S.r.l. (Italy); Luca Maresi, Matteo Taccola, European Space Research and Technology Ctr. (Netherlands)

The increasing number of Earth Observation missions launched over the last decade has fostered the development of a large number of satellite instruments delivering rich imagery supporting ever growing and expanding applications. Recent advances in electronics, optical manufacturing and remote sensing are now enabling smaller instruments that are at the basis of new mission concepts that can affordably be extended to satellite constellations for improved temporal resolution.

We present the development of STREEGO, an innovative multispectral optical payload for Earth Observation from microsatellites. STREEGO is an athermal, fully reflective telescope based on a three mirror anastigmat optical design with 200 mm aperture, 1.2 m focal length, 2° FoV, and 20 kg mass, including electronics. Leveraging on a large format two-dimensional CMOS sensor with a pixel size of 5.5 μm and 9-band multispectral filter, STREEGO delivers a nominal modulation transfer function (MTF) of 64% at Nyquist frequency and a ground sampling distance of 2.75 m from an orbit of 600 km. Extensive straylight and tolerancing analyses and a worst-case thermal model ensure optimal image quality under operational conditions. A fully functional Engineering Model of STREEGO has been built and tested in laboratory with excellent results, such as wavefront error of 43 nm RMS, MTF better than 30% at Nyquist, and 1% linearity. An environmental test campaign has been planned to complete the qualification tests. The design of the instrument and the results of the characterization and qualification tests are presented in details.

10402-11, Session 2

Technical and cost advantages of silicon-carbide telescopes for small-satellite imaging applications

Keith Kasunic, Optical Systems Group LLC (United States); Dave Aikens, Savvy Optics Corp. (United States); Dean Szwabowski, Chip Ragan, Flemming Tinker, Aperture Optical Sciences Inc. (United States)

Small satellites (“SmallSats”) are a growing segment of the Earth imaging market. Designed to be relatively low cost and with performance tailored to specific end-use applications, they are driving changes in optical telescope assembly (OTA) requirements.

OTAs implemented in silicon carbide (SiC) provide performance advantages for space applications but have been predominately limited to large programs. A new generation of lightweight and thermally-stable designs is becoming commercially available, expanding the application of SiC to small satellites. This paper reviews the cost and technical benefits of an OTA designed using SiC for small satellite platforms.

Taking into account faceplate fabrication quilting and surface distortion after gravity release, an optimized open-back SiC design with a lightweighting of 70% for a 125-mm class primary mirror has an estimated area density of 2.8 kg/m2 and an aspect ratio of 40:1. In addition, the thermally-induced surface error of such optimized designs is estimated at ?/150 RMS per watt of absorbed power. Cost benefits of SiC include reductions in launch mass, thermal-management infrastructure, and manufacturing time based on allowable assembly tolerances.

10402-12, Session 3

MOS+P: A combined spectrometer and polarimeter optimized for ocean color

William S. Good, Rainer Illing, Derek Sabatke, Ball Aerospace & Technologies Corp. (United States); Nicholas Tufillaro, Oregon State Univ. (United States)

A significant challenge for ocean color retrievals is atmospheric correction due to the strong atmospheric reflectance and relatively weak ocean color signal. Aerosol measurements coincident with spectral radiance can improve ocean color retrievals by providing appropriate inputs to atmospheric models for aerosol loading and type. Polarimeters provide those aerosol measurements but often are limited in the number of spectral bands and require a separate instrument from the spectral radiance sensor. The Multi-slit Optimized Spectrometer and Polarimeter, MOS+P, includes three linear polarization channels and an un-polarized channel that are all imaged onto a single focal plane. This compact instrument design exhibits low stray light and provides simultaneous measurements of scene polarization across the visible to NIR spectral band. Results from a laboratory characterization will be compared to modeled performance to determine the linear polarization sensitivity of each pixel. This sensitivity can be used to determine scene polarization sensitivity which can provide valuable inputs for atmospheric retrieval models. The MOS+P airborne instrument was flown for NASA in the 2016 KORUS-AQ and OC campaigns based in South Korea. Initial results of measured scene polarizations over the Yellow Sea and Sea of Japan and a comparison of atmospheric retrievals with and without the polarization channels will be presented.

10402-13, Session 3

Radiometric and spectral stray light correction for the portable remote imaging spectrometer (PRISM) coastal ocean sensor

Justin M. Haag, Byron E. Van Gorp, Pantazis Mouroulis, David R. Thompson, Jet Propulsion Lab. (United States)

The airborne Portable Remote Imaging Spectrometer (PRISM) instrument is based on a fast (F/1.8) Dyson spectrometer operating at 350-1050 nm and a two-mirror telescope combined with a Teledyne HyViSI 6604A detector array. Raw PRISM data contain electronic and optical artifacts that must be removed prior to radiometric calibration. We provide an overview of the process transforming raw digital numbers to calibrated radiance values. Electronic panel artifacts are first corrected using empirical relationships developed from laboratory data. The instrument spectral response functions (SRF) are reconstructed using a measurement-based optimization technique. Removal of SRF effects from the data improves retrieval of true spectra, particularly in the typically low-signal near-ultraviolet and near-infrared regions. As a final step, radiometric calibration is performed using

corrected measurements of an object of known radiance. Implementation of the complete calibration procedure maximizes data quality in preparation for subsequent processing steps, such as atmospheric removal and spectral signature classification.

10402-14, Session 3

High altitude hyperspectral remote sensing in the thermal infrared: recent instrument improvements

William R. Johnson, Simon Hook, Jet Propulsion Lab. (United States)

Spectroscopy has been a key part of this scientific exploration because of its ability to remotely determine elemental and mineralogical composition. Mineralogy in particular is critical, because the presence and configuration of minerals within a geologic setting can reveal environmental conditions (e.g., temperature, pressure) at the time of formation and/or evolution. Spectroscopy allows the discrimination of minerals such as olivine, pyroxene, plagioclase, quartz, clays, sulfates, and carbonates. For example, mineralogy can provide key constraints on processes such as internal differentiation and alteration by water. Many key gas species such as methane, ammonia, sulfur, etc. also have vibrational bands which show up in the thermal infrared spectrum above the background response.

The Hyperspectral thermal emission spectrometer (HyTES) has transitioned to NASA's ER-2 platform. We discuss the transition as well as specific challenges faced with installation, operation and calibration. For example, the sensor is outside the pressurized zone of the ER-2 to eliminate a 2nd window. We discuss the large temperature swings and how this affects the calibration (performed pre and post flight on the ground). HyTES uses sensing technology based on the quantum well infrared photodetector (QWIP). The sensor is currently transitioning to a new complementary barrier infrared photodetector (CBIRD) which has a slightly longer wave cut-off and increased sensitivity. We expect this to expand the wide application base of the instrument.

10402-15, Session 3

Imaging spectroscopy using embedded diffractive optical arrays

Michele Hinnrichs, Bradford R. Hinnrichs, Pacific Advanced Technology, Inc. (United States)

We have developed a very small robust infrared imaging spectrometer using and area array of diffractive optical elements embedded in the cold-shield of the sensor and actuated with a piezo motor. This approach allows rapid imaging spectroscopy with multiple spectral images collected and processed each frame of the camera.

This paper will present our optical mechanical design approach including the gray scale photolithographic technique for the fabrication of the diffractive optical elements. And show results of the images collected and processed in real-time on target such as hydrocarbon gases.

The diffractive optical elements are blazed gratings where each lenslet in the array in tuned for a different spectral bandpass. The lenslets are configured in an area array placed a few millimeters above the focal plane and embedded in the cold-shield to reduce the background signal.

We have developed various systems using a different number of lenslets in the area array. Depending on the size of the focal plane and the diameter of the lenslet array will determine the spatial resolution. A 2 x 2 lenslet array will image four different spectral images of the scene each frame and when coupled with a 512 x 512 focal plane array will give spatial resolution of 256 x 256 pixel each spectral image. Another system that we developed uses a 4 x 4 lenslet array on a 1024 x 1024 pixel element focal plane array which gives 16 spectral images of 256 x 256 pixel resolution each frame.

10402-16, Session 3

Assembly and test of a visible and near-infrared imaging spectrometer with a Shack-Hartmann wavefront sensor

Jun Ho Lee, Sung Lyoung Hwang, Kongju National Univ. (Korea, Republic of); Jin Suk Hong, Young Soo Kim, Hanwha Systems Co., Ltd. (Korea, Republic of); Yeon Soo Kim, Hyun Sook Kim, Agency for Defense Development (Korea, Republic of)

We report an assembly procedure and performance evaluation of a visible and near-infrared spectrometer in the region of 400 ~ 900 nm in wavelength, which is later to be combined with a fore-optics i.e. a telescope to form a f/2.5 imaging spectrometer with a field of view of ±7.68°. The detector at the final image plane is a 640?480 pixel charge-coupled device of 24?24 ?m pitch. The spectrometer is an Offner relay configuration consisting of two concentric spherical mirrors, the secondary of which is replaced by a convex grating mirror. A double pass test method with an interferometer is mostly applied in assembly procedures of precision optics but was excluded in our study due to large residual wavefront error (WFE) in optics design i.e. 210nm (0.35? at 600 nm) in root mean squared (RMS). This results in a single-path test method with a Shack-Hartmann sensor. The final assembly was tested to have the RMS WFE increasement of less than 90 nm over the entire field of view, the keystone 0.08 pixel, the smile 0.13 pixel and the spectral resolution 4.32 nm. During the procedure, we confirmed the validity of the use of the Shack-Hartmann as an alignment monitor in the assembly of an Offner-like spectrometer.

10402-17, Session 3

Curved focal plane array for hyperspectral imaging system

Mohammad A. Saleh, Corning Incorporated (United States)

Prior work has demonstrated that curved focal plan arrays (FPA) enable lenses for traditional cameras with improved image quality and fewer elements as compared to existing flat image planes. There is an increasing interest in the development of curved focal planes for other imaging applications using a variety of surface contours. In this work, the potential performance improvements of a hyperspectral imaging system (HSI) with a curved FPA are explored using Corning's existing hyperspectral designs. We evaluated the effect of curved FPAs for spectrometers from the free-space and monolithic Offner class as well as the Dyson form. While these designs are already optimized with aspheric mirrors, the addition of the curved FPA provided additional performance improvements.

Surface types considered for the FPA include aspheric, toroidal, anamorphic and free-forms. The surfaces providing optimum performance offer guidelines for future curved FPA development. We found that multiple design parameters, such as size, weight, f-number, field of view and relative cost can be improved compared with current state-of-the-art flat FPAs. A free-space Offner spectrometer, for example, can be reduced 30% in size, or improved by 20% in f-number. Our initial findings indicate that while a curved FPA improves instrument performance, the aspheric mirror surfaces cannot be removed from the spectrometer designs since they compensate for aberrations that are not diminished by the curved FPA.

10402-18, Session 3

Imaging gratings: Technology and applications for spectrometers

Peter Triebel, Tobias Moeller, Carl Zeiss Microscopy GmbH (Germany); Torsten Diehl, Carl Zeiss Spectroscopy GmbH (Germany); Alexandre Gatto, Alexander Pesch, Lars Erdmann, Matthias Burkhardt, Alexander Kalies, Carl Zeiss Jena GmbH (Germany)

For imaging spectrometers beside the polarization sensitivity and efficiency the imaging quality of the diffraction grating is essential. Low aberration imaging quality of the grating is required not to limit the overall imaging quality of the instrument. The wavefront aberration of an optical grating is a combination of the substrate wavefront and the grating wavefront. During the manufacturing process of the grating substrate different processes can be applied in order to minimize the wavefront aberrations. The imaging performance of the grating is also optimized due to the recording setup of the holography and a special technique to apply blazed profiles also in photoresist of curved substrates.

This technology of holographically manufactured gratings is used for transmission and reflection gratings on different types of substrates like prisms, convex and concave spherical and aspherical surface shapes, free-form elements. All the manufactured gratings are monolithic and can be coated with high reflection and anti-reflection coatings. Prism substrates were used to manufacture monolithic GRISM elements for the UV to IR spectral range preferably working in transmission. Besides of transmission gratings, numerous spectrometer setups (e.g. Offner, Rowland circle, Czerny-Turner system layout) working on the optical design principles of reflection gratings. The present approach can be applied to manufacture high quality reflection gratings for the EUV to the IR.

In this paper we report our latest results on manufacturing lowest wavefront aberration gratings based on holographic processes in order to enable at least diffraction limited complex spectrometric setups over certain wavelength ranges. Beside the results of low aberration gratings the latest achievements on improving efficiency together with less polarization sensitivity and multi-band performance of diffractive gratings will be shown.

10402-19, Session 4

Analysis of a commercial small unmanned airborne system (sUAS) in support of the Radiometric Calibration Test Site (RadCaTS) at Railroad Valley

Jeffrey S. Czapla-Myers, Nikolaus J. Anderson, College of Optical Sciences, The Univ. of Arizona (United States)

The Radiometric Calibration Test Site (RadCaTS) is an automated facility developed by the Remote Sensing Group (RSG) at the University of Arizona to provide radiometric calibration data for airborne and satellite sensors. RadCaTS uses stationary ground-viewing radiometers (GVRs) to spatially sample the surface reflectance of the site. The number and location of the GVRs is based on previous spatial, spectral, and temporal analyses of Railroad Valley. With the increase in high-resolution satellite sensors, there is renewed interest in examining the spatial uniformity the 1-km2 RadCaTS area at scales smaller than a typical 30-m sensor. RadCaTS is one of the four instrumented sites currently in the CEOS WGCV Radiometric Calibration Network (RadCalNet), which aims to harmonize the post-launch radiometric calibration of satellite sensors through the use of a global network of automated calibration sites. A better understanding of the RadCaTS spatial uniformity as a function of pixel size will also benefit the RadCalNet work. RSG has recently acquired a commercially-available small unmanned airborne system (sUAS) system, with which preliminary spatial homogeneity measurements of the 1-km2 RadCaTS area were made. This work describes an initial assessment of the airborne platform and integrated camera for spatial studies of RadCaTS using data that were collected in 2016 and 2017.

10402-20, Session 4

Calibration and use of an ultra-portable field transfer radiometer for automated vicarious calibration

Kurtis J. Thome, NASA Goddard Space Flight Ctr. (United States); Jeffrey S. Czapla-Myers, The Univ. of Arizona (United States); Brian N. Wenny, Science Systems and Applications, Inc. (United States); Nikolaus J. Anderson, The Univ. of Arizona (United States)

A small portable transfer radiometer has been developed as part of an effort to ensure the quality of upwelling radiance at automated test sites used for vicarious calibration in the solar reflective. The test sites, such as the one located at Railroad Valley, are used to predict top-of-atmosphere reflectance relying on ground-based measurements of the atmosphere and surface. The portable transfer radiometer is designed for one-person operation for on-site field calibration of the instrumentation used to determine ground-leaving radiance. The current work describes the laboratory-based calibration of the transfer radiometer highlighting the expected accuracy and SI-traceability. Results from recent field deployments of the transfer radiometer are presented to show how the sensor is to be used for 1) evaluating the health of the automated site radiometers, 2) characterizing the surface being measured at the automated test sites, and 3) assessing the error budget for top-of-atmosphere reflectance prediction from the test site characterization. Additionally, results from using the transfer radiometer for a radiance-based calibration of the Operational Land Imager are presented.

10402-22, Session 5

Updates of MODIS On-orbit calibration uncertainty assessments

Xiaoxiong J. Xiong, NASA Goddard Space Flight Ctr. (United States); Amit Angal, Hongda Chen, Science Systems and Applications, Inc. (United States); Kwofu Chiang, Science Systems and Applicaitons, Inc. (United States); Xu Geng, Yonghong Li, Kevin A. Twedt, Zhipeng Wang, Truman Wilson, Aisheng Wu, Science Systems and Applications, Inc. (United States)

Terra and Aqua MODIS have successfully operated for more than 17 and 15 years, respectively, and continuously provided many science products that have significantly improved various studies of the earth's system and its key environmental parameters of land, oceans, and atmosphere. The MODIS level 1B (L1B) calibrated data products include TOA reflectance factors for the reflective solar bands (RSB), radiances for both the RSB and thermal emissive bands (TEB), and the associated uncertainty indices. The uncertainty indices are reported as unsigned integers, which can be converted to the uncertainties in percentage using coefficients provided in the L1B metadata. At launch, most contributors to the L1B uncertainties were estimated from pre-launch calibration and characterization and the use of its on-board calibrators (OBC). Starting from collection 6 (C6), the L1B uncertainties, which are represented via a set of time-dependent parameters, have included contributors estimated from ground observations. As both Terra and Aqua MODIS continue to operate beyond their design lifetime, changes in each instrument's performance and behavior need to be fully characterized and addressed in the L1B algorithms, including the uncertainties. This paper provides an overview of MODIS on-orbit calibration uncertainty assessments, its L1B uncertainty algorithm and implementation, lessons learned for the VIIRS L1B data products. It also discusses the updates resulting from recent changes in sensor characteristics and future improvements.

10402-23, Session 5

Crosstalk effect and its mitigation in Aqua MODIS middle wave infrared bands

Junqiang Sun, Global Science & Technology, Inc. (United States); Sriharsha Madhavan, Science Systems and Applications, Inc. (United States); Menghua Wang, Ctr. for Satellite Applications and Research (United States)

The MODerate-resolution Imaging Spectroradiometer (MODIS) is one of the primary instruments in the National Aeronautics and Space Administration (NASA) Earth Observing System (EOS). The first MODIS instrument was launched in December 1999 on-board the Terra spacecraft. A follow on MODIS was launched on an afternoon orbit in 2002 and is aboard the Aqua

spacecraft. Both MODIS instruments are very akin, has 36 bands, among which bands 20 to 25 are Middle Wave Infrared (MWIR) bands covering a wavelength range from approximately 3.750 ?m to 4.515 ?m. It was found that there was severe contamination in these bands early in mission but the effect has not been characterized and mitigated at the time. The crosstalk effect induces strong striping in the Earth View (EV) images and causes significant retrieval errors in the EV Brightness Temperature (BT) in these bands. An algorithm using a linear approximation derived from on-orbit lunar observations has been developed to correct the crosstalk effect and successfully applied to mitigate the effect in both Terra and Aqua MODIS Long Wave Infrared (LWIR) Photovoltaic (PV) bands. In this paper, the crosstalk effect in the Aqua MWIR bands is investigated and characterized by deriving the crosstalk coefficients using the scheduled Aqua MODIS lunar observations for the MWIR bands. It is shown that there are strong crosstalk contaminations among the five MWIR bands and they also have significant crosstalk contaminations from Short Wave Infrared (SWIR) bands. The crosstalk correction algorithm previously developed is applied to correct the crosstalk effect in these bands. It is demonstrated that the crosstalk correction successfully reduces the striping in the EV images and improves the accuracy of the EV BT in the five bands as was done similarly for LWIR PV bands. The crosstalk correction algorithm should thus be applied to improve both the image quality and radiometric accuracy of the Aqua MODIS MWIR bands Level 1B (L1B) products.

10402-24, Session 5

Improvements to Terra MODIS L2 science products through using crosstalk corrected radiances

Christopher C. Moeller, Richard A. Frey, Eva Borbas, W. Paul Menzel, Cooperative Institute for Meteorological Satellite Studies, Univ. of Wisconsin-Madison (United States); Truman Wilson, Aisheng Wu, Xu Geng, Science Systems and Applications, Inc. (United States)

Terra MODIS PVLWIR band 27 – 30 radiances have been increasingly contaminated by electronic crosstalk through the mission lifetime. In recent years, the contamination has been recognized as compromising the climate quality status of several MODIS L2 science products that depend on the PVLWIR bands. In response to this, the MODIS Characterization Support Team (MCST) has undertaken an effort to generate a crosstalk correction algorithm for use in the operational L1B radiance product algorithm. The correction algorithm has matured and crosstalk corrected L1B radiances have been applied in several Terra MODIS L2 science product algorithms, including MOD35 (Cloud Mask), MOD06 (Cloud Fraction, Cloud Particle Phase, Cloud Top Properties), and MOD07 (Water Vapor). This paper will discuss and document the L1B and L2 product improvements as a result of the crosstalk correction. The crosstalk correction itself is documented in other literature.

10402-25, Session 5

The performance of DC restoration function for MODIS thermal emissive bands

Zhipeng Wang, Science Systems and Applications, Inc. (United States); Xiaoxiong J. Xiong, NASA Goddard Space Flight Ctr. (United States); Ashish Shrestha, NASA Goddard Space Flight Ctr. (United States) and Science Systems and Applications, Inc. (United States)

The DC restore (DCR) process of MODIS instrument maintains the output of a detector at focal plane assembly (FPA) within the dynamic range of subsequent analog-to-digital converter, by adding a specific offset voltage to the output. The DCR offset value is adjusted per scan, based on the comparison of the DN values collected from the blackbody (BB) view with target DN saved as an on-board look-up table. In this work, the MODIS DCR mechanism is revisited, with the trends of DCR offset provided for thermal emissive bands (TEB). Noticeable changes have been occasionally found which coincide with significant detector gain change due to various reasons such as instrument safe-mode anomaly, south Atlantic anomaly and FPA temperature fluctuation. In general, MODIS DCR functionality has been effective and the change of DCR offset has no impact to the quality of MODIS data. One exception is the EV data saturation of Aqua MODIS LWIR bands 33, 35 and 36 during BB warm-up cool-down (WUCD) cycle observed since 2008. The BB view of their detectors saturate when the BB temperature is above certain threshold so the DCR cannot work as designed. Therefore, the dark signal DN fluctuates with the cold FPA (CFPA) temperature and saturate for a few hours per WUCD cycle, which also saturate all data sectors within the scan. The CFPA temperature fluctuation peaked in 2012 and has been reduced in recent years. While the saturation phenomenon has been easing accordingly, it demonstrates the importance of DCR to data production.

10402-26, Session 5

AIRS visible light channels: Lessons from 15 years of using internal calibration sources, vicarious calibration, and the use of deep convective clouds

Steven E. Broberg, Hartmut H. Aumann, Evan M. Manning, Jet Propulsion Lab. (United States)

The Atmospheric Infrared Sounder (AIRS) on the EOS Aqua Spacecraft was launched on May 4, 2002 and is currently fully operational. AIRS, in addition to the infrared system comprised of 2378 channels with wavelengths ranging from 3.7-15.4 um, has 4 Visible/Near-Infrared channels and an on-board calibration source utilizing 3 independent lamps to characterize the change in the visible response over time.

One of the key measurements related to climate change is the measurement of the Reflected Short-Wave Solar radiation (RSW). The AIRS visible light channels can be used to accurately measure the stability of the RSW. We describe our experience from 15 years of AIRS data with using internal calibration lamps, vicarious calibration, MODIS cross-calibration, and Deep Convective Clouds (DCCs) for the calibration and stabilization of the AIRS visible light data. The result is the DCC stabilized anomaly trend of the RSW measured with AIRS.

10402-27, Session 5

A strategy to assess the pointing accuracy of the CERES FM1-FM5 scanners

Nathaniel P. Smith, Z. Peter Szewczyk, Phillip C. Hess, Susan Thomas, Science Systems and Applications, Inc. (United States); Kory J. Priestley, NASA Langley Research Ctr. (United States)

The Clouds and the Earth's Radiant Energy System (CERES) scanning radiometer is designed to measure the solar radiation reflected by the Earth and thermal radiation emitted by the Earth. Five CERES instruments are currently in service; two aboard the Terra spacecraft, launched in 1999; two aboard the Aqua spacecraft, launched in 2002; and one instrument about the Suomi-NPP spacecraft, launched in 2011. Verifying the pointing accuracy of the CERES instruments is required to assure that all earth viewing data is correctly geolocated. The CERES team has developed an on-orbit technique for assessing the pointing accuracy of the CERES sensors that relies on a rapid gradient change of measurements taken over a well-defined and known Earth target, such as a coastline, where a strong contrast in brightness and temperature exists. The computed coastline is then compared with World Bank II map to verify the accuracy of the measurement location. This paper briefly restates the algorithm used in the study, describes the collection of coastline data, and summarizes the results of the study for each of the five CERES instruments currently in operation.

10402-28, Session 6

Initial post-launch radiometric calibration performance of GOES-16 ABI

Fangfang Yu, ERT, Inc. (United States); Xiangqian Wu, NOAA NESDIS Office of Satellite and Product Operations (United States); Hyelim Yoo, National Oceanic and Atmospheric Administration (United States) and ERT, Inc. (United States); Xi Shao, ERT, Inc. (United States)

The first NOAA next-generation geostationary weather satellites, GOES-R was successfully launched on 19 November 2016 and became GOES-16 when it reached the geostationary orbit on 29 November 2016. The satellite is currently parking at 89.5W about 35,000km above the Equator and undergoing intensive instrument performance tests. The main payload instrument on-board is Advanced Baseline Imager (ABI), which has 16 multi-spectral bands covering the spectrum between 0.47μm and 13.3 μm to provide continuous data stream for weather forecasting, disaster monitoring, and long-term climate research. This instrument, for the first time for the NOAA GOES satellites, is housed with a solar diffuser and a temperature-controlled blackbody to provide accurate on-orbit radiometric calibration for the 6 visible and near-infrared (VNIR) bands and 10 infrared (IR) bands, respectively. A series of methods and tools are being used at NOAA/STAR to validate and assess the ABI radiometric calibration accuracy. In this study, we will report the ABI radiometric calibration performance during the post-launch product tests (PLPT) period, including the results of using the ray-matching method to compare the ABI radiance with SNPP/VIIRS for the VNIR bands, and with SNPP/CrIS and Metop/IASI for the IR bands, desert observations to characterize the ABI VNIR imaging bands calibration stability, and lunar tracing images to validate VNIR spatial uniformity. Some other early results related to the instrument performance will also be reported at the meeting.

10402-29, Session 6

Calibration/validation status for GOES-16 products

Jon P. Fulbright, Arctic Slope Technical Services (United States); Elizabeth Kline, Science and Technology Corp. (United States); David R. Pogorzala, Integrity Applications, Inc. (United States); Wayne MacKenzie, Kathryn Mozer, Jamese Sims, Matthew Seybold, NOAA NESDIS Office of Satellite and Product Operations (United States)

The Geostationary Operational Environmental Satellite-R series (GOES-R) will be the next generation of NOAA geostationary environmental satellites. The first satellite in the series, GOES-16, was in November 2016. The satellite carries six instruments dedicated to the study of the Earth's weather (ABI), lightning mapping (GLM), solar observations (EXIS and SUVI), and space weather monitoring (MAG and SEISS). By August 2017, the product calibration/validation and instrument characterization plans for these six instruments should be past the Provisional product maturity threshold. These cal/val plans were created to advance the products through well-characterized states following an aggressive maturity schedule. In this talk, we give an update of the GOES-16 products, the path forward to Full product validation status, and a look forward to any changes to the cal/val plans GOES-S (to be launched in 2018).

10402-30, Session 6

Evaluation of GOES-16 ABI geospatial calibration accuracy using SNO method

Fangfang Yu, Xi Shao, ERT, Inc. (United States); Xiangqian Wu, National Oceanic and Atmospheric Administration (United States) and National Environmental Satellite, Data, and Information Service (United States) and Ctr. for Satellite Application and Research (United States); Vladimir Kondratovich, ERT, Inc. (United States)

The Advanced Baseline Imager (ABI) onboard the GOES-16 satellite is the first next-generation geostationary weather imager operated by NOAA. It has 6 solar reflective and 10 emissive bands for weather forecasting, natural disaster tracking and meteorological and climatic research. Compared to the legacy GOES weather instruments, ABI has improved spectral, spatial and temporal resolutions and the imagery of the 16 spectral bands are produced on a fixed-grid, which is referenced to an ideal location in space located in the earth's equatorial plane. To meet these challenging requirements for accurate geospatial calibration, a set of new technologies are applied for the ABI image navigation and registration (INR) processing. In this study, we evaluate the ABI navigation and band-to-band registration (BBR) accuracies for all the spectrally matched bands between ABI and the Suomi National Polar-orbiting Partnership (SNPP) Visible Infrared Imaging Radiometric Suite (VIIRS), using simultaneous nadir observations (SNO) data between these two instruments. The ABI resampling algorithm and kernels are used to simulate ABI observations using the spectrally matched VIIRS data. The navigation and BBR accuracies at VIIRS I and M band sub-pixel levels are derived using VIIRS geo-location as reference and transfer, respectively. Unlike the traditional INR evaluation method, which relies on clear sky images at coastline or river edges, this method works at heterogenic area with cloudy surface at the sub-satellite area. It will serve as a complementary and independent method to the Landsat imagery based INR algorithms to validate, evaluate and monitor ABI INR accuracies.

10402-31, Session 6

Sentinel 2B: the image quality performances at the beginning of the mission

Thierry L. Trémas, Vincent Lonjou, Arthur Dick, Florie Languille, Angélique Gaudel, Bruno Vidal, Ctr. National d'Études Spatiales (France)

Launched on March 6th, 2017 from Kourou, Sentinel 2B has passed the phase of commissioning. Sentinel 2B will work together with Sentinel 2A launched in June 2015. The building and implementation of the satellite has been realized under the responsibility of ESA, for the European Commission.

The subset of Image Quality commissioning was delegated by ESA to CNES, referring to the experience of the French Space Agency on previous imagers. This phase lasted 4 months after the launch, a little longer than the formal In Orbit Calibration period conducted by ESA, some Image Quality parameters requiring several months before converging to a stable state. This paper presents the status of the satellite, from an IQ prospective, just before it entered its operational phase. The radiometric and geometric performances are listed, including: the absolute radiometric calibration, the equalization, the SNR, the absolute and the multi-temporal location accuracy. The performances of both satellites Sentinel and Sentinel 2B working together, will be addressed. A particular focus will be done on multi-temporal location performances, homogeneity of radiometric inter calibrations. The accomplishment of the Global Reference Image over Europe is evoked as well.

The IQ commissioning phase ended on June 2017. From this date, the monitoring of IQ parameters is under the responsibility of ESA/ESRIN. Nevertheless, CNES continues to support ESA to survey the accuracy of S2A and S2B performances. The article ends by dealing with the prospective offered by the couple Sentinel 2A + Sentinel 2B.

10402-32, Session 6

Compact, on-demand broad spectral range (visible to long wave infrared) calibrator

James Chow, Edward Ward Jr., Raytheon Space and Airborne Systems (United States)

First, the emission wavelengths from visible to short-wave infrared are generated by Light Emitting Diodes (LEDs) and phosphors which spectrally down convert the higher energy photons from the LED to a lower energy photon distribution. This process is analogous to the commercial lighting industry where blue LEDs are down converted into a distribution that resembles variations of white light. Second, several formats of carbon materials have been combined together into a multi-layer structure so that a highly uniform temperature interface feeds a high emissivity surface of vertically aligned carbon nanotubes. Finally, both of these technologies give rise to a thin profile, layered structure which can be easily mounted on a paddle for movement in and out of the optical path.

10402-33, Session 7

Rapid acquisition, processing, and delivery of advanced infrared and microwave sounder data from polar orbiting satellites for numerical weather prediction and other time-sensitive applications

Liam Gumley, Univ. of Wisconsin-Madison (United States)

The current and future satellites of the US Joint Polar Satellite System (JPSS) in low earth orbit provide advanced sounder observations from the Cross-track Infrared Sounder (CrIS) and the Advanced Technology Microwave Sounder (ATMS) for applications including numerical weather prediction, weather forecasting, and aviation hazard detection. NOAA has funded the deployment and operation of a network of satellite ground stations across North America and the Pacific to acquire sounder data from these satellites in real-time, and in conjunction with Cooperative Institute for Meteorological Satellite Studies (CIMSS) at the University of Wisconsin-Madison, has established a system for processing the data with low latency and delivering it to the National Weather Service for assimilation in rapid-refresh numerical weather prediction (NWP) models. The data are also delivered to EUMETSAT for retransmission via satellite to NWP centers in Europe. This presentation will outline the features of the space-borne sensors, the ground receiving stations, the processing system, and the delivery networks which allow advanced infrared and microwave sounder data to be delivered to end users within minutes of the end of a satellite passing over the ground station. This presentation will also describe recent efforts to cut the data latency from the order of minutes to seconds, by using novel processing techniques at the ground station while a satellite is passing overhead.

10402-34, Session 7

Comparison between point-based and line-based parallel-projection transformation models in rectifying satellite images

Ahmed Elaksher, California State Polytechnic Univ., Pomona (United States)

The quick advance in remote sensing technologies established the potential to gather accurate and reliable information about the Earth surface using high resolution satellite images. Remote sensing satellite images of less than one-meter pixel size are currently used in large-scale mapping. Rigorous photogrammetric equations are usually used to describe the relationship between the image coordinates and ground coordinates. These equations require the knowledge of the exterior and interior orientation parameters of the image that might not be available. On the other hand, the parallel projection transformation could be used to represent the mathematical relationship between the image-space and object-space coordinate systems and provides the required accuracy for large-scale mapping using fewer ground control features. This article investigates the differences between point-based and line-based parallel projection transformation models in rectifying satellite images with different resolutions. The point-based parallel projection transformation model and its extended form are presented and the corresponding line-based forms are developed. Results showed that the RMS computed using the point- or line-based transformation models are equivalent and satisfy the requirement for large-scale mapping. The differences between the transformation parameters computed using the point- and line-based transformation models are insignificant. The results showed high correlation between the differences in the ground elevation and the RMS.

10402-35, Session 7

Integrating satellite images and LIDAR data for shoreline mapping

Ahmed Elaksher, California State Polytechnic Univ., Pomona (United States)

Shorelines are imperative for coastal ecosystems and activities. Despite this simplicity, accurate and precise extraction of these features is a challenging task due to the complicity of water bounding zones. Shoreline mapping has been carried out through a variety of techniques such as traditional surveying and aerial mapping. As spatial resolution and geospatial mapping technologies improved in the last few years, satellite images and active remote sensing systems have also been introduced to produce high quality shorelines. The focus of this research is on generating reliable shorelines from satellite images and LIDAR datasets. Different classification algorithms were implemented and tested followed by a number of image processing techniques to vectorize shoreline pixels. The completeness and geometric accuracy of the results are presented and evaluated. They show the benefits of adding ranging data in improving both shoreline recognition quality and mapping accuracy.

10402-36, Session 7

Satellite-based shoreline change detection analysis using operational land imager data

Wasim Pervez, Shoab Ahmad Khan, National Univ. of Sciences and Technology (Pakistan)

Remote sensing change detection remains a challenging problem. Change detection techniques using pre-classification provide changes but do not provide information on the nature of that change. Post classification change detection technique is most commonly used technique due to its inherent advantages as well as its compensation for variation in atmospheric correction. Post classification change detection technique provides its suitability for medium and high resolution data and minimizes impact of misregistration, inconsistencies in classification. Hence is suitable for change detection analysis of Operational Land Imager (OLI) data. This paper investigated OLI suitability for post classification change detection analysis for shoreline changes due to its enhanced features over previous Landsat series. This paper evaluated OLI data classification using support vector machine (SVM) by using data for the four seasons (i.e., spring, summer, autumn and winter) and were compared for the change detection results of the six cases: (1) spring to summer; (2) spring to autumn; (3) spring to winter; (4) summer to autumn; (5) summer to winter; (6) autumn to winter. The results confirmed that OLI SVM classified data is appropriate for shoreline post-classification change detection analysis of the study area.

10402-37, Session 7

Applicability of Distrad technique for downscaling of thermal images in different seasons over Raipur city and its surroundings

Subhanil Guha, Himanshu Govil, National Institute of Technology, Raipur (India); Sandip Mukherjee, TERI Univ. (India)

Land surface temperature (LST) considers a number of biophysical processes associated with the interaction between earth surface features and atmosphere. The present study analysed the applicability of the DisTrad thermal sharpening method to correlate land surface temperature over different types of land surface indices. Water body, Vegetation, Bare land and built-up area were considered as different categories of land cover. Landsat and MODIS satellite data of different seasons having various spatial and temporal resolutions were used for evaluating thermal sharpening. Raipur city and its surroundings were selected for the entire work. High resolution land surface temperature can be retrieved from low resolution sensors using DisTrad based on impervious percentage relationship with the urban land surface temperature. Downscaled land surface temperature at higher resolutions presents a higher correlation compare to the observed land surface temperature. DisTrad technique with impervious percentage always shows a higher correlation with land surface temperature in comparison with NDVI for all the seasons. This thermal sharpening technique allows an improved estimation of urban heat island (UHI) mapping.

10402-38, Session 7

HT-FRTC: Fast radiative transfer using Gaussian processes

Gerald J. Wong, Stephan Havemann, Met Office (United Kingdom)

The Havemann-Taylor Fast Radiative Transfer Code (HT-FRTC) is a principal component (PC) based code that can be used across the whole electromagnetic spectrum to calculate transmittance, radiance and flux spectra. The PCs cover the spectrum at very high spectral resolution, allowing very fast line-by-line, hyperspectral and broadband simulations for satellite-based, airborne and ground-based sensors. The PCs are derived during a code training phase from line-by-line simulations for a diverse set of atmosphere and surface conditions. The derived PCs are sensor independent, with no extra training required to include additional sensors.

The HT-FRTC code is an integral part of the Met Office's Tactical Decision Aids such as NEON, playing an important part in the prediction of environmental impacts on sensors such as IR cameras and night-vision goggles. Moreover, the HT-FRTC has been incorporated into a one-dimensional variational (1D-Var) retrieval system that also works solely in PC space. This reduces the dimensions of the matrices involved, which are important for computational efficiency. Examples of the above applications will be presented, including the retrievals of surface and cloud properties.

10402-40, Session 8

High efficiency signal acquisition

Xiteng Liu, QualVisual Technology (Canada)

This paper presents a new mathematical method for high efficiency signal acquisition. The new method makes revolutionary improvement as compared with compressed sensing. It dispenses with both sparsity and convex optimization on which compressed sensing relies. Convex optimization techniques such as linear programming and orthogonal matching pursuit employ iterative computations and may become very slow and unstable in high dimensional systems. Doing without convex optimization, the new method dramatically improves both computing speed and computing stability. It is eligible for real time applications. Even better, the new method doesn't require signals to have sparse representations. A signal can be recovered in perceptually lossless quality from its as few as 25% samples. Experimental results manifest that our new method may overwhelmingly outperform compressed sensing methods. Demo software and testing data are all downloadable at the website http://qualvisual.net.

10402-41, Session 8

Experimentally validated modification to Cook-Torrance BRDF model for improved accuracy

Samuel D. Butler, Air Force Institute of Technology (United States); James A. Ethridge, Air Force Institute of Technology (United States) and Southwestern Ohio Council for Higher Education (United States); Stephen E. Nauyoks, Air Force Institute of Technology (United States) and Oak Ridge Institute for Science and Education (United States); Michael A. Marciniak, Air Force Institute of Technology (United States)

The bidirectional reflectance distribution function (BRDF) describes material reflectance by relating incident irradiance to scattered radiance. One popular class of BRDF models is the microfacet model, which assumes geometric optics but is computationally simpler than wave optics models, and thus more readily applicable to remote sensing. One drawback of this geometric optics model is the need for a cross section conversion term, which diverges at large angles. This problem is only partially addressed by adding a geometric attenuation (shadowing and masking) term to conserve energy, while still neglecting wave optics effects. In 2003, Matusik measured 100 materials in the MERL database. In 2015, Butler measured several rough materials in the IR at multiple wavelengths with higher fidelity using the SMS CASI®. Butler also proposed a theoretical approximation to replace the geometric attenuation and cross section conversion terms in the microfacet model with the closed-form polarization factor, Q, present in wave optics models such as Rayleigh-Rice. In this work, this theoretical approximation is validated using experimental results from Matusik's MERL measurements and Butler's IR measurements. These BRDFs are fitted to a novel version of the Cook-Torrance model using the polarization factor, and the error in the fits are compared to the standard Cook-Torrance model. The overall error is decreased when using the novel model, particularly for large incident and scattered angles. These experimental results suggest incorporating the polarization factor in the microfacet model in the way previously posited by Butler to improve the quality of fit consistently for several rough materials.

10402-42, Session 8

Wave optics simulation of statistically rough surface scatter

Ann Lanari, Samuel D. Butler, Michael A. Marciniak, Air Force Institute of Technology (United States); Mark F. Spencer, Air Force Research Lab. (United States)

The Bidirectional Reflectance Distribution Function (BRDF) describes optical scatter from surfaces by relating the incident irradiance to the exiting radiance over the entire hemisphere. Laboratory verification of BRDF models and experimentally populated BRDF databases are hampered by sparsity of monochromatic sources and ability to statistically control the surface features. Numerical methods are able to control surface features, have wavelength agility, and via Fourier methods of wave propagation, may be used to fill the knowledge gap. Monte-Carlo techniques, adapted from turbulence simulations, generate Gaussian distributed and correlated surfaces with an area of 1 cm2, RMS surface height of 2.5 μm, and correlation length of 100 μm. The surface is centered inside a Kirchhoff absorbing boundary with an area of 16 cm2 to prevent wrap around aliasing in the far field. These surfaces are uniformly illuminated at normal incidence with a

unit amplitude plane-wave varying in wavelength from 3 μm to 5 μm. The resultant scatter is propagated to a detector in the far field utilizing multi-step Fresnel Convolution and observed at angles from -2μrad to 2μrad. The far field scatter is compared to both a physical wave optics BRDF model (Modified Beckmann Kirchhoff) and two microfacet BRDF Models (Priest, and Cook-Torrance). Modified Beckmann Kirchhoff, which accounts for diffraction, is consistent with simulated scatter for multiple wavelengths for RMS surface heights greater than ?/2. The microfacet models, which assume geometric optics, are less consistent across wavelengths. Both model types over predict far field scatter width for RMS surface heights less than ?/2.

10402-43, Session 9

The Sentinel 4 focal plane subsystem

Rüdiger Hohn, Airbus Defence and Space (Germany); Michael Skegg, Airbus Defence and Space (Germany); Markus Hermsen, Airbus Defence and Space (Germany); Christian Williges, Ralf Reulke, Deutsches Zentrum für Luft- und Raumfahrt e.V. (Germany)

The Sentinel 4 instrument is an imaging spectrometer, developed by Airbus under ESA contract in the frame of the joint European Union (EU)/ESA COPERNICUS program with the objective of monitoring trace gas concentrations. SENTINEL 4 will provide accurate measurements of key atmospheric constituents such as ozone, nitrogen dioxide, sulfur dioxide, formaldehyde, as well as aerosol and cloud properties.

SENTINEL 4 is unique in being the first geostationary UVN mission. The SENTINEL 4 space segment will be integrated on EUMETSAT's Meteosat Third Generation Sounder satellite (MTG-S). Sentinel 4 will provide coverage of Europe and adjacent regions.

The Sentinel 4 instrument comprises, as a major element, two Focal Plane Subsystems (FPS) covering the wavelength ranges 305nm to 500 nm (UVVIS) and 750 to 775 nm respectively.

The paper describes the Focal Plane Subsystems, comprising the detectors, the optical bench and the control electronics. Further the design and development approach will be presented as well as first measurement results of FPS Qualification Model.

10402-44, Session 9

The Sentinel-4 UVN focal plane assemblies

Jürgen Hinger, Rüdiger Hohn, Airbus Defence and Space (Germany); Ralf Reulke, Deutsches Zentrum für Luft- und Raumfahrt e.V. (Germany)

The Sentinel-4 UVN Instrument which is a dispersive imaging spectrometer covering the UV-VIS and the NIR wavelength is developed and built under an ESA contract by an industrial consortium led by Airbus DS GmbH.

It will be accommodated on board of the MTG-S (Meteosat Third Generation - Sounder) satellite that will be placed in a geostationary orbit over Europe sampling data for generating two-dimension maps of a number of atmospheric trace gases.

The light reflected by a scan mirror into a common telescope passes a slit and a polarization scrambler and is split by a dichroic beam splitter in the NIR and UV-VIS band. The UV-VIS part of the light (305-500 nm) is dispersed by a combination of a grating and a prism inside the UV-VIS spectrometer and detected by a dedicated CCD accommodated inside the UV-VIS Focal Plane Assembly (FPA).

The near infra-red (NIR) light (750-775 nm) which is dispersed by a reflective grating in the NIR spectrometer is detected by the NIR-CCD inside the NIR FPA. Both CCD detectors acquire spectral channels and spatial sampling in two orthogonal directions and will be operated at about 215 K mainly to minimize random telegraph signal effects and to reduce dark current. Stringent detector temperature as well as alignment stability requirements of less than ±0.1 K per day respectively of less than 2 micrometers/2 arcseconds from ground to orbit are driving the FPA thermo-mechanical design. A special FPA design features is the redundant LED-calibration system for bad pixel detection as well as pixel gain and linearity monitoring.

This paper reports on the design and qualification of the Focal Plane Assemblies with emphasis on thermo-mechanical as well as alignment stability verification.

10402-45, Session 9

The Sentinel-4 detectors: Architecture and performance

Michael Skegg, Markus Hermsen, Rüdiger Hohn, Airbus Defence and Space (Germany); Christian Williges, Deutsches Zentrum für Luft- und Raumfahrt e.V. (Germany); Charles Woffinden, e2v technologies plc (United Kingdom); Yves Levillain, European Space Research and Technology Ctr. (Netherlands); Ralf Reulke, Deutsches Zentrum für Luft- und Raumfahrt e.V. (Germany)

The Sentinel-4 instrument is an imaging spectrometer, developed by Airbus under ESA contract in the frame of the joint European Union (EU)/ESA COPERNICUS program. SENTINEL 4 will provide accurate measurements of trace gases from geostationary orbit, including key atmospheric constituents such as ozone, nitrogen dioxide, sulfur dioxide, formaldehyde, as well as aerosol and cloud properties.

Key to achieving these atmospheric measurements are the two CCD detectors, covering the wavelengths in the ranges 305 nm to 500 nm (UVVIS) and 750 to 775 nm (NIR) respectively. The paper describes the architecture, and operation of these two CCD detectors, which have an unusually high full-well capacity and a very specific architecture and read-out sequence to match the requirements of the Sentinel-4 instrument. The key performance aspects and their verification through measurement are presented, with a focus on an unusual, bi-modal dark signal generation rate observed during test.

10402-46, Session 9

The Sentinel 4 detector electrical system integration

Markus Hermsen, Rüdiger Hohn, Michael Skegg, Airbus Defence and Space (Germany); Christian Williges, Deutsches Zentrum für Luft- und Raumfahrt e.V. (Germany); Charles Woffinden, e2v technologies plc (United Kingdom); Ralf Reulke, Deutsches Zentrum für Luft- und Raumfahrt e.V. (Germany)

The detectors of the Sentinel 4 multi spectral imager are operated in flight at 215K while the analog electronics is operated at ambient temperature. As the cooling power is highly limited no active component has been allowed in the cooled area closest to the detector. Electrically a short connection between detector and electronics is ideal. From mechanical and from thermal point of view the connection requires a certain minimum length. The selected solution supports all these aspects but had to approach the limits of what is electrically feasible. Such constraints manifested a severe challenge in the design as no sacrifice on the technical system performance is acceptable. The physical separation between CCD detector and the Frontend Electronics, the adverse EMI environment in which the instrument will be operated in (the location of the instrument on the satellite is in vicinity to a downlink K-band communication antenna of the S/C and no effective shielding means are given on the satellite to protect from these signals) and the extreme cleanliness requirements for the detector in manufacturing and assembly are some examples for specific challenges to overcome.

This paper describes how in Sentinel 4 the given issues have been overcome, how the limited load drive capability of the detector component

has been considered on a flex length of about 20cm (~8") and how EMC shielding of the highly sensitive analogue signals of the detector has been realized. Also covered are design/manufacturing aspects and a glance on testing results.

The result is an Instrument, based on CCD detectors which are proven to be ruggedized versus strong RF signals and which allows to read out the detector signals with 13,5 bit effective resolution at a pace of 1,42MHz.

10402-47, Session 9

Verification of the Sentinel-4 focal plane subsystem

Christian Williges, Mathias Uhlig, Stefan Hilbert, Hannes Rossmann, Kevin Buchwinkler, Steffen Babben, Llse Sebastian, Deutsches Zentrum für Luft- und Raumfahrt e.V. (Germany); Rüdiger Hohn, Airbus Defence and Space (Germany); Ralf Reulke, Deutsches Zentrum für Luft- und Raumfahrt e.V. (Germany)

The Sentinel-4 payload is a multi-spectral camera system which is designed to monitor atmospheric conditions over Europe. The German Aerospace Center (DLR) Berlin conducted the verification campaign of the Focal Plane Subsystem (FPS) on behalf of Airbus Defense and Space GmbH. The FPS consists of two Focal Plane Assemblies, one for the UV-VIS spectral range (305 nm ... 500 nm), the second for NIR (750 nm ... 775 nm). In this publication, we will present the laboratory set-up of the verification campaign of the Sentinel-4 Qualification Model which will also be used for the upcoming Flight Model verification.

The test campaign consists mainly of radiometric tests performed with an integrating sphere as homogenous light source, as well as a cross-talk test with a 635 nm Diode-Laser as point source. A MTF test will be performed on the Sentinel-4 Engineering Model detector which is identical to the QM.

The FPS has to be operated at 215 K, making it necessary to employ a thermal vacuum chamber (TVC) for the test accomplishment. This publication focuses on the challenge to remotely illuminate both Sentinel-4 detectors as well as a reference detector homogeneously over a distance of approximately 1 m from outside the TVC. Furthermore we will report on the additional set-up for remote illumination with a Laser and the MTF test set-up.

Aside the opto-mechanical test set-up, the publication presents a way to automate numerous tests. Due to the vast amount of measurements to be performed during the test campaign a high grade of automatization is necessary.

10402-48, Session 9

RTS effect detection in Sentinel-4 data

Henrique Candeias, Xavier Gnata, Maximilian Harlander, Markus Hermsen, Rüdiger Hohn, Stefan Riedl, Michael Skegg, Airbus Defence and Space (Germany); Ralf Reulke, Deutsches Zentrum für Luft- und Raumfahrt e.V. (Germany)

The future ESA Earth Observation Sentinel-4/UVN is a high resolution spectrometer intended to fly on board a Meteosat Third Generation Sounder (MTG-S) platform, placed in a Geostationary orbit. The main objective of this optical mission is to continuously monitor the air quality over Europe in near-real time.

The Sentinel-4/UVN instrument operates in three wavelength bands: Ultraviolet (UV: 305-400 nm), Visible (VIS: 400-500 nm) and Near-infrared (NIR: 750-775 nm). Two dedicated CCD detector have been developed to be used in the Focal Plane Subsystems (FPS), one for the combined UV and VIS band, the other covering the NIR band.

Being an high resolution spectrometer with challenging radiometric accuracy requirements, both on spectral and spatial dimensions, an effect such the Random Telegraph Signal (RTS) can represent a relevant contribution for the complete system accuracy.

In this work we analyze the RTS effect on data acquired during the FPS testing campaign with qualification models for the Sentinel-4/UVN detectors, performed in late 2016. The strategy for the impact assessment of RTS was to measure the effect at room temperature and then to extrapolate the results to the at instrument operational temperature. This way very-long lasting data acquisitions could be avoided.

A technique for RTS effect detection has been developed in order to characterize the signal levels amplitude and flipping rate frequencies.

We demonstrate the residual impact of the RTS on the global In-Orbit Sentinel-4/UVN instrument performance and products accuracy.

10402-21, Session 10

A reflectance-based cross calibration of the Landsat archive

Cibele Teixeira Pinto, South Dakota State Univ. (United States); Sandeep Chittimalli, NASA Goddard Space Flight Ctr. (United States); Larry Leigh, Timothy Ruggles, Dennis L. Helder, South Dakota State Univ. (United States)

First launched in 1972, the Landsat satellite sensors have provided the longest continuous record of high quality images of the Earth's surface that are used in both civilian and military applications. Extraction of quantitative information (e.g., surface reflectance) from the Landsat image data is only possible through a well-performed absolute radiometric calibration. Typically, this calibration has been performed as a radiance based cross-calibration between sensors. However, to convert radiance to reflectance an accurate estimate of solar exoatmospheric irradiance is critical; and there are several solar models currently available which estimate exoatmospheric irradiance with varying levels of accuracy. A TOA reflectance-based approach, independent of exoatmospheric irradiance, has been developed to provide a consistent cross calibration of the entire Landsat series (from Landsat 8 OLI to Landsat 1 MSS), based on analysis of coincident and near-coincident scene pairs acquired with each sensor. With this method, the Landsat-8 OLI reflectance measurements are used as the starting point (reference), as they are estimated with a 3% uncertainty (compared to the 5% uncertainty associated with radiance measurements). A set of radiometric coefficients has been estimated based on the equations presented in this paper, which allows direct conversion of the digital numbers from the image data to TOA reflectance. The results obtained from application of these coefficients show significant improvement in consistency of reflectance measurements between the Landsat sensors.

10402-49, Session 10

Radiometric characterization of Landsat Collection 1 products

Esad Micijevic, Md. Obaidul Haque, U.S. Geological Survey (United States) and SGT, Inc. (United States); Nischal Mishra, U.S. Geological Survey (United States) and Virtuoso Technologies Inc. (United States)

Landsat data in the U.S. Geological Survey (USGS) archive are being reprocessed to generate a tiered collection of consistently geolocated and radiometrically calibrated products that are suitable for time series analyses. With the implementation of the collection management, no major updates will be made to calibration of the Landsat sensors within a collection. Only calibration parameters needed to maintain the established calibration trends without an effect on derived environmental records will be regularly updated, while all other changes will be deferred to a new collection. This first collection, Collection 1, incorporates various radiometric calibration updates to all Landsat sensors including absolute and relative gains for Landsat 8 Operational Land Imager (OLI), stray light correction for Landsat 8 Thermal Infrared Sensor (TIRS), absolute gains for Landsat 4 and 5 Thematic Mappers (TM), recalibration of Landsat 1-5 Multispectral Sensors (MSS) to ensure radiometric consistency among different formats

of archived MSS data, and a transfer of Landsat 8 OLI reflectance based calibration to all previous Landsat sensors. It is important to note that, although still available for download from the USGS web pages, the products generated using the pre-collection processing do not benefit from the latest radiometric calibration updates.

In this paper, we are assessing radiometry of Landsat Collection 1 products through analysis of trends in pseudo invariant site (PICS) responses and comparisons with the pre-collection products.

10402-50, Session 10

Using earth data to evaluate Landsat 8 collection-1 products radiometric uniformity stability of the focal plane array sensor chips

Raviv Levy, NASA Goddard Space Flight Ctr. (United States) and Science Systems and Applications, Inc. (United States); Brian L. Markham, NASA Goddard Space Flight Ctr. (United States)

The Operational Land Imager (OLI) and Thermal Infrared Sensor (TIRS) aboard the Landsat-8 satellite were rigorously characterized prior to launch to assure flat response at any illumination level and spectra. In this paper we demonstrate how to use in-orbit routine earth data collects processing for extracting information about the sensor chip-to-chip response uniformity across the focal plane array (FPA) field of view (FOV). We evaluate the stability of the response uniformity overtime and against factors such as mean signal level or solar azimuth.

10402-51, Session 10

Statistical relative gain calculation for Landsat 8

Cody Anderson, SGT, Inc. (United States); Dennis L. Helder, Drake Jeno, South Dakota State Univ. (United States)

The Landsat 8 Operational Land Imager (OLI) is an optical multispectral push-broom sensor with a focal plane consisting of over 7000 detectors per spectral band. Each of the individual imaging detectors contributes one column of pixels to an image. It is therefore important to ensure each detector's response is consistent with the responses of each of the other detectors. Any difference in the response between neighboring detectors may result in a visible stripe or band in the imagery. Assuming a detector's response is linear, matching detector responses requires a bias and a relative gain. The gain is called a relative gain since it is matching a detector's response to the spectral band average and not estimating the actual input output response curve. Several methods exist for estimating a detector's relative gain including on-board calibration systems, i.e. a solar diffuser, or special spacecraft maneuvers, i.e. a 90 degree yaw/side slither. This paper describes a procedure for estimating relative gains which uses only normally acquired Earth viewing statistics. The primary idea behind the procedure is that over a "long enough" period of time each detector should receive the same distribution of radiance levels, and if the input is the same for every detector, the output can be equalized by equalizing the means of the output distributions. Things to be considered are how long of time period, i.e. number of scenes, is needed and which scenes provide the best results.

10402-52, Session 10

Landsat-8 TIRS radiometric calibration status

Julia A. Barsi, Brian L. Markham, NASA Goddard Space Flight Ctr. (United States); Matthew Montanaro, Rochester Institute of Technology (United States); Simon Hook, Jet Propulsion Lab. (United States) and NASA Goddard Space Flight Ctr. (United States); John R. Schott, Nina G. Raqueno, Aaron D. Gerace, Rochester Institute of Technology (United States)

The Thermal Infrared Sensor (TIRS) instrument is the thermal-band imager on the Landsat-8 platform. Unlike previous Landsat satellites, there are two thermal bands on Landsat-8 but they are included on a separate instrument from the reflective bands of the Operational Land Imager (OLI). The OLI and TIRS are operated jointly on a single platform to provide a data product continuous with the previous sensors, but the new design of the TIRS instrument has led to calibration problems.

The absolute calibration of the TIRS instrument began immediately after launch by teams from NASA/JPL and the Rochester Institute of Technology. Using measurements from buoys over large water bodies, the predicted sensor-reaching radiance is compared to the radiance provided by TIRS. The initial calibration estimates showed large average errors in both bands, -0.29 and -0.51 W/m2 sr um or -2.1K and -4.4K at 300K in Band 10 and 11, respectively, as well as high variability in the errors, 0.87K (1 sigma) and 1.67K (one sigma), respectively. The average bias error was corrected in operational processing in January 2014, though this adjustment did not account for the variability.

Using scans of the moon as a source , it was determined that stray light originating from far outside the nominal field of view was the origin of the calibration error and variability. An algorithm for modeling the stray light effect was developed and implemented in the Landsat-8 processing system in February 2017. The new process has improved the overall calibration of the two TIRS bands, such that it reduces the residual variability in the calibration from 0.87K to 0.52K at 300K for Band 10 and from 1.67K to 0.91K at 300K for Band 11.

10402-53, Session 10

Landsat 8 TIRS calibration with external sensors

Yue Wang, Emmett J. Ientilucci, Nina G. Raqueno, John R. Schott, Rochester Institute of Technology (United States)

This paper describes a methodology to calibrate stray light error for the Landsat 8 TIRS sensor with data from external sensors, such as Geostationary Operational Environmental Satellite (GOES) and Meteosat Second Generation Satellite (MSG). We utilized the near-coincident thermal image data from these external sensors as the source of stray light radiance (i.e., ghost radiance). Necessary slant path and sensor response corrections were implemented to those sensors before gathering the ghost radiance. Previous studies have proposed an optical model to indicate the ghosting source locations and relative magnitude of the ghost. Once the out-of-field radiance values were collected, two different algorithms are proposed. One method utilizes the magnitude provided by the optical model while the second method uses regression technics to re-estimate stray light errors. Moderate Resolution Imaging Spectroradiometer (MODIS) Sea Surface Temperature (SST) product coupled with water temperatures measured by Buoys were two metrics used to evaluate results. The top-of-atmosphere (TOA) radiance from target water bodies was derived from the measured temperature and the model of the atmosphere at the time of image acquisition. The differences between the calculated TOA radiance and the derived TIRS radiance represents the absolute radiometric calibration error for the sensor. Initial experiments have shown the absolute calibration error has been reduced from 2K to 0.5K when this correction method is implemented.

10402-54, Session 10

Assessing the potential to use the split window technique to retrieve surface temperature with Landsat 8's thermal infrared sensor (TIRS)

Aaron D. Gerace, Matthew Montanaro, Rochester Institute of Technology (United States); Ronald A. Morfitt, U.S. Geological Survey (United States)

Since the launch of the Landsat 8 Thermal Infrared Sensor (TIRS) in early 2013, the utility of its image data for surface temperature retrieval has been hindered by a stray light effect within the instrument. In the subsequent years, a stray light removal algorithm was developed and approved by the Landsat Calibration and Validation team to be incorporated into the USGS ground system. In February 2017, all TIRS data were reprocessed to remove stray light effects, significantly improving the radiometric quality of the data. Considering its dual-band design, and its improved radiometric quality, TIRS exhibits the potential to be used for surface temperature retrieval using the Split-Window technique.

This work investigates the renewed interest for TIRS data to be used to derive surface temperature. A modeling analysis is conducted to assess the accuracy of the Split-Window technique as a function of a sensor's absolute radiometric fidelity. The Split-Window technique is then applied to actual TIRS image data, both before and after the stray light correction, to retrieve surface temperature and compared to MODIS-derived surface temperature. Considering Terra/MODIS is outperforming its absolute radiometric accuracy requirement of 0.5% for the bands corresponding to TIRS, its data is used as a reference. Results of the studies presented here indicate that the stray light removal algorithm significantly improves the utility of TIRS data with surface temperature retrieval accuracies that are in-line with Terra/MODIS.

10402-55, Session 11

JPSS-1 VIIRS RSB sensor spectral response calibration and its applications

Jinan Zeng, Fibertek Inc. (United States) and NASA Goddard Space Flight Ctr. (United States); James J. Butler, Xiaoxiong J. Xiong, NASA Goddard Space Flight Ctr. (United States); Hassan Oudrari, Jeffery McIntire, Thomas Schwarting, Qiang Ji, Science Systems and Applications, Inc. (United States)

We present system-level responsivity calibration results of the visible and near infrared channels of JPSS-1 VIIRS in the reflective solar band (RSB) from bands M1(412 nm) to M7 (865 nm). A monochromator-based method based on the Spectral Measurement Assembly (SpMA), and a laser-based calibration method based on Travelling-Spectral Irradiance and Radiance responsivity Calibrations using Uniform Sources (T-SIRCUS) were applied to determine the relative and absolute spectral responses (RSR and ASR). These responsivities are provided for both the single pixel/detector and band-averaged cases for each band. Differences in RSR results from the two methods, SpMA and T-SIRCUS, are compared. The contribution of spectral features in the RSRs is also examined through a comparison to the component-level spectral transmittance of the VIIRS bandpass filters. The potential effects of detector-to-detector RSR variations on image quality are also investigated. The two calibration methods using different configurations provide the opportunity to separate optical and electrical cross-talk as well as contributions from out-of-band which is estimated at about 3 %. We also utilize the ASRs to verify the gain coefficients derived from an independent radiometric calibration test using a broadband source. The system-level responsivity measurement methodologies presented in this paper demonstrate a more accurate, NIST-traceable calibration, which can be used to validate/verify conventional radiometric calibration tests.

10402-56, Session 11

Atmospheric correction for JPSS-2 VIIRS response versus scan angle measurements

Jeffrey McIntire, Science Systems and Applications, Inc. (United States); Christopher C. Moeller, Univ. of Wisconsin-Madison (United States); Hassan Oudrari, Science Systems and Applications, Inc. (United States); Xiaoxiong J. Xiong, NASA Goddard Space Flight Ctr. (United States)

The Joint Polar Satellite System 2 (JPSS-2) Visible Infrared Imaging Radiometer Suite (VIIRS) includes one spectral band centered in a strong atmospheric absorption region. As much of the pre-launch calibration is performed under laboratory ambient conditions, accurately accounting for the absorption, and thereby ensuring the transfer of the sensor calibration to on-orbit operations, is necessary to generate science quality data products. This work is focused on the response versus scan angle (RVS) measurements, which characterize the relative scan angle dependent reflectance of the JPSS-2 VIIRS instrument optics. The spectral band of interest, centered around 1378 nm, is within a spectral region strongly effected by water vapor absorption. The methodology used to model the absolute humidity and the atmospheric transmittance under the laboratory conditions is detailed. The application of this transmittance to the RVS determination is then described including an uncertainty estimate; a comparison to the pre-launch measurements from earlier sensor builds is also performed.

10402-57, Session 11

VIIRS pre-launch near field response characterization

Thomas Schwarting, Jeffrey McIntire, Hassan Oudrari, Science Systems and Applications, Inc. (United States); Xiaoxiong J. Xiong, NASA Goddard Space Flight Ctr. (United States)

The Visible Infrared Imaging Radiometer Suite (VIIRS) is a scanning radiometer sensor containing 22 spectral bands that is currently taking data aboard the Suomi-NPP satellite. A second flight unit is set to launch aboard the JPSS-1 satellite in the 4th quarter of 2017 followed by a third one aboard JPSS-2 in 2022. The VIIRS sensor is designed to obtain high quality data products over a variety of conditions including high contrast scenes like bright clouds over ocean for example. In the pre-launch test program the vendor, Raytheon, makes measurements to determine the contamination from Near Field Response (NFR), which is scattered light from bright targets, to characterize these features and compare them against the structured scene requirement. As of now prelaunch testing has been completed on the first three VIIRS flight units, S-NPP, JPSS-1 and JPSS-2, with independent analyses performed by the NASA VCST team. We present this NFR characterization including derivation of the Harvey-Shack coefficients and impacts from other contamination such as retro reflections off the dewar to the cold focal planes. Impact of these effects to the on-orbit products will be explored as well.

10402-58, Session 11

Spectralon solar diffuser BRDF variation for NPP, JPSS J1, and JPSS J2

Vijay Murgai, Lindsay H. Johnson, Staci N. Klein, Raytheon Space and Airborne Systems (United States)

The Visible/Infrared Imaging Radiometer Suite (VIIRS) is a key sensor on the Suomi National Polar-orbiting Partnership (NPP) satellite as well as the upcoming Joint Polar Satellite System (JPSS). VIIRS collects Earth radiometric and imagery data in 22 spectral bands from 0.4 to 12.5

?m. Radiometric calibration of the reflective bands in the 0.4 to 2.5 ?m wavelength range is performed by measuring the sunlight reflectance from Spectralon®. Reflected sun light is directly proportional to the Bidirectional Reflectance Distribution Function (BRDF) of the Spectralon®. This paper presents the BRDF measurements of the Spectralon® for JPSS J2 in the 0.4 – 1.63 ?m wavelength using PASCAL (Polarization And Scatter Characterization Analysis of Lambertian materials) with an uncertainty better than 1.2%. PASCAL makes absolute measurements of BRDF in an analogous fashion National Institute of Standards and Technology (NIST) Spectral Tri-function Automated Reflectance Reflectometer (STARR) facility. Unique additional features of this instrument include the ability to vary the sample elevation and roll / clock the sample about its normal allowing measuring BRDF in the as use geometry. Comparison of BRDF in the as use configuration for NPP, J1, and J2 shows variation of up to 3%. The sign of the change from panel to panel depends on the angle of incidence and view angle. The results demonstrate lot to lot variability in Spectralon® and emphasize the necessity of characterizing each panel. A pattern in the BRDF variation is also presented.

10402-59, Session 11

Establishing BRDF calibration capabilities through shortwave infrared

Georgi T. Georgiev, NASA Langley Research Ctr. (United States); James J. Butler, Kurtis J. Thome, NASA Goddard Space Flight Ctr. (United States); Catherine C. Cooksey, National Institute of Standards and Technology (United States)

Satellite instruments operating in the reflective solar wavelength region require accurate and precise determination of the Bidirectional Reflectance Distribution Functions (BRDFs) of the laboratory and flight diffusers used in their pre-flight and on-orbit calibrations. Challenges in making high accuracy BRDF measurements in the ShortWave InfraRed (SWIR) above 1700nm has led to the assumption that Directional Hemispherical Reflectance (DHR), a measurement confidently made with high accuracy, scales linearly with BRDF and can be used to derive BRDF. The work of Yoon et al. questioned the validity of that assumption. This paper advances that initial work and presents a comparison of spectral BRDF and DHR on Spectralon, a common material for laboratory and on-orbit flight diffusers. A new measurement setup for BRDF measurements from 900 nm to 2500 nm located at NASA Goddard Space Flight Center is described. The NASA setup employs an extended indium gallium arsenide detector, bandpass filters, and a supercontinuum light source. Comparisons of the NASA BRDF measurements in the SWIR with those made by the NIST Spectral Tri-function Automated Reference Reflectometer (STARR) are presented. The Spectralon samples used in this study included 2 inch diameter, 99% white pressed and sintered PTFE targets. The control sample was optical grade Spectralon while the second sample was space grade Spectralon. The BRDF results are discussed and compared to empirically generated BRDF data from a linear model based on NIST certified values of 6o DHR from 900 nm to 2500 nm and to NIST BRDF measurements. The NASA/NIST BRDF comparison measurements were made at an incident angle of 0o and viewing angle of 45o. Additional BRDF data not compared to NIST are presented at additional incident and viewing angle geometries. The total combined uncertainty for BRDF in the SWIR range is less than 1% (k=1). This study is in support of current and future NASA remote sensing missions operating across the reflected solar wavelength region.

10402-500, Session Plen

Demonstrating Technologies for Hyperspectral Infrared Remote Sensing from Space on a CubeSat

Thomas S. Pagano, Jet Propulsion Lab. (United States)

CubeSats offer a low cost platform for remote sensing and in-situ measurements in space. Not only is the cost of the spacecraft low, but also the cost of the launch since typically CubeSats are secondary payloads to the primary satellite being launched. Despite the low available volume, mass and power and a typically less than ideal orbit, the platform can be ideal for demonstrating technology and even achieving certain science quality measurements. In this talk we discuss the CubeSat Infrared Atmospheric Sounder (CIRAS) a new project at NASA JPL designed to demonstrate key technologies for hyperspectral infrared measurements of atmospheric temperature and water vapor from space.

10402-60, Session 12

Operational correction and validation of the VIIRS TEB longwave infrared band calibration bias during blackbody temperature changes

Wenhui Wang, ERT, Inc. (United States); Changyong Cao, National Oceanic and Atmospheric Administration (United States) and National Environmental Satellite, Data, and Information Service (United States) and Ctr. for Satellite Applications and Research (United States); Bin Zhang, ERT, Inc. (United States); Likun Wang, Univ. of Maryland, College Park (United States)

The Suomi NPP VIIRS thermal emissive bands (TEB) have been performing very well since the data became available on January 20, 2012. The longwave infrared bands at 11 and 12 um (M15 and M16) are primarily used for sea surface temperature (SST) retrievals. However, a long standing anomaly has been observed during the quarterly warm-up-cool-down (WUCD) events. During such event the SST product becomes anomalous with a warm bias shown as a spike in the SST time series on the order of 0.3K. Analysis shows that this is primarily due to warm biases in M15 (~0.12K) and M16 (~0.07K) during the blackbody cooling phase of the WUCD, which are further amplified by the SST retrieval algorithm. A correction algorithm known as Ltrace has been developed based on analysis of the operational calibration algorithm and traceability to prelaunch. This study presents the evaluation and the implementation of the correction algorithm towards the operational processing in generating VIIRS SDR. Sample reprocessing of the data have been performed with the correction algorithm, and the corrected data have been compared with CrIS observations as independent verification with positive results. Preliminary results from the SST users also indicate positive changes. Our implementation minimizes the impacts to the current operational system and the correction is automatically triggered during the blackbody temperature changes. Analysis of historical data shows that the algorithm is applicable to all WUCD events with the same correction parameters. The algorithm is expected to be implemented in operations in the near future.

10402-61, Session 12

Electronic crosstalk effect in SNPP VIIRS thermal emissive bands

Junqiang Sun, Global Science & Technology, Inc. (United States); Menghua Wang, Ctr. for Satellite Applications and Research (United States)

The Visible Infrared Imaging Radiometer Suite (VIIRS) onboard the Suomi National Polar-orbiting Partnership (SNPP) spacecraft has been on orbit for more than five years. Pronounced striping in Earth view (EV) images and obvious discontinuity in the EV brightness temperature (BT) of the thermal emissive bands (TEB) during the blackbody (BB) warm-up cool-down (WUCD) calibration have been found since launch but the root-cause of the phenomena has not yet been identified. Meanwhile, recent studies of the MODerate-resolution Imaging Spectroradiometer (MODIS) long-wave infrared (LWIR) photovoltaic (PV) bands demonstrate that crosstalk effect induces the same erroneous features. In this paper, it is shown that there is, indeed, a remarkable crosstalk contamination in SNPP VIIRS TEB. The

crosstalk effect is quantitatively characterized by deriving the crosstalk coefficients from the scheduled lunar observations and the established lunar imagery analysis. Among all SNPP VIIRS TEB, band M14 is shown to have the largest crosstalk contamination from Band M15, while bands M13, M15, M16, and I5 have pronounced crosstalk effect as well. The crosstalk effect is distinctively different for the odd and even detectors within each affected band during to the pattern of the placement of the odd and the even detectors of the band on the focal plane assembly (FPA). The crosstalk coefficients are applied to mitigate the crosstalk effect and the improvements to both the BB calibration and EV retrieval are presented and addressed.

10402-62, Session 12

Suomi-NPP VIIRS thermal emissive bands calibration stability monitoring using Dome C

Zhipeng Wang, Science Systems and Applications, Inc. (United States); Xiaoxiong J. Xiong, NASA Goddard Space Flight Ctr. (United States); Aisheng Wu, Yonghong Li, Science Systems and Applications, Inc. (United States)

The thermal emissive bands (TEB) of VIIRS are radiometrically calibrated on a scan-by-scan basis in reference to an on-board blackbody (BB) regularly operated at approximately 292.5 K. The calibration stability at other temperature ranges can be independently evaluated using remote targets with stable surface properties. Dome Concordia (Dome C), Antarctic (75°06?S, 123°21?E) is a high plateau homogeneous dry scenes with its surface temperatures varying from 190 to 250 K from winter to summer, which are constantly measured on site. Close to South Pole, Dome C is frequently viewed by Suomi-NPP nearly 10 times per day at various scan angles, providing continuous time series TEB data throughout its mission. In this study, the brightness temperatures (BT) of the Dome C surface retrieved from the data generated by NASA Land Science Investigator-led Processing System (SIPS) is trended to monitor the calibration stability of VIIRS TEB. The trending is performed in detector level at various scan angles. Results show that the radiometric calibration of all TEB detectors has been stable since the instrument's launch in 2011. There is also no noticeable BT drift at different scan angles, indicating no significant response versus scan-angle (RVS) drift for TEB. We further analyzed the data by inter-band comparison and in-band (inter-detector) comparison and found no sign of anomaly such as electric crosstalk. The study confirms that Dome C can serve as a valuable calibration reference site at a temperature range far colder than the BB operating temperature.

10402-63, Session 13

Monitoring of VIIRS ocean clear-sky brightness temperatures against CRTM simulation in ICVS for TEB/M bands

Xingming Liang, National Oceanic and Atmospheric Administration (United States) and ERT, Inc. (United States); Ninghai Sun, Quanhua Liu, National Oceanic and Atmospheric Administration (United States); Wenhui Wang, ERT, Inc. (United States) and National Oceanic Atmospheric Administration (United States); Bin Zhang, National Oceanic and Atmospheric Administration (United States) and ERT, Inc. (United States); Taeyoung J. Choi, National Environmental Satellite, Data, and Information Service (United States) and ERT, Inc. (United States); Fuzhong Weng, National Oceanic and Atmospheric Administration (United States); Alexander Ignatov, National Environmental Satellite, Data, and Information Service (United States); Changyong Cao, National Oceanic and Atmospheric Administration (United States)

NOAA Integrated Calibration/Validation System (ICVS) for Long-Term Monitoring is a real-time environmental satellite performance monitoring system. It is used to ensure high-quality satellite imagery and to deliver accurate Sensor Data Record (SDR) products for weather forecasts and environmental monitoring. The Visible Infrared Imaging Radiometer Suite (VIIRS) is one of key sensors monitored in the ICVS. With the development of faster and more accurate radiative transfer models (RTM), validating sensor radiometric accuracy against RTM simulation has become a more important requirement by both SDR and Environmental Data Record (EDR) users. In this presentation, monitoring of VIIRS ocean clear-sky Observations (brightness temperatures, BTs) against the NOAA Community Radiative Transfer Model (CRTM) Simulations (O-S) for thermal emissive M Bands was set up in ICVS. This monitoring builds upon another NOAA system, Monitoring of IR Clear-sky Radiances over Ocean for SST (MICROS) to support VIIRS calibration and validation. To minimize O-S mean biases and uncertainties, model data are calculated on a pixel-by-pixel basis using the CRTM in conjunction with European Center for Medium range Weather Forecasting (ECMWF) atmospheric profiles and Canadian Meteorological Center (CMC) sea surface temperature (SST) analysis as inputs. A modified clear-sky mask employed in the NOAA Advanced Clear-Sky Processor for Oceans (ACSPO) SST system was used to remove cloud contamination. The preliminary results show that the nighttime O-S biases and standard deviations are exemplary stable for all bands. Also the system detects VIIRS warm-up-cool-down (WUCD) event effects in the bands M12, M13 M14 and M15. More efforts are needed to unscramble and fix anomalies in M13, which show large mean biases (~-0.55K) and satellite view zenith angle dependence with an amplitude of ~0.3 K by collaborating with CRTM and VIIRS sensor calibration Teams. Future work will be to extend functionalities to prepare for the upcoming Joint Polar Satellite System 1 (JPSS1, J1) operations.

10402-64, Session 13

Improvements in the calibration of the SNPP VIIRS day-night band

Junqiang Sun, Global Science & Technology, Inc. (United States); Menghua Wang, Ctr. for Satellite Applications and Research (United States)

We present improvements to the on-orbit calibration of the day-night band (DNB) of the Visible Infrared Imaging Radiometer Suite (VIIRS) on the Suomi National Polar-orbiting Partnership (SNPP) satellite. Most important among the improvements is the expansion of the "sweet spot" from 4 o to 7.8o to increase the number of the fully illuminated scans for calcuation. This allows for the completion of the on-orbit calibration using the solar diffuser (SD) within one orbit instead multiple orbits as required in the current standard approach. The bidirectional reflectance factor (BRF) of the SD and the vignetting function (VF) describing the transmission of the attenuation screen in front of the SD port are also examined and improved. Additional enhancements include the analysis of the out-of-band (OOB) contribution of the relative spectral response (RSR) and the adaptation of the previously improved SD degradation. The result shows that the improved DNB calibration coefficients are more stable, smooth and less noisy.

10402-65, Session 13

Prediction of S-NPP VIIRS DNB gains and dark offsets

Chengbo Sun, Global Science & Technology, Inc. (United States); Thomas Schwarting, Hongda Chen, Kwofu Chiang, Science Systems and Applications, Inc. (United States); Xiaoxiong J. Xiong, NASA Goddard Space Flight Ctr. (United States)

We describe the methodology for predicting the S-NPP VIIRS Day-Night-Band (DNB) detector gains and dark offsets. During the first 5 years of

operation, the DNB has shown recognizable patterns in these calibration parameters. These patterns can be decomposed into two distinctive components: degradation and oscillation. We fit the historical data using a periodic function of time superimposed on an exponential function of time to capture both sources of the variation. The results of the fit showed good agreements with historical measured data, indicating the functions may be useful as a forward model for predicting these calibration parameters in operation. As a test, predictions made in April, 2016 were examined against newly obtained measurement data collected at monthly intervals. Through December of 2016, the prediction errors have been smaller than 1.5% and 0.5% in gains and offsets respectively, with the largest errors seen in the end-of-scan aggregation modes of the high-gain stage. The oscillatory features seen in the measured gains will be analyzed to isolate its possible causes and to determine the relevance of its inclusion in the model. Comparisons among the results from using the existing predictions of the gain and offset Look-Up-Tables (LUTs) will be presented.

10402-66, Session 13

Suomi-NPP VIIRS initial reprocessing improvements and validations in the reflective solar bands (RSBs)

Taeyoung J. Choi, National Environmental Satellite, Data, and Information Service (United States); Junqiang Sun, Global Science & Technology, Inc. (United States) and National Oceanic and Atmospheric Administration (United States) and Ctr. for Satellite Application and Resarch (United States); Bin Zhang, National Environmental Satellite, Data, and Information Service (United States) and Univ. of Maryland (United States); Zhuo Wang, National Oceanic and Atmospheric Administration (United States) and Univ. of Maryland (United States); Changyong Cao, National Oceanic and Atmospheric Administration (United States); Fuzhong Weng, National Environmental Satellite, Data, and Information Service (United States); Menghua Wang, National Oceanic and Atmospheric Adminstration (United States) and National Environmental Satellite, Data, and Information Service (United States)

Over five years of the Suomi National Polar orbiting Partnership (S-NPP) Visible Infrared Imaging Radiometer Suite (VIIRS) Sensor Data Records (SDR) production, there were mutual demands of the lifetime VIIRS SDR reprocessing to alleviate operational changes and user oriented suggestions. Meanwhile, the NOAA Ocean Color (OC) team through its independent effort has achieved the robust calibration of the S-NPP VIIR Reflective Solar Bands (RSBs) – including improved radiometric accuracies, minimized annual oscillations and mitigated growing bias for long-term radiometric stability – leading to the institutional decision to use the OC calibration results as the official Look-Up Tables (LUTs) for operational mission-long reprocessing to provide enhanced radiometric accuracy for Environmental Data Records (EDR) productions. The SDR reprocessing team has applied the most recent calibration coefficients LUTs provided by the OC Team to the current VIIRS reprocessing. This paper briefly summarizes the efforts of the SDR reprocessing team, the related entire life reprocessing issues and the initial results in the RSBs. It will show that the quality and accuracy of the SDR reprocessed with the new LUTs are significantly improved. It will also demonstrate the remarkable improvements of the VIIRS EDR for various applications and higher-level science products by using the reprocessed SDR as their inputs.

10402-67, Session 14

Reflective solar bands calibration improvements and look up tables for SNPP VIIRS operational mission-long SDR reprocessing

Menghua Wang, Ctr. for Satellite Applications and Research (United States); Junqiang Sun, Global Science & Technology, Inc. (United States)

The Suomi National Polar-orbiting Partnership (SNPP) Visible Infrared Imaging Radiometer Suite (VIIRS) has been on orbit for more than five years. Through independent efforts by the NOAA OC Team, the radiometric calibration of reflective solar bands (RSBs) recently has reached a mature stage. Numerous improvements have been made in the standard RSB calibration methodology for the sensor data records (SDR), which is the starting for the higher-level environmental data records (EDR) and science products. These improvements have helped the EDR ocean color products that demand stringent accuracy to reach maturity. The success of the OC EDR performance has further led to the institutional decision to use the calibration results generated by the OC Team, in the form of the look-up-tables (LUTs), as the official input for the operational SDR reprocessing, which are to be the official release to be used by all science groups and communities. The OC LUTs delivered for the operational SDR reprocessing is the latest update containing further improvements over the current LUTs used for the OC reprocessing and forward processing. This presentation will address the following: the good performance of the SNPP VIIRS RSBs, the inadequacies in the current operational forward SDR generated by the Interface Data Processing Segment (IDPS), the RSB calibration improvements made by the NOAA OC Team, the success of the RSB SDR reprocessing for ocean color EDR using the improved RSB LUTs, and finally, the use of the OC LUTs as the official LUTs for VIIRS RSB SDR operational reprocessing.

10402-68, Session 14

On-orbit noise characterization of the SNPP VIIRS reflective solar bands

Kevin A. Twedt, Ning Lei, Science Systems and Applications, Inc. (United States); Xiaoxiong J. Xiong, NASA Goddard Space Flight Ctr. (United States)

The Visible Infrared Imaging Radiometer Suite (VIIRS) aboard the Suomi National Polar-orbiting Partnership satellite has 14 reflective solar bands (RSBs) covering a spectral range from 410 nm to 2250 nm. We provide an overview of the noise characterization of the VIIRS RSB from pre-launch through more than five years of on-orbit operation. On orbit, the noise is measured as the variation in the signal level observed at the sunlit solar diffuser (SD) within each instrument scan. The SD signal level changes from scan to scan as the solar angle changes during the SD illumination time period of each orbit, allowing us to establish a functional dependence of the noise on signal level. The signal-to-noise ratio for all RSB has been slowly decreasing on-orbit, but remains above specification performance values (given at fixed typical radiance for each band) and is projected to remain above specification for at least five more years based on the current trends in the performance of the electronic and optical sub-systems. We show a comparison to pre-launch measurements, and also discuss the importance of data quantization and sample aggregation in the interpretation of the SNR values.

10402-69, Session 14

RSB calibration of SNPP VIIRS using solar diffuser illuminated by scattered light

Junqiang Sun, Global Science & Technology, Inc. (United States) and Ctr. for Satellite Applications and Research (United States); I-Wen Mike Chu, Menghua Wang, Ctr. for Satellite Applications and Research (United States)

We present a different approach to the on-orbit calibration of the reflective solar bands (RSBs) using solar diffuser (SD) for SNPP VIIRS. Instead of following the standard methodology that uses full solar illumination occurring in the short window of time right before the satellite reaches the terminator, we use light scattered off the earth scenes coming through the nadir port as the source of the illumination for the SD. This alternative to the standard approach is shown to be viable, and in fact demonstrates more stable calibration results due to having more data volume. We describe the methodology, present the results, make comparison with the current standard method, and discuss its advantages. The methodology is applicable to other instruments employing a similar SD-based calibration strategy, such as MODIS, and can serve as a viable replacement.

10402-70, Session 14

Suomi-NPP visible infrared imaging radiometer suite (VIIRS) calibration uncertainty its effect on trends in the ocean color data record

Kevin R. Turpie, NASA Goddard Space Flight Ctr. (United States) and Univ. of Maryland (United States); Robert E. Eplee Jr., NASA Goddard Space Flight Ctr. (United States) and SAIC (United States); Gerhard Meister, Bryan A. Franz, NASA Goddard Space Flight Ctr. (United States)

The NASA Ocean Color calibration team continued to reanalyze and improve on their approach to the on-orbit calibration of the Visible Infrared Imaging Radiometer Suite (VIIRS), aboard the Suomi National Polar-orbiting Partnership (NPP) satellite, now five years into its Earth Observation mission. As the calibration was adjusted for changes in ocean band responsitivity with time, the team also observed the variance and autocorrelation properties of calibration trend fit residuals, which appeared to have a standard deviation within a few tenths of a percent. Autocorrelation was observed to be different between bands at the blue end of the spectrum and bands at the red/NIR end, which are affected by significant changes in responsitivity stemming from mirror contamination. This residual information offered insight into the effect of small calibration biases, which can cause significant trend uncertainties in regional time series of surface reflectance and derived products. This work involves modeling spurious trends that are inherent to the calibration over time and that also arise between reprocessing efforts because of extrapolation of the time-dependent calibration table. Uncertainty in calibration trends was estimated using models of instrument and calibration system trend artifacts and correlated noise models using Monte Carlo techniques. Combined table reprocessing and extrapolation biases are presented for the first time. Calibration trend uncertainty is then propagated through to ocean color remote sensing reflectance and chlorophyll-a concentration time series. The results quantify the smallest trend observable in these oceanic parameters. This quantification furthers our understanding of uncertainty in measuring regional and global biospheric trends in the ocean using VIIRS, and better defines the roles of records in climate research.

10402-71, Session 14

Advances in the on-orbit calibration of SNPP VIIRS for ocean color applications

Robert E. Eplee Jr., NASA Goddard Space Flight Ctr. (United States); Kevin R. Turpie, Univ. of Maryland, Baltimore (United States); Gerhard Meister, Frederick S. Patt, Bryan A. Franz, NASA Goddard Space Flight Ctr. (United States)

The NASA Ocean Biology Processing Group has continued monitoring the SNPP VIIRS on-orbit calibration since the derivation of the calibration for Reprocssing 2014.0 of the VIIRS ocean color data set. A key technique involves evaluation of globally-derived anomaly plots of remote sening reflectance for the ocean color bands. Updates to the on-orbit calibration have produced ocean color data retrievals that show trends in the anomaly plots for bands M1 (412 nm), M4 (555 nm), and M5 (672 nm). Consequently, the OBPG has re-examined the effects of the prelaunch calibration (counts-to-radiance conversion) of SNPP VIIRS on the on-orbit calibration. Two cases were compared to the baseline linear function of counts: a quadratic function of counts, and a focal plane temperature-dependent quadratic function of counts. The quadratic function, compared to the baseline, showed a 0.2% effect on band M7 (862 nm) over the mission. The temperature-dependent quadratic function, compared to the baseline, showed the following effects over the mission: 0.5% on band M1 (412 nm), 0.6% on band M4 (555 nm), 0.2% on band M6 (748 nm) and 0.6% on band M7 (862 nm). The OBPG has produced an on-orbit calibration based on the temperature-dependent quadratic counts-to-radiance conversion and has reprocessed the mission-long solar and lunar calibration time series using our standard approach for deriving lunar adjustments to the solar-derived radiometric gains. The impact of this new on-orbit calibration of SNPP VIIRS on global ocean color data retrievals will be reported.

10402-72, Session 14

Assessment of S-NPP VIIRS band-to-band registration using Earth-scene features

Daniel Link, Zhipeng Wang, Science Systems and Applications, Inc. (United States); Xiaoxiong J. Xiong, NASA Goddard Space Flight Ctr. (United States)

The Visible Infrared Imaging Radiometer Suite (VIIRS) is currently operating onboard the Suomi National Polar-orbiting Partnership (S-NPP) spacecraft. VIIRS records Earth imagery with spectral bands ranging from 0.4 to 12.2 micrometers at a combination of resolutions. Five imaging bands (I1-5) have a 375 m spatial resolution at nadir, which is half of the 750 m resolution of the 16 moderate resolution bands (M1-16). These bands are mounted according to their wavelengths among three separate Focal Plane Assemblies (FPA).

The proper spatial registration between imaging bands is required to create multi-spectral images and analyses. Measurement of the band-to-band registration (BBR) is a determination of how well these bands are coincident. Using an external target such as the moon has proven to be a valid method and has been thoroughly investigated using VIIRS raw data record (RDR). Calibrated VIIRS radiometric data has been investigated using normalized mutual information (NMI) for BBR and shown stable results, by focusing on high-contrast shoreline sites. However, these results focus on a relatively small number of observations. We have previously reported analyses using earth-scene targets to determine BBR for MODIS instruments. This approach focuses on an African Desert site with high contrast spots generated through agricultural pivot irrigation. Using the near-daily observations provided by the VIIRS instrument, we investigate a large data set and track the BBR stability over the VIIRS mission. We discuss our results as they relate to pre-launch measurements and design specifications.

10402-85, Session PWed

Design and implementation of JOM-3 Overhauser magnetometer analog circuit

Xiao Zhang, Xue Jiang, Jianchang Zhao, Shuang Zhang, Xin Guo, Tingting Zhou, Jilin Univ. (China)

Overhauser magnetometer, a kind of static-magnetic measurement system based on the Overhauser effect, has been widely used in archaeological exploration, mineral resources exploration, oil and gas basin structure detection, prediction of engineering exploration environment, earthquakes and volcanic eruotions, object magnetic measurement and underground buried booty exploration. Overhauser magnetometer plays an important role in the application of magnetic field measurement for its characteristics of small size, low power consumption and high sensitivity. This paper researches the design and the application of the analog circuit of JOM-3 Overhauser magnetometer. First, the Larmor signal output by the probe is very weak. In order to obtain the signal with high SNR, the design of pre-amplifier circuit is the key to improve the quality of the system signal. Second, in this paper, the effectual step which could improve the frequency characters of bandpass filter amplifier circuit were put forward, and theoretical analysis was made for it. Third, the shaping circuit shapes the amplified sine signal into a square wave signal which is suitable for detecting the rising edge. Fourth, this design elaborated the optimized choice of coordination capacitor circuit, so the measurement range of the magnetic field can be covered. Last, integrated analog circuit testing system was formed to obtain waveform of each module. By calculating the standard deviation, the sensitivity of the improved Overhauser magnetometer is close to 0.05nT for Earth's magnetic field observation. Experimental results show that the new magnetometer is sensitive to earth field measurement.

10402-86, Session PWed

The curious case of the intersensor radiometric comparison of SNPP VIIRS M11 with Aqua MODIS B7

I-Wen Mike Chu, Ctr. for Satellite Applications and Research (United States) and Cooperative Institute for Research in the Atmosphere (United States) and ERT, Inc. (United States); Junqiang Sun, Global Science & Technology, Inc. (United States) and Ctr. for Satellite Applications and Research (United States); Menghua Wang, Ctr. for Satellite Applications and Research (United States)

The radiometric performance of the Visible Infrared Imaging Radiometer Suite (VIIRS) onboard the Suomi National Polar-orbiting Partnership (SNPP) satellite is often carried out against the Moderate-resolution Imaging Spectrometer (MODIS) onboard Aqua satellite utilizing simultaneous nadir overpasses (SNOs). The comparison of SNPP VIIRS Band M11 (2257 nm) versus Aqua MODIS B7 (2130 nm), however, suffers from widely varying and inconsistent result unusable for further evaluation of the radiometric performance. This investigation presents the first successful radiometric comparison between SNPP VIIRS M11 and Aqua MODIS B7. It is shown that the non-overlapping relative spectral responses (RSRs) are the cause of the widely varying comparison coming from the mix of snow and cloudy scenes with each having different reflectance in different part of the spectrum. A targeted selection procedure using both geolocation and statistics seek out the more stable surface snow scenes as the viable targets of comparison. The resulting comparison time series, with about 50 sufficiently robust SNO events, of Aqua MODIS B7 radiance over the SNPP VIIRS M11 radiance is shown to be stable at 0.4 with a ~5% range and no obvious drift.

10402-87, Session PWed

Bridging the thermal band comparison between LEO-LEO sensors and between GEO-GEO sensors

Tiejun Chang, Graziela R. Keller, Science Systems and Applications, Inc. (United States); Xiaoxiong J. Xiong, NASA Goddard Space Flight Ctr. (United States)

The MODIS onboard the Terra and Aqua satellites have operated since 1999 and 2002, respectively. The inter-comparison between their thermal emissive bands is a useful tool in assessing their calibration consistency and enhancing their product quality. One application of the comparison is to assess the MODIS thermal band cross-talk. However, the comparison is hindered by the time difference of their measurements, since Terra is in the morning orbit and Aqua is in the afternoon orbit.

GOES-R was launched on November 19, 2016 and Himawari 8 was launched on October 7, 2014. The Advanced Baseline Imager (ABI) onboard GOES-R and the Advanced Himawari Imager (AHI) onboard Himawari are in the same class and have almost identical thermal spectral bands. Their comparison will be very useful for sensor calibration assessment. However, the comparison is challenged by the fact that they image different regions of the Earth.

This work focuses on bridging the thermal band comparison between LEO-LEO sensors and between GEO-GEO sensors. The double difference method is applied to assess the BT measurements between the two MODIS instruments using the GOES imager as a bridge. The comparison between ABI and AHI can also be performed with bridging by either MODIS or VIIRS measurements. GOES-R and Himawari are both positioned over tropical ocean regions. Thus, the comparison with simultaneous nadir overpass can provide assessments for BT measurements for this type of scenery. The comparison can also be extended to simultaneous off-nadir measurement for various types of sites and for a broad BT range.

10402-88, Session PWed

Status of the MODIS spatial and spectral characterization and performance after recent SRCA operational changes

Daniel Link, Zhipeng Wang, Kevin A. Twedt, Science Systems and Applications, Inc. (United States); Xiaoxiong J. Xiong, NASA Goddard Space Flight Ctr. (United States)

There are two nearly identical MODIS instruments currently operating on-board the NASA EOS Terra and Aqua spacecraft. Each MODIS is equipped with several on-board calibrators (OBCs) including a Spectro-Radiometric Calibration Assembly (SRCA). The SRCA is a multi-configuration calibrator that aids in determining the performance parameters of MODIS detectors on-orbit. Depending on its configuration, scheduled operations of the SRCA provide measurements to assess the on-orbit radiometric, spatial, and spectral performance. The SRCA was designed to utilize various combinations of three 10 Watt lamps and one 1 Watt lamp and included a spare of each type. Lamp failures reduced the available number of 10 Watt lamps from four to two for each mission by 2006.

Over the past year, each instrument experienced an issue on-orbit. The nadir door of Terra MODIS closed as the instrument was autonomously commanded into safe-mode after a spacecraft commanding issue. The instrument and spacecraft were successfully recovered. For Aqua, a failure occurred for one of the two remaining 10 Watt lamps. We investigate each issue as it relates to the SRCA's operation and its ability to properly characterize MODIS detector performance. For Terra MODIS, we present changes in MODIS spectral and spatial performance due to changes in the instrument environment. In the case of Aqua MODIS, losing a lamp reduces the output potential of the SRCA. We present the results from this impact and the adjustments made to calibration activities to maximize the effectiveness of the remaining lamps.

10402-89, Session PWed

CrIS sub-pixel level VIIRS radiance clustering analysis

Haibing Sun, I. M. Systems Group, Inc. (United States); Walter Wolf, Ctr. for Satellite Applications and Research (United States); Thomas S. King, Shanna Sampson, I. M. Systems Group, Inc. (United States)

The Visible Infrared Imaging Radiometer Suite (VIIRS) and Cross-track Infrared Sounder (CrIS) are two key infrared instruments onboard JPSS for observing the Earth's weather, climate, and environment. Their observations and products provide information with different spectral and spatial resolution. NOAA/NESDIS/STAR satellite observation collocation algorithms are used to spatially match observations or products from different sensors. The spatially matched and integrated satellite datasets are widely used in integrated satellite retrievals, satellite instrument inter-calibration and satellite observation validation. The VIIRS instrument has multi-band imaging capabilities to support the acquisition of high-spatial resolution atmospheric imagery. The VIIRS measurements collocated within the CrIS file of view (FOV) can provide sub-pixel level scene VIIRS radiances and cloud information. These data have been used for CrIS cloud-clearing algorithms and sub-pixel observation selection. The currently operational CrIS and VIIRS collocation processing algorithm was updated to generate a radiance clustering analysis. This analysis is performed on the co-located VIIRS pixels to identify localized areas of similar radiance clusters within the CrIS FOV, the assumption being that these clusters correspond to different scene types. The algorithm is based on the K-means clustering method using all available VIIRS channels. The CrIS sub-pixel VIIRS clustering product consists of the mean radiance, the standard deviation, and the coverage of the class within the CrIS FOV. The radiance clustering analysis product provides the inhomogeneity knowledge within the CrIS field of view. This knowledge is helpful to define the scene type and provide an accurate guess estimate of the decomposition parameters for the cloud clearing processing. In this paper, the CrIS sub-pixel radiance clustering algorithm and its operational implementation is presented. The product, parameter selection, and the validation results are presented in detail.

10402-90, Session PWed

MTF analysis using lunar observations for Himawari-8/AHI

Graziela R. Keller, Tiejun Chang, Zhipeng Wang, Science Systems and Applications, Inc. (United States); Xiaoxiong J. Xiong, NASA Goddard Space Flight Ctr. (United States)

The modulation transfer function (MTF) is a common measure of image fidelity, which has been historically characterized on-orbit using high contrast images of the lunar limb obtained by remote sensing instruments onboard both low-orbit and geostationary satellites.

Himawari-8, launched in 2014, is a Japanese geostationary satellite that carries the Advanced Himawari Imager (AHI), a near-identical copy of the Advanced Baseline Imager (ABI) instrument onboard the GOES-16 satellite. In this paper, we apply a slanted-edge method for deriving the MTF from lunar images, first verified by us on simulated test images, to Himawari-8/AHI L1A and L1B data. The MTF is derived along both the North/South and East/West directions separately and we assess the impact of the relative movement between the Moon and the spacecraft on the edge profiles.

The AHI L1A images used in the characterization of the MTF are obtained from scheduled lunar observations routinely acquired for validating the radiometric calibration. The L1B data, on the other hand, come from serendipitous lunar observations where the Moon appears close to the Earth's disk and spanning different Moon phases. We developed and implemented an algorithm to identify such occurrences using the SPICE/Icy package to predict the times where the Moon is visible in the L1B imagery and demonstrate their use for MTF derivation. AHI L1B data is spatially re-sampled and this application allows the impact of the AHI re-sampling algorithm on the MTF to be assessed at different North/South and East/West positions on the images.

10402-91, Session PWed

Prediction of S-NPP VIIRS DNB stray light correction

Chengbo Sun, Global Science & Technology, Inc. (United States); Thomas Schwarting, Hongda Chen, Kwofu Chiang, Science Systems and Applications, Inc. (United States); Xiaoxiong J. Xiong, NASA Goddard Space Flight Ctr. (United States)

The VIIRS Day-Night-Band (DNB) is a panchromatic band with three gain stages used for delivering imagery under a variety of conditions ranging from daylight to low light nighttime scenes. Early in the S-NPP mission a gray haze was observed in some nighttime DNB imagery with the cause determined to be stray light contamination. This effect was characterized along with a proposed correction algorithm. The correction algorithm was subsequently included in operational data processing and re-processing. However, in order to process real-time data, prediction of the stray light correction is necessary. In this paper we present a new method to predict the DNB stray light correction Look-Up-Tables (LUTs). Since measurements suitable for characterizing the stray light contamination are sparse (about once a month during new-Moon), and because some of the measurements might not be accurate due to the presences of unaccounted light sources, such as algae glow and lightening, we have applied additional constraints to the model by assuming that certain patterns of the stray light are repeatable. Comparisons of the LUT parameters produced by the prediction algorithm with those from the measurements will be presented along with the impact on the derived Earth View products.

10402-92, Session PWed

MODIS solar diffuser degradation at short-wave infrared band wavelengths

Kevin A. Twedt, Amit Angal, Science Systems and Applications, Inc. (United States); Xiaoxiong J. Xiong, NASA Goddard Space Flight Ctr. (United States); Xu Geng, Hongda Chen, Science Systems and Applications, Inc. (United States)

The MODIS instruments aboard the Terra and Aqua spacecraft have 20 reflective solar bands (RSB) with wavelengths spanning 0.412 μm to 2.13 μm. The primary on-board calibration source for the RSB is a sunlit solar diffuser (SD), with its degradation tracked by a SD stability monitor (SDSM). The SDSM measurements show that the decrease in SD reflectance over time has a strong wavelength dependence, with longer wavelengths showing less degradation. The SDSM has 9 detectors to track the SD degradation at wavelengths from 0.412 μm to 0.936 μm, but is not designed to track the degradation at SWIR wavelengths. In recent years, the SDSM has measured non-negligible degradation in the SD reflectance at 0.936 μm for both Terra (>2%) and Aqua (>0.5%) MODIS. In addition, comparison of SD calibration results to earth view targets suggests that smaller but non-negligible SD degradation also exists at the SWIR band wavelengths.

In this paper, we review the current status of the MODIS SD degradation as measured by the SDSM, and discuss the challenges involved in calibration. We present efforts to extend the SD degradation measurements to the SWIR band wavelengths (1.2 μm to 2.1 μm) by fitting a wavelength-dependent model to the SDSM results from the NIR wavelength detectors. The predicted degradation results are used to correct the MODIS SWIR band degradation, and comparisons are made with that determined using the pseudo-invariant earth targets. Results are presented for both Terra and Aqua MODIS.

10402-93, Session PWed

Prism spectrometer analysis for field use

Adam Abdelatif, Nikolaus J. Anderson, College of Optical

Sciences, The Univ. of Arizona (United States); Oscar Hernandez, The Univ. of Arizona (United States); Jeffrey S. Czapla-Myers, College of Optical Sciences, The Univ. of Arizona (United States)

The Spectrometer Arduino Mega (SpAM) is a prism spectrometer that has been designed and fabricated by the Remote Sensing Group (RSG) at the College of Optical Sciences of the University of Arizona. SpAM is designed to be a low budget, stand alone, solar powered field spectrometer. RSG plans to use SpAM to measure the reflectance of natural surfaces in the field. After verification of the accuracy and performance of SpAM, it will be deployed to the Radiometric Calibration Test Site (RadCaTS) at Railroad Valley, where network capabilities and data logging devices will allow RSG to remotely download spectral radiance measurements.

SpAM measures and records the spectral composition of a light source or light reflected from a surface. The prism inside of SpAM refracts the input light on to a linear array of 512 silicon detectors. The detector-prism combination produces a spectral resolution of ~2 nm, and the overall spectral range is 433–760 nm. The spectral radiometric measurements produced by SpAM are stored and processed by an Arduino mega micro controller with network capabilities for field applications. SpAM will be used to analyze the spectral reflectance of Railroad Valley, Nevada, and its accuracy and performance will be determined by a comparison with more precise radiometers that have been produced by RSG.

This work presents the design and instrumentation of SpAM, and an assessment of its ability to provide radiometric results for satellite calibration and other radiometric measurement applications.

10402-94, Session PWed

Site selection and characterization at Uyuni desert for the calibration and validation of GOES solar reflective bands

Hyelim Yoo, National Oceanic and Atmospheric Administration (United States); Fangfang Yu, ERT, Inc. (United States) and National Oceanic and Atmospheric Adminstration (United Kingdom); Xianqian Wu, National Oceanic and Atmospheric Administration (United States)

Uyuni desert (-20.8 to -19.6 in latitude, -68.2 to -66.8 in longitude) covered by a few meters of salt can be a good target for Earth observation satellite with its flatness and high altitude. Also, the Uyuni desert is the closest desert to the sub-satellite point of GOES-East satellites and we can validate the accuracy of GOES-16 ABI visible and near-IR bands using the Uyuni desert as a reference. An selection of uniform scenes over the Uyuni desert using a number of space-borne observational datasets is a main objective.

It is critical to identify the geospatially, temporally, and spectrally uniform area with at least 3 km x 3 km in size for ABI band 2 and 7 km x 7 km for ABI band 1,3,4,5,and 6. For radiometric and temporal stability, GOES-15 Imager visible data obtained near the satellite noon time is used. Reflectance is calculated by applying the post-launch calibration for each image using calibration coefficients generated by Yu et al.(2014) and projected them to the ABI fixed grid position in order to identify the area with low standard deviation reflectance pixels. In terms of spatial stability, SNPP Visible Infrared Imaging Radiometer Suite (VIIRS) data is compared to find the uniform scenes with low coefficient of variance of reflectance over the radiometric and temporal stable areas. The Hyperion data is used to minimize atmospheric effect and examine the desert spectral variability over a long-term period. The spectral band adjustment factor is calculated as the ratio of GOES-13 Imager visible and VIIRS I band 1 reflectance.

Such findings are expected to help validate the accuracy of ABI visible and near infrared bands by providing high and stable reflectance information. We will cross-check these results with the results of the Sonoran desert.

10402-95, Session PWed

The space-borne hyperspectral imager (SPARK) based on curved prisms

Juanjuan Jing, Jinsong Zhou, Academy of Opto-Electronics, CAS (China) and Univ. of Chinese Academy of Sciences (China); Lei Feng, Academy of Opto-Electronics, CAS (China) and Univ. of Chinese Academy of Sciences (China); Guifeng Zhang, Academy of Opto-Electronics, CAS (China)

The space borne hyperspectral imager, SPARK, the payloaded of microsatellite, has been developed by Academy of Opto-electronics, Chinese Academy of Sciences, China. It has been launched on 22, Dec, 2016, and now deployed for commercial operations around the world. The compact Offner spectrometer featuring two curved prisms are designed to disperse the incident light in optical system with the benefits of low smile, keystone and lateral distortion. All surfaces of mirrors and prisms are spherical. It features a pushbroom imaging spectrometer with more than 148 channels covering a spectral range from 420 to 1000nm. The ground sampling distance is as low as 50m @700km, and the swath width is 100km. But the weight is only 12.8kg, the outer dimensions of SPARK are 362mm (X)* 343mm (Z)*139 mm (Y). The spectrometer has an F-number of 4.5. Because prisms are used for imaging spectrometry, the spectral sampling distance varies with wavelength. The width of the spectral response function varies from 1nm to 12nm. The mean bandwidth is less than 5nm. The SPARK sensor has achieved high performance levels in terms of signal to noise ratio(SNR), spectral calibration and image quality. The SNR is better than 110, the relative calibration precision is better than 5%, and the absolute calibration precision is better than 10%. It can be used for environmental and disaster monitoring.

10402-96, Session PWed

El Niño southern oscillation: Nonlinear modeling, satellite data, and Fourier analysis

Nour Hadjih, Ahmed Hassebo, The City College of New York (United States); Yasser Y. Hassebo, The City College of New York (United States) and LaGuardia Community College (United States); Frank Wang, LaGuardia Community College (United States) and The City College of New York (United States)

The El Niño Southern Oscillation (ENSO) is considered one of the most prominent signal of interannual climate variability. For instance, an investigation provided evidence of the El Niño events impact in determining the ecosystem conditions. El Niño events are characterized by positive Sea Surface Temperature (SST). In this study, Sixty six-year of SST anomalies data of the Niño 3.4 region were analyzed to understand the El Niño-Southern Oscillation (ENSO) phenomenon quantitatively through an elementary nonlinear model using Fast Fourier Transform (FFT) algorithm. A key element in this model is the inclusion of the effects of equatorially trapped oceanic waves (Kelvin and Rossby waves) propagating in a closed basin through a time delayed element. The relationship between this element and the temporal oscillation variability was examined. Results showed that when the time delay was small, there was no oscillation; which explain the lack of El Niño in the Atlantic Ocean compared to the Pacific Ocean. FFT of the Oceanic Niño Index revealed multiple peaks centered on a period of 3.7 years. Range of parameters that cause drastic qualitative changes in the climate system, i.e. bifurcation, was investigated. The model was extended by including external influences such as annual forcing, global warming, and stochastic effects. Study revealed that when the global warming rate was too high, the oscillations disappeared. Self-sustained oscillations under certain conditions was discussed. To validate the model results, four stages of data correction of 5-year Satellite data of Earth Surface Temperature (EST) for Niño 3.4 (5N-5S, 170W-120W) were performed.

10402-97, Session PWed

Principle and analysis of a rotational motion Fourier transform infrared spectrometer

Qisheng Cai, Huang Min, Wei Han, Yixuan Liu, Lulu Qian, Xiangning Lu, Academy of Opto-Electronics, CAS (China)

Fourier transform infrared spectroscopy is an important technique in studying molecular energy levels, analyzing material compositions, and environmental pollutants detection. A novel rotational motion Fourier transform infrared spectrometer with high stability and ultra rapid scanning advantages is proposed in this paper. The basic principle, the optical path difference calculations, and the tolerance analysis are elaborated. The optical path difference of this spectrometer varies with the continuously rotational motion of a pair of parallel mirrors instead of the translational motion in traditional Michelson interferometer. Because of the rotational motion, it avoids the tilt problems occurred in the translational motion Michelson interferometer. There is a cosine function between the optical path difference and the rotating angle of the parallel mirrors. The NUFFT (Non-Uniform Fast Fourier Transform) needs to be used to recover the input spectrum. The vibration of the parallel mirrors, the parallelism of the two rotating mirrors, and the alignment of the two fixed end mirrors are analyzed. The vibration of the parallel mirrors is the main error during the rotation. An optical model is setup in non-sequential mode of the ZEMAX software, and the interferogram of a monochromatic light is simulated using ray tracing method. The simulated interferogram is consistent with the theoretically calculated interferogram. This high stability and ultra rapid scanning Fourier transform infrared spectrometer is a suitable candidate for airborne and space-borne remote sensing spectrometer.

10402-98, Session PWed

Impact of fluorescence on the underwater polarized light field: Comparison of theory and field measurements

Ahmed El-Habashi, Robert Foster, Carlos Carrizo, Thomas Legbandt, Sam Ahmed, The City College of New York (United States)

We have examined, in earlier work, the relationship between naturally induces chlorophyll fluorescence and the underwater polarized oceanic light field. This shows the un-polarized fluorescence causes a reduction in the degree of polarization over the fluorescence spectral range. Theory shows that the peak of the reduction in polarization occurs at or near the fluorescence peak. Furthermore, it also shows that the magnitude of this reduction in degree of polarization can be related to both the magnitude of the fluorescence as well as the intensity of the underwater light field over the fluorescence spectral range. To examine this relationship in detail, a vector radiative transfer code (VRTE) for the coupled atmosphere-ocean system was employed for a variety of oligotrophic and eutrophic water conditions. The VRTE used measured inherent optical properties (IOPs) for these water conditions as inputs to simulate the complete elastic and in-elastic components of the underwater light field, as well as the degree of linear polarization (DoLP) associated with it. These theoretical predictions were then compared with the results of DoLP measurements carried out using by our multi-angular hyperspectral polarimeter. A comparison of the measured reduction in degree polarization of the underwater light field over the fluorescence spectral range, and the magnitude of the fluorescence causing it, confirmed the validity of our theoretical relationship, and the feasibility of determining the natural fluorescence existing in an underwater light field from polarization measurements.

10402-73, Session 15

The updated intersensor radiometric comparison of SNPP VIIRS M1-M8 with Aqua MODIS bands through June 2017

I-Wen Mike Chu, Ctr. for Satellite Applications and Research (United States) and Cooperative Institute for Research in the Atmosphere (United States) and ERT, Inc. (United States); Menghua Wang, Ctr. for Satellite Applications and Research (United States)

The radiometric inter-sensor comparison of the Visible Infrared Imaging Radiometer Suite (VIIRS) onboard Suomi National Polar-orbiting Partnership (SNPP) satellite with the Moderate-resolution Imaging Spectrometer (MODIS) onboard Aqua satellite in the visible and near-infrared spectral range (410 – 1238 nm) is updated and presented. The methodology and statistical analyses have been improved since the preceding report. The radiometric comparison time series are updated and extended through June 2017, and are shown to be more robust and complete. All comparison time series achieve an overall precision under 1% with no obvious long-term drift. The SNPP VIIRS SDR version generated by the NOAA Ocean Color Team, with numerous important calibration improvements, demonstrates through inter-sensor comparison with Aqua MODIS the continual radiometric stability of SNPP VIIRS Bands M1?M8 bands as well as the very robust calibration achieved. The inter-sensor comparison of SNPP VIIRS M11 (2257 nm) versus Aqua MODIS B7 (2130 nm), the first-ever successful comparison achieved via a targeted study over the snowy scene, is a new result included in this report. The overall result demonstrates the long-term radiometric stability of the SNPP VIIRS bands that are presented in this update.

10402-74, Session 15

GEO-LEO reflectance band inter-comparison with BRDF and atmospheric scattering corrections

Tiejun Chang, Science Systems and Applications, Inc. (United States); Xiaoxiong J. Xiong, NASA Goddard Space Flight Ctr. (United States); Graziela R. Keller, Science Systems and Applications, Inc. (United States); Xiangqian Wu, National Oceanic and Atmospheric Administration (United States) and Ctr. for Satellite Applications and Research (United States)

The inter-comparison of reflective solar bands between the sensors onboard a geostationary orbit satellite and a low Earth orbit satellite is very helpful to assess their calibration consistency. GOES-R was launched on November 19, 2016 and Himawari 8 was launched October 7, 2014. Unlike previous GOES instruments, the Advanced Baseline Imager on GOES-R and the Advanced Himawari Imager on Himawari have onboard calibrators for the reflective solar bands. The assessment of calibration is important for their product quality enhancement. MODIS and VIIRS provide good references. The SNO and ray-matching are widely used inter-comparison methods for reflective solar bands.

In this work, the inter-comparisons are performed over pseudo-invariant targets. The use of stable and uniform calibration sites provides comparison with appropriate reflectance level, accurate adjustment for band spectral coverage difference, reduction of impact from pixel mismatching, and consistency assessment from long-term trending. The sites in this work include deserts in Australia, New Mexico, and Mexico. Due to the difference in solar and view angles, two corrections are applied to have comparable measurements. First, the satellite sensor measurements are top of atmosphere reflectance. The scattering, especially Rayleigh scattering, should be removed allowing the ground reflectance to be derived. Secondly, the angle differences magnify the BRDF effect. The ground reflectance should be corrected to have comparable measurements. The atmospheric correction is performed using a vector version of the Second Simulation of a Satellite Signal in the Solar Spectrum modeling and BRDF correction is performed using a semi-empirical model.

10402-76, Session 15

Validation of VIIRS with CrIS by taking into account the sub-pixel cloudiness and viewing geometry

Jun Li, Univ. of Wisconsin-Madison (United States); Changyong Cao, National Environmental Satellite, Data, and Information Service (United States); Zhenglong Li, Xinya Gong, Univ. of Wisconsin-Madison (United States); Wenhui Wang, ERT, Inc. (United States); Christopher C. Moeller, Univ. of Wisconsin-Madison (United States)

The Cross-track Infrared Sounder (CrIS) onboard Suomi NPP (SNPP) and JPSS series has high radiometric accuracy, which can be used for validating some infrared bands of Visible Infrared Imaging Radiometer Suite (VIIRS) onboard the same platform. The collocated CrIS and VIIRS sensor data record (SDR) along with the VIIRS cloud mask product from 19 to 21 September 2016 (during a period of blackbody warm-up cool-down, or WUCD) are used for inter-comparisons. This study addresses the questions on how the sub-pixel cloud presence and the local zenith angle impact the radiometric differences between CrIS and VIIRS. Both VIIRS brightness temperature (BT) bias and standard deviation for I5, M13, M15 and M15 whose spectral response functions (SRFs) have the full coverages over the CrIS spectral regions, are analyzed over the clear and cloudy skies, respectively. Results show good agreement between VIIRS and CrIS, cloud presence has substantial impact on STD, and also impact on BIAS, local zenith angle has also substantial impact on STD, but impact on bias is small. Both bias and STD are large in DCC (deep convective cloud) areas. The study clearly shows the VIIRS scene temperature bias during WUCD, as well as the bias removal after reprocessing the M15 and M16 with the improved calibration bias correction algorithm. The methodology can be applied to monitor and validate the imager with advanced infrared (IR) sounder onboard the same platform, such as CrIS for VIIRS (SNPP, JPSS), IASI for AVHRR (Metop), and GIIRS for AGRI (FengYun-4).

10402-77, Session 15

Using AIRS level-1c for AIRS/CrIS full-resolution longwave band comparisons

Evan M. Manning, Hartmut H. Aumann, Jet Propulsion Lab. (United States)

In order to make long-term records from AIRS and CrIS radiance spectra, the spectra must first be made compatible in spectral resolution and sampling. We illustrate this with the CrIS LW band, which has resolution comparable to AIRS. The first step is to use the new AIRS Level-1C product to eliminate spectral gaps and bad channels in the AIRS data. We illustrate this with real AIRS data. The second step is to re-sample the AIRS spectra on the CrIS sample grid. The third step is to match the AIRS and CrIS (apodized) spectral resolution. We illustrate and provide a statistical evaluation of the second and third steps with calculated clear spectra.

10402-78, Session 15

AIRS/CrIS data continuity: Evaluation for extreme conditions

Hartmut H. Aumann, Evan M. Manning, Jet Propulsion Lab. (United States)

AIRS and CrIS have been in the same orbit, with the same footprint size and the same scan pattern for the past four years. On average, and for spatially homogeneous scenes, AIRS and CrIS radiometry agrees at the 100 mK level. This agreement does not assure that the measurements of extremes agree. We evaluate daily extremes using data from the 900 cm-1 channel of AIRS and CrIS. The choice of the 900 cm-1 channel suppresses spectral resolution and sampling differences. For measurements of extremes AIRS and CrIS statistically disagree significantly. For example, the daily frequency of clouds colder than 225K in the tropical zone identified by CrIS is 5% larger that than for AIRS. The daily maximum 900 cm-1 brightness temperature is typically 330K for day tropical land, but for CrIS it is 0.3±0.1 K warmer than for AIRS. If AIRS and CrIS data were not obtained for the same time period, the observed differences would be misinterpreted as climate change effects. The differences are significant for the continuity of the data record established by AIRS, to be continued with CrIS on NPP and future satellites. We evaluate if the observed differences are related to scene temperature or scene contrast dependent radiometric calibration differences or due to more subtle differences in what appear to be "the same" conditions.

10402-79, Session 15

Intercomparisons of IASI on METOP and infrared multi-spectral instruments

Bertrand Theodore, Mayte Vasquez, Dorothee Coppens, K. Dieter Klaes, EUMETSAT (Germany)

Since the launch of the second Metop platform in September 2012, two IASI (Infrared Atmospheric Sounding Interferometers) instruments are flying on the same orbit, overflying the same area with 50 minutes delay. This provides a unique opportunity to perform multiple inter-comparisons and cross-monitoring. To do so, different methodologies have been implemented to provide complementary results giving qualitative and quantitative information on both instruments in terms of radiometric and spectral inter-calibration. This includes comparisons between the two IASI but also with other instruments covering infrared regions flying on the same platform like AVHRR and HIRS; comparisons with CrIS flying on Suomi/NPP have also been performed both using SNOs which occur every seven weeks and also on a daily basis using double differences.

We will present an overview this monitoring which, besides giving us confidence on the intercalibration of both IASI, provides a way to detect the slightest differences between IASI and other infrared multispectral instruments

10402-80, Session 16

The stars: An absolute radiometric reference for the on-orbit calibration of PLEIADES-HR satellites

Aimé Meygret, Gwendoline Blanchet, Ctr. National d'Études Spatiales (France); Flore Mounier, Capgemini Sud (France); Christian Buil, Ctr. National d'Études Spatiales (France)

The accurate on-orbit radiometric calibration of optical sensors has become a challenge for space agencies who gather their effort through international working groups such as CEOS/WGCV or GSICS with the objective to insure the consistency of space measurements and to reach an absolute accuracy compatible with more and more demanding scientific needs. Different targets are traditionally used for calibration depending on the sensor or spacecraft specificities: from on-board calibration systems to ground targets, they all take advantage of our capacity to characterize and model them. But achieving the in-flight stability of a diffuser panel is always a challenge while the calibration over ground targets is often limited by their BDRF characterization and the atmosphere variability. Thanks to their agility, some satellites have the capability to view extra-terrestrial targets such as the moon or stars. The moon is widely used for calibration and its albedo is known through ROLO (RObotic Lunar Observatory) USGS model but with a poor absolute accuracy limiting its use to sensor drift monitoring or cross-calibration. Although the spectral irradiance of some stars is known with a very high accuracy, it was not really shown that they could provide an absolute reference for remote sensors calibration. This paper shows that high resolution optical sensors can be calibrated with a high absolute accuracy using stars. The agile-body PLEIADES 1A satellite is used for this demonstration. The star based calibration principle is described and the

results are provided for different stars, each one being acquired several times. These results are compared to the official calibration provided by ground targets and the associated error budget is discussed.

10402-81, Session 16

Absolute, SI-traceable lunar irradiance tie-points for the USGS Lunar Model

Steven W. Brown, Keith R. Lykke, National Institute of Standards and Technology (United States); Robert E. Eplee Jr., Xiaoxiong J. Xiong, NASA Goddard Space Flight Ctr. (United States)

The USGS ROLO model predicts the top-of-the atmosphere lunar irradiance as a function of lunar phase and libration angles over the spectral range from 350 nm to 2350 nm. The current uncertainties in the lunar irradiance predicted by the ROLO model are too large for the Moon to be used as an absolute, exo-atmospheric, satellite sensor calibration source. In this work two low uncertainty, absolute SI-traceable top-of-the atmosphere measurements of the lunar irradiance at phase angles of 7o and 17o are used to scale the output of the ROLO model in the visible to near infrared spectral region. The corrected ROLO output is SI-traceable with quantified uncertainties an order of magnitude less than the estimated uncertainties in the current ROLO model.

In addition, empirical corrections to the phase and libration angle dependence of the output of the ROLO model using lunar observation data from Earth remote sensing satellite sensors are presented. Including corrections in the output of the ROLO model for lunar phase and libration angles enables the development of an empirical correction to the output of the ROLO model for phase and libration angles relevant to Earth remote sensing sensors over this wavelength range.

Implications of the empirical correction to the output of the ROLO Model for transitioning the Moon toward an absolute, exo-atmospheric, SI-traceable satellite sensor calibration source with uncertainties commensurate with science data product requirements will be discussed.

10402-82, Session 16

Improving ROLO lunar albedo model using PLEIADES-HR satellites extra-terrestrial observations

Aimé Meygret, Gwendoline Blanchet, Ctr. National d'Études Spatiales (France); Stéphane Colzy, Capgemini Sud (France)

The accurate on orbit radiometric calibration of optical sensors has become a challenge for space agencies which have developed different technics involving on-board calibration systems, ground targets or extra-terrestrial targets. The combination of different approaches and targets is recommended whenever possible and necessary to reach or demonstrate a high accuracy. Among these calibration targets, the moon is widely used through the well-known ROLO (RObotic Lunar Observatory) model developed by USGS. A great and worldwide recognized work was done to characterize the moon albedo which is very stable. However the more and more demanding needs for calibration accuracy have reached the limitations of the model. This paper deals with two mains limitations: the residual error when modelling the phase angle dependency and the absolute accuracy of the model which is no more acceptable for the on orbit calibration of radiometers.

Thanks to PLEIADES high resolution satellites agility, a significant data base of moon and stars images was acquired, allowing to show the limitations of ROLO model and to characterize the errors. The phase angle residual dependency is modelled using PLEIADES 1B images acquired for different quasi-complete moon cycles with a phase angle varying by less than 1°. The absolute albedo residual error is modelled using PLEIADES 1A images taken over stars and the moon. The accurate knowledge of the stars spectral irradiance is transferred to the moon spectral albedo using the satellite as a transfer radiometer.

This paper describes the data set used, the ROLO model residual errors and their modelling, the quality of the proposed correction and show some calibration results using this improved model.

10402-83, Session 16

MODIS and VIIRS reflective solar calibration inter-comparisons using lunar observations

Xiaoxiong J. Xiong, NASA Goddard Space Flight Ctr. (United States); Junqiang Sun, Global Science & Technology, Inc. (United States); Zhipeng Wang, Amit Angal, Science Systems and Applications, Inc. (United States); Jon P. Fulbright, ASTS (United States)

The reflective solar bands (RSB) of both MODIS and VIIRS, covering wavelengths from 0.41 to 2.1 microns, are calibrated on-orbit by a sunlit solar diffuser (SD) panel placed behind an attenuation screen (optional for MODIS). In addition, near-monthly scheduled lunar observations have been performed through the entire mission of each instrument and used to validate and improve its RSB on-orbit calibration, particularly in term of its long-term radiometric calibration stability. MODIS and VIIRS lunar observations have also been used for other applications, including characterization of crosstalk, optical leak, and sensor spatial performance. In this paper, we provide an overview of MODIS and VIIRS solar and lunar calibration strategies and methodologies and present calibration inter-comparison results based on their lunar observations. A lunar irradiance model, such as the USGS ROLO model, is used in the lunar calibration inter-comparisons to correct for the differences due to sensors' relative spectral response (RSR) and their lunar viewing geometries. Also discussed in this paper are key uncertainty contributors associated with current lunar calibration inter-comparisons and potential improvements in future work.

10402-84, Session 16

In-orbit verification of MHS spectral channels co-registration using the moon

Roberto Bonsignori, European Organisation for the Exploitation of Meteorological Satellites (Germany)

In-orbit verification of the co-registration of channels in a scanning microwave or infrared radiometer can in principle be done during normal in-orbit operation, by using the regular events of lunar intrusion in the instrument cold space calibration view. A technique of data analysis based on best fit of data across lunar intrusions has been used to check the mutual alignment of the spectral channels of the MHS instrument. MHS (Microwave Humidity Sounder) is a cross-track scanning radiometer in the millimetre-wave range flying on EUMETSAT and NOAA polar satellites, used operationally for the retrieval of atmospheric parameters in numerical weather prediction and nowcasting.

This technique does not require any special operation or manoeuvre and only relies on analysis of data from the nominal scanning operation. The use of earth landmarks for this purpose would not be possible on the sounding channels due to the effect of the atmosphere.

The analysis reported in this paper shows an achievable accuracy below 0.5 mrad against a beam width at 3dB and spatial sampling interval of about 20 mrad. In-orbit results for the MHS instrument on Metop-B are also compared with the pre-launch instrument characterisation, showing a good correlation.

Conference 10403: Infrared Remote Sensing and Instrumentation XXV

Monday - Tuesday 7 –8 August 2017

Part of Proceedings of SPIE Vol. 10403 Infrared Remote Sensing and Instrumentation XXV

10403-1, Session 1

Integrated optical filters on chip for miniature spectrometer *(Invited Paper)*

Shao-Wei Wang, Wei Lu, Shanghai Institute of Technical Physics of the Chinese Academy of Sciences (China) and Shanghai Engineering Research Ctr. of Energy-Saving Coatings (China)

We proposed the concept of integrated narrow bandpass filter array in 2003 and realized in 2004, which can totally match with detectors array with very high spectral resolution and high structure & spectrum flexibility. The structure of corresponding spectrometer or imaging is simple with small volume and high reliability. We developed the combinatorial etching technique and combinatorial deposition technique for fabrication of such devices. A concept of a high-resolution miniature spectrometer has been demonstrated by using an integrated filter array. Such a device has already been successfully used in a multi-spectral luminescence imaging for plant growth research setup of Shijian ten satellite launched in 2016.

10403-2, Session 1

Research on active imaging information transmission technology of satellite borne quantum remote sensing

Siwen Bi, Institute of Remote Sensing and Digital Earth (China) and Beijing Institute of Space Mechanics and Electricity (China); Ming Zhen, Institute of Remote Sensing and Digital Earth (China); Song Yang, Xuling Lin, Zhiqiang Wu, Beijing Institute of Space Mechanics and Electricity (China)

According to the needs of the development and application of Remote Sensing Science and technology, Prof. Siwen Bi proposed quantum remote sensing. Firstly, the background of Quantum Remote sensing, The research status of quantum remote sensing theory, information mechanism, imaging experiments and principle prototype, the related research at home and abroad are briefly introduced. Then, the basic principles of the squeezing operator and the single mode squeezing operator of the quantum remote sensing radiation field are, Active imaging experiment of information transmission and preparation of quantum optical field squeezed light imaging experiments are described. Finally, the scheme of satellite active imaging information transmission is proposed, The composition and working principle of the active imaging system of the satellite borne quantum remote sensing are mainly included, Active imaging compression light preparation and injection device and quantum noise amplifying device. In order to realize the active imaging technology of satellite borne quantum remote sensing, the scheme and technical basis are provided. The use of quantum field technology is higher than that of coherent light imaging resolution results of 2-3 times, it can significantly improve the quantum information transmission of the remote sensing image SNR and spatial resolution. It provides the technical basis for the development of quantum remote sensing imaging engineering prototype.

10403-3, Session 1

Narrowband infrared emitter constructed with metal-DBR cavity

Shao-Wei Wang, Shanghai Institute of Technical Physics of the Chinese Academy of Sciences (China) and Shanghai Engineering Research Ctr. of Energy-Saving Coatings (China); Mingfei Wu, Shanghai Institute of Technical Physics of the Chinese Academy of Sciences (China) and Shanghai Engineering Research Ctr. of Energy-Saving Coatings (China) and Shanghai Normal Univ. (China); Jialiang Lu, Shanghai Institute of Technical Physics of the Chinese Academy of Sciences (China); Xingxing Liu, Shanghai Institute of Technical Physics of the Chinese Academy of Sciences (China) and Shanghai Engineering Research Ctr. of Energy-Saving Coatings (China); Zhiwei Li, Shanghai Institute of Technical Physics of the Chinese Academy of Sciences (China); Huafen Li, Shanghai Institute of Technical Physics of the Chinese Academy of Sciences (China) and Shanghai Engineering Research Ctr. of Energy-Saving Coatings (China); Jiaming Hao, Shanghai Institute of Technical Physics of the Chinese Academy of Sciences (China); Wei Lu, Shanghai Institute of Technical Physics of the Chinese Academy of Sciences (China) and Shanghai Engineering Research Ctr. of Energy-Saving Coatings (China)

We developed a narrowband infrared emitter constructed with Metal and Dielectric Bragg Reflector (DBR) cavity. The center wavelength and Q factor of emitter can be easily tuned by changing the thickness of dielectric cavity layer and the number of DBR stack. It was demonstrated that an infrared emitter centered at 10.4 ?m with emission of 92% and Q factor larger than 100, fabricated with thin film deposition equipment on 4 inch Si substrate. Such a simple structure can be easily fabricated in a large scale and can be applied in many fields.

10403-4, Session 2

Long wavelength interband cascade lasers on GaSb substrates *(Invited Paper)*

Anne Schade, Julius-Maximilians-Univ. Würzburg (Germany); Sven Höfling, Julius-Maximilians-Univ. Würzburg (Germany) and Univ. of St. Andrews (United Kingdom)

Interband Cascade Lasers (ICLs) are semiconductor laser sources emitting photons in the mid-infrared wavelength region. In the GaSb material system, ICLs cover the ~2.7 μm to ~5.6 μm wavelength range operating in continuous wave mode. In this spectral region, the low power consumption of ICLs is unrivaled compared to diode lasers and quantum cascade lasers emitting in this region. Many important gases like hydrocarbons have strong absorption lines in this wavelength region. ICLs are therefore suitable for gas sensing applications like tunable laser absorption spectroscopy (TLAS) for the detection of various gases. ICLs combine the cascading of active stages from quantum cascade lasers with interband transitions of diode lasers enabled by the semimetallic interface between InAs and GaSb. Beyond 5.6 μm important gases like nitrogen oxides have strong absorption lines making long wavelength GaSb ICLs interesting. We show the realization of long wavelength emitting ICLs optimized by reducing the number of electron injector quantum wells and improving doping in the active region, increasing thicknesses of the separate confinement layer and cladding layer. The devices emit at 5.72 μm and 6.00 μm, with pulsed mode characteristic temperatures of 47 K and threshold current densities of 1194 A/cm2 and 778 A/cm2 with voltage drops of 1.29 V and 1.33 V respectively.

10403-5, Session 2

Antimonide-based resonant tunneling photodetectors for mid infrared wavelength light detection *(Invited Paper)*

Fabian Hartmann, Andreas Pfenning, Georg Knebl, Robert Weih, Andreas Bader, Monika Emmerling, Martin Kamp, Julius-Maximilians-Univ. Würzburg (Germany); Sven Höfling, Julius-Maximilians-Univ. Würzburg (Germany) and Univ. of St. Andrews (United Kingdom); Lukas Worschech, Julius-Maximilians-Univ. Würzburg (Germany)

The semiconductors of the so-called 6.1 Å family, GaSb, InAs and AlSb, enable a broad range of bandgap energies and bandgap alignments which make them particularly suitable for mid-infrared optoelectronic devices. Resonant tunneling diode (RTD) photodetectors based on 6.1 Å family semiconductors allow to transfer the photodetection principle of RTDs from the visible and near infrared to the mid-infrared wavelength region. The RTD photodetection principle originates from the modulation of the majority carrier resonant tunneling current via Coulomb interaction of photogenerated minority charge carriers with the benefit of low voltage operation, high amplification factors and low noise operation. Here, we show room temperature operation of antimonide-based resonant tunneling photodetectors with GaSb/AlAsSb double barrier structures and pseudomorphically grown prewell emitter structures comprising the ternary compound semiconductors GaInSb and GaAsSb. The AlSb/GaSb double barrier RTS resembles conventional GaAs based RTDs and provides a type-I band alignment with large band offsets. We show that the electronic transport properties of AlSb/GaSb RTDs with emitter prewells lead to large peak-to-valley current ratios that are caused by an increased ?-L-valley energy separation and consequently an increased population of electrons at the ?-point. At room temperature the peak-to-valley current ratios reaches up to 2.4 for samples with incorporation of GaAsSb prewell emitters. RTD photodiodes with cut-off wavelength up to 3 μm are realized by integration of a lattice-matched quaternary GaInAsSb absorption layer. Due to the well-pronounced region of negative differential conductance, we are able to demonstrate a variety of different operation modes of the RTD photodetectors.

10403-6, Session 2

Trace gas spectroscopy using state-of-the- art mid-infrared semiconductor laser sources: Progress, status, and applications *(Invited Paper)*

Frank K. Tittel, Rice Univ. (United States)

Broadband spectroscopy is a useful tool for measuring trace gas species simultaneously. In this report basic techniques and their implementation as well as applications for laser absorption spectroscopy (LAS) and quartz-enhanced photoacoustic spectroscopy (QEPAS) will be reviewed. The design and performance characteristics of sensor systems based on absorption spectroscopy including laser sources, absorption cells and detection methods will be described. Potential future advances in techniques and applications of LAS and QEPAS relevant to the petrochemical industry, in life sciences and biomedical applications as well as environmental monitoring, atmospheric chemistry will be described.

The authors acknowledge the support from National Science Foundation (NSF) (ERC MIRTHE award), USA Robert Welch Foundation (C-0586), NSF Phase II SBIR (IIP-1230427DE DE), DOE ARPA-E awards (DE-0000545, DE-0000547).

10403-7, Session 2

Mid infrared DFB interband cascade lasers *(Invited Paper)*

Johannes Koeth, Robert Weih, Marc O. Fischer, nanoplus Nanosystems and Technologies GmbH (Germany); Martin Kamp, Sven Höfling, Julius-Maximilians-Univ. Würzburg (Germany)

The mid infrared spectral range (MIR) is of great interest for a variety of industrial, medical and environmental applications since numerous molecules have strong absorption lines therein. Interband cascade lasers (ICLs) have the ability to cover the entire MIR almost independently from the bandgap of the utilized semiconductors. Combined with a DFB technology which is applicable for most kinds of interband transition based semiconductor lasers the spectral range between 2.8 and 5.9 μm could be covered with application grade single mode devices with low power consumption. Recent optimizations regarding the layer design as well as the device processing yielded DFB laser chips with improved performance that will pave the way for a variety of applications that benefit from reasonable output power.

10403-8, Session 2

A GaAs-based up-converter for mid-infrared detection utilizing quantum cascade transport

Zhibiao Hao, Lili Xie, Chao Wang, Yaqi Liu, Lai Wang, Jian Wang, Bing Xiong, Changzheng Sun, Yanjun Han, Hongtao Li, Yi Luo, Tsinghua Univ. (China)

The next generation infrared (IR) detection technology demands for very-large-format focal plane arrays (FPAs) with high performance. Semiconductor up-converters can convert IR photons to near-infrared (NIR) photons, and can be a potential candidate for large-format IR imaging since the mechanical bonding with read-out circuit can be avoided. However, previously reported up-converters and corresponding up-conversion systems suffer from low detectivity because of the trade-off between responsivity and dark current. To solve this issue, a cascade infrared up-converter (CIUP) is demonstrated in this work. Based on a quantum cascade transport mechanism, higher IR responsivity is achieved while the dark current is maintained fairly low. A 4-?m InGaAs/AlGaAs CIUP has been fabricated, and both the CIUP and up-conversion system are under background-limited infrared performance (BLIP) regime below 120 K. The up-conversion efficiency is 2.1 mW/W at 3.3 V and 78 K. Taking shot noise as the main noise in the up-conversion system, the BLIP detectivity of the system is 2.4E9 Jones at 3.3 V and 78 K, higher than the semiconductor up-converters at similar wavelengths reported so far. To further improve the CIUP performance, AlInP hole-blocking layer is introduced taking place of AlAs layer . AlInP/GaAs has larger valence band discontinuity than AlAs/GaAs, showing the advantage of tightly confining injected holes into the emission quantum well. By adopting the AlInP hole-blocking layer, the quantum efficiency and detectivity of the up-conversion system can be enhanced.

10403-9, Session 3

High bit depth infrared image compression via low bit depth codecs *(Invited Paper)*

Evgeny A. Belyaev, Claire Mantel, Søren O. Forchhammer, Technical Univ. of Denmark (Denmark)

Future infrared remote sensing systems, such as monitoring of the Earth's environment by satellites, infrastructure inspection by unmanned airborne vehicles etc., will require 16 bit depth infrared images to be compressed and stored or transmitted for further analysis. Such systems are equipped with

low power embedded platforms where image or video data is compressed by a hardware block called video processing unit (VPU). However, in many cases using two 8-bit VPUs can provide advantages compared with using one higher bit depth image compression directly. We propose to compress 16 bit depth images via 8 bit depth codecs in the following way. First, an input 16 bit depth image is mapped into 8 bit depth images, e.g., the first image contains only the most significant bytes (MSB image) and the second one contains only the least significant bytes (LSB image). Then each image is compressed by an image or video codec with 8 bits per pixel input format. We analyze how the compression parameters for both MSB and LSB images should be chosen to provide the maximum objective quality for a given compression ratio. Finally, we apply the proposed infrared image compression method utilizing JPEG and H.264/AVC codecs, which are usually available in efficient implementations, and compare their rate-distortion performance with JPEG2000, JPEG-XT and H.265/HEVC codecs supporting direct compression of infrared images in 16 bit depth format. A preliminary result shows that two 8 bit AVC codecs can achieve similar result as 16 bit HEVC codec for far-IR images.

10403-10, Session 3

Observation and analysis of modulation and noise in visible and near-infrared diffuse ambient daylight

John Kielkopf, Elijah Jensen, Frank O. Clark, Univ. of Louisville (United States); Jeff Hay, RDI Technologies (United States)

We report on observations of low level noise and modulation in natural sky light and in sunlit scenes. Data were taken with various clear sky and partly cloudy conditions of the sky itself, as a function of altitude and angular resolution, and of naturally illuminated scenes. Different optical and sensor configurations were employed to explore the contributions of natural signal fluctuation to the remote sensing of vibrations through modulation of optical and near infrared diffusely scattered light and temporal imaging of partially resolved high contrast features. Low noise InGaAs high dynamic range photodiodes and cameras, and silicon image sensors were used with real time and post-processing to identify the noise floor, and to establish practical limits on light level and viewing distance in the use of these methods for remote structural health and vibration monitoring.

10403-11, Session 3

Flexible thermistors: MCNO films with low resistivity and high TCR deposited on flexible organic sheets by RF magnetron sputtering

Jing Wu, Zhiming Huang, Yanqing Gao, Shanghai Institute of Technical Physics of the Chinese Academy of Sciences (China)

Because of its large temperature coefficient of resistivity and good chemical stability, Mn-Co-Ni-O (MCNO) spinel is an attractive ternary system for thermistor applications, and for infrared detecting bolometers. However, conventional MCNO chip or ceramic thermistors are usually be fabricated using a solid-state reaction and sintering above 1100 ? high temperature.1 Although there are many reports on MCNO film deposition techniques, including pulsed laser deposition, chemical solution deposition, sputtering, screen printing,2-5 all those methods require 600-1200 ? high temperature treatment ((including post-annealing) to achieve sufficient crystal quality and good properties for high performance. High temperature treatment has severely hindered MCNO films to be used in standard semiconductor industry process, and also have prevented MCNO thermistor from being prepared on flexible organic substrates so as to develop wearable healthcare devices.

Meanwhile, in order to achieve lower noise and higher responsivity of bolometers, researchers have made a great effort to pursue MCNO films expected to have lower resistivity and higher TCR. For the past several decades, people considered that MCNO ternary system has a resistivity minimum as ~250?cm at room temperature.

In this work, we have used $MnCO_3$, Co_2O_3, Ni_2O_3 as original materials to sinter MCNO target under an oxygen-enriched ambient and employed RF magnetron sputtering method to directly deposit MCNO on polyethylene terephthalate (PET) and polyimide (PI) sheets at room temperature. For the first time, we have reached the lowest resistivity among the results have ever been reported for MCNO ternary system. We have achieved flexible MCNO film thermistor with resistivity 110?cm and TCR -3.1% at 295 K.

10403-12, Session 3

Nanoantenna integrated infrared pixels

Fei Yi, Huazhong Univ. of Science and Technology (China)

The concept of the antenna is widely used in the microwave regime to convert freely propagating electromagnetic waves into localized energy, and vice versa. By simple scaling down of antennas, through “scale-invariance” of Maxwell’s equations and ignoring kinetic inductance, one gets an antenna for light that has nanoscale dimensions commensurate with the much shorter optical wavelengths. Unlike conventional photonic devices (lenses, mirrors and diffractive elements) which redirect the wave front of optical radiation through the reflection and refraction of electromagnetic waves, resonantly excited optical antennas support localized surface plasmon resonances(LSPR), or the collective oscillation of electron plasma at the surface of nanostructured metals. Since metals are usually not perfect conductors at optical frequencies, the oscillating electron plasma in the optical antenna can cause high losses to the electromagnetic energy and the high optical absorption has led to the demonstration of absorbers for radiation from THz frequencies to the visible region. The electromagnetic energy dissipated in plasmonic absorber is eventually turned into heat and the thermal effects of plasmonic absorbers have enabled the investigation of such structures as nanoscale heat sources in many applications.

In this presentation I will talk about our recent works on nanoantenna integrated thermomechanical infrared pixels towards spectral selective mid-infrared detector free of discrete optics such as optical filters and polarizers. I will also talk about our proposed thermal infrared pixel array integrated with narrowband nanoantenna absorbers towards on-chip infrared spectroscopy.

10403-13, Session 4

Assessing the GOES-16 ABI onboard calibration using deep convective cloud *(Invited Paper)*

Hyelim Yoo, National Oceanic and Atmospheric Administration (United States) and ERT, Inc. (United States); Fangfang Yu, ERT, Inc. (United States) and National Oceanic and Atmospheric Administration (United States); Xianqian Wu, Ctr. for Satellite Applications and Research (United States) and National Oceanic and Atmospheric Administration (United States)

Tropical deep convective clouds (DCCs) are thick, bright, and cold and their reflectance is considered stable. Thus, DCCs can be used to calibrate visible/near infrared channels of satellite instruments. Previous studies report that how DCCs are identified by providing specific brightness temperature thresholds and are used for calibration purpose as an invariant target for solar channels.

On 19 November 2016, the Geostationary Operational Environment Satellite-R Series (GOES-R) has been successfully launched and became GOES-16 after reached the geostationary orbit on 29 November 2016. The Advanced Baseline Imager (ABI) instrument on-board GOES-R has 16 multi-spectral bands (0.47 - 13.3 um) which can provide more accurate and frequent radiometric calibration information than previous GOES satellite series.

Assessment and monitoring of the GOES-16 ABI visible/near infrared channel calibration using DCC method is a main objective of this study. The calibration stability of the ABI visible/near infrared channels will be examined and compared the results with other method (e.g., ray-matching, desert). In this study, we use the improved DCC identification method and characterize DCC temporal and spatial variation by selecting the identification thresholds to get only DCC cores. The target region is a 20°N-20°S and 109.5°W-69.5°W centered on the GOES-16 ABI check-out spatial domain. This work can be expected to provide useful information of the ABI radiometric calibration stability.

10403-14, Session 4

Preliminary study of the on-orbit radiometric traceability and artifacts for the VIIRS longwave infrared channels during blackbody temperature changes

Changyong Cao, National Environmental Satellite, Data, and Information Service (United States); Wenhui Wang, ERT, Inc. (United States)

The Longwave infrared channels (thermal emissive bands or TEB) of the Suomi NPP VIIRS are primarily used for retrieving sea surface temperatures globally. Since the VIIRS TEB data became available in January, 2012, its calibration has gone through several stages and the data reached validated maturity on March 18, 2014. While overall the validation has shown that these channels are very stable based on comparisons with CrIS, MODIS, and aircraft campaigns, with an estimated absolute uncertainty on the order of 0.1K, there is a remaining issues that persisted over the years. A calibration bias on the order of 0.1 K is introduced during the quarterly blackbody warm-up-cool-down (WUCD), and the bias is further amplified by the SST retrieval algorithm up to 0.3K in the SST products which causes an apparent spike in the SST time series. Our investigation reveals that this bias is related to a fundamental and theoretical assumption in the radiometric traceability of the VIIRS calibration equation, which states that the shape of the calibration curve is assumed unchanged from prelaunch to postlaunch, although not supported by test data from either prelaunch or postlaunch. On the other hand, the VIIRS calibration is otherwise stable when the blackbody temperature is well maintained at the designed 292.5K, during which this assumption has limited effects. In this study, after extensive analysis, we present a correction algorithm (known as Ltrace) to reconcile the calibration curve shape assumption so that the calibration bias is removed during the WUCD with minimal impacts to the operations.

10403-15, Session 4

Millikelvin thermal dynamics of infrared scenes

Nathan Hagen, Utsunomiya Univ. (Japan)

Imaging the thermal changes in a scene at the millikelvin level reveals a fascinating world that we normally cannot see. Wind passing over the ground produces dynamic striations that indicate the wind direction and speed. A person's pulse rate and blood flow can be seen from the thermal changes visible even at the surface of the skin. Material defects normally invisible to the eye become visible through the changes they induce in a surface's dynamic thermal response. We show example videos and discuss the underlying measurement principles.

10403-45, Session 4

Utilizing the precessing orbit of TRMM to produce hourly corrections of geostationary infrared imager data with the VIRS sensor

Benjamin R. Scarino, Science Systems and Applications, Inc. (United States); David R. Doelling, NASA Langley Research Ctr. (United States); Conor O. Haney, Science Systems and Applications, Inc. (United States); Kristopher M. Bedka, Univ. of Wisconsin-Madison (United States); Patrick Minnis, NASA Langley Research Ctr. (United States); Arun Gopalan, Rajendra Bhatt, Science Systems and Applications, Inc. (United States)

It is important that consistent calibration coefficients across satellite platforms are made available to the remote sensing community, and that calibration anomalies are recognized and mitigated. One such anomaly is the infrared imager brightness temperature (BT) drift that is caused by solar heating of some geostationary satellite (GEOsat) instruments near local midnight. Currently the GSICS community uses hyperspectral IASI data to uniformly inter-calibrate GEOsat IR imagers to a common reference. The IASI sensors are located on the MetOp sun-synchronous satellites, which have a local equator crossing time (LECT) of 21:30 hours on the ascending node. Similarly, the hyperspectral AIRS sensor, another viable reference, on the Aqua platform has a 01:30 LECT. Thus, the combination of IASI and AIRS observations is unable to completely resolve the GEOsat midnight BT bias. The precessing orbit of the TRMM VIRS sensor, however, allows sampling of all local hours over 46 days. Thus, VIRS has the capability of providing hourly temperature adjustments in order to mitigate the midnight anomaly observed in the 3.8-, 11-, and 12-?m channels of concurrent GEOsat sensors. In order to achieve this goal, the VIRS IR measurements are first assessed for temporal stability between 2002 and 2012 via direct comparisons with Aqua-MODIS. Furthermore, VIRS IR calibration artifacts are corrected by inter-calibrating with the IASI GSICS reference standard. The validity of this methodology is tested through direct comparisons of GEOsat and VIRS hourly-adjusted temperatures with measurements from IASI and AIRS, as well as with GEOsat measurements resulting from official GSICS calibration.

10403-32, Session PMon

Thermal pulse propagation in the search of subcutaneous masses

Marija Strojnik, Centro de Investigaciones en Óptica, A.C. (Mexico)

The irradiation of matter with laser pulse is important for determining the material surface characteristics and to form them, upon absorption of energy. The knowledge of the physical phenomena, taking place during the surface interaction with radiation directly impacts the amount of energy transmitted through the interface. This is of particular interest when assessing the tissue non-homogeneities with a probing propagating pulse, for tissue growth with modified characteristics. We simulate the thermal pulse propagation in a partially absorbing and in a partially scattering material. We compare the results to the case of pulse propagation inside the non-absorbent and non-scattering medium.

10403-33, Session PMon

Noncoding sequences classification based on wavelet transform analysis

Omar Paredes, Rebeca Romo Vázquez, Hugo Vélez Pérez, J. Alejandro Morales, Univ. de Guadalajara (Mexico); Radu Ranta, Univ. de Lorraine (France) and Ecole Nationale

Supérieure d'Electricité et de Mécanique - Nancy (France); Guillermo Garcia-Torales, Univ. de Guadalajara (Mexico); Marija Strojnik, Univ. de Guadalajara (Mexico) and Centro de Investigaciones en Óptica, A.C. (Mexico)

DNA sequences in human genome can be divided into the coding and noncoding ones. Coding sequences are those that are read during the transcription. The identification of coding sequences is widely described in literature due to its much studied periodicity. Noncoding sequences represent the majority of the human genome. They play an important role in gene regulation and differentiation among the cells. However, noncoding sequences do not exhibit periodicities that correlate to their functions. The ENCODE (Encyclopedia of DNA elements) and Epigenomic Roadmap projects have cataloged the human noncoding sequences into specific functions. We study characteristics of noncoding sequences with wavelet analysis of genomic signals. We hypothesize that noncoding sequences have characteristic periodicities related to their function. We describe identification of these characteristic periodicities using wavelet analysis. Our results show that three groups of noncoding sequences, each one with different biological function are differentiated by their wavelet coefficients within specific frequency range.

10403-34, Session PMon

Optical spectral characterization of leaves for endemic species from La Primavera forest

Roberto Carlos Barragan Campos, Antonio Rodríguez Rivas, Guillermo Garcia-Torales, Univ. de Guadalajara (Mexico); Francisco Javier González Contreras, Univ. Autónoma de San Luis Potosí (Mexico); Marija Strojnik, Univ. de Guadalajara (Mexico) and Centro de Investigaciones en Óptica, A.C. (Mexico)

La Primavera forest is the main climate regulator in the metropolitan area of Guadalajara, the second most populated megalopolis in Mexico with approximately 4.4 million people. This forest area has been a focus of fires in the last decade and it is deteriorating the quality of life of the inhabitants. Leaves from the endemic forest provide information about their biochemical composition and physiology. This information is enclosed in the spectral range of the visible band to the middle infrared (400 nm at 2500 nm). In this paper we examine the reflectance of six endemic species leaves of La Primavera forest, considering the measurement in fresh and dry samples. Measurements will be obtained with a Vis-NIR spectrometer which uses a calibrated light source. A formal collection of the optical properties of tree leaves in La Primavera forest does not exist, but it is important to classify about the type of vegetation in the area. In addition, it will provide information to generate vegetation inventories, provide data to the forest fire prevention systems, pest control and erosion in the area.

10403-35, Session PMon

Solar irradiance forecasting with an artificial vision system for Shor-time horizons

Cesar Mauricio M. Peña Martinez, Manuel I. Peña-Cruz, Centro de Investigaciones en Óptica, A.C. (Mexico)

Solar resource assessment is a subject of great importance for any technological application that wants to exploit this resource; e.j, photovoltaic technology, solar thermal, agriculture, meteorology, etc. In this paper, detailed information about solar irradiance and its variations due to climate conditions is given for Aguascalientes, Mexico. This development was achieved through an artificial vision system that analyse earth-sky dynamics. The prototype consist of image acquisition system mounted on a convex mirror that reflects the sun and sky dome over the CCD sensor. The prototype was designed with the intention of capturing wide horizon images and sun position at all times. From the images taken, shape, thickness and cloud displacements (cloud vector) can be identified, as well as the positions of the sun throughout the day. A digital image processing algorithm was designed to obtain Global Horizon Irradiance values (GHI) and compare it through a correlation with data from a traditional thermopile pyranometer. From cloud classification and cloud vector, mathematical expressions that predicts overlapping between clouds and sun was found. The developed prototype is capable of obtaining the value of GHI as accurate as those sensors in highly sophisticated solarimetric stations. It also provides a great tool for solar irradiance short-time forecasting.

10403-36, Session PMon

High precision phase shifter modulator in a shearing interferometric system

Alejandro Reynoso Alvarez, Guillermo Garcia-Torales, Univ. de Guadalajara (Mexico); Marija Strojnik, Univ. de Guadalajara (Mexico) and Centro de Investigaciones en Óptica, A.C. (Mexico); Jorge Luis Flores Nuñez, Univ. de Guadalajara (Mexico)

Shearing interferometers measure small angular variations such as the angle between a star and a planet measured from the Earth. The detected intensity pattern usually presents few fringes or less, often just a fraction of a fringe that may be interpreted as a misalignment error. Exact alignment is a challenge in the calibration of an interferometer. The optical components frequently introduce tilt making it very difficult to retrieve the phase. Spatial light modulators (SLM) are traditionally used to shift the phase to compensate small amounts of tilt, improving the accuracy of the phase measurement. We implement a phase retrieving algorithm to evaluate the accuracy of the phase shifter based on a SLM in a vectorial shearing interferometer (VSI). Our VSI is based on a Mach-Zehnder configuration. With the SLM we are able to compensate the phase error due to the alignment and the fabrication errors. Our results also demonstrate that we may correct error in the OPD and the magnitude of the tilt in the observation plane.

10403-37, Session PMon

Differential shearing interferometer

Guillermo Garcia-Torales, Univ. de Guadalajara (Mexico); Marija Strojnik, Univ. de Guadalajara (Mexico) and Centro de Investigaciones en Óptica, A.C. (Mexico); Azael Mora-Nuñez, Beethoven Bravo-Medina, Univ. de Guadalajara (Mexico)

We present a novel interferometer that we call the differential shearing interferometer (DSI). It incorporates a set of Risley prisms in a Sagnac interferometer. The Risley prisms deviate the beam in both directions. This interferometer interferes two beams displaced in the same direction, but with different magnitudes. The resultant interferogram is the directional derivative of the wavefront. The interferometer sensitivity depends on the difference between the beam deviations. This deviation is controlled by the position of the Risley prisms inside the path and their angular orientation. The advantages of quasi-common-path configuration include its low sensitivity to vibrations.

10403-38, Session PMon

Alignment of a shearing interferometer for faint sources detection using a spatial light modulator

Guillermo Garcia-Torales, Marija Strojnik, Roberto Carlos Barragan Campos, Alejandro Reynoso Alvarez, Jorge Luis

Flores Nuñez, Univ. de Guadalajara (Mexico)

Perfect alignment of shearing system is crucial for the optimal detection and analysis of wave fronts from faint and remote sources. This paper describes a method for optical misalignment detection using an intensity pattern obtained in the calibration process using a spatial light modulator. The key of the misalignment correction is the comparison of a reference intensity pattern, against a sheared interferogram. We apply digital filters used in a numerical correlator, which results in a simple and robust calibration system. Experimental and simulated work is presented.

10403-39, Session PMon

Tracking pointer using Risley Prisms

Guillermo Garcia-Torales, Univ. de Guadalajara (Mexico); Marija Strojnik, Univ. de Guadalajara (Mexico) and Centro de Investigaciones en Óptica, A.C. (Mexico); Anuar B. Beltran-Gonzalez, Jorge Luis Flores Nuñez, Univ. de Guadalajara (Mexico)

Risley prisms system has been used in scientific and technological approaches and pointing for alignment. This system is able to mark the path of a moving object by the proper combination of the angular position of a prisms pair. In this work the performance of the Risley prism model is compared with a robotic arm with two degrees of freedom model. The system is able to track an object in movement with precision and obtain the spatial coordinates in near real time.

10403-40, Session PMon

Three-dimensional shape profiling by projection of binary patterns: generated by a deterministic optimization approach

Adriana Silva, Antonio Muñoz, Jorge Luis Flores Nuñez, Univ. de Guadalajara (Mexico); Jesus Villa, Univ. Autónoma de Zacatecas (Mexico)

Three-dimensional shape profiling by sinusoidal phase-shifting methods are affected by the non-linearity of the projector. To overcome this problem, the defocused projection of binary patterns has become an important alternative to generate sinusoidal fringe patterns. In this paper, we present an efficient technique to generate binary fringe patterns where we use the symmetry and periodicity properties of binary-coded sinusoidal wavefront. This reduces the search-space for the optimization problem. The patterns are projected out-of-focus to generate quasi-sinusoidal patterns, which can be used together with a phase-shifting algorithm to retrieve 3D shape measurements. Simulations and experimental results show the feasibility of the proposed scheme.

10403-41, Session PMon

Online 3D measurement by an efficient iterative algorithm

Jorge Luis Flores Nuñez, Antonio Muñoz, Guillermo Garcia-Torales, Sotero Ordoñes Nogales, Adán Cruz, Univ. de Guadalajara (Mexico)

Online three-dimensional shape measurement has been an important procedure in many fields of the science and technology. In this work, we propose a novel technique to retrieve the 3D shape of dynamic objects by the simultaneous projection of a fringe pattern and a homogeneous white light pattern, they are both coded in an RGB image. The first one is used to retrieve the phase by an iterative least-square method. The last one is used to match pixels from the object in consecutive images, which are acquired at different positions. The proposal successfully overcome the requirement of projecting different frequency fringes: one to extraction of the object information and the other to retrieve phase. Simulations and experimental results show the feasibility of the proposed method.

10403-42, Session PMon

Piezoresistive method for a laser induced shock waves detection on solids

J. R. Gonzalez Romero, Guillermo Garcia-Torales, Gilberto Gomez-Rosas, Univ. de Guadalajara (Mexico); Marija Strojnik, Univ. de Guadalajara (Mexico) and Centro de Investigaciones en Óptica, A.C. (Mexico)

A laser shock wave is a mechanical high-pressure impulse with a duration of a few nanoseconds induced by a high power laser pulse. We performed wave pressure measurements in order to build and check mathematical models. They are used for wave applications in material science, health, and defense, to list a few. Piezoresistive methods have been shown to be highly sensitive, linear, and highly appropriate for practical implementation, compared with piezoelectric methods employed in shock wave pressure measurements. In this work, we develop a novel method to obtain the sensitivity of a piezoresistive measurement system. The results shows that it is possible to use a mechanical method to measure pressure of a laser induced shock wave in nanosecond range. Experimental pressure measurements are presented.

10403-43, Session PMon

Experiments to measure salient feature characteristics of laser-induced shock waves

Gilberto Gomez Rosas, J. R. Gonzalez Romero, Guillermo Garcia-Torales, Univ. de Guadalajara (Mexico)

Laser induced shock waves are mechanical waves of pressure of extraordinary magnitude with duration of a few nanoseconds that travel at high velocities through a material. Shock waves have been used extensively in material science to improve physical properties of material as to fatigue, strength, wear resistance, corrosion resistance, to list just a few. The shock wave induces a compressive residual stress on the target material that plastically deforms it. In this work, a piezoelectric method is used for superficial shock wave characterization near the area of the incidence of the laser pulse. It can be shown that the shock wave propagation is spherical and the velocity reduction is not linear. Experimental results with different geometrical configuration of the sensor are presented.

10403-44, Session PMon

The detection of heat emission to solar cell using drone-based thermal infrared sensor and GIS technology

Geun Sang Lee, VISION Univ. of Jeonju (Korea, Republic of)

Many studies have been implemented to manage solar plant being supplied widely in recent years. This study analyzed heat emission of solar cell using UAV-based thermal infrared sensor, and major conclusions are as below. Firstly, orthomosaic image and DSM data were acquired using UAV-based RGB sensor, and solar light module layer necessary to analyze the heat emission of solar cell was constructed by these data. Also as a result of horizontal error into validation points using VRS survey for evaluating the location accuracy of solar light module layer, higher location accuracy could be acquired like standard error of dx=±2.4cm and dy=±3.2cm. And this study installed rubber patch to test the heat emission of solar cell and could analyzed efficiently the location of rubber patch being emitted heat using UAV-based thermal infrared sensor. Also standard error showed as

±3.5% in analysis between calculated cell ratio by rubber patch and analyzed cell ratio by UAV-based thermal infrared sensor. Therefore, it could be efficiently analyzed to heat emission of solar cell using UAV-based thermal infrared sensor. Also efficient maintenance of solar plant could be possible through extracting the code of solar light module being emitted of heat automatically.

10403-16, Session 5

Rosetta's studies of comet 67P: A review after the end of the mission *(Invited Paper)*

Gabriele E. Arnold, Deutsches Zentrum für Luft- und Raumfahrt e.V. (Germany)

ESA's cornerstone mission Rosetta ended with landing the orbiter at comet 67P/Churyumov-Gerasimenko in September 2016. It acquired an enormous amount of scientific data, which have increased our knowledge about these pristine Solar system objects. The paper summarizes some the outstanding results of this mission.

10403-17, Session 5

The Venus emissivity mapper *(Invited Paper)*

Joern Helbert, Gabriele E. Arnold, Ingo Walter, Dennis Wendler, Deutsches Zentrum für Luft- und Raumfahrt e.V. (Germany); Thomas Widemann, Lab. d'Etudes Spatiales et d'Instrumentation en Astrophysique (France); Gabriel Guignan, Emmanuel Marcq, LATMOS (France); Anko Börner, Judit Jänchen, Deutsches Zentrum für Luft- und Raumfahrt e.V. (Germany)

Based on experience gained from using the VIRTIS instrument on Venus Express to observe the surface of Venus and the new high temperature laboratory experiments, we have developed the multi-spectral Venus Emissivity Mapper (VEM) to study the surface of Venus. VEM imposes minimal requirements on the spacecraft and mission design and can therefore be added to any future Venus mission. Ideally, the VEM instrument will be combined with a high-resolution radar mapper to provide accurate topographic information, as for example the NASA Discovery VERITAS mission or the ESA EnVision M5 proposal.

10403-18, Session 5

Fourier spectrometer TIRVIM/ACS aboard ExoMars 16 orbiter *(Invited Paper)*

Alexei V. Grigoriev, Alexey Shakun, Boris E. Moshkin, Dmitry V. Patsaev, Alexander V. Zharkov, Victor Shashkin, Andrey S. Kungurov, Alexander Santos-Skripko, Fedor G. Martynovich, Igor A. Stupin, Dmitry Merzlyakov, Vladislav Makarov, Oleg M. Sazonov, Yuryi Nikolskyi, Nikolai I. Ignatiev, Igor A. Maslov, Dmitry Gorinov, Elena Efremenkova, Alexander Terentiev, Oleg Korablev, Space Research Institute (Russian Federation)

Fourier-spectrometer TIRVIM is a part of ACS spectral complex aboard Mars-Express orbiter spacecraft. TIRVIM spectral range is 2–16 micron. It can operate as a spectrometer – with the Sun as a standard radiation source ("occultation" mode) or as a spectro-radiometer ("nadir" mode). In occultation mode the spectral resolution is 0.2 cm-1, in nadir mode – 1.3 cm-1. The main scientific objective of the occultation mode is to search for atmosphere minor constituents, of the nadir mode – to monitor the Mars atmosphere vertical thermal profile (by 15-micron CO_2 band). The occultation mode is self-calibrated. For absolute calibration in the nadir mode TIRVIM has a rotating inlet flat mirror (single-axis foreoptic) able to point the FOV (2º) to nadir, space, built-in black-body or to another direction in the plane. TIRVIM mass is 12 kg, the power consumption is 15 W.

10403-19, Session 6

Directional ringlet intensity feature transform (DRIFT) based object tracking in IR imagery *(Invited Paper)*

Theus H. Aspiras, Evan W. Krieger, Vijayan K. Asari, Univ. of Dayton (United States)

Current object tracking implementations utilize different feature extraction techniques to obtain salient features to track objects of interest which change in different types of imaging modalities and environmental conditions. Challenges in infrared imagery for object tracking include object deformation, occlusion, background variations, and smearing, which demands high performance algorithms. We propose the directional ringlet intensity feature transform to encompass significant levels of detail while being able to track low resolution targets. The algorithm utilizes a weighted circularly partitioned histogram distribution method which outperforms regular histogram distribution matching by localizing information and utilizing the rotation invariance of the circular rings. The image also utilizes directional edge information created by a Frei-Chen edge detector to improve the ability of the algorithm in different lighting conditions. We find the matching features using a weighted Earth Mover's Distance (EMD), which results in the specific location of the target object. The algorithm is fused with image registration, motion detection from background subtraction and motion estimation from Kalman filtering to create robustness from camera jitter and occlusions. It is found that the DRIFT algorithm performs very well under different operating conditions in IR imagery and yields better results as compared to other state-of-the-art feature based object trackers. The testing is done on two IR databases, a collected database of vehicle and pedestrian sequences and the Visual Object Tracking (VOT) IR database.

10403-20, Session 6

Automatic building change detection through linear feature fusion and difference of Gaussian classification

Daniel Prince, Vijayan K. Asari, Univ. of Dayton (United States)

Many applications in infrastructure planning and maintenance are currently aided by the collection of aerial image data and manual examination by human analysts. The increasing availability and quality of this image data presents an opportunity for computer vision and machine learning techniques to aid in infrastructure planning and maintenance. Due to the immense effort required for human analysts to view and organize the data, there is great demand for computer automation of these tasks. A strategy for detecting changes in known building regions in multi-temporal visible and near-infrared imagery based on a linear combination of independent features and a difference of Gaussian based classification approach is being developed. Initial building candidates are discovered using a linear combination of features representing vegetation intensity, image texture, shadow intensity and distance from known road areas. The resulting building candidates are classified by shape using a unique difference of Gaussians technique and a standard Support Vector Machine classifier. Building regions reported in the reference data set from the prior observation time are revisited using the same classification approach to minimize the number of false positive detections from the feature fusion strategy. The effectiveness of the proposed technique is evaluated on five wide area real-world images. Ground truths for the building regions in all five images are manually created and used to measure the accuracy of the building detection and change detection results. Detection statistics and visualized results of the proposed algorithm are presented, and it is observed that the results are promising compared to the manually created ground truth.

10403-21, Session 6

Spectrum modeling of mid-infrared flare considering realistic measurement environment

Kiwook Han, Yonsei Univ. (Korea, Republic of); Wondong Lee, Korea Military Academy (Korea, Republic of) and Yonsei Univ. (Korea, Republic of); Jae W. Hahn, Yonsei Univ. (Korea, Republic of)

Evaluating the performance of infrared (IR) flare as an active countermeasure, the similarity between an actual signal of flare and emission of an aircraft exhaust plume is important. In order to predict the actual signal of flame, exact knowledge of theoretical modeling of the flare spectrum considering realistic measurement environment is required. In this study, we conduct a line-by-line modeling of IR flare. We calculate the spectral line parameters of IR flare using high-temperature molecular spectroscopic database (HITEMP) and chemical parameters using ICT thermodynamic code in thermodynamic equilibrium condition. We consider a collisional broadening of the spectral lines under atmospheric pressure, and instrument function of spectrometer. Also, we apply an atmospheric transmission with varying altitudes, measurement angles, and humidity based on moderate resolution atmospheric transmission database (MODTRAN). Finally, we verify our modeling of IR flare by comparing with experimental results. The normalized RMS deviation between the measured and modeled data is calculated to be about 6.7%.

Acknowledgement: This work was supported by the Low Observable Technology Research Center program of Agency for Defense Development (ADD).

10403-22, Session 6

Object parameters optimization on pure and mixed pixels in thermal hyperspectral imagery

Xinyuan Miao, Ye Zhang, Junping Zhang, Sheng Wei Zhong, Harbin Institute of Technology (China)

The hyperspectral image in thermal infrared domains provide information, such as temperature and emissivity, about different kinds of materials. These information can be used for a wide number of applications such as mineral mapping, bathymetry, indoor and outdoor detection of chemicals. But because of the limitation of spatial resolution and the characteristics of thermal infrared sensor, there are many mixed pixels in the data, whose temperature?emissivity and abundance of different components can be hard to estimated. In this paper, a new method to estimate the parameters in pure and mixed pixels is proposed based on linear and nonlinear optimization. Firstly, the standard temperature and emissivity separation (TES) algorithm is applied on pure pixels of different materials selected by supervise or unsupervised methods to get the initial temperature. Secondly, the emissivity in different bands can be retrieved by minimizing the reconstruction error, which the more accurate temperature is optimized with. The emissivity in one band is trained by the samples in the same band but in different pixels, while the temperature is trained by different bands in one pixel. Lastly, the abundance and temperature of components in mixed pixels are estimated based on a linear mixture model of the bottom of atmosphere radiance as full constraint linear optimization problem and nonlinear optimization problem. The method is also analyzed with respect to sensitivity to the noise and different parameters' influences on estimation errors.

10403-23, Session 7

Sentinel-5, the new generation European operational atmospheric chemistry mission in polar orbit *(Invited Paper)*

Abelardo Pérez Albiñana, Didier D. Martin, Matthias Erdmann, Norrie Wright, European Space Research and Technology Ctr. (Netherlands); Markus Melf, Peter Bartsch, Wolfgang Seefelder, Airbus Defence and Space (Germany)

Sentinel-5 is an Earth Observation instrument to be flown on the MetOp Second Generation satellites with the fundamental objective of monitoring atmospheric composition from polar orbit. The Sentinel-5 instrument consists of five spectrometers to measure the solar spectral radiance backscattered by the earth atmosphere in five bands within the UV (270nm) to SWIR (2385nm) spectral range. The data obtained with Sentinel-5 will allow obtaining the distribution of important atmospheric constituents such as ozone on a global daily basis and at a finer spatial resolution than its precursor instruments on the first generation of MetOp satellites. The launch of the first MetOp Second Generation satellite is foreseen for 2021. The Sentinel-5 instrument is being developed by Airbus DS under contract to the European Space Agency. The Sentinel-5 mission is part of the Copernicus program Space Component, a joint initiative by ESA, EUMETSAT and the European Commission. The Preliminary Design Review (PDR) for the Sentinel-5 development was successfully completed in 2015. This paper provides a description of the Sentinel-5 instrument design and data calibration.

10403-25, Session 7

Design and characterization of a low cost CubeSat multi-band optical receiver to map water ice on the lunar surface for the Lunar Flashlight mission

Quentin Vinckier, Jet Propulsion Lab. (United States); Karlton Crabtree, Photon Engineering LLC (United States); Christopher G. Paine, Paul O. Hayne, R. Glenn Sellar, Jet Propulsion Lab. (United States)

The Lunar Flashlight mission is an innovative NASA CubeSat mission dedicated to mapping water ice in the permanently shadowed regions of the Moon, which may act as cold traps for volatiles. To this end, a multi-band reflectometer will be sent to orbit around the Moon. This instrument consists of an optical receiver aligned with four lasers, each of which emits sequentially at a different wavelength in the near-infrared between 1μm and 2μm. The receiver measures the laser light reflected from the lunar surface and continuum/absorption band ratios are then analyzed to quantify water ice in the illuminated spot. Here we present the current state of the optical receiver design. To optimize the optical signal-to-noise ratio, we have designed the receiver so as to maximize the laser signal collected, while minimizing the stray light reaching the detector from solar-illuminated areas of the lunar surface outside the FOV, taking into account the lunar topography. Calibration and test plans are also discussed. This highly mass- and volume-constrained mission will demonstrate several firsts, including being one of the first CubeSats performing science measurements beyond low Earth orbit.

10403-30, Session 7

Tissue characterization by transillumination interferometry

Brenda Guzman Valdivia, Marija Strojnik, Centro de Investigaciones en Óptica, A.C. (Mexico)

In this research, we demonstrate the feasibility of an optical method, based on transillumination interferometry, to detect anomalies in biological tissues. By light tissue interference, tree phenomena may occur when a light beam interacts with a tissue: absorption, scattering, and the un-deviated passage of light through the sample (ballistic photons). The method uses the ballistic photons property to preserve their coherence and phase, so they can participate in interference. We develop equations that describe the transmission of a beam light that pass through multiple tissues. We obtain the expressions that describes the interference pattern between both beams of an interferometer. We simulate the transillumination and the interference by considering biological tissues. The interference pattern contains information about the tissue transmission characteristics. With this information, we determine the existence of anomalies within the tissue. An experimental setup, that consist in a modified Mach-Zehnder interferometer, is presented. Such an arrangement is used to obtain the interference pattern when using a simulated tissue. The simulation results demonstrate that the method can detect anomalies in absorption and scattering coefficients in tissues. The experimental results show that the experimental arrangement is capable to characterize biological tissues. The potential of the method to be used in detecting abnormalities in biological tissues is demonstrated.

10403-27, Session 8

Millimeter-wave/terahertz detection and photonic double-mixing by transistors *(Invited Paper)*

Akira Satou, Taiichi Otsuji, Tohoku Univ. (Japan)

Development of high-performance devices for millimeter-wave (MMW)/terahertz (THz) frequencies is emerging for MMW/THz wireless communication networks and remote sensing networks. For this purpose, two-dimensional (2D) plasmons in the channels of transistor structures, specifically, InP HEMTs and graphene FETs, have been extensively investigated. The detection of MMW/THz waves can be accomplished by excitation of the 2D plasmons with the generation of rectified photocurrent due to their hydrodynamic nonlinearities as well as the nonlinear transfer characteristics of the transistors. Also, the downconversion of an optical data signal to an MMW/THz IF signal, the so-called photonic double-mixing, can be accomplished by the transistors. A local MMW/THz signal is generated in the channel of a transistor by the photomixing of the optical data and an optical subcarrier signal as a beat note signal, and then the LO signal is input to the gate, leading to the mixing of the beat note and LO signal due to the nonlinearities and, in turn, leading to the generation of the MMW/THz IF signal.

In this paper, we review the two types of MMW/THz devices we have developed; the grating-gate InP HEMTs for detection and single-gate InP HEMTs/graphene FETs for photonic double-mixing. We experimentally demonstrate the ultra-high internal responsivity of the detectors, and we discuss about their response speed to modulated data signals. For photonic double-mixing, we experimentally verify the down-conversion of 10-Gbps-class optical data to the MMW IF band using InP HEMTs and graphene FETs. We also address a possibility of photonic double-mixing in the THz frequencies.

10403-28, Session 8

Generation of ultra-stable signal twins and idler twins by coupled optical parametric oscillators: Applications in remote sensing *(Invited Paper)*

Pengda Hong, Yujie J. Ding, Lehigh Univ. (United States)

We will summarize the progress made on investigation of coupled optical parametric oscillators using a single pair of nonlinear-optical crystals forming the twins. A single signal is split into signal twins whereas a single idler is split into two idler twins. Such twins are ultrastable since their frequency difference is insensitive to the change of the pump wavelength and temperature fluctuation. It exhibits the inverse proportionality of the frequency separation on the length of each of the crystals and difference of the group indices of the signal and idler waves. What is unique about such coupled optical parametric oscillators lies in the fact that the frequency separation can be scaled to a few 100 GHz from a few THz by using just a single pair of the twins. Such a significant reduction opens up novel applications of such coupled optical parametric oscillators in remote sensing by heterodyning the output beams generated by the ultrastable twins in a photodiode.

Conference 10404: Infrared Sensors, Devices, and Applications VII

Wednesday - Thursday 9 –10 August 2017

Part of Proceedings of SPIE Vol. 10404 Infrared Sensors, Devices, and Applications VII

10404-2, Session 1

Noise and detectivity of InAs/GaSb T2SL 4.5 um IR detectors

Andrzej Kolek, Lukasz Ciura, Rzeszów Univ. of Technology (Poland); Krzysztof Czuba, Iwona Sankowska, Janusz B. Kaniewski, Institute of Electron Technology (Poland); Jaroslaw Jurenczyk, Institute of Electron Technology (Poland) and VIGO System S.A. (Poland); Agata Jasik, Institute of Electron Technology (Poland)

Infrared detectors operating under bias may suffer from 1/f noise in the low frequency (LF) range. Then, their LF detectivity is no longer determined by thermal or shot noise but instead by 1/f noise. This noise must be experimentally determined because there is no universal model allowing for its theoretical estimation. In the paper, the measurements of LF noise of type-II superlattice (T2SL) detectors are reported and used to describe detectors' performance and gain the knowledge on noise phenomena in these devices. Devices under test (DUTs) have p-i-n architecture and were formed from 10 ML/10 ML InAs/GaSb T2SL material grown using MBE technology. They reach maximum responsivity of 0.8 A/W, with 50% cutoff at 4.5 um.

The noise versus temperature and bias voltage was measured with low-noise transimpedance amplifier. These measurements enable one to draw a maps of noise limitations and frequency/voltage-dependent detectivity of DUTs. It occurs that the common approach to describe detectivity, based on theoretical estimation of shot or thermal noise, is valid only in a very limited region. Much more wider are the areas, where detector is limited by either 1/f noise or noise of the amplifier. The latter has the performance (1 nV/Hz^1/2/15 fA/Hz^1/2) better than modern read-out integrated circuits, so this limitation holds in real detection systems.

The insights into phenomena governing the noise in the studied devices, were gained employing the modeling to decompose dark current into its components and correlating them with the measured 1/f noise. We have found no 1/f noise related to the diffusion current. The generation-recombination and shunt currents contribute to the total 1/f noise power as ?_gr*I_gr^2 and ?_sh*I_sh^2, and the coefficients ?_gr, ?_sh were estimated. The coefficient ?_sh can be so large that shunt-originated noise dominates even in the high temperature region, in which current is limited by generation-recombination and diffusion components. Tunneling currents also add a contribution to 1/f noise (at high reverse bias); however, its dependence on the bias current is weaker, i.e. noise power ~ ?_tun*I_tun.

One more issue connected with the LF noise is the possibility of detecting traps that generate random processes. In our DUTs, the traps were found, that generate processes with thermally activated kinetics. The activation energies of these traps were determined.

10404-3, Session 1

Resonantly enhanced infrared detectors based on type-II superlattice absorbers

Michael D. Goldflam, Emil A. Kadlec, Benjamin V. Olson, John F. Klem, Samuel D. Hawkins, S. Parameswaran, Wesley T. Coon, Gordon A. Keeler, Torben R. Fortune, Anna Tauke-Pedretti, Joel R. Wendt, Eric A. Shaner, Paul S. Davids, Jin K. Kim, David W. Peters, Sandia National Labs. (United States)

Recent improvements in measured dark current and minority carrier lifetimes in type-II superlattice infrared detectors have positioned these materials as possible competitors to mercury cadmium telluride. We have demonstrated a resonantly enhanced sub-2 ?m thick type-II superlattice long-wavelength infrared detector with gold nanoantennas on its top surface. Enhanced quantum efficiency in this device results from increased fields from both the patterned metal surface, as well as the Fabry-Pérot cavity formed by the active region of the detector structure. Coupling of these two resonances results in spectral selectivity of the detector, as well as a peak quantum efficiency exceeding 50%, nearly four times that of a comparable non-resonant device. This increase in quantum efficiency is possible in spite of the thin active region, which has a thickness a fraction of the free-space light wavelength. Through modification of only the nanoantenna structure, the device spectral response can be tailored to include multiple peaks or to shift a single peak by up to 2 ?m. Ultimately, use of thinned detector structures has the potential to reduce dark current, thereby improving signal-to-noise, while alleviating the expected decrease in quantum efficiency that results from a smaller absorbing volume. The mechanisms used here to improve detector functionality are detector-material agnostic suggesting their utility with alternative materials such as mercury cadmium telluride. These resonantly enhanced detectors show promise for future applications as sensitive frequency-agile solid-state sensors as well as two-color detector systems.

10404-4, Session 1

Theoretical simulation of mid-wave type-II InAs/GaSb superlattice interband cascade photodetector

Piotr Martyniuk, Klaudia Hackiewicz, Jaros?aw Rutkowski, Tetina Manyk, Andrzej Kowalewski, Wojskowa Akademia Techniczna im. Jaroslawa Dabrowskiego (Poland)

In this paper, the performance of a HOT interband type-II mid-wave (MWIR) InAs/GaSb superlattice (T2SLs) cascade detector is presented. Detailed analysis of the detector's performance (dark current and detectivity) versus bias voltage and operating temperatures reached by thermoelectrical cooling T= 200?230 K is shown. The bulk analytical base model to include surface current contribution is used while absorption coefficient and carrier effective masses are calculated by APSYS platform. It was assumed that cascade detector is composed of N stages where active layer length, d ~156 nm in each stage are equal to the same value. The carrier's diffusion length, L and absorber's length meet the requirement d << L. Simulated structure exhibits a cut-off wavelength ~ 4.8 μm at 200 K. The absorber region is non-intentionally doped and is made of 9 ML InAs/9 ML GaSb T2SLs. Responsivity, and detectivity, of the structure without immersion lens and zero bias reaches ~ 0.25 A/W and ~ 3e9 Jones for T = 230 K respectively. The proper compatibility between experimental and measured results was reached.

10404-5, Session 1

Effects of 4.5 MeV and 63 MeV proton irradiation on carrier lifetime of InAs/InAsSb type-II superlattices

Emil A. Kadlec, Michael D. Goldflam, Edward Bielejec, Jin K. Kim, Benjamin V. Olson, John F. Klem, Samuel D. Hawkins, Johnathan Moussa, Peter A. Schultz, Sandia National Labs. (United States); Christian P. Morath, Geoffery D. Jenkins, Vincent M. Cowan, Air Force Research Lab. (United States); Eric A. Shaner, Sandia National Labs. (United States)

Type-II strained-layer superlattices (T2SLs) are receiving increased interest as mid-wave infrared (MWIR) and long-wave infrared detector absorbers due to their potential Auger suppression and ability to be integrated into

complex device structures. Although T2SLs show promise for use as infrared detectors, further investigation into the effects of high energy particle radiation is necessary for space-based applications. In this presentation, the effects of both 4.5 MeV and 63 MeV proton radiation on the carrier lifetime of MWIR InAs/InAsSb T2SLs will be shown. The 63 MeV proton radiation study will focus on the carrier lifetime of MWIR InAs/InAsSb T2SL samples of varying donor density. These results reveal a Shockley-Read-Hall (SRH) lifetime associated with a radiation induced defect level, which is not dependent on the donor density of the T2SL. Using 4.5 MeV proton radiation, the dependence of carrier lifetime on relative trap density in MWIR T2SLs samples is studied by varying the particle fluence. A comparison of these two radiation studies shows similar lifetime effects that will be discussed in detail. These results give insight into the viability of Ga-free T2SLs for space applications.

10404-6, Session 1

Extraction of minority carrier diffusion length of MWIR type-II superlattice nBp detector

Zahra Taghipour, The Univ. of New Mexico (United States); Alireza Kazemi, The Ohio State Univ. (United States); Stephen Myers, SKINfrared LLC (United States); Priyalal S. Wijewarnasuriya, U.S. Army Research Lab. (United States); Sen Mathews, The Univ. of New Mexico (United States); Elizabeth Steenbergen, Christian P. Morath, Vincent M. Cowan, Gamini Ariyawansa, John Scheihing, Air Force Research Lab. (United States); Sanjay Krishna, The Ohio State Univ. (United States) and Univ. of New Mexico (United States) and SKInfrared LLC (United States)

We present a model to extract the minority carrier diffusion length (Ln) of an unipolar nBp InAs/GaSb Type II superlattice (T2SL) mid-wave infrared (MWIR) detector. The detector consists of a p-doped 10ML InAs/10ML GaSb SL absorber with a 50% cut-off wavelength of 4.5 μm at 80 K and zero bias. The detector was designed with an n-type doped InAs/AlSb SL barrier to reduce the operating bias. The device was fully turned on at 0 V. The external quantum efficiency (EQE) was measured to be 62% at 80 K, using front side illuminated devices with no anti-reflection (AR) coating. The dark current density, at the same temperature and operating bias, was measured to be 3.05?10-8 A/cm2. By fitting the experimentally measured EQE data to the theoretically calculated QE based on Hovel expressions, Ln can be extracted if the absorption coefficients are known accurately. The absorption coefficient was measured using an FTIR microscope and found to be 1600 cm-1 at 4.5 μm at 80 K. In addition, a reduced background concentration of 1.6?1016 cm?3 and a built-in potential of 150 meV were extracted by utilizing a capacitance-voltage measurement technique. Combining these results with the minority carrier lifetime measured via time-resolved-photoluminescence (TRPL), we were able to obtain an estimate of the diffusion length in this T2SL detector with a 4 μm thick absorber. This work was sponsored by the Army Research Office (ARO) under the contract W911NF-16-2-0068.

10404-7, Session 2

Active modulation of surface plasmon polaritons at degenerate semiconductor interfaces

Raj K. Vinnakota, Dentcho A. Genov, Louisiana Tech Univ. (United States)

The prospective of plasmonics to bridge the gap between electronics and photonics is well recognized by the scientific community with a large number of investigators working in the field of plasmonics. The Surface Plasmon Polaritons (SPPs), charge-density waves propagating at metal-dielectric and/or semiconductor-dielectric interfaces have tighter spatial confinement and higher local field intensity, can possess the key to offer the bandwidths of photonic devices and physical dimensions shared with nanoscale electronics. Here, we present an opto-electric switching element for plasmonic interconnects and circuits by electronically controlling highly confined SPPs at the metallurgic interfaces of degenerate semiconductor materials. The opto-electric SPP switch uses heavily doped sandwich of p and n-type semiconductor. In the operation the SPPs propagating at the interface of the p-n junction are switched by forward biasing the p-n junction by an external voltage. Two figure of merits are introduced and parametric study has been performed identifying the device optimal operation range. For high optical confinement, reduced system size and fast operation Indium Gallium Arsenide (In0.53Ga0.47As) is identified as the best semiconductor material. The opto-electric SPP switching element is shown to operate at signal modulation up to -24dB and switching rates surpassing 100GHz, thus possibly providing a path towards bridging the gap between photonic and electronic devices.

10404-8, Session 2

Distance and temperature dependent plasmon-enhanced carrier generation and diffusion in InAs/InGaAs/GaAs near-infrared photodetectors

Terefe Habteyes, Sharmin Haq, Sadhvikas Addamane, Ganesh Balakrishnan, The Univ. of New Mexico (United States); Danhong Huang, Air Force Research Lab. (United States)

Compared to the highly sensitive silicon based affordable visible light detectors, infrared photodetectors require significant improvement. Localized surface plasmon resonances of metal nanoparticles can be utilized for increasing the absorption efficiency of semiconductors suited for detection of infrared radiation. In this presentation, plasmonic gold nanorods (AuNRs) are used to enhance generation of charge carriers and photon emission by InAs/InGaAs/GaAs quantum dots-in-a-well structures. Comparison of measured and calculated scattering spectra reveals that the AuNRs on GaAs exhibit red to green colors depending on their proximity to the GaAs surface. On the other hand, theoretical and experimental near-field optical characterization show that the electric field is tightly localized at the AuNR-GaAs interfacial regions, creating a convenient platform for investigating localized carrier generation and diffusion by monitoring the emission of InAs QDs. The carrier generation and photon emission enhancement is studied as a function of the GaAs thickness (distance) and temperature. Analysis of the InAs quantum dot emission enhancement as a function of distance reveals a Förster radius of 3.85 ± 0.15 nm, a near-field decay length of 4.8 ± 0.1 nm and an effective carrier diffusion length of 64.0 ± 3.0 nm. These distance parameters indicate two emission enhancement mechanisms: plasmon enhanced carrier generation inside the GaAs layer and diffusion to the InAs quantum dots, and direct near-field excitation of the InAs/InGaAs. The emission enhancement increases with temperature, confirming the importance of charge carrier diffusion from the GaAs to the InAs quantum dots, where recombination and photon emission takes place.

10404-9, Session 3

The photonic device for integrated evaluation of collateral circulation of lower extremities in patients with local hypertensive-ischemic pain syndrome

Volodymyr S. Pavlov, Vinnitsa State Technical Univ. (Ukraine); Yurii O. Bezsmernyi, SRI of Invalid Rehabilitationon on the base of National Pirogov Memorial Medical University (Ukraine); Sergey M. Zlepko, Vinnitsa State Technical Univ. (Ukraine); Halyna V. Bezsmertna, SRI of Invalid Rehabilitationon on the base of National Pirogov Memorial Medical University (Ukraine)

Non-invasive diagnostic methods with optical registration and transformation of biomedical information extensive have been extensively developed for the last few years. Laser photoplethysmography (LPPG) relates to one method of non-invasive optical diagnostics peripheral circulation.

The purpose is the evaluation of LPPG diagnostic value in examination of patients with chronic ischemia of lower extremities.

Method can improve the reliability of the control and peripheral circulation diagnostics and identify the effects on the autonomic nervous system, can serve for evaluation of sympathetic innervations of the skin, can be used in the diagnostics of Reynaud's disease, early forms of atherosclerosis, thrombosis, etc. Besides, LPPG has additional diagnostic and prognostic value in the study of many cardiovascular and neurological diseases that are the most common causes of death and disability in young age. Therefore, effective processing of LPPG information is very important.

Photonic device is developed to determine the level of the peripheral blood circulation, which determines the basic parameters of peripheral blood circulation and saturation level. Device consists of two sensors: infrared sensor, which contains the infrared laser radiation source and photodetector, and the red sensor, which contains the red radiation source and photodetector. The outputs of amplifiers connected to the inputs of the microcontroller.

LPPG method allows to determined pulsatility of blood flow in different areas of the foot and lower leg, the degree of compensation and conservation perspectives limb and of amputation level. LPPG is the highly informative method to evaluation the pulsatility of blood flow in a specific area.

10404-10, Session 3

In vivo noninvasive detection of blood glucose by near-infrared spectroscopy with machine learning techniques

Siman Zhang, Siqi Liu, Ting Xie, Peng Sun, Chang Wang, Huaye Li, Zhenrong Zheng, Zhejiang Univ. (China)

Blood glucose level (BGL) has been regarded as an indicator of diabetes mellitus, hypoglycemia and metabolism disorders for patients. In this paper, we presented a system for in vivo noninvasive BGL detection using near-infrared (Near-IR) diffuse-reflectance spectroscopy combined with machine learning (ML) algorithms. Compared with conventional BGL detection devices, this system could release the pain of patients associated with the frequent pricking of skin for taking blood samples. The system was consisted of an illumination module, a noninvasive detection module based on Near-IR spectrometer and a data processing module. Method underlying the system was that there was functional relationship between Near-IR spectra and BGL. Near-IR spectra were collected separately from thirty volunteers at the fingertip during glucose tolerance tests. Calibration models were generated from two-thirds of the spectra data to predict BGL using multilayer perceptron neural network, support vector machine and random forest ML techniques. Unlike traditional chemometrics methods which were used to model linear relationships, ML algorithms performed better in representing BGL via Near-IR spectra due to the presence of nonlinearity. The performance of the calibration models were examined by evaluating the accuracy of glucose predictions from the remaining third spectral data using correlation coefficient of prediction, mean error percentage of prediction and root mean square error of prediction (RMSEP). The best results were obtained with random forest technique. Results showed that with the designed system, blood glucose could be detected with a high correlation coefficient of 92.4%, mean error percentage of 14.49% and RMSEP of 0.52 mmol/L.

10404-11, Session 3

Photoacoustic signal detection using interferometric fiber-optic ultrasound transducers

Amanda D. Salas-Caridad, Geminiano Martinez-Ponce, Rodolfo Martinez Manuel, Centro de Investigaciones en Óptica, A.C. (Mexico)

Photoacoustics is a hybrid technique driven by the photoacoustic effect. This effect is based on the sensitive detection of acoustic waves launched by the absorption of pulsed or modulated radiation by means of transient localized heating and expansion in a gas, liquid, or solid. This effect is due to the transformation of at least part of the excitation energy into kinetic (translational) energy by energy exchange processes between different degrees of freedom. Consequently, the absorption of pulsed radiation generates an acoustic signal that is acquired by an ultrasonic piezoelectric transducer or optically with a contact-free method. It is an interesting technique which combines the advantages of optics and acoustics. The optics field provides with high resolution, while acoustics provides higher spreading range. The technique caught the special attention of biomedical researchers, as the optical absorption of some tissue components such as hemoglobin, oxy-hemoglobin, melanin, bilirubin, lipids and water, allows them to process information regarding their presence.

This work aims to propose the design of a fiber-optic interferometric sensors array which localizes the origin of an acoustic signal generated by an infrared light absorption center inside the volume of a semi-opaque medium. The characterization and evaluation of the performance for ultrasonic transductors (hydrophones) based in fiber-optic interferometric sensors must be made in order to develop an accurate inverse algorithm for the localization of an acoustic signal from its spatial and temporal behavior. Also, an experimental method to determine the optimal distribution of four ultrasonic transductors can be developed as well.

10404-13, Session 4

Improved performance of GaAs photocathodes using effective activation technique

Yijun Zhang, Jingzhi Zhang, Cheng Feng, Nanjing Univ. of Science and Technology (China); Hongchang Cheng, Science and Technology on Low-Light-Level Night Vision Lab. (China); Xiang Zhang, Yunsheng Qian, Nanjing Univ. of Science and Technology (China)

Up to now, negative-electron-affinity (NEA) GaAs-based photocathodes have found widespread applications in photoelectric detectors for night observation and electron sources for high-energy physics. To achieve NEA state, the atomically clean cathode surface is usually activated by cesium and oxygen. In view of the required computer-control of evaporation flow rates, the solid oxygen dispenser instead of gaseous oxygen is used just as the regular Cs dispenser. Two types of solid oxygen dispensers composed of barium peroxide powder and silver oxide powder are chosen to activate GaAs photocathodes. By residual gas detection during degassing, it is found that the barium peroxide-based O dispenser can release more oxygen than silver oxide-based one. The appropriate evaporation current passing through the O dispenser of silver oxide should exceed 7.8A. Through a series of Cs-O activation experiments, there exists an unsatisfactory feature that the silver oxide-based O dispenser released effectual oxygen gas more slowly than the barium peroxide-based O dispenser, which was adverse to the first Cs/O alternate activation. Therefore, an effective activation technique was proposed to ameliorate the unfavorable phenomenon for silver oxide-based O dispenser, which could bring out the desired symmetry of photocurrent curve shape during the whole Cs/O alternate activation process. Whereas, compared with the silver oxide-based O dispenser, the barium peroxide-based one can bring a higher activation photocurrent for GaAs photocathodes, which accordingly resulted in a better spectral response. The effective activation technique using solid dispensers can provide guidance for the optimization of activation craft.

10404-14, Session 4

Extended wavelength InGaAs SWIR FPAs with high performance

Xue Li, Xiu-Mei Shao, HaiMei Gong, Xianliang Zhu, Shanghai Institute of Technical Physics of the Chinese Academy of Sciences (China)

The extended InGaAs short wavelength infrared (SWIR) detector covers 1.0-2.5μm wavelength, which plays an important role in weather forecast, resource observation, low light level systems, and astronomical observation and so on. In order to fabricate the high performance extended InGaAs detector, materials structure and parameters were characterized by using Scanning Capacitance Microscopy(SCM), Scanning Spreading Resistance Microscopy (SSRM) and Photoluminescence Spectroscopy(PL), the spreading of minority carriers and lattice quality were obtained. Mesa etching parameters, etching damage restoration and low temperature passivation were used in the fabrication of the extended InGaAs detector. The improvement of material structure and device process was studied by using different perimeter-to-area (P/A) photodiodes and MIS structure device, respectively. The dark current of the extended InGaAs detector obviously decreases, about 1nA/cm2 at 170K temperature. The 512?256 FPAs were fabricated, the peak detectivity and the quantum efficiency of which are 5?1011cmHz1/2/W and 80% , respectively. The staring image yielded of the 512?256 FPAs is shown, which demonstrates very good imaging quality.

10404-15, Session 4

640x512 pixel InGaAs FPAs for short-wave infrared and visible light imaging

Xiu-Mei Shao, Bo Yang, Songlei Huang, Yang Wei, Xue Li, Xianliang Zhu, Tao Li, HaiMei Gong, Shanghai Institute of Technical Physics of the Chinese Academy of Sciences (China)

The spectral irradiance of moonlight and air glow is mainly in the wavelength region from visible to SWIR band. The imaging for very low background applications during this wavelength range is of great significance in civil safety and defense field. In this paper, 640?512 visible-SWIR InGaAs FPAs were studied for night vision and short-wave infrared (SWIR) imaging. A special epitaxial wafer structure with etch-stop layer was designed and developed. Planar-type 640?512 InGaAs detector arrays were fabricated. The photosensitive arrays were bonded with readout circuit through Indium bumps. The FPAs were tested at the temperature of 293K. The relative spectral response is in the range of 900nm to 1700nm. Then, the InP substrate was removed with low damage by mechanical thinning and chemical wet etching. Multilayer anti-reflection films were designed and deposited on the backside-illuminated surface. The quantum efficiency is approximately 15% at 500nm, 30% at 700nm, 50% at 800nm, 90% at 1550nm. The visible irradiance can reach InGaAs absorption layer and then to be detected. As a result, the detection spectrum of the InGaAs FPAs has been extended toward visible spectrum from 500nm to 1700nm. The average peak detectivity is higher than 3?10^12cm•Hz^1/2/W at room temperature with a integrated time of 10ms.The Visible-SWIR InGaAs FPAs were applied to an imaging system with good resolution for SWIR and visible light imaging.

10404-16, Session 4

Life test of the InGaAs focal plane arrays detector for space applications

Xianliang Zhu, HaiYan Zhang, Xue Li, ZhangCheng Huang, HaiMei Gong, Shanghai Institute of Technical Physics of the Chinese Academy of Sciences (China)

Compared to tactical applications, IR detectors for space applications require far fewer quantities, and reliability and photoelectric performances must be extraordinarily high. Therefore, the research of its reliability is very difficult because of the little amount and high price.

Hybrid Infrared focal plane array (IRFPA) is the core component of the third generation infrared detection systems, which consists of infrared detector chip, readout integrated circuit (ROIC), and flip-chip bonding interconnection by Indium bump. In order to satisfy space application requirements for failure rates or Mean Time to Failure (MTTF), which can only be demonstrated with the large number of detectors manufactured, the single pixel in short-wavelength infrared InGaAs focal plane array is chose as the research object in this paper.

As the InGaAs FPAs are usually operated around room temperature, they will not go through thousands times of temperature cycles, so hot temperature is the suitable accelerated stress. Through step-stress accelerated life test, the maximum temperature stress of InGaAs FPAs under the same failure mechanism has been obtained, and it was found that Indium bump is the most possible weakness of the FPAs. According to the results of step-stress accelerated life test, choosing the single pixel in InGaAs FPAs as research object, the constant-stress accelerated life test has been carried out at 70??80??90?and100?. The bad pixels increased gradually during more than 10000 hours at each elevated temperatures. Statistical analysis on the experimental data shows that the activation energy is about 0.46eV, and the average lifetime of a single pixel in InGaAs FPAs will be more than 1E+7h at the operating temperature(5?).

10404-17, Session 5

Mid-infrared photo detector using pyroelectric response of LiNbO3

Kavitha K. Gopalan, ICFO - Institut de Ciències Fotòniques (Spain); Davide Janner, Politecnico di Torino (Italy); Sebastien Nanot, Romain Parret, Mark B. Lundeberg, Frank H. L. Koppens, Valerio Pruneri, ICFO - Institut de Ciències Fotòniques (Spain)

Photodetectors (PDs) in the mid infrared (mid-IR) wavelength region are of great interest as they are essential components in many applications, e.g. vibrational spectroscopy and thermal imaging. The majority of current PDs in the mid-IR are limited by the fact that they operate at cryogenic temperatures. We demonstrate a room temperature photodetector working in the 6-10 ?m range based on graphene on z-cut LiNbO3 pyroresistive platform. Infrared radiation absorbed in the LiNbO3 crystal leads to an increase in temperature, which subsequently induces polarization (bound) charges at the crystal surface via the pyroelectric effect. These cause doping into graphene which in turn changes its carrier density and hence the electrical conductivity.The characteristics of such pyro-resistive detectors are in between conventional pyroelectric detectors and bolometers that are used in IR detection, thus enabling an optimum trade-off between both these classes of detectors. Detectivities of about 10^5cm√HzW-1 in the 6 to 10 ?m region are demonstrated. We also show that up to two orders of magnitude larger detectivity can be achieved by optimising the geometry and operating in vacuum, thus opening the path to a new class of mid-IR photo-detectors that can challenge classical HgCdTe devices, especially in real applications where cooling is to be avoided and low cost is crucial.

10404-18, Session 5

Low dark current p-on-n technology for space applications

Nicolas Péré-Laperne, SOFRADIR (France); Nicolas Baier, Cyril Cervera, Jean-Louis Santailler, Clément Lobre, CEA-LETI (France); Christine Cassillo, Jocelyn Berthoz, Vincent Destefanis, Diane Sam-Giao, Adrien Lamoure, SOFRADIR (France)

Space applications are requiring low dark current in the long wave infrared at low operating temperature for low flux observation. The applications

envisioned with this type of specification are namely scientific and planetary missions. Within the framework of the joint laboratory between Sofradir and the CEA-LETI, a specific development of a TV format focal plane array with a cut-off wavelength of 12μm at 40K has been carried out.

For this application, the p on n technology has been used. It is based on an In doped HgCdTe absorbing material grown by Liquid Phase Epitaxy (LPE) and an As implanted junction area. This architecture allows decreasing both dark current and series resistance compared to the legacy n on p technology based on Hg vacancies.

In this paper, the technological improvements are briefly described. These technological tunings led to a 40% decrease of dark current in the diffusion regime. CEA-LETI and Sofradir demonstrated the ability to use the p on n technology with a long cutoff wavelength in the infrared range.

10404-19, Session 5

Germanium photodetectors fabricated on 300 mm silicon wafers for near-infrared focal plane arrays

Ashok K. Sood, John W. Zeller, Magnolia Optical Technologies, Inc. (United States); Caitlin Rouse, Pradeep Haldar, Harry Efstathiadis, SUNY Polytechnic Institute (United States); Nibir K. Dhar, U.S. Army Night Vision & Electronic Sensors Directorate (United States)

Germanium near-infrared (NIR) photodetectors operating a room temperature have certain advantages compared to conventional III-V and HgCdTe based infrared detectors in relation to ease of fabrication, cost, and size, weight and power (SWaP), aided by recent improvements in techniques for epitaxially depositing layers of pure Ge. While Ge based detectors have traditionally been limited to operating up to ~1.6 ?m, this detection limit may be extended to longer wavelengths through incorporation of tensile strain. Scanning transmission electron microscopy (STEM) based fast Fourier transform (FFT) modeling of atomic-scale lattice periodicity of the cross-sectional device structure has been performed to determine the location and extent of tensile strain in the detectors, as well as the nature of material coalescence at the Si-Ge junction. Ge-based p-i-n photodetectors have been fabricated on 300 mm silicon wafers, taking advantage of complementary metal-oxide semiconductor (CMOS) technology. The fabrication is based on a specialized two-step low/high temperature growth process taking into account the significant difference in thermal expansion coefficients between Ge and Si, designed to minimize formation of threading dislocations. Bright-field STEM analysis showed the Ge seed and intrinsic layers to be of high quality with limited defects and dislocations. In addition, measured I-V photoresponse behavior of photodetector devices at room temperature under dark and illuminated conditions demonstrated significant photocurrent enhancement for visible-NIR radiation at reverse biases, and relatively high zero-bias response. These Ge p-i-n detectors were designed to function as elements in an NIR imager focal plane array (FPA).

10404-1, Session PWed

Effect of antimony segregation on the electronic properties of InAs/InAsSb superlattices

Heather J. Haugan, Frank Szmulowicz, John J. Hudgins, Logan E. Cordonnier, Gail J. Brown, Air Force Research Lab. (United States)

There has been great progress in recent years in advancing the state-of-the-art of Ga-free InAs/InAsSb superlattice (SL) materials for infrared detector applications, spurred by the observation of long minority carrier lifetimes in this material system. However, compositional and dimensional changes through Sb segregation alter the detector properties from those originally designed. Therefore, in this work, epitaxial conditions that can mitigate this segregation were explored in order to produce high-quality SL materials for optimum detector performance. A nominal SL structure of 7.7 nm InAs/3.5 nm InAs0.7Sb0.3 tailored for an approximately six-micron response at 5 K was used to optimize the epitaxial parameters. Since the growth of mixed AsSb alloys is complicated by the potential reaction of As with Sb surfaces, the authors vary the substrate temperature (Ts) in order to control the As surface reaction on a Sb surface. Experimental results indicate that the SL sample grown at the lowest investigated Ts produces the highest Sb-mole fraction x of ~0.3 in InAs1-xSbx layers, which then decreases by 21 % as the Ts increases from 395 to 440 °C. This reduction causes an approximately 30 meV blueshift in the position of the excitonic photoluminescence (PL) peak. This finding differs from the results obtained from the Ga-containing InAs/GaSb SL equivalents, where the PL peak position remains constant at about 220 meV, regardless of Ts. The Ga-free SLs generally generate a broader PL linewidth than the corresponding Ga-containing SLs due to the higher spatial Sb distribution at the hetero-interfaces engendered by Sb segregation.

10404-12, Session PWed

Improved calibration-based non-uniformity correction method for uncooled infrared camera

Chengwei Liu, Xiubao Sui, Nanjing Univ. of Science and Technology (China)

With the latest improvements of microbolometer focal plane arrays (FPAs), uncooled infrared (IR) cameras become the most widely devices in thermography, especially in handheld devices. While the influences derived from changing ambient condition and the non-uniform response of the sensors make it more disturbing to correct the non-uniformity of uncooled infrared camera. In this paper, based on the infrared radiation characteristic in the TEC-less uncooled infrared camera, a novel model was proposed for calibration-based non-uniformity correction. In this model, we introduce the FPA temperature, together with the responses of microbolometer under different ambient temperature to calculate the correction parameters. Based on the proposed model, we can work out the correction parameters with the calibration measurements under controlled ambient condition and uniform blackbody. All correction parameters can be determined after the calibration process and then be used to correct the non-uniformity of the infrared camera in real time. This paper present the detail of the compensation procedure and the performance of the proposed calibration-based non-uniformity correction method. And our method was evaluated on realistic IR images obtained by a 384?288 pixels uncooled long wave infrared (LWIR) camera operation under changed ambient condition. The results show that our method can exclude the influence caused by the changed ambient condition, and ensure that the infrared camera has a stable performance.

10404-23, Session PWed

Chalcogenide based rib waveguide for compact on-chip supercontinuum sources in mid-infrared domain

Than Singh Saini, Umesh K. Tiwari, Central Scientific Instruments Organisation (India); Ravindra K. Sinha, Delhi Technological Univ. (India)

Mid-infrared supercontinuum generation (i.e the broadening in the intense laser pulses when they pass through the highly nonlinear medium) is very exciting research field because of its applications in diverse fields such as spectroscopy, medical imaging, security and sensing. The broadening of the supercontinuum spectrum depends on both strong nonlinearity and dispersion characteristic, which leads to solitonic effects and efficient four-wave mixing. The highly nonlinear materials such as chalcogenide glasses are promising platform for the realization of compact, on-chip mid-infrared supercontinuum sources. To date, various chalcogenide glass systems have been explored and their potential applications have been estimated. Recently, a novel chalcogenide glass system, Ga–Sb–S, is reported which has a very high nonlinearity (n2 = ~12.4?10–14 cm2/W at 1.55 μm) and wide

transparent window of ~0.8–14 μm. Because of these favorable properties this chalcogenide glass system supposed to be promising materials for mid-infrared nonlinear applications such as thermal imaging, nonlinear optics, and mid-infrared lasers. In this work, we have designed and analyzed a highly nonlinear rib waveguide structure in recently reported Ga-Sb-S based chalcogenide glass for mid-infrared supercontinuum generation ranging from 2 – 10 μm. The proposed waveguide structure possesses a very high nonlinear coefficient and can be used for compact on-chip supercontinuum sources in mid-infrared domain.

10404-37, Session PWed

High security Infrared biometrics authentication system for financial application

Xiaofeng Jin, Sun Yat-Sen Univ. (China); Tiancai Liang, Research Institute of GRG Banking Equipment Co., Ltd. (China); Biao Wang, Sun Yat-Sen Univ. (China); Ming Li, Jun Xu, Research Institute of GRG Banking Equipment Co., Ltd. (China); Jianfeng Sun, Shanghai Institute of Optics and Fine Mechanics (China)

Based on infrared Finger-vein Recognition technology, security chip and hardware encryptor, this paper provides secure and trusted solution for identity authentication. In order to guarantee the safe running environment of the Finger-vein device, a security chip was embedded to process triple DES algorism for sensitive biometric information encryption and storage. And the device to be self-defensive, once destructed, all the information inside the chip will gone. Besides the hardware encryptor was adopted to be with the server of the platform, to generate all the keys running in the system and decryption the key during communication. The digital signature was applied to guarantee the integrity of biometric information, which is unable to be manipulated. So we can support the process of Finger-vein authentication to meet with financial-level security standard.

10404-38, Session PWed

A comparison of approximate and exact modes in few-mode micro-optical fibres

José Á. Flores-Bravo, Fernando Martínez-Piñón, Ctr. de Investigación e Innovación Tecnológica (Mexico); Grethell G. Pérez-Sánchez, Univ. Autónoma Metropolitana (Mexico)

An analysis of different cases of few-mode micro-optical fibers from 10 to 1 microns in diameter is performed based on solving the eigenvalue equation using both the weak guidance approximation (scalar LP modes) when the refractive index difference is small, and the exact full eigenvalue equation (vector TE, TM, HE and EH modes), when the refractive index difference is large, for example having air or a gas as the surrounding medium. One of the objectives of this analysis is to show at what point the propagation constant and optical field intensity of the fundamental modes LP01 and HE11 differ significantly depending of the refractive index difference, the other objective is to find out the evolution of the other modes along the final tapered section in a few mode fiber taper. The graphical behavior of the solutions of the eigenvalue equation is presented and the optical intensity distributions are calculated for different sizes, as for example in adiabatic tapers to evaluate the extent of the evanescent field. In general, the propagation constant and effective refractive index depends on the size of the core waveguide diameter, the refractive index difference and the wavelength. This analysis is useful to calculate the extension of the evanescent field in liquids or gases for optical fiber sensors that can be used to model, for example, fluorescent optical fiber sensors for biological or industrial applications. Additionally, the propagation characteristics of the few-mode micro optical fiber could be controlled or tuned by changing the refractive index of the surrounding media by changing, for example, its temperature.

10404-39, Session PWed

Elongation-based fiber optic tunable filter

Grethell G. Pérez-Sánchez, José A. Mejía-Islas, Edgar A. Andrade-González, Univ. Autónoma Metropolitana (Mexico); José R. Pérez-Torres, Tecnológico de Estudios Superiores de Coacalco (Mexico)

Fiber optic filters are devices that allow selecting certain wavelengths transmitted in a fiber optic and rejecting the others. Such devices are highly used in both fiber optic communications networks, and in fiber optic testing and monitoring systems as sensors. The main applications of optical filters in optical communication systems include: elimination of noise; equalization of the response of optical amplifiers, selection of channels in WDM systems. Communications systems have the need of tunable filters to be able to select different wavelengths that are propagated in the same transmission medium, also require devices with a large dynamic range that allow to explore of effects and system responses at different wavelengths.

This paper focuses on introducing the results of a model using a control system for an optical fiber Bragg grating filter with central wavelength at 1557 nm that can be tuned, using a solution that employs, an elongation control system. At the first stage, the optical characterization of the filter was made, then the stepper motors were chosen for the desired wavelength selection with a couple of pulleys which produce the grating elongation and, as a consequence, the wavelength shifting The pulleys diameters were calculated to produce 0.08 nm shift for each step on the stepper motors. At the last stage the user can define the filtering wavelenght using a control program.

10404-41, Session PWed

Laser goniometer used for remote non-contact measurement of angular position and movement

Nkpoikanke Eno, Saint Petersburg Electrotechnical Univ. “LETI” (Russian Federation)

Laser Goniometer and other standard devices operate in remote non-contact mode of measuring object’s angular positions. This article is devoted to error’s analysis, results and new methods of measuring wider angles of 15-30degs with 0.1arcs accuracy

10404-21, Session 6

Wave study of compound eyes for efficient infrared detection

Takiyettin O. Kilinc, Roketsan A.S. (Turkey) and TOBB Univ. of Economics and Technology (Turkey); Zeki Hayran, Hamza Kurt, TOBB Univ. of Economics and Technology (Turkey)

Improving sensitivity in the infrared spectrum is a challenging task. Detecting or imaging infrared light over wide band width and at low power consumption is very important. Novel solutions can be acquired by mimicking biological eyes such as compound eye with many individual lenses inspired from nature. Nature provides many ingenious approaches of sensing and detecting the surrounding environment. Even though compound eye consists of small optical units, it can detect wide-angle electromagnetic waves and it has high transmission and low reflection loss. Insects have eyes that are superior compared to human eyes (single-aperture eyes) in terms of compactness, robustness, wider field of view, higher sensitivity of light intensity and being cheap vision systems. All these desired properties are accompanied by an important drawback: lower spatial resolution. The first step to investigate the feasibility of bio-inspired optics in photodetectors is to perform light interaction with the optical system that gather light and detect it. The most common method used

in natural vision is ray analysis. Light wave characteristics are not taken into consideration in such analyses, such as the amount of energy at the focal point or photoreceptor site, the losses caused by reflection at the interfaces and absorption cannot be investigated. In this study, we present a bio-inspired wave analysis of infrared detection of light. We numerically model the wave analysis based on Maxwell equations from the viewpoint of efficient light detection and reveal the light journey after intercepting the first interface of the eye towards the photoreceptor site.

10404-22, Session 6

Probing infrared detectors through energy-absorption interferometry

Dan Moinard, Stafford Withington, Christopher N. Thomas, Univ. of Cambridge (United Kingdom)

We introduce an interferometric technique capable of fully characterizing the optical response of few-mode and multi-mode detectors, including the amplitude and phase patterns of their individual modes, using solely power measurements. Describing detectors' outputs as the contraction of the external field correlation tensor and detector response tensor representing their respective coherence states, the latter can be recovered using Energy-Absorption Interferometry. EAI is essentially a generalization of holography, and allows the reconstruction of the individual degrees of freedom through which the detector can absorb energy, including their relative sensitivities and spatial forms. Coupling mechanisms into absorbing structures and their underlying solid-state phenomena can therefore be studied, with direct applications in improving current infrared detector technology. In particular, material properties such as the absorber's spatial coherence length are directly obtained.

EAI yields an experimental procedure where the system under test is excited with two external coherent sources, and the fringe in the total power dissipated is measured as the relative phase between the sources is varied. Iterating for multiple source positions, the fringes' complex visibilities allow the two-point detector response function to be retrieved: this correlation function can then be decomposed into a set of natural modes.

We describe the theoretical basis of EAI, examine a room-temperature 1550nm-wavelength infrared experiment we have constructed and present our preliminary results. Finally, we discuss how EAI is applicable to detector arrays, and more broadly to many-body structures as varied as spin systems and energy-harvesting absorbers.

10404-24, Session 6

Frequency-selective surfaces for infrared imaging

Emeline Lesmanne, François Boulard, CEA-LETI (France); Roch Espiau de Lamaestre, MINATEC (France); Giacomo Badano, CEA-LETI (France)

In the past decade, the infrared detector industry has developed a multitude of solutions for multicolor detection. The general idea behind them is to stack up two or more diodes per pixel, each tuned to the target wavelength range. That involves the fabrication of multilayer structures and results in quite complex and expensive devices of superior performance. Bayer matrices have attracted attention as an inexpensive albeit less performant approach, whereby wavelength selection is achieved by filters deposited on top of an existing detector. In this work, we developed a 4 color Bayer matrix of filters that operates in the mid-infrared range (MWIR). Our filters consist of metasurfaces of transverse-electric resonators : a thin metallic sheet is punctured with apertures filled with a high-index dielectric material. Each aperture behaves as a separate resonator. The aperture size determines the transmission waveband. Two or more arrays of such apertures can be juxtaposed to create a multicolor filter, without cross-talk between the adjacent colors. Using an original approach based on the temporal coupled mode theory, we show that metallic loss is negligible in the infrared range, as long as the filter bandwidth is large enough (typically >?/10). To get this result, we develop closed form expression for the radiative and dissipative loss rates and show that the transmission of the filter depends solely on their ratio. Next, we present a prototype infrared detector functionalized with one such array of filters and characterize it by electro-optical measurements.

10404-25, Session 6

Plasmo-thermomechanical suspended nanowire array detectors for mid-infrared spectrum

Qiancheng Zhao, Mohammad W. Khan, Univ. of California, Irvine (United States); Parinaz Sadri-Moshkenani, Univ. of California Irvine (United States); Rasul Torun, Imam-Uz Zaman, Ozdal Boyraz, Univ. of California, Irvine (United States)

We propose a plasmo-thermomechanical mid-infrared detector operating at 4.3 μm wavelength. The design utilizes an array of the bimetallic fishbone nanowires that are suspended 50 nm above a 1.5 μm x 0.3 μm silicon nitride waveguide to create a leaky wave radiation. Moreover, the thermo-mechanically actuated nanowire will induce evanescent wave modulation that can be detected by the leaky wave or transmitted power of the waveguide. The antenna has a strip length of 1.76 μm and can yield an absorption coefficient of 35.57% with a period of 3.1 μm. Six unit cells are connected by a nanowire, and the fishbone-like nanowires are clamped at the two ends, leaving the center free to bend. The mid-infrared energy is absorbed by the resonant metallic antennas, resulting in a temperature increment. The mismatch of the thermal expansion coefficients of the bimetallic materials, gold and nickel, actuates the nanowire, and thus changes the gap between the nanowire and the waveguide. The deformation of the nanowire modulates the waveguide evanescent field, and hence alternates the transmitted power as well as the leak wave power. With a normal incident power of 10 μW/μm2, the temperature in the center of the nanobridge can be increased over 133 K above the ambient temperature, leading to an elevation of 29.9 nm in the center and thus weakening the evanescent modulation strength. The difference of S21 caused by the gap change is 0.111. This methodology can be applied in other spectrums and the fabrication progress will be reported later.

10404-26, Session 6

PbS and HgTe quantum dots for SW IR devices

Witold Palosz, Sudhir Trivedi, Brimrose Corp. of America (United States); Gregory Meissner, Kimberley Olver, Eric DeCuir Jr., Priyalal S. Wijewarnasuriya, U.S. Army Research Lab. (United States); Janet Jensen, U.S. Army Edgewood Chemical Biological Ctr. (United States)

HgTe and PbS Colloidal Quantum Dots with first excitonic absorption peak of about 2 ?m and shorter (down to about 1 ?m) have been synthesized and characterized. A wide range of growth conditions, in particular the growth temperature and temperature timeline, type and concentration of the reagents, and growth time, were tested. Post-growth purification conditions and procedures were also investigated. The synthesized CQDs were characterized using FTIR spectroscopy and TEM technique. The nanomaterials were tested for photo-electrical properties with PC devices. The devices were fabricated by drop-casting a suspension of the QDs on a fan-out, followed by solid ligand exchange, and then spectral and electrical photoresponse of the device was measured. The device fabrication parameters were the number of deposited layers, the thickness of individual layers, the type of the substituting ligand, and the ligand exchange duration. The solid ligand exchange process was evaluated thru absorption spectra of test samples. (The tests were done by forming QD layers on a CdF2 substrate and then conducting the ligand exchange.) For selected devices Quantum Efficiency was also determined.

10404-27, Session 7

Innovations in imaging technology and NASA/ESTO investments in technology development *(Invited Paper)*

Sachidananda R. Babu, NASA Goddard Space Flight Ctr. (United States)

Imaging technology is one of the fastest evolving areas in the consumer market, due to the penetration of imaging instruments into our everyday life. NASA has specific interest in space and earth imaging requirements. Therefore, there is a big push in consumer needs that is advancing the technology at explosive rate. Some of the technologies of particular interest to NASA applications are dual gain pixel design, wafer level integration of the imagers and mass production of high resolution imagers. We are also looking at ways to operate the existing imaging sensors in innovative ways to extract more information.

This talk will focus on the imaging technology developments in professional and consumer application areas and its relevance to NASA imaging needs. Some of the ESTO investments in innovative use of existing technology and our recent investments in new technology applications will be also presented.

10404-28, Session 7

Target detection in sun glint using the improved MWIR polarization technique

Ji Zheng, Huijie Zhao, Yansong Li, BeiHang Univ. (China); Xiaofeng Sun, Pengfei Song, Shitao Wang, China Academy of Space Technology (China); Chi Cheng, BeiHang Univ. (China)

When detecting target in sun glint by a mid-infrared detector, the target could be submerged in its intense background noises due to detector saturation.The traditional technique based on the single horizontal linear polarizer was one of the common methods to reduce the sun glint by eliminating its s-polarized component, nevertheless, the residual p-polarized component of sun glint could be still too strong to saturate the detector in some cases. Therefore, we further improve the sun glint countermeasure and propose the sun glint suppression method based on two rotatable polarizers, which is presented in this paper. Firstly, the brief theoretical analysis methods employed in different detection scenarios that whether the single or two polarizers should be used to further eliminate the p-polarized component of the sun glint is described. Secondly, the formula and its derivation for the optimum angle between the two polarizers is provided in case that the second polarizer is required. Thirdly,the MWIR polarization imaging system design with two rotatable and dismountable polarizers is described. Then, the field experiments and results under two different experimental conditions are presented, demonstrating that the improved polarization technique can significantly reduce sun glint and can enhance the contrast of target images in both cases. Combined with the commonly used image processing algorithm,the targets in sun glint can be identified, confirming the effectiveness of the improved MWIR polarization technology.

10404-29, Session 7

Temperature measurements on fast-rotating objects using a thermographic camera with an optomechanical image derotator

Bettina Altmann, Christian Pape, Eduard Reithmeier, Leibniz Univ. Hannover (Germany)

Increasing requirements concerning the quality and lifetime of machine parts in industrial and automotive applications require comprehensive investigations of the components in conditions close to the application. Irregularities in heating of mechanical parts reveal regions with increased loading of pressure, draft or friction. In the long run this leads to damage and failure of the component. Thermographic measurements of rotating objects like roller bearings, brakes and clutches present an approach to investigate those defects. However, it is challenging to measure fast-rotating objects accurately. Currently one contact-free approach is performing stroboscopic measurements using an aerial infrared sensor. The data acquisition would be triggered so that the image is taken once per revolution. This leads to a huge loss of information on the majority of the movement and motion blur. The objective of this research is using an optomechanical image derotator together with a thermographic camera. The derotator follows the rotation of the measurement object so that quasi-stationary thermal images of the whole movement can be acquired by the infrared sensor. Unlike conventional derotators which use a glass prism to achieve this effect, the derotator within this work is equipped with a sophisticated mirror-assembly. These mirrors are made of aluminum to transfer infrared radiation emitted by the rotating object. Because of the resulting stationary thermal image, the operation can be monitored seamlessly even for fast-rotating objects. The field of view can also be set to a small off-axis region of interest which then can be investigated with higher resolution or frame rate. To depict the potential of this approach, thermographic measurements on various roller bearings and their rolling elements are presented to show differences in the heating and problem areas during different operating states.

10404-30, Session 7

Modeling of IR spectra for nerve agent-sorbent binding

Michael R. Papantonakis, Courtney A. Roberts, Andrew Shabaev, Youngchan Kim, R. Andrew McGill, Christopher A. Kendziora, Robert Furstenberg, Samuel G. Lambrakos, U.S. Naval Research Lab. (United States)

An inverse analysis of experimentally measured absorption spectra for the custom sorbent polymer SiFA4H, nerve agent simulant DMMP and molecular structure SiFA4H-DMMP is presented. These molecular structures and their associated IR spectra provide general understanding of the process of nerve agent detection based on spectral analysis. The inverse analysis presented provides estimates of permittivity functions, which when combined with the Claussius-Mossotti relation, can predict molecular polarizabilities associated with the SiFA4H-SiFA4H and SiFA4H-DMMP interactions. Molecular polarizabilities deduced from measured absorption coefficients are modeled using molecular dynamics simulations.

10404-31, Session 8

NDIR gas sensing using high performance AlInSb mid-infrared LED as light source

Edson G. Camargo, Yuji Goda, Osamu Morohara, Hromi Fujita, Hirotaka Geka, Koichiro Ueno, Yoshihiko Shibata, Naohiro Kuze, Asahi Kasei Microdevices Corp. (Japan)

Global warming has become a pressing issue worldwide and high performance sensors for environmental gas monitoring have being required. Particularly, CO2 sensors have been used for optimal control of indoor air quality reducing around 30% the energy consumption in heating, ventilation and air conditioning systems. An important element of these gas sensors is low power consumption, which is possible to be achieved by short current pulse driving of the light source.

To allow pulsed driving, we developed a high performance mid-infrared LEDs using MBE grown AlInSb active/barrier layers. The structure was grown on a semi-insulating GaAs (001) substrate using a Riber MBE-49 system, having a 0.5 μm thick n+-InSb buffer layer which improved the crystal quality of the AlxIn1-xSb (0.039≤x≤0.076) active layer. The LED consists on several junctions connected in series and its design was optimized so that maximum efficiency could be achieved at a desirable voltage/current condition.

The developed LEDs showed the highest performance until reported (75% higher emission than commercial LEDs for the 4.2 μm wavelength) and together with already reported mid-infrared photovoltaic detectors [1] allowed the realization of high performance and low power consumption CO2 gas sensors.

Moreover, a new technique was developed for temperature and/or output drift compensation, by referencing the LED output with a detector on the same substrate, leading us to realize high precision and long term stability measurements.

The developed technology is believed to be promising not only for CO2 but also for other environmental gas sensing systems.

[1] E. G. Camargo; K. Ueno; Y. Kawakami; Y. Moriyasu; K. Nagase; M. Sato; H. Endo; K. Ishibashi; N. Kuze, Opt. Eng. 47(1) (2008)

10404-33, Session 8

Development of nanostructured antireflection coatings for infrared technologies and applications

Gopal G. Pethuraja, John W. Zeller, Roger E. Welser, Ashok K. Sood, Magnolia Optical Technologies, Inc. (United States); Pradeep Haldar, Harry Efstathiadis, SUNY Polytechnic Institute (United States); Eric DeCuir Jr., Priyalal Wijewarnasuriya, U.S. Army Research Lab. (United States); Nibir K. Dhar, U.S. Army Night Vision & Electronic Sensors Directorate (United States)

Infrared (IR) sensing technologies and systems operating from near-infrared (NIR) to long-wave infrared (LWIR) spectrum are being developed for a variety of defense and commercial system applications. Loss of a significant portion of the incident optical signal due to reflection limits the performance of IR sensing systems. One critical technology that will overcome this limitation and enhance the performance of IR sensing systems is the development of advanced antireflection (AR) coatings. Magnolia is actively working on the development and advancement of ultra-high performance AR coatings for a wide variety of defense and commercial applications. Ultrahigh performance nanostructured AR coatings have been demonstrated for ultraviolet (UV) to LWIR spectral bands on various substrates. The AR coatings enhance the transmission of light through optical components and devices by significantly minimizing reflection losses, a substantial improvement over conventional thin-film AR coating technologies.

Nanostructured AR coatings have been fabricated using a tunable self-assembly process on substrates transparent for a given spectrum of interest, ranging from UV to LWIR. The nanostructured multilayer structures have been designed, developed and optimized for various optoelectronic applications. The optical properties of AR-coated optical components and sensor substrates have been measured and fine-tuned to achieve a predicted high level of performance. In this paper, we review our latest work on high quality nanostructure-based AR coatings, including recent efforts for the development of the nanostructured AR coatings on IR-transparent substrates.

10404-34, Session 8

Long wavelength infrared (LWIR) acousto-optical (AOTF) and acousto-optic modulators (AOM) using Hg2Br2 crystals *(Invited Paper)*

Priyanthi Amarasinghe, Joo-Soo Kim, Feng Jin, Sudhir Trivedi, Brimrose Technology Corp. (United States); Syed Qadri, U.S. Naval Research Lab. (United States); Jolanta Soos, Mark Diestler, Brimrose Technology Corp. (United States); Neelam Gupta, U.S. Army Research Lab. (United States); Janet Jensen, James O. Jensen, U.S. Army Edgewood Chemical Biological Ctr. (United States)

High quality large single crystals of mercurous bromide were grown by physical vapor transport method (PVT). The crystalline quality and the orientation of the crystals were determined using high resolution x-ray diffraction (HRXRD) technique. The full width at half maximum (FWHM) of the rocking curve of mecurous iodide crystals was measured as 0.13 degrees for (004) reflection, which is the best that has been achieved so far. Due to their high figure of merit and wide transmission range (0.35 um – 30 um) mercurous bromide is considered as an excellent material for acousto-optic tunable filter (AOTF) and Acousto-optic modulators (AOM) operating in strategic long wavelength infrared (LWIR) region. The paper will discuss performance of the crystals as acousto-optic tunable filter (AOTF) and acousto-optic modulator (AOM). Application of the AOTF for the long wavelength infrared (LWIR) imaging will be discussed. The results indicate the grown mercurous halide crystals are excellent materials for above device fabrication. The diffraction efficiencies of the AOTF device was found to be 26% at 10.6 um wavelength which to the best of our knowledge is the highest ever, reported.

10404-35, Session 8

Overview of detector technologies and IRFPA's for various sensor applications *(Invited Paper)*

Siva Sivananthan, Univ. of Illinois at Chicago (United States) and EPIR Technologies Inc. (United States)

No Abstract Available

10404-36, Session 8

Thermal sensitivity of the fundamental natural frequency of a resonant MEMS IR detector pixel

Sedat Pala, Kivanc Azgin, Middle East Technical Univ. (Turkey)

This paper presents the effect of temperature on the natural frequency of (1,1) mode shape of a resonant MEMS IR detector pixel in the range of 295-340 K. For the first time in literature, closed form equation of the temperature effect on the frequency of mode (1,1) is presented for silicon as the structural material.

The resonating plate is supported at its geometric center, enabling more robust pixels with 98% fill factor and less complicated fabrication process. In this work, we focused on the thermal sensitivity of the frequency of the fundamental (1,1) mode shape of the pixel structure shown in Figure 1. Higher mode shapes and corresponding frequency equations can also be derived with an acceptable error compared to FE simulations and test results [1]

Mechanical structure of the pixel is composed of a plate and a post as shown in Figure 2. It is shown that mode shapes and corresponding frequencies can be found using Rayleigh-Ritz energy method including electrostatic softening effect [1]. Inserting the thermal coefficient of mechanical properties (e.g. thermal coefficient of expansion and the thermal coefficient of Young's modulus) into the frequency equation, thermal effects are modelled as well (Eqn. 1).

Fabrication flow is given in Figure 5 as they can be found in [2]. Figure 3 shows SEM images of the fabricated pixels. Temperature range of 295-340 K is tested and selected frequency sweeps are presented in Figure 6. Test results and the model behave in the same manner (Figure 4), with some expected discrepancy due to undamped mathematical model.

References:

[1] P. Sedat and A. Kıvanç, "A MEMS square Chladni plate resonator," Journal of Micromechanics and Microengineering", vol. 26, p. 105016, 2016.

[2] M. M. Torunbalci, S. E. Alper, and T. Akin, "Advanced MEMS Process for Wafer Level Hermetic Encapsulation of MEMS Devices Using SOI Cap Wafers With Vertical Feedthroughs," Microelectromechanical Systems, Journal of, vol. 24, pp. 556-564, 2015.

10405-1, Session 1

Use of artificial neural network and satellite data to predict Boro rice yield in Bangladesh

Kawsar A. Akhand, The City Univ. of New York (United States); Mohammad Nizamuddin, Leonid Roytman, The City College of New York (United States); Felix Kogan, National Oceanic and Atmospheric Administration (United States)

Rice is the main staple food that plays a crucial role in the agro-based economy of Bangladesh. Due to increasing population and decreasing agricultural land in every year, rice production plays a key role in national economy because this sector is in under pressure of increasing demand of food to maintain food security for its large population of Bangladesh. In addition, Bangladesh is faced with production constraints such as drought, flooding, salinity, lack of irrigation facilities and lack of modern technologies. To maintain self sufficiency in rice, Bangladesh will have to continue to expand rice production by increasing yield at a rate that is at least equal to the rate of population growth until the demand of rice has stabilized. The first and foremost responsibility of the country is to ensure an uninterrupted supply of food to all people at all times to ensure dependable food security. At present, rice yield prediction is an important area of study because its potential contribution to food security to ensure adequate and stable supply of safe and nutritious food at all times for an active and healthy life. This paper tries to develop a reliable rice yield prediction model by using Artificial Neural Network (ANN) and satellite data. Advanced Very High Resolution Radiometer (AVHRR)-based vegetation health (VH) indices (Vegetation Condition Index (VCI) and Temperature Condition Index (TCI)) are used as input variables and official statistics of Boro rice yield is used as target variables for ANN prediction model. The result obtained with ANN method shows a great promise and the error of prediction is less than 10%. Therefore, this prediction model can serve as an important tool to the planners, policy makers, economists, analysts, academics, educationists, researchers, and others stakeholders.

10405-2, Session 1

Using deep recurrent neural network for direct beam solar irradiance cloud screening

Maosi Chen, John M. Davis, Zhibin Sun, Colorado State Univ. (United States); Chaoshun Liu, East China Normal Univ. (China); Melina Maria Zempila, Wei Gao, Colorado State Univ. (United States)

Cloud screening is an essential procedure for in-situ calibration and atmospheric properties retrieval on Multi-Filter Rotating Shadowband Radiometer (MFRSR). Previous study has explored a cloud screening algorithm for direct-beam MFRSR raw voltage measurements based on the stability assumption on a long time period (typically a half day or a whole day). Although the algorithm was not too complex, to design such an algorithm and to implement it on codes was not a trivial task. It requires the detailed understanding of physical properties and the delicate strategy of data manipulation. Recent rapid developments on deep neural network and GPU have opened a window for modeling complicated End-to-End systems with a standardized strategy. In this study, a three-layer dynamic bidirectional Long Short-Term Memory was chosen for determining the cloudiness on each point based on the daily raw direct beam voltages and the corresponding airmasses inputs. This sequence to sequence network was trained and tested at two stations of the USDA UV-B Monitoring and Research Program. The size of the training set was around 6000 days per station, while the size of testing set was around 500 days per station. The final accuracy of the network was around 95-97% depending on the testing station.

10405-3, Session 1

Comparison of two satellite imaging platforms for monitoring quasi-circular vegetation patch in the Yellow River Delta, China

Qing-sheng Liu, Li Liang, Gaohuan Liu, Chong Huang, Institute of Geographic Sciences and Natural Resources Research (China)

Vegetation often exists as patch in arid and semi-arid region throughout the world. Vegetation patch can be effectively monitored by remote sensing images. However, not all satellite platforms are suitable to study quasi-circular vegetation patch. This study compares fine (GF-1, launched in Jiuquan Satellite Launch Center on April 26, 2013) and coarse (CBERS-04, launched in Taiyuan Satellite Launch Center on December 7, 2014) resolution platforms, specifically focusing on the quasi-circular vegetation patches in the Yellow River Delta (YRD), China. Vegetation patch features (area, shape and location) were extracted from GF-1 and CBERS-04 imagery using unsupervised classifier (K-Means), supervised classifier (Maximum Likelihood) and object-based approach in order to analyze vegetation patterns. These features were then compared using image overlay and differencing, and the Root Mean Squared Error (RMSE) was used to determine if the mapped vegetation patches were significantly different. It was found that CBERS-04 is a sufficient data source when studying patch patterns within a regional scale, but smaller vegetation patches identified from GF-1 data were not capable of being extracted in the data sourced from CBERS-04. This means that for studies concerned with the quasi-circular vegetation patch patterns in the YRD, CBERS-04 is sufficient. But in studies where the area, shape and dynamics of small patches are required, a fine resolution such as GF-1 is required. However, in the future, finer resolution platforms such as Worldview are needed in order to gain more detailed insight on the patch structures and components and to study the formation mechanism.

10405-41, Session 1

Retrieval of crop leaf area index from SPOT-5 data using a look-up-table approach based on PROSAIL

Xiaohua Zhu, Academy of Opto-Electronics, CAS (China)

Leaf Area Index (LAI) is a key structural characteristic of vegetation and plays a significant role in global change researches. Several methods and remotely sensed data have been evaluated for LAI estimation. The objective of this article is to study on retrieval and scale effect analysis of crop LAI based on PROSAIL model and SPOT-5 data, mainly focusing on: i) establishment and evaluation of a new LUT approach for crop LAI estimation in northwestern China; ii) scale effect analysis during LAI retrieval from different scale data; and iii) integration of scale information into LUT to improve accuracy of LAI estimation. The LAI inversion result of LUT method was validated by in-situ LAI measurements, indicating that the LUT generated based on PROSAIL model was suitable for crop LAI estimation, with a root mean square error (RMSE) of approximately 0.31 m2/m2 and determination coefficient (R2) of 0.65. The spatial scale effect of crop LAI was analyzed based on Taylor expansion theory, indicating that when the SPOT data aggregated by 200 by 200 pixel, the relative error is significant with 13.7%. Finally, a new LUT method integrated with scale information was proposed in this article, improving the inversion accuracy with RMSE of 0.20 m2/m2 and R2 of 0.83.

10405-4, Session 2

Using feature information in neural networks for ultraviolet retrieval in the USA

Zhibin Sun, Colorado State Univ. (United States); Ni-Bin Chang, Univ. of Central Florida (United States); Wei Gao, Maosi Chen, Melina Maria Zempila, Colorado State Univ. (United States)

In neural networks, the training/predicting accuracy and algorithm efficiency can be improved significantly via accurate input feature extraction and weight determination. In this study, some spatial features of several important factors in retrieving surface ultraviolet (UV) are extracted, and the input weights are determined via the local information of those factors. A single hidden layer feedforward network (SLFN) is used to retrieve the surface UV of 2013 in the United States, using the extracted features and input weights. The results are analyzed by comparing with the retrieval results using extreme learning machine (ELM).

10405-5, Session 2

Introducing a new total ozone column retrieval algorithm: Evaluation at Mauna Loa station

Melina Maria Zempila, USDA UV-B Monitoring and Research Program (United States); Konstantinos Fragkos, National Institute of R&D for Optoelectronics (Romania); John Davis, Zhibin Sun, Maosi Chen, Wei Gao, USDA UV-B Monitoring and Research Program (United States)

The USDA UV-B Monitoring and Research Program (UVMRP) comprises of 36 climatological sites along with 4 long-duration research sites, in 27 states, one Canadian province, and the south island of New Zealand. Each station is equipped with an Ultraviolet multi-filter rotating shadowband radiometer (UV-MFRSR) which can provide response weighted irradiances at 7 wavelengths (300, 305.5, 311.4, 317.6, 325.4, and 368 nm) with a nominal full width at half maximun of 2 nm. These UV irradiance data from the long term monitoring station at Mauna Loa, Hawaii, are used as inputs to a retrieval algorithm in order to derive high time frequency total ozone columns. The sensitivity of the algorithm to the different wavelength inputs is tested and the uncertainty of the retrievals is assessed based on error propagation methods. For the validation of the method, collocated hourly ozone data from the Network for the Detection of Atmospheric Composition Change (NDACC) for the period 2010-2016 are used.

Acknowledgement: MMZ. would like to thank Dr. Russell C. Schnell as the MAUNA LOA station representative.

10405-6, Session 2

An integrated hyperspectral and SAR small satellite constellation for environment monitoring

Jinnian Wang, CHINARS SHENZHEN Institute for Satellite Applications Innovation (China)

A fully-integrated, Hyperspectral optical and SAR (Synthetic Aperture Radar) constellation of small earth observation satellites will be deployed over multiple launches from last December to next five years. The Constellation is expected to comprise a minimum of 16 satellites (8 SAR and 8 optical) flying in two orbital planes, with each plane consisting of four satellite pairs, equally-spaced around the orbit plane. Each pair of satellites will consist of a hyperspectral/mutispectral optical satellite and a high-resolution SAR satellite (X-band) flying in tandem. The constellation is expected to offer a number of innovative capabilities for environment monitoring. As a pre-launch experiment, two hyperspectral earth observation minisatellites, Spark 01 and 02 were launched as secondary payloads together with Tansat in December 2016 on a CZ-2D rocket. The satellites feature a wide-range hyperspectral imager. The ground resolution is 50 m, covering spectral range from visible to near infrared (420 nm - 1000 nm) and a swath width of 100km. The imager has an average spectral resolution of 5 nm with 148 channels, and a single satellite could obtain hyperspectral imagery with 2.5 million km2 per day, for global coverage every 16 days. This paper describes the potential applications of constellation image in environment monitoring.

10405-7, Session 3

Deep and fast learning for feature extraction of merged or fused satellite remote sensing images to observe lake eutrophication *(Invited Paper)*

Ni-Bin Chang, Univ. of Central Florida (United States)

In this presentation, two advanced feature extraction methods with fast and deep learning algorithms will be discussed for environmental monitoring in all-weather conditions with convergent and divergent thinking. One is the newly developed novel Spectral Information Adaptation and Synthesis Scheme (SIASS) and the other is the newly invented SMart Information Reconstruction (SMIR) method to support the Integrated Data Fusion and Mining (IDFM) research. Whereas the former is organized to generate cross-mission consistent ocean color reflectance by merging observations from several different satellites to recover the cloudy pixels, the latter is designed to reconstruct cloud contaminated pixel values from the time-space-spectrum continuum with the aid of a machine learning tool. For the purpose of demonstration, Lake Nicaragua located at Central America is selected as a study site which is a very cloudy area year round. In this case study, merging observations from MODIS-Terra, MODIS-Aqua, and VIIRS over Lake Nicaragua will be presented for the 2012-2015 time period. Then the performance of SMIR will be performed after the merging operation by reconstructing the missing remote sensing reflectance values derived from the Moderate Resolution Imaging Spectroradiometer (MODIS) on board the Terra satellite over Lake Nicaragua. The SIASS algorithm is proven to have the capability not only in eliminating incompatibilities for those matchup bands but also in reconstructing spectral information for those mismatching bands among sensors. For the recovery of those missing pixel values after merging three satellite images, experimental results from SMIR show that the extreme learning machine may perform well with simulated memory effect due to linking the complex time-space-spectrum continuum between cloud-free and cloudy pixels. Final water quality assessment will be generated based on the integrative algorithm of the two with bio-optical models for eutrophication assessment in Lake Nicaragua.

10405-8, Session 3

Quality assurance of the UV irradiances of the UV-B monitoring and research program: the Mauna Loa test case

Melina Maria Zempila, John M. Davis, George T. Janson, Elizabeth Olson, Maosi Chen, Bill Durham, Scott Simpson, Jonathan Straube, Zhibin Sun, Wei Gao, USDA UV-B Monitoring and Research Program (United States)

The USDA UV-B Monitoring and Research Program (UVMRP) is an ongoing effort aiming to achieve a better understanding of climate change driven variations in the Ultra Violet (UV) solar radiation, and their impacts on agriculture. By providing high quality radiometric measurements of UV solar radiation, UVMRP is focusing on advancing science for agricultural, forest, and range systems in order to mitigate climate impacts. Within these foci, the goal of the present study is to validate the accuracy of the erythemal measurements and response-weighted irradiances at 6 UV channels from a

YES UVB-1 radiometer and an ultraviolet multi-filter rotating shadowband radiometer (UV-MFRSR) respectively at the calibration site of Mauna Loa. Uncertainties during the calibration procedures are discussed, while collocated ground-based measurements from a Brewer spectrophotometer along with model simulations are used as a baseline for the validation of the data. Besides this quantitative research, the limitations and merits of the existing UVMRP methods are considered and further improvements are analyzed.

Acknowledgements: M.M.Z would like to thank Drs. R. McKenzie and V. Fioletov for providing the Brewer data used in this study.

10405-9, Session 3

Spatio-temporal anomaly detection for environmental impact assessment: A case of an abandoned coal mine site in Turkey

Hilal Soydan, Alper Koz, Hafize Sebnem Duzgun, Middle East Technical Univ. (Turkey)

The main purpose of this research is to determine the anomalies regarding with the coal mining operations in an abandoned coal mine site in central Anatolia by multi-temporal image analysis of Landsat 4-5 surface reflectance data. A well-known hyperspectral anomaly detection algorithm, Reed-Xioli (RX), which calculates Mahalanobis distance metrics to calculate the likelihood ratios by normalizing the difference between the test pixel and the background to allocate anomaly pixels, was implemented across the time series.The high score anomaly pixels in the output image sets are selected using multi-thresholding technique based on Otsu method, as the technique presents extra information of segmentation metric for performance evaluation.An additional false alarm removal was applied with the baseline anomaly signal calculated with pre-mining imagery anomaly pixels. The high score abnormalities in the region with this additional removal of false alarms are appointed as the deviations due to mining operations. According to the initial results, the anomaly scores are allocated in the open-pit, coal storage, excavations & area of disturbances of the land, dumpsites starting with the mining operations throughout the multi-temporal images, which reveal the differentiations on earth surface across the years. The preliminary studies point out especially the profound land use – land cover change in the field in time series, exposing some critical regions that need an immediate rehabilitation action. Presenting such an invaluable potential to observe the anomalies in multi-temporal fashion, Landsat reflectance images seem to be bringing out the abnormalities with a great contrast despite its spatial resolution limitations.

10405-10, Session 3

Remote hybrid electro-optic biosensor with fluorescent fiber optic for cephalosporins determination in water

Ramona M. Galatus, Technical Univ. of Cluj Napoca (Romania); Cecilia Cristea, Bogdan Feier, Iuliu Hatieganu Univ. of Medicine and Pharmacy (Romania); Nunzio Cennamo, Luigi Zeni, Seconda Univ. degli Studi di Napoli (Italy)

Antibiotics are extensively used not only in human, for prophylactic and treatment purposes, but also in animals and in agriculture and it leads gradually to environmental contamination and drug resistance. The present research propose a hybrid electro-optical platform capable of sensitive detection for one major class of most used drugs in water (drinking water and waste water), ?-lactams antibiotics (cephalosporines). The analytical technique is based on an integrated solution with Raspberry Pi with remote analysis capabilities of the results. The platform integrates the results from the D-shape surface plasmon resonance plastic optical fiber (SPR-POF) [R. Galatus et.al, SAS-2016], with the electrochemical sensors, for flow injection analysis of cephalosporines in water [Bogdan Feier, Cecilia Cristea, et.al, Analytica Chimica Acta-2017, under review]. This new approach use multiplexed fluorescent plastic optical fibers, as light source for SPR, instead of the halogen lamp, for broadband wavelength biosensing analysis. The solution assure low-power consumption and low-heating capabilities of the sensing platform. For direct electrochemical detection, due to the extreme oxidation potential of antibiotics only boron-doped-diamond (BDD) could be used as working electrode, that is a quite expensive method. For label-free fast low-cost SPR-POF method, the effective refractive-index variations of the sample (water) are determined by the resonance wavelength and related to the binding of non–labeled molecules on the sensing area. The bioreagents for the detection of ?-lactams are CCK-BSA (cholecystokinin receptor ligands bind to bovine serum albumin); RSA (rat serum albumin), bioreceptor; anti-RSA, polyclonal antibody from rabbit. SPR sensitivity is about 1,200(nm/RIU).

10405-11, Session 3

Effects of microphysics parameterization on simulations of summer heavy precipitation in the Yangtze-Huaihe Region, China

Yu Kan, East China Normal Univ. (China); Bo Chen, Air Traffic Management Bureau of East China (China); Tao Shen, Shanghai Shixi High School (China); Chaoshun Liu, Fengxue Qiao, East China Normal Univ. (China)

The Yangtze-Huaihe region (YHR) is an extremely important area in China, densely populated and economically developed, but during the summer, heavy rainfall events frequently occur over this region causing devastating damages and considerable socio-economic consequences. However, it is still a challenge for current weather/climate models to accurately predict the summer precipitation over this region due to model uncertainty related to key precipitation processes such as microphysics parameterization. This study first examines all the weather patterns causing regional persistent heavy precipitation in summer over the YHR during 2008-2012, and classifies them into three types of rain: the type I associated with stationary front, the type II directly associated with typhoon or with its spiral rain band, and the type III associated with strong convection along the edge of Subtropical High. Sixteen groups of comparative experiments are conducted for three representative cases from the above different types, using the WRF v3.5.1 model with eight different microphysics schemes (Kessler, Purdue Lin, WSM3, WSM5, Eta Ferrier, WSM6, Goddard and Thompson) and two cumulus parameterization schemes (KF and BMJ). The study focuses on examining the effects of microphysics parameterization on the simulation of different type of heavy precipitation over the YHR with respect to different cumulus schemes. A local short-time rainstorm event in Shanghai is used to compare with the regional persistent heavy rainfall events. Major results are: (1) Two cumulus parameterization schemes have systematic but different impacts on the simulations of different type of rain. The BMJ cumulus scheme shows better capability than the KF scheme in simulating the spatial pattern of precipitation for the type I and III, while the KF scheme is better than the BMJ scheme for the type II. (2) The microphysics parameterization has large but different impacts on the location and intensity of regional heavy precipitation centers. For type I, Ferrier-BMJ scheme most realistically simulates the pattern of rainbands with the rain center location and intensity. For type II, Thompson-KF scheme not only accurately simulates the precipitation areas, center position and intensity, but also has higher predictive skills than others for daily precipitation. For type III, Lin-BMJ scheme shows clear advantages over others in simulating the rainbands and heavy rain centers for regional persistent heavy rainfall events, while WSM5-BMJ scheme shows better capability than others in simulating the heavy rain centers for the short-time rainstorm in Shanghai with the similar weather pattern of type III.

10405-12, Session 3

Assessment and verification of rainfall threshold through antecedent soil-moisture model in Lambagarh and Pipalkoti landslides (Chamoli District) of Garhwal Himalaya, in Gis & remote sensing environment

Mahesh K. Tripathi, Himanshu Govil, National Institute of Technology, Raipur (India); Prashant K. Chamapatiray, Indian Institute of Remote Sensing (India); Monkia Besoya, National Institute of Technology, Raipur (India)

Landslide is among the major hydro-geological hazards that affect the large part of India; especially the Himalayas. Landslide inventory is a major way of assessment of study of landslide hazard. Geospatial techniques and satellites images providing many advantageous information about landslides along with some other factors like as rainfall, soil-moisture, geological, geographical, climatological and anthropogenic which initiate the order of increment of occurrences of landslides. In this study landslide inventory of Alaknanda catchment was prepared with the help of LISS III, LISS IV satellite images for subsequent years (2007, 2008, 2009, and 2010). A soil-moisture index table was prepared through TRMM rainfall data (25x25 km.) to assess and verify, rainfall threshold for initiation of landslides occurrences. Assessment of rainfall threshold (3-days prior and 15-days cumulative) with soil-moisture shows a direct relationship among landslides occurrence, regolith thickness, drained porosity, porosity, evapotranspiration, rainfall, of the study area. The regolith thickness, drained porosity, total porosity, evapotranspiration, effective rainfall, directly interrelated to initiation of landslide occurrences, as well as intensity of rainfall and soil-moisture is also main important variable of intensity of occurrences of landslides in the study area. A process based (soil- moisture) approach verify the rainfall threshold in initiation of landslide.

10405-13, Session 3

Watershed management using geospatial data: A case study of Beas upper catchment of India

Monkia Besoya, Himanshu Govil, National Institute of Technology, Raipur (India); Sagar Salunkhe, Regional Remote Sensing Service Ctr. (India) and National Remote Sensing Ctr., Government of India (India); Mahesh K. Tripathi, National Institute of Technology, Raipur (India)

Watershed play a critical role in the natural functioning of the Earth, thus consider as one of the primary planning units in the field of natural resource Management.

In this study watershed delineation and morphometric analysis of Beas Upper Catchment in India was carried out using Geospatial Techniques. ASTER DEM & Cartosat-1 version 3 DEM (30m) used for watershed delineation and morphometric analysis and satellite image of IRS LISS-IV (Resourcesat-2) was used for study area map preparation, threshold analysis and morphometric analysis. Different morphometric parameters i.e. stream, basin, relief parameters (highest & lowest point, drainage density,etc.) including slope and aspect analyses were carried out through measurement of linear, aerial and relief aspects of the catchment.

Total 10 watersheds were delineated using ASTER & Cartosat DEM using Arc GIS hydrological tool. Using ASTER DEM areas were found to be ranging from 324.51 to 850.34 km2 and using Cartosat DEM 322.27 to 850.03 km2. The basin area is found to be 5800 m and 5412 m delineated and the catchment is of 7th order and 8th order in drainage map prepared using ASTER and Cartosat DEM respectively. By calculating Drainage density, Bifurcation ratio, Ruggedness number etc. indicates the area is moderate drainage, extremely rugged with high relief and is more prone to soil erosion.

Hence, from the research, it can be concluded Digital Elevation Model and Satellite data coupled with GIS techniques have proven as a robusting tool in watershed management.

10405-14, Session 3

The relationship of Aleutian low and sea surface heat flux

Junqiang Gong, East China Normal Univ. (China)

Using the observed data from NCEP, this paper evaluates the climate features of Aleutian low, heat flux in winter. SVD method has been used to analyse the relations between Aleutian low and heat flux in north Pacific. The results show that the intensity of Aleutian low and heat flux in central north pacific have positive correlation, while having negative correlation with heat flux in western coast of north America.

10405-15, Session PWed

Remote sensing estimates of reclamation-induced carbon loss in coastal wetland of Yangtze River estuary

Jinquan Ai, East China Normal Univ. (China); Wei Gao, Colorado State Univ. (United States); Zhiqiang Gao, Yantai Institute of Coastal Zone Research (China); Runhe Shi, Chao Zhang, East China Normal Univ. (China); Fuxiang Xu, Yantai Institute of Coastal Zone Research (China); Debin Song, Yantai Institute of Coastal Zone Researches, (China)

Coastal wetland reclamation directly changes the structure and function of wetland ecosystem, causing potential ecological consequences. In this study, we estimated the total emissions and carbon sequestration of the coastal wetlands in the Yangtze River before reclamation and after reclamation to other land cover types using GF-1 WFV imagery. Results showed that the converted coastal wetland area occupied up to 55.5% between 2013 and 2016. Carbon estimation indicated that the coastal wetland before reclamation had greater contribution to the global warming mitigation than the wetland reclamation to other land cover types. This study further demonstrated that the coastal wetland loss in the Yangtze River would lead to 3.2 ?104 CO2 eq/yr of net sequestration loss and may cause the further climate warming.

10405-16, Session PWed

Comparison of snow depth retrieval algorithm in Northeastern China based on AMSR2 and FY3B-MWRI data

Xintong Fan, Lingjia Gu, Ruizhi Ren, Tingting Zhou, Jilin Univ. (China)

The snow accumulation has a very important influence on the natural environment and human activities. Meanwhile, the high-precision passive microwave snow depth retrieval has been a hotspot currently. Northeastern China is a typical snow study area including a large area of farmland, forest and other surface types. Especially, there is relatively stable snow accumulation in January. With the Global Change Observation Mission 1st Water (GCOM-W1) launched on May 18, 2012?Japan Standard Time?, the 2-year (2013-2014) observations of brightness temperature by the Advanced Microwave Scanning Radiometer 2 (AMSR2) on GCOM-W1 and those by the FengYun3B Microwave Radiation Imager (FY3B-MWRI) in the same period are selected in the research. Snow depth retrieval algorithms, considering different land cover types, are used in this paper. Therefore, the results of snow depth retrieval using AMSR2 standard algorithm and Jiang's FY operational algorithm are compared in the research. To further validate the accuracy of the two algorithms, the retrieval results are compared with

the snow depth data observed at the national meteorological stations in Northeastern China. In order to analyze the difference between the retrieval results and the standard snow products, the retrieval snow depth (SD) using AMSR2 and FY3B-MWRI data are compared with AMSR2 and FY standard snow depth products, respectively.

10405-17, Session PWed

Research on snow cover monitoring of northeast China using Fengyun geostationary satellite

Tong Wu, Jilin Univ. (China); Lingjia Gu, Ruizhi Ren, TIngting Zhou, Jilin Univ. (China)

Snow cover information has great significance for monitoring and preventing snowstorms. With the development of satellite technology, geostationary satellites are playing more important roles in snow monitoring. Currently, cloud interference is a serious problem for obtaining accurate snow cover information. Therefore, the cloud pixels located in the MODIS snow products are usually replaced by cloud-free pixels around the day, which ignores snow cover dynamics. FengYun-2(FY-2) is the first generation of geostationary satellite in our country which complements the polar orbit satellite. The snow cover monitoring of Northeast China using FY-2G data in January and February 2016 is introduced in this paper. First of all, geometric and radiometric corrections are carried out for visible and infrared channels. Secondly, snow cover information is extracted according to its characteristics in different channels. Multi-threshold judgment methods for the different land types and similarity separation techniques are combined to discriminate snow and cloud. Furthermore, multi-temporal data is used to eliminate cloud effect. Finally, the experimental results are compared with the MOD10A1 (MODIS daily snow cover) product. The MODIS product can provide higher resolution of the snow cover information in cloudless conditions. Multi-temporal FY-2G data can get more accurate snow cover information in cloudy conditions, which is beneficial for monitoring snowstorms and climate changes.

10405-18, Session PWed

Analysis of relationships between NDVI and land surface temperature in coastal area

Jicai Ning, Yantai Institute of Coastal Zone Research (China)

Relationships between NDVI and Land Surface Temperature (LST) variations were analyzed using Landsat imagery in the Yellow River Delta (YRD). The area has increased substantially due to the deposited sediment carried by the Yellow River from upper reach during nearly 30 years. Qin's mono-window algorithm was used to retrieve the regional LST. There was a regular connection between LST, NDVI, ANDVI, SAVI and other relevant vegetation indices, and there was a positive correlation, as well as a negative correlation, between different threshold ranges.

10405-19, Session PWed

Study of waterline extraction based on object-oriented method

Yuanyuan Zhang, Yantai Institute of Coastal Zone Research (China)

The coastal zone is a dynamic land reserve resource. Taking Shandong Bohai rim as the study area, the paper combined with TM and HJ1A/1B satellite images under the help of time series built by MODIS images, using Ecognition software platform to realize the waterline extraction based on object-oriented method. The result shows that this method can make full use of the existing image resources to realize the batch processing of the waterline extraction, and the accuracy is well which means that the method is applicable and can be popularized.

10405-20, Session PWed

Temporal and spatial characteristics of macroalgae blooms in the Yellow Sea based on MODIS data

Fuxiang Xu, Yantai Institute of Coastal Zone Research (China); Zhiqiang Gao, Yantai Institute of Coastal Zone Research (China) and East China Normal Univ. (China); Jicai Ning, Xiangyu Zheng, Yantai Institute of Coastal Zone Research (China); Jinquan Ai, Yantai Institute of Coastal Zone Research (China) and East China Normal Univ. (China); Debin Song, Yantai Institute of Coastal Zone Research (China)

We conducted a comprehensive utilization of aerial images, in situ data, and MODIS dynamic monitoring of the green tide in 2016, to reveal the source and spatial-temporal characteristics of green tide in the Yellow Sea. The dynamic monitoring of green tide by MODIS indicates that the Yellow Sea green tide first moved northwards, then moved in the northeast direction along the coastline of Shandong Peninsula, and finally became stranded in the sea areas near Qingdao and Weihai in 2016. Our goal is to provide a reference for monitoring, prevention, control and research of green tide.

10405-21, Session PWed

Multi-resource data-based research on remote sensing monitoring over the green tide in the Yellow Sea

Zhiqiang Gao, Yantai Institute of Coastal Zone Research (China)

This paper conducted dynamic monitoring over the green tide (large green alga—Ulva prolifera) occurred in the Yellow Sea in 2014 to 2016 by the use of multi-source remote sensing data, including GF-1 WFV, HJ-1A/1B CCD, CBERS-04 WFI, Landsat-7 ETM+ and Landsta-8 OLI, and by the combination of VB-FAH (index of Virtual-Baseline Floating macroAlgae Height) with manual assisted interpretation based on remote sensing and geographic information system technologies.

10405-22, Session PWed

Correlation analysis between green tide evolution and secchi disk depth variation in south Yellow Sea

Xuerong Li, Qianguo Xing, Yantai Institute of Coastal Zone Research (China)

Secchi disk depth (SDD), which can directly reflect the clarity and turbidity of coastal seawater, is a measure of seawater visibility and an important parameter to describe the optical properties of water. Green tides is the marine algae in the formation of explosive growth and aggregation of algal blooms phenomenon. 2007-2016, the south Yellow Sea for 10 years outbreak of Enteromorpha algae species as the green tide disaster. The outbreak of enteromorpha cannibalis seriously damaged the ecological balance of the southern Yellow Sea and brought serious impact to the economic and social development of the southern coast of Shandong Peninsula. Based on the MODIS remote sensing reflectance data and the three-band model, the SDD was analyzed and the green-tide drift trajectory was formed to form the SDD change images based on year, month and week. In the spring, the

Enteromorpha proliferates first in the form of small-scale floating green algae in the north of Jiangsu, and gradually drifts northwards and under the effect of wind and sea current, and finally accumulates in the coast of Shandong Peninsula in August. In 2008, large-scale Macroalgal blooms broke out in Qingdao, focusing on the changes of SDD from the origin to the end of the green-tide outbreak. And the change rule of SDD in the process of green tide evolution is revealed.

10405-23, Session PWed

Spectrum analysis of plants growing in the oil-fields

Ekaterina A. Selezneva, Elena V. Timchenko, Pavel E. Timchenko, Nikolay V. Tregub, Yana Fedorova, Anna S. Tyumchenkova, Samara Univ. (Russian Federation)

Currently, for the oil industry of many countries more and more raises the matter of replenishment of hydrocarbon resource base and discovery of new energy feedstock sources. Exploration activity of hydrocarbon accumulation is a difficult task and, above all, expensive. Therefore, the development of quick and cheap way to detect oil and gas fields is priority. For operational evaluation of oil-and-gas content with minimal cost and time use biogeochemical technique. Biogeochemical prospecting of mineral deposits based on the research study of the chemical composition of biological objects, usually plants.

The studies were carried out in two phases. First of all were carried out laboratory experiments based on the theory that oil affects on the plants Raman spectra. Then, field studies have been carried out.

Raman spectroscopy method was used as a method of research, realized with the help of experimental stand described in the work. Processing of Raman spectra were carried out in software environment Mathematica'8. Method of error did not exceed 5.84%. The highest statistical dispersion of the optical parameters of plant facilities within a single zone of investigation is 7.93%.

Green pea (Pisum sativum) and soft wheat (Tríticum aestívum) was chosen as the object of laboratory tests. The samples were divided into five groups; each group was grown in 3 pots. The first and second group of samples was a control; plants were grown in soil (without adding hydrocarbons). These groups of samples were located near the samples of the third and fourth groups. Into the pots with plants of third and fourth groups was added pure oil at a concentration of 1 g / kg. This concentration of oil is equal to the MRL for pure oil in the soil. The fifth group of plants had been growing in 6 pots in separate rooms in order to eliminate the influence of oil vapor on the spectral characteristics of plants. Dandelion ordinary (Taráxacum officinále) was chosen as the object of field research. Plants of this type are good bioindicators of environmental conditions.

The features of Raman spectra of plants growing in the field of oil deposits were obtained as a result of research studies. Major changes were documented at wave numbers 605 cm-1, 1440 cm-1 and 1547 cm-1 corresponding to the stretching vibrations of bromide ions, boron and chlorophyll "a" in plant leaves.

On the basis reasoning from two-dimension analysis of optical coefficients (H1, H2 and H3) were input criteria of plants separation growing in the oil-field area and outside of the oil-field area.

10405-24, Session PWed

The extraction of coastal windbreak forest information based on UAV remote sensing images

WeiTao Shang, Zhiqiang Gao, XiaoPeng Jiang, Yantai Institute of Coastal Zone Research (China)

Unmanned aerial vehicle(UAV) have been increasingly used for natural resource applications in recent years as a result of their greater availability, the miniaturization of sensors, and the ability to deploy UAV relatively quickly and repeatedly at low altitudes. UAV remote sensing offer rich contextual information, including spatial, spectral and contextual information. In order to extract the information from these UAV remote sensing images, we need to utilize the spatial and contextual information of an object and its surroundings. If pixel based approaches are applied to extract information from such remotely sensed data, only spectral information is used. Thereby, in Pixel based approaches, information extraction is based exclusively on the gray level thresholding methods. To extract the certain features only from UAV remote sensing images, this situation becomes worse. To overcome this situation an object-oriented approach is implemented. By object-oriented thought, the coastal windbreak forest information are extracted by the use of UAV remote sensing images. Firstly, the images are segmented. And then the spectral information and object geometry information of images objects are comprehensively applied to build the coastal windbreak forest extraction knowledge base. Thirdly, the results of coastal windbreak forest extraction are improved and completed. The results show that better accuracy of coastal windbreak forest extraction can be obtained by the proposed method, in contrast to the pixel-oriented method. In this study, the overall accuracy of classified image is 0.94 and Kappa accuracy is 0.92. The classification overall accuracy is based on TTA mask (training and test area mask) and it is 0.98 and Kappa accuracy is 0.96.

10405-25, Session PWed

A GIS-based health assessment of marine ecosystem in the Bohai Sea

Debin Song, Zhiqiang Gao, Fuxiang Xu, Xiangyu Zheng, Yantai Institute of Coastal Zone Research (China); Jinquan Ai, East China Normal Univ. (China)

Based on the index system of 22 indicators including water environment, sedimentary environment, ecosystem obtained from the investigation data of several voyage in the Bohai Sea during 2014 to 2016, the ecosystem health in the Bohai Sea was assessed by using Analytic Hierarchy Process (AHP) method and GIS technology. The results show the CEI value of marine ecosystem health is 0.643 and its health level is middle, which indicate the ecosystem health around the Bohai Sea are in an sub-health state. The maritime area with poor ecosystem performance were mainly located in Laizhou Bay, Bohai Bay and its adjacent area of the Yellow River Delta. The ecosystem health of offshore waters and high-seas area nearby Tangshan, Qinhuangdao and Huludao generally in an intermediate level. The central study area along with Bohai Straits displayed a relatively better health state. Be familiar with the assessment result, this paper carried out analysis on the health stress factors in Laizhou Bay and Bohai Bay, and obtained the following result: land-based input and reclamation. Based on these stress factors, countermeasures is studied to provide decision support in the management of the Bohai Sea.

10405-26, Session PWed

Monitoring of coastal zone pollution using unmanned aerial vehicle remote sensing system

XiaoPeng Jiang, Zhiqiang Gao, WeiTao Shang, Yantai Institute of Coastal Zone Research (China)

As an important complement to satellite observation, the technique of Unmanned Aerial Vehicle (UAV) shows great advantages because of its high spatiotemporal resolutions, low cost and risk. With the development of technology related to UAV, its research was increasingly enhanced and has been applied to many fields such as environmental monitoring. Taking a coastal zone of Yantai city as study area, this paper utilized the UAV system to capture aerial images and monitor the pollutant status of the study area, then analyzed the effects to coastal environment. The results showed that there were some different types of pollution in the study area, including solid waste (industrial refuse, house refuse), waste water (industrial and living sewage), which had a bad effect on the air, sea and

beach environment. This research on the application of UAV will provide the good base for coastal environment protection.

10405-27, Session PWed

The trend of the Tropospheric NO2 over the Yangtze River delta and the impact of the rapid urbanization on it

Ming-Liang Ma, East China Normal Univ. (China); Yue Song, Shanghai Shixi High School (China); Qiyang Liu, Runhe Shi, Wei Gao, East China Normal Univ. (China)

Over the past few decades, China has experienced a rapid increase in urbanization, especially in the Yangtze River delta. The urban built-up areas (population) in this region increase a lot from 1995 to 2015. In the same time, the dramatic economic development also has led to tremendous increases in energy consumption and put millions of cars on the roads. In this paper, we use satellite retrieval data to quantify the trend of the Tropospheric NO2 over the Yangtze River delta and the effects of rapid urbanization on the yearly and seasonal changes in tropospheric nitrogen dioxide (NO2) over this area.

10405-28, Session PWed

Remote sensing of atmospheric aerosols by MFRSR

Xiaoli Wei, Wei Gao, Runhe Shi, East China Normal Univ. (China)

Multi-filter rotating shadow-band radiaometer (MFRSR)is a ground-based instrument and it is used to measure irradiance and aerosol. It use automated rotating shadow-band technique to alternatively measure total horizontal and diffuse horizontal irradiance at seven wavelengths simultaneously, and then deduce direct normal irradiance. This paper uses two ground-based stations' data which avoid the influence of cloud. It is necessary to use the satellite data and AERONET data to check its accuracy.

10405-29, Session PWed

A study of long-term ground settlement behavior of muddy coastal lands in Shanghai with time-series InSAR

Hongbin Dong, Shanghai Shixi High School (China); Qing Zhao, East China Normal Univ. (China) and ECNU-CSU Joint Research Institute for New Energy and the Environment (China)

As the global warming problem is becoming seriously in recent decades, the global sea level is continuously rising. This will cause damages to the coastal deltas with the characteristics of low-lying land, dense population, and developed economy. Continuously reclamation costal intertidal and wetland areas is making Shanghai, the mega city of Yangtze River Delta, more vulnerable to sea level rise. In the paper, we investigate the ground settlement temporal evolution of patterns and processes on a stretch of muddy coast located between the Yangtze River Estuary and Hangzou Bay with differential synthetic aperture radar interferometry (DInSAR) analysis. By exploiting a set of 31 SAR images acquired by the ENVISAT/ASAR sensor from February 2007 to May 2010 with persistent scatters and small baseline approaches, coherent point targets with ground settlement velocity and time series are identified and densely distributed in the coastal region. The ground settlement time series and velocity are analyzed with multiple regression analysis and regression equation by SPSS to obtain a time-dependent settlement model. With the DInSAR constrained ground settlement model, we predict the ground settlement trend and the expected cumulative settlement in 2015 and 2020. Ground settlements retrieved with the high resolution SAR sensor, X-band COSMO-SkyMed, are used for validation purpose. With the ground settlement predictions and digital elevation model (DEM), we analyze the combined risk of ground settlement and sea level rise on the coastal areas of Shanghai. The potential flooded areas are mapped under different scenarios.

10405-30, Session PWed

Effects of climate change on peanut's yield in China

Hanqing Xu, Shanghai Institute of Technology (China) and Shanghai Climate Ctr., Shanghai Meteorological Bureau (China); Zhan Tian, Shanghai Institute of Technology (China) and Shanghai Climate Ctr., Shanghai Meteorological Bureau (China); Dongli Fan, Shanghai Institute of Technology (China); Runhe Shi, East China Normal Univ. (China)

Peanut production is one of the main sources of edible vegetable oil and feed protein in China. In recent years the demand for peanut products has been increasing much faster than its domestic production, which has resulted in massive imports and reduced self-reliance. Peanut cultivation faces a wide range of production conditions in china and is rather sensitive to climate change. It is critical to evaluate the climate change impact on peanut and production and its impact to the oil industry and security in China. In this research, we calibrate DSSAT based on available research data covering 31 years (1981-2011) of site-specific observations of peanut growth and development. We simulate the peanut production under climate projections from 5 General Circulation Models (GCMs) with 4 representative concentration paths (RCPs) in 2011-2040 (2020s), 2041-2070 (2050s) and 2071-2010 (2080s). Then we develop a probabilistic estimation to present an analysis that combines outputs from a wide range of General Circulation Models (GCMs) with observational data to produce more detailed projections of local climate suitable for assessing the impact on peanut yield. This assessment will help to evaluate the climate change impact on peanut and production and its in the food security of China.

10405-31, Session PWed

Residual settlements detection of ocean reclaimed lands with multi-platform SAR time series and SBAS technique: A case study of Shanghai Pudong International Airport

Lei Yu, East China Normal Univ. (China) and ECNU-CSU Joint Research Institute for New Energy and the Environment (China); Tianliang Yang, Ministry of Land and Resources (China) and Shanghai Institute of Geological Survey (China); Hongbin Dong, Shanghai Shixi High School (China); Qing Zhao, East China Normal Univ. (China) and ECNU-CSU Joint Research Institute for New Energy and the Environment (China); Antonio Pepe, Istituto per il Rilevamento Elettromagnetico dell'Ambiente (Italy)

Shanghai Pudong International airport(PVG) is one of three major international airports in china. The airport is located at the Yangtze estuary which is a sensitive belt of sea and land interaction region. The majority of the buildings and facilities of Pudong International airport are built on ocean reclaimed lands and silt tidal flat. Residual ground settlement could probably occur after the completion of the airport construction. The current status of the ground settlement at PVG and whether it is within a safe range are necessary to be investigated. In order to continuously monitor the ground settlement of the airport, we employed with high resolution SAR satellite TerraSAR-X(TSX) and the new generation SAR satellite Sentinel-1, which was launched by European Space Agency(ESA) in April 2014. Three

SAR time series, acquired by C-band TerraSAR-X(TSX) and TanDEM-X (TDX) sensor from December 2009 to December 2010 and from April 2013 to July 2015, and C-band Sentienl-1A(S1A) from February 2015 to December 2016, were used for obtaining the ground deformation of PVG with SBAS/DInSAR technique. The maximum ground settlement rate of the three SBAS results are as high as -48, -42, and -35 mm/y respectively. Ground settlement maps of the Pudong International Airport are generated with the multiplatform SBAS results. It shows continuous ground settlement occurred in this region. The results are consistent with field surveying records and implying that attention should be paid to impacts of ocean processes on the stability of newly reclaimed lands in recent years.

10405-32, Session PWed

The estimation model of chlorophyll content based on spectral index of Spartina alterniflora leaf

Jiapeng Wang, Runhe Shi, Chao Zhang, Pudong Liu, Yuyan Zeng, East China Normal Univ. (China)

The content of chlorophyll is an indicator of photosynthesis ability ?growth and development for vegetation. It is one of the important indexes to monitor the health status of vegetation growth. Spartina alterniflora is one of the most important invasive species in the coastal wetland in China, its chlorophyll content information is an important basic data for the research of wetland ecosystem. Taking Chongming Dongtan wetland, the Yangtze Estuary as the study area, we measured the leaf spectral reflectance with Field SpecHandHeld spectrometer and the content of chlorophyll with spectrophotometer indoor. In the base of these data sources, the relationship model(linear, logarithmic, exponential, quadratic, cubic, power model) is established by using correlation analysis and univariate fitting analysis, including the model of chlorophyll content and spectral index as well as trilateral parameters, then Cross Validation was used to test the accuracy of the estimation model.

10405-33, Session PWed

Calculation of mean solar exo-atmospheric irradiances of GF-4 data

Chunying Guo, Runhe Shi, East China Normal Univ. (China)

Mean Solar Exo-atmospheric Irradiances (ESUN) is an important parameter to calculate the appearance reflectance according the DN value of satellite receiving.GF-4 were launched in 2015.However,the ESUN of this satellite has not been released publicly. To determine which solar spectrum curves is good for GF satellite, this paper calculated the ESUN of GF-1,using 7 solar spectrum curves and spectral response curve of GF-1.And we compared and verified the result with official results. At last we calculate the ESUN of GF-4 with this solar spectrum curve.

10405-34, Session PWed

Vegetation dynamics and their response to climatic variability in Yangtze River watershed region

Bowen Zhang, Shanghai Institute of Technology (China); Linli Cui, Jun Shi, Shanghai Meteorological Bureau (China); Peipei Wei, Shanghai Institute of Technology (China)

Based on SPOT/NDVI and meteorological data, NDVI and their response to temperature and precipitation in the watershed region between Changjiang River and Huaihe River were investigated over the period 1998--2013 by using the maximum value composite, linear regression and the method based on Pearson correlation coefficient. The results show that the average value of NDVI have a significant increasing trend for the whole area in the past 16 years. And the annual mean temperature of Yangtze River watershed region has a slightly increasing, while the annual average precipitation has a slightly decreasing in the past 16 years. Accordingly the values exist evidently variations in month and season. Correlation analysis shows that monthly averaged NDVI variations are generally determined by temperature but not precipitation. Positive correlations appear between NDVI and temperature, and the correlations are more significant in spring and autumn. Significant negative correlations are found in summer and winter between NDVI and precipitation. Spatial heterogeneity analysis shows that NDVI is more vulnerable to climate change for the middle basin than other regions. Finally, it can be demonstrated that NDVI can currently responds to temperature with a lag of 1 month. With respect to precipitation, the strongest response may occur 2 months. In addition, human activities also had profound effect to the NDVI trends in some regions. This study contributes to ongoing investigations of the effects of climate change on vegetation activity.

10405-35, Session PWed

Effects of distribution density of 3D vegetation model on canopy NDVI simulation

Zhu Tao, Runhe Shi, East China Normal Univ. (China)

The 3D model is an important part of simulated remote sensing for earth observation. In the study of small-scale spatial extent of DART software, both the details of the model itself and the number of models of the distribution have an important impact on the scene canopy NDVI. Taking the phragmites australis of Changjiang Estuary wetland as an example, this paper studied the effect of the phragmites model on the canopy NDVI, based on the previous studies of the model precision, mainly from the cell dimension of the DART software and the density distribution of the phragmites model in the scene , As well as the choice of the density of the phragmites model under the cost of computer running time in the actual simulation. The DART Cell dimensions and the density of the scene model were set by using the optimal precision model in the existing research results. The simulation results of NDVI with different model densities under different cell dimensions were analyzed by error analysis. By studying the relationship between relative error, absolute error and time costs, we have mastered the density selection method of phragmites model in the simulation of small-scale spatial scale scene. Experiments show that the number of phragmites in the simulated scene need not be the same as in the real environment due to the difference between the 3D model and the real plant. The best simulation results can be obtained by keeping the density ratio of about 40 trees per square meter, simultaneously, of the visual effects.

10405-36, Session PWed

Comparison of satellite hyperspectral infrared sounder temperature and relative humidity profiles with ECMWF reanalysis datasets and radiosonde observations in East China

Yaru Gu, East China Normal Univ. (China); Yan-An Liu, Chaoshun Liu, East China Normal Univ. (China) and ECNU-CSU Joint Research Institute for New Energy and the Environment (China); Runhe Shi, East China Normal Univ. (China); Wei Gao, ECNU-CSU Joint Research Institute for New Energy and the Environment (China); Siying Cao, Shanghai Shixi High School (China)

The temperature and humidity profiles that come from different data sources are of different characteristics?Reasonable scientific use can help improve the accuracy of numerical models?This study focuses on East China during the summer 2015?and the AIRS retrievals? radiosonde

data and the European Center for medium Range Forecast (ECMWF) data are in intercomparison to analysis the pros and cons of different datasets?This study compares the difference between AIRS AIRX2RET data and AIRS2RET data as well?Results of the entire intercomparison reveal that the RMSE of temperature profiles are in very good agreement with all cases?whilst the relative humidity RMSE show larger difference?It's basically distributed within 30% while it appears to be more than 40% in little upper troposphere?When AIRX2RET retrievals and ECMWF data are compared with RAOBs?The temperature RMSE difference of AIRX2RET and ECMWF range from 1.02? to 2.49? and from 0.74? to 1.53??respectively?Apparentl y?the ECMWF temperature data is superior to AIRX2RET? with respect to temperature biases? the situation remains the same?As for relative humidity profiles?The ECMWF bias and RMSE are better than AIRX2RET under 400 hPa while the case is opposite in upper troposphere?Besides these?Probably influenced by AMSU?There is no more than 10% relative humidity RMSE difference between AIRX2RET and AIRS2RET data?As the AMSU is more sensitive to water vapor?Overall?ECMWF and AIRS data show wetter in high levels?It is necessary to do error description during model applications in the future?

10405-37, Session PWed

The preliminary analysis of the occultation atmospheric products of FY-3C satellite

Zhenxiang Shen, Chaoshun Liu, East China Normal Univ. (China); Yan Chen, Shanghai Shixi High School (China)

FY-3 is the second-generation polar orbit meteorological satellite in China and the purpose is to realize all-weather, multi-spectral and three-dimensional observation of the global atmospheric and geophysical elements. The FY-3C successfully launched in Taiyuan on the morning of September 23, 2013. The Global Navigation Satellite System Occultation Sounder (GNOS) is the first new civilian payload to detect the neutral atmosphere and ionospheric atmosphere by occultation in FY-3C. The detector can realize the atmospheric and ionospheric detection and it can be more comprehensive and accurate determination of the atmospheric and ionospheric profiles, so as to provide more high-precision technical support to China's space weather monitoring and weather forecasting. GNOS can receive Global Positioning System (GPS) navigation satellites and China's Beidou navigation satellite signal and we can get a global range of atmospheric products (including refractive index, density, temperature and humidity profile) of the neutral atmosphere and ionospheric atmosphere after inversion. In this paper, the atmospheric products (including refractive index, density, temperature, and humidity profile) of the GNOS receiver is examined by the ECMWF profile data. The results show that the difference in temperature was very small between the 200 hPa and 600 hPa near the mid-troposphere, and significantly different in temperature at the tropospheric top at 200 hPa and above. The basic range of bias is between -2% and 1%. In the whole troposphere, the bias of humidity a greater degree of dispersion and basically maintained at -40% to 40%.

10405-38, Session PWed

Assessing the potential productivity of summer maize using WOFOST in north China plain

Mingnuo Jiang, Chaoshun Liu, East China Normal Univ. (China)

The North China Plain(NCP) region is an important maize producing area in China.This study simulated the potential and water-limited yield of summer maize in the region using the reanalysis data of 30 yrars with the help of WOFOST model, and analyzed the yield gaps between the actual and potential production.The aims are to reveal the yield potential and its spatial and temporal variation,identify the limiting facters affecting crop growth, and indicate room to increase the yield of summer maize.The results show that:1)potential and water-limited yield of summer maize in the NCP region 5384-11876kg/ha and 2987-7798kg/ha.respectively. 2)Annual variation of potential yield is relatively lower in the middle and southern parts,while it is higher in the northeastern region. 3)The region has a high potential room to increase the yield of summer maize by improving the crop managemment and irrigation systems.

10405-39, Session PWed

Satellite observations of autumn-winter floating brown macroalgae blooms drifted from the Yellow Sea to the East China Sea

Qianguo Xing, Xuerong Li, Yantai Institute of Coastal Zone Research (China)

At the end of December, 2016, massive macroalgae blooms caused by floating brown macroalgae (Sargassum honeri) beat the seaweed aquaculture at the Jiangsu Shoal, China, and led to the largest direct economic loss due to Sargassum honeri blooms in China. In this study, high resolution satellite images were used to monitor the drifting path and development of the brown macroalgae blooms. For the first time, we showed that brown macroalgal blooms first occurred at the middle of October in the western Yellow Sea (YS) near the south coast of the Shandong Peninsula, arrived at the Jiangsu Shoal and damaged the local seaweed aquaculture at the middle of December, and finally drifted into the East China Sea (ECS). This kind of southward drifting path from the YS to the ECS, is also verified by the winter-spring macroalgal blooms in previous years.

10405-40, Session PWed

Measurement of changes in the land cover and classification of regions of interest

Wendy Barrera Garcia, Juan Carlos Valdiviezo Navarro, Univ. Politécnica de Tulancingo (Mexico); César Joel Camacho Bello, Univ. Tecnológica de Tulancingo (Mexico)

The study and interpretation of changes on Earth´s surface have become the main topic of interest for different researches around the globe. Thanks to the availability of satellite data acquired by different missions, now a days it is possible to analyze the evolution of land surface changes at a certain interval of time as satellite time series. The research here outlined presents a novel technique to analyze satellite time series registered from natural reserves and water bodies in Mexico. With the aim to delineate land use changes, our method is applied to various collections of Landsat images acquired in the period from 1980 to 2015. For this purpose, each satellite image set is analyzed by means of two different approaches. Fist, the Hurst Exponent (H), which measures the distortion in the curve of some time series through windows of different dimensions, is computed. In a previous research we demonstrated the relation between Hurst exponent values and changes in land use. Hence, a decreasing H value can be associated with alterations in land surface. Second, the well known normalized difference vegetation index (NDVI) and the normalized difference water index (NDWI) are computed for each image in the series to segment areas of the corresponding natural resources. The segmented images are then compared at small windows, located at the same position along the series, in order to mark out the differences. At the end of the procedure we have a global estimation of H, NDVI, and NDWI values for each image in the set. In addition, an image indicating the positions where land use changes occurred is also produced by the algorithm. According to our preliminary results, decreasing H, NDVI, and NDWI values state that the Earth´s surface has been significantly modified. We remark that our method facilitates precise classification of the regions analyzed, minimizing confusion in any interpretation of the data.

10405-42, Session PWed

A sampling strategy based on CGM for LAI measurements over non-uniform surface

Xiaohua Zhu, Lingling Ma, Yongguang Zhao, Academy of Opto-Electronics, CAS (China)

Currently, the remotely sensed product compared by measurements of field reference targets is still the basic means for validation. Limited by the representativeness of point sampling, all of the field measurements covering the whole region should be collected, which is impossible. Taking the cost of field measurement into account, more representative points with minimum number should be selected during remotely sensed product validation. There are several sampling strategies are used for remotely sensed product validation, including simple random sampling strategy, spatial uniform sampling strategy, Prior knowledge-based sampling strategy and so on. However, without fully considering the influence of the surface spatial heterogeneity, those sampling strategies often reduce the reliability of products validation. In this paper, a new sampling strategy based on computational geometry model (CGM) is proposed for leaf area index (LAI) ground measurement over non-uniform surface, as shown in Figure 1. Firstly, a correlation index (CI) is calculated based on high-resolution LAI image to choose the points of field measurement. Secondly, based on the first selected field measurements, the CGM model is used for simulating low-resolution LAI. Thirdly, the points of field measurement are decided according to the gaps between the simulated LAI and the aggregated LAI from high resolution. If the gap is accepted, the sampling strategy is finally established for field measurement. Otherwise, the field measurements should be re-selected and analyzed until the gap is accepted.

10405-43, Session PWed

About remote monitoring systems for aquatic environment

Ferdenant A. Mkrtchyan, Kotel'nikov Institute of Radio Engineering and Electronics of Russian Academy of Sciences (Russian Federation)

The technique of detection offered in given work and identification of the abnormal phenomena in the aquatic environment (microwave and optical) combines presence with application of possibilities of remote measurements algorithmic and the software, allowing to solve measurement and detection problems in real time. The effective decision of these problems is impossible without wide introduction in practice of researches of the automated systems of gathering, storage and data processing on the basis of modern computer systems with application of technology of open systems. Already created methods and algorithms possess ability to overcome such difficulties, as scantiness and not stationary information, presence small statistically non-uniform samples. It is obvious that complex research of the given land and remote measurements can raise reliability of estimations of parameters of natural systems and solve a problem of planning of these measurements. Application of means of remote monitoring in many cases is connected with acceptance of the statistical decision on presence on a surveyed part of studied space of this or that phenomenon. One of features of conditions of gathering of the information for such decision is the impossibility of reception statistical samples great volumes. Therefore working out and research of optimum algorithms of distinction of the casual signals characterized by samples of the limited volume, in the conditions of parametrical aprioristic indefinite are necessary.

Conference 10406: Lidar Remote Sensing for Environmental Monitoring 2017

SPIE. OPTICS+ PHOTONICS OPTICAL ENGINEERING+ APPLICATIONS

Tuesday - Wednesday 8 –9 August 2017

Part of Proceedings of SPIE Vol. 10406 Lidar Remote Sensing for Environmental Monitoring 2017

10406-1, Session 1

A survey of enabling active remote sensing technologies for NASA's Earth science observations *(Keynote Presentation)*

George J. Komar, NASA Headquarters (United States)

Recently conducted NASA Earth Science Technology Office (ESTO) review of current science challenges related to NASA's Earth science measurement goals highlighted the technology needs that would make future Earth observations possible. New investments in lidar technology and a review of state-of-the-art transmitter, receiver, and information technologies as they pertain to lidar systems will enable successful new capabilities that will give researchers a better understanding of the Earth system. This presentation will cover the needs and technology advancements that will make advanced science measurements from space possible.

10406-2, Session 2

Progress on development of an airborne two-micron IPDA lidar for water vapor and carbon dioxide column measurements *(Invited Paper)*

Upendra N. Singh, Mulugeta Petros, Tamer Refaat, Jirong Yu, Charles W. Antill, Bryant D. Taylor, Ruben G. Remus, Teh-Hwa Wong, Karl Reithmaier, Jane Lee, Syed Ismail, NASA Langley Research Ctr. (United States)

An airborne 2-?m triple-pulse integrated path differential absorption (IPDA) lidar is currently under development at NASA Langley Research Center (LaRC). This lidar targets both atmospheric carbon dioxide (CO2) and water vapor (H2O) column measurements, simultaneously. Advancements in the development of this IPDA lidar are presented in this paper. Updates on advanced two-micron triple-pulse high-energy laser transmitter will be given including packaging and lidar integration status. In addition, receiver development updates will also be presented. This includes a state-of-the-art detection system integrated at NASA Goddard Space Flight Center. This detection system is based on a newly developed HgCdTe (MCT) electron-initiated avalanche photodiode (e-APD) array. Future plan for IPDA lidar system for ground integration, testing and flight validation will be discussed.

10406-3, Session 2

GreenLITE: A new laser-based tool for near-real-time monitoring and mapping of CO2 and CH4 concentrations on scales from 0.4-25 km2

Jeremy T. Dobler, Nathan Blume, Michael Braun, Harris Corp. (United States); Scott Zaccheo, Timothy G. Pernini, Atmospheric and Environmental Research, Inc. (United States)

In 2013, Harris and Atmospheric and Environmental Research developed the greenhouse-gas laser imaging tomography experiment (GreenLITE™) under a cooperative agreement with the National Energy Technology Laboratory of the Department of Energy. The system uses a pair of high precision intensity modulated continuous wave (IMCW) transceivers and a series of retroreflectors to generate overlapping atmospheric density measurements from absorption of a particular greenhouse gas (e.g. CO2 or CH4), to provide an estimate of the 2-D spatial distribution of the gas within the area of interest. The system is capable of making the measurements over areas from approximately 0.4 to 25 km2 (~200 m X 200 m, up to ~5 km X 5 km). Multiple GreenLITE™ CO2 demonstrations have been carried out to date, including a full year, November 04, 2015, to November 14, 2016, deployment over ~25 km2 area of downtown Paris, France. In late 2016 the GreenLITE™ system was converted to provide similar measurements for CH4. Recent experiments showed that GreenLITE™ CH4 concentration retrievals agreed with an in situ instrument, calibrated with World Meteorological Organization traceable gas purchased from the NOAA Earth Systems Research Laboratory, to within approximately 0.5% of background or ~10-15 parts per billion. Several experiments are planned in 2017 to further evaluate the accuracy of the CH4 and CO2 retrieved concentration values compared to the calibrated in situ instrument and to demonstrate the feasibility of GreenLITE™ for environmental and safety monitoring of CO2 and CH4 in industrial applications.

10406-4, Session 2

New semiconductor laser technology for gas sensing applications in the 1650nm range

Milan L. Mashanovitch, Gordon Morrison, Paul O. Leisher, Jeremy Thomas, Freedom Photonics, LLC (United States); Mark Stephen, Kenji Numata, Stewart Wu, Haris Riris, NASA Goddard Space Flight Ctr. (United States)

Atmospheric methane (CH4) is the second most important anthropogenic greenhouse gas with approximately 25 times the radiative forcing of carbon dioxide (CO2) per molecule. CH4 also contributes to pollution in the lower atmosphere through chemical reactions leading to ozone production. Recent developments of LIDAR measurement technology for CH4 have been previously reported by Goddard Space Flight Center (GSFC). The instrument has a tunable, narrow-frequency light source and photon-sensitive detector to make continuous measurements from orbit, in sunlight and darkness, at all latitudes and can be relatively immune to errors introduced by scattering from clouds and aerosols. To further improve and simplify the instrumentation used, advances in tunable laser technology used are required.

In this paper, we report on a novel, high-performance tunable semiconductor laser technology developed by Freedom Photonics for the 1650nm wavelength range operation, and for LIDAR detection of CH4. Devices described are monolithic, with simple control, and compatible with low-cost fabrication techniques. They are based on distributed Bragg reflector laser implementations, and exhibit >70nm of tuning. They can thus also be used for CO2 and water vapor detection. The fabrication platform is radiation hard, allowing for simplified space deployment.

10406-5, Session 2

Compact, highly efficient, single-frequency 25W,2051nm Tm Fiber-based MOPA for Co2 trace-gas laser space transmitter

Doruk Engin, Fibertek, Inc. (United States); Ti Chuang, Fibertek (United States); Mark Storm, Fibertek, Inc. (United States)

Fibertek has developed and demonstrated a high output power, low risk, low SWAP (size, weight and power) 2051nm laser design meeting the lidar requirements for satellite-based global measurement of CO2. The laser design provides a path to space for either a coherent lidar approach being developed by NASA JPL or an Integrated Path Differential Absorption (IPDA) lidar approach. The IPDA approach has been implemented using RF

modulation and is being flown as part of a NASA Earth Venture suborbital mission - NASA's Atmospheric Carbon and Transport – America. The thulium fiber laser amplifies a < 500 kHz linewidth DFB laser up to 25W average power in a polarization maintaining fiber. The design manages and suppresses deleterious non-linear effect that can cause linewidth broadening or amplified spontaneous emission and meets the laser transmitter requirements for the identified lidar programs. We believe the core laser components, architecture and design margins can support a coherent or IPDA lidar for a 10 year space-based mission. We would be able to adapt an existing space-based, TRL-6, 20 W erbium fiber laser package for this thulium design and enable a near term space mission with an electrical to optical efficiency of > 20 %.

10406-6, Session 2

Wide area methane emissions mapping with airborne IPDA lidar

Jarett Bartholomew, Philip Lyman, Carl Weimer, Lyle Ruppert, Ball Aerospace & Technologies Corp. (United States)

Methane emissions from natural gas production, storage and transportation are a potential source of greenhouse gas emissions. Leaks also constitute revenue loss potential from operations. Since 2013, Ball Aerospace has been developing advanced airborne sensors using integrated path differential absorption (IPDA) LIDAR instrumentation to identify methane, propane and longer-chain alkanes in the lowest region of the atmosphere. Additional funding has come from the U.S. Department of Transportation, Pipeline and Hazardous Materials Administration (PHMSA) to upgrade instrumentation to broader swath coverage of 0.3 km while maintaining high spatial sampling resolution and geolocation accuracy. Wide area coverage allows efficient mapping of emissions from gathering and distribution networks, processing facilities, landfills, natural seeps, and other distributed methane sources. This paper summarizes benefits of advanced instrumentation for aerial methane emission mapping, describes the operating characteristics and design of this upgraded IPDA instrumentation, and reviews technical challenges encountered during development and deployment.

10406-7, Session 2

Single frequency Er:YAG methane/water vapor DIAL source

Patrick M. Burns, Moran Chen, Dave Pachowicz, Jeremy E. Young, Fran Fitzpatrick, Nicholas Sawruk, Fibertek, Inc. (United States)

Fibertek is developing injection locked, resonantly pumped Er:YAG laser systems for use in methane and water vapor differential absorption lidar (DIAL) systems. Accurate measurements of methane and water vapor are critical to understanding global energy transport and climate change. Current state-of-the-art lidar sources for DIAL measurements of these constituents are based on less efficient non-linear parametric conversion of diode pumped Nd:YAG systems. Er:YAG offers an avenue for a more compact, efficient system that can interrogate both methane and water vapor spectra. Fibertek's approach uses VBG stabilized 1532nm fiber coupled diodes minimizing the quantum defect and thermal loading while generating tunable single frequency output at 1.645 to 1.646μm. Single frequency operation is achieved through an injection seeded ring laser architecture with a Pound Drever Hall (PDH) locking technique. Laser systems from 1kHz to 10kHz are being studied with powers in the 4 to 10W range at the fundamental. Further work is being done on doubling this output to the 822nm regime for water vapor Lidar with a target of 3-5W.

10406-8, Session 3

Application of Doppler wind lidar observations to hurricane analysis and prediction *(Invited Paper)*

Robert M. Atlas, National Oceanic and Atmospheric Administration (United States); George D. Emmitt, Simpson Weather Associates, Inc. (United States); Lisa Bucci, Kelly Ryan, Jun A. Zhang, National Oceanic and Atmospheric Administration (United States)

Winds are among the most important variables in the atmosphere. They transport all the other variables of the atmosphere and govern the exchanges of mass, energy, and momentum. Currently, winds make up a very small fraction of the observations that are used in data assimilation systems. Many of the winds that are available are created by tracking features in the cloud or water vapor field. These atmospheric motion vectors are valuable, but they are an indirect measurement and have inherent height uncertainties. In contrast, Doppler Wind Lidars (DWLs) directly measure the line-of-sight wind by observing the Doppler shift in the lidar signal returned by a volume of atmospheric scatterers.

Impact experiments with real data, termed Observing System Experiments (OSEs), are conducted with and without one observing system to quantify the impact of that observing system. Similar experiments with simulated data are termed Observing System Simulation Experiments (OSSEs). In OSSEs a long forecast is taken to be the "truth" or nature run. The present study complements previous space-based DWL OSSEs by examining the impact of DWL observations on hurricanes and by beginning to evaluate the impact of having an existing DWL on NOAA's Hurricane Hunter aircraft. An airborne DWL was flown for the first time in 2015 on the NOAA P3 Orion Hurricane Hunter aircraft into Atlantic Tropical Storms Danny and Erika, and then again during the 2016 hurricane season. The impacts of the airborne DWL data that was obtained will be presented at the conference.

10406-9, Session 3

Status of pulsed coherent-detection wind lidars at NASA LaRC and recent airborne science campaign results

Michael J. Kavaya, NASA Langley Research Ctr. (United States); George D. Emmitt, Simpson Weather Associates, Inc. (United States); Zhaoyan Liu, Upendra N. Singh, NASA Langley Research Ctr. (United States)

NASA LaRC is developing high-energy 2-micron lasers and coherent-detection wind lidar systems to advance technology that is needed for global wind measurements from space. The wind measurements have been endorsed by the NRC in its Earth Science "Decadal Survey", and by NOAA for improved forecasting. LaRC began laser development in the 1990s, wind lidar development with the high-energy lasers in 2002, and airborne wind lidar systems in 2005. The wind lidar systems utilized the advanced laser technology available at the time in the development progress. The first 2-micron airborne wind lidar system was developed over 2005 – 2010. The Doppler Aerosol WiNd (DAWN) lidar system featured a 250 mJ, 10 Hz, 190 ns laser, an optical wedge-based conical scanner approximately centered on nadir, and a 15-cm receiver aperture. DAWN has flown in three science campaigns to date: the NASA hurricane Genesis and Rapid Intensification Processes (GRIP) in 2010, the NASA Polar Winds campaign based at Greenland in 2014, and the Polar Winds campaign based in Iceland in 2015. We are planning to fly DAWN in NASA's Convective Processes Experiment (CPEX) in May-June 2017. In preparation for CPEX, DAWN is being upgraded to improve its photon efficiency and to permit more operator test and alignment options in the field. NASA LaRC is also developing a second generation airborne lidar system that will have a different laser operating point to reduce risk, to greatly decrease the heat to be removed from the laser, and to improve the science product from future use in space. The status of the wind lidar systems, and aircraft science campaign results will be presented.

10406-10, Session 3

Efficient, space-based, 100W thulium fiber laser for pumping Q-switched 2um Ho:YLF for global winds and carbon dioxide lidar

Doruk Engin, Brian Mathason, Mark Storm, Fibertek, Inc. (United States)

Space-based global wind and CO2 measurements are critically needed to improve and extend NOAA weather forecasting that impacts U.S. crop production, hurricane forecasting, flooding, and FEMA disaster planning. NASA, NOAA, and the 2007 National Research Council (NRC) Earth Science Decadal Survey have identified space-based, global wind measurements as critical for improving both weather prediction as well as longer term climate change research. Researchers at NASA Langley have conducted aircraft-based coherent wind lidar measurements using 2 um Ho:YLF lasers that have demonstrated the ability of the lidar system to provide both wind and CO2 measurements. Extending the lidar system design to a space-qualifiable version requires the development of a robust and efficient pump source for the required 2 μm laser. Fibertek has designed and demonstrated a high-efficiency, 100 W average power continuous wave 1940 nm thulium-doped fiber laser breadboard system that meets the performance requirements for a space-qualifiable, 2 μm Ho:YLF pump laser source. Our preliminary design shows that it is possible to package the pump laser for high reliability, spaceflight operation in an ultra-compact ~2”x8”x14” volume and weight <8.5 lbs. Our 100 W polarization maintaining Tm laser provides a key component for the development of a space-qualified, Q-switched, 2 μm Ho:YLF laser with 30-80 mJ/pulse at 100-200 Hz repetition rates.

10406-11, Session 3

Fast widely-tunable single-frequency 2-micron laser for remote sensing applications

Sammy W. Henderson, Charles P. Hale, Beyond Photonics (United States)

We describe a fast frequency–tunable diode-pumped solid-state laser we have developed, called the SWIFT laser. The laser architecture is compatible with operation using many different solid state laser crystals for access of various emission lines between 1 and 2.1 micron. We initially demonstrated the laser using a Tm,Ho:YLF laser crystal near 2.05 micron wavelength and achieved up to 100 mW of output power and up to 50 GHz fast PZT-actuated tuning range. The fast frequency tuning range can be centered at any wavelength from 2047-2059 nm using the Tm,Ho:YLF crystal, making the laser compatible with path-integrated or range-resolved differential absorption lidar systems for atmospheric CO2 or H20-vapor concentration measurements. Other laser crystals will allow access to other molecular absorption lines, e.g., Er:YAG for CH4. The frequency stability and power are sufficient to serve as the local oscillator laser in long-range (e.g., space-based) coherent lidar systems for measurement of atmospheric winds or tracking and characterization of hard targets.? The SWIFT laser and its performance will be described in detail in the paper and presentation. We also have demonstrated that a miniature Q-switched laser of similar design to the SWIFT laser can produce 20 microJoule pulses at 5-10 kHz PRF. We will also describe lidar modeling which predicts that such low energy laser pulses are sufficient to allow for range-resolved wind measurements in the atmospheric boundary layer to a few km range.

10406-12, Session 4

First principle calibration of water vapor Raman lidars *(Invited Paper)*

Valentin B. Simeonov, Ecole Polytechnique Fédérale de Lausanne (Switzerland)

Raman lidars exploit the proportionality between the intensity of scattered by Raman process laser radiation and the number density of scattering molecules. Water vapor-air mixing ratio is proportional to the ratio of the measured intensities of Raman scattering from water vapor and nitrogen molecules. The coefficient of proportionality, denoted as calibration constant, depends on instrument parameters and spectroscopic parameters of the scattering molecules and is primary factor defining lidar measurement accuracy. Derivation of the calibration constant using above mentioned parameters is possible but leads to high uncertainty. Therefore Raman lidars are calibrated against reference instrument- radio sonde or microwave radiometer. The accuracy of such calibration is thus limited by the accuracy of the reference instrument.

The new method for calibration of water vapor Raman lidars proposed here is based on first principles. The calibration constant is derived from set of water vapor and nitrogen Raman backscatter signals measured with the lidar receiver in a cell filled with reference humidity mixture.

The reference humidity mixture is prepared gravimetrically. The water vapor mixing ratio is calculated directly as a ratio of the mass of water to the mass of air. Since mass is a fundamental quantity, this method yields an absolute value of water vapor mixing ratio which translates to the lidar calibration constant.

A lidar calibrated with the method has the potential to become reference instrument for atmospheric profiling of water vapor and can be used for validation and calibration of other instruments, such as microwave radiometer, balloon sonde, and GPS.

10406-13, Session 4

Greater than 2mJ pulse energy and 65kW peak power single frequency fiber laser at 1.03 micron

Shibin Jiang, AdValue Photonics, Inc. (United States)

All-fiber monolithic laser sources are highly desirable for airborne and space borne applications because fiber laser sources offer a much more compact and robust solution compare to free-space solid state lasers. However, the pulse energy and peak power of the fiber amplifiers are limited because of the stimulated Brillouin scattering (SBS). The pulse energy is generally limited to near 0.5mJ level.

We developed multi-component non-silica glasses as the host of the rare-earth ions, which permit a higher doping concentration because of their less-defined glass network as compared to silica glass. Yb doped glasses were fabricated as the core glasses, and a large core single mode fiber was developed. A singe frequency fiber laser with pulse energy of greater than 2mJ and peak power of greater than 65kW will be presented.

10406-14, Session 4

Stabilized diode seed laser for flight and space-based remote lidar sensing applications

Shirley McNeil, Phillip Battle, AdvR, Inc. (United States); Floyd Hovis, Joe Rudd, Fibertek, Inc. (United States)

AdvR, through support of the NASA SBIR program, has developed fiber-based components and sub-systems that are routinely used on NASA’s flight-based missions, and is now developing an environmentally hardened, diode-based, locked wavelength, seed laser for future space-based high

spectral resolution lidar applications. The seed laser source utilizes a fiber coupled diode laser, a fiber coupled calibrated iodine cell module to provide an absolute wavelength reference, and an integrated dual-element nonlinear optical waveguide component for second harmonic generation, spectral formatting and wavelength locking. The seed laser operates over a range close to 1064.5nm, provides for stabilization of the seed to the desired iodine transition and allows for a highly efficient, fully integrated seed source that is well-suited for use in flight and space-based environments. A summary of component level environmental testing and spectral purity measurements with a seeded Nd:YAG laser will be presented. A direct diode, wavelength locked seed laser will reduce the overall size weight and power (SWaP) requirements of the laser transmitter thus directly addressing the need for developing compact, efficient, lidar component technologies for use in flight and space-based environments.

10406-15, Session 4

Development of a wing-beat-modulation scanning lidar system for insect studies

Martin J. Tauc, Montana State Univ. (United States); Kurt M. Fristrup, U.S. National Park Service (United States); Joseph A. Shaw, Montana State Univ. (United States)

The spatial distributions of flying insects are not well understood since most sampling methods -- Malaise traps, sticky traps, vacuum traps, light traps -- are not suited to documenting movements or changing distributions of various insects on short time scales. These methods also capture and kill the insects. To noninvasively monitor the spatial distributions of flying insects, we developed and implemented a scanning lidar system that measured wing-beat-modulation. Transmitting and receiving optics were mounted to a telescope that was attached to a scanning mount. As it scanned, the lidar collected and analyzed the light scattered from insect wings of various species. Mount position and pulse time-of-flight determined spatial location and spectral analysis of the backscattered light provided clues to insect identity. During one day of a four day field campaign at Grand Teton National Park in June of 2016, 76 insects were detected, with a maximum range to the insect of 87.6 m.

10406-16, Session 4

1550 nm eye-safe wavelength watt-level laser transmitter for space communication and lidar

Ray R. Y. Tang, Ramadas Pillai, NuPhoton Technologies, Inc. (United States)

A master-oscillator power amplifier (MOPA) based 1550 nm wavelength fiber laser transmitter has been developed for Space-to-Earth communication application, utilizing Telcordia rated 1550 nm seed laser, pump lasers, and fiber optics. With adequate pre-screening of electrical components, the fiber laser transmitter has been in operation since its original launch in April 2014 for more than 28 months. This presents as a relatively cost-effective route for low-earth-orbit optical communication as well as LIDAR application.

10406-17, Session 4

The Scheimpflug lidar method

Mikkel Brydegaard, Elin Malmqvist, Samuel Jansson, Jim Larsson, Sandra Török, Lund Univ. (Sweden); Guangyu Zhao, South China Normal Univ. (China)

The recent several years we developed the Scheimpflug lidar method. We combined an invention from the 19th century with modern optoelectronics such as diode lasers and CMOS array from the 21st century. The approach exceeds expectations of background suppression, sensitivity and resolution beyond known from time-of-flight lidars. We accomplished multiband elastic atmospheric lidars for resolving single particles and aerosol plumes from 405 nm to 1550 nm. We pursued hyperspectral differential absorption lidar for molecular species. We demonstrated a simple method of inelastic hyperspectral lidar for profiling aquatic environment and vegetation structure. Not least, we have developed polarimetric Scheimpflug lidar with multi-kHz sample rates for remote modulation spectroscopy and classification of the aerofauna. All these advances thanks to the scheimpflug principle. Here we give a tour of how far we came, we shed light on the limitations and opportunities for future directions. In particular we show how the biosphere can be resolved with unsurpassed resolution in space and time, and share our expectation on how this can revolutionize ecological analysis and management in relation to agricultural pests, disease vectors and pollinator problematics.

10406-18, Session PWed

A photon-efficient method based on curve fitting for photon counting 3D imaging lidar

Ling Ye, Guohua Gu, Weiji He, Wenye Yin, Jie Lin, Jian Fang, Nanjing Univ. of Science and Technology (China)

For using Geiger mode avalanche photodiode (Gm-APD) and the technique of time correlated single photon counting (TCSPC), a direct-detection 3D imaging lidar has high sensitivity in low-light-level (LLL) scene. Conventionally, traditional method needs long fixed dwell time to collect thousands of photons to find accurate range and mitigate Poisson noise at each pixel. We present a new method, which acquires accurate depth images using much less detected photons and has quantitative analysis to estimate whether results are in the confidence interval. Based on the shape of emitted laser and the response curve of the detector, we use one order of magnitude back-reflected photons less than traditional method, fitting a curve of laser-return pulse by nonlinear least-squares fitting to obtain the range. The condition of moving to next pixel in our method is acquiring a fixed number of back-reflected photons, instead of sampling for a fixed time. Low-reflection areas have more time to acquire enough photons. This adaptive jump condition is able to speed up the scanning without generating distortion. The results are analyzed with chi-square test to determine whether the curve we fit has enough credibility. This quantitative analysis provides a important judgment condition for our method to recover the depth image. Experimental results demonstrate our method obtained the millimeter-accuracy depth image in the confidence interval using one tenth photons of traditional method each pixel. Thus our method will be of considerable value to fast 3D imaging in LLL scene, such as remote sensing and military reconnaissance.

10406-19, Session PWed

11 years of Rayleigh lidar observations of gravity wave activity above the southern tip of South America (Río Gallegos, Argentina, 51.6ºS, 69.3ºW)

Jacobo O. Salvador, Instituto de Investigaciones Científicas y Técnicas para la Defensa (Argentina) and CONICET (Argentina); Pablo Llamedo Soria, Univ. Austral (Argentina); Jonathan Quiroga, Consejo Nacional de Investigaciones Científicas y Técnicas (Argentina); Eduardo Quel, Instituto de Investigaciones Científicas y Técnicas para la Defensa (Argentina); Peter Alexander, Univ. de Buenos Aires (Argentina); Rodrigo Hierro, Alejandro de la Torre, Univ. Austral (Argentina)

Gravity wave (GW) activity is analyzed using Temperature (T) data retrieved from a Rayleigh Lidar at Río Gallegos, Argentina (51.6ºS, 69.3ºW). GW characteristics are derived from 302 observations providing more than 960

of high-resolution lidar data between 20 km and 56 km height between August 2005 and December 2015.

Temperature measurements from the Rayleigh scattering are evaluated through a DIAL system (Differential Absorption Lidar). Rayleigh backscattered photons are emitted by an Excimer (XeCl) laser at 308 nm (300 mJ maximum energy) and the third harmonic of Nd-YAG laser at 355 nm (130 mJ maximum energy). This lidar is the southernmost outside Antarctica. Located 300 km leeward of the southern Andes and 70 km North of the strait of Magellan. Río Gallegos is an exceptional place to observe large amplitude GW where the principal sources are the orography and the spontaneous adjustment processes around the jet in the stratosphere.

During the spring (September to November) the polar vortex weakens and advances northward surpassing Río Gallegos and rapidly changing the conditions for GW.

The mean specific potential energy (PE) is a proxy for GW activity. PE statistical differences inside, outside and in the edge of the polar vortex are analyzed. Also, the sensitivity of T perturbation to different integration time of backscattered signals is studied.

10406-20, Session PWed

Potential of UAV LIDAR systems for geospatial mapping

Ahmed Elaksher, Subodh Bhandari, California State Polytechnic Univ., Pomona (United States)

Shorelines are imperative for coastal ecosystems and activities. Despite this simplicity, accurate and precise extraction of these features is a challenging task due to the complicity of water bounding zones. Shoreline mapping has been carried out through a variety of techniques such as traditional surveying and aerial mapping. As spatial resolution and geospatial mapping technologies improved in the last few years, satellite images and active remote sensing systems have also been introduced to produce high quality shorelines. The focus of this research is on generating reliable shorelines from satellite images and LIDAR datasets. Different classification algorithms were implemented and tested followed by a number of image processing techniques to vectorize shoreline pixels. The geometric accuracy and the completeness of the results are presented and evaluated. Results show the benefits of adding ranging data in improving both shoreline recognition and accuracy.

10406-21, Session PWed

Lidar observations of long range dust transport over Mauna Loa Observatory

Jalal-ud-din Butt, Nimmi C. P. Sharma, Central Connecticut State Univ. (United States); John E. Barnes, National Oceanic and Atmospheric Administration (United States)

A bistatic CCD camera lidar (CLidar) was used at the National Oceanic and Atmospheric Administration's Mauna Loa Observatory (MLO) to map aerosol light scattering. Laser light from a 532 nm, 20 watt, Nd:YAG laser was vertically transmitted into the atmosphere and the scatter off clouds, aerosols and air molecules was detected using a CCD camera with wide angle optics and a laser line filter. The intensity of each CCD camera pixel imaging the beam was normalized to a molecular scattering model in an aerosol free region for subtraction of molecular scattering. Aerosol extinction was derived using a column average aerosol phase function derived from AERONET sun photometer measurements at MLO. The CLidar design allows measurements of aerosol scattering all the way to the ground without an overlap correction. MLO, at 3397 m.a.s.l., typically receives free tropospheric air. Though during spring months, prevailing winds can transport dust from Asian sources with high dust activity over MLO. Aerosol scattering measurements were taken by the CLidar during spring months at MLO and revealed extinction peaks at mid-range altitudes. Back trajectories of these peaks were conducted using NOAA's Hybrid Single Particle Lagrangian Integrated Trajectory (HYSPLIT) model and found their origins to be Eastern Asian sources of high dust activity. Relative humidity data from radiosondes and the NOAA lidar's water vapor channel were examined to differentiate aerosol scattering from tenuous cloud scattering. This paper presents aerosol extinction data with observations of Asian dust as measured by the CLidar during spring months at MLO.

10406-22, Session PWed

Applications of synergistic combination of remote sensing and in-situ monitoring of urban air quality

Adrian Diaz Fortich, NOAA-CREST (United States)

Understanding the spatial distribution of aerosols can shed light on atmospheric dynamics, aerosol transport and particulate pollution. Moreover, due to the harmful effects of particulate pollution on human health, it is of special interest to monitor air quality at high resolution in populated urban areas. In this study, multiple remote sensing and in-situ measurements are combined in order to obtain a more comprehensive understanding of the aerosol distribution in New York City. Measurement of the horizontal distribution of aerosols is performed using a scanning eye-safe elastic-backscatter mini micro-pulse lidar. Vertical distribution of aerosols is measured with a multi-wavelength lidar. Wind measurements are obtained from multiple meteorological stations and available wind profiler data for New York City. Our analysis also includes in-situ measurements of particulate matter (PM2.5) from sampling stations throughout the area of interest. These observations are combined to understand dynamics of the boundary layer and inhomogeneous distribution and transport of aerosols.

Conference 10407: Polarization Science and Remote Sensing VIII

Tuesday - Wednesday 8 –9 August 2017

Part of Proceedings of SPIE Vol. 10407 Polarization Science and Remote Sensing VIII

10407-1, Session 1

A fast Stokes polarimeter

Israel J. Vaughn, The Univ. of New South Wales (Australia); Andrey S. Alenin, J. Scott Tyo, UNSW Canberra (Australia)

Designing polarimetric systems directly in the channel space has provided insight into how to design new types of polarimetric systems, including systems which use carriers in hybrid domains of space, time, or spectrum. Utilizing linear systems theory, we present a full Stokes imaging polarimeter design which has the potential to operate at the full frame rate of the imaging sensor of the system by utilizing a hybrid spatio-temporal carrier design. The design places channels on the faces and the edges of the Nyquist cube resulting in the potential for the temporal Nyquist limit to be achieved, provided that the spatial frequency of the objects being imaged are bandlimited to less than 0.25 cycles per pixel. If the objects are not spatially bandlimited, then the achievable temporal bandwidth is more difficult to analyze. However, a spatio-temporal tradeoff still exists allowing for increased temporal bandwidth. We present the design of a ``Fast Stokes'' polarimeter and some simulated images using this design.

10407-2, Session 1

Real-time Stokes polarimeter using three polarized beam splitter

Shuhei Shibata, Utsunomiya Univ. (Japan); Shuichi Kawabata, Tokyo Polytechnic Univ. (Japan); Yukitoshi Otani, Utsunomiya Univ. (Japan)

This paper describes real-time, very small and cheap Stokes polarimeter using three polarized beam splitters (PBSs). Each s1, s2 and s3 of Stokes parameters is measured by the PBSs. However this technique has to separate three beams keeping unknown incidental polarization state. To overcome this problem, three same normal beam splitters (BSs) are possible to separated two beams keeping polarized state. An alignment of three BSs is set orthogonal in transmission part and reflection part. In transmission part, the polarization state after two BSs can be canceled change of polarization state of first BS by change of second orthogonal BS. In reflection part is same theory. If you set two pear of this keeping polarization beam splitter, you can separate three beams keeping incidental polarization state. After separated beams, three PBS can measure Stokes parameters easily. At first we checked effect of the keeping polarization beam splitter using spectoscopic Mueller matrix polarimeter. We got Mueller matrixes having max 3.3% value of transmission and reflection from unit matrix during from 450nm to 700nm. In second we checked Stokes parameters after a rotating polarizer and a quarter wave plate in this Stokes polarimeter. In two condition results, an error had 5.6%. Finally we checked measurement speed of this real-time Stokes polarimeter using rotating quarter wave plate. From this result this Stokes polarimeter is possible to measure Stokes parameter in 15Hz. This measurement speed depends on detection speed of six PIN photodiodes and transfer speed of AD convertor.

10407-3, Session 1

Snapshot spatially heterodyned imaging Fourier transform spectropolarimeter

Eddie J. Youngs, Michael W. Kudenov, Michael J. Escuti, North Carolina State Univ. (United States); Jim Schwiegerling, The Univ. of Arizona (United States)

The development, calibration, and implementation of a snapshot spatially heterodyned imaging fourier transform spectropolarimeter (SHIFT) is detailed. While conventional scanning, imaging fourier transform spectroscopy techniques incorporate a Michelson interferometer and modulation mirrors, the described SHIFT utilizes a set of common-path, mechanically robust birefringent prisms to generate a set of interference fringes. By leveraging the data provided by these fringes, per pixel spectral and polarimetric data across the entire imaged scene is obtained. Incident light is first passed through an analyzer array, which directs the top-half of the imaged scene through a quarter-wave plate and the bottom-half through a linear polarizer. A lenslet array then images both halves into a series of subimages. These subimages are propagated through a set of common-path birefringent prisms to generate interference fringes which overlay onto the subimages. These fringes are heterodyned by a pair of polarization gratings and passed onto a focal plane array. Mathematically, the set of subimages can be rearranged into a cube. Each x,y location on this cube represents a pixel location, whereas the z-axis at this location corresponds to a sampled version of the interferogram for this pixel. The sample locations in the interferogram are different for each pixel, with the same sampled resolution providing identical spectral information. By leveraging the data provided by these fringes, per pixel spectral and polarimetric data across the entire imaged scene is obtained. To achieve this, a theoretical model for the system was developed and validated with data from proof of concept experiments. With this model, a prototype assembly has been designed and calibrated via multiple techniques, including exposing the sensor to a target spectrum of monochromatic light in multiple polarization states. A variety of scenes was then measured with the calibrated prototype to demonstrate its functionality. Applications for this sensor includes high-resolution spectroscopy and polarimetry in biomedical imaging, remote sensing, and machine vision.

10407-4, Session 1

Intrinsic coincident full-Stokes polarimeter using stacked organic photovoltaics and architectural comparison of polarimeter techniques

Ruonan Yang, Pratik Sen, Brendan T. O'Connor, Michael W. Kudenov, North Carolina State Univ. (United States)

An intrinsic coincident full-Stokes polarimeter is demonstrated by using stain-aligned polymer-based organic photovoltaics (OPVs) which can preferentially absorb certain polarized states of incident light. The photovoltaic-based polarimeter is capable of measuring four stokes parameters by cascading four semitransparent OPVs in series along the same optical axis. Two wave plates were incorporated into the system to modulate the S3 stokes parameter so as to reduce the condition number of the measurement matrix. The model for the full-Stokes polarimeter was established and validated from radiometric calibration which showed an average RMS error of 0.84%. The optimization based on minimizing the condition number of the 4-cell OPV design showed that a condition number of 2.4 is possible. The performance of this in-line polarimeter concept was compared with other polarimeter techniques (Division of Time (DoT), Division of Amplitude (DoAm), Division of Focal Plane (DoFP) and Division of Aperture (DoA) Polarimeter) from signal collection abilities and signal-to-noise ratio (SNR) perspective. This in-line polarimeter concept has the potential to enable both high temporal (as compared with DoT polarimeter) and high spatial resolution (as compared with DoFP and DoA polarimeter) at the same time. It has the same SNR advantage as the DoAm polarimeter theoretically, twice as much as other techniques, but the former is significantly more compact than the latter.

10407-5, Session 1

Characterization of cameras for all-sky polarization measurements during the 2017 solar eclipse

Taiga Hashimoto, Hokkaido Univ. (Japan); Laura M. Dahl, Seth A. Laurie, Joseph A. Shaw, Montana State Univ. (United States)

A solar eclipse is one of the most famous natural phenomena and on 21 August 2017 we will measure the skylight polarization during a total solar eclipse in Rexburg, Idaho. Previous research has shown that during totality the sky polarization pattern is altered significantly to become nominally symmetric about the zenith. However, there are still questions remaining about the details of how surface reflectance near the eclipse observation site and aerosol properties influence the totality sky polarization pattern. We will study how skylight polarization in a solar eclipse changes through each phase and how surface and atmospheric features affect the measured polarization signatures. During this solar eclipse, the estimated time for totality is under three minutes. With the short window of time to take measurements and the drastic change from day to totality conditions, instrument limitations can be problematic. Therefore, fully characterizing the cameras and fisheye lenses is critical. These measurements include finding the camera sensitivity and its relationship to the required exposure times, the camera's spectral response function, and angular pixel mapping with the fisheye lens. Additional steps include comparing daytime polarimetric images to an existing polarimetric radiative transfer model and taking measurements during twilight and nighttime.

10407-6, Session 2

Advances in modeling polarimeter performance *(Invited Paper)*

Russell A. Chipman, College of Optical Sciences, The Univ. of Arizona (United States) and Airy Optics, Inc. (United States)

Polarization modeling methods developed for the NASA MSPI, MAIA, and several Mueller matrix imaging polarimeters will be discussed. This algorithm development culminated in the Polaris-M polarization analysis program. Polarimeter design requires attention to issues of wavelength and angle sensitivities of polarization elements, as well as target or sample polarization, polarization aberrations of imaging systems, and thermal and mechanical effects. The realistic modeling of polarization elements involves precise crystal optics models, rigorous coupled wave analysis with anisotropic materials, ghost reflection analysis, and the athermalization of polarization properties such as retardance.

Artifacts in polarimeters are apparent polarization features which are not real but result from the systematic errors in the polarimeter. The polarization artifacts are very different between division of focal plane, spectral, and time modulation polarimeters. Artifacts result from many sources such as source properties, micropolarizer arrays, coatings issues, vibrations, and stress birefringence. Modeling examples will be presented including the athermalization of retarders and polarization aberration analyses for polarimeters.

10407-7, Session 2

Modeling the polarization aberrations of optical elements

Kyle Hawkins, Russell A. Chipman, Airy Optics, Inc. (United States)

Conventional ray tracing calculates the shape of wavefronts, but not their amplitudes or polarization states. Thin films, polarizers, diffraction gratings, crystals and even lenses, in addition to affecting the shape of wavefronts make contributions to the relative phase and amplitude of the light in an Optical System.

These contributions will vary with polarization, field, and pupil position, adversely affecting the system performance. For sensitive optical systems, it is necessary to design around these effects with polarization ray tracing algorithms which are not only related to the optical path length, but include polarization dependent surface effects. This is done by supplementing the optical path length with calculations of the polarization ray tracing matrix (PRT).

The adverse effects can then be described as the deviations from an identity Jones Pupil (polarization aberration), and Zernike polynomials can then be used to provide a simplified generalization of the polarization aberration that is still accurate. The Zernike terms will describe the amplitude transmission along the ray paths, the amplitude aberration, which is normally unavailable with a geometrical ray trace, and the Zernike terms will have the relative phase accumulations along ray paths, that describe phase variation with polarization state.

Three different optical elements will be modeled: a wire grid polarizer, an anisotropic diffraction grating, and an injection molded lens with the polarization ray tracing software, Polaris-M. For each optical element, the polarization aberrations will be calculated and fit to Zernike polynomials. The effects of the aberrations on system performance will then be discussed and categorized.

10407-8, Session 2

End-to-end multi-scale simulations of optical systems containing isotropic and anisotropic components with arbitrary geometries using full vector wave propagation

Steven Bos, Sebastiaan Haffert, Christoph Keller, Leiden Observatory (Netherlands)

Precise three-dimensional modelling of the (off-axis) point spread function (PSF) to identify geometrical and polarization aberrations is important for many optical systems. In order to characterise the PSF of the system in all Stokes parameters, an end-to-end multi-scale simulation has to be performed that includes all relevant physics.

We present the first results of a python code that we are developing to perform end-to-end wave propagation (no ray-tracing), including all relevant physics: vector diffraction in isotropic and anisotropic materials, reflection and refraction of arbitrary surfaces and interference effects. The code will operate on multiple scales: from meter size (e.g. telescope mirrors) to structures on the order of wavelengths (e.g. waveguides). Current capabilities of the code are: near- and far-field vector diffraction effects of propagating waves in homogeneous isotropic and anisotropic materials, refraction and reflection of flat parallel surfaces. Next steps in the development are to include reflection and refraction of arbitrarily shaped surfaces and interference effects in thin films.

An example application is the accurate modelling of the PSFs of future space and ground-based telescopes. These will try to perform the first observations of Earth-like exoplanets ten billion times fainter than their host star. To evaluate the performance of the entire system including advanced coronagraphic, spectroscopic, polarimetric and adaptive optics techniques, where an end-to-end characterisation on all scales is needed.

10407-9, Session 2

Polarization fringe modeling for the DKIST retarders

David M. Harrington, National Solar Observatory (United States)

We present polarization fringe models based on a new application of the Berreman calculus. The new 4m Daniel K. Inouye Solar Telescope has very challenging specifications for retarders. The optic must operate in a 300W beam with flux from <320nm to >25 micron wavelength and a clear aperture over 105mm. Thermal performance and polarization fringes represent a major challenge for accurate calibration of instruments operating at 380nm to 5000nm wavelength and large fields of view. Predicting fringe behavior, field dependence, temperature dependence and allowing trade studies on the impacts of various anti-refelction coatings have been enabled with the new fringe models. We also create models for retarders other solar and night-time spectropolarimeters and compare with observations to verify the models.

10407-10, Session 3

Statistics for linear Stokes polarimetry

Nathan Hagen, Utsunomiya Univ. (Japan)

We present a method of calculating analytic formulas for the second-order statistics --- the signal, variance, and SNR --- of a variety of linear Stokes polarization measurement techniques. The advantage of the method is that it is easy to perform and produces simpler formulas than previously published methods. Using the resulting formulae, we compare a number of different polarimetric designs and discuss how these can be used to optimize instrumentation.

10407-11, Session 3

Single image super-resolution via regularized extreme learning regression for imagery from microgrid polarimeters

Garrett C. Sargent, Univ. of Dayton (United States); Bradley M. Ratliff, Univ. of Dayton Research Institute (United States); Vijayan K. Asari, Univ. of Dayton (United States)

The advantage of division of focal plane imaging polarimeters is their ability to obtain temporally synchronized intensity measurements across a scene; however, they sacrifice spatial resolution in doing so due to their spatially modulated arrangement of the pixel-to-pixel polarizers and often result in aliased imagery. This shortcoming is largely overcome through advanced demosaicing strategies that minimize the effects of false polarization while preserving as much high frequency content as possible. While these techniques can yield acceptable imagery, they tend to be computationally complex and the spatial resolution is often reduced below the native capabilities of the focal plane array. Here we propose a super resolution method based upon previously trained extreme learning machines (ELM) that attempt to recover missing high frequency content beyond the spatial resolution of the sensor while suppressing false polarization signatures resulting from pixel-to-pixel misalignment. For each channel of an image, the proposed method utilizes two ELM models: the first predicts the missing high frequency components, whereas the second predicts the pixel-to-pixel alignment errors associated with the low frequency components of each channel. Adding the results of the two ELM models together yields a sharper image with minimized false polarization artifacts. This provides a fast and computationally simple way of demosaicing raw microgrid polarimetric imagery while simultaneously improving image resolution. The technique is applied to both visible and long-wave infrared data.

10407-12, Session 3

Channeled linear imaging polarimetry using iterative reconstruction

Dennis J. Lee, Charles F. LaCasse IV, Julia M. Craven, Sandia National Labs. (United States)

Channeled linear imaging polarimeters amplitude modulate the linear stokes parameters onto spectrally broadband interference fringes. The Stokes parameters are demodulated by performing a 2D Fourier transform on the intensity pattern and applying 2D filters to isolate channels for further processing. A disadvantage of processing the fringes in the frequency domain is that reconstruction of the Stokes parameters suffers from high sensitivity to noise. Noise or cross talk between channels will degrade the quality of reconstruction. We propose an iterative reconstruction approach to improve on Fourier domain processing and achieve a more accurate and noise robust calculation of the Stokes parameters. This work will outline the theoretical approach and demonstrate simulated results.

10407-13, Session 4

Moving towards more intuitive display strategies for polarimetric image data

Bradley M. Ratliff, Univ. of Dayton Research Institute (United States); J. Scott Tyo, UNSW Canberra (Australia)

The display of polarimetric image data has been a subject of considerable debate. Display strategies range from direct display of the Stokes vector images (or their derivatives) to false color representations. In many cases, direct interpretation of polarimetric image data using traditional display strategies is not intuitive and can at times provide confusion as to what benefit polarimetric information is actually providing. Here we investigate approaches that attempt to augment the s0 image with polarimetric information, rather than directly display it, as a means of enhancing the baseband s0 image. The benefit is that the polarization-enhanced visible or infrared image maintains a familiar look without the need for complex interpretation of the meaning of the polarimetric data, thus keeping the incorporation of polarimetric information transparent to the end user. We take a more subjective approach to image enhancement than current techniques employ by simply seeking to improve contrast and shape information for polarized objects within a scene. We find that such approaches provide clear enhancement to the imagery when polarized objects are contained within the scene without the need for complex interpretation. We investigate these display strategies using both visible and infrared data.

10407-14, Session 4

Engaging Montana high school students in optical sciences with a polarization photo contest

Martin J. Tauc, Montana State Univ. (United States); Jim Boger, Flathead Valley Community College (United States); Andrew Hohne, Laura M. Dahl, Paul W. Nugent, David W. Riesland, Benjamin Moon, Carol L. Baumbauer, Orrin Boese, Joseph A. Shaw, Wataru Nakagawa, Montana State Univ. (United States)

Getting students interested in science, specifically in optics and photonics, can be a significant challenge. We developed and implemented an outreach campaign which sought to engage high school students in the science of polarized light. The outreach was motivated and paid for by a NASA-sponsored project to investigate the use of nanostructure-based, polarization-selective bandpass filters for atmospheric science applications. Over the course of a few months, we traveled to Montana high schools and gave a presentation on the polarization of light. The presentation covered the physics of light, the ways that it becomes polarized, how polarization is useful, and how to take pictures with linear polarizers to see polarization. Students were given polarizers and instructions to take pictures that show polarization in either a natural setting or a contrived scene. Each participant submitted his or her entry - a photo along with an explanation of how polarization was involved - for evaluation by a panel of judges. A good photograph illustrated polarization in a well composed and interesting manner. The paragraph-long writing component was judged on how the photo was taken, the scientific explanation of how polarization was present, and why it was interesting. The contest was open to all high school students in the state. We visited 13 high schools, and presented live to approximately 450 students. A video version of the presentation and other resources for the contest were also made available online through the Montana Space Grant Consortium website.

10407-16, Session 5

Polarization-selective infrared bandpass filter based on a two-layer subwavelength metallic grating

Andrew Hohne, Benjamin Moon, Carol L. Baumbauer, Tristan Gray, James Dilts, Joseph A. Shaw, David L. Dickensheets, Wataru Nakagawa, Montana State Univ. (United States)

We present the design, fabrication, and optical characterization of a polarization-selective infrared bandpass filter based on a two-layer subwavelength metallic grating for use in cloud polarimetric imaging. Gold nanowires were deposited via physical vapor deposition (PVD) onto a silicon surface-relief grating that was fabricated using electron beam lithography. Optical characterization with a broad-spectrum tungsten halogen light source and a grating spectrometer showed normalized peak TM transmission of 53% with a full-width half-maximum (FWHM) of 122 nm, which was consistent with rigorous coupled-wave analysis (RCWA) simulations. The peak TM transmission wavelength was shifted by as much as 200 nm by changing the period of the grating by less than 100 nm. This device was designed to operate at a wavelength of 1.55-μm, but by altering only the lithography step, multiple gratings sensitive to different wavelengths can be created on the same substrate. Simulation results suggested that device operation relies on suppression of the TM transmission caused by surface plasmon polariton (SPP) excitation at the gold-silicon interface and an increase in TM transmission caused by a Fabry-Perot (FP) resonance in the cavity between the gratings. TE rejection occurs at the initial air-gold interface. We also present simulation results of an improved design based on a two-dielectric grating where two different SPP resonances allowed us to improve the shape of the passband by suppressing the side lobes. This newer design resulted in improved side-band performance, increased peak TM transmission, and a more reliably fabricated device.

10407-17, Session 5

Achromatic and chromatic liquid crystal polymer films at near-infrared wavelengths

Nathaniel Z. Warriner, Michael J. Escuti, Shuojia Shi, Kathryn J. Hornburg, North Carolina State Univ. (United States)

Certain wavelengths bands, especially Y, J, H, and K, have become the main measurement pathway for many of the world's largest telescopes. Additionally, the study of stellar light within of near-infrared (NIR) bands has become the staple in the field of direct imaging. Because of this, there is a growing necessity for customized broadband optics in the near infrared to meet the needs of the astronomers and allow for more precise measurements. We report on complex birefringent films developed for NIR operation, useful to implement wave-plates, vector apodizing phase plates, and polarization gratings. The combination of multi-twist retarders (MTRs) with both direct-write laser scanning or holographic lithography, and allows us to fabricate arbitrary phase patterns via a geometric phase effect and achromatic, super-achromatic, and highly chromatic (dual-band) spectra from 0.5 to 5 microns. MTRs are complex birefringent films with an optic axis variation along 1D/2D/3D. They consist of two or more chiral liquid crystal (LC) layers on a single substrate and with a single photo-alignment layer. Importantly, subsequent LC layers are aligned directly by prior layers, allowing simple fabrication, achieving automatic layer registration, and resulting in a monolithic film with a continuously varying optic axis. MTRs can be used for a wide range of remote optical sensing, both earth- and space-based. Here, we will review our current and prior MTR films being used for NIR astronomical observation, and discuss the realistic opportunities and limitations ahead for improved precision and design-complexity for retardation and wavefront(phase).

10407-18, Session 5

Polarization conversion systems based on geometric-phase microlenses

Jihwan Kim, Michael W. Kudenov, Michael J. Escuti, North Carolina State Univ. (United States)

Many optical devices and systems require polarized light for operation. However, preferable light sources are unpolarized, including LED, CCFL, incandescent lamps, and natural light. While many polarizing elements, including sheet polarizers or various birefringent prisms, can convert unpolarized light into polarized, they are inherently lossy, since they operate by either absorbing the unwanted light or redirecting it in an unwanted direction, which leads to more than 50% loss of optical power. We report on a new polarization conversion system (PCS) based on geometric phase holograms (GPHs) and a patterned retarder (PR). The first GPH acts essentially as thin-film polarizing lens that can separate (i.e., converge/diverge) unpolarized light into two orthogonal circular polarizations with high efficiency. The PR is a birefringent optical element having two patterned regions, designed to alter the separated polarization states into a target output polarization. The second GPH located next to the PR homogenizes and recollimates the output light. A simple arrangement of these elements results in a thin, monolithic, and flat surface device, with the ability to convert unpolarized input into linearly polarized output across most of the visible bandwidth. We experimentally demonstrate GPH-PCS that manifests about 70% conversion efficiency for ±10 degrees input light divergence. Here, we describe the concept and characterize our first prototypes by evaluating conversion efficiency, correct polarization transmittance, and divergence/uniformity of the output light. We also discuss the realistic opportunities and limitations for this approach.

10407-19, Session 5

Fraunhofer line optical correlator for improvement of initial orbit determination

Brett A. Pantalone, Michael W. Kudenov, North Carolina State Univ. (United States)

The design of a Fraunhofer line optical correlator is detailed. The instrument described herein correlates a reflected solar spectrum against multiple Fraunhofer absorption lines to estimate the velocity of the reflecting body. By using a spatial light modulator (SLM) as a photomask for known solar absorption lines in the range of 512-552 nm, the ratio of Doppler shifted solar energy to the total received energy can be calculated. Although the reflected light from targets in high orbit is relatively weak, signal-to-noise ratio (SNR) is enhanced by the measurement of multiple Fraunhofer lines in a single snapshot image. Simulations indicate that prediction of orbital parameters is improved by incorporation of this velocity information, and in some cases the number of line-of-sight measurements can be reduced from three to two.

10407-40, Session 5

Adaptive display strategies for polarization data

J. Scott Tyo, UNSW Canberra (Australia); Bradley M. Ratliff, Univ. of Dayton Research Institute (United States); Andrey S. Alenin, Israel J. Vaughn, UNSW Canberra (Australia)

Display of polarization information has always been a challenge. Since the human vision system cannot directly perceive polarization, systems are forced to represent polarization information in a visual channel that is

normally used for something else: e.g. color, texture, or motion. A handful of strategies are widely used with polarization data, one of which is a mapping that places angle of polarization (AOP), degree of linear polarization (DoLP), and s0 into the color channels hue saturation and value. We recently presented an extension of that mapping that provides significant benefits in areas of a polarization scene that have high DoLP but low s0. The circumstance of high DoLP and low s0 is relatively common in both emissive and reflective polarimetry, so this problem can be important. Our new strategy uses the local spatial statistics of AOP as metric of confidence in the polarization measurement; regions of high AOP variability tend to imply noisy polarization measurements. In this poster presentation, we will demonstrate our new system with data from several different sensors, and we will compare its properties with other popular polarization rendering schemes.

10407-20, Session 6

A nine-channeled partial Mueller matrix polarimeter

Andrey S. Alenin, Israel J. Vaughn, J. Scott Tyo, UNSW Canberra (Australia)

We have recently introduced channeled-partial Mueller matrix polarimeters as a potential design for measuring a limited number of Mueller elements for remote sensing discrimination. Because the polarization information in such systems is modulated in space or spectrum, the corresponding carrier domain ends up sharing two different types of information, thus leading to a reduction of bandwidth for each. In this work, we concentrate on an efficient nine-channel/nine-reconstructables design, which reduces the noise power in the reconstructed measurements and limits the associated resolution loss by limiting the overall complexity of the system. Employing structured decomposition techniques allows us to produce a system description that provides an analytically deducible set of reconstructables that include m00, any two linear combinations of the elements within the diattenuation vector, any two linear combinations of the elements within the polarizance vector, as well as the linear combinations specified by the Kronecker product of the diattenuation and polarizance vectors. Finally, we optimize the available polarimeter parameters to align the nine reconstructables with the desirables derived from sample data. Though class separability is impacted, the ability to discriminate between different objects is maintained.

10407-21, Session 6

Hyperspectroscopic Mueller-matrix polarimeter based on channeled polarimetry

Kazuhiko Oka, Kodai Sayama, Hiroshi Michida, Hokkaido Univ. (Japan)

We describe the principle and the demonstrative experiment of a novel hyperspectroscopic Mueller-matrix polarimeter based on channeled polarimetry. The channeled polarimetry is a method for measuring polarimetric parameters using a cosinusoidally-modulated spectrum. We previously reported on a snapshot spectroscopic Mueller-matrix polarimeter based on channeled polarimetry. In this presentation, we describe its expansion for the hyperspectroscopic Mueller-matrix measurement. The developed method uses both spectrally and spatially modulated spectrum. A light from a polychromatic source first passes through a spectral polarization state modulator, consisting of a polarizer and two high-order retarders, and is then impinges upon a sample under measurement. The light emerging from the sample is fed into a polarization state analyzer using spatial carriers, including two Savart plates. The hyperspectral image obtained from the system is cosinusoidally modulated along both wavenumber- and space-axes, and the respective spatio-spectral frequency components carry the information of the sixteen Mueller-matrix elements of the sample. The Fourier analysis of the hyperspectral image allows us to demodulate the spatio-spectrally resolved Mueller matrix of the sample. This method has a feature that it requires neither mechanical nor active components for polarization modulation. For the experimental demonstration, two different types of experimental systems were assembled. The first system uses a pushbroom-type hyperspectrometer using a grating spectrometer with a two-dimensional CCD sensor, whereas the second system is based on the wavelength-scanning type hyperspectrometry using a wavelength-scanning laser. Both systems demonstrated the feasibility of the present principle in the visible region.

10407-22, Session 7

Remote sensing of atmospheric aerosols and clouds using the AirMSPI imaging polarimeter

Gerard van Harten, David J. Diner, Feng Xu, Brian E. Rheingans, Jet Propulsion Lab. (United States); Mick Tosca, The School of the Art Institute of Chicago (United States) and Jet Propulsion Lab. (United States); Felix C. Seidel, Jet Propulsion Lab. (United States)

Ambient particulate matter is a major global environmental risk factor, causing millions of premature deaths per year. In addition, the direct interaction of aerosols with sunlight, and the indirect effect through their impacts on cloud formation, contribute large uncertainties to the degree of warming expected in a future climate. The spatial heterogeneity of aerosols and short atmospheric lifetimes motivate the need for global observations of their amount and spatial distribution, their optical and microphysical properties (such as particle size distribution), and composition. Particle abundances, microphysical properties, and optical proxies for composition (such as the complex refractive index) are retrievable from multi-angle, multi-wavelength, radiometric and polarimetric observations of scattered sunlight. High spatial resolution enables observations of aerosol spatial gradients. A key technical challenge is high polarimetric accuracy (~0.005 in the degree of linear polarization) in a multispectral imager over a broad spectral range. JPL's Airborne Multiangle SpectroPolarimetric Imager (AirMSPI) instrument has demonstrated the capability of meeting this objective using a dual photoelastic-modulator-based measurement technique. The data processing pipeline, on-ground and in-flight polarimetric calibrations, and performance comparisons with the NASA Research Scanning Polarimeter (RSP) and the SRON Spectropolarimeter for Planetary EXploration (SPEX) will be discussed, along with example aerosol and cloud droplet size retrievals from recent airborne field campaigns. The AirMSPI modulated polarization technique is employed in JPL's future Multi-Angle Imager for Aerosols (MAIA) satellite instrument, currently in development. MAIA is scheduled for launch around 2020-2022 and will study the health effects of different aerosol components in major cities across the globe.

10407-23, Session 7

Cloud thermodynamic phase detection using an all-sky polarimeter

Laura M. Dahl, Martin J. Tauc, Joseph A. Shaw, Montana State Univ. (United States)

Clouds strongly influence weather and climate, as they shade the surface from direct sunlight, increase the greenhouse effect, and regulate surface precipitation, thereby contributing to a net warming or cooling effect on the Earth's radiation budget. Knowing the cloud thermodynamic phase, if the cloud is composed of ice crystals or liquid particles, can help in accurately simulating the cloudy atmosphere to better understand how clouds influence Earth's climate. Clouds containing liquid particles, such as cumulus clouds, are generally optically thick and tend to have a net cooling effect. Thin cirrus clouds on the other hand, have a net warming effect on the Earth's radiation budget. Knobelspiesse et al. (Atmos. Meas. Tech., 8, 1537–1554, 2015) showed that for zenith observations, the direction of linear polarization (the sign of the S1 Stokes parameter) can be used to detect cloud thermodynamic phase when observed with a ground-based passive polarimeter. A positive S1 value indicates a liquid cloud, while a negative S1 values indicates an ice cloud. In this paper, we show results from a ground-based, all-sky imaging Stokes polarimeter used to detect cloud thermodynamic phase by analyzing the sign of the measured S1 parameter. We used our all-sky polarimeter, operating in 10 nm band wavelengths at 450 nm, 530 nm, and 780 nm, to detect liquid, ice, and mixed layered clouds. The thermodynamic phase was independently verified with a dual-polarization lidar.

10407-24, Session 7

Polarimetric time-lapse imaging of aurorae with DSLR color cameras

Frans Snik, Michael J Wilby, Louis Martin, Felix C. M. Bettonvil, Leiden Observatory (Netherlands); Michiel Rodenhuis, Ramón Navarro, Netherlands Research School for Astronomy (Netherlands); Hervé Lamy, Belgian Institute for Space Aeronomy (Belgium)

We present the design and first results from a polarimetric instrument for time-lapse imaging of the aurora. The auroral red line is polarized because of the anisotropic electron flux that bombards the upper atmosphere during a geomagnetic storm, and can therefore be used to study the local effects of such a storm. The aurora consists of three main spectral features: the green and red lines (due to atomic oxygen), and the blue band (due to molecular nitrogen). Regular color cameras with RGB filters can therefore constrain the spectral content of the auroral signal. We have constructed a polarimeter from two synchronized Canon 6D cameras with regular polarization filters in front of the identical objective lenses to deliver the first two Stokes parameters. We use the background stars to map pairs of frames onto each other, and bin down to reduce the effects of pixel gain variations to the polarimetric sensitivity. We have performed auroral observations at Skibotn Observatory (Norway) in March 2016, and detect a clear polarization signal for the red line at a level of ~2%, perpendicular to the magnetic field lines. This low-cost set-up therefore provides the first imaging polarimetry of aurorae, and can easily be upgraded to furnish tomographic measurements from several locations.

10407-25, Session 8

The hand-hold polarization-sensitive spectral domain optical coherence and its applications

Hao Liu, Nanjing Univ. of Science and Technology (China)

The advantages of polarization-sensitive spectral domain optical coherence tomography (PSOCT) include that PSOCT is able to measure the polarization properties of samples, such as phase-retardation, diattenuation, depolarization, and optical axis orientation. In contrast to conventional OCT, PSOCT provide a convenient method to distinguish the differences between the diseased area and normal area in tissues with additional contrast in images. Conventionally, the sample arm of PSOCT is fixed on the stage where biomedical tissues or models is placed, and the OCT images is acquired by scanning with galvanomer-based mirrors. While this method provides accurate imaging quality, the clinical experiments are limited by stationary of sample arm. To be applied in the practical diagnosis, a promising way is to design a hand-hold device. To this end, it is required that probe is assembled with a small volume to allow for comprehensively imaging large tissues areas at a microscopic scale, and is available to move on different samples to be acquired quickly with negligible motion artifacts. Meanwhile, the probe should be manufactured wih well stability to avoid system jitter error while it is used to detect the biological tissues in vivo. In this work, a design of a hand-hold fiber-based PSOCT is described, the parameters that influence the performance of the system are considered. The images of several examples are presented to demonstrate the capability of the system.

10407-26, Session 9

Polarimetric LIDAR with FRI sampling for target characterization

Erandi Wijerathna, Charles D. Creusere, David G. Voelz, New Mexico State Univ. (United States); Juan Castorena, Ford Motor Co. (United States)

Polarimetric LIDAR is a significant tool for current remote sensing applications. Extensive developmental and field studies have been conducted with polarimetric LIDARs such as MAPL (Multiple-wavelength Airborne Polarimetric LIDAR) for target identification and characterization in agriculture and vegetation settings. The conventional Nyquist sampling used in most implementations, however, requires vast data collection and storage to achieve satisfactory depth and spatial resolutions. To address this problem, we previously introduced an FRI (Finite Rate of Innovations) model for application to third generation full-waveform (FW) LIDAR systems. The concept is to detect time resolved 1D signals produced by laser pulses reflecting from the intercepted targets and use the FRI approach to effectively sample and record the signals at sub-Nyquist rates. We have demonstrated that laboratory targets within the beam footprint can be identified and ranged with high accuracy (i.e. sub spot-size target localization). Here, we describe the latest results with the FRI approach and extend the capability of the laboratory system to characterize targets with differing polarization signatures. Targets with different retardance characteristics are illuminated by a linearly polarized laser beam and the return pulse intensities are observed with a 3-channel, time division, polarimetric setup. The return signals are resolved using the FRI model analysis and Stokes vectors are constructed. The Stokes vectors are then used to identify the retardance properties of the targets within limitations. Hence, the proposed FRI based LIDAR approach can be used to achieve sub laser spot size target localization and to resolve target characteristics within the spot.

10407-27, Session 9

Active infrared polarimetric imaging demonstrator by orthogonality breaking sensing

Francois Parnet, Julien Fade, Institut de Physique de Rennes (France); Noé Ortega-Quijano, Deneb Medical, S.L. (Spain); Ludovic Frein, Goulc'hen Loas, Mehdi Alouini, Institut de Physique de Rennes (France)

Polarimetric imaging systems are likely to reveal contrasts that are not visible on classical intensity images. This ability is especially important in target detection applications where manufactured objects are hidden in a surrounding natural environment. Since their polarization behavior differs strongly from the background, polarimetry may enhance their visibility and improve detection performances. Standard active techniques are mainly based on a fixed polarization state at the illumination and several polarization orientations at the analysis by performing either sequential (division of time techniques) or simultaneous acquisitions (division of amplitude, division of focal plane techniques). We have developed an alternative approach to probe polarization effects, which revisits the standard way of performing polarimetric images.

We report the design of a free-space active infrared polarimetric imaging demonstrator based on the orthogonality breaking technique. With this non-conventional approach, a scene is enlightened by raster scanning with a specific Dual-Frequency Dual-Polarization beam, obtained from a fibered source developed at 1.55 μm. The light backscattered and detected on an avalanche photodiode in a confocal configuration produces an intensity signal comprises a continuous part and a modulated part (beatnote at the frequency difference between the two optical frequencies) whose amplitude is directly linked to the polarization behavior of the targeted point on the scene. Finally, Raw images are built-up digitally on a computer and, polarimetric contrast maps are obtained on homemade scenes within limited acquisition time (~1s). Based on experimental test scenes, we

compare this technique with standard full-field approaches and discuss its benefits and drawbacks.

10407-28, Session 9

Polarization vector signatures for target identification

Diane Beamer, Ujitha A. Abeywickrema, Partha P. Banerjee, Univ. of Dayton (United States)

Objects distant enough to be unresolved images have been studied and manipulated in different ways to attempt to recognize the object based on various characteristics. Most of the effort to recognize objects from space or in space has focused on imaging and spectral analysis, and only a fraction of work has been performed using polarimetry for target identification. Yet in the work that has been performed, it has been demonstrated that polarization signatures do exist, and appear to carry more information and can more easily differentiate between unresolved objects. In recent work, it has been demonstrated that polarization signatures are more distinctive than intensity signatures alone. This work was based on using two of the four Stokes parameters, S0 and S1, to create a vector signature which could be obtained from recording polarization states of reflected sunlight. This work proposes to use full Stokes polarimetry to create vector spaces that can be associated with the object observed. A novel analysis is proposed based on astronomy's color-color technique of analyzing wavelength band intensity of reflected light from objects in space. The proposed vector-vector spaces will provide a method to analyze and statistically compare polarization signatures to a library of objects so that target recognition can be obtained. This work will be based on experimental observations of near field objects to demonstrate the signature methodology.

10407-29, Session 9

Surface parameter based image estimation from application of a scattering model to polarized light measurements

Hanyu Zhan, New Mexico State Univ. (United States) and Research Institute of Highway, Ministry of Transport (China); Hanwan Jiang, New Mexico State Univ. (United States) and Research Institute of Highway, Ministry of Transportation (China); David G. Voelz, New Mexico State Univ. (United States); Zhan Li, Research Institute of Highway, Ministry of Transportation (China); Pengfei Li, Research Institute of Highway, Ministry of Transportation (China); Shoushan Cheng, Research Institute of Highway, Ministry of Transportation (China)

An importance task for remote sensing applications is the characterization of material properties, which can be accomplished by estimating physics-based parameters from optical scattering off a target's surface. In a recent paper, we present a theoretical development of a modified polarimetric bidirectional reflectance distribution function (pBRDF) incorporating both surface and diffuse scattering components.The model is applied to Stokes parameters measurements of scattered light for jointly estimating the complex refractive index (?), slope variance roughness (?2) and diffuse scattering coefficient (?d) of a surface. The parameter estimation results and synthetic Stokes parameters curves generated by the proposed pBRDF models shows close correspondence to the associated measurement values. In the work presented here, we describe a novel approach to estimate surface parameters and generate parameter-based images by extending the modified pBRDF model to the multispectral Stokes parameter-based imaging measurements collected with the University of Arizona's MultiangleSpectroPolarimetric Imager (MSPI). In particular, we analyze the measured Stokes parameters values as a function of time of day and wavelength. Values for ?, ?2 and ?d for each pixel are jointly estimated and statistics associated the estimated values are presented. Multispectral imagesconsisting of the parameter values are generated by using the relevant results for each pixel at different wavelengths and optimized by contrast-ratio enhancement algorithms. The approach offers significant potential for remote targets analysis and novel imaging technology development.

10407-30, Session 10

High contrast observations of circumstellar disks with the Gemini Planet Imager's polarimetry mode *(Invited Paper)*

Maxwell A. Millar-Blanchaer, Jet Propulsion Lab. (United States); Marshall D. Perrin, Space Telescope Science Institute (United States); Bruce A. Macintosh, Stanford Univ. (United States); James R. Graham, Univ. of California, Berkeley (United States); Michael P. Fitzgerald, Univ. of California, Los Angeles (United States); Paul R. Kalas, Univ. of California, Berkeley (United States); Jeffrey K. Chilcote, Dunlap Institute for Astronomy & Astrophysics (Canada); Jason J. Wang, Univ. of California, Berkeley (United States); Li-Wei Hung, Univ. of California, Los Angeles (United States); Sloane J. Wiktorowicz, The Aerospace Corp. (United States); Sebastian Bruzzone, Western Univ. (Canada)

The Gemini Planet Imager (GPI) is a near-infrared high-contrast imager on the 8-m Gemini South telescope, optimized for the direct detection and characterization of extrasolar Jovian-mass planets and circumstellar disks. The instrument includes a dual-channel polarimetry mode designed to image the inherently polarized light scattered off faint debris disks and protoplanetary disks. In the three and half years that it has been operational, GPI has imaged over two dozen circumstellar disks — detecting some for the first time in scattered-light — and carried out polarimetric measurements of brown dwarfs and exoplanets. These observations have let us study the locations and conditions in which exoplanets form in protoplanetary disks, increased our understanding of the composition of extrasolar debris disks, and allowed for the characterization of disk-planet interactions. Here, we review the design, implementation and performance of GPI's polarimetry mode, and highlight a selection of significant scientific results it has enabled.

10407-31, Session 10

Visible, near infrared spectropolarimeter for characterization of the DKIST optical system and polarization properties

Stacey R. Sueoka, David M. Harrington, National Solar Observatory (United States)

We have developed a laboratory spectropolarimeter built to characterize the transmissive and reflective polarization properties of the Daniel K. Inouye Solar Telescope (DKIST) optical components. This includes the full Mueller matrix of retarders, polarizers, mirrors, dichroic coatings, and other optical elements that introduce polarization effects. Characterization is performed at various angles of incidence from 400nm to 1650nm with ~9nm spectral resolution and statistical noise limits >5000 using many automated stages. With this data set, we present tolerance analysis of typical as-built DKIST optics.

10407-32, Session 11

Controlling the spatial coherence and polarization of a quasi-homogeneous, planar electromagnetic source for remote sensing applications

Oscar G. Rodríguez-Herrera, Univ. Nacional Autónoma de México (Mexico)

We present the design and characterization of a quasi-homogeneous, planar electromagnetic source to produce beam-like optical fields with controllable spatial coherence and polarization properties. Dynamic control of the second-order correlation properties of an optical beam is achieved by controlling the spectral density and polarization state distributions at the source plane, as described by the generalized van Cittert-Zernike theorem for the cross-spectral density matrix of a quasi-homogeneous, planar electromagnetic source.

In the proposed design, the spectral density distributions of orthogonal linear polarization components at the quasi-homogeneous source are controlled using a spatial light modulator. The beam generated in this way propagates to the far-field region yielding the desired spatial coherence and polarization state distributions. With this source we can generate an optical beam that is unpolarized in the usual one-point polarization sense, but polarized in the two-point mutual polarization sense. That is, the beam has a polarization distribution where two orthogonal linear polarization components at two points, within the aperture of the beam, separated by a set vector, given by the spectral density distribution at the source, are fully correlated. A beam with that polarization distribution may be used to perform the measurements required by variable coherence polarimetry, which can be applied to estimate the polarimetric bidirectional reflectance distribution function from monostatic measurements, with promising applications in remote sensing.

10407-33, Session 11

Statistics of partially-polarized fields: Beyond the Stokes vector and coherence matrix

Mikhail I. Charnotskii, Consultant (United States)

Traditionally, the partially-polarized light is characterized by the four Stokes parameters. Equivalent description is also provided by correlation tensor of the optical field. These statistics specify only the second moments of the complex amplitudes of the narrow-band two-dimensional electric field of the optical wave. Electric field vector of the random quasi monochromatic wave is a nonstationary oscillating two-dimensional real random variable. We introduce a novel statistical description of these partially polarized waves: the Period-Averaged Probability Density Function (PA-PDF) of the field. PA-PDF contains more information on the polarization state of the field than the Stokes vector. In particular, in addition to the conventional distinction between the polarized and depolarized components of the field PA-PDF allows to separate the coherent and fluctuating components of the field. We present several model examples of the fields with identical Stokes vectors and very distinct shapes of PA-PDF. In the simplest case of the nonstationary, oscillating normal 2-D probability distribution of the real electrical field and stationary 4-D probability distribution of the complex amplitudes, the newly-introduced PA-PDF is determined by 13 parameters that include the first moments and covariance matrix of the quadrature components of the oscillating vector field. PA-PDF can be measured by simultaneous heterodyne detection of the optical field. It provides additional information about the polarization state of the wave that is hidden from the classic Stokes vector description. Potential application of this theoretical development include terrestrial and atmospheric remote sensing, environmental monitoring, radar meteorology, biomedical optics particle characterization and astrophysics.

10407-34, Session 12

Estimating the relative water content of leaves in a cotton canopy

Vern C. Vanderbilt, NASA Ames Research Ctr. (United States); Craig S. T. Daughtry, U.S. Dept. of Agriculture (United States); Meredith K. Kupinski, Christine L. Bradley, College of Optical Sciences, The Univ. of Arizona (United States); Andrew N. French, Kevin Bronson, U.S. Arid-Land Agriculture Research Ctr. (United States); Russell A. Chipman, College of Optical Sciences, The Univ. of Arizona (United States); Robert P. Dahlgren, NASA Ames Research Ctr. (United States)

Remotely sensing plant canopy water status remains a long term goal of remote sensing research. Established approaches to estimating canopy water status — the Crop Water Stress Index, the Water Deficit Index and the Equivalent Water Thickness — involve measurements in the thermal or reflective infrared. Here we report plant water status estimates based upon analysis of polarized visible imagery of a cotton canopy measured by ground Multi-Spectral Polarization Imager (MSPI). Such estimators potentially provide access to the plant hydrological photochemistry that manifests scattering and absorption effects in the visible spectral region.

Twice during one day, +/- 3 hours from solar noon, we collected polarized imagery and relative water content data on a cotton test plot located at the Arid Land Agricultural Research Center, United States Department of Agriculture, Maricopa, AZ. The test plot, a small portion of a large cotton field, contained stressed plants ready for irrigation. The evening prior to data collection we irrigated several rows of plants within the test plot. Thus, ground MSPI imagery from both morning and afternoon included cotton plants with a range of water statuses.

Data analysis includes classifying the polarized imagery into sunlit reflecting, sunlit transmitting, shaded foliage and bare soil. We estimate the leaf surface reflection and interior reflection based upon the per pixel polarization and sun/view directions. We compare our cotton results with our prior polarization results for corn and soybean leaves measured in the lab and corn leaves measured in the field.

10407-35, Session 12

A high-sensitivity circular spectropolarimeter for remote sensing of homochirality in photosynthetic organisms

Lucas Patty, Vrije Univ. Amsterdam (Netherlands); Frans Snik, Luuk Visser, Leiden Observatory (Netherlands)

We describe the design and performance of a spectropolarimetric instrument, called TreePol, that is dedicated to remote sensing of the circular polarization signatures due to homochirality in photosynthetic organisms. To ensure high polarimetric sensitivity to observe such signatures, we combine rapid modulation offered by a Ferroelectic Liquid Crystal with a dual-beam spectrometer that incorporates fast line-detectors. The latter also furnishes relatively short measurement times through spectral multiplexing. We introduce several mitigation steps to correct for potential cross-talk from much stronger linear polarization signals into the measured circular polarization spectra. We present first laboratory results for (decaying) leaves and microbes, and we provide an outlook for field-work. In addition to providing a unique look into chiral photosystems of life on Earth, we aim to pave the way towards a unique detection method for extraterrestrial life.

10407-36, Session PWed

Passive millimeter-wave polarization characteristics of several common structures

Yayun Cheng, Fei Hu, Liangqi Gui, Huazhong Univ. of Science and Technology (China)

Passive millimeter-wave (PMMW) imaging has been widely adopted in security and military applications. Objects emit and reflect the MMW radiation just as they do in the visible and infrared regimes. Polarization is an important feature of electromagnetic waves and is affected by surface features, shapes, shading, materials, local curvature, and roughness. To obtain more information about the interested objects, polarimetric measurement is an important approach. In this paper, the polarization characteristics of several common structures (e.g., sphere, cone, and periodic surface) have been analyzed theoretically and the corresponding physical meanings have been revealed. The analyzed polarization feature parameters include Stokes vector, angle of polarization, degree of linear polarization, degree of polarization, linear polarization ratio and so on. The considered structure parameters include the radius of sphere, the radius and height of cone, and the curve function of periodic surface.

The ambient radiation can affect the polarization characteristics in PMMW imaging, which may be from sky, ground, water, building, mountain, or human. Different ambient radiations not only have different brightness temperatures, but also may have different polarization states. The indoor and outdoor simulations have been conducted to investigate the effect of ambient radiation. The relationship between polarization feature parameters and ambient polarization states are obtained.

The polarization characteristics discussed in this paper can provide some intrinsic mechanisms to acquire objects information (e.g., three-dimensional feature, contour, and material composition). In future work, we will further investigate the extraction methods of object information for several practical applications.

10407-37, Session PWed

Active polarization imaging system based on optical heterodyne balanced receiver

Qian Xu, Jianfeng Sun, Zhiyong Lu, Yu Zhou , Zhu Luan, Peipei Hou, Liren Liu, Shanghai Institute of Optics and Fine Mechanics (China)

Active polarization imaging technology has recently become the hot research field all over the world, which has great potential application value in the military and civil area. By introducing active light source, the Mueller matrix of the target can be calculated according to the incident light and the emitted or reflected light. Compared with conventional direct detection technology, optical heterodyne detection technology have higher receiving sensitivities, which can obtain the whole amplitude, frequency and phase information of the signal light. In this paper, an active polarization imaging system will be designed. Based on optical heterodyne balanced receiver, the system can acquire the real part and imaginary part of reflected optical field simultaneously, which contain the polarization characteristic of the target. Besides, signal to noise ratio and imaging distance can be greatly improved.

10407-38, Session PWed

A partial Mueller matrix polarimeter using two photoelastic modulator and polarizer pairs

Nia Natasha Tipol, Utsunomiya Univ. (Japan); Shuichi Kawabata, Tokyo Polytechnic Univ. (Japan); Yukitoshi Otani, Utsunomiya Univ. (Japan)

A partial Mueller matrix polarimeter using two photoelastic modulators and polarizer pairs is introduced. Photoelastic modulators (PEMs) are commonly used in various kinds of polarization measurement techniques for many years. The advantage of instruments that works using PEMs is the high-sensitivity and high-speed measurement of polarization properties due to its light modulation by specific resonant frequency. A polarized light beam passing through the center of the fused quartz bar will experience a periodic phase retardation because of the photoelastic effect which is the basis operation of PEM. In the two PEM-polarizer pairs, Mueller matrix elements of a sample are determined based on the analysis of the frequencies of the time-dependent light beam. Each PEM is operated at different resonant frequencies of 50 kHz and 60 kHz and are oriented 45° apart. Mueller algebra is used to analyze the optical configuration of the proposed system. The changing variables inside the proposed system will be only the orientations of the azimuthal angle of polarizer and analyzer whereas orientations for both PEMs are fixed. The polarization information that are to be represented by Mueller matrix is distributed based on combinations of two resonant frequencies of operating PEMs. Polarization information such as total retardation can be retrieved instantaneously by using the partial Mueller matrix information based on the proposed polarimeter. Experimental results of a quarter wave plate and a variable linear retarder will be presented showing the characteristics of the implementation.

10407-39, Session PWed

System of Mueller-Jones matrix polarizing mapping of blood plasma films in breast pathology

Natalia I. Zabolotna, Kostiantyn O. Radchenko, Mykola H. Tarnovskiy, Vinnytsia National Technical Univ. (Ukraine)

With the latest laser polarimetry methods used for the diagnosis of optical-anisotropic objects, it's possible to obtain fundamentally new results on the structure and condition of facilities, including blood plasma.

The combined method of Jones-Mueller matrix mapping and blood plasma films analysis based on the system that proposed in this paper. Based on the obtained data about the structure and state of blood plasma samples the diagnostic conclusions can be made about the state of breast cancer patients (“normal” or “pathology”).

The proposed method of mapping of blood plasma films is to receive, in particular algorithm, the coordinate distributions of real and imaginary components of the Jones matrix and Mueller matrix elements.

Then, by using the statistic and correlation analysis obtain statistical and correlational moments for every coordinate distributions; these indicators are served as diagnostic criterias. The final step is to comparing results and choosing the most effective diagnostic indicators.

This method is implemented on the existing experimental automated multiparameter system of laser polarimetry. It consists of a semiconductor laser, quarter-wave plates, collimator optics, a polarizer and an analyzer, a micro lens, a research sample and a CCD camera connected to the computer.

It was developed the specialized software that allows to implement algorithms for system management, processing, analysis of the obtained distributions of blood plasma films parameters of anisotropy, and decision support for diagnosis of breast diseases.

The paper presents the results of Mueller-Jones matrix mapping of optically thin (?≤0.1) plasma layers.

On the basis of the obtained data was performed differentiation of samples to “norm-pathology” and were made conclusions regarding the availability of pathological changes in the breast of each patient.

10408-1, Session 1

Testing of a compact 10G Lasercomm system for maritime platforms *(Invited Paper)*

Juan C. Juarez, Katherine T. Souza, Dustin D. Nicholes, James L. Riggins II, Hala J. Tomey, Radha A. Venkat, Johns Hopkins Univ. Applied Physics Lab., LLC (United States)

Lasercomm systems have gained increasing interest for both defense an commercial applications due to their ability to provide secure, long-distance, high-bandwidth communications channels. This paper will present field test results for a reduced SWAP Lasercomm system developed for highly scintillated links such as terrestrial communications.

The link architecture utilizes a multilayered approach to ensuring robust data transport through long-distance, highly scintillated links while operating on mobile platforms. The reduced size terminal leverages a 2x2 simultaneous transmit and receive spatial diversity scheme to mitigate scintillation fades. A demonstrator system suitable for operation on mobile surface platforms is being developed for mobile land and maritime platforms. The optical terminal utilizes an inertially stabilized gimbal to host the optical payload and provide the geo-pointing function of the pointing, acquisition, and tracking system.

In addition, a 10-Gbps layer 2 retransmission system has been integrated with previously developed high-sensitivity, high dynamic range optical modems demonstrated during the DARPA FOENEX program. The retransmission system implements a Rateless Round Robin error control protocol that applies several key principles to address the demanding requirements of a FSO link. The methods involve always efficiently filling the link with unique data, performing positive acknowledgement on data segments received and providing edge buffering. The current hardware is designed to support a 10 GbE client interface with channel loads exceeding 9 Gbps.

10408-2, Session 1

Phase and amplitude modification of a laser beam by two deformable mirrors using conventional 4f image encryption techniques

Chensheng Wu, Jonathan Ko, John R. Rzasa, Christopher C Davis, Univ. of Maryland, College Park (United States)

The image encryption and decryption technique using lens components and random phase screens has attracted a great deal of research interest in the past few years. In general, the optical encryption technique can translate a positive image into an image with nearly a white speckle pattern that is impossible to decrypt. However, with the right keys as conjugated random phase screens, the white noise speckle pattern can be decoded into the original image. We find that the fundamental ideas in image encryption can be borrowed and applied to carry out beam corrections through turbulent channels. Based on our detailed analysis and laboratory experiments, we show that by using two deformable mirrors arranged in similar fashions as in the image encryption technique, a large number of controllable phase and amplitude distribution patterns can be generated from a collimated Gaussian beam. Such a result can be further coupled with wavefront sensing techniques to achieve laser beam correction against turbulence distortions. In application, our approach leads to a new type of phase conjugation mirror that could be beneficial for directed energy systems.

10408-3, Session 1

Design and flight test results of high speed optical bidirectional link between stratospheric platforms for aerospace applications

Simone Briatore, Rustam Akhtyamov, Skolkovo Institute of Science and Technology (Russian Federation); Alessandro Golkar, Skolkovo Institute of Science and Technology (Russian Federation)

As small and nanosatellites become increasingly relevant in the aerospace industry, the need of efficient, lightweight and cost-effective networking solutions drives the need for the development of lightweight and low cost networking and communication terminals.

In this paper we propose the design and prototype results of a hybrid optical and radio communication architecture developed to fit nanosatellites, tested through a proxy flight experiment on a stratospheric flight. This system takes advantage of the higher data-rate offered by optical communication channels while relying on the more mature and stable technology of conventional radio systems for link negotiation and low-speed data exchange.

Such architecture allows the user to overcome the licensing requirements and scarce availability of high data-rate radio frequency channels in the commonly used bands.

Outlined are the architecture, development and test of the mentioned terminal, with focus on the communication part and supporting technologies, including the navigation algorithm, the developed fail-safe approach, and the evolution of the pointing system.

The system has been built with commercial-off-the-shelf components and demonstrated on a stratospheric balloon launch campaign.

The paper outlines the results of the main flight demonstration, where the two platforms successfully established an optical link at stratospheric altitudes. The results are then analyzed and contextualized in plans of future work for nanosatellite implementations.

10408-5, Session 1

Overwater ultraviolet non-line-of-sight communication channel modeling and experiment verification

Tian Lang, Crystal Han, Juan Marquez, Gang Chen, Univ. of California, Riverside (United States)

In this study, the characteristics of overwater non-line-of-sight (NLOS) ultraviolet (UV) communication channel which include scattering and turbulence effect are modeled using Monte Carlo multiple scattering simulation. In addition, experimental measurements of turbulence effect and path loss at distances of up to 500 meters are reported and analyzed where communication distance, transmitting angles, along with airborne humidity and temperature are taken into considerations as key parameters which affect the distribution of the receiving signals. These channel modeling and experimental results will be valuable for studying overwater NLOS UV communication performance.

10408-6, Session 2

Experimental evaluation and determination of free space optical link at 532nm wavelength under rain conditions and comparison with the link performance at 850nm wavelength

Gaurav Soni, Amritsar College of Engineering and Technology (India)

Free Space Optics (FSO) communication is a demanding efficient wireless technology which have been accepted due to its low power and mass requirements, high data rates and unlicensed spectrum. Atmospheric disturbances have a significant impact on performance of FSO Link which causes to degrade the laser beam. The effect of rain on the visible light communication has taken two different cases of rain attenuation on the FSO link that depends on the rain drop sizes. in this proposed experimental research based on FSO experimental work transmitter is based on green laser and a LDR is used at the receiver side. The medium used is free space on which the rain is falling and across it attenuation that will produced that will be noticed and compared with the 850nm wavelength laser.The assumption is taken that the same change in current is produced at the case of 850nm wavelength laser.To determine the variation in current a multimeter is used at the receiver side. The calculation of the attenuation is based upon the attenuation formula on decibel scale.The attenuation calculation for the wavelength is taken on different-different exposed lengths and rain rates. In this paper, the analysis and investigation based on experimental set-up for a Free Space optical communication link at wavelength of 532nm and 850nm is being carried out to evaluate and further improvement in link performance is done by experimental arrangement. The FSO link in case of 532nm tolerate attenuation up to 66.12 dB/km at the loss of -0.04 dB and rain rate of 2.3592mm/min. whereas 850nm tolerate attenuation up to 17.5 dB/km at the loss of -0.01 dB and at the same rain rate as in 532nm. The experimental investigation is carried out by analyzing the receiver current, exposed length and rain rate conditions. It is concluded that the proposed FSO link of 532nm having more attenuation than 850nm wavelength and in the both the cases loss is assumed of -0.01 dB. There is a increase in attenuation when rain rate increases. The rain rate over the exposed lengths depends on the different-different rain drop sizes. So it can be say that visible wavelengths due to its low cost, low power consumption and easy detection is good for short range communication purposes than infrared wavelengths.

10408-7, Session 2

Performance analysis of stationary Hadamard matrix diffusers in free-space optical communication links

Derek J. Burrell, Christopher T. Middlebrook, Michigan Technological Univ. (United States)

Wireless communication systems that employ free-space optical links in place of radio/microwave technologies carry substantial benefits in terms of data throughput, network security and design efficiency. Along with these advantages comes the challenge of counteracting signal degradation caused by atmospheric turbulence in free-space environments. A fully coherent laser source experiences random phase delays along its traversing path in turbulent conditions forming a speckle pattern and lowering the received signal-to-noise ratio upon detection. Preliminary research has shown that receiver-side speckle contrast may be significantly reduced and signal-to-noise ratio increased accordingly through the use of a partially coherent light source. While dynamic diffusers and adaptive optics solutions have been proven effective, they also add expense and complexity to a system that relies on accessibility and robustness for successful implementation. The goal of the research being performed is to experimentally demonstrate and quantify improvement of signal-to-noise ratio for turbulence scenarios using a custom Hadamard diffractive matrix design to statically induce partial coherence in a transmitted beam. Atmospheric phase screens are generated using an open-source software package and subsequently loaded into a spatial light modulator using nematic liquid crystals to modulate the phase.

10408-8, Session 2

Simulating the performance of adaptive optics techniques on FSO communications through the atmosphere

Noelia Martínez, Luis Fernando Rodríguez-Ramos, Instituto de Astrofísica de Canarias (Spain)

The Optical Ground Station (OGS), installed in the Teide Observatory since 1995, was built as part of ESA efforts in the research field of satellite optical communications to test laser telecommunication terminals on board of satellites in Low Earth Orbit and Geostationary Orbit. As far as one side of the link is settled on the Earth, the laser beam (either in the uplink or in the downlink) has to bear with the atmospheric turbulence. Within the framework of designing an Adaptive Optics system to improve the performance of the Free-Space Optical Communications at the OGS, turbulence conditions regarding uplink and downlink have been simulated within Matlab as well as the possible utilization of a Laser Guide Star to measure the wavefront in this context and even to perform optical communications with it. Simulations have been carried out by reducing available atmospheric profiles regarding both night-time and day-time measurements and by having into account possible seasonal changes. An AO proposal to reduce atmospheric aberrations and, therefore, ameliorate FSO links performance is presented and analysed in this paper.

10408-9, Session 2

Capacity and outage performance of multiple-input multiple-output free space optical system over double-Weibull atmospheric turbulence channel and weather conditions

Omar Hasan, Princess Sumaya Univ. for Technology (Jordan)

We investigate ergodic capacity and outage probability performance of multiple-input multiple-output (MIMO) free space optical system operating over moderate to strong turbulence channel conditions. The MIMO optical system employees intensity modulation direct detection with on-off signaling (IMDD/OOK), with equal gain combining techniques at the receiver receiver. We derive novel closed form expressions for two system metrics; ergodic capacity, probability of outage. Expressions derived here are based on the Double-Weibull channel model, which is based on scintillation theory that assumes that the irradiance of the received optical wave is modeled as the product of small-scale and large scale turbulence eddies. In addition, the Double-Weibull stochastic is modeled as the product of two Weibull random variables. The results for the two system metrics performance are evaluated for plane wave transmission and displayed for different values of received signal-to-noise ratios, moderate to strong turbulence conditions, several values of transmit / receive diversity and different weather conditions.

10408-10, Session 3

Atmospheric propagation of coherently and incoherently combined quantum cascade lasers *(Invited Paper)*

Robert J. Grasso, EOIR Technologies (United States)

Quantum Cascade Lasers represent one of the most significant advances in solid state lasers. Their ability to generate mid-IR through THz wavelengths

have found numerous applications in IR Countermeasures and Remote Sensing for defence, security, and commercial application. In many practical defence and security applications, to achieve the desired power levels many beams must be combined to form a single focused beam. This paper examines both coherent and incoherent beam combining of multi-kilowatt lasers and the effects imposed by atmospheric turbulence and atmospheric aerosols on the propagation of these combined beams. In this paper beam centroid wander and beam spread are analyzed and their contribution to eventual laser spot size to obtain the energy/power on target at range for varying turbulence values. In this analysis it is found that there is little difference between the energy/power delivered to a target whether coherently or incoherently combined beams. Additionally, it was found that there is a maximum intensity that can be propagated to a target that is independent of initial beam quality and size for km-type ranges in moderate turbulence.

10408-11, Session 3

A study on the effect of anisotropy on a propagating beam

Melissa Beason, Larry C. Andrews, Ronald L. Phillips, Townes Institute Science and Technology Experimentation Facility, Univ. of Central Florida (United States)

General anisotropy leads to different effects along the horizontal axis of a propagating beam than along the vertical axis. To better understand these effects, we developed theoretical models for mean intensity, spatial coherence radius, and covariance function of intensity. With different anisotropic conditions in each direction, these statistical quantities exhibit an elliptical shape in the plane of the receiver. Both weak and strong fluctuation regimes will be considered.

10408-12, Session 3

Beam control of the ultra-short laser pulse in turbid medium

Vladimir Markov, Anatoliy Khizhnyak, Advanced Systems & Technologies, Inc. (United States); Phillip Sprangle, Univ. of Maryland, College Park (United States)

An effective power delivery of the high energy ultra-short laser pulse (USLP) on a distant target through turbulent atmosphere requires adaptive control of the outgoing beam. Adaptive Optics allows compensation of integral perturbations of the USLP wavefront and on-target power delivery with the intensity distribution similar to that of a beacon. However, at its propagation through the range the wavefront of the USLP beam replicates scintillations incurred by the beacon-generated reference wave. This may results in early self-focusing and filamentation of the USLP beam. This presentation discusses possible solutions to this problem and methods to address issues critical for optimal beam propagation and focusing.

10408-13, Session 3

Analysis of the covariance function and aperture-averaged fluctuations of irradiance to calculate Cn2

Galen Cauble, David T. Wayne, SPAWAR Systems Ctr. Pacific (United States)

Deep fading of an optical communication system over long propagation paths can be reduced with a large aperture receiver. Aperture averaging reduces scintillation effects on an optical detector and increases signal to noise ratio. We report on the design and testing of a new instrument that simultaneously records the spatial intensity pattern at the entrance pupil of a telescope and the aperture-averaged temporal intensity fluctuations of a laser beam propagating through turbulence. A camera records the pupil plane turbulence images, while a photodetector records aperture averaged intensity fluctuations. Using weak turbulence theory we relate aperture averaged scintillation and the covariance function derived from the pupil plane imagery to BLS900 Cn2 values over a 500m path using two wavelengths, 1064nm and 633nm.

10408-14, Session 3

Optimization of wavefront-sensorless adaptive optics for horizontal laser beam propagation in a realistic turbulence environment

Max Segel, Esdras Anzuola, Szymon Gladysz, Karin U. Stein, Fraunhofer-Institut für Optronik, Systemtechnik und Bildauswertung (Germany)

Unconventional wavefront sensing strategies are being developed to provide alternatives for measuring the wavefront deformation of a laser beam propagating through strong turbulence and/or along a horizontal-path. In this paper we present a modified wavefront-sensorless adaptive optical (AO) system, where the well-known stochastic parallel gradient descent (SPGD) approach is extended with a-priori knowledge of the spatial and temporal statistics related to atmospheric turbulence. Here, a modal implementation of the correction algorithm allows us to exploit the decreasing phase variance of high-order Zernike modes in a distorted wavefront, as well as the different temporal characteristics of each mode. We also propose an implementation of a modal decomposition based on Karhunen-Loève polynomials instead of the common Zernike polynomials. The performance evaluation of this modified wavefront-sensorless AO system is carried out in a realistic turbulence environment and the results are compared against traditional SPGD algorithms.

10408-15, Session 4

Cloud free optical link probabilities to satellites from multiple ground stations

Lindsey Willstatter, Taylor A. Page, Christopher I. Moore, Jake Griffiths, Linda M. Thomas, U.S. Naval Research Lab. (United States)

The availability of a cloud free line of sight (CFLOS) for a ground-space free space optical (FSO) link is strongly dependent on a satellite's orbit and cloud cover spatial and temporal statistics. A diverse network of multiple ground stations at locations with minimal and uncorrelated cloud cover can be used to maximize the availability of a CFLOS to multiple satellite orbits. Historic cloud cover data for this availability study is extracted from the ERA-Interim database which is generated, updated, and maintained by the European Center for Medium-Range Weather Forecast (ECMWF). The database contains worldwide data in 6 hour time segments from 1970 to the present. For our analysis, cloud cover data, ground station locations, and satellite ephemerides are conjointly analyzed to determine ground-space link availabilities. The results of this analysis will be presented.

10408-16, Session 4

Modeling of ground based laser propagation to low earth orbit object for maneuver

Matthew M. Bold, Liam Smith, Lockheed Martin Space Systems Co. (United States)

The Space Environment Research Centre (SERC) endeavors to demonstrate the ability to maneuver high area to mass ratio objects using ground based

lasers. Lockheed Martin has been leading system performance modeling for this project that includes high power laser propagation through the atmosphere, target interactions and subsequent orbital maneuver of the object. This paper will describe the models used, model assumptions and performance estimates for laser maneuver demonstration and discuss how the end to end model has already impacted design considerations for the demonstration.

10408-46, Session 4

Atmospheric applications of intense ultrashort-pulse lasers

Pavel Polynkin, College of Optical Sciences, The Univ. of Arizona (United States)

Ultrashort-pulse laser beams with multi-gigawatt peak power propagate in the air in the self-channeling regime leaving behind traces of dilute plasma. This propagation regime, termed laser filamentation, has several potential applications. This presentation discusses two of them. The first application is the so-called air lasing. The concept of air lasing is based on the utilization of the constituents of the air itself for the generation of standoff, impulsive laser action. While both forward-propagating and backward-propagating laser emissions can be generated, the backward-propagating emission is of the most practical significance, as it enables single-ended remote sensing schemes and guide stars. The paper will review recent results on air lasing from singly ionized nitrogen molecular ions N2+, pumped through femtosecond laser filamentation in air. So far, lasing has been demonstrated only in the forward direction and the mechanisms that enable population inversion have been controversial. The second potential applications of air plasma is for the guidance of electrical breakdown of air. The diluteness and sub-nanosecond lifetime of the plasma limits the extent of the guidance. I will discuss approaches that help alleviate these limitations.

10408-47, Session 4

Polarized photon transport through fog

Brett H. Hokr, U.S. Army Space and Missile Defense Command (United States); Jonathan Farmer, Eikon Research, Inc. (United States); Christopher M. Persons, IERUS Technologies, Inc. (United States); Robert Desilva, James H. Kirkland, Eikon Research, Inc. (United States); Greg A Finney, IERUS Technologies, Inc. (United States); Kirk A. Fuller, The Univ. of Alabama in Huntsville (United States)

Anyone who has driven through fog understands the detrimental effect scattering can have on your ability to see. When light interacts with a scattering center, in this case a fog droplet, it is scattered into a new direction, ultimately turning the world around you into a dull gray haze. In some fogs, visibility can be less than 100 meters. It would be possible to see through turbid media like fog if you can separate the scattered light from the unscattered, or ballistic, light; however, we must understand the light transport properties of the atmosphere to determine the optimum scheme. Here, we present an end-to-end simulation for polarized light transport through fog. Our approach can be summarized in three steps: compute the Mueller matrix for a single scattering interaction, ensemble average a distribution of sizes and shapes, and solve the light transport using a Monte Carlo simulation. For small spherical particles, such as fog, we use Mie theory to calculate the single scattering Mueller matrix, but this approach can be generalized to non-spherical particles using ray tracing for large particles or a T-matrix approach for smaller particles. Through this simulation, we are able to determine a backscattering Mueller matrix and a forward scattering Mueller matrix response function for the atmosphere as a function of position and detection angle.

10408-19, Session 5

Wavefront analysis of optical vortices propagating through terrestrial atmospheric turbulence *(Invited Paper)*

Jaime A. Anguita, Gustavo Funes, Univ. de los Andes (Chile)

Increasing the aggregate capacity of FSO systems by taking advantage of the available degrees of freedom of light, like orbital angular momentum (OAM), may contribute to cost-effective high-speed network access if the generation and detection of OAM is properly managed in turbulent propagation conditions. Although several theoretical schemes and laboratory demonstrations with OAM, there is still a wide technological gap to be covered to make these technologies available for terrestrial FSO links in the presence of turbulence, specifically due to broadening of beams and OAM crosstalk as they propagate in turbulent media.

We investigate the use of Laguerre-Gauss (LG) beams with the purpose of increasing the security and link distance of FSO communications. For such beams, alignment and phase structure are crucial to ensure adequate signal detection. Using numerical propagation models including atmospheric turbulence and realistic diffraction devices, we evaluate the distorted received field of LG beams under several propagation distances and turbulence strength to determine beam wander and OAM mode spreading using phase retrieval algorithms. We explore the effectiveness of beam shaping at the transmitter side to reduce scintillation at the receiver side to reduce the bit-error rate in a OAM-based communication system. Transmitter and receiver adaptive corrections are analyzed according to their complexity and effectiveness in reducing outage probability in a OOK and PPM-modulated link for several turbulence regimes and distances.

We also describe and demonstrate our 400m OAM propagation testbed and show the effects of turbulence on a wide range of OAM states, including OAM crosstalk and scintillation.

10408-20, Session 5

OAM of beam waves in random inhomogeneous medium

Mikhail I. Charnotskii, Consultant (United States)

For paraxial propagation of scalar waves classic electromagnetic theory definitions of transverse linear (TLM) and orbital angular (OAM) momenta of beam waves are simply related to the wave coherence function in the coherent. This allows the extension of the TLM and OAM density concepts to the case of partially coherent waves when phase is indeterminate. We show on several examples that there no direct connection between the intrinsic OAM and optical vorticity. Namely, neither the presence of the optical vortices is necessary for the intrinsic OAM, nor the presence of the optical vortices warrants the non-zero intrinsic OAM. We examine OAM for two classes of partially-coherent beam waves and show that Simon and Mukunda's Twisted Gaussian beam has an intrinsic OAM with per unit power value that can be continuously changed by varying the twist parameters. Using the parabolic propagation equation for the coherence function, we show that both total TLM and OAM are conserved for the free space propagation, but not for propagation in inhomogeneous medium in general. Under Markov Approximation (MA), in the presence of the random statistically homogeneous medium the total TLM and OAM are conserved in average. Based on the MA parabolic equation for the fourth-order coherence function, we examine for evolution of the total OAM variance. Perturbation solution of this equation shows that the OAM fluctuations in general grow approximately linearly with the propagation path length. However, this growth appears to be slower for the beams with rotation-symmetric irradiance.

10408-21, Session 5

Shack-Hartmann measurements of the transverse linear and orbital angular momenta after propagation through turbulence

Mikhail I. Charnotskii, Consultant (United States); Terry J. Brennan, Prime Plexus, LLC (United States)

Theory presented in the companion paper [M. Charnotskii, "OAM of beam waves in random inhomogeneous medium"] reveals that for paraxial propagation of scalar waves transverse linear momentum (TLM) and orbital angular momentum (OAM) of beam waves are simply related to the wave coherence function, and that the TLM and OAM densities can be measured by a conventional Shack-Hartman sensor, which is typically used for the phase measurements. Here we report the TLM and OAM measurements derived from the data obtained by the Hartman Turbulence Sensor (HTS) during the field measurement campaign in 2009-10 and data produced by wave optics simulation of the HTS. We estimate dependence of the mean TLM and OAM densities on the turbulent conditions on the propagation path. We calculate the variance and spatial and temporal covariances of the of the TLM and OAM fluctuations. We also examine the statistics of the total TLM and OAM intercepted by the wave front sensor aperture. We compare the OAM measurements to the optical vorticity data derived from the phase slopes estimates that the WFS routinely delivers, and attempt to estimate the vortex and asymmetry OAM components introduced by Bekshaev, Soskin and Vasnetsov [JOSA A 2003], and dependence of both components on the turbulent propagation conditions.

10408-22, Session 6

Image blurring due to turbulent wakes for airborne systems: Flight tests

Stanislav V. Gordeyev, Univ. of Notre Dame (United States); Yakov Diskin, Matthew R. Whiteley, MZA Associates Corp. (United States); Aaron Archibald, Air Force Institute of Technology (United States); Nicholas G. De Lucca, Eric J. Jumper, Univ. of Notre Dame (United States)

In addition to blurring effects caused by atmospheric turbulence, airborne imaging systems can also be negatively affected by turbulent flows formed by the aircraft. To study and eventually mitigate these effects, simultaneous measurements of the instantaneous wavefronts due to the turbulent flow, and the resulted blurred images were performed in-flight using Airborne Aero-Optics Laboratory (AAOL-T). It consists of two planes flying 50 meters apart to minimize the atmospheric aberrations. A divergent point laser source from one aircraft was transmitted to a second aircraft, where the laser beam was received by an optical turret, protruding from the aircraft. The turbulent wake, formed by the turret, imposed spatially-temporally-evolving optical distortions, which were measured by a wavefront sensor at the sampling rate of 25 kHz. A target board, derived from USAF1951, was placed around the divergent laser beam of the first aircraft. Images of the board, blurred by the turbulent wake, were recorded by a second high-speed camera at 500 fps. The laser radiation was filtered out before going to the imaging camera. Both cameras shared the same optical path to guarantee one-to-one relation between the wavefronts and the blurred images.

Series of flights were performed at altitudes between 15,000 and 29,000 ft at Mach numbers between 0.5 and 0.8. Relative position of both planes was varied to study wavefronts and resulted images by different regions of the turbulent wake. Statistics of wavefronts (OPDrms, spatial length etc) were computed. The relation between these quantities and MTF, extracted from images, is presented and discussed.

10408-23, Session 6

Image blurring due to turbulent wakes for airborne systems: Simulation and modeling

Yakov Diskin, David J. Goorskey, Matthew R. Whiteley, Richard Drye, MZA Associates Corp. (United States); Nicholas G. De Lucca, Stanislav V. Gordeyev, Univ. of Notre Dame (United States); Eric J. Jumper, MZA Associates Corp. (United States)

We present our findings from a modeling and simulation effort in which we analyzed the imaging performance of a turreted laser beam director/telescope on a transonic aircraft platform. We used real wavefront sensor (WFS) data collected by the Airborne Aero-Optics Laboratory (AAOL) test platform at Mach 0.8. Using these WFS data, we quantified the imaging point spread function (PSF) for a variety of line-of-sight (LOS) angles. The LOS angle values sweep from forward-looking angles imaging through the shock wave to backward-looking imaging through the turbulent wake. Our simulation results show Strehl ratios from 4% to 50% with substantial scattering of energy out to many time larger than the diffraction-limited core. For each LOS angle, we analyze the imaging modulation transfer function (MTF) which shows a rapid reduction of contrast for low-to-mid range spatial frequencies. We reaffirm that practical limits to usable spatial frequencies require higher imaging signal to noise ratio in the presence of aero-optical disturbances at high Mach number. The presented MTF analysis speaks to the degradation of image-contrast-based tracking algorithms that rely on illuminator laser propagating through aero-optical aberrations. In conclusion, we discuss the AAOL imaging flight test campaigns and the anticipated imaging performance of AAOL turret.

10408-24, Session 6

Motion deblurring of simulated light-field images

Shuo Wang, Jeremy P. Bos, Michigan Technological Univ. (United States)

We have developed a light field rendering model in PBRT [1] that allows us to generate a sampled four dimensional light field based on the two-plane parameterization popularized by Adelson and Wang [2]. From this data cube we can perform common post-processing tasks like perspective shifts and varying the focus and depth of field. We are able to simulate motion blur by shifting the camera perspective linearly and averaging over the dataset. Dansereu [3] has demonstrated a technique for motion deblurring of light field images using simple image sets featuring Lambertian sources. In this work, we explore the interplay between spatial and angular sampling. Also, we explore the possibility of extending the idea of motion deblurring to the case where a static scene is imaged through a turbulence volume.

[1] Pharr, M., Jakob, W., & Humphreys, G. (2016). Physically based rendering: From theory to implementation. Morgan Kaufmann.

[2] Adelson, E. H., & Wang, J. Y. (1992). Single lens stereo with a plenoptic camera. IEEE transactions on pattern analysis and machine intelligence, 14(2), 99-106.

[3] Dansereau, D. G., Eriksson, A., & Leitner, J. (2016). Motion Deblurring for Light Fields. arXiv preprint arXiv:1606.04308.

10408-25, Session 7

Atmospheric characterization on the Kennedy Space Center Shuttle Landing Facility

Jonathan Ko, Univ. of Maryland, College Park (United States); Joseph T. Coffaro, Univ. of Central Florida (United States); Chensheng Wu, Christopher C. Davis, Univ. of Maryland, College Park (United States)

Large temperature gradients are a known source of strong atmospheric turbulence conditions. Often times these areas of strong turbulence conditions are also accompanied by conditions that make it difficult to conduct long term optical atmospheric tests. The Shuttle Landing Facility (SLF) at the Kennedy Space Center (KSC) provides a prime testing environment that is capable of generating strong atmospheric turbulence yet is also easily accessible for well instrumented testing. The Shuttle Landing Facility features a 3 mile long and 300 foot wide concrete runway that provides ample space for measurements of atmospheric turbulence as well as the opportunity for large temperature gradients to form as the sun heats the surface. We present the results of our large aperture LED scintillometer and a thermal probe RTD system that were used to calculate a path averaged and a point calculation of Cn2. In addition, we present the results of our Plenoptic Sensor that was used to measure wavefront distortions as well as to calculate a path averaged Cn2 value. These measurements were conducted over a multi-day continuous test with supporting atmospheric and weather data from the University of Central Florida.

10408-26, Session 7

A machine learning approach for predicting atmospheric aerosol size distributions

Joshua J. Rudiger, Kevin Book, SPAWAR Systems Ctr. Pacific (United States); Brooke Baker, SPAWAR Systems Ctr. Atlantic (United States); John S. deGrassie, Stephen Hammel, SPAWAR Systems Ctr. Pacific (United States)

An accurate model and parameterization of aerosol concentration is needed to predict the performance of electro-optical imaging systems. Current models have been shown to vary widely in their ability to accurately predict aerosol size distributions and subsequent scattering properties of the atmosphere. One of the more prevalent methods for modeling particle size spectra consists of fitting a modified gamma function to measurement data, however this limits the distribution to a single mode. Machine learning models have been shown to predict complex multimodal aerosol particle size spectra. Here we establish an empirical model for predicting aerosol size spectra using machine learning techniques. This is accomplished through careful measurements of aerosols in controlled laboratory environments and measuring aerosol particle size distributions in outdoor, littoral environments. The machine learning based model is shown to extend the functionality of Advanced Navy Aerosol Model (ANAM), developed to model the size distribution of aerosols in the maritime environment.

10408-27, Session 7

Climatological assessment of maritime atmospheric profiles: model-based and LIDAR-based approaches

Kevin M. McBryde, SPAWAR Systems Ctr. Pacific (United States)

Local meteorological conditions drive variability of vertical extinction profiles over both short and long timescales. Wind speed and relative humidity, in particular, are associated with production modes for maritime aerosols. Climatological variability of profiles are modeled based upon surface layer historical measurements of meteorological parameters. We have generated a database of profiles using the SPAWAR ClimoCube methodology. This distinct methodology is discussed, and model-based climatological vertical extinction profiles are compared with a new, separate, database of profiles from the CALIPSO satellite LIDAR experiment. We analyze similarities and discrepancies between the two databases.

10408-28, Session 7

Variability of refractive index structure parameter and aerosols in the marine atmospheric boundary layer

Qing Wang, Naval Postgraduate School (United States); Denny P. Alappattu, Moss Landing Marine Labs. (United States); Benjamin J. Wauer, Ryan T. Yamguchi, Naval Postgraduate School (United States); John A. Kalogiros, National Observatory of Athens (Greece); Haflidi Jonsson, Naval Postgraduate School (United States)

Electro-optical (EO) and infrared (IR) signals propagating through the atmosphere exhibit intensity fluctuations caused by atmospheric turbulence, a phenomenon known as scintillation. Scintillation is directly related to the refractive index structure parameter Cn2 defined as the refractive index structure function scaled to for the turbulence inertial subrange. Quantifying Cn2 is essential to evaluate and predict scintillation effects on EO/IR systems. Meanwhile, aerosols in the lower atmosphere absorb and scatter EO/IR energy, resulting in attenuation, aliasing, and blurring.

We will present initial results on Cn2 and aerosol variability in the coastal zone using simultaneous measurements from a Twin Otter research aircraft, two instrumented ocean vessels [R/V John Martin and a rigid hull inflatable boat (RHIB)] , and a coastal land site. All measurements were taken as part of the Coastal Electro-Optical PropagaTion eXperiment (CEOPTeX) conducted in April/May 2016 offshore of Moss Landing, CA. Aerosol concentration, scattering, and absorption were obtained from the research aircraft in the atmospheric boundary layer. Cn2 was derived from measurements of temperature and humidity sampled at 20 Hz from all platforms/site. Two level Cn2 measurements were also taken when the R/V John Martin and the RHIB were co-located. We will discuss the spatial/temporal variability of the measured quantities, and the difference between the Cn2 at the coastal region and those predicted by surface layer similarity theory and the measured bulk quantities.

10408-29, Session 8

Determination of accurate vertical atmospheric profiles of extinction and turbulence

Stephen Hammel, Eric Hallenborg, SPAWAR Systems Ctr. Pacific (United States); James R. Campbell, U.S. Naval Research Lab. (United States)

Our ability to generate an accurate vertical profile characterizing the atmosphere from surface to a point above the boundary layer top is quite rudimentary. The region from a land or sea surface to an altitude of 3000 meters is dynamic and particularly important to the performance of many active optical systems. In this paper we discuss efforts to measure both turbulence and extinction for this region of interest.

Measurement of these profiles in the field is a problem, and we will present a discussion of recent field test activity to address this issue. Our approach comprises measurement techniques and models, and we describe the instruments that provide data for a variety of models that in turn generate the vertical profiles of absorption, scattering, and turbulence. These three profiles are the core requirements for an accurate assessment of laser beam propagation.

10408-30, Session 8

Investigation of the height dependency of optical turbulence in the surface layer over False Bay (South Africa)

Detlev Sprung, Fraunhofer-Institut für Optronik, Systemtechnik und Bildauswertung (Germany); Alexander M. J. van Eijk, TNO Defence, Security and Safety (Netherlands); Willem H. Gunter, Institute for Maritime Technology (South Africa); Derek J. Griffith, Council for Scientific and Industrial Research (South Africa); Christian Eisele, Erik Sucher, Karin U. Stein, Fraunhofer-Institut für Optronik, Systemtechnik und Bildauswertung (Germany)

Atmospheric turbulence impacts on the propagation of electro-optical radiation. Typical manifestations of optical turbulence are scintillation (intensity fluctuations), beam wander and (for laser systems) reduction of beam quality. For longer propagation channels, it is important to characterize the vertical and horizontal distribution (inhomogeneity) of the optical turbulence. In the framework of the First European South African Transmission ExpeRiment (FESTER) optical turbulence was measured between June 2015 and February 2016 over a 2 km over-water link over False Bay. The link ran from the Institute of Maritime Technology (IMT) at Simons Town to the lighthouse at Roman Rock island. Three Boundary layer scintillometers (BLS900) allowed assessing the vertical distribution of optical turbulence at three different heights between 7 and 14 m above the water surface. The expected decrease with Cn2 with height is not always found. These results are analyzed in terms of the meteorological scenario, and a comparison is made with a fourth optical link providing optical turbulence data over a 8.7 km path from IMT to Kalk Bay, roughly 36° shifted to the three 2 km paths.

10408-31, Session 8

In-situ and path-averaged measurements of aerosol optical properties over False Bay (South Africa)

Sven A. van Binsbergen, TNO Defence, Security and Safety (Netherlands); Peter Grossmann, Fraunhofer-Institut für Optronik, Systemtechnik und Bildauswertung (Germany); Faith J. February, Institute for Maritime Technology (South Africa); Leo H. Cohen, TNO Defence, Security and Safety (Netherlands); Alexander M. J. van Eijk, TNO Defence, Security and Safety (Netherlands) and Fraunhofer-Institut für Optronik, Systemtechnik und Bildauswertung (Germany); Karin U. Stein, Fraunhofer-Institut für Optronik, Systemtechnik und Bildauswertung (Germany)

Atmospheric aerosols adversely affect the propagation of electro-optical radiation through scattering and absorption processes. Consequently, knowledge of the aerosol concentration and composition is required to predict the performance of electro-optical sensor systems in the operational theatre. A study is reported of aerosol properties over the False Bay area, near Cape Town in South Africa. Aerosol properties were measured by in-situ optical particle counters and a transmissometer, operating at 7 wavelengths between the visible and far-infrared, set up for a 7.8 km over-water path. The transmissometer receiver was collocated with the optical particle counters. The aerosol properties are discussed in terms of meteorological scenario (wind speed, wind direction, etc), and the path-averaged results are compared to the in-situ measurements.

10408-32, Session 8

Determination of the spectral behaviour of atmospheric soot using different particle models

Krzysztof Skorupski, Wroclaw Univ. of Science and Technology (Poland)

Soon after emission black carbon particles tend to connect to each other, what leads to the creation of complex geometries, namely aggregates. In the atmosphere, they interact with both organic and inorganic matter. In many studies such aggregates are modelled as monodisperse spheres positioned in point contact. Such a simplification might lead to many inaccuracies in light scattering simulations. The goal of this study was to compare the spectral behavior of different, commonly used soot particle models. The simplest one was a ball with two external layers (inorganic and organic). The most complex model was composed of a black carbon aggregate with inorganic particles attached to it. The geometry was covered by an external organic layer. In the study, the volume of each material was always the same, regardless of the model used. For light scattering simulations the ADDA algorithm was used. The incident wavelength varied from 400nm to 800nm and results were orientationally averaged. The ADDA settings were adapted from the work by Skorupski. The number of dipoles per wavelength was always larger than 250. The refractive index for black carbon was based on the work by Chang et al., for organic matter (organic acid) on the work by Myhre et al. and the refractive index for inorganic matter (sulfate) was adapted from the OPAC database. The results prove that the relative extinction cross section error, in some cases, can be even larger than 20%. Therefore, before starting excessive simulations, it is important to know what error is expected.

10408-33, Session 9

Saturation of anisoplanatic error in horizontal imaging scenarios

Jeffrey R. Beck, Jeremy P. Bos, Michigan Technological Univ. (United States)

Our approach extends work completed by Stone [1] and seeks to understand the performance of speckle imaging systems over fields of view much larger than the isoplanatic patch size [2] . One possibility is that the piston-removed anisoplanatic error saturates to a value much smaller than 1 when the aperture size is small. In [1] Stone shows that this is true for a 0.5m aperture using the HV5-7 model pointing at nadir when both tilt and piston are removed. There is good cause to believe that as D/r0 approaches unity the piston anisoplanatic error may saturate to values smaller than one. This work will start by evaluating Stone's expressions for anisoplanatic error over 1 km paths for values of D/r0 between 1 and 5. Results will be compared to those produced by phase screen models such as those used in [3].

[1] Stone, J., Hu, P. H., Mills, S. P., & Ma, S. (1994). Anisoplanatic effects in finite-aperture optical systems. JOSA A, 11(1), 347-357.

[2] Bos, J. P., & Roggemann, M. C. (2012). Robustness of speckle-imaging techniques applied to horizontal imaging scenarios. Optical Engineering, 51(8), 083201-1.

[3] Bos, J. P., & Roggemann, M. C. (2012). Technique for simulating anisoplanatic image formation over long horizontal paths. Optical Engineering, 51(10), 101704-1.

Chicago

10408-34, Session 9

Hybrid wavefront sensing and image correction algorithm for imaging through turbulent media

Chensheng Wu, John R. Rzasa, Jonathan Ko, Christopher C. Davis, Univ. of Maryland, College Park (United States)

It is well known that passive image correction of turbulence distortions often involves using geometric dependent deconvolution algorithms. On the other hand, active imaging techniques using adaptive optics corrections would use the distorted wavefront information for guidance. Our work shows that a hybrid hardware-software approach is possible to reveal accurate and high detail images through turbulent media. The processing algorithm also takes much fewer iteration steps in comparison with conventional image processing algorithms. In our proposed approach, a plenoptic sensor is used as a wavefront sensor to guide post-stage image correction on a high-definition zoomable camera. Reversely, we show that given the ground truth of the high detailed image and the plenoptic imaging result, we can generate an accurate prediction of the blurring image on a traditional zoomable camera. Similarly, the ground truth combined with the blurred image from the zoomable camera would provide the wavefront condition. In application, our hybrid approach can be used as an effective way to conduct object recognition in a turbulent environment where the target has been significantly distorted or is even unrecognizable.

10408-36, Session 9

Numerical simulation and analysis of aero-optical effect of the 3D side window

Yi Liu, Ming Liu, Yuejin Zhao, Liquan Dong, Lingqin Kong, Mei Hui, Xiaohua Liu, Beijing Institute of Technology (China)

When the flight with an optical window is flying in a high speed, the temperature and the refractive index of the air around it will be changed because of the friction, and this will make the image on the detector blurring and shifting, which will degrade the detecting precision greatly.

At present, research on 2D aerodynamics simulation and optical transmission has been relatively comprehensive, but the analysis of 3D environment remains imperfect, especially of a plane side window.

This paper chose a classic kind of side window model for the research. Ansys was used to simulate the discretionary temperature field around the dome and the window instead of the assumptive grid information by expressions. So the refractive index of the air around the flight could be worked out. On this basis, the offset and the blur of the image could be figured out using the ray tracing method. Considering of the huge amount of data, fixed step length tracing method and interpolation method were used in order to shorten the run time and guarantee computational precision at the same time instead of the adaptive variable step method and complicated mesh construction method. In this study, 3D simulation and programming results under different working conditions were discussed. The results clearly showed the relationship between the image quality and the flight speed, wavelength and incident angle of the entering ray. Wind tunnel experiment data indicates the validity of the analysis and proves the applicability of the method this paper used.

10408-4, Session PWed

Hemispherical optical dome for underwater communication

Ron Shiri, Patrick L. Coronado, Emily L. Lunde, NASA Goddard Space Flight Ctr. (United States)

The underwater wireless optical communication has a narrow field-of-view. In this work, we employ hemispherical optical domes fitted with spherical lenses to increase the field-of-view.

10408-37, Session PWed

Coherent optical communication detection device based on modified balanced optical phase-locked loop

Bo Zhang, Jianfeng Sun, Guangyu Cai, Mengmeng Xu, Guangyuan Li, Guo Zhang, Hongyu He, Chenzhe Lao, Zhiyong Lu, Liren Liu, Shanghai Institute of Optics and Fine Mechanics (China) and Key Lab. of Space Laser Communication and Detection Technology, Univ. of Chinese Academy of Sciences (China)

In the field of satellite communication, space laser communication technology is famous for its high communication rate, good confidentiality, small size, low power consumption and so on. The design of coherent optical communication detection device based on modified balanced optical phase-locked loop (OPLL) is presented in the paper. It combined by local oscillator beam, modulator, voltage controlled oscillator, signal beam, optical filter, 180 degree hybrid, balanced detector, loop filter and signal receiver. Local oscillator beam and voltage controlled oscillator trace the phase variation of signal beam simultaneously. That taking the advantage of voltage controlled oscillator which responses sensitively and tunable local oscillator laser source with large tuning range can trace the phase variation of signal beam rapidly and achieve phase locking. The demand of the phase deviation is very low, and the system is easy to adjust. When the transmitter transmits the binary phase shift keying (BPSK) signal, the receiver can demodulate the baseband signal quickly, which has important significance for the free space coherent laser communication.

10408-38, Session PWed

The integration of laser communication and ranging

Mengmeng Xu, Jianfeng sun, Bo Zhang, Guangyu cai, Guo Zhang, Guangyuan Li, Shanghai Institute of Optics and Fine Mechanics (China)

In the field of satellite communication, space laser communication technology is famous for its high communication rate, good confidentiality, small size, low power consumption and so on. Integration of laser communication and ranging is proposed , which can make the aircraft complete various tasks with the same load, so as to reduce the requirement of volume, power consumption, and improve the performance of thesystem. the ranging code which has the uniqueness, good auto-correlation and cross-correlation propertiesand the communication datas transport with with series tranmission by encoding, which can realize high speed two one-way laser communications.And making use of the ranging code good auto-correlation properties, in the receiver B, the received ranging code correlates with local ranging code to relize the coarse measurement. and utilizing the phase difference between recovery of local clock and receiving clock to achieve the precise measurement in one ranging chip.the we can get the timission time t1, similarly,we can get another timission time t2 in the sender A , so the distance between A and B is(t1+t2)*c/2 ,c is the speed of light. so in the whole precess,we can achieve high precision measurement without the high speed A/D conversion. Through the above mentioned?we can realize the integration of laser high speed communication and high precision ranging.

Integration of laser communication and ranging is proposed in this paper. we use the ranging code embed in thecommmunication data ,making the ranging code and the communication datas transport with with series tranmission by encoding, which can realize high speed two one-way laser communications.And making use of the ranging code good auto-correlation properties, at the receiver the received ranging code correlates with local ranging code to relize the coarse measurement , and utilizing the phase difference between recovery of local clock and receiving clock to achieve the precision of the distance .

10408-39, Session PWed

Radial partially coherent beams for free-space optical communications

Minghao Wang, Xiuhua Yuan, Huazhong Univ. of Science and Technology (China)

In this study, a special class of nonuniformly correlated partially coherent beams with radially symmetric coherence distributions, called radial partially coherent beams (RPCBs), is introduced. By spatially modulating a uniformly correlated phase screen used for generating conventional Gaussian Schell-model beams, RPCBs with arbitrary distributions of degree of coherence can be easily produced. RPCBs whose degree of coherence decreases from the beam center along the radial direction were found to self-focus in free-space propagation, leading to higher optical intensity near the beam center. Meanwhile, the scintillation mitigation ability of RPCBs remains significant. By means of wave optics simulation, free-space and atmospheric propagation properties of RPCBs with various coherence distributions and amplitude profiles are numerically analyzed. Simulation results show that, when there exists a flat-topped central fully coherent area, the RPCB will focus repeatedly during propagation, resulting into much higher on-axis intensity and smaller beam spread in the far field. Moreover, it is noticeable that the enhanced intensity can be achieved without compromise of scintillation reduction. Therefore, even though the multi-focusing effects may be slightly suppressed in atmospheric propagation, the RPCB can provide a substantial improvement for the SNR of an optical receiver with small aperture. The remarkable propagation properties as well as easy implementation of RPCB make it a valuable source option for free-space optical communications.

10408-40, Session PWed

A variable rate communicate method for self-differential coherent DPSK

Chenzhe Lao, Jianfeng Sun, Guangyu Cai, Guangyuan Li, Guo Zhang, Bo Zhang, Mengmeng Xu, Hongyu He, Shanghai Institute of Optics and Fine Mechanics (China)

In the satellite-to-ground laser communication, there are many adverse factors in the Atmospheric channel. At present, self-differential coherent DPSK is proved that could overcome atmospheric turbulence effects. Nevertheless, there is still the unsatisfactory detecting result when the atmospheric channel quality is extremely poor. In this case, full rate communication is not very easy to achieve. In this paper, a new method called digital coherence is presented, which superposes several same encoding to reduce the BER; that is to say, it reduces the communication rate to achieve higher quality. Compared to the general method, this method doesn't need to change the original communication rate, reduces the complexity of the system to a great extent. The theory of this method has been discussed that the SNR is increased by 3dB when the rate is reduced to half. An experimental setup was constructed to verify the proposed theoretical analysis. The offline process and results are presented.

10408-41, Session PWed

Optical axis stability system based on acousto-optic deflector

Peipei Hou, Jianfeng Sun, Yu Zhou, Qian Xu, Wei Lu, Zhiyong Lu, Zhu Luan, Lijuan Wang, Liren Liu, Shanghai Institute of Optics and Fine Mechanics (China)

An adaptive space optical coupling system for free-space optical communication is proposed in BPSK coherent laser communication link. Nutation principle is used. The position of the light spot relative to the center of the detector is determined by theory. The signal lights passing through acousto-optic frequency shifter and acousto-optic deflector are deflected by output control signal. The signal lights received by optical receiving system pass through acousto-optic deflector, and then coupled with local signal lights when they incident to 2 * 4 90 ° optical hybrid. The acousto-optic deflector is controlled by phase error signal, which is output from 2*4 90 ° optical hybrid. And high coupling efficiency for local signal light and free space light is obtained. The system has a strong ability to filter out the background light, and can achieve a relatively good space optical communication transmission channel.

10408-42, Session PWed

Fine track system of space coherent optical communication without position detector

Hongyu He, Jianfeng Sun, Liren Liu, Shanghai Institute of Optics and Fine Mechanics (China)

Fine tracking technology is one of the key technologies in space optical communication systems based on coherent detection. Traditional fine tracking system use CCD as the position detector of signal light. In order to simplify the system and improve accuracy, we propose a fine tracking system without position detector and theoretically prove that the system is feasible. Meanwhile corresponding space optical communication system was built, experiment on tracking the signal light with random jitter was done.

10408-43, Session PWed

Condition for keeping polarization invariance on propagation in space-to-ground optical communication downlink

Jiajie Wu, Jing Ma, Liying Tan, Siyuan Yu, Harbin Institute of Technology (China)

Based on the extended Huygens–Fresnel principle, the expression of cross-spectral density matrix of a GSM laser beam at receiver plane in a space-to-ground optical communication downlink is obtained. According to the expression, the sufficient condition for Gaussian Schell-model (GSM) beam to keep the polarization properties unchanged in a space-to-ground optical communication downlink is derived analytically. The results indicate when three coherence lengths (?xx, ?yy and ?xy) are equal to each other, the GSM beam maintains the polarization properties on propagation. With full consideration of the source parameters and the zenith angle, both the DOP and SOP on propagation are investigated. The results of this work provide a design basis of the polarization shift keying optical communication system with GSM laser beam.

10408-44, Session PWed

Multiple wavelength spectral system simulating background light noise environment in satellite laser communications

Wei Lu, Jianfeng Sun, Peipei Hou, Qian Xu, Yueli Xi, Yu Zhou, Funan Zhu, Liren Liu, Shanghai Institute of Optics and Fine Mechanics (China)

Performance of satellite laser communications between GEO and LEO satellites will be influenced by background light noise appeared in the field of view of optical terminals due to sunlight or planets and some comets. Such influences should be studied on the ground testing platform before the space application. In this paper, we introduce a simulator that can simulate the real case of background light noise in space environment during the data talking via laser beam between two lonely satellites. This simulator can not only simulate the effect of multiple wavelength spectrum, but also the effects of adjustable angles of field-of-view, large range of adjustable optical

power and adjustable deflection speeds of light noise in space environment. We integrate these functions into a device with small and compact size for easily mobile use. Software control function is also achieved via personal computer to adjust these functions arbitrarily.

10408-45, Session PWed

A survey of POAM in starlight

Stephen Grulke, Jeremy P. Bos, Michigan Technological Univ. (United States)

This work is an extension of the work done by Oesch and Sanchez [1-4] and relies on analysis of historical site monitoring data from the AFRL's Starfire Optical Range (SOR). Initial analysis of this data by Oesch and Sanchez provided preliminary evidence of POAM static across multiple observations. They hypothesize that this POAM is the result of nearby interstellar media. This work presents initial results of a large-scale survey of site monitoring data for evidence of residual POAM that may be attributable to the interstellar medium.

1. Oesch, Denis; Sanchez, Darryl. Photonic orbital angular momentum in starlight, Further analysis of the 2011 Starfire Optical Range Observations. EDP Sciences, 2014

2. Oesch, Denis; Sanchez, Darryl. Orbital angular momentum in optical waves propagating through distributed turbulence. Optical Society of America, 2011

3. Oesch, Denis; Sanchez, Darryl; Gallegos, Anita; Holzman, Jason; Brennan, Terry; Smith, Julie; Gibson, William; Farrell, Tom; Kelly, Patrick. Creation of photonic orbital angular momentum by distributed volume turbulence. Optical Society of America, 2013

4. Oesch, D. W.; Sanchez, D. J.; Reynolds, O. R. The creation of photonic orbital angular momentum in the electromagnetic waves propagating through turbulence. EDP Sciences, 2013

10409-1, Session 1

Applications of photon-number-resolving measurements for quantum interferometry and quantum state tomography *(Invited Paper)*

Olivier Pfister, Aye Win, Rajveer Nehra, Univ. of Virginia (United States); Sae-Woo Nam, Thomas Gerrits, National Institute of Standards and Technology (United States)

Photon-number-resolving measurements allow one to address quantum optics from the corpuscular angle of quantum physics. A number of classically non-intuitive features are typically expected from working in the photon-number Fock eigenbasis, such as nonpositive Wigner functions. In this talk, we report on the progress of two applications of photon-number-resolving measurements in quantum optics: quantum interferometry with photon-subtracted twin beams and quantum state tomography of Fock states created by heralded parametric downconversion.

10409-2, Session 1

Coincidence rates and permutation symmetry *(Invited Paper)*

Hubert de Guise, Lakehead Univ. (Canada); Barry C. Sanders, Univ. of Calgary (Canada) and Canadian Institute for Advanced Research (Canada)

We discuss the importance that photon permutation symmetry has on coincidence rates at interferometer outputs, how permutations naturally lead partition the many-photon space, and how permutation symmetry reveals the connection between partial distinguishability, matrix immanants and the complexity of the coincidence landscape.

10409-3, Session 1

Photon number statistics of entanglement generated by multiple single photon sources *(Invited Paper)*

Junyi Wu, Holger F. Hofmann, Hiroshima Univ. (Japan)

Multiphoton interference results in a wide variety of non-classical photon number statistics, including characteristic signatures of entanglement between two or more sets of optical modes. Here, we consider the photon number statistics observed after applying discrete Fourier transformations (DFTs) to bipartite entangled states generated using single photon sources and beam splitters. It is shown that the output photon number states of DFTs are eigenstates of a translational mode shifting operator in the input. The complex eigenvalues of the mode shift can be identified by a phase number k obtained from the output photon distribution. For each output distribution, the possible input states are limited to mode shift eigenstates with the same k-value. Using this mode shift rule, we can identify the quantum coherence between different photon number distributions in the input with experimentally observable k-values in the output of the DFT. In the case of multi-photon entanglement obtained by post-selection and beam splitting single photons, this coherence is non-local, resulting in correlated pairs of k-values that always sum up to zero. We can therefore observe both the correlations between the input photon number distributions and a complementary correlation between the output photon numbers of two DFTs to obtain a reliable characterization of the entanglement between the two multi-mode multi-photon systems. Importantly, the k-value allows a classification of large sets of possible photon number distributions, resulting in a significant simplification of the experimental evaluation of the multi-photon output statistics and opening up the road towards more efficient applications of non-classical multi-photon states.

10409-4, Session 1

Entanglement detection with single Hong-Ou-Mandel interferometry *(Invited Paper)*

Joonwoo Bae, Hanyang Univ. (Korea, Republic of); Leong-Chuan Kwek, Nanyang Technological Univ. (Singapore); Simone Felicetti, Lab. Matériaux et Phénomènes Quantiques (France); Chang Jian Kwong, Univ. of Darmstadt (Germany)

Entanglement is not only fundamental for understanding multipartite quantum systems but also generally useful for quantum information applications. Despite much effort devoted so far, little is known about minimal resources for detecting entanglement and also comparisons to tomography which reveals the full characterization. Here, we show that all entangled states can in general be detected in an experimental scheme that estimates the fidelity of two pure quantum states. An experimental proposal is presented with a single Hong-Ou-Mandel interferometry in which only two detectors are applied regardless of the dimensions or the number of modes of quantum systems. This shows measurement settings for entanglement detection are in general inequivalent to tomography: the number of detectors in quantum tomography increases with the dimensions and the modes whereas it is not the case in estimation of fidelity which detects entangled states.

10409-5, Session 1

Erasing the orbital angular momentum information of a photon

Isaac M. Nape, Bienvenu I. Ndagano, Melanie McLaren, Andrew Forbes, Univ. of the Witwatersrand (South Africa)

The traditional variations of quantum eraser use interferometric schemes (double slits or beams splitters) that rely on physical path interference to acquire and remove path information. For example when, orthogonal polarisations mark the independent paths, no interference pattern is observed. However, performing a complementary projection of the polarisation recovers the interference pattern due to the paths of the photon interfering. Interestingly, the expression of the entangled system after going through the marked slits shows an entanglement between the spatial degree of freedom (path) of one photon and the polarisation of its entangled twin. The entanglement of photons between their degrees of freedom is called hybrid entanglement.

Here we show that the orbital angular momentum (OAM) of photons is an alternative degree of freedom to explore besides path. We exploit the geometric phase of light using a locally birefringent material called the q-plate to generate hybrid entanglement from entangled photons prepared via spontaneous parametric down conversion. Using OAM to polarisation conversion in one of the entangled photons, hybrid entanglement is established between the polarisation and OAM of the entangled pair. Therefore the polarisation control of one photon determines the OAM information of its twin. Just as in Young's experiment, we show that the paths (OAM) marked with polarisation do not lead to interference. However, a complimentary projection of the polarisation causes the OAM (paths) to interfere, leading to the formation of azimuthal fringes whose frequency is proportional to the OAM content carried by the photon.

10409-6, Session 2

Optical hybrid quantum teleportation and its applications *(Invited Paper)*

Shuntaro Takeda, Masanori Okada, Akira Furusawa, The Univ. of Tokyo (Japan)

Quantum teleportation is the act of transferring unknown quantum information from a sender to a spatially distant receiver without transmitting the physical carrier of information itself. It is the essence of many sophisticated protocols for quantum communication and computation. Quantum teleportation has been experimentally realized both in discrete-variable (DV; such as qubits) and continuous-variable (CV) systems in quantum optics, but both approaches have pros and cons. DV teleportation transfers photonic qubits with high fidelity, albeit probabilistically and post-selectively. In contrast, CV teleportation deterministically transfers quadrature variables of electromagnetic fields, though the fidelity is relatively low due to the imperfection of CV entanglement.

Here we take a "hybrid" approach to overcome the current limitations: CV quantum teleportation of DVs. When the classical channel gain is optimally tuned, the CV teleporter acts as a pure loss channel, while dual-rail photonic qubits are robust against photon loss and hence can be reliably teleported even with imperfect CV entanglement. This approach enabled the first realization of deterministic quantum teleportation of photonic qubits without post-selection. We also applied the hybrid scheme to entanglement swapping, where DV two-mode entanglement was robustly transferred by means of CV quantum teleportation. To overcome the photon-loss error in the hybrid scheme, we are now working on CV teleportation of two-photon qutrits, a pair of which can form a quantum error correction code against photon loss. Our hybrid approach will stimulate the development of optical hybrid quantum information processing with the potential to enable high-fidelity, highly efficient universal quantum computation.

10409-7, Session 2

Quantum interference in topological photonic circuits

Jean-Luc Tambasco, RMIT Univ. (Australia); Giacomo Corrielli, Politecnico di Milano (Italy); Robert Chapman, RMIT Univ. (Australia); Andrea Crespi, Politecnico di Milano (Italy); Oded Zilberberg, ETH Zürich (Switzerland); Roberto Osellame, CNR-Istituto di Fotonica e Nanotecnologie (Italy); Alberto Peruzzo, RMIT Univ. (Australia)

Quantum technologies hold great promise for developing extremely powerful quantum computers and unattackable communication systems, and for achieving the ultimate precision measurements. The platforms used to manipulate quantum states typically suffer high loss and introduce noise, limiting their scalability and application. Topology introduces the idea of robust states known as edge-states and recently, topological states have been demonstrated in engineered photonic systems and used to effectively transport light. We report quantum interference of edge-states in an array of ten photonic waveguides with the coupling coefficients following the Aubry-André-Harper (AAH) model of topological edge states. High control over the circuit layout is achieved using femtosecond laser-written waveguides in glass. Two edge states, initially at either sides of the array, are adiabatically transferred to the centre where they interfere. After interfering, the states are returned to the outsides of the array, where they are protected again. By tuning the interference region to implement a 50:50 beamsplitter, we measure near unit visibility Hong-Ou-Mandel (HOM) photon bunching of the topological edge states. Our results demonstrate on-chip quantum state transfer and quantum interference of photonic topological states, providing a route to robust quantum information processing.

10409-8, Session 2

Towards the strong-coupling regime with a trapped ion coupled to a fiber cavity *(Invited Paper)*

Klemens Schüppert, Florian R. Ong, Pierre Jobez, Florian Kranzl, Konstantin Friebe, Dario A. Fioretto, Moonjoo Lee, Markus Teller, Univ. Innsbruck (Austria); Konstantin T. Ott, Jakob Reichel, Lab. Kastler Brossel (France); Rainer Blatt, Univ. Innsbruck (Austria) and Institut für Quantenoptik und Quanteninformation (Austria); Tracy E. Northup, Univ. Innsbruck (Austria)

Single atoms coupled to optical cavities can be used to build up quantum interfaces between stationary and flying qubits in a quantum network. These interfaces are compelling candidates for quantum repeaters, which would enable fiber-based quantum communication over long distances. By using fiber-based optical cavities, we expect to reach the strong coupling regime of cavity quantum electrodynamics with single trapped ions. Operating in this regime would enable protocols for quantum communication over long distances to be carried out with enhanced fidelity and efficiency.

The challenge in integrating fiber cavities with ion traps is that the dielectric fibers should be far enough from the ions so that they do not significantly alter the trap potential. On the other hand, larger cavity mode volumes reduce the coupling rate. Additionally, small deviations from the mirrors' ideal spherical shape introduce optical losses. Therefore, we have developed new CO_2-laser ablation techniques for improved fiber-mirror structures. With the resulting fibers, we have constructed optimized fiber cavities with finesses up to 70,000 at a length of 550 microns. To integrate these fiber cavities with ions, we have built a miniaturized calcium ion trap in the proven "Innsbruck" linear design. Both fibers are mounted on separate nanopositioners, enabling us to adjust the cavity length and optimize its alignment in vacuum. By developing procedures to control the charges trapped on the fibers' dielectric surfaces, we were able to couple an ion to cavities with lengths of about 500 microns and with finesses in excess of 30,000.

10409-9, Session 2

PPLN-waveguide-based polarization entangled QKD simulator

John Gariano, Ivan B. Djordjevic, The Univ. of Arizona (United States)

We have developed a comprehensive simulator to study the polarization entangled quantum key distribution (QKD) system, which takes various imperfections into account. We assume that a type-II SPDC source using a PPLN-based nonlinear optical waveguide is used to generate entangled photon pairs and implements the BB84 protocol, using two mutually unbiased basis with two orthogonal polarizations in each basis. The entangled photon pairs are then simulated to be transmitted to both parties; Alice and Bob, through the optical channel, imperfect optical elements and onto the imperfect detector. It is assumed that Eve has no control over the detectors, and can only gain information from the public channel and the intercept resend attack. The secure key rate (SKR) is calculated using an upper bound and by using actual code rates of LDPC codes implementable in FPGA hardware. After the verification of the simulation results, such as the pair generation rate and the number of error due to multiple pairs, for the ideal scenario, available in the literature, we then introduce various imperfections. Then, the results are compared to previously reported experimental results where a BBO nonlinear crystal is used, and the improvements in SKRs are determined for when a PPLN-waveguide is used instead.

10409-10, Session 2

Hamiltonian dynamics for entanglement distribution in quantum networks

Laszlo Gyongyosi, Budapest Univ. of Technology and Economics (Hungary) and Hungarian Academy of Sciences (Hungary); Sandor Imre, Budapest Univ. of Technology and Economics (Hungary)

Quantum entanglement is a necessity for future quantum communication networks, quantum internet, and long-distance quantum key distribution. The current approaches of entanglement distribution require high-delay entanglement transmission, entanglement swapping to extend the range of entanglement, high-cost entanglement purification, and long-lived quantum memories. We introduce a protocol for establishing entanglement in quantum communication networks. The proposed scheme does not require entanglement transmission between the nodes, high-cost entanglement swapping, entanglement purification, or long-lived quantum memories. The protocol reliably establishes a maximally entangled system between the remote nodes via dynamics generated by local Hamiltonians. The method eliminates the main drawbacks of current schemes allowing fast entanglement establishment with a minimized delay. Our solution provides a fundamental method for future long-distance quantum key distribution, quantum repeater networks, quantum internet, and quantum-networking protocols.

10409-11, Session 3

Discrimination of coherent-state phase-shift-keys with quantum non-demolition sequential measurements *(Invited Paper)*

Si-Hui Tan, Singapore Univ. of Technology & Design (Singapore)

Sequential decoding is a decoding procedure that uses a series of measurements to discern encoded information in a quantum channel. It has been shown by Giovannetti, Lloyd, and Maccone that a sequential decoder implementing only projective measurements at every step is able to achieve Holevo bound asymptotically. One of the main components of their scheme is a YES-NO projective measurement, which projects the received state into either one of the codewords, or the orthogonal subspace. Here I study the performance of a YES-NO projective measurement, the vacuum-or-not (VON) measurement, for discriminating the states of a M-ary coherent-state phase-shift-key (PSK) constellation. The VON measurement is a quantum non-demolition measurement that projects a state either onto the vacuum state or its complement. For guessing one of M possible coherent states of this constellation, one first selects a hypothesis, then displaces the received state by the inverse of the phase shift of that hypothesis, and finally performs a VON measurement. If vacuum is detected, one concludes that the guessed hypothesis is the correct hypothesis. Otherwise, these steps are iterated for all the hypotheses of the constellation until VON measurement yields vacuum in which case one concludes that the guessed hypothesis for that round is the correct hypothesis. The error probability of this sequential decoder is calculated explicitly for some specific M values, and compared to the performance of known sub-optimal and near-optimal receivers for M-ary PSK.

10409-12, Session 3

Quantum communication with spectrally correlated photons

Piotr L. Kolenderski, Mikolaj Lasota, Karolina Sedziak, Nicolaus Copernicus Univ. (Poland)

Single-photon sources are crucial components for the implementation of quantum communication protocols. However, photons emitted by some of the most popular types of realistic sources are spectrally broadband. Due to this drawback, the signal emitted from such sources is typically affected by the effect of temporal broadening during its propagation through telecommunication fibers which exhibit chromatic dispersion. Such problem can be observed e.g. when using sources based on the process of spontaneous parametric down-conversion (SPDC). In the case of long-distance quantum communication temporal broadening can significantly limit the efficiency of temporal filtering. It is a popular method, which is based on the reduction of the duration time of the detection window, used for decreasing the number of registered errors.

In this work we analyzed the impact of the type of spectral correlation within a pair of photons produced by the SPDC source on the temporal width of those photons during their propagation in dispersive media. We found out that in some situations the width can be decreased by changing the typical negative spectral correlation into positive one or by reducing its strength. This idea can be used to increase the efficiency of the temporal filtering method. Therefore it can be applied in various implementations of quantum communication protocols.

As an example of the application we subsequently analyzed the security of a quantum key distribution (QKD) scheme based on single photons. It was realized in the configuration with the source of photons located in the middle between the legitimate participants of a QKD protocol (called typically Alice and Bob). We demonstrated that when the information about the emission time of the photons produced by the SPDC source is not distributed to Alice and Bob, the maximal security distance can be considerably extended by using positively correlated photons, while in the opposite case strongly (no matter positively or negatively) correlated photons are optimal. We also found out that the results of our calculation may be very sensitive to the spectral widths of the photons produced by the SPDC source. In addition, we concluded that in realistic situation Alice and Bob would have to optimize their source over both the spectral widths of the generated photons and the type of spectral correlation in order to maximally extend the security distance.

The results of our work are, in particular, important for the QKD systems utilizing commercial telecom fibers populated by strong classical signals. In those systems temporal filtering method can be used to reduce not only the dark counts registered by the detection system, but also the channel noise originating from the process of Raman scattering, which is the main factor limiting their performance.

10409-13, Session 3

Approaches to a global quantum key distribution network *(Invited Paper)*

Md Tanvirul Islam, Robert Bedington, National Univ. of Singapore (Singapore); Doug K. Griffin, Russell Boyce, UNSW Canberra (Australia); Christian Kurtsiefer, National Univ. of Singapore (Singapore); Alexander Ling, Ctr. for Quantum Technologies (Singapore)

Progress in quantum computers and computational power threatens to weaken existing public key encryption. A global quantum key distribution (QKD) network can play a role in computational attack-resistant encryption. Such a network could use a constellation of airships and satellites as trusted nodes to facilitate QKD between any two points on the globe on demand. This requires both satellite-to-ground and inter-satellite links. However, the prohibitive cost of traditional satellite based development limits the experimental work demonstrating relevant technologies. To accelerate progress towards a global network, we use an emerging class of shoe-box sized spacecraft known as CubeSats. We have designed an entangled photon pair source that can operate on board CubeSats.

The robustness and miniature form factor of the entanglement source makes it especially suitable for performing pathfinder missions. Using this design, we have performed a feasibility study for a satellite-to-satellite QKD demonstration mission in collaboration with the University of New South Wales; Canberra. This mission concept uses two 6U CubeSats in low Earth orbit and aims to demonstrate QKD between them over varying separations.

10409-14, Session 3

On photonic spectral entanglement improving quantum communication

Piotr L. Kolenderski, Karolina Sedziak, Mikolaj Lasota, Nicolaus Copernicus Univ. (Poland)

Let us consider the experimental setup where SPDC source generates photon pairs which are subsequently coupled to single-mode fibers (SMFs). We assume that there are three parties involved: 1) Alice, possessing the photon pair source, detection system and the fiber connecting them, 2) Bob, who monitors the output of the second, long-distance fiber and 3) Eve, who can perform the most general collective attacks in order to acquire information which Alice and Bob wish to transfer. Typically, in fiber-based communication the chromatic dispersion is considered to be an obstacle, limiting the maximal distance at which information carrier can be securely transmitted. This phenomenon forces the trusted parties to define longer detection windows to avoid losing signal photons and increases the amount of detection noise that is being registered.

We consider standard BB84 quantum key distribution protocol, based on the SPDC source located in between Alice and Bob. The parameters of standard realistic telecommunication fibers (SMF28e+) are take into account. The source emits photon which apart of being entangled in polarization degree of freedom are entangled in spectral domain. This is the key feature which allows one to reduce detection noise by manipulating the spectral correlation between the produced photons. In this way the maximal security distance can be increased by around 10%.

10409-15, Session 3

The design of a continuous variable quantum repeater *(Invited Paper)*

William J. Munro, Fabian Furrer, NTT Basic Research Labs. (Japan); Kae Nemoto, National Institute of Informatics (Japan)

Quantum repeaters are well known as a necessary tool for large-scale quantum network and any future quantum internet. Typically such repeaters have relied on the transmission of single photons along long optical fibres. There is however a natural compatibility issue however as our current 'classical' telecommunication networks use multi-photon pluses of light. A natural question arises whether we can design quantum repeaters using these multi-photon pluses of light. In this talk we will present a CV QR scheme that has a success probability scaling polynomial in the distance and that can distribute entangled EPR states with arbitrary squeezing and fidelity over arbitrarily long distances. Further we will show that this distribution of pure two-mode (entangled) squeezed states can occur over arbitrarily long distances with a polynomial resource scaling.

10409-16, Session 3

The rise of silicon carbide as a promising integrated quantum nanophotonics platform *(Invited Paper)*

Stefania Castelletto, RMIT Univ. (Australia); Alexander Lohrmann, The Univ. of Melbourne (Australia); Takeshi Ohshima, National Institutes for Quantum and Radiological Science and Technology (Japan); Jeffrey C. McCallum, Brett C. Johnson, The Univ. of Melbourne (Australia)

Silicon carbide (SiC) is rising as a versatile platform for quantum optics and spin sensing due its integrated optically and spin active atomic size centres [1], with the additional opportunity to advance integrated quantum nanophotonics devices, due to its mature nanofabrication, synthesis and device engineering. Recently, we have demonstrated formation of optically active centres in SiC with excellent characteristics for broadband single photon generation at room temperature in the visible spectral range and very favourable for integration into nanophotonic/plasmonics devices.

In this presentation, I will review some of recent results on the controlled formation of single defects in silicon carbide in different polytypes, responsible for single photon emission in a broad spectral range of zero phonon lines. We have found that they can be formed in all technologically relevant polytypes of SiC, including 3C-SiC, a relevant polytype in micro and nano-electromechanical sensors and for optical micro-cavity fabrication. Further, I will focus on their integration in nanomaterials, electrically controlled devices and microdisks. An outlook on current efforts to achieve integrated quantum nanophotonics based on silicon carbide hyperbolic metamaterials with engineered single defects will be provided.

[1] A. Lohrmann, B.C. Johnson, J. McCallum, S. Castelletto "A review on Single photon sources in silicon carbide", Reports on Progress in Physics 80 034502 (2017) http://dx.doi.org/10.1088/1361-6633/aa5171

10409-17, Session 3

Experimental investigation of security parameters of Y-00 quantum stream cipher transceiver with randomization technique: Part I *(Invited Paper)*

Fumio Futami, Kentaro Kato, Osamu Hirota, Tamagawa Univ. (Japan)

Y-00 cipher is a quantum cipher disabling an eavesdropper from reading ciphertext of mathematical encryption (M-E) box correctly. Ciphertext are generated by mapping binary signals to multilevel signals by M-E box, and the cipher signals for Eve suffer error in their discrimination by quantum noise of coherent state. On the other hand, security against the brute force attack is ensured by the quantum no-cloning theorem.

The authors developed a Y-00 cipher transceiver in which randomization technique was incorporated. Last year in this conference, an irregular mapping as the randomization technique of the Y-00 cipher transceiver was experimentally demonstrated, and an application of the transceiver to secure optical fiber transmission of GbE signals was reported.

We have been also investigation the security performance of the transceiver. Our theoretical security analysis showed, for higher security, it is desirable that the signal power distribution after converting into multilevel signals in the optical domain should be uniform, even when the bit sequence of plaintext has any form of non-uniformity. Consequently, it is required to measure an optical signal power distribution of the Y-00 cipher transceiver for evaluating its security levels. In this research, we experimentally measure powers of multi-level optical signals and calculate the numbers of the signals over and under the average power. In the experiments, we employ various kinds of information sequences as input signals, and confirm that the distributions are uniform for most sequences. In the conference, the meaning of this security analysis is introduced and experimental results of the measurements are reported. In addition, an improving method is discussed.

10409-18, Session 3

Permutation modulation for quantization and information reconciliation in CV-QKD systems *(Invited Paper)*

Fred Daneshgaran, California State Univ., Los Angeles (United States); Marina Mondin, California State Univ., Los Angeles (United States) and Politecnico di Torino (Italy); Khashayar Olia, California State Univ., Los Angeles (United States)

Coding over higher and higher dimensions is always advantageous when it comes to Information Reconciliation (IR) for Continuous Variable Quantum

Key Distribution (CV-QKD) schemes. Let X be the d-dimensional vector of Gaussian samples at Alice, X' be the corresponding vector of samples at Bob and Y the corresponding m-bit quantized version of X'. Then the Theorem by Slepian-Wolf provides a bound on the achievability region of rate for the correlated sources and states that disclosing r=?H(K(X)?Y))+1/d? bits of the quantization label is enough to obtain the remaining (m-r)-bits with arbitrary low error probability, where K(X) is the key function that generates the secret key given the continuous valued Gaussian samples in X. Given this setup, the main problem here is how do you quantize a d-dimensional Gaussian vector when d can potentially be very large? Standard vector quantization may not be efficient, and different techniques may be devised. In this regard, this paper presents the use of Permutation Modulation (PM) techniques to perform the quantization of the Gaussian vector where d can be as high as several thousands. Monte Carlo simulation is used to assess the effectiveness of the technique and establish the error rates associated with the labels of the quantized samples.

10409-19, Session 3

A unified analysis of optical signal modulation formats for quantum enigma cipher *(Invited Paper)*

Kentaro Kato, Tamagawa Univ. (Japan)

A framework of the quantum enigma cipher was reported as a generalization of the quantum stream cipher by Y00 protocol that aims to break the Shannon limit of symmetric key encryption systems with the help of quantum noise of light last year. Development of criteria in designing of optical signal modulation formats is of importance to realize such physical encryption systems for secure fiber-optic communications, for controlling the net amount of the signal masking effect caused by quantum noise of light. In this study, we focus on this problem.

So far, we have proposed a variety of optical signal modulation formats for the quantum stream cipher. However, no unified analysis of the basic features of optical signal modulation formats for the quantum enigma cipher has been done. Fortunately, recent progress of the computation algorithms for optimal discrimination problems of quantum state signals enables us to handle a large-scale and complicated case such as the minimax discrimination of multi-ary non-symmetric quantum states. This helps us to seek possibilities of other new optical signal modulation formats. By using such algorithms for optimal quantum signal detection problem, the signal masking effect caused by quantum noise of light is evaluated in some modulation formats. From the analysis of the signal masking effect, some tradeoff relations between security level and communication performance will be observed. Moreover, a comparison of optical signal modulation formats for the quantum enigma cipher will be done, and some useful criteria for designing modulation formats in the quantum enigma cipher will be given.

10409-20, Session 4

The first sub shot noise wide field microscope *(Invited Paper)*

Marco Genovese, Istituto Nazionale di Ricerca Metrologica (Italy)

In the last years several proof of principle experiments have demonstrated the advantages of quantum technologies respect to classical schemes. The present challenge is to overpass the limits of proof of principle demonstrations to approach real applications. In this talk, following a general introduction, we present such an achievement in the field of quantum enhanced imaging. In particular, we describe the realization of a sub-shot noise wide field microscope based on spatially multi-mode non-classical photon number correlations in twin beams. The microscope produces real time images of 8000 pixels at full resolution, for (500μm)2 field-of-view, with noise reduced to the 80% of the shot noise level (for each pixel), suitable for absorption imaging of complex structures. By fast post-elaboration, specifically applying a quantum enhanced median filter, the noise can be further reduced (less than 30% of the shot noise level) by setting a trade-off with the resolution, demonstrating the best sensitivity per incident photon ever achieved in absorption microscopy. We will also discuss possible conjugation of ghost imaging techniques to this method.

10409-21, Session 4

Cancelling out aberrations through high order correlations *(Invited Paper)*

Juarez G. Silva, Eduardo J. S. Fonseca, Alcenisio J. de Jesus Silva, Univ. Federal de Alagoas (Brazil)

The imaging through optical systems may have distortions called aberrations. It can be chromatic aberrations, an effect resulting from dispersion due to the impossibility to focus all colors to the same point or monochromatic aberrations, where the rays emerging from one object point will not all meet at a single image point. Thanks to an analogy between the quantum and classical intensity light correlations, the previous studies explored the ghost imaging under both viewpoint. Although, the first approach was the use of correlated-photon imaging for the cancellation of phase aberrations, some authors have suggested theoretical models for the cancellation of phase aberrations using classical light in the ghost-imaging scheme. However, a detailed experimental study of the cancelation of phase aberrations using classical light intensity correlation is still missing in the literature. In this work, we show that exploring correlations of fluctuations in speckle intensity it is possible to cancel out aberrations that may exist in the Fraunhofer plane of an optical system. The aberrations cancelation occurs independently of its shape and it does not need coordinate inversion. We use high-order intensity correlations to obtain high visibility. Therefore, we extended the quantum-classical analogy to the study of cancelation of phase aberrations showing an interesting and useful distinction from the quantum case. It is possible to embed images into speckle patterns, and to recover it though the spatial correlation function. Therefore, this effect can be useful in imaging through random media and microscopy, canceling inherent aberrations than can cause distortions in the image.

10409-22, Session 4

Squeezed light enhanced sensing of a micro-mechanical oscillator *(Invited Paper)*

Ulrik Lund Andersen, Technical Univ. of Denmark (Denmark)

Ultra-precise measurements of various parameters such as the mass of nano-particles, magnetic fields or gravity can be attained by probing the phononic modes of a micro-mechanical oscillator with light. The sensitivity of such measurements is in part governed by the noise of the phononic mode as well as the noise of the probing light mode, so by decreasing the noise of the probe beam an enhanced sensitivity can be expected. We demonstrate this effect by using squeezed states of light where the quantum uncertainty of the relevant quadrature is reduced below the shot noise level. Using this squeezing-enhanced sensitivity effect, we demonstrate 1) improved feedback cooling of a phononic mode in a microtoroidal cavity and 2) improved sensing of a magnetic field using the coupling to a microtoroidal phononic mode via a magnetorestrictive material. We present our recent experimental results and discuss future directions.

10409-23, Session 4

Future outlook for diamond-based quantum information devices *(Invited Paper)*

Philip R. Hemmer, Texas A&M Univ. (United States)

In recent years there has been substantial progress in solid-state quantum information demonstrations based on diamond. This ranges from room-temperature multi-qubit quantum registers to spin-photon entanglement to loophole-free Bell tests. Most of these demonstrations are done with the nitrogen-vacancy (NV) center. Recently however the silicon-vacancy (SiV) center has shown a much better coupling to photons, owing to the suppression of spectral diffusion. Still more recently the germanium-vacancy (GeV) has shown much higher quantum efficiency the SiV. However there are tradeoffs. In this talk I will review the various options for quantum information devices in diamond. I will also discuss new options for the future, including designer color centers made possible by novel diamond growth techniques.

10409-24, Session 4

Verification of quantum entanglement of two-mode squeezed light source towards quantum radar and imaging

Genta Masada, Tamagawa Univ. (Japan)

Two-mode squeezed light is an efficient resource for quantum entanglement and shows non-classical correlation between quadrature phase amplitudes in each optical mode. We are developing a high-quality two-mode squeezed light source to explore the possibility of quantum radar based on the quantum illumination theory. It is expected to improve error probability for discrimination of target presence or absence even in a lossy and noisy environment. We are also expecting apply two-mode squeezed light source to quantum imaging. In this work we generate two-mode squeezed light source and verify its quantum entanglement property towards quantum radar and imaging.

Firstly we generate two independent single-mode squeezed light beams utilizing two sub-threshold optical parametric oscillators which include periodically-polled potassium titanyl phosphate crystals for the second order nonlinear interaction. They are combined by using a half mirror with a relative optical phase of 90 degrees between each optical field. Then entangled two-mode squeezed light beams can be generated. We observe correlation variances between quadrature phase amplitudes in entangled two-mode fields by balanced homodyne method. Finally we verify quantum entanglement property of two-mode squeezed light source based on Duan's inseparability criteria. In quantum radar or quantum imaging system, a turbulent atmosphere degrades quantum entanglement of a light source and affects performance of target detection. An optical loss is one of the simplest and most probable examples of environmental factors. In this work we also investigate quantum entanglement under the influence of an optical loss and optimum conditions of the two-mode squeezed light source for realizing quantum radar.

10409-25, Session 4

Superresolution via structured illumination quantum correlation microscopy *(Invited Paper)*

Girish Agarwal, Texas A&M Univ. (United States)

We propose to use intensity correlation microscopy in combination with structured illumination to image quantum emitters that exhibit antibunching with a spatial resolution reaching far into the sub-classical regime. Combining intensity measurements and intensity auto correlations up to order m creates an effective PSF with FWHM shrunk by the factor pm. Structured Illumination microscopy on the other hand introduces a resolution improvement of factor 2 by use of the principle of moiré fringes. Here, we show that for linear low-intensity excitation and linear optical detection the simultaneous use of both techniques leads to an in theory unlimited resolution power with the improvement scaling favorably as m+sqrtm in dependence of the correlation order m. Hence, yielding this technique to be of the utmost interest for biological imaging. We present the underlying theory and simulations demonstrating the highly increased spatial superresolution, and point out requirements for an experimental implementation.

10409-26, Session 5

Quantum walks with twisted classical light *(Invited Paper)*

Bereneice Sephton, Council for Scientific and Industrial Research (South Africa) and Univ. of the Witwatersrand (South Africa); Angela Dudley, CSIR National Laser Ctr. (South Africa); Andrew Forbes, Univ. of the Witwatersrand (South Africa)

In the avid search for means to increase computational power in comparison to that which is currently available, quantum walks (QWs) have become a promising option with derived quantum algorithms providing an associated speed up compared to what is currently used for implementation in classical computers. It has additionally been shown that the physical implementation of QWs will provide a successful computational basis for a quantum computer. It follows that considerable drive for finding such means has been occurring over the 20+ years since its introduction with phenomena such as electrons and photons being employed. Principal problems encountered with such quantum systems is the vulnerability to environmental influence as well as scalability of the systems. Here we perform the QW classically, due to interference characteristics inherent in the phenomenon, to mitigate these challenges. We utilize the properties of classical vector beams to physically implement such a walk in orbital angular momentum space by manipulating polarization and exploiting the non-separability of such beams. We show that with this method it is possible to achieve a physical QW with the advantage of robust properties that are associated with many classical systems.

10409-27, Session 5

Sum uncertainty relations for compact classical Lie algebra *(Invited Paper)*

Namrata Shukla, Institute for Quantum Science and Technology (Canada); Lorenzo Maccone, Univ. degli Studi di Pavia (Italy); Hubert de Guise, Lakehead Univ. (Canada); Barry C. Sanders, Univ. of Calgary (Canada)

The sum uncertainty relations are useful because they provide us with a state-independent non- trivial bound. We describe the construction of sum uncertainty relations for compact classical Lie algebras of the type su(n), so(2n), so(2n+1) and sp(n). Then we present resulting uncertainty relations explicitly for the su(2), su(3) and su(4) cases. In order to verify the bounds for general irreps of su(2) and su(3) and su(4), we develop and run a computer program that checks that the relations are correct for general states. Our method uses as a starting point the quadratic Casimir operator of the algebra, which can be recognized as a sum of variances of the generators using elementary observations. We discuss what type of states saturate the su(n) bound, and compare these states with states that saturate more familiar products of uncertainties. Our method is valuable for extending sum uncertainty relations to su(n) and beyond su(n) algebras. We also discuss our results in the context of multi-level atoms and squeezing.

10409-28, Session 5

Optical trapping and control of levitated nanoparticles *(Invited Paper)*

David Grass, Uros Delic, Nikolai Kiesel, Univ. Wien (Austria); Daniel R. Ladiges, John E. Sader, The Univ. of Melbourne (Australia); Markus Aspelmeyer, Univ. Wien (Austria)

The coupling of a levitated nanoparticle to an optical cavity field promises access to unprecedented parameter regimes for macroscopic quantum experiments at room temperature. We report our current progress on the combination of an optical tweezer trap [1] with a Fabry-Perot cavity for

optomechanical control [2] towards quantum cavity-optomechanics with levitated nanoparticles.

For fast and clean delivery of nanoparticles into ultra-high vacuum we have developed a hollow core photonic crystal fiber based conveyor belt [3]. An optical read-out allows monitoring the three-dimensional motion of the particle over the entire fiber length and is used for radiation pressure based feedback cooling. We utilize read-out and feedback cooling to investigate the local pressure along the fiber when a pressure gradient is applied. We compare the measurements with predictions from a direct simulating Monte Carlo method of the nonlinear Boltzmann equation.

[1] Gieseler, J. et al. PRL 109, 103603 (2012)

[2] Kiesel, N. et al. PNAS 110, 14180 (2013)

[3] Grass, D. et al. APL 108, 221103 (2016)

10409-29, Session 5

A repository for quantum measurement trajectories *(Invited Paper)*

Durga B. Rao Dasari, Univ. Stuttgart (Germany); Sen Yang, The Chinese Univ. of Hong Kong (China); Jörg Wrachtrup, Univ. Stuttgart (Germany)

Revealing the quantum mechanical nature of system-bath interactions has gained lot of prominence due to its connection to the foundational aspects of quantum mechanics and also to upcoming quantum technologies where a good control over such interactions is a prerequisite. Though a theoretical description of such interactions has always been quantum mechanical, assumptions on the nature of the coupling and the bath-evolution has led to effective master equations that describe only the dynamics of the system alone. As most experimental settings can only achieve a high degree control and readout of the system alone, characterizing the bath on a similar level of detail as contained in a quantum model has not been achieved. Here we develop protocols that certify the quantum nature of the bath and effects that cannot be reproduced by classical descriptions of the same. Based on measurement correlations of subsequent readouts of the quantum system we show back-action effects on the bath, by imprinting on it the measurement trajectory of the quantum system and storing it for few seconds. For both experiments and theory we have used single defect centers in diamond as our quantum system and the surrounding nuclear spin-bath as our environment. The experiments are performed at low temperatures where the optical excited states of the defect are well-resolved allowing for projective readout of the quantum defect.

Conference 10410: Unconventional and Indirect Imaging, Image Reconstruction, and Wavefront Sensing 2017

SPIE. OPTICS+ PHOTONICS OPTICAL ENGINEERING+ APPLICATIONS

Wednesday - Thursday 9 –10 August 2017

Part of Proceedings of SPIE Vol. 10410 Unconventional and Indirect Imaging, Image Reconstruction, and Wavefront Sensing 2017

10410-1, Session 1

Impact of beacon anisochromatatism on phase-compensation performance

Colleen T. Gross, Air Force Insititute of Technology (United States); Mark F. Spencer, Air Force Research Lab. (United States)

This study evaluates the effects of beacon anisochromatatism on phase-compensation performance. In general, beacon anisochromatatism occurs at the system level because the beacon-illuminator laser (BIL) and high-energy laser (HEL) are often at different wavelengths. Such is the case, for example, when using an aperture sharing element to isolate the beam-control sensor suite from the blinding nature of the HEL. With that said, this study uses the WavePlex toolbox in MATLAB to model ideal spherical wave propagation through various atmospheric turbulence conditions. In order to quantify phase-compensation performance, we also model a nominal adaptive-optics (AO) system. We achieve low-order correction from a centroid tracker and fast-steering mirror and higher-order correction from a Shack-Hartmann wavefront sensor and continuous-face-sheet deformable mirror using least-squares phase reconstruction in the Fried geometry. To this end, we plot the normalized power in the bucket as a function of BILL-HEL wavelength difference. Our initial results show that positive BILL-HEL wavelength differences achieve better phase compensation performance compared to negative BIL-HEL wavelength differences (i.e., red BILs outperform blue BILs). This outcome is consistent with past results.

10410-2, Session 1

Adaptive optics using a MEMS deformable mirror for a segmented mirror telescope

Norihide Miyamura, Meisei Univ. (Japan)

For small satellite remote sensing missions, a large aperture telescope more than 400mm is required to realize less than 1m GSD observations. However, it is difficult or expensive to realize the large aperture telescope using monolithic primary mirror with high surface accuracy. A segmented mirror telescope should be studied especially for small satellite missions. Generally, not only high accuracy of optical surface but also high accuracy of optical alignment is required for large aperture telescope. For a segmented mirror telescopes, the alignment is more difficult and more important. For conventional systems, optical alignment is adjusted before launch to achieve desired imaging performance. However, it is difficult to adjust the alignment for large sized optics in high accuracy. Furthermore, thermal environment in orbit and vibration in launch vehicle cause the misalignments of the optics. We are developing an adaptive optics system using a MEMS deformable mirror for earth observing remote sensing sensor. Image based adaptive optics system compensate the misalignments and wavefront aberration of optical elements using deformable mirror by feedback of observed images. Because, it is difficult to use a reference point source unless the satellite controls its attitude toward a star for earth observing systems. Furthermore, total amount of incident light can enter an image sensor. We propose the control algorithm of the deformable mirror for a segmented mirror telescope by using of observed image. The experimental results show that misalignment and wavefront aberration of the segmented mirror telescope are corrected and image quality is improved.

10410-3, Session 1

Deep turbulence wavefront sensing using digital holographic detection in the phase-shifting recording geometry

Douglas E. Thornton, Air Force Institute of Technology (United States); Mark F. Spencer, Air Force Research Lab. (United States); Glen P. Perram, Air Force Institute of Technology (United States)

The effects of distributed-volume or “deep” turbulence in long range imaging applications presents unique challenges to properly measure and correct for aberrations incurred along the atmospheric path. Digital holography can detect the volumetric wavefront distortions caused by deep-turbulence to resolve the aberrations. Different recording geometries of the hologram offer different benefits depending on the application and previous studies have evaluated the performance off-axis and image plane recording geometries for wavefront sensing. This study models digital holographic detection in the phase-shifting recording geometry in the presence of deep-turbulence using wave optics simulations. In particular, the analysis models spherical-wave propagation through varying deep-turbulence conditions to estimate phase screens along the horizontal propagation path and the performance is evaluated by calculating the field-estimated Strehl ratio. Altogether, the results show digital-holographic detection in the phase-shifting recording geometry is an effective wavefront sensing method in the presence of deep turbulence.

10410-4, Session 1

Shack-Hartmann electronic densitometer (SHED)

Anthony R. Valenzuela, U.S. Army Research Lab. (United States); Aaron Schweinsberg, Oak Ridge Institute for Science & Education (United States)

The Shack-Hartmann Electron Densitometer (SHED) is a novel method to diagnose ultrashort pulse laser–produced plasmas by measuring the phase change to a probe laser beam. Using the Shack-Hartmann method, the phasefront of a probe laser is measured through a lenslet array onto a camera. Small changes in the location of the individual focal points on the camera plane are translated into changes in the probe beam’s wavefront. These wavefront distortions arise from refractive index variations caused by the free electrons. This method allows for superior performance in measuring minute variations in the electron density in 2 dimensions, single-shot, with sub-picosecond time resolution. The data taken with SHED demonstrated the ability to diagnose plasmas with densities of the order of 1019 cm-3 and show the temporal evolution of the plasma long after the driving laser pulse has left. The method can be further improved by enclosing the probe beam and adding a second axis to allow for tomographic reconstruction of the electron density in 3 dimensions. By using SHED in a pump/probe setup, we are able to obtain temporally synchronized, ultrashort snap shots of the evolution of free electrons in laser-induced ionization of air and other transparent media.

10410-5, Session 1

Simultaneous measurements of density field and wavefront distortions in high speed flows

Jacob George, Thomas P. Jenkins, James D. Trolinger, MetroLaser, Inc. (United States); Benjamin D. Buckner, Spectabit Optics, LLC (United States); Cecil F Hess, MetroLaser (United States)

The primary objective of this study is towards the development of optical sensors and hence it is important to know the effects on an optical beam as it traverses the flow field, and thus relate measured wavefront distortions to the specific flow structure of the time varying flow field. The motivation behind this research rests in the fact that the performance of laser based and guided systems is strongly affected by aero-optical effects. These effects limit the capability of the systems in resolving images with high resolution as well as projecting high optical energy densities. When an optical wavefront passes through an aerodynamic flow, its phase and amplitude are modulated, resulting in distortion and loss of optical information and energy. Depending on the beam size relative to the turbulence scales, the degradation results in adverse effects such as defocus, beam jitter, beam steering, etc. Thus, it is pertinent to measure the density structures and their spatial extent, flow statistics, and density fluctuations since they are directly related to index of refraction fluctuations. In this study, simultaneous measurements of density, using Rayleigh scattering (RS) and wavefronts using a wavefront sensor is carried out in ambient conditions in a high speed compressible jet flow. These experiments should help in greater understanding of the connection between a flowfield and the associated optical degradation by correlating features of the flow with the distorted wavefronts. Also, it will help in developing models that describe relationships between turbulence and optical aberrations.

10410-49, Session 1

Horizontal atmospheric turbulence, beam propagation, and simulation using collected data and predictive techniques

Christopher C. Wilcox, Freddie Santiago, Ty Martinez, K. Peter Judd, Sergio R. Restaino, U.S. Naval Research Lab. (United States)

The turbulent effect from the Earth's atmosphere degrades the performance of an optical imaging system. Many studies have been conducted in the study of beam propagation in a turbulent medium. Horizontal beam propagation and correction presents many challenges when compared to vertical due to the far harsher turbulent conditions and increased complexity it induces. We investigate the collection of beam propagation data, analysis, and use for building a mathematical model of the horizontal turbulent path and the plans and designs for an adaptive optical system to use this information to correct for horizontal path atmospheric turbulence.

10410-6, Session 2

Using optical interferometry for GEO satellites imaging: An update *(Invited Paper)*

Sergio R. Restaino, J. Thomas Armstrong, Ellyn K. Baines, Henrique R. Schmitt, James H. Clark III, U.S. Naval Research Lab. (United States)

We describe updates in both hardware and software at the Navy Precision Optical Interferometer (NPOI) and our continuous work to expand and extend the capabilities of this instrument for potential Space Situational Awareness (SSA) technological demonstration. The main new topics with respect to our previous work are a campaign of observations carried out in March and then repeated in June and the results of these campaigns. The second area is the procurement of three one-meter diameter telescopes in order to increase the sensitivity of the instrument. Description of the ongoing work for the deployment of these telescopes will be described.

10410-7, Session 2

Improving spatial resolution of the light field microscope with Fourier ptychography

Yoshitake Tani, Tomohiro Suzuki, Kenjiro Takai Miura, Shizuoka Univ. (Japan)

Light field microscope (LFM) is an optical microscope capable of obtaining images having large depth of field with different viewpoints. By using the parallax of these multi-view images, it is possible to reconstruct the 3D sample. However, the sampling interval of this multi-viewpoint image depends on the pitch interval of the microlens array, so the spatial resolution is low, and the accuracy of the 3D sample to be reconstructed is also low.

Conventional research has a method of increasing the spatial resolution by subpixel-shifted multiple images. However, this method has problems such as the necessity of mechanical operation and high cost.

Therefore, we propose applying Fourier ptychography to the LFM. Fourier ptychography is a technique to obtain high spatial resolution images by joining images obtained by irradiating samples from different angles using LED arrays in Fourier space. Fourier ptychography does not require mechanical scanning and is high throughput and low cost. In addition, Fourier tycoography is possible to obtain phase information on a sample, and it is also possible to obtain a fine 3D sample. We propose a method to generate high spatial resolution multiview images using Fourier ptychography and reconstruct highly accurate 3D sample from those images. In this research, we experiment with the original LFM and verify the effect.

10410-8, Session 2

System compression theory and application

Xiteng Liu, QualVisual Technology (Canada)

In this paper, we introduce the concept and rationale of system compression and its application to signal recovery in high quality and high speed. Essentially different from compressed sensing, system compression dispenses with signal sparsity and convex optimization on which compressed sensing relies. Convex optimization such as linear programming and orthogonal matching pursuit depend on iterative computations and become very slow and unstable in high dimensional systems. Doing without convex optimization, system compression dramatically improves both computation speed and stability and hence is eligible for real-time applications. Even better, it doesn't require signals to be sparse. A high-quality signal can be recovered in numerically or perceptually lossless manner with as few as 25% measurements. Experimental results manifest that system compression overwhelmingly outperforms existing methods for signal recovery. Demo software and testing data are all downloadable at the website http://qualvisual.net.

10410-9, Session 3

Synthetic-aperture direct-detection coherent imaging *(Invited Paper)*

James R. Fienup, Univ. of Rochester (United States)

This paper describes an approach to coherent aperture synthesis and fine-

resolution image reconstruction employing phase retrieval from intensity measurements. A Gerchberg-Saxton algorithm is used on a pair of intensity measurements to obtain the fields for each telescope at each position of the telescopes without a reference beam. These are combined into a larger synthetic aperture, and a cross-correlation is used to sense and correct for piston, tip and tilt phases of each of the sub-apertures with respect one another. Results of simulations, including the effects of speckle, are shown, and practical considerations are evaluated.

10410-10, Session 3

Method and algorithm for efficient calibration of compressive hyperspectral imaging system based on a liquid crystal retarder

Liat Revah, Yaniv Oiknine, Isaac Y. August, Adrian Stern, Ben-Gurion Univ. of the Negev (Israel)

Recently we presented a Miniature Compressive Ultra-spectral Imaging System (MUSI). This system consists of a single Liquid Crystal (LC) phase retarder as a spectral modulator and a gray scale sensor array to capture a multiplexed signal of the imaged scene. By designing the LC spectral modulator in compliance with the Compressive Sensing (CS) guidelines and applying appropriate algorithms we demonstrated reconstruction of spectral (hyper/ ultra) datacubes from an order of magnitude fewer samples than taken by conventional sensors. The LC modulator is designed to have an effective width of a few tens of micrometers, therefore it is prone to imperfections and spatial nonuniformity. In this work, we present the study of this nonuniformity and present a mathematical algorithm that allows the inference of the spectral transmission over the entire cell area from only a few calibration measurements.

10410-11, Session 3

Drift in correlation tracking algorithms

David C. Dayton, Applied Technology Associates (United States)

All image correlation based tracking algorithms exhibit some sort of deleterious drift problems. This presentation examines this issue and steps to mitigate it.

10410-12, Session 3

Efficiency measurements for a digital-holography imaging system

Matthias T. Banet, MZA Associates Corp. (United States); Mark F. Spencer, Air Force Research Lab. (United States) and Air Force Institute of Technology (United States)

This paper compares efficiency measurements to efficiency predictions for a digital-holography imaging system operating in the off-axis image plane recording geometry. In practice, we use a highly-coherent 532 nm laser source and an extended Spectralon® object. To compare our efficiency measurements to our efficiency predictions, we make use of an expression for the signal-to-noise ratio (SNR), which contains many multiplicative terms with respect to total-system efficiency. The results show that the polarization and the fringe-integration efficiency terms play the largest role in the total-system efficiency for the digital-holography imaging system.

10410-50, Session 3

Local sharpening and subspace wavefront correction with predictive dynamic digital holography

Sennan Sulaiman, Steve Gibson, Univ. of California, Los Angeles (United States)

Digital holography holds several advantages over conventional imaging and wavefront sensing, chief among these being significantly fewer and simpler optical components and the retrieval of complex field. Consequently, many imaging and sensing applications including microscopy and optical tweezing have turned to using digital holography. A significant obstacle for digital holography in real-time applications, such as wavefront sensing for high energy laser systems and high speed imaging for target tracking, is the fact that digital holography is computationally intensive; it requires iterative virtual wavefront propagation and hill-climbing to optimize some sharpness criteria. It has been shown recently that minimum-variance wavefront prediction can be integrated with digital holography and image sharpening to reduce significantly large number of costly sharpening iterations required to achieve near-optimal wavefront correction. This paper demonstrates further gains in computational efficiency with localized sharpening in conjunction with predictive dynamic digital holography for real-time applications. The method optimizes sharpness of local regions in a detector plane by parallel independent wavefront correction on reduced-dimension subspaces of the complex field in a spectral plane.

10410-13, Session 4

Use of (N-1)-D expansions for N-D phase unwrapping in MRI

Philip J. Bones, Laura J. King, Rick P. Millane, Univ. of Canterbury (New Zealand)

In MRI the presence of metal implants causes severe artifacts in images and interferes with the usual techniques used to separate fat signals from other tissues. In the Dixon method three images are acquired at different echo times to enable the variation in the magnetic field to be estimated. However, the estimate is represented as the phase of a complex quantity and therefore suffers from wrapping. High field gradients near the metal mean that the phase estimate is undersampled and therefore challenging to unwrap.

We have developed POP, phase estimation by onion peeling, an algorithm which unwraps the phase along 1-D paths for a 2-D image. The unwrapping is initially performed along a closed path enclosing the implant and well separated from it. The recovered phase is expanded using a smooth periodic basis along the path. Then, path-by-path, the estimate is applied to the next path and then the expansion coefficients are estimated to best fit the wrapped measurements. We have successfully tested POP on MRI images of specially constructed phantoms and on a group of patients with hip implants.

In principle, POP can be extended to 3-D imaging. In that case, a smooth basis for phase would be applied over a series of surfaces enclosing the implant (the "onion skins"), again beginning the phase estimation well away from the implant.

Results are presented for fat and water separation for 2-D images of phantoms and actual patients. The practicality of the method and its employment in clinical MRI are discussed.

10410-14, Session 4

High resolution depth reconstruction from monocular images and sparse point clouds using deep convolutional neural network

Martin Dimitrievski, Peter Veelaert, Wilfried Philips, Univ. Gent (Belgium)

Understanding the 3D structure of the environment is advantageous for many tasks in the field of robotics and autonomous vehicles. From the robot's point of view, 3D perception is often formulated as a depth image reconstruction problem. In the literature, dense depth images are often recovered deterministically from stereo image disparities. Other systems use an expensive LiDAR sensor to produce accurate, but semi-sparse depth images. With the advent of deep learning there have also been attempts to estimate depth by only using monocular images. In this paper we combine the best of the two worlds, focusing on a combination of monocular images and low cost LiDAR point clouds. We explore the idea that very sparse depth information accurately captures the global scene structure while variations in image patches can be used to reconstruct local depth to a high resolution. The main contribution of this paper is a supervised learning depth reconstruction system based on a deep convolutional neural network. The network is trained on RGB image patches reinforced with sparse depth information and the output is a depth estimate for each pixel. Using image and point cloud data from the KITTI vision dataset we are able to learn a correspondence between local RGB information and local depth, while at the same time preserving the global scene structure. Our results are evaluated on sequences from the KITTI dataset and our own recordings using a low cost camera and LiDAR setup.

10410-16, Session 4

Improving 3D registration by up-sampling of sparse point cloud through fusion with high-resolution 2D image

Hyukseong Kwon, Kyungnam Kim, HRL Labs., LLC (United States); Jean J. Dolne, Boeing Co. (United States)

No Abstract Available

10410-17, Session 4

Rapid 3D registration using local subtree caching in iterative closest point (ICP) algorithm

Ryan Uhlenbrock, Kyungnam Kim, Heiko Hoffmann, HRL Labs., LLC (United States); Jean J. Dolne, Boeing Co. (United States)

No Abstract Available

10410-18, Session PWed

An edge sensitive 3D measurement using two directional laser stripe scanning with a MEMS scanner

Dong Li, Xiang Zhou, Chang da Xu, Chao Wang, Jia yu Guo, Rui Jin, Xi'an Jiaotong Univ. (China)

The width of the laser stripe is physically difficult to compress, when the measured object has a mutually perpendicular edge (X axis and Y axis direction, respectively, containing the edge), this traditional measurement method will only accurately measure a certain direction of the edge, so using traditional measurement methods requires two directions to scan separately and a rotation device. Obviously, the traditional laser stripe measurement method is inefficient and complex.

This work proposes an edge sensitive 3D measurement system which is fast and accurate, using two directional laser stripe scanning with a MEMS scanner. This method for scanning the edges(x direction and y direction) of an object has the advantages of high efficiency, high speed and edges with high precision.

The 3D measurement system consists of four cameras and a MEMS scanner, four cameras which are named , , , and array around the MEMS scanner. Firstly, we should calibrate the system parameters of cameras and determine the matrix transformation relationship between calibration plate coordinate system and the camera coordinate system. Secondly, the picture captured by group (and) cameras are Fourier transformed, to determine the mask of the region of interest. Then to perform inverse Fourier transform, and to extract laser stripe center. Matrix of laser stripe center is multiplied by mask, and we can get the effective zone of the laser stripe center matrix. Using the same method, we can get the effective zone of the laser stripe center matrix of group (and). Lastly, according to calibration parameters and matrix of laser stripe center, with binocular stereo reconstruction technique, we can get the 3D point cloud model of group cameras and cameras. The two sets of point cloud models are converted to the calibration plate coordinate system, we can get 3D model with fine edge step.

10410-36, Session PWed

Three dimensional interferometric synthetic aperture ladar based on Pseudo-random Code

Guangyuan Li, Zhiyong Lu, Jianfeng Sun, Yu Zhou, Guo Zhang, Bo Zhang, Mengmeng Xu, Chenzhe Lao, Hongyu He, Liren Liu, Shanghai Institute of Optics and Fine Mechanics (China)

In order to get the three dimensional information of the target, and satisfy the requirement of high speed imaging, the three dimensional interferometric synthetic aperture ladar(SAL) based on the pseudo-random code was proposed, without local reference delay time, which can get fine resolution and overcome the speed mismatch problem between the pulse repetition frequency and the chirp rate of the linear frequency modulation signal. The phase modulation method of the three dimensional SAL is pseudo-random code modulation. M sequence is adopted as the pseudorandom code for its superior performance in code compression to get the range direction information. The azimuth direction information was obtained by doppler frequency shift of the return signal. The interferometric image of the two cross-track apertures was used to get the height information. The principle of the three dimensional interferometric SAL based on pseudorandom code was theoretical deduced in detail, and the simulation results were given. The feasibility of the three dimensional interferometric SAL is verified.

10410-37, Session PWed

Imaging processing with bidirectional modulation in down-looking synthetic aperture imaging ladar

Zhiyong Lu, Yu Zhou, Jianfeng Sun, Zhu Luan, Lijuan Wang, Qian Xu, Liren Liu, Shanghai Institute of Optics and Fine Mechanics (China)

Down-looking synthetic aperture imaging ladar have bidirectional (positive and negative direction) modulation in the orthogonal direction of travel during phase modulation. The return signal can be also collected in the two direction. The imaging processing with bidirectional modulation is used and demonstrated. The signal-to-noise ratio can be enhanced in this mode synthetic aperture imaging ladar. Meanwhile, the velocity of

carrying-platform can be faster. In the experiment, the return signals with bidirectional modulation are stacked and rebuilt. Compared to the unidirectional modulation imaging, the faster and clearer imaging is realized with bidirectional modulation. This technique has a great potential for applications in extensive synthetic aperture imaging ladar fields.

10410-38, Session PWed

Influence of polarization features of target reflection on synthetic aperture imaging ladar

Qian Xu, Zhiyong Lu, Jianfeng Sun, Lijuan Wang, Peipei Hou, Wei Lu, Liren Liu, Shanghai Institute of Optics and Fine Mechanics (China)

Synthetic aperture imaging ladar (SAIL) is one of the most possible optical active imaging methods to achieve superresolution in a long distance and break the diffraction limit. Two-dimensional reconstructed images of the laser cooperative targets have been obtained successively by many institutes. Nevertheless, natural target reconstructed images by the SAILs have not been achieved. The polarization state of return optical field will be changed due to the interaction of incident polarized light and materials of the target, furthermore, it would affect the intermediate frequency signal which the SAILs imaging needed. The Mueller matrices can describe the complex polarization features of the target reflection and treat this interaction. In this paper, the influence on resolution element imaging in side-looking and down-looking SAILs will be theoretically analyzed.

10410-39, Session PWed

A three dimensional point cloud registration method based on rotation matrix eigenvalue

Chao Wang, Xiang Zhou, Xi'an Jiaotong Univ. (China); Zixuan Fei, Xiaofei gao, Rui Jin, Xi'an Jiaotong Univ. (China)

We usually need to measure an object at multiple angles in the traditional optical three-dimensional measurement method, due to the reasons for the block, and then use point cloud registration methods to obtain a complete three-dimensional shape of the object. The point cloud registration based on a turntable is essential to calculate the coordinate transformation matrix between the camera coordinate system and the turntable coordinate system. We usually calculate the transformation matrix by fitting the rotation center and the rotation axis normal of the turntable in the traditional method, which is limited by measuring the field of view. The range of exact feature points used for fitting the rotation center and the rotation axis normal is approximately distributed within an arc less than 120 degrees, resulting in a low fit accuracy. In this paper, we proposes a better method, based on the invariant eigenvalue principle of rotation matrix in the turntable coordinate system and the coordinate transformation matrix of the corresponding coordinate points. First of all, we control the rotation angle of the calibration plate with the turntable to calibrate the coordinate transformation matrix of the corresponding coordinate points by using the least squares method. And then we use the feature decomposition to calculate the coordinate transformation matrix of the camera coordinate system and the turntable coordinate system. Compared with the traditional previous method, it has a higher accuracy, better robustness and it is not affected by the camera field of view. In this method, the coincidence error of the corresponding points on the calibration plate after registration is less than 0.1mm.

10410-40, Session PWed

A multi-resolution texture fusion algorithm

Yuqin Li, Xiang Zhou, Xi'an Jiaotong Univ. (China); Jia yu Guo, Tao Yang, Zixuan Fei, Xi'an Jiaotong Univ. (China)

Texture fusion is essential for 3D photo-realistic texture model reconstruction. multi-resolution texture fusion mainly is applied to reconstruct three-dimensional models that the local texture are very realistic. This paper presents a multi-resolution texture fusion algorithm based on digital image processing.

The technique utilizes the depth camera to obtain range data and the texture camera to obtain the local interested high-resolution texture of the object. And each point of the range images a pixel of the picture corresponding to this view should be found, so the map between high-resolution texture and local 3D points could be obtained by using the SURF to register the local high-resolution texture with the low resolution texture collected by the depth camera. Then the light source correction of textures is applied to remove the systematic differences such as black edges which are achieved by computing the HIS difference between each point's colors. Finally, ICP is applied to register models, and mapping different-resolution textures onto three-dimensional models. The global correction is applied to refine the observable variations in color that may still exist near the fusion boundaries. These corrections will utilize the grid triangle vertex color as a constraint to drive texture fusion to remove discontinuities from different resolutions.

The advantage of this technique is that it utilizes the light source correction and global correction to fuse different resolutions textures. Experiments with this technique indicate that it significantly corrects the observable discontinuities within the overlapping areas, which are given from different resolutions, lighting change, non-lambertian object surface, etc.

10410-41, Session PWed

A novel 360-degree shape measurement using a simple setup with two mirrors and a laser MEMS scanner

Rui Jin, Xi'an Jiaotong Univ. (China); Xiang Zhou, Xi'an Jiaotong Univ. (China); Tao Yang, Dong Li, Xi'an Jiaotong Univ. (China); Chao Wang, Xi'an Jiaotong Univ. (China)

There is no denying that 360-degree shape measurement technology plays an important role in the field of three-dimensional optical metrology. Traditional optical 360-degree shape measurement methods are mainly two kinds: the first kind, by placing multiple scanners to achieve 360-degree measurements; the second kind, through the high-precision rotating device to get 360-degree shape model. The former increases the number of scanners and costly, while the latter using rotating devices lead to time consuming.

This paper presents a low cost and fast optical 360-degree shape measurement method, which possesses the advantages of full static, fast and low cost. The measuring system consists of two mirrors with a certain angle, a laser projection system, a stereoscopic calibration block, and two cameras. As the need to capture the virtual image of objects presented in the mirror, the projector needs a great depth of field. We have successfully developed an optical module called laser MEMS scanner by using the laser MEMS scanning technology that can produce always-in-focus images in long distance, so this problem is solved. At the same time, the laser MEMS scanner can achieve precise movement of laser stripes without any movement mechanism, improving the measurement accuracy and efficiency.

What's more, a novel stereo calibration technology presented in this paper can achieve point clouds data registration, and then get the 360-degree model of objects. A stereoscopic calibration block with special coded patterns on six sides is used in this novel Stereo calibration method. Through this novel stereo calibration technology we can quickly get the 360-degree models of objects.

10410-42, Session PWed

Enhancement of incoherent imaging through turbulence by using multi-aperture receivers

Vadim V. Dudorov, Anna S. Eremina, V.E. Zuev Institute of Atmospheric Optics (Russian Federation)

Possibilities of the image quality enhancement by using multi-aperture systems are investigated numerically for incoherent imaging through atmospheric turbulence. We compare the quality of images formed by a single aperture and images synthesized by an array of N*N subapertures (N = 2–15). The use of multi-aperture systems have advantage by means of local tip-tilt compensation of image-forming wavefront distorted by turbulence - image tip-tilt displacement for each subaperture. In so synthesized images, residual turbulent distortions are almost isoplanatic in a wide range of atmospheric conditions, which allows a significant increase in the image quality via computer object restoration. The results of correction of images synthesized are compared with images without correction and with traditional images formed by a single aperture. The effect of the number and size of subapertures on the quality of the image restored is analyzed. It is shown that if the size of a multi-aperture system is constant, then there is an optimal number of subapertures, which depends on the turbulence intensity and diffraction effect. Optimal conditions for the use of multi-aperture imaging versus the atmosphere conditions and distance are found.

10410-43, Session PWed

Super-resolution imaging with one complex filter based on compressive sensing

Yicheng Sun, Nanjing Univ. of Science and Technology (China) and NRIEE (China); Guohua Gu, Xiubao Sui, Nanjing Univ. of Science and Technology (China); Yuqi Li, NRIEE (China)

Super-resolution is being considered as one of the important goals for optical imaging and image processing. In this paper, we present a novel imaging technique that exceeds the limit of resolving power of diffraction-limited optical system to achieve super-resolution imaging, by combining the advantages of compressive sensing and complex annular filters. This technique is realized by utilizing a classical 4F optical system with a phase-only spatial light modulator. Furthermore, the feasibility of this technique is theoretically analyzed, and physically validated by laboratory experiments. Experimental results have demonstrated that the technique improves the resolving power of diffraction-limited optical system by approximately times, and the intensity image of high-resolution object can be recovered from of the total number of measurements.

10410-44, Session PWed

Optical method of separating of isotropic and anisotropic parts of polymer-dispersed liquid crystals images

Andriy L. Nehrych, Peter P. Maksimyak, Yuriy Fedkovych Chernivtsi National Univ. (Ukraine)

We have investigated the spatial-frequency filtering on PDLC. Partial beams passed through LC droplets and polymer matrix may be considered as plane waves passing different optical pathes and interfering in the far zone. Changing the voltage results in changeing the LC effective refractive index leading to a change of the path difference between the interfering beams. The effect of interference decreases of some spectral components of the radiation passing through PDLC sample can be used for space-frequency filtering of images.

We have used LC E7 by Merck, dispersed in the polymer NOA 65 by Norland Inc. as the object of research.

Scattering indicatrix is modulated with a periods of 2.5o and 10o, which is clearly recognized at small angles. At small angles of scattering indicatrix, significant redistribution of the radiation intensity is observed depending on the applied voltage to PDLC.

In the absence of applied voltage, PDLC passes high and low spatial frequencies. At a voltage of 2 V, the regular component formed at low spatial frequencies is quenching by interference, while the PDLC sample strongly scatters radiation. This phenomenon has been studied in detail in our previous works. When the voltage of 6 V is applied to PDLC, the scattering is almost absent because the refractive index of LC drops is close to the refractive index of the polymer matrix. Therefore, the scattered radiation containing high spatial frequencies is filtered by PDLC, and low spatial frequencies passes through the sample. These features of the scattering indicatrix provide the possibility of spatial frequency filtering of images.

10410-45, Session PWed

Adaptive compressed photon counting 3D imaging based on wavelet trees and Hadamard multiplexing

Huidong Dai, Guohua Gu, Nanjing Univ. of Science and Technology (China); Weiji He, Nanjing Univ. of Science and Technology (China) and Key Lab. of Intelligent Perception and Systems for High-Dimensional Information (China); Ling Ye, Nanjing Univ. of Information Science & Technology (China); Tianyi Mao, Qian Chen, Nanjing Univ. of Science and Technology (China)

A photon counting 3D imaging system with short-pulsed structured illumination and a single-pixel photon counting detector are built. The proposed multiresolution photon counting 3D imaging technique acquires a high-resolution 3D image from a coarse image and details at successfully finer resolution sampled by hadamard multiplexing along the wavelet trees. The detected power is significant increased thanks to the hadamard multiplexing method. Both the required measurements and the reconstruction time can be significant reduced, which makes the proposed technique suitable for scenes with high spatial resolution. Since the depth map is retrieved through an inverse wavelet transform instead of the computational intensive optimization problems performed in CS, the time consumed to retrieve the depth map can be also reduced, and thus it will be suitable for applications of real-time compressed 3D imaging such as object tracking. even though the resolution of the final 3D image can be high, the number of measurements remains small due to the adaptivity of the wavelet-trees-based sampling strategy. The adaptive sampling technique is quality oriented, allowing more control over the image quality. The experimental results indicate that both the reflectivity and depth map of a scene at resolutions up to pixels can be acquired and retrieved with practical times as low as 14 seconds.

10410-46, Session PWed

Using virtual reality to test the regularity priors used by the human visual system

Eric Palmer, Purdue Univ. (United States); TaeKyu Kwon, The Ohio State Univ. (United States); Zygmunt Pizlo, Purdue Univ. (United States)

Virtual reality applications provide opportunity to test human vision in well-controlled scenarios that would be difficult to generate in real physical spaces. This study is intended to evaluate the importance of regularity priors used by the human visual system. Using a CAVE simulation, subjects viewed virtual objects in a variety of experimental manipulations. In the

first experiment, the subject was asked to count the objects in a scene that was viewed right-side-up or upside-down for 4 seconds. The subject counted more accurately in the right-side-up viewing condition regardless of the presence of binocular disparity or color. In the second experiment, the subject was asked to reconstruct the scene from a different viewpoint. Reconstructions were accurate, but the position and orientation error was twice as high when the scene was rotated by 45°, compared to 22.5°. Similarly to the first experiment, there was little difference between monocular and binocular viewing. In the third experiment, the subject was asked to adjust the position of one object to match the depth extent to the frontal extent among three objects. Performance was best when symmetrical objects were used and became poorer when asymmetrical objects were used and poorest with only small circular markers on the floor. Finally, in the fourth experiment, we demonstrated reliable performance in monocular and binocular recovery of 3D shapes of objects standing naturally on the simulated horizontal floor. Based on these results, we conclude gravity, horizontal ground, and symmetry priors play an important role in veridical perception of scenes.

10410-47, Session PWed

Ghost imaging using shifted speckles and bucket detection

Tianyi Mao, Qian Chen, Weiji He, Guohua Gu, Nanjing Univ. of Science and Technology (China)

Computational ghost imaging (CGI), which is based on the quantum or classical correlation of fluctuating light fields, for the last decades, has opened new avenues for computational light microscopy, remote sensing, optical encryption and so on. The resolution of CGI is determined by the speckle's transverse size on the object plane and the numerical aperture of the projection optics. In many applications, it is enough to get the periphery of the object, which is called "edge enhancement" in image processing. However, poor imaging quality of CGI limits the edge detection, which is important for target recognition and localization in remote sensing and biological imaging. In this paper, we proposed ghost imaging using shifted speckles and bucket detection. In our simulations and experiments, it is hard for us to recognize the detected object by using "ghost" images. It has been demonstrated that using the proposed method dramatically limits the reconstruction noise and enhances the edges continuously at the sacrifice of contrast. The edge detection using this technique with Sobel operator, Standard operator and Laplacian operator were demonstrated theoretically and experimentally. The results show that the method using Sobel operator is robust in noisy environments. It is noted that the potential applications of ghost imaging are remote sensing and biological imaging, where complex photoelectric systems and high-speed sampling will cause much noise in detection. The robust indicates that the proposed method using Sobel operator is much appropriate in real applications. It is noticeable that the technique overcomes the disadvantages of edge detection in ghost imaging without any addition of hardware and complex computation. Combining the proposed method with other proposed applications of CGI, especially in remote sensing and biological applications, will improve the success rate of target recognition and localization.

10410-48, Session PWed

Shape from shading using a linear filtering approach

Oscar E. Castillo, Jorge Luis Flores Nuñez, Univ. de Guadalajara (Mexico)

There is a vast variety of algorithms for the resolution of the shape from shading problem; most of these algorithms rely on basic assumptions about the surface reflective properties, camera projection and location, and the light source distribution; nevertheless, real models do not follow those real assumptions and therefore modifications must be made to the existing algorithms in orger to get useful results. In this paper, we implemented an algorithm based on a linear filtering approach to obtain surface estimation from a single image. We tested the algorithm with images generated synthetically and also with images from a real object. Further, perspective projection and a combination of a Lambertian and specular reflectance is employed in our algorithm. We were able to obtain the shape of objects with different geometries, although the algorithm has problems when discontinuities are present.

10410-19, Session 5

Phase retrieval in the presence of multiplicative noise *(Invited Paper)*

Joe P. J. Chen, Richard A. Kirian, Arizona State Univ. (United States)

An additional step to traditional iterative phase retrieval algorithms is described that allows the reconstruction of an image from the product of its sufficiently sampled far-field diffraction intensity and a second signal. The iterative phasing algorithm with this added step attempts to recover both the image and the multiplicative signal at the same time. Simulations show that reasonable reconstructions of both the original image and the multiplicative signal can be attained in many cases.

10410-20, Session 5

Fast adaptive optical system for the high-laser power laser beam correction in the atmosphere

Alexis V. Kudryashov, Institute of Geosphere Dynamics (Russian Federation) and Institute of Atmospheric Optics (Russian Federation); Ann Lylova, Vadim Samarkin, Julia V. Sheldakova, Alexey Rukosuev, Institute of Geosphere Dynamics (Russian Federation)

No Abstract Available

10410-21, Session 5

Laser beam focusing through the atmosphere aerosol

Alexis V. Kudryashov, Institute of Geosphere Dynamics (Russian Federation) and Institute of Atmospheric Optics (Russian Federation); Ilya Galaktionov, Julia V. Sheldakova, Vadim Samarkin, Alexander N. Nikitin, Institute of Geosphere Dynamics (Russian Federation)

No Abstract Available

10410-22, Session 5

Phase retrieval for crystalline specimens

Romain Arnal, Rick P. Millane, Univ. of Canterbury (New Zealand)

The phase retrieval problem for a single object is known to have a unique solution in two or more dimensions, and iterative projection algorithms are generally an effective reconstruction method. More difficult situations arise when diffraction data are collected from crystalline specimens, since the diffraction amplitudes are then undersampled. Three-dimensional crystalline specimens are necessary in x-ray diffraction imaging of biological molecules in order to obtain measurable diffraction, but the phase retrieval problem does not have a unique solution and some ancillary information is needed to solve the problem. However, with the recent availability of high intensity x-ray sources such as x-ray free-electron lasers, there is the possibility

of measuring diffraction data from 1D or 2D crystals. For these crystals, the effects of undersampling are reduced. The solvability, or uniqueness, of a phase problem can be characterised by an appropriately calculated "constraint ratio," that measures the independent data-to-parameter ratio. The constraint ratio provides information in the 1D and 2D crystal cases, but because of the structured sampling of the diffraction amplitude that results, there are additional considerations that are needed to in order characterise uniqueness. We show that uniqueness in these cases depends on particular properties of the support of the object in the crystal. In cases where a unique solution is expected, iterative projection algorithms can be appropriately adapted to invert the data. Uniqueness results will be illustrated by examples and reconstruction algorithms by simulation. Specific applications in coherent diffraction imaging will be described.

10410-24, Session 5

Advances in shadow imaging of geosynchronous satellites

Dennis M. Douglas, Bobby R. Hunt, David Sheppard, Integrity Applications, Inc. (United States)

Shadow imaging is a technique to obtain highly resolved silhouettes of resident space objects (RSOs) which would otherwise be unattainable using conventional terrestrial based imaging approaches. This is done by post processing the measured irradiance pattern (shadow) cast onto the Earth as the RSO occults a star. Here, we present ongoing research efforts pertaining to shadow imaging of geosynchronous (GEO) satellites. Resolution limits are shown to be independent of wavelength for monochromatic collections. Resolution limits are then quantified based on the spectral bin width of the collected diffraction pattern for polychromatic observations. Sub meter resolution is shown to be readily achievable for anticipated observing scenarios using source stars brighter than mv = 11. Image reconstruction is performed using a Fresnel integral based phase retrieval algorithm and use of Babinet's principle. We also present refinements to our shadow prediction model that further quantify the number of shadow events and greatly reduce the shadow ground track uncertainties. Finally, we outline our current efforts to physically collect a GEO shadow by implementing our shadow prediction model and simulation based radiometric limits.

10410-25, Session 6

Opportunities for sub-wavelength imaging based on motion in structured illumination *(Invited Paper)*

Kevin J. Webb, Qiaoen Luo, Vivek RAghuram, Yulu Chen, Purdue Univ. (United States)

We describe the concept of controlled or natural motion of an object in a spatially varying field magnitude as the basis for coherent optical sensing and imaging. Examples presented are for microscopy with interfering laser beams and speckle formed by scatter from a random medium. Biomedical and environmental applications are presented and resolution limits discussed.

A method to extract far-subwavelength geometry and dielectric constant information based on precisely controlled object motion with structured light illumination and far-field measurement data is illustrated with simulated measurements. The principle is that far-field measurements with controlled motion in a spatially varying incident field add information about nanometer-scale dimensions and material properties. We show example results with sensitivity to the properties of a film on a substrate.

We present and demonstrate a coherent imaging and sensing method that can provide high resolution images of objects moving inside an essentially arbitrarily thick and heavily scattering medium, limited only by the medium stability or characterization and the detector noise. The speckle intensity correlations have short-range, wavelength-scale features, and longer range decorrelations. These provide a simple basis for identification of moving objects, and upon phase reconstruction, an object function that serves as an image can be obtained.

10410-26, Session 6

Long-range speckle imaging theory, simulation, and brassboard results

Jim F. Riker, the Optical Sciences Co. (United States); Glenn A. Tyler, Jeffrey L. Vaughn, the Optical Sciences Co. (United States)

In the SPIE 2016 Unconventional Imaging session, the authors laid out a breakthrough new theory for active array imaging that exploits the speckle return to generate a high-resolution picture of the target. Since then, we have pursued that theory even in long-range (>1000-km) engagement scenarios and shown how we can obtain that high-resolution image of the target using only a few illuminators, or by using many illuminators. There is a trade of illuminators versus receivers, but many combinations provide the same synthetic aperture resolution. We will discuss that trade, along with the corresponding radiometric and speckle-imaging Signal-to-Noise Ratios (SNR) for geometries that can fit on relatively small aircraft, such as an Unmanned Aerial Vehicle (UAV). Furthermore, we have simulated the performance of the technique, and we have created a laboratory version of the approach that is able to obtain high-resolution speckle imagery. The principal results presented in this paper are the Signal to Noise Ratios (SNR) for both the radiometric and the speckle imaging portions of the problem, and the simulated and experimental results obtained for representative arrays.

10410-27, Session 6

An underwater turbulence degraded image restoration algorithm

Md Hasan Furhad, Murat Tahtali, Andrew J. Lambert, UNSW Canberra (Australia)

Underwater turbulence occurs due to random fluctuations of temperature and salinity in the water. These fluctuations are responsible for the alteration in water density, refractive index variation and attenuation in light direction. These impose random geometric distortions, spatio-temporal varying blur, limited range visibility and limited contrast on the acquired images (Thomas Stephan et al, Proc SPIE, 8791, 2013). We propose here an image restoration algorithm to restore underwater-degraded images. There are some restoration techniques developed to address this problem, such as image registration based, lucky region based and centroid-based image restoration algorithms. Although these methods demonstrate better results in terms of removing turbulence, they require computationally intensive image registration, higher CPU load and memory allocations. We propose a simple patch based dictionary-learning algorithm to restore the image by alleviating the computational intensive image registration step, which requires lower computational load compared to conventional restoration algorithms and shows better results.

Dictionary learning is a machine learning technique, which builds a dictionary of non-zero atoms derived from the sparse representation of an image or signal. The image is divided into several patches and we detect the sharp patches from them. Next, we perform dictionary learning across these sharp patches to update the image frames, and finally we average the frames with updated dictionaries to estimate the restored image. These averages are performed to eliminate any existing artefacts in the individual frames. Finally, we employ an image deconvolution algorithm on the estimated restored image to remove noise that still exists.

10410-28, Session 6

Object detection from images obtained through underwater turbulence medium

Md Hasan Furhad, Murat Tahtali, Andrew J. Lambert, UNSW Canberra (Australia)

Imaging through underwater experiences severe distortions due to

random fluctuations of temperature and salinity in water, which produces underwater turbulence through diffraction limited blur, and lights reflecting from objects of an image perturbs and attenuates contrast, making the recognition of objects of interest difficult (Kalyan K. Halder et al, Proc SPIE, 9622, 2015). Thus, in underwater imaging, the information available for detecting objects of interest is a challenging task because they have inherent confusion among the background, foreground and other image properties. In this study, we propose a saliency based approach to detect the objects acquired through underwater turbid medium. Saliency based approach is one of the most popular and efficient techniques which makes an object or pixel stand out and capture our attention. This approach has drawn attention among a wide range of computer vision applications, such as image retrieval, artificial intelligence, neuro-imaging and object detection.

In this study, we propose a framework to detect the objects through a fused saliency technique. First, we pre-process the image through deblurring in order to remove the underwater turbulence induced blur. Next, we employ a visual saliency technique on this image for object detection. In this step, first we estimate the region of the object of interest automatically through an optimized support vector machine (SVM) saliency map. After the regions are estimated, we propose a graph based model to extract the object regions for more precise object detection. Finally, we fuse these two maps into one and detect the objects from the fused map.

10410-29, Session 7

GPU-enhanced computational platform for performance evaluation of atmospheric optical systems

Svetlana L. Lachinova, Mathieu Aubailly, Morris Maynard, Optonicus (United States); Mikhail A. Vorontsov, Optonicus (United States) and Univ. of Dayton (United States); Mark F. Spencer, Air Force Research Lab. (United States)

We present a user-friendly computational platform for numerical analysis and performance assessment of a wide range of optical systems for imaging and laser projection applications. The wave-optics-based software package, referred to as the Wave-Optics Joint Estimation Toolbox (WaveJET), exploits advantages of GPU/CUDA technologies and allows one to quickly and accurately simulate atmospheric turbulence effects on various systems using the combination of different computational techniques and algorithms for wavefront sensing and imaging. The WaveJET software also takes into account critical system engineering design constraints including system architecture, diffraction, turbulence propagation, adaptive optics control, and coherent/incoherent beam combining.

10410-30, Session 7

ANN-based model to compensate for the error phase in the 3D reconstruction of small objects

Carlos Andrés Madrigal González, Instituto Tecnológico Metropolitano (Colombia); Alejandro Restrepo Martínez, John W. Branch Bedoya, Univ. Nacional de Colombia Sede Medellín (Colombia)

To get accurate 3D reconstruction of small objects using structured light, it is necessary to modify the optics of commercial projection systems. However, this addition of lenses increases the aberrations, distortions, and nonlinearities in the projection. This generates errors in the phase unwrapping. In this paper we propose an ANN-based model to compensate for phase errors due to nonlinearities such as gamma effect, defocusing and illumination changes. The ANN is used to approximate the nonlinear distortion curve. This curve is obtained by projecting and capturing a range of gray levels at different levels of defocusing. This is achieved by varying the position of the calibration plane every 2mm and with 3 different lighting conditions. From the ideal phase, computed with a four-step phase-shifting algorithm and its phase distorted by the estimated model, a compensation map is determined. The proposed method is compared with the passive and active methods most used in the literature. The experimental results show that our proposal reduces the effects of nonlinearities, achieving accurate 3D reconstructions. This is important for the automatic visual inspection community when detecting surface defects on small objects since if phase errors due to nonlinearities are not compensated, the errors in 3D reconstruction are easily mixed and confused with the defects.

10410-31, Session 7

Simulation of the effects that lead to the degradation of the images obtained using a ground based telescope

Youness Bentahar, Univ. Hassan II Mohammedia - Casablanca (Morocco)

The atmospheric turbulence is the biggest obstacle to terrestrial astronomical observations. The objective of this study is to estimate these parameters the case of observation of the sun by the statistical analysis of arrival angle fluctuation and this can be directly obtained from the observations of the solar edge.

10410-32, Session 7

Unconventional imaging with contained granular media

Marco B. Quadrelli, Jet Propulsion Lab., California Institute of Technology (United States); Erkin Sidick, Jet Propulsion Lab., California Institute of Technology (United States)

Typically, the cost of a space-borne imaging system is driven by the size and mass of the primary aperture. The solution that we propose uses a method to construct an imaging system in space in which the nonlinear optical properties of a cloud of micron-sized particles, shaped into a specific surface by electromagnetic means, and allows one to form a very large and lightweight aperture of an optical system, hence reducing overall mass and cost. Recent work at JPL has investigated the feasibility of a granular imaging system, concluding that such a system could be built and controlled in orbit. We conducted experiments and simulation of the optical response of a granular lens. In all cases, the optical response, measured by the Modulation Transfer Function (MTF), of hexagonal reflectors was closely comparable to that of a conventional spherical mirror. We conducted some further analyses by evaluating the sensitivity to fill factor and grain shape, and found a marked sensitivity to fill factor but no sensitivity to grain shape. We have also found that at fill factors as low as 30%, the reflection from a granular lens is still excellent. Furthermore, we replaced the monolithic primary mirror in an existing integrated model of an optical system (WFIRST Coronagraph) with a granular lens, and found that excellent contrast levels are provided by the granular lens that can be useful for exoplanet detection. We will present our testbed and simulation results in this paper.

10410-33, Session 7

Modeling coherence propagation in a homogenizing light pipe for speckle mitigation

Robert Raynor, Mark F. Spencer, Trevor Moore, Air Force Research Lab. (United States)

Speckle elimination via coherence reduction is currently being investigated as a means of improving the quality of images obtained with laser illumination. Homogenizing light pipes provide one avenue of altering the spatial coherence properties of a laser source for this purpose. This paper models the propagation of a partially coherent source in a light pipe via propagation of the cross-spectral density. Though direct numerical

propagation of the cross-spectral density is computationally burdensome, immense simplifications are possible for the class of partially coherent sources known as Schell-model sources. The cross-spectral density of a Schell-model source may be represented as the convolution of a coherent "mode" with a weighting function. Mathematically, propagation of this mode can precede evaluation of the convolution. Discretization and numerical evaluation of the convolution casts this approach as a "finite-element source" approach, wherein individual identical modes are propagated and superposed to obtain the propagated cross-spectral density. The end result is that the 4-dimensional integral needed to propagate the cross-spectral density is replaced by the 2-dimensional integral needed to propagate the individual mode. In this paper, this method of propagation is baselined to analytic results for free space propagation, and then used to model the evolution of coherence within a homogenizing light pipe. The conditions necessary to achieve uniform illumination via projection of the waveguide exit field are discerned and discussed, and the speckle mitigation capabilities of the setup are modeled and assessed.

10410-34, Session 7

Incoherent image simulation through atmospheric turbulence with ray optics

Xifeng Xiao, Erandi Wijerathna, Thomas A. Underwood, David G. Voelz, New Mexico State Univ. (United States); Andreas Muschinski, NorthWest Research Associates (United States)

The simulation of optical imaging through distributed atmospheric turbulence has played an important role in studying system performance for application such as inspection, mapping, target identification, and tracking. Our interest is the simulation of a series of short-exposure image realizations which allows the study of the dynamic nature of turbulence and its effect on imaging. Several methods based on numerical wave optics propagation and split-step turbulence screen modeling have been used to generate short-exposure images through distributed turbulence. However, the coherent nature of these methods generally requires a significant number of propagation repetitions and averaging in the image plane to approach an incoherent result. This process is time and resource demanding. Here, we consider replacing the wave optics propagation with a geometrical optics approach where rays are traced through the split-step turbulence screens to create incoherent imagery. Ray tracing is computationally efficient and propagation repetition and averaging are not required so a considerable speedup in calculation time is possible compared to wave optics calculations. A few examples of this concept exist in the literature such as a brightness function approach that has been used successfully to create incoherent image video simulations. Ray optics, however, does not account for diffractive effects, which can limit its applicability. We review the limitations of geometric optics for turbulence scenarios and identify the parameter regimes where ray tracing may be valid for incoherent image simulation. We present a ray tracing approach and demonstrate the computation time speedup compared to wave optics. We also discuss concepts that extend the basic ray tracing method, such as the brightness function approach, and consider algorithmic options for approximating the effects of diffraction in the resulting imagery.

10410-35, Session 7

Crosswind measurements based on the turbulent distortions analysis in incoherent images

Vadim V. Dudorov, Anna S. Eremina, V.E. Zuev Institute of Atmospheric Optics (Russian Federation)

The possibilities of passive crosswind profiling on a remote-object observing path based on video imaging are studied. The method suggested is based on the analysis of image distortion evolution caused by the wind drift of turbulent air inhomogeneities. The main advantage of the method based on the analysis of two adjacent frames in incoherent video images is a high speed due to no need to accumulate any statistics measured. We investigate numerically the distorting effect of atmospheric turbulent layers located along the observing path as well as a possibility of determining the drift speed of these layers based on the analysis of turbulent distortions. We suggest an algorithm for image distortion filtering, which allows one to distinguish distortions caused by turbulent inhomogeneities located at a different distance from the observer. A possibility of determining the wind speed for several (at least three) turbulent layers located at a different distance between the object observed and the receiving optical system is shown numerically. The test results of the method based on processing real object (a fragment of deciduous forest) video at an atmospheric path 500 m long are presented. Based on the comparison with contact measurements (using 10 acoustic anemometers along the path) of a wind speed, the method showed satisfactory accuracy in determining the wind speed for atmospheric layers close to the observer, as well as the average wind speed along the entire observation path.